

THE PROCEEDINGS OF THE PHYSICAL SOCIETY

Section A

VOL. 67, PART 1

1 January 1954

No. 409A

EDITORIAL

The total number of communications accepted and published in parts A and B of the *Proceedings* amounted to 370, this number being made up of 243 Papers, 35 Research Notes and 76 Letters to the Editor. 15% of the manuscripts submitted for publication were rejected on the advice of referees. To give the average time required for publication of material can be misleading, since as much as a few months' delay may occur in cases where an author is carrying out an extensive revision which he feels the referees' reports require. A better indication of the speed of publication is the three to four months which is required by a well prepared manuscript which meets with no serious criticisms of content from referees.

As previously, Papers have normally been sent to two referees, and Research Notes and Letters to one, additional referees being consulted only in cases where a dispute or doubt arises.

The policy of the Papers Committee with regard to Letters to the Editor is that announcements of a preliminary nature prior to full publication will not normally be accepted for the *Proceedings*, and referees are asked not to recommend publication of such communications unless a strong case exists.

A recent Notice to Members, which was circulated to Fellows of the Society, was worded in a manner which could easily be misinterpreted. To avoid any doubt which may exist, the Papers Committee desires it to be repeated that both Fellows and Non-Fellows of the Society may submit their own manuscripts for publication. There is no obligation for any author to have a manuscript communicated by a Fellow of the Society. When an article is communicated by a Fellow of the Society, it is of assistance to the Papers Committee and referees to know whether the communicator of the paper personally knows the work described and whether he also recommends it for publication.

H. H. HOPKINS,
Honorary Papers Secretary.

A Calculation of the Eigenvalues of Electronic States in Metallic Lithium by the Cellular Method

By B. SCHIFF

Department of Mathematics, Imperial College, London

Communicated by H. Jones; MS. received 25th August 1953

Abstract. A potential function is computed for the lithium ion core, and is used to calculate the cohesive energy of metallic lithium, which is found to be in good agreement with experiment. Eigenvalues for conduction electrons in metallic lithium are calculated for points of high symmetry in the Brillouin zone, using the improved cellular method of Howarth and Jones, in which boundary conditions are applied at a large number of points on the surface of the atomic polyhedron; the merits of this type of boundary condition are discussed. The energy gap at the centre of a face of the zone is found to be 2.57 eV, the lowest state at that point having a p-like symmetry, and the interpretation of the soft x-ray emission spectrum of lithium is discussed in the light of this result.

§ 1. INTRODUCTION

THE energy of the lowest state of a conduction electron in metallic lithium has been calculated by Seitz (1935), and Millman (1935) has obtained the energies of electrons in excited states, using the method of Slater (1934). However, as Shockley (1937) has shown, Slater's method frequently leads to errors of 20% in the empty lattice test. In this paper the more accurate method of von der Lage and Bethe (1947), as developed by Howarth and Jones (1952), is used to calculate the energies of electrons at points of high symmetry in the Brillouin zone of metallic lithium. The energy gap at the centre of a face of the zone is found to be 2.57 eV; the energy of the N_s state* lying above that of the N_p^1 state. The interpretation of the soft x-ray emission spectrum of lithium in the light of this last result is discussed in § 4.

The work involved in a calculation of this kind is considerable, and only the use of the symmetry properties of the wave functions, as mentioned above, has kept the labour necessary within reasonable bounds. In the present case thirty-five integrations of the radial Schrödinger equation are required. Considerable further computation is involved in the determination of the eigenvalues, as described in § 3.

§ 2. POTENTIAL FUNCTION FOR THE LITHIUM ION CORE

The potential function for the lithium ion core given by Seitz is tabulated only at fairly wide intervals of the radius r , which makes interpolation rather

* Throughout this paper the notation of Howarth and Jones (1952) will be used to indicate electronic states. The first Brillouin zone for a body-centred cubic lattice is a regular dodecahedron, and the points Γ , N , H lie at the zone centre, the centre of a zone face, and a corner point at which four faces of the zone meet, respectively. The subscript letters denote the symmetry of the function, e.g. Γ_s is a state at the centre of the zone with no nodal planes through the atomic nucleus. Superscript numbers, e.g. H_d^1 , are used to distinguish between states at the same point of the zone with similar symmetries.

difficult and, as Silverman and Kohn (1950) have pointed out, the published potential is in error; the correct potential has not yet been published. In view of these facts it was decided to calculate a smooth potential function of analytic form, which we denote by $V(r)$, using the method of Prokofiew over as large a portion of the range of r as possible. As Seitz has pointed out, it is not possible to determine a consecutive series of parabolaes for $r^2V(r)$ over the whole range of r in the case of lithium. However, the two parabolaes (2) and (3) given below, calculated from the 2p and 3d terms respectively, are found to cover the range $1.2 \leq r \leq 7.22$. For values of r greater than 7.22 the coulombic potential $V = -2/r$ is a sufficiently good approximation. Since $V(r)$ tends to $-6/r$ Ryd as r tends to zero, and to $-2/r$ Ryd as r tends to infinity the form $rV = -2 - 4 \exp[-\{ar + br^2 + cr^3\}]$ is assumed for values of r less than 1.2. The constant a is chosen to have the value 3 in order that the function may approximate to the Hartree-Fock potential given by Fock and Petrashen (1935) near the origin. The requirement that the function should fit the Prokofiew parabola (2) smoothly at $r = 1.2$ gives $b = 0.1738$ and $c = -0.4475$.

Thus the potential function over the whole range of r is as follows:

$$r^2V = -2r - 4r \exp\{-3r - 0.1738r^2 + 0.4475r^3\}, \quad r < 1.2 \quad \dots\dots(1)$$

$$r^2V = -0.02446r^2 - 1.7972r - 0.4296, \quad 1.2 < r < 4.02 \quad \dots\dots(2)$$

$$r^2V = -0.00096r^2 - 1.9861r - 0.0500, \quad 4.02 < r < 7.22 \quad \dots\dots(3)$$

$$r^2V = -2r, \quad 7.22 < r \quad \dots\dots(4)$$

where $V(r)$ is in Rydberg units.

Hartree's method (1928) is employed to calculate the energy of the 2s electron in the free atom, i.e. the ionization potential, which is found to be -0.3661 Ryd, compared with the experimental value -0.3965 Ryd, an error of 0.0305 Ryd. The above potential function is chosen in preference to the Hartree-Fock function, since the latter leads to a considerably greater error in the value of the ionization potential.

§ 3. DETERMINATION OF THE EIGENVALUES

The energy of the Γ_s state is found by means of the Wigner-Seitz method (1933) to be -0.615 Ryd. The method used to determine the eigenvalues of the states N_s , N_p^1 , H_s , H_p and H_d^1 is described by Howarth and Jones, who give the expansions for the corresponding wave functions. For example, the wave function for the N_s state is

$$\psi(N_s) = R_0 + AR_2P_2(\cos \theta) + BR_4P_4(\cos \theta) + CR_6P_6(\cos \theta), \quad \dots\dots(5)$$

which contains three arbitrary constants. The radial wave functions are obtained by integration for several values of the energy ϵ , and three boundary conditions are used to calculate the values of these constants for various values of ϵ . From the large number of particular boundary conditions applicable to the state N_s eleven examples are given by Howarth and Jones as being most suitable. If three of them are used to calculate the constants in (5), a determination of the eigenvalue may be made from each of the remaining eight conditions, the eight determinations forming a 'set'. Other sets are obtained by calculating the constants from a different choice of three boundary conditions.

The consistency of the various determinations of the eigenvalue of a given state is affected by the expansion used for the wave function and by the particular

group of point boundary conditions employed. Groups of boundary conditions not fully independent of one another will yield incorrect eigenvalues. Apart from these cases, however, experience shows that when sufficient terms are taken in the expansion, very consistent results are obtained for all groups of conditions. On the other hand if the expansion is terminated at too low a value of l , no group of boundary conditions will give a good eigenvalue. This is evidently because there are no values of the arbitrary constants A , B , C , etc. which will make the expansion an adequate representation of the wave function if the essential high harmonics are omitted. This shows that none of the elaborate average boundary conditions which have been suggested by various authors can give good wave functions if the expansion is too limited, and there appears to be no real reason why they should give good eigenvalues in this case. On the other hand, when sufficient terms are taken in the expansion, the very easily applied point boundary conditions appear to give excellent results, as demonstrated below.

The most consistent results are obtained for the H_d^1 state, five separate determinations giving the value $\epsilon = +0.202$ Ryd, which is taken as the eigenvalue. Eight determinations (taken from four sets) for the H_p state yield the values $\epsilon = -0.119$, -0.120 , or -0.121 , giving a mean of -0.120 Ryd. The eigenvalue

Table 1

Conditions used	Eigenvalue (Ryd)
(i), (vi), (viii), (ix), (vii)	-0.122
(i), (vi), (viii), (ix), (x)	-0.122
(i), (vi), (viii), (ix), (xi)	-0.112
(viii), (ix), (x), (xi), (ii)	-0.109
(viii), (ix), (x), (xi), (i)	-0.114
(viii), (ix), (x), (xi), (iv)	-0.107
(viii), (ix), (x), (xi), (vi)	-0.111
(i), (vi), (x), (xi), (ii)	-0.122
(i), (vi), (x), (xi), (viii)	-0.109

of the H_s state is found to lie well outside the range of energy covered by the integrations, which are carried out at $\epsilon = -0.3$, -0.15 , 0 , and $+0.2$ Ryd. The eigenvalue for this state probably lies between $\epsilon = +0.45$ Ryd and $\epsilon = +0.65$ Ryd, and is not of sufficient interest to justify the considerable extra number of integrations which would be needed to determine it accurately.

The symmetry at the point N in the Brillouin zone is lower than that at the point H, and it is therefore to be expected that the accuracy of the results for the states at the point N will be less than for those at the point H. Nevertheless, the results for the N_p^1 state are almost as consistent as those obtained by Howarth and Jones for the corresponding state in sodium. Six determinations lie in the range -0.302 to -0.307 , which gives a mean of -0.304 Ryd. The results for the N_s state, using the expansion (5) are less satisfactory, and the determinations can be divided into two distinct groups lying near to -0.10 and -0.13 respectively. The expansion (5) is not the full one for $l \leq 6$, as terms $P_l^m(\cos \theta) \cos m\phi$, with l and m both even, can also occur. The inclusion of these terms, giving nine arbitrary constants in all, leads to no significant improvement in the results. If, however, the next term $DR_8P_8(\cos \theta)$ in the expansion is included, the effect is to bring the two groups together, as shown in table 1, in which the figures in parentheses refer to the boundary conditions

given by Howarth and Jones. The determinations lie in the range -0.107 to -0.122 , which gives a mean of -0.114 Ryd.

The results for the N_s state would seem to indicate that for the body-centred cubic lithium structure the consistency of the determinations is improved, as would be expected, by the addition of terms with higher values of l , but that the inclusion of terms dependent on ϕ does not result in any significant improvement.

The final results are summarized in table 2, which includes the energies of free electrons at the points N and H measured relative to the ground state energy, -0.615 Ryd.

Table 2

State	Eigenvalue (Ryd)	State	Eigenvalue (Ryd)
Γ_s	-0.615	H_d^1	$+0.202$
N_p^1	-0.304	H_s	$\sim +0.55$
N_s	-0.114	Free electrons at N	-0.166
H_p	-0.120	Free electrons at H	$+0.283$

The energy gap at the centre of the zone face is thus 0.190 Ryd (2.57 ev), and the largest deviations from the mean for the N_s and N_p^1 states amongst the consistent determinations of the eigenvalues are 0.008 Ryd and 0.003 Ryd respectively, so that the total error is almost certainly well below 5% of the size of the energy gap.

§ 4. DISCUSSION OF RESULTS

In view of the soft x-ray emission spectrum of lithium, the most interesting feature of the results given in § 3 is the order of the energies of the N_s and N_p^1 states. The emission spectra for sodium and lithium have been measured by O'Bryan and Skinner (1934) and are illustrated in figure 1, which is taken from

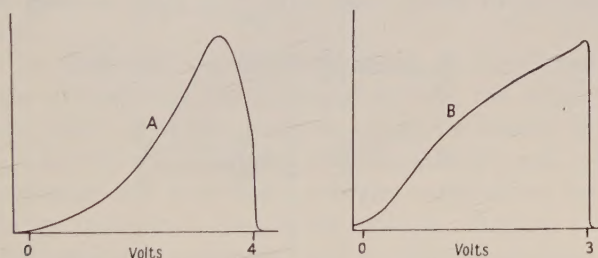


Figure 1 (after Skinner 1938). Curves showing the relative densities of soft x-ray emission for transitions of conduction electrons to the K shell of lithium (A) and to the L shell of sodium (B).

a review article by Skinner (1938). The curves A and B arise from transitions of electrons in the conduction band to the $1s$ state in lithium, and to the $2p$ state in sodium, respectively. It will be noticed that the curve for lithium begins to drop before the cut-off at the top of the Fermi distribution, whilst that for sodium rises steadily until the cut-off is reached. If n_E is the number of electrons whose energy lies in the range E to $E + dE$, and f_E is the transition probability per unit time, the number of transitions is given by

$$I_E = n_E f_E \quad \begin{array}{l} E < E_{\max} \\ E > E_{\max} \end{array}$$

$$= 0$$

where E_{\max} is the energy of an electron at the top of the Fermi distribution. Jones, Mott and Skinner (1934) consider the case of a simple cubic lattice, and show that the wave function for points along the line joining the origin in k -space to the centre of the zone face may be expressed in the form $\psi_k = a_s \psi_s + a_p \psi_p$, where ψ_s and ψ_p are the zero order s and p wave functions for electrons in the lattice. For these electrons I_E will be proportional to $n_E |a_s|^2$ if the final state is an s-state and to $n_E |a_p|^2$ if it is a p-state, as the value of l must change by unity. For the body-centred cubic lattice, the state at the centre of the zone is Γ_s , an s-state. Let us suppose that the state at the point N, at the boundary of the first zone, also has s symmetry. In this case, as we go along the line ΓN in the zone, a_p , the proportion of p-state present, will be zero at either end, having a maximum near the middle of the line, and may be decreasing at the top of the Fermi distribution, agreeing with the curves shown. It was on these grounds that Mott (1953) suggested that the lowest state at the point N should be an s-state for lithium, as well as for sodium. The results obtained would seem to indicate that no simple explanation of the difference between the soft x-ray emission spectra of lithium and sodium can be given in terms of these transition probabilities.

A comparison of the energy levels for sodium and for lithium is given in figure 2. The levels are measured in electron volts, relative to the Γ_s state of

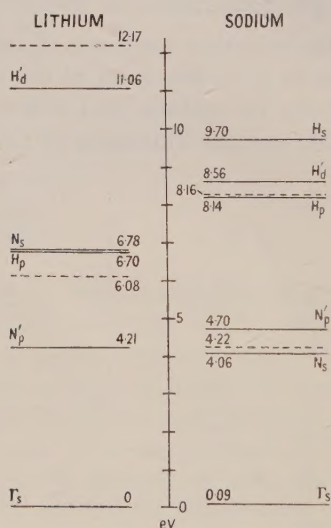


Figure 2. Comparison of the energy levels of corresponding states in lithium and sodium. The energies are in eV relative to the ground state Γ_s of lithium. The broken lines represent the energies of free electrons at N and H respectively.

lithium, which differs from the corresponding state of sodium by 0.09 eV. The main difference is the size of the energy gap at N and the large depression of the H_p state of lithium below its free electron value. In sodium the H_p energy lies well above the higher energy at N_s , whereas for lithium it lies just below the energy of the N_s state. This would have the effect of drawing the energy contours nearer towards the corner point H than in the case of sodium, suggesting that,

although the valence electrons in lithium are by no means free, the energy contours may not be far from spherical throughout most of the occupied part of the first zone.

§ 5. COHESIVE ENERGY

In view of the use of a different potential function from that given by Seitz, the cohesive energy has been calculated again, using the field given in § 2. The rapid variation of the effective mass with interatomic distance has been noted by Bardeen (1938). His method gives the value 0.5559 for α , the reciprocal of the effective mass, at the observed lattice constant of 3.4492 Å quoted by Silverman and Kohn (1950). The latter have also computed the cohesive energy, using the correct Seitz field, and a comparison of the results is given in table 3. In view of the uncertainty about the values of the coulomb, exchange,

Table 3

	Field chosen	Seitz field
α	0.5559	0.7270
E_0 (Ryd)	-0.6148	-0.6832
E_I (Ryd)	+0.3661	+0.3965
E_F (Ryd)	+0.1188	+0.1554
$E_0 + E_I + E_F$ (Ryd)	-0.1299	-0.1313

and correlation energies, the values of the sum $E_0 + E_I + E_F$ have been compared, where E_0 is the ground state energy, E_F is $2.21 \alpha/r_s^2$, the Fermi energy for electrons of effective mass $1/\alpha$, and E_I is the ionization potential. The energies are given in Rydberg units, and have been evaluated for a lattice constant of 3.4492 Å, which gives a value of 3.2156 Bohr units for r_s , the radius of the equivalent sphere.

It will thus be seen that the different values of the Fermi energy almost exactly cancel the difference in the values of $E_0 + E_I$, the values of $E_0 + E_I + E_F$ differing by only 0.0014 Ryd per electron, or approximately 0.5 kg cal mole⁻¹. If we add to $E_0 + E_I + E_F$ the quantities $1.2/r_s$, $-0.916/r_s$ and $-0.576/(r_s + 5.1)$, the coulomb, exchange and correlation energies respectively for free electrons, the cohesive energy amounts to 34.5 kg cal mole⁻¹. Herring (1951) has added corrections to the coulomb, exchange, and correlation energies to compensate for the use of the free electron values. These corrections depend on the effective mass, their sum amounting to approximately 1.5 kg cal mole⁻¹ for $\alpha = 0.7270$, so that for the value of α quoted above the corrections would add up to nearer 3 kg cal mole⁻¹, thus bringing the cohesive energy somewhere near the most recent experimental value of 37.9 kg cal mole⁻¹ quoted by the National Bureau of Standards (*Selected Values of Chemical Thermodynamic Properties*, March 1952).

ACKNOWLEDGMENTS

I would like to express my thanks to Professor H. Jones for his constant advice and encouragement throughout the work. I am also indebted to the Senate of the University of London for the award of a Postgraduate Studentship.

REFERENCES

- BARDEEN, J., 1938, *J. Chem. Phys.*, **6**, 367.
FOCK, V., and PETRASHEN, M. J., 1935, *Phys. Z. Sowjet*, **8**, 547.
HARTREE, D. R., 1928, *Proc. Camb. Phil. Soc.*, **24**, 89.
HERRING, C., 1951, *Phys. Rev.*, **82**, 282.
HOWARTH, D. J., and JONES, H., 1952, *Proc. Phys. Soc. A*, **65**, 355.
JONES, H., MOTT, N. F., and SKINNER, H. W. B., 1934, *Phys. Rev.*, **45**, 379.
VON DER LAGE, F. C., and BETHE, H. A., 1947, *Phys. Rev.*, **71**, 612.
MILLMAN, J., 1935, *Phys. Rev.*, **47**, 286.
MOTT, N. F., 1953, *Phil. Mag.*, **44**, 187.
O'BRYAN, H. M., and SKINNER, H. W. B., 1934, *Phys. Rev.*, **45**, 370.
PROKOFIEW, W., 1929, *Z. Phys.* **58**, 255.
SEITZ, F., 1935, *Phys. Rev.*, **47**, 400.
SHOCKLEY, W., 1937, *Phys. Rev.*, **52**, 866.
SILVERMAN, R., and KOHN, W., 1950, *Phys. Rev.*, **80**, 912.
SKINNER, H. W. B., 1938, *Rep. Progr. Phys.*, **5**, 257 (London: Physical Society).
SLATER, J. C., 1934, *Phys. Rev.*, **45**, 794.
WIGNER, E., and SEITZ, F., 1933, *Phys. Rev.*, **43**, 804.

Momentum Distribution of Electrons in Solids: Results for some Metals using the Thomas-Fermi Method

By N. H. MARCH

Department of Physics, The University, Sheffield

MS. received 3rd September 1953

Abstract. Experimental results giving the shape of the Compton profile in x-ray scattering show that the momentum distribution of the electrons in metallic Li and Be differs markedly from that given by wave-mechanical calculations for isolated atoms.

As the starting point of a detailed theoretical investigation the present paper is concerned with examining the momentum distribution of electrons in metals on the basis of the Thomas-Fermi theory. Quantitative results are presented for Li, Be, Na, K and Rb, and a considerable broadening of the Compton line due to the interaction of atoms in a lattice is unmistakably shown. Agreement with experiment is, however, poor for Li, and it is concluded that the momentum distribution of the valence electrons in metallic Li differs considerably from a free electron distribution. For Be there is surprisingly good agreement with experiment, but unfortunately no experimental results exist as yet for the other metals.

The effect of introducing exchange is examined in detail for Na and some additional broadening of the Compton line is found. Finally the concept of free electrons in the Thomas-Fermi theory is discussed.

§ 1. INTRODUCTION

MUCH attention has been given in recent years to the problem of calculating wave-mechanically the momentum distribution of electrons in isolated atoms and molecules such as exist in the gaseous phase. A useful summary of some of this work, due largely to Coulson and Duncanson, has been given in a book by Sneddon (1951), where a number of references can also be found. The importance of the momentum distribution lies in the fact that it determines the shape of the Compton line in x-ray scattering and also the energy distribution of inelastically scattered electrons.

The most accurate calculations for atoms have been made using the analytical wave functions of Morse, Young and Haurwitz (1935) for the elements H to Ne, and the wave functions of Slater (1930) for those from Na to K. Whilst direct comparison with experiment is only possible for He and Ne, in which cases agreement is satisfactory, the accurate values for the other atoms are valuable in the sense that they provide a means of estimating the effect of the binding of atoms in a molecule or crystal.

For molecules the situation with regard to quantitative results is less satisfactory than for atoms, as one would expect, since molecular wave functions are in general known with less precision than those for atoms, and even in cases

where accurate space wave functions are known the difficulties involved in the transformation to momentum space are often formidable. With regard to the general effect of molecular binding on the momentum distribution it will be useful to bear in mind in what follows that in forming a diatomic molecule, for example, the half width of the Compton profile is increased by about 15 to 25%.

Although numerous theoretical results exist for isolated atoms and molecules, very little work has been done on the momentum distribution of electrons in solids. In fact, when the present investigation was begun the writer was not aware of any previous attempt to make quantitative calculations for a solid. Since then, however, Duncanson and Coulson (1952) have published a paper in which they have calculated the momentum distribution in graphite. Experimental results in this case show a broadening of the Compton line by about 35%, whilst the calculations of Duncanson and Coulson, using the tight-binding approximation, lead to a predicted increase of 22%, though the authors show that the introduction of a plausible scale factor in the atomic wave functions can lead to much better agreement.

The broadening of the Compton line noted above for graphite is similar to, though somewhat larger than, that occurring in isolated molecules. However, an examination of the experimental results for metallic Li (Kappeler 1936) and Be (Dumond 1933) indicates that for these solids the broadening is very much greater, for Li about 350% and for Be about 160%. It was the observation of this striking broadening which prompted the present investigation.

In this paper, as the starting point of a detailed theoretical discussion, the momentum distribution of electrons in metals is examined on the basis of the Thomas-Fermi (TF) theory. A qualitative discussion of the results to be expected in this case has indeed already been given by Slater (1934). The purpose of this paper is to present detailed quantitative results for a number of metals and to compare with existing experimental data. The TF method has the considerable advantage over a completely wave-mechanical treatment that one does not have to handle separate space or momentum wave functions for each electron, but can simply deal with the total spatial electron density obtained from a proper TF treatment of the metallic problem, as discussed by Slater and Krutter (1935), and can transform this into momentum space to obtain directly the momentum distribution function required for calculation of the shape of the Compton line.

The results of the TF method for atoms have already been investigated in detail by Coulson and March (1950). In this case, although a useful overall description of the momentum distribution function resulted, and the variation of mean momentum with atomic number was in good agreement with wave-mechanical calculations, the results, on the whole, were rather disappointing, due to the fact that the Compton profile was of quite the wrong shape. This defect could however be traced back to the incorrect form of the momentum distribution function for small momenta. The reason for this wrong behaviour near the origin in momentum space resides in the fact that electrons with small momenta are found, in the main, at large distances from the nucleus, and in these regions the fundamental assumptions of the theory break down, as indicated by the fall-off of the electron density as r^{-6} instead of exponentially. However, the method can be used with more confidence in the metallic case, since here this defect is not present, the electron density in any atomic polyhedron (replaced

by a sphere in the Slater and Krutter treatment) joining smoothly on to that in the neighbouring polyhedra without ever becoming very small.

The TF method is, however, limited in its application and, in consequence of the basic assumptions, it will be most appropriate to describe the alkali metals (see, for example, Seitz 1940).^{*} We have restricted ourselves therefore to these metals, with the single exception that we have made calculations also for Be, since this is one of the two metals for which experimental results exist at the moment. It is not suggested that the application of the method is really very appropriate in this case, but it will be seen later that at any rate some understanding of the experimental results for Be is possible along these lines.

§ 2. MOMENTUM DISTRIBUTION USING THE UNMODIFIED TF METHOD

The method of setting up the equations giving the momentum distribution has been discussed in detail by Coulson and March (1950) and, therefore, it will be sufficient to quote the results here. If $I(p) dp$ is the probability of an electron having momentum of magnitude between p and $p + dp$, then we have the equations

$$\left. \begin{aligned} I(p) dp &= \frac{32\pi^2}{3h^3Z} R^3 p^2 dp && \text{for } p < p_0(R) \\ &= \frac{32\pi^2}{3h^3Z} r^3(p) p^2 dp && \text{for } p \geq p_0(R) \end{aligned} \right\} \dots\dots(1)$$

where $r(p)$ is defined for this purpose by

$$p(x) = \left(\frac{2me^2Z}{b} \right)^{1/2} \left(\frac{\phi(x)}{x} \right)^{1/2} \dots\dots(2)$$

$$\text{with} \quad r = bx = \left(\frac{3}{32\pi^2} \right)^{2/3} \frac{h^2}{2me^2Z^{1/3}} x. \dots\dots(3)$$

In these equations $p_0(r)$ represents the maximum momentum at a distance r from the nucleus, $R(=bx_0)$ is the radius of the spherical cell and $\phi(x)$ is the appropriate solution of the TF equation in its customary dimensionless form

$$d^2\phi/dx^2 = \phi^{3/2}/x^{1/2}. \dots\dots(4)$$

As Slater and Krutter first pointed out, the solution representing the metallic state in the TF theory is defined by the boundary conditions $\phi(0)=1$, $(d\phi/dx)_{x_0}=\phi(x_0)/x_0$. The first of these simply ensures that as we approach a nucleus of charge Ze the potential $V \rightarrow Ze/r$. The second is the condition characteristic of the metallic problem and can be obtained either from the requirement of electrical neutrality or from the condition that the potential V has the correct periodicity, that is $(dV/dr)_R=0$.

As the TF model does not predict a position of metallic binding, the obvious procedure is to choose the cell radius in accordance with the experimental lattice constant. Thus, as soon as $\phi(x)$ is known, the corresponding momentum distribution can be calculated in a straightforward manner.

Now a number of solutions of the TF equation of the form required here have been given recently by the writer in the course of a discussion of the TF method

^{*} Further evidence in support of this will be given in a forthcoming paper by the writer in which the cohesion of the alkali metals will be discussed by means of the TF method including exchange.

for molecules (March 1952). In table 1 of this paper the solutions with $\phi(x_0)=0.1806$, $x_0=5.229$, and $\phi(x_0)=0.2463$, $x_0=4.330$ correspond to lattice constants differing by only 1 and 2% from the observed values for Li and Be respectively. For our purposes this is quite adequate as calculations show that the momentum distribution and width of the Compton profile are not particularly sensitive to small changes in the lattice constant. For Na the existing solution nearest to the experimental lattice constant is that given by Feynman, Metropolis and Teller (1949) and defined by $\phi(x_0)=0.0599$, $x_0=9.565$ (for some comments on these solutions see March 1952). The lattice constant in this case differs from the experimental value by about 4%, which, as we shall see later, is still good enough for our purpose. The curves of $I(p)$ thus obtained for Li, Be and Na from eqns (1) and (2) are shown in figure 1. The general shape of these curves agrees with that given previously by Slater (1934), to whose paper the reader is referred for a very interesting qualitative discussion.

§ 3. MOMENTUM DISTRIBUTION USING THE THOMAS-FERMI-DIRAC MODEL

Before going on to discuss the calculation of the Compton profiles it is of some interest to consider the effect of exchange on the momentum distribution. The equations required to discuss the momentum distribution on the basis of the Thomas-Fermi-Dirac (TFD) model are essentially the same as for the unmodified TF method, except that eqn (2) must be replaced by

$$p(x) = \left(\frac{2me^2Z}{b} \right)^{1/2} \left[\alpha + \left(\frac{\phi}{x} \right)^{1/2} \right] \quad \dots\dots(5)$$

where

$$\alpha = 6^{1/3}/4(\pi Z)^{2/3} \quad \dots\dots(6)$$

and $\phi(x)$ is now the appropriate solution of the TFD equation

$$\frac{d^2\phi}{dx^2} = x \left[\alpha + \left(\frac{\phi}{x} \right)^{1/2} \right]^3. \quad \dots\dots(7)$$

Detailed calculations have been carried out only for Na, for which the writer has recently obtained a solution of the TFD equation corresponding to a lattice constant which differs from the experimental value by about 4%. The momentum distribution using this solution is shown in curve IV of figure 1. The results with and without exchange are not quite directly comparable since the lattice constants differ slightly. But it can be seen that the momentum distribution in the neighbourhood of the peak of the curve is quite appreciably altered. This is mainly due to the fact that inclusion of exchange has a marked effect on the electron density near the boundary of the atomic sphere. The general effect of exchange is to spread the momentum distribution curve out somewhat, which is reasonable when it is remembered that a contraction of the charge cloud results when exchange is introduced.

§ 4. COMPTON PROFILES

As we have already mentioned, it is the momentum distribution of the electrons in the scatterer which determines the form of the Compton modified line for x-rays. The calculations are most easily carried out by finding

$$J(q) = \frac{1}{2} \int_q^\infty \frac{I(p)}{p} dp \quad \dots\dots(8)$$

which can be regarded as giving the Compton profile in a convenient form in which all incident wavelengths and all scattering angles are included (see, for example, Duncanson and Coulson 1945). Using the momentum distributions shown in curves I, II and III of figure 1, the Compton profiles have been found and are displayed in curves I-III of figure 2. The total widths of the profiles at half maximum provide a convenient means of comparison with experiment,

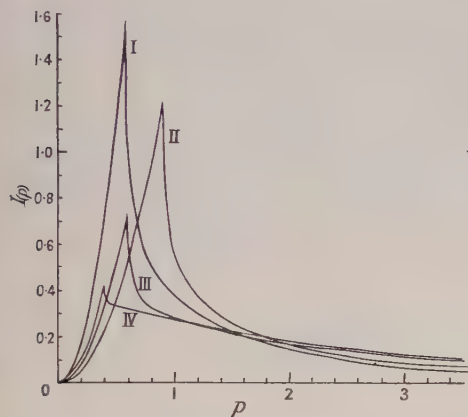


Figure 1. Momentum distribution function $I(p)$ (atomic units used). I, Li; II, Be; III, Na; IV, Na including exchange.

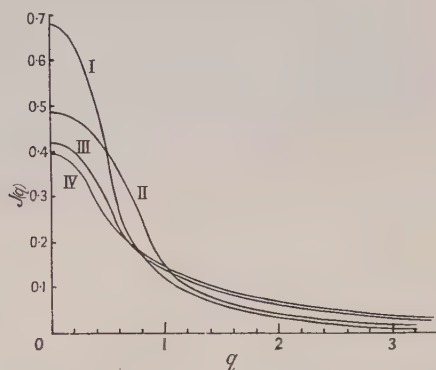


Figure 2. Compton profiles (atomic units used). I, Li; II, Be; III, Na; IV, Na including exchange.

and are recorded in the table. For Na, to ascertain the effect on the width of small changes in the lattice constant, three solutions have been used, and the width corresponding to the observed lattice constant has been found by interpolation to be 1.25 A.U. This value differs by 4% from the value recorded in the table, a difference which will be almost certainly quite unimportant in view of the more fundamental limitations of the TF model.

Half Widths of Compton Profiles (in atomic units)

	Li	Be	Na	K	Rb
TF	1.08	1.61	1.30	—	—
TFD	—	—	1.40	1.65	2.11
Isolated atom	0.57	0.77	0.80	1.06	—
Experiment	2.6	2.0	—	—	—

In the case when exchange is included, the Compton profile for Na is shown in curve IV of figure 2 and the half width is recorded in the table. Interpolating from the results without exchange to find the half width for the same lattice constant as in the case when exchange is considered it is found that the half width is increased by the inclusion of exchange by about 16%. We can infer, then, that the general effect of exchange will be to broaden the Compton profile somewhat, which is as we would expect from the fact that the momentum distribution becomes more diffuse. It can be seen from curves III and IV of figure 2 that the form of the Compton profile is not markedly changed even though, as we have seen, the effect of exchange on the momentum distribution is quite large near the peak of the curve.

It is worth while to consider here the results to be expected on the basis of the TF theory (including exchange) for K and Rb. The half widths can be obtained by interpolation from the result obtained here for Na, and the half widths obtained for A and Kr by Coulson and March (1950) using Jensen's interpretation for the isolated atom in the TFD model (Jensen 1935).^{*} The results thus obtained for the half widths are given in the table.

§ 5. COMPARISON OF COMPTON PROFILES WITH EXPERIMENT

We are now in a position to compare our results with experiment. Unfortunately the only results that exist at the moment are for Li and Be, and we have recorded the values of the half widths obtained experimentally for these metals in the table, together with the values calculated wave-mechanically for isolated atoms.

It will be seen immediately, by comparing the results given in the first two rows of the table with those in the third row, that a very definite broadening of the Compton line is predicted when atoms are bound in a lattice. The broadening decreases from about 100% for Li to 50% for K. A decrease is qualitatively reasonable when one remembers that the number of electrons in K which are appreciably disturbed by metallic binding is a much smaller fraction of the total number than in the case of Li. However, the width for Li, though twice as great as that indicated by wave-mechanical calculations for an isolated atom, is still only about two-fifths of the experimentally determined width. (An estimate of the effect of exchange for Li shows that agreement between theory and experiment is not significantly improved by its inclusion.) The agreement is much better for Be but, as we have already mentioned, it is unlikely that the TF model is a good one for this metal, and it seems that the degree of agreement in this case is at least partly fortuitous. The result for Li, we feel, is of more significance. It is true that the TF model will give a somewhat poor description of the ion-core of Li (this is true of course also for Be) and this will affect the results for the momentum distribution. But the experimental results show that the actual momentum distribution in metallic Li must be very considerably different from that calculated on the basis of the TF model, and the difference is so large that it seems to us very unlikely that it can be attributed solely to the shortcomings of the TF description of the ion-core. We believe therefore that our results indicate that the momentum distribution of the valence electrons in metallic Li is considerably different from that of free electrons since the TF method ought to be able to describe a momentum distribution resembling that due to free electrons with some accuracy. This conclusion is perhaps not too surprising, even for Li, in view of the astonishing complexity of the momentum eigenfunctions found in some cases by Slater (1952) in his recent discussion of the Mathieu problem. It would be very helpful to have experimental results for the other alkalis considered here, and particularly so for Na, since the method used should be most appropriate in this case.

^{*} Further justification for using these solutions will be given in the forthcoming paper on the TFD method applied to the cohesion of the alkali metals. For the moment it will suffice to note that the solutions correspond to lattice constants not differing very much (about 12% for K and Rb) from the observed values.

§ 6. CONCEPT OF FREE ELECTRONS IN THE TF THEORY

It is worth while here, whilst on the subject of momentum distribution, to say a little about the concept of free electrons in the TF model. As Slater (1934) has pointed out, there is a sharp distinction between bound and free electrons in this theory. Those electrons which have sufficiently high energies to pass over the potential barrier between atoms are free electrons, in the sense that they may travel throughout the metal, whilst those with insufficient energy to surmount the barrier are bound electrons. As Slater also pointed out, it is incorrect to suppose however that all the electrons within the sphere of discontinuity in momentum space defined by $0 \leq p \leq p_0(R)$ are free electrons, even though in this region the momentum distribution is of exactly the form that holds for perfectly free electrons. Slater contended though that the number of electrons within this sphere is exactly equal to the number of free electrons. This did not appear to the writer to be at all obvious, and it seemed worth while to clear up the point and to see in a particular case what value one would obtain for the number of free electrons.

In the TF model all energies are allowed up to a maximum E_0 . Now the maximum value of the potential energy occurs at $r=R$, the value being $U(R)$, say. Thus the number of free electrons is the number having energies between $U(R)$ and E_0 . To find this number we require first of all the number of electrons, say $N(E)dE$, in the energy range E to $E+dE$. This can be obtained in a quite straightforward manner. $N(E)dE$ is obviously zero for $E > E_0$, and otherwise it is given by

$$N(E)dE = \frac{32\pi^2(2m^3)^{1/2}}{h^3} \int \{E - U(r)\}^{1/2} r^2 dr dE \quad \dots\dots(9)$$

where the limits of the r integration are such that $E - U(r)$ is always positive. We require to obtain the number of free electrons

$$\int_{U(R)}^{E_0} N(E) dE.$$

The limits of E here are such that $E - U$ is positive for all r from 0 to R , and hence these are the required limits of integration. Interchanging the order of integration, the integration over E can be performed but the remaining integral must be evaluated numerically. This has been done for Li using the solution defined in §2, and the number found is 1.3. On the other hand the number of electrons within the sphere of discontinuity in momentum space is 0.9, and we can only conclude that Slater's contention is not correct. Whilst we attach no great significance to the number of 'free' electrons obtained from a model such as this, in which classical mechanics is used, and we are thus enabled to distinguish sharply between free and bound electrons, it is somewhat gratifying that a sensible value around unity is obtained.

§ 7. CONCLUSIONS

The results we have presented here show clearly that a very considerable increase in the half width of the Compton profile results from metallic binding, in general agreement with experiment. The results for Li show, however, that the TF model is not adequate to explain quantitatively the very broad profile found experimentally. We conclude that, although some of the difference

between theory and experiment is doubtless due to the somewhat poor description of the ion-core that the TF method will give in this case, the discrepancy is so large that it seems very likely that the momentum distribution of the valence electrons in metallic Li is markedly different from that of perfectly free electrons. This, though somewhat surprising for Li, is not incompatible with some recent results of Slater concerning the Mathieu problem, which showed that in many cases the momentum eigenfunctions were unexpectedly complex. The better agreement obtained in the case of Be, whilst interesting, is not very convincing as the assumptions of the theory are not likely to be well satisfied in this case.

In view of the results for Li, the writer, in conjunction with Dr. B. Donovan, is at present undertaking completely wave-mechanical calculations of the momentum distribution for this metal. It is hoped to report the results of this work in a later paper.

ACKNOWLEDGMENT

The writer wishes to thank Professor C. A. Coulson for reading and commenting on a preliminary manuscript of this paper.

REFERENCES

- COULSON, C. A., and MARCH, N. H., 1950, *Proc. Phys. Soc. A*, **63**, 367.
 DUMOND, J. W. M., 1933, *Rev. Mod. Phys.*, **5**, 1.
 DUNCANSON, W. E., and COULSON, C. A., 1945, *Proc. Phys. Soc.*, **57**, 190; 1952, *Proc. Phys. Soc. A*, **65**, 825.
 FEYNMAN, R. P., METROPOLIS, N., and TELLER, E., 1949, *Phys. Rev.*, **75**, 1561.
 JENSEN, H., 1935, *Z. Phys.*, **93**, 232.
 KAPPELER, H., 1936, *Ann. Phys., Lpz.*, **27**, 129.
 MARCH, N. H., 1952, *Proc. Camb. Phil. Soc.*, **48**, 665.
 MORSE, P. M., YOUNG, L. A., and HAURWITZ, E. S., 1935, *Phys. Rev.*, **48**, 948.
 SEITZ, F., 1940, *Modern Theory of Solids* (New York: McGraw-Hill), p. 384.
 SLATER, J. C., 1930, *Phys. Rev.*, **36**, 57; 1934, *Rev. Mod. Phys.*, **6**, 209; 1952, *Phys. Rev.*, **87**, 807.
 SLATER, J. C., and KRUTTER, H. M., 1935, *Phys. Rev.*, **47**, 559.
 SNEDDON, I. N., 1951, *Fourier Transforms* (New York: McGraw-Hill), p. 362.

Riesz Potential and the Elimination of Divergences from Quantum Electrodynamics *

By L. S. KOTHARI

Cavendish Laboratory, Cambridge

MS. received 7th September 1953

Abstract. Using a modified definition of Riesz potential it is shown that the divergences arising in quantum electrodynamics from (i) the point nature of charge, (ii) the electron self energy and (iii) the vertex part of a Feynman graph, can be eliminated in a consistent way, without having to introduce any cut-off factors or auxiliary fields.

§1. INTRODUCTION

SOME time back Riesz (1949) developed an elegant method for solving the hyperbolic equation by the analytic continuation of an integral which is an analytic function of a parameter α (α real or complex). This method has been successfully used by various authors to avoid some of the divergences in electrodynamics and meson theory. Most of the work has been carried out using Fremberg's definition (1946) of the 'Riesz potential' which is a suitable generalization of the Maxwell potential (or the usual meson potential) in the α -plane. Ma (1947) has proved the equivalence of this definition and the λ -limiting process, whereas the equivalence of Riesz potential to the method of contour integration has been demonstrated by Auluck and Kothari (1949).

So far the application of Riesz potential to quantum electrodynamics has been considered mainly by Gustafson (1945, 1946) and Nilsson (1949). While Gustafson has introduced photons of both positive and negative energy for removing the electron self-energy divergence, Nilsson has obtained what might be regarded as a generalization of the λ -limiting process. He succeeds in removing the electron self-energy divergence without having to introduce any negative energy photons.

For the electromagnetic field a new definition of Riesz potential in momentum space was recently given by Auluck and Kothari (1951, to be referred to as AK). Kothari and Bhatnagar (1952) showed explicitly that the new definition represents a generalization of the Wentzel potential in the α -plane and hence makes it possible to obtain a direct connection between Riesz potential and the work of Feynman, Dyson, and others in quantum electrodynamics. It has also been pointed out (Kothari 1952) that by using Riesz potential as defined by AK, one is in fact working with a field that has a continuous mass spectrum. Only photons of rest mass zero remain when finally continuation to $\alpha=0$ is carried out.

Recently a number of methods have been devised for evaluating the divergent integrals occurring in quantum electrodynamics. Feynman (1949) and Pauli and Villars (1949) have given rules for evaluating such integrals by introducing fields with auxiliary masses. A more consistent account of auxiliary fields has been

* Submitted to the University of Cambridge in partial fulfilment of the requirements for the Ph.D. degree.

presented by Gupta (1953). In all such attempts, though the fields are introduced explicitly, it is ensured by suitable boundary conditions that the particles corresponding to such fields never show up in the free state. The purpose of the present paper is to show that the explicit introduction of the auxiliary fields is not necessary. By using the Riesz potential instead of the usual electromagnetic potential one can evaluate the divergent integrals in a consistent way. In this paper we consider the divergences arising from the point nature of charge, the self energy of an electron and the vertex part of a Feynman graph. (Though here we have considered a third order vertex graph only, the method developed is applicable to higher order irreducible vertex graphs as well.) To treat the photon self-energy divergence one has to generalize the solution of the Dirac equation in the α -plane. This problem will be studied in a subsequent paper.

In §2 we quantize the Riesz potential and then proceed to eliminate the longitudinal part of the electromagnetic potential from the Dirac equation. The divergence due to the point nature of charge that normally arises in this problem is removed. In §4 we consider the self energy of an electron (lowest order graph). The last section is devoted to the study of the divergence arising from the vertex part of a Feynman graph.

§2. QUANTIZATION OF RIESZ POTENTIAL

We define a metric tensor $g_{\mu\nu}$ as $g_{00}=1$, $g_{11}=g_{22}=g_{33}=-1$, $g_{\mu\nu}=0$ for $\mu \neq \nu$. \mathbf{c} and \hbar are taken to be unity. The scalar product of two four vectors A_μ , B_μ is denoted by $[AB]$:

$$[AB] = A_\mu B^\mu = A_0 B_0 - A_1 B_1 - A_2 B_2 - A_3 B_3 = A_0 B_0 - (AB)$$

where (AB) is the three-dimensional scalar product of the space parts of A_μ and B_μ . The positive length of the space part of A_μ is denoted by $|A|$. Greek suffixes take the values 0, 1, 2, 3 while the Latin suffixes run from 1 to 3.

We define the Riesz potential $A_\mu^\alpha(x)$ at any point x as

$$A_\mu^\alpha(x) = H(\alpha) l_0^\alpha \int_D \chi^{\alpha-2} \{ A_{k\mu} e^{i[kx]} + \bar{A}_{k\mu} e^{-i[kx]} \} d^4k, \quad \dots\dots(1)$$

where

$$H(\alpha) = 2/\Gamma(\tfrac{1}{2}\alpha)\Gamma(1-\tfrac{1}{2}\alpha) = 2/\pi \sin \tfrac{1}{2}\pi\alpha$$

$$\chi^2 = k_0^2 - |k|^2. \dagger$$

$A_{k\mu}$'s are so far arbitrary. The domain of integration D is the region bounded by $k_0 > 0$, $[kk]=0$, k_μ being the momentum four vector of the field. l_0 is a constant with dimensions of length, introduced to make the dimensions of $A_\mu^\alpha(x)$ independent of α . With a suitable choice of $A_{k\mu}$, it readily follows that (for details see AK),

$$\frac{\partial A_\mu^\alpha(x)}{\partial x_\mu} = -\sum_i e_i \mathcal{D}^\alpha(x-z_i), \quad \dots\dots(2)$$

where

$$\mathcal{D}^\alpha(x) = \frac{H(\alpha)}{2\pi^2} l_0^\alpha \int_D \chi^{\alpha-2} \sin[kx] d^4k, \quad \dots\dots(3)$$

and $z_i = z_i(\tau_i)$ is the world line of the i th electron with charge e_i and proper time τ_i . It has also been shown that in classical electrodynamics the potential $A_\mu^\alpha(x)$ satisfies the following Poisson bracket relation

$$[A_\mu^\alpha(x), A_\nu^\alpha(x')] = g_{\mu\nu} \mathcal{D}^\alpha(x-x') \quad \dots\dots(4)$$

† For convenience we have slightly changed our notation from that of AK.

Transition to quantum theory can be made in the usual way (Dirac 1947) by treating the potentials in (4) as operators satisfying commutation relation instead of the corresponding Poisson bracket relation. Therefore from henceforth we will consider (4) as a commutation relation between $A_{\mu}^{\alpha}(x)$ and $A_{\nu}^{\alpha}(x')$. Further, eqn (2) has to be replaced by a supplementary condition

$$R^{\alpha}(x)\psi\rangle_F=0, \quad \dots\dots(5)$$

$$\text{where} \quad R^{\alpha}(x)=\frac{\partial A_{\mu}^{\alpha}(x)}{\partial x_{\mu}}+\sum_i e_i \mathcal{D}^{\alpha}(x-z_i), \quad \dots\dots(6)$$

and $\psi\rangle_F$ represents the state of the system, ψ being a power series in the operators $A_{k1}, A_{k2}, A_{k3}, \bar{A}_{k0}$ whose coefficients are wave functions in the z -variables and the spin variables. \rangle_F is the standard ket of the whole radiation field, and satisfies the relations

$$A_{k0}\rangle_F=0, \quad \bar{A}_{kr}\rangle_F=0. \quad \dots\dots(7)$$

The above supplementary condition is consistent with the commutation relations (4) only for $\alpha=0$. In order that they may be consistent for all values of α , one has to modify the commutation relations, and this modification is introduced a little later.

To get the commutation relations between the various Fourier components $A_{k\mu}$, we substitute for the potential from (1) in the left-hand side of (4) and obtain on a little simplification

$$\begin{aligned} H(x)H(x')l_0^{\alpha+\alpha'}\int_D\int_{D'}\chi^{\alpha-2}\chi'^{\alpha'-2}\{\exp(i[kx]-i[k'x'])-\exp(-i[k'x]+i[kx'])\}\times \\ \times[A_{k\mu},\bar{A}_{k'\nu}]d^4k\,d^4k' \\ =\frac{H(\alpha)}{2\pi^2}l_0^{\alpha}g_{\mu\nu}\int\chi^{\alpha-2}\sin[kx]\,d^4k. \end{aligned} \quad \dots\dots(8)$$

Here we have made use of the following facts, (i) the commutation relation between $A_{k\mu}$ and $\bar{A}_{k'\nu}$ is symmetric in μ and ν (since the right-hand side of (8) is symmetric in μ and ν), and (ii) since Riesz potential has finally to reduce to the usual electromagnetic potential, we have taken

$$[A_{k\mu},A_{k'\nu}]=[\bar{A}_{k\mu},\bar{A}_{k'\nu}]=0. \quad \dots\dots(9a)$$

It can now be readily verified that the commutation relations

$$[A_{k\mu},\bar{A}_{k'\nu}]=-\frac{i}{4\pi^2}g_{\mu\nu}\frac{\delta_4(k-k')}{H(\alpha)l_0^{\alpha}\chi^{\alpha-2}}, \quad \dots\dots(9b')$$

satisfy eqn (8). However we will work with slightly different commutation relations instead of (9b'). We assume

$$[A_{k0},\bar{A}_{k'0}]=-\frac{i}{4\pi^2}\frac{\delta_4(k-k')}{H(\alpha)l_0^{\alpha}\chi^{\alpha-2}}, \quad \dots\dots(9b)$$

$$[A_{ki},\bar{A}_{k'j}]=\frac{i}{4\pi^2}\delta_{ij}\frac{\delta_4(k-k')}{H(\alpha)l_0^{\alpha}\chi^{\alpha-2}}\frac{k_0^2}{|k|^2}. \quad \dots\dots(9c)$$

The introduction of the factor $k_0^2/|k|^2$ in (9c) is essential (in working with Riesz potential one cannot assume $k_0=|k|$ for photons) in order to carry out the elimination of the longitudinal waves in a consistent way. Further, as can easily be seen, with this modification the commutation relations (9) and the supplementary condition (4) are consistent for all α . As it stands, this makes relations (9b) and (9c) non-relativistic, though in the limit $\alpha\rightarrow 0$ the theory is Lorentz invariant.

§ 3. ELIMINATION OF LONGITUDINAL WAVES

To eliminate the longitudinal waves from the electromagnetic potential $A_\mu(x)$ we write, following Dirac (1947),

$$A_\mu^\alpha(x) = L_\mu^\alpha(x) + M_\mu^\alpha(x), \quad \dots\dots(10)$$

where $L_\mu^\alpha(x)$ is the potential of the longitudinal waves and $M_\mu^\alpha(x)$ that of the transverse waves. The longitudinal waves are made up of the Fourier components A_{k0} and $A_{k\kappa}$, $A_{k\kappa}$ being the component along the wave vector of the space part of $A_{k\mu}$. We define

$$L_0^\alpha(x) = A_0^\alpha(x) \quad \dots\dots(11 a)$$

$$L_r^\alpha(x) = H(\alpha) l_0^\alpha \int_D \chi^{\alpha-2} k_r k_0^{-2} \{ (k A_k) e^{i[kx]} + (k \bar{A}_k) e^{-i[kx]} \} d^4 k. \quad \dots\dots(11 b)$$

These equations determine the longitudinal part of the potential and the transverse part is given by

$$M_0^\alpha(x) = 0 \quad \dots\dots(12 a)$$

$$M_r^\alpha(x) = A_r^\alpha(x) - L_r^\alpha(x) \quad \dots\dots(12 b)$$

The supplementary condition (5), with the help of eqns (1) and (3), can be written in the form

$$\left\{ k^\mu A_{k\mu} - \frac{1}{4\pi^2} \sum_i e_i \exp(-i[kz_i]) \right\} \psi \rangle_F = 0, \quad \dots\dots(13 a)$$

$$\left\{ k^\mu \bar{A}_{k\mu} - \frac{1}{4\pi^2} \sum_i e_i \exp(i[kz_i]) \right\} \psi \rangle_F = 0. \quad \dots\dots(13 b)$$

Further, if for the time being we assume that k takes on discrete values only, the commutation relations (9 b) and (9 c) become

$$[A_{k0}, \bar{A}_{k'0}] = -\frac{i}{4\pi^2} \frac{s_k \delta_{kk'}}{H(\alpha) l_0^\alpha \chi^{\alpha-2}}, \quad \dots\dots(14 a)$$

$$[A_{ki}, \bar{A}_{k'j}] = \frac{i}{4\pi^2} \frac{s_k \delta_{kk'} \delta_{ij}}{H(\alpha) l_0^\alpha \chi^{\alpha-2} |k|^2}, \quad \dots\dots(14 b)$$

s_k being the density of discrete k values. With the help of the above two relations and (7) one arrives at the following result

$$\begin{aligned} \frac{1}{4\pi^2} \frac{k_0 s_k}{H(\alpha) l_0^\alpha \chi^{\alpha-2}} \frac{\partial \psi}{\partial \bar{A}_{k0}} \rangle_F - \left\{ (k A_k) + \frac{1}{4\pi^2} \sum_i e_i \exp(-i[kz_i]) \right\} \psi \rangle_F &= 0, \\ \frac{1}{4\pi^2} \frac{k_0^2 s_k}{H(\alpha) l_0^\alpha |k|^2 \chi^{\alpha-2}} \left(k_r \frac{\partial \psi}{\partial A_{kr}} \right) \rangle_F - \left\{ k_0 A_{k0} - \frac{1}{4\pi^2} \sum_i e_i \exp(i[kz_i]) \right\} \psi \rangle_F &= 0. \end{aligned}$$

The solution of these equations is of the form

$$\psi = e^S \phi_1 \quad \dots\dots(15)$$

where

$$\begin{aligned} S &= 4\pi^2 H(\alpha) l_0^\alpha \sum_k k_0^{-1} s_k^{-1} \chi^{\alpha-2} \\ &\times \left\{ \bar{A}_{k0} (k A_k) + \frac{\bar{A}_{k0}}{4\pi^2} \sum_i e_i \exp(-i[kz_i]) - \frac{(k A_k)}{4\pi^2 k_0} \sum_i e_i \exp(i[kz_i]) \right\}, \end{aligned}$$

and ϕ_1 is independent of \bar{A}_{k0} and $A_{k\kappa}$. Returning to continuous k values we have

$$\begin{aligned} S &= 4\pi^2 H(\alpha) l_0^\alpha \int k_0^{-1} \chi^{\alpha-2} \left\{ \bar{A}_{k0} (k A_k) + \frac{\bar{A}_{k0}}{4\pi^2} \sum_i e_i \exp(-i[kz_i]) \right. \\ &\quad \left. - \frac{(k A_k)}{4\pi^2 k_0} \sum_i e_i \exp(i[kz_i]) \right\} d^4 k. \quad \dots\dots(16) \end{aligned}$$

We can look upon ϕ_1 as a wave function from which the longitudinal waves have been eliminated. To get the wave equation for ϕ_1 we proceed as follows.

We have

$$p_{\mu j} e^S = e^S p_{\mu j} + i e^S \frac{\partial S}{\partial z_j^\mu}, \quad \dots\dots (17)$$

where $p_{\mu j}$ is the momentum of the j th electron. Substituting for S from (16) and using (11) and (13) we obtain after some simplification

$$\{p_{\mu j} - e_j L_\mu(z_j)\} \psi \rangle_F = e^S \{p_{\mu j} - e_j B_\mu(z_j)\} \phi_1 \rangle_F, \quad \dots\dots (18)$$

where

$$B_0(z_j) = \frac{H(\alpha)}{4\pi^2} l_0^\alpha \sum_i e_i \int k_0^{-1} \chi^{\alpha-2} \exp(-i[k, z_i - z_j]) d^4 k,$$

$$B_r(z_j) = -\frac{H(\alpha)}{4\pi^2} l_0^\alpha \sum_i e_i \int k_r k_0^{-2} \chi^{\alpha-2} \exp(i[k, z_i - z_j]) d^4 k.$$

We now introduce another transformation

$$\phi_1 = e^T \phi, \quad \dots\dots (19)$$

where

$$T = -\frac{H(\alpha)}{8\pi^2} l_0^\alpha \sum_{i,j} e_i e_j \int \cos[k, z_i - z_j] k_0^{-2} \chi^{\alpha-2} d^4 k.$$

With the help of this, eqn (18) can be written in the form

$$\{p_{\mu j} - e_j L_\mu(z_j)\} \psi \rangle_F = e^{S+T} \{p_{\mu j} - e_j b_\mu(z_j)\} \phi \rangle_F, \quad \dots\dots (20)$$

where

$$b_\mu(z_j) = B_\mu(z_j) - \frac{i}{e_j} \frac{\partial T}{\partial z_j^\mu}$$

$$= \pm \frac{H(\alpha)}{4\pi^2} l_0^\alpha \sum_i e_i \int k_\mu k_0^{-2} \chi^{\alpha-2} \cos[k, z_i - z_j] d^4 k, \quad \dots\dots (21)$$

the positive sign being taken when $\mu=0$ and the negative sign otherwise.

We are now in a position to write down the wave equation for an electron interacting with electromagnetic field from which longitudinal waves have been eliminated. The wave equation for the j th electron interacting with a general electromagnetic field is

$$\{p_{0j} - e_j A_0(z_j) + (\alpha_j, p_j - e_j A(z_j)) + \beta_j m_j\} \psi \rangle_F = 0, \quad \dots\dots (22)$$

α_j, β_j being the Dirac matrices for the j th electron having a mass m_j . With the help of eqns (10) and (21) we can rewrite this as

$$\{p_{0j} - e_j b_0(z_j) + (\alpha_j, p_j - e_j b(z_j) - e_j M(z_j)) + \beta_j m_j\} \phi \rangle_F = 0. \quad \dots\dots (23)$$

The variables describing the longitudinal waves no longer appear in the equation. The effect of longitudinal waves appears here through the functions $b_\mu(z_j)$, which have already been evaluated in AK:

$$b_0(z_j) = \frac{1}{2} \sum_{i \neq j} \frac{e_i}{|z_j - z_i|}, \quad \dots\dots (24a)$$

$$b_r(z_j) = -\frac{1}{2} \sum_{i \neq j} \frac{e_i (z_{0j} - z_{0i})(z_{rj} - z_{ri})}{|z_j - z_i|^3}. \quad \dots\dots (24b)$$

For single time formalism $b_r(z_j) = 0$ and $b_0(z_j)$ gives the usual coulomb interaction term.

§ 4. SELF ENERGY OF AN ELECTRON

It is well known that the self energy of an electron diverges logarithmically in the hole theory. One method of getting a finite and physically significant result is to introduce a suitable cut-off factor in the integral for the matrix element. We will show that the introduction of any cut-off factor is not necessary if one works with the modified definition of the Riesz potential. We propose to work in the Feynman-Dyson formalism and hence before proceeding with the actual problem, it is essential to generalize the Feynman D_F -function in the α -plane. For this we consider the function $\mathcal{D}^\alpha(x)$ defined by eqn (3). By changing the variables of integration from k_0, k_1, k_2, k_3 to $\chi = (k_0^2 - |k|^2)^{1/2}$, $K_i = k_i$; we can write it as

$$\begin{aligned}\mathcal{D}^\alpha(x) &= \frac{H(\alpha)}{2\pi^2} l_0^\alpha \int_0^\infty \chi^{\alpha-1} d\chi \int \sin \{x_0(\chi^2 + |K|^2)^{1/2} - (Kx)\} \frac{d^3K}{(\chi^2 + |K|^2)^{1/2}} \\ &= H(\alpha) l_0^\alpha \int_0^\infty \chi^{\alpha-1} D_\chi(x) d\chi, \quad \dots\dots (25)\end{aligned}$$

where $D_\chi(x)$ is the usual D function referring to a particle of mass χ , and satisfies the equation $(\square + \chi^2)D_\chi(x) = 0$.

From eqn (25) it is now simple to see that

$$\begin{aligned}\mathcal{D}_F^\alpha(x) &= H(\alpha) l_0^\alpha \int_0^\infty \chi^{\alpha-1} D_{F\chi}(x) d\chi \\ &= \frac{H(\alpha)}{4\pi^2} l_0^\alpha \int_0^\infty \chi^{\alpha-1} d\chi \int \frac{e^{-i[kx]} d^4k}{k^2 - \chi^2}. \quad \dots\dots (26)\end{aligned}$$

To obtain a finite result from an otherwise logarithmically divergent integral we have to assume α to be a complex quantity (Nilsson 1949) and instead of taking $l_0^\alpha \chi^{\alpha-1}$ as the 'weight factor' in eqn (26) we take

$$g_\alpha(\chi) = \frac{1}{2}(l_0^\alpha \chi^{\alpha-1} + l_0^{\alpha*} \chi^{\alpha*-1}) \quad \dots\dots (27)$$

as the weight factor. The need for this assumption will become clear later on.

Thus we define

$$\mathcal{D}_F^\alpha(x) = \frac{H(\alpha)}{4\pi^2} \int_0^\infty g_\alpha(\chi) d\chi \int \frac{e^{-i[kx]} d^4k}{k^2 - \chi^2}. \quad \dots\dots (28)$$

Using $\mathcal{D}_F^\alpha(x)$ as defined by eqn (28) instead of the usual D_F function, we write the matrix for the self energy graph between the states \bar{u} and u of the electron:

$$\frac{e^2 H(\alpha)}{4\pi^3 i} \int_0^\infty g_\alpha(\chi) d\chi \int \gamma^\mu \frac{(\mathbf{p} - \mathbf{k}) + m}{(p - k)^2 - m^2} \gamma^\mu \frac{d^4k}{k^2 - \chi^2}, \quad \dots\dots (29)$$

where $\mathbf{p} = [\gamma p]$, p_μ being the momentum of the electron, $p^2 = m^2$. The γ -matrices satisfy the following relations

$$\left. \begin{aligned}\gamma_\mu \gamma_\nu + \gamma_\nu \gamma_\mu &= 2g_{\mu\nu}, \\ \gamma_\mu \gamma^\mu &= 4, \\ \gamma_\mu \mathbf{A} \gamma^\mu &= -2\mathbf{A}.\end{aligned} \right\} \quad \dots\dots (30)$$

To evaluate (29) we consider the integral (in Feynman notation)

$$I^\alpha = H(\alpha) l_0^\alpha \int_0^\infty \chi^{\alpha-1} d\chi \int \frac{(1 : k_\sigma) d^4k}{\{(p - k)^2 - m^2\} \{k^2 - \chi^2\}}. \quad \dots\dots (31)$$

This is convergent over χ for $0 < \alpha < 2$. Integrating by parts over χ in this range of α we obtain

$$I^\alpha = -\frac{2H(\alpha)}{\alpha} l_0^\alpha \int_0^\infty \chi^{\alpha+1} d\chi \int \frac{(1:k_\sigma) d^4k}{\{k^2 - 2[kp]\}\{k^2 - \chi^2\}^2}.$$

Now integration over k can be carried out and it yields

$$\begin{aligned} I^\alpha &= -\frac{2\pi^2 H(\alpha)}{i\alpha} l_0^\alpha \int_0^\infty \chi^{\alpha+1} d\chi \int_0^1 \frac{(1:(1-x)p_\sigma)x dx}{\{\chi^2 x + m^2(1-x)^2\}}, \\ &= -\frac{2\pi^2 H(\alpha)}{i\alpha} l_0^\alpha \int_0^1 (1:(1-x)p_\sigma)x dx \left[\int_0^K \frac{\chi^{\alpha+1} d\chi}{\chi^2 x + m^2(1-x)^2} \right. \\ &\quad \left. + \frac{1}{x} \int_K^\infty \chi^{\alpha-1} d\chi - \int_K^\infty \left\{ \frac{1}{\chi^2 x} - \frac{1}{\chi^2 x + m^2(1-x)^2} \right\} \chi^{\alpha+1} d\chi \right]. \quad \dots\dots(32) \end{aligned}$$

The first integral over χ , on the right-hand side of (32), is convergent and we can put $\alpha=0$ before evaluating it ($H(\alpha)/\alpha \rightarrow 1$, as $\alpha \rightarrow 0$). It gives

$$\frac{1}{2x} \log \frac{K^2 x + m^2(1-x)^2}{m^2(1-x)^2}.$$

The second integral is convergent for $\alpha < 0$, and gives

$$\frac{l_0^\alpha}{x} \int_K^\infty \chi^{\alpha-1} d\chi = -\frac{l_0^\alpha K^\alpha}{x\alpha} = -\frac{1}{x} \left(\frac{1}{\alpha} + \log Kl_0 + O(\alpha) \right).$$

Since in the limit $\alpha \rightarrow i0$, $1/\alpha + 1/\alpha^* \rightarrow 0$, we have

$$\text{cont} \frac{1}{x} \int_K^\infty g_\alpha(\chi) d\chi = -\frac{1}{x} \log Kl_0.$$

The last integral is zero for $K \rightarrow \infty$.

Combining the above results and substituting them in (32) we obtain, for $K \rightarrow \infty$,

$$\begin{aligned} I^0 &= i\pi^2 \int (1:(1-x)p_\sigma) dx \log \frac{x}{l_0^2 m^2 (1-x)^2}, \\ &= i\pi^2 \left\{ 1 + \log \frac{1}{l_0^2 m^2} : p_\sigma \left(\frac{1}{2} \log \frac{1}{l_0^2 m^2} - \frac{1}{4} \right) \right\}. \end{aligned}$$

The matrix element (29) therefore becomes

$$\begin{aligned} (29) &= \frac{e^2}{4\pi} \gamma^\mu \left[(\mathbf{p} + m) \left(\log \frac{1}{l_0^2 m^2} + 1 \right) - \mathbf{p} \left(\frac{1}{2} \log \frac{1}{l_0^2 m^2} - \frac{1}{4} \right) \right] \gamma_\mu \\ &= \frac{e^2}{8\pi} \left[8m \left(\log \frac{1}{l_0^2 m^2} + 1 \right) - \mathbf{p} \left(2 \log \frac{1}{l_0^2 m^2} + 5 \right) \right]. \quad \dots\dots(33) \end{aligned}$$

To calculate the self energy we note that $\mathbf{p}u = mu$, and this gives

$$\frac{\Delta m}{m} = \frac{e^2}{2\pi} \left(3 \log \frac{1}{l_0 m} + \frac{3}{4} \right). \quad \dots\dots(34)$$

§5. VERTEX PART OF A GRAPH

To illustrate the use of Riesz potential in eliminating the divergence arising from the vertex part of a Feynman graph we consider, as an example, the scattering of a free electron by an external electromagnetic potential $A_\mu^{(e)}(x)$, which is assumed to vary as $a(q)e^{i[qx]}$ in space and time. If p_1 and p_2 respectively denote the initial and final momenta of the electron, then $p_1^2 = p_2^2 = m^2$.

The correction to the scattering matrix element from the 'vertex graph', apart from a numerical factor, is

$$I_V^\alpha = H(\alpha) \int g_\alpha(\chi) d\chi \int \gamma_\mu \frac{(\mathbf{p}_2 - \mathbf{k}) + m}{(p_2 - k)^2 - m^2} \gamma_\nu \frac{(\mathbf{p}_1 - \mathbf{k}) + m}{(p_1 - k)^2 - m^2} \gamma^\mu \frac{d^4k}{k^2 - \chi^2}. \quad \dots\dots(35)$$

To evaluate this we consider the following integral

$$I^\alpha = H(\alpha) l_0^\alpha \int \chi^{\alpha-1} d\chi \int \frac{(1:k_\sigma:k_\sigma k_\tau) d^4k}{\{(p_2-k)^2-m^2\}\{(p_1-k)^2-m^2\}\{k^2-\chi^2\}} \dots\dots(36)$$

This integral is divergent over k but converges over χ for $0 < \alpha < 2$. As before we first integrate by parts over χ , obtaining

$$I^\alpha = -\frac{2H(\alpha)}{\alpha} l_0^\alpha \int \chi^{\alpha+1} d\chi \int \frac{(1:k_\sigma:k_\sigma k_\tau) d^4k}{\{(p_2-k)^2-m^2\}\{(p_1-k)^2-m^2\}\{k^2-\chi^2\}^2}.$$

The integration over k can now easily be carried out by introducing Feynman variables. One gets

$$I^\alpha = -\frac{2i\pi^2 H(\alpha)}{\alpha} l_0^\alpha \int_0^\infty \chi^{\alpha+1} d\chi \int_0^1 \int_0^1 \frac{x(1-x) dx dy}{\{x^2 p_y^2 + \chi^2(1-x)\}^2} \\ \times (1: x p_{y\sigma}: x^2 p_{y\sigma} p_{y\tau} - \frac{1}{2} g_{\sigma\tau} \{x^2 p_y^2 + \chi^2(1-x)\}), \dots\dots(37)$$

where $p_y = p_1 y + p_2(1-y)$. Analytic continuation to $\alpha=0$ gives

$$I^0 = -\frac{i\pi^2}{2} \int \frac{dy}{p_y^2} \left(\log \frac{1}{\epsilon^2} : 2p_{y\sigma}: p_{y\sigma} p_{y\tau} + \frac{1}{4} p_y^2 - \frac{1}{2} g_{\sigma\tau} p_y^2 \log \frac{1}{l_0^2 p_y^2} \right) \dots\dots(38)$$

where integration over x has already been carried out. For integration over y Feynman's paper may be referred to.

The slight difference between result (38) and the corresponding result obtained by Feynman will be noticed. If we put $\alpha=0$ in (37) before integrating it over χ , the first term, (1), of $(1:k_\sigma:k_\sigma k_\tau)$ gives $x^{-2} p_y^{-2}$ and this leads to a divergent integral over x as $x \rightarrow 0$. Feynman overcomes this difficulty by putting a lower limit χ_{\min} to the integral over χ (his λ). However in our case the contribution to the integral over χ from $x=0$ vanishes and the integral over x has to be taken between $\epsilon < x < 1$ with $\epsilon \rightarrow 0$.

ACKNOWLEDGMENTS

I wish to express my thanks to Mr. J. Hamilton for his interest in the work and to Professor M. Riesz for some stimulating discussions and for glancing through the present paper. I am also indebted to the Atomic Energy Commission, Government of India, for the award of a scholarship.

REFERENCES

- AULUCK, F. C., and KOTHARI, D. S., 1949, *Proc. Roy. Soc. A*, **198**, 170.
 AULUCK, F. C., and KOTHARI, L. S., 1951, *Proc. Camb. Phil. Soc. A*, **47**, 436.
 DIRAC, P. A. M., 1947, *Quantum Mechanics* (Oxford: University Press).
 FEYNMAN, R. P., 1949, *Phys. Rev.*, **76**, 769.
 FREMBERG, N. E., 1946, *Medd. Lunds Univ. Mat. Sem.*, **7**, 1.
 GUPTA, S. N., 1953, *Proc. Phys. Soc. A*, **66**, 129.
 GUSTAFSON, T., 1945, *Fysiogr. Sallsk. Lund Forh.*, **15**, 277; 1946, *Ark. Mat. Astr. Fys. A*, **34**, 1.
 KOTHARI, L. S., 1952, *Phys. Rev.*, **87**, 536.
 KOTHARI, L. S., and BHATNAGAR, P. L., 1952, *Proc. Nat. Inst. Sci., India*, **18**, 171.
 MA, S. T., 1947, *Phys. Rev.*, **71**, 787.
 NILSSON, S. B., 1949, *Ark. Fys.*, **1**, 369.
 PAULI, W., and VILLARS, F., 1949, *Rev. Mod. Phys.*, **21**, 434.
 RIESZ, M., 1949, *Acta Math.*, **81**, 1 (references to his earlier papers are given here).

On the Electron Affinities of Atomic Fluorine, Oxygen and Lithium

By B. L. MOISEIWITSCH

Department of Applied Mathematics, Queen's University of Belfast

Communicated by D. R. Bates; MS. received 21st September 1953

Abstract. The Ritz variational method in conjunction with an extrapolation procedure has been employed to calculate the electron affinities of atomic fluorine, oxygen and lithium, the values obtained being 3.05, 1.12 and 0.74 eV respectively. In the case of fluorine the accord with the value 3.57 eV found by using the Born-Haber cycle is reasonable. The electron affinity of oxygen obtained from collision experiments is 2.2 ± 0.2 eV, which is considerably larger than the value calculated in this paper. No comparison data are available for lithium.

§ 1. INTRODUCTION

THE electron affinity of atomic hydrogen has been calculated by many investigators using the Ritz variational method, the most accurate of these calculations being performed by Henrich (1943) with an eleven parameter trial wave function. Because of the computational difficulties involved such an elaborate treatment is not practicable for more complex systems. However, Glockler (1934) and Bates (1947) obtained useful results by extrapolating the experimental values for the ionization potentials of the neutral atom and positive ions isoelectronic with the negative ion under consideration keeping second differences constant. For instance, they found that this procedure gives a very good approximation to the electron affinity of atomic hydrogen $A(H)$ and for helium it gives $A(He)$ to be less than zero which is in agreement with the fact that He^- has never been observed.

Although reliable laboratory data are rather scanty for the heavier atoms, the evidence available suggests that parabolic extrapolation (i.e. extrapolation keeping second differences constant) seriously underestimates the electron affinities. In the case of oxygen, for example, the error is apparently as much as 1.1 eV which is surprisingly large in view of the fact that the second differences for the higher members of the isoelectronic series are remarkably constant. Conceivably, however, an error of such magnitude might arise from the fundamental difference that exists between negative ions on the one hand and neutral atoms and positive ions on the other hand. An attempt has been made in this paper to investigate the matter further by performing variational calculations on the series isoelectronic with H^- , Li^- , O^- and F^- respectively. The first two series were chosen because their relative simplicity permits the effects of polarization and non-separability to be studied and the last two series because of their intrinsic importance. A summary of the values of the deduced electron affinities and a comparison with the results obtained by other methods are given in table 5.

§2. THE VARIATIONAL METHOD AND TRIAL FUNCTIONS ASSUMED

The Hamiltonian of an atom or ion consisting of N electrons moving in the field of a nucleus of charge Z is

$$H = - \sum_{i=1}^N \nabla_i^2 - \sum_{i=1}^N \frac{2Z}{r_i} + \sum_{i,j=1}^N \frac{2}{r_{ij}} \quad \dots\dots(1)$$

where r_i is the distance of the i th electron from the nucleus and r_{ij} is the distance between the i th and j th electrons in Hartree units. If Ψ is a suitable trial wave function which depends on a number of arbitrary parameters C_k , an upper bound to the total energy of the atom or ion in its ground state can be obtained by minimizing the expression

$$W = \int \Psi^* H \Psi d\tau / \int \Psi^* \Psi d\tau \quad \dots\dots(2)$$

and this upper bound gives a good approximation to the true value of the energy provided the trial wave function is sufficiently flexible.

A convenient form to take for Ψ is the set of N -electron Slater determinants for which the orthonormal one-electron wave functions (with the spin functions factorized out) are

$$u(nlm | r\theta\phi) = R(nl | r) Y(lm | \theta\phi) \quad \dots\dots(3)$$

where $Y(lm | \theta\phi)$ is a normalized spherical harmonic and the first three normalized radial wave functions are those used by Fock and Petraschen (1934):

$$\left. \begin{aligned} R_\alpha(10 | r) &= (4\alpha^3)^{1/2} e^{-\alpha r}, \\ R_\beta(20 | r) &= \left(\frac{12\beta^5}{\alpha^2 - \alpha\beta + \beta^2} \right)^{1/2} \{1 - \frac{1}{3}(\alpha + \beta)r\} e^{-\beta r}, \\ R_\gamma(21 | r) &= \left(\frac{4\gamma^5}{3} \right)^{1/2} r e^{-\gamma r}. \end{aligned} \right\} \quad \dots\dots(4)$$

As Slater (1929) has shown W depends on the one- and two-electron integrals

$$\left. \begin{aligned} I(nl; nl) &= - \int_0^\infty R(nl | r) \left[\frac{d}{dr} \left(r^2 \frac{d}{dr} \right) - l(l+1) + 2Zr \right] R(nl | r) dr \\ F'(nl; n'l') &= 2 \int_0^\infty \int_0^\infty R(nl | r_1) R(n'l' | r_2) \frac{r_{>}^t}{r_{>}^{l+1}} R(nl | r_1) R(n'l' | r_2) r_1^2 r_2^2 dr_1 dr_2 \\ G'(nl; n'l') &= 2 \int_0^\infty \int_0^\infty R(nl | r_1) R(n'l' | r_2) \frac{r_{<}^t}{r_{>}^{l+1}} R(n'l' | r_1) R(nl | r_2) r_1^2 r_2^2 dr_1 dr_2 \end{aligned} \right\} \quad \dots\dots(5)$$

where $r_{<}$, $r_{>}$ are the lesser and the greater of r_1 and r_2 . It is convenient to express these integrals as functions of α and the ratios $x = \beta/\alpha$, $y = \gamma/\alpha$ because then W can be written in the form (see Appendix)

$$W = \alpha^2 T(x, y) - \alpha V(x, y) \quad \dots\dots(6)$$

so that for given values of x and y the minimum value of W corresponds to $\alpha = V/2T$ in which case $W = -V^2/4T$ and only the minimization with respect to x and y need be done numerically.

It is also of interest to investigate the effect of using trial wave functions which are not simply Slater determinants. This can be done comparatively

easily for the H^- and Li^- isoelectronic series. Thus, in the case of the H^- series, in addition to the Slater determinant given by

$$\left. \begin{aligned} \Psi &= R_\alpha(10|r_1)R_\alpha(10|r_2) & A \\ \Psi &= R_\alpha(10|r_1)R_\beta(10|r_2) + R_\beta(10|r_1)R_\alpha(10|r_2), & B \\ \Psi &= R_\alpha(10|r_1)R_\alpha(10|r_2)\{1 + \gamma r_{12}\} & C \end{aligned} \right\} \dots\dots (7)$$

For the Li^- series not only has a four-electron Slater determinant been used but also wave functions which are analogous to B and C. These are discussed in more detail in the next section.

§3. DISCUSSION OF THE RESULTS

3.1. H^- Series

Table 1 shows the values of the parameters and the total binding energy W_{\min} for H^- , He, Li^+ and Be^{2+} in the ground $(1s)^2\ ^1S$ state corresponding to the wave functions A, B and C respectively.† The total binding energy for a member of the series isoelectronic with hydrogen is given by $-Z^2$ in Hartree units, where Z is the nuclear charge. Consequently the calculated ionization potential for a member of the H^- series is $-Z^2 - W_{\min}$. Also listed in table 1 are the experimental ionization potentials‡ of He, Li^+ and Be^{2+} . The difference

Table 1. The calculated values for the binding energies of H^- , He, Li^+ , Be^{2+} corresponding to the trial functions A, B and C

Atom or ion	A		B			C			(I.P.) _{exp}
	α	E_{calc}	α	x	E_{calc}	α	y	E_{calc}	
H^-	11/16	— 0.945	1.04	0.27	— 1.027	0.83	0.30	— 1.018	
He	27/16	— 5.695	2.19	0.54	— 5.751	0.93	0.10	— 5.782	1.808
Li^+	43/16	— 14.445	3.30	0.63	— 14.498	0.95	0.059	— 14.536	5.562
Be^{2+}	59/16	— 27.195	4.39	0.68	— 27.246	0.96	0.041	— 27.288	11.317

α , x , y parameters; E_{calc} calculated total energy (Hartree units); (I.P.)_{exp} experimental ionization potentials (Hartree units).

between the calculated and experimental ionization potentials can be extrapolated to give the electron affinity of hydrogen by assuming the second differences are constant. Corresponding to the wave functions A, B and C respectively, A(H) is found in this way to be 0.73 ev, 1.03 ev and 0.57 ev. Thus the wave function A gives a value for A(H) which is in very good agreement with the value of 0.749 ev found by Henrich with an eleven parameter trial function. On the other hand A(H) is overestimated by the wave function B and underestimated by the wave function C. The same value 0.73 ev found by using

† Note that the trial wave functions B and C are not normalized.

‡ Some of these have been calculated previously by Hylleraas (1929, 1930), Zener (1930), Eckart (1930) and Chandrasekhar (1944).

§ The experimental values for the ionization potentials which are used in this paper have been taken from the compilation of Charlotte Moore (1949), with the exception of Ne^+ for which the ionization potential is not well determined. In this case a value was obtained by interpolating the experimental results for F, Na^{2+} and Mg^{3+} .

the wave function A can also be obtained by parabolic extrapolation of the experimental values only for the ionization potentials of He, Li^+ and Be^{2+} .

3.2. Li^- Series

Summarized in table 2 are the values of the parameters and the total binding energy for Li^- , Be, B^+ and C^{2+} in the ground $(1s)^2(2s)^2\ ^1\text{S}$ state. Two types of wave function, chosen by analogy to the trial functions A and B respectively, were used to calculate the total energies for the members of this isoelectronic series. The first type was just a four-electron Slater determinant; the second type was obtained by replacing all products of the form $R_\beta(20|r_3)R_\beta(20|r_4)$ which occur in the Slater determinant by $R_\beta(20|r_3)R_\gamma(20|r_4) + R_\gamma(20|r_3)R_\beta(20|r_4)$. Also shown in table 2 are the values of the parameters and the total binding energy corresponding to a trial wave function which is simply a three-electron Slater determinant for Li, Be^+ , B^{2+} and C^{3+} in the ground $(1s)^2(2s)\ ^1\text{S}$ state. Using these values for the energy, the electron affinity of Li and the ionization potentials of Be, B^+ and C^{2+} can be calculated. By parabolic extrapolation of the difference between the calculated and the experimental ionization potentials, the type A wave function gives 0.74 eV and the type B wave function gives

Table 2. The calculated values for the binding energies of Li^- , Be, B^+ , C^{2+} corresponding to trial functions of type A and type B and also the calculated values for the binding energies of Li, Be^+ , B^{2+} , C^{3+} corresponding to a three-electron Slater determinant trial function

Atom or ion	A			B				(I.P.) _{exp}	Atom or ion			
	α	x	E_{calc}	α	x	y	E_{calc}			α	x	E_{calc}
Li^-	2.70	0.20	-14.790	2.69	0.30	0.10	-14.833		Li	2.69	0.28	-14.828
Be	3.71	0.31	-29.060	3.70	0.40	0.22	-29.104	0.686	Be^+	3.70	0.36	-28.512
B^+	4.71	0.36	-48.379	4.71	0.44	0.28	-48.427	1.850	B^{2+}	4.69	0.40	-46.706
C^{2+}	5.72	0.39	-72.714	5.70	0.47	0.31	-72.765	3.521	C^{3+}	5.69	0.42	-69.404

α , x , y parameters; E_{calc} calculated total energy (Hartree units); (I.P.)_{exp} experimental ionization potentials (Hartree units).

0.80 eV for A(Li). A similar calculation for Li^- was performed previously by Ta-You Wu (1936) using Slater determinants only. He obtained the value of 0.54 eV for A(Li) which differs from the corresponding value obtained in this paper because he used earlier values for the experimental ionization potentials given by Bacher and Goudsmidt (1932).†

Allowance can be made for polarization between the electrons in the 2s shell in a similar manner to the way the wave function C makes allowance for polarization between the 1s electrons. This was done without an excessive amount of calculation by assuming that the motion of the 1s electrons is unaffected by the presence of the 2s electrons. The wave function A was used for the 1s electrons while wave functions given by $R_\beta(20|r_3)R_\beta(20|r_4)$ and $R_\beta(20|r_3)R_\beta(20|r_4)\{1 + \gamma r_{34}\}$ were used for the 2s electrons. The results obtained with these two types of wave function are given in columns A and C respectively in table 3. By making a comparison with the values of the total energy given by the four-electron Slater determinant for the Li^- series

† By interpolating the experimental results for Be, C^{2+} and N^{3+} Edlén has recently revised the value of the ionization energy of B^+ (cf. Moore 1949).

extrapolation of the results obtained with the polarization type wave function gives $A(\text{Li})$ to be 0.67 ev. Thus the Slater determinant trial wave function gives a value for $A(\text{Li})$ which is the arithmetic mean of the values of the affinity given by the type B wave function and the polarization type of wave function. It may be noted that the effects are similar to those found for hydrogen but that the spread in the results is less. Extrapolation of the experimental values only for the ionization potentials of Be, B^+ and C^{2+} gives for $A(\text{Li})$ the value 0.38 ev. This differs from the result obtained by using the four-electron Slater determinant by 0.36 ev.

Table 3. The calculated values for the binding energies of Li^- , Be, B^+ , C^{2+} assuming that the motion of the 1s electrons is unaffected by the presence of the 2s electrons

Atom or ion	Calculated energy (Hartree units)	
	A	C
Li^-	-14.783	-14.841
Be	-29.006	-29.101
B^+	-48.255	-48.376
C^{2+}	-72.513	-72.654

Columns A and C respectively refer to calculations in which polarization between the 2s electrons has been neglected and has been taken into account.

3.3. O^- and F^- Series

Table 4 gives the parameters and the total binding energy for O, F^+ , Ne^{2+} , Na^{3+} in the ground $(1s)^2(2s)^2(2p)^4\ ^3\text{P}$ state; for O^- , F, Ne^+ , Na^{2+} , Mg^{3+} in the ground $(1s)^2(2s)^2(2p)^5\ ^2\text{P}$ state; and for F^- , Ne, Na^+ , Mg^{2+} in the ground $(1s)^2(2s)^2(2p)^6\ ^1\text{S}$ state, corresponding to trial wave functions which are simply eight-, nine- and ten-electron Slater determinants respectively. By parabolic extrapolation of the difference between the calculated and experimental ionization potentials, the electron affinities of O and F are found to be 1.12 ev and 3.05 ev respectively.† The values for $A(\text{O})$ and $A(\text{F})$ obtained by extrapolating the experimental values for the ionization potentials are 0.97 ev and 2.93 ev respectively. Thus the results obtained by the two extrapolation procedures are almost the same. This at least suggests that they are not seriously in error, for any major discontinuity in passing along an isoelectronic series to the negative ion would be expected to be revealed by variation with Slater type wave functions (particularly as the use of more elaborate wave functions in the case of H^- and Li^- made very little difference).

Experiments to determine the electron affinity of oxygen have been carried out by Lozier (1934), by Hagstrum and Tate (1941), and by Metlay and Kimball (1948). These investigators obtained the value 2.2 ± 0.2 ev for $A(\text{O})$. A detailed discussion of the experiments is given by Massey (1950) and by Gaydon (1953).

It is also possible to calculate $A(\text{F})$ by using the Born-Haber cycle for the alkaline fluorides (Mayer and Helmholtz 1932). Until fairly recently the value of the electron affinity obtained was 4.13 ev using the old value of $63.5 \text{ kcal mole}^{-1}$ for the dissociation energy of F_2 . However, a new value of $37.7 \text{ kcal mole}^{-1}$ for

† A value of 3.17 ev for $A(\text{F})$ has been obtained by Johnston (1951) using perturbation methods.

the dissociation energy of F_2 has been obtained by Doescher (1951) and by Barrow and Caunt (1953) which gives $A(F)$ to be 3.57 ev (Bernstein and Metlay 1951). This value is in good agreement with the experimentally determined value 3.6 ± 0.2 ev for $A(F)$ (which was previously considered unreliable) obtained by Metlay and Kimball (1948).

Table 4. The calculated values for the binding energies of the members of the series isoelectronic with O, F and Ne using Slater determinants as trial wave functions

Atom or ion	α	κ	γ	E_{calc}	(I.P.) _{exp}
O	7.71	0.36	0.29	-148.786	
F ⁺	8.70	0.38	0.32	-196.816	
Ne ²⁺	9.70	0.39	0.34	-251.882	
Na ³⁺	10.69	0.40	0.35	-313.972	
O ⁻	7.71	0.35	0.26	-148.254	
F	8.71	0.37	0.29	-197.501	1.281
Ne ⁺	9.70	0.38	0.32	-254.310	3.014
Na ²⁺	10.70	0.39	0.34	-318.658	5.270
Mg ³⁺	11.70	0.40	0.35	-390.533	
F ⁻	8.72	0.35	0.26	-196.938	
Ne	9.71	0.37	0.29	-255.138	1.586
Na ⁺	10.71	0.38	0.32	-321.400	3.478
Mg ²⁺	11.69	0.39	0.33	-395.703	5.893

α , κ , γ parameters; E_{calc} calculated total energy (Hartree units); (I.P.)_{exp} experimental ionization potentials (Hartree units).

Table 5. Calculated and experimental values of electron affinities

Atom	Electron affinities (ev)		
	(i)	(ii)	(iii)
H	0.73	0.73	0.749
He	-0.53	—	<0
Li	0.38	0.74	—
N	-0.66	(-0.51)	≤ 0
O	0.97	1.12	2.2
F	2.93	3.05	3.57

In column (i) are given the values calculated by a purely extrapolation procedure; in column (ii) are given the values calculated by using the variational method with Slater determinants as trial functions in conjunction with an extrapolation procedure; and in column (iii) are given the values obtained by experiment and by the variational method in the case of hydrogen.

The differences between the experimental values of $A(O)$ and $A(F)$ and those calculated in this paper are 1.08 ev and 0.52 ev respectively.† In comparison with the latter the former difference is unexpectedly large as is at once apparent when consideration is given to the next member of the Periodic Table. For it seems highly probable that N^- does not exist in a stable form because although a careful search has been made for it by Tüxen (1936) with

† If the estimated value for the ionization potential of Ne^+ given by Moore (1949) is used, $A(O)$ is found to be 0.85 ev which makes the anomaly between the experimental and calculated values of $A(O)$ even more acute.

a mass spectrograph its presence was not detected. If this is correct $A(N)$ is less than zero. Now the extrapolation procedure first used by Glockler and later by Bates gives $A(N)$ to be -0.66 ev and the extrapolation procedure used in this paper is likely to raise this value by about 0.15 ev. Thus the error made by the latter procedure is less than 0.5 ev in the case of $A(N)$ as in the case of $A(F)$ so that it is very peculiar that for $A(O)$ it should seemingly be as much as 1.1 ev. Indeed it is almost tempting to suppose that the error in the calculated electron affinity is *not* greater than this amount and consequently that $A(O)$ is smaller than 1.7 ev (unless indeed the original value of $A(F)$ is in fact correct). However, though the anomaly is at least sufficiently suggestive to make further laboratory work seem desirable, too much weight should not be attached to it. Even should the true value of $A(O)$ be as low as 1.7 ev both it and $A(F)$ would still be some 0.5 ev above the calculated values. While such a difference is not of course unduly large the corresponding difference in the case of the simpler extrapolation procedure is only 0.15 ev higher. Apparently therefore the improvement brought about by the variational refinement is slight. The reason for this is not understood so it would seem that the electron affinities may depend on some more subtle factor than any which have been considered.

ACKNOWLEDGMENT

In conclusion I would like to express my thanks to Professor D. R. Bates for suggesting this problem and for many helpful discussions.

APPENDIX

Let us consider an atom or ion in the ground state with configuration $(1s)^{n_1} (2s)^{n_2} (2p)^{n_3}$ where $0 \leq n_1 \leq 2$, $0 \leq n_2 \leq 2$, $0 \leq n_3 \leq 6$. The energy W is given in terms of the one- and two-electron integrals by the expression

$$\begin{aligned} W = & n_1 I(10; 10) + \frac{1}{2} n_1 (n_1 - 1) F^0(10; 10) + n_2 I(20; 20) + \frac{1}{2} n_2 (n_2 - 1) F^0(20; 20) \\ & + 2n_2 F^0(10; 20) - n_2 G^0(10; 20) \\ & + n_3 I(21; 21) + \frac{1}{2} n_3 (n_3 - 1) F^0(21; 21) - \frac{1}{6} \delta F^2(21; 21) \\ & + 2n_3 F^0(10; 21) + 2n_3 F^0(20; 21) - \frac{1}{3} n_3 G^1(10; 21) - \frac{1}{3} n_3 G^1(20; 21) \end{aligned}$$

where

$$\begin{aligned} \delta = & \frac{1}{2} n_3 (n_3 - 1) \quad \text{if } 0 \leq n_3 \leq 3 \\ = & \frac{1}{2} (n_3 - 3)(n_3 - 4) + 3 \quad \text{if } 4 \leq n_3 \leq 6. \end{aligned}$$

With the wave functions specified in the main text (eqns (4)) we obtain:

$$\begin{aligned} I(10; 10) &= \alpha^2 - 2Z\alpha \\ I(20; 20) &= \left\{ \frac{x^2}{3} + \frac{2x^4}{1-x+x^2} \right\} \alpha^2 - Z \left\{ x - \frac{(1-2x)x^2}{1-x+x^2} \right\} \alpha \\ I(21; 21) &= y^2 \alpha^2 - Zy\alpha \\ F^0(10; 10) &= \frac{5}{4} \alpha \\ F^0(20; 20) &= \frac{1}{128(1-x+x^2)^2} \{93x - 244x^2 + 438x^3 - 420x^4 + 245x^5\} \alpha \\ F^0(21; 21) &= \frac{93}{128} y\alpha \end{aligned}$$

$$\begin{aligned}
 F^0(10; 20) &= \left\{ x - \frac{(1-2x)x^2}{1-x+x^2} - \frac{(5+3x)x^5}{(1-x+x^2)(1+x)^3} \right\} \alpha \\
 F^0(10; 21) &= \left\{ 2 - \frac{2}{(1+y)^2} - \frac{3y}{(1+y)^3} - \frac{3y^2}{(1+y)^4} - \frac{2y^3}{(1+y)^5} \right\} \alpha \\
 F^0(20; 21) &= \frac{x(1-2x+3x^2)}{1-x+x^2} \alpha \\
 &\quad - \frac{x^5}{1-x+x^2} \left[\frac{3}{(x+y)^2} \left\{ 2 + \frac{3y}{x+y} + \frac{3y^2}{(x+y)^2} + \frac{2y^3}{(x+y)^3} \right\} \right. \\
 &\quad \left. - \frac{(1+x)}{(x+y)^3} \left\{ 4 + \frac{9y}{x+y} + \frac{12y^2}{(x+y)^2} + \frac{10y^3}{(x+y)^3} \right\} \right. \\
 &\quad \left. + \frac{(1+x)^2}{(x+y)^4} \left\{ 1 + \frac{3y}{x+y} + \frac{5y^2}{(x+y)^2} + \frac{5y^3}{(x+y)^3} \right\} \right] \alpha \\
 F^2(21; 21) &= \frac{45}{128} y \alpha \\
 G^0(10; 20) &= \frac{8x^5}{(1-x+x^2)(1+x)^5} \alpha \\
 G^1(10; 21) &= \frac{56y^5}{(1+y)^7} \alpha \\
 G^1(20; 21) &= \frac{4x^5y^5}{3(1-x+x^2)(x+y)^7} \left\{ 126 - 294 \frac{1+x}{x+y} + 185 \frac{(1+x)^2}{(x+y)^2} \right\} \alpha.
 \end{aligned}$$

REFERENCES

- BACHER, R. F., and GOUDSMIDT, S., 1932, *Atomic Energy States* (New York : McGraw-Hill).
 BARROW, R. F., and CAUNT, A. D., 1953, *Proc. Roy. Soc. A*, **219**, 120.
 BATES, D. R., 1947, *Proc. R. Irish Acad. A*, **51**, 151.
 BERNSTEIN, R. B., and METLAY, M., 1951, *J. Chem. Phys.*, **19**, 1612.
 CHANDRASEKHAR, S., 1944, *Astrophys. J.*, **100**, 176.
 DOESCHER, R. N., 1951, *J. Chem. Phys.*, **19**, 1070.
 ECKART, C., 1930, *Phys. Rev.*, **36**, 882.
 FOCK, V., and PETRASCHEN, MARY J., 1934, *Phys. Z. Sowjet*, **6**, 368.
 GAYDON, A. G., 1953, *Dissociation Energies*, 2nd Edn (London : Chapman and Hall).
 GLOCKLER, G., 1934, *Phys. Rev.*, **46**, 111.
 HENRICH, L. R., 1943, *Astrophys. J.*, **99**, 59.
 HAGSTRUM, H. D., and TATE, J. T., 1941, *Phys. Rev.*, **59**, 354.
 HYLLERAAS, E. A., 1929, *Z. Phys.*, **54**, 347; 1930, *Ibid.*, **60**, 624.
 JOHNSTON, R. H., 1951, *J. Chem. Phys.*, **19**, 1391.
 LOZIER, W. W., 1934, *Phys. Rev.*, **46**, 268.
 MASSEY, H. S. W., 1950, *Negative Ions*, 2nd Edn (Cambridge : University Press).
 MAYER, J. E., and HELMHOLZ, L., 1932, *Z. Phys.*, **75**, 19.
 METLAY, M., and KIMBALL, G. E., 1948, *J. Chem. Phys.*, **16**, 779.
 MOORE, CHARLOTTE, 1949, *Atomic Energy Levels, National Bureau of Standards Circular 467* (Washington : U.S. Government Printing Office).
 SLATER, J. C., 1929, *Phys. Rev.*, **34**, 1293.
 TÜXEN, O., 1936, *Z. Phys.*, **103**, 463.
 WU, TA-YOU, 1936, *Phil. Mag.*, **22**, 837.
 ZENER, C., 1930, *Phys. Rev.*, **36**, 51.

Self-Consistent Spin-Wave Theory for the Ferromagnetic Exchange Problem

By M. R. SCHAFROTH

Department of Theoretical Physics, University of Liverpool

Communicated by H. Fröhlich; MS. received 19th June 1953,

Abstract. A self-consistent improvement of Bloch's spin-wave treatment of the ferromagnetic exchange problem at low temperatures is developed. This leads to appreciable corrections to the spontaneous magnetization.

§1. INTRODUCTION

THE limiting solutions of the three-dimensional ferromagnetic exchange problem for high and low temperatures are well known. In the former case (Opechowski 1937) the thermodynamic functions can be computed by consistent expansion in descending powers of the temperature. For the latter case, Bloch (1930) by his famous spin-wave method was able to give an expansion in ascending powers of temperature, of which the first term can certainly be trusted. It does not, however, appear to be known up to which term this series is correct, i.e. how strongly the spin-wave solution deviates from the exact one at very low temperatures.* The purpose of the present paper is to deal with that question by introducing a refined, self consistent spin-wave method which allows the determination of the next higher terms in the above-mentioned expansion. The main result will be that Bloch's expression for the spontaneous magnetization of the lattice

$$M = M_0(1 - c_1 T^{3/2} + \dots)$$

has to be supplemented by terms of the orders $T^{7/4}$, T^2 , ..., whereas the classical spin-wave theory would give as a next term one in $T^{5/2}$. This result indicates that the spin-waves interact quite strongly with each other and that care is required in applying the results of Bloch's original theory to actual experimental results as the $T^{7/4}$ term will usually not be negligible compared with the $T^{3/2}$ term.

§2. CALCULATIONS

We wish to calculate the low-temperature thermodynamic behaviour, in particular the spontaneous magnetization M , of a lattice occupied by spins of magnitude S with nearest-neighbour exchange interaction, i.e. of a system with Hamiltonian

$$\mathcal{H} = -I \sum_{\langle jk \rangle} (\mathbf{S}_j \mathbf{S}_k) - \mu g H \sum_j S_j^z \quad \dots\dots (1)$$

where $I > 0$ is the exchange integral, μ the Bohr magneton, g the g -factor, H the magnetic field, acting in the z direction, and $\langle jk \rangle$ means that the sum is to be

* Kramers and Opechowski (1937), by a different approach, have pointed out already that the second term of Bloch's expansion cannot be trusted.

extended over all nearest-neighbour pairs. The well-known substitution (Holstein and Primakoff 1940, Kubo 1952)

$$\left. \begin{aligned} S_j^x + iS_j^y &= (2S)^{1/2} f_s(n_j) a_j & n_j &\equiv a_j^* a_j \\ S_j^x - iS_j^y &= (2S)^{1/2} a_j^* f_s(n_j) & f_s(n_j) &= (1 - n_j/2S)^{1/2} \\ S_j^z &= S - n_j \end{aligned} \right\} \dots\dots(2)$$

brings \mathcal{H} to the form

$$\begin{aligned} \mathcal{H} = & -\frac{1}{2}NzIS^2 - Ng\mu SH + (zIS + \mu gH)\sum_j n_j \\ & + IS \sum_{\langle jk \rangle} n_j n_k - IS \sum_{\langle jk \rangle} \{a_j^* f_s(n_j) f_s(n_k) a_k + a_k^* f_s(a_k) f_s(a_j) a_j\}, \dots\dots(3) \end{aligned}$$

where N is the total number of lattice points and z the number of nearest neighbours to a lattice point.

The operators a_j and a_j^* as defined by (2) satisfy the commutation relations of absorption and emission operators:

$$[a_j, a_k^*] = \delta_{jk} \dots\dots(4)$$

Hence $n_j = a_j^* a_j$ has the properties of an occupation number operator with positive integer eigenvalues.

Bloch's (1930) spin-wave approximation consists in replacing in (3) $f_s(n_j)$ by unity and neglecting the term $IS \sum_{\langle jk \rangle} n_j n_k$. The justification for this lies in our expectation of finding ferromagnetic ordering at low temperatures, i.e. a value of

$$\nu \equiv \langle \sum_j n_j / N \rangle_{av} \dots\dots(5)$$

differing from the ground-state value $\nu_0 = 0$ by an amount independent of N in the limit of large N and vanishing as $T \rightarrow 0$. This expectation can then be checked in a self-consistent way by computing the value of ν which is obtained in this approximate treatment: it is found (Bloch 1930) that for lattices of dimensions equal to or greater than three ν has the required properties, whereas for dimensions less than or equal to two ν is not independent of N for large N (which fact is then to be interpreted as an indication that no ferromagnetic ordering exists, contrary to the initial assumption).

A further point needs some care: in applying the spin-wave approximation we destroy the invariant splitting of the Hilbert space of the eigenfunction of (n_1, \dots, n_j, \dots) into two disconnected parts $0 \leq n_j \leq 2S$, $n_j > 2S$, of which only the first one corresponds in a one-to-one manner to the state vectors of the initial spin representation. However, though this point has an important bearing on the theory of antiferromagnetism (Kubo 1952), it is here of no importance as the average excitation of all n_j is small compared with S .

It is thus clear that Bloch's method will give a correct approximation for the spontaneous magnetization of a ferromagnetic three-dimensional lattice. The well-known result is

$$M = Ng\mu S(1 - a_1(kT/I)^{3/2} + \dots) \dots\dots(6)$$

The next term of the expansion, which would be proportional to $T^{5/2}$, can, however, not be trusted as the deviation of the $f_s(n)$ from unity and the neglected term $IS \sum_{\langle jk \rangle} n_j n_k$ will have an influence. Our aim is to correct this shortcoming by carrying out a self-consistent improvement of the spin-wave method.

We shall replace the exact Hamiltonian (3) by an approximate Hamiltonian of form

$$\mathcal{H}' = -\frac{1}{2}NzIS^2 - Ng\mu SH + (zIS + \mu gH)\sum_j n_j + \frac{1}{2}NzIS\beta - IS\sigma \sum_{\langle jk \rangle} \{a_j^* a_k + a_k^* a_j\}. \quad \dots\dots(7)$$

Here σ and β are two adjustable parameters which we allow to be functions of the temperature and which are to be determined by the self-consistency requirement

$$\left. \begin{aligned} \beta &= \frac{2}{Nz} \langle \sum_{\langle jk \rangle} n_j n_k \rangle \\ \sigma &= \langle \sum_{\langle jk \rangle} a_j^* f_s(a_j) f_s(a_k) a_k \rangle / \langle \sum_{\langle jk \rangle} a_j^* a_k \rangle \end{aligned} \right\} \quad \dots\dots(8)$$

where $\langle \rangle$ means averaging over the canonical ensemble of the Hamiltonian \mathcal{H}' .

We expect, of course, that for vanishing temperature β tends to zero and σ to unity, so that our procedure should agree with Bloch's results as far as the lowest term in the expansion in the temperature is concerned.

The diagonalization of \mathcal{H}' is easily achieved in the usual way by introducing the Fourier transforms

$$a_\lambda = \frac{1}{\sqrt{N}} \sum_j a_j e^{ij\lambda}; \quad a_\lambda^* = \frac{1}{\sqrt{N}} \sum_j a_j^* e^{-ij\lambda} \quad \left\{ \begin{aligned} [a_\lambda, a_{\lambda'}^*] &= \delta_{\lambda\lambda'} \\ a_\lambda^* a_\lambda &\equiv n_\lambda \end{aligned} \right\} \quad \dots\dots(9)$$

where λ runs over a reciprocal lattice of N points. One then gets

$$\mathcal{H}' = -\frac{1}{2}NzIS(S - \beta) - Ng\mu SH + zIS \sum_\lambda n_\lambda \left(1 + \frac{\mu gH}{zIS} - \sigma \gamma_\lambda \right) \quad \dots\dots(10)$$

where γ_λ is defined by

$$\gamma_\lambda = \frac{1}{z} \sum_\delta e^{i\lambda\delta} \quad \dots\dots(11)$$

δ running over all z lattice vectors connecting a lattice point to its nearest neighbours. As in the case of Bloch, the 'spin waves' (9) form a Bose-Einstein gas with energy function in the magnetic field

$$\epsilon_\lambda = \epsilon_\lambda^0 + \mu gH/zIS. \quad \dots\dots(12)$$

The field-free energy (13) $\epsilon_\lambda^0 = 1 - \sigma \gamma_\lambda$ may be expanded in terms of λ , retaining only the second-order term in λ , since it may easily be shown that the higher terms give only contributions to M of order higher than $T^{5/2}$. We write

$$\gamma_\lambda = 1 - \tau \lambda^2 \quad \dots\dots(14)$$

and

$$\epsilon_\lambda^0 = (1 - \sigma) + \sigma \tau \lambda^2. \quad \dots\dots(15)$$

Our first task is to compute the self-consistent values of the parameters β and σ . For this purpose we do not need the magnetic field which will be introduced as a perturbation for the actual calculation of the free energy; we thus put $H=0$. In order to evaluate β we need first the diagonal elements

$$\langle (n_\lambda) | IS \sum_{\langle jk \rangle} n_j n_k | (n_\lambda) \rangle = \frac{zIS}{2N} \sum_{\lambda\mu} n_\lambda n_\mu (1 + \gamma_{\lambda-\mu}) \quad \dots\dots(16)$$

as is easily seen by Fourier transformation. Thus

$$\beta = \frac{zIS}{2N} \sum_{\lambda\mu} \langle n_\lambda n_\mu \rangle (1 + \gamma_{\lambda-\mu}), \quad \dots\dots(17)$$

$\langle n_\lambda n_\mu \rangle$ may be replaced by $\langle n_\lambda \rangle \langle n_\mu \rangle$, since fluctuations exist only for $\lambda = \mu$, and thus give rise only to corrections of the relative order $1/N$. Hence

$$\beta = \frac{IS}{N^2} \left\{ \left(\sum_{\lambda} \langle n_{\lambda} \rangle \right)^2 + \sum_{\lambda \mu} \langle n_{\lambda} \rangle \langle n_{\mu} \rangle \gamma_{\lambda-\mu} \right\} \quad \dots\dots (18)$$

where we have to put

$$\langle n_{\lambda} \rangle = [\exp(zIS\epsilon_{\lambda}^0/kT) - 1]^{-1}. \quad \dots\dots (19)$$

Replacing the summations by integrals

$$\sum_{\lambda} \rightarrow \frac{N}{(2\pi)^3} \int d^3\lambda$$

leads to

$$\sum_{\lambda} \langle n_{\lambda} \rangle = N \left(\frac{kT}{4\pi zIS\sigma\tau} \right)^{3/2} Z_{3/2}(x), \quad \dots\dots (20)$$

$$\sum_{\lambda \mu} \langle n_{\lambda} \rangle \langle n_{\mu} \rangle \gamma_{\lambda-\mu} = N^2 \left(\frac{kT}{4\pi zIS\sigma\tau} \right)^3 \left\{ [Z_{3/2}(x)]^2 - \frac{3kT}{zIS\sigma} Z_{3/2}(x) Z_{5/2}(x) \right\} \quad \dots\dots (21)$$

where

$$x \equiv \frac{zIS}{kT} (1 - \sigma) \quad \dots\dots (22)$$

and

$$Z_n(x) = \frac{1}{\Gamma(n)} \int_0^{\infty} du u^{n-1} (e^{u+x} - 1)^{-1}. \quad \dots\dots (23)$$

(The properties of this function are collected in the Appendix.) Finally we find

$$\beta = IS \left(\frac{kT}{4\pi zIS\sigma\tau} \right)^3 \left\{ 2[Z_{3/2}(x)]^2 - \frac{3kT}{zIS\sigma} Z_{3/2}(x) Z_{5/2}(x) \right\}. \quad \dots\dots (24)$$

The calculation of σ is quite similar. We write

$$\sigma \langle \sum_{\langle jk \rangle} a_j^* a_k \rangle = \langle \sum_{\langle jk \rangle} a_j^* f_s(n_j) f_s(n_k) a_k \rangle \quad \dots\dots (8a)$$

and expand $f_s(n)$ about $n=0$ keeping only the first-order term; this is easily seen to be permissible, the neglected terms giving to σ only contributions proportional to T^3 . Hence

$$\sigma \langle \sum_{\langle jk \rangle} a_j^* a_k \rangle = \langle \sum_{\langle jk \rangle} a_j^* \left(1 - \frac{n_j}{2S} \right) \left(1 - \frac{n_k}{2S} \right) a_k \rangle$$

or
$$1 - \sigma = \frac{1}{2S} \langle \sum_{\langle jk \rangle} (a_j^* a_j^* a_j a_k + a_j^* a_k^* a_k a_k) \rangle \bigg/ \langle \sum_{\langle jk \rangle} a_j^* a_k \rangle. \quad \dots\dots (25)$$

Fourier transformation of the right-hand side leads easily to

$$1 - \sigma = \frac{(2z/N) \sum_{\lambda} \langle n_{\lambda} \rangle \sum_{\mu} \langle n_{\mu} \rangle \gamma_{\mu}}{zS \sum_{\lambda} \langle n_{\lambda} \rangle \gamma_{\lambda}} = \frac{2}{S} \frac{\sum_{\lambda} \langle n_{\lambda} \rangle}{N}, \quad \dots\dots (26)$$

which finally gives
$$1 - \sigma = \frac{2}{S} \left(\frac{kT}{4\pi zIS\sigma\tau} \right)^{3/2} Z_{3/2}(x), \quad \dots\dots (27)$$

with x given by (22). This is our self-consistency equation for σ . Equation (26) can also be written, using $M = \mu g(NS - \sum_{\lambda} n_{\lambda})$,

$$M = M_0 \{ 1 - \frac{1}{2}(1 - \sigma) \} = M_0(1 + \sigma)/2, \quad \dots\dots (28)$$

which shows that σ is directly related to the spontaneous magnetization. The fact that the definition (25) reduces to the simple form (28) is again related to the vanishing of fluctuation terms for large N . Equation (28) together with

Bloch's result for M leads us to expect $(1-\sigma)/kT$ to be small for small T ; we therefore expand the right-hand side of (27) in powers of $x = (zIS/kT)(1-\sigma)$. Using eqn (A 4) (see Appendix) we obtain

$$(1-\sigma) = \frac{2}{S} \left(\frac{kT}{4\pi zIS\sigma\tau} \right)^{3/2} \left\{ \zeta\left(\frac{3}{2}\right) - \frac{\pi}{\Gamma\left(\frac{3}{2}\right)} \left[\frac{zIS}{kT} (1-\sigma) \right]^{1/2} - \zeta\left(\frac{1}{2}\right) \frac{zIS}{kT} (1-\sigma) + O(x^2) \right\}. \quad \dots\dots(27a)$$

Solving this equation for $1-\sigma$ by iteration we find

$$1-\sigma = \frac{2}{S} \left(\frac{kT}{4\pi zIS\tau} \right)^{3/2} \zeta\left(\frac{3}{2}\right) \times \left\{ 1 - \left(\frac{kT}{4\pi zIS\tau} \right)^{1/2} \left(\frac{2}{S\tau\zeta\left(\frac{3}{2}\right)} \right)^{1/2} + \left(\frac{kT}{4\pi zIS\tau} \right)^{1/2} \frac{2\pi - \zeta\left(\frac{1}{2}\right)\zeta\left(\frac{3}{2}\right)}{2\pi\zeta\left(\frac{3}{2}\right)S\tau} + O(T^{4/3}) \right\}. \quad \dots(29)$$

Introducing this into (24) and confining ourselves to the first term of the expansion, we obtain for β

$$\beta = 2IS \left(\frac{kT}{4\pi zIS\tau} \right)^3 [\zeta\left(\frac{3}{2}\right)]^2 \{1 + O(T^{1/4})\}. \quad \dots\dots(30)$$

With the self-consistent values (29) and (30) of the parameters σ and β the Hamiltonian \mathcal{H}' , eqn (7), is now fully defined and we can easily calculate by standard methods its partition function in the presence of a magnetic field. We find for the free energy

$$F = -\frac{1}{2}NzIS(S-\beta) - Ng\mu SH - N \frac{(kT)^{5/2}}{(4\pi zIS\sigma\tau)^{3/2}} Z_{5/2} \left(x + \frac{\mu gH}{kT} \right). \quad \dots\dots(31)$$

Expansion in powers of the magnetic field yields, using eqn (A 6),

$$F = -\frac{1}{2}NzIS(S-\beta) - Ng\mu SH - N \frac{(kT)^{5/2}}{(4\pi zIS\sigma\tau)^{3/2}} Z_{5/2}(x) + N \frac{\mu gH}{kT} \frac{(kT)^{5/2}}{(4\pi zIS\sigma\tau)^{3/2}} Z_{3/2}(x) + O(H^2) \quad \dots\dots(32)$$

from which all interesting quantities may be derived. Especially for the magnetization we get, using $M = -(\partial F/\partial H)_T$,

$$M = Ng\mu S \left\{ 1 - \frac{1}{S} \left(\frac{kT}{4\pi zIS\sigma\tau} \right)^{3/2} Z_{3/2}(x) \right\} = M_0 \{1 - \frac{1}{2}(1-\sigma)\},$$

in accordance with (28). Inserting the expansion (29) we find

$$M = Ng\mu S \left\{ 1 - \frac{\zeta\left(\frac{3}{2}\right)}{S} \left(\frac{kT}{4\pi zIS\tau} \right)^{3/2} + \frac{1}{S} \left(\frac{2\zeta\left(\frac{3}{2}\right)}{S\tau} \right)^{1/2} \left(\frac{kT}{4\pi zIS\tau} \right)^{7/4} - \frac{1}{S} \frac{2\pi - \zeta\left(\frac{1}{2}\right)\zeta\left(\frac{3}{2}\right)}{2\pi\zeta\left(\frac{3}{2}\right)S\tau} \left(\frac{kT}{4\pi zIS\tau} \right)^2 + O(T^{9/4}) \right\}. \quad \dots\dots(33)$$

Up to $T^{3/2}$ this expression is identical with Bloch's, but the remaining two terms are due to deviations from the original spin-wave model. One can easily see that they represent quite noticeable corrections by considering some special case, e.g. the simple cubic lattice with $S = \frac{1}{2}$ ($z = 6, \tau = \frac{1}{6}$). One finds for this case

$$M = Ng\mu S \left\{ 1 - 0.33 \left(\frac{kT}{I} \right)^{3/2} + 0.63 \left(\frac{kT}{I} \right)^{7/4} - 0.37 \left(\frac{kT}{I} \right)^2 + \dots \right\} \quad \dots\dots(33a)$$

ACKNOWLEDGMENTS

The author is greatly indebted to Professor Fröhlich for kind hospitality in his Department and to the Swiss 'Arbeitsgemeinschaft für Stipendien in Mathematik und Physik' for financial support.

APPENDIX

The Function $Z_\nu(x)$

We define

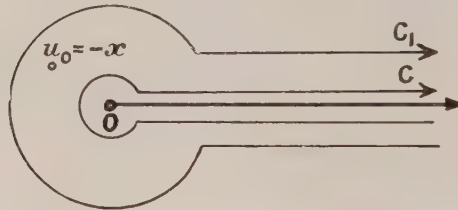
$$Z_\nu(x) \equiv [\Gamma(\nu)]^{-1} \int_0^\infty du u^{\nu-1} (e^{x+u} - 1)^{-1} \quad (\Re \nu > 0). \quad \dots\dots (A1)$$

For non-integral ν this can be written

$$Z_\nu(x) = \frac{1}{(1 - e^{2\pi i})\Gamma(\nu)} \int_C du u^{\nu-1} (e^{x+u} - 1)^{-1}, \quad \dots\dots (A2)$$

with C shown in the figure. We obtain the expansion of $Z_\nu(x)$ for small x by replacing the integral over C by one over C_1 and a residue at $u_0 = -x$:

$$\begin{aligned} Z_\nu(x)(1 - e^{2\pi i})\Gamma(\nu) &= \int_{C_1} du u^{\nu-1} (e^{x+u} - 1)^{-1} + \oint dt (t-x)^{\nu-1} (e^t - 1)^{-1} \\ &= \int_{C_1} du u^{\nu-1} (e^{x+u} - 1)^{-1} + 2\pi i e^{i\pi(\nu-1)} x^{\nu-1}. \quad \dots\dots (A3) \end{aligned}$$



Integration paths in the u -plane.

The integral over C_1 can be expanded by expanding the integrand, which finally gives

$$Z_\nu(x) = \frac{\pi}{\sin \pi \nu} \frac{x^{\nu-1}}{\Gamma(\nu)} + \sum_{\lambda=0}^{\infty} \frac{(-1)^\lambda}{\lambda!} \zeta(\nu-\lambda) x^\lambda, \quad \dots\dots (A4)$$

where $\zeta(\nu)$ is Riemann's ζ -function. The series clearly converges for all non-integral values of ν and $|x| < 2\pi$. (For integral values of ν the singularities in the term in x^1 cancel, but we need not enter into this question here.)

From (A2) or (A4) it follows at once that

$$Z_\nu'(x) = -Z_{\nu-1}(x) \quad \dots\dots (A5)$$

which enables us to write down the expansion of $Z_\nu(x)$ about a point $x \neq 0$:

$$Z_\nu(x+\xi) = \sum_{\lambda=0}^{\infty} \frac{(-1)^\lambda}{\lambda!} Z_{\nu-\lambda}(x). \quad \dots\dots (A6)$$

REFERENCES

- BLOCH, F., 1930, *Z. Phys.*, **61**, 206.
 HOLSTEIN, T., and PRIMAKOFF, H., 1940, *Phys. Rev.*, **58**, 1908.
 KRAMERS, H. A., and OPECHOWSKI, L., 1937, *Physica*, **4**, 715.
 KUBO, R., 1952, *Phys. Rev.*, **86**, 929.
 OPECHOWSKI, L., 1937, *Physica*, **4**, 181.

Isotopic Spin and Coulomb Forces II: Excited States of Light Nuclei

By L. A. RADICATI

Department of Mathematical Physics, University of Birmingham

Communicated by R. E. Peierls; MS. received 6th August 1953

Abstract. The isotopic-spin purity of some low-lying excited states in light nuclei is calculated in first order perturbation theory. Special attention is given to the odd parity states in even nuclei. The isotopic spin impurity caused by coulomb forces is shown to be sufficient to account for the electric dipole transition in ^{16}O between the 7.12 mev excited state and the ground state.

§ 1. INTRODUCTION

IN the last few months the isotopic-spin purity of many excited states in light nuclei has been measured in order to test the validity of the isotopic-spin selection rules (Jones and Wilkinson 1953 a, b, Wilkinson 1953, unpublished). The accuracy of these measurements is still not very high. However, it seems worth while to investigate the amount of mixing between excited states of different isotopic-spin caused by coulomb forces in order to see to what extent the violation of the isotopic-spin selection rules might be considered to disprove the charge independence hypothesis.

To calculate the coulomb mixing in the excited states one needs a fairly detailed knowledge of the quantum numbers and of the configuration to which these states belong, together with a knowledge of the location of the states that can be mixed. Owing to the uncertainties in these factors one cannot hope to get very accurate results, but in many cases the order of magnitude can be obtained.

To calculate the isotopic-spin purity of the excited state we will use the same method already applied to the ground state (Radicati 1953, to be referred to as I).

In particular if T is the isotopic spin of a state with energy E_T on the assumption of purely charge independent forces, we will take $\alpha_T^2(T')$ as a measure of the amount of mixing introduced by the coulomb forces, where

$$\alpha_T(T') = \frac{H_{TT'}}{E_T - E_{T'}} \quad \dots\dots(1)$$

and $H_{TT'}$ is the matrix element of the coulomb energy between the two states T and T' .

In § 2 we will consider briefly the purity of the low-lying states which can be assigned to the same configuration as the ground state. § 3 will be devoted to establishing a formula for the matrix element $H_{TT'}$ for states of $T=0$ and odd parity in light even nuclei, i.e. for states whose configuration can be written $p^n l$ (n odd, l even). These states are important because an E1 transition from them to the ground state is forbidden by the isotopic-spin selection rule (Radicati 1952) even if it is allowed by angular momentum consideration. It is

therefore important to know the isotopic-spin purity of such states in order to decide the extent to which the isotopic-spin selection rule might be expected to be satisfied. In §4 we will apply the formulae previously established to the discussion of the state at 5.11 MeV ($J=2, -$) in ^{10}B discussed by Jones and Wilkinson (1953 b). Finally (§5) we evaluate the purity of the state at 7.12 MeV ($J=1, -$) in ^{16}O whose E1 decay to the ground state constitutes a striking violation of the isotopic-spin selection rule.

§ 2. PURITY OF THE STATES BELONGING TO THE SAME CONFIGURATION AS THE GROUND STATE

To calculate the coulomb mixing in these states we can use the same formulae established in I for the ground state.

We consider, in particular, the lowest states $J=2$ in ^8Be and ^{12}C . These states can be identified with the states ^{11}D of the lowest Wigner super-multiplet in the configurations p^4 and p^8 respectively. It has been shown in I that the ground state of these configurations (^{11}S) cannot be mixed with any state of $T=1$ in the same configuration, the only possible mixing arising from mixed configurations. This is no longer true for the state ^{11}D , which can be mixed by coulomb forces to a state ^{31}D of the p -configuration belonging to the next excited supermultiplet. We expect therefore that the admixture of $T=1$ will be slightly larger in the state ^{11}D than in the state ^{11}S .

In this connection we will mention the case of the first $T=1$ level in ^{10}B at 1.74 MeV ($J=0, +$).

The knowledge of the purity of this state is important in the discussion of the ratio between the cross sections for the reactions $^9\text{Be}(d, p)^{10}\text{B}^*$ and $^9\text{Be}(d, n)^{10}\text{B}^*$ (Adair 1952). It seems reasonable to suppose that a state with such a low excitation energy belongs mainly to the lowest Wigner super-multiplet. In this case the isotopic-spin $T=0$ and the total angular momentum $J=0$ fix uniquely the orbital angular momentum $L=0$. It is easy to verify that in the p^6 configuration there is no other state with $S=0$, $L=0$ and $T=0$ which could be mixed with this state. The mixing between $T=1$ and $T=0$ will therefore mainly occur through interconfigurations mixing with a matrix element $H_{10}^c \sim 0.12$ MeV. Using this value for H_{10}^c we can set an upper limit to $\alpha_0^2(1)$: since no state below 5.58 MeV is known with $J=0, +$ ($T=0$) we will put $E_1 - E_0 > 5.58$ in (1). We get in this way $\alpha_0^2(1) < 9 \times 10^{-4}$.

§ 3. COULOMB MIXING IN THE CONFIGURATION $p^n l$

States of odd parity in even nuclei may be assigned to configurations like $p^n l$ (n odd, l even). In this section we want to establish a formula for the evaluation of the matrix element of H^c between states with a different T .

By specifying all the required quantum numbers, the matrix element $H_{TT'}^c$ is written

$$H_{TT'}^c = \langle p^n([\alpha_1]T_1S_1L_1)\{\beta\}TSL, M_T M_S M_L | H^c | p^n([\alpha_2]T_2S_2L_2)\{\beta'\}T'SL, M_T M_S M_L \rangle \dots\dots (2)$$

where $[\alpha_1]$, $[\alpha_2]$ denote the representations of the unitary group $U(3)$ for the p -nucleons. $T_1S_1L_1$, $T_2S_2L_2$ are the isotopic-spin, the spin, the orbital angular momentum for the p -nucleons in the initial and final state respectively.

$\{\beta\}$, $\{\beta'\}$ specify the representation of the symmetric group S_{n+1} for the $n+1$ nucleons. T , T' , S , L are the resultant isotopic-spin, spin and orbital angular momentum of the $n+1$ nucleons. $M_T M_S M_L$ are the components of T , S and L . The contributions to this matrix element come (i) from the interactions between pairs of p-particles, (ii) from the interactions between each p-particle and the l or l' -particle.

We will examine these contributions separately.

(i) *Interactions between pairs of p-particles.*

Each of the wave functions in the matrix element (2) can be written in the form

$$\begin{aligned} & |p^n(z_1) T_1 S_1 L_1 l \{\beta\} T S L, M_T M_S M_L \rangle \\ &= \frac{1}{\sqrt{(n+1)}} \sum_i^{n+1} (-1)^{P_i} \sum_{M_{T_1} M_{S_1} M_{L_1}} C_{M_{T_1} m_{T_1} M_{T_1}}^{T_1 \frac{1}{2} T} C_{M_{S_1} m_{S_1} M_{S_1}}^{S_1 \frac{1}{2} S} C_{M_{L_1} m_{L_1} M_{L_1}}^{L_1 l L} \mathcal{S}_\beta \\ &\times |p^n[\alpha_1] T_1 S_1 L_1, M_{T_1} M_{S_1} M_{L_1} \rangle |l m_T m_S m_L \rangle \dots\dots (3) \end{aligned}$$

where P_i is the parity of the permutation exchanging the l -particle with the i th p-particle, and \mathcal{S}_β is the operator which chooses the wave function corresponding to the space symmetry $\{\beta\}$ among all those with appropriate T , S , L . The C 's are the Wigner coefficients.

By inserting expression (3) (and a similar expression for the second wave function) into eqn (2) it is easy to verify that the contributions from the interactions between particles can be cast in the form

$$\begin{aligned} & \delta_{ll'} \delta_{\beta\beta'} \sum_{M_{T_1}} C_{M_{T_1} m_{T_1} M_{T_1}}^{T_1 \frac{1}{2} T} C_{M_{T_1} m_{T_1} M_{T_1}}^{T_2 \frac{1}{2} T'} \\ & \times \langle p^n[\alpha_1] T_1 S_1 L_1 M_{T_1} M_{S_1} M_{L_1} | H^c | p^n[\alpha_2] T_2 S_2 L_2 M_{T_2} M_{S_2} M_{L_2} \rangle \dots\dots (4) \end{aligned}$$

The two δ factors take into account the orthogonality of the single particle wave functions with different l and the orthogonality of the total wave functions for the $n+1$ particles when the representations $\{\beta\}$ and $\{\beta'\}$ of the symmetric group S_{n+1} are different. The two Wigner coefficients C arise from the coupling of the odd particle to the state of the n p-particles.

(ii) *Interactions between unlike particles.*

With an obvious extension of the methods developed by Racah (1943) one can easily show that the contribution of these terms to the matrix element (2) is given by

$$\begin{aligned} & n \sum_{\alpha'' T'' S'' L''} \langle l^{n-1}(\alpha'' T'' S'' L'') \rangle l^{n\alpha_1} T_1 S_1 L_1 \rangle \langle l^{n\alpha_2} T_2 S_2 L_2 \rangle l^{n-1}(\alpha'' T'' S'' L'') \rangle \\ & \times U(T'' \frac{1}{2} T_2', T_1 1) U(T'' \frac{1}{2} T_2', T_2 1) U(S'' \frac{1}{2} S_2', S_1 S''') \\ & \times U(S'' \frac{1}{2} S_2', S_2 S''') U(L'' 1 L_1, L_1 L''') U(L'' 1 L_1', L_2 L''') \\ & \times C_{M_{T''} - \frac{1}{2} M_T}^{T'' - \frac{1}{2} T} C_{M_{T''} - \frac{1}{2} M_T}^{T'' - \frac{1}{2} T'} \\ & \times \langle p l 1 S''' L''', -1 M_{S'''} M_{L'''} | H^c | p l 1 S''' L''', -1 M_{S'''} M_{L'''} \rangle \dots\dots (5) \end{aligned}$$

where $U(abcd, ef) = W(abcd, ef) \{(2e+1)(2f+1)\}^{1/2}$ and W is the Racah function. The fractional parentage coefficients $\langle \dots \rangle$ for the p-shell have been tabulated by Jahn and van Wieringen (1951).

§ 4. ISOTOPIC SPIN PURITY OF THE STATE AT 5.11 MEV IN ^{10}B

We will apply now the formulae established in the previous section to the state at 5.11 mev in ^{10}B . The angular distribution of the neutrons in the reaction $^9\text{Be}(\text{d}, \text{n})^{10}\text{B}^*$ (Ajzenberg 1952) fixes the parity and the angular momentum $J=2$ for one of the two states at 5.11 and 5.17 in ^{10}B , without allowing one to distinguish between the two. By measuring the excitation function of the reaction $^6\text{Li}(\alpha, \gamma)^{10}\text{B}$ Jones and Wilkinson (1953 b) conclude that the state at 5.11 should be given $J=2$, odd parity and isotopic-spin $T=0$. It is our purpose to investigate the isotopic-spin purity of this state assuming for T , J , and for the parity the values proposed by Wilkinson. The angular distribution in the reaction $^9\text{Be}(\text{d}, \text{n})^{10}\text{B}^*$ is consistent with the assumption that the proton is captured in an s-state (Ajzenberg 1952). To specify completely the state in the configuration p^5s we have still to fix L , S , the symmetry symbol $\{\beta\}$ and the same quantities for the configuration p^5 . We will fix these quantities by making some assumptions, namely: (i) the symmetry $\{\beta\}$ corresponds to the lowest Wigner super-multiplet, i.e. $\{\beta\} = \{42\}$. (ii) The incoming s-particle does not modify the state of the five nucleons in the ground state of ^9Be , i.e. $[\alpha_1] = [41]$, $T_1 = \frac{1}{2}$, $S_1 = \frac{1}{2}$, $L_1 = 1$. (iii) The s-particle is captured in such a way that its spin is added to the intrinsic spin of ^9Be , i.e. $S = 1$, whereas its isotopic-spin gives with the isotopic spin of ^9Be a state of resultant $T=0$. This amounts to assuming that the order of levels in the configuration p^5s is the same as in the configuration p^6 , namely, that the first level with $S=1$, $T=0$ corresponds to the lowest energy.

Having chosen (assumption (i)) the symmetry $\{\beta\}$ it is easy to see that there are no states belonging to the same super-multiplet with the same S and a different T . Therefore in the matrix element (2) we will have $\{\beta\} \neq \{\beta'\}$, so that the expression (3) vanishes, and the only contribution to the matrix element H_{01}^c will be given by (4). It remains to fix the quantities $[\alpha_2]T_2S_2L_2$ in the matrix element (2). We will take $[\alpha_2] = [\alpha_1]$, $T_2 = T_1$, $S_2 = S_1$, $L_2 = L_1$. A different choice will tend to decrease the matrix element. Finally we will put $l=l'=0$. The justification for doing so is that the first state of negative parity and with the appropriate values of J and T above the state at 5.11 is a state at 7.48 which appears to be formed by s-capture of protons on ^9Be (Ajzenberg and Lauritsen 1952).

After inserting in the expression (5) the values corresponding to our assumption, the matrix element of the coulomb interaction between the state $T=0$ and $T=1$ is

$$\begin{aligned} H_{01}^c &= \langle \text{p}^5([41]_{\frac{1}{2}\frac{1}{2}}1)\text{s}\{42\}011 | H^c | \text{p}^5([41]_{\frac{1}{2}\frac{1}{2}}1)\text{s}\{411\}111 \rangle \\ &= \frac{1}{3} \langle \text{ps}111 | H^c | \text{ps}111 \rangle. \end{aligned} \quad \dots\dots(6)$$

The two-particles matrix element in eqn (6) is

$$\langle \text{ps}111 | H^c | \text{ps}111 \rangle = F^0 = G^1$$

where F^0 and G^1 are the radial integrals defined by Condon and Shortley (1951). The evaluation of this matrix element is not very sensitive to the choice of individual particle wave functions. For the sake of comparison with the calculations in I the same wave functions (gaussians) have been used, with the same parameters. The result is

$$\langle \text{ps}111 | H^c | \text{ps}111 \rangle \sim 0.33 \text{ mev},$$

which is slightly less than the interaction between two p-particles in an S state (~ 0.51 Mev).

The matrix element of the coulomb interaction is therefore $H_{01}^c \sim 0.11$ Mev. The amount of mixing of the state $T=1$ is given by eqn (1), in which we will put $E_1 = 7.48$ Mev in accordance with the previous discussion. We get in this way $\alpha_0^2(1) \sim 2.0 \times 10^{-3}$, in good agreement with Wilkinsen's (1953, unpublished) estimate ($\alpha_0^2(1) < 3 \times 10^{-3}$). This shows that the main assumption used in this calculation, i.e. that the state belongs to the first Wigner super-multiplet, is essentially correct.

§ 5. THE ELECTRIC DIPOLE TRANSITION BETWEEN THE 7.12 MeV STATE AND THE GROUND STATE IN ^{16}O

We will now investigate the isotopic spin purity of the state at 7.12 ($J=1, -$) in ^{16}O . We do not have any indication of the possible configuration to which this state belongs. For the sake of argument we assume the wave function to be of the type $|p^{11}([443]_{\frac{1}{2}, \frac{1}{2}}1)d\{444\}001\rangle$, which is consistent with the observed total angular momentum and the parity. A different choice (for example to assume an s-level) would not appreciably modify the results. Again, there is no state in the super-multiplet $\{444\}$ with spin zero and isotopic spin 1, so that the mixing can only occur with a state belonging to another super-multiplet. Therefore (see § 2) there is no contribution to the coulomb matrix element from the interaction between two p-nucleons.

After inserting the appropriate values for the fractional parentage coefficients, and for the Racah functions, one gets $H_{01}^c \sim 0.30$ Mev.

We do not exactly know where the state $T=1$ of this configuration is located, so we shall insert the energy of the first state of $T=1$ in ^{16}O which is around, 12.8 Mev. We get in this way for the amount of mixing $\alpha_0^2(1) \sim 3.6 \times 10^{-3}$.

This value for $\alpha_0^2(1)$ is greatly in excess of the lower limit ($\alpha_0^2(1) > 4 \times 10^{-6}$) set by Jones and Wilkinson (1953 a) in their discussion of the branching ratio between the transition

$$7.12 \text{ Mev } (J=1, -) \rightarrow \text{ground } (J=0, +)$$

and

$$7.12 \text{ Mev } (J=1, -) \rightarrow 6.14 \text{ Mev } (J=3, -).$$

This shows that the coulomb forces alone may be sufficient to account for this electric dipole transition, which constitutes one of the most striking violations of the isotopic spin selection rule.

ACKNOWLEDGMENT

It is a pleasure to thank Dr. D. H. Wilkinson for several discussions and for making the results of his experiments available to me in advance of publication.

REFERENCES

- ADAIR, R. K., 1952, *Phys. Rev.*, **87**, 1041.
 AJZENBERG, F., 1952, *Phys. Rev.*, **88**, 298.
 AJZENBERG, F., and LAURITSEN, T., 1952, *Rev. Mod. Phys.*, **24**, 321.
 CONDON, U., and SHORTLEY, G. H., 1951, *The Theory of Atomic Spectra* (Cambridge : University Press).
 JAHN, H. A., and VAN WIERINGEN, J. S., 1951, *Proc. Roy. Soc. A*, **209**, 502.
 JONES, G. A., and WILKINSON, D. H., 1953 a, *Phil. Mag.*, **44**, 542; 1953 b, *Phys. Rev.*, **90**, 722.
 RACAH, G., 1943, *Phys. Rev.*, **63**, 367.
 RADICATI, L. A., 1952, *Phys. Rev.*, **87**, 521; 1953, *Proc. Phys. Soc. A*, **66**, 139.

The Absorption Spectrum of Bismuth Oxide

BY N. K. BRIDGE AND H. G. HOWELL

The British Rayon Research Association, Urmston, Nr. Manchester

MS. received 22nd May 1953, and in amended form 7th October 1953

Abstract. The absorption spectrum produced when bismuth is heated in a furnace up to 1500°C has been analysed. It extends from 2450 Å to 3800 Å. Evidence is given to attribute it to the diatomic molecule BiO. The bands are grouped into four systems and there is evidence of the existence of a fifth.

The vibrational constants proposed for these systems are:

ν_e	ω_e	$x_e\omega_e$	ν_e	ω_e	$x_e\omega_e$
40930	770		30220	487	
38551.8	769.3	6.2	28739.5	487.0	6.5
30500	—		0	695.9	4.9

The ground state is considered to be the lower component of a case $a^2\Pi$ with probable $\omega-\omega$ coupling and the doublet splitting is estimated to be between the limits 8000 and 13 500 cm^{-1} . The relation of the absorption spectrum to the emission spectrum is considered and an attempt is made to account for the energy levels in terms of electron configurations.

§ 1. INTRODUCTION

DURING a study of the absorption spectra of the antimony halides, it was observed that when a little bismuth was introduced into the absorption tube a strong band system was produced in the 2200–2700 Å region. Preliminary measurements of this suggested that the molecule responsible was either the oxide BiO or the nitride BiN, the former being the more probable. A survey of the relevant literature shows that our knowledge of the spectra of the oxide molecules of Group V is least satisfactory in the case of BiO. A number of papers report work on this molecule, but the net result has been to produce a state of confusion. All previous investigations have been concerned with the red-degraded bands in the visible which are produced in a carbon arc when fed with metallic bismuth or BiCl_3 . First measured by Mecke and Guillery (1927), they were later analysed by Ghosh (1933) into four singlet systems. However, the work of Saper (1931) and Morgan (1936) showed that some of these bands coincided with known bands of BiCl. This was confirmed by Ray (1942) who also pointed out that the spectrum did indeed contain a number of bands which could not be allocated to BiCl and were probably due to BiO. In the latest investigation into these residual bands Sen Gupta (1944) gives new measurements for 17 of them, and fits them into a single system having the wave-number equation: $\nu(\text{head}) = 15194.5 + 500.0(v' + \frac{1}{2}) - 3.10(v' + \frac{1}{2})^2 - 702.1(v'' + \frac{1}{2}) + 5.20(v'' + \frac{1}{2})^2$.

The present paper describes new systems for this molecule and discusses the probable nature of the electronic energy levels involved.

§ 2. EXPERIMENTAL

The absorption described here is that due to the vapour produced by placing metallic bismuth in an open-ended vitreosil tube of diameter 1 cm. Temperatures up to 1500°C were used with a Johnson, Matthey T.53 furnace. The source was a high pressure xenon gas arc for the ultra-violet and a 500 w filament lamp for the visible region. A Hilger Intermediate quartz spectrograph was used for the initial survey work whilst the Hilger automatic-focusing E.492 provided the more detailed spectrograms.

The experimental procedure was to set the furnace at some fixed temperature and then to charge the absorption cell with bismuth. A continuous spectrogram was then taken covering the whole plate of the Intermediate quartz by racking down the plateholder with a variable-speed motor. The xenon source is sufficiently intense over the whole region 2200–8000 Å to enable the plate to be exposed continuously over varying periods from 1 second upwards. By this means it is possible to detect absorption of any short-lived radicals which may be formed during the contact of the heated vapour with the oxygen and nitrogen of the air. This process was now repeated for a range of temperatures so that the optimum conditions for the production of any given part of the spectrum could be determined, after which the work was transferred to the larger spectrograph.

The ultra-violet bands already mentioned were found to appear first at about 1100°C, in the shape of a narrow absorption region near 2600 Å. This extends in both wavelength directions as the temperature is raised. The actual working temperatures ranged from 1300 to 1450°C, the lower being necessary to bring out detail in the strongest bands and the higher to record the weakest bands. Exposures of the order of 15 seconds were made on Kodak P.1500 plates. At higher temperatures, up to and slightly above 1500°C a second system in the region 3200–3700 Å was observed and photographed on Ilford Rapid Process Panchromatic plates. The visible region was also investigated and much Bi₂ absorption was found. Occasionally a few violet-degraded bands were also observed.

Wavelength measurements were made on a Hilger Comparator using iron arc standards.

§ 3. ANALYSES

3.1. *The 2600 Å Bands*

A photograph of this strong system taken under low dispersion is shown in figure 1(a) (Plate). It consists of five groups of bands having an obvious sequence-type structure which appear reasonably sharp. However, on higher dispersion (3 Å mm⁻¹) each sequence reveals so much structure that the eventual sorting out into individual bands proved more troublesome than was at first expected. Up to six branches can be detected in the strong bands, three branches in each being usually stronger than the others. None have really sharp heads and some appear as fairly narrow absorption lines. Narrow transmission regions indicating origin gaps are also occasionally observed. These are of varying width and not suitable for very accurate setting in wavelength measurements. Whilst the sequences are degraded to short wavelengths most of the individual branches are headless, suggesting near equality of the vibrational frequencies. The branches in most

bands are very short with maxima well separated from each other due to the high temperature of the absorbing vapour. There is no sign of rotational structure in any of these bands.

The vibrational analysis does not present much difficulty and with the exception of five, all the bands were originally represented in the quantum scheme of table 1 as a single system, the measurements referring to the first strong branch of each

Table 1. Vibrational Analysis of 2600 Å System of BiO

v''	0	1	2	3	4
v'					
0	38588 (10) 2382 40970 (2) 755 —	685 674 758 744	37903 (6) 2393 40296 (3) 758 751	674 671 758 751	37229 (1) 2396 39625 (1)
1	39343 (8) — — 746 —	682 — — 746 —	38661 (7) 2379 41040 (2) 739 —	674 664 746 —	37987 (4) 2389 40376 (2) 749 —
2	40089 (3) —	689 —	39400 (6) —	667 —	38733 (1) —
			748 —	669 —	38064 (3) —
3			40148 (2) —	651 —	37413 (2) —

band. Those which did not fit into this scheme are marked with a cross in figure 1(a). They are very similar in general appearance to the main bands but as observation and measurement have been confined to low dispersion plates nothing can be said about the branch structure. They have approximately the same vibrational differences and may well be the other component of a doublet system and are accordingly included in table 1 as such. The doublet separation is of the order of 2385 cm^{-1} . The following quantum equation has been derived for the wave numbers of the bands of the main component:

$$\nu = 38551.8 + 769.3(v' + \frac{1}{2}) - 6.2(v' + \frac{1}{2})^2 - 696.7(v'' + \frac{1}{2}) + 5.7(v'' + \frac{1}{2})^2.$$

Although the observations are only presented to the nearest wave number it is, of course, necessary to deal with the first decimal in order to represent the data mathematically.

3.2. The 3500 Å System

This is shown in figure 1(b) and has quite a different appearance from the other system. The bands are all red-degraded, have well-defined heads and form progressions. Table 2 shows the proposed Déslandres scheme, which is

bounded by the two strongest progressions. At first the analysis was limited to the first member of the doublet pair in the table but, as in the previous case, it was later found that a number of unallocated bands revealed differences of the same order as those in the main system and they were then provisionally included as the second component of a doublet system having $\Delta\nu_E$ approximately 1480 cm^{-1} .

The main bands have been fitted to the equation

$$\nu = 28739.5 + 487.0(v' + \frac{1}{2}) - 6.5(v' + \frac{1}{2})^2 - 695.0(v'' + \frac{1}{2}) + 4.0(v'' + \frac{1}{2})^2.$$

The constants for the ground state differ slightly from those obtained from the other system. The mean values are $\omega_e'' = 695.9$ and $x_e''\omega_e'' = 4.9$.

This analysis still leaves a number of unallocated bands which are given in table 3. The first four form a v'' progression and probably represent a fragment of another weak system with an origin about $30\,500\text{ cm}^{-1}$.

Table 3. Unallocated Bands of BiO (cm^{-1})

29791	29131	28471	27812
	660	660	659
28309	27840	27022	

§ 4. DISCUSSION

4.1. Nature of the Absorbing Molecule

As the method of production in this case does not indicate unambiguously the nature of the molecule responsible for the spectrum it is necessary to find other evidence for ascribing it to BiO and this is provided from considerations of the magnitude of ω_e'' . The value found here is much too large for Bi_2 which might have some claim to be the absorbing molecule, but is perhaps of the right order for BiN. However, as Rochester (1936) first pointed out, the ω_e values of corresponding pairs of Group IV and V oxide molecules are very nearly equal. This leads to the expectation of ω_e for BiO to be nearly the same as that for PbO, viz. 720 cm^{-1} , which agrees quite well with the value of 695 cm^{-1} here determined. Against BiN being responsible it should be noted that although emission spectra of the similar molecules PN, AsN and SbN are known, they are relatively simple, involving one singlet transition in the ultra-violet, quite unlike the complex structure found for the present molecule. Again a study of the ω_e values of all the nitride molecules indicates a value of at least 800 cm^{-1} to be expected for BiN. Consequently, it is with some confidence that, apart from any knowledge of the emission spectrum, the absorbing molecule is stated to be BiO. It is now relevant to consider the emission bands, for the lower state of which Sen Gupta obtained a value for ω_e of 702 cm^{-1} . In view of the confused past history of the emission bands this ω_e value by itself would not be completely convincing evidence for BiO being the emitting molecule, but taken in conjunction with the present work it is clear that the emission data support the view that BiO is responsible and also that the absorption work broadly confirms the analysis of the emission spectrum.

4.2. Energy Levels of BiO

It is established from rotational analyses that the ground state of the simplest molecules of this type NO and PO is $^2\Pi$ and it is inferred from vibrational analyses that the molecules AsO and SbO also have such a ground state. The electronic separation of these states are given in table 4 which also includes that for similar $^2\Pi$ states of the iso-electronic fluorides.

Table 4. Electronic Separations of $^2\Pi$ Ground States (cm^{-1})

NO	PO	AsO	SbO	BiO	CF	SiF	GeF	SnF	PbF
120	224	1026	2272	—	77	161	935	2317	8266

BiO can be expected to have a similar $^2\Pi$ ground state based upon the probable electron configuration $\sigma^2\pi^4\pi$. Sen Gupta estimated the doublet separation of BiO to be $4000\text{--}4500\text{ cm}^{-1}$ and hence was led to expect that the origin of the other component of his singlet emission system should be at either 5200 \AA or 9000 \AA . He could not detect any bands in the former region and consequently assumed them to be in the infra-red. An examination of table 4 shows that his figure is much too low and that a minimum value of 8000 cm^{-1} is to be expected. In the present discussion a value of $10\,000\text{ cm}^{-1}$ will be assumed and this has enabled the energy level diagram of figure 2 to be drawn. This includes the

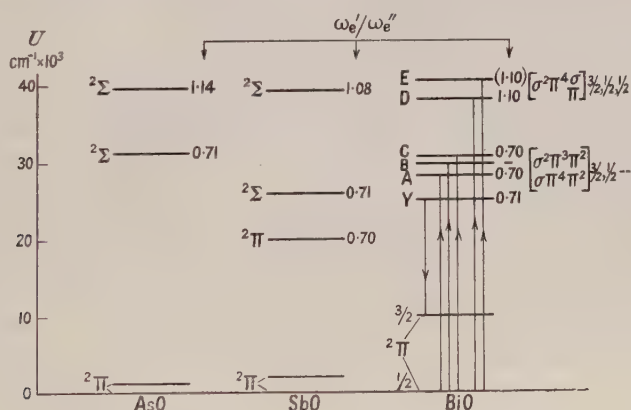


Figure 2. Energy levels of AsO, SbO and BiO.

level marked C representing the upper state of the fragmentary v'' progression previously mentioned. From the magnitude of the doublet separation of the ground states it is certain that the coupling is case *a* with an increasing tendency to ω - ω coupling from AsO to BiO in which only Ω retains its significance. In spite of this the designations $^2\Sigma$, $^2\Pi$, etc. are retained (usually in brackets) as the relation of the state to a particular electron configuration is thereby made clearer.

As there is no sign of the emission bands in absorption, the lower state of these cannot be the ground state $^1(^2\Pi)$ and, accordingly, is here taken to be the $^3(^2\Pi)$ component, which fixes the position of the emission upper state Y at about $25\,000\text{ cm}^{-1}$. Against this supposition is the fact that there is no sign of any absorption in this region, the nearest being to the A level at $28\,700\text{ cm}^{-1}$. Consequently, the following alternative must be considered possible, viz. that

Y and A are identical, A then being the upper state of the emission system. The difference in the quoted ω_e values for Y and A may not be significant when it is remembered that they are derived in each case from a small number of bands. This interpretation now gives the ground state separation $\frac{3}{2} - \frac{1}{2}(2\Pi)$ as 13 500.

The ratio of ω_e'/ω_e'' is given in figure 2 as this is often very helpful in sorting out corresponding states in a group of similar molecules. It will be observed that the levels fall into one of two classes: (i) $\omega_e'/\omega_e'' < 1$; (ii) $\omega_e'/\omega_e'' > 1$. This suggests that the levels arise from two different electron configurations in which on excitation there is in class (i) a decrease and in class (ii) an increase in bonding. Now in the ground state $\sigma^2\pi^4\pi^*$, the π^* electron is in an anti-bonding orbital and so any excitation from the bonding (or even non-bonding) orbitals to this Π^* orbital will give a reduction in bonding so that the complex of levels Y, A, B and C probably belong to one of the configurations

$$\begin{array}{l} \sigma^2\pi^3\pi^{*2}, \quad {}^2\Pi_1, {}^2\Pi_r, {}^2\Pi_1 4\Pi_b \\ \sigma\pi^4\pi^{*2}, \quad {}^2\Sigma^+, {}^2\Sigma^-, {}^2\Delta, {}^4\Sigma^- \end{array}$$

Now in table 2 the bands are represented as belonging to an electronic doublet, presumably of the ${}^2\Pi - {}^2\Pi$ type because of the simple rotational structure with no obvious Q branch, but in the case of $\omega - \omega$ coupling there is no distinction between components of a multiplet and other levels arising from the same configurations (apart from their Ω values). They are all separate levels and in the present case they can best be described as arising from the complex

$$\left[\begin{array}{l} \sigma^2\pi^3\pi^{*2} \\ \sigma\pi^4\pi^{*2} \end{array} \right] \frac{3}{2}(4), \frac{1}{2}(5),$$

the figures in round brackets giving the probable number of states likely to be concerned, having the given Ω value. As the transition to, or from, the ground state appears to be of the form $\Delta\Omega = 0$, i.e. $\frac{1}{2} - \frac{1}{2}$, the description of these levels can thus probably be defined more closely. The electronic separation given in table 2 is probably then a difference between two $\frac{1}{2}$ states of the above complex.

Essentially the same remarks apply to the separation shown in table 1 for the bands of the farther ultra-violet systems. Here the main bands have the apparent complexity of transition of the type ${}^2\Sigma \leftarrow {}^2\Pi$ or ${}^2\Delta \leftarrow {}^2\Pi$. As the upper state has a greater bonding than the ground state the electron configuration must be of the type $\sigma^2\pi^4\sigma$, $\frac{1}{2}({}^2\Sigma)$ or $\sigma^2\pi^4\pi$, $\frac{1}{2}$, $\frac{3}{2}({}^2\Pi)$ where the anti-bonding π^* electron has been replaced by a bonding or non-bonding one—more probably the latter as the increase in ω_e'' is not very great. This suggests the state to be of a Rydberg type similar to the upper state of the NO γ -bands. Table 5 gives the wavelengths of the strongest bands (intensity of 5 and over based upon visual estimates) together with the observed—calculated (O—C) values of the wave numbers.

Table 5. Strongest Bands of BiO Absorption

2600 Å Bands			3500 Å Bands		
(Å)	I	O—C (cm ⁻¹)	(Å)	I	O—C (cm ⁻¹)
2537	6	-4	3238.4	6	-4
2541.0	8	-2	3283.0	8	-2
2585.8	7	1	3330.4	9	0
2590.7	10	0	3381.0	10	-1
2637.5	6	0	3434.4	10	0
			3576.7	5	2

ACKNOWLEDGMENTS

This work was done in the laboratories of the British Rayon Research Association, Manchester, where one of us (N. K. B.) was undergoing a training in spectroscopy. We are indebted to the Government Grants Committee of the Royal Society for a grant (to H. G. H.) which enabled the work to be completed. We also thank Miss I. Phillip for much experimental assistance.

REFERENCES

- GHOSH, C., 1933, *Z. Phys.*, **86**, 241.
MECKE, R., and GUILLERY, M., 1927, *Phys. Z.*, **28**, 514.
MORGAN, F., 1936, *Phys. Rev.*, **49**, 41.
RAY, S. K., 1942, *Ind. J. Phys.*, **16**, 35.
ROCHESTER, G. D., 1936, *Proc. Roy. Soc. A*, **153**, 407.
SAPER, P. G., 1931, *Phys. Rev.*, **37**, 1710.
SEN GUPTA, A. K., 1944, *Ind. J. Phys.*, **18**, 182.

Correlation Energy in Metals and the Cohesive Energy of Metallic Sodium

By S. RAIMES

Department of Mathematics, Imperial College, London

MS. received 22nd September 1953

Abstract. The method of Wigner and Seitz for calculating the cohesive energy of metallic sodium is compared with a recent method of Löwdin, and reasons are given for preferring the former. A simple calculation shows that Löwdin's use of the LCAO method in constructing his one-electron functions must give rise to an error in the energy greater than the correlation energy as estimated by Wigner, so that Löwdin's results should not be used in assessing the accuracy of Wigner's formula.

IN calculating the cohesive energy of metallic sodium Wigner and Seitz (1934) implicitly assumed a total wave function consisting of a single determinant of Bloch-type molecular spin orbitals, the latter being approximations whose nature will be discussed more fully below, to the solutions of lowest energy of the Hartree-Fock equations for the valence electrons in the crystal. It is well known that such a wave function takes no account of correlations between the positions of electrons with antiparallel spins, so that, unless this effect is negligible, accurate agreement with experiment can only be expected when allowance is made for such correlations by including in the energy an additional term, generally known as the *correlation energy*. Wigner (1934) has estimated the correlation energy for a system of free electrons, and his result may be expressed in the form (Wigner 1938, cf. Seitz 1940, p. 343)

$$-0.576/(r_s + 5.1) \quad \dots\dots (1)$$

for the correlation energy in rydberg units per electron, where r_s , in Bohr units, is the atomic radius, or the radius of a sphere whose volume is the total volume of the system divided by the number of electrons. Although this expression was obtained for *free* electrons it may be expected to apply with reasonable accuracy to the *valence* electrons in many metals and, in particular, to those in sodium, which are certainly very nearly free; and Wigner and Seitz, in fact, obtained a good value for the cohesive energy of sodium when this term was included. The value of expression (1) is small compared with the total energy of the valence electrons, but it is nearly as large as the cohesive energy, so that, if Wigner's estimate is correct, it is of considerable importance in calculations of the latter quantity. It is not our purpose at present to establish the accuracy of expression (1), which Wigner himself puts at only 20%, but it is certainly true that in all calculations of the cohesive energies of metals, by the Wigner-Seitz and closely related methods, agreement with experiment would be

considerably worsened if the correlation energy were found to be much smaller than Wigner's estimate.

More recently, however, Löwdin (1951) has calculated the cohesive energy of metallic sodium by a method which differs in certain important respects from that of Wigner and Seitz and obtains very good agreement with experiment, at least for the cohesive energy and lattice parameter, without including a term of any kind to represent the correlation energy. The fact that Löwdin obtains a poor value for the compressibility, while Wigner and Seitz obtain a good one, is an indication that his method should be treated with reserve, and indeed the author himself states that the accuracy of his other results may be somewhat fortuitous. Slater (1953), however, takes the opposite view and quotes Löwdin's results in support of his opinion that Wigner's value for the correlation energy is much too large and that, in fact, the numerical accuracy of the calculation of Wigner and Seitz for sodium, using this correlation term, is probably fortuitous. It is the purpose of the present note to show that Löwdin's calculation is quantitatively not sufficiently reliable for any conclusions to be drawn from it regarding the magnitude of the correlation energy.

The total wave function assumed by Löwdin also consists of a single determinant of Bloch-type molecular spin orbitals. The latter, however, unlike those employed by Wigner and Seitz, are formed by linear combination of atomic orbitals (LCAO), the atomic orbitals used by Löwdin being valence electron 3s functions situated at the lattice points, or orthogonal localized functions constructed from these. The method is thus similar to that known in the theory of metals as the *approximation of tight binding*, with one important difference: the tight binding method, as its name implies, has only been considered in relation to electrons which are tightly bound, so that, with considerable simplification in the mathematics, it is justifiable to neglect overlap effects except between nearest neighbours, while in metallic sodium the valence electrons are far from being tightly bound and, in fact, Löwdin finds it necessary to consider overlap effects from no less than 136 first neighbours of a given atom. This would normally result in the mathematically inconvenient occurrence of a very large number of three-centre and four-centre integrals, and the importance of Löwdin's work lies in the fact that by ingenious manipulation and the introduction of what he calls *combined atomic orbitals* he has been able to reduce all the integrals occurring to two-centre integrals. In this way the computational problem, although still formidable, is reduced to manageable proportions, and Löwdin has been able to complete the calculation for sodium. Without detracting from the magnitude of this accomplishment it must nevertheless be pointed out that the molecular orbitals employed by Löwdin are not solutions of the Hartree-Fock equations for the valence electrons in the crystal and, what is more relevant, they are undoubtedly worse approximations to such solutions than are the functions used by Wigner and Seitz. Furthermore, an attempt will now be made to show, by comparison of the orbitals of lowest energy, that the difference in the energies given by the two methods *due to the different one-electron functions alone* is greater than Wigner's estimate of the correlation energy.

The Wigner-Seitz function of lowest energy, which we shall denote by ψ_0 , is obtained, within an atomic cell, by solving the equation

$$H\psi_0 = \epsilon_0\psi_0 \quad \dots\dots (2)$$

subject to the condition that the normal derivative of ψ_0 vanish on the surface of the atomic sphere, H being given by

$$H = -\frac{d^2}{dr^2} - \frac{2}{r} \frac{d}{dr} + V(r), \quad \dots\dots (3)$$

where $V(r)$ is the potential function of the ion-core. Elementary considerations suggest, and more detailed investigation confirms, that ψ_0 is, in spite of the simplified boundary conditions employed in its calculation, a very good approximation to the correct solution of lowest energy. Of course the use of the simple Hamiltonian H involves approximations in addition to that of the spherical symmetry of ψ_0 , but these hardly affect the present discussion. The fact that ψ_0 is approximately constant over the greater portion of the atomic sphere led Wigner and Seitz to use free-electron functions in calculating all energy terms except ϵ_0 and the Fermi energy (cf. Bardeen 1938), and the reasonableness of this procedure is amply demonstrated by the work of von der Lage and Bethe (1947) and of Howarth and Jones (1952), which shows that the valence electrons in metallic sodium are almost completely free.

Löwdin's function of lowest energy, which we shall denote by $\psi_0^{(L)}$, is, apart from a normalizing constant, simply the sum of atomic 3s functions situated at all the lattice points: it has, of course, the periodicity of the lattice, but within a given atomic cell it is almost spherically symmetrical, and it is sufficient for our present purposes if we take it, like ψ_0 , to be exactly so. The function used in the calculation below, and shown in figure 1 (b), was taken

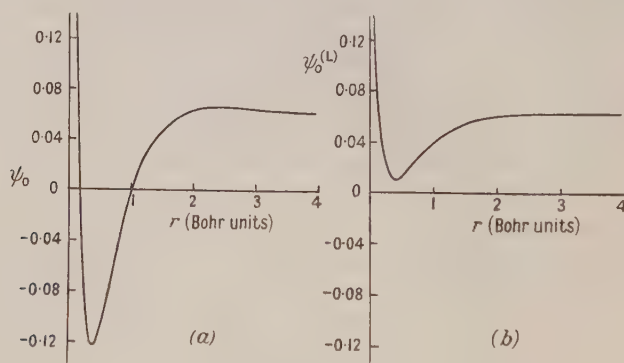


Figure 1. One-electron functions of lowest energy for metallic sodium: (a) according to Wigner and Seitz (1934); (b) according to Löwdin (1951). Both functions are normalized to unity in an atomic sphere of radius 3.96 Bohr units.

from figure 6 of Löwdin's paper, except for that part between the origin and the position of the minimum—here measurement of Löwdin's small graph was unsatisfactory and the function was therefore calculated, accurately enough, assuming that the total contribution from all atoms but the central one is constant in this region.

The two functions ψ_0 and $\psi_0^{(L)}$ display certain similarities: in particular they are both approximately constant over the greater portion of the atomic cell. Of more significance for this discussion, however, are their differences, which are very pronounced in the region lying inside the ion-core, whose radius is about 2 Bohr units. In this region the function of lowest energy is expected

to resemble the atomic 3s function, and the Wigner-Seitz function does so, while the Löwdin function does not, since it has no spherical nodes. This alone, quite apart from the arguments presented above, should lead one to prefer the Wigner-Seitz function and to regard the other with suspicion. Now, although at first sight the two methods appear to be quite different, they are in principle similar, and furthermore several approximations are common to them both—for instance, exchange and correlation interactions between valence and core electrons are assumed to be the same in the metal as in free atoms; the occupied region of \mathbf{k} -space is assumed to be a sphere; and Löwdin assumes spherical symmetry for his combined atomic orbitals for the same reason that Wigner and Seitz assume it for ψ_0 , namely, the high symmetry of the body-centred cubic lattice. The principal difference between the two methods, then, lies in the type of molecular orbital employed, and since any error in the orbital of lowest energy will in both cases be reflected in those of higher energy a comparison of the energies of ψ_0 and $\psi_0^{(L)}$ should give a good indication of how the calculated cohesive energies will differ in the two methods.

The energy of ψ_0 , namely ϵ_0 , is found by solution of eqn (2) to be -0.61 Ryd. For comparison purposes the energy of $\psi_0^{(L)}$ was taken to be

$$\epsilon_0^{(L)} = \int \psi_0^{(L)} H \psi_0^{(L)} d\tau \quad \dots\dots (4)$$

where the integration is over the atomic sphere of radius 3.96 Bohr units, $\psi_0^{(L)}$ is normalized to unity in this sphere, and H is given by eqn (3). It should be noted that the potential function $V(r)$ used in this calculation was the Prokofjew (1929) function, since this was used in calculating ϵ_0 ; Löwdin, of course, uses the ion-core field of Hartree and Hartree (1948), but since we only wish to find the difference between ϵ_0 and $\epsilon_0^{(L)}$, the choice of field is unimportant so long as the same one is used in calculating both quantities. In this way $\epsilon_0^{(L)}$ was found to be -0.76 Ryd.

Thus we see that the energy of the Löwdin function $\psi_0^{(L)}$ is 0.15 Ryd *lower* than that of the Wigner-Seitz function ψ_0 , which is undoubtedly the better approximation. Since the correlation energy given by Wigner's formula (1) is only -0.06 Ryd it is not surprising that Löwdin, without including this term, obtains a lower total energy (i.e. a larger cohesive energy) than Wigner and Seitz; indeed it is rather surprising that Löwdin does not obtain a cohesive energy about twice as great as his present result. What has been established with some certainty is that the error to be expected from Löwdin's use of the LCAO method in constructing his molecular orbitals is greater than the correlation energy as estimated by Wigner, and therefore Löwdin's results are of no help at all in judging the accuracy of Wigner's formula.

Certain conclusions of greater generality come out of the present discussion, and these may be worth emphasizing. There are two main disadvantages in applying the Bloch (or crystal orbital -LCAO) method, as Löwdin has done, to the valence electrons in metals. First, the large overlap creates computational difficulties, which Löwdin has managed to overcome. Secondly, the large overlap results in orbitals which are rather poor approximations to the true Hartree-Fock functions. This latter disadvantage could in principle be resolved by considering, not one, but several atomic orbitals at each lattice point and applying the variational method; the labour involved would certainly be

immense, however, and if a great many atomic orbitals had to be used, as seems likely, the calculation would probably prove impracticable. It should be noted that the importance of the second difficulty, in metals, is due to the large number of near neighbours of a given atom, which means that the small overlap from a single neighbouring atom is multiplied many times: this difficulty will be by no means so pronounced in small molecules—for instance, in a hypothetical Na_2 molecule the overlap could never remove the spherical nodes of the atomic 3s functions, as is the case in the metal. Of course, if the overlap were small, as for more tightly bound electrons, the molecular orbitals formed by LCAO, using only one kind of atomic orbital, would be much better approximations, so that the second difficulty would be reduced—the first difficulty would be correspondingly reduced, however, and the simple tight binding method might be expected to suffice. None the less, Löwdin's method would probably be more reliable quantitatively, and more useful practically, if applied, say, to the d-shells of the transition metals. The problem of the correlation energy would remain, however, and indeed in an aggravated form, since even Wigner's formula could not be used for electrons which are not at least approximately free.

REFERENCES

- BARDEEN, J., 1938, *J. Chem. Phys.*, **6**, 367.
HARTREE, D. R., and HARTREE, W., 1948, *Proc. Roy. Soc. A*, **103**, 299.
HOWARTH, D. J., and JONES, H., 1952, *Proc. Phys. Soc. A*, **65**, 355.
VON DER LAGE, F. C., and BETHE, H. A., 1947, *Phys. Rev.*, **71**, 612.
LÖWDIN, P. O., 1951, *J. Chem. Phys.*, **19**, 1579.
PROKOFJEV, W., 1929, *Z. Phys.*, **58**, 255.
SEITZ, F., 1940, *Modern Theory of Solids* (New York: McGraw-Hill).
SLATER, J. C., 1953, *Rev. Mod. Phys.*, **25**, 199.
WIGNER, E., 1934, *Phys. Rev.*, **46**, 1002; 1938, *Trans. Faraday Soc.*, **34**, 678.
WIGNER, E., and SEITZ, F., 1934, *Phys. Rev.*, **46**, 509.

The Auger Effect and Negative Meson Capture

BY A. H. DE BORDE*

Department of Physics, University College, London

MS. received 2nd September 1953

Abstract. Previous work on the mesonic Auger effect is extended to meson capture in non-circular orbits, and to Auger emission of L shell electrons. Corrections to the theoretical results are discussed and calculations made of the probable Auger emission from heavy elements for capture in photographic emulsions. The results are compared with observations and reasons suggested for a deviation.

§ 1. INTRODUCTION

IT is now generally accepted that negative mesons stopped in matter tend to eject an atomic electron forming a system in which the meson is bound to the atom. Owing to the large mass of a meson compared with that of an electron such a system is likely to be formed in a highly excited state. The meson then cascades to its ground state either by radiative or radiationless transitions, direct interaction with the nucleus being improbable in the excited states. Experimental support for this picture has been provided both by observations of γ -rays emitted in the radiative transitions (Chang 1949, Hincks 1951) and of slow electrons emitted in Auger transitions which are the most important of the radiationless processes (Cosyns *et al.* 1949, Fry 1951, 1953). It is of some interest to make calculations concerning the probable number of electrons emitted in such processes on the basis of a pure electromagnetic interaction as a confirmation of the general picture of the capture process.

A previous simplified theory of the mesonic Auger effect has been presented (Burbidge and de Borde 1953). This theory was unsatisfactory in several respects. In particular, (i) the theory was based on the assumption that the meson was initially captured into a state with azimuthal quantum number $l=n-1$, (ii) ejection of Auger electrons from L and higher electronic shells was neglected, (iii) no account was taken of a possible reduction in the Auger transition rates due to depletion of the number of electrons in the K shell.

These objections to the theory are removed in the present paper. It will be shown that the theory can only be reconciled with experiment by either assuming that the initial atomic capture takes place predominantly into states of low angular momentum or by assuming that a high degree of ionization arises in transitions to the meson ground state.

§ 2. CALCULATION OF TRANSITION RATES

The first step required in a detailed theory of the mesonic Auger effect is the calculation of the Auger and radiative transition rates between meson states of low quantum numbers. These calculations follow the same lines as described in the

* Now at the Department of Natural Philosophy, University of Glasgow.

earlier paper (Burbidge and de Borde 1953) and the same notation will be used. Since the calculations are somewhat lengthy, they will not be described in full.*

For transitions with emission of K shell electrons, the angular integrations may be simply performed as described therein. The radial integrals, however, are more complicated as, in general, a polynomial in r_1 replaces the single term occurring for transitions between circular orbits. If, however, the terms I_1 , I_2 are ignored, the integral over r_1 may be transformed into the same form as that occurring in the evaluation of the radial integral for the dipole matrix element for hydrogen. The evaluation of this integral has been fully discussed by Gordon (1929).

A correction for the neglected terms may also be deduced with the same approximation as described previously, and using the methods of Gordon to evaluate the integral over r_1 .

The evaluation of the transition rates for emission of L shell electrons is similar but rather more complicated as the ejection of both 2s and 2p electrons has to be considered. However, it is found that the contribution of this type of transition to the observable electron emission is much smaller than those with ejection of K shell electrons. The rates are thus required less accurately and the correcting terms have been neglected.

It is found that to a first approximation the Auger transition rates involve the same selection rules as dipole radiation. The final formulae obtained are

$$P_{K,L}^{\pm} = \left(\frac{Z}{Z_1}\right)^2 G_{K,L}(y) F^{\pm}(n_1, n_2, l_1) (1 - C_{K,L}^{\pm})^2 \quad \dots\dots(1)$$

$$P_R^{\pm} = Z_1^4 R F^{\pm} \quad \dots\dots(2)$$

where $P_{K,L}^{\pm}$, R are respectively the transition rates for emission of K shell electrons, L shell electrons and dipole radiation in the transitions $(n_1, l_1) \rightarrow (n_2, l_1 \pm 1)$. Here

$$G_K = \left(\frac{\pi m e^4}{3 \hbar^3 \mu^2}\right) \left(\frac{y^2}{1+y^2}\right) \frac{\exp\{y(4 \tan^{-1} y - \pi)\}}{\sinh \pi y} \quad \dots\dots(3)$$

$$G_L = \left(\frac{\pi m e^4}{6 \hbar^3 \mu^2}\right) \frac{y^2(4+5y^2)(4+3y^2)}{(4+y^2)^3} \left\{ \frac{\exp\{y[4 \tan^{-1}(y/2) - \pi]\}}{\sinh \pi y} \right\} \quad \dots\dots(4)$$

$$F^- = \frac{2l_1}{2l_1+1} \frac{(n_1+l_1)!(n_2+l_1-1)!}{(n_1-l_1-1)!(n_2-l_1)!} \frac{(4n_1n_2)^{2l_1+2}}{[(2l_1-1)!]^2} \frac{(n_1-n_2)^{2n_1+2n_2-4l_1-4}}{(n_1+n_2)^{2n_1+2n_2}} \\ \times \left[{}_2F_1\left(l_1+1-n_1, l_1-n_2; 2l_1; -\frac{4n_1n_2}{(n_2-n_1)^2}\right) - \left(\frac{n_1-n_2}{n_1+n_2}\right)^2 {}_2F_1\left(l_1-1-n_1; l_1-n_2; 2l_1; -\frac{4n_1n_2}{(n_2-n_1)^2}\right) \right]^2 \quad \dots\dots(5)$$

$$R = \frac{\mu m c^3}{3e^2} \left(\frac{e^2}{\hbar c}\right)^6 \frac{(n_1^2 - n_2^2)^3}{(2n_1n_2)^6} \quad \dots\dots(6)$$

$$C_K^- = \frac{1}{5\mu^2} \left(\frac{Z}{Z_1}\right)^2 \left(\frac{1+y^2}{y^2}\right) \left(\frac{n_1n_2}{n_1^2-n_2^2}\right)^2 \{6(n_1^2+n_2^2) - 5l_1(n_1^2-n_2^2)\} \\ \times \exp\{y(\pi - 2 \tan^{-1} y)\}. \quad \dots\dots(7)$$

F^+ , C_K^+ can be deduced from F^- , C_K^- by interchanging n_1 and n_2 , writing l_1+1 for l_1 , and, in the former case, multiplying by $(2l_1+3)/(2l_1+1)$ to allow for the different degeneracy of the final states.

* The detailed calculation will be described in a thesis for the degree of Ph.D. to be submitted to the University of London.

§ 3. CHARACTERISTICS OF TRANSITION RATES

Using the above formulae all possible transition rates have been calculated up to $n_1=8$ for bromine and selected rates up to $n_1=14$, the remaining rates required being obtained by logarithmic interpolation.

Figure 1 shows the variation of the total radiative and Auger transition rates (summed over n_2) for various values of n_1 , and for $l_1=1$ and n_1-1 . The radiative rate falls off rapidly as n_1 increases, while the Auger rate increases, except for a slight fall at $n_1=9$, where emission of K shell electrons ceases to be energetically possible. The Auger rate becomes comparable with the radiative rate for $n_1=6$ when $l_1=n_1-1$, but when $l_1=1$ this does not occur until $n_1=14$. Thus Auger transitions are of much greater importance when l_1 is large.

Figure 2 shows certain transition rates of the type ($l_1 \rightarrow l_1-1$) from the states $n_1=8$ as a function of n_2 . For Auger transitions the highest rate is that for which $n_2=n_1-1$, while for radiative transitions lower values of n_2 are much more probable. These characteristics are shown generally for other values of n_1 .

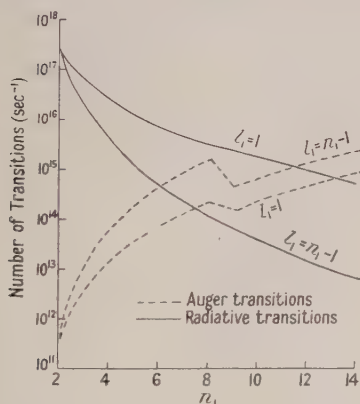


Figure 1. Total transition rates from a given level, n_1 (bromine).

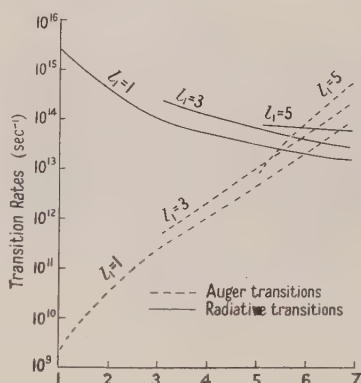


Figure 2. Some transitions with $n_1=8$ (bromine).

The Auger rates are to a first approximation independent of Z_1 while the radiative rates vary directly as Z_1^4 . Thus Auger transitions will be of importance for lower values of n_1 for lighter elements. The ejected electrons will, however, be of lower energy.

§ 4. CORRECTION FOR K SHELL DEFICIENCY

Once an Auger transition has taken place ejecting an inner shell electron, that shell is deficient of one electron and the Auger rate is reduced. This effect is likely to be more significant for the electrons ejected from the K shell, since the rate is cut by half until the shell is refilled.

Assuming that the K shell can be refilled from outer shells, a modified transition rate can be calculated as follows. Let P_1 be the unmodified K Auger transition rate, P_2 the total transition rate by other processes out of a given state and let P_3 be the total rate at which the K shell is replenished from other shells. Suppose that, after time t , the respective probabilities of the meson remaining in its

initial state or, having passed out of that state, by K Auger or other transitions respectively, are χ_0 , χ_1 , χ_2 . Then

$$\frac{d\chi_1}{dt} = \left(\frac{P_1}{2}\right) \{2 - \exp(-P_3 t)\} \chi_0$$

$$\frac{d\chi_2}{dt} = P_2 \chi_0$$

$$\frac{d\chi_0}{dt} = - \left(\frac{d\chi_2}{dt} + \frac{d\chi_1}{dt} \right) = \left\{ -(P_1 + P_2) + \left(\frac{P_1}{2}\right) \exp(-P_3 t) \right\} \chi_0.$$

Integrating,

$$\chi_0 = \exp - [(P_1 + P_2)t + (P_1/2P_3)\{\exp(-P_3 t) - 1\}].$$

Hence

$$\begin{aligned} \chi_2(\infty) &= P_2 \int_0^\infty \chi_0 dt \\ &= \frac{P_2}{P_2 + P_1} {}_1F_1 \left(1; 1 + \frac{P_1 + P_2}{P_3}; \frac{P_1}{2P_3} \right) \end{aligned} \quad \dots\dots(8)$$

by repeated integration by parts.

In the limit $P_3 \rightarrow \infty$ the modified probability is

$$\chi_2(\infty) = P_2/(P_2 + P_1). \quad \dots\dots(9)$$

Thus to calculate the number of Auger electrons P_1 may be replaced by a modified Auger transition rate P_1' such that

$$\frac{P_2}{P_1' + P_2} = \frac{P_2}{P_2 + P_1} {}_1F_1 \left(1; 1 + \frac{P_1 + P_2}{P_3}; \frac{P_1}{2P_3} \right). \quad \dots\dots(10)$$

§ 5. ATOMIC CAPTURE CROSS SECTION OF MESONS

With the transition rates calculated it is now possible to make an estimate of the probable number of Auger electrons, providing suitable assumptions are made as to the orbit of capture of the meson. A complete solution of the problem would require the evaluation of the cross section for capture for a large number of states with different values of n and l and at several energies of the incident meson. However, it is reasonable to expect that the largest cross sections will occur at low energies of the incident meson and, if a K shell electron is ejected, maximum overlap of the wave functions for the meson and electron will be secured when the Bohr radii for the meson and electron are approximately equal, that is for $n \sim \sqrt{\mu} \sim 15$ for μ -mesons.

A few calculations have been made of the capture cross section in atomic hydrogen for this value of n , and for an energy of the incident meson of 6.45 ev. The results are given in table 1.

The Born approximation breaks down completely and gives values in excess of the limit set by the conservation theorem in many cases. The distorted wave approximation has been tried for two states and gave values well below the conservation limit. In view of the calculations of Massey and Mohr (1952), based on a schematic model, it seems probable that these latter results are reasonably accurate. However, large cancellations occur during the calculation and high accuracy is required in the numerical work. Thus the labour involved in calculations for a large number of states and energies seems prohibitive.

In view of these results, and those of Burbidge (1951), who also explored the method of the perturbed stationary state, and again found the labour involved in obtaining suitable wave functions too great, it is unlikely that a complete solution of the capture problem will be attained in the near future.

Table 1. Calculated cross section for capture of 6.45 ev μ -meson into states of quantum number, $n=15$ and various values of l , by various methods (in units of $\pi a_0^2/100$)

l	(1)	(2)	(3)
0	1	0.1	—
1	3	9	—
2	5	0.2	—
3	7	22	—
4	9	0.1	—
5	11	35	—
6	13	4	—
7	15	42	—
8	17	27	—
9	19	26	—
10	21	87	—
11	23	0.4	0.1
12	25	120	—
13	27	189	—
14	29	61	17

(1) Limiting cross section (conservation theorem); (2) cross section (Born approximation); (3) cross section (distorted wave method).

The calculations carried out suggest that coupling between the incident meson wave and the states $n=15$ is sufficiently strong for the cross section to rise to an appreciable fraction of the theoretical limit $(2l+1)\lambda^2/4\pi$ (λ is the wavelength for the incident meson). The lower values arise from interference phenomena which might be expected to average out when other energies are considered. Thus the most plausible assumption in default of further information is to assume that the probability of capture in a state with given value of l is proportional to its degeneracy, $2l+1$.

§ 6. AUGER EMISSION PROBABILITIES

The total Auger emission probability Π_{n_1, l_1} for transitions from a state (n_1, l_1) to the ground state is given by

$$\Pi_{n_1, l_1} = \frac{\sum_{\pm} \sum_{n_2 < n_1} \{ \Pi_{n_2, l_1 \pm 1}^{\pm} P_K^{\pm} + (P_L^{\pm} + P_R^{\pm}) \Pi_{n_2, l_1 \pm 1}^{\pm} + P_K^{\pm} + P_L^{\pm} \}}{\sum_{\pm} \sum_{n_2 < n_1} \{ P_K + P_L + P_R \}}. \quad \dots\dots (11)$$

Π_{n_1, l_1}^{\pm} is calculated by replacing P_K by P_K' everywhere. This ignores the possibility of decay before reaching the ground state, and all transitions other than the dominant transitions, $l_1 \rightarrow l_1 \pm 1$. Similar formulae can be written down for emission in a given energy range. The probabilities were calculated numerically for a number of energy ranges, for μ -mesons in bromine ($Z_1=35$) the work being checked by calculating the total emission probability independently.

An estimate of the rates for silver was then made as follows. In general the major contributions to the Auger probability occur from states with l_1 close to n_1-1 . A detailed calculation was therefore made for the case in which the meson is captured in the state $n=14$, $l=13$ in silver. The ratio of the number of Auger

electrons in each energy range compared with the corresponding number for bromine was then used as a correction factor to be applied to the bromine results for other orbits of capture. This procedure is not likely to be very accurate for low values of l , but since these in general give very much smaller values for the Auger emission, and since, in obtaining the average emission, weight $2l+1$ will be given to the states of different l , the final error should be small.

Table 2 illustrates the variation with the n value of the state of capture of the total Auger emission probability and the emission probability in the range 15–70 keV for bromine. It is clear that a small increase in the n value of the state of capture would not greatly affect the emission in the observable range, although the total emission might be expected to increase rapidly. Both values would fall off rapidly for values of n less than 9. Table 3 illustrates the variation in both these quantities with the l value of the state of capture. The time of descent to the meson 1s state is also shown.

The second and third columns of table 4 illustrate the variation of the Auger emission in a given energy range for a weighted mean, silver and bromine being given equal weight, the results being compared with the experimental results of Fry (1951). It should be observed that the total number of observed electrons will be very sensitive to the exact value of the lower cut-off energy.

Table 2. Variation of total Auger emission per stopped μ -meson and emission in energy range 15–70 keV from bromine for μ -meson captured into state with quantum number n (weighted mean of possible l values)

n	14	12	10
Total emission	5.3	3.7	2.4
Emission in range 15–70 keV	0.585	0.594	0.578

Table 3. Variation in total Auger emission, emission in energy range 15–70 keV, and time of descent to ground state with quantum number l of state of capture for μ -meson captured in quantum states $n=15$ in bromine

l	13	10	7	4	1
Total emission	8.1	5.8	3.9	2.4	1.1
Emission in range 15–70 keV	0.84	0.73	0.42	0.16	0.05
Time of descent to ground state (10^{-13} sec)	10.2	8.0	6.3	4.4	2.3

It is clear from table 4 that while the predicted number of electrons per stopped μ -meson is in reasonable agreement at high energies, for low energies agreement is poor. It is possible that the procedure adopted in estimating the emission from silver may have over-estimated the emission in the 15–20 keV range since the correction factor applied to the bromine results for this energy range is large. However, if a correction factor for the range 15–70 keV is obtained as previously described and applied directly, a new value for the total emission in the range 15–70 keV of 0.84 is obtained. This result indicates that high accuracy cannot be expected from the procedure adopted, but since both results are of the same order of magnitude it is clear that more refined procedure of estimating the silver emission would still result in disagreement.

The assumption of hydrogen-like wave functions for the meson is likely to be quite accurate as for the significant rates, the functions are large only inside the K shell of heavy atoms, where screening will only make a proportionate change in the effective nuclear charge. The effect of the finite size of the nucleus will clearly be insignificant except for meson s states. Thus the distortion of the wave functions is unlikely to make an appreciable change in the transition rates except possibly for transitions involving states with high values of $n-l-1$, where the number of nodes is likely to make the rates rather sensitive to the precise form of the function. These states, however, give a very small contribution to the Auger emission probability.

Table 4. Number of emitted electrons in given energy ranges per stopped μ -meson in silver, bromine. Experimental results of W. F. Fry compared with various theoretical estimates:

- (a) Assuming L shell can be refilled. Capture in states $n=14$ and weight $(2l+1)$ given to state l .
- (b) Circular orbits only. L shell full.
- (c) Circular orbits only. One L shell electron only left at $n_1=8$.
- (d) Circular orbits only. No L shell electrons left at $n_1=8$.

Energy range (kev)	Experimental	Theoretical			
		(a)	(b)	(c)	(d)
15-20	0.08	0.56	—	—	—
20-30	0.13	0.29	0.36	0.18	0.15
30-50	0.08	0.06	0.13	0.13	0.09
50-70	0.05	0.09	0.16	0.09	0.05
>70	—	0.05	0.05	0.02	0.01

The possibility of de-excitation by processes in which energy is transferred to other atoms can be readily ruled out. Even if a cross section πa_0^2 is assumed for this process* and the atom is assumed to possess an energy of the order of 10 eV, as a result of the capture process the number of collisions is approximately $5 \times 10^{12} \text{ sec}^{-1}$. Since the calculated time of descent to the ground state is less than 10^{-14} second it is clear that no significant reduction can take place through this process.

Thus to reconcile the observed number of slow electrons with the theory it seems necessary to postulate a very high probability for capture of the meson into orbits of high angular momentum. This appears to contradict the distorted wave calculations. However, one further possibility must be examined.

§ 7. THE EFFECT OF A HIGH DEGREE OF IONIZATION

It has also been suggested that Auger emission of observable electrons might be reduced when the meson is captured in an orbit well out from the K shell. The atom might then become almost completely ionized in the earlier transitions and the later observable Auger transitions become impossible.

This possibility is difficult to discuss in detail. Without knowledge of the variation of the capture cross section with and without detailed wave functions only approximate calculations may be made. However, some discussion can be

* This is almost certainly an over-estimate since the meson is supposed to be tightly bound within the K shell of an atom of high nuclear charge.

carried out on the following points: (a) energetic possibility of complete ionization, (b) probability of complete ionization of the M and L shells, (c) resulting probability of Auger emission.

We restrict ourselves first to transitions between circular orbits, i.e. of the type $(n_1, n_1-1) \rightarrow (n_1-1, n_1-2)$. Considering (a), it has already been shown that for transitions of this type emission of K shell electrons is only possible for $n_1 \leq 8$. There will be 8 electrons in the L shell and 18 in the M shell. For at least one transition for $n_1 \geq 8$ we must expect the radiative rates to be dominant (see table 6). Thus for an appreciable probability of complete ionization of the L and M shells, L transitions must be possible for $n_1 \geq 17$ and M transition for $n_1 \leq 35$.

For calculating the amount of energy released in a transition we suppose that the energy of the state n_1 is given by the hydrogen-like formula

$$E_{n_1} = -13.55 \left(\frac{Z_{\text{eff}}}{n_1} \right)^2 \mu \quad (\text{ev}).$$

We suppose that $Z_{\text{eff}} = Z - F$, the screening factor F being determined as

$$F = \sum_{\lambda} \int_V \phi_{\lambda}^2 dV$$

the volume V being taken as a sphere equal to the appropriate Bohr radius of the meson, and the summation over the electron wave functions ϕ_{λ} of the atom being taken over all occupied states giving a significant contribution in the volume V (in practice over the K and L shells, hydrogen-like wave functions being assumed).

Table 5. Estimated energy difference ΔE (kev) between meson states with quantum numbers n_1 and n_1-1 and L and M ionization energies I_L and I_M for silver and bromine

	$n_1=16$	ΔE $n_1=17$	I_L	$n_1=35$	ΔE $n_1=34$	I_M
Silver	3.5	2.9	3.2	0.30	0.34	0.37
Bromine	1.9	1.7	1.5	0.17	0.19	0.16

Table 6. Auger rates for ejection of one 2s or 2p electron and radiative rates for transition $(n_1, n_1-1) \rightarrow (n_1-1, n_1-2)$ in silver and bromine

n	14	11	10	9
Auger rate (sec ⁻¹) (2s electron)	3.9×10^{14}	1.6×10^{14}	1.4×10^{14}	1.1×10^{14}
Auger rate (sec ⁻¹) (2p electron)	2.7×10^{14}	9.3×10^{13}	5.2×10^{13}	2.8×10^{13}
Radiative rate (sec ⁻¹) (bromine)	6.5×10^{12}	2.3×10^{13}	3.7×10^{13}	6.4×10^{13}
Radiative rate (sec ⁻¹) (silver)	2.1×10^{13}	7.4×10^{13}	1.2×10^{14}	2.1×10^{14}

Table 7. Probability of different states of ionization of L shell in silver when K Auger transitions become possible

Number of electrons in L shell at $n_1=11$	2	3
Probability of 0 electrons in L shell at $n_1=8$	0.30	0.04
Probability of 1 electron in L shell at $n_1=8$	0.58	0.44

Transition energies for certain transitions in silver and bromine calculated on this basis together with the estimated lowest L and M shell ionization energies are shown in table 5. These were taken as the L III and M IV absorption edges for palladium ($Z=46$) in the case of silver to allow for the extra screening of the meson. For bromine the ionization energies were taken as the L III edge for selenium ($Z=34$) and the ionization potential for Se VII. It will be seen that, for bromine, M shell transitions can clearly take place for $n_1 \leq 35$ while L shell transitions can take place for $n_1 \leq 17$, and hence complete ionization to the K shell can easily take place by the time the μ -meson has reached $n_1=8$. The situation for silver is more doubtful. M shell transitions are apparently not energetically possible until $n_1=33$ and L transitions until $n_1=16$. Thus complete ionization to the K shell does not appear possible before $n_1=8$, and hence the emission of Auger electrons would not be so greatly reduced.

It should be remembered, however, that the energy estimates are very crude when the meson is outside the K shell. Since only small changes in the estimated energy values are required, better values might show that complete M and L shell ionization is possible before the meson reaches $n_1=8$ in silver.

Considering point (b), it is only necessary to consider silver, since in this case the transition rates are least favourable for the occurrence of complete ionization. In table 4 a few selected transition rates are shown for radiative and L shell Auger rates on the assumption that only one electron remains in the L shell. The Auger rates are of course increased if more than one electron is in the shell. The ratio of Auger to radiative rate increases rapidly with n_1 . For $n_1=11$, if two electrons only remain in the L shell the probability of Auger emission is greater than 70%, and for greater n_1 , with more electrons remaining in the L shell, the radiative rates will be negligible. Thus if we suppose that the L shell is not refilled it will contain two or three electrons, according to whether L transitions are possible at $n_1=17$ or $n_1=16$. These are most likely to be 2p electrons. Table 7 shows the probability that either 0 or 1 electrons will be left in the L shell in both these assumptions. It is clear that the probability of a high degree of ionization of the L shell is critically dependent on whether L Auger transitions are possible for n_1 greater than 16.

With regard to the outer electrons, it seems probable that they should be regarded as belonging to the crystal as a whole rather than localized on a particular atom. If so the outer shell could never become exhausted and it is necessary to check that the transition rate from the upper band system is small enough for the lower shells to be depleted.

An estimate of this rate can be obtained by regarding it as a process of radiative capture of electrons by a bare nucleus of charge $+Ze$. The calculations of Bates, Buckingham, Massey and Unwin (1939) can then be used. They found that, for sufficiently low energies, the cross section for this process behaves like (Q_0/ϵ) where Q_0 is a constant and ϵ is the energy of the electron, falling off more rapidly at higher energies. Estimates based on these calculations should probably be regarded as upper limits, since the long tail of the coulomb potential will be considerably distorted by the presence of neighbouring ions, and it would be expected that, for low energies, this would result in a considerable reduction of the magnitude of the wave function close to the nucleus.

Using the low-energy limit for the radiative capture cross section, assuming an electron density of 18 electrons per atom with a Fermi energy distribution,

upper limits of 3.8×10^{13} and 3.6×10^{13} per second are derived for the transition rates to empty L and K shells in silver. A comparison with table 6 shows that, even if this limit is attained, the possibility of empty L and K shells cannot be excluded.

Concerning (c), calculations have been carried out assuming that complete ionization of the L shell has taken place at $n_1=8$ in bromine, and that 0 or 1 electrons are left in the L shell of silver. The results, together with circular orbit calculations for a complete L shell, are shown in table 4. No results are shown for the energy range 15–20 keV, as these would only arise for transitions with n_1 greater than 8. The results show that a reduction in the Auger probability of the right order of magnitude is produced if the L shell becomes completely ionized.

The experimental and theoretical results on Auger emission following the capture of μ -mesons in the heavy elements of a photographic emulsion can thus be reconciled if either (i) practically no mesons are captured in states of high angular momentum, (ii) mesons captured in such states have very high initial excitation, and strip the atom to its K shell in subsequent Auger processes.

§ 8. AUGER EMISSION IN THE LIGHT ELEMENTS

The above concepts lead to some difficulties when applied to the light elements of the emulsion. As shown previously, the only transitions contributing significantly to the Auger emission amongst the light elements are those for $n_1=3$ in carbon, nitrogen and oxygen giving electrons of 14, 19 and 25 keV respectively. Fry (1953) observed 18 low energy electrons from 358 μ -meson tracks showing a decay electron and therefore attributed to capture in the light elements. The energy of all low energy electrons was in the range 10–25 keV. This gives an Auger probability of 50%. Assuming the probability of capture in H:C:N:O is as 56:22:5:17 and that the K shell is refilled immediately, consideration of circular orbit transitions only leads to an Auger probability of 8.5%. However, if it is supposed that the K shell cannot be refilled, the probability of emission of an observable electron is completely negligible. For the light elements it is probable that the molecular binding of the atoms is important both when considering the initial capture of the meson and its subsequent descent to the ground state. In particular, since the refilling of the K shell can only take place from valence electrons it is difficult to make any reliable estimate of the Auger emission. The figure of 8.5% is almost certainly an over-estimate, but is probably the best estimate that can be obtained theoretically without a considerable amount of labour.

It should be noted that non-observation of electrons of higher energy is only consistent with theoretical predictions if either complete ionization occurs or if an electron of low ionization energy remains, when the meson reaches the 2s state. For since this state is metastable to radiative transitions, electrons of 70–130 keV should be observed in carbon, nitrogen or oxygen from the 2s–1s Auger transition, as suggested by Wheeler (1949), unless the 2s 2p transition can take place. Wheeler showed that the radiative 2s–2p is very slow for the light elements, but Ioffe and Pomeranchuk (1952) pointed out that this transition could take place as an Auger transition with ejection of a valence electron, the rate for this process being considerably greater than that for the 2s–1s transition.

If ionization of the outer shells occurs without complete ionization of the K shell, electrons in this energy range should again be observed.

Fry (1953) also secured a track with two slow electrons and a fast decay electron, and Cosyns observed a similar event. These events should be very rare (less than 1 in 200 cases of single emission should show a second track if we allow that the events do take place in the light elements) and, in addition, the second electron should have greater energy than 70 kev, in disagreement with Fry's observations. It seems possible that these cases might be explained as arising from meson decays taking place during capture by the heavy elements, although it can be deduced by Wheeler's law and the observed Auger emission probabilities that such events should not occur with a frequency of greater than 1 in 800 cases of capture in the heavy elements.

ACKNOWLEDGMENTS

I should like to express my gratitude to Professor H. S. W. Massey for suggesting this problem and for helpful discussions concerning atomic capture, and to Dr. E. H. S. Burhop for very many suggestions and comments concerning Auger transitions. I should also like to acknowledge the receipt of a grant from the Ministry of Education.

REFERENCES

- BATES, D. R., BUCKINGHAM, R. A., MASSEY, H. S. W., and UNWIN, J. J., 1939, *Proc. Roy. Soc. A*, **170**, 322.
BURBIDGE, G. R., 1951, *Thesis*, University of London.
BURBIDGE, G. R., and DE BORDE, A. H., 1953, *Phys. Rev.*, **89**, 189.
CHANG, W. Y., 1949, *Rev. Mod. Phys.*, **21**, 166.
COSYNS, M. G. E., DILWORTH, C. C., OCCHIALINI, G. P. S., SCHOENBERG, M., and PAGE, N., 1949, *Proc. Phys. Soc. A*, **62**, 801.
FRY, W. F., 1951, *Phys. Rev.*, **83**, 594; 1953, *Nuovo Cim.*, **10**, 490.
GORDON, W., 1929, *Ann. Phys., Lpz.*, **2**, 1031.
HINCKS, E. P., 1951, *Phys. Rev.*, **81**, 313.
IOFFE (Joffe)*, L., and POMERANCHUK, I., 1952, *J. Exp. Theor. Phys., U.S.S.R.*, **23**, 123.
MASSEY, H. S. W., and MOHR, C. B. O., 1952, *Proc. Phys. Soc. A*, **65**, 845.
WHEELER, J. A., 1949, *Rev. Mod. Phys.*, **21**, 133.

* Transliteration in accordance with Royal Society's scheme.

The Ultra-Violet Spectrum of a Diatomic Hydride Excited in Hydrogen-Potassium Fluoride Hollow-Cathode Discharges

BY R. F. BARROW AND A. D. CAUNT

Physical Chemistry Laboratory, University of Oxford

MS. received 26th August 1953

Abstract. A many-lined spectrum in the region 2200 to 2600 Å has been obtained in hollow-cathode discharges in hydrogen in the presence of potassium fluoride. A rotational analysis has shown this to be a $v' = \text{constant}$ progression of a $\Sigma - \Sigma$ transition, probably singlet. The emitter has not been identified.

§ 1. INTRODUCTION

A PRELIMINARY note on the analysis of a many-lined spectrum appearing in hollow-cathode discharges in hydrogen in the presence of potassium fluoride has recently been given (Caunt and Barrow 1952). Further experiments carried out with a view to identifying the emitter have not been successful owing to the difficulty of reproducing the conditions of excitation. A full account of the experimental details and analysis is given in this paper.

§ 2. EXPERIMENTAL

The apparatus consisted of a vertical quartz tube at the bottom of which was a high-temperature steel hollow cathode. The latter was supported from below on a steel rod and was open at the top so that solids could be introduced into the cathode and held there without danger of being ejected by the violence of the discharge. The anode, made from nickel sheet, was placed about four centimetres above the cathode. Light from the cathode passed through the anode and out through a quartz window, and was reflected into the spectrograph by a right-angle quartz prism.

The discharge was run from a 1200 volt d.c. generator with a 500 ohm series resistance at currents varying from 0.2 to 0.5 amp. The hydrogen used was obtained from a cylinder and the pressure in the discharge tube maintained in the range 1 to 5 mm Hg. The cathode was allowed to become red hot, and sometimes additional heating from an external furnace was found helpful.

The most successful conditions for exciting the spectrum were as follows: A 50:50 mixture of KF and KHF₂, both freshly dried by heating in nickel crucibles, was placed in the cathode. The discharge was begun at low hydrogen pressure; the cathode glow became deep red as the temperature rose and much of the HF was driven off. An exposure was taken when the gas pressure had decreased and the cathode glow turned reddish grey. It was found that a true hollow-cathode discharge could be maintained for $\frac{1}{4}$ hour provided the current was kept lower than about 0.4 amp. The final photographs under these conditions of excitation were taken on Ilford 'Process' plates using a Hilger E 478 spectrograph (quartz optics), focused for the region 2200 to 2600 Å. The reciprocal dispersion per millimetre varies from 46.5 cm⁻¹ at 2600 Å to 34 cm⁻¹ at 2200 Å.

The iron arc spectrum was used as a standard. A reproduction of the spectrum is given in the plate.

It should be possible to derive the mass of the heavy atom of this emitter from an analysis of the corresponding deuteride spectrum. We therefore decided to search for a reliable and strong source.

No discharges were found to produce the spectrum if fluorides were absent. Attempts were made to produce a strong source by introduction of carbon (as K_2CO_3 , CH_4 , grease, wax or soot), nitrogen (as NH_3 , N_2), oxygen (as H_2O) or silicon into the discharge in the presence of KF , but no success was achieved.

A weak source was obtained in the absence of KF using a mixture of hydrogen and hydrogen fluoride, but this proved too weak to use in deuterium experiments. In fact as the work proceeded even the best sources were found, for reasons unknown to us, to fail. No experiments with deuterium were made.

§ 3. ANALYSIS

After a number of false starts, three pairs of branches were picked out. These are degraded strongly to longer wavelengths, and no heads are apparent. Each pair was assumed to consist of a P and an R branch, for if one were a Q and the other, say, a P branch no lines which might form a sensible R branch could be found. The bands were analysed as a $^1\Sigma-^1\Sigma$ transition (see Herzberg 1950), and from combination differences it became obvious that the bands form a $\tau' = \text{constant}$ progression, the upper-state level being presumably $v' = 0$. It was assumed that the first band observed on the high-frequency side of the system was the 0, 0 band. The J numbering of the rotational levels could be deduced without ambiguity.

Accurate values of the rotational constants of the upper state were calculated from averages of the combination differences $R(J) - P(J) = \Delta_2 F'(J)$ of the five bands observed. $\{\Delta_2 F'(J)/(J + \frac{1}{2}) - 12H_0'(J + \frac{1}{2})^4\}$ was then plotted against $(J + \frac{1}{2})^2$, the small H_0' term being chosen by trial and error to produce a straight line. From the slope and intercept of this line B_0' and D_0' were calculated. The upper-state term values were then deduced from the formula

$$F_0'(J) = B_0'J(J+1) - D_0'J^2(J+1)^2 + H_0'J^3(J+1)^3.$$

Good support for the correctness of the analysis is derived from the fact that the calculated and observed $\Delta_2 F'(J)$ values differ with a standard deviation of only 0.2 cm^{-1} , which is of the same order as the error in line measurement.

The lower-state rotational constants and the band origin were calculated from the accurately known upper-state term values by the formula

$$R(J-1) + P(J) = 2\nu_0 + 2(B' - B'')J^2 + 2(D' - D'')J^2(J^2 + 1) + 2(H' - H'')J^4(J^2 + 3).$$

Plots of $R(J-1) + P(J)$ against J^2 gave curves which could be made linear by trial-and-error methods, first by trying suitable $D' - D''$ values for low J values and then by bringing the high J -value lines to fit with an $H' - H''$ term. The accuracy of this procedure can be judged from the $R(J)$ and $P(J)$ (observed - calculated) columns in table 1, where the calculated line frequencies were derived from the band origins and term values.

Values for B_e'' , α_e'' and γ_e'' were obtained from successive differences of B_v'' values and ω_e'' , $x_e''\omega_e''$ and $y_e''\omega_e''$ were found similarly from the band-origin values. The Kratzer relation, $\omega_e'^2 \simeq 4B_e'^3/D_e'$, afforded a rough estimate of the upper-state vibration frequency. The results are presented in table 2.

Table 1. Wave Numbers of Rotation Lines

0, 0 Band. $\nu_0=46399.4 \text{ cm}^{-1}$				
J	R(J) observed	P(J) observed	R(J) obs - calc	P(J) obs - calc
16	44462.6	44204.0	+0.3	+0.1
17	227.7	43954.9	+0.3	+0.6
18	43982.2	694.8	-0.1	+0.2
19	727.9	—	+0.5	—
20	464.2	148.1	+0.2	+0.5
21	192.6	42862.2	+0.4	+0.1
22	42914.1	570.1	-0.3	+0.2
23	629.5	271.1	-0.4	-0.1
24	340.0	41968.1	-0.2	-0.4
25	045.9	660.8	-0.9	-0.9
26	41749.4	351.1	-0.8	-0.9
27	451.4	040.2	-0.5	-0.7
28	153.1	40729.2	+0.1	-0.1
29	40856.7	420.0	+1.8	+1.2
30	563.4	114.7	+4.6	+4.2
0, 1 Band. $\nu_0=44350.2 \text{ cm}^{-1}$				
7	44009.8	43889.2	-0.1	-0.9
8	43903.2	767.7	-1.0	-0.8
9	784.1	633.1	-0.9	-0.8
10	652.7	485.9	-0.7	-0.6
11	508.5	326.1	-0.6	-0.5
12	352.8	154.8	0.0	-0.1
13	184.9	42971.8	0.0	+0.1
14	006.2	777.6	+0.2	-0.1
15	42816.7	573.3	-0.1	-0.1
16	618.1	359.5	+0.4	+0.2
17	409.7	136.5	+0.1	0.0
18	193.3	41905.5	+0.1	0.0
19	41969.0	666.9	0.0	0.0
20	738.2	422.1	-0.1	+0.2
21	501.9	171.3	+0.6	+0.1
22	260.4	40916.4	-0.2	+0.3
23	015.6	657.3	0.0	+0.4
24	40768.2	396.4	+0.3	+0.2
25	519.3	134.6	+0.4	+0.8
29	271.3	39873.2	+1.7	+1.8
27	025.4	614.2	+3.9	+3.7
28	39783.6	359.8	+7.8	+7.7
29	548.7	112.4	+14.5	+14.3
30	322.1	38873.6	+23.8	+23.6
0, 2 Band. $\nu_0=42471.5$				
1	42474.6	42451.0	+0.1	+0.6
2	456.4	416.2	-0.2	-0.2
3	425.7	369.2	0.0	-0.3
4	382.1	309.7	+0.2	-0.1
5	325.4	237.3	-0.1	-0.1

(Table 1 *continued*)0, 2 Band. $\nu_0=42471.5$

J	R(J) observed	P(J) observed	R(J) obs—calc	P(J)
6	42256.4	42152.5	-0.4	-0.3
7	175.6	055.6	-0.1	-0.3
8	082.8	41947.1	-0.1	-0.1
9	41978.3	826.8	-0.1	-0.3
10	862.6	695.6	0.0	-0.3
11	736.5	554.2	+0.1	+0.3
12	600.0	402.2	+0.2	+0.3
13	454.0	240.4	+0.6	+0.2
14	298.2	069.9	+0.4	+0.4
15	134.3	40891.3	+0.3	+0.7
16	40963.2	704.7	+0.8	+0.7
17	784.3	511.4	+0.5	+0.7
18	599.5	312.0	+0.3	+0.5
19	409.4	107.6	+0.1	+0.4
20	215.4	39898.9	0.0	-0.1
21	018.2	687.5	+0.1	-0.5
22	39819.3	474.6	-0.7	-0.9
23	619.7	261.5	-1.1	-0.6
24	421.5	049.6	-0.5	-1.2
25	226.3	38841.6	-0.3	+0.1
26	036.6	638.6	+2.0	+2.2
27	38855.3	444.3	+7.1	+7.1
28	685.5	261.5	+16.1	+15.8

0, 3 Band. $\nu_0=40779.4 \text{ cm}^{-1}$

1	40784.3		+0.1	
2	769.8	40729.2	+0.1	-0.3
3	744.1	687.9	+0.1	+0.1
4	707.4	635.0	+0.2	-0.1
5	659.6	571.2	0.0	-0.3
6	601.3	497.1	+0.1	-0.1
7	532.1	412.3	-0.4	-0.4
8	453.5	317.9	-0.3	-0.2
9	365.0	213.9	-0.2	0.0
10	267.3	100.6	-0.1	+0.1
11	161.1	39978.2	+0.3	+0.1
12	046.0	848.2	0.0	+0.1
13	39923.3	710.5	-0.2	+0.2
14	794.4	565.7	+0.3	-0.1
15	658.8	415.5	+0.2	+0.3
16	518.0	259.7	+0.1	+0.2
17	373.0	100.1	+0.3	+0.5
18	224.2	38936.9	-0.3	+0.1
19	073.8	771.8	+0.1	0.0
20	38922.2	606.0	-0.6	-0.4

Table 1 (*continued*)

0, 3 Band. $\nu_0=40779.4 \text{ cm}^{-1}$				
J	R(J) observed	P(J) observed	R(J)	P(J) obs—calc
21	38771.8	38441.5	+0.1	-0.1
22	623.4	279.0	-0.5	-0.4
23	479.8	121.7	+0.5	+1.1
24	343.7	37971.9	+3.3	+3.2
25	218.6	833.6	+9.3	+9.4
26	? 096.2		?+8.2	

0, 4 Band. $\nu_0=39291.4 \text{ cm}^{-1}$				
0	39299.3		-0.1	
1	297.9	39274.2	-0.2	+0.2
2	287.6	247.3	+0.2	+0.1
3	267.6	211.2	+0.2	0.0
4	237.9	166.1	-0.3	0.0
5	200.1	112.4	-0.2	+0.2
6	153.7	049.6	+0.2	+0.1
7	098.2	38978.6	-0.2	-0.1
8	035.3	899.9	-0.2	+0.1
9	38964.6	813.1	-0.2	-0.4
10	887.1	720.0	-0.1	-0.3
11	803.1	620.5	0.0	-0.1
12	713.3	515.3	0.0	-0.1
13	618.4	405.0	+0.1	-0.1
14	518.9	290.7	-0.3	-0.2
15	416.9	173.3	-0.1	-0.3
16	312.4	054.3	-0.2	+0.1
17	207.0	37934.5	-0.2	+0.4
18	102.3	814.8	0.0	+0.2

Table 2. Spectroscopic Constants

$$\nu_{0,0}=46399.4 \text{ cm}^{-1}$$

Band Origins and Ground-State Constants

	ν_0	B_v''	D_v''	H_v''
0, 0	46399.4	12.049 ₈	$1.71_5 \times 10^{-3}$	-1.0×10^{-7}
0, 1	44350.2	11.324 ₀	$1.80_0 \times 10^{-3}$	-1.5×10^{-7}
0, 2	42471.5	10.532 ₅	$1.86_4 \times 10^{-3}$	$-3.1_3 \times 10^{-7}$
0, 3	40779.4	9.665 ₇	$1.94_9 \times 10^{-3}$	$-5.8_8 \times 10^{-7}$
0, 4	39291.4	8.718 ₅	$2.21_4 \times 10^{-3}$	-8.6×10^{-7}

$$B_v'' = 12.383_3 - 0.648_3 (v'' + \frac{1}{2}) - 0.036_9 (v'' + \frac{1}{2})^2$$

$$G_v'' = 2203.4 (v'' + \frac{1}{2}) - 72.5_3 (v'' + \frac{1}{2})^2 - 2.8 (v'' + \frac{1}{2})^3$$

Upper-State Constants

$$B_0' = 4.016_6; \quad D_0' = 1.89_6 \times 10^{-4}; \quad H_0' = +4.2 \times 10^{-9}; \quad \omega' \simeq 1170 \text{ cm}^{-1}$$

§ 4. DISCUSSION

Since no signs of a Q branch were detected and no Λ -doubling was found even at high J values, we assumed that the transition is Σ - Σ . There is less certainty about the multiplicity of the system, although a splitting of about 1 cm^{-1} would have been resolved. The extent of the line splitting for multiplet Σ - Σ transitions would be very small if the spin-splitting constants of the upper and lower states were about the same.

The B value of the lower state is so large that it seems unlikely that the emitter is a hydride of any other than a first-row element in the periodic table. Although it may be HF or HF^+ , the difficulty of excitation and the ultimate disappearance of the spectrum after several experiments seem to suggest that the emitter was present as an impurity.

Since the reduced masses of hydrides do not vary greatly from carbon onwards, we can calculate approximate interatomic distances from the B values. With $\mu_{\text{A}} = 0.943$, the mean value of the reduced masses of CH and HF, we get $r_0'' = 1.22$ and $r_0' = 2.11\text{ \AA}$. Such a great disparity in distances for the two states means that the system must be relatively weak, which may account for some of the trouble experienced in trying to excite it.

The upper state has a much smaller force constant than the lower, and the level $v' = 0$ cannot be far removed from a dissociation limit. The two electronic states appear to dissociate to give atomic products in different states of excitation with an energy difference of about $40\,000\text{ cm}^{-1}$ ($\nu_{0,0} - D_0'' + F'(30)$; see below for D_0''). This seems to rule out NH and HF as possible emitters, unless very highly excited atomic states are involved.

The positions of the last two or three lines of each band do not agree well with those calculated from the rotational constants, and terms in $F''(J)$ of order $(J + \frac{1}{2})^4$ and perhaps $(J + \frac{1}{2})^5$ would be necessary to reproduce them. The anomaly for each band sets in at about $10\,000\text{ cm}^{-1}$ above the level $v'' = 0$, indicating that there may be some sort of perturbation at this level. The vibration levels of the lower state converge rapidly to a dissociation limit at $v'' \simeq 9$, from which we get $D_0'' \simeq 10\,900\text{ cm}^{-1} = 31.1\text{ kcal}$. Whether the anomalous positions of the last rotation lines are due to this dissociation or to perturbation by another state is uncertain.

The $46\,400\text{ cm}^{-1}$ band is assumed to be the $0, 0$ transition, but it is possible that a band further out in the ultra-violet has been missed due to the insensitivity of the photographic plates below 2200 \AA .

Further progress in the elucidation of this spectrum clearly awaits the discovery of a reproducible source.

ACKNOWLEDGMENT

One of the authors (A. D. C.) wishes to thank Imperial Chemical Industries Limited for the award of a Research Fellowship.

REFERENCES

- CAUNT, A. D., and BARROW, R. F., 1952, *Proc. Phys. Soc. A*, **65**, 373.
HERZBERG, G., 1950, *Molecular Spectra and Molecular Structure*, Vol. 1 (New York: Van Nostrand).

On the Theory of Optical Absorption in Metals and Semiconductors

By R. WOLFE

H. H. Wills Physical Laboratory, University of Bristol

Communicated by N. F. Mott; MS. received 15th May 1953, resubmitted after amendment 18th August 1953

Abstract. A quantum-mechanical method is described for calculating the effect on the optical absorption of metals and semiconductors of any of the factors responsible for electrical resistance. In this method the electrons which are scattered by imperfections in the crystal lattice are considered to absorb light by a photoelectric process. The calculation is carried out for the case where the conduction electrons are scattered by dissolved impurities. A first order approximation method is used. The results obtained are compared with those of the semi-classical theory used in existing textbooks, in which the current set up by the light is assumed to be damped by the impurities. It is found that the two methods give very similar results for metals. For semiconductors, on the other hand, the approximate method used here gives considerably less absorption than the semi-classical method. The use of exact wave functions for the very slow electrons in semiconductors would give greatly increased absorption coefficients because the intensity of these wave functions is high near the scattering centres. It is suggested that in this way the high absorption of infra-red radiation in semiconductors can be explained.

§ 1. INTRODUCTION

THE theory of the absorption of light in metals has been treated in the past by a semi-classical method. This method makes use of the classical relationship between the absorption coefficient and the resistivity of a metal, quantum mechanics being used, if at all, only in calculating the resistivity. In the long wavelength region of the spectrum where the period of the light is large compared with the relaxation time of the electrons in the metal, the result obtained—the Hagen–Rubens relation—is in good agreement with experiment. For light of shorter wavelengths, the agreement is not good. In this paper a quantum-mechanical method for calculating the absorption coefficient of a metal is described. The mechanism of absorption is assumed to be an internal photoelectric effect: a conduction electron absorbs a photon, and its energy is raised from one conduction level to a higher level in the same band. Such transitions, which are forbidden in a perfect crystal, have a finite probability in a crystal with lattice irregularities. The method could be applied to find the absorption due to thermal vibration or lattice defects. For mathematical simplicity the procedure is carried through here only for a metal containing a small proportion of dissolved foreign atoms of valence different from that of the solvent.

Although the expression obtained for the absorption coefficient differs from that derived by the semi-classical method, the two results become identical for long wavelengths. In a typical example the numerical results of the two methods are very similar for a wide range of conditions. It seems probable that this similarity of results would also be found if the calculation were carried out for lattice vibrations or other crystal imperfections.

The absorption coefficient of a semiconductor can be calculated by the same methods, but in this case there are many fewer conduction electrons and the distribution of their velocities is different from that of the metallic electrons. The quantum-mechanical calculation is carried out here for a semiconductor containing charged impurity centres using wave functions obtained by the same first-order approximation as was used in the case of metals. The result is in general much smaller than that obtained by the semi-classical method. The approximations used in this calculation have, however, been found to be inadequate in the case of electrons of very low energy. Much higher absorption coefficients would be obtained for semiconductors if accurate wave functions were used in the calculations. The results are then of the same order of magnitude as those which have been found in recent experiments on infra-red absorption in germanium and silicon.

§ 2. SEMI-CLASSICAL ABSORPTION COEFFICIENT

In the semi-classical method, classical electromagnetic theory is used to find an expression for the absorption coefficient in terms of the optical constants of the metal. These optical constants are then related to the resistivity which is the only quantity that is calculated by a quantum-mechanical method. In a perfect lattice in which the atoms are at rest, the resistivity and absorption coefficient are zero. In a perturbed lattice, electrons are scattered by the irregularities and the resistivity is greater than zero.

The absorption coefficient η is defined as the rate of absorption of energy per unit thickness of the material divided by the energy flux. In an absorbing medium with refractive index n and extinction coefficient k the time average of the energy flux \bar{S} is

$$\bar{S} = \frac{cn}{4\pi} \bar{\mathcal{E}}^2 \exp(-2k\omega z/c)$$

where $\bar{\mathcal{E}}^2$ is the mean square of the electric vector of the light which is propagated in the z direction with angular frequency ω , and c is the velocity of light in a vacuum.

Therefore
$$\eta = -\frac{\partial \bar{S}}{\partial z} / \bar{S} = \frac{2k\omega}{c}. \quad \dots\dots(1)$$

The classical optical constants satisfy the equation

$$2nk = \frac{4\pi N e^2}{m} \frac{1}{\omega\tau} \left(\omega^2 + \frac{1}{\tau^2} \right)^{-1} \quad \dots\dots(2)$$

where N is the number of electrons per unit volume, e is the electronic charge, m the mass of an electron, and τ is the relaxation time (Mott and Jones 1936). τ is related to the resistivity for steady currents ρ_0 by the formula

$$\tau = m/\rho_0 N e^2. \quad \dots\dots(3)$$

Combining eqns (1), (2) and (3) we obtain

$$\eta = \frac{4\pi}{nc} \left(\frac{N e^2}{m} \right)^2 \rho_0 \left(\omega^2 + \rho_0^2 \frac{N^2 e^4}{m^2} \right)^{-1}. \quad \dots\dots(4)$$

If the metal contains a small proportion of dissolved foreign atoms which scatter the conduction electrons, the residual resistance in e.s.u. is given by:

$$\rho_0 = \frac{m}{N e^2} \frac{vx}{100 \Omega_0} A, \quad \dots\dots(5)$$

where v is the velocity of the electrons at the top of the Fermi distribution, Ω_0 is the volume per atom, x is the percentage of foreign atoms in the metal, and A is the effective area presented by each foreign atom. The Born approximation of collision theory gives for A

$$A = \int_0^\pi (1 - \cos \theta) \left| \frac{2\pi m}{\hbar^2} \int \psi_k^* U \psi_k d\tau \right|^2 2\pi \sin \theta d\theta \quad \dots\dots(6)$$

where U is the difference between the potentials in the dissolved and solvent atoms.

Mott (1936) has calculated the resistivity of a monovalent metal containing dissolved atoms with $Z+1$ electrons outside closed shells. He used for U a screened coulomb potential with screening constant q :

$$U = Ze^2 e^{-qr}/r. \quad \dots\dots(7)$$

He obtained for the resistivity due to x per cent of foreign metal in solid solution:

$$\rho_0 = \frac{x}{100} \frac{2\pi Z^2 e^2}{mv^3} \left\{ \log \left(1 + \frac{1}{y} \right) - \frac{1}{1+y} \right\} \quad \dots\dots(8)$$

where $y = q^2 \hbar^2 / 4m^2 v^2$. Substitution in eqn (4) gives the 'semi-classical' absorption coefficient:

$$\eta_c = \frac{x}{100} \frac{8\pi^2}{nc} \frac{Z^2 N^2 e^6}{m^3 v^3} \left(\omega^2 + \rho_0^2 \frac{N^2 e^4}{m^2} \right)^{-1} \left\{ \log \left(1 + \frac{1}{y} \right) - \frac{1}{1+y} \right\} \quad \dots\dots(9)$$

§3. QUANTUM-MECHANICAL METHOD—THE INTERNAL PHOTOELECTRIC EFFECT

If $\overline{A^2}$ is the mean square value of the vector potential of the incident light on a plane within the metal perpendicular to the light beam, the energy incident on unit area of this plane in unit time is

$$n\pi v^2 \overline{A^2} / c. \quad \dots\dots(10)$$

When some of this light is absorbed in the metal we assume that for each photon absorbed, an electron in an occupied energy level is raised to an empty level in the conduction band, the difference between the initial and final energies being $\hbar\nu$, the energy of the photon. Let P be the probability, per unit volume per unit time, of allowed transitions between all pairs of states which satisfy this condition. Then the energy absorbed per unit area per unit time in a thickness dx is

$$P\hbar\nu dx. \quad \dots\dots(11)$$

The absorption coefficient η is defined as $\frac{\text{Energy absorbed per unit thickness}}{\text{Incident energy}}$

$$\text{which in this case gives} \quad \eta = \frac{P\hbar\nu}{n\pi v^2 \overline{A^2} / c}. \quad \dots\dots(12)$$

The problem of finding the absorption coefficient therefore reduces to the calculation of P .

We assume that the energy difference between the top of the highest full band and the lowest empty levels in the conduction band is so large than no transitions will be possible between the bands for the optical frequencies considered. In a perfect lattice we assume that the electrons behave like free electrons, so that transitions from one conduction level to another are forbidden. We must therefore consider the perturbations of the crystal lattice and calculate the probability of transitions between the corresponding perturbed wave functions.

§4. CALCULATION OF THE TRANSITION PROBABILITY

We consider a monovalent metal at a temperature 0°K , so that there are no thermal oscillations. Some of the atoms of the otherwise perfect lattice are replaced by foreign atoms with $Z+1$ electrons outside closed shells. These foreign atoms are so far apart that their interaction may be neglected. We assume that the conduction electrons, one per atom, behave like free electrons perturbed by the added potential around each foreign atom. For this perturbing potential we take the screened coulomb form:

$$U = Ze^2 e^{-ar}/r. \quad \dots\dots(13)$$

In the absence of any impurity atoms the electron wave functions would satisfy the free electron wave equation:

$$\nabla^2\psi + k^2\psi = 0 \quad \dots\dots(14)$$

where $k^2 = 2mE/\hbar^2$ and E is the energy of the electron. If the metal is in the form of a large sphere of radius R , the appropriate solutions of this equation are

$$\psi = D(kr)^{1/2} J_{l+1/2}(kr) P_l^{|m|}(\cos\theta) e^{im\varphi} \quad \dots\dots(15)$$

where $J_{l+1/2}$ is a Bessel function of the first kind, $P_l^{|m|}$ is an associated Legendre polynomial, and D is a normalizing constant. l and m are integers and the condition that ψ shall vanish on the surface of the sphere determines the allowed value of k . The reason for choosing these unperturbed wave functions instead of plane waves will appear below.

If there is one foreign atom at the centre of the sphere, the wave equation becomes

$$\nabla^2\psi' + k'^2\psi' = \frac{2m}{\hbar^2} U\psi'. \quad \dots\dots(16)$$

The angular part of a solution ψ'_i of this equation is identical with that of ψ_i , the corresponding solution of eqn (14), since U is a spherically symmetrical potential. The radial part of ψ'_i differs from that in eqn (15) only by small added terms, since U is small everywhere except near the origin, and for fixed l_i and m_i the wave functions ψ_i are non-degenerate. The perturbation has little effect on the quantized energy of an electron since R is large. The state characterized by quantum numbers (k'_i, l_i, m_i) has the energy $E_i = \hbar^2 k'^2_i / 2m$, and k'_i is very close to the corresponding k_i .

We now consider the probability of transitions between two perturbed states due to the incident light. Without loss of generality we may assume that the light is incident in the x direction and is polarized in the z direction. The only non-zero component of the vector potential is then A_z , and \bar{A}_z is its root mean square value. (Although we have assumed that the sphere of metal is large compared with the interatomic distance, we also assume that it is small enough so that \bar{A}_z may be considered to be constant throughout the metal.) First order time-dependent perturbation theory (Heitler 1944) gives for the probability per unit time of a transition from a state ψ_1 , with quantum numbers (l_1, m_1) and energy E_1 to a state ψ_2 with quantum numbers (l_2, m_2) and energy near E_2 :

$$w_{12} = (2\pi/\hbar) n(E_2) |H_{12}|^2 \quad \dots\dots(17)$$

where $n(E_2)$ is the density of states of energy E_2 with quantum numbers (l_2, m_2) and

$$|H_{12}| = \left| \frac{ie\hbar}{mc} \int \psi_2'^* \mathbf{A} \cdot \text{grad} \psi_1' d\tau \right| = \left| \frac{e\hbar}{mc} \frac{\bar{A}_z}{\sqrt{2}} \int \psi_2'^* \frac{\partial}{\partial z} \psi_1' d\tau \right| \quad \dots\dots(18)$$

The region of integration is the sphere of radius R . In the derivation of eqn (18) it is assumed that the wave vector of the light is negligibly small compared with that of a conduction electron.

Making use of a well-known theorem, we replace

$$\int \psi_2'^* \frac{\partial}{\partial z} \psi_1' d\tau \quad \text{by} \quad \frac{1}{E_1 - E_2} \int \psi_2'^* \frac{\partial U}{\partial z} \psi_1' d\tau.$$

In the latter integral we may replace $\psi_2'^*$ and ψ_1' by the corresponding unperturbed wave functions ψ_2^* and ψ_1 and the resulting error will be of the second order since $\partial U/\partial z$ is small except at the origin. This procedure is valid because the wave functions ψ_1 and ψ_2 which we have chosen are non-degenerate. This would not have been the case if plane waves had been used instead of Bessel functions.

The probability per unit time of transitions from all states with energy near E_1 to all states with energy near E_2 is obtained by multiplying w_{12} in eqn (17) by the density of states with energy E_1 and quantum numbers $(l_1 m_1)$, and summing over all values of l_1, l_2, m_1 and m_2 :

$$W_{12} = \frac{2\pi}{\hbar} \left(\frac{e\hbar \bar{A}_z}{mc\sqrt{2}} \right)^2 \frac{1}{(E_1 - E_2)^2} Q \quad \dots\dots (19)$$

where

$$Q = \sum_{l_1 l_2 m_1 m_2} n(E_1) n(E_2) \left| \int \psi_2^* \frac{\partial U}{\partial z} \psi_1 d\tau \right|^2. \quad \dots\dots (20)$$

For any potential U the quantity Q may be considered to correspond to some physical property of free electrons confined to a large sphere on the surface of which the wave functions vanish. This property of the electrons would remain unchanged if they were confined to a large rectangular box with periodic boundary conditions at its surfaces. In a box of volume V the normalized free-electron wave functions are $V^{-1/2} \exp(i\mathbf{k}_i \cdot \mathbf{r})$, where \mathbf{k}_i is the wave vector of the electron ($E_i = \hbar^2 k_i^2/2m$). The quantity which corresponds to Q in this case is

$$Q' = \int \int \int n'(E_1) n'(E_2) V^{-2} \left| \int \exp(-i\mathbf{k}_2 \cdot \mathbf{r}) \frac{\partial U}{\partial z} \exp(i\mathbf{k}_1 \cdot \mathbf{r}) d\tau \right|^2 \\ \times \sin \theta_1 \sin \theta_2 d\theta_1 d\theta_2 d\phi_1 d\phi_2 \quad \dots\dots (21)$$

where $(\theta_i \phi_i)$ are the polar angles of \mathbf{k}_i . $n'(E_i)$ is now the density of states with energy E_i per unit solid angle in \mathbf{k}_i -space. The summations over the quantum numbers in (20) are replaced by integrations over all directions of the wave vectors \mathbf{k}_1 and \mathbf{k}_2 . The equality of Q and Q' which is suggested by the physical argument above can be proved by a rigorous mathematical argument† if the integrations with respect to $d\tau$ in each case are taken over all space. The errors thus introduced are negligible since $\partial U/\partial z$ is very small far from the origin.

We now evaluate Q' using the potential defined in eqn (13). This evaluation is feasible only because we have replaced the Bessel functions in Q by exponentials and the summations by integrations. First we perform the integration with respect to $d\tau$ over all space:

$$\int \int \int \exp \{-i(\mathbf{k}_2 - \mathbf{k}_1) \cdot \mathbf{r}\} \frac{\partial (Ze^2 e^{-qr}/r)}{\partial z} r^2 \sin \theta dr d\theta d\phi = -4\pi Ze^2 \cos \Theta \frac{K}{K^2 + q^2} \\ \dots\dots (22)$$

† The proof of this theorem, due to Dr. J. S. Plaskett, will not be reproduced here.

where Θ is the angle between \mathbf{K} and the z axis and $\mathbf{K} = \mathbf{k}_2 - \mathbf{k}_1$. Substituting in eqn (21) we obtain

$$Q' = f(k_1, k_2) \int \int \int \frac{(k_2 \cos \theta_2 - k_1 \cos \theta_1)^2 \sin \theta_1 \sin \theta_2 d\theta_1 d\theta_2 d\phi_1 d\phi_2}{[k_1^2 + k_2^2 - 2k_1 k_2 \{\cos \theta_1 \cos \theta_2 + \sin \theta_1 \sin \theta_2 \cos(\phi_1 - \phi_2)\} + q^2]^2} \dots \dots (23)$$

where $f(k_1, k_2) = n'(E_1) n'(E_2) V^{-2} (4\pi Z e^2)^2$. Integration with respect to ϕ_1 and ϕ_2 from 0 to 2π gives

$$Q' = 4\pi^2 f(k_1, k_2) \int \int \frac{(k_1 x - k_2 y)^2 (C - 2k_1 k_2 xy)}{[(C - 2k_1 k_2 xy)^2 - 4k_1^2 k_2^2 (1 - x^2)(1 - y^2)]^{3/2}} dx dy \dots \dots (24)$$

where x is written for $\cos \theta_1$, y for $\cos \theta_2$ and C for $(k_1^2 + k_2^2 + q^2)$. The limits of integration with respect to x and y are 1 to -1 .

The x and y integrations are simplified if we integrate at this stage with respect to C and differentiate later:

$$\int Q' dC = -4\pi^2 f(k_1, k_2) \int \int \frac{(k_1 x - k_2 y)^2}{[(C - 2k_1 k_2 xy)^2 - 4k_1^2 k_2^2 (1 - x^2)(1 - y^2)]^{1/2}} dx dy. \dots \dots (25)$$

The x and y integrations can now be performed, giving

$$\int Q' dC = -4\pi^2 f(k_1, k_2) \left[\frac{4}{3} + \frac{1}{3} \frac{k_1^2 + k_2^2 - C}{k_1 k_2} \log \frac{C + 2k_1 k_2}{C - 2k_1 k_2} \right]. \dots \dots (26)$$

Differentiating with respect to C :

$$Q' = -\frac{4}{3} \pi^2 f(k_1, k_2) \left[\frac{4q^2}{C^2 - 4k_1^2 k_2^2} - \frac{1}{k_1 k_2} \log \frac{(k_1 + k_2)^2 + q^2}{(k_1 - k_2)^2 + q^2} \right]. \dots \dots (27)$$

In all possible transitions due to the absorption of light of frequency ν , the initial energy of the electron E_1 must be less than or equal to the Fermi energy (occupied states) and the final energy must be greater than the Fermi energy (vacant states). The difference $E_2 - E_1$ must be equal to the energy of an absorbed photon $\hbar\nu$. The total transition probability W for a sample of metal containing one foreign atom is obtained by integrating W_{12} over all allowed values of the initial energy:

$$W = \frac{1}{2} \int W_{12} dE_1. \dots \dots (28)$$

The limits of integration are $F - \hbar\nu$ and F where F is the Fermi energy (or 0 and F if $\hbar\nu > F$). The factor $\frac{1}{2}$ is introduced because only those transitions in which the direction of the electron spin is preserved are allowed.

If there are x per cent of non-interacting foreign atoms in the metal, the total transition probability per unit volume for light of frequency ν is obtained by multiplying the value for one foreign atom by the number of foreign atoms per unit volume:

$$P = (Nx/100) W. \dots \dots (29)$$

The density of states $n'(E)$ per unit solid angle in \mathbf{k} -space is given in this case as for a free electron gas (Seitz 1940) by

$$n'(E) = V(2m)^{3/2} E^{1/2} / \hbar^3 = 2mV\hbar k / \hbar^3. \dots \dots (30)$$

In eqns (19), (27), (28), (29) and (30) we have all the information necessary for the determination of P . Combining these equations we find (since $dE_1 = (\hbar^2/m) k_1 dk_1$)

$$P = \frac{Nx}{100} \left(\frac{2mV\hbar}{\hbar^3} \right)^2 \frac{\pi}{\hbar} \left(\frac{e\hbar\bar{A}_z}{mc} \right)^2 \frac{1}{(\hbar\nu)^2} \left(-\frac{4}{3}\pi^2 \right) (4\pi Ze^2)^2 V^{-2} \frac{1}{2} I \quad \dots\dots (31)$$

where

$$I = \frac{\hbar^2}{m} \int k_1^2 k_2 \left[\frac{4q^2}{C^2 - 4k_1^2 k_2^2} - \frac{1}{k_1 k_2} \log \frac{(k_1 + k_2)^2 + q^2}{(k_1 - k_2)^2 + q^2} \right] dk_1 \quad \dots\dots (32)$$

This integration with respect to k_1 is simplified by the substitutions

$$k_1 = t - \mu/t, \quad k_2 = t + \mu/t; \quad \mu = m\hbar\nu/2k^2.$$

The result may be written in the form

$$I = -\hbar\nu \{Y_b - Y_a\} \quad \dots\dots (33)$$

where

$$Y = \frac{1}{4} \left(\frac{G^2}{\hbar\nu} + \frac{\hbar\nu}{G^2} + \frac{q^2\hbar^2}{m\hbar\nu} \right) \log \left\{ \left(\frac{G^2}{\hbar\nu} + \frac{q^2\hbar^2}{2m\hbar\nu} \right) / \left(\frac{\hbar\nu}{G^2} + \frac{q^2\hbar^2}{2m\hbar\nu} \right) \right\} - \frac{1}{2} \left(\frac{G^2}{\hbar\nu} - \frac{\hbar\nu}{G^2} \right)$$

and

$$G_a = F^{1/2} + (F - \hbar\nu)^{1/2} \quad \text{if } \hbar\nu < F$$

$$= F^{1/2} \quad \text{if } \hbar\nu > F$$

$$G_b = F^{1/2} + (F + \hbar\nu)^{1/2}.$$

Substitution of this value into eqn (31) gives

$$P = \frac{16\pi^2}{3} \frac{Nx}{100} \frac{(Ze^3\bar{A}_z)^2}{c^2\hbar^4\nu} \{Y_b - Y_a\}. \quad \dots\dots (34)$$

The quantum-mechanical absorption coefficient η_Q is now obtained by substituting this value for P in eqn (12):

$$\eta_Q = \frac{16\pi}{3} \frac{Nx}{100} \frac{Z^2 e^6}{n\hbar^3\nu^2} \{Y_b - Y_a\}. \quad \dots\dots (35)$$

§5. COMPARISON OF QUANTUM-MECHANICAL AND SEMI-CLASSICAL RESULTS

The number of electrons per unit volume N , and the velocity of an electron at the top of the Fermi distribution are both related to the Fermi energy F (Seitz 1940):

$$F = \frac{\hbar^2}{2m} \left(\frac{3N}{8\pi} \right)^{2/3} = \frac{1}{2} m v^2. \quad \dots\dots (36)$$

In eqn (9) the term $\rho_0^2 N^2 e^4 / m^2$ is small compared with ω^2 for visible and ultra-violet light. Even for infra-red light this term may be neglected if x and Z are small and q is not too small. To this approximation, and using eqn (36), eqn (9) may be replaced by:

$$\eta_0 = \frac{16\pi}{3} \frac{Nx}{100} \frac{Z^2 e^6}{n\hbar^3\nu^2} \left\{ \log \left(1 + \frac{1}{y} \right) - \frac{1}{1+y} \right\}. \quad \dots\dots (37)$$

The factor in front of the bracket is identical with that in eqn (35). If we consider the limiting case of low frequency light so that $\hbar\nu \ll F$ and terms of order $(\hbar\nu/F)^2$ may be neglected, the expression in braces in eqn (35) reduces to precisely the form of that in braces in eqn (37). Therefore if the screening constant is not too small, and the concentration of foreign atoms is not too great, the two methods give identical expressions for the absorption coefficient at low frequencies. If q is infinite both coefficients become zero for all frequencies (i.e. no light is absorbed if the electrons are not scattered in the metal). However, if $q=0$, each foreign atom being surrounded by a coulomb potential, the semi-classical absorption coefficient becomes infinitely large, but the quantum-mechanical value remains finite.

In table (a) the results obtained by the two methods are shown for a typical example. The solvent metal is copper ($F=7.04$ eV) and it contains 1% of some divalent metal such as zinc. The value of $1/q$ is assumed to be one atomic unit (0.529×10^{-8} cm), and n is taken to be unity. When $\lambda=1760$ Å in this example, the condition $h\nu = F$ is satisfied. In the quantum-mechanical method, the slope of the curve of η_Q plotted against λ should have a discontinuity at this point. In this example the discontinuity is not noticeable. The agreement between the two results is excellent in the infra-red region, as expected. Throughout the whole range of wavelengths extending into the ultra-violet the agreement remains surprisingly good.

In table (b) the variation of the two absorption coefficients with q is shown for the same example, with λ fixed at 7300 Å. The difference between the two results remains small until q becomes very close to zero.

The semi-classical and quantum-mechanical absorption coefficients
of copper containing 1% of zinc.

(a) Variation with λ for $1/q = 1$ A.U.				(b) Variation with $1/q$ for $\lambda = 7300$ Å		
ω (A.U.)	λ (Å)	$\eta_C(10^{-5} \text{ Å}^{-1})$	$\eta_Q(10^{-5} \text{ Å}^{-1})$	$1/q$ (A.U.)	$\eta_C(10^{-5} \text{ Å}^{-1})$	$\eta_Q(10^{-5} \text{ Å}^{-1})$
0.04	11400	129.9	129.3	0	0	0
0.08	5700	32.46	32.17	0.1	0.010	0.005
0.12	3790	14.43	14.16	0.2	0.144	0.084
0.16	2850	8.12	7.83	0.4	1.73	1.76
0.20	2280	5.19	4.88	1.0	20.77	20.48
0.24	1900	3.61	3.25	2.0	62.00	59.53
0.2586	1760	3.11	2.70	4.0	118.34	116.46
0.28	1625	2.65	2.38	10.0	201.61	181.00
0.32	1425	2.03	1.91	100.0	415.04	214.90
0.36	1265	1.60	1.57			
0.40	1140	1.30	1.34	∞	∞	215.37

§6. OPTICAL ABSORPTION IN SEMICONDUCTORS

In extending the method of §§ 3 and 4 to include semiconductors we make most of the same simplifying assumptions which were used above. We consider only absorption due to the presence of ionized impurity atoms with valence differing by Z from that of the solvent. The current carriers are treated as free negative or positive electrons of mass m^* which may be different from the actual electronic mass, and only transitions within the conduction band (for electrons) or within the valence band (for holes) are considered. The screened coulomb potential around each impurity atom is (cf. eqn (13))

$$U = Ze^2 e^{-qr} / \epsilon r \quad \dots\dots (38)$$

where ϵ is the dielectric constant of the semiconductor.

With a low density of free carriers it is no longer a good approximation to assume that all energy levels up to the Fermi energy are occupied and all higher levels are vacant. We must consider the energy distribution of the free carriers which is given to a good approximation by the classical distribution function. The densities per unit solid angle in \mathbf{k} -space of occupied states of energy E_1 and of unoccupied states of energy E_2 are (cf. eqn (30))

$$\begin{aligned} n(E_1) &= (2m^*)^{3/2} V E_1^{1/2} h^{-3} B \exp(-E_1/kT) \\ n(E_2) &= (2m^*)^{3/2} V E_2^{1/2} h^{-3} \{1 - B \exp(-E_2/kT)\} \end{aligned} \quad \dots\dots (39)$$

where $B = \hbar^3 N_T / 2(2\pi m^* \mathbf{k} T)^{3/2}$. N_T is the number of free carriers at absolute temperature T . The energy of the initial state may have any value from 0 to ∞ . Since B is small for semiconductors the term in B^2 may be neglected in the product $n(E_1)n(E_2)$.

The procedure for calculating the absorption coefficient is identical with that used above. The change in the potential introduces a factor $1/\epsilon^2$ in Q' of eqns (23) to (27) and therefore in the absorption coefficient. Using the new density of states, we must replace I of eqn (32) by

$$I' = \frac{\hbar^2}{2m^*} \int_0^\infty k_1^2 k_2 \left[\frac{4q^2}{C^2 - 4k_1^2 k_2^2} - \frac{1}{k_1 k_2} \log \frac{(k_1 + k_2)^2 + q^2}{(k_1 - k_2)^2 + q^2} \right] B \exp(-E_1/\mathbf{k} T) dk_1. \quad \dots\dots (40)$$

This integration is difficult to perform in the general case. However, since the density of free carriers is small, the screening of the coulomb potential around each impurity atom will be very weak. The screening constant is of the order of the reciprocal of the average distance between neighbouring foreign atoms (Conwell and Weisskopf 1950). By completing the calculation with $q=0$ we shall obtain an upper bound for the absorption coefficient.

With $q=0$, eqn (40) becomes

$$I' = -\frac{\hbar^2}{2m^*} B \int_0^\infty k_1 \log \frac{(k_1 + k_2)^2}{(k_1 - k_2)^2} \exp(-k_1^2/s) dk_1 \quad \dots\dots (41)$$

where

$$s = 2m^* \mathbf{k} T / \hbar^2.$$

Expressing k_2 in terms of k_1 , as above:

$$k_2^2 = k_1^2 + 4\mu; \quad \mu = m^* \hbar \nu / 2\hbar^2$$

and integrating by parts we obtain

$$I' = -\frac{\hbar^2}{m^*} B s \int_0^\infty \exp(-k_1^2/s) (k_1^2 + 4\mu)^{-1/2} dk_1 = -\frac{\hbar^2}{2m^*} B s \exp\left(\frac{2\mu}{s}\right) \mathcal{K}_0\left(\frac{2\mu}{s}\right) \quad \dots\dots (42)$$

where \mathcal{K}_0 is the modified Bessel function of order zero. Substituting in eqns (31) and (12) we obtain

$$\eta_Q' = \frac{8}{3} N_T \frac{N_x}{100} \frac{\hbar^2 Z^2 e^6}{n \epsilon^2 m^* \mathbf{c}} \frac{1}{(2\pi m^* \mathbf{k} T)^{1/2}} \frac{1}{(\hbar \nu)^3} \exp\left(\frac{\hbar \nu}{2\mathbf{k} T}\right) \mathcal{K}_0\left(\frac{\hbar \nu}{2\mathbf{k} T}\right). \quad \dots\dots (43)$$

The function $\exp(\hbar \nu / 2\mathbf{k} T) \mathcal{K}_0(\hbar \nu / 2\mathbf{k} T)$ decreases slowly as $\hbar \nu / 2\mathbf{k} T$ increases. Its value is less than unity when $\hbar \nu / 2\mathbf{k} T$ is greater than 1.36 (Watson 1945). Therefore, under normal experimental conditions,

$$\eta_Q' < \frac{8}{3} N_T \frac{N_x}{100} \frac{\hbar^2 Z^2 e^6}{n \epsilon^2 m^* \mathbf{c}} \frac{1}{(2\pi m^* \mathbf{k} T)^{1/2}} \frac{1}{(\hbar \nu)^3}. \quad \dots\dots (44)$$

The semi-classical absorption coefficient may be calculated by the same method which was used above for metals. Instead of the velocity of the electrons at the top of the Fermi distribution we must now use the average velocity of the electrons, given by

$$\frac{1}{2} m^* v^2 = 3\mathbf{k} T / 2 \quad \dots\dots (45)$$

and we must use the potential of eqn (38) instead of eqn (13). Neglecting the term in ρ_0^2 , we obtain in this case instead of eqn (9)

$$\eta_C' = \frac{8\pi^2}{\mathbf{c}} N_T \frac{N_x}{100} \frac{Z^2 e^6}{n \epsilon^2 m^{*3} v^3} \frac{1}{\omega^2} \log \left\{ \left(1 + \frac{1}{y} \right) - \frac{1}{1+y} \right\}. \quad \dots\dots (46)$$

As above, this gives infinite absorption when $q=0$. For small non-zero values of q , the term $\log \{(1+1/y) - 1/(1+y)\}$ is greater than unity even for low temperatures. Therefore

$$\eta_c' > \frac{8\pi^2}{c} N_T \frac{Nx}{100} \frac{Z^2 e^6}{n \epsilon^2 m^{*3} v^3} \frac{1}{4\pi^2 v^2}. \quad \dots\dots(47)$$

Comparing eqns (44) and (47) and making use of eqn (45) we find

$$\frac{\eta_Q'}{\eta_c'} < 4 \left(\frac{2}{3\pi} \right)^{1/2} \frac{\frac{1}{2} m^* v^3}{h\nu}. \quad \dots\dots(48)$$

Therefore this quantum-mechanical method gives a smaller value for the absorption coefficient of a semiconductor than the semi-classical method.

§ 7. DISCUSSION

The use of free electron wave functions instead of the accurate wave functions in calculating the transition probabilities is not a good approximation when the energy of the electrons is very low ($Ze^2/\hbar v$ large), as it is in semiconductors. In their calculation of the absorption coefficient of hydrogen negative ions in the Sun's atmosphere, Chandrasekhar and Breen (1946) found that the use of Hartree wave functions instead of plane waves increased their result by a factor of ten. In our problem, which is similar, the difference would be much greater since we are interested in laboratory temperatures instead of solar temperatures. We can make a rough estimate of our errors for an unscreened coulomb potential. In this case, the exact wave functions are known. Near the scattering centre their amplitude is greater than that of plane waves by a factor $[2\pi\alpha/(e^{2\pi\alpha}-1)]^{1/2}$ where $\alpha = ZZ'e^2/\hbar v$; $Z'e$ is the charge of the free carriers ($Z' = \pm 1$) and v is their velocity (Heitler 1944, p. 167). Therefore, in an accurate calculation, the absorption coefficient would differ by a factor of the order of

$$2\pi\alpha_1 2\pi\alpha_2 / [\exp(2\pi\alpha_1) - 1][\exp(2\pi\alpha_2) - 1]$$

from that found in § 6. The magnitude of α is large for slow electrons or holes. If Z and Z' have the same sign α is positive and this factor is very small. In the more important cases where Z and Z' are of opposite sign (scattering of electrons by positive centres or of holes by negative centres) α is negative and the factor is large. In our case α_1 corresponds to thermal energies (if $Z=1$, $\alpha_1 \sim 20$ at 300°K) and α_2 corresponds to optical energies (if $Z=1$, $\alpha_2 \sim 5$ for infra-red radiation of wavelength 2μ). The multiplying factor is therefore of the order of 4000.

Experiments on germanium and silicon (Fan and Becker 1951, Gibson 1953) have shown that the infra-red absorption coefficients are proportional to the number of free carriers and increase with wavelength but that their magnitudes are greater by a factor of 1000 than those predicted by semi-classical theory. The calculation in § 6 increases the discrepancy between theory and experiment. However, a similar calculation using the accurate electron wave functions should give results of the same order of magnitude as the experimental values.

ACKNOWLEDGMENTS

I am pleased to express my gratitude to Professor N. F. Mott for suggesting this problem and for his guidance during the course of the work, and to Dr. J. S. Plaskett for several helpful and stimulating discussions.

REFERENCES

- CHANDRASEKHAR, S., and BREEN, F. H., 1946, *Astrophys. J.*, **104**, 430.
CONWELL, E., and WEISSKOPF, V. F., 1950, *Phys. Rev.*, **77**, 388.
FAN, H. Y., and BECKER, M., 1951, *Semi-Conducting Materials*, Ed. H. K. Henisch (London : Butterworths Scientific Publications), p. 132.
GIBSON, A. F., 1953, *Proc. Phys. Soc. B*, **403**, 588.
HEITLER, W., 1944, *The Quantum Theory of Radiation*, 2nd Edn (Oxford : University Press).
MOTT, N. F., 1936, *Proc. Camb. Phil. Soc.*, **32**, 281.
MOTT, N. F., and JONES, H., 1936, *The Theory and Properties of Metals and Alloys* (Oxford : University Press).
SEITZ, F., 1940, *The Modern Theory of Solids* (New York : McGraw-Hill).
WATSON, G. N., 1945, *Theory of Bessel Functions*, 2nd Edn (New York : Macmillan).

Inelastic Magnetic Scattering of Neutrons from a Ferromagnetic Crystal

By W. MARSHALL

Mathematical Physics Department, University of Birmingham

*Communicated by R. E. Peierls; MS. received 2nd July 1953,
and in amended form 17th October 1953*

Abstract. The wave functions and energy eigenvalues of a ferromagnetic crystal at low temperature are obtained assuming a model of two electrons localized on each atom. The results are applied to the problem of inelastic scattering of neutrons following Moorhouse. The effect of assuming two electrons per atom is quite unimportant. However, a more realistic estimate of the exchange integral leads to narrower peaks than predicted by Moorhouse and therefore tends to make the effect easier to observe.

§ 1. INTRODUCTION

THE inelastic magnetic scattering of slow neutrons (2.5×10^{-3} eV) by a ferromagnetic crystal was considered by Moorhouse (1951) using the Heisenberg-Bloch model with one electron per atom. However, since the saturation moment in iron approximates closely to two magnetons per atom it is of interest to generalize the treatment to the case of two electrons per atom. To apply this model consistently we must consider these two electrons as coupled with their spins parallel, and so we have essentially a problem involving unit spin per atom.

It is well known that the Heisenberg-Bloch model is an idealization that, in some respects, is in conflict with the observed properties of ferromagnetics, but this paper, like Moorhouse's, is concerned with studying neutron scattering from this model since comparison with experiment may then further clarify the validity or the limitations of the model.

§ 2. THE FERROMAGNETIC CRYSTAL

The intrinsic magnetization of a ferromagnet results from the exchange interaction of the spin 'carriers'. The relevant part of the Hamiltonian, assuming that only coupling between nearest neighbours is effective and that the exchange integrals for such neighbours are the same, is (Van Vleck 1945)

$$H = -2J \sum_{\text{adjacent pairs}} \mathbf{S}_i \cdot \mathbf{S}_j, \quad \dots\dots(2.1)$$

where \mathbf{S}_i and \mathbf{S}_j are spin operators expressed in units of \hbar .

For the case of spin $\frac{1}{2}$ per atom Bloch (1940) has obtained an approximate solution of the three-dimensional problem and Bethe (1931) has shown how in principle the one-dimensional problem may be solved exactly, though the algebraic difficulties involved become great for more than two 'wrong' spins. Both these solutions involve the concept of spin waves. Near saturation most spins have $S = \frac{1}{2}$, and the wrong spins, those with $S = -\frac{1}{2}$, jump from atom to atom and

travel through the crystal-like waves. Bloch's treatment breaks down at high temperatures because he has to assume that the spin waves are non-interacting. This is a good approximation only at low temperatures when there are only a few waves. Møller (1933) considered the case $S > \frac{1}{2}$, but since his method is very general and not very transparent we give here the solution for the $S = 1$ case.

We suppose that the crystal, which is nearly saturated in the z direction, has N atoms, upon each of which is localized a spin of one. The atoms are at lattice points $\mathbf{r}_1, \mathbf{r}_2, \dots, \mathbf{r}_N$. We consider only a cubic lattice with $N_1 \times N_2 \times N_3$ unit cells each with side a . Each atom has z nearest neighbours. The individual spin matrices we shall call α, β and γ , corresponding to z -components of 1, 0 and -1 respectively, i.e. $\mathbf{S}^z \alpha = \alpha$; $\mathbf{S}^z \beta = 0$; $\mathbf{S}^z \gamma = -\gamma$.

Since we may easily see that the total z -component of spin, $\sum_{i=1}^N \mathbf{S}_i^z$, commutes with H we can diagonalize this operator and the Hamiltonian simultaneously. We need therefore only consider the eigenvalues of this operator one at a time. Let ψ_t be a stationary state eigenfunction corresponding to a total z component of spin $= N - t$, i.e. $\sum_{i=1}^N \mathbf{S}_i^z \psi_t = (N - t) \psi_t$. Our problem is to determine the ψ_t 's and the corresponding energy eigenvalues E_t of each value of t .

$t = 0$. ψ_0 , the eigenfunction of the completely saturated state, is obviously $\alpha(1) \alpha(2) \alpha(3) \dots \alpha(N)$. Then

$$H\psi_0 = -JNz\psi_0 \quad \text{and} \quad E_0 = -JNz. \quad \dots\dots(2.2)$$

$t = 1$. In this case one of the atoms has $S^z = 0$. Suppose it is at \mathbf{r}_n . The corresponding wave function is $\phi(\mathbf{r}_n) = \alpha(1) \alpha(2) \dots \beta(n) \dots \alpha(N)$. The stationary state eigenfunction will be a linear sum of such terms.

$$\text{Let} \quad \psi_1 = \sum_n c(\mathbf{r}_n) \phi(\mathbf{r}_n). \quad \dots\dots(2.3)$$

$$\text{Now} \quad H\phi(\mathbf{r}_n) = -2J(\tfrac{1}{2}Nz - z)\phi(\mathbf{r}_n) - 2J\sum \phi(\mathbf{r}_n') \quad \dots\dots(2.4)$$

where the sum goes over all atoms \mathbf{r}_n' which are nearest neighbours of \mathbf{r}_n .

$$\text{Then} \quad H\psi_1 = -2J\sum_n c(\mathbf{r}_n) [\tfrac{1}{2}Nz - z]c(\mathbf{r}_n) + \sum c(\mathbf{r}_n')], \quad \dots\dots(2.5)$$

$$(H - E_1)\psi_1 = 0; \text{ therefore}$$

$$\{2J(\tfrac{1}{2}Nz - z) + E_1\}c(\mathbf{r}_n) + 2J\sum c(\mathbf{r}_n') = 0. \quad \dots\dots(2.6)$$

$$\text{This is satisfied by} \quad c(\mathbf{r}_n) = \exp(i\mathbf{k} \cdot \mathbf{r}_n) \quad \dots\dots(2.7)$$

$$\text{and} \quad E_1 = -JNz + 2Jz - 2J \exp(-i\mathbf{k} \cdot \mathbf{r}_n) \sum \exp(i\mathbf{k} \cdot \mathbf{r}_n'). \quad \dots\dots(2.8)$$

\mathbf{k} satisfies the conditions

$$k_x = \frac{2\pi}{aN_1} n_1; \quad k_y = \frac{2\pi}{aN_2} n_2; \quad k_z = \frac{2\pi}{aN_3} n_3$$

where

$$n_1 = 0, 1, 2, \dots, N_1 - 1; \quad n_2 = 0, 1, 2, \dots, N_2 - 1; \quad n_3 = 0, 1, 2, \dots, N_3 - 1. \quad \dots(2.9)$$

For the simple cubic structure

$$\exp(-i\mathbf{k} \cdot \mathbf{r}_n) \sum \exp(i\mathbf{k} \cdot \mathbf{r}_n') = 2\{\cos ak_x + \cos ak_y + \cos ak_z\} = 6 - a^2 \mathbf{k}^2 \quad \dots(2.10)$$

for ak_x, ak_y and ak_z small enough.

It is easily shown that for the body-centred and face-centred cubic structures this expression reduces to $z - a^2 \mathbf{k}^2$. So for all cases

$$E_1 = -JNz + 2Ja^2 \mathbf{k}^2 \quad \dots\dots(2.11)$$

and

$$\psi_1 = \sum_n \exp(i\mathbf{k} \cdot \mathbf{r}_n) \alpha(1) \alpha(2) \dots \beta(n) \dots \alpha(N). \quad \dots\dots(2.12)$$

$t \geq 2$. So far our solution is exactly analogous to Bloch's solution of the spin $\frac{1}{2}$ problem, but now we have the possibility of having two sorts of spin waves, ' β -waves' with $S^z = 0$ and ' γ -waves' with $S^z = -1$. However, we expect the β -waves to be predominantly important for two reasons.

Firstly, the density of states for β -waves is much higher than for γ -waves. Although it is not evident from (2.11), which is valid only near the bottom of the range, it can be seen from (2.10) and (2.8) that E_t can have values ranging between $-JNz$ and $-JNz + 4Jz$. In general E_t will have a range of about $4Jzt$. In this range we must fit $N!/t!(N-t)!$ states if we have only β -waves or $N!/(\frac{1}{2}t)!(N-\frac{1}{2}t)!$ states if we have only γ -waves. The density of states in the first case is therefore greater, by a factor of the order of $N^{t/2}$, than in the second case provided $t \ll N$. Most of the wrong spins will therefore go into β -wave states.

Secondly, we know we will have to ignore the scattering of β -waves by each other, and we know this is a good approximation at low temperatures. But a γ -wave can only be created by the interaction of two β -waves and, therefore, to be consistent, if we treat the β -waves as non-interacting we must also ignore all γ -waves. However, we could put in γ -waves with coefficients which account for some interactions but not all. This presumably would be a little closer to the truth, but since, as we have seen above, we expect the effect to be $N^{-t/2}$ of the main effect, this is not really very important. Now let us consider this case in more detail.

$$t = 2. \quad \text{Define } \phi(\mathbf{r}_l, \mathbf{r}_m) = \alpha(1)\alpha(2) \dots \beta(l) \dots \beta(m) \dots \alpha(N) \dots \dots (2.13)$$

$$\chi(\mathbf{r}_l) = \alpha(1)\alpha(2) \dots \gamma(l) \dots \alpha(N) \dots \dots (2.14)$$

$$\text{and set} \quad \psi_2 = \frac{1}{2} \sum_{l, m \neq l} c(\mathbf{r}_l, \mathbf{r}_m) \phi(\mathbf{r}_l, \mathbf{r}_m) + \sum_n b(\mathbf{r}_n) \chi(\mathbf{r}_n) \dots \dots (2.15)$$

from which it follows that

$$\begin{aligned} H\psi_2 = & -2J \sum_{\text{non-adjacent pairs}} \phi(\mathbf{r}_l, \mathbf{r}_m) [(\frac{1}{2}Nz - 2z)c(\mathbf{r}_l, \mathbf{r}_m) + \Sigma c(\mathbf{r}_l', \mathbf{r}_m')] \\ & - 2J \sum_{\text{adjacent pairs}} \phi(\mathbf{r}_l, \mathbf{r}_m) [(\frac{1}{2}Nz - 2z + 1)c(\mathbf{r}_l, \mathbf{r}_m) + \Sigma' c(\mathbf{r}_l', \mathbf{r}_m') + b(\mathbf{r}_l) + b(\mathbf{r}_m)] \\ & - 2J \sum_{\mathbf{r}_l} \chi(\mathbf{r}_l) [(\frac{1}{2}Nz - 2z)b(\mathbf{r}_l) + \Sigma c(\mathbf{r}_l, \mathbf{r}_l')] \dots \dots (2.16) \end{aligned}$$

where $\Sigma c(\mathbf{r}_l', \mathbf{r}_m')$ means the sum over \mathbf{r}_l' , the nearest neighbours of \mathbf{r}_l , and over \mathbf{r}_m' , the nearest neighbours of \mathbf{r}_m , taken one at a time, and $\Sigma' c(\mathbf{r}_l', \mathbf{r}_m')$ is a similar sum excluding the terms $c(\mathbf{r}_l, \mathbf{r}_l)$ and $c(\mathbf{r}_m, \mathbf{r}_m)$ which arise when \mathbf{r}_l and \mathbf{r}_m are nearest neighbours.

Hence the coefficients satisfy the equations

$$\left(\frac{Nz}{2} - 2z + \frac{E_2}{2J}\right) c(\mathbf{r}_l, \mathbf{r}_m) + \Sigma c(\mathbf{r}_l', \mathbf{r}_m') = 0 \dots \dots (2.17)$$

if \mathbf{r}_m is not a neighbour of \mathbf{r}_l , and

$$\left(\frac{Nz}{2} - 2z + 1 + \frac{E_2}{2J}\right) c(\mathbf{r}_l, \mathbf{r}_m) + \Sigma' c(\mathbf{r}_l', \mathbf{r}_m') + b(\mathbf{r}_l) + b(\mathbf{r}_m) = 0. \dots \dots (2.18)$$

if \mathbf{r}_l and \mathbf{r}_m are neighbours. Also

$$\left(\frac{Nz}{2} - 2z + \frac{E_2}{2J}\right) b(\mathbf{r}_l) + \Sigma c(\mathbf{r}_l, \mathbf{r}_l') = 0. \dots \dots (2.19)$$

These equations cannot be simultaneously solved exactly but we can easily find a solution of (2.17), so let us consider the error involved in E_2 in ignoring (2.18) and (2.19), which are concerned with the interactions of β -waves and transitions to γ -wave states. From (2.16)

$$E_2 = \frac{\psi_2^* H \psi_2}{\psi_2^* \psi_2} = -2J \left(\frac{1}{2} N z - 2z \right) - 2J \{c(\mathbf{r}_b, \mathbf{r}_m)\}^{-1} \sum c(\mathbf{r}_l', \mathbf{r}_m')$$

$$\times \frac{-2J}{\frac{1}{2} \sum_{l, m \neq l} |c(\mathbf{r}_b, \mathbf{r}_m)|^2 + \sum |b(\mathbf{r}_l)|^2}$$

$$\times \left\{ \begin{array}{l} \sum_{\text{adjacent pairs}} c^*(\mathbf{r}_b, \mathbf{r}_m) [c(\mathbf{r}_b, \mathbf{r}_m) - c(\mathbf{r}_b, \mathbf{r}_l) - c(\mathbf{r}_m, \mathbf{r}_m) + b(\mathbf{r}_l) + b(\mathbf{r}_m)] \\ + \sum_l b^*(\mathbf{r}_l) [\sum c(\mathbf{r}_b, \mathbf{r}_l') - b(\mathbf{r}_l) \{c(\mathbf{r}_b, \mathbf{r}_m)\}^{-1} \sum c(\mathbf{r}_l', \mathbf{r}_m')] \end{array} \right\} \dots\dots (2.20)$$

The third term is small, of the order of N^{-1} , because the numerator contains approximately N terms while the denominator contains the sum of approximately N^2 positive terms. If we could choose the coefficients so that (2.18) and (2.19) were satisfied the third term would be zero, but we see the error involved is of the order of N^{-1} (i.e. $N^{-1/2}$), which is negligible whatever our choice of coefficients. For the case $t=2$, therefore, we are certainly justified in neglecting γ -wave and β -wave interactions.

We therefore select

$$c(\mathbf{r}_b, \mathbf{r}_m) = \exp \{i(\mathbf{k}_1 \cdot \mathbf{r}_l + \mathbf{k}_2 \cdot \mathbf{r}_m)\} + \exp \{i(\mathbf{k}_2 \cdot \mathbf{r}_l + \mathbf{k}_1 \cdot \mathbf{r}_m)\} \dots\dots (2.21)$$

which is a solution of (2.17) giving

$$E_2 = -JNz + 4Jz - 2J \{ \exp i(\mathbf{k}_1 \cdot \mathbf{r}_l + \mathbf{k}_2 \cdot \mathbf{r}_m) + \exp i(\mathbf{k}_2 \cdot \mathbf{r}_l + \mathbf{k}_1 \cdot \mathbf{r}_m) \}^{-1}$$

$$\times \sum \{ \exp i(\mathbf{k}_1 \cdot \mathbf{r}_l' + \mathbf{k}_2 \cdot \mathbf{r}_m') + \exp i(\mathbf{k}_2 \cdot \mathbf{r}_l' + \mathbf{k}_1 \cdot \mathbf{r}_m') \}. \dots\dots (2.22)$$

\mathbf{k}_1 and \mathbf{k}_2 obey (2.9).

The expression for E_2 reduces to

$$E_2 = -JNz + 2Ja^2(\mathbf{k}_1^2 + \mathbf{k}_2^2) \dots\dots (2.23)$$

for ak_1^x, ak_1^y , etc. small enough, and ψ_2 can be written

$$\psi_2 = \sum_{\mathbf{r}_l, \mathbf{r}_m \neq \mathbf{r}_l} \exp \{i(\mathbf{k}_1 \cdot \mathbf{r}_l + \mathbf{k}_2 \cdot \mathbf{r}_m)\} \alpha(1)\alpha(2) \dots \beta(l) \dots \beta(m) \dots \alpha(N).$$

$$\dots\dots (2.24)$$

$t > 2$. For t not too large the solution is evidently

$$\psi_t = \sum_{\mathbf{r}_a, \mathbf{r}_b, \dots, \mathbf{r}_t} \exp \{i(\mathbf{k}_1 \cdot \mathbf{r}_a + \mathbf{k}_2 \cdot \mathbf{r}_b + \dots \mathbf{k}_t \cdot \mathbf{r}_t)\}$$

$$\times \alpha(1)\alpha(2) \dots \beta(a) \dots \beta(b) \dots \beta(t) \dots \alpha(N) \dots (2.25)$$

where $\mathbf{r}_a, \mathbf{r}_b, \dots, \mathbf{r}_t$ are all different.

$$E_t = -JNz + 2Ja^2 \sum_{n=1}^t \mathbf{k}_n^2. \dots\dots (2.26)$$

For comparison the spin $\frac{1}{2}$ formula for t wrong spins is

$$E_t = -\frac{1}{4}JNz + Ja^2 \sum_{n=1}^t \mathbf{k}_n^2. \dots\dots (2.27)$$

After constructing the partition function the variation of the magnetization with temperature can be found. A calculation like that in Bloch's paper gives

$$\frac{M}{M_0} = 1 - \frac{1}{N_e} \left(\frac{kT}{2J} \right)^{3/2} \frac{1}{2\pi^2} \int_0^\infty \frac{\sqrt{y} dy}{e^y - 1} \dots\dots (2.28)$$

where N_v is the number of magnetic electrons in a volume a^3 , i.e. $N_v = 2, 4$ or 8 for the simple, body-centred or face-centred cubic lattices respectively for $S = 1$. In the spin $\frac{1}{2}$ formula the factor $(kT/2J)^{3/2}$ is replaced by $(kT/J)^{3/2}$ and, of course, N_v becomes 1, 2 or 4 respectively.

§ 3. VALUE OF THE EXCHANGE INTEGRAL

We now wish to estimate J . For convenience define $J = gkT_C$ where T_C is the ferromagnetic Curie temperature, and now we wish to know g . The simplest way is to assume that the law (2.28) holds up to the Curie temperature and for $T = T_C$ set $M = 0$. This is the method used by Moorhouse. Equation (2.28) gives $g = 0.0476$ for a body-centred cubic and spin 1; $g = 0.0300$ for a face-centred cubic and spin 1. The values obtained by Moorhouse using $\frac{1}{2}$ formula are $g = 0.151$ and $g = 0.095$ respectively.

However, we do not expect (2.28) to hold up to high temperatures, and experiment shows that they do not, so we cannot regard these values as being very accurate. As we expect our model of the ferromagnet to be a better one than that used by Moorhouse it seems worth while to obtain a better estimate of g than can be given by this method.

Weiss (1934) verified the $T^{3/2}$ law and he found that it was obeyed accurately up to 150°K for nickel and up to 300°K for iron. The best method to estimate g therefore seems to be to compare the slopes of his graphs of M against $T^{3/2}$ over these ranges with the slopes predicted by (2.28). This gives $g = 0.197$ for iron (body-centred cubic) and spin 1; $g = 0.113$ for nickel (face-centred cubic) and spin 1. The value $g = 0.197$ is the one used in the calculations for iron in the next section. For comparison this method would give $g = 0.624$ and $g = 0.358$ for iron and nickel respectively in the spin $\frac{1}{2}$ case.

§ 4. SCATTERING CROSS SECTION

Moorhouse's calculation of the scattering from iron now follows through exactly except that his equation (2.6) becomes

$$\hbar^2(\mathbf{p}^2 - \mathbf{p}'^2)/2M = -2Ja^2\mathbf{k}^2 \quad \dots\dots(4.1)$$

$$\text{so we redefine his } \alpha = 4MJ a^2/\hbar^2 = 139 \text{ using the value } g = 0.197. \quad \dots\dots(4.2)$$

The limits on θ , where 2θ is the angular spread of a peak, now become $5^\circ > \theta > 0$ and we obtain, using his notation,

$$\sigma_n = \frac{3.16 \times 10^{-3} Q a p_1 / 2\pi}{\exp \{0.406(a p_1 / 2\pi) Q (288/T)\} - 1} \text{ barns for } \mathbf{n}^2 = 2. \quad \dots\dots(4.3)$$

where σ_n is the integrated cross section of the scattered peak centred on the direction \mathbf{n} , \mathbf{p}_1 is a reduced wave number and Q is a quantity defined in Moorhouse's paper and is of order 1. The values of σ_n at 288° corresponding to different values of \mathbf{n} are shown in the table which is given for just two values of the incident neutron wave number \mathbf{p} . Using the known lattice constant of iron, we therefore see that for $\kappa = \frac{1}{2}$, where $p = 2\pi\kappa/a$, the neutron energy is approximately $2.5 \times 10^{-3} \text{ ev}$. Energies much greater than this cannot be used since diffraction peaks would occur for $\kappa \geq 1/\sqrt{2}$, and these would completely mask the small 'spin wave scattered' peaks. In the limit $\kappa = 0$ then the direction of the incoming neutrons is unimportant and we easily see that $\sigma_n = 3.6 \times 10^{-3}$ barns and the cross section per steradian $= 0.16$ for all the \mathbf{n} and for all incident directions.

Cross Sections for $\mathbf{p} = \frac{2\pi}{a}(\kappa, 0, 0)$

\mathbf{n}	$\left(\frac{a\mathbf{p}_1}{2\pi}\right)^2$	for $\kappa = \frac{1}{2}$	Q	for $\kappa = \frac{1}{2}$	$a^2\mathbf{k}^2$	for $\kappa = \frac{1}{2}$	$\sigma_{\mathbf{n}}$ (barns) at 288°A for $\kappa = \frac{1}{2}$	Cross section per steradian $= \frac{\sigma_{\mathbf{n}} a}{\pi Q}$
$(1, 1, 0)$	$2 - 2\kappa + \kappa^2$	$\frac{5}{4}$	$\frac{2 - 2\kappa}{2 - 2\kappa + \kappa^2}$	$\frac{4}{5}$	$\frac{4\pi^2}{\alpha}(2 - 2\kappa)$	0.29	5.7×10^{-3}	0.32
$(0, 1, 1)$	$2 + \kappa^2$	$\frac{9}{4}$	$\frac{2}{2 + \kappa^2}$	$\frac{8}{9}$	$\frac{8\pi^2}{\alpha}$	0.58	3.3×10^{-3}	0.17
$(-1, 1, 0)$	$2 + 2\kappa + \kappa^2$	$\frac{13}{4}$	$\frac{2 + 2\kappa}{2 + 2\kappa + \kappa^2}$	$\frac{12}{13}$	$\frac{4\pi^2}{\alpha}(2 + 2\kappa)$	0.87	2.2×10^{-3}	0.11

Cross sections for $\mathbf{p} = 2\pi/a\sqrt{3}(\kappa, \kappa, \kappa)$

$(1, 1, 0)$	$2 + \kappa^2 - 2.31\kappa$	1.10	$\frac{2 - 2.31\kappa}{2 - 2.31\kappa + \kappa^2}$	0.764	$\frac{4\pi^2}{\alpha}\left(2 - \frac{4\kappa}{\sqrt{3}}\right)$	0.24	6.2×10^{-3}	0.36
$(1, -1, 0)$	$2 + \kappa^2$	2.25	$\frac{2}{2 + \kappa^2}$	$\frac{8}{9}$	$\frac{8\pi^2}{\alpha}$	0.58	3.3×10^{-3}	0.17
$(-1, -1, 0)$	$2 + \kappa^2 + 2.31\kappa$	3.40	$\frac{2 + 2.31\kappa}{2 + 2.31\kappa + \kappa^2}$	0.93	$\frac{4\pi^2}{\alpha}\left(2 + \frac{4\kappa}{\sqrt{3}}\right)$	0.90	2.1×10^{-3}	0.10

In each line of the table just one typical value of \mathbf{n} is given, and similar peaks will be found in directions obtained by simply rotating the given direction about \mathbf{p} , e.g. in the first line $(1, 1, 0)$ stands for $(1, 1, 0), (1, 0, 1), (1, -1, 0), (1, 0, -1)$.

\mathbf{p} is the incident neutron wave vector; $\mathbf{p}_1 = \mathbf{p} - 2\pi\mathbf{n}/a$; $Q = (a\mathbf{p}/2\pi)^2 \mathbf{n}^2 \cdot (a/\pi)\mathbf{p} \cdot \mathbf{n}$. \mathbf{k} is the wave vector of the absorbed spin wave. σ is the integrated cross section of the peak centred about \mathbf{n} .

The peaks are now narrower than Moorhouse predicted, so it should be easier to distinguish experimentally between scattering from spin waves and phonons. If they could be observed we would have a direct method of testing the details of the spin-wave model. Examination of the calculation shows it should produce a maximum error of about 15%, so that anything outside this limit must be due to deficiencies in our model of a ferromagnet.

It is easily seen from (4.3) that σ_n increases almost linearly with T , but it is undesirable to perform the experiment at temperatures much above room temperature because then the approximation of neglecting the interaction between spin waves is certainly not good. In addition, the behaviour of the electronic specific heats of the ferromagnetics shows that at high temperatures a band model is better than the Heitler-London model used here. But the band model could not give scattered peaks like those we have calculated. We would therefore expect (4.3) to hold up to about 300°K, but for σ_n gradually to fall below the predicted values for temperatures greater than this.

A similar calculation for the spin $\frac{1}{2}$ case, using the value $g=0.624$, shows that σ_n is reduced by a factor of 0.63 compared with the spin 1 case. The peaks are slightly narrower ($4^\circ > \theta > 0$) and the cross sections per steradian remain the same. The effect of assuming two spins per atom is therefore quite unimportant, and the differences between these results and those of Moorhouse are due almost entirely to the different estimate of J . The similarity between the spin $\frac{1}{2}$ and the spin 1 results leads us to expect that they will be good also for the actual case of a mean spin of 1.1 atom.

We expect to obtain the same kind of peaks from nickel because the values of g do not differ very much from those of iron. But since the $T^{3/2}$ law only holds up to about 150°K for nickel, our model is probably not a very good one at room temperature.

ACKNOWLEDGMENTS

The author would like to acknowledge the receipt of a maintenance allowance from the Department of Scientific and Industrial Research during the tenure of which this work was carried out. It is a pleasure to thank Professor R. E. Peierls for his continual help and guidance and the referee for several helpful suggestions.

REFERENCES

- BETHE, H., 1931, *Z. Phys.*, **71**, 205.
- BLOCH, F., 1930, *Z. Phys.*, **61**, 206.
- MØLLER, C., 1933, *Z. Phys.*, **82**, 559.
- MOORHOUSE, R. G., 1951, *Proc. Phys. Soc. A*, **64**, 1097.
- VAN VLECK, J. H., 1945, *Rev. Mod. Phys.*, **17**, 27.
- WEISS, P., 1934, *C.R. Acad. Sci., Paris*, **198**, 1893.

LETTERS TO THE EDITOR

Scattering of High Energy Nucleons and Electrons by Carbon

The nuclear model with a uniform density distribution has been found inadequate from the point of view of nuclear shell structure (Born and Yang 1950, Yang 1951), the nuclear scattering of high energy nucleons (Gatha and Riddell 1952, Mathur and Gatha 1953) and electrons (Lyman, Hanson and Scott 1951). The following two analytically simple nuclear models with non-uniform density distributions have been proposed:

$$(1) \rho = \rho_0 \exp \{-(r-R_0)^2/a^2\} \quad \text{for } r > R_0 \text{ (Born and Yang 1950),}$$

$$(2) \rho = \rho_0 \exp \{-(r-R_0)/a\} \quad \text{for } r > R_0 \text{ (Jastrow and Roberts 1952),}$$

while $\rho = \rho_0$ for $r \leq R_0$ for both.

These density distributions have already been examined from the points of view of their correlation with nuclear shell structure by Yang as well as by Mathur and Gatha and for the scattering of high energy electrons by heavy nuclei by the latter. In the present investigation we have examined the validity of these nuclear models for the nuclear scattering of 345 mev nucleons and 15.7 mev electrons by carbon. We have found that Jastrow's model gives a better fit with the experimental data than the Born-Yang model. Hence we are presenting our results for Jastrow's model only. Since the wavelength of 345 mev nucleons is much smaller than that of 15.7 mev electrons, we have regarded the nuclear scattering of 345 mev nucleons as a more reliable source of information on nuclear structure than the nuclear scattering of 15.7 mev electrons. Therefore we have determined the parameters R_0 and a for Jastrow's nuclear model from the former and have observed that they are not inconsistent with the latter.

We have used the Born approximation after testing its validity for our problem. In this approximation the differential cross section is given by

$$\sigma(\theta) = [\{1 - \beta^2 \sin^2 \theta/2\} / \{1 - \beta^2\}] |f(\theta)|^2.$$

The scattering amplitude for the neutron scattering has been derived from the complex potentials

$$V = -[(E^2 - M^2 c^4) n_0 \exp \{-(r-R_0)/a\}] / E \quad \text{for } r > R_0$$

$$V = -[(E_2 - M^2 c^4) n_0] / E \quad \text{for } r \leq R_0$$

where $n_0 = \{k_1 + iK/2\}/k$ is the maximum complex refractive index with

$$k_1 = (\pi \rho_0 / k) \{f_{nn}(0) + f_{np}(0)\} \quad \text{and} \quad K = (\rho_0 / 2) \{\sigma_{nn} + \sigma_{np}\}$$

as usually employed, while $k_1, k \ll 1$ and $K/2k \ll 1$ and other symbols have their usual meanings. This leads to

$$f_n(\theta) = \{2M(E^2 - M^2 c^4) n_0\} [P \sin(\omega R_0) + Q \cos(\omega R_0)] / E \hbar^2 \omega^3$$

$$\text{where} \quad P = \{1 + 3a^2 \omega^2 + R_0 a \omega^2 (1 + a^2 \omega^2)\} / (1 + a^2 \omega^2)^2$$

$$Q = \{2a^3 \omega^3 - \omega R_0 (1 + a^2 \omega^2)\} / (1 + a^2 \omega^2)^2$$

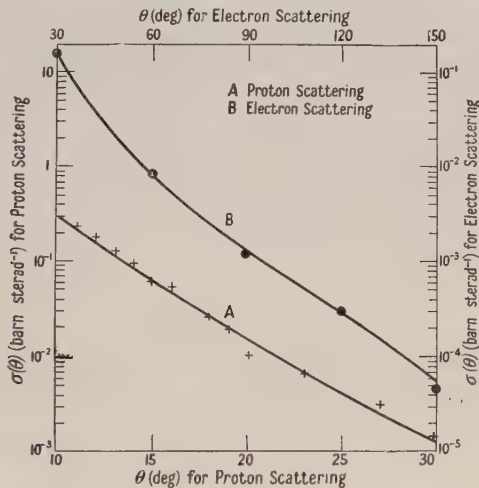
$$\omega = 2k \sin \theta/2.$$

Since the coulomb effects are negligible for carbon for the angular range under consideration we have used for the proton scattering $f_p(\theta) = f_n(\theta)$.

In the figure we have shown the experimental values of $\sigma(\theta)$ for the elastic scattering of 345 mev protons (Richardson, Ball, Leith and Moyer 1952). We have calculated $\sigma(\theta)$ theoretically for various values of R_0 and a and compared the same with the above experimental diffraction pattern, adjusting each time the value of $|n_0|^2$ to give the best fit. As a result of this comparison we have found that a reasonable approximate fit is obtained if we take $0 < R_0 < 0.6 \times 10^{-13}$ cm and $a \simeq 1 \times 10^{-13}$ cm. Increasing the value of R_0 beyond the above range gives rise to significant deviations even if we use the most optimum values of a . However, the agreement remains about the same if we restrict R_0 within the above range. Therefore, for simplicity, we take $R_0 = 0$. With this value of R_0

$$f_n(\theta) = \{4M(E - M^2c^4)a^3n_0\} / \{E\hbar^2(1 + a^2\omega^2)^{\frac{1}{2}}\}.$$

Calculating $\sigma(\theta)$ on the basis of the above expression we find that the best agreement with the experimental observations is obtained by taking $a = 1 \times 10^{-13}$ cm and $|n_0|^2 = 0.035$. We have also found that about 15% change in a from this value gives rise to noticeable deviations. The theoretical diffraction pattern for these parameters is shown in the figure. We have also calculated for these parameters the total elastic cross section, which turns out to be 101 mbn, in close agreement with the value of 98 mbn given by Richardson and others.



For Jastrow's model with $R_0 = 0$ one obtains $\rho_0 = A/8\pi a^3$, while for a uniform model one has $\rho = 3A/4\pi R^3$, where A is the nuclear mass number while R is the radius of the uniform nucleus. Using these density expressions we have obtained $|n_0|^2$ for the uniform nucleus, taking $R = 1.28 \times 10^{-13} \times A^{1/3}$ cm after Gatha and Riddell. Using their value $K = 3 \times 10^{12}$ cm $^{-1}$ we obtain $k_1 = 1.2 \times 10^{12}$ cm $^{-1}$. This value of k_1 lies between the values $k_1 = 0.9 \times 10^{12}$ cm $^{-1}$ and $k_1 = 1.9 \times 10^{12}$ cm $^{-1}$ as calculated by us using the Jastrow and the Christian models respectively for the nucleon-nucleon scattering and the experimental data on the same at 345 mev.

Regarding the nuclear scattering of 15.7 mev electrons by carbon we have shown in the figure the experimental results (Lyman, Hanson and Scott 1951). However, it has been suggested (Acheson 1951) that at this energy no unambiguous information about the nuclear density distribution can be obtained from the nuclear scattering of electrons. This is being further confirmed (Elton 1953, Vachaspati 1953, private communication) on a more quantitative basis. It appears that any

nuclear model with suitable parameters can give a good agreement with the experimental observations. Hence we have used these experimental observations to check that the parameters we have selected for Jastrow's model are not inconsistent from the point of view of electron scattering. We have in this case

$$f_c(\theta) = -[16\pi mZe^2\rho_0 a^3]/[A\hbar^2\omega^2(1+a^2\omega^2)^2].$$

The theoretical diffraction pattern calculated from the above is also shown in the figure.

Thus we have found that suitable parameters can be assigned to Jastrow's nuclear model so as to obtain an approximate agreement between the theoretical and the experimental angular distributions for the nuclear scattering by carbon of 345 mev nucleons and 15.7 mev electrons. We are now examining the validity of this nuclear model for other elements, the results of which will be published later.

M.G. Science Institute,
Navrangpura, Ahmedabad 9, India.
24th July 1953.

G. Z. SHAH.
N. J. PATEL.
K. M. GATHA.

- ACHESON, L. K., Jr., 1951, *Phys. Rev.*, **82**, 488.
BORN, M., and YANG, L. M., 1950, *Nature, Lond.*, **166**, 399.
ELTON, L. R. B., 1953, *Proc. Phys. Soc. A*, **66**, 806.
GATHA, K. M., and RIDDELL, R. J., 1952, *Phys. Rev.*, **86**, 1035.
JASTROW, R., and ROBERTS, J. E., 1952, *Phys. Rev.*, **85**, 757.
LYMAN, E. M., HANSON, A. O., and SCOTT, M. B., 1951, *Phys. Rev.*, **84**, 626.
MATHUR, A. L., and GATHA, K. M., 1953, *Proc. Phys. Soc. A*, **66**, 773.
RICHARDSON, R. E., BALL, W. P., LEITH, C. E., Jr., and MOYER, B. J., 1952, *Phys. Rev.*, **86**, 29.
YANG, L. M., 1951, *Proc. Phys. Soc. A*, **64**, 632.

Triplet Electronic States of Aluminium Monofluoride

The band spectrum of AlF has formed the subject of several recent investigations in which have been studied both the emission spectrum excited in hollow-cathode discharges (Rowlinson and Barrow 1953 a, Naudé and Hugo 1953) and the absorption spectrum in the Schumann region (Rowlinson and Barrow 1953 b). As a result of this work, values of the vibrational constants for a number of singlet states have been determined (Rowlinson and Barrow 1953 a, b) and Naudé and Hugo have evaluated the rotational constants for the states $c^1\Sigma^+$ and $A^1\Pi$. So far the vibrational analysis of only one triplet system, probably $b^3\Sigma^- - a^3\Pi$, has been given (Rowlinson and Barrow 1953 a). We have now succeeded in analysing the vibrational structure of two further triplet systems.

The new systems (system (2) of Naudé and Hugo) were photographed in emission from hollow-cathode discharges as before: they lie in the regions 2550 to 2650 Å and 2700 to 2912 Å respectively. They arise from transitions from what appear to be $^3\Sigma$ states to a common lower state $a^3\Pi_r$, which is also the lower state of the triplet system lying at 3450 to 3750 Å. The B values of the upper and lower states are in each case approximately equal, resulting in large head-origin separations, and for the 2700–2912 Å system a detailed calculation of head-origin separations has been carried out showing that $B' - B'' \simeq 0.04 \text{ cm}^{-1}$.

The B values of the $^3\Sigma$ states are all higher than that of the $^3\Pi$ state, which therefore has a greater r_e , in agreement with its lower ω_e value. The constants obtained from the analyses are given below.

Constants of the Triplet States of AlF

State	T_0^*	ω_e	$x_e\omega_e$	$\Delta G_{1/2}$
d($^3\Sigma$)	a + 38623.7	—	—	939.4
c($^3\Sigma$)	a + 36017.3	—	—	930.7
b($^3\Sigma$)	a + 27719.3	933.5	4.9	—
a($^3\Pi_r$)	a	828.8	4.1	—

$$A(a^3\Pi) = +46.8$$

* The values of T_0 are referred to $v''=0$ of $a^3\Pi_1$.

The intercombination system $a^3\Pi-x^1\Sigma^+$ is still being sought and several systems, notably one overlapping the $D^1\Delta-A^1\Pi$ system at about 5700 Å, remain to be analysed.

Physical Chemistry Laboratory,
Oxford University.
10th November 1953.

P. G. DODSWORTH.
R. F. BARROW.

NAUDÉ, S. M., and HUGO, T. J., 1953, *Phys. Rev.*, **90**, 318.

ROWLINSON, H. C., and BARROW, R. F., 1953 a, *Proc. Phys. Soc. A*, **66**, 437 ; 1953 b, *Ibid.*, **66**, 771.

The E-X Band System of SiS in Emission and the Dissociation Energy of SiS

The E-X band system of SiS, which consists of red-degraded bands in the region 2100 to 2500 Å, was first discovered in absorption (Vago and Barrow 1946). Further spectrograms of this system in absorption were taken with longer path lengths by Thomas (1947) who extended the system and showed that the values of v' given by Vago and Barrow should be increased by one. He derived the following constants:

$$\nu_e = 41923.5 \text{ cm}^{-1},$$

$$G_{v'}' = 403.5_4 u' - 1.4_0 u'^2 - 0.032_9 u'^3 - 1.1_5 \times 10^{-5} u'^5,$$

where $u = v + \frac{1}{2}$. This expression is valid for $v' \leq 18$.

We have recently discovered that this system is strongly excited in an electrodeless discharge run from a valve oscillator operating at about 50 m through a stream of silicon tetrachloride vapour to which a small amount of carbon disulphide is added. The spectrum of this source has been photographed as far as 1995 Å with a Hilger small quartz spectrograph on Ilford Q1 plates. About forty new bands have been assigned to the system. The vibrational term values with respect to $v''=0$ of $x^1\Sigma^+$ are given in the table.

Values of the vibrational intervals in the E state are now known as low as about 180 cm^{-1} , as compared with $\Delta G'_{1/2} = 401 \text{ cm}^{-1}$. Thus, even though the highest four levels observed vary rather irregularly, not more than a short extrapolation is necessary to reach what should be a reliable limit at about 52000 cm^{-1} above $v''=0$, which corresponds to 148.6 kcal.

The products of dissociation must be $\text{Si}(^3\text{P}) + \text{S}(^3\text{P})$, but which sub-levels of the ^3P states are involved is uncertain. However, the excitation energy of $\text{Si}(^3\text{P}_2)$ is only 0.64 kcal and that of $\text{S}(^3\text{P}_0)$ 1.64 kcal, so that the uncertainty on this account is only ± 1.2 kcal. It seems that the error in the extrapolation is

Vibrational Term Values for the E State of SiS

v'	$\nu_{v',0}$	v'	$\nu_{v',0}$
0	41750.3	16	47664.5
1	42151.6	17	985.6
2	548.9	18	48300.5
3	943.5	19	605.3
4	43334.4	20	895.2
5	720.1		
6	44105.1	21	49175.5
7	482.0	22	434.2
8	857.6	23	680.5
9	45227.1	24	912.8
10	592.0	25	50102.8
11	953.4	26	307.5
12	46308.3	27	495.5
13	658.7	28	670.5
14	47002.2		
15	337.9		

unlikely to exceed ± 1.5 kcal; the final result may be given as $D_0'' = 147.4 \pm 3.0$ kcal (6.39 eV). This is not very different from the result ($D_0'' = 6.4_7$ eV) obtained by Lagerqvist, Nilheden and Barrow (1952) from the less certain extrapolation from $v' = 18$.

Physical Chemistry Laboratory,
Oxford University.
9th November 1953.

S. J. Q. ROBINSON.
R. F. BARROW.

LAGERQVIST, A., NILHEDEN, G., and BARROW, R. F., 1952, *Proc. Phys. Soc. A*, **65**, 419.
THOMAS, D. M., 1947, *Thesis*, University of Oxford.
VAGO, E. E., and BARROW, R. F., 1946, *Proc. Phys. Soc.*, **58**, 538.

REVIEWS OF BOOKS

Exercises in Experimental Physics, edited by N. C. B. ALLEN and L. H. MARTIN.
Pp. xiii + 237. (Melbourne : University Press, 1952). 30s.

This work is a collection of experiments designed to supplement the second-year courses of physics in the University of Melbourne. The experiments described would be suitable in general for an ordinary B.Sc. course or for the less advanced parts of an honours course in Universities in England.

The book is described as being essentially the sixth edition of *Practical Physics*, in which the laboratory exercises were assembled by Professor Laby and the text was prepared by members of the staff of the Physics Department of Melbourne University.

The fact that the book has been written especially to conform to the needs of a particular group of students of necessity limits its usefulness as a textbook for other courses which may extend beyond its bounds. But the same remark would apply to any such work of reasonable size.

A more serious limitation is that it is written for undergraduates at a particular stage in their studies. This gives the appearance of omission and lack of balance. Thus, in a brief account of experiments on elasticity, nearly one half of the space is devoted to the interference method of measuring Poisson's ratio. The chapters on the measurements of inductances and capacitances are brief and incomplete and the necessity for shielding, the use of non-inductive resistances and pure harmonic oscillators could with advantage be more strongly emphasized.

On the other hand there are many useful hints scattered throughout the book, such as those on the choice of a galvanometer.

An important feature is the inclusion of a chapter on observations and statistical theory, with two experiments as illustrations.

The properties of vacuum tubes, the construction of a power supply unit and the use of the Geiger counter are described and illustrated in a well chosen series of experiments, designed to explain the principles of these instruments without emphasis at the expense of other fundamental parts of this course.

H. T. FLINT.

Progress in Metal Physics, Volume 3, by B. CHALMERS (Ed.). Pp. viii + 334.
(London : Pergamon Press, 1952.) 48s.

The regular appearance of these volumes, each containing up-to-date accounts of many aspects of metal physics, shows how successfully and rapidly the subject is now developing. The volume with which this notice is concerned, number three of the series, contains articles on a wide variety of topics. These may be roughly classified as, first, those dealing with the equilibrium properties of more or less perfect metallic crystals, i.e. electrical, structural and magnetic properties, and, secondly, those dealing with the properties of the secondary structure (crystal boundaries etc.) and crystallographic transformations. The articles in the first category are written against a background of a highly developed theory : the electron theory of metals based on wave mechanics. In the second category

the articles are largely descriptive and empirical, and where theory is introduced it is phenomenological rather than fundamental. To any reader who attempts to study the whole book this difference between the two main branches of the subject quickly makes itself felt. Chapters 2, 3 and 5, which deal respectively with the properties of metals at low temperatures, recent advances in the electron theory of metals, and ferromagnetism, have a certain coherence which enables the reader to see relations between the observational data discussed and to view each subject as a whole. The articles dealing with what the editor refers to as the "dynamic effects", on the other hand, call for a disciplined effort on the reader's part to assimilate the large number of individual observations, the relations between which are not always easy to see. In the absence of a firm theoretical background the selection of the definitive observations is difficult to make and the authors are compelled to record faithfully all the experimental data available, and this may result in an article such as, for example, that dealing with x-ray diffraction in strained metals, which reads almost like the minutes of some committee meeting.

In a short notice of this kind it is not possible to deal with each of the eight articles individually, but special mention may be made of one or two. The book opens with an excellent account of the crystallography of transformations by J. S. Bowles and C. S. Barrett. This article deals with martensite transformations and the atomic movements which take place in these phase changes. Although the account is clear and complete, the reader new to the subject will find that a considerable effort is called for to follow the details of the geometry of the different transformations which have been proposed to explain the observational data. The physical (as distinct from the purely crystallographic) nature of the process is also discussed, but it cannot be said that the theory, as presented in this article, is very satisfactory; many gaps, according to the authors, remain to be filled.

Two other chapters which may be specially mentioned are Chapters 3 and 7. Chapter 3 deals with recent advances in the electron theory of metals and is written by N. F. Mott. As indicated by the title, this is not a critical account of established theory, but largely a description of newly developed ideas. It is, perhaps, too much to hope that all of these, or even the greater part of them, will survive without substantial modification in the future. Chapter 7, by J. E. Burke and D. Turnbull, is concerned with recrystallization and grain growth. A clear account of experimental results, expressed in terms of the concepts of nucleation and growth, is followed by some pages of physical theory dealing with the kinetics of boundary migrations. This admirable article of some 70 pages can be comfortably read without prior knowledge of this particular subject.

One minor criticism of the production of the whole book is that the proof reading does not appear to have been done with sufficient care. For example, in the article just referred to the letters t and τ are used rather indiscriminately although they are intended to have quite distinct meanings. More remarkable, perhaps, is the slip in the editor's foreword where we find the word 'phrases' where 'phases' is intended. These, however, are small blemishes which do not seriously detract from the great value of this volume. Some idea of the extent of the information contained within its covers is indicated by the fact that there are altogether 770 references to published papers, all of which are dealt with in the text.

H. JONES.

Data for X-Ray Analysis, Vols. I and II (Eindhoven: Philips' Technical Library, 1953; London agent: Cleaver-Hume Press, London.)

Vol. I. Charts for Solution of Bragg's Equation (d versus θ and 2θ), by W. PARRISH and B. W. IRWIN. Pp. 99. 15s.

Most workers using x-ray powder photography for identification purposes have made themselves charts for conversion from θ values to d values, but few can have done so in such a convenient or satisfactory form as has been reproduced in this volume. For some purposes d can be plotted directly against s (the film measurement), but if such a chart is required for a particular camera it may readily be constructed from these graphs, which, in addition, provide a model lay-out for their more specialized counterparts.

The spacings are given in ångströms and the internationally agreed wavelengths have been used in the calculations. The Bragg angle θ can be read to 0.01° directly and the d -values to 0.01 \AA in the θ -range 3° to about 18° , and to 0.001 \AA at higher angles. A weighted average wavelength is used for low angles, supplemented by values for α_1 and α_2 in the medium range and for the higher angles values are plotted for α_1 and α_2 only. Charts are given for Mo, Cu, Co, Fe and Cr $K\alpha$ wavelengths. In addition a useful table for converting minutes into decimals of a degree is included.

Vol. II. Tables for Computing the Lattice Constant of Cubic Crystals, by W. PARRISH, M. G. EKSTEIN and B. W. IRWIN. Pp. 81. 15s.

Tables of $\sqrt{N\lambda/2}$ for the $K\alpha_1$, $K\alpha_2$ and $K\beta$ wavelengths of Cu, Ni, Co, Fe and Cr are tabulated in a convenient and extremely readable form. Tables of $\sin^2\theta$ and $\frac{1}{2}(\cos^2\theta/\sin\theta + \cos^2\theta/\theta)$, for extrapolation purposes, are included as is also a table of lattice constants of cubic substances and figures showing graphically the representative cubic powder patterns. A short description of the procedure for using the tables in computing the lattice constant is given in the introduction.

J. W. JEFFERY.

Le rôle de la régularité dans le calcul numérique, by PIERRE VERNOTTE. Pp. xii + 33 (Paris: Publications Scientifiques et Techniques du Ministère de l'Air (Notes Techniques No. 45), 1952.) 350 fr.

Les principes physiques de la formulation des lois expérimentales, conséquences pour la philosophie des sciences, calcul effectif de différents types de lois, by PIERRE VERNOTTE. Pp. v + 256 + xxxii. (Paris: Publications Scientifiques et Techniques du Ministère de l'Air (No. 271), 1952.) 1800 fr.

CONTENTS OF SECTION B

	PAGE
Editorial	1
Dr. D. G. AVERY. Further Measurements on the Optical Properties of Lead Sulphide, Selenide and Telluride	2
Dr. A. MANY. Measurement of Minority Carrier Lifetime and Contact Injection Ratio on Transistor Materials	9
Mr. R. LAWRENCE. The Temperature Dependence of the Drift Mobility of Injected Holes in Germanium	18
Prof. L. F. BATES and Mr. D. HUGHES. The Magnetic Susceptibility of Metallic Uranium	28
Mr. A. W. SIMPSON and Mr. R. H. TREDGOLD. Intrinsic Magnetization in Platinum Cobalt Alloys	38
Dr. W. RAILSTON. The Temperature Decay Law of a Naturally Convected Air Stream	42
Dr. G. P. RUNDLE, Mr. J. ELLIS, Dr. T. C. GRIFFITH and Mr. H. S. TOMLINSON. The Design and Operation of a Double Magnetic Lens Beta-Ray Spectrometer	52
Dr. L. E. LAWLEY. The Absorption of Sound in Carbon Dioxide contained in Narrow Tubes	65
Mr. A. W. PRYOR and Dr. R. ROSCOE. The Velocity and Absorption of Sound in Aqueous Sugar Solutions	70
Reviews of Books	82
Contents of Section A	88

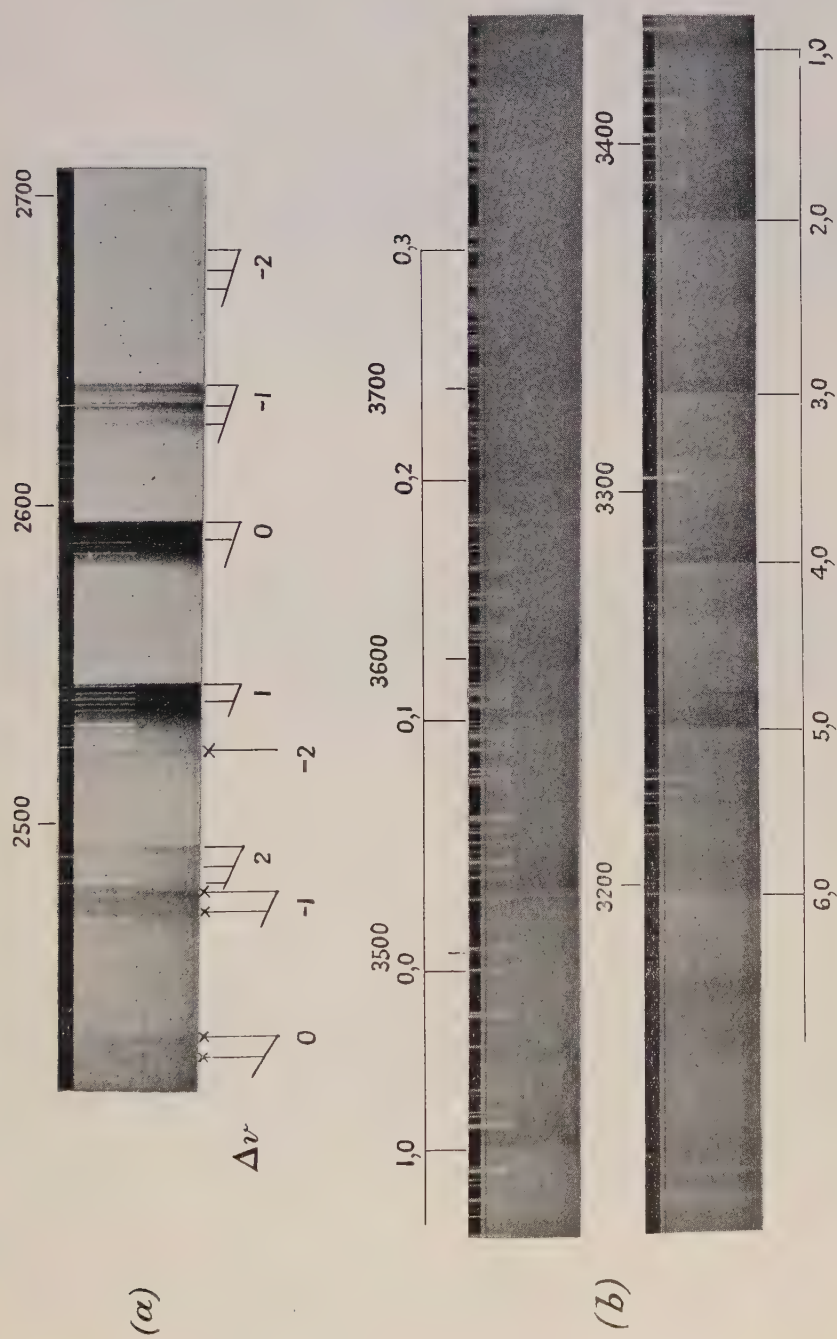
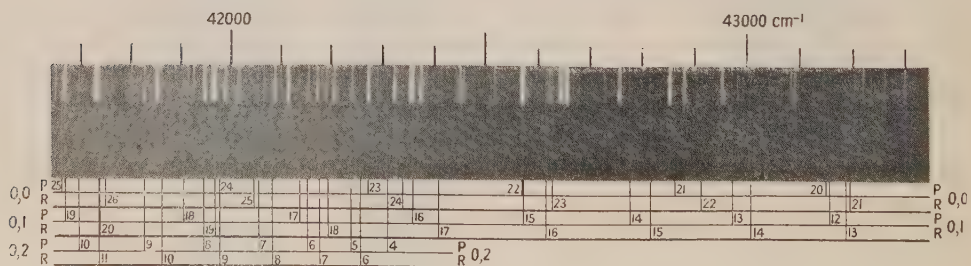
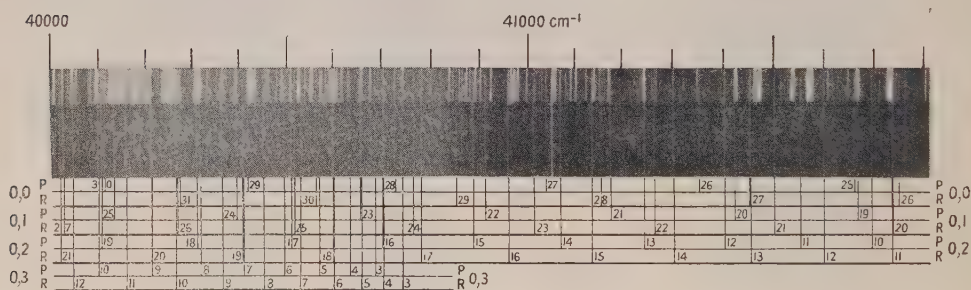
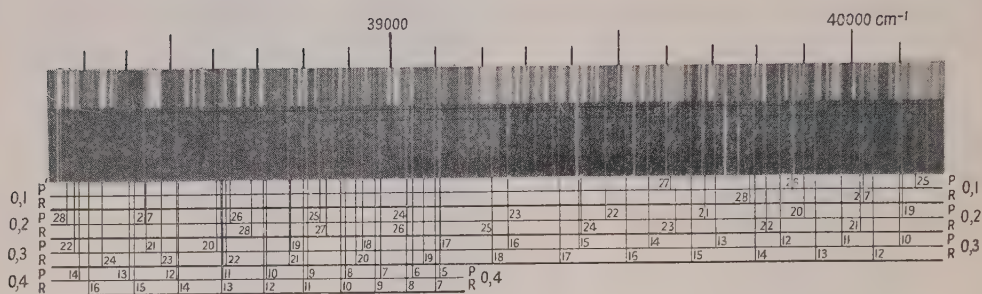


Figure 1. Absorption spectrum of BiO.



The hydride spectrum photographed on Hilger E.478 quartz Littrow spectograph;
Fe arc comparison spectrum.

γ -Radiation from the Reaction $^{27}\text{Al}(\text{p}, \gamma)^{28}\text{Si}$

By J. G. RUTHERGLEN, P. J. GRANT, F. C. FLACK
AND W. M. DEUCHARS

Department of Natural Philosophy, The University, Glasgow

MS. received 31st August 1953

Abstract. The spectra of γ -radiation at the resonances for proton capture in ^{27}Al occurring at $E_p = 404, 503, 630, 652$ and 677 kev have been studied with a sodium iodide scintillation spectrometer. The angular distributions of the more prominent γ -ray components have been determined at each resonance. Spin and parity assignments to levels in ^{28}Si are made on the basis of these and other measurements.

§ 1. INTRODUCTION

IN the region of proton energies below 800 kev the reaction $^{27}\text{Al}(\text{p}, \gamma)^{28}\text{Si}$ has been investigated by Tangen (1946), Brostrom, Huus and Tangen (1947), Rae, Rutherglen and Smith (1951), Rutherglen and Smith (1953) and Casson (1953).

Tangen, and Brostrom *et al.* measured accurately the position and yield of a large number of γ -ray resonances over a wide range of proton energies. Rae *et al.* used a magnetic pair spectrometer to study the spectrum of γ -radiation from bombardment of a thick aluminium target with protons of energy 750 kev. They deduced a Q -value for the reaction and proposed a decay scheme in terms of known levels in ^{28}Si . Rutherglen and Smith determined the excitation curve for the reaction, together with that of the competing reaction $^{27}\text{Al}(\text{p}, \alpha)^{24}\text{Mg}$, in the range of proton energies 400–750 kev and showed that while all resonances produced γ -radiation, α -particle emission was forbidden at several of them. Casson examined the thick-target γ -ray spectra from resonances below 450 kev by means of a sodium iodide scintillation spectrometer.

The present paper describes measurements made with a sodium iodide scintillation spectrometer on the γ -ray spectra and angular distributions from five resonances in the range of proton energies 400–700 kev. The results enable spin and parity assignments to be made to a number of levels in ^{28}Si . With knowledge of the γ -ray spectra from individual resonances it is possible to use the thick-target results of Rae *et al.* to deduce an amended Q -value for the reaction. This is in excellent agreement with the figure deduced from other reactions.

I. MEASUREMENTS OF γ -RAY SPECTRA

§ 2. EXPERIMENTAL PROCEDURE

Targets were made from pure aluminium evaporated on to a brass backing and were bombarded with proton currents of up to $70 \mu\text{A}$. The target thickness used was normally about 15 kev.

The γ -radiation was detected by a sodium iodide crystal, about 1.3 in. cube, with an E.M.I. 5311 photomultiplier tube. The crystal was packed with dry magnesium oxide in an airtight aluminium container fitted with a quartz window; optical contact between the crystal and the window was obtained by a thin film of silicone vacuum grease. Pulses from the photomultiplier, after amplification, were fed into a five-channel pulse analyser.

Calibration of the pulse height in terms of γ -ray energy was carried out using the 2.62 MeV γ -ray from ThC'' and γ -radiation from the reactions $^{19}\text{F}(\text{p}, \alpha)^{16}\text{O}^*$ (6.13 MeV), $^{11}\text{B}(\text{p}, \gamma)^{12}\text{C}$ (4.45 and 11.8 MeV) and $^{13}\text{C}(\text{p}, \gamma)^{14}\text{N}$ (8.06 MeV). In the low energy region (< 3 MeV) a single γ -ray produces three separate peaks which can be resolved from each other. The peak of highest energy corresponds to total capture of the γ -ray energy in the crystal, the second to Compton collisions in which the scattered quantum escapes from the crystal together with pair production in which one annihilation quantum escapes, and the third corresponds to pair production with escape of both annihilation quanta. There is little difficulty in determining γ -ray energies in this region except when overlapping occurs of the peaks from two separate γ -rays. As the quantum energy is raised the three peaks merge into one, and for this region a calibration curve was constructed showing γ -ray energy plotted against pulse height at the peak, using the γ -rays of known energy from the reactions mentioned above.

§ 3. RESULTS

Gamma-ray spectra from the resonances at proton energies of 404, 503 and 630 keV are shown in figures 1–3. Figures 1(a)–3(a) show the high energy region down to about 3.5 MeV. Figures 1(b)–3(b) were taken with the amplifier gain increased by a factor of four and show the spectra in the energy range from 0.8–3.5 MeV. The high energy spectra at the 652 and 677 keV resonances are similar to those at the 630 keV resonance except that the 10.5 MeV gamma-ray is of slightly lower intensity and that the 652 keV resonance shows a very weak ground-state transition.

More detailed examination of the spectra illustrated, in the region 2–4 MeV, has shown the presence at the 630 keV resonance of two components, of energies 2.8 and 3.5 MeV. The energies and intensities are summarized in table 1. The energies of those γ -rays which were well resolved are accurate to within 3%. The intensities were estimated from the areas under the curves, using the line shapes measured for the mono-energetic calibration gamma-rays, and are accurate to within about 20%.

It will be seen that only the resonance at $E_p = 503$ keV produces the 12 MeV ground-state γ -radiation with significant intensity, and we estimate that its intensity is sufficient to account for all the radiation of energy 12.12 ± 0.10 MeV observed in the experiment of Rae *et al.* Thus a centre-of-mass bombarding energy of 490 keV instead of 610 keV should be used in evaluating the Q -value. The amended figure is $Q = 11.63 \pm 0.10$ MeV.

This is in good agreement with that calculated from the nuclear masses given by Li (1952), $Q = 11.59 \pm 0.05$ MeV, and that given by Feather (1953), $Q = 11.56 \pm 0.03$ MeV. We shall adopt the value $Q = 11.60$ MeV.

The γ -ray energies are consistent with the level scheme for ^{28}Si , deduced from the reaction $^{27}\text{Al}(\text{d}, \text{n})^{28}\text{Si}$ (Peck 1949).

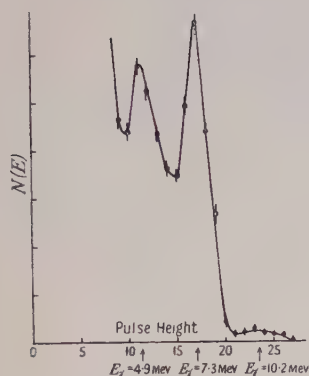


Figure 1 (a). Pulse height spectrum of γ -rays at $E_p = 404$ kev.

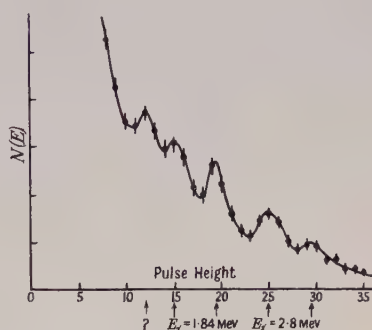


Figure 1 (b). Pulse height spectrum of low-energy γ -rays at $E_p = 404$ kev.

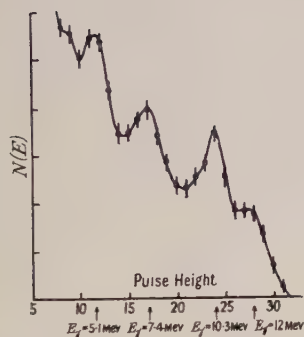


Figure 2 (a). Pulse height spectrum of γ -rays at $E_p = 503$ kev.

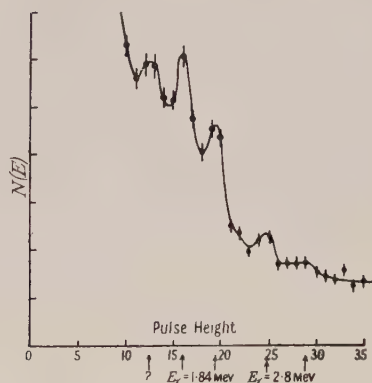


Figure 2 (b). Low energy spectrum at $E_p = 503$ kev.

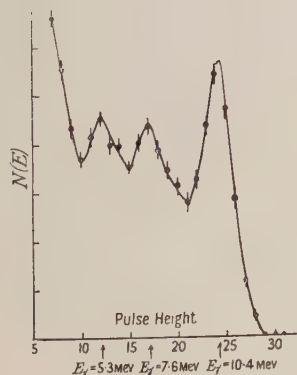


Figure 3 (a). Pulse height spectrum of γ -rays at $E_p = 630$ kev.

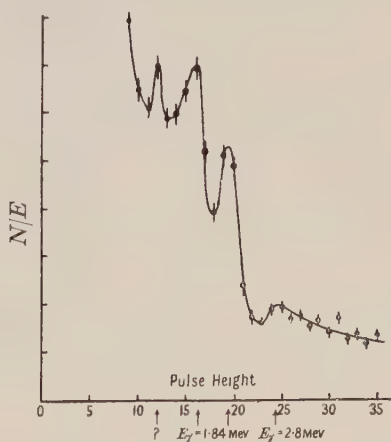


Figure 3 (b). Low energy spectrum at $E_p = 630$ kev.

Table 1
(All energies in mev)

Reson. energy	²⁸ Si excit. energy	E_γ	Rel. int.	Interpretation
0.404	11.99	10.2	0.05	$11.99 \rightarrow 1.8$
		7.3	1.0*	$\left\{ \begin{array}{l} 11.99 \rightarrow 4.6 \\ 11.99 \rightarrow 5.2 \end{array} \right.$
		5.1	0.35	$\left\{ \begin{array}{l} 11.99 \rightarrow 7.1 \\ 7.1 \rightarrow 1.8 \end{array} \right.$
		2.8	1.0	$\left\{ \begin{array}{l} 5.2 \rightarrow 1.8 \\ 4.6 \rightarrow 1.8 \end{array} \right.$
		1.84	1.0*	$1.8 \rightarrow 0$
		1.13?		?
0.503	12.09	12.1	0.9	$12.09 \rightarrow 0$
		10.3	1.0*	$12.09 \rightarrow 1.8$
		7.3	0.54	$\left\{ \begin{array}{l} 12.09 \rightarrow 4.6 \\ 12.09 \rightarrow 5.2 \end{array} \right.$
		5.1	0.60	$\left\{ \begin{array}{l} 12.09 \rightarrow 7.1 \\ 7.1 \rightarrow 1.8 \end{array} \right.$
		2.8	0.3	$\left\{ \begin{array}{l} 5.2 \rightarrow 1.8 \\ 4.6 \rightarrow 1.8 \end{array} \right.$
		1.84	1.0*	$1.8 \rightarrow 0$
		1.18?		?
0.630	12.21	10.4	1.0*	$12.21 \rightarrow 1.8$
		7.6	0.21	$\left\{ \begin{array}{l} 12.21 \rightarrow 4.6 \\ 12.21 \rightarrow 5.2 \end{array} \right.$
		5.1	0.10	$\left\{ \begin{array}{l} 12.21 \rightarrow 7.1 \\ 7.1 \rightarrow 1.8 \end{array} \right.$
		3.5	0.21	$\left\{ \begin{array}{l} 5.2 \rightarrow 1.8 \\ 4.6 \rightarrow 1.8 \end{array} \right.$
		2.8		
		1.84	1.0*	$1.8 \rightarrow 0$
		1.13?		?
0.652	12.23	12.2	0.07	$12.23 \rightarrow 0$
		10.4	1.0*	$12.23 \rightarrow 1.8$
		7.5	0.74	$\left\{ \begin{array}{l} 12.23 \rightarrow 4.6 \\ 12.23 \rightarrow 5.2 \end{array} \right.$
		5.1	0.19	$\left\{ \begin{array}{l} 12.23 \rightarrow 7.1 \\ 7.1 \rightarrow 1.8 \end{array} \right.$
		Low energy region not measured		
0.677	12.25	10.4		$12.25 \rightarrow 1.8$
		7.5		$\left\{ \begin{array}{l} 12.25 \rightarrow 4.6 \\ 12.25 \rightarrow 5.2 \end{array} \right.$

* This figure was adopted as the standard of comparison for each spectrum. The intensity figures for different spectra are not directly comparable.

II. ANGULAR DISTRIBUTIONS

§4. EXPERIMENTAL PROCEDURE

The crystal and photomultiplier assembly used in the spectrum measurements was mounted on a movable arm pivoted on the line through the centre of the target and moving in a plane containing the direction of the incident beam. Targets, of about 15 kev thickness, were made from aluminium evaporated on to 0.005 in. or 0.01 in. copper foil. γ -ray absorption in the target backing could thus be neglected except in the approximate direction of the plane of the target, where a copper 'stiffener' round the edge produced a measurable absorption. To avoid this effect in the region 100° to -20° to the direction of the proton beam, the range of angle over which measurements were normally taken, the plane of the target was set at an angle of about 110° to the proton beam. The beam was accurately centred on the target by two molybdenum defining slits 1 mm wide separated by a distance of about 15 cm.

Counts in the movable detector were recorded for a definite number of counts in a fixed monitor counter, which also consisted of a sodium iodide crystal and photomultiplier, and were thus independent of fluctuations in the proton beam current hitting the target.

The accuracy desired in the angular distribution measurements was to about 1%. To obtain an accuracy of this order the pulse analyser was set to cover the peak of the γ -ray under observation and the total counts in four channels recorded. (The fifth 'channel' recorded all counts above the top of the fourth channel.) Since the peaks were roughly symmetrical and could be placed centrally over the four channels, small changes in gain or drifts of the analyser were by this means made less important. Other precautions taken were: (a) the voltage on the photomultiplier tube was checked regularly by measuring a small fraction of it with a vernier potentiometer, the voltage on the monitor photomultiplier being similarly checked; (b) the mains supply to each amplifier was kept constant by means of a Variac variable transformer on each mains input; (c) counts at the different angular positions were taken in a random order for short counting periods, the measured distribution being the sum of a number of short runs. In this way errors due to residual drifts in the amplifiers or the pulse analyser were avoided.

A slight anisotropy of the apparatus was found and a correction determined by measuring the angular distribution of the γ -radiation from bombardment of fluorine with protons of energy 340 kev. This radiation is known to be isotropic (Devons and Hine 1949).

When the angular distribution of γ -radiation other than the component of highest energy was being determined it was necessary to subtract the contributions from higher-energy components. This required knowledge not only of the angular distributions of the more energetic γ -rays, but also of the shape of the pulse height spectrum of single γ -rays of the appropriate energy. The latter information was obtained by measurements of the γ -radiation from the reactions $^{11}\text{B} + p$, $^{13}\text{C} + p$ and $^{19}\text{F} + p$.

§5. RESULTS

Angular distributions obtained at the various resonances are shown in figures 4-8. In each case the curve was fitted to the experimental points by the

method of least squares, assuming it to be of the form $W(\theta) = 1 + A \cos^2 \theta$. There appears to be no evidence for terms of higher order in these distributions. The experimental points are corrected for slight instrumental anisotropies, the

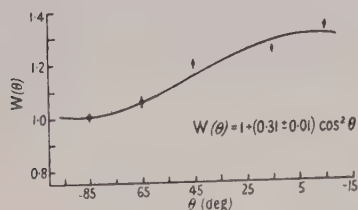


Figure 4. 7.3 MeV γ -ray component at $E_p = 404$ keV.

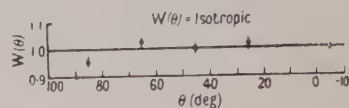


Figure 5. 10.3 MeV γ -ray component at $E_p = 503$ keV.

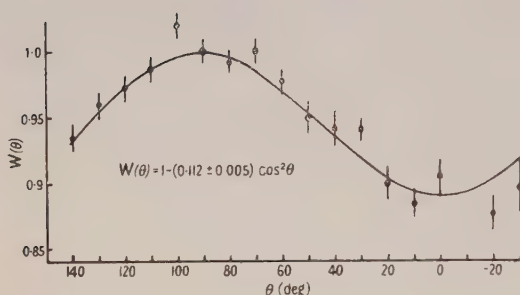


Figure 7 (a). 10.4 MeV γ -ray component at $E_p = 652$ keV.

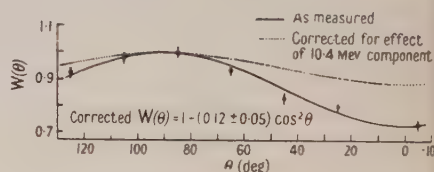


Figure 7 (b). 7.5 MeV γ -ray component at $E_p = 652$ keV.

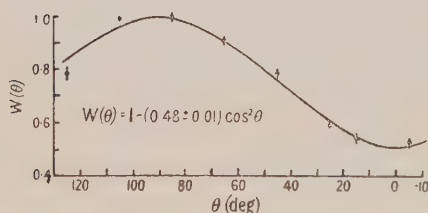


Figure 6. 10.4 MeV γ -ray component at $E_p = 630$ keV.

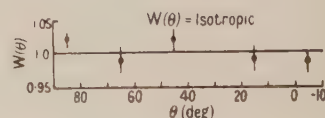


Figure 8. 10.4 MeV γ -ray component at $E_p = 677$ keV.

Figures 4–8. $^{27}\text{Al}(p\gamma)^{28}\text{Si}$. Angular distributions.

correction being in no case greater than 3%. No correction has been made for the finite solid angle of acceptance of the crystal detector since the correction was not greater than about 0.5%.

Table 2 summarizes the results obtained, both as regards the emission of γ -radiation of a given energy from a particular resonance and its angular distribution, if measured. The angular distribution of the 1.8 MeV radiation at the 630 keV resonance was estimated by observations at 90° and 0° only. Also

included are the results of Rutherglen and Smith on the emission of α -particles from these resonances.

§ 6. DISCUSSION

One general conclusion can be drawn immediately from table 2, namely that there is no evidence that protons having an orbital angular momentum greater than unity take part in the reaction at any of the five resonances. (The assumption of d-wave protons would not, in any case, help to explain the results.

Table 2

Resonance (kev)	404	503	630	652	677
α	No	Yes	Yes	No	No
γ_{12}	No	Yes	No	Very little	No
		Isotropic			
$\gamma_{10.4}$	Very little	Yes	Yes	Yes	Yes
		Isotropic	$1-0.11 \cos^2 \theta$	$1-0.48 \cos^2 \theta$	Isotropic
$\gamma_{7.5}$	Yes	Yes	Yes	Yes	Yes
	$1+0.31 \cos^2 \theta$		$1+0.10 \cos^2 \theta$	$1-0.12 \cos^2 \theta$	
$\gamma_{1.8}$	Yes	Yes	Yes	Yes	Yes
			$1+0.13 \cos^2 \theta$		

^{27}Al has a nuclear spin $J=5/2$ in its ground-state, and we shall assume the shell-model prediction to be correct, that it is a state of even parity. With this assumption the possible states that can be formed by proton capture are as follows: s-wave, $l=0$, $J=2(+)$, $3(+)$; p-wave, $l=1$, $J=1(-)$, $2(-)$, $3(-)$, $4(-)$. Of these, the $2(+)$, $1(-)$ and $3(-)$ states could emit α -particles to the ground-state of ^{24}Mg , which has spin zero with even parity, while the others could not. From this we may proceed to an assignment of spins and parities to all five resonance levels:

503 keV resonance. This must produce a state $J=2(+)$ since it emits α -particles and emits γ -rays isotropically.

677 keV resonance. It is reasonable to assign $J=3(+)$ to this state since it emits γ -rays isotropically, but does not emit α -particles.

These two assignments are consistent with the fact that the 503 keV resonance produces γ -radiation to the ground-state of ^{28}Si ($E2$, $2(+)\rightarrow 0(+)$) while the 677 keV resonance does not ($3(+)\rightarrow 0(+)$ would be M3). The other three resonances all have anisotropic γ -ray distributions and cannot therefore be formed by s-wave proton capture. Of the four possible states which might be formed by capture of p-wave protons, the $1(-)$ state does not appear to correspond to an experimentally observed level since it should emit ground-state γ -radiation ($E1$, $1(-)\rightarrow 0(+)$).

630 keV resonance. This must lead to a $3(-)$ state in ^{28}Si since it emits α -particles to ^{24}Mg . It is unlikely (as stated above) to be a $1(-)$ state since no ground-state γ -radiation is emitted.

652 keV resonance. Since this resonance does not emit α -particles it must have $J=2(-)$ or $4(-)$. The fact that a detectable ground-state transition occurs limits the choice to $J=2(-)$, since the M4 transition, $4(-)\rightarrow 0(+)$, would be very highly forbidden.

404 keV resonance. This resonance must also have $J=2(-)$ or $4(-)$ and since it has a γ -ray spectrum very different from that of the 652 keV resonance, in particular showing no observable ground-state transition and only a very weak transition to the first excited level at 1.8 MeV, we assign $J=4(-)$ to this resonance.

From the fact that the 404 keV resonance produces very little γ -radiation to the 1.8 MeV excited level in ^{28}Si we may say that this level cannot have J greater than 2 with even parity or J greater than 1 with odd parity. $J=1$ seems unlikely, firstly from consideration of the β -decay of ^{28}Al , in which the transition to the ground-state of ^{28}Si is highly forbidden compared with the less energetic transition to the 1.8 MeV level, and secondly because a low-lying dipole level in an even-even nucleus has not hitherto been observed. It is also thought unlikely on theoretical grounds (Touschek 1950). We are left with the assignment $J=2(+)$ to this level, which is consistent with all the experimental data on γ -ray intensities.

We now consider in detail the γ -ray angular distributions. The calculation of the theoretical distributions is a straightforward procedure, and we shall not discuss it in detail. One point, however, should be mentioned: in calculating the transformation coefficients for the formation of the states $J=2(-)$ or $J=3(-)$ by adding a proton ($s=\frac{1}{2}$ $l=1$) to ^{27}Al ($5/2+$) there are two possible 'routes', by the addition of $l=1$ to either 'channel spin' $j=2$, ($\frac{5}{2}-\frac{1}{2}$), or $j=3$, ($\frac{5}{2}+\frac{1}{2}$). The two routes to a given J lead to different angular distributions, so that the theoretical distributions for these two states are not absolutely determined, but can each lie within certain limits. It has been pointed out by Christy (1953) that this indeterminacy is a consequence of lack of knowledge of the wave function describing the compound state and could be removed by assuming, for example, either $j-j$ or $L-S$ coupling between the incoming proton and the target nucleus. If we define the channel-spin ratio

$$F = \frac{\text{number of states formed by } j=3}{\text{number of states formed by } j=2}$$

then the values of F required to fit the experimental data (J being known from other evidence) may give further information about the compound state. In the formation of the states $J=2(+)$, $J=3(+)$ and $J=4(-)$ (also $J=1(-)$ if it were observed) there is no uncertainty, only one 'route' being possible.

630 keV resonance ($J=3(-)$). This has a strong γ -ray component to the 1.8 MeV level. The theoretical distribution for a transition $3(-) \rightarrow 2(+)$ is

$$W(\theta) \sim 5F(17 + 9 \cos^2 \theta) + 4(28 - 9 \cos^2 \theta),$$

giving the limiting distribution functions:

$$F=0, W(\theta) \sim 1 - 0.32 \cos^2 \theta; \quad F=\infty, W(\theta) \sim 1 + 0.53 \cos^2 \theta.$$

The experimental distribution is $W_{\text{exp}}(\theta) \sim 1 - (0.112 \pm 0.01) \cos^2 \theta$, which can be fitted by $F=3/7$.

Using this value of F , the calculated distribution for the 1.8 MeV transition ($2(+) \rightarrow 0(+)$) which belongs to the same cascade, is $W(\theta) \sim 1 + 0.18 \cos^2 \theta$. This is in satisfactory agreement with the experimental distribution

$$W_{\text{exp}}(\theta) \sim 1 + (0.13 \pm 0.05) \cos^2 \theta.$$

This resonance also produces γ -radiation to the levels at 4.6 and 5.2 MeV, which has an angular distribution $W_{\text{exp}}(\theta) \sim 1 + (0.10 \pm 0.05) \cos^2 \theta$. This result may be explained by assigning $J=3$ to one level of the doublet and $J=2$ or $J=4$ to the other. The theoretical distributions, for dipole transitions and $F=3/7$, are

$$3(-) \rightarrow 3(\pm) \quad W(\theta) \sim 1 + 0.15 \cos^2 \theta$$

$$3(-) \rightarrow 2(\pm) \quad W(\theta) \sim 1 - 0.11 \cos^2 \theta$$

$$3(-) \rightarrow 4(\pm) \quad W(\theta) \sim 1 - 0.05 \cos^2 \theta.$$

Combination in suitable proportions of the first of these with either of the others will readily explain the experimental result.

652 keV resonance ($J=2(-)$). The γ -radiation leading to the 1.8 MeV level is markedly anisotropic: $W_{\text{exp}}(\theta) \sim 1 - (0.485 \pm 0.01) \cos^2 \theta$. The theoretical distributions for the transition $2(-) \rightarrow 2(+)$, dipole are

$$F=0, W(\theta) \sim 1 - 0.44 \cos^2 \theta; \quad F=\infty, W(\theta) \sim 1 + 0.16 \cos^2 \theta.$$

The distribution for $F=0$ thus gives fair agreement with the experimental result, although the fit is not as good as might be expected. The difference, which is outside the experimental error, may be due to a small admixture of M2 radiation with the predominant E1 type.

There appears to be radiation to both the 4.6 and 5.2 MeV levels from this resonance. The angular distribution of this radiation is

$$W_{\text{exp}}(\theta) \sim 1 - (0.12 \pm 0.05 \cos^2 \theta).$$

The theoretical angular distributions for $F=0$ are

$$2(-) \rightarrow 3(\pm), \text{ dipole}, \quad W(\theta) \sim 1 + 0.16 \cos^2 \theta,$$

$$2(-) \rightarrow 2(\pm), \text{ dipole}, \quad W(\theta) \sim 1 - 0.44 \cos^2 \theta,$$

$$2(-) \rightarrow 4(\pm), \text{ quadrupole}, \quad W(\theta) \sim 1 - 0.20 \cos^2 \theta.$$

A suitable mixture of the first of these with either of the others may easily be made to fit the experimental result.

404 keV resonance ($J=4(-)$). The angular distribution of the radiation to the 4.6 and 5.2 MeV levels is $W_{\text{exp}}(\theta) \sim 1 + (0.31 \pm 0.01) \cos^2 \theta$. The calculated distributions are:

$$4(-) \rightarrow 3(\pm), \text{ dipole}, \quad W(\theta) \sim 1 - 0.26 \cos^2 \theta,$$

$$4(-) \rightarrow 2(\pm), \text{ quadrupole}, \quad W(\theta) \sim 1 + 0.49 \cos^2 \theta,$$

$$4(-) \rightarrow 4(\pm), \text{ dipole}, \quad W(\theta) \sim 1 + 0.48 \cos^2 \theta.$$

Once more a suitable mixture will explain the experimental result.

§ 7. DECAY SCHEME

The proposed decay scheme with spin and parity assignments is shown in figure 9. It provides a good explanation of all the experimentally observed γ -ray intensities and angular distributions, but further evidence from γ - γ correlation experiments is necessary before it can be regarded as definitely

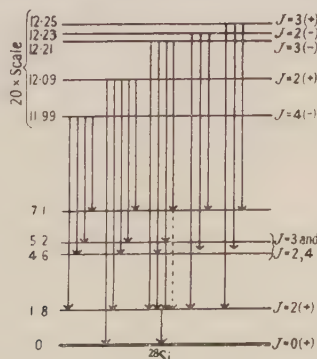


Figure 9. Decay scheme (energies in MeV)

established. Such experiments might also serve to remove the uncertainties in spin and parity assignment to the 4.6 and 5.2 mev levels. By consideration of the theoretical γ -ray transition probabilities it is possible to derive spin and parity assignments for both these levels, but in view of the uncertainty of the theory it is felt that this is of very doubtful value, and the correlation method seems the more promising.

ACKNOWLEDGMENTS

One of us (F. C. F.) wishes to acknowledge the award of an Imperial Chemical Industries Research Fellowship and one (W. M. D.) the receipt of a grant from the Department of Scientific and Industrial Research during the course of this work.

REFERENCES

- BROSTROM, K. J., HUUS, T., and TANGEN, R., 1947, *Phys. Rev.*, **55**, 27.
CASSON, H., 1953, *Phys. Rev.*, **89**, 809.
CHRISTY, R. F., 1953, *Phys. Rev.*, **89**, 839.
DEVONS, S., and HINE, M. G. N., 1949, *Proc. Roy. Soc. A*, **199**, 56.
FEATHER, N., 1953, *Advances in Physics (Phil. Mag. Suppl.)*, **2**, 141.
LI, C. W., 1952, *Phys. Rev.*, **88**, 1038.
PECK, R. A., 1949, *Phys. Rev.*, **76**, 1279.
RAE, E. R., RUTHERGLEN, J. G., and SMITH, R. D., 1951, *Proc. Phys. Soc. A*, **64**, 906.
RUTHERGLEN, J. G., and SMITH, R. D., 1953, *Proc. Phys. Soc. A*, **66**, 800.
TANGEN, R., 1946, *K. Norske Vidensk. Selsk. Skr.*, No. 1.
TOUSCHEK, B. F., 1950, *Phil. Mag.*, **41**, 849.

Investigation of Triplet Neutron-Proton Scattering in the Low Energy Region using the Eckart and Bargmann Potentials

By J. S. TURNER

School of Physics, University of Sydney, Sydney, Australia

Communicated by H. S. W. Massey; MS. received 13th March 1953, and in amended form 6th August 1953

Abstract. It is pointed out that the extension of some results obtained for a special form of potential by Bargmann leads to an especially simple expression for the asymptotic phase of the scattered S waves. The expansion of $k \cot \eta_0$ in terms of energy contains two terms only, the third coefficient P and all later coefficients being identically zero. The procedure for fitting experimental results is easier since the unmodified effective range theory is now exact for the Bargmann potentials. Graphs are drawn to illustrate the types of potential chosen by this method and to compare them with the conventional forms. Other Bargmann potentials for which P is not zero are discussed more briefly and fitted to the low-energy data, and some conclusions are drawn about the implications of the coefficient P .

§ 1. INTRODUCTION

IT is well known that the analysis of neutron-proton scattering data may be conveniently carried out by considering the expansion in terms of energy

$$k \cot \eta_0 = -1/a + \frac{1}{2} r_0 k^2 - Tk^4 + \dots \quad (1.1)$$

Blatt and Jackson (1949, denoted hereafter by BJ) showed that for the interpretation of low-energy data (below 10 mev) only S wave scattering is of importance and that only two parameters are necessary to fit the experimental results, namely a the 'scattering length at zero energy' and r_0 the effective range. For the experimental data available at that time it was therefore impossible to distinguish between the four types of potential well which are usually assumed, since in the expression for each of them are two adjustable parameters which can be found from the experimental values of a and r_0 once the form of well has been chosen.

Blatt and Jackson discussed further the effect of the third term in (1.1) and concluded that for all reasonable well shapes the coefficient $P \equiv Tr_0^{-3}$ is so small as to make this term negligible at low energies. P does, however, give the first indication of the shape of the well as the BJ plot of P against αr_0 ($\alpha = 1/a$) shows; P is positive for the Yukawa and exponential wells, and negative for the gaussian and square wells.

As experimental data become accurate enough to allow a determination of P it will be of some interest to examine further the implications of this coefficient. In particular a set of potentials will be treated here which makes P exactly zero; this is in any case small and as yet of unknown sign. A number of results obtained in BJ as approximations and later modified by the inclusion of P will become exact for potentials of this type, and it will therefore be easier to refer low-energy experimental results to them than to one of the four conventional types.

§ 2. THE ECKART AND BARGMANN POTENTIALS

The potentials to be considered here were first discussed by Eckart (1930) and later generalized and applied to scattering problems by Jost (1947) and Bargmann (1949 a, b). We shall use the notation of the latter two authors and assume some familiarity with their papers.

Bargmann was interested in what he called phase equivalent potentials, and for this purpose used the function $f(k)$, related to the phase by

$$e^{i\eta(k)} = f(k)/|f(k)|. \quad \dots\dots(2.1)$$

We need to carry his work one step further and to use the expression for $\cot \eta$ implicit in (2.1), namely

$$\cot \eta = \mathcal{H}f(k)/\mathcal{I}f(k). \quad \dots\dots(2.2)$$

Since we have in mind a possible application to n-p scattering we shall consider only the two Bargmann potentials $V_3(r)$ and $V_4(r)$, viz.

$$V_3(r) = \frac{-2(\rho/\sigma)(\rho+\sigma)^2 e^{-(\rho+\sigma)r}}{\{1+(\rho/\sigma) e^{-(\rho+\sigma)r}\}^2} \quad \dots\dots(2.3)$$

$$V_4(r) = \frac{-\rho\sigma\{4\rho\sigma + (\rho-\sigma)^2 \cosh(\rho+\sigma)r + (\rho+\sigma)^2 \cosh[(\rho-\sigma)r - 2\theta]\}}{\{\sigma \cosh(\rho r - \theta) + \rho \cosh(\sigma r + \theta)\}^2} \quad \dots\dots(2.4)$$

where θ is a parameter taking any value $-\infty < \theta < \infty$ and $\rho > \sigma > 0$.

We shall see that some of these are attractive over all the range and some have repulsive* portions, but they always are attractive for large r . $V_1(r)$ and $V_2(r)$ of Bargmann have been excluded as physically unreasonable, since they represent repulsive potentials at large values of r .

When $\theta = -\infty$, $V_4(r)$ reduces to $V_3(r)$, which is a special case of the Eckart potential. Parameters $\beta = \rho/\sigma$ and $\lambda = \rho + \sigma$ can be conveniently used when discussing $V_3(r)$.

For both (2.3) and (2.4) $f(k)$ is independent of θ :

$$f(k) = \frac{2k + i(\rho - \sigma)}{2k - i(\rho + \sigma)} \quad \dots\dots(2.5)$$

hence using (2.2)

$$\left. \begin{aligned} k \cot \eta &= (\sigma^2 - \rho^2)/4\rho + k^2/\rho \\ &= -(\beta - 1)\lambda/4\beta + (\beta + 1)k^2/\lambda\beta. \end{aligned} \right\} \quad \dots\dots(2.6)$$

The potentials have one bound state with energy $E = -\frac{1}{4}(\rho - \sigma)^2$.

§ 3. FITTING OF POTENTIALS TO THE SCATTERING DATA

Attempts to define an intrinsic range for these potentials, following the methods of BJ for the conventional shapes, will be unsatisfactory because a change in range or depth will in the present case also modify the shape. It is unnecessary to do so, however, since we may evaluate the parameters ρ and σ or λ and β directly by comparing (1.1) and (2.6). Equating coefficients and solving for the parameters we obtain

$$\rho = 2/r_0, \quad \sigma = (2/r_0)(1 - 2\alpha r_0)^{1/2}. \quad \dots\dots(3.1)$$

$$\lambda = (2/r_0)\{1 + (1 - 2\alpha r_0)^{1/2}\}, \quad \beta = (1 - 2\alpha r_0)^{-1/2}. \quad \dots\dots(3.2)$$

* The term 'repulsive' is used here to denote a region where the gradient of V is negative, and should not be taken to mean necessarily that V is positive.

Now in practice r_0 for triplet scattering is determined by using the value of a obtained from scattering cross section measurements together with the experimental binding energy of the deuteron. This procedure is especially simple for the case where only two terms are present in the expansion of $k \cot \eta$.

The expression of the form (1.1) may be extended to bound states by replacing k by $-i\gamma$, where γ^{-1} is the 'radius of the deuteron', related to the binding energy E by $E = \hbar^2 \gamma^2 / 2m$. We arrive at the form

$$\gamma = \alpha + \frac{1}{2} r_0 \gamma^2, \quad \dots\dots(3.3)$$

This relation for r_0 is exact if the n-p interaction is assumed to be of the form (2.3) or (2.4). We may therefore write ρ and σ directly in terms of γ and a thus:

$$\rho = \frac{\gamma}{1 - \alpha/\gamma}, \quad \sigma = \frac{(2\alpha/\gamma - 1)\gamma}{1 - \alpha/\gamma} \quad \dots\dots(3.4)$$

with similar forms for β and λ .

In obtaining the numerical values of the parameters we have used two sets of data to show what effect changes in the current best experimental values will have on the potentials chosen. BJ gave the values for the radius of the deuteron and triplet scattering length as

$$\gamma^{-1} = 4.332 \times 10^{-13} \text{ cm}, \quad a_t = 4.28 \pm 0.13 \times 10^{-13} \text{ cm}, \quad \dots\dots(A)$$

leading to $r_{0t} = 1.56 \pm 0.13 \times 10^{-13} \text{ cm}$ for the effective range.

More recent values quoted by Salpeter (1951) and by Feshbach and Schwinger (1951), which are a combination of results of various observers, are

$$a_t = 5.39 \pm 0.03 \times 10^{-13} \text{ cm}, \quad r_{0t} = 1.72 \pm 0.04 \times 10^{-13} \text{ cm}. \quad \dots\dots(B)$$

Taking the unit of length at 10^{-13} cm we find the following values, using (3.4) with data (A) and (3.1) with data (B)

$$(A) \quad \rho = 1.28, \quad \sigma = 0.82; \quad \beta = 1.56, \quad \lambda = 2.10 \quad (\text{see fig. 5}).$$

$$(B) \quad \rho = 1.16, \quad \sigma = 0.69; \quad \beta = 1.67, \quad \lambda = 1.85 \quad (\text{see fig. 4}).$$

§ 4. BEHAVIOUR OF THE POTENTIALS AS THE PARAMETERS ARE VARIED

We will now look at the forms of potentials which are obtained by our present fitting procedure.

4.1. Eckart Potentials

Figures 1 to 3 illustrate the behaviour of the Eckart potentials for various β and λ . They have a turning point where

$$r_1 = (1/\lambda) \log \beta, \quad \dots\dots(4.1)$$

so if $\beta < 1$ there is no turning point for positive r , if $\beta = 1$ there is a minimum at $r = 0$, and if $\beta > 1$ there is a minimum at the value of r given by (4.1). The value of V at the minimum is $-\lambda^2/2$.

In fig. 1, β is constant and equal to 1, in fig. 2, λ is constant and equal to 2, and in fig. 3 the depth of all potentials at the origin is constant and equal to 4.

The potentials may be attractive over the whole range, or repulsive out to a distance r_1 , then attractive. The potentials given by fitting $V_3(r)$ to the experimental data of the last section have this latter property, since the parameter $\beta > 1$.

4.2. The More General Potential

In fig. 4 potentials of the form $V_4(r)$ having different values of θ are compared, with the other parameters fixed at $\rho = 1.16$, $\sigma = 0.69$.

All the potentials have the same depth at the origin. It will be noticed that for θ negative there is a repulsive portion of the potential near the origin but it is always attractive out further; the asymptotic form is given in Bargmann's second paper. For θ positive the potential is attractive for small r , but for a value of θ about 0.9 a

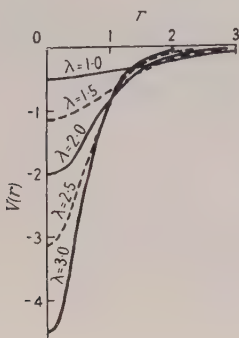


Fig. 1. Eckart potentials with $\beta=1$ and various λ .

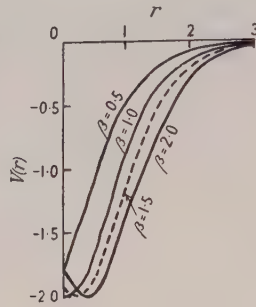


Fig. 2. Eckart potentials with $\lambda=2$ and various β .

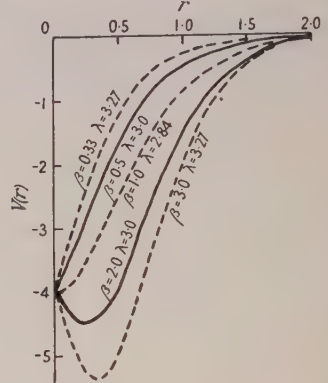


Fig. 3. Eckart potentials with depth at origin constant and equal to 4.

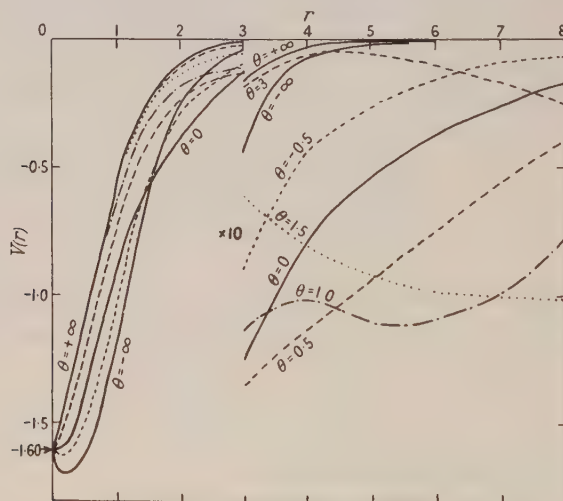


Fig. 4. Potentials of the form $V_4(r)$ with parameters chosen to fit the values of a_t and r_{0t} given by Feshbach and Schwinger (1951).

repulsive portion of the potential appears. The maximum depth of this portion decreases as θ increases further, and its position moves outwards. Thus only those potentials with θ lying between 0 and 0.9 are attractive over the whole range; but of course the whole family of phase equivalent potentials of fig. 4 give an equally good fit to the low energy n-p scattering data.

In fig. 5 we compare three curves of the form (2.4), chosen to fit the BJ experimental data (A), with the four standard well shapes computed from the same data using the method outlined in BJ for the shape independent approximation. The

curves with other values of θ will be similar to those in fig. 4; the most obvious effect of a change in ρ and σ will be to change the depth of the wells without altering very much the relation between the curves.

The depth at the origin of the potentials we have considered is about the same as that of the corresponding gaussian potential, but they have a much longer tail which is finally exponential in form.

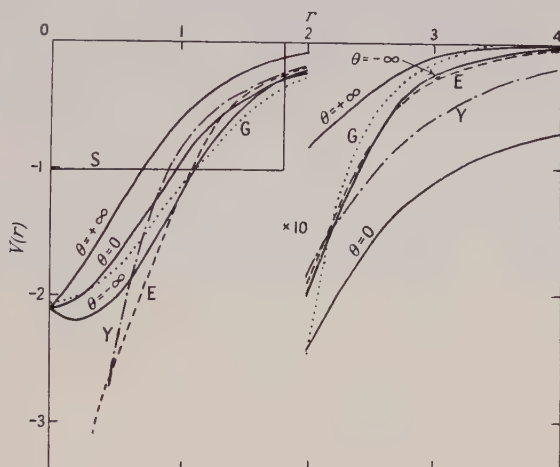


Fig. 5. Potentials of the form $V_4(r)$ compared with the conventional well shapes, all potentials being chosen to fit the values of a_t and r_{0t} quoted by Blatt and Jackson (1949).

§ 5. FURTHER TERMS IN THE EXPANSION OF $k \cot \eta$

It is clear that for the conventional types of potential well containing only two parameters the third term in the expansion of $k \cot \eta$ in powers of energy cannot be fixed independently once these parameters have been chosen. It would be desirable therefore to have available potentials defined by three parameters, which will allow of a direct fitting of three terms.

The effect of a small non-zero third term in the expansion on the results of the previous sections will be investigated here, using the form of potential which Bargmann (1949 b) called the 'quadratic type', without the restriction which previously made all terms after the second in that expansion zero. We will sketch briefly the method used and indicate the forms of the potentials obtained before attempting to draw any conclusions as to the significance of the coefficient P .

The most general potential considered by Bargmann arises from the assumption of a special form for $f(k)$, namely

$$f(k) = \frac{4k^2 + 2ika_0 + b_0}{2k^2 + 2ika_\infty + b_\infty} \quad \dots\dots (5.1)$$

where $a_0, b_0, a_\infty, b_\infty$ are constants which Bargmann has expressed in terms of the four parameters defining the corresponding potential. An expression for $k \cot \eta$ can be obtained from (5.1) using (2.2) and writing the result as a series in ascending powers of k^2 . It is easily verified that the earlier form (2.6) arises as a special case when the parameters are restricted in such a way as to give the potential (2.4).

The next step seemed to be to test the effect of putting the fourth term zero (the succeeding terms also become zero since the same factor occurs in all of them). This condition is too stringent; the potentials obtained by fitting the first two terms as given by experimental results, and various assumed values of P are found

to be unsuitable for the present application since they are all repulsive at large distances and very different from $V_3(r)$ and $V_4(r)$. This case will not be discussed further.

If, however, the first three terms are fitted without making any assumptions about later terms, physically reasonable potentials are obtained. It is a matter of straightforward but tedious algebra to equate coefficients and solve for the parameters defining the potentials, in terms of α , r_0 and P . There is still one variable parameter, so that there may be a family of potentials satisfying a given set of conditions. It was found most convenient in the calculation first to fix this arbitrary parameter, and also α and r_0 at the experimental values, and to express each of the other parameters in terms of P .

The corresponding potentials will vary continuously from those displayed in fig. 4 as P is increased from zero. They can only be obtained, however, for small *positive* values of P , i.e. negative values of the third coefficient, there being no real sets of parameters when P is negative. The variation from the potentials having P zero is small. For example, if we choose the arbitrary parameter so as to give a turning point at the origin, there are two potentials having $T \equiv Pr_0^3 = +0.5$, and these have depths of 1.75 and 1.89 units at the origin, compared with 1.60 units for the Bargmann potentials with $P=0$. The forms for large r are also very little different; they are both exponential with a rate of decrease in one case slightly greater, and in the other slightly less than that for the potential of fig. 4 having $\theta=0$.

§ 6. CONCLUSIONS

Any conclusions which we may draw can of course only strictly apply to the Bargmann potentials, but they do suggest results of more general interest. The fact that it is impossible to find similar potentials for *negative* P supports the conclusion in BJ that the sign of P is determined by the nature of the tail of the potential and that the long (exponential) tail in the present case is responsible for restricting P to a positive or zero value.

On the other hand we have seen that positive values of P of the same order as that found by BJ for the Yukawa well lead to potentials which are not very different from those having $P=0$; the depth at the origin is increased very little and is certainly still finite, and the form for large r is exponential. This shows that although an accurate value for the magnitude of P would allow us to distinguish between the exponential and Yukawa wells it would give no definite information about the actual form either at the origin or at infinity.

ACKNOWLEDGMENTS

The author wishes to express his indebtedness to Dr. R. E. B. Makinson for suggesting this problem for research and for his advice and encouragement as it proceeded. He is also grateful to Dr. F. C. Barker for some helpful discussions and criticisms.

The work was carried out during the tenure of a Research Studentship at the University of Sydney.

REFERENCES

- BARGMANN, V., 1949 a, *Phys. Rev.*, **43**, 253; 1949 b, *Rev. Mod. Phys.*, **21**, 488.
- BLATT, J. M., and JACKSON, J. D., 1949, *Phys. Rev.*, **76**, 18.
- ECKART, C., 1930, *Phys. Rev.*, **35**, 1303.
- FESHBACH, H., and SCHWINGER, J., 1951, *Phys. Rev.*, **84**, 194.
- JOST, R., 1947, *Helv. Phys. Acta*, **20**, 256.
- SALPETER, E. E., 1951, *Phys. Rev.*, **82**, 60.

Electron-Neutrino Angular Correlation Functions in the Theory of Beta Decay

BY G. N. FOWLER

Physical Laboratories, University of Manchester

Communicated by L. Rosenfeld; MS. received 23rd February 1953, and in amended form 18th August 1953

Abstract. The angular correlation functions have been calculated for linear combinations of interactions (excluding combinations of scalar and vector interactions or of tensor and axial vector interactions) in the first and second forbidden approximations with neglect of the coulomb field corrections.

§ 1. INTRODUCTION

THE angular correlation functions have been calculated for the first and second forbidden transitions, with neglect of the coulomb field correction, using those linear combinations of the five interactions which are not excluded by the experimental results on allowed energy spectra. These results allow us to omit consideration of any combination of scalar and vector or tensor and axial vector. Since this work was completed the results of Greuling and Meeks (1951) have been published on the coulomb effect on the angular correlation functions. They have shown that the Z dependent terms can dominate the results even for $A \sim 40$. It is necessary, therefore, to point out that this must be borne in mind when applying the results of the present work.

However, it is found that for first forbidden tensor and axial vector transitions with $\Delta J = 2$ the correlation function is independent of Z , and one may infer a similar result for higher degrees of forbiddenness, for this particular type of transition, since the same type of combinations of electron wave functions will occur in every case, the only difference being in the permitted values of $k = \pm(j + \frac{1}{2})$ (see Greuling and Meeks, eqn. (36)). Thus measurement of angular correlation functions would afford further opportunities of distinguishing between the tensor and axial vector interactions in the rather numerous class of $\Delta J = n + 1$ transitions.

§ 2. GENERAL FORMULAE

The notation used is that of Konopinski and Uhlenbeck (1941) and Hamilton (1947), and the method used is very similar to that used by the former authors in the calculation of the energy spectrum.

In the units used $\hbar = c = m = 1$.

The probability of decay with a given angle θ between the electron and neutrino directions and a given electron energy E is given by

$$P(E, \theta) \sin \theta \, d\theta \, dE = \frac{G^2}{4\pi^3} p E q^2 W_n(\theta) \sin \theta \, d\theta \, dE$$

where n is the degree of forbiddenness and $p = (E^2 - 1)^{1/2}$, $q = E_0 - E$, $r^2 = p^2 + q^2$ and E_0 is the maximum decay energy.

For $n=1$:

$$W_1 = A_1 + B_1 \cos \theta + C_1 \cos^2 \theta$$

$$\text{where } A_1 = r^2 M_1 + q(M_3 + M_5/E) + (p^2/E)(M_4 + qM_7) + M_6/E + M_8$$

$$B_1 = pq(2M_1 + M_4/E) + p(M_3 + M_5/E + M_9/E) + (p/E)r^2 M_2$$

$$C_1 = (p^2 q/E)(2M_2 - M_7)$$

$$\text{with } M_1 = (C_T^2 + C_A^2) \left\{ \frac{1}{12} \sum_{ij} |B_{ij}|^2 + \frac{1}{6} \left| \int \boldsymbol{\sigma} \wedge \mathbf{r} \right|^2 + \frac{1}{9} \left| \int \boldsymbol{\sigma} \cdot \mathbf{r} \right|^2 \right\} + \frac{1}{3} (C_S^2 + C_V^2) \left| \int \mathbf{r} \right|^2$$

$$M_2 = (C_A^2 - C_T^2) \left\{ \frac{1}{9} \left| \int \boldsymbol{\sigma} \cdot \mathbf{r} \right|^2 - \frac{1}{6} \left| \int \boldsymbol{\sigma} \wedge \mathbf{r} \right|^2 - \frac{1}{60} \sum_{ij} |B_{ij}|^2 \right\} + \frac{1}{3} (C_V^2 - C_S^2) \left| \int \mathbf{r} \right|^2$$

$$M_3 = \frac{1}{3} (C_V^2 - C_S C_T) \left(i \int \mathbf{r}^* \int \boldsymbol{\alpha} + \text{c.c.} \right) - \frac{1}{3} (C_T^2 - C_V C_A) \left(\int \boldsymbol{\sigma} \wedge \mathbf{r}^* \int \boldsymbol{\alpha} + \text{c.c.} \right) \\ + \frac{1}{3} (C_A^2 - C_T C_P) \left(i \int \boldsymbol{\sigma} \cdot \mathbf{r}^* \int \gamma_5 + \text{c.c.} \right)$$

$$M_4 = \frac{1}{3} (C_V^2 + C_S C_T) \left(i \int \mathbf{r}^* \int \boldsymbol{\alpha} + \text{c.c.} \right) - \frac{1}{3} (C_T^2 + C_V C_A) \left(\int \boldsymbol{\sigma} \wedge \mathbf{r}^* \int \boldsymbol{\alpha} + \text{c.c.} \right) \\ + \frac{1}{3} (C_A^2 + C_T C_P) \left(i \int \boldsymbol{\sigma} \cdot \mathbf{r}^* \int \gamma_5 + \text{c.c.} \right)$$

$$M_5 = \frac{1}{3} C_V C_T \left\{ \left(i \int \mathbf{r}^* \int \boldsymbol{\alpha} + \text{c.c.} \right) - \left(\int \boldsymbol{\sigma} \wedge \mathbf{r}^* \int \boldsymbol{\alpha} + \text{c.c.} \right) \right\} \\ + \frac{1}{3} C_A C_P \left(i \int \boldsymbol{\sigma} \cdot \mathbf{r}^* \int \gamma_5 + \text{c.c.} \right)$$

$$M_6 = 2C_A C_P \left| \int \gamma_5 \right|^2 + 2C_V C_T \left| \int \boldsymbol{\alpha} \right|^2$$

$$M_7 = (C_A^2 - C_T^2) \left\{ \frac{1}{60} \sum_{ij} |B_{ij}|^2 - \frac{1}{6} \left| \int \boldsymbol{\sigma} \wedge \mathbf{r} \right|^2 + \frac{2}{9} \left| \int \boldsymbol{\sigma} \cdot \mathbf{r} \right|^2 \right\}$$

$$M_8 = (C_T^2 + C_V^2) \left| \int \boldsymbol{\alpha} \right|^2 + (C_A^2 + C_P^2) \left| \int \gamma_5 \right|^2$$

$$M_9 = \frac{1}{3} (C_T^2 - C_V^2) \left| \int \boldsymbol{\alpha} \right|^2 + (C_A^2 - C_P^2) \left| \int \gamma_5 \right|^2$$

For $n=2$:

$$W_2 = A_2 + B_2 \cos \theta + C_2 \cos^2 \theta + D_2 \cos^3 \theta$$

$$\text{where } A_2 = r^2 \{ r^2 M_1 + (p^2/E)(qM_3 + M_4) + q(M_5 + M_9/E) + M_6 \} + (p^2 q/E) M_8$$

$$B_2 = r^2 \{ p r^2 M_2/E + p q (4M_1 + M_4/E) + p (M_5 + M_7/E) \} \\ + 2p^3 q \{ q(M_3/E + M_4/E) + 2p q \{ q(M_9/E + M_5) + M_6 \} \}$$

$$C_2 = 2p^2 q \{ q(2M_1 + M_4/E) + M_5 + M_7/E - M_8/2E \} + (p^2 q^3/E)(4M_2 - M_3) \\ + (p^4 q/E)(4M_2 - M_3)$$

$$D_2 = (2p^3 q^2/E)(2M_2 - M_3)$$

$$\text{with } M_1 = (C_T^2 + C_A^2) \left\{ \frac{1}{1080} \sum_{ijk} |S_{ijk}|^2 + \frac{1}{180} \sum_{ij} |T_{ij}|^2 \right\} + \frac{1}{30} (C_V^2 + C_S^2) \sum_{ij} |R_{ij}|^2$$

$$M_2 = (C_T^2 - C_A^2) \left\{ \frac{1}{7560} \sum_{ijk} |S_{ijk}|^2 + \frac{1}{180} \sum_{ij} |T_{ij}|^2 \right\} + \frac{1}{30} (C_V^2 - C_S^2) \sum_{ij} |R_{ij}|^2$$

$$M_3 = (C_A^2 - C_T^2) \left\{ \frac{1}{3780} \sum_{ijk} |S_{ijk}|^2 - \frac{1}{180} \sum_{ij} |T_{ij}|^2 \right\}$$

$$M_4 = -\frac{1}{60} (C_T^2 + C_V C_A) \left(\sum_{ij} A_{ij}^* T_{ij} + \text{c.c.} \right) \\ - \frac{1}{30} (C_V^2 + C_S C_T) \left(i \sum_{ij} A_{ij}^* T_{ij} + \text{c.c.} \right)$$

$$\begin{aligned}
M_5 &= -\frac{1}{60}(C_T^2 - C_V C_A)(\sum_{ij} A_{ij}^* T_{ij} + \text{c.c.}) \\
&\quad - \frac{1}{30}(C_V^2 - C_S C_T)(i \sum_{ij} A_{ij}^* R_{ij} + \text{c.c.}) \\
M_6 &= (C_V^2 + C_T^2) \left\{ \frac{1}{12} \sum_{ij} |A_{ij}|^2 + \frac{1}{6} \left| \int \boldsymbol{\alpha} \wedge \mathbf{r} \right|^2 \right\} + \frac{1}{3}(C_A^2 + C_P^2) \left| \int \gamma_5 \mathbf{r} \right|^2 \\
&\quad + (C_V C_T / E) \left\{ \frac{1}{6} \sum_{ij} |A_{ij}|^2 + \frac{1}{3} \left| \int \boldsymbol{\alpha} \wedge \mathbf{r} \right|^2 \right\} + (2C_A C_P / 3E) \left| \int \gamma_5 \mathbf{r} \right|^2 \\
M_7 &= (C_T^2 - C_V^2) \left\{ \frac{1}{60} \sum_{ij} |A_{ij}|^2 + \frac{1}{6} \left| \int \boldsymbol{\alpha} \wedge \mathbf{r} \right|^2 \right\} + \frac{1}{3}(C_A^2 - C_P^2) \left| \int \gamma_5 \mathbf{r} \right|^2 \\
&\quad - \frac{1}{30} C_V C_T \left\{ (i \sum_{ij} A_{ij}^* R_{ij} + \text{c.c.}) + \frac{1}{2} \sum_{ij} A_{ij}^* T_{ij} + \text{c.c.} \right\} \\
M_8 &= (C_T^2 - C_V^2) \left\{ \frac{1}{6} \left| \int \boldsymbol{\alpha} \wedge \mathbf{r} \right|^2 - \frac{1}{60} \sum_{ij} |A_{ij}|^2 \right\} \\
M_9 &= -\frac{1}{30} C_V C_T \left\{ (i \sum_{ij} A_{ij}^* R_{ij} + \text{c.c.}) + \frac{1}{2} (\sum_{ij} A_{ij}^* T_{ij} + \text{c.c.}) \right\}.
\end{aligned}$$

In the particular case, already referred to above, with $\Delta J = \pm 3$ with no parity change, one finds

$$W_2(\theta) \propto (7 \pm p \cos \theta / E) |p + q|^4 \mp p^2 q \sin^2 \theta |p + q|^2 / E$$

where the upper and lower signs refer respectively to the tensor and axial vector interactions.

In every case, on integrating over θ , one recovers the usual energy spectra given by Greuling and Meeks, and also the cross terms given by Pursey (1951) in the approximation $Z \sim 0$.

§ 3. REDUCTION OF THE FORMULAE

In order to make these results more readily visualizable they have been classified according to the different selection rules which the various matrix elements satisfy. The different matrix elements have then been eliminated using relations between them based, for the most part, on the Mayer shell model, a restriction on the generality of the results in particular for the lighter nuclei.

The relations used have been derived by Pursey (1951), (1)–(3), Greuling (1942), (4) and (5), Fowler (1952), (6)–(8), Ahrens and Feenberg (1952), (9), and Ahrens, Feenberg and Primakoff (1952), (10).

- (1) $(f | \boldsymbol{\alpha} | i) = i\kappa(f | \mathbf{r} | i)$
- (2) $(f | \beta \boldsymbol{\alpha} | i) = \epsilon(f | \boldsymbol{\alpha} | i)$
- (3) $(f | \beta \boldsymbol{\sigma} \wedge \mathbf{r} | i) = -(f | \boldsymbol{\sigma} \wedge \mathbf{r} | i) = i\epsilon(f | \mathbf{r} | i)$
- (4) $\sum_{ij} |B_{ij}|^2 = \frac{5}{3} |(f | \mathbf{r} | i)|^2$
- (5) $\sum_{ijk} |S_{ijk}|^2 = \frac{7}{3} \sum_{ij} |R_{ij}|^2$
- (6) $(f | A_{ij} | i) = iy(f | R_{ij} | i)$
- (7) $(f | \beta A_{ij} | i) = t(f | A_{ij} | i)$
- (8) $(f | \beta T_{ij} | i) = i\epsilon(f | R_{ij} | i) = -(f | T_{ij} | i)$
- (9) $(f | \boldsymbol{\sigma} \cdot \mathbf{r} | i) = -3is(f | \gamma_5 | i)$
- (10) $(f | \beta \gamma_5 | i) = \frac{1}{6M_S} (f | \gamma_5 | i).$

Here $k = \beta(\sigma \cdot \mathbf{l} + 1)$

$$\epsilon = k_f - k_i$$

$$x = (E_i - E_f) - (M_n - M_p) + Z\alpha/R - 15A^{-4/3}(N - Z)(1 - 3A^{-2/3}) \\ + 55\epsilon A^{-1/3}(1.07 - 3.6A^{-2/3})$$

$$y = (E_i - E_f) - (M_n - M_p) + Z\alpha/R - 30A^{-4/3}(N - Z)(1 - A^{-1/3}) \\ + 55\epsilon A^{-1/3}(1.07 - 3.6A^{-2/3})$$

$$\Lambda = 1 + (E_i - E_f - 2.5)A^{1/3}/Z + (-1)^{Z+1}\delta/A, \quad A \text{ even} \\ + 0, \quad A \text{ odd}$$

$$R = 1.4 \times 10^{-13} A^{1/3} \text{ cm.}$$

$$s = 2R/3\Lambda\alpha Z$$

$$t = \epsilon - (l_f^2 - l_i^2)/(k_f + k_i)$$

M = nucleon mass.

The quantity δ , occurring in Λ , may be estimated from the data given by Feenberg (1947).

The following formulae were found:

$$n = 1:$$

(i) $\Delta J = 0$ ($0 \rightarrow 0$) with parity change.

$$A_1 = s^2 \left(r^2 - \frac{2p^2q}{E} \right) C_T^2 + \left\{ s^2 \left(r^2 + \frac{2p^2q}{E} \right) - 2s \left(q + \frac{p^2}{E} \right) + 1 \right\} C_A^2 \\ + \frac{1}{36s^2M^2} C_P^2 - \frac{1}{3M} \left(q - \frac{p^2}{E} \right) C_T C_P + \frac{1}{3M} \left(q + \frac{1}{s} \right) \frac{1}{E} C_A C_P \\ \frac{1}{p} B_1 = s^2 \left(2q - \frac{r^2}{E} \right) C_T^2 + \left\{ s^2 \left(2q + \frac{r^2}{E} \right) - 2s \left(1 + \frac{q}{E} \right) + \frac{1}{E} \right\} C_A^2 \\ - \frac{1}{36s^2M^2} \frac{1}{E} C_P^2 - \frac{1}{3M} \left(1 - \frac{q}{E} \right) C_T C_P - \frac{1}{3M} \frac{1}{E} C_A C_P$$

$$C_1 = 0.$$

(ii) $\Delta J = \pm 1$ with parity change (not $1 \rightleftharpoons 0$).

$$A_1 = \frac{1}{3}(a_{SS}C_S^2 + a_{VV}C_V^2 + a_{TT}C_T^2 + a_{AA}C_A^2 + a_{ST}C_SC_T + a_{VA}C_VC_A + a_{VT}C_VC_T)$$

where

$$a_{SS} = r^2$$

$$a_{VV} = r^2 - 2x \left(q + \frac{p^2}{E} \right) + 3x^2$$

$$a_{TT} = -2\epsilon^2x \left(q + \frac{p^2}{E} \right) + 3\epsilon^2x^2 \\ + \frac{1}{2}\epsilon^2 \left(r^2 + \frac{p^2q}{E} \right) + \frac{1}{12} \left(5r^2 - \frac{p^2q}{E} \right)$$

$$a_{AA} = \frac{1}{2}\epsilon^2 \left(r^2 - \frac{p^2q}{E} \right) + \frac{1}{12} \left(5r^2 + \frac{p^2q}{E} \right)$$

$$a_{ST} = a_{VA} = -2\epsilon x \left(q - \frac{p^2}{E} \right)$$

$$a_{VT} = -2\epsilon x(q - 3x) \frac{1}{E}.$$

$$B_1 = \frac{p}{3} (b_{SS} C_S^2 + b_{VV} C_V^2 + b_{TT} C_T^2 + b_{AA} C_A^2 + b_{ST} C_S C_T + b_{VA} C_V C_A + b_{VT} C_V C_T)$$

where

$$\begin{aligned} b_{SS} &= 2q - \frac{r^2}{E} \\ b_{VV} &= 2q + \frac{r^2}{E} - 2x \left(1 + \frac{q}{E} \right) - x^2 \frac{1}{E} \\ b_{TT} &= -2\epsilon^2 x \left(1 + \frac{q}{E} \right) + \epsilon^2 x^2 \frac{1}{E} \\ &\quad + \frac{1}{2} \epsilon^2 \left(2q + \frac{r^2}{E} \right) + \frac{1}{12} \left(10q + \frac{r^2}{E} \right) \\ b_{AA} &= \frac{1}{2} \epsilon^2 \left(2q - \frac{r^2}{E} \right) + \frac{1}{12} \left(10q - \frac{r^2}{E} \right) \\ b_{ST} &= b_{VA} = -2\epsilon x \left(1 - \frac{q}{E} \right) \\ b_{VT} &= -4\epsilon x \frac{1}{E}. \end{aligned}$$

$$C_1 = \frac{2p^2 q}{3E} \left\{ -C_S^2 + C_V^2 + \frac{1}{4} (\epsilon^2 + \frac{1}{2}) (C_T^2 - C_A^2) \right\}.$$

$n=2$.

(i) $\Delta J=2$ without parity change (not $2 \Rightarrow 0$).

$$A_2 = \frac{r^2}{30} (a_{SS} C_S^2 + a_{VV} C_V^2 + a_{TT} C_T^2 + a_{AA} C_A^2 + a_{ST} C_S C_T + a_{VA} C_V C_A + a_{VT} C_V C_T)$$

$$\begin{aligned} a_{SS} &= r^2 \\ a_{VV} &= r^2 - 2y \left(q + \frac{p^2}{E} \right) + \frac{y^2}{2r^2} \left(5r^2 + \frac{p^2 q}{E} \right) \\ a_{TT} &= -yt\epsilon \left(q + \frac{p^2}{E} \right) + \frac{y^2 t^2}{2r^2} \left(5r^2 - \frac{p^2 q}{E} \right) \\ &\quad + \frac{1}{6} \epsilon^2 \left(r^2 + \frac{p^2 q}{E} \right) + \frac{1}{54} \left(\frac{7}{2} r^2 - \frac{p^2 q}{E} \right) \\ a_{AA} &= \frac{1}{6} \epsilon^2 \left(r^2 - \frac{p^2 q}{E} \right) + \frac{1}{54} \left(\frac{7}{2} r^2 + \frac{p^2 q}{E} \right) \\ a_{ST} &= -2yt \left(q - \frac{p^2}{E} \right); \quad a_{VA} = -y\epsilon \left(q - \frac{p^2}{E} \right) \\ a_{VT} &= -2y \left\{ q \left(t + \frac{1}{2} \epsilon \right) - \frac{5}{2} yt \right\} \frac{1}{E}. \end{aligned}$$

$$B_2 = \frac{\dot{p}}{30} (b_{SS}C_S^2 + b_{VV}C_V^2 + b_{TT}C_T^2 + b_{AA}C_A^2 + b_{ST}C_SC_T + b_{VA}C_VC_A + b_{VT}C_VC_T)$$

$$b_{SS} = r^2 \left(4q - \frac{r^2}{E} \right)$$

$$b_{VV} = r^2 \left(4q + \frac{r^2}{E} \right)$$

$$-2y \left\{ (r^2 + 2q^2) + \frac{q(r^2 + 2p^2)}{E} \right\} + \frac{1}{2}y^2 \left(10q - \frac{r^2}{E} \right)$$

$$b_{TT} = -yt\epsilon \left\{ (r^2 + 2q^2) + \frac{q(r^2 + 2p^2)}{E} \right\} + \frac{1}{2}y^2t^2 \left(10q + \frac{r^2}{E} \right) \\ + \frac{2}{3}\epsilon^2 \left(qr^2 + \frac{r^4 + 2p^2q^2}{4E} \right) + \frac{1}{27} \left(7qr^2 + \frac{r^4 - 4p^2q^2}{4E} \right)$$

$$b_{AA} = \frac{2}{3}\epsilon^2 \left(qr^2 - \frac{r^4 + 2p^2q^2}{4E} \right) + \frac{1}{27} \left(7qr^2 - \frac{r^4 - 4p^2q^2}{4E} \right)$$

$$b_{ST} = -2yt \left\{ (r^2 + 2q^2) - \frac{q(r^2 + 2p^2)}{E} \right\}$$

$$b_{VA} = -y\epsilon \left\{ (r^2 + 2q^2) - \frac{q(r^2 + 2p^2)}{E} \right\}$$

$$b_{VT} = -2y \left\{ (r^2 + 2q^2)(t + \frac{1}{2}\epsilon) - 5qty \right\} \frac{1}{E}.$$

$$C_2 = \frac{\dot{p}^2q}{15} (c_{SS}C_S^2 + c_{VV}C_V^2 + c_{TT}C_T^2 + c_{AA}C_A^2 + c_{ST}C_SC_T + c_{VA}C_VC_A + c_{VT}C_VC_T)$$

$$c_{SS} = 2 \left(q - \frac{r^2}{E} \right)$$

$$c_{VV} = 2 \left(q + \frac{r^2}{E} \right) - 2y \left(1 + \frac{q}{E} \right) - \frac{3}{4}y^2 \frac{1}{E}$$

$$c_{TT} = -yt\epsilon \left(1 + \frac{q}{E} \right) + \frac{3}{4}y^2t^2 \frac{1}{E} \\ + \frac{1}{3}\epsilon^2 \left(q + \frac{3r^2}{4E} \right) + \frac{1}{27} \left(\frac{7}{2}q + \frac{3r^2}{4E} \right)$$

$$c_{AA} = \frac{1}{3}\epsilon^2 \left(q - \frac{3r^2}{4E} \right) + \frac{1}{27} \left(\frac{7}{2}q - \frac{3r^2}{4E} \right)$$

$$c_{ST} = -2yt \left(1 - \frac{q}{E} \right); \quad c_{VA} = -y\epsilon \left(1 - \frac{q}{E} \right)$$

$$c_{VT} = -2y \left(t + \frac{1}{2}\epsilon \right) \frac{1}{E}.$$

$$D_2 = \frac{2p^3q^2}{15E} \left\{ -C_S^2 + C_V^2 + \frac{1}{12} \left(\epsilon^2 + \frac{2}{9} \right) (C_T^2 - C_A^2) \right\}.$$

It will be seen from these formulae that the results will, in general, depend rather sensitively on the sign of ϵ , that is to say, on whether $\Delta J < \text{or} > 0$. This is a consequence of relations (1), (2), (6) and (8) in particular, and is therefore connected with the extreme one-particle model of the nucleus.

§4. EVALUATION FOR A TYPICAL CASE

Finally, these formulae were evaluated for a typical case in which the relevant parameters have been chosen to make the coulomb effect small. The values chosen for the various quantities are the following:

$$A=27, \quad W_0=7 mc^2, \quad Z=10=\frac{1}{3}Z_{\text{crit}}$$

where $Z_{\text{crit}}=1.6 W_0^{3/2}$ and $|q/p|=2$. This last quantity has been chosen with a view to satisfying certain experimental requirements discussed, for example, by Sherwin (1951).

The results are approximately as follows:

 $n=1$.

(i) $\Delta J=0$ with parity change.

When it is assumed that $C_T \sim C_A \sim C_P$ the terms proportional to C_P and C_P^2 play no role because of the occurrence of the factors $1/M$ and $1/M^2$ in the expression (8). The results are therefore the same as those given by Hamilton for this particular case, i.e.

$$W_A \propto 1 + \frac{3}{4} \cos \theta; \quad W_T \propto 1 - \frac{1}{3} \cos \theta.$$

With an approximately equal mixture of the interactions concerned one finds

(ii) (a) $\Delta J = +1$ with parity change ($\epsilon = +1$)

$$W_V + W_A \sim W_V \propto 1 - \frac{2}{3} \cos \theta$$

$$W_S + W_T \propto 1 + \frac{1}{4} \cos \theta$$

$$W_V + W_T \propto 1 - \frac{1}{6} \cos \theta$$

$$W_S + W_A \propto 1 - \frac{1}{2} \cos^2 \theta$$

(b) $\Delta J = -1$ with parity change ($\epsilon = -1$)

$$W_V + W_A \propto 1 + \frac{1}{2} \cos \theta$$

$$W_S + W_T \propto 1 + \frac{1}{2} \cos \theta$$

$$W_V + W_T \propto 1 + \frac{2}{3} \cos \theta$$

$$W_S + W_A \propto 1 - \frac{1}{2} \cos^2 \theta.$$

$n=2$. $t = \epsilon - (l_f^2 - l_i^2)/(k_f + k_i)$ has been taken to be ~ 1 .

(a) $\Delta J = +2$ without parity change ($\epsilon = +2$)

$$W_V + W_A \sim W_V \propto 1 + \frac{1}{3} \cos \theta - \frac{1}{3} \cos^2 \theta$$

$$W_S + W_T \sim W_T \propto 1 + \frac{3}{4} \cos \theta$$

$$W_V + W_T \propto 1 + \frac{1}{2} \cos \theta$$

$$W_S + W_A \propto 1 + \cos \theta - \cos^2 \theta - \frac{1}{2} \cos^3 \theta.$$

(b) $\Delta J = -2$ without parity change ($\epsilon = -2$)

$$W_V + W_A \sim W_V \propto 1 + \cos \theta$$

$$W_S + W_T \propto 1 + \frac{1}{2} \cos \theta$$

$$W_V + W_T \propto 1 + \frac{2}{3} \cos \theta$$

$$W_S + W_A \propto 1 + \cos \theta - \cos^2 \theta - \frac{1}{2} \cos^3 \theta.$$

It should be added that these results do not depend at all sensitively on the values of the parameters A , Z , W_0 and $|q/p|$ subject only to the restrictions $Z < Z_{\text{crit}}$.

ACKNOWLEDGMENTS

Thanks are due to Professor L. Rosenfeld for his interest and encouragement and to the Department of Scientific and Industrial Research for a grant.

REFERENCES

- AHRENS, T., and FEENBERG, E., 1952, *Phys. Rev.*, **86**, 64.
AHRENS, T., FEENBERG, E., and PRIMAKOFF, H., 1952, *Phys. Rev.*, **87**, 663.
FEENBERG, E., 1947, *Rev. Mod. Phys.*, **19**, 239.
FOWLER, G. N., 1952, *Thesis*, University of Manchester.
GREULING, E., 1942, *Phys. Rev.*, **61**, 568.
GREULING, E., and MEEKS, M. L., 1951, *Phys. Rev.*, **82**, 531.
HAMILTON, D. R., 1947, *Phys. Rev.*, **71**, 456.
KONOPINSKI, T. J., and UHLENBECK, G. E., 1941, *Phys. Rev.*, **60**, 308.
PURSEY, D., 1951, *Phil. Mag.*, **42**, 1193.
SHERWIN, C. W., 1951, *Phys. Rev.*, **82**, 52.

Absorption Cross Sections for 134 MeV Protons

By J. M. CASSELS* AND J. D. LAWSON

Atomic Energy Research Establishment, Harwell, Didcot, Berks.

MS. received 14th September 1953

Abstract. The absorption cross sections for 134 MeV protons of carbon, aluminium, copper, cadmium and lead have been measured by a transmission method. The results are consistent with the predictions of the usual optical theory for high energy nuclear cross sections.

§ 1. INTRODUCTION

THE interaction of high energy nucleons with nuclei is often described in optical terms (Bethe 1940, Fernbach, Serber and Taylor 1949). The gross properties of nuclear matter, as seen by the incoming nucleon waves, are represented by a refractive index. This index has to be complex, because some nucleons are absorbed while others are scattered elastically.

It is usually assumed that the nuclei are spheres with a moderately well defined surface and a constant density, and therefore index, throughout the interior. There are then only three parameters entering into the situation, the nuclear radius R and the real and imaginary parts of the refractive index. It is convenient to specify the real part in terms of k_1 , defined so that the nucleon wave number changes from k outside to $k+k_1$ inside the nucleus. The imaginary part is specified by K , the reciprocal of the mean free path of the nucleon inside the nucleus.

The actual values of R can be found in many ways, although not all the results are concordant. The value of K for protons can be estimated from the results of free two-body scattering experiments (Goldberger 1948), provided that many-body forces acting on the incoming proton can be neglected. To calculate K for neutrons it is necessary to assume that the n - n and p - p interactions are equal, but this is probably justified to the order of accuracy required. On the other hand, the value of k_1 is difficult to forecast, because it involves combinations of the free two-body scattering amplitudes (Jastrow 1951) which are not directly observable (Mandl and Skyrme 1953).

The absorption cross section σ_a , which includes partial cross sections for all kinds of inelastic scattering, is a simple function of R and K . The elastic, or 'diffraction', cross section σ_d is a function of R , K and k_1 , and it depends rather sensitively on $k_1 R$ (Lawson 1953). The total cross section σ_t is the sum of these two cross sections and is, therefore, also a sensitive function of the 'unpredictable' parameter k_1 .

So far the most accurate experimental data available for comparison with the theory have been the neutron total cross sections of several elements at various neutron energies, sometimes well defined (Taylor and Wood 1953), but the theoretical analyses of these results have not been very convincing, just because k_1

* Now at Nuclear Physics Research Laboratory, University of Liverpool.

is arbitrarily adjustable. Some neutron absorption cross sections have been measured (DeJuren and Knable 1950, DeJuren 1950), but the results given are admittedly only lower limits and the neutron energies were not very well defined.

The purpose of the present paper is to describe some measurements of proton absorption cross sections at 134 meV, and to compare the results with the theory. A counter technique was used, so that a fully representative range of elements could be examined. In this respect the experiment improves upon an earlier photographic plate investigation of the same problem (Lees, Morrison, Muirhead and Rosser 1953).

§ 2. APPARATUS

The experimental apparatus is shown in figure 1. A beam of 147 ± 1 meV protons from the 110 in. Harwell cyclotron emerged into the air through a thin copper window A. The central part of the beam passed through two collimating holes (diameter 1 and $1\frac{1}{2}$ cm respectively) in the copper-tungsten alloy blocks B, C, and these protons were detected by gas counters D, E connected in double coincidence (resolving time $\frac{1}{2}$ μ sec). Both counters had 46 mg cm^{-2} copper windows at front and back, and were filled with A-CO₂ mixture. The liquid scintillation counter F was made by hollowing out an aluminium block, sealing to it a glass window with thermo-setting Araldite, and filling the 5 in. diameter cavity with a

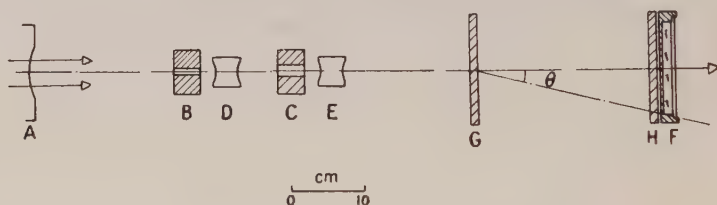


Figure 1. Experimental apparatus. A, end of proton beam tube; B, C, collimating holes; D, E, gas counters; F, liquid scintillation counter; G, attenuator; H, copper absorber.

solution of p-terphenyl in benzene (2 g litre^{-1}). It was viewed by an E.M.I. photomultiplier. The aluminium wall in front of the scintillating liquid was 0.86 g cm^{-2} thick. The double coincidence pulses DE were delayed by $\frac{3}{4}$ μ sec and then gated by $1\frac{1}{2}$ μ sec anti-coincidence pulses from F.

Attenuators G made of carbon, aluminium, copper, cadmium, or lead could be placed between E and F. The thickness of each attenuator was such that the protons passing through it were slowed down from 147 meV to 121 meV, and the effective energy is therefore given as 134 meV. Since the cross sections vary slowly with energy, the values found must certainly be those appropriate to an energy within 4 meV of this figure. When an attenuator was in position a proton which had registered a double coincidence DE could make a nuclear collision in the attenuator and so give rise to an anti-coincidence DE, - F. This happened if the event was an elastic scattering collision through an angle greater than θ , or an absorptive collision in which no charged secondary was emitted at an angle less than θ with energy sufficient to reach the scintillator.

The cross section for making a collision causing an anti-coincidence will be called the loss cross section σ_1 ; it is clearly a function of θ or, more conveniently, of the solid angle Ω subtended by the scintillator at the attenuator.

Measurements were made with each attenuator at various distances from the scintillator, so that σ_1 was found for several values of Ω ranging from 0.096 to 2.08 steradians ($10^\circ \leq \theta \leq 48^\circ$). The number of charged secondaries collected, and hence σ_1 , depended also on the thickness of material in front of the scintillator counter. Sometimes a 5.81 g cm⁻² copper absorber H was put immediately in front of the counter to stop short range secondaries.

The intensity of the primary proton beam was also varied, and a small correction for accidental anti-coincidences was found to be necessary.

§ 3. PRINCIPLE OF THE EXPERIMENT

To find σ_a from the measured data, the part of σ_1 due to absorptive collisions has to be recognized and then extrapolated to the $\Omega = 0$ axis, so as to eliminate altogether the effect of charged secondaries. The process is made possible by the fact that at the energy of this experiment the angular spread of the diffraction pattern ($\sim \lambda/2\pi R$) is much smaller than that of the secondaries from absorptive collisions. The r.m.s. width of the diffraction pattern of copper, for example, is about 8° , whereas the r.m.s. angle of emission of secondaries is 30° or more (Hadley and York 1950, Miller, Sewell and Wright 1951, Snowden 1952, Hofmann and Strauch 1953).

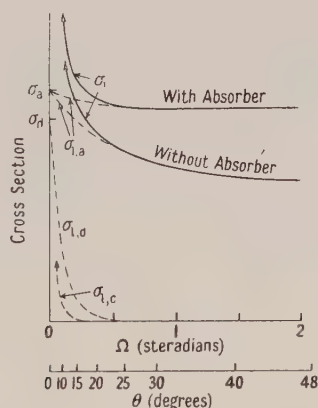


Figure 2. Typical behaviour of the three contributions to the loss cross section.

Figure 2 shows the expected behaviour of the various components. When $\Omega = 0$, the contribution $\sigma_{1,a}$ of absorptive collisions to σ_1 is of course equal to σ_a , the total absorption cross section. As Ω increases, $\sigma_{1,a}$ drops slowly because charged secondaries are collected in increasing numbers, determined in part by the absorber in front of the scintillation counter. Again, when $\Omega = 0$, the diffraction contribution $\sigma_{1,d}$ is equal to σ_d , the total diffraction cross section. It falls much more rapidly than $\sigma_{1,a}$, as already mentioned. Finally, there is a small angle contribution $\sigma_{1,c}$ caused by coulomb scattering, especially in the heavy elements. The full lines show $\sigma_1 = \sigma_{1,a} + \sigma_{1,d} + \sigma_{1,c}$ with and without the absorber H; it is these lines that are actually determined by experiment.

When working back to σ_a from measured values of σ_1 as a function of Ω , the necessary extrapolation is closely guided by the following considerations:

(i) The diffraction contribution $\sigma_{1,d}$ should have an appropriate angular spread. For the present purpose it is quite accurate enough (Bratenahl, Fernbach,

Hildebrand, Leith and Moyer 1950) to assume that the differential diffraction scattering cross section is proportional to $[J_1(2kr \sin \frac{1}{2}\theta)/(kr \sin \frac{1}{2}\theta)]^2$ where $2\pi r^2$ is the neutron total cross section at 134 mev of the element concerned.

(ii) From the definition of $\sigma_{1,a}$ it is clear that $-\dot{\sigma}_{1,a}/d\Omega$ at any angle is nearly equal to the differential cross section at that angle for the emission of charged secondaries with range sufficient to reach the scintillator. The correspondence is not quite exact for two reasons; in some events a secondary was lost by nuclear absorption, and in others two charged particles from the same collision reached the scintillator. But $-\dot{\sigma}_{1,a}/d\Omega$ certainly has to change quite slowly as Ω increases, and its value at $\Omega = 0$ must be comparable with the differential cross section for the production of neutron secondaries at about the same energy (Randle, Cassels, Pickavance and Taylor 1953). The results of Snowden (1952), and others, show that it should fall to about half its initial value at $\theta = 25^\circ$ (absorber H out) or 15° (absorber H in). In practice these conditions severely restrict the maximum value of σ_a allowed by the experimental data.

(iii) A useful lower limit to σ_a is set by the value of σ_1 for large Ω , with the absorber in.

§4. EVALUATION OF LOSS CROSS SECTIONS

Ideally the fraction of the double coincidences accompanied by an anti-coincidence should have been $1 - \exp(-n\sigma_l)$ when an attenuator of surface density n atoms cm^{-2} was in position, and zero otherwise. A typical value of $n\sigma_1$ was about 5%. In fact, however, there was a background of anti-coincidences with the attenuator out; these were caused by losses in the aluminium wall of the scintillation counter ($\sim 0.45\%$) and slit scattering at BC ($\sim 0.95\%$). Moreover the slit scattering also produced some ($\sim 0.65\%$) abnormally low energy protons which had sufficient range to reach the scintillator only if no attenuator was present. This pernicious type of background was shown up by re-measuring the attenuation of a sample with some scattering material placed at A to increase the amount of slit scattering. A correction could then be calculated by making the reasonable assumption that the number of low energy protons produced was proportional to the number lost altogether.

When the absorber was placed in front of the scintillation counter, an additional correction had to be made for losses there. Most of these were the result of nuclear collisions in the copper, but some were caused by the slit scattering effect already discussed. The correction for the nuclear collisions was so chosen that the differences in loss cross sections, measured with and without absorber, tended to zero at $\Omega = 0$. In the light of the results of the whole experiment, the correction turns out to be quite consistent with the loss cross section to be expected for copper at approximately 100 mev and $\Omega = 2\pi$.

The corrections for low energy slit scattered protons were of the order of 15%, and it seemed reasonable to give the loss cross sections a standard error of 6% on that account. The statistical errors of counting were relatively small.

A further substantial allowance for error was made when extrapolating $\sigma_{1,a}$ to the $\Omega = 0$ axis. This was more important for the smallest nuclei, whose diffraction patterns had the largest angular spread. It was considered that the extrapolation was unreasonable when $-\dot{\sigma}_{1,a}/d\Omega$, without absorber, fell to half its value at $\theta = 15^\circ$. The change in σ_a brought about by such an extrapolation was regarded as a standard error, which was compounded with the other errors in the usual way.

§ 5. RESULTS

The results of the measurements are displayed in figures 3(a)–(e), which should be compared with figure 2 and the discussion of § 3. The extrapolations shown lead to the values of σ_a given in the table, where all cross sections are given in millibarns (1mb (or mbn) = 10^{-27} cm). The table also contains the results of Lees *et al.* for the light and heavy constituents of photographic emulsion; the two sets of results seem to be in tolerable agreement.

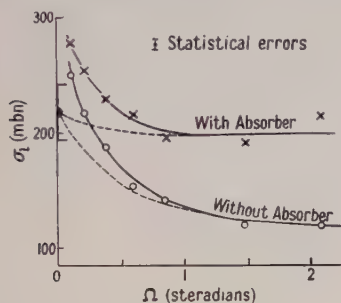


Figure 3(a). Carbon.

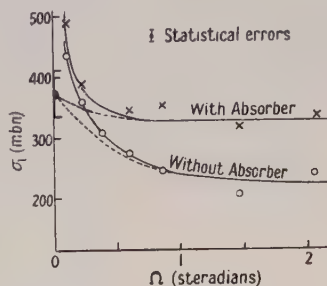


Figure 3(b). Aluminium.

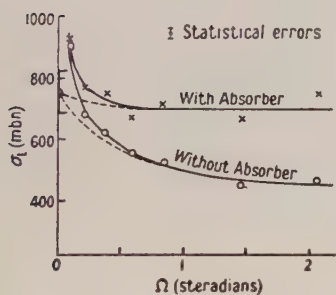


Figure 3(c). Copper.

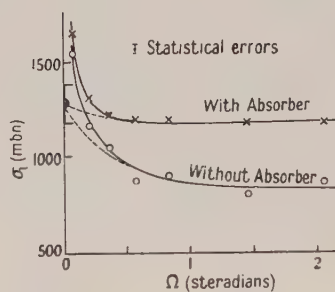


Figure 3(d). Cadmium.

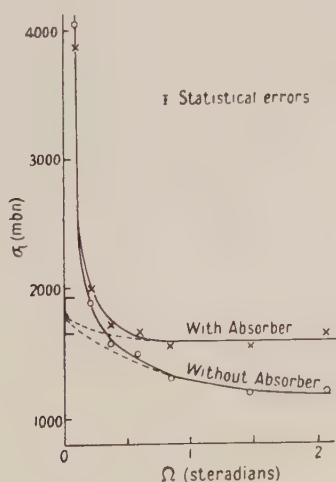


Figure 3(e). Lead.

Figures 3(a)–(e). Experimental loss cross sections for carbon, aluminium, copper, cadmium and lead.

Element	A	Energy (MeV)	Reference	Absorption cross section (mbn)
Carbon	12	134 ± 4	This paper	220 ± 24
Aluminium	27	134 ± 4	" "	373 ± 37
Copper	63.6	134 ± 4	" "	752 ± 68
Cadmium	112.4	134 ± 4	" "	1286 ± 103
Lead	207.2	134 ± 4	" "	1782 ± 143
Photographic emulsion				
Light (C, N, O)	12, 14, 16	130	Lees <i>et al.</i>	160 ± 70
Heavy (Br, Ag)	79.9, 107.9	130	" "	1280 ± 160

§ 6. DISCUSSION

According to the optical calculations reviewed in § 1, the absorption cross section should be given by the equation (Bethe 1940, Fernbach *et al.* 1949).

$$\sigma_a = \pi R^2 \left(1 - \frac{W}{E}\right) \left[1 - \frac{1 - (1 + 2KR)e^{-2KR}}{2K^2 R^2}\right] \dots\dots(1)$$

where E is the energy of the bombarding protons and $W = Ze^2/R$ is the coulomb barrier height. Skyrme (private communication) has suggested the inclusion of the factor $1 - W/E$ to correct approximately for the small effect of coulomb repulsion ($\sim 10\%$ for lead); classically, a proton of impact parameter $R(1 - W/E)^{1/2}$ passes at a distance R from a nucleus of charge Z . It should be remarked that the same formula (1) could be obtained by a purely classical argument, since the wavelength of the protons (and hence \hbar) does not enter explicitly into it. This is in contrast to the corresponding expression for σ_d , which is not required, however, in the present paper.

The theoretical value of K , as deduced from free two-body scattering data, is given by

$$K_{th} = \frac{3}{4\pi R^3} [(A - Z) \sigma_{np} \alpha_{np} + Z \sigma_{pp} \alpha_{pp}] \dots\dots(2)$$

where σ_{np} and σ_{pp} are the total cross sections for free n, p and p, p scattering respectively, and α_{np}, α_{pp} are factors which allow for the effect of the exclusion principle on the motion of nucleons inside the nucleus.

Goldberger (1948) has described how these exclusion principle factors may be evaluated, albeit by a very crude classical argument. If the free two-body scattering is isotropic, as p - p scattering actually is at this energy (Birge, Kruse and Ramsey 1951, Cassels, Stafford and Pickavance 1952), then

$$\alpha_{pp} = 1 - \frac{7}{5} \left(\frac{F_p}{E + F_p + B} \right) \dots\dots(3)$$

where F_p is the Fermi energy of the protons in the nucleus, $(\hbar^2/2M)(9\pi Z/4R^3)^{2/3}$, and B is the binding energy of the incoming proton.

The estimation of α_{np} was complicated by the fact that n - p scattering is anisotropic, with maxima at 0° and 180° , just where the effect of the exclusion principle is most serious. After inspection of the experimental angular distribution at about this energy (Randle, Taylor and Wood 1952) it seemed reasonable to put

$$\alpha_{np} = 1 - \frac{7}{5} \left(\frac{0.64F_n}{E + F_p + B} + \frac{0.96F_p}{E + F_p + B} \right) \dots\dots(4)$$

with F_n the Fermi energy of the neutrons in the nucleus $(\hbar^2/2M)[9\pi(A - Z)/4R^3]^{2/3}$.

The two terms in the brackets refer to scattering near 0° and 180° respectively, and the numerical factors are intended to take into account the increase, as compared with σ_{np} , 4π , of the n, p differential cross section in the regions of interest.

The internal n - p collisions take place with relative momenta corresponding to a considerable range of energy around $E + F_p + B$, and the average σ_{np} over this range was taken to be 50 mbn (Taylor, Pickavance, Cassels and Randle 1951, Taylor and Wood 1953). The value of σ_{pp} was put at $2\pi \times 4.9 = 31$ mbn (Cassels *et al.* 1952). If it is less than this (Chamberlain, Segrè and Wiegand 1951), K_{th} would not be very seriously affected because the n, p term in (2) is the more important one.

Figure 4 shows the nuclear radius as a function of $A^{1/3}$ according to an analysis by Feshbach and Weisskopf (1949) of 14 and 25 mev neutron total cross sections (Amaldi, Bocciarelli, Cacciapuotì and Trabacchi 1946, Sherr 1945). The

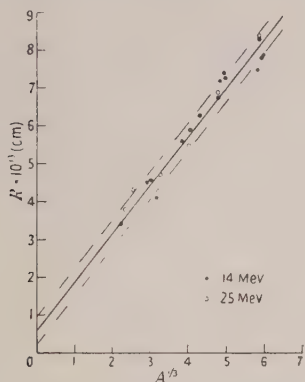


Figure 4. Nuclear radii deduced from 14 and 25 mev neutron total cross sections.

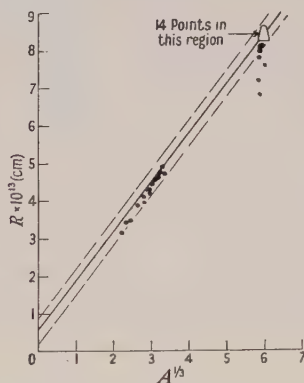


Figure 5. Nuclear radii deduced from coulomb energies of mirror nuclei, and lifetimes against α -decay. The lines are taken from figure 4.

straight line, $R = (0.57 + 1.30 A^{1/3}) \times 10^{-13}$ cm, was fitted by the method of least squares, and the broken lines indicate the standard deviation of the individual points. These lines are included in later figures to act as a standard of comparison.

Some recent measurements (Nereson and Darden 1953) of fast neutron total cross sections up to 12 mev seem to need a theoretical interpretation qualitatively different from that generally accepted in 1949. It is reasonable to hope that, when these results are fully understood, the deduced nuclear radii will not be very much changed.

Figure 5 shows the nuclear radii suggested by studies of 13 mirror nuclei (Wilson 1952, Table III, column 5) and 22 α -active nuclei (Blatt and Weisskopf 1952). The agreement with the data of figure 4 is good, apart from a few exceptions among the α -active nuclei, which are thought to be caused by difficulties of interpretation rather than real anomalies in radius.

Figure 6 shows the nuclear radii implied by the present inelastic cross section results, if it is assumed that K is in fact equal to the K_{th} given in eqn (2). It will be seen that these radii are perfectly consistent with those shown in figures 4 and 5. It follows that the optical theory as usually developed has given results in excellent agreement with observation.

In order to investigate the sensitivity of this test, the nuclear radii were twice recalculated, with the assumptions that $K = 1.4 K_{th}$ and $K = 0.7 K_{th}$ respectively.

The results are shown in figures 7 and 8, where the fit might be described as just tolerable.

Some recent experiments on mesic atoms (Rainwater and Fitch 1953) suggest that the effective radii of nuclei are about 15% smaller than those given in figures 4-6. If this should be confirmed, then it would be necessary to increase K very considerably, and even then a perfect fit for lead could not be obtained within the framework of the present theory, because the inelastic cross section (1) cannot be greater than $\pi R^2(1 - W/E)$.

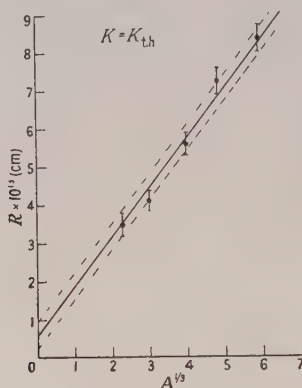


Figure 6. Nuclear radii deduced from the inelastic cross sections given in the table, on the assumption that $K = K_{th}$. The lines are taken from figure 4.

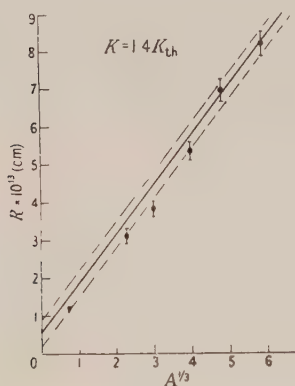


Figure 7.

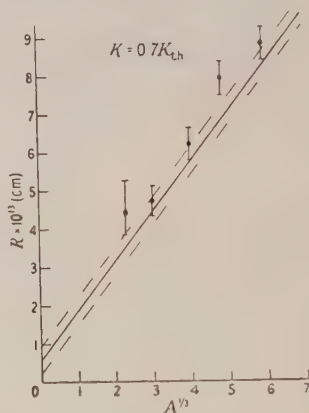


Figure 8.

Figures 7 and 8. Nuclear radii deduced on the assumptions that $K = 1.4 K_{th}$ and $K = 0.7 K_{th}$ respectively.

An increase in K would of course correspond to a decrease of the mean free path of high energy protons inside nuclei. This might be the result of many-body interactions, which have not been taken into account in (1). With the usual nuclear radii the present results suggest that many-body interactions are unimportant, but the point will have to be looked at again when the mesic atom results have been collated with the rest of the data concerning nuclear radii.

The discussion given here has been based on the assumption that the density inside a nucleus is more or less uniform. Obviously some surface shading must occur, and it is indeed assumed in the optical calculations so that the reflection of incoming nucleons at the surface can be neglected. Some recent electron scattering

experiments (Hofstadter *et al.* 1953) suggest an exponential distribution of the nuclear protons with radius to explain the absence of secondary diffraction maxima. At first sight this seems to conflict with the proton scattering work of Richardson, Ball, Leith and Moyer (1952), but at any rate there is more than a possibility that the density of nuclei is quite non-uniform. The effective radius (i.e. that radius which is calculated on the assumption of uniform density) will then depend on the process by which it is determined. It is probable that the effective radii for fast neutron cross sections, for α -decay, and for the present inelastic cross sections will remain quite closely equal. An example concerning the coulomb energy of mirror nuclei has already been worked out by Wilson (1952). However, this whole question also needs examination, in the light of the electron scattering results.

ACKNOWLEDGMENTS

The authors wish to thank Mr. P. H. Bowen for much assistance in taking the measurements, and Mr. A. O. Edmunds and the cyclotron crew for their willing co-operation. They have enjoyed valuable discussions of the results with Drs. F. Mandl and T. H. R. Skyrme, and with the Director, Atomic Energy Research Establishment.

This paper is published by permission of the Director, A.E.R.E.

REFERENCES

- AMALDI, E., BOCCIARELLI, D., CACCIAPUOTI, B. N., and TRABACCHI, G. C., 1946, *Nuovo Cim.*, **3**, 203.
 BETHE, H. A., 1940, *Phys. Rev.*, **57**, 1125.
 BIRGE, R. W., KRUSE, U. E., and RAMSEY, N. F., 1951, *Phys. Rev.*, **83**, 274.
 BLATT, J. M., and WEISSKOPF, V. F., 1952, *Theoretical Nuclear Physics* (New York : Wiley).
 BRATENAHL, A., FERNBACH, S., HILDEBRAND, R. H., LEITH, C. E., and MOYER, B. J., 1950, *Phys. Rev.*, **77**, 597.
 CASSELS, J. M., STAFFORD, G. H., and PICKAVANCE, T. G., 1952, *Proc. Roy. Soc. A*, **214**, 262.
 CHAMBERLAIN, O., SEGRÈ, E., and WIEGAND, C., 1951, *Phys. Rev.*, **83**, 923.
 DEJUREN, J., 1950, *Phys. Rev.*, **80**, 27.
 DEJUREN, J., and KNABLE, N., 1950, *Phys. Rev.*, **77**, 606.
 FERNBACH, S., SERBER, R., and TAYLOR, T. B., 1949, *Phys. Rev.*, **75**, 1352.
 FESHBACH, H., and WEISSKOPF, V. F., 1949, *Phys. Rev.*, **76**, 1550.
 GOLDBERGER, M. L., 1948, *Phys. Rev.*, **74**, 1269.
 HADLEY, J., and YORK, H., 1950, *Phys. Rev.*, **80**, 345.
 HOFMANN, J. A., and STRAUCH, K., 1953, *Phys. Rev.*, **90**, 449.
 HOFSTADTER, R., FECHTER, H. R., and MCINTYRE J. A., 1953, *Phys. Rev.*, **91**, 422.
 JASTROW, R., 1951, *Phys. Rev.*, **82**, 261.
 LAWSON, J. D., 1953, *Phil. Mag.*, **44**, 102.
 LEES, C. F., MORRISON, G. C., MUIRHEAD, H., and ROSSER, W. G. V., 1953, *Phil. Mag.*, **44**, 304.
 MANDL, F., and SKYRME, T. H. R., 1953, *Phil. Mag.*, **44**, 1028.
 MILLER, R. D., SEWELL, D. C., and WRIGHT, R. W., 1951, *Phys. Rev.*, **81**, 374.
 NERESON, N., and DARDEN, S., 1953, *Phys. Rev.*, **89**, 775.
 RAINWATER and FITCH, 1953, Press release reviewed in *Nature, Lond.*, **171**, 1097.
 RANDLE, T. C., CASSELS, J. M., PICKAVANCE, T. G., and TAYLOR, A. E., 1953, *Phil. Mag.*, **44**, 425.
 RANDLE, T. C., TAYLOR, A. E., and WOOD, E., 1952, *Proc. Roy. Soc. A*, **213**, 392.
 RICHARDSON, R. E., BALL, W. P., LEITH, C. E., and MOYER, B. J., 1952, *Phys. Rev.*, **86**, 29.
 SHERR, R., 1945, *Phys. Rev.*, **68**, 240.
 SNOWDEN, M., 1952, *Phil. Mag.*, **43**, 285.
 TAYLOR, A. E., PICKAVANCE, T. G., CASSELS, J. M., and RANDLE, T. C., 1951, *Phil. Mag.*, **42**, 328.
 TAYLOR, A. E., and WOOD, E., 1953, *Phil. Mag.*, **44**, 95.
 WILSON, R. R., 1952, *Phys. Rev.*, **88**, 350.

Emission of Electron-Positron Pairs from Light Nuclei I: Monopole Transition in ^{16}O *

BY S. DEVONS, G. GOLDRING† AND G. R. LINDSEY‡

Department of Physics, Imperial College, London

MS. received 21st August 1953, and in amended form 30th October 1953

Abstract. An apparatus is described for measuring the angular correlation of electron-positron pairs from light nuclei. The apparatus has been used to study the pairs emitted in the mono-pole transition from the first excited state of ^{16}O . Measurements are also described of the excitation function for this state of ^{16}O in the reaction $^{19}\text{F}(\text{p}, \alpha)^{16}\text{O}$, and of the absolute probability (half-life) of the mono-pole transition.

§ 1. INTRODUCTION

THE study of electron pair creation in high-energy electromagnetic transitions in light nuclei is a direct, and in principle generally applicable, method of studying the properties of such transitions. The probability of pair emission is, however, very small compared with that of γ -radiation for typical transition energies (up to 20 mev), which makes the measurements technically difficult. Previous work (e.g. Thomas and Lauritsen 1952) has been concerned mainly with measuring the relative probabilities for γ and pair-emission, 'pair-coefficient', either averaged over all positron-electron energies, or differentially by spectrometric analysis of the positron continuum. These methods require careful absolute measurements since the pair coefficient changes only by some 10 to 20 per cent for different successive multipole orders. Moreover when, on account of the method of excitation, the intensity of radiation from the emitting nucleus is not isotropic, the ordinarily calculated pair coefficient is insufficient if the pair emission is only measured in a particular direction.

In the present work, which is concerned with transitions immediately following nuclear reactions, we have concentrated our attention on the angular correlation of electrons and positrons, since this characteristic does not involve absolute intensity measurements, and, in some respects, provides better discrimination than these latter, between different multipole transitions. The theory of this correlation has been given by Rose (1949) in a general form involving approximations which should be well satisfied for the particular processes we have measured. The calculations have been extended to include cases where the radiation is not emitted isotropically (Goldring 1953). For the transition energies and nuclei with which we shall be concerned, the theory indicates that by far the major part of the electromagnetic field which is effective in producing pairs is outside the nucleus, where the usual multipole representation of the field is a good approximation, and that there is only a small contribution to the process from the

* This work was begun at the Cavendish Laboratory, Cambridge, and completed at Imperial College, London.

† Now at the Hebrew University, Jerusalem.

‡ Now at National Defence Research Council, Ottawa, Canada.

internal field. Neglecting this latter, a transition from a definite initial quantum-mechanical state (including magnetite quantum number) to a similar final one is characterized by a definite relative probability of γ -radiation to pair emission and specific angular correlation of electrons and positrons, the undefined quantity being the absolute probability, or lifetime, for the process.

In one particular case, a transition between two states both $J=0$ and even parity, there is no electromagnetic field external to the nucleus, and the internal field is of a very simple form—purely radial. Also for this special ‘mono-pole’ transition many detailed refinements of the theory have been evaluated (Dalitz 1951), and the absence of competing γ -radiation for the transition, together with the consequent high intensity of pairs, makes this a very favourable case for which to make accurate comparison with the theory. However, it should be pointed out that agreement with theory in this case provides no justification for at least one approximation made in the general case—neglect of the contribution from the internal field. There may be other approximations which have differing validity for the spherically symmetrical and general multipole field.

§ 2. EXCITATION OF PAIR-EMITTING STATE OF ^{16}O

The well-known first excited state of ^{16}O ($J=0$, even, at 6.06 mev, see Ajzenberg and Lauritsen 1952) goes to the ground state by pair emission. This transition, which can be readily excited in the reaction $^{19}\text{F}(\text{p}, \alpha)^{16}\text{O}^*$, was chosen for a detailed study of the angular correlation of the pairs. The absolute probability of this process was also measured. With proton energies in the range 0.5–1.5 mev the above reaction is accompanied to some degree by the reactions $^{19}\text{F}(\text{p}, \alpha)^{16}\text{O}^+$, where $^{16}\text{O}^+$ represents one of the γ -emitting levels of ^{16}O in the energy range 6–7 mev. The variation of cross section with proton energy is quite different for the two processes, but since the maximum cross section for production of $^{16}\text{O}^+$ is many times greater than that for $^{16}\text{O}^*$, it is necessary to find the optimum proton energy, where the disturbance produced by the γ -radiation from $^{16}\text{O}^+$ is a minimum. It is necessary to know the magnitude and nature of this disturbance if accurate measurements are attempted. Detailed measurements were therefore made of the cross section for the two processes.

A simple arrangement of target and counters was used as shown in figure 1. The target (CaF_2) was deposited by vacuum-evaporation on a thin foil of aluminium (0.15 mg cm^{-2}). The target foil was then mounted in an aluminium cylinder, with wall thickness, in the centre portion of 0.1 mm. This was thin enough to allow most of the electrons and positrons to pass through and be detected in the Geiger counters a, b. These were of very light construction, to reduce their response to γ -radiation, and with wall thickness of 0.1 mm at the sensitive region. The counters were arranged to detect coincidence counts, and a third similar counter c was used in anti-coincidence, to avoid registering as pairs, single electrons which have scattered in the walls of one of the counters a, b, and detected in both. The intensity of γ -radiation was monitored simultaneously with these measurements of the pairs, and since the accurate values of the proton energies for resonances emitting γ -rays have been published by several investigators, an accurate energy scale could be established in this way. The proton beam was magnetically analysed and was mono-energetic to about $\pm 1 \text{ kev}$.

To determine the absolute cross section for the process $^{19}\text{F}(\text{p}, \alpha)^{16}\text{O}^*$ it was necessary to estimate the thickness of the targets used. These were about

3 kev stopping power (for 873 kev protons), and the most reliable estimates of thickness were obtained by comparing the yield of γ -radiation from them at the 873 kev γ -resonance with the yield from thick CaF_2 targets. In addition, the effective solid angles and efficiencies of the Geiger counters were also required. To within the accuracy that was significant these factors could be determined by comparison of the actual coincident counting rate ($a+b$) with the single electron counting rate (a or b), together with a measurement of the variation of the coincidence rate with θ , the angle between the radii from the target to the centres of the two counters. (This latter measurement gave a preliminary result for the angular correlation of electron and positron, but a much more accurate measurement is described below.) The calibration of these counters was, of course, made at a proton energy where the ratio of cross sections for pair production and γ -radiation was most favourable (about 840 kev), and effects in the electron counters were due almost entirely to pairs.

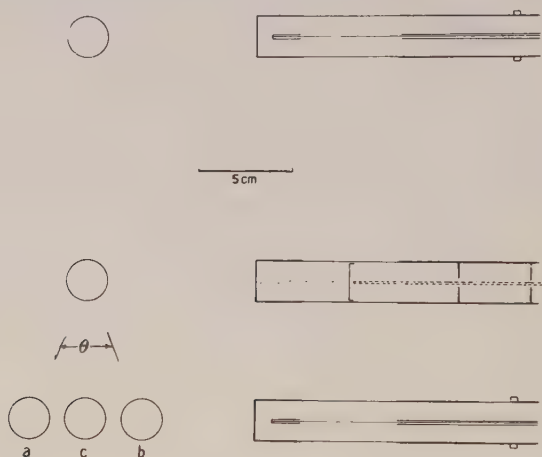


Figure 1. Apparatus for measuring the excitation function for pair production.

The results of these measurements for protons of 600–1300 kev are shown in figure 2. Proton beams of about $1 \mu\text{A}$ were used and measured with a calibrated current integrator (accuracy to within about 2%). The simultaneous measurements of the γ -radiation yield, after allowance has been made for the radiation emitted from the supporting aluminium foil, is shown in the same diagram.

The results are in general agreement with previous measurements (Streib *et al.* 1941, Phillips and Heydenburg 1951), although they reveal more detail: in particular, the peak at about 780 kev was observed with all sufficiently thin targets. The variation of the cross section for pair-production shows clearly superimposed on an excitation function which we interpret as that for $^{19}\text{F}(p, \alpha)^{16}\text{O}^*$, peaks associated with the γ -emitting states $^{16}\text{O}^+$, due to internal-conversion electrons in these transitions. There is also a small contribution ($\sim 10\%$) at these energies due to externally produced pairs in the walls of the target chamber. One cannot, from these measurements alone, exclude the possibility that the peaks in the pair cross section at the energies of the γ -resonances contain some contribution from excitation of the pair-emitting state $^{16}\text{O}^*$. Comparison of the relative cross sections, and remembering that

the internal pair coefficients are of the order 10^{-3} , shows, however, that the relative probability, for these resonances, of producing $^{16}\text{O}^+$ and $^{16}\text{O}^*$ must be at least 2000:1.

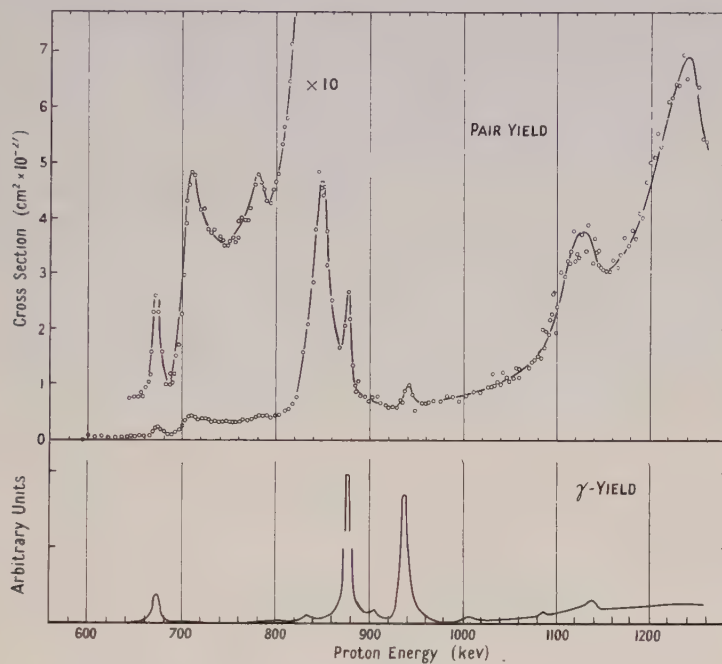


Figure 2. Excitation function for pair production.

Our interest here is primarily with the choice of a suitable proton energy for studying the $^{16}\text{O}^* \rightarrow ^{16}\text{O}$ transition, with as little interference as possible from γ -radiation and associated pairs. A proton energy of 840 kev was chosen for most of these measurements.

§ 3. ANGULAR CORRELATION OF ELECTRONS AND POSITRONS

To eliminate, as far as possible, the scattering of the pair particles in material in the neighbourhood of the emitting source (the target of CaF_2) the whole of the source and detecting apparatus, including the beam defining slits, target support and Geiger counters, was arranged inside a large evacuated chamber. To reduce still further any disturbing effects, the electrons were detected by a pair of simple counter telescopes, each composed of two cylindrical thin-walled counters. The general arrangement is shown in figure 3.

The vacuum envelope consisted of a heavy steel plate A, 20 in. diameter and 1 in. thick, to which a removable spun-aluminium dome ($\frac{1}{8}$ in. thick) was sealed with a neoprene gasket. The proton beam entered through the centre of the base plate and was defined, by the slits S, to within ± 1.5 mm of the central axis, and normally fills this aperture uniformly. The target support T was an aluminium foil of thickness 0.2 mg cm^{-2} mounted on two parallel nichrome wires 0.002 in. diameter and 2 in. apart. These wires were attached at one end to a drum D which could be rotated from outside the vacuum vessel, and at the other end were held taut by a spring. In this way the part of the target material being bombarded

could be readily changed, either because the target spot had deteriorated under prolonged bombardment or to measure some background effect; and the position of the target was accurately located despite the flimsy nature of its support. The proton beam struck the target foil at 45° .

One pair of the electron detecting counters, c, C, was mounted on an arm that could be rotated from outside about an axis coincident with the proton bombarding beam, and the other pair was mounted in a fixed position. All four counters were mounted on light Perspex guides, enabling them to be accurately aligned, and permitting their radial positions to be varied. A fifth counter, G, shielded with 1 cm thickness of lead and mounted some distance away from the target, was used to monitor the intensity of γ -radiation during the observations. The vacuum chamber was fitted with a small movable furnace E, which could be used to evaporate material on to the target foil *in situ*, and withdrawn after use. It was not used for evaporation in the present experiments, and the furnace was replaced by a small rectangular brass strip, mounted on a light wire frame, which could be brought into a position between the target spot and the movable counter telescope. This arrangement was used to measure certain 'background' corrections described below.

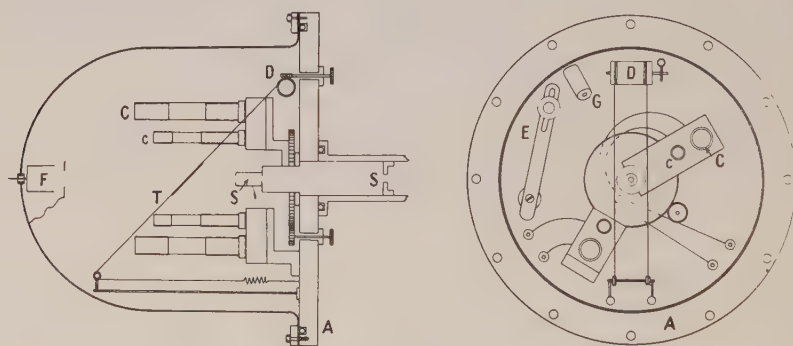


Figure 3. Apparatus for measuring the angular correlation.

The target current was monitored by a Faraday cup F (with an arrangement of guard rings for eliminating the effects of secondary electron emission) connected to 'earth' through a 2 megohm resistance, the voltage across which was amplified and continuously observed on an oscilloscope.

Each electron-detecting telescope consisted of an inner and an outer counter with diameters 2.1 cm and 3.1 cm and effective lengths 5 cm and 7.5 cm respectively. The counter walls were of aluminium 0.3 mm thick, thinned down to 0.1 mm and 0.15 mm respectively over the sensitive region, and internally electroplated with copper to a thickness of 0.005 mm. The actual length of the counters was more than twice the effective length so as to keep the more solid material at the ends, where electrons could be produced or scattered, as far as possible from the sensitive volume.

Since the angular correlation function expected is not completely independent of the partition of energy between electron and positron, it was necessary to know the relative efficiency of the counter telescopes for electrons of different energy, particularly for those of low energy. Measurements of these characteristics were made with a magnetic lens β -spectrometer and a radioactive source of

electrons. The electrons emerged from the spectrometer in an annular cone and traversed the counters at a mean angle equal to that occurring in the actual experiments. Strictly speaking, the efficiency of the counter telescopes should be considered as a function of position and angle of traversal of the counters as well as energy, but it is quite sufficient for the present purpose to consider an average over these variables. The variation of efficiency was measured by comparing both the number n_1 of counts in the front counter, and the number n_2 of coincident counts between the two counters with the number n_0 recorded in a thin (7 mg cm^{-2}) window end-window counter. The minimum electron energy for detection by the end-window counter is much less than for the cylindrical counters, either in coincidence or singly, and it was assumed that its efficiency was constant in the energy region of interest. Hence the quantity $n_2/n_1 \times n_1/n_0$ gives us the required efficiency as a function of energy. Figure 4 shows the experimental measurements. These results require some correction to allow for the additional material between the β -spectrometer proper and the counters, namely the exit window of the spectrometer and 10 cm path in air, a total of 15 mg/cm^{-2} . To make this correction an additional foil of similar superficial density was placed between the exit window and the counters and the modified ratios n_2'/n_0 as function of energy were obtained. By extrapolation the relative efficiency of the arrangement used in the angular correlation experiments was obtained.

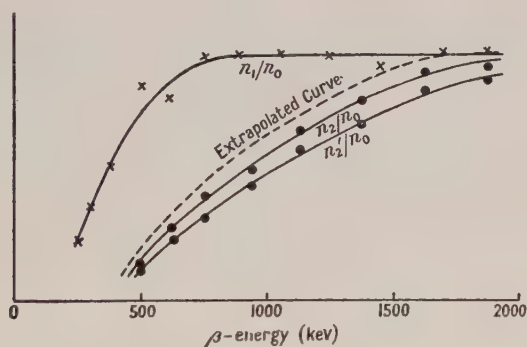


Figure 4. Variation of efficiency with energy of the electron telescopes.

Two different arrangements of counters were used for the correlation measurements. In the first ('close position') the inner counter was 7 cm and the outer 10.5 cm from the target spot, and in the second the distances were 10 cm and 15 cm respectively, so that for both arrangements each counter subtended approximately the same solid angle at the target spot. Coincidences in each pair of counters (resolving time $1 \mu\text{sec}$) and coincidences between the two telescopes were recorded. Random coincidences were estimated by two methods: (a) by introducing a fixed delay time into one channel of a coincidence pair, so as to destroy any real coincidence counts, and measuring the residual coincidence rate; (b) from the observed variation in the intensity of the beam, and the single counting rates in the members of a coincident pair, and the knowledge of the resolving times, the random rate could be estimated. With the actual, small, fluctuations in beam current that occurred during most of the measurements, the second method proved most reliable. Random coincidences only accounted for a small fraction of the total number recorded, and in all cases

the error introduced by the uncertainty in making this correction was much less than the statistical fluctuation in the number of counted pairs.

To measure the angular correlation, the number of counts in the fixed and moving telescopes (F , M) and the number of coincidences T between them

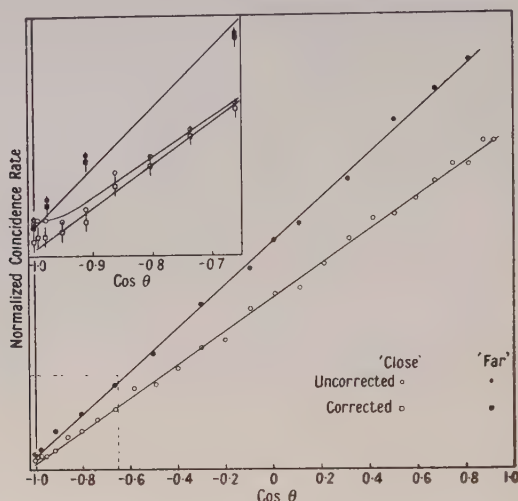


Figure 5. Electron-positron angular correlation.

were measured as a function of θ . This angle was changed frequently and in large steps so as to avoid any systematic errors, such as might arise from small movements of the target spot and slight changes in counting efficiency. These are, in addition, to some extent compensated for in the normalized quantity $T/\frac{1}{2}(F + M)$ which was taken to be the experimental angular correlation function. The experimental results for the two counter arrangements are shown in figure 5. Before comparing these experimental results with theoretical predictions the following corrections and possible sources of error must be considered.

(i) *Scattering in target foil and support.*

The plane of the target foil was 45° to the plane of rotation of counters, an orientation which represented a compromise between minimum material traversed by the electrons, and a small angle between the normal to the foil and the proton beam. With the fixed counter telescope in a suitable position the average thickness of the aluminium target foil traversed was $1.5 \times$ the foil thickness, and the mean angle of scattering, averaged over all electrons of energies which the counters could detect, was estimated to be less than 1° . Since this scattering was symmetrical ($\pm \delta\theta$) its effect on the angular correlation function was quite negligible with the experimental accuracy achieved. Pair production in the target foil and supports by γ -radiation present was of quite negligible intensity.

(ii) *Geometry.*

The counters were aligned parallel to the beam axis to within $\frac{1}{2}\%$, the distance of the counters from the centre of the target spot was set to 0.02 cm, and the angle θ between the radii to the two telescopes could be read to $\frac{1}{3}^\circ$ or better. The effective centre of the target spot was estimated to move at most 0.05 cm from the mean position. Systematic errors due to these factors were considered negligible. Random errors are revealed in the individual observations.

(iii) *Cosmic radiation.*

Discharges of all four counters, due to cosmic radiation and other background radiation not arising from the target bombardment, were measured for several hours. To reduce the contribution from this source to a minimum the apparatus was arranged so that when all four counters were collinear they were in a horizontal plane.

(iv) *Background from target support.*

The effects produced when the aluminium foil, without evaporated CaF_2 , was bombarded were found to be less than 1/2000 of the pairs from the target itself.

(v) *'Stray' electrons.*

Spurious coincidences between the two telescopes could be produced (a) if one member of a pair passes through one telescope and either this electron or its partner, after scattering in the counter walls or neighbouring material, passes through the other telescope, (b) an electron or pair created in the surroundings by the background γ -radiation passed through both telescopes. Both these effects are absolutely greatest near $\theta = \pi$, when all four counters are collinear, and here also the true effect is smallest. To obtain reliable data near $\theta = \pi$ it was necessary to establish the magnitude of these stray effects with an accuracy comparable with that of the measured total effect. This was done by interposing a small brass plate $1 \text{ cm} \times 2.5 \text{ cm}$ and 2 mm thick between the target spot and the movable telescope, placed in the $\theta = \pi$ position. Viewed from the target spot, this plate completely obscured the movable counter telescope (in fact it reduced the counting rate in this telescope by a factor of 25), whereas viewed from most other, distant, points which might act as sources or scattering points for electrons it only obscured about one quarter of this telescope. Coincidence counts between the two telescopes with this 'shadow' plate in position are due, then, chiefly to electrons passing through the fixed telescope, together with a few true pairs. Other effects could be estimated, and appeared to contribute less than 10% of this source of stray coincidences. Measurements of the variation of the number of stray coincidences with and without the 'shadow' plate, near $\theta = \pi$, and for both the 'close in' and 'far out' counter positions, confirmed this interpretation of the origin of the major part of these stray effects and allowed the proper corrections to be made.

(vi) There is a very small contribution to the observed pairs from internally converted γ -rays from the reaction $^{19}\text{F}(\text{p}, \alpha)^{16}\text{O}^+$, although the proton energy chosen was well removed from the γ -resonance. From the monitored intensity of γ -radiation and from estimates of the number and angular correlation of the pairs associated with these γ -transitions a correction of adequate accuracy could be applied.

The result of correcting the observations for cosmic-ray background, 'stray' electrons, background from the aluminium foil, and pairs associated with γ -transitions ((iii), (iv), (v) and (vi)) are shown in figure 5. Results for both geometrical arrangements are consistent with a correlation function of the form $A(1 + \alpha_{\text{exp}} \cos \theta)$. The values of α_{exp} are :

$$\alpha_{\text{exp, F}} = 0.980 \pm 0.009 \quad (\text{'far out'})$$

$$\alpha_{\text{exp, C}} = 0.948 \pm 0.012 \quad (\text{'close in'}).$$

Comparison with Theory

Assuming both excited state $^{16}\text{O}^*$ and ground state ^{16}O have even parity, and the interaction with the electron-positron field is electromagnetic, the correlation function for the zero-pole transition is (Oppenheimer 1941, Dalitz 1951), in first order :

$$P(\theta) dW_+ d\Omega = \frac{e^4 \langle M \rangle^2}{9\pi} p_+ p_- (W_+ W_- - 1 + p_+ p_- \cos \theta) dW_+ d\Omega$$

where p_{\pm} , W_{\pm} are the momenta and energies (rest mass of electron m_0 and velocity of light c both unity) of electron and positron. $\langle M \rangle$ is the nuclear matrix element, independent of θ , $W_0 (= W_+ + W_-)$ is the energy of the nuclear transition.

The measured correlation function is given by

$$\int d\Omega_+ d\Omega_- dW_+ \eta(W_+) \eta(W_-) P(\theta); \quad W_+ + W_- = W_0$$

where $\eta(W_{\pm})$ represents the (relative) efficiency of each counter telescope as a function of energy, and the integrations are over the whole range of energies and solid angles, and θ corresponding to the actual sizes of the counters used. The result of calculating these integrals by approximate and numerical methods is that the correlation function to be expected with the given counters and geometry is of the form $P'(\theta) = A\{1 + (0.9937 - \delta)\cos\theta\}$. δ depends on the geometry alone ($\delta=0$ for infinitesimally small counters), and the theoretically predicted results are :

$$P_F'(\theta) \propto 1 + (0.974 \pm 0.002) \cos \theta \quad (\text{'far out'})$$

$$P_C'(\theta) \propto 1 + (0.955 \pm 0.003) \cos \theta \quad (\text{'close in'}).$$

The errors in the 'theoretical' results are mainly due to uncertainties in the exact dimensions of the sensitive areas of the telescopes.

Comparing these results with the experimental ones, we see that both measurements are separately consistent with theoretical prediction, and the mean difference between theory and experiment in the value of α , -0.002 ± 0.008 , is not significantly different from zero. Earlier measurements of this correlation function (Devons and Lindsey 1949, Phillips and Heydenburg 1951) had indicated the possibility of some discrepancy between theory and experiment, which must, in the light of the present experiments, be attributed to the inadequacy of the experimental arrangements used.

The theoretical expression for $P(\theta)$ quoted above is derived from the Dirac equation for electrons and positrons. Refinements in the theory, including radiation corrections occurring in current quantum-electrodynamics, have been calculated and examined in detail by Dalitz (1951). He finds that the corrections to $P(\theta)$ are very small, of the order $0.002P(\theta)$ at most angles, although an order of magnitude larger, very near $\theta=0$ and near $\theta=\pi$. The increase at $\theta \sim 0$ is due to interaction between electron and positron, and that at $\theta \sim \pi$ is associated with creation of an electron-positron pair together with a photon of comparable energy. Unfortunately, the region near $\theta=0$ is inaccessible with the present technique and the measurements near $\theta=\pi$ are subject to such considerable experimental correction that a test of these small deviations from the Dirac theory was not attempted. The modified theoretical correlation function $P'(\cos\theta)$ is no longer strictly of the form $1 + \alpha \cos\theta$, but if the best fit using a function of this type were taken (neglecting the regions $\theta \sim 0, \pi$), α would only differ from the value in the simple theory by the

order 0.001, and the departure from the simple form would not be detectable with the present experimental accuracy. An increase in accuracy of the order 10 or more, which appears feasible, should enable one at least to discriminate between the simple and refined theories, both of which are consistent with the present experimental results.

§ 4. ABSOLUTE TRANSITION PROBABILITY FOR PAIR EMISSION†

An upper limit to the absolute probability of pair emission can be obtained by measuring the lifetime of the pair-emitting state and, in so far as other competing processes ‡ are not likely to be of comparable probability, this limit will approximate to the actual value. Theoretically, the absolute probability is a measure of the matrix element $\langle M \rangle$, and therefore depends on the details of the nuclear states involved. An order of magnitude estimate of $\langle M \rangle$ on the basis of nuclear dimensions indicates a value of the order 10^{-11} sec for the half-life of the pair-emitting state. The experimental method adopted was capable of measuring a half-life of this order or greater, and consisted essentially of measuring the mean distance travelled by the recoiling $^{16}\text{O}^*$ nucleus, produced in the process $^{19}\text{F}(\text{p}, \alpha)^{16}\text{O}^*$, before emitting the electron pair.

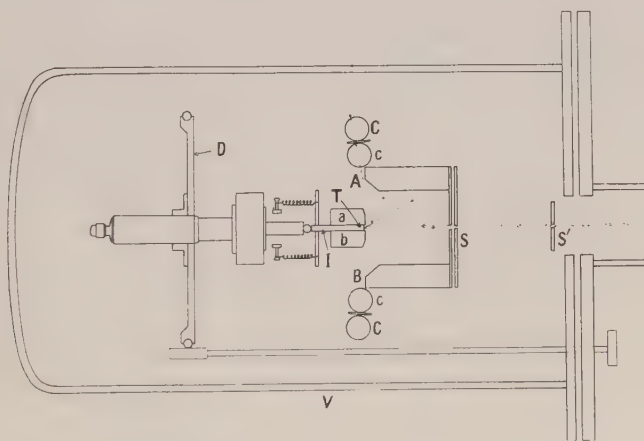


Figure 6. Apparatus for measuring the lifetime for pair emission.

The essential features of the experimental arrangements, which are shown diagrammatically in figure 6, are the defining apertures Aa and Bb, which are accurately coplanar and with parallel edges (in the plane perpendicular to the paper) 5 cm long, and the movable target face T also parallel to the plane Aa Bb; the target was an evaporated layer of CaF_2 on to the face T, which was the end of the invar bar I. The movement of I could be accurately controlled by a micrometer arrangement (operated from outside the vacuum envelope V of the apparatus) so that the plane of T could be brought into coincidence with the aperture plane or withdrawn by a distance of up to several millimetres. The position of the target plane, relative to the aperture plane, could be determined

† A preliminary account of this work has been published (Devons, Hereward and Lindsey 1949).

‡ Double quantum emission is theoretically the most likely competitor. Preliminary measurements (R. Latham and others, unpublished) indicate that probability of this process is at most 10% of that of pair emission.

to about 0.005 mm. The materials and construction of the apertures and target mounting was such that this accuracy was not destroyed by the temperature changes occurring during proton bombardment. The proton beam was defined by the slits S, S' so as to have a cross section of 1.5 mm \times 6 mm on striking centrally the target support T, the cross section of which was 3 mm \times 10 mm.

Electrons passing through the apertures A, B at small angles to the plane AB were detected by the counter pairs cC. Apart from scattered electrons and other stray effects, such electrons could only come from ^{16}O nuclei which were to the right of the plane AB when the pair was emitted. A fifth thin-walled counter (not shown) was placed in a position to the right of the target so as to receive a large flux of electrons. It acted as a monitor of the number of pairs emitted from the target and the change in its solid angle for electron detection, due to small movements in the target, was quite negligible. On the other hand, the number of $^{16}\text{O}^*$ nuclei which can send electrons into the detecting counters clearly depends on the distance of the target face T behind the plane AB, since as this depth increases a larger fraction of the $^{16}\text{O}^*$ nuclei recoiling to the right will have emitted pairs before reaching this plane AB, and also the solid angle subtended by the counting apertures increases with increasing distance beyond the plane at which pair-emission occurs. The actual rate of this decrease with Z (distance of T from AB) is dependent on the mean lifetime τ of the $^{16}\text{O}^*$ state, and hence, by observing the rate of change of the number of electrons detected in cC, as a function of Z , we could obtain a value for τ .

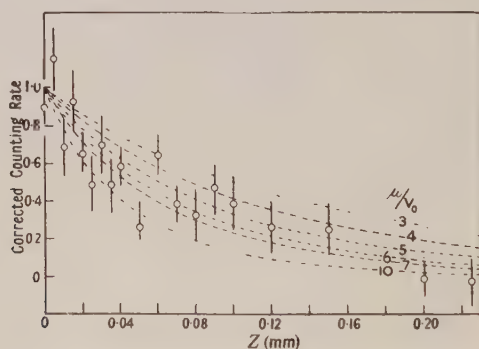


Figure 7. Typical results obtained in the lifetime measurement.

The targets used were about 2 kev thick for the proton energy, 840 kev, used. The proton beam current was of the order $1\mu\text{A}$. The counting rate in cC, normalized by the counting rate in the monitor counter, was measured as a function of Z in some ten independent sets of observations. In all cases the counting decreased with increasing Z from zero to about $\frac{1}{4}$ mm and then remained constant at about half the maximum rate. This 'background' rate was attributed to secondary electrons produced by the substantial background of γ -radiation inevitably present, and, indeed, the change in this background when the proton energy, and thus the γ -intensity, was changed confirmed this.

In figure 7 results are given for a typical set of observations in which the 'background', obtained by measurements at several large values of Z , has been subtracted.

To verify that the observed effects were in fact due to recoiling $^{16}\text{O}^*$ nuclei a thin layer of aluminium, about 0.4 mg cm^{-2} , was evaporated over a normal CaF_2 target. No recoil nuclei would be expected to penetrate such a film, but as far as the proton beam is concerned the effect would be simply to shift the energy scale by some 80 kev. Increasing the proton energy by this amount should result in the reaction proceeding as before, except now no pairs from $^{16}\text{O}^*$ should reach the counters cC. With this arrangement it was, indeed, found that the background remained much as before, but the initial decrease in counting rate for Z between 0 and 0.25 mm did not occur.

In order to translate the experimental results into an actual lifetime for $^{16}\text{O}^*$ a straightforward, but somewhat lengthy, calculation was made of the expected variation in counting rate in the counter pairs as a function of Z . In this calculation it was assumed that the compound nucleus ^{20}Ne dissociates into $^{16}\text{O}^* + \alpha$ -particle in an isotropic manner (in centre-of-mass frame). It was also found that as a result of the small average distance ($\sim 0.05\text{ mm}$) traversed by the $^{16}\text{O}^*$ nucleus before emitting a pair, as compared with the dimensions of T, aA, AB, the solid angle subtended by the apertures A, B at the pair-emitting $^{16}\text{O}^*$ nucleus could be taken as proportional to distance of the nucleus to the right of the plane AB. The variation in velocity V of the $^{16}\text{O}^*$ nucleus with the angle to the proton beam, due to the momentum of the proton, was taken into account, and the mean loss of energy of the ^{16}O nuclei in traversing part of the CaF_2 target was estimated, as a function of direction of motion, using the data of Blackett and Lees (1932).

We can express the expected counting rate as

$$N(Z, \mu, E) = \sigma(E)\mu \int \exp\left\{-\frac{\mu r}{V(\theta, S, E)}\right\} \frac{\Omega}{V} p(\theta, E) \sin \theta dS dr d\theta$$

where $1/\mu = \tau$, S is the depth of the layer in the target film at which the (p, α) reaction occurs, E is the proton bombarding energy, θ the angle between the ^{16}O recoil and the proton beam, Ω the solid angle subtended by the counting aperture at the $^{16}\text{O}^*$ nucleus (r, θ), and V the velocity of this nucleus. $\sigma(E)p(\theta, E)$ is the differential cross section for the (p, α) reaction. With the approximation of $\Omega \propto (r \cos \theta - Z)$, $E = 840\text{ kev}$, the relationship between N and Z (apart from constant factors) was computed for several values of the parameter μ/V_0 , V_0 being the velocity in the centre-of-mass system of the $^{16}\text{O}^*$ nucleus, recoiling along the Z axis (to the right) before any slowing down in the target film has occurred. The calculations for six values of μ/V_0 from 30 to 100 cm^{-1} are shown in figure 7 (broken lines). For each set of experimental observations the best fitting theoretical curve was estimated, by inspection, and the results obtained are:

Experiment	1	2	3	4	5	6	7	8	9	10
Target number		1				2			3	
$\mu/V_0\text{ (cm}^{-1}\text{)}$	55	40	65	60	50	40	50	60	60	60

The weighted mean is $55 \pm 5\text{ cm}^{-1}$, corresponding to a mean path of the $^{16}\text{O}^*$ nucleus before de-excitation of 0.18 mm and a half-life of $5.0 \pm 0.5 \times 10^{-11}\text{ second}$. The error is estimated from the consistency of the results in the above table. There is an additional uncertainty due to the assumption of isotropy in the reaction $^{19}\text{F(p, } \alpha)^{16}\text{O}^*$. For example, a distribution (in centre-of-mass frame) of the type $1 + \alpha \cos^2 \theta$ would reduce the value of the half-life by 3% for $\alpha = 0.5$

and 7% for $\alpha = 1$. A comparison with the angular distribution of the competing reaction $^{19}\text{F}(p, \alpha)^{16}\text{O}$ at this energy indicates a relatively small anisotropy, and the error in the half-life due to this factor is probably less than 5%.

For the comparison of this result with theoretical estimates it is quite sufficient to use the 'first order' theory. Expressions for the absolute rate of pair emission in monopole transitions have been given by Oppenheimer and Schwinger (1939) and Dalitz (1951). The two expressions are slightly different numerically, the difference being apparently due to some approximations used by the first authors.

From Dalitz's results the absolute rate, μ (natural units) is[†]:

$$P = \frac{8e^4}{27\pi} \langle M \rangle^2 \frac{(\frac{1}{2}W_0 - 1)^3 (\frac{1}{2}W_0 + 1)^2}{10S^3} \\ \times [S^2\{6 + 5(S + S^{-1}) - 2(S + S^{-1})^2\}E(S) - (1 - S^2)(S^2 + 5S - 2)K(S)]$$

where $S = (W_0 - 2)/(W_0 + 2)$ and K , E are the first and second elliptic integrals. With $W_0 = 11.8 m_0 c^2$ and c.g.s. units μ becomes

$$485 \left(\frac{m_0^5 e^4 c^4}{\hbar^7} \right) \langle M \rangle^2 = 0.97 \cdot 10^{61} \langle M \rangle^2 \text{ sec}^{-1}.$$

The nuclear matrix element $\langle M \rangle$ is given by

$$\int \psi_0^* \sum_p r_p^2 \psi_1 d\tau$$

where ψ_0 , ψ_1 are the initial and final nuclear wave functions and the summation \sum_p is over all protons whose positions are r_p . If we write the matrix elements as ρ^2 , where ρ is a characteristic length, then comparison of the theoretical and experimental results gives a value of ρ of 1.95×10^{-13} cm, which is of the order of r_p for a single proton.

The value of this half-life is of interest in connection with the difficulty in explaining the existence of a low-level of ^{16}O with $J=0$ and even parity (see, for example, the discussion by Inglis (1953)). The state must be symmetrical with respect to neutrons and protons ($T=0$), but the low-lying states obviously predicted by the shell model due to excitation of a neutron and proton from P to D orbits also predicts a large value of the spin. The above expression for the matrix element gives, of course, a value zero for the excitation of two particles of an *independent* particle model, and hence for the actual transition one might expect a much smaller value of $\langle M \rangle$ than that corresponding to single particle excitation. The possibility of half-neutron and half-proton excitation from ^1P to ^2P orbits could also result in a $T=0$ state of the correct spin and parity, but the energy of such a state has not been estimated. It should, perhaps, be borne in mind that we are dealing here with an almost unique example, and comparison with other calculations based on the shell model may be misleading. This level of ^{16}O is possibly the only case of a first excited state of a symmetrical ($T=0$) nucleus with both neutron and proton closed shells and for which the coulomb effects are negligible.

In view of the uncertainties in interpreting this level in terms of the shell model it is of interest to look at the α -particle model (cf. Inglis 1953). Following the procedure of Wheeler (1937) we assume a tetrahedral model and quasi-elastic

[†] There is a misprint in equation (4.5) in Dalitz's paper. The term $(S^2 + 5S - 2)$ is misprinted $(S^2 + 5S - 3)$.

forces between pairs of α -particles, i.e. a potential $V = V(r_0) + \frac{1}{2}k(r - r_0)^2$, where r_0 represents the mean position of the α -particles. The mode of vibration of interest to us is isotropic dilation and contraction, and the energy of first excited state of this mode will be $\hbar(k/M)^{1/2}$, where M is the proton mass. If we identify this mode with the level at 6.0 mev we obtain a value for k immediately. The matrix element for the transition to the ground state can be evaluated simply by using the corresponding harmonic-oscillator wave functions. The numerical estimate with $r_0 = 4 \times 10^{-13}$ cm is 3.8×10^{-49} cm⁴ for $\langle M \rangle^2$, corresponding to a value of μ of 3.7×10^{12} sec⁻¹ as compared with the experimental 1.4×10^{10} sec⁻¹. The large theoretical value arises primarily from the fact that all eight protons take part in the oscillation.

The matrix element is proportional to $r_0^2(\hbar^2/M\epsilon_0)$, where ϵ_0 is the level energy (6 mev). It is clear that adjustment of r_0 cannot account for the big divergence between experimental and predicted values; k does not enter explicitly since it is given in terms of ϵ_0 . It appears then that the α -particle model cannot adequately describe this first state of ¹⁶O.

ACKNOWLEDGMENTS

We would like to thank Drs. A. Folkierski and R. Latham for valuable technical assistance during the course of these experiments.

REFERENCES

- AJZENBERG, F., and LAURITSEN, T., 1952, *Rev. Mod. Phys.*, **24**, 321.
 BLACKETT, P. M. S., and LEES, C. H., 1932, *Proc. Roy. Soc. A*, **134**, 658.
 DALITZ, R. H., 1951, *Proc. Roy. Soc. A*, **206**, 521.
 DEVONS, S., HERWARD, H. G., and LINDSEY, G. R., 1949, *Nature, Lond.*, **164**, 586.
 DEVONS, S., and LINDSEY, G. R., 1949, *Nature, Lond.*, **164**, 539.
 GOLDRING, G., 1953, *Proc. Phys. Soc. A*, **66**, 341.
 INGLIS, D. R., 1953, *Rev. Mod. Phys.*, **25**, 451.
 OPPENHEIMER, J. R., 1941, *Phys. Rev.*, **60**, 164.
 OPPENHEIMER, J. R., and SCHWINGER, J., 1939, *Phys. Rev.*, **56**, 1066.
 PHILLIPS, G. C., and HEYDENBURG, N. P., 1951, *Phys. Rev.*, **83**, 184.
 ROSE, M. E., 1949, *Phys. Rev.*, **76**, 678.
 STREIB, J. F., FOWLER, W. A., and LAURITSEN, C. C., 1941, *Phys. Rev.*, **59**, 523.
 THOMAS, R. G., and LAURITSEN, T., 1952, *Phys. Rev.*, **88**, 966. See also HARRIES, G., and DAVIES, W. T., 1952, *Proc. Phys. Soc. A*, **65**, 564.
 WHEELER, J. A., 1937, *Phys. Rev.*, **52**, 1083.

A Modified Form of Heisenberg's Theory of Ferromagnetism

BY R. H. TREDGOLD

Department of Physics, University of Nottingham

Communicated by L. F. Bates; MS. received 22nd October 1953

Abstract. The Heisenberg theory of ferromagnetism is extended to include exchange interactions between atoms other than nearest neighbours. The calculation is carried through as far as the third approximation and a general expression for the susceptibility above the Curie point is obtained. A particular law of variation of exchange interaction with distance is investigated and it is shown that the results obtained reproduce the general features of the susceptibility versus temperature curves of real ferromagnetic materials.

§ 1. INTRODUCTION

IN a former paper (Tredgold 1953, to be referred to as I) a method was given for extending the Heisenberg (1928) theory of ferromagnetism to higher approximations than the second. In particular an expression for the magnetization as a function of temperature was obtained in terms of the moments of the spin dependent energy (the k th moment being defined as the mean k th power of the energy). It was shown how to obtain a high temperature expansion for the inverse of the susceptibility above the Curie temperature without the necessity of inverting a series. The calculation was carried through explicitly as far as the third approximation for the case of a face-centred cubic lattice having one unpaired electron per lattice site and involving exchange interactions only between nearest neighbours. The variation of susceptibility with temperature so obtained was found to be in poor agreement with the behaviour of real ferromagnetic materials and as far as could be judged the expressions obtained showed little likelihood of converging on the results of the molecular field theory which are known to give reasonably good agreement with experimental results.

It was evident from the form of the expressions obtained that a model involving exchange interactions extending somewhat further than to nearest neighbours would lead to material improvement in the results. It therefore seemed desirable to ascertain whether a law of interaction could be found which would extend sufficiently far to lead to a satisfactory variation of susceptibility with temperature and which at the same time would be consistent with a Heitler–London type of model.

It is obviously possible to postulate any arbitrary localized wave functions and adjust their extension by means of some parameter in such a way that agreement with the behaviour of real materials is obtained in the susceptibility–temperature curve. This, however, would not be a valid approach because it is necessary to use orthogonal wave functions if the spin operation treatment of ferromagnetism is to be employed. The errors in neglecting the non-orthogonality integrals even in the conventional Heisenberg treatment can be quite great, as has been pointed out by Slater (1953).

The longest range interaction consistent with orthogonality which can be obtained in the Heisenberg type of model is arrived at by the employment of Wannier (1937) functions. An exact evaluation of the variation of exchange

interaction with distance using these functions would be extremely difficult and would have little significance unless one possessed a precise knowledge of the band structure of the material under consideration. It is possible, however, to obtain a rough idea of the law of interaction by evaluating the overlap integrals for the square of the 'free electron' Wannier functions. The expressions so obtained should at least set an upper limit to the 'range' of interactions possible for a model of the type discussed. Further consideration of this point is delayed until § 4 (see also the Appendix).

§ 2. THE STATISTICAL TREATMENT

The spin dependent internal energy may be written

$$E = -2J' \sum_{i,j}' g(\mathbf{n}_i - \mathbf{n}_j) \mathbf{s}_i \cdot \mathbf{s}_j \quad \dots\dots(1)$$

where J' is a constant, $\mathbf{n}_i, \mathbf{n}_j$ define the i th and j th lattice sites, $g(\mathbf{n}_i - \mathbf{n}_j)$ is proportional to the exchange interaction between orbitals centred about the i th and j th lattice sites and $\mathbf{s}_i = \frac{1}{2}\boldsymbol{\sigma}_i$ where $\boldsymbol{\sigma}_i$ is the Pauli spin operator representing the spin of the electron located on the i th lattice site.

The first three moments of this energy may be expressed in terms of the mean values of various products of the spin operators (expressed as functions of the relative magnetization) which were evaluated in I and in terms of the following four sums:

$$\left. \begin{aligned} a &= \sum_j' g(\mathbf{n}_i - \mathbf{n}_j), & b &= \sum_j' g^2(\mathbf{n}_i - \mathbf{n}_j), & c &= \sum_j' g^3(\mathbf{n}_i - \mathbf{n}_j) \\ d &= \sum_{j,k}''' g(\mathbf{n}_i - \mathbf{n}_j) g(\mathbf{n}_j - \mathbf{n}_k) g(\mathbf{n}_k - \mathbf{n}_i), \end{aligned} \right\} \quad \dots\dots(2)$$

the primes denoting that terms involving $\mathbf{n}_i = \mathbf{n}_j$, etc. are to be omitted.

Making use of the moments so obtained and eqn (14) of I and proceeding as in I, one finally obtains the following expression for the inverse of the susceptibility per atom above the Curie temperature:

$$\frac{1}{\chi} = \frac{J'at}{\beta^2} \left[1 - \frac{1}{t} \left(\frac{1}{2} \right) + \frac{1}{t^2} \left(\frac{b}{2a^2} \right) + \frac{1}{t^3} \left(\frac{5d}{24a^3} - \frac{c}{3a^3} \right) + \dots \right] \quad \dots\dots(3)$$

where $t = kT/J'a$ and β is the Bohr magneton. It is of interest to note that the somewhat involved expressions occurring in the derivation of (3) can be checked by putting $a=b=c=12$ and $d=48$ and comparing them with the analogous expressions employed in obtaining eqn (19) of I.

§ 3. A PARTICULAR MODEL

For initial simplicity the treatment given here is confined to the simple cubic lattice. The law of interaction chosen in the light of the discussion given above has the following form (see Appendix):

$$\left. \begin{aligned} g(\mathbf{n}_i - \mathbf{n}_j) &= \frac{1}{(n_{i1} - n_{j1})^2 (n_{i2} - n_{j2})^2 (n_{i3} - n_{j3})^2} \\ &\quad n_{i1} \neq n_{j1} \quad n_{i2} \neq n_{j2} \quad n_{i3} \neq n_{j3} \\ g(\mathbf{n}_i - \mathbf{n}_j) &= \frac{2\pi^2}{3(n_{i2} - n_{j2})^2 (n_{i3} - n_{j3})^2} \\ &\quad n_{i1} = n_{j1} \quad n_{i2} \neq n_{j2} \quad n_{i3} \neq n_{j3} \\ g(\mathbf{n}_i - \mathbf{n}_j) &= \frac{4\pi^4}{9(n_{i3} - n_{j3})^2} \\ &\quad n_{i1} = n_{j1} \quad n_{i2} = n_{j2} \quad n_{i3} \neq n_{j3} \\ &\quad \text{etc.} \end{aligned} \right\} \quad \dots\dots(4)$$

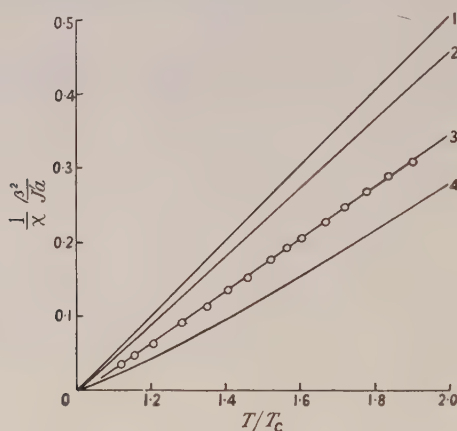
where the suffixes 1, 2 and 3 refer to the three-coordinate axis. On evaluating the sums a , b , c and d defined by (2) for this particular law of interaction it is found that

$$\left. \begin{aligned} a &= \frac{665\pi^6}{945} & b &= \frac{21^6\pi^{12}}{945^3} \\ c &= \frac{474768\pi^{18}}{945^3} & d &= \frac{1660422\pi^{18}}{945^3} \end{aligned} \right\} \dots\dots(5)$$

Using (3) and (5) it is found that

$$\frac{1}{\chi} = \frac{J'at}{\beta^2} \left[1 - \frac{0.5}{t} + \frac{0.01398}{t^2} + \frac{0.0006383}{t^3} + \dots \right] \dots\dots(6)$$

This function is shown in the figure together with the experimental points obtained for nickel by Sucksmith and Pearce (1938). The susceptibility-temperature curve calculated to the same degree of approximation for a face-centred cubic lattice



The inverse of susceptibility plotted against reduced temperature for: 1, the Heisenberg first approximation; 2, the modified Heisenberg theory taken to the third approximation for the simple cubic lattice; 3, the experimental values for nickel after Sucksmith and Pearce (1938); 4, the simple Heisenberg theory for the face-centred cubic lattice taken to the third approximation.

in which only nearest neighbour interactions are taken into account is also shown. For ease in comparison the temperature scales are adjusted to make the Curie temperatures obtained from the different treatments coincident.

The values of the Curie temperature obtained by equating the right-hand side of (6) to zero and solving for t are as follows: first approximation $t_C=0.5$, second approximation $t_C=0.4711$, third approximation $t_C=0.4669$. Since it is impossible to obtain the general term of the series for $1/\chi$ by the methods employed here it is not possible to prove convergence, nevertheless the values of t_C obtained from the first three approximations indicate that it is reasonable to take eqn (6) as being a good approximation to the correct expression for the susceptibility for the model considered.

§ 4. DISCUSSION

That the variation of $1/\chi$ with temperature obtained from the model discussed does not fit the experimental points for nickel is hardly surprising, as the law of interaction assumed has the longest 'range' which would be consistent with a

Heitler-London-Heisenberg type of model and therefore represents a limiting case.

As will be seen from the figure the experimental points for nickel lie between the theoretical curve obtained from the present treatment and the theoretical curve obtained in I for a model involving only nearest neighbour exchange interactions. It should therefore be possible to reproduce the experimental curve for nickel fairly accurately by choosing a law of interaction between these two limiting cases. This suggestion is moreover supported by the fact that 'nearest neighbour' model over-estimates the difference between the ferromagnetic and paramagnetic Curie points, whereas the model discussed in this paper tends to under-estimate this quantity. It is thus felt that the Heisenberg type of treatment, suitably modified to take into account exchange interaction between atoms other than nearest neighbours, is capable of giving quite a good description of the high temperature behaviour of ferromagnetic materials. That the low temperature behaviour may be treated adequately by this method is, of course, well known (Bloch 1930).

As has been pointed out by Slater (1953) a model based on one-electron wave functions will never be entirely satisfactory, as it will not take account of the important influence of the correlation effect. However, the immense complications involved in applying the configurational interaction technique as any equivalent method to even simple problem indicate that even if this method could be applied to the problem of ferromagnetism it would be very difficult to formulate any clear qualitative picture which would assist in the interpretation of experimental results.

One is thus left with the problem of whether the modified Heisenberg model as proposed here or the collective electron model (see, for example, Stoner 1948, Wohlfarth 1953) gives the best approximate description of real ferromagnetic materials. To find the answer to this question it seems necessary to find the conditions necessary to establish ferromagnetism in a metal and then, within the limits of these conditions, to find which model leads to the lowest free energy at some finite temperature. An attempt to solve this problem for a simple model for a metal is now being made and it is hoped to publish the results at a future date.

ACKNOWLEDGMENTS

The author would like to take this opportunity of thanking Professor L. F. Bates for his interest and encouragement and Dr. J. M. Ziman of the Clarendon Laboratory, Oxford, for a helpful consultation.

APPENDIX

The general expression for a Wannier function located about the i th lattice site is:

$$a(\mathbf{r}-\mathbf{n}_i) = \frac{1}{N^{1/2}} \sum_{\mathbf{k}} \exp(-i\mathbf{k} \cdot \mathbf{n}_i) b(\mathbf{k}, \mathbf{r}) \quad \dots\dots (A1)$$

where N is the number of atoms in the crystal and $b(\mathbf{k}, \mathbf{r})$ is the Bloch function characterized by the wave vector \mathbf{k} .

For nearly free electrons Bloch functions in a cubic lattice one obtains:

$$a(\mathbf{r}-\mathbf{n}_i) = \frac{\sin \pi(x-n_{ix}) \sin \pi(y-n_{iy}) \sin \pi(z-n_{iz})}{\pi^3(x-n_{ix})(y-n_{iy})(z-n_{iz})} \quad \dots\dots (A2)$$

It may easily be shown that this expression decreases more slowly for increasing x , y and z than do Wannier functions derived from any other type of Bloch function. To find the largest range type of interaction consistent with the Heisenberg type of model it is thus required to evaluate the exchange integral between the functions $a(\mathbf{r}-\mathbf{n}_i)$ and $a(\mathbf{r}-\mathbf{n}_j)$ as defined by eqn (A 2). It may be seen that the exchange charge density will have a number of strong maxima separated by nodes. Since the contributions to the exchange integral arising from the two electrons being in the region of the same maxima will be considerably larger than contributions arising from the electrons being located in the regions of different maxima it is possible to obtain a reasonable approximation to the variation of exchange with $\mathbf{n}_i-\mathbf{n}_j$ by writing

$$J_{ij} \simeq \text{const} \int a^2(\mathbf{r}-\mathbf{n}_i) a^2(\mathbf{r}-\mathbf{n}_j) d\tau, \quad \dots\dots (A 3)$$

and from (A 2) and (A 3) eqn (4) is obtained.

REFERENCES

- BLOCH, F., 1930, *Z. Phys.*, **61**, 206.
 HEISENBERG, W., 1928, *Z. Phys.*, **49**, 619.
 SLATER, J. C., 1953, *Rev. Mod. Phys.*, **25**, 199.
 STONER, E. C., 1948, *Rep. Progr. Phys.*, **11**, 43 (London : Physical Society).
 SUCKSMITH, W., and PEARCE, R. R., 1938, *Proc. Roy. Soc. A*, **167**, 189.
 TREDGOLD, R. H., 1953, *Proc. Phys. Soc. A*, **66**, 421.
 WANNIER, G. H., 1937, *Phys. Rev.*, **52**, 191.
 WOHLFARTH, E. P., 1953, *Rev. Mod. Phys.*, **25**, 211.

A Cloud Chamber Study of Internal Pairs from $^{12}\text{C}^*$

By G. HARRIES †

Clarendon Laboratory, Oxford

Communicated by E. P. George; MS. received 4th August 1953, and in amended form 6th November 1953

Abstract. The nature and multipolarity of the 4.45 mev γ -ray from carbon-12* are obtained from the angular distribution of the positrons and electrons of internal conversion pairs photographed in a cloud chamber. The transition is found to be of electric quadrupole origin. Accordingly, a spin of 2^+ is ascribed to the first excited level in ^{12}C and a decay scheme is proposed for $^{12}\text{C}^*$ at the lower energies.

A transformation formula is given which relates the spatial angular distribution of cloud-track pairs to the distribution of pair-angles projected on to a plane of reference.

§1 INTRODUCTION

THE nature and multipolarity of gamma transitions can be found from the distribution of angles in internal conversion pairs; this possibility has been discussed by Horton (1948) and Rose (1949). If the energy of a γ -transition exceeds $2mc^2$ the emission of internal pairs is a mode of decay of an excited nucleus which competes with the γ -emission and electron conversion; the pair formation coefficient is largest when the electron conversion is smallest.

The total pair formation coefficients are sensitive to change of multipole order, and many transitions have been studied in this way (see Burhop 1952). However, for high energy transitions the ratio of total pair coefficients for successive multipoles of the same nature approaches unity because for small wavelengths pair formation takes place in the outer zone of the radiation field of the nucleus and the dependence on multipolarity consequently disappears.

The angular distribution of pairs is also sensitive to change of multipole, and in the energy range, say, above $5mc^2$ the angular distribution is a more sensitive indication of the multipolarity.

Rose (1949) has also suggested an abbreviated form of the angular distribution investigation. As the pairs are predominantly emitted with small angles it should be possible to establish the multipole order of the transition by measuring the ratio of the positron-electron coincidence rates at pair-angles of 0° and, say, 90° . (At 180° the coincidence rate is extremely small.) However, the sensitive surfaces of electron counters are too large to allow the subtended solid angle to be narrow and well defined; and a source far removed from the counters improves the geometry at the expense of counting rate.

Using a cloud chamber it has been found possible to examine the spectrum of internal conversion pair-angles in the range 0° to 120° . The shape of the spectrum agrees with the theoretical distribution given by Rose (1949) and differs, according to theory, from the distribution of *total* internal conversion

† Now at Admiralty Gunnery Establishment, Teddington, Middlesex.

pairs found by Devons and Lindsay (1949). In general, unlike internal pairs, there is a greater tendency for the components of total internal conversion pairs to be formed with equal energies.

§ 2. CARBON-12*

2.1. Angular Distribution of Internal Pairs

A Po-Be source was used in the investigation of the internal pairs formed from the 4.45 MeV level in ^{12}C . On to a strip of platinum 0.01 inch thick 300 mc of polonium was electrolytically deposited over 1 cm square. This was prepared in nitrogen to prevent oxidation, and consequent thickening, of the polonium. A beryllium strip (25 mg cm^{-2}) covered the polonium, and the source was accommodated in an evacuated source holder with a mica window 5 mg cm^{-2} thick. The radiation from the source was admitted to the cloud chamber through a mica window (5 mg cm^{-2}) in the chamber wall. The arrangement was such that the source was in the field of view of both cameras of a stereo pair. This facilitated the identification of associated pair particles. The chamber, in a field of 550 gauss, contained air at a pressure of 50–60 cm and was expanded at 1 minute intervals.

The cloud chamber photographs record the high x-ray activity from polonium. The short dense tracks of photoelectrons diffuse rapidly and the smear of the ionization of tracks admitted to the chamber an appreciable time before the expansion produced a high level of ion background. The effect in air is shown in figures 1 and 2 (Plate). In an investigation of the γ -rays from polonium Grace *et al.* (1951) report, in addition to the 0.8 MeV γ -ray, 16 keV radiation which may be attributed to L-radiation of lead and also 75 keV K-radiation of lead. The short tracks photographed are presumably due to the L-radiation. It was not possible to reduce the number of undesirable photoelectron tracks without introducing an absorber of high Z which would have produced a high yield of unwanted external pairs. The possibility of recording external pairs formed by the interaction of the γ -ray with the platinum support of the source may be neglected since these would need to be scattered through about 180° and, as in the case of internal pairs, they are formed with a strong predominance in the direction of the gamma-ray.

1520 pairs of stereo photographs were taken and 72 pairs of total energy $4.4 \pm 0.5 \text{ MeV}$ were accepted for measurement. A typical photograph of an internal positron-electron pair is reproduced in the photograph, figure 1. The theoretical curves for the distribution of pair-angles projected on to a plane are considered in § 3 and the projected distributions for the conversion of the 4.45 MeV line for electric dipole and electric quadrupole transitions are given in figure 3. The theoretical curves have been normalized to give ordinate values of

$$Q(x) / \int_0^\pi Q(x) dx$$

where $Q(x)$ is the pair formation probability. Numbers of pairs are plotted at intervals of 15° and the experimental points fitted to the curves are consistent with a transition of electric quadrupole origin.

The angular distributions for magnetic dipole and electric quadrupole transitions lie very closely together, and a very high experimental resolution is

required to be able to distinguish between these two modes of emission with any certainty. But magnetic dipole radiation is improbable. Seed and French (1952) ascribe a value of 2^- to the compound nucleus $^{16}\text{O}^*$ from the angular

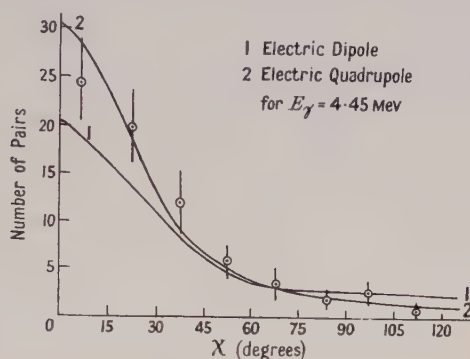


Figure 3. Projected angular distribution of internal pairs.

correlation between the α -particles and the subsequent γ -rays at the 898 keV resonance in the reaction $^{15}\text{N}(p, \alpha\gamma)^{12}\text{C}$. This result agrees with an α emission with $l=1$ to a 2^+ first excited level in ^{12}C .

Lewis (1952) has shown that the angular correlation of the successive γ -rays in the reaction $^{11}\text{B}(p; \gamma_1, \gamma_2)^{12}\text{C}$ is also consistent with a spin 2^+ for the 4.45 MeV excited state of ^{12}C , and the result has been confirmed in a similar experiment by Hubbard, Nelson and Jacobs (1952).

2.2. The 7 MeV Level

During the investigation of the pairs from the 4.45 MeV level seven pairs with a total energy of 7.0 ± 0.6 MeV were found, a brief account of which has appeared earlier (Harries and Davies 1952). A description of the pairs is given in table 1 and a photograph of a typical pair in figure 2. In the absence of evidence for a γ -ray of this energy it is suggested that the level has zero spin and even parity and that the pairs observed result from total internal conversion. In the special case of a transition $I=0$ to $I=0$ the conversion is confined to the intranuclear field, and γ -radiation is completely forbidden.

Table 1

	1	2	3	4	5	6	7
W_+ positron energy (MeV)	2.8	2.6	3.5	3.5	3.0	3.8	1.9
W_- electron energy (MeV)	4.25	4.5	3.5	3.5	4.0	3.0	4.1
E_γ total energy (MeV)	7.05	7.1	7.0	7.0	7.0	6.8	6.0
χ projected pair-angle (deg.)	10	35	10	5	8	24	4

The possibility of these pairs being combinations of internal pairs which have undergone considerable multiple scattering or that they are random associations of a positron with a Compton electron has been examined. The probability of these processes is too low to account for the number of high energy pairs photographed, and these processes would produce a greater deviation in total pair energies.

2.3. Level Scheme in $^{12}\text{C}^*$

The experimental results indicate that the spin and parities of the levels are:

$^{12}\text{C}^*$	0	4.45 Mev	7 Mev
I	0	2	0
Parity	+	+	+

Although the high-energy level decays to the ground state by pair emission only, the scheme suggests that decay should also be possible by the emission of a 2.55 Mev γ -ray in cascade with the 4.45 Mev γ -ray, both transitions being considered electric quadrupole.

However, assuming that the population of the 4.45 Mev level is eight times that of the 7 Mev state (Guier *et al.* 1952), and that the ratio of 4.45 Mev pairs to 7 Mev pairs is 10, then the intensity ratio of 2.5 Mev γ -rays to 4.45 Mev γ -rays is 0.1. It is possible that this weak line has escaped detection. These results have been incorporated in the ^{12}C level scheme by Ajzenberg and Lauritsen (1952).

§ 3. THEORETICAL

The angles between positron-electron pairs in a cloud chamber are usually measured by the reprojection of stereoscopic photographs. However, for comparison with a theoretical distribution the photographs may be more conveniently analysed if the distribution of angles projected on to a plane is adopted; then the theoretical distribution of the angles in space needs to be suitably transformed. From $\Gamma(\Theta)$, the theoretical probability of finding pair components at an angle Θ in space, we determine $Q(\chi)$, the probability of pair formation in the illuminated region of the cloud chamber, where χ is the projection of Θ on to the plane of the photographic image.

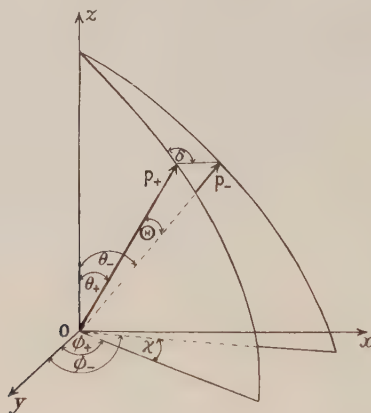


Figure 4.

3.1. Projection of Internal Pairs

The form of the spatial angular distribution is determined by the nature and multipolarity of the transition. The probability of the emission of an electron (figure 4) with direction between (θ_-, ϕ_-) and $(\theta_- + d\theta_-, \phi_- + d\phi_-)$ and a positron between (θ_+, ϕ_+) and $(\theta_+ + d\theta_+, \phi_+ + d\phi_+)$ is given by

$$P(\theta_+, \phi_+, \theta_-, \phi_-) \sin \Theta \sin \theta_+ d\theta_+ d\phi_+ d\theta_- d\phi_- \dots (1)$$

where Θ is the angle between the pair and δ the dihedral formed by the planes (\mathbf{p}_+, z) and $(\mathbf{p}_+, \mathbf{p}_-)$. Rose (1949) has evaluated the expression $\gamma(\Theta)$, the probability per unit solid angle when the energies W_{\pm} are fixed:

$$\gamma(\Theta) = \int_0^{\pi} d\theta_+ \int_0^{2\pi} d\phi_+ \int_0^{2\pi} d\delta P(\theta_+, \phi_+, \theta_-, \phi_-) \sin \theta_+ \quad \dots\dots(2)$$

For isotropic emission $P(\theta_+, \phi_+, \theta_-, \phi_-)$ depends only on Θ , therefore

$$P(\theta_+, \phi_+, \theta_-, \phi_-) = \gamma(\Theta)/8\pi^2. \quad \dots\dots(3)$$

If χ be the angle between the projected directions of \mathbf{p}_+ and \mathbf{p}_- on to the $z=0$ plane, i.e. $\chi = \phi_+ - \phi_-$, then the probability of creation of a pair with the projected angle within χ and $\chi + d\chi$ is

$$F(\chi)d\chi = (d\chi/8\pi^2) \int_0^{\pi} d\theta_+ \int_0^{\pi} d\theta_- \int_0^{2\pi} d\phi_+ \gamma(\Theta) \sin \theta_+ \sin \theta_- \quad \dots\dots(4)$$

since the integration is performed over all angles with χ fixed.

$$\cos \Theta = \sin \theta_+ \sin \theta_- \cos \chi + \cos \theta_+ \cos \theta_- \quad \dots\dots(5)$$

$$F(\chi)d\chi = (1/4\pi) d\chi \int_0^{\pi} d\theta_+ \int_0^{\pi} d\theta_- f(\sin \theta_+ \sin \theta_- \cos \chi + \cos \theta_+ \cos \theta_-) \sin \theta_+ \sin \theta_- \quad \dots\dots(6)$$

But the geometry of the cloud chamber does not permit θ_+ and θ_- to range from 0 to π . Only tracks with projected lengths greater than an arbitrary minimum L can be measured with sufficient accuracy. With the source in the central plane of the illuminated region of depth $2a$, θ_+ and θ_- are confined to regions defined by $\frac{1}{2}\pi \pm \Delta$ where $\Delta = a/L < 1$. If $\theta_{\pm} = \frac{1}{2}\pi - \xi_{\pm}$ and Δ is small,

$$F(\chi) = (1/\pi)\Delta^2\gamma(\Theta)\{1 - (\Delta^2/3)(1 + \cos \Theta\gamma'(\Theta)/\gamma(\Theta))\}. \quad \dots\dots(7)$$

The probability over all partition energies of the electrons is

$$Q(\chi) = \int_1^{k-1} F(\chi)dW_+ \quad \dots\dots(8)$$

where k is the quantum energy in units of mc^2 and W_+ is the positron energy.

The correction term $(\Delta^2/3)\{1 + \cos \Theta\gamma'(\Theta)/\gamma(\Theta)\}$ in (7) is small for large L and shallow light beams. In the experimental arrangement used above $L = 5$ cm and $a = 1$ cm, and for $k = 9$ mc^2 the correction term for electric quadrupole is not greater than 10%. Only a small proportion of tracks ($\sim \Delta^2/2$) has to be rejected by this method.

ACKNOWLEDGMENTS

The author is indebted to Professor Lord Cherwell for providing the experimental facilities and to Drs. W. T. Davies, H. Davies and H. Halban for helpful discussion and advice.

REFERENCES

- AJZENBERG, F., and LAURITSEN, T., 1952, *Rev. Mod. Phys.*, **24**, 356.
 BURHOP, E. H. S., 1952, *The Auger Effect* (Cambridge : University Press).
 DEVONS, S., and LINDSAY, G. R., 1949, *Nature, Lond.*, **164**, 539.
 GRACE, M. A., ALLEN, R. A., WEST, D., and HALBAN, H., 1951, *Proc. Phys. Soc. A*, **64**, 481.
 GUIER, W. H., BERTINI, H. W., and ROBERTS, J. H., 1952, *Phys. Rev.*, **85**, 426.
 HARRIES, G., and DAVIES, W. T., 1952, *Proc. Phys. Soc. A*, **65**, 564.
 HORTON, G. K., 1948, *Proc. Phys. Soc.*, **60**, 457.
 HUBBARD, T. P., JR., NELSON, E. B., and JACOBS, J. A., 1952, *Phys. Rev.*, **87**, 378.
 LEWIS, G. M., 1952, *Phil. Mag.*, **43**, 690.
 ROSE, M. E., 1949, *Phys. Rev.*, **76**, 678.
 SEED, J., and FRENCH, A. P., 1952, *Phil. Mag.*, **43**, 1214.

Three Dimensional Theory of Electron-Photon Showers

BY B. A. CHARTRES AND H. MESSEL

School of Physics, University of Sydney, Sydney, Australia

MS. received 26th May 1953

Abstract. The method developed by Messel and Green of solving the diffusion equation of the general mixed cascade for the moments of the distribution functions is applied to an electron-photon cascade initiated by a single electron or photon when provision is made for loss of electron energy by ionization. Exact solutions for the Mellin transform of the $2n$ th angular and $2n$ th radial moments are given. It is shown that the $2n$ th radial moment increases asymptotically as n^{4n} and that the radial distribution function is of the form $\exp(-ar^{1/2})$ for all but the core of the shower. Numerical results are given for the lower moments and compared with previous results.

§ 1. INTRODUCTION

VARIOUS attempts have been made to calculate the radial distribution function or the lower moments of the function for the electron-photon cascade. A criticism of the various methods employed can be found in the paper by Green and Messel (1952). It is sufficient to point out here that the approximation common to all previous investigations is to use the second moment only of the coulomb scattering cross section. This has made it impossible to estimate the higher moments of the radial distribution with any precision at all.

In the paper mentioned above a technique is given for obtaining exact values of all moments of the radial and angular distribution functions for media in which the number density of the constituent atoms may vary in an arbitrary manner. This is done by expanding the distribution function in a series of derivatives of the Dirac delta function, the coefficients of which are the required moments. Ionization loss was not allowed for, although provision was made for its inclusion at a later date.

Messel and Green (1953, to be referred to as MG) have since developed a simpler and more powerful technique for obtaining the various moments. It involves taking a fourfold Fourier transform of the distribution function and then expanding it as a power series in the transformed variables, the coefficients giving the required moments. This technique has been used to solve the difficult problem of the radial spread of a mixed cascade, in which the soft component is continuously generated by the decay of mesons arising from the nucleon cascade. In this paper we apply this technique to the problem of an electron-photon cascade initiated by a single electron or photon, when energy loss due to ionization by electrons is accounted for. Provision is made for ionization loss by use of the Bhabha-Chakrabarty expansion (Bhabha and Chakrabarty 1943, 1948). Expressions are given for the functions required to calculate all the angular and radial moments using the first term only of this

expansion. The necessary functions for the second and further terms can be written down from our recursion formula (27), but they are too lengthy to be worth including in this paper.

We have given numerical values for the second radial moment for a uniform medium and the second angular moment, both in approximation A, for a cascade initiated by an electron. They are given in graphical form in figures 1 and 2. The higher moments and the ionization correction terms will be calculated on an electronic computer in the near future.

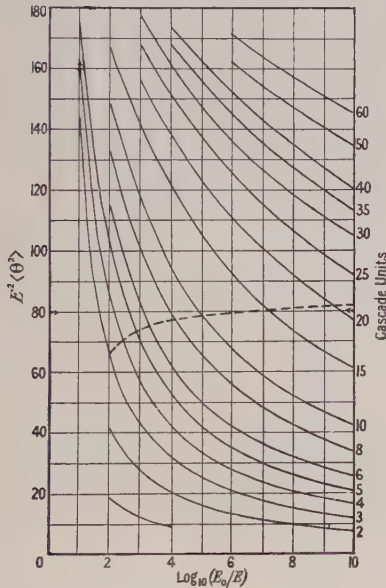


Figure 1. Curves of $E^2\langle\theta^2\rangle$ in approximation A for electrons of energy greater than E Mev in a shower initiated by an electron of energy E_0 , where θ is measured in radians. These curves are valid for all media. The broken curve gives the values of $E^2\langle\theta^2\rangle$ at the shower maximum for different values of E_0/E . The arrows indicate the value obtained for the shower maximum by Roberg and Nordheim.

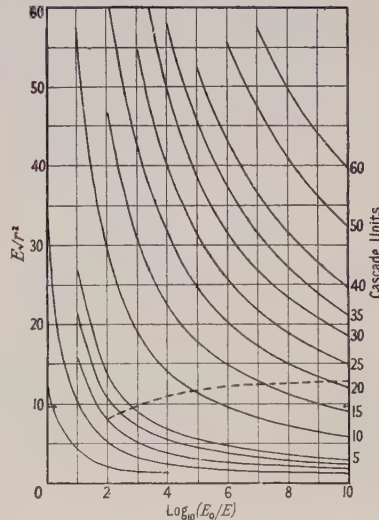


Figure 2. Curves of $E\sqrt{r^2}$ in approximation A for electrons of energy greater than E Mev in a shower initiated by an electron of energy E_0 , where r is measured in cascade units. These curves are valid for all media of constant density. The broken curve gives the values of $E\sqrt{r^2}$ at the shower maximum for different values of E_0/E . The arrows indicate the value obtained for the shower maximum by Roberg and Nordheim.

§ 2. THE TRANSFORMED DIFFUSION EQUATION

The fundamental equation for the angular-radial distribution function $f^{(i)}$ is given by Green and Messel (1952):

$$\begin{aligned}
 & -\frac{1}{q'(z)} \left[-\frac{\partial}{\partial z} + \mathbf{t} \cdot \frac{\partial}{\partial \mathbf{r}} \right] f^{(i)}(E, \mathbf{t}, \mathbf{r}, z) + [\alpha^{(i)} + \alpha \delta_{i,1}] f^{(i)}(E, \mathbf{t}, \mathbf{r}, z) \\
 & = \beta \frac{\partial f^{(i)}}{\partial E} \delta_{i,1} + \int_E^\infty \left[w^{(3-i)} \left(\frac{E}{E'} \right) f^{(3-i)}(E') + w^{(i)} \left(1 - \frac{E}{E'} \right) f^{(i)}(E') \delta_{i,1} \right] \frac{dE'}{E'} \\
 & + \int w(E, |\mathbf{t}' - \mathbf{t}|) f_{\frac{1}{2}}^{(i)}(E, \mathbf{t}', \mathbf{r}, z) \frac{d\mathbf{t}'}{2\pi} \delta_{i,1}.
 \end{aligned}
 \tag{1}$$

The vector \mathbf{t} is of length $\tan \theta$, where θ is the angle between the direction of motion of the shower particle and that of the primary initiating particle. We shall assume that t can be taken as equal to θ . This is equivalent to assuming that the lateral spread of the shower has no effect on its longitudinal development, an assumption that has been implicitly made in all previous work on the longitudinal development of a shower.

We now apply the fourfold Fourier transform

$$g^{(i)}(E, \mathbf{l}, \mathbf{k}, z) = (2\pi)^{-2} \int d\mathbf{t} \int d\mathbf{r} \exp \{i[\mathbf{l} \cdot \mathbf{t} - \mathbf{k} \cdot \mathbf{r}]\} f^{(i)}(E, \mathbf{t}, \mathbf{r}, z) \dots (2)$$

to the diffusion equation (1) and obtain (see MG)

$$\begin{aligned} -\frac{1}{q'(z)} \left[-\frac{\partial}{\partial z} + \mathbf{k} \cdot \frac{\partial}{\partial \mathbf{l}} \right] g^{(i)}(E) + \alpha^{(i)} g^{(i)}(E) &= \beta \frac{\partial g^{(i)}}{\partial E} \delta_{i,1} \\ + \int_E^\infty \left[w^{(3-i)} \left(\frac{E}{E'} \right) g^{(3-i)}(E') + w^{(i)} \left(1 - \frac{E}{E'} \right) g^{(i)}(E') \delta_{i,1} \right] \frac{dE'}{E'} \\ + \sum_{r=1}^\infty w_r l^{2r} (r!)^{-2} (-4)^{-r} E^{-2r} g^{(i)}(E, \mathbf{l}, \mathbf{k}, z) \delta_{i,1}. \end{aligned} \dots (3)$$

Now our original distribution function $f^{(i)}(E, \mathbf{t}, \mathbf{r}, z)$ is actually a function only of E, t, r, z (or q) and the angle between \mathbf{t} and \mathbf{r} . Consequently the transformed function $g^{(i)}$ is a function of E, l, k, q and the angle between \mathbf{l} and \mathbf{k} . Let l_1 and l_2 be the components of \mathbf{l} parallel and perpendicular respectively to \mathbf{k} . Then $g^{(i)}(E, \mathbf{l}, \mathbf{k}, z) = g^{(i)}(E, l_1, l_2, k, q)$ and $\mathbf{k} \cdot \partial/\partial \mathbf{l} = k \partial/\partial l_1$. We can now expand the transformed distribution function in a series of powers of the transformed variables. Let

$$g^{(i)}(l_2=0) = \sum_{a=0}^\infty \sum_{b=0}^\infty g_{a,b}^{(i)}(E, q) l_1^a k^b. \dots (4)$$

Substituting the expansion (4) into the diffusion equation (3) and equating powers of l_1 and k gives the following differential recursion equation

$$\begin{aligned} \frac{\partial}{\partial q} g_{a,b}^{(i)}(E, q) - \frac{a+1}{q'(z)} g_{a+1,b-1}^{(i)}(E) + \alpha^{(i)} g_{a,b}^{(i)}(E) &= \beta \frac{\partial}{\partial E} g_{a,b}^{(i)}(E) \delta_{i,1} \\ + \int_E^\infty \left[w^{(3-i)} \left(\frac{E}{E'} \right) g_{a,b}^{(3-i)}(E') + w^{(i)} \left(1 - \frac{E}{E'} \right) g_{a,b}^{(i)}(E') \delta_{i,1} \right] \frac{dE'}{E'} \\ + \sum' w_r (r!)^{-2} (-4E^2)^{-r} g_{a-2r,b}^{(i)}(E) \delta_{i,1} \end{aligned} \dots (5)$$

in which \sum' signifies summation from $r=1$ to $a/2$ if a is even, or $(a-1)/2$ if a is odd. The integral over E' is now eliminated in the usual way (Jánossy 1950) by taking the Mellin transform

$$h_{a,b}^{(i)}(v, q) = \int_0^\infty \left(\frac{E}{E_0} \right)^{v-1} g_{a,b}^{(i)}(E, q) dE \dots (6)$$

which gives us

$$\begin{aligned} \frac{\partial}{\partial q} h_{a,b}^{(i)}(v, q) - B^{(i)}(v) h_{a,b}^{(3-i)}(v) + D^{(i)}(v) h_{a,b}^{(i)}(v) &= \frac{a+1}{q'(z)} h_{a+1,b-1}^{(i)}(v) \\ - (v-1) \frac{\beta}{E_0} h_{a,b}^{(i)}(v-1) \delta_{i,1} + \sum' w_r (r!)^{-2} (-4E_0^2)^{-r} h_{a-2r,b}^{(i)}(v-2r) \delta_{i,1}. \end{aligned} \dots (7)$$

The connection between the coefficients $h_{a,b}^{(i)}(v, q)$ and the moments of the original distribution function can now be established (see MG). We have defined

$$h^{(i)}(v, l_1, l_2, k, q) = \int_E^\infty dE \left(\frac{E}{E_0} \right)^{v-1} (2\pi)^{-2} \int dt \int d\mathbf{r} \exp i[\mathbf{l} \cdot \mathbf{t} - \mathbf{k} \cdot \mathbf{r}] f^{(i)}(E, \mathbf{t}, \mathbf{r}, z). \quad \dots\dots(8)$$

$$\text{Therefore } h^{(i)}(l_1=0, l_2=0) = \sum_{b=0}^\infty h_{0,b}^{(i)}(v, q) k^b$$

$$\begin{aligned} &= \int_E^\infty dE \left(\frac{E}{E_0} \right)^{v-1} (2\pi)^{-2} \int dt \int d\mathbf{r} \exp [-i\mathbf{k} \cdot \mathbf{r}] f^{(i)}(E, \mathbf{t}, \mathbf{r}, z) \\ &= \sum_{n=0}^\infty (-4)^{-n} (n!)^{-2} k^{2n} \int_E^\infty dE \left(\frac{E}{E_0} \right)^{v-1} f_{0,2n}^{(i)}(E, q) \quad \dots\dots(9) \end{aligned}$$

where $f_{0,2n}^{(i)}$ is the $2n$ th radial moment of the distribution function. We therefore have

$$f_{0,2n}^{(i)}(E, q) = (-4)^n (n!)^2 (2\pi i E_0)^{-1} \int_{v_0-i\infty}^{v_0+i\infty} \left(\frac{E_0}{E} \right)^v h_{0,2n}^{(i)}(v, q) dv \quad \dots\dots(10)$$

with an exactly analogous expression for the $2n$ th angular moment $f_{2n,0}^{(i)}(E, q)$, obtained by putting $l_2=0, k=0$ in (8).

§ 3. IONIZATION LOSS

Equations (7) and (10) are all that is needed to solve for the various moments if we are willing to neglect the effect of the ionization term β . In order to allow for the effect of ionization we first expand the coefficients $h_{a,b}^{(i)}(v, q)$ in a power series in β/E_0 , and then transform this series to the Bhabha-Chakrabarty expansion. The full details of this method can be found in a paper by Messel (1951). Expand

$$h_{a,b}^{(i)}(v, q) = \sum_{n=0}^\infty h_{(n)a,b}^{(i)}(v, q) \left(-\frac{\beta}{E_0} \right)^n. \quad \dots\dots(11)$$

Inserting this expansion into (7) and equating the powers of β/E_0 gives

$$\begin{aligned} &\frac{\partial}{\partial q} h_{(n)a,b}^{(i)}(v, q) - B^{(i)}(v) h_{(n)a,b}^{(i)}(v) D^{(i)}(v) h_{(n)a,b}^{(i)}(v) \\ &= \frac{a+1}{q'(z)} h_{(n)a+1,b-1}^{(i)}(v) + (v-1) h_{(n-1)a,b}^{(i)}(v-1) \delta_{i,1} \\ &\quad + \sum' w_r (r!)^{-2} (-4E_0^2)^{-r} h_{(n)a-2r,b}^{(i)}(v-2r) \delta_{i,1}. \quad \dots\dots(12) \end{aligned}$$

Equation (10) now expands to

$$f_{0,2n}^{(i)}(E, q) = (-4)^n (n!)^2 (2\pi i E_0)^{-1} \sum_{m=0}^\infty \int_{v_0-i\infty}^{v_0+i\infty} \left(\frac{E_0}{E} \right)^v \left(\frac{-\beta}{E_0} \right)^m h_{(m)0,2n}^{(i)}(v, q) dv \quad \dots\dots(13a)$$

or

$$F_{0,2n}^{(i)}(E, q) = (-4)^n (n!)^2 (2\pi i)^{-1} \sum_{m=0}^\infty \int_{v_0-i\infty}^{v_0+i\infty} \left(\frac{E_0}{E} \right)^{v-1} \left(\frac{-\beta}{E_0} \right)^m h_{(m)0,2n}^{(i)}(v, q) \frac{dv}{v-1} \quad \dots\dots(13b)$$

$$\text{where } F_{0,2n}^{(i)}(E, q) = \int_E^\infty f_{0,2n}^{(i)}(E, q) dE.$$

This series is then transformed into the following rapidly convergent series:

$$F_{0,2n}^{(i)}(E, q) = (-4)^n (n!)^2 \sum_{m=0}^{\infty} F_{(m)0,2n}^{(i)}(E, q) \quad \dots\dots (14a)$$

and

$$F_{2n,0}^{(i)}(E, q) = (-4)^n (n!)^2 \sum_{m=0}^{\infty} F_{(m)2n,0}^{(i)}(E, q) \quad \dots\dots (14b)$$

where

$$F_{(m)a,b}^{(i)}(E, q) = \frac{1}{2\pi i} \int_{v_0-i\infty}^{v_0+i\infty} \left(\frac{E_0}{\beta}\right)^{v-1} \left[\frac{\beta}{E + \beta r_{a,b}^{(i)}(v, q)} \right]^{v+m-1} \\ \times \frac{\Gamma(v+m)}{\Gamma(v)} P_{(m)a,b}^{(i)}(v, q) \frac{dv}{v+m-1} \quad \dots\dots (15a)$$

$$P_{(m)a,b}^{(i)}(v, q) = \sum_{\mu=0}^m (-1)^\mu \frac{\Gamma(v)}{\Gamma(v+\mu)} h_{(\mu)a,b}^{(i)}(v, q) [r_{a,b}^{(i)}(v, q)]^{m-\mu} [(m-\mu)!]^{-1} \quad \dots\dots (15b)$$

$$\left. \begin{aligned} P_{(1)a,b}^{(i)}(v, q) &\equiv 0 \\ r_{a,b}^{(i)}(v, q) &= \frac{\Gamma(v)}{\Gamma(v+1)} \frac{h_{(1)a,b}^{(i)}(v, q)}{h_{(0)a,b}^{(i)}(v, q)} \end{aligned} \right\} \quad \dots\dots (15c)$$

We anticipate that for most energy ranges and depths of physical interest the first term $F_{(0)a,b}^{(i)}$ or at most the first and third terms, $F_{(0)} + F_{(2)}$, will be sufficient, and so we include in this paper only those solutions necessary to calculate the various moments from the first term only, although solutions for the higher terms can be written down quite simply from our recursion formula (27).

§ 4. SOLUTION OF THE EQUATION

We must solve the differential recursion equation (12) for the coefficients $h_{(n)a,b}^{(i)}(v, q)$, which can then be inserted in eqns (14) and (15) to give the various radial and angular moments. Now

$$h_0^{(j,i)}(v, q) = G_{\theta}^{(j,i)}(v) \exp [-qa_{\theta}(v)] \quad \dots\dots (16)$$

is the solution of (12) with the right-hand side omitted, and has the boundary value $h_0^{(j,i)}(v, q=0) = \delta_{j,i}$. (For definitions of $G_{\theta}^{(j,i)}(v)$ and $a_{\theta}(v)$ see Green and Messel 1952.) Writing $Q_{(n)a,b}^{(i)}(v, q)$ for the right-hand side of (12), the general solution is

$$h_{(n)a,b}^{(i)}(v, q) = h_0^{(j,i)}(v, q) h_{(n)a,b}^{(j)}(v, q=0) + \int_0^q h_0^{(j,i)}(v, q-t) Q_{(n)}^{(j)}(v, t) dt. \quad \dots\dots (17)$$

In the case of a single incident particle of type α and energy E_0 we have

$$h_{(n)a,b}^{(j)}(v, q=0) = \delta_{j,\alpha} \delta_{n,0} \delta_{a,0} \delta_{b,0}. \quad \dots\dots (17a)$$

We then obtain the following solutions for the average numbers and second moments with ionization loss:

$$h_{(0)0,0}^{(i)}(v, q) = G_{\theta}^{(\alpha,i)} \exp [-qa_{\theta}(v)] \quad \dots\dots (18)$$

$$h_{(1)0,0}^{(i)}(v, q) = (v-1) G_{\theta_1}^{(1,i)}(v) G_{\theta_2}^{(\alpha,1)}(v-1) \exp [-qa_{\theta_1}(v)] \\ \times \int_0^q dq \exp [q\{a_{\theta_1}(v) - a_{\theta_2}(v-1)\}] \quad \dots\dots (19)$$

$$h_{(0)2,0}^{(i)}(v, q) = -\frac{v_1}{4E_0^2} G_{\theta_1}^{(1,i)}(v) G_{\theta_2}^{(\alpha,1)}(v-2) \exp [-qa_{\theta_1}(v)] \\ \times \int_0^q dq \exp [q\{a_{\theta_1}(v) - a_{\theta_2}(v-2)\}] \quad \dots\dots (20)$$

$$\begin{aligned}
h_{(1)2,0}^{(i)}(v, q) = & -(v-3) \frac{w_1}{4E_0^2} G_{\theta_1}^{(1,i)}(v) G_{\theta_2}^{(1,1)}(v-2) G_{\theta_3}^{(\alpha,1)}(v-3) \exp[-qa_{\theta_1}(v)] \\
& \times \int_0^q dq \exp[q\{a_{\theta_1}(v) - a_{\theta_2}(v-2)\}] \int_0^q dq \exp[q\{a_{\theta_2}(v-2) - a_{\theta_3}(v-3)\}] \\
& - (v-1) \frac{w_1}{4E_0^2} G_{\theta_1}^{(1,i)}(v) G_{\theta_2}^{(1,1)}(v-1) G_{\theta_3}^{(\alpha,1)}(v-3) \exp[-qa_{\theta_1}(v)] \\
& \times \int_0^q dq \exp[q\{a_{\theta_1}(v) - a_{\theta_2}(v-1)\}] \int_0^q dq \exp[q\{a_{\theta_2}(v-1) - a_{\theta_3}(v-3)\}] \\
& \dots\dots(21)
\end{aligned}$$

$$\begin{aligned}
h_{(1)0,2}^{(i)}(v, q) = & -\frac{w_1}{2E_0^2} G_{\theta_1}^{(1,i)}(v) G_{\theta_2}^{(\alpha,1)}(v-2) \exp[-qa_{\theta_1}(v)] \int_0^q \frac{dq}{q'(z)} \int_0^q \frac{dq}{q'(z)} \\
& \times \int_0^q dq \exp[q\{a_{\theta_1}(v) - a_{\theta_2}(v-2)\}] \\
& \dots\dots(22)
\end{aligned}$$

$$\begin{aligned}
h_{(1)0,2}^{(i)}(v, q) = & -(v-3) \frac{w_1}{2E_0^2} G_{\theta_1}^{(1,i)}(v) G_{\theta_2}^{(1,1)}(v-2) G_{\theta_3}^{(\alpha,1)}(v-3) \exp[-qa_{\theta_1}(v)] \\
& \times \int_0^q \frac{dq}{q'(z)} \int_0^q \frac{dq}{q'(z)} \int_0^q dq \exp[q\{a_{\theta_1}(v) - a_{\theta_2}(v-2)\}] \\
& \times \int_0^q dq \exp[q\{a_{\theta_2}(v-2) - a_{\theta_3}(v-3)\}] \\
& - (v-1) \frac{w_1}{2E_0^2} G_{\theta_1}^{(1,i)}(v) G_{\theta_2}^{(1,1)}(v-1) G_{\theta_3}^{(\alpha,1)}(v-3) \exp[-qa_{\theta_1}(v)] \\
& \times \left\{ \int_0^q \frac{dq}{q'(z)} \int_0^q \frac{dq}{q'(z)} \int_0^q dq \exp[q\{a_{\theta_1}(v) - a_{\theta_2}(v-1)\}] \right. \\
& + \int_0^q \frac{dq}{q'(z)} \int_0^q dq \exp[q\{a_{\theta_1}(v) - a_{\theta_2}(v-1)\}] \int_0^q \frac{dq}{q'(z)} \\
& + \left. \int_0^q dq \exp[q\{a_{\theta_1}(v) - a_{\theta_2}(v-1)\}] \int_0^q \frac{dq}{q'(z)} \int_0^q \frac{dq}{q'(z)} \right\} \\
& \times \int_0^q dq \exp[q\{a_{\theta_2}(v-1) - a_{\theta_3}(v-3)\}]. \\
& \dots\dots(23)
\end{aligned}$$

The curves in figures 1 and 2 were calculated by us from eqns (18), (20), (22) and (13b) with $m=0$, and so apply only to the high-energy region, where ionization loss can be neglected. The complex integration was carried out by the method of steepest descents.

§ 5. THE GENERAL 2nth MOMENTS

The solution of (12) can be obtained rather more elegantly by throwing it into a matrix form. This also enables us to write down expressions for the general angular and radial moments, which would be too cumbersome to handle in the superfix notation. We shall use the following matrices:

$$\begin{aligned}
\mathbf{B}(v) &= \begin{bmatrix} D^{(1)}(v) & -B^{(1)}(v) \\ -B^{(2)}(v) & D^{(2)} \end{bmatrix} & \mathbf{H}_{(n)a,b}(v, q) &= \begin{bmatrix} h_{(n)a,b}^{(1)} \\ h_{(n)a,b}^{(2)} \end{bmatrix} \\
\mathbf{R} &= \begin{bmatrix} 1 & 0 \\ 0 & 0 \end{bmatrix} & \mathbf{S}^{(1)} &= \begin{bmatrix} 1 \\ 0 \end{bmatrix} & \mathbf{S}^{(2)} &= \begin{bmatrix} 0 \\ 1 \end{bmatrix} \\
\mathbf{S}_\theta(v) &= \begin{bmatrix} G_{\theta}^{(1,1)} & G_{\theta}^{(2,1)} \\ G_{\theta}^{(1,2)} & G_{\theta}^{(2,2)} \end{bmatrix}.
\end{aligned}$$

Then $a_1(v)$ and $a_2(v)$ are the eigenvalues of $\mathbf{B}(v)$ and

$$\mathbf{G}_\theta(v) = [\mathbf{B}(v) - a_{3-\theta}(v)\mathbf{E}]\{a_\theta(v) - a_{3-\theta}(v)\}^{-1}. \quad \dots\dots(24)$$

We shall also use the following matrix operators:

$$\mathbf{J}(v) = \exp \{-\mathbf{B}(v)q\} \int_0^q dq \exp \{\mathbf{B}(v)q\}; \quad \mathbf{K}(v) = \mathbf{J}(v) \frac{1}{q'(z)}.$$

The solutions we shall obtain in matrix form can be converted back to the $G_\theta^{(i,j)}$ form by application of Sylvester's theorem (Frazer *et al.* 1938), which reduces in this instance to

$$f\{\mathbf{B}(v)\} = \mathbf{G}_\theta(v)f\{a_\theta(v)\} \quad \dots\dots(25a)$$

$$\mathbf{G}_{\theta_1}(v)\mathbf{G}_{\theta_2}(v) = \mathbf{G}_{\theta_1}(v)\delta_{\theta_1, \theta_2}. \quad \dots\dots(25b)$$

Converted to matrix form, eqn (12) now becomes

$$\begin{aligned} \frac{\partial}{\partial q} \mathbf{H}_{(n)a, b}(v, q) + \mathbf{B}(v) \mathbf{H}_{(n)a, b}(v) &= \frac{a+1}{q'(z)} \mathbf{H}_{(n)a+1, b-1}(v) \\ &+ (v-1)\mathbf{R}\mathbf{H}_{(n-1)a, b}(v-1) + \sum' w_r(r!)^{-2}(-4E_0^2)^{-r} \mathbf{R}\mathbf{H}_{(n)a-2r, b}(v-2r). \end{aligned} \quad \dots\dots(26)$$

The solution of this equation is

$$\begin{aligned} \mathbf{H}_{(n)a, b}(v, q) &= (a+1)\mathbf{K}(v) \mathbf{H}_{(n)a+1, b-1}(v) + (v-1)\mathbf{J}(v)\mathbf{R}\mathbf{H}_{(n-1)a, b}(v-1) \\ &+ \sum' w_r(r!)^{-2}(-4E_0^2)^{-r} \mathbf{J}(v)\mathbf{R}\mathbf{H}_{(n)a-2r, b}(v-2r) + \exp[-\mathbf{B}(v)q] \mathbf{H}_{(n)a, b}(v, q=0). \end{aligned} \quad \dots\dots(27)$$

By an iteration process it is possible to obtain from this equation expressions for all angular and radial moments and for all the terms in the Bhabha-Chakrabarty expansion. We here give the expressions needed to calculate all moments using the first term only of the expansion.

$$\mathbf{H}_{(0)0, 0}(v, q) = \exp[-\mathbf{B}(v)q] \mathbf{S}^{(\alpha)}. \quad \dots\dots(28)$$

$$\mathbf{H}_{(1)0, 0}(v, q) = (v-1)\mathbf{J}(v)\mathbf{R}\mathbf{H}_{(0)0, 0}(v-1, q) \quad \dots\dots(29)$$

$$\mathbf{H}_{(0)2n, 0}(v, q) = (-4E_0^2)^{-n} \sum_{p(n)} \left\{ \prod_{i=1}^k \left[\frac{w_{a_i}}{(a_i!)^2} \mathbf{J}(v) \mathbf{R} \mathbf{I}_v^{-2a_i} \right] \right\} \mathbf{H}_{(0)0, 0}(v, q) \quad \dots\dots(30)$$

$$\begin{aligned} \mathbf{H}_{(1)2n, 0}(v, q) &= (-4E_0^2)^{-n} \sum_{p(n)} \sum_{m=0}^k \left\{ \prod_{i=1}^k \left[\frac{w_{a_i}}{(a_i!)^2} \right] \prod_{i=1}^m [\mathbf{J}(v) \mathbf{R} \mathbf{I}_v^{-2a_i}] (v-1) \right. \\ &\times \left. \mathbf{J}(v) \mathbf{R} \mathbf{I}_v^{-1} \prod_{i=m+1}^k [\mathbf{J}(v) \mathbf{R} \mathbf{I}_v^{-2a_i}] \right\} \mathbf{H}_{(0)0, 0}(v, q) \end{aligned} \quad \dots\dots(31)$$

$$\begin{aligned} \mathbf{H}_{(0)0, 2n}(v, q) &= (-4E_0^2)^{-n} \prod_{j=1}^{2n} \left[\sum_{b_j=0}^{[\frac{1}{2}(j-1)]-C_{j-1}} C_{j-1} \right] \prod_{j=1}^{2n} (j-2C_j) \\ &\times \prod_{j=1}^{2n+1} \left[\sum_{p(b_j)} \left\{ \prod_{i=1}^k \left[\frac{w_{a_i}}{(a_i!)^2} \mathbf{J}(v) \mathbf{R} \mathbf{I}_v^{-2a_i} \right] \right\} \mathbf{K}(v) \right] \\ &\times \mathbf{K}^{-1}(v) \mathbf{H}_{(0)0, 0}(v, q) \end{aligned} \quad \dots\dots(32)$$

$$\begin{aligned} \mathbf{H}_{(1)0, 2n}(v, q) &= (-4E_0^2)^{-n} \prod_{j=1}^{2n+1} \left[\sum_{b_j=0}^{[\frac{1}{2}(j-1)]-C_{j-1}} C_{j-1} \right] \sum_{m=0}^{2n} \prod_{j=1}^m (j-2C_j) \prod_{j=m+2}^{2n+1} \\ &\times (j-2C_j-1) \prod_{j=1}^{m+1} \left[\sum_{p(b_j)} \left\{ \prod_{i=1}^k \left[\frac{w_{a_i}}{(a_i!)^2} \mathbf{J}(v) \mathbf{R} \mathbf{I}_v^{-2a_i} \right] \right\} \mathbf{K}(v) \right] \mathbf{K}^{-1}(v)(v-1) \\ &\times \mathbf{J}(v) \mathbf{R} \mathbf{I}_v^{-1} \prod_{j=m+2}^{2n+2} \left[\sum_{p(b_j)} \left\{ \prod_{i=1}^k \left[\frac{w_{a_i}}{(a_i!)^2} \mathbf{J}(v) \mathbf{R} \mathbf{I}_v^{-2a_i} \right] \right\} \mathbf{K}(v) \right] \mathbf{K}^{-1}(v) \\ &\times \mathbf{H}_{(0)0, 0}(v, q) \end{aligned} \quad \dots\dots(33)$$

where $\sum_{p(n)}$ means sum over all different partitions of n , $\sum_{i=1}^k a_i = n$, $a_i \geq 1$, \mathbf{I}_v^{-a} is the operator defined by $\mathbf{I}_v^{-a} f(v) = f(v-a) \mathbf{I}_v^{-a}$; $[\frac{1}{2}j]$ means the integral part of $\frac{1}{2}j$, i.e. either $\frac{1}{2}j$ or $(j-1)/2$; $C_j = \sum_{i=1}^j b_i$; in (32) $C_{2n+1} = n$; in (33) $C_{2n+2} = n$.

§ 6. ASYMPTOTIC VALUES OF THE MOMENTS AND THE RECONSTRUCTION OF THE DISTRIBUTION FUNCTIONS

As Messel and Green (1952) and Green and Messel (1953) have shown, it is possible to reconstruct the angular and radial distribution functions, if given the numerical values of the first few moments and the asymptotic behaviour of the $2n$ th moment. From eqns (30) and (32) we can easily show that the $2n$ th angular moment increases asymptotically as $(n!)^2$ or n^{2n} and the $2n$ th radial moment as $(n!)^2(2n)!$ or n^{4n} . If we define $\Omega^{(i)}(E, t, q)t dt$ to be the angular distribution function and $R^{(i)}(E, r, q)r dr$ the radial function so that

$$\Omega^{(i)}(E, t, q) = (2\pi)^{-1} \int d\mathbf{r} f^{(i)}(E, \mathbf{t}, \mathbf{r}, q)$$

$$R^{(i)}(E, r, q) = (2\pi)^{-1} \int d\mathbf{t} f^{(i)}(E, \mathbf{t}, \mathbf{r}, q)$$

then we have

$$\Omega^{(i)}(E, t, q) = w^{(i)}(E, q; t) \exp [-w_0^{(i)}(E, q) \cdot t]$$

$$R^{(i)}(E, r, q) = r^{(i)}(E, q; r) \exp [-r_0^{(i)}(E, q) \cdot r^{1/2}]$$

where $w^{(i)}(E, q; t)$ and $r^{(i)}(E, q; r)$ are polynomials in t^2 and r^2 respectively, in which the coefficient of t^{2s} (or r^{2s}) depends on the values of all the moments up to the $2s$ th. If the numerical values of all moments up to the $2n$ th are available the procedure is to find all the coefficients up to the $(n-1)$ th and then calculate $w_0^{(i)}$ (or $r_0^{(i)}$) to give the $2n$ th moment correctly. As we have only calculated, so far, the second moments it is impossible to make any estimate of the number of moments required to give a fair approximation to the actual distribution functions.

If, however, in addition to the above information, we know the true behaviour of the distribution functions near the origin (small r or t) then the functions may be approximated to great accuracy by use of only one or two moments and the asymptotic value of the higher moments.

§ 7. DISCUSSION

We have given in this paper a simple method for obtaining all the angular and radial moments exactly and the distribution functions themselves to any required degree of accuracy for all depths of penetration for an electron-photon shower in which energy losses due to ionization are taken into account in any medium. Our technique is mathematically simpler than those used by others (for instance Eyges and Fernbach 1951, Roberg and Nordheim 1949) to obtain much less information, usually the so-called track length distribution, which is the lateral distribution integrated over the entire length of the shower.

In figure 1 we have plotted the mean square angular spread $\langle \theta^2 \rangle$ for an electron producing electrons $[\langle \theta^2 \rangle = F_{2,0}/F_{0,0}]$ multiplied by the square of the energy E in Mev, against $\log_{10}(E_0/E)$ for various values of the depth, measured

in cascade units. It will be remembered that the angular spread is independent of the number density distribution of the medium concerned, hence the results are valid for all media. We have also plotted on the same figure the curve for the angular spread at the shower maximum. It will be noted that this curve is not independent of primary energy as assumed by previous authors: for instance we have also included the point given by Roberg and Nordheim (1949); this value is only approximately valid for $\log_{10}(E_0/E) > 6$. The behaviour of the curves for various depths is that which would be expected from straightforward qualitative reasoning; the mean square spread increasing with increasing depth and decreasing E_0/E . It may easily be shown that each curve cuts the $E^2 \langle \theta^2 \rangle$ axis at the point $w_1 q$, and hence the curves do not pass through a maximum.

In figure 2 we have plotted the curves for the root mean square radial spread multiplied by the energy E , for electrons producing electrons in a medium of constant density, against $\log_{10}(E_0/E)$ for various values of the depth variable. $E\sqrt{r^2}$ is measured in mev cascade units and is defined by $E\sqrt{r^2} = E(F_{0,2}/F_{0,0})^{1/2}$. Here again the value of $E\sqrt{r^2}$ increases with increasing depth and decreasing value of E_0/E . For $E \rightarrow E_0$ the curves approach the value $12.1q^{1.5}$. The behaviour of the curves for media of constant density is very different from that found for the case of variable density (see Green and Messel 1952). We have also plotted the curve for $E\sqrt{r^2}$ at the shower maximum and given the point found by Roberg and Nordheim. It appears, assuming that our work is correct, that even in this limited case these authors were in considerable error.

ACKNOWLEDGMENT

One of us (B. A. C.) wishes to express his thanks to the Research Committee of the University of Adelaide for the provision of a Research Fellowship.

REFERENCES

- BHABHA, H. J., and CHAKRABARTY, S. K., 1943, *Proc. Roy. Soc. A*, **181**, 267; 1948, *Phys. Rev.*, **74**, 1352.
 EYGES, L., and FERNBACH, S., 1951, *Phys. Rev.*, **82**, 23.
 FRAZER, R. A., DUNCAN, W. J., and COLLAR, A. R., 1938, *Elementary Matrices* (Cambridge : University Press).
 GREEN, H. S., and MESSEL, H., 1952, *Phys. Rev.*, **88**, 331; 1953, *Quart. J. Appl. Maths.*, in the press.
 JÁNOSSY, L., 1950, *Cosmic Rays* (Oxford : University Press).
 MESSEL, H., 1951, *Phys. Rev.*, **83**, 21.
 MESSEL, H., and GREEN, H. S., 1952, *Phys. Rev.*, **87**, 738; 1953, *Proc. Phys. Soc.*, **66**, 1009.
 ROBERG, J., and NORDHEIM, L. W., 1949, *Phys. Rev.*, **75**, 444.

Studies in Intermediate Coupling—II: Radiative Transitions in Light Nuclei

BY A. M. LANE* AND L. A. RADICATI

Department of Mathematical Physics, University of Birmingham

Communicated by R. E. Peierls ; MS. received 7th September 1953

Abstract. Formulae are presented for the matrix elements of the various types of radiative transitions of low multipolarity that are frequently met in light nuclei. These formulae are derived on the basis of the nuclear shell-model. First of all, extreme L - S coupling and extreme j - j coupling are considered with a view to seeing if either can give an adequate account of the experimental data. It is found, in fact, that neither extreme mode of coupling can do this, but that an intermediate coupling probably could. As an example, the radiative transitions in ^{13}N are studied in detail in intermediate coupling and are found to give considerable support to this contention.

§ 1. INTRODUCTION

WEISSKOPF (1951) has given expressions for the matrix elements of radiative transitions in nuclei. These expressions assume that only one particular nucleon in a nucleus is responsible for a transition, and the presence of the other particles is ignored. This drastic assumption has the consequence that all the matrix elements of transitions of a given multipole character are predicted to be constant for all nuclei, except for some slight dependence upon the size of the nucleus. Wilkinson (1953 a) has examined the experimental data on E1 and M1 transitions in light elements and has tabulated values of $(2J+1)|M|^2$, where J is the spin of the emitting state and $|M|^2$ is the ratio of the experimental to the single-particle radiative width. The variation in the values for E1 transitions is by about a factor of six and, for M1 transitions, about a hundred. Kinsey (1953) has reached similar conclusions from a study of medium nuclei.

Even accepting that the E1 transitions are in reasonable accord with the single-particle model, the M1 transitions clearly are not. Furthermore there are suspected E1 transitions in light elements whose matrix elements would increase the spread of values in the Wilkinson tabulation considerably.

From the theoretical point of view, some cases of severe disagreement of the single-particle model with experiment are to be expected. The nuclear shell-model in its correct form does not allow one, in general, to isolate a particular particle in a nucleus for the purpose of explaining certain effects. The wave functions of states containing 'equivalent' particles (particles in the same shell) must be correctly constructed according to the Pauli principle, and no one particle can be given any special significance. These considerations apply, *a fortiori*, to other nuclear models which assume a more strongly coupled

* Now at Theoretical Physics, Atomic Energy Research Establishment, Harwell, Didcot, Berks.

motion of the nucleons. Such a point of view has already been adopted by Flowers (1952) and Umezawa (1952) in their analysis of the magnetic moments of nuclei. They show that the discrepancies between the observed values and those predicted by the single-particle (Schmidt) model can often be reduced by taking account of all nucleons present.

The single-particle model may serve as a convenient standard for comparing experimental data but, because of its oversimplified nature, it cannot be used as a true test of the shell-model. On the other hand, a shell-model taking all nucleons into account (the 'individual particle model') can provide such a test, and also make possible conclusions about the mode of coupling (L - S , j - j or intermediate) existing in nuclei. Only in special circumstances, such as those of a single hole or single particle outside a closed shell, can the single particle model be expected to give a true picture of a nucleus.

The present paper describes how the single-particle predictions for radiative transitions must be corrected according to the ideas of the individual particle model. In the following section we present formulae for the matrix elements of $E1$, $M1$ and $E2$ transitions in L - S and in j - j coupling. These are the only types of transition that one is likely to find frequently in light nuclei. The next section contains an analysis of experimentally observed transitions in the light of the formulae. Finally the situation of intermediate coupling is examined in the specific cases of the $E1$ and $M1$ transitions in ^{13}N .

§ 2. MATRIX ELEMENTS FOR RADIATIVE TRANSITIONS IN THE INDIVIDUAL PARTICLE MODEL

We can express the radiative width for a transition of multipolarity k as follows (Weisskopf 1951)

$$\Gamma_k = \frac{8\pi(k+1)}{k[(2k+1)!]^2} \left(\frac{E}{\hbar c}\right)^{2k+1} \sum_q |\langle JM | H_q^{(k)} | J' M' \rangle|^2 \quad \dots (1)$$

where J, J' are the spins of the initial and final states, M, M' are the corresponding magnetic quantum numbers, $H_q^{(k)}$ is the electromagnetic interaction operator of multipolarity k inducing change q in the magnetic quantum numbers between the initial and final states. The summation is over q , $M (= M' + q)$ being fixed (the value of Γ_k does not depend on M). E is the energy change in the transition and \hbar, c have their usual meaning.

Simple relations exist between the various matrix elements of tensor operators such as $H_q^{(k)}$:

$$\frac{\langle JM | H_q^{(k)} | J' M' \rangle}{C_{q M' M}^{k J' J}} = \frac{\langle JM | H_0^{(k)} | J' M \rangle}{C_{0 M M}^{k J' J}} = (-)^{k+J'-J} \langle J || H^{(k)} || J' \rangle. \quad \dots (2)$$

In this equation, the denominators are Wigner coefficients and $\langle J || H^{(k)} || J' \rangle$ is a 'reduced matrix element' into which a normalizing factor $(2J+1)^{1/2}$ that occurs in the usual definition (Racah 1943) is incorporated for convenience. The reduced matrix elements do not depend upon magnetic quantum numbers, and the summation over q in (1) can be reduced simply to $|\langle J || H^{(k)} || J' \rangle|^2$. We shall now evaluate the reduced matrix elements for various types of transition assuming a shell model.

In general we shall be dealing with states involving equivalent particles and so, as already mentioned, we cannot resort to a single-particle model. In

order to evaluate the matrix elements in such cases we use the theory of fractional parentage of nuclear states, introduced by Racah (1943) and developed for L - S coupling by Jahn and van Wieringen (1951), and for j - j coupling by Flowers and Edmonds (1952). We shall not give details of the algebra encountered in finding expressions for the matrix elements because this is of the usual type used in the manipulation of Wigner and Racah coefficients.

The operator $H_q^{(k)}$ is a 'single-particle operator' in the sense that it is a sum of terms, $\sum_i H_{q_i}^{(k)}$ each of which operates on one nucleon, i , only. (An immediate consequence of this is the general selection rule that all radiative transitions are strictly forbidden between two states differing in configuration by more than one particle.) By far the most common type of transition that is met in practice in light elements can be written in L - S coupling as

$$l^{n-1}l_0(\alpha TSL, J) \rightarrow l^{n-1}l_1(\alpha' T'S'L', J') \quad \dots\dots(3a)$$

i.e. a nucleon in the l_0 orbit goes into the l_1 orbit in the presence of $n-1$ equivalent nucleons in the l orbit. As special cases, any two of l, l_0, l_1 may be equal, or even all three. T, S, L denote the total isotopic spin, ordinary spin and orbital angular momentum of the emitting state, and α denotes any other quantum numbers needed to specify the state. The dash denotes corresponding quantities for the final state.

Corresponding to (3a) in j - j coupling we have:

$$j^{n-1}j_0(\alpha TJ) \rightarrow j^{n-1}j_1(\alpha' T'J') \quad \dots\dots(3b)$$

and the same remarks apply except that now, of course, we speak about different j -orbits j, j_0, j_1 instead of l -orbits.

We can divide all the operators with which we shall be dealing into 'space' and 'spin' operators. The first type only operates on the space variables and so, for instance, cannot alter the total ordinary spin S in L - S coupling. The second type cannot alter the total orbital angular momentum L and so, in L - S coupling, each of the two types has special selection rules. This means that certain transitions that are allowed in j - j coupling will be forbidden in L - S coupling. On the other hand there are other transitions, allowed in L - S coupling, that are forbidden in j - j coupling due to the previously mentioned selection rule forbidding transitions between two states differing in configuration by more than one particle (a situation more likely to arise in j - j coupling because two particles in the same orbit - equivalent in L - S coupling - may have different j -values and so be inequivalent in j - j coupling). It is clear that matrix elements in general will be very sensitive to the predominant mode of coupling in nuclei.

Using the theory of fractional parentage, we can express the matrix elements as a sum over all parent states $p \equiv (\alpha_p T_p S_p L_p)$ of l^{n-1} . For *space* operators in L - S coupling, the reduced matrix elements in (2) are:

$$\begin{aligned} \langle J(LS) || H^{(k)}(\text{space}) || J'(L'S') \rangle \\ = \delta_{SS'} (-)^{k_n} [\sum_p U(kl_1 L L_p, l_0 L') U(kL' J S, L J') \langle \alpha_p || \alpha \rangle \langle \alpha_p || \alpha' \rangle (\frac{1}{2} \delta_{TT'} - \mathcal{F}_p)] \\ \times \langle l_0 || H_i^{(k)}(\text{space}) || l_1 \rangle \quad \dots\dots(4) \end{aligned}$$

where $\langle \alpha_p || \alpha \rangle$ is written for the full fractional parentage coefficients

$$\langle l^{n-1}(\alpha_p T_p S_p L_p) l_0 || l^{n-1} l_0(\alpha TSL) \rangle$$

the values of which are discussed in the next section. The $\langle l_0 || H_i^{(k)}(\text{space}) || l_1 \rangle$

are reduced matrix elements, as defined in eqn (2), for the spatial motion of a single particle i . The quantities U are related to Racah functions by

$$U(abcd, ef) = \{(2e+1)(2f+1)\}^{1/2} W(abcd, ef).$$

The radiative effects of spatial motion that we are considering can only arise from charged particles (protons), and so the spatial operator contains a factor $(\frac{1}{2} - t_z)$ for each nucleon, t_z having eigenvalues $+\frac{1}{2}$ for neutrons, $-\frac{1}{2}$ for protons. This gives rise to the factor we have written $(\frac{1}{2}\delta_{TT'} - \mathcal{T}_p)$ in eqn (4), \mathcal{T}_p being defined as:

$$\mathcal{T}_p = \sum_{m_t} C_{M_T p}^{T_p \frac{1}{2} T} C_{M_T p}^{T_p \frac{1}{2} T'} m_t = (-)^{2T_p - T - T'} \frac{\sqrt{3}}{2} U(1\frac{1}{2} T T_p, \frac{1}{2} T') C_{0 M_T M_T}^{1 T' T}.$$

The reduced matrix elements of *spin* operators in L - S coupling can be written:

$$\begin{aligned} \langle J(LS) || H^{(k)}(\text{spin}) || J'(L'S') \rangle \\ = \delta_{LL'} (-)^{k+J'-J+S-S'} n [\sum_p U(kS'JL, SJ') U(kSS_p, sS') \langle \alpha_p || \alpha \rangle \langle \alpha_p || \alpha' \rangle \\ \times \{ (\frac{1}{2}\delta_{TT'} - \mathcal{T}_p) \langle s || H_{i=p}^{(k)}(\text{spin}) || s \rangle + (\frac{1}{2}\delta_{TT'} + \mathcal{T}_p) \langle s || H_{i=n}^{(k)}(\text{spin}) || s \rangle \}]. \end{aligned} \quad (5)$$

where the $\langle s || H_i^{(k)}(\text{spin}) || s \rangle$ are reduced matrix elements for the spin s ($=\frac{1}{2}$), of a single particle i ($i=p$ for proton, $=n$ for neutron).

In j - j coupling the space and spin operators give respectively:

$$\begin{aligned} \langle J(j^{n-1}j_0) || H^{(k)}(\text{space}) || J'(j^{n-1}j_1) \rangle \\ = (-)^{k+l_0+l_1} n [\sum_p U(kj_1JJ_p, j_0J') U(kl_1j_0s, l_0j_1) \langle \alpha_p || \alpha \rangle \langle \alpha_p || \alpha' \rangle \\ \times \langle \alpha_p || \alpha' \rangle (\frac{1}{2}\delta_{TT'} - \mathcal{T}_p) \langle l_0 || H_i^{(k)}(\text{space}) || l_1 \rangle] \dots\dots\dots (6) \\ \langle J(j^{n-1}j_0) || H^{(k)}(\text{spin}) || J'(j^{n-1}j_1) \rangle \\ = \delta_{l_0l_1} (-)^{k+1} n [\sum_p U(kj_1JJ_p, j_0J') U(ksj_1l_0, sj_0) \langle \alpha_p || \alpha \rangle \langle \alpha_p || \alpha' \rangle \\ \times \{ (\frac{1}{2}\delta_{TT'} - \mathcal{T}_p) \langle s || H_{i=p}^{(k)}(\text{spin}) || s \rangle + (\frac{1}{2}\delta_{TT'} + \mathcal{T}_p) \langle s || H_{i=n}^{(k)}(\text{spin}) || s \rangle \}]. \end{aligned} \quad (7)$$

In all formulae throughout the present work, the phase conventions of Racah (1943) are used. We shall now specify the single-particle operators $H_{0i}^{(k)}$ and evaluate the single-particle reduced matrix elements in the case of E1, E2 and M1 transitions.

For E1 and E2 transitions, the total operator consists of a spin and a space part. The contribution of the former is very much less than the latter (unless the latter is forbidden for some reason) and will be ignored (Gell-Mann and Telegdi 1953). Since an E1 transition ($k=1$) leads to a change in parity and a change in orbital momentum of one unit, $l_0 = l_1 \pm 1$. An E2 transition ($k=2$) does not change parity, so $l_0 = l_1$ or $l_1 \pm 2$. The single particle (space) operator for these electric transitions is:

$$H_{0i}^{(k)}(\text{space}) = e r^k Y_{k0}(\theta, \phi) \dots\dots\dots (8)$$

where Y_{k0} is a normalized spherical harmonic, (r, θ, ϕ) are radial coordinates and e is the unit of electric charge.

For E1 radiation this means that (using eqn (2)):

$$\langle l_0 || H^{(1)}(\text{space}) || l_1 \rangle = e \sqrt{\frac{3}{4\pi}} \frac{\langle l_0 0 | r \cos \theta | l_1 0 \rangle}{C_{000}^{1l_1l_0}} \dots\dots\dots (9)$$

and for E2 radiation:

$$\langle l_0 || H^{(2)}(\text{space}) || l_1 \rangle = e \sqrt{\frac{5}{16\pi}} \frac{\langle l_0 0 | (3 \cos^2 \theta - 1) r^2 | l_1 0 \rangle}{C_{000}^{2l_1l_0}} \dots\dots\dots (10)$$

Both expressions depend upon the radial wave functions and so there is some uncertainty in their numerical evaluation depending upon the potential well we choose.

For M1 transitions there is no change in parity and no particle can change its orbit, so $l_0 = l_1$. The operators for M1 transitions are:

$$H_{0i}^{(1)}(\text{space}) = \left(\frac{3}{4\pi}\right)^{1/2} \frac{e\hbar}{2Mc} l_{zi}; \quad H_{0i}^{(1)}(\text{spin}) = \left(\frac{3}{4\pi}\right)^{1/2} \frac{e\hbar}{2Mc} g_i s_{zi} \quad \dots\dots (11)$$

where g_i is the gyromagnetic ratio ($i = p$ for a proton, n for a neutron) in nuclear magnetons $e\hbar/2Mc$, and s_{zi} is the spin component operator with eigenvalues $\pm \frac{1}{2}$. One can now show that, for M1 transitions (space):

$$\langle l_0 || H^{(1)}(\text{space}) || l_0 \rangle = - \{l_0(l_0 + 1)\}^{1/2} \frac{e\hbar}{2Mc} \left(\frac{3}{4\pi}\right)^{1/2} \quad \dots\dots (12)$$

and for M1 transitions (spin):

$$\langle s || H^{(1)}(\text{spin}) || s \rangle = - \frac{\sqrt{3}}{2} g_i \frac{e\hbar}{2Mc} \left(\frac{3}{4\pi}\right)^{1/2} \quad \dots\dots (13)$$

Unlike the corresponding expressions for the E1 and E2 transitions, these quantities do not depend upon the radial wave functions and so there is no uncertainty in their numerical values from this source.

Finally, having expressed the matrix elements for general transitions in terms of these for single particles, we draw attention to the several sum-rules that can be formulated for the squares of matrix elements of transitions between two configurations involving several particles. They are too numerous and of insufficient practical consequence to give here. They are easily derived from the orthonormality properties of the Racah and fractional parentage coefficients and are closely related to the sum rules of atomic spectroscopy (Condon and Shortley 1951). It suffices to mention that the sums can be considered as upper limits to the matrix elements of particular transitions.

§ 3. COMPARISON WITH EXPERIMENTAL DATA IN LIGHT NUCLEI

Before we can compare the predictions from our formulae with experiment we must discuss the values to be used for the fractional parentage coefficients $\langle x_p || x \rangle$ in eqns (4)–(7) and the values to be used for the radial integrals in (9) and (10).

For states consisting of n equivalent particles only, the fractional parentage coefficients in extreme L – S or extreme j – j coupling do not depend on the detailed nature of the nuclear forces and can be given explicit numerical values (for L – S coupling see Jahn and van Wieringen (1951); for j – j coupling see Flowers and Edmonds (1952)). For states consisting of $n-1$ equivalent particles and one odd particle, however, the coefficients will generally depend upon the nuclear forces and, in particular, upon the ratio of the interaction matrix elements between particles in different orbits to those between particles in the same orbit. If this ratio is small then, to each state of the mixed configuration $l^{n-1}l_0$ we can assign a unique parent state p of l^{n-1} and then, according to the normalization implied by the factor n in eqns (4)–(7), the fractional parentage coefficient for this parent is $n^{-1/2}$, and all other coefficients are zero. There is a certain amount of evidence that this approximation is a good one in light nuclei. This is perhaps surprising in view of the fact that it is long-range forces that tend to make inter-orbit interactions weak, whereas nuclear forces are short-range ones and

so there is no strong theoretical justification for assuming that particles in different orbits interact much less strongly than those in the same orbit. There are cases, however, where the low-lying states of the parent nucleus belonging to l^{n-1} are widely spaced and the inter-orbit interaction may not be strong enough to mix these states. One of the best examples of this is the ^{12}C nucleus in its ground state which is the parent state of the first excited states in ^{13}C and ^{13}N . The latter states have the configuration $1p^8 2s^1$ and unpublished calculations by one of us (Lane) show that all the features of these states (reduced width, coulomb shift, etc.) are consistent with the assumption that the ^{12}C 'core' is in its ground state and almost undisturbed by the presence of the 2 particle, which 'sees' it as a simple potential well. This would seem to be due to the fact that the first excited state that could be an alternative parent state is at a high excitation of 7.68 mev. (It is interesting that there appears to be another state of $1p^8 2s^1$ in ^{13}C at 7.75 mev, and this may have this 7.68 mev state in ^{12}C as its parent.) We shall thus tentatively make the approximation that each state of $l^{n-1}l_0$ has a unique parent state of l^{n-1} , with a corresponding value of the fractional parentage coefficient of $n^{-1/2}$. The corresponding approximation for the $j-j$ configurations $p_{3/2}^n p_{1/2}$ has been discussed by Inglis (1953).

The values of the radial integrals in (9) and (10) can only be estimated after assuming some kind of potential well for the single particle wave functions. In order to make such an estimate we first consider the first excited state of ^{13}N . As explained above, one can fit all the observed data on this state by assuming that the odd 2s-proton moves in a square well with a certain depth and radius. Using this well to estimate the single-particle radial integrals, we find for the most commonly met cases of E1 and E2 transitions:

$$\left. \begin{aligned} \frac{\langle 2s, 0 | r \cos \theta | 1p, 0 \rangle}{C_{000}^{110}} &= - \int \psi_{2s}(r) r \psi_{1p}(r) dr = 1.80 \times 10^{-13} \text{ cm} \\ \frac{\langle 1d, 0 | r \cos \theta | 1p, 0 \rangle}{C_{000}^{112}} &= \sqrt{\frac{2}{5}} \int \psi_{1d}(r) r \psi_{1p}(r) dr = 2.0 \times 10^{-13} \text{ cm} \\ \frac{\langle 1p, 0 | r^2 (3 \cos^2 \theta - 1) | 1p, 0 \rangle}{C_{000}^{211}} &= - \sqrt{\frac{8}{5}} \int \psi_{1p}^2(r) r^2 dr = -1.15 \times 10^{-25} \text{ cm}^2. \end{aligned} \right\} \dots (14)$$

These numerical values may be sensitive to the choice of well, especially the first case in which the value depends on a difference of positive and negative contributions to the radial integral. In order to check the dependence on well shape, the matrix elements were recalculated using a harmonic oscillator well. It was found that all values agreed with those of (14) to within 15%. For other nuclei near $A=13$ one expects that the values for the integrals are not very different from (14)—perhaps the error may be as large as a factor of 30%.

In tables 1, 2 and 3 are given lists of the observed E1, M1 and E2 transitions in nuclei of the 1p shell ($A=5$ to 16). The first seven columns give the emitting and final states with their believed spins, parities and isotopic spins. The next column gives the observed radiation width, and the following one gives a dimensionless quantity containing the square of the reduced matrix element extracted from the observed radiation width. For E1 and E2 transitions this quantity is

$$\Lambda = \frac{|\langle J || H^{(k)} || J' \rangle|^2}{|\langle l_0 || H_i^{(k)} || l_1 \rangle|},$$

Table 2. M1 Transitions

(1)	(2)	(3)	(4)	(5)	(6)	(7)	(8)	(9)	(10)	(11)	(12)	(13)	
${}^7\text{Li}$	0.478	$\frac{1}{2}-$	$\frac{1}{2}$	0	$\frac{1}{2}-$	$\frac{1}{2}$	0.003	9.8	$\begin{Bmatrix} 22\text{P} \\ 13\text{P} \\ 33\text{P} \end{Bmatrix}$	18.36	$\begin{Bmatrix} [\frac{1}{2} \frac{1}{2}] \\ [\frac{3}{2} \frac{1}{2}] \\ [1 \ 1] \end{Bmatrix} p_{1/2}$	$\begin{Bmatrix} [\frac{1}{2} \frac{1}{2}] \\ [0 \ 0] \\ [0 \ 0] \end{Bmatrix}$	2.70
${}^8\text{Be}$	17.63	$1+$	$\begin{Bmatrix} 0 \\ 1 \end{Bmatrix}$	0	$0+$	0	17	1.15	$\begin{Bmatrix} 11\text{S} \\ 11\text{S} \end{Bmatrix}$	0	$\begin{Bmatrix} [\frac{3}{2} \frac{1}{2}] \\ [1 \ 1] \end{Bmatrix} p_{1/2}$	$\begin{Bmatrix} [0 \ 0] \\ [0 \ 0] \end{Bmatrix}$	$\begin{Bmatrix} 1.09 \\ 0.94 \end{Bmatrix}$
${}^8\text{Be}$	17.63	$1+$	$\begin{Bmatrix} 0 \\ 1 \end{Bmatrix}$	2.9	$2+$	0	8.3	0.97	$\begin{Bmatrix} 11\text{D} \\ 11\text{D} \end{Bmatrix}$	0	$\begin{Bmatrix} [\frac{3}{2} \frac{1}{2}] \\ [1 \ 1] \end{Bmatrix} p_{1/2}$	$\begin{Bmatrix} [2 \ 0] \\ [2 \ 0] \end{Bmatrix}$	
${}^{10}\text{B}$	4.78	$1+$	0	0.72	$1+$	0	~ 0.15	0.79	$\begin{Bmatrix} 13\text{S} \\ 13\text{S} \end{Bmatrix}$	0	$\begin{Bmatrix} [\frac{3}{2} \frac{1}{2}] \\ [\frac{5}{2} \frac{1}{2}] \end{Bmatrix} p_{1/2}$	$\begin{Bmatrix} [1 \ 0] \\ [1 \ 0] \end{Bmatrix}$	
${}^{10}\text{B}$	5.16	$2+$	1	0	$3+$	0	~ 0.03	~ 0.1	$\begin{Bmatrix} 13\text{D}_{\text{I(II)}} \\ 13\text{D}_{\text{I(II)}} \end{Bmatrix}$	0	$[2 \ 0]$	$[3 \ 0]$	6.42
${}^{10}\text{B}$	5.16	$2+$	1	0.72	$1+$	0	~ 0.15	~ 0.7	$\begin{Bmatrix} 13\text{S} \\ 13\text{S} \end{Bmatrix}$	$\begin{Bmatrix} 0 \\ 0 \end{Bmatrix}$	$[2 \ 0]$	$[1 \ 0]$	7.36
${}^{10}\text{B}$	5.16	$2+$	1	2.15	$1+$	0	~ 0.4	~ 6	$\begin{Bmatrix} 13\text{D}_{\text{II(II)}} \\ 13\text{D}_{\text{I(II)}} \end{Bmatrix}$	0	$\begin{Bmatrix} [2 \ 0] \\ [2 \ 0] \end{Bmatrix}$	$\begin{Bmatrix} [\frac{3}{2} \frac{1}{2}] \\ [\frac{5}{2} \frac{1}{2}] \end{Bmatrix} p_{1/2}$	
${}^{10}\text{B}$	7.56	$0+$	0	0.72	$1+$	0	5.6	6.1	$\begin{Bmatrix} 13\text{P} \\ 33\text{P} \end{Bmatrix}$	$\begin{Bmatrix} 0 \\ 0.44 \end{Bmatrix}$	$\begin{Bmatrix} [\frac{1}{2} \frac{1}{2}] \\ [\frac{3}{2} \frac{1}{2}] \end{Bmatrix} p_{1/2}$	$\begin{Bmatrix} [1 \ 0] \\ [1 \ 0] \end{Bmatrix}$	$\begin{Bmatrix} 19.6 \\ 1.67 \end{Bmatrix}$
${}^{12}\text{C}$	16.10	$2+$	1	4.43	$2+$	0	18	4.2	$\begin{Bmatrix} 11\text{D} \\ 11\text{D} \end{Bmatrix}$	0	$\begin{Bmatrix} [\frac{3}{2} \frac{1}{2}] \\ [\frac{5}{2} \frac{1}{2}] \end{Bmatrix} p_{1/2}$	$\begin{Bmatrix} [3 \ 0] \\ [3 \ 0] \end{Bmatrix} p_{1/2}$	1.88
${}^{13}\text{N}$	3.51	$\frac{3}{2}-$	$\frac{1}{2}$	0	$\frac{1}{2}-$	$\frac{1}{2}$	0.70	5.7	$\begin{Bmatrix} 22\text{P} \\ 33\text{P} \end{Bmatrix}$	9.22	$\begin{Bmatrix} [\frac{3}{2} \frac{1}{2}] \\ [\frac{5}{2} \frac{1}{2}] \end{Bmatrix} p_{1/2}^2$	$\begin{Bmatrix} [\frac{1}{2} \frac{1}{2}] \\ [\frac{3}{2} \frac{1}{2}] \end{Bmatrix}$	2.82
${}^{14}\text{N}$	8.62	$0+$	1^*	0	$1+$	0	0.73	0.42	$\begin{Bmatrix} 13\text{S} \\ 13\text{D} \end{Bmatrix}$	0.66	$\begin{Bmatrix} p_{3/2}^{-2} \\ p_{3/2}^{-2} \end{Bmatrix} p_{1/2}^4$	$\begin{Bmatrix} p_{1/2}^2 \\ p_{1/2}^2 \end{Bmatrix}$	0
${}^{14}\text{N}$	8.62	$0+$	1^*	3.95	$1+$	0	3.1	11.1	$\begin{Bmatrix} 13\text{D} \\ 13\text{S} \end{Bmatrix}$	0.83	$\begin{Bmatrix} p_{3/2}^{-2} \\ p_{3/2}^{-2} \end{Bmatrix} p_{1/2}^4$	$\begin{Bmatrix} p_{3/2}^{-1} \\ p_{3/2}^{-1} \end{Bmatrix} p_{1/2}^3$	34.3
${}^{14}\text{N}$	8.98	$1+$	0^*	0	$1+$	0	0.04	0.02	$\begin{Bmatrix} 11\text{P} \\ 13\text{S} \end{Bmatrix}$	0	$\begin{Bmatrix} p_{3/2}^{-2} \\ p_{3/2}^{-2} \end{Bmatrix} p_{1/2}^4$	$\begin{Bmatrix} p_{3/2}^{-2} \\ p_{3/2}^{-2} \end{Bmatrix} p_{1/2}^4$	0

(1) Nucleus; (2) emitting state (mev); (3) J ; (4) T ; (5) final state (mev); (6) J' ; (7) T' ; (8) observed radiation width (ev); (9) value of Λ from previous column; (10) character of states in $L-S$ coupling; (11) predicted value of Λ from $L-S$ coupling; (12) character of states in $j-j$ coupling; (13) predicted value of Λ from $j-j$ coupling.

The characters of the states in $L-S$ and $j-j$ coupling have been assigned largely on the basis of the discussion given by Inglis (1953).

*Assignment uncertain.

Table 3. E2 Transitions

(1)	(2)	(3)	(4)	(5)	(6)	(7)	(8)	(9)	(10)	(11)	(12)	(13)				
${}^7\text{Be}$	7.16	$\frac{5}{2}-$	$\frac{1}{2}$	0.430	$\frac{1}{2}-$	$\frac{1}{2}$	—	—	$\left\{ \begin{array}{l} {}^{22}\text{F} \\ {}^{11}\text{D} \\ {}^{22}\text{F} \\ {}^{33}\text{P} \\ {}^{22}\text{P} \end{array} \right.$	224/75	$\left\{ \begin{array}{l} [\frac{5}{2} \frac{1}{2}] \\ [2 0] \\ [\frac{3}{2} \frac{1}{2}] \\ [\frac{3}{2} \frac{1}{2}] \\ [\frac{3}{2} \frac{1}{2}] \end{array} \right.$	(13)				
${}^8\text{Be}$	2.94	2+	0	0	0+	0	—	—		224/75			$\left\{ \begin{array}{l} [\frac{1}{2} \frac{1}{2}] \\ [0 0] \\ [\frac{3}{2} \frac{1}{2}] \\ [0 0] \\ [\frac{1}{2} \frac{1}{2}] \end{array} \right.$	36/25		
${}^9\text{Be}$	2.43	$\frac{7}{2}-$	$\frac{1}{2}$	0	$\frac{3}{2}-$	$\frac{1}{2}$	—	—		84/25					$\left\{ \begin{array}{l} [\frac{1}{2} \frac{1}{2}] \\ [0 0] \\ [\frac{3}{2} \frac{1}{2}] \\ [0 0] \\ [\frac{1}{2} \frac{1}{2}] \end{array} \right.$	6/5
${}^{12}\text{C}$	16.10	2+	1	0	0+	0	0.72	0.052		16/25						
${}^{13}\text{N}$	3.51	$\frac{3}{2}-$	$\frac{1}{2}$	0	$\frac{1}{2}$	$\frac{1}{2}$	—	—	0	$\left\{ \begin{array}{l} [\frac{5}{2} \frac{1}{2}] \\ [\frac{3}{2} \frac{1}{2}] \\ [\frac{3}{2} \frac{1}{2}] \\ [\frac{3}{2} \frac{1}{2}] \\ [\frac{3}{2} \frac{1}{2}] \end{array} \right.$	27/25					

(1) Nucleus; (2) emitting state (mev); (3) J ; (4) T ; (5) final state (mev); (6) J' ; (7) T' ; (8) observed radiation width (ev); (9) value of Λ from previous column; (10) character of states in L - S coupling; (11) predicted value of Λ from L - S coupling; (12) character of states in j - j coupling; (13) predicted value of Λ from j - j coupling.

Only one transition given has been observed experimentally. The others represent an arbitrary selection of theoretically possible transitions, and one sees that the transition strengths Λ can be increased by a factor of 3 or more above the single-particle one as a result of coupling between nucleons in the same shell.

i.e. the ratio of the squares of the observed to the theoretical single-particle reduced matrix elements. The (exact) equations used in deriving values of these quantities are :

$$\Lambda = \begin{cases} \frac{\Gamma(\text{ev})}{0.25 \times E^3(\text{Mev}) \times \left| \frac{\langle l_0 0 | r \cos \theta | l_1 0 \rangle}{C_{000}^{1l_1 l_0}} \times 10^{13} \right|^2} & \text{for E1 transitions} \\ & \dots\dots(15) \\ \frac{\Gamma(\text{ev})}{8.08 \times 10^{-6} \times E^5(\text{Mev}) \times \left| \frac{\langle l_0 0 | r^2 (3 \cos^2 \theta - 1) | l_1 0 \rangle}{C_{000}^{2l_1 l_0}} \times 10^{25} \right|^2} & \text{for E2 transitions} \\ & \dots\dots(16) \end{cases}$$

where we insert the values given in (14). For M1 transitions, we list

$$\Lambda = \frac{|\langle J || H^{(1)} || J' \rangle|^2}{(\epsilon \hbar / 2 M c)(3/4\pi)^{1/2}}$$

which can be extracted from the observed widths by :

$$\Lambda = \frac{\Gamma(\text{ev})}{2.76 \times E^3(\text{Mev}) \times 10^{-3}} \dots\dots(17)$$

The final columns contain the suspected characters of the states involved in the transitions in L - S and j - j coupling, and the predicted values for the above dimensionless quantities in the two cases. Many of the characters stated are tentative, in which case we often give two or more alternatives. In these columns and throughout the tables, an asterisk means that there is no definite evidence for, or there is some dispute about, the assignment. We have attempted to give only transitions between levels whose spins have not been assigned from data on radiative transitions, but from independent evidence. The previously mentioned compilation of Wilkinson (1953 a) has been widely used with certain exclusions (the transitions in ^{11}B , for example, about the character of which there is some doubt in the light of recent parity assignments from deuteron stripping (Parkinson 1953)) and with certain additions (transitions in ^{12}C —from spin assignments suggested by A. P. French (1953, private communication)).

One of the striking features of the last columns containing the predictions of L - S and j - j coupling is the large variation of the various values given. Apart from the zero values for forbidden transitions, the 'allowed' transitions exhibit values of the squares of the reduced matrix elements from some larger than the single-particle ones to others much less (sometimes by a factor of a hundred or more). Theoretically, within the scope of the sum-rules, such large variations are to be expected. If groups of particles in a shell move in phase then the matrix elements will be large. On the other hand considerable reductions can be caused by the fractional parentage coefficients or the Racah coefficients being small (or, in physical terms, by the need in some transitions for a severe recoupling of the spins of the nucleons and the orbital momenta).

When we compare the observed matrix element in the tables with the predicted ones we find very little basis for believing that one extreme mode of coupling or the other predominates in the nuclei concerned. On the other hand there is a *correlation* between the observed values and the pairs of predicted values, which indicates that an intermediate coupling model may be more successful. One cannot say more than this without examining specific cases in the light of intermediate coupling. It is important to realize that *the predictions from the two extremes*

do not impose limits on the τ values from intermediate coupling (cf. figure 2 in the next section).

In all but one case, the E2 transitions that are listed have not been observed experimentally. Although the experimental widths are not known, we include these in order to have some idea of the magnitudes expected for the reduced matrix elements of E2 transitions and especially to see if the transitions can, in some cases, be much stronger than single-particle ones. It can be seen from table 3 that the shell-model can, in fact, predict such strong transitions, and so it is not necessary to use a surface oscillation model (Bohr and Mottelson 1953) to obtain this result.

Finally we add some remarks about selection rules. If a transition is forbidden in both coupling extremes, then it will be very weak in intermediate coupling in general. If, on the other hand, the transition is only forbidden in one extreme coupling, it is quite unjustified to assume that the intermediate coupling matrix elements will necessarily be small (cf. figure 1 in the next section). Thus, if intermediate coupling is the true situation in nuclei, the selection rules peculiar to L - S or j - j coupling are of little use. On the other hand the selection rule forbidding transitions between states differing in orbital configuration by more than one nucleon is still a 'strict' one. It is strict in so far as each state has a pure configuration. This is an idealized situation and, in practice, there will be weak transitions between such pairs of states due to configuration mixing in the states. This fact could be useful in estimating 'the purity' of nuclear configurations. We do not know any definite examples of these transitions in light nuclei, but we might expect to find them in ^8Be , ^{12}C , ^{16}O where (Inglis 1953) there are believed to be low levels, mainly of spins $0+$, $2+$, arising from configurations other than p^4 , p^8 , p^{12} . It may be significant that Titterton (1953) finds transitions from the $17.63 (1+)$ level in ^8Be that are much weaker than the well-known M1 transitions to the $2.9 (2+)$ and ground $(0+)$ states.

Instances of the special isotopic spin selection rules on E1 transitions have been discussed by Wilkinson (1953 b). The only transitions in table 1 that are suppressed by this rule are those from the $5.11 (2-)$ state in ^{10}B . This selection rule is not implied by eqns (4) and (6), which are not valid for transitions that the rule forbids. The shell-model, upon which (4) and (6) are based, obscures the centre-of-mass motion of the nucleus which is responsible for the selection rule. Taking account of this motion means that, for E1 transitions, the term $\delta_{TT'}$ in (4) and (6) should be omitted.

§ 4. THE RADIATIVE TRANSITIONS IN ^{13}N IN INTERMEDIATE COUPLING

As an instance of an intermediate coupling calculation we consider the E1 and M1 transitions in ^{13}N from the first ($\frac{1}{2}+$) and second ($\frac{3}{2}-$) excited states respectively to the ground state ($\frac{1}{2}-$). The case of the M1 transition has already been discussed in a previous paper (Lane 1953, to be referred to as I), and in figure 1 we merely present the result, viz. the variation in the predicted value of Λ as the mode of coupling in the nucleus changes from L - S to j j coupling. The abscissa is a modified intermediate coupling parameter $y = a/(a + 5K)$, which is more suitable for plotting than a/K itself (a/K being the ratio of the spin-orbit parameter to the exchange integral which is zero in L - S coupling, infinite in j - j coupling). Just as we have derived formulae for matrix elements in L - S and j j coupling, so we can

do this in intermediate coupling. As always with intermediate coupling problems, however, the expressions are distinctly more cumbersome than their correspondents in L - S and j - j coupling. We shall merely present here the intermediate coupling formula for the space part of the matrix element of the transition $l^{n-1}l_0 \rightarrow l^n$ ($l \neq l_0$) of multipolarity k . This includes the most common type of E1 transition in light nuclei. The formula is:

$$\begin{aligned} & \langle J \| H^{(k)} \| J' \rangle \\ &= (-)^{l-J+1} n^{1/2} \left\{ \frac{(2J_p+1)(2J'+1)(2l_0+1)}{2k+1} \right\}^{1/2} \langle l_0 \| H^{(k)} \| l_1 \rangle (\tfrac{1}{2}\delta_{TT'} - \mathcal{F}_p) \\ & \times \sum_{\substack{L'S' \\ L_p S_p}} \left\{ \frac{2S'+1}{2S_p+1} \right\}^{1/2} \langle J_p \| L_p S_p \rangle \langle J' \| L' S' \rangle \langle \alpha T_p S_p L_p | \alpha' T' S' L' \rangle \\ & \times \left(\sum_f \frac{(-)^f}{2f+1} U(sS' J_p L_p, S_1 f) U(l L_p J' S', L' f) U(l_0 s J J_p, j_0 f) U(J J' l_0 l, k f) \right) \\ & \dots (18) \end{aligned}$$

where it has been assumed that the l_0 nucleon is spin-orbit coupled (j value: j_0) before being coupled to the 'core' nucleus (spin J_p), which is assumed to be undisturbed by the addition.

$\langle J_p \| L_p S_p \rangle$, $\langle J' \| L' S' \rangle$ are the transformation coefficients for the parent (core) state J_p of l^{n-1} and for the final state J' of l^n in terms of the complete sets of L - S wave functions (see I). f is a dummy summation suffix taking the values $l \pm \frac{1}{2}$. We have assumed, in the light of the discussion in a previous section, that there is a unique parent state J_p of l^{n-1} in the state $(l^{n-1} l_0)_J$ and so we have only one fractional parentage coefficient in our expression and no summation over parent states J_p .

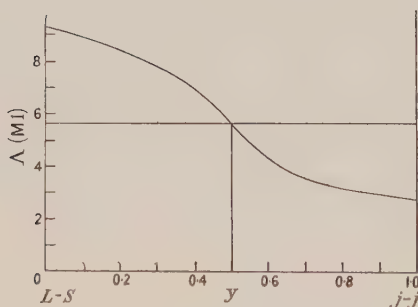


Figure 1. The theoretical variation in Λ for the M1 transition in ^{13}N in intermediate coupling. (Note. The curve given in figure 5 of paper I is incorrect and has been rectified here.)

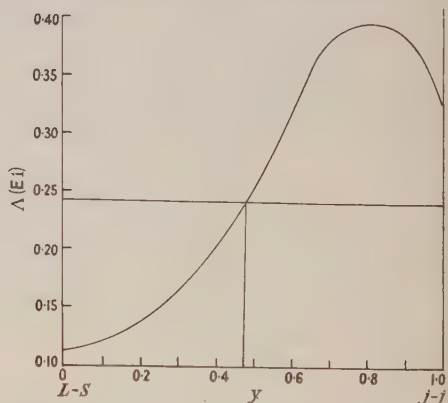


Figure 2. The theoretical variation in Λ for the E1 transition in ^{13}N in intermediate coupling. (Note. Ordinate values should be divided by 4.)

Making use of (18) we can construct figure 2 showing the variation in Λ for the E1 transition in ^{13}N as the mode of coupling is changed from one extreme to the other. In figures 1 and 2 the horizontal lines represent the observed transition strengths, assuming the radial integral in the latter case to be 1.80×10^{-13} cm. One can see that both observed transitions can be explained in intermediate coupling with $y = 0.50$ or $a/K = 5$. As has been shown in I, these values can also explain

three other independent experimental data and so one has very strong evidence that the correct mode of coupling in the nuclear shell model is intermediate—at least for nuclei in the region of $A=13$.

We should mention that it may be fortuitous that the observed value of the E1 transition picks out a value of γ so close to the others. This is because of the indefiniteness in the value of the single-particle radial integral. As mentioned, 15% seems a reasonable estimate of this uncertainty in the case of ^{13}N . Such an uncertainty does not limit the essential conclusions that we have drawn, but it does bring attention to the fact that E1 and E2 transitions are not so reliable in examining the shell-model as M1 transitions. A second reason why M1 transitions are preferable in this type of work is that, since they usually take place between states of the same equivalent particles I^n we do not have to make assumptions about the magnitudes of the fractional parentage coefficients which are uniquely determined and tabulated for such states in $L-S$ and $j-j$ coupling.

§ 5. CONCLUSIONS

It has been customary in the past to restrict discussion of the shell-model to its prediction about the 'static' features of nuclear levels such as the spins and magnetic moments. One of the main purposes of the present and previous (I) papers is to point out that the shell-model also makes predictions about what may be called the 'dynamical' features of nuclei—the reduced widths and radiative transition probabilities. The only practical difficulty that one meets is in assigning the characters of the energy levels in $L-S$ or $j-j$ coupling, the trouble being that the levels are often at a high excitation where levels are beginning to crowd together. With this reservation, one can say that comparison of the observed values of 'dynamical' nuclear constants with theory can give just as crucial a test of the shell-model and its mode of coupling as the 'static' constants.

A second purpose of the present paper is to demonstrate the shortcomings of the single-particle model in explaining radiative transitions. In the original paper presenting this model, Weisskopf (1951) remarked that this model can only be expected to provide very crude estimates of the radiation matrix elements. We have shown that the model can not only over-estimate matrix elements by a factor ten or more, but can also under-estimate them in certain cases. These variations are especially marked for transitions involving equivalent particles near the middle of a shell. In general, one should be suspicious of assignments to the character of a transition from its radiation width alone without any independent evidence on the spins of the states involved.

Finally, in investigating the observed radiation widths in light elements, we have shown that there is a strong suggestion for an intermediate coupling model of the (light) nucleus with a/K of the order of 5. Only one specific nucleus has been examined in detail in intermediate coupling and there is clearly much scope for further work in this field.

ACKNOWLEDGMENTS

One of us (A.M.L.) is indebted to the Department of Scientific and Industrial Research for a maintenance grant. We would also like to thank Dr. D. H. Wilkinson of the Cavendish Laboratory, Cambridge, for generous assistance in collecting the experimental data.

REFERENCES

- BOHR, A., and MOTTELSON, B. R., 1953, *Phys. Rev.*, **89**, 316.
CONDON, E. U., and SHORTLEY, G. H., 1951, *The Theory of Atomic Spectra*, 2nd Edn (Cambridge: University Press), chap. IX.
FLOWERS, B. H., 1952, *Phil. Mag.*, **43**, 1330.
FLOWERS, B. H., and EDMONDS, A. R., 1952, *Proc. Roy. Soc. A*, **214**, 515.
GELL-MANN, M., and TELEGI, V. L., 1953, *Phys. Rev.*, **91**, 169.
INGLIS, D. R., 1953, *Rev. Mod. Phys.*, **25**, 390.
JAHN, H. A., and VAN WIERINGEN, H., 1951, *Proc. Roy. Soc. A*, **209**, 502.
KINSEY, B. B., 1953, *Report of Birmingham Conference on Nuclear Physics*.
LANE, A. M., 1953, *Proc. Phys. Soc. A*, **66**, 977.
PARKINSON, W. C., 1953, *Report of Birmingham Conference on Nuclear Physics*.
RACAH, G., 1943, *Phys. Rev.*, **63**, 367.
TITTERTON, E. W., 1953, *Report of Birmingham Conference on Nuclear Physics*.
UMEZAWA, M., 1952, *Prog. Theor. Phys.*, **8**, 509.
WEISSKOPF, V., 1951, *Phys. Rev.*, **83**, 1073.
WILKINSON, D. H., 1953 a, *Phil. Mag.*, **44**, 542; 1953 b, unpublished notes, and *Phys. Rev.*, **90**, 721.

Isotope Shifts in the Atomic Spectrum of Calcium

By ANNE PERY

Clarendon Laboratory, Oxford

Communicated by H. G. Kuhn; MS. received 13th October 1953

Abstract. The isotope shift in several spectral lines of ^{40}Ca and ^{48}Ca has been measured. A triplet of the arc spectrum shows a specific mass effect a little larger than the normal mass effect and in the opposite direction. In the resonance line and a doublet of the spark spectrum the specific mass shift is very small and in the same direction as the normal shift. Comparison with analogous transitions in magnesium indicates that the specific mass effect shows a similar behaviour in both elements.

§ 1. INTRODUCTION

THE isotope shift in spectral lines of the lighter elements is caused mainly by the difference in mass of their nuclei. In hydrogen-like atoms the term difference ΔT between isotopes of masses M_1 and M_2 is, according to both Bohr's theory and wave mechanics,

$$\Delta T = m \frac{\Delta M}{M_1 M_2} T \quad \dots\dots(1)$$

where m is the mass of the electron.

In all other spectra the wave mechanical calculation of the mass effect is very difficult. Hughes and Eckart (1930) showed that if spin-orbit coupling is neglected the effect can be expressed as the sum of the normal (hydrogen-like) mass shift given by (1) and a 'specific' shift, and they calculated the latter for atoms with two and three electrons. The theory was extended to many-electron atoms by Bartlett and Gibbons (1933) and by Vinti (1939), using Hartree wave functions to evaluate the integrals in the calculation of specific shifts. Discrepancies between theory and experiment can always be attributed to inaccuracies in the wave functions used, and at present it is these inaccuracies which limit the useful application of the theory. The incomplete knowledge of the specific mass effect has proved to be a serious handicap in the study of the so-called 'volume effect', which is connected with nuclear charge distribution; Brix and Kopfermann (1951) and Foster (1951) have recently summarized the problem.

The isotope shift in calcium should be almost entirely a mass effect, for one would expect the volume effect to contribute very little to the isotope shift in such a light element. This paper describes measurements of the shift between ^{40}Ca and ^{48}Ca in the resonance line and a triplet of the arc spectrum and in a doublet of the spark spectrum. This work was primarily undertaken to help in an investigation of the hyperfine structure of ^{43}Ca , and it is for this reason that the measurements were made on these particular lines and not extended further.

§ 2. EXPERIMENTAL METHOD

Calcium has isotopes of mass numbers 40, 42, 43, 44 and 48. Since ^{40}Ca forms 97% of natural calcium, no structure can be resolved without the use of enriched isotopes. For the purposes of this experiment the Atomic Energy Research Establishment at Harwell kindly provided about 3 mg of heavily enriched ^{48}Ca (whose natural abundance is about 0.18%). Even if this had been mixed with ordinary calcium, the large Doppler width of the spectral lines would have prevented the measuring of any shift in some cases. Hence the experiment was designed to compare the line from each isotope separately with a reference line from another element.

The calcium spectrum was excited in a hollow-cathode discharge tube, which was a slightly modified form of that described by Kuhn and Woodgate (1951). The principal change was that the cathode piece was made of beryllium instead of aluminium. The calcium, in the form of a chloride solution, was spread around the inside of the cavity with considerable care, for the efficiency of this 'smearing' process appeared to have a large effect on the intensity of the spectral lines; in fact only about $\frac{3}{4}$ mg of the rare isotope was needed for the whole experiment. Currents of up to 30 ma were used, with neon or krypton as the carrier gas, and the discharge was cooled in liquid oxygen. In these conditions the Doppler width was about 0.021 cm^{-1} in the red lines and 0.034 cm^{-1} in the violet.

The high resolution instrument employed was a Fabry-Perot interferometer, in conjunction with a one-metre Littrow spectrograph. Most of the measurements were made with a 3 cm spacer, although a smaller spacer was also used as a check.

Intensity measurements showed that the sample of ^{48}Ca contained about 25% of ^{40}Ca , and the two isotopes were resolved in the arc resonance line $\lambda 4227$ and in the spark doublet $\lambda 3968, 3933$. In a strongly exposed photograph the shift could be measured directly, though not very accurately, and this was the method used for the resonance line. For the other lines greater accuracy was achieved by photographing the fringes from each isotope separately and comparing the ring diameters with those of a nearby line from another element. It is, of course, essential that the etalon remain steady for this comparison, so the reference line was photographed both before and after the calcium line, and any plate in which this comparison showed a shift of more than $1/40$ order was rejected. Moreover, as the exposures for the two isotopes could not be taken on the same day, one must allow for the variations of the effective spacing of the etalon with differences in pressure and temperature. Such variations cause a relative shift of the calcium and reference lines which is proportional to their difference in wavelength. The appropriate corrections are easily made and were in fact very small. Finally, the reference fringes must be formed by the same part of the etalon as are the calcium fringes; errors due to bad adjustment of the etalon and imperfections in its plates are thus avoided. This requirement was automatically met for the arc triplet, $\lambda 6103, 6122$ and 6162 , which was excited with krypton as carrier gas: here it was possible to use for reference the krypton line $\lambda 6056$ directly from the hollow-cathode discharge. The spark doublet, $\lambda 3933$ and 3968 , was compared with a mercury line at 3906 \AA , for which purpose a small mercury discharge tube was set up in the position of an image of the hollow cathode. The illumination conditions could then be satisfied with suitable aperture stops.

§ 3. RESULTS

Table 1 shows the isotope shifts found in each of the six lines measured. The value for the line 4227 Å may be in error by 0.002 cm^{-1} , but the other values, for each of which about 15 fringes of each isotope were measured, should be correct to 0.001 cm^{-1} , which is three times the standard deviation. In two plates the shift in $\lambda 3933$ was also measured directly, and the result lay well

Table 1. Position of ^{48}Ca Component with respect to ^{40}Ca Component (in cm^{-1})

Line (Å)	Transition	Measured shift	Normal mass shift (calc)	Difference	Est. vol. shift	Resid. (spec. mass) shift
Ca I						
4227	$4s^2\ ^1S_0-4s4p\ ^1P_1$	$+0.050_8$	$+0.0537$	-0.002_9	-0.005	$+0.002$
Ca I						
6103	$4s4p\ ^3P_0-4s5s\ ^3S_1$	-0.004_1	$+0.0372$	-0.041_3	$+0.003$	-0.044
6122	$4s4p\ ^3P_1-4s5s\ ^3S_1$	-0.002_6	$+0.0372$	-0.039_8	$+0.003$	-0.043
6162	$4s4p\ ^3P_2-4s5s\ ^3S_1$	-0.003_3	$+0.0372$	-0.040_5	$+0.003$	-0.043
Ca II						
3933	$4s\ ^2S_{1/2}-4p\ ^2P_{3/2}$	$+0.059_0$	$+0.0577$	$+0.001_3$	-0.008	$+0.009$
3968	$4s\ ^2S_{1/2}-4p\ ^2P_{1/2}$	$+0.060_1$	$+0.0577$	$+0.002_4$	-0.008	$+0.010$

within the limit of error of the more accurate indirect measurement. Of course no such check could be made on the very small shift in the triplet lines; here a small correction was applied for the influence of the completely unresolved component of ^{40}Ca on the position of that of ^{48}Ca . The measured value can be taken as the centre of gravity of the two components, whose intensity ratio is known.

The normal mass shift calculated for each line is also given in table 1. The residual shift cannot be ascribed entirely to the specific mass effect, because the volume-dependent shift is probably not quite negligible. A rough estimate of the latter has been made, but as the isotope shift constant can be predicted only by extrapolating the results for heavy elements the estimated shift may well be in error by a factor of two. However, the ratios of the shifts in different lines should be quite accurate.

When the best possible allowance has been made for the volume effect, the residual shift, given in the last column of table 1, must be attributed to the specific mass effect. Its accuracy is obviously limited by the uncertainties in the calculation of the volume shift. For the resonance line $\lambda 4227$ one can only say that the specific shift must be small (less than, say, 0.01 cm^{-1}). The spark doublet, too, has a fairly small specific shift, of about 0.01 cm^{-1} ; this is definitely in the same direction as the normal shift and is approximately equal for both members. On the other hand, the specific shift in the triplet is slightly larger than the normal shift and in the opposite direction; for all three components it lies between 0.04 and 0.05 cm^{-1} . In both multiplets the shift is the same, within the limit of error, for all components, which is in accordance with theory.

§ 4. DISCUSSION OF RESULTS

No attempt has been made to calculate the specific shift in calcium. The calculation would be difficult and the result of little value, because the approxi-

mations in the methods hitherto employed are such that accurate results cannot be expected. In the few atoms, all simpler than calcium, for which theoretical and experimental results have been compared the agreement has usually been poor. At present, measurements of the specific shift in calcium are useful less as a test of theory than as a basis for predicting the order of magnitude of the specific effect in other spectra. With this in view these shifts have been compared with those in similar transitions of a few other elements.

Of the two elements preceding calcium in the second column of the periodic table, beryllium has only one isotope, but magnesium should furnish a useful analogy. The electron configuration of the ground state of magnesium is $1s^2 2s^2 2p^6 3s^2$; in calcium the $3p$ and $4s$ shells are also filled. The measured shifts and the normal mass shifts, together with the specific mass shifts derived from these, are compared for the three transitions in table 2. Since the values

Table 2. Isotope Shifts for $\Delta M=2$ (in cm^{-1})

	$^1S_0-^1P_1$			$^3P_{0,1,2}-^3S_1$			$^2S_{1/2}-^2P_{3/2,1/2}$		
	$\Delta\nu_{\text{obs}}$	$\Delta\nu_N$	$\Delta\nu_S$	$\Delta\nu_{\text{obs}}$	$\Delta\nu_N$	$\Delta\nu_S$	$\Delta\nu_{\text{obs}}$	$\Delta\nu_N$	$\Delta\nu_S$
Ca	+0.0127	+0.0134	0.000	-0.0009	+0.0093	-0.011	+0.0149	+0.0144	+0.000
Mg	+0.053	+0.0611	-0.008	-0.0136	+0.0337	-0.047	+0.1021	+0.0624	+0.040
K							+0.0076	+0.0087	0.000

obtained for calcium refer to a mass difference of eight units, they have here been divided by four to bring them into line with results quoted for $\Delta M=2$. The shift quoted for the magnesium resonance line is that found by Fisher (1942); for the other two transitions ($3s3p^3P-3s4s^3S$ and $3s^2S-3p^2P$) the values are given by Crawford, Kelly, Schawlow and Gray (1949). The spark doublet is also compared with the iso-electronic transition in potassium studied by Jackson and Kuhn (1938). Their value for the specific shift has been roughly corrected for the volume effect just as was done for calcium.

There is a certain rough similarity in the specific shifts shown by the three elements. The resemblance is more marked when one takes into account that all the shifts are larger in magnesium because of its smaller mass, so that the fairest basis for comparison is probably the ratio of the specific to the normal shift. This quantity agrees very roughly for calcium and magnesium in the first two transitions, but in the third one it is considerably larger for magnesium than for calcium and potassium.

A comparison with zinc is less justifiable; zinc differs from calcium by the filling of the $3d$ electron shell, and it seems that d electrons may make rather a large contribution to the specific shift. Crawford, Gray, Kelly and Schawlow (1950) found a shift for $\Delta M=2$ of $+0.016\text{ cm}^{-1}$ in the resonance line, the normal shift being $+0.011\text{ cm}^{-1}$. If the volume effect is estimated on the same assumptions as for calcium the specific shift turns out to be about $+0.010\text{ cm}^{-1}$, which does not bear much resemblance to the analogous shifts in calcium and magnesium.

These comparisons indicate that the specific mass effect has the same general tendencies in similar spectra, but only if the similarity is close. In none of the transitions considered here is the specific mass shift appreciably larger than the normal shift.

ACKNOWLEDGMENTS

I should like to express my sincere thanks to Dr. H. G. Kuhn for his constant help and to St. Hugh's College, Oxford, for a scholarship.

REFERENCES

- BARTLETT, J. H., and GIBBONS, J. J., 1933, *Phys. Rev.*, **44**, 538.
BRIX, P., and KOPFERMANN, H., 1951, *Akad. Wiss., Göttingen*, 2nd Centenary number, p. 17.
CRAWFORD, M. F., GRAY, W. M., KELLY, F. M., and SCHAWLOW, A. L., 1950, *Canad. J. Res. A*, **28**, 138.
CRAWFORD, M. F., KELLY, F. M., SCHAWLOW, A. L., and GRAY, W. M., 1949, *Phys. Rev.*, **76**, 1527.
FISHER, R. A., 1942, *Rev. Mod. Phys.*, **14**, 79.
FOSTER, E. W., 1951, *Rep. Progr. Phys.*, **14**, 288 (London : Physical Society).
HUGHES, D., and ECKART, C., 1930, *Phys. Rev.*, **36**, 694.
JACKSON, D. A., and KUHN, H., 1938, *Proc. Roy. Soc. A*, **165**, 303.
KUHN, H., and WOODGATE, G. K., 1951, *Proc. Phys. Soc. A*, **64**, 1090.
VINTI, J. P., 1939, *Phys. Rev.*, **56**, 1120.

RESEARCH NOTES

A Note on the Ultra-Violet Band Spectra of CCl and SiCl

BY R. F. BARROW, G. DRUMMOND AND S. WALKER

Physical Chemistry Laboratory, Oxford University

MS. received 9th November 1953

§1. THE SPECTRUM OF CCl

DISCHARGES at low current density of the kind designed by Schüller (1950) are capable of giving very clean spectra, and it was with the hope of extending the analysis of the well-known CCl band system at 2800 Å (Venkateswarlu 1950) that we examined a Schüller discharge in carbon tetrachloride vapour. Although no new information about the 2800 Å system was obtained, weak, red-degraded bands in the region 2360 to 2440 Å were discovered in emission from a discharge running at about 30 mA. Measurements of the new bands are given below.

Table 1. Red-Degraded Bands in Low Current Discharge through Carbon Tetrachloride

λ (Å)	ν (cm ⁻¹)	Intensity
2367.8	42220	10
2383.9	41935	9
2400.6	41644	5
(2434.0)	(41070)	0 ?

The source emitted simultaneously the CCl system at 2800 Å and bands of the $2\Sigma^-2\Pi$ system of HCl^+ : the intensity of the new bands was not more than about 10% of that of the main CCl system. The appearance of the new bands suggests that they constitute a 0,0 sequence; unfortunately attempts to locate other sequences largely failed, apart from the rather doubtful observation of a candidate for the 0,1 band at 2434 Å. No multiplet structure was detected, so that the most likely interpretation of the bands—if they arise from a diatomic molecule—is that they represent a $2\Sigma^-2\Sigma$ transition in CCl or a singlet-singlet transition in CCl^+ .

Discharges at low current density through a number of other chlorine containing molecules such as CHCl_3 , CCl_3CHO , $\text{C}_6\text{H}_5\text{CCl}_3$, $\text{C}_6\text{H}_5\text{CHCl}_2$, $\text{C}_6\text{H}_5\text{CH}_2\text{Cl}$ were also examined. These all gave emission from HCl^+ , and for the first three molecules there was also emission of the 2800 Å system of CCl, but the new bands were absent. The bands are also absent in discharges at higher current density through CCl_4 .

The absorption spectra of the products of pyrolysis of carbon tetrachloride and of chloroform at temperatures up to about 2000°C in a carbon-tube furnace have also been photographed. No absorption attributable to CCl was observed, in agreement with the results of Wieland and Heise (1952).

§2. THE SPECTRUM OF SiCl

Three band systems of SiCl are known with certainty (Jevons 1936). No special difficulties arise about the vibrational analyses of the systems $c(^2\Delta \text{ or } ^2\Pi)-x^2\Sigma$ and $D(^2\Sigma)-x^2\Pi$, but the analysis of bands at the short wavelength end of the system $B(^2\Sigma)-x^2\Pi$ is not yet established. Garg (1950) has attempted to resolve this problem by postulating the existence of a further system, $A-x^2\Pi$, of SiCl, but his solution is unattractive, for his suggested vibrational scheme has $\omega' \simeq \omega''$, and yet the strongest bands in the scheme are assigned quantum numbers 3, 4 and 2, 3.

We hoped that observations of the spectrum of SiCl in absorption would help to settle this question. We found that the B-x system of SiCl is readily observed in absorption from the pyrolysis of silicon tetrachloride vapour in a carbon-tube furnace at about 1600°C with a path length of about 15 cm (see also Wieland and Heise 1952, Wieland 1952). The same system was photographed in thermal emission at about 1700°C. In both cases the intensity distribution of the bands in the system is quite normal, and the impression is that there is only *one* system in the region 2640 to 3020 Å, although the low wavelength limit of this region is far below that for the limit of bands certainly attributable to the B-x system in emission (2850 Å).

The interpretation of the bands which appear in emission in discharges through silicon tetrachloride vapour at moderately low pressures (1 mm) in the region 2700–2850 Å is still doubtful.

It is difficult to be certain of the presence or absence of these bands in the absorption spectrum, although there are a number of wavelength coincidences; however, plates taken of the electrodeless discharge through silicon tetrachloride vapour by Dr. E. B. Andrews show clearly that the intensity of the strong bands measured by Jevons in this region does *not* vary from exposure to exposure in proportion to the intensity of the main bands of the B-x system. The simplest conclusion is that these emission bands arise from a different emitter, perhaps SiCl^+ , but it seems unlikely that this question will be settled without high dispersion spectrograms with isotopically pure chlorine.

REFERENCES

- GARG, S. N., 1950, *Proc. Nat. Acad. Sci., India*, A, **19**, 23.
JEVONS, W., 1936, *Proc. Phys. Soc.*, **48**, 563.
SCHÜLER, H., 1950, *Spectrochim. Acta*, **4**, 85.
VENKATESWARLU, P., 1950, *Phys. Rev.*, **77**, 676.
WIELAND, K., 1952, *Z. Phys.*, **133**, 229.
WIELAND, K., and HEISE, M., 1952, *Boll. Sci. Fac. Chim. Ind., Bologna*, **10**, 12.

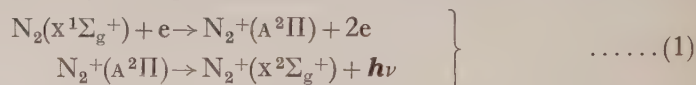
Excitation Conditions for the Infra-Red Auroral Bands of Ionized Nitrogen

BY D. T. STEWART, P. W. F. GRIBBON AND K. G. EMELÉUS

Physics Department, Queen's University of Belfast

MS. received 3rd November 1953

THE near infra-red $A^2\Pi-X^2\Sigma_g^+$ bands of N_2^+ were first recognized by Meinel (1950) in the spectrum of an aurora. Shortly after, they were found by Dalby and Douglas (1951) and Herman (1951) in the spectra of discharges through helium containing a trace of nitrogen, and in this laboratory (Sayers 1952) in the spectrum of some discharges through almost pure nitrogen. Douglas (1953) has recently obtained grating spectra of a number of the bands. In this Note we consider briefly the mechanism of production of the bands from a number of sources, particularly some employing pure nitrogen. It will be assumed that the main process responsible for forming N_2^+ ions in the excited state in our experiments has been collision of electrons with neutral N_2 molecules in the $x^1\Sigma_g^+$ ground state, i.e. that the excitation of the bands may be represented by



The first condition for producing the bands is that the exciting electrons shall have at least the energy required by (1), about 17 ev. This rules out use of an uncondensed positive column discharge, where most of the electrons have energy less than 10 ev. The negative glow of an ordinary cold cathode glow discharge is, however, a possible source, since although the majority of the plasma electrons again have energy less than 10 ev, faster electrons are present with energies which may approach that corresponding to free fall through the potential difference across the cathode dark space. Investigation of the light from a negative glow in nitrogen at a pressure of about 0.2 mm Hg, with a cathode fall of 400 v (Sayers 1952) has shown the presence of the (2, 0) and (3, 1) bands near 7850 Å and 8100 Å, which are the most intense in Meinel's auroral spectrum. This source has, nevertheless, the disadvantage that it emits strongly the First Positive bands $B^3\Pi-A^3\Sigma_u^+$ of N_2 . Although the most intense First Positive bands in this region are between 7500 Å and 7750 Å and clear of the Meinel bands, a number of other First Positive bands, at longer and shorter wavelengths, partly overlap them.

The First Positive bands have been suppressed by Dalby and Douglas, and by Herman, by diluting the nitrogen with helium. We have also found that the First Positive bands can be greatly reduced in relative intensity in pure nitrogen by designing sources based on the probable forms of the cross-section curves for electron excitation of the $A^2\Pi$ state of N_2^+ , and the $B^3\Pi$ state of N_2 , from the ground state of N_2 . From the electronic structures of the molecular states involved the former should have a broad maximum at energy of order of 100 ev, and the latter a sharp peak at energy between 12 and 30 ev. In the negative glow both the Meinel bands and First Positive bands are excited because of the wide range of electron energies. In sources for exciting the Meinel bands predominantly most of the electrons should have energy greater than about 50 ev.

One such source is a hollow cathode discharge through nitrogen at low pressure (~ 0.01 mm Hg), with a cathode fall of potential of 1000 v or more. A narrow blue pencil of light emerges axially from the cathode under these conditions; it is presumably produced in a similar way to the pencils which come out of 'sandwich-cathodes' (Goldstein 1914). This form of discharge has not been completely analysed, but the pencils are unlikely to be ordinary plasmas and probably contain cathode rays with energy up to a large fraction of that corresponding to the potential difference between anode and cathode. Examination of the spectrum of a pencil showed the presence of the strongest Meinel bands, with the First Positive bands relatively weak.

The most controllable source of the Meinel bands has however proved to be not a self-maintained discharge, but an equipotential collision box with a thermionic source of electrons outside the collision chamber. When used with nitrogen (preferably streaming, to minimize accumulation of products of electron impact) at a pressure of less than 10^{-2} mm Hg, so that the electron free path is at least comparable with the linear dimensions of the box, an approximately monoenergetic beam can be fired through it. Formation of a plasma can be avoided by keeping the beam current well below 1 ma. With electron energy above about 20 ev, the spectrum of the beam includes the Meinel bands, and they appear with comparative freedom from First Positive bands above about 50 v. This arrangement was used in a crude form by Sayers (1952); in the present work the electrode system has been improved, and the trace of oxygen present in Sayers' tube has been eliminated. All the bands recorded by Meinel (1951) have now been obtained, with about the same relative intensities as in Meinel's auroral spectrum.

These experiments can unfortunately give little direct information about conditions in the aurora. The spectra taken using the collision box with different electron energies show that the relative intensities of the Meinel bands and First Positive bands in the aurora are what would result from excitation of both by collisions of electrons of between 30-35 ev energy with N_2 molecules in the ground state, but a given intensity ratio for two different spectra can be produced by a wide range of excitation conditions.

One other observation with the collision box may be mentioned. It has been found previously (Thompson and Williams 1934) that the visible bands and some infra-red bands of the First Positive system are emitted for a considerable distance outside the electron beam. We have confirmed this behaviour of the First Positive bands, but find that both the negative bands and Meinel bands are much more closely confined to the beam. This observation does not in itself show that the Meinel bands arise from N_2^+ , as the Second Positive bands of N_2 do not spread.

ACKNOWLEDGMENTS

We are indebted to Professor D. R. Bates and Miss N. D. Sayers for discussion of the work.

REFERENCES

- DALBY, F. W., and DOUGLAS, A. E., 1951, *Phys. Rev.*, **84**, 843.
DOUGLAS, A. E., 1953, *Astrophys. J.*, **117**, 380.
GOLDSTEIN, E., 1914, *Verh. Dtsch. Phys. Ges.*, **16**, 545.
HERMAN, R., 1951, *C. R. Acad. Sci., Paris*, **233**, 926.
MEINEL, A. B., 1950, *C. R. Acad. Sci., Paris*, **231**, 1049; 1951, *Astrophys. J.*, **114**, 431.
SAYERS, N. D., 1952, *Proc. Phys. Soc. A*, **65**, 152.
THOMPSON, N., and WILLIAMS, S. E., 1934, *Proc. Roy. Soc. A*, **147**, 583.

The Continuous Absorption of Light in Calcium Vapour

By P. J. JUTSUM

Physics Department, University of Reading

Communicated by R. W. Ditchburn; MS. received 9th October 1953

THE absorption cross section for calcium vapour has been measured over a wavelength range from the vicinity of the series-limit (2026 Å) to 1950 Å. The technique employed was substantially the same as that described in connection with similar experiments on sodium vapour (Ditchburn, Jutsum and Marr 1953).

An iron tube of low carbon content was used to contain the absorbing column. Initial experiments using a nickel absorption tube showed that the calcium vapour was removed by some reaction, apparently by the formation of a nickel calcium solution at the temperatures required to produce a sufficiently high vapour pressure. The absorption spectrum, although observable on first heating, rapidly disappeared. The use of an iron tube overcame this difficulty satisfactorily, and no diminution in absorption was observed over periods of the order of an hour, while the reservoir temperatures were maintained constant.

Only one centrally placed calcium reservoir was used, instead of two widely spaced ones, as in earlier experiments. Although the use of two reservoirs is more satisfactory, in that the length of the absorption tube requires a smaller correction in order to find the effective length, the very good agreement that has been obtained between the two arrangements in the experiments on sodium justifies the calculations that are necessary in the simpler case. This simplification was desirable in that the construction of a furnace having the necessary temperature distribution at the high temperatures required (about 1150 Å) presented far less difficulty than would otherwise have been the case.

The accuracy of measurement in experiments of this type depends directly upon the accuracy with which the vapour pressure of the substance under investigation is known. The vapour pressure equations used in the present work were: $\log_{10} p = 8.84 - 9259/T$ over the liquid and $\log_{10} p = 9.48 - 9947/T$ over the solid; p is in mm Hg, T in degrees absolute. The melting point of calcium is about 1100 Å, and the experiments extended over a range which includes this temperature. These equations were obtained by considering published data (Ditchburn and Gilmour 1941), together with unpublished work carried out by P. E. Douglas and independently by D. H. Tomlin in this laboratory. An accuracy to $\pm 10\%$ is attributed to values calculated from them. The errors arising from other sources, i.e. temperature and photometric measurements, are considered not to exceed $\pm 10\%$.

Molecular absorption in the region investigated appears to be negligible, in that the absorption observed is proportional to the concentration of vapour (figure 1). Also, the absorption measured between the series lines is negligible. The absorption cross section measured was $0.45 \times 10^{-8} \text{ cm}^2$ at the series-limit, and the variation with wavelength over the range investigated is shown in figure 2.

Bates and Massey (1941) have calculated a value of $2.5 \times 10^{-17} \text{ cm}^2$ for the absorption cross section of calcium, and predict the variation with wavelength to be as λ^3 . The fall off in absorption measured is very much more rapid than this. A power law is not appropriate to express the variation but the rate of change of absorption with wavelength (at 2026 \AA) is proportional to λ^{47} . The shape of the curve obtained is not subject to any errors in vapour pressure measurement or temperature measurement. The f -value for the continuum,

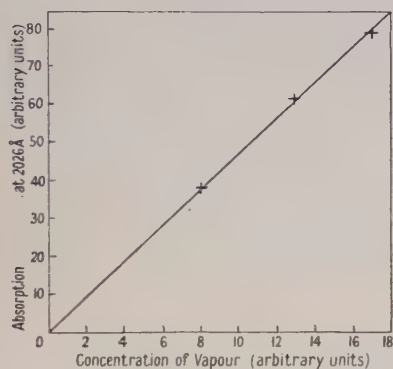


Figure 1.

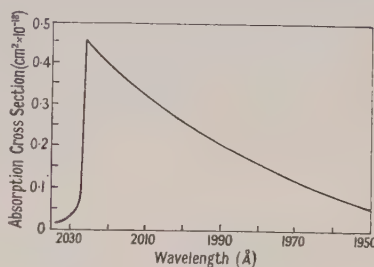


Figure 2.

as far as measurements have been made, is lower than that predicted by a factor of several hundred and is of the order of 5×10^{-4} . However, there may well be a minimum of absorption at wavelengths below the range of measurement as is the case for sodium and potassium. Professor D. R. Bates has informed the writer that a new calculation, which is in progress, is likely to yield a lower theoretical value than that obtained by Bates and Massey (1941). The rapid fall near the series-limit is likely to be associated with a low absolute value.

§

ACKNOWLEDGMENTS

I wish to thank Professor R. W. Ditchburn for advice on experimental methods and Professor D. R. Bates for a discussion of the theory.

REFERENCES

- BATES, D. R., and MASSEY, H. S. W., 1941, *Proc. Roy. Soc. A*, **177**, 329.
 DITCHBURN, R. W., and GILMOUR, J. C., 1941, *Rev. Mod. Phys.*, **13**, 310.
 DITCHBURN, R. W., JUTSUM, J. P., and MARR, G. V., 1953, *Proc. Roy. Soc. A*, **219**, 89.

LETTERS TO THE EDITOR

Red-Shifts in the Spectra of Celestial Bodies*

Stars of high surface temperature, that is B-stars ($T \sim 20\,000^\circ\text{K}$) and O-stars ($T \sim 30\,000^\circ\text{K}$), show a very marked red-shift of their spectral lines. This is especially noticeable in the case of the stars embedded in the Orion Nebula, since in that case it is possible to deduct from the observed red-shifts the red-shift due to the recession of the system as a whole. If one considers these stars, it is found that, relative to the Orion Nebula itself, the B-stars show a systematic red-shift corresponding to a recession velocity of 11.4 km sec^{-1} and a similar discussion of O-stars gives a red-shift corresponding to 17.6 km sec^{-1} .†

In earlier discussions it was suggested that this red-shift might be due to the relativistic gravitational effect. From the known masses and radii of B-stars it follows, however, that the gravitational effect would only lead to red-shifts of the order of 1.2 km sec^{-1} , which are by a factor 10 smaller than the observed red-shifts.

While the observed red-shifts in the case of B- and O-stars are by far larger than the relativistic red shifts, in the case of the sun the situation is just the opposite. In this case most detailed and accurate data are available, but while the theory of relativity predicts a red-shift $\Delta\lambda/\lambda = 2 \times 10^{-6}$, the red-shift in the centre of the solar disc is only 8×10^{-7} , although the relativistic value is reached, and even surpassed, at the limb. A careful analysis of the red-shift in the solar spectrum shows that it follows the law $\Delta\lambda/\lambda = a + b \sec \theta$, where θ is the angle between the line of sight and the solar radius to the point where the line of sight cuts the solar surface.

It is tempting to try to account for all these red-shifts by one process and we suggest the following formula:

$$\Delta\lambda/\lambda = AT^4l, \quad A = 2 \times 10^{-29} \text{ cm}^{-1} \text{ deg}^{-4}, \quad \dots\dots(1)$$

In eqn (1) $\Delta\lambda/\lambda$ is the relative red-shift, T the temperature of the radiation field through which the light has passed and l the length of its path through the radiation field. The constant A is chosen in such a way that $\Delta\lambda/\lambda = 3 \times 10^{-5}$ for $T = 20\,000^\circ\text{K}$, $l = 10^7\text{ cm}$, which are the values for a B-star. Formula (1) implies that the red-shift is due to a loss of energy in the intense radiation field, perhaps due to photon-photon interactions.

It turns out that eqn (1) can well account for most of the observed red-shifts. For the sun we get $\Delta\lambda/\lambda = 2.7 \times 10^{-7} \sec \theta$, while the observed value of b is 3.0×10^{-7} . The constant term a may be due to a gravitational effect, which in that case would be about five times smaller than the theoretically predicted constant red-shift.‡

In the case of A-stars eqn (1) predicts a red-shift of about 0.6 km sec^{-1} , while the observed red-shifts lie between 0.1 and 0.9 km sec^{-1} . In the case of

* A more detailed account of the subject matter of the present note can be found elsewhere (Freundlich 1954 a, b).

† I would like to express my thanks to T. B. Slebarski for critically discussing the available data.

‡ It is of interest to note that the red-shift in Sirius B, which can only be due to a gravitational effect, is also about five times smaller than the theoretical value.

supergiant M-stars T is very small, but their enormous atmospheres—about a thousand times more extensive than the solar atmosphere—lead to expected red-shifts of about 5 km sec^{-1} . It is found that lines formed at the top of the atmosphere are, indeed, displaced by about 5 km sec^{-1} to the violet with respect to lines formed at the bottom of the atmosphere. In the case of Wolf-Rayet stars ($T \gtrsim 40\,000^\circ\text{K}$) eqn (1) leads to red-shifts of the order of 100 km sec^{-1} , which also have been observed (Wilson 1949).

Finally, it seems tempting to apply formula (1) to the case of the cosmological red-shift or Hubble effect. In that case $\Delta\lambda/\lambda$ is about 0.0008 for every million parsec ($= 3 \times 10^{24} \text{ cm}$). Using eqn (1) this leads to an intergalactic temperature of about 1.5°K , which does not seem to be an unreasonable value.

The Observatory,
University of St. Andrews.
7th December 1953.

E. FINLAY-FREUNDLICH.

FREUNDLICH, E. F., 1954 a, *Göttinger Nachr.*, No. 7; 1954 b, *Phil. Mag.*, **45**, in the press.
WILSON, O., 1949, *Astrophys. J.*, **109**, 76.

On the Interpretation of Freundlich's Red-Shift Formula

Freundlich (1954) has suggested that his red-shift formula $\Delta\nu/\nu = -AT^4l$ ($A = 2 \times 10^{-29} \text{ cm}^{-1} \text{ deg}^{-4}$) may be interpreted as an effect of photon-photon collisions. I have investigated whether this is possible. The first step is to write the equation in a dimensionless form,

$$\frac{\Delta\nu}{\nu} = -C \frac{l}{l_0} \frac{u}{u_0} \quad \dots\dots(1)$$

where $u = aT^4$ ($a = 7.66 \times 10^{-15} \text{ erg cm}^{-3} \text{ deg}^{-4}$) is the radiation density according to Stefan's law. If one takes for l_0 and u_0 the atomic constants

$$\left. \begin{aligned} l_0 &= \frac{\lambda_0}{2\pi} = \frac{\hbar}{mc} & (\lambda_0 = \text{Compton wavelength}) \\ u_0 &= \frac{mc^2}{l_0^3} = \frac{\hbar c}{l_0^4} & (\text{one electron per cube } l_0^3) \end{aligned} \right\} \quad \dots\dots(2)$$

$$\text{one has} \quad l_0 u_0 = \frac{\hbar c}{l_0^3} = 5.54 \times 10^{14} \text{ erg cm}^{-2} \quad \dots\dots(3)$$

$$\text{and obtains} \quad C = \frac{l_0 u_0}{a} A = 1.45, \quad \dots\dots(4)$$

a value so near to unity that the assumptions (2) seem to be justified.

A simple analysis of (1) then leads to the result that it can be written in the form

$$\Delta\lambda/\lambda = -\Delta\nu/\nu = CN\lambda_0/\bar{\lambda}, \quad N = l_0^2 n \quad \dots\dots(5)$$

where n is the number of photons per unit volume and $\bar{\lambda}$ the wavelength corresponding to the mean frequency of the radiation field defined by $u = n\hbar\bar{\omega}$.

Hence the red-shift can be explained as a sequence of N photon-photon collisions with an effective cross section l_0^2 , each of which produces a small change in wavelength or frequency

$$\delta\lambda/\lambda = C\lambda_0/\bar{\lambda}, \quad \delta\nu = -C\nu\bar{\nu}/\nu_0. \quad \dots\dots(6)$$

If Freundlich's explanation of the Hubble effect is accepted, these frequency (energy) changes should not be accompanied by deflections (changes of momentum).

An effect like this is of course not in agreement with current theory. It has, however, an attractive consequence. A simple application of the conservation laws of energy and momentum shows that a collision of this kind is only possible if a pair of particles with opposite momenta is created. The energy of one of these is $h\nu' = -\frac{1}{2}h\delta\nu$, where $\delta\nu$ is given by (6). If the secondary particles are photons their frequency is of the order of radar waves (for the sun $\nu' \sim 2 \times 10^9 \text{ sec}^{-1}$, $\lambda' \sim 15 \text{ cm}$). Thus the red-shift is linked to radio-astronomy. A simple estimate of the efficiency leads to the result that it is very high; one has to assume that only a small part of the secondary particles are photons or are observed as photons. Thus it seems possible that the strong radar emission of sun spots and flares and of other celestial objects may be explained by this new effect.

The secondary radiation for two colliding primary x-ray beams of $\lambda \sim 10 \text{ \AA}$ would be visible ($\lambda' \sim 6000 \text{ \AA}$). But it seems to be hardly possible to observe this effect because of the smallness of the cross section.

This theory would indicate the appearance of an absolute length in the field equations for the vacuum, and as the laws of general relativity do not contain such a length they ought to be modified. Therefore the predictions of relativity about the red-shift cannot be used as an argument against Freundlich's formula and its interpretation indicated here.

A more detailed account will soon appear in *Göttinger Nachrichten*.

Department of Mathematical Physics,
University of Edinburgh.
7th December 1953.

MAX BORN.

FINLAY-FREUNDLICH, E., 1954, *Proc. Phys. Soc. A*, **67**, 192.

The Thermal Conductivity of Monovalent Metals

According to the Bloch theory, the thermal conductivity of a pure metal at low temperatures ($T \ll \theta$) should be inversely proportional to the square of the absolute temperature. To obtain the multiplicative constant in that relationship, an integral equation must be solved. This has been done by Sondheimer (1950), but it can be shown that the solution is of such a form that it cannot be well represented by a polynomial of a small number of terms, which is Sondheimer's trial function. Thus doubt is thrown on his result, but since he used a variational method, leading to a stationary expression for the conductivity, his final result may be accurate, even though his trial function cannot adequately represent the true solution.

In order to clarify this point, the author has solved the integral equation numerically, using two different methods which led to the same result. In one the integral equation was replaced by a finite set of linear algebraic equations; the other was an iterative procedure. The result of these numerical calculations was renormalized by the variational method, and used in a stationary expression for the thermal conductivity. The renormalization correction was only 0.4%, and the conductivity is judged to be accurate to at least the same limit. The result exceeds Sondheimer's value by 11%.

Since the expression for the conductivity contains parameters which are difficult to calculate, it is usual, for purposes of comparing the theory with the results of experiments, to eliminate some of them by intercomparing two conductivities. The result of the present calculation can thus be expressed as

$$\kappa(T) = \kappa(\infty)(\theta/T)^2(64.0 N^{2/3})^{-1}, \quad T \ll \theta \quad \dots\dots(1)$$

where κ is the thermal conductivity, θ the Debye temperature and N the actual number of electrons per atom in the conduction band, the Fermi surface being assumed spherical.

There are well known discrepancies between eqn (1) and the thermal conductivity observed at low temperatures (Hulm 1950, 1952, Andrews, Webber and Spohr 1951, Berman and MacDonald 1951, 1952, White 1953) which are hardly reduced by the results of the present calculation. Using as θ -value the Debye temperature derived from the specific heat and putting $N=1$, they range from 5 to 6 for the monovalent metals sodium, copper, silver and gold. In all these cases $\kappa(T)$ as found experimentally is too high compared with $\kappa(\infty)$.

It is not clear, however, whether the discrepancy in (1) is due to an error in the theory of $\kappa(T)$ or $\kappa(\infty)$. It has been generally assumed that the theory is wrong in respect of the low-temperature thermal conductivity. However, there are considerable uncertainties in the theory of the electrical and thermal conductivity at high temperatures, because of the occurrence of Umklapp-processes at high temperatures, and because of the dispersion of the lattice waves. Both these effects are disregarded in the Bloch theory, and their inclusion would increase the high temperature resistance, thus reducing and possibly eliminating the discrepancy in (1).

However, the uncertainty of the theory at high temperatures can be avoided by intercomparing the thermal and electrical resistivity at low temperatures. Using the Bloch-Grüneisen expression for the temperature dependence of the electrical resistivity, and making use of the Wiedemann-Franz law at high temperatures, one obtains from (1)

$$\frac{W(T)}{T^2} = \frac{64.0}{497.6} N^{2/3} \frac{\theta^2}{L} \frac{R(T)}{T^5}, \quad T \ll \theta \quad \dots\dots(2)$$

where W is the thermal and R the electrical resistivity, and

$$L = (\pi K/e)^2/3 = 2.45 \times 10^{-8} \text{ watt-ohm deg}^{-2}.$$

Equation (2) should hold irrespective of any deviations of the phonon spectrum from the Debye theory and of Umklapp-processes.

The Bloch theory assumes that the conduction electrons interact only with longitudinal phonons, so that the appropriate θ -value in (2) is θ_L , the Debye temperature of the longitudinal lattice waves, introduced by Blackman (1951). Comparing (2) with the observed ratio of the electrical to the thermal resistance, there is a discrepancy of a factor of 5 for sodium, and of from 10 to 14 for the noble metals, the observed ratio being too high. This is a clear indication that the quasi-free electron model is inadequate.

The discrepancy is reduced if it is assumed that conduction electrons interact with transverse as well as with longitudinal waves, so that the appropriate θ -value in (2) is the Debye temperature as deduced from the low-temperature specific heat. The discrepancy for sodium is then 1.7, and ranges from 4.2 to 5.4 for the noble metals. There is support for this assumption from the lattice component of the thermal conductivity at low temperatures, the magnitude of

which is very sensitive to the nature of the electron-phonon interaction (Klemens 1954).

The remaining discrepancy in (2) may be explained by assuming that the Fermi surface is non-spherical. This will not alter the effective relaxation time for the case of thermal conduction because each electron-phonon interaction changes the energy of the electron, but does not significantly change its direction. The electrical resistance, on the other hand, is due to processes taking electrons in momentum space from a point on the Fermi surface to one on the opposite side. At low temperatures this will be a diffusion process, the electron moving on the surface in many small steps. Hence the effective relaxation time is sensitive to the shape of the Fermi surface. This effect will be particularly marked if the Fermi surface touches the zone boundary. Electrons can then diffuse to the nearest point of contact and reappear on the opposite side of the zone. On the average the distance to be covered is about halved, so that there will be an additional contribution to the resistance of about four times that due to normal diffusion.

It thus appears that the discrepancies in the relative magnitudes of the electrical and thermal resistances at low temperatures may be explained in the case of the noble metals in terms of the Fermi surface touching the zone boundary. This may also explain the anomalous sign of their thermoelectric power, and agrees with conclusions derived from the effect of strain on the thermoelectric power (Smit 1952, Mortlock 1953). The Fermi surface of sodium, on the other hand, does not seem to touch the zone boundary.

Division of Physics,
Commonwealth Scientific and
Industrial Research Organization,
Sydney, Australia.

P. G. KLEMENS.

23rd November 1953.

ANDREWS, F. A., WEBBER, R. T., and SPOHR, D. A., 1951, *Phys. Rev.*, **84**, 994.

BERMAN, R., and MACDONALD, D. K. C., 1951, *Proc. Roy. Soc. A*, **209**, 368; 1952, *Ibid.*, **211**, 122.

BLACKMAN, M., 1951, *Proc. Phys. Soc. A*, **64**, 681.

HULM, J. K., 1950, *Proc. Roy. Soc. A*, **204**, 98; 1952, *Proc. Phys. Soc. A*, **65**, 227.

KLEMENS, P. G., 1954, *Aust. J. Phys.*, **7**, January.

MORTLOCK, A. J., 1953, *Aust. J. Phys.*, **6**, 410.

SMIT, J., 1952, *Physica*, **18**, 587.

SONDHEIMER, E. H., 1950, *Proc. Roy. Soc. A*, **203**, 75.

WHITE, G. K., 1953, *Proc. Phys. Soc. A*, **65**, 559, 844.

A Note on the Absorption of Light by Indium Vapour

The atomic absorption cross sections in the region of the photo-ionization threshold have been experimentally determined for the alkali metals (Ditchburn, Jutsum and Marr 1953), for calcium (Jutsum 1954), for magnesium (Ditchburn and Marr 1953) and for thallium (Marr 1954). The author has recently attempted to obtain similar measurements for indium, but owing to temperature limitations of the apparatus it was not possible to observe the series limit absorption. However, with a path length of 150 cm and a pressure of 0.003 mm of indium

vapour, absorption was observed due to the auto-ionization line at 1758 \AA and an atomic cross section of about 10^{-16} cm^2 was calculated for this region.

Garton (1950) used a short carbon absorption tube in a King-type furnace and observed this line with a furnace temperature of 950°C , while a temperature of 1400°C was required to observe the series limit. Because of uncertainties in the effective length of his absorbing column he was unable to measure any atomic cross section. Since an accurate determination of the cross section at the series limit seems unlikely in the near future, the following estimation of the order of magnitude to be expected appears justified.

The atomic cross section at 1758 \AA may be used to calculate the effective path length in Garton's experiment, and after allowing for the differences in furnace temperature, etc. a value of 8 cm was obtained. Garton's results may now be used to estimate the atomic cross section at the series limit and it appears probable that it has a value between 10^{-18} and 10^{-19} cm^2 .

This result may be compared with that of thallium ($4.5 \times 10^{-18} \text{ cm}^2$) which has the same electron configuration in the outer shell, while calcium and magnesium also have atomic cross sections of about 10^{-18} cm^2 .

The Physics Research Laboratories,
Reading University.
13th November 1953.

G. V. MARR.

DITCHBURN, R. W., JUTSUM, P. J., and MARR, G. V., 1953, *Proc. Roy. Soc. A*, **219**, 89.

DITCHBURN, R. W., and MARR, G. V., 1953, *Proc. Phys. Soc. A*, **66**, 655.

GARTON, W. R. S., 1950, *Nature, Lond.*, **166**, 150.

JUTSUM, P. J., 1954, *Proc. Phys. Soc. A*, **67**, 190.

MARR, G. V., 1954, in the press.

CORRIGENDUM

γ -Radiation from the Reaction $^{27}\text{Al}(p, \gamma)^{28}\text{Si}$ by J. G. RUTHERGLEN, P. J. GRANT, F. C. FLACK and W. M. DEUCHARS (*Proc. Phys. Soc. A*, 1954, **67**, 101).

Figures 6 and 7 (a) should be interchanged.

REVIEWS OF BOOKS

Grundversuche der Physik in historischer Darstellung, by CARL RAMSAUER. Vol. I. *Von den Fallgesetzen bis zu den elektrischen Wellen*. Pp. viii + 190. (Berlin, Göttingen, Heidelberg : Springer-Verlag, 1953.) DM. 19.80.

In the introduction to his excellent book Professor Ramsauer draws attention to one of those well-known facts that have a way of escaping attention, namely that the standard histories of physics by Poggendorff, by Heller and by Gerland contain no illustrations—and the illustrations in Rosenberger's history are so few that he might have added that work. Gerland and Traumüller's *Geschichte der physikalischen Experimentierkunst* is a valuable work which is copiously illustrated but stresses the apparatus rather than the advances made with its aid, and is little concerned with work after 1800. Professor Ramsauer, who is known to physicists for his fundamental investigations in electronics, including the effect known by his name, has set himself the task of describing certain well-chosen fundamental experiments in physics and the way in which they were carried out, writing throughout as an experimenter. This means, of course, that he has always gone to the original accounts and has read them with a full realization of the conditions of the times in question. The result is a book that will be of the greatest interest to all physicists with historical leanings. Probably any experimental physicist who picks up the book and starts reading will find that he has historical leanings.

The experiments range from those of Galileo on the law of fall to Hertz's investigations of electric waves, although one or two are included that fall outside the dates so determined. For instance, in discussing the history of the law of gravitation, the author takes together Tycho Brahe—somewhat before Galileo—Kepler and Newton. He admits that Newton's work in this field is scarcely experimental, but effectively defends its inclusion. Typical of his attitude is that Professor Ramsauer points out the fundamental importance of the accuracy which Tycho obtained with the instruments on which he lavished so much care. These instruments had open, not telescopic, sights, but Kepler estimated that Tycho's error in angle did not exceed two minutes of arc: such was his confidence in this precision that a discrepancy of eight minutes between Tycho's observation and a calculation of the orbit of Mars which he, Kepler, had carried out on an early scheme of his was sufficient to lead him to abandon this scheme and turn to work that culminated in the discovery of the elliptic orbit. Professor Ramsauer is, perhaps, a little over-kind to Kepler's notions on the mechanics of the heavens—Kepler's 'magnetic' force had no resemblance to a gravitational force, for he said quite plainly *non est attractoria sed promotoria*—but he rightly stresses his immense services.

Exceeding the limiting date at the other end is the account of Lebedew's experiments on the pressure of light, no doubt included as clinching Maxwell's theory of light and because the experimental elegance strongly appealed to the author. To give some notion of the scope of the book, the other experiments on light which are to be found here are those of Römer (perhaps hardly experimental), Fizeau and Foucault on the velocity of light, Newton's work on the

decomposition of white light, Fresnel on interference, Malus on polarization and the chief optical work of Fraunhofer, Kirchhoff and Bunsen. The account of the experimental proofs of the kinetic theory of gases, dealing with the work of Robert Brown ('Brownian-movement Brown'), O. E. Meyer and Maxwell, is completed by a short description of the experiments which Stern carried out in 1920.

The careful discussion of the early experiments on the gas laws, going up to Regnault, disposes of Mariotte's claim to be included with Boyle. We are glad to see Andrews' fundamental experiments on the critical point included in the work on gases. The experiments on electricity and magnetism comprise, besides those that would at once occur to the reader, Rowland's work on the magnetic effect of a moving charge, a difficult and fundamental achievement. The book concludes with an account of Feddersen's investigations of the oscillatory discharge, a fascinating piece of work, and Hertz's discovery of electric waves, of which the author says that since Faraday's discovery of electromagnetic induction there has been no experimental discovery of such genius.

This book is written with a lifetime's knowledge of experimental physics and with an unabated enthusiasm for ingenuity of experimental method. It should meet with a warm welcome, not least wherever physics is taught. We look forward to a second volume which is announced, to cover the period from Röntgen rays to wave mechanics.

E. N. DA C. ANDRADE.

Ferroelectricity, by E. T. JAYNES. (Investigations in Physics No. 1.) Pp. viii + 136. (Princeton: University Press; Oxford: University Press, 1953.) \$2.00.

This book, which is an expansion of a doctoral thesis, is concerned mainly with the theory of ferroelectricity. It opens with a short account of the properties of Rochelle salt, and this is followed by a discussion of the dielectric theories of Lorentz, Onsager and others and of the conditions under which spontaneous polarization can take place. Mueller's interaction theory is then described. Except for a short note on KH_2PO_4 the rest of the book is devoted to BaTiO_3 and allied compounds. After an account of the main properties of BaTiO_3 there is a description of the theories of Mason and Matthias, Devonshire, and Slater followed by a more detailed account of the author's electronic theory. In the last two chapters the author discusses his original work on internal fields in crystals and the conditions for saturation polarization.

The material of the book falls into two classes: general accounts of ferroelectric theory and accounts of the author's original work. Although the latter is of considerable interest a full account of it in a work of this nature tends to make the book as a whole rather unbalanced. Nevertheless, it can be recommended as a useful and readable introduction to the subject. One error should be mentioned since it has often been repeated, namely the statement that Onsager's dielectric theory does not lead to spontaneous polarization; Pirenne showed in 1949 (*Helv. Phys. Acta*, **22**, 479) that, contrary to Onsager's statement, it does, but his paper seems to have been overlooked by later writers.

A. F. DEVONSHIRE.

CONTENTS OF SECTION B

	PAGE
Dr. A. S. LODGE and Dr. H. G. HOWELL. Friction of an Elastic Solid	89
Dr. M. J. DUMBLETON. Discontinuous Flow in Zinc Crystals and its Relationship to Strain Ageing	98
Dr. E. PITTS. The Application of Radiative Transfer Theory to Scattering Effects in Unexposed Photographic Emulsions	105
Mr. J. J. BENBOW. The Dynamic Mechanical Properties of some Organic Glasses	120
Mr. D. G. COLE, Dr. P. FELTHAM and Mr. E. GILLAM. On the Mechanism of Grain Growth in Metals, with Special Reference to Steel	131
Dr. R. C. FAUST. The Determination of the Refractive Indices of Inhomogeneous Solids by Interference Microscopy	138
Miss NORA E. HILL. The Dielectric Relaxation of Polar Molecules in Solution .	149
Research Notes :	
Dr. P. M. DAVIDSON. A Note on the Formula for the Mobility of Electrons with Mean Free Path varying with Velocity	159
Dr. P. A. C. MORTIER and Mr. J. F. ROOSE. Velocity of Discharge Propagation in Self-Quenching Geiger-Müller Counters	161
Dr. G. C. FARNELL. Scattering of Light in Photographic Emulsion Layers .	164
Reviews of Books	166
Contents of Section A	168

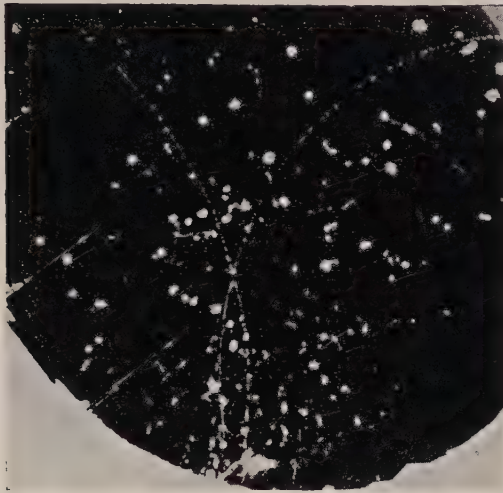


Figure 1. 4.5 mev internal pair from $^{12}\text{C}^*$. Magnification $\times \frac{2}{5}$.



Figure 2. 7 mev positron-electron pair from $^{12}\text{C}^*$. Magnification $\times \frac{2}{5}$.

Reisz Potential and the Elimination of Divergences from Quantum Electrodynamics : II

By L. S. KOTHARI*

Clarendon Laboratory, Oxford

MS. received 6th November 1953

Abstract. The solution of Dirac equation in interaction representation and the Feynman function S_F are generalized in the β -plane, β being a parameter characteristic of the Reisz potential. It is then shown that by using the generalized function $\mathcal{S}_F^\beta(x)$ instead of S_F , divergence arising from the lowest order photon self-energy graph can be eliminated, though the result obtained is not gauge invariant and contains the Wentzel term.

§ 1. INTRODUCTION

IN quantum electrodynamics, as Dyson (1949) has shown, there are only three types of primitive divergent graphs: those of (i) electron self-energy, (ii) irreducible vertex parts and (iii) the photon self-energy. Apart from these one has also to deal with infra-red divergence and the divergence arising from the point nature of charge. These two divergences are, however, easily avoided and a number of methods are known for removing them. To remove the divergences arising from the primitive divergent graphs Dyson has developed a subtraction procedure, while Feynman (1949) uses a cut-off technique. In an earlier paper (Kothari 1954, to be referred to as I) we have shown that in quantum electrodynamics the divergences arising from the point nature of charge, the electron self-energy and the vertex part of a Feynman graph can as well be eliminated by working with modified Reisz potential instead of the usual electromagnetic potential. In the present paper we propose to discuss the divergence from the lowest order photon self-energy graph.

The solution of the Dirac equation in Schrödinger representation has been generalized in the β -plane, β being an arbitrary parameter, real or complex, by Reisz (1939) and Gustafson (1946). Reisz considers the case $m=0$, m being the mass of the electron. The case $m \neq 0$ has been treated by Gustafson. Their generalization, however, is not suited for the present purpose. In order to link the method of analytic continuation with the technique of Feynman and Dyson it is necessary to obtain the generalization of the solution of the Dirac equation in interaction representation and of the Feynman function, S_F , in the β -plane. After obtaining the generalization in the next section, we proceed to consider the photon self-energy in § 3.

§ 2. GENERALIZATION OF S_F IN β -PLANE

Even in the presence of electromagnetic field the Dirac equation in interaction representation is†

$$(i\nabla - m)\psi(x) = 0, \quad \dots\dots(1)$$

$$\text{where} \quad \nabla = \gamma_\mu \frac{\partial}{\partial x_\mu}, \quad \nabla^2 = \square, \quad \dots\dots(2)$$

γ_μ are the Dirac matrices and $\psi(x)$ is the wave function of the electron.

* Present address: Tata Institute for Fundamental Research, Apollo Pier Road, Bombay 1.

† Notation in this paper is the same as used in I.

We define a function $\mathcal{S}^\beta(x)$ as

$$\mathcal{S}^\beta(x) = (-i\nabla - m)\mathcal{D}_m^\beta(x) \quad \dots\dots(3)$$

$$= \frac{H(\beta)l_0^\beta}{2\pi^2} \int_{D'} (\chi^2 - m^2)^{(\beta-2)/2} (-i\nabla - m) \sin[kx] d^4k, \quad \dots\dots(4)$$

D' being the region defined by $\chi^2 \geq m^2$; $k_0 > 0$. $\mathcal{D}_m^\beta(x)$, which was introduced in an earlier paper (Kothari 1952), is a generalization in the β -plane of the D-function referring to a particle of mass m , and satisfies the equation

$$(\square + m^2)\mathcal{D}_m^\beta(x) = l_0^{-2}\mathcal{D}_m^{\beta+2}(x). \quad \dots\dots(5)$$

From (4) it follows that

$$\mathcal{S}^\beta(x) = H(\beta)l_0^\beta \int_{\chi > m} (\chi^2 - m^2)^{(\beta-2)/2} \chi (-i\nabla - m) D_\chi(x) d\chi. \quad \dots\dots(6)$$

Further, on operating with $(i\nabla - m)$ from the left, equation (3) becomes, using (5),

$$(i\nabla - m)\mathcal{S}^\beta(x) = (\square + m^2)\mathcal{D}_m^\beta(x) = l_0^{-2}\mathcal{D}_m^{\beta+2}(x).$$

When analytically continued to $\beta=0$, the right-hand side reduces to zero and we obtain

$$(i\nabla - m)S(x) = 0, \quad \dots\dots(7)$$

where $S(x) \equiv \lim_{\beta \rightarrow 0} \mathcal{S}^\beta(x)$ is the usual propagation function for an electron of mass m and satisfies the Dirac equation. The generalized wave function $\psi^\beta(x)$ for the electron can be written in terms of the Green's function (3). When analytically continued to $\beta=0$, $\psi^\beta(x)$ would represent the solution of the Dirac equation in interaction representation. We now assume the following anti-commutation relation for the wave functions

$$\{\psi^\beta(x), \bar{\psi}^\beta(x')\} = i\mathcal{S}^\beta(x - x'), \quad \dots\dots(8)$$

and define the vacuum for the present field by the relation

$$\psi^{+\beta}(x)\Psi_0 = 0, \quad \dots\dots(9)$$

where $\psi^{+\beta}(x)$ represents the positive frequency part of $\psi^\beta(x)$ and Ψ_0 is the vacuum state vector. From (9) and (8) it follows that

$$\langle P(\psi^\beta(x), \bar{\psi}^\beta(x')) \rangle_0 = -\epsilon(x, x')\mathcal{S}_F^\beta(x - x'), \quad \dots\dots(10)$$

where $\epsilon(x, x') = \pm 1$ according as $x_0 > x'_0$ or $x_0 < x'_0$, and

$$\mathcal{S}_F^\beta(x) = \frac{H(\beta)l_0^\beta}{(2\pi)^2} \int_{\chi > m} (\chi^2 - m^2)^{(\beta-2)/2} \chi d\chi \int \frac{(\mathbf{k} + m) e^{-i[kx]}}{k^2 - \chi^2} d^4k. \quad \dots\dots(11)$$

By putting $\chi^2 - m^2 = t^2$ we can rewrite (11) as

$$\mathcal{S}_F^\beta(x) = \frac{H(\beta)l_0^\beta}{(2\pi)^2} \int_0^\infty t^{\beta-1} dt \int \frac{(\mathbf{k} + m) e^{-i[kx]}}{k^2 - m^2 - t^2} d^4k.$$

As in I, here also it is necessary to change the 'weight factor' in the above relation from $l_0^\beta t^{\beta-1}$ to $g_\beta(t) = \frac{1}{2}(l_0^\beta t^{\beta-1} + l_0^{\beta*} t^{\beta*-1})$ in order to evaluate an otherwise logarithmically divergent integral.

Thus we finally have

$$\mathcal{S}_F^\beta(x) = \frac{H(\beta)}{(2\pi)^2} \int_0^\infty g_\beta(t) dt \int \frac{(\mathbf{k} + m) e^{-i[kx]}}{k^2 - m^2 - t^2} d^4k. \quad \dots\dots(12)$$

$\mathcal{S}_F^\beta(x)$ is the generalization in the β -plane of the usual Feynman function S_F .

§3. SELF ENERGY OF PHOTON

We now consider the self-energy of a photon. Instead of using the usual S_F function, we write out the matrix element for the lowest order photon self-energy graph using the generalized function $\mathcal{O}_{F^\beta}(x)$. Apart from a numerical factor, the matrix element for a photon of momentum \mathbf{p} (p^2 not necessarily zero) is

$$J_{\mu\nu}^{\beta\beta'} = - \frac{e^2 H(\beta) H(\beta')}{(2\pi)^4} \int_0^\infty \int_0^\infty g_\beta(t) g_{\beta'}(t') dt dt' \\ \times \int \frac{\text{Sp}[\gamma_\mu(\mathbf{p} + \mathbf{k} + m) \gamma_\nu(\mathbf{k} + m)]}{\{(p+k)^2 - m^2 - t^2\} \{k^2 - m^2 - t'^2\}} d^4k. \quad \dots\dots(13)$$

Evaluating the spur and integrating by parts with respect to t and t' once, we obtain

$$J_{\mu\nu}^{\beta\beta'} = - \frac{e^2 H(\beta) H(\beta')}{\pi^4 \beta \beta'} \int_0^\infty \int_0^\infty g_\beta(t) t^2 g_{\beta'}(t') t'^2 dt dt' \\ \times \int \frac{m^2 g_{\mu\nu} + p_\mu k_\nu + p_\nu k_\mu - [kp] g_{\mu\nu} + 2\bar{k}_\mu k_\nu - k^2 g_{\mu\nu}}{\{k^2 + p^2 + 2[kp] - m^2 - t^2\}^2 \{k^2 - m^2 - t'^2\}^2} d^4k. \quad \dots\dots(14)$$

Now consider the integral

$$I = \int \frac{(1 : k_\mu : k_\mu k_\nu) d^4k}{\{k^2 + p^2 + 2[kp] - m^2 - t^2\}^2 \{k^2 - m^2 - t'^2\}^2}. \quad \dots\dots(15)$$

It is convergent over k and can be evaluated by introducing a Feynman variable. We get

$$I = i\pi^2 \int_0^1 \frac{x(1-x)}{\Lambda^2} (1 : -p_\mu x : x^2 p_\mu p_\nu - \frac{1}{2} g_{\mu\nu} \Lambda) dx, \quad \dots\dots(16)$$

where $\Lambda = m^2 - p^2 x(1-x) + t^2 x + t'^2(1-x)$. Hence

$$J_{\mu\nu}^{\beta\beta'} = - \frac{ie^2 H(\beta) H(\beta')}{\pi^2 \beta \beta'} \iint g_\beta(t) t^2 g_{\beta'}(t') t'^2 dt dt' \\ \times \int_0^1 \frac{x(1-x)}{\Lambda^2} \{m^2 g_{\mu\nu} + x(1-x)(p^2 g_{\mu\nu} - 2p_\mu p_\nu) + g_{\mu\nu} \Lambda\} dx. \quad \dots\dots(17)$$

To carry out the integration over t and t' we write

$$J_{\mu\nu}^{\beta\beta'} \equiv J_1^{\beta\beta'} + J_2^{\beta\beta'}, \quad \dots\dots(18)$$

where

$$J_1^{\beta\beta'} = - \frac{ie^2 H(\beta) H(\beta')}{\pi^2 \beta \beta'} \iint g_\beta(t) t^2 g_{\beta'}(t') t'^2 dt dt' \\ \times \int_0^1 \frac{x(1-x)}{\Lambda^2} \{m^2 g_{\mu\nu} + x(1-x)(p^2 g_{\mu\nu} - 2p_\mu p_\nu)\} dx. \quad \dots\dots(19)$$

The integral is convergent over one of the variables t or t' for β or $\beta' = 0$. Therefore we put, say, $\beta' = 0$ and integrate over t' . After this, continuation to $\beta = 0$ can be carried out without any difficulty. We finally obtain

$$J_1^{00} = - \frac{ie^2}{4\pi^2} \int_0^1 \{m^2 g_{\mu\nu} + x(1-x)(p^2 g_{\mu\nu} - 2p_\mu p_\nu)\} \log \frac{x l_0^2}{m^2 - p^2 x(1-x)} dx. \quad \dots\dots(20)$$

Now consider $J_2^{\beta\beta'}$,

$$J_2^{\beta\beta'} = - \frac{ie^2 H(\beta) H(\beta') g_{\mu\nu}}{\pi^2 \beta \beta'} \int_0^\infty \int_0^\infty g_\beta(t) t^2 g_{\beta'}(t') dt dt' \int_0^1 \frac{x(1-x)}{\Lambda} dx. \quad \dots\dots(21)$$

Continuing the right-hand side to, say, $\beta' = 0$, we get

$$J_2^{\beta 0} = -\frac{ie^2 H(\beta) g_{\mu\nu}}{2\pi^2 \beta} \int_0^\infty g_\beta(t) t^2 dt \int_0^1 x dx \log \frac{(1-x)l_0^{-2}}{m^2 - p^2 x(1-x) + t^2 x}. \quad \dots\dots (22)$$

To integrate (22) over t , let us consider

$$\begin{aligned} I_1 &= l_0^\beta \int_0^\infty t^{\beta+1} dt \log \frac{(1-x)l_0^{-2}}{xt^2 + A} \\ &= l_0^\beta \int_0^K + \int_K^\infty t^{\beta+1} dt \log \frac{(1-x)l_0^{-2}}{xt^2 + A}, \quad \dots\dots (23) \end{aligned}$$

where K is any large number. The first integral in (23) is convergent over t for $\beta=0$ and we can therefore put $\beta=0$ before integrating it. It yields

$$\frac{1}{2x} [xK^2 \log(1-x) - (A + xK^2) \log(A + xK^2)l_0^2 + A \log Al_0^2 + xK^2]. \quad \dots\dots (24)$$

The second integral reduces to

$$-\frac{1}{2}K^2 \log(1-x) - l_0^\beta \int_K^\infty t^{\beta+1} dt \log(A + xt^2)l_0^2. \quad \dots\dots (25)$$

Putting
$$I_2 = l_0^\beta \int_K^\infty t^{\beta+1} dt \log(A + xt^2)l_0^2, \quad \dots\dots (26)$$

we find that this integral converges for sufficiently large negative values of β . We therefore differentiate both sides with respect to A and obtain, on a little modification,

$$\frac{\partial I_2}{\partial A} = l_0^\beta \int_K^\infty t^{\beta+1} dt \left\{ \frac{1}{xt^2} + \left(\frac{1}{A + xt^2} - \frac{1}{xt^2} \right) \right\}.$$

In evaluating the right-hand side for $\beta=0$ we note that the contribution of the term $1/\beta$ would vanish when the conjugate term is added to get the value of the integral in (22) and $\beta \rightarrow i0$.

This gives

$$\frac{\partial I_2}{\partial A} = \frac{1}{2x} \log x - \frac{1}{2x} \log(A + xK^2)l_0^2$$

or
$$I_2 = \frac{A}{2x} \log x - \frac{1}{2x} [(A + xK^2) \log(A + xK^2)l_0^2 - (A + xK^2)].$$

Combining these results

$$J_2^{00} = \frac{ie^2 g_{\mu\nu}}{4\pi^2} \int \{m^2 - p^2 x(1-x)\} \left[1 + \log \frac{x l_0^{-2}}{m^2 - p^2 x(1-x)} \right] dx. \quad \dots\dots (27)$$

From equations (18), (20) and (27) it follows that

$$\begin{aligned} J_{\mu\nu}(p) = J_{\mu\nu}^{00} &= -\frac{ie^2}{2\pi^2} (g_{\mu\nu} p^2 - p_\mu p_\nu) \int x(1-x) \log \frac{x l_0^{-2}}{m^2 - p^2 x(1-x)} dx \\ &\quad + \frac{ie^2 g_{\mu\nu}}{4\pi^2} \left(m^2 - \frac{1}{6} p^2 \right). \quad \dots\dots (28) \end{aligned}$$

The second term in (28) makes the result non gauge invariant. For free photons $p^2=0$, and this term reduces to

$$\frac{ie^2}{4\pi^2} g_{\mu\nu} m^2, \quad \dots\dots (29)$$

a result which was obtained earlier by Wentzel (1948) using Schwinger's method.

Feynman, by suitably modifying his cut-off factors, avoids any such term and gets only the first term of (28). In the present case the extra term arises on account of the fact that the electron, in going round the closed loop, changes its mass at each photon vertex. However, apart from this physically unimportant term, (28) gives the correct finite value for the matrix element. In order to obtain a completely gauge invariant result it seems that one may have to modify the formalism a little.

ACKNOWLEDGMENTS

I am thankful to Mr. J. Hamilton for his interest in the present work, which was carried out while at Cambridge on a Government of India Scholarship. I would also like to thank Professor Pryce for facilities to work at the Clarendon Laboratory.

REFERENCES

- DYSON, F. J., 1949, *Phys. Rev.*, **75**, 1736.
FEYNMAN, R. P., 1949, *Phys. Rev.*, **76**, 769.
GUSTAFSON, T., 1946, *Ark. Mat. Astr. Fys. A*, **34**, 1.
KOTHARI, L. S., 1952, *Proc. Phys. Soc. A*, **65**, 930; 1954, *Ibid.*, **67**, 17.
REISZ, M., 1939, Conference à la Réunion internationale de Mathématique à Paris en Juillet 1937.
WENTZEL, G., 1948, *Phys. Rev.*, **74**, 1070.

Justification of the Use of Perturbation Theory in Metallic Conductivity

BY J. S. VAN WIERINGEN*

Department of Mathematical Physics, The University, Birmingham

Communicated by R. E. Peierls; MS. received 16th October 1953

Abstract. In metals at high temperatures the time τ spent by an electron between two consecutive scatterings is smaller than the duration of the collision t_c , if one defines t_c as that time after which one can be sure that the interaction with the scattering centre (or lattice wave) is less than kT . Hence the customary theory of conductivity is not justified *a priori* because it considers the scatterings to be independent. Yet its results are confirmed by experiment. In this paper the correction terms for scattering by two centres are calculated. They are shown to be negligible for a Fermi gas.

§1. INTRODUCTION

IN the customary theory of electrical conductivity in metals use is made of perturbation theory (Bloch 1928). Its validity for this problem has been questioned (Kretschmann 1934, Peierls 1934 a, b, c). Therefore in this paper it is intended to clarify the question by calculating the next higher order perturbation theory.

First it is useful to give a brief outline of the usual theory. In an applied external electric field F the electrons in the metal are accelerated. Their velocity does not increase indefinitely, however, because they collide with lattice impurities or thermal lattice waves. Mathematically this is expressed in the Boltzmann equation. It says that in the steady state $(\partial f / \partial t)_{\text{coll}}$ the change of the number of particles in a volume element of \mathbf{k} -space under the influence of the collisions is cancelled by $(\partial f / \partial t)_F$, the corresponding change under the influence of the field F ; or

$$\left(\frac{\partial f}{\partial t}\right)_{\text{coll}} + \left(\frac{\partial f}{\partial t}\right)_F = 0. \quad \dots\dots(1)$$

Hence in the steady state the number of particles in a volume element of \mathbf{k} -space does not change. This paper is concerned with the first term of (1). Usually it is calculated with second order time dependent perturbation theory. Kretschmann (1934) remarked that this assumes transitions between well-defined levels. Hence, roughly speaking, the 'unsharpness' of the levels due to their finite lifetime τ should be less than the distances between them. The latter, at high temperatures ($T \gg \theta$), are of the order $k\theta$ because most phonons have an energy of this order. Here θ is the Debye temperature and τ is the average time between collisions. Hence $\hbar/\tau \ll k\theta$ or

$$\tau \gg \hbar/k\theta. \quad \dots\dots(2)$$

This condition is not satisfied by actual metals (if τ is taken to be the relaxation time, which is the case at high temperatures). Kretschmann thought he could

* Present address : Philips Research Laboratories, Eindhoven, Netherlands

prove condition (2) by a critical review of Bloch's calculation, but his proof contains a mistake which was pointed out by Peierls (1934 a, b, c).

In a classical theory of the collision process a similar condition would be required if the collisions are described as separate scatterings by single scattering centres. In that case the time between subsequent scatterings τ should be long compared with the duration of the collision t_c , i.e. the time during which the electron is under the influence of the scattering centre. If this were not true the electron would be scattered by complexes of two (or more) scattering centres and not by single ones. Thus in the quantum mechanical scattering theory $\hbar/k\theta$ plays the role of t_c .

Peierls (1934 a, b, c) showed that the condition (2) is too stringent by considering time dependent perturbation theory more carefully. As is well known, the change of the probability of finding an electron in a state k is

$$w_k(t+t_c) - w_k(t) = \sum_{k'} B_{kk'} \{w_k(t) - w_{k'}(t)\} \frac{1 - \cos(E_k - E_{k'} - \hbar\omega)t_c/\hbar}{(E_k - E_{k'} - \hbar\omega)^2} \dots\dots (3)$$

where the $B_{kk'}$ are proportional to the square of the matrix elements of the perturbing energy (lattice vibrations or imperfections). The last factor of (3) is replaced by $\delta(E_k - E_{k'} - \hbar\omega)$, i.e. when integrating over $E_{k'}$ the other factors are supposed to be constant. For $B_{kk'}$ this is usually approximately true, but w_k changes appreciably over an interval of the order of kT . Thus the last factor should be different from zero in a region less than kT . This requires $t_c \gtrsim \hbar/4kT$. Thus the new condition becomes

$$\tau > \hbar/4kT. \dots\dots (4)$$

Although (4) is a less severe restriction than (2) it is not satisfied in some metals (e.g. in Cu) at high temperatures. Yet the customary theory of conductivity has been quite successful in describing, for example, the temperature dependence of the resistance of metals (Sondheimer 1950, Rhodes 1950). Hence it seems that not only (2) but even (4) is too stringent a condition.

Landau (Peierls 1934 b) has proved that (4) may be replaced by

$$\tau > \hbar/E_F \dots\dots (5)$$

(where E_F is the Fermi energy), but the details of his proof have never been published. Condition (5) is satisfied in all metals. It may be visualized as follows. If one wants to describe the scattering as a series of independent collisions with one impurity (or lattice wave) at a time, the distance between the impurities should be large compared with the de Broglie wavelength. This gives $v\tau \gg \hbar/mv$ or $\hbar/2\tau \ll \frac{1}{2}mv^2$. Only electrons near the Fermi surface contribute to the conductivity. Hence $\frac{1}{2}mv^2 \simeq E_F$, which leads again to $\tau > \hbar/2E_F$.

In the following we want to study in detail what happens during a collision. Therefore perturbation theory will be pushed one step further, i.e. to fourth order in the perturbing potential. It will be shown that this introduces no new effects provided $kT \ll E_F$, which is all right for all ordinary metals.

§2. FOURTH ORDER PERTURBATION THEORY FOR SCATTERING BY POTENTIAL WELLS DISTRIBUTED AT RANDOM (or lattice waves with random phases)

The unperturbed wave functions of an electron in a crystal lattice are $\psi(\mathbf{x}, \mathbf{k}, t) = u(\mathbf{x}, \mathbf{k}) \exp(i\mathbf{k} \cdot \mathbf{x}) \exp(-iEt/\hbar)$ where $u(\mathbf{x}, \mathbf{k})$ has the periodicity of the lattice (Seitz 1940). The wave function Ψ of the particle in a perturbing

potential V that starts acting on it at $t=0$ will be expanded in the unperturbed wave functions

$$\Psi(\mathbf{x}, t) = \int \psi(\mathbf{k}, \mathbf{x}) a(\mathbf{k}, t) \exp(-iE_{\mathbf{k}}t/\hbar) d\mathbf{k}. \quad \text{.....(6)}$$

If this is inserted in the Schrödinger equation one gets

$$\dot{a}(\mathbf{k}, t) = -(i/\hbar) \int (\mathbf{k} | V | \mathbf{k}') a(\mathbf{k}', t) \exp\{-i(E' - E)t/\hbar\} d\mathbf{k}'.$$

If V is small a good solution will be found by iteration:

$$a(\mathbf{k}, t) = a^{(0)}(\mathbf{k}, t) + a^{(1)}(\mathbf{k}, t) + a^{(2)}(\mathbf{k}, t) + \dots$$

where $a^{(0)}(\mathbf{k})$ describes the situation at $t=0$ when V starts to disturb the system, while the further terms follow from

$$\dot{a}^{(n)}(\mathbf{k}, t) = -(i/\hbar) \int (\mathbf{k} | V | \mathbf{k}') a^{(n-1)}(\mathbf{k}', t) \exp\{-i(E - E')t/\hbar\} d\mathbf{k}'.$$

Thus one gets

$$\dot{a}^{(1)}(\mathbf{k}, t) = -(i/\hbar) \int (\mathbf{k} | V | \mathbf{k}') a^{(0)}(\mathbf{k}') \exp\{-i(E - E')t/\hbar\} d\mathbf{k}' \quad \text{.....(7a)}$$

$$a^{(1)}(\mathbf{k}, t) = \int (\mathbf{k} | V | \mathbf{k}') a^{(0)}(\mathbf{k}') \frac{\exp\{-i(E - E')t/\hbar\} - 1}{E - E'} d\mathbf{k}' \quad \text{.....(7b)}$$

and so on till

$$\begin{aligned} a^{(3)}(\mathbf{k}, t) = & \int (\mathbf{k} | V | \mathbf{k}') (\mathbf{k}' | V | \mathbf{k}'') (\mathbf{k}'' | V | \mathbf{k}''') a^{(0)}(\mathbf{k}''') \\ & \times \left\{ \frac{\exp\{-i(E - E''')t/\hbar\} - 1}{(E - E''')(E' - E''')(E'' - E''')} + \frac{\exp\{-i(E - E'')t/\hbar\} - 1}{(E - E'')(E' - E'')(E'' - E'')} \right. \\ & \left. + \frac{\exp\{-i(E - E')t/\hbar\} - 1}{(E - E')(E'' - E')(E''' - E')} \right\} d\mathbf{k}' d\mathbf{k}'' d\mathbf{k}'''. \quad \text{.....(7c)} \end{aligned}$$

The matrix aa^* if averaged over phases is nothing but the density matrix (Dirac 1947, Tolman 1938) and the formulae (7) can equally well be derived from the equation of motion of this dynamical variable. In our case the density matrix is exceptionally simple, however, for we want to show later that once it is diagonal it remains diagonal. Hence it may be assumed diagonal and can simply be interpreted as giving the numbers of particles in each state.

The general expressions (7) can be simplified in the special case under consideration. We are interested either in a random distribution of scattering centres (impurities in the crystal) or in deformation waves without phase relations (thermal vibration of the crystal). In the first case the potential $v(\mathbf{r} - \mathbf{r}_n)$ of the n th scattering centre is expanded in a Fourier integral:

$$v(\mathbf{r} - \mathbf{r}_n) = \int d\mathbf{k} v(\mathbf{k}) \exp\{-i\mathbf{k} \cdot (\mathbf{r} - \mathbf{r}_n)\}. \quad \text{.....(8a)}$$

Then one gets for N centres

$$V(\mathbf{r}) = \int d\mathbf{k} V(\mathbf{k}) \exp(-i\mathbf{k}\mathbf{r}) = \sum_{n=1}^N v(\mathbf{r} - \mathbf{r}_n) = \sum_{n=1}^N \int d\mathbf{k} v(\mathbf{k}) \exp\{-i\mathbf{k}(\mathbf{r} - \mathbf{r}_n)\}. \quad \text{.....(8b)}$$

Thus $(\mathbf{k} | V | \mathbf{k}') = \int d\mathbf{r} u(\mathbf{k}, \mathbf{r}) \exp(i\mathbf{k} \cdot \mathbf{r}) V(\mathbf{r}) \exp(-i\mathbf{k}' \cdot \mathbf{r}) u^*(\mathbf{k}', \mathbf{r})$

$$\begin{aligned} &= \sum_n \int d\mathbf{k}'' d\mathbf{r} u(\mathbf{k}, \mathbf{r}) u^*(\mathbf{k}', \mathbf{r}) v(\mathbf{k}'') \\ &\quad \times \exp\{-i(\mathbf{k}'' - \mathbf{k} + \mathbf{k}') \cdot \mathbf{r}\} \exp(i\mathbf{k}' \cdot \mathbf{r}_n) \\ &= \int d\mathbf{r} u(\mathbf{k}, \mathbf{r}) u^*(\mathbf{k}', \mathbf{r}) v(\mathbf{k} - \mathbf{k}') \sum_n \exp\{i(\mathbf{k} - \mathbf{k}') \cdot \mathbf{r}_n\} \quad \text{....(9)} \end{aligned}$$

† For brevity we have left out the density factor $L_x L_y L_z / (2\pi)^3$ in all integrals over \mathbf{k} throughout.

owing to the δ -function character of $\int \exp \{-i(\mathbf{k}'' - \mathbf{k} + \mathbf{k}') \cdot \mathbf{r}\} d\mathbf{k}''$. If the scattering centres are distributed at random

$$\sum_n \exp \{i(\mathbf{k} - \mathbf{k}') \cdot \mathbf{r}_n\} = N\delta_{\mathbf{k}\mathbf{k}'} \quad \dots\dots (10)$$

but by a suitable choice of the zero point of the potential $v(0) = 0$ and hence

$$(\mathbf{k} | V(\mathbf{r}) | \mathbf{k}') = 0. \quad \dots\dots (11a)$$

A product of matrix elements becomes

$$\begin{aligned} (\mathbf{k} | V | \mathbf{k}')(\mathbf{k}' | V | \mathbf{k}'') &= \iint d\mathbf{r} d\mathbf{r}' u(\mathbf{k}, \mathbf{r}) u^*(\mathbf{k}', \mathbf{r}) u(\mathbf{k}', \mathbf{r}') u^*(\mathbf{k}'', \mathbf{r}') v(\mathbf{k} - \mathbf{k}') v(\mathbf{k}' - \mathbf{k}'') \\ &\times \sum_{n, m} \exp \{i(\mathbf{k} - \mathbf{k}') \cdot \mathbf{r}_n + i(\mathbf{k}' - \mathbf{k}'') \cdot \mathbf{r}'_m\}. \quad \dots\dots (12) \end{aligned}$$

In the double sum only the terms for which $n = m$ give a contribution; its value is

$$(\mathbf{k} | V | \mathbf{k}')(\mathbf{k}' | V | \mathbf{k}'') = \left\{ \int d\mathbf{r} u(\mathbf{k}, \mathbf{r}) u^*(\mathbf{k}', \mathbf{r}) \right\}^2 |v(\mathbf{k} - \mathbf{k}')|^2 N\delta_{\mathbf{k}\mathbf{k}''}. \quad \dots\dots (11b)$$

Similarly

$$\begin{aligned} &(\mathbf{k} | V | \mathbf{k}')(\mathbf{k}' | V | \mathbf{k}'')(\mathbf{k}'' | V | \mathbf{k}''') \\ &= \int d\mathbf{r} u(\mathbf{k}) u^*(\mathbf{k}') \int d\mathbf{r} u(\mathbf{k}') u^*(\mathbf{k}'') \\ &\times \int d\mathbf{r} u(\mathbf{k}'') u^*(\mathbf{k}''') v(\mathbf{k} - \mathbf{k}') v(\mathbf{k}' - \mathbf{k}'') v(\mathbf{k}'' - \mathbf{k}''') N\delta_{\mathbf{k}''', \mathbf{k}} \quad \dots\dots (11c) \end{aligned}$$

$$\begin{aligned} &(\mathbf{k} | V | \mathbf{k}')(\mathbf{k}' | V | \mathbf{k}'')(\mathbf{k}'' | V | \mathbf{k}''')(\mathbf{k}''' | V | \mathbf{k}^{iv}) \\ &= \int d\mathbf{r} u(\mathbf{k}) u^*(\mathbf{k}') \int d\mathbf{r} u(\mathbf{k}') u^*(\mathbf{k}'') \int d\mathbf{r} u(\mathbf{k}'') u^*(\mathbf{k}''') \\ &\times \int d\mathbf{r} u(\mathbf{k}''') u^*(\mathbf{k}^{iv}) v(\mathbf{k} - \mathbf{k}') v(\mathbf{k}' - \mathbf{k}'') v(\mathbf{k}'' - \mathbf{k}''') v(\mathbf{k}''' - \mathbf{k}^{iv}) N\delta_{\mathbf{k}^{iv}, \mathbf{k}} \\ &+ N^2 \left[\left\{ \int d\mathbf{r} u(\mathbf{k}) u^*(\mathbf{k}') \int d\mathbf{r} u(\mathbf{k}) u^*(\mathbf{k}''') \right\}^2 |v(\mathbf{k} - \mathbf{k}')|^2 |v(\mathbf{k} - \mathbf{k}''')|^2 \delta_{\mathbf{k}'', \mathbf{k}'} \delta_{\mathbf{k}^{iv}, \mathbf{k}} \right. \\ &+ \left\{ \int d\mathbf{r} u(\mathbf{k}) u^*(\mathbf{k}') \int d\mathbf{r} u(\mathbf{k}') u^*(\mathbf{k}'') \right\}^2 |v(\mathbf{k} - \mathbf{k}')|^2 |v(\mathbf{k}' - \mathbf{k}'')|^2 \delta_{\mathbf{k}'', \mathbf{k}'} \delta_{\mathbf{k}^{iv}, \mathbf{k}} \\ &+ \int d\mathbf{r} u(\mathbf{k}) u^*(\mathbf{k}') \int d\mathbf{r} u(\mathbf{k}') u^*(\mathbf{k}'') \int d\mathbf{r} u(\mathbf{k}'') u^*(\mathbf{k}''') \int d\mathbf{r} u(\mathbf{k}''') u^*(\mathbf{k}^{iv}) \\ &\times |v(\mathbf{k} - \mathbf{k}')|^2 |v(\mathbf{k}' - \mathbf{k}'')|^2 \delta_{\mathbf{k} - \mathbf{k}', \mathbf{k}'' - \mathbf{k}'''} \delta_{\mathbf{k}' - \mathbf{k}'', \mathbf{k}'' - \mathbf{k}^{iv}} \left. \right]. \quad \dots\dots (11d) \end{aligned}$$

The terms proportional to N arise when the scattering centres are taken separately ($n = m$, $n = m = \sigma$, $n = m = \sigma = s$ in the sum occurring in the products of 2, 3, 4 matrix elements respectively). Hence they describe successive approximations of the scattering by a single centre. We assume that the scattering potentials are so weak that the first approximation is sufficient to treat the scattering by a single centre.† The physically interesting term is the one proportional to N^2 in the last line. It describes the interference in the scattering by two centres, and this is the stumbling block on which the ordinary conductivity theory might break down. It is this interference effect that will be shown to be negligible if $\hbar T \ll E_F$.

† A stronger potential can be treated by replacing it by an effective weak potential which gives the same scattered wave.

If the scattering is caused by the lattice vibrations of a perfect crystal the perturbing potential is

$$W = \sum_{\alpha=-\pi}^{\pi} \sum_{\mathbf{k}, j} A_{\mathbf{k}, j} \exp(i\alpha_{\mathbf{k}, j}) \exp(i\mathbf{k} \cdot \mathbf{x} - i\omega_{\mathbf{k}} t)$$

where $j=1, 2, 3$ labels the two transverse and longitudinal waves, $A_{-\mathbf{k}j} = A_{\mathbf{k}j}^*$, $\omega_{\mathbf{k}} = 2\pi \times \text{frequency}$, $\omega_{-\mathbf{k}} = -\omega_{\mathbf{k}}$; $\alpha_{\mathbf{k}j}$ is the phase ($\alpha_{\mathbf{k}j} = -\alpha_{-\mathbf{k}j}$). The phases of the lattice waves are arbitrary, so one must average over them. Thus

$$\begin{aligned} (\mathbf{k} | W | \mathbf{k}') &= \int d\mathbf{r} \psi(\mathbf{k}, \mathbf{r}) W \psi^*(\mathbf{k}', \mathbf{r}) \\ &= \sum_{\mathbf{k}'', j, \alpha} \int A_{\mathbf{k}'', j} \exp(i\alpha_{\mathbf{k}'', j}) u(\mathbf{k}, \mathbf{r}) u^*(\mathbf{k}', \mathbf{r}) \exp\{-i(\mathbf{k}'' - \mathbf{k} + \mathbf{k}') \cdot \mathbf{r}\} \\ &\quad \times \exp(-i\omega_{\mathbf{k}''} t) d\mathbf{r} \\ &= \sum_{j, \alpha} A_{\mathbf{k}-\mathbf{k}', j} \exp(i\alpha_{\mathbf{k}-\mathbf{k}', j}) \int d\mathbf{r} u(\mathbf{k}, \mathbf{r}) u^*(\mathbf{k}', \mathbf{r}) \exp(-i\omega_{\mathbf{k}-\mathbf{k}'} t). \end{aligned} \quad (13)$$

This leads to expressions similar to (11)

$$(\mathbf{k} | W | \mathbf{k}') = 0 = (\mathbf{k} | W | \mathbf{k}') (\mathbf{k}' | W | \mathbf{k}'') (\mathbf{k}'' | W | \mathbf{k}''') \dots \dots (14a, c)$$

$$(\mathbf{k} | W | \mathbf{k}') (\mathbf{k}' | W | \mathbf{k}'') = \sum_j |A_{\mathbf{k}-\mathbf{k}', j}|^2 N \left\{ \int d\mathbf{r} u(\mathbf{k}, \mathbf{r}) u^*(\mathbf{k}', \mathbf{r}) \right\}^2 \delta_{\mathbf{k}, \mathbf{k}''}. \quad (14b)$$

N has now a different physical meaning; it gives the number of waves of a definite wave number but phases distributed at random.

$$\begin{aligned} &(\mathbf{k} | W | \mathbf{k}') (\mathbf{k}' | W | \mathbf{k}'') (\mathbf{k}'' | W | \mathbf{k}''') (\mathbf{k}''' | W | \mathbf{k}^{iv}) \\ &= N^2 \left[\sum_j |A_{\mathbf{k}-\mathbf{k}', j}|^2 |A_{\mathbf{k}-\mathbf{k}'', j}|^2 \left| \int uu'^* \int uu'''^* \right|^2 \delta_{\mathbf{k}'', \mathbf{k}} \delta_{\mathbf{k}^{iv}, \mathbf{k}} \right. \\ &\quad + \sum_j |A_{\mathbf{k}-\mathbf{k}', j}|^2 |A_{\mathbf{k}'-\mathbf{k}'', j}|^2 \left| \int uu'^* \int u'u'''^* \right|^2 \delta_{\mathbf{k}', \mathbf{k}'''} \delta_{\mathbf{k}, \mathbf{k}^{iv}} \\ &\quad + \sum_j |A_{\mathbf{k}-\mathbf{k}', j}|^2 |A_{\mathbf{k}'-\mathbf{k}'', j}|^2 \int uu'^* \int u'u'''^* \int u''u'''^* \int u''''u^{iv*} \\ &\quad \times \delta_{\mathbf{k}-\mathbf{k}', \mathbf{k}''-\mathbf{k}'''} \delta_{\mathbf{k}'-\mathbf{k}'', \mathbf{k}'''-\mathbf{k}^{iv}} \left. \right] \dots \dots (14d) \\ &\int uu'^* \equiv \int d\mathbf{r} u(\mathbf{r}, \mathbf{k}) u^*(\mathbf{r}, \mathbf{k}'). \end{aligned}$$

§3. COMPARISON BETWEEN EXACT FOURTH ORDER TERMS AND SIMILAR TERMS IN THE CUSTOMARY THEORY

The second order Bloch calculation describes only single collisions. If it is extended over longer times it will give rise to terms containing fourth powers of the perturbing potential. In the following they will be called 'Bloch terms'. They represent consecutive single collisions with no interference between them.

Part of our fourth order terms come from these consecutive single collisions, i.e. they can be found by extending the second order Bloch treatment. This part describes nothing new so it must be separated from the rest. The Bloch-Dirac method assumes that at $t=0$ the phases of the amplitudes $a(\mathbf{k}, t)$ in (6) are distributed at random, i.e. there are no relations between the phases of different $a(\mathbf{k}, 0)$'s. Equations (7) show that in course of time phase relations are developed, but it is assumed that they are destroyed again after each collision.

Thus the life of a particle is cut up into intervals each of which contains one collision and knows nothing of the phase relations during the previous intervals. Using this picture one can calculate what happens during two collisions after the particle had been in a well defined state \mathbf{k}_0 at $t=0$. Now we want to compare this with the situation that results if the phase relations are not destroyed after the first collision. The Bloch method assumes a time proportional transition probability $c(\mathbf{k}_0, \mathbf{k}) = c(\mathbf{k}, \mathbf{k}_0)$ from a state \mathbf{k}_0 (or \mathbf{k}) to a state \mathbf{k} (or \mathbf{k}_0). The resulting change in the distribution function $g(\mathbf{k})$ is

$$\begin{aligned} \frac{d}{dt}g(\mathbf{k}) &= \int c(\mathbf{k}, \mathbf{k}')g(\mathbf{k}')[1-g(\mathbf{k})]d\mathbf{k}' - \int c(\mathbf{k}, \mathbf{k}')g(\mathbf{k})[1-g(\mathbf{k}')]d\mathbf{k}' \\ &= \int c(\mathbf{k}, \mathbf{k}')g(\mathbf{k}')d\mathbf{k}' - g(\mathbf{k}) \int c(\mathbf{k}, \mathbf{k}')d\mathbf{k}'. \end{aligned} \quad \dots\dots(15)$$

If at $t=0$, $g(\mathbf{k}) = \delta(\mathbf{k} - \mathbf{k}_0)$ iteration gives

$$\begin{aligned} \dot{g}(\mathbf{k}) &= - \int c(\mathbf{k}_0, \mathbf{k}')d\mathbf{k}' + t \left[\int c(\mathbf{k}_0, \mathbf{k}')^2 d\mathbf{k}' \right. \\ &\quad \left. - c(\mathbf{k}, \mathbf{k}_0) \left\{ \int c(\mathbf{k}', \mathbf{k}_0) d\mathbf{k}' - \int c(\mathbf{k}, \mathbf{k}') d\mathbf{k}' \right\} \right] + \dots \end{aligned} \quad \dots\dots(16)$$

$$\begin{aligned} \dot{g}_{\mathbf{k} \neq \mathbf{k}_0}(\mathbf{k}) &= c(\mathbf{k}, \mathbf{k}_0) + t \left[\int c(\mathbf{k}, \mathbf{k}')c(\mathbf{k}', \mathbf{k}_0) d\mathbf{k}' \right. \\ &\quad \left. - c(\mathbf{k}, \mathbf{k}_0) \left\{ \int c(\mathbf{k}', \mathbf{k}_0) d\mathbf{k}' + \int c(\mathbf{k}, \mathbf{k}') d\mathbf{k}' \right\} \right] + \dots \end{aligned} \quad \dots\dots(17)$$

If one knows how a distribution $g(\mathbf{k}) \equiv \delta(\mathbf{k} - \mathbf{k}_0)$ changes in course of time, the change of a general distribution $g(\mathbf{k})$ can be calculated simply by adding the changes for every \mathbf{k} separately. This is justified because there are no phase relations between states of different \mathbf{k} . We shall assume a distribution $\delta(\mathbf{k} - \mathbf{k}_0)$ at $t=0$ in the following.

Before we embark on the calculation of the fourth order elements of the matrix g we want to prove that it is sufficient to consider its diagonal elements. It can namely be shown easily that—in our special case—a density matrix that is diagonal will always remain diagonal. In fact $(d/dt)g(\mathbf{k}_1, \mathbf{k}_2, t) = 0$ because it contains a factor $(\mathbf{k}_1 | V | \mathbf{k}')(\mathbf{k}' | V | \mathbf{k}'') \dots (\mathbf{k}^{(n)} | V | \mathbf{k}_2) = 0$ if $\mathbf{k}_1 \neq \mathbf{k}_2$ according to (11).

The diagonal elements are (cf. (7))

$$\dot{g}^{(0)}(\mathbf{k}) = 0 \quad \dots\dots(18a)$$

$$\dot{g}^{(1)}(\mathbf{k}) = a^{(0)}\dot{a}^{(1)*} + \dot{a}^{(1)}a^{(0)*} + \dot{a}^{(0)}a^{(1)*} + a^{(1)}\dot{a}^{(0)*} = 0 = \dot{g}^{(3)}(\mathbf{k}) \quad \dots\dots(18b)$$

$$\begin{aligned} \dot{g}^{(2)}(\mathbf{k}) &= a^{(0)}\dot{a}^{(2)*} + \dot{a}^{(2)}a^{(0)*} + \dot{a}^{(0)}a^{(2)*} + a^{(1)}\dot{a}^{(1)*} + \dot{a}^{(1)}a^{(1)*} \\ &= 2R\{a^{(0)}\dot{a}^{(2)*}\} + a^{(1)}\dot{a}^{(1)*} + \dot{a}^{(1)}a^{(1)*} \end{aligned} \quad \dots\dots(18c)$$

$$= \frac{2}{\hbar} \int d\mathbf{k}' |(\mathbf{k} | V | \mathbf{k}')|^2 \frac{\sin(E - E')t/\hbar}{E - E'} \{g(\mathbf{k}') - g(\mathbf{k})\}$$

and thus if $g^{(0)}(\mathbf{k}) = \delta(\mathbf{k} - \mathbf{k}_0)$

$$\dot{g}^{(2)}(\mathbf{k}_0) = - \frac{2}{\hbar} \int d\mathbf{k}' |(\mathbf{k} | V | \mathbf{k}')|^2 \frac{\sin(E_0 - E')t/\hbar}{E_0 - E'} \quad \mathbf{k}' \neq \mathbf{k}_0 \quad \dots\dots(19)$$

$$\dot{g}_{\mathbf{k} \neq \mathbf{k}_0}^{(2)}(\mathbf{k}) = \frac{2}{\hbar} |(\mathbf{k} | V | \mathbf{k}_0)|^2 \frac{\sin(E_0 - E')t/\hbar}{E_0 - E'}. \quad \dots\dots(20)$$

Comparison with (16) and (17) shows that

$$c(\mathbf{k}, \mathbf{k}') = \frac{2}{\hbar} |(\mathbf{k}' | V | \mathbf{k})|^2 \frac{\sin(E - E')t/\hbar}{E - E'} \quad \dots\dots(21)$$

which has a limit $(2/\hbar) |(\mathbf{k} | V | \mathbf{k}')|^2 \delta(E - E')$ as $t \rightarrow \infty$.

$$\begin{aligned} \dot{g}^{(4)}(\mathbf{k}) &= 2R\{a^{(0)}\dot{a}^{(4)*}\} + 2R\{a^{(4)}\dot{a}^{(0)*}\} + 2R\{a^{(1)}\dot{a}^{(3)*}\} + 2R\{a^{(3)}\dot{a}^{(1)*}\} + 2R\{a^{(2)}\dot{a}^{(2)*}\} \\ &= 2R\{a^{(1)}\dot{a}^{(3)*}\} + 2R\{a^{(3)}\dot{a}^{(1)*}\} + 2R\{a^{(2)}\dot{a}^{(2)*}\} \end{aligned}$$

if $\mathbf{k} \neq \mathbf{k}_0 \quad (g^{(0)}(\mathbf{k}) = \delta(\mathbf{k} - \mathbf{k}_0)).$

In the following we shall write for brevity

$$\begin{cases} E - E_0 = u & E - E' = v & E_0 - E' = v - u = w \\ E - E'' = x & E_0 - E'' = x - u = y \\ E' - E'' = x - v = y - w = z. \end{cases}$$

It follows from (11) that (the products of 4 matrix elements are real, see (11)):

$$\begin{aligned} \dot{g}_{\mathbf{k} \neq \mathbf{k}_0}^{(4)}(\mathbf{k}) &= \frac{2}{\hbar} \int d\mathbf{k}' d\mathbf{k}'' (\mathbf{k} | V | \mathbf{k}') (\mathbf{k}' | V | \mathbf{k}'') (\mathbf{k}'' | V | \mathbf{k}_0) (\mathbf{k}_0 | V | \mathbf{k}) \\ &\times \left\{ \frac{\sin ut/\hbar}{u} \left(\frac{1}{vx} + \frac{1}{wy} \right) + \frac{\sin wt/\hbar}{uvz} - \frac{\sin yt/\hbar}{uxz} - \frac{\sin vt/\hbar}{uwx} + \frac{\sin xt/\hbar}{uyz} \right\} \\ &+ \frac{2}{\hbar} \int d\mathbf{k}' d\mathbf{k}'' (\mathbf{k} | V | \mathbf{k}') (\mathbf{k}' | V | \mathbf{k}_0) (\mathbf{k}_0 | V | \mathbf{k}'') (\mathbf{k}'' | V | \mathbf{k}) \\ &\times \left\{ \frac{\sin ut/\hbar - \sin xt/\hbar}{uwy} + \frac{\sin wt/\hbar}{vwy} - \frac{\sin yt/\hbar}{uwy} + \frac{\sin zt/\hbar}{vwy} \right\}. \quad \dots\dots(22) \end{aligned}$$

According to (11d) the products of 4 matrix elements are non-zero only if $\mathbf{k}' = \mathbf{k}_0$, $\mathbf{k}'' = \mathbf{k}$ or $\mathbf{k} - \mathbf{k}' = \mathbf{k}_0 - \mathbf{k}''$ in the first integral and $\mathbf{k}'' = \mathbf{k}'$ or $\mathbf{k} - \mathbf{k}' = \mathbf{k}'' - \mathbf{k}_0$ in the second integral. In the first case $\mathbf{k}' = \mathbf{k}_0$, the first integral becomes

$$\begin{aligned} &\frac{2}{\hbar} \int d\mathbf{k}'' |(\mathbf{k} | V | \mathbf{k}_0)|^2 |(\mathbf{k}_0 | V | \mathbf{k}'')|^2 \\ &\times \left\{ \frac{\sin ut/\hbar}{u} \left(\frac{1}{ux} - \frac{1}{y^2} \right) - \frac{(t/\hbar) \cos ut/\hbar}{uy} - \frac{\sin yt/\hbar}{uxy} + \frac{\sin xt/\hbar}{uy^2} \right\}. \quad \dots\dots(23) \end{aligned}$$

The factor in brackets is finite everywhere, including at $y=0$ and $x=0$. By using the well known formulae for sin and cos of sums or differences of two variables, it may be written in the form

$$\begin{aligned} &\left\{ \frac{\sin ut/\hbar}{u} \frac{\cos yt/\hbar - 1}{y^2} + \frac{\cos ut/\hbar}{u^2} \frac{\sin xt/\hbar}{x} - \frac{\sin yt/\hbar}{u^2 y} + \frac{\cos ut/\hbar}{u} \frac{\sin yt/\hbar - yt/\hbar}{y^2} \right. \\ &\quad \left. + \frac{\sin ut/\hbar}{u^2} \frac{1 - \cos xt/\hbar}{x} \right\}. \quad \dots\dots(24) \end{aligned}$$

In the limit $t \rightarrow \infty$ integration gives

$$\int \left\{ -\frac{\sin ut/\hbar}{u} \pi \frac{t}{\hbar} - \frac{1}{u^2} \pi + \frac{\cos ut/\hbar}{u^2} \pi \right\} du = -\frac{2\pi^2}{\hbar} t. \quad \dots\dots(25)$$

This leads to

$$-\frac{4\pi^2 t}{\hbar^2} |(\mathbf{k} | V | \mathbf{k}_0)|^2 \delta(E - E_0) \int d\mathbf{k}'' |(\mathbf{k}_0 | V | \mathbf{k}'')|^2 \delta(E_0 - E''), \quad \dots\dots(26)$$

i.e. the second Bloch term in (17). (The last two terms of (24) give no contribution because they are odd.)

Similarly, in the second case of the first integral (22) $\mathbf{k}'' = \mathbf{k}$ it becomes

$$\frac{2}{\hbar} \int d\mathbf{k}' |(\mathbf{k} | V | \mathbf{k}_0)|^2 |(\mathbf{k} | V | \mathbf{k}')|^2 \left\{ -\frac{\sin ut/\hbar}{u} \left(\frac{1}{v^2} + \frac{1}{uv} \right) + \frac{(t/\hbar) \cos ut/\hbar}{uv} - \frac{\sin wt/\hbar}{uv^2} + \frac{\sin vt/\hbar}{uvw} \right\} \dots\dots (27)$$

or

$$\frac{2}{\hbar} \int d\mathbf{k}' |(\mathbf{k} | V | \mathbf{k}_0)|^2 |(\mathbf{k} | V | \mathbf{k}')|^2 \left\{ \frac{\sin ut/\hbar}{u} \left(\frac{\cos vt/\hbar - 1}{v^2} + \frac{\cos wt/\hbar - 1}{uvw} \right) - \frac{\sin vt/\hbar}{u^2 v} + \frac{\cos ut/\hbar}{u} \left(\frac{\sin wt/\hbar}{uvw} - \frac{\sin vt/\hbar - vt/\hbar}{v^2} \right) \right\} \dots\dots (28)$$

which is again finite everywhere. In the limit $t \rightarrow \infty$ this gives

$$-\frac{4\pi^2 t}{\hbar^2} |(\mathbf{k} | V | \mathbf{k}_0)|^2 \delta(E - E_0) \int d\mathbf{k}' |(\mathbf{k} | V | \mathbf{k}')|^2 \delta(E - E') \dots\dots (29)$$

which is the third Bloch term in (17).

By the same procedure one gets for the first case of the second integral (22) $\mathbf{k}'' = \mathbf{k}'$

$$\frac{2}{\hbar} \int d\mathbf{k}' |(\mathbf{k} | V | \mathbf{k}')|^2 |(\mathbf{k}_0 | V | \mathbf{k}')|^2 \left\{ \frac{\sin ut/\hbar}{uvw} - \frac{\sin vt/\hbar}{uvw} + \frac{\sin wt/\hbar}{uvw} - \frac{\sin wt/\hbar}{uw^2} \right\} \dots\dots (30)$$

or

$$\frac{2}{\hbar} \int d\mathbf{k}' |(\mathbf{k} | V | \mathbf{k}')|^2 |(\mathbf{k}_0 | V | \mathbf{k}')|^2 \left\{ \frac{\sin vt/\hbar}{v} \frac{1 - \cos wt/\hbar}{w^2} + \frac{\sin ut/\hbar}{u} \frac{1 - \cos wt/\hbar}{w^2} + \frac{\cos vt/\hbar}{v} \frac{\sin wt/\hbar}{w^2} - \frac{\sin wt/\hbar}{w^2} \frac{1 + \cos ut/\hbar}{u} \right\} \dots\dots (31)$$

which gives in the limit $t \rightarrow \infty$

$$\frac{4\pi^2 t}{\hbar^2} \int d\mathbf{k}' |(\mathbf{k} | V | \mathbf{k}')|^2 |(\mathbf{k}' | V | \mathbf{k}_0)|^2 \delta(E - E') \delta(E - E_0), \dots\dots (32)$$

i.e. the first term of (17).

§ 4. DISCUSSION OF THE NEW INTERFERENCE TERMS

The whole of (17) has now been accounted for but there are still two terms left, namely

$$\frac{2}{\hbar} \int d\mathbf{k}' |(\mathbf{k} | V | \mathbf{k}')|^2 |(\mathbf{k}_0 | V | \mathbf{k})|^2 \left\{ \frac{\sin ut/\hbar}{u} \left(\frac{1}{vx} + \frac{1}{wy} \right) + \frac{\sin wt/\hbar}{uvw} - \frac{\sin yt/\hbar}{uxz} - \frac{\sin vt/\hbar}{uvw} + \frac{\sin xt/\hbar}{uyz} \right\} \delta(\mathbf{k} - \mathbf{k}_0 - \mathbf{k}' + \mathbf{k}'') \dots\dots (33)$$

$$\frac{2}{\hbar} \int d\mathbf{k}' |(\mathbf{k} | V | \mathbf{k}')|^2 |(\mathbf{k}_0 | V | \mathbf{k}')|^2 \left\{ \frac{\sin ut/\hbar}{uvy} - \frac{\sin xt/\hbar}{uvy} + \frac{\sin wt/\hbar}{vwy} - \frac{\sin yt/\hbar}{uvw} + \frac{\sin zt/\hbar}{vwy} \right\} \delta(\mathbf{k} - \mathbf{k}' - \mathbf{k}'' + \mathbf{k}_0). \dots\dots (34)$$

They describe interference effects that are not covered by the Bloch-Dirac method. If the wave of an incoming particle is scattered by two scattering centres or two lattice waves a and b the outgoing scattered wave is composed of the waves that result from successive scatterings b and a or a and b (i.e. the three terms (26), (29) and (32)) and additional interference terms (33) and (34).

The function $f(p) = (\sin pt/\hbar)/p$ is such that

$$\lim_{t \rightarrow \infty} \int_a^\infty \frac{\sin pt/\hbar}{p} dp = 0 \text{ for any fixed } a > 0$$

and a similar property holds for

$$\frac{\sin pt/\hbar}{p+b}; \quad \lim_{t \rightarrow \infty} \int_0^\infty \frac{\sin pt/\hbar}{p+b} dp = 0$$

if $p+b$ has no zero in the integration interval. Hence, owing to the denominators u , v and w and the oscillatory numerators, the integral of (33) is in general small outside an area where $E' \simeq E_0$, $E \simeq E'$ and $E' \simeq E''$. This area is ring-shaped in \mathbf{k} space (see figure 1). In (33) \mathbf{k} and \mathbf{k}_0 are kept fixed, because of the last factor $\mathbf{k}' - \mathbf{k}'' = \mathbf{k} - \mathbf{k}_0$. As $E' \simeq E_0$ the end point of \mathbf{k}' lies on and near a closed surface round the end point of \mathbf{k}_0 and similarly for \mathbf{k}'' and \mathbf{k} . Thus for long t the area of integration is confined to the ring-shaped intersection of the two surfaces.

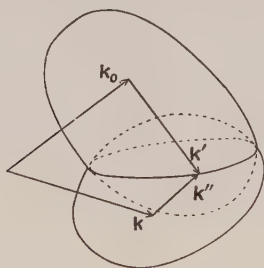


Figure 1. Ring-shaped path of integration used in formula (31).

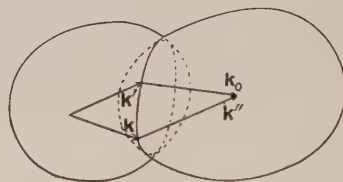


Figure 2. Ring-shaped path of integration used in formula (32).

The integrands of the Bloch terms were appreciable on a whole closed surface (on a sphere if the electrons are free or quasi-free, i.e. $E \sim \mathbf{k}^2$). Hence (33) is small compared with the Bloch terms unless $\mathbf{k} = \mathbf{k}_0$ and $\mathbf{k}' = \mathbf{k}''$, so that the two surfaces coincide. In the limit $E', E'', E \rightarrow E_0$ the energy factor becomes the same as for the (29) Bloch term (proportional to t^3), but at the same time $|(\mathbf{k}_0 | V | \mathbf{k})|^2 \rightarrow 0$, and thus this term is negligible compared with the corresponding Bloch term.

In the same way in (34) the integration over \mathbf{k}' is over two rings at most ($E' \simeq E_0$, $E' \simeq E$), and the only case in which this term can become important is for $-\mathbf{k} = \mathbf{k}_0$, $\mathbf{k}' = -\mathbf{k}'$ (see figure 2). In the latter case it extends over a closed surface because $E_{-\mathbf{k}} = E_{\mathbf{k}}$ quite generally. If $\mathbf{k} = -\mathbf{k}_0$, $u=0$, $x=y$, $v=w$, $z \rightarrow 0$, $x \rightarrow v$. Consequently the energy factor reduces to $(t/\hbar)(1 - \cos vt/\hbar)/v^2$ and (34) becomes

$$t^2 \frac{2\pi}{\hbar^3} \int d\mathbf{k}' |(-\mathbf{k}_0 | V | \mathbf{k}')|^2 |(\mathbf{k}_0 | V | \mathbf{k}')|^2 \delta(E_0 - E') \quad \mathbf{k} = -\mathbf{k}_0, \dots\dots (35)$$

This is exactly the same as the Bloch term for $-\mathbf{k}_0$.

We shall now derive the condition for this term to be small. If at $t=0$ the distribution function had a peak $\delta(\mathbf{k}-\mathbf{k}_0)$ at $\mathbf{k}=\mathbf{k}_0$ the situation after a time dt and up to the second order in dt would be as shown in figure 3: part of the peak is smoothly spread out over the states of about the same energy (because of the factor $\delta(E-E_0)$), but there is a hump round $-\mathbf{k}_0$. The δ -function has a breadth $\hbar t$. In first approximation the stationary distribution function is the Fermi distribution which depends only on E . Therefore all the N states in the energy interval $E_F, E_F + \hbar/t$ contain the same number of electrons. Any state \mathbf{k} in this interval receives 'Bloch particles' from N states and 'non-Bloch particles' from one of them (viz. $-\mathbf{k}$). Consequently the contribution of the non-Bloch term is small if $N \gg 1$. Now N can be easily estimated for free electrons. Then $dE = dk_0^2/2m \simeq \hbar/t$ and in \mathbf{k} space the states of equal energy are lying on circles. N is the ratio of the volume of the shell with radius k_0 ($k_0^2/2m \simeq E_F = \text{Fermi energy}$) and thickness dk_0 to the volume of the little sphere with radius dk_0 round $-\mathbf{k}_0$ (figure 4). The ratio of these volumes is

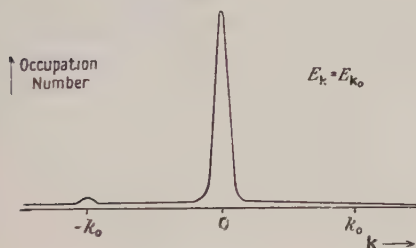


Figure 3. The occupation number in \mathbf{k} -space as a function of the wave number \mathbf{k} a short time after it has started as a δ -function at $\mathbf{k}=\mathbf{k}_0$.

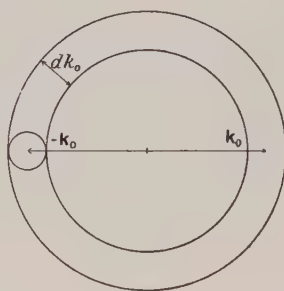


Figure 4. Spheres of equal energy of quasi-free electrons in \mathbf{k} -space.

$4\pi^2 k_0^2 dk_0 / \frac{4}{3}\pi (dk_0)^3 = 3E_F / (\hbar/t) = N \gg 1$ or $\hbar/t \ll E_F$, and this is satisfied in all cases of practical interest. It is clear that this proof is valid only for free electrons or for electrons with an apparent mass that does not differ in order of magnitude from the electron mass.

The same argument for a Boltzmann gas would lead to $\hbar/t \ll kT$, i.e. the same condition as for the validity of the approximation to second order in W . Thus the validity of the Bloch treatment in cases where $\tau > \hbar/4kT$ depends on the Fermi statistics of the electron gas. At low temperatures the change in the energy of the electron cannot be neglected. Then one gets, according to (13),

$$\begin{aligned} \dot{a}(\mathbf{k}, t) = & -\frac{i}{\hbar} \int d\mathbf{k}_1 \sum_{\alpha, j} A_{\mathbf{k}-\mathbf{k}_1, j} \exp(i\alpha_{\mathbf{k}-\mathbf{k}_1, j}) \\ & \times \int u_{\mathbf{k}} u_{\mathbf{k}_1}^* a(\mathbf{k}, t) \exp\{-i(E_1 - E + \hbar w_{\mathbf{k}-\mathbf{k}_1})t/\hbar\}. \end{aligned}$$

Hence all formulae remain the same provided $E_1 - E_2$ is replaced by $E_1 - E_2 + \hbar w_{\mathbf{k}_1 - \mathbf{k}_2}$ everywhere. If a particle was originally in a state \mathbf{k}_0 the states into which it can make a transition are no longer on a sphere of equal energy but on two closed surfaces (because a transition of the whole system

electrons + lattice vibrations should satisfy the laws of conservation of energy and momentum). However, the changes in energy are of the order $kT \ll E \simeq E_F$, so that the two closed surfaces are quite near the sphere of radius $(2mE_F)^{1/2}$ and the whole argument can be repeated. This case is only of academic interest though, for as we saw in the beginning there is no reason to doubt the validity of Bloch's method for low temperatures.

If both impurities and lattice waves are present it is well known that deviations from Matthiessen's rule may occur. This rule states that residual resistance and temperature dependent resistance are additive. The cause of the deviation is that the same electrons undergo two kinds of collisions—elastic ones by the impurities and inelastic ones by the thermal waves. Thus the Bloch integral equation becomes more complicated. It is clear, however, that at high temperatures where—as we saw before—the scattering by the lattice vibrations may be considered as elastic, Matthiessen's rule will hold. By solving the Bloch equation for combined impurity and lattice wave scattering at low temperature Wilson (1937) could prove that in this case the rule was valid as well, the corrections being of the order 10^{-4} . Hence the only deviations occur in the intermediate region $T \simeq \theta$. These deviations from Matthiessen's rule are thus a result of the nature of the Bloch integral equation and have nothing to do with our problem. It might be conceivable, however, that the fourth order terms considered here would introduce new interference effects between the two types of scattering and thus lead to a new type of deviations from Matthiessen's rule. The result of a tedious calculation, along the same lines as above, but now for a case where two kinds of scattering are present, is that these new effects are negligible for a Fermi gas.

ACKNOWLEDGMENTS

The author wishes to express his thanks to Professor R. E. Peierls for suggesting the problem and constant help and encouragement, and to the British Council for the award of a scholarship.

REFERENCES

- BLOCH, F., 1928, *Z. Phys.*, **52**, 555.
 DIRAC, P. A. M., 1947, *Principles of Quantum Mechanics*, 3rd Edn (Oxford: Clarendon Press), p. 130.
 KRETSCHMANN, E., 1934, *Z. Phys.*, **87**, 518.
 PEIERLS, R. E., 1934 a, *Z. Phys.*, **88**, 786; 1934 b, *Helv. Phys. Acta*, **7**, 24 (Sonderheft); 1934 c, *Conf. Intern. des Sc. Math.*, Genève, Oct. 1934.
 RHODES, P., 1950, *Proc. Roy. Soc. A*, **202**, 466.
 SEITZ, F., 1940, *Modern Theory of Solids* (New York and London: McGraw-Hill), p. 272.
 SONDHEIMER, E. H., 1950, *Proc. Roy. Soc. A*, **203**, 75.
 TOLMAN, R. C., 1938, *The Principles of Statistical Mechanics* (Oxford: University Press), p. 327.
 WILSON, A. H., 1937, *Proc. Camb. Phil. Soc.*, **33**, 371.

Nuclear Magnetic Resonance in Metallic Lithium and Sodium

BY H. JONES AND B. SCHIFF

Department of Mathematics, Imperial College, London

MS. received 19th November 1953

Abstract. The magnitude of the change in the nuclear magnetic resonance frequencies in metals, with respect to the resonance frequencies of the same nuclei in chemical compounds, depends upon the nature of the electronic states at the surface of the Fermi distribution. In this paper it is shown that the observed 'Knight-shifts' are in good agreement with the results of cellular-type calculations of the electronic states in metallic lithium and sodium.

THE interesting discovery by Knight (1949) that nuclear magnetic resonance frequencies are slightly displaced in metals, relative to the resonance frequencies of the same nuclei in chemical compounds, provides a means of obtaining information regarding the nature of the electronic states in metals at the top of the Fermi distribution. A recent calculation by Schiff (1954) has shown that in lithium the state of lowest energy at a centre of a face of the Brillouin zone has a p-like character, in contrast to the case of sodium where the same state is s-like (Howarth and Jones 1952). It is the purpose of this paper to show that nuclear magnetic resonance data on lithium and sodium are in good agreement with this interesting result.

The frequency shift, according to Townes, Herring and Knight (1950), arises in the following way: The constant magnetic field H acting on the nucleus is increased by the spin paramagnetism of the metal to a much greater extent than might at first be supposed. If the wave functions of the electrons at the top of the Fermi distribution are s-like in character the magnetic moment per unit volume, in the immediate neighbourhood of the nucleus, is much larger than the susceptibility times the external field, because the spin density near the nucleus is much greater than its average value over the atomic polyhedron.

A straightforward application of Dirac's relativistic theory shows that the magnetic field at the nucleus due to one electron in an s-state and given spin state is equal to $8\pi\beta|\psi(0)|^2/3$ to a high degree of approximation, where β is the Bohr magneton of the electron and ψ the ordinary Schrödinger wave function.

Let dS be an element of the surface of the Fermi distribution in \mathbf{k} -space, then $dS/|\text{grad}_{\mathbf{k}} E|$ is the contribution to the density of states function $N(E)$ arising from dS , if the wave vector \mathbf{k} is so defined that $\hbar\mathbf{k}$ is the momentum of the electron. Hence the number of electrons with unbalanced spins parallel to H and lying in dS is $2\beta H dS/|\text{grad}_{\mathbf{k}} E|$. If we divide this number by the total number of nuclei per unit volume Ω^{-1} , where Ω is the atomic volume, we obtain the probability that at any nucleus we have an electron with unbalanced spin parallel to the field. Thus the additional magnetic field ΔH at any nucleus, due to the aligned spins, is given by

$$\Delta H = \frac{16\pi}{3} \beta^2 H \Omega \int \frac{|\psi_{\mathbf{k}}(0)|^2 dS}{|\text{grad}_{\mathbf{k}} E|} = \frac{16\pi}{3} \beta^2 H \Omega N(E_0) \langle |\psi_m(0)|^2 \rangle \dots\dots (1)$$

where $N(E_0)$ is the number of states per unit energy range per unit volume for a given spin state at the Fermi surface, and the average quantity $\langle |\psi_m(0)|^2 \rangle$ is to be regarded as defined by (1).

In the original theory of Townes *et al.*, and of Kohn and Bloembergen (1951), the spin paramagnetic susceptibility was introduced in place of $N(E)$. Unfortunately, reliable experimental values of this susceptibility are not available in the case of lithium, where widely different values are given by different observers. Equation (1) is equivalent to using Pauli's formula for the spin paramagnetism in Townes' expression. Sampson and Seitz (1940) have tried to improve the theory of the paramagnetism of lithium by including terms arising from the exchange and correlation between electrons, but it now seems possible that exchange effects should not be included without some modification, just as they must not be included in the calculation of the electronic specific heats (cf. Wohlfarth 1950, Bohm and Pines 1953). Equation (1) is, therefore, probably the best form for ΔH .

It is useful to combine equation (1) with Fermi's formula for the hyperfine splitting of s-states, viz.

$$\Delta\nu = \frac{8\pi}{3} \left(\frac{2I+1}{I} \right) \frac{\beta^2 \mu(n)}{1837 hc} |\psi_a(0)|^2, \quad \dots\dots (2)$$

where $\mu(n)$ is the magnetic moment of the nucleus expressed in nuclear magnetons, I is the nuclear spin quantum number, and ψ_a the atomic wave function.

First, however, we use (2) to calculate $|\psi_a(0)|^2$, and to compare the result with Hartree type calculations of the wave function. Table 1 gives the necessary data.

Table 1

	$\Delta\tilde{\nu} (\text{cm}^{-1})$	I	$\mu(n)$	$ \psi_a(0) ^2 (\text{cm}^{-3})$
Li	0.0268	3/2	3.25586	1.56×10^{24}
Na	0.0596	3/2	2.21711	5.10×10^{24}

Numerical integration of the wave equation, using self-consistent fields for the ions, gives for $|\psi_a(0)|^2$ the values $0.96 \times 10^{24} \text{ cm}^{-3}$ for Li and $3.56 \times 10^{24} \text{ cm}^{-3}$ for Na. These values are, therefore, 30 to 40% less than those given by (2). The most likely reason for this discrepancy is that $|\psi_a(0)|^2$ is exceptionally sensitive to small inaccuracies of the central field. This can be seen as follows: Let ϕ_1 and ϕ_2 be two unnormalized solutions of the Schrödinger equation, for somewhat different central fields, with the same starting values at $r=0$. The ratio of the normalized $|\psi(0)|^2$ for these two fields will then clearly be $\int \phi_2^2 d\tau / \int \phi_1^2 d\tau$. In the neighbourhood of the maximum of the wave functions, and for greater values of r , small differences in the central field can produce appreciable differences between ϕ_1 and ϕ_2 , and it is just these regions which contribute most to the normalizing integrals. It may be noticed that if ϕ_1 and ϕ_2 are each normalized the resulting wave functions will be very similar everywhere except in the neighbourhood of $r=0$, so that for most purposes small inaccuracies in the central field are not serious. For this reason it is advisable to combine formulae (1) and (2) and to calculate the ratio $\langle |\psi_m(0)|^2 \rangle / |\psi_a(0)|^2$, which we will denote by R for convenience, and which would not, presumably, suffer from excessive sensitivity to the central field in calculations of the Hartree type.

The most uncertain quantity in the calculation of R from (1) and (2) is the density of states function $N(E)$. If the energy surfaces within the first Brillouin

zone may be regarded as spherical, then whatever the effective mass of the electrons we can write, for monovalent metals,

$$N(E_0) = 3/4\Omega E_0. \quad \dots\dots(3)$$

No difficulty arises in the case of sodium, where calculations show that E_0 is almost exactly the value given by the free electron approximation. In the case of lithium, however, where the conduction electrons behave very differently from free electrons, the value of E_0 is not so certain. Schiff finds $E_0 = 2.69$ ev, but Bardeen's calculation (1938) based on a central field prepared by Seitz gives $E_0 = 3.52$ ev. We shall assume Schiff's value in the following, but it is clear that there is here an uncertainty of several per cent.

Introducing numerical values for the universal constants, (1) and (2) can be combined to give

$$\Omega N(E_0) R = 2.7408 \times 10^{12} \left(\frac{\Delta H}{H} \right) \left(\frac{2I+1}{2I} \right) \frac{\mu(n)}{\Delta \tilde{\nu}}. \quad \dots\dots(4)$$

In table 2 the values of $\Delta H/H$ are taken from the data of Gutowsky and McGarvey (1952) and the $\Delta \tilde{\nu}$ given in table 1 are from the work of Fox and Rabi (1935). The figures in column 2 are obtained from (3), using the value of E_0 quoted for Li, and the free electron value in the case of Na. To see the physical meaning of these

Table 2

	$\Delta H/H$	$\Omega N(E)$ (erg ⁻¹)	R
Li	0.0261×10^{-2}	1.740×10^{11}	0.666
Na	0.112×10^{-2}	1.483×10^{11}	1.027

two values of R we proceed as follows: Let $\psi_1(r)$ and $\psi_2(\mathbf{r})$ be two normalized solutions of the Schrödinger equation which have s- and p-like symmetries within the atomic polyhedron, then to a rather rough approximation we can write

$$\psi_{\mathbf{k}}(\mathbf{r}) = (|a_s|^2 + |a_p|^2)^{-1/2} (a_s \psi_1(r) + a_p \psi_2(\mathbf{r})), \quad \dots\dots(5)$$

where the right-hand side can be regarded as the first two terms in the well-known expansion used in the cellular method for $\psi_{\mathbf{k}}(\mathbf{r})$. If $\phi_s(r)$ is the s-atomic wave function which has the same starting values as $\psi_1(r)$ at $r=0$, and if $\psi_s(r)$ is the normalized atomic wave function, then

$$|\psi_s(0)|^2 = |\phi_s(0)|^2 / \int |\phi_s|^2 d\tau. \quad \dots\dots(6)$$

Since $\psi_2(0) = 0$ and $\psi_1(0) = \phi_s(0)$ we have

$$\frac{|\psi_{\mathbf{k}}(0)|^2}{|\psi_s(0)|^2} = \frac{|a_s|^2}{|a_s|^2 + |a_p|^2} N \quad \dots\dots(7)$$

where $N = \int |\phi_s|^2 d\tau$.

Although we do not know the function $\psi_1(r)$, and therefore cannot determine ϕ_s , we can approximate to N very satisfactorily by using the Wigner-Seitz wave function $\psi_0(r)$ for the state of lowest energy in the conduction band. Thus approximately

$$N = \int_0^\infty r^2 \phi_s^2(r) dr / \int_0^{r_s} r^2 \psi_0^2(r) dr, \quad \dots\dots(8)$$

where $\psi_0(r)$ is not necessarily normalized but $\phi_s(0) = \psi_0(0)$, and r_s is the radius of the atomic sphere. Hence

$$R = \left\{ \frac{|a_s|^2}{|a_s|^2 + |a_p|^2} \right\}_{\text{av}} N, \quad \dots\dots(9)$$

where the subscript *av* means an average taken over all values of **k** on the Fermi surface.

Numerical integration shows that for sodium $N=1.572$ and for lithium $N=2.688$. Hence we find

$$\left\{ \frac{|a_s|^2}{|a_s|^2 + |a_p|^2} \right\}_{av} = 0.248 \text{ for Li,} \\ = 0.653 \text{ for Na.}$$

Thus, as we should expect from the calculations of Howarth and Jones, the states at the Fermi surface in sodium are mainly s-like in character, whilst for lithium they are predominantly p-like, in accordance with Schiff's calculations.

Existing data on the soft x-ray emission spectrum from metallic lithium (Skinner 1940) do not seem to be compatible with the calculated electronic states of the conduction band. Although the widths of the observed bands are approximately the same as the calculated widths, in the case of lithium the shape of the band is not what might be expected on a simple theory. The observed band shows a falling off of intensity just before the final drop at the Fermi surface is reached, whereas the calculated states suggest that the transition probability should increase steadily up to the Fermi limit. A possible explanation of this discrepancy is as follows: the x-ray emission takes place at an atom which has already lost one 1s electron, and thus such x-ray spectra do not give direct information about the normal electronic states in metals, but only about states which are strongly perturbed in the neighbourhood of the emitting atom.

ACKNOWLEDGMENT

One of us (B.S.) is indebted to the Senate of the University of London for the award of a Postgraduate Studentship.

REFERENCES

- BARDEEN, J., 1938, *J. Chem. Phys.*, **6**, 367.
 BOHM, D., and PINES, D., 1953, *Phys. Rev.*, **92**, 609.
 FOX, M., and RABI, I., 1935, *Phys. Rev.*, **48**, 746.
 GUTOWSKY, H. S., and MCGARVEY, B. R., 1952, *J. Chem. Phys.*, **20**, 1472.
 HOWARTH, D. J., and JONES, H., 1952, *Proc. Phys. Soc. A*, **65**, 355.
 KNIGHT, W. D., 1949, *Phys. Rev.*, **76**, 1259.
 KOHN, W., and BLOEMBERGEN, N., 1950, *Phys. Rev.*, **80**, 913; 1951, *Ibid.*, **82**, 283.
 SAMPSON, J. B., and SEITZ, F., 1940, *Phys. Rev.*, **58**, 633.
 SCHIFF, B., 1954, *Proc. Phys. Soc. A*, **67**, 2.
 SKINNER, H. W. B., 1940, *Phil. Trans.*, **239**, 95.
 TOWNES, C. H., HERRING, C., and KNIGHT, W. D., 1950, *Phys. Rev.*, **77**, 852.
 WOHLFARTH, E. P., 1950, *Phil. Mag.*, **41**, 534.

On the Exchange Interaction in the Collective Electron Approximation

By R. H. TREDGOLD

Department of Physics, University of Nottingham

MS. received 12th November 1953

Abstract. A brief discussion of the previous work on the subject is given. A general expression for the exchange integral in the collective electron approximation is obtained in terms of the Fourier coefficients of the exchange charge density. These coefficients are evaluated for a particular case of tightly bound electrons and it is shown that the exchange integral is a strong function of the difference of the wave vectors characterizing the two states between which exchange is considered. The significance of this result is discussed and the inadequacies of the collective electron approximation in dealing with problems involving exchange are pointed out.

§ 1. INTRODUCTION

STATISTICAL treatments of solid state phenomena based on the collective electron approximation usually appear to ignore the effect of the exchange energy. Those treatments which do not ignore this energy take for the exchange integral between states characterized by wave vectors \mathbf{k}_i and \mathbf{k}_j the expression obtained by Bethe (1930) for the case of nearly free electrons, viz.

$$J_{ij} = \frac{4\pi}{V|\mathbf{k}_i - \mathbf{k}_j|^2}, \quad \dots\dots(1)$$

V being the volume of the crystal under consideration. In particular Wohlfarth (1950) has calculated the low temperature electronic specific heat of various metals, and Lidiard (1951) has calculated the magnetic properties of an assembly of electrons. Both these authors obtain results differing considerably from those which experiment would lead one to expect. It is evident that their results would be far more satisfactory if the exchange integral was a weakly varying function of $\mathbf{k}_i - \mathbf{k}_j$ instead of the strong function given in (1). Both these authors point out this fact and also suggest that if an adequate allowance for the correlation of the position of the electrons were made the result would be formally equivalent to the exchange integral being a weak function of $\mathbf{k}_i - \mathbf{k}_j$.

Wohlfarth (1953) suggested that an exchange integral based on the correct wave functions for a solid instead of free electron functions would lead to an expression of the required form and attempted to calculate this quantity using the approximation of tight binding. Unfortunately, the expression he obtains involves a lattice sum of the form $\exp[i(\mathbf{k}_i - \mathbf{k}_j) \cdot \mathbf{r}]/r$. It has not so far been found possible to evaluate sums of this form for a three-dimensional lattice, and to circumvent this difficulty he drops all but the leading terms of the series, justifying this procedure by the assumption that the effect of the other terms on the total exchange energy of the solid will be small. Thus his treatment never actually

leads to an explicit expression for the exchange integral which may be compared with the expression for the case of free electrons.

It is thus desirable to obtain an expression for the exchange integral based on wave functions similar to those obtained from the tight-binding approximation in order to be able to judge how far the discrepancies between theory and experiment are due to the assumption of too simple a type of one-electron wave functions and how far they are due to a neglect of the correlation effect. It is the purpose of the present work to obtain such an expression.

§ 2. A GENERALIZED EXPRESSION FOR THE EXCHANGE INTEGRAL

It is desirable in the first place to evaluate the integral

$$I = \frac{1}{V^2} \iint \frac{\exp[i\mathbf{k}_p \cdot \mathbf{r}_1 + i\mathbf{k}_q \cdot (\mathbf{r}_2 - \mathbf{r}_1)]}{|\mathbf{r}_2 - \mathbf{r}_1|} d\tau_2 d\tau_1 \quad \dots\dots(2)$$

$\mathbf{k}_p \neq \mathbf{k}_q$, V being the volume of the crystal and the integration being taken throughout it.

Putting $\mathbf{r}_2 - \mathbf{r}_1 = \mathbf{r}$ and changing to spherical polar coordinates one has

$$\left. \begin{aligned} I &= \frac{2\pi}{V^2} \int d\tau_1 \int_0^L \int_1^{+1} \frac{\exp[i\mathbf{k}_p \cdot \mathbf{r}_1 + i\mathbf{k}_q r \cos \theta] r^2}{r} d(\cos \theta) dr \\ &= \frac{4\pi}{V^2 k_q^2} \int \exp[i\mathbf{k}_p \cdot \mathbf{r}_1] [1 - \cos k_q L(\mathbf{r}_1)] d\tau_1 \\ &= \frac{4\pi}{V k_q^2} \text{ when } \mathbf{k}_p = 0, \quad \text{and } 0 \text{ when } \mathbf{k}_p \neq 0. \end{aligned} \right\} \quad \dots\dots(3)$$

Terms in $1/V^2$ are neglected. Here $L(\mathbf{r}_1)$ is the mean distance from \mathbf{r}_1 to the boundary. In particular, if $\mathbf{k}_q = \mathbf{k}_i - \mathbf{k}_j$ and $\mathbf{k}_p = 0$, one obtains equation (1). The method used here to deal with the indeterminate definite integral occurring in the derivation of (1) differs somewhat from the method used by Bethe (1930) and appears to the author to be more satisfactory as it takes account of the fact that the crystal is of finite extent.

One may now turn to the case of an actual crystal. For convenience the lattice parameter is taken as unity. Let \mathbf{R} be a principal vector in the lattice, let \mathbf{K} be a principal vector in the reciprocal lattice (the factor 2π is included in \mathbf{K}). Summations over \mathbf{R} or \mathbf{K} are taken to be over the whole of the lattice or the reciprocal lattice as the case may be.

The Bloch function characterized by the wave vector \mathbf{k}_i may now be written as

$$\psi_i(\mathbf{r}) = \frac{1}{N^{1/2}} \mu_i(\mathbf{r}) \exp[i\mathbf{k}_i \cdot \mathbf{r}] = \frac{1}{N^{1/2}} \exp[i\mathbf{k}_i \cdot \mathbf{r}] \sum_{\mathbf{K}} b(\mathbf{K}, \mathbf{k}_i) \exp[i\mathbf{K} \cdot \mathbf{r}], \quad \dots\dots(4)$$

where N is the number of atoms in the crystal and $\mu_i(\mathbf{r})$ has the periodicity of the lattice and is normalized over one primitive unit cell.

The exchange integral between states characterized by the wave numbers \mathbf{k}_i and \mathbf{k}_j is then

$$J_{ij} = \frac{1}{N^2} \iint \frac{\mu_i^*(\mathbf{r}_1) \mu_j(\mathbf{r}_1) \mu_j^*(\mathbf{r}_2) \mu_i(\mathbf{r}_2) \exp[i(\mathbf{k}_i - \mathbf{k}_j) \cdot (\mathbf{r}_2 - \mathbf{r}_1)]}{|\mathbf{r}_2 - \mathbf{r}_1|} d\tau_1 d\tau_2. \quad \dots\dots(5)$$

One may now put

$$\mu_i^*(\mathbf{r}) \mu_j(\mathbf{r}) = \sum_{\mathbf{K}} a(\mathbf{K}, \mathbf{k}_i, \mathbf{k}_j) \exp[i\mathbf{K} \cdot \mathbf{r}], \quad \dots\dots(6)$$

when from (3), (4) and (6) it is found that

$$J_{ij} = \frac{4\pi}{V} \sum_{\mathbf{K}} \frac{|a(\mathbf{K}, \mathbf{k}_i, \mathbf{k}_j)|^2}{|\mathbf{k}_i - \mathbf{k}_j - \mathbf{K}|^2}. \quad \dots\dots(7)$$

From (4) and (6) it may be shown that

$$a(\mathbf{K}, \mathbf{k}_i, \mathbf{k}_j) = \sum_{\mathbf{K}'} b^*(\mathbf{K}', \mathbf{k}_i) b(\mathbf{K} + \mathbf{K}', \mathbf{k}_j). \quad \dots\dots(8)$$

It is of interest to note that the b 's are equivalent to the momentum eigenfunction as employed by Slater (1952).

§ 3. A PARTICULAR CASE

As the form of the exchange integral for nearly free electrons is already known it is of interest to attempt to obtain an explicit expression for this quantity for the opposite extreme, namely the case of tightly bound electrons.

The case considered is that of a simple cubic lattice having atomic wave functions of the form $\exp[-\alpha^2 r^2]$ located on the lattice points. This is equivalent to the case of tightly bound electrons in the lowest band in the Mathieu function problem investigated by Slater (1952).

According to the tight binding approximation the wave functions are then of the form

$$\psi_i(\mathbf{r}) = \frac{\alpha^{2/3}}{N^{1/2}} \left(\frac{2}{\pi}\right)^{3/4} \sum_{\mathbf{R}} \exp[-\alpha^2(\mathbf{r} - \mathbf{R})^2 + i\mathbf{k}_i \cdot \mathbf{R}] = \frac{1}{N^{1/2}} \mu_i(\mathbf{r}) \exp[i\mathbf{k}_i \cdot \mathbf{r}]. \quad \dots\dots(9)$$

It is found that the Fourier coefficients of $\mu_i(\mathbf{r})$ are given by

$$b(\mathbf{K}, \mathbf{k}_i) = \alpha^{3/2} \left(\frac{2}{\pi}\right)^{3/4} \sum_{\mathbf{R}} \exp[i\mathbf{k}_i \cdot \mathbf{R}] \int \exp[-\alpha^2(\mathbf{r} - \mathbf{R})^2 - i(\mathbf{k}_i + \mathbf{K}) \cdot \mathbf{r}] d\mathbf{r}, \quad \dots\dots(10)$$

where the integration is taken over one atomic polyhedron.

If α is large, as in the case of tight binding, two approximations may be made without serious error: (i) only the leading term ($\mathbf{R}=0$) need be considered, (ii) the integration over the atomic polyhedron may be replaced by an integration over all space. To this approximation it is found that

$$b(\mathbf{K}, \mathbf{k}_i) = \left(\frac{2\pi}{\alpha^2}\right)^{3/4} \exp\left[-\left(\frac{\mathbf{K} + \mathbf{k}_i}{2\alpha}\right)^2\right]. \quad \dots\dots(11)$$

The use of this expression is equivalent to assuming that the binding is so tight that the Wannier (1937) functions degenerate to the atomic functions.

From (8) and (11) it is found that

$$a(\mathbf{K}, \mathbf{k}_i, \mathbf{k}_j) = \left(\frac{2\pi}{\alpha^2}\right)^{3/2} \sum_{\mathbf{K}'} \exp\left[-\left(\frac{\mathbf{K}' + \mathbf{k}_i}{2\alpha}\right)^2 - \left(\frac{\mathbf{K} + \mathbf{K}' + \mathbf{k}_j}{2\alpha}\right)^2\right]. \quad \dots\dots(12)$$

Since α is assumed large this series will converge slowly. It may however be transformed into the following rapidly convergent series (see Appendix)

$$a(\mathbf{K}, \mathbf{k}_i, \mathbf{k}_j) = \exp\left[-\frac{(\mathbf{k}_i - \mathbf{k}_j - \mathbf{K})^2}{8\alpha^2}\right] \sum_{\mathbf{R}} \exp\left[-\frac{\alpha^2 R^2}{2} + i\mathbf{R} \cdot \mathbf{D}\right], \quad \dots\dots(13)$$

where $\mathbf{D} = \frac{1}{2}(\mathbf{K} + \mathbf{k}_i + \mathbf{k}_j)$.

Making an approximation exactly equivalent to approximation (1) one may neglect all terms except the leading term of this series. It is then found that

$$J_{ij} = \frac{4\pi}{V} \sum_{\mathbf{K}} \frac{\exp[-\{(\mathbf{k}_i - \mathbf{k}_j - \mathbf{K})/2\alpha\}^2]}{|\mathbf{k}_i - \mathbf{k}_j - \mathbf{K}|^2}. \quad \dots\dots(14)$$

Now $\mathbf{k}_i - \mathbf{k}_j$ can range over a zone having twice the linear dimensions of the first Brillouin zone. $J_{ij} \rightarrow \infty$ as $\mathbf{k}_i - \mathbf{k}_j \rightarrow 0$, and will also tend to infinity as $\mathbf{k}_i - \mathbf{k}_j$ approaches any of the 26 reciprocal lattice points lying on the boundary of the allowed range of $\mathbf{k}_i - \mathbf{k}_j$. It may thus be seen that even in the case of tight binding the exchange integral will be a strong function of $\mathbf{k}_i - \mathbf{k}_j$. Although equation (14) represents the results for a special case it is evident that the results will be qualitatively the same for any tightly bound system of electrons.

§ 4. DISCUSSION

From the foregoing considerations it appears reasonable to conclude that the weakness in the existing treatments of solid state phenomena based on equation (1) lies not so much in the assumption of the wrong form of exchange integral as in neglecting the influence of electron correlations. The method employed by Wigner and Seitz (1934, see also Wigner 1934) to estimate the effect of electron correlation on cohesive energy is, unfortunately, not applicable to the type of problems discussed here and is moreover, as was pointed out by Wigner (1934), only a rough approximation.

It thus appears that the collective electron theory of metals in its present form is not suitable for dealing with problems in which exchange interaction plays a prominent part.

ACKNOWLEDGMENTS

The author would like to take this opportunity to thank Professor L. F. Bates for his interest and encouragement and Dr. M. E. Noble for several helpful discussions.

APPENDIX

Equation (12) may be written as

$$a(\mathbf{K}, \mathbf{k}_i, \mathbf{k}_j) = \left(\frac{2\pi}{\alpha^2}\right)^{3/2} F_x(K_x, k_{ix}, k_{jx}) F_y(K_y, k_{iy}, k_{jy}) F_z(K_z, k_{iz}, k_{jz}), \dots (A1)$$

where

$$\begin{aligned} F_x &= \sum_{l'=-\infty}^{+\infty} \exp \left[- \left(\frac{2\pi l' + k_{ix}}{2\alpha} \right)^2 - \left(\frac{2\pi l + 2\pi l' + k_{jx}}{2\alpha} \right)^2 \right] \\ &= \exp \left[- \frac{(k_{ix} - k_{jx} - 2\pi l)^2}{8\alpha^2} \right] \sum_{l'=-\infty}^{+\infty} \exp \left[- \frac{2\pi^2}{\alpha^2} (l' + d)^2 \right], \dots (A2) \end{aligned}$$

where $d = \frac{1}{2}l + (k_{ix} + k_{jx})/4\pi$.

The series obtained is periodic in d and may accordingly be expressed as a Fourier series giving

$$F_x = \frac{\alpha}{2} \left(\frac{2}{\pi} \right)^{1/2} \exp \left[- \frac{(k_{ix} - k_{jx} - 2\pi l)^2}{8\alpha^2} \right] \sum_{q=-\infty}^{+\infty} \exp \left[- \frac{\alpha^2 q^2}{2} + 2\pi i q d \right]. \dots (A3)$$

From (A1) and (A3) one may easily obtain (13).

REFERENCES

- BETHE, H., 1930, *Ann. Phys., Lpz.*, **5**, 325.
- LIDIARD, A. B., 1951, *Proc. Phys. Soc. A*, **64**, 814.
- SLATER, J. C., 1952, *Phys. Rev.*, **87**, 807.
- WANNIER, G., 1937, *Phys. Rev.*, **52**, 191.
- WIGNER, E., 1934, *Phys. Rev.*, **46**, 1002.
- WIGNER, E., and SEITZ, F., 1934, *Phys. Rev.*, **46**, 509.
- WOHLFARTH, E. P., 1950, *Phil. Mag.*, **41**, 534; 1953, *Rev. Mod. Phys.*, **25**, 211.

Static Magnetic Fields in General Relativity

By W. B. BONNOR

Department of Applied Mathematics, The University, Liverpool

MS. received 20th July 1953, and in amended form 16th October 1953

Abstract. A theorem is proved which enables a class of known electrostatic solutions of the field equations to be adapted to the magnetostatic case. Exact solutions referring to a uniform magnetic field and to a magnetic dipole are given.

The solution for a circular loop of wire carrying a steady current is considered, and it is shown that if the mass of the wire be neglected, both the magnetic and gravitational fields at great distances are equivalent to those of a magnetic dipole.

The paper concludes with a short discussion of the significance of the solutions presented here, and in an earlier paper, for relativistic electromagnetic theory.

§ 1. INTRODUCTION

IN a previous paper (Bonnor 1953, hereafter denoted by I) certain solutions of the field equations of general relativity with an electrostatic field were obtained.

These were of two types: one describing electric fields corresponding closely to classical electric fields, with accompanying gravitational fields of expected nature having regard to the sources of the electric field; and the second type referring to electric fields not predicted at all by classical theory.

The present work extends the investigation to static magnetic fields, and shows that two types of solution, similar to those mentioned above, again exist. In §§ 2 and 3 we show how some known electrostatic solutions may be adapted to the magnetic case, and in § 4 we consider briefly certain magnetic fields arising from steady currents.

§ 2. A THEOREM CONNECTING ELECTRIC AND MAGNETIC SOLUTIONS

The field equations for regions of space-time containing electromagnetic fields but no matter are (Eddington 1924, chap. VI, § 77)

$$G_{ij} = -8\pi E_{ij}, \quad \dots\dots(2.1)$$

$$E_j^i = -F^{ia} F_{ja} + \frac{1}{4} \delta_j^i F^{ab} F_{ab}, \quad \dots\dots(2.2)$$

where G_{ij} is the contracted Riemann-Christoffel tensor, and F_{ij} is the (anti-symmetrical) electromagnetic field tensor which satisfies Maxwell's equations for empty space if

$$F_{ij;k} + F_{jk;i} + F_{ki;j} = 0, \quad \dots\dots(2.3)$$

$$F^{ij}_{;j} = 0, \quad \dots\dots(2.4)$$

the semi-colon denoting covariant differentiation.

We shall first prove a result which enables solutions of the equations (2.1)–(2.4) referring to purely electric fields in empty space to be adapted to corresponding magnetic fields. The result may be stated as follows:

Theorem. If g_{ij} , F_{ij} are tensors satisfying the field equations (2.1)–(2.4), then g_{ij} , F^*_{ij} also satisfy them, where

$$F^*_{ij} = \frac{1}{2} \eta^{ijkl} F_{kl}. \quad \dots\dots(2.5)$$

The expression η_{ijkl} is defined by

$$\eta_{ijkl} = \epsilon_{ijkl} (-g)^{1/2}, \quad \dots\dots (2.6)$$

where ϵ_{ijkl} is the usual permutation symbol, and g is the determinant of the metric tensor g_{ij} ; η_{ijkl} is a covariant tensor with respect to transformations with positive Jacobian, and it has zero covariant derivative, a fact which will be used later.

The theorem will be proved if we show that

$$E^{*i}_{;j} = E^i_j, \quad \dots\dots (2.7)$$

$$F^{*i}_{;j;k} + F^{*j}_{;k;i} + F^{*k}_{;i;j} = 0, \quad \dots\dots (2.8)$$

and

$$F^{*ij}_{;j} = 0, \quad \dots\dots (2.9)$$

where E^{*i}_j is the electromagnetic energy tensor formed from the F^{*}_{ij} in accordance with (2.2).

We shall need in the proof the following, which are easily deduced from (2.6):

$$\eta^{ijkl} = -\epsilon_{ijkl} (-g)^{-1/2},$$

$$\eta_{ijkl} \eta^{ijmn} = -2\delta^{mn}_{kl}, \quad \dots\dots (2.10)$$

$$\eta_{ijkl} \eta^{imnp} = -\delta^{mnp}_{jkl}. \quad \dots\dots (2.11)$$

To prove (2.7) we first calculate the E^{*i}_j , using the formula (2.5) for the F^{*ij} .

$$\begin{aligned} E^{*i}_j &= -F^{*ia} F^{*}_{ja} + \frac{1}{4} \delta^i_j F^{*ab} F^{*}_{ab}, \\ &= -\frac{1}{4} \eta^{iakl} \eta^{bcmn} g_{jb} g_{ac} F_{kl} F_{mn} \\ &\quad + \frac{1}{16} \delta^i_j \eta^{abcd} \eta^{mnpq} g_{am} g_{bn} F_{cd} F_{pq}, \\ &= -\frac{1}{4} \eta^{iakl} \eta_{japq} F^{pq} F_{kl} + \frac{1}{16} \delta^i_j \eta^{mnpq} \eta_{mnef} F_{ef} F_{pq}. \end{aligned}$$

Using (2.10) and (2.11), we have

$$E^{*i}_j = \frac{1}{4} \delta^{ikl}_{jpq} F^{pq} F_{kl} - \frac{1}{8} \delta^i_j \delta^{pq}_{ef} F^{ef} F_{pq},$$

which, because of the antisymmetry of the F_{ij} , reduces to

$$E^{*i}_j = \frac{1}{4} \delta^{ikl}_{jpq} F^{pq} F_{kl} - \frac{1}{4} \delta^i_j F^{ab} F_{ab}.$$

It is easily verified that this gives

$$E^{*i}_j = -F^{ia} F_{ja} + \frac{1}{4} \delta^i_j F^{ab} F_{ab} = E^i_j.$$

It is clear that (2.8) will be proved if we can show that $\eta^{ijkl} F^{*}_{ij;k} = 0$.

Now, using (2.5),

$$\begin{aligned} \eta^{ijkl} F^{*}_{ij;k} &= \frac{1}{2} \eta^{ijkl} \eta^{abcd} g_{ia} g_{jb} F_{cd;k} \\ &= \frac{1}{2} \eta^{ijkl} \eta_{ijef} F^{ef}_{;k}; \end{aligned}$$

and, using (2.10), we obtain

$$\eta^{ijkl} F^{*}_{ij;k} = -\delta^{kl}_{ef} F^{ef}_{;k} = -2 F^{kl}_{;k} = 0$$

from (2.4). Hence (2.8) is established.

Finally, (2.9) follows at once on using (2.5), because $F^{*ij}_{;j} = \frac{1}{2} \eta^{ijkl} F_{kl;j} = 0$ from (2.3). This completes the proof of the theorem.

We shall be concerned with static solutions of the field equations, i.e. solutions in which the g_{ij} are not functions of x_4 , and in which $g_{i4} = 0$. Such solutions correspond to purely electric fields if the components of F_{ij} (or F^{ij}) are zero unless i or j equals 4, and to purely magnetic fields if the components F_{i4} are zero. Let us take a purely electric solution, with metric tensor g_{ij} , and write

$$(X, Y, Z) = (F^{14}, F^{24}, F^{34}).$$

From the above theorem it follows that there exists a purely magnetic solution in which g_{ij} is unchanged, and the components of F_{ij} (obtained by lowering suffices in (2.5)) are

$$\left. \begin{aligned} F_{12} = -F_{21} = (-g)^{1/2} Z, \quad F_{31} = -F_{13} = (-g)^{1/2} Y, \quad F_{23} = -F_{32} = (-g)^{1/2} X, \\ F_{14} = F_{24} = F_{34} = 0. \end{aligned} \right\} \dots\dots (2.12)$$

Consider now a space-like two-dimensional surface V_2 and let λ^i, μ^i be unit vectors orthogonal to it, λ^i being time-like; then the electric and magnetic intensities normal to the V_2 may be taken as (Synge 1936)

$$\left. \begin{aligned} E(\mu, \lambda) &= F^{ij} \mu_i \lambda_j, \\ H(\mu, \lambda) &= \frac{1}{2} \eta^{ijkl} F_{kl} \mu_i \lambda_j, \end{aligned} \right\} \dots\dots (2.13)$$

where F_{ij} is the electromagnetic field tensor satisfying (2.3) and (2.4), which may contain both electric and magnetic components. Let us now suppose that the parametric line of x_4 is normal to V_2 , so that $\lambda_\alpha = 0$ ($\alpha = 1, 2, 3$). Then if the relation (2.12) exists between the components of F_{ij} we have

$$\left. \begin{aligned} H(\mu, \lambda) &= \frac{1}{2} \eta^{i4kl} F_{kl} \mu_i \lambda_4, \\ &= -F^{i4} \mu_i \lambda_4, \\ &= -E(\mu, \lambda). \end{aligned} \right\} \dots\dots (2.14)$$

Hence the electric and magnetic intensities normal to a V_2 at rest in the coordinate system are numerically equal; and therefore the fluxes of these intensities across an element dS of V_2 , defined as $H(\mu, \lambda) dS$ and $E(\mu, \lambda) dS$, are numerically equal.

From the above it follows that *to every purely electric solution g_{ij}, F^{i4} of the field equations (2.1)–(2.4) there corresponds a purely magnetic solution in which the g_{ij} are the same, and the F_{ij} are given in terms of the F^{i4} by (2.12); and the electric and magnetic fluxes across any two-dimensional surface at rest are numerically equal in the two solutions.*

The above results hold only in regions where the electric charge and current-density vanish. Moreover, in applying them we must bear in mind the fact that there is not an equivalence between sources of the static electric and magnetic fields; by this is meant that whereas the electrostatic field in empty space may be considered to arise from point-charges, the magnetostatic field must arise from magnetic dipoles, or from stationary electric currents. (In § 4 we shall give some justification for taking the magnetic dipole as a source equivalent to a stationary electric current.) For example, the relativistic solution for a charged mass-point (Eddington 1924, § 78) yields, on applying the above theorem, a solution referring to a magnetic pole with mass, which we must reject on physical grounds. But with these provisos we may use the results of this section to derive solutions for magnetostatic fields in empty space from known electrostatic solutions.

§ 3. CERTAIN MAGNETOSTATIC SOLUTIONS

First, we may adapt to the magnetic case the class of electrostatic solutions discovered by Majumdar (1947), and independently by Papapetrou (1947). This class is given by

$$\left. \begin{aligned} ds^2 &= -(1+\psi)^2 (dx^2 + dy^2 + dz^2) + (1+\psi)^{-2} dt^2, \\ \phi &= \psi/(1+\psi), \\ \frac{\partial^2 \psi}{\partial x^2} + \frac{\partial^2 \psi}{\partial y^2} + \frac{\partial^2 \psi}{\partial z^2} &= 0 \quad \text{and} \quad F_{i4} = -\frac{1}{2} \pi^{-1/2} \frac{\partial \phi}{\partial x_i} \end{aligned} \right\} \dots\dots (3.1)$$

where

For electrostatic fields the electric flux across a spatial surface S on which the position of points is described by parameters u, v is (Whittaker 1935)

$$\iint_S \left\{ F_{41} \frac{\partial(x_2, x_3)}{\partial(u, v)} + F_{42} \frac{\partial(x_3, x_1)}{\partial(u, v)} + F_{43} \frac{\partial(x_1, x_2)}{\partial(u, v)} \right\} (-g)^{1/2} du dv, \dots (3.2)$$

a result which follows also from (2.13). In the case of the solution (3.1), this reduces to

$$-\frac{1}{2} \pi^{-1/2} \iint_S \left\{ \frac{\partial \psi}{\partial x_1} \frac{\partial(x_2, x_3)}{\partial(u, v)} + \frac{\partial \psi}{\partial x_2} \frac{\partial(x_3, x_1)}{\partial(u, v)} + \frac{\partial \psi}{\partial x_3} \frac{\partial(x_1, x_2)}{\partial(u, v)} \right\} du dv$$

which is proportional to the electric flux across S arising from the classical potential ψ . Hence it is reasonable to suppose that the electric field of (3.1) is that which arises from the potential ψ in Maxwell's theory.

From § 2 the magnetostatic solution corresponding to (3.1) is

$$\left. \begin{aligned} ds^2 &= -(1 + \psi)^2 (dx^2 + dy^2 + dz^2) + (1 + \psi)^{-2} dt^2, \\ F_{12} &= \frac{1}{2} \pi^{-1/2} \frac{\partial \psi}{\partial x_3}, \quad F_{31} = \frac{1}{2} \pi^{-1/2} \frac{\partial \psi}{\partial x_2}, \quad F_{23} = \frac{1}{2} \pi^{-1/2} \frac{\partial \psi}{\partial x_1}. \end{aligned} \right\} \dots (3.3)$$

Further, we know that the magnetic flux for (3.3) is proportional to that in the electric, and therefore in the classical case.

Papapetrou (1947) has considered in detail the special case of (3.1) which refers to a set of point charges, and it is clear that the masses of the points are all proportional to their charges, the constant of proportionality being one in the units being used here. The solution, in fact, refers to a set of charged mass-points in which the gravitational and electric forces just balance so that the set remains in equilibrium. For this reason the solution for the electric case is not of great physical interest, and the same may be said of the magnetic solution (3.3). Examples exist of (3.3) corresponding, for instance, to magnetic dipoles, but these must carry mass dipoles with moment proportional to the magnetic dipole moment.

Another set of electrostatic solutions was given by Weyl (1917). This refers to fields with axial symmetry, for which the line-element may be taken in the form

$$ds^2 = -e^\lambda (dx_1^2 + dx_2^2) - e^{-\rho} x_2^2 dx_3^2 + e^\rho dt^2, \dots (3.4)$$

the origin of coordinates O being taken on the axis of symmetry Ox_1, x_2 and x_3 being radial and angular coordinates respectively, and λ and ρ being functions of x_1 and x_2 only. For electric fields containing no matter or charge except at singularities Weyl's solution is

$$\left. \begin{aligned} e^\rho &= A + B\phi + \phi^2, \\ \int \frac{d\phi}{A + B\phi + \phi^2} &= \psi, \\ \frac{\partial^2 \psi}{\partial x_1^2} + \frac{\partial^2 \psi}{\partial x_2^2} + \frac{1}{x_2} \frac{\partial \psi}{\partial x_2} &= 0, \\ F_{4i} &= \frac{1}{2} \pi^{-1/2} x_2 \frac{\partial \phi}{\partial x_i}; \end{aligned} \right\} \dots (3.5)$$

and specification of ψ fixes not only ϕ and ρ but also λ . From (3.2) it is found that the electric flux across a given surface for this solution is proportional to that of the classical electric field arising from the potential ψ .

The magnetostatic solution corresponding to that of Weyl is given by (3.4) and (3.5) together with

$$F_{12} = F_{4i} = 0; \quad F_{31} = \frac{1}{2} \pi^{-1/2} x_2 \frac{\partial \psi}{\partial x_2}; \quad F_{23} = \frac{1}{2} \pi^{-1/2} x_2 \frac{\partial \psi}{\partial x_1}. \dots (3.6)$$

The magnetic flux is proportional to that corresponding to the potential ψ .

Two axially symmetric fields of physical interest are those corresponding to a uniform magnetic field, and to the field of a magnetic dipole. The solution for a uniform magnetic field may be written down from that in I for a uniform electric field, using (2.12) to obtain the components of the magnetic field :

$$\left. \begin{aligned} ds^2 &= -\exp \{C^2(1-b^2)x_2^2\} [X^{-3}dx_1^2 + X^{-1}dx_2^2] - x_2^2 X^{-1}dx_3^2 + X dt^2, \\ F_{12} &= F_{31} = 0, \quad F_{23} = \frac{1}{2}\pi^{-1/2} Cx_2, \\ X &= 1 + 2Cbx_1 + C^2x_1^2. \end{aligned} \right\} \quad (3.7)$$

It was shown in the electrostatic case that the field corresponding to this solution arises from charged mass-points at infinity, the constant Cb representing mass and C the field strength. It therefore has no physical significance in the magnetic case unless b is put equal to zero, which abolishes the mass; we may then regard the solution as referring simply to a uniform field produced by a solenoid without mass.

Solutions corresponding to magnetic dipoles may be obtained from (3.5) and (3.6) by using the classical potential $\psi = \mu x_1/r^3 + c$, where $r^2 = x_1^2 + x_2^2$ and μ and c are constants. There are two cases :

$$(i) \quad \left. \begin{aligned} A &= \frac{1}{4}B^2, \quad e^e = Ke^{-\lambda} = \left(c + \frac{\mu x_1}{r^3}\right)^{-2}, \\ \phi &= -\frac{1}{2}B - \left(c + \frac{\mu x_1}{r^3}\right)^{-1}, \end{aligned} \right\} \quad \dots\dots (3.8)$$

$$(ii) \quad A - \frac{1}{4}B^2 = D^2 \text{ (where } D \text{ may be real or imaginary),} \\ \left. \begin{aligned} e^e &= D^2 \sec^2 \left[D \left(c + \frac{\mu x_1}{r^3} \right) \right], \\ e^\lambda &= K \cos^2 \left[D \left(c + \frac{\mu x_1}{r^3} \right) \right] \exp \left[2D^2\mu^2 \left(\frac{2x_2^2}{r^6} - \frac{9x_2^4}{4r^8} \right) \right], \\ \phi &= -\frac{1}{2}B + D \tan \left[D \left(c + \frac{\mu x_1}{r^3} \right) \right]. \end{aligned} \right\} \quad \dots (3.9)$$

In the above K is an arbitrary constant, and e^λ has been found from the field equations given in I.

Solution (3.8) is a special case of (3.1) and, as already mentioned, solutions of this type refer to distributions of charges (magnetic or electric) associated with masses numerically equal to the charges. In the case of (3.9), taking D real, we can make the line-element tend to Galilean form as x_1, x_2 tend to infinity by choosing

$$K = D^{-2}, \quad D^2 \sec^2(Dc) = 1. \quad \dots\dots (3.10)$$

If we do this, and expand g_{44} in powers of $\mu x_1/r^3$, we find that

$$g_{44} \rightarrow 1 \pm \frac{2\mu(1-D^2)^{1/2}x_1}{r^3} + \frac{\mu^2(3-2D^2)x_1^2}{r^6} + \dots$$

The solution now contains two arbitrary constants D and μ , and it is clear that $\pm(1-D^2)^{1/2}\mu$ is to represent the strength of a mass-dipole present together with the electric (or magnetic) dipole of strength μ . Thus the solution for an electric or magnetic dipole only is obtained by putting $D=1$, and the asymptotic form of g_{44} is then

$$g_{44} \sim 1 + \mu^2 x_1^2/r^6. \quad \dots\dots (3.11)$$

With this interpretation the solution corresponding to (3.10) allows mass-dipoles of strengths between $\pm\mu$; another solution giving mass-dipoles of strengths

numerically greater than μ is obtained by taking D in (3.9) to be imaginary. The solution for a mass-dipole of strength μ is given by (3.8).

From the observational point of view some interest might be attached to a solution of the field equations representing a mass-point carrying a magnetic dipole as a model for a star or planet with a magnetic field of the type found on earth. No solution of this type exists in the class (3.5) as can be verified by using the appropriate form of ψ (which is $\psi = er^{-1} + \mu x_1 r^{-3} + c$) and trying to adjust the constant D so as to obtain a term representing a mass-point without mass-dipole. However, it seems probable from (3.11) that the asymptotic form of g_{44} for this solution must be

$$g_{44} \sim 1 - \frac{2m}{r} + \frac{\mu^2 x_1^2}{r^6}, \quad \dots\dots(3.12)$$

where m represents the mass and μ the magnetic dipole strength. In this case the contribution of the magnetic field to the gravitational field will be quite negligible, even for strong dipoles. For example, for the ratio of the third and second terms on the right of (3.12) at the surface of the sun, supposing a magnetic field there of about 1000 gauss, one finds, paying due regard to the units, a value of order 10^{-16} .

In I were given certain electrostatic solutions of the field equations which have no classical analogy. Similar solutions exist also in the magnetostatic case and they may be written down from the electrostatic solutions by the use of the theorem of §2. For example, there is the solution referring to a field symmetrical about an axis Ox_1 in which the line-element has the form (3.4) with

$$\left. \begin{aligned} e^\lambda = e^\rho &= (1 + \frac{1}{4} C^2 x_2^2)^2, \\ \text{and } F_{12} = F_{13} &= 0; \quad F_{23} = -F_{32} = C x_2 e^{-e}, \end{aligned} \right\} \quad \dots\dots(3.13)$$

where C is an arbitrary constant. The field represented by (3.13) has properties similar to those of the corresponding electrostatic field described in I; the magnetic field is everywhere parallel to Ox_1 but is not a uniform field in the classical sense; and this magnetic field generates an orthogonal gravitational field which for large x_2 is equal to that of a line-mass of unit density along Ox_1 .

§4. MAGNETIC FIELDS OF CERTAIN STEADY CURRENTS

Solutions for certain axially symmetric fields of steady currents may be written down from (3.5) if the magnetic field be represented by the scalar magnetic potential for the magnetic shell equivalent to a current wire.

As an example, let us consider a circular loop of wire carrying a steady current j . If we take the centre of the circle at the origin of coordinates, and $x_1 = 0$ as the plane of the loop, Weyl's form of the line-element (3.4) may be used and g_{44} is given by (3.5), in which ψ is the classical potential corresponding to the equivalent magnetic shell. Evaluating the integral in (3.5) and putting $A - \frac{1}{4} B^2 = D^2$, we find

$$e^e = D^2 \sec^2 [D(\psi + c)], \quad \dots\dots(4.1)$$

where c is a constant of integration. For the multi-valued potential ψ we may write $\psi = \psi_0 + 4n\pi j$, where ψ_0 is the single-valued part of ψ and n is an integer. Assuming that the g_{ij} , which determine the line-element, must be single-valued, we must replace ψ in (4.1) by ψ_0 , so that

$$g_{44} = D^2 \sec^2 [D(\psi_0 + c)]. \quad \dots\dots(4.2)$$

To obtain the complete solution it would be necessary to find λ from the field equations associated with (3.5). It was shown in I that a function λ always exists when ρ and ϕ are given by (3.5), but we do not bother to determine it here since it will not be needed in what follows.

For large x_1, x_2 we know that $\psi_0 \sim \pi a^2 j x_1 (x_1^2 + x_2^2)^{-3/2}$, and by choosing $D=1, c=0$ we find that (4.2) gives $g_{44} \sim 1 + \psi_0^2$. This is of the same form as (3.11), and it shows that the gravitational field of a current loop without mass is the same at large distances as that of a magnetic dipole without mass. We cannot use this method to obtain a solution for a current loop with mass because a different choice of arbitrary constants D and c gives a solution referring to a field whose mass source is a mass dipole shell. However, as in the case of a magnetic dipole, it seems plausible to suppose that the asymptotic form of g_{44} for a current loop of mass m is

$$g_{44} \sim 1 - \frac{2m}{r} + \frac{\pi^2 a^4 j^2 x_1^2}{r^6},$$

which is similar to (3.12) for a magnetic dipole with mass. This suggests that we may extend to gravitational fields the well-known classical result concerning the equivalence at great distances of a magnetic dipole and a current loop.

One might expect that there would be a solution of the field equations corresponding to an infinite straight wire carrying a steady current. Indeed, Mukherji (1938) gave a solution which he considered to refer to this case. Using pseudo-cylindrical coordinates and supposing the wire to lie along the axis of symmetry Oz , Mukherji assumed that the field depended only on the radial coordinate r , and took the line-element in the form

$$ds^2 = -e^\lambda dz^2 - e^\mu (dr^2 + r^2 d\theta^2) + e^e dt^2, \quad \dots\dots(4.3)$$

where λ, μ and ρ depend on r only. The only non-zero component of F_{ij} is $F_{12} (= -F_{21})$, and this also depends only on r . Mukherji obtained the most general solution of the field equations (2.1)–(2.4) on these assumptions, and this involved three significant arbitrary constants M, a and j , which were interpreted as the mass per unit length of the wire, the radius, and the current respectively. It seems reasonable to impose as boundary conditions, first, that the components of the Riemann–Christoffel tensor shall tend to zero as $r \rightarrow \infty$, and secondly, that for large r the magnetic flux shall be that of a classical line-current and the gravitational field that of a line-mass. If one does this, one finds that the first condition is satisfied, but the magnetic flux in the solution does not tend to the classical value, and an application of the relativistic form of Gauss's theorem (Whittaker 1935) shows that M cannot be interpreted as the mass per unit length. Moreover, it does not seem to be possible to transform the solution into a form in which these difficulties are removed without introducing singularities to which no meaning can be attached.

I tried to find a more satisfactory solution corresponding to a line-current first by allowing λ, μ and ρ in (4.3) to depend on θ as well as on r and, secondly, by taking the line-element in the form

$$ds^2 = -e^\lambda (dr^2 + dz^2) - r^2 e^\mu d\theta^2 + e^e dt^2 \quad \dots\dots(4.4)$$

and allowing λ, μ and ρ to depend on r and z ; in both cases F_{12} was assumed to be a function of r only. In the first case the general solution of the field equations was found, and although it could be made to satisfy the boundary conditions given

above, the g_{ij} were found to be multivalued or to have singularities to which no physical significance could be ascribed. With the second approach I did not succeed in obtaining the general solution corresponding to the line-element (4.4), but I found that no satisfactory solutions exist in which each of the g_{ij} is a product of a function of r and a function of z .

§ 5. CONCLUSION

It is relevant to consider the present status of the relativistic electromagnetic theory which is given by the field equations (2.1)–(2.4). The usual objections to it are that it does not satisfactorily weld together gravitation and electromagnetism because the electromagnetic field, which is introduced in a rather artificial way by means of the tensor E_{ij} , does not arise naturally from the field variables g_{ij} ; and that it does not describe any of the phenomena of the quantum theory. The second criticism is irrelevant if one regards the scope of the theory as the unification of gravitation and Maxwell's theory, which seems to be a reasonable first objective for a unified theory, and one which might lead to measurable predictions, not on the atomic scale, but perhaps of an astrophysical nature. The first objection still holds, but in the absence of a successful, more coherent union of the gravitational and electromagnetic fields, the theory would still be of value if it could be shown to describe satisfactorily the phenomena with which it is concerned; and it might help to indicate the lines on which a better theory could be constructed. It is well known that the theory gives Maxwell's equations in first approximation, reduces to general relativity in the absence of electromagnetic fields, and entails the Lorentz equations of motion.

Considering the work described here, and also in I, from this point of view, we observe that, among the static fields, there is a wide range of solutions which correspond with classical theory. These include the point electric charge, electric and magnetic dipoles, uniform fields, and other members of the classes (3.3) and (3.5) which apply, with appropriate modifications, to both electric and magnetic fields. No satisfactory solution referring to the field of an infinite line-current has been found, but a solution has been shown to exist for a circular current loop without mass, and this corresponds at large distances with that of a magnetic dipole, as in classical theory.

There is also a number of solutions, of which (3.13) is an example, which have no classical analogues. The physical circumstances in which these could apply are obscure, but they do not at present involve any conflict with observation and so need not be considered as a serious fault in the theory.

It therefore appears that the description by relativistic electromagnetic theory of the fields considered here may be regarded as adequate.

REFERENCES

- BONNOR, W. B., 1953, *Proc. Phys. Soc. A*, **66**, 145.
 EDDINGTON, A. S., 1924, *The Mathematical Theory of Relativity* (Cambridge: University Press).
 MAJUMDAR, S. D., 1947, *Phys. Rev.*, **72**, 390.
 MUKHERJI, B. C., 1938, *Bull. Calcutta Math. Soc.*, **30**, 95.
 PAPAPETROU, A., 1947, *Proc. Roy. Irish Acad.*, **51**, 191.
 SYNGE, J. L., 1936, *Proc. Roy. Soc. A*, **157**, 434.
 WEYL, H., 1917, *Ann. Phys., Lpz.*, **54**, 117.
 WHITTAKER, E. T., 1935, *Proc. Roy. Soc. A*, **149**, 384.

The Mayer Theory of Condensation Tested Against a Simple Model of the Imperfect Gas

By H. N. V. TEMPERLEY

King's College, Cambridge, and University of Nebraska

MS. received 10th April 1953, and in final form 21st October 1953

Abstract. A very simple model of an imperfect gas, analogous to the Weiss model of a ferromagnetic, is used to check various conflicting conclusions about the relationship between the condensation of an imperfect gas and the divergence of Mayer's virial series. For this model, the divergence of the virial series has *no* physical significance, and the interpretations of this divergence suggested by Mayer and by Born and Green are both incorrect. The model also turns out to be one for which care is necessary in going to the limit of a very large assembly.

§ 1. INTRODUCTION

A FUNDAMENTAL advance was made by Mayer and his collaborators (Mayer 1937, Mayer and Harrison 1938, Mayer and Goeppert-Mayer 1940), by showing that the phenomenon of condensation was closely related to the singularities of power series expansions of the partition function. The mathematical treatment was improved by Born and Fuchs (1938) and a number of other papers on the same problem have been published by other workers, e.g. Kahn and Uhlenbeck (1938), Fowler and Guggenheim (1939), Born and Green (1947 a, b), Rodriguez (1949), Zimm (1951), Katsura and Fujita (1951), Yang and Lee (1952) but there are many points of disagreement about the interpretation of the results.

Much of this disagreement seems to result from the fact that the partition function has never been precisely evaluated in any case of physical interest. One important feature, the behaviour of the partition function as a function of density, becomes a matter of conjecture as soon as the liquid state is approached. It therefore seems opportune to call attention to the fact that there does exist a simple physical model, not too far removed from physical reality, for which precise conclusions can be drawn about some of these controversial matters. The model is analogous to the Weiss model of a ferromagnetic, and will be shown to be practically equivalent to that of attracting rigid spheres.

It seems to be clearly established that the isotherms of the imperfect gas can be described by means of the equations

$$P = kT \sum_i b_i Z^i \quad \dots\dots(1a)$$

where Z is determined by

$$1 = \sum_i i b_i Z^i. \quad \dots\dots(1b)$$

These equations may be shown to be mathematically equivalent to

$$Pv = kT \left[1 - \sum_k \frac{k}{k+1} \beta_k v^{-k} \right] \quad \dots\dots(2a)$$

$$Z = \frac{1}{v} \exp \left(- \sum_k \beta_k v^{-k} \right) \quad \dots\dots(2b)$$

as long as all these series are convergent. In these equations $v = V/n$ and the b_i 's and β_k 's are the cluster integrals and irreducible cluster integrals defined by the Mayers (1940). The points at issue seem to be:

(a) The physical interpretation of the densities and temperatures at which the series (1) and (2) diverge. For a given T , the two types of series will not necessarily diverge at the same value of v .

(b) The question whether it is mathematically and physically correct to treat the b 's and β 's as independent of n .

(c) The mathematical form of the isotherms in the neighbourhood of the critical temperature.

The Mayers (1940) attempt to answer these questions by guessing the probable behaviour of the b 's and β 's as functions of temperature, while Born and Green (1947 a, b) derived approximate expressions for the β 's from their integral equation. Unfortunately, the two pictures of the critical region differ widely, and, although other workers have directed attention to important points, Kahn and Uhlenbeck (1938), Born and Fuchs (1938), Zimm (1951), Katsura and Fujita (1951), further progress with the problem seems unlikely in the absence of physically reasonable models for which precise information about the cluster integrals can be obtained.

Yang and Lee (1952) work with such a model, 'the lattice gas', analogous to the Ising model of a ferromagnet, the vessel being supposed divided into compartments of size V/N , ($n < N$) the interaction energy between two molecules being supposed to be positive infinite if they are in the same compartment, negative if they are in neighbouring compartments and zero otherwise. This is a crude approximation to a Lennard-Jones type of interaction, but the explicit results obtainable with the two-dimensional version of this model are physically very suggestive. They show that the critical and condensation temperatures are indeed determined by the divergence of series (1), and that in the liquid region, these series can be replaced by algebraically equivalent series in *inverse* powers of the variable Z , and they thus avoid having to consider explicitly any possible variation of the b 's with N . They also show that singularities of the series (1) can only occur on the unit circle of the variable Z , and this seems to rule out, for this special model, the possibility of a 'lower' critical temperature associated, in the manner suggested by the Mayers (1940), with the divergence of series (2). Unfortunately, the b 's and β 's are not known explicitly, so we cannot yet say whether, in this special model, series (2) always diverge at the same density as series (1), or whether, as in the model we shall consider below, series (2) only diverge in the physically irrelevant case in which all compartments are filled ($n = N$).

It has further been shown (Temperley 1952) that this model has a finite 'boundary tension' (the two-dimensional analogue of surface tension) that persists right up to the critical temperature. The Mayers' suggestion (1940) of the existence of a lower critical temperature (the surface tension vanishing before the densities become equal) is therefore untenable for this special model.

§ 2. THE 'LATTICE GAS' MODEL WITH LONG RANGE INTERACTIONS

It seems of interest to examine the consequences of the 'lattice gas' model in which, in contrast to Yang and Lee (1952), we assume the attractive forces between molecules to be of *very long* range. In other words, we suppose the

volume V to be divided into N compartments as before, and that it contains n molecules, the interaction energy between any two of which is $+\infty$ when they are in the same compartment, $-\epsilon$ when they are in different compartments. To get sensible physical results, it is necessary to suppose that, as N and V become large, $N\epsilon$ remains constant and equal to E_0 , which is comparable with kT_c . (A similar assumption is implied in the Weiss theory of ferromagnetism, where we assume that the 'effective field' is independent of the size of the assembly.) On this understanding we can calculate explicitly the limiting form of the irreducible cluster integrals, assuming that V/N remains constant as $N \rightarrow \infty$. For this model the integrals change in an obvious way to sums, integration over the coordinates of a molecule being replaced by placing it in turn in all possible compartments. We must remember to consider configurations where two or more molecules are in the same compartment, because the Mayer expression

$$f_{ij} = \exp(E_{ij}/kT) - 1$$

is then -1 and not zero. For β_1 we have

$$\beta_1 = \frac{1}{V} \left[(-1)V \frac{V}{N} + \left\{ \exp\left(\frac{\epsilon}{kT}\right) - 1 \right\} V \left(V - \frac{V}{N}\right) \right]$$

because, when two molecules are in the same compartment the first may be anywhere in the volume, but integration over the coordinates of the second molecule then contributes a factor V/N , while, if they are known to be in different compartments, the corresponding factors are V and $V - V/N$. Thus we have

$$B_1 = -\frac{V}{N} \left[1 - \frac{E_0}{kT} + O\left(\frac{1}{N}\right) \right] \quad \text{where } E_0 = N\epsilon.$$

For β_2 we have

$$\begin{aligned} \beta_2 &= \frac{1}{2V} \left[(-1)V \left(\frac{V}{N}\right)^2 + 3 \left\{ \exp\left(\frac{\epsilon}{kT}\right) - 1 \right\}^2 (-1)V \frac{V}{N} \left(V - \frac{V}{N}\right) \right. \\ &\quad \left. + \left\{ \exp\left(\frac{\epsilon}{kT}\right) - 1 \right\}^3 V \left(V - \frac{V}{N}\right) \left(V - \frac{2V}{N}\right) \right] \\ &= -\frac{1}{2} \left(\frac{V}{N}\right)^2 \left[1 + O\left(\frac{1}{N}\right) \right]. \end{aligned}$$

Continuing this process, we can show quite generally that, as $N \rightarrow \infty$, the only significant contribution to β_k is $-k^{-1}(V/N)^k$ which arises when all $k+1$ molecules are in a single compartment. If we remove one molecule to another compartment, we gain a factor N in the integration, but we at the same time introduce at least two extra factors $\exp(\epsilon/kT) - 1$ because, in the irreducible clusters (with the single exception of β_1), every molecule is bound to the remainder of the cluster by at least two links, and since ϵ/kT is of order $1/N$ we lose, on balance, a factor of at least N .

We recall the analogous problem in magnetism, given n 'positive' magnets and $N-n$ 'negative' magnets of moment μ in an external field H , I being proportional to the total magnetization or to $(2n-N)/N$. The solution of this problem is well known to be given by

$$\begin{aligned} I/N\mu &= \tanh\left(\frac{\mu H + \mu \lambda I}{kT}\right) \\ \text{or} \quad \frac{(2N-4n)\lambda\mu^2 - 2\mu H}{kT} &= \log\left(1 - \frac{n}{N}\right) - \log\left(\frac{n}{N}\right). \end{aligned}$$

The corresponding result for the lattice gas is eqn (2b) and we make transcriptions (analogous to those deduced by Yang and Lee (1952) for nearest neighbour interactions) $n \rightarrow V/v$, $\exp \{(2\mu H - 2N\mu^2\lambda)/kT\} \rightarrow ZV/N$, $4N\mu^2\lambda \rightarrow E_0$.

From this we deduce
$$Z = \frac{1}{v} \exp \left(- \sum_k \beta_k v^{-k} \right) \quad \dots (3a)$$

with
$$\beta_1 = -\frac{V}{N} \left(1 - \frac{E_0}{kT} \right), \quad \beta_k = -\frac{1}{k} \left(\frac{V}{N} \right)^k \quad \text{for } k > 1.$$

The corresponding virial equation may be written in the form

$$P + \frac{a}{v^2} = -\frac{kT}{b} \log \left(1 - \frac{b}{v} \right), \quad \text{with } a = \frac{1}{2} \frac{E_0 V}{N}, \quad b = \frac{V}{N} \quad \dots (3b)$$

which resembles the van der Waals equation or that for rigid spheres.

§ 3. THERMODYNAMIC PROPERTIES OF THIS CRUDE MODEL

Our derivation has shown that eqns (3a) and (3b) should really be supplemented by the condition that, for a finite assembly, the β 's must be corrected by terms of order $1/N$. We recall the Mayers' relation (1940) between the two types of cluster integral

$$l^2 b_l = \sum_{n_k} \frac{(l\beta_1)^{n_1}}{n_1!} \frac{(l\beta_2)^{n_2}}{n_2!} \dots \quad \text{with } \sum_k k n_k = l - 1.$$

This shows that the omission of these correcting terms in the β 's *may* affect the values of the b_l 's as soon as l becomes comparable with N , because the product of N factors of the type $1 + O(1/N)$ is not necessarily equal to unity. The fact that in a 'hard-core' type of model there is a limit, N , to the permissible number of molecules in a cluster, also leads us to expect that the analytic form of b_l should change as l approaches the value of N .

A further reason for expecting such a dependence of the higher b_l 's on the density was pointed out by Kahn and Uhlenbeck (1938) and by Yang and Lee (1952). If we suppose that all the b_l 's are density-independent, the theory predicts a flat isotherm down to $v=0$, that is, an infinite density for the liquid phase. This difficulty disappears if we admit that the higher b_l 's are *always* functions of the density. Such b_l 's do not affect any physical results until we are actually in the condensation region, series (1b) being 'just about to' diverge. Put in another way, if we express the isotherms in the form (2a), it does not necessarily follow that we omit the correcting terms in the β_k 's, even though any *one* such correction vanishes as the assembly becomes very large. Although the correcting terms vanish at least as fast as $1/N$, the series that they form *may* have a singularity for a value of v at which the series formed by the main terms in (2a) still converges, so that we can reach no conclusion about the temperature at which $\partial P/\partial v$ first becomes discontinuous. The isotherm in the form (1a) is based on a proper averaging over *all* regions of configuration space. As has been pointed out by many workers, such a process can predict only *one* value for such a quantity as the pressure at any given temperature and density.

It remains to consider what status is to be accorded to equations such as (2) and (3). They are clearly correct for the entire vapour phase, that is until series (1b) is about to diverge, because the treatments in term of the b 's and β 's are mathematically equivalent as long as both types of series converge. Born and Green (1947a,b) and Rodriguez (1949) maintain that appropriate analytic

continuations of the virial series can be used to describe the vapour and liquid phases even after this series diverges, and they interpret the density and temperature at which divergence occurs as representing the extreme limits of survival for a superheated liquid. The Mayers (1940) identify the divergence of the series (3*b*) as heralding the appearance of surface tension. For the model we have just considered neither of these contentions can possibly be correct and they therefore cannot be relied on in general, the series (3*b*) remaining perfectly convergent down to $v=b$, the lowest permissible value of v . At low enough temperatures, (3*b*) includes a physically impossible rising portion, but not any actual singularity for $v>b$.

In mathematical language, we have two distinct limiting processes to carry out, namely making our number of molecules very large and making our vessel very large, these operations corresponding respectively to $n \rightarrow \infty$ and N or $V \rightarrow \infty$ (Kahn and Uhlenbeck 1938, Katsura and Fujita 1951). Physically, these limiting processes should be carried out in such a way that V/n remains constant. If we could do this, proper account of the correcting terms in the β 's would be automatically taken and we would probably be led to an isotherm of Mayer rather than van der Waals type. If, however, we let N and n tend to infinity independently, the correcting terms in the β 's are neglected, and we are led to eqn (3*b*) which is of a kind that cannot arise from an absolutely correct averaging over configuration space. (This incorrect method of taking limits includes configurations for which $n>N$, which are impossible for any 'rigid core' model.) We therefore assert that (a) equations such as (3) *need* not have any significance in the liquid region, because they cannot be validly deduced from (1) unless these series converge, (b) their divergence *need* not have any physical significance whatever.

We have used the extremely crude model just discussed as a 'particular negative', to show that certain conjectures and assertions are certainly *not* correct for *all* models that predict a condensation phenomenon. It should be emphasized that none of this discussion invalidates Mayer's formal results. It remains true that Mayer *et al.* have, in principle, solved the problem of the imperfect gas and liquid. All the equilibrium properties follow if the cluster integrals are known, and they can, in principle, all be calculated. What does emerge is that mistakes may arise if we use the limiting form of these cluster integrals for a very large assembly in attempting to discuss a finite one. We have thus confirmed, with an actual *model*, the validity of the point made by Katsura and Fujita (1951). (They give only a *set of functions* whose behaviour resembles that of a set of cluster integrals.)

§ 4. CONCLUSIONS

1. The generally accepted result that the condensation of a vapour is associated with the appearance of singularities in series such as those appearing in eqn (1) is confirmed. In principle, actual discontinuities in the shape of the isotherm may occur here, or at a lower temperature.

2. The use of a series such as (2) is not necessarily even an approximation for the liquid phase unless explicit account of the variation of the cluster integrals with density can be taken.

3. The divergence of series such as (2) does not necessarily have any physical significance, and the two suggested interpretations of it are incorrect for the model studied, so neither can be of *general* validity.

ACKNOWLEDGMENTS

This work was carried out during my stay at Yale for part of the academic year 1952/3. I wish to thank the Chemistry Department for its hospitality and Professors J. G. Kirkwood and L. Onsager for helpful discussions. I also wish to thank the United States Congress and King's College, Cambridge, for research grants.

Note added in proof. The recent work of Schneider and Attack, reported at the Paris Conference on Phase Changes in 1952, strongly suggests that there would be no 'two-density, no meniscus' region of temperature observed experimentally if the effect of gravity could be eliminated. This work, in conjunction with the work of Yang and Lee (1952) on attractive forces of *very short* range, and with that of the present paper on attractive forces of *very long* range, seems to make the hypothesis of a second critical temperature unnecessary.

REFERENCES

- BORN, M., and FUCHS, K., 1938, *Proc. Roy. Soc. A*, **166**, 391.
BORN, M., and GREEN, H. S., 1947 a, *Proc. Roy. Soc. A*, **189**, 103; 1947 b, *Ibid.*, **190**, 455.
FOWLER, R. H., and GUGGENHEIM, E. A., 1939, *Statistical Thermodynamics* (Cambridge: University Press).
KAHN, B., and UHLENBECK, G. E., 1938, *Physica*, **5**, 399.
KATSURA, S., and FUJITA, H., 1951, *Progr. Theor. Phys.*, **6**, 498.
MAYER, J. E., 1937, *J. Chem. Phys.*, **5**, 399.
MAYER, J. E., and GOEPPERT-MAYER, M. G., 1940, *Statistical Mechanics* (New York: Wiley).
MAYER, J. E., and HARRISON, S. F., 1938, *Chem. Phys.*, **6**, 87.
RODRIGUEZ, A. E., 1949, *Proc. Roy. Soc. A*, **196**, 73.
TEMPERLEY, H. N. V., 1952, *Proc. Camb. Phil. Soc.*, **48**, 683.
YANG, C. N., and LEE, T. D., 1952, *Phys. Rev.*, **87**, 404, 410.
ZIMM, B. H., 1951, *J. Chem. Phys.*, **19**, 1019.

Spherical Tensors in Physics

By M. E. ROSE

Oak Ridge National Laboratory, Oak Ridge, Tennessee, U.S.A.

MS. received 19th October 1953

Abstract. Irreducible tensors in the spherical coordinate representation, in contrast to the cartesian representation, are discussed. The greater simplicity of this representation, especially when one deals with eigenstates of particles or radiation fields of sharp angular momentum, is emphasized. Applications to the theory of beta-transitions, gamma-ray emission, angular correlation and the static interaction of a multipole with a surrounding spin system or field are considered.

§ 1. INTRODUCTION

IT is customary in physics to think of a tensor defined in terms of its cartesian components. Very familiar examples are the stress or strain tensors of elasticity theory, the dipole, quadrupole and other multipole moments of a charge distribution and the operators which occur in the theory of forbidden beta-transitions (Konopinski and Uhlenbeck 1941). In fact, there seems to be a fairly widespread misconception that, by definition, a tensor must necessarily be represented in cartesian form. Actually, for most problems of current interest, this is not the convenient representation, and an equivalent and far more appropriate representation is obtained by using the spherical tensors. This is especially the case wherever one deals with states of sharp angular momentum and properties of the eigenstates under three-space rotations and inversion (conservation of angular momentum and parity) are relevant. A general definition of a tensor in the spherical representation is given below in eqns (5) and (6). At this point we may remark that these are not new constructs, and various special forms of these tensors, in one form or another, have been used on a number of occasions. Apart from the rather trivial case of spherical surface or solid harmonics, which constitute one particular variety of spherical tensor, we make special mention of tensors introduced in the work of Racah (1942) wherein the algebra appropriate for these tensors was established. The pertinence of the Racah algebra is not diminished by the fact that the tensors he defined explicitly are less general than those considered below. Although Racah's chief concern was the application to atomic spectroscopy, his results, of course, apply with equal force to a large variety of problems. Explicit use of the spherical tensors in the theory of angular correlation has been made by Biedenharn and Rose (1953)—see below. The full scale introduction of these tensors in the theory of beta-decay has been made by Rose and Osborn (1954 a, b) and, from this work, it is apparent that the theory of γ -ray emission is, in a sense, a special case of the beta-decay theory and is most simply expressed in terms of the spherical

tensor representation. The application of these tensors in the theory of beta-decay also appears in the work of Spiers and Blin-Stoyle (1952). Further applications, including the static interaction of a nuclear spin with a surrounding field, will be found in §3.

§2. PROPERTIES OF THE SPHERICAL TENSORS

We begin by considering the spherical tensors in a special context. As is customary, we define a tensor of first rank as a set of (three) functions which transform under the three-space group like the components of the coordinate vector. The spherical components of any vector \mathbf{A} , or first rank tensor, are A_μ where

$$A_{\pm 1} = \mp \frac{1}{\sqrt{2}}(A_x \pm iA_y); \quad A_0 = A_z, \quad \dots\dots(1)$$

which can be thought of as the new components of a vector, the original components of which are A_x, iA_y, A_z , after a rotation about the z axis. Thus the coordinate vector \mathbf{r} can be written as

$$r_\mu = \left(\frac{4\pi}{3}\right)^{1/2} y_1^\mu(\mathbf{r}), \quad \dots\dots(2)$$

where y_L^M is one of the $2L+1$ solid harmonics of degree L . For $y_L(\mathbf{A})$ when the components of the vector \mathbf{A} do not commute one must complete the definition by what amounts to a symmetrization prescription. This is done below in §3. The definition of y_L^M is $r^L Y_L^M$, where the surface harmonic Y_L^M differs from that used in many places (Rose 1937) by a factor $(-)^M$. Under rotation we have

$$r_\mu' = \sum_m r_m D_{m\mu}^1(\alpha\beta\gamma) \quad \dots\dots(3)$$

where the prime indicates the components in the rotated system and $D_{m\mu}^1$ are the elements of the three-dimensional representation of the rotation group (Wigner 1931). In (3) α, β, γ are the Euler angles of the rotation. Similarly any tensor of first rank will transform under D^1 . Thus $y_1^\mu(\mathbf{A})$ for any vector \mathbf{A} is a first rank tensor.

To generate tensors of higher rank one uses the transformation rule for direct products of lower rank tensors. However the only interest in the present case is in irreducible tensors. Thus for the coordinate vector the irreducible second rank tensor is

$$R_{ij} = x_i x_j - \frac{1}{3} r^2 \delta_{ij} \quad \dots\dots(4)$$

or, more generally,

$$T_{ij} = \frac{1}{2}(a_i b_j + a_j b_i - \frac{2}{3} \mathbf{a} \cdot \mathbf{b} \delta_{ij}) \quad \dots\dots(4')$$

where a_i, b_j , etc. are cartesian components of first rank tensors. Both R_{ij} and T_{ij} transform with D^2 , the five dimensional representation of the rotation group.

We may proceed to the general case at once by asserting that if a tensor of rank one is defined, one can obtain all tensors of higher rank from the definition

$$T_\lambda^M = \sum_{M_1} C(L_1 L_2 \lambda; M_1 M_2) T_{L_1}^{M_1} T_{L_2}^{M_2}. \quad \dots\dots(5)$$

Here $C(L_1 L_2 \lambda; M_1 M_2)$ is a vector addition or Clebsch-Gordan coefficient (Condon and Shortley 1935). In another notation this coefficient is identical with $(L_1 L_2 M_1 M_2 | L_1 L_2 \lambda M_1 + M_2)$ and the alternative notation is adopted in the interest of brevity. Note that in (5) $C=0$ unless $M_1 + M_2 = M$. The C -coefficients are real and unitary. Equation (5) defines a tensor of rank λ in

terms of two tensors of rank L_1 and L_2 and, for the purpose of the definition, $L_{1,2} < \lambda$. To complete the definition we set

$$T_1^M(\mathbf{A}) = \mathcal{Y}_1^M(\mathbf{A}). \quad \dots\dots(6)$$

The linear combination of $T_{L_1} T_{L_2}$ which appears in (5) assures the property of irreducibility: T_λ^M transforms under D^λ , the $(2\lambda + 1)$ -dimensional representation of the rotation group. Thus with

$$(T_{L_1}^{M_1})' = \sum_{\mu_1} T_{L_1}^{\mu_1} D_{\mu_1 M_1}^{L_1}$$

and similarly for $T_{L_2}^{M_2}$ we have

$$(T_\lambda^M)' = \sum_{M_1 M_2} C(L_1 L_2 \lambda; M_1 M_2) D_{\mu_1 M_1}^{L_1} D_{\mu_2 M_2}^{L_2} T_{L_1}^{\mu_1} T_{L_2}^{\mu_2}.$$

We use the Clebsch-Gordan series:

$$D_{\mu_1 M_1}^{L_1} D_{\mu_2 M_2}^{L_2} = \sum_\nu C(L_1 L_2 \nu; \mu_1 \mu_2) C(L_1 L_2 \nu; M_1 M_2) D_{\nu M}^\nu$$

with $\mu = \mu_1 + \mu_2$, $M = M_1 + M_2$. The sum over M_1 with fixed M can be done at once with

$$\sum_{M_1} C(L_1 L_2 \lambda; M_1 M_2) C(L_1 L_2 \nu; M_1 M_2) = \delta_{\lambda \nu}$$

and then

$$\begin{aligned} (T_\lambda^M)' &= \sum_{\mu_1 \mu_2} D_{\mu M}^\lambda C(L_1 L_2 \lambda; \mu_1 \mu_2) T_{L_1}^{\mu_1} T_{L_2}^{\mu_2} \\ &= \sum_\mu T_\lambda^\mu D_{\mu M}^\lambda \quad \dots\dots(7) \end{aligned}$$

which is the required result.

Two additional remarks need to be made concerning (5). The restriction $L_1, L_2 < \lambda$ is convenient for purposes of definition, but with any possible set of L_1, L_2 and λ eqn (5) is a valid relation between spherical tensors. The possible values of L_1, L_2 and λ are those for which these three numbers form a triangle: $|L_1 - L_2| \leq \lambda \leq L_1 + L_2$. This condition, which is briefly referred to as $\Delta(L_1 L_2 \lambda)$, is implied by the C -coefficient. Secondly, the tensor T_λ^M should carry a number of additional indices. Thus T_λ^M depends on L_1 and L_2 , and the tensors $T_{L_1}^{M_1}$, $T_{L_2}^{M_2}$ also depend on additional (angular momentum) indices, depending on their manner of construction. It is clear that such a complete notation would be very cumbersome and is actually unnecessary for most purposes. In addition, our notation, at this point, does not explicitly indicate the fact that T_λ^M depends on one or more vector arguments. For instance, if $T_{L_1}^{M_1}$ depends on $\mathbf{A}_1, \mathbf{A}_2 \dots \mathbf{A}_{n_1} (n_1 \leq L_1)$ and $T_{L_2}^{M_2}$ depends on $\mathbf{B}_1, \mathbf{B}_2 \dots \mathbf{B}_{n_2} (n_2 \leq L_2)$, then T_λ^M depends on the indicated $n_1 + n_2$ vector arguments. In the present context it is unnecessary to encumber the notation with this complication.

The parity of T_λ^M can be ascertained immediately when the argument vectors are specified. Thus, let $\pi(\mathbf{A}_i)$ be the parity of \mathbf{A}_i and similarly for $\pi(\mathbf{B}_i)$. Then the parity of T_λ^M is

$$\pi = \pi^{n_1}(\mathbf{A}_1) \pi^{n_2}(\mathbf{A}_2) \dots \pi^{m_1}(\mathbf{B}_1) \pi^{m_2}(\mathbf{B}_2) \dots$$

where now n_i, m_i represent the number of times $\mathbf{A}_i, \mathbf{B}_i$ occur in $T_{L_1}^{M_1}, T_{L_2}^{M_2}$ respectively. That is, each of these tensors is a homogeneous function of $\mathbf{A}_i \dots$ and $\mathbf{B}_i \dots$ of degree n_i and m_i respectively.

It is important to realize just how the tensors will appear in any given physical problem. In many cases one is interested in an interaction between components of a system. Specific cases are the beta-decay interaction where the coupling between nucleon sources and electron-neutrino field is the prime consideration,

the coupling between charged particles (with or without spin) and an electromagnetic field and the static coupling to a multipole field of a particle with spin. These are all rotationally invariant and the interaction will appear in the form

$$\sum_M (-)^M T_\lambda^M(\mathbf{A} \dots) T_\lambda^{-M}(\mathbf{B} \dots) \quad \dots\dots(8)$$

where $\mathbf{A} \dots$ and $\mathbf{B} \dots$ represent two (in general, different) sets of vector operators. Alternatively, one may have

$$\sum_M T_\lambda^M(\mathbf{A} \dots) T_\lambda^{M*}(\mathbf{B} \dots) \quad \dots\dots(9)$$

where * means complex conjugate. That both (8) and (9) are invariant follows immediately from (7) and the unitary property of the D -matrices: $DD^+ = D^+D = 1$. A special case of (8) is the scalar product of two first rank tensors

$$\mathbf{A} \cdot \mathbf{B} = \sum_m (-)^m A_m B_{-m}.$$

The parity π of the operators (8) or (9) is, of course, the product of the parities of the operators occurring therein. Thus $\pi = 1(-1)$ implies that states of the same (different) parity are connected.

It is also of interest to recognize the manner in which the tensor operators enter in a particular theory. The theory of β -decay is sufficiently illustrative and, since details are presented elsewhere (Rose and Osborn 1954a), we indicate the mechanisms of the calculations in brief outline. The beta-coupling is represented in terms of an operator of the form

$$\sum_k \omega_k \cdot L(\omega') \delta(\mathbf{r} - \mathbf{r}_k) \quad \dots\dots(10)$$

where ω_k is a Dirac operator in the space of the k th nucleon (i.e. $\omega = 1, \beta, \sigma, \beta\sigma, \alpha, \beta\alpha, \gamma_5, \beta\gamma_5$). In the non-relativistic representation (Rose and Osborn 1954a) the operators $\alpha, i\beta\alpha$ and γ_5 are replaced by $(Mc)^{-1}$ times $-\mathbf{p}, \sigma \times \mathbf{p}, \sigma \cdot \mathbf{p}$ acting on the nuclear wave function, with M the nucleon mass, and $\beta\gamma_5$ is replaced by $\sigma \cdot \mathbf{p}$ acting on $L(\beta\gamma_5)$. In (10) $L(\omega')$ is a lepton covariant, $L(\omega') = \psi^* \omega' \phi$ where ψ and ϕ represent an electron, say, and a charge-conjugate neutrino, while ω' is the same as ω_k but in the lepton space. The non-relativistic approximation, referred to above, is obviously applicable only to the nucleons. Since both ψ and ϕ in a central field involve $y_L^m(\mathbf{r})$, and using the coupling rule

$$y_{l_1}^{m_1}(\mathbf{r}) y_{l_2}^{m_2}(\mathbf{r}) = \sum_L \left[\frac{(2l_1+1)(2l_2+1)}{4\pi(2L+1)} \right]^{1/2} C(l_1 l_2 L; 00) C(l_1 l_2 L; m_1 m_2) \\ \times r^{l_1+l_2-L} y_L^{m_1+m_2}(\mathbf{r}) \quad \dots\dots(11)$$

the lepton covariants can be expressed as a linear combination of $y_L^m(\mathbf{r})$. Noting that the operator ω occurs linearly and using

$$\omega_\mu = \left(\frac{4\pi}{3} \right)^{1/2} y_1^\mu(\omega) \quad \dots\dots(12)$$

one has

$$y_1^\mu(\omega) y_L^m(\mathbf{r}) = \sum_\lambda C(1L\lambda; \mu m) T_{\lambda L}^{m+\mu}(\mathbf{r}, \omega) \quad \dots\dots(13)$$

which is the inversion formula corresponding to (5). Here we have attached a second index L to the tensor T_λ to indicate the parity; thus $\pi = (-)^L \pi(\omega)$. In all cases with the exception of the pseudoscalar interaction ω and \mathbf{r} are to be regarded as commuting observables. The β -decay interaction is thereby expressed as a sum of irreducible tensors of rank λ . If the nuclear spins of

initial and final states are J_i and J_f one has $\Delta(J_i J_f \lambda)$ and $\Delta(1 L \lambda)$, so that $L = \lambda \pm 1, \lambda$. The major contribution to the β -transition occurs for the lowest value of L consistent with the parity change.

We may note at this point that the tensors introduced by Biedenharn and Rose (1953) in the discussion of angular correlations involving β -particles are essentially the tensors given above. Thus, writing

$$\Phi_{L, L-1}^M = [L(2L+1)]^{-1/2} (r \nabla + L \mathbf{r}_1) Y_L^M$$

$$\Phi_{L, L}^M = [L(L+1)]^{-1/2} (-i \mathbf{r} \times \nabla) Y_L^M$$

$$\Phi_{L, L+1}^M = [(L+1)(2L+1)]^{-1/2} (r \nabla - (L+1) \mathbf{r}_1) Y_L^M$$

where \mathbf{r}_1 is a unit vector, one finds

$$\sigma \cdot \Phi_{\lambda L}^M = \left(\frac{4\pi}{3} \right)^{1/2} T_{\lambda L}^M(\mathbf{r}_1, \sigma).$$

Incidentally $\Phi_{L, L-1}$ and $\Phi_{L, L}$ are respectively the angular part of the vector potentials of an electric 2^L and magnetic 2^L pole electromagnetic wave.

The same procedure is followed for the case of γ -ray emission. Here the interaction is

$$\mathcal{H}' = -\frac{e}{Mc} \left(\mathbf{A} \cdot \mathbf{p} + \frac{\mu \hbar}{2} \sigma \cdot \mathbf{H} \right) \quad \dots\dots(14)$$

for a particle with charge e and magnetic moment $\mu \hbar / 2Mc$. In (14) \mathbf{A} is the vector potential of a (polarized) plane wave and $\mathbf{H} = \text{curl } \mathbf{A}$. Using the well-known expansion of \mathbf{A} (and therefore \mathbf{H}) into multipole fields (Goertzel 1946) one finds

$$\mathcal{H}' = \left(\frac{16\pi^3 \hbar}{3\omega} \right)^{1/2} \frac{e}{M} \sum_{LM} \frac{(ik)^L D_{MP}^L(\mathbf{k}_1)}{(2L-1)!!} [i \mathcal{H}^m(LM) + P \mathcal{H}^e(LM)] \quad \dots\dots(15)$$

and $P = +1$ (-1) refers to a left (right) circularly polarized wave. In (15) ω is the frequency of the radiation $k = \omega/c$ and \mathbf{k}_1 is a unit vector in the propagation direction. Also $(2x+1)!! = 1.3.5 \dots (2x+1)$. The first and second terms in the square brackets in (15) refer to the contribution of magnetic and electric 2^L -poles respectively.

$$\begin{aligned} \mathcal{H}^m(LM) = & -i(2L+1)^{-1/2} T_{LL}^M(\mathbf{r}, \mathbf{p}) - \frac{1}{2} \mu \hbar \left[(L+1)^{1/2} T_{L, L-1}^M(\mathbf{r} \sigma) \right. \\ & \left. + \frac{k^2 L^{1/2}}{(2L+1)(2L+3)} T_{L, L+1}^M(\mathbf{r} \sigma) \right] \quad \dots\dots(15a) \end{aligned}$$

$$\begin{aligned} \mathcal{H}^e(LM) = & -\frac{i}{k} \left[(L+1)^{1/2} T_{L, L-1}^M(\mathbf{r}, \mathbf{p}) - \frac{k^2 L^{1/2}}{(2L+1)(2L+3)} T_{L, L+1}^M(\mathbf{r} \mathbf{p}) \right] \\ & - \frac{1}{2} \mu \hbar k (2L+1)^{-1/2} T_{LL}^M(\mathbf{r} \sigma). \quad \dots\dots(15b) \end{aligned}$$

The separate contributions due to the charge and spin are, of course, easily identified. Not all the terms in (15a) and (15b) will be equally important; in the practical case $kR \ll 1$, where R is the nuclear radius. Thus the $T_{L, L+1}$ contribution is unimportant compared with that of the $T_{L, L-1}$ contribution unless selection rules permit the matrix element of the former to exist but make that of the latter vanish.

In (15) we have the special tensors

$$T_{\lambda L}^M(\mathbf{r}, \mathbf{B}) = \sum_{\mu} C(1L\lambda; -\mu, \mu + M) \mathcal{Y}_L^{\mu+M}(\mathbf{r}) \mathcal{Y}_1^{-\mu}(\mathbf{B}) \quad \dots\dots(16)$$

with $\mathbf{B} = \sigma$ or $\mathbf{p} = -i\hbar \nabla$. In the former case the parity is $\pi = (-)^L$ and for $\mathbf{B} = \mathbf{p}$, $\pi = (-)^{L-1}$. Hence $\mathcal{H}^m(LM)$ and $\mathcal{H}^e(L \pm 1, M)$ can mix, as expected.

There will be no interference between these, however, in the total intensity. This is a direct result of the unitary property of $D^L(\mathbf{k}_1)$. It will be recognized that \mathcal{H}' is an invariant. This is evident since from the group property of the rotation matrices $D_{MP}^L(\mathbf{k}_1)$, for fixed P , is itself a tensor of rank L in \mathbf{k}_1 space. Of course (16) is a special case of (5) with $L_1=1$ due to the linear dependence of \mathcal{H}' on $\boldsymbol{\sigma}$ and \mathbf{p} . The matrix elements of these operators (15a) and (15b) have been evaluated in the j - j coupling model (Rose and Osborn 1954b).

It will be seen that for the interaction of a particle of intrinsic spin $1/2$ with a field the only operators which are apt to occur are \mathbf{r} , $\boldsymbol{\sigma}$ and \mathbf{p} . Combinations of these can conceivably enter and indeed, in β -decay, one does have the tensors $T_{\lambda, \lambda-1}(\mathbf{r}, \boldsymbol{\sigma} \times \mathbf{p})$ in the T interaction. Here $\lambda=n$, where n is the forbiddenness order. In the T and A interactions one has $T_{11}(\mathbf{r}, \boldsymbol{\sigma})$ where

$$T_{11}^M(\mathbf{A}, \mathbf{B}) = -\frac{i}{\sqrt{2}} \frac{3}{4\pi} (\mathbf{A} \times \mathbf{B})_M$$

which can be expressed in the alternative forms

$$T_{11}^M(\mathbf{A}, \mathbf{B}) = -i \left(\frac{3}{8\pi} \right)^{1/2} \mathcal{Y}_1^M(\mathbf{A} \times \mathbf{B}) = -i \left(\frac{3}{2} \right)^{1/2} T_{10}^M(\mathbf{C}, \mathbf{A} \times \mathbf{B}),$$

where \mathbf{C} is arbitrary. More generally, the T and A interactions involve $T_{\lambda\lambda}(\mathbf{r}, \boldsymbol{\sigma})$ where $\lambda=n$. In the A interaction of β -decay one also has the tensor $\mathcal{Y}_\lambda(\mathbf{r})\boldsymbol{\sigma} \cdot \mathbf{p}$ which is irreducible, of rank λ and parity $(-)^{\lambda-1}$. Here $\lambda=n-1$. Generally, if in (5) either L_1 or $L_2=0$

$$T_\lambda^M = T_0^0 T_{L_i}^{M_i} \delta_{MM_i} \delta_{\lambda L_i}$$

where $L_i \neq 0$ necessarily and T_0^0 is a scalar.

Returning to the general tensor T_λ^M of (5), but with $T_{L_i}^{M_i} = \mathcal{Y}_{L_i}^{M_i}(\mathbf{r})$, there arises the question of uniqueness of the tensor $T_\lambda^M(\mathbf{r})$. That is, if different values are given to L_1 and L_2 consistent with the condition $\Delta(L_1 L_2 \lambda)$ does one get essentially different tensors? Using eqn (11) one sees readily that, in the space of the unit vector \mathbf{r}_1 , $T_\lambda^M(\mathbf{r})$ is unique. The unitary property of the C -coefficients enables one to deduce that

$$T_\lambda^M(\mathbf{r}) = \left[\frac{(2L_1+1)(2L_2+1)}{4\pi(2\lambda+1)} \right]^{1/2} C(L_1 L_2 \lambda; 00) r^{L_1+L_2-\lambda} \mathcal{Y}_\lambda^M(\mathbf{r}). \quad \dots\dots (17)$$

All these tensors have the same rank and parity, and in most considerations only the smallest value of L_1+L_2 will be of interest. In this connection note that the C -coefficient requires the parity rule $L_1+L_2+\lambda = \text{even integer}$.

Finally, we observe that the matrix element of T_λ^M between states of sharp angular momentum can always be written (Wigner 1931)

$$(Jm | T_\lambda^M | J'm') = C(J'\lambda J; m'M)(J || T_\lambda || J') \quad \dots\dots (18)$$

which is the Wigner-Eckart theorem. The reduced matrix element $(J || T_\lambda || J')$ is independent of the magnetic quantum numbers m' , M and $m=m'+M$. The hermitian conjugation properties are not necessarily simple. However, if in (5) one writes $T_{L_i}^{M_i} = \mathcal{Y}_{L_i}^{M_i}(\mathbf{A}_i)$ and \mathbf{A}_1 commutes with \mathbf{A}_2 , it follows that

$$T_\lambda^{M*} = (-)^{M+L_1+L_2-\lambda} T_\lambda^{-M}. \quad \dots\dots (19)$$

This implies that

$$(2J'+1)^{1/2} (J' || T_\lambda || J)^* = (-)^{J'-J+\lambda+L_1+L_2} (2J+1)^{1/2} (J || T_\lambda || J') \quad \dots\dots (20)$$

where the symmetry relations of the C -coefficients have been used (Rose, Biedenharn and Arfken 1952).

§3. FURTHER APPLICATIONS OF THE SPHERICAL TENSORS

The concept of polarized harmonics has been discussed by Weyl (1949) and applied by Falkoff and Uhlenbeck (1950) to the problem of angular correlation. The relation between polarized harmonics and the spherical tensors discussed above is fairly obvious. We consider two 'polarization' processes.

The first is exemplified by the electrostatic potential due to a system of charges such that no lower moments than a 2^L pole moment exist. This potential is

$$\phi_L = (4\pi)^{1/2} (-)^L e \prod_1^L (\mathbf{a}_n \cdot \nabla) \mathfrak{D}_0(\mathbf{r}) \quad \dots\dots(21)$$

where

$$\mathfrak{D}_0(\mathbf{r}) = r^{-L-1} Y_0^L(\mathbf{r}_1) = r^{-L-1} (4\pi)^{-1/2}, \quad (L=0)$$

and $\mathbf{a}_1 \mathbf{a}_2 \dots \mathbf{a}_L$ are L arbitrary vectors. We use

$$\begin{aligned} \nabla_m Y_L^M \psi(r) &= \left(\frac{L+1}{2L+3} \right)^{1/2} C(L1L+1; Mm) Y_{L+1}^{M+m} D_- \psi \\ &\quad - \left(\frac{L}{2L-1} \right)^{1/2} C(L1L-1; Mm) Y_{L-1}^{M+m} D_+ \psi \end{aligned} \quad \dots\dots(22)$$

where ψ is any radial function and

$$D_- = \frac{d}{dr} - \frac{l}{r}; D_+ = \frac{d}{dr} + \frac{l+1}{r}. \quad \dots\dots(22')$$

It is clear that in the present instance only the first term of (22) contributes. One now defines a sequence of irreducible tensors by

$$T_\lambda^M(\mathbf{a}_1 \dots \mathbf{a}_\lambda) = \sum_\mu C(1\lambda-1\lambda; -\mu, \mu+M) y_1^{-\mu}(\mathbf{a}_\lambda) T_{\lambda-1}^{M+\mu}(\mathbf{a}_1 \dots \mathbf{a}_{\lambda-1}) \quad \dots\dots(23)$$

with $T_0^0 = 1$. Thus

$$T_1^M(\mathbf{a}_1) = y_1^M(\mathbf{a}_1)$$

and

$$T_2^M(\mathbf{a}_1 \mathbf{a}_2) = T_{21}^M(\mathbf{a}_1 \mathbf{a}_2) = T_2^M(\mathbf{a}_2 \mathbf{a}_1), \quad \dots\dots(23')$$

where $T_{21}(\mathbf{a}_1 \mathbf{a}_2)$ is defined by (16). Clearly, (23) represents the 2^λ pole moment of a charge configuration characterized by the vectors $\mathbf{a}_1, \mathbf{a}_2 \dots \mathbf{a}_\lambda$. The results (23') express the well-known symmetry of the quadrupole moment tensor, and from (21) it is clear that symmetry of $T_\lambda^M(\mathbf{a}_1 \dots \mathbf{a}_\lambda)$ with respect to any permutation of the \mathbf{a}_n holds. It is now a straightforward matter to obtain the result

$$\phi_L = (4\pi)^{1/2} e \left(\frac{4\pi}{3} \right)^{L/2} \left[\frac{L! (2L-1)!!}{(2L+1)} \right]^{1/2} \sum_M (-)^M T_L^{-M}(\mathbf{a}_1 \mathbf{a}_2 \dots \mathbf{a}_L) \mathfrak{D}_L^M(\mathbf{r}) \quad \dots(24)$$

where $\mathfrak{D}_L^M(\mathbf{r}) = r^{-L-1} Y_L^M(\mathbf{r}_1)$.

When $\mathbf{a}_1 = \mathbf{a}_2 = \dots = \mathbf{a}_L = \mathbf{r}'$ one finds the standard result

$$\phi_L = (4\pi)^{1/2} (-\mathbf{r}' \cdot \nabla)^L \mathfrak{D}_0 = L! \frac{r'^L e}{r^{L+1}} P_L(\cos \theta) \quad \dots\dots(24')$$

where θ is the angle between \mathbf{r} and \mathbf{r}' .

The second problem to be considered in this section involves the polarization process as it is usually defined. Thus we consider $T_L^M = \mathbf{l} \cdot \nabla y_L^M(\mathbf{r})$ where \mathbf{l} is a vector operator. From (22) one sees that only the second term contributes and

$$T_L^M = \left[\frac{4\pi}{3} L(2L+1) \right]^{1/2} \sum_m C(1L-1L; -m, m+M) y_1^{-m}(\mathbf{l}) y_L^{m+M}(\mathbf{r}). \quad \dots\dots(25)$$

If \mathbf{l} and \mathbf{r} commute this becomes

$$T_L^M = \left[\frac{4\pi}{3} L(2L+1) \right]^{1/2} T_{LL-1}^M(\mathbf{r}, \mathbf{l}). \quad \dots\dots(25')$$

In any case (25) defines an irreducible spherical tensor of rank L , parity $(-)^{L-1}\pi(\mathbf{l})$.

The problem of an arbitrary spin \mathbf{l} interacting with a field can now be treated. We define a new tensor $T_L^M(\mathbf{l})$ by

$$T_L^M(\mathbf{l}) = (\mathbf{l} \cdot \nabla)^L \mathcal{Y}_L^M(\mathbf{r}). \quad \dots\dots(26)$$

Again, using (22), and with the definition

$$\mathcal{J}_{\lambda\lambda-1}^\mu(\mathbf{l}) = \sum_m C(1\lambda-1\lambda; -m, \mu+m) \mathcal{J}_{\lambda-1}^{\mu+m}(\mathbf{l}) \mathcal{Y}_1^{-m}(\mathbf{l}) \quad \dots\dots(27)$$

and with $\mathcal{J}_{10}^\mu(\mathbf{l}) = \mathcal{Y}_1^\mu(\mathbf{l})$ one finds that

$$T_L^M(\mathbf{l}) = \left(\frac{4\pi}{3} \right)^{L/2} \left[\frac{L!(2L+1)!!}{4\pi} \right]^{1/2} \mathcal{J}_{L, L-1}^M(\mathbf{l}) \quad \dots\dots(28)$$

which is a tensor of rank L . In the above we have made use of the fact that \mathbf{l} and the ∇ operator commute but it has not been assumed that the components of \mathbf{l} commute with each other. For $L=2$ the tensor (28) is

$$T_2^M(\mathbf{l}) = \left(\frac{40\pi}{3} \right)^{1/2} \mathcal{J}_{21}^M(\mathbf{l}) \quad \dots\dots(29)$$

where

$$\begin{aligned} \mathcal{J}_{21}^M(\mathbf{l}) &= \sum_m C(112; -m, M+m) \mathcal{Y}_1^{M+m}(\mathbf{l}) \mathcal{Y}_1^{-m}(\mathbf{l}) \\ &= T_{21}^M(\mathbf{l}, \mathbf{l}) \end{aligned} \quad \dots\dots(29a)$$

and in this case the order of the two first degree solid harmonics $\mathcal{Y}_1(\mathbf{l})$ is irrelevant. The individual components of $\mathcal{Y}_{21}^M(\mathbf{l})$ are

$$\begin{aligned} \mathcal{J}_{21}^{\pm 2}(\mathbf{l}) &= \frac{3}{4\pi} (I_{\pm 1})^2 \\ \mathcal{J}_{21}^{\pm 1}(\mathbf{l}) &= \frac{1}{\sqrt{2}} \frac{3}{4\pi} (I_0 I_{\pm 1} + I_{\pm 1} I_0) \\ \mathcal{J}_{21}^0(\mathbf{l}) &= \frac{3}{8\pi} \left(\frac{2}{3} \right)^{1/2} (3I_0^2 - \mathbf{l}^2). \end{aligned} \quad \dots\dots(29b)$$

These correspond to the *symmetrized* second degree spherical harmonics of the spin vector \mathbf{l} .

Note that the commutation rule $\mathbf{l} \times \mathbf{l} = i\mathbf{l}$, in terms of the spherical components, takes the form

$$I_\mu I_\nu - I_\nu I_\mu = I_{\mu, \nu} \quad \mu < \nu.$$

For the interaction of two spin systems \mathbf{l} and \mathbf{j} the coupling energy will be

$$\mathcal{H}' = K \sum_M (-)^M T_L^M(\mathbf{l}) T_L^{-M}(\mathbf{j}) \quad \dots\dots(30)$$

where K is a constant. For $L=2$ this is the coupling of a (nuclear) quadrupole with a spin system (surrounding electrons) of spin \mathbf{j} (Casimir 1936).

For a (nuclear) spin embedded in a crystal lattice the system to which the spin \mathbf{l} is coupled may be treated classically (Pound 1950) and the interaction energy has the form (30) with $T_L^M(\mathbf{j})$ replaced by its expectation value. This tensor, $\langle T_L^M(\mathbf{j}) \rangle$, is simply the magnetic field for $L=1$, the gradient of the electric field for $L=2$ and higher rank tensors for $L>2$.

Of course with L equal to the tensor rank one has $L \leq 2I$. This condition is automatically expressed by the C -coefficients when one considers the matrix element of the operator (28) between two states of sharp angular momentum, I and I' . Thus, by (18), the matrix element is

$$(Im_i | T_L^M(\mathbf{I}) | I'm_i') = C(I'LI; m_i'M)(I || T_L(\mathbf{I}) || I'). \quad \dots\dots(31)$$

The reduced matrix element may be evaluated by considering a special case, and it is convenient to take $M=L$ and $m_i=I$. Then (Wigner 1931)

$$C(ILI; I-LL) = (-)^L \left[\frac{(2I+1)!(2L)!}{(2I+L+1)!L!} \right]^{1/2}.$$

Also, in (27) only $m = -1$ contributes and

$$(Im | \mathcal{Y}_1^1(I) | I'm') = - \left[\frac{3}{8\pi} (I-m_i')(I+m_i'+1) \right]^{1/2} \delta_{II'} \delta_{m_i m_i' + 1}. \quad \dots\dots(31')$$

With the value of m considered, $m_i' = I - L$ and we obtain, by repeated use of (31'), the result

$$(Im_i | T_L^M(\mathbf{I}) | I'm_i') = \delta_{II'} \delta_{m_i m_i' + M} \frac{L!}{2L} \left[\frac{1}{4\pi} \frac{2L+1}{2I+1} \frac{(2I+L+1)!}{(2I-L)!} \right]^{1/2} C(ILI; m_i'M). \quad \dots\dots(32)$$

For $L=2$ the result (32) yields the quadrupole matrix elements previously given by Pound (1950). For the interaction (30) the matrix elements are given by a product of (32) and a similar result with M replaced by $-M$ and I replaced by J . For $L=1$ the matrix elements of \mathcal{H}' are (within the constant K) just those of $(3/4\pi)\mathbf{I} \cdot \mathbf{J}$, which gives the usual hyperfine structure coupling. It is clear that the foregoing results can be directly applied to the interaction of an octupole or higher multipole with a surrounding field.

The examples of the application of spherical tensors given above are meant to be illustrative. It is evident that many other cases could be cited for which the use of these tensors would be appropriate and would greatly facilitate the calculations.

REFERENCES

- BIEDENHARN, L. C., and ROSE, M. E., 1953, *Rev. Mod. Phys.*, **25**, 729.
 CASIMIR, H. B. G., 1936, *Archives der Musée Teyler*, Series III, VIII.
 CONDON, E. U., and SHORTLEY, G. H., 1935, *Theory of Atomic Spectra* (Cambridge : University Press).
 FALKOFF, D. L., and UHLENBECK, G. E., 1950, *Phys. Rev.*, **79**, 323.
 GOERTZEL, G., 1946, *Phys. Rev.*, **70**, 897.
 KONOPINSKI, E. J., and UHLENBECK, G. E., 1941, *Phys. Rev.*, **60**, 308.
 POUND, R. V., 1950, *Phys. Rev.*, **79**, 685.
 RACAH, G., 1942, *Phys. Rev.*, **62**, 438.
 ROSE, M. E., 1937, *Phys. Rev.*, **51**, 484.
 ROSE, M. E., BIEDENHARN, L. C., and ARFKEN, G. B., 1952, *Phys. Rev.*, **85**, 5.
 ROSE, M. E., and OSBORN, R. K., 1954 a, *Phys. Rev.*, in the press; 1954 b, *Ibid.*, in the press.
 SPIERS, J. A., and BLIN-STOYLE, R. J., 1952, *Proc. Phys. Soc. A*, **65**, 801.
 WEYL, H., 1939, *The Classical Groups* (Princeton : University Press).
 WIGNER, E. P., 1931, *Gruppentheorie* (Braunschweig : Vieweg).

The Scattering of Slow Neutrons by Ferromagnetic Crystals

By G. L. SQUIRES

Atomic Energy Research Establishment, Harwell, Didcot, Berks.

MS. received 20th November 1953

Abstract. A beam of filtered neutrons with an average wavelength of 7.0 \AA has been used to measure the total cross section of iron as a function of temperature from 290°K to 1170°K . The cross section is found to have a sharp peak at the Curie temperature, 1043°K . At this temperature the measured scattering cross section is 8.6 barns, while the calculated value of the cross section due to nuclear scattering alone is 3.8 barns.

A similar experiment carried out for nickel reveals only a slight increase in the cross section at the Curie temperature, 631°K . At this temperature the calculated value for the nuclear scattering cross section is 7.5 barns. The observed additional scattering is (0.11 ± 0.05) barn.

§1. INTRODUCTION

A THEORETICAL treatment of the scattering of slow neutrons by the nuclei in a crystal was first given by Weinstock (1944). Measurements with aluminium (Cassels 1951) and magnesium (Squires 1952) show that Weinstock's theory, as extended by Cassels (1950) and Squires (1952), gives results in good agreement with observation. In the case of iron, however, the observed cross sections are larger than those predicted by the theory. This is because the theory takes account only of nuclear scattering, i.e. scattering due to the interaction of the neutron with the nuclei. The additional scattering observed in iron is due to the interaction of the magnetic moment of the neutron with the magnetic moments of the iron atoms. The success of the theory in its application to non-magnetic crystals indicates that the nuclear scattering can be calculated correctly. Measurements with iron may therefore be used to obtain information about the magnetic scattering. The cross section σ_{ns} for nuclear scattering is calculated and, on the assumption that the nuclear and magnetic scattering are not coherent, the difference between the measured scattering cross section and σ_{ns} is taken to be the magnetic cross section σ_{ms} .

The total cross section of iron for neutrons in the wavelength range 4.6 to 12 \AA has been measured by Latham and Cassels (1952), Palevsky and Hughes (1953) and by Squires (1953, unpublished). In all three experiments a neutron velocity selector was used. However, with present neutron fluxes the counting rates obtained by this method are comparatively small so that, to obtain a cross section accurate to 1% for neutrons with a wavelength of 5 \AA , it is necessary to count for about 1 hour. It is not easy to keep the temperature of the specimen constant for periods of this order. The technique is therefore unsatisfactory for iron at temperatures in the region 950°K to 1100°K where the cross section has been found to vary rapidly with temperature.

The experiments described in this paper have been carried out with a beam of thermal neutrons filtered through lead. The flux is sufficiently high to enable an accuracy to 1% in the total cross section to be attained in 40 seconds. The filtered neutrons have been used to measure the cross section of iron from 290°K to 1170°K and of nickel from 290°K to 930°K.

The effect of the lead filter is to remove neutrons with wavelengths less than 5.7 Å from the thermal beam. The relatively large range of wavelengths in the filtered beam is not a disadvantage provided the variation of cross section with wavelength is known throughout the range. For iron and nickel this condition is satisfied. Velocity selector measurements indicate that, apart from a small constant term, the cross section is directly proportional to wavelength in both cases.

§ 2. DESCRIPTION OF EXPERIMENT

2.1. Incident Neutron Beam

Two cylinders (A in figure 1), one of solid lead and one filled with lead shot were used as a filter. The thickness of lead was equivalent to 600 g cm⁻². The filter was placed in a hole in the Harwell pile, BEPO.

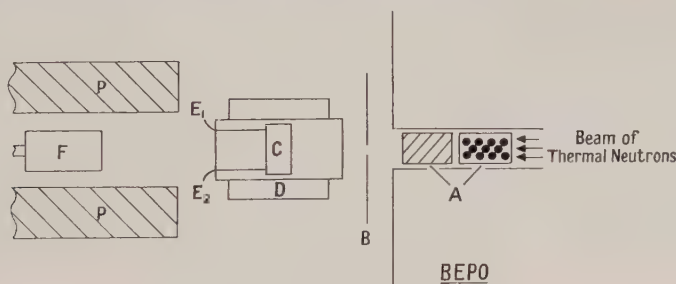


Figure 1. Arrangement of scattering apparatus. (The furnace is shown in the 'in' position.) P (shaded) consist of a mixture of paraffin wax and borax glass to shield counter from stray neutrons.

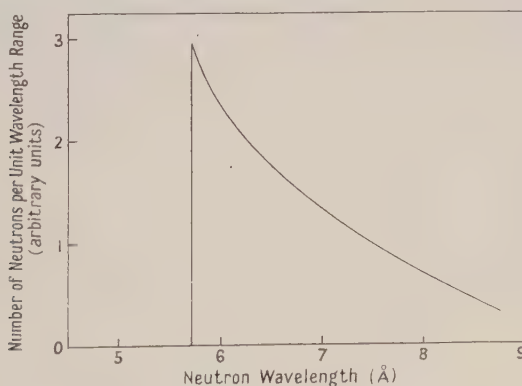


Figure 2. Wavelength distribution of neutrons emerging from lead filter.

The wavelength distribution of the neutrons emerging from the filter is shown in figure 2. To obtain the average wavelength λ_{av} the attenuation of the neutrons by a plate of gold was measured. In the wavelength range that includes

7 Å the relation between the total cross section σ_{Au} of gold and the wavelength λ has been given by Carter *et al.* (1953) as $\sigma_{\text{Au}} = (54.3 \pm 0.2)\lambda$ where σ_{Au} is in barns and λ in ångströms. This relation together with the attenuation measurements gave $\lambda_{\text{av}} = (7.00 \pm 0.04)$ Å.

In arriving at the value of λ_{av} allowance was made for the fact that the gold absorbed neutrons with long wavelengths more than those with short wavelengths. Thus the measured total cross section of the gold corresponded to a wavelength slightly less than λ_{av} . For the same reason the effective wavelength λ_{eff} , defined as the wavelength of a beam of monoenergetic neutrons for which the measured cross section would be the same as that actually obtained with the filtered beam, was slightly less than λ_{av} in the iron and nickel measurements. A small correction of the order of 2% was therefore made to the measured cross sections so that all the final cross sections given in figures 3 to 7 relate to λ_{av} .

The diameter of the beam was cut down to $\frac{1}{2}$ in. by the cadmium sheet B (figure 1). In this condition the counting rate when the beam was uninterrupted by the specimen was about 2000 counts per second.

2.2. Temperature Control and Measurement

The scattering specimen was in the shape of a disc, 2.7 in. in diameter. The iron was 99.97% pure and its mass per unit area was 7.09 g cm^{-2} . The nickel was 99.78% pure and its mass per unit area was 8.75 g cm^{-2} .

The specimen (C in figure 1) was placed in an electric furnace D which was mounted on wheels and could be set in one of two positions. In one position the beam was uninterrupted and in the other it passed through the specimen. The ends of the furnace were sealed with thin plates of aluminium so that the specimen could be immersed in an atmosphere of argon. This prevented oxidation which occurs rapidly for iron in air at temperatures above about 800°K . Argon was not used for the measurements with nickel.

The temperature was measured by means of two chromel–alumel thermocouples E_1 and E_2 , welded at their hot junctions, and screwed into the ends of a diameter in the specimen. The cold junctions were maintained in melting ice.

The thermocouples were calibrated in a subsequent experiment by screwing the hot junction of a standard platinum–13% rhodium–platinum thermocouple into the centre of the specimen and varying the temperature of the furnace. In this way any systematic error due to temperature variation across the diameter of the specimen was eliminated. From the internal consistency of the results of the calibration experiment, the error in the calibration of the chromel–alumel thermocouples relative to the standard thermocouple was estimated to be $1\frac{1}{2}^\circ\text{K}$. The error in the standard thermocouple, given by the manufacturers of the platinum–rhodium–platinum wires, was 1°K . Combining these two independent errors we obtain 2°K as the maximum systematic error in the temperature measurements.

2.3. Measurements of Cross Section

The cross section was obtained from the ratio of the counts obtained with the sample in and out of the beam. Small corrections were made for the effect of the aluminium end plates and for the fact that the beam was attenuated less by the column of air or argon in the furnace than by the same length of air when the furnace was in the 'out' position. These corrections amounted to about 2%.

They were calculated from published data and also measured directly by repeating the neutron measurements without the specimen in the furnace. The two estimates of the correction agreed to within 5%. A further correction was made for the fact that, due to the dead-time in the counting system, some counts were lost, and these were proportionately greater for the 'out' than for the 'in' counts. The error due to background neutrons and to neutrons in the incident beam with energies greater than thermal was obtained by covering the aperture in B (figure 1) with cadmium. The correction due to dead-time and the last two effects was less than 1%.

The counter F subtended a semi-angle θ of 2° at the specimen. Thus there was no contribution to the measured cross section from small angle scattering of the type reported by Hughes *et al.* (1949). Measurements were also made with $\theta = \frac{1}{2}^\circ$ and the results did not differ significantly from those with $\theta = 2^\circ$.

§3. RESULTS AND DISCUSSION

The results for iron are given in figures 3 and 4. Figure 3 shows the total cross section σ_{exp} plotted against temperature over the whole range for which measurements were made. The cross section at 90°K was not measured with filtered neutrons. The value shown in the figure was obtained from measurements with a velocity selector. The results in the neighbourhood of the Curie temperature are shown in figure 4.

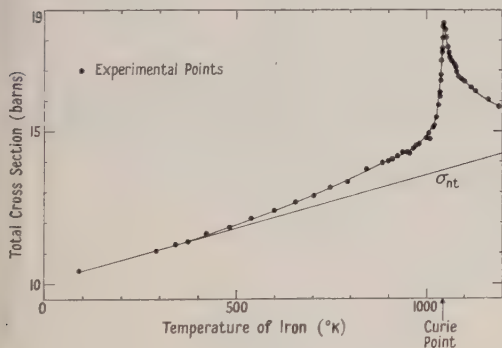


Figure 3. Iron: total cross section plotted against temperature. The r.m.s. error in each point is 0.08 barn.

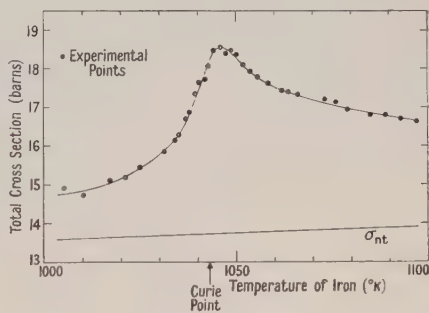


Figure 4. Iron: total cross section plotted against temperature in the neighbourhood of the Curie point. The r.m.s. error in each point is 0.10 barn.

In order to fix the temperature T_{max} , at which the cross section is a maximum, as accurately as possible and to determine whether there is any hysteresis effect, measurements were made on six occasions as the iron was taken through the Curie temperature. On four of these the temperature was rising and on two it was falling. The mean value of T_{max} for rising temperature differed by only 1°K from its value for falling temperature. The mean value of all six measurements was $(1044 \pm 3)^\circ\text{K}$, where the error of 3°K includes both the random error and the possible systematic errors mentioned above.

The theoretical curve for the total nuclear cross section σ_{nt} is shown in figures 3 and 4. σ_{nt} is the sum of the absorption cross section σ_{abs} , which does not vary with temperature, and σ_{ns} the scattering cross section due to the

interaction of the neutrons with the nuclei in the iron. σ_{ns} has been calculated by the methods given by Squires (1952) and includes the cross sections due to multiphonon processes. The curve for σ_{nt} in figures 3 and 4 is based on the values given in the table.

	Iron	Nickel
Nuclear constants (barns)		
Ordered (coherent) cross section S	11.4	13.4
Disordered (incoherent) cross section s	0.4	4.6
σ_{abs} at 7.00 Å	9.9	17.0
Atomic constants		
Debye temperature ($^{\circ}\text{K}$)	420	370

The quantities S and s are defined by Cassels (1950). Their values are taken from Hughes (1953). The quantities $\sigma_{\text{fa}}(A+1)^2/A^2$ and σ_{coh} , defined by Hughes on p. 350 of his book, are related to S and s by

$$\sigma_{\text{fa}}(A+1)^2/A^2 = S + s$$

$$\sigma_{\text{coh}} = S.$$

The values of σ_{abs} are discussed in the text. They are within the limits given by Pomerance (1952). The Debye temperatures are taken from Borelius (1935).

Halpern and Johnson (1939) have shown that for unpolarized neutrons, such as have been used in the present experiments, the nuclear and magnetic scattering are incoherent. The difference between σ_{exp} and σ_{nt} may therefore be taken to equal σ_{ms} , the magnetic scattering cross section. σ_{ms} and σ_{ns} are plotted against temperature in figure 5. It must be pointed out that the values of σ_{ms} , as arrived at by this method, depend on the values of the nuclear constants given in the table. The value of σ_{abs} has been chosen so that σ_{ms} is zero at low temperatures.

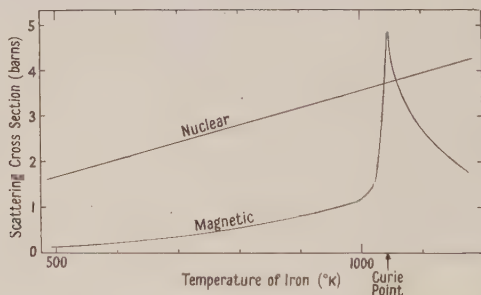


Figure 5. Iron : scattering cross sections plotted against temperature.

As far as the writer is aware no theoretical calculations on neutron scattering at temperatures in the region of the Curie point have been published so far. Moorhouse (1951) has calculated the cross section for magnetic inelastic scattering but his theory, based on the Bloch model of spin waves, is not expected to be valid at temperatures greater than about one third of the Curie temperature.

The experimental results for nickel are given in figures 6 and 7. Figure 6 shows the results from 90 $^{\circ}\text{K}$ to 930 $^{\circ}\text{K}$ —as with iron the result at 90 $^{\circ}\text{K}$ was obtained with a velocity selector—and figure 7 shows the results in the neighbourhood of the Curie temperature. The calculated curve for σ_{nt} , based on the values given in the table, is shown also. The value of σ_{abs} used in the calculation was chosen to give the best fit between σ_{nt} and the experimental points at low temperatures.

It can be seen from figure 7 that there is little change in the cross section as the temperature passes through the Curie point. The maximum deviation from the curve representing σ_{nt} is equal to (0.11 ± 0.05) barn and occurs at a temperature of $(628 \pm 4)^\circ\text{K}$.

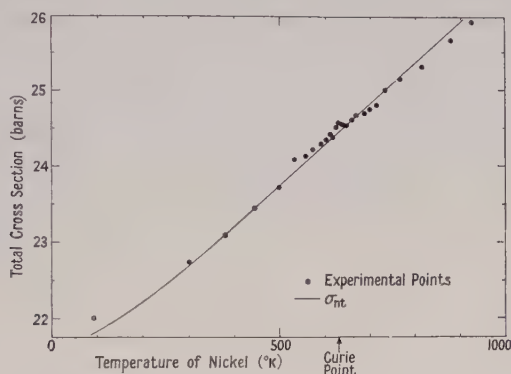


Figure 6. Nickel : total cross section plotted against temperature. The r.m.s. error is 0.3 barn in the point at 90°K and 0.04 barn in the other points.

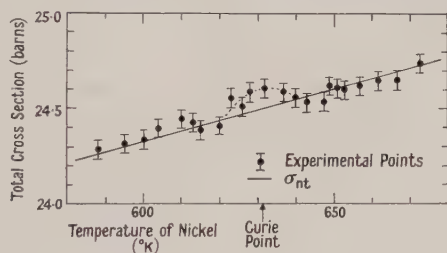


Figure 7. Nickel : total cross section plotted against temperature in the neighbourhood of the Curie point.

ACKNOWLEDGMENTS

The iron and nickel specimens used in these experiments were kindly provided by the British Iron and Steel Research Association, and the Mond Nickel Company, respectively.

The writer wishes to thank Mr. P. Egelstaff and Mr. S. Pease for providing the lead filter and the curve of the wavelength distribution given in figure 2. He is indebted to the Director of the Atomic Energy Research Establishment for permission to publish this paper.

REFERENCES

- BORELIUS, G., 1935, *Handbuch der Metallphysik*, Band 1, Teil 1 (Leipzig : Akad. Verlag), p. 252.
- CARTER, R. S., PALEVSKY, H., and MYERS, V. W., 1953, *Phys. Rev.*, **91**, 450.
- CASSELLS, J. M., 1950, *Progr. Nucl. Phys.*, **1**, 185; 1951, *Proc. Roy. Soc. A*, **208**, 527.
- HALPERN, O., and JOHNSON, M. H., 1939, *Phys. Rev.*, **55**, 898.
- HUGHES, D. J., 1953, *Pile Neutron Research* (Cambridge, Mass. : Addison-Wesley).
- HUGHES, D. J., BURG, M. T., HELLER, R. B., and WALLACE, J. W., 1949, *Phys. Rev.*, **75**, 565.
- LATHAM, R., and CASSELLS, J. M., 1952, *Proc. Phys. Soc. A*, **65**, 241.
- MOORHOUSE, R. G., 1951, *Proc. Phys. Soc. A*, **64**, 1097.
- PALEVSKY, H., and HUGHES, D. J., 1953, *Phys. Rev.*, **92**, 202.
- POMERANCE, H., 1952, *Phys. Rev.*, **88**, 412.
- SQUIRES, G. L., 1952, *Proc. Roy. Soc. A*, **212**, 192.
- WEINSTOCK, R., 1944, *Phys. Rev.*, **65**, 1.

The Decay of ^{203}Pb and the Energy Levels of ^{203}Tl

By J. R. PRESCOTT*

Clarendon Laboratory, Oxford

MS. received 5th September 1953 and in final form 27th October 1953

Abstract. The electron capture decay of ^{203}Pb has been studied with a scintillation spectrometer using coincidence techniques. Gamma-rays of energy 280 ± 5 , 400 ± 7 and 685 ± 10 keV are found in the approximate proportions 1:0.047:0.0087. The whole of the spectrum is in coincidence with the x-rays following electron capture and the 280 and 400 keV gamma-rays are in coincidence. A level scheme with shell model configurations is suggested for ^{203}Tl ; it is: ground, $s_{1/2}$; 280 keV, $d_{3/2}$; 685 keV, $d_{5/2}$. The angular correlation between the 280 and 400 keV gamma-rays is discussed in relation to the published internal conversion data on the 280 keV gamma-ray. Evidence is presented that part of the decay goes by L-capture. There is no appreciable electron capture to the ground state of ^{203}Tl —this enables the shell model assignment $f_{5/2}$ to be made to the ground state of ^{203}Pb .

§1. INTRODUCTION

STABLE ^{203}Tl is the daughter nucleus in the decay of ^{203}Hg and ^{203}Pb . In the former case, a beta-ray of energy 210 keV is followed by a single gamma-ray whose energy is given as 278 ± 3 keV (Wilson and Curran 1951) 297 ± 2 keV (Slätis and Siegbahn 1949) or 286 ± 5 keV (Saxon 1949) with a total internal conversion coefficient of the order of 0.25 and a K/L ratio of the order of 3. The best values appear to be those of Wilson and Curran (1951) who give 0.247 and 3.71 for these quantities. Beta-decay to the ground state, if it occurs at all, is less than 0.5% (Wilson and Curran).

Fifty-two hour ^{203}Pb decays by electron capture. Lutz, Pool and Kurbatov (1944) find electrons in the beta-ray spectrograph of 185, 255 and 267 keV, which certainly result from the K, L and M conversion of the 280 keV gamma-ray found also in the decay of ^{203}Hg , and an electron of 308 keV which they interpret as a Compton electron from a gamma-ray of energy 470 keV. Maurer and Ramm (1942) find gamma-rays of energy 270 and 420 keV by absorption measurements, as well as the 70 keV x-rays following K-capture. O'Kelley (1951) with a beta-ray spectrograph finds internal conversion lines corresponding to gamma-ray energies 153, 269 and 424 keV and suggests a decay scheme in which the two former are in cascade and the latter a cross-over transition.

In the present experiments, the decay of ^{203}Pb has been investigated. The results are used in conjunction with the shell model (Mayer 1950) to make spin, parity and orbital angular momentum assignments to the energy levels of ^{203}Tl .

§2. RESULTS

2.1. Experimental Technique

^{203}Pb was prepared both as the daughter of ^{203}Bi (produced by bombarding natural lead with 25 MeV protons in the Harwell cyclotron) and by bombarding natural thallium with 20 MeV deuterons in the Birmingham cyclotron. In the former case the ^{203}Pb was extracted with the target lead by standard chemical

* Now at the Physics Department, University of Melbourne, Melbourne, Australia.

methods; in the second, the lead was extracted carrier-free by paper chromatography (see for example Burstall *et al.* 1950).

The gamma-rays from ^{203}Pb were examined with a scintillation spectrometer using a 1-in. cube of NaI(Tl) as the detector with an EMI 6260 photomultiplier. The electronic equipment was mainly of standard 'Harwell' pattern and analysis was performed with either a single or 25 channel analyser and by photographing a pulse spectrum on a cathode-ray screen.

The crystal, well polished and surrounded by an aluminium reflector, was mounted in a sealed aluminium can of wall thickness 0.01 in. with a glass window of thickness 0.15 cm, metallic sodium being included in the can as a drying agent. Apart from a film of medicinal paraffin to make optical contact between the crystal and the window, the crystal was mounted dry. This method of mounting gave resolution equal to any obtained using MgO as a backing for the crystal and certainly superior to any in which the crystal was wholly immersed in paraffin. In addition, this mounting preserves the condition of the crystal indefinitely. No deterioration in performance has been found during a period of more than 12 months' constant use.

For coincidence measurements involving the detection of x-rays, a 2-mm slice of NaI(Tl) crystal was used, mounted in a similar manner. This crystal had a calculated efficiency of 91% for the x-rays produced in the decay of ^{203}Pb and less than 2% of the counts recorded in this region were due to other agencies (Compton detection of higher energy gamma-rays, etc.).

The calibration curve for the relative efficiency of the 1-in. NaI(Tl) cube was determined as a function of energy by two independent methods:

(i) Four sources having a pair of gamma-rays of known relative intensity (^{65}Zn , ^{22}Na , ^{60}Co , ^{46}Sc) were selected and the ratios of the areas under the photo peaks found by graphical methods from spectra obtained under conditions of high resolution. These ratios were then adjusted by trial and error to give a smooth energy response curve in the region 0.5 to 1.33 mev.

(ii) The relative areas under the photo and Compton peaks for a number of single gamma-rays were obtained (^{203}Hg , 279 kev; ^{202}Tl , 435 kev; ^{137}Cs , 660 kev; ^{46}Sc , 890 kev; ^{65}Zn , 1.11 mev; ^{22}Na , 1.28 mev). These were then compared with theoretical ratios calculated from the geometry of the crystal, using the absorption coefficients of Davisson and Evans (1952) and considering primary absorption processes only. The empirical ratios of photo peak area to Compton area were larger than the theoretical ratios, as expected, an indication of the well-known effect of primary Compton events being transferred under the photo peak through secondary and higher order absorption processes. The theoretical absorption curves for the Compton and photo processes were then mutually adjusted to give the empirical ratios. This process takes care of both secondary and higher collisions, which are difficult to allow for in an explicit calculation, and possible errors introduced by any simplifying geometrical assumptions in the primary calculation.

The energy response calibration curves obtained by the two methods were in excellent agreement and agreed well with corresponding response curves of Maeder and Wintersteiger (1952 and private communication).

2.2. The Gamma-Ray Spectrum

The radiation from ^{203}Pb , as examined with the scintillation spectrometer, showed radiation of about 70 kev energy, identifiable as the x-rays following

K-capture and internal conversion. The decay curve obtained by counting this radiation in fixed geometry gave a half-life of 52 ± 1 hours which confirms the nucleus as ^{203}Pb . In addition to x-rays, gamma-rays of energy 280 ± 5 kev, 400 ± 7 kev and 685 ± 10 kev were found. The single crystal scintillation spectrum obtained with a single channel kicksorter is shown in figure 1.

As might be expected, the 280 kev gamma-ray was indistinguishable in energy from the 280 kev gamma-ray following the decay of a sample of ^{203}Hg . The presence of the 400 kev gamma-ray shows that the 308 kev electron observed by Lutz *et al.* (1944) is almost certainly the K-conversion electron of this gamma-ray.* The 685 kev gamma-ray was observed in sources from three separate irradiations. Since the 400 and 280 kev gamma-rays are in coincidence (§2.3), a series of runs with a wide range of source-to-crystal distances was taken to determine that the observed 685 kev gamma-ray was not a 'sum line' due to accidental coincidences between the two former gamma-rays.

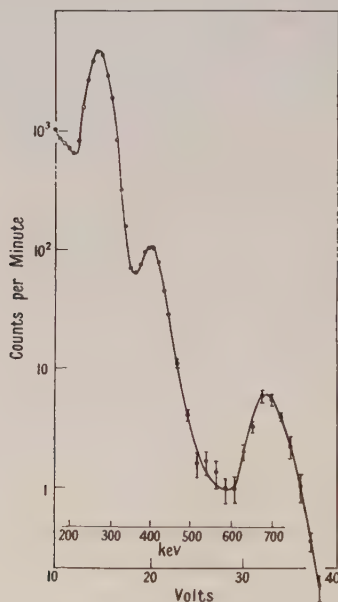


Figure 1. The gamma-ray spectrum of ^{203}Pb obtained with scintillation counter and single channel kicksorter.

The relative abundances of the gamma-rays were $1:0.047 \pm 0.003:0.0087 \pm 0.001$ in the order 280, 400, 685 kev, uncorrected for internal conversion but corrected for the counting efficiency of the crystal (§2.1).

A search was made for gamma-rays of energy greater than about 0.9 mev by setting a discriminator to count all pulses greater than a voltage corresponding to this energy and counting for periods of about 24 hours. The counts obtained on alternate days were $19.7 (\pm 0.5\%)$; 19.4; 19.5; 19.3 counts per minute. The fact that the counts are almost constant shows that there is no appreciable high

* The energies (185, 255, 267 kev) of the K, L and M internal conversion electrons observed by Lutz *et al.* give a gamma-ray energy of 271 kev as opposed to 279 kev from the ^{203}Hg data. Allowing for this difference, the 308 kev electron corresponds to a gamma-ray energy of 405 kev.

energy radiation of 52-hour half-life. If we assume that there may have been a small amount of ^{203}Pb contributing to the count at the beginning of the series of observations, say equal to the experimental error, then any high energy gamma-ray from this nucleus certainly has an intensity less than 1 in 10^4 of the 280 kev gamma-ray*.

High energy gamma-rays are unlikely in any case, since the decay energy of ^{203}Pb can be estimated to be about 800 kev, in the following way: though no decay cycle is available, an empirical cycle can be closed using neutron binding energies. This is shown in figure 2. The binding energy of the neutron in ^{204}Tl is 6.52 ± 0.15 mev (Harvey 1951); ^{204}Tl decays to ^{204}Pb by beta emission with energy 0.765 mev (der Mateosian and Smith 1952). No binding energy has been measured for the neutron in ^{204}Pb but it can be estimated from the semi-empirical mass formula quoted by Harvey (1951) as 7.5 mev, to which must be added about 0.6 mev (Harvey 1951, figure 8) to correct for the increased binding energy associated with the approaching closure of the 126 neutron shell.

The above cycle gives a decay energy (ground to ground) for ^{203}Pb of 800 kev with an error of about ± 250 kev.

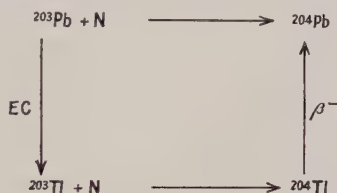


Figure 2. Energy cycle for estimating the electron capture decay energy of ^{203}Pb .

2.3. Coincidence Measurements

The fact that the energy of the 685 kev gamma-ray is equal, within the experimental error, to the sum of the two lower energy gamma-rays, suggests that it represents a cross-over transition from a level at 685 kev to ground and that the 280 and 400 kev gamma-rays are in coincidence. These coincidences were found, using two sodium iodide crystals, both by direct coincidence techniques and by gating one crystal with the other.

The whole of the spectrum was in coincidence with the K-capture x-rays. In particular, it is possible, by coincidence measurements, to set an upper limit for the lifetime of the level from which the 400 and 685 kev gamma-rays originate, which will be of material assistance in making an assignment of spin and parity to this level.

In the absence of L-capture, the coincidence rates $Q_{K\gamma_1}$, $Q_{K\gamma_2}$ between K x-rays and the 400 and 280 kev gamma-rays (γ_1 , γ_2 respectively) are related to the single crystal counting rates C_1 , C_2 for these gamma-rays by the relations:

$$Q_{K\gamma_1}/C_1 = e_K p_1(\tau) \left\{ \frac{k_2 + 2\alpha_2 k_2 + \alpha_2}{k_2 + \alpha_2 k_2 + \alpha_2} \right\} \dots\dots (2.1)$$

$$Q_{K\gamma_2}/C_2 = e_K p_2(\tau) \left\{ 1 + \frac{(1-x)k_1\alpha_1}{k_1 + \alpha_1 k_1 + \alpha_1} \right\} \dots\dots (2.2)$$

* The 1.45 mev gamma-ray reported by *Nuclear Data* (1951) is not in fact mentioned in any of the references there quoted.

where e_K is the experimental detection efficiency of x-rays; $p_1(\tau)$, $p_2(\tau)$ are the respective probabilities that γ_1 and γ_2 follow the x-ray within the resolving time τ of the apparatus; α_1 , α_2 are the K internal conversion coefficients of γ_1 and γ_2 ; k_1 , k_2 are the K/L ratios for γ_1 and γ_2 ; x is the fraction of decays ($\sim 95\%$) that give γ_2 directly*.

In the present case the lifetime of γ_1 can be determined with reference to that of γ_2 . The lifetime of the latter has been measured by Deutsch and Wright (1950) as less than 3×10^{-9} sec and by McGowan (1952) as less than 0.4×10^{-9} sec. For a resolving time of anything greater than $0.1 \mu\text{sec}$ $p_2(\tau)$ can therefore be taken as unity and e_K determined from expression (2.2).† By repeating the experiment in identical geometry with γ_1 we can then estimate $p_1(\tau)$ from expression (2.1), where α_2 and k_2 are already known (§1).

The result obtained is: $p_1(\tau) = 0.94 \pm 0.03$, i.e. 94% of γ_1 follows the x-ray within the resolving time $0.36 (\pm 2\%) \mu\text{sec}$. If the true value of $p_1(\tau)$ is 0.88, i.e. 0.94 less two probable errors (probability less than 0.005), then the probability that the half-life of γ_1 exceeds 1.2×10^{-7} sec is less than 0.005.

In fact, in the above experiment, L-capture has been neglected altogether. This has the effect of setting the lifetime upper limit too high so that the estimate 1.2×10^{-7} sec is certainly too generous; this strengthens the subsequent argument.

2.4. The Energy Levels of ^{203}Tl

^{203}Tl has 122 neutrons and 81 protons, i.e. one less than a closed shell. The measured spin and magnetic moment show that the ground state is $s_{1/2}$, in agreement with the predictions of the shell model (Klinkenberg 1952). The energy levels available for the excited states according to the shell model for a single hole in the 82 proton shell are $d_{3/2}$, $h_{11/2}$, $d_{5/2}$, $g_{7/2}$. . . not necessarily in that order, though the first excited state might be expected to be $d_{3/2}$ (Klinkenberg 1952). Goldhaber and Sunyar (1951) show, on the basis of the internal conversion data, that the 280 kev gamma-ray from ^{203}Hg must be interpreted as mixed M1 and E2 in the proportions 1:3. Using the more recent internal conversion data of Wilson and Curran (1951) one obtains a 24:76 mixture of M1 + E2. Taken with the fact that the 280 kev gamma-ray is the only one observed in the decay of ^{203}Hg , this definitely places the $d_{3/2}$ level at 280 kev above ground. This is consistent with the measured lifetime of less than 3×10^{-9} sec (Deutsch and Wright 1950) or 0.4×10^{-9} sec (McGowan 1952).

The coincidence measurements show that the next observed level is at 685 kev above ground; $h_{11/2}$ can be discarded, since even if it were excited it would have a lifetime for transition to the ground state of the order of 10^5 sec and to the $d_{3/2}$ level of the order of 10^4 sec, using the nomogram of Montalbetti (1952) based on the Weisskopf lifetime relations. This is contrary to the findings of §2.3. The two shell-model alternatives are (a) $d_{5/2}$ and (b) $g_{7/2}$. Figure 3 shows the two schemes; the multipolarities of the gamma-rays are indicated and they are labelled γ_1 , γ_2 , γ_3 for convenience of reference.

* Possible branching to the ground state is immaterial since it does not enter into the evaluation of the formulae.

† For the present purposes (of finding an upper lifetime limit) we can neglect the second expression in the brackets, containing the as yet unknown α_1 and k_1 . The maximum possible error is 5% and actual error is, in fact, less than 1%; see §2.4.

The lifetime limit set for γ_1 in §2.3 enables us to distinguish between these two alternatives. In that section the half-life of the 685 keV level was shown to be certainly less than 10^{-7} second. Since the level decays by the cross-over transition γ_3 in about 15% of the cases, γ_3 will have a partial half-life of less than about 10^{-6} sec. An M3 transition of this energy, scheme (b), would have a half-life of the order of 10^{-3} sec (Montalbetti 1952). This scheme is thus ruled out, leaving $d_{5/2}$, scheme (a) for the 685 keV level; and γ_1 is M1 or possibly mixed M1 and E2.

It does not seem possible to reconcile this suggested decay scheme with that of O'Kelley (1951). O'Kelley places levels at 153 and 422 keV, the upper level being de-excited either by a 269 + 153 keV two-stage cascade or by a 422 keV cross-over. The 269 and 422 keV gamma-rays may correspond to γ_2 and γ_1 of the present experiments but no evidence was found for a gamma-ray of 153 keV which would need to be present in considerable strength in the scintillation measurements if O'Kelley's scheme is correct.

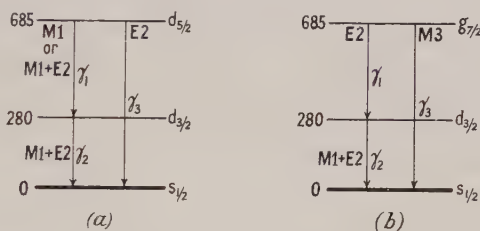


Figure 3. Alternative level schemes for ^{203}Tl .

The angular correlation between γ_1 and γ_2 has been measured in this laboratory* ; it is

$$W(\theta) = 1 + 0.07(\pm 0.008) \cos^2 \theta.$$

Examination of the angular correlation tables of Lloyd (1951) shows that this angular correlation is precisely what one would expect for the pure dipole-dipole case $5/2 \rightarrow 3/2 \rightarrow 1/2$; (no other combination of pure multipoles is possible if the final spin state is $1/2$). Now Goldhaber and Sunyar (1951) show that the 280 keV gamma-ray (γ_2) is certainly mixed M1 + E2. The presence of mixed multipole emission introduces additional 'interference terms' into the angular correlation (Ling and Falcoff 1949, Lloyd 1952) which will, as a consequence, generally be different from the pure multipole correlation. If we assume that γ_1 is pure M1, then we can use the observed angular correlation to estimate the relative amounts of M1 and E2 present in γ_2 , for comparison with the proportions deduced from the internal conversion data.

The theoretical angular correlations for M1 followed by M1 + E2 were worked out from the formulae of Ling and Falcoff (1949) with the sign correction indicated by Lloyd (1952) and are shown in figure 4 where A , the coefficient of $\cos^2 \theta$, is plotted against the percentage of mixture of E2 in γ_2 . The two curves correspond to the two possible choices of phase in evaluating the relations.

The observed angular correlation is obtained either if γ_2 is pure dipole or an 'out of phase' mixture containing $76(\pm 2)\%$ E2. This is apparently an

* The author is extremely grateful to Mr. H. R. Lemmer for allowing him to quote his result prior to publication and to use it in the discussion in this paper.

excellent confirmation of the conclusion of Goldhaber and Sunyar. It is probable however that not very great significance can be attached to the absolute estimate of 76% since this figure is obtained under the assumption that γ_1 is pure M1 whereas it too may well be a mixture.

The angular correlation to be expected in the present case for two successive mixed transitions was worked out for the author by Mr. G. R. Satchler (to whom the author expresses his great appreciation) from the general angular correlation formulae given by Lloyd (1952). Evaluation of this formula shows that the amount of mixture in γ_2 can vary over fairly wide limits by adding less than 1% of E2 to γ_1 . The formula also leads to the observed angular correlation if the amount of E2 in γ_1 is of the order of 90% and upwards, when there is more than about 20% of E2 in γ_2 . In particular, if we take as correct the proportion found from the internal conversion data (viz. 76% E2 in γ_2), then the observed angular correlation indicates that γ_1 is either pure M1 (as already shown above) or contains 95% E2.

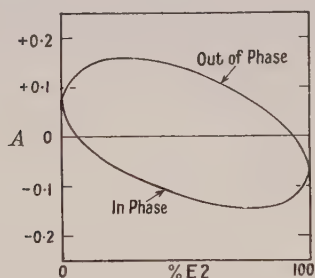


Figure 4. Asymmetry coefficient for a mixed multipole angular correlation in ^{203}Tl .

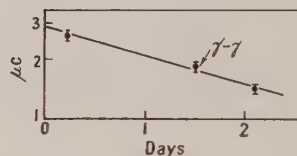


Figure 5. Electron capture into the ground state of ^{203}Tl —comparative source strength determinations.

The latter possibility receives some support from the fact that the 685 keV (E2) cross-over transition is stronger by a factor of roughly ten than is expected from Weisskopf's formula, assuming γ_1 to be pure M1. On the other hand, theory (Blatt and Weisskopf 1952) suggests that M1 should be favoured for an odd proton transition of this type (where $\Delta l = 0$). A measurement of the internal conversion coefficient or K/L ratio for γ_1 should be able to resolve this point. In either case the lifetime of the 685 keV level is estimated to be less than 2×10^{-9} sec (Montalbetti 1952).

Absence of definite knowledge (either direct or indirect) of the above internal conversion data introduces a small degree of uncertainty in estimating the relative proportions of the gamma-rays that follow the various branches, since it is not possible to correct for the internal conversion of the 400 keV radiation.

The shell model suggests that the configuration $h_{11/2}$ should be available for a low-lying state of ^{203}Tl ; if it exists, it will be an isomeric state with a half-life in the region of a few hours to several days. Such a state was sought for in the present experiments but no evidence for or against it was found. It appears unlikely, however, that it could be formed in the electron-capture decay of ^{203}Pb because of the second-forbidden nature of the transition (see §2.6).

2.5. Evidence for L-capture in ^{203}Pb

If relations (2.1) and (2.2) are modified to take account of L-capture, they become (in the same notation):

$$\frac{Q_{K\gamma_1}}{C_1} = e_K \left\{ y_1 + \frac{\alpha_2 k_2}{k_2 + \alpha_2 k_2 + \alpha_2} \right\} \dots\dots (2.3)$$

$$\frac{Q_{K\gamma_2}}{C_2} = e_K \left\{ xy_2 + (1-x)y_1 + \frac{(1-x)k_1\alpha_1}{k_1 + \alpha_1 k_1 + \alpha_1} \right\} \dots\dots (2.4)$$

where y_1, y_2 are respectively the fractions of the decay in each branch that go by K-capture and $p_1(\tau), p_2(\tau)$ have been set equal to unity, as justified in the previous section.

Relations (2.3) and (2.4) enable us to evaluate y_1 and y_2 provided we know e_K , the detection efficiency per K-capture of the x-ray crystal. We may write $e_K = \epsilon f_K (1 - a_K) \Omega / 4\pi$ where ϵ is the intrinsic efficiency of the crystal per x-ray entering it, Ω is the solid angle, f_K the fluorescence yield of the K-shell of thallium, and a_K the fraction of x-rays lost by absorption in the material between source and crystal. ϵ was calculated to be 0.91 from the geometry of the crystal and the absorption coefficients for x-rays (*Handbook of Chemistry and Physics* 1951). No measurement has been made for the K fluorescence yield of Tl but Broyles (1952) gives 94.6 (± 0.8)% for Hg which is only one unit of Z removed. A round figure of 95% was taken; a_K was determined in a separate experiment as 0.03 and the effective value of Ω by a comparison count in well-defined geometry. This gives $0.84\Omega/4\pi$ for e_K and from relations (2.3) and (2.4) the proportions of K-capture into the 685 and 280 kev levels are respectively 0.74 ± 0.05 and 0.87 ± 0.05 , the balance being attributable to L-capture.

Rose and Jackson (1949) and Marshak (1942) have calculated the amount of L-capture to be expected in electron-capture processes. For lead ($Z=82$) Rose and Jackson's figures show that L-capture should account for at least 13% of the decays at high energies and progressively more as the energy available decreases.

The figures 0.74 and 0.87 obtained above imply (including the errors) available decay energies of 230 (+70 or -40) kev and greater than 450 kev respectively for *allowed* transitions, in which the ratio of L- to K-capture varies as the square of the ratio of the neutrino energies (Rose and Jackson 1949, Marshak 1942), i.e. a total decay energy of about 800-900 kev which is in agreement with the value of 800 ± 250 kev obtained in §2.2. However, it will be shown in §2.6 that the decay is almost certainly first-forbidden and in this case the energy variation in the ratio of L- to K-capture is a fourth power law. A plausible extrapolation of Marshak's first-forbidden relation to $Z=82$ gives decay energies of 570 ± 120 kev and greater than 1.1 mev, i.e. a total decay energy of greater than about 1.4 mev. This seems significantly outside the experimental error and is difficult to understand.

2.6. Branching to the Ground State of ^{203}Tl and the Spin of ^{203}Pb

Two alternative methods of determining the 'source-strength' of a ^{203}Pb source are available: (a) gamma-gamma coincidences between the 280 kev and 400 kev gamma-rays; (b) coincidences between the K-capture x-ray and γ_2 .

Using both methods, we can find out how much of the decay goes direct to the ground state, for if K-capture occurs direct to the ground state, the

'source-strength' found by method (b) will be greater than that found by method (a), since (a) measures only the strength of that part of the source decay in which the 280 keV gamma-ray participates whereas (b) includes additionally x-rays from the ground-state transition for which there is no corresponding 280 keV gamma-ray.

In the present experiments, a source-strength determination by gamma-gamma coincidences was bracketed with determinations by x-ray-gamma coincidences with γ_2 . The former determination (a) is straightforward and gives the source strength in the standard form $N = C_1 C_2 / Q_{1,2}$ (Barnothy and Forro 1951, with a small additional correction for the angular correlation) where one coincidence channel is set on the photo peak of γ_1 and the other on γ_2 by means of kicksorters. Method (b) gives

$$N' = \frac{C_2' C_K'}{Q_{K\gamma_2}} F(\alpha_1, \alpha_2; k_1, k_2; y_1, y_2; x)$$

where $F(\alpha_1, \alpha_2; k_1, k_2; y_1, y_2; x)$ is a function including the effects of internal conversion and L-capture. In practice the terms containing α_1 and k_1 can be neglected, which avoids the necessity for knowing these quantities; y_1 and y_2 were estimated in the previous section.

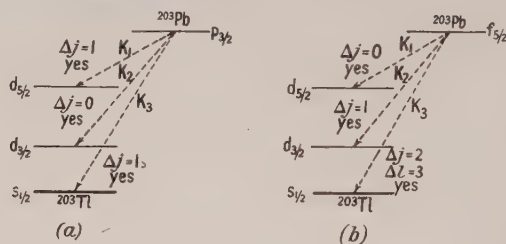


Figure 6. Alternative decay schemes for the decay ^{203}Pb to ^{203}Tl .

The results of the source-strength determinations are shown in figure 5, where a line representing a 52-hour decay has been drawn through the experimental points. There is no evidence for any excess of x-rays in the source, indeed the results indicate an apparent deficiency. In statistical terms it is extremely improbable that K-capture to the ground state exceeds 10% of the total decays.

This fact enables us to make an assignment to the ground state of ^{203}Pb with reasonable certainty on the basis of the shell model. ^{203}Pb has a closed shell of protons and five less than a closed shell of neutrons. The most likely states for ^{203}Pb are $p_{3/2}$ or $f_{5/2}$. Other alternatives are $p_{1/2}$, $i_{13/2}$, $f_{7/2}$, but the $p_{1/2}$ state is known to take the last two neutrons in this shell; high spin states, such as $i_{13/2}$, do not occur as ground states; and the $f_{7/2}$ states must already be filled before the $f_{5/2}$ (Klinkenberg 1952, Mayer 1950).

Figure 6 (a) and (b) shows the two possible K-capture decay schemes; for scheme (a) ^{203}Pb has a $p_{3/2}$ ground state, for scheme (b) the ground state is $f_{5/2}$. Angular momentum and parity changes are indicated by the side of each transition which are labelled K_1 K_2 K_3 in order of increasing transition energy. Inspection of the schemes reveals that, under Fermi selection rules, all transitions are first-forbidden except K_3 in scheme (b) which is third-forbidden. Under Gamow-Teller rules, all the transitions are first-forbidden although K_3 in

scheme (b) involves a change in orbital angular momentum of 3 and must be expected to be correspondingly less probable. Thus, Mayer *et al.* (1951) show that for transitions of the type $\Delta l=1$, $\Delta j=0$, 1 which covers all except the latter case, $\log ft$ values lie between 6 and 8 whereas for the one known case where $\Delta l=3$, $\Delta j=2$ (^{187}Re) the $\log ft$ value is 17.7. Other things being equal, the lifetime of K_3 in scheme (b) will be long and therefore it will be absent from the decay.

In scheme (a), on the other hand, transitions K_2 and K_3 are both first-forbidden, the latter (ground state) transition being energetically favoured by 280 kev. Assuming a total decay energy (ground to ground) of 800 kev (§ 2.2) K_3 should exceed K_2 by a factor of two or three assuming a square-law dependence on energy (see, for example, Feenberg and Trigg 1950). Even if the figure of 800 kev is greatly in error, more decays should go via K_3 than K_2 . However, it was shown above that it is extremely improbable that electron capture to the ground state (K_3) exceeds 10%. Scheme (a) is therefore ruled out and the ground state of ^{203}Pb must be $f_{5/2}$, as in scheme (b).

This conclusion receives further support from the decay of ^{203}Hg which has three neutrons less than a closed shell and which must be $f_{5/2}$ since decay to the ground state of ^{203}Tl is absent (Wilson and Curran 1951) and from ^{207}Pb which has one neutron less than a closed shell. Here the ground state is $p_{1/2}$ but the first excited state is $f_{5/2}$ instead of the expected $p_{3/2}$ (Pryce 1952). These facts seem to indicate an abnormally large spin-orbit splitting for the $p_{3/2}$ - $p_{1/2}$ doublet, whereas Klinkenberg (1952) suggests that the splitting is abnormally small. One might guess on the basis of the above evidence that the ground state of ^{205}Pb (with a three-neutron deficit) is $f_{5/2}$; this would account for its apparently long life.

ACKNOWLEDGMENTS

The author wishes to express his appreciation to Professor Lord Cherwell for affording him the facilities of the Clarendon Laboratory, to Dr. P. F. D. Shaw for advice on chemical problems, to Mr. C. H. Collie and Professor M. H. L. Pryce for valuable discussions, and to the Executive of the Commonwealth Scientific and Industrial Research Organization, Australia, for leave of absence. Financial assistance was received from the Australian National University and the Nuffield Foundation.

REFERENCES

- BARNOTHY, J., and FORRO, M., 1951, *Rev. Sci. Instrum.*, **22**, 415.
BLATT, J. M., and WEISSKOPF, V. F., 1952, *Theoretical Nuclear Physics* (New York: John Wiley), Ch. XII.
BROYLES, C. D., 1952, *Nuclear Sci. Abstr.*, **6**, 5912.
BURSTALL, F. H., DAVIES, G. R., LINSTEAD, R. P., and WELLS, R. A., 1950, *J. Chem. Soc.*, 516.
DAVISSON, C. M., and EVANS, R. D., 1952, *Rev. Mod. Phys.*, **24**, 79.
DEUTSCH, M., and WRIGHT, W. E., 1950, *Phys. Rev.*, **77**, 139.
FEENBERG, E., and TRIGG, G., 1950, *Rev. Mod. Phys.*, **22**, 399.
GOLDHABER, M., and SUNYAR, A. W., 1951, *Phys. Rev.*, **83**, 906.
Handbook of Chemistry and Physics, 33rd Edn, 1951 (Cleveland: Chemical Rubber Publishing Co.).
HARVEY, J. R., 1951, *Phys. Rev.*, **81**, 353.
KLINKENBERG, P. F. A., 1952, *Rev. Mod. Phys.*, **24**, 63.

- LING, D. S., and FALCOFF, D. L., 1949, *Phys. Rev.*, **76**, 1639.
LLOYD, S. P., 1951, *Phys. Rev.*, **83**, 716; 1952, *Phys. Rev.*, **85**, 904.
LUTZ, A. L., POOL, M. L., and KURBATOV, J. D., 1944, *Phys. Rev.*, **65**, 61 (A).
MCGOWAN, F. K., 1952, *Phys. Rev.*, **85**, 142.
MAEDER, D., and WINTERSTEIGER, V., 1952, *Helv. Phys. Acta*, **25**, 465; *Phys. Rev.*, **87**, 537.
MARSHAK, R. E., 1942, *Phys. Rev.*, **61**, 431.
DER MATEOSIAN, E., and SMITH, A., 1952, *Phys. Rev.*, **88**, 1186.
MAURER, W., and RAMM, W., 1942, *Z. Phys.*, **119**, 602.
MAYER, M. G., 1950, *Phys. Rev.*, **78**, 16, 22.
MAYER, M. G., MOSZKOWSKI, S. A., and NORDHEIM, L. W., 1951, *Rev. Mod. Phys.*, **23**, 315.
MONTALBETTI, R., 1952, *Canad. J. Phys.*, **30**, 660.
Nuclear Data, 1950, *U.S. National Bureau of Standards Circular* No. 499, and supplements.
O'KELLEY, G. D., 1951, *University of California, Radiation Laboratory Report* 1243.
PRYCE, M. H. L., 1952, *Proc. Phys. Soc. A*, **65**, 773.
ROSE, M. E., and JACKSON, J. L., 1949, *Phys. Rev.*, **76**, 1540.
SAXON, D., 1949, *Phys. Rev.*, **74**, 849.
SLÄTIS, H., and SIEGBAHN, K., 1949, *Phys. Rev.*, **75**, 318; *Ark. Mat. Astr. Fys.*, **36**, no. 21.
WILSON, R., and CURRAN, S. C., 1951, *Phil. Mag.*, **42**, 762.

Lens Spectrometer Study of the Disintegration of MsTh_2

BY THE LATE W. D. BRODIE*

Department of Natural Philosophy, University of Edinburgh

Communicated by N. Feather; MS. received 30th October 1953

Abstract. Measurements have been made (i) of the absolute intensities of the internal conversion lines of the 57, 78, 97, 127 and 184 keV γ -rays of MsTh_2 and (ii) of the absolute intensity of the associated L-Auger electrons. The K/L conversion ratios for the 127 and 184 keV transitions are respectively 0.023 ± 0.005 and 4.7. Difficulties are encountered in attempting to attribute spins and parities to the two lowest excited levels of the RdTh nucleus.

§ 1. INTRODUCTION

MESOTHORIUM 2 grows from the long-lived mesothorium 1 and decays by β -emission to radiothorium with a half-value period of 6.13 hours. The internal conversion electrons emitted by MsTh_2 were photographed by Black (1924), who used a semicircular magnetic spectrometer and deduced the presence of eight γ -rays, and by Yovanovitch and d'Espine (1927) using the direct deviation method. Some of the γ -rays of MsTh_2 were detected by Thibaud (1926), who studied the 'external' spectrum of photoelectrons from a lead radiator. Yovanovitch and Proca (1926) carried the investigation of the MsTh_2 spectrum into the very low energy region and reported the presence of lines down to about 3 keV. More recently Lecoin, Perey and Teillac (1949) made a cloud-chamber study of the disintegration and Lecoin, Perey and Riou (1949) determined the intensity of the L x-rays using the method of selective absorption.

A study of the β - and γ -rays of MsTh_2 has recently been completed in this department by Kyles, Campbell and Henderson (1953). The present work was intended to be complementary to their investigation. The objectives were to map the β -particle spectrum in the momentum range 600 to 2000 gauss cm, to measure the intensities of the internal conversion lines within this range, and then to examine the energy region of the L-Auger lines.

The apparatus used was a magnetic lens β -spectrometer incorporating a post-focusing electron accelerator. With this apparatus electron spectra could be observed down to 4 keV energy. A thin-windowed Geiger-Müller counter was used as detector. Details of the spectrometer have already been published (Butt 1949, 1950).

§ 2. SOURCE PREPARATION

The earlier sources were prepared 'carrier-free', using the method of Peterson (M.D.D.C. 1709, U.S.A.E.C.) in which cerium is initially used as

* Dr. W. D. Brodie died on 27th June 1953 at the age of 30 of an incurable disease. This paper was prepared from his own rough draft by Dr. M. A. S. Ross, whom I wish to thank on behalf of Dr. Brodie's many friends in the Department of Natural Philosophy at Edinburgh.—N.F.

carrier and subsequently removed by oxidation to the four-valent state and precipitation with iodate ion. In this connection, ammonium persulphate plus nitrate was found to be superior to the silver oxide recommended as oxidant. However, difficulties were encountered in the complete removal of the cerium, and the method was later abandoned, at the suggestion of Dr. N. Miller of this Department, in favour of one using a very small ($15\mu\text{g}$) quantity of iron carrier which carried the MsTh_2 completely and yielded sources having sufficiently small mass.

The sources were deposited by evaporation of a single drop of dilute nitric acid solution on thin foils of aluminium or gold, which, following Langer, Motz and Price (1950), had previously been wetted with a 10% solution of insulin (40 units per ml.). The resulting source was normally 1 mc in strength and was distributed over a circle about 3 mm in diameter with a superficial mass of about 0.1 mg per cm^2 . Each source was used for about ten hours of counting.

§3. GENERAL SURVEY OF THE SPECTRUM

Table 1 shows the $H\rho$ values of the lines observed and, for comparison, the corrected* values of Black (1924). Approximate values are entered for poorly resolved lines.

Table 1

Line No.	Author		Black	
	$H\rho$ (gauss cm)	Intensity (%)	$H\rho$ (gauss cm)	Intensity (%)
1	665	44	665	9.4
2	693		696	8.0
3	789		790	6.1
4	815	15	816	4.2
5	837	~0.1	836	0.56
6	—	—	864	0.38
7	900	~0.1	900	1.5
8	950	8.0	946	4.7
9	975		975	3.3
10	1070		1069	1.5
11	1099	1.3	—	—
12	1165	5.6	1162	3.3
13	1185		1183	2.3
14	1260		1248	2.1
15		1267	0.56	
16	—	—	1299	0.3
17	—	—	1336	—
18	1460	1.3	1459	1.9
19	1550		1528	0.56
20	—		1681	—
21	1725	~0.2	—	—
22	1770	~0.2	1770	0.7

The intensities in column 3, giving the number of electrons per 100 disintegrations, were measured by comparison with the extrapolated continuous spectrum. The work of Kyles, Campbell and Henderson (1953) shows that the

* Black based his measurements on the $H\rho$ values for the lines of Ra (B+C) obtained by Ellis and Skinner (1924). In table 1, Black's values have been altered to agree with the later measurements on Ra (B+C) made by Ellis (1934).

β -continuum of MsTh_2 includes six partial spectra having end-points between 0.469 and 2.18 mev and relative intensities as given in their table 2. From the Fermi plots of these six partial spectra they were able to reconstruct an entire continuous spectrum, from zero to the ultimate end-point, which fitted their direct measurements down to their lower limit of observation on the continuum at 2000 gauss cm. The present survey extended up to about 2500 gauss cm, and from 1600 to 2500 gauss cm the spectrum is substantially free from lines. The continuous spectrum of Kyles *et al.* could therefore be fitted to our observations with confidence—and a good fit was, in fact, obtained. The area under this fitted continuous spectrum was taken to represent one electron per disintegration.

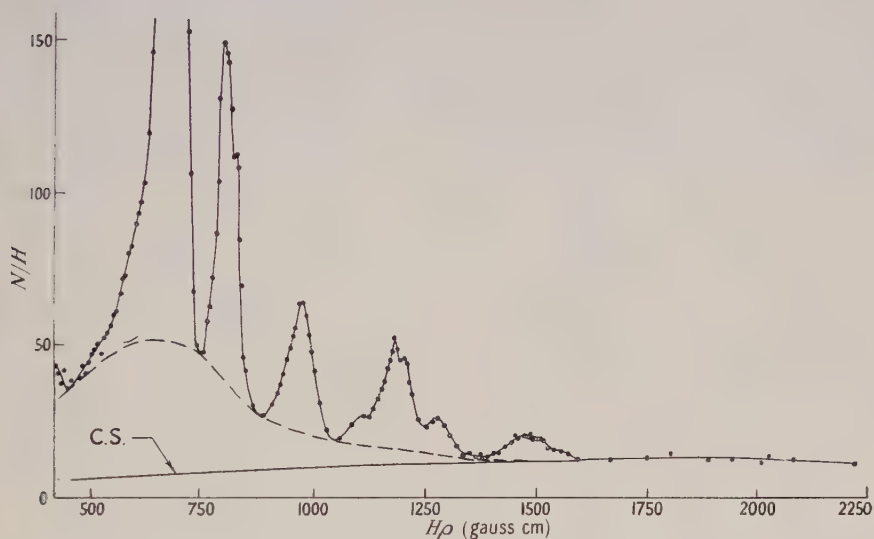


Figure 1. MsTh_2 spectrum from source on aluminium leaf.

The areas under the profiles of the low-energy lines include back-scattered electrons from the source mounting, and two different experiments were carried out in an attempt to correct for this effect, one tending to underestimate, and the other to overestimate the back-scattering correction. In the first, the source was produced by the Peterson method and was almost carrier-free. It was mounted on an aluminium leaf 0.2 mg per cm^2 in thickness. The spectrum obtained is shown in figure 1. The curve marked C.S. is the normalized continuous spectrum of Kyles, Campbell and Henderson. The region between the broken line in figure 1 and the continuous spectrum is assumed to be due to scattered electrons. The shape of this region is consistent with the view that the back-scattered electrons are increasingly subject to absorption in the source as their energy decreases. The line intensities were measured on the figure with a planimeter, using the broken curve as base. The results obtained are given in column 2 of table 2.

The second experiment was made using a source mounted on gold leaf 0.22 mg per cm^2 in thickness. In this case a calculated line shape was used and the area under each line was estimated down to the extrapolated continuous spectrum. The measured intensity of each line then included its own quota of

back-scattered electrons together with a small quota from the continuous spectrum. The observations were then corrected for back-scattering using the correction factor (55%) determined by Butt and Brodie (1951) for saturation back-scattering from a gold source backing of the stated thickness, and for the solid angle conditions obtaining in this spectrometer. Hamilton and Gross (1950) have given formulae for the energy below which saturation back-scattering takes place and the energy at which back-scattering begins for a given foil. These formulae show that lines Nos. 1 to 9 of table 1 are in the energy range of saturation back-scattering, while lines No. 18 and above are beyond the range in which back-scattering is appreciable. Accordingly, the measured intensities of the lines have been corrected by the factors shown in table 2, column 4, yielding the corrected absolute intensities of column 5. The main sources of error in this method arise in dividing up the observed continuum of back-scattered electrons between the various lines, and in estimating the correction factors for lines in the energy range of non-saturation back-scattering. The first error is greatest for lines Nos. 1 to 4 and the second for lines Nos. 10 to 13. The use of 55% correction for lines 1 and 2 may represent over-correction.

Table 2

Line No.	Aluminium backing Intensity (%)	Gold backing		
		Obs. Rel. Int.	Corrn. Factor (%)	Corr. Int. (%)
1 and 2	49.5	893	-55	39
3 „ 4	13.5	364	-55	16
8 „ 9	7.7	190	-55	8.3
10 „ 11	1.0	33	-40	1.6
12 „ 13	5.5	110	-30	5.7
14 „ 15	1.7	34	-15	2.0
18	—	~20	- 0	~1.3

The intensity measurements obtained by the two methods and given in columns 2 and 5 of table 2 show reasonable agreement, and their mean values have been entered in table 1; it is these values which have been used by Kyles, Campbell and Henderson. A comparison with the intensities (also shown in table 1) which Black obtained from visual estimates of photographic blackening,* shows that Black's results for the four lines of lowest energy are too low. This is not unexpected and is probably due to the variation of photographic blackening with electron energy.

§ 4. INTERPRETATION OF THE INTERNAL CONVERSION LINES

An analysis of the low- and medium-energy internal conversion lines of MsTh_2 is given in table 3, which shows 16 lines, 15 interpreted in terms of five γ -rays and one as a K-Auger line. The energies and intensities of lines 1 to 19 are those measured in the present investigation. In the case of unresolved pairs of lines such as 1 and 2, the measured intensities have been divided in the ratio given by Black.

Lines Nos. 16, 17 and 20 were found by Black, but were not observed in the present work and are not shown in table 3. Lines Nos. 11 and 21 were observed

* Black's relative intensities have been normalized to agree with our absolute intensity for the pair of lines Nos. 8 and 9.

in the present work, but are not included in the table because their interpretation is not certain; they correspond to lines numbered 17 and 30 by Kyles, Campbell and Henderson (1953), to whose paper reference is also made for the analysis of lines of higher energy.

Table 3

Line No.	$H\rho$ (gauss cm)	E (kev)	Conv. shell	Intensity (%)	γ -ray Energy (kev)	Mean γ -energy (kev)	Total Conv. Int. (%)
1	665	37.5	L _{II}	24	57.2	57.0	59
2	693	40.6	L _{III}	20	56.9		
3	789	52.16	M _{II}	15	57.0		
4	815	55.4	N _I		56.7		
5	837	58.3	L _{II}	~0.1	78.0	78.1	
6	864	61.9	L _{III}		78.2		
7	900	66.9		~0.1	(K-Auger Line)		
9	975	77.7	L _I or II	3.3	97.4	97.4	4
10	1069	92.2	M _I	—	97.4		
12	1165	108.0	L _{II}	3.3	127.7	127.5	7.4
13	1185	111.5	L _{III}	2.3	127.8		
14	1248	122.4	M _I	1.8	127.6		
15	1267	125.8	N _I		127.1		
8	950	74.04	K	4.7	183.6	183.7	6
18	1460	161.9	L _I	1.3	182.4		
19	1550	179.8	M _I		185.0		

Assumed binding energies in kev: K, 109.6; L_I , 20.50; L_{II} , 19.68; L_{III} , 16.30; M_I , 5.18; M_{II} , 4.81; N_I , 1.32.

§5. DISCUSSION OF THE INTENSITY MEASUREMENTS

In the cloud-chamber investigation of Lecoin, Perey and Teillac (1949) electron tracks were divided into two categories, 'soft' and 'hard', dividing at about 60 kev and containing respectively 920 and 946 tracks. By using a source of MsTh_1 in equilibrium, of which the disintegration rate was known, these authors deduced that MsTh_2 emits roughly two electrons per disintegration, one in each of the 'soft' and 'hard' groups. In the γ -ray and x-ray absorption experiment of Lecoin, Perey and Riou (1949) two electromagnetic radiations were observed, a hard component having a mean energy of 460 kev and corresponding to the mean energy of the known γ -rays, and a soft component which was shown by selective absorption to consist of the L x-radiation of thorium. Since the absolute efficiency of their counter was known, Lecoin, Perey and Riou were able to deduce that the number of L-photons emitted per disintegration of MsTh_2 was 0.30 ± 0.06 . It is possible to show that these rather imprecise conclusions are in agreement with the present intensity measurements.

Working from the data given in table 3 and by Kyles *et al.*, we find that the numbers of K, L and (M + N) conversion electrons emitted per hundred disintegrations of MsTh_2 are respectively 7.8, 55.0 and 17.8, giving a total of 0.806 internal conversion electrons per disintegration. The electrons which would be counted in the cloud-chamber experiments include also the K- and L-Auger electrons. The K-Auger electrons, represented only by the weak line No. 7 in table 3, may for present purposes be neglected. Kinsey (1948) has estimated

the fluorescence yield of each of the L shells using the best available measurements of the total width of x-ray lines and absorption edges for heavy elements and radiation widths calculated relativistically by Massey and Burhop (1936). He gives 15, 56 and 39%, respectively, for the fluorescence yields of the L_I , L_{II} and L_{III} shells. From table 3 the primary ionizations produced by internal conversion in the L_I , L_{II} , L_{III} shells are respectively 3.75, 28.9 and 22.3%. In deducing these figures, the L-conversion of the higher energy γ -rays (from Kyles *et al.*) has been assumed to take place entirely in the L_I shell. This approximation will introduce at most a small error since the intensities of these lines are low. The primary L_{II} and L_{III} ionizations are increased by the transfer of ionization from the K-shell by K x-ray emission and by the transfer of L_I vacancies to the L_{III} shell by the Coster-Krönig effect. Taking Massey and Burhop's (1936) figures for the relative intensities of the K x-rays, and Kinsey's (1948) estimate of 60% for the fraction of L_I ionization transferred to L_{III} by the Coster-Krönig effect, the final absolute ionization intensities in the L_I , L_{II} and L_{III} shells are respectively 1.5, 30.8 and 28.7 per 100 disintegrations. Introducing Kinsey's values for the L_I , L_{II} and L_{III} fluorescence yields, the total L-Auger intensity then amounts to $0.9 + 13.5 + 17.5$ or 31.9 per hundred disintegrations.

The total number of electrons emitted per disintegration of $MsTh_2$ including the nuclear β -particle but excluding the very low energy M- and N-Auger electrons, is therefore $1.0 + 0.806 + 0.319 \simeq 2.1$, in good agreement with the cloud chamber results. To check the numbers of electrons in the 'soft' and 'hard' groups as defined by Lecoin, Perey and Teillac, the total electron spectrum consisting of the continuous spectrum, and internal conversion electrons and the L-Auger electrons may be divided at 60 keV. The resulting calculation gives 1.0 electrons in the low energy group, and 1.1 in the high energy group, in excellent agreement with the cloud chamber result. Also, since there are 32 Auger electrons from a total of 61 L-shell ionizations, there must be 29 L x-ray photons per hundred disintegrations. This figure lies in the centre of the rather wide limits (30 ± 6) given by Lecoin, Perey and Riou for the L x-ray intensity.

The large measure of agreement which has been shown now to exist among these three independent intensity measurements of the electronic and electromagnetic radiations from $MsTh_2$ suggests that the absolute intensities listed in table 3 are fairly accurate.

§ 6. THE LOW-ENERGY SPECTRUM OF $MsTh_2$

Figure 2 shows the electron spectrum of $MsTh_2$ between 250 and 500 gauss cm. Of the seven lines visible in the figure, six are considered to be L-Auger lines and the seventh an internal conversion line. Taking the conversion line first, reference to table 3 shows that lines 12, 13, 14 and 15 are interpreted as the L-, M- and N-conversion electrons of a γ -ray of 127.5 keV. As the binding energy of the K-shell of radiothorium is 109.6 keV, an electron line due to internal conversion of this γ -ray in the K shell should be observed at about 18 keV. In figure 2 a weak line, No. 7, appears at 460 gauss cm (18.2 keV) and this is considered to be the K-shell conversion line of the 127 keV γ -ray. The intensity of the line on the scale of table 3 is about 0.13 so the K/L conversion ratio (α_K/α_L) for the 127 keV γ -ray may be given as 0.023 ± 0.005 .

Lines 1 to 6 of figure 2 have been interpreted as L-Auger lines. Because of the large number of possible transitions involving the L, M and N levels and the

relatively low resolution of the experiment, it is not possible to identify the transitions which give rise to these lines purely on energy considerations. The calculations of the preceding section have shown, however, that about 0.9, 13.5 and 17.5 Auger electrons per 100 disintegrations should originate in the L_I , L_{II} and L_{III} shells respectively, so that the strong lines should be associated with the L_{II} and L_{III} shells. Also, on theoretical grounds, the transitions representing internal conversion of the strong x-ray lines should be favoured. The application of these principles lead to the assignments shown in table 4, each assignment being regarded merely as representing the strongest single contribution to the peak in question.

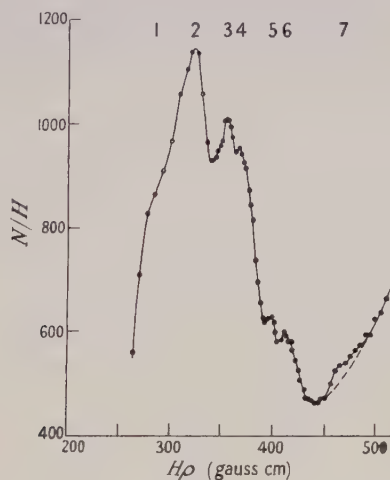


Figure 2. Low-energy spectrum of $MsTh_2$.

Table 4

Line No.	$H\rho$ (gauss cm)	Observed Energy (kev)	Assignment	Calculated Energy (kev)
1	~ 285	7.1	$L_{III} \rightarrow M_{III}M_I$	7.09
2	323 ± 2	9.09 ± 0.10	$\left\{ \begin{array}{l} L_{III} \rightarrow M_{III}M_{III} \\ L_{III} \rightarrow M_{III}M_{IV} \end{array} \right.$	$\begin{array}{l} 8.95 \\ 9.50 \end{array}$
3	355 ± 2	10.97 ± 0.12	$L_{II} \rightarrow M_{IV}M_I$	11.04
4	367 ± 3	11.71 ± 0.19	$L_{III} \rightarrow M_VN_I$	11.67
5	398 ± 2	13.76 ± 0.14	$L_{II} \rightarrow N_{IV}M_I$	13.83
6	413 ± 2	14.79 ± 0.14	$L_{II} \rightarrow M_{IV}N_I$	14.91

An attempt was made to obtain a direct measure of the total intensity of the L-Auger lines by taking a set of observations over the range 250 to 900 gauss cm and comparing planimeter measurements of the Auger peak and the (L + M) conversion lines of the 57 kev γ -ray. All the lines in question should be equally affected by back-scattering but losses due to self-absorption of the Auger electrons were anticipated. For intensity reasons, a source thickness of about 0.1 mg per cm^2 was necessary and this thickness is an appreciable fraction of the mean range (about 0.25 mg per cm^2) of the Auger electrons. The result of the measurement was 22 Auger electrons per 100 disintegrations which is considerably below the figure of 32 Auger electrons reached by calculation. It may be noted that the

difference between the two estimates is equivalent to the loss of all back-scattered electrons, and it is reasonable to assume that self-absorption would almost entirely remove these electrons. The measurements are therefore regarded as supporting the accuracy of the calculated result.

§ 7. CONCLUSIONS

The main results established by the present experiments on the disintegration of MsTh_2 are the absolute intensities of the conversion lines of the 57, 78, 97, 127 and 184 keV γ -rays. The values of these are given in table 3. The total intensity of the L-Auger lines is 32 per 100 disintegrations. The ratios of conversions in the K and L shells (α_K/α_L) for the 127 and 184 keV transitions are respectively 0.023 and 4.7. These results were made available to Kyles, Campbell and Henderson (1953) and were used by them in their discussion of the MsTh_2 disintegration.

The outstanding problem which has appeared as a result of the present measurements concerns the spins and parities of the first two excited states of the RdTh nucleus, at 57 and 184 keV. As Kyles, Campbell and Henderson point out, the evidence strongly favours the assignment E2 to the 57 and 127 keV transitions, but if these assignments are accepted difficulties arise concerning the cross-over transition of 184 keV which has some of the attributes of M1. Possibly Thibaud's identification of this radiation in emission is in error (there is some evidence for the existence of a transition of 179 keV which might explain such an error) and the 184 keV state, like the ground state, should be classified $0+$. Further experiment is obviously required to elucidate the situation.

REFERENCES

- BLACK, D. H., 1924, *Proc. Roy. Soc. A*, **106**, 632.
 BUTT, D. K., 1949, *Proc. Phys. Soc. B*, **62**, 551; 1950, *Proc. Phys. Soc. A*, **63**, 986.
 BUTT, D. K., and BRODIE, W. D., 1951, *Proc. Phys. Soc. A*, **64**, 791.
 ELLIS, C. D., 1934, *Proc. Roy. Soc. A*, **143**, 350.
 ELLIS, C. D., and SKINNER, H. W. B., 1924, *Proc. Roy. Soc. A*, **105**, 165.
 HAMILTON, D. R., and GROSS, L., 1950, *Rev. Sci. Instrum.*, **21**, 912.
 KINSEY, B. B., 1948, *Canad. J. Res. A*, **26**, 404, 421.
 KYLES, J., CAMPBELL, C. G., and HENDERSON, W. J., 1953, *Proc. Phys. Soc. A*, **66**, 519.
 LANGER, L. M., MOTZ, J. W., and PRICE, H. C., 1950, *Phys. Rev.*, **77**, 798.
 LECOIN, M., PEREY, M., and RIOU, M., 1949, *J. Phys. Radium*, **10**, 390.
 LECOIN, M., PEREY, M., and TEILLAC, J., 1949, *J. Phys. Radium*, **10**, 33.
 MASSEY, H. S. W., and BURHOP, E. H. S., 1936, *Proc. Camb. Phil. Soc.*, **32**, 461.
 THIBAUD, J., 1926, *Ann. Phys., Paris*, **5**, 73.
 YOVANOVITCH, D.-K., and D'ESPINE, J., 1927, *J. Phys. Radium*, **8**, 276.
 YOVANOVITCH, D.-K., and PROCA, A., 1926, *C. R. Acad. Sci., Paris*, **183**, 878.

Absolute Magnitudes of (d, p) Scattering Cross Sections

By G. ABRAHAM

Department of Theoretical Physics, The University of Liverpool

Communicated by R. Huby; MS. received 22nd September 1953

Abstract. A formula is given for the absolute magnitudes of (d, p) reactions on the basis of the single particle model (square-well potential) of the nucleus and the Butler stripping theory. On comparison with experimental data for the reaction $^{28}\text{Si}(\text{d}, \text{p})^{29}\text{Si}$ it is seen to give cross sections which are too large, but there is reasonable agreement on relative values. This is consistent with the recent work on absolute magnitudes of Horowitz and Messiah and of Thomas. The stripping cross section given here leads to a simple single particle formula for the reduced width, which is approximately the same as the Wigner sum-rule limit for resonance reduced widths.

THERE have been many experiments recently on the absolute magnitudes of (d, p) scattering cross sections. It is interesting to compare these with theoretical estimates. The Butler theory provides the required formula if one assumes some model for the nucleus. In this paper the simplest model is chosen, namely the representation of the nucleus by a square-well potential. Calculation shows the theoretical cross sections are too large, but there is reasonable agreement in the relative magnitudes of single particle levels. The absolute magnitude of stripping on Butler's theory can be expressed in terms of the reduced neutron width of the final nucleus. The assumption here of the square-well model gives a simple formula for this reduced width.

In the Butler theory (Butler 1951) the cross section is given by

$$\sigma_{l,j}(\mathbf{k}_{ps}) = 4\pi \frac{k_{ps}^3}{K_d} \int |\chi_{l,j}^{m_j}(\mathbf{k}_{ps}, r_n)|^2 r_n^2 dr_n. \quad \dots\dots(1)$$

Here $\chi_{l,j}^{m_j}(\mathbf{k}_{ps}, r_n)$ is the residue (at the singularity $k_p = k_{ps}$, corresponding to a bound state level) of the neutron wave function $\psi_{l,j}^{m_j}(\mathbf{k}_p, r_n)$ for total angular momentum j, m_j and orbital angular momentum l . Having now a model to represent the interaction of the neutron with the nucleus, we can determine the neutron wave function completely. It is identical with Butler's for r_n in the neighbourhood of r_0 and for $r_n > r_0$, where r_0 is the radius for the capture of the neutron; and it is a regular square-well wave function for $r_n < R$, where R is the radius of the well, which is taken a little less than r_0 . There are, of course, two sets of boundary conditions to be satisfied now, one at $r_n = R$ and the usual one at $r_n = r_0$. The integrals over r_n in the cross section are evaluated by the use of standard Bessel-function formulae to give

$$\left. \begin{aligned} \sigma_{l,j}(\mathbf{k}_{ps}) &= 8\pi C^2 (2j+1) \frac{k_{ps}}{K_d R} \left\{ \frac{1}{K^2 + \alpha^2} - \frac{1}{K^2 + (\alpha + \beta)^2} \right\}^2 \left(1 + \frac{E_n}{V} \right) F_l \\ F_l &= \frac{\{Zr_0 g_l(\kappa r_0) j_{l-1}(Zr_0) + \kappa r_0 g_{l-1}(\kappa r_0) j_l(Zr_0)\}^2}{g_{l+1}(\kappa R) g_{l-1}(\kappa R)}, \quad l > 0 \\ F_0 &= \frac{\{\cos Zr_0 + (\kappa/Z) \sin Zr_0\}}{g_1(\kappa R) g_0(\kappa R)} \end{aligned} \right\} \quad \dots\dots(2)$$

where

$$\left. \begin{aligned} i_l(x) &= \left(\frac{\pi}{2x}\right)^{1/2} J_{l+1/2}(x) \\ g_l(x) &= \exp(\kappa r_0 - x) \sum_{r=0}^l \frac{(l+r)!}{(l-r)! r! (2x)^r} \end{aligned} \right\} \dots\dots(2')$$

If the initial spin of the nucleus is not zero, the factor $2j+1$ has to be replaced by $(2J_B+1)/(2J_A+1)$ where J_A, J_B are the spins of the initial and final nuclei.

The cross section (2) is calculated for the reaction $^{28}\text{Si}(d, p)^{29}\text{Si}$ (Holt and Marsham 1953) and the results tabulated below. ^{28}Si , being made up of complete shells, is specially suitable for representation by a potential well. The following values are assumed for the parameters R, r_0 and V .

(a) $R=r_0=5.4 \times 10^{-13}$ cm, $V=30$ Mev.

(b) $R=4.2 \times 10^{-13}$ cm, $r_0=5.7 \times 10^{-13}$ cm, $V=35$ Mev.

The angular distribution is dependent on r_0 , but not on R , and r_0 is taken in (a) to be the best value found by Holt and Marsham to fit the angular distribution. The large value of r_0 in (b) does not affect the curve-fitting appreciably. There is no restriction on the choice of R , except that we expect $r_0 - R$ to be small compared with R . We shall see that the total cross section depends sensitively on $r_0 - R$. V depends on R and the bound state energies E_{ns} which are given experimentally, and is fixed by the vanishing of the coefficients $b(\mathbf{k}_{ps})$ in Butler's equation (20).

Maximum differential cross sections for the reaction $^{28}\text{Si}(d, p)^{29}\text{Si}$

Proton Group	Excitation (mev)	<i>l</i>	Max. Diff. Cross section (Millibarns)			Suggested Shell Model Orbit
			Experi- mental	Theoretical (Relative)		
				(a)	(b)	
p ₀	0	0	63	51	45	2s _{1/2}
p ₁	1.278	2	6.3	6.5	5.1	1d _{3/2}
p ₂	2.027	2	2.4	6.5	6.8	
p ₄	3.070	2	1.3	6.8	8.1	
p ₅	3.623	3	4	8.5	5.1	1f _{7/2}
p ₉	4.934	1	55	42	66	2p _{3/2}
p ₁₂	6.380	1	33	29	62	2p _{1/2}

Since this gives a different V for each l , an average value is taken for each choice of R ; V occurs explicitly only in the last factor of the cross section, which changes very little with V . But the large difference $r_0 - R$ in (b) reduces the cross section by a factor of 5 because of the factor $\exp\{\kappa(r_0 - R)\}$ in $g_l(\kappa R)$. The results are tabulated above. In both cases the theoretical cross sections are too large and the tabulated values are divided by 20 in (a) and by 4 in (b). This over-estimate of the stripping cross section by the Butler theory is in line with the indications of other recent work. Horowitz and Messiah (1953) find a reduction by a factor varying from 2 to 5 when the potential scattering of the proton is taken into account. Thomas (1953), in calculating reduced widths by the stripping theory, obtains values which are four times too small when compared with resonance experiments.

The tabulated relative magnitudes of the theoretical cross sections support the conclusion of Holt and Marsham that the levels p_2, p_4 are not single-particle levels.

To obtain a theoretical expression for the reduced width γ_l^2 of single-particle levels, the formula (2) is compared with the stripping formula of Huby (1953). One gets, taking $R=r_0$,

$$\left. \begin{aligned} \frac{mR}{2\hbar^2\{1+(E_n/V)\}} \gamma_l^2 &= \frac{g_l^2(\kappa R)}{g_{l+1}(\kappa R)g_{l-1}(\kappa R)}, & l > 0 \\ &= \frac{1}{g_1(\kappa R)}, & l = 0. \end{aligned} \right\} \dots\dots (3)$$

From the definition (2') of $g_l(\kappa R)$, it follows that the right-hand side of (3) is less than 1; for most bound levels in light nuclei, it does not vary greatly with l or κ and does not assume a value much less than 1. This estimate of the reduced width for single particle levels agrees therefore with the Wigner sum-rule limit for the resonance reduced width, which is $3\hbar^2/2mR$.

ACKNOWLEDGMENTS

I am indebted to Dr. R. Huby for suggesting this investigation and for many valuable discussions, and also to Drs. Holt and Marsham for access to their calculations on the angular distributions in the reaction $^{28}\text{Si}(d, p)^{29}\text{Si}$. I also wish to acknowledge a grant from the Department of Scientific and Industrial Research for the period during which this work was done.

REFERENCES

- BUTLER, S. T., 1951, *Proc. Roy. Soc. A*, **208**, 559.
 HOLT, J. R., and MARSHAM, T. N., 1953, *Proc. Phys. Soc. A*, **66**, 467.
 HOROWITZ, J., and MESSIAH, A. M. L., 1953, *J. Phys. Radium*, **14**, 695.
 HUBY, R., 1953, *Progr. Nucl. Phys.*, **3**, 177.
 THOMAS, R. G., 1953, *Phys. Rev.*, **91**, 453.

RESEARCH NOTES

The De-Excitation of Helium Metastable Atoms in Helium

By E. H. S. BURHOP

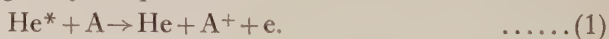
Department of Physics, University College, London

MS. received 30th October 1953

§ 1. THE EXPERIMENTAL OBSERVATIONS

PHelps AND MOLNAR (1953) have measured the rate of destruction of $\text{He}(2^3\text{S})$ metastable atoms in the afterglow of a pulsed discharge in very pure helium using an optical absorption technique. Biondi (1952) has measured the change of electron concentration in a similar afterglow using a microwave method and was able to estimate the rate of helium metastable destruction from an interpretation of the rather complicated variation of the electron concentration which increased at first after the discharge was interrupted and then decreased exponentially. Recently Phelps (1953) has employed both techniques on the same afterglow and has shown that under these conditions $\text{He}(2^1\text{S})$ metastable atoms are rapidly converted to the $\text{He}(2^3\text{S})$ state in super-elastic collisions with slow electrons so that Biondi's measurements almost certainly referred to the destruction of $\text{He}(2^3\text{S})$ metastable atoms also.

Evidence of the destruction of helium metastable atoms by collision with normal helium atoms without the production of ionization has been obtained by Jesse and Sadauskis (1952) in a very different type of experiment. They measured the energy per ion pair in the passage of alpha-particles through helium contaminated with very small amounts of argon and other gases. For many years the experimental value of this quantity for alpha-particles in helium has been found to be about 30 ev while the best calculated value is about 43 ev (Erskine 1953). Jesse and Sadauskis showed that when stringent precautions were taken to use very pure helium in these experiments a value of the energy per ion pair close to the theoretical value was obtained but the addition of a few parts per ten thousand of argon led to the much lower value observed earlier. They interpreted their result by supposing that in the presence of argon helium metastable atoms were capable of ionizing argon by the process



But in very pure helium the observation of the high value of the energy per ion pair implies that the excitation of helium metastable atoms is disposed of by collision with other helium atoms in a way that does not produce any ionization and Jesse and Sadauskis were able to estimate the cross section for such a process.

§ 2. PROCESSES EFFECTIVE IN THE DESTRUCTION OF HELIUM METASTABLES IN HELIUM

The following processes may produce the observed destruction of helium metastable atoms in helium:

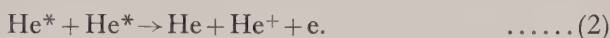
(i) In collisions with energetic normal atoms the helium metastable may be raised to a state from which radiation can occur. For helium, however, the nearest

radiating level (2^1P) lies 1.4 eV and 0.6 eV above the 2^3S and 2^1S metastable levels respectively and the number of atoms which would possess sufficient kinetic energy at room temperature to produce the necessary excitation is much too small to account for the observations.

(ii) As a result of the perturbation due to a collision with a normal helium atom the optical selection rule may break down and a radiative transition to the ground state may occur (collision induced radiation).

(iii) Molecular He_2 may be formed in an excited state as a result of a three-body collision between a metastable and two normal helium atoms. Radiative transitions could then occur to the ground state of He_2 leading to immediate dissociation.

(iv) In discharges in which the metastable concentration is high (greater than 10^{10} cm^{-3}) two-body collisions between metastables may occur leading to the de-excitation of one and the ionization of the other in the process



Let σ_d be the cross section for the destruction processes (ii) and (iii) which do not lead to ionization and ν_d the corresponding collision frequency, related to σ_d by the expression $\nu_d = n\bar{v}\sigma_d$ where n is the gas concentration and \bar{v} the mean velocity of relative motion between the two particles.

Similarly let σ_i be the cross section for process (iv) and α_i the corresponding collision frequency per unit metastable concentration given by $\alpha_i = \bar{v}^*\sigma_i$ where \bar{v}^* is the mean relative velocity of two metastable atoms. If D_m is the metastable diffusion coefficient, the metastable concentration M in an afterglow at time t after the interruption of the discharge satisfies the equation

$$\frac{\partial M}{\partial t} = D_m \nabla^2 M - \nu_d M - 2\alpha_i M^2. \quad \dots\dots(3)$$

(The factor 2 in the last term of this equation which has been omitted in previous discussions of this problem is necessary because two metastable atoms are destroyed in each collision of type (iv).)

The lowest mode solution of this equation is

$$M = \{M_0 \exp(-t/T_m)\} / \{1 + 2\alpha_i M_0 T_m [1 - \exp(-t/T_m)]\} \quad \dots\dots(4)$$

where M_0 is the initial metastable concentration and $1/T_m = \nu_d + D_m/\Lambda^2$, Λ being the characteristic diffusion length of the container.

At a temperature of $300^\circ K$ and for a range of pressures from 20 to 100 mmHg Phelps and Molnar found $\nu_d = 0.2 p^2 \text{ sec}^{-1}$, where p is the gas pressure expressed in mmHg leading to a cross section,

$$\sigma_d = 3 \times 10^{-23} p \text{ cm}^2. \quad \dots\dots(5)$$

This form of variation of ν_d with pressure indicates that the destruction of metastables in pure helium when the metastable density is less than 10^{10} cm^{-3} occurs predominantly through the three-body process (iii), and the two-body process (ii) is relatively unimportant. A conclusion different from this was reached by Biondi who interpreted his results to lead to a value $\sigma_d = 9.6 \times 10^{-21} \text{ cm}^2$ for the process (ii). Biondi's measurements, however, referred to afterglows in which the metastable density was very large ($> 10^{10} \text{ cm}^{-3}$) and his results can be interpreted equally well by assuming the cross section for process (ii) to be very small and most of the loss of metastables in his case to be due to process (iv).

Using eqn (4) his measurements can be interpreted by assuming the cross section for process (iv) to be approximately 10^{-14} cm^2 . This cross section is very high but a similar high estimate was obtained independently by Phelps and Molnar.

From their measurements of the energy per ion pair in helium-argon mixtures Jesse and Sadauskis (private communication) estimated the cross section σ_d for the destruction of He^* in He at a pressure of 850 mm Hg to be $\sigma_d = 1.55 \times 10^{-20} \text{ cm}^2$. The value expected from eqn (5) is $2.5 \times 10^{-20} \text{ cm}^2$. The agreement is very satisfactory particularly when it is remembered that not only 2^1S but more highly excited metastables were probably also present in their case.

§ 3. THE DESTRUCTION OF HELIUM METASTABLES IN THREE-BODY COLLISIONS

In a recent theoretical investigation Buckingham and Dalgarno (1952) have calculated the form of the interaction between normal and metastable helium atoms. They found that molecule formation is possible for the $1\Sigma_u$ and $3\Sigma_u$ states of the combined system. The dissociating ground state of He_2 is $1\Sigma_g$ and radiative transitions are allowed from the $1\Sigma_u$ to the ground $1\Sigma_g$ state.

It is more difficult to understand how the triplet metastables can be disposed of. But if the curves E_A' , E_A of figure 1 in Buckingham and Dalgarno's paper are plotted so as to lead to the correct energies of $\text{He} + \text{He}^*(1\text{S})$ and $\text{He} + \text{He}^*(3\text{S})$ for infinite separation it is observed that they cross so that in principle one might expect some transformation from $3\Sigma_u$ to $1\Sigma_u$ on collision. Of course such a transition would violate the Wigner spin conservation rule. But such violations have been well established in other cases of collisions of excited helium atoms (Massey and Burhop 1952, pp. 428-431), so that it seems possible also to dispose of helium triplet metastables without ionization.

The cross section for the three-body process can be estimated by a method exactly analogous to the Thomson theory of recombination. According to this theory molecule formation can occur by collision stabilization if one of the colliding systems suffers a collision with a third body when within a critical distance r_0 apart. Thomson took $r_0 = 2e^2/3kT$ which is reasonable for the collision of two charged particles.

Buckingham and Dalgarno showed the existence of a potential barrier in the interaction between normal and metastable helium which would have to be surmounted before the atoms could come together to form a molecule. It is clear that in the present case r_0 should be taken as the separation corresponding to the top of the potential barrier ($r_0 \simeq 2 \times 10^{-8} \text{ cm}$).

The effective cross section for molecular formation (and thence for collision de-excitation of the helium metastables) is given then by

$$\sigma = \frac{1}{2} \exp(-\Delta E/kT) (S_1 + S_2) \pi r_0^2$$

$$S = 1 + 2 \left\{ \frac{e^{-g}}{g^2} + \frac{e^{-g}}{g} - \frac{1}{g^2} \right\}; \quad g = \frac{2r_0}{l} \quad \dots\dots (6)$$

where S_1 and S_2 are associated with l_1 and l_2 , the mean free paths for collisions of normal and metastable helium atoms in helium (Massey and Burhop 1952, p. 623) and ΔE is the height of the potential barrier. The factor $\frac{1}{2}$ arises because formation of the Σ_u and the dissociating excited Σ_g molecular states are equally probable. Under the conditions of the experiments discussed above $2r_0 \ll l$ and

$$\sigma = \frac{2}{3} \exp\left(\frac{-\Delta E}{kT}\right) \pi r_0^3 \left(\frac{1}{l_1} + \frac{1}{l_2}\right) \quad \dots\dots (7)$$

For collisions between normal helium atoms $l_1 = 0.014/p$ (Kennard 1938, p. 149). For collisions between metastable and normal helium atoms the interactions calculated by Buckingham and Dalgarno give $l_2 = 0.012/p$ so that (7) can be written

$$\sigma_d = 325 p \exp(-\Delta E/kT) r_0^3 \text{ cm}^2. \quad \dots\dots(8)$$

The parameters r_0 , ΔE were not determined uniquely by Buckingham and Dalgarno because of the difficulty of carrying out the second order perturbation calculations. At separations of importance in the present considerations they give for the interaction energy

$$V(R) = V_1(R) - C/R^6 \quad \dots\dots(9)$$

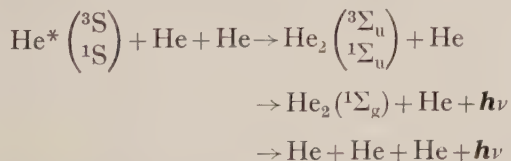
where $V_1(R)$ is the interaction given by a first order perturbation calculation and C a constant estimated as $2 \times 10^{-59} \text{ erg cm}^6$ and $3 \times 10^{-59} \text{ erg cm}^6$ using two different methods of calculation. The second term in (9) affects the critical distance r_0 only slightly but has a marked effect on the barrier height ΔE .

Equation (8) becomes consistent with the results of Phelps and Molnar (eqn (5)) if $\Delta E = 0.115 \text{ ev}$, $r_0 = 2.2 \times 10^{-8} \text{ cm}$. These values would be obtained by substituting $C = 3 \times 10^{-59} \text{ erg cm}^6$ in eqn (9).

There remains one inconsistency in this interpretation. Phelps and Molnar measured the destruction cross section σ_d when their afterglow tube was surrounded by liquid nitrogen and found a value 67 times smaller than at room temperature. As they point out this greatly reduced cross section suggests the importance of an activation energy for collisions between He^* and He . The height of the corresponding barrier would be only 0.04 ev . This assumes, however, that the gas temperature is equal to 77°K when the discharge tube is surrounded by liquid nitrogen. Owing to the continual dissipation of energy in the discharge one would expect the actual gas temperature to be higher than this, leading to an increased activation energy. It is difficult to say whether this effect would be sufficient to account for the discrepancy without more data about the discharge conditions in Phelps and Molnar's experiments. Gas heating in the discharge at room temperature would also lead to a difference between the cross section deduced from the experiments of Jesse and Sadauskis and Phelps and Molnar in the direction observed.

§ 4. CONCLUSION

It is concluded that the experimental data on the destruction of metastable helium atoms in helium are consistent with the interpretation that two processes are important, viz. $\text{He}^* + \text{He}^* \rightarrow \text{He} + \text{He} + e$ with a cross section of 10^{-14} cm^2 and



with a cross section of $3 \times 10^{-23} p \text{ cm}^2$ (p in mm Hg). This three-body process can be interpreted along similar lines to the Thomson recombination theory and is consistent with a potential barrier of height 0.125 ev at a separation of $2.2 \times 10^{-8} \text{ cm}$ in the interaction between normal and metastable helium atoms.

ACKNOWLEDGMENTS

I am indebted to Prof. H. S. W. Massey and Dr. R. A. Buckingham for useful discussion and to Dr. W. P. Jesse for sending me details of his experimental results on He-A mixtures prior to publication.

REFERENCES

- BIONDI, M. I., 1952, *Phys. Rev.*, **88**, 660.
 BUCKINGHAM, R. A., and DALGARNO, A., 1952, *Proc. Roy. Soc. A*, **213**, 327.
 ERSKINE, G. A., 1953, *Thesis*, University of London.
 JESSE, W. P., and SADAUSKIS, J., 1952, *Phys. Rev.*, **88**, 417.
 KENNARD, E. H., 1938, *Kinetic Theory of Gases* (London: McGraw-Hill).
 MASSEY, H. S. W., and BURHOP, E. H. S., 1952, *Electronic and Ionic Impact Phenomena* (Oxford: Clarendon Press).
 PHELPS, A. V., 1953, *Phys. Rev.*, **91**, 436A.
 PHELPS, A. V., and MOLNAR, J. P., 1953, *Phys. Rev.*, **89**, 1202.

The Disintegration of Cobalt 57

BY D. E. ALBURGER* AND M. A. GRACE†

* Nobel Institute of Physics, Stockholm, Sweden; National Science Foundation Fellow now returned to Brookhaven National Laboratory.

† Clarendon Laboratory, Oxford.

MS. received 27th October 1953

THE γ -rays of ^{57}Fe excited during the decay of ^{57}Co have been studied by a number of authors (Plesset 1942, Elliott and Deutsch 1943, Cheng, Dick and Khurbatov 1952) and the principal features of the decay scheme are indicated in figure 1. The 14 keV γ -ray (γ_3) has been identified as an

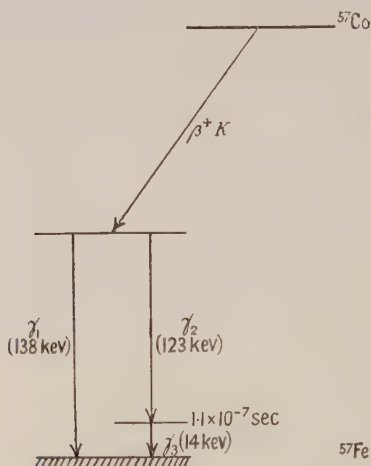


Figure 1. Decay scheme of ^{57}Co .

M1 transition by Goldhaber and Sunyar (1951) from a lifetime measurement by Deutsch and Wright (1950). The multipole character of the other γ -rays has not been determined reliably although evidence that for both the internal conversion coefficient α_K is about 1 and the K/L ratio about 6 was obtained by

Cheng, Dick and Khurbatov (1952); this suggested that the transitions might be M2 or E3. The object of the present experiments was to establish the multipole character of γ_1 and γ_2 .

A source of ^{57}Co contaminated by about 10% ^{56}Co was available, as a residue from the deuteron bombardment of an iron target; this was used throughout the experiments. A preliminary measurement involving rapid chemical separation of iron from cobalt activities showed that no half-life of 7 seconds or greater was present in the iron. This suggested that neither γ -ray could be higher than quadrupole unless these transitions were about 100 times faster than values given by Goldhaber and Sunyar (1951).

In figure 2 is shown a characteristic pulse height distribution obtained using a xenon-filled proportional counter (Rothwell and West 1950); the 'escape' peak arises from photoelectric absorption of the γ -ray quantum with subsequent escape from the counter of K x-radiation of xenon, whereas the primary peak corresponds to the total energy of the radiation. This gives values for the energy of γ_1 and γ_2 of 138 ± 1 kev and 123 ± 1 kev respectively; the counter was calibrated with the 59.8 ± 0.02 kev γ -ray of ^{241}Am (Browne and Perlman 1952).

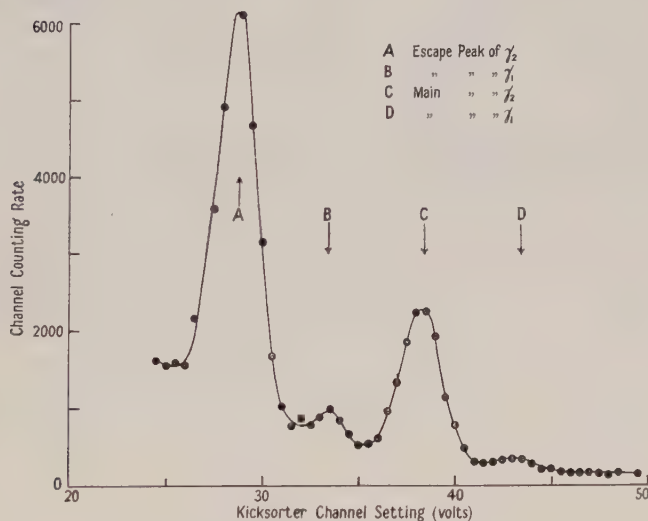


Figure 2. Pulse height distribution on proportional counter of γ -rays of ^{57}Co .

These values of energy were confirmed by β -ray spectrometer measurements where energies of 137.6 ± 0.5 kev and 122.8 ± 0.5 kev were obtained: in this case the K conversion line of the 184.1 ± 0.2 kev γ -ray from ^{206}Bi (Alburger, unpublished) was used as a calibration. These values are significantly higher than those obtained by earlier authors, namely 131 and 119 kev. From the areas lying under the peaks and the stopping power of xenon in this energy range, a value of 15 ± 7 for the branching ratio $I(\gamma_2)/I(\gamma_1)$ for the unconverted γ -rays was found. The large error enters through the uncertainty in the contribution of the background to the γ_1 peak: from the known general form of the background the upper limit of this ratio is favoured. There was no indication of γ -radiation from the highly converted γ_3 (14 kev) transition.

Measurements made on the internal conversion lines of γ_1 and γ_2 using the double focusing β -spectrometer at the Nobel Institute are reproduced in figure 3.

The source (approx 1 mg cm^{-2} thick) was obtained by plating the cobalt activities on to a platinum foil. With a resolution of about $\frac{1}{2}\%$ the K and L conversion lines are well resolved. From the heights of the peaks, making a small correction for the M conversion peak, the $K/(L+M)$ ratios are found to be 7.7 for γ_1 and 8.2 for γ_2 . Although these values are accurate to about 10% the $K/(L+M)$ ratio in this energy region is very insensitive to multipole order and it is only possible to conclude that the radiation is octupole or lower.

From approximate values for the transmission of the spectrometer the numbers of electrons in the K peaks were found to be 4×10^4 and $3.5 \times 10^4 \text{ sec}^{-1}$ respectively. These should be correct to within a factor of 2, the uncertainty arising from scattering in the source thickness and backscattering in the foil as indicated by the low energy tail (figure 3). The γ -ray strength of the same source ($108 \pm 14 \mu\text{C}$) was determined with a scintillation counter using a 1 in. NaI crystal; the error in this case enters through uncertainty in the amount of scattered radiation which was detected. From these figures values for α_K are obtained and these together with values extrapolated from the figures of Rose *et al.* (1951) are shown below.

	Obs	E1	M1	E2	M2	E3	M3
$\gamma_1=138 \text{ kev}$	1.4×10^{-1}	1.6×10^{-2}	1.5×10^{-2}	1.5×10^{-1}	1.2×10^{-1}	1.2	1.0
$\gamma_2=123 \text{ kev}$	1.1×10^{-2}	1.3×10^{-2}	1.2×10^{-2}	1.1×10^{-1}	1.0×10^{-1}	0.8	0.7

This shows that γ_1 is quadrupole and γ_2 is dipole. Because the absolute value of α_K could be in error by a factor of 2 it is not possible to identify the electric or magnetic character from these measurements alone.

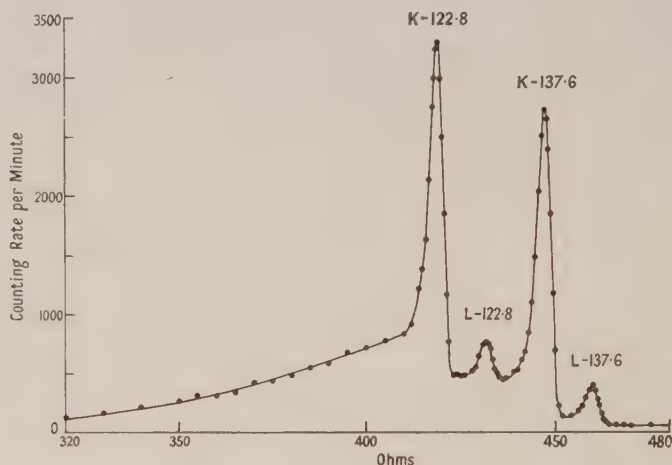


Figure 3. Internal conversion electron spectrum of γ -rays of ^{57}Co .

Since γ_3 is an M1 transition γ_1 and γ_2 must involve the same change in parity. Therefore the transitions must be either E2 and M1 or M2 and E1. From the observed strengths of the two transitions γ_1 and γ_2 the former choice seems to be preferable and it is concluded that no change in parity occurs. On this assumption the ground state and the two excited states in ^{57}Fe are all of the same parity: this is in accord with the shell model which predicts that low-lying levels will be configurations of an odd number of particles in $p_{3/2}$ or $f_{5/2}$ states with the first even parity state $g_{9/2}$ lying at higher excitation.

ACKNOWLEDGMENTS

We are indebted to Mr. D. West and the Director, Atomic Energy Research Establishment, Harwell, for the provision of facilities for the proportional counter measurements, and to the Nuffield Cyclotron Group at Birmingham for the target irradiation. We are especially grateful to Dr. P. F. D. Shaw for his generous assistance in preparing the sources.

We wish to thank Lord Cherwell for his interest in this work, and the Director of the Nobel Institute, Stockholm, where some of the measurements were made.

REFERENCES

- BROWNE, C. I., and PERLMAN, I., 1952, *Phys. Rev.*, **85**, 758.
CHENG, L. S., DICK, J. L., and KHURBATOV, J. D., 1952, *Phys. Rev.*, **88**, 887.
DEUTSCH, M., and WRIGHT, W. E., 1950, *Phys. Rev.*, **77**, 139.
ELLIOTT, L. G., and DEUTSCH, M., 1943, *Phys. Rev.*, **64**, 321.
GOLDHABER, M., and SUNYAR, A. W., 1951, *Phys. Rev.*, **83**, 906.
PLESSET, E. H., 1942, *Phys. Rev.*, **62**, 181.
ROSE, M. E., GOERTZEL, G. H., SPINRAD, B. I., HARR, J., and STRONG, P., 1951, *Phys. Rev.*, **83**, 79.
ROTHWELL, P., and WEST, D., 1950, *Proc. Phys. Soc. A*, **63**, 539.

A Search for ^{205}Pb

By P. F. D. SHAW AND J. R. PRESCOTT

Clarendon Laboratory, Oxford

MS. received 13th October 1953

§ 1. INTRODUCTION

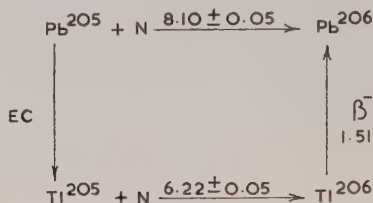
LEAD 205 has been sought by Templeton, Howland and Perlman (1947) in the $\text{Tl}(d, 2n)\text{Pb}$ reaction; they estimate its life to be greater than 500 years by comparison with ^{203}Pb , assuming it to be counted with comparable efficiency.

In the present experiments ^{205}Pb was sought for as the daughter of ^{205}Bi which decays by electron capture to ^{205}Pb ; and in the irradiation of thallium with deuterons, where ^{205}Pb should be produced from ^{205}Tl with almost the same cross section as ^{203}Pb from ^{203}Tl .

§ 2. POSSIBLE MODES OF DECAY OF ^{205}Pb

We first determine the decay energy of ^{205}Pb as a pointer to the kind of results we may expect. This energy can be found from the closed cycle shown in the figure. It involves neutron binding energies and the data required are shown on the figure, energies being expressed in MeV (Wapstra 1953, Alburger and Friedlander 1951). From the figure the available energy for the decay of ^{205}Pb is 370 ± 100 keV; Feather (1952) estimates this energy to be 250 ± 200 keV. ^{205}Pb is thus expected to decay by electron capture to stable ^{205}Tl , and any gamma-radiation appearing in the decay will be determined by the energy levels in the latter.

We can infer something about the level scheme of ^{205}Tl from that of ^{203}Tl and ^{207}Tl . ^{203}Tl has a ground state $s_{1/2}$, and its first excited state at 280 kev is $d_{3/2}$ (Klinkenberg 1952, Wilson and Curran 1951, Prescott 1954). Pryce (1952) has suggested that the ground and the first excited states of ^{207}Tl are $s_{1/2}$ and $d_{3/2}$ respectively, but recent measurements at 350 kev by Gorodetsky (private communication to Prof. M. H. L. Pryce) are more consistent with an inversion of these levels. If the two lowest levels (ground and first excited states) of ^{203}Tl and ^{207}Tl are either $s_{1/2}$ or $d_{3/2}$, it is probable that these correspond to the lowest levels in ^{205}Tl since this differs from the former nuclei by two neutrons. The ground state of ^{205}Tl is $s_{1/2}$ from its spin and magnetic moment (Klinkenberg 1952), and it therefore seems probable that its first excited state is $d_{3/2}$.



Energy scale for estimating the electron-capture decay energy of ^{205}Pb .

In a previous paper one of the authors (Prescott 1954) has shown that the ground state of ^{203}Pb is probably $f_{5/2}$ and has suggested that the ground state of ^{205}Pb is $f_{5/2}$ also. If this is the case, the electron capture transition $f_{5/2} \rightarrow s_{1/2}$ to the ground state is of the type $\Delta l = 3$, $\Delta j = 2$ which, though technically first forbidden, is strongly l-forbidden and of long life (Mayer *et al.* 1951). If it occurred, the transition $f_{5/2} \rightarrow d_{3/2}$ to the first excited state would be of the normal first forbidden type and would correspond to a half-life of the order of several days to a few months (Moszkowski 1951).

In seeking evidence of the decay of ^{205}Pb we should look for the x-rays following electron capture and possibly a gamma-ray of less than 400 kev. If the decay to the first excited state is energetically forbidden, then the only radiation observable will be K and L x-rays.

§ 3. ^{205}Pb IN ASSOCIATION WITH ^{203}Pb

Natural thallium ($^{203}\text{Tl} : ^{205}\text{Tl} = 29 : 71$) was bombarded with 20 mev deuterons in the Birmingham cyclotron. ^{205}Tl differs from ^{203}Tl only in a pair of neutrons, and it is reasonable to assume roughly the same yield for the (d, 2n) reaction in each isotope. This assumption is supported by the few analogous cases for which yields have been estimated: ^{191}Ir (d, 2n) (Wilkinson 1949), $^{128,130}\text{Te}$ (d, 2n) (Livingood and Seaborg 1938), $^{63,65}\text{Cu}$ (d, 2n) (Clarke and Irvine 1946). Assuming equal yields, ^{205}Pb and ^{203}Pb were present after irradiation in the proportions 2.5 : 1.

The lead was extracted as a thin source and the ^{203}Pb content found by coincidence counting (Prescott 1954) and extrapolating back to the time of irradiation. This activity was $820 \pm 50 \mu\text{C}$. After allowing the ^{203}Pb to decay out for several months, the remaining lead was re-separated by paper chromatography (see, for example, Balston and Talbot 1952) with Whatman no. 542

filter paper using 5% conc. HCl in methanol as the solvent. In this separation the lead remains in the starting strip. Care was taken in the re-separation of the lead to avoid contamination from other possible electron-capture nuclei. Carriers were added for all likely contaminants, and to prevent any loss of lead, platinum containers were used. Previous experience showed that trace amounts of lead tended to stick to glass containers.

The strip containing the lead was examined with an NaI(Tl) scintillation spectrometer over the energy region 0–350 kev. There was no evidence for peaks either in the x-ray region or at higher energies, though in the absence of the former the latter is not to be expected.

A number of 12-hour counts were taken with a kicksorter set on the x-ray region. The average background count (three runs) was $6.09 (\pm 2\%) \text{ min}^{-1}$ and the average count with lead (four runs) was $6.53 (\pm 2\%)$; the errors include statistical errors and a 'consistency' error estimated from similar long runs in other experiments. The increase with lead is statistically significant. If we assume that the difference, 0.44 count per minute, is due to ^{205}Pb we can estimate the half-life by comparison with ^{203}Pb in the following way.

From the known efficiency of the crystal (Prescott 1954) and the solid angle, 0.44 count per minute represents $5 \times 10^{-6} \mu\text{C}$. Under the assumptions of the first paragraph in this section, the proportion of ^{205}Pb to ^{203}Pb is 2.5 to 1. The initial activity of the ^{203}Pb was $820 \pm 50 \mu\text{C}$, and the specific activities are in the inverse ratio of the half-lives. From this it follows that the half-life of ^{205}Pb is 3×10^6 years. However, since the observed count is only just of statistical significance, probably only the order of magnitude can be taken seriously.

§ 4. ^{205}Pb FROM ^{205}Bi

Natural lead was irradiated as a thick target in the Harwell cyclotron for 24 hours at 25 mev at an approximate beam current of protons of $2 \mu\text{A}$. Immediately after irradiation the bulk of the inactive lead was chemically separated, and the active bismuth extracted by paper chromatography using n-butyl alcohol saturated with 3N HCl as the solvent; the bismuth was then left on the paper for five months. During this time the x-rays from an aliquot were counted, giving the bismuth decay curve. The activity contained a substantial amount of 14.5-day ^{205}Bi , though 6.4-day ^{206}Bi was evident at the beginning and 56-year ^{207}Bi at the end. From the decay curve we find the ratio of ^{205}Bi to ^{207}Bi originally present in the sample. When substantially all of the ^{205}Bi had decayed out to ^{205}Pb , the chromatogram was run off and the remaining bismuth recovered; in this process the daughter lead remains behind at the original location of the bismuth. The bismuth, consisting now of ^{207}Bi , was counted and the source strength determined. This gives the initial amount of ^{205}Bi when combined with the ratio measurement on the aliquot. There was $800 \pm 50 \mu\text{C}$ of ^{205}Bi originally present. The lead was then washed out of the chromatogram, re-separated three more times by paper chromatography* and finally counted. The average count was $4.35 (\pm 2\%) \text{ min}^{-1}$ with a background

* The efficiency of separation of the method varies somewhat with the amount of material placed originally on the chromatogram and with the solvent. The first three separations (with the butyl alcohol-HCl mixture) gave 98.5%, 99.5% and 99% separations respectively. The fourth, with methanol-HCl mixture, could not be measured because of the negligible activity.

count of $4.17 (\pm 2\%)$. The difference is not statistically significant. We can place a lower limit to the half-life of ^{205}Pb if we assume that up to three probable errors of the background count (0.25 min^{-1}) are due to ^{205}Pb . The calculation is identical, *mutatis mutandis*, with that in the previous section, and the half-life of ^{205}Pb found in this way is 8.5×10^6 years.

§ 5. DISCUSSION

Although the counting rate for the supposed ^{205}Pb is in both cases greater than background, the difference is not sufficiently significant to justify actually attributing it to ^{205}Pb , if only for the reason that it is impossible to be certain that a count of the order of 0.5 per minute is not due to some contamination imperfectly removed. For this reason the half-life estimates are best regarded as lower limits, and in this they agree that the half-life of ^{205}Pb is greater than a figure lying between 10^6 and 10^7 years. For the reasons given in § 2 we therefore conclude: (a) that the first excited state of ^{205}Tl cannot be much lower than about 400 keV, and (b) that the assignment $f_{5/2}$ for the ground state of ^{205}Pb is plausible.

ACKNOWLEDGMENTS

The authors wish to express their appreciation to Professor Lord Cherwell for making available the facilities of the Clarendon Laboratory. One of us (J. R. P.) is indebted to the Executive of the Commonwealth Scientific and Industrial Research Organization, Australia, for leave of absence and to the Australian National University and the Nuffield Foundation for financial assistance.

REFERENCES

- ALBURGER, D. F., and FRIEDLANDER, G., 1951, *Phys. Rev.*, **82**, 977.
 BALSTON, J. N., and TALBOT, B. E., 1952, *A Guide to Filter Paper and Cellulose Powder Chromatography* (London: Reeve Angel).
 CLARKE, E. T., and IRVINE, J. W., Jr., 1946, *Phys. Rev.*, **70**, 893.
 FEATHER, N., 1952, *Proc. Roy. Soc., Edinb.*, **63**, 242.
 KLINKENBERG, P. F. A., 1952, *Rev. Mod. Phys.*, **24**, 63.
 LIVINGOOD, J. J., and SEABORG, G. T., 1938, *Phys. Rev.*, **54**, 775.
 MAYER, R. G., MOSZKOWSKI, S. A., and NORDHEIM, L. W., 1951, *Rev. Mod. Phys.*, **23**, 315.
 MOSZKOWSKI, S. A., 1951, *Phys. Rev.*, **82**, 35.
 PRESCOTT, J. R., 1954, *Proc. Phys. Soc. A*, **67**, 254.
 PRYCE, M. H. L., 1952, *Proc. Phys. Soc. A*, **65**, 773.
 TEMPLETON, D. H., HOWLAND, J. J., and PERLMAN, I., 1947, *Phys. Rev.*, **72**, 766.
 WAPSTRA, A. H., 1953, *Thesis*, University of Amsterdam, p. 71, *Physica*, **17**, 628.
 WILKINSON, G., 1949, *Phys. Rev.*, **75**, 1019.
 WILSON, R., and CURRAN, S. C., 1951, *Phil. Mag.*, **42**, 762.

Isomerism in ^{46}Ti

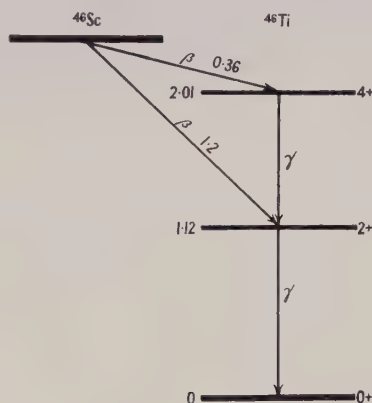
By H. S. MURDOCH AND A. J. WEBB

School of Physics, University of Sydney, Sydney, Australia

Communicated by R. E. B. Makinson; MS. received 27th October 1953

THE decay scheme of ^{46}Sc to ^{46}Ti is now well established (Goldhaber and Hill 1952), and is shown in the figure. The relative intensity of the 1.2 MeV β -ray is 0.2% (Schmidt and Keister 1953). The first excited state (then considered to be 0.89 MeV) was reported as metastable with a half-life

12.15 μsec by Nag, Sen and Chatterjee (1950). The spins of the two excited states are shown in the figure and are supported by angular correlation measurements (Brady and Deutsch 1950), polarization-direction correlation measurements (Metzger and Deutsch 1950) and by internal conversion coefficient measurements (Moon, Waggoner and Roberts 1950). The expected half-life calculated from Weisskopf's formula (Weisskopf 1951) is of the order of 10^{-12} second. Whilst this formula is only approximate, such a large divergence cannot be expected, and a half-life of 12 μsec is quite incompatible with a spin of 2 but would rather indicate a spin of 4.



Decay scheme of ^{46}Sc (energies in MeV)

By the use of the delayed coincidence method we have found that no half-life greater than 1 μsec exists. A delay of 2 μsec was used which was sufficient to eliminate any instantaneous coincidences. The respective widths τ_1 and τ_2 of the non-delayed and delayed pulses were 0.2 and 22 μsec . The value chosen for $\tau_1 + \tau_2$ is the optimum value for the detection of a half-life of 12.2 μsec (Murdoch 1953).

Sufficient absorber was placed in front of counter 2 to eliminate the 0.36 MeV β -ray, and in front of counter 1 to eliminate also the high energy β -ray. A very weak source was used in order to obtain an adequate ratio of true to chance coincidences. The results obtained were as follows:

$$\text{Observed coincidence rate} = 0.00053 \pm 0.00011 \text{ sec}^{-1}$$

$$\text{Chance coincidence rate} = 0.00048 \pm 0.00001 \text{ sec}^{-1}$$

$$\text{True coincidence rate} = 0.00005 \pm 0.00011 \text{ sec}^{-1}$$

The true coincidence rate with no artificial delay introduced was 0.0066 sec^{-1} . The proportion of delayed coincidences of half-life 12.2 μsec which would be recorded with the value of τ_2 used is 0.6. On the above figures there is a probability of only 1% that more than 5% of the coincidences recorded should be delayed, whereas, on the basis of the result of Nag, Sen and Chatterjee, all such coincidences should be delayed. A similar experiment was carried out with no absorber in front of counter 2, and this eliminated the possibility of the presence of a metastable state following the 0.36 MeV β -ray.

Different values of τ_2 were also used, which gave equally sensitive negative results for half-lives down to $1\mu\text{sec}$.

The authors would like to thank Drs. R. E. B. Makinson and K. Landecker for their interest in this work.

REFERENCES

- BRADY, E., and DEUTSCH, M., 1950, *Phys. Rev.*, **78**, 558.
 GOLDHABER, M., and HILL, R. D., 1952, *Rev. Mod. Phys.*, **24**, 179.
 METZGER, F., and DEUTSCH, M., 1950, *Phys. Rev.*, **78**, 551.
 MOON, M. L., WAGGONER, M. A., and ROBERTS, A., 1950, *Phys. Rev.*, **79**, 905.
 MURDOCH, H. S., 1953, *Proc. Phys. Soc. A*, **66**, 944.
 NAG, B. D., SEN, S., and CHATTERJEE, S., 1950, *Indian J. Phys.*, **72**, 888.
 SCHMIDT, F. H., and KEISTER, G. L., 1953, *Phys. Rev.*, **91**, 483.
 WEISSKOPF, V. F., 1951, *Phys. Rev.*, **83**, 1073.

On Momentum Distribution in Nuclei

By N. H. MARCH

Department of Physics, The University, Sheffield

MS. received 2nd November 1953

THE momentum distribution of the particles in the nucleus is of some importance in current nuclear problems. For example, the details of the production of mesons by bombarding nuclei with photons depend on the momentum distribution of the particles in the target nuclei (Lax and Feshbach 1951).

The purpose of this note is to point out that the Thomas-Fermi (TF) model of the nucleus will provide an approximation to the momentum distribution and to examine the validity of the results thus obtained.* It is true that certain recent work using the TF method to predict the 'magic numbers' of nuclei (Yang 1951, Ivanenko and Rodichev 1950) has been severely criticized (Paneth 1951, Jensen and Luttinger 1952, referred to hereafter as JL). Nevertheless it is clear from the work of JL that the TF method is useful for certain applications and that, as Yang had initially believed, some light is thus thrown on the form of the nuclear density. JL were concerned with the angular momentum distribution in the nucleus, and with a particular choice of density they showed that the results obtained for the mean square angular momentum using the TF model were in good agreement with the results of the shell model.

Once the choice of nuclear density is made, a consistent carrying-through of the assumptions of the model allows the linear momentum distribution to be obtained unambiguously. Similar calculations in the atomic case have been made by Coulson and March (1950); the method of obtaining the momentum distribution is given there and hence need not be repeated here. For a given proton density† the probability $I(p)dp$ that a proton will have momentum of magnitude between p and $p+dp$ can thus be obtained.

* Thanks are due to a referee for suggestions which have helped to clarify this latter part of the work.

† Exactly similar considerations apply to the neutrons.

JL assume the proton density to be given by

$$\frac{8\pi}{3\hbar^3} [P_0 f(x)]^3.$$

Here $x=r/R$, r being the distance from the centre of the nucleus and R being of the order of magnitude of the nuclear radius; P_0 is the maximum proton momentum at the centre of the nucleus, and $f(x)$ is given by

$$f(x) = \begin{cases} 1 & \text{for } x < 1, \\ \exp(-\{x-1\}^2/3\beta) & \text{for } x > 1. \end{cases}$$

The choice of β and R is discussed in detail by JL. If we accept this density, then it is easily shown that the corresponding momentum distribution is given by

$$I(p) = \begin{cases} \frac{32\pi^2 R^3}{3\hbar^3 Z} \left[1 + \left(3\beta \ln \frac{P_0}{p} \right)^{1/2} \right]^3 p^2 & \text{for } p \leq P_0, \\ 0 & \text{for } p > P_0. \end{cases} \quad \dots\dots(1)$$

In an attempt to investigate the validity of this approximation to the momentum distribution of nucleons we have examined the case of particles moving in an oscillator potential. The TF method has been used to transform the wave mechanical densities into momentum space, and a comparison has been made with the exact wave mechanical results. The nuclear densities for 20, 58 and 92 particles are shown in figure 1, whilst the results obtained for the momentum distribution are displayed in figure 2. In both figures convenient

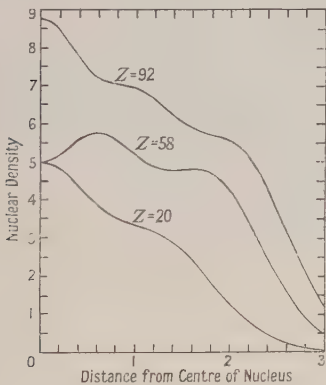


Figure 1. Nuclear densities for 20, 58 and 92 protons in oscillator potential.

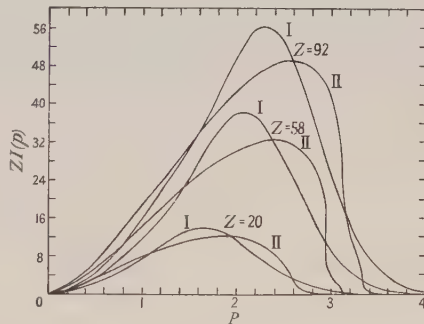


Figure 2. Momentum distributions for oscillator potential. Curve I, Exact wave mechanical result. Curve II, TF result.

dimensionless units are used, which need not be specified here. It can be seen from figure 2 that the overall agreement between the exact and approximate curves is quite good. However, apart from obvious differences in the detailed shapes of the curves, two defects are introduced by the TF procedure of transforming into momentum space. First, the momentum density $I(p)/4\pi p^2$ is infinite at the origin according to the approximate method and finite from the exact treatment. Secondly, the approximate distribution is of finite extent, whilst the exact distribution extends to infinity.

It is immediately clear from eqn (1) that the momentum distribution given there suffers from these two defects. Even so, in view of the results for the oscillator potential, it does not seem too optimistic to suppose that eqn (1) will give a useful overall description of the momentum distribution of nucleons in medium and heavy nuclei.

REFERENCES

- COULSON, C. A., and MARCH, N. H., 1950, *Proc. Phys. Soc. A*, **63**, 367.
 IVANENKO, D., and RODICHEV, V., 1950, *C. R. Acad. Sci., U.S.S.R.*, **70**, 605.
 JENSEN, J. H. D., and LUTTINGER, J. M., 1952, *Phys. Rev.*, **86**, 907.
 LAX, M., and FESHBACH, H., 1951, *Phys. Rev.*, **81**, 189.
 PANETH, H. R., 1951, *Proc. Phys. Soc. A*, **64**, 937.
 YANG, L. M., 1951, *Proc. Phys. Soc. A*, **64**, 632.

The Thermal Conductivity of Metals

By R. E. B. MAKINSON

School of Physics, The University of Sydney, Sydney, Australia

MS. received 21st October 1953

SONDHEIMER (1950) has evaluated the thermal conductivity of a monovalent metal, taking account of impurities and lattice vibrations, by solving for $c^{(n)}(\eta)$ an integral equation (Wilson 1937)

$$E^n = Lc^{(n)}(\eta), \quad n = 3/2, 5/2. \quad \dots\dots(1)$$

The function $c^{(n)}$ is represented by a power series in η , the first few coefficients $c_\mu^{(n)}$ in this trial function being determined by a variation principle.

The expression used by Sondheimer for the thermal conductivity is

$$\kappa = \{ \mathcal{K}_{3/2, 3/2} \mathcal{K}_{5/2, 5/2} - \mathcal{K}_{3/2, 5/2}^2 \} / \mathcal{K}_{3/2, 3/2} T \quad \dots\dots(2)$$

where

$$\mathcal{K}_{m, n} = \lambda \int_{-\infty}^{\infty} E^m c^{(n)}(\eta) \frac{\partial f_0}{\partial \eta} d\eta. \quad \dots\dots(3)$$

λ is a constant at given temperature and f_0 is the Fermi function $(e^\eta + 1)^{-1}$ of $\eta = (E - \xi)/kT$.

The expression used for the electrical conductivity $\sigma = e^2 \mathcal{K}_{3/2, 3/2}$ is stationary for arbitrary small variations of $c^{(n)}$ from its correct value which are subject to the normalizing condition imposed

$$\int_{-\infty}^{\infty} c^{(n)} L(c^{(n)}) \frac{\partial f_0}{\partial \eta} d\eta = \int_{-\infty}^{\infty} E^n c^{(n)} \frac{\partial f_0}{\partial \eta} d\eta. \quad \dots\dots(4)$$

One may therefore have some confidence in the accuracy of the result obtained for σ even if the first few terms used of the power series for $c^{(n)}$ represent that function rather poorly.

On the other hand the expression (2) is *not* stationary because of the term in $\mathcal{K}_{3/2, 5/2}$ and it is not clear from Sondheimer's treatment that similar confidence may be attached to the accuracy of his values for the thermal conductivity.

It is the purpose of this note to point out that although (2) is not stationary for arbitrary small variations of $c^{(n)}$ subject to (3), the method of choosing the coefficients $c_\mu^{(n)}$ actually used by Sondheimer does in fact so restrict the trial

function that (2) is stationary against small variations of $c^{(n)}$ due to change in the number of terms included in the power series.

If (as appears to be the case) the breaking-off of infinite determinants in his procedure is exactly equivalent to terminating the power series at corresponding terms, one may regard the closest approximation for κ he found manageable as having some claim to accuracy even though the representation of the $c^{(n)}$ by a polynomial of a few terms is poor (Klemens, to be published). The same applies to the absolute thermo-electric power.

To prove this we note that

$$\lambda \int_{-\infty}^{\infty} \{c^{(m)} E^n + c^{(n)} E^m - c^{(n)} E c^{(m)}\} \frac{\partial f_0}{\partial \eta} d\eta$$

is stationary at $\mathcal{K}_{m,n} = \mathcal{K}_{n,m}$ for $c^{(n)}$, $c^{(m)}$ satisfying (1) against arbitrary small variations of either, as is easily shown using Kohler's theorem. If we use this expression for $\mathcal{K}_{3/2, 5/2}$ in (2) in place of (3), inserting as approximations for the $c^{(n)}$ the terminated series

$$\bar{c}^{(n)} = \sum_{\mu=0}^M \bar{c}_{\mu}^{(n)} \eta^{\mu}$$

with the coefficients determined from equations

$$\sum_{\mu=0}^M d_{\nu\mu} \bar{c}_{\mu}^{(n)} = \alpha_{\nu}^{(n)}, \quad \nu = 0, 1, 2, \dots, M \quad \dots\dots(5)$$

(cf. Sondheimer's equation (13)), we obtain as expressions for $\mathcal{K}_{3/2, 5/2}$ correct to the first order

$$\lambda \sum_0^M \alpha_{\mu}^{(3/2)} \bar{c}_{\mu}^{(5/2)} = \lambda \sum_0^M \alpha_{\mu}^{(5/2)} \bar{c}_{\mu}^{(3/2)} = \lambda \sum_0^M \sum_0^M d_{\mu\nu} \bar{c}_{\mu}^{(3/2)} \bar{c}_{\nu}^{(5/2)}.$$

But this is exactly the result obtained by Sondheimer (his equation (16) with the series terminated) from the non-stationary expression (3).

It may be remarked that this is so because the trial functions $\bar{c}^{(n)}$ satisfy (5) which includes but is more restrictive than (4).

I wish to acknowledge the value of discussions with Dr. P. G. Klemens.

REFERENCES

- SONDHEIMER, E. H., 1950, *Proc. Roy. Soc. A*, **203**, 75.
WILSON, A. H., 1937, *Proc. Camb. Phil. Soc.*, **33**, 371.

The Absorption Spectrum of Lutetium

By L. F. H. BOVEY* AND W. R. S. GARTON †

* Emission Spectroscopy Group, Atomic Energy Research Establishment,
Harwell, Didcot, Berks.

† Department of Astrophysics, Imperial College, London

MS. received 27th November 1953

IN the course of work (in collaboration with Professor R. W. B. Pearse) by one of the authors (L.F.H.B.) on the term analysis of lutetium it was thought desirable to examine the high temperature absorption spectrum of the metal. The furnace described by Garton (1952) was used with a heated tube of length four inches and a maximum operating temperature of approximately 2400°C.

The spectrum was taken in the second order on a Hilger Compact 3-metre Spectrograph (Model E 661) over the region 2600–6050 Å; the light sources were a Siemens Xenon High Pressure Arc for the ultra-violet and an over-run 12 v, 48 w car bulb for the remaining regions. In order to increase the intensity of the weaker absorption lines, the work was repeated (3080–6050 Å) at Imperial College with a larger furnace containing a twelve-inch tube; higher resolution was also obtained by use in the second order of the 21-foot grating instrument (1.3 Å mm^{-1}).

The results are detailed in the table. The wavelengths were obtained generally by approximate measurement and comparison with the M.I.T. wavelength tables (Harrison 1939) but a few of the weaker lines were accurately measured. The main impurities arising from the Johnson Matthey 'Specpure' lutetium oxide appeared to be thulium and ytterbium of which former rare earth some fifteen lines were recorded.

Wavelength	Strength	Wavelength	Strength	Wavelength	Strength
2615.42	S	3081.47	S	4112.67	W
2670.78	VW	3118.43	S	4124.73	M
2685.08	S	3171.36	M	4154.08	M
2685.54	S	3278.97	M	4309.57	W
2692.35	VW	3280.50	VW	4450.81	VW
2703.13	VW	3281.74	VS	4498.85	W
2715.94	M	3312.11	VS	4518.58	VS
2719.11	S	3359.56	M	4658.03	VS
2728.95	S	3376.51	VS	4716.70	VW
2765.74	VS	3385.53	S	4815.05	M
2845.13	VS	3396.82	S	4904.88	M
2881.89	W	3507.39	W	4942.34	M
2885.14	W	3508.42	S	5001.14	M
2886.04	VW	3546.39	M	5135.09	VS
2903.05	VS	3567.84	S	5206.47	VW
2912.70	S	3620.31	VW	5402.57	S
2949.73	M	3636.25	VS	5736.55	S
2989.27	S	3647.77	S	6004.52	W
3020.54	S	3841.18	S	6055.03	W
3063.51	W	3968.47	M		
3080.11	S	4054.45	M		

VS, very strong; S, strong; M, medium; W, weak; VW, very weak.

A detailed discussion of the experimental data will be given with results of the term analysis but it is interesting to note how far the work confirms the preliminary analysis by Meggers and Scribner (1930). All the pairs of lines arising from the ground state 2D are obtained. (We have confirmed King's (1931) finding that the line 3968.47 Å belongs to the lutetium spectrum. There appears to be a misprint in that paper since the line 1994 cm^{-1} from this is 4309.57 Å and not 4518.58 Å as stated.) Some additional 30 absorption lines are present and it is hoped that these will lead to the identification of further low-lying levels in the lutetium spectrum. An alternative explanation may be that some of these lines arise from other than deep levels and can show considerable strength in absorption because a high transition probability compensates for the low population factor.

ACKNOWLEDGMENTS

The authors would like to thank the Director of the Atomic Energy Research Establishment for permission to publish this work which was partly carried out whilst one of us (W.R.S.G.) was acting as a University Vacation Consultant. They also appreciate the co-operation of Mr. A. R. Powell of Johnson, Matthey Ltd. in supplying relatively large quantities of pure lutetium oxide.

REFERENCES

- GARTON, W. R. S., 1952, *Proc. Phys. Soc. A*, **65**, 268.
HARRISON, G. R., 1939, *M.I.T. Wavelength Tables* (New York : John Wiley).
KING, A. S., 1931, *Astrophys. J.*, **74**, 328.
MEGGERS, W. F., and SCRIBNER, B. F., 1930, *J. Res. Nat. Bur. Stand.*, **5**, 73 (RP. 187)

LETTERS TO THE EDITOR

A Chemical Approach to the Treatment of Electronic Spin in Semiconductors

The effect of electronic spin, associated with impurity quantum states, on the equilibrium distribution of electrons and holes, first treated by Mott and Gurney (1940) in the classical approximation, has recently been generalized by a number of workers to include degenerate statistics. Landsberg (1952) essentially generalized the approach of Mott and Gurney, James (1952) solved the problem generally using the method of grand partition functions and Guggenheim (1953) used a straightforward application of statistics employing the concept of absolute activity. The purpose of this note is to point out another very simple approach, based on the method of Fowler (1933), which at the same time is very effective for most applications. Unfortunately this approach loses its simplicity when the electron or hole gas becomes degenerate but, even then, it will give correct results if properly used. In the following only the non-degenerate case will be considered.

In his method, which we shall call the chemical approach, Fowler (1933) treated electrons and both neutral and ionized donors as chemical entities. Thus, if the free electrons are non-degenerate, one may write a chemical equilibrium equation for the dissociative equilibrium of the donor

$$\frac{n_e N_{D^+}}{N_D} = K(T) = \frac{Q_e Q_{D^+}}{Q_D} \quad \dots\dots(1)$$

where n_e is the concentration of free electrons, N_{D^+} and N_D are the concentrations of ionized and neutral donors and the Q_i 's are the respective partition functions. If the energy zero is chosen at the bottom of the conduction band (lowest quantum state of a free electron), the partition functions become†

$$\left. \begin{aligned} Q_e &= \omega_e \frac{(2\pi m_e kT)^{3/2}}{h^3} \\ Q_{D^+} &= \omega_{D^+} N_D^0 \\ Q_D &= \omega_D N_D^0 \exp(-\epsilon_D/kT) \end{aligned} \right\} \quad \dots\dots(2)$$

where ω_i is the degeneracy of the i th state ($\omega_e=2$), N_D^0 is the total donor concentration, and ϵ_D is the energy of the un-ionized donor (usually negative). If the neutral donor contains an unpaired s electron $\omega_D=2$ and $\omega_{D^+}=1$ (Case I) while the converse is true if the donor contains only paired electrons (Case II). Equations (1) and (2) with the additional relations $N_{D^+}=N_D^0-N_D$ and $n_e=2(2\pi m_e kT/h^2)^{3/2} \exp(\xi/kT)$ give for these two cases:

$$\text{Case I} \quad N_D = N_D^0 \{1 + \frac{1}{2} \exp[(\epsilon_D - \xi)/kT]\}^{-1} \quad \dots\dots(3)$$

$$\text{Case II} \quad N_D = N_D^0 \{1 + 2 \exp[(\epsilon_D - \xi)/kT]\}^{-1} \quad \dots\dots(4)$$

In order to investigate the parameter β introduced by Landsberg (1952) as the generalized coefficient of the exponential term, one may consider a mixture

† The vibrational contributions to Q_{D^+} and Q_D have been neglected in this formulation. These contributions are assumed to be identical for both the donor and its ion, a good assumption for a homopolar crystal particularly if the dielectric constant is large.

of donors of type I and type II with the same energy ϵ_D . The total concentration of un-ionized donors is then

$$N_D = N_D(I) + N_D(II) = \frac{N_D^0(I)}{1 + \frac{1}{2} \exp[(\epsilon_D - \zeta)/kT]} + \frac{N_D^0(II)}{1 + 2 \exp[(\epsilon_D - \zeta)/kT]} \quad (5)$$

Equation (5) may be put into the form of equation (5) of Landsberg's treatment, i.e.

$$N_D = \frac{N_D^0(I) - N_D^0(II)}{1 + \beta \exp[(\epsilon_D - \zeta)/kT]} \quad \dots\dots(6)$$

with β given by

$$\beta = 2/(4 - 3f) \quad \dots\dots(7)$$

where f is the fraction of the electrons which come from paired sites. The β of equation (7) does not agree with the corresponding result of Landsberg's paper. This is a result of the fact that Landsberg does not count the two types of levels as distinguishable with respect to spin in the entropy of mixing term. When the two types of levels are accounted for properly, the method of Landsberg agrees with equation (7) of this Letter.

Oak Ridge National Laboratory,
Oak Ridge, Tennessee, U.S.A.

J. H. CRAWFORD, JR.
D. K. HOLMES.

8th October 1953, in revised form 29th December 1953.

FOWLER R. H., 1933, *Proc. Roy. Soc. A*, **140**, 505.

GUGGENHEIM, E. A., 1953, *Proc. Phys. Soc. A*, **66**, 121.

JAMES, H. M., 1952, *Third Quarterly Report of the Purdue Research Foundation to the United States Signal Corps*, Jan. 1, PRF 746, p. 8 (unpublished).

LANDSBERG, P. T., 1952, *Proc. Phys. Soc. A*, **65**, 604.

MOTT, N. F., and GURNEY, R. W., 1940, *Electronic Processes in Ionic Crystals* (Oxford: University Press), p. 157.

Collective Electron Antiferromagnetism

In a recent letter, Lidiard (1953) has given a collective electron treatment of antiferromagnetism which indicates a possible reason for the apparent inconsistency of the results of experiments made to investigate the magnetic ordering of the transition metals. Lidiard's treatment is, however, incomplete. Although, in the more complete development sketched below, Lidiard's qualitative conclusions are not affected, the actual quantitative results show an interesting difference.

The case of $2N$ electrons distributed in an energy band of the form $\nu'(\epsilon) = a\epsilon''$ is considered. In the presence of an externally applied field \mathbf{H} the expression for the exchange energy, together with the energy of interaction with the field is taken to be (cf. Lidiard 1953)

$$-\frac{J(\zeta)}{2N} = \frac{k\theta'}{8} [\zeta_1^2 + \zeta_2^2] - \frac{k\phi'}{4} \zeta_1 \cdot \zeta_2 + \frac{\mu}{2} \mathbf{H} \cdot \zeta_1 + \frac{\mu}{2} \mathbf{H} \cdot \zeta_2 \quad \dots\dots(1)$$

The partition function for the system may be written as

$$Z = \sum_{\zeta_1} \sum_{\zeta_2} \left[\exp\left(-\frac{J}{kT}\right) \left\{ \sum_{\sum n_r = (1+\zeta_1)N/2} \exp\left(-\frac{\sum n_r \epsilon_r}{kT}\right) \right\} \left\{ \sum_{\sum n_r = (1-\zeta_1)N/2} \exp\left(-\frac{\sum n_r \epsilon_r}{kT}\right) \right\} \right. \\ \times \left. \left\{ \sum_{\sum n_r = (1+\zeta_2)N/2} \exp\left(-\frac{\sum n_r \epsilon_r}{kT}\right) \right\} \left\{ \sum_{\sum n_r = (1-\zeta_2)N/2} \exp\left(-\frac{\sum n_r \epsilon_r}{kT}\right) \right\} \right] \quad \dots\dots(2)$$

The individual sums in curly brackets may be evaluated by the method of steepest descents and then substituted into (2) when Z may be differentiated logarithmically to obtain its largest term. The equations determining the equilibrium magnetization are found to be

$$\left. \begin{aligned} (1 + \zeta_1) &= (m+1) \tau^{m+1} F_m \{ \eta + \beta' \zeta_1 - \alpha' \zeta_2 \cos(\delta_1 - \delta_2) + \beta \cos \delta_1 \} \\ (1 - \zeta_1) &= (m+1) \tau^{m+1} F_m \{ \eta - \beta' \zeta_1 + \alpha' \zeta_2 \cos(\delta_1 - \delta_2) - \beta \cos \delta_1 \} \\ (1 + \zeta_2) &= (m+1) \tau^{m+1} F_m \{ \eta + \beta' \zeta_2 - \alpha' \zeta_1 \cos(\delta_1 - \delta_2) + \beta \cos \delta_2 \} \\ (1 - \zeta_2) &= (m+1) \tau^{m+1} F_m \{ \eta - \beta' \zeta_2 + \alpha' \zeta_1 \cos(\delta_1 - \delta_2) - \beta \cos \delta_2 \} \\ \alpha' \zeta_1 \zeta_2 \sin(\delta_1 - \delta_2) - \beta \zeta_1 \sin \delta_1 &= 0 \\ \alpha' \zeta_1 \zeta_2 \sin(\delta_1 - \delta_2) + \beta \zeta_2 \sin \delta_2 &= 0 \end{aligned} \right\} \quad (3)$$

where
$$F_m(\eta) = \int_0^\infty x^m [1 + \exp(x - \eta)]^{-1} dx,$$

and $\beta' = \theta'/T$, $\alpha' = \phi'/T$, $\beta = \mu H/kT$, $\tau = kT/\epsilon_0$, and δ_1 and δ_2 are the angles ζ_1 , H and ζ_2 , H .

In zero applied field ($\beta = 0$), and for an applied field parallel to the antiferromagnetic axis ($\delta_1 = 0$, $\delta_2 = \pi$), equations (3), for $m = 1, 2$, lead to the equations given by Lidiard (1953, equation (2) and above).

For a vanishingly small applied field perpendicular to the antiferromagnetic axis and considering only the case where the resultant magnetization and field are parallel, $\delta_1 = \delta$, $\delta_2 = 2\pi - \delta$, $\delta_1 - \delta_2 = 2(\delta - \pi)$, when either of the last two of equations (3) give the susceptibility directly. From (3),

$$\frac{\mu H}{\zeta \epsilon_0} = \frac{1}{\chi} \cdot \frac{2N\mu^2}{\epsilon_0} = \frac{k\phi^1}{\epsilon_0}, \quad \dots\dots(4)$$

independent of the temperature.

As already mentioned, Lidiard implicitly considers only the case where \mathbf{H} is parallel to the antiferromagnetic axis and derives the result that $\chi(0)/\chi(T_c) = 0$ for $\zeta_{01} = 1$, and $1 \geq (\chi(0)/\chi(T_c)) \geq 0$ for $0 \leq \zeta_{01} \leq 1$. The theoretical quantity comparable with the susceptibility as determined experimentally is, however, the weighted mean of $\chi_{||}$ and χ_{\perp} (see, for example, Van Vleck 1941.) From the above it turns out that

$$\left. \begin{aligned} \text{for } 0 \leq \zeta_{01} \leq 1, \text{ i.e. } \frac{1}{m+1} \leq \frac{k(\theta' + \phi')}{2\epsilon_0} \leq 2^{-m/(m+1)}, \\ \text{then} \quad 1 \geq \overline{\chi(0)/\chi(T_c)} \geq 2/3 \end{aligned} \right\}, \quad \dots\dots(5)$$

$$\text{whilst for } k(\theta' + \phi')/2\epsilon_0 > 2^{-m/(m+1)}, \quad \overline{\chi(0)/\chi(T_c)} = 2/3. \quad \dots\dots(6)$$

On the other hand, provided not more than one antiferromagnetic axis is assumed (cf. Anderson 1950) the Heitler-London models predict that $\overline{\chi(0)/\chi(T_c)} = 2/3$. Moreover, both the neutron and x-ray diffraction data are usually interpreted as being consistent with the idea of a single antiferromagnetic axis. In general, however, the experimental values for the ratio $\overline{\chi(0)/\chi(T_c)}$ (e.g. for FeO, CoO, etc.) are greater than $2/3$ and less than 1. This is just the range of possible values predicted by the present treatment. It is to be noted that values $\overline{\chi(0)/\chi(T_c)}$ greater than $2/3$ arise from the possibility that the antiferromagnet is unsaturated at absolute zero, this situation never occurring in the Heitler-London treatments.

Thus, although the collective electron treatment is more appropriate to metallic rather than non-metallic antiferromagnets, it is perhaps of heuristic value more generally.

Department of Natural Philosophy,
Marischal College, Aberdeen.
4th January 1954.

E. W. ELCOCK.

ANDERSON, P. W., 1950, *Phys. Rev.*, **79**, 705.

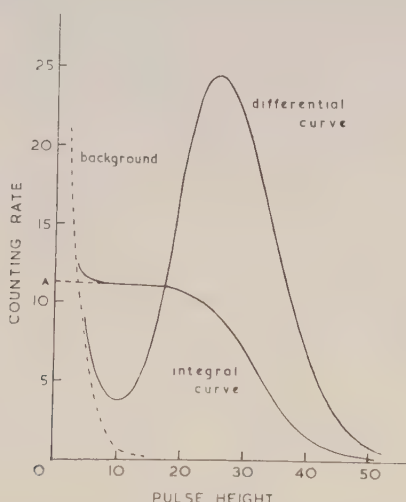
LIDIARD, A. B., 1953, *Proc. Phys. Soc. A*, **66**, 1188.

VAN VLECK, J. H., 1941, *J. Chem. Phys.*, **9**, 85.

Absolute Alpha Standardization with Liquid Scintillators

Counting of all the alpha-particles emitted by a source is almost impossible due to self-absorption in the source. Especially in the case of long-lived radio-isotopes, where the specific activity is correspondingly lower, the required source thickness causes an indeterminable amount of absorption. Absolute counting with gas-filled counters or solid phosphor scintillation counters is therefore liable to considerable inaccuracy.

The difficulty of self-absorption can be surmounted by dissolving the alpha-emitter in a liquid phosphor. Raben and Bloembergen (1951) estimated low energy beta-emitters by incorporating them in compounds soluble in the solvent used for the scintillating material. Farmer and Bernstein (1952) employed p-dioxane, saturated with p-terphenyl, as liquid scintillator suitable for both organic and water-soluble materials. As much as 20% water could be added to the p-dioxane without decreasing the counting efficiency.



Differential and integral pulse distributions for 5.3 mev alpha-particles from polonium dissolved in a liquid phosphor. The integral curve extrapolated to zero pulse height gives the absolute disintegration rate, A.

In the case of alpha-emitters this method offers even bigger possibilities as all the alpha-particles are emitted with the same energy, forming a definite peak in the pulse-height distribution. With a selected photomultiplier and good

optical coupling, an efficient phosphor should give a peak reasonably far removed from the background, without need of cooling or coincidence arrangements for decreasing the background. The figure gives the distribution of pulses from polonium dissolved in a solution of 2, 5 diphenyloxazole (Hayes, Hiebert and Schuch 1952) in p-dioxane (3 grammes litre) with 3% water, as observed by a RCA 5819 photomultiplier. Extrapolation of the integral counting rate to zero bias can be done quite accurately and gives the absolute disintegration rate of the sample. This has been verified by measurement of a uranium sample, immediately after methyl isobutyl ketone extraction from its decay products. A chemical analysis corresponded to within 3%*. The solution in ketone was added directly to a phosphor consisting of 2 g p-terphenyl per litre of phenylcyclohexane, the concentration of the ketone in the phosphor being about 1% by weight. As the size of the pulses, due to alpha-particles, are only about one-fifteenth of that for beta-particles of the same energy (Birks 1951), the resulting pulse-height distribution has a much larger half-width and the background can be quite disturbing. It is therefore of importance to find liquid scintillators of higher efficiency.

The authors would like to express their indebtedness to the South African Council for Scientific and Industrial Research for permission to publish this note.

National Physical Laboratory,
Pretoria, Union of South Africa.
21st December 1953.

J. K. BASSON.
J. STEYN.

BIRKS, J. B., 1951, *Proc. Phys. Soc. A*, **64**, 874.

FARMER, E. C., and BERNSTEIN, I. A., 1952, *Science*, **115**, 460.

HAYES, F. N., HIEBERT, R. D., and SCHUCH, R. L., 1952, *Science*, **116**, 140.

RABEN, M. S., and BLOEMBERGEN, N., 1951, *Science*, **114**, 363.

* Determined by Mr. Strelow of the National Chemical Research Laboratory.

REVIEWS OF BOOKS

Ultraviolet Radiation, by L. R. KOLLER. Pp. ix+270. (New York : John Wiley; London: Chapman and Hall, 1952.) 52s.

This book is likely to be of particular utility to workers who lack specialized knowledge of the topics treated, but need to refer to certain basic data relevant to the use of ultra-violet radiation as a research or routine tool. Detailed descriptions of the characteristics of commercial ultra-violet sources available in the United States follow upon brief and simply written expositions of the fundamental physics involved. The latter feature, and the space devoted in other chapters to medical, germicidal and other biological effects of the ultra-violet, seem to indicate that the author has sought particularly to serve the needs of workers in such fields.

A valuable feature of more general interest is the inclusion of extensive data, presented numerically and graphically, on such things as reflection and transmission coefficients, the performance of ultra-violet filters, the spectral characteristics of detectors and of intensity measuring devices.

While the general tone of the book is up to date, some important topics receive scant mention. Thus there is little mention of the region of the vacuum ultra-violet and, related to this, although a long chapter is headed Solar radiation, there is practically no mention of the important results of recent experiments with rocket-borne spectrographs. The important subjects of fluorescence analysis and oxalate actinometry are dealt with very briefly and without references.

The book is excellently produced and illustrated, apart from the regrettable exception of being almost completely lacking in reproductions of spectra of the light sources discussed.

W. R. S. GARTON.

Physical Formulae, by T. S. E. THOMAS. Pp. vii+118. (London : Methuen, 1953.) 8s. 6d.

A useful addition to the well-known series of Monographs on Physical Subjects, containing formulae, short explanations of principles and statements of laws in all the branches of physics encountered in an Honours degree course and also formulae in mathematics and statistics. Both graduates and undergraduates will find this little book a reliable source of reference.

In a future edition it would be worth while to add more data on M.K.S. units and to include tables comparing formulae in electricity and magnetism using unrationalized and rationalized units.

J. YARWOOD.

Radioactivity and Radioactive Substances, by Sir JAMES CHADWICK. 4th Edn (revised and supplemented by Professor J. ROTBLAT). Pp. xv+120. (London : Pitman, 1953.) 12s. 6d.

When the study of radioactivity was anything but a branch of technology this little book was first published as one of Pitman's Technical Primers. Now that the subject has developed into the technological field we have the fourth edition of the book, still a 'primer' according to Professor Rotblat's preface, but no longer one of the original series. In larger format—but with only four more pages than previously—it stands on its own feet, with more dignity perhaps,

but with a fivefold increased price on its dust jacket (the publishers make the strange mistake of labelling the 1931 preface as of the second edition—it was in fact that of the third edition of that date—and, it seems to this reviewer, the unnecessary gesture of suppressing the initial ‘E’ in the signature to the foreword written by Rutherford for the first edition of 1921).

Much of the text of the last cheap edition has been retained in this new version. The original was written with such clarity and with such respect for ascertained fact that it could not easily have been improved upon as an authoritative and unadorned presentation for the student who was not proposing for the moment to probe more deeply into the subject. A new chapter on nuclear structure has been added, the chapter on the β - and γ -rays has been divided into two and modernized, something has been said regarding new experimental techniques and the tables of experimental data have been revised, but the character of the book has been retained. It is a pity that it could not have been put on sale at a lower price: the market to which it is chiefly addressed may find it rather an expensive luxury. It deserves a better fate than to languish for reasons of economics alone.

In the new matter a few ambiguities of expression would repay attention at some future date, and two definitions certainly are not correct as they stand: the definition of proportional counter behaviour on page 21 and that of Avogadro’s number on page 116. Strictly—and importantly even for the general student—the concept of atomic absorption cross section should have been introduced to form the basis of the statements concerning the variation of absorption coefficient with γ -ray quantum energy and with atomic number (page 54). Otherwise these statements are imprecise.

N. FEATHER.

Introduction to Tensors, Spinors, and Relativistic Wave-Equations, by E. M. CORSON. Pp. xii + 221. (Glasgow: Blackie and Son, 1953.) 55s.

The search for equations consistent with the special relativity principles and which may describe the behaviour of new elementary particles has always been a fascinating one and very many theoretical physicists have been attracted to studies in this field. The outstandingly successful equation was that proposed by Dirac for the electron. Suitable wave equations were also given for particles of spin 0 (Klein–Gordon) and of spin 1 (Proca). Kemmer’s achievement in formulating these latter theories in a form close to that of the Dirac equation then stimulated a great deal of research into generalizations of the Dirac equation, especially by Bhabha and Harish-Chandra. However, all the further theories proposed have been in some way defective; for example, most of the theories cannot be satisfactorily quantized since, in the c -number theory, both the total charge and the total energy of the field have non-definite sign. On the other hand, experiments have not yet identified any particle requiring description by such a higher spin theory—the few particles of known spin have spin 0 or $1/2$, and the heavier mesons, of which little is known at present, may well be composite particles for which the implications of the description ‘elementary particle’ may not apply.

Studies in elementary particle theory necessarily bring together widely differing considerations. The theory of the Lorentz group of transformations is clearly essential, as well as the mathematical and physical principles of

relativistic field theories, both classical and quantum ; a considerable knowledge of algebras and their representations is also appropriate. The purpose of the book under review is to give a connected account of many of these underlying aspects of fundamental particle theory, leading on to a study of the progress in this theory to the present. The first two chapters summarize some necessary points in tensor analysis and give a detailed account of two-spinors, four-spinors, the Dirac spinor matrices and expinors, and their relation with the representations of the proper Lorentz group. The reader is assumed to have a working familiarity with the theory of the Lorentz group, although references are generally given. A chapter is next given to the physical principles of a classical Lagrangian field theory with special emphasis on the relation of the conservation laws to the invariance properties of the Lagrangian. The canonical Hamiltonian formalism is set up in preparation for the quantization of the theory. The simple field theories mentioned above are then discussed in considerable detail both in the wave (i.e. spinor or tensor) formalism and in the particle (i.e. matrix-algebraic) formalism since their properties provide the basis for the generalizations considered. The relation between spin and statistics is derived, following the arguments of Pauli.

The final chapter is concerned with the generalization of the 'particle' form of these theories, i.e. with the equation $(\alpha^\mu \partial_\mu - i\kappa)\psi = 0$. The restrictions on the α -matrices arising from the requirement of Lorentz-covariance of the theory are analysed, following Bhabha, and the further restrictions implied by the requirement of unique rest mass or of positive definite energy are obtained. The algebraic problem of obtaining all irreducible representations of the α -matrices is discussed in detail and illustrated by a variety of examples from the literature. It concludes with a brief discussion of the manifolds irreducible under the inhomogeneous Lorentz group.

The book is well produced and gives an almost complete account of researches in this field of linear wave equations. Their extent is exemplified by the fact that even the twelve-page bibliography given is not quite complete. The book provides a very useful introduction for the advanced mathematical physicist who is not familiar with this field, and will be invaluable to those wishing to find their way amongst the many theories encountered in the literature. These researches have not yet been fruitful physically, although they have led to a much sharper appreciation of the virtues of the theories of spin 0, 1/2 and 1. Some beautiful mathematics has resulted from these attempts, deserving collection and preservation as a whole on aesthetic grounds alone. Furthermore, physicists will operate within the framework of special relativity for a long time yet and the techniques developed in the study of these covariant systems of equations will undoubtedly have many applications yet before them.

R. H. DALITZ.

Notes on the Quantum Theory of Angular Momentum, by E. FEENBERG and G. E. PAKE. Pp. vii + 56. (Cambridge, Mass. : Addison-Wesley, 1953.) \$2.00.

In the 56 pages of this book a self-contained account is given of some aspects of angular momentum in quantum mechanics, using elementary methods throughout and sufficient for the derivation of some frequently quoted results

concerning magnetic and quadrupole interactions, total transition probabilities and the description of supermultiplets in nuclei. The first chapter summarizes the quantum-mechanical principles and notation necessary later. The angular momentum operators are characterized by their commutation relations, from which their eigenvalues and matrix elements are deduced and the eigenvalues of two coupled angular momenta derived. The matrix elements of scalar, vector and second-rank tensor operators between angular momentum eigenstates are obtained algebraically for every possible case and these are applied in the final chapter to the physical problems mentioned above.

The atomic physicist will find considerable use for this book; its treatment is straightforward and many important formulae are given a simple and direct derivation. For the student of theoretical physics, it will be a good introductory text, providing a solid basis for the appreciation of the more general treatments he will need for a more complete understanding of this field. As the Clebsch-Gordan coefficient is not defined or even mentioned in the book, very little indication has been given of the close and important relationships connecting the many formulae obtained. Also a book of this size could scarcely be expected to show how the systematic development of its methods can greatly simplify the calculation of nuclear and atomic properties, of angular correlations in nuclear processes and the description of oriented nuclear systems. This is unfortunate, since the techniques underlying these developments can now be found only in scattered scientific papers and their systematic exposition in a uniform notation would be most welcome.

R. H. D.

Complex Variable Theory and Transform Calculus, by N. W. McLACHLAN.
Pp. xi + 388. 2nd Edn (Cambridge: University Press, 1953). 55s.

This is a revised edition of the book published in 1939 under the title of *Complex Variable and Operational Calculus with Technical Applications*, dealing with the use of Laplace transforms and the Mellin inversion theorem in solving certain types of differential equation which arise in technical problems. There are some omissions and additions but, in general, the book follows the first edition fairly closely.

An important feature of the book is the large section devoted to those parts of complex variable theory, namely complex integration, power series expansions, Cauchy's theorem, evaluation of residues and infinite integrals and the Bromwich contour, which are necessary for an understanding of operational methods. Little previous acquaintance with complex variable theory is required of the reader and, although the treatment is more rigorous than in the first edition, it is still suited to those who are not primarily concerned with the mathematical niceties of the subject. One chapter is devoted to the properties of gamma, Bessel and error functions, which are of frequent occurrence in later applications, and another to differentiation and integration under the integral sign.

Part II establishes the main theorems of operational calculus (with illustrative examples), and their application to the solution of differential equations. Impulses are also treated and the section on frequency spectra has been amplified.

The last part, which takes up nearly half the book, covers a wide range of applications, including electrical circuits, filters and transmission lines, vibrating

systems, bending beams, radio and television amplifiers, microphones and loudspeakers and diffusion problems.

The number of examples to be worked out by the reader has been increased to more than a hundred and about fifty references have been added to bring the list up to date. There is also a new appendix in which the convergence of the series which occur in the text is considered.

When the first edition was written there were very few textbooks on the practical use of transform theory and it was probably the best. Now that competition is keener, this new edition still maintains its place. A. N. GORDON.

Actes du Colloque International des Vibrations non Lineaires, Ile de Porquerolles
1951. Pp. ii+296. (Paris: Publications Scientifiques et Techniques du
Ministère de l'Air (No. 281), 1953.) 1,800 fr.

Régularité et séries divergentes, by PIERRE VERNOTTE. Pp. 52+xi. (Paris:
Publications Scientifiques et Techniques du Ministère de l'Air (No. 282),
1953.) 800 fr.

Modellversuche zur thermischen Konvektion, by GÜNTER SKIEB. Vol. III, No. 20
of *Abhandlungen des meteorologischen und hydrologischen Dienstes der
Deutschen Demokratischen Republik*. Pp. 56. (Berlin: Akademie-Verlag,
1953.) \$ 5.28.

CONTENTS OF SECTION B

	PAGE
Prof. F. A. VICK and Dr. C. A. WALLEY. Negative Ion Emission from Oxide-Coated Cathodes : I	169
Dr. W. GRATTIDGE and Dr. A. A. SHEPHERD. Negative Ion Emission from Oxide-Coated Cathodes : II	177
Dr. T. J. LEWIS. The Work Function of Irregular Metal Surfaces	187
Mr. J. J. POLLING and Dr. A. CHARLESBY. Analysis of the Formation Current in Electrolytic Oxidation of Zirconium	201
Dr. F. MINOZUMA and Mr. H. ENOMOTO. The Mechanism and Distribution of Short Period Fading under Conditions of Ionospheric Turbulence	211
Mr. J. L. MONTEITH. Error and Accuracy in Thermocouple Psychrometry	217
Dr. D. A. BELL. Statistics of a Population with Creation and Recombination Dependent on Existing Numbers	227
Mr. D. BROWN. A Shearing Interferometer with Fixed Shear and Its Application to some Problems in the Testing of Astro-Optics	232
Dr. M. COCKS. The Effect of Compressive and Shearing Forces on the Surface Films present in Metallic Contacts	238
Dr. D. TABOR. Mohs's Hardness Scale—A Physical Interpretation	249
Research Notes :	
Mr. C. H. L. GOODMAN. Semiconducting Compounds and the Scale of Electronegativities	258
Mr. N. LOUAT and Mr. M. HATHERLEY. The Behaviour of Aluminium Deformed under Alternating Stresses	260
Dr. E. W. J. MITCHELL and Mr. E. G. S. PAIGE. On the Formation of Colour Centres in Quartz	262
Letters to the Editor :	
Mr. D. E. WESTON. The Effect of Slip on Sound Propagation	265
Dr. F. E. HOARE and Mr. B. YATES. The Elastic Constants and Density of Palladium Silver Alloys	266
Mr. J. A. REYNOLDS. A Method of Measuring the Dielectric Constant of Isotropic Powders	267
Dr. J. N. HODGSON. The Infra-Red Properties of Bismuth	269
Dr. B. V. ROLLIN and Mr. I. M. TEMPLETON. Noise in Germanium Filaments at Very Low Frequencies	271
Reviews of Books	272
Corrigendum (P. M. Davidson)	279
Contents of Section A	280

The Magneto-Resistance Effect in Metals at High Frequencies

By B. DONOVAN

Department of Physics, Northern Polytechnic, London

MS. received 20th November 1953

Abstract. An examination is made of the effect of a magnetic field on the surface impedance of a metal in which there are two overlapping bands of normal form. In general it is not possible to express the surface resistance, as a function of frequency and field strength, in convenient analytical form, but the results are depicted graphically for a number of special cases.

At low frequencies the relative change in the surface resistance due to the field is independent of frequency and its variation with field strength is very similar to that obtained in d.c. experiments. At high frequencies it is shown that in all cases the magneto-resistance effect ultimately drops to zero. The frequency region in which this phenomenon occurs is determined by the relaxation time and lies in the far infra-red for normal metals. From a comparison with the available experimental results for bismuth it is inferred that the relaxation time in bismuth is abnormally large.

§ 1. INTRODUCTION

THE change in electrical conductivity due to a magnetic field has been extensively investigated in metals and semiconductors in the case of direct currents, but comparatively little attention has been given to the corresponding phenomenon at high frequencies. A small amount of experimental evidence is available for bismuth but, so far as the author is aware, there are no published results for any other element.* Experiments in the radio-frequency region have been briefly reported by Blunt (1948) and no appreciable departure from the d.c. behaviour was observed with alternating currents of frequencies up to 3.5 Mc/s. In the case of optical and infra-red frequencies several attempts have been made to deduce the behaviour of the conductivity from observations of the reflection or absorption coefficients in a magnetic field. These experiments (Heaps 1926, McLennan *et al.* 1932, Englert and Schuster 1932) all failed to reveal any magneto-resistance effect. More recently Heaps (1950) measured the power loss in a bismuth cavity and found that the change in resistivity at 3000 Mc/s was of the order of half the d.c. value.

The significant general feature would thus appear to be the existence of a transition region in which the magneto-resistance change drops to zero. So far no theory has been put forward to explain this effect. The purpose of the present paper is to apply the electron theory of metals to the elucidation of magneto-resistance phenomena at high frequencies and to show that the disappearance of the magneto-resistance effect follows as a general result.

* Cooke (1948) has investigated the Hall effect at 3 cm in iron, nickel and various ferromagnetic alloys as well as in bismuth. The theory of the Hall effect at high frequencies will be dealt with in a subsequent paper.

This calculation is based on a model in which the electrons occupy two overlapping partially filled bands, in each of which the energy is proportional to the square of the wave-number. It is assumed that an isotropic time of relaxation exists for the conduction electrons. Although a time of relaxation may be defined rigorously only at high temperatures such that $(\theta/T)^2$ may be neglected, where θ is the Debye temperature, this restriction is not a serious one for the purposes of the present paper. The calculation is essentially classical and no account is taken of the anomalous skin effect discussed by Pippard (1947) and by Reuter and Sondheimer (1948, subsequently referred to as RS). The latter authors have shown that deviations from the classical theory become more pronounced when the mean free path is very long and thus very low temperatures are excluded from the scope of the present paper.

For the description of the properties of metals at high frequencies it is convenient to introduce the complex surface impedance Z , of which the real and imaginary parts are designated the surface resistance R and surface reactance X respectively. The surface resistance is directly accessible to experimental determination since it is proportional to the absorption coefficient and hence is obtainable from measurements on the reflection of electromagnetic waves. Before discussing the two-band model the results for the special case of free electrons are given in § 3; a preliminary note on this case has already been published (Donovan and Sondheimer 1953).

§ 2. CALCULATION OF THE SURFACE IMPEDANCE

We use the well-known model with two overlapping bands of standard form, band 1 being normal and band 2 inverted. In general the effective mass m and time of relaxation τ of the electrons in the two bands will be different and these will be distinguished by suffixes as usual. It will be assumed that the bands may be treated separately and that each contributes independently to the total current.

A semi-infinite metal is considered whose surface corresponds to the plane $z=0$, the positive z -axis being directed into the metal. The alternating electric field is specified by $(\mathcal{E}_x(z), \mathcal{E}_y(z), 0) e^{i\omega t}$, where ω is the angular frequency, and the *constant* magnetic field H is parallel to the z -axis. The calculation of the current density $(J_x(z), J_y(z), 0)$ is carried through by the usual method (cf. Sondheimer and Wilson 1947, Wilson 1953, p. 210). As is apparent from the form of the Boltzmann equation, the distinguishing feature of the present analysis is that $1/\tau$ is replaced by $(1+i\omega\tau)/\tau$, and the components of the current density are found to be

$$J_x = \frac{e^2}{3\pi^2\hbar^4} (P\mathcal{E}_x - Q\mathcal{E}_y), \quad \dots\dots(1)$$

$$J_y = \frac{e^2}{3\pi^2\hbar^4} (Q\mathcal{E}_x + P\mathcal{E}_y), \quad \dots\dots(2)$$

where

$$P = \frac{\hbar\tau_1 m_1(1+i\omega\tau_1)(2m_1\zeta_1)^{3/2}}{\alpha_1^2\tau_1^2 + (1+i\omega\tau_1)^2} + \frac{\hbar\tau_2 m_2(1+i\omega\tau_2)(2m_2\zeta_2)^{3/2}}{\alpha_2^2\tau_2^2 + (1+i\omega\tau_2)^2}, \quad \dots\dots(3)$$

$$Q = \frac{\hbar\alpha_1\tau_1^2/m_1(2m_1\zeta_1)^{3/2}}{\alpha_1^2\tau_1^2 + (1+i\omega\tau_1)^2} - \frac{\hbar\alpha_2\tau_2^2/m_2(2m_2\zeta_2)^{3/2}}{\alpha_2^2\tau_2^2 + (1+i\omega\tau_2)^2}, \quad \dots\dots(4)$$

and $\alpha = eH/mc$. In these expressions ζ_1 and ζ_2 specify the position of the Fermi energy level relative to the bottom of band 1 and the top of band 2 respectively.

The surface impedance is derived by using Maxwell's equations to obtain a second relation between \mathcal{E} and \mathbf{J} . Neglecting the displacement current this relation may be written (in gaussian units)

$$\frac{d^2 \mathcal{E}}{dz^2} = \frac{4\pi i \omega}{c^2} \mathbf{J}, \quad \dots\dots(5)$$

which may be combined with (1) and (2) to give

$$\frac{d^2 \mathcal{E}_x}{dz^2} = i\gamma(P\mathcal{E}_x - Q\mathcal{E}_y) \quad \dots\dots(6)$$

and

$$\frac{d^2 \mathcal{E}_y}{dz^2} = i\gamma(Q\mathcal{E}_x + P\mathcal{E}_y), \quad \dots\dots(7)$$

where

$$\gamma = 4\omega e^2 / 3\pi \hbar^4 c^2.$$

In dealing with (6) and (7) we must ensure that the *total* transverse current is zero and we therefore impose the condition

$$\int_0^\infty J_y dz = 0, \quad \text{i.e. } d\mathcal{E}_y/dz = 0 \quad \text{when } z=0. \quad \dots\dots(8)$$

The solutions of (6) and (7) are found to be

$$\mathcal{E}_x = a_1 \exp(-\mu_1 z) + a_2 \exp(-\mu_2 z), \quad \dots\dots(9)$$

$$\mathcal{E}_y = -i\{a_1 \exp(-\mu_1 z) - a_2 \exp(-\mu_2 z)\}, \quad \dots\dots(10)$$

where

$$\mu_1 = (1+i)[\frac{1}{2}\gamma(P+iQ)]^{1/2}, \quad \dots\dots(11)$$

$$\mu_2 = (1+i)[\frac{1}{2}\gamma(P-iQ)]^{1/2}, \quad \dots\dots(12)$$

and a_1 and a_2 are arbitrary constants.

The surface impedance is given by

$$Z = \frac{\mathcal{E}_x(0)}{\int_0^\infty J_x dz} = -\frac{4\pi i \omega}{c^2} \frac{\mathcal{E}_x(0)}{(d\mathcal{E}_x/dz)_0}$$

and using (8), (9) and (10) we find

$$Z = \frac{4\pi i \omega}{c^2} \left(\frac{\mu_1 + \mu_2}{2\mu_1 \mu_2} \right). \quad \dots\dots(13)$$

Substituting from (11) and (12) one obtains the final expression for the surface impedance in terms of frequency and applied magnetic field:

$$Z(\omega, H) = (1+i) \frac{2\pi \omega}{c^2} \left[\frac{P + (P^2 + Q^2)^{1/2}}{\gamma(P^2 + Q^2)} \right]^{1/2}. \quad \dots\dots(14)$$

Our concern is with the surface resistance $R(\omega, H)$ which in general must be extracted from (14) by numerical methods. In describing the magneto-resistance effect at high frequencies we shall evaluate the relative change in the surface resistance, i.e. $[R(\omega, H) - R(\omega, 0)]/R(\omega, 0)$, and this will be denoted by $\Delta R/R(0)$.

In dealing with the expression (14) it is convenient to introduce the number of electrons per unit volume in band 1 and the number of positive holes per unit volume in band 2. Denoting these respectively by n_1 and n_2 we have (Wilson 1953, p. 213)

$$n_1 = \frac{(2m_1\zeta_1)^{3/2}}{3\pi^2\hbar^3}, \quad n_2 = \frac{(2m_2\zeta_2)^{3/2}}{3\pi^2\hbar^3}. \quad \dots\dots(15)$$

Finally we shall require the d.c. conductivity which, for the general two-band model, is given by

$$\sigma_0 = e^2 \left(\frac{n_1\tau_1}{m_1} + \frac{n_2\tau_2}{m_2} \right). \quad \dots\dots(16)$$

§ 3. THE FREE-ELECTRON MODEL

Before investigating the behaviour of the two-band model it is of interest to consider the implications of the expression (14) for the case of perfectly free electrons. For this model the formulae (3), (4) and (16) contain only one term each and no suffix is needed. Substituting for P and Q in (14) and making use of (15) we find

$$Z(\omega, H) = \frac{(1+i)}{\sqrt{2}} \left[\frac{2\pi\omega}{c^2\sigma_0} \right]^{1/2} (1+i\omega\tau)^2 \left[1 + \left\{ 1 + \left(\frac{\alpha\tau}{1+i\omega\tau} \right)^2 \right\}^{1/2} \right]^{1/2}. \quad \dots\dots(17)$$

Putting $\alpha=0$ the surface impedance in zero magnetic field is seen to be

$$Z(\omega, 0) = (1+i) \left[\frac{2\pi\omega}{c^2\sigma_0} \right]^{1/2} (1+i\omega\tau)^{1/2}, \quad \dots\dots(18)$$

which agrees with RS, equation (23), when the displacement current is neglected. The surface resistance in zero field is

$$R(\omega, 0) = R_n \{ -\omega\tau + (1 + \omega^2\tau^2)^{1/2} \}^{1/2}, \quad \dots\dots(19)$$

where $R_n = [2\pi\omega/c^2\sigma_0]^{1/2}$, the limiting value in the non-relaxation region ($\omega\tau \ll 1$).

The real part of (17) cannot in general be represented by a convenient expression; in the non-relaxation region, however, we have

$$R(\omega, H) = \frac{R_n}{\sqrt{2}} [1 + \{1 + \alpha^2\tau^2\}^{1/2}]^{1/2}, \quad \dots\dots(20)$$

and $\Delta R/R(0)$ is independent of frequency. It is of some significance that the present theory predicts a non-zero magneto-resistance effect at high frequencies for the free-electron model, since it is well known that this model gives a zero d.c. change. Experimental evidence on this point would be extremely useful.

At first sight the *constant* magneto-resistance change implicit in (20) appears to be inconsistent with the zero d.c. change. This apparent contradiction is resolved, however, when it is recalled that the present treatment refers to a semi-infinite metal. In effect this means that the dimensions of the specimen must be large compared with the penetration depth and it is therefore not permissible to extrapolate to zero frequency. The surface impedance in zero field, as given by (18), is itself subject to the same limitation. Thus according to (19), $R \rightarrow 0$ as $\omega \rightarrow 0$ whereas for a specimen of finite dimensions R is non-zero at $\omega = 0$. As a simple illustration, for a cylindrical specimen of radius a , the d.c. value of the surface resistance is easily seen to be $2\rho/a$, where ρ is the resistivity. Thus it is evident that $R \rightarrow 0$ as $a \rightarrow \infty$.

Returning to (17), the behaviour of $R(\omega, H)$ at very high frequencies ($\omega\tau \gg 1$) is determined by $(\alpha/\omega)^2$, which indicates that the magneto-resistance effect must ultimately disappear at sufficiently high frequencies. In order to demonstrate the frequency variation of the magneto-resistance effect $R(\omega, H)$ has been evaluated from (17) taking $\alpha = 2 \times 10^{12}$, corresponding to $H = 1.1 \times 10^5$ oersteds, and $\tau = 3 \times 10^{-14}$ sec, which is the room temperature value for sodium. In figure 1 curve *a* the relative change $\Delta R/R(0)$ is plotted as a function of the frequency $\omega/2\pi$ and of the product $\omega\tau$; it will be seen that a steep drop occurs, following a maximum at $\omega\tau \sim \frac{1}{2}$. This peak is due to the fact that although $R(\omega, H)/R_n$ and $R(\omega, 0)/R_n$ both tend to zero as $\omega \rightarrow \infty$, the latter expression decreases more quickly after the non-relaxation region. The steep drop in

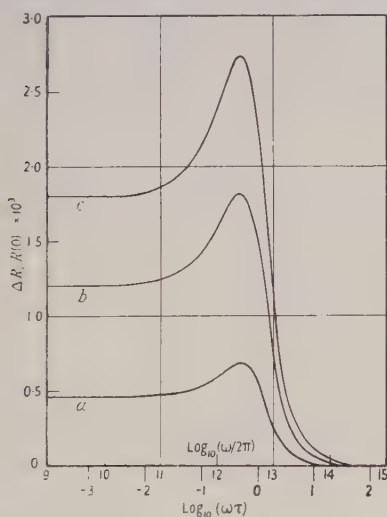


Figure 1. Variation of magneto-resistance effect with frequency for: *a*, free-electron model ($\xi=1$); *b*, two-band model with $\xi=\frac{2}{3}$; *c*, two-band model with $\xi=0$. In all three cases $\alpha\tau=0.06$.

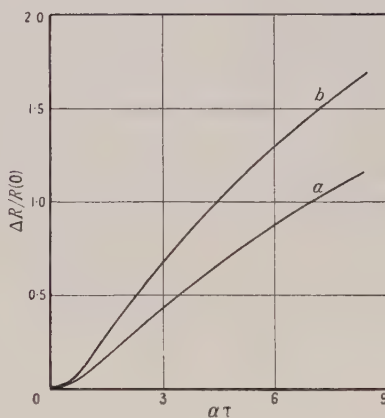


Figure 2. Variation of magneto-resistance effect with field strength for free-electron model: *a*, in low-frequency region $\omega\tau \ll 1$; *b*, at $\omega\tau = \frac{1}{2}$.

$\Delta R/R(0)$ occurs in the frequency range $\omega\tau \sim \frac{1}{2}$ to $\omega\tau \sim 4$, which, for the particular value of τ chosen, corresponds to the far infra-red, between the approximate limits 100μ and 20μ . For shorter wavelengths $\Delta R/R(0)$ decreases less rapidly, but is negligible for $\omega\tau \sim 10$, i.e. for wavelengths less than 5μ . The disappearance of the magneto-resistance effect at high frequencies is thus seen to be essentially a relaxation effect and the critical region in which $\Delta R/R(0)$ drops to zero is determined by the time of relaxation.

The variation of the magneto-resistance effect with field strength at constant frequency is illustrated in figure 2. In the non-relaxation region one obtains from (20) in the case of weak fields ($\alpha\tau \ll 1$)

$$\frac{\Delta R}{R(0)} = \frac{1}{8} \left(\frac{eH\tau}{mc} \right)^2, \quad \dots\dots(21)$$

showing that the quadratic variation, well known in d.c. magneto-resistance experiments, emerges also from the present theory. In very strong fields ($\alpha\tau \gg 1$), $\Delta R/R(0) \propto \sqrt{H}$ but under these circumstances the Boltzmann equation

would no longer be valid and it would be necessary to consider the quantization of the electronic orbits. Figure 2 curve *a* shows the variation of $\Delta R/R(0)$ in the non-relaxation region and figure 2 curve *b* shows the result obtained at $\omega\tau = \frac{1}{2}$, which corresponds approximately to the peak in figure 1 curve *a*.

§ 4. THE TWO-BAND MODEL ($\tau_1 = \tau_2$)

We now take up the case of the two-band model by examining the behaviour of (14) when the more general expressions for P and Q are used. In view of the number of parameters involved, some specialization is clearly desirable and for the remainder of this paper we shall regard the effective masses in the two bands as equal and write $m_1 = m_2 = m$. In the present section we shall in addition consider the relaxation times to be equal, thus $\tau_1 = \tau_2 = \tau$. Accordingly two possibilities arise, depending on whether n_1 is equal to, or different from n_2 .

Case (i) $n_1 = n_2$

Here we have $Q = 0$ and thus (14) gives

$$Z(\omega, H) = (1+i)R_n \left[\frac{\alpha^2\tau^2 + (1+i\omega\tau)^2}{1+i\omega\tau} \right]^{1/2}, \quad \dots\dots (22)$$

which reduces to the expression (18) in zero magnetic field.

At low frequencies ($\omega\tau \ll 1$) the surface resistance is given by

$$R(\omega, H) = R_n(1 + \alpha^2\tau^2)^{1/2}, \quad \dots\dots (23)$$

and this expression, like (20), indicates a constant magneto-resistance change.

The real part of (22) has been evaluated numerically, using the same values of H and τ as in § 3, and the frequency variation of $\Delta R/R(0)$ is shown in figure 1 curve *c*. It will be seen that the curve is very similar in form to that obtained with the free-electron model and the peak occurs at precisely the same frequency.

The variation of $\Delta R/R(0)$ with field strength for this model is illustrated in figure 3. In the non-relaxation region (23) shows that the usual quadratic

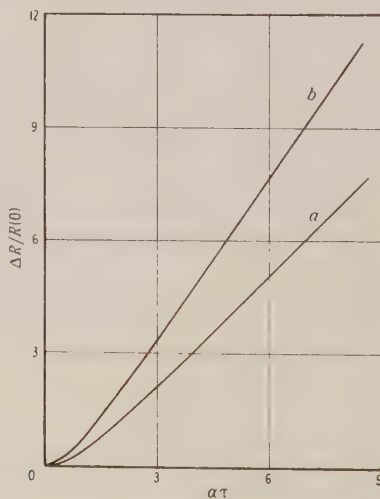


Figure 3. Variation of magneto-resistance effect with field strength for two-band model ($n_2/n_1 = 1$, $\tau_2/\tau_1 = 1$): *a*, in low-frequency region $\omega\tau \ll 1$; *b*, at $\omega\tau = \frac{1}{2}$.

variation is obtained in weak fields:

$$\frac{\Delta R}{R(0)} = \frac{1}{2} \left(\frac{eH\tau}{mc} \right)^2, \quad \dots\dots (24)$$

and this is just four times as large as the corresponding free-electron value given by (21). In strong fields $\Delta R/R(0)$ tends to a linear variation H with, thus exhibiting a further analogy with observed d.c. magneto-resistance behaviour (cf. Kapitza 1929).

Case (ii) $n_1 \neq n_2$

Here we may write $n_1 = \kappa n_2$ so that the d.c. conductivity, from (16), is $\sigma_0 = n_2 e^2 \tau (\kappa + 1)/m$. Substituting for P and Q in (14) we may derive the surface impedance in the form

$$Z(\omega, H) = \frac{(1+i)}{\sqrt{2}} R_n \left[\frac{(1+i\omega\tau)^2 + \alpha^2 \tau^2}{(1+i\omega\tau)^2 + \alpha^2 \tau^2 \xi^2} \right]^{1/2} [\{(1+i\omega\tau)^2 + \alpha^2 \tau^2 \xi^2\}^{1/2} + (1+i\omega\tau)]^{1/2}, \quad \dots\dots (25)$$

where $\xi = (\kappa - 1)/(\kappa + 1)$.

This expression reduces to (22) if $\xi = 0$ ($\kappa = 1$) and reduces to the free-electron form (17) if $\xi = 1$ (κ infinite, i.e. band 2 absent). The effect of replacing κ by $1/\kappa$ is simply to replace ξ by $-\xi$ and, as only ξ^2 appears in (25), we see that the results are unaffected if n_1/n_2 is replaced by n_2/n_1 .

In order to illustrate the behaviour of (25) the surface resistance has been evaluated with $|\xi| = 2/3$ ($\kappa = 5$ or $1/5$); the same values of H and τ have been used as in the previous calculations. The frequency variation of $\Delta R/R(0)$ is shown in figure 1 curve *b* and is entirely similar to the two cases previously discussed. We may note that curves *a* and *c* of figure 1 represent in fact the limiting forms of the magneto-resistance effect implicit in the general expression (25).

§ 5. THE TWO-BAND MODEL ($\tau_1 \neq \tau_2$)

In view of the special significance of the relaxation time in the present theory it is of particular interest to consider a more general model in which the relaxation times for the two bands are different. A detailed discussion would seem scarcely to be justified at present and, accordingly, in this section, we restrict ourselves to a simple special case and put $n_1 = n_2 = n$.

If we write $\tau_1 = \lambda \tau_2$, the d.c. conductivity from (16) is $\sigma_0 = ne^2 \tau_2 (\lambda + 1)/m$. Substituting for P and Q in (14) we obtain, after some reduction,

$$Z(\omega, H) = \frac{(1+i)}{\sqrt{2}} R_n \times \left[\frac{A_1 A_2 (\lambda + 1) \{ (\lambda W_1 A_2 + W_2 A_1) + [(\lambda W_1 A_2 + W_2 A_1)^2 + \alpha^2 \tau_2^2 (\lambda^2 W_2^2 - W_1^2)^2]^{1/2} \}}{(\lambda W_1 A_2 + W_2 A_1)^2 + \alpha^2 \tau_2^2 (\lambda^2 W_2^2 - W_1^2)^2} \right]^{1/2} \quad \dots\dots (26)$$

where

$$W_j = 1 + i\omega\tau_j, \quad A_j = \alpha^2 \tau_j^2 + W_j^2 \quad (j = 1, 2).$$

If $\lambda = 1$, the distinction between the suffixes disappears and the expression in square brackets reduces to $2A/W$. Thus (26) goes over to the correct form (22), for the case of equal relaxation times. For zero magnetic field (26) reduces to

$$Z(\omega, 0) = \frac{(1+i)}{\sqrt{2}} R_n \left[\frac{2(\lambda + 1) W_1 W_2}{\lambda W_2 + W_1} \right]^{1/2} \quad \dots\dots (27)$$

and this expression goes over to the correct form (18) when $\lambda = 1$.

In order to examine the implications of (26) and (27) the real parts of these expressions have been extracted by numerical methods, taking $\lambda=0.1$. This large difference between the relaxation times is not, perhaps, very plausible, but will serve to illustrate the new features of the present model. In figure 4 $R(\omega, 0)$, calculated from (27), is shown as a function of $\omega\tau_2$, together with the curve given by (19), which applies to the free-electron model and to the two-band model with equal relaxation times. The main point of interest is the subsidiary maximum, which occurs approximately at $\omega\tau_2=10$, i.e. $\omega\tau_1=1$. In practice the two relaxation times are hardly likely to be separated so widely and the subsidiary maximum is therefore likely to be less prominent. Moreover, unless exceptional values of the relaxation times are involved, this phenomenon is confined to the far infra-red and experimental verification is likely to be very difficult.

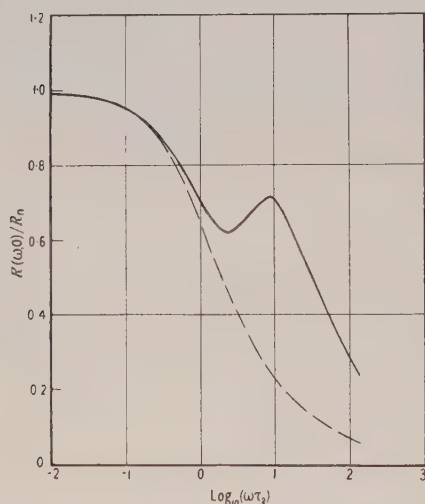


Figure 4. Variation of surface resistance with frequency for two-band model ($n_2/n_1=1$, $\tau_2/\tau_1=10$). The broken line shows the corresponding free-electron curve.

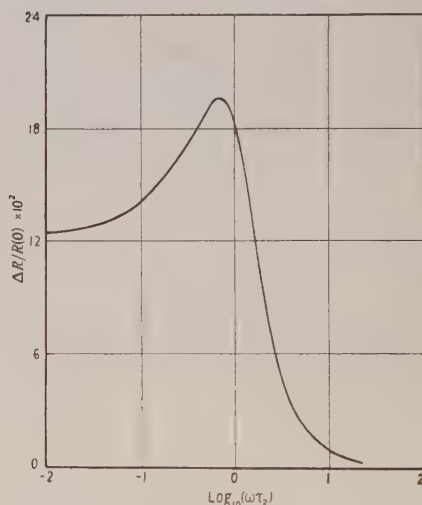


Figure 5. Variation of magneto-resistance effect with frequency for two-band model ($n_2/n_1=1$, $\tau_2/\tau_1=10$, $\alpha\tau_2=1$).

In view of the frequency variation of $R(\omega, 0)$ it is somewhat striking that the magneto-resistance effect, represented by $\Delta R/R(0)$, exhibits no anomaly. As a specific example $R(\omega, H)$ has been calculated from (26), taking $\lambda=0.1$, $\alpha\tau_2=1$, $\alpha\tau_1=0.1$. The frequency variation of $\Delta R/R(0)$ is shown in figure 5 and in general shape the curve is seen to be indistinguishable from those of figure 1. The occurrence of the maximum at $\omega\tau_2=0.7$, as compared to $\omega\tau=0.5$ in figure 1, is explained by the fact that in our rather artificial example band 2 carries ten times as much current as band 1. The peak would occur nearer the position $\omega\tau_1=0.5$ if band 1 carried the greater part of the current. As a further consequence of this extremely unequal division of the current, it is perhaps not surprising that the order of magnitude of $\Delta R/R(0)$ should be comparable with that given by the free-electron model.

§ 6. APPLICATION TO BISMUTH

The properties of bismuth indicate a very small number of conduction electrons and, for ideally *pure* bismuth, an equal number of positive holes. It is therefore reasonable to suppose that the two-band model would be applicable in this case and, indeed, this model was used by Jones (1936) in his discussion of d.c. galvano-magnetic phenomena in bismuth.

The significant experimental results are those of Heaps (1950), who deduced the magneto-resistance effect from measurements of the power loss in a bismuth cavity. (The power loss is proportional to the surface resistance but Heaps has interpreted his results in terms of a change in resistivity.) At 3000 Mc/s $\Delta\rho/\rho(0)$ was found to be of the order of half the d.c. value. Now on the basis of the present theory no appreciable decrease in the magneto-resistance change should be observed for frequencies lower than that corresponding (roughly) to $\omega\tau \sim 1$. This limit corresponds to a wavelength of about 50μ , if one takes $\tau = 3 \times 10^{-14}$ sec, which is the room temperature value for sodium or copper. The wavelength used in Heaps' experiments was 9.2 cm and, although there are insufficient data for a quantitative discussion, this suggests strongly that in bismuth the relaxation time is very much larger than in the monovalent metals.

Sondheimer (1952) has pointed out that in metals containing a very small number of conduction electrons the relaxation time, and hence the mean free path, should be abnormally large, and our conclusion gives further support to this suggestion. According to recent measurements (Pippard and Chambers 1952, Chambers 1953) the value of the mean free path in bismuth at room temperature is in the neighbourhood of 6μ , i.e. about 150 times larger than for copper. Thus one might reasonably expect the relaxation time in bismuth to be greater than that in copper by a factor of about 100–200, but a factor of 1000, as suggested by Heaps' results, would appear to be rather surprising. Further experiments, particularly in the millimetre and far infra-red regions, would be extremely valuable in helping to clarify the position.

§ 7. CONCLUSION

In the foregoing sections the two-band model has been used to interpret the frequency variation of the magneto-resistance effect, represented by the relative change in the surface resistance in a magnetic field. Although by no means exhaustive, our discussion has demonstrated the importance of the relaxation time and, in particular, the conclusion has been reached that in all cases the magneto-resistance effect should be independent of frequency in the region $\omega\tau \ll 1$. At higher frequencies, the disappearance of the magneto-resistance effect has been shown to follow as a general result, and is to be expected in all metals. When the two relaxation times are equal, the curve of $\Delta R/R(0)$ versus frequency shows a peak corresponding to $\omega\tau \sim \frac{1}{2}$ and a subsequent rapid decrease to zero. When the two relaxation times are not equal the exact positions of the peak and the steep decline will depend upon the division of the current between the two bands. In this connection the relative magnitudes of the carrier density n and effective mass m must be borne in mind. Variations in these parameters will not, however, affect the general conclusions and it does not seem worth while to pursue the matter in great detail until further experimental evidence becomes available.

ACKNOWLEDGMENT

During the course of the work on this problem, which was commenced at the University of Sheffield and continued at the Northern Polytechnic, London, the author learned that certain non-relaxation formulae for the free-electron model had been derived independently by Dr. E. H. Sondheimer. A joint note was accordingly published, summarizing the results for the free-electron model. It is a pleasure to thank Dr. Sondheimer for several subsequent discussions and for many valuable suggestions.

REFERENCES

- BLUNT, R. F., 1948, *Phys. Rev.*, **73**, 654.
CHAMBERS, R. G., 1953, *Physica*, **19**, 365.
COOKE, S. P., 1948, *Phys. Rev.*, **74**, 701.
DONOVAN, B., and SONDHEIMER, E. H., 1953, *Proc. Phys. Soc. A*, **66**, 849.
ENGLERT, E., and SCHUSTER, K., 1932, *Z. Phys.*, **79**, 194.
HEAPS, C. W., 1926, *Phys. Rev.*, **27**, 764; 1950, *Ibid.*, **80**, 892.
JONES, H., 1936, *Proc. Roy. Soc. A*, **155**, 653.
KAPITZA, P., 1929, *Proc. Roy. Soc. A*, **123**, 292.
MCLENNAN, J. C., ALLIN, E. J., and BURTON, A. C., 1932, *Phil. Mag.*, **14**, 508.
PIPPARD, A. B., 1947, *Proc. Roy. Soc. A*, **191**, 385.
PIPPARD, A. B., and CHAMBERS, R. G., 1952, *Proc. Phys. Soc. A*, **65**, 955.
REUTER, G. E. H., and SONDHEIMER, E. H., 1948, *Proc. Roy. Soc. A*, **195**, 336.
SONDHEIMER, E. H., 1952, *Proc. Phys. Soc. A*, **65**, 561.
SONDHEIMER, E. H., and WILSON, A. H., 1947, *Proc. Roy. Soc. A*, **190**, 435.
WILSON, A. H., 1953, *The Theory of Metals* (Cambridge: University Press).

X-Ray Diffraction from Built-up Multilayers Consisting of only a few Monolayers

By D. C. BISSET* AND J. IBALL†

University of St. Andrews, Carnegie Laboratory of Physics, University College, Dundee

MS. received 28th December 1953

Abstract. Experiments are described which show that there is an exact similarity between optical diffraction from a plane grating containing only a few lines and x-ray diffraction from a built-up multilayer, of barium stearate for instance, when the multilayer consists of a few monolayers. The diffraction maxima given by Bragg's law are accompanied by subsidiary maxima equal in number to $N-2$ where N is the number of 'unit cells' (i.e. the number of repeat distances in the direction perpendicular to the plane of the monolayers). The formulae for the x-ray case are given and several experimental examples are cited.

§ 1. INTRODUCTION

SINCE the early experiments of Langmuir (1920) on monolayers of fatty acids at the air-liquid interface and the discovery of Blodgett (1935) that successive monolayers of these acids could be deposited on a glass slide by repeated dippings through the interface, many workers have investigated the diffraction of x-rays by such built-up multilayers. Clark, Sterret and Leppla (1935) found that fatty acids spread on a solution of a calcium salt gave a multilayer of a calcium soap. X-ray measurements of the repeat distance in the multilayer agreed with those found in the normal crystalline soap. Built-up multilayers of barium stearate were examined by optical and x-ray methods by Halley and Bernstein (1936, 1937). More recent investigations were those of Stenhagen (1938), Alexander (1939) and Knott, Schulman and Wells (1940). Most of these workers used multilayers containing a large number (often some hundreds) of monolayers, though Clark and Leppla (1936) reported having obtained good x-ray diffraction patterns from as few as three layers of lead stearate; they did not, however, observe any unusual effects such as are described below.

A discussion of the diffraction effects to be expected when the diffracting crystal is very small, i.e. contains only a few unit cells is given by James (1948) but he states (p. 545) that "It is not possible to observe the effects characteristic of the diffraction of x-rays by very small single crystals, for the intensities involved are far too small". He then goes on to give examples of some of the effects produced when electron beams are diffracted by very small crystals. The case of optical diffraction by gratings consisting of a few elements is discussed in textbooks of physical optics, and Bragg and Lipson (1943) give some examples of the subsidiary maxima obtained. It is the purpose of this paper to show,

* Now at Monsanto Chemicals Ltd., Ruabon, North Wales.

† British Empire Cancer Campaign Research Fellow.

by using multilayers as a 'one-dimensional grating', that the diffraction of x-rays by a small number of unit cells can be observed very simply, and that there is a close similarity between x-rays and optics in this respect. With the methods described below, it is in many ways easier to illustrate the effect with x-rays than it is with light, but as far as the authors are aware this is the first time these effects have been demonstrated with x-rays.

§2. EXPERIMENTAL METHODS

2.1. *Preparation of Specimens*

Multilayers of stearates and palmitates of calcium, magnesium, strontium and barium were prepared by spreading pure fatty acids on aqueous solutions of the metal salts and then depositing the films of soap on to narrow strips of glass cut from rectangular microscope cover glasses. The technique was developed by Blodgett (1935) and is quite standard. The pH of the aqueous solutions on which the films were spread was adjusted to 8.5 in order to obtain a monolayer consisting almost entirely of neutral soap. It is often the practice, in building a multilayer consisting of a large number of monolayers, to make the surface of glass or metal hydrophobic initially. This can be done by melting a little ferric stearate on the glass surface and then rubbing it down to a monolayer. In the present work this could not be done as the whole purpose was to study the diffraction effects from a small number of layers. Consequently the process of building the multilayer had to begin with a clean glass surface which is hydrophilic and in order to deposit the first layer it is necessary to immerse the glass strip in the water of the spreading trough before spreading the film of soap. When the glass is withdrawn through the surface one monolayer is deposited and the surface is now hydrophobic. Subsequently monolayers are deposited in pairs, one on the down trip through the surface and one on the up trip. Consequently the multilayers studied consist of an odd number of layers in most cases.

2.2. *X-Ray Cameras*

A flat film camera was normally used on a specially constructed stand which was rigidly attached to the x-ray tube housing and which carried rails on which the film holder could be moved to vary the specimen-to-film distance. The stand carried the collimating system, which consisted of three narrow slits parallel to the line focus of the x-ray tube, which, in the case of the particular tube used, was horizontal. The glass strips on which the multilayers were deposited were mounted horizontally on a stage which could be oscillated with reference to the x-ray beam by means of cams. A specimen-to-film distance of 12 cm was found to be convenient for most purposes when a large number of orders of reflection was recorded. It was found advantageous to place the nickel filter (when using $\text{CuK}\alpha$ radiation) immediately in front of the film in the film holder, instead of near the x-ray tube window which is the more usual place for it. The films are much less affected by scattered radiation and any fluorescent radiation which may be caused is absorbed. When the diffraction pattern in the range of Bragg angle 0 to 1.5° was being studied a special vacuum camera could be placed on the stand without disturbing the specimen, and this provided specimen-to-film distances of 33 cm and more. A detailed description of this vacuum camera and the method of calibration is given elsewhere (Bisset and Iball 1954). In most of

these investigations involving specimens containing a small number of monolayers, barium stearate and barium palmitate were used as they give better diffraction patterns than any other material of this kind, but the same kinds of effects as were observed for the barium soaps were obtained with other metal soaps and with multilayers containing no metal atoms, as for example, octadecylamine.

§ 3. THEORETICAL

3.1. *The Diffracting Material*

The scattering power of barium atoms, atomic number 56, is so much greater than that of any other atoms (e.g. carbon, atomic number 6) in a barium soap, that the multilayers can be regarded, to a first approximation at any rate, as being planes of barium atoms with a separation of approximately 50 Å and the diffraction caused by the carbon chains will be negligible in comparison. These multilayers can be regarded as one-dimensional single crystals of barium with a repeat distance of approximately 50 Å. Since the multilayers can be built up of any number of monolayers, it is possible to construct 'crystals' of as many 'unit cells' as desired. As far as the diffraction in a plane perpendicular to the plane of the layers is concerned, the variation of intensity with number of unit cells can be treated as a one-dimensional problem.

3.2. *The Interference Function for a Unidimensional Crystal*

The total intensity of reflection of x-rays from a crystal is given by the product of the structure factor and the interference function which depends on the number of unit cells in the crystal specimen. In the present case the crystal is regarded as consisting of a distribution of scattering matter along a line perpendicular to the layers with a pronounced maximum at intervals of approximately 50 Å. As stated above, with a substance like barium stearate the scattering power of the barium atoms is so great compared with the other atoms present, that a multilayer can be considered to a first approximation as layers of barium atoms 50 Å apart separated by a transparent continuous medium.

The general expression for the intensity of the scattered beam from a three-dimensional crystal lattice is given by James as

$$J = \frac{|\Phi|^2}{R^2} I_0(\xi, \eta, \zeta)$$

where the first factor depends on the scattering power of an individual lattice-unit, and the second factor I_0 (the interference function) is expressed

$$I_0(\xi, \eta, \zeta) = \frac{\sin^2(\pi N_1 \xi)}{\sin^2(\pi \xi)} \frac{\sin^2(\pi N_2 \eta)}{\sin^2(\pi \eta)} \frac{\sin^2(\pi N_3 \zeta)}{\sin^2(\pi \zeta)}$$

where N_1, N_2, N_3 are the number of repeat units in the directions of the translation vectors of the elementary parallelepiped.

In the case of built-up multilayers, in so far as the reflections from the layers are concerned, we are dealing with a one-dimensional lattice and the interference function is

$$I_0(\xi) = \sin^2(\pi N_1 \xi) / \sin^2(\pi \xi)$$

which is of the same form as in the case of an optical grating (Wood 1919).

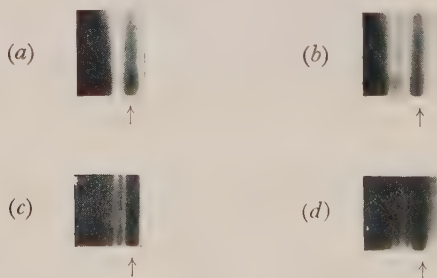
The principal maxima will occur when $\xi = h$ where h is any integer, and this is of course the case which corresponds to the reflection when the Bragg law holds.

When N_1 is large, which is assumed to be the case for the Bragg law to hold, then the principal maxima are narrow and intense. When N is small, however, the principal maxima are broad, and in between them there will be subsidiary maxima of appreciable intensity. The number of such subsidiary maxima is $N-2$ and the two on either side of a principal maximum will have an intensity of approximately 5% of that of the principal maximum, but the other subsidiary maxima will decrease in intensity very rapidly. The positions of the subsidiary maxima are given by the above expression and when N is greater than 8 the subsidiary maxima can be taken as lying midway between the minima given by $\sin(\pi\xi) = n\lambda/Nd$ where n is an integer not a multiple of N , λ is the wavelength of the x-rays used, and d is the spacing of the planes. For smaller values of N the positions of the subsidiary maxima are best obtained graphically using the equation $\tan(N\pi\xi) = N \tan(\pi\xi)$ (cf. Wood 1919).

§ 4. RESULTS

4.1. Barium Stearate Multilayers

X-ray diffraction patterns were obtained from multilayers consisting of 3, 5, 7, 9 . . . 17, 19 and 23 monolayers. These correspond to 1, 2, 3, 4, . . . 8, 9, 11 'unit cells'. This is due to the fact that the layers are deposited as follows, $\longleftrightarrow\longleftrightarrow\longleftrightarrow\longleftrightarrow$ where an arrow represents a monolayer and the arrow-head represents the metal atom. With three monolayers therefore we have a layer of single metal atoms attached to the glass plate and layer of twice as many metal atoms separated from the single layer by a distance equal to the length of two carbon chains. With five monolayers there will be three layers of metal atoms, again one of the layers having only half the number of metal atoms. Thus with five monolayers there are only two repeat distances or 'unit cells' as far as the metal atoms are concerned. With seven monolayers there will be three 'unit cells' and so on. The principal and subsidiary maxima are observed as predicted by the theory. The figure shows some examples of the photographs taken on the



Diffraction from multilayers of barium stearate. (a) 7 monolayers, (b) 9 monolayers, (c) 15 monolayers, (d) 19 monolayers. Specimen-to-film distance 33cm. $\text{CuK}\alpha$ —The arrow indicates the position of the 1st principal maximum (Bragg spacing 50 Å).

vacuum camera at 33 cm from the specimen. The positions were measured and compared with those calculated from the interference function as indicated above. The results are given in table 1. The agreement is satisfactory especially with the thicker specimens; with the very thin specimens the lines on the films are diffuse and it is difficult to locate the maximum with any great accuracy.

Table 1 refers to the subsidiary maxima lying between the position of the main beam and the first principal maximum. Subsidiary maxima were also observed between the higher orders of the principal maxima and these can be seen on photographs taken at a specimen-to-film distance of 12 cm. They are much fainter of course but it was confirmed that there are always $N-2$ subsidiary maxima present.

It will be noticed in table 1 that when the number of unit cells is very small the value of the Bragg angle for the first principal maximum changes slightly as the number of layers is increased and tends towards the value obtained when a

Table 1. Comparison of Observed and Calculated Angles of Diffraction for Barium Stearate Multilayers, Specimen-to-Film Distance 33 cm. $\text{CuK}\alpha$ Radiation

(1)	(2)	(3)	(4)	(5)	(6)
9	4	47'	22'	17' 36"	19' 42"
			34'	29' 18"	32' 48"
13	6	49'	—	10' 12"	10' 56"
			22'	20' 24"	21' 50"
			30'	28' 33"	30' 36"
			38'	38' 45"	41' 30"
17	8	49'	—	9' 12"	9' 48"
			—	15' 18"	16' 24"
			23'	21' 24"	23' 0"
			28'	27' 30"	29' 30"
			35'	33' 39"	36' 6"
			41'	39' 48"	42' 38"
23	11	52'	—	7' 8"	7' 9"
			—	11' 48"	11' 56"
			19'	16' 30"	16' 42"
			22'	21' 15"	21' 28"
			26'	25' 57"	26' 14"
			31'	30' 42"	31' 0"
			35'	35' 24"	35' 48"
			39'	40' 6"	40' 33"
			45'	44' 50"	45' 20"

(1) No. of monolayers; (2) No. of 'unit cells'; (3) principal maximum; (4) subsidiary maxima (observed); (5) subsidiary maxima (calculated); (6) subsidiary maxima (calculated).

Column (5) gives the values calculated on the basis of a layer spacing calculated from the observed principal maximum of column (3). The values of column (6) are calculated on the basis of the spacing obtained for a multilayer containing a large number of monolayers (i.e. principal maximum at 52' 30").

large number of layers is used (52' 30"). This could mean that the actual spacing of the planes is changing or that the refractive index for x-rays is changing. At these small glancing angles the effect of refractive index is appreciable. It is noticed in addition that the observed positions of the secondary maxima for small numbers of layers, agree better with the positions calculated on the assumption that the spacing is the same for a small number of layers as for a large number (column (6)), than with the positions calculated using the value of spacing given by the *observed* first principal maxima in each individual film (column (5)). No very satisfactory explanation of these slight changes can be put forward at present.

4.2. *Mixed Multilayers*

A large number of experiments was carried out on composite films made by sandwiching monolayers of one substance between monolayers of another, for example, octadecylamine monolayers between barium stearate layers. Tables 2 (*a*) and 2 (*b*) give the results obtained with such films composed respectively of (*a*) alternating double layers of the two substances, (*b*) two double layers of octadecylamine sandwiched between double layers of barium stearate. The results in the tables were obtained with a specimen-to-film distance of 12 cm but photographs were also taken at 33 cm with the vacuum camera, and on these photographs the first four orders of specimen (*a*) were observed and the first seven orders of specimen (*b*). With specimen (*b*) at 12 cm the first order at 153 Å spacing is not observed since it is not resolved from the primary beam but it is clearly seen at 33 cm.

Table 2 (*a*). Observed Spacings and Estimated Intensities of Orders of Diffraction from a Mixed Multilayer: Barium Stearate-Octadecylamine Alternating Double Layers, 25 Double Layers of Each. Specimen-to-Film Distance 12 cm

Order	1	2	3	4	5	6	7	8	9	10	11	12	13	14
Spacing (Å)	97.1	56.4	34.4	25.7	21.05	17.45	14.8	12.95	11.45	10.25	9.45	8.65	8.0	7.4
Intensity	M	VS	MW	M	MW	S	MW	W	W	M	W	W	W	W

Table 2 (*b*). As for Table 2 (*a*) but Double Layers of Barium Stearate Alternating with *two* Double Layers of Octadecylamine, 25 Double Layers of Stearate to 50 Double Layers of Octadecylamine

Order	1	2	3	4	5	6	7	8	9	10	11	12	13	14	15	21
Spacing (Å)	(153)	75.2	50.4	37.6	30.6	25.5	22.2	19.6	16.9	15.2	13.8	12.8	11.75	10.95	10.15	7.30
Intensity	—	M	VS	MW	MW	M	MW	MW	S	W	W	W	W	W	M	W

(The first order is present but merges with the main beam; the orders between 15 and 21 are not missing but are too weak to be measured.)

VS S MS M MW indicate intensities, ranging from very strong, strong to weak.

Table 2 (*a*) shows that the observed diffraction maxima correspond to different orders of reflection from planes of spacing 103 Å and the results of table 2 (*b*) correspond to a spacing of approximately 153 Å. The orders corresponding to the barium stearate spacing (even orders in table 2 (*a*) and every third order in table 2 (*b*)) are always stronger than the others. Stenhagen (1940-41) reported similar results with composite films of ethyl stearate and barium eicosoate.

It was confirmed that with multilayers consisting of octadecylamine alone the subsidiary maxima appeared when the number of layers was small, but the intensity of the whole diffraction pattern is less than in the case of a metal salt.

4.3. *Intensities of Subsidiary Maxima*

An attempt was made to estimate the relative intensities of the diffraction maxima when changes were made in the composition of the multilayers. The intensities of the subsidiary maxima, and of course those of the principal maxima, will be affected by the composition and arrangement of the molecules in the monolayers, and it was decided in the first instance to investigate the effect of changing the metal atom in the monolayers. Intensities were estimated by eye, using a calibrated scale. The accuracy is probably not better than 20%. The results given in table 3 show, however, that while the intensities of the principal maxima change in the manner expected as the metal atom changes, there is not the same change in the intensities of the subsidiary maxima.

Table 3. Relative Intensities of Principal and Subsidiary Maxima for Multilayers Composed of 13 Monolayers of Palmitates of Four Different Metals. Specimen-to-film Distance 12 cm

Principal maxima (Å)	Subsidiary maxima (Å)	Relative intensities			
		Ba	Sr	Ca	Mg
	71.9	16	16	8-16	8-16
	57.1	16	16	8-16	8-16
45.9		80	56	48	40
22.9		8-16	4	4	3
15.3		16	8	8	4
11.5		2	1	1	1
9.2		3	2	1	1

§5. CONCLUSIONS

It has been shown that x-ray diffraction from a multilayer consisting of a small number of monolayers gives the same phenomenon of subsidiary maxima as is observed with optical diffraction from a line grating of a few lines. In the case of x-ray diffraction the intensity of the subsidiary maxima can be quite appreciable compared with the intensity of the principal maxima. The presence of small angle diffraction maxima in an x-ray pattern need not mean that there is a repeat distance of the corresponding spacing in the diffracting specimen. With some biological specimens the small angle maxima observed, which indicate large spacings if interpreted as Bragg reflections, may well be subsidiary maxima due to a small number of repeat units in the specimen. One such case is on record. Bernal and Fankuchen (1941) when investigating x-ray diffraction from tobacco mosaic virus preparations, observed extra reflections which on the basis of the assumed unit cell dimensions would have to be assigned fractional Millar indices. They suggested rather tentatively that these 'extra' reflections are due to *intra*-molecular repeat distances of which there will be only a small number per virus particle and consequently the assumption that there is an infinite number of repeat distances, which is inherent in the Bragg law, is not valid. They go on, "The theory (for the case of a small number of unit cells) is here necessarily complicated and has not up to now been attempted largely because no known experimental examples of it existed". They compare the phenomenon to the case of electron diffraction from very thin crystals but it seems to us that the proper comparison is to physical optics and, as is shown in the present paper, the theory of diffraction which explains the observations of optics applies to x-rays, provided the analogous physical conditions apply in both cases.

It is hoped that investigations of thin specimens where these subsidiary maxima appear will make it possible to use the diffraction data to throw light on the structure of the specimen. The technique thus developed may then be used in the elucidation of the structure of materials which are obtainable *only* in thin layers such as protein membranes and adsorbed layers.

ACKNOWLEDGMENTS

We wish to acknowledge grants in support of this work from the British Empire Cancer Campaign and the Royal Society. One of us (D.C.B.) is indebted to the Department of Scientific and Industrial Research for a maintenance grant and we wish to thank Professor G. D. Preston for his continued interest and support.

REFERENCES

- ALEXANDER, A. E., 1939, *J. Chem. Soc.*, 777.
BERNAL, J. D., and FANKUCHEN, I., 1941, *J. Gen. Physiol.*, **25**, 111.
BISSET, D. C., and IBALL, J., 1954, *J. Sci. Instrum.*, **31**, 55.
BLODGETT, K. B., 1935, *J. Amer. Chem. Soc.*, **57**, 1007.
BRAGG, W. L., and LIPSON, J., 1943, *J. Sci. Instrum.*, **20**, 110.
CLARK, G. L., and LEPLA, P. W., 1936, *J. Amer. Chem. Soc.*, **58**, 2199.
CLARK, G. L., STERRET, R. R., and LEPLA, P. W., 1935, *J. Amer. Chem. Soc.*, **52**, 330.
HOLLEY, C., and BERNSTEIN, S., 1936, *Phys. Rev.*, **49**, 403; 1937, *Ibid.*, **52**, 525.
JAMES, R. W., 1948, *The Optical Principles of the Diffraction of X-rays* (London : Bell).
KNOTT, G., SCHULMAN, J. H., and WELLS, A. F., 1940, *Proc. Roy. Soc. A*, **176**, 534.
LANGMUIR, I., 1920, *Trans. Faraday Soc.*, **15**, 68.
STENHAGEN, E., 1938, *Trans. Faraday Soc.*, **34**, 1328; 1940-41, *Arkiv Kemi. Min. Geol.*, **14A**, No. 10.
WOOD, R. W., 1919, *Physical Optics* (London : Macmillan).

The Binding Energy of the Alpha Particle

By A. C. CLARK†

Department of Theoretical Physics, University of Liverpool

Communicated by K. J. Le Couteur; MS. received 16th December 1953

Abstract. The method of Morpurgo is extended to deal with both central and tensor forces, each having Yukawa-type radial dependence. The method is applied to calculate the binding energy of ${}^4\text{He}$ for one set of Pease-Feshbach force parameters. It is shown that the inclusion of a second D state in the trial wave function leads to a large increase in binding energy.

§ 1. INTRODUCTION

IN default of a consistent theory of the origin of the nuclear forces, the phenomenological approach still retains much of its interest. The point of view adopted here is to consider only static, two-body forces to be acting, the force depending on the separation r_{ij} of the two particles according to some simple law (Yukawa, exponential, etc.). The strength and range are then chosen so that the experimental data on the two-particle system (low-energy scattering and properties of the deuteron) are reproduced. The theory of the effective range shows that these properties are largely independent of the law of force, so it is necessary to find some other check on the theory. It appears that the properties of the ground states of light nuclei provide such a check. In fact it was formerly the custom to use the binding energy of the triton to determine some of the force parameters. The inadequacy of this practice only became obvious when it was found that the tensor force had a large effect on the binding of light nuclei.

Forces which contain a large tensor component are not easy to handle by traditional theoretical methods. The only approach hitherto is by the variational method, and it is found that the calculated binding energy increases steadily as further terms are added to the linear variation function. A first step in the research for a new variation function was taken by Irving (1951), who used exponential functions of an argument R , given by $R^2 = \sum r_{ij}^2$. His results are not substantially better than those given by gaussian functions of R .

Recently Morpurgo (1952) made a major advance by his introduction of a function $\psi(R)$ with no adjustable parameters, the form of the function ψ itself being variable. He found that ψ must satisfy a certain second-order differential equation of the one-dimensional Schrödinger type. He was able to solve this equation by an elegant device and obtained, with much less labour, results as good as Margenau's with 11 variational parameters. Morpurgo ignored the tensor forces in his work, and as it stands his technique is not well adapted to handle two-body forces with a singularity such as the Yukawa potential.

It is the purpose of this note to describe an adaptation of Morpurgo's method which overcomes the defects mentioned above. The method is applied to

† Now at the Ministry of Supply, Sellafield, Cumberland.

calculate the binding energy of ${}^4\text{He}$ for Yukawa forces with one set of Pease-Feshbach parameters, and the result is compared with Irving's for the same forces.

§ 2. THE METHOD OF MORPURGO

First we consider Morpurgo's work in a general way in order to establish its connection with the traditional variational method. For definiteness take the case of four nucleons in mutual interaction, with Hamiltonian H . The trial wave function representing the ground state of ${}^4\text{He}$ is

$$|\Psi\rangle = |\chi\rangle \psi(\rho) \rho^{-4} \quad \dots\dots(1)$$

where $|\chi\rangle$ depends only on the spin coordinates of the nucleons, and ρ is given by

$$\rho^2 = \frac{1}{4} \sum r_{ij}^2. \quad \dots\dots(2)$$

The function ψ is then determined by minimizing $\langle \Psi | H | \Psi \rangle$ with respect to variations $\delta\psi$ of ψ , subject to $\delta\langle \Psi | \Psi \rangle = 0$. The integrations implicit in these expressions can all be performed, when H is given, with the exception of a single integration over ρ in each case. The equation for ψ then takes the form

$$\frac{d^2\psi}{d\rho^2} + \epsilon\psi - V(\rho)\psi = 0. \quad \dots\dots(3)$$

This is an eigenvalue problem to determine ψ and ϵ subject to the usual boundary conditions at $\rho=0$ and $\rho=\infty$. The function $V(\rho)$ is given explicitly, usually as an integral representation, and depends on the assumed form of the nuclear forces.

The trick adopted by Morpurgo to solve (3) is to consider an entirely different equation, namely

$$\frac{d^2\psi_0}{d\rho^2} + \epsilon_0\psi_0 - U_0(\alpha_i; \rho)\psi_0 = 0. \quad \dots\dots(4)$$

Here $U_0(\alpha_i; \rho)$ is a simple analytic function which contains a certain number of parameters α_i and which permits (4) to be solved for ψ_0 and ϵ_0 explicitly. The parameters α_i are then chosen so that $|V - U_0|$ shall be as small as possible. This is not difficult. By adding to U_0 a small perturbing potential $\Delta U_0 = V - U_0$ (4) is converted into (3). Hence by perturbation theory

$$\epsilon \simeq \epsilon' \equiv \epsilon_0 + \langle \psi_0 | \Delta U_0 | \psi_0 \rangle. \quad \dots\dots(5)$$

From (4) and (5) we can eliminate ϵ_0 , getting

$$\begin{aligned} \epsilon' &= \langle \psi_0 | -\frac{d^2}{d\rho^2} + U_0 | \psi_0 \rangle + \langle \psi_0 | \Delta U_0 | \psi_0 \rangle \\ &= \langle \psi_0 | -\frac{d^2}{d\rho^2} + V | \psi_0 \rangle. \end{aligned} \quad \dots\dots(6)$$

But from (3) we have

$$\epsilon = \langle \psi | -\frac{d^2}{d\rho^2} + V | \psi \rangle. \quad \dots\dots(7)$$

Equation (7) is merely the expression of the variation principle with the 'exact' wave function ψ ; equation (6) is the same thing with the approximate function ψ_0 . This conclusion does not affect the value of the method, since it is very much easier to choose the α_i to make $V - U$ small than it is to choose them to minimize the right-hand side of (6).

§ 3. THE CHOICE OF WAVE FUNCTION

The interaction between any two nucleons i and j is taken to be

$$V_{ij} = -\mathcal{V}_0 \left\{ 1 + \frac{1}{2} g (\boldsymbol{\sigma}_i \cdot \boldsymbol{\sigma}_j - 1) \right\} J(r/r_c) - \gamma \mathcal{V}_0 S_{ij} J(r/r_t) \quad \dots\dots(8)$$

where $r = r_{ij} = |\mathbf{r}_i - \mathbf{r}_j|$, $J(x) = x^{-1} e^{-x}$ and S_{ij} is the usual tensor-force operator. Sets of values of the parameters \mathcal{V}_0 , g , γ , r_c and r_t which satisfy the two-body data have been published by Pease and Feshbach (1951) and by Feshbach and Schwinger (1951).

The possible terms in the ${}^4\text{He}$ wave function are S , P and D and have been listed by Gerjuoy and Schwinger (1942). Of these, Irving retains only the principal S state and the principal D state. In the following, however, we shall use the principal S state and two D states in order to estimate the effect of the higher D states.

The trial wave function is taken to be

$$|\Psi\rangle = N_0(|s\rangle - N_1\lambda\rho^{-2}|d_1\rangle + N_2\mu\rho^{-4}|d_2\rangle)\rho^{-4}\psi \quad \dots\dots(9)$$

where ψ , λ and μ are functions of ρ which we have to determine. Particles 1 and 2 are neutrons, 3 and 4 protons. The spin functions are as follows :

$$\begin{aligned} |s\rangle &= \frac{1}{2}(\alpha_1\beta_2 - \beta_1\alpha_2)(\alpha_3\beta_4 - \beta_3\alpha_4) \\ |d_1\rangle &= |\boldsymbol{\rho}_1, \boldsymbol{\rho}_2\rangle \\ |d_2\rangle &= (\boldsymbol{\rho}_2 \cdot \mathbf{r})|\boldsymbol{\rho}_1, \mathbf{r}\rangle + (\boldsymbol{\rho}_1 \cdot \mathbf{r})|\boldsymbol{\rho}_2, \mathbf{r}\rangle \end{aligned} \quad \dots\dots(10)$$

in which

$$|\mathbf{a}, \mathbf{b}\rangle = \{3(\boldsymbol{\sigma}_1 \cdot \mathbf{a})(\boldsymbol{\sigma}_3 \cdot \mathbf{b}) + 3(\boldsymbol{\sigma}_1 \cdot \mathbf{b})(\boldsymbol{\sigma}_3 \cdot \mathbf{a}) - 2(\mathbf{a} \cdot \mathbf{b})(\boldsymbol{\sigma}_1 \cdot \boldsymbol{\sigma}_3)\}|s\rangle \quad \dots\dots(11)$$

the relative coordinates being

$$\boldsymbol{\rho}_1 = \mathbf{r}_2 - \mathbf{r}_1; \quad \boldsymbol{\rho}_2 = \mathbf{r}_4 - \mathbf{r}_3; \quad \mathbf{r} = \frac{1}{2}(\mathbf{r}_4 + \mathbf{r}_3 - \mathbf{r}_2 - \mathbf{r}_1). \quad \dots\dots(12)$$

Further, $N_0^2 = 105/32\pi^4$, $N_1^2 = 11/80$, $N_2^2 = 429/224$, which choice simplifies the normalization integral :

$$\langle \Psi | \Psi \rangle = \int_0^\infty \psi^* \psi \Gamma d\rho \quad \dots\dots(13)$$

where

$$\Gamma = 1 + \lambda^2 + \mu^2 - 4\kappa\lambda\mu \quad \dots\dots(14)$$

and $\kappa^2 = 15.182$. The ultimate calculations are simplified by defining $\phi = \Gamma^{1/2}\psi$ and using the dimensionless independent variable $x = a\rho = \sqrt{2}\rho/r_c$.

The expectation value of the kinetic energy turns out to be

$$\langle \Psi | T | \Psi \rangle = -\frac{\hbar^2 a^2}{2M} \int \phi^* (\phi'' - V_1\phi - V_2\phi) d\rho \quad \dots\dots(15)$$

where M is the mass of a nucleon, and the primes denote differentiation with respect to x . Also

$$V_1 = \frac{12}{x^2} + \frac{2}{\Gamma x^2} \left(9\lambda^2 + \frac{124}{7}\mu^2 - 36\kappa\lambda\mu \right) \quad \dots\dots(16)$$

and

$$V_2 = \frac{1}{\Gamma^2} \left\{ (\lambda')^2 \left(1 + \frac{61}{91}\mu^2 \right) + (\mu')^2 \left(1 + \frac{61}{91}\lambda^2 \right) - 2\lambda'\mu' \left(2\kappa + \frac{61}{91}\lambda\mu \right) \right\}. \quad \dots(17)$$

The expectation value of the potential energy is somewhat more complicated, and may be written

$$\langle \Psi | V | \Psi \rangle = -\frac{\hbar^2 a^2}{2M} \int \phi^* \phi \Gamma^{-1} (A + B\lambda + C\mu + D_1\lambda^2 + E_1\lambda\mu + F_1\mu^2) d\rho$$

where A, B, C, D_1, E_1 and F_1 are certain functions of x which are defined in the Appendix, where also may be found an indication of the way in which they are obtained.

§ 4. THE WAVE EQUATION AND ITS SOLUTION

According to the variation principle, we now seek to minimize $\langle \Psi | T + V | \Psi \rangle$. If for the moment we keep λ and μ as fixed functions of x and allow only ψ to vary, we easily obtain

$$\phi'' + \epsilon\phi - \left(\frac{12}{x^2} + V_2 \right) \phi + V_0 \phi = 0 \quad \dots\dots(18)$$

where $V_0 = \Gamma^{-1}(A + B\lambda + C\mu + D\lambda^2 + E\lambda\mu + F\mu^2) \quad \dots\dots(19)$

and $D = D_1 - 18/x^2$; $E = E_1 + 72\kappa/x^2$; $F = F_1 - 248/7x^2$. $\epsilon = -2MW/\hbar^2 a^2$ is the eigenvalue, W being the binding energy.

Equation (19) differs from Morpurgo's equation in that it contains the unknown functions λ and μ . These can easily be found by the following considerations. If they are assumed to be only slowly varying functions, then V_2 will be very small, since it depends on the derivatives λ' and μ' . Accordingly we neglect V_2 and choose λ and μ so as to minimize the effective potential energy integral, i.e.

$$\delta \int \phi^* V_0 \phi dx = 0. \quad \dots\dots(20)$$

Strictly ϕ should be determined from (18) and thus depends on λ and μ , but to a high order of approximation we can neglect this fact, and (20) becomes

$$\partial V_0 / \partial \lambda = \partial V_0 / \partial \mu = 0. \quad \dots\dots(21)$$

Substituting (19) into (21) we obtain two algebraic equations for λ and μ . In the general case considered here they can be reduced to a cubic equation in λ and a relation between λ and μ linear in μ .

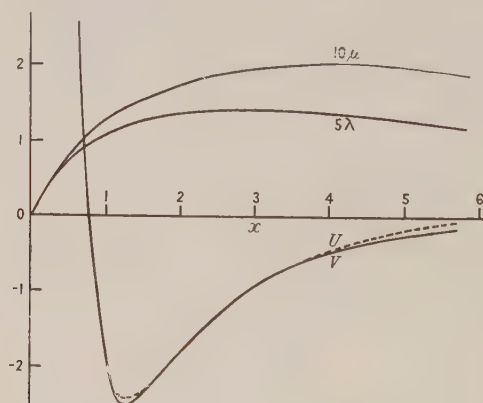


Figure 1.

From this point all the calculations were done numerically, the force parameters used being as follows (from Pease and Feshbach 1951) :

$$\begin{aligned} \mathcal{V}_0 &= 42.7 \text{ MeV}; & \gamma &= 0.69 \\ g &= -0.044; & r_c &= 1.184 \times 10^{-13} \text{ cm} \\ & & r_t &= 1.58 \times 10^{-13} \text{ cm}. \end{aligned} \quad \dots\dots(22)$$

The functions A, B, C, D, E and F were calculated for values of x between 0 and 5.6 at intervals of 0.4. This enabled λ and μ to be calculated at these points as described above. The resulting function $V = 12/x^2 - V_0$ is shown in figure 1, together with λ and μ .

It turns out that V_0 has rather a strong term of the type x^{-1} near $x=0$. For this reason the comparison potential U_0 adopted by Morpurgo gives a very poor fit to V . It was found that an excellent fit could be obtained with a potential of the form U , with

$$\frac{U}{\alpha^2} = \frac{p(p-1)}{\sinh^2 t} - \frac{q(q+1)}{\cosh^2 t} + \frac{\beta b^2 c e^{-bt}(1 + \beta c e^{-bt})}{(1 + \beta e^{-bt})^2} - \frac{2\beta b c e^{-bt}}{1 + \beta e^{-bt}} (p \coth t - q \tanh t) \dots\dots (23)$$

where $t = \alpha x$.

The solution of our comparison equation

$$\phi_0'' + \epsilon_0 \phi_0 - U \phi_0 = 0 \dots\dots (24)$$

corresponding to the ground state is

$$\phi_0 = (1 + \beta e^{-bt})^c \sinh^p t \cosh^{-q} t \dots\dots (25)$$

with $\epsilon_0 = -\alpha^2(q-p)^2$ which gives the approximate binding energy as

$$W_0 = 29.59 \alpha^2 (q-p)^2 \text{ Mev.} \dots\dots (26)$$

In (22) and (24) α , β , b , c , p and q are all adjustable parameters. If we set $c=0$, our equations reduce to Morpurgo's, and then α , p and q are the available parameters.

The method adopted for finding the parameters was to find approximate values of α , p and q which gave slightly too large values of $-U$ in the neighbourhood of $x=3.0$. The right-hand side of (22) was then expanded in powers of x , and β , b and c found by fitting the first few terms to V at $x=0.4$, 0.8 and 1.2 . Thus having approximate values of all the parameters permitted a revised estimate of α and q to be made.

The finally adopted values are $\alpha=0.5$, $p=4.0$, $q=6.0$, $\beta=1.618$, $b=2.557$, $c=3.120$, which give $W_0=29.59$ Mev and the first-order perturbation energy $\langle \phi_0 | V - U | \phi_0 \rangle$ is found to be -0.37 Mev. Taking into account the effect of V_2 (equation (17)), also by first-order perturbation theory, reduces the binding energy by 0.09 Mev. Thus the final value for the binding energy of ^4He is 29.87 Mev.

§ 5. COMPARISON WITH IRVING'S RESULTS

In the last section an estimate of the binding energy of ^4He was made using a wave function representing the principal S state and two D states. The only other calculations taking account of the tensor forces are by Irving (1953), who used a wave function with only one D state. For the sake of comparison it would seem desirable to use the present method with only one D state in the wave function.

This is a simple matter; we merely set $\mu=0$ in all equations. The best value of the function λ will be denoted by λ_0 and is given by

$$\lambda_0 = u + (1 + u^2)^{1/2} \dots\dots (27)$$

where $u = (D - A)/B$. The effective potential is then

$$V = V_\lambda = \frac{12}{x^2} + \frac{(\lambda_0')^2}{(1 + \lambda_0^2)^2} - \frac{A + B\lambda_0 + D\lambda_0^2}{1 + \lambda_0^2} \dots\dots (28)$$

A comparison potential of the form (22) was used with the following parameters: $\alpha=0.5$, $p=4.0$, $q=5.8$, $\beta=1.035$, $b=2.248$, $c=4.344$, which give $W_0=23.97$ Mev.

V_λ , U and λ_0 are shown in figure 2. The expectation value of $V_\lambda - U$ is 3.11 mev, and that of V_2 is 0.01 mev, giving a final binding energy of 20.85 mev.

This result is not greatly superior to Irving's value of 19.5 mev.

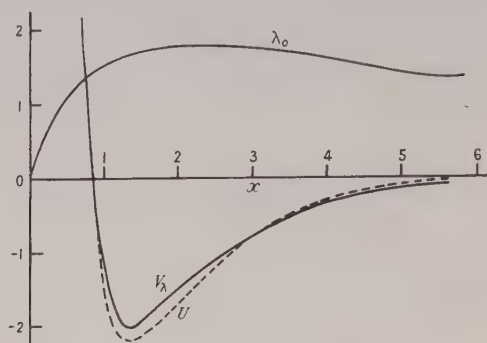


Figure 2.

§ 6. SUMMARY AND DISCUSSION

The binding energy of ${}^4\text{He}$ has been calculated by a method essentially the same as Morpurgo's, with suitable modifications to deal with both central and tensor forces, both having a Yukawa-type radial dependence. Using the forces given by a certain set of Pease-Feshbach parameters, binding energies of 20.85 mev and 29.87 mev were obtained when one and two D states were included in the trial wave function, respectively. The former value is to be compared with Irving's 19.5 mev, obtained by conventional methods but using the same nuclear forces.

Referring to figure 2, for the case of only one D state, it will be seen that U and V_λ do not fit as well as the corresponding curves in figure 1, which relate to a trial wave function with two D states. Now the argument of § 2 shows that the greatest binding energy is obtained when these curves fit each other exactly. From the point of view of perturbation theory large values of $|V - U|$ mean that the second and higher orders of perturbation must be considered in equation (5). These extra terms will increase the value of the calculated binding energy. In the present treatment it is not possible to include them because of the formidable mathematical difficulties. Thus our value of 20.85 mev for the case of one D state is too low, that is, a better comparison function U would yield better results. It is hard to estimate the error, but it probably does not exceed 2 mev.

Even with this generous estimate the effect of including a second D state is surprising. Of the six D states listed by Gerjuoy and Schwinger only one is completely symmetric in the space coordinates. This was taken here, and in Irving's work, as the principal D state. The effect has been found (not reported in this paper) of taking the second D state as the only one. This leads to a binding energy of only about 16 mev. Thus the principal D state, of the two considered, is certainly the most important for the calculation of the binding energy. The high binding energy obtained with two D states confirms the results of Hu and Hsu (1950) and Pease and Feshbach (1951), who found that the binding energy increases steadily as more and more D states are added. The extra binding energy appears to come from the interaction between the various D states, coupled by the tensor forces, and depends critically on the choice of wave function to represent the D states. This explains why the method here presented is so successful, the

introduction of variable functions being equivalent to having a trial wave function with an infinite number of variable parameters.

There seems no reason why more than two D states should not be employed, except for the amount of labour required. The number of D states was kept down to two in the present work in order to preserve the simplicity of the method. Most of the effort required lies in computing the effective potential V .

Since the calculated binding energy is a little greater than the experimentally known binding energy of 28.2 mev, it is clear that the nuclear forces (8) with parameters given by (22) are at least adequate to explain the binding of ${}^4\text{He}$. It is, however, impossible to say without further calculation what would be the effect of additional D states. If it were negligible, the assumed nuclear forces would lead to no contradiction with experiment. If it were not negligible, it would probably still be possible to find a set of Pease-Feshbach parameters which would give agreement with experiment.

ACKNOWLEDGMENTS

It is a pleasure to express my thanks to Professor H. Fröhlich, to Dr. K. J. Le Couteur and to Dr. G. Abraham for their interest in and helpful criticism of this work.

Financial support was provided by the Department of Scientific and Industrial Research.

APPENDIX

THE CALCULATION OF V_0

We require the expectation value of the potential energy $\Sigma V_{ij} + e^2/r_{34}$ with V_{ij} given by (8) with respect to the wave function (9). Most of the spin matrix elements needed are given by Irving (1953); the remaining ones can easily be found by his method. It is found that V_0 consists of a sum of terms, corresponding to the different terms in (9). We consider the simplest term, namely the contribution arising from the central force in (8) and the S state in (9).

Neglecting for the moment the Coulomb forces, we have, after integration over the spin coordinates,

$$V_c = -\mathcal{V}_0 N_0^2 \langle s | \Sigma (1 + \frac{1}{2}g(\boldsymbol{\sigma}_i \cdot \boldsymbol{\sigma}_j - 1)) J_{ij} | s \rangle \\ = -2\mathcal{V}_0 N_0^2 \int \psi^* \psi \rho^{-8} \{ (1-2g)J_{12} + (2-g)J_{13} \} d\mathbf{x}_1 d\mathbf{x}_2 d\mathbf{x}_3 \quad \dots\dots (A1)$$

where $J_{ij} = J(r_{ij}/r_c)$ and $\sqrt{2}x_1 = \boldsymbol{\rho}_1$; $\sqrt{2}x_2 = \boldsymbol{\rho}_2$; $\mathbf{x}_3 = \mathbf{r}$. Now make the orthogonal transformation $\mathbf{r}_2 \leftarrow \mathbf{r}_3$ in the second term on the right-hand side of (A1), giving

$$V_c = -6\mathcal{V}_0 N_0^2 (1-g) \int \psi^* \psi J_{12} \rho^{-8} d\mathbf{x}_1 d\mathbf{x}_2 d\mathbf{x}_3. \quad \dots\dots (A2)$$

After performing the angular integrations in (A2), transform to spherical polar coordinates in the x_1, x_2, x_3 space, noting that $\rho^2 = x_1^2 + x_2^2 + x_3^2$. This gives, after a simple integration,

$$V_c = -\frac{315}{4} (1-g) \mathcal{V}_0 \int_0^\infty \psi^* \psi \rho \, d\rho \int_0^{\pi/2} J(a\rho \cos \theta) \cos^2 \theta \sin^5 \theta \, d\theta. \quad \dots\dots (A3)$$

Inserting the Yukawa expression for J , and with $a\rho = x$, $t = \cos \theta$, we readily find

$$V_c = -\frac{315}{4}(1-g)\mathcal{V}_0 \int_0^\infty \psi^* \psi \frac{1}{x} (A_1 - 2A_3 + A_5) d\rho \quad \dots\dots (A 4)$$

where
$$A_n = A_n(x) = \int_0^1 e^{-xt} t^n dt. \quad \dots\dots (A 5)$$

The contribution of the Coulomb potential to this case is

$$V_c = \frac{35e^2}{16r_c} \int_0^\infty \psi^* \psi x^{-1} d\rho. \quad \dots\dots (A 6)$$

Thus
$$A = \frac{315}{4}(1-g)fx^{-1}(A_1 - 2A_3 + A_5) - fhx^{-1} \quad \dots\dots (A 7)$$

where $f = M\mathcal{V}_0 r_c^2 / \hbar^2$ and $h = 35e^2 / 16\mathcal{V}_0 r_c$.

The remaining functions are as follows:

$$B = 630 \sqrt{\left(\frac{11}{80}\right)} \frac{f\gamma}{\tau x} (B_3 - 2B_5 + B_7) \quad \dots\dots (A 8)$$

where
$$B_n = B_n(x) = A_n(\tau x), \quad \tau = r_c / r_t. \quad \dots\dots (A 9)$$

$$C = 105 \sqrt{\left(\frac{429}{224}\right)} \frac{f\gamma}{\tau x} (5B_3 - 21B_5 + 27B_7 - 11B_9) \quad \dots\dots (A 10)$$

$$D_1 = \frac{693}{256} fx^{-1} (25A_1 - 20A_3 - 74A_5 + 108A_7 - 39A_9) \\ - \frac{693}{16} \frac{f\gamma}{\tau x} (7B_3 - 19B_5 + 17B_7 - 5B_9) - \frac{33}{40} fhx^{-1} \quad \dots\dots (A 11)$$

$$E_1 = -\frac{693}{256} \sqrt{\left(\frac{65}{42}\right)} fx^{-1} (27A_1 - 5A_3 - 330A_5 + 846A_7 \\ - 817A_9 + 279A_{11}) \\ + \frac{1155}{8} \sqrt{\left(\frac{39}{70}\right)} \frac{f\gamma}{\tau x} (7B_3 - 33B_5 + 63B_7 - 55B_9 + 18B_{11}) \\ + \frac{11}{8} \sqrt{\left(\frac{39}{70}\right)} fhx^{-1}. \quad \dots\dots (A 12)$$

$$F_1 = \frac{6435}{4096} fx^{-1} (53A_1 - 70A_3 - 285A_5 + 524A_7 + 427A_9 \\ - 1254A_{11} + 605A_{13}) \\ - \frac{1287}{512} \frac{f\gamma}{\tau x} (259B_3 - 875B_5 + 110B_7 + 2810B_9 \\ - 3745B_{11} + 1441B_{13}) - \frac{429}{448} fhx^{-1}. \quad \dots\dots (A 13)$$

REFERENCES

- FESHBACH, H., and SCHWINGER, J., 1951, *Phys. Rev.*, **84**, 194.
 GERJUOY, E., and SCHWINGER, J., 1942, *Phys. Rev.*, **61**, 138.
 HU, T., and HSU, K., 1950, *Proc. Roy. Soc. A*, **204**, 476.
 IRVING, J., 1951, *Phil. Mag.*, **42**, 338; 1953, *Proc. Phys. Soc. A*, **66**, 17.
 MORPURGO, G., 1952, *Nuovo Cim.*, **9**, 461.
 PEASE, R. L., and FESHBACH, H., 1951, *Phys. Rev.*, **81**, 142.

Ionization by Relativistic μ -Mesons in Oxygen

BY S. K. GHOSH*, THE LATE G. M. D. B. JONES AND J. G. WILSON†

The Physical Laboratories, University of Manchester

MS. received 23rd November 1953

Abstract. The specific ionization in oxygen near atmospheric pressure has been measured over the momentum range $3 \times 10^8 \text{ ev/c} < p < 3 \times 10^{10} \text{ ev/c}$, excluding collisions involving energy transfers greater than 1 kev. The measurement was based upon drop counts in the positive ion column of tracks in a cloud chamber independent of the system used to measure momentum. Modification of ionization due to polarization phenomena is shown to become important at momenta greater than about $6 \times 10^9 \text{ ev/c}$.

§ 1. INTRODUCTION

THE ionization produced when fast charged particles pass through matter has recently attracted particular attention, with special reference to the polarization effects to be expected when the possible range of effective ionization extends to distances from the particle trajectory which are large compared with the mean spacing of molecules in the material traversed. These effects are likely to cause a modification of direct ionization along the particle trajectory under conditions very similar to those leading to the emission of Cerenkov radiation, and the relation between the two phenomena has proved of considerable interest.

The possibility of ionization at considerable distances from the particle trajectory essentially arises from the relativistic contraction of the field of the particle, and leads to an expected slow increase of ionization with increasing particle energy. This slow 'logarithmic increase' of ionization, although certainly well founded from a theoretical standpoint, had until recently only been observed experimentally in a rather qualitative way. Within the last year or two, however, concordant measurements in gases have been reported by Hereford (1948), the present authors (1952), Carter and Whittemore (1952), Becker *et al.* (1952), McClure (1953), Parry *et al.* (1953) and Price *et al.* (1953), and of these measurements Ghosh *et al.* (1952) and Parry *et al.* (1953) further provide evidence of the modification of the 'logarithmic increase' by the onset of polarization effects. Parallel results have been reported by several groups for the variation with energy of the ionization produced in photographic emulsion as measured by the number of grains rendered developable along particle trajectories: these refer to conditions in a 'condensed medium' as opposed to the extended configuration of a gas, and, as is to be expected, demonstrate the relatively early onset of polarization phenomena.

* Now at the Institute of Nuclear Physics, Calcutta.

† Now at the University of Leeds.

A preliminary note of the main results of the work now described has already been given (Ghosh *et al.* 1952). The present account incorporates additional data, and in particular a large group of new measurements near the minimum of ionization which provides a homogeneous group of results in which the track-to-track fluctuations of the measured ionization can be examined. Further, the standardization of technique, upon which the reliability of the work is based, is treated in greater detail.

§2. EXPERIMENTAL METHOD

Ionization was measured by means of drop counts, along the trajectories in a cloud chamber, of particles for which momentum was determined outside the chamber, and for which evidence of identification was almost entirely dependent upon data external to the chamber. The design and manipulation of the cloud chamber was then governed only by the requirements of the ionization measurement, and the conflicting claims of this measurement and that of momentum on a single track segment, which was one of the major difficulties of earlier work, was avoided. A consistently low level of background condensation was of primary importance, and for this purpose a relatively slow expansion was used, and metal parts were, except for the field electrodes, excluded from the active part of the chamber. Maximum drop growth time and photography at a scattering angle of 45° were used to obtain the greatest possible intensity of scattered light from each drop, and in this way to allow the maximum depth of focus to be used.

For most of the work the identification of particles and measurement of momentum were carried out in the Manchester magnetic spectrograph under the conditions described in detail by Hyams *et al.* (1950). The design of the spectrograph, however, did not allow the important particle group in the neighbourhood of the minimum of ionization to be efficiently selected, and measurements in this group were therefore made on particles selected as having a range in lead between 15 and 35 cm.

The selection methods are considered in detail in the following section: they permitted measurements of ionization over the momentum range 3×10^8 ev/c to 3×10^{10} ev/c; that is to say, for p/mc between about 3 and 300.

Drop counting was carried out using a projection microscope magnifying about 70 times, the field of view of which accommodates the whole of a unit cell of the counting procedure (§4 (iv)). The drop images within such a cell, numbering from about 20 to 70 (figure 2), were then counted and recounted as might be necessary. The cell divisions were permanently marked and numbered upon the photographic plates, and counting checks by different observers and at different times were shown to be concordant.

The control of gas composition and of condensation efficiency are discussed in §4 below.

§3. MEASUREMENT OF MOMENTUM, AND THE IDENTIFICATION OF PARTICLES

As has been indicated above, the present work is based upon particles selected in two ways: (i) particles, $p > 6 \times 10^8$ ev/c, for which momentum is measured in the magnetic spectrograph, and (ii) particles in the momentum

range $3 \times 10^8 \text{ ev/c} < p < 6 \times 10^8 \text{ ev/c}$ which were selected by means of a range technique.

The nature of the selection and the grounds for assuming that the measured particles are μ -mesons without any significant admixture of particles of other kinds is now examined.

3.1. Particle Selection in the Magnetic Spectrograph

The operation of the spectrograph, and the classification of particles according to momentum, have been described in detail by Hyams *et al.* (1950). For the work now described the spectrograph was used at maximum deflecting field, in which the highest momentum group (category 0) has a mean momentum of about $3 \times 10^{10} \text{ ev/c}$ and in which the output becomes very low below momentum $6 \times 10^8 \text{ ev/c}$. It is shown by Hyams and his colleagues that spurious responses of the spectrograph do not occur as frequently as once in 500 measurements; in the present work we require, in addition, the presence of a single cloud track in the correct position and orientation in the drop-counting cloud chamber together with the operation of the independent counting system associated with this chamber; with these further conditions we regard the possibility of misidentification of the track examined to be negligible.

Protons formed the most serious contamination of the meson beam, for it was possible to exclude substantially all electrons. According to Williams (1939), less than 1% of the incident cosmic ray beam, $p > 6 \times 10^8 \text{ ev/c}$, will consist of electrons. The effect of even this component is drastically reduced by the introduction of a 1.2 cm lead plate below the drop-counting chamber and immediately above the spectrograph, the fraction of primary electrons which give rise beneath this lead to a single secondary of energy in the measuring range of the spectrograph being extremely small.

The work of Mylroï and Wilson (1951) provides data for estimating the possible proton contamination and also establishes that π -mesons will (quite apart from the fact that the difference of their ionization from that of μ -mesons is small throughout the relativistic region) be very much rarer than protons. Proton contamination can only be serious at momenta appreciably below about $1.5 \times 10^9 \text{ ev/c}$, the value of momentum at which the ionization by protons and mesons is the same. At higher momenta the difference of ionization is never more than 20% and the percentage of protons is less than 1%; the effect of the possible presence of protons will then be negligible. Thus the second momentum group of table 2 ($6 \times 10^8 \text{ ev/c} < p < 10^9 \text{ ev/c}$) is the only one which is seriously liable to proton contamination. In this range of momentum the data of Mylroï and Wilson indicate that between 3 and 4% of all the particles will be protons, and accordingly it is about equally probable that no proton or one proton will be included in the tabulated data of this group, and less likely that two or more protons have been measured. However, these protons would on average ionize about 80% above the minimum, and would be expected to be detectable by inspection. Our conclusion, based on the detailed examination of this group, is that no protons were in fact measured. It is true that the average ionization measured for the group is high, being one and a half standard errors from the probable curve (figure 4), but the particular track contributing most to this high value is that of a negative particle. We conclude that proton contamination has played no part in determining the results of table 2.

3.2. Particle Selection in the Range $3 \times 10^8 \text{ ev/c} < p < 6 \times 10^8 \text{ ev/c}$

This group, in the neighbourhood of the minimum of ionization of μ -mesons, is not conveniently taken from the spectrograph, for both the incident intensity of particles is beginning to diminish at this low momentum and also the instrumental efficiency is rapidly falling. The group was therefore selected by a range measurement; it includes particles which penetrate 15 cm of lead but stop in a further 20 cm. The arrangement is shown schematically in figure 1; the required counter response is (1, 2, 3, -A). The counters, 3, are shielded against particles coming from the side, and it is clear that the further requirement that a particle shall be seen to traverse the cloud chamber in the plane defined by counters 1 and 2 adds greatly to the confidence of identification, virtually excluding electron complexes.

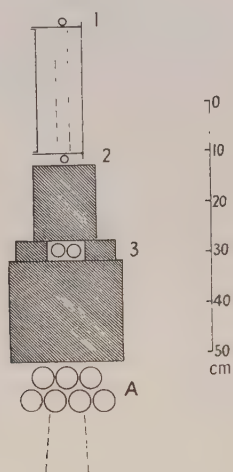


Figure 1. Schematic arrangement of cloud chamber and lead absorber for range selection of mesons near the minimum of ionization. The parallel broken lines in the cloud chamber indicate the depth of focus; the diverging broken lines below counter group A show the purely geometrical spread of the particle flux defined by counters 1 and 2.

Here, the most serious possible contamination will arise from μ -mesons of higher momentum brought in by inefficiency of the anticoincidence counter layer, A. The performance of such a tray was examined by Mylroi and Wilson, the internal evidence of whose work placed the overall inefficiency as less than $\frac{1}{2}\%$, and showed that the inefficiency occurred preferentially at low momenta (probably from scattering at the lowest levels of absorber). Of the 101 particles listed in the first group of table 2 it is accordingly unlikely that more than one, or at most two, came from outside the desired range, while even these would be likely to be of only slightly higher momentum. It is unlikely that the mean ionization of the group as a whole could be affected by as much as 0.2%.

§4. CONDITIONS OF ACCURATE DROP-COUNTS

The aim was to make the number of drops counted in a selected segment of track as closely as possible an accurate measure of the number of ion pairs formed,

under specified conditions, in that segment. In addition, the medium in which ionization took place was controlled so that corrections arising from variation of physical condition or from changes of composition were always small and well established to the measuring accuracy. The features involved are conveniently discussed under four headings: (i) the control of gas composition, (ii) the control of condensation, (iii) the conditions of photography and the treatment of overlap of drop images, (iv) the selection and rejection of track segments.

(i) *The Control of Gas Composition*

The gas used in the present work was oxygen with an alcohol-water mixture as condensant. Before expansion the gas was maintained at a temperature $(20 \pm 1)^\circ\text{C}$ and was at atmospheric pressure, the latter condition being achieved by connecting a partially inflated rubber balloon through a slow leak to the active part of the cloud chamber. A record of the time of each photograph then allowed the relevant pressure before expansion to be determined subsequently. The condensant was introduced with 65% by volume of alcohol, but alcohol vapour was found to diffuse through the rubber back of the chamber, and the concentration of water increased as time went on. When the concentration of alcohol fell to 40% by volume, the supply was replenished to bring the liquid in the chamber back to the original composition. It is shown below (§ 4.2) that the total difference of ionization between the saturated gas used and dry oxygen at the same pressure is of the order 1%, and that the variation of this difference in the course of an experimental run in which the alcohol concentration falls, from the maximum used to the minimum after which it was replenished, is still smaller. A single correction was accordingly applied which corresponded to a mean composition of the liquid condensant, and the variations of composition of condensant were ignored as leading to corrections too small to be of significance.

There seemed no strong reasons to undertake this work with one gas rather than another, although a pure gas of simple composition was probably desirable for comparison with any theoretical treatment of the problem. Under these circumstances oxygen, which is well known to lead to satisfactory chamber operation, was an obvious choice.

(ii) *The Control of Condensation*

When an alcohol-water mixture is used as condensant, condensation takes place preferentially upon positive ions (not, as with pure water, upon negative ions). It is valuable to separate the columns of positive and negative ions before condensation takes place, in part to avoid the doubled number of drops to be counted without any statistical advantage, but mainly because the ratio of the number of drops found in the column of negative ions to that found in the column of positive ions forms a most sensitive indication of the completeness of condensation in the positive column. From previous work it appeared that condensation would be virtually complete in the positive column if any appreciable condensation at all was found in the negative column. For example, Hazen (1944) reported that in a mixture containing 75% alcohol more than 95% condensation took place on positive ions when n_-/n_+ was of the order 0.1, and substantially 100% condensation when this ratio was greater than 0.2. For a very large range of composition of the condensant 100% condensation took place on positive ions when n_-/n_+ was greater than 0.5.

Recent work by Nielsen and Needels further establishes that substantially 100% condensation in the positive column is attained for $n_-/n_+ > 0.3$ over the whole range of condensant used in our work.*

The internal evidence of our work confirms these criteria and is summarized in table 1. There is some indication that for $n_-/n_+ < 0.3$ some reduction of condensation in the positive column has taken place; the next group of measurements, for which $0.3 < n_-/n_+ < 0.4$, shows no significant reduction of condensation on positive ions as compared with the groups with $n_-/n_+ > 0.4$, and our main observations were accordingly restricted to tracks for which the ratio n_-/n_+ was measured to be greater than 0.3.

Table 1. Condensation per centimetre at standard pressure in the positive ion column of tracks at the minimum of ionization, in oxygen saturated at 20°C with water-alcohol condensant, as a function of the ratio n_-/n_+ of the condensation in the negative and positive ion columns. Of the two figures in brackets (column 2) the first gives the number of tracks actually measured at the minimum of ionization, while the second gives the number measured at other momenta and subsequently reduced to the equivalent value at the minimum.

n_-/n_+	Number of tracks	Condensation cm^{-1} (positive ions)
< 0.2	16 (12 + 4)	39.3 ± 1.0
$0.2-0.3$	26 (18 + 8)	39.4 ± 0.6
$0.3-0.4$	34 (10 + 24)	40.7 ± 0.8
$0.4-0.6$	46 (15 + 31)	41.2 ± 0.6
> 0.6	60 (43 + 17)	41.0 ± 0.5

This lower limit of conditions leading to full condensation on positive ions is of particular importance because of the advantage of working, for drop counts in well-diffused tracks, with the lowest possible density of background condensation. The examples reproduced (see plates) are typical of the standard which was sought, with background condensation less than one drop per cubic centimetre; this very low level of background condensation was only exceptionally reached when n_-/n_+ was greater than about 0.8. An adequate estimate of the effect of this low background condensation upon the actual drop counts in tracks is readily derived from observations of the distance from track centre, in each unit one centimetre cell, of the nearest recognizable background droplet. A correction for the inclusion of background drops in the track counts is made in the final column of table 2; it reduces the average ionization at all momenta by 0.3 drops cm^{-1} .

There seems no reason to doubt that the condensation achieved on positive ions, with the criterion $n_-/n_+ > 0.3$, is substantially complete for ions which are recognizably part of the track at the moment when the critical supersaturation for drop growth is reached. The recombination which may previously have taken place is unlikely to be large or to vary significantly with the total density of condensation.

* Private communication: we are most grateful to Professor G. E. Nielsen for this information.

(iii) Conditions of Photography and the Treatment of the Overlap of Drop Images

The problems of optics and photography are governed by the small amount of light which is scattered, even under favourable conditions, from a single cloud droplet. This amount was made as large as possible in the present work by allowing the drops to grow for as long as possible before photography, and by making use of the light scattered in the forward direction (at 45° to the direction of incident light). The use of forward scattering increases the available light by a factor of about ten over that scattered at right angles. Since curvature measurement upon the cloud tracks was not used for the determination of momenta, the available drop-growth time was considerable, for it could be increased until distortion in length of trajectories became important; it was in fact made about 0.4 second.

Even with the increased light made available by these measures it was necessary to use a fairly rapid emulsion if a useful depth of focus (~ 2 cm) was to be attained. With such emulsions the 'in focus' drop images were about 50μ diameter and, since the size of the image is determined by turbidity rather than by grain-density, were well-defined discs. The diameter of these discs, together with the actual distribution of drops in a track image, determine suitable conditions of diffusion and optical magnification and the degree of image overlap which is then to be expected.

Tracks were photographed at a magnification of about $1/4$ and were allowed to diffuse to a breadth of about 0.3 cm before the onset of condensation. This track breadth corresponds to a diffusion time of about 0.08 sec, and the necessary separation of the positive and negative ion columns (about 0.8 cm) could readily have been achieved by maintaining an electrostatic field of suitable magnitude across the chamber for the whole of this time. It was found to yield a notable improvement, however, if a much stronger field was applied and removed a relatively short time after the passage of the particles to be recorded, on account of the considerable reduction in the numbers of diffuse old tracks in the photographs. A field of 40 volts cm^{-1} was accordingly applied between wire grids and removed 0.01 sec after the passage of the controlling particle. Under these conditions only one or two background tracks of any sort were normally photographed, and, because these were never of great age and heavily diffused, very little of the track under measurement was ever obscured by them.

Because of the well-defined shape of drop images it was possible to lay down clear criteria of drop overlap, and to determine from the internal evidence of the photographs the actual correction to be made to measured drop counts to take account of drop images lost by overlapping. If r_0 is the limiting separation of the centres of drop images below which the images are not resolved, and $n(r_0)$ is the number of occasions per centimetre of track in which drop images lie within the distance r_0 , while $n(r, r + \delta r)$ is the corresponding number of occasions in which the centres of drops will be separated by distances between r and $r + \delta r$, then for a random distribution of images,

$$\frac{n(r_0)}{n(r, r + \delta r)} = \frac{r_0^2}{(2r + \delta r)\delta r}.$$

Inspection of photographs suggested that r_0 was in fact the image radius. The number $n(r, r + \delta r)$ was determined for $r = 2r_0$, $\delta r = r_0/2$, and it was found that

$$n(r_0) = 0.44 n(2r_0, 2.5r_0) \sim 2 \text{ drops cm}^{-1}.$$

This analysis requires a random distribution of images only over distances of the order $2r_0$ ($=50\mu$) in the photograph and, since the breadth of the diffuse track in the photograph is of the order 700μ , the condition is adequately met except perhaps in the centre of dense clusters.

(iv) *The Selection and Rejection of Track Segments*

When satisfactory track photographs in which drops are adequately resolved have been obtained, it remains necessary to reject certain parts of the tracks. Some reasons for rejection are purely technical—evidence of incomplete condensation (§4(ii) above), presence of background condensation or of overlapping unwanted track images—and need not be considered in detail since they merely lead to loss of material. It is also necessary, however, to reject the large blobs of secondary ionization which are formed when large energy transfers take place at an act of primary ionization. This procedure is a technical necessity, since for a sufficiently large transfer of energy some part of the resulting condensation will not be countable, but it also represents an advantage of the drop-counting techniques, as opposed to measurements of ionization in proportional counters in which no breakdown of the processes of ionization is possible.

In the present work no energy transfers of more than about 1 kev are included, while the mean ionization for each momentum range in table 2 is based upon a total energy transfer from fast primaries of at least 130 kev (and, with one exception, of much more). The phenomenon studied does not therefore include the possibility of single transfers of energy which are of the same order as the total observed transfer, and the high energy 'tail' occurring in the treatments of total energy transfer by Landau (1944) and by K. R. Symon (as quoted by Rossi (1952)) and in the experimental studies of fluctuations of ionization by Rothwell (1951), West (1953) and others does not arise.

The rejection of a drop cluster corresponding to a large energy transfer involves the complete removal of a segment of the track photograph, for the large cluster will in fact obscure the normal ionization in its neighbourhood. It is not satisfactory to do this by a selection of limits by inspection for each segment of track which is to be excised, and we have instead adopted the procedure of dividing each track image, by lines ruled upon the developed plate, into a series of cells each of which corresponds to about one centimetre of the original track. The whole of each cell which is judged to be in any way affected by some feature which meets the criterion for exclusion is then rejected. The degree of uncertainty in deciding how long a segment of track is to be rejected is greatly reduced in this way. In the two examples reproduced, sharp horizontal lines represent the cell rulings; in plate I the track shows no disturbing feature, in plate II the third cell from the top and the bottom cell would both be rejected.

§ 5. RESULTS

The variation of ionization by mesons as a function of momentum is summarized in table 2, which is discussed below. It will be seen from the table that for each momentum range the measurement is based on a total track length of about 3 metres except for the range centred upon the minimum of ionization for which about 16 metres of track were measured, and for the range of very high momentum ($\sim 3 \times 10^{10}$ ev/c) for which rather less than 1 metre of track was available. These total track lengths were recorded in single tracks of which the

measurable part was on average rather more than 15 cm long and were analysed in cells of length (1.0 ± 0.1) cm. The main work was carried out by the exclusion (as described in §4) of clusters of more than 30 drops: a cluster of 30 drops was adequately resolved under the condition of photography. It is convenient to discuss the fluctuations of ionization in the measured sections of track as it bears upon the significance of the mean values given in table 2.

5.1. Fluctuations of Ionization in Finite Segments of Track

The fluctuation in the drop counts in 1 cm cells and in single tracks (normalized to a unit length of 25 cm) are shown for the largest homogeneous group of data (which refers to the minimum of ionization) in figures 2 and 3.

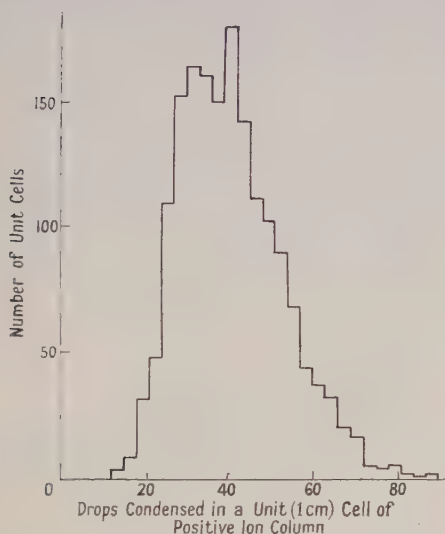


Figure 2. Drop counts in 1 cm cells covering about 16 metres of minimum ionization track. Cells including any part of a cluster of more than 30 drops have been rejected.

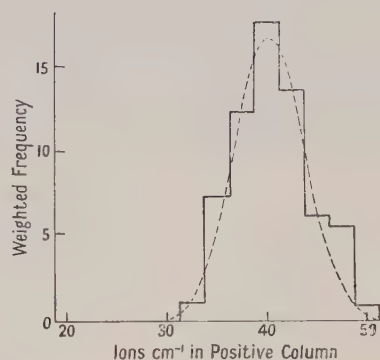


Figure 3. Ionization in 101 tracks near the minimum of ionization weighted according to track length. The broken curve, $I = 40.2 \pm 4.2$ ions cm^{-1} , is referred to in the text.

Since the maximum accepted energy transfer, corresponding to the formation of a cluster of 30 ion pairs, is a large fraction of the average transfer in a 1 cm cell, we expect the distribution of drop counts in figure 2 to be asymmetric with a marked 'tail', and this is seen to be the case. For single tracks this condition no longer obtains: the total transfer corresponds to the formation of upwards of 600 ion pairs while the largest single transfer remains unchanged. The distribution is now (figure 3) seen to be more symmetrical with only a slight trace of 'tail'. It is therefore appropriate to derive the accuracy of the average ionization measured in each homogeneous group of data by a root mean square over the deviations of the ionization in individual tracks from the group average, and this procedure has been followed (§5.2 below).

In figure 3 the broken curve shows the gaussian distribution (40.2 ± 4.2) ions cm^{-1} in the positive column which fits well the experimental determinations, and the breadth of which we may compare with the expected fluctuations. In

the homogeneous group plotted, the average track length for which measurements were possible was about 16 cm, and for this length the expected fluctuation is about 40 ion pairs from close collisions and a similar number from resonance collisions. A resultant fluctuation per centimetre of rather less than four ions follows, in fair agreement with the observed distribution. While the average measurable length of each track is 16 cm, variations from this average will tend slightly to increase the total fluctuations.

5.2. Reduction of Mean Ionization to Standard Conditions

Measurements refer to ionization in oxygen saturated with a mixed vapour of water and alcohol at the prevailing barometric pressure and at a temperature $(20 \pm 1)^\circ\text{C}$. These have been reduced to standard temperature and pressure, and to a value appropriate for pure oxygen. (Throughout the table the largest correcting factor is the (constant) factor passing from the operating temperature to 0°C .)

For the small correcting terms involved we assume that the number of ions produced in oxygen, alcohol and water is proportional to the respective electron densities. This assumption is essentially based on the approximate equality of the mean energy for production of an ion pair in these gases. Then the specific ionizations, I_0 , I_a , I_w , at standard pressure are connected by the relations $I_a = 1.6 I_0$, $I_w = 0.6 I_0$; and at pressure p with the partial pressures p_0 , p_a , p_w the observed specific ionization $I(p)$ will be

$$I(p) = I_0(p_0 + 1.6p_a + 0.6p_w).$$

The partial pressure p_a , p_w may be derived from the results of Gautier and Ruark (1940),* and, at the extreme concentrations of the condensant, $I(p)$ takes the values $1.012 I_0$ and $1.007 I_0$ respectively. The changes of condensant are thus not significant, and an average correction of rather less than 1% is applied throughout.

Table 2. Average specific ionization by μ -mesons in collisions involving energy transfers up to 1000 ev, in oxygen at S.T.P. as a function of meson momentum

Momentum range (ev/c)	No. of tracks	Meas. track length (cm)	Total no. of drops (+ve col.)	Average ionization (cm^{-1})	
				Observed	Reduced to O_2
3.10^8 – 6.10^8	101	1601.7	63978	40.2 ± 0.4	44.3 ± 0.4
6.10^8 – 10^9	15	228.7	9861	43.6 ± 0.9	48.0 ± 1.0
10^9 – 2.10^9	27	407.1	18080	45.2 ± 0.9	49.8 ± 1.0
2.10^9 – 3.10^9	24	354.5	16964	48.5 ± 1.0	53.5 ± 1.1
3.10^9 – 4.10^9	24	384.8	19100	50.0 ± 0.8	55.2 ± 0.9
4.10^9 – 10^{10}	16	266.6	13832	52.0 ± 1.2	57.5 ± 1.3
$\sim 1.5.10^{10}$	14	219.2	11690	52.8 ± 1.1	58.3 ± 1.2
$\sim 3.10^{10}$	5	85.1	4641	55.1 ± 2.8	60.5 ± 3.1

Minimum of ionization: 44.0 ± 0.4

5.3. Ionization as a Function of Momentum

The measurements of average ionization as a function of momentum are summarized in table 2, in which the measured tracks have been grouped into convenient momentum ranges. The first group, $3 \times 10^8 \text{ ev/c} < p < 6 \times 10^8 \text{ ev/c}$,

* The relevant values at 20°C are: at 65% alcohol, $p_a = 24 \text{ mm}$, $p_w = 14 \text{ mm}$; at 40% alcohol, $p_a = 19 \text{ mm}$, $p_w = 15 \text{ mm}$.

was selected by a range technique (§3.2) and the remaining groups correspond to combinations of momentum categories of the magnetic spectrograph.

The uncertainties of the two last columns are derived from the actual variation of the ionization in single tracks from the group average, on the assumption that these may be described by a gaussian distribution around the group average. The justification for this procedure is seen in §5.1 (figure 3). The values obtained in this way, however, are all in excellent agreement with those to be expected from the details of the ionization process. For example, in the momentum range $10^9 \text{ ev/c} < p < 2 \times 10^9 \text{ ev/c}$ the positive ion condensation of approximately 4 metres of track was counted. For this track length the fluctuation of total number of ion pairs is estimated to be 280 or 0.7 cm^{-1} . The observed fluctuation, 1.0 cm^{-1} , however, also includes the effect of actual variations of the average specific ionization between momenta 10^9 ev/c and $2 \times 10^9 \text{ ev/c}$, which has extreme values $\pm 2.0 \text{ cm}^{-1}$ from the mean, and these two effects together can completely account for the observed spread of measurements on single tracks.

The measurement in the neighbourhood of the minimum of ionization refers to a broad band of momenta extending from $3 \times 10^8 \text{ ev/c}$ to $6 \times 10^8 \text{ ev/c}$. Over this band the variation of ionization is small, and we are able to estimate the minimum value to the accuracy of our work without detailed knowledge of the momentum spectrum through this band of particles. The minimum value is about $0.3 \text{ ion pair cm}^{-1}$ lower than the average over the measured band, and accordingly $I_{\min} = 44.0 \pm 0.4 \text{ ion pairs cm}^{-1}$.

§6. DISCUSSION

The numerical values quoted are for the average specific ionization, excluding that which arises from primary transfers of more than about 1000 ev. With the low background condensation which obtained it seems established that no appreciable further contribution to track ionization can be attributed to radiation re-absorbed at distances from the particle trajectory which are large compared with the diffusion breadth of the tracks. The work leads to no estimate of the extent to which recombination may have reduced the number of ions before condensation took place, and the available work on the subject only allows rough estimates of recombination to be made. These are sufficient, however, to show that this effect must be very small.

Since the publication of the preliminary results of this work, theoretical treatments of the problem for the conditions to which our measurements refer have been given along essentially similar lines by Huybrechts and Schönberg (1952), Budini (1953) and Sternheimer (1953), while a difficulty pointed out by Huybrechts and Schönberg has been clarified in a paper by one of us (G. M. D. B. J.) and G. N. Fowler (Fowler and Jones 1953). While the general agreement of these treatments is good, the precision of the measurement is insufficient to give useful indications upon the differences in detail of treatment. For example, the measurements are not at present adequate to distinguish between the two rather extreme assumptions concerning breadth of absorption bands examined by Budini (figure 4). For this purpose the ratio of ionization at the minimum to that at $p \cdot mc \sim 100$ is required to an accuracy of within 1%. Using mesons, this implies work to this accuracy under the rather slow operating conditions under which momenta of the order 10^{10} ev/c are measured with

confidence. It may well be that the fine detail of behaviour will most effectively be studied using electrons.

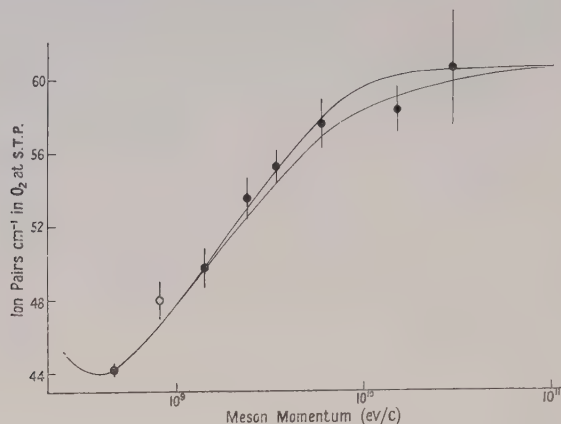


Figure 4. Average specific ionization in oxygen at S.T.P. arising in encounters of energy transfer less than 1 kev. The curves are those for two extreme assumptions made by Budini (1953), normalized to the experimental value near the minimum of ionization. These curves show the extent to which the present measurements fail to distinguish between details of theoretical treatment.

ACKNOWLEDGMENTS

The authors are indebted to Professor P. M. S. Blackett, in whose laboratory the work was carried out, for the facilities made available and for his constant interest, and to the other workers with the magnetic spectrograph, in particular Dr. B. G. Owen, for much assistance throughout the work.

REFERENCES

- BECKER, J., CHANSON, P., NAGEOTTE, E., TREILLE, P., PRICE, B. T., and ROTHWELL, P., 1952, *Proc. Phys. Soc. A*, **65**, 437.
 BUDINI, P., 1953, *Nuovo Cim.*, **10**, 236.
 CARTER, R. S., and WHITEMORE, W. L., 1952, *Phys. Rev.*, **87**, 494.
 FOWLER, G. N., and JONES, G. M. D. B., 1953, *Proc. Phys. Soc. A*, **66**, 597.
 GAUTIER, T. N., and RUARK, A. E., 1940, *Phys. Rev.*, **57**, 1040.
 GHOSH, S. K., JONES, G. M. D. B., and WILSON, J. G., 1952, *Proc. Phys. Soc. A*, **65**, 68.
 HAZEN, W. E., 1944, *Phys. Rev.*, **65**, 259.
 HEREFORD, F. L., 1948, *Phys. Rev.*, **74**, 574.
 HUYBRECHTS, M., and SCHÖNBERG, M., 1952, *Nuovo Cim.*, **9**, 764.
 HYAMS, B. D., MYLROI, M. G., OWEN, B. G., and WILSON, J. G., 1950, *Proc. Phys. Soc. A*, **63**, 1053.
 LANDAU, L., 1944, *J. Phys. U.S.S.R.*, **8**, 201.
 MCCLURE, G. W., 1953, *Phys. Rev.*, **90**, 796.
 MYLROI, M. G., and WILSON, J. G., 1951, *Proc. Phys. Soc. A*, **64**, 404.
 PARRY, J. K., RATHGEBER, H. D., and ROUSE, J. L., 1953, *Proc. Phys. Soc. A*, **66**, 541.
 PRICE, B. T., WEST, D., BECKER, J., CHANSON, P., NAGEOTTE, E., and TREILLE, P., 1953, *Proc. Phys. Soc. A*, **66**, 167.
 ROSSI, B., 1952, *High Energy Particles* (New York: Prentice-Hall Inc.), p. 32.
 ROTHWELL, P., 1951, *Proc. Phys. Soc. B*, **64**, 911.
 STERNHEIMER, R. M., 1953, *Phys. Rev.*, **91**, 256.
 WEST, D., 1953, *Proc. Phys. Soc. A*, **66**, 306.
 WILLIAMS, E. J., 1939, *Proc. Roy. Soc. A*, **172**, 194.

Approximate Molecular Orbitals I: The $1\sigma_g$ and $2p\sigma_u$ States of H_2^+

BY A. DALGARNO AND G. POOTS

Department of Applied Mathematics, Queen's University of Belfast

Communicated by D. R. Bates; MS. received 3rd December 1953

Abstract. The variational method is used to obtain approximate wave functions for the $1\sigma_g$ and $2p\sigma_g$ states of H_2^+ . Their accuracy is assessed by comparing various quantities computed using the approximate wave functions with the exact values of these quantities. The dependence of the total kinetic and potential energies on the nuclear separation is briefly discussed.

§ 1. INTRODUCTION

APPROXIMATE molecular wave functions have usually been obtained by the application of the Rayleigh-Ritz variational principle. Owing to the lack of proper comparison data in the past, no precise estimates have been made of their accuracy when used for the determination of molecular properties other than the energy. The recent publication of the exact wave functions of the hydrogen molecular ion (Bates, Ledsham and Stewart 1953) and their use in the evaluation of its quadrupole moment (Bates and Poots 1953) and oscillator strengths (Bates 1951, Bates, Darling, Hawe and Stewart 1953) supplies the necessary data in the case of H_2^+ . This paper, which is itself concerned with the $1\sigma_g$ and $2p\sigma_u$ states† of H_2^+ , is the first of a series in which it is intended to determine by variational methods approximate molecular orbitals and to use them for the evaluation of various quantities which can be compared with the exact results of Bates and his collaborators. It is hoped that these approximate molecular orbitals will provide a convenient basis for the development of analytic approximations to other molecules for which electron correlation must be taken into account.

§ 2. CHOICE OF WAVE FUNCTIONS

Many approximations appropriate to the 1σ and $2p\sigma$ states of H_2^+ have been used previously but none of them is both sufficiently accurate at all nuclear separations and capable of easy generalization to excited states. The simplest approximations which take account of the symmetry are (Pauling 1928)

$$\Psi(1\sigma) = \exp(-r_a) + \exp(-r_b) \quad \dots\dots(1a)$$

$$\Psi(2p\sigma) = \exp(-r_a) - \exp(-r_b) \quad \dots\dots(1b)$$

where r_a, r_b are the position vectors of the electron relative to the nuclei A and B respectively. These were improved by the introduction of a screening parameter (Finkelstein and Horowitz 1928, Coulson 1937):

$$\Psi(1\sigma) = \exp(-\alpha r_a) + \exp(-\alpha r_b) \quad \dots\dots(2a)$$

$$\Psi(2p\sigma) = \exp(-\alpha r_a) - \exp(-\alpha r_b) \quad \dots\dots(2b)$$

† In the separated atoms notation these are designated $\sigma(1s)$ and $\sigma^*(1s)$ respectively.

α , of course, being varied to obtain the minimum energy. Dickinson (1933) investigated the effect of adding a polarization term in the $1s\sigma$ case,

$$\Psi(1s\sigma) = \exp(-\alpha r_a) + \exp(-\alpha r_b) + p\{r_a \exp(-\beta r_a) \cos \theta_a + r_b \exp(-\beta r_b) \cos \theta_b\}, \quad \dots\dots(3a)$$

and found that the resulting value for the dissociation energy was inferior to that obtained by Guillemin and Zener (1929), who took

$$\Psi(1s\sigma) = \exp(-\alpha r_a - \beta r_b) + \exp(-\beta r_a - \alpha r_b). \quad \dots\dots(4a)$$

The function

$$\Psi(1s\sigma) = \exp\{-\alpha(r_a + r_b)\}\{1 + p(r_a - r_b)^2\} \quad \dots\dots(5a)$$

was used by James (1935), but it led to no improvement in the computed energies over those obtained by Guillemin and Zener. Recently, Pritchard and Skinner (1951) have computed the $1s\sigma$ energy using the function (3a) with $\alpha = 1$ and $\beta = \frac{1}{2}$. Their results, which are given graphically, are of course less accurate than those of Dickinson.

Of the various $1s\sigma$ wave functions, (2a), (3a) and (4a) have the correct form for both zero and infinite separations R of the nuclei, but none of the $2p\sigma$ wave functions is correct at both limits. This desirable characteristic may most easily be achieved by writing the wave function as a linear combination of a function which takes the correct form at $R = \infty$ and another function which takes the correct form at $R = 0$. Thus we choose

$$\Psi(1s\sigma) = \exp\{-\alpha(r_a + r_b)\} + p\{\exp(-\beta r_a) + \exp(-\beta r_b)\} \quad \dots\dots(6a)$$

$$\Psi(2s\sigma) = (r_a \cos \theta_a - r_b \cos \theta_b) \exp\{-\frac{1}{2}\alpha(r_a + r_b)\} - p\{\exp(-\beta r_a) - \exp(-\beta r_b)\}. \quad \dots\dots(6b)$$

Functions of this type do not seem to have been used previously. Besides behaving correctly at the two limits, they lend themselves to straightforward generalization to excited states; and, as will be seen later, they are more accurate than any other wave function of comparable simplicity that has been suggested.

§ 3. DESCRIPTION OF CALCULATIONS

Values of the parameters α , β and p over a wide range of R have been determined by minimization of the electronic energy of the system

$$E = - \int \Psi^* \left(\nabla^2 + \frac{2}{r_a} + \frac{2}{r_b} \right) \Psi \, d\mathbf{r}$$

where Ψ is now, and for the remainder of the paper, the normalized wave function. The functions studied were of the type (6a), (6b) with

- (i) $p = \infty$, $\beta = 1$.
- (ii) $p = \infty$, β variable.
- (iii) $p = 0$, $\alpha = 1$.
- (iv) $p = 0$, α variable.
- (v) $\alpha = 1 = \beta$, p variable.
- (vi) α as determined by (iv) and β by (ii), p variable.
- (vii) α , β and p all variable.

Some of these have been employed by other authors but, unfortunately, the published results are not given with sufficient accuracy, so that it was necessary

to repeat all of the earlier work. Exact values of E are tabulated by Bates, Ledsham and Stewart (1953).

Using the seven functions (i) . . . (vii) the integrals

$$\overline{X^2} = \int \Psi^* x^2 \Psi d\mathbf{r}, \quad \overline{Z^2} = \int \Psi^* z^2 \Psi d\mathbf{r}$$

where (x, y, z) are the cartesian coordinates of the electron referred to the mid-point of AB with the z -axis lying along AB, have been evaluated. The integrals occur in the calculation of the quadrupole moment, and for the $1s\sigma$ state have been computed exactly by Bates and Poots (1953); for the $2p\sigma$ state it was necessary to compute them using the exact wave functions.

The $1s\sigma-2p\sigma$ transition integrals, Q , have also been computed using the functions (i) . . . (vii), the $1s\sigma$ and $2p\sigma$ functions being always of the same type. Both the dipole length and dipole velocity forms for Q were used:

$$Q_L = \left| \int \Psi(1s\sigma) \mathbf{r} \Psi(2p\sigma) d\mathbf{r} \right| \quad (\text{dipole length})$$

$$Q_V = \frac{2}{\Delta E} \left| \int \Psi(1s\sigma) \nabla \Psi(2p\sigma) d\mathbf{r} \right|$$

$$= \frac{2}{\Delta E} \left| \int \Psi(2p\sigma) \nabla \Psi(1s\sigma) d\mathbf{r} \right| \quad (\text{dipole velocity})$$

where ΔE is the photon energy of the radiation. The exact values are given by Bates (1951).

Finally the potential energy of the electron in the field of the two nuclei has been computed:

$$V = - \int \Psi^* \left(\frac{2}{r_a} + \frac{2}{r_b} \right) \Psi d\mathbf{r}.$$

Knowledge of the variation of V with R provides additional insight into the mechanism of molecular bonding so that it is useful to assess how accurately approximate functions can reproduce it. Exact values of V were derived from the exact values of E by use of the quantal virial theorem (Slater 1933).

§ 4. RESULTS

Because they may be of use in other connections, the values of α , β and p obtained for (ii), (iv), (v), (vi) and (vii) are given in table 1 for the $1s\sigma$ state and in table 2 for the $2p\sigma$ state. The total and potential energies (excluding the nuclear-nuclear interaction contribution) corresponding to the functions (i) . . . (vii) are compared with the exact values in tables 3, 4 and tables 5, 6 respectively. In addition, some energy values obtained by Dickinson using the function (3a), by Guillemin and Zener using the function (4a) and by Bell and Long (1950) using (5a)[†] are included in table 3. Tables 7, 8 compare the integrals $\overline{X^2}$, and 9, 10 the integrals $\overline{Z^2}$, whilst table 11 gives the $1s\sigma-2p\sigma$ transition integrals Q_L and Q_V computed using the dipole length and dipole velocity formulae.

All quantities are measured in Hartree units (a_0 for length, $e^2/2a_0$ for energy).

[†] The values reported by Bell and Long are rendered suspect by the fact that their table contains a value of the energy which is less than the exact, in violation of the variation theorem.

§ 5. DISCUSSION

Some comments are desirable concerning the accuracy of the wave functions in relation to the work involved in obtaining them. Functions (iii), (iv) are particularly convenient since the energies (and in fact all the quantities considered in this paper) are expressible as rational functions of R . They are simpler and apparently more accurate than the usual united-atom approximation (cf. Matsen 1953), and it is to be anticipated that functions of this type (appropriately generalized) will be even better for excited states. The separated-atom approximations (i), (ii) are rather more complicated to use, but the necessary work is still not great. The accuracy of the LCAO wave function (i) has been discussed by Bates, Ledsham and Stewart (1953) and the accuracy with which (ii) reproduces the energy by Coulson (1937). Functions (v), (vi) cause little additional trouble, the energy being merely the solution of a quadratic equation with no explicit variation necessary, but function (vii) is distinctly more laborious (though the fact that the parameter α is insensitive to changes in β eases the computational task). The improvement in the derived energy values compared with (vi) is slight, especially for the excited $2p\sigma$ state, so that it appears likely that for most occasions functions of the type (vi) should suffice.

It may be worth pointing out that in the $1s\sigma$ case $\alpha \simeq 2\beta$ over a wide range of R . The function (vii) is then essentially equivalent to the unusual type of function (5a) introduced by James (1935).

The integrals X^2 , Z^2 depend upon the wave functions at distances from the nuclei greater than those which effectively determine the energy, so that the accuracy of X^2 , Z^2 when evaluated using (vi), and especially (vii), is encouraging; the error is never greater than 5% and 2% respectively. The functions (i) to (v) are much less accurate although in view of its simplicity (iv) is remarkably good over a wide range of R . The commonly used LCAO (i) may be considerably in error unless high values of R are concerned. It is of interest to note that in general the correct values of X^2 and Z^2 lie between the corresponding values obtained using the united-atom approximations (iii) or (iv) and the separated-atom approximations (i) or (ii).

It is apparent from the tabulated transition integrals that the evaluation of the probability of the $1s\sigma$ – $2p\sigma$ transition is not especially sensitive to details of the wave functions (as is frequently the case). The comparative success of the LCAO approximation (i) (which has been discussed elsewhere (Bates 1951)) should not therefore be given too much weight. The inclusion of a variable parameter leads to little improvement, and similarly (iv) is not greatly better than the unvaried function (iii). This behaviour is different from the case of X^2 , Z^2 , whose values were much improved by the introduction of screening factors. The use of a linear combination yields much greater accuracy, which progressively improves using (v), (vi), (vii), the values corresponding to (vii) being essentially correct. It is again true in general that the correct values of Q_L or Q_V lie between the approximate values calculated using (i) and (iii) or (ii) and (iv). With certain exceptions, the dipole velocity expression is more accurate than the dipole length in the range of R studied, but a better value can usually be obtained by choosing Q equal to $\frac{1}{2}(Q_L + Q_V)$. It must be stressed that these remarks may not be correct when considering other transitions.

As is to be expected, the potential energies are much less precise than the total energies except at equilibrium separation (the accuracy of the total energy arising

from a cancellation of errors in the potential and kinetic energies). The approximate wave functions usually underestimate the magnitude of both the potential and kinetic energies, although in the $1s\sigma$ case, function (ii), and in the $2p\sigma$ case, function (i), overestimates them. A marked improvement in the values results from the inclusion of screening factors, and the accuracy of the linear combinations (v), (vi), (vii) increases regularly with their complexity, (vii) being correct to within 0.5%.

The behaviour of the potential energy $V' = V + 2/R$ and the kinetic energy T as R decreases is of considerable interest. Their behaviour and that of $E' = E + 2/R$ are illustrated in figures 1, 2 for the $1s\sigma$ and $2p\sigma$ states respectively. As the atoms

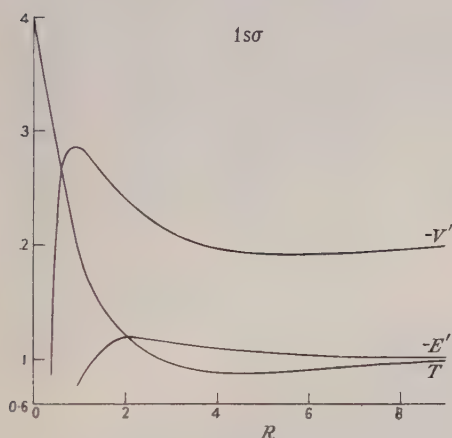


Figure 1. $-V'$, T , $-E'$ as functions of R for the $1s\sigma$ state.

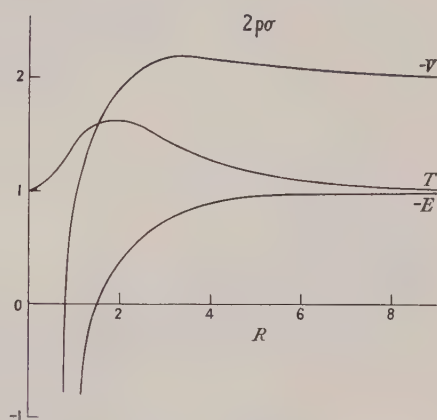


Figure 2. $-V'$, T , $-E'$ as functions of R for the $2p\sigma$ state.

approach in the $1s\sigma$ state T passes through a minimum and V' through a maximum. T then steadily increases to a finite limit at $R=0$ whilst V' decreases to a deep minimum. Eventually the $2/R$ term dominates and V' becomes infinite. (This behaviour has been described previously on the basis of approximate wave functions (Coulson and Bell 1945).) The variation of V' , T is quite different in the repulsive $2p\sigma$ state, for which T passes through a maximum and V' through a shallow minimum as the two atoms approach. It may be that an initial decrease in kinetic energy is a decisive factor in the formation of a one-electron bond (cf. Slater 1933).

Table 1. Parameters of the $1s\sigma$ Wave Functions

Internuclear distance R		0.0	0.4	0.8	1.2	1.6	2.0	2.4	3.0	4.0
Function (ii)	β	2.000	1.833	1.627	1.460	1.333	1.239	1.168	1.095	1.028
Function (iv)	α	1.000	0.920	0.831	0.763	0.710	0.667	0.631	0.588	0.533
Function (v)	p	0.0000	0.0261	0.0652	0.102	0.133	0.155	0.166	0.163	0.125
Function (vi)	p	0.250	0.276	0.304	0.333	0.368	0.412	0.468	0.575	0.844
Function (vii)	α	1.000	0.921	0.834	0.767	0.716	0.677	0.645	0.611	0.580
	β	2.000	1.840	1.665	1.533	1.433	1.354	1.288	1.216	1.126
	p	0.250	0.276	0.304	0.328	0.352	0.375	0.394	0.438	0.499

Table 2. Parameters of the $2p\sigma$ Wave Functions

Internuclear distance R		0.0	0.4	0.8	1.2	1.6	2.0	2.4	3.0	4.0
Function (ii)	β	0.400	0.488	0.598	0.717	0.822	0.900	0.952	0.995	1.015
Function (iv)	$\frac{1}{2}\alpha$	0.500	0.517	0.563	0.622	0.670	0.696	0.705	0.701	0.674
Function (v)	p	0.000	0.357	0.939	1.896	3.488	6.340	12.569	86.84	37.22
Function (vi)	p	0.000	0.389	0.741	0.985	1.189	1.569	2.221	2.876	2.970
Function (vii)	$\frac{1}{2}\alpha$	0.500	0.519	0.566	0.621	0.665	0.685	0.702	0.715	0.745
	β	0.400	0.488	0.617	0.733	0.835	0.916	0.962	1.001	1.020
	p	0.000	0.396	0.750	0.994	1.213	1.595	2.148	2.598	1.980

Table 3. Total Electronic Energies, $-E$, of the $1s\sigma$ State

Function \ R	0.0	0.4	0.8	1.2	1.6	2.0	2.4	3.0	4.0
(i)	3.0000	2.8902	2.6849	2.4715	2.2770	2.1075	1.9624	1.7848	1.5737
(ii)	4.0000	3.5977	3.0931	2.6985	2.4006	2.1732	1.9957	1.7956	1.5747
(iii)	4.0000	3.5762	3.0116	2.5564	2.2067	1.9355	1.7211	1.4737	1.1868
(iv)	4.0000	3.6000	3.1013	2.7067	2.4010	2.1595	1.9644	1.7331	1.4538
(v)	4.0000	3.5929	3.0863	2.6974	2.4070	2.1854	2.0116	1.8126	1.5875
(vi)	4.0000	3.6009	3.1081	2.7229	2.4289	2.2010	2.0209	1.8153	1.5859
(vii)	4.00000	3.60105	3.10833	2.72406	2.43142	2.20489	2.02612	1.82153	1.59194
(3a)	4.0000					2.2011			
(4a)	4.0000					2.20451*	2.025	1.820	1.592
(5a)†	4.0000					2.2042		1.8211	
Exact	4.00000	3.60157	3.10895	2.72461	2.43186	2.20525	2.02642	1.82178	1.59216

* This value is taken from Rahman (1953).

† Cf. footnote on p. 345.

Table 4. Total Electronic Energies, $-E$, of the $2p\sigma$ State

Function \ R	0.0	0.4	0.8	1.2	1.6	2.0	2.4	3.0	4.0
(i)	-1.0000	0.1396	0.7261	1.0455	1.2235	1.3217	1.3733	1.4018	1.3898
(ii)	0.8000	0.9111	1.0349	1.1571	1.2593	1.3316	1.3754	1.4018	1.3900
(iii)	1.0000	1.0199	1.0681	1.1258	1.1794	1.2222	1.2523	1.2749	1.2674
(iv)	1.0000	1.0209	1.0807	1.1673	1.2553	1.3217	1.3606	1.3769	1.3403
(v)	1.0000	1.0214	1.0837	1.1735	1.2635	1.3325	1.3755	1.4018	1.3899
(vi)	1.0000	1.0215	1.0851	1.1766	1.2665	1.3343	1.3765	1.4025	1.3908
(vii)	1.00000	1.02150	1.08522	1.17671	1.26653	1.33437	1.37659	1.40255	1.39096
Exact	1.00000	1.02158	1.08548	1.17722	1.26721	1.33507	1.37715	1.40285	1.39110

Table 5.* Electronic Potential Energies, $-V$, of the $1s\sigma$ State

Function \ R	0.0	0.4	0.8	1.2	1.6	2.0	2.4	3.0	4.0
(i)	6.000	3.854	3.584	3.311	3.074	2.880	2.707	2.563	2.410
(ii)	8.000	6.684	5.286	4.373	3.766	3.346	3.028	2.745	2.466
(iii)	8.000	7.152	6.023	5.113	4.413	3.871	3.423	2.947	2.374
(iv)	8.000	6.667	5.306	4.376	3.723	3.240	2.850	2.455	1.982
(v)	8.000	6.773	5.371	4.392	3.734	3.287	2.962	2.685	2.433
(vi)	8.000	6.673	5.298	4.375	3.744	3.298	2.956	2.648	2.354
(vii)	8.000	6.671	5.341	4.453	3.845	3.412	3.226	2.771	2.468
Exact	8.000	6.671	5.339	4.448	3.840	3.409	3.223	2.772	2.468

* It is believed that all quantities are correct to 0.1% but, due to the difficulty of assessing precisely the sensitivity of these quantities to p , the error may occasionally be as much as 0.2% in case of functions (vi) and (vii). This applies also to tables 6-11.

Table 6. Electronic Potential Energies, $-V$, of the $2p\sigma$ State

Function \ R	0.0	0.4	0.8	1.2	1.6	2.0	2.4	3.0	4.0
(i)	4.000	3.911	3.737	3.545	3.361	3.194	3.047	2.860	2.631
(ii)	1.600	1.940	2.320	2.659	2.870	2.948	2.939	2.850	2.669
(iii)	2.000	2.015	2.047	2.080	2.103	2.111	2.105	2.072	1.978
(iv)	2.000	2.084	2.315	2.610	2.828	2.904	2.876	2.741	2.447
(v)	2.000	2.062	2.144	2.575	2.819	2.928	2.934	2.848	2.550
(vi)	2.000	2.078	2.320	2.634	2.855	2.939	2.927	2.835	2.636
(vii)	2.000	2.086	2.344	2.650	2.860	2.947	2.941	2.851	2.664
Exact	2.000	2.087	2.335	2.642	2.857	2.943	2.937	2.851	2.664

Table 7. \bar{X}^2 for $1s\sigma$ State

Function \ R	0.8	1.2	1.6	2.0	2.4	3.0
(i)	1.01 ₈	1.03 ₅	1.05 ₃	1.06 ₈	1.08 ₀	1.08 ₉
(ii)	0.39 ₂	0.49 ₇	0.60 ₄	0.70 ₆	0.79 ₇	0.90 ₈
(iii)	0.28 ₂	0.31 ₁	0.34 ₄	0.37 ₉	0.41 ₅	0.47 ₁
(iv)	0.39 ₆	0.49 ₈	0.60 ₈	0.72 ₄	0.84 ₆	1.03 ₆
(v)	0.42 ₇	0.55 ₁	0.66 ₆	0.76 ₄	0.83 ₇	0.92 ₃
(vi)	0.39 ₅	0.49 ₈	0.60 ₇	0.71 ₆	0.82 ₃	0.95 ₅
(vii)	0.38 ₅	0.47 ₄	0.56 ₃	0.64 ₉	0.73 ₀	0.83 ₈
(5a)				0.65 _†		0.83 _†
Exact	0.38 ₀	0.46 ₈	0.55 ₆	0.64 ₂	0.72 ₂	0.82 ₈

† These values are taken from Hirschfelder (1935) who used function (5a).

Table 8. \bar{X}^2 for the $2p\sigma$ State

Function \ R	0.8	1.2	1.6	2.0	2.4	3.0
(i)	0.63 ₈	0.67 ₀	0.70 ₄	0.73 ₈	0.77 ₁	0.81 ₇
(ii)	1.72 ₄	1.25 ₀	1.00 ₆	0.89 ₀	0.84 ₁	0.82 ₄
(iii)	1.50 ₃	1.50 ₈	1.51 ₇	1.52 ₉	1.54 ₆	1.57 ₉
(iv)	1.18 ₆	0.97 ₈	0.85 ₅	0.80 ₈	0.80 ₇	0.84 ₉
(v)	1.34 ₈	1.14 ₄	1.00 ₄	0.89 ₉	0.84 ₇	0.82 ₆
(vi)	1.27 ₆	1.06 ₉	0.92 ₉	0.86 ₁	0.83 ₁	0.83 ₀
(vii)	1.25 ₀	1.05 ₄	0.92 ₁	0.85 ₁	0.81 ₉	0.81 ₅
Exact	1.23 ₈	1.03 ₉	0.90 ₄	0.83 ₆	0.80 ₅	0.80 ₃

Table 9. \bar{Z}^2 for $1s\sigma$ State

Function \ R	0.8	1.2	1.6	2.0	2.4	3.0
(i)	1.11 ₇	1.26 ₇	1.48 ₂	1.77 ₃	2.14 ₅	2.87 ₃
(ii)	0.49 ₆	0.74 ₃	1.06 ₂	1.45 ₂	1.91 ₄	2.74 ₈
(iii)	0.32 ₀	0.38 ₃	0.47 ₂	0.57 ₉	0.70 ₃	0.92 ₁
(iv)	0.42 ₈	0.57 ₀	0.73 ₆	0.92 ₄	1.13 ₄	1.48 ₆
(v)	0.47 ₅	0.67 ₄	0.92 ₈	1.24 ₂	1.62 ₃	2.34 ₃
(vi)	0.45 ₅	0.64 ₅	0.89 ₂	1.20 ₂	1.57 ₉	2.31 ₁
(vii)	0.44 ₇	0.62 ₀	0.84 ₃	1.12 ₂	1.46 ₆	2.12 ₆
(5a)				1.11 _†		2.13 _†
Exact	0.44 ₀	0.612	0.83 ₄	1.11 ₁	1.45 ₂	2.10 ₆

† These values are taken from the work of Hirschfelder (1935) who used the function (5a).

Table 10. \bar{Z}^2 for $2p\sigma$ State

R	0.8	1.2	1.6	2.0	2.4	3.0
Function						
(i)	2.01 ₃	2.23 ₆	2.52 ₃	2.87 ₃	3.28 ₆	4.02 ₉
(ii)	5.26 ₈	3.97 ₂	3.42 ₂	3.32 ₁	3.48 ₇	4.04 ₉
(iii)	4.57 ₇	4.67 ₈	4.82 ₄	5.01 ₇	5.25 ₆	5.70 ₂
(iv)	3.62 ₇	3.08 ₉	2.86 ₉	2.85 ₄	3.03 ₉	3.51 ₂
(v)	4.12 ₀	3.69 ₃	3.38 ₀	3.31 ₈	3.48 ₄	4.05 ₇
(vi)	3.90 ₁	3.38 ₈	3.12 ₈	3.15 ₈	3.38 ₂	3.96 ₉
(vii)	3.83 ₃	3.34 ₃	3.10 ₅	3.12 ₈	3.35 ₁	3.93 ₁
Exact	3.81 ₈	3.34 ₈	3.12 ₀	3.14 ₇	3.34 ₉	3.91 ₁

Table 11. Transition Integrals Q for the $1s\sigma-2p\sigma$ Transition†

R		0.8	1.2	1.6	2.0	2.4	3.0
Function							
(i)	$\left\{ \begin{array}{l} Q_L \\ Q_V \end{array} \right\}$	0.939	1.016	1.117	1.235	1.370	1.601
		0.510	0.581	0.672	0.768	0.868	1.015
(ii)	$\left\{ \begin{array}{l} Q_L \\ Q_V \end{array} \right\}$	0.617	0.827	1.018	1.187	1.351	1.597
		0.554	0.675	0.771	0.849	0.917	1.019
(iii)	$\left\{ \begin{array}{l} Q_L \\ Q_V \end{array} \right\}$	0.420	0.458	0.518	0.573	0.630	0.718
		0.543	0.692	0.888	1.141	1.464	2.116
(iv)	$\left\{ \begin{array}{l} Q_L \\ Q_V \end{array} \right\}$	0.597	0.737	0.857	0.963	1.057	1.203
		0.604	0.789	0.987	1.205	1.453	1.941
(v)	$\left\{ \begin{array}{l} Q_L \\ Q_V \end{array} \right\}$	0.636	0.815	0.959	1.102	1.248	1.485
		0.583	0.741	0.894	1.034	1.167	1.375
(vi)	$\left\{ \begin{array}{l} Q_L \\ Q_V \end{array} \right\}$	0.614	0.781	0.940	1.090	1.241	1.480
		0.592	0.744	0.883	1.010	1.135	1.330
(vii)	$\left\{ \begin{array}{l} Q_L \\ Q_V \end{array} \right\}$	0.607	0.764	0.914	1.060	1.212	1.446
		0.597	0.754	0.904	1.047	1.199	1.431
Exact	$Q_L=Q_V$	0.59 ₇	0.75 ₃	0.90 ₄	1.04 ₉	1.19 ₇	1.43 ₂

† Q_L is evaluated using the dipole length expression and Q_V using the dipole velocity expression (with the exact energies).

ACKNOWLEDGMENTS

The authors take pleasure in thanking Professor D. R. Bates for reading this paper and for his interest throughout the course of this work. They are indebted to Dr. A. L. Stewart for helpful discussions on the behaviour of the exact wave functions.

REFERENCES

- BATES, D. R., 1951, *J. Chem. Phys.*, **19**, 1122.
 BATES, D. R., DARLING, R. T. S., HAWE, S. C., and STEWART, A. L., 1953, *Proc. Phys. Soc. A*, **66**, 1124.
 BATES, D. R., LEDSHAM, K., and STEWART, A. L., 1953, *Phil. Trans. Roy. Soc. A*, **246**, 215.
 BATES, D. R., and POOTS, G., 1953, *Proc. Phys. Soc. A*, **66**, 784.
 BELL, R. P., and LONG, D. A., 1950, *Proc. Roy. Soc. A*, **203**, 364.
 COULSON, C. A., 1937, *Trans. Faraday Soc.*, **33**, 1479.
 COULSON, C. A., and BELL, R. P., 1945, *Trans. Faraday Soc.*, **41**, 141.
 DICKINSON, B. N., 1933, *J. Chem. Phys.*, **1**, 317.
 FINKELSTEIN, B. N., and HOROWITZ, G. E., 1928, *Z. Phys.*, **48**, 118.
 GUILLEMIN, V., and ZENER, C., 1929, *Proc. Nat. Acad. Sci., Wash.*, **15**, 314.
 HIRSCHFELDER, J. O., 1935, *J. Chem. Phys.*, **3**, 555.
 JAMES, H. M., 1935, *J. Chem. Phys.*, **3**, 9.
 MATSEN, F. A., 1953, *J. Chem. Phys.*, **21**, 928.
 PAULING, L., 1928, *Chem. Rev.*, **5**, 173.
 PRITCHARD, H. O., and SKINNER, H. A., 1951, *J. Chem. Soc.*, 945.
 RAHMAN, A. V., 1953, *Physica*, **19**, 377.
 SLATER, J. C., 1933, *J. Chem. Phys.*, **1**, 687.

Energy Levels of Triatomic Molecules

By S. DATTA MAJUMDAR

Department of Physics, University College of Science, Calcutta, India

MS. received 15th December 1953

Abstract. The mathematical theory of the asymmetrical top and of triatomic molecules has been considerably simplified by removing two of the Eulerian angles from the wave equation by a special artifice. Asymptotic expressions for the eigenvalues of the former and the centrifugal and Coriolis corrections to be applied to the energy levels of the latter have been obtained in closed forms for values of J exceeding 9 without solving any secular equation.

§ 1. INTRODUCTION

AN exact treatment of the asymmetrical top by wave mechanics leads to Wang's secular equation of degree $2J+1$ in energy. For each value of the asymmetry parameter the secular equation can be factored into four equations of roughly $J/2$ degree. As J increases the evaluation of Wang's determinant becomes increasingly laborious, and for values of J exceeding 10 the numerical work involved becomes almost prohibitive. But such high J values frequently occur experimentally. In the recent work on microwave and infra-red spectra it is not unusual to come across values of J up to 30 or 40. The actual situation is, however, much worse than this. A molecule is a deformable structure with internal degrees of freedom. The determination of the levels of the *rigid* asymmetrical top therefore solves the problem only partially. A comparison with experiment is not possible without adequately taking into account the shifts caused by the gyroscopic forces. In an important paper Wilson and Howard (1936) have delineated a very convenient method for calculating these finer interactions between rotation and vibration. Their method again leads to a secular determinant similar to Wang's with two additional sub-diagonals. The method, as it stands, not only entails a large amount of numerical work but also fails to reveal the nature of the interaction terms.

It is therefore desirable to find a simpler method of calculating the higher energy levels of polyatomic molecules, a method which will be sufficiently accurate but will spare us the trouble of evaluating a secular determinant. With this end in view several authors have made fresh attacks on the problem with considerable success. In this connection, the investigations of King (1947) and Golden (1948a) deserve special attention. King makes no attempt to calculate the interaction terms and using the old quantum theory obtains an asymptotic expression for the rotational levels of the rigid molecule for large J -values. It will be seen in § 3 that his formula agrees almost exactly with the first approximation of the BWK method.

Golden adopts an entirely different procedure. By studying the energy matrix of the asymmetrical top he finds that the limiting form it assumes, when J is indefinitely increased, differs only slightly from that arising in the characteristic

value problem of Mathieu's equation. He, therefore, takes Mathieu's equation as a substitute for the zeroth order Hamiltonian. To get better approximations the equation is then modified by adding to it suitable perturbation operators which take account of the smaller elements of the matrix. He applies the same technique to the computation of the interaction (Golden 1948 b) terms and, thus, in a way solves the problem completely.

Although the approach is altogether different, Golden's method and ours have one feature in common, namely, the reduction to a one-variable problem. In the following section it will be shown how this reduction can be carried out. The success of the method rests on the fact that from certain combinations of the angular momentum operators the Eulerian angle θ can be removed by giving θ the special value $\pi/2$. The *exact* differential equation in one variable obtained in this way closely resembles Mathieu's equation confirming Golden's investigations. The same method has been used to compute the interaction terms in triatomic molecules by a perturbation treatment. They come out as integrals over an eigenfunction of the ordinary differential equation to which the problem of the rigid top has been reduced. For the highest and the lowest energy levels corresponding to a particular value of J the results assume surprisingly simple forms, if, for the eigenfunction, the first approximation of the BWK solution is used, and some other simplifications are introduced.

The results given in this paper are only asymptotically correct, and begin to be valid as J approaches 10. On the other hand, just at this stage the numerical solution of the secular equations becomes laborious.

§ 2. REDUCTION OF THE HAMILTONIAN FOR THE ASYMMETRICAL TOP

In terms of the Eulerian angles θ , ϕ , χ , the components \hat{P}_x , \hat{P}_y , \hat{P}_z of the total angular momentum are

$$\begin{aligned}\hat{P}_x &= \frac{\hbar}{i} \left[\sin \phi \frac{\partial}{\partial \theta} + \cot \theta \cos \phi \frac{\partial}{\partial \phi} \right] \\ \hat{P}_y &= \frac{\hbar}{i} \left[\cos \phi \frac{\partial}{\partial \theta} - \cot \theta \sin \phi \frac{\partial}{\partial \phi} \right], \quad \hat{P}_z = \frac{\hbar}{i} \frac{\partial}{\partial \phi}\end{aligned}$$

if $\partial/\partial\chi=0$. The Hamiltonian of the asymmetrical top and of triatomic molecules (see § 4) involves only the operators \hat{P}_x^2 , \hat{P}_y^2 , \hat{P}_z^2 , $\hat{P}_x\hat{P}_y + \hat{P}_y\hat{P}_x$ and \hat{P}_z . From these five operators the Eulerian angle θ can be removed by giving θ the fixed value $\pi/2$ and making use of the total angular momentum equation

$$P_x^2 + P_y^2 + P_z^2 + J(J+1) = 0 \quad \dots\dots(1)$$

where, for simplicity, we have written P_x , P_y , P_z for $i\hat{P}_x/\hbar$, $i\hat{P}_y/\hbar$, $i\hat{P}_z/\hbar$ respectively. It is clear that this simplification is not possible for an arbitrary combination of P_x , P_y , P_z . Carrying out the reduction, we have

$$\begin{aligned}P_x^2 &= -\sin^2 \phi \left(\frac{\partial^2}{\partial \phi^2} + F \right) - \frac{1}{2} \sin 2\phi \frac{\partial}{\partial \phi} \\ P_y^2 &= -\cos^2 \phi \left(\frac{\partial^2}{\partial \phi^2} + F \right) + \frac{1}{2} \sin 2\phi \frac{\partial}{\partial \phi} \\ P_x P_y + P_y P_x &= -\sin 2\phi \left(\frac{\partial^2}{\partial \phi^2} + F \right) - \cos 2\phi \frac{\partial}{\partial \phi} \\ P_z^2 &= \frac{\partial^2}{\partial \phi^2}, \quad \text{with} \quad F = J(J+1).\end{aligned}$$

The wave equation

$$-\frac{\hbar^2}{2} \left(\frac{P_x^2}{A} + \frac{P_y^2}{B} + \frac{P_z^2}{C} \right) u = Eu$$

for the asymmetrical top with moments of inertia A, B, C then reduces to an ordinary differential equation in ϕ . This only means that we are confining our attention to the value of the wave function on the equatorial line $\theta = \pi/2$. The function defined by these values will obviously be an eigenfunction of the ordinary differential equation, and hence *some* of the eigenvalues of the latter must be identical with those of the asymmetrical top. This argument fails only when the wave function vanishes identically for $\theta = \pi/2$. We are therefore to search for the eigenvalues of the asymmetrical top among those of the ordinary differential equation, which, on introduction of the asymmetry parameter $k = (b-a)/(2c-a-b)$ and the reciprocal moments $a = \hbar^2/2A, b = \hbar^2/2B, c = \hbar^2/2C$, assumes the simple form

$$\left[g \left(\frac{d^2}{d\phi^2} + F \right) + \frac{1}{2} g' \frac{d}{d\phi} + \mu \right] u = 0 \quad \dots\dots(2)$$

where

$$g = 1 - k \cos 2\phi, \mu = (E - cF) / \{c - \frac{1}{2}(a+b)\}. \quad \dots\dots(3)$$

Equation (2) possesses an infinite number of eigenvalues which are all different if $k \neq 0, +1, -1$. To make the appropriate selection we consider the limiting case of the symmetrical top for which $k=0$. Equation (2) then reduces to $u'' + (F + \mu)u = 0$ which has the eigenvalues $F + \mu = m^2$ for arbitrary integral values of m . But it is known that only the lowest $J+1$ of them give the energy levels of the symmetrical top. Since the eigenvalues vary continuously with k , the same holds for the asymmetrical top whose levels are obtained from the lowest $2J+1$ eigenvalues of equation (2).

The eigenfunctions of equation (2) can be obtained by putting $\pi/2$ for θ in the complete wave functions involving both θ and ϕ . The latter are of two types:

$$\sum a_{J-2i} P_J^{J-2i}(\cos \theta) \frac{\cos}{\sin} (J-2i)\phi \quad \text{and} \quad \sum a_{J-2i-1} P_J^{J-2i-1}(\cos \theta) \frac{\cos}{\sin} (J-2i-1)\phi.$$

Evidently the functions of the second type vanish for $\theta = \pi/2$, and so we cannot say, without further examination, whether the corresponding eigenvalues are contained in those of equation (2). Substitution of the series $\sum a_r \frac{\cos}{\sin} r\phi$ in this equation leads to the recurrence relations

$$a_{r-2} \frac{1}{2} k f(r-2) + a_r (r^2 - F - \mu) + a_{r+2} \frac{1}{2} k f(r+1) = 0 \quad \dots\dots(4)$$

where $f(r) = F - r(r+1)$. The possible values of μ are the roots of the finite determinant formed by the coefficients of a_r . This determinant can be transformed into the Wang form

$$E_{r,r} = r^2 - F - \mu, \quad E_{r,r+2} = E_{r+2,r} = \frac{1}{2} k [f(r)f(r+1)]^{1/2}.$$

It is evident from the recurrence relations (4) that solutions of equation (2) of the form

$$\sum a_{J-2i-1} \frac{\cos}{\sin} (J-2i-1)\phi$$

with only a finite number of terms do not exist. This, combined with the fact that the wave functions of the second type vanish identically for $\theta = \pi/2$, leads one to doubt whether all the eigenvalues of the asymmetrical top can be obtained

from equation (2). The situation, however, becomes clear by the substitution $u = g^{1/2}w$, when the differential equation for w is found to be satisfied by a function of the type

$$\sum a_{J-2i-1} \frac{\cos}{\sin} (J-2i-1)\phi$$

with exactly Wang's secular equation for μ .

Values of the Asymmetry Parameter

In the actual computation of the energy levels from equation (2) it will certainly be advantageous to keep the value of k as small as possible. If we take B to be the intermediate moment of inertia and assume, without loss of generality, that $|c-b| \geq |b-a|$, then the values of k will always lie between 0 and $\frac{1}{3}$. But this restriction is not necessary, and any permutation of A, B, C in equation (2) must lead to the same energy values arranged in a different order. Interchanging, for instance, A and C , we have a differential equation of the same form with k' and μ' replacing k and μ , where

$$k' = (1-k)/(1+3k), \mu' = (E-aF)/\{a-\frac{1}{2}(c+b)\}.$$

If the eigenvalues are arranged in a decreasing order, and if their positions are indicated by an index τ which runs from $+J$ to $-J$, then we have, from equation (3),

$$E = \frac{1}{2}(a+b)F + G_{\tau}(k)\{c - \frac{1}{2}(a+b)\} = \frac{1}{2}(c+b)F + G_{\tau}(k')\{a - \frac{1}{2}(c+b)\}$$

where $G_{\tau} = F + \mu_{\tau}$. Since the quantities $c - \frac{1}{2}(a+b)$ and $a - \frac{1}{2}(c+b)$ have opposite signs, it follows that $\tau' = -\tau$ and

$$2G_{-\tau}(k) + (1+3k)G_{\tau}(k') = (1+k)F. \quad \dots\dots(5)$$

For $k = \frac{1}{3}$ this reduces to $G_{-\tau}(\frac{1}{3}) + G_{\tau}(\frac{1}{3}) = \frac{2}{3}F$.

Equation (5) connects the lowest levels for a k lying between 0 and $\frac{1}{3}$ with the highest levels for some k' lying between 1 and $\frac{1}{3}$. This apparently trivial transformation completely changes the character of the eigenfunction and extends the domain of applicability of the results of this paper to the lowest levels for a given J .

§ 3. ASYMPTOTIC SOLUTION OF THE WAVE EQUATION

The substitution $u = g^{-1/4}v$ transforms equation (2) into Hill's equation

$$v'' + \left[\frac{3k^2}{4g^2} \sin^2 2\phi + 1 + J(J+1) + \frac{\mu-1}{g} \right] v = 0 \quad \dots\dots(6)$$

which, for large J -values, differs but little from Mathieu's equation, and confirms Golden's observation that a rough estimate of the eigenvalues may be obtained from a table of characteristic values of the latter. But, because of the slow convergence of their Fourier expansions, Mathieu functions do not form a convenient basis for a perturbation calculation. Since the problem has been reduced to the solution of a one-dimensional equation with periodic coefficients, the methods available for approximately handling such equations may be used. In this paper Jeffreys' method (or the so-called BWK method) will be used, partly because of its simplicity, and partly because it leads to very simple expressions for the centrifugal and Coriolis corrections to the energy levels of triatomic molecules. Moreover, calculations will be carried out only for the highest and the lowest levels for which the results assume particularly simple

forms. At least half of the energy levels for a given J will thus be covered by the present theory. For the intermediate levels the coefficient of v in equation (6) approaches zero, and it becomes necessary to change the technique of solution. This question and an improved method of solution will be taken up in a future paper.

Returning to equation (6) we see that if the coefficient of v remains everywhere large, then a good approximation to the solution is obtained by neglecting the second term and writing with Jeffreys

$$v = \left(1 - \frac{\nu}{fg}\right)^{-1/4} \frac{\cos}{\sin} \int_0^\phi \left(f - \frac{\nu}{g}\right)^{1/2} d\phi, \quad \text{where} \quad \begin{matrix} f=1+F \\ -\nu=\mu-1 \end{matrix} \dots\dots (7)$$

If the integrand is expanded in a Fourier series the condition of periodicity leads to the equation

$$\frac{1}{2\pi} \int_0^{2\pi} \left(f - \frac{\nu}{g}\right)^{1/2} d\phi = m, \quad \text{an integer}, \quad \dots\dots (8)$$

for the determination of ν . As J increases, this approximation improves, while the evaluation of Wang's determinant becomes increasingly laborious.

Introducing the symbols $p^2 = f - \nu$, $w = \nu k/p^2$, we have

$$f - \nu/g = p^2(1 - w \cos 2\phi/g).$$

Considering only values of ν for which

$$w \leq \frac{1}{4}, \quad \dots\dots (9)$$

expanding the integrand in a power series and retaining the first three terms, we have, from equation (8), the following approximate formula for the determination of p :

$$\frac{m}{p} = 1 - \frac{k^2}{16} \left[\left(\frac{f}{p^2} + 1\right)^2 - 4 \right] - \frac{k^4}{64} \left[\left(\frac{3f}{p^2} - 1\right)^2 - 4 \right].$$

It is instructive, at this stage, to compare equation (8) with the eigenvalue equation obtained by King by the use of the old quantum theory. Equation (6) of his paper (King 1947), written in our notation, is

$$\frac{1}{2\pi} \int_0^{2\pi} (F + \mu/g)^{1/2} d\phi = m$$

and this agrees satisfactorily with equation (8). This is only to be expected, since the first approximation of the BWK method yields the Bohr-Sommerfeld quantization rule.

It is well known that the expression (7) for v is only the first term of an asymptotic expansion of which the higher terms can be calculated by the method suggested by Wentzel (1926). But an unlimited degree of accuracy cannot be attained by this method, since the addition of successive terms leads ultimately to a divergent series. This is clearly brought out by the fact that pairs of eigenvalues corresponding to an odd and an even function remain coincident in all higher approximations, whereas it is known that no two of the energy levels of the asymmetrical top coincide exactly, although pairs of them often come very close to one another. The treatment given below is therefore applicable only to the highest and the lowest energy levels which are essentially degenerate. Comparing the results with the exact values tabulated by Hainer, Cross and King (1949), we can also form an idea of the highest accuracy attainable

in this way. In the following paragraphs we shall not attempt to explore the full possibilities of this method, but shall be content to work out the second approximation which is likely to yield a highly accurate value for energy. Following Wentzel we therefore write

$$v = \chi^{-1/4} \exp \left\{ \pm i \int_0^\phi \left[\chi^{1/2} + \frac{5}{32} \chi^{-5/2} (\chi')^2 - \frac{1}{8} \chi^{-3/2} \chi'' \right] d\phi \right\}$$

where χ is the coefficient of v in equation (6). It is convenient to divide χ into two parts

$$\chi = \chi_0 + \chi_1, \quad \chi_0 = f - \frac{\nu}{g}, \quad \chi_1 = \frac{3k^2}{4g^2} \sin^2 2\phi$$

and write approximately

$$v = \chi^{-1/4} \exp \left\{ \pm i \int_0^\phi \left[\chi_0^{1/2} + \frac{1}{2} \chi_0^{-1/2} \chi_1 + \frac{5}{32} \chi_0^{-5/2} (\chi_0')^2 - \frac{1}{8} \chi_0^{-3/2} \chi_0'' \right] d\phi \right\}.$$

Eigenvalues are now obtained from the condition that the constant term in the Fourier expansion of the integrand must be an integer, that is, from the equation

$$\begin{aligned} m &= \frac{1}{2\pi} \int_0^{2\pi} \left[\chi_0^{1/2} + \frac{1}{2} \chi_0^{-1/2} \chi_1 - \frac{1}{48} \chi_0^{-3/2} \chi_0'' \right] d\phi \\ &= \frac{1}{2\pi} \int_0^{2\pi} \left[\chi_0^{1/2} + \chi_0^{-1/2} \left\{ \frac{k^2}{24} \frac{\sin^2 \theta}{g^2} + \frac{k \cos \theta}{3g} \right\} - \frac{\nu}{12} \frac{k \cos \theta}{g^2} \chi_0^{-3/2} \right] d\theta, \quad \theta = 2\phi. \end{aligned}$$

.....(10)

The transformations necessary to reduce these elliptic integrals to standard forms are given in the Appendix. We will adopt here the simpler (and perhaps more useful) procedure of expanding the integrand in a series and integrating term by term. Thus

$$\frac{1}{2\pi} \int_0^{2\pi} \chi_0^{1/2} d\theta = p \left[1 + \sum C_r^{1/2} \left(\frac{\nu}{p^2} \right)^r \frac{1}{2\pi} \int_0^{2\pi} \left(\frac{k \cos \theta}{g} \right)^r d\theta \right]$$

where the $C_r^{1/2}$ are the coefficients in the binomial expansion of $(1-x)^{1/2}$. The integrals involving θ are evaluated most conveniently with the help of Legendre's formula. If (i, j) denotes the value of the integral

$$\frac{1}{2\pi} \int_0^{2\pi} \frac{(k \cos \theta)^i}{g^j} d\theta$$

then, for $i \leq j$,

$$(i, j) = \frac{1}{2\pi} \int_0^{2\pi} \frac{(1-g)^i}{g^j} d\theta = \frac{1}{2\pi} \sum \int_0^{2\pi} \frac{a_r}{g^r} d\theta = \sum a_r \beta^r p_{r-1}(\beta)$$

where $\beta = (1-k^2)^{-1/2}$. But for a constant term ± 1 which occurs only when $i=j$, (i, j) comes out as a polynomial in odd powers of β . This is the form most suitable for numerical work. To solve the algebraic equation for p , we write equation (10) in the form

$$p^2 = m^2 / [1 + f(p^2)]^2 \quad \text{.....(10')}$$

and make use of the fact that $f(p^2)$ is of the nature of a correction term small compared with unity. Starting from a trial value of p^2 we can get in a few steps a highly accurate value by repeated substitution in the right-hand side of equation (10').

For the case of maximum asymmetry corresponding to $k=\frac{1}{3}$, the series has the form

$$10^3 \times f(p^2) = -30.330\,086x - 8.990\,294x^2 - 1.201\,758x^3 - 0.422\,269x^4 \\ - 0.117\,746x^5 - 0.043\,04x^6 + \frac{1}{p^2} [22.747\,56 + 1.055\,83x \\ - 8.990\,29x^2 - 3.567\,42x^3 - 2.3631x^4 - 1.141x^5]$$

with $x = \nu/p^2$. The energies of sixteen out of the twenty-five levels for $J=12$ have been calculated by this formula and are given in table 1. The results are found to be in excellent agreement with the exact values given by Hainer, Cross and King (1949).

Table 1. Values of p^2 for $J=12$, $k=\frac{1}{3}$

Level	Exact	Our values	King
12 ₁₂	144.717 59	144.717 58	144.7000
12 ₁₁	144.717 59		
12 ₁₀	123.171 69	123.171 66	123.1470
12 ₉	123.171 68		
12 ₈	103.693 89	103.6934	103.6376
12 ₇	103.693 30		
12 ₆	86.374 71	86.365	86.2866
12 ₅	86.359 43		

The figures in the second and fourth columns are taken from Hainer, Cross and King (1949).

§ 4. REDUCTION OF THE WILSON-HOWARD HAMILTONIAN FOR TRIATOMIC MOLECULES

Wilson and Howard (1936) have shown how to write the quantum mechanical Hamiltonian of a vibrating and rotating polyatomic molecule in a convenient form. The procedure suggested by them will be closely followed in our treatment of the triatomic molecule.

If the z -axis of the moving coordinates is taken to be perpendicular to the plane of the molecule, two of the products of inertia vanish, and the motion of the atoms remains confined to the xy plane, so that the angular momentum relative to the moving system can have no component in this plane. If the moving x - and y -axes are next chosen in such a way that this angular momentum vanishes to a first approximation, then the classical kinetic energy of a triatomic molecule assumes the simple form

$$2T = \mu_{xx} \dot{P}_x^2 + 2\mu_{xy} \dot{P}_x \dot{P}_y + \mu_{yy} \dot{P}_y^2 + \mu_{zz} (\dot{P}_z - p_z)^2 + \sum p_k^2$$

where the p_k are momenta conjugate to the normal coordinates q_k , p_z is the vibrational angular momentum, and the $\mu_{\alpha\beta}$ are certain functions of q_k whose exact forms depend on the structure of the molecule and its force constants. The corresponding Hamiltonian operator is

$$H = -\frac{1}{2}\hbar^2 [\mu_{xx} P_x^2 + \mu_{xy} (P_x P_y + P_y P_x) + \mu_{yy} P_y^2] \\ + \frac{1}{2}\mu^{1/2} \left(\frac{\hbar}{i} P_z - p_z \right) \mu_{zz} \mu^{-1/2} \left(\frac{\hbar}{i} P_z - p_z \right) + \frac{1}{2}\mu^{1/2} \sum_k p_k \mu^{-1/2} p_k + V \quad \dots (11)$$

where μ is the determinant of $\mu_{\alpha\beta}$.

We notice that in the Hamiltonian (11) the operators P_x , P_y , P_z occur only in the combinations P_x^2 , P_y^2 , P_z^2 , $P_x P_y + P_y P_x$ and P_z . It is this remarkable

circumstance which leads to the possibility of applying the method of §2 to triatomic molecules. A glance at the formulae listed there shows that if we set $\theta = \pi/2$, and make use of the total angular momentum equation (1), then the Hamiltonian is reduced to a form in which the coordinate θ no longer occurs. According to our previous arguments, some of the eigenvalues of the reduced Hamiltonian must be identical with those of (11). The task of finding out the energy levels of triatomic molecules by a perturbation treatment thus becomes considerably simplified because, instead of having to solve a formidable secular equation, which gives us no insight whatsoever into the nature and magnitude of the correction terms, we need only take averages of operators of the type P_x^2 , P_z^4 , etc. over an eigenfunction of equation (2). Moreover, since these correction terms are always small an approximate evaluation of the integrals will be sufficient in almost all cases.

Following the customary procedure we can write the reduced Hamiltonian as a sum of three parts $H^{(0)}$, $H^{(1)}$, $H^{(2)}$ of which $H^{(0)}$ is separable in the vibrational and the rotational coordinates. The solution of the equation $(H^{(0)} - E^{(0)})\psi^{(0)} = 0$ is the product $\psi_V^0 \psi_R^0$ of an eigenfunction of equation (2) and three harmonic oscillator functions corresponding to the three modes of vibration of the molecule. When these are taken as the basis for a perturbation calculation, it is found that the first-order correction $E^{(1)}$ to energy vanishes exactly. The second-order correction $E^{(2)}$ has the value

$$E^{(2)} = \int (\psi_V^0 \psi_R^0)^* H^{(2)} \psi_V^0 \psi_R^0 \\ + \sum'_{R''V''} \left[\int (\psi_V^0 \psi_R^0)^* H^{(1)} \psi_{V''}^0 \psi_{R''}^0 \int (\psi_{V''}^0 \psi_{R''}^0)^* H^{(1)} \psi_V^0 \psi_R^0 \right] / (E_{VR}^{(0)} - E_{V''R''}^{(0)}).$$

In evaluating the series on the right-hand side great simplification is achieved by setting $E_{VR}^{(0)} - E_{V''R''}^{(0)}$ equal to $E_V^{(0)} - E_{V''}^{(0)}$ because the summation over the rotational functions for a particular value of V'' can then be conveniently carried out by means of the formula

$$\sum_{\sigma''} (\sigma | T | \sigma'') (\sigma'' | S | \sigma) = (\sigma | TS | \sigma)$$

with the result that $E^{(2)}$ assumes the particularly simple form

$$E^{(2)} = \rho + \sigma_\alpha \bar{P}_\alpha + \tau_{\alpha\beta} \bar{P}_\alpha \bar{P}_\beta, \quad (\alpha, \beta = 1, 2, 3, 4) \quad \dots\dots (12)$$

where, for brevity, we have written P_1, P_2, P_3, P_4 for $P_x^2, P_y^2, P_z^2, P_x P_y + P_y P_x$ respectively. The bars indicate averages over the rotational function, and ρ, σ_α and $\tau_{\alpha\beta}$ are combinations of integrals over the vibrational functions. A careful examination shows that in equation (12) we can set $\tau_{\alpha\beta} = \tau_{\beta\alpha}$, $\sigma_4 = 0$, and $\tau_{4\alpha} = 0$ for $\alpha \neq 4$, partly because P_z and P_4 convert odd functions into even and vice versa.

The method outlined above is applicable to the general triatomic molecule of the XYZ type. For symmetric molecules of the XY_2 type the coefficients $\rho, \sigma_\alpha, \tau_{\alpha\beta}$ have been evaluated by Shaffer and Nielsen (1939) in terms of the molecular constants. Their work, supplemented by the results of the following section, puts the theory of symmetric triatomic molecules in a very convenient form. We have now an analytic formula for the energy levels analogous to that for diatomic molecules.

§ 5. ANALYTIC EXPRESSIONS FOR THE CORRECTION TERMS FOR LARGE J -VALUES

In calculating the average values of the various operators we observe that the eigenfunctions u of equation (2) are orthogonal with the weight factor $g^{-1/4}$, so that it is necessary to multiply the integrand in every case by $g^{-1/2}$. For example,

$$\overline{P}_3 = N^2 \int_0^{2\pi} g^{-1/2} u \frac{d^2 u}{d\phi^2} d\phi \quad \text{where} \quad 1/N^2 = \int_0^{2\pi} g^{-1/2} u^2 d\phi.$$

Using equation (2) and integrating by parts, we have

$$\overline{P}_3 = -N^2 \int g^{-1} v^2 \left[\left(f - \frac{\nu}{g} \right) - 1 + \frac{1}{g} + \frac{3}{8} \left(\frac{g'}{g} \right)^2 - \frac{1}{4} \frac{g''}{g} \right] d\phi \quad \dots\dots(13)$$

and
$$1/N^2 = \int g^{-1} v^2 d\phi$$

where $v = g^{1/4} u$ is a solution of equation (6).

To a first approximation, all other terms in the integrand can be neglected in comparison with $f - \nu/g$, which predominates over the rest for large J -values. Moreover, since we are dealing with small correction terms the approximate form of v given in equation (7) may be used without any serious error. With this form of v ,

$$v^2 = \frac{1}{2} \left(f - \frac{\nu}{g} \right)^{-1/2} \left[1 \pm \cos 2 \int_0^\phi \left(f - \frac{\nu}{g} \right)^{1/2} d\phi \right] \quad \dots\dots(14)$$

which contains a rapidly oscillating function of ϕ . It will be convincingly demonstrated in the next section that in carrying out the integrations this oscillatory part can always be neglected if J exceeds 9 and ν satisfies the inequality (9). This is a lucky state of affairs, for if the situation were otherwise it would not be possible to carry out the integrations (even numerically) and give neat analytical expressions for the correction terms.

Introducing all these simplifications we get the surprisingly simple result

$$\overline{P}_3 = -\frac{1}{2} N^2 \int_0^{2\pi} g^{-1} \chi_0^{1/2} d\phi, \quad \text{with} \quad \frac{1}{N^2} = \frac{1}{2} \int_0^{2\pi} g^{-1} \chi_0^{-1/2} d\phi;$$

similarly

$$\overline{P}_1 = -\frac{1}{2} N^2 \nu \int_0^{2\pi} g^{-2} \sin^2 \phi \chi_0^{-1/2} d\phi, \quad \overline{P}_2 = -\frac{1}{2} N^2 \nu \int_0^{2\pi} g^{-2} \cos^2 \phi \chi_0^{-1/2} d\phi.$$

It is, however, unnecessary to calculate the correction terms involving σ_α separately, as their effects can be fully taken into account by introducing effective moments of inertia which depend in a simple manner on the vibrational quantum numbers. The centrifugal expansion terms, quartic in the components of angular momentum, cannot be disposed of so easily. To a good approximation these seven terms can be represented by simple analytic expressions of the type

$$\overline{P}_3^2 = \frac{1}{2} N^2 \int_0^{2\pi} g^{-1} \chi_0^{3/2} d\phi. \quad \dots\dots(13')$$

Correlation with Experiment

The analysis of the far infra-red spectrum of water vapour by Randall, Dennison, Ginsburg and Weber (1937) affords a means of testing the correctness of the theoretical results obtained here. After making the best choice of the

effective moments of inertia they find, for the higher energy levels, a discrepancy which they attribute to the centrifugal distortion suffered by the molecule during rotation. In the highest level for $J=11$ it amounts to 279 cm^{-1} , that is, 8.7% of the term value. The present work makes it possible to calculate this difference theoretically with the help of simple formulae of the type (13') for $\overline{P_\alpha P_\beta}$. An elaborate comparison of the theory with the experimental findings of these authors has been undertaken, but is being delayed by certain unavoidable factors. The results of a *rough* calculation for the highest two pairs of levels 11_{11} , 11_{10} and 11_9 , 11_8 of H_2O are given below and are seen to be quite encouraging.

In carrying out the calculations we have made free use of the valuable formulae placed at our disposal by Shaffer and Nielsen (1939). It can be easily shown that any permutation of the operators P_x , P_y , P_z in the equation (35) of their paper leaves the values of energy unaltered. To make the numerical value of k smaller than $\frac{1}{3}$ we interchange P_x and P_z , and observe that in the resulting expression the term involving P_z^4 makes by far the largest contribution to the energy of the highest levels. Neglecting the contributions from the remaining six terms we therefore get the following rough estimate of the correction $E^{(2)}$ to energy:

$$E^{(2)} = 4 \left(\frac{h}{8\pi^2 A_0 c} \right)^3 \left(\frac{\cos^2 \gamma}{\nu_1^2} + \frac{\sin^2 \gamma}{\nu_2^2} \right) \overline{P_3^2} \text{ cm}^{-1}$$

where $\nu_1 = 3825\text{ cm}^{-1}$, $\nu_2 = 1654\text{ cm}^{-1}$, $h/8\pi^2 A_0 c = 27.33\text{ cm}^{-1}$. If we use the potential constants given by Herzberg (1951), the value of γ comes out to be $-50^\circ 38'$. An examination of equation (13') shows that, for the highest levels, $\overline{P_3^2}$ is very nearly equal to the fourth power of an integer. Inserting all these values in the above expression we have

$$E^{(2)} = 294\text{ cm}^{-1}, \text{ for the levels } 11_{11}, 11_{10}$$

and

$$E^{(2)} = 201\text{ cm}^{-1}, \text{ for the levels } 11_9, 11_8$$

to be compared with the experimental values 279 cm^{-1} and 194 cm^{-1} respectively. For an accurate calculation of $E^{(2)}$ the small contributions from the remaining six terms must be added to them.

§ 6. AN ESTIMATE OF THE INTEGRAL (15) BY THE SADDLE-POINT METHOD

The method outlined in the previous section for computing the correction terms would be of little practical use if the value of the integral

$$\begin{aligned} 2\pi \mathcal{J} &= \int_{-\pi}^{+\pi} \left[\cos 2 \int_0^\phi \chi_0^{1/2} d\phi \right] d\phi = \int_{-\pi}^{+\pi} \left[\exp \left\{ i \sqrt{f} \int_0^\theta \left(1 - \frac{a}{1-k \cos \theta} \right)^{1/2} d\theta \right\} \right] d\theta \\ &= \int_{-\pi}^{+\pi} \exp \{ F(\theta) \} d\theta \end{aligned} \quad \dots\dots(15)$$

were not negligible compared with unity for the range of energy levels considered in this paper. This, fortunately, turns out to be the case, enabling us to avoid the most troublesome part of the calculations. The difficulty would not be so great if a tolerably accurate value of the integral could be obtained by the numerical method. But the rapid oscillations of the function on the real axis make even a numerical integration impracticable.

To show that the integral has a negligible value we apply Debye's saddle-point method in a slightly modified form. Since the integrand has a period 2π , it is possible to shift the line of integration along the imaginary axis without altering the value of the integral until a point is reached where $F'(\theta)$ vanishes. According to the customary procedure the path of integration is to be a curve passing through this point and satisfying the equation, $\text{Im } F(\theta) = \text{const}$. In the present case the analytic form of $\text{Im } F(\theta)$ turns out to be so complicated that it is found more convenient to choose a straight path of integration parallel to the real axis. On this line L the real part of $F(\theta)$ becomes large and negative and an upper limit to the absolute value of the integral can be set without much difficulty. In the majority of cases this upper limit comes out to be so small that it is only under exceptional circumstances that a closer investigation by the numerical method becomes necessary. These points are clearly brought out by the following discussions.

Let $\theta = u + iv$, and let $\theta_0 = iv_0 = i \cosh^{-1} \{ (1-a)/k \} = i \cosh^{-1} (b/k)$ be the saddle point. For $0 < u < \pi$, and $0 < v < v_0$, the imaginary part of $(-1 + a/g)$ is negative, and therefore the point representing $(-1 + a/g)^{1/2}$ in the complex plane lies either in the second or the fourth quadrant. To decide between the two we observe that, for $u = 0$, the point lies on the positive part of the imaginary axis. Because of continuity the point cannot leave the second quadrant as u changes from 0 to π , and hence the real part of $(-1 + a/g)^{1/2}$ must always be negative except at the extreme points iv and $\pi + iv$ where it vanishes. The real part of the integral $\int_0^u (-1 + a/g)^{1/2} du$ on L , therefore, attains its maximum value at $u = 0$, and hence $\exp\{F(iv_0)\}$ may be taken to be an upper limit to the value of $|\mathcal{J}|$. We now show by concrete examples that in the majority of cases, this upper limit is quite small.

It is easily seen that the value of the integral

$$I = \int_0^{v_0} [1 - a/(1 - k \cosh v)]^{1/2} dv \quad \dots\dots(16)$$

steadily decreases as a and k increase. Since in the discussion of the rigid top levels, a and k were subjected to the restriction $\nu k (f - \nu) \leq \frac{1}{4}$, that is, $a \leq 1/(1 + 4k)$, an extreme case will arise for $k = \frac{1}{3}$ and $a = \frac{3}{7}$. Although an exact integration can be carried out with the help of elliptic functions, the simpler procedure of replacing $\cosh v$ in (16) by $1 + sv$, with $s = (b/k - 1)/v_0$, may sometimes be adopted with advantage if it does not lead to too low an estimate for I . Introducing this simplification we can write

$$I > I' = \int_0^{v_0} \left[1 - \frac{a}{1 - k(1 + sv)} \right]^{1/2} dv = \frac{a}{ks} \left[\{z(z+1)\}^{1/2} - \sinh^{-1} \sqrt{z} \right]_0^{(b-k)/a}.$$

For $k = \frac{1}{3}$, $a = \frac{3}{7}$, this simplified integral has the value 0.490. Since $f \geq 111$ we have, finally, $|\mathcal{J}| < \exp(-10.5 \times 0.490) = 1/171$. If this is not considered sufficiently small the limit can be pushed down further by using the exact expression for I given in the Appendix. For the same pair of values of a and k we find, after some numerical work, that $I = 0.562$, which gives the upper limit $|\mathcal{J}| < 1/365$, and this is already so small that the integration along L becomes unnecessary. It is evident from the behaviour of the function on L that, if this integration is performed, the value of $|\mathcal{J}|$ will drop to a small fraction of this.

Our discussions will be incomplete without some remarks about the integration along L which becomes necessary, sometimes, for the following two reasons. The multiplier of $\cos 2 \int_0^\phi \chi_0^{1/2} d\phi$ in the equations (13) and (13') is never a constant but a slowly varying function of ϕ , which, on Fourier expansion, yields terms of the type $\cos 2r\phi$ with rapidly decreasing coefficients. Secondly, the restriction (9) on the values of a and k , necessary for an accurate determination of the rigid top levels, may be somewhat relaxed in the computation of the correction terms. For $k = \frac{1}{3}$, $a = \frac{1}{2}$, for instance, we have $I' = 0.339$, $|\mathcal{J}| < 1/35.5$; $I = 0.399$, $|\mathcal{J}| < 1/66.7$. Thus an increase in the value of a by so small a fraction as $1/14$ raises the upper limit by a factor 5.47. We therefore set down below the formulae required for an approximate integration. The real part of

$$F'(\theta) = -\frac{\sqrt{f}}{\sqrt{2}} \left[-1 + \frac{a(1-b\cos u)}{M^2} + \frac{2\sin \frac{1}{2}u}{M} (b^2 - k^2 \cos^2 \frac{1}{2}u)^{1/2} \right]^{1/2} \dots\dots (17)$$

where $M^2 = a^2 + 4\sin^2 \frac{1}{2}u(b - k^2 \cos^2 \frac{1}{2}u)$. The expression (17) behaves like $-[fu(b^2 - k^2)^{1/2}/(2a)]^{1/2}$ near $u=0$, vanishes again at $u=\pi$, and passes through one minimum between these two points. For $a = \frac{1}{2}$, $k = \frac{1}{3}$ the values are given in table 2.

Table 2. Values of $\text{Re } F'(\theta)/\sqrt{f}$ on L for $a = \frac{1}{2}$, $k = \frac{1}{3}$

u	$\pi/12$	$\pi/4$	$\pi/3$	$\pi/2$
Values	-0.246	-0.218	-0.177	-0.108

The function (17) is too complicated to admit of even an approximate analytical integration. By a closer study of this function, however, it appears quite possible to construct another simpler function which at every point has a higher value and at the same time gives a good estimate of $|\mathcal{J}|$. But until that is done we have no other alternative but to resort to the numerical method. It is evident that this second estimate will also be an upper limit much higher than the actual value of $|\mathcal{J}|$ because it has been obtained by setting the imaginary part of $F(\theta)$ equal to zero.

A rough estimate of $|\mathcal{J}|$, which is likely to be of the right order of magnitude, can be obtained by replacing the function (17) by its approximate form near $u=0$, and extending the domain of integration to infinity. Thus

$$\begin{aligned} |\mathcal{J}| &\simeq \exp(-\sqrt{f}I) \frac{1}{\pi} \int_0^\infty \exp \left[-\frac{2}{3} \left\{ \frac{f}{2a} (b^2 - k^2)^{1/2} \right\}^{1/2} u^{3/2} \right] du \\ &= \exp(-\sqrt{f}I) \frac{1}{\pi} \left\{ \frac{3f}{4a} (b^2 - k^2)^{1/2} \right\}^{-1/3} \Gamma\left(\frac{2}{3}\right). \end{aligned}$$

For $a = \frac{1}{2}$, $k = \frac{1}{3}$, $J = 10$, this has the value $0.107 \exp(-\sqrt{f}I)$.

The foregoing discussions leave little room for doubt that in the calculation of the correction terms of §5 the error caused by neglecting the troublesome part of the wave function will always lie below those arising from other approximations in the theory.

ACKNOWLEDGMENT

For interest and encouragement I offer my sincerest thanks to Professors S. N. Bose and M. N. Saha.

APPENDIX

All the integrals occurring in this paper can be evaluated exactly in terms of elliptic functions. Out of them we select only the following two for a detailed discussion.

$$I_1 = \int_0^{\cosh^{-1} b/k} [1 - a/(1 - k \cosh v)]^{1/2} dv \quad \dots\dots (18)$$

$$I_2 = \int_0^\pi [1 - a/(1 - k \cos \theta)]^{1/2} d\theta. \quad \dots\dots (19)$$

The first of these is identical with the integral (16) of the last section and the second, multiplied by $\sqrt{f/\pi}$, is the dominant term in the eigenvalue equation (10). The remaining integrals involve the same irrational function, and, therefore, require the same elliptic function substitution for a reduction to standard forms.

As they differ very slightly in form, the two integrals can be considered simultaneously. Rationalizing the numerator and writing $y = k \cosh v$ in (18) and $y = k \cos \theta$ in (19) we have

$$I_1 = \int_k^b (b-y)/[(y-1)(y-b)(y^2-k^2)]^{1/2} dy$$

$$I_2 = \int_{-k}^{+k} (b-y)/[(y-1)(y-b)(k^2-y^2)]^{1/2} dy.$$

The two can be brought into the common form

$$I = \int (b-y)/[\pm (y-1)(y-b)(y^2-k^2)]^{1/2} dy$$

where the limits of integration in the two cases are, of course, different, and the upper sign is to be taken for I_1 and the lower for I_2 . The homographic substitution $t = (y-\alpha)/(y-\beta)$ transforms I into

$$I = -\sqrt{2(\alpha-\beta)} \int \frac{t dt}{(1-t^2)E} + \sqrt{2(b-\beta)} \int \frac{dt}{E} - \sqrt{2(\alpha-\beta)} \int \frac{dt}{(1-t^2)E}$$

$$= I^{(1)} + I^{(2)} + I^{(3)}$$

where

$$E = [\pm (A_1 t^2 - B_1)(-A_2 t^2 + B_2)]^{1/2}.$$

α, β are the roots of the quadratic equation

$$(1+b)x^2 - 2(b+k^2)x + (1+b)k^2 = 0$$

α being greater than β . $A_1 = 1+b-2\beta$, $B_1 = 1+b-2\alpha$, $A_2 = \beta$, $B_2 = \alpha$.

$I^{(1)}$ is an elementary integral, while $I^{(2)}$ and $I^{(3)}$ are elliptic integrals of the first and third kinds respectively. The following results can now be easily established, if $0 < k < b < 1$:

- (i) $\alpha\beta = k^2$,
- (ii) $b < \alpha < 1$,
- (iii) $k^2 < \beta < k$,
- (iv) $A_1 = \{(1-k^2)^{1/2} + (b^2-k^2)^{1/2}\}^2/(1+b) > 0$,
- (v) $B_1 = \{(1-k^2)^{1/2} - (b^2-k^2)^{1/2}\}^2/(1+b) > 0$,
- (vi) $A_1 B_2 - A_2 B_1 = (1+b)(\alpha-\beta) > 0$.

It will therefore be possible to rationalize the denominator by the substitution $(A_2/B_2)^{1/2} t = dn u$ where the square of the complementary modulus $\kappa'^2 = A_2 B_1 / A_1 B_2$.

When this substitution is made, and the limits of integration are determined, we have

$$\begin{aligned}
 I_1^{(2)} &= \left(\frac{2}{A_1 B_2} \right)^{1/2} (b - \beta) K, & I_2^{(2)} &= \left(\frac{2}{A_1 B_2} \right)^{1/2} (b - \beta) 2K' \\
 I_1^{(3)} &= \left(\frac{2}{A_1 B_2} \right)^{1/2} \beta \int_{2iK'}^{K+2iK'} \left(1 - \frac{\alpha}{\alpha - \beta} \kappa^2 \operatorname{sn}^2 u \right)^{-1} du \\
 I_2^{(3)} &= - \left(\frac{2}{A_1 B_2} \right)^{1/2} 2\beta i \int_0^{iK'} \left(1 - \frac{\alpha}{\alpha - \beta} \kappa^2 \operatorname{sn}^2 u \right)^{-1} du.
 \end{aligned}$$

It can be shown by very simple arguments that for the above limits of integration both $I_1^{(1)}$ and $I_2^{(2)}$ vanish.

To bring $I^{(3)}$ into the standard form we write

$$\kappa \operatorname{sn} \gamma = \left(\frac{\alpha - \beta}{\alpha} \right)^{1/2} \quad \text{with} \quad 0 < \gamma < K.$$

This is permissible, since $\alpha - \beta / \kappa^2 \alpha = (1 + b - 2\beta) / (1 + b) < 1$. With this meaning of γ ,

$$I_1^{(3)} = -KZ(\gamma), \quad I_2^{(3)} = -2K'Z(\gamma) + \pi(1 - \gamma/K)$$

where $Z(\gamma)$ is Jacobi's zeta-function.

The final results are thus quite simple and can be used with advantage in numerical work. The correctness of these expressions can be tested by giving b and k special values which make an elementary integration possible. The values chosen by the author were $b = 1$, $k = 0$, $b = k$.

REFERENCES

- GOLDEN, S., 1948 a, *J. Chem. Phys.*, **16**, 78; 1948 b, *Ibid.*, **16**, 250.
 HAINER, R. M., CROSS, P. C., and KING, G. W., 1949, *J. Chem. Phys.*, **17**, 826.
 HERZBERG, G., 1951, *Molecular Spectra and Molecular Structure*, Vol. 2, pp. 229, 230, 488, 489 (New York: Van Nostrand).
 KING, G. W., 1947, *J. Chem. Phys.*, **15**, 820.
 RANDALL, H. M., DENNISON, D. M., GINSBURG, N., and WEBER, L. R., 1937, *Phys. Rev.*, **52**, 160.
 SHAFFER, W. H., and NIELSEN, H. H., 1939, *Phys. Rev.*, **56**, 188.
 WENTZEL, G., 1926, *Z. Phys.*, **38**, 518.
 WILSON, E. B., and HOWARD, J. B., 1936, *J. Chem. Phys.*, **4**, 260.

Rotational Analysis of the β Band System of the NS Molecule

By R. F. BARROW, G. DRUMMOND AND P. B. ZEEMAN*

Physical Chemistry Laboratory, Oxford University

* Merensky Institute for Physics, University of Stellenbosch

MS. received 5th January 1954

Abstract. Rotational analyses of the 1,0,0,0 and 0,1 bands of the β system of NS have been carried out. It is found that the transition is ${}^2\Delta$ - ${}^2\Pi$ and not ${}^2\Pi$ - ${}^2\Pi$ as has hitherto been supposed. The rotational constants of the state $A^2\Delta$ are: $B_v = 0.6960_4 - 0.0069_5(v + \frac{1}{2})$; $r_e = 1.576_8 \text{ \AA}$. In the same spectral region there occur the $c^2\Sigma$ - $x^2\Pi$ system (γ -bands) and other weaker bands which may belong to a system $B({}^2\Pi)$ - $x^2\Pi$.

§ 1. INTRODUCTION

FOWLER and BAKKER (1932) obtained two systems of NS in emission, and designated them γ and β on the grounds of their general similarity to the γ and β systems of NO. The vibrational analyses showed that both systems have the same lower state: that this state is the ground state of NS has been shown by the observation of the 1,0 and 0,0 bands of the γ system in absorption (Barrow, Downie and Laird 1952). The double double-headed violet-degraded bands of the γ system were attributed to a $B^2\Sigma^+ - x^2\Pi$ transition, and this was later confirmed by the independent rotational analyses of Zeeman (1951) and Barrow, Downie and Laird (1952). Fowler and Bakker's vibrational analysis of the red-degraded pairs of bands of the β system was confirmed by Zeeman.

There are in addition a number of red-degraded bands in the region 2380 to 2770 \AA , whose intensities appear to bear a constant relation to those of the β system, but which do not fit into the vibrational analysis of this system. These bands have been obtained under a variety of conditions and seem also to arise from NS.

For many years it has been considered that the β system of NS, by analogy with NO, arises from a ${}^2\Pi$ - ${}^2\Pi$ transition. However, a comparison reveals certain differences which lead one to doubt whether the two systems are indeed analogous. For example: (i) The ratio of the force constants of the upper states to the ground states, taking the mean values for the doublet components, are 0.61 and 0.30 for NS and NO respectively; thus there is much stronger binding in the upper state relative to the ground state for NS than for NO. (ii) The vibrational constants for the two doublet components of the upper state in NO are nearly equal, but in NS they differ appreciably. This produces an anomalous effect in NS, since with the ground state doublet separation 223 cm^{-1} the doublet separation in the upper state A is approximately 38 cm^{-1} when obtained from the $v' = 0$ level and approximately 24 cm^{-1} from the $v' = 1$ level.

Barrow, Downie and Laird (1952), from a partial rotational analysis of the β system based on moderate dispersion plates, have suggested that the transition may be ${}^2\Delta-{}^2\Pi$. No rotational analysis of a ${}^2\Delta-{}^2\Pi$ transition between states in Hund's coupling case *a* appears yet to have been made, and the authors' interest was aroused in a complete analysis of the β NS system from high dispersion plates. In addition, an analysis of one of the unassigned bands could lead to the identification of the transition responsible for this groups of bands. Plates photographed on 4th, 6th and 8th orders of a 21-ft concave grating (Zeeman 1951) were used for the analysis.

§ 2. INTERPRETATION OF THE ROTATIONAL STRUCTURE OF THE β SYSTEM

The ${}^2\Pi$ ground state has $A \sim 223 \text{ cm}^{-1}$ and $Y \sim 288$, and approximates to Hund's case *a*. The observed separation from the band-heads with $v' = 0$ is 185 cm^{-1} , so that the splitting in the upper state is $223 - 185 = 38 \text{ cm}^{-1}$ (low-lying inverted states are not expected). This doublet separation is large enough to suggest that the state is fairly close to case *a* at least for low J values. If the selection rules $\Delta\Lambda = 0, \pm 1$ and $\Delta S = 0$ hold, then the possible transitions for the β systems are

$${}^2\Sigma-{}^2\Pi(a), \quad {}^2\Pi(a)-{}^2\Pi(a), \quad {}^2\Delta(a)-{}^2\Pi(a).$$

The first, however, is ruled out since the observed doublet separation is too big for a Σ state, so there remain the other two possibilities. ${}^2\Pi(a)-{}^2\Pi(a)$ will consist of the sub-bands ${}^2\Pi_{3/2}-{}^2\Pi_{3/2}$ and ${}^2\Pi_{1/2}-{}^2\Pi_{1/2}$, each possessing strong P and R branches and weak Q branches. All the rotational lines are subject to Λ -doubling.

For ${}^2\Delta(a)-{}^2\Pi(a)$ the sub-bands are ${}^2\Delta_{5/2}-{}^2\Pi_{3/2}$ and ${}^2\Delta_{3/2}-{}^2\Pi_{1/2}$, each consisting of Λ -doubled P, Q and R branches with the Q branches the most intense.

Preliminary Examination

Examination of the 0, 0 band revealed the following features: (i) The short-wavelength sub-band shows distinct doubling away from the head, which is not obvious in the long-wavelength sub-band. This suggests that the former is ${}^2\Delta_{3/2}-{}^2\Pi_{1/2}$ or ${}^2\Pi_{1/2}-{}^2\Pi_{1/2}$, and that the upper doublet state is regular. (ii) A series of strong lines seem to form one branch, and there appear to be two other branches, one of them fairly weak. The strong branch is probably a Q branch, and the transition ${}^2\Delta-{}^2\Pi$.

Detailed Analysis

The 0, 0, 1, 0 and 0, 1 bands were measured on the sixth order plates, where the dispersion was about 0.42 \AA mm^{-1} and in a favourable case two lines 0.25 cm^{-1} apart were just resolved. The measured lines and their assignments appear in tables 1-6.

The analysis proceeded on the assumption that the transition is ${}^2\Delta(a)-{}^2\Pi(a)$. Some difficulty was experienced in the identification of the branches in parts of the 1, 0 ${}^2\Delta_{3/2}-{}^2\Pi_{1/2}$, ${}^2\Delta_{5/2}-{}^2\Pi_{3/2}$, and 0, 1 ${}^2\Delta_{5/2}-{}^2\Pi_{3/2}$ sub-bands due to overlapping by the 0, 2 γ band, 2, 1 β band and 1, 2 β band respectively. The Q branch in each sub-band was easily picked out since it consisted of most of the stronger lines. The analysis was then carried out without difficulty: it was confirmed by a comparison of values of $\Delta_1 F''(J)$ with those calculated from Zeeman's (1951) figures for B''_{eff} and D'' . The agreement between the $\Delta_1 F''(J)$ values is such as to leave no doubt that the transition is correctly ${}^2\Delta-{}^2\Pi$ and that the present

identification of the branches is correct. Unfortunately the structure right up to the R heads is not clearly resolved, so that it is not possible to confirm the nature of the transition by the criterion of missing lines.

Evaluation of Rotational Constants

In view of the good agreement of the values of $\Delta_1 F''(J)$ and of $\Delta_2 F''(J)$, Zeeman's values for the rotational constants for the ground state were accepted.

Table 1. 0, 0 Band ${}^2\Delta_{5/2}-{}^2\Pi_{3/2}$

J	P(J)	Q(J)	R(J)	J	P(J)	Q(J)	R(J)
$3\frac{1}{2}$		39688.78		$33\frac{1}{2}$	39557.59	39604.53	39652.99*
$4\frac{1}{2}$	39682.22*	88.18*		$34\frac{1}{2}$	51.31	599.53	49.31
$5\frac{1}{2}$	79.78	87.30		$35\frac{1}{2}$	44.92*	94.48*	45.37
$6\frac{1}{2}$	77.01	86.36*		$36\frac{1}{2}$	38.12*	89.10*	41.67
$7\frac{1}{2}$	74.62*	84.95		$37\frac{1}{2}$	31.59	83.98	37.58
$8\frac{1}{2}$	72.45*	83.80	39696.81H	$38\frac{1}{2}$	24.45	78.29	33.44
$9\frac{1}{2}$	68.81	82.22*	96.81H	$39\frac{1}{2}$	17.50	72.56	29.10
$10\frac{1}{2}$	65.73*	80.53*		$40\frac{1}{2}$	10.19	66.79	24.63
$11\frac{1}{2}$	62.54*	78.65*		$41\frac{1}{2}$	02.94	60.78	19.77
$12\frac{1}{2}$	59.27*	76.68		$42\frac{1}{2}$	495.36	54.55	15.16
$13\frac{1}{2}$	55.70	74.62*		$43\frac{1}{2}$	87.60	48.25	09.89
$14\frac{1}{2}$	52.14	72.45*	94.06	$44\frac{1}{2}$	79.79	41.70	04.89
$15\frac{1}{2}$	48.28	69.97	93.27	$45\frac{1}{2}$	71.71	35.12	599.89
$16\frac{1}{2}$	44.47	67.57	92.02	$46\frac{1}{2}$	63.60	28.42	94.48*
$17\frac{1}{2}$	40.43	64.92	90.62	$47\frac{1}{2}$	55.36	21.29	89.10*
$18\frac{1}{2}$	36.26	61.96	89.50	$48\frac{1}{2}$	46.84	14.21	83.02
$19\frac{1}{2}$	31.85	59.27*	88.18*	$49\frac{1}{2}$	38.15	06.99	77.55
$20\frac{1}{2}$	27.64	56.27*	86.36*	$50\frac{1}{2}$	29.26	499.92*	71.18
$21\frac{1}{2}$	22.98*	52.99*	84.66	$51\frac{1}{2}$	20.79	92.13	64.83
$22\frac{1}{2}$	18.55*	49.75	82.65	$52\frac{1}{2}$		84.20	58.21
$23\frac{1}{2}$	13.39	46.32	80.53*	$53\frac{1}{2}$	02.15	76.31	51.81
$24\frac{1}{2}$	08.42	42.73	78.65*	$54\frac{1}{2}$	392.59	68.29	44.92*
$25\frac{1}{2}$	03.13	39.07	76.35	$55\frac{1}{2}$	83.08	59.84	38.12*
$26\frac{1}{2}$	598.03	35.26	73.94	$56\frac{1}{2}$	73.10	51.36	31.07
$27\frac{1}{2}$	92.73	31.24	71.26	$57\frac{1}{2}$		42.64	23.54
$28\frac{1}{2}$	87.18	27.20	68.54	$58\frac{1}{2}$		33.86	15.99
$29\frac{1}{2}$	81.56	22.98*	65.73*	$59\frac{1}{2}$		24.86	08.18
$30\frac{1}{2}$	75.86	18.55*	62.54*	$60\frac{1}{2}$		15.42	499.92*
$31\frac{1}{2}$	69.92	14.03	59.27*	$61\frac{1}{2}$		05.93	91.48
$32\frac{1}{2}$	63.83	09.27	56.27*	$62\frac{1}{2}$		396.10	83.27
				$63\frac{1}{2}$		85.95	73.99
				$64\frac{1}{2}$		75.39	65.61

* = blended line.

The best methods of evaluating the upper state constants is to utilize the strong Q branches. The calculations were done in two ways:

(1) For case a we have, neglecting terms in ΔD ,

$$Q_1(J) = \nu_0^{(1)} + \Delta B_{\text{eff}}^{(1)} J(J+1)$$

$$Q_2(J) = \nu_0^{(2)} + \Delta B_{\text{eff}}^{(2)} J(J+1)$$

where $\Delta B_{\text{eff}} = [B'_{\text{eff}} - (B''_{\text{eff}} + \delta_c)]$ and $Q_1(J)$ is the mean of the Λ doublets for the ${}^2\Delta_{3/2}-{}^2\Pi_{1/2}$ sub-band.

Table 2. 0, 0 Band ${}^2\Delta_{3/2}-{}^2\Pi_{1/2}$

J	$P_{cd}(J)$	$P_{dc}(J)$	$Q_d(J)$	$Q_c(J)$	$R_{cd}(J)$	$R_{dc}(J)$
$2\frac{1}{2}$			39875.12		39879.11*	
$3\frac{1}{2}$			74.39		80.30*	
$4\frac{1}{2}$	39867.34*		73.82*		81.04*	
$5\frac{1}{2}$			72.90		—	
$6\frac{1}{2}$	63.02		71.79*		81.90	
$7\frac{1}{2}$	60.22		70.30*		81.90H	
$8\frac{1}{2}$	57.33		68.98		81.90	
$9\frac{1}{2}$	54.34*		67.34*		—	
$10\frac{1}{2}$	51.51*		65.78*		81.04*	
$11\frac{1}{2}$	48.06*		63.55*		80.30*	
$12\frac{1}{2}$	44.66		61.31		79.77	
$13\frac{1}{2}$	—		59.23		79.11*	
$14\frac{1}{2}$	36.91		56.79		77.93	
$15\frac{1}{2}$	32.71		54.34*		76.88	
$16\frac{1}{2}$	29.33		51.51*		75.57	
$17\frac{1}{2}$	24.59		48.63		73.82*	
$18\frac{1}{2}$	20.19		45.45*		71.79*	
$19\frac{1}{2}$	15.53		42.04*		70.30*	
$20\frac{1}{2}$	10.66		38.65*		67.98	
$21\frac{1}{2}$	05.36*		35.15		65.78*	
$22\frac{1}{2}$	00.37		31.36		63.55*	
$23\frac{1}{2}$	795.15*		27.31		60.74	
$24\frac{1}{2}$	89.76*		23.27		58.41	
$25\frac{1}{2}$	84.36		19.09		55.24	
$26\frac{1}{2}$	78.10		14.53		52.24	
$27\frac{1}{2}$	72.30		09.92		49.10	
$28\frac{1}{2}$	66.43	66.06	05.36*	05.20	45.45*	
$29\frac{1}{2}$	59.98	59.65	00.37	00.16	42.04*	
$30\frac{1}{2}$	53.51	53.03	795.47	795.15	38.65*	
$31\frac{1}{2}$	47.11	46.73	89.97	89.76*	34.45	
$32\frac{1}{2}$	40.18	39.70	84.67	84.36*	30.52	
$33\frac{1}{2}$	33.39	33.09	79.41	79.06	26.35	
$34\frac{1}{2}$	26.28	25.94	73.66	73.37	21.98	
$35\frac{1}{2}$	19.02	18.75	67.88	67.51	17.83	
$36\frac{1}{2}$	12.60	11.67	61.82	61.45	12.84	12.42
$37\frac{1}{2}$	04.49	04.15	55.88	55.30	08.02	08.02
$38\frac{1}{2}$			49.42	49.07	03.50	03.01
$39\frac{1}{2}$			43.09	42.66	798.07	797.54
$40\frac{1}{2}$			36.49	36.04	93.47	92.91
$41\frac{1}{2}$			29.80	29.39	87.94	87.54
$42\frac{1}{2}$			23.01	22.45	82.25	82.09
$43\frac{1}{2}$			15.82	15.29	76.60	76.60
$44\frac{1}{2}$			08.76	08.13	71.00	70.54
$45\frac{1}{2}$			01.29	00.77		

* = blended line.

A preliminary value of ΔB_{eff} was first found for each sub-band by plotting $Q_1(J)$ and $Q_2(J)$ respectively against $J(J+1)$. Attempts were then made to adjust ΔB until a constant value of ν_0 was obtained for all Q lines in a given sub-band. It was found unnecessary to introduce a ΔD term, so that $D' \sim D''$. However, the values of the ν_0 derived in this way are not constant with J .

 Table 3. 0, 1 Band ${}^2\Delta_{5/2}-{}^2\Pi_{3/2}$

J	P(J)	Q(J)	R(J)	J	P(J)	Q(J)	R(J)
$4\frac{1}{2}$		38484.16		$34\frac{1}{2}$	38355.02	38403.29*	38452.99*
$5\frac{1}{2}$		83.56*		$35\frac{1}{2}$	48.91	398.62*	49.57*
$6\frac{1}{2}$		82.44		$36\frac{1}{2}$	42.88	93.80*	46.16*
$7\frac{1}{2}$		81.39		$37\frac{1}{2}$	36.54	88.88*	42.73*
$8\frac{1}{2}$		80.20*		$38\frac{1}{2}$	30.04	83.84*	39.13
$9\frac{1}{2}$		78.62*	38493.31H	$39\frac{1}{2}$	23.38	78.61	35.17
$10\frac{1}{2}$		77.32	93.31H	$40\frac{1}{2}$	16.72	73.21	31.33
$11\frac{1}{2}$		75.67		$41\frac{1}{2}$	09.92	67.77	27.16
$12\frac{1}{2}$	38456.28*	73.86		$42\frac{1}{2}$	02.95	62.12	22.86
$13\frac{1}{2}$	52.99*	71.89*		$43\frac{1}{2}$	295.75	56.35	18.55
$14\frac{1}{2}$	49.57*	69.82*	91.25	$44\frac{1}{2}$	88.47	50.53	13.71
$15\frac{1}{2}$	46.16*	67.55*	90.68	$45\frac{1}{2}$	81.13	44.43	09.16
$16\frac{1}{2}$	42.34	65.39	89.81	$46\frac{1}{2}$	73.60	38.22	04.43
$17\frac{1}{2}$	38.39	62.97	88.80	$47\frac{1}{2}$	65.96	32.03	399.14
$18\frac{1}{2}$	34.49	60.48	87.72	$48\frac{1}{2}$	57.99	25.48	94.13
$19\frac{1}{2}$	30.58	57.73	86.64	$49\frac{1}{2}$	49.63	18.77	89.39
$20\frac{1}{2}$	26.19	54.97	85.11	$50\frac{1}{2}$	41.55	12.31	83.84*
$21\frac{1}{2}$	22.16	52.06	83.56*	$51\frac{1}{2}$		05.10	77.81*
$22\frac{1}{2}$	17.55	49.13	82.05	$52\frac{1}{2}$		297.92	72.27*
$23\frac{1}{2}$	13.00	45.93	80.20*	$53\frac{1}{2}$		90.71	66.45
$24\frac{1}{2}$	08.28	42.73*	78.62*	$54\frac{1}{2}$		83.34	60.09
$25\frac{1}{2}$	03.29*	39.33	76.50	$55\frac{1}{2}$		75.78	53.88
$26\frac{1}{2}$	398.62*	35.88	74.27	$56\frac{1}{2}$		68.16	47.35
$27\frac{1}{2}$	93.80*	32.24	71.89*	$57\frac{1}{2}$		60.07	40.58
$28\frac{1}{2}$	88.88*	28.41	69.82*	$58\frac{1}{2}$		51.69	33.85
$29\frac{1}{2}$	83.14	24.58	67.55*	$59\frac{1}{2}$		43.22	
$30\frac{1}{2}$	77.81*	20.58	64.72				
$31\frac{1}{2}$	72.27*	16.41	62.06				
$32\frac{1}{2}$	66.73	12.19	59.19				
$33\frac{1}{2}$	60.90	07.73	56.28*				

* = blended line.

Although there is a considerable range of J values over which ν_0 is constant for the 0, 0 and 0, 1 bands, there is in particular a drift at high J values, which occurs in opposite senses for the two sub-bands. The fact that identical deviations are observed for the 0, 0 and 0, 1 bands confirms the rotational analyses for these bands. The values of ν_0 calculated for the 1, 0 band are still more

Table 4. 0, 1 Band ${}^2\Delta_{3/2}-{}^2\Pi_{1/2}$

J	$P_{cd}(J)$	$P_{dc}(J)$	$Q_d(J)$	$Q_c(J)$	$R_{cd}(J)$	$R_{dc}(J)$
$3\frac{1}{2}$			38670.59*			
$4\frac{1}{2}$			69.73			
$5\frac{1}{2}$			68.89*			
$6\frac{1}{2}$			67.92			
$7\frac{1}{2}$	38656.31*		66.72		38678.21H	
$8\frac{1}{2}$	53.49		65.09*		78.21H	
$9\frac{1}{2}$	50.82		64.09			
$10\frac{1}{2}$	47.57		62.39*			
$11\frac{1}{2}$	44.87		60.34*			
$12\frac{1}{2}$	41.49		58.97			
$13\frac{1}{2}$	37.80		56.31*		76.68	
$14\frac{1}{2}$	33.87*		54.46		75.59	
$15\frac{1}{2}$	30.47*		51.59		74.28	
$16\frac{1}{2}$	26.45*		49.04		73.19	
$17\frac{1}{2}$	22.59*		46.48*		71.72	
$18\frac{1}{2}$	18.25		43.48*		70.59*	
$19\frac{1}{2}$	13.58		40.35*		68.89*	
$20\frac{1}{2}$	08.92*		37.25	37.10*	66.72	
$21\frac{1}{2}$	04.41*		33.87*	33.87*	65.09*	
$22\frac{1}{2}$	599.71		30.47*	30.47*	62.39*	
$23\frac{1}{2}$	94.54*		26.45*	26.45*	60.34*	
$24\frac{1}{2}$	89.21*		22.92	22.59*	57.81	
$25\frac{1}{2}$	84.60*	84.14*	19.12	18.94	55.54	
$26\frac{1}{2}$	78.79*	78.37	15.01	14.31	52.69	
$27\frac{1}{2}$	73.28*	72.66	10.72	10.37	49.77	
$28\frac{1}{2}$	67.49	67.08	06.36	05.87	46.48*	
$29\frac{1}{2}$	61.22	61.22	01.90	01.55	43.48*	42.98*
$30\frac{1}{2}$	55.44	55.44	597.12	596.58	40.35*	40.35*
$31\frac{1}{2}$	48.92*	48.92*	92.42	91.86	37.10*	36.57
$32\frac{1}{2}$	42.93*	42.36*	87.42	87.20	32.73	32.73
$33\frac{1}{2}$	36.61*	36.06*	82.17	81.83	29.31	29.31
$34\frac{1}{2}$	29.85*	29.85*	77.19	76.60	25.49	25.49
$35\frac{1}{2}$	23.24*	22.72	71.66	71.17	21.26	20.96
$36\frac{1}{2}$	16.03	16.03	66.14	65.83	17.54	17.25
$37\frac{1}{2}$	09.28	09.28	60.61	60.25	12.75	12.75
$38\frac{1}{2}$	02.08	01.72	54.71	54.14	08.92*	08.49
$39\frac{1}{2}$			48.92*	48.31	04.41*	03.91
$40\frac{1}{2}$			42.93*	42.36*	599.41	598.88
$41\frac{1}{2}$			36.61*	36.06*	94.54*	94.54*
$42\frac{1}{2}$			30.48	29.85*	89.21	89.21*
$43\frac{1}{2}$			23.85	23.24*	84.60*	84.14*
$44\frac{1}{2}$			17.34	16.72	78.79*	78.79*
$45\frac{1}{2}$			10.36	09.89	73.91	73.28*
$46\frac{1}{2}$			03.41	02.99		
$47\frac{1}{2}$			496.52	495.95		

* = blended line.

irregular, and the values of ν_0 can only be estimated approximately. It seemed possible that the drift at high values of J might arise from spin uncoupling in the upper state.

(2) The application of the Hill and Van Vleck equations (Herzberg 1950) for any degree of spin uncoupling was therefore considered. In the present case

$$\frac{1}{2}[\mathbf{Q}_1(J) + \mathbf{Q}_2(J)] = \bar{\nu}_0 + \Delta B_v J(J+1) - \frac{15}{4}B_v' + \frac{3}{4}B_v'' - \frac{1}{2}\Delta D_v[(J+1)^4 + J^4]$$

where $\bar{\nu}_0$ is the origin of the whole band, $\Delta B_v = B_v' - B_v''$ and $\Delta D_v = D_v' - D_v''$.

 Table 5. 1, 0 Band ${}^2\Delta_{5/2} - {}^2\Pi_{3/2}$

J	P(J)	Q(J)	R(J)	J	P(J)	Q(J)	R(J)
$7\frac{1}{2}$			40628.09H	$28\frac{1}{2}$	40518.30*	40558.34	40598.47
$8\frac{1}{2}$		40614.82*	28.09H	$29\frac{1}{2}$	12.93*	53.62	96.16
$9\frac{1}{2}$	40599.78*	13.22	28.09H	$30\frac{1}{2}$	06.45*	48.70*	92.98
$10\frac{1}{2}$	97.18*	11.62	28.09H				
				$31\frac{1}{2}$	00.22	44.27*	89.55
$11\frac{1}{2}$	94.53*	10.21*		$32\frac{1}{2}$	493.90	38.95	85.50*
$12\frac{1}{2}$	90.77	08.25		$33\frac{1}{2}$	87.39	33.83	82.05*
$13\frac{1}{2}$	87.45	06.35	26.73	$34\frac{1}{2}$	80.62	28.29	77.56
$14\frac{1}{2}$	84.00	04.31	25.96	$35\frac{1}{2}$	73.53	22.63	73.13
$15\frac{1}{2}$	80.18	02.17*	25.17	$36\frac{1}{2}$	66.57	16.80	68.67*
$16\frac{1}{2}$	76.48	599.78*	24.10	$37\frac{1}{2}$	59.05	10.90	64.06*
$17\frac{1}{2}$	72.62	97.18*	23.11	$38\frac{1}{2}$	51.59	04.64	59.45
$18\frac{1}{2}$	68.67*	94.53*	21.69	$39\frac{1}{2}$	44.10	498.28	54.33
$19\frac{1}{2}$	64.06*	91.61	20.26	$40\frac{1}{2}$	36.02	91.74	48.70*
$20\frac{1}{2}$	59.89	88.45	18.74				
				$41\frac{1}{2}$	27.91	85.00	44.27*
$21\frac{1}{2}$	55.43	85.50*	16.74	$42\frac{1}{2}$	19.75	78.38	38.14
$22\frac{1}{2}$	50.38	82.05*	14.82*	$43\frac{1}{2}$	11.14	70.99	32.11
$23\frac{1}{2}$	45.54	78.36	12.85	$44\frac{1}{2}$	02.47	63.58	25.98
$24\frac{1}{2}$	40.47	74.76	10.21*	$45\frac{1}{2}$	393.76	56.01	18.30*
$25\frac{1}{2}$	35.30	70.91	07.97	$46\frac{1}{2}$		48.20	12.93*
$26\frac{1}{2}$	29.75	66.81	05.37	$47\frac{1}{2}$		40.25	06.45*
$27\frac{1}{2}$	24.29	62.64	02.17*	$48\frac{1}{2}$		31.74	
				$49\frac{1}{2}$		22.93	

* = blended line.

Using this expression it should be possible to obtain a value of ΔB which with a reasonable value of ΔD leads to a constant origin in each band. The calculated value of $\bar{\nu}_0$ still showed deviations at high J values, implying that the drift in ν_0 was not entirely due to spin uncoupling: this is considered below (§ 3).

The results of these calculations are collected in table 7. The values of B_v' obtained by the two treatments are seen to be in good agreement. The values of $\Delta G''_{1/2}(1) = 1204.1_2 \text{ cm}^{-1}$ and $\Delta G''_{1/2}(2) = 1204.0_3$ agree well with Zeeman's values, 1204.1_0 and 1204.1_9 cm^{-1} , respectively, from the analysis of the γ -bands. The value of $\Delta G''_{1/2}$ from $\bar{\nu}_0$ is satisfactorily close to these values, confirming that the origins of the 0, 0 and 0, 1 sub-bands have been correctly chosen.

Table 6. 1, 0 Band ${}^2\Delta_{3/2}-{}^2\Pi_{1/2}$

	$P_{cd}(J)$	$P_{dc}(J)$	$Q_d(J)$	$Q_c(J)$	$R_{cd}(J)$	$R_{dc}(J)$
$2\frac{1}{2}$					40824.19	
$3\frac{1}{2}$			40818.80		24.96	
$4\frac{1}{2}$	40811.81*		18.06*			
$5\frac{1}{2}$	09.68*		17.02			
$6\frac{1}{2}$	06.88*		15.81*		26.19H	
$7\frac{1}{2}$	03.93*		14.18*		26.19H	
$8\frac{1}{2}$	01.04		12.54			
$9\frac{1}{2}$	798.04		10.29		24.96	
$10\frac{1}{2}$	94.35		08.54		24.19	
$11\frac{1}{2}$	90.96		06.33		23.07	
$12\frac{1}{2}$	87.12		03.93*		21.99	
$13\frac{1}{2}$	83.08		01.36*		20.64	
$14\frac{1}{2}$	79.19		798.53*			
$15\frac{1}{2}$	74.67		95.66*		18.06*	
$16\frac{1}{2}$	69.96*		92.45		15.81*	
$17\frac{1}{2}$	65.56*		89.17		14.18*	
$18\frac{1}{2}$	61.14*		85.87		11.81*	
$19\frac{1}{2}$	56.00		82.18		09.68*	
$20\frac{1}{2}$	50.59		78.00		06.88*	
$21\frac{1}{2}$	44.89		74.07		03.93*	
$22\frac{1}{2}$	39.55*	39.24*	69.96*		01.36*	
$23\frac{1}{2}$	33.72*	33.31*	65.56*		798.53*	
$24\frac{1}{2}$	27.98*	27.98*	61.14*		95.66*	
$25\frac{1}{2}$	22.34*	21.91*	56.54		91.82	
$26\frac{1}{2}$	16.21*	15.72*	51.29		88.30	
$27\frac{1}{2}$	09.38*	09.38*	46.56		84.99	
$28\frac{1}{2}$	02.89*	02.89*	41.43		81.31	
$29\frac{1}{2}$	696.29	696.29	36.22	35.93	77.25	
$30\frac{1}{2}$	89.41	89.07	30.53	30.23	73.42	72.74
$31\frac{1}{2}$	82.07	81.81	25.00	24.70	69.11	68.49
$32\frac{1}{2}$	74.91	74.91	18.98	18.45	64.29	64.29
$33\frac{1}{2}$	67.32	67.32	13.16	12.66	59.71	59.21
$34\frac{1}{2}$	60.04	60.04	06.90	06.45	54.55	54.55
$35\frac{1}{2}$	52.35	52.35	00.39	00.03		
$36\frac{1}{2}$	44.29	44.29	694.15	694.15	44.89	44.46
$37\frac{1}{2}$	36.94	36.47	87.57	86.97	39.55*	39.24*
$38\frac{1}{2}$			80.33	80.00	33.72*	33.31*
$39\frac{1}{2}$			73.42	72.95	27.98*	27.54
$40\frac{1}{2}$			66.07	65.73	22.34*	21.91*
$41\frac{1}{2}$			58.58	58.58	16.21*	15.72*
$42\frac{1}{2}$			51.50	50.64	10.28	09.38*
$43\frac{1}{2}$			43.55	43.14	03.61	02.89*
$44\frac{1}{2}$			35.84	35.11		

* = blended line.

Table 7. Constants for the $A \ ^2\Delta-X \ ^2\Pi$ system of NS (cm^{-1})

Band	ν head	ν_0	$\bar{\nu}_0$
0, 0	$^2\Delta_{5/2} - ^2\Pi_{3/2}$	39881.90	39875.70
	$^2\Delta_{3/2} - ^2\Pi_{1/2}$	696.81	688.05
0, 1	$^2\Delta_{5/2} - ^2\Pi_{3/2}$	38678.21	38671.58
	$^2\Delta_{3/2} - ^2\Pi_{1/2}$	493.31	484.02
1, 0	$^2\Delta_{5/2} - ^2\Pi_{3/2}$	40826.19	40819.56
	$^2\Delta_{3/2} - ^2\Pi_{1/2}$	628.09	622.47
Band	$B'_{\text{eff}}^{(1)}$	$B'_{\text{eff}}^{(2)}$	B_v' (mean of $^{(1)}$ and $^{(2)}$)
0, 0	0.6839 ₆	0.7010 ₉	0.6925 ₂
0, 1	0.6840 ₄	0.7010 ₉	0.6925 ₆
1, 0	0.6742 ₇	0.6969 ₂	0.6855 ₉
		$\Delta G''_{1/2} \cdot \nu_{0,0}^{(1)} - \nu_{0,1}^{(1)} = 1204.1_2$	
		$\nu_{0,0}^{(2)} - \nu_{0,1}^{(2)} = 1204.0_3$	
		$\bar{\nu}_{0,0} - \bar{\nu}_{0,1} = 1204.1_8$	
		$\Delta G'_{1/2} \cdot \nu_{1,0}^{(1)} - \nu_{0,0}^{(1)} = 943.8_6$	
		$\nu_{1,0}^{(2)} - \nu_{0,0}^{(2)} = 934.4_2$	
		$\bar{\nu}_{1,0} - \bar{\nu}_{0,0} = 938.4_7$	

NOTE: The constants ν_0 and B'_{eff} were obtained from treatment (1); $\bar{\nu}_0$ and \bar{B}' from treatment (2). See pp. 367, 371.

§ 3. PERTURBATIONS

A deviation of either the upper or ground state rotational levels from the rotational formula will be reflected in the values of ν_0 and of $\bar{\nu}_0$. The $^2\Pi$ ground state levels are unperturbed, so that any variation in ν_0 or $\bar{\nu}_0$ must be attributed to perturbations in the upper state rotational levels.

The observed rotational effects may be summarized as follows:

$^2\Delta_{5/2}$	Perturbations	
$\nu' = 0$	$J \leq 20.5$	$J \geq 47.5$
$\nu' = 1$	$J \leq 20.5$	$J \geq 31.5$

In neither of the sub-bands involving $^2\Delta_{5/2}$ does the observed head-origin separation agree with the calculated separation, thus:

Band	Head-origin separation (cm^{-1})	
	calc.	obs.
0, 0	7.52	8.76
0, 1	8.17	9.29

In $v' = 1$ the difference between observed and calculated separations indicates a perturbation of about 1.4 cm^{-1} of the lines forming the head. There are also intensity anomalies in lines coming from this sub-level.

${}^2\Delta_{3/2}$	Perturbations	
$v' = 0$	$J \geq 30.5$	
$v' = 1$	$J \leq 9.5$	$J \geq 26.5$

In $v' = 0$ the calculated head-origin separation agrees with that observed; in $v' = 1$ the separations indicate a head-shift of about 1 cm^{-1} .

The Upper State Vibrational Intervals

The values $\Delta G'_{1/2}{}^{(1)} = 943.8_6$ and $\Delta G'_{1/2}{}^{(2)} = 934.4_2 \text{ cm}^{-1}$ call for some comment. Indeed the vibrational constants for the ${}^2\Delta$ state are anomalous. Bands to $v' = 2$ are known; the constants derived from band-head measurements are as follows:

	ω_0	$x_0\omega_0$
${}^2\Delta_{5/2}$	935.60	4.80
${}^2\Delta_{3/2}$	953.35	8.65

Small differences in ω have been established between the ${}^2\Pi_{1/2}$ and ${}^2\Pi_{3/2}$ sub-states of such molecules as ScO, YO, CaF, SrF, etc., but these differences do not exceed 2 cm^{-1} . For no molecule with small doublet splitting have the vibrational constants for the sub-states been found to differ as widely as they do in the present case.* The effect may be seen most clearly from the values of A for the different vibrational levels of the ${}^2\Delta$ state: they are 35.3_8 , 25.9_4 and 18.1 cm^{-1} for $v = 0, 1$ and 2 respectively.

The most natural explanation of these anomalies is that they are caused by perturbations which shift not only the lines of low J value but the origins of the sub-bands themselves. Since no abnormal Λ -doubling effects have been observed (see §4), it appears that the perturbing state is most probably ${}^2\Pi$ or ${}^2\Delta$. The unexpected regular variation of A with v in the state ${}^2\Delta$ suggests that if only one perturbing state is responsible for the variation, then its vibrational intervals are comparable with those of the ${}^2\Delta$ state.

It is doubtful if further progress in the elucidation of these effects can be made without very high resolution spectrograms at low rotational temperatures.

§4. Λ -DOUBLING

No Λ -doubling is observed in any line of the ${}^2\Delta_{5/2}$ - ${}^2\Pi_{3,2}$ sub-bands, as might have been expected. Λ -doubling certainly exists in the ${}^2\Delta_{3/2}$ - ${}^2\Pi_{1/2}$ sub-bands and since it has already been shown that doubling occurs in the ${}^2\Pi_{1/2}$ state, it remains to be shown whether or not there is any in the ${}^2\Delta_{3/2}$ state. The examination of suitable differences led, in fact, to the conclusion that no Λ -doubling could be detected in ${}^2\Delta_{3/2}$. The Λ -doubling in the ${}^2\Pi_{1/2}$ state is therefore given directly for each J level by the separations

$$Q_d(J) - Q_c(J) = \Delta\nu_{cd}(J) = P_{cd}(J) - P_{dc}(J) = R_{cd}(J) - R_{dc}(J).$$

* Considerable differences in the values of ω may of course arise for molecular states of large splitting approaching Hund's case c .

For the case of pure precession, for a single electron, the theoretical treatment (Mulliken and Christy 1931) leads to

$$p = \pm \frac{2A}{B_v} l(l+1)/\nu(\Pi\Sigma). \quad \dots\dots(1)$$

Here B_v is the value for the state $x^3\Pi$ and $\nu(\Pi\Sigma)$ is the energy of the interacting $^2\Sigma$ state above the $^2\Pi$ state: the + sign goes with a $^2\Sigma^+$ state, the - sign with $^2\Sigma^-$. For $^2\Pi_{1/2}$ in case *a*

$$\Delta\nu_{dc} \simeq \pm p(J + \frac{1}{2}) \quad \dots\dots(2)$$

where the minus sign goes with a positive value of A .

Using relation (2), we obtain

$$p(v''=0) = +0.011, \quad p(v''=1) = +0.013 \text{ cm}^{-1}.$$

Zeeman's measurements on the γ system yield

$$p(v''=0) = +0.011, \quad p(v''=1) = +0.009,$$

in satisfactory agreement.

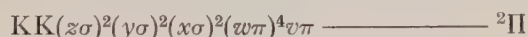
Since the Π state is the ground state, $\nu(\Pi\Sigma)$ is negative: A is positive and the right-hand side of (1) must therefore have a negative sign introduced, indicating that the interaction of the $^2\Pi$ state is not with the known upper state $c^2\Sigma^+$, as might have been expected, but with an unknown $^2\Sigma^-$ state. It is therefore impossible to calculate p from equation (1).

A similar situation occurs in NO (Mulliken and Christy 1931), and it may be noted that the value of p found for NS is much the same as the experimental value of $+0.015 \text{ cm}^{-1}$ for NO.

§ 5. THE ELECTRON CONFIGURATION OF NS

Information about the electronic states of NS is collected in table 8.

A lead in treating the states of this molecule is given by first considering the analogous molecule NO. The ground state is represented by Mulliken (1932) as



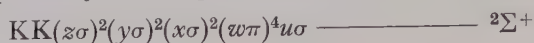
corresponding approximately to one σ bond and $1\frac{1}{2}\pi$ bonds. The $^2\Sigma^+$ state when compared with the ground state shows a marked increase in stability, and this indicates that the $v\pi$ antibonding electron of the normal $^2\Pi$ state has been replaced by a bonding electron, which must be some sort of a σ electron.

Table 8. Summary of Spectroscopic Constants for the NS Molecule

State	T_0	ω_e	$x_e\omega_e$	B_0	α_e	$D_e \times 10^6$	r_e
C $^2\Sigma^+$	43388.1	1403.5	8.7 ₆	$B_0=0.8267_0$		1.1 ₈	$r_0=1.446_9$
B $\left(\begin{smallmatrix} ^2\Pi_{3/2} \\ ^2\Pi_{1/2} \end{smallmatrix} \right)$	$\begin{pmatrix} 43181.4 \\ 43082.7 \end{pmatrix}$	(780)	—	$B_0 \sim 0.66_2$		—	$r_0 \sim 1.62$
A $^2\Delta_{5/2}$	39911.08	940.4	4.8 ₀	0.6960 ₄	0.0069 ₆	1.4 ₇	1.576 ₈
A $^2\Delta_{3/2}$	39875.70	970.6 ₅	8.6 ₅				
X $^2\Pi_{3/2}$	223.0 ₃	1219.1	7.5	0.7736 ₄	0.0061 ₂	1.2 ₅	1.495 ₇
X $^2\Pi_{1/2}$	0						

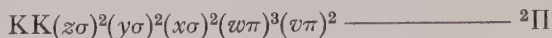
The values of D_e are calculated from Kratzer's relation, $D_e=4B_e^3/\omega_e^2$.

The $^2\Sigma^+$ state is probably to be represented by



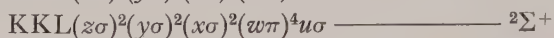
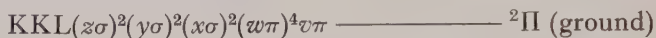
with one σ bond and two π bonds, which is in accord with an increase of 55% in the force constant relative to the ground state.

The excited $^2\Pi$ state has a much larger r_e , and smaller ω_e than the $^2\Pi$ ground state, and this indicates that a bonding electron from the ground state has gone over into an antibonding orbital in agreement with

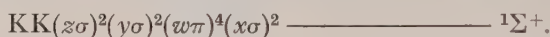


where there is one σ bond and $\frac{1}{2}\pi$ bond, the force constant being decreased by 70%.

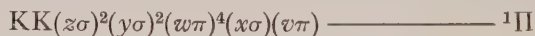
The molecule NS should behave similarly to NO except that there is an additional L shell due to the sulphur atom. Accordingly:



The increase in force constant in going to $^2\Sigma^+$ is only 30%, which is somewhat lower than in NO, but the above configuration seems the best representation of the $^2\Sigma^+$ state. The upper state of the β bands has been shown to be $^2\Delta$, and this cannot be formed by the same electron configuration as given for the $^2\Pi$ excited state of NO. The related molecule CO is helpful here. The ground state of CO, which has one electron less than NS if the L shell be neglected, is

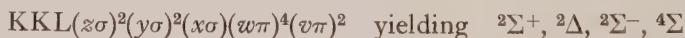


The first excited singlet state $^1\Pi$ is given by



where an electron has been moved from the $x\sigma$ to a π orbital and in so doing the force constant is reduced by about 50%.

A similar procedure in NS would give



with one π bond, and $\frac{1}{2}\sigma$ bond and this would imply weaker bonding relative to the ground state than in the NO $^2\Pi$ state. It is found, however, that in NS there is a decrease of only 39% as compared with 70% in NO. A possible explanation is that the NS $^2\Delta$ state has been stabilized relative to the ground state by resonance with a triply bonded Δ state arising from a conversion of a sulphur 3d electron into a δ electron, e.g. $KKL(z\sigma)^2(y\sigma)^2(x\sigma)^2(w\pi)^4(\delta)$.

Such a process would mean an increased dipole moment in the $^2\Delta$ state as compared with the ground state, which might lead to an increased transition moment for the $^2\Delta \rightarrow ^2\Pi$ system relative to the $^2\Pi \rightarrow ^2\Pi$ transition which occurs for NO. The above idea is of course only very tentative. By analogy with NO a $^2\Pi \rightarrow ^2\Pi$ transition would be expected to occur, and it may be that some of the unidentified bands in the NS spectrum arise from just such a transition.

§ 6. UNIDENTIFIED BANDS

There are observed in emission a number of red-degraded bands which bear a constant intensity ratio to the β and γ bands, and which thus appear to arise from NS. Measurements were made of the heads of some of these bands from a fourth order plate.

The four strongest heads measured can be fitted into a scheme as follows:

43082.72	1203.61	41879.11
124.34		126.96
42958.38	1206.23	41752.15
0		1

The differences of 1204 and 1206 cm^{-1} agree with the value of $\Delta G''_{1/2}$ for the $^2\Pi$ ground state of NS. The separation of 125 cm^{-1} , if the heads are correctly assigned, indicates that the doublet separation of the upper state is approximately 100 cm^{-1} .

An approximate value of r' for the unidentified state was obtained from measurements of the strongest branch of the band at 2387.1 Å. Successive differences were plotted against a running number, and from the slope there was obtained $\Delta B = -0.10$; this value, in conjunction with the value of $B'_{\text{eff}}^{(1)}$ for $v'' = 1$, gives $B'_{\text{eff}}^{(1)} = 0.662$. If $B'_{\text{eff}}^{(1)}$ is taken to be approximately equal to B' then r' is approximately 1.61 \AA . The likely assumption, that the unknown state is a regular doublet, is made in the above calculation.

r_e and ω_e for the known states of NS are related empirically according to $r_e = 1.829 - 2.719 \times 10^{-4} \omega_e$ (where r_e is in Å and ω_e in cm^{-1}). Extrapolation of this expression to $r_e = 1.61\text{\AA}$ gives $\omega_e \sim 780 \text{ cm}^{-1}$. This corresponds to a value of the force constant approximately equal to 30% of the value for the ground $^2\Pi$ state, and it is noteworthy that a similar percentage holds for the $^2\Pi$ excited and $^2\Pi$ ground states of NO. This suggests that the hitherto unidentified state in NS may be $^2\Pi$, but confirmation of this must await a complete rotational analysis.

ACKNOWLEDGMENTS

We should like to thank Dr. L. E. Orgel for helpful discussion about the electron configurations in NS, and the Department of Scientific and Industrial Research for the award of a maintenance grant to one of us (G.D.).

REFERENCES

- BARROW, R. F., DOWNIE, A. R., and LAIRD, R. K., 1952, *Proc. Phys. Soc. A*, **65**, 70.
 FOWLER, A., and BAKKER, C. J., 1932, *Proc. Roy. Soc.*, **136**, 28.
 HERZBERG, G., 1950, *Molecular Spectra and Molecular Structure*, Vol. I (New York: Van Nostrand).
 MULLIKEN, R. S., 1932, *Rev. Mod. Phys.*, **4**, 7.
 MULLIKEN, R. S., and CHRISTY, A., 1931, *Phys. Rev.*, **38**, 87.
 ZEEMAN, P. B., 1951, *Canad. J. Phys.*, **29**, 174.

RESEARCH NOTES

Extended Thomas-Fermi Methods

By R. A. BALLINGER AND N. H. MARCH

Department of Physics, The University, Sheffield

MS. received 17th December 1953

THE Thomas-Fermi (TF) method provides a very practicable and useful approximation to the solution of many-body problems in quantum mechanics. However, the method has associated with it certain shortcomings which restrict its applicability quite considerably. If, to be specific, we consider the important application to isolated atoms, then the following well-known defects arise: (i) the electron density at the nucleus becomes infinite as $r^{-3/2}$, r being the distance from the nucleus, whereas the correct wave-mechanical density remains finite; (ii) the density falls off at large distances from the nucleus as r^{-6} instead of exponentially; (iii) the method leads to a smooth curve for the radial charge distribution in atoms, and thus fails to resolve the well-known peaks associated with the various electronic shells. From a practical point of view the method is sufficiently attractive to warrant further investigation to ascertain whether it is possible to remove any, or all, of these defects, whilst still keeping the amount of labour involved down to a very small fraction of that involved in Hartree self-consistent field calculations.

Two generalizations of the TF method which in principle appear to be capable of removing some of the defects of the original treatment have been proposed by Weizsäcker (1935) and Plaskett (1953). Little attention has been given to Weizsäcker's proposal, however, probably because of its somewhat uncertain theoretical basis, and as yet no practical application of the method developed in the recent paper by Plaskett has been attempted.

In order to see the general nature of the improvements to be expected from the proposed generalizations of the TF method, we have considered the case of the linear harmonic oscillator with the first ten levels singly occupied. Curve I of the figure shows the exact wave-mechanical density ρ obtained by summing the squares of the wave functions. (The figure is plotted in terms of $\rho/\alpha^{1.2}$ and $\alpha^{1.2}x$ where $\alpha = 4\pi^2 m\nu_0/\hbar$ and ν_0 is the classical frequency of the oscillator.) In curve II we have plotted for comparison the results of the simple TF approximation. It can be seen that this gives a quite good overall description of the density, although the TF density cuts off at a finite distance from the origin and is given by a smooth curve. These two limitations in this one-dimensional problem can be regarded as analogous to the defects (ii) and (iii) for atoms referred to previously.

We have now studied the results of applying the methods of Weizsäcker and Plaskett to this problem. Both methods lead to a second order differential equation relating the density ρ to the potential energy V . These differential equations are superficially of very similar form although, as we shall see, the types of solution are quite different.

Plaskett's equation for the density ρ is

$$\frac{\hbar^2}{8m} \rho^2 + V + \frac{\hbar^2}{4m} \frac{\rho''}{\rho} - \frac{3\hbar^2}{8m} \frac{\rho'^2}{\rho^2} = E_N \quad \dots\dots(1)$$

and in our case $V = 2\pi^2 m v_0^2 x^2$ and $E_N = 19\hbar v_0/2$. This rather formidable looking equation can in fact be handled without great difficulty by making use of a result first obtained by Milne (1930) and utilized by Plaskett in his work. In our case this tells us that we can write solutions of (1) in the form

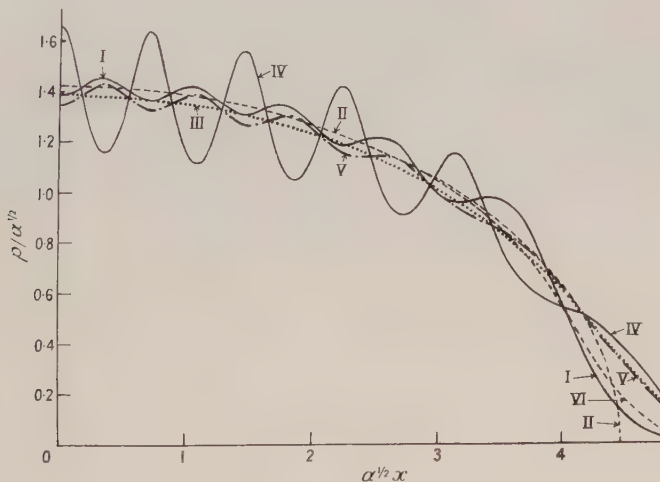
$$\pi\rho = W/(\psi_1^2 + \psi_2^2) \quad \dots\dots(2)$$

where ψ_1 and ψ_2 are two independent solutions of the equation

$$\frac{d^2\psi}{dx^2} + \frac{2m}{\hbar^2} \left(\frac{19}{2} \hbar v_0 - 2\pi^2 m v_0^2 x^2 \right) \psi = 0, \quad \dots\dots(3)$$

and W is the non-zero constant $\psi_2(d\psi_1/dx) - \psi_1(d\psi_2/dx)$. One of these solutions can conveniently be chosen to be the usual harmonic oscillator wave function. The second can be developed as an even power series from which starting values can be calculated, the solution then being most conveniently extended outwards by numerical integration. Knowing ψ_1 and ψ_2 we can now use (2) to construct a solution of (1). However, if ψ_2 is a solution of (3) then so is $c\psi_2$, where c is an arbitrary constant, and hence other solutions of (1) are given by

$$\pi\rho = cW/(\psi_1^2 + c^2\psi_2^2). \quad \dots\dots(4)$$



Densities for harmonic oscillator.

Curve I. Wave-mechanical. Curve II. TF. Curves III-V. Plaskett.
Curve VI. Weizsäcker.

All these solutions satisfy equally well the physical conditions of the problem

$$\rho'(0) = 0, \quad \rho(\infty) = 0, \quad \int_{-\infty}^{+\infty} \rho dx = 10.$$

In other words, Plaskett's method in its present form does not lead to a unique density. This does not mean that it may not be possible to choose c uniquely in

the future by some method such as setting up an energy expression* and minimizing it with respect to c . It is, nevertheless, of some interest to consider the kind of results that Plaskett's method in principle can lead to, and to illustrate this we have plotted in curves III, IV and V of the figure solutions corresponding to three different values of c . It can be seen that the method can yield a quite smooth curve III or a violently oscillatory curve IV. Curve V, which is certainly the most interesting, shows that with a particular choice of c a very remarkable degree of correlation with the wave-mechanical density is possible. Unfortunately, as we have said, we see no reason to prefer one value of c rather than another at present, although it seems to us that the agreement between curves I and V is so remarkable that it is hardly likely to be completely fortuitous.

In view of this degree of arbitrariness associated with Plaskett's method it is clearly of interest to enquire whether a similar situation obtains in Weizsäcker's treatment. For the present case, Weizsäcker's equation can be written

$$\frac{\hbar^2}{8m}\rho^2 + 2\pi^2 m v_0^2 x^2 - \frac{\hbar^2}{4m} \frac{\rho''}{\rho} + \frac{\hbar^2}{8m} \frac{\rho'^2}{\rho^2} = E'. \quad \dots (5)$$

The substitution $\rho = w^2$ leads to an equation involving only w and w'' . We have now solved this equation numerically for a number of different values of E' , and in each case we have found that there is only one solution which tends to zero at infinity, and hence this is the only one which is physically acceptable. We have found that the choice $E' = 10\hbar v_0$ leads to a density which is normalized correctly to our numerical accuracy, and this density, which is quite smooth, is shown in curve VI of the figure. It is indistinguishable from the TF curve out to $\alpha^{1/2}x \sim 3$.

These results for the harmonic oscillator are not very encouraging, though it would appear that if some information about the energy were forthcoming in the future, then Plaskett's method might be capable of giving remarkably good results. Weizsäcker's method, it is true, leads to a unique solution, but our results indicate that it is incapable of following the fluctuations in the exact wave-mechanical density.

When we consider the application to atoms, however, a further serious difficulty arises in Plaskett's treatment. First of all, we would have to handle separate equations for s, p, d, . . . states, which would greatly complicate the numerical calculations even if the arbitrariness which would occur in the solutions of each of these equations could be resolved. But even more discouraging is the fact that for s states the density becomes infinite at the nucleus as r^{-2} , and thus Plaskett's method accentuates, rather than removes, defect (i) referred to previously. It is clearly then of little value to proceed further in this case.

With Weizsäcker's treatment we have only to handle one differential equation for the total density, and by investigating this it appears that the method is capable in principle of removing defects (i) and (ii) of the TF method. Whilst it seems clear that one could also obtain a unique electron density by this method (though we believe it may be necessary to use the energy expression in this case in order to do so), our results for the harmonic oscillator indicate that the defect (iii) will almost certainly remain. This, coupled with the rather uncertain theoretical basis of the method, leads us to conclude that the results of generalizing the TF

* Dr. J. S. Plaskett (private communication) has informed us that he has had ideas along similar lines. Like us, however, he has so far been unable to obtain a useful expression for the energy.

treatment for atoms in this way are most unlikely to justify the heavy numerical calculations which would be involved. We have therefore discontinued our attempts to improve the TF method for atoms along these lines.

ACKNOWLEDGMENTS

The authors are grateful to Dr. J. S. Plaskett for a helpful correspondence. One of us (R.A.B.) also wishes to acknowledge the award of an Ellison Fellowship by the University of Sheffield.

REFERENCES

- MILNE, W. E., 1930, *Phys. Rev.*, **35**, 863.
 PLASKETT, J. S., 1953, *Proc. Phys. Soc. A*, **66**, 178.
 VON WEIZSÄCKER, C. F., 1935, *Z. Phys.*, **96**, 431.

The Approach to Saturation Magnetostriction

By E. W. LEE

University of Nottingham

Communicated by L. F. Bates; MS. received 25th January 1954

IN high fields, where apart from increase in intrinsic magnetization the only magnetic process is the turning of domain vectors into the field direction against the forces of internal anisotropy, the magnetostriction of a polycrystal can be expressed as a function of the external field by

$$\frac{dl}{l} = A + BH^{-1} + CH^{-2} + \dots \quad \dots\dots(1)$$

The coefficient B has been calculated by Rüdiger and Schlechtweg (1941) for the case in which the anisotropy is magnetocrystalline. One would expect this to be the dominant term in equation (1) since both B and C have the same origin. However, in a previous paper (Lee 1952a, to be referred to as I) experiments were described which seemed to indicate that for nickel the H^{-2} term is the dominant one in fields below 600 oersteds. Later work (Lee 1952 b) showed that in such fields both H^{-1} and H^{-2} terms are needed to describe the behaviour completely. It is the purpose of this note to point out the conditions under which the H^{-2} term is of real importance. Only the barest details will be given of the calculation, which takes as its starting point the treatment by Becker and Döring (1939, Section 13a, pp. 167-71) of the approach to saturation magnetization. We shall use a number of their results and adhere strictly to their notation.

For a single domain, the magnetostriction is

$$\frac{dl}{l} = \frac{3}{2}\lambda_{100}(\alpha_1^2\beta_1^2 + \alpha_2^2\beta_2^2 + \alpha_3^2\beta_3^2 - \frac{1}{3}) + 3\lambda_{111}(\alpha_1\alpha_2\beta_1\beta_2 + \alpha_2\alpha_3\beta_2\beta_3 + \alpha_3\alpha_1\beta_3\beta_1)$$

where $(\alpha_1, \alpha_2, \alpha_3)$ and $(\beta_1, \beta_2, \beta_3)$ are the direction cosines of the magnetization vector and the magnetic field with respect to the cubic axes of the crystal. This may be written

$$\frac{dl}{l} = -\frac{1}{2}\lambda_{100} + \frac{3}{2}(\lambda_{100} - \lambda_{111}) \sum \alpha_i^2 \beta_i^2 + \frac{3}{2}\lambda_{111} \cos^2 \theta \quad \dots\dots(2)$$

where $\cos \theta = \sum \alpha_i \beta_i$.

Following Becker and Döring we express the difference $\alpha_i - \beta_i$ as a power series in η , where $\eta = (HI_s)^{-1}$. Thus

$$\alpha_i = \beta_i + \eta A_i + \eta^2 B_i + \dots \quad \dots\dots(3)$$

in which A_i and B_i are coefficients to be determined. Using the results of Becker and Döring, in particular their equations (9), (12) and (13), we find

$$A_i = \beta_i \sum_k F_k \beta_k - F_i \quad \dots\dots(4)$$

$$B_i = - \sum_k F_{ik} A_k - \frac{1}{2} \beta_i \sum_i A_i^2 + \beta_i \sum_{i,k} F_{ik} A_k \beta_i + A_i \sum_i F_i \beta_i \quad \dots\dots(5)$$

where

$$\begin{aligned} F_i &= -2K\beta_i^3 \\ F_{ik} &= -6K\beta_i^2 \quad (i=k) \\ &= 0 \quad (i \neq k) \end{aligned}$$

K being the crystal anisotropy constant.

It can be shown (Becker and Döring, eqn (10)) that $\cos \theta = 1 - \frac{1}{2} \eta^2 \sum A_i^2$ and hence, to the approximation with which we are concerned,

$$\cos^2 \theta = 1 - \eta^2 \sum A_i^2. \quad \dots\dots(6)$$

The remaining variable term in equation (2) is $\sum \alpha_i^2 \beta_i^2$. Using equation (3) to eliminate α_i we have

$$\sum \alpha_i^2 \beta_i^2 = \sum \beta_i^4 + 2\eta \sum A_i \beta_i^3 + \eta^2 (\sum A_i^2 \beta_i^2 + 2 \sum B_i \beta_i^3). \quad \dots\dots(7)$$

The coefficients of η and η^2 in equations (6) and (7) can now be evaluated using (4) and (5). We find

$$\begin{aligned} \sum A_i \beta_i^3 &= 2K(S_6 - S_4^2) & \sum A_i^2 \beta_i^2 &= 4K^2(S_4^3 + S_8 - 2S_4 S_6) \\ \sum A_i^2 &= 4K^2(S_6 - S_4^2) & \sum B_i \beta_i^3 &= 6K^2(3S_4^3 + 2S_8 - 5S_4 S_6) \end{aligned}$$

where $S_4 = \sum \beta_i^4$, etc. Thus

$$\begin{aligned} \cos^2 \theta &= 1 - 4K^2(S_6 - S_4^2)\eta^2 \\ \sum \alpha_i^2 \beta_i^2 &= S_4 + 4K(S_6 - S_4^2)\eta + 4K^2(10S_4^3 + 7S_8 - 17S_4 S_6)\eta^2. \end{aligned}$$

Replacing S_4 , S_6 , etc. by their mean values, corresponding to a random polycrystal we finally obtain from (2)

$$\frac{dl}{l} = \frac{1}{5}(2\lambda_{100} + 3\lambda_{111}) + (\lambda_{100} - \lambda_{111}) \left(\frac{8}{5.7} K\eta - \frac{32}{7.11.13} K^2\eta^2 \right) - \lambda_{111} \frac{8}{5.7} K^2\eta^2.$$

If the magnetostriction is isotropic $\lambda_{100} = \lambda_{111}$ and the coefficient of the term in H^{-1} vanishes. This is the case envisaged in I.

For nickel $\lambda_{100} = -46 \times 10^{-6}$, $\lambda_{111} = -24 \times 10^{-6}$ (Bozorth and Hamming 1953), $K = -6 \times 10^4$ erg cm⁻³, $I_s = 500$, and for $H < 130$ oersteds the H^{-2} term is greater than the H^{-1} term. For iron $\lambda_{100} = 20 \times 10^{-6}$, $\lambda_{111} = -21 \times 10^{-6}$ (Carr and Smoluchowski 1952), $K = 5 \times 10^5$ erg cm⁻³, $I_s = 1720$, and the H^{-2} term exceeds the H^{-1} term only for $H < 100$ oersteds, i.e. in fields below which the approximations used to derive equation (2) may be considered to hold.

The effect of magnetic interactions between crystal grains has not been taken into account. This has been dealt with by Holstein and Primakoff (1941) in a related problem. As far as this particular problem is concerned the effect of interactions may be included by replacing the applied field H by a total internal field H' where

$$\left(\frac{H}{H'} \right)^2 = \frac{1}{2} \left[1 + \frac{\alpha}{2(1+\alpha)} + \frac{\alpha^2}{4(1+\alpha)^{3/2}} \ln \frac{(1+\alpha)^{1/2} + 1}{(1+\alpha)^{1/2} - 1} \right]$$

in which $4\pi I_s \alpha = H$.

It follows from the above considerations that the procedure sometimes adopted of obtaining the saturation magnetostriction by plotting dl/l against H^{-1} and extrapolating to $H = \infty$ is usually valid but ceases to be so when the magnetostriction is nearly isotropic.

REFERENCES

- BECKER, R., and DÖRING, W., 1939, *Ferromagnetismus* (Berlin : Springer), p. 167.
 BOZORTH, R. M., and HAMMING, R. W., 1953, *Phys. Rev.*, **89**, 865.
 CARR, W. J., and SMOLUCHOWSKI, R., 1952, *Phys. Rev.*, **83**, 1236.
 HOLSTEIN, T., and PRIMAKOFF, H., 1941, *Phys. Rev.*, **59**, 388.
 LEE, E. W., 1952 a, *Proc. Phys. Soc. B*, **65**, 162; 1952 b, *Thesis*, University of Nottingham.
 RÜDIGER, O., and SCHLECHTWEIG, H., 1941, *Ann. Phys., Lpz.*, **39**, 1.

Perturbation Theory for the One-Dimensional Wave Equation

BY P. J. PRICE

Watson Laboratory, Columbia University, New York, N.Y., U.S.A.

MS. received 2nd December 1953

IN a recent paper on perturbation methods for the one-dimensional Schrödinger equation, Makinson and Turner (1953) remark (§ 6) that their formulation makes possible a solution of the eigenvalue problem, to second order, explicitly in terms of the unperturbed wave function only. The following method gives such an explicit solution, for the ground state, to any required order.

For definiteness, consider the real solutions in (a, b)

$$\left. \begin{aligned} H\psi_0(x) &= E_0\psi_0 \\ [H + v(x)]\psi(x) &= (E_0 + \epsilon)\psi \end{aligned} \right\} \dots\dots(1)$$

where ψ_0 and ψ are zero at $x = a, b$ and nowhere else in the interval, and

$$H \equiv -d^2/dx^2 + V(x). \dots\dots(2)$$

Then we may find ψ and ϵ in terms of ψ_0^2 and v only, by setting

$$\psi = \psi_0 \exp \left[\int_a^x \Omega(x') dx' \right]. \dots\dots(3)$$

Substituting (3) in (1),

$$(\epsilon - v + \Omega^2)\psi_0 + \psi_0 d\Omega/dx + 2\Omega d\psi_0/dx = 0. \dots\dots(4)$$

If the perturbation v is not such as to alter the character of the solution (e.g. both ψ_0 and ψ tend to zero as $(x-a)^n$ and $(x-b)^m$), then $\Omega(a)$ and $\Omega(b)$ are finite. Hence, multiplying (4) by ψ_0 and integrating,

$$\left. \begin{aligned} \Omega(x)\rho_0(x) &= - \int_a^x [\epsilon - v(x') + \Omega^2(x')] \rho_0(x') dx' \\ \epsilon &= \int_a^b (v - \Omega^2) \rho_0 dx \end{aligned} \right\} \dots\dots(5)$$

where

$$\rho_0 \equiv \psi_0^2, \quad \int_a^b \rho_0 dx = 1. \dots\dots(6)$$

We obtain a perturbation series solution of (5) by replacing v by λv and expanding formally :

$$\left. \begin{aligned} \epsilon &= \sum_1^{\infty} \lambda^n \epsilon_n, \quad \Omega = \sum_1^{\infty} \lambda^n \Omega_n(x); \\ \Omega^2 &= \sum_2^{\infty} \lambda^n \theta_n, \quad \theta_n = \sum_{r=1}^{n-1} \Omega_r \Omega_{n-r}; \\ \Omega_n(a), \Omega_n(b) &\text{ are finite.} \end{aligned} \right\} \dots\dots(7)$$

Then the solution of (5) is given by

$$\left. \begin{aligned} \epsilon_1 &= \int_a^b v \rho_0 dx & \Omega_1 \rho_0 &= - \int_a^x [\epsilon_1 - v(x')] \rho_0(x') dx' \\ \epsilon_2 &= - \int_a^b \Omega_1^2 \rho_0 dx & \Omega_2 \rho_0 &= - \int_a^x [\epsilon_2 + \Omega_1^2] \rho_0 dx' \\ \epsilon_3 &= - \int_a^b 2\Omega_1 \Omega_2 \rho_0 dx & \Omega_3 \rho_0 &= - \int_a^x [\epsilon_3 + 2\Omega_1 \Omega_2] \rho_0 dx' \\ \dots\dots\dots & & \dots\dots\dots & \\ \epsilon_n &= - \int_a^b \theta_n \rho_0 dx & \Omega_n \rho_0 &= - \int_a^x [\epsilon_n + \theta_n] \rho_0 dx' \end{aligned} \right\} \dots\dots(8)$$

The restriction on Ω then requires $(x-a)(x-b)v(x)$ to be bounded in the closed interval (a, b) . The solution (3)–(8) applies equally where the domain is semi-infinite or infinite, and also with ‘periodic boundary conditions’. It is restricted to the ground state, where zeros of ψ_0 are zeros of ψ and conversely. For the general Sturm–Liouville equation the Ansatz (3) yields equations generalizing (4)–(8), but there the interest is normally in the effects of singularities in the coefficients.

The above method may be applied to ‘perturbations’ of the phase-shifts of the waves scattered by a central potential, for example, to the expansion of the S-phase $\delta^0(k)$ about $k=0$. If the S-wave function is $\psi^0(r)$, and $\phi = r\psi^0$, we have

$$-\partial^2 \phi / \partial r^2 + V(r) \phi = k^2 \phi(k, r) \quad \dots\dots(9)$$

where ϕ is real, $\phi(k, 0) = 0$, and for large r

$$\phi = (kr)^{1/2} J_{1/2}(kr + \delta^0). \quad \dots\dots(10)$$

Set

$$\phi(k, r) = \phi(0, r) \exp \left[\int_0^r \Omega(x) dx \right] \quad \dots\dots(11)$$

(which is now possible for $r < R_1(k)$, where the first zero of ϕ comes at R_1). Then

$$(k^2 + \Omega^2)f = -\partial(\Omega f)/\partial r, \quad f \equiv \phi^2(0, r). \quad \dots\dots(12)$$

Expand $\Omega = \sum_1^{\infty} k^{2n} \Omega_n(r)$ and define θ_n as in (7). Then, integrating (12) from 0 to $R < R_1$,

$$\Omega_1 f(R) = -k^2 \int_0^R f(r) dr \quad \dots\dots(13)$$

$$\Omega_n f(R) = - \int_0^R \theta_n(r) f(r) dr. \quad \dots\dots(14)$$

Since

$$\Omega = \frac{\partial \phi(k, r) / \partial r}{\phi(k, r)} - \frac{\partial \phi(0, r) / \partial r}{\phi(0, r)},$$

equation (13) is equation (7) of Bethe and Peierls (1935), and thus leads to the Barker-Peierls (1949) formula for $\cot \delta^0$. Evidently the latter might be generalized, by means of (14) above, to higher powers of k^2 . In a similar way the effect, at fixed k , of perturbations in $V(r)$ may also be calculated in terms of $\phi^2(k, r)$.

ACKNOWLEDGMENTS

The solution (3)–(8) was obtained in January 1951, the work being supported by an award from the Department of Scientific and Industrial Research. The scattering variant, at Duke University, was supported by the U.S. Office of Naval Research.

REFERENCES

- BARKER, F. C., and PEIERLS, R. E., 1949, *Phys. Rev.*, **75**, 312.
 BETHE, H. A., and PEIERLS, R. E., 1935, *Proc. Roy. Soc. A*, **149**, 176.
 MAKINSON, R. E. B., and TURNER, J. S., 1953, *Proc. Phys. Soc. A*, **66**, 857.

The Electrical Properties of Indium Antimonide at Low Temperatures

BY J. HATTON AND B. V. ROLLIN

The Clarendon Laboratory, Oxford

MS. received 1st December 1953

MEASUREMENTS have been made of the resistivity, the Hall coefficient and the magneto resistance coefficients of the semiconducting compound indium antimonide over the temperature range 300°K to 1°K . The specimen was of polycrystalline material which had been extensively purified by the zone melting technique (Pfann 1952). The dimensions of the specimen were about $10\text{ mm} \times 2\text{ mm} \times 2\text{ mm}$. The faces were ground and contacts soldered directly to the specimen. The results obtained in the intrinsic region at room temperature are in good agreement with those reported by other investigators (Pearson and Tanenbaum 1953, Tanenbaum and Maita 1953). The Hall and magneto resistance measurements at room temperature indicate an electron mobility of about $2.5 \times 10^4\text{ cm}^2\text{ sec}^{-1}\text{ V}^{-1}$. At 90°K the specimen is p-type, the hole concentration being about $3 \times 10^{16}\text{ cm}^{-3}$ and the mobility about $3 \times 10^3\text{ cm}^2\text{ sec}^{-1}\text{ V}^{-1}$.

At temperatures below 90°K it is found that the conductivity decreases nearly linearly with temperature. The Hall coefficient reaches a maximum between 90°K and 20°K and decreases rapidly at lower temperatures (figure 1).

The transverse magneto resistance coefficient at room temperature varies nearly quadratically with the field up to 9000 gauss (figure 2) and the longitudinal coefficient is only of the order of 1% of the transverse coefficient. At lower temperatures, however, the transverse effect approaches more nearly a linear variation with field above 4000 gauss and there is an appreciable longitudinal effect.

At temperatures below 20°K there is a considerable drop in the magneto resistance effect, and at 4.2°K it is so small that it could be measured only in the highest field.

It is difficult to find adequate explanation for the small magnitude of the Hall coefficient and magneto resistance effect at the lowest temperatures. The results suggest that, at these temperatures, the dominant conduction process is associated with a high density of charge carriers of low mobility and it is perhaps possible that the conduction takes place mainly along the surface of the specimen or over the grain boundaries where the properties of the material may be expected to differ from those of the bulk specimen.

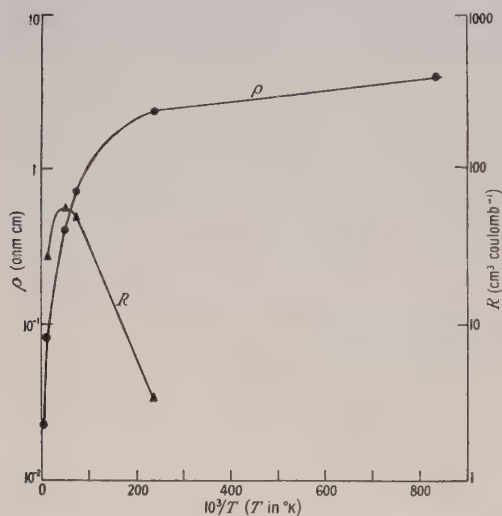


Figure 1. Variation of resistivity ρ and Hall constant R with temperature T .

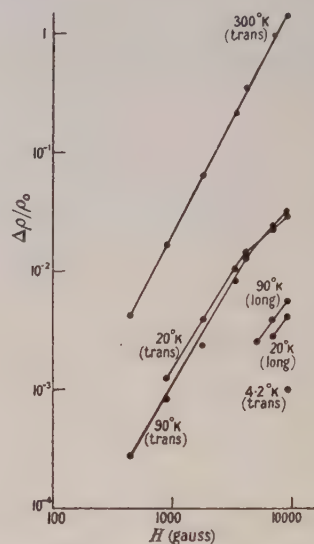


Figure 2. Variation of magneto resistance effect $\Delta\rho/\rho_0$ with field H at different temperatures.

ACKNOWLEDGMENTS

The indium antimonide was prepared at the Services Electronic Research Laboratory and we are indebted to Mr. I. M. Ross for supplying us with the specimen. We wish to record our thanks to Mr. E. Watson for his assistance with some of the measurements. This work has been assisted by an Admiralty research contract.

REFERENCES

- PEARSON, G. L., and TANENBAUM, M., 1953, *Phys. Rev.*, **90**, 153.
 PFANN, W. G., 1952, *J. Metals*, **4**, 747.
 TANENBAUM, M., and MAITA, J. P., 1953, *Phys. Rev.*, **91**, 1009.

The Optical Constants of Tin below the Superconducting Transition Temperature

By N. G. MCCRUM AND C. A. SHIFFMAN

Clarendon Laboratory, Oxford

Communicated by K. Mendelssohn ; MS. received 11th January 1954

MEASUREMENTS of the high-frequency surface impedance of superconductors indicate that there is a mechanism of absorption of energy at temperatures well below the transition point at sufficiently high frequencies. The measurements of Fawcett (1953) at 36 000 Mc/s and of

Daunt, Keeley and Mendelssohn (1937) and Ramanathan (1952) in the infra-red region have set upper and lower limits to the onset frequency for this absorption. Both of the experiments in the infra-red region used calorimetric techniques, and it was felt that a direct optical determination would consolidate the position at the high-frequency end. Our measurements at 5890 Å do not therefore set a new upper limit to the onset frequency but help to verify the previous measurements by an independent method.

If plane polarized light be incident upon a metallic surface the reflected vectors vibrate with a phase difference Δ' and amplitude ratio $\tan \psi'$. A knowledge of the angle of incidence, the orientation of the incident plane of polarization and the optical constants of the reflector enable Δ' and ψ' to be calculated. It has been shown theoretically (Drude 1889) that the presence of a thin dielectric layer causes the ellipse parameters to become Δ and ψ , given by

$$2\psi - 2\psi' = \sin 2\psi' \frac{4\pi}{\lambda} \frac{\cos \phi \sin^2 \phi \alpha'}{(\cos^2 \phi - \alpha)^2 + \alpha'^2} (1 - n_1^2 \cos^2 \phi) \left(1 - \frac{1}{n_1^2}\right) l \dots\dots (1)$$

$$\Delta - \Delta' = \frac{4\pi \cos \phi \sin^2 \phi (\cos^2 \phi - \alpha)}{\lambda (\cos^2 \phi - \alpha)^2 + \alpha'^2} \left(1 - \frac{1}{n_1^2}\right) l \dots\dots (2)$$

$$\alpha = \frac{1 - \kappa^2}{\nu^2(1 + \kappa^2)^2}, \quad \alpha' = \frac{2\kappa}{\nu^2(1 + \kappa^2)^2}$$

where ϕ is the angle of incidence, n_1 the index of refraction of the film of thickness l , and the complex refractive index of the metal $n = \nu(1 - i\kappa)$. By the deposition of uniform layers of dielectric on to a polished metallic surface a half shade technique has been developed (Rothen and Hanson 1948) which permits very sensitive detection of changes in ellipticity. Small resulting changes of ellipticity caused by an increase of l in (1) and (2) can be accurately detected. This method has been used to measure the helium II superfluid film (Burge and Jackson 1951) and the helium II adsorption isotherm (McCrum and Mendelssohn 1954). Alternatively, any variation of κ will cause Δ' and ψ' and Δ and ψ to change. We have used this method to investigate the optical constants of a superconductor.

The specimen was a tin film of Johnson Matthey 3921 with a purity of 99.997%. It was evaporated on to a glass optical flat in vacuum. Its thickness was 1900 Å, measured by a multiple beam technique (Tolansky 1947). Since we were unable to anneal the specimen *in situ* it undoubtedly had a large amount of surface strain. However, the measurements of Fairbank (1949) at 9400 Mc s and for different surface conditions indicate that this would make little difference, particularly near the transition temperature, where the change in surface impedance with temperature would be most marked. The measurements were made by switching on and off a sufficiently large magnetic field normal to the plane of the specimen while observing the position of balance of the analysing nicol. This method, while having the advantage of allowing the magnet to be placed where it would not interfere with the optical apparatus, made it necessary to raise the temperature above the transition point after the application and removal of the field because of the large frozen-in moments which were left in the specimen on removing the field (Andrew and Lock 1950). Measurements made at different temperatures were not compared as the variation of glass strain due to change of pressure in the cryostat made the interpretation of the results difficult.

Barium stearate layers were deposited on the tin from an Adam-Langmuir tray (Blodgett and Langmuir 1937). The specimen was mounted in a glass

envelope which was thoroughly pumped, filled with helium gas at a pressure of 2 cm and then sealed off. The source was a sodium lamp and the incident beam polarized at 45° to the vertical by means of a large nicol prism. The analyser consisted of a mica quarter-wave plate of 59° retardation and a nicol prism mounted on an engraved circular scale.

The theoretical sensitivity of the experiment has been calculated, using equations (1) and (2), on the assumption that the optical constants were $\nu = 1.12$ and $\kappa = 4.03$ (*International Critical Tables*, V, 248). Our measurements indicate that in a transition from the superconducting to the normal state any change in the absorption coefficient at 5890 \AA is less than 0.3%, the limit of our accuracy.

ACKNOWLEDGMENT

We should like to thank Dr. Mendelssohn for his constant interest and encouragement.

REFERENCES

- ANDREW, E. R., and LOCK, J. M., 1950, *Proc. Phys. Soc. A*, **63**, 13.
 BLODGETT, K., and LANGMUIR, I., 1937, *Phys. Rev.*, **51**, 964.
 BURGE, E. J., and JACKSON, L., 1951, *Proc. Roy. Soc. A*, **205**, 270.
 DAUNT, J. G., KEELEY, T. C., and MENDELSSOHN, K., 1937, *Phil. Mag.*, **23**, 264.
 DRUDE, P., 1889, *Ann. Phys. u. Chem.*, **36**, 865.
 FAIRBANK, W. M., 1949, *Phys. Rev.*, **76**, 1106.
 FAWCETT, E., 1953, *Proc. Phys. Soc. A*, **66**, 1071.
 MCCRUM, N. G., and MENDELSSOHN, K., 1954, *Phil. Mag.*, **45**, 102.
 RAMANATHAN, K. G., 1952, *Proc. Phys. Soc. A*, **65**, 532.
 ROTHEN, A., and HANSON, M., 1948, *Rev. Sci. Instrum.*, **19**, 839.
 TOLANSKY, S., 1947, *Multiple Beam Interferometry* (Oxford: Clarendon Press).

Volume Changes in a Substitutional Alloy

BY D. TER HAAR AND A. W. ROSS

Department of Natural Philosophy, The University, St. Andrews

MS. received 21st December 1953

ONE would not expect the equilibrium distance between two atoms to be independent of the choice of the two atoms and it therefore follows that one would expect volume changes to accompany order-disorder transitions in a substitutional alloy. Although Nix and Shockley (1938) have mentioned this, the effect does not seem to have been investigated, and we felt that it might be worth while to do so. Although a linear chain does not exhibit an order-disorder transition, the main features of the volume change effect can be seen from a consideration of such a linear chain and it is this case which is treated below. It is hoped to treat the more complicated two- and three-dimensional cases later.

Consider a linear chain consisting of $\frac{1}{2}N$ A atoms and $\frac{1}{2}N$ B atoms. In the first rather trivial model we assume an A-A pair, an A-B pair and a B-B pair to be associated with the constant distances apart r_1 , r_2 and r_3 and the constant energies V_{AA} , V_{AB} and V_{BB} respectively. For simplicity we take r_3 equal to r_1 . We define V by the equation $V = \frac{1}{2}(V_{AA} + V_{BB}) - V_{AB}$ and we assume that $V > 0$ in order to obtain the ordered structure ABABABAB... at the absolute zero.

Let Q_{AA} , Q_{AB} and Q_{BB} be the number of nearest neighbour pairs which are A-A, A-B, or B-B pairs. The energy associated with a given distribution Q_{AA} , Q_{AB} , Q_{BB} is $E = Q_{AA}V_{AA} + Q_{BB}V_{BB} + Q_{AB}V_{AB}$. From the relations $Q_{AB} = \text{const} - 2Q_{AA} = \text{const} - 2Q_{BB}$ it follows that $E = -VQ_{AB} + \text{const}$. Taking the energy of the completely ordered state as the zero of energy, we have, since $Q_{AA} + Q_{AB} + Q_{BB} = N$,

$$E = VN(1 - Q_{AB}/N). \quad \dots\dots(1)$$

The length of the chain is given by the equation

$$L = (Q_{AA} + Q_{BB})r_1 + Q_{AB}r_2 = Nr_1 - Q_{AB}(r_1 - r_2).$$

Substituting the value of Q_{AB} given by equation (1) gives finally

$$L = Nr_2 + (E/V)(r_1 - r_2). \quad \dots\dots(2)$$

In the case of a linear chain E is found to have the value (e.g. Kramers and Wannier 1941)

$$E = \frac{1}{2}NV - \frac{1}{2}NV \tanh X, \text{ where } X = V/2kT.$$

Substituting this value of E in equation (2) we obtain

$$L = Nr_2 + \frac{1}{2}N(1 - \tanh X)(r_1 - r_2),$$

which gives us the length of the chain as a function of temperature. Thus the rate of change of length with temperature, which in this case is proportional to the specific heat, is

$$dL/dT = \frac{Nk}{V} (r_1 - r_2) X^2 / (\cosh X)^2.$$

The variation of dL/dT with temperature is shown in figure 1, curve *a*.

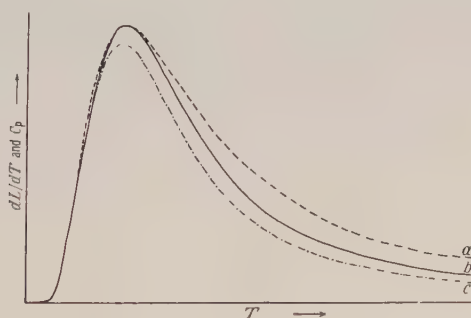


Figure 1.

Since this model, containing two different lengths r_1 and r_2 , cannot be applied to the case of a square net, or a three-dimensional lattice, we have considered the following slightly different model. If we assume a uniform spacing r between successive atoms in the chain, then the value of r as a function of T will follow from the thermodynamical condition of minimum free energy. Furthermore, we assume the energy associated with an A-A or a B-B pair to be

$$V_{AA} = V_{BB} = V_0' + D'(r - r_1)^2$$

and with an A-B or a B-A pair to be

$$V_{AB} = V_{BA} = V_0 + D(r - r_2)^2.$$

This variation of the energies with r was chosen as representing reasonably well the lower part of the potential energy function of an atomic pair such as is given for instance by a Morse potential.

We assume $r_1 > r_2$, corresponding to the experimental evidence that ordering is usually accompanied by a diminution of volume (Nix and Shockley 1938, p. 51), and for simplicity $D' = D$, corresponding to the fact that the frequencies in most diatomic systems are of the same order of magnitude. Since, as before, we are considering the case where the arrangement of the atoms at the absolute zero is ABABABAB..., it follows that $V_0' - V_0 > D(r_1 - r_2)^2$. To simplify our calculations we have assumed the relation $V_0' - V_0 = 2D(r_1 - r_2)^2$. With values of D , r_1 and r_2 to be expected from data about potential energy functions, $V_0' - V_0$ turns out to be (at most) of the order of 0.1 ev, which seems a reasonable value (cf. Nix and Shockley 1938).

We shall call the lattice sites occupied by A atoms in the state of complete order α -sites and the lattice sites occupied by B atoms β -sites, so that the arrangement of sites is $\alpha\beta\alpha\beta\alpha\beta\dots$. We call N_{YZ} the number of nearest neighbour pairs which consist of a Y atom on an α -site and a Z atom on a β -site. In the case where there are equal numbers of A and B atoms the following relations hold (cf. ter Haar 1954, § XII 4): $N_{AA} = N_{BB}$, $N_{AB} = N_{BA}$, $N_{AA} = \frac{1}{2}N - N_{AB}$. The number of ways of obtaining a distribution N_{AA}, \dots is the compound probability

$$W = \frac{N!}{N_{AA}! N_{BB}! N_{AB}! N_{BA}!}$$

and the entropy of the chain is thus

$$S = k \ln W = k [N \ln N - 2(\frac{1}{2}N - N_{AB}) \ln (\frac{1}{2}N - N_{AB}) - 2N_{AB} \ln N_{AB}].$$

The energy of the chain is

$$\begin{aligned} E &= N_{AA}V_{AA} + N_{BB}V_{BB} + N_{AB}V_{AB} + N_{BA}V_{BA} \\ &= NV_{AA} - 2N_{AB}(V_{AA} - V_{AB}), \end{aligned} \quad \dots\dots(4)$$

and for the free energy we have

$$\begin{aligned} F &= E - TS = NV_{AA} - 2N_{AB}(V_{AA} - V_{AB}) \\ &\quad - kT [N \ln N - 2(\frac{1}{2}N - N_{AB}) \ln (\frac{1}{2}N - N_{AB}) - 2N_{AB} \ln N_{AB}]. \end{aligned}$$

Minimizing F with respect to N_{AB} and r gives finally the results

$$N_{AB} = \frac{NdV_{AA}/dr}{2(dV_{AA}/dr - dV_{AB}/dr)} \quad \dots\dots(5)$$

and

$$V_{AB} - V_{AA} = kT \ln \left(- \frac{dV_{AB}}{dr} / \frac{dV_{AA}}{dr} \right),$$

or, by substituting from (3),

$$D(r - r_2)^2 - D(r - r_1)^2 - 2D(r_1 - r_2)^2 = kT [\ln(r - r_2) - \ln(r_1 - r)]. \quad \dots\dots(6)$$

We introduce the quantity m by the equation $r = r_2 + m(r_1 - r_2)$, and equation (6) becomes

$$\frac{2m - 3}{\ln m - \ln(1 - m)} = x, \quad \text{where } x = cT \text{ (} c = \text{constant)}.$$

We see that m approaches the value $1/2$ asymptotically, in agreement with the fact that the state of greatest disorder has as many A-A or B-B pairs as it has A-B or B-A pairs.

The length of chain is given by $L = Nr = Nr_2 + N(r_1 - r_2)m$, and its variation with T is shown in figure 2. Its rate of change with temperature is given by the equation

$$dL/dT = N(r_1 - r_2)(dm/dT) \propto dm/dx.$$

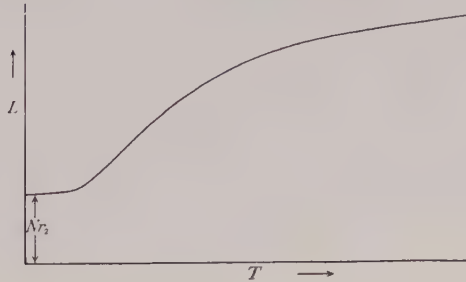


Figure 2.

The variation of dL/dT with T is shown in figure 1, curve b . The energy of the chain follows from equations (4) and (5) and is given by

$$E = N[V_0 + \frac{1}{2}(V_0' - V_0)(3 - m)m],$$

so that the specific heat, C_p , is given by

$$C_p = H(3 - 2m)(dm/dx) \text{ where } H \text{ is a constant.}$$

The variation of C_p with T is shown also on figure 1 (curve c). It is seen from a comparison of curves a and b of figure 1 that there is not a great deal of difference between the two models which we have considered and, although C_p is no longer proportional to dL/dT as was the case in our first model, the two functions are still very similar and the maxima of C_p and dL/dT occur at approximately the same temperature. We therefore expect that in the case of a two- or three-dimensional substitutional alloy the expansion coefficient may show a discontinuity at the Curie point.

ACKNOWLEDGMENT

We would like to express our thanks to the Department of Scientific and Industrial Research for the award of a maintenance grant to one of us (A.W.R.).

REFERENCES

- TER HAAR, D., 1954, *Elements of Statistical Mechanics* (New York : Rinehart).
- KRAMERS, H. A., and WANNIER, G. H., 1941, *Phys. Rev.*, **60**, 252.
- NIX, F. C., and SHOCKLEY, W., 1938, *Rev. Mod. Phys.*, **10**, 1.

LETTERS TO THE EDITOR

The Coupling of Angular Momenta in the Reaction $^{27}\text{Al}(\text{p}, \gamma)^{28}\text{Si}$

In the reaction $^{27}\text{Al}(\text{p}, \gamma)^{28}\text{Si}$ it is possible to deduce the spins and parities of five resonance levels, at proton energies of 404, 503, 630, 652 and 677 kev, without considering in detail the angular distribution of the γ -rays (Rutherglen *et al.* 1954). At two of the resonances (630 and 652 kev) two 'channel spins' may produce the resonant state, and thus at each resonance the relative contributions of parallel and antiparallel spin states may be deduced from the observed angular distribution. These two resonances can provide further evidence of the kind considered by Christy (1953) on the type of coupling between the angular momenta of the incident proton and the target nucleus.

Calculations have been made of the angular distributions expected for (a) j - j coupling in which only one of the two possible j -values of the incident proton takes part, and (b) L - S coupling. The results are given below, where F is defined as the ratio

$$\frac{\text{number of states formed via channel spin 3}}{\text{number of states formed via channel spin 2}},$$

and the ground state of ^{27}Al is assumed to be $d_{5/2}$.

630 kev resonance, $J=3(-)$. The angular distribution of the γ -radiation to the first excited state ($J=2(+)$) of ^{28}Si is given by $W_{\text{exp}}(\theta) \sim 1 - 0.12 \cos^2 \theta$, corresponding to $F=3/7$. The calculated values are:

j - j	$j_p = 1/2$	$F = 4/5$	$W(\theta) \sim \text{isotropic}$
	$j_p = 3/2$	$F = 5/4$	$W(\theta) \sim 1 + 0.093 \cos^2 \theta$
L - S	$^{28}\text{Si}^* = {}^1\text{F}_3$	$F = 0$	$W(\theta) \sim 1 - 0.321 \cos^2 \theta$
	${}^3\text{F}_3$	$F = 5/16$	$W(\theta) \sim 1 - 0.158 \cos^2 \theta$
	${}^3\text{D}_3$	$F = 20$	$W(\theta) \sim 1 + 0.477 \cos^2 \theta$

652 kev resonance, $J=2(-)$. The angular distribution of the γ -radiation to the $2(+)$ level of ^{28}Si is given by $W_{\text{exp}}(\theta) \sim 1 - 0.48 \cos^2 \theta$. The best fit is obtained with $F=0$, giving $W(\theta) \sim 1 - 0.447 \cos^2 \theta$. The calculated values are:

j - j	$j_p = 1/2$	$F = 7/2$	$W(\theta) \sim \text{isotropic}$
	$j_p = 3/2$	$F = 2/7$	$W(\theta) \sim 1 - 0.333 \cos^2 \theta$
L - S	$^{28}\text{Si}^* = {}^3\text{D}_2$	$F = 14/25$	$W(\theta) \sim 1 - 0.259 \cos^2 \theta$
	${}^3\text{F}_2$	$F = 1/14$	$W(\theta) \sim 1 - 0.415 \cos^2 \theta$
	${}^1\text{D}_2$	$F = 0$	$W(\theta) \sim 1 - 0.447 \cos^2 \theta$

At both resonances the j - j coupling calculations are in disagreement with experiment, while the L - S results provide a good fit (${}^3\text{F}_3$ and ${}^1\text{D}_2$ respectively). At the 630 kev resonance the difference between the theoretical (5/16) and experimental (3/7) values of F is not significant. A mixture of M2 radiation, with an intensity 6×10^{-3} of that of the E1 radiation and in phase with it, is sufficient to give agreement with the experimental distribution. This figure is consistent with the result at the 652 kev resonance where a mixture of M2

radiation, of intensity 1.5×10^{-3} of that of the E1 radiation and in phase with it, provides a fit with the experimental result. This mixture is required independently of any assumptions about the coupling of the angular momenta.

The L - S coupling description of the five resonance levels is: 404 kev, ${}^3F_4(-)$; 503 kev, ${}^1D_2(+)$; 630 kev, ${}^3F_3(-)$; 652 kev, ${}^1D_2(-)$; 677 kev, ${}^3D_3(+)$.

I would like to thank Dr. K. V. Roberts of King's College, Cambridge, for advice on some of these calculations.

Department of Natural Philosophy,
Glasgow University.
28th December 1953.

P. J. GRANT.

CHRISTY, R. F., 1953, *Phys. Rev.*, **89**, 839.

RUTHERGLEN, J. G., GRANT, P. J., FLACK, F. C., and DEUCHARS, W. M., 1954, *Proc. Phys. Soc. A*, **67**, 101.

Spectroscopic Isotope Shifts and Electron Scattering by Nuclei

Recent experiments on the scattering of 125 mev electrons by nuclei (Hofstadter, Fechter and McIntyre 1953) have indicated that the nuclear charge may be concentrated towards the centre of the nucleus. These authors and Schiff (1953) have shown that with the use of the Born approximation to calculate the scattering the experimental results may be fitted equally well to either of the charge distributions

$$\rho = \rho_0 e^{-r/\alpha} \quad \dots\dots(1)$$

or

$$\rho = \rho_0 \left(1 + \frac{r}{\beta}\right) e^{-r/\beta} \quad \dots\dots(2)$$

where ρ is the charge density at a distance r from the centre, and α and β are adjusted to give the best fit with experiment.

Another method giving information about nuclear charge distribution is the study of spectroscopic isotope shifts in heavy elements. In an attempt to correlate the results of scattering experiments and those of isotope shift measurements, the isotope shift ΔT due to the nuclear volume effect was calculated for the above two charge distributions by the following method.

The first order perturbation method of Rosenthal and Breit (1932) was used as a first approximation. This result was then corrected for the distortion of the electronic wave function inside the nucleus by multiplying by the ratio

$$\frac{\Delta T \text{ perturbation}}{\Delta T \text{ non-perturbation}}$$

given by Bodmer (1953) for a uniform volume distribution of nuclear charge. Bodmer's calculations show that this ratio does not depend very critically on the charge distribution. For lead, the ratio for uniform charge distribution differs from that for inverse square charge distribution by about 5%. It was assumed in the present calculation that α and β are proportional to $A^{1/3}$, where A is the mass number. The measured value of the isotope shift in lead was used to calculate the values of α and β for lead. In the following table these

results are compared with the values of α and β deduced from the electron scattering experiments by Hofstadter *et al.* (1953) and Schiff (1953).

Values of α and β for lead		
	$\alpha \times 10^{13}$	$\beta \times 10^{13}$
Scattering	2.36 ± 0.3	1.3 ± 0.2
Isotope shift	1.35 ± 0.3	1.15 ± 0.3

It is very difficult to estimate the errors in the isotope shift values of α and β , but they are unlikely to exceed those quoted.

It appears from these calculations that while the results of scattering experiments so far can be made to fit either of the charge distributions (1) or (2), the consideration of both isotope shift measurements and electron scattering experiments discriminates in favour of the modified exponential distribution (2), that is, a distribution that is smooth at the origin.

Clarendon Laboratory,
Oxford.
29th January 1954.

W. R. HINDMARSH.

BODMER, A. R., 1953, *Proc. Phys. Soc. A*, **66**, 1041.

HOFSTADTER, R., FECHTER, H. R., and MCINTYRE, J. A., 1953, *Phys. Rev.*, **92**, 978.

ROSENTHAL, J. E., and BREIT, G., 1932, *Phys. Rev.*, **41**, 459.

SCHIFF, L. I., 1953, *Phys. Rev.*, **92**, 988.

CORRIGENDUM

Lens Spectrometer Study of the Disintegration of $MsTh_2$. By the late W. D. BRODIE (*Proc. Phys. Soc. A*, 1954, **67**, 265).

P. 271. Table 4, lines 2 and 3 of column 4 *should read*

$$\begin{cases} L_{III} \rightarrow M_V M_{III} \\ L_{III} \rightarrow M_V M_{IV} \end{cases}$$

REVIEWS OF BOOKS

Introduction to Electric Theory, by R. G. FOWLER. Pp. xii + 390. (Cambridge, Mass. : Addison-Wesley, 1953.) \$7.50.

This book is designed as a text appropriate to certain mathematics and physics curricula of American universities. Its standard is roughly that of the pass degree of British universities. It is generally recognized that there is a great need for electricity textbooks of this kind. Simultaneously there is a great need for expositions which place theoretical electricity on a rigorous, logical footing and are free of the fallacies and pitfalls for which the subject is notorious. The 'tidying-up' of classical electricity, however, still lies largely on the research level, and to attempt to combine this with a didactic account at the undergraduate level at the present time is a difficult task indeed. This is what the author has attempted. It is therefore sufficient commendation that he should have achieved a fair measure of success, and although much remains that one might criticize, no critic would wish to be unduly harsh—especially one who has himself had the experience of teaching such a course.

Regarding the treatment on its didactic merits, the outstanding characteristic is the unparalleled beauty, clarity and simplicity of exposition, making the subject not only understandable but alive and fascinating to the student grappling with its difficulties for the first time. Points which, as shown by experience, the student finds particularly difficult (e.g. the potential) are discussed at great length, leaving no room whatsoever for uncertainty or misunderstanding. Where possible, topics are illustrated by worked examples, and each chapter ends with a large number of examples for the student to do, with answers at the end of the book. This is in accordance with a plan of the author's to exploit the application to physics of the American student's parallel mathematical training, but no one will deny that its desirability is general. The text is well illustrated, a striking feature being the use of beautiful shaded diagrams for depicting complex, especially three-dimensional, situations. Vectors are introduced as a basic concept, but, appropriately so at this level, vector analysis is not used as a method of calculation; only vector summaries of results are given. A general system of units is used throughout, and is specialized where necessary, as in problems.

As already indicated, the scope of the book is roughly that of a pass degree course, so that a detailed description is unnecessary. The order differs from the conventional wherever this is necessary to meet the demands of an improved logical continuity. Features of special interest are the thorough use of Kelvin cavities for overcoming the difficulties of static field theory in polarized media, the introduction of convection and displacement currents at an early stage in order to provide a complete, although elementary, idea of the electromagnetic field, and the excellent and extensive treatments of special but useful topics such as networks and alternating current circuits.

Unfortunately the book could not serve as a complete text for the type of course usually given in British universities since, as indicated by the title, only the theory of electricity is treated; the experimental aspects are scarcely touched upon. More unfortunate, perhaps, is the fact that the average student may not feel able to pay such a high price for a text dealing with a limited part of his course. However, in all other respects the book can be highly recommended to both teacher and student. A reviewer cannot allow for the individual tastes of teachers, but it is a book that the teacher must see and judge for himself.

R. CADE.

CONTENTS OF SECTION B

	PAGE
Mr. H. MYKURA. Interference Microscopy at High Wedge Angles	281
Dr. B. T. M. WILLIS and Mr. H. P. ROOKSBY. Magnetic Transitions and Structural Changes in Hexagonal Manganese Compounds	290
Dr. D. MADOC JONES and Prof. E. A. OWEN. Experimental Study of the Variation of the Degree of Order with Temperature in a Copper-Palladium Alloy	297
Dr. M. V. WILKES. A Table of Chapman's Grazing Incidence Integral $Ch(x, \chi)$	304
Mr. J. DYSON and Dr. W. HIRST. The True Contact Area Between Solids	309
Dr. ALAN POWELL. The Reduction of Choked Jet Noise	313
Mr. A. LEMPICKI and Mr. C. WOOD. Observations on a Form of Breakdown in Germanium Diodes	328
Dr. F. C. ROESLER and Mr. J. R. A. PEARSON. Determination of Relaxation Spectra from Damping Measurements	338
Dr. J. L. ROGERS and the late Prof. F. C. CHALKLIN. A Geiger Counter Vacuum Spectrometer and its Use for the Study of Soft X-Ray Lines.	348
Research Notes :	
Dr. U. W. ARNDT, Mr. W. A. COATES and Dr. A. R. CRATHORN. A Gas-Flow X-Ray Diffraction Counter	357
Dr. AJIT RAM VERMA. Interferometric Observation of Mosaic Structure on the (111) Face of a Single Crystal of Germanium	359
Mr. H. J. GOLDSMID. On the Thermal and Electrical Conductivity of Semiconductors	360
Reviews of Books	364
Contents of Section A	368



PLATE I.



PLATE II.

Lens Spectrometer Study of the Disintegration of ^{233}Pa

BY THE LATE W. D. BRODIE*

Department of Natural Philosophy, University of Edinburgh

Communicated by N. Feather; MS. received 2nd December 1953

Abstract. The electron spectrum of ^{233}Pa has been studied over the energy range 4 keV to 570 keV. The energies of the observed conversion lines agree well with those (19 keV and over) of Keller and Cork and confirm the existence of the weak 272 keV γ -ray. The low-energy spectrum includes L-conversion lines of the 28.7 keV γ -ray, and M, N and O conversions of the predicted 17.2 keV γ -ray.

The intensities of the observed lines are in good agreement with the observations (37 keV and over) of Elliott and Underhill. The main part of the continuum consists of three partial spectra with end-points at 568 ± 5 , 256 ± 4 , and 140 ± 14 keV, and intensities of 5, 57 and 38% respectively. A decay scheme is proposed which requires that the partial spectrum of lowest energy is a close doublet.

^{233}Pa yields a total of 2.0 ± 0.15 electrons of 4 keV and over per disintegration.

§1. INTRODUCTION

THE first evidence for the existence of a 27.4 day activity in protactinium was obtained by Meitner, Strassmann and Hahn (1938). Two of these workers, namely Hahn and Strassmann (1940), later questioned the assignment of the 27.4 day activity to protactinium and suggested that it belonged to a zirconium isotope. The final assignment to an isotope of protactinium of mass number 233 was made and verified by other investigators (Seaborg, Gofman and Kennedy 1941, Grosse, Booth and Dunning 1941).

Several workers have studied the radiations from ^{233}Pa by absorption and spectroscopic methods. Haggström (1941) and Levy (1947), using 180° constant-radius β -ray spectrometers, found that the end-point of the β -spectrum was masked by conversion lines and estimated it to be at about 200 keV. Fulbright (1944) concluded that there is also a β -component with an end-point in the neighbourhood of 700 keV.

A careful investigation was made by Keller and Cork (1950) who used a permanent-magnet type β -spectrograph. The field strengths were chosen so that the range from 19 keV to 1.5 MeV could be covered. Keller and Cork observed 46 internal conversion lines and three weak K-Auger lines, all having energies below 411 keV. They also carried out an absorption experiment, using lead absorbers, which revealed no γ -ray harder than about 400 keV. They concluded from absorption experiments using beryllium and aluminium that the β -ray end-point was in the 200 keV region and found no trace of a component of higher energy as reported by Fulbright. The spectrometer used by Keller and Cork was a high resolution instrument capable of resolving the L-shell fine structure in the lower energy region. They found lines due to internal

* Dr. W. D. Brodie died on 27th June 1953. This paper was prepared from his Ph.D. thesis by Dr. M. A. S. Ross at the request of Professor N. Feather.

conversion in the L_I and L_{II} shells, but did not detect any L_{III} conversion. A list of the γ -rays found by these workers, showing the observed internal conversions is given in table 1. The nuclear level scheme suggested by them required a 17.4 keV γ -ray (not observed) to make it self-consistent.

After much of the work to be described below had been carried out, a report on ^{233}Pa by Elliott and Underhill (1952) became available. These workers used a magnetic lens spectrometer and studied the spectrum above 37 keV. They found that the main part of the β -continuum ends at about 260 keV and that about 8% extends to 570 keV. They observed internal conversion lines corresponding to nine γ -rays of energies 76, 88, 105, 298, 310, 339, 398, 415 and 474 keV. The presence of the last of these was deduced from a single very weak conversion line.

Table 1

γ -ray energy (keV)	Conversion lines observed	γ -ray energy (keV)	Conversion lines observed
28.9	M, N, O.	301.5	K, L, M.
40.6	L_{II} , M, N.	313.1	K, L, M, N.
58.1	L_I , L_{III} .	342	K, L, M, N.
75.7	L_I , L_{II} , M, N, O.	376.5	K, L.
87.1	L_I , L_{II} , M, N, O.	399.9	K, L, M.
104.5	L_I , L_{II} , M, N, O.	416.4	K, L, M.
272.6	K, L.		

Some of these γ -rays were also found in the external photoelectron spectra from silver and gold radiators. Elliott and Underhill carried out a coincidence experiment using two lens spectrometers arranged end to end. One was focused on the intense K internal conversion line of the 310 keV γ -ray, while the other was set on selected points in the spectrum. The 76, 88 and 105 keV transitions, as well as about 75% of the continuum, were found to be correlated with the 310 keV transition. These facts, together with the intensities of the γ -rays in external and internal conversion, led them to suggest the disintegration scheme shown in figure 4(b). It will be noticed that the main part of the β -spectrum (i.e. below 260 keV) has been divided amongst six β -transitions.

The objects of the present work were to re-examine the spectrum of ^{233}Pa , using a lens spectrometer with postfocusing acceleration (Butt 1949, 1950), extending the observations below the limit of Keller and Cork's apparatus. Since there are many K- and L-conversion lines in the ^{233}Pa spectrum, an L-Auger spectrum must be present in the region between 7 and 17 keV. Also, if the interpretation of Keller and Cork is correct, some very low energy internal conversion lines should be found. In particular, L-conversion electrons of the 28.9 and 40.6 keV transitions should appear at about 7 and 19 keV, respectively, and if a 17.4 keV γ -ray exists, M, N and O conversion electrons may be seen.

§2. EXPERIMENTS WITH SOURCE NO. 1

The ^{233}Pa was produced at the Atomic Energy Research Establishment, Harwell, by slow neutron bombardment of ^{232}Th followed by β -decay (half-value period = 23.5 min). It was purified chemically at the Radiochemical Centre, Amersham, and delivered in the form of the complex with thenol tri-fluoro acetone in benzene solution. The protactinium was extracted with 25% efficiency from the benzene solution by treatment with concentrated HCl,

After boiling off the excess HCl one drop of solution was placed on gold leaf 0.2 mg cm^{-2} in thickness which had previously been wetted with insulin solution. For extra strength the gold leaf was backed with a nylon film of superficial mass $20 \mu\text{g cm}^{-2}$. The diameter of the prepared source was 0.4 cm .

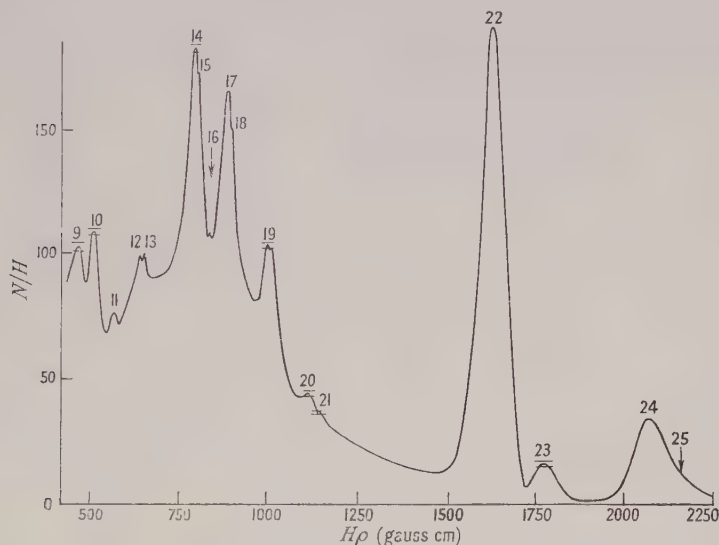


Figure 1. Electron spectrum of ^{233}Pa above 16 keV taken with source no. 1. Statistical errors are indicated.

Figure 1 shows the spectrum in the energy range above 16 keV. The observations were made at 300 different $H\rho$ values selected to give good definition of the lines. The statistical error (not constant throughout the spectrum) is indicated for chosen points on the curve. An accelerating potential of 7.0 kv was used in investigating the lower-energy half of the spectrum, the counter window being about 0.1 mg cm^{-2} in thickness. The continuum appears to end at approximately 1900 gauss cm. It will be shown later, however, that there is a weak β -ray continuum extending to a higher energy end-point.

Since the product nucleus of the β -decay is uranium, the K-L-M . . . energies to be used in interpreting the line spectrum are those of element 92. They were calculated from the term values given in the 'Landolt-Börnstein' tables (1950), and are shown in table 2.

Table 2

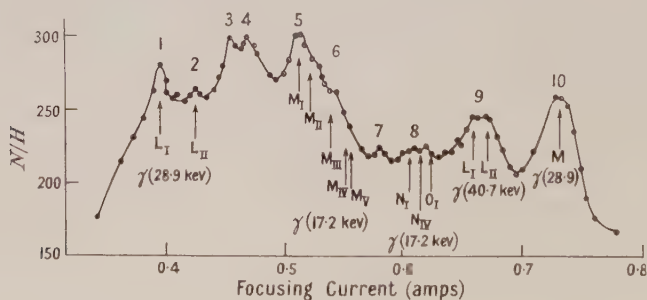
	K	L _I	L _{II}	L _{III}	M _I	M _{II}	M _{III}	M _{IV}	M _V
$E \text{ (kev)}$	115.8	21.80	20.99	17.20	5.56	5.19	4.31	3.73	3.56
			N _I	N _{II}	N _{III}	N _{IV}	N _V	N _{VI}	N _{VII}
$E \text{ (kev)}$			1.44	1.27	1.04	0.78	0.74	0.39	0.38

The conversion lines have been analysed in table 3, which shows the momenta in gauss cm, the energies in kev, the shells in which conversion is assumed to take place and the corresponding γ -ray energies. The results agree well with those of Keller and Cork shown in table 1—except that the weak γ -ray of 272 kev energy was not observed and the γ -rays of 301 and 313 kev were not resolved.

Table 3

No. of line	$H\rho$ (gauss cm)	E (keV)	Level of conversion	Energy of γ -ray (keV)
9	472	19.3	L_I and L_{II}	40.7
10	518	23.1	M	28.7
11	571	27.9	N	29.3
12	641.5	35.0	M	40.6
13	656	36.5	L_I	58.3
14	804	54.0	L_I	75.8
15	811	54.9	L_{II}	75.9
16	839	58.6	L_{III}	75.8
17	888	65.3	L_I	87.1
18	895	66.2	L_{II}	87.2
19	1010	83	L_I and L_{II}	104.4
20	1112	99.2	M	104.8
21	1142	104	N	105.4
22	1640	198	K	313.8
23	1777	227	K	342.8
24	2073	293	L	314
25	~ 2185	~ 320	L	342

An examination was next made of the low-energy region of the spectrum. The accelerating potential was maintained at 7.0 kv, and four runs were taken between $H\rho = 240$ and $H\rho = 550$ gauss cm. The first and third runs were started at the upper momentum limit and the second and fourth at the lower momentum limit. A plot of the 'raw counts' was made for each run, and these four plots were found to be closely similar, peaks appearing at very nearly the same positions in the four cases. In view of this consistency it is very unlikely that any of the peaks is due to a chance statistical fluctuation. The averaged and normalized low-energy spectrum is shown in figure 2.

Figure 2. The low-energy spectrum of ^{233}Pa .

The interpretation of the low-energy lines is rendered uncertain by the fact that both Auger and internal conversion lines are present. Moreover, since the relative intensities of internal conversion in the three L shells are not known, it is difficult to make an estimate of the relative intensities of the Auger lines originating in L_I , L_{II} and L_{III} . However, an examination of figure 1 and table 3 indicates that internal conversion in L_{III} is low, while that in L_{II} , although smaller than in L_I , is certainly not negligible. Anticipating the results of table 5 we can assume that the relative intensities of internal conversion in the K, L and (M+N) shells are approximately as 113:85:14.5. In whatever ratios the 85 units in the L shells are divided among L_I , L_{II} and L_{III} (always remembering

that $L_I \geq L_{II} \geq L_{III}$) it turns out that ultimately the ionization in L_{III} considerably exceeds that in L_I and L_{II} . The reasons for this are, firstly, that the x-ray transition $K \rightarrow L_I$ is forbidden, and the K-Auger transition $K \rightarrow L_I L_I$ of small intensity (virtually all of the K-shell ionization being transferred to L_{II} , L_{III} and the M shells), and secondly that the Coster-Krönig transitions transfer a large fraction of the direct L_I ionization to the L_{III} shell.

Two calculations have been made using the K x-ray intensities calculated by Massey and Burhop (1936) and the Coster-Krönig coefficient calculated by Kinsey (1948). For the first, the initial L-shell ionization was assumed to be divided among L_I , L_{II} and L_{III} in the ratios 76:8:1, and for the second in the ratios 45:35:5. The final relative L-shell ionization intensities are 30.4:35.8:105.8 and 18.0:62.8:91.2 for the two cases. Hence, using Kinsey's (1948) calculated fluorescence yields for the three shells, the relative numbers of Auger electrons originating from ionization in L_I , L_{II} and L_{III} are 18.3:14.7:62.4 and 8.8:25.8:53.8, respectively, corresponding to the two sets of initial assumptions. Thus, whatever the true ratio of the numbers of L_I and L_{II} internal conversion electrons, most of the observed L-Auger electrons must be due to the filling of vacancies in the L_{III} shell. L_I - and L_{II} -Auger lines should also be observed, but with smaller intensity.

With this conclusion in mind, the ten lines of figure 2 have been interpreted as shown in table 4.

Table 4

No. of line	$H\rho$ (gauss cm)	E (keV)	Interpretation
1	282	7.0	L_I conversion of γ -ray 28.8 keV
2	302	7.9	L_{II} conversion of γ -ray 28.9 keV
3	324	9.2	Auger $L_{III} \rightarrow M_V M_{III}$ (9.3 keV)
4	335	9.8	Auger $L_{III} \rightarrow M_V M_{IV}$ (9.9 keV)
5	365	11.6	M conversion of γ -ray 17.2 keV + Auger $\begin{cases} L_{II} \rightarrow M_{IV} M_I & (11.7 \text{ keV}) \\ L_{III} \rightarrow M_V N_I & (12.2 \text{ keV}) \end{cases}$
6	387	12.9	M conversion of γ -ray 17.2 keV + Auger $L_{II} \rightarrow M_{IV} M_{III}$ (12.95 keV)
7	413	14.8	Auger $L_I \rightarrow M_I N_I$ (14.8 keV) or Auger $\begin{cases} L_{II} \rightarrow N_{IV} M_I & (14.65 \text{ keV}) \\ L_{II} \rightarrow N_{IV} M_{II} & (15.0 \text{ keV}) \end{cases}$
8	438	16-17	N+O conversion of γ -ray 17.2 keV + Auger $L_{II} \rightarrow M_{IV} N_I$ (15.8 keV)
9	$\begin{cases} 469 \\ 478 \end{cases}$	$\begin{cases} 19.0 \\ 19.7 \end{cases}$	L_I conversion of γ -ray 40.8 keV L_{II} conversion of γ -ray 40.7 keV
10	522	23.4	M conversion of γ -ray 28.9 keV

Lines 1 and 2 are due to conversion in the L_I and L_{II} shells of a 28.9 keV γ -ray, already known from its M and N conversion electrons (see table 3). Lines 3 and 4 are interpreted as Auger lines corresponding to the transitions $L_{III} \rightarrow M_V M_{III}$ and $L_{III} \rightarrow M_V M_{IV}$. The same transitions appeared in the L-Auger spectra of RaE and RdTh (Butt and Brodie 1951, Brodie 1954), although in neither of these cases were the two lines resolved. Lines 9 and 10 are also easily interpreted. The former is due to conversion of the 40.6 keV γ -ray in the L_I and L_{II} shells, the two lines being incompletely resolved, and the latter to the M-shell conversion of the 28.9 keV γ -ray (see also figure 1).

Regarding the remaining four lines, if numbers 5 and 6 are due to Auger electrons, the most likely transitions appear to be $L_{II} \rightarrow M_{IV} M_I$ and $L_{III} \rightarrow M_{IV} M_{III}$, and, in view of the conclusions reached above about the relative intensities of the L_{II} and L_{III} Auger electrons, the observed intensities seem rather high. Further, the shape of the high-energy side of the group of lines 5 and 6 suggests that the main contribution to the observed distribution is from the conversion of a single γ -ray in the five M shells. The arrows in figure 2 show the calculated positions of M conversion electrons of a 17.2 keV γ -ray, and it is clear that this interpretation fits the observations. It is assumed that the Auger lines, for example those due to the transitions $L_{II} \rightarrow M_{IV} M_I$ and $L_{III} \rightarrow M_{IV} N_I$ which are expected on the basis of the results for $MsTh_2 \rightarrow RdTh$ (Brodie 1954), are submerged in this complex group.

If lines 5 and 6 are indeed due to internal conversion of a 17.2 keV γ -ray, it is to be expected that conversion in the N and O shells would also show up. The broad line number 8 in figure 2 is very probably due to these conversions, together with an Auger line due to the transition $L_{II} \rightarrow M_{IV} N_I$. The calculated positions of these lines are shown on the figure. Finally, line 7 in figure 2 may be due to the Auger transition $L_I \rightarrow M_I N_I$, or to a combination of two lines resulting from the transitions $L_{II} \rightarrow N_{IV} M_I$ and $L_{III} \rightarrow N_{IV} M_{II}$.

The conclusions to be drawn from this study of the low-energy region of the ^{233}Pa spectrum are therefore as follows:

1. The 28.9 keV γ -ray reported by Keller and Cork in M, N and O conversion has been confirmed by the detection of its conversion electrons in the L_I and L_{II} shells at 7.0 and 7.9 keV respectively.
2. L_I and L_{II} conversion lines of the 40.6 keV γ -ray have been found. Previously L_{II} was the only L-shell conversion reported since the apparatus of Keller and Cork cut off at just over 19 keV.
3. While the existence of the 'hypothetical' 17 keV γ -ray of Keller and Cork cannot be said to have been proved beyond all doubt, strong circumstantial evidence for its existence has been obtained from lines attributed to M, N and O conversion.
4. As regards the lines which have been interpreted as due to Auger electrons, the transitions postulated agree with those suggested to explain similar lines in the spectra of RaE and RdTh.

§3. EXPERIMENTS WITH SOURCE NO. 2

Because of back-scattering from the gold leaf on which it was mounted, source no. 1 could not give satisfactory information about the shape of the continuous β -spectrum or about the relative intensities of the internal conversion lines. Moreover, the resolving power obtainable with this source was not sufficiently good in the high-energy region; in particular, the K conversion lines of the 301 and 313 keV γ -rays were not resolved. To try to remove these defects a new source was prepared with the following objectives in mind: (i) the backing to be as thin and light as possible to reduce scattering, (ii) the source to be as thin as possible, despite loss of intensity, so as to reduce scattering and absorption in the source material, (iii) the area of the source to be smaller than before, to improve resolution.

To ensure that no organic matter was left in the source, it was prepared by the following method. The protactinium compound was dissolved in benzene,

evaporated to dryness in a platinum crucible and ignited. The residue was dissolved in 12N HCl, evaporated to a small volume and one drop of the solution was placed on a collodion film, previously wetted with insulin solution in the usual way. The collodion film was about $20\ \mu\text{g cm}^{-2}$ in thickness. The drop of solution was evaporated under an infra-red lamp, using gentle heat, the remainder of the film being protected by a piece of aluminium foil. In colour the source was a brownish deposit. Since all organic matter had been removed in the ignition process, the residue must have been an inorganic impurity. The source was about one tenth as strong as no. 1 and was too weak to be used in the very low energy region. Its diameter was 0.3 cm. No attempt was made to 'earth' this source to the spectrometer. With such a weak source the conductivity of the collodion can generally be relied on to prevent the source from charging up to such an extent that the energies of the lines are measurably affected. In fact, no evidence of source charging was found—the energies of the observed lines agreed closely with the values found with source no. 1 over the energy range covered (i.e. above 23 kev).

The spectrum obtained with source no. 2 showed considerably improved resolving power at the higher energies. The K-conversion line of the 301 kev γ -ray was clearly seen. At the lower energies the statistical error was too large for the L-shell fine structure to be revealed. The energies of the observed lines are given in table 5. They agree well with those in table 3 even at the lower energies, where the effects of source charging are likely to be most serious.

Table 5

Line no.	Energy (kev)	Level of conversion	γ -ray energy	Conversion line intensity	Elliott's conversion line intensity
9*	19.19.7	L	40.7	5	—
10	22.9	M	28.6	10	—
11	27.3	N	28.7	1.5	—
13	36.4	L	58	4	—
14	53.8	L	75.6	21	20
17	65.2	L	87	17.4	24
18a	70.5	M, N	76	1	5
19	82.3	L	104.1	10.4	11
20	99.2	M	104.7	2	3
22a	185.8	K	301.6	4	10
22	198	K	313.8	100	100
23	228	K	343	8	10
24	292	L	313.8	25	25
25	319	L	340	4†	2.5

* The data for this line were obtained from figure 2. Its intensity was estimated by comparison with the M conversion of the 28.7 kev γ -ray.

† Includes the K conversion of 415 kev γ -ray—not resolved.

A 'continuous spectrum' was sketched in under the lines so that an estimate of the line intensities could be made. The results of the relative intensity measurements, made with a planimeter, are included in table 5, the intense 198 kev line being arbitrarily assigned an intensity of 100. Keller and Cork did not measure the intensities of their lines, but table 5 shows the figures given by Elliott and Underhill. Agreement between their results and ours is good, with the exception of line 22a (which was not completely resolved) and the weak line 18a.

A Fermi plot of the continuous β -spectrum, as far as it could be observed in the presence of the internal conversion lines, is shown in figure 3. Six of the points, corresponding to energies between 140 and 210 keV, lie on a straight line which, on extrapolation, cuts the energy axis at about 252 keV. This

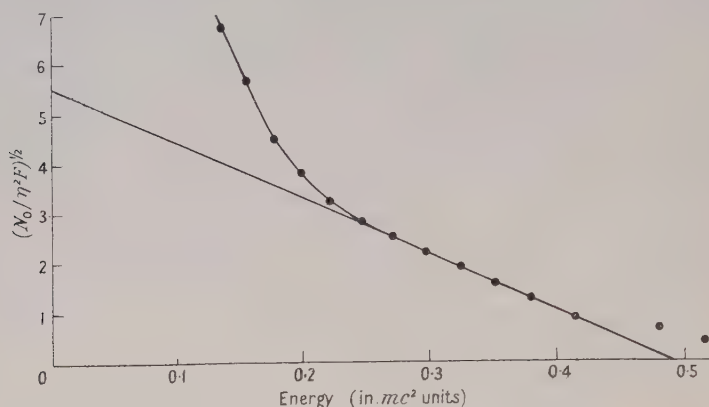


Figure 3. The Fermi plot obtained from the spectrum of source no. 2. N_0 is the number of electrons per unit momentum interval, η is the momentum of the electrons in mc units and F is the Fermi function for $Z=92$.

agrees well with the value of 260 keV given by Elliott and Underhill for the end-point of the main component of the β -spectrum. Below 140 keV the Fermi plot curves upwards and, while this curvature may in part arise from scattered electrons, it is probably due in the main to the presence of one or more partial β -spectra with end-points lower than 250 keV. The two points at the high energy end of the plot lie well above the straight line. These points are subject to considerable error, but they suggest that the β -continuum does, in fact, have a low intensity component with an end-point considerably higher than 250 keV.

§4. PRELIMINARY DISCUSSION OF THE DECAY SCHEME

On the whole the γ -rays deduced from the observations reported above agree well with those reported by Keller and Cork, and some evidence has been found for a γ -ray of about 17 keV. The 272 and 377 keV γ -rays of these authors have not been found. This measure of agreement does not necessarily confirm the level scheme of Keller and Cork (hereafter referred to as I), as will now be shown. The scheme suggested by Elliott and Underhill, reproduced in figure 4(b) and designated II, can accommodate the 29, 41, 59 and 17 keV γ -rays, which are shown by dotted lines in the diagram as they were not observed by these workers: in fact there are two possible 59 keV transitions. Moreover, the presence of these γ -rays, the first three of which have been confirmed beyond doubt, may remove the need for some of the partial β -spectra suggested by Elliott and Underhill.

Basically there are four levels which are common to the two suggested schemes. To make this clear, Keller and Cork's scheme, I, has been drawn inverted in figure 4(a), with the energies of the levels suitably reallocated. Clearly, apart from the fact that I is inverted, the only differences are that there is no level corresponding to B in II, and that levels b and g do not appear in I. Level B is missing from II because Elliott and Underhill did not detect the 40.6, 272 and 376 keV γ -rays, all of which involve level B in I. But to

accommodate their 298 kev γ -ray, Elliott and Underhill introduced level b and fed it directly by a partial β -spectrum. It is noteworthy, however, that the energy difference between b and d is 41 kev, so that one of the 'missing' γ -rays can be accommodated in II. Clearly, to confirm the existence of B it is necessary to confirm either the 272 or the 376 kev γ -ray. This point will be dealt with in a later section.

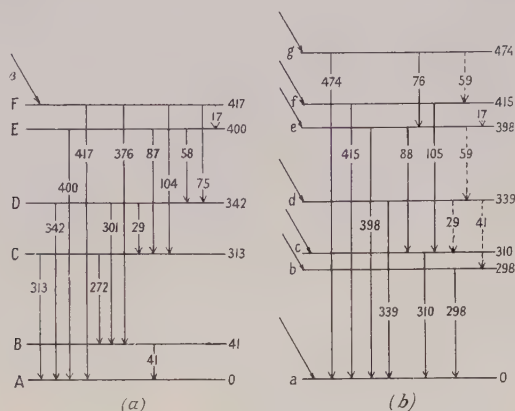


Figure 4. A comparison between (a) the inverted level scheme of Keller and Cork and (b) the level scheme as given by Elliott and Underhill.

Turning now to level g, we recall that the existence of a 474 kev γ -ray appeared, on the basis of Elliott and Underhill's spectrum, to be a little doubtful. Further, since the difference between levels f and d is 76 kev, the transition $g \rightarrow e$ can be replaced by $f \rightarrow d$. As Elliott and Underhill did not observe the 29 kev γ -ray they could not use the transition $f \rightarrow d$, because it would violate their experiment showing coincidence in time between the 76 and 310 kev γ -rays. However, as the 29 kev γ -ray has now been established, it is possible that the 76, 29 and 310 kev transitions occur in cascade. We conclude, therefore, that further experimental evidence is required before the existence of the 474 kev level can be accepted as proved.

The remaining point of disagreement between schemes I and II concerns the ultimate β -particle end-point in the ^{233}Pa disintegration. The work of Elliott and Underhill suggests an end-point at 570 kev, which fits satisfactorily into their decay scheme, but the only other report of a high-energy end-point places it at 700 kev (Fulbright 1944). The present work, as described so far, shows some indication of a β -component with an end-point higher than 250 kev, but the precise position of this end-point remains uncertain.

To provide evidence on the points discussed above, further experiments were performed.

§5. EXPERIMENTS WITH SOURCE NO. 3

Search for Conversion Electrons of a 272 kev γ -Ray

A much stronger source was prepared from a new and chemically purer supply of ^{233}Pa . It was mounted in the usual way on gold foil 0.2 mg cm^{-2} in thickness. A search was then made for the 272 kev γ -ray reported by Keller and Cork. According to these workers the K-conversion line has an energy

of 156.6 keV, corresponding to a momentum of 1430 gauss cm. In all, ten runs were made over the region between 1270 and 1525 gauss cm, about 50 000 counts being taken on each point. The curve obtained is shown in figure 5, in which the statistical error on each point corresponds to about $\pm 0.4\%$. The only departure from an otherwise smooth curve occurs at about 1430 gauss cm, where there seems to be a very weak line. It has about the expected width for a line of this momentum, and its energy (156 keV) suggests that it is, in fact, the K-conversion line of a γ -ray of 272.6 keV. On the basis of this evidence, together with the fact that Keller and Cork, using a semicircular spectrometer with photographic detection (which is possibly the most sensitive method of detecting weak lines), reported finding both K- and L-conversion electrons of this γ -ray, the existence of this transition may be said to be established. This implies that level B of figure 4(a) must be included in the scheme, and so favours the level scheme of Keller and Cork, either inverted or as originally published.

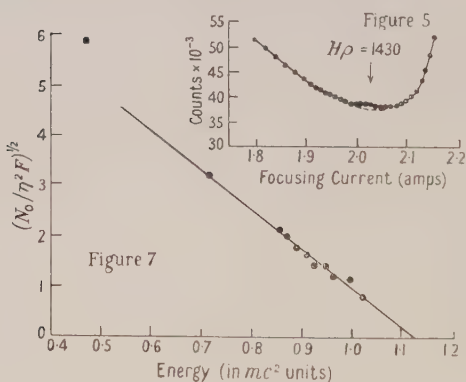
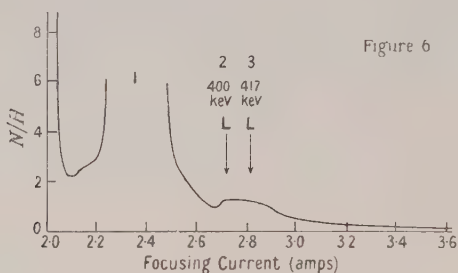


Figure 5. Electron spectrum obtained from source no. 3 in the search for K-conversion electrons of a 272 keV γ -ray.

Figure 6. The high energy 'tail' of the β -spectrum of ^{233}Pa obtained from source no. 3.

Figure 7. Fermi plot of the spectrum in figure 6.

The Continuous β -Spectrum of ^{233}Pa at High Energies

In all the experiments so far reported the spectrometer had been set for high collecting power, with a source-to-counter distance of about 50 cm. Under these conditions the maximum momentum which could be focused was about 2500 gauss cm. With a strong source available it became possible to increase the source-to-counter distance to 80 cm, allowing the coil to focus electrons having momenta up to about 3400 gauss cm.

With this arrangement the high energy tail of the β -spectrum was examined carefully from about 235 kev upwards. The spectrum so obtained is shown in figure 6. The group of lines marked 1 consists of the L- and M-conversion electrons of the 313 kev transition, and the L line of the 342 kev γ -ray. The weak lines 2 and 3 at 2430 and 2500 gauss cm respectively, not previously detected in this work, are interpreted as the L-conversion lines of γ -rays of 400 and 417 kev respectively. The K-conversion lines of these transitions are in the group of lines 1 and are not resolved from the other lines present. This interpretation is in agreement with both Keller and Cork and Elliott and Underhill.

A Fermi plot of the high-energy continuum was made by selecting points between the conversion lines. The result is shown in figure 7, from which it can be seen that the last ten points lie very nearly on a straight line. The end-point, deduced by the method of least squares, is 568 kev, in good agreement with the value of 570 kev given by Elliott and Underhill.

The spectrum obtained with this source down to about 90 kev is shown in figure 8, the sharp rise of the continuum in the region of the strong conversion lines being evident. The complete Fermi plot obtained from this set of

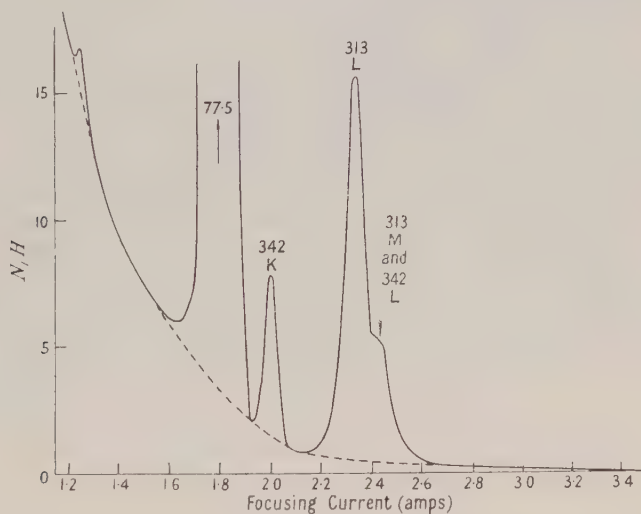


Figure 8. β -spectrum of ^{233}Pa from source no. 3.

observations is shown in figure 9, while the inset on the same diagram shows a tracing of the Fermi plot published by Elliott and Underhill. Clearly the two are almost identical. The end-points of the three partial spectra in figure 9 are 565, 256 and ~ 140 kev. The first two of these have already been measured in the present work as 568 and 252 kev, respectively; the third must be regarded as approximate since the Fermi plot might well be distorted on account of back-scattering at low energies.

Assuming that all three partial spectra have shapes which approximate to the allowed shape, then the relative intensities deduced from the extrapolated Fermi plots of the three spectra, in the order given above, are approximately

5 : 45 : 50. These ratios are liable to error on account of departures from assumed spectral shape and of distortion of the Fermi plot due to back-scattering, but the figures may be taken as a guide in an attempt to build up a disintegration scheme.

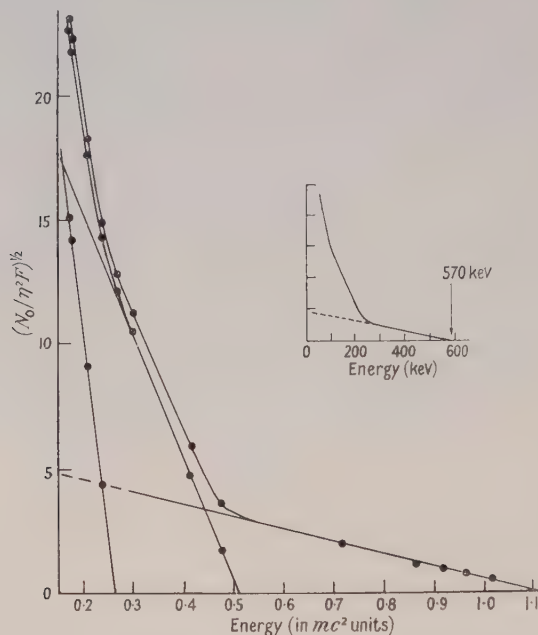


Figure 9. Fermi plot obtained from spectrum in figure 8 compared with the Fermi plot (inset) published by Elliott and Underhill.

Search for K-Conversion Electrons of a 474 keV γ -Ray

The K-conversion line of the 474 keV γ -ray would appear between lines 1 and 2 in figure 6. A search was therefore made in this region but, because the counting rate was low and less than three times the γ -ray background, the statistical accuracy was only about 3%. No line of intensity comparable with the weak lines 2 and 3 of figure 6 was found, and it is estimated that a line one-third as intense as line 2 would just have been observed. According to Elliott and Underhill the ratio of the intensities of the two lines was roughly 1 : 3.

The experiment was therefore inconclusive, so that the existence of a 474 keV level in the ^{233}U nucleus is still in doubt.

§6. SUGGESTED DECAY SCHEME FOR $^{233}\text{Pa} \rightarrow ^{233}\text{U}$

The data which have to be used in building up a disintegration scheme are as follows:

1. The energies of the transitions occurring in the ^{233}U nucleus, as given in earlier sections.
2. The relative intensities of the internal conversion electrons, as listed in table 5.
3. The end-points of the partial β -spectra.
4. The relative intensities of the partial β -spectra.
5. The internal conversion coefficients of the γ -rays.
6. The absolute intensity of the 313 keV transition.

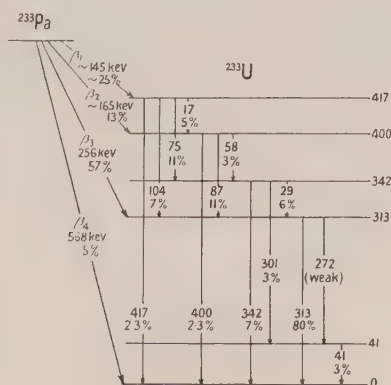
Items 5 and 6 were taken from the results of Elliott and Underhill, except that the intensity of 75% which they give for the 313 keV transition had to be increased to 80% to make the scheme self-consistent.

The data on the transitions in the daughter nucleus, ^{233}U , are summarized in table 6, the absolute intensities having been deduced from the measured relative intensities of the internal conversion lines and the internal conversion coefficients, assuming a total intensity of 80% for the 313 keV transition.

Table 6

No. of γ -ray	Transition energy (keV)	Intensity of internal conversion electrons		Remarks	Absolute intensity of transition (%)
		Rel.	Abs. (%)		
1	17.2	?			?
2	28.7	(M and N only)	4	Allow 2% for L conversion and unconverted γ -ray—based on figure 2	6
		12			
3	40.7	5	2	Relative intensity from figure 2	3
4	58	4	2		3
5	76	22	7.5	Using Elliott's conversion coefficients	11
6	87	17	6	ditto	11
7	104	12	4	ditto	7
8	272	—	—	Very weak	—
9	301	5	2	Using Elliott's conversion coefficients	3
10	313	125	43	ditto	80
11	342	10	3	ditto	7
12	400	—	—	Elliott's intensity	2.3
13	417	—	—	ditto	2.3

The end-points of the partial β -spectra are finally taken to be 568 ± 5 , 256 ± 4 and ~ 140 keV. The accuracy of the third figure is probably no better than 10%. The intensities of the three β -spectra are provisionally 5%, 45% and 50% respectively.


 Figure 10. Suggested disintegration scheme for $^{233}\text{Pa} \rightarrow ^{233}\text{U}$.

On the basis of these data the disintegration scheme of figure 10 is suggested. The levels in the ^{233}U nucleus correspond to an inversion of the scheme of

Keller and Cork; the details of the partial β -spectra and the relative intensities of table 6 forbid its use in the original form. The intensities of the transitions in the ^{233}U nucleus which are shown in figure 10 are those listed in table 6, and it can be seen that the scheme adequately meets the requirement that the total intensity arriving at any level is equal to that leaving the level. It has been necessary to assume that the least energetic of the partial β -spectra is split into two having end-points differing by 17 kev. If this is not done, an intensity of 18% must be assumed for the 17 kev transition. This was not found, and in the scheme a value of 5% has been suggested as the probable maximum intensity for this transition. The intensities suggested in the scheme for the partial β -spectra are 5%, 57% and $(13+25)\%$. These show reasonable agreement with the provisional values 5%, 45% and 50%, which were accurate enough only to serve as a guide.

While figure 10 fits the observations satisfactorily, it is not claimed to be unique. In particular, the weak 474 kev transition suggested by Elliott and Underhill has not been conclusively proved to be absent. If it is present, a 474 kev level must be included in the ^{233}U nucleus, fed by a β -spectrum having an end-point at about 95 kev. As has been indicated in figure 4, such a level would allow an alternative position for the 75 kev transition. It would also require some modification of the intensities of the partial β -spectra.

Further experiment is required to establish a final decay scheme. The 474 kev transition is, at best, very weak, and the most fruitful method would probably be to search for line-to-line coincidences among the 87, 75 and 58 kev transitions, using a double spectrometer or electron sensitive nuclear emulsions. Figure 10 would forbid all such coincidences, whereas Elliott and Underhill's scheme (figure 4(b)) would show the 76 kev transition in coincidence with the 88 kev, and possibly also with the 59 kev transition. Useful information might also be obtained by finding the end-points of the partial β -spectra in coincidence with the various γ -rays.

§7. THE COUNTING EFFICIENCY OF ^{233}Pa

Counting efficiency has been defined (see, for example, Karraker 1951) as "the ratio of observed counts to actual disintegrations under specified counting conditions". If a counter insensitive to electromagnetic radiations is used under suitable solid angle conditions the counting efficiency gives a measure of the total number of electrons per disintegration. This quantity has been measured by Karraker (1951) using a direct counting method, and by Seaborg *et al.* (1942), the respective results being 2.7 and 2.3 electrons per disintegration. Since the probable error quoted by Karraker is 10%, he claims substantial agreement with Seaborg.

An estimate of the number of electrons per disintegration can be made from the results of the present work with an accuracy of the same order as that claimed by Karraker, provided the number of Auger electrons can be assessed. As has been explained in §2, there is not enough information available concerning the relative intensities of the L_I , L_{II} and L_{III} conversion electrons to enable an accurate estimate of the intensity of the L-Auger electrons to be made. However, a rough value can be obtained by assuming a value for the total fluorescence yield of all three L shells.

From table 6 the total number of internal conversion electrons is 0.73 per disintegration. This result is unlikely to be greatly in error in view of the satisfactory way in which the intensities fit into the decay scheme. Further, it agrees well with the value of 0.72 deduced from the results of Elliott and Underhill, although the latter figure ought perhaps to be increased slightly to take account of the low-energy transitions which they did not detect. The value 0.73 ± 0.08 has been assumed. This figure was divided among the K, L, M and N shells according to the measured relative intensities of the internal conversion electrons. After taking account of the transfer of ionization from the K to the L and M shells by K x-ray emission, the number of L-Auger electrons was found to be 0.31 ± 0.08 . This assumes a total L-shell fluorescence yield of 0.52, a value based upon the calculations of Kinsey (1948). The total number of electrons emitted per disintegration of ^{233}Pa is thus 2.0 ± 0.15 .

In making this estimate no account has been taken of the K-Auger electrons since the K-shell fluorescence yield for uranium is very high, nor any account of the M- or N-Auger electrons. The M-Auger electrons would have energies of about 2 kev and, since Karraker used a windowless counter in determining the absorption curve of ^{233}Pa , it is possible that electrons of 2 kev could have been counted. Moreover, the sensitivity of his counter to the soft M x-rays could have been appreciable. These considerations may explain at least some of the difference between Karraker's result and the present one.

§ 8. CONCLUSIONS

1. *γ -rays and internal conversion electrons.* In the region above 19 kev 12 γ -rays have been identified from a study of their internal conversion electrons. The energies of the γ -rays agree well with those given by Keller and Cork (1950) who, however, list one additional weak γ -ray of 377 kev. The relative intensities of the internal conversion electrons have been measured and the results agree well with the values given by Elliott and Underhill (1952).

2. *The spectrum at low energies.* Interpretation of the L-Auger spectrum is complicated by the presence of internal conversion electrons, but the transitions suggested to explain those lines definitely identified as Auger lines are in agreement with transitions occurring in the spectra of RaE or RdTh or both. L-conversion electrons of the 28.7 kev γ -ray have been identified in the 7 kev region, and some evidence has been obtained for a 17.2 kev γ -ray.

3. *The continuous β -spectra.* The main part of the primary β -spectrum of ^{233}Pa ends at 256 kev, but there is a low-intensity partial spectrum extending to 568 kev. These results agree very well with those of Elliott and Underhill. The main part of the continuum has been shown to consist of three partial β -spectra, the intensities of which have been roughly estimated.

4. *Disintegration scheme.* The energies and intensities of the β -spectra and of the γ -rays and internal conversion electrons fit satisfactorily into the decay scheme given in figure 10.

5. *The number of electrons emitted per disintegration of ^{233}Pa .* The number of electrons emitted per disintegration of ^{233}Pa , excluding M- and N-Auger electrons, was found to be 2.0 ± 0.15 . This is lower than the figures published by Karraker (1951) and by Seaborg *et al.* (1942), but it is suggested that their values may include the M-Auger electrons and possibly an appreciable fraction of the M x-rays.

REFERENCES

- BUTT, D. K., 1949, *Proc. Phys. Soc. B*, **62**, 551; 1950, *Ibid.*, A, **63**, 986.
BUTT, D. K., and BRODIE, W. D., 1951, *Proc. Phys. Soc. A*, **64**, 791.
BRODIE, W. D., 1954, *Proc. Phys. Soc. A*, **67**, 265.
ELLIOTT, L. G., and UNDERHILL, A. B., 1952, *Atomic Energy Research Establishment Library*, Harwell, Report HAR 761.
FULBRIGHT, H. W., 1944, *Plutonium Project Report*, CP-1954.
GROSSE, A. V., BOOTH, E. T., and DUNNING, J. R., 1941, *Phys. Rev.*, **59**, 322.
HAGGSTRÖM, E., 1941, *Phys. Rev.*, **59**, 322.
HAHN, O., and STRASSMANN, F., 1940, *Naturwissenschaften*, **28**, 543.
KARRAKER, D. G., 1951, *University of California Radiation Laboratory Report* AECD 3154.
KELLER, H. B., and CORK, J. M., 1950, *Phys. Rev.*, **79**, 1030.
KINSEY, B. B., 1948, *Canad. J. Res. A*, **26**, 404, 421.
LANDOLT-BÖRNSTEIN, 1950 *Zahlenwerte und Funktionen*, Part 1, 6th Edn (Berlin: Springer), p. 288.
LEVY, P. W., 1947, *Phys. Rev.*, **72**, 352.
MASSEY, H. S. W., and BURHOP, E. H. S., 1936, *Proc. Camb. Phil. Soc.*, **32**, 461.
MEITNER, L., STRASSMANN, F., and HAHN, O., 1938, *Z. Phys.*, **109**, 538.
SEABORG, G. T., GOFMAN, J. W., and KENNEDY, J. W., 1941, *Phys. Rev.*, **59**, 321.
SEABORG, G. T., GOFMAN, J. W., and STOUGHTON, R. W., 1942, *University of California Radiation Laboratory*, Report A 192.

Emission of Electron-Positron Pairs from Light Nuclei II: γ -Transitions in ^8Be , ^{10}B and ^{16}O

BY S. DEVONS AND G. GOLDRING*

Department of Physics, Imperial College, London

MS. received 3rd November 1953

Abstract. The angular correlation of internally produced electron-positron pairs has been measured in the γ -transitions of several light nuclei. The measured correlation functions are compared with the theoretically predicted values and other information regarding the multipole character of the transitions.

§ 1. INTRODUCTION

IN a previous paper (Devons, Goldring and Lindsey 1954, subsequently referred to as I) apparatus has been described for measuring the angular correlation of internally produced electron-positron pairs, and its application to a study of the monopole transition in the ^{16}O nucleus. The present paper describes measurements of the pairs associated with some high energy γ -transitions in light nuclei. The transitions investigated were:

$^7\text{Li}(p, \gamma)^8\text{Be}$ (440 keV); $^9\text{Be}(p, \gamma)^{10}\text{Be}$ (998 keV); $^{19}\text{F}(p, \alpha\gamma)^{16}\text{O}$ (340 keV).

The energies are those of the bombarding protons. In all these transitions the γ -transition energy (k , measured in units of m_0c^2) is sufficiently large (>12) and the charge of the radiating nucleus ($Z < 8$) sufficiently small for the usual approximations, as made for example in the calculations of Rose (1949) and Goldring (1953), to be justified.

For transitions in which the radiating nucleus has the normal, random population of sub-states (i.e. isotropic radiation), the probability per quantum of pair emission with angle θ between positron and electron, and with positron and electron energies ω_+k, ω_-k ($\omega_+ + \omega_- = 1$), can be expressed as $\gamma_l^k(\theta, \omega_+)\Omega_+\Omega_-$ where l denotes the multipole character of the radiation and Ω_+, Ω_- are the solid angles for detection of positron and electron. $\gamma_l^k(\theta, \omega_+)$ as a function of θ has, for $k \gg 1$, a sharp peak around $\theta = 0$ which increases with k . One can specify this region as $\theta \ll \theta_0$, where θ_0 is given by $1 - \cos \theta_0 = 1/k$, and in this range $\gamma_l^k(\theta, \omega_+)$ is nearly independent of multipolarity l , but strongly dependent on the energy k . On the other hand for large values of θ , $\theta > \theta_0$, $\gamma_l^k(\theta, \omega_+)$ is nearly independent of k but strongly dependent on multipolarity l . Roughly speaking the large peak at small angles corresponds to pairs emitted in the radiation zone of the transition field, whereas the pairs emitted with large angular separation are those 'produced' close to the nucleus. At high energies then, most of the pairs are produced with small angular separation, and since this region is independent of l the total pair conversion coefficient is not very sensitive to multipolarity (cf. Rose 1949). The angular correlation on the other hand is sensitive to l for all energies, and in particular the integrated angular correlation

$$g_l^k(\theta) = \int_{\omega_+=1/k}^{\omega_+=1-1/k} \gamma_l^k(\theta, \omega_+) d\omega_+,$$

* Now at the Department of Physics, Hebrew University, Jerusalem.

which is, approximately, the quantity measured in the experiments, is almost independent of transition energies over the range of angles used, $\theta_1 < \theta < \pi$, $\theta_1 > \theta_0$.

The angular correlation functions g_l^k for high energy transitions of the electric 2^l -pole and magnetic 2^{l-1} -pole are very nearly, but not exactly, identical, so that it is convenient to refer, for the present purposes, to an 'order' Λ of a transition. $\Lambda = l$ for electric El , and $l+1$ for magnetic Ml transitions.

§ 2. EXPERIMENTAL

The difficulties and sources of error arising in measurements of angular correlation of the pairs in a monopole (radiationless) transition have been described in detail in I. Some additional difficulties are encountered in γ -transitions.

(a) The diffuse electron radiation in the vacuum chamber is relatively more intense, because, apart from scattered electrons it contains electrons produced by γ -radiation in the walls of the chamber. In particular, there will be a background of 'stray' coincidences counts due to these externally produced electrons, the most important process being the passage of such an electron right through all four counters when these are approximately collinear, i.e. in the region $\theta \simeq \pi$. For angles appreciably different from π , this process, as well as the background effects discussed in I, are negligible.

(b) External pairs produced in the target or target backing distort the correlation function. This distortion is roughly of the same order of magnitude as that caused by scattering, which as indicated in I, is negligible for the aluminium foils (approximately 0.2 mg cm^{-2}), which were used as target supports in all cases. In all the γ -transitions investigated, the yield of internal pairs was very much smaller than in the case of the transition measured in I, and the statistical accuracy of the measurements was correspondingly lower. To the accuracy of the present measurements then, the distortion due to both scattering the pair production in the target and supporting foils, was quite negligible.

(c) The geometrical correction due to the finite angular aperture of the counters is a function of the angle θ ; for small θ the correction rises rapidly with decreasing θ , and a limit is set in this way to the smallest angle that can be usefully employed. In all our measurements (apart from one case which will be mentioned specifically) the smallest angle was $\pi/4$. With the counter geometry used, the largest correction, that at $\pi/4$, could be estimated to better than 2%. With the limited statistical accuracy obtained the errors involved in estimating the geometrical correction were insignificant for angles between $\pi/4$ and π .

The apparatus was set up so that the axis, about which the counter telescopes rotated, coincided with the axis of the proton beam. This was most convenient for practical reasons; in addition it is the most advantageous arrangement for investigating anisotropic transitions (Goldring 1953).

The experimental arrangements were not particularly suited to measurements of the absolute pair-coefficient (i.e. the relative probability of pair and γ -emission). Uncertainties in the beam current (due to scattering), the counter telescope efficiencies, and absolute γ -flux measurements resulted in absolute intensity measurements of overall accuracy between 10% and 20%, which is inadequate for unambiguous assignment of multipolarity of high energy transitions. Consequently only the correlation functions are discussed below. In all cases the absolute intensities were estimated and were found to be consistent (to within the above accuracy) with the information that could be derived from the angular correlations.

§ 3. MEASUREMENTS

3.1. ${}^7\text{Li}(p, \gamma){}^8\text{Be}$

LiH was used as a target. This substance is unstable in air, and was therefore evaporated *in situ*. The measurements were carried out with two different separations between the inner and outer counters: (a) inner counter 7 cm and outer counter 10 cm from the target, (b) inner counter 7 cm and outer counter 12.5 cm from the target. The correlation curves obtained were found to be identical within the statistical accuracy. As in I, this is taken as a confirmation that 'stray' background coincidence counts, if at all appreciable, are due to the causes listed above and can be ignored except near $\theta = \pi$. The number of 'stray' coincidences at $\theta = \pi$ can be estimated on the basis of the shadow measurements described in I.

The results of both sets of measurement, arbitrarily normalized, are shown in figure 1. N is proportional to $T/\frac{1}{2}(F+M)$, where T is the number of total coincidences, and F, M are the number of counts in the fixed and moving telescopes respectively.

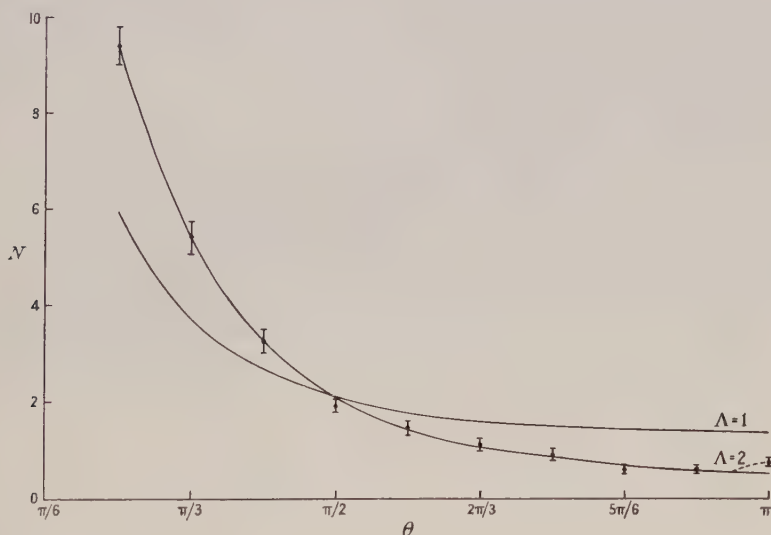


Figure 1. Angular correlation of pairs from ${}^7\text{Li}(p, \gamma)$. The curves are theoretically calculated for $\Lambda=1$ and $\Lambda=2$, normalized to be equal at $\pi/2$.

The radiation consists mainly of two components of energies $k=28.2$ and $k=34.5$ (Hornyak *et al.* 1950). There has been some uncertainty about the parity of the excited level in ${}^8\text{Be}$ in which these transitions originate. The anomalous scattering of protons in ${}^7\text{Li}$ at 440 keV can be interpreted as due to p-wave scattering (Hornyak *et al.* 1950). Since the ground state of ${}^7\text{Li}$ has odd parity, this means that the resonance level in ${}^8\text{Be}$ has even parity. On the other hand, the near-isotropy of both γ -radiation components at resonance is most naturally accounted for by the assumption that the level is produced by s-protons (Devons and Hine 1949). Devons and Lindsey (1950) have pointed out that a p-wave excitation will result in isotropic radiation, if the channel spins are mixed in a certain definite ratio. In particular, such a mixture may be due either to a pure $p_{1/2}$ proton wave, or to the ${}^8\text{Be}$ state being an S_1 state (Christy 1953). All the evidence about the state is consistent with the assumption that its angular momentum is equal to one. The two final states after γ -emission, i.e. the ground

state and the first excited state of ^8Be , are assumed to be 0^+ and 2^+ (Hornyak *et al.* 1950). If the $J=1$ state has odd parity (1^-), the transitions will be E1, and if it has even parity (1^+), they will be M1 and M1 + E2. The pair emission will therefore be of the order $\Lambda=1$ for odd parity, and of the order $\Lambda=2$ for even parity. In both cases the angular correlations for the two γ -ray components are nearly the same, and it is sufficient to evaluate the theoretical curve for the more intense component ($k=34.5$). The appropriate theoretical expressions:

$$\int_{2.5/34.5}^{32/34.5} \gamma_l^{34.5}(\theta, \omega_+) d\omega_+ \quad (l \rightarrow \text{E1, E2 or M1})$$

have been evaluated numerically and are also shown, suitably normalized, in figure 1. The 'cut-off' energy $\omega_+ = 2.5/34.5$ (corresponding to an electron kinetic energy of 0.75 mev) has been introduced to represent the reduction in sensitivity of the telescopes at low energies (see I). The γ -transitions are slightly anisotropic; strictly speaking, the outgoing electromagnetic waves do not even have well-defined angular momenta or parities, because of the interference between the two ^8Be levels (Devons and Hine 1949), but the effect on the correlation functions is expected to be negligible compared with the statistical accuracy, and isotropic correlation functions have been used in calculating the curves in figure 1. The dotted line represents the contribution due to 'stray' background counts (as a correction to the $\Lambda=2$ curve).

It is seen that the results quite definitely establish the order of the transition as $\Lambda=2$. This result confirms the conclusion that the $^7\text{Li} + p$ reaction is produced by p-wave protons, and that the γ -radiation is magnetic dipole (M1).

The pair-emission calculations on which our discussions are based assume that all the pairs are created outside the nucleus. This assumption is not strictly true, since some of the pairs are created inside the nucleus in a manner similar to the monopole pairs; the relative number of these pairs (in the region of large angles) increases with k . For $k=34.5$, and with reasonable assumptions about the electromagnetic field inside the nucleus ^8Be , the number of these pairs at any angle is estimated to be of the order, or less than, $1.5(1 - \cos\theta)\%$ of the total number observed. The error due to neglect of this factor is therefore much smaller than the statistical accuracy of the measurement. For the other transitions investigated k , the transition energy, is smaller, and the production of pairs inside the nucleus should be relatively less important than in the ^8Be case.

3.2. $^{19}\text{F}(p, \alpha\gamma)^{16}\text{O}$

Thin evaporated targets of both CaF_2 and LiF were used. For a given proton current a LiF target provides a higher yield of pairs. This advantage was partially offset by the fact that lower currents had to be used with LiF targets, since the current density was determined by the highest current that the target material could stand without destruction, and the dissociation temperature for LiF is much lower than that for CaF_2 ; the maximum yield per unit area of target determined in this way is slightly higher for LiF than for CaF_2 .

In early experiments rather thick targets were used. By examining the angular correlation, it was found that a large fraction of the pairs was due to a monopole transition. On varying the proton bombarding energy, it was established that whereas the γ -ray intensity dropped to a very small value outside a certain voltage range, the electron intensity (measured in the fixed telescope) remained at a finite and almost constant value. This was attributed to an

appreciable cross section for the reaction $^{19}\text{F}(p, \alpha e_+ e_-)^{16}\text{O}$, even at these low proton energies. In later experiments care was taken to produce targets not much thicker than the level thickness (1.7 kev). With these targets the monopole pair background, inferred from the difference in the excitation curves for counts in a γ -counter and in a single electron telescope, was as low as 2% of the total number of pairs. Since both the target thickness and the bombarding energy were liable to vary with time, the monopole pair background was frequently checked. The measured values were corrected according to the background found in the corresponding time interval.

In figure 2 two sets of measurements (with arbitrary normalization) with different counter geometries are shown. The point at $\theta = 0.2\pi$ is outside the range where accurate geometrical corrections can be applied, but the calculated correction which has been applied at this angle is believed to be accurate to better than 10%.

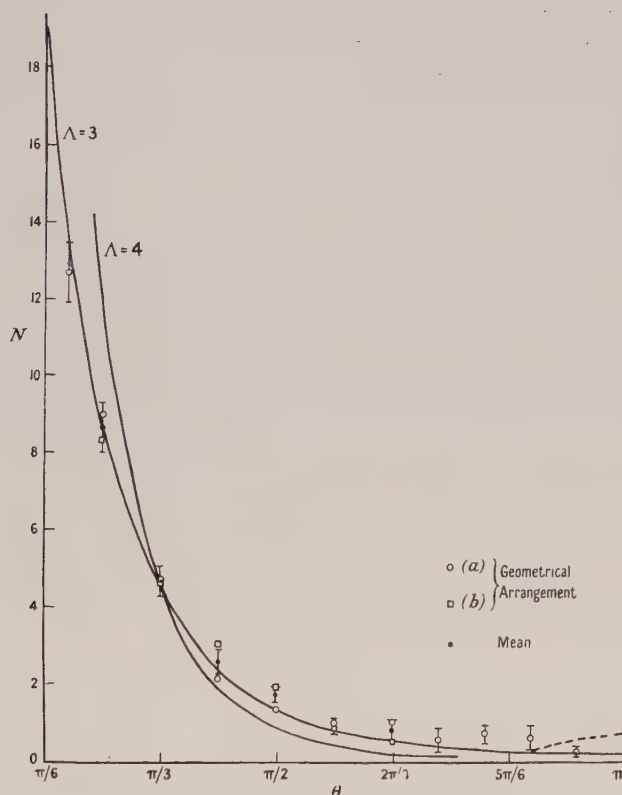


Figure 2. Angular correlation of pairs from $^{19}\text{F}(p, \alpha\gamma)$. The two theoretical curves are for $\Lambda=3, 4$, normalized to be equal at $\pi/3$.

The transition in ^{16}O is of energy $k = 12.06$; this transition had already been established as $E3: 3^- \rightarrow 0^+$ (Seed and French 1952). The present results confirm this assignment. The 'E3' curve in figure 2 has been drawn as $0.96E3 + 0.04E1$, in order to take into account the weak 7.1 Mev component (Seed and French 1952, Hornyak *et al.* 1950). The difference between the combination and the pure E3 is almost negligible; only near $\theta = \pi$ is the contribution from E1 appreciable.

It has so far been assumed that the approximation using plane wave functions for both electrons gives an accurate representation of the pair formation process. A very rough estimate of the relative error ϵ involved by using this approximation is $\epsilon \sim 10^{-3}Z$ irrespective of energy (for $k \gg 2$), where Z is the atomic number. This estimate is valid in the large angle region. Of all the nuclei investigated in the present work, ^{16}O has the largest Z , but even in this case ϵ is less than 1%, and may be ignored.

3.3. $^9\text{Be}(p, \gamma)^{10}\text{B}$

Evaporated Be metal was used for the targets. The targets were, at first, consistently found to contain traces of F (the monopole pairs were conspicuous in the angular correlation). The impurity was completely eliminated by interposing a mica shield between the evaporating boat and the aluminium foil. The shield was withdrawn only after the mica had started to show signs of a Be deposit.

A large number of counts was registered in the inner counters and was ascribed to x-rays excited in the target material. Although these counts did not affect the telescope counting rates, they were harmful because they drove the counters into multiple discharges and eventually completely choked the coincidence circuit. Tin foil, 13 mg cm^{-2} thick, covering the front of the inner counters, stopped almost all of these counts.

At a proton energy of 1000 keV the plain Al foils were found to emit a pair radiation which was about 8% of the Be pair radiation. These pairs are probably due primarily to radiation from the ^{28}Si resonance level excited by protons of energy 986 keV, and the yield did in fact drop to about 15% of that at 1000 keV when the proton energy was reduced to 950 keV. In order to avoid this radiation, care was taken to prepare Be targets thick enough (some 50 to 100 keV) to reduce the proton energy to less than 950 keV after passing through the Be layer. The narrow resonance level at 1087 keV proton energy can easily be avoided by keeping the bombarding voltage low enough, and in any case the yield from this level is so small that, even if it were included in the measurement, the effect would hardly be discernible.

Since the results of this measurement were rather surprising (see below), some check measurements were made; it was established that:

(i) The variation of the γ -ray yield with energy was in satisfactory agreement with the expected curve.

(ii) The angular correlations with and without the tin foil absorbers were quite consistent.

(iii) The angular correlation was shown to be independent of bombarding voltage over a range of 90 keV in the neighbourhood of the resonance.

The experimentally observed correlation is shown in figure 3. The transition has been reported as $E1: 2^+ \rightarrow 3^-$ (Devons and Hine 1949). The angular distribution of the γ -radiation is also given by these authors as $I(\theta) \sim 1 + 0.09 \sin^2 \theta$.

The theoretical curves for E1 and E2 transitions shown in figure 3 have both been calculated with the correct anisotropic terms as explained in detail in Goldring (1953). The difference between the correct and isotropic functions for these pure multipole transitions is not more than a few per cent. Neither theoretical curve separately fits the results. The constant value of the experimental correlation function at large angles clearly indicates that E1 radiation is present, since the correlation functions for all other orders decrease rapidly in this

region. If we draw the complete theoretical E1 curve to fit the experimental values at large angles, and examine the difference between this and the actual experimental values, we find that a mixture of $\Lambda = 1$ and $\Lambda = 3$ is consistent with the results.

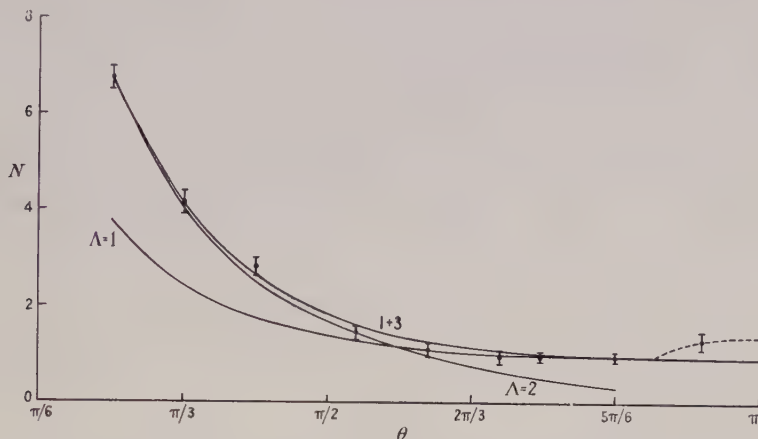


Figure 3. Angular correlation of pairs from ${}^9\text{Be}(p, \gamma){}^{10}\text{B}$. The theoretical curves $\Lambda=1$, $\Lambda=2$ have been normalized to fit the experimental values at large and small angles respectively.

One can try to interpret this departure from a simple correlation function in several ways: (a) a background radiation of intensity comparable to the ${}^{10}\text{B}$ radiation is present, (b) cascade γ -transitions occur from the resonance level of ${}^{10}\text{B}$ in competition with the direct ground state transition, (c) the transition to the ground state is a mixed E1, E3 or M2 multipole, (d) interference between components of a mixed multipole together with the anisotropy of the γ -radiation gives rise to effects of uncertain magnitude. None of these possibilities is free from difficulties.

(a) This interpretation appears very unlikely in view of measurements (i) above and the check experiments with blank aluminium foils.

(b) The only intense γ -component of sufficient energy from the 998 keV resonance level seems to be the 7.5 MeV transition to the ground state of ${}^{10}\text{B}$ (Hornyak and Coor 1953, Ajzenberg and Lauritsen 1952). Measurement (ii) above further indicates even if any pairs from cascade γ -radiation were present, the radiation would have to contain one component of energy comparable with 7.5 MeV. Such a transition, starting from the resonance, would, if of higher multipolarity than the E1 transition to the ground state, be as difficult to interpret as (c) below. If the transition followed a low-energy transition from the resonance level, then we would be faced with the difficulty of explaining the roughly equal competition of two transitions of very unequal energy and the higher energy one E1.

(c) The absolute γ -radiation width can be deduced from the yield of γ -radiation. If half the radiation is attributed to E1 the width for this component is quite reasonable, about 0.03 of the width predicted by the single particle model (Blatt and Weisskopf 1952), but the width for E3 or M2 (both $\Lambda=3$) would be about 10^3 times larger than that predicted by either the single particle or liquid-drop model.

(d) It has been shown by Goldring (1953) that no interference in the electron-pair correlation is to be expected in a mixed El' , Ml transition if both electron momenta are at right angles to the beam of bombarding particles, and if the energy-sensitivities of the two detectors are identical. In mixed El , El' transitions, there are however finite interference terms proportional to the correlation functions for pure $E(l+l')/2$ transitions. There is, therefore, some uncertainty in the theoretical correlations arising from the limited accuracy with which the anisotropic terms can be deduced from the experimental angular distribution of the γ -radiation, and also from the unknown strength of the interference term. Moreover, if the population of the various substates of the radiating ^{20}B , were to be very different from the random one, an additional uncertainty will be introduced due to the fact that the detectors are not strictly confined to the equatorial plane.

§4. CONCLUSIONS

The measurement of the angular correlation of electrons and positrons, as a means of studying γ -transitions, by the method described above, is of limited applicability. It is necessary for the spectrum of the γ -radiation to be reasonably simple, so that either the average correlation, or that of the highest energy γ -component can be studied and interpreted; in addition the intensity of radiation must be sufficient for reasonable statistical accuracy to be obtained. Using the type of target support described, bombarding currents are severely limited, and as a result a yield of the order 10^{-8} γ -transitions per proton, or more, is necessary. Many reactions in light nuclei, particularly deuteron induced reactions, have γ -yields far in excess of the above figure, but the γ -spectra are usually quite complex. The introduction of reasonable energy resolution into the apparatus, without loss in detection efficiency is quite feasible and should extend the scope of this type of measurement quite considerably.

REFERENCES

- AJZENBERG, F., and LAURITSEN, T., 1952, *Rev. Mod. Phys.*, **24**, 321.
BLATT, J. M., and WEISSKOPF, V., 1952, *Theoretical Nuclear Physics* (New York: John Wiley; London: Chapman and Hall), Chap. XII.
CHRISTY, R. F., 1953, *Phys. Rev.*, **89**, 839.
DEVONS, S., GOLDRING, G., and LINDSEY, G. R., 1954, *Proc. Phys. Soc. A*, **67**, 134.
DEVONS, S., and HINE, M. G. N., 1949, *Proc. Roy. Soc. A*, **199**, 56.
DEVONS, S., and LINDSEY, G. R., 1950, *Proc. Phys. Soc. A*, **63**, 1202.
GOLDRING, G., 1953, *Proc. Phys. Soc. A*, **66**, 341.
HORNYAK, W. F., *et al.*, 1950, *Rev. Mod. Phys.*, **22**, 291.
HORNYAK, W. F., and COOR, T., 1953, *Phys. Rev.*, **91**, 463.
ROSE, M. E., 1949, *Phys. Rev.*, **76**, 678; 1950, *Phys. Rev.*, **78**, 184 (erratum).
SEED, J., and FRENCH, A. P., 1952, *Phys. Rev.*, **88**, 1007.

Cosmic Radiation : Ionization Intensity and Specific Ionization in Air at Sea Level

By P. R. J. BURCH

Department of Medical Physics, University of Leeds

Communicated by W. V. Mayneord ; MS. received 9th October 1953

Abstract. The lack of agreement between different estimates of the cosmic radiation ionization intensity under similar conditions at sea level is pointed out, and arguments supported by experiment are advanced in favour of J. Clay's procedure for interpreting high-pressure ionization chamber data. An average specific ionization is obtained from the ionization intensity and a recently published value for the absolute particle intensity. The significance of the result is discussed and compared with the value computed from formulae for the energy loss by ionization.

§ 1. INTRODUCTION

THE values quoted in the literature for the cosmic radiation ionization intensity in air are based on early experiments, and there is, unfortunately, a wide measure of disagreement between them, as is shown in table 1. Johnson (1938) and D. J. X. Montgomery (1949) have both concluded that little reliance can be placed upon ionization-chamber determinations.

Table 1

(All measurements were carried out in the Northern Hemisphere
at a geomagnetic latitude of 41° N or greater)

Investigators	Filtration	I_{sl}	I_{fa}
Millikan (1931)	11 cm Pb+		
	0.3 cm Fe (min)	1.75	
	0.3 cm Fe (min)	2.48	
Compton & Turner (1937)	10.7 cm Pb+		
	2.1 cm Fe	1.22	
	2.1 cm Fe	1.92	
Millikan & Neher (1936)	0.8 cm Fe (av)	2.88 (modified by Neher (1952) to 2.74)	
Clay & Clay (1938)	1.3 cm Fe (min)	$1.69_5 \pm 0.05^*$	1.93
Author (1952)	0.62 cm Fe (min)	$1.77 \pm 0.10^\dagger$	1.88
	1.1 cm Fe (min)	$1.73 \pm 0.10^\dagger$	1.94

I_{sl} = Ionization at sea level (76 cm Hg) ion pairs $\text{cm}^{-3} \text{sec}^{-1}$, standard air; I_{fa} = Ionization in free air (see text).

* The published result has been reduced to standard air and a further correction of $-1\frac{1}{2}\%$ applied for the barometric coefficient: For an unshielded chamber this was assumed by Clay and Clay to be -5% per cm Hg and the observations were made at an atmospheric pressure of 77.0 cm Hg. Measurements by the author (Burch 1952) with an ionization chamber under a light roof and ceiling and by Duperier (1944) with lightly shielded G-M counters show that this correction is, on the average, about $-3\frac{1}{2}\%$ per cm Hg. Clay and Clay will therefore have over-corrected for the barometric coefficient by $1\frac{1}{2}\%$.

† Semi-independent measurements with two different groups of chambers. Errors quoted are estimated standard errors.

Apart from the physical importance of this quantity, it is also of some interest to the biologist when deriving the normal background radiation dosage to living organisms. Under typical sea-level conditions cosmic radiation is responsible for about a quarter of this dosage in human beings.

§ 2. INTERPRETATION OF IONIZATION-CHAMBER DATA

Pressurized ionization chambers were used in each of the above determinations, and the discrepancies noted reflect the lack of an agreed procedure for interpreting results obtained in this way.

The salient factors which must be considered are as follows.

2.1. Ionization Recombination

The types of recombination which may be encountered in this kind of work are intra-track recombination and volume or general recombination. Preferential recombination is only likely to occur at higher pressures than are usually employed (Wilkinson 1950).

Volume recombination is usually negligible at background intensities as indicated by the following experiment: The phenomenon was investigated in a large cylindrical ionization chamber of 20.6 cm internal diameter with a fine central electrode of 0.1 mm diameter; the chamber was filled with commercial nitrogen at a pressure of 45 atmospheres. A collecting voltage of 640 was applied to the chamber wall and the decay of a radioactive source (^{24}Na) was observed. This appeared accurately exponential over a wide range of ionization intensities, but at the highest intensities a departure was observed. It may be shown that the fraction of ions recombining, $r = ai^2/(1 + ai^2)$ where a is a constant and i the ionization current. Thus for small values of recombination the percentage recombination is proportional to i^2 . The maximum recombination obtained was 5% and, putting $r = ci^x$, the exponent x was found to be 2.04 ± 0.19 , by a method of least squares analysis. 1% volume recombination occurred at 54 times the background intensity, hence volume recombination at the background ionization rate would be only $1/54^2$ %. Starting at the point on the decay curve at which volume recombination was 0.17%, the remaining corrected points at lower intensities, extending over 3.7 half-lives, were analysed by the method of least squares to obtain the half-life of ^{24}Na . This was found to be (14.973 ± 0.015) hours; the standard error of ± 0.015 includes both statistical and systematic errors. This result is in complete agreement with the most accurate recent determination (Lockett and Thomas 1953) of (14.97 ± 0.02) hours.

There has been some dispute as to whether intra-track recombination should be treated by the columnar theory (Jaffé 1913, Zanstra 1935) or by the cluster theory (Lea 1934). J. Clay and his co-workers (see numerous papers in *Physica* from 1935 to 1940) and Taylor and Singer (1940) applied with apparent success the Jaffé-Zanstra (JZ) theory of columnar recombination to their results, which involved altogether various gases and x-, γ - and cosmic radiations. The validity of this approach was however questioned by Kara-Michailova and Lea (1940) who suggested that the Jaffé theory, intended originally to deal with the phenomenon of recombination in heavily ionizing tracks (α -particles, slow protons, etc.), was generally inapplicable to sparsely ionizing tracks such as those produced by high energy γ -radiation or cosmic rays. They assumed that ionization occurred

in widely separated clusters, for which Lea (1934) had evolved a theory of recombination. In the 1940 paper Kara-Michailova and Lea applied this theory to published experimental data, and found that, where this was suitable for testing, fairly consistent results were obtained. In reply, Clay and Kweiser (1940) applied both cluster and columnar theories to a wide selection of their experimental results and showed that the JZ theory invariably yielded the better results although differences were seldom very marked. Both extrapolation procedures involve constants for which there are insufficient data to permit an accurate independent derivation, and in practice these constants are adjusted to yield linear extrapolation curves. The Lea theory (as adapted by Clay and Kweiser) involves two such constants and the Jaffé theory only one.

Further consideration will be given to this problem in § 3.

2.2. The Effect of the Chamber Wall

2.2.1. 'Multiplication' processes. The relation between i_s , the saturation ionization, and ρ , the gas density, is usually of the form shown in figure 1 (curve

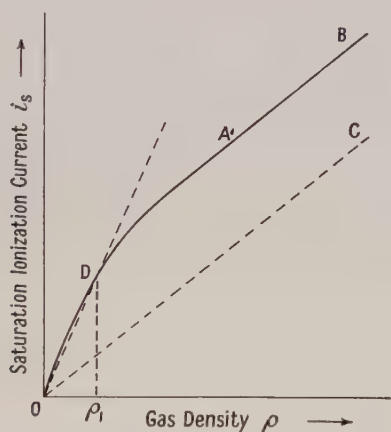


Figure 1. Theoretical relationship between saturation ionization current and gas density (atomic number of chamber wall > atomic number of gas).

ODAB). Under the appropriate conditions (atomic number of wall material > atomic number of gas) this characteristic is exhibited by cosmic, x- and γ -radiations. Indeed, investigators (Millikan 1931, Compton and Turner 1937) have used the more easily observed (i_s, p) curves for radium γ -radiation to convert the cosmic radiation ionization found at a high gas pressure to the ionization at atmospheric pressure. (Any α -particle contamination of the material of the chamber complicates the interpretation of the *background* ionization at low pressures). Because of the complex spectrum and behaviour of the cosmic-ray flux, it is easier to consider the way in which the (i_s, ρ) curve is built up for quantum radiations.

In the region of ρ or $p = 0$ the chamber may be regarded as a 'cavity chamber', providing the source-to-chamber distance is very much greater than chamber dimensions; $di_s/d\rho$ in this region may be obtained from the Bragg-Gray principle (see, for example, Gray 1949 for a comprehensive treatment) which states that

i_m , the ionization per unit mass of gas in the cavity, is related to E_m , the electronic energy dissipated per unit mass of the medium immediately surrounding the cavity by

$$(i_m)_{\rho \simeq 0} = \frac{E_m}{\overline{SW}} \propto \left(\frac{di_s}{d\rho} \right)_{\rho \simeq 0}.$$

\overline{SW} is the mean value of the product of S , the mass-stopping power of the solid relative to the gas, and W the energy required to form one ion pair.*

Under ideal cavity conditions ionization is caused entirely by those electrons which originate in the wall material (as the result of the absorption of quanta there) and cross the gas cavity; the direct absorption of quanta in the gas is infinitesimally small. At high gas pressures the situation is reversed, and nearly all the ionization is caused by the direct absorption of quanta by the gas. Hence,

$$(i_m)_{\rho \text{ large}} \simeq \frac{E_g}{\overline{W}} \propto \left(\frac{di_s}{d\rho} \right)_{\rho \text{ large}}$$

where E_g is the electronic energy dissipated per unit mass of gas and \overline{W} is the average energy required to form one ion pair.

For radium γ -radiation, a chamber wall of steel and a nitrogen or air filling, $E_g \simeq E_m$, but $\overline{S} < 1$. Hence

$$\left(\frac{di_s}{d\rho} \right)_{\rho \simeq 0} > \left(\frac{di_s}{d\rho} \right)_{\rho \text{ large}},$$

that is, slope OD > slope AB, and there will be an intermediate region of intermediate slope. When we require the ionization and energy absorption by the gas we are therefore concerned with the AB portion of the curve of ionization against density (or pressure, for perfect gases). Although the absorption of radiation is exponential in form, the percentage absorption in the gas is usually so small that it is virtually linear with pressure; we should find, then, that the portion of AB well beyond the 'knee' is linear.

For cosmic radiation, the phenomena are more complex and the wall multiplication effect may be regarded as the ionization-chamber analogue of the shower or Rossi transition curves obtained in counter experiments.

The magnitude of the wall multiplication effect at a given pressure depends on the nature of the radiation, the gas, the wall material and the dimensions of the chamber. In the case of x- and γ -radiations it increases with the divergence of the radiation beam through the chamber.

2.2.2. Attenuation. The wall will absorb those low-energy particles (e.g. δ -tracks branching from high-energy particles passing near, but not through the chamber) whose range is less than the wall thickness. It is difficult to make an accurate allowance for this wall-attenuation effect because the soft-electron differential-range spectrum rises sharply for filtrations less than 10 g cm^{-2} , and previous investigators have apparently avoided this correction. If we try to approach the problem experimentally by reducing the wall thickness, a point will be reached where we begin to decrease the wall multiplication effects. To determine these effects we need to carry out (i_s, ρ) tests over a large density range, and for vanishingly thin walls this becomes impossible. It may be thought that G-M counter-telescope absorption results would afford a way out of this dilemma, but the issue is far from clear. As we reduce the total filtration with such an

* The theory of the ionization in integrating chambers will be discussed in detail elsewhere. The formula for \overline{SW} obtained by the author differs from that given by Gray (1949); in most cases the difference will be quantitatively unimportant.

apparatus, we begin to count more and more low-energy δ -tracks as individual particles, and indeed a completely rigorous (if impracticable) extrapolation to zero filtration would result in counting every ionizing event as a single particle! If this reasoning is accepted then it is evident that some standard condition other than zero filtration should be used for the expression of cosmic-radiation particle intensities. The figures in the last column of the table were based on what should be a reasonable extrapolation of Clay's (1936) cosmic radiation absorption measurements using steel ionization chambers and steel absorbers. Account has been taken of the curvature of the chamber walls.

2.3. Radioactive Contaminations of Chamber and Surroundings

These effects may be analysed by well-established methods and raise no special points of contention (see, for example, Compton and Hopfield 1932, Hess and Vancour 1949).

§ 3. CONCLUSIONS REGARDING INTERPRETATION OF IONIZATION-CHAMBER DATA

We may sum up §§ 2.1 and 2.2.1 by considering the following requirements which must be met by a treatment of experimental data:

(a) At pressures high enough to avoid the wall multiplication influence the slope of the (i_s, ρ) curve must be linear for x- and γ -radiations. (Strictly, it should be exponential, but the percentage absorption of radiation in the gas is usually so small that departures from linearity are negligible.) Linearity at high pressures is also observed with cosmic radiation.

(b) The slope of this linear portion must be of the correct value. This is perhaps most conveniently tested by obtaining the saturation-ionization rate produced per unit mass of gas at different pressures by a standard γ -ray source for which the energy absorption may be predicted, e.g. a known quantity of Ra or of, say, ^{60}Co , calibrated by β - γ coincidences. This was done by Clay and Tijn (1937) and by Taylor and Singer (1940); the latter paper contains some extremely accurate and convincing proofs of the validity of the Jaffé-Zanstra extrapolation procedure, both for Ra- γ , and 300 kv x-radiations.

(c) The magnitude of the wall effect must be correctly indicated. This is difficult to calculate precisely, but in special cases (e.g. distant γ -source of known spectrum or known composition and mass electronic stopping powers of wall and gas) a fairly reliable estimate may be made. Thus for a steel chamber with a nitrogen or air filling and a distant source of radium it is calculated that at a density ρ_1 , where the direct absorption of radiation by the gas accounts for 5% of the total ionization, the ratio of the gradients of OD and OC should be approximately 1.2₃ (see figure 1).

In figure 6 of Clay and Kweiser's (1940) paper this ratio is 1.33 on the JZ extrapolation and 2.0 on the Lea extrapolation. From figure 9 of the same paper the ratios are 1.49 (JZ) and 1.75 (Lea). The experimental conditions were not specified in either case, but short source-to-chamber distances would account for the values being greater than theoretical.

The author found that when a carnotite source (radium + uranium γ -radiation with rather high internal source absorption) was placed at right angles to the long axis of a cylindrical chamber, the ratio was 1.28 for a ratio of (source distance from chamber centre) to (chamber radius) of 5.6; when this latter ratio was reduced to 2.0, the ratio of the gradients of OD and OC was raised to 1.52.

Where the interpretation of cosmic radiation ionization curves is concerned, several possibilities remain for the introduction of small errors. Thus when the gas density is raised, particles in the cosmic-ray spectrum of low enough energy will fail to penetrate the gas space completely and the ionization per unit mass of gas will diminish slightly with increasing density. This will produce a slightly exaggerated wall effect and an underestimated slope for AB. Judging from the differential momentum spectrum of all particles (Glaser *et al.* 1950) and from absorption experiments, this effect will be trivial. There is also a possibility that the wall will produce a multiplication of high-energy particles and, therefore, an increased ionization which would not be revealed by the wall effect as deduced above. Although very high-energy particles are found in showers, this transition effect is not likely to be very important for the usual experimental arrangement and the above method of interpretation.

§ 4. PROCEDURE ADOPTED FOR DERIVING THE COSMIC-RADIATION IONIZATION INTENSITY

The experimental work was not aimed primarily at a determination of this quantity, and the corrections made necessary are larger than those which would normally be encountered in a direct attack on the problem. Two groups of steel cylindrical chambers were used, one set consisting of seven chambers, 165 cm overall length and 20.6 cm internal diameter, the other group of four, of 215 cm overall length and 29.2 cm internal diameter. All chambers were fitted with 0.1 mm diameter stainless steel electrodes and filled with commercial nitrogen.

At pressures above a few atmospheres it was impossible to use field strengths high enough to achieve the low $f(x)$ values needed for an accurate extrapolation with the Jaffé-Zanstra plot. However, it was possible to utilize the conclusion of § 3 (a) to arrive at a fairly reliable value for the saturation current by the following trial-and-error method: A trial value was adopted for the percentage columnar recombination at the highest pressure and the JZ theory was used to calculate the recombination at the lower pressures. This process was repeated until the derived i_s values, when plotted against pressure, gave the best straight line over the pressure range above the knee caused by the wall effect (figures 2 and 3).

The experiments were performed within a water-shielded cavity and the intensity (20%) of the residual local γ -radiation background was determined from independent experiments with a small high-pressure ionization chamber and lead shielding. Corrections for the attenuation of cosmic radiation by the shielding above the apparatus were based on Clay's (1936) curves, and the γ -radiation intensity from the vertical overhead direction was investigated with the small chamber. Despite the rather complex derivation, involving a fairly wide margin of error, the results are in good agreement with and are probably sufficiently accurate to confirm the value obtained by Clay and Clay (1938).

§ 5. CONCLUSIONS REGARDING COSMIC-RADIATION IONIZATION INTENSITY AT SEA LEVEL

J. Clay and his co-workers were the first to provide an adequate treatment of the factors discussed in §§ 2.1 and 2.2.1, and results prior to that of Clay and Jongen (1937) are consequently unreliable. Although the lower three results of the table are in excellent harmony, differences of up to a few per cent at the same

atmospheric pressure are to be expected with changes in atmospheric temperature, etc. The estimated 'free air' values in the last column, although less reliable than the directly determined values of the previous column, are unlikely to be as much as 10% in error.

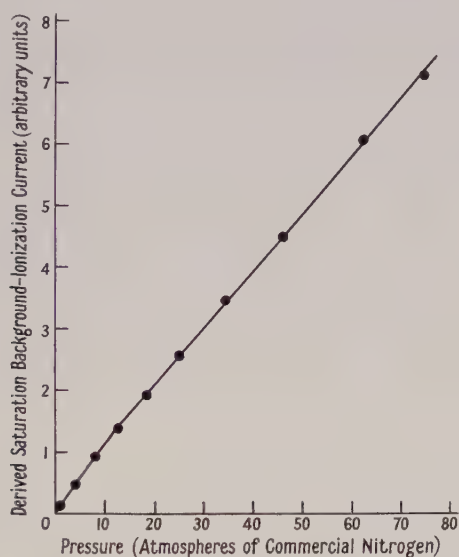


Figure 2. Saturation background ionization current (from application of Jaffé-Zanstra theory of columnar recombination to observed non-saturation values) plotted against gas pressure. Cylindrical chamber 20.6 cm internal diameter.

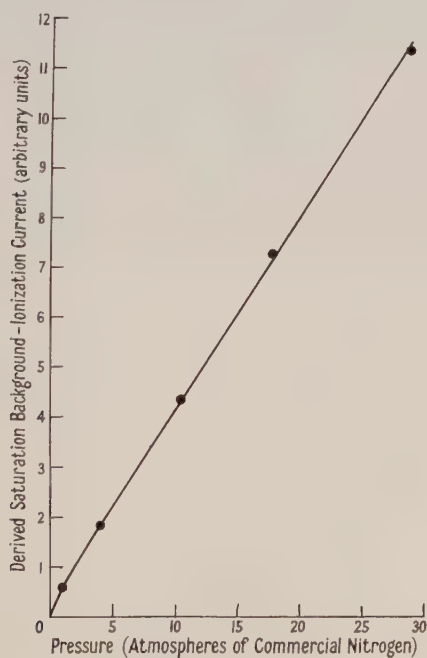


Figure 3. As figure 2. Cylindrical chamber 29.4 cm internal diameter.

§ 6. AVERAGE SPECIFIC IONIZATION OF COSMIC-RAY PARTICLES AT SEA LEVEL

If we know J the omnidirectional particle intensity referred to unit sphere (particles $\text{sec}^{-1}\text{cm}^{-2}$ projected area), and I the ionization intensity (ion pairs $\text{cm}^{-3}\text{sec}^{-1}$) caused by the *same particles*, then \bar{N} an average specific ionization may be defined by $\bar{N} = I/J$ ion pairs cm^{-1} .

The precise significance of \bar{N} is not immediately apparent for it is difficult to decide what upper energy limit of δ -tracks is involved. In cloud-chamber observations a 'probable specific ionization' N_p is adopted in which an upper limit of energy transfer of the order of 10^3 ev is usually imposed, because of the impossibility of resolving individual ions in large clusters. On the other hand, the 'total specific ionization' N_t of a particle will involve all δ -tracks associated with it, and for high-energy particles large energy transfers are possible. N_t may be obtained from theoretical calculations of the ionization energy loss.

As far as the present problem is concerned, if the energy transfer to the secondary and its angular spread from the parent track are both large enough, then in counter observations we shall be dealing with two particles and \bar{N} will be less than N_t . I and J have been calculated for a planar filtration of 5.5 g cm^{-2} , thus secondary particles capable of penetrating this filtration (that is, electrons of rather more than 10 mev) will usually appear as independent particles.

Value for J . The most recent and probably the most accurate measurement of the omnidirectional particle intensity is that of Palmatier (1952). This result has been corrected to sea level and, by using the absorption results of R. A. Montgomery (1949), reduced to a planar filtration of 5.5 g cm^{-2} . This gave the value 2.17×10^{-2} particles $\text{sec}^{-1}\text{cm}^{-2}$. The standard error is here assumed to be $\pm 3\%$.

Value for I . This was obtained from the weighted mean of the last three results of the table. These results should be corrected for that ionization caused (a) by the quantum component which produces secondary electrons with a range less than 5.5 g cm^{-2} , and (b) by short-range heavy particles produced in nuclear interactions ('stars'). Cerenkov radiation will introduce a small error in the opposite direction. There are insufficient data on which to base an accurate estimate of these effects but the net correction is probably about -2% .

The corrected value of I corresponding to that of J above is 1.77 ± 0.06 ion pairs $\text{cm}^{-3}\text{sec}^{-1}$. Thus $\bar{N} = I/J = 81.5 \pm 3.5$ ion pairs (cm^{-1} standard air) for sea-level cosmic-ray particles with an upper limit of δ -track energy of the order of 10 mev .

§ 7. THEORETICAL VALUE OF AVERAGE SPECIFIC IONIZATION

If the types of particles in the cosmic-radiation flux and their energy or momentum spectra are known, it is possible to calculate the average ionization energy loss per centimetre of track $\overline{dE/dx}$ from theoretical formulae and then to deduce the average specific ionization. This calculation was performed using the following data: (a) the differential momentum spectrum for μ -mesons was taken from figure 2 of Glaser *et al.* (1950); (b) the energy spectrum for electrons ($>10\text{ mev}$) was obtained from Palmatier (1952); (c) Sternheimer's (1952) 'density' (polarization) effect correction was applied to the ionization energy-loss formulae quoted in his later paper (Sternheimer 1953); the 'average ionization potential' for air occurring in these formulae was taken to be 80.5 ev and the rest

mass for μ -mesons to be 107 mev; (d) it was assumed that knock-on electrons (δ -tracks) of energy greater than 10 mev arriving at the counter telescope would be recorded as individual particles. This means that the value calculated for $\overline{dE/dx}$ is slightly less than the average *total* ionization loss, which involves knock-on electrons of all energies up to the maximum.

The average value obtained for $(dE/dx)/\rho$ was $2.09 \text{ mev g}^{-1} \text{ cm}^2$.

Now $\bar{N} = (\overline{dE/dx})/W$ where W is the average energy required to form one ion pair. Reviewing the available evidence, Gray (1949) concluded that W for energetic electrons ($> 8 \text{ kev}$) is $(32.5 \pm 1.0) \text{ ev}$ per ion pair. The recent work of Valentine (1952) is in disagreement with some of the evidence used by Gray and suggests that W at 46.7 kev is not less than $33.3 \pm 0.5 \text{ ev}$ and may be as high as $(35.0 \pm 0.5) \text{ ev}$, the value found by Valentine for electrons with an average energy of 2.61 kev .

There are theoretical grounds and experimental evidence for believing that W for argon W_A is constant with respect to the velocity of the ionizing particle. If we avail ourselves of this property we may obtain a crude value for W_{air} by comparing the ionization produced by cosmic radiation in air and in argon and then substituting in the following approximate relationship:

$$\frac{I_A}{I_{\text{air}}} \simeq \frac{(\overline{dE/dx})_A W_{\text{air}}}{(\overline{dE/dx})_{\text{air}} W_A}.$$

From the experimental results of Clay and Jongen (1937) and Clay and Oosthuizen (1937) for the cosmic radiation ionization intensity in air and argon and assuming $W_A = (27.0 \pm 0.5) \text{ ev}$ (Valentine 1952) we find $W_{\text{air}} = (33.2 \pm 1.8) \text{ ev}$.

The position is obviously unsatisfactory, but calculating \bar{N} for the 'extreme' W_{air} values of 32.5 and 35.0 ev we obtain 83.2 and 77.3 ion pairs ($\text{cm}^{-1} \text{ air}$) respectively. These agree with the experimental figure of 81.5 ± 3.5 .

Alternatively, we may use the experimental average specific ionization in conjunction with the semi-theoretical value of $\overline{dE/dx}$ to determine W approximately. We obtain $W = (33.2 \pm 1.6) \text{ ev}$.

§ 8. CONCLUSIONS REGARDING AVERAGE SPECIFIC IONIZATION OF COSMIC-RAY PARTICLES

Johnson (1938) gives a summary of experimental determinations of specific ionization. Even when the methods are similar and the same significance may be attached to the result, there are often large discrepancies. When specific ionization is derived from separate ionization and particle intensity measurements it is obviously important to ensure that it is the ionization of the recorded particles which is being obtained. The mean filtration in both experiments must be the same, and the average specific ionization will depend upon the magnitude of this filtration, which determines at what energy δ -tracks appear as independent particles.

For a mean filtration of 5.5 g cm^{-2} the value of \bar{N} given by the most reliable ionization and particle intensity measurements is 81.5 ± 3.5 ion pairs (cm^{-1} standard air) at sea level. It is shown that this is well supported by considerations of the theoretical energy loss of particles by ionization.

Under rather similar conditions of filtration (6.2 g cm^{-2}) Neher (1952) gives $\bar{N} = 114$ ion pairs cm^{-1} from $I = 2.74$ ion pairs cm^{-3} , and $J = 0.0241$ particle $\text{cm}^{-2} \text{ sec}^{-1}$ (sea-level conditions). J is almost certainly too high (by about 10%) for the conditions under which I was measured, hence it may be concluded that

the latter has been considerably overestimated. This discrepancy in \bar{N} is regarded as constituting further strong evidence in favour of Clay's basic procedure for interpreting high-pressure ionization chamber data.

ACKNOWLEDGMENTS

This work was carried out during the course of an investigation of the natural γ -radioactivity of the human body and was supported by the Medical Research Council. I wish to thank Professor F. W. Spiers for his interest and support and Professor J. G. Wilson for advice concerning the form of this publication. I am grateful for technical assistance with the apparatus construction and assembly given by Messrs. D. B. Appleby and S. Taylor of this department.

REFERENCES

- BURCH, P. R. J., 1952, *Thesis*, University of Leeds.
 CLAY, J., 1936, *Physica*, **3**, 332.
 CLAY, J., and CLAY, P. H., 1938, *Physica*, **5**, 898.
 CLAY, J., and JONGEN, H. F., 1937, *Physica*, **4**, 245.
 CLAY, J., and KWEISER, M., 1940, *Physica*, **7**, 721.
 CLAY, J., and OOSTHUIZEN, K., 1937, *Physica*, **4**, 527.
 CLAY, J., and v. TIJN, M. A., 1937, *Physica*, **4**, 648.
 COMPTON, A. H., and HOPFIELD, J. J., 1932, *Phys. Rev.*, **41**, 593.
 COMPTON, A. H., and TURNER, R. N., 1937, *Phys. Rev.*, **52**, 799.
 DUPERIER, A., 1944, *Nature, Lond.*, **153**, 529.
 GLASER, D. A., HAMERMESH, B., and SAFONOR, G., 1950, *Phys. Rev.*, **80**, 625.
 GRAY, L. H., 1949, *Brit. J. Radiol.*, **22**, 677.
 HESS, V. F., and VANCOUR, R. P., 1949, *Phys. Rev.*, **76**, 1205.
 JAFFÉ, G., 1913, *Ann. Phys., Lpz.*, **42**, 303.
 JOHNSON, T. H., 1938, *Rev. Mod. Phys.*, **10**, 193.
 KARA-MICHAILOVA, E., and LEA, D. E., 1940, *Proc. Camb. Phil. Soc.*, **36**, 101.
 LEA, D. E., 1934, *Proc. Camb. Phil. Soc.*, **30**, 80.
 LOCKETT, E. E., and THOMAS, R. H., 1953, *Nucleonics*, **11**, 14.
 MILLIKAN, R. A., 1931, *Phys. Rev.*, **39**, 397.
 MILLIKAN, R. A., and NEHER, H. V., 1936, *Phys. Rev.*, **50**, 15.
 MONTGOMERY, D. J. X., 1949, *Cosmic Ray Physics* (Princeton : University Press), p. 181.
 MONTGOMERY, R. A., 1949, *Phys. Rev.*, **75**, 1407.
 NEHER, H. V., 1952, *Progress in Cosmic Ray Physics*, Ed. J. G. Wilson (Amsterdam : North Holland Publishing Co.), p. 257.
 PALMATIER, E. D., 1952, *Phys. Rev.*, **88**, 761.
 STERNHEIMER, R. M., 1952, *Phys. Rev.*, **88**, 851 ; 1953, *Ibid.*, **91**, 256.
 TAYLOR, L. S., and SINGER, G., 1940, *Amer. J. Roentgenol.*, **44**, 428.
 VALENTINE, J. M., 1952, *Proc. Roy. Soc. A*, **211**, 75.
 WILKINSON, D. H., 1950, *Ionization Chambers and Counters* (Cambridge : University Press), p. 55.
 ZANSTRA, H., 1935, *Physica*, **2**, 817.

Statistical Errors at Background Intensities in Integrating Ionization Chambers

By P. R. J. BURCH

Department of Medical Physics, University of Leeds

Communicated by W. V. Mayneord ; MS. received 9th October 1953 and in amended form 22nd January 1954

Abstract. A theoretical analysis of the statistical errors in cylindrical integrating ionization chambers is carried out, attention being given to the different types of ionizing particles encountered at background intensities. The conclusions are compared with experimental data and used to derive a parameter related to the specific ionization and 'shower' properties of cosmic-ray particles. Independent considerations show that the value obtained for this parameter is satisfactory. Some practical suggestions are made concerning the minimization of statistical errors.

§ 1. INTRODUCTION

WITH the recent and extending use of large cylindrical high-pressure ionization chambers in the measurement of the γ -radioactivity of the human body (e.g. Sievert 1951, Spiers and Burch 1952, Burch and Spiers 1953, Henriques and Taylor 1953) a theoretical guide is needed to predict the magnitude of the statistical fluctuations which impose a limiting factor upon the performance of such an apparatus. The most comprehensive and rigorous analysis performed so far (Evans and Neher 1934) was applied to a spherical ionization chamber, which, unlike the cylindrical chamber, is insensitive to the directional distribution of the penetrating cosmic radiation particles and consequently presents a simpler problem.

In this paper, the case of cylindrical ionization chambers with hemispherical ends is treated, with attention to cosmic-ray shower phenomena (after Evans) and the 'soft' components of the background radiations. Predictions are compared with experimental results obtained with a differential form of apparatus. When balanced appropriately this experimental arrangement ensures that the differential current is not appreciably affected by systematic variations in the cosmic radiation intensity such as those which accompany changes in atmospheric or geomagnetic conditions.

Because statistical fluctuations depend not only upon the number and distribution of tracks, but also upon the amount of ionization along them (and therefore upon the energy and type of particle), it follows that, in considering the errors of any particular apparatus, one must first possess a knowledge of the distinctive components of the background ionization. These will normally consist of (a) radioactive contamination of the chamber wall (mainly an α -particle effect), (b) residual γ -radiation transmitted through the apparatus shielding and arising from presence of the natural radioactive species in the environment, (c) cosmic radiation, with a complex particle and photon energy spectrum.

In high pressure chambers component (c) will generally contribute the greater part of the statistical fluctuations.

§ 2. THEORETICAL ANALYSIS OF STATISTICAL ERRORS

2.1. Internal α -particle Contamination

We use the following notation: $E_{\alpha, \text{rms}}$ is the r.m.s. energy (in ev) of tracks in the sensitive volume of the chamber (i.e. allowing for partial absorption of α -particles by wall), r_{α} is the fraction of ions undergoing recombination, i_{α} the ionization current (in amps) contributed by α -particles at the pressure concerned, and W_{α} the average energy (in ev) required to form one ion pair. The electronic charge is taken as 1.6×10^{-19} coulomb.

Then it is easily shown that the value of the standard deviation observed from this source for exposures of t seconds duration is

$$\pm \left\{ \frac{1.6i_{\alpha}E_{\alpha, \text{rms}}(1-r_{\alpha}) \times 10^{-19}}{W_{\alpha}t} \right\}^{1/2} \text{ amp.}$$

At atmospheric pressure and typical collecting fields, r_{α} is usually small (up to a few per cent), and i_{α} may easily be very much larger than the ionization current from all other background sources. With gases such as air or commercial impure nitrogen, r_{α} increases rapidly with pressure; thus, with large diameter chambers (20 to 30 cm) a fine central electrode and collecting potentials in the region of 200 volts, r_{α} rises from a few per cent at one atmosphere to about 0.8 (80%) at 15 atmospheres and to 0.9 at 30 atmospheres.

If we neglect the small amount of recombination at one atmosphere and call the α -particle ionization current at this pressure i'_{α} , the standard deviation at any pressure for which the fraction of ions recombining is r_{α} is

$$\pm \left\{ \frac{1.6i'_{\alpha}E_{\alpha, \text{rms}}(1-r_{\alpha})^2 \times 10^{-19}}{W_{\alpha}t} \right\}^{1/2} \text{ amp.}$$

$$\text{i.e.} \quad \pm (1-r_{\alpha}) \left(\frac{1.6i'_{\alpha}E_{\alpha, \text{rms}} \times 10^{-19}}{W_{\alpha}t} \right)^{1/2} \text{ amp.}$$

Whereas this quantity decreases with increasing pressure, the standard deviation for radiations (b) and (c) (expressed in terms of current) increases with pressure. Therefore, by raising the pressure sufficiently, errors caused by α -particle contamination may be made negligibly small compared with other statistical errors.

2.2. Residual γ -Radiation

Similarly, if $E_{\gamma, \text{rms}}$ is the r.m.s. energy loss of the secondary electron tracks in the sensitive volume of the chamber arising from the absorption of quanta, using a notation similar to that in the previous section, the standard deviation arising from the γ -component is

$$\pm \left\{ \frac{1.6i_{\gamma}E_{\gamma, \text{rms}}(1-r_{\gamma}) \times 10^{-19}}{W_{\gamma}t} \right\}^{1/2} \text{ amp.}$$

$E_{\gamma, \text{rms}}$ is not constant with pressure, for at low pressures most tracks will be cut short by the chamber walls. At high pressures most of the ionization will be caused by the direct absorption of quanta in the chamber gas, and only a small proportion of these will be terminated by the walls. At intermediate pressures the ionization contributions of electrons originating in the wall and those originating in the gas will be of the same order of magnitude, and an

appreciable proportion of tracks will be shortened by the wall. Under these conditions it would be difficult to calculate $E_{\gamma, \text{rms}}$.

In §3.2 an experimental value for $E_{\gamma, \text{rms}}$ under fairly high pressure conditions is compared with the calculated value.

2.3. Cosmic Radiation

Cosmic radiation presents a much more complicated problem than the two previous radiations and in an apparatus designed for high sensitivity it will be responsible for the major proportion of the overall error. Both quanta and particles, each with a complex energy spectrum, are involved. (Only about 1% of the equilibrium ionization results from the low-energy quantum component.)

At this stage the assumption is made that particles (mainly mesons and electrons) have sufficient energy to traverse completely the gas space of the chamber. The complication caused by 'showers' or genetically related simultaneous particles is treated later in this section. Where cylindrical chambers are involved, it is necessary to know the directional distribution of these particles and it is assumed that at sea level the intensity follows the ' \cos^2 ' law (the small azimuth effect may be ignored). The calculation is performed for a cylindrical ionization chamber with hemispherical ends and with the long axis horizontal.

As in the cases of the local gamma- and alpha-particle components, if we neglect 'shower' phenomena, the standard deviation of the cosmic-ray component over a given period is given by (number of particles through apparatus) $^{1/2} \times$ (r.m.s. ionization per particle). For a high-energy particle the amount of ionization produced in the ionization chamber is, on the average, proportional to the length of track. Hence, ignoring for a moment the rather small variations in average specific ionization with particle energy, statistical fluctuations are approximately proportional to (track length) $_{\text{rms}}$.

The analytical difficulty in calculating directly the (track length) $_{\text{rms}}$ for a cylindrical chamber is severe, and the following more tractable course is adopted: (a) Calculate the total path length through the sensitive volume of the chamber per unit time for all tracks. (b) Calculate the total number of particles intercepted by the sensitive volume of the chambers in unit time. (c) Dividing (a) by (b) gives the algebraic average path length: an approximate value for the standard deviation may be obtained from (total number particles) $^{1/2} \times$ (average track length \times average specific ionization). (d) We are concerned with the r.m.s. ionization per particle and the approximate value for the standard deviation given in (c) should be multiplied by a correction factor to allow for the difference in r.m.s. and algebraic averages. This correction factor has two components: the first follows from the fact that the r.m.s. track length will be slightly greater than the algebraic average track length, while the second arises from the variability in energy loss of a particle as it traverses the chamber. The first component amounts to 1.04 for a cylinder and 1.06 for a sphere. As far as the second component is concerned, since the larger energy losses involving 'knock-on' electrons are accounted for by the 'shower factor' (see below), this correction will be only very slightly greater than 1. In principle, it could be calculated from an appropriately modified version of the Landau theory. (e) So far the radiation has been regarded as being purely random in character. The effect of the frequency and multiplicity of genetically connected ionizing events is considered.

(a) *Total track length per second.*

Cylindrical section. Let J_0 be the vertical intensity of particles on a plane normal to direction of incidence (unit solid angle) $^{-1}$ cm $^{-2}$ sec $^{-1}$. Then for particles from a direction making an angle θ with zenith, $J_\theta = J_0 \cos^2 \theta$. Other symbols are as in figure 1. It may be shown that the total track length per second is

$$4\pi J_0 l r^2 \int_0^{\pi/2} \int_{-\pi/2}^{\pi/2} \sin \theta \cos^2 \theta \cos^2 \phi \, d\theta \, d\phi = \frac{2}{3} \pi^2 J_0 l r^2.$$

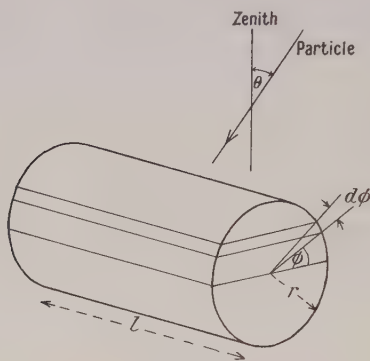


Figure 1.

Hemispherical ends. These ends may be brought together to form a complete sphere for analytical purposes. The total track length per second traversing this sphere is

$$4\pi^2 J_0 r^3 \int_0^{\pi/2} \int_0^{\pi/2} \sin \theta \cos^2 \theta \cos^2 \phi \, d\theta \, d\phi = \frac{8}{9} \pi^2 J_0 r^3.$$

Thus the total track length per second in the chamber is

$$\frac{\pi^2 J_0 r^2}{9} (6l + 8r) = 1.096 J_0 r^2 (6l + 8r).$$

(b) *Total number of intercepted particles per second.*

The effective sphere always presents the same projected area normal to the particles irrespective of zenith or azimuth angles.

Thus it may be shown that total number of particles entering both hemispherical surfaces per second is

$$2\pi^2 J_0 r^2 \int_0^{\pi/2} \sin \theta \cos^2 \theta \, d\theta = \frac{2}{3} \pi^2 J_0 r^2 = 6.57 J_0 r^2.$$

In the case of the cylindrical portion the analysis is rather more complicated but reduces to

$$\begin{aligned} & 2J_0 l r \int_0^{\pi/2} \int_0^{2\pi} \sin \theta \cos^2 \theta (1 - \sin^2 \theta \sin^2 \psi)^{1/2} \, d\theta \, d\psi \\ &= 8J_0 l r \int_0^{\pi/2} \int_0^{\pi/2} \cos^2 \theta (1 - \sin^2 \theta \sin^2 \psi)^{1/2} \, d(\cos \theta) \, d\psi. \end{aligned}$$

ψ is the azimuth angle measured from a line at right angles to the major axis of the chamber. Now

$$\int_0^{\pi/2} (1 - \sin^2 \theta \sin^2 \psi) d\psi$$

for constant θ is a complete elliptic integral of the second kind and its values for different $\sin^2 \theta$ were obtained from tables, multiplied by the appropriate value for $\cos^2 \theta$ and plotted against $\cos \theta$. In this way, the solution to the above double integral was obtained graphically, giving $0.459 \times 8J_0lr$. Hence the total number of particles intercepted by chamber per second is $J_0r(6.57r + 3.67l)$.

(c) *Approximate standard deviation.*

For t seconds exposures the approximate standard deviation is

$$\pm \left\{ \frac{1.096rs(6l + 8r)}{6.57r + 3.67l} \right\} \{J_0rt(6.57r + 3.67l)\}^{1/2} \text{ ions}$$

where s is the r.m.s. specific ionization at the gas pressure in the chamber (taking recombination into account).

This is

$$\pm 1.096rs(6l + 8r) \left\{ \frac{J_0rt}{6.57r + 3.67l} \right\}^{1/2} \text{ ions}$$

or, in terms of current (putting electronic charge = 1.6×10^{-19} coulomb),

$$\pm 1.615rs(6l + 8r) \left\{ \frac{J_0r}{t(6.57r + 3.67l)} \right\}^{1/2} \times 10^{-19} \text{ amp.} \quad \dots\dots (1)$$

For the 'cos² distribution' of particles it may be shown that

$$J_0 = \frac{3}{2\pi} J_* \quad \dots\dots (2)$$

where J_* is the omnidirectional particle intensity (particle sec⁻¹ cm⁻² projected area). Further,

$$J_* = \frac{I}{\bar{N}} \quad \dots\dots (3)$$

where I is the ionization intensity (ion pairs sec⁻¹ cm³) and \bar{N} the average specific ionization (ion pairs) cm⁻¹ both at chamber gas pressure.

From equations (1), (2) and (3)

$$\text{Approximate S.D.} = \pm 1.615rs(6l + 8r) \left\{ \frac{1.5Ir}{\pi t \bar{N}(6.57r + 3.67l)} \right\}^{1/2} \times 10^{-19} \text{ amp.}$$

(d) *Correction factor to (c).*

Since s , the r.m.s. specific ionization, will be only slightly greater than \bar{N} we may treat $s = \bar{N}$ in the above equation, and regard s as a parameter to be determined experimentally. That is,

$$\text{Approximate S.D.} = \pm 1.615r(6l + 8r) \left\{ \frac{1.5Irs}{\pi t(6.57r + 3.67l)} \right\}^{1/2} \times 10^{-19} \text{ amp.} \quad (4)$$

Turning now to the problem of the r.m.s. track length, consider first the correction necessary for particles in planes at right angles to the long axis of the cylinder. Let the particles be of vertical incidence, there being n particles per second crossing each square centimetre of horizontal area.

If we perform the approximate type of analysis used in §2.3 (c) above, then the algebraic average path length of the particles is $\frac{1}{2}\pi r$.

The total number of particles passing through the cylinder per second is

$$4\pi nr^2 l \int_0^{\pi/2} \sin^2 \phi \, d\phi = \pi nr^2 l.$$

Hence for 1 second intervals, the approximate S.D. = $\pm \pi(nl)^{1/2} sr^{3/2}/\sqrt{2}$. Now consider the rigorous analysis. The standard deviation for particles passing through the strip PQRS for 1 second intervals (figure 2) is

$$\pm (nrl \sin \phi \, d\phi)^{1/2} 2rs \sin \phi$$

and S.D. for whole chamber is

$$\pm (4\pi r^3 s^2 l \int_0^{\pi/2} \sin^3 \phi \, d\phi)^{1/2} = \frac{4}{\sqrt{3}} (nl)^{1/2} sr^{3/2}.$$

Hence,

$$\frac{\text{Rigorous S.D.}}{\text{Approximate S.D.}} = \frac{4/\sqrt{3}}{\pi/\sqrt{2}} = 1.04.$$

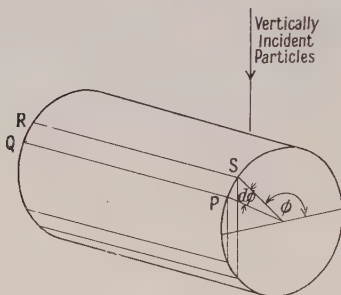


Figure 2.

If the plane of the particles is now inclined at an angle θ to the zenith, remaining at right angles to the vertical plane through the long axis of the chamber, the track lengths are all multiplied by $\sec \theta$, and the same correction factor still applies.

If we now consider the correction factor for particles in planes parallel to the long axis, then for the \cos^2 distribution law the factor is again found to be 1.04. Thus 1.04 may be regarded as the correction factor for the cylindrical section. Similarly, it may be shown that in the case of a sphere, the correction factor is 1.06.

If therefore we are concerned with a chamber in which $l \gg r$, the approximate formulae in 2.3(c) should be multiplied by 1.04. When $l \simeq r$, the correction factor is 1.05.

(e) *The effect of 'showers' or simultaneous, genetically related ionizing events.*

J_0 and J_* are quantities measured in G-M telescope experiments and we may consider the latter quantity to give the total number of particles (independent and genetically related) per unit sphere per second. Palmatier (1952) shows that with his telescope (which is typical) the correction which should be applied to his results from the simultaneous travel of two genetically related particles on parallel tracks is negligibly small.

Suppose the number of single particle events (in the same units as J_*) is J_1 , the number of simultaneous genetically related double events is $J_2 \dots$ etc.,

then

$$J_* = J_1 + 2J_2 + \dots + nJ_n + \dots$$

i.e.

$$J_* = \sum nJ_n.$$

We have shown in § 2.3 (c) that when shower events are ignored

$$(\text{S.D.})^2 \propto J_* s^2 \text{ (from equations (1) and (2))}$$

where s is taken to represent the r.m.s. specific ionization of a single track. When we take into account genetically related events

$$(\text{S.D.})^2 \propto s^2(J_1 + 4J_2 + \dots n^2J_n + \dots).$$

(A single event comprising a double track, each track with a r.m.s. specific ionization s is the equivalent for analytical purposes of an event with a r.m.s. ionization of $2s$.)

That is

$$(\text{S.D.})^2 \propto s^2 \Sigma n^2 J_n$$

or

$$(\text{S.D.})^2 \propto s^2 J_* \frac{\Sigma n^2 J_n}{\Sigma n J_n}.$$

The factor $\Sigma n^2 J_n / \Sigma n J_n$ by which it is necessary to multiply J_* may be described as the 'shower factor' F .

(The magnitude of F will be a function of the shielding and the size of the apparatus. For an infinitesimal apparatus $F \rightarrow 1$. It is shown in § 4 that an F value of approximately 1.9 derived from cloud-chamber observations appears to apply reasonably well to the ionization chamber apparatus described in the next section.)

Incorporating corrections (d) and (e) in equation (4) we have

$$\text{S.D.} = \pm 1.68r(6l + 8r) \left\{ \frac{1.5IFrs}{l(6.57r + 3.67l)} \right\}^{1/2} \times 10^{-19} \text{ amp.}$$

§ 3. EXPERIMENTALLY OBSERVED ERRORS

The layout of the differential apparatus used for measurements of body γ -radioactivity is illustrated in figure 3 and the block circuit arrangement in

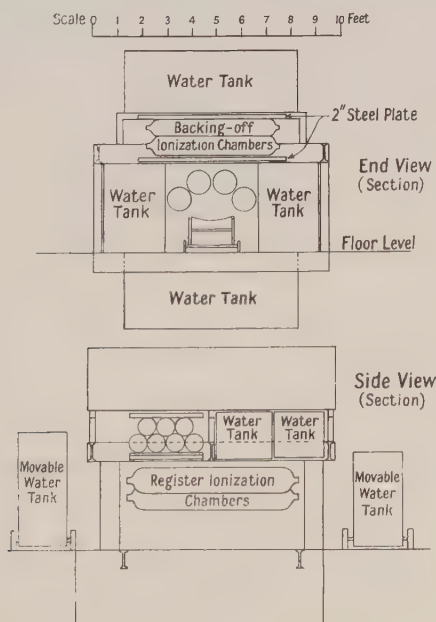


Figure 3. Layout of differential ionization chamber apparatus and shielding. Details of lead and water shielding at sides and ends of backing-off chambers omitted. (Designed for measurement of gamma-radioactivity of human beings.)

figure 4; a detailed description will appear elsewhere. The disposition of chambers is not ideal for a comparison between experimental and theoretically predicted errors because, with the overlap between the two layers of the upper group of chambers, some degree of randomness in the penetrating cosmic-ray particles is lost; this is however counteracted by the overlap between the upper and lower groups and it is considered that these two opposing effects will very nearly cancel each other.

Two methods have been used for observing the differential background current.

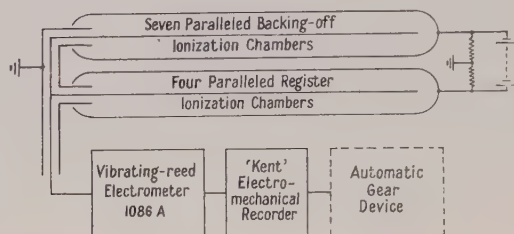


Figure 4.

(The automatic gear device gives average current when the grid-resistor input to the vibrating reed electrometer is used.)

3.1. Rate-of-Drift

Here the final pen-recorded display consisted of a series of dots printed at $33\frac{1}{3}$ second intervals, the distance between successive dots representing the voltage increment during that interval. The mean current was positive and when a dot was printed above 0.9 f.s.d. the input to the vibrating-reed electrometer was short-circuited for an instant and the potential of the central-electrode system returned to zero indicated volts. This record was exceedingly tedious to analyse, but in all 2086 intervals were measured. It was found (both with this method and the grid-resistor method) that the vast majority of points fell on a smooth gaussian distribution (see figures 5 and 6) but that occasionally a point fell outside the normal error limits. These points, representing an energy dissipation in the chamber of the order of 10^9 ev, were caused, presumably, either by nuclear disintegrations ('stars') or by dense extensive showers affecting one group of chambers predominantly. Such an energy absorption would occur for approximately 500 meson or electron tracks, for example, at the normal average specific ionization for fast particles. These 'anomalous' points were excluded when determining the standard deviation. For an average gas pressure of 28.6 atmospheres of commercial nitrogen in the upper chambers and 17.9 atmospheres in the lower group, the standard deviation was found to be $\pm(2.69 \pm 0.11) \times 10^{-14}$ amp for intervals of $33\frac{1}{3}$ seconds. The error of ± 0.11 (the 'S.D. of the S.D.') applies to the randomness of the sampling procedure only; the actual error may be slightly greater. Thus, although the atmospheric pressure was nearly constant for the period of the analysis, chamber gas pressures were such that a small change in differential current did accompany changes in atmospheric pressure. Systematic changes in cosmic-ray intensity uncorrelated with atmospheric pressure (e.g. atmospheric temperature effects) would tend to produce an exaggerated standard deviation.

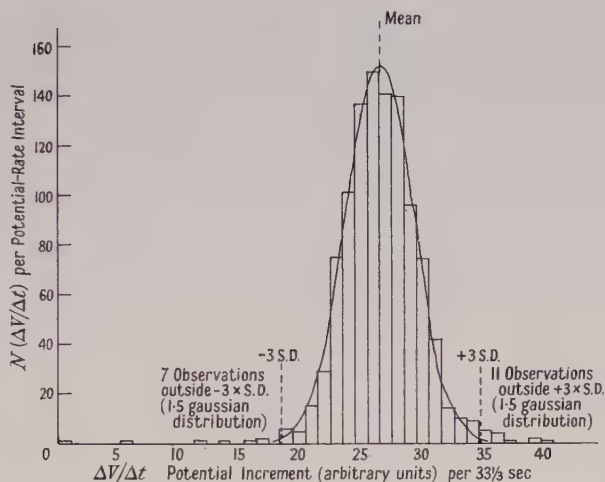


Figure 5. Histogram of 10 hr 20 min of differential background current record (rate-of-voltage-drift method). Potential increment in $33\frac{1}{3}$ sec, $\Delta V/\Delta t$, plotted against frequency of occurrence $N(\Delta V/\Delta t)$ per potential-rate interval. Smooth curve represents gaussian error distribution.

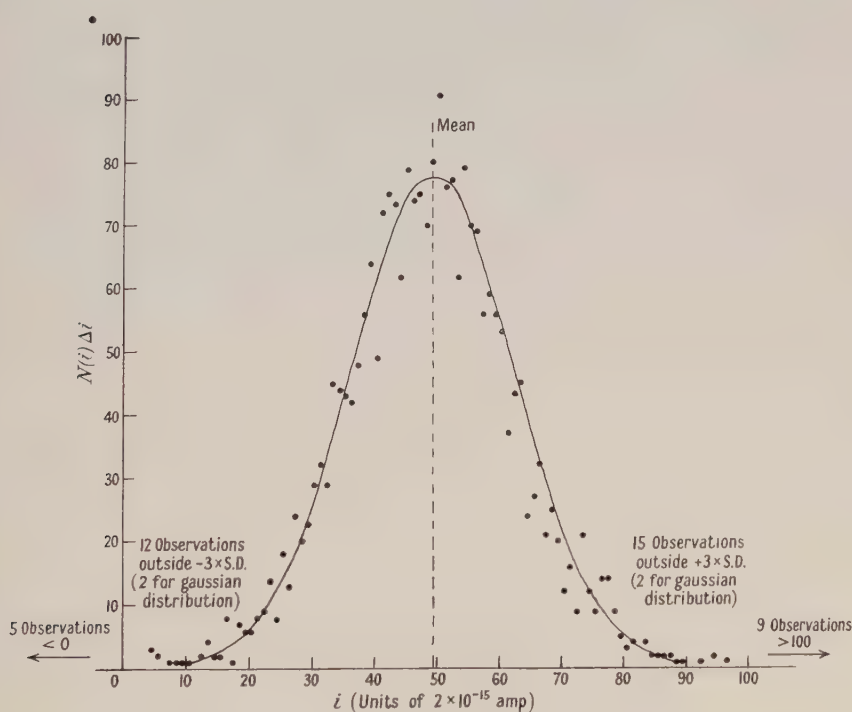


Figure 6. Histogram of 23.5 hours of differential background-current record (grid resistor method). Instantaneous current i (at regular $33\frac{1}{3}$ second intervals) plotted against frequency of occurrence $N(i)\Delta i$. Smooth curve represents gaussian error distribution.

3.2. Grid Resistor

In this method, a 10^{12} ohm grid resistor was used and the printed record gave the 'instantaneous current' at $33\frac{1}{3}$ second intervals. It was obvious that the spread of these current indications was a function of the 'effective time constant' of the whole apparatus, although it was not clear to what time interval (by analogy with the rate-of-drift method) these fluctuations corresponded.

Accordingly, the following independent time constants were determined experimentally: (i) that involved by the slow mobility of ions in the chambers (separately, for each group of chambers), (ii) the 'C-R' time constant of the input circuit to the vibrating-reed electrometer (with the 10^{12} ohm grid resistor in circuit), (iii) the time constant of the recorder.

An 'effective time constant' for the whole apparatus under differential background conditions was computed from $\tau_{\text{eff}} = (\Sigma \tau^2)^{1/2}$.

The assumption was made that the current fluctuations were of the magnitude which would be observed under rate-of-drift conditions taken at intervals of τ_{eff} . This was tested in two ways: (a) At a pressure of 14.9 atmospheres in the lower chambers and 28.6 atmospheres in the upper group, it was found from the analysis of 2513 current indications that the standard deviation for a $33\frac{1}{3}$ second interval on the above assumptions was $\pm (2.36 \pm 0.08) \times 10^{-14}$ amp. On the basis of the rate-of-drift record (obtained at slightly different pressures), the expected standard deviation was calculated to be $\pm (2.45 \pm 0.10) \times 10^{-14}$ amp. (b) Statistical errors were observed firstly for the normal background radiation (σ_1), and then with a radium needle placed outside the shielding so that the current in each group of chambers was approximately doubled (σ_2). The difference in standard deviations, $(\sigma_2^2 - \sigma_1^2)^{1/2}$ was caused by the radium γ -radiation and was used to obtain a value for the r.m.s. energy of the secondary electron tracks. This was found to be 0.82 ± 0.08 mev. Cormack and Johns' (1952) calculations were used to obtain the r.m.s. value of the secondary electron tracks produced by the radium γ -spectrum in water, and this procedure gave 0.86₃ mev. The low atomic number filtration introduced by the experimental arrangement caused some degradation of the quantum energy of the beam as a result of scattered radiation entering the chambers, and about 10% of the ionization was caused by secondary electrons from the wall (of a lower r.m.s. energy). Both these factors will cause the measured value to be less than 0.86₃ mev.

Thus within the limits of experimental error we may conclude that where the grid-resistor technique is used to determine the ionization current, the spread of the statistical variations is characterized by the 'effective time constant' of the apparatus as defined above.

§ 4. COMPARISON OF THEORETICAL AND EXPERIMENTAL ERRORS

The composition of the background radiation was investigated with the aid of lead shielding and a small high-pressure ionization chamber developed by Spiers (1949). At the pressures used for the observations of statistical error, α -contamination effects were negligibly small. The experimental standard deviation for a $33\frac{1}{3}$ second interval, assumed to be $(2.40 \pm 0.08) \times 10^{-14}$ amp, was equated with the theoretical expressions and after taking out the errors caused by the local γ -radiation, the product sF was derived and found to be 119.5 ± 9 ion pairs $\text{cm}^{-1} \text{atm}^{-1}$ (nitrogen). For air, we would expect sF to be 126 ± 10 ion pairs $\text{cm}^{-1} \text{atm}^{-1}$.

It is in principle possible to obtain F the 'shower factor' from random cloud-chamber exposures under similar filtration conditions, the apparatus covering a similar area. There does not appear to be a really comprehensive set of data available which would give a reasonable statistical accuracy. Combining all the results quoted by Evans and Neher (1934), representing 1010 exposures, $F=1.8_4$, whereas using Anderson's observations alone (815 exposures), made under very similar conditions of filtration to those used here but over a smaller area, $F=1.9_2$.

Taking $F \simeq 1.9$, we obtain in the case of air, $s \simeq 67$ ion pairs $\text{cm}^{-1} \text{atm}^{-1}$.

This corresponds to the specific ionization which would be found along the average cosmic-ray track involving all δ -tracks up to about 10^5 ev and is the kind of result we would anticipate.

A similar result was obtained by Evans and Neher (1934) who concluded that their analysis dictated an upper limit for s of 70 ± 10 ion pairs $\text{cm}^{-1} \text{air}$. Johnson (1938) estimates from their data that s is probably a little greater than 65.

It is assumed here and in Evans' treatment that the individual tracks described in the cloud-chamber observations would have sufficient energy (in the present case $\simeq 1.5 \text{ MeV}$) to traverse completely the gas space of the ionization chambers. The existence of the wall 'multiplication' effect (Burch 1954) shows that this is not always the case, and the neglect of this aspect will cause s to be underestimated. On the other hand, the larger area covered by this apparatus should involve an F value greater than the 1.9 given by the cloud-chamber experiments. For practical purposes however we are concerned only with the product sF ; this will vary with filtration, but for air, under the conditions described here, the value 126 ± 10 ion pairs cm^{-1} would appear to be justified.

§ 5. SOME PRACTICAL CONSIDERATIONS

It is useful to compare the relative magnitudes of the statistical errors contributed by the different radiations. The table applies to the apparatus considered in this paper.

Chambers	Radiation component	% total ionization	S.D. (arbitrary units)	(S.D.) ²
$4 \times (12 \text{ in. outside diameter})$	Local γ -radiation	20	} 5.9	35
	Soft quantum-component, cosmic	1		
	Penetrating cosmic	79		
$7 \times (9 \text{ in. outside diameter})$	Local γ -radiation	26	} 5.9	35
	Soft quantum-component, cosmic	1		
	Penetrating cosmic	73		

Under these conditions it is clear that the penetrating component of the cosmic radiation is by far the most important contributor to statistical error.

Minimization of Errors

Since the minimization of errors is of some practical importance, the following suggestions may be made concerning their reduction.

(a) With suitably designed shielding (e.g. 5 to 6 feet of water) there would be little difficulty in reducing the local γ -radiation intensity to very low proportions.

(b) By the use of gases with high recombination coefficients (air or impure nitrogen) and a suitably high gas pressure (say, above 10 atmospheres) the effects of α -contamination of the chambers may be made negligibly small.

(c) Cosmic radiation presents the most obtuse problem, and while theoretical considerations point to the desirability of an underground situation, there are few such sites which are sufficiently attractive for semi-routine measurements on human subjects who may, for example, be suspected of radioactive contamination. One possible method of minimizing the effects of penetrating particles would be to use an 'anti-coincidence' technique with specially constructed chambers (figure 7).

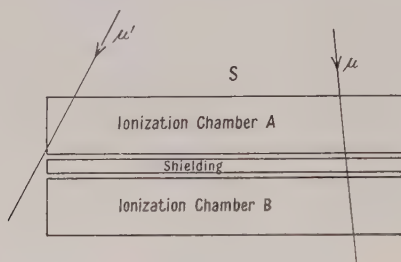


Figure 7. Ionization chambers in 'anti-coincidence'.

Two similar box-shaped chambers with a high breadth-to-depth ratio may be placed one above the other with sufficient shielding (e.g. 2 to 3 in. Fe) between them to attenuate the γ -radiation from a source S, so that chamber B would be almost unaffected by S. The majority of penetrating particles (e.g. μ , in figure 7) would then produce roughly equal amounts of ionization in A and B, and the statistical fluctuations from these particles would be reduced. Such an arrangement would have little influence on fluctuations arising from the soft component (apart from compensation for systematic variations) and the ionization from penetrating particles such as μ' would be uncompensated. With a well-shielded apparatus, the standard deviation should be reduced by a factor of from 2 to 3 by the use of the 'anti-coincidence' technique.

REFERENCES

- BURCH, P. R. J., 1954, *Proc. Phys. Soc. A*, **67**, 421.
 BURCH, P. R. J., and SPIERS, F. W., 1953, *Nature, Lond.*, **172**, 519.
 CORMACK, D. V., and JOHNS, H. E., 1952, *Brit. J. Radiol.*, **25**, 369.
 EVANS, R. D., and NEHER, H. V., 1934, *Phys. Rev.*, **45**, 144.
 HENRIQUES, O. M., and TAYLOR, D., 1953, Paper presented at Seventh International Congress of Radiology, Copenhagen.
 JOHNSON, T. H., 1938, *Rev. Mod. Phys.*, **10**, 193.
 PALMATIER, E. D., 1952, *Phys. Rev.*, **88**, 761.
 SIEVERT, R. M., 1951, *Ark. för Fys.*, **3**, 337.
 SPIERS, F. W., 1949, *Brit. J. Radiol.*, **22**, 169.
 SPIERS, F. W., and BURCH, P. R. J., 1952, *Biological Hazards of Atomic Energy*, Ed. A. Haddow (Oxford: Clarendon Press), p. 203.

The Determination of the Resonant Energies for Proton Capture by ^{24}Mg and ^{25}Mg below 550 keV, and Measurement of the Half Lives of ^{25}Al and ^{26}Al

By S. E. HUNT, W. M. JONES, J. L. W. CHURCHILL
AND D. A. HANCOCK

Research Laboratory, Associated Electrical Industries Ltd., Aldermaston, Berkshire

Communicated by D. R. Chick ; MS. received 3rd November 1953 and in amended form
14th January 1954

Abstract. The energy of the proton beam from an air insulated Van de Graaff generator was measured absolutely by an electrostatic analyser, and the resonant energies for proton capture by ^{24}Mg and ^{25}Mg were determined by observing the positron yields. The following resonances were observed:

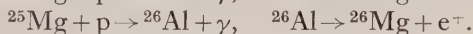
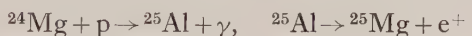
$^{24}\text{Mg}(p, \gamma)^{25}\text{Al}$ 225.5 ± 0.3 and 418.4 ± 0.4 keV of half widths 6.0 ± 1.0 and 2.5 ± 0.5 keV respectively.

$^{25}\text{Mg}(p, \gamma)^{26}\text{Al}$ 316.7 ± 0.7 , 391.5 ± 0.5 , 495.6 ± 0.6 , 513.4 ± 0.7 and 530.4 ± 0.7 keV, of half widths 12.0 ± 1.0 , 8.0 ± 1.0 , 5.0 ± 1.0 , 3.0 ± 1.0 and 3.0 ± 1.0 keV respectively.

The half lives of the positron decay of ^{25}Al and ^{26}Al were measured as 7.62 ± 0.13 and 6.68 ± 0.11 seconds respectively.

§ 1. INTRODUCTION

ON irradiating an unseparated magnesium target with protons both ^{24}Mg and ^{25}Mg produce aluminium isotopes which decay by positron emission:



Magnesium targets were irradiated with protons of energy accurately determined by an absolute electrostatic analyser (Hunt 1952) and the positron yields were measured as a function of the proton energy. In the energy range where the presence of a mass 2 beam could cause confusion, a deflecting magnet was placed after the electrostatic analyser to select the proton beam only (Hunt and Jones 1953).

The half lives for the decay of ^{25}Al and ^{26}Al are comparable so that in order to distinguish between resonances due to the two isotopes, targets of separated ^{24}Mg and ^{25}Mg were irradiated.

§ 2. TARGETS

Unseparated magnesium targets of thickness in energy units of 0.5 to 3.0 keV were prepared by evaporation *in vacuo* (Hunt and Jones 1953). In order to prevent the deposition of carbon during irradiation the targets were heated and a liquid nitrogen trap was placed immediately in front of them (Hunt 1952). Carbon deposits are undesirable in that they produce displacements in the apparent position of the resonance and also high positron background counts in the region of the 456.8 keV carbon resonance.

It was impossible to heat the large disc targets used for the continuous irradiation method to a sufficiently high temperature because of their proximity to the Geiger-Müller counter, and some increase in background in the carbon resonance region was observed. It was shown, however, by repeated determinations of the 418.4 keV resonance that the rate of carbon deposition was less than 0.05 keV per hour.

Separated ^{24}Mg and ^{25}Mg targets were prepared by mass spectrographic deposition of the materials on to copper backings by the Isotope Division, Atomic Energy Research Establishment, Harwell. As it was impossible to estimate accurately the thickness or uniformity of these targets, they were used only to assign the resonances to the correct isotope.

§ 3. DETECTION

The target and counter arrangement is shown in figure 1. The end window type counter was found to operate satisfactorily *in vacuo*. The two following methods were used to measure the positron yields.

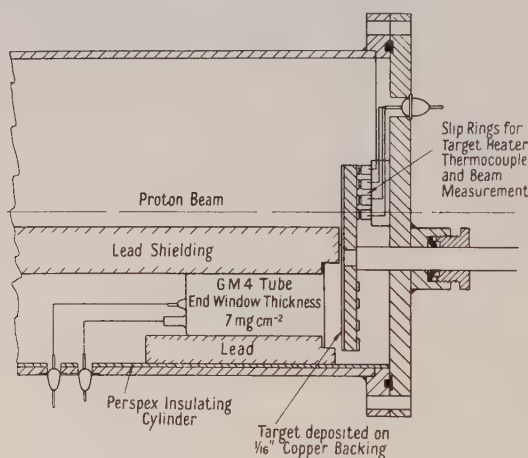


Figure 1. Target and counter assembly.

(i) Decay Method

A small area of the disc target was irradiated for 30 seconds, in which time 95% of the equilibrium activity was built up. The target was then rotated through 180° so that the active portion of the target was about 0.25 inch from the counter window. The electrostatic generator was automatically shorted to cut out x-ray background and counts occurring in the following 20 seconds were recorded. After an interval of 30 seconds the counts occurring in a further 20 seconds period were used as a background correction, since by this time the activity due to the aluminium isotopes had become negligible, whilst that due to ^{13}N produced by proton capture in ^{12}C contamination had not decayed appreciably. Target currents of about $10\ \mu\text{A}$ were used and the uncertainty in target current readings produced an error of approximately $\pm 5\%$ in the yield estimations.

The optimum counting time is discussed in the Appendix.

For the present resonance determinations 20 seconds was sufficiently close to this optimum.

(ii) *Continuous Irradiation Method*

In this method the disc was rotated and irradiated continuously. An active ring was thus built up on the target and positrons coming from a sector (figure 1) were counted. The lead shield reduced bremsstrahlung from the target and the counting rate due to x-ray background from the generator and γ -rays from stronger $^{26}\text{Mg}(p, \gamma)^{27}\text{Al}$ resonances. It can be shown that after near equilibrium target activity has been built up the relative cross section for the reaction is proportional to the number of true counts recorded per unit beam charge, if the time of the irradiation is long compared with the half-life of the activity. Counting times of about one minute were therefore used after an initial irradiation of 30 seconds.

The background due to bremsstrahlung, γ -rays and positrons from the decay of ^{13}N was estimated by irradiating a stationary target with the same total charge in approximately the same time. A period of 30 seconds was allowed for the original aluminium positron activity to fall to a negligible level between the irradiations with the target rotating and those with the target stationary.

(iii) *Comparison of Decay and Continuous Irradiation Methods*

In the continuous irradiation method the aluminium activity was always observed near its equilibrium value and irradiation and observation were simultaneous, whilst in the decay method the activity fell during observation from near equilibrium level to approximately one eighth of this, and the irradiation and observation was done consecutively. However, in the former method it was possible to observe only one quarter of the active ring at any instant, whilst the whole active portion of the target could be observed in the decay method. The number of true counts observed in a given time was about 50% higher when the continuous irradiation method was used. The relative usefulness of the two methods depended on the respective background counting rates. In general the continuous irradiation method was preferable except very close to the $^{26}\text{Mg}(p, \gamma)^{27}\text{Al}$ resonances and in the region of the strong $^{12}\text{C}(p, \gamma)^{13}\text{N}$ resonance. The requirements in the constancy of the beam current were also less stringent.

It was necessary to use the decay method for the separated isotope targets since these could not be deposited over the larger target surface required for the continuous irradiation method.

§ 4. DETERMINATION OF THE MEAN LIVES

(i) *Method*

Separated ^{24}Mg and ^{25}Mg targets were irradiated for about 30 seconds by beams of energy 419 kev and 392 kev respectively. The target was then rotated so that the activated part was presented to the counter as described in § 3 (i). An automatic switch (§ 4 (ii)) connected the counter successively to scaling circuits for nine equal periods of two seconds.

Peierls (1935) has shown that the most rigorous method for determining τ (the mean life) is from the formula:

$$1 - S/\tau = (T/\tau) [\exp(T/\tau) - 1]$$

where S is the mean time of the pulses counted reckoned from the beginning of the total counting time T .

A block diagram of the equipment is shown in figure 2. The timing circuit was controlled by the frequency of the mains supply and the paralysis and delay signals guarded against incorrect operation due to a count indicated during the change-over period between scalars. The statistical accuracy achieved in the counting experiments was within about 3%, and as the drifts in supply frequency were found to be an order less than this, their effects on the accuracy of the timing were ignored. A more detailed description of the circuits is reported elsewhere (Churchill and Evans 1954).

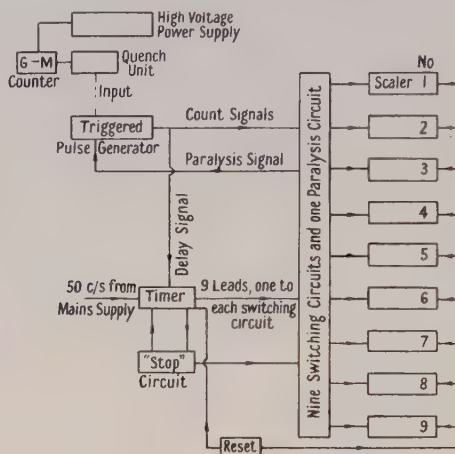


Figure 2. Block diagram of equipment for determination of mean lives.

The irradiations were repeated until the required statistical accuracy was obtained and mean lives were determined by Peierls' method.

(ii) Results

One hundred and ninety irradiations were carried out on ^{24}Mg and three hundred on ^{25}Mg . This gave a total number of recorded counts in each case of approximately twenty thousand.

The results are summarized in figure 3 for the two aluminium isotopes. The computation of the mean lives yielded values of 11.00 ± 0.19 seconds for

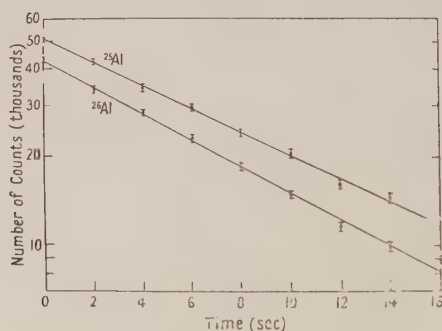


Figure 3. Graph of results for the decay of aluminium 25 and aluminium 26.

^{25}Al and 9.64 ± 0.16 seconds for ^{26}Al . These correspond to half-lives of 7.62 ± 0.13 seconds and 6.68 ± 0.11 seconds respectively.

§ 5. THE RESONANCE MEASUREMENTS

The resonance measurements are summarized in the table, together with those obtained by Tangen (1946). The γ -ray yield of the 418.4 keV resonance

Tangen		Present work		Identification
Resonance	Half width	Resonance	Half width	
222 ± 1	< 1 keV	225.5 ± 0.2	6.0 ± 1	^{24}Mg
310 ± 3		316.7 ± 0.7	12.0 ± 1	^{25}Mg
392 ± 4		391.5 ± 0.5	8.0 ± 1	^{25}Mg
417 ± 4		418.4 ± 0.4	2.5 ± 0.5	^{24}Mg
492 ± 5		495.6 ± 0.6	5.0 ± 1	^{25}Mg
508 ± 5		513.4 ± 0.7	3.0 ± 1	^{25}Mg
525 ± 6		530.4 ± 0.7	3.0 ± 1	^{25}Mg

has been measured (Hunt and Jones 1953). It was found to be one two thousandth of that of the strong $^{19}\text{F}(p, \gamma)^{20}\text{Ne}$ resonance at 340.4 keV, which has been estimated to have a yield of 0.174 quantum per 10^7 incident protons (Ajzenberg and Lauritsen 1952). The relative yields of other resonances are shown in figure 4. It should be noted that this curve refers to the yield from natural magnesium targets so that the yield of the ^{25}Mg resonances should be multiplied by approximately seven because of the lower abundance of this isotope.

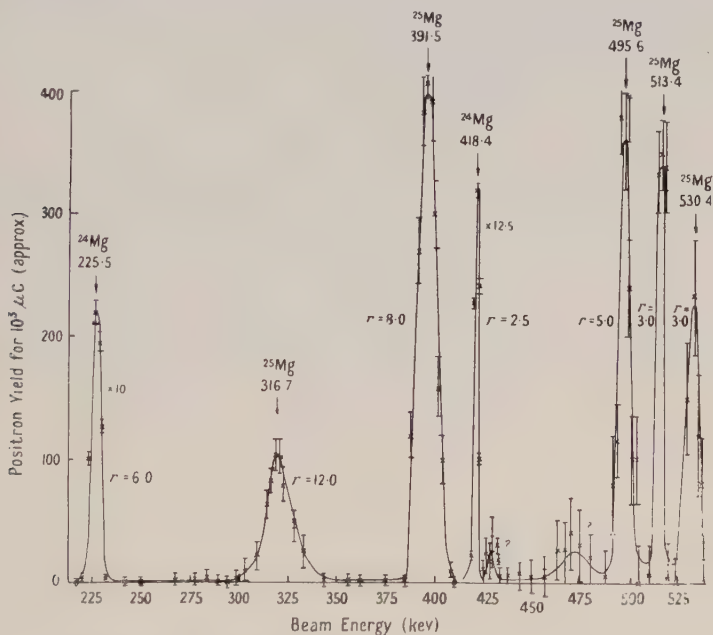


Figure 4. Magnesium resonances observed by continuous irradiation method.

By irradiating a thick magnesium target with protons of energy 220 keV it was shown that no resonance of yield greater than one five hundredth of that of the 418.4 keV resonance existed below this energy.

§ 6. DISCUSSION OF RESULTS

Of the present resonance measurements only the 225.5 keV and 316.7 keV values disagree with those obtained by Tangen by more than the combined

limits of error. Tangen initially ascribed all the resonances to the ^{25}Mg isotope, but subsequently Grottdal *et al.* (1950) observed resonances at 222 and 417 keV on separated ^{24}Mg targets.

The present work confirms Grottdal's results. Russel *et al.* (1952) have observed resonances on separated ^{25}Mg targets at 386, 489 and 508 keV. The errors associated with their measurements appear to be about 10 keV (Taylor *et al.* 1952) and their results are therefore consistent with the assignment of the 391.5, 495.6 and 513.4 keV resonances to ^{25}Mg in the present work. The 316.7 and 530.4 keV resonances have not previously been assigned to the ^{25}Mg isotope.

Tangen measured the half width of the lowest energy resonance only and obtained a value of less than 1 keV, which does not agree with that obtained in the present work. The other half widths have not been measured previously. Frisch (1934) first measured the half life of ^{26}Al as 7.0 seconds. It has since been determined by Bradner and Gow (1948), who obtained a value of 6.3 seconds, Perlman and Friedlander (1948) 7.0 seconds, Allan and Wilkinson (1948) 7.0 ± 0.2 , Wäffler and Hirzel (1948) 7.2 seconds and Katz and Cameron (1951) 6.5 ± 0.1 seconds. The present value is in good agreement with the latter precise determination.

Before separated isotope targets were used the proximity of the half life of ^{25}Al to that of ^{26}Al led to some confusion, as it was not possible to separate the two activities (White *et al.* 1939). The only other measurement of the half life of ^{25}Al is that of Bradner and Gow (1948) who obtained a value of 7.3 seconds.

ACKNOWLEDGMENTS

The authors would like to thank Professor Peierls, Professor Rotblat and Mr. D. R. Chick for helpful discussions in the course of this work. Mr. R. M. Payne and Mr. W. W. Evans have also given valuable assistance. We should also like to thank Dr. R. H. V. M. Dawton and Dr. M. L. Smith of the Atomic Energy Research Establishment, who prepared the separated isotope targets. Thanks are also due to Dr. T. E. Allibone for permission to publish this paper.

APPENDIX

Calculation of the Optimum Counting Time in the Decay Method

The number of true counts recorded in t seconds is $EN[1 - \exp(-t/\tau)]$ where E is the efficiency of detection and N the initial number of radioactive nuclei.

Assuming gaussian errors, the fractional statistical error S in the true counts is given by:

$$S = [EN\{1 - \exp(-t/\tau)\} + 2\beta t]^{1/2} / EN[1 - \exp(-t/\tau)].$$

Differentiating we obtain:

$$dS/dt = [-4t/\tau - 2\{1 - \exp(t/\tau)\} - R_0\{1 - \exp(-t/\tau)\}/\beta]P$$

where P is a finite positive term for $t/\tau > 0$ and R_0 is the initial true counting rate, β is the background counting rate.

It may be shown that $dS/dt=0$ is satisfied for only one finite positive value of t/τ and that this value corresponds to a minimum in S . The equation $dS/dt=0$

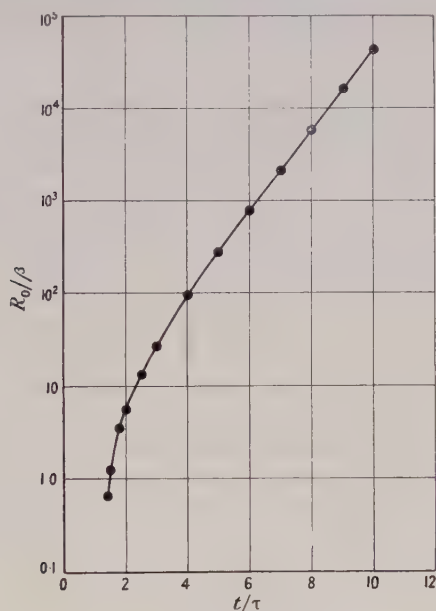


Figure 5. Graph of R_0/β against t/τ .

is not analytically soluble for t/τ but may be solved for R_0/β and the function obtained is plotted in figure 5. The optimum value of t/τ can be read from figure 5 for values of R_0/β in the range 1 to 10^4 .

REFERENCES

- AJZENBERG, F., and LAURITSEN, T., 1952, *Rev. Mod. Phys.*, **24**, 321.
 ALLAN, H. R., and WILKINSON, C. A., 1948, *Proc. Roy. Soc. A*, **194**, 131.
 BRADNER, H., and GOW, J. D., 1948, *Phys. Rev.*, **74**, 1559.
 CHURCHILL, J. W., and EVANS, W. W., 1954, *Nucleonics*, in the press.
 FRISCH, O., 1934, *Nature, Lond.*, **133**, 721.
 GROTDAL, T., LÖNSJÖ, O. M., TANGEN, R., and BERGSTRÖM, I., 1950, *Phys. Rev.*, **77**, 296.
 HUNT, S. E., 1952, *Proc. Phys. Soc. A*, **65**, 982.
 HUNT, S. E., and JONES, W. M., 1953, *Phys. Rev.*, **89**, 1283.
 KATZ, L., and CAMERON, A. G. W., 1951, *Phys. Rev.*, **84**, 1115.
 PEIERLS, R., 1935, *Proc. Roy. Soc. A*, **149**, 467.
 PERLMAN, M. L., and FRIEDLANDER, G., 1948, *Phys. Rev.*, **74**, 442.
 RUSSEL, L. N., WARREN, E. T., and COOPER, J. N., 1952, *Phys. Rev.*, **86**, 653 A.
 TANGEN, R., 1946, *K. Norske Vidensk. Selsk. Skr.* No. 1.
 TAYLOR, W. E., RUSSEL, L. N., COOPER, J. N., and HARRIS, J. C., 1952, *Phys. Rev.*, **86**, 630.
 WÄFFLER, H., and HIRZEL, O., 1948, *Helv. Phys. Acta*, **21**, 200.
 WHITE, M. G., DELSASSO, L. A., FOX, J. G., and CREUTZ, E. C., 1939, *Phys. Rev.*, **56**, 512.

Hyperfine Structures in the Atomic Spectrum of Calcium

By F. M. KELLY*, H. KUHN AND ANNE PERY

Clarendon Laboratory, Oxford

MS. received 2nd February 1954

Abstract. The spectrum of calcium was excited in a hollow cathode tube cooled with liquid hydrogen. The use of a sample of calcium enriched in the isotope 43 allowed hyperfine structures to be resolved in the arc line $\lambda 6103 (4s4p\ ^3P_0-4s5s\ ^3S_1)$ and the spark lines $\lambda 3933 (4s\ ^2S_{1/2}-4p\ ^2P_{3/2})$ and $\lambda 3968 (4s\ ^2S_{1/2}-4p\ ^2P_{1/2})$, from which an approximate value of -1.2 nuclear moments (n.m.) for the nuclear magnetic moment was derived. The intensity ratio of the components of the arc line was found to be affected by self-absorption due to the metastability of the lower term. After correction for this effect, the measured intensity ratio agreed best with a value of $7/2$ for the nuclear spin. After publication of the value of the gyromagnetic ratio by Jeffries, the measurements of the width of splitting of the spark lines allowed the nuclear spin to be determined conclusively as $I = 7/2$, in agreement with the predictions from the shell model and the value deduced from the strength of the nuclear resonance signal. The splitting of the ground term, $0.109 \pm 0.002\text{ cm}^{-1}$, is 4% smaller than the value calculated from the gyromagnetic ratio by the use of the formulae of Goudsmit, Fermi, Segrè, Breit and Racah.

§ 1. INTRODUCTION

NATURAL calcium consists almost entirely of even isotopes, of which that of mass number 40 is the most abundant. The only stable, odd isotope, of mass number 43, has an abundance of only 0.15% . When the Atomic Energy Research Establishment at Harwell kindly supplied a sample of 2 mg of calcium containing 75% of the odd isotope, the investigation of hyperfine structures in the optical spectrum was undertaken in order to determine the nuclear spin I and magnetic moment μ of Ca43. After approximate values of both these quantities had been found, and experiments to obtain more definite results were nearly finished, Jeffries (1953) published the results of nuclear resonance experiments on Ca43, giving a very accurate value of the nuclear g -factor $g_I = \mu/I = -0.3758$ n.m. The value of I , which by this method must be deduced from the amplitude of the signal, was found to agree with the value $7/2$ predicted by the nuclear shell model (Schawlow and Townes 1951, Davidson 1952). In the later stages of the present work it was possible to use the resonance value of the nuclear g -factor to determine the spin from the hyperfine structure by an independent method and to compare the observed term splitting in the ground state of the ion with that calculated from the value of μ .

The smallness of the splitting in all the lines made it necessary to cool the discharge in liquid hydrogen.

§ 2. EXPERIMENTAL METHODS

(a) *The Choice of Lines*

The widest hyperfine structure was to be expected in the term $4s5s\ ^3S_1$. Provided the value of I is greater than $\frac{1}{2}$, this term consists of three components

* Postdoctorate Overseas Fellow from the National Research Council of Canada. Present address Department of Physics, University of Manitoba.

($F = I + 1$, I , and $I - 1$). The transition from this state to the structureless term $4s4p\ ^3P_0$, $\lambda 6103$, should therefore form a triplet (see figure 1). It should be possible to determine the nuclear spin, either from the ratio of the two intervals or from the ratio of the intensities of the components. The middle component, is,

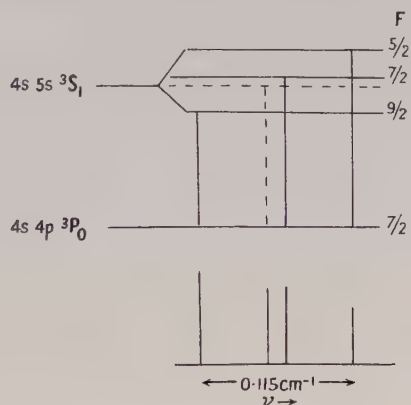


Figure 1. Term diagram of $\lambda 6103$.

however, blended with the line produced by the residual even isotopes; thus the interval rule can only be used if the position of the even component and the isotopic composition of the sample are accurately known. A separate series of experiments was carried out to determine the isotope shift in this and other lines of the calcium spectrum, using a sample of calcium highly enriched in the isotope 48. These experiments have been described in an earlier paper (Pery 1954). It was found that in the line $\lambda 6103$ the normal mass effect is almost exactly cancelled by the specific mass effect, and the residual shift is negligible.

Once the intensity and position of the even isotope component are known, it should be possible to find the spin from the interval rule. Unfortunately, however, the chance combination of a term with $J = 1$, a line of negligible isotope shift and a sample of calcium enriched to 75% is found to give rise to a pattern which, whatever the value of I , appears as three equally spaced components. The determination of I from the interval ratio was therefore impossible.

A promising method appeared to be the measurement of the intensity ratio of the two outer components; this ratio is equal to $(2I + 3)/(2I - 1)$, and thus should have the values 3, 2, 1.67 and 1.50 for the spin values $3/2$, $5/2$, $7/2$, and $9/2$ respectively. A reliable measurement of intensities is, however, not possible unless the lines are well resolved so that the correction for overlap is small; this could be achieved only by cooling the light source with liquid hydrogen.

The structure of the lines of the alkali-like spark spectrum appeared of special interest because it is possible to calculate the nuclear magnetic moment from it. The resonance lines $\lambda 3933$ ($4s\ ^2S_{1/2} - 4p\ ^2P_{3/2}$) and $\lambda 3968$ ($4s\ ^2S_{1/2} - 4p\ ^2P_{1/2}$) were expected to show a resolvable hyperfine doublet, due to the splitting of the S term, with a third line between them caused by the even isotopes. In principle, it is possible to use these lines, too, to find I , but for large values of I , the measurement of the intensity ratio in a hyperfine doublet is not a sensitive method for this. The same objection applies to the determination of I from the ratio of the distances of the components from their centre of gravity, as derived from the position of the even isotope line. The latter method also involves the influence of the unresolved splitting of the P terms.

In conjunction with the known value of the gyromagnetic ratio, however, the measurement of the splitting of the spark lines offered a simple and reliable means of determining the spin. Cooling with liquid hydrogen again proved necessary to achieve sufficient resolution.

(b) *The Light Source*

The calcium spectrum was excited in a hollow cathode discharge tube which was a modified form of that described by Kuhn and Woodgate (1951). It was specially designed for work with enriched isotopes; the cathode block containing the isotope can be easily and quickly lifted in and out without displacement of the discharge tube, good thermal contact is assured and the precious material is easily recovered. Since no metal parts protrude through the surface of the coolant, the tube is well suited for use with liquid hydrogen; the consumption of hydrogen was, in fact, found to be almost entirely due to the electric power consumed by the discharge. The technique of cooling with liquid hydrogen was similar to that described by Kuhn and Series (1950).

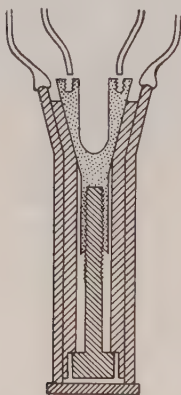


Figure 2. Hollow cathode.

Figure 2 shows the details of the cathode. Inside the upper cylinder of a commercial copper-glass seal is soldered a copper sleeve, machined to fit the conical part of a removable cathode piece. The bottom of the cathode is bored and tapped so that it can be screwed down on to a steel bolt with a rectangular head. The bolt is then free to tip but not to turn, and the cone can be pulled down into really good thermal contact with its socket. A two-pronged screwdriver fits into a pair of small holes in the top of the cathode piece for the screwing operation, and two threaded rods can be screwed into a second pair of holes to lift the cathode piece in and out of the discharge tube.

The cathode piece itself was made of beryllium, which appears to sputter rather less than aluminium. The main cavity, 10 mm deep and 5 mm in diameter, contained the calcium. Experiments with ordinary calcium showed that even spread of the material over the walls of the cavity was most important. This was achieved by spreading a concentrated solution of the chloride around the cavity while the cathode was gently heated until the water had evaporated. With this technique it was found possible to perform long series of experiments with a filling of only $\frac{1}{2}$ mg of the isotope. A glass sleeve, whose lower end is shown in the figure, was placed over the cavity; for recovery of the material, only the cathode

block and the glass sleeve need be removed. Neon, at a pressure of about 1 mm Hg, was used to carry the discharge and was kept clean by a few pieces of charcoal in a side tube which was cooled with liquid air.

(c) The Spectrograph and Interferometer

An autocollimating spectrograph of focal length 1 metre and aperture 1/13 was used for separating the calcium lines from those of neon. With a 30° prism, the dispersion was 13 Å per mm for violet light. For exposures in the red, the dispersion was increased to 22 Å per mm by the addition of a 60° prism.

The Fabry-Perot interferometer had silica plates 6 cm in diameter. In the final experiments, these had silver coatings of 89% reflection and 8% transmission in the red, and aluminium coatings of 79% reflection and 10% transmission in the violet. These values were chosen to make the instrumental width, with the spacers finally used (2.5 and 3 cm respectively) about half the Doppler width. In view of the long exposures, it was necessary not only to control the temperature of the room, but also to eliminate the effect of changes in atmospheric pressure by enclosing the etalon in an airtight box.

(d) The Filter Etalon

In the investigation of the line at 6103 Å an additional problem was presented by a strong neon line at 6096 Å, which was so overexposed as to spread into the neighbouring calcium line. The difficulty was overcome by introducing a second etalon to act as a high-order interference filter (Edser-Butler plate) in suppressing the neon line. With the comparatively large spacing (0.15 mm) required to produce a maximum of transmission at 6103 Å and a minimum at 6096 Å, the permissible variation of the angle of incidence is very small. The etalon could therefore not be used in front of the slit, like an ordinary interference filter, but was placed in the collimated beam immediately in front of the main etalon. In contrast to a double etalon, however, the centre of the ring system of the filter etalon was made to coincide with the centre of the slit, not with the centre of the ring system of the other etalon. The arrangement is thus intermediate between a double etalon and an interference filter combined with a single etalon. With very light silver coating on the filter etalon, the intensity of the neon line was reduced by a factor of about 50, and that of the calcium line by just over 2. Ilford Rapid Process Panchromatic plates proved to be most suitable for the red line, on account of their fine grain and comparatively high sensitivity. Their threshold value was raised by pre-fogging.

Intensity marks were made on each plate by photographing a neutral step filter close to the image of the slit. The densities of the filter steps were measured by means of a microphotometer whose response was known to be linear.

§ 3. RESULTS

When the discharge tube was cooled in liquid oxygen and operated at currents of 20 mA, with a voltage drop of 200 to 300 volts, the hyperfine triplet was resolved in the line λ 6103 (see figure 3(a)), but it was clear that intensity measurements would require considerable corrections for the overlapping of the components. In the spark lines, the even isotope line was not properly resolved from the long wavelength component of the hyperfine doublet.

The advantage gained by cooling with liquid hydrogen is shown by comparing figure 3(a) with figure 3(b) which is the tracing from a 9 hour exposure with liquid

hydrogen cooling, at a current of 20 mA. Lower currents would probably have reduced the line width still further but would have made the time of exposure too long. The resolving power of the etalon in figure 3 (b) is slightly larger than that in figure 3 (a) owing to the use of a larger spacer, but most of the gain in resolution is certainly due to the reduction in Doppler width.

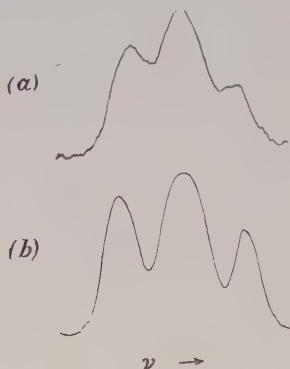


Figure 3. Photometer tracing of $\lambda 6103$ ($4s4p\ ^3P_0-4s5s\ ^3S_1$), (a) with liquid air cooling, (b) with liquid hydrogen cooling.

As expected, the blend forming the central component was found to be exactly half-way between the outer components whose separation was found to be 0.115 cm^{-1} .

For the measurement of the intensity ratio, the photometer tracings were converted into plots of intensity against wave-number. The effects of overlapping of the wings and of scattered light were calculated from the intensity between orders, i.e. from the empirically determined intensity distribution in the outer wings of the two outer components. Eleven fringes from four photographs gave very consistent results, with an average of 1.52 for the corrected value of the ratio (uncorrected 1.42). It was noticed, however, that the lines were wider than expected, and the presence of self-absorption was suspected. At such small current densities, self-absorption is not usually observed except in resonance lines; but the term 3P_0 is highly metastable, owing to the rule forbidding transition of J from 0 to 0, and moreover the reduction of Doppler width increases the effect of self-absorption.

The fact that the term 3P_1 is not metastable made it possible to test for the presence of self-absorption in the line $\lambda 6103$ ($4\ ^3P_0-5\ ^3S_1$) by measuring the ratio of its intensity to that of the line $\lambda 6122$ ($4\ ^3P_1-5\ ^3S_1$), in exposures taken without any etalon. At a current of 10 mA the intensity ratio was found to be about 3.0, in agreement with the intensity rule for a triplet; at 20 mA, however, the value rose to about 3.35, indicating self-absorption in the line connected with the metastable term. From these results, an estimate of the influence of self-absorption on the hyperfine structure components could be made and was found to raise the value of the intensity ratio from 1.52 to about 1.64 (with a lower limit of 1.60 and an upper limit of 1.68). Though the intensity ratio is thus found to support the value $7/2$ for the nuclear spin (see § 2 (a)), the presence of self-absorption makes the method rather unsatisfactory.

The hyperfine structure in the spark line $\lambda 3933$ was just resolved and that in the line $\lambda 3968$ well resolved with liquid hydrogen cooling at currents between 13 and

10 mA, and the splitting of the outer components, i.e. the doublet components of the odd isotope, was measured in eleven fringes from two plates for each of the lines. The mean values found were 0.104 cm^{-1} for $\lambda 3933$ ($^2S_{1/2}-^2P_{3/2}$) and 0.114 cm^{-1} for $\lambda 3968$ ($^2S_{1/2}-^2P_{1/2}$). The exposures lasted 8 to 18 hours.

The difference between these two values is due to the unresolved splitting of the P terms. It is easy to calculate the influence of this splitting from the known ratio of the splittings of two doublet terms $^2P_{3/2}$ and $^2P_{1/2}$ (Jackson 1934) and one finds that the splitting of the S term is exactly the arithmetical mean of the widths of splitting of the two lines. We thus find $\Delta S_{1/2} = 0.109 \pm 0.002 \text{ cm}^{-1}$. The values of the splitting of the P terms estimated from the difference of the splittings of the two lines agree well with those calculated from the value of g_I .

The width of the hyperfine structure of a $^2S_{1/2}$ term of an alkali-like atom can be written as

$$\Delta\nu = \frac{H_0}{2hc} g_I (2I + 1) = \frac{H_0}{2hc} \mu \frac{2I + 1}{I} \quad \dots\dots(1)$$

where H_0 , the magnetic field strength at the nucleus, can be calculated by means of the well-known formulae of Goudsmit, Fermi, Segrè, Breit and Racah (see, for example, Kopfermann 1940). From numerous applications, these formulae are known to be accurate to about 5%.

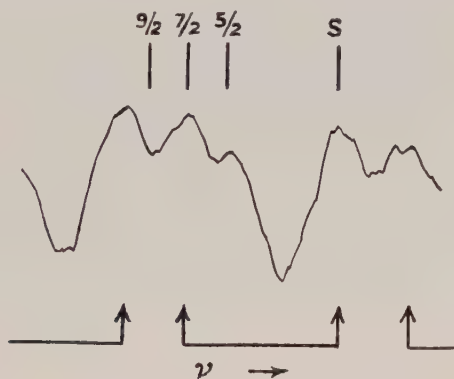


Figure 4. Photometer tracing of $\lambda 3968$ ($4^2S_{1/2}-4^2P_{1/2}$).

Equation (1) shows that $\Delta\nu$, when expressed as function of μ , depends little on I , for not too small values of the latter. Even without an exact knowledge of I , an approximate value of μ could thus be derived from the observed width of splitting. The value found, $\mu = -1.2 \text{ n.m.}$, agreed well with the prediction from the nuclear shell model (Schawlow and Townes 1951, Davidson 1952) in sign and magnitude.

When the value of g_I was known, the observed splitting $\Delta\nu$ could be used for determining I by means of (1). For the spin values $5/2$, $7/2$ and $9/2$, the calculated values of $\Delta\nu$ are 0.085 , 0.113 and 0.142 cm^{-1} . Any value except $I = 7/2$ is thus found to give a splitting whose value differs from the experimental result by far more than the errors of either experiment or calculation.

Figure 4 shows a photometer tracing of the line $\lambda 3968$ from an exposure with liquid hydrogen cooling, with an etalon spacer of 3 cm. The bracketed arrows indicate the doublet components belonging to the same order; the three vertical

lines give the positions of the long-wave component, relative to the short-wave component s , calculated for different values of I . The smaller peak between the doublet components is due to the even isotopes.

The difference between the observed value of the splitting $\Delta\nu = 0.109 \text{ cm}^{-1}$, of the ground term, and the value of 0.113 cm^{-1} derived from g_I is of similar magnitude and the same sign as that found in other alkali-like spectra. In the iso-electronic spectrum of K, the calculation gives the value 0.0165 cm^{-1} , while direct measurement gives 0.0154 cm^{-1} .

The effect of the volume distribution of the nuclear charge on the width of splitting (Rosenthal and Breit 1932) is included in the values quoted for Ca^+ and K; it is less than 1% of the splitting. The effect of the volume distribution of the nuclear magnetic moment (Bohr and Weisskopf 1950) is entirely negligible. The correction factor $(1 - d\sigma/dn)$ was calculated by means of the method described by Crawford and Schawlow (1949). It appears that the formula of Goudsmit, Fermi and Segrè gives systematically slightly too high values for the splitting.

ACKNOWLEDGMENT

One of the authors (A. P.) wishes to express her gratitude to St. Hugh's College for the award of a senior scholarship.

REFERENCES

- BOHR, A., and WEISSKOPF, V. F., 1950, *Phys. Rev.*, **77**, 94.
CRAWFORD, M. F., and SCHAWLOW, A. L., 1949, *Phys. Rev.*, **76**, 1310.
DAVIDSON, J. P., 1952, *Phys. Rev.*, **85**, 432.
JACKSON, D. A., 1934, *Proc. Roy. Soc. A*, **147**, 500.
JEFFRIES, C. D., 1953, *Phys. Rev.*, **90**, 1130.
KOPFERMANN, H., 1940, *Kernmomente* (Leipzig : Akad. Verl. Ges.).
KUHN, H., and SERIES, G. W., 1950, *Proc. Roy. Soc. A*, **202**, 127.
KUHN, H., and WOODGATE, G. K., 1951, *Proc. Phys. Soc. A*, **64**, 1090.
PERY, ANNE, 1954, *Proc. Phys. Soc. A*, **67**, 181.
ROSENTHAL, J. E., and BREIT, G., 1932, *Phys. Rev.*, **41**, 459.
SCHAWLOW, A. L., and TOWNES, C. H., 1951, *Phys. Rev.*, **82**, 269.

Approximate Molecular Orbitals II : The $2p\pi_u$ and $3d\pi_g$ States of H_2^+

BY B. L. MOISEWITSCH AND A. L. STEWART

Department of Applied Mathematics, The Queen's University of Belfast

Communicated by D. R. Bates ; MS. received 13th January 1954

Abstract. The variational method is used to obtain approximate wave functions for the $2p\pi_u$ and $3d\pi_g$ states of H_2^+ . Their accuracy is assessed by comparing the values of various quantities computed from them with the corresponding values computed from the exact wave functions. The dependence of the total kinetic and potential energies on the nuclear separation is briefly discussed.

§ 1. INTRODUCTION

THIS paper is the second of a series in which it is intended to determine by the Rayleigh-Ritz variational principle approximate molecular orbitals and to use them for the evaluation of various quantities which have been or can be exactly determined. It is hoped, with this comparison available, that these approximate molecular orbitals will provide a convenient basis for the development of analytic approximations to other more complex molecules. Paper I (Dalgarno and Poots 1954, to be referred to as I) was concerned with the $1s\sigma_g$ and $2p\sigma_u$ states of H_2^+ ; in the present paper the $2p\pi_u$ and $3d\pi_g$ states† are dealt with analogously.

§ 2. CHOICE OF WAVE FUNCTIONS

The problem of obtaining approximate molecular orbitals for the $2p\pi$ and $3d\pi$ states of H_2^+ has received much less attention from theorists than the similar problems for the $1s\sigma$ and $2p\sigma$ states. The simplest approximations which take account of the symmetry are

$$\Psi(2p\pi) = r_a \sin \theta_a \cos \phi_a \{ \exp(-\frac{1}{2}r_a) + \exp(-\frac{1}{2}r_b) \} \quad \dots\dots(1a)$$

$$\Psi(3d\pi) = r_a \sin \theta_a \cos \phi_a \{ \exp(-\frac{1}{2}r_a) - \exp(-\frac{1}{2}r_b) \} \quad \dots\dots(1b)$$

where r_a and r_b are the position vectors of the electron relative to the nuclei A and B respectively. This linear combination of atomic orbitals (LCAO) approximation has been applied to the $2p\pi$ state by Lennard-Jones (1929) and by Dooling (1953), who has considered also a linear combination of the orbital (1a) and the next higher excited orbital. No attempt seems to have been made to improve (1a) and (1b) by including a screening parameter

$$\Psi(2p\pi) = r_a \sin \theta_a \cos \phi_a \{ \exp(-\frac{1}{2}\alpha r_a) + \exp(-\frac{1}{2}\alpha r_b) \}, \quad \dots\dots(2a)$$

$$\Psi(3d\pi) = r_a \sin \theta_a \cos \phi_a \{ \exp(-\frac{1}{2}\alpha r_a) - \exp(-\frac{1}{2}\alpha r_b) \} \quad \dots\dots(2b)$$

and minimizing the energy.

For small internuclear separations one may write

$$\Psi(2p\pi) = r \sin \theta \cos \phi \exp(-r), \quad \dots\dots(3a)$$

$$\Psi(3d\pi) = r^2 \sin \theta \cos \theta \cos \phi \exp(-\frac{2}{3}r) \quad \dots\dots(3b)$$

† In the separated atoms notation these are designated $\pi(2p_x)$ and $\pi^*(2p_x)$ respectively.

where \mathbf{r} is the position vector of the electron with respect to the centre of charge of the nuclei A and B. The energy matrix element derived with this approximation includes the zero order and first order terms in the energy series obtained by applying perturbation theory to the wave functions of the united atom (the atom to which the molecule reduces at zero separation of the nuclei). Dooling (1953) found that the energy series converged much too slowly when he sought to improve the energy by including terms of higher order. The functions (3a) and (3b) can, of course, be improved by the inclusion of a screening parameter (cf. Matsen 1953).

Of the various wave functions mentioned only (2a) has the correct form for both zero and infinite separations, R , of the nuclei. This desirable characteristic may be achieved (following I) by taking

$$\begin{aligned}\Psi(2p\pi) = & \left(\frac{\alpha^5}{16N_1^2\pi} \right)^{1/2} r_a \sin \theta_a \cos \phi_a \exp\left\{-\frac{1}{4}\alpha(r_a + r_b)\right\} \\ & + p \left\{ \frac{\beta^5}{64(1+S)\pi} \right\}^{1/2} r_a \sin \theta_a \cos \phi_a \left\{ \exp\left(-\frac{1}{2}\beta r_a\right) + \exp\left(-\frac{1}{2}\beta r_b\right) \right\},\end{aligned}\quad \dots\dots (4a)$$

$$\begin{aligned}\Psi(3d\pi) = & \left(\frac{\alpha^7}{6561N_2^2\pi} \right)^{1/2} r_a \sin \theta_a \cos \phi_a (r_a \cos \theta_a - r_b \cos \theta_b) \exp\left\{-\frac{1}{6}\alpha(r_a + r_b)\right\} \\ & + p \left\{ \frac{\beta^5}{64(1-S)\pi} \right\}^{1/2} r_a \sin \theta_a \cos \phi_a \left\{ \exp\left(-\frac{1}{2}\beta r_a\right) - \exp\left(-\frac{1}{2}\beta r_b\right) \right\}\end{aligned}\quad \dots\dots (4b)$$

with

$$\begin{aligned}N_1^2 = & \left\{ 2 + (\alpha R) + \frac{1}{5}(\alpha R)^2 + \frac{1}{60}(\alpha R)^3 \right\} \exp\left(-\frac{1}{2}\alpha R\right), \\ N_2^2 = & \frac{1}{2187} \left\{ 4374 + 1458(\alpha R) + \frac{1539}{7}(\alpha R)^2 \right. \\ & \left. + \frac{135}{7}(\alpha R)^3 + \frac{36}{35}(\alpha R)^4 + \frac{1}{35}(\alpha R)^5 \right\} \exp\left(-\frac{1}{3}\alpha R\right)\end{aligned}$$

and

$$S = \left\{ 1 + \frac{1}{2}(\beta R) + \frac{1}{10}(\beta R)^2 + \frac{1}{120}(\beta R)^3 \right\} \exp\left(-\frac{1}{2}\beta R\right)$$

so that $\Psi(2p\pi)$ and $\Psi(3d\pi)$ are normalized for $p=0$ and $p=\infty$ at all internuclear distances R .

§ 3. DESCRIPTION OF CALCULATIONS

Values of the parameters α , β and p over a wide range of R have been determined by minimization of the electronic energy E of the system

$$E = - \int \Psi^* \left(\nabla^2 + \frac{2}{r_a} + \frac{2}{r_b} \right) \Psi d\mathbf{r} \quad \dots\dots (5)$$

where Ψ is the normalized wave function. The functions studied were of the type (4a) and (4b) with

- (i) $p = \infty$, $\beta = 1$.
- (ii) $p = \infty$, β variable.
- (iii) $p = 0$, $\alpha = 2$.
- (iv) $p = 0$, α variable.
- (v) $\alpha = 2$, $\beta = 1$, p variable.
- (vi) α as determined by (iv) and β by (ii), p variable.

No study has been made of the function with α , β and p all variable since it appears unlikely from the work of Dalgarno and Poots that the improvement over (vi) would justify the extra labour. Exact values of E are provided by Bates, Ledsham and Stewart (1953).

$$\text{The integrals } \overline{X^2} = \int \Psi^* x^2 \Psi d\mathbf{r} \text{ and } \overline{Z^2} = \int \Psi^* z^2 \Psi d\mathbf{r} \quad \dots\dots(6)$$

where (x, y, z) are the cartesian coordinates of the electron referred to the mid-point of AB with the z -axis lying along AB, occur in the evaluation of the quadrupole moment and depend upon the wave functions at distances from the nuclei greater than those which effectively determine the energy. They have been evaluated using functions (i) to (vi) and the exact wave functions of Bates, Ledsham and Stewart. Comparison of the results provides a severe test of the approximations.

A further test is to evaluate the $2p\pi-3d\pi$ transition integral Q with functions (i) to (vi) in the dipole length form

$$Q_L \mathbf{t} = \int \Psi^* (2p\pi) \mathbf{r} \Psi (3d\pi) d\mathbf{r} \quad \dots\dots(7)$$

and in the dipole velocity form

$$Q_V \mathbf{t} = -\frac{2}{\Delta E} \int \Psi^* (2p\pi) \nabla \Psi (3d\pi) d\mathbf{r} \quad \dots\dots(8)$$

where ΔE is taken as the exact value of the vertical excitation energy and \mathbf{t} is some unit vector, and compare with the exact value of Q given by Bates, Darling, Hawe and Stewart (1953).

Orbitals such as (i) to (vi), which have been derived in such a way as to minimize the total energy, naturally reproduce the potential energy

$$V = - \int \Psi^* \left\{ \frac{2}{r_a} + \frac{2}{r_b} \right\} \Psi d\mathbf{r} \quad \dots\dots(9)$$

much less accurately. Exact values of V can be derived from the exact values of E by use of the quantal virial theorem (Slater 1933) and, besides providing comparison data, are useful in themselves in that the variation of V with R gives some insight into the mechanism of molecular bonding.

§ 4. RESULTS

The values of α , β and p obtained for (ii), (iv), (v) and (vi) are given in tables 1 and 2 for the $2p\pi$ and $3d\pi$ states respectively. Tables 3 and 4 compare the total energies derived using the functions (i) to (vi) with the exact energies, a similar comparison for the potential energies being rendered in tables 5 and 6. The integrals $\overline{X^2}$ and $\overline{Z^2}$ are found in tables 7 and 8, and 9 and 10 respectively, whilst table 11 gives the $2p\pi-3d\pi$ transition integrals. All quantities are measured in Hartree units (the unit of energy being $e^2/2a_0$, i.e. one rydberg).

§ 5. DISCUSSION

It can be seen by referring to the tables that the usual LCAO approximation given by function (i) is, in general, unsatisfactory, except for very large values of the internuclear distance R . The introduction of a screening parameter β as in function (ii) gives rather better results, especially in the case of the $2p\pi$ state, for which the function has the correct asymptotic form both for small and large values of R . However, for the $3d\pi$ state, function (ii) fails to give the true total energy at $R=0$ and, furthermore, the values of the $\overline{X^2}$ and $\overline{Z^2}$ integrals at $R=0$ are in error by as much as 30%.

Table 1*. Parameters of the $2p\pi$ Wave Functions

Function	R	0.0	0.4	0.8	1.2	1.6	2.0	3.0	4.0	5.0
(ii)	β	2.0000	1.9802	1.9312	1.8663	1.7942	1.7203	1.5484	1.4088	1.3009
(iv)	α	2.0000	1.9805	1.9341	1.8772	1.8184	1.7615	1.6348	1.5302	1.4433
(v)	p^{-1}	∞	75.45	20.55	9.983	6.093	4.190	2.144	1.333	0.922
(vi)	p^{-1}	—	3.903	3.795	3.614	3.423	3.229	2.752	2.317	1.937

Table 2*. Parameters of the $3d\pi$ Wave Functions

Function	R	0.0	0.4	0.8	1.2	1.6	2.0	3.0	4.0	5.0
(ii)	β	0.8571	0.8637	0.8799	0.9012	0.9253	0.9504	1.0094	1.0536	1.0800
(iv)	α	2.0000	2.0044	2.0168	2.0357	2.0590	2.0841	2.1407	2.1719	2.1752
(v)	p^{-1}	∞	102.6	24.65	10.41	5.512	3.294	1.208	0.6106	0.4831
(vi)	p^{-1}	∞	116.4	30.25	13.70	7.847	5.103	2.299	1.201	0.7285

*The charge parameters α and β , obtained as solutions of the equations $\partial E(\alpha)/\partial\alpha=0$ and $\partial E(\beta)/\partial\beta=0$ (where $E(\beta)$ refers to function (ii) and $E(\alpha)$ to function (iv)), are accurate to the figures given. Due to the lack of sensitivity of the energy to α and β , these determine the minimum in the $E(\alpha)$ or $E(\beta)$ curve to many more figures than are given in tables 3 and 4. p was similarly obtained as the solution of $\partial E(p)/\partial p=0$ with α and β as given in this table and $E(\alpha)$ and $E(\beta)$ as given in tables 3 and 4.

Table 3. Total Electronic Energies $-E$ of the $2p\pi$ State

Function	R	0.0	0.4	0.8	1.2	1.6	2.0	3.0	4.0	5.0
(i)		0.75000	0.74803	0.74237	0.73363	0.72248	0.70954	0.67270	0.63376	0.59587
(ii)		1.00000	0.98989	0.96393	0.92917	0.89076	0.85181	0.76152	0.68645	0.62577
(iii)		1.00000	0.98983	0.96326	0.92695	0.88614	0.84416	0.74468	0.65957	0.58904
(iv)		1.00000	0.98992	0.96433	0.93058	0.89380	0.85683	0.77109	0.69832	0.63754
(v)		1.00000	0.98987	0.96378	0.92891	0.89067	0.85229	0.76469	0.69278	0.63461
(vi)		1.00000	0.98993	0.96436	0.93070	0.89409	0.85736	0.77254	0.70104	0.64182
Exact		1.00000	0.98993	0.96439	0.93078	0.89422	0.85755	0.77289	0.70165	0.64277

Table 4. Total Electronic Energies $-E$ of the $3d\pi$ State

Function	R	0.0	0.4	0.8	1.2	1.6	2.0	3.0	4.0	5.0
(i)		0.41667	0.41954	0.42578	0.43302	0.44002	0.44613	0.45623	0.45938	0.45732
(ii)		0.42857	0.43008	0.43344	0.43782	0.44254	0.44715	0.45627	0.46025	0.45912
(iii)		0.44444	0.44489	0.44614	0.44799	0.45018	0.45243	0.45690	0.45818	0.45575
(iv)		0.44444	0.44489	0.44617	0.44813	0.45053	0.45312	0.45869	0.46071	0.45826
(v)		0.44444	0.44489	0.44617	0.44813	0.45052	0.45306	0.45835	0.46008	0.45780
(vi)		0.44444	0.44489	0.44618	0.44818	0.45066	0.45336	0.45926	0.46175	0.46009
Exact		0.44444	0.44490	0.44618	0.44819	0.45069	0.45340	0.45937	0.46191	0.46023

Table 5†. Electronic Potential Energies $-V$ of the $2p\pi$ State

Function	R	0.0	0.4	0.8	1.2	1.6	2.0	3.0	4.0	5.0
(i)		1.000	0.997	0.990	0.978	0.964	0.947	0.900	0.852	0.808
(ii)		2.000	1.961	1.865	1.747	1.625	1.511	1.274	1.103	0.980
(iii)		2.000	1.980	1.927	1.854	1.772	1.688	1.489	1.319	1.178
(iv)		2.000	1.961	1.867	1.754	1.639	1.531	1.304	1.131	0.997
(v)		2.000	1.970	1.893	1.792	1.681	1.571	1.327	1.140	1.002
(vi)		2.000	1.961	1.867	1.752	1.636	1.526	1.296	1.123	0.991
Exact		2.000	1.961	1.868	1.754	1.641	1.534	1.312	1.145	1.019

† It is believed that all quantities are correct to 0.1% but, due to the difficulty of assessing precisely the sensitivity of these quantities to p , the error may occasionally be as much as 0.2% in the case of function (vi). This applies also to tables 6–11.

Table 6. Electronic Potential Energies $-V$ of the $3d\pi$ State

R Function	0.0	0.4	0.8	1.2	1.6	2.0	3.0	4.0	5.0
(i)	1.000	0.998	0.993	0.984	0.974	0.961	0.925	0.887	0.849
(ii)	0.857	0.863	0.875	0.890	0.904	0.917	0.933	0.926	0.902
(iii)	0.889	0.889	0.888	0.887	0.885	0.883	0.872	0.855	0.833
(iv)	0.889	0.891	0.896	0.903	0.911	0.919	0.930	0.921	0.894
(v)	0.889	0.890	0.892	0.894	0.897	0.899	0.895	0.874	0.844
(vi)	0.889	0.891	0.895	0.902	0.911	0.919	0.931	0.923	0.899
Exact	0.889	0.891	0.896	0.903	0.912	0.921	0.932	0.925	0.903

Table 7. $\overline{X^2}$ for $2p\pi$ State

R Function	0.0	0.4	0.8	1.2	1.6	2.0	3.0	4.0	5.0
(i)	18.00	18.0 ₁	18.0 ₄	18.0 ₆	18.1 ₅	13.2 ₃	18.4 ₆	18.7 ₁	18.9 ₃
(ii)	4.50	4.6 ₀	4.8 ₇	5.2 ₅	5.7 ₃	6.2 ₈	7.8 ₇	9.6 ₀	11.3 ₂
(iii)	4.50	4.5 ₂	4.5 ₈	4.6 ₇	4.7 ₉	4.9 ₃	5.3 ₆	5.8 ₆	6.3 ₉
(iv)	4.50	4.6 ₁	4.8 ₉	5.2 ₈	5.7 ₁	6.2 ₅	7.6 ₆	9.2 ₁	10.8 ₆
(v)	4.50	4.5 ₉	4.8 ₅	5.2 ₄	5.7 ₅	6.3 ₅	8.1 ₂	9.9 ₉	11.7 ₂
(vi)	4.50	4.6 ₁	4.8 ₉	5.2 ₇	5.7 ₄	6.2 ₆	7.7 ₂	9.3 ₁	11.0 ₅
Exact	4.50	4.6 ₀	4.8 ₅	5.2 ₁	5.6 ₁	6.1 ₀	7.3 ₈	8.7 ₅	10.1 ₄

Table 8. $\overline{X^2}$ for $3d\pi$ State

R Function	0.0	0.4	0.8	1.2	1.6	2.0	3.0	4.0	5.0
(i)	12.86	12.8 ₇	12.9 ₂	13.0 ₀	13.1 ₁	13.2 ₃	13.6 ₁	14.0 ₅	14.5 ₁
(ii)	17.50	17.2 ₅	16.6 ₇	15.9 ₈	15.2 ₇	14.6 ₁	13.3 ₇	12.7 ₄	12.6 ₀
(iii)	13.50	13.5 ₁	13.5 ₂	13.5 ₃	13.5 ₉	13.6 ₅	13.8 ₃	14.0 ₉	14.4 ₂
(iv)	13.50	13.4 ₅	13.3 ₀	13.0 ₈	12.8 ₃	12.5 ₈	12.1 ₂	12.0 ₄	12.3 ₃
(v)	13.50	13.5 ₀	13.5 ₀	13.5 ₁	13.5 ₂	13.5 ₅	13.7 ₂	14.0 ₅	14.4 ₆
(vi)	13.50	13.4 ₇	13.3 ₃	13.2 ₄	13.0 ₅	12.8 ₅	12.4 ₄	12.3 ₂	12.4 ₆
Exact	13.50	13.4 ₁	13.3 ₄	13.1 ₆	12.9 ₄	12.7 ₁	12.2 ₃	12.0 ₃	12.1 ₂

Table 9. $\overline{Z^2}$ for $2p\pi$ State

R Function	0.0	0.4	0.8	1.2	1.6	2.0	3.0	4.0	5.0
(i)	6.00	6.0 ₃	6.1 ₁	6.2 ₄	6.4 ₃	6.6 ₇	7.5 ₄	8.8 ₃	10.6 ₀
(ii)	1.50	1.5 ₆	1.7 ₂	1.9 ₇	2.3 ₀	2.7 ₂	4.1 ₄	6.0 ₅	8.4 ₅
(iii)	1.50	1.5 ₁	1.5 ₅	1.6 ₁	1.6 ₉	1.7 ₉	2.1 ₁	2.5 ₂	3.0 ₂
(iv)	1.50	1.5 ₄	1.6 ₅	1.8 ₁	2.0 ₁	2.2 ₃	2.8 ₇	3.6 ₄	4.5 ₁
(v)	1.50	1.5 ₄	1.6 ₄	1.8 ₀	2.0 ₃	2.3 ₁	3.2 ₁	4.5 ₃	6.2 ₀
(vi)	1.50	1.5 ₅	1.6 ₇	1.8 ₄	2.0 ₇	2.3 ₄	3.1 ₉	4.3 ₀	5.7 ₁
Exact	1.50	1.5 ₄	1.6 ₆	1.8 ₂	2.0 ₄	2.2 ₈	3.0 ₇	4.1 ₀	5.4 ₀

Table 10. $\overline{Z^2}$ for $3d\pi$ State

R Function	0.0	0.4	0.8	1.2	1.6	2.0	3.0	4.0	5.0
(i)	12.86	12.9 ₀	13.0 ₂	13.2 ₁	13.4 ₈	13.8 ₁	14.9 ₅	16.4 ₉	18.4 ₂
(ii)	17.50	17.2 ₈	16.7 ₇	16.1 ₉	15.6 ₄	15.1 ₉	14.7 ₁	15.1 ₉	16.5 ₆
(iii)	13.50	13.5 ₂	13.5 ₈	13.6 ₇	13.8 ₁	13.9 ₈	14.5 ₁	15.5 ₀	16.5 ₀
(iv)	13.50	13.4 ₈	13.3 ₅	13.2 ₀	13.0 ₄	12.9 ₁	12.8 ₇	13.3 ₇	14.4 ₁
(v)	13.50	13.5 ₁	13.5 ₆	13.6 ₄	13.7 ₈	13.9 ₄	14.7 ₄	16.0 ₆	17.7 ₆
(vi)	13.50	13.4 ₈	13.4 ₄	13.3 ₆	13.2 ₈	13.2 ₂	13.3 ₆	14.1 ₄	15.6 ₁
Exact	13.50	13.4 ₈	13.4 ₂	13.3 ₅	13.2 ₇	13.2 ₃	13.4 ₀	14.1 ₄	15.4 ₆

Table 11. Transition Integrals Q for the $2p\pi$ - $3d\pi$ Transition†

R		0.0	0.4	0.8	1.2	1.6	2.0	3.0	4.0	5.0
Function										
(i)	$\{Q_L$	2.24	2.24	2.26	2.29	2.33	2.38	2.55	2.78	3.06
	$\{Q_V$	0.81	0.82	0.85	0.90	0.95	1.01	1.18	1.36	1.54
(ii)	$\{Q_L$	1.01	1.04	1.13	1.25	1.39	1.55	1.99	2.43	2.85
	$\{Q_V$	1.04	1.06	1.11	1.18	1.25	1.32	1.47	1.57	1.64
(iii)	$\{Q_L$	1.06	1.07	1.08	1.10	1.13	1.16	1.27	1.40	1.54
	$\{Q_V$	1.06	1.08	1.13	1.21	1.30	1.41	1.75	2.18	2.71
(iv)	$\{Q_L$	1.06	1.09	1.15	1.23	1.32	1.42	1.67	1.90	2.12
	$\{Q_V$	1.06	1.08	1.15	1.23	1.33	1.45	1.78	2.15	2.58
(v)	$\{Q_L$	1.06	1.09	1.15	1.24	1.35	1.47	1.78	2.12	2.47
	$\{Q_V$	1.06	1.08	1.14	1.21	1.31	1.41	1.68	1.95	2.23
(vi)	$\{Q_L$	1.06	1.09	1.15	1.24	1.34	1.46	1.76	2.07	2.38
	$\{Q_V$	1.06	1.08	1.14	1.22	1.32	1.42	1.70	1.98	2.26
Exact	$Q_L=Q_V$	1.06	1.08	1.14	1.22	1.32	1.43	1.71	2.01	2.32

† Q_L is evaluated using the dipole length expression and Q_V using the dipole velocity expression (with the exact energies).

Functions (iii) and (iv) are both satisfactory in the neighbourhood of $R=0$, but at $R=5$ function (iii) results in an error of about 40% in the \bar{X}^2 and \bar{Z}^2 integrals for the $2p\pi$ state. However, function (iv), in view of the relative ease with which it enables all the quantities considered in this paper to be evaluated, is remarkably accurate even for quite large values of R . Thus the total electronic energy is in error by not more than 1% at $R=5$ for both the $2p\pi$ and $3d\pi$ states. The \bar{X}^2 and \bar{Z}^2 integrals impose a much more severe test upon function (iv). For the $2p\pi$ state the error at $R=5$ is about 10% for the former and about 15% for the latter integral, the corresponding errors being rather less for the $3d\pi$ state.

Due to the higher orbital quantum numbers of the $2p\pi$ and $3d\pi$ states it is to be expected that the results obtained with functions (iii) and (iv) for these states would be superior to those obtained for the $1s\sigma$ and $2p\sigma$ states respectively. This is indeed found to be the case.

The values of the transition integral Q corresponding to the dipole length and dipole velocity formulae for the various functions (i) to (vi) are displayed in table 11. The results are less sensitive to the details of the wave functions than are those for the \bar{X}^2 and \bar{Z}^2 integrals. It can be seen that the dipole velocity formula is usually more accurate than the dipole length formula, but that the correct value of the transition integral lies nearer to the mean of Q_L and Q_V than to either. Further, the exact value of Q falls between the approximate values calculated by using the functions (i) and (iii) or (ii) and (iv). It is worth noting that in general this is also true for the \bar{X}^2 and \bar{Z}^2 integrals.

The variation with R of the potential energy, $V' = V + 2/R$, and the kinetic energy T of the $2p\pi$ and $3d\pi$ states is illustrated in figures 1 and 2. Essentially the same features as were found for the $1s\sigma$ and $2p\sigma$ states by Dalgarno and Poots appear. Although neither extremum lies in the range of R covered, it is clear that in the case of the attractive $2p\pi$ state T must pass through a shallow minimum and V' through a maximum; but for the repulsive $3d\pi$ state there is, in contrast, a maximum in T and a minimum in V' . This adds further weight to the hypothesis (cf. Slater 1933) that an initial decrease in kinetic energy as the nuclei approach is a decisive factor in the formation of a one-electron bond.

ACKNOWLEDGMENTS

It gives us great pleasure to thank Professor D. R. Bates and Dr. A. Dalgarno for helpful discussions.

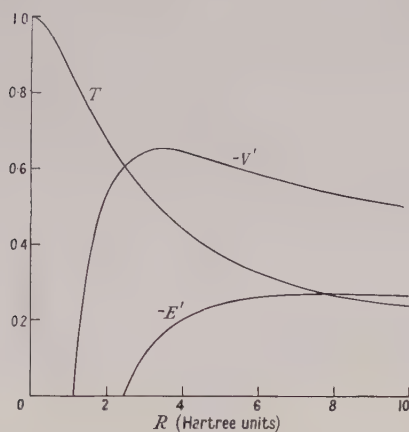


Figure 1. Potential energy V' , kinetic energy T , and total energy E' (in rydbergs) as functions of R in Hartree units for the $2p\pi$ state.

The minimum in the E' curve is at $R=7.93a_0$ and the depth of the potential well is 0.0190 rydberg, i.e. 0.259 ev. The kinetic energy tends to 0.25 rydberg at $R=\infty$ while at $R=10a_0$ $T=0.238$ rydberg.

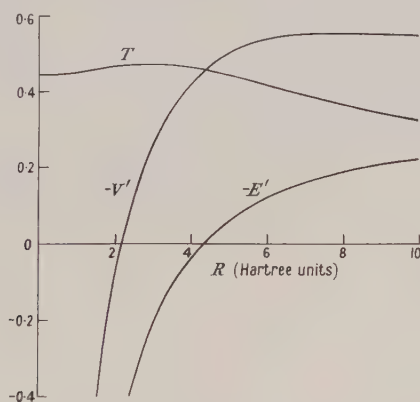


Figure 2. Potential energy V' , kinetic energy T , and total energy E' (in rydbergs) as functions of R in Hartree units for the $3d\pi$ state.

REFERENCES

- BATES, D. R., DARLING, R. T. S., HAWE, S. C., and STEWART, A. L., 1953, *Proc. Phys. Soc. A*, **66**, 1124.
 BATES, D. R., LEDSHAM, K., and STEWART, A. L., 1953, *Phil. Trans. Roy. Soc. A*, **246**, 215.
 DALGARNO, A., and POOTS, G., 1954, *Proc. Phys. Soc. A*, **67**, 343.
 DOOLING, J. S., 1953, *J. Chem. Phys.*, **21**, 859.
 LENNARD-JONES, J. E., 1929, *Trans. Faraday Soc.*, **25**, 668.
 MATSEN, F. A., 1953, *J. Chem. Phys.*, **21**, 928.
 SLATER, J. C., 1933, *J. Chem. Phys.*, **1**, 687.

RESEARCH NOTES

Free Electron Diamagnetism and Susceptibilities of the Alkali Metals

BY N. H. MARCH* AND B. DONOVAN†

* Department of Physics, The University, Sheffield

† Department of Physics, Northern Polytechnic, London

MS. received 9th February 1954

SOME years ago Sampson and Seitz (1940, subsequently referred to as SS) computed the magnetic susceptibilities of metallic Li and Na, emphasizing in particular the need for including exchange and correlation effects in calculating the spin paramagnetism which appeared to be the dominant contribution in determining the resultant susceptibility. Two possible criticisms of their treatment which might be put forward concern the use of (a) the Wigner correlation energy formula in calculating the spin paramagnetism and (b) the Landau value for the diamagnetic susceptibility.

Considerable progress in dealing with correlation effects in a free electron gas has been made recently (see especially Bohm and Pines 1953, Pines 1953). The work of Pines leads to a correlation energy in agreement with Wigner's result to well within the accuracy of the two treatments, and it would therefore seem that the spin paramagnetism calculated by SS (at absolute zero) cannot be seriously in error, and we shall assume this here.

As we pointed out previously (March and Donovan 1953) there are, however, several points in connection with the diamagnetism which warrant further discussion. The effect of exchange was considered in some detail by SS, who showed that at low temperatures the susceptibility became very large and positive, with a logarithmic singularity at $T=0$. SS believed it unlikely that the effect of correlation would entirely remove the singularity. As the free electron diamagnetism was quite small anyway in the neighbourhood of room temperatures, and since no correlation correction could be made at the time, SS finally adopted the Landau value. However, in the case of Na, the magnitude of the Landau diamagnetic contribution is about one third of the total susceptibility, and it is clear that any marked departure from it may impair the quantitative agreement obtained in this case.

The main purpose of the present note is to show that correlation effects do in fact oppose the effects of exchange in such a way as to restore the diamagnetic susceptibility to the neighbourhood of the Landau value at $T=0$. The procedure of SS can thus be justified to a certain extent since it is clear that the temperature dependence will be negligible up to room temperature. The diamagnetic susceptibility may readily be derived from the Peierls-Wilson formula (cf. SS, footnote 7) when the one-electron energy $\epsilon(k)$ is known. Thus, using Pines' results, one can obtain an expression demonstrating the effect of the long-range

correlations on the diamagnetism (cf. Pines' discussion of specific heat)[†]. The result for $T=0$ is

$$\chi = \chi_{\text{Landau}} \left[1 - \frac{1}{6\pi k_0} \left\{ 2 \ln \frac{2}{\beta} + \frac{3}{2} \beta^2 - 4 \right\} \right] \dots\dots(1)$$

where k_0 is the maximum momentum of the electrons (in atomic units), β is as defined by Pines, and values for the alkali metals can be taken from table 1 of his paper. The square bracket in (1) has the following values:

Li	Na	K	Rb	Cs
1.10	1.13	1.16	1.17	1.19

The experimental results for the susceptibilities of the alkali metals are so diverse that there is little point in making a detailed comparison at this stage. We shall therefore merely summarize briefly a few points which seem to be of some interest.

(i) The quantitative agreement for Na obtained by SS is unimpaired. It is actually slightly improved by the small increase in the diamagnetic susceptibility, though this has probably little significance in view of the neglect of the short-range correlations in calculating the diamagnetism and of possible errors in the spin paramagnetism.

(ii) For Li, SS obtained a susceptibility which was considerably higher than the (very inconsistent) experimental values, and the small change in the diamagnetism is quite negligible. There is some doubt, however, about the best value to take for the effective mass m^* in this case, Silverman and Kohn (1950), Parmenter (1952) and Schiff (1954) having obtained values of $1.38m$, $1.24m$ and $1.80m$ respectively. Using Parmenter's value, the agreement with experiment is improved very considerably, and this seems satisfactory since his calculations appear to us to be the most reliable yet made for this metal. Accurate experimental results would be very valuable in clarifying the position.

(iii) For K, with $m^* = m$, the susceptibility appears to be rather larger than the experimental value, and reducing the effective mass somewhat would improve the agreement. The value $m^* = 0.58m$ calculated by Gorin (1936) seems to be too low, however, the susceptibility becoming diamagnetic.

REFERENCES

- BOHM, D., and PINES, D., 1953, *Phys. Rev.*, **92**, 609.
 GORIN, E., 1936, *Phys. Z. Sowjet*, **9**, 328.
 LANDSBERG, P. T., 1949, *Proc. Phys. Soc. A*, **62**, 49.
 MARCH, N. H., and DONOVAN, B., 1953, *Proc. Phys. Soc. A*, **66**, 1104.
 PARMENTER, R. H., 1952, *Phys. Rev.*, **86**, 552.
 PINES, D., 1953, *Phys. Rev.*, **92**, 626.
 SAMPSON, J. B., and SEITZ, F., 1940, *Phys. Rev.*, **58**, 633.
 SCHIFF, B., 1954, *Proc. Phys. Soc. A*, **67**, 2.
 SILVERMAN, R. A., and KOHN, W., 1950, *Phys. Rev.*, **80**, 912.
 WOHLFARTH, E. P., 1950, *Phil. Mag.*, **41**, 534.

[†] Before the appearance of Pines' paper essentially the same conclusions had been reached by calculations on the basis of the empirical treatment of correlation suggested by Landsberg (1949) and Wohlfarth (1950).

Energy Levels in ^{10}B and ^8Be

By G. C. REID

Department of Natural Philosophy, University of Edinburgh

Communicated by N. Feather; MS. received 23rd November 1953

A NEW type of fast neutron spectrometer, based on an earlier design of Kinsey, Cohen and Dainty (1948), has been employed in a partial investigation of the energy spectra of neutrons from the reactions $^9\text{Be}(d, n)^{10}\text{B}$ and $^7\text{Li}(d, n)^8\text{Be}$. The spectrometer consists of a triple coincidence proportional counter telescope recording those recoil protons from a thin film of polythene $[(\text{CH}_2)_n]$ which are projected in the same direction as the neutron beam, and thus have the full energy of the incident neutrons. Aluminium absorbers can be inserted between the first and second counters of the telescope, and the heights of the pulses appearing on the second counter when a coincidence occurs can be measured. Since this is a specific ionization method, it possesses high resolution only over a fairly small range of recoil proton energy, but by varying the amount of absorption a large energy range may be covered in successive runs. The amplified output of the second counter is applied to the Y-plates and the coincidence output to the grid of an oscilloscope, so that only those pulses causing a triple coincidence are made visible. These pulses are photographed on a moving film. A series of runs carried out with different absorbers can then be pieced together to form the complete recoil proton spectrum. From this the spectrum of the incident neutrons can be obtained by correction for the variation of the n - p scattering cross section.

The instrument has been calibrated by examining the neutrons from the D-D reaction at 110° to the deuteron beam, using the value obtained by Livesey and Wilkinson (1948) for the energy release, viz. 3.25 ± 0.02 mev. The pulse-height distribution obtained is shown in figure 1.

Figure 2 shows the neutron spectrum obtained from the reaction $^9\text{Be}(d, n)^{10}\text{B}$ at an angle of 0° to the deuteron beam of 750 kev provided by the University of Edinburgh Cockcroft-Walton (Philips) generator. There are seen to be six neutron groups, of respective energies 1.50, 2.12, 2.78, 3.16, 4.34 and 4.86 mev (estimated probable error ± 0.10 mev), and a broad group at about 3.6 mev attributable to the D-D neutrons. When a small correction is applied for the finite thickness of the polythene radiator, these observations yield Q -values of 0.86, 1.47, 2.14, 2.52, 3.73 and 4.28 mev, respectively. The first, third, fifth and sixth of these groups are well known (Staub and Stephens 1939, Powell 1943, Ajzenberg 1951), and the second and fourth provide confirmation of groups found by Ajzenberg 1951 and by Dyer and Bird (1953). The second group, somewhat doubtful from figure 2, was also found in observations at 90° to the beam.

If the Q -value for the ground-state transition be taken as 4.35 mev, as deduced from the nuclear mass values, the group of Q -value 1.47 mev shows the existence of a level in ^{10}B at 2.88 ± 0.10 mev. The existence of such a level was previously suspected from the observation of a gamma-ray of energy 2856 kev in this reaction (Rasmussen, Hornyak and Lauritsen 1949).

Runs with three different absorbers have been carried out on the reaction ${}^7\text{Li}(d, n){}^8\text{Be}$ covering the neutron energy range from about 9 meV to about 11 meV, again at an angle of 0° with 750 keV deuterons. Previous work on this neutron spectrum had yielded some evidence for the existence of a level in ${}^8\text{Be}$ at 4.9 meV excitation (Richards 1941, Green and Gibson 1949), and this was supported by the discovery of a 4.9 meV gamma-ray from the same reaction (Bennett *et al.* 1941)

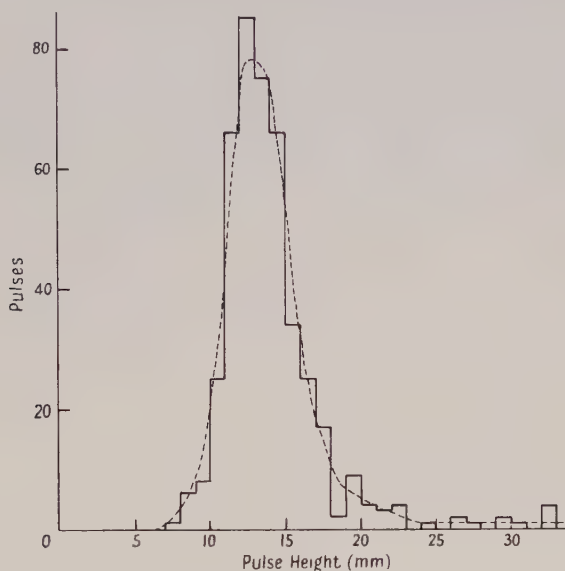


Figure 1.

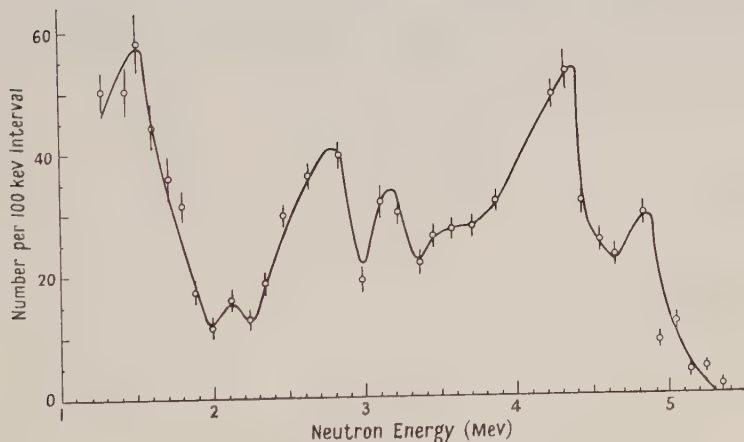


Figure 2.

The existence of this gamma-ray would imply that the level is of odd parity, since even parity states of ${}^8\text{Be}$ break up directly into two alpha-particles. Recent work by Titterton and others (1953), however, has shown evidence of a broad level at about 5.3 meV of even parity, and no evidence for the 4.9 meV level.

Our results (see figure 3) show a broad neutron group centred at about 9.9 mev, giving a Q -value of 9.60 ± 0.10 mev. Taking the Q -value for the ground-state transition as 15.04 mev, the value obtained from the nuclear masses, this implies the existence of a level in ^8Be at 5.44 ± 0.10 mev. As can be seen, there is no significant indication of a level at 4.9 mev, which would appear as a neutron group at about 10.4 mev.

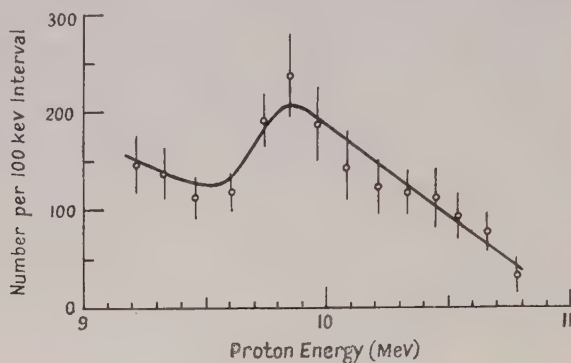


Figure 3.

Whilst these results cannot be regarded as decisive evidence in favour of the new level, since no other neutron groups are present to afford a check on the energy allocations, they are in line with the results of Titterton. A further experiment is being planned to examine the gamma-ray spectrum in the region of 5 mev.

ACKNOWLEDGMENTS

My thanks are due to Professor N. Feather and to Mr. J. Dainty, Mr. R. M. Sillitto and Mr. M. D. Carter of the University of Edinburgh for facilities and advice during the course of this work, and to the Department of Scientific and Industrial Research for the award of a grant.

REFERENCES

- AJZENBERG, F., 1951, *Phys. Rev.*, **82**, 43.
 BENNETT, W. E., BONNER, T. W., RICHARDS, H. T., and WATT, B. E., 1941, *Phys. Rev.*, **59**, 904.
 DYER, A. J., and BIRD, J. R., 1953, *Aust. J. Phys.*, **6**, 45.
 GREEN, L. L., and GIBSON, W. M., 1949, *Proc. Phys. Soc. A*, **62**, 407.
 KINSEY, B. B., COHEN, S., and DAINITY, J., 1948, *Proc. Camb. Phil. Soc.*, **44**, 96.
 LIVESEY, D. L., and WILKINSON, D. H., 1948, *Proc. Roy. Soc. A*, **195**, 123.
 POWELL, C. F., 1943, *Proc. Roy. Soc. A*, **181**, 344.
 RASMUSSEN, V. K., HORNYAK, W. F., and LAURITSEN, T., 1949, *Phys. Rev.*, **76**, 581.
 RICHARDS, H. T., 1941, *Phys. Rev.*, **59**, 796.
 STAUB, H., and STEPHENS, W. E., 1939, *Phys. Rev.*, **55**, 131.
 TITTERTON, E. W., 1953, *Report of the Birmingham Conference on Nuclear Physics*, p. 11.

Cross Sections for the Reaction ${}^7\text{Li}(\gamma p){}^6\text{He}$ at 17.6 and 14.8 Mev and the First Excited State of ${}^6\text{He}$

By E. W. TITTERTON AND T. A. BRINKLEY

Australian National University, Canberra

MS. received 25th January 1954

THE reaction ${}^7\text{Li}(\gamma p){}^6\text{He}$ was first observed in lithium loaded photographic emulsions by Titterton (1950). Recently the excitation function in the range from threshold to 20 mev has been measured in this laboratory (Titterton and Brinkley 1953) and shows a typical giant resonance centring on 15.6 mev. In order to normalize these relative cross section measurements an experiment has been performed to determine the cross sections at 17.6 and 14.8 mev using the resonance radiation from the reaction ${}^7\text{Li}(p\gamma){}^8\text{Be}$. As in the earlier experiments, Ilford Type E1 emulsions loaded with lithium sulphate and 200μ thick were employed. The number-energy histogram for the 160 events (which are identified by the usual methods of energy and momentum balances and the scattering of the tracks) which are wholly contained in the emulsion is given in figure 1(a). Because of the short range of the ${}^6\text{He}$ recoil

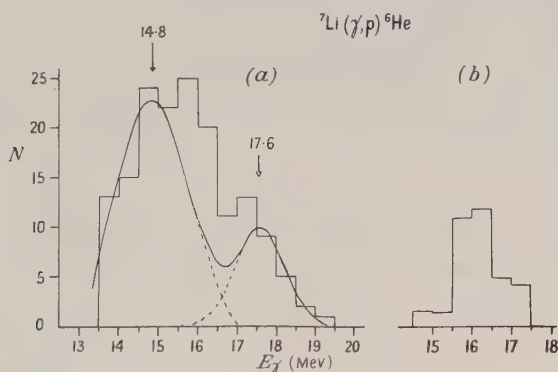


Figure 1. (a) Number-energy histogram; (b) Difference between fitted curve and histogram.

the resolution of the experiment is not as good as could be desired, the experimental half-width being $\Gamma_{\text{exp}} = 1.5$ mev. The Walker-McDaniel (1949) experiment shows the main components of the ${}^7\text{Li}(p\gamma)$ spectrum to be a narrow line at 17.6 mev and a line having $\Gamma = 2$ mev at 14.8 mev. Corrections were made for the variation of cross section over the width of the 14.8 mev line using the measured excitation function and for the geometrical losses of events from the emulsion, and a fit to the distribution was calculated. It is given as the full line in figure 1(a) and it will be seen that, in the region of 16 mev, there is an excess of events over the computed value. If differences are taken between the histogram and the calculated curve the events group about 16 mev, as is indicated by figure 1(b). This behaviour is what would be expected if, in some of the events induced by the 17.6 mev γ -ray, the recoiling ${}^6\text{He}$ nucleus

is left with an energy of 1.6 ± 0.2 mev which it loses by γ -ray emission. The first excited state of ${}^6\text{He}$ has been identified by Dewan *et al.* (1952) as lying at 1.71 ± 0.01 mev from a study of the reaction ${}^7\text{Li}(\text{t}\alpha){}^6\text{He}$, but more recently Crews (1952) has given the energy as 1.94 ± 0.08 mev. The result given above would be compatible with the measurement of Dewan *et al.* but not with that of Crews.

This indication, that the 1.71 mev state of ${}^6\text{He}$ de-excites by γ -ray emission, if correct, is surprising since, in the absence of a selection rule against it, the state would be expected to lead to disintegration into either $(\alpha + \text{dineutron})$ or $(\alpha + n + n)$, the disintegration $({}^6\text{He} + n)$ being excluded on energy grounds. The experiment precludes the first of these possibilities for, if it occurred, there could be no momentum balance; the proton and the recoil would not, in general, be collinear as is observed. The three-body break-up, where only a small amount of energy is available for sharing among three particles already moving in the recoil, could, however, lead to events with two collinear tracks $(p + \alpha)$ which might satisfy the selection requirements for ${}^7\text{Li}(\gamma p){}^6\text{He}$ events. For these reasons the indication that the first excited state of ${}^6\text{He}$ de-excites by γ -ray emission should be treated with reserve until it can be verified by an α - γ coincidence experiment using the reaction ${}^7\text{Li}(\text{t}\alpha){}^6\text{He}$.

Taking the experiment at its face value and accepting the Walker-McDaniel figure for the intensity ratio of the 17.6 and 14.8 mev lines at resonance as 2 : 1, cross sections can be calculated in terms of the cross section for ${}^{12}\text{C}(\gamma 3\alpha)$ taken as 2.4×10^{-28} cm² at 17.6 mev (Glättli, Seippel and Stoll 1952). They are :

$$\sigma_{14.8} {}^7\text{Li}(\gamma p){}^6\text{He} (\text{ground state}) = (2.2 \pm 0.25) \times 10^{-27} \text{ cm}^2$$

$$\sigma_{17.6} {}^7\text{Li}(\gamma p){}^6\text{He} (\text{ground state}) = (6.8 \pm 0.9) \times 10^{-28} \text{ cm}^2$$

$$\sigma_{17.6} {}^7\text{Li}(\gamma p){}^6\text{He} (1.71 \text{ mev state}) = (5.44 \pm 0.9) \times 10^{-28} \text{ cm}^2.$$

These values, although they confirm the general trend of the excitation function, cannot be compared with it directly. If the 1.71 mev level de-excites by γ -emission and the probability of its formation is energy dependent (as the present experiment suggests), then the excitation function, which is derived by determining the number of events corresponding to a γ -ray energy of $E_\gamma = E_{{}^6\text{He}} + E_p + 10.1$ mev, would contain events to which an incorrect E_γ had been assigned; this would tend to sharpen the curve. Recently the Saskatchewan betatron group (Katz 1953, private communication) has determined the excitation function for ${}^7\text{Li}(\gamma p){}^6\text{He}$ by examining the ${}^6\text{He}$ β emission as a function of peak machine energy. The measurement obtained by this method, although it also shows a maximum at 15 mev, is somewhat broader than that obtained by the photographic plate method as illustrated in figure 2, where the curves are matched at their maxima. The discrepancy on the high-energy side qualitatively supports the idea that a state of ${}^6\text{He}$ de-exciting by photon emission is formed, the probability of formation increasing with incident γ -ray energy. On the low-energy side the rapid rise of cross section observed by the Saskatchewan group would be difficult to observe by the photographic plate method as, with very little energy in the ${}^6\text{He}$ recoil, its identification would be impossible.

Tucker and Gregg (1953) recently determined the excitation function for the reaction ${}^7\text{Li}(\gamma p){}^6\text{He}$. Their result disagrees with both the Saskatoon and Canberra measurements as shown in figure 2; they find the cross section rising

rapidly in the region between 17 and 19 mev, where the other two experiments show it to be falling.*

Their cross section at 17.6 mev is approximately twice the value of 14.8 mev, which is in sharp disagreement with the present measurement, where the cross section at 14.8 mev is found to be larger than that at 17.6 mev.

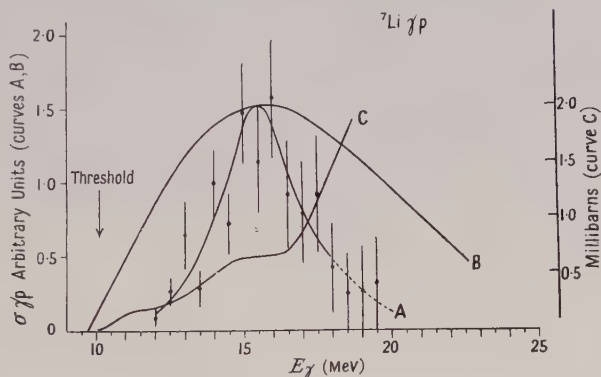


Figure 2. Excitation function.

A. Canberra result.

B. Saskatoon result.

C. Case Institute measurement.

* Note added in proof. In a private communication Dr. B. L. Tucker states that re-evaluation of their earlier data showed the monitoring to be subject to some question. The experiment was repeated along with a comparison $^{63}\text{Cu}(\gamma n)^{62}\text{Cu}$ run. The new result is similar to the earlier one up to 16 mev, but a resonance peak appears at 17.5 mev, ~ 2 mev higher than in the Canberra and Saskatoon results.

REFERENCES

- CREWS, 1952, quoted in AJZENBERG, F., and LAURITSEN, T., 1952, *Rev. Mod. Phys.*, **24**, 321.
 DEWAN, J. T., PEPPER, T. P., ALLEN, K. W., and ALMQVIST, E., 1952, *Phys. Rev.*, **86**, 416.
 GLÄTTLI, H., SEIPPEL, O., and STOLL, P., 1952, *Helv. Phys. Acta*, **25**, 491.
 TITERTON, E. W., 1950, *Proc. Phys. Soc. A*, **63**, 915.
 TITERTON, E. W., and BRINKLEY, T. A., 1953, *Proc. Phys. Soc. A*, **66**, 194.
 TUCKER, B. L., and GREGG, E. C., 1953, *Phys. Rev.*, **91**, 1579.
 WALKER, R. L., and MCDANIEL, B. D., 1949, *Phys. Rev.*, **74**, 315.

Some Remarks on Radiative Capture and Stripping Reactions

By G. R. SATCHLER

Clarendon Laboratory, Oxford

MS. received 8th February 1954

FORMULAE for the angular distribution of γ -rays following nucleon capture or stripping reactions when the nuclei obey $j-j$ or $L-S$ coupling rules have been published (Satchler 1953, to be referred to as S). We now give explicitly the absolute magnitudes of the parameters used in S and indicate how we may treat intermediate coupling. The angular distribution depends on nuclear structure through the relative amounts taking part of the two possible

incoming 'channel spins' (spins of target and nucleon parallel or antiparallel), or alternatively of the two possible total angular momenta of the captured particle ($j=l\pm\frac{1}{2}$). The extreme j - j model, for example, would require only one value of j to take part. Information from this source† may then be correlated with that from energy levels, magnetic moments, etc. (Inglis 1953, Lane 1953).

In practice only a moderate number of direct capture processes are of use, due to the high excitation produced and the complexity of the ensuing decay scheme. In stripping reactions, however, nucleons may be introduced directly into low-lying excited levels. The angular correlation between the γ -rays and outgoing particles gives similar information about the coupling.

The differential cross section for single-level resonance capture of a nucleon with wave number k is (summing over $j, j', l, l',$ and ν)

$$\frac{d\sigma}{d\omega} = \frac{2J_e + 1}{(2J_i + 1)8k^2} \frac{\Gamma(L)}{(E - E_e)^2 + \frac{1}{4}\Gamma^2} \sum B(jl)B^*(j'l')\eta_\nu(jj'J_iJ_e)F_\nu(LJ_fJ_e)P_\nu(\cos\theta) \dots\dots(1)$$

where $\Gamma(L)$ is the radiative width for 2^L -pole γ -emission. We use the notation of S; suffixes i, e, f refer to initial, excited, and final nuclear states. The η_ν are tabulated in S, the F_ν by Biedenharn and Rose (1953). The mixture parameters $B(jl)$ ('reduced matrix elements' in perturbation theory) are simply related to the partial reduced widths $\gamma^2(jl)$ for nucleon emission, and are real apart from the coulomb and 'potential' phase, $\exp i\xi_l$ (Blatt and Weisskopf 1952, Ch. VIII):

$$B(jl) = \pm \exp i\xi_l \Gamma(jl)^{1/2} = \exp i\xi_l (2k v_l R)^{1/2} \gamma(jl), \dots\dots(2)$$

v_l is the penetration factor evaluated at the nuclear surface, $r=R$.

When the capture goes via a stripping process (say (d, p) for definiteness), besides the intrinsic neutron capture probability we have factors dependent on the emission direction of the proton. In the simple stripping theory (using the notation of Bhatia *et al.* 1952) these are the 'availability' $G(K)$ of a neutron of the required energy and momentum in the incident deuteron, and the probability of order $j_l(kR)$ of this neutron reaching the nuclear surface, $r_n=R$. Apart from constant factors, $G^2 j_l^2$ gives the proton angular distribution; curves for many cases have been published. The arguments of these factors depend on the angle θ_p between \mathbf{k}_d and \mathbf{k}_p (both centre-of-mass system), the wave vectors of incident deuteron and outgoing proton; if the target nucleus has mass A ,

$$K^2 = \frac{1}{4}k_d^2 + k_p^2 - k_p k_d \cos \theta_p; \quad k^2 = k_d^2 + \left(\frac{A}{A+1}\right)^2 k_p^2 - \frac{2A}{A+1} k_p k_d \cos \theta_p.$$

The p - γ correlation cross section is then

$$\sigma(\theta_p, \gamma) = \frac{M_p^* M_d^*}{4\pi^2 \hbar^4} \frac{k_p}{k_d} \frac{2J_e + 1}{2J_i + 1} G^2(K) \sum B(jl)B^*(j'l')\eta_\nu(jj'J_iJ_e)F_\nu(LJ_fJ_e)P_\nu(\cos\gamma) \dots\dots(3)$$

summing over ν, j, j', l, l' . γ is now the angle between the γ -ray and the recoil axis $\mathbf{k} = \mathbf{k}_d - \{A/(A+1)\}\mathbf{k}_p$, the dependence on θ_p being contained in k and K . The reduced matrix elements are real, and in Born approximation (Bhatia *et al.* 1952) given by (summing over M_i, m, μ)

$$B(jl) = j_l(kR) i^l \sum C(J_i j J_e; M_i M_e - M_i) C(l \frac{1}{2} j; m \mu) \langle f | V | i l m \mu \rangle;$$

† Emission of α -particles (since spin-less) is as useful as γ -emission provided they carry away only one value of orbital angular momentum.

hence we see that $\Lambda_l j_l^2(kR) = (2J_c + 1) \Sigma_j B^2(jl)$. In the Butler (1951) formalism, with $\gamma^2(jl)$ the reduced width, they become

$$B(jl) = i(\epsilon_n R^3)^{1/2} \gamma(jl) [(k/k_n) j_{l-1}(kR) - j_l(kR) h_{l-1}^{(1)}(k_n R) / h_l^{(1)}(k_n R)] \dots (4)$$

which is approximately equal to $(\epsilon_n R^3)^{1/2} \gamma(jl) j_l(kR)$ for a tightly bound capture state with neutron binding energy $\epsilon_n = -\hbar^2 k_n^2 / 2M_n^*$. The Born approximation expression reduces to an analogous form.

The angular dependent $G(K)$ only affects the overall magnitude of the cross section, whereas the spherical Bessel function $j_l(kR)$ depends also on l , the orbital momentum transfer. This is important when mixtures of l are investigated; the relative contribution of one component can be raised or depressed by suitable choice of the proton counter position. If the admixture is small it is the interference term depending on the *amplitude* of mixing which is important in the p - γ correlation experiment; the relative intensity of this varies with θ_p as $j_l(kR)/j_l(kR)$.

If we use the channel spin s (vector sum of initial spins, $\mathbf{s} = \mathbf{J}_i + \frac{1}{2}\boldsymbol{\sigma}$) then $\Sigma_{j'} BB^* \eta_{j'}$ in (1) and (3) has to be replaced by

$$\sum_s A(sl) A^*(sl') (-)^{s-J} Z(lJ_e l' J_e; s\nu).$$

There are relations similar to (2), (4) between $A(sl)$ and the reduced width $\gamma^2(sl)$. The Z functions are tabulated by Biedenharn (1952). The two representations are related by (9) of S:

$$B(jl) = \sum_s (-)^{j-l-1/2} [(2j+1)(2s+1)]^{1/2} W(\frac{1}{2} l J_i J_e; js) A(sl).$$

If extreme j - j coupling held we should find only one non-zero $B(jl)$, with the reduced width for an n -nucleon excited state configuration:

$$\gamma(jl) = (n\hbar^2/2MR)^{1/2} u_l(R) \langle J_e | \} J_i j \rangle. \dots (5)$$

$u_l(R)$ R is the single-particle radial wave function evaluated at the nuclear surface, $r=R$, and $\langle | \rangle$ is the coefficient of fractional parentage appropriate to the initial and excited states (Flowers and Edmonds 1952).

On the other hand, extreme L - S coupling for these two states would give

$$\gamma(jl) = \gamma(l) [(2J_i + 1)(2j + 1)(2L_e + 1)(2S_e + 1)]^{1/2} X(J_e L_e S_e; J_i L_i S_i; jl \frac{1}{2}) \dots (6a)$$

or

$$\gamma(sl) = \gamma(l) [(2J_i + 1)(2s + 1)(2L_e + 1)(2S_e + 1)]^{1/2} W(L_i S_i s \frac{1}{2}; J_i S_e) W(S_e s L_e l; L_i J_e) \dots (6b)$$

where

$$\gamma(l) = u_l(R) (n\hbar^2/2MR)^{1/2} \langle J_e | \} J_i l \rangle.$$

The coefficient of fractional parentage is now that appropriate to L - S coupling (Jahn and van Wieringen 1951). Expressions analogous to (5) and (6b) have been given independently by Lane (1953).

It seems the coupling actually realized is intermediate between these two extremes. In that case we may follow Lane (1953, to which reference should be made for further details) and expand the actual nuclear wave functions in terms of L - S eigenfunctions

$$|JM\rangle = \sum_{LS\alpha} |JM, LS\alpha\rangle \langle LS\alpha || J \rangle.$$

We then have a sum of factors like (6) weighted with the expansion coefficients for initial and excited states.

The expressions from the simple stripping theory given above are modified by the coulomb field and any 'scattering' interaction of the outgoing proton with the nucleus. These effects will be dealt with in a future communication.

ACKNOWLEDGMENT

The author is indebted to Dr. J. A. Spiers for advice on this problem.

Note added in proof. The author is indebted to Dr. A. M. Lane for comments on this paper. It should be stressed that the extreme 'one-level approximation' has been used in the interests of simplicity, so neglecting the distortion of the simple relation between observed and reduced widths due to far-away levels (Thomas and Lane 1954). Similarly the level-shift variation with energy has been ignored in equations (2) and (4), although its effect may not be small (Thomas 1952). However, these corrections only alter the magnitude and energy dependence of the $B(jl)$; their relative values, which are of interest for the γ angular distribution, remain unaffected.

REFERENCES

- BHATIA, A. B., KUN HUANG, HUBY, R., and NEWNS, H. C., 1952, *Phil. Mag.*, **43**, 485.
 BIEDENHARN, L. C., 1952, *Tables of Racah Coefficients* (Oak Ridge National Laboratory Report 1098).
 BIEDENHARN, L. C., and ROSE, M. E., 1953, *Rev. Mod. Phys.*, **25**, 729.
 BLATT, J. M., and WEISSKOPF, V. F., 1952, *Theoretical Nuclear Physics* (New York: John Wiley).
 BUTLER, S. T., 1951, *Proc. Roy. Soc. A*, **208**, 559.
 FLOWERS, B. H., and EDMONDS, A. R., 1952, *Proc. Roy. Soc. A*, **214**, 515.
 INGLIS, D. R., 1953, *Rev. Mod. Phys.*, **25**, 390.
 JAHN, H. A., and VAN WIERINGEN, H., 1951, *Proc. Roy. Soc. A*, **214**, 502.
 LANE, A. M., 1953, *Proc. Phys. Soc. A*, **66**, 977, *Phys. Rev.*, **92**, 839.
 SATCHLER, G. R., 1953, *Proc. Phys. Soc. A*, **66**, 1081.
 THOMAS, R. G., 1952, *Phys. Rev.*, **88**, 1109.
 THOMAS, R. G., and LANE, A. M., 1954, *Rev. Mod. Phys.*, in the press.

Pressure Broadening in the Spectrum of NO and its Photodissociation

By A. G. GAYDON AND A. R. FAIRBAIRN

Department of Chemical Engineering, Imperial College, London S.W.7

MS. received 22nd January 1954

IT has been reported (Lambrey 1929, 1930, Naudé 1930) that the bands of the γ system of NO show an abnormally large pressure broadening, and Wulf (1934) suggested that this might be due to induced predissociation. This suggestion has recently been repeated by Moore, Wulf and Badger (1953) who have shown that there is some photodissociation on exposure to light in the region of the γ bands. Naudé stated that with nitric oxide in nitrogen at 44 cm pressure "every rotational line is broadened so much that the absorption becomes complete". This seems at variance with studies (Gaydon 1944) of the γ bands in emission in an ozonizer discharge through nitrogen containing a trace of oxygen at atmospheric pressure. This emission showed normal

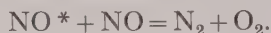
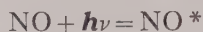
rotational structure, and one of the old plates, taken on a medium quartz spectrograph is enlarged and reproduced in strip *a* of the plate. The true width in emission and absorption should obviously be the same under similar conditions; the emission was actually at higher pressure and similar temperature. In view of this discrepancy we have now made an examination of the absorption spectrum of nitric oxide. The subject is of considerable importance because of its bearing on the dissociation energies of NO and N₂. Most recent evidence (Gaydon 1953) favours the high value of 9.76 eV for $D(\text{N}_2)$, but, if proved, the induced predissociation would require the low value 7.38 eV.

Preliminary observations were made with a medium quartz spectrograph using a xenon high-pressure arc as background source. With a 15 cm absorption tube and the spectrograph in good focus it was found that the (0, 0) and (1, 0) γ bands could be observed with about 2 mm pressure of nitric oxide (see strip *b* of the plate). On adding pure nitrogen to bring the pressure up to 1 atmosphere the NO absorption appeared to be strengthened (strip *c*) but the rotational structure of the bands still appeared sharp. Photographs were then taken of this same absorption using a large two-prism Littrow-type quartz spectrograph having a dispersion of 1.1 Å/mm at 2269 Å. These show that the NO absorption lines are quite sharp (see strip *d*). In an absorption spectrum of this type it is difficult accurately to estimate the true half-breadth of a line, but from study of the less heavy lines we can say that it is less than 0.025 Å or 0.5 cm⁻¹. Nitric oxide is a paramagnetic gas and Professor J. O. Hirschfelder (private communication) has suggested that it might have a relatively large collision cross section. Anyhow it is clear that there is no abnormally large pressure broadening.

The divergence between our observations and those of Naudé are no doubt mainly due to the excessive amount of absorbing gas which he used—about 60 times our optical path of NO. His long exposure times of 6 to 12 hours may have contributed to some loss of definition. For a more detailed understanding of the divergence and for the explanation of the apparent increase in strength of absorption when nitrogen is added, we must consider the change in line contour due to pressure broadening. It is well known that with pure Doppler broadening the lines have comparatively narrow 'wings'. With pressure broadening there is some increase in the half-breadth of the line, but the main change is a strengthening and extension of the 'wings'. With limited resolving power it is difficult to observe in absorption the very fine lines of a cool gas with pure Doppler broadening, and to obtain a record of the spectrum it may be necessary to use enough gas to get appreciable absorption in the weak 'wings' even though the absorption in the line centre may be extremely strong. Slight pressure broadening, by strengthening the 'wings' and weakening the centre, will then cause an apparent increase in absorption.

If we are to reject the induced predissociation, then it is necessary to re-examine the interpretation of the photodissociation. Flory and Johnston (1935) studied the photodissociation using a mercury arc and metal sparks. They found that the active region was at short wavelengths and was probably mainly located in a band of the δ system at 1830 Å. Gaydon (1953) failed to detect any action in the region of the γ bands. In this experiment nitric oxide was exposed through quartz to an iron arc at a distance of about 2 in. for two days, and no NO₂ formation was detected. Moore, Wulf and Badger point out that the iron arc is weak in this region, but this does not seem to be so to the extent their

plate might lead one to think. Our iron arc, on 220 volts, was adequately exposed in one minute using a fine (0.009 mm) slit on the large quartz spectrograph (strip *d* of plate). The iron lines at 2259.511, 2267.080 and 2267.465 Å coincide fairly well with lines of NO. The experiments of Moore *et al.* using N₂O₃ to detect photochemical action are probably more sensitive, and we do not doubt their results in this respect. It does however seem clear that the action in this region of the spectrum must be very slight and have a low quantum efficiency. It seems that this small amount of dissociation can easily be explained by the secondary reaction



This is similar to the explanation put forward (Gaydon 1953) for the photodissociation of carbon monoxide. Now that it is established that there is no abnormal pressure broadening and therefore no induced predissociation in nitric oxide, it seems that this weak photodissociation is not important in the discussion of the dissociation energies of NO and N₂.

ACKNOWLEDGMENTS

One of us (A.G.G.) is indebted to the Royal Society for a Warren Fellowship, and the other (A.R.F.) to the Gas Council for a research scholarship.

REFERENCES

- FLORY, P. J., and JOHNSTON, H. L., 1935, *J. Amer. Chem. Soc.*, **57**, 2641.
 GAYDON, A. G., 1944, *Proc. Phys. Soc.*, **56**, 95; 1953, *Dissociation Energies*, 2nd Edn (London: Chapman and Hall).
 LAMBREY, M., 1929, *C. R. Acad. Sci., Paris*, **189**, 574; 1930, *Ibid.*, **190**, 261, 670; *Ann. Phys., Paris*, **14**, 95.
 MOORE, G. E., WULF, O. R., and BADGER, R. M., 1953, *J. Chem. Phys.*, **21**, 2091.
 NAUDÉ, S. M., 1930, *Phys. Rev.*, **36**, 333.
 WULF, O. R., 1934, *Phys. Rev.*, **46**, 316.

The Absorption Spectrum of Thulium

By L. F. H. BOVEY* AND W. R. S. GARTON†

* Emission Spectroscopy Group, Atomic Energy Research Establishment, Harwell, Berks.

† Department of Astrophysics, Imperial College, London S.W.7

MS. received 4th March 1954

WHEN the absorption spectrum of lutetium was examined (Bovey and Garton 1954) it was noted that some fifteen lines of thulium were apparently present. In order to confirm this, a sample of thulium oxide was used in the King furnace and the absorption spectrum taken in the range 2500–6000 Å on a 3-metre Hilger spectrograph.

Some eighty-five lines were obtained and are detailed in the table; absorption lines from lutetium and ytterbium were also present. Most wavelengths were assigned by reference to the M.I.T. Wavelength Tables or to the series of charts by Gatterer and Junkes (1945). A few of the weaker lines were accurately measured.

Absorption Lines of Thulium

Wavelength	Strength	Wavelength	Strength	Wavelength	Strength
2601.09	W	3416.61	M	3887.35	VS
2622.27	VW	3425.08	W	3896.62	S
2660.10	VW	3428.62	VW	3916.47	S
2854.15	M	3429.34	VW	3949.27	S
2907.17	VW	3441.51	VW	4007.75	VW
2914.83	M	3453.67	VW	4044.47	VW
2932.97	M	3462.21	W	4094.18	VS
2973.23	S	3487.40	W	4105.84	VS
3015.30	VW	3499.97	VW	4138.36	M
3046.87	M	3500.92	M	4187.62	VS
3081.13	W	3514.06	M	4203.75	S
3107.16	W	3517.62	VW	4222.66	VW
3122.54	W	3563.89	S	4359.93	S
3131.26	W	3567.36	S	4386.43	S
3133.89	VW	3568.13	S	4394.42	VW
3151.04	VW	3624.20	VW	4599.00	S
3172.82	M	3638.42	VW	4724.25	S
3179.84	W	3646.71	VW	4733.32	S
3180.54	W	3700.27	VW	5060.89	S
3233.75	M	3701.36	VW	5113.96	S
3241.53	VW	3717.92	VS	5307.12	W
3246.96	W	3744.07	VS	5631.41	VS
3299.12	M	3751.82	S	5675.85	VS
3302.45	VW	3761.33	VW	5764.29	M
3323.22	VW	3761.91	VW	5895.63	S
3349.99	W	3781.14	S	5971.27	S
3362.61	W	3795.77	VW	VS=Very Strong	
3380.60	W	3807.72	M	S=Strong	
3385.03	W	3826.36	S	M=Medium	
3410.05	M	3848.02	W	W=Weak	
3412.61	VW	3883.13	VS	VW=Very Weak	

The term analysis of thulium is very incomplete but the ground state level is thought to be $^2F^0$ (Meggers 1942) with a doublet separation of 8771.3 cm^{-1} . All the lines arising from the lower level ($^2F^0_{7/2}$) were observed in absorption but only two (the strongest in emission) from the upper level ($^2F^0_{5/2}$) were found. It is possible that at the furnace temperature (approximately 2400°C) insufficient atoms were available in the upper level to give rise to absorption. Indirect evidence for this assumption can be based on the experimental observation that the absorption lines of iron, present as an impurity and shown on the same spectrum, arose entirely from levels below about 7000 cm^{-1} .

The frequencies corresponding to the absorption line data were examined for sets of constant differences. No sets with more than three equal differences were found. Until further experimental information is available it is not proposed to attempt the term analysis.

This work was partly carried out whilst one of us (W.R.S.G.) was acting as a University Vacation Consultant.

REFERENCES

- BOVEY, L. F. H., and GARTON, W. R. S., 1954, *Proc. Phys. Soc. A*, **67**, 291.
 GATTERER, A., and JUNKES, J., 1945, *Specola Vaticana, Citta del Vaticana*.
 MEGGERS, W. F., 1942, *Rev. Mod. Phys.*, **14**, 96.

LETTERS TO THE EDITOR

Isotope Shifts in the Atomic Spectra of Tin and Cadmium

Isotope shifts in the optical spectra of elements near the middle of the periodic table are generally small, and therefore difficult to measure, but the occurrence of large numbers of isotopes in many of these elements offers possibilities of an extensive study of the relative values of the shifts within one element and, in some cases, of the comparison of relative shifts in iso-neutronic isotopes of different elements.

The isotope shifts were measured in the line $5s^2 6s^2 S_{1/2} - 5s^2 6p^2 P_{3/2}$, λ 6454, of the spark spectrum of tin with the use of highly enriched samples of all the even isotopes. By due attention to the uniform illumination of the Fabry-Perot etalon it was possible to obtain results whose accuracy was better than $\pm 0.001 \text{ cm}^{-1}$, as judged by the consistency of the results for different etalon spacers. After corrections for isotopic impurities, the following results were found.

Isotope mass numbers	112-114	114-116	116-118	118-120	120-122	122-124
Isotope shifts ($\nu_{\text{light}} - \nu_{\text{heavy}}$)	6.7	6.1	4.4	4.4	1.2	1.7
$\times 10^3 \text{ cm}^{-1}$						

Owing to the lack of a mass analysis for Sn_{122} , the difference between the shifts given for the last two pairs is not claimed to be genuine.

In cadmium, isotope shifts have so far been observed only with the use of the natural element (Schüler and Westmeyer 1933, Brix and Steudel 1950). The published values are therefore confined to the abundant even isotopes 110, 112, and 114. In the spark line $4d^{10} 5p^2 P_{3/2} - 4d^9 5s^2 D_{5/2}$, λ 4416, the component due to Cd_{116} has been observed (Steudel, private communication), and the spacing 114-116 found to be smaller than 112-114. The unknown positions of the components due to the odd isotopes made any quantitative data unreliable. With the use of highly enriched isotopes the following isotope shifts were measured in the line λ 4416:

Isotope mass numbers	110-112	112-114	114-116
Isotope shifts $\times 10^3 \text{ cm}^{-1}$	-53.3	-47.9	-34.4

The accuracy is to $\pm 1.5 \times 10^{-3} \text{ cm}^{-1}$.

In the following table the normal mass shift has been subtracted and the shift between isotopes with neutron numbers 62 and 64 defined as unit.

Neutron numbers	62-64	64-66	66-68	68-70	70-72	72-74
Isotope shifts: Tin	1.00	0.93	0.72	0.72	0.32	0.39
Cadmium	1.00	0.90	0.63			

The specific mass shift, which would not cause 'jumps' in the isotope shifts, has been ignored.

It is seen that the relative shifts between iso-neutronic pairs of isotopes show marked similarity. It is tempting to associate the irregularity after neutron number 66 with the completion of the $5g_{7/2}$ shell of neutrons and the beginning of the $6h_{11/2}$ shell in the level scheme quoted by Flowers (1953). A similarly simple interpretation of the irregularity observed in tin after neutron number 70 cannot be given. Shifts for the neutron numbers 68-74 have been reported in tellurium by Murakawa and Ross (1952); they do not agree with those measured in tin.

The isotope shift constant C was calculated for tin, assuming that the shift in the line $\lambda 6454$ is due to the 6s electron in the lower term, and using the measured value of the hyperfine structure of the odd isotopes (Tolansky 1934) in conjunction with the nuclear resonance value of the nuclear magnetic moment (Proctor 1949) to evaluate the atomic wave function. The value found was $C = 44 \times 10^{-3} \text{ cm}^{-1}$ for the pair Sn_{112} and Sn_{114} .

Work is now in progress on the remaining stable isotopes of cadmium and tin.

We are indebted to the electromagnetic group and the mass spectrometry group of the Atomic Energy Research Establishment, Harwell, for the provision of samples of separated isotopes and their mass analyses.

The Clarendon Laboratory,
Oxford.
25th February 1954.

W. R. HINDMARSH.
H. KUHN.
S. A. RAMSDEN.

- BRIX, P., and STEUDEL, A., 1950, *Z. Phys.*, **128**, 260.
FLOWERS, B. H., 1953, *Progr. Nucl. Phys.*, **2**, 252.
MURAKAWA, K., and ROSS, J. S., 1952, *Phys. Rev.*, **85**, 559.
PROCTOR, W. G., 1949, *Phys. Rev.*, **76**, 684.
SCHÜLER, H., and WESTMEYER, H., 1933, *Z. Phys.*, **82**, 685.
TOLANSKY, S., 1934, *Proc. Roy. Soc. A*, **144**, 574.

Measurement of the End Point Energy of Positrons from ^{25}Al

Aluminium 25 was produced by irradiating thick natural magnesium targets with protons of slightly greater energy than that of the lowest $^{24}\text{Mg}(p, \gamma)^{25}\text{Al}$ resonance at 225.5 keV. The yield of ^{26}Al , which is also a positron emitter of comparable half-life, for the irradiation energy used is negligible (Hunt *et al.* 1954).

The level of activity of the targets was estimated by feeding the target current into a microammeter which was shunted by a resistance-capacity circuit of time constant equal to the previously measured mean life of the ^{25}Al activity (Churchill *et al.* 1953). After the required activity had been built up the irradiation was stopped and positrons from the decay of ^{25}Al were detected by Geiger-Müller counter of window thickness 7 mg cm^{-2} mounted close to the target inside the vacuum system.

Aluminium foils of known thickness were placed in front of the Geiger window and the counts recorded for a given target activity were plotted as a function of foil thickness. It was necessary to repeat the irradiations ten or twenty times for each foil thickness in order to obtain a sufficiently high statistical accuracy, and as a check on the reproducibility of the results irradiations with zero foil thickness were repeated several times during the experiment.

The absorption curve obtained is shown in figure 1, and has been analysed by the method proposed by Katz and Penfold (1952). This method involves the assumption that y , the fractional transmission, is related to E_0 , the end point energy, by the equation $y^{1/n} = K_2(E_0 - E)$ where n is a positive number and E the energy of a positron just absorbed by a foil thickness for which the fractional transmission for the spectrum under investigation is y . The number n is determined by plotting $\log y$ against $\log(E_0' - E)$ where E_0' is an initial estimate of the end point energy by inspection of the absorption curve, and the final value of E_0 is obtained by a process of successive approximation (figure 2).

The value giving the best fit was 3.17 meV with a probable error ± 0.15 meV due to statistical uncertainties. This value is in good agreement with the value 3.1 meV due to Van Patter quoted by Goldberg (1953). The slight upward curvature of the graph near the low energy end may indicate the presence of a positron group of lower energy. Efforts were made to confirm the presence of a lower energy group, corresponding to a transition to an excited state of ^{25}Mg by measuring the coincidence rate between positrons and γ -rays. The result indicates that the abundance of a low energy positron group producing isotropic γ -rays in the energy range 1 to 2.5 meV was $9 \pm 8\%$, but, due to possible coincidences from annihilation radiation, this figure must be taken as an upper limit.

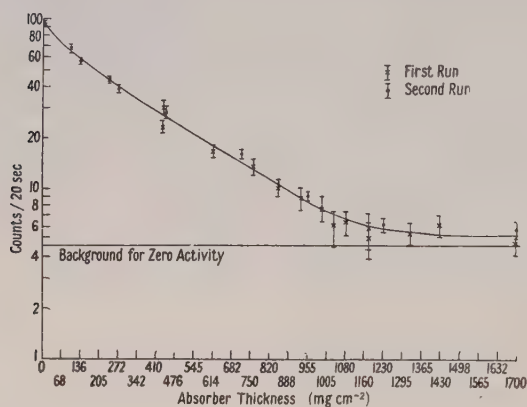


Figure 1. Absorption curve for positrons from ^{25}Al .

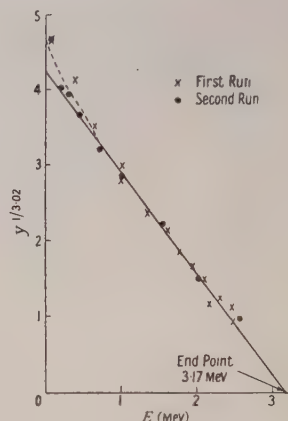


Figure 2. Plot of $y^{1/3.02}$ against E for positrons from ^{25}Al .

Using the mass values for ^{25}Al and ^{25}Mg given by Goldberg (1953) and Li (1952) the end point of the positron spectrum for a transition to the ^{25}Mg ground state would be 3.23 ± 0.10 meV. The closeness of this value to the one observed indicates that the measured end point energy corresponds to a transition to the ^{25}Mg ground state.

In order to check the accuracy of the end point determination, the target was replaced by a ^{32}P source and an absorption curve taken, keeping the same geometry. The end point determination of 1.80 ± 0.1 meV was in essential agreement with published results (Hollander *et al.* 1953).

The authors wish to acknowledge the help of Dr. A. J. Salmon and Messrs. D. A. Hancock, W. W. Evans and M. Kerridge. Thanks are also due to Dr. T. E. Allibone for permission to publish this letter.

Research Laboratory,
Associated Electrical Industries Ltd.,
Aldermaston, Berkshire.
19th February 1954.

S. E. HUNT.
W. M. JONES.
J. L. W. CHURCHILL.

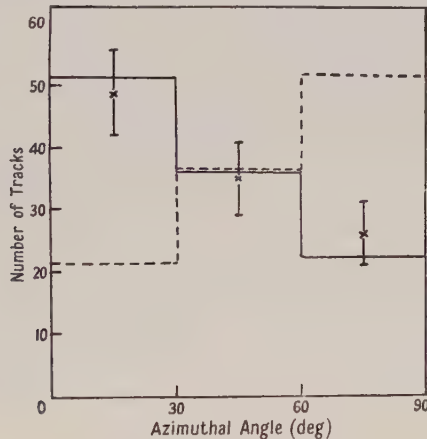
- CHURCHILL, J. L. W., JONES, W. M., and HUNT, S. E., 1953, *Nature, Lond.*, **172**, 460.
GOLDBERG, E., 1953, *Phys. Rev.*, **89**, 760.
HOLLANDER, J. M., PERLMAN, I., and SEABORG, G. T., 1953, *Rev. Mod. Phys.*, **25**, 469.
HUNT, S. E., JONES, W. M., CHURCHILL, J. L. W., and HANCOCK, D. A., 1954, *Proc. Phys. Soc. A*, **67**, 443.
KATZ, L., and PENFOLD, A. S., 1952, *Rev. Mod. Phys.*, **24**, 28.
LI, C. W., 1952, *Phys. Rev.*, **88**, 1038.

Polarization of the 10.4 Mev Gamma-Ray in the Reaction $^{27}\text{Al}(\text{p}\gamma)^{28}\text{Si}$

The polarization of the 10.4 mev gamma-ray from the transition between the 12.23 mev and 1.80 mev levels in ^{28}Si , excited at the 652 kev resonance in the reaction $^{27}\text{Al}(\text{p}\gamma)^{28}\text{Si}$, has been measured by the method of photodisintegration of the deuteron in nuclear emulsions (Wilkinson 1952).

200 and 300 micron G.5 emulsions were loaded with heavy water and exposed to gamma-rays produced by the bombardment of thin (10 kev) aluminium targets with 660 kev protons. The plates were scanned over areas where the gamma-rays were approximately at normal incidence to the plane of the emulsion and at 90° to the proton beam, this being the most favourable arrangement for detection of the polarization. 110 proton tracks were found having a range corresponding to disintegration of a deuteron by the 10.4 mev gamma-ray, and the distribution of the azimuthal angles of these tracks was measured relative to the plane of the gamma-ray and the proton beam.

The results of Rutherglen *et al.* (1954) showed that the gamma-radiation was of the dipole type with an angular distribution $W(\theta) \sim 1 - 0.48 \cos^2 \theta$. By adopting the shell-model assignment of even parity to ^{27}Al it was deduced that the radiation was from an electric dipole transition.



In the figure the full-line histogram, drawn in 30° intervals for comparison with the experimental results, shows the expected distribution in azimuthal angle of the photoprotons at polar angle $\theta = 90^\circ$ for an electric dipole transition. For a magnetic dipole transition the distribution would be given by the dotted histogram.

The experimental points enable a clear choice to be made in favour of the electric dipole transition and thus help to confirm that the shell model is correct in assigning even parity to ^{27}Al .

Department of Natural Philosophy,
Glasgow University.
11th February 1954.

I. S. HUGHES.
P. J. GRANT.

WILKINSON, D. H., 1952, *Phil. Mag.*, **43**, 659.

RUTHERGLEN, J. G., GRANT, P. J., FLACK, F. C., and DEUCHARS, W. M., 1954, *Proc. Phys. Soc. A*, **67**, 101.

REVIEWS OF BOOKS

Flames: Their Structure, Radiation and Temperature, by A. G. GAYDON and H. G. WOLFARD. Pp. xi + 340. (London: Chapman and Hall, 1953.) 55s.

Physicists, physical chemists and engineers can find common ground in the field of flame studies, which is bound up with both widespread industrial applications and fundamental problems of gas flow and chemical reaction. In any such field the literature in the form of published papers is both voluminous and widely scattered, which makes very welcome the appearance of a monograph such as this one. Its particular merit lies in the fact that both authors are actively engaged in research in the most promising aspects of the subject, which has given the book a most useful experimental approach.

It is broadly limited to a discussion of burner flames, which fall into the two main classes of premixed flames, where the fuel and oxidant are well mixed before burning, and diffusion flames, in which the fuel, emerging from the burner, mixes with the oxidant in the body of the flame. The first class has a well-defined reaction zone, usually conical in form, and is associated with a characteristic parameter of burning velocity. A useful account is given of the photographic study of the flow pattern in such cases, and of methods of measuring the burning velocity. This leads to a theoretical discussion of the reaction and preheating zones in the light of thermal and diffusion hypotheses. The more difficult topic of diffusion flames is then dealt with, including an excellent account of the elucidation of the chemical reactions in flat diffusion flames by spectroscopic methods.

The latter part of the book contains a most valuable discussion of the radiation from flames and flame temperatures. The various methods of measurement of temperature, in particular the line-reversal method, are very adequately described, and there is a useful account of thermodynamic calculations of temperature and of composition of flame gases. Lack of equilibrium and departures from equipartition are also discussed, and possibly should have been treated at greater length. This is, however, by far the best account of flame temperatures known to the reviewer.

The book also includes a short section on ionization in flames, which is rather obscure, and ends with a stimulating account of some unusual flames and some current problems. It cannot be recommended too highly for any research worker on flames or cognate subjects.

T. M. SUGDEN.

Tables of 10^x (Antilogarithms to the base 10). NATIONAL BUREAU OF STANDARDS APPLIED MATHEMATICS SERIES, No. 27. Pp. viii + 543. (Washington: U.S. Government Printing Office, 1953.) \$3.50.

The main table gives values of 10^x to 10 decimal places, at intervals of 0.00001, for the complete range from 0 to 1.

There is a subsidiary table, by help of which it is possible to compute antilogarithms to 15 decimal places.

The table was compiled by correcting Dodson's table of 1742, and is printed from typescript. Differences are not tabulated.

J. H. AWBERY.

Les Applications de la Mécanique Ondulatoire à l'Étude de la Structure des Molécules. Pp. 223. (Paris: Editions de la Revue d'Optique Théorique et Instrumentale, 1953.) 1600 fr.

This is a collection of some eleven lectures arranged in a series, and given under the general presidency of L. de Broglie in 1951. Some of the papers are essentially experimental, others entirely theoretical. As might be expected, the styles of the essays are different for different authors, and so also is the level of difficulty. But there are one or two common threads which link the individual contributions together. Among the experimental papers the full account of Mme Ramart-Lucas on steric effects in ultra-violet spectra is quite outstanding. And the discussion of dipole moments, particularly in terms of the difficulty of distinguishing the various elements which contribute to their calculation, is well brought out by Trinh, Lumbroso and Laforgue. It is inevitable that in a series like this some of the contributions should be largely didactic. So far as these are concerned the gap of $2\frac{1}{2}$ years in publication is not very serious. But for the original work, such as that of Ramart-Lucas and Pacault, it is rather a pity. This collection of papers is a useful—if not terribly thrilling—addition to the available literature on the subject.

C. A. COULSON.

Structure Reports for 1945–1946, Vol. 10, edited by A. J. C. WILSON. Pp. viii + 325. (Utrecht: Oesthook (for International Union of Crystallography), 1953.) 45 Dutch fl. 84s.

This volume is one more welcome contribution to filling the gap in recording crystal structures between the last issue of the pre-war *Strukturbericht* and the later volumes of the new *Structure Reports* which are now fast catching up on current researches. The decision was taken by the International Union of Crystallography, at the start of the new venture, to work backwards from that date as well as forwards. This accounts for volume 10 appearing after volumes 11 and 12, in what is apparently the wrong order in time. This publication is of the greatest importance to all those who are concerned with the crystalline state and is an essential part of any serious library of reference. It is also a fine example of book production.

D. P. RILEY.

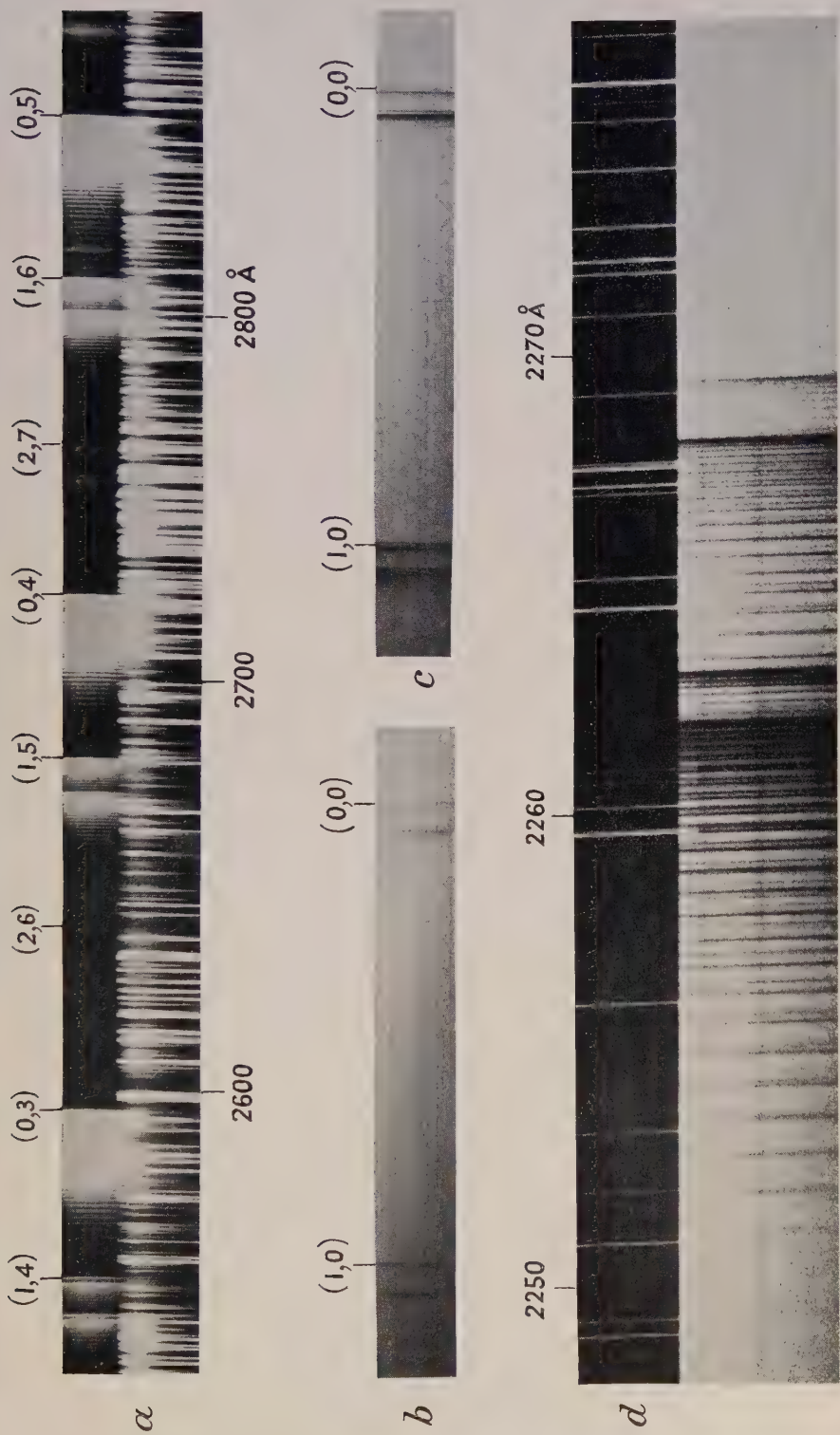
Static Electrification: a Symposium held by the Institute of Physics in London, 25th–27th March, 1953. British Journal of Applied Physics Supplement No. 2. Pp. iv + 104. (London: Institute of Physics, 1953.) 25s.

Those who are concerned with static electrification, either from interest or because of its nuisance value, find the literature scattered through a great variety of journals, and going back many years, if, indeed, they find it at all. The symposium held on the subject by the Institute of Physics in March 1953 brought out the importance of its various ramifications and led to valuable discussions arising from different points of view. This is reflected in the papers now published in book form, covering the hazards of static, useful applications, what little is known about the physics of the phenomena, and the design of electrostatic machinery. Turning over the pages of this admirably produced book, one can hardly fail to find something of importance for any immediate problem, and the references to earlier work, though far from complete, form the most useful collection available.

W. R. HARPER.

CONTENTS OF SECTION B

	PAGE
Dr. S. WAGENER. Reactions between Oxide Cathodes and Gases at Very Low Pressures	369
Miss C. M. LOVETT. Some Measurements of the Electrical Conductivity, Thermoelectric Power and other Properties of the Coating in the Oxide-Coated Cathode	387
Mr. G. F. N. CALDERWOOD and Dr. E. W. J. MARDLES. Viscometry—The Meniscus Resistance in Capillary Flow of Liquids	395
Dr. J. ROLFE. A Micro-Method for the Measurement of Self-Diffusion Coefficients of Solutions	401
Mr. J. B. GUNN. Measurement of the Surface Properties of Germanium	409
Dr. R. BECHMANN and Mrs. S. AYERS. Elastic and Piezoelectric Coefficients of Dipotassium Tartrate (DKT)	422
Dr. A. N. STROH. Constrictions and Jogs in Extended Dislocations	427
Research Notes :	
Mr. J. MARRIOTT, Mr. R. THORBURN and Dr. J. D. CRAGGS. Negative Ion Formation in CCl_4 and TiCl_4	437
Dr. P. N. DAYKIN and Mr. D. A. WRIGHT. Oxide Cathodes in Accelerating Fields	439
Letters to the Editor :	
Dr. G. F. J. GARLICK and Dr. M. J. DUMBLETON. Phosphors Emitting Infra-Red Radiation	442
Reviews of Books	444
Contents of Section A	448



a. NO γ bands in emission from ozonizer-type discharge at 1 atm. Medium quartz. $1\frac{1}{2}$ hr on Zenith plate. Fe arc comparison. *b.* Absorption by 15 cm NO at 2 mm pressure; medium quartz. *c.* Similar to *b* but 2 mm partial pressure NO in 1 atm of N_2 . *d.* Absorption from Xe lamp by 15 cm NO at 2 mm partial pressure in N_2 at 1 atm, showing absence of pressure broadening. Quartz Littrow. 4 min on Ilford Q2 plate. Fe comparison 1 min.

The Inertia of Heat Flow in Liquid Helium II

BY H. E. HALL

Royal Society Mond Laboratory, Cambridge

MS. received 25th January 1954

Abstract. Measurements have been made of the mechanical reaction on a source of heat in liquid helium II. On the two-fluid model this reaction is due to the inertia of the fluids. The results are consistent with the predictions of the two-fluid model, although the conditions of the experiment were chosen so that dissipative effects were present which are not given by that model in its present form. This result gives experimental justification for retaining the two-fluid model under such conditions.

§ 1. INTRODUCTION

THE two-fluid model (Landau 1941, Tisza 1947) of liquid helium II has proved adequate to explain periodic phenomena such as second sound and the Andronikashvili (1948) experiment and, with the addition of a critical velocity for superfluidity, flow in the film and in very narrow slits. But for steady state phenomena in the bulk liquid such as heat conduction (Keesom, Saris and Meyer 1940) and capillary flow (Atkins 1951) the two-fluid theory, if it is to be used at all, must be supplemented by further hypotheses such as the force of mutual friction postulated by Gorter and Mellink (1949). The extension of the Andronikashvili experiment to larger amplitudes (Hollis-Hallett 1952) and the rotating cylinder viscometer (Hollis-Hallett 1953) show that while such a force may be necessary it is certainly not sufficient. On the other hand the absence of appreciable attenuation of second sound (Osborne 1951) makes the inclusion of mutual friction an embarrassment in this case. In such a situation it must be considered whether any extension of the two-fluid theory is justifiable. For it is quite conceivable that, under conditions such that the simple two-fluid model is no longer adequate, the internal structure of the helium changes in such a way that the division into two fluids becomes meaningless. Alternatively the two fluids might persist, but with quantities such as ρ_n profoundly modified.

The obvious way to check this point experimentally is to measure, under conditions where the simple two-fluid theory is known to be inadequate, some quantity which depends only on the division into two fluids and is unaffected by any extra terms we may add to the equations of motion. Such a quantity is the mechanical inertia associated with flow of heat. It can be measured by the momentum flux $\rho \mathbf{v} \cdot \mathbf{v}$ associated with each fluid. Thus in a linear flow of heat there is a reaction pressure $\rho_s v_s^2 + \rho_n v_n^2$ on the source due to the inertia of the fluids. Both fluids give positive contributions as positive momentum is associated with a positive velocity and negative momentum with a negative velocity. Using the relations of two-fluid theory: heat flow per unit area $= w = \rho S T v_n$ and $\rho_s v_s + \rho_n v_n = 0$ for no flow of matter, we obtain

$$\rho_s v_s^2 + \rho_n v_n^2 = \frac{\rho_n w^2}{\rho_s \rho T^2 S^2}.$$

For comparison of theory and experiment it is convenient to use the velocity of second sound as a lumped constant given by

$$u_2^2 = \frac{\rho_s}{\rho_n} \frac{TS^2}{C}$$

so that

$$\rho_s v_s^2 + \rho_n v_n^2 = \frac{w^2}{u_2^2 \rho CT}. \quad \dots\dots(1)$$

The function $1/u_2^2 \rho CT$ is shown in figure 4.

The mechanical reaction on a source of heat has already been measured in the pioneer experiments of Kapitza (1941). The heat left a thermally isolated bulb via a capillary tube, and the flow was shown to be a well-defined jet by means of a small vane placed across it. The reaction on the source was equal to the force on a sufficiently large vane. His results are disquieting in that the power dependence is nearly linear rather than quadratic, and the size of the effect decreases monotonically with increasing temperature from 1.7°K to 2.1°K. An apparatus in which contraction at the end of the capillary was carefully avoided gave forces about twice as large at high power and a rather more nearly quadratic power dependence at lower power flows. The pressure was always less than $\rho_s v_s^2 + \rho_n v_n^2$ except possibly at the lowest power used, where it approached equality. Thus it seems that the shape of the capillary mouth may be critical. From a quantitative point of view Kapitza's geometry is subject to the criticism that while the force on the vane indicates a jet of normal fluid, the superfluid flow pattern is not clear. A jet of both fluids cannot be stable in the presence of dissipative forces, as a temperature gradient would be required inside it but not outside, giving rise to lateral forces on the two fluids. Variations in the superfluid flow combined with possible mutual friction terms can give rise to an unknown difference in hydrostatic pressure between the interior of the jet at emergence and the bath. This adds on to the reaction pressure calculated above. In view of the importance of this experiment as a test for the validity of the two-fluid theory it was decided to repeat the experiment with a geometry not subject to these criticisms.

The quantity $\rho_s v_s^2 + \rho_n v_n^2$ is also measured by the thermal Rayleigh disc (Pellam and Hanson 1952). But for second sound at their frequency (about 100 c/s) the two-fluid theory is already known to apply, and it would indeed have been surprising if any other result had been obtained. It may well be, as Pellam and Hanson remark, that the result in the form $w^2/u_2^2 \rho CT$ can be derived merely from the existence of second sound, without explicit reference to a two-fluid model. But for the steady state (zero frequency) the equations of propagation of second sound are known experimentally not to apply, so there is probably no special significance in expressing the result in the form $w^2/u_2^2 \rho CT$.

§2. APPARATUS

Figure 1 shows in section an idealized apparatus to measure the force of reaction on a heat source emitting heat in one direction. The source is mounted on a flat plate impermeable to heat, suitably suspended at the end of an insulated tube which guides the heat flow. The thermally isolated chamber at the back of this plate serves only to transmit hydrostatic pressure. This arrangement has the important difference from Kapitza's that there can be no flow of matter or heat to the helium round that part of the suspended source which is not

emitting heat. Consequently dissipative forces cannot give rise to a pressure difference between the isolated chamber and the region of heat flow, but the possible effect of Bernoulli forces must be considered. The equations of motion without any dissipative terms may be written:

$$-\frac{\rho_n}{\rho} \text{grad } p - \rho_s S \text{ grad } T - \frac{\rho_n \rho_s}{2\rho} \text{grad } (v_n - v_s)^2 = \rho_n \frac{\partial \mathbf{v}_n}{\partial t} + \rho_n (\mathbf{v}_n \cdot \text{grad}) \mathbf{v}_n \quad \dots\dots(2)$$

$$-\frac{\rho_s}{\rho} \text{grad } p + \rho_s S \text{ grad } T + \frac{\rho_n \rho_s}{2\rho} \text{grad } (v_n - v_s)^2 = \rho_s \frac{\partial \mathbf{v}_s}{\partial t} + \rho_s (\mathbf{v}_s \cdot \text{grad}) \mathbf{v}_s. \quad \dots\dots(3)$$

The third term in these equations, the kinetic energy of relative motion, appears only in the derivations of Landau (1941) and Zilsel (1950), and is controversial. However, it disappears on adding and integrating to obtain the Bernoulli equation for a stationary flow:

$$p + \frac{1}{2} \rho_n v_n^2 + \frac{1}{2} \rho_s v_s^2 - \int (\rho_n \mathbf{v}_n \times \text{curl } \mathbf{v}_n + \rho_s \mathbf{v}_s \times \text{curl } \mathbf{v}_s) \cdot d\mathbf{s} = \text{const.} \quad \dots\dots(4)$$

where the integration is from some fixed point to the point under consideration.

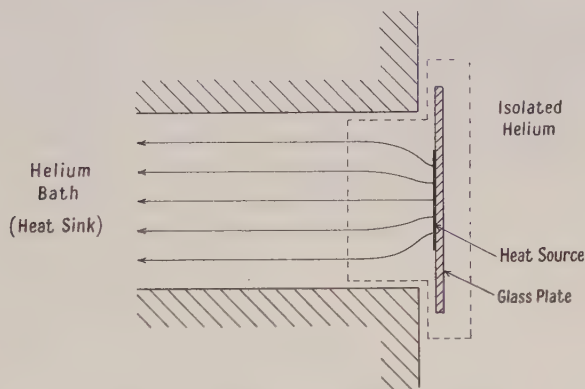


Figure 1. Geometry of the experiment.

To calculate the force on the plate in figure 1 pressure and momentum flux are summed over some convenient control surface such as that shown by dotted lines in the figure. Whatever the detailed flow patterns, equation (4) shows that any pressure difference between the isolated chamber and the region of heat flow must take the form $a\rho_s v_s^2 + b\rho_n v_n^2$, where the velocities are average values over the cross section of the tube, so that with momentum flux added the net force is seen to be of the form

$$\alpha \rho_s v_s^2 + \beta \rho_n v_n^2 = \left(\alpha \frac{\rho_n}{\rho} + \beta \frac{\rho_s}{\rho} \right) \frac{w^2}{u_2^2 \rho C T}. \quad \dots\dots(5)$$

If the flow patterns of the two fluids are identical $\alpha = \beta$. Two special cases will be considered here:

(a) Heater filling the end of the tube, so that flow is completely uniform with a velocity discontinuity between the stream and the liquid in the isolated chamber. Provided the discontinuity surface is plane, the integral in equation (4) just cancels the $\frac{1}{2} \rho v^2$ terms, so that the pressures are equal. Thus the net force is $A(\rho_s v_s^2 + \rho_n v_n^2)$ where A is the area of the tube. This has the

advantage that Bernoulli pressures do not affect the result, but on the other hand the postulated plane discontinuity surface may well not be realized in practice.

(b) Heater smaller than the end of the tube, and a curl-free flow as shown in figure 1. In this case there is a stagnation line at the corner between tube and suspended plate, so the pressure in the isolated chamber is greater than that in the uniform stream by $\frac{1}{2}(\rho_s v_s^2 + \rho_n v_n^2)$ giving a net reaction force of $\frac{1}{2}A(\rho_s v_s^2 + \rho_n v_n^2)$. This arrangement has the advantage that the ideal flow for a tube closed at one end is not likely to be appreciably perturbed by the gap between tube and plate, as this is situated at a stagnation point.

With a viscous fluid there is also a tangential force on the control surface of figure 1 from the boundary layer at the edge of the tube. But with a viscosity of 10^{-5} poise this force is less than 1% of the expected force at the largest power used even for a boundary layer as thin as 10^{-2} cm.

The actual form of apparatus used is shown in section in figure 2(a). Forces are measured by observation of Newton's rings formed between the suspended

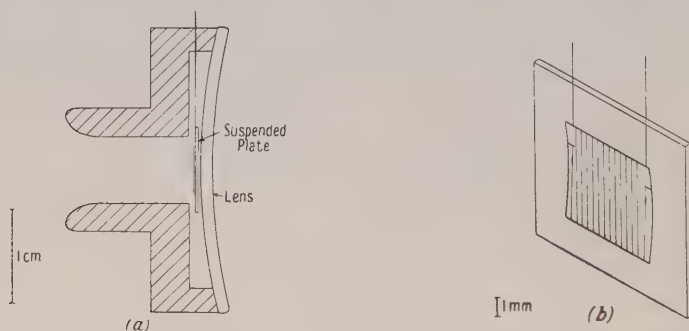


Figure 2. (a) The apparatus.

(b) Suspended plate with heater.

glass plate and a convex lens. The main body of the apparatus is constructed from bakelized paper (a sufficiently good thermal insulator) and the isolated chamber behind the heater is closed off by the weak convex lens required to form the interference fringes, which is secured with spring clips and cemented with shellac. This joint only needs to be sufficiently tight to present a thermal resistance much greater than the short tube used to guide the flow. This tube has a 7 mm square cross section. Figure 2(b) shows the construction of the heater. It is wound of 50 s.w.g. eureka on a square of stiff paper, opposite edges of which have been nicked at about $\frac{1}{3}$ mm intervals with a razor blade. The wire is entirely on the front of the paper except for the short turns that go just round the edge through the nicks. Leads of 48 s.w.g. copper, which act as a suspension, are soldered on and taken behind the paper. This heater is secured to a glass plate about $9 \times 9 \times \frac{1}{3}$ mm by spots of Durofix at the centre of the paper former and at the points where the leads leave the plate. The completed heater is suspended by soldering the leads to two relatively thick copper wires passing through the top of the isolated chamber. To facilitate levelling of the apparatus it is suspended from three micrometers in the cryostat cap. It is also necessary to take fairly elaborate precautions to avoid vibration, despite the fact that the small gap between lens and plate gives some viscous damping. The glass plate was prevented from sticking to the lens by taking precautions to avoid the condensation of frost on the apparatus during pre-cooling.

The advantages of interferometry for force measurement are high sensitivity and small displacement of the heated plate. The technique of measurement is to view the fringes by reflected sodium light through a telescope and measure the heater power required to displace integral numbers of fringes. As this merely requires the pattern of rings to be restored to its original appearance distortion caused by viewing through two dewars is unimportant, and it is easy to count the fringes as they appear at the centre of the pattern. It is easily seen that the application of a horizontal force F ($\ll mg$ where m is the mass of the suspended plate with heater) is equivalent to tilting the force of gravity through an angle F/mg , and will therefore produce the same displacement of the plate relative to the lens as tilting the apparatus through this angle. So the apparatus can be calibrated by tilting smoothly through a known angle while counting fringes.

§ 3. RESULTS

The first experiments used a heater consisting of a layer of Aquadag painted on a 1 mm thick glass plate and over the suspending wires, which passed right round the ends of the plate for mechanical strength. This gave the unexpected result that the heater was pulled into the heat current, in the opposite sense to the expected force, and with a force proportional to W at low powers and increasing rather less rapidly at high power. The heat input was only about 10 mW and the force varied from $\frac{1}{2}$ dyn/mW at 1.4°K to $\frac{1}{20}$ dyne/mW at 2°K with no marked rise near the λ -point. A similar effect, but only about 5% of the magnitude, was later found with a wire heater which, on becoming loose, had been stuck down firmly all over with Durofix and acetone. In view of the qualitative discrepancy with the other experiments with wire heaters, these results are attributed to some of the heat leaving the heater via the isolated chamber behind it. In helium I, under a pressure greater than the vapour pressure to avoid boiling on the heater, similar results were obtained with subsequent wire heaters. This is the form expected for the radiometer effect in normal liquids. It was to make quite certain that no heat flowed via the isolated chamber that the heater form of figure 2(b), in which the heater wire is totally surrounded by helium, was adopted.

With the wire heaters various heater areas were tried with the edge of the guide tube at 1.3 mm and 0.3 mm from the suspended plate, and without a guide tube. With the largest heater one run was made with the heater surrounded by a paper guard projecting about 1 mm from the glass plate, so that the isolated chamber was connected to the heat stream by a slit nearly 1 mm in front of the heater. This modification produced no significant change in the result. Experiments were also tried with a heater of very small area consisting of a strip of pencil lead $1\frac{1}{4}$ mm long and $\frac{1}{4}$ mm diameter, suspended from its leads in front of the glass plate. But this heater merely produced unsteadiness of the plate with no definite deflection. It is possible that boiling on the heater set in, as the heat current at the heater surface was quite large. Measurements using the heater form of figure 2(b) were made up to about 0.4 W cm^{-2} in the temperature range from 1.5°K to the λ -point. At higher powers it was difficult either to count fringes accurately or to control the temperature. Near the λ -point a sudden instability set in at powers corresponding to $v_s \sim 10 \text{ cm sec}^{-1}$ but this may have been due to a thin layer of helium I on the heater rather than

to a critical velocity. In helium I under its vapour pressure boiling on the heater occurred at the smallest heat inputs. At lower temperatures the apparatus became more susceptible to vibration, partly because it was more directly coupled to the pump via returning gas when the control valve was wide open. Also it became difficult to control the temperature sufficiently closely in the presence of a changing heat input.

Two important generalizations can be made from the results of these experiments.

(1) The heater is repelled from the heat current with a force proportional to W^2 . A specimen set of results illustrating this is presented in figure 3. Such

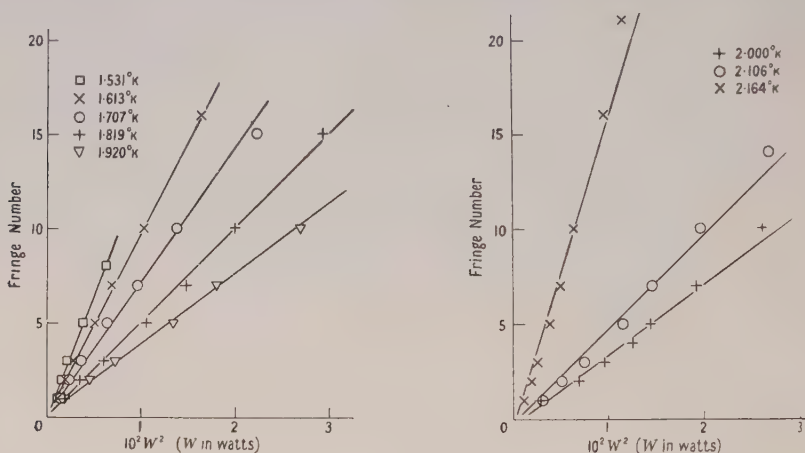


Figure 3. Dependence of the force on heat flow. $a/A=0.55$.

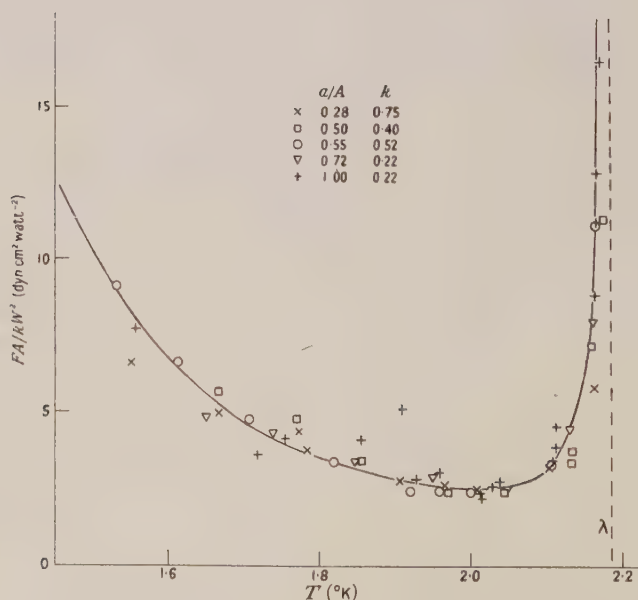


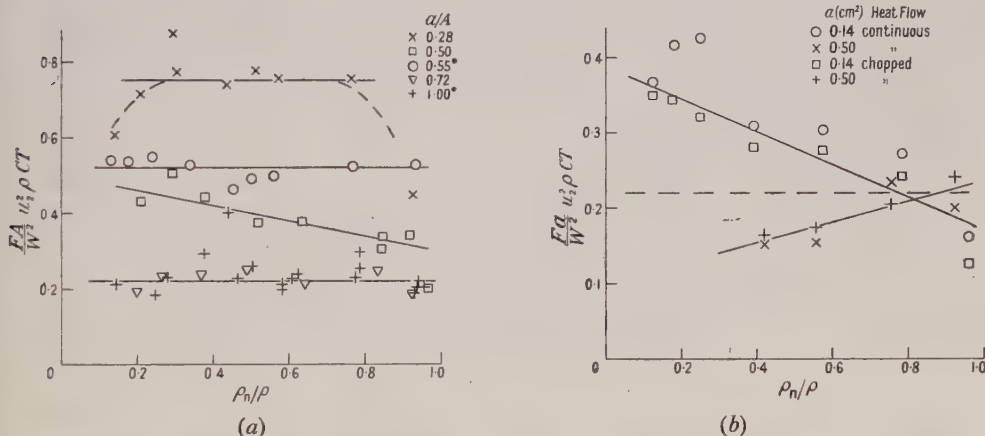
Figure 4. Dependence of the force on temperature. Full curve: $1/(u_s^2 \rho CT)$.

a power dependence is characteristic of the counterflow mechanism of heat transport.

(2) The temperature dependence of the force follows closely that of the function $1/u_2^2 \rho CT$. Figure 4 shows the temperature dependence of the observed force for all measurements with a guide tube. Results for different heater areas have been brought to a common curve by means of an arbitrary scaling factor k of order $\frac{1}{2}$ which is discussed further below. In computing the theoretical curve, the second sound velocity measurements of Peshkov (1948) and the specific heat measurements of Kramers *et al.* (1952) have been used. This temperature dependence contains the ratio ρ_n/ρ_s showing that such a quantity is still significant in a steady heat flow.

Both these features of the results differ from Kapitza's, but are in agreement with the predictions of two-fluid theory.

The dependence of the force on geometrical factors is shown in figures 5 and 6. Here A =tube area, a =heater area. Figure 5(a) shows $k=(FA/W^2)u_2^2 \rho CT$



* For these measurements the suspended plate was 1.3 mm from the end of the guide tube; otherwise the distance was 0.3 mm.

Figure 5. Dependence of the force on geometry and temperature.

(a) With guide tube.

(b) Without guide tube. Broken line: results for same heaters with guide tube.

plotted as a function of ρ_n/ρ for the measurements using a guide tube. Equation (5) shows that for a given geometry the result should be a straight line, horizontal if $\alpha=\beta$. With the possible exception of the results for $a/A=0.50$ it appears that $\alpha=\beta=k$ for these measurements. This indicates a tendency for $\rho_s v_s + \rho_n v_n = 0$ to be satisfied everywhere rather than as an average over the cross section. It is probably due to the fact that this relation must be satisfied for each part of the heater separately and to the dominance of inertial forces. Figure 5(b) shows $(Fa/W^2)u_2^2 \rho CT$ as a function of ρ_n/ρ for the measurements without a guide tube, in which a direct comparison of steady state and second sound conditions was made by repeating the measurements with the heater current chopped on and off for equal periods at about 30 c/s by means of a commutator. There is no substantial difference between the results based on

the average value of W^2 in the two cases. But there is distinct evidence that when the guide tube is removed $\alpha \neq \beta$, i.e. the flow patterns are different for the two fluids. The trend of the corresponding measurements with a guide tube is also shown in the figure, and shows that the order of magnitude of the effect is unchanged. These results are important in showing the correspondence between steady heat flow and second sound, but further discussion of the absolute magnitude of the effect will be confined to the measurements with a guide tube. Unfortunately it was not possible to compare steady state and second sound conditions in these measurements, as chopping of the d.c. heater current merely caused the suspended plate to vibrate irregularly, at larger amplitudes as the power was increased.

The effect of altering heater area and the gap between guide tube and suspended plate is summarized in figure 6. It is seen that the primary

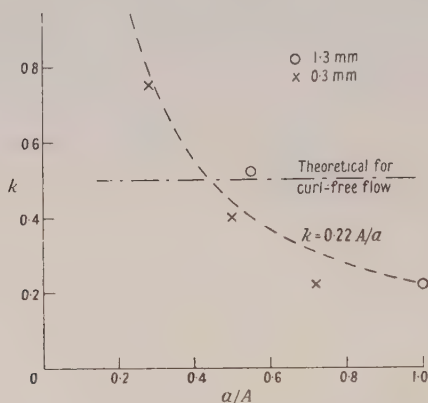


Figure 6. Dependence of the force on geometry. Suspended plate at 1.3 mm and at 0.3 mm from end of guide tube.

geometrical factor is the heater area, and the dependence on this is roughly represented by $k(=FA/W^2)u_2^2\rho CT)=0.22 A/a$, i.e.

$$\frac{Fa}{W^2} = \frac{0.22}{u_2^2\rho CT}.$$

It was shown in §2 that $k=\frac{1}{2}$ for a curl-free flow; therefore such a flow certainly does not hold at the larger heater areas and possibly not at all. For a well-defined jet equal in area to the heater, inverse proportionality to heater area is expected but with a constant 1.0 rather than 0.22. In any case, as was mentioned in the discussion of Kapitza's results in §1, a jet of both fluids is unstable. So it becomes necessary to consider more general flows in which the integral term of equation (4) must be evaluated. As the flow patterns of the two fluids are experimentally the same, equation (4) permits the motion of a single fluid to be considered instead. The Reynolds number of the flow is large compared with unity (indeed so large that laminar flow may not persist far beyond the heater), so that the contribution of dissipative forces to the pressure distribution in the interesting region near the heater can be neglected and the equation of motion becomes that of an ideal fluid:

$$\mathbf{v} \times \text{curl } \mathbf{v} = \text{grad} \left(\frac{p}{\rho} + \frac{v^2}{2} \right). \quad \dots\dots(6)$$

As the velocity is necessarily parallel to the insulating boundaries $\mathbf{v} \times \text{curl } \mathbf{v}$ must be perpendicular to them so that $p + \frac{1}{2}\rho v^2$ is constant on these boundaries, as may also be seen from the fact that the boundary is a limiting stream line. Consider for convenience the case of a cylindrical tube and suppose that when the stream lines have become parallel to the axis, the velocity is of the form $v_0 + \gamma r^2$. For parallel stream lines equation (6) shows that the pressure is constant in a plane normal to the stream lines. So adding up pressure and momentum flux over the control surface of figure 1 gives the net reaction force on the suspended plate for a general flow as:

$$F = (\overline{\rho v^2} - \frac{1}{2}\rho v_1^2)A = k\rho(\bar{v})^2A$$

where the bar denotes averaging over the cross section of the tube and v_1 is the velocity at the edge, but outside any viscous boundary layer. For the special velocity profile under consideration it is possible to put $v_0 = \bar{v}(1-x)$, $v_1 = \bar{v}(1+x)$, giving $k = \frac{1}{2} - x - \frac{1}{6}x^2$ where $x = (v_1 - v_0)/2\bar{v}$ is a convenient parameter to represent the vorticity of the flow.

It is plausible that when the heater area is small the velocity should be greater at the centre than the edge, giving $k > \frac{1}{2}$ but it is less easy to see how a larger velocity at the edge, as required for $k < \frac{1}{2}$ can arise. A possible cause is the method of winding the heater shown in figure 2(b), which necessitates about 10% of the wire being along the nicked edges of the paper former. The consequent increased source strength at the edge of the heater might give rise to a stronger heat current at the edge of the tube when the heater nearly filled the end, as vorticity generated by the heater will be practically conserved throughout the interesting region owing to the predominance of inertial forces. If the change of velocity at the edge is more rapid than the parabolic form assumed above a smaller difference between axial and peripheral velocity is required for a given change in k .

§ 4. CONCLUSIONS

It must be borne in mind when considering these results that the accuracy is not high, about 10% for a single value of F/W^2 under good conditions. There is a further possibility of a systematic error of this order in the results of a single run due to uncertainties in the calibration. Also geometrical constants such as the heater area cannot be very precisely defined. Within these limits of accuracy the following conclusions can be drawn:

(i) The power dependence, temperature dependence, and order of magnitude of the observed force are in agreement with the predictions of the two-fluid theory.

(ii) Where simultaneous observations with steady heat flow and with second sound have been possible no appreciable difference has been found between the force in the two cases.

(iii) The dependence on heater area and other geometrical factors shows that the flow is not curl free, but can probably be accounted for in terms of the distribution of heat source over the heater. At any rate the geometrical dependence appears to be explicable in principle.

The essential point that emerges is that the observed power and temperature dependence and reasonable absolute magnitude of the effect, supported by the direct comparison with second sound, show that the division into two fluids remains a meaningful concept in steady heat flow, with ρ_n and S substantially

unchanged. This gives some experimental justification for retaining the two-fluid model in dealing with irreversible phenomena, and attempting to describe them by the addition of dissipative terms to the equations of motion.

ACKNOWLEDGMENTS

I am grateful to Dr. D. Shoenberg for encouraging this research, to Dr. D. V. Osborne and Dr. A. B. Pippard for many helpful discussions, and to Mr. W. F. Vinen for assistance with the experiments. The work was supported by the Department of Scientific and Industrial Research.

REFERENCES

- ANDRONIKASHVILI, E. L., 1948, *J. Exp. Theor. Phys.*, U.S.S.R., **18**, 424, 429.
ATKINS, K. R., 1951, *Proc. Phys. Soc. A*, **64**, 833.
GORTER, C. J., and MELLINK, J. H., 1949, *Physica*, **15**, 285.
HOLLIS-HALLETT, A. C., 1952, *Proc. Roy. Soc. A*, **210**, 404; 1953, *Proc. Camb. Phil. Soc.*, **49**, 717.
KAPITZA, P. L., 1941, *J. Phys. U.S.S.R.*, **4**, 181.
KEESOM, W. H., SARIS, B. F., and MEYER, L., 1940, *Physica*, **7**, 817.
KRAMERS, H. C., WASSCHER, J. D., and GORTER, C. J., 1952, *Physica*, **18**, 329.
LANDAU, L. D., 1941, *J. Phys. U.S.S.R.*, **5**, 71.
OSBORNE, D. V., 1951, *Proc. Phys. Soc. A*, **64**, 114.
PELLAM, J. R., and HANSON, W. B., 1952, *Phys. Rev.*, **85**, 216.
PESHKOV, V., 1948, *J. Exp. Theor. Phys.*, U.S.S.R., **18**, 951.
TISZA, L., 1947, *Phys. Rev.*, **72**, 838.
ZILSEL, P. R., 1950, *Phys. Rev.*, **79**, 309.

A Possible Model of Liquid He_3

By H. N. V. TEMPERLEY

King's College, Cambridge

MS. received 10th June 1953, and in final form 5th February 1954

Abstract. It is shown that many of the properties of liquid He_3 , *including its two changes of state*, are predicted semi-quantitatively by a model in which one applies corrections of van der Waals type to the free energy of a perfect Fermi gas. Various other models are also discussed in the light of available experimental evidence.

§ 1. INTRODUCTION

VARIOUS writers, Buckingham and Temperley (1950), Pomeranchuk (1950), Lifshitz (1951), Singwi (1951), Chen and F. London (1953), have suggested that liquid He_3 may behave like an 'imperfect Fermi gas', and there is some experimental support for this view. For example, the viscosity of the liquid is of the order of magnitude, and has the trend with temperature to be expected for such a gas (Buckingham and Temperley 1950), and the entropy of the liquid, calculated as if it were a perfect Fermi gas of the observed density, is reasonably consistent with existing data on the vapour pressure of the liquid (Weinstock *et al.* 1953 a, equations (7) and (10), Lifshitz 1951, Singwi 1952).

In this paper we study the properties of a model obtained by applying corrections of van der Waals type to the perfect Fermi gas model. It turns out that a surprisingly complete and accurate picture of the properties of He_3 can be given, it being possible to choose the van der Waals parameters so that many of the properties of the liquid, *including its two changes of state*, are reproduced, some accurately, while others are of the correct order of magnitude. It is suggested that the available evidence is consistent with the view that the nuclear spins are aligned antiparallel in the solid as well as in the liquid. By 'aligned antiparallel' we mean primarily that the wave functions can be regarded as 'one-particle' ones with reasonable accuracy, and that they are mainly occupied in pairs, one of each pair being associated with each spin direction. Apart from this hypothesis of virtually complete antiparallel alignment in both solid and liquid, there are at least two other possible views, one being that, at 'helium' temperatures, there is a *random* distribution of spin directions in both solid and liquid (a situation that has not yet been explored theoretically). Another idea is the 'hybrid' one that the spins are aligned antiparallel in the liquid but less markedly so in the solid. The evidence discussed by Chen and F. London (1953), and by Weinstock *et al.* (1953 a), did *not* enable us to decide whether at, say, 0.2°K the entropy of the liquid is still $k \ln 2$ per atom, or whether it is approaching zero, as would be expected for a 'nearly perfect' Fermi gas. Further definite evidence on this point has recently become available from measurements of the heat capacity of the liquid, of the vapour pressure at lower temperatures, and of the magnetic susceptibility. We now put on record some of the consequences of the

hypothesis of nearly complete antiparallel alignment in both solid and liquid. It is possible to develop these in more detail than the consequences of either of the last two.

§ 2. THE 'GAS-LIKE' MODEL

The justification for trying a 'gas-like' model seems to be that the potential barriers in the liquid are probably small or non-existent (due to its low density). For not too strong interactions we make the familiar assumption that the new energy levels are distributed like the perfect gas ones but that, due to the attractive forces, they begin at a lower energy and that they may have a different energy spacing (that is, the excitations may have an 'effective mass' that differs from the atomic mass). Finally, we suppose that the volume accessible to a typical atom is less than the total volume of liquid, and thus we take account of the repulsive portion of the interactions between atoms. In the Appendix we show that the two-atom distribution for a *perfect Fermi gas* at low temperatures strongly resembles that for a classical *liquid*.

We therefore assume the following form for the free energy of the assembly (for T small) by modifying the standard formulae for a Fermi gas:

$$F = \frac{3}{5} N \mu_0 \left[1 - \frac{5\pi^2}{12} \left(\frac{kT}{\mu_0} \right)^2 + \frac{\pi^4}{48} \left(\frac{kT}{\mu_0} \right)^4 + \dots \right] - \frac{aN^3}{V^2} \dots \dots (1)$$

with
$$\mu_0 = \frac{\hbar^2}{8m^*} \left(\frac{3N}{\pi(V-b)} \right)^{2/3}.$$

§ 3. CHOICE OF THE CONSTANTS

We have now three adjustable constants, a , b and m^* , and we choose these in the following way. The term aN^3/V^2 represents the effect of inverse-sixth power interactions between the atoms. Assuming spinless He_4 atoms and various types of lattice arrangement, F. London (1936) estimated this energy to be $7-10 \times 10^{-44} N^2/V^2$ calories/mole. For He_3 we shall assume the smaller value $2-2.5 \times 10^{-44} N^2/V^2$ calories/mole, the reduction being made in an attempt to allow for the fact, pointed out by Pomeranchuk (1950), that the attraction between a pair of atoms whose spin functions are antisymmetrical should be nearly the same as that between spinless atoms, but that there is likely to be less attraction, perhaps even a repulsion, between a pair of atoms with a symmetrical spin function.

By differentiation of (1) we get the following equations:

$$P = \frac{2}{5} \frac{N\mu_0}{V-b} + \frac{Nk^2 T^2 \pi^2}{6\mu_0(V-b)} \dots - \frac{2aN^3}{V^3} \dots \dots (2)$$

$$S = Nk \left[\frac{\pi^2}{2} \frac{kT}{\mu_0} - \frac{\pi^4}{20} \left(\frac{kT}{\mu_0} \right)^3 \dots \right] \dots \dots (3)$$

$$\mu = \mu_0 - \frac{\pi^2 (kT)^2}{12 \mu_0} - \frac{\pi^4 (kT)^4}{80 \mu_0^3} \dots - \frac{3aN^2}{V^2} \dots \dots (4)$$

Choice of the Constant a

To determine the vapour-pressure curve we equate μ , given by equation (4) to the partial potential of a perfect gas of He_3 atoms, a step justified on p. 500. This potential is (see Chen and London 1953, equation (2))

$$\mu_{\text{ideal}} = kT \{ \ln(P_m/T^{5/2}) - 5.325 \}$$

where P_m is the pressure expressed in millimetres of mercury. The vapour-pressure equation is then

$$\log_{10}(P_m/T^{5/2}) = 2.313 - \frac{1.3}{T} - 0.072T - 0.0042T^3 \quad \text{'van der Waals'} \quad \dots\dots(5)$$

This is to be compared with the equation obtained empirically by Weinstock *et al.* (1950) from their measurement:

$$\log_{10}(P_m/T^{5/2}) = 1.916 - \frac{0.978}{T} - 0.0003T^3 \quad \text{'WAO'} \quad \dots\dots(6)$$

and with the equation proposed by Chen and London (1953), on the basis of the same measurements, together with the hypothesis that the entropy vanishes as $T \rightarrow 0$. (Coefficients in (6) and (7) have been 'rounded off.')

$$\log_{10}(P_m/T^{5/2}) = 2.313 - \frac{1.156}{T} - 0.253T - 0.0067T^2 + 0.0527T^3 - 0.0121T^4 \quad \text{'CL'} \quad \dots\dots(7)$$

It is known (Chen and London 1953) that both equations (6) and (7) agree very closely with the experimental data between 1° and 2.5°K . Further powers of T would be required as one approaches the critical region. Between 1° and 0.47°K , it has very recently been reported (Sydoriak and Roberts 1953) that equation (7) agrees much better with the data than does equation (6).

The constants in equation (5) were arrived at as follows. It was first assumed that the degeneracy temperature μ_0/k was the same as that for the perfect Fermi gas of an equal density (4.85°K), which fixes the terms in T and T^3 . The reason for this choice will be explained in a moment. The coefficient of T^{-1} was then chosen so that equations (5) and (7) should agree at 1°K , which choice calls for an assumed interaction energy of $2.1 \times 10^{-44} N^2/V^2$ calories/mole, which is of the calculated order of magnitude as noted above. Equation (5) gives too high a vapour pressure at 'high' temperatures, but this is to be expected, since we are approaching both the critical and the degeneracy temperatures, so it is no longer correct to treat the vapour phase as 'ideal'.

Choice of the Degeneracy Temperature μ_0/k

The expression (3) for the entropy, if we assume $\mu_0 = k \times 4.85^\circ$, gives us

$$S/Nk = 1.02T - 0.043T^2 \dots \quad \text{'van der Waals'} \quad \dots\dots(8)$$

which has to be compared with the following two estimates. One was arrived at by Weinstock *et al.* (1953 a) from their vapour-pressure data, together with the hypothesis that the entropy is proportional to T as $T \rightarrow 0$. Their equation (7) reads

$$S/Nk = 0.978T - 0.053T^2 \quad \text{'WAO'} \quad \dots\dots(9)$$

while Chen and London (1953) calculate from their vapour-pressure equation (our equation (7)) that

$$S/Nk = 1.163T + 0.046T^2 - 0.485T^3 + 0.139T^4 \dots \quad \text{'CL'} \quad \dots\dots(10)$$

Equation (8), having been arrived at by assuming that μ_0 is the same for the perfect Fermi gas of the same density, is in satisfactory agreement with (9)

and (10). Sydoriak and Roberts (1953) represent their measurements of the specific heat of the liquid by an empirical formula equivalent to

$$S/Nk = 1.41T - 0.78T^2 + 0.22T^3 \quad \text{'SR',} \quad \dots\dots(11)$$

Measurements of the specific heat in approximate agreement with Sydoriak and Roberts have also been reported by de Vries and Daunt (1954) and by Weinstock *et al.* (1953 b). (The decision to use the 'perfect Fermi' degeneracy temperature was originally made on the basis of the close agreement between equations (8) and (9).) There is also qualitative agreement with equations (10) and (11), but these are hard to interpret on a 'Fermi-like' model because of the presence of terms in T^2 .

This assumption about the degeneracy temperature calls for the following relationship between the effective mass m^* and the van der Waals constant b ,

$$(m^*/m)^{3/2} = V/(V-b) \quad \text{where} \quad V \simeq 12.5 \text{ cm}^3 \text{ g}^{-1} \quad \dots\dots(12)$$

as can be easily checked from equation (1).

The Melting Curve

We notice that equation (2) is still of van der Waals form even at $T=0$. We may treat it exactly like this equation by suppressing any portion for which $\partial P/\partial V$ is positive, then assuming that the two remaining portions correspond to distinct phases and then determining the equilibrium value of P by the use of the rule of equal areas. This is automatically equivalent to equating partial potentials, since both portions of the curve are derived from the same free energy (1).

Provided that the attractive forces are not too great, we are led to the prediction $P = P_0 + AT^2$ as the limiting form for the transition curve as $T \rightarrow 0$, this form following that of the first two terms in equation (2), and this is just the type of law reported for the melting curve of He_3 by Weinstock *et al.* (1953 b). The values of a and μ_0 that we have just chosen seem to be just about on the borderline at which such a transition ceases to be possible, but there is no difficulty in getting agreement with the observed P_0 if one makes the not unrealistic assumption that the power law of the attractive term in (2) varies as the volume diminishes (and it is often claimed that attractive forces of van der Waals type need more than one term to describe them properly). As an example, if we replaced the V^{-3} type law in (2) by a V^{-4} type law, there is no difficulty in getting a P_0 of the observed 25–30 atmospheres if we assumed b to be approximately 12 cm^3/mole (which would imply a melting density of about 20 cm^3/mole), but these results are so sensitive to the precise assumptions made that they can only be regarded as qualitative. Further progress must await actual knowledge of the density of liquid and solid along the melting curve, together with the form of this curve itself below 0.5°K, which is still unknown. It seems fair to claim that an expression for the free energy of the type (1) is capable of giving qualitative predictions of both the melting and vapour-pressure curves, though it is almost certainly not possible to describe all the data quantitatively with any one choice of the constants. This is almost always what happens with a van der Waals type theory.

If we assume provisionally that the melting curve can be derived from an equation of the type (2), it would mean that, near the melting curve, the solid,

as well as the liquid could be approximately described by an *energy spectrum* of 'one-particle' type (though the *wave functions* may well differ considerably from 'gas-like' ones). This suggestion is due to Chen and London (1953, also private communication). A not dissimilar situation exists for Fermi particles in metals and nuclei, where crude models of 'one-particle' type give useful results even in the presence of strong interactions.

Choice of the Constant b

The constant b was actually estimated by an intuitive argument which seems worth putting on record for a reason that will appear in a moment. If we assume that the relative change of density of liquid between melting and boiling points is of the same order of magnitude in He_3 and He_4 , we may guess a melting density of 0.1 g cm^{-3} , which would call for a value of b of the order of $25 \text{ cm}^3/\text{mole}$. In turn, this would call for a value of m^*/m of about 3 for the liquid, in order to get a μ_0 equal to the 'perfect Fermi gas' value (see equation (12)). This estimate was made on the basis of the melting and vapour pressure curves, before the magnetic measurements reported by Fairbank *et al.* (1953) had been begun. These workers find that the susceptibility departs considerably from that expected from the perfect Fermi-gas model, their observed points still following a Curie law down to 1.25°K , at which temperature the discrepancy with the perfect Fermi-gas model is a factor of approximately 3. This *can* be interpreted as evidence against a 'Fermi-like' model, but the discrepancy would be almost exactly removed if $m^* \simeq 3m$, as was concluded on quite other evidence. It seems entirely reasonable that this ratio should slowly rise (from a value of unity in the vapour) as the density increases and the potential barriers in the liquid become higher. This would certainly mean that the 'liquid' wave functions do differ very considerably from 'perfect-gas' ones.

A variation of m^* with density may be helpful for another reason (p. 501).

§ 4. COMPARISON OF CALCULATED AND OBSERVED CRITICAL CONSTANTS

We have stated that our model predicts *two* distinct transitions. The first was obtained from an equation of the type (2), and would be between two *dense* phases. The existence of a second transition can best be established by replacing equation (2) by the corresponding result for 'high' temperatures. This is, again, modifying standard formulae appropriately:

$$P = \frac{NkT}{V-b} [1 + 0.177y - 0.0033y^2 \dots] - \frac{2aN^3}{V^3} \quad \dots\dots(13)$$

with $y = Nh^3/2(2\pi m^*kT)^{3/2}(V-b)$.

Let us first neglect the terms in $y, y^2 \dots$ in (3), which then becomes practically the same as the classical van der Waals equation and can be treated in the same way. We can allow for the effect of these neglected terms by successive approximation, a process which seems to converge rapidly even near the predicted critical region, so equation (13) can be used safely to calculate the 'high-temperature' portion of the vapour-pressure curve and, in particular, to predict the position of the critical point. As with the classical form of van der Waals' equation, one of the phases never differs greatly from a perfect gas.

We have to justify the derivation of the 'low-temperature' portion of the vapour-pressure curve by equating, as we have done, expression (4) for the partial potential of the liquid at 'low' temperatures with the partial potential of a nearly perfect gas. As noted above, our constants were chosen in order to reproduce this part of the observed vapour-pressure curve. Equation (13) is the correct consequence of the model near the critical point, where the densities of the two phases are the same, but, as we travel down the vapour-pressure curve, the liquid becomes denser, which means that, at *some* stage, equation (2) becomes more appropriate for the liquid than equation (13), while the vapour phase approaches nearer to perfection as we go further from the critical point, as happens with ordinary vapours. Equation (13) therefore describes the isotherms, and can correctly be used to obtain the vapour-pressure curve, for a short region below the critical point, but at the 'low-temperature end' the simplest method of determining the vapour-pressure curve is to equate μ , given for the dense phase by expression (4), to the partial potential of a nearly perfect vapour.

The theoretical vapour-pressure curve is thus obtained by applying the rule of equal areas to equation (13) in the 'high-temperature' region, while in the 'low-temperature' region it will be practically identical with equation (5). Since this curve passes through ($P=0$, $T=0$) it is quite distinct from the phase-boundary obtained from an equation like (2), which begins at a finite pressure at $T=0$.

By the process used by van der Waals we can calculate the critical constants from equation (5), and after inserting the values of m^* , a and b that we have already chosen we compare in the table the calculated and observed critical

	Calculated	Observed
P_c (atmospheres)	2.8	1.15
T_c ($^{\circ}\text{K}$)	2.0	3.34
V_c ($\text{cm}^3 \text{g}^{-1}$)	18	24

constants, the observed values being those of Grilly, Hammel and Sydoriak (1949). This comparison reveals a familiar situation. Using a theory of van der Waals type, it has proved possible to reproduce some observed features (the 'low-temperature' part of the vaporization curve) quantitatively, while others are predicted qualitatively and are of the right order of magnitude (the melting curve and the critical constants). (As a matter of fact, no possible choice of a , b and m^* could fit all three critical constants, but they were actually chosen in the manner explained above.)

We have thus shown that the imperfect Fermi gas is capable of at least two transitions of the first order, and it is extremely tempting to identify the two corresponding (P , T) curves with the melting and vaporization curves of He_3 .

We must not let the undoubted successes of a simple model in reproducing many of the facts obscure what we have already mentioned above, namely that there *are* other assumptions which seem equally capable, in principle, of accounting for the observed facts.

The first possible assumption is that the effect of the interactions is strong enough to destroy completely the 'Fermi-gas' behaviour of the assembly and, in particular, to prevent any appreciable alignment of spins in both the solid and liquid at 'helium' temperatures. The 'entropy of spin disorder' $Nk \ln 2$

would then persist down to 'magnetic' temperatures. Weinstock *et al.* (1953 a) showed that such behaviour, assuming similar behaviour for the entropy of the solid, was perfectly compatible with what was then known about both the vapour pressure and the melting curves, but it now seems practically ruled out by the extension of the vapour-pressure measurements to lower temperatures (Sydoriak and Roberts 1953).

A 'hybrid' assumption, due to Pomeranchuk (1951), is that the solid loses spin entropy *more slowly* with falling temperature than does the liquid. Pomeranchuk made this assumption in an extreme form, namely that at 'helium' temperatures the solid preserves its spin entropy intact while the liquid is losing it rapidly. Weinstock *et al.* (1953 a) showed that this last assumption cannot be reconciled simultaneously with the melting and vapour-pressure curves, though the milder assumption (that the solid has lost *some* of its spin entropy) would still be permissible.

Let us assume, for the moment, the approximate validity of treating the *solid* as an imperfect Fermi gas. If the effective mass, m^* , were the same for solid and liquid, the Fermi temperature of the solid would *always* be higher than that of the liquid, because of the higher density, and the entropy at a given temperature and pressure would always be smaller for the solid. If the effective masses are *not* the same, and vary with density, see p. 499, it is then, in principle, possible for the liquid to lose entropy with falling temperature *faster* than does the solid, which would result in there being some point on the melting curve at which the entropies were equal, the melting curve having a minimum at this point. Such a result, though peculiar, is by no means thermodynamically impossible. As an example of a transition curve behaving in a similar way, we may mention the mixing curve of nicotine and water. This system has a *closed* solubility curve so that, for a given composition, it may be possible to find *two* temperatures, at one of which heat has to be *supplied* to cause a break-up into two layers, while, at the other, *cooling* is necessary for this.

It should be mentioned that the experiments of Weinstock *et al.* (1952) on the melting curve are quite compatible with the existence of such a minimum. Since they were using a 'blocked capillary' technique it follows that, at a pressure corresponding to that at the minimum, the capillary would still block, not now *in* the bath, but at some point between the bath and the gauge at room temperature. Such a situation was indicated by their original experiments (1952), and they state (private communication) that further experiments, using greatly improved heat contact, confirm it.

It is instructive to discuss the argument that led Pomeranchuk (1950) to believe that, as in other solids, there is no appreciable nuclear alignment in solid He_3 and yet at the same time to accept a 'Fermi-like gas' model for the liquid. The discussion throws some light on the question whether such a model is likely to succeed for the solid. Pomeranchuk's argument runs as follows: (a) The liquid cannot solidify until the amplitude of the vibrations of an atom about its equilibrium position is small compared with the lattice distance. (b) If this ratio *is* small, exchange effects cannot occur in the solid to any marked extent, and the distribution of spin directions will therefore be nearly random down to 'magnetic' temperatures.

Unfortunately, both of these points, though they are probably valid for other substances, seem to be suspect for He_3 . Point (a) is certainly incorrect

for He_4 . A simple calculation by Domb (1953) shows that the ratio of amplitude to lattice distance is of the order of 0.3 on the melting curve of He_4 , which means that close encounters between neighbours would be very frequent. (For most other solids the ratio is only about 0.1.) Even if we could grant point (a), it must be remembered that He_3 and He_4 differ from other solids in that the de Broglie wavelength, associated with the motion of an atom of helium at the freezing temperature, is comparable with the lattice distance. This opens up possibilities of spin exchange effects that do not exist for other solids because of the larger masses and higher temperatures.

This combination of exceptional circumstances, large amplitudes of oscillation and large de Broglie wavelength, probably combined with rather low potential barriers, make it possible that a 'Brillouin zone' type of treatment might be more appropriate for solid or liquid He_3 than for other liquids and solids, the effects of the interactions being taken care of by the van der Waals constants a and b , and by the effective mass m^* . If we allow for the possible effect of higher potential barriers in the solid, m^* might be significantly larger in the solid than in the liquid, which could conceivably over-compensate for the effect of the higher density. If m^* varied strongly enough with density, we *could* get a crossing of the entropy curves and thus a melting curve of the kind predicted by Pomeranchuk (1950). Thus this effect, too, if its existence is finally confirmed, receives a natural interpretation on the basis of the 'imperfect Fermi gas' treatment, though we must emphasize once again that the possibility that the interactions are strong enough to invalidate such a treatment of either or both phases has by no means been ruled out. However, it is known that extremely crude models of other assemblies of 'fermions', e.g. atomic nuclei or electrons in metals, give worth-while results, so *this* crude treatment seems of interest also.

§ 5. CONCLUSIONS

(a) The assumptions that He_3 can be treated as a 'van der Waals-Fermi' gas seem capable of correlating all that is at present known about the equilibrium properties of this substance, including the melting curve. The treatment will not be invalidated should existing indications of a minimum in the melting curve be confirmed.

(b) The assumption that spins are oriented at random in both liquid and solid at helium temperatures seems not quite as capable as (a) of accounting for the facts as they are at present known.

What is now known about the vapour pressure and specific heat of the liquid is difficult to reconcile with assumption (b), but the magnetic data are easier to interpret on that basis.

A tentative explanation of the magnetic data on the basis of assumption (a) is available. One can only await the extension of the magnetic work to lower temperatures.

ACKNOWLEDGMENTS

This work was mainly carried out during my stay at Yale during part of the academic year 1952/3. I wish to thank the Sterling Chemistry Laboratory for hospitality, and the United States Congress and King's College, Cambridge, for research grants. I also wish to thank Drs. Abraham, Weinstock and Osborne

for the interesting discussions that started this investigation, and for telling me their new results before publication. I also wish to thank Drs. F. London and W. M. Fairbank for helpful discussions.

REFERENCES

- BUCKINGHAM, R. H., and TEMPERLEY, H. N. V., 1950, *Phys. Rev.*, **78**, 482.
 CHEN, T. C., and LONDON, F., 1953, *Phys. Rev.*, **89**, 1038.
 DOMB, C., 1953, *Report on Paris Conference on Phase Changes*, p. 338.
 FAIRBANK, W. M., ARD, W. B., DEHMELT, H. G., GORDY, W., and WILLIAMS, S. R., 1953, *Phys. Rev.*, **92**, 208.
 GRILLY, E. R., HAMMEL, E. F., and SYDORIAK, S. G., 1949, *Phys. Rev.*, **75**, 303, 1103.
 LIFSHITZ, E. M., 1951, *Jour. Exp. Theor. Phys.*, U.S.S.R., **21**, 659.
 LONDON, F., 1936, *Proc. Roy. Soc. A*, **153**, 576.
 POMERANCHUK, R., 1950, *Jour. Exp. Theor. Phys.*, U.S.S.R., **20**, 919.
 SINGWI, K. S., 1952, *Phys. Rev.*, **87**, 540.
 SYDORIAK, S. G., and ROBERTS, K. R., 1953, *Low Temperature Conference at Rice Institute, Texas*.
 DE VRIES, G., and DAUNT, J. G., 1954, *Phys. Rev.*, **93**, 631.
 WEINSTOCK, B., ABRAHAM, B. M., and OSBORNE, D. W., 1950, *Phys. Rev.*, **80**, 366; 1952, *Ibid.*, **85**, 158; 1953 a, *Ibid.*, **89**, 787; 1953 b, *Low Temperature Conference at Rice Institute, Texas*.
 WIGNER, E., and SEITZ, F., 1933, *Phys. Rev.*, **43**, 804.

APPENDIX

THE 'TWO-ATOM' DISTRIBUTION FUNCTION FOR A PERFECT FERMI GAS

The following result, showing that, at very low temperatures, the Fermi gas would approach a structure very similar to that of a classical *liquid* does not seem to have been explicitly noted before. We make the one-dimensional calculation explicitly, but it is readily extended to three dimensions without introducing any new physical features, and could be extended to any Fermi assembly described by 'one-particle' wave functions.

Consider $2N+1$ atoms in a *ring* of length L . For simplicity we only allow each level to be occupied once, that is we neglect spin effects. The elementary wave functions are $\frac{\sin}{\cos}(2r\pi x/L)$, (r integral), so that the ground-state wave function for the whole assembly is

$$\Delta = \begin{vmatrix} \sin(2\pi x_1/L), & \sin(4\pi x_1/L), & \sin(6\pi x_1/L) \dots & \cos(2\pi x_1/L) \dots \\ \sin(2\pi x_2/L), & \sin(4\pi x_2/L), & \dots & \dots & \cos(2\pi x_2/L) \dots \\ \sin(2\pi x_3/L), & \sin(4\pi x_3/L), & \dots & \dots & \dots & \dots \\ \dots & \dots & \dots & \dots & \dots & \dots \end{vmatrix} \dots \quad (A1)$$

We expand this determinant from the first row, square, and then integrate with respect to x_1 from 0 to L . The cross terms contribute nothing because of the orthogonality, and we have

$$\frac{2}{L} \int_0^L \Delta^2 dx_1 = \begin{vmatrix} \sin(4\pi x_2/L), & \sin(6\pi x_2/L) \dots \\ \sin(4\pi x_3/L), & \dots & \dots \\ \dots & \dots & \dots \end{vmatrix}^2 + \begin{vmatrix} \sin(2\pi x_2/L), & \sin(6\pi x_2/L) \dots \\ \sin(2\pi x_3/L), & \sin(6\pi x_3/L) \dots \\ \dots & \dots & \dots \end{vmatrix}^2 + \dots \dots \dots (A2)$$

Further integrations can be carried out on the squared determinants in (A 2) by the same process. We repeat over the coordinates of all except two particles (p and q , say). We find

$$\int_0^L \dots \int \Delta^2 dx_1 \dots \propto \sum_{s=0}^N \sum_{t=0}^N \left| \frac{\sin(2s\pi x_p/L)}{\sin(2t\pi x_p/L)}, \frac{\sin(2s\pi x_q/L)}{\sin(2t\pi x_q/L)} \right|^2 + \dots + \dots \quad \dots (A 3)$$

In forming the wave function (A 1) we need $2N+1$ different elementary wave functions corresponding to the smallest possible total energy. These are obtained by letting r run from 0 to N for the cosine functions, and from 1 to N for the sine functions. In passing from (A 1) to (A 2) we shall have one minor determinant corresponding to each of these $2N+1$ functions, each of which gives rise to $2N$ further minors when integrated with respect to x_s , and in (A 3) we have $\binom{2N+1}{2}$ different types of term corresponding to all possible ways of selecting two states out of $2N+1$, each term being repeated $(2N-1)!$ times. Expression (A 3) is, by definition, proportional to the probability that two particles will be simultaneously found near the points x_p, x_q , after averaging over all possible locations of the remaining particles. This is identical with the two-particle distribution function often used to describe liquid structure. The summations in (A 3) are understood to run over both sine and cosine types of function. No harm is done by letting $s=t$ because such determinants vanish. Performing these summations we find

$$g(x_p, x_q) \propto 2(N+1)^2 - \frac{1}{2} \left\{ \frac{\sin[(2N+1)\pi(x_p - x_q)/L]}{\sin[\pi(x_p - x_q)/L]} + 1 \right\}^2 \quad \dots (A 4)$$

which is an 'upside down' version of the function describing the intensity of light diffracted by a slit, intensity maxima in the diffraction pattern corresponding to minima in the distribution function, and zeroes in the diffraction pattern to cusp-like maxima in the distribution function. At finite temperatures the cusps will 'round off', and we have a function vanishing for $x_{pq}=0$ and, for x_{pq} large oscillating with diminishing amplitude and period $L/(2N+1)$ about a constant value, thus reproducing qualitatively all the properties of the distribution function of a classical liquid.

Result (A 4) depends only on the interparticle distance x_{pq} and similar results hold in two and three dimensions, as long as we use periodic boundary conditions. The results for 'particles in a box' are much more complicated because the wave functions have to vanish on the walls, and the simple physical interpretation that can be given to (A 4) is not nearly so apparent.

Note added in proof. The three-dimensional version of (A 4) is given by Wigner and Seitz (1933). $g(r)$ still oscillates with r , but with a relatively small amplitude.

Calculations of the First Ferromagnetic Anisotropy Coefficient, Gyromagnetic Ratio and Spectroscopic Splitting Factor for Nickel

By G. C. FLETCHER

Department of Mathematics, University College of the South West, Exeter

MS. received 28th August 1953, and in amended form 20th January 1954

Abstract. Calculations are made of the first anisotropy coefficient K_1 and of the spectroscopic splitting factor g for nickel, based on the collective electron theory of the corresponding effects due to Brooks and the calculations of the author of the $N(E)$ curve for the 3d electrons in nickel. Brooks' theory is reviewed, the underlying assumptions and approximations examined, some minor errors are corrected and it is extended to provide a formula for the gyromagnetic ratio g' . The value of $-5 \times 10^7 \text{ erg cm}^{-3}$ obtained for K_1 is considerably larger than the best available experimental value of $-8 \times 10^5 \text{ ergs cm}^{-3}$ for nickel at 0°K and Brooks' estimate of $-8 \times 10^5 \text{ erg cm}^{-3}$. The values of 2.14 and 1.84 are obtained for g and g' respectively as compared with experimental values of 2.19–2.42 and 1.93. Possible reasons for the discrepancies are discussed. Finally Brooks' theory is formally extended to remove one of the major approximations.

§ 1. INTRODUCTION

THE problem of ferromagnetic anisotropy has been treated theoretically by a number of authors, the early work being critically summarized by Van Vleck (1937). The experimental results, showing that ferromagnetic crystals are generally magnetized more easily along certain crystal directions than others, can be interpreted formally by assuming that the free energy per unit volume of a cubic crystal has the form

$$F = F_0 + K_1(\alpha_1^2\alpha_2^2 + \alpha_2^2\alpha_3^2 + \alpha_3^2\alpha_1^2) + K_2\alpha_1^2\alpha_2^2\alpha_3^2, \quad \dots\dots(1)$$

where $(\alpha_1, \alpha_2, \alpha_3)$ are the direction cosines of the direction of domain magnetization relative to the crystal axes and K_1, K_2 are termed the first and second anisotropy coefficients respectively. To explain their experimental values some mechanism must be found for coupling the atomic spins in a metal to the crystal axes. Bloch and Gentile (1931) first suggested that this might be provided by spin-orbit interaction together with the coupling of the electronic orbits to the crystal by the crystal field. The only treatment indicating clearly how spin orbit interaction can provide the requisite coupling and lead to anisotropy coefficients of the correct sign and probably the right order of magnitude is that of Brooks (1940). Briefly the crystal field in a ferromagnetic is sufficiently strong to maintain a definite orientation of the orbital momenta of the d electrons, which are mainly responsible for ferromagnetism, relative to the crystal axes even in the presence of an external magnetic field. Due to spin-orbit interaction the electron spins are also affected slightly by the crystal field so that the energy of the electrons in a magnetic field is not quite independent of spin orientation and anisotropy results. Quantitatively the anisotropy would be far too large if the degeneracy of the d electrons in the free atom were not largely removed in the metal by the crystal field.

Unfortunately Brooks was unable to carry his theory, which is based on the collective electron model, through to a satisfactory quantitative conclusion owing to lack of available data on the energy distribution of d electrons in the ferromagnetic metals. Since such data have recently been provided by the author (Fletcher 1952) in the case of nickel, it was decided to evaluate K_1 for this metal, utilizing Brooks' theory, thereby providing also a further test of the calculations involved in the author's previous work. The main assumptions in the theory are as follows:

(i) Spin-orbit interaction can be treated as a small perturbation compared with the effect of the crystal field and exchange forces.

(ii) Matrix elements of this interaction between Bloch functions are approximately the same as those between the corresponding free atom wave functions.

(iii) Interatomic exchange effects can be treated by the usual approximation of an additional energy $\pm \delta$ per electron according to the direction of the electron spin, i.e. non-diagonal elements of the relevant operator are ignored and the wave functions are assumed unaltered.

(iv) For the anisotropic effect for the whole crystal summation can be carried out over the occupied states of the Fermi distribution without spin-orbit interaction, i.e. the latter is assumed not to alter this distribution of states.

(v) The two atomic d functions

$$\phi_4 = (x^2 - y^2)f(r)/2r^2 \quad \text{and} \quad \phi_5 = (3z^2 - r^2)f(r)/2\sqrt{3}r^2$$

can be ignored and the calculation based on the Γ_5 band derived from the other three. This assumption is not fundamental to the theory as is demonstrated in § 9. In carrying out the calculation these assumptions have been critically surveyed. Suggestions of possible explanations of the large temperature variation of K_1 are made in § 10 but no attempt is made to consider K_1 for iron, the second anisotropy coefficient K_2 or the variation of K_1 in alloys, points considered by Brooks.

Brooks also considers the related effect of ferromagnetic resonance measured by the spectroscopic factor g . This and the gyromagnetic ratio g' (which Brooks purports to calculate rather than g) depend on the magnetic moment and total angular momentum of the metal in a magnetic field. The spins of the electrons concerned are almost completely free to reorient themselves in such a field whereas their orbital momenta are almost unable to do so owing to the crystal field maintaining their orientation. If the spins were quite free and the orbital momenta completely fixed, g and g' would both have the value 2. Owing to spin-orbit interaction, however, the reorientation of the spins reorients the orbital momenta slightly also and, conversely, the reorientation of the spins is not quite free. As is seen in § 6, this makes g slightly more than 2 and g' slightly less, as is found experimentally. As for K_1 , these effects would be much too large if the crystal field did not largely remove the degeneracy of the free atom d functions.

For the same reasons as above it was decided to calculate g for nickel, utilizing Brooks' theory, and it was also possible to provide a theory of g' on the collective electron model and to evaluate g' for nickel. A similar assumption to (iv) above is made in both cases, i.e. that to calculate g , g' for the whole crystal summation can be carried out over the states occupied when there is zero magnetic field. This very drastic assumption is considered in §§ 6 and 8.

In order to indicate clearly the approximations of the methods used and for comparison purposes between the original theory and its extension in § 9, it has

been necessary to reproduce, with some modifications and corrections, Brooks' derivation of the secular equation (8) and expressions (9), (10) and (22).

§ 2. THE HAMILTONIAN OF THE PROBLEM

The Hamiltonian involved in the problem will first be considered in order to clarify the method of procedure. For a single electron in the metal subject to an external magnetic field \mathfrak{H} , vector potential \mathbf{A} , it may be written in the form

$$H = -(\hbar^2/2m)\nabla^2 + U(r) + V(\mathbf{r}) - U(r) + \mathcal{E} + O - (ie\hbar/mc)\nabla \cdot \mathbf{A} \\ + (e/mc)\mathfrak{H} \cdot \mathbf{S} + (e^2/2mc^2)\mathbf{A}^2 \quad \dots\dots(2)$$

where U is the potential for the free atom, V is the electrostatic potential in the solid metal, \mathcal{E} , O are operators representing exchange and spin-orbit interaction respectively and \mathbf{S} is the spin of the electron. The effects of $V-U$, \mathcal{E} and O are considered successively as perturbations of the free atomic energy levels, and this procedure will be discussed briefly. Consideration of the remaining terms in (2) will be deferred to § 6.

(i) The atomic functions which form the starting point of the present calculations were obtained by the Hartree self-consistent field method (Hartree and Hartree 1936, see Fletcher 1952). In this spin-orbit interaction was neglected but the effect of intra-atomic exchange was included. The corresponding states are completely degenerate and are characterized by n , l , m_l , s and m_s .

(ii) The first perturbation considered, $V-U$, represents the effect of the crystal field, for which the approximations have already been given in detail (Fletcher 1952). The corresponding states are largely non-degenerate and are characterized by n , l , \mathbf{k} , s and m_s , being still degenerate in m_s .

(iii) The second perturbation \mathcal{E} represents interatomic exchange only, if it is assumed that (ii) has not affected the intra-atomic exchange considered in (i). This is valid provided the interatomic forces are insufficient to destroy the quantization of the spin of each atom (Van Vleck 1932, Ch. XII), as has been assumed in (ii), where the calculation was made independent of spin direction. The interatomic forces can only affect the spin of each atom through the spin-orbit coupling, and it is seen in § 7 that the effect is very small. \mathcal{E} is therefore assumed to represent interatomic exchange only, and for this the usual approximation has been made here of assuming that these exchange forces in the metal may be formally represented by an additional energy contribution per electron of $\pm\delta = \pm k\theta'\zeta$ according as the electron's spin is antiparallel or parallel to the total spin of the crystal (Heisenberg 1928, Stoner 1938), which itself will be antiparallel to the field \mathfrak{H} . Here ζ is the relative magnetization I/I_0 (I_0 =saturation intensity) and θ' a parameter of dimensions temperature, giving a measure of the exchange energy of the d electrons in the metal.

The corresponding states will be unaffected in n , l , s and \mathbf{k} , but now s will be quantized along the field direction.

(iv) The third perturbation O represents the spin-orbit interaction. Dirac's relativistic theory of an electron in a central field, potential U , leads, subject to one approximation which has little effect on d states, to a term

$$(2m^2c^2r)^{-1}(\partial U/\partial r)\mathbf{S} \cdot \mathbf{L} = \xi(r)\mathbf{S} \cdot \mathbf{L}$$

in the Hamiltonian, where \mathbf{L} , \mathbf{S} are the orbital and spin angular momentum operators for the electron and obviously $\xi(r) \sim r^{-3}$. Condon and Shortley (1936,

p. 120 ff.) show that an additional term of the form $\sum_s \pi(\mathbf{r}, \mathbf{s}) \mathbf{S} \cdot \mathbf{L}_s$, summed over all other electrons of the free atom, should be included. It has the effect of reducing the nuclear field U in the original term, being unimportant except for s states, so that for d electrons an operator $\xi(r) \mathbf{S} \cdot \mathbf{L}$, where $\xi(r)$ falls off rather more rapidly than r^{-3} , should be accurate enough. In the metal the spin of an electron on a given atom will also interact with the orbital magnetic fields of electrons on other atoms. Near any atom the field due to a complete shell of electrons on another atom will be zero; the field due to incomplete shells on other atoms will also be small owing to their symmetrical arrangement about the atom considered. Since d electrons spend most of their time in orbits around the atoms in a metal, it therefore seems a valid approximation to neglect any such interaction in their case; the point is discussed further in §8. Using Bloch-type wave functions, however, it is necessary to allow for the fact that the electron may be located on any atom at a given instant by forming the operator (Brooks 1940, equation 13)

$$O = \sum_{\mathbf{l}} \xi(|\mathbf{r} - \mathbf{al}|) \mathbf{S} \cdot \mathbf{L}(\mathbf{r} - \mathbf{al}), \quad \dots\dots(3)$$

where $\mathbf{L}(\mathbf{r} - \mathbf{al})$ is the angular momentum operator about the atom at \mathbf{al} and operates only on that part of a wave function representing motion about that atom.

§3. SPIN-ORBIT SECULAR EQUATION

The first step in Brooks' theory is to obtain the matrix elements of O in the system of representation in which the band + exchange energy is diagonal, i.e. with respect to the crystal wave functions $\psi_{\tau}(\mathbf{k}; \mathbf{r})$ with spin quantized along the field direction. Here

$$\psi_{\tau}(\mathbf{k}; \mathbf{r}) = \sum_n a_{\tau n}(\mathbf{k}) \phi_{nk} = N^{-1/2} \sum_n a_{\tau n}(\mathbf{k}) \sum_{\mathbf{l}} \exp(i\mathbf{al} \cdot \mathbf{k}) \phi_n(\mathbf{r} - \mathbf{al}) \quad \dots\dots(4)$$

(cf. Ψ_n in Fletcher 1952), where $\phi_1, \phi_2, \dots, \phi_5$ are the atomic d functions. O has the period of the lattice and is hence rigorously diagonal in \mathbf{k} (Mott and Jones 1936, p. 59); also it is easily shown that

$$(n\mathbf{k}m_s | O | n'\mathbf{k}m_s') = \sum_{\mathbf{l}} \exp(-i\mathbf{al} \cdot \mathbf{k}) \int \phi_n^*(\mathbf{r} - \mathbf{al}) \xi(r) \mathbf{S} \cdot \mathbf{L} \phi_n(\mathbf{r}) d\tau. \quad \dots\dots(5)$$

Without the factor $\xi(r)$ the integrals for $\mathbf{l} \neq 0$ would be non-orthogonality integrals such as have already been neglected in considering the perturbation $V - U$, i.e. in the energy band calculation of Fletcher (1952). Since $\xi(r) \sim r^{-3}$ it therefore seems justifiable to neglect all integrals here except that for $\mathbf{l} = 0$, i.e. the matrix elements of O with respect to the Bloch functions ϕ_{nk} are assumed to be the same as between the corresponding atomic functions ϕ_n . Thus

$$(n\mathbf{k}m_s | O | n'\mathbf{k}m_s') \simeq \int \phi_n^*(\mathbf{r}) \xi(r) \mathbf{S} \cdot \mathbf{L} \phi_n(\mathbf{r}) d\tau = A(nm_s | \mathbf{S} \cdot \mathbf{L} | n'm_s') \quad \dots\dots(6)$$

where A is the spin-orbit interaction parameter for an individual electron in the free atom, corresponding to a_l in Goudsmit's notation (Goudsmit 1928).

The derivation of the requisite secular equation then proceeds as follows: (a) The matrix elements $(n\mathbf{k}m_s | O | n'\mathbf{k}m_s')$ with spin quantized along the z axis are obtained in terms of A by (6). (b) The elements $(\tau\mathbf{k}m_s | O | \tau'\mathbf{k}m_s')$ with respect to the crystal wave functions $\psi_{\tau}(\mathbf{k}; \mathbf{r})$ are deduced in terms of the coefficients $a_{\tau n}$. (c) Similar elements, but with respect to wave functions $\psi_{\tau}(\mathbf{k}; \mathbf{r})$ having their spin

quantized in the direction $(\alpha_1, \alpha_2, \alpha_3)$ or (θ, ϕ) relative to the crystal axes, are obtained by a spinor transformation. (d) With Brooks' assumption that only the three wave functions ϕ_1, ϕ_2 and ϕ_3 need be considered and ϕ_4, ϕ_5 ignored, the resulting expressions can be greatly simplified by defining a new set of rectangular Cartesian axes

$$\mathbf{i}' = (a_{11}, a_{12}, a_{13}); \quad \mathbf{j}' = (a_{21}, a_{22}, a_{23}); \quad \mathbf{k}' = (a_{31}, a_{32}, a_{33}) \quad \dots\dots(7)$$

for each wave vector \mathbf{k} . If the direction of quantization of spin relative to these axes is $(\alpha'_1, \alpha'_2, \alpha'_3)$ or (θ', ϕ') and the directions $(\cos \theta \cos \phi, \cos \theta \sin \phi, -\sin \theta)$ and $(-\sin \phi, \cos \phi, 0)$ similarly become $(\beta'_1, \beta'_2, \beta'_3)$ and $(\gamma'_1, \gamma'_2, \gamma'_3)$ respectively, the secular equation for the energy, including the effect of the crystal field, exchange and spin-orbit interactions, appears finally in the form

$$\begin{vmatrix} E_1 + \delta - E & iA\alpha'_3 & -iA\alpha'_2 & 0 & A(-\gamma'_3 - i\beta'_3) & A(\gamma'_2 + i\beta'_2) \\ -iA\alpha'_3 & E_2 + \delta - E & iA\alpha'_1 & A(\gamma'_3 + i\beta'_3) & 0 & A(-\gamma'_1 - i\beta'_1) \\ iA\alpha'_2 & -iA\alpha'_1 & E_3 + \delta - E & A(-\gamma'_2 - i\beta'_2) & A(\gamma'_1 + i\beta'_1) & 0 \\ 0 & A(\gamma'_3 - i\beta'_3) & A(-\gamma'_2 + i\beta'_2) & E_1 - \delta - E & -iA\alpha'_3 & iA\alpha'_2 \\ A(-\gamma'_3 + i\beta'_3) & 0 & A(\gamma'_1 - i\beta'_1) & iA\alpha'_3 & E_2 - \delta - E & -iA\alpha'_1 \\ A(\gamma'_2 - i\beta'_2) & A(-\gamma'_1 + i\beta'_1) & 0 & -iA\alpha'_2 & iA\alpha'_1 & E_3 - \delta - E \end{vmatrix} = 0. \quad \dots\dots(8)$$

Here E_1, E_2, E_3 are the energies obtained from the band calculation, i.e. including the effect of the crystal field but not exchange or spin-orbit interaction. They and the matrix $\{a_{\tau n}\}$ are functions of the wave vector \mathbf{k} and hence all elements of (8) are also. In carrying out the simplification in (d) Brooks implies that $\cos \theta \cos \phi$ becomes $\cos \theta' \cos \phi'$, $\cos \theta \sin \phi$ becomes $\cos \theta' \sin \phi'$ and so on, but this will not in general be true. Also the phase factors $\exp(\pm i\phi)$ in his formulae (17) should be $\exp(\pm i\phi')$, but in any case they may be dropped as they have no effect on the physical results obtained. The differences in sign between (8) and Brooks' secular equation appear to be caused by his definition of $(\tau \mathbf{k}_s | \mathbf{O} | \tau' \mathbf{k}_s)$ as

$$\int \psi_{\tau}(\mathbf{m}_s') \mathbf{O} \psi_{\tau'}(\mathbf{m}_s) d\tau.$$

Since for most wave vectors the off-diagonal elements of (8) are small compared with the differences between diagonal ones, the solutions of the secular problem may be expanded in powers of the spin-orbit parameter A by successive orders of perturbation theory. For certain values of \mathbf{k} , however, two or more of the energies $E_{\tau} \pm \delta$ are degenerate or nearly so; such cases will be considered later.

§ 4. DERIVATION OF ANISOTROPY COEFFICIENT K_1

Using the collective electron model, only information about an 'average atom' is available, e.g. one with 9.46 electrons and 0.54 hole in the d band in the case of nickel. For a physical quantity referring to the whole crystal or to unit volume the contribution from an average atom is simply multiplied by the number of atoms in the crystal or per unit volume respectively. An equation such as (8) will give the contributions from individual electronic states, and these must be summed over all occupied states in the Fermi distribution to obtain the contribution from an average atom. With cubic symmetry there are 48 wave vectors \mathbf{k} with the same set of band energies E_1, E_2, E_3 . Any set of 48 states with such equivalent wave vectors and the same energy E_{τ} will be termed equivalent states. Then it is easily

shown that the average value per state for such a set of a term such as $\alpha_i'^2 f(E_1, E_2, E_3, \delta)$ is $\frac{1}{3} f(E_1, E_2, E_3, \delta)$ and that the average values of terms involving $\alpha_i', \alpha_i' \alpha_j', \alpha_i'^3, \alpha_i'^2 \alpha_j'$ or $\alpha_1' \alpha_2' \alpha_3'$ are zero.

For this reason, on applying perturbation theory to the secular equation (8), the fourth-order correction to the energy of an average atom is the first to exhibit anisotropy. If the fourth-order correction to the band energy level $E_3(\mathbf{k}) + \delta$ is considered, the average correction per state for the corresponding set of equivalent states then proves to be

$$\frac{1}{3} A^4 \sum_{\mu < \nu} A_{\mu\nu} (1 - 5J_{\mu\nu}) (\alpha_1'^2 \alpha_2'^2 + \alpha_2'^2 \alpha_3'^2 + \alpha_1'^2 \alpha_3'^2) \dots\dots (9)$$

where

$$\left. \begin{aligned} A_{12} &= \left\{ \frac{1}{\epsilon_1'^2} - \frac{1}{\epsilon_2'^2} - \frac{1}{(\epsilon_1 + 2\delta)^2} + \frac{1}{(\epsilon_2 + 2\delta)^2} \right\} \left\{ \frac{1}{\epsilon_1} - \frac{1}{\epsilon_2} - \frac{1}{\epsilon_1 + 2\delta} + \frac{1}{\epsilon_2 + 2\delta} \right\} \\ &\quad + \frac{1}{2\delta} \left\{ \frac{1}{\epsilon_1} - \frac{1}{\epsilon_2} - \frac{1}{\epsilon_1 + 2\delta} + \frac{1}{\epsilon_2 + 2\delta} \right\}^2 \\ A_{23} &= \left\{ \frac{1}{\epsilon_2} - \frac{1}{\epsilon_2 + 2\delta} + \frac{1}{2\delta} + \frac{1}{\epsilon_1} + \frac{1}{\epsilon_1 + 2\delta} \right\} \left\{ \frac{1}{\epsilon_1} - \frac{1}{\epsilon_1 + 2\delta} \right\}^2 \\ A_{13} &= \left\{ \frac{1}{\epsilon_1} - \frac{1}{\epsilon_1 + 2\delta} + \frac{1}{2\delta} + \frac{1}{\epsilon_2} + \frac{1}{\epsilon_2 + 2\delta} \right\} \left\{ \frac{1}{\epsilon_2} - \frac{1}{\epsilon_2 + 2\delta} \right\}^2 \end{aligned} \right\} \dots\dots (10)$$

$$\epsilon_1 = E_3 - E_1; \quad \epsilon_2 = E_3 - E_2; \quad J_{\mu\nu} = \sum_j a_{\mu j}^2 a_{\nu j}^2$$

Expression (9) must now be summed over all occupied states of the Fermi distribution to obtain the first anisotropic energy term for an average atom. But, if all states were occupied, this would involve for any given \mathbf{k} all six states $E_\tau \pm \delta$, and by the diagonal sum rule the sum of their energy corrections to any order is zero. Hence

$$\Sigma (\text{occupied states}) = -\Sigma (\text{unoccupied states}).$$

Hence the first anisotropy coefficient for a cubic metal is finally given by

$$K_1 = -\frac{n}{3} A^4 \sum_u \sum_{\mu < \nu} A_{\mu\nu} (1 - 5J_{\mu\nu}) \text{ erg cm}^{-3} \dots\dots (11)$$

where n is the number of atoms per cubic centimetre, A and the ϵ_τ are expressed in ergs, and Σ_u denotes summation over the unoccupied states of the Fermi distribution.

§5. EVALUATION OF K_1 FOR NICKEL

To obtain a numerical value for nickel the calculations of Fletcher and Wohlfarth (1951) and Fletcher (1952) of the 3d energy band for nickel were utilized. Since (8) has been obtained by ignoring the atomic wave functions ϕ_4 and ϕ_5 , it appeared most consistent to consider all the holes in the d band as occurring in the Γ_5 band obtained by a band calculation using ϕ_1, ϕ_2, ϕ_3 only, i.e. one obtained from the solutions of the cubic secular equation of Fletcher and Wohlfarth (1951). Argyres and Kittle (1935) have recently pointed out that the usual assumption of 0.6 holes per atom in the d band for nickel is open to criticism since this value has been deduced from saturation magnetization data, assuming the effects to be entirely due to electron spin and unaffected by the orbital motion of the electrons. Due to spin-orbit interaction this is not so, as is demonstrated by the deviation of g, g' from the value 2 (see §6). On the theory of ferromagnetic resonance due to Kittel (1949a) and Van Vleck (1950) the value 0.6 should be multiplied by $2/g$, and

Argyres and Kittel obtain 0.54 effective magnetic electrons per atom, corresponding to $g = 2.22$, for nickel, and this value has been used here. K_1 for nickel was therefore calculated by summation over the 0.54 highest energy states in the Γ_5 band. To avoid numerical integration in three dimensions it was considered sufficiently accurate, in view of other approximations, to adopt a summation procedure over the wave vectors, for which E_1 , E_2 , E_3 were already known, instead.

In so doing it was found that for certain wave vectors the energy levels $E_\tau \pm \delta$ were degenerate ($\epsilon_1 = 0$ say) or nearly so ($\epsilon_1 + 2\delta < A$). In such cases formulae (10) must be replaced by others deduced by degenerate perturbation theory (Condon and Shortley 1936). In the first case, however, it may be noted that, if $\epsilon_1 = 0$, the two states corresponding to the energies E_1 and E_3 will either both be occupied or both unoccupied and may therefore be considered together. Also such cases only occur on the (100) axis of the Brillouin zone, for which $J_{\mu\nu} = 0$. It is then found that the total contribution to K_1 from both states $E_1 + \delta$, $E_3 + \delta$ is the same, whether non-degenerate or degenerate theory is used. This justifies the use of (10) in cases where ϵ_1 is small, the contributions from the two states being separately large but of opposite sign.

In order finally to evaluate K_1 for nickel it was necessary to estimate values of the exchange energy δ and the spin-orbit parameter A . For consistency with the remainder of the work it seemed best to estimate δ from the author's Γ_5 band. A calculation of the type made by Stoner (1938) for a parabolic band and Wohlfarth (1951) for a rectangular band was considered impracticable at present. On plotting q against E for the Γ_5 band, where q is the number of states between E and the top of the band, the graph proved to be very nearly a straight line. It would be exactly so for a rectangular band and therefore Wohlfarth's formula $(E_{0P}/k\theta') = 1 - \exp(-E_{0P}/k\theta')$ for such a band was used, where θ is the Curie temperature and E_{0P} the energy difference between the top of the band and the paramagnetic Fermi limit (0.27 holes of each spin). With $\theta = 631^\circ\text{K}$ and assuming $\zeta = 1$, this gave

$$\delta = k\theta'\zeta = 0.215 \text{ ev}, \quad \dots\dots(12)$$

which value was therefore used. It may be remarked that this is much larger than Wohlfarth's estimate of 0.1 ev. In fact a value almost identical with this is obtained from the most accurate band calculated by the author (Fletcher 1952), involving all five atomic d functions, but use of this value would neither be consistent with the remainder of the present calculation nor with the assumption that $\zeta = 1$, since the unfilled portion of the Γ_5 band in the ferromagnetic state is of width 0.4 ev $\gg 2 \times 0.1$ ev, i.e. there would be occupied states of one spin of considerably higher energy than unoccupied ones of the other.

Goudsmit (1928), in a consideration of the effect of spin-orbit interaction on atomic spectra, outlined a method of estimating the parameter A for particular electrons of a given atom from spectroscopic data. Using these methods and the latest available data (Moore 1952), values of A were estimated for a 3d electron in nickel in the configurations $3d^7 4s^3$, $3d^8 4s^2$ and $3d^9 4s$, and by extrapolation a value of 590 cm^{-1} was deduced for the 'configuration' $3d^9.46 4s^{0.54}$, which value was used. By so doing some allowance was made for the location of the atom in the metal since for a free nickel atom the normal configuration is $3d^8 4s^2$. Further justification for this procedure is afforded by the fact that addition of 4s electrons to a given configuration $3d^n$ scarcely alters the relevant value of A for the 3d electrons at all, so that the completely different distribution of the 4s electrons in the metal is

unlikely to have any noticeable effect. Finally, as already stated, the 3d electrons spend most of their time in orbits round the atoms in the metal, so that the above value of A should be a good approximation to that relevant to the present problem.

Using the above values for δ and A and $n = 9.25 \times 10^{22}$ atoms cm^{-3} , the value obtained for K_1 for nickel at 0°K was

$$K_1 = -5 \times 10^7 \text{ erg cm}^{-3}. \quad \dots\dots(13)$$

§ 6. THEORY OF g AND g' ON THE COLLECTIVE ELECTRON MODEL

Consider a specimen of material, for which the Hamiltonian H_0 and eigenfunctions ψ_n are known, placed in a magnetic field \mathfrak{H} , vector potential \mathbf{A} . The Hamiltonian may be written

$$H = H_0 + (e/2mc)\mathfrak{H} \cdot (\mathbf{L} + 2\mathbf{S}) + (e^2/2mc^2)\mathbf{A}^2 \quad \dots\dots(14)$$

where \mathbf{L} , \mathbf{S} are the total orbital and spin momenta of the specimen. Since no effect of $O(\mathfrak{H}^2)$ is observed in normal fields, the last term may be ignored, and for the same reason the changes in energy levels due to the field will be given by the diagonal matrix elements $(e\mathfrak{H}/2mc)(n|L_H + 2S_H|n)$, where the suffix H refers to the field direction. Similarly the changes in total angular momentum in this direction are given by the elements $(n|L_H + S_H|n) = (n|J_H|n)$.

Hence, if ΔM_H , ΔJ_H are the changes in magnetic moment and angular momentum of a specimen, initially in the state ψ_n , observed in a gyromagnetic experiment, then the gyromagnetic ratio

$$g' = (2mc/e)(\Delta M_H/\Delta J_H) = (n|L_H + 2S_H|n)/(n|L_H + S_H|n). \quad \dots\dots(15)$$

Obviously $g' < 2$ if there is a positive contribution from \mathbf{L} .

If a small alternating field \mathbf{h} is applied to a ferromagnetic specimen subject to a large constant field \mathfrak{H} perpendicular to \mathbf{h} , it is found that for given \mathfrak{H} there is a critical value of the frequency ν of \mathbf{h} , for which the energy adsorption by the material exhibits a large peak. The spectroscopic splitting factor g is defined by $\nu = g(e/2mc)\mathfrak{H}'$, where \mathfrak{H}' is the effective field in the material corresponding to \mathfrak{H} . (Kittel 1949) describes the effect as being due to the quantum of energy $\hbar\nu$ becoming equal to the separation between adjacent eigenvalues of the energy of the specimen in the field \mathfrak{H} . Van Vleck (1950) puts this another way when he says that such experiments determine g in the formula $E = E_0 + \mathcal{S}_H g(e/2mc)\mathfrak{H}$ for the Zeeman energy states, \mathcal{S}_H being the total spin of the specimen. Hence one obtains

$$g = (n|L_H + 2S_H|n)/\mathcal{S}_H \quad \dots\dots(16)$$

and $g > 2$ if there is a positive contribution from \mathbf{L} .

On the collective electron model, as explained in § 4, values of M_H , L_H , S_H for the whole crystal will be simply N times the values for an average atom, if there are N atoms in the crystal. From the one-electron Hamiltonian (2), ignoring the last term for the reasons given above, the first-order contribution to M_H of the average atom, for instance, from an electron in the state Ψ_τ will be $(2/\mathfrak{H})(\tau|-i\hbar\nabla \cdot \mathbf{A} + \mathfrak{H} \cdot \mathbf{S}|\tau)$ where Ψ_τ is an eigenfunction of the Hamiltonian

$$H_0 = -(\hbar^2/2m)\nabla^2 + V(\mathbf{r}) + \mathcal{E} + O,$$

i.e. Ψ_τ is obtained by solution of the secular equation (8). Then M_H for the average atom is found by summation over all occupied states of the Fermi distribution.

With regard to this argument it is to be noted that the vector potential \mathbf{A} is linear in the coordinates and cannot therefore be treated as a small perturbation throughout the crystal, i.e. the zero-field energy levels and wave functions given by (8) are so altered by the field that they should not be used to calculate J_H and M_H in the way outlined. Since, however, it is only M_H for the whole crystal which is required, Peierls (1933) has shown that under certain conditions use of the zero-field levels and functions gives a good approximation. Thus the Bloch functions ϕ_{nk} of the original band calculation should be replaced by

$$\phi_{nk}' = N^{-1/2} \sum_l \exp(i\mathbf{a}l \cdot \mathbf{k}) \exp[-(ie/\hbar c)\mathbf{A}_l \cdot \mathbf{r}] \phi_n(\mathbf{r} - \mathbf{a}l) \quad \dots\dots(17)$$

where \mathbf{A}_l is the value of the vector potential at the lattice point $\mathbf{a}l$. It is easily shown that

$$H\phi_{nk}' = (H_0 + H_1')\phi_{nk}' \quad \dots\dots(18)$$

where H_1' now represents a small perturbation but, of course, (17) is no longer a Bloch function. Assuming, however, the conditions given by Peierls (see § 8), the phase factor $\exp[-(ie/\hbar c)\mathbf{A}_l \cdot \mathbf{r}]$ may be dropped and (18) reduces to

$$H\phi_{nk} = (H_0 + H_1')\phi_{nk}$$

which is equivalent to saying that the solutions of the zero-field problem may be used to calculate the quantities required as explained above.

§ 7. CALCULATION OF g AND g' FOR NICKEL

Applying perturbation theory to equation (8), the first-order approximation to the wave function arising from the energy level $E_3 + \delta$, for instance, is

$$\Psi_{3+} = \psi_{3+} - \frac{iA\alpha_2'}{\epsilon_1} \psi_{1+} + \frac{iA\alpha_1'}{\epsilon_2} \psi_{2+} - \frac{A(\gamma_2' - i\beta_2')}{\epsilon_1 + 2\delta} \psi_{1-} + \frac{A(\gamma_1' - i\beta_1')}{\epsilon_2 + 2\delta} \psi_{2-} \quad \dots(19)$$

where the ψ_r are the wave functions (4) obtained from the band calculation and the suffixes \pm are an obvious spin notation. Taking $(\alpha_1, \alpha_2, \alpha_3)$ as the direction of the field \mathcal{H} , it is easily shown that

$$(3^+ | L_H | 3^+) = 2A\hbar \left(\frac{\alpha_2'^2}{\epsilon_1} + \frac{\alpha_1'^2}{\epsilon_2} \right) + O(A^2) \quad \dots\dots(20)$$

$$(\tau^+ | S_H | \tau^+) = \frac{1}{2}\hbar + O(A^2); \quad (\tau^- | S_H | \tau^-) = -\frac{1}{2}\hbar + O(A^2). \quad \dots\dots(21)$$

In summing over the Fermi distribution it is again simpler first to average these results over equivalent states as before. Also it can again be shown by direct calculation that

$$\Sigma (\text{occupied states}) = -\Sigma (\text{unoccupied states}).$$

Finally it is obvious that for the average atom

$$\mathcal{S}_H = \Sigma(\tau | S_H | \tau) = 0.54(\hbar/2)$$

so that, cancelling the factors N which now occur in (15) and (16),

$$g = 2 + \frac{1}{0.54} \frac{4}{3} A \Sigma_u \left(\frac{1}{\epsilon_1} + \frac{1}{\epsilon_2} \right) + O(A^2) \quad \dots\dots(22)$$

$$g' = \frac{0.54 + \frac{2}{3} A \Sigma_u \left(\frac{1}{\epsilon_1} + \frac{1}{\epsilon_2} \right)}{0.27 + \frac{2}{3} A \Sigma_u \left(\frac{1}{\epsilon_1} + \frac{1}{\epsilon_2} \right)} + O(A^2). \quad \dots\dots(23)$$

In his paper Brooks purports to calculate g' but, by comparison with the above, he actually calculates g . However, he obtains $g < 2$; Van Vleck (1950) considers that this is caused by taking A as positive when summing over the unoccupied states, arguing that the spin-orbit parameter is of opposite sign for a nearly full electron shell as compared with a nearly empty one. However, Brooks stresses that his parameter A is for a single electron and not for a shell, so that it is essentially of the same sign in either case. His error arises simply from a mistake in sign in his formula for ΔE , corresponding to (20) above. Another point is that in his final formula for $g-2$ he obtains a factor $2/3$ whereas it should be $4/3$ (see (22)), so that his final value for $g-2$ should be doubled.

As in the calculation of K_1 , cases of degeneracy in the energy levels $E_\tau \pm \delta$ arise and must be dealt with by degenerate perturbation theory. Again, however, it is found that the total contribution to L_H or S_H for the average atom from two degenerate states $E_1 + \delta$, $E_3 + \delta$ is the same, whether calculated by non-degenerate or degenerate theory. This justifies the use of the non-degenerate formulae in cases where ϵ_1 is small.

Since it was found that the results obtained gave $g-2 \simeq 2-g'$, in disagreement with experiment, it was decided to extend the above theory to include terms of $O(A^2)$. The functions Ψ_τ were therefore calculated to this order, and it is then easily shown that

$$\begin{aligned} (3^+ | L_H | 3^+) &= 2A\hbar \left(\frac{\alpha_2'^2}{\epsilon_1} + \frac{\alpha_1'^2}{\epsilon_2} \right) \\ &\quad + 2A^2\hbar \left(\frac{\alpha_2'^2}{\epsilon_1(\epsilon_2 + 2\delta)} + \frac{\alpha_1'^2}{\epsilon_2(\epsilon_1 + 2\delta)} - \frac{\alpha_3'^2}{(\epsilon_1 + 2\delta)(\epsilon_2 + 2\delta)} \right) \\ (3^+ | S_H | 3^+) &= \frac{1}{2}\hbar - A^2\hbar \left(\frac{1 - \alpha_2'^2}{(\epsilon_1 + 2\delta)^2} + \frac{1 - \alpha_1'^2}{(\epsilon_2 + 2\delta)^2} \right). \end{aligned}$$

Again summation may be carried out over unoccupied states, and the non-degenerate formulae may be used in cases where ϵ_1 is small.

For the actual numerical evaluation of g and g' for nickel the Γ_5 band derived from the calculations of the author was used with the same assumptions and summation procedure as for K_1 . With the same values of δ and A the final results were

$$\text{To } O(A) \quad g = 2.18 \quad g' = 1.85 \quad \dots\dots(24a)$$

$$\text{To } O(A^2) \quad g = 2.14 \quad g' = 1.84 \quad \dots\dots(24b)$$

§ 8. CONSIDERATION OF RESULTS

The best available experimental figure for the first anisotropy coefficient for nickel at 0°K is $-8 \times 10^5 \text{ erg cm}^{-3}$ (Kittel 1949 b), so that the value obtained here is about 50 times too large. Possible reasons for this will be considered later. Brooks obtains a rough estimate for K_1 of $-8 \times 10^5 \text{ erg cm}^{-3}$, assuming that (i) $a_{\tau n} \simeq \delta_{\tau n}$ so that $1 - 5J_{\mu\nu} \simeq 1$, (ii) $A = 630 \text{ cm}^{-1}$, (iii) $\delta = 4000 \text{ cm}^{-1}$, (iv) $\epsilon_1 = \epsilon_2$, an average value for either being 10000 cm^{-1} . Strict comparison with the present value for K_1 is rendered impossible by Brooks' final assumption, which entirely alters the character of expressions (10) for the $A_{\mu\nu}$. It is worth noting, however, that his estimates of δ and the average value of ϵ_τ are based on the energy band for nickel calculated by Slater (1936), which has twice the width of that used here.

His δ is therefore about twice the value (12), which would explain part of the discrepancy in K_1 , but on the other hand 10000 cm^{-1} is rather a low value for the average value of ϵ_r .

The respective experimental values for g and g' for nickel are 2.19–2.42 and 1.93 (Kittel 1949a) so that fair agreement has been obtained here for g but not for g' . Both Kittel (1949) and Van Vleck (1950) have obtained the result $g-2 \sim 2-g'$, admittedly by very approximate methods, whereas this is not confirmed by experiment. If the first-order effect of spin-orbit interaction gives $g=2+a$, then on either treatment $g'=(2+a)/(1+a) \simeq 2-a$ if a is small, as it is in practice. Since the theory used here is the same as that of Kittel, modified to fit the collective electron model, the results were bound to give $g-2 \sim 2-g'$. The second-order effect of spin-orbit interaction is probably considerably larger than Van Vleck expected but, as he pointed out, it acts in the wrong direction, decreasing both g and g' . Brooks made a rough estimate of $g-2$ as A ('mean bandwidth'), using values of 500 and 20000 cm^{-1} for A and the 'mean bandwidth' respectively. Allowing for the mistakes in sign and numerical factor mentioned, this gives the value $g \sim 2.05$, considerably less than the comparable value ($24a$). Apart from the fact that Brooks' estimate is a very rough one, the main reason for the discrepancy is that his 'mean bandwidth' is based on Slater's wider energy band.

The approximations and assumptions made in arriving at the value (13) for K_1 for nickel will now be considered.

(i) The validity of the assumption that the operator \mathcal{E} represents interatomic exchange only depends on the magnitude of the spin-orbit coupling. It is seen from (21) that the effect of spin-orbit interaction on the quantization of spin of an atom is very small and hence the interatomic forces are unlikely to affect the intra-atomic exchange already considered in calculating the free atom wave functions ϕ_n . Thus this assumption regarding \mathcal{E} appears valid.

(ii) For certain wave vectors two band wave functions $\psi_r, \psi_{r'}$ are very similar linear combinations of the atomic functions, e.g. $2^{-1/2}(\phi_1 \pm \phi_2)$, so that the off-diagonal elements of \mathcal{E} would be comparable with the diagonal ones. The effect of neglect of the former will not be large, however, since in such cases $E_r \sim E_{r'} \gg \delta$, but will be comparable with the spin-orbit effect since $\delta \sim A$. These cases are infrequent, however, and contribute little to K_1 (since again $A \ll E_r \sim E_{r'}$), so that the usual diagonal approximation to the exchange energy seems reasonable.

(iii) The neglect of terms of the form

$$\exp(-ia\mathbf{l} \cdot \mathbf{k}) \int \phi_n^*(\mathbf{r}-a\mathbf{l}) \xi(r) \mathbf{S} \cdot \mathbf{L} \phi_n'(\mathbf{r}) d\tau$$

in calculating the matrix elements $(n\mathbf{k}m_s | \mathcal{O} | n'\mathbf{k}m_s')$ should introduce a similar error to that caused by the neglect of non-orthogonality integrals in the author's band calculation (Fletcher 1952), viz. $\sim 8\%$. Also the diagonal elements of \mathcal{O} would no longer be zero, although small, if these terms were included.

(iv) With regard to the order in which the various perturbations are considered, both A and δ are much smaller than the free atom energy level separations and would therefore not affect these levels or the corresponding wave functions appreciably. Since only summations over the Fermi distribution are of physical interest on the collective electron model and since Σ (occupied

states) = $-\Sigma$ (unoccupied states), \mathcal{E} and O may be regarded as small perturbing operators compared with $V - U$, since the effect of the latter is much larger than δ or A for all unoccupied states. Finally, although $A \sim \delta$, O may be considered as a smaller perturbing operator than \mathcal{E} since it has zero diagonal matrix elements. The cases where this argument breaks down, i.e. $\epsilon_1 = 0$ and $\epsilon_1 + 2\delta \sim 0$, have been dealt with; the latter is considered again in (vii).

(v) The effect of using the Γ_5 band for all calculations and the assumption that all 0.54 holes occur in it will be discussed in §9.

(vi) The spin-orbit interaction parameter A used here corresponds to an electron having spin-orbit interaction energy $AL \cdot S$ when travelling in its orbit in the free atom but not interacting with other orbits (Russell-Saunders coupling). In fact the energy will be less than this due to such interaction; also the field, in which the electron moves, will be smaller in the metal than in the free atom, both due to increased screening by the conduction electrons and because the electron moves from atom to atom. These points have been discussed in §§2 and 5, and it is considered that the relevant value for A for a 3d electron in the metal will only be slightly less than the value used here.

(vii) If a metal is only just magnetized to saturation, states with the same wave vector, of opposite spin and with very nearly the same energy (ignoring spin-orbit interaction), seem bound to occur near the Fermi surface, i.e. one just occupied and one just unoccupied. Then spin-orbit interaction is sufficient to cause transference of electrons between these states. In other words, although the effect is small, it may distort the Fermi surface considerably, as indicated by the fact that on the treatment used here the wave functions become of the form $2^{-1/2}[\psi_3^+ - \exp(-i\chi)\psi_1^-]$, i.e. with spin no longer quantized along the direction of magnetization. Spin-orbit interaction could not be included in a band calculation as would seem desirable, however, without also including the exchange effect, and a separate calculation would have to be made for each direction of domain magnetization.

All the above remarks apply also to the calculations of g and g' . In addition a serious approximation is involved in the use of Peierls' method of gauge transformation. Peierls points out that the zero-field energy levels may be used in such a calculation if (a) the field \mathcal{H} is small and the temperature not too low and (b) the zero-field energy surfaces in \mathbf{k} -space have not too great a curvature anywhere. His treatment applied to diamagnetism and its application to a ferromagnetic, where effective fields are large, is dubious. Also in all calculations here there is the implicit assumption of very low temperature, e.g. it is assumed that the energy band of one spin is full and the other contains all 0.54 holes. Condition (b) is necessary because of the movement of an electron between atoms, and the effect is small for tightly bound electrons. Although the relevant curvature is fairly large at certain points of the region of the Brillouin zone considered in the present case, these large values are sometimes positive and sometimes negative, and the effect is considered far less important than (a).

§9. EXTENSION OF THEORY TO COMPLETE d BAND

One of the worst approximations in the above theory, as Brooks remarks, is the neglect of the atomic wave functions ϕ_4 and ϕ_5 . This is unnecessary for an analytic solution of the problems, as will be shown. The same procedure is adopted as in §§3, 4 and 7 except that no simplification by redefining of axes

(cf. (7)) is possible as $\{a_{\tau n}\}$ is now a 5×5 matrix. Putting

$$\begin{aligned}\mathcal{A}_{\tau\tau'} &= (a_{\tau 1}a_{\tau' 2} - a_{\tau 2}a_{\tau' 1}) + 2(a_{\tau 3}a_{\tau' 4} - a_{\tau 4}a_{\tau' 3}) \\ \mathcal{B}_{\tau\tau'} &= -(a_{\tau 1}a_{\tau' 3} - a_{\tau 3}a_{\tau' 1}) - (a_{\tau 2}a_{\tau' 4} - a_{\tau 4}a_{\tau' 2}) + \sqrt{3}(a_{\tau 2}a_{\tau' 5} - a_{\tau 5}a_{\tau' 2}) \\ \mathcal{C}_{\tau\tau'} &= -(a_{\tau 1}a_{\tau' 4} - a_{\tau 4}a_{\tau' 1}) - \sqrt{3}(a_{\tau 1}a_{\tau' 5} - a_{\tau 5}a_{\tau' 1}) + (a_{\tau 2}a_{\tau' 3} - a_{\tau 3}a_{\tau' 2}) \\ G_{\tau\tau'} &= \mathcal{A}_{\tau\tau'}^2 + \mathcal{B}_{\tau\tau'}^2 + \mathcal{C}_{\tau\tau'}^2; H_{1\tau} = \mathcal{A}_{1\tau}^2 \mathcal{B}_{1\tau}^2 + \mathcal{B}_{1\tau}^2 \mathcal{C}_{1\tau}^2 + \mathcal{C}_{1\tau}^2 \mathcal{A}_{1\tau}^2 \\ L_{1\tau} &= \mathcal{A}_{1\tau}^2 \mathcal{A}_{\tau\tau'}^2 + \mathcal{B}_{1\tau}^2 \mathcal{B}_{\tau\tau'}^2 + \mathcal{C}_{1\tau}^2 \mathcal{C}_{\tau\tau'}^2; M_{1\tau} = \mathcal{A}_{1\tau} \mathcal{A}_{\tau\tau'} + \mathcal{B}_{1\tau} \mathcal{B}_{\tau\tau'} + \mathcal{C}_{1\tau} \mathcal{C}_{\tau\tau'}\end{aligned}$$

and, for instance,

$$\begin{aligned}N_{12\ 34}^{24\ 13} &= \mathcal{A}_{12} \mathcal{A}_{24} \mathcal{A}_{34} \mathcal{A}_{13} + \mathcal{B}_{12} \mathcal{B}_{24} \mathcal{B}_{34} \mathcal{B}_{13} + \mathcal{C}_{12} \mathcal{C}_{24} \mathcal{C}_{34} \mathcal{C}_{13} \\ P_{234} &= 2 \left[M_{24\ 13}^{12\ 34} + M_{34\ 13}^{12\ 24} + M_{13\ 34}^{12\ 24} + M_{23\ 14}^{13\ 24} + M_{14\ 23}^{13\ 24} + M_{23\ 14}^{13\ 24} \right. \\ &\quad \left. - M_{23\ 34}^{12\ 14} - M_{34\ 14}^{12\ 23} - M_{14\ 23}^{12\ 34} - 5N_{24\ 13}^{12\ 34} - 5N_{14\ 24}^{13\ 23} + 5N_{23\ 34}^{12\ 14} \right]\end{aligned}$$

the average contributions to K_1 from the 48 equivalent states of energy $E_1 + \delta$ is

$$\begin{aligned}\frac{1}{3}A^4 \left\{ \sum_{\tau=2}^5 (2G_{1\tau}^2 - 10H_{1\tau}) \left(\frac{1}{\epsilon_\tau} - \frac{1}{\epsilon_\tau + 2\delta} \right)^2 \left(\frac{1}{\epsilon_\tau} + \frac{1}{\epsilon_\tau + 2\delta} + \frac{1}{2\delta} \right) \right. \\ + \sum_{\tau < \tau'} \left(5L_{1\tau'} - G_{1\tau} G_{1\tau'} - 2M_{1\tau'}^2 \right) \left(\frac{1}{\epsilon_\tau} - \frac{1}{\epsilon_\tau + 2\delta} \right) \left(\frac{1}{\epsilon_{\tau'}} - \frac{1}{\epsilon_{\tau'} + 2\delta} \right) \\ \times \left(\frac{1}{\epsilon_\tau} + \frac{1}{\epsilon_\tau + 2\delta} + \frac{1}{\epsilon_{\tau'}} + \frac{1}{\epsilon_{\tau'} + 2\delta} + \frac{2}{2\delta} \right) \\ + \sum_{\tau \neq \tau'} \left(G_{1\tau} G_{\tau\tau'} + 2M_{1\tau'}^2 - 5L_{1\tau'} \right) \left(\frac{1}{\epsilon_\tau} - \frac{1}{\epsilon_\tau + 2\delta} \right)^2 \left(\frac{1}{\epsilon_{\tau'}} - \frac{1}{\epsilon_{\tau'} + 2\delta} \right) \\ \left. + \sum_{\tau < \tau' < \tau''} P_{\tau\tau'\tau''} \left(\frac{1}{\epsilon_\tau} - \frac{1}{\epsilon_\tau + 2\delta} \right) \left(\frac{1}{\epsilon_{\tau'}} - \frac{1}{\epsilon_{\tau'} + 2\delta} \right) \left(\frac{1}{\epsilon_{\tau''}} - \frac{1}{\epsilon_{\tau''} + 2\delta} \right) \right\} \quad (25)\end{aligned}$$

where $\epsilon_\tau = E_1 - E_\tau$. It is easily shown that when three energy bands only are of interest, as in §4, this expression reduces to (9). As regards cases of degeneracy, some consideration has been given to the case of $\epsilon_2 = 0$, although the application of fourth-order degenerate perturbation theory proves extremely complicated. As before, the two states corresponding to the degenerate levels $E_1 + \delta$, $E_2 + \delta$ may be considered together as they will be both occupied or both unoccupied. The sum of their contributions appears to be the same on use of degenerate or non-degenerate formulae as was found before provided their wave vector lies along the (100) axis, but not otherwise. The $\epsilon_2 + 2\delta = 0$ type of degeneracy has not been investigated.

In a similar manner the following expressions may be obtained for g and g' :

$$\begin{aligned}g &= 2 + \frac{1}{0.54} \frac{4}{3} A \sum_u \sum_{\tau=2}^5 \frac{\mathcal{A}_{\tau 1}^2 + \mathcal{B}_{\tau 1}^2 + \mathcal{C}_{\tau 1}^2}{\epsilon_\tau} + O(A^2) \\ g' &= \frac{0.54 + \frac{2}{3} A \sum_u \sum_{\tau=2}^5 \{(\mathcal{A}_{\tau 1}^2 + \mathcal{B}_{\tau 1}^2 + \mathcal{C}_{\tau 1}^2)/\epsilon_\tau\}}{0.27 + \frac{2}{3} A \sum_u \sum_{\tau=2}^5 \{(\mathcal{A}_{\tau 1}^2 + \mathcal{B}_{\tau 1}^2 + \mathcal{C}_{\tau 1}^2)/\epsilon_\tau\}} + O(A^2). \quad \dots\dots (26)\end{aligned}$$

It proves permissible to use these formulae for degenerate and near-degenerate states ($\epsilon_2 = 0$) as before; since the theory has not been extended to terms of $O(A^2)$, near-degeneracy of the type $\epsilon_2 + 2\delta < A$ has not been investigated.

The possible effects of the use of (25) and (26) on the numerical values of K_1 , g and g' for nickel will now be considered.

(i) The Fermi surface occurs at a considerably higher energy value in the complete (quintic) energy band (Fletcher 1952) than in the Γ_5 band used in §§ 5 and 7, so that the relevant value of δ is of the order of 0.1 eV, i.e. less than half the value used before.

(ii) A greater proportion of the unoccupied states than before occur in the highest constituent energy band, for which all $\epsilon_r \geq 0$ and hence $\epsilon_r + 2\delta \gg A$.

(iii) Apart from actual degeneracy ($\epsilon_2 = 0$) on the (100) axis of the Brillouin zone, such as occurred before, cases also occur now for other wave vectors, and there are other states where $\epsilon_2 < A$. Otherwise the ϵ_r for the unoccupied states will generally be rather larger than before, owing to the general 'spreading' effect on the eigenvalues observed in the exact solution of the quintic secular equation of Fletcher (1952) as compared with the approximate one.

It seems possible that use of (25) might reduce the calculated value of K_1 , since factors of the form $1/\epsilon_r - 1/(\epsilon_r + 2\delta)$ will be reduced by a factor of the order of $\frac{1}{2}$ by virtue of (i) above, although there will be far more terms involved than in (9). For the latter reason it seems most likely that the calculated values of $g - 2$ and $2 - g'$ would be increased to $O(A)$. It is worth noting that the greatest contribution to all these quantities arises from degenerate and nearly degenerate states, and more of these would be involved than before if the full quintic band was used. No numerical calculation involving (25) and (26) has been attempted owing to the formidable computational labour involved, but evaluation of these formulae for certain special wave vectors, e.g. on the (100) axis of the Brillouin zone, would seem worth while.

§ 10. SUMMARY

The calculations described here were carried out for two reasons. Firstly some test against experiment of the calculations of Fletcher and Wohlfarth (1951) and Fletcher (1952) was desired, apart from those which could be made directly from the $N(E)$ curve obtained for nickel. Secondly it seemed of interest to carry the only theory of ferromagnetic anisotropy so far proposed on the collective electron model through to a quantitative stage, since suitable data for so doing were not available to Brooks when he formulated the theory, and similarly for his theory of the spectroscopic splitting factor g . In so doing a few minor errors in Brooks' original derivation have been corrected, and it has been possible to consider the gyromagnetic ratio g' also and to extend the theory formally to remove one of the major approximations. The assumptions involved in the theory and difficulties which arise in its quantitative application have been considered in detail.

The numerical value of $-5 \ll 10^7$ ergs cm^{-3} obtained for the first anisotropy coefficient K_1 for nickel is rather large compared with experiment. A possible reason for this is that a large proportion of this value arises from degenerate and nearly degenerate states ($\epsilon_r = 0$). The usual diagonal approximation to the exchange energy does not separate these states and a more rigorous treatment of exchange might modify this result considerably. The question of the order in which the various perturbing effects are considered seems vital, as has already been indicated, and both these points would be even more important if the full quintic energy band were used for computation. It is worth noting that if the band, as calculated by the author, is too narrow, as suggested by recent work by Howarth (1953), then the above value would be reduced by a factor of about $(2.7/3.4)^3 \simeq \frac{1}{2}$.

Regarding the temperature variation of K_1 , one consideration is that $\delta = k\theta'\zeta$ is a function of temperature and the value of K_1 is fairly sensitive to variations in δ owing to the states where $\epsilon_\tau + 2\delta$ is small. This effect, however, appears inadequate to explain the very large decrease in $-K_1$ for nickel between 0°K and room temperature for instance. On Brooks' theory the facts seem explicable only if most of the degeneracy and near degeneracy is removed by an increase of temperature above 0°K. The use of Fermi-Dirac statistics at finite temperature would have a similar effect by reducing the importance of these degenerate states, since they are mainly the states of highest energy.

As regards the numerical values obtained for g and g' for nickel, there seems no reason to ignore $O(A^2)$ terms, so that agreement with experiment is not particularly good. The calculations have not led to any suggestion of an explanation of the difference between $g-2$ and $2-g'$; the fault here appears to lie with the general theory of the two effects, although in their interpretation on the collective electron model the straightforward use of Peierls' method of gauge transformation seems open to strong criticism.

ACKNOWLEDGMENTS

I wish to express my gratitude to Professor H. Brooks of Harvard University for the provision of a copy of his unpublished Ph.D. thesis (Harvard 1940), on which the paper referred to was based. I also wish to thank Dr. E. P. Wohlfarth for suggesting the problem and providing much helpful advice, and Professor H. Jones and Professor V. C. A. Ferraro for supervising this work. The work described forms part of the author's Ph.D. thesis (London 1953).

REFERENCES

- ARGYRÉS, P., and KITTEL, C., 1953, *Acta Metallurgica*, **1**, 241.
 BLOCH, F., and GENTILE, G., 1931, *Z. Phys.*, **70**, 395.
 BROOKS, H., 1940, *Phys. Rev.*, **58**, 909.
 CONDON, E. U., and SHORTLEY, G., 1936, *Theory of Atomic Spectra* (Cambridge : University Press).
 FLETCHER, G. C., 1952, *Proc. Phys. Soc. A*, **65**, 192.
 FLETCHER, G. C., and WOHLFARTH, E. P., 1951, *Phil. Mag.*, **42**, 106.
 GOUDSMIT, S., 1928, *Phys. Rev.*, **31**, 946.
 HARTREE, D. R., and HARTREE, W., 1936, *Proc. Roy. Soc. A*, **157**, 490.
 HEISENBERG, W., 1928, *Z. Phys.*, **49**, 619.
 HOWARTH, D. J., 1953, *Proc. Roy. Soc. A*, **220**, 513.
 KITTEL, C., 1949 a, *Phys. Rev.*, **76**, 743; 1949 b, *Rev. Mod. Phys.*, **21**, 541.
 MOORE, C., 1952, *Atomic Energy Levels*, Vol. II (American National Bureau of Standards).
 MOTT, N. F., and JONES, H., 1936, *Properties of Metals and Alloys* (Oxford : Clarendon Press).
 PEIERLS, R. E., 1933, *Z. Phys.*, **80**, 763.
 SLATER, J. C., 1936, *Phys. Rev.*, **49**, 537, 931.
 STONER, E. C., 1938, *Proc. Roy. Soc. A*, **165**, 372.
 VAN VLECK, J. H., 1932, *Electric and Magnetic Susceptibilities* (Oxford : Clarendon Press); 1937, *Phys. Rev.*, **52**, 1178; 1950, *Ibid.*, **78**, 266.
 WOHLFARTH, E. P., 1951, *Phil. Mag.*, **42**, 374.

A Nuclear Method for the Estimation of Traces of Light Water in Heavy Water

By G. L. SQUIRES

Atomic Energy Research Establishment, Harwell, Berks.

MS. received 7th January 1954, and in final form 26th February 1954

Abstract. A method has been developed for estimating traces of light water in heavy water. The transmission of slow neutrons through a sample of the water is compared with that through a standard sample. The method gives an accuracy to 0.006% in the heavy water content after 3 hours' counting.

§1. INTRODUCTION

OWING to the comparatively high value of the neutron-proton capture cross section, traces of light water in the moderator of a heavy water reactor have a pronounced effect on the performance of the reactor. With the advent of this type of reactor the estimation of traces of light water in heavy water has assumed some importance. Several methods are available for carrying out such an estimation (Kirschenbaum 1951). The present paper describes a further method based on the difference in the total cross sections of light and heavy water for slow neutrons. The number of neutrons that pass undeflected through a sample of water can be made a measure of the amount of light water present.

Denote the fraction of heavy water molecules in a mixture of light and heavy water by α and the mean total cross section per molecule by σ . Consider a sample with α close to unity and suppose that when slow neutrons are incident on the sample a fraction ϕ passes through, the rest being scattered and absorbed. The value of ϕ depends on the value of α and the length of the sample.

The present method does not entail the measurement of ϕ itself. Instead, the procedure adopted is to measure the ratio ρ of the number of neutrons that pass through the sample to the number that pass through a roughly equal length of standard heavy water. It can readily be shown that α is obtained most accurately by this method when the length of the sample is so chosen that $\phi = e^{-2}$, and that, when this condition is satisfied, a change $\Delta\alpha$ in α gives rise to a change in ρ of $F\rho\Delta\alpha$, where $F = (2/\sigma)d\sigma/d\alpha$. The fact that the cross section of light water is much larger than that of heavy water results in a high value for F when α is close to unity, and makes the slow neutron method of determining α a very sensitive one. For $\alpha = 1$ and neutrons of wavelength 7 Å the values of σ and $d\sigma/d\alpha$ are about 22 and 210 barns respectively. These values give $F \simeq 20$. Therefore to measure α to, say, 0.01% it is only necessary to measure ρ to 0.20%.

In considering the accuracy of ρ we may distinguish between the error due to statistics in counting neutrons, and other errors. The latter, which will be called E errors, arise from the following effects: (i) the counting of stray neutrons, i.e. neutrons that have not passed through the sample, (ii) variation

in effective length of the sample, (iii) variation in sample density due to changes in temperature, (iv) moisture collecting on the ends of the sample holders, (v) variation in counting efficiency due to effects either in the neutron counter itself or in the associated electronic circuits. The design of the apparatus and the procedure for making measurements are largely governed by the need to eliminate these errors or to reduce them to such an extent that they are small compared with the statistical error.

§ 2. DESCRIPTION OF METHOD

The neutron beam was obtained by placing a cylinder of lead shot (A in figure 1) in a flux of thermal neutrons in the Harwell pile, BEPO. Neutrons with wavelength less than 5.7 \AA were scattered out of the beam, and the average wavelength of the neutrons emerging from the lead was 7.0 \AA . The beam was collimated by the cadmium discs B.

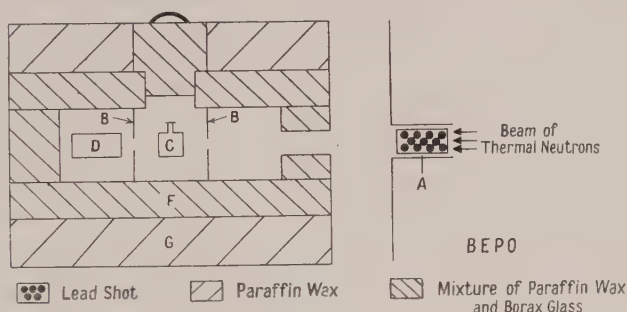


Figure 1. Arrangement of apparatus.

A quartz glass vessel C, containing 15 cm^3 of the sample to be analysed, was placed in the filtered beam, and the neutrons that passed undeflected through the sample were counted by the BF_3 counter D. The length of C, about 3 cm, was chosen so that the fraction of neutrons transmitted was close to e^{-2} . After a period of 100 seconds, during which about 100 000 neutrons were counted, C was removed and replaced by the standard sample which was contained in a vessel S similar to C. Neutrons were again counted for 100 seconds. The counting periods were timed by means of a crystal controlled oscillator with a frequency of 10 kc/s. The process of counting with C and S alternately in the beam was repeated several times.

The ratio ρ of the two sets of counts is a measure of the difference in α between the samples in C and S. If the same sample is kept in S and different samples are placed in C, the relation between ρ and the α value of the sample in C is

$$\log \rho = A\alpha + B. \quad \dots (1)$$

The two constants A and B may be determined by measuring ρ for two or more known values of α . The value of an unknown α in C is then obtained by measuring its ρ . The linear relation between $\log \rho$ and α only holds if the mean total cross section per molecule varies linearly with α . The results shown in figure 2 demonstrate the validity of equation (1), at least for α greater than 0.99.

In effect the basis of the method is the correlation of the number of neutrons that pass through C with the α value of the sample in C. The purpose of the sample in S is to reduce the E errors. Provided C and S are kept in proximity and treated alike, e.g. placed in the same container when not in position in the scattering apparatus, effects due to changes in temperature and to moisture on the end-plates of the sample holders are negligible, for any effect they have on the transmission of C is almost duplicated in S. Further, provided C and S are placed in the beam with a repetition time τ short compared with the period of fluctuation of counting efficiency—a condition fairly easily satisfied—effects due to such fluctuations are negligible. It may be noted that the value of α for the sample in S must stay constant but need not be known.

Variations in the length of the sample must be kept to a minimum. Variations in length due to temperature changes have little effect, for they are almost equal in C and S. However, the effective length may vary for another reason. The sample is placed in the beam many times and a variation of its position with respect to the neutron beam may give rise to a variation in path length. This error was reduced by rigidly mounting each sample vessel in a brass support with guide bars that fitted into corresponding slots in the scattering apparatus. Thus the vessel was always in the same position relative to the cadmium discs B that defined the neutron beam. In addition, the two end-plates of the vessels were effectively parallel, so that even if the beam had passed through a different part of the vessel the difference in the thickness of sample traversed would have been small.

Finally, the effect of stray neutrons was reduced by surrounding the scattering apparatus with an inner shield F, 4 in. thick, consisting of a mixture of paraffin wax and borax glass, and an outer shield G, 6 in. thick, consisting of paraffin wax alone. In these circumstances the number of stray neutrons recorded by the counter was 0.01% of the total count.

Originally, a separate neutron counter was used to monitor the incident beam, but it was discovered that for periods of the order of an hour the flux of neutrons from the pile varied very little. The flux was therefore assumed constant and the monitor discarded. This was only permissible because the repetition time τ was short compared with the period of fluctuation of the incident neutron flux.

§ 3. RESULTS AND DISCUSSION

Known samples of different α were made by mixing and were placed in C; ρ was measured as a function of α for eleven such samples. The results are shown in figure 2 where $\log \rho$ is plotted against α . The 'best' linear relation between $\log \rho$ and α was found by a least squares analysis. From the 'best' line and the measured ρ for each sample the value of α given by the method was obtained and compared with the known value. Denote the difference by $\Delta\alpha$. The r.m.s. value of $\Delta\alpha$ was found to be

$$\overline{\Delta\alpha_{\text{obs}}} = 5.8 \times 10^{-5}. \quad \dots\dots(2)$$

The calculated r.m.s. value of $\Delta\alpha$ due to statistical error alone was

$$\overline{\Delta\alpha_{\text{stat}}} = 3.1 \times 10^{-5}. \quad \dots\dots(3)$$

Before considering the significance of the difference between the observed value of $\overline{\Delta\alpha}$ and the calculated statistical value we shall describe a further set of measurements that were made.

A third sample S' was employed. Like S , it was filled initially with heavy water and remained unchanged. Neutrons were counted with C , S and S' successively in the beam. Thus, in addition to ρ , a second quantity ρ' , equal to the ratio of the number of neutrons that passed through S' and S , was

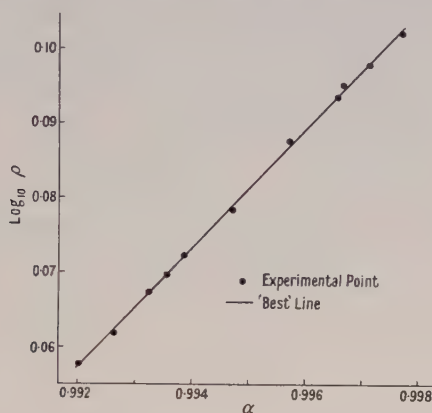


Figure 2. $\log \rho$ plotted against α .

Note. Experimental points are obtained after 3 hours' counting.

obtained. At the same time that ρ was measured for each sample in C , ρ' was measured also. As the samples in S and S' were the same throughout, differences in the eleven values of ρ' were due solely to errors, both statistical and type E. The r.m.s. value of the difference between each ρ' and the mean value of ρ' was found and translated into a difference in α . The value of the latter, which we denote by $\overline{\Delta\alpha'}$, was found to be

$$\overline{\Delta\alpha'_{\text{obs}}} = 3.6 \times 10^{-5}. \quad \text{.....(4)}$$

The calculated r.m.s. value of $\Delta\alpha'$ due to statistical error alone was

$$\overline{\Delta\alpha'_{\text{stat}}} = 3.1 \times 10^{-5}. \quad \text{.....(5)}$$

The difference between $\overline{\Delta\alpha'_{\text{obs}}}$ and $\overline{\Delta\alpha'_{\text{stat}}}$ is due to E errors. Equations (4) and (5) show that the difference is less than 20%, and this is reasonably small.

Returning now to equations (2) and (3), we may remark that the only difference between the measurements of ρ and ρ' lay in the fact that the former was obtained with a sample that was changed and the latter with one that was not. Thus the difference between $\overline{\Delta\alpha_{\text{obs}}}$ and $\overline{\Delta\alpha'_{\text{obs}}}$ may be attributed either to errors in mixing the sample or to contamination of the sample while it was being mixed and introduced into the holder C . The contaminant may have been light water or some neutron-absorbing impurity. The contribution to $\overline{\Delta\alpha_{\text{obs}}}$ from errors in mixing the samples is estimated to be about 1×10^{-5} .

The overall accuracy of the method is summarized by the relation

$$\overline{\Delta\alpha} = \left(25 + \frac{35}{t}\right)^{1/2} \times 10^{-5} \quad \text{.....(6)}$$

where $\overline{\Delta\alpha}$ is the r.m.s. error in α obtained after making measurements for t hours. The error is the total observed error. 80% of the time t represents counting time and the remaining 20% the time taken to record the counts and change the samples. Equation (6) indicates that an accuracy to 0.02% can be obtained after a period of 6 minutes and to 0.006% after 3 hours. Comparable figures

for the accuracy of other methods of measuring α are 0.01% for the mass spectrometer (Reynolds and Loveridge 1953) and 0.003% for infra-red absorption methods (Gaunt 1953).

The advantages and disadvantages of the neutron method may be stated briefly. The chief advantages are accuracy and simplicity. No preliminary treatment of the sample is necessary, and the neutron measurements can be carried out by an unskilled operator. The method can be adapted to enable a supply of heavy water to be monitored continuously.

The chief disadvantage is that neutron-absorbing impurities in the heavy water result in the measured value of α being too low. In the particular application of the method to the analysis of heavy water in reactors this is not a serious disadvantage because separate measurements are made to determine the concentration of these impurities, and their effects can be allowed for. Alternatively, the slow neutron measurements may be regarded as giving an overall check on the suitability of the heavy water as a moderator.

Slow neutron measurements can be used generally to estimate the amount of deuteration in deuterated compounds. With some compounds it may be difficult to obtain samples of known deuteration for calibration purposes, in which case it is preferable to use neutrons with energies of a few electron volts. For such neutrons the cross section is simply the sum of the cross section for each nucleus in the molecule. (This is not the case with the very slow neutrons used in the heavy water estimation, for their wavelengths are of the order of the distance between the nuclei in a molecule, and interference between the scattered neutron waves occurs.) From the measured cross section and the published data on free atom cross sections the average cross section per hydrogen atom is calculated and is assumed to vary linearly with the percentage deuteration.

ACKNOWLEDGMENTS

The writer wishes to thank Dr. B. Loveridge for mixing the samples, Mr. R. Bennett for constructing the apparatus, and Dr. J. Freeman for helpful comments on the manuscript. He is indebted to the Director of the Atomic Energy Research Establishment for permission to publish this paper.

REFERENCES

- GAUNT, J., 1953, *A.E.R.E. Report C/R 1264* (Atomic Energy Research Establishment, Harwell).
KIRSCHENBAUM, I., 1951, *Physical Properties and Analysis of Heavy Water* (New York: McGraw-Hill).
REYNOLDS, P., and LOVERIDGE, B. A., 1953, *A.E.R.E. Report GP/R 1282* (Atomic Energy Research Establishment, Harwell).

The Magnetic Susceptibility of Nitric Oxide in a Clathrate Compound

By A. H. COOKE AND H. J. DUFFUS *

Clarendon Laboratory, Oxford

MS. received 23rd February 1954

Abstract. The magnetic susceptibility of nitric oxide enclosed in a β -quinol lattice has been measured at temperatures from 10°K to 300°K. The susceptibility, which obeys Curie's law at room temperature, approaches a temperature-independent value at low temperatures. This behaviour is compared with that predicted for the free gas by Van Vleck.

WE have measured the magnetic susceptibility of a nitric oxide 'clathrate' compound over a range of temperature from 10°K to 300°K, using the Faraday method.

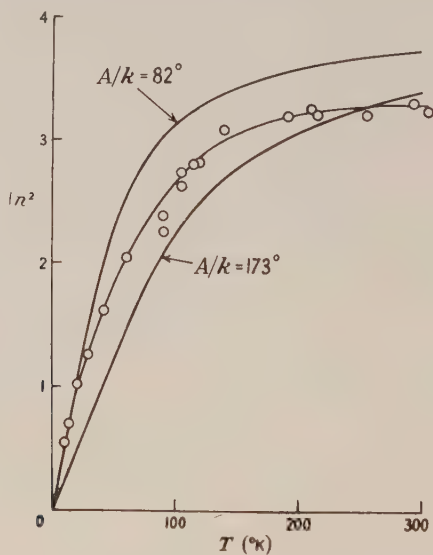
The structure and chemical properties of a number of adducts formed by quinol with molecules or atoms of suitable dimensions have been described by Powell (1948) and his collaborators. In these clathrate compounds each trapped molecule is totally enclosed in a cage formed by the molecular arrangement of the β -quinol lattice. Of the common paramagnetic gases, oxygen and nitric oxide are the only ones having molecules of suitable size which do not react with quinol. Evans and Richards (1952) synthesized clathrate compounds of these gases and found their room temperature susceptibilities to be very nearly those of the free gases. They then proposed that the clathrate compounds might offer a means of examining the susceptibilities of 'free' molecules below the temperature at which they would normally liquefy. We have therefore extended the measurements on the nitric oxide clathrate to 10°K. Measurements are also being made on the oxygen compound.

Measurements were made on a powder specimen of nitric oxide clathrate sealed in a glass phial in order to delay chemical decomposition of the nitric oxide. To cover a large range of temperatures we used a Sucksmith ring balance adapted for work with liquid helium, hydrogen or oxygen. The specimen was connected by a quartz rod to a phosphor-bronze ring whose deflection was magnified by a beam of light reflected from two plane mirrors attached to it. Because the compound was so weakly paramagnetic it was necessary to increase the sensitivity of the balance by using a split selenium photocell to show the position of the light beam. To avoid error from changes in the elastic modulus of the system a null method of measurement was used, the magnetic field at the specimen being varied until the force on the specimen exactly balanced the effect of removing a 4 mg rider from the balance. An absolute calibration of the balance was obtained by comparing the susceptibility of the clathrate with that of three 'standard' specimens of manganous ammonium sulphate. The diamagnetic deflection due to the glass phial and Perspex specimen mount was

* Now at the Pacific Naval Laboratory, British Columbia.

measured, and that due to the quinol was calculated, taking the specific susceptibility of quinol to be $-0.60 \pm 0.02 \times 10^{-5}$ e.m.u./gm (Evans and Richards 1952). Analysis of our sample showed that 38.5% of the available holes were filled with nitric oxide molecules. Two observations of the susceptibility of the specimen at 20°C gave 0.87×10^{-6} e.m.u./gm and 0.95×10^{-6} e.m.u./gm, corresponding to a susceptibility per gramme of nitric oxide of 45×10^{-6} e.m.u. and 47×10^{-6} respectively. This is slightly less than the value 51.6×10^{-6} e.m.u./gm obtained by Evans and Richards using the Gouy method, though it is close to the values found for free nitric oxide gas by various observers, viz. 47.2×10^{-6} (Burris and Hause 1943), 48.7×10^{-6} (Bauer, Weiss and Piccard 1918) and 48.8×10^{-6} (Soné 1922). The value calculated for nitric oxide by Van Vleck (1932) is 47.7×10^{-6} e.m.u./gm at 20°C. In view of the difficulty of making absolute measurements of susceptibility on such a weakly paramagnetic substance we do not attach any significance to this discrepancy. Our measurements could not easily be repeated because the analysis to determine the percentage of holes filled entails the destruction of part of the specimen. Furthermore, the clathrate compound is difficult to synthesize, and decomposes slowly even when sealed in a capsule.

The results of the measurements, corrected for the diamagnetism of the glass phial, the Perspex mount, and the quinol lattice, are shown in the diagram, in which the square of the effective magneton number n is plotted against the absolute temperature. n is defined from $n^2 = 3\chi kT / N\beta^2$, where χ is the molar susceptibility at an absolute temperature T , k is Boltzmann's constant, N is Avogadro's number, and β is the Bohr magneton.



Dependence of effective magneton number on temperature, for nitric oxide in a clathrate compound.

The normal state of the nitric oxide molecule is known to fall under Hund's case *a* as a $^2\Pi$ doublet of separation $A = 120.9 \text{ cm}^{-1}$ (Jenkins, Barton and Mulliken 1927). The lower doublet component has $\Sigma = -\frac{1}{2}$ and $\Lambda = 1$, and is therefore diamagnetic. If the susceptibility of the gas could be observed over a sufficient range of temperature it would exhibit a gradual transition from a susceptibility

inversely proportional to temperature to a susceptibility independent of temperature. Van Vleck (1932) gives the following formula for the dependence of the effective magneton number on temperature:

$$n^2 = \frac{4(1 - e^{-x} + xe^{-x})}{x + xe^{-x}}$$

where $x = A/kT$. In the diagram are given graphs of this equation for $A/k = 173^\circ$ ($A = 120.9 \text{ cm}^{-1}$) and for $A/k = 82^\circ$ (to fit the low temperature end of our experimental curve). It will be seen that no single value of the parameter A will fit the experimental curve, though it must be noted that small changes in the diamagnetic correction would alter the shape of our curve at high temperatures. Despite the quantitative discrepancy, it is evident that nitric oxide in the clathrate behaves magnetically very much as would a free gas, but over a range of temperature well below the liquefaction point of the free gas. The diamagnetic level $\Sigma = -\frac{1}{2}$, $\Lambda = 1$ is clearly lower than the paramagnetic level $\Sigma = \frac{1}{2}$, $\Lambda = 1$, but there may be an interaction between the orbital moment of the nitric oxide molecule and the electric field of the quinol cage which decreases the doublet separation relative to that of the free molecule. Further information on this point would be obtained from measurements on single crystals, but at present it is not possible to grow sufficiently large clathrate crystals to study the magnetic anisotropy. Attempts to observe paramagnetic resonance absorption in a powder specimen have given no result.

ACKNOWLEDGMENTS

We acknowledge gratefully the help and advice of Dr. D. F. Evans and Dr. R. E. Richards, who prepared and analysed the specimen. One of us (H.J.D.) was supported by the National Research Council of Canada.

REFERENCES

- BAUER, E., WEISS, P., and PICCARD, A., 1918, *C. R. Acad. Sci., Paris*, **167**, 484.
 BURRIS, A., and HAUSE, C. D., 1943, *J. Chem. Phys.*, **11**, 442.
 EVANS, D. F., and RICHARDS, R. E., 1952, *J. Chem. Soc.*, 3295.
 JENKINS, F. A., BARTON, H. A., and MULLIKEN, R. S., 1927, *Phys. Rev.*, **30**, 150.
 POWELL, H. M., 1948, *J. Chem. Soc.*, 61.
 SONE, T., 1922, *Sci. Rep. Tôhoku Univ.*, **11**, (3), 139.
 VAN VLECK, J. H., 1932, *The Theory of Electric and Magnetic Susceptibilities* (Oxford: University Press).

The Ultra-Violet Emission Spectra of the Gaseous Monofluorides of Gallium and Indium

By R. F. BARROW, J. A. T. JACQUEST AND E. W. THOMPSON

Physical Chemistry Laboratory, University of Oxford

MS. received 26th February 1954

Abstract. The emission spectra of GaF and InF may be excited conveniently in hot hollow-cathode tubes, the cathode containing a mixture of the respective metal with aluminium trifluoride. The emission spectra are similar to those observed in absorption, but many more bands of the $^3\Pi-^1\Sigma$ systems of InF have been observed. The Ga isotope effect in GaF has been resolved, and improved constants are derived for the two molecules.

§ 1. INTRODUCTION

THE strongest features in the ultra-violet spectra of GaF and of InF consist of three band systems, $C\ ^1\Pi-X\ ^1\Sigma^+$ and $A\ ^3\Pi_0+, B\ ^3\Pi_1-X\ ^1\Sigma^+$. These were first observed and analysed from plates of the spectra taken in absorption (Welti and Barrow 1952). The successful production of the emission spectrum of AlF in hot hollow-cathode discharge tubes (Rowlinson and Barrow 1953a) suggested that the examination of similar discharges for the excitation of the emission spectra of GaF and InF might be fruitful.

§ 2. EXPERIMENTAL

Discharge tubes in which vertical high-temperature steel cathodes which could be filled with mixtures of Ga + AlF₃ or In + AlF₃ were used. Additional, external heating of the cathode was provided, and dry hydrogen was used as carrier gas to start the discharge, which was run from 1000 or 2000 v d.c. generators. The GaF spectrum was photographed on a large quartz Littrow instrument (Hilger E 478): the InF spectrum was also photographed in a first order of a 2.4 m grating instrument giving a reciprocal dispersion on the plate of about 7.4 Å per mm, and on a Hilger small quartz spectrograph.

§ 3. RESULTS

In general, the emission spectra were similar in appearance to the absorption spectra, but the $^3\Pi_1, ^3\Pi_1-^1\Sigma$ systems of InF were much more strongly developed, and many more bands of these systems were observed. The emission sources proved also to be more convenient to operate, so that it was possible to use higher resolution than in the case of the absorption spectra.

The results are summarized in tables 1-6. The following comments may be made:

- (1) The observation of the vibrational isotope effect between Ga⁶⁹F and Ga⁷¹F satisfactorily confirms the analyses.
- (2) No pre-dissociation was observed, either in GaF or in InF.

(3) In the emission spectrum of InF there appears a weak system of apparently double-headed bands degraded to longer wavelengths: the strongest heads are at 2185.8 and 2187.1 Å (table 6). Unfortunately it has been possible to observe only two sequences of this system. The most plausible arrangement of the bands leads to $\Delta G''_{1/2} = 610$, $\Delta G'_{1/2} = 550$ cm⁻¹. They may arise from a transition between two excited states of InF not yet known; other possible emitters are InO, or some unidentified fluoride. Against the latter possibility is the fact that the system was not observed in the experiments with GaF, so it is likely that the emitter contains In. It is noteworthy that there are other emission systems which have not yet satisfactorily been explained in the spectra of other molecules of this group, for example in GaCl (Levin and Winans 1951) and in TlCl (Miescher 1941).

Table 1. Band Heads of the $A^3\Pi_0-x^1\Sigma$ System of GaF

v', v''	λ_{air}	ν_{vac}	$\nu(\text{Ga}^{69}\text{F}) - \nu(\text{Ga}^{71}\text{F})$	
			obs.	calc.
0, 0	3018.90*	33115.0	—	+0.1
1, 1	15.14*	156.3	—	+0.2
2, 2	11.41	197.4	+0.9	+0.3
3, 3	08.07*	235.4	—	+0.4
4, 4	04.82*	270.2	—	+0.5
1, 0	2960.52	768.0	+1.4	+2.0
2, 1	57.58	801.6	+1.6	+2.1
3, 2	54.75	834.5	+1.5	+2.2
4, 3	51.55*	871.1	—	+2.3

Note: The measurements refer to P heads: an asterisk (*) indicates that only an unresolved blend of the bands of Ga⁶⁹F and Ga⁷¹F was measured.

Table 2. Band Heads of the $B^3\Pi_1-x^1\Sigma$ System of GaF

v', v''	λ_{air}	ν_{vac}	$\Delta\nu(Q-P)$	$\nu(\text{Ga}^{69}\text{F}) - \nu(\text{Ga}^{71}\text{F})$	
				obs.	calc.
0, 1	3044.84	32832.9	9.1	-1.5	-1.8
1, 2	40.22*	880.7	7.9*	—	-1.6
2, 3	35.98*	928.7	9.2*	—	-1.5
3, 4	31.85*	973.1	7.8*	—	-1.3
0, 0	2988.79*	33448.6	11.0*	—	-0.1
1, 1	85.05*	491.0	11.5*	—	+0.2
2, 2	81.50*	530.4	11.1*	—	+0.3
3, 3	77.87	571.3	12.4	+1.7	+0.4
4, 4	75.12*	602.3	—	—	+0.4
5, 5	72.77*	628.9	5.1*	—	+0.3
1, 0	31.18	34106.0	14.0	+2.4	+2.1
2, 1	28.23	140.4	14.3	+2.0	+2.1
3, 2	25.48	172.9	15.0	+2.2	+2.1
4, 3	23.18	199.3	11.3	+2.1	+2.0
5, 4	21.86*	214.8	7.5*	—	+2.0
6, 5	20.95*	225.5	—	—	+1.8

Note: The measurements refer to Q heads; an asterisk (*) indicates that only an unresolved blend of the bands of Ga⁶⁹F and Ga⁷¹F was measured.

(4) The discovery of a number of band systems in the absorption spectrum of AlF at wavelengths lower than the system $A^1\Pi-X^1\Sigma^+$ (Rowlinson and Barrow 1953 b) prompted a re-examination of the absorption plates of GaF and InF. In the latter case two weak bands degraded to the red were found at 2103.0 and 2126.6 Å which are separated by the ground-state vibrational interval for InF. It seems likely that these bands constitute the 0,0 and 0,1 bands of a new system $D-X^1\Sigma^+$.

Table 3. Band Heads of the $c^1\Pi-X^1\Sigma$ System of GaF

v', v''	λ_{air}	λ_{vac}	Degradation	$\Delta\nu$, R-Q or Q-P	$\nu(\text{Ga}^{69}\text{F})-\nu(\text{Ga}^{71}\text{F})$ obs.	calc.
2, 1	2094.56*	47727.5	R	11.8*	—	+0.9
3, 2	2100.76*	586.7	R	7.4*	—	+0.2
4, 3	08.10*	421.0	R	5.4*	—	-0.6
0, 0	12.37*	325.1	R	46.5*	—	-0.5
1, 1	16.64*	229.7	R	26.6*	—	-0.5
2, 2	21.70	117.1	R	15.9	-0.8	-0.9
3, 3	27.80	46982.0	R	10.4	-1.3	-1.5
4, 4	35.01	823.4	R	6.5	-2.4	-2.4
0, 1	40.28	708.1	V	—	-2.2	-2.0
5, 5	43.69	633.8	R	(4.3)	(-4.3)	-3.3
1, 2	44.34	619.7	R	35.6	-2.6	-2.3
2, 3	49.24	513.4	R	21.4	-2.8	-2.7
3, 4	55.16	385.6	R	12.5	-3.0	-3.3
4, 5	62.28	232.9	R	7.9	-5.1	-4.0
0, 2	68.58	098.6	V	20.0	-3.8	-3.8
5, 6	70.65	054.6	R	(4.7)	—	-4.7
1, 3	72.19	022.0	R	—	-3.8	-4.1
1, 3	72.42	017.1	V	—	-4.3	-4.1
2, 4	77.15	45917.2	R	31.4	-4.2	-4.4
3, 5	82.92	795.8	R	17.1	-5.1	-4.9
4, 6	89.98	648.2	R	9.4	-5.8	-5.7
5, 7	98.59	469.5	R	6.2	-7.0	-6.7

Note: The measurements refer to Q heads; an asterisk (*) indicates that only an unresolved blend of the bands of Ga^{69}F and Ga^{71}F was measured.

Table 4. Band Heads of the $A^3\Pi_0-X^1\Sigma$ System of InF

v', v''	λ_{air}	ν_{vac}	v', v''	λ_{air}	ν_{vac}
0, 2	3400.05	29402.9	1, 1	3278.35	30494.4
1, 3	3394.51	450.9	2, 2	74.64	528.9
2, 4	89.27	496.4	3, 3	71.14	561.6
3, 5	84.30	539.8	4, 4	67.75	593.3
4, 6	79.54	581.4	1, 0	22.59	31022.0
5, 7	74.86	622.4	2, 1	19.38	052.9
7, 9	66.52	695.8	3, 2	16.54	080.4
0, 1	40.34	928.5	4, 3	13.73	107.5
1, 2	35.66	970.5	5, 4	11.23	131.8
2, 3	31.13	30011.2	6, 5	19.94	154.0
3, 4	26.95	048.9	7, 6	06.78	174.9
4, 5	22.84	086.1	8, 7	04.90	193.2
5, 6	19.04	120.6	9, 8	03.32	208.6
6, 7	15.35	154.1	10, 9	01.95	222.0
7, 8	11.93	185.2	11, 10	00.91	232.1
0, 0	3282.50	455.8	12, 11	00.03	240.7

Note: The measurements refer to P heads.

Table 5. Band Heads of the $B^3\Pi_1-X^1\Sigma$ System of InF

v', v''	λ_{air}	ν_{vac}	$\Delta\nu, Q-P$	v', v''	λ_{air}	ν_{vac}	$\Delta\nu, Q-P$
2, 5	3354.87	29798.9	—	2, 3	3243.13	30825.5	6.8
3, 6	49.17	849.6	—	3, 4	39.15	863.4	6.6
4, 7	43.80	897.5	—	4, 5	35.30	900.1	6.6
5, 8	38.76	942.6	—	5, 6	31.80	933.6	6.8
6, 9	34.35	982.3	—	6, 7	28.48	965.4	—
7, 10	30.36	30018.2	—	7, 8	25.83	990.9	—
0, 2	08.37	217.7	5.1	0, 0	3196.93	31271.0	7.2
1, 3	03.21	264.9	—	1, 1	93.17	307.8	7.0
2, 4	3298.20	310.9	4.9	2, 2	89.54	343.4	6.8
3, 5	93.61	353.1	5.4	1, 0	40.04	837.5	7.9
4, 6	88.95	396.1	6.0	2, 1	37.04	868.0	9.5
5, 7	84.85	434.0	5.6	4, 3	31.65	922.8	7.1
0, 1	51.75	743.8	6.4	5, 4	29.34	946.4	7.7
1, 2	47.37	785.3	6.4	6, 5	27.23	967.9	—

Table 6. Unidentified System Observed in the Emission Spectrum of InF

λ_{air}	ν_{vac}	Int.	Suggested assignment	λ_{air}	ν_{vac}	Int.	Suggested assignment
2227.19	44885.7	2	4, 5	2196.19	45519.1	4	3, 3 Q
24.49	940.2	2	3, 4	95.27	538.1	2	3, 3 R
21.65	997.6	2	2, 3	92.95	586.4	7	2, 2 Q
19.22	45046.8	1	1, 2	92.03	605.4	3	2, 2 R
18.49	061.6	1	?	89.99	648.0	9	1, 1 Q
16.66	098.8	1	0, 1	88.86	671.5	4	1, 1 R
2199.54	449.9	2	4, 4 Q	87.06	709.1	10	0, 0 Q
98.72	466.8	0	4, 4 R	85.77	736.1	5	0, 0 R

Note: All bands are degraded to longer wavelengths.

§ 4. DISCUSSION

The values derived for the molecular constants are collected together in table 7. The most interesting question relates to the determination of the energies of dissociation of these molecules. In the case of GaF we have to rely on the

Table 7
Constants for Ga⁶⁹F

State	T_0	ω_e	$x_e\omega_e$	$y_e\omega_e$
C $^1\Pi$	47325.1	542.8	9.7	-0.56
B $^3\Pi_1$	33448.6	663	1.8	-0.4
A $^3\Pi_0+$	33126.6	661	3.4	—
X $^1\Sigma+$	0	623.8	3.4	—

Constants for InF

State	T_0	ω_e	$x_e\omega_e$	$y_e\omega_e$
D	(47536)	535	—	—
C $^1\Pi$	42771.6	463.9	7.35	-0.5
B $^3\Pi_1$	31271.0	571.3	2.63	-0.095
A $^3\Pi_0+$	30463.9	575.7	3.66	—
X $^1\Sigma+$	0	534.7	2.56	—

extrapolation of the vibrational constants for the state $c^1\Pi$. The new values for the constants of this state lead to $D_0(c^1\Pi) = 3915 \text{ cm}^{-1}$, corresponding to a dissociation limit at 51240 cm^{-1} above $v'' = 0$. The arguments (Welti and Barrow 1952) which lead us to believe that this state probably dissociates into $\text{Ga}(^2P_{3/2}) + \text{F}(^2P)$ need not be rehearsed here. If this view is correct, there is obtained $D_0''(\text{GaF}) = 50210 \pm 203 \text{ cm}^{-1}$ (where the figure $\pm 203 \text{ cm}^{-1}$ corresponds to uncertainty in the state of F between $^2P_{3/2}$ and $^2P_{1/2}$). This is equivalent to $D_0'' = 143.5 \pm 0.6 \text{ kcal}$.

The constants for $c^1\Pi$ of InF are unchanged. Extrapolation gives $D_0(c^1\Pi) = 3500 \text{ cm}^{-1}$, corresponding to a limit at 46270 cm above $v'' = 0$. Subtracting the excitation energy of $\text{In}(^2P_{3/2})$, we obtain, as before, $D_0''(\text{InF}) = 43850 \pm 203 \text{ cm}^{-1}$ or $125.4 \pm 0.6 \text{ kcal}$. A much longer extrapolation from $B^3\Pi_1$ gives a limit at 43700 cm^{-1} , suggesting that this state dissociates into $\text{In}(^2P_{1/2}) + \text{F}(^2P)$. No reliable value can be obtained from $A^3\Pi_0$, in view of the uncertain, but probably by no means negligible, head-origin separations.

It has been pointed out previously that the true values for the dissociation energies of these molecules may be somewhat lower, for there may be maxima in the potential energy curves for these states $c^1\Pi$ (Rowlinson and Barrow 1953 a).

REFERENCES

- LEVIN, F. K., and WINANS, J. G., 1951, *Phys. Rev.*, **84**, 431.
MIESCHER, E., 1941, *Helv. Phys. Acta*, **14**, 148.
ROWLINSON, H. C., and BARROW, R. F., 1953 a, *Proc. Phys. Soc. A*, **66**, 437; 1953 b, *Ibid.*, **66**, 771.
WELTI, D., and BARROW, R. F., 1952, *Proc. Phys. Soc. A*, **65**, 629.

Properties of the Hydrogen Molecular Ion
IV: Oscillator Strengths of the Transitions Connecting the Lowest Even
and Lowest Odd σ -States with Higher σ -States

By D. R. BATES, R. T. S. DARLING, S. C. HAWE AND A. L. STEWART

Department of Applied Mathematics, The Queen's University of Belfast

MS. received 3rd February 1954

Abstract. The oscillator strengths associated with the $1s\sigma_g-3p\sigma_u$, $1s\sigma_g-4p\sigma_u$, $1s\sigma_g-4f\sigma_u$, $2p\sigma_u-2s\sigma_g$, $2p\sigma_u-3s\sigma_g$ and $2p\sigma_u-3d\sigma_g$ transitions of H_2^+ are computed from the exact two-centre wave functions. It is found that some of the transition integrals vary rapidly with the internuclear separation. The significance of this in connection with the calculation of relative intensities in band systems is briefly discussed. A comparison is made with the values of the oscillator strengths obtained using the l.c.a.o. approximation.

§ 1. INTRODUCTION

THE oscillator strengths of a number of the transitions of the hydrogen molecular ion have already been calculated from the exact two-centre wave functions (Bates 1951, Bates, Darling, Howe and Stewart 1953). Table 1 lists the transitions which have been treated describing them in the united atom designation (which is used hereafter as in the case of H_2^+ it is especially appropriate: cf. Herzberg 1950) and also in the separated atoms designation (which is favoured in the chemical literature: cf. Coulson 1952).

Table 1. Transitions of H_2^+ investigated previously

United atom designation	Separated atoms designation
$1s\sigma_g-2p\sigma_u$	$\sigma(1s)-\sigma^*(1s)$
$1s\sigma_g-2p\pi_u$	$\sigma(1s)-\pi(2p_x)$
$2p\sigma_u-3d\pi_g$	$\sigma^*(1s)-\pi^*(2p_x)$
$2p\pi_u-3d\pi_g$	$\pi(2p_x)-\pi^*(2p_x)$

As can be seen, all are either of the so-called charge-transfer type (Mulliken 1939) or tend to strong atomic transitions in *both* the united and the separated limits. Because of this the associated oscillator strengths are in general rather large. They are also comparatively slowly varying functions of R , the internuclear separation. Their computed values are, moreover, not unduly sensitive to the precise form of the wave functions adopted (Bates 1951, Dalgarno and Poots 1954, Moiseiwitsch and Stewart 1954). The transitions are thus representative only of a restricted class. To provide further accurate information on molecular oscillator strengths a study is made in the present paper of the transitions shown in table 2. Apart from the general interest attached to them, the oscillator strengths of these transitions are required in connection with a certain collision problem (cf. Bates, Massey and Stewart 1953). We wish to thank Professor H. S. W. Massey for many helpful discussions on this aspect of the investigation.

Table 2. Transitions of H_2^+ investigated in present paper

United atom designation	Separated atoms designation†
$1s\sigma_g-3p\sigma_u$	$\sigma(1s)-\sigma^*(2s, 2p_z)$
$1s\sigma_g-4p\sigma_u$	$\sigma(1s)-\sigma^*(3s, 3p_z, 3d_z)$
$1s\sigma_g-4f\sigma_u$	$\sigma(1s)-\sigma^*(2s, 2p_z)$
$2p\sigma_u-2s\sigma_g$	$\sigma^*(1s)-\sigma(2s, 2p_z)$
$2p\sigma_u-3s\sigma_g$	$\sigma^*(1s)-\sigma(3s, 3p_z, 3d_z)$
$2p\sigma_u-3d\sigma_g$	$\sigma^*(1s)-\sigma(2s, 2p_z)$

† The symbols within the brackets represent the atomic orbitals which of course belong to both nuclei. Odd (u) σ states are indicated with an asterisk and even (g) σ states are left plain. (The reverse is done for odd and even π states.)

§ 2. CALCULATIONS

Taking the nuclei as stationary, the oscillator strength connecting a lower electronic state A to an upper electronic state B is

$$f(A-B|R) = \frac{1}{3} E(A-B|R) G(A-B) |Q(A-B|R)|^2 \quad \dots\dots(1)$$

where $E(A-B|R)$ is the vertical energy difference (or photon energy) measured in rydbergs, $G(A-B)$ is the orbital degeneracy factor and $Q(A-B|R)$ is the transition integral (Mulliken 1939). This transition integral is given by

$$Q(A-B|R)\mathbf{t} = \int \chi_B^*(\mathbf{r}|R) \mathbf{r} \chi_A(\mathbf{r}|R) d\mathbf{r} \quad (\text{length}) \quad \dots\dots(2)$$

$$= -\frac{2}{E(A-B|R)} \int \chi_B^* \nabla \{\chi_A(\mathbf{r}|R)\} d\mathbf{r} \quad (\text{velocity}) \quad \dots\dots(3)$$

$$= \frac{4}{\{E(A-B|R)\}^2} \int \chi_B^* (\mathbf{r}|R) \nabla \{V(\mathbf{r}|R)\} \chi_A(\mathbf{r}|R) d\mathbf{r} \quad (\text{acceleration}) \quad \dots\dots(4)$$

where \mathbf{t} is some unit vector, \mathbf{r} is the position vector of the electron, $\chi_A(\mathbf{r}|R)$ and $\chi_B(\mathbf{r}|R)$ are the wave functions of the states indicated and $V(\mathbf{r}|R)$ is the potential of the electron in the field of the nuclei, all in atomic units (Chandrasekhar 1945). The three expressions are of course not identical if approximate wave functions are used. When necessary the Q 's and f 's derived from them will be distinguished by the superscripts L, V and A respectively.

The exact two centre wave functions of the σ -states of the hydrogen molecular ion may be written in the form

$$\chi(\mathbf{r}|R) = \Lambda(\lambda|R)M(\mu|R) \quad \dots\dots(5)$$

where λ and μ are the usual elliptical coordinates (cf. Mott and Sneddon 1948) and Λ and M (both of which are real) are expressible in terms of parameters tabulated by Bates, Ledsham and Stewart (1953). With the aid of these functions the required matrix elements may readily be evaluated. The dipole length formula (2) is much the most convenient to use. As may readily be seen (cf. Bates, Öpik and Poots 1953), the double integration entailed reduces to single integrations over λ (which must be done numerically) and single integrations over μ (which may be done analytically). The severe cancellation occurring in many cases causes the results to be disproportionately affected by small numerical errors. It was desirable therefore to obtain some check on the computational work. This was

achieved by re-calculating the majority of the matrix elements from the dipole acceleration formula (4)† which, when expressed in elliptical coordinates, becomes

$$Q(A-B|R) = \frac{8\pi R}{\{E(A-B|R)\}^2} \int_1^\infty \int_{-1}^1 \Lambda_B M_B \left\{ \frac{(1-\lambda\mu)(\lambda+\mu)}{(\lambda-\mu)^2} \right\} \Lambda_A M_A d\lambda d\mu \dots (6)$$

for σ - σ transitions. The M 's are normally represented by a sum of the Legendre polynomials, but this sum can of course be converted to the power series

$$M = \sum_{t=0}^{\infty} c(t) \mu^t \dots\dots (7)$$

the c 's being known constants for a given state and a given internuclear separation. Substitution in (6) yields

$$Q(A-B|R) = \frac{8\pi R}{\{E(A-B|R)\}^2} \int_1^\infty \Lambda_A \Lambda_B \sum_{t_1 t_2} c_A(t_1) c_B(t_2) \alpha(t_1+t_2) d\lambda \dots\dots (8)$$

where

$$\alpha(n) = \int_{-1}^1 \mu^n \left\{ \frac{(1-\lambda\mu)(\lambda+\mu)}{(\lambda-\mu)^2} \right\} d\mu \dots\dots (9)$$

which may be evaluated using the recurrence relation

$$\alpha(n) = 2\lambda\alpha(n-1) - \lambda^2\alpha(n-2) + \begin{cases} 2(1-\lambda^2)/n & n \text{ odd} \\ 4\lambda/(n^2-1) & n \text{ even} \end{cases} \dots\dots (10)$$

and noting that

$$z(0) = -6\lambda + (3\lambda^2 - 1) \ln \left(\frac{\lambda+1}{\lambda-1} \right), \quad \alpha(1) = 2 - 10\lambda^2 + (5\lambda^3 - 3\lambda) \ln \left\{ \frac{\lambda+1}{\lambda-1} \right\} \dots (11)$$

The integration over λ must be carried out by numerical methods. In all cases the agreement with the results obtained by the alternative procedure (using formula (2)) was found to be essentially perfect.

For comparison purposes the oscillator strengths associated with the transitions to the states which have principal quantum 2 in the separated atoms limit were also evaluated, taking for the wave functions the appropriate l.c.a.o. approximation: that is, taking

$$\chi_A = \{\phi(\mathbf{r}_1|1s) \pm \phi(\mathbf{r}_2|1s)\} / (2 \pm 2S)^{1/2}, \quad S = (1 + R + \frac{1}{3}R^2) \exp(-R) \dots\dots (12)$$

$$\chi_B = a_s \{\phi(\mathbf{r}_1|2s) \pm \phi(\mathbf{r}_2|2s)\} + a_p \{\phi(\mathbf{r}_1|2p) \pm \phi(\mathbf{r}_2|2p)\} \dots\dots (13)$$

in which the upper signs are adopted for the even states and the lower for the odd states; the ϕ 's are normalized hydrogenic wave functions based on nucleus 1 or 2 as indicated (the polar angles θ_1 and θ_2 being measured in opposite senses from the molecular axis); and a_s and a_p are parameters determined using the variational theorem (Gilbert 1933). Only the dipole length and velocity formulae were applied, the dipole acceleration formulae being of less interest since the heavy weighting it gives the region near the nuclei renders particularly doubtful whether any conclusions which might be drawn from the results for the special case of H_2^+ would be valid for complex molecules (for which in any event it is not commonly employed). The final expressions obtained for Q^L and Q^V are rather cumbersome and need not be presented since they may easily be recovered, the integrals involved being simply combinations of the J -functions of Coulson (1942).

† The dipole velocity formula (3) could of course also have been used and is rather simpler. However, it provides a less exacting test of the wave functions themselves.

§ 3. RESULTS

3.1

Figures 1, 2 and 3 give the transition integrals Q as functions of the internuclear separation R for the six transitions investigated. As may be seen, the fractional variation may be very marked. Thus in the case of the $1s\sigma_g-3p\sigma_u$, $1s\sigma_g-4p\sigma_u$ and $2p\sigma_u-3s\sigma_g$ transitions Q is of different sign in the united and separated limits and

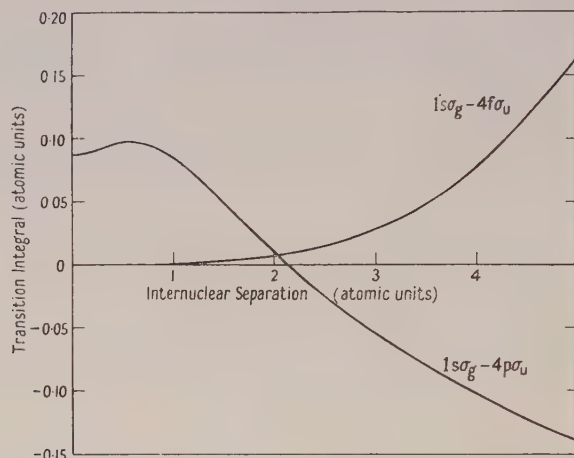


Figure 1. $1s\sigma_g-4p\sigma_u$ and $1s\sigma_g-4f\sigma_u$ transition integrals calculated from the exact wave functions.

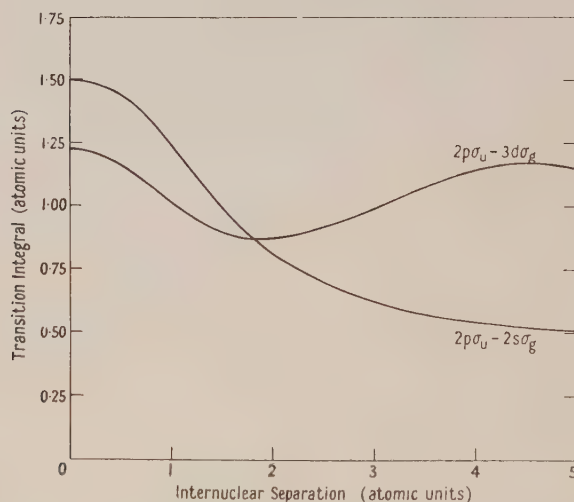


Figure 2. $2p\sigma_u-2s\sigma_g$ and $2p\sigma_u-3d\sigma_g$ transition integrals calculated from the exact wave functions.

passes through zero at some intermediate value of R ; and in the case of the $1s\sigma_g-4f\sigma_u$ transition, which is forbidden in the united limit but allowed in the separated limit, Q increases extremely rapidly with R , as would be expected. Such variation is of importance in connection with the calculation of the relative intensities in band systems.

The spontaneous transition probability between the levels v_a and v_b of two electronic states A and B is given by

$$\mathcal{A} = C\nu(v_b, B - v_a, A)^3 G(B-A) \left| \int P(R|v_a, A) Q(A-B|R) P(R|v_b, B) dR \right|^2 \quad (14)$$

where C is an atomic constant which need not be specified, ν is the frequency of the radiation emitted, $G(B-A)$ is the orbital degeneracy factor and the P 's are the vibrational wave functions (cf. Mulliken 1939). It is customary to assume that Q is a slowly varying function of R and to take it outside the integral sign so that (14) becomes

$$\mathcal{A} \simeq C\nu(v_b, B - v_a, A)^3 G(B-A) Q(A-B)^2 p(v_b, B - v_a, A) \quad \dots\dots (15)$$

with

$$p(v_b, B - v_a, A) = \left| \int P(R|v_a, A) P(R|v_b, B) dR \right|^2.$$

The dimensionless quantity p appearing in (15) is sometimes referred to as the *Franck-Condon factor*[†] of the band concerned.

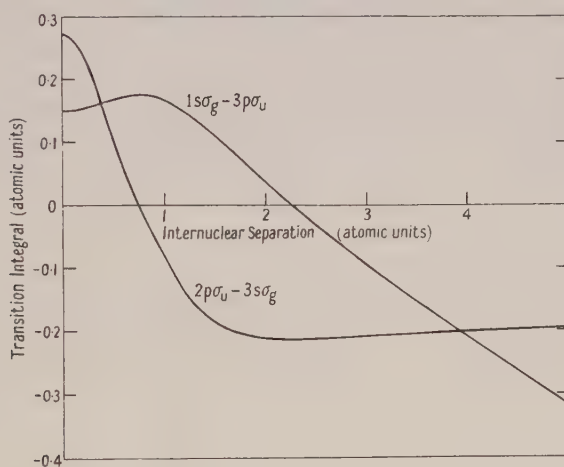


Figure 3. $1s\sigma_g-3p\sigma_u$ and $2p\sigma_u-3s\sigma_g$ transition integrals calculated from the exact wave functions.

In recent years much effort has been devoted to the computation of the Franck-Condon factors of the bands of many systems. It is clear, however, that caution must be exercised before using these in deriving relative intensities. For though the value of the integral in (14) is not so sensitive to the dependence of Q on R as it might at first be thought to be (cf. Bates 1949, Poots 1953), nevertheless a variation such as occurs for some of the H_2^+ transitions would certainly make (15) a very poor approximation. In particular the passage of Q through zero in the R -range of relevance would render the approximation almost worthless. As Shuler (1952) has emphasized it is desirable that consideration should be given to the possible variation in all detailed calculations on relative intensities. Special care is required with transitions which are forbidden in either the united or separated limits (or in both) since with these the variation is likely to be rapid: for example, naïve use of Franck-Condon factors appears to lead to quite erroneous relative intensities in the case of the $A^2\Sigma^+ - X^2\Pi$ transition of the hydroxyl radicle (Shuler 1950).

[†] The phrase *relative transition probability* is also sometimes used but is not altogether satisfactory since $\mathcal{A}(v_b, B - v_a, A)$ also depends on $\nu(v_b, B - v_a, A)$; and in addition, by its descriptive nature it gives the number p a significance which may be misleading.

Table 3. Photon Energies E and Oscillator Strengths f of some Transitions of the Hydrogen Molecular Ion

R	E	$1s\sigma_g-3p\sigma_u$			E	$1s\sigma_g-4f\sigma_u$			exact f
		f^L	l.c.a.o. approx.	exact f		f^L	l.c.a.o. approx.	exact f	
0.0	3.5556	2.2×10^{-1}	5.9×10^{-2}	$2.6_4 \times 10^{-2}$	3.7500	1.0	5.6×10^{-2}	0	
0.4	3.1508	5.4×10^{-2}	3.3×10^{-2}	$2.8_3 \times 10^{-2}$	3.3514	1.1	8.5×10^{-2}	$1.2_9 \times 10^{-8}$	
0.8	2.6409	3.7×10^{-3}	8.8×10^{-3}	$2.6_5 \times 10^{-2}$	2.8584	1.0	1.1×10^{-1}	$3.2_4 \times 10^{-7}$	
1.2	2.2359	1.7×10^{-2}	7.9×10^{-4}	$1.6_3 \times 10^{-2}$	2.4735	1.0	1.1×10^{-1}	$2.5_1 \times 10^{-6}$	
1.6	1.9281	3.4×10^{-2}	1.9×10^{-4}	$6.0_2 \times 10^{-3}$	2.1798	1.0	1.0×10^{-1}	$1.1_7 \times 10^{-5}$	
2.0	1.6944	4.5×10^{-2}	2.0×10^{-3}	$8.2_4 \times 10^{-4}$	1.9520	1.1	8.6×10^{-2}	$4.0_7 \times 10^{-5}$	
3.0	1.3154	5.6×10^{-2}	9.6×10^{-3}	$4.1_1 \times 10^{-3}$	1.5640	1.4	5.2×10^{-2}	$4.4_2 \times 10^{-4}$	
4.0	1.1019	6.1×10^{-2}	1.9×10^{-2}	$1.6_1 \times 10^{-2}$	1.3273	1.9	3.0×10^{-2}	$2.6_7 \times 10^{-3}$	
5.0	0.9767	6.5×10^{-2}	5.1×10^{-2}	$3.2_5 \times 10^{-2}$	1.1730	2.5	2.5×10^{-2}	$1.0_7 \times 10^{-2}$	

R	E	$2p\sigma_u-2s\sigma_g$			E	$2p\sigma_u-3d\sigma_g$			exact f
		f^L	l.c.a.o. approx.	exact f		f^L	l.c.a.o. approx.	exact f	
0.0	0	0	∞	0	0.5556	4.8×10^{-3}	8.8×10^{-1}	$2.7_8 \times 10^{-1}$	
0.4	0.0734	3.5×10^{-3}	1.7×10^{-1}	$5.2_7 \times 10^{-2}$	0.5762	5.4×10^{-3}	8.2×10^{-1}	$2.6_9 \times 10^{-1}$	
0.8	0.2077	1.0×10^{-2}	6.6×10^{-2}	$1.2_4 \times 10^{-1}$	0.6373	7.0×10^{-3}	7.0×10^{-1}	$2.4_6 \times 10^{-1}$	
1.2	0.3606	1.8×10^{-2}	4.2×10^{-2}	$1.5_6 \times 10^{-1}$	0.7241	9.4×10^{-3}	5.7×10^{-1}	$2.2_0 \times 10^{-1}$	
1.6	0.5020	2.6×10^{-2}	3.3×10^{-2}	$1.5_2 \times 10^{-1}$	0.8064	1.2×10^{-2}	4.7×10^{-1}	$2.1_1 \times 10^{-1}$	
2.0	0.6133	3.2×10^{-2}	3.0×10^{-2}	$1.3_6 \times 10^{-1}$	0.8635	1.5×10^{-2}	4.0×10^{-1}	$2.1_9 \times 10^{-1}$	
3.0	0.7651	4.3×10^{-2}	3.0×10^{-2}	$1.0_0 \times 10^{-1}$	0.8878	1.8×10^{-2}	3.0×10^{-1}	$2.9_1 \times 10^{-1}$	
4.0	0.8141	4.7×10^{-2}	3.3×10^{-2}	$8.1_0 \times 10^{-2}$	0.8196	1.7×10^{-2}	2.5×10^{-1}	$3.5_9 \times 10^{-1}$	
5.0	0.8236	5.0×10^{-2}	3.7×10^{-2}	$7.0_7 \times 10^{-2}$	0.7426	1.2×10^{-2}	2.2×10^{-1}	$3.2_8 \times 10^{-1}$	

R	E	$1s\sigma_g-4p\sigma_u$			E	$2p\sigma_u-3s\sigma_g$			exact f
		f^L	l.c.a.o. approx.	exact f		f^L	l.c.a.o. approx.	exact f	
0.0	3.7500			$9.6_6 \times 10^{-3}$	0.5556			$1.3_6 \times 10^{-2}$	
0.4	3.3489			$1.0_0 \times 10^{-2}$	0.5927			$4.5_7 \times 10^{-3}$	
0.8	2.8493			$8.3_2 \times 10^{-3}$	0.6784			$1.0_8 \times 10^{-4}$	
1.2	2.4570			$4.3_3 \times 10^{-3}$	0.7898			$5.3_4 \times 10^{-3}$	
1.6	2.1591			$1.2_1 \times 10^{-3}$	0.8969			$1.1_4 \times 10^{-2}$	
2.0	1.9306			$5.5_4 \times 10^{-5}$	0.9797			$1.4_8 \times 10^{-2}$	
3.0	1.5511			$1.5_5 \times 10^{-3}$	1.0776			$1.5_7 \times 10^{-2}$	
4.0	1.3296			$4.6_8 \times 10^{-3}$	1.0891			$1.4_6 \times 10^{-2}$	
5.0	1.1950			$7.8_1 \times 10^{-3}$	1.0712			$1.3_7 \times 10^{-2}$	

3.2

The oscillator strengths based on the exact wave functions and on the l.c.a.o. approximation† for them are displayed in table 3.

A striking feature of the exact values is that when R is close to $2a_0$ all those associated with transitions from the $1s\sigma_g$ state are abnormally small. This feature is an immediate consequence of the fact that the oscillator strength of the $1s\sigma_g-2p\sigma_u$ transition is here almost $\frac{1}{3}$ (Bates 1951), which is the value given by the Thomas-Kuhn rule for the *sum* of the oscillator strengths of all $1s\sigma_g-nl\sigma_u$ transitions. It is interesting to note that the required smallness of the oscillator strengths is achieved by the corresponding (Q, R) curves crossing the zero line. This crossing phenomenon may well be a characteristic of many spectral series and would seem particularly likely if a member has an oscillator strength near the maximum possible.

Since the oscillator strength of the $2p\sigma_u-1s\sigma_g$ transition is negative, its large magnitude when R equals $2a_0$ does not necessitate that the oscillator strengths of the upward transitions $2p\sigma_u-nl\sigma_g$ be small. On the contrary it necessitates that at least certain of them be considerable since their sum must be almost $\frac{2}{3}$ for the Thomas-Kuhn sum rule to be satisfied.

Inspection of the tables reveals that the results obtained with the l.c.a.o. approximation are sometimes not even of the right order. The dipole velocity formula is usually (but not always) rather more successful than is the dipole length formula. On the limited evidence available it would of course be unwise to assume that the same is true in the case of complex molecules. With either formula the l.c.a.o. approximation yields correct predictions as to whether or not a particular transition integral passes through zero, but this may be fortuitous.

REFERENCES

- BATES, D. R., 1949, *Proc. Roy. Soc. A*, **196**, 217; 1951, *J. Chem. Phys.*, **19**, 1122.
 BATES, D. R., DARLING, R. T. S., HAWE, S. C., and STEWART, A. L., 1953, *Proc. Phys. Soc. A*, **66**, 1124.
 BATES, D. R., LEDSHAM, K., and STEWART, A. L., 1953, *Phil. Trans. Roy. Soc. A*, **246**, 215.
 BATES, D. R., MASSEY, H. S. W., and STEWART, A. L., 1953, *Proc. Roy. Soc. A*, **216**, 437.
 BATES, D. R., ÖPIK, U., and POOTS, G., 1953, *Proc. Phys. Soc. A*, **66**, 1113.
 CHANDRASEKHAR, S., 1945, *Astrophys. J.*, **102**, 223.
 COULSON, C. A., 1942, *Proc. Camb. Phil. Soc.*, **38**, 210; 1952, *Valence* (Oxford: Clarendon Press), p. 90.
 DALGARNO, A., and POOTS, G., 1954, *Proc. Phys. Soc. A*, **67**, 343.
 GILBERT, C., 1933, *Phil. Mag.*, **14**, 929.
 HERZBERG, G., 1950, *Molecular Spectra and Molecular Structure*, 2nd Edn, **1**, *Spectra of Diatomic Molecules* (London: Macmillan), p. 330.
 MOISEWITSCH, B. L., and STEWART, A. L., 1954, *Proc. Phys. Soc. A*, **67**, 457.
 MOTT, N. F., and SNEDDON, I. N., 1948, *Wave Mechanics and its Applications* (Oxford: Clarendon Press), p. 184.
 MULLIKEN, R. S., 1939, *J. Chem. Phys.*, **7**, 14, 20.
 POOTS, G., 1953, *Proc. Phys. Soc. A*, **66**, 1181.
 SHULER, K. E., 1950, *J. Chem. Phys.*, **18**, 1221; 1952, *Proc. Phys. Soc. A*, **65**, 70.

† The exact photon energies were used even with the l.c.a.o. approximation.

The Decay of ^{207}Bi and the Energy Levels of ^{207}Pb

By J. R. PRESCOTT *

The Clarendon Laboratory, Oxford

MS. received 16th September 1953, and in final form 2nd March 1954

Abstract. The electron-capture decay of ^{207}Bi has been studied by scintillation counter coincidence techniques. Gamma-rays of energy 0.57, 1.07, 1.76 and 2.47 MeV were found in the relative abundances 1.57:1:0.16:0.0072. 'Prompt' coincidences were observed between the three former and the K-capture x-ray. The following percentages of the gamma-rays were prompt: 0.57:19%; 1.07:6%; 1.76:7%. There is some evidence for a prompt gamma-ray of 1.46 MeV. The 1.76 and 1.07 MeV gamma-rays are in coincidence with the 0.57 MeV gamma-ray. The results are discussed in relation to the level scheme of ^{207}Pb .

§ 1. INTRODUCTION

EXPERIMENTAL information about the energy levels of stable ^{207}Pb comes from a variety of sources which are quoted in detail in § 2. The greater part of this information was available to Pryce (1952), who constructed a level scheme using the shell model to make definite spin, parity and orbital angular momentum assignments to many of the levels.

The present work is an extension of that on ^{207}Bi (which decays to ^{207}Pb by electron capture) reported earlier (Grace and Prescott 1951) and was designed to clarify details of Pryce's level scheme. For this reason it will be an advantage first to summarize the existing experimental data (§ 2). In § 3 the results of the present experiments are given. Discussion is presented in § 4.

§ 2. PREVIOUS WORK ON THE LEVELS OF ^{207}Pb

2.1. *Experimental*

(i) The spin and magnetic moment of the ground state of ^{207}Pb show that it has the configuration $p_{1/2}$ (Klinkenberg 1952).

(ii) The short-range alpha groups from ^{211}Po , which decays to ^{207}Pb , indicate levels at 0.54 ± 0.04 ; 0.88 ± 0.04 and 1.11 ± 0.06 MeV (Neumann and Perlman 1951, Spiess 1951). However, the 6.34 MeV alpha-particle corresponding to the level at 1.11 MeV is not found in a more recent investigation by Hoff and Asaro (1953).

(iii) A weak gamma-ray of energy 0.870 MeV is found by Surugue (1946) in the decay ^{207}Tl to ^{207}Pb .

(iv) Neumann and Perlman (1951) also find gamma-rays following the electron-capture decay of ^{207}Bi (from conversion electron measurements in the beta-ray spectrograph) of energy 0.565, 1.063, 1.46, 2.05, 2.20, 2.33 and 2.49 MeV and one of low energy, either 0.137 or 0.064 MeV. Wapstra (1953) finds conversion electrons for gamma-rays of energy 0.565 and 1.063 MeV and identifies Neumann and Perlman's low-energy electron as the KLL Auger line. Scintillation counter measurements have been made by Grace and Prescott (1951) and Wapstra (1953) showing gamma-rays of energy 0.56 and 1.06 MeV. At least some of these are in coincidence.

* Now at the Physics Department, University of Melbourne.

(v) An isomeric state of ^{207}Pb , of lifetime 0.82 sec, is associated with gamma-rays of 0.52 and 1.05 mev (Campbell and Goodrich 1950, Campbell and Nelson 1953, Hopkins 1952, Lascoux and Vendryes 1951). These gamma-rays are to be identified with the 1.06 and 0.56 mev gamma-rays in the decay of ^{207}Bi . Goldhaber and Sunyar (1951) show that the lifetime is determined by the 1.06 mev gamma-ray which is an M4 transition. This assignment is confirmed by measurements of the internal conversion coefficient and K/L ratio (Wapstra 1953). The 0.56 mev gamma-ray follows the 1.06 mev gamma-ray and is E2 (Wapstra 1953, Grace and Prescott 1951).

(vi) The $^{206}\text{Pb}(\text{d}, \text{p})^{207}\text{Pb}$ and $^{208}\text{Pb}(\text{d}, \text{t})^{207}\text{Pb}$ reactions have been studied by Harvey (1953). He finds unresolved groups in the region 0.5–1 mev and interprets them as due to levels at 0.61 and 0.95 or, alternatively, by fitting to the lower energy, at 0.56 and 0.89 (0.90 for the (d, t) reaction). The (d, t) reaction shows a level at 1.63 and one at 2.33, while the (d, p) reaction reveals further levels at 2.75, 3.60, 4.42, 4.66 and 5.28 mev.

2.2. A Level Scheme for ^{207}Pb

A consistent level scheme (figure 1) can be set up from the above data. The arguments that lead to it are substantially those of Pryce (1952) modified, where necessary, to take account of more recent data.

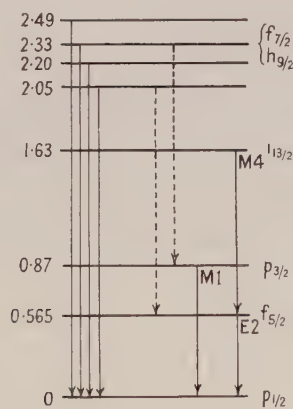


Figure 1. Level scheme for ^{207}Pb (after Pryce). Full lines show probable gamma transitions, dotted lines show possible transitions discussed in the text.

Lead 207 has a closed shell (82) of protons and one less (125) than a closed shell of neutrons. The shell model indicates that the configurations available for the ground and excited states will be those corresponding to the single hole in this 126 neutron shell, and they will follow approximately inversely the order in which the levels were filled. The configurations available are $p_{1/2}$, $p_{3/2}$, $f_{5/2}$, $i_{13/2}$, $f_{7/2}$, $h_{9/2}$ and possibly $g_{9/2}$, which is the first level in the next shell. The ground state is $p_{1/2}$, as expected.

The decay energy of ^{207}Tl is low and suggests that the 0.870 mev gamma-ray goes to ground, implying a level at 0.87 mev, corresponding to the alpha-group level at 0.88 ± 0.04 mev. The 1.06 mev isomeric transition is M4 and is followed by a further gamma-ray of energy 0.565 mev. It can only be $i_{13/2}$ to $f_{5/2}$ and cannot be to ground; the $i_{13/2}$ level is thus at least 1.63 mev above ground.

Below this are experimental levels at 0.54 and 0.87.* $h_{9/2}$ cannot be below $i_{13/2}$ since the $i_{13/2}$ to $h_{9/2}$ (M2) transition would eliminate the observed M4 transition. The beta-decay selection rules for ^{207}Tl require that the 0.87 mev level be $p_{3/2}$. This leaves $f_{5/2}$ or $f_{7/2}$ to be assigned to the remaining level. The level at about 0.54 mev is clearly $f_{5/2}$, making the 0.565 mev gamma-ray a ground-state transition from this level, in agreement with its E2 character, and the $i_{13/2}$ level is at 1.63 mev, where the (d, t) measurements locate a level.

The four gamma-rays of energy greater than 2 mev found by Neumann and Perlman are shown by them to be most likely ground-state transitions and must correspond to levels at these energies; they probably arise from configurations in which at least one nucleon is excited to the next shell or in which the core itself is excited.

The position of the $f_{7/2}$ and $h_{9/2}$ levels is undetermined. The ^{208}Pb (d, t) ^{207}Pb reaction is expected to give rise to levels corresponding to one neutron hole and the level at 2.33 is therefore probably $h_{9/2}$ or $f_{7/2}$. This cannot be the same as the level found at this energy by Neumann and Perlman since this radiates to the ground state. Harvey assigns $f_{7/2}$ to his 2.33 mev level. Harvey also makes shell model assignments to his high-energy levels; these are not shown in figure 1 since they will not be available to the decay of ^{207}Bi , which is the primary concern of the present paper.

§ 3. RESULTS

3.1. *Experimental Technique*

The ^{207}Bi was prepared by bombarding natural lead with 25 mev protons in the Harwell cyclotron. The bismuth was extracted either as BiOCl with the addition of carrier, or carrier-free by paper chromatography (see e.g. Balston and Talbot 1952). The decay was followed until the activity due to ^{205}Bi was negligible (about nine months) before measurements were begun.

All measurements were carried out by scintillation counting. For gamma-ray measurements 1 in. cubes of NaI(Tl) were used. Some details of the apparatus and the method of obtaining the energy calibration of the crystal in terms of photo-peak area have been described in an earlier publication (Prescott 1954). Recording was by single-channel kicksorter or 25-channel kicksorter of the 'gated oscillator' type (hereinafter referred to as SKS and MKS respectively) or by photographing the pulse-height distribution on a cathode-ray screen. For experiments where detection of x-rays was required, a slice of NaI(Tl) , 2 mm thick, was used. The efficiency of this for detecting Pb K x-rays was calculated to be 0.89 from the absorption coefficients (*Handbook of Chemistry and Physics*, 1951). After including the effect of absorption in the crystal housing and fluorescent yield† the net efficiency per K-shell vacancy is 0.825. It was calculated (data from Davisson and Evans 1952) that the maximum contribution to the count under the x-ray peak from the gamma-rays of ^{207}Bi did not exceed 2%, and this was confirmed by observation.

* The work of Neumann and Perlman (1951) on the short-range alphas from ^{211}Po requires a level at 1.11 mev. However, the corresponding alpha-particle is not found by Hoff and Asaro (1953). Harvey (1953) finds no evidence from (d, p) and (d, t) reactions for a level at this energy, and its existence must be regarded as extremely doubtful.

† The fluorescent yield was taken as 0.95 from the measurement of Broyles (1952) on mercury, viz. 0.946 ± 0.008 ; the theoretical value is 0.955 (Burhop 1952).

Coincidence measurements were carried out in three ways: Setting an SKS on the required region of the scintillation spectrum and either (i) causing it to gate the output of a second crystal into MKS, (ii) using it to trigger an oscillograph to which the second crystal output was fed, (iii) feeding the output into a Harwell type 1036 coincidence unit together with the output of a second SKS set on the output from the second crystal.

All three methods were used in coincidence measurements reported here. The gating crystal will be designated 'crystal I' and the gated crystal 'crystal II'. Methods (i) and (iii) were used to obtain quantitative results.

3.2. The Gamma-Ray Spectrum

The radiations from the ^{207}Bi as examined with a single crystal scintillation spectrometer showed radiation of about 70 kev which was identified as the expected K x-radiation of lead by critical absorption in Ir and Os.

Figure 2 shows typical scintillation spectra. The spectrum to 2 mev was obtained with SKS, and above this energy by MKS because of the low counting rates. There are four readily distinguishable lines: 0.57 ± 0.01 ; 1.07 ± 0.01 ;

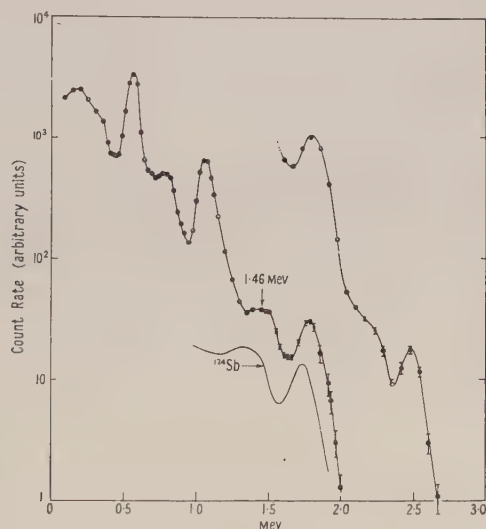


Figure 2. Gamma-ray scintillation spectrum of ^{207}Bi .

1.76 ± 0.02 ; 2.47 ± 0.05 mev. The first two are well known (see §2). The 1.76 mev line is not reported by Neumann and Perlman (1951). A long-lived gamma-ray of 1.77 mev has been found by Wapstra (1953) both in the scintillation spectrum and in the beta-ray spectrometer, though he does not assign it to ^{207}Bi . Gamma-rays of very closely similar energy were also found in the present experiments in the spectra of ^{206}Bi and ^{205}Bi . The 2.47 mev line presumably corresponds to the 2.49 mev line found by Neumann and Perlman. It is not possible to distinguish the 2.05, 2.20 and 2.33 mev lines of Neumann and Perlman in the present spectrum. Any one of them might have an intensity up to one-fifth of that of the 2.47 mev gamma-ray. There is no evidence in the spectrum for the 0.137 or 1.46 mev gamma-rays of Neumann and Perlman or the 0.870 mev gamma-ray of Surugue (1946). The 0.137 mev gamma-ray was

looked for using the thin crystal to reduce the count from the higher energy gamma-rays. If it occurs it is certainly less than about 5% of all disintegrations. The 0.870 mev gamma-ray is not expected to occur in the decay of ^{207}Bi because the level from which it originates can only be reached by a highly forbidden electron capture (see §4). The absence of the 1.46 mev gamma-ray presents a puzzle. Its location is indicated by an arrow in figure 2. Comparison with the line-shape of the 1.71 mev gamma-ray in ^{124}Sb , drawn immediately below, shows that, if present, the 1.46 mev gamma-ray cannot exceed 10% of the intensity of the 1.76 mev gamma-ray. Wapstra (1953) also finds no evidence for it. Now the observed K/L ratio (2.8) of the 1.46 mev gamma-ray (Neumann and Perlman) indicates that its multipolarity is either E4 or E5 (or possibly E3 or M4 if we permit an error of 100%). α_K for E4 and E5 transitions of this energy are respectively 9.9×10^{-3} and 1.66×10^{-2} . The observed K-conversion electrons of the 1.06 and 1.46 mev gamma-rays (Neumann and Perlman 1951) are in the ratio 34:1. Taking the 1.06 mev gamma-ray as M4 (§2) with $\alpha_K = 0.103$ (Rose *et al.* 1951), then the ratio of the intensities of the 1.07 and 1.46 mev gamma-rays should be 3.2 and 5.5 for E4 and E5 transitions respectively. A 1.46 mev gamma-ray of this intensity would be readily identified. Assignment of any other multipolarity to the 1.46 mev gamma-ray requires that it should be even more intense.

We are obliged to conclude either that the 1.46 mev gamma-ray of Neumann and Perlman does not belong to ^{207}Bi or that their internal conversion data are seriously in error.

The observed relative intensities of the four prominent gamma-rays are: $1.57 \pm 0.06 : 1.016 \pm 0.01 : 0.0072 \pm 0.0008$ in the order 0.57, 1.07, 1.76, 2.47 mev. They are corrected for the efficiency of the crystal but not for internal conversion. The errors are composed partly of the error in the efficiency calibration and partly of the standard deviation of the mean of a number of determinations of each photo-peak area.* The relative intensities of the first two agree reasonably well with those of Wapstra (1953) and the 1.76 mev gamma-ray is of the same relative intensity as the long-lived 1.77 mev gamma-ray of Wapstra (1953 and private communication).

3.3. Coincidences with X-Rays—Region less than 1.3 mev

Figure 3 shows the spectrum of gamma-rays, in the energy region 0.35–1.3 mev, which are in coincidence with K x-rays, with an ungated spectrum for comparison. This covers the region containing the two prominent lines at 0.57 and 1.07 mev and was obtained by setting SKS on the x-ray photo-peak in the small crystal and using it to gate crystal II into MKS.

It is clear from figure 3 that at least some of *both* the 0.57 and the 1.07 mev gamma-rays are in *prompt* coincidence with the x-rays. The former can be readily understood since K-capture direct to the 0.565 mev level (figure 1) would give this gamma-ray. The presence of prompt coincidences involving the 1.07 mev gamma-ray, however, is quite unexpected since this line has been identified (§2) as an isomeric transition of 0.8 sec lifetime. Since the gate has a resolving time of about $1.5 \mu\text{sec}$, prompt coincidences between the isomeric

* In an earlier publication (Grace and Prescott 1951) the 0.57 and 1.07 mev lines were reported to be about equal in intensity, but the calibration error was then considerable.

gamma-ray and x-rays should be negligible (less than 1 in 10^5). In fact, the coincidence rates show that $9.5 (\pm 0.5)\%$ of the '1.07' mev gamma-rays are in prompt coincidence with the x-rays.

The result was obtained by all three of the coincidence methods described in §3.1 and the two alternative quantitative methods were consistent. Two different ^{207}Bi sources gave similar results. Since the result is of some importance, a careful examination of all possible sources of spurious coincidences was made:

(i) *Accidentals*. The accidental rate was obtained by removing the x-ray crystal and photomultiplier and operating them with an independent x-ray source, leaving the source and crystal II in the original geometry. This avoids the necessity of knowing resolving times accurately. Accidentals account for 0.5% in the above figure.

(ii) *Internal Conversion*. Some coincidences will take place with the x-rays following internal conversion of the 0.57 mev gamma-ray since this is in coincidence with the 1.07 mev gamma-ray (Grace and Prescott 1951, Wapstra 1953, and §3.5). The internal conversion coefficient is 1.8×10^{-2} (Rose *et al.* 1951), so that at most this contributes 1.8% to the original figure of 9.5%. Internal conversion *electrons* cannot give coincidences.

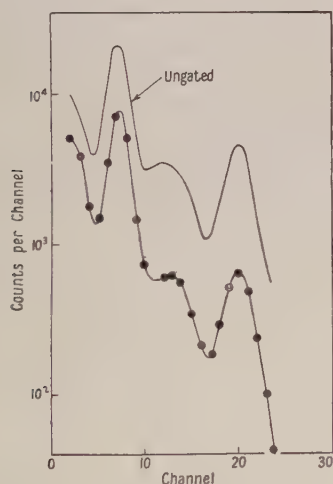


Figure 3. Gamma-rays in coincidence with K x-rays in ^{207}Bi ; energy region 0.35–1.3 mev.

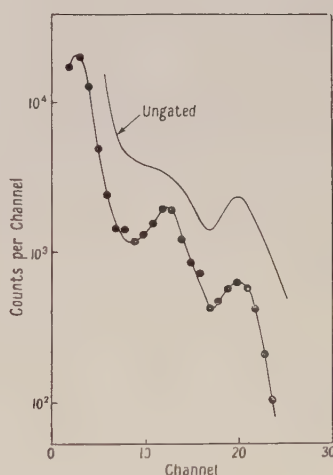


Figure 4. Gamma-rays in coincidence with K x-rays in ^{207}Bi ; energy region above 1.1 mev.

(iii) *Gamma-gamma coincidences*. Some 0.57 mev gamma-rays are directly detected by Compton effect under the x-ray peak and give coincidences. The fraction was calculated to be 1.2%.

(iv) *Scattering*. Radiation of 0.57 mev is scattered by the surroundings into a lower energy with a correspondingly higher probability of detection by the x-ray crystal. In the geometry of the present experiments the only significant scattering could have been backscattering in crystal II, and in these circumstances the energy release in this crystal does not fall under the 1.07 mev photo-peak, nor does it do so for backscattering of the 1.07 mev gamma-ray itself.

Allowing for all the above sources of coincidences, $6(\pm 0.5)\%$ of the '1.07' mev gamma-rays remain as prompt. In fact this is a lower limit since possible L-capture has been neglected; in bismuth L-capture should account for a minimum of 13% of decays (Rose and Jackson 1949, Marshak 1942). The result means that there are two gamma-ray lines close together at about 1.06–1.07 mev. Even if their energies are not very close together, the prompt one may well have been missed in beta-spectrograph measurements since the intensity of its K-conversion electron relative to that from the isomeric 1.063 mev transition is less than about 1% for any reasonable choice of multipolarity.

In a similar way, $19.3(\pm 1.8)\%$ of the 0.57 mev gamma-rays are found to be prompt, neglecting L-capture.

3.4. Coincidences with X-Rays—Region greater than 1.1 mev

Figure 4 extends the coincidence spectrum to include the region of the 1.76 mev gamma-ray; an ungated spectrum is included for comparison. At channel 20 is the photo-peak of the 1.76 mev gamma-ray, and there is clear evidence for a further gamma-ray at about channel 12 corresponding to an energy of 1.46 ± 0.03 mev—possibly the 1.46 mev gamma-ray of Neumann and Perlman. The intensity of the 1.46 mev gamma-ray in the coincidence spectrum is $1.2(\pm 10\%)$ times that of the 1.76 line. The fact that the gated and ungated spectra are different shows that the 1.46 and 1.76 mev gamma-rays do not originate from the same level, for this would require the same coincidence efficiency for each.

The most interesting quantitative feature of figure 4 is that only $7.0(\pm 0.4)\%$ of the 1.76 mev gamma-rays are in coincidence with K x-rays. This means that the level from which this gamma-ray originates is either an isomeric state of 10–20 μ sec half-life or it is fed substantially by L-capture.

The first alternative was checked by direct coincidence methods in the following way: Coincidences between the 1.76 mev gamma-ray and K x-rays gave $7.4(\pm 0.6)\%$ of coincidences (in agreement with the gated spectrum figure). The experiment was then repeated with the high energy gamma-ray in ^{206}Bi given by Alberger and Friedlander (1951) as 1.72 mev and measured in the present experiments as 1.70 mev. This gamma-ray is known to be prompt (Alberger and Friedlander 1951) and the fraction in coincidence with the x-ray was $86(\pm 4)\%$. The fact that this is not 100% is presumably due to L-capture, which is of about the amount predicted by theory (Rose and Jackson 1949). This measurement establishes that there is no instrumental bias in recording coincidences in this energy region and establishes confidence that the figure of 7.4% for ^{207}Bi is correct. A 6 μ sec delay was now inserted in the x-ray channel and the measurement on ^{207}Bi repeated. The only coincidences observed were those to be expected from accidentals ($\sim 10\%$ of the coincidence rate without the delay); nor did alteration of resolving time affect the net coincidence rate. It is concluded that the 1.76 mev gamma-ray is not from an isomeric transition and that the low observed coincidence rate results from L-capture. Unfortunately it was not possible to look for coincidences between L x-rays and the 1.76 mev gamma-ray, but it is hoped to perform this experiment at a later date.

Attempts to establish coincidences between x-rays and the gamma-rays of energy greater than 2 mev were inconclusive, due to lack of source strength. The

levels from which these originate are probably also fed partly by L-capture. No evidence was found in the coincidence spectrum for either the 0.064 or 0.137 mev gamma-ray of Neumann and Perlman (1951).

3.5. Gamma-Gamma Coincidences

Figure 5 (curve A) shows the spectrum of gamma-rays in coincidence with the 1.76 mev gamma-ray (in comparison with an ungated spectrum). It is clear that the latter is in coincidence with the 0.57 mev gamma-ray. This confirms that the 1.76 mev gamma-ray belongs to ^{207}Bi and suggests that at least some of the long-lived gamma-rays of this energy found by Wapstra (1953) should be assigned to this nuclide.

Figure 5 (curve B) shows the spectrum obtained when the gating kicksorter was set in the region 1.34–1.58 mev, i.e. to include any possible 1.46 mev gamma-ray, the experimental arrangement for figure 5 being chosen to minimize false coincidences due to backscattering. The 1.46 mev gamma-ray will fit into the level scheme of figure 1 between the 2.05 mev and the 0.565 mev level or the 2.33 mev and 0.870 mev level, and will therefore be in coincidence either with a

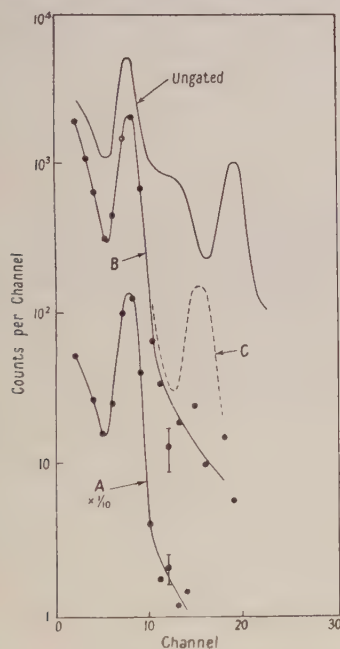


Figure 5. Gamma-gamma coincidence spectra; energy region 0.3–1.3 mev; for details see text.

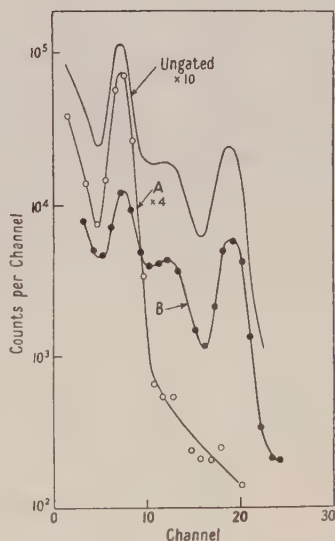


Figure 6. Gamma-gamma coincidence spectra; energy region 0.3–1.3 mev. Curve A is gated on the region of the 1.07 mev gamma-ray, curve B on the region of the 0.57 mev gamma-ray.

0.57 or 0.87 mev gamma-ray. There is no evidence in the gated spectrum for a gamma-ray of 0.87 mev. The previous section showed a 1.46 mev gamma-ray of total intensity 10% of the 1.76 mev gamma-ray (neglecting the unknown coincidence efficiency for the former). If it were in coincidence with a 0.87 mev gamma-ray the spectrum would appear as in curve C. The conclusion is that the 1.46 mev gamma-ray is in coincidence with the 0.57 mev gamma-ray.

Figure 6 shows the coincidence spectra involving the isomeric transition. Curve A is the spectrum gated on the 1.07 mev line and curve B on the region of the 0.57 mev line. These curves give the well-known result (Grace and Prescott 1951, Wapstra 1953) that at least some of the 0.57 and 1.07 mev gamma-rays are in coincidence. In addition, curve B forms quite a sensitive test for the existence of cascades involving two or more (unresolved) gamma-rays of energy about 0.57 mev.

Consider the idealized ^{207}Bi spectrum shown in figure 7. We are to gate on the region G in crystal I and observe the spectrum in coincidence with these

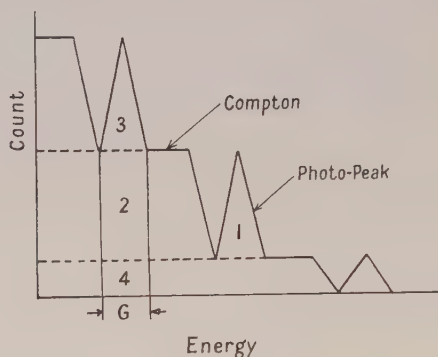


Figure 7. Idealized gamma-ray scintillation spectrum of ^{207}Bi .

pulses in crystal II. If we denote by Q_1 and Q_3 respectively the counts in the 1.07 and 0.57 mev photo-peaks in the *gated* spectrum, then an elementary calculation shows that

$$Q_3/Q_1 = k + fRx. \quad \dots\dots(1)$$

In this expression k is a constant depending on the width of the gating limits and is essentially the ratio of the areas 2 and 1 (figure 7). It can therefore be found with reasonable accuracy from a standard 1.07 mev spectrum. A small correction ($\sim 1\%$) involves the ratio of the areas 4 and 1. R , in expression (1), is the ratio ($2.35 (\pm 3\%)$) of the efficiencies of the crystals to 0.57 and 1.07 mev gamma-rays; x is the intensity (relative to that of the 1.07+0.57 mev cascade) of any cascade involving two or more '0.57' mev gamma-rays. The factor f assumes the values 2, 6, 12 . . . according as the cascade is two-, three-, four- . . . stage. The expression is valid so long as the gating limits are wide enough to include all of the 0.57 mev photo-peak.

In table 1 experimental values Q_3/Q_1 are compared with the estimated values

Table 1

Run	Exptl Q_3/Q_1	Estimated k
C49	1.07 ± 0.03	1.08 ± 0.03
C5	1.07 ± 0.03	1.08 ± 0.03
C51	1.13 ± 0.04	1.14 ± 0.04
B58	1.44 ± 0.05	1.40 ± 0.07

of k . Both were obtained graphically and the errors, which are estimated on the basis of many similar measurements, represent the limitations of this method.

Counting statistics were negligible in all cases. The larger errors in run B58 were due to poor resolution in the gating crystal. Table 1 shows no evidence for any contribution from possible multi-stage cascades. The probability that the term fRx in expression (1) exceeds 4% of k is only 0.005. At the same level of probability a three-stage cascade cannot exceed 0.3% and a two-stage cascade 0.9% of the intensity of the $1.07 + 0.57$ cascade.

§ 4. DISCUSSION

4.1. Summary of Experimental Results

The results of the previous section can be summarized as follows:

(i) The relative intensities of the gamma-rays observed with a scintillation spectrometer are given in table 2, uncorrected for internal conversion.

Table 2. Intensities of Gamma-Rays in ^{207}Bi

MeV	0.57	1.07	1.46	1.76	2.47
Total intensity	1.57 ± 0.06	1	not resolved	0.16 ± 0.01	0.0072 ± 0.0008
Coincident with with K x-rays	0.303 ± 0.03	0.06 ± 0.005	0.013 ± 0.002	0.011 ± 0.001	—

(ii) Implicit in table 2 is the following information: There are prompt gamma-rays of energy 0.57 and 1.07 mev. Only 7% of the 1.76 mev gamma-rays are in coincidence with K x-rays—the conclusion being that the level from which they originate is fed mainly by L-capture.

(iii) No evidence has been found for gamma-rays of energy 0.87 and 0.137 (or 0.064). Failure to find the latter is to be expected if Wapstra's explanation (1953) of the corresponding 'conversion electron' as the KLL Auger electron is correct.

(iv) The 1.07, 1.76 and plausibly 1.46 mev gamma-rays are in coincidence with the 0.57 mev gamma-ray.

(v) There are no two-fold or three-fold cascades involving gamma-rays of energy about 0.57 mev.

4.2. An Alternative Level Scheme for ^{207}Pb

We now examine these results in relation to the level scheme of figure 1.

From (iv) it is reasonable to infer that 1.07, 1.46 and 1.76 mev gamma-rays all go to the $f_{5/2}$ level at 0.57 mev. This puts levels at 1.64, 2.03 and 2.33 mev where levels are already located. However, the 2.03 mev level cannot be the same as that in the original scheme, for this level also radiates to ground. Since the ground state is $p_{1/2}$ one would expect the level to decay also to the $p_{3/2}$ state, followed by a gamma-ray of 0.87 mev. The level cannot have a unique spin that permits it to radiate to the $p_{1/2}$ and $f_{5/2}$ levels and prohibits it radiating to the $p_{3/2}$ level. The same argument applies to the 2.33 mev level. The prompt 0.57 mev gamma-ray is made up partly of 0.57 mev gamma-rays in coincidence with the prompt 1.07, 1.46 and 1.76 mev gamma-rays. The balance must be made up only of transitions following direct electron capture into the $f_{5/2}$ level.

A difficulty arises when we attempt to assign the prompt 1.07 mev gamma-ray to the level scheme of figure 1 for, apart from the isomeric transition, there are no transitions of this energy available. The observations can be accounted for only by introducing a new level for which the shell-model assignments $f_{7/2}$ and $h_{9/2}$ (or possibly even $g_{9/2}$) are available.

The only locations possible for such a level are at 1.07, 1.63 or 1.94 mev, i.e. 1.07 mev higher than existing levels. The last of these would be followed by a gamma-ray of 0.87 mev, and since no such prompt gamma-ray is observed it must be excluded. A level at 1.07 mev decaying direct to the ground state is not possible since, with any of the shell-model assignments available, it would decay preferentially via the $f_{5/2}$ level with a probability exceeding 10^5 to 1 (Montalbetti 1952). This, incidentally, introduces a further argument against the existence of a level at 1.11 mev (Neumann and Perlman 1951, cf. § 2), for such a level would also decay by a cascade of two gamma-rays of energy about 0.57 mev. Such a cascade was shown to be absent in the previous section. The only possible location for the new level is thus at 1.63 mev, i.e. close to the $i_{13/2}$ level already located at that energy. There are now two cascades of 1.07 + 0.57 mev, one of which is 'prompt' and the other 'isomeric'.

We now have to decide between the assignments $f_{7/2}$, $h_{9/2}$ and $g_{9/2}$ for this level. The latter, however, is the first single particle level in the next shell; Pryce (1952) shows that about 3.4 mev is needed to lift a single neutron into the next shell, and Harvey (1953) places the $g_{9/2}$ assignment at 2.75 mev. There remain $f_{7/2}$ and $h_{9/2}$ for the new level.

To resolve this question let us consider the selection rules governing electron capture into the various levels. The ground state of ^{207}Bi is almost certainly $h_{9/2}$ (odd proton) by analogy with ^{209}Bi (Klinkenberg 1952). Table 3 shows, *inter alia*, the spin and parity changes involved in the possible decay

Table 3. Electron Capture ^{207}Bi to ^{207}Pb —Initial Level $h_{9/2}$

Final level	Δl	Δj	Parity change	Degree of forbiddenness	Fraction of decays
$h_{9/2}$	0	0	no	allowed	0.10
$i_{13/2}$	1	2	yes	first 'special'	0.65
$f_{7/2}$	2	1	no	allowed, <i>l</i> -forbidden	0.04
$f_{5/2}$	2	2	no	second	0.19
$p_{3/2}$	4	3	no	second, <i>l</i> -forbidden	nil
$p_{1/2}$	4	4	no	fourth	nil
others	—	—	—	—	0.02

branches. It shows that electron-capture transitions to the $p_{1/2}$ or $p_{3/2}$ levels are not to be expected because of higher degrees of forbiddenness. The table also shows that the new level at 1.63 mev cannot be $h_{9/2}$ since $h_{9/2}$ to $h_{9/2}$ is an allowed transition which would compete too strongly with the first-forbidden transition to the $i_{13/2}$ level. The transition to the $f_{7/2}$ level is also allowed, though at the same time *l*-forbidden (Mayer *et al.* 1951, Konopinski and Langer 1953), which might slow it down sufficiently to allow capture into the $i_{13/2}$ level to predominate. On the other hand, the latter transition is of the type $\Delta l = 1$; $\Delta j = 2$, which is characterized by abnormally large *ft* values as well as unique spectral shape (Mayer *et al.* 1951, Konopinski and Langer 1953). This feature is in accord with the fact that the *second*-forbidden transition to the $f_{5/2}$ level occurs in an appreciable fraction of the decays, and that the total half-life is long (56 years).

In all of the transitions considerable internal rearrangement is necessary, involving a double transition in the daughter nucleus and the breaking into a closed sub-shell. This might well exert a considerable influence on the transition probabilities, but nevertheless the presence of the $f_{7/2}$ level at 1.63 mev is embarrassing.

We nevertheless are obliged to locate the $f_{7/2}$ level at 1.63 mev and tentatively assign the $h_{9/2}$ level to 2.33 mev. This makes the 1.76 mev gamma-ray E2. An alternative mode of de-excitation of this level is to the $f_{7/2}$ level at 1.63 mev. This is M1 or E2 or both, but the energy available is less.

Figure 8 shows the revised level scheme for ^{207}Pb suggested by the results of this paper. The fractions of the decay (neglecting L-capture) that go to the various levels are shown in the last column of table 3.

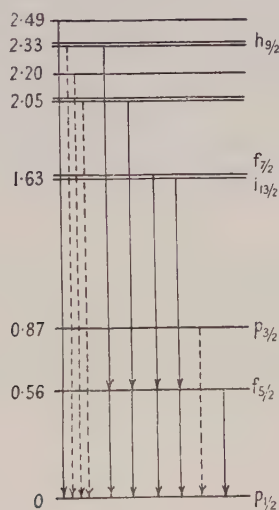


Figure 8. Revised level scheme for ^{207}Pb . Full lines show gamma transitions suggested by the present work ; dotted lines show gamma-rays observed by other workers.

4.3. Conclusions

The experimental data enable a consistent level scheme for ^{207}Pb to be constructed along the lines originally suggested by Pryce (1952). The existence of a prompt gamma-ray of 1.07 mev in the decay of ^{207}Bi , reported here, requires the $f_{7/2}$ level in ^{207}Pb to be located at 1.63 mev. This leads to difficulties however ; in particular, it results in a rather small spacing of the $(f_{5/2}, f_{7/2})$ doublet. According to the shell-model this spacing should be about three times that of the $(p_{3/2}, p_{1/2})$ doublet, whereas it is only 1.2 of this. Analogy with other doublets suggests that the $f_{7/2}$ level should be located at about 2–2.5 mev (Harvey 1953).

Further, the level scheme of figure 8 would appear to require a much greater electron capture into the $f_{7/2}$ level than is actually observed. For this reason an independent verification of the existence of the prompt 1.07 mev gamma-ray appears to be desirable. The 1.46 mev gamma-ray of Neumann and Perlman is not found by Wapstra (1953) and only indirect evidence for it is found in the present experiments. A new search for this gamma-ray seems to be justified.

ACKNOWLEDGMENTS

The author wishes to express his great appreciation to Professor Lord Cherwell for making available the facilities of the Clarendon Laboratory, to Mr. C. H. Collie for originally drawing attention to the problem and for his guidance during the course of the experiments, to Professor M. H. L. Pryce and Dr. M. A. Grace for valuable discussions, and to the executive of the Commonwealth Scientific and Industrial Research Organization, Australia, for leave of absence. Financial assistance was received from the Australian National University and the Nuffield Foundation.

REFERENCES

- ALBERGER, D. E., and FRIEDLANDER, G., 1951, *Phys. Rev.*, **81**, 523.
 BALSTON, J. N., and TALBOT, B. E., 1952, *A Guide to Filter Paper and Cellulose Powder Chromatography* (London: Reeve Angel).
 BROYLES, C. D., 1952, *Nuclear Sci. Abstr.*, **6**, 5912.
 BURHOP, E. H. S., 1952, *The Auger Effect* (Cambridge: University Press).
 CAMPBELL, E. C., and GOODRICH, M., 1950, *Phys. Rev.*, **78**, 640 (A).
 CAMPBELL, E. C., and NELSON, F., 1953, *Bull. Amer. Phys. Soc.*, **28**, No. 3, 75.
 DAVISSON, C. M., and EVANS, R. D., 1952, *Rev. Mod. Phys.*, **24**, 79.
 GOLDBABER, M., and SUNYAR, A. W., 1951, *Phys. Rev.*, **83**, 906.
 GRACE, M. A., and PRESCOTT, J. R., 1951, *Phys. Rev.*, **84**, 1059.
Handbook of Chemistry and Physics, 33rd Edn, 1951 (Cleveland: Chemical Rubber Publishing Co.).
 HARVEY, J. R., 1953, *Canad. J. Phys.*, **31**, 278.
 HOFF, R. W., and ASARO, F., 1953, private communication to HOLLANDER, J. M., PERLMAN, I., and SEABORG, G. T., *Rev. Mod. Phys.*, 1953, **25**, 469.
 HOPKINS, N. J., 1952, *Phys. Rev.*, **88**, 680.
 KLINKENBERG, P. F. A., 1952, *Rev. Mod. Phys.*, **24**, 63.
 KONOPINSKI, E. J., and LANGER, L. M., 1953, *Annual Review of Nuclear Science*, Vol. 2 (Stanford: Annual Reviews Inc.), p. 261.
 LASCoux, J., and VENDRYES, G., 1951, *C. R. Acad. Sci. Paris*, **233**, 858.
 MARSHAK, R. E., 1942, *Phys. Rev.*, **61**, 431.
 MAYER, M. G., MOSZKOWSKI, S. A., and NORDHEIM, L. W., 1951, *Rev. Mod. Phys.*, **23**, 315.
 MONTALBETTI, R., 1952, *Canad. J. Phys.*, **30**, 660.
 NEUMANN, H. M., and PERLMAN, I., 1951, *Phys. Rev.*, **81**, 958.
 PRESCOTT, J. R., 1954, *Proc. Phys. Soc. A*, **67**, 254.
 PRYCE, M. H. L., 1952, *Proc. Phys. Soc. A*, **65**, 773.
 ROSE, M. E., and JACKSON, J. L., 1949, *Phys. Rev.*, **76**, 1540.
 ROSE, M. E., GOERTZEL, G. H., SPINRAD, B. I., HARR, J., and STRONG, P., 1951, *Phys. Rev.*, **83**, 79.
 SPIESS, F. N., 1951, *University of California Radiation Laboratory*, Report No. 1494.
 SURUGUE, J., 1946, *J. Phys. Radium*, **7**, 145.
 WAPSTRA, A. H., 1953, *Thesis*, University of Amsterdam.

Note added in proof. D. E. Alberger (*Phys. Rev.*, 1953, **92**, 1257) has searched with a beta spectrometer in the energy region $1064 \text{ keV} \pm 25\%$ at 0.75 and 0.4% resolution for the K electrons associated with the 'prompt' 1.07 MeV transition suggested by the work in this paper. He places an upper limit of 1.5% intensity relative to K-1064 on such a line unless it falls on one of the 1064 keV conversion lines. This observation does not exclude the existence of such a line since its intensity is predicted to be less than 1% of K-1064. (§3.3.)

RESEARCH NOTES

The Intensity of High Angle Kikuchi Bands

BY M. BLACKMAN AND I. A. KHAN

Department of Physics, Imperial College, London

§ 1

IN the patterns obtained on reflection of electrons (of energy about 30 kev) from the surface of single crystals, Kikuchi bands are found which extend with measurable intensity to high angles relative to the incident beam (Rupp and von Meibom 1933, Boersch 1937). In a recent investigation (Alam, Blackman and Pashley 1954, to be referred to as I), a systematic study was made of this phenomenon. The relative intensity of the scattered electrons was measured over an angular region of scattering of 5° to 164° measured from the incident beam. The angular variation of the intensity was found to change systematically, for crystals possessing the rock salt structure, under identical experimental conditions. Cleavage surfaces were used, the angle of incidence, the azimuthal direction and the energy of the beam being kept fixed. The variation of intensity, with angle of scattering, was relatively small for crystals containing the heaviest ions. It was about 25 : 1 between 10° and 164° for potassium iodide, the energy of the incident electrons being 30 kev and the glancing angle of incidence 5° . For lithium fluoride, on the other hand, the variation was about 1000 : 1 under the same experimental conditions.

The Kikuchi bands for lead sulphide and potassium iodide were not merely visible at the highest scattering angles, but the clarity of the pattern (see I) suggested that a large fraction of the scattered electrons had sensibly the same energy. Further, the measurement of the width of the Kikuchi bands at the highest scattering angles showed that the energy of these electrons did not differ from that of the incident beam by more than the experimental error associated with the measurement of the band width. This error is, at the most, 10%.

It appears therefore that there is an efficient mechanism responsible for turning electrons of energy 30 kev through large angles without appreciable loss of energy. It was suggested in I that multiple elastic scattering was the main factor, but this involved the assumption that the probability of such scattering processes was distinctly higher than one would have expected from a consideration of the (atomic) cross sections for elastic and inelastic scattering.

It is the purpose of this paper to describe an experimental investigation into one aspect of this scattering mechanism, namely whether it is induced by the crystalline nature of the substances examined. For this purpose the intensities of the scattered electrons from natural quartz and from fused quartz were compared.

§ 2

The experimental arrangement was the same as that described in I, a cylindrical camera being used which allowed the Kikuchi band pattern to be recorded on a photographic film up to an angle of scattering of 164° (relative to the incident beam).

A natural quartz crystal was cut at a random angle and the resulting surface was optically polished. The pattern from this crystal was that to be expected from a single crystal, well-defined Kikuchi bands being observed. The purpose of polishing a random surface was to reproduce as closely as possible the surface topography which would be found on the fused quartz specimen which was also cut and optically polished.

The relative intensity of the scattered electrons was measured for each crystal with a fixed angle of incidence and a fixed energy of the incident electrons. The procedure used to calibrate the photographic film was the same as that described in I, the measurements being taken over the centre portion of the film.

As only relative intensities are measured, the intensity curves for the natural and the fused quartz have been fitted at a selected point. Two values of the glancing angle of incidence were chosen, these being 5° and 15° respectively. The energy of the incident electrons was 20 kev. This low value of the energy was chosen since it was expected that the variation of the intensity of the scattered electrons with scattering angle would be relatively small for the natural quartz at a glancing angle of incidence of 15° . It is under these conditions that the difference, if any, between the crystalline and the amorphous solid would be expected to be most pronounced.

The two pairs of intensity curves found experimentally are shown in figures 1 and 2. There is no significant difference between the curves for the natural

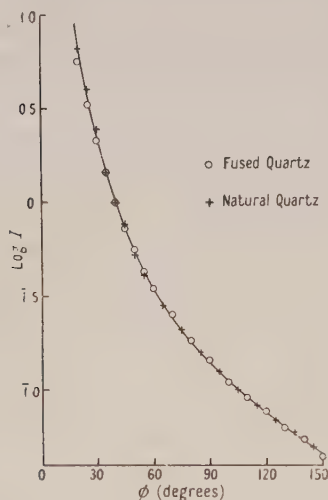


Figure 1. The variation of the intensity I of the scattered electrons as a function of scattering angle ϕ . The glancing angle of incidence on the crystal surface was 5° , the energy of the incident electrons 20 kev.

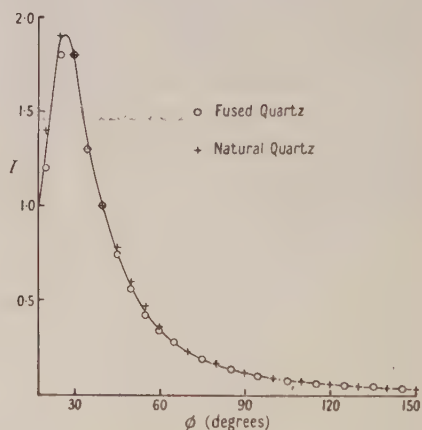


Figure 2. The variation of the intensity I of the scattered electrons as a function of the scattering angle ϕ . The glancing angle of incidence was 15° , the energy of the incident electrons 20 kev.

quartz and the fused quartz (what differences there are, being within the experimental error). Some differences might have been expected, partly because of the different density of fused and natural quartz and partly because the surface topography will not be identical. This latter point is expected to influence the shape of the intensity curve at low scattering angles.

The agreement is particularly noteworthy in the case of figure 2 as the change in intensity between the peak value (at about 30°) and that at the highest scattering angle measured (155°) is only about 40 : 1. In figure 1 which pertains to the case of a 5° glancing angle of incidence, the extreme variation is about 200 : 1.

It should be pointed out that it has been tacitly assumed that the energy spectrum of the scattered electrons is not significantly different for the two specimens. The agreement found in two very different cases suggests that this assumption is reasonable.

It is concluded from these experiments that the mechanism which produces the high intensity at large scattering angles is not a 'lattice' effect.

The authors are indebted to Messrs. B. K. Johnson and E. Menage who were responsible for cutting and polishing the quartz specimens.

REFERENCES

- ALAM, N. R., BLACKMAN, M., and PASHLEY, D. W., 1954, *Proc. Roy. Soc. A*, **221**, 224.
BOERSCH, H., 1937, *Z. tech. Phys.*, **18**, 574.
RUPP, E., and VON MEIBOM, R., 1933, *Z. Phys.*, **82**, 690.

The α -Activity Induced in Gold by Bombardment with Nitrogen Ions

By W. E. BURCHAM

Department of Physics, University of Birmingham

MS. received 9th March 1954

§ 1. INTRODUCTION

THE production of alpha-particle activity by the bombardment of gold with nitrogen ions ($^{14}\text{N}^{6+}$) has already been briefly reported (Chackett, Fremlin and Walker 1953). If the nitrogen nucleus as a whole unites with a nucleus of gold the compound nucleus ^{211}Em is formed, and subsequent evaporation of particles may lead to α -active isotopes of emanation, astatine, polonium and possibly other elements. The object of the present work was to identify the observed α -emitting isotopes.

§ 2. EXPERIMENTAL METHOD

Gold foils of thickness 15 microns were bombarded in the internal nitrogen beam of the 60 in. Nuffield cyclotron of the University of Birmingham. The foils were mounted on the outside of an electrically screened probe at a distance of 63.5 cm from the centre of the cyclotron, and the heavy ion current was measured after passing through the gold foil and also through a 25-micron aluminium foil forming part of the wall of the probe. The nitrogen ions reaching a radius of 63.5 cm have a continuous distribution in energy up to 120 mev (Walker, Fremlin, Link and Stephens 1954), but only those of initial energy greater than 75 mev contribute to the current measured after passage through the foils. These are just the ions with sufficient energy to surmount the potential barrier of approximately 80 mev in the laboratory system between nuclei of nitrogen and of gold. Bombardments of one hour or less with recorded currents of 10^{-8} to 10^{-9} ampere gave sufficient activity for most of the work.

Gross decay curves were taken by mounting the irradiated foil in an ionization chamber and following the counting rate using a low discriminator bias. The ionization chamber was of the electron-collection type described by Cranshaw and Harvey (1948), and was filled to a pressure of 35 lb in⁻² with a mixture of argon and 2% carbon dioxide. The chamber was also used to find the energies of α -particle groups associated with particular elements extracted from the irradiated foils. For this purpose a photographic record was made of the pulse height distribution from a thin source of the unknown material and compared with that from a freshly prepared source of ^{210}Po ($E_\alpha = 5.298$ mev). The linearity of the amplifier and recording equipment was checked with a pulse generator and attenuator. Figure 1 shows typical pulse size distributions obtained; the width of the Po calibration peak is normally about 100 kev. It was usually possible to start counting about 5 minutes after the end of an irradiation, plus any time necessary for processing.

Emanation isotopes were extracted by melting the irradiated gold foil in a chamber filled with air at a pressure of 100 μ . The evolved gases were passed through a spiral immersed in a mixture of dry ice and methylated spirits at a temperature of -71°C to remove astatine as far as possible, and emanation isotopes were fixed to a platinum plate by the glow-discharge method (Momyer 1953). This procedure occupied about 10 minutes.

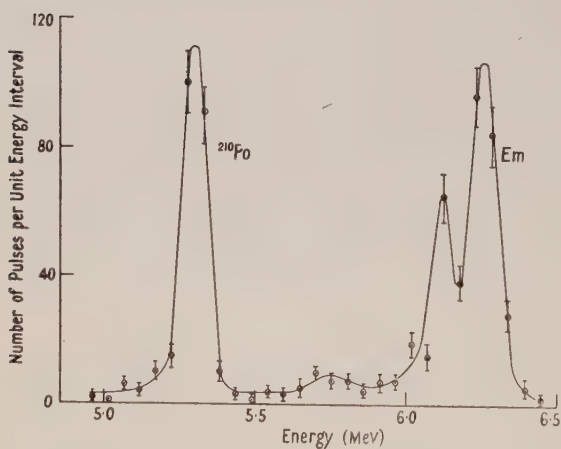


Figure 1 (a). Pulse size distribution for ^{210}Po and Em.

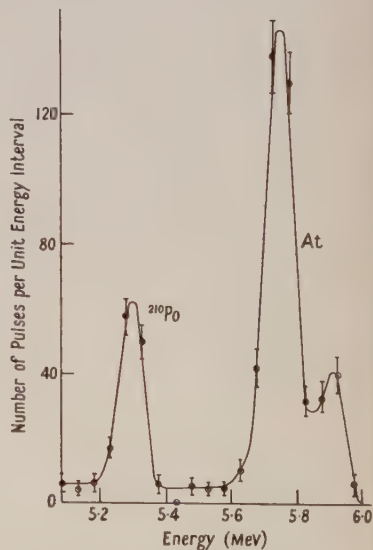


Figure 1 (b). Pulse size distribution for ^{210}Po and At.

Astatine was investigated by dissolving the irradiated foil in lead or bismuth at a temperature just above the melting point and collecting the evolved halogen on a silver foil. Tracer experiments with ^{210}Po showed that less than 0.2% of any polonium isotopes present would be carried over to the silver collector. The presence of astatine was also confirmed by a double evaporation process in which the gold foil was melted in a silica tube with a collector cooled in liquid air just above the sample. The collector was removed to a second chamber containing a silver foil and allowed to warm up to room temperature.

The α -activity found on the silver foil was assumed to be due to astatine (Wahl and Bonner 1951), although the method does not necessarily discriminate against polonium daughters of emanation isotopes condensed on the cold surface.

Polonium was studied by dissolving the gold foil in aqua regia, boiling to expel emanation and astatine as far as possible and extracting the gold into ethyl acetate. Tracer experiments showed that about 15% of the polonium could be deposited by evaporation of the inorganic phase on a platinum foil.

No systematic study of lighter elements was made.

§ 3. RESULTS

The gross decay curve for α -activity showed periods of approximately 7 minutes, 30–50 minutes, 110 minutes and 10 days; no attempt was made to find the periods accurately from these curves. A search was made, using a special apparatus, for periods between 7 minutes and 0.1 second, but none was found. The results of separating these activities and of determining the corresponding α -particle energies are shown in the table, which gives the average of a number of observations; accepted values of half-lives and energies are taken from the article by Hollander, Perlman and Seaborg (1953).

α -Emitters Observed in the Reaction $^{197}\text{Au} + ^{14}\text{N}$

Element separated	Half-life	α -particle energy (mev)	Probable mass number	Accepted values	
				Half-life	Energy (mev)
Em	6.5 ± 0.5 min	6.25 ± 0.05	206	—	—
	11.0 ± 1.0 min	6.09 ± 0.05	207	—	—
At	25 ± 2 min	5.90 ± 0.04	205	25 min	5.90
	108 ± 5 min	5.75 ± 0.04	207	120 min	5.75
Po	56 ± 5 min	5.61 ± 0.05	202	52 min	5.59
	10.4 ± 1 days	*	206	9 days	5.21

* This activity was followed only in the gross decay curve and no energy measurement was made.

The activity ascribed in the table to astatine was extracted from gold foils after one-hour bombardments. It appeared to decay initially with a period of about 87 minutes, but experiments in which the decay was followed over eight half-lives showed that the decay curve could be resolved into periods of 25 minutes and 108 minutes. The energies of the associated alpha-particle groups (figure 1 (b)) confirm the assignments made in the table. No evidence for the production of ^{209}At or ^{208}At was obtained; if the latter isotope had been responsible for more than one twentieth of the total astatine activity, the daughter activity of ^{208}Po would have been observed according to the figures given by Hyde, Ghiorso and Seaborg (1950). No 7-minute period was observed after rapid evaporations of astatine to a silver foil.

The main α -activity of the gold foils immediately after a short bombardment is due to emanation isotopes. The α -particle energy spectrum of the emanation activity (figure 1 (a)) shows groups of 6.09 and 6.25 mev which decay at different rates. The period observed for the total emanation activity was 7.6 ± 0.5

minutes, and the periods for the two separate groups were determined rather less accurately as shown in the table. Platinum foils on which the emanation activity had been allowed to decay showed a residual α -activity of energy 5.76 ± 0.04 mev and period 85 ± 10 minutes. This activity was not found when the gold foils were left for 60 minutes before the emanation was extracted. The properties of this residual activity are in fair agreement with those of ^{207}At and indicate the presence of electron-capturing ^{207}Em in the emanation deposit; this isotope has not previously been reported. The α -activity of the emanation deposit extrapolated back to the time of preparation of the source was 80 ± 10 times that of the residual activity extrapolated back to the same time.

§ 4. DISCUSSION

An incident nitrogen nucleus of energy 120 mev captured by ^{197}Au would produce an excitation energy of about 90 mev according to the empirical masses given by Metropolis and Reitwiesner (1950). The corresponding temperature of the nucleus ^{211}Em before particle emission is 2.9 mev (Blatt and Weisskopf 1952). Allowing for evaporation energy, it seems possible for as many as seven neutrons to be emitted, but since most of the incident ions have energies less than 120 mev the highest yields will be obtained for evaporation of fewer particles. Excitation energies of ^{211}Em of less than 50 mev are unlikely because of the coulomb barrier, so that the formation of ^{208}Em and heavier isotopes is unfavoured. These arguments suggest that ^{207}Em , ^{206}Em and ^{205}Em might be formed by the (N, 4n), (N, 5n) and (N, 6n) reactions under the conditions of the experiment. All the α -activities observed, as will be seen from the table, may be ascribed to these isotopes or to their decay products. The astatine and polonium isotopes may of course also be formed directly by the reactions $\text{Au}(\text{N}, \text{pxn})\text{At}$ and $\text{Au}(\text{N}, \alpha\text{xn})\text{Po}$.

Assignment of the 6.25 mev group of α -particles to ^{206}Em is based on predictions from α -decay systematics (Perlman, Ghiorso and Seaborg 1950, Pryce 1950, Momyer 1953). The daughter activity of ^{202}Po was not observed after decay of the emanation but, since the electron capture to α -decay branching ratio of ^{202}Po is not known, no conclusion can be drawn from this fact. The 6.09 mev group of α -particles could come from ^{207}Em according to the systematics. If this is so the electron capture to α -decay branching ratio for this isotope is found to be 2.6 ± 0.3 and the partial half-life for α -emission is about 40 minutes. This is only 2.5 times that for an even-even emanation nucleus of the same decay energy and not specially forbidden, according to the curves given by Perlman, Ghiorso and Seaborg (1950). Such a small 'departure factor' is unusual for an odd mass nucleus with less than 126 neutrons.

Observation of the electron-capturing daughters and subsequent products of the emanation isotopes will be necessary in order to confirm the assignments to ^{206}Em and ^{207}Em . No attempt to follow these activities was made in these experiments because of low intensities and also because of the presence of β - and γ -emitting fission products which were not necessarily removed by the separation procedures.

ACKNOWLEDGMENTS

I am grateful to Miss D. Latham for analysing the film records and to Mr. M. Winn for the use of his photographic recording equipment.

REFERENCES

- BLATT, J. B., and WEISSKOPF, V. F., 1952, *Theoretical Nuclear Physics* (New York : John Wiley), p. 372.
- CHACKETT, K. F., FREMLIN, J. H., and WALKER, D., 1953, *Proc. Phys. Soc. A*, **66**, 495.
- CRANSHAW, T. E., and HARVEY, J. A., 1948, *Canad. J. Res. A*, **26**, 243.
- HOLLANDER, J. M., PERLMAN, I., and SEABORG, G. T., 1953, *Rev. Mod. Phys.*, **25**, 469.
- HYDE, E. K., GHIORSO, A., and SEABORG, G. T., 1950, *Phys. Rev.*, **77**, 765.
- METROPOLIS, N., and REITWIESNER, G., 1950, *Table of Atomic Masses*, U.S. Atomic Energy Commission Report, No. NP 1980.
- MOMYER, F. F., 1953, *Thesis*, Radiation Laboratory, University of California (UCRL 2060).
- PERLMAN, I., GHIORSO, A., and SEABORG, G. T., 1950, *Phys. Rev.*, **77**, 26.
- PRYCE, M. H. L., 1950, *Proc. Phys. Soc. A*, **63**, 692.
- WAHL, A. C., and BONNER, N. A., 1951, *Radioactivity applied to Chemistry* (New York : John Wiley), p. 203.
- WALKER, D., FREMLIN, J. H., LINK, W. T., and STEPHENS, K. G., 1954, *Brit. J. Appl. Phys.*, in the press.

The Anomalous Scattering of μ Mesons

By D. A. TIDMAN

School of Physics, University of Sydney, New South Wales

Communicated by H. Messel; MS. received 15th February 1954

RECENTLY a number of authors (George, Redding and Trent 1953, Leontic and Wolfendale 1953) have published results of measurements on the scattering of μ -mesons using the cosmic radiation. The present experimental data are not conclusive, but there seems to be some indication that the cross sections obtained are inconsistent with coulomb scattering from a nucleus with an extended charge distribution.

We give here results of calculations made in an attempt to explain the anomalously large scattering cross section. The contribution to the scattering of μ -mesons, arising from the anomalous magnetic moment (A.M.M.) of the nucleon and from a possible A.M.M. of the μ -meson, has been worked out.

The lowest-order process for this scattering in weak-coupling theory is shown.

$$e\gamma_\mu + \frac{Ke}{2m} \frac{1}{2} (\mathbf{q}\gamma_\mu - \gamma_\mu \mathbf{q}) \left\langle \begin{array}{c} \text{muon} \\ \text{-----} \\ \mathbf{q} \end{array} \right\rangle \left\langle \begin{array}{c} \text{nucleon} \\ \text{-----} \\ \mathbf{q} \end{array} \right\rangle e\gamma_\mu + \frac{ke}{2M} \frac{1}{2} (\mathbf{q}\gamma_\mu - \gamma_\mu \mathbf{q}) \dots (1)$$

where $ke/2M$ = nucleon A.M.M., $Ke/2m$ = μ -meson A.M.M.

We can separate the cross section σ out into four parts :

$$\sigma = \sigma_0 + \sigma_\mu + \sigma_p + \sigma_{\mu p}$$

σ_0 = ordinary point-charge scattering.

σ_μ = contributions from μ -meson A.M.M.

σ_p = contributions from proton A.M.M.

$\sigma_{\mu p}$ = contributions from the A.M.M.-A.M.M. interaction.

$\sigma_{\mu p}$ can be neglected.

We find

$$\sigma_0 = \frac{e^4}{4m^2\beta^4c^4} \operatorname{cosec}^4 \frac{1}{2}\theta (1 - \beta^2 \sin^2 \frac{1}{2}\theta) (1 - \beta^2) \quad \dots\dots (2)$$

$$\frac{\sigma_\mu}{\sigma_0} = K\beta^2 \sin^2 \frac{1}{2}\theta (1 - \beta^2 \sin^2 \frac{1}{2}\theta)^{-1} \left(2 + \frac{K\beta^2}{1 - \beta^2} \right) \quad \dots\dots (3)$$

$$\frac{\sigma_p}{\sigma_0} = \frac{E^2}{M^2} \left(\frac{2k \tan^2 \frac{1}{2}\theta \sin^2 \frac{1}{2}\theta + k^2 \sin^2 \frac{1}{2}\theta}{1 + (2E/M) \sin^2 \frac{1}{2}\theta + (2E^2/M^2) \tan^2 \frac{1}{2}\theta \sin^2 \frac{1}{2}\theta} \right) \quad \dots\dots (4)$$

θ is the angle of scattering in the laboratory, E is the total energy of μ -meson, $\beta = v/c$ and M is the nucleon mass.

The effect of the nucleon A.M.M. is negligible. The magnetic moment of the μ -meson is unknown, but a value of K greater than 1 for the μ -meson A.M.M. would be inconsistent with data on burst production (Peaslee 1952).

We find the following values :

$$\begin{aligned} \sigma_\mu/\sigma_0 &= 0.6 \text{ for } K=1, \theta=20^\circ, E=400 \text{ mev} \\ &= 0.3 \text{ for } K=1, \theta=20^\circ, E=200 \text{ mev} \end{aligned}$$

This effect is thus too small since we require at large angles (20°) an anomalous scattering cross section of about ten times the ordinary electromagnetic one.

Other electromagnetic effects, for example incoherent scattering from nuclei, have been considered in detail by other authors (Gatto 1953). They are too small to account for the anomalous scattering cross section.

Some non-electromagnetic couplings are known, such as that involving the neutrino in the π and μ decays. However, these have extremely small coupling constants and hence give rise to negligible contributions to μ -meson scattering.

In the light of the above considerations we were led to consider a direct coupling between μ -mesons and nucleons. Of the theoretically possible couplings pair coupling is the simplest one not in obvious disagreement with experiment.

The interaction Hamiltonian used was

$$H_i = G \int (\bar{\Psi} O \Psi)(\bar{\Phi} O \Phi) dx^3 \quad \dots\dots (5)$$

where Ψ is the nucleon field, Φ the charged muon field, and

$$O = 1, \gamma_5, \gamma_5 \gamma_\mu, \gamma_\mu \gamma_\nu, \gamma_\mu$$

This Hamiltonian gives rise to unrenormalizable divergencies in higher-order processes using the weak-coupling theory.

The scattering cross sections of μ -mesons from nucleons in the Born approximation have been worked out and rise indefinitely with increasing μ -meson energy so that this approximation is obviously a very poor one. Using the Heitler equation for radiation damping, this cross section can be made eventually to decrease with increasing energy. However, the cross section is still so large that one should observe nuclear disintegrations with a frequency very much higher than that measured in the underground radiation. The cross sections, worked out using various approximations for the above five couplings, can be found in the literature (Tannenwald 1952).

George, Redding and Trent give a cross section of $4 \times 10^{-27} \text{ cm}^2/\text{nucleon}$ for scattering of μ -mesons with energies of 100–300 mev through angles greater than 15° . To fit this cross section one requires to take $G/m^2 \sim 0.3$ in equation (5) for scalar coupling. This coupling constant is unreasonably large.

One would expect such an interaction to make itself apparent in the μ -mesic atom. However, by choosing pseudoscalar coupling in equation (5) which gives matrix elements proportional to v/c one can avoid an inconsistency with the recent μ -mesic atom results of Fitch and Rainwater (1953), provided one takes the interaction to refer only to charged μ -mesons.

In view of the breakdown in the approximation methods used in pair coupling, one could use an empirical cut-off of the interaction as for example, was done in Wentzel's μ -pair theory of the charged π mesons (Wentzel 1950). However, this destroys the relativistic invariance of the theory.

It is interesting to note, though possibly of not much significance, that using such a violent cut-off in the same energy range as used by Wentzel, one can make pair production of μ -mesons in nucleon-nucleon improbable, and prevent a rise in the scattering cross section past the region where experimentally it seems to be at a maximum.

In view of all the difficulties inherent in the use of a coupling between μ -mesons and nucleons, it would seem very worth while to repeat the experiments on the scattering of μ -mesons under more controlled conditions.

ACKNOWLEDGMENTS

I would like to express my gratitude to Dr. E. P. George for many helpful discussions and to the University of Sydney Research Committee for a grant which made this work possible.

REFERENCES

- FITCH, V. L., and RAINWATER, J., 1953, *Phys. Rev.*, **92**, 789.
GATTO, R., 1953, *Nuovo Cim.*, **10**, 1560.
GEORGE, E. P., REDDING, J. L., and TRENT, P. T., 1953, *Proc. Phys. Soc. A*, **66**, 533.
LEONTIC, B., and WOLFENDALE, A. W., 1953, *Phil. Mag.*, **44**, 1101.
PEASLEE, D. C., 1952, *Nuovo Cim.*, **9**, 56.
TANNENWALD, L. M., 1952, *Phys. Rev.*, **86**, 332.
WENTZEL, G., 1950, *Phys. Rev.*, **79**, 710.

LETTERS TO THE EDITOR

A Note on the Band Structure of Silicon

Recently several papers have been published describing theoretical calculations on the electronic band structure of the diamond-type crystals of carbon, silicon and germanium. Herman (1952) and Herman and Callaway (1953) have used the method of orthogonalized plane waves to study diamond and germanium, while Zehler (1953) has investigated diamond by both the cellular and plane wave methods. These workers agree that the lowest state of the conduction band at the origin of \mathbf{k} space is triply degenerate and derived from a p-type atomic state; in general, the quantitative agreement of their results with experiment is good. On the other hand, calculations on silicon by the cellular method (Mullaney 1944, Holmes 1952, Yamaka and Sugita 1953) follow earlier work on diamond (Kimball 1935) in making the lowest conduction band state non-degenerate; of these calculations, only that of Yamaka and Sugita obtains a reasonable value for the energy gap.

Since all three crystals would be expected to have similar band structures, it is interesting that our investigation of silicon agrees with the most recent work on diamond and germanium, with triply degenerate states bounding the forbidden energy gap above and below at $\mathbf{k}=0$. As in the other calculations on silicon we have used the cellular method, expressing the one-electron wave function in each cell as a sum of solutions of a Schrödinger equation. The spherically symmetric potential used in the equation is the simple Hartree field given by Mullaney (1944) in which the effect of exchange is neglected. However, instead of obtaining the energy levels by point matching conditions we have made use of a variation principle proposed by Kohn (1952) and developed by Jenkins and Pincherle (1954). In this approach the energy levels of an electron in a crystal are determined by minimizing an expression related to the familiar Ritz variation integral, but containing an additional surface integral which expresses the continuity condition on the wave function.

We approximate to the wave function of wave vector \mathbf{k} and energy $E(\mathbf{k})$ by

$$\psi(\mathbf{k}) = \sum_s A_s \phi_s(\lambda)$$

inside a cell containing one silicon atom, and this determines the form of the wave function in all other cells. The $\phi_s(\lambda)$ satisfy

$$[-\frac{1}{2}\nabla^2 + V - \lambda]\phi_s(\lambda) = 0$$

where the potential V has spherical symmetry, and we can determine the angular parts of the ϕ_s appropriate to a given \mathbf{k} by group theory (see, for example, Bell 1954). The condition determining the coefficients A_s (in general complex) and $E(\mathbf{k})$ is that the function

$$J(A_s, \lambda) = [\lambda - E(\mathbf{k})] \sum_s \bar{A}_s A_s + \sum_s \sum_t \bar{A}_s A_t K_{st}(\mathbf{k}, \lambda)$$

shall be stationary for variation of the A_s and λ . Here K_{st} is a sum of surface integrals of the form given in Jenkins and Pincherle (1954), where it is also shown that the stationary problem can be treated in two ways: (a) obtaining $\lambda - E(\mathbf{k})$ as the latent root of the K_{st} matrix for each value of λ and using variations of λ

to determine the best value of $E(\mathbf{k})$; (b) assuming that the best value of λ is $E(\mathbf{k})$ so that $E(\mathbf{k})$ is equal to that value of λ for which the determinant of the K_{st} matrix vanishes. The determinant criterion is theoretically less sound, and as far as possible we have supplemented its results by the more laborious latent root technique, good agreement being obtained between the two methods.

Our results for $\mathbf{k}=0$ are shown in the table, the notation for the energy levels being that of Bouckaert, Smoluchowski and Wigner (1936), while the symbols for the angular functions used are taken from Von der Lage and Bethe (1943).

Energy level type:	${}^1\Gamma_1$	${}^3\Gamma'_{25}$ ${}^3\Gamma_{15}$	${}^1\Gamma'_2$
Angular functions used:	α_0, β_3	$\delta_1, \delta_3, \epsilon_2, \epsilon_4$	α_0, β_3
Energy in ev:	-13.7	-0.85 0.45	2.3

The convergence of the triply degenerate energy levels as the number of terms in the wave function is increased was sufficiently good to suggest that our values will not be greatly altered by including more terms. The difference between the ${}^3\Gamma'_{25}$ and ${}^3\Gamma_{15}$ levels is 1.3 ev compared with the experimental energy gap of 1.12 ev, but preliminary calculations in the (1, 0, 0) direction suggest that one of the p-type conduction bands has a negative curvature (cf. Herman 1952, Herman and Callaway 1953). We are continuing this investigation since it may throw an interesting light on the electrical properties of silicon, and further details will be published shortly.

Acknowledgment is made to the Chief Scientist, Ministry of Supply, and the Controller of Her Majesty's Stationery Office, for permission to publish this letter.

Ministry of Supply,
Radar Research Establishment,
St Andrew's Road,
Malvern,
Worcestershire.
10th March 1954.

D. G. BELL.
R. HENSMAN.
D. P. JENKINS.
L. PINCHERLE.

- BELL, D. G., 1954, *Rev. Mod. Phys.*, in the press.
BOUCKAERT, L. P., SMOLUCHOWSKI, R., and WIGNER, E., 1936, *Phys. Rev.*, **50**, 58.
HERMAN, F., 1952, *Phys. Rev.*, **88**, 1210.
HERMAN, F., and CALLAWAY, J., 1953, *Phys. Rev.*, **89**, 518.
HOLMES, D. K., 1952, *Phys. Rev.*, **87**, 782.
JENKINS, D. P., and PINCHERLE, L., 1954, *Phil. Mag.*, **45**, 93.
KIMBALL, G. E., 1935, *J. Chem. Phys.*, **3**, 560.
KOHN, W., 1952, *Phys. Rev.*, **87**, 472.
MULLANEY, J. F., 1944, *Phys. Rev.*, **66**, 326.
VON DER LAGE, F. C., and BETHE, H., 1947, *Phys. Rev.*, **71**, 612.
YAMAKA, E., and SUGITA, T., 1953, *Phys. Rev.*, **90**, 992.
ZEHLER, V., 1953, *Ann. Phys., Lpz.*, (6) **13**, 229.

The Deuteron Bombardment of Oxygen

Recently it has been shown that if the assumptions in the theory of the stripping process (Butler 1951) are modified so as to include an interaction between the proton and the bombarded nucleus (Horowitz and Messiah 1953), the absolute magnitude of the differential cross section is reduced considerably. The relation between this absolute magnitude and the reduced width of the level of the nucleus formed in the reaction has been determined when the assumptions used are those of Butler (Fairbairn 1953), and in favourable cases the absolute cross sections can be predicted.

Such a case is the (d, p) reaction in which ^{17}O is formed, because the ^{17}O nucleus consists of a single neutron outside closed shells in either $j-j$ or $L-S$ coupling. Because the spin of ^{16}O is zero the two modes of coupling give the same result, and if the reduced neutron width is taken to have its one-body value, viz. $\hbar^2/(M_n r_0^2)$, the absolute cross sections can be predicted. In either coupling the two lowest levels of ^{17}O are formed by adding a neutron to ^{16}O in its ground state configuration, and therefore these two levels offer a means of testing Butler's assumptions.

The experimental results with which comparisons are made are those performed at 7.73 Mev (Burge *et al.* 1951) and at 19.1 Mev (Freemantle *et al.* 1953) for the incident deuteron energy in the laboratory system. When ^{17}O is formed in its ground state (Q -value 1.93 Mev) the neutron must have $l_n=2$, and when the first excited state is formed (Q -value 1.04 Mev) the neutron must have $l_n=0$; these restrictions on the angular momentum of the neutron follow from the spins and the parities of the nuclei involved as given by $j-j$ coupling and confirmed by experiment. The value $r_0=4.8 \times 10^{-13}$ cm $= (1.7 + 1.22A^{1/3})10^{-13}$ cm was used to calculate the theoretical results shown in the accompanying table.

State of ^{17}O	At 7.73 Mev					At 19.1 Mev				
	(i)	(ii)	(iii)	(iv)	(v)	(ii)	(iii)	(iv)	(v)	
Ground	2	35°	30	130	0.18	20°	20	120	0.13	
First excited	0	15°	50	80	0.51	15°	15	40	0.27	

Column (i) l_n -value; (ii) angle (c.m.s.) at which the measurement was taken; (iii) experimental differential cross section in mbn sterad $^{-1}$; (iv) theoretical differential cross section in mbn sterad $^{-1}$; (v) reduced width (in units of $\hbar^2/M_n r_0^2$) which would give the experimental cross section.

An examination of the results in the table shows that for each of the reactions considered the experimental cross section is smaller than that predicted from the theory by a factor of the order 2-6. This is outside the limits of experimental error. It should be added that with the quoted value for r_0 the theoretical angular distributions for the protons are in good agreement with experiment in each reaction, and that the error seems, therefore, to occur only for the absolute magnitudes of the cross sections.

Although the hypothesis that the reduced width has its one-body value might be questioned, the necessity for such a nuclear constant to be invariant under the changing of the incident deuteron energy, and the differing values which would be required to give the experimental cross sections, show that there must be another source for the discrepancy. The previously quoted work of Horowitz and Messiah offers a guide as to where the error lies.

These authors have shown that the introduction of the proton-nucleus interaction leaves unaltered the form of the angular distribution in a (d, p) reaction, but reduces by a substantial factor the magnitude of the cross section. This reduction factor depends on the values of l_p , the angular momentum of the proton, which are involved, and also on the energy of the bombarding deuteron. Such angular momentum and energy considerations give correctly the relative reductions in the above four reactions. It is hoped to do the more accurate calculations shortly.

This work was done at the University of Birmingham, and the receipt of a Department of Scientific and Industrial Research maintenance allowance is gratefully acknowledged.

The Mathematics Department,
University of Glasgow.
3rd March 1954.

W. M. FAIRBAIRN.

BURGE, E. J., BURROWS, H. B., GIBSON, W. M., and ROTBLAT, J., 1951, *Proc. Roy. Soc. A*, **210**, 534.

BUTLER, S. T., 1951, *Proc. Roy. Soc. A*, **208**, 559.

FAIRBAIRN, W. M., 1953, *Thesis*, University of Birmingham.

FREEMANTLE, R. G., GIBSON, W. M., PROWSE, D. J., and ROTBLAT, J., 1953, *Phys. Rev.*, **92**, 1268.

HOROWITZ, J., and MESSIAH, A. M. L., 1953, *J. Phys. Radium*, **14**, 695.

REVIEWS OF BOOKS

The Printing of Mathematics, by T. W. CHAUNDY, P. R. BARRETT and CHARLES BATEY. Pp. ix+105. (Oxford: University Press, 1954.) 15s.

Most physicists know that it is easier, and therefore cheaper, to print $(a+x)/(b+y)$ than $\frac{a+x}{b+y}$, and $\sqrt{(x+y)}$ than $\sqrt{x+y}$. They might be in doubt whether e^{ax} is any more difficult than e^{ax} , and most would be surprised to learn that x_1^2 is cheaper than x_1^2 .

Here is a book which makes the reasons clear, by actually describing the processes of composing on a monotype machine and by hand. The authors are men of quite exceptional experience in the field of mathematical printing, and have written an account which cannot fail to interest anyone of enquiring mind; but they have gone further, and provide a reference work in which the author pressed for symbols may see what is available in different founts, whether a letter can easily be printed with a dot, bar, accent or tilde over it, and can even see a specimen legible handwriting for Latin and Greek letters.

It would have been great fun to mention a misprint, but this reviewer, at least, has failed to find one.

J. H. AWBERY.

Four-Place Tables of Transcendental Functions, by W. FLÜGGE. Pp. 136. (London: Pergamon Press, 1954.) Price 25s.

Professor Flügge has prepared this book with a view to making the practical use of some of the transcendental functions easier, and therefore commoner. In addition to the trigonometric and hyperbolic functions, he has chosen to include the exponential function and its inverse, the logarithm; the two kinds, J and Y, of Bessel functions, of zero and first order, and their representatives for imaginary argument, I and K; the functions ber, bei, ker and kei, which give the real and imaginary parts of $J(x\sqrt{i})$ and $K(x\sqrt{i})$; the first derivatives of the last four; the elliptic integrals of the first and second kind; the error function; Fresnel's integrals; the sine, cosine and exponential integrals, of which the last is $\int_x^x (e^\beta/\beta) d\beta$; and finally, the gamma function.

The tables are in nearly all cases to four significant figures, and great care has been taken to ensure that interpolation is simple; in every case, means of calculating values outside the range of tabulated arguments are given. There are also collections of formulae.

The lay-out of the tables seems to the present reviewer to have aimed at too much economy in printing. The first figures of an entry are not printed if they are the same as in the line or lines above, and copious use is made of asterisks to denote that in fact these unprinted figures are to be taken from the following, and not the preceding, line. Considerable use, too, is made of the device of taking out a power of 10. This leads to entries which are sometimes difficult to unravel.

J. H. AWBERY.

Bessel Functions and Formulae, compiled by W. G. BICKLEY. Pp. 12.
(Cambridge: University Press, 1953.) 3s. 6d.

This is a collection of about two hundred formulae reprinted without change from the introduction to Volume X of the British Association Tables.

The various kinds of function are defined and all main formulae are listed, e.g. recurrence relations, asymptotic expansions, addition formulae, integral representations, etc.

A. N. GORDON.

Progress in Nuclear Physics, Vol. 3, edited by O. R. FRISCH. Pp. vii + 279.
(London: Pergamon Press, 1953.) 63s.

The continued expansion of research in physics is reflected by the growth of publications in which progress is summarized and expounded by specialists in different branches. It is interesting to trace their development from the separate reports sponsored by Physical Societies a generation ago. The best-known examples in English are the *Reviews of Modern Physics*, which include summaries as well as articles that are largely original work, and the annual *Reports on Progress in Physics*, where invited articles of a survey character are traditional. During the past few years publications have begun to appear which are closely similar to the Physical Society's annual *Reports*, but are restricted to a single branch of physics. When such a publication appears for three years without change of character or loss of quality it may be reckoned well established; such is the situation as regards *Progress in Nuclear Physics*, published by the Pergamon Press under the editorship of Professor O. R. Frisch.

The third annual volume contains nine articles, all of high merit though diverse in character. One group is formed by the accounts of diffusion cloud chambers by M. Snowden, of energy measurements with proportional counters by D. West, of Čerenkov radiation by J. V. Jelley, and of solid conduction counters by F. C. Champion, together with an article on the production of intense ion beams by P. C. Thonemann. These provide very useful summaries of phenomena and of techniques based upon them, and are naturally written by experimenters for experimenters. The articles on oriented nuclear systems (R. J. Blin-Stoyle, M. A. Grace and H. Halban) and on the annihilation of positrons (M. Deutsch) deal with subjects in which theoretical considerations are inseparable from the description of experimental advances; they are both written in concentrated style and assume the reader to be well grounded in theoretical principles, though they contain nothing that can be described as advanced or difficult.

The article on stripping reactions by R. Huby is more definitely theoretical in character, though experimental methods and results are given. The final article, on the collision of deuterons with nucleons, by H. S. W. Massey, is concerned with pointing a way to future progress even more than with reporting what has already been achieved. It develops the thesis that the loose binding of the deuteron "makes possible the development of approximate theories which relate the effects to be expected in high energy collisions of nucleons with deuterons to those which arise in the corresponding collisions between nucleons".

P. B. MOON.

CONTENTS OF SECTION B

	PAGE
Mr. J. DAIN and Mr. I. A. D. LEWIS. Adiabatic Theory of an Electron Gun for Crossed Field Devices	449
Prof. E. A. OWEN and Dr. D. MADOC JONES. Effect of Grain Size on the Crystal Structure of Cobalt	456
Prof. S. TOLANSKY and Mr. V. R. HOWES. Optical Studies of Ring Cracks on Glass	467
Prof. S. TOLANSKY and Dr. A. HALPERIN. Oriented Ring Cracks on Diamond .	473
Mr. F. L. WARBURTON. Variations in Normal Colour Vision in Relation to Practical Colour Matching	477
Dr. G. ECKER. Theory of the Positive Column	485
Research Notes :	
Mr. D. A. RICHARDS. Newton's Rings of High Visibility	492
Letters to the Editor :	
Prof. K. G. EMELÉUS. Dissociative Recombination at Surfaces	495
Dr. P. W. RANBY and Dr. S. T. HENDERSON. Cascade Excitation of Phosphors by Ultra-Violet Radiation	496
Dr. R. W. HOFFMAN, Dr. R. D. DANIELS and Mr. E. C. CRITTENDEN, Jr. The Cause of Stress in Evaporated Metal Films	497
Reviews of Books	501
Contents of Section A	512

The Molar Heats of Lead Sulphide, Selenide and Telluride in the Temperature Range 20°K to 260°K

By D. H. PARKINSON AND J. E. QUARRINGTON

Ministry of Supply, Radar Research Establishment, Great Malvern, Worcs.

MS. received 14th January 1954, and in amended form 24th March 1954

Abstract. An apparatus suitable for calorimetry at low temperatures is described. With it, the molar heats of lead sulphide, selenide and telluride have been measured between 20°K and 260°K. These salts show a normal family of molar heat curves, from which the usual thermodynamic functions have been calculated. An analysis of corrections required with the method of calorimetry used, is given in an Appendix.

§ 1. INTRODUCTION

THE electrical properties of lead sulphide, selenide and telluride and other semiconductors have been under investigation in this laboratory for a number of years. More recently work has been extended to their thermal properties. This paper deals with an investigation of the molar heats of the lead salts from 20°K to 260°K, which will be extended to lower temperatures in due course.

The present specimens were collections of synthetic single crystals prepared by Mr. W. D. Lawson. The sulphide, selenide and telluride crystals weighed 34.43, 38.11 and 61.97 grammes respectively; at 290°K their specific conductivities were ~ 150 , ~ 500 and $\sim 100 \text{ ohm}^{-1} \text{ cm}^{-1}$ respectively and the concentrations of free charge carriers were $\sim 2 \times 10^{18}$, $\sim 3 \times 10^{18}$ and 10^{18} respectively, all deduced from Hall constant measurements carried out by Dr. E. H. Putley. Each collection of crystals contained about equal weights of p- and n-type, but any resulting differences in heat capacity can be expected to be masked by the experimental errors in this work.

A well-known technique for determining heat capacities was used. The calorimeter was suspended in a high vacuum enclosure, the shield, kept at a constant temperature near to that of the calorimeter, the temperature drift of which was recorded before and after the heating period. By extrapolation into the heating period the corresponding temperature rise could be obtained. This method has been used frequently in the hydrogen and helium ranges of temperature but in the experiments described here it was used up to 260°K. At these comparatively high temperatures the thermal isolation from the surroundings began to deteriorate. This necessitated corrections which are dealt with in the Appendix.

A particularly simple construction for the calorimeter was followed so that the temperature recorded was that of its walls and not necessarily that of the contained specimen. This facilitates the analysis leading to the corrections in question.

§ 2. EXPERIMENTAL

The calorimeter used in these experiments was a cylinder 3 cm long, 3 cm in diameter, of wall thickness 0.1 mm and with domed end. The bottom was sealed in position with soft solder; Wood's metal was used to seal the top, to which was attached the thin-walled (0.1 mm) spiral cupro-nickel tube F (figure 1), 20 cm

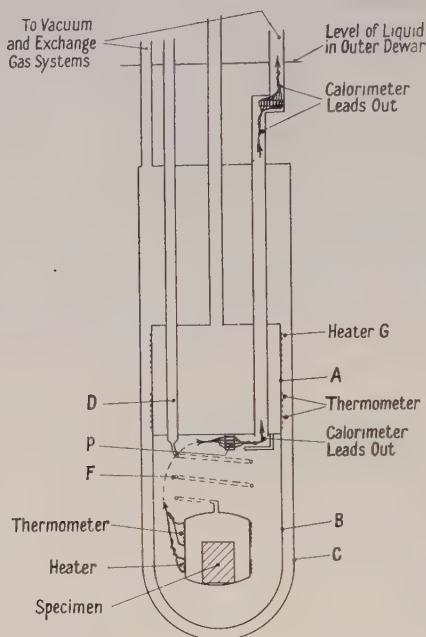


Figure 1. Schematic layout of cryostat.

long \times 1 mm o.d. Thermometer and heater coils were wound non-inductively on the outside of the drum, insulated electrically, held in place and covered by araldite varnish. The heater was a 475 ohm coil of 40 s.w.g. constantan. The thermometer was of platinum annealed electrically at a bright red heat in air before winding. It was wound by hand so as to avoid kinks and strains. Leads of constantan, 42 s.w.g. for the thermometer and 34 s.w.g. for the heater, were used.

The tube F and thermometer leads were regarded as an integral part of the calorimeter, so that to dismount it they were detached from the binding post P and the tube D at fixed points. The specimens were sealed into the calorimeter by breaking and remaking the Wood's metal seam at its top. The weights of solder and Wood's metal used in all operations were carefully recorded.

Figure 1 shows schematically a calorimeter mounted in position in the cryostat. The general layout is very similar to that described by Parkinson, Simon and Spedding (1950, to be referred to as I) and also by Hill (1953). In figure 1, B and C are both vacuum cases. For operation in the temperature ranges of liquid hydrogen, nitrogen or oxygen the vessel A was filled with the liquid concerned and the calorimeter cooled to the normal boiling point by using exchange gas in B. This gas was then removed and more gas condensed in D in the usual way (I). The liquid formed ran into the calorimeter and was there

available for vapour pressure calibrations of the thermometers. The liquid in the calorimeter was finally removed by pumping and using the calorimeter heater to keep the temperature just above its triple point. Alternatively, when vapour pressure calibrations were not required, cooling by exchange gas only was used, with the vessel A pumped to the required temperature. During heat capacity measurements the vessel A, and consequently the inner vacuum case or shield B, was held at a fixed temperature by controlling the vapour pressure in A.

At temperatures between or above those ranges already dealt with the coolant liquid was placed in the outer dewar and the temperature of A and hence B raised to the required level, using the constantan heater G. The heat dissipated in G just balanced all losses by conduction etc. to the cooling liquid in the outer dewar. The current through G was controlled automatically using a platinum resistance thermometer wound on A. The control circuit, which is of orthodox design is shown in figure 2. The platinum thermometer forms part of a non-

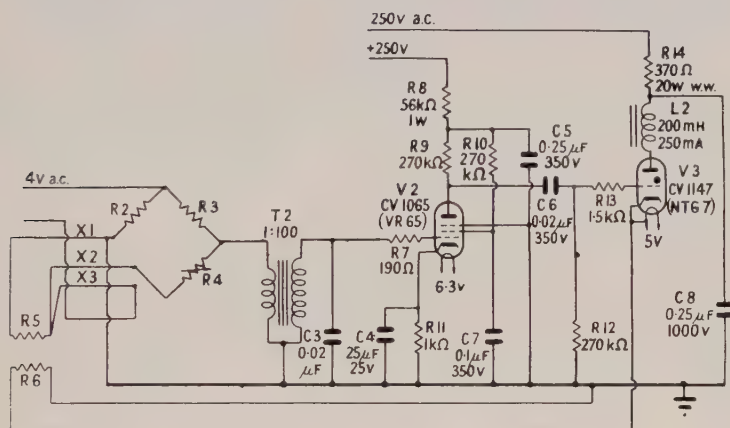


Figure 2.

inductive 50 c/s a.c. bridge. The out-of-balance signal of the bridge is then amplified and used to operate a thyatron controlling the heater current. As arranged here the required temperature is set using the resistance box R4 and the circuit with the components indicated is suitable for handling large out-of-balance signals when it is necessary to move the temperature of A and B quickly. Their temperature can in fact be swept through 50°K and be balanced at its final point in approximately 10 minutes. At the balance point the temperature of A shows a short period overall fluctuation (about 1 min) of approximately $1/60^{\circ}\text{K}$ superimposed on a longer period overall fluctuation (about 20 min) of $1/25^{\circ}\text{K}$.

In all temperature ranges measurements were made with the calorimeter within a few degrees of the temperature of B. The normal procedure of observing the temperature drifts before and after heating until internal equilibrium was achieved, as shown by linear drifts, was followed. The circuit for observing and recording temperatures was identical with that described in I, using a five-decade Tinsley Wheatstone bridge type 3352. The heater resistance was determined as a function of temperature in subsidiary experiments and the heating current measured using a Tinsley potentiometer type 3387B. The heating interval was measured on a calibrated stopwatch reading to $1/5$ second which was mechanically controlled by the heater current switch.

Calibration of the thermometer was carried out using the vapour pressures of hydrogen, nitrogen and oxygen, together with CO_2 point and ice point determinations. Interpolation for the intervening ranges of temperature was carried out using the procedure described in I. The ice point 90°K and 20°K resistances were 142.587Ω , 34.645Ω and 0.817Ω respectively.

In these experiments the heat capacity of the calorimeter was first measured in an independent series of experiments. Then followed the experiments with the lead salts; with all three a certain amount of contamination of the calorimeter was observed after the experiment. This was most marked with the sulphide, and seemed to be due to the formation of a film of copper sulphide. The loss in weight of the sulphide specimen was less than 0.005 gramme. With the selenide and telluride the contamination was progressively less. The specimens were not heated appreciably while the Wood's metal seal of the calorimeter was made. After mounting, the calorimeter was always kept with a few millimetres of helium gas inside.

§ 3. RESULTS

The method of correcting heat capacities is dealt with in the Appendix.

In figure 3 the corrected molar heats of all three salts are shown. The molar heat of lead sulphide has been investigated earlier in this temperature range

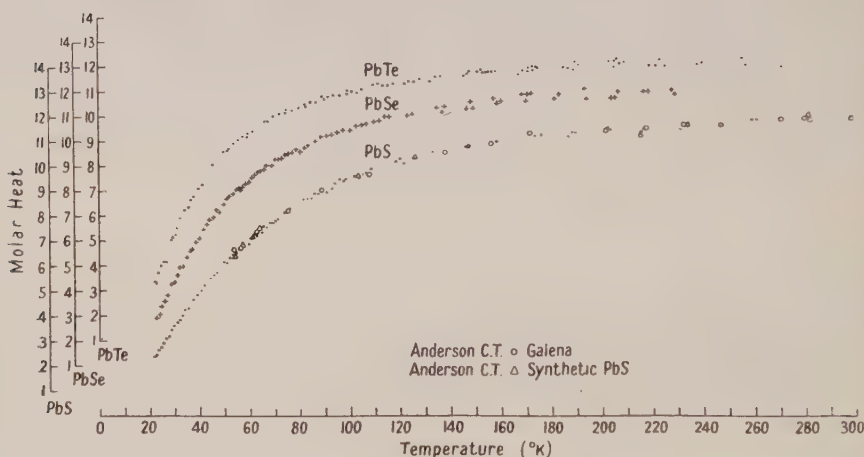


Figure 3. Molar heats of lead salts.

by Eastman and Rodebush (1918) and by Anderson (1932). Of these, the more recent work of Anderson is likely to be more precise and is much more complete; his points are shown in figure 3 both for galena and synthetic crystals. The agreement with the present work is highly satisfactory.

The results for lead selenide and telluride are as consistent as those of the sulphide. In view of the number of points available it is permissible to smooth by eye using large-scale graphs. Taking into account the observed scatter the smoothed results should be correct to $\frac{3}{4}\%$ below 100°K and to $1\frac{1}{2}\%$ at 200°K provided there is no unforeseen systematic error present. Table 1 shows the smoothed molar heats of these salts with the corresponding values of C_V and θ_D , the Debye temperature.

The correction of C_p to C_v with lead sulphide has been made using the normal thermodynamic equation and using the expansion coefficient (Sharma 1951) and compressibility (Bridgman 1925). Extrapolation to the low temperature range was made using the expression $C_p - C_v = AC_p^2 T$. With lead selenide and telluride the value of A was calculated using the melting point formula of Schrödinger (1919).

θ_D has been calculated from each value of C_v shown in table 1; above 200°K the values of θ_D are so sensitive to small changes in C_v that they are not shown, for no significance can be attached to their variation. The variation in the range

Table 1

T (°K)	PbS			PbSe			PbTe		
	C_p	C_v	θ_D	C_p	C_v	θ_D	C_p	C_v	θ_D
20	1.96		149				2.82		127
25	2.81		159	8.44		144	4.24		128
30	3.63		167	4.48		148	5.45		130
35	4.34		176	5.41		152	6.41	6.40	131
40	4.99		184	6.24	6.23	154	7.28	7.26	132
45	5.58	5.57	190	7.03	7.01	155	8.03	8.00	133
50	6.13	6.11	197	7.64	7.62	157	8.58	8.55	134
55	6.61	6.59	202	8.10	8.07	160	9.04	9.00	135
60	7.05	7.03	206	8.49	8.46	163	9.40	9.35	136
65	7.45	7.42	210	8.85	8.81	164	9.71	9.65	136
70	7.82	7.78	214	9.19	9.14	165	9.99	9.93	137
75	8.16	8.12	217	9.48	9.43	166	10.2	10.1	137
80	8.50	8.45	218	9.73	9.67	167	10.4	10.3	139
85	8.80	8.75	219	9.96	9.89	167	10.6	10.5	139
90	9.06	9.00	220	10.2	10.1	168	10.7	10.6	138
95	9.28	9.21	222	10.4	10.3	167	10.8	10.7	138
100	9.50	9.42	223	10.5	10.4	165	11.0	10.9	136
105	9.68	9.60	223	10.7	10.6	166	11.1	10.9	138
110	9.84	9.75	225	10.8	10.7	165	11.2	11.0	135
115	10.0	9.90	225	10.9	10.8	162	11.2	11.1	138
120	10.1	10.0	227	11.0	10.9	163	11.3	11.2	136
130	10.3	10.2	230	11.2	11.1	160	11.5	11.3	135
140	10.6	10.5	227	11.3	11.2	156	11.6	11.4	130
150	10.8	10.7	227	11.5	11.3	150	11.7	11.5	125
160	11.0	10.8	226	11.6	11.4	144	11.8	11.6	121
170	11.1	10.9	226	11.7	11.5	139	11.9	11.6	117
180	11.2	11.0	227	11.8	11.6	139	11.9	11.7	115
190	11.3	11.1	228	11.8	11.6	137	11.9	11.7	118
200	11.4	11.2	227	11.8	11.6	138	11.9	11.7	125
210	11.4	11.2		11.9	11.6		12.0	11.7	
220	11.5	11.3		11.9	11.7		12.0	11.7	
230	11.6	11.3		11.9	11.7		12.0	11.7	
240	11.6	11.3		11.9	11.7		12.0	11.7	
250	11.7	11.4					12.0	11.7	
260	11.7	11.4					12.0	11.7	

Units of C_p and C_v are cal mol⁻¹ deg⁻¹.

20°K to 100°K is significant; as the weight of the atom combined with lead decreases, the divergence from a Debye law increases. This is to be expected from general lattice theory, and apart from this these salts show, so far, a normal family of C_p/T curves. There is no result which can be used immediately to explain the fact that the infra-red lattice absorption edges are not in the order of increasing molecular weight (Gibson 1952). When the course of the molar heats has been measured down to 1–2°K an analysis leading to the form of the Debye spectrum will be possible; unfortunately the accuracy with which this can be done is not high.

Table 2 shows for each salt the thermodynamic functions entropy $S - S_{20}$ and internal energy $U - U_{20}$.

Table 2

	PbS		PbSe		PbTe	
$T(^{\circ}\text{K})$	$S - S_{20}$	$U - U_{20}$	$S - S_{20}$	$U - U_{20}$	$S - S_{20}$	$U - U_{20}$
50	3.58	126.7	4.41	157.0	5.46	185.3
100	9.03	527.6	10.77	619.5	12.36	685.0
150	13.15	1033	15.24	1166	16.97	1247
200	16.35	1581	18.63	1743	20.38	1828
250	18.93	2145	21.29	2326	23.06	2412
300*	21.07	2716	23.52	2913	25.29	2996

Units of entropy are cal (g mol)⁻¹ deg⁻¹.

Units of internal energy are cal (g mol)⁻¹.

* Extrapolated values.

ACKNOWLEDGMENTS

The authors wish to express their thanks to Miss M. Davies for her assistance in the experiments and the arithmetical computation and to Mr. W. A. Hoyes and other members of the staff who produced the liquid hydrogen. They are also indebted to the Chief Scientist, Ministry of Supply, and to the Controller, H.M. Stationery Office, for permission to publish this paper.

REFERENCES

- ANDERSON, C. T., 1932, *J. Amer. Chem. Soc.*, **54**, 107.
 BRIDGMAN, P. W., 1925, *Amer. J. Sci.*, **10**, 483.
 DEVJATAKOVA, E. D., MESLAKOVITZ, Y. P., and SOMNINSKI, I., 1941, *Bull. Acad. Sci. U.R.S.S., Sér. Phys.*, **5**, 409.
 EASTMAN, E. D., and RODEBUSH, W. H., 1918, *J. Amer. Chem. Soc.*, **40**, 496.
 GIBSON, A. F., 1952, *Proc. Phys. Soc. B*, **65**, 378.
 HILL, R. W., 1953, *J. Sci. Instrum.*, **30**, 331.
 KEESOM, W. H., and KOK, J. A., 1932, *Proc. Acad. Sci. Amst.*, **35**, 294.
 PARKINSON, D. H., SIMON, F. E., and SPEDDING, F. H., 1950, *Proc. Roy. Soc. A*, **207**, 137.
 SCHRÖDINGER, E., 1919, *Phys. Z.*, **20**, 452.
 SHARMA, S. S., 1951, *Proc. Indian Acad. Sci. A*, **34**, 76.

APPENDIX

Keesom and Kok (1932) have dealt with the calculation of heat capacities under the comparatively simple conditions where the thermometer, specimen and calorimeter are at all times in equilibrium with each other. Owing to the nature of many specimens of which the heat capacity is required (e.g. a collection of

crystals) it is quite impossible to construct a calorimeter in which internal equilibrium can always be guaranteed, and this is obviously so when it is necessary to rely on a few millimetres of helium exchange gas to establish thermal contact. Under these circumstances the specimen and calorimeter do not necessarily follow the same temperature course.

Figures 4(a) and 4(b) show the nature of the temperature-time curves which are observed during heat capacity determinations and relate specifically to the type of construction used in the preceding paper. The fact that overheating at Q in figure 4(a) is very small even for high heating rates shows that thermometer, heater and calorimeter are in very close thermal contact. In the analysis which follows it is assumed that the thermometer measured the true calorimeter temperature at all times and that the heater was very closely coupled to the calorimeter.

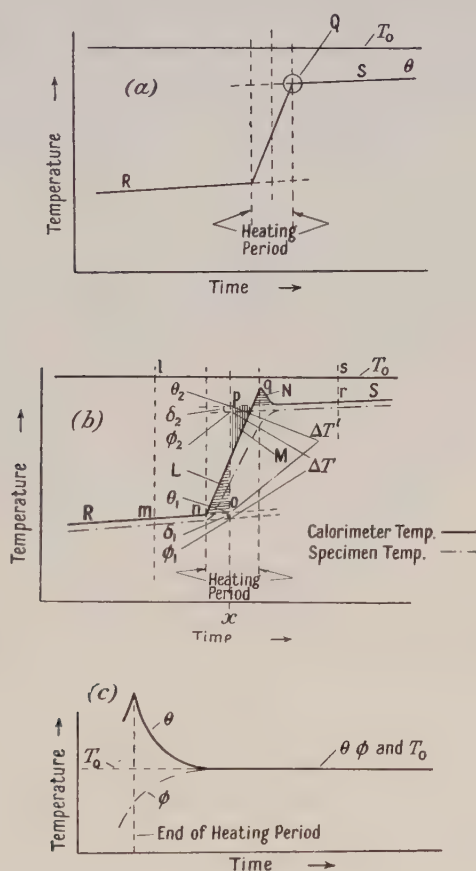


Figure 4.

In figure 4(b) over-heating is shown. This can always be observed under the right conditions when the calorimeter and specimen are linked by thermal exchange gas only. In experiments the calorimeter can always be isolated thermally from the surroundings sufficiently well for the portions R and S of temperature-time curves to appear as straight lines over periods of at least ten minutes. They are in fact parts of shallow exponential curves.

It is assumed that the rate at which heat can be exchanged between shield and calorimeter is proportional to the temperature difference and that it is characterized by a 'thermal exchange coefficient' k (units, $\text{cal deg}^{-1} \text{sec}^{-1}$). A similar coefficient K is defined for the exchange between the calorimeter and specimen. k is usually small compared with K but may well be up to some 6 to 8% of it.

The linear portions R and S of the measured calorimeter temperature-time curves are extrapolated into the heating interval. Now the heat lost or gained from the shield by the calorimeter in any interval $t_2 - t_1$ is given by

$$k \int_{t_1}^{t_2} \{T_0 - F(t)\} dt$$

where $F(t)$ represents the variation of calorimeter temperature with time. This integral is represented by the area $lmnqrs$ in figure 4(b); the point x in time at which to measure the temperature rise $\Delta T'$ must then be such that area $lmoprs = \text{area } lmnqrs$ or such that the areas $L + N = \text{area } M$. It follows at once that where over-heating exists x occurs sooner than the mid-point of the heating interval. If an automatic recorder is used to trace the temperature time curve, x can be found graphically, very rapidly and with sufficient accuracy. Otherwise it is very convenient to get a first estimation of $\Delta T'$ by taking x at the mid-point of the heating interval. If the error in time by so doing is δt , it follows that the error ϵ in $\Delta T'$ is given by $\epsilon = \delta t(d\theta_1/dt - d\theta_2/dt)$. In the linear ranges R and S it is reasonable to make the approximation that the temperature curves for calorimeter and specimen are parallel; this follows from the condition that k is small compared with K . Therefore $(c+s) d\theta_1/dt = k(T_0 - \theta_1)$ and similarly for $d\theta_2/dt$, whence $\epsilon = \delta t k(\theta_2 - \theta_1)/(c+s)$ or $\epsilon = \delta t k \Delta T''/(c+s)$. $\Delta T''$ in this equation is the rise in temperature at the mid-point of the heating interval; c and s are the heat capacities of calorimeter and specimen. $\Delta T''$ is always smaller than $\Delta T'$, consequently the heat capacities are systematically over-estimated by taking x at the mid-point of the heating interval. However, ϵ is very small at low temperatures since $k \sim 10^{-4}$ or less and the ratio $\Delta T''/(c+s)$ is usually of the order of unity. δt depends chiefly on the height of the over-heating peak at Q. This can be reduced by choosing a suitably small heating rate and lengthening the heating interval. In all the experiments described in the preceding paper the temperature rise has been calculated at the centre of the heating period, but the resulting bias is negligibly small at low temperatures and at the highest temperatures is less than $\frac{1}{3}\%$ ($k \sim 10^{-3}$, $\delta t < 10 \text{ sec}$ and $\Delta T''/(c+s) \sim 0.3$).

Now assume that the heat capacity c of the calorimeter is accurately known and $\Delta T'$ has been found as above, then the apparent heat capacity s' of the specimen can be and has frequently been calculated assuming that calorimeter and specimen rise through the same temperature, i.e. $H = (c+s')\Delta T'$, where H is the total heat generated in the heater. In fact $H = c\Delta T' + s\Delta T$ whence $s\Delta T = s'\Delta T'$, and provided the ratio $\Delta T'/\Delta T$ can be found s' can be converted to s . From figure 4(b) it can be clearly seen that ΔT is always greater than $\Delta T'$, so the apparent specimen heat capacity s' is always greater than s .

$\Delta T'/\Delta T$ can be calculated sufficiently accurately without a detailed analysis of the differential equations governing the temperatures of specimen and calorimeter with only the conditions given above, namely k is small compared with K , the ranges R and S can be treated as linear, and in these ranges the specimen and calorimeter temperatures follow parallel lines.

Using the symbols shown in figure 4(b),

$$\Delta T - \Delta T' = \delta_1 - \delta_2. \quad \dots\dots(1)$$

The equations governing the calorimeter at o and p are

$$k(T_0 - \theta_1) - K\delta_1 = c d\theta_1/dt \quad \text{and} \quad k(T_0 - \theta_2) - K\delta_2 = c d\theta_2/dt.$$

Subtracting, we have

$$k(\theta_2 - \theta_1) - K(\delta_1 - \delta_2) = c(d\theta_1/dt - d\theta_2/dt)$$

whence from (1)

$$k\Delta T' - K(\Delta T - \Delta T') = c(d\theta_1/dt - d\theta_2/dt). \quad \dots\dots(2)$$

Then the if linear parts of the calorimeter and specimen temperature curves are taken as parallel,

$$d\theta_1/dt = k(T_0 - \theta_1)/(c + s) \quad \dots\dots(3)$$

with a similar expression for $d\theta_2/dt$. Subtracting these expressions,

$$d\theta_1/dt - d\theta_2/dt = k(\theta_2 - \theta_1)/(c + s) = k\Delta T'/(c + s).$$

Substituting in (2) and re-arranging,

$$\Delta T/\Delta T' = \{1 + ks/K(c + s)\} \quad \text{and} \quad s = s'/\{1 + ks/K(c + s)\}. \quad \dots\dots(4)$$

Since the correction is not large, s' can be written for s in the right of equation (4).

k and K can be found from the recorded calorimeter temperature curve. In equation (3) s' can be used for s without serious error, and θ_1 , $d\theta_1/dt$, T_0 and c are known for any series of determinations about a given T_0 . Hence k can be calculated as a function of temperature with reasonable precision. It is to be expected that k will only depend on the calorimeter and its coupling to the shield, including radiation. In figure 5 values of k derived from the three series

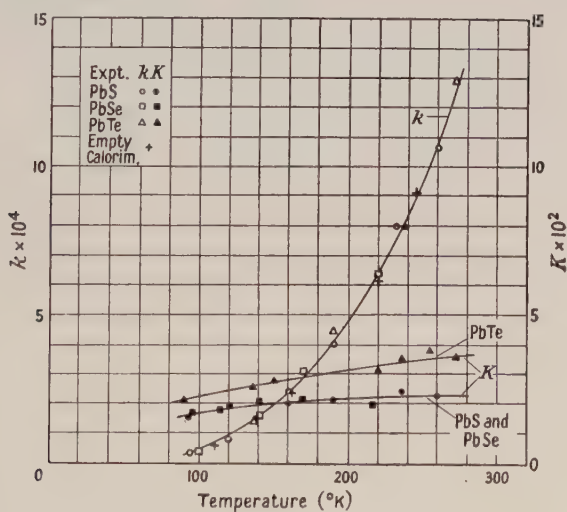


Figure 5.

of experiments described and also from the empty calorimeter heat capacity determinations are shown. They are in satisfactory agreement with each other and behave as expected. Above 120° radiation becomes the predominating factor; as its contribution to k becomes more important the assumption of heat exchange proportional to the temperature difference will begin to break down;

but since the temperature difference between calorimeter and shield is rarely more than 2°K in the high temperature range, the consequent errors are very small.

K can be derived readily from the over-heating portions of the curves. Consider for simplicity those drift curves in which the final calorimeter temperature is equal to that of the shield, then in the linear range $T_0 = \theta = \phi$. In figure 4(c) for all the temperature range shown $c(\theta - T_0) = s(T_0 - \phi)$, neglecting any losses to the shield, which are very small under these circumstances. Thus $\phi = T_0 - (\theta - T_0)c/s$. But the full equation for the variation of θ is

$$c \, d\theta/dt + K(\theta - \phi) + k(\theta - T_0) = 0 \quad \dots\dots(5)$$

whence $c \, d\theta/dt + \{K + (Kc/s) + k\}(\theta - T_0) = 0$. The solution to this equation is

$$(\theta - T_0) = A \exp(-\beta/ct) \quad \text{where} \quad \beta = \{K + (Kc/s) + k\}.$$

It follows that if θ and t are known for two points in the over-heating period, A can be eliminated and

$$\beta/c = (Ks + Kc + ks)/sc = (\ln(\theta' - T_0)/(\theta'' - T_0))/(t' - t'')$$

$$\text{or} \quad K = sc/(s + c)[\{\ln(\theta' - T_0)/(\theta'' - T_0)\}/(t' - t'') - k/c].$$

k/c is a small term which can usually be neglected, which confirms the initial assumption that the loss to the shield is negligible, in which case the term involving k in (5) could have been omitted.

Values of K , which can be quickly deduced from the experiments, are shown in figure 5. At 250°K k has risen to about 6% of K in all experiments. K depends on the internal geometry of the calorimeter, its internal surface, the surface of the specimen, their effective separation and the filling of helium exchange gas (2 mm at 300°K). Of these, the surface areas of the specimens are likely to be considerably different, likewise the effective separations, and it is fortuitous that the values of K for the sulphide and selenide agree with each other.

It has been tacitly assumed throughout that the specimen is of reasonably high thermal conductivity, so that it is possible to regard it as being at one temperature at any time. If the surface area of the specimen is, say, 20 cm^2 , the average rate of transfer of heat through the surface is $10^{-3} \text{ cal cm}^{-2} \text{ sec}^{-1}$. Devjatakova *et al.* (1941) give values of the order of $10^{-2} \text{ cal cm}^{-1} \text{ deg}^{-1}$ for the thermal conductivities of the sulphide and selenide. Taking into account the minimum dimensions of the crystals, the conditions of the analysis are sufficiently nearly approached in the experiments. If this were not so the over-heating part of the temperature-time curve would not be a simple exponential but would contain a contribution depending on the thermal conductivity of the specimen. This was not observed in these experiments.

The correction $s = s'\Delta T/\Delta T$ becomes appreciable at about 120°K , where it is rather less than $\frac{1}{2}\%$ and progressively increases up to 260°K , where it is approximately 4%. An important point arises here, namely, that the appearance or not of 'over-heating' is no criterion for the necessity of this correction, for it is always possible to choose a small enough heating current so that the over-heating is inappreciable. The presence of over-heating simply gives a convenient way of measuring K . The ratio of k/K is the important criterion; here this decreases very rapidly as the temperature falls to 100°K , and the resulting correction is negligible down to 30°K . In the lower temperature ranges this need not be so, particularly if the vacuum conditions about the calorimeter are not perfect. Consideration of this correction in the helium and hydrogen temperature ranges will be made in a later paper.

The heat generated in the heater leads cannot be divided equally between the calorimeter and shield, as in the adiabatic method, unless it can be shown that during the heating interval the temperature of the centre of the leads becomes considerably higher than that of either the calorimeter or shield. The proper course is to make this unwanted heat generation as small as possible: here it was $\frac{1}{2}\%$ of that in the heater. An order of magnitude calculation shows that to add half the heat generated in the leads to that generated in the calorimeter is only a crude approximation, and the errors arising from this are likely to lead to an overall scatter of the order of $\frac{1}{2}\%$. In the higher temperature range in fact it increases to about 2%. This is due to the residual lack of constancy in the shield temperature combined with the increase in the value of k .

Conditions are reasonably good with the present apparatus up to 150°K. To improve the consistency at higher temperatures a smaller variation in the shield temperature is required combined with the conventional highly polished foil around the outside of the calorimeter to reduce k . In this way the size of the corrections can be reduced as well as the overall scatter.

Riesz Potential and the Elimination of Divergences from Meson Theory

By L. S. KOTHARI

Tata Institute of Fundamental Research, Apollo Pier Road, Bombay 1

MS. received 28th January 1954

Abstract. Using a modified definition of Riesz potential for the neutral vector meson field, the potential on the world line of a nucleon is calculated. The 'lower order' meson potential corresponding to $\alpha = -2$ is given.

Finally the self-energy of a nucleon in direct interaction with neutral vector mesons as well as with pseudoscalar mesons is evaluated. A finite expression is obtained without having to introduce any cut-off factors or auxiliary fields.

§ 1. INTRODUCTION

IN two earlier papers (Kothari 1954 a, to be referred to as II; 1954 b) the method of analytic continuation, first developed by Riesz, was applied to quantum electrodynamics. It was shown that the divergences associated with the self-energy of an electron, vertex part of a Feynman graph and the photon self-energy could be eliminated in a consistent way without having to introduce any arbitrary cut-off factors or any auxiliary fields. The purpose of the present paper is to extend the method to meson theory and to show how some of the divergences arising here can also be eliminated. For the greater part of this paper we will confine ourselves to neutral vector mesons, though it is not difficult to extend the results to other renormalizable meson theories.

The method of analytic continuation was first used in meson theory by Fremberg (1946). He and, later, Majumdar and Gupta (1949) used this method for deriving the equation of motion of a nucleon in a meson field. For evaluating the meson potential and the field tensor on the world line of the nucleon the Riesz potential at any point x is defined by them in terms of an integral in coordinate space which, as in the electromagnetic case, is an analytic function of an arbitrary parameter α (α real or complex). Fremberg considers a single neutron of mesic charge g and mass χ_0 describing the world line with a velocity v_μ , and defines the Riesz potential $\mathcal{A}_\mu^\alpha(x)$ for this case as

$$\mathcal{A}_\mu^\alpha(x) = \frac{\chi_0^{(\alpha+2)/2} g}{2^{-\alpha/2} \Gamma(1 - \frac{1}{2}\alpha)} \int_{-\infty}^{\tau_{\text{ret}}} v_\mu(z') r^{-(\alpha+2)/2} J_{-(\alpha+2)/2}(\chi_0 r) d\tau' \quad \dots\dots (1)$$

where τ is the proper time of the particle and $r_\mu = x_\mu - z_\mu'$, $r^2 = (x_0 - z_0')^2 - |x - z'|^2$. The above integral converges for $\alpha < 0$.

A modified definition of the Riesz potential for the neutral vector meson field was given some time back by Kothari (1952, to be referred to as I). He works in momentum space and, as he has shown, the new definition represents a generalization in the α -plane of meson potential in interaction representation. Here we will discuss some of its consequences. We will show how the method of analytic continuation can be linked up with the techniques of Feynman and Dyson, and then successfully employed to eliminate the divergences arising in renormalizable meson theories.

In the next section, after introducing the modified Riesz potential for the neutral vector meson field, we evaluate the potential on the world line of an arbitrarily moving point particle. As we shall be working in the interaction representation, the meson potential, instead of being defined by the retarded expression everywhere, is defined differently in different parts of the light cone of z . The various expressions have been worked out and it is shown that only in the region outside the light cone of z the potential in the interaction representation reduces to the retarded potential. In § 3 'lower order' potential is discussed. In the last section a generalization of the Feynman function $D_{F\chi_0}$ is obtained in the α -plane and the self-energy of a nucleon in direct interaction with neutral vector meson and with pseudoscalar meson fields is evaluated.

§ 2. POTENTIAL ON THE WORLD LINE OF A POINT PARTICLE

The modified Riesz potential for the neutral vector meson field due to a point source is defined in I and is given by (notation used is the same as that in I, except that here we have replaced k by χ and χ by χ_0),

$$A_\mu^\alpha(x) = g \int_{-\infty}^z v_\mu(z') \mathcal{D}_{\chi_0}^\alpha(x - z') d\tau' \quad \dots\dots (2)$$

where

$$\mathcal{D}_{\chi_0}^\alpha(x) = \frac{H(\alpha) l_0^\alpha}{2\pi^2} \int_D (\chi^2 - \chi_0^2)^{(\alpha-2)/2} \sin[kx] d^4k, \quad \dots\dots (3)$$

$$\chi^2 = k_0^2 - |k|^2,$$

and l_0 is a constant of the dimensions of length, introduced to make the dimensions of $A_\mu^\alpha(x)$ independent of α . (This appears in some of the final results and introduces a certain arbitrariness. This arbitrariness, however, is not peculiar to the method of the Riesz potential. In the theory of Feynman and others the cut-off factor introduces the same arbitrariness.) We have also shown in I that the right-hand side of (3) can be partly integrated and yields

$$\mathcal{D}_{\chi_0}^\alpha(x) = - \frac{H(\alpha) l_0^\alpha}{|x|} \frac{\partial}{\partial |x|} \int_{\chi_0}^\infty (\chi^2 - \chi_0^2)^{(\alpha-2)/2} \chi U(\chi^s) d\chi \quad \dots\dots (4)$$

where

$$U(\chi^s) = \begin{cases} J_0(\chi^s) & \text{for } x_0 > |x| \\ 0 & \text{for } |x| > x_0 > -|x| \\ -J_0(\chi^s) & \text{for } -|x| > x_0, \end{cases} \quad \dots\dots (5)$$

$$s^2 = x_0^2 - |x|^2.$$

If the field point x lies outside the light cone of z , i.e.

$$|x - z| > (x_0 - z_0) > -|x - z|,$$

it follows from (2), (4) and (5), after putting $t = (\chi^2 - \chi_0^2)^{1/2}$, that

$$A_\mu^\alpha(x) = H(\alpha) l_0^\alpha g \int_{-\infty}^{\tau_{\text{ret}}} \frac{v_\mu(z')}{r} d\tau' \frac{\partial}{\partial r} \int_0^\infty t^{\alpha-1} J_0[r(\chi_0^2 + t^2)^{1/2}] dt. \quad \dots\dots (6)$$

The integration over t can be carried out by using Sonine's formula (Watson 1944), and it is readily seen that (6) reduces to (1). Thus the new definition for the Riesz potential reduces to Fremberg's definition in the region outside the light cone of z .

To evaluate the potential at any point x due to a point particle moving along the world line $z = z(\tau)$ we substitute for $\mathcal{D}_{\chi_0}^\alpha(x - z')$ from (4) and (5) in (2) and analytically continue the whole expression to $\alpha = 0$, obtaining,

$$A_\mu(x) \equiv A_\mu^0(x) = g \int_{-\infty}^z v_\mu(z') \left\{ \Delta(x - z') + \frac{1}{r} \frac{\partial}{\partial r} U(\chi_0 r) \right\} d\tau', \quad \dots\dots(7)$$

where it is now understood that $U(\chi_0 r) = 0$ on the light cone, the Δ singularity of the function $\partial U(\chi_0 r)/\partial r$ having been explicitly written down in (7). If the point x lies outside the light cone of the point z , i.e. if

$$[x - z, x - z] < 0, \quad \dots\dots(8)$$

we can write $A_\mu(x)$ as

$$A_\mu(x) = \left. \frac{g v_\mu}{[v, x - z]} \right|_{\text{ret}} - g \chi_0 \int_{-\infty}^{\tau_{\text{ret}}} v_\mu(z') r^{-1} J_1(\chi_0 r) d\tau'. \quad \dots\dots(9)$$

The integral in (9) is to be taken along the world line of the particle from the point $z(\tau' = -\infty)$ to the 'retarded point of $x - z(\tau_{\text{ret}})$ ', i.e. the point where the retrograde cone with its vertex at x intersects the world line of the particle.

In the case where x lies in the future part of the light cone of z , i.e. if

$$[x - z, x - z] > 0, \quad x_0 - z_0 > 0, \quad \dots\dots(10)$$

we have

$$A_\mu(x) = -g \chi_0 \int_{-\infty}^z v_\mu(z') r^{-1} J_1(\chi_0 r) d\tau'. \quad \dots\dots(11)$$

If the point x lies in the past part of the light cone of z , i.e. if

$$[x - z, x - z] > 0, \quad x_0 - z_0 < 0, \quad \dots\dots(12)$$

then

$$A_\mu(x) = \left. \frac{g v_\mu}{[v, x - z]} \right|_{\text{ret}} - \left. \frac{g v_\mu}{[v, x - z]} \right|_{\text{adv}} - g \chi_0 \int_{-\infty}^{\tau_{\text{ret}}} v_\mu(z') r^{-1} J_1(\chi_0 r) d\tau' + g \chi_0 \int_{\tau_{\text{adv}}}^z v_\mu(z') r^{-1} J_1(\chi_0 r) d\tau' \quad \dots\dots(13)$$

where $z(\tau_{\text{adv}})$ is 'the advanced point of x '.

The meson potential outside the world line of the particle is given by the expression (9). This agrees with the result deduced by Fremberg and others. The potential on the world line of the particle is given by the average value of the potential in the future part (11) and in the past part (13) of the light cone of z :

$$A_\mu^{\text{w.l.}} = \frac{g}{2} \left\{ \left. \frac{v_\mu}{[v, x - z]} \right|_{\text{ret}} - \left. \frac{v_\mu}{[v, x - z]} \right|_{\text{adv}} \right\} - g \chi_0 \int_{-\infty}^{\tau_{\text{ret}}} v_\mu(z') r^{-1} J_1(\chi_0 r) d\tau', \quad \dots\dots(14)$$

as $x - z \rightarrow 0$. The limit of the first two terms on the right-hand side of (14) as $x - z \rightarrow 0$ can be shown to be $g dv_\mu/d\tau$. Thus we have

$$A_\mu^{\text{w.l.}} = g dv_\mu/d\tau - g \chi_0 \int_{-\infty}^{\tau_{\text{ret}}} v_\mu(z') r^{-1} J_1(\chi_0 r) d\tau'. \quad \dots\dots(15)$$

The expression on the right-hand side agrees with the result generally obtained for the potential on the world line of the particle.

§ 3. 'LOWER ORDER' POTENTIALS

The usual meson (or electromagnetic) potential is a particular case, corresponding to $\alpha=0$, of the more general Riesz potential $A_\mu^\alpha(x)$. For all $\alpha=2m$ ($m=1, 2, \dots$) the potential $A_\mu^\alpha(x)$ vanishes. However, for negative integral values of α it is not necessarily zero. It is of some interest to consider the potential $A_\mu^{-2}(x)$, where $A_\mu^{-2}(x)$ represents the analytic continuation of $A_\mu^{\alpha-2}$ to $\alpha=0$.

It is easily seen that (2) satisfies the equation

$$(\square + \chi_0^2)A_\mu^{\alpha-2} = l_0^{-2}A_\mu^\alpha, \quad \dots\dots(16)$$

When α is made to tend to zero we obtain

$$A_\mu(x) \equiv A_\mu^0(x) = l_0^2(\square + \chi_0^2)A_\mu^{-2}(x), \quad \dots\dots(17)$$

i.e. the usual meson potential $A_\mu(x)$ is defined in terms of a 'lower order' potential (the term 'lower' or 'higher' is relative and depends upon the notation). To evaluate $A_\mu^{-2}(x)$ we consider (2) and (3) with α replaced by $\alpha-2$:

$$A_\mu^{\alpha-2}(x) = \frac{H(\alpha-2)l_0^{\alpha-2}g}{2\pi^2} \int_D \int_{-\infty}^z v_\mu(z')(\chi^2 - \chi_0^2)^{(\alpha-4)/2} \sin[k, x - z'] d^4k d\tau'. \quad \dots\dots(18)$$

It readily follows that in the space-time region defined by $(x_0 - z_0) > |x - z|$

$$A_\mu^{\alpha-2}(x) = H(\alpha)l_0^{\alpha-2}g \int_0^\infty \int_{-\infty}^{\tau_{\text{ret}}} t^{\alpha-3}(t^2 + \chi_0^2)^{1/2} r^{-1} J_1[r(t^2 + \chi_0^2)^{1/2}] dt dz'_\mu, \quad \dots\dots(19)$$

($dz'_\mu = v_\mu d\tau$). Continuing to $\alpha=0$, we obtain

$$A_\mu^{-2}(x) = \frac{1}{2}gl_0^{-2} \int_{-\infty}^{\tau_{\text{ret}}} J_0(\chi_0 r) dz'_\mu. \quad \dots\dots(20)$$

For the electromagnetic case $J_0(\chi_0 r) = 1$, and we have, replacing g by e ,

$$A_\mu^{-2}(x) = \frac{1}{2}el_0^{-2}z_\mu|_{\text{ret}} \quad (\text{electromagnetic case}), \quad \dots\dots(21)$$

a result which has been obtained earlier by Riesz (1949).

§ 4. SELF-ENERGY OF A NUCLEON

We will now evaluate the self-energy of a nucleon in meson field. Treating from now on the meson potentials $A_\mu^\alpha(x)$ as operators instead of c -numbers, as in classical theory, we define the commutation relation

$$[A_\mu^\alpha(x), A_\nu^\alpha(x')] = g_{\mu\nu} \mathcal{D}_{\chi_0}^\alpha(x - x'), \quad \dots\dots(22)$$

The vacuum for the field can be defined by

$$A_\mu^{+\alpha}(x)\Psi_0 = 0 \quad \dots\dots(23)$$

where $A_\mu^{+\alpha}(x)$ is the positive frequency part of $A_\mu^\alpha(x)$ and Ψ_0 is the vacuum state vector. From (22) and (23) it readily follows that

$$\langle P(A_\mu^\alpha(x), A_\nu^\alpha(x')) \rangle_0 = -ig_{\mu\nu} \mathcal{D}_{\chi_0}^\alpha(x - x') \quad \dots\dots(24)$$

where

$$\mathcal{D}_{\chi_0}^\alpha(x) = H(\alpha)l_0^\alpha \int_0^\infty t^{\alpha-1} D_{F(t^2 + \chi_0^2)^{1/2}}(x) dt = \frac{H(\alpha)l_0^\alpha}{(2\pi)^2} \int_0^\infty t^{\alpha-1} dt \int \frac{e^{-i[k,x]} d^4k}{k^2 - t^2 - \chi_0^2}.$$

In order to eliminate logarithmic divergences, it is found necessary (Nilsson 1949) to change the 'weight factor' in the above relation from $l_0^\alpha t^{\alpha-1}$ to

$$g_\alpha(t) = \frac{1}{2}(l_0^\alpha t^{\alpha-1} + l_0^{\alpha*} t^{\alpha*-1}), \quad \dots\dots(25)$$

so that we finally have

$$\mathcal{D}_{F_{\chi_0}}^{\alpha}(x) = \frac{H(\alpha)}{(2\pi)^2} \int_0^{\infty} g_{\alpha}(t) dt \int \frac{e^{-i[kx]} d^4k}{k^2 - t^2 - \chi_0^2}. \quad \dots\dots (26)$$

$\mathcal{D}_{F_{\chi_0}}^{\alpha}(x)$ is the generalization in the α -plane of the usual Feynman function $D_{F_{\chi_0}}$.

Using $\mathcal{D}_{F_{\chi_0}}^{\alpha}(x)$ instead of the usual $D_{F_{\chi_0}}$ function we write out the matrix element for the second order self-energy graph between states \bar{u} and u of the nucleon:

$$\frac{g^2 H(\alpha)}{4\pi^3 i} \int_0^{\infty} g_{\alpha}(t) dt \int \gamma_{\mu} \frac{\mathbf{p} - \mathbf{k} + M}{(p-k)^2 - M^2} \gamma^{\mu} \frac{d^4k}{k^2 - t^2 - \chi_0^2} \quad \dots\dots (27)$$

where $\mathbf{p} = [\gamma p]$, p_{μ} being the momentum of the nucleon, $p^2 = M^2$. The γ -matrices satisfy the following relations:

$$\left. \begin{aligned} \gamma_{\mu} \gamma_{\nu} + \gamma_{\nu} \gamma_{\mu} &= 2g_{\mu\nu} \\ \gamma_{\mu} \gamma^{\mu} &= 4 \\ \gamma_{\mu} \mathbf{A} \gamma^{\mu} &= -2\mathbf{A} \end{aligned} \right\}. \quad \dots\dots (28)$$

To evaluate (27) we consider the integral (in Feynman notation)

$$I^{\alpha}(1: k_{\sigma}) = H(\alpha) l_0^{\alpha} \int_0^{\infty} t^{\alpha-1} dt \int \frac{(1: k_{\sigma}) d^4k}{\{(p-k)^2 - M^2\} \{k^2 - t^2 - \chi_0^2\}} \quad \dots\dots (29)$$

Integrating first by parts over t for $0 < \alpha < 2$, and then over k , we obtain

$$I^{\alpha}(1: k_{\sigma}) = -\frac{2\pi^2 H(\alpha)}{i\alpha} \int_0^{\infty} t^{\alpha+1} dt \int_0^1 \frac{x(1-x)p_{\sigma} dx}{t^2 x + \chi_0^2 x + M^2(1-x)^2} \quad \dots\dots (30)$$

where x is the Feynman variable. Analytic continuation of the integral over t to $\alpha = 0$ can be carried out as shown in II, and we get

$$I^0(1: k_{\sigma}) = i\pi^2 \int_0^1 (1-x)p_{\sigma} dx \log \frac{x l_0^{-2}}{\chi_0^2 x + M^2(1-x)^2}. \quad \dots\dots (31)$$

Integration over x is fairly simple to carry out. Substituting the result in (27), we obtain, after some simplification, for the case of a free nucleon:

$$\begin{aligned} \frac{\Delta M}{M} = \frac{g^2}{2\pi} \left[\frac{3}{4} + 3 \log \frac{1}{l_0 M} + \frac{1}{2} \frac{\chi_0^2}{M^2} - \frac{1}{4} \frac{\chi_0^4}{M^4} \log \frac{\chi_0^2}{M^2} \right. \\ \left. - \frac{1}{4} \frac{\chi_0^2}{M^2} \left(4 - \frac{\chi_0^2}{M^2} \right) \left(2 + \frac{\chi_0^2}{M^2} \right) \int_0^1 \frac{M^2 dx}{\chi_0^2 x + M^2(1-x)^2} \right]. \quad \dots\dots (32 V) \end{aligned}$$

The above expression gives the contribution to the mass of a free nucleon arising from the lowest order self-energy graph when the mesons considered are neutral vector mesons.

The theory of pseudoscalar mesons in direct interaction with the nucleons is also renormalizable. If we consider neutral mesons, the matrix element for the second order self-energy graph between states \bar{u} and u of the nucleon is

$$\frac{g^2 H(\alpha)}{4\pi^3 i} \int_0^{\infty} g_{\alpha}(t) dt \int \gamma_5 \frac{\mathbf{p} - \mathbf{k} + M}{(p-k)^2 - M^2} \gamma_5 \frac{d^4k}{k^2 - t^2 - \chi_0^2}. \quad \dots\dots (33 \text{ Ps})$$

This leads to an additional mass for a free nucleon, given by

$$\begin{aligned} \frac{\Delta M}{M} = \frac{g_0^2}{4\pi} \left[-\frac{1}{4} + \log \frac{1}{l_0 M} + \frac{1}{2} \frac{\chi_0^2}{M^2} + \frac{1}{2} \frac{\chi_0^2}{M^2} \log \frac{\chi_0^2}{M^2} \right. \\ \left. - \frac{1}{4} \frac{\chi_0^4}{M^4} \log \frac{\chi_0^2}{M^2} - \frac{1}{4} \frac{\chi_0^4}{M^4} \left(4 - \frac{\chi_0^2}{M^2} \right) \int_0^1 \frac{M^2 dx}{\chi_0^2 x + M^2(1-x)^2} \right]. \quad \dots\dots (34 \text{ Ps.N}) \end{aligned}$$

On the symmetric theory the change in the mass of a neutron is

$$\frac{\Delta M_N}{M} = \frac{5g^2}{8\pi} \left[-\frac{1}{4} + \dots \right] \dots\dots (35\text{Ps.S})$$

while that of a proton is

$$\frac{\Delta M_P}{M} = \frac{3g^2}{8\pi} \left[-\frac{1}{4} + \dots \right] \dots\dots (36\text{Ps.S})$$

We note that on the symmetric theory the contribution of the second order self-energy graph to the neutron mass is different from that to the proton mass. However, it is not possible to rely on the numerical values, because the applicability of perturbation theory itself, especially to the case of pseudoscalar mesons, is rather doubtful. Further, one expects higher order contributions also be of the same order of magnitude.

The present method can readily be applied to evaluate the contribution of any vertex part of a Feynman graph. The calculations are very similar to those presented in II, and will not be repeated here.

ACKNOWLEDGMENTS

The present work was carried out while at Cambridge on a Government of India Scholarship. I am also grateful to Professor M. H. L. Pryce for facilities to work for a few months at the Clarendon Laboratory.

REFERENCES

- FREMBERG, N. E., 1946, *Medd. Lunds Univ. mat. Semin.*, **7**, 1.
 KOTHARI, L. S., 1952, *Proc. Phys. Soc. A*, **65**, 930; 1954 a, *Ibid.*, **67**, 17; 1954 b, *Ibid.*, **67**, 201.
 MAJUMDAR, R. C., and GUPTA, S., 1949, *Phys. Rev.*, **75**, 1788.
 NILSSON, B. S., 1949, *Ark. Fys.*, **1**, 369.
 RIESZ, M., 1949, *Acta Math.*, **81**, 1.
 WATSON, G. N., 1944, *Theory of Bessel Functions* (Cambridge : University Press), p. 412.

Statistics of Nuclear Levels †

BY J. M. B. LANG AND K. J. LE COUTEUR
Department of Theoretical Physics, University of Liverpool

Communicated by H. Fröhlich; MS. received 16th February 1954

Abstract. All the available experimental evidence relating to the statistical distribution of dense nuclear levels is collected together and analysed. The simplest adequate nuclear equation of state is

$$U = \frac{1}{11}At^2 - t + \frac{1}{8}A^{2/3}t^{7/3} \text{ Mev}$$

which leads to

$$D_0 = 0.11A^2(U+t)^2 \exp - \left\{ 2 \left(\frac{AU}{11} \right)^{1/2} + \frac{3}{32}(11U)^{2/3} \right\} \text{ Mev}$$

for the spacing of levels of zero angular momentum. The significance of these formulae is discussed.

An appendix refines the theoretical level density formula for a Fermi gas with a fixed number of particles; this analysis incidentally yields a slightly more accurate form of the simple Hardy-Ramanujan asymptotic formula for the number of partitions of a positive integer.

§ 1. INTRODUCTION

BECAUSE a heavy nucleus has many degrees of freedom, at sufficiently high excitation energies the nuclear states become too numerous to treat individually and only a statistical description is possible. Densities P and ρ are defined so that $P(A, U)dU$ is the total number of states of a nucleus of mass A within the range dU of excitation energy, and, more specifically, $\rho(A, J, U)dU$ is the number of levels of a particular total angular momentum J . Then

$$P(A, U) = \sum_J (2J+1) \rho(A, J, U). \quad \dots\dots(1)$$

The essential assumption of the statistical theory is that P and ρ can be treated as smoothly varying functions of energy; usually to obtain results of useful scope the variation with A also is treated as smooth. In principle the densities could depend on the neutron excess $N-Z=A\theta$, but theoretically the effect is small (Le Couteur 1950, eqn 37) and practically this refinement is beyond the scope of the experimental data.

Statistical thermodynamics provides some guide to the behaviour of P (Bethe 1937). The variable $F(A, \beta)$ defined by

$$\exp(-\beta F) = \int P(A, U') \exp(-\beta U') dU' \quad \dots\dots(2)$$

may be identified with the thermodynamic free energy of the nucleus A at temperature $t=1/\beta$, and inversion of this Laplace transform leads to

$$P(A, U) = \frac{1}{2\pi i} \int_{\gamma-i\infty}^{\gamma+i\infty} d\beta \exp \beta(U-F). \quad \dots\dots(3)$$

† A preliminary account was communicated to the Birmingham Conference of July 1953.

The integrand has a saddle point at the value $\beta(U)$ of β defined by

$$U = d(\beta F)/d\beta \quad \text{.....(4)}$$

where the exponent has the value

$$S(A, U) = \beta(U - F) = \int_0^U \beta' dU' \quad \text{.....(5)}$$

since $dS = \beta dU$ follows from (4). Integration by the method of steepest descent yields Bethe's theorem

$$P(A, U) = e^S / (-2\pi dU/d\beta)^{1/2} \quad \text{.....(6)}$$

which may be considered to define the statistical scale of nuclear temperature. Specifically

$$\frac{d}{dU} \log P = \frac{1}{t} - \frac{1}{2} \frac{d}{dU} \log \left(t^2 \frac{dU}{dt} \right) \quad \text{.....(7)}$$

but in practical applications the last term is usually negligible, so the experimental scale of nuclear temperature and applications of nuclear evaporation theory are always based on the equation

$$(d/dU) \log P = 1/\tau. \quad \text{.....(8)}$$

Always $\tau > t$, but only for light nuclei at low excitation energies is the difference between τ and t significant.

All the simple nuclear models which have been used to calculate the functional relationship between U and t lead to results of the form $U \propto t^\delta$ and $S \propto t^{\delta-1} \propto U^{1-1/\delta}$ with exponents δ ranging between 2 for the Fermi gas model and 4 for a continuous fluid model. Thus it is qualitatively predicted that P must increase very rapidly with U .

To get quantitative information about P it is best to proceed by direct analysis of experiments. It is essential to take a broad view of the evidence because the power of the statistical approach lies in its wide scope rather than in the accuracy to be expected at any point. For example, the fluctuations with A of the observed level densities are not represented by any smooth formula for $P(A, U)$, which can only represent the general trend. Also anomalies must be expected at low excitation energies where the symmetry properties of nuclear configurations play an essential role. For all these reasons it is essential to survey a large range of A and U .

There are essentially two logically distinct different types of experiment, which will be treated in §§2 and 3 respectively: (i) measurements of ratios of level densities at neighbouring excitation energies of the same nucleus, leading through equation (8) to assignments of nuclear temperature, (ii) direct measurement of level density ρ , mostly at the excitation energy of about 8 mev provided by slow neutron capture.

§ 2. NUCLEAR TEMPERATURE AND EVAPORATION

The probability per unit time that an excited nucleus *a* decays, by emission of a particle or fragment of mass M and spin s with kinetic energy T , to leave a residual nucleus *b* with excitation energy in the range dU_b , is given by Weisskopf's (1937) evaporation formula

$$p(T) dT = \frac{(2s+1)M\sigma}{\pi^2 \hbar^3} T \frac{P(b)}{P(a)} dU_b \quad \text{.....(9)}$$

where σ is the cross section for the inverse process. Simple approximations to σ suffice to calculate the relative probabilities of emission of different types of particle and the energy spectrum of each type. This treatment of the disintegration of a stands apart from the often more difficult (Feshbach, Porter and Weisskopf 1953) consideration of how it was excited; useful results can be obtained even when, as with cosmic rays (Le Couteur 1950), the mechanism of excitation is not understood. However, caution is required whenever this method predicts a very small probability for a particular process, since a larger contribution may come from some mechanism other than compound nucleus formation: obvious examples are d , p and γ , p reactions.

For emission of a single neutron use of the geometrical cross section $\sigma = \pi R^2$ in (9) gives Weisskopf's (1937) normalized energy spectrum

$$\left. \begin{aligned} n(T) dT &= T e^{-T/\tau} dT/\tau^2 \\ \bar{T} &= 2\tau, \quad \sigma^2(T) \equiv \bar{T}^2 - (\bar{T})^2 = 2\tau^2 \end{aligned} \right\} \dots\dots (10)$$

where τ , defined by (8), is the temperature of the residual nucleus at its average energy, which for reasons given in §1 should not be less than 2 or 3 mev if this simple formula is to hold. If several neutrons can be emitted in succession while the temperature falls as $U^{1/\delta}$ from an initial value τ_m to zero, the resultant energy spectrum is (Le Couteur 1952, §4)

$$\left. \begin{aligned} n(T) dT &= T^{l-1} \exp(-T/\tau^*) dT/\tau^{*l} \\ \bar{T} &= l\tau^*, \quad \sigma^2(T) = l\tau^{*2} = (\bar{T})^2/l \end{aligned} \right\} \dots\dots (11)$$

with $l = 16/11$, $\tau^* = 11\tau_m/12$ for $\delta = 2$. Strictly τ_m is the nuclear temperature at excitation energy $\frac{1}{2}Q$ below the initial value, where Q is the average energy removed from the nucleus by the first neutron emitted.

2.1. Temperature at $U \simeq 50$ Mev

An example of a neutron evaporation spectrum, due to Mrs. Skyrme at Harwell, is shown in figure 1; it represents evaporation of about 3 neutrons from a silver nucleus. Experimentally $\bar{T} = 2.58$ mev, so from (11) the average value of τ_m must be $\bar{\tau}_m = \frac{3}{4}\bar{T} = 1.94$ mev.

To interpret this result the mechanism of nuclear excitation must be discussed. The bombarding particle was a 150 mev proton, and Bernardini, Booth and Lindenbaum (1952) have treated its interaction with a silver nucleus by the Monte Carlo method. We are grateful to Dr. Lindenbaum for sending us the values of excitation energy U transferred to the silver nucleus in a study of 198 events; these statistics are represented by the frequency distribution $f(U)d(U)$ of figure 2, which is consistent with our experimental knowledge of the energy spectrum of the fast particles emitted in the forward direction. For comparison with Mrs. Skyrme's experiment $f(U)$ must be weighted by the number n_n of neutrons emitted from a nucleus with excitation U , which was taken from table 2 of Le Couteur (1952), to yield the sharply peaked curve $n_n f$ of figure 2. The measured value $\bar{\tau}_m = 1.94$ mev is an average over this distribution and so corresponds to a mean excitation energy \bar{U}_m given by $\bar{U}_m^{1/\delta} = \text{av}(U - 5)^{1/\delta}$; for $\delta = 2$ this is $\bar{U}_m = 50.6$ mev, but because $n_n f$ has a strong maximum the average is not sensitive to δ . The theoretical spectrum plotted in figure 1 is an average

of (11) over the distribution $n_n f$, assuming that τ_m varies as $(U-5)^{1/2}$, and is therefore slightly wider than the spectrum (11) corresponding to $\tau_m = 1.94$ mev.

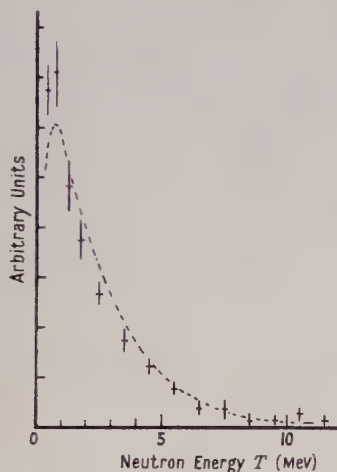


Figure 1. Experimental and theoretical energy distributions of neutrons evaporated in the backward direction from a silver target bombarded by 150 mev protons.

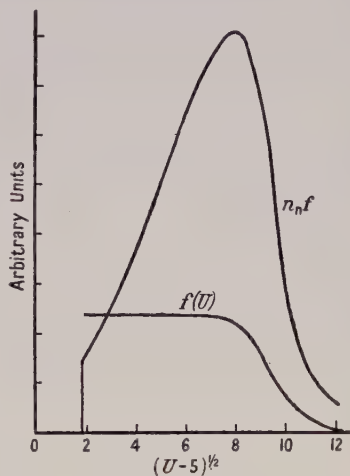


Figure 2. The frequency distribution $f(U)dU$ of excitation energy U transferred to a silver nucleus by a 150 mev proton and the distribution $n_n f$ of the number of neutrons afterwards evaporated.

It may be mentioned that the theoretical spectrum could be increased by about 30% at energies below $\frac{1}{2}$ Mev by allowance for the finite wavelength of the emitted neutron; that is, by using $\sigma = \pi(R + \lambda/2\pi)^2$ instead of $\sigma = \pi R^2$, which leads to the simple formula (10).

Similar experiments have been done by Skyrme and Williams (1951) for tungsten and by Skyrme for aluminium, and we have calculated the energy transfer U for these materials. Altogether we gain the following data:

^{27}Al	$U_m = 24$ mev	$T_m = 3.09$ mev
^{107}Ag	51 mev	1.94 mev
^{182}W	65 mev	1.78 mev

Because the incident proton generates a small cascade within nuclear matter, the energy loss per unit depth increases with depth. Accordingly our detailed calculations yield excitation energies which increase from aluminium to tungsten slightly faster than the nuclear radius.

2.2. Temperature at $U \simeq 200$ MeV

Detailed calculations of Le Couteur (1950, 1952) represent the behaviour of the low energy particles emitted from cosmic-ray stars in terms of nuclear evaporation, assuming $U = \frac{1}{4}\tau^2\Lambda^2$ with Λ^2 between $A/3.3$ and $A/2.9$ mev $^{-1}$. Most of the experimental data concern stars in silver or bromine with about 400 mev total excitation energy, so this formula must be a good representation of τ for $A \simeq 100$ and $U \simeq 250$ mev.

2.3. Temperature at $U \simeq 10$ Mev

Gugelot (1951) measured energy spectra of neutrons from (p, n) reactions induced by 16 mev protons. If only one neutron can be emitted, a logarithmic plot of $n(T)/T$ gives a direct measure of temperature τ ; if emission of 2 neutrons is energetically possible this distorts the low energy end of the spectrum and was allowed for by special arguments. For $U \simeq 9$ mev Gugelot assigned temperatures 0.95, 0.85, 0.8, 0.78 ± 1 mev to ^{56}Co , ^{103}Pd , ^{197}Hg , ^{205}Pb , respectively, also $\tau = 2.3$ to ^9B at 5.5 mev. It is surprising that the $^9\text{Be}(p, n)^9\text{B}$ reaction can be represented so; actually Gugelot derived $\tau = 2.3$ mev from the spectrum of neutrons with kinetic energy above 7 mev, and the spectrum also has a distinct low energy component with $\tau \simeq 0.9$ mev which we attribute to the $^9\text{Be}(p, pn)^8\text{Be}$ reaction. The neutron spectrum from bombardment of Al also seems to have two components; because the Q of $^{27}\text{Al}(p, n)^{27}\text{Si}$ is -5.4 mev the favoured reaction $^{27}\text{Al}(p, pn)^{26}\text{Al}$ probably contributes most of the low energy neutrons rather than $^{27}\text{Al}(p, n)^{27}\text{Si}$; the latter must, however, provide all neutrons with kinetic energy above 3 mev, and these have $\tau = 1.75$ mev, which we attribute to ^{27}Si at $U \simeq 5.5$ mev.†

Further work of Gugelot (1954) on (p, p) reactions with 18 mev protons assigns temperatures 2.3, 1.35, 1.3, 1.05, 0.95, 0.7 mev to Al, Ni, Cu, Ag, Au, Pt at $U \simeq 12$ mev.

§ 3. NUCLEAR EQUATION OF STATE

In the upper part of figure 3 the data assembled in § 2 are used to examine the dependence of τ on U for $A = 27, 103, 200$. The values for $A = 103$ are based on Br, Ag, Pd; for $A = 200$ on W, Pt, Hg, Pb, proportionality of U to A being assumed for small differences of A . Evidently U varies approximately as τ^2 ; the lines drawn on the graph represent the simple law

$$U = A\tau^2/\epsilon \quad \dots\dots(12)$$

with $\epsilon = 10.5$ mev empirically determined as the average of $A\tau^2/U$ over all the data.

The dependence of τ on A is shown in the upper part of figure 4. In addition to Gugelot's results, we have plotted results of Graves and Rosen's (1953) study of inelastic scattering of 14 mev neutrons on Fe, Cu, Zn, Ag, Cd, Sn, Pb, Bi (their temperature assignments have been corrected by Dr. Rosen to allow for the distortion of the low energy and of the neutron spectrum by the n, 2n process and so differ from the published values). To conform with these authors' presentation of their results the quantity plotted is $a = 4U/\tau^2$ and, since we found $U \propto \tau^2$, this procedure has the advantage of allowing us to show the high energy data on the same diagram. Again equation (12) represents the material reasonably. The low values of a found by Graves and Rosen for ^{206}Pb and ^{209}Bi are presumably due to closure of the neutron shell in ^{206}Pb ; Gugelot's experiments do not encounter this closed shell.

Although from an individual experiment only τ can be determined, knowledge of the variation with U now allows us to calculate t from (7). Since $t < \tau$ for small A the data of figure 3 would be slightly better represented by (12) if τ was replaced by t . For $U \propto t^2$ equations (7) and (8) give

$$\frac{1}{\tau} = \frac{1}{t} - \frac{3}{4U}, \quad t = \tau - \frac{3\tau^2}{4U} \quad \dots\dots(13)$$

† This is the only experimental result which we have modified in this analysis.

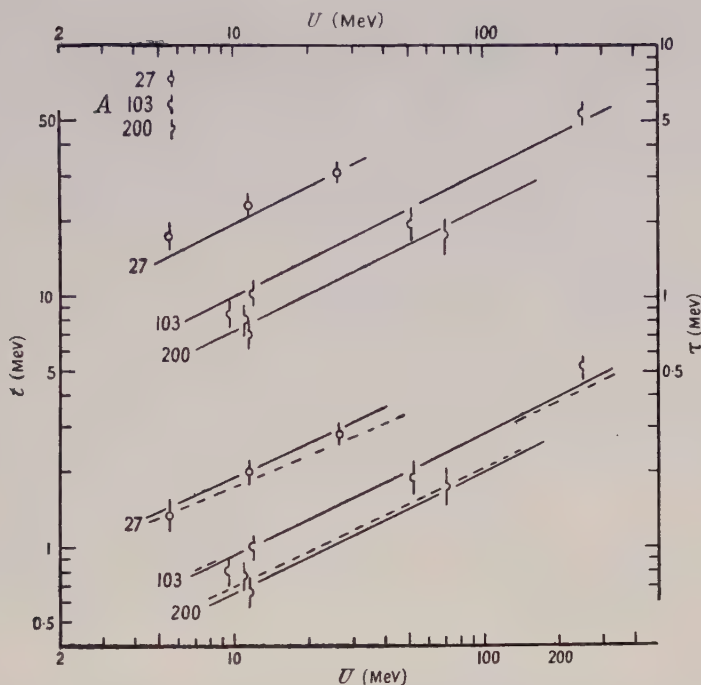


Figure 3. Top : experimental values of energy U and temperature τ for $A=27, 103, 200$ compared with the formula $U=A\tau^2/10.5$ MeV.

Bottom : values of U and temperature t compared with the formulae

$$U = \frac{1}{8}At^2 - t \quad (\text{full line})$$

$$U = \frac{1}{11}At^2 - t + \frac{1}{8}A^{2/3}t^{7/3} \quad (\text{broken line}).$$

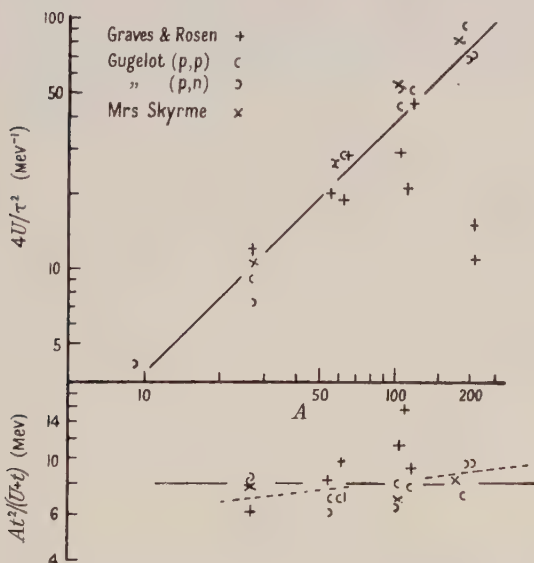


Figure 4. Top : experimental values of $4U/\tau^2$ compared with $U/\tau^2=A/10.5$.

Bottom : the derived values of $At^2/(U+t)$ compared with equation (14) with $f=8$ MeV (full line) and equation (19) with $f'=11$ MeV (broken line).

so the difference between t and τ is easily read off figure 4 and the values of t plotted in the lower half of figure 3 may be compared with the corresponding values of τ in the upper half. Equation (12) strongly suggests a neutron-proton gas model, for which the appropriate theoretical equations of state are (see Appendix A)

$$U = \frac{At^2}{f} - t, \quad P = \frac{\pi^{1/2}}{12} \left(\frac{f}{A}\right)^{3/2} t^{-5/2} \exp 2 \left(\frac{AU}{f}\right)^{1/2} \dots\dots(14)$$

where f is a convenient constant defined by

$$A/f = \pi^2 g/6 \dots\dots(15)$$

since g , the number of individual neutron and proton states per unit energy at the top of the zero temperature Fermi distribution, is proportional to A if nuclear matter is assumed to be homogeneous. To estimate the constants we calculate

$$4A/f = 4(U+t)/t^2 = 4U/\tau^2 + 10/\tau \dots\dots(16)$$

for every point, and the values of f are shown in figure 4. The scatter of the points is quite consistent with the experimental difficulties; there is no regular variation of f with U or A from the mean value

$$f = 8 \text{ Mev.} \dots\dots(17)$$

In contrast the values of ϵ deduced from (12) decrease slightly with A and decrease by about 20% from the low to the high energy data: thus (14) represents the experiments better than (12). It is tempting to regard this as a triumph of thought over empiricism, but the accuracy is hardly sufficient. However, (14) has the advantage that, being derived from a model, it predicts the absolute level density, whereas (12) only gives the variation of P with U .

Theoretically the equation of state should show some surface effects. In particular it has been predicted that (Devons 1949, §21.2) surface waves contribute

$$U_s = \frac{1}{8} A^{2/3} t^{7/3} \text{ Mev} \dots\dots(18)$$

to the excitation energy, the coefficient $\frac{1}{8}$ being calculated from the empirical nuclear surface tension. The variation of U_s with t is consistent with figure 3, but the variation with A is too little and, with the coefficient $\frac{1}{8}$, U_s represents only about one third of the observed energy. While the interplay of surface and volume effects is not well understood, it may be a sufficient approximation to add the corresponding excitation energies (18) and (14) to obtain

$$U = \frac{At^2}{f'} - t + \frac{1}{8} A^{2/3} t^{7/3} \dots\dots(19)$$

and presumably, as in (15),

$$A/f' = \pi^2 g'/6 \dots\dots(20)$$

determines the density g' of individual particle states in this model. As shown in figures 3 and 4, the data are reasonably well represented by

$$f' = 11 \text{ Mev} \dots\dots(21)$$

but the material does not permit a choice between (14) and (19).

§4. DISTRIBUTION OF LEVELS OVER ANGULAR MOMENTUM

For comparison with the experimental results of §5 the density ρ of equation (1) must be calculated.

If a nucleus has total excitation energy U and Z component of angular momentum J_z , the energy available as heat is $U - J_z^2/2c$, where $c\hbar^2$ is the moment of inertia of the assembly of particles carrying the angular momentum. According to (8) this reduces the density of such states to

$$P(A, U, J_z) = P(A, U, J_z = 0) \exp(-J_z^2/2c\tau). \quad \dots\dots(22)$$

The density $\rho(A, J, U)$ and spacing $D(A, J, U)$ of levels of total angular momentum J and either parity are derived from (22) as

$$\begin{aligned} D^{-1}(A, J, U) &\equiv \rho(A, J, U) = P(A, U, J_z = J) - P(A, U, J_z = J + 1) \\ &= D_0^{-1}(A, U)(2J + 1) \exp(-(J + \frac{1}{2})^2/2c\tau) \quad \dots\dots(23) \end{aligned}$$

where the factors independent of J have been combined into $D_0(A, U)$, which may be identified by use of equation (1) to give

$$D_0^{-1}(A, U) = \pi^{-1/2}(2c\tau)^{-3/2}P(A, U) \quad \dots\dots(24)$$

assuming $2c\tau \geq 1$. The average value of J is thus about $(2c\tau)^{1/2}$.

If for the moment of inertia we use the classical value for a sphere $c\hbar^2 = \frac{2}{5}MAR^2$, these results agree with those of Bethe (1937, eqn 300) for a gas of non-interacting nucleons. However, Mrs. Mayer (1950) has established the existence of a pairing energy between nucleons which favours states of low J , and this suggests that in (23) c should be reduced below the value for non-interacting particles: alternatively, following Teller and Wheeler (1938) and Bohr and Mottelson, (1953) we can argue that the existence of some closed shells within the nucleus reduces the moment of inertia by some factor which we call B^2 . Then

$$c = \frac{2}{5}B^2A^{5/3}Mr_0^2/\hbar^2 = B^2A^{5/3}/75 \text{ meV}^{-1} \quad \dots\dots(25)$$

for $r_0 = 1.2 \times 10^{-13}$ cm. Bitter and Feshbach's (1953) radius is used since it represents measurements of $\int \rho r^2 dr$.

If equation (14) is accepted, (24) gives

$$D_0(A, U) = 12(2cA/f)^{3/2}t^4 \exp - 2(AU/f)^{1/2} \quad \dots\dots(26a)$$

$$= 0.054B^3f^{1/2}A^2(U+t)^2 \exp - 2(AU/f)^{1/2} \quad \dots\dots(26b)$$

after use of (25) and (14). The alternative assumption (19) gives (see Appendix B)

$$D(A, U) = 0.054B^3\frac{f^{3/2}}{f'}A^2(U+t)^2 \exp - \left\{ 2(AU/f')^{1/2} + \frac{3}{32}(Uf')^{2/3} \right\}. \quad \dots\dots(27)$$

§5. ABSOLUTE MEASUREMENT OF LEVEL DENSITY

Hughes, Garth and Levin (1953, see also Hughes 1953) measured absorption cross sections of 1 meV neutrons in many elements and deduced level spacings from the formula

$$\sigma(n, \gamma) = 2\pi^2(\lambda/2\pi)^2\Gamma_\gamma/D \quad \dots\dots(28)$$

where Γ_γ is the mean radiation width and D the mean spacing of the levels of the compound nucleus formed by incoming neutrons with $l=0$. They used Heidmann and Bethe's (1951) average values $\bar{\Gamma}$ of Γ_γ which vary smoothly with A and are mainly based on neutron capture to odd mass nuclei. Therefore the

experiments strictly determine $D\bar{\Gamma}/\Gamma_\gamma$ and the results are plotted in figure 5, together with the corresponding excitation energies.

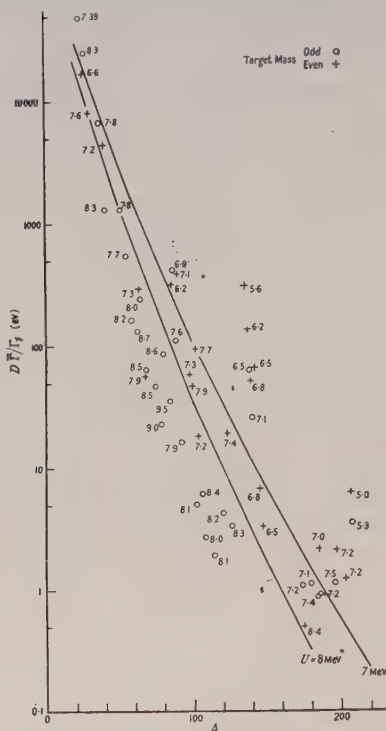


Figure 5. Experimental spacings of nuclear levels formed by absorption of 1 mev neutrons to give compound nuclei with the excitation energies indicated in mev. The curves are calculated from equation (27) for $U=7$ and $U=8$ mev.

The states of the compound nucleus are formed with the same parity as the target and with spin J determined by conservation of angular momentum, so we should find

$$(D\bar{\Gamma}/\Gamma_\gamma)_{\text{obs}} = 2(2J+1)^{-1}D_0(A, U)\bar{\Gamma}/\Gamma_\gamma \quad \dots\dots(29a)$$

$$= D_0(A, U)\bar{\Gamma}/\Gamma_\gamma \text{ for even mass targets} \quad \dots\dots(29b)$$

$$= 0.37 D_0(A, U) \text{ for odd mass targets} \quad \dots\dots(29c)$$

because the average spin of the odd mass targets concerned is about $5/2$ and the derivation of $\bar{\Gamma}$ implies $\bar{\Gamma}/\Gamma_\gamma \approx 1$ for odd mass target nuclei. For comparison with the experimental values of $D\bar{\Gamma}/\Gamma_\gamma$ in figure 5 we plot $0.37 D_0(A, U)$ evaluated from (27) with $B=0.55$. Although β had to be chosen arbitrarily to give the correct mean value of D , it is satisfactory that (19) and (21), which were based on independent experiments, lead to a formula which follows the variation of D with A from 10^5 to 1 ev.

In view of the $2J+1$ factor in (29) it is at first sight surprising that the observed values of $D\bar{\Gamma}/\Gamma_\gamma$ for even mass targets do not lie systematically above those for odd mass. Probably the level spacing formula, like the empirical mass formula, should contain a correction term to differentiate between odd and even nuclei, but this should wait until the J -dependence and values of Γ_γ have been checked.

It is difficult to interpret figure 5 as all the points have different energies, so, to test these formulae more precisely, we combine (27), (29) and (21) as

$$D \frac{\bar{\Gamma}}{\Gamma_\gamma} A^{-2} \exp 2 \left(\frac{AU}{11} \right)^{1/2} = 0.02 B^3 \frac{f^{3/2}}{f'} (U+t)^2 \exp \left\{ -\frac{3}{32} (Uf')^{2/3} \right\} \text{ Mev} \dots (30)$$

and the right-hand side is $0.54B^3$ with negligible variation over the small range of U covered by the experiment. The observed values of the left-hand side of (30) are plotted in figure 6 and the averages are 0.08 and 0.1 mev for odd

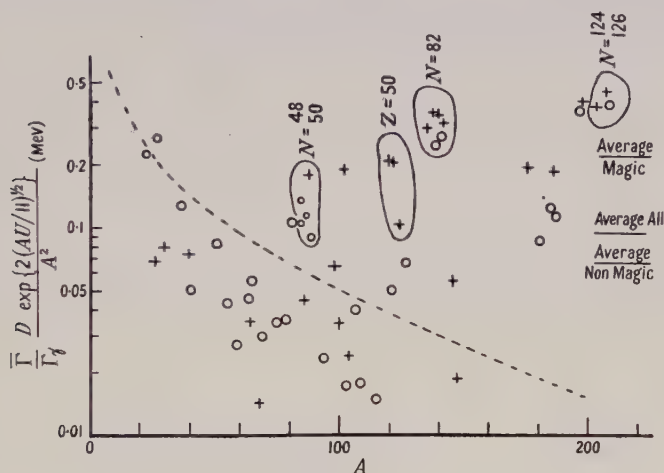


Figure 6. Experimental values of $D(\bar{\Gamma}/\Gamma_\gamma)A^{-2} \exp 2(AU/11)^{1/2}$; according to (27) they should be constant; according to (26) they should vary as the broken line.

and even mass targets respectively; these are not significantly different, showing conclusively that, as already discussed, some effect must compensate the different spin factors in (29). The average over all points is 0.093 mev, from which we deduce from (30)

$$B = 0.55. \dots (31)$$

Although the data of § 3 did not allow us to choose between equations (14) and (19), the present material decides in favour of (27) and so (19) rather than (26) and (14). For (26) predicts that the experimental points of figure 6 should vary as $\exp 2[(AU/11)^{1/2} - (AU/8)^{1/2}]$, which is plotted as a broken line, for $U=8$ mev. On this evidence (26) can be excluded; it gives too much variation of D with A .

Figure 6 establishes that (27) correctly represents the average decrease of D with A , but since Hughes *et al.* estimate the probable error of their measurement of D as about a factor 2, it is unjustified to analyse the material in much more detail. We have, however, ballooned the points with $N=48, 50, 82, 124, 126$ target neutrons, which give compound nuclei with magic ± 1 neutrons; also the points with the magic number 50 protons. These have significantly high values of D : the averages of $DA^{-2} \exp 2(AU/11)^{1/2}$ for near magic and for other nuclei differ by a factor 3, being 0.22 mev and 0.066 mev respectively. Figure 6, however, suggests that the magic nuclei are not so much singular points as maxima of some curve winding about the average value 0.093 mev. This view would require f' to vary by about $\pm 10\%$ from its mean value 11 mev, which,

according to (20), means that close to the magic numbers the spacing $1/g'$ of the individual proton and neutron levels is about 10% above its smooth average $11\pi^2/6A$, and midway between magic numbers is about 10% below this average. This is plausible enough, and the effect is too slight to be detected from the material discussed in §3.

§ 6. DISCUSSION

The extensive data collected together show some consistency between the interpretation of widely different experiments; much greater accuracy would be required to assess the significance of the discrepancies.

Figure 3 shows that it would be useful to have some temperature assignments at high energy for nuclei other than silver and bromine; these might be provided by synchro-cyclotron work with heavy targets. Much of the error in the temperature measurements at $U \simeq 10$ mev arises from the difficulty of allowing for the effect of competing processes; some of these might be eliminated if the bombarding energy was slightly reduced, e.g. for inelastic scattering of neutrons to a value just below the threshold of the $(n, 2n)$ process.

The discussion of §5 suggests that it would be desirable to have some more direct measurement of D or more extensive measurements of Γ_γ , because deviations of these quantities from their average behaviour may be so correlated as not to be detected by measurement of D/Γ_γ . It might then be possible to check the dependence of level spacing on angular momentum.

Since equations (14) and (17) are connected with specific nuclear models, significance can be attached to the values of f and f' in these equations. If the nucleons are treated as free particles in a box we find $g = g_1 + g_2 = 3A/2\zeta$, where ζ is the kinetic energy of the particles at the top of the zero temperature Fermi distribution. For $r_0 = 1.47 \times 10^{-13}$ cm we find $\zeta = 22$ mev, and then from (15) $f = 4\zeta/\pi^2 = 8.9$ mev, which is not far from the empirical value $f = 8$ mev. However, we saw that (19) and (27) represent the experiments better than (14) and these have $f' = 11$ mev, which according to (20) implies that the spacing $1/g'$ between successive individual particle states exceeds the difference of kinetic energy on the free particle model by a factor $11/8.9 = 1.24$. In the notation of Le Couteur (1950, §2.3) we can write this as

$$\frac{d\epsilon}{dk^2} = \frac{d(\epsilon_{\text{kin}} + \epsilon_{\text{pot}})}{dk^2} = \frac{\hbar^2}{2M} \gamma \quad \dots\dots (32)$$

with $\gamma = 1.24$. The assumption of pure exchange forces within the nucleus suggested $\gamma \simeq 2$; mixed forces like Serber's would give a value closer to 1. The assumption that the average potential energy of a particle in a nucleus increases with its kinetic energy does not change the order of individual particle levels, which is important for shell structure, since (32) is formally equivalent to a change of mass to the effective value M/γ .

There is independent experimental evidence for (32).

(i) If a μ^- meson is absorbed in a heavy nucleus in the reaction $\mu^- + P \rightarrow N + \nu$ the average energy transfer to the nucleus is proportional to γ , and Lang's (1952) analysis shows that the observed neutron emission requires $\gamma > 1$.

(ii) The neutron cross section experiments of Taylor and Wood (1953), interpreted by us according to the optical model of Fernbach, Serber and Taylor (1949) or, more elaborately, by Mandl and Skyrme (1953), imply that $\epsilon_{\text{pot}} = -V$

changes from about -30 to -11 mev as ϵ changes from 60 to 150 mev, which is equivalent to $\gamma = 1.27$, in remarkable agreement with our value.

It is encouraging to find that all the numerical coefficients in our final equation of state (19) can be correlated with nuclear properties independent of the nuclear level distribution.

The lowest nuclear levels are currently interpreted as mainly individual particle levels together with a few of collective motion, so when the degeneracy is taken into account the smoothed density of states must be approximately in agreement with our formulae: Appendix A shows that just above the ground state (26) gives the correct density of states for excitation of an individual particle, and (27) adds a few widely spaced levels of collective surface oscillation. While the application of statistical formulae to the lowest levels has little interest, this argument suggests that our formulae remain valid at lower energies than are covered by the evidence we discussed.

ACKNOWLEDGMENTS

We are much indebted to Mrs. D. M. Skyrme for carrying out the experiment referred to and for keeping us informed of her results, to Dr. Lindenbaum for supplying unpublished details of Monte Carlo calculations, and to Dr. Gugelot for advance information of experimental results.

Note added in proof. Recent measurements of slow neutron resonances suggest that the experimental level spacings shown in figure 5 are too small. The discrepancy is removed if, instead of using (28), the spacing D' of levels formed by capture of $l=0$ neutrons is calculated from the formula

$$\sigma(n, \gamma) = 2\pi^2 (R + \lambda/2\pi)^2 \Gamma_\gamma / D', \quad \dots (28')$$

which is appropriate (Blatt and Weisskopf, p. 478) for 1 mev neutrons. Comparison with (28) gives

$$D = D' / (1 + kR)^2,$$

so for comparison of experimental and theoretical values the right-hand side of (30) should be divided by $(1 + kR)^2$ and comes to $0.15B^3$, $0.086B^3$, $0.07B^3$ for $A=27$, 125, 216, respectively. With $B=1$ these values are consistent with the experimental points plotted in figure 6; thus this interpretation of the data has the merit of allowing one to use the classical value of the nuclear moment of inertia, which is the most natural thing to do. In this sense our final formulae involve only one adjustable constant f' . Our value $f' = 11$ mev corresponds to a nuclear radius $r_0 = 1.3 \times 10^{-13}$ cm, which is consistent with recent evidence. So the argument of § 6, based on $r_0 = 1.47 \times 10^{-13}$ cm, may be unnecessary.

APPENDIX A

Level Density of a Fermi Gas

The main exponential term in P is well known, but there is a disagreement in the literature (Bethe 1937, Sneddon and Touschek 1948) about the multiplying factors appropriate to the case of a fixed number of nucleons which must be cleared up before the interpretation of measured absolute level densities is meaningful.

A state of a mixture of neutrons with available individual levels a_s and protons with available levels b_s is defined by the corresponding occupation numbers n_s, z_s which in particular give the total energy and particle numbers as

$$E = \sum a_s n_s + b_s z_s, \quad N = \sum n_s, \quad Z = \sum z_s. \quad \dots (A 1)$$

The grand partition function is defined (e.g. Schrödinger 1948) as

$$\begin{aligned} \exp -\beta\Phi(\beta, \mu_1, \mu_2) &= \sum \exp \beta(\mu_1 N' + \mu_2 Z' - E') \\ &= \sum_{N'Z'} \int dE' P(E', N', Z') \exp \beta(\mu_1 N' + \mu_2 Z' - E') \quad \dots (A 2) \end{aligned}$$

where the summation extends over all states of the mixture and reduces by (A 1) to

$$\exp -\beta\Phi = \prod_s \sum_{n_s} \exp \beta(\mu_1 - a_s) n_s \sum_{z_s} \exp \beta(\mu_2 - b_s) z_s$$

summed over all allowed occupation numbers. So for Fermions

$$-\beta\Phi = \sum_s \log [1 + \exp \beta(\mu_1 - a_s)] + \sum_s \log [1 + \exp \beta(\mu_2 - b_s)]$$

and the first sum can be evaluated by Sommerfeld's method as

$$\sum_{a_s \leq \mu_1} \beta(\mu_1 - a_s) + \log [1 + \exp \beta(a_s - \mu_1)] + \sum_{a_s > \mu_1} \log [1 + \exp \beta(\mu_1 - a_s)].$$

Evaluation of the sums as integrals using the densities $g_1(\epsilon)$ and $g_2(\epsilon)$ of individual neutron and proton states yields

$$-\beta\Phi = \frac{\pi^2}{6\beta} [g_1(\mu_1) + g_2(\mu_2)] + \beta \int_0^{\mu_1} (\mu_1 - \epsilon) g_1 d\epsilon + \beta \int_0^{\mu_2} (\mu_2 - \epsilon) g_2 d\epsilon. \quad \dots (A 3)$$

Now inversion of (A 2) gives the density for a particular N as

$$\begin{aligned} \sum_{Z'} \int dE' P(E', N, Z') \exp \beta(\mu_2 Z' - E') &= \frac{1}{2\pi i} \int_{\gamma-i\infty}^{\gamma+i\infty} \exp -\beta(\Phi + \mu_1 N) d(\beta\mu_1) \\ &= \beta^{1/2} (2\pi g_1)^{-1/2} \exp -\beta(\Phi + \mu_1 N) \quad \dots (A 4) \end{aligned}$$

after integration over the saddle point located by

$$N = -\partial\Phi/\partial\mu_1 = \int_0^{\mu_1} g_1 d\epsilon \quad \dots (A 5)$$

which defines the value of μ_1 to be substituted in (A 4). Repetition of this procedure yields

$$\int dE' P(E', N, Z) \exp (-\beta E') = \beta(2\pi g_1)^{-1/2} (2\pi g_2)^{-1/2} \exp \{ -\beta(\Phi + \mu_1 N + \mu_2 Z) \}$$

which, by use of (A 3), can more simply be expressed in terms of the excitation energy,

$$U' = E' - \int_0^{\mu_1} \epsilon g_1 d\epsilon - \int_0^{\mu_2} \epsilon g_2 d\epsilon,$$

$$\begin{aligned} \text{as} \quad \int dU' P(U', N, Z) \exp (-\beta U') &= \exp \left\{ \frac{\pi^2}{6\beta} (g_1 + g_2) + \log \frac{\beta}{2\pi g_1^{1/2} g_2^{1/2}} \right\} \\ &\dots (A 6) \end{aligned}$$

By comparison with equation (2) of § 1 the exponent is identified with $-\beta F$ for the system of N neutrons and Z protons, and then if we write $t = 1/\beta$ and $g = g_1 + g_2$ equation (4) gives the equation of state as

$$U = \frac{1}{6} \pi^2 g t^2 - t \quad \dots (A 7)$$

which is equation (14). Of course (A 6, 7) are valid only for $t \geq g^{-1}$; combined, they give

$$S = \beta(U - F) = 2\left(\frac{1}{6} \pi^2 g t - \frac{1}{2}\right) + \log \frac{\beta}{2\pi g_1^{1/2} g_2^{1/2}} \quad \dots (A 8)$$

and then, using (A 7), equation (8) leads to

$$P(U, N, Z) = \left(\frac{8}{3}\pi^5 g g_1 g_2 t^5\right)^{-1/2} \exp 2\left(\frac{1}{6}\pi^2 g U + \frac{1}{4}\right)^{1/2} \dots\dots (A 9)$$

which agrees with (14) if we approximate $4g_1 g_2 = g^2$. If t is calculated from (A 7) this becomes

$$P(U, N, Z) = \frac{1}{12} \left(\frac{6}{g}\right)^{1/4} (U+t)^{-5/4} \exp 2\left(\frac{\pi^2}{6} g U\right)^{1/2} \dots\dots (A 10)$$

Though (26 *a*) and (A 9) agree with Bethe's (1937) results, at low temperatures (26 *b*) and (A 10) are less than his. Sneddon and Touschek's density exceeds (A 10) by a factor $(6gU)^{1/2}$.

For a gas with just N particles of one type the results are slightly simpler :

$$U = \frac{1}{6}\pi^2 g t^2 - \frac{1}{2}t \dots\dots (A 11)$$

$$P(U, N) = \frac{1}{4\sqrt{3}(U + \frac{1}{2}t)} \exp 2\left(\frac{1}{6}\pi^2 g U\right)^{1/2} \dots\dots (A 12)$$

To test this formula put $g=1$, so taking the difference between successive individual particle levels as the unit of energy. Then U must be an integer, and it is known that $P(U, N)$ should equal the number of partitions of U into not more than N different parts, which was calculated for large N by Hardy and Ramanujan (1918) and also from statistical mechanics by Auluck and Kothari (1946) as

$$\omega(U) = \frac{1}{4\sqrt{3}U} \exp 2\left(\frac{1}{6}\pi^2 U\right)^{1/2} \dots\dots (A 13)$$

The exact value $p(U)$ was evaluated numerically by Major MacMahon.

Table 1

U	$p(U)$	ω/p	P/p
1	1	1.8	1.23
3	3	1.33	1.064
10	42	1.145	1.012
80	15796476	1.051	1.006

The different results are compared in table 1, which shows that (A 12) is better than (A 13) for small U and converges faster towards the correct value as U increases. Of course (A 12) does not compete with the really sophisticated formulae of Hardy and Ramanujan, but these results justify the appearance of the term $\frac{1}{2}t$ in (A 10) and (A 11).

With a little more labour (A 9) for the neutron-proton gas can be tested numerically. Again put $g=1$ so that the individual neutron or proton levels, and therefore the levels of the whole nucleus, increase in steps of 2.

Table 2

U	$P(U, N, Z)$	$2\bar{P}$	No. of states
1	0.672	—	—
2	1.05	2.19	2
3	1.62	—	—
4	2.42	4.97	5
5	3.48	—	—
6	4.98	10.2	10
7	7.0	—	—

The last column of table 2 shows the computed number of states with excitation 2, 4, 6 . . . which it is appropriate to compare with

$$2\bar{P}(U) = \frac{1}{2}P(U-1) + P(U) + \frac{1}{2}P(U+1)$$

since our asymptotic formula P increases continuously with U . As before the agreement shows that the appearance of the term t in (A 7) and (A 10) is justified and that our simple formulae represent their model with unexpected accuracy.

APPENDIX B

Mixed Surface and Volume Effects

If we write (19) in the form

$$U = at^2 - t + bt^{7/3} \quad \dots\dots (B 1)$$

with

$$a = A/f', \quad b = \lambda A^{2/3} \quad \dots\dots (B 2)$$

the last term in U contributes $7bt^{4/3}/4$ to the entropy which, added to (A 8), gives

$$\begin{aligned} S &= 2(at - \tfrac{1}{2}) - \log \pi g' t + \tfrac{7}{4}bt^{4/3} \\ &= 2\{(a + bt^{1/3})U + \tfrac{1}{4}\}^{1/2} - \tfrac{1}{4}bt^{4/3} - \log \pi g' t \\ &= 2(aU)^{1/2} + b(U/a)^{1/2}t^{1/3} - \tfrac{1}{4}bt^{4/3} - \log \pi g' t \\ &= 2(aU)^{1/2} + \tfrac{3}{4}b(U/a)^{2/3} - \log \pi g' t \\ &= 2(AU/f')^{1/2} + \tfrac{3}{4}\lambda(Uf')^{2/3} - \log \pi g' t \quad \dots\dots (B 3) \end{aligned}$$

where terms involving $(bt^{1/3}/a)^2 = (\lambda f' A^{-1/3})^2$ have been neglected. For $\lambda = \frac{1}{8}$, $f' = 11$ this is justifiable, and in the rather unfavourable case $A = 27$, $t = 1.6$, $U = 8.04$ mev the error in S is only 0.2. From this expression for S (27) follows like (26) if for simplicity the factors t^4 in (26 a) are expressed in terms of U using (14) rather than (19); this is permissible since at the energy concerned the formula gives the same numerical results.

REFERENCES

- AULUCK, F., and KOTHARI, D., 1946, *Proc. Camb. Phil. Soc.*, **42**, 272.
 BERNARDINI, G., BOOTH, E., and LINDENBAUM, S., 1952, *Phys. Rev.*, **88**, 1017.
 BETHE, H., 1937, *Rev. Mod. Phys.*, **9**, 69.
 BITTER, F., and FESHBACH, H., 1953, *Phys. Rev.*, **92**, 837.
 BLATT, J., and WEISSKOPF, V., 1952, *Theoretical Nuclear Physics* (New York: John Wiley).
 BOHR, A., and MOTTELSON, B. R., 1953, *Mat. Fys. Medd.*, **27**, No. 16.
 DEVONS, S., 1949, *Excited States of Nuclei* (Cambridge: University Press).
 FERNBACH, S., SERBER, R., and TAYLOR, T., 1949, *Phys. Rev.*, **75**, 1352.
 FESHBACH, H., PORTER, C. E., and WEISSKOPF, V., 1953, *Phys. Rev.*, **90**, 166.
 GUGELOT, P. C., 1951, *Phys. Rev.*, **81**, 51; 1954, *Ibid.*, **93**, 425.
 GRAVES, E., and ROSEN, L., 1953, *Phys. Rev.*, **89**, 343.
 HARDY, G. H., and RAMANUJAN, S., 1918, *Proc. Lond. Math. Soc.*, **17**, 75.
 HEIDMAN, J., and BETHE, H., 1951, *Phys. Rev.*, **84**, 274.
 HUGHES, D. J., 1953, *Pile Neutron Research* (Cambridge, Mass: Addison-Wesley).
 HUGHES, D. J., GARTH, R. C., and LEVIN, J. S., 1953, *Phys. Rev.*, **91**, 1423.
 LANG, J., 1952, *Proc. Phys. Soc. A*, **65**, 905.
 LE COUTEUR, K. J., 1950, *Proc. Phys. Soc. A*, **63**, 259; 1952, *Ibid.*, **65**, 718.
 MAYER, M. G., 1950, *Phys. Rev.*, **78**, 16.
 MANDL, F., and SKYRME, T. H. R., 1953, *Phil. Mag.*, **44**, 1028.
 SCHRÖDINGER, E., 1948, *Statistical Thermodynamics* (Cambridge: University Press).
 SKYRME, D. M., and WILLIAMS, W., 1951, *Phil. Mag.*, **42**, 1187.
 SNEDDON, I., and TOUSCHEK, D., 1948, *Proc. Camb. Phil. Soc.*, **44**, 391.
 TAYLOR, A., and WOOD, E., 1953, *Phil. Mag.*, **44**, 95.
 TELLER, E., and WHEELER, J., 1938, *Phys. Rev.*, **53**, 778.
 WEISSKOPF, V., 1937, *Phys. Rev.*, **52**, 295.

Resonant Scattering of Gamma-Rays in ^{63}Cu and ^{56}Fe

By K. ILAKOVAC

Department of Physics, The University of Birmingham

Communicated by P. B. Moon; MS. received 18th November 1953

Abstract. The 0.96 MeV gamma-radiation following the decay of ^{63}Zn is selectively scattered by copper. The intensity of elastic scattering from copper at 90° is several times greater than from iron, provided that the ^{63}Zn source is in solution; with a solid source, only slight evidence of resonant scattering has been found.

These results are interpreted as resonant nuclear scattering by ^{63}Cu , and are analysed in terms of the displacement and broadening of the emission line by nuclear recoil, which persists longer in the liquid than in the solid.

The mean life of the 0.96 MeV excited state of ^{63}Cu is estimated to be of the order of 6×10^{-13} second.

From the absence of any observable selective scattering by iron of the gamma-rays following the decay of ^{56}Mn , the mean life of the 0.84 MeV excited state of ^{56}Fe is estimated to exceed 8×10^{-12} second.

§ 1. INTRODUCTION

THE difficulties involved in experiments on resonance scattering of gamma-rays by nuclei are mainly caused by the narrowness of the resonances, which at a typical energy of 10^6 eV seldom have a natural line-width of more than 10^{-3} eV. At energies in the 10 MeV range very broad resonances may occur, making it possible to observe the scattering from a continuous (bremsstrahlung) spectrum, but in the 1 MeV region it is necessary to use a line source, which in practice means gamma-rays emitted by nuclei of the same type as the scatterer. These, though normally off resonance because of the energy lost to nuclear recoils, may be restored to resonance by the Doppler effect if the source nuclei are moving towards the scatterer. In favourable circumstances this can be achieved by mechanical motion (Moon 1951, Moon and Storruste 1953, Davey and Moon 1953) or by heating the source, which increases the random thermal motions (Malmfors 1952).

The Doppler effect of a preceding β -ray recoil has previously been tried (Pollard and Alburger 1948, Metzger 1951, Metzger and Todd 1953), but with negative results. In the present experiments 0.96 MeV gamma-rays of ^{63}Cu are found to be selectively scattered by copper. The additional scattering is clearly detectable if the ^{63}Zn source is in solution, but not if a solid source is used; this difference is ascribed to the longer persistence of β -ray recoil in the liquid.

§ 2. THEORY

If an excited nucleus of mass M is moving with velocity V before emitting a gamma-ray at an angle α , considerations of energy and momentum show that the energy of the gamma-ray is given, to the first order in V/c and in E_0/Mc^2 , by

$$E_\gamma = E_0 + E_0 \frac{V}{c} \cos \alpha - \frac{E_0^2}{2Mc^2} \dots\dots (1)$$

where E_0 is the difference of energy between the initial and final nuclear levels. The second term on the right represents the Doppler shift, while the last term is the energy lost to nuclear recoil.

If the gamma-ray strikes a stationary nucleus of identical type in the final level (in practice, the ground state) resonant scattering will occur if

$$E_\gamma = E_0 + E_0^2/2Mc^2. \quad \dots\dots(2)$$

The term $E_0^2/2Mc^2$ represents the energy required to provide the nuclear recoil when the photon excites the scattering nucleus.

The condition for resonant scattering may thus be written as

$$\frac{V}{c} \cos \alpha = \frac{E_0}{Mc^2}. \quad \dots\dots(3)$$

If the emitting nuclei are moving in random directions, as the result of a previous recoil, the emission line will be broadened in a manner that is calculable if the distribution of recoil momenta is known. We may suppose the fraction of the intensity between energy E and $E + dE$ to be $F(E) dE$.

$F(E)$ will be symmetrical about the central energy $E_0 - E_0^2/2Mc^2$ (see equation (1)); what is required is its value $F(E_0 + E_0^2/2Mc^2)$ at the energy specified by equation (2), and the condition that there shall be any intensity at this energy is that the maximum recoil velocity shall exceed the velocity specified by equation (3).

If Γ is the width of the resonance as usually defined, its effective width for abstracting energy from a uniform continuous spectrum is $\frac{1}{2}\pi\Gamma$. The energy distribution due to recoil is very broad in comparison with Γ , therefore if σ_{\max} is the scattering cross section at exact resonance, the effective cross section is

$$\sigma_{\text{eff}} = \sigma_{\max} \frac{1}{2}\pi\Gamma F(E_0 + E_0^2/2Mc^2). \quad \dots\dots(4a)$$

It may be noted that $\sigma_{\max} = (\lambda^2/2\pi)g_1/g_2$, where λ is the wavelength and g_1 and g_2 are the respective multiplicities of the upper and lower states.

The intrinsic width Γ is connected with the mean life τ of the excited state by the uncertainty relation $\tau\Gamma = \hbar/2\pi$, so that equation (4a) may be written as

$$\sigma_{\text{eff}} = \sigma_{\max} \frac{\hbar}{4\tau} F\left(E_0 + \frac{E_0^2}{2Mc^2}\right). \quad \dots\dots(4b)$$

For the 0.96 MeV γ -ray of ^{63}Cu the velocity required for exact resonance is about $5 \times 10^5 \text{ cm sec}^{-1}$, while the preceding 1.4 MeV positron transition gives initial velocities distributed over the range $\pm 9.6 \times 10^5 \text{ cm sec}^{-1}$. These speeds are high enough to make thermal agitation negligible.

From the measured K-conversion coefficient (Huber *et al.* 1947) the transition is likely to be a dipole; the mean life for a magnetic dipole would probably lie between 10^{-14} and 10^{-12} sec, during which time a nucleus recoiling at $5 \times 10^5 \text{ cm sec}^{-1}$ in a solid or liquid would make several collisions. Those nuclei which originally have the correct recoil velocity will be effective only to the extent that they radiate before making a collision, but others that start with too high a velocity will pass through the correct velocity during the process of degradation. The situation is very complicated but may be approached by using an equivalent time t_0 in which about half these faster nuclei are slowed below resonance, and making the rough approximation that the number of excited nuclei having the correct value of $V \cos \alpha$ remains constant during this time and then falls suddenly to zero.

Equation (4b) then becomes

$$\sigma_{\text{eff}} = \sigma_{\text{max}} \frac{h}{4\tau} F_0 \left(E_0 + \frac{E_0}{2Mc^2} \right) \{1 - \exp(-t_0/\tau)\}$$

where F_0 is the distribution function due to the initial β^+ recoil. If t_0 is less than τ this is approximately

$$\sigma_{\text{eff}} = \sigma_{\text{max}} \frac{h}{4} F_0 \frac{t_0}{\tau^2} \quad \dots\dots(5)$$

If $t_0 \gg \tau$ we have the case of free recoil, which gives higher intensity and avoids the difficulty of estimating t_0 ; with t_0 less than τ , as in the present examples, the difficulty is to some extent offset by the possibility of changing t_0 by altering the medium in which the recoil takes place, and by the fact that errors in measuring σ_{eff} or estimating F_0 and t_0 lead to proportional errors only in τ^2 and not in τ itself.

§ 3. EXPERIMENTAL METHODS AND RESULTS

The apparatus (figure 1) consists of a source holder mounted on the top of a 25 cm lead cone, below which a NaI (Tl) crystal was placed on the photomultiplier tube. Pulses were taken to a cathode follower and subsequently amplified.

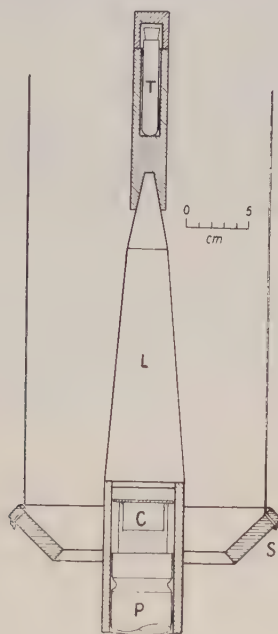


Figure 1. Section through apparatus.

- T—source tube.
- L—lead shield.
- C—NaI(Tl) crystal in Perspex container.
- P—photomultiplier.
- S—scatterer.

A discriminator (E. C. Park, to be published) was used to select pulses in the region of the photoelectric peak. Two scatterers, an iron one and a copper one (the latter being about 5% heavier), were hung one below the other by four strings. By pulling the strings the two scatterers could be easily and quickly interchanged.

They should give closely similar intensities of Rayleigh, nuclear, Thomson and any other non-specific elastic scattering.

As only 8% transitions in 38.3 min ^{63}Zn pass through the 0.96 mev state (Huber, Medicus, Preiswerk and Steffen 1947), and almost all give positrons (there are only about 8% of K-capture transitions), there are about 22 times as many annihilation quanta as 0.96 mev γ -rays. The holder of the source was made with an aluminium wall 6 mm thick to stop all positrons above the lead shield, thus preventing annihilation quanta from being generated in the air and going straight into the counter. Even so a very large number of these rays were Compton-scattered into the detector, and gave a very large number of pulses at low bias of the discriminator. There was also a possibility of overlapping pulses which would have given additional counts in a selected channel; a lead absorber 6 mm thick was therefore placed round the detector, and this reduced low-energy γ -rays by a factor of about ten and the 0.96 mev γ -rays to about 65%.

The ^{63}Zn sources, usually of several hundred millicuries, were made by 5 mev proton bombardment in the cyclotron. For experiments with a solid source a copper tube was bombarded and used when cut off the holder. Liquid sources were obtained by dissolving a layer of the target in nitric acid.

Though the bias curve of weak sources in preliminary experiments showed definite photoelectric peaks at a bias corresponding to 0.96 mev, the scattered radiation showed a steadily decreasing bias curve with a flattening at the positron of photoelectric peak, the intensity here being considerably higher than the calculated Rayleigh scattering. This seems to be caused by bremsstrahlung of photo-electrons ejected in the scatterers and surroundings. For this reason it is not possible to obtain the absolute nuclear resonance cross section by comparison with Rayleigh scattering.

Rayleigh and Compton scattering, as well as bremsstrahlung, should be very nearly the same for the two scatterers, apart from the small correction due to the difference in weight; the copper scatterer was therefore expected to show additional counts due to nuclear resonance scattering of 0.96 mev γ -rays in copper. This additional scattering should be larger for the liquid than for the solid source since the corresponding times t_0 , in which nuclei lose their energy from previous β^+ recoil, are considerably different for the two cases. This gave an opportunity of proving that the difference of scattering from copper and from iron was due to resonance scattering.

Counting was done with no scatterer, iron, and copper scatterer round the detector, interchanging every five minutes. Thus three separate decay curves were obtained in each experiment. The half-periods obtained were always about 10% shorter than the accepted value 38.3 minutes and the value 38 minutes obtained with a small part of the source with another counter. This was explained by slow changes in amplification of the photomultiplier tube.

After subtraction of the counting rate with no scatterer, the ratios of the scattering from copper to scattering from iron for three experiments with the liquid source were 4.5 ± 1.6 , 2.6 ± 0.5 , 3.8 ± 1.4 , with an average value 3.6 ± 0.9 . The actual results obtained in the third experiment are shown in figure 2(a).

In two experiments with the solid source the following results for the copper to iron ratio were obtained: 1.0 ± 1.1 , 2.2 ± 0.8 , with an average value 1.6 ± 0.7 , which is significantly lower than that for the liquid source. Figure 2(b) shows the detailed results for the second of these experiments.

In the calculation of experimental cross section for resonance scattering only results from the liquid source experiments are used.

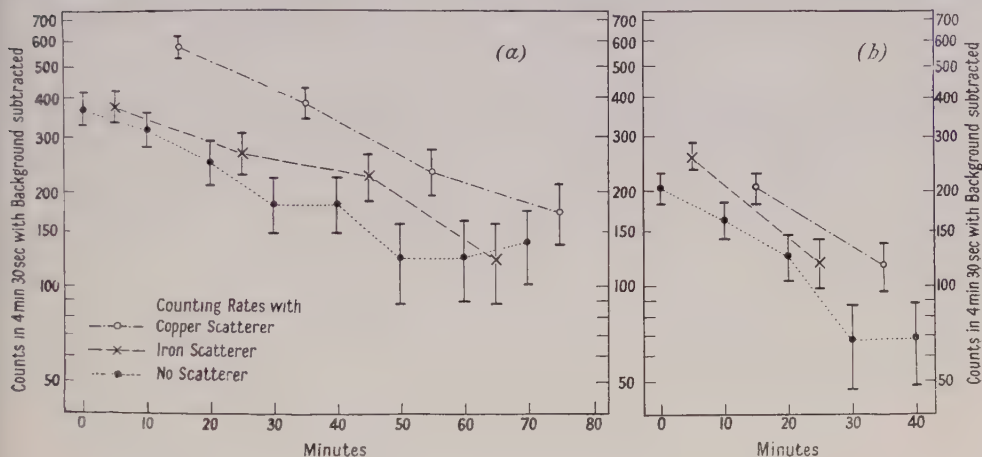


Figure 2. Counting rates.
(a) third experiment with the liquid source.
(b) second experiment with the solid source.

§ 4. ANALYSIS OF RESULTS

The experimental cross section for nuclear resonance scattering, σ_{exp} , was calculated from the geometry of the apparatus and from a comparison of the counting rate due to the selective scattering with the direct counting rate measured when the source was placed at a known distance from the detector. With this procedure the absolute sensitivity of the counter is not required. When the isotopic abundance of ^{63}Cu (69%) and the absorption in the scatterer were taken into account, the following results were obtained for the three experiments: $(6.1 \pm 1.9) \times 10^{-27} \text{ cm}^2$, $(11 \pm 2.1) \times 10^{-27} \text{ cm}^2$, $(8.1 \pm 1.7) \times 10^{-27} \text{ cm}^2$, with an average value $\sigma_{\text{exp}} = (8.4 \pm 1.4) \times 10^{-27} \text{ cm}^2$.

To obtain the mean life the following further data have been calculated and estimated: the cross section for exact resonance is, omitting the statistical weight factor, which is not far from unity, $\sigma_{\text{max}} = \lambda^2/2\pi = 0.27 \times 10^{-20} \text{ cm}^2 = 2700 \text{ barns}$, the distance of the copper atoms from surrounding atoms in the solution is about $3 \times 10^{-8} \text{ cm}$ and their speed, with energy 7.8 eV (which is needed for resonance), about $5 \times 10^5 \text{ cm sec}^{-1}$. These atoms would therefore collide after about $6 \times 10^{-14} \text{ sec}$, and would not give γ -rays having the resonance energy at greater times after the positron emission. Faster moving copper atoms collide after a shorter time, but some of them would still, after one collision, have sufficiently high energy. One can therefore estimate t_0 as about $6 \times 10^{-14} \text{ second}$. For the solid source t_0 would be halved on account of the closer atomic spacing and further reduced by the smaller persistence of velocity after the first collision.

From the positron spectrum the distribution of the unidirectional components of recoil momenta of Cu nuclei has been calculated, assuming no angular correlation between neutrinos and positrons. The maximum recoil momentum is $3.75mc$, corresponding to an energy of 28 eV. This distribution, with a scale giving the corresponding γ -ray energies, is shown in figure 3. For the ordinate $F_0(E)$ the scale is chosen so that the area under the curve is unity. Therefore the

ordinates in this scale represent directly values of $F_0(E)$. For $E - E_0 = 7.8$ ev one obtains $F_0(E_0 + 7.8 \text{ ev}) = 0.02 (\text{ev})^{-1}$.

Inserting the values of σ_{\max} , t_0 and $F_0(E_0 + 7.8 \text{ ev})$ into equation (4b), one obtains

$$\tau = \left[\frac{\sigma_{\max}}{\sigma_{\exp}} \frac{h}{4} F_0(E_0 + 7.8 \text{ ev}) t_0 \right]^{1/2} = 6 \times 10^{-13} \text{ sec}$$

with a rather large error, which is difficult to estimate because of the uncertainty of the value of t_0 , but may well amount to a factor of 2 or 3.

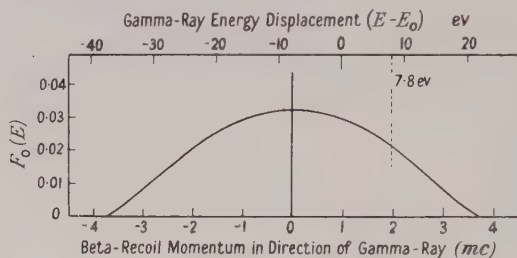


Figure 3. Profile of emission line for freely-recoiling ^{63}Cu -nuclei.

While the measured K-conversion coefficient (Huber *et al.* 1947) corresponds to an M1 transition, Weisskopf's (1951) theory gives 4×10^{-14} sec for an M1 transition and 2.6×10^{-11} for E2. The present result may thus be taken to suggest either a slow M1 or a fast E2 transition. Three M1 transitions in other odd- Z even- N nuclei have been measured by Graham and Bell (1953) and, in relation to their energies, are even slower than the one reported here; one (Elliott and Bell 1949) is even faster than the theoretical prediction.

§ 5. EXPERIMENT WITH ^{56}Fe

Using the same technique and the same apparatus, another experiment on nuclear resonance scattering has been done with 0.84 MeV γ -rays produced in the decay of ^{56}Mn . This time additional scattering due to resonances of ^{56}Fe nuclei was expected from the iron scatterer. No such effect was observed. The ratio of scattering from iron to scattering from copper was calculated without subtracting the counting rate without the scatterer (as it was relatively rather smaller than in experiments with ^{63}Zn). It is 0.97 ± 0.03 .

The possible value less than one can be explained by the difference in weight of the two scatterers.

From the geometry of the apparatus, the strength of the source and the above-mentioned experimental error we obtain for the upper limit for experimental cross section $2.5 \times 10^{-28} \text{ cm}^2$. In this case $\sigma_{\max} = 0.34 \times 10^{-20} \text{ cm}^2$, $t_0 \approx 0.5 \times 10^{-13} \text{ sec}$, $F_0 \approx 0.01 (\text{ev})^{-1}$. Therefore the estimated lower limit for the mean life is $0.8 \times 10^{-11} \text{ second}$. It is thought to be an electric quadrupole or higher order transition.

§ 6. DISCUSSION

The use of the recoil caused by a β - or γ -ray preceding the γ -ray whose nuclear resonance scattering is observed seems to give a possibility of observing that process for many nuclei. If sources in the liquid state are used, transitions with a

mean life shorter than about 5×10^{-12} sec could be measured, though not very accurately. The use of sources in the gaseous state would greatly improve the accuracy in that region, and also extend the possibility of observation of nuclear resonance scattering with much longer mean lives.

ACKNOWLEDGMENTS

I should like to thank Professor P. B. Moon for suggesting the general methods of experiment and analysis as well as for assistance in the preparation of the paper, and the Nuffield cyclotron team for their work in producing isotopes for these experiments. I am grateful for a grant from the Yugoslav Academy of Science.

REFERENCES

- DAVEY, W. G., and MOON, P. B., 1953, *Proc. Phys. Soc. A*, **66**, 956.
ELLIOTT, L. G., and BELL, R. E., 1949, *Phys. Rev.*, **76**, 168.
GRAHAM, R. L., and BELL, R. E., 1953, *Canad. J. Phys.*, **31**, 377.
HUBER, O., MEDICUS, H., PREISWERK, P., and STEFFEN, R., 1947, *Helv. Phys. Acta*, **20**, 495.
MALMFORS, K. G., 1952, *Ark. Fys.*, **6**, 49.
METZGER, F. R., 1951, *Phys. Rev.*, **83**, 842.
METZGER, F. R., and TODD, W. B., 1953, *Phys. Rev.*, **91**, 1286.
MOON, P. B., 1951, *Proc. Phys. Soc. A*, **63**, 76.
MOON, P. B., and STORRUSTE, A., 1953, *Proc. Phys. Soc. A*, **66**, 585.
POLLARD, E. C., and ALBURGER, D. E., 1948, *Phys. Rev.*, **74**, 926.
WEISSKOPF, V. F., 1951, *Phys. Rev.*, **83**, 1073.

Note on the Applicability of the Free-Electron Network Model to Metals

By C. A. COULSON

Mathematical Institute, Oxford

MS. received 10th December 1953

Abstract. The free-electron model of a conjugated molecule is extended to apply to a metal. When each conduction electron is allowed to move freely along the set of one-dimensional lines (i.e. bonds) joining adjacent atoms, a band-structure appears. This is shown to be almost identical with the shape predicted by the conventional tight-binding approximation. The particular example of the π -electrons in a graphite layer is worked out in detail. No empirical parameters are used except the interatomic distance and the crystal structure.

§ 1. INTRODUCTION

THE so-called 'free-electron model' has recently been applied to conjugated and aromatic molecules with great success (Ruedenberg and Scherr 1953, Scherr 1953). Calculations of resonance energy, bond order, free valence, excitation energy and other similar properties agree quite extraordinarily closely—often to within only 2 or 3%—with those obtained with the more usual, tight-binding, i.e. molecular-orbital, method. At first sight, it would appear strange that this should be so, since the essential step in the m.o. method is an expansion of an electronic wave function in terms of suitable atomic orbitals, whereas in the free-electron model, the molecule is replaced by a network of straight lines joining adjacent atoms, and the assembly of valence (or π -) electrons are supposed to move entirely freely along these various one-dimensional paths. But the present writer has shown (Coulson 1953) that in most cases these two apparently different models must give very nearly equivalent results for the wave functions and energies: and Griffith (1953 b) and Ruedenberg and Scherr (1953) have shown a similar relationship for the charges associated with each nucleus. In view of all this agreement we may reasonably expect a corresponding similarity between the familiar tight-binding approximation for metals and the free-electron network approximation. We shall find it convenient to refer to this later as the network approximation, since the term 'free-electron model' is commonly applied to the early Sommerfeld treatment of a metal. It is the purpose of this note to show that this is indeed so. We shall do this by considering in § 2 a simple cubic lattice, in § 3 the more general cubic lattice and in § 4 a graphite layer.

§ 2. SIMPLE CUBIC LATTICE

Figure 1 shows a simple cubic lattice—more precisely it shows only two of the three dimensions, the third axis lying perpendicular to the plane. We are to treat the electrons as free to move over this whole network of lines under no potential energy except that which keeps them on the lines. With an obvious notation let us label the unit cells by the three indices (ijk) and let A_{ijk} , B_{ijk} , C_{ijk}

stand for the wave function ψ of an electron in the three basic directions of the (ijk) cell. Then these functions must satisfy the following conditions:

$$(a) \quad \frac{d^2 A}{dx^2} + q^2 A = 0, \text{ and similarly for } B \text{ and } C,$$

$$\text{where} \quad q^2 = 8\pi^2 mE/\hbar^2, \quad \dots\dots(1)$$

and E is the energy of the electrons, supposed wholly kinetic.

$$(b) \quad A_{ijk} = B_{ijk} = C_{ijk} \text{ at their common meeting point.}$$

$$(c) \quad A_{ijk} = A_{i-1,j,k} \text{ etc. at their common point.}$$

(d) $\Sigma \text{grad} \psi = 0$ at each joint, where the gradient is measured along each line of the network, away from the joint.

(e) $\psi = e^{i\mathbf{k} \cdot \mathbf{r}} u(\mathbf{r})$, where \mathbf{k} is the wave vector ($k_x k_y k_z$) and $u(\mathbf{r})$ is periodic with the period \mathbf{l} of the lattice.

Condition (a) is the Schrödinger equation; (b) and (c) are continuity conditions, (d) is the conservation of current (Griffith 1953a) and (e) is the usual Bloch condition for periodic lattices.

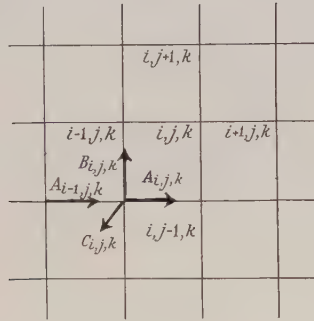


Figure 1. Nomenclature for wave functions along the bonds of a simple cubic lattice.

From (a) and (b) we can write

$$\left. \begin{aligned} A_{ijk} &= \cos qx + a \sin qx \\ B_{ijk} &= \cos qy + b \sin qy \\ C_{ijk} &= \cos qz + c \sin qz \end{aligned} \right\}, \quad \dots\dots(2)$$

where x, y, z are measured from an origin at the corner of the ijk cell, and a, b, c are three constants to be determined. Next, condition (e) shows that

$$A_{i-1,j,k} = \{\exp(-ik_x l)\}(\cos qx' + a \sin qx'), \quad \dots\dots(3)$$

x' being measured from an appropriate origin in the $i-1, j, k$ cell. Condition (c) which applies at the point $x' = l, x = 0$, gives

$$\{\exp(-ik_x l)\}(\cos ql + a \sin ql) = 1. \quad \dots\dots(4)$$

There are two other equations analogous to (4), but involving k_y and k_z instead of k_x , and b and c instead of a .

Condition (d) may be applied in the same way. It yields

$$a + \{\exp(-ik_x l)\}(\sin ql - a \cos ql) + \dots + \dots = 0, \quad \dots\dots(5)$$

where the two omitted terms are obtained from the first term by the cyclic permutation $a \rightarrow b \rightarrow c, k_x \rightarrow k_y \rightarrow k_z$.

We have now obtained four linear equations in a, b, c ; three of them come from (4) and the last one comes from (5). Their mutual consistency requires that the determinant obtained by elimination of a, b, c should vanish identically. The result is an equation (6) which expresses the variation of the energy E with wave vector \mathbf{k} :

$$3 \cos ql = \cos k_x l + \cos k_y l + \cos k_z l, \quad \dots\dots (6)$$

where

$$q^2 = 8\pi^2 m E / \hbar^2.$$

We wish to make two comments on this relation. In the first place q is only defined with modulo $2\pi/l$, so that (6) leads to a zone structure. In the second place we may compare (6) with the tight-binding equation (e.g. Mott and Jones 1936, p. 68)

$$\frac{E_0 - \alpha - E}{2\beta} = \cos k_x l + \cos k_y l + \cos k_z l. \quad \dots\dots (7)$$

In this last equation E_0 and α are constants associated with one atom and β is a resonance integral between neighbouring atoms. Now apart from a trivial change in zero of E , (6) and (7) are identical provided that (i) we may replace $\cos ql$ by $1 - q^2 l^2 / 2$ and (ii) $\beta = \hbar^2 / 24\pi^2 m l^2$. The first of these conditions is entirely similar to the condition recently obtained by the author (Coulson 1953) for molecules; and is satisfied well enough in the lower half of the lowest conduction band. It does, however, become progressively less well satisfied for higher energies in this band. Other bands than the lowest are dealt with by replacing $\cos ql$ by $1 - q^{*2} l^2 / 2$, where q^* is the reduced value of q . This is the quantity lying in the range 0 to $2\pi/l$ such that $\cos q^* l = \cos ql$. The second condition above, which is one of absolute magnitude and not just of form, has already been met in the work of Ruedenberg and Scherr (1953) and others, where it has been found to be reasonably well satisfied for carbon-carbon bonds. It is, of course, unlikely to hold for all interatomic distances, though a variation of β as proportional to l^{-2} is in general agreement with the detailed study of molecules by Mulliken (1949) over the physically interesting range of atomic distances. Now if the relations between E and \mathbf{k} are almost identical in the two theories, so also must the density distribution of energies within a band. Hence we conclude that the band distribution of the network model is exceedingly similar to that of the usual tight-binding approximation.

§ 3. GENERAL CUBIC LATTICE

It is easy to extend the previous analysis. Thus, if we consider a more general cubic lattice, in which any one atom has neighbours at vector distances $\pm \mathbf{l}_i$ ($i = 1, 2, \dots, n$) it may be shown that (6) becomes

$$\sum \frac{\cos ql_i}{\sin ql_i} = \sum \frac{\cos \mathbf{k} \cdot \mathbf{l}_i}{\sin ql_i}. \quad \dots\dots (8)$$

The analysis leading to (8) is omitted, since it follows the same lines as in § 2. However, certain particular cases of (8) are worth mentioning.

(a) For a simple cubic (8) reduces at once to (6), since there are three vector displacements \mathbf{l}_i all equal in length to l , and directed along the three coordinate axes.

(b) For a body-centred cubic, all the \mathbf{l}_i are again equal, and if we put $l_i^2 = 3a^2$, so that $2a$ is the side of the unit cell, then

$$4 \cos ql = 4 \cos k_x a \cos k_y a \cos k_z a.$$

This is exactly equivalent to the tight-binding formula if we may replace $\cos ql$ by $1 - q^2 l^2 / 2$ and use the appropriate value for the resonance integral. In fact, with

the notation of Mott and Jones (1936, p. 68) in which the resonance integral is called γ , $\gamma = \hbar^2/32\pi^2 ml^2$.

(c) For a face-centred cubic, putting $l_i^2 = 2a^2$, so that $2a$ is the side of the unit cell, we have

$$3 \cos ql = \cos k_x a \cos k_y a + \cos k_y a \cos k_z a + \cos k_z a \cos k_x a.$$

Once again this agrees with the tight-binding formula in Mott and Jones provided that $\gamma = \hbar^2/48\pi^2 ml^2$.

(d) Other cases, such as that of a simple cubic with unequal lattice vectors, are soon written down from (8). The only situation where the method appears to break down badly is the linear chain. Here, since there is nothing to mark out where the atoms are, it reduces to the Sommerfeld free-electron model.

§ 4. A GRAPHITE LAYER

Our example is a graphite layer with interatomic distance l , as in figure 2, in

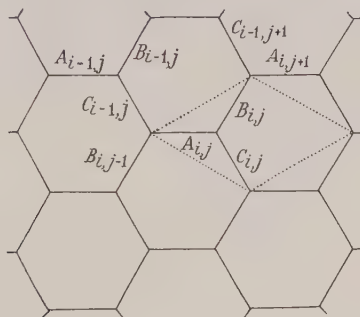


Figure 2. Nomenclature for wave functions along the bonds of a plane graphite layer. The ij unit cell is shown dotted.

which the free electrons are the familiar π -electrons of organic chemistry. These electrons have a wave function antisymmetric in the layer plane, but, as Ruedenberg and Scherr (1953) have shown for the analogous situation in molecules like benzene and naphthalene, we may discuss their distribution in the coordinates xy of the plane without reference to the z coordinate perpendicular to the plane. We know that these π -electrons are much more mobile than the σ -electrons whose wave functions are symmetric in the layer plane. Thus it is reasonable to suppose that our free electron network treatment will be more applicable to the π -electrons than to the σ -electrons. Our calculations therefore relate only to the π -electrons, and not at all to the σ -electrons, which were the only ones considered by Hund and Mrowka (1953) in their discussion of graphite by means of the tight-binding approximation.

For a single graphite layer, each unit cell, such as that shown in dotted lines, contains three bonds. Let us call the wave function in these three bonds A_{ij} , B_{ij} , C_{ij} as shown in the figure. Then A_{ij} , B_{ij} and C_{ij} are given by analytical expressions identical with (2) provided that x , y , z denote distances, in the plane, along the three bond directions, away from their common point near the middle of the unit cell. Continuity of current at this point further requires that $a + b + c = 0$. There are three other conditions to be satisfied. These are best expressed in terms of a wave vector measured in terms of its components in reciprocal space. This has been discussed within the tight-binding approximation by Coulson and Taylor

(1952). If the lattice vectors for the unit cell of figure 2 are called \mathbf{a}_1 and \mathbf{a}_2 with lengths $a_1 = a_2 = \sqrt{3}l$ then the reciprocal vectors are \mathbf{b}_1 and \mathbf{b}_2 related to \mathbf{a}_1 and \mathbf{a}_2 as in figure 3. A point \mathbf{r} in coordinate space is then represented by $\mathbf{r} = r_1\mathbf{a}_1 + r_2\mathbf{a}_2$,

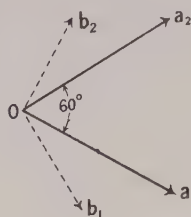


Figure 3. Lattice vectors \mathbf{a}_1 \mathbf{a}_2 and reciprocal lattice vectors \mathbf{b}_1 \mathbf{b}_2 for a graphite layer.

and a point \mathbf{k} in reciprocal space by $\mathbf{k} = k_1\mathbf{b}_1 + k_2\mathbf{b}_2$. The three extra conditions now are:

$$\begin{aligned} B_{ij}(y=l) &= \{\exp(ik_2a_2)\}A_{ij}(x=l), \\ C_{ij}(z=l) &= \{\exp(ik_1a_1)\}A_{ij}(x=l), \\ \left(\frac{dA_{ij}}{dx}\right)_{x=l} + \left(\frac{dC_{i-1,j}}{dz}\right)_{z=l} + \left(\frac{dB_{i,j-1}}{dy}\right)_{y=l} &= 0. \end{aligned}$$

We have now a total of four conditions, all linear in a, b, c . Their mutual consistency requires that their eliminant vanishes, just as in § 2. After some reduction the exceedingly simple result is obtained

$$\cos ql = \pm g/3, \quad \dots\dots(9)$$

where $g^2(k_1k_2) = 3 + 2 \cos k_1a + 2 \cos k_2a + 2 \cos (k_1 - k_2)a. \quad \dots\dots(10)$

This result may be compared with the tight-binding result of Coulson and Taylor, in which overlap integrals between neighbouring atomic orbitals are neglected:

$$E - E_0 = g\beta,$$

where g is given by precisely the same formula as (10). Once again, therefore, we have a close correspondence between the two theories, which is exact provided that (i) we may neglect overlap integrals in the tight-binding calculation, (ii) we may put $\cos ql = 1 - q^2l^2/2$ and (iii) $\beta = \hbar^2/12\pi^2ml^2$. This numerical value of the resonance integral is 1.28 eV; it may be compared with the value of about 1 eV which is needed in the tight-binding method for agreement with experimental resonance energies for molecules like benzene and naphthalene with six-rings similar to those in graphite. It is satisfying that the two values of β are so close, since no empirical data except the bond length appears in (iii).

In view of the current interest in graphite, we have thought it worthwhile to compute the density distribution $N(E)$ using the network model. This distribution is easily found from the distribution function $\mathcal{N}(g)$ which has already been used by Coulson and Taylor (1952). This is defined by the fact that $\mathcal{N}(g)dg$ is the number of k -values for which $g(k_1k_2)$ lies between g and $g + dg$, allowance being made for the existence of electron spin by normalizing $\mathcal{N}(g)$ in such a way that

$$\int_0^3 \mathcal{N}(g) dg = 1. \quad \dots\dots(11)$$

This corresponds to exactly one half of the total band, the total spread of g -values being from -3 to $+3$. The definition (11) shows us that in the tight-binding approximation, with neglect of overlap integrals, the density of states is $\beta\mathcal{N}[(E - E_0)/\beta]$. This is the function which Coulson and Taylor plotted in figure 4(a) of their paper.

It is perfectly straightforward to show, from (1) and (9), that

$$dg = \frac{(9-g^2)^{1/2}}{2 \cos^{-1}(g/3)} d(E/\beta'), \quad \dots\dots(12)$$

where β' is used for the quantity $\hbar^2/8\pi^2 ml^2$, whose dimensions are those of energy. Numerically $\beta' = 1.92$ eV, independently of any model. It follows from (12) and the definitions of $N(E)$ and $\mathcal{N}(g)$ that

$$N(E/\beta') = \frac{(9-g^2)^{1/2}}{2 \cos^{-1}(g/3)} \mathcal{N}(g). \quad \dots\dots(13)$$

In figure 4 we show the graph of $\beta' N(E/\beta')$ as a function of E/β' . This curve shows

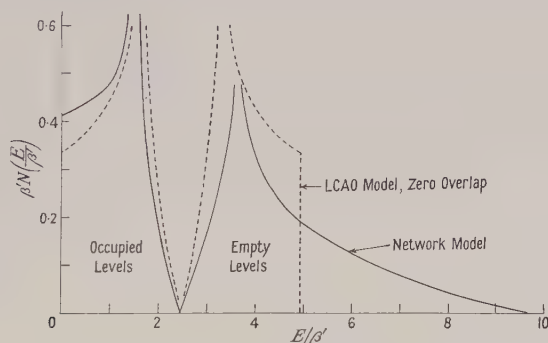


Figure 4. Density function of levels for a single graphite layer as a function of energy. $N(E)$ is normalized to give just one level per atom in the occupied half of the band.

the characteristic zero in the middle of the band just as does the curve obtained by Coulson and Taylor, which is also shown in the figure. In drawing this latter curve, the unknown resonance integral β (but not of course β' which is fixed) is chosen so that the width of the lower half-band agrees with that calculated for the network model. In the normal state of the layer, since there is one π -electron per atom, all levels up to the zero are filled, all above it are empty. It is really quite astonishing that the two curves agree so closely, even as regards such details as the positions of the infinities and the shape near the zero value at $E/\beta' = 2.47$. The only serious disagreement is for large values of E/β' . But this is completely irrelevant, since for E/β' greater than about 5, no l.c.a.o. model would be expected to be significant on account of the intrusion of higher atomic orbitals such as the $3p\pi$ and $3d\pi$, in the manner suggested by Coulson, Craig and Jacobs (1951). However, it is perhaps worth drawing attention to the fact that even in this high energy region the $N(E)$ curve is closely similar to the l.c.a.o. curve, when overlap integrals are included in the latter. This may be seen at once by comparison of the $N(E)$ curve in figure 4 with figure 4(b) in the paper by Coulson and Taylor. If it were permissible to take the overlap integral S between neighbouring $2p\pi$ atomic orbitals equal to about $1/8$, the agreement would be within about 10% over almost all the range of E . But such a value for S is rather smaller than that (about 0.25) obtained using Slater-type wave functions.

§ 5. CONCLUSIONS

The general conclusions which emerge from this study are quite easy to state. In all cases (other than a one-dimensional chain, or line, of atoms) the free-electron network model gives energies and band distributions in close agreement with those

obtained by former theories. When it is realized, for example, that in a graphite layer, this agreement is found with both the tight-binding approximation of Bloch and also with the bond-orbital approximation of the present writer (1954) it becomes even more clear than it was before, that the density function $N(E)$ must be determined in quite large degree by the geometry of the lattice. Probably the general shape of the $N(E)$ curve would be given correctly by almost any theory that was at all plausible. In one sense we can see this as follows. In all theories the energy E must be given as a certain function of the wave vector \mathbf{k} , i.e. $E = f(\mathbf{k})$. Now the shape of the lattice permits certain translations and rotations and inversions which leave it unchanged. These symmetry operations must therefore leave $f(\mathbf{k})$ unchanged. The translational symmetry operations show that $f(\mathbf{k})$ will be an expression involving periodic functions of \mathbf{k} , so that we expect trigonometrical rather than algebraic functions to appear. And the existence of the rotational symmetry operations implies that $f(\mathbf{k})$ must involve certain invariant combinations of these trigonometric quantities. We shall not pursue the details of this argument here, but it is fairly clear from the way in which $f(\mathbf{k})$ is calculated, that the simplest invariants are likely to be the most important ones. This is precisely what is found. For example, in graphite, the function $g(k_1 k_2)$ defined in (11) is the simplest invariant for rotations of $2\pi/3$: and the energy is given in terms of g even if we include interactions between first- and second-nearest neighbours. It is only when third-nearest neighbours are considered (Coulson and Taylor 1952, p. 823) that a second invariant is required as well. This means that the general shape of the band distribution is likely to be substantially the same for all theories, since it is always governed by the first invariant.

There are two further comments to make. The first is that the free-electron network model is only applicable to pure metals, since in the presence of atoms of different kinds it is absurd to suppose that the potential function for a conduction electron is even approximately constant along the network. The second comment is that the type of analysis described in this note may have its greatest utility as a kind of interpolation formula, in the manner suggested by Slater (1954). In this scheme, much more accurate calculations are made for certain values of \mathbf{k} which permit an easier handling of the wave equation (due to increased symmetry, etc.). These accurate calculations enable us to calibrate our more approximate distribution, and so to use it for those intermediate values of \mathbf{k} for which really accurate calculations would be prohibitively complicated.

REFERENCES

- COULSON, C. A., 1953, *Proc. Phys. Soc. A*, **66**, 652; 1954, *Paper read at International Conference in Physics, Kyoto, Japan*, to be published in Report of Conference.
- COULSON, C. A., CRAIG, D. P., and JACOBS, J., 1951, *Proc. Roy. Soc. A*, **206**, 297.
- COULSON, C. A., and TAYLOR, R., 1952, *Proc. Phys. Soc. A*, **65**, 815.
- GRIFFITH, J. S., 1953 a, *Trans. Faraday Soc.*, **49**, 345; 1953 b, *Proc. Camb. Phil. Soc.*, **49**, 650.
- HUND, F., and MROWKA, B., 1935, *Ber. Saechs. Akad. Wiss.*, **87**, 185, 325.
- MOTT, N. F., and JONES, H., 1936, *Properties of Metals and Alloys* (Oxford: University Press).
- MULLIKEN, R. S., 1949, *J. Chim. Phys.*, **46**, 497.
- RUEDENBERG, K., and SCHERR, C. W., 1953, *J. Chem. Phys.*, **21**, 1565.
- SCHERR, C. W., 1953, *J. Chem. Phys.*, **21**, 1582.
- SLATER, J. C., 1954, *Paper read at International Conference in Physics, Kyoto, Japan*, to be published in Report of Conference.

Two-Group Perturbation Theory in Neutron Transport Theory

BY J. H. TAIT

Atomic Energy Research Establishment, Harwell, Berks.

MS. received 3rd February 1954, and in amended form 26th March 1954

Abstract. This paper describes the application of perturbation theory to two-velocity-group neutron problems. We consider the exact integral equations satisfied by the neutron densities. The treatment is, therefore, not restricted to systems whose dimensions are large compared with the relevant mean free paths, and is more general than that reported by Glasstone and Edlund. The latter describe a theory, due to Wigner, in which it is assumed that the neutron densities satisfy the diffusion equations, i.e. the theory is applicable only to large systems.

The eigenfunctions of the integral equations do not form an orthogonal set. They are orthogonal to the eigenfunctions of the adjoint equations. The first part of the paper deals with the construction of these latter equations. The variation of the eigenvalue of the integral equations with small changes in the system is calculated. Finally formulae are obtained for the multiplication of a source of neutrons in a system near to critical.

The theory described in this paper is a generalization of that given by Fuchs for application to one-group-theory problems. The pattern of the analysis is similar, but deviates in the treatment of the effect of a change in the neutron mean free path in the system.

§ 1. INTRODUCTION

AN account of multi-group perturbation theory as applied to reactor problems is given in the book by Glasstone and Edlund (1953). The treatment described is due to Wigner, and is applied to one- and two-velocity-group problems in which the neutron density satisfies the diffusion equation. The theory is, therefore, applicable to systems which are large compared with the relevant neutron mean free paths.

Fuchs (1949) has given an account of perturbation theory as applied to one-group neutron problems without the restriction that the size of the system is large compared with the mean free path. This theory is developed by an expansion in the system of orthogonal solutions of the exact integral equation, as distinct from an expansion in terms of the orthogonal functions of the diffusion equation.

In this paper Fuchs' treatment is extended to two-group theory. In general the pattern of the analysis is similar. It deviates, however, in the treatment of the effect of a change in the total mean free path on the system. To describe this effect, Fuchs first considered the multiplication in a sub-critical system containing anisotropic sources. In this paper it will be shown that this step can be dispensed with.

§ 2. THE INTEGRAL EQUATIONS

Let $n_1(\mathbf{r})$ and $n_2(\mathbf{r})$ be the neutron densities in the two groups. $n_1(\mathbf{r})$ and $n_2(\mathbf{r})$ satisfy the following equations:

$$v_1 n_1(\mathbf{r}) = v_1 \int \beta_{11}(\mathbf{r}') K_1(\mathbf{r}, \mathbf{r}') n_1(\mathbf{r}') dv' + v_2 \int \beta_{21}(\mathbf{r}') K_1(\mathbf{r}, \mathbf{r}') n_2(\mathbf{r}') dv' + \int q_1(\mathbf{r}') K_1(\mathbf{r}, \mathbf{r}') dv' \quad \dots\dots(2.1)$$

$$v_2 n_2(\mathbf{r}) = v_1 \int \beta_{12}(\mathbf{r}') K_2(\mathbf{r}, \mathbf{r}') n_1(\mathbf{r}') dv' + v_2 \int \beta_{22}(\mathbf{r}') K_2(\mathbf{r}, \mathbf{r}') n_2(\mathbf{r}') dv' + \int q_2(\mathbf{r}') K_2(\mathbf{r}, \mathbf{r}') dv' \quad \dots\dots(2.2)$$

where

$$K_s(\mathbf{r}, \mathbf{r}') = \exp(-\alpha_s |\mathbf{r} - \mathbf{r}'|) / 4\pi |\mathbf{r} - \mathbf{r}'|^2 = K_s(\mathbf{r}', \mathbf{r}).$$

s numbers the group and can be 1 or 2. K_s is the probability that a neutron of group s emitted at \mathbf{r} with velocity v_s arrives at \mathbf{r}' without a collision.

α_s is the inverse total mean free path for neutrons in group s . β_{ss}/α_s and β_{st}/α_s are the probable number of neutrons of velocities v_s and v_t produced when a neutron of velocity v_s undergoes a collision. $q_s(\mathbf{r}')$ is the source strength per unit volume for neutrons of group s at a point \mathbf{r}' .

Equations (1) and (2) can be written in matrix form as follows:

$$n = Mn + s \quad \dots\dots(2.3)$$

where $n = \|n_s\|$, $M = \|M_{st}\|$ and $s = \|s_s\|$. $\dots\dots(2.4)$

The elements of the matrix $\|M_{st}\|$ are defined as follows:

$$M_{st} = \frac{v_t}{v_s} \int \beta_{ts}(\mathbf{r}') K_s(\mathbf{r}, \mathbf{r}') \dots dv'. \quad \dots\dots(2.5)$$

§ 3. ADJOINT EQUATION

Let us consider the source free equation

$$n = \lambda Mn. \quad \dots\dots(3.1)$$

Let λ_i be an eigenvalue of the equation and n_i the corresponding eigen solution.

In general the eigenfunctions do not form an orthogonal set. They are orthogonal to the eigenfunctions of the adjoint equation

$$n^+ = \lambda M^+ n^+ \quad \dots\dots(3.2)$$

where $n^+ = \|n_s^+\|$ and $M^+ = \|M_{st}^+\|$

The elements of the matrix $\|M_{st}^+\|$ are defined as follows:

$$M_{st}^+ = \frac{v_s}{v_t} \beta_{ts}(\mathbf{r}) \int K_t(\mathbf{r}, \mathbf{r}') \dots dv'. \quad \dots\dots(3.3)$$

The eigenvalues of (3.2) are the same as those of (3.1). We shall later assume that the set n_i is complete.

The orthogonality property is easily demonstrated. Let ${}_t n_i^+$, ${}_t n_i$ denote the transposed vectors (n_{1i}^+, n_{2i}^+) and (n_{1i}, n_{2i}) .

$$\int {}_t n_j^+ n_i dv = \lambda_i \int {}_t n_j^+ M n_i dv = \lambda_i \int {}_t n_i M^+ n_j^+ dv$$

because, for example,

$$\begin{aligned} \int n_{1j}^+ M_{11} n_{1i} dv &= \int \int n_{1j}^+(\mathbf{r}) \beta_{11}(\mathbf{r}') K_1(\mathbf{r}, \mathbf{r}') n_{1i}(\mathbf{r}') dv' dv \\ &= \int n_{1i}(\mathbf{r}') \beta_{11}(\mathbf{r}') \int n_{1j}^+(\mathbf{r}) K_1(\mathbf{r}', \mathbf{r}) dv' dv \\ &= \int n_{1i}(\mathbf{r}') M_{11}^+ n_{1j}^+(\mathbf{r}') dv', \text{ etc.} \end{aligned}$$

Therefore
$$\begin{aligned} \int {}_t n_j^+ n_i dv &= \lambda_i \int {}_t n_i M^+ n_j^+ dv \\ &= \frac{\lambda_i}{\lambda_j} \int {}_t n_i n_j^+ dv = \frac{\lambda_i}{\lambda_j} \int {}_t n_j^+ n_i dv, \end{aligned}$$

i.e.
$$\int {}_t n_j^+ n_i dv = \delta_{ij} \quad \text{where} \quad \delta_{ij} = 0, \quad i \neq j, \\ = 1, \quad i = j.$$

if the n 's are normalized.

§ 4. VARIATION THEORY

Consider the equation
$$n_i = \lambda_i M n_i. \quad \dots\dots(4.1)$$

Let the system vary to a slight extent. Such a variation may be expressed as changes δK_n and $\delta \beta_{nm}$ ($n, m = 1, 2$), all incorporated in a change δM in M ,

i.e.
$$\delta n_i = \delta \lambda_i M n_i + \lambda_i \delta M n_i + \lambda_i M \delta n_i. \quad \dots\dots(4.2)$$

Multiply (4.2) by ${}_t n_i^+$ and integrate.

Then

$$\int {}_t n_i^+ \delta n_i dv = \delta \lambda_i \int {}_t n_i^+ M n_i dv + \lambda_i \int {}_t n_i^+ \delta M n_i dv + \lambda_i \int {}_t n_i^+ M \delta n_i dv. \quad \dots\dots(4.3)$$

Now
$$\lambda_i \int {}_t n_i^+ M \delta n_i dv = \lambda_i \int {}_t \delta n_i M^+ n_i^+ dv = \int {}_t \delta n_i n_i^+ dv.$$

Therefore
$$\frac{\delta \lambda_i}{\lambda_i} = - \frac{\int {}_t n_i^+ \delta M n_i dv}{\int {}_t n_i^+ M n_i dv}, \quad \dots\dots(4.4)$$

i.e.
$$\frac{\delta \lambda_i}{\lambda_i^2} = - \frac{\int {}_t n_i^+ \delta M n_i dv}{\int {}_t n_i^+ n_i dv} = - \int {}_t n_i^+ \delta M n_i dv.$$

§ 5. EFFECT ON λ DUE TO A CHANGE OF α AND β IN A SMALL REGION

The expression $\int {}_t n_i^+ \delta M n_i dv$ is now evaluated when α and β change in a small region. The suffix i will be dropped from the expressions for the sake of convenience.

$$\begin{aligned} \int {}_t n^+ \delta M n dv &= \int n_1^+ \delta M_{11} n_1 dv + \int n_1^+ \delta M_{12} n_2 dv + \int n_2^+ \delta M_{21} n_1 dv + \int n_2^+ \delta M_{22} n_2 dv \\ &\dots\dots(5.1) \end{aligned}$$

where

$$\begin{aligned} \int n_1^+ \delta M_{11} n_1 dv &= \int \int n_1^+(\mathbf{r}) \delta \beta_{11}(\mathbf{r}') K_1 n_1(\mathbf{r}') dv' dv + \int \int n_1^+ \beta_{11}(\mathbf{r}') \delta K_1 n_1(\mathbf{r}') dv' dv. \\ &\dots\dots(5.2) \end{aligned}$$

From (3.2) and (3.3) we obtain the following equations :

$$\lambda D \int K_s(\mathbf{r}, \mathbf{r}') n_s^+(\mathbf{r}') dv = \beta_{st} n_s^+(\mathbf{r}) - \frac{v_s}{v_t} \beta_{st} n_t^+ \quad (s \neq t) \quad \dots\dots (5.3)$$

where

$$D = |\beta_{st}|. \quad \dots\dots (5.4)$$

Therefore the first term on the right-hand side of (5.2) is given by

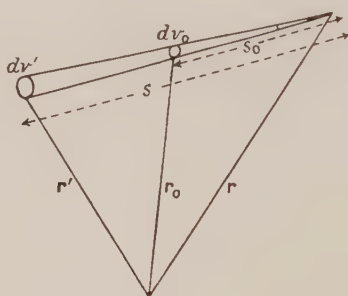
$$\begin{aligned} \int \int n_1^+(\mathbf{r}) \delta \beta_{11}(\mathbf{r}') K_1(\mathbf{r}, \mathbf{r}') n_1(\mathbf{r}') dv' dv &= \int \delta \beta_{11}(\mathbf{r}') n_1(\mathbf{r}') \int n_1^+(\mathbf{r}) K_1(\mathbf{r}, \mathbf{r}') dv dv' \\ &= \frac{1}{\lambda} \int \frac{\delta \beta_{11}(\mathbf{r}')}{D} n_1(\mathbf{r}') \left(n_1^+ \beta_{22} - \frac{v_1}{v_2} \beta_{12} n_2^+ \right) dv' \\ &= \frac{\delta \beta_{11}(\mathbf{r}_0)}{\lambda D(\mathbf{r}_0)} n_1(\mathbf{r}_0) \left[n_1^+ \beta_{22} - \frac{v_1}{v_2} \beta_{12} n_2^+ \right] dv_0 \quad \dots\dots (5.5) \end{aligned}$$

if the change in β occurs in an elementary volume dv_0 at \mathbf{r}_0 .

We now simplify the second term occurring in (5.2). It will be convenient to combine two of these terms occurring in (5.1), namely

$$\begin{aligned} \int \int n_1^+ \beta_{11}(\mathbf{r}') \delta K_1(\mathbf{r}, \mathbf{r}') n_1 dv' dv + \frac{v_2}{v_1} \int \int n_1^+(\mathbf{r}') \beta_{21}(\mathbf{r}') \delta K_1 n_2(\mathbf{r}') dv' dv \\ = \int n_1^+ \int \left\{ \beta_{11}(\mathbf{r}') n_1(\mathbf{r}') + \frac{v_2}{v_1} \beta_{21}(\mathbf{r}') n_2(\mathbf{r}') \right\} \delta K_1(\mathbf{r}, \mathbf{r}') dv' dv. \quad \dots\dots (5.6) \end{aligned}$$

We introduce the following quantities, $N_1(\mathbf{r}, \Omega)$ and $N_2(\mathbf{r}, \Omega)$. $N_1(\mathbf{r}, \Omega)$ is the density of neutrons in the first group whose directions lie in the solid angle $d\Omega$ around Ω . $N_2(\mathbf{r}, \Omega)$ is a similar quantity for neutrons of group 2. We shall reduce (5.6) to a sum of integrals of the type $\int N_1^+(\mathbf{r}, -\Omega) N_1(\mathbf{r}, \Omega) d\Omega$. The change in K is due to a change in α in a volume dv_0 at \mathbf{r}_0 . To assess the effect on K we consider all directions passing through \mathbf{r}_0 .



Let the volume element dv_0 at \mathbf{r}_0 in which the change in α occurs be $s_0^2 d\Omega ds_0$ where $s_0 = |\mathbf{r}_0 - \mathbf{r}|$ and $d\Omega$ is the solid angle subtended by the volume element dv_0 at \mathbf{r} . The element of volume dv' at \mathbf{r}' (see figure) such that all neutrons from this volume element in the direction $\mathbf{r}' - \mathbf{r}$ pass through dv_0 is given by $s^2 d\Omega ds$, where $s = |\mathbf{r}' - \mathbf{r}|$, and

$$s^2 d\Omega ds = \frac{s^2}{s_0^2} \frac{dv_0}{ds_0} ds. \quad \dots\dots (5.7)$$

The value of δK , which is the change in the probability that a neutron proceeds from \mathbf{r}' to \mathbf{r} without a collision, is

$$-\delta\alpha_1 ds_0 K_1(\mathbf{r}, \mathbf{r}') = -\delta\alpha_1 ds_0 K_1(\mathbf{r}_0, \mathbf{r}) \exp[-\alpha_1(s-s_0)] \frac{s_0^2}{s^2}$$

where $\delta\alpha_1$ is the change in α_1 in the volume dv_0 .

Therefore,

$$\begin{aligned} & \int \left\{ \beta_{11}(\mathbf{r}') n_1(\mathbf{r}') + \frac{v_2}{v_1} \beta_{21}(\mathbf{r}') n_2(\mathbf{r}') \right\} \delta K_1(\mathbf{r}, \mathbf{r}') dv' \\ &= -\delta\alpha_1 K_1(\mathbf{r}_0, \mathbf{r}) dv_0 \int_0^\infty \left\{ \beta_{11}(\mathbf{r}_0 + s_1 \Omega) n_1(\mathbf{r}_0 + s_1 \Omega) \right. \\ & \quad \left. + \frac{v_2}{v_1} \beta_{21}(\mathbf{r}_0 + s_1 \Omega) n_2(\mathbf{r}_0 + s_1 \Omega) \right\} \exp[-\alpha_1 s_1] ds_1 \quad \dots\dots (5.8) \end{aligned}$$

where $\Omega = (\mathbf{r}' - \mathbf{r})/|\mathbf{r}' - \mathbf{r}|$, $s_1 = s - s_0$, and where we have used the relation (5.7). The term $(1/4\pi) \{v_1 \beta_{11}(\mathbf{r}_0 + s_1 \Omega) n_1(\mathbf{r}_0 + s \Omega) + v_2 \beta_{21}(\mathbf{r}_0 + s \Omega) n_2(\mathbf{r}_0 + s_1 \Omega)\}$ represents the neutrons at $(\mathbf{r}_0 + s \Omega)$, scattered into group 1 and travelling towards \mathbf{r}_0 . $\exp[-\alpha_1 s_1]$ is their chance of arrival at \mathbf{r}_0 without a collision. Therefore the integral on the right-hand side of (5.8) is equal to

$$4\pi N_1(\mathbf{r}_0, -\Omega). \quad \dots\dots (5.9)$$

Therefore the right-hand side of (5.6) is given by

$$-4\pi \delta\alpha_1 dv_0 \int n_1^+ N_1(\mathbf{r}_0, -\Omega) K_1(\mathbf{r}_0, \mathbf{r}) dv. \quad \dots\dots (5.10)$$

This result could have been obtained assuming

$$K_1 = \frac{1}{4\pi |\mathbf{r}' - \mathbf{r}|^2} \exp \left\{ - \int_0^{|\mathbf{r}' - \mathbf{r}|} \alpha_1(\mathbf{r} + s \Omega) ds \right\},$$

i.e. α_1 a function of position.

(5.10) is equal to

$$-4\pi \delta\alpha_1 dv_0 \int N_1(\mathbf{r}_0, -\Omega) \int_0^\infty n_1^+(\mathbf{r}_0 - s \Omega) K_1(\mathbf{r}_0, \mathbf{r}_0 - s \Omega) s^2 ds d\Omega.$$

Let N_1^+ and N_2^+ be the angular distributions of densities in the two groups in the adjoint equations. In the integral occurring on the right-hand side of (5.3) the neutrons travelling to points \mathbf{r} in a direction Ω make a contribution equal to

$$d\Omega \int_0^\infty s^2 ds K_s(\mathbf{r}, \mathbf{r} - s \Omega) n_s^+(\mathbf{r} - s \Omega) ds.$$

Therefore, from (5.3), with s equal to 1,

$$\beta_{22} N_1^+(\mathbf{r}_0, \Omega) - \frac{v_1}{v_2} \beta_{12} N_2^+(\mathbf{r}_0, \Omega) = \lambda D \int_0^\infty n_1^+(\mathbf{r}_0 - s \Omega) K_1(\mathbf{r}_0, \mathbf{r}_0 - s \Omega) s^2 ds.$$

The integral (5.10) is given by

$$\begin{aligned} & -\delta\alpha_1 \frac{4\pi \beta_{22}(\mathbf{r}_0) dv_0}{\lambda D(\mathbf{r}_0)} \int N_1(\mathbf{r}_0, -\Omega) N_1^+(\mathbf{r}_0, \Omega) d\Omega \\ & \quad + \delta\alpha_1 \frac{4\pi v_1 \beta_{12}(\mathbf{r}_0) dv_0}{v_2 \lambda D(\mathbf{r}_0)} \int N_1(\mathbf{r}_0, -\Omega) N_2^+(\mathbf{r}_0, \Omega) d\Omega. \end{aligned}$$

It is therefore possible to evaluate the expressions occurring in (5.1).

Expression (5.1) becomes

$$\begin{aligned} & \frac{dv_0}{v_1 v_2 \lambda D} (v_2 n_1^+ \beta_{22} - \beta_{12} v_1 n_2^+) (v_1 \delta \beta_{11} n_1 + v_2 \delta \beta_{21} n_2) \\ & + \frac{dv_0}{v_1 v_2 \lambda D} (v_1 n_2^+ \beta_{11} - v_2 \beta_{21} n_1^+) (v_1 \delta \beta_{12} n_1 + n_2 \delta \beta_{22} v_2) \\ & - \delta \alpha_1 \frac{\beta_{22}}{\lambda D} g_{11} n_1^+ n_1 dv_0 + \delta \alpha_1 \frac{v_1 \beta_{12}}{v_2 \lambda D} g_{12} n_2^+ n_1 dv_0 \\ & - \frac{\delta \alpha_2 \beta_{11}}{\lambda D} g_{22} n_2 n_2^+ dv_0 + \frac{\delta \alpha_2 v_2 \beta_{21}}{\lambda D v_1} g_{21} n_2 n_1^+ dv_0 \end{aligned} \quad \dots\dots (5.11)$$

where

$$g_{st} = \frac{\int N_s^+(\mathbf{r}_0, \mathbf{\Omega}) N_t(\mathbf{r}_0, -\mathbf{\Omega}) d\Omega}{4\pi n_s^+(\mathbf{r}_0) n_t(\mathbf{r}_0)} \quad \dots\dots (5.12)$$

The effect of a change in α and β over a finite volume can be obtained by integration of (5.11) with respect to dv_0 . The change in the eigenvalue can then be computed from equation (4.4). With the aid of formula (5.12) one can determine the changes in α and β which leave λ_i unaltered, i.e. leave the system in a critical state.

§ 6. MULTIPLICATION PROBLEMS

Let us return to equation (2.5), i.e.

$$n = Mn + s, \quad \dots\dots (6.1)$$

Let us expand the neutron density in terms of the eigenfunctions n_i of the equation (3.1),

$$n_i = \lambda_i M n_i, \quad \text{i.e. } n = \sum [n_i] n_i(\mathbf{r}),$$

where $[n_i] = \int n_i^+ n dv$. Multiply equation (6.1) by n_i^+ and integrate.

$$\text{Then} \quad [n_i] = \int n_i^+ M n dv + \int n_i^+ s dv = \frac{1}{\lambda_i} \int n_i n_i^+ dv + \int n_i^+ s dv.$$

Therefore

$$n = \sum \frac{\lambda_i n_i(\mathbf{r})}{\lambda_i - 1} \int n_i^+ s dv. \quad \dots\dots (6.2)$$

The expression $\int n_i^+ s dv$ occurring in (6.2) can be further simplified, for

$$\begin{aligned} \int n_i^+ s dv &= \int \|n_{si}^+\| \cdot \left\| \frac{1}{v_s} \int q_s(\mathbf{r}') K_s(\mathbf{r}, \mathbf{r}') dv' \right\| dv \quad (s=1, 2) \\ &= \frac{1}{v_1} \iint q_1(\mathbf{r}') K_1(\mathbf{r}, \mathbf{r}') n_{1i}^+(\mathbf{r}) dv dv' + \frac{1}{v_2} \iint q_2(\mathbf{r}') K_2(\mathbf{r}', \mathbf{r}) n_{2i}^+(\mathbf{r}) dv dv'. \end{aligned} \quad (6.3)$$

Substituting from (5.3) into (6.3), we find

$$\begin{aligned} \lambda_i \int n_i^+ s dv &= \int \frac{q_1(\mathbf{r}')}{D(\mathbf{r}')} \left[\frac{1}{v_1} \beta_{22} n_{1i}^+(\mathbf{r}') - \frac{1}{v_2} n_{2i}^+ \beta_{12} \right] dv' \\ &+ \int \frac{q_2(\mathbf{r}')}{D(\mathbf{r}')} \left[\frac{1}{v_2} \beta_{11} n_{2i}^+(\mathbf{r}') - \frac{1}{v_1} \beta_{21} n_{1i}^+(\mathbf{r}') \right] dv'. \end{aligned} \quad \dots\dots (6.4)$$

§ 7. THE MULTIPLICATION

Let E_1 and E_2 be the number of neutrons in the two groups that emerge from a surface S enclosing a volume V , containing sources given by distributions $q_1(\mathbf{r}')$ and $q_2(\mathbf{r}')$. The multiplication of these source neutrons is given by a matrix

$$E = \|E_s\| = \|A_{st}\| \|n_s(\mathbf{r})\| + \left\| \int q_s(\mathbf{r}') dv' \right\| \quad \dots\dots(7.1)$$

where $A_{st} = \int v_t \{\beta_{ts} - \alpha_s \delta_{st}\} \dots dv$.

$$\text{Let } \|q_s(\mathbf{r})\| = \Sigma_i B_i \| \beta_{1s} v_1 n_{1i} + \beta_{2s} v_2 n_{2i} \| \quad \dots\dots(7.2)$$

If this equation be multiplied by

$$\frac{1}{D} \left(-\frac{1}{v_2} n_{2i} + \beta_{12} + \frac{1}{v_1} n_{1i} + \beta_{22}, \quad \frac{1}{v_2} n_{2i} + \beta_{11} - \frac{1}{v_1} \beta_{21} n_{1i} + \right)$$

and integrated over dv , it is easily shown that

$$B_i = \lambda_i \int v_i n_i + s dv.$$

Substituting from (6.2) we find that

$$E = \sum_i \frac{\lambda_i \int v_i n_i + s dv}{\lambda_i - 1} \|B_{s1} n_{1i} + B_{s2} n_{2i}\|$$

$$\text{where } B_{st} = \int v_t \{\lambda_i \beta_{ts} - \delta_{st} \alpha_s\} \dots dv \quad \dots\dots(7.3)$$

ACKNOWLEDGMENTS

I wish to thank Dr. B. Davison and Dr. B. H. Flowers for helpful criticism in the preparation of this paper.

REFERENCES

- FUCHS, K., 1949, *Proc. Phys. Soc. A*, **62**, 791.
GLASSTONE, S., and EDLUND, M. C., 1953, *The Elements of Nuclear Reactor Theory* (London: Macmillan).

Spectroscopic Isotope Shift and Nuclear Deformations

By A. R. BODMER†

Department of Theoretical Physics, University of Manchester

Communicated by L. Rosenfeld; MS. received 4th December 1953, and in final form 29th March 1954

Abstract. With a method developed in a previous paper the isotope shift due to a difference in nuclear deformation of two isotopes is calculated, making certain simplifying assumptions about the nuclear charge distribution. If both isotopes have a spectroscopic quadrupole moment these may then be used to make an estimate of the deformations. It is found that the difference between the intrinsic and spectroscopic quadrupole moments is quite crucial and that when this is taken into account the anomalously large isotope shift of Eu is satisfactorily explained with the experimentally determined quadrupole moments. Using available data on quadrupole and magnetic moments, a tentative examination of other isotope shift data in terms of the deformation dependent isotope shift indicates that this may perhaps explain the large observed variations.

§ 1. INTRODUCTION

THE volume dependent spectroscopic isotope shift (I.S.) has till recently been considered as due to a difference in charge distribution between two isotopes arising from a change in volume between these. Brix and Kopfermann (1949, 1951) however have suggested that if the two isotopes are considered as non-spherical there will in addition be a distinct contribution arising from a difference in shape. The effective potential energy of an $s_{1/2}$ or $p_{1/2}$ electron in the nuclear interior will in all cases be obtained by averaging the non-spherical nucleus over all directions. If the isotopes have a spin $I \geq 1$ they will also possess a spectroscopic quadrupole moment defined with respect to fixed axes in space for the substate $M=I$. Brix and Kopfermann have assumed that if these quadrupole moments are too large to be due to the motion of a single proton it is not too unreasonable to describe the nuclear charge distribution by a uniformly charged ellipsoid of revolution. It then becomes possible to make a quantitative estimate of the deformation from spherical shape and hence, also, of the extra potential arising from this. It will be shown that it is of crucial importance when interpreting the experimental data to take account of the fact that the spectroscopic quadrupole moment may be considerably smaller than the intrinsic quadrupole moment referred to the symmetry axis of the nucleus. This difference will have an important influence, especially for smaller I , since the deformation occurs as the square in the extra potential to which it gives rise.

A modification of the individual particle model of nuclear structure in which a well-defined deformation such as has been considered above plays a central

† Now at the Armament Design Establishment, Fort Halstead, Sevenoaks, Kent.

role, and which is capable of explaining the large observed quadrupole moments, has recently been suggested by Rainwater (1950) and Bohr (1951, 1952) and Bohr and Mottelson (1953). The nucleons in unclosed shells are considered as exerting a centrifugal pressure on the nuclear wall which, together with the action of surface tension and the coulomb forces, leads to a deformation of the nucleus.

Brix and Kopfermann have especially considered the connection of the I.S. between ^{150}Sm and ^{152}Sm with the quadrupole moments of ^{151}Eu and ^{153}Eu which have one additional proton. Both I.S. are exceptionally large. It is especially noteworthy that the former is nearly twice the already large I.S. between any other two adjacent even Sm isotopes, thus the relative spacings of the Sm I.S. are

^{144}Sm	^{147}Sm	^{148}Sm	^{149}Sm	^{150}Sm	^{152}Sm	^{154}Sm
0	≥ 1.41	2	≤ 2.26	3.14	4.81	5.72

Brix and Kopfermann assume that the deformations of ^{150}Sm and ^{152}Sm are approximately the same as those of the corresponding Eu isotopes. They then calculate the deformations of the latter from their known quadrupole moments and are then able to obtain an estimate of the deformation dependent part of the I.S. between ^{151}Eu and ^{153}Eu and hence also of that between ^{150}Sm and ^{152}Sm . They find that this is rather smaller than the difference of the I.S. between ^{150}Sm and ^{152}Sm and that between other adjacent even Sm isotopes. Their interpretation is, then, that in view of the uncertainties involved just this I.S. jump can be explained as due to a difference in deformation.

In the following the deformation dependent I.S. is calculated with the method developed in a previous paper (Bodmer 1953, referred to as A), using the same model as Brix and Kopfermann of a uniformly charged nucleus deformed into a rotational ellipsoid of the same volume as the undeformed spherical nucleus but also taking into account the difference between the spectroscopic and intrinsic quadrupole moments. It is found that the deformation dependent I.S. of Eu is of the order of magnitude of the whole of its anomalously large I.S. and hence, with the above assumptions of Brix and Kopfermann, regarding the deformations of ^{150}Sm and ^{152}Sm also of the order of magnitude of the whole of the I.S. between these.

A tentative attempt is made to examine other I.S. data, more especially the large observed variations, in terms of the deformation dependent I.S. using available data on quadrupole and magnetic moments.

§ 2. CALCULATION OF POTENTIALS

We consider the nuclear charge distribution to be described by a uniformly charged body of revolution whose surface \mathbf{r}_0' is given by

$$r_0' = r_0[1 + \epsilon u(\theta) + \epsilon^2 w(\theta) + \dots]. \quad \text{.....(1)}$$

Here θ is the angle between the axis of revolution and the radius vector from the origin to a point on the surface, the origin being taken as the centre of the sphere, radius r_0 , which is obtained in the limit $\epsilon=0$; ϵ is a measure of the deformation of the body relative to this sphere. In the following it is assumed

that ϵ is sufficiently small that only powers up to ϵ^2 need be retained. Expanding in terms of spherical harmonics, we write

$$\begin{aligned}u(\theta) &= \sum_{n=0}^{\infty} \alpha_n P_n(\cos \theta) \\w(\theta) &= \sum_{n=0}^{\infty} \beta_n P_n(\cos \theta) \\u^2(\theta) &= \sum_{n=0}^{\infty} \delta_n P_n(\cos \theta).\end{aligned}$$

Taking the volume to be the same as that of the sphere, radius r_0 , and assuming that the charge density ρ is constant,

$$\rho = \frac{3}{4\pi} \frac{Ze}{r_0^3}.$$

The total charge is then Ze . The potential energy of an electron at a point \mathbf{r} in the interior of the nucleus ($r < r_0$) is

$$V(\mathbf{r}) = V^{(0)}(r) - 3 \frac{Ze^2}{r_0} \sum_{n=0}^{\infty} \frac{P_n(\cos \theta)}{2n+1} \left(\frac{r}{r_0}\right)^n \{\epsilon \alpha_n + \epsilon^2 [\beta_n + \frac{1}{2} \delta_n (1-n)]\} \dots\dots(2)$$

$$\text{where} \quad V^{(0)}(r) = -\frac{3}{2} \frac{Ze^2}{r_0} \left[1 - \frac{1}{3} \left(\frac{r}{r_0}\right)^2\right] \dots\dots(3)$$

is the potential energy due to the uniformly charged sphere, radius r_0 . For a $s_{1/2}$ or $p_{1/2}$ electron the effective potential energy $V(r)$ is obtained by averaging $V(\mathbf{r})$ over all directions.

$$V(r) = V^{(0)}(r) + V_{\epsilon}(r)$$

$$\text{where} \quad V_{\epsilon}(r) = -3 \frac{Ze^2}{r_0} [\epsilon \alpha_0 + \epsilon^2 (\beta_0 + \frac{1}{2} \delta_0)] \dots\dots(4)$$

is the potential energy due to the deformation. We now suppose more specifically that the nucleus may be described by an ellipsoid of revolution of semi-axes a , b along and perpendicular to the axis of revolution respectively. The deformation may then be described in terms of the parameter $\epsilon = (a-b)/r_0$ which is positive for a prolate and negative for an oblate ellipsoid of revolution. Using the equation for the surface of an ellipsoid, it is easily found that $\alpha_0 = 0$, $\beta_0 = -4/45$, $\delta_0 = 4/45$ for both a prolate and an oblate ellipsoid. Hence from (4)

$$V_{\epsilon}(r) = \frac{2}{15} \frac{Ze^2}{r_0} \epsilon^2. \dots\dots(5)$$

The difference of potential energy in the nuclear interior between two isotopes is then

$$\delta V = \delta V_v + \delta V_{\epsilon} + \delta V_{\epsilon, v}$$

$$\text{where} \quad \delta V_v = \frac{3}{2} \frac{Ze^2}{r_0} \frac{\delta r_0}{r_0} \left[1 - \left(\frac{r}{r_0}\right)^2\right]$$

is the usual change in potential energy of a uniformly charged spherical nucleus, radius r_0 , due to an increase of volume specified by a change of radius δr_0 . The change in potential energy δV_{ϵ} due to differing deformations ϵ_1 , ϵ_2 of the lighter and heavier isotopes respectively is

$$\delta V_{\epsilon} = \frac{Ze^2}{r_0} F \quad \text{where} \quad F = \frac{2}{15} (\epsilon_2^2 - \epsilon_1^2) \dots\dots(6)$$

and is independent of r . δV_ϵ may either increase or decrease the I.S. due to δV_v , depending on whether $\epsilon_2 > \epsilon_1$ or $\epsilon_1 > \epsilon_2$ respectively.

$$\delta V_{\epsilon, v} = -\frac{2}{15} \frac{Ze^2 \delta r_0}{r_0} \epsilon_2^2$$

is a small correction to the volume dependent change of potential δV_v arising from the fact that for an ellipsoidal nucleus the charge is effectively concentrated more towards the centre. Even for $\epsilon = \frac{1}{4}$ the I.S. due to $\delta V_{\epsilon, v}$ is less than 2% of that due to δV_v , and can therefore be safely neglected.

The deformation ϵ is related to the intrinsic quadrupole moment Q_0 which is defined with respect to the symmetry axis of the nucleus by

$$Q_0 = \frac{4}{5} \epsilon Z r_0^2. \quad \dots\dots (7)$$

If the nucleus has a spin $I \geq 1$ it will also have a spectroscopic quadrupole moment which may be used to calculate ϵ if the relation between Q and Q_0 is known. Q_0 will be larger than Q by a quantum mechanical projection factor γ_I which will depend to some extent on the coupling of the angular momenta in the nucleus. We take for γ_I the value given by considering the nucleus as a symmetric top:

$$Q_0 = \gamma_I Q, \quad \gamma_I = \frac{(I+1)(2I+3)}{I(2I-1)}. \quad \dots\dots (8)$$

When I becomes large γ_I tends to one, but for small I , γ_I may be much larger. For $I=0, \frac{1}{2}$, Q is zero whatever the value of Q_0 . It may be mentioned (see Bohr 1951) that the same value of γ_I as above is obtained for a single nucleon whose total angular momentum is I and which is strongly coupled to a deformed core of the remaining nucleons. If, however, the spin-orbit coupling of the nucleon is weak compared with the coupling of its orbital angular momentum L to the core a larger value of γ_I for $I = L + \frac{1}{2}$ from the above is obtained. This is not however sufficiently different to affect any of the conclusions reached. In general it can be expected that for other coupling schemes γ_I will be larger than given by (7) and that therefore the qualitative conclusions will remain unchanged. If both isotopes have a spectroscopic quadrupole moment

$$F = \frac{5}{24} \frac{\gamma_{I_2}^2 Q_2^2 - \gamma_{I_1}^2 Q_1^2}{Z^2 r_0^4}. \quad \dots\dots (9)$$

Thus for small I , γ_I will have a very large effect on δV_ϵ since it occurs as the square in the above expression. In fact the omission of this factor will be quite crucial.

Even if the nucleus does not have a spectroscopic quadrupole moment it may still have a deformation, i.e. an intrinsic quadrupole moment with respect to the internal symmetry axis. Hence, also, for even and spin $\frac{1}{2}$ nuclei δV_ϵ need not be zero. In this case, however, ϵ can only be obtained on the basis of some nuclear model such as Bohr's, which allows for deformations. The importance of nuclei which have observable spectroscopic quadrupole moments and for which the I.S. is also known is that ϵ , and hence the I.S. due to δV_ϵ may be estimated from the spectroscopic quadrupole moments and that, therefore, a comparison with the experimentally observed I.S. may be made involving only a minimum of hypothesis. Such a comparison should give a rather direct indication of the significance of nuclear deformations for the I.S.

§ 3. CALCULATION OF THE DEFORMATION DEPENDENT I.S.

We first calculate the I.S. due to δV_ϵ using the simple perturbation theory due to Rosenthal and Breit (1932) and Racah (1932). If the I.S. corresponding to δV_v , δV_ϵ is denoted by $\delta(\Delta E_v)$, $\delta(\Delta E_\epsilon)$ respectively it is easily found that

$$D_{\epsilon, \text{pert}} = \frac{\delta(\Delta E_\epsilon)_{\text{pert}}}{\delta(\Delta E_v)_{\text{pert}}} = \frac{2\sigma + 3}{3} \frac{r_0}{\delta r_0} F \quad \dots\dots(10)$$

where $\sigma = (1 - \alpha^2 Z^2)^{1/2}$; $\alpha = e^2/\hbar c$. This is essentially the result already obtained by Brix and Kopfermann (1949). It was shown in A that, avoiding the uncertainties of the perturbation theory arising from the neglect of the distortion of the electronic wave function in the nuclear interior, the I.S. depends only on

$$S = \int_0^r V r'^2 dr'$$

and the change in S between the two isotopes, r being outside the charge distribution (in our case $r \geq r_0$). The change δS_ϵ corresponding to δV_ϵ is

$$\delta S_\epsilon = \frac{Ze^2}{3} F r_0^2. \quad \dots\dots(11)$$

On the other hand the change in S due to a change in radius δr_ϵ is

$$\frac{Ze^2}{5} r_0^2 \frac{\delta r_\epsilon}{r_0}. \quad \dots\dots(12)$$

Equating (11) and (12) we obtain the equivalent change in radius δr_ϵ , which gives the same I.S. as δV_ϵ :

$$\frac{\delta r_\epsilon}{r_0} = \frac{5}{3} F. \quad \dots\dots(13)$$

It was shown in A that the I.S. is proportional to the equivalent change in radius obtained from δS as above. Thus if the change in radius corresponding to $\delta(\Delta E_v)$ is δr_0 , and since the radius itself is r_0 for both $\delta(\Delta E_v)$ and $\delta(\Delta E_\epsilon)$,

$$D_\epsilon = \frac{\delta(\Delta E_\epsilon)}{\delta(\Delta E_v)} = \frac{\delta r_\epsilon}{\delta r_0} = \frac{5}{3} F \frac{r_0}{\delta r_0}. \quad \dots\dots(14)$$

It is seen that the perturbation expression (10) reduces to this in the limit $Z \rightarrow 0$. We have

$$\frac{D_\epsilon}{D_{\epsilon, \text{pert}}} = \frac{5}{3 + 2\sigma}. \quad \dots\dots(15)$$

For Pb this is 1.1, and thus $D_{\epsilon, \text{pert}}$ is a rather good approximation. Also from (15), $\delta(\Delta E_\epsilon)/(\delta\Delta E_\epsilon)_{\text{pert}} \simeq 0.85$ for Pb if the value of $\delta(\Delta E_v)/\delta(\Delta E_v)_{\text{pert}}$ obtained for a uniform charge distribution in A is used.

With $r_0 = 1.4 \times 10^{-13} A^{1/3}$ and $\delta r_0/r_0 = 2/3A$, which is the model Brix and Kopfermann have used as a standard for comparison in presenting the I.S. data (denoted by the index N), we have from (9) and (14),

$$D_{\epsilon, N} = \frac{\delta(\Delta E_\epsilon)}{\delta(\Delta E_v)_N} = 1.35 \times 10^3 \frac{\gamma_{I_2}^2 Q_2^2 - \gamma_{I_1}^2 Q_1^2}{Z^2 A^{1/3}} \quad \dots\dots(16)$$

where Q is expressed in barns.

§ 4. RESULTS AND DISCUSSION

The I.S. data, apart from rather uncertain corrections of the order of unity due to the shielding of the inner electrons by the optical electron (see Humbach 1952),

have been presented by Brix and Kopfermann in the form $D_N = \delta(\Delta E) / \delta(\Delta E_v)_N$ where $\delta(\Delta E)$ is the experimentally determined I.S. In their most recent presentation (1951, 1952) the correction due to the distortion of the electronic wave function as calculated by Humbach (1952) has been included (see also A). If we assume that the effects of nuclear polarization as discussed by Breit, Arfken and Clendenin (1950) are small, we may write,

$$d = \frac{\delta(\Delta E_v)}{\delta(\Delta E_v)_N} = D_N - D_{\epsilon, N}.$$

Thus in order to test the theory of the deformation dependent I.S. it must be seen whether a reasonable value is obtained for d , the actual value of which must be assumed to be positive, if $D_{\epsilon, N}$ is determined from (16) and D_N is obtained from the observed data.

We first consider the I.S. between the two Eu isotopes ($Z=63$). The spin of both is $5/2$ and therefore from (7), $\gamma_{5/2}^2 \simeq 8$. The hyperfine structure and I.S. have recently been very thoroughly re-investigated by Brix (1952) who gives $s = Q(^{153}\text{Eu}) / Q(^{151}\text{Eu}) = 2.0$ and $D_N = 2.3$, where this value includes an estimate of the effect of the shielding of the inner electrons by the optical electron. Schuler and Korsching (1936) give $Q(^{151}\text{Eu}) = 1.2$ barns, which is considered somewhat uncertain as the electronic terms which can be used for its determination are perturbed, the error being of the order of 20%; however, s , the ratio of the quadrupole moments, is known much more accurately since it does not involve this uncertainty. Hence from (16)

$$D_{\epsilon, N} = 0.5(s^2 - 1)Q^2(^{151}\text{Eu}) \simeq 2.2 \pm 0.9$$

and $d = 2.3 - 2.2 = 0.1 \pm 1.0$.

The error indicated is that due to the error in the quadrupole moment. In view of the large errors involved in $Q(^{151}\text{Eu})$ and D_N and the uncertainties of the assumptions regarding the nuclear charge distribution the actual numerical value of d obtained cannot be considered as significant. However, the above results show very clearly that the anomalously large I.S. between the Eu isotopes can be readily explained as due to a difference in deformations. The whole, and not merely the jump, of the exceptionally large I.S. between ^{150}Sm and ^{152}Sm ($Z=62$) is then also readily explained if the deformations in this case are assumed to be somewhat less than those of the corresponding Eu isotopes. The still larger I.S. between ^{151}Eu and ^{153}Eu would then indicate that the extra proton increases the already large deformations of the Sm isotopes. In connection with the latter it is interesting to consider the application of an empirical rule given by Bohr (1951) to the isotopes ^{147}Sm , ^{149}Sm . This states that for two isotopes which differ by two neutrons and have the same value of I , the nucleus with the numerically smallest quadrupole moment has a magnetic moment closest to the appropriate Schmidt value. The theoretical justification is, according to Bohr, that the greater the deformation of the nucleus the more important will be the influence of the coupling of the angular momentum of the nucleons in unclosed shells with the motion of the core of the remaining nucleons, and the greater, consequently, is likely to be the deviation of the magnetic moment from the Schmidt value.

The spins of the odd neutron nuclei ^{147}Sm , ^{149}Sm are both $7/2$, while the magnetic moments are -0.3 and -0.25 nuclear magnetons respectively, the quadrupole moments not being known. The I.S. is approximately the same

as that between the other Sm isotope pairs (excepting ^{150}Sm and ^{152}Sm), and therefore rather large. The spins and magnetic moments agree with the configurations $(f_{7/2})^3$ and $(f_{7/2})^5$ predicted by the shell model, the magnetic moment of ^{147}Sm lying rather closer to the appropriate Schmidt value than that of ^{149}Sm . Bohr's rule thus predicts that $|Q(^{149}\text{Sm})| > |Q(^{147}\text{Sm})|$, and that therefore the deformation dependent I.S. tends to increase the volume dependent part. This would support the explanation of these rather large I.S. as due to a deformation dependent effect which then become exceptionally large for ^{150}Sm , ^{152}Sm and ^{151}Eu , ^{153}Eu .

The conjunction between the neutron numbers 88 and 90 of the I.S. jump observed both for Sm and for Nd ($Z=60$), together with the exceptionally large difference in quadrupole and magnetic moments of the Eu isotopes, seems to suggest that there is some change in the neutron configurations on the addition of the 45th pair of neutrons.

The only other isotopes for which both the spectroscopic quadrupole moments and the I.S. are known are ^{185}Re and ^{187}Re ($Z=75$). The spin of both is $5/2$. Schuler and Korsching (1937) give the two values $Q(^{185}\text{Re})/Q(^{187}\text{Re})=1.08$ and 1.02 which are obtained from different terms, the former being claimed as the more accurate; $Q(^{187}\text{Re})=2.6$ barns, there being good agreement between the values obtained from the two terms. The deformation dependent I.S. will thus act in the opposite direction to the volume dependent part. If we write $Q(^{185}\text{Re})/Q(^{187}\text{Re})=1+\beta$, $\beta \ll 1$, then

$$D_{\epsilon, N} = -4.6\beta = \begin{cases} -0.37, & \beta = 0.08, \\ -0.09, & \beta = 0.02. \end{cases}$$

On the other hand Brix and Kopfermann, using the data of Schuler and Korsching, give $D_N=0.35$. Thus $d=0.72$, $\beta=0.08$; $d=0.46$, $\beta=0.02$. There is thus in general the possibility, also present for isotopes without spectroscopic quadrupole moments, that the deformation dependent I.S. is sufficiently negative to reduce the I.S. to a very small or perhaps even negative value. This may then be the reason for the rather small I.S. of the elements from W ($Z=74$) to Pt ($Z=78$) inclusive.

Brix and Kopfermann have also suggested that the difference in the Re quadrupole moments may be connected with the decrease in the I.S. of the corresponding W isotopes, ^{184}W and ^{186}W . The relative spacing of the I.S. of the W isotopes is

^{180}W	^{182}W	^{184}W	^{186}W
-0.91	0	1	1.89

With the larger and more accurate value 1.08 for $Q(^{185}\text{Re})/Q(^{187}\text{Re})$ it would seem however that with deformations for ^{184}W , ^{186}W of approximately the same value as those of the corresponding Re isotopes, and including the difference between the spectroscopic and intrinsic quadrupole moments, $D_{\epsilon, N}$ is too large to account for just the rather small jump in the I.S. It seems more likely to suppose, as for the Sm isotopes, that the somewhat small I.S. of the W as well as of the Re isotopes is due to a negative deformation dependent I.S. and that the small I.S. jump between ^{184}W and ^{186}W is due to a change in this.

A case of some interest regarding the possibility of a very small I.S. is that of the iodine isotopes ^{127}I , ^{129}I ($Z=53$) for which the quadrupole moments but not the I.S. are known. The spin of ^{127}I is $5/2$ and $Q(^{127}\text{I})=-0.75$ barn, the corresponding quantities for ^{129}I being $7/2$ ($\gamma_{7/2}^2=4.6$) and $Q(^{129}\text{I})=-0.43$ barn.

From (16), $D_{\epsilon, N} = -0.35$. It must be remarked that the model of an ellipsoidal nucleus is not likely to be a very good description in this case as the quadrupole moments are rather near the single particle values expected on the basis of the simple shell model. The order of magnitude of the deformation dependent I.S. obtained is nevertheless likely to be correct and the I.S. between ^{127}I and ^{129}I can be expected to be rather small.

The reason for the very small I.S. of the elements Xe ($Z=54$) and Ba ($Z=56$) which follow iodine may then be due to a large negative deformation dependent I.S. In this connection it is interesting to consider the application of Bohr's rule to the odd neutron isotopes ^{135}Ba and ^{137}Ba . These each have a spin of $3/2$ and the magnetic moments 0.832 and 0.936 nuclear magneton respectively, the quadrupole moments not being known. The values are not far from the $d_{3/2}$ Schmidt value, suggesting the neutron configuration $(d_{3/2})^1$ and $(d_{3/2})^3$, which are in good agreement with the prediction of the shell model. The magnetic moment of ^{137}Ba is nearest the Schmidt value, this isotope having just one neutron less than the magic number 82. Bohr's rule predicts that $|Q(^{137}\text{Ba})| < |Q(^{135}\text{Ba})|$, and that therefore the deformation dependent I.S. will act in the opposite direction to the volume dependent part. This would seem to support the explanation that the deformation dependent I.S. may be partly responsible for the small I.S. of Ba. It would be of great interest to know the quadrupole moments of ^{135}Ba and ^{137}Ba .

Certain indications about deformations may be obtained from the I.S. and magnetic moments of isotopes with a spin $\frac{1}{2}$, which of course have no spectroscopic quadrupole moment, if a plausible extension of Bohr's rule is made by considering the nuclear deformation rather than the quadrupole moment. The only two isotopes with a spin $\frac{1}{2}$ which come into consideration at present are those of the odd proton elements Ag ($Z=47$) and Tl ($Z=81$). The magnetic moments of ^{107}Ag , ^{109}Ag are -0.159 and -0.086 nuclear magneton respectively, both being near the $p_{1/2}$ Schmidt value, in good agreement with the shell model. That of ^{109}Ag is somewhat closer to the Schmidt value, and therefore the deformation dependent I.S. should be negative. It is not however likely that this is very appreciable in view of the normal value of the I.S. and also of the fact that since the magnetic moments of both isotopes are rather close to the Schmidt value their deformations will probably be small. The magnetic moments of ^{203}Tl and ^{205}Tl are 1.596 and 1.612 nuclear magnetons respectively and are somewhat closer to the $s_{1/2}$ than the $p_{1/2}$ Schmidt value, which is reconcilable with the shell model. The magnetic moment of the heavier isotope is closest to the Schmidt value and the deformation dependent I.S. should be negative. There is no indication from the experimental I.S. that this is significant. This is perhaps not surprising in view of the very nearly equal magnetic moments, suggesting that their deformations also differ little.

Finally we mention two cases which are of interest:

1. The spins of ^{121}Sb and ^{123}Sb ($Z=51$) are $5/2$ and $7/2$ respectively. The quadrupole moments have very recently been redetermined spectroscopically by Sprague and Tomboulion (1953), who find $Q(^{121}\text{Sb}) = -1.3$ and $Q(^{123}\text{Sb}) = -1.7$ barns. These are very different from those accepted previously. The I.S. is not known. From (16) $D_{\epsilon, N} = -0.023$ which is small, and thus the I.S. can be expected to have a normal value. This might indicate that the unknown I.S. between Cd and Xe have values of the order of those expected by linearly interpolation between the values for Cd and Xe.

2. The two isotopes ^{171}Yb , ^{173}Yb ($Z=70$) have spins of $1/2$ and $5/2$ respectively. $Q(^{173}\text{Yb}) = +3.9$ barns and is exceptionally large. $D_N \simeq 0.3$, and although somewhat on the small side, is not abnormally so, thus $D_{\epsilon, N}$ cannot be expected to be numerically very large and will almost certainly be less than 0.5 in magnitude. One obtains

$$\frac{\epsilon(^{171}\text{Yb})}{\epsilon(^{173}\text{Yb})} \simeq 1 - \frac{1}{12} D_{\epsilon, N}.$$

This shows that even though the deformation of ^{173}Yb is so large, $\epsilon(^{173}\text{Yb}) \simeq 1/3$, that of ^{171}Yb can only differ very little. In fact since the relative spacings of the I.S. are

^{171}Yb	^{172}Yb	^{173}Yb	^{174}Yb	^{176}Yb
0	0.62	1	1.38	2.1

the deformations of all the isotopes must be very nearly the same, which seems rather remarkable in view of the estimated large magnitude of these. It should however be mentioned that although the spin of ^{173}Yb would be in agreement with the shell model configuration $(f_{5/2})^3$, the magnetic moment is nearer the wrong Schmidt value. This may perhaps be due to an error in its determination, which is based on optical hyperfine structure measurements, in which case the same uncertainty would apply to the quadrupole moment.

From the foregoing, and in particular the example of the Eu isotopes, it must be considered as established, even in view of the rather large uncertainties involved, that a difference in the deformations of two isotopes can have an effect on the I.S. comparable, or even larger, in magnitude than the volume dependent part. The possibility must also be strongly entertained that the large variations observed in the I.S. may be due to this deformation dependent effect. The I.S. data could then be used to give information about the variation of nuclear deformations, providing a valuable test for theories of nuclear structure which involve a deformed core. Of special interest in this connection are the I.S. of a sequence of isotopes which all have a rather large or small I.S. This must then be taken as indicating that the deformations continuously increase or decrease respectively from one isotope to the next, and not that merely the difference in deformation between any two isotopes remains approximately the same. Thus the large I.S. of the Sm isotopes would indicate that all the isotopes from ^{144}Sm to ^{154}Sm have successively large deformations with an exceptionally large increase between ^{150}Sm and ^{152}Sm .

In conclusion it may be remarked that it is perhaps possible to explain the odd-even staggering of the I.S. as a deformation dependent effect. We consider the successive addition of neutrons into a shell of angular momentum j , the remaining nucleons being in closed shells. In the limit of strong coupling between the extra core neutrons and the deformation of the nuclear core these neutrons will move independently of each other, each having a definite component m_i of angular momentum along the symmetry axis. The deformation of the core is then given by

$$\epsilon \simeq -K \sum_i \frac{3m_i^2 - j(j+1)}{j(j+1)} \quad \dots\dots (17)$$

where K depends on the coupling constant and the deformability of the core, and the summation is over the extra core neutrons. In the ground state all the neutrons will be paired in an even neutron nucleus and all except one paired in an odd neutron nucleus. It follows that, for an even number of neutrons n ,

$$\epsilon_{n+2} - \epsilon_n = 2(\epsilon_{n+1} - \epsilon_n) \quad \dots\dots (18)$$

for if in the odd neutron nucleus the odd neutron is in the level (j, m) the additional neutron in the heavier nucleus will occupy the level $(j, -m)$. From (18) we get

$$\epsilon_{n+1}^2 = \frac{1}{2}(\epsilon_{n+2}^2 + \epsilon_n^2) - (\epsilon_n - \epsilon_{n+2})^2.$$

Assuming that the volume dependent part of the I.S. is the same for each of the neutrons added, the condition for odd-even staggering in the direction observed is $\epsilon_{n+1}^2 < \frac{1}{2}(\epsilon_{n+2}^2 + \epsilon_n^2)$, and we see that this is satisfied in the strong coupling limit. In this model there will also be differences between the isotope shifts of adjacent even-even (or odd-even) nuclei, which will in general be of the same order as the odd-even staggering.[†]

The direct interactions between the extra core neutrons will tend to couple these together to give a good total angular momentum leading to a smaller deformation of the core in even-even than in odd-even nuclei. In fact, when the direct coupling is very strong the deformation is of the first order in the coupling constant in odd-even nuclei, whereas it is a second-order effect in even-even nuclei (J. Rowlands, private communication). In this case there will also be an odd-even staggering but in the opposite direction to that when the coupling with the core is predominant. The direct interactions will thus in general tend to reduce any odd-even staggering due to the deformation of the core. Whether the variations of the nuclear deformation can actually explain consistently the odd-even staggering of any particular series of isotopes will require a more detailed investigation which would also have to take into account the possibility that the successive neutrons may not all go into the same shell.

ACKNOWLEDGMENTS

I am grateful to Professor L. Rosenfeld for the interest he has taken in this work and for helpful discussions. I would also like to express my gratitude to Professor J. H. D. Jensen for several interesting discussions. To Mr. J. Rowlands I would like to express my indebtedness for helping to clarify my ideas on the odd-even staggering of the I.S. and also with help on the presentation of this point. I am indebted to the British Rayon Research Association for a research grant which made this investigation possible.

REFERENCES

- BODMER, A. R., 1953, *Proc. Phys. Soc. A*, **66**, 1041, referred to as A.
 BOHR, A., 1951, *Phys. Rev.*, **81**, 134; 1952, *K. Danske Vidensk. Selsk. Dan. Mat. Fys. Medd.*, **26**, 14.
 BOHR, A., and MOTTELSON, B. R., 1953, *K. Danske Vidensk. Selsk. Dan. Mat. Fys. Medd.*, **27**, 16.
 BREIT, G., ARFKEN, G. B., and CLENDENIN, W. W., 1950, *Phys. Rev.*, **78**, 390.
 BRIK, P., 1952, *Z. Phys.*, **132**, 579.
 BRIK, P., and KOPFERMANN, H., 1949, *Z. Phys.*, **126**, 344; 1951, *Festschrift Akad. Wiss. Gött., Math.-Physik. Kl.*, 17; 1952, *Phys. Rev.*, **85**, 1050.
 HUMMACH, W., 1952, *Z. Phys.*, **133**, 589.
 RACAH, G., 1932, *Nature, Lond.*, **129**, 723.
 RAINWATER, J., 1950, *Phys. Rev.*, **79**, 432.
 ROSENTHAL, J. E., and BREIT, G., 1932, *Phys. Rev.*, **41**, 459.
 SCHULER, H., and KORSCHING, H., 1936, *Z. Phys.*, **103**, 434; 1937, *Ibid.*, **105**, 168.
 SPRAGUE, G., and TOMBOULIAN, D. H., 1953, *Phys. Rev.*, **92**, 105.
 WILETS, L., HILL, D. L., and FORD, K. W., 1953, *Phys. Rev.*, **91**, 1488.

[†] Essentially the same explanation of the odd-even staggering of the I.S. as above has been suggested by Wilets, Hill and Ford (1953).

On Bose-Einstein Functions

By J. CLUNIE

Department of Mathematics, University College of North Staffordshire,
Keele, Staffordshire

Communicated by P. T. Landsberg; MS. received 12th April 1954

Abstract. Asymptotic expansions are found for the integral $G_k(\eta)$ defined by

$$\int_0^\infty \frac{x^k dx}{\exp(x-\eta)-1} \quad \text{if } \eta \leq 0,$$

and as the Cauchy principal part of the same integral if $\eta > 0$. A table is constructed for $k = \frac{1}{2}$, and the ranges $-3 \leq \eta \leq -0.6$ (0.2), $-0.5 \leq \eta \leq 0.5$ (0.1), $0.6 \leq \eta \leq 20$ (0.2).

§ 1. INTRODUCTION

THIS paper generalizes some numerical results on Bose-Einstein functions which have recently been given by Robinson (1951). If P denotes the Cauchy principal part (Whittaker and Watson 1924, § 6.23), we consider the function

$$G_k(\eta) \equiv \begin{cases} \int_0^\infty \frac{x^k dx}{e^{x-\eta}-1}, & \eta \leq 0, & \dots\dots(1.1) \\ P \int_0^\infty \frac{x^k dx}{e^{x-\eta}-1}, & \eta > 0, & \dots\dots(1.2) \end{cases}$$

for $k > 0$. Expression (1.1) arises in connection with the usual theory of the perfect Bose-Einstein gas above its transition temperature; it also arises in the theory of ferromagnetism (Schafroth 1954 and references given there). Expression (1.2) has not so far had any important physical application, although integrals of this form would arise if the occupation probabilities of the states of a perfect Bose-Einstein gas of N particles were taken in the form

$$\frac{1}{e^{x-\eta}-1} = \frac{N+1}{e^{(x-\eta)(N+1)}-1}, \quad x \equiv \frac{E}{kT},$$

where η can assume positive values (Sommerfeld 1942, cf. also Landsberg 1954 and references given there).

Asymptotic formulae for $G_k(\eta)$ are presented for the case of large $|\eta|$, and for $k = \frac{1}{2}$ a numerical table is given for the range $-3 \leq \eta \leq 20$ within which the asymptotic formulae are not applicable. The results are tabulated at intervals of 0.2 outside the range $-0.5 \leq \eta \leq 0.5$. Within the latter range the interval has been taken as 0.1 because of the rapid variation of $G_{1/2}(\eta)$ in the neighbourhood of the origin.

§ 2. EVALUATION OF $G_k(\eta)$ FOR $\eta > 0$

Let

$$F_k(\eta) = \int_0^\infty \frac{x^k dx}{e^{x-\eta}+1}, \quad k > 0,$$

be a Fermi-Dirac integral. It may be shown that

$$G_k(\eta) = \sum_{r=0}^{n-1} 2^{-kr} F_k(2^r \eta) + 2^{-kn} G_k(2^n \eta), \quad \dots\dots(2.1)$$

It follows that if an asymptotic expansion is available for $G_k(\eta)$ then these integrals can easily be calculated from the table of Fermi-Dirac integrals for small η .

The behaviour of $G_k(\eta)$ for large η is derived as follows. By suitable changes in the variable of integration we have

$$G_k(\eta) = -\frac{\eta^{k+1}}{k+1} + \int_0^\infty \frac{(\eta+x)^k - (\eta-x)^k}{e^x - 1} dx + \int_\eta^\infty \frac{x^k dx}{e^x - 1}. \quad \dots\dots(2.2)$$

From the binomial theorem with integral remainder it follows that

$$(\eta \pm x)^k = \eta^k \sum_{r=0}^n \frac{k(k-1)\dots(k-r+1)}{r!} (\pm x/\eta)^r + R_n(\pm x), \quad \dots\dots(2.3)$$

where

$$R_n(\pm x) = \frac{k(k-1)\dots(k-n)}{n!} \left(\pm \frac{x}{\eta}\right)^{n+1} \int_0^1 (1-y)^n \left(1 \pm \frac{x}{\eta} y\right)^{k-n} dy. \quad \dots\dots(2.4)$$

If we take the maximum values of the integrands in (2.4) and assume that $x \leq \eta$ in $R_n(-x)$ and $k \leq n$ in $R_n(+x)$ we have

$$|R_n(+x)| < \frac{|k(k-1)\dots(k-n)|}{(n+1)!} \left(\frac{x}{\eta}\right)^{n+1} \quad \dots\dots(2.5)$$

and

$$|R_n(-x)| < \frac{|k(k-1)\dots(k-n)|}{n!} \left(\frac{x}{\eta}\right)^{n+1}. \quad \dots\dots(2.6)$$

From (2.2), (2.3) and (2.4) we get

$$G_k(\eta) = -\frac{\eta^{k+1}}{k+1} + 2\eta^k \sum_{r=0}^{n-1} \frac{k(k-1)\dots(k-2r)}{\eta^{2r+1}} \zeta(2r+2) + \mathcal{R}_n, \quad \dots\dots(2.7)$$

where

$$\begin{aligned} \mathcal{R}_n = & \eta^k \int_0^\infty \frac{R_{2n}(+x)}{e^x - 1} dx + \eta^k \int_0^\infty \frac{R_{2n}(-x)}{e^x - 1} dx \\ & + \eta^k \int_\eta^\infty \sum_{r=0}^{2n-1} (-)^r \frac{k(k-1)\dots(k-r+1)}{r!} \left(\frac{x}{\eta}\right)^r \frac{dx}{e^x - 1}. \quad \dots\dots(2.8) \end{aligned}$$

From (2.5) and (2.6) the first two terms in (2.8) have an absolute value not exceeding

$$\eta^k |k(k-1)\dots(k-2n)| (2n+z) \frac{\zeta(2n+2)}{\eta^{2n+1}}. \quad \dots\dots(2.9)$$

If

$$k(m) = \max_{1 \leq r \leq m} \left\{ 1, \frac{|k(k-1)\dots(k-r)|}{(r-1)!} \right\}, \quad \dots\dots(2.10)$$

then the third term in (2.8) is less in absolute value than

$$\frac{k(2n-1)(2n)! \eta^{k-2n+1}}{e^\eta - 1} \left\{ 1 + \eta + \frac{\eta^2}{2!} + \dots + \frac{\eta^{2n-1}}{(2n-1)!} \right\}. \quad \dots\dots(2.11)$$

From (2.9), (2.10) and (2.11) it is found that when $k = \frac{1}{2}$ the remainder after three terms in (2.7) amounts to less than half a unit in the third decimal place for $\eta \geq 20$.

§ 3. EVALUATION OF $G_k(\eta)$ FOR $\eta \leq 0$

When $\eta = 0$ then $G_k(0) = \Gamma(k+1) \zeta(k+1)$ (3.1)

When $\eta < 0$ we again use (2.1), but the asymptotic behaviour of $G_k(\eta)$ is now obtained as follows. It is not difficult to show that

$$G_k(\eta) = \sum_{r=1}^{n-1} \frac{\Gamma(k+1)}{r^{k+1}} e^{r\eta} + \int_0^\infty \frac{x^k e^{-n(x-\eta)}}{e^{x-\eta} - 1} dx. \quad \dots\dots(3.2)$$

Since

$$\int_0^\infty \frac{x^k e^{-n(x-\eta)}}{e^{x-\eta} - 1} dx < \frac{e^{-n|\eta|} \Gamma(k+1)}{|\eta| n^{k+1}}, \quad \dots\dots(3.3)$$

we see that in (3.2) the remainder after three terms is less than half a unit in the sixth decimal place, and after two terms is less than half a unit in the fourth decimal place for $k = \frac{1}{2}$, $\eta \leq -3$.

§ 4. EVALUATION OF $G_k(\eta)$ NEAR $\eta = 0$

The following details are taken from Robinson (1951). If

$$F(\sigma, \alpha) = \frac{1}{\Gamma(\sigma)} \int_0^\infty \frac{x^{\sigma-1}}{e^{x+\alpha} - 1} dx, \quad \sigma > 1, \quad \alpha > 0, \quad \dots\dots(4.1)$$

then the Mellin transform of $F(\sigma, \alpha)$ with respect to α is

$$\mathcal{F}(\sigma, s) = \int_0^\infty F(\sigma, \alpha) \alpha^{s-1} d\alpha = \Gamma(s) \zeta(\sigma+s). \quad \dots\dots(4.2)$$

By the inversion formula for the Mellin transform we have

$$\begin{aligned} F(\sigma, \alpha) &= \frac{1}{2\pi i} \int_{c-i\infty}^{c+i\infty} \mathcal{F}(\sigma, s) \alpha^{-s} ds \\ &= \frac{1}{2\pi i} \int_{c-i\infty}^{c+i\infty} \alpha^{-s} \Gamma(s) \zeta(\sigma+s) ds, \quad c > 0 \quad \dots\dots(4.3) \end{aligned}$$

when the contour ($c-i\infty$, $c+i\infty$) is suitably distorted. It follows that

$$F(\sigma, \alpha) = \Gamma(1-\sigma) \alpha^{\sigma-1} + \sum_{n=0}^\infty \frac{(-)^n}{n!} \zeta(\sigma-n) \alpha^n. \quad \dots\dots(4.4)$$

By analytic continuation this result holds for all non-integral σ . If $\sigma = m$, a positive integer, then

$$F(m, \alpha) = \frac{(-1)^{m-1}}{\Gamma(m)} \left\{ \gamma + \frac{\Gamma'(m)}{\Gamma(m)} - \log \alpha \right\} \alpha^{m-1} + \sum_{n=m-1}^\infty \frac{(-)^n}{n!} \zeta(m-n) \alpha^n, \quad \dots\dots(4.5)$$

where γ is Euler's constant.

The series expression is easily shown to be convergent for $|\alpha| < 2\pi$. Hence it follows that

$$\begin{aligned} G_k(\eta) &= \Gamma(k+1) F(k+1, -\eta), \quad -2\pi \leq \eta \leq 0 \\ &= \Gamma(k+1) \{ F(k+1, -\eta) - \Gamma(-k) (-\eta)^k \}, \quad 0 < \eta \leq 2\pi \quad k \neq m, \dots\dots(4.6) \end{aligned}$$

For $k = \frac{1}{2}$ it can be shown that neglect of

$$\sum_{n=5}^\infty \frac{(-)^n}{n!} \zeta\left(\frac{3}{2}-n\right) \alpha^n$$

will produce an error of at most one unit in the sixth decimal place.

Table of $G_{1/2}(\eta)$

$$G_{1/2}(\eta) \equiv \begin{cases} \int_0^\infty \frac{x^{1/2}}{e^{x-\eta}-1} dx, & \eta \leq 0, \\ \lim_{\delta \rightarrow 0} \left(\int_0^{\eta-\delta} + \int_{\eta+\delta}^\infty \right) \frac{x^{1/2}}{e^{x-\eta}-1} dx, & \eta > 0. \end{cases}$$

η	$G_{1/2}(\eta)$	η	$G_{1/2}(\eta)$	η	$G_{1/2}(\eta)$
-3.0	0.0449	4.0	-4.4810	12.2	-27.9362
-2.8	0.0551	4.2	-4.9085	12.4	-28.6415
-2.6	0.0676	4.4	-5.3441	12.6	-29.3524
-2.4	0.0831	4.6	-5.7879	12.8	-30.0688
-2.2	0.1022	4.8	-6.2396	13.0	-30.7908
-2.0	0.1260	5.0	-6.6997	13.2	-31.5181
-1.8	0.1558	5.2	-7.1673	13.4	-32.2510
-1.6	0.1938	5.4	-7.6426	13.6	-32.9892
-1.4	0.2403	5.6	-8.1258	13.8	-33.7327
-1.2	0.3012	5.8	-8.6165	14.0	-34.4816
-1.0	0.3790	6.0	-9.1149	14.2	-35.2357
-0.8	0.4839	6.2	-9.6207	14.4	-35.9951
-0.6	0.6253	6.4	-10.1340	14.6	-36.7597
-0.5	0.7183	6.6	-10.6546	14.8	-37.5294
-0.4	0.8314	6.8	-11.1825	15.0	-38.3043
-0.3	0.9745	7.0	-11.7175	15.2	-39.0843
-0.2	1.1654	7.2	-12.2597	15.4	-39.8694
-0.1	1.4502	7.4	-12.8089	15.6	-40.6595
0.0	2.3154	7.6	-13.3651	15.8	-41.4547
0.1	2.1849	7.8	-13.9282	16.0	-42.2548
0.2	2.0526	8.0	-14.4982	16.2	-43.0598
0.3	1.9185	8.2	-15.0749	16.4	-43.8698
0.4	1.7825	8.4	-15.6582	16.6	-44.6847
0.5	1.6445	8.6	-16.2483	16.8	-45.5045
0.6	1.5047	8.8	-16.8448	17.0	-46.3290
0.8	1.2190	9.0	-17.4481	17.2	-47.1584
1.0	0.9254	9.2	-18.0575	17.4	-47.9926
1.2	0.6236	9.4	-18.6734	17.6	-48.8315
1.4	0.3136	9.6	-19.2956	17.8	-49.6751
1.6	-0.0046	9.8	-19.9242	18.0	-50.5237
1.8	-0.3311	10.0	-20.5594	18.2	-51.3765
2.0	-0.6661	10.2	-21.2002	18.4	-52.2342
2.2	-1.0095	10.4	-21.8472	18.6	-53.0965
2.4	-1.3614	10.6	-22.5002	18.8	-53.9634
2.6	-1.7220	10.8	-23.1592	19.0	-54.8349
2.8	-2.0909	11.0	-23.8242	19.2	-55.7110
3.0	-2.4682	11.2	-24.4950	19.4	-56.5916
3.2	-2.8540	11.4	-25.1718	19.6	-56.4767
3.4	-3.2482	11.6	-25.8543	19.8	-58.3663
3.6	-3.6508	11.8	-26.5426	20.0	-59.2610
3.8	-4.0618	12.0	-27.2366		

§ 5. CONSTRUCTION OF TABLE

The table was constructed by using (2.1) with $2^n\eta \geq 20$ for η positive and $2^n\eta \leq -3$ for η negative, in conjunction with the table of Fermi-Dirac integrals of McDougall and Stoner (1938). In the latter table the error is less than one unit in the fifth decimal place from which it follows that the error in ours is certainly less

than one unit in the fourth decimal place. The values in $-0.5 \leq \eta \leq 0.5$ were also calculated by means of (4.1) and this provided an independent check on the results in this range. The other results were checked by means of differences.

ACKNOWLEDGMENT

This paper is the result of discussions with Dr. P. T. Landsberg, of the University of Aberdeen, Scotland, and I am indebted to him for advice and criticism.

REFERENCES

- LANDSBERG, P. T., 1954, *Proc. Camb. Phil. Soc.*, **50**, 65.
MCDUGALL, J., and STONER, E. C., 1938, *Phil. Trans. Roy. Soc. A*, **237**, 67.
ROBINSON, J. E., 1951, *Phys. Rev.*, **83**, 678.
SCHAFROTH, M. R., 1954, *Proc. Phys. Soc. A*, **67**, 33.
SOMMERFELD, A., 1942, *Ber. dtsh. chem. Ges.*, **75**, 1988.
WHITTAKER, E. T., and WATSON, G. N., 1924, *Modern Analysis* (Cambridge : University Press).

RESEARCH NOTES

Note on the Positive Temperature Coefficient of the Cosmic Radiation

By J. C. BARTON

University College of the West Indies

MS. received 26th March 1954

ALTHOUGH the explanation given by Duperier (1948) for the positive upper-air temperature effect of the cosmic radiation has been verified qualitatively, the experimental results have been higher than those predicted theoretically. One possible explanation of this discrepancy has recently been suggested by Trefall (1953), who has shown that any difference between the mean height of production and the reference height used for the meteorological data may greatly affect the theoretically predicted value. This analysis is still not entirely satisfactory as it is assumed that all the mesons arise at the one height. A more detailed analysis of this type, assuming that the mesons are produced throughout the atmosphere and allowing for the temperature variation at each level, would appear to be very difficult. Olbert (1953) has made some progress in this direction, but only by ignoring completely the effects of π -meson decay and interaction.

It seems to be preferable to avoid the very complicated variations which the atmosphere displays in its daily behaviour and instead to work in terms of monthly averages. It is then very nearly true that the height of any particular pressure level depends only on the temperature throughout the atmosphere and the sea-level pressure, so that there is one less term in the correlation analysis. This has the further advantage that we can make use of the method of Barrett *et al.* (1952), who take account of the distributed production of mesons by means of an 'effective temperature'. The experimental result of these workers, who were making measurements at 1574 m water equivalent, is double the value expected, but the statistical accuracy is such that this difference is not necessarily significant. Sherman (1954), observing for a longer period at a depth of 846 m water equivalent, obtained a result in reasonable agreement with that expected.

Since this method of calculation appears to be the most reliable yet used it is interesting to apply it to the observations of MacAnuff (1951) who, working in London at a depth of 60 m water equivalent, found a temperature coefficient of $+0.058 \pm 0.010\%$. The temperature used in the analysis was that of the 100 mb layer, and the only other variable was the sea-level pressure. The theory for this depth predicts a positive temperature effect of 0.08% due to π -decay and a negative effect of 0.06% due to μ -decay, giving an expected value of $+0.02\%$. The discrepancy with the experimental value is considerable and it does not seem possible to explain it on the lines of Trefall's suggestion.

The main purpose of this note is to point out a possible way of reconciling this discrepancy. Since the variations in monthly averages of temperature at various heights in the troposphere over England are not very different from the

variation at 100 mb, using the 'effective temperature' would not appear to alter the results greatly. Recently, however, it has been established that there are very large changes of temperature in the lower stratosphere. At heights above 20 km Scrase (1951) has found that the seasonal temperature variation increases rapidly with height; it is more than three times greater at 30 km than at 20 km, and has roughly the same phase. It is of course true that this part of the atmosphere is above the region of maximum meson production, and that more of the mesons found here decay before they reach sea level, but the temperature variation is so great that it will certainly make an appreciable difference to the expected temperature coefficient, particularly for the more energetic mesons observed underground.

The effects to be expected from both π - and μ -decay will thus be different from those calculated using the temperature variation of the 100 mb layer. Using the 'effective temperature' of Barrett *et al.* (1952) for the π -decay effect, where

$$T_{\text{eff}} = \frac{\int_{x=0}^{h_0} T(x)e^{-x/\lambda} dx}{\int_{x=0}^{h_0} e^{-x/\lambda} dx},$$

we find that Scrase's data leads to an effective temperature variation which is roughly double that of the 100 mb layer. For the μ -decay it seems again reasonable to define an effective temperature which is now given by

$$T'_{\text{eff}} = \frac{\int_{z=\infty}^0 T(x)(1 - e^{-x/\lambda}) dz}{\int_{z=\infty}^0 (1 - e^{-x/\lambda}) dz}.$$

Since μ -decay occurs predominantly in the lower part of the atmosphere, the fluctuations near sea level become of importance comparable with those in the stratosphere. Putting in figures for the whole atmosphere gives a value of T'_{eff} about 50% greater than the temperature variation of the 100 mb layer.

Thus the final theoretical value for the temperature effect is

$$2 \times 0.08 - 1.5 \times 0.06 = 0.07\%$$

which is in better agreement with the experimental result.

The above considerations are far from precise, but they do indicate the importance of temperature variations in the atmosphere. In fact their importance has still been underestimated, since no allowance has been made for particles arriving at an angle to the vertical or for those mesons produced by heavy nuclei in the primary radiation. The calculations were made assuming $\lambda = 120 \text{ g cm}^{-2}$, which is certainly not correct for other than hydrogen primaries. It hardly seems worth trying to estimate the magnitude of these corrections with the scanty data at present available.

It is not certain how far other measurements of the positive temperature coefficient can be interpreted in a similar way. From the meteorological data quoted by Barrett *et al.* the atmosphere over New York appears to behave in a more complicated way than that over London. There is however again an indication of increasing temperature variations in the stratosphere. Similarly the day to day behaviour which is analysed in Duperier's work cannot be treated

in terms as simple as those used for MacAnuff's results. But we suggest that any analysis which ignores the variations in the stratosphere may well lead to spurious results.

I am indebted to Dr. E. P. George for discussions of this problem.

REFERENCES

- BARRETT, P. H., BOLLINGER, L. M., COCCONI, G., EISENBERG, Y., and GREISEN, K., 1952, *Rev. Mod. Phys.*, **24**, 133.
 DUPERIER, A., 1948, *Proc. Phys. Soc.*, **61**, 34.
 MACANUFF, J. W., 1951, *Thesis*, University of London.
 OLBERT, S., 1953, *Phys. Rev.*, **92**, 454.
 SCRASE, F. J., 1951, *Quart. J. R. Met. Soc.*, **77**, 483.
 SHERMAN, N., 1954, *Phys. Rev.*, **93**, 208.
 TREFALL, H., 1953, *Nature, Lond.*, **171**, 888.

Non-Equilibrium Thermodynamics of Thermal Transpiration of a Dissociating Gas

BY R. P. RASTOGI* AND R. C. SRIVASTAVA†

Departments of Chemistry* and Physics†, Lucknow University, India

MS. received 9th March 1954

IT has been shown by kinetic methods (Srivastava 1940) that when two vessels containing a dissociating gas are connected by a narrow opening, the diameter of which is smaller than the mean free path, the usual transpiration relation and the law of mass action cannot be satisfied simultaneously. The phenomenon cannot be treated by classical thermodynamics. Accordingly we have employed the 'thermodynamics of irreversible processes' developed considerably in recent years (de Groot 1952, Denbigh 1951). De Groot has investigated the thermomolecular pressure effect involving isomeric reactions, particularly in liquid He II. Following de Groot, it is found that for a reaction of the type $X_n \rightleftharpoons nX$ we have for the stationary state of the first order when ΔT is fixed

$$\Delta P/\Delta T = (h + c_1 L_1 + c_2 L_2)/vT \quad \dots\dots(1)$$

$$\Delta c_1/\Delta T = \frac{c_2}{vT} [v_2(h_1 + L_1) - v_1(h_2 + L_2)] / \left(\frac{\partial \mu_1}{\partial c_1} \right)_{T,P} \quad \dots\dots(2)$$

and the affinity for the two chambers is given by

$$\frac{A^I}{T^I} \frac{1}{\Delta T} = \frac{L_{cc}'}{L_{cc} + L_{cc}'} \frac{1}{T^2} [nL_2 - L_1]; \quad \frac{A^{II}}{T^{II}} \frac{1}{\Delta T} = \frac{-L_{cc}}{L_{cc} + L_{cc}'} \frac{1}{T^2} [nL_2 - L_1] \quad \dots\dots(3)$$

where

$$L_1 = \frac{nL_{cc}L_{cc}'(L_{2V} + nL_{1V}) + (L_{cc} + L_{cc}')(L_{1V}L_{22} - L_{2V}L_{12})}{(L_{cc} + L_{cc}')(L_{12}^2 - L_{11}L_{22}) - L_{cc}L_{cc}'(n^2L_{11} + 2nL_{12} + L_{22})}$$

$$L_2 = \frac{L_{cc}L_{cc}'(L_{2U} + nL_{1V}) + (L_{cc} + L_{cc}')(L_{2U}L_{11} - L_{1V}L_{12})}{(L_{cc} + L_{cc}')(L_{12}^2 - L_{11}L_{22}) - L_{cc}L_{cc}'(n^2L_{11} + 2nL_{12} + L_{22})}$$

and $h = c_1 h_1 + c_2 h_2$; $v = c_1 v_1 + c_2 v_2$. In these expressions the subscript 1 refers to the species X_n and 2 to the species X ; c represents the concentration, h and v denote the specific enthalpy and specific volume. The L 's are the

phenomenological coefficients. L_{cc} and L_{cc}' are the phenomenological coefficients associated with the chemical reaction in Chambers I and II respectively. Chamber II is maintained at a higher temperature. It may be stressed that from kinetic considerations it can be shown that L_{cc} and L_{cc}' are different in the two chambers (Srivastava *et al.* 1954).

For testing the theory these expressions are hardly useful as they all involve so many coefficients which are difficult to determine. But on eliminating L_1 and L_2 the above equations yield for the affinity the relation

$$\frac{A^I}{T^I \Delta T} = \frac{L_{cc}'}{L_{cc} + L_{cc}'} \frac{1}{T^2} \left[T \left(\frac{\Delta P}{\Delta T} \right) (nv_2 - v_1) + T \left(\frac{\partial \mu_1}{\partial c_1} \right) \left(\frac{\Delta c_1}{\Delta T} \right) \left(1 - \frac{nc_1}{c_2} \right) + (h_1 - nh_2) \right]. \quad \dots\dots(4)$$

For a mixture of perfect gases and binary dissociation this simplifies to

$$\frac{A^I}{T^I \Delta T} = \frac{L_{cc}'}{L_{cc} + L_{cc}'} \frac{R}{T} \left[\frac{3}{2M_2} \frac{\Delta \log P}{\Delta \log T} + \left(1 - \frac{2c_1}{c_2} \right) \frac{\Delta \log c_1}{\Delta \log T} - \frac{15}{4M_2} \right]. \quad \dots\dots(5)$$

Thus the observed pressure, temperature and concentration differences can give the value of the affinity in either chamber, thereby indicating the shift in equilibrium. This can provide a check for the theory when the results are compared with those obtained from thermal or equilibrium data. It may be pointed out that Denbigh and Raumann (1952) have been able to show only a partial correspondence between theory and experiment because of difficulty in estimating the heats of transfer from theoretical considerations.

Experiments are being set up and the detailed paper will be published elsewhere.

Our thanks are due to Prof. B. N. Srivastava for suggesting the problem and for useful advice.

REFERENCES

- DENBIGH, K. G., 1951, *Thermodynamics of the Steady State* (London: Methuen).
 DENBIGH, K. G., and RAUMANN, G., 1952, *Proc. Roy. Soc. A*, **210**, 377, 518.
 DE GROOT, S. R., 1952, *Thermodynamics of Irreversible Processes* (Amsterdam: North-Holland Publishing Company).
 SRIVASTAVA, B. N., 1940, *Proc. Roy. Soc. A*, **175**, 474.
 SRIVASTAVA, B. N., RASTOGI, R. P., and VARMA, A. S., 1954, in the press.

The Effect of Contaminating Gases on the Energy per Ion Pair in Helium

BY G. A. ERSKINE

Physics Department, University College, London

Communicated by H. S. W. Massey; MS. received 10th March 1954

RECENT measurements by Jesse and Sadauskis (1952) show that when small amounts of A, Kr, Xe, or CO₂ are added to helium the energy W per ion pair for incident α -particles falls, and continues to fall, until a saturation value is reached, beyond which there is no further change as the concentration of contaminating gas is increased. The ionization potentials of these four gases are each less than the least excitation potential of helium, and Jesse and Sadauskis suggest that the observed drop in W is caused by the production of ion pairs in

two-body collisions between excited helium atoms and atoms of the contaminant gas X :



This process is likely to account for the de-activation of most of the long-lived metastable helium atoms. Owing to the trapping of resonance radiation, the effective lifetime of all excited helium atoms may be very long, and the majority of excitation collisions between α -particles and helium atoms may lead eventually to the production of ion pairs through the de-activation process (1). In calculating W for comparison with the 'saturation' value measured in the presence of a contaminant we therefore consider two alternative assumptions :

- (a) That each metastable helium atom can be counted as an ion pair.
- (b) That *every* excited helium atom can be counted as an ion pair.

Assumption (b) provides a lower bound to the calculated value of W in the presence of a contaminant.

If N is the number of helium atoms per cm^3 , and Q_1 is the cross section for the ionization of helium by α -particles, the total number of ion pairs produced per cm of α -particle path in pure helium is $N(Q_1 + Q_1')$, where NQ_1' is the number produced by secondary, tertiary, etc., electrons. Denoting by $N(EQ)_{\text{ex}}$ and $N(EQ)_i$ the energy loss per cm in discrete excitation collisions and ionizing collisions respectively, W for pure helium is given by

$$W = \frac{(EQ)_{\text{ex}} + (EQ)_i}{Q_1 + Q_1'}. \quad \dots\dots(2)$$

If the value of W in the presence of a contaminant is calculated using assumption (a) above, it is necessary to calculate the total number of metastable helium atoms, $\rho(x)$, produced when an electron with energy x is absorbed in helium. The energy per ion pair is then

$$W_a = \frac{(EQ)_{\text{ex}} + (EQ)_i}{Q_1 + Q_1' + Q_m + Q_m'} \quad \dots\dots(3)$$

where Q_m is the cross section for the production of a helium metastable by collision with an α -particle and

$$Q_m' = \int Q(E_\alpha, x) \rho(x) dx. \quad \dots\dots(4)$$

Here $Q(E_\alpha, x) dx$ is the differential cross section for the ejection from a helium atom of an electron with energy between x and $x + dx$, the energy of the incident α -particle being E_α . All the terms occurring in (2), (3) and (4) except $\rho(x)$, Q_m and Q_m' have been evaluated in connection with a detailed calculation of W for pure helium (Erskine 1954).

The function $\rho(x)$ satisfies the integral equation

$$\rho(x) = p_m^{\text{ex}}(x) + p_{\text{ex}}^{\text{ex}}(x) \rho(x - 22) + \int_0^{x-1} \pi(x, y) [\rho(x - I - y) + \rho(y)] dy \quad \dots\dots(5)$$

which differs from equation (15) of the pure helium calculation of Erskine (1954) only in having $p_m(x) = q_m(x)/q_{\text{in}}(x)$ in place of $p_i(x)$. For $q_m(x)$ we use Dorrestein's (1942) cross section for the production of helium metastables by electrons. The integral equation is then solved numerically.

In case (b), the function $\sigma(x)$ which gives the number of helium ions *plus* the number of excited helium atoms produced by an electron with energy x satisfies the

integral equation obtained from (5) by replacing $p_m(x)$ on the right-hand side by 1. Then, on defining

$$Q'_{ex+i} = \int Q(E_\alpha, x) \sigma(x) dx,$$

the energy per ion pair corresponding to assumption (b) is

$$W_b = \frac{(EQ)_{ex} + (EQ)_i}{Q_i + Q_{ex} + Q'_{ex+i}}.$$

The data required for the calculation of σ from the integral equation which it satisfies are exactly the same as those used in calculating the function J from equation (15) of the pure helium calculation (Erskine 1954).

The calculations were carried out at α -particle energies of 1, 2, . . . , 6 mev, yielding the following values :

E_α (mev)	1	2	3	4	5	6	Av. calc. W	Meas. W (0.5-3 mev)
W (pure He) (ev)	40.3	41.1	41.2	41.4	41.1	41.5	41.1	42.7
W_a (ev)	34.4	35.1	35.4	35.5	35.1	35.6	35.2	} 29.7
W_b (ev)	28.4	28.8	29.4	29.6	29.6	29.9	29.3	
								(He + A)

The measured values are those of Jesse and Sadauskis (1952), $W = 29.7$ ev being the saturation value corresponding to an argon concentration of 0.13%. The experimental values refer to the complete absorption of a polonium α -particle, i.e. to α -particle energies from 5.3 mev down to zero. The calculated values refer to α -particles of an exactly specified energy.

These results show that, on the assumption that the increase in ionization resulting from the addition of a contaminant to helium is due entirely to the process (1), the calculated W can be reduced to that measured by Jesse and Sadauskis for an argon contaminant only by assuming that *all* excited helium atoms lead eventually to ion pairs. The alternative assumption, that only metastable atoms are involved in the production of additional ion pairs, does not appear to reduce the calculated W sufficiently. When krypton or xenon is used in place of argon as a contaminant the saturation value of W (Kr 28.7 ev, Xe 28.4 ev) lies slightly below the calculated 'lower bound' $W_b = 29.3$ ev. The uncertainty of the data used in the theoretical calculations is such that the calculated values might well be in error by as much as 1 ev; and there does not, therefore, appear to be any serious discrepancy between Jesse and Sadauskis' measurements and the calculation based on the assumption that all the energy expended in exciting helium atoms is eventually dissipated in the process (1).

ACKNOWLEDGMENTS

I wish to thank Dr. E. H. S. Burhop for his advice on this problem, and the University of London for the award of an I.C.I. Research Fellowship.

REFERENCES

- DORRESTEIN, R., 1942, *Physica*, **9**, 447.
 ERSKINE, G. A., 1954, *Proc. Roy. Soc. A*, in the press
 JESSE, W. P., and SADAUSKIS, J., 1952, *Phys. Rev.*, **88**, 417. (The values of W quoted above are as revised by Jesse in a Quarterly Report of the Argonne National Laboratory, Chicago, U.S.A., November 1952.)

The Principal Magnetic Susceptibilities of the Maleic Acid Molecule HOOC·HC : CH·COOH

By M. P. GUPTA

Department of Physics, Patna University, India

Communicated by K. Lonsdale ; MS. received 7th April 1954

LONSDALE and KRISHNAN (1936) have shown that the principal magnetic susceptibilities of a molecule can be calculated if the principal crystal susceptibilities are measured and if the orientations of the molecules in the crystal lattice are known by x-ray methods or otherwise. The present note gives the values of the principal susceptibilities of the maleic acid molecule, the molecular and the crystal structure of which have recently been established, using x-ray diffraction data, by Shahat (1952). The calculations are based on the values of the principal crystal susceptibilities as measured by Lonsdale (1939):

$$\chi_1 = -43.34 \times 10^{-6}, \quad \chi_2 = -62.32 \times 10^{-6}, \quad \chi_3 = -42.90 \times 10^{-6}$$

$$\bar{\chi} = \frac{\chi_1 + \chi_2 + \chi_3}{3} = -49.52 \times 10^{-6} \text{ c.g.s. e.m.u.}$$

(001) is the plane of χ_1, χ_3 , the crystals being magnetically nearly uniaxial.

Shahat (1952) gives the following values for the angles χ, ϕ, ω which the molecule makes with the a, b and c crystallographic axes respectively of the crystal:

	L	M	N
χ (deg.)	108.0	19.6	88.5
ϕ (deg.)	18.0	70.4	88.5
ω (deg.)	121.3	121.4	31.3

The L axis is the line in the molecular plane bisecting the C=C bond at right angles. It is a line of pseudo-mirror symmetry. The M axis is the line parallel to C=C and the N axis is perpendicular to the L, M axes. Using the above data, and following the treatment of such data as given by Lonsdale and Krishnan (1936), one obtains the following values for the principal molecular susceptibilities of the maleic acid molecule:

$$X_L = -41.99 \times 10^{-6}, \quad X_M = -44.27 \times 10^{-6}, \quad X_N = -62.32 \times 10^{-6} \text{ c.g.s. e.m.u.}$$

These values may be compared with the values obtained for related molecules by Lonsdale (1938, 1939):

	X_L	X_M	X_N
Oxalic acid	-53.13	-52.73	-62.40×10^{-6}
Succinic acid	-53.11	-48.58	-60.67
Benzoquinone	-24.3	-28.7	-67.1

The anisotropy in the plane of the maleic acid molecule must be a dimensional effect. The susceptibility is numerically greater along the longer axis. The big anisotropy $X_N - X_M$, almost one-half that of benzoquinone and about one-third that of benzene itself, must be associated with some degree of mesomerism in the molecule, which has a ring structure of which one side is an internal H bond, 2.46 Å in length.

It would be interesting to see how this anisotropy compares with that of the trans-isomer, fumaric acid, which has the same double bonds and in which the molecules are certainly joined externally by H bonds, but in which the individual molecules have no ring structure. Fumaric acid, however, forms poor small crystals and neither its magnetic susceptibilities nor its crystal structure have as yet been adequately determined.

REFERENCES

- LONSDALE, K., 1938, *J. Chem. Soc.*, 364; 1939, *Proc. Roy. Soc. A*, **171**, 541.
LONSDALE, K., and KRISHNAN, K. S., 1936, *Proc. Roy. Soc. A*, **156**, 597.
SHAHAT, M., 1952, *Acta Cryst., Camb.*, **5**, 763.

A Modified Scintillation Pair Spectrometer

BY B. HIRD AND C. WHITEHEAD

The Clarendon Laboratory, Parks Road, Oxford

Communicated by C. H. Collie; MS. received 1st April 1954

THE three-crystal scintillation pair spectrometer (Johansson 1952) is more efficient than the magnetic deflection type. It is thus suitable for examining γ -ray spectra of high energy and low intensity.

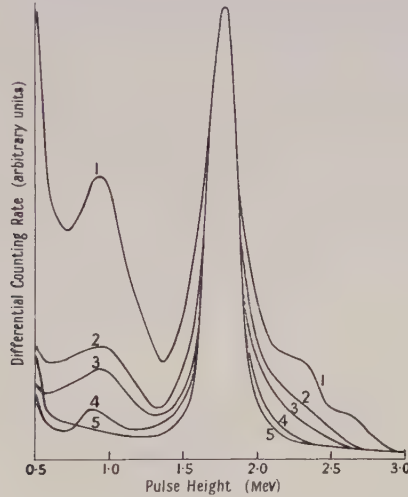
However, in these circumstances Johansson's method suffers from a practical defect. Since the spectrum measured with a single crystal is only difficult to interpret when more than one γ -ray is emitted, the pair spectrometer will be most useful in the analysis of complex spectra. In such spectra it is probable that some of the γ -rays will be emitted in cascade, and unless the side crystals are shielded from direct radiation more coincidences will be produced than those due to the pair production process in the centre crystal. A pair of γ -rays in cascade can cause an unwanted triple coincidence if the Compton electron and the Compton scattered photon of one γ -ray are captured in different crystals. In this way Compton edges appear in the pulse height distribution, thus defeating the purpose of the three-crystal method. The unwanted effect can be eliminated by collimating the γ -ray beam to fall only on the centre crystal but if this is to be done effectively the source must be placed at least 10 cm from the crystal, which then reduces the already low counting rate by a large factor.

We have modified the spectrometer so as to discriminate against unwanted coincidences; weak sources can then be used near the centre crystal. The side crystal pulses are accepted only if they are of a height corresponding to annihilation radiation, both larger and smaller pulses being rejected.

A ^{24}Na source was chosen to test the apparatus because it emits two γ -rays in coincidence, and they are in the energy region where the Compton effect predominates. The spectrum was examined with different pulse height apertures for the side crystals, these apertures being identical for the two side crystals.

The results are shown graphically in the figure. Each curve is normalized to give the same number of counts in the 2.76 MeV γ -ray pair peak. The source was placed 1 cm from the centre crystal in all cases; it decayed from 5 μC to 2 μC during the experiment.

With no rejection of larger pulses from the side crystals the Compton distributions of the 1.38 Mev and the 2.76 Mev γ -rays are prominent (curve 1). As expected, their intensity relative to the pair peak decreases as the aperture is narrowed. Since annihilation radiation is detected about equally as full energy pulses and as Compton scatter pulses the pair counting rate was expected to fall to one quarter when the aperture was narrowed to exclude these Compton pulses in the side crystals (curve 3).



With a still narrower aperture (curve 4) a six-fold rejection of the Compton edges, relative to the pair peak, was obtained at the expense of a seven-fold decrease in the pair spectrometer efficiency.

In order to compare results with the distribution when Compton pulses were completely absent curve 5 was obtained by using a strong well-collimated source.

1-inch cubic NaI (Tl) crystals were used with EMI 6260 photomultipliers and with a resolving time for the side crystals of $0.2 \mu\text{sec}$ and of $1.1 \mu\text{sec}$ for the centre crystal.

REFERENCE

JOHANSSON, S. A. E., 1952, *Phil. Mag.*, **43**, 249.

LETTERS TO THE EDITOR

The Spontaneous Fission Rate of ^{240}Pu

This note, which is published as a result of a recent security de-classification, contains a summary of experiments, carried out some years ago at Harwell, in which the spontaneous fission rate of ^{240}Pu was measured. Two samples were used, both composed predominantly of ^{239}Pu . The first (A) contained 3.86% and the second (B) 5.58% of ^{240}Pu , determined by mass spectrometer analysis. Both samples also contained small amounts of ^{241}Pu , detected with the mass spectrometer, and of ^{238}Pu , found by α -particle pulse analysis.

The specific α -particle activities (disintegrations $\text{sec}^{-1} \mu\text{g}^{-1}$) of the two samples were measured. This made it possible to determine the masses of plutonium used in the main experiments by α -particle counting. The spontaneous fission rates were measured in a simple ionization chamber. Almost the whole of the observed rate can be attributed to ^{240}Pu , since the rate for ^{239}Pu is known to be so low (Segrè 1952) that its contribution can be neglected, while that from the trace of ^{238}Pu is small and can be allowed for.

The ^{240}Pu content of the samples was measured with a mass spectrometer in which the plutonium sample was mounted on a tungsten strip filament, and steady production of plutonium oxide ions was ensured by a method similar to that described by Hand (1953). The filament was first treated with Sauereisen cement, and about $10 \mu\text{g}$ of plutonium nitrate solution was then pipetted on to the surface. When the filament was heated the nitrate decomposed, and, at about 1000°C ion beams of PuO_2^+ , PuO^+ and Pu^+ were detected. These are produced by a thermal ionization process at the tungsten surface. Only the PuO_2^+ ion beams were large enough for successful analysis, although confirmatory results were obtained with PuO^+ beams. More than twenty measurements of the ratios in height of the peaks corresponding to ^{239}Pu , ^{240}Pu and ^{241}Pu were made. Corrections for the presence of ^{17}O and ^{18}O were applied.

The results, expressed in atoms per cent, were

	Sample A	Sample B
^{239}Pu	95.88	94.03
^{240}Pu	3.86 ± 0.06	5.58 ± 0.08
^{241}Pu	0.26 ± 0.02	0.39 ± 0.02

It has been possible to compare the results from one of the samples with analyses made in two other laboratories using mass spectrometers of somewhat different design, and agreement within 1% was found.

An α -particle analysis was also performed on suitable sources from samples of A and B using a low-geometry methane proportional counter (Hurst and Hall 1952) together with a 30-channel pulse analyser, the channel widths of which were set to correspond to about 30 keV in α -particle energy. Two peaks were observed in the α -particle spectrum, the higher corresponding to ^{238}Pu , and the lower containing both ^{239}Pu and ^{240}Pu , whose α -particle energies are almost identical. Although the contribution of ^{238}Pu to the α -particle activity is easily measurable, this represents a negligible amount by weight. Because of the high spontaneous fission rate of this isotope a correction must nevertheless

be applied. The following figures are based on a half-life for α -decay of 90 years, and a spontaneous fission rate of $5.1 \times 10^6 \text{ g}^{-1} \text{ h}^{-1}$:

Sample	A	B
$\% \text{ } ^{238}\text{Pu} \left\{ \begin{array}{l} \text{by } \alpha\text{-activity} \\ \text{by weight} \end{array} \right.$	2.48 ± 0.4 0.0097	4.16 ± 0.05 0.017
Spontaneous fissions ($\text{mg}^{-1} \text{ h}^{-1}$)	0.50	0.87

Uniform deposits containing about 0.2 to 0.3 mg cm^{-2} of plutonium on strips of platinum foil were prepared. The technique was similar to that described by Rossi and Staub (1949) and Glover (1954). The foils used for fission counting were stamped out of these strips.

The mass of plutonium on the foils was determined by counting the α -particles in the low-geometry counter. To convert the α -disintegration rate to a mass of plutonium it is necessary to know the specific activity of each sample. This cannot be calculated accurately from the known half-lives and the isotopic compositions and must be found experimentally. Accordingly the concentration of the plutonium in the stock solution used for each foil was determined for sample A by a gravimetric method, in which the plutonium was weighed as dioxide, and for sample B, by spectrophotometric analysis (Hall and Herniman 1952). The α -particle emission rates of aliquot parts of the solutions were measured in the low-geometry counter, and the overall specific activities were obtained. The value for the mass of plutonium on the foil A was $0.86 \pm 0.01 \text{ mg}$ and on foil B $0.42 \pm 0.01 \text{ mg}$.

The spontaneous fission rates of the two samples were measured in a simple ionization chamber similar to that described by Barclay and Whitehouse (1953). The chamber was surrounded by cadmium and placed inside a cube of paraffin wax to eliminate the possibility of neutron-induced fissions in ^{239}Pu . Small corrections, each of the order of 1% or less, were made for the dead time of the apparatus, for the slope of the bias curve, and for the fragments absorbed in the foil. The precautions against spurious pulses (e.g. photographing oscilloscope traces of the fission pulses) and the statistical checks mentioned by Barclay and Whitehouse (1953) were also applied. The corrected fission rates, after subtracting the contributions from ^{238}Pu , were 52.7 ± 2.0 per hour for foil A and 38.2 ± 0.5 per hour for foil B.

From the values of the fission rates, the weights of plutonium on the foils and the percentages of ^{240}Pu , the spontaneous fission rates may be calculated: sample A $(1.59 \pm 0.07) \times 10^6 \text{ g}^{-1} \text{ h}^{-1}$, sample B $(1.63 \pm 0.05) \times 10^6 \text{ g}^{-1} \text{ h}^{-1}$. The weighted mean of these results is $(1.62 \pm 0.04) \times 10^6 \text{ fissions g}^{-1} \text{ h}^{-1}$. A value of 1.66×10^6 has recently been published (Chamberlain, Farwell and Segrè 1954). This result is in accord with the approximate linear relation reported by Seaborg (1952) and by Whitehouse and Galbraith (1952) between the spontaneous fission rates of even-even nuclei and the value of Z^2/A (see also Huizenga 1954).

Atomic Energy Research Establishment,
Harwell,
Didcot,
Berkshire.
6th May 1954.

F. R. BARCLAY.
W. GALBRAITH.
K. M. GLOVER.
G. R. HALL.
W. J. WHITEHOUSE.

- BARCLAY, F. R., and WHITEHOUSE, W. J., 1953, *Proc. Phys. Soc. A*, **66**, 447.
 CHAMBERLAIN, O., FARWELL, G. W., and SEGRÈ, E., 1954, *Phys. Rev.*, **94**, 156.
 GLOVER, K. M., 1954, *Atomic Energy Research Establishment Report C/R. 1359*.
 HALL, G. R., and HERNIMAN, P. D., 1952, *Atomic Energy Research Establishment Report C/R. 975*.
 HAND, J. E., 1953, *Rev. Sci. Instr.*, **24**, 181.
 HUIZENGA, J. R., 1954, *Phys. Rev.*, **94**, 158.
 HURST, R., and HALL, G. R., 1952, *Analyst*, **77**, 790.
 ROSSI, B. B., and STAUB, H. H., 1949, *Ionization Chambers and Counters* (New York : McGraw-Hill).
 SEABORG, G. T., 1952, *Phys. Rev.*, **85**, 157.
 SEABORG, G. T., and KATZ, J. J., 1954, *The Actinide Elements* (New York : McGraw-Hill) Chap. 20.
 SEGRÈ, E., 1952, *Phys. Rev.*, **86**, 21.
 WHITEHOUSE, W. J., and GALBRAITH, W., 1952, *Nature, Lond.*, **169**, 494.

The Temperature Dependence of Ferromagnetic Resonance in Colloidal Nickel

The measurements of ferromagnetic resonance in colloidal suspensions (Bagguley 1953) have been extended to investigate the temperature dependence of the line width and spectroscopic splitting factor g for nickel between 20°K and 750°K. For these colloids the line width is half the measured separation in magnetic field between points of maximum slope for the absorption line and the g value is obtained directly from the relation

$$h\nu = g\beta H \quad \dots\dots (1)$$

when anisotropy effects are neglected.

From measurements on nickel foil Bloembergen (1950) concluded that the g value was constant between room temperature and the Curie point (631°K). Our measurements, shown in figure 1, give a more accurate confirmation of this

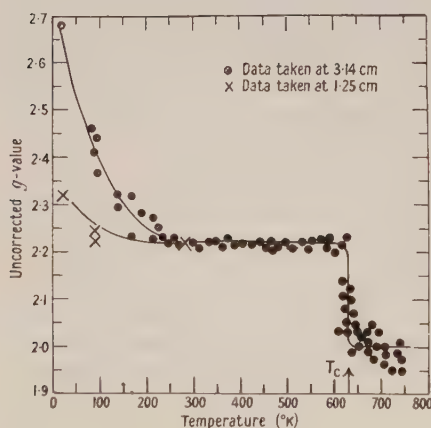


Figure 1. Uncorrected g value plotted against temperature for colloidal nickel.

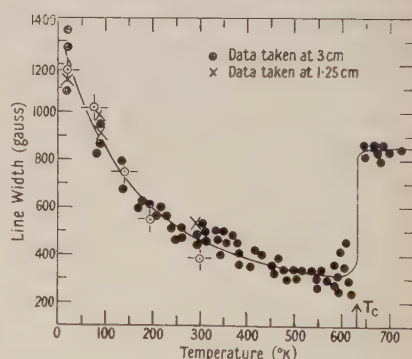


Figure 2. Line width plotted against temperature for nickel colloid.

—○— from anisotropy data.

suggestion and show that in addition a discontinuity occurs at the Curie point where the g value falls from 2.22 ± 0.02 to 2.00 ± 0.05 . Below room temperature, the g value obtained from equation (1) is frequency dependent and increases

continuously down to 20°K. The measured line width, given in figure 2, has an anomaly near the Curie point where it increases rapidly from a minimum value of 350 gauss $\pm 10\%$ to about 850 gauss $\pm 30\%$ in the paramagnetic region.

A first order expansion of the general resonance condition (Van Vleck 1950) shows that for an assembly of randomly oriented, non-interacting, spherical crystallites the effect of magnetic anisotropy is to broaden the resonance line and to shift the resonance peak. The order of magnitude for each effect is $K_1/2M_s$, where K_1 is the first order anisotropy constant and M_s is the saturation magnetization and so effects due to anisotropy will be particularly important below room temperature where K_1 is known to be large (Brukhatov and Kirensky 1937, Bozorth 1951). Since the displacement of the resonance peak is a constant field deviation, the g value derived from equation (1) will be frequency dependent and only approach the true value at the higher measuring frequencies. The g values given in figure 1 are in qualitative agreement with this interpretation but the displacement of the resonance peak, although of the correct sign, is somewhat less than $K_1/2M_s$ if the true g value is taken to be constant and equal to 2.22 below the Curie point. Quantitative agreement would be fortuitous however as the shift is also dependent on the single crystal line width.

The measured line width is broader than that for a single crystal because of the contribution $K_1/2M_s$ from anisotropy. Representative values of $K_1/2M_s$ have been plotted in figure 2 and good agreement is obtained by assuming that the single crystal line width is about 350 gauss and independent of temperature. Above room temperature the anisotropy constants are not well established but the continuous decrease in measured line width is consistent with the usual trend of these quantities towards zero at the Curie point.

The considerable change in the g value which occurs at the Curie point is unexpected and is not readily explained by the present theories of ferromagnetism. It seems likely that both the g value and the line width for a single crystal are constant below this temperature and there do not appear to be any changes in the line width due to the spin-lattice relaxation. Further measurements on other substances are in progress.

One of us (N.J.H.) wishes to acknowledge a fellowship from the National Research Council of Canada.

Clarendon Laboratory,
Oxford.
15th April 1954.

D. M. S. BAGGULEY.
N. J. HARRICK.

BAGGULEY, D. M. S., 1953, *Proc. Phys. Soc. A*, **66**, 765.

BLOEMBERGEN, N., 1950, *Phys. Rev.*, **78**, 572.

BOZORTH, R. M., 1951, *Ferromagnetism* (New York: D. Van Nostrand Co.).

BRUKHATOV, N. L., and KIRENSKY, L. V., 1937, *Phys. Z. Sowjet*, **12**, 602.

VAN VLECK, J. H., 1950, *Phys. Rev.*, **78**, 266.

REVIEWS OF BOOKS

Experimental Nuclear Physics, Vols. 1 and 2, edited by E. SEGRÈ. Pp. ix + 789, viii + 600. (New York: John Wiley; London: Chapman and Hall, 1953.) 120s. and 96s.

It appears much more difficult to write a coherent and integrated account of a vast and growing scientific subject from an experimental than from a theoretical standpoint. Theory represents, or should do, the logically connected framework of the subject, whereas experiment may include large sprawling areas of investigation, as yet uncoordinated, but possibly of great significance in the future of the subject. Moreover the techniques of experiment are so varied, and real familiarity with any one takes so long to acquire, that an individual can usually only write authoritatively on one or two topics; and the more rapid the growth and range of experimental technique the more specialized the experimentalist becomes.

Experimental nuclear physics, with its prodigious progress of the past couple of decades, presents these difficulties to the would-be textbook writer in a marked degree, and they are fully in evidence in the present volumes. The problem of specialization has been solved by abandoning the attempt to present the *whole* subject from a single viewpoint (apart from the extent to which this is achieved by the editorial choice of content). The first two volumes contain some half-dozen complete, independent monographs, ranging in standard and style and with little *direct* relation to each other.

It is not possible for the reviewer to judge the comprehensiveness of the work as a whole, since at least one further volume is in preparation, and even then the nature of the compilation does not ensure, or necessarily aim at presenting, a complete picture of the subject. Rather can he judge each article separately in relation to the purpose stated in the editor's preface: to "bring the experimenter up to date in experimental technique, point out to him the important facts and data, and indicate the broad lines of theoretical interpretation". The individual contributors have, as might have been expected, devoted varying proportions of their attentions to these three distinct aims.

The first article, on "Detection Methods", by H. H. Staub, is very much in the textbook style that is so useful to newcomers to a field of research or a technique. Unfortunately this subject has moved so rapidly since 1950, when the article was written, that the relative amounts of space devoted to such subjects as ionization chambers and scintillation counters, or cloud chambers and photographic emulsions, no longer reflects the relative importance of these subjects in "up-to-date experimental technique". The decision to include circuit instrumentation must have been a difficult one to make, and it can hardly be expected that the treatment should be more than introductory in less than 50 pages. This article provides a particularly good introductory account of the physical principles involved in particle detection, and also of many of the more detailed techniques as they stood some three or four years ago.

The article of H. A. Bethe and J. Ashkin on the "Passage of Radiation through Matter" is of a very different type. The whole subject, both theory and

experiment, is treated as part of the experimental nuclear physics. Experimental material is presented but the article is dominated by the theoretical outlook. It contains, as we have come to expect from the first author, a wealth of most useful charts and tables concerning the passage of heavy particles, mesons, electrons and γ -radiation through matter. It is an exhaustive, professional survey article summarizing the present state of the subject matter rather than introducing one to it. It concludes with a very useful bibliography with some 500 references.

The third article, by N. F. Ramsay, treats the subject of "Nuclear Moments and Statistics" with roughly equal space devoted to theory, technique and results. Some of the theoretical arguments appear a trifle unconvincing, possibly due to an attempt to compress and simplify the material. The account of experimental technique, particularly the molecular beam work, provides a good overall picture of this field, but does not perhaps quite convey the 'atmosphere' of the actual experiments. This article ends with a useful, although inevitably dated, table of mechanical, electric and magnetic nuclear moments, a very brief indication of the significance of this data, and a list of no less than 700 references.

Part IV, also by N. F. Ramsay, appears a little out of place in this series. It is a short (90 pages) article on the "Nuclear Two-Body Problem and the Elements of Nuclear Structure", most of which is devoted to the *theory* of nucleon-nucleon interaction. One might have expected that an account of the direct experimental study of nucleon-nucleon interaction would have provided sufficient material for a much fuller article, and that the very cursory account (13 pages) of the structure of complex nuclei could have been omitted.

The last part of volume I contains two really very different, although connected, articles by K. T. Bainbridge: "Charged Particle Dynamics and Optics", and "Relative Isotopic Abundances of the Elements and Atomic Masses". Some 50 pages are devoted to the general theory of particle focusing and its application to particular cases. About 70 pages are devoted to a *detailed* account of the techniques of mass spectrometry as applied to measurements of isotopic abundances and exact masses. This article is, perhaps, the only place in either of the two volumes in which the reader really feels he is somewhere near the laboratory. He is told, not only of the experimental 'methods' and results, but also something of the elusive 'gremlins' which are certainly not exclusive to mass spectrometry. The account is completed by 85 pages of tables of Q -values, isotopic abundances, atomic masses and some 800 references.

One third of volume II is occupied by an article by P. Morrison in which the *theory* of nuclear reactions is surveyed. No attempt is made to describe or discuss the experimental methods in detail and only occasional references are made to particular experimental results. The theory is presented rather sketchily and the argument is not always free from minor slips and careless mis-statements. Although this article presents a useful and readable account of some aspects of nuclear theory, one is a little puzzled to understand its place in a volume entitled *Experimental Nuclear Physics*, and when, moreover, much of the material is dealt with in the companion volume, *Theoretical Nuclear Physics*. The references at the end of this article are helpfully classified according to subject, a procedure which might well have been followed in some of the very extensive bibliographies at the end of other articles.

The remaining two-thirds of volume II is an extensive article by B. Field on "The Neutron". In it is an account of such matters as neutron scattering, capture and disintegrations; production of neutrons and techniques for their detection; diffusion of neutrons and the elements of pile theory; the coherent scattering of neutrons in solids, liquids and gases, and, in particular, the use of the intense beams of neutrons from piles as a tool in the study of the solid state.

The balance between experimental methods, results and theoretical interpretation is well kept throughout, although there are times when somewhat more intimate description of experimental methods would be welcome, perhaps at the expense of some of the theory presented. The classification of neutrons as 'slow', 'intermediate', 'fast', 'very fast' and 'ultrafast' is hardly elegant, and a more explicitly quantitative notation would not be too difficult to invent or too clumsy to use. This article is written in a loose colloquial style (e.g. "... there is observed, superposed on the evaporated neutrons, a strong forward peak of ultrafast neutrons...") which is, perhaps, more disturbing to English than American sensibilities. The article concludes with an impressive, but unclassified, collection of some 700 references.

The collection of articles contained in the first two volumes of this work will certainly be of great value, particularly to young research workers starting experimental investigation in nuclear physics. As 'permanent' textbooks they suffer from too wide a range of interest, style and viewpoint in the individual contributions. The extensive bibliographies (some 3500 references in all, mostly unclassified) are of limited value when one considers the inevitable two years that must elapse between compilation and utilization. Much shorter, selected bibliographies, with some guide to help the student find his way through the immense literature, would be more appropriate to a 'textbook', leaving the exhaustive lists of references for the less permanent journal review article. If this work, or its future editions, is to fulfil a definite need, and is to take its place in the 'permanent' literature of the subject, then the editor and contributors might well consider how they can adhere more clearly to their defined aim, and share a more uniform level of presentation.

S. DEVONS.

Nuclear Theory, by ROBERT G. SACHS. Pp. xi+283 (Cambridge, Mass.: Addison-Wesley Publishing Co., 1953). \$7.50.

Professor Sachs begins his book with a statement that the end product of nuclear physics should be a quantitative description of nuclear interactions. However pessimistic one may feel about this view—for one might be hard put to it to deduce the inverse-square law from the spectra of molecules, for example—the author consistently presents his material with this idea in mind. That is, he concerns himself mainly with the interpretation of complex nuclear phenomena in terms of simple concepts such as the static two-body potential, and takes pains to show to what extent such concepts may be sufficient.

It is consequently not surprising to find that over one-third of the book is devoted to a thorough and up-to-date account of the two-body problem, supplemented by an appendix which contains numerical results of the deuteron ground state problem including tensor forces. This part of the book by itself constitutes a most useful monograph.

The author goes on to treat the structure of complex nuclei, again with the problem of nuclear forces uppermost in mind. He includes a short account of

the shell model, and a full discussion of the restrictions put upon an exchange potential by the requirements of saturation. There follows an excellent chapter on the electromagnetic properties of nuclei; here, as elsewhere in the book, the author gives us the full benefit of his special knowledge of exchange currents in nuclei. There is an omission in this otherwise complete chapter in that no mention is made of internal pair production in $0 \rightarrow 0$ transitions.

The chapter on nuclear reactions is disappointing, being mainly a condensed version of the dispersion theory of Wigner and Eisenbud. Condensation has here led to a measure of unintelligibility happily lacking in the rest of the book. A more simplified treatment, containing fewer purely formal and bewildering manipulations, and combined with a fuller discussion of the validity of the one-level formula, might have been more in keeping with the author's general purpose. It is also disappointing to find such useful concepts as the isotopic spin selection rules so summarily dismissed in two brief paragraphs. The final section of this chapter, however, treats briefly, but with great clarity, the deuteron stripping reactions. One general criticism of the whole book is particularly pertinent here: this difficult chapter contains not a single diagram.

The final chapter deals fully with the allowed β -transition. Following the general tenor of the book, it ends with an attempt to deduce some of the constants of the β -interaction from the allowed ft -values of the lightest nuclei. No mention is made of forbidden transitions; nor is there any attempt to correlate ft -values with nuclear models, except for the brief remark that some support for the shell model has been provided in this way.

One gets the impression that the book is lacking in balance and that the author has put together a number of monographs. For example, the standard of prior knowledge required of the reader fluctuates considerably. Certainly the density of diagrams decreases as the book proceeds, with an ensuing lack of clarity. A few more diagrams in the latter chapters, a little less about the two-body system, and a little more about β -decay would have improved the balance greatly.

Some of the appendices are of doubtful worth, but the index is excellent, as, too, is the printing.

B. H. F.

Experimental Nucleonics, by E. BLEULER and G. J. GOLDSMITH. Pp. xv + 393. (London: Pitman, 1953.) 30s.

This laboratory manual was published in the United States in 1952 and has now been re-issued, without revision, in an English edition. It consists of twenty-four experiments, each preceded by a long explanatory section. The range of subjects covered is wide, and, apart from the Introduction, is divided into sections entitled General, Chemical, and Physical Techniques. It would be quite impossible to mention all the topics covered by these experiments, but a few examples will illustrate the scope of the book. The student is instructed how to separate his own radioactive material from natural sources, such as spent radon tubes, or from pile- or cyclotron-irradiated targets. (Nearly all the experiments can be done with natural sources, with the aid of a small neutron source, or with radioactive isotopes obtainable from the U.S. Atomic Energy Commission or from Harwell.) In the general section there is a very thorough series of experiments on counting methods, and on the measurement of the energies of β -particles and γ -rays by absorption. There are also several experiments with

neutron sources, illustrating the effect of a moderator, neutron activation, resonance capture, and so on. The chemical section includes, among other subjects, separation by solvent extraction, by ion exchange and by electrochemical means, the Szilard-Chalmers reaction, and a short section on radioelements as tracers. The physical section includes experiments on the range-energy relations of α -particles, the use of nuclear emulsions, and introduces the student to fairly advanced methods for investigating decay schemes by coincidence and absorption methods, and by simple magnetic analysis. There is also a short, probably inadequate, section on cosmic radiation. Any student who works through the experiments will acquire an excellent grounding from which to start research in nuclear physics, reactor technology or in the applications of radioactive isotopes.

The instructions for carrying out the experiments are usually clear, precise and adequate, and, although referring exclusively to American components and techniques (what is the *cookie sheet*, referred to on p. 34 ?), should be followed quite easily by English readers. Some experiments of historical importance are included, for which, quite rightly, old-fashioned or improvised apparatus is recommended, but in general the apparatus and methods described are commendably up to date. The well-written explanatory sections are not strictly confined to the subject in hand and, taken together, contain enough matter for a good textbook. The method of presentation adopted might, however, make it difficult to read up any topic in a systematic way.

Any criticisms of this book tend to be little more than expressions of personal prejudice, since it would be difficult to strengthen some sections without either weakening others, or adding inordinately to the length. The reviewer thought that the introductory sections on laboratory techniques and health precautions were hardly adequate for anyone who was faced with the responsibility of running a laboratory. On the other hand they did not take the form of a clear set of rules which the student might be expected to learn and obey. For instance, the tolerance levels for inhaled or ingested radioactive material, and their effects on the body, are hardly mentioned. The methods of handling radioactive waste are treated very briefly, and the advice given on p. 15, "Accumulated waste is to be buried", might be positively dangerous.

The methods for 'absolute' β -particle counting based upon calibrations with RaD, RaE and UX, which are used in some of the experiments, are not very reliable, and have in the past led to considerable errors. The student is not clearly warned against these. Coincidence methods for absolute measurements of disintegration rates are adequately treated later in the book. The technique of ' 4π ' counting is not employed, although it was well developed by the time the book was published, and has proved to be one of the most useful. The less reliable methods which depend upon finding the solid angle subtended by the counter are mentioned in several places, but the arrangements suggested are not the best. Thus the student is not left with a really sound grounding in methods of standardization, which is a pity, because the correct methods are not fundamentally more difficult than the incorrect.

The reviewer thought the subject of Radioelements as Tracers was inadequately treated. Although it is described in a general way in the introductory section to Experiment 15, the student is only given one experiment (to measure the solubility of PbSO_4). Even this does not illustrate the fundamental properties of isotopic tracers, as the authors admit when they say "the information can be

gained more accurately through the use of conventional techniques, but probably not so easily and quickly".

These, however, are only the opinions of a single reader. There is little doubt that this is the best laboratory course in the group of subjects covered by the name Nucleonics. It should be useful when planning the experimental work for an Honours Course in Physics. The standard of work is fairly high, and some of the experiments may be too much for technical college students, or even for post-graduate students working outside their own subjects. Nevertheless the book is almost a necessity to anyone who is training either technicians or potential users of radioactive tracers.

W. J. WHITEHOUSE.

Physikalisches Wörterbuch, by W. H. WESTPHAL. Pp. v + 833 + 795. (Berlin : Springer-Verlag, 1952.) D.M. 148.

When one reads in such an authoritative work as the *Oxford Dictionary* that an interference fringe is "one of a series of alternate light and dark bands produced by a diffraction grating", the need for specialist technical dictionaries is more than apparent. Moreover, a little thought is sufficient to show that a dictionary of physics must be radically different from a dictionary of words. To describe the adjectival use of 'Hamiltonian' by the phrase "pertaining to or invented by the Irish mathematician, Sir William Rowan Hamilton", is semantically impeccable so far as the conventional lexicographer is concerned, but the meanings that the word carries for the physicist are left unmentioned. More often than not the understanding of the meaning of a word or phrase in physics entails learning new facts and merely accepting the word or phrase as the accepted label for the given phenomenon.

In English there appears to be only the *Dictionary of Applied Physics*, and this is now very much out of date—but pure physics lacks even this. It is regrettable therefore that linguistic considerations may prevent many English-speaking physicists from possessing the volume under discussion. A person who knows the German word 'Ergodenhypothese', for example, is more than likely to know enough about statistical mechanics not to need to refer to a short dictionary article. However, a good English-German scientific dictionary used as an intermediary, not to mention the almost completely international word vocabulary of physics, should make the use of this *Physikalisches Wörterbuch* quite practicable.

The material of the book has been prepared by some eighty collaborators under the editorship of Professor Westphal. The list of contributors, all but three of whom are from Germany, contains a reassuring number of workers with international reputations. There are more than 1600 pages, of large format, and well printed in double columns on excellent paper. The number of entries exceeds 10 000, and the text contains 1595 figures. The material is very up to date, and an emphasis seems to have been given (unexpectedly) to theoretical and mathematical physics. Recent attempts to formulate a divergence-free quantum electrodynamics, for example, are described and references given.

The binding of the book is of a quality most of us long thought forgotten. A sample of entries revealed in most cases clarity and concise description. Every library, and many individuals, should possess a copy.

H. H. HOPKINS.

CONTENTS OF SECTION B

	PAGE
Dr. P. W. TREZONA. Additivity of Colour Equations: II	513
Dr. J. C. BURFOOT. Third-Order Aberrations of 'Doubly Symmetric' Systems .	523
Dr. C. G. WYNNE. The Primary Aberrations of Anamorphic Lens Systems .	529
Dr. A. HALPERIN. The Formation of Trigon on Diamonds	538
Dr. G. ECKER and Prof. K. G. EMELÉUS. Cathode Sputtering in Glow Discharges .	546
Dr. H. A. WHALE. A Rotating Interferometer for the Measurement of the Directions of Arrival of Short Radio Waves	553
Mr. C. RUBENSTEIN. The Influence of Creep on the Measured Hardness of Soft Metals	563
Dr. G. BLACK. Ray Tracing on the Manchester University Electronic Computing Machine	569
Mr. J. B. GUNN. The Theory of Rectification and Injection at a Metal-Semi- conductor Contact	575
Research Notes :	
Dr. D. B. HODGES. A Comparison of the Rates of Change of Current in the Step and Return Processes of Lightning Flashes	582
Mr. J. E. GOULD and Dr. M. McCAIG. Anhysteretic Magnetization of Alcomax III	584
Letters to the Editor :	
Mr. J. E. PARROTT. The Effects of Heat Flow on Thermoelectric Power in Semiconductors	587
Mr. G. G. E. LOW. Properties of Point Contacts on Cobaltite	589
Reviews of Books	591
Corrigendum (GOLDSMID)	599
Contents of Section A	600



PROFESSOR R. WHIDDINGTON, C.B.E., M.A., D.Sc., F.R.S.
President of the Physical Society 1952–54.

(The Presidential Address is published in the August issue of the
Proceedings, B, page 601.)

The Scattering of 15.7 MeV Neutrons by ^4He

By M. H. ALSTON, A. V. CREWE, W. H. EVANS,
L. L. GREEN AND J. C. WILLMOTT

Nuclear Physics Research Laboratory, University of Liverpool

Communicated by H. W. B. Skinner; MS. received 2nd March 1954

Abstract. The angular distribution of the α -particles from collisions with 15.7 MeV neutrons has been studied using a diffusion cloud chamber. The results indicate that a $D_{5/2}$ phase shift slightly smaller than the hard sphere value must be used to obtain the best fit.

§ 1. INTRODUCTION

THE scattering of neutrons by α -particles has been studied for the neutron energies 0.4 to 2.73 MeV by Adair (1952) using a proportional counter, and for neutrons up to 4.14 MeV by Huber and Baldinger (1952) using an ionization chamber. An attempt has been made by Dodder and Gammel (1952) to explain the results of these experiments and similar ones on p - α scattering in terms of virtual levels in the mirror nuclei ^5He , ^5Li . They have calculated the phase shifts to be expected in each case assuming the same nuclear parameters for ^5He and ^5Li . However, these data only fix the position and widths of the ground states and first excited states, which are $P_{3/2}$ and $P_{1/2}$ respectively, and give no information about the D-wave phase shifts. A study of n - α scattering at higher energies should provide some information about the D-wave phase shifts, and hence about the existence of the $D_{5/2}$ and $D_{3/2}$ levels in ^5He .

In the present work the angular distribution of the α -particles from collisions with 15.7 MeV neutrons has been studied using a diffusion cloud chamber. This method has the advantage that with one gas pressure all angles except small neutron scattering angles may be studied, and much of the background of scattered particles can be eliminated by a suitable choice of reprojection system.

§ 2. EXPERIMENTAL METHOD

A Philips 1 MeV accelerator was used to produce a beam of 700 keV deuterons, which struck a tritium target. The neutrons produced in this reaction entered a diffusion cloud chamber at 44° to the direction of the deuteron beam. The chamber was placed with its beam entry port 20 inches away from the target and was filled with a mixture of helium and nitrogen. The neutrons entering the chamber had an energy of 15.7 MeV and produced α -particle recoils of range 10 cm in the forward direction. The cloud chamber would not operate successfully if the background radiation was much greater than normal cosmic radiation level, and consequently the h.t. set was pulsed. The deuteron beam was allowed to strike the target for 0.2 second every 15 seconds.

Stereoscopic photographs of the scattering events were taken on 100-foot lengths of 70 mm film (Ilford 5G91). In the present experiment seven reels of

film were taken, providing 1223 photographs with a total of 3061 measurable scattering events. The recoil particles were examined by means of a reprojection apparatus which was designed to facilitate the measurement of scattering angles and the ranges of scattered particles: only those scattered particles which were produced by neutrons entering the chamber through the beam entry port were accepted for measurement.

The diffusion chamber has already been described (Crewe and Evans 1952, Alston, Crewe and Evans 1954). It is of mild steel, 18 in. in diameter, with a top glass 12 in. in diameter. The chamber was illuminated through side ports 10 in. wide and $2\frac{1}{2}$ in. high, and the particles entered the chamber through a beam entry port $1\frac{3}{4}$ in. in diameter mid-way between the two illumination ports. The tracks were photographed through the glass top plate. The base of the chamber was cooled by acetone which flowed through copper tubes soldered to the base and also through a tank containing a mixture of dry ice and methanol. The inside of the chamber was covered with black velvet, and a pool of methanol was maintained on the base in order to smooth out any temperature variations in the velvet, and also to provide a good photographic background.

For the present experiment the chamber was filled with $3\frac{1}{2}$ atmospheres of helium and $\frac{1}{4}$ atmosphere of nitrogen. With methanol as the vapour, a sensitive depth of $2\frac{1}{2}$ –3 inches could be maintained, provided that the level of background radiation was not much greater than normal cosmic-ray level. This particular mixture of gases was chosen in order to make the range of the recoil α -particles of reasonable value and at the same time to ensure stable conditions in the chamber.

The accelerator was required to produce its full beam of $80\mu\text{A}$ of deuterons for a short time, of the order of $1/10$ second, approximately every 10 seconds. During the recovery time of the diffusion chamber the background from the set had to be reduced to a level which would not disturb the recovery of the cloud chamber. Both the length of the pulse and the interval between pulses had to be variable in order to obtain the best conditions in the chamber.

Deuterons from a radio-frequency ion source were accelerated vertically downwards, and then steered into the vacuum box of a resolving magnet in the room below by two sets of deflector plates. The beam was turned through 90° into a horizontal direction by the magnet, and focused on to the target.

In view of the proximity of the cloud chamber to the set, it was decided that a mechanical pulsing mechanism would be inadequate, and that the only satisfactory method would be to pulse the radio-frequency source. This pulse had to be fitted to the normal sequence of events in the cloud-chamber control equipment, and it was necessary for the cloud-chamber control to initiate the sequence.

A signal from the cloud-chamber control equipment opened the shutter of a camera lens which sent a beam of light up the inside of one of the supporting columns of the h.t. set. This light beam was directed on to a photomultiplier, which energized a high-speed relay. This relay, in turn, operated the ion source.

The shutter was used in position 'B' and the shutter arm was operated by the armature of a relay, which was energized when the contacts of a second high-resistance relay closed. The length of time for which this relay was on was controlled by a condenser-resistance circuit, as shown in figure 1, and this in turn determined the length of the pulse from the ion source. Additional contacts on the high resistance relay were used to remove the voltage from the deflector plates when the ion source was not switched on. This prevented any residual

beam from striking the target, and was found to be essential if the background was to be reduced to the level of cosmic radiation. The ion source output was most easily removed by switching off the 2 kv extractor potential. With the extractor potential at zero and all other voltages on the ion source and focusing electrodes normal it was found that there was a residual beam approximately 0.1% of the normal resolved beam of $80\text{ }\mu\text{A}$. This small residual beam was removed from the target to a well-shielded region above the magnet box some six feet from the chamber by shorting the deflector plate voltage which directed the beam into the magnet-box aperture during the 'on' period.

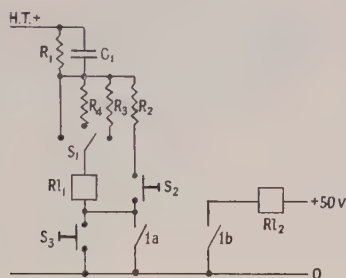


Figure 1. $R_1=1\text{ M}\Omega$, $R_2=50\text{ k}\Omega$, $R_3=100\text{ k}\Omega$, $R_4=50\text{ k}\Omega$, $C=1\text{ }\mu\text{F}$. The switches S_1 and S_2 control the length of the 'on' period of relay RL_1 ($50\text{ k}\Omega$). Contact 1b of this relay operates the relay RL_2 ($30\text{ }\Omega$). The switch S_3 is the contact in the cloud-chamber control apparatus.

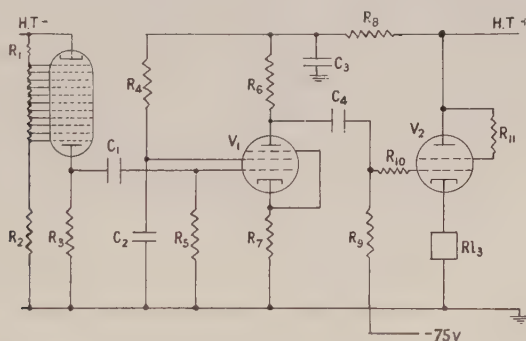


Figure 2. $R_1=R_3=R_9=1\text{ M}\Omega$, $R_2=2\text{ M}\Omega$, $R_4=100\text{ k}\Omega$, $R_5=10\text{ M}\Omega$, $R_6=33\text{ k}\Omega$, $R_7=100\text{ }\Omega$, $R_8=10\text{ k}\Omega$, $R_{10}=R_{11}=270\text{ }\Omega$, $C_1=C_4=1\text{ }\mu\text{F}$, $C_2=8\text{ }\mu\text{F}$, $C_3=16\text{ }\mu\text{F}$. V_1 type 6SJ7; V_2 , type 12E1. RL_3 is the coil of the high speed relay.

The light signal from the lamp, operated by the cloud-chamber control system, fell on to the light-sensitive surface of an RCA multiplier situated in the 1 mV electrode which contained the ion source assembly. With 350 volts across the electrode of the photomultiplier the light flash would produce a pulse across $1\text{ M}\Omega$ sufficient to cut off a pentode. The positive pulse at the anode of this valve was applied to the grid of a 12E1 valve (figure 2) acting as a cathode follower with the coil of a relay as the cathode load. This relay had heavy duty contacts. With this arrangement the relay could be made to close and open with a light pulse which varied in length from 1/100 second to 10 seconds.

The h.t. set itself was stabilized to 1 kv by an electronic stabilizer which was well able to control the surges produced by the beam pulses.

Six pulse lengths from 55 to 320 milliseconds were available and each of these times remained constant within 5 milliseconds. This range could be extended, and the system remain reliable down to a beam pulse length of 10 milliseconds. These pulse lengths, together with the normal controls of the h.t. set, were sufficient to control the number of events seen in the cloud chamber and maintain the background at an extremely low level. With the ion source switched off the appearance of the cloud chamber was indistinguishable from the appearance with the whole set switched off.

§ 3. RESULTS

The reprojection apparatus (Alston, Crewe and Evans, to be published later) was such that pairs of images were made to coincide when the direction of the track was coplanar with a line drawn from the target to the beginning of the track; this line was engraved on the reprojection surface. Each photograph was inspected for measurable tracks, and for each event the scattering angle and range were noted, and whether it was scattered to the left or to the right. A range histogram was then constructed for each 5-degree interval (in the laboratory system). Tracks were accepted only if their ranges lay within reasonable limits.

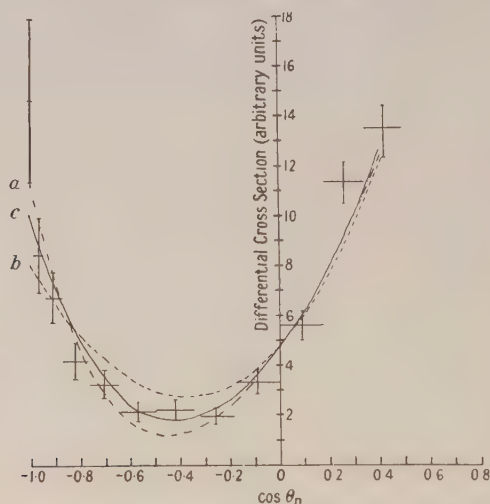


Figure 3. The differential cross section plotted against $\cos \theta_n$. The curves were calculated from phase-shift data. *a*, $D_{3/2} = D_{5/2} = -14^\circ$; *b*, $D_{3/2} = -14^\circ$, $D_{5/2} = 0^\circ$; *c*, $D_{3/2} = -14^\circ$, $D_{5/2} = -7^\circ$.

The spread in the measured ranges is due to three effects: (*a*) The track was only placed within a 5 degree interval, which allows a small variation in energy. (*b*) The temperature of the gas-vapour mixture in which the recoil occurs varied from -65°C at the bottom of the sensitive region to about -10°C at the top. This allows a considerable variation in range for any one energy of recoil particle. (*c*) The accuracy of range measurement was 0.1 cm and that of scattering angle varies from $\pm 1^\circ$ in the forward direction to $\pm 5^\circ$ at 80° in the laboratory system. The magnitude of each of these effects can be readily evaluated and the limits imposed on the range histogram were calculated in this way.

The results obtained are shown in figure 3 and the table. It was necessary to make a small correction for background, and this is also shown in the table. The

statistics were not considered sufficiently good to warrant a phase-shift analysis; instead the results are compared with theoretical curves drawn from various assumed phase shifts.

θ_α (deg)	θ_n (deg)	Range (cm)	N	$N-N_B$	σ
0-4	180-170	7.0-8.8	26	22	1466 ± 330
5-9	170-160	6.6-8.6	46	38	845 ± 154
10-14	160-150	6.4-8.4	57	50	676 ± 103
15-19	150-140	5.8-7.6	54	42	420 ± 74
20-24	140-130	5.2-7.2	50	40	325 ± 58
25-29	130-120	4.4-6.2	40	31	216 ± 44
30-34	120-110	3.6-5.4	48	35	222 ± 44
35-39	110-100	2.6-4.4	44	33	197 ± 34
40-44	100- 90	1.8-3.6	69	58	334 ± 49
45-49	90- 80	1.2-2.8	111	97	560 ± 61
50-54	80- 70	0.6-1.8	208	190	1130 ± 86
55-59	70- 60	0.4-1.4	227	213	1345 ± 95

θ_α , scattering angle of α -particle in laboratory system; θ_n , scattering angle of neutron in centre-of-mass system; N , total number of events recorded in laboratory system; N_B , estimated number of background events in laboratory system; σ , differential cross section (centre-of-mass system) in arbitrary units.

Since this experimental work was completed a paper has been published by Seagrave (1953) reporting results obtained for neutron energies up to 14.3 MeV, using a proportional counter. Seagrave compares his experimental phase-shifts with the theoretical values worked out by Dodder and Gammel (1952) for the p - α case. Excellent agreement is obtained for the S and P phase-shifts; consequently the S and P phase-shifts were taken from the calculated curves given by Seagrave, and not varied, and curves were plotted for the following values of the D phase-shifts: *a*, $D_{3/2} = D_{5/2} = -14^\circ$ (the hard sphere value); *b*, $D_{3/2} = -14^\circ$, $D_{5/2} = 0^\circ$; *c*, $D_{3/2} = -14^\circ$, $D_{5/2} = -7^\circ$.

It will be seen that case *c* fits the experimental results much better than either of the other cases, indicating that a $D_{5/2}$ phase-shift must be employed, but of a smaller value than that given by a hard sphere of 2.9×10^{-13} cm radius.

The total cross section measurements in the region from 12 to 16 MeV as reported in Seagrave's paper also indicate that the D-wave phase-shifts are not the hard sphere values. The measured values of the total cross section are smaller than those predicted assuming that there are no levels in ^5He between the $P_{1/2}$ level at 2.6 MeV excitation and the $J = 3/2$ level at 16.64 MeV excitation. A $D_{5/2}$ resonance somewhat above the 15.7 MeV neutron bombarding energy used in this work would depress the $D_{5/2}$ phase shift below the hard sphere value, in agreement with our results, and also produce a corresponding reduction in the total cross section at this energy.

Using the phase shifts quoted above we have calculated the polarization for neutrons scattered at 90° in the centre-of-mass system using the formula given by Lepore (1950) and the result is 86% polarization. No detectable left-right asymmetry was observed in the number of α -particles scattered at 45° in the laboratory system, indicating that neutrons from the D-T reaction at 700 keV bombarding energy have little or no polarization under the conditions of our experiment.

ACKNOWLEDGMENTS

We are indebted to Professor H. W. B. Skinner for much helpful discussion of this paper, and one of us (M.H.A.) is indebted to the Department of Scientific and Industrial Research for the award of a maintenance grant.

REFERENCES

- ADAIR, R. K., 1952, *Phys. Rev.*, **86**, 155.
 ALSTON, M. H., CREWE, A. V., and EVANS, W. H., 1954, *Rev. Sci. Instrum.*, in the press.
 CREWE, A. V., and EVANS, W. H., 1952, *Atomics*, **3**, 221.
 DODDER, D. C., and GAMMEL, J. L., 1952, *Phys. Rev.*, **88**, 520.
 HUBER, P., and BALDINGER, E., 1952, *Helv. Phys. Acta*, **25**, 435.
 LEPORE, J. V., 1950, *Phys. Rev.*, **79**, 137.
 SEAGRAVE, J. D., 1953, *Phys. Rev.*, **92**, 1093.

Inelastic Collisions between Heavy Particles

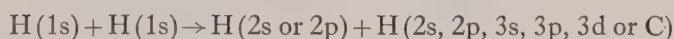
II : Contributions of Double-Transitions to the Cross Sections associated with the Excitation of Hydrogen Atoms in Fast Encounters with other Hydrogen Atoms

BY D. R. BATES AND G. W. GRIFFING†

Department of Applied Mathematics, The Queen's University of Belfast

MS. received 5th March 1954

Abstract. Born's approximation is used to calculate the cross sections of the processes



where C represents the continuum. The results are presented mainly in graphical form. It is found that these *double*-transition collisions are together much more effective at high impact energies than are simple single-transition collisions such as



An asymptotic formula for the total inelastic cross section is also obtained.

§ 1. INTRODUCTION

IN paper I of this series (Bates and Griffing 1953) calculations were carried out on the cross section for the excitation of a hydrogen atom A by a high energy incident hydrogen atom B which itself remained unaffected by the collision,



It was pointed out, however, that the reaction path



might also be followed and that such double-transitions might be of importance.

Clearly if the cross section for process (2) is $Q(1s - nl; 1s - n'l')$ then the total cross section describing the excitation of A to the (nl) -state is

$$Q(1s - nl; 1s - \Sigma) = \sum_{n'l'} Q(1s - nl; 1s - n'l') \quad \dots\dots(3)$$

where the summation involves also integration over the continuum; that describing the excitation of B to the (nl) -state is naturally the same; that describing the excitation of *either or both* atoms to this state is

$$\mathcal{Q}((1s)^2 - (nl, \Sigma)) = 2Q(1s - nl; 1s - \Sigma) - Q(1s - nl; 1s - nl); \quad \dots\dots(4)$$

and that describing all inelastic collisions is

$$\mathcal{Q}((1s)^2 - (\Sigma, \Sigma')) = Q(1s - 1s; 1s - \Sigma') + \sum'_{nl \neq 1s} Q(1s - nl; 1s - \Sigma) \quad \dots\dots(5)$$

† Affiliated to the Cambridge Geophysics Research Directorate of the United States Air Force.

which of course includes the contribution

$$\mathcal{Q}((1s)^2 - (1s, \Sigma')) = 2 \sum'_{nl \neq 1s} \mathcal{Q}(1s - nl; 1s - 1s) \quad \dots\dots(6)$$

from encounters giving rise only to single transitions.

The present paper is devoted mainly to the determination of the influence of double transitions on the cross sections associated with the excitation of the 2s and 2p states.

§ 2. THEORY

2.1. Neglecting exchange effects and using the Born approximation (cf. Mott and Massey 1949), it may be seen that the cross section for process (2) is given by

$$\mathcal{Q}(1s - nl; 1s - n'l') = \frac{8\pi^3 M^2}{K_i^2 h^4} \int_{K_{\min}}^{K_{\max}} |\mathcal{N}(1s - nl; 1s - n'l')|^2 K dK \quad \dots\dots(7)$$

with

$$\begin{aligned} \mathcal{N}(1s - nl; 1s - n'l') = e^2 \iiint |\mathbf{R} - \mathbf{r}_a + \mathbf{r}_b|^{-1} \exp(i\mathbf{R} \cdot \mathbf{K}) \chi^*(\mathbf{r}_a | 1s) \chi^*(\mathbf{r}_b | 1s) \\ \times \chi(\mathbf{r}_a | nl) \chi(\mathbf{r}_b | n'l') d\mathbf{r}_a d\mathbf{r}_b d\mathbf{R} \quad \dots\dots(8)^\dagger \end{aligned}$$

$$\mathbf{K} = \mathbf{K}_f - \mathbf{K}_i, \quad \mathbf{K}_i = 2\pi M \mathbf{v}_i / h, \quad \mathbf{K}_f = 2\pi M \mathbf{v}_f / h \quad \dots\dots(9)$$

where M is the reduced mass, \mathbf{R} is the relative position vector of the two protons, \mathbf{r}_a and \mathbf{r}_b are the position vectors of the electrons with respect to them (the subscript a referring to one electron-proton system, the subscript b to the other); the χ 's are the wave functions of the states indicated, and \mathbf{v}_i and \mathbf{v}_f are the initial and final velocities of relative motion. After integration over \mathbf{R} -space, formula (8) reduces to

$$\mathcal{N}(1s - nl; 1s - n'l') = \frac{4\pi a_0^2 e^2}{t^2} \mathcal{J}(1s - nl) \mathcal{J}(1s - n'l') \quad \dots\dots(10)$$

$$\text{where} \quad \mathcal{J}(1s - nl) = \int \exp(i\mathbf{t} \cdot \mathbf{r}) \chi^*(\mathbf{r} | 1s) \chi(\mathbf{r} | nl) d\mathbf{r} \quad \dots\dots(11)$$

$$\mathbf{t} = \mathbf{K} a_0 \quad \dots\dots(12)$$

and \mathbf{r} is in atomic units. Substitution in (7) then yields

$$\mathcal{Q}(1s - nl; 1s - n'l') = \left[\frac{8}{s^2} \int_{t_{\min}}^{t_{\max}} |\mathcal{J}(1s - nl)|^2 |\mathcal{J}(1s - n'l')|^2 t^{-3} dt \right] \pi a_0^2 \dots(13)$$

$$\text{with} \quad s^2 = \frac{1}{2} m v_i^2 / I_H \quad \dots\dots(14)$$

m being the electronic mass and I_H being the ionization potential of hydrogen. The \mathcal{J} 's defined in (11) also arise in the calculations on the cross sections of the single-transition collisions, (1), and expressions for them are given in paper I for the cases 1s-2s, 2p, 3s, 3p, 3d and C (where C represents the continuum).

The integration in (13) is generally best done by numerical methods. Transitions to the discrete states can indeed be treated analytically but the resulting formulae are cumbersome and awkward to evaluate unless the final principal

[†] Terms of the interaction potential not involving \mathbf{r}_a and \mathbf{r}_b explicitly have been omitted since, owing to orthogonality effects, they give no contribution to the matrix elements associated with double-transition collisions.

quantum numbers are equal. Such equality brings about great simplification, for example

$$Q(1s-2s; 1s-2s) = \left[\frac{2^{30}}{495s^2} (880x^2 + 396x + 81)(4x+9)^{-11} \right] \pi a_0^2 \quad \dots\dots(15)$$

$$Q(1s-2p; 1s-2p) = \left[\frac{2^{30} \times 3^4}{11s^2} (4x+9)^{-11} \right] \pi a_0^2 \quad \dots\dots(16)$$

$$Q(1s-2s; 1s-2p) = \left[\frac{2^{29} \times 3^2}{55s^2} (44x+9)(4x+9)^{-11} \right] \pi a_0^2 \quad \dots\dots(17)$$

$$\text{with} \quad x = \frac{9}{16s^2} \left[1 + \frac{3m}{4Ms^2} + \dots \right] \quad \dots\dots(18)$$

It will be observed that according to the Born approximation the cross sections are initially extremely rapidly increasing functions of E , the energy of relative motion: thus $Q(1s-2s; 1s-2s)$, $Q(1s-2p; 1s-2p)$ and $Q(1s-2s; 1s-2p)$ initially increase as E^8 , E^{10} and E^9 respectively as compared with $Q(1s-2s; 1s-1s)$ and $Q(1s-2p; 1s-1s)$ which initially increase as E^4 and E^5 respectively (cf. paper I).

2.2. The summation over the separate cross sections to get $Q(1s-nl; 1s-\Sigma)$ may readily be effected since the series converges rapidly. A closed asymptotic formula may also be obtained. At sufficiently high energies it is permissible to take t_{\max} as infinite and t_{\min} as zero so that

$$Q(1s-nl; 1s-\Sigma) \sim Q(1s-nl; 1s-1s) + \left[\frac{8}{s^2} \int_0^\infty |\mathcal{J}(1s-nl)|^2 \sum_{n'l' \neq 1s} |\mathcal{J}(1s-n'l')|^2 t^{-3} dt \right] \pi a_0^2 \quad \dots\dots(19)$$

Using the expression for $Q(1s-nl; 1s-1s)$ given in paper I (eqn (17)), noting that

$$\sum_{n'l'} |\mathcal{J}(1s-n'l')|^2 = 1 \quad \dots\dots(20)$$

(Bethe 1930) and that

$$|\mathcal{J}(1s-1s)|^2 = 256/(4+t^2)^4 \quad \dots\dots(21)$$

it may be seen that

$$Q(1s-nl; 1s-\Sigma) \sim \left[\frac{16}{s^2} \int_0^\infty |\mathcal{J}(1s-nl)|^2 \left\{ 1 - \frac{16}{(4+t^2)^2} \right\} t^{-3} dt \right] \pi a_0^2 \quad \dots(22)$$

which is easy to evaluate in any particular case: thus

$$\begin{aligned} Q(1s-2s; 1s-\Sigma) &\sim \left[\frac{2^{21}}{s^2} \int_0^\infty \frac{t}{(4t^2+9)^6} \left\{ 1 - \frac{16}{(4+t^2)^2} \right\} dt \right] \pi a_0^2 \\ &\sim [0.172_0 s^{-2}] \pi a_0^2; \quad \dots\dots(23) \end{aligned}$$

and

$$\begin{aligned} Q(1s-2p; 1s-\Sigma) &\sim \left[\frac{3^2 \times 2^{19}}{s^2} \int_0^\infty \frac{t^{-1}}{(4t^2+9)^6} \left\{ 1 - \frac{16}{(4+t^2)^2} \right\} dt \right] \pi a_0^2 \\ &\sim [0.848_3 s^{-2}] \pi a_0^2. \quad \dots\dots(24) \end{aligned}$$

Similarly it may be seen from (6) that

$$\begin{aligned} Q((1s)^2 - (1s, \Sigma')) &\sim \left[\frac{16}{s^2} \int_0^\infty \left\{ 1 + \frac{16}{(4+t^2)^2} \right\} \left\{ 1 - \frac{16}{(4+t^2)^2} \right\}^3 t^{-3} dt \right] \pi a_0^2 \\ &\sim [116/35s^2] \pi a_0^2; \quad \dots\dots(25) \end{aligned}$$

and from (5) that

$$\begin{aligned} \mathcal{Q}((1s)^2 - (\Sigma, \Sigma')) &\sim \left[\frac{8}{s^2} \int_0^\infty \left\{ 1 + \frac{16}{(4+t^2)^2} \right\} \left\{ 1 - \frac{16}{(4+t^2)^2} \right\}^2 \left\{ 3 - \frac{16}{(4+t^2)^2} \right\} t^{-3} dt \right] \pi a_0^2 \\ &\sim [881/105s^2] \pi a_0^2. \end{aligned} \quad \dots\dots (26)$$

The major contribution to the first of these cross sections comes from single-ionization collisions and the major contribution to the second from double-ionization collisions. As may readily be verified, formula (25) is in harmony with the detailed calculations, reported in paper I, on the cross sections for the separate processes involved, and thus provides a useful check on the computational work. Combined with formula (26) it gives for the cross section describing a *specified* one of the atoms being excited or ionized (the other being unaffected by the collision or being also excited or ionized),

$$Q(1s - \Sigma'; 1s - \Sigma) \sim [101/15s^2] \pi a_0^2 \quad \dots\dots (27)$$

which is in fair accord with the rather similar semi-classical formula of Bohr (1948), this latter having 8 instead of 101/15 as the numerical factor.

§ 3. RESULTS

With the aid of formula (13) calculations were carried out on the cross sections $Q(1s - 2s; 1s - 2s, 2p, 3s, 3p, 3d \text{ or } C)$ and $Q(1s - 2p; 1s - 2s, 2p, 3s, 3p, 3d \text{ or } C)$ for various values of \mathcal{E} , the energy of the *incident* atom (the other atom being taken to be at rest). The results are shown on a log-log scale in figures 1 and 2 respectively. It will be observed that for given azimuthal quantum numbers the cross sections fall off rapidly with increasing values of the principal quantum numbers; that for given principal quantum numbers the cross sections are in general greatest

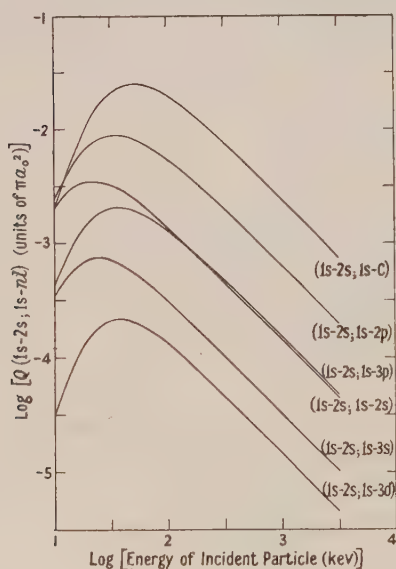
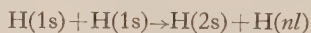


Figure 1. (Cross section, energy) curves for the collision



where nl represents 2s, 2p, 3s, 3p, 3d or C (the continuum).

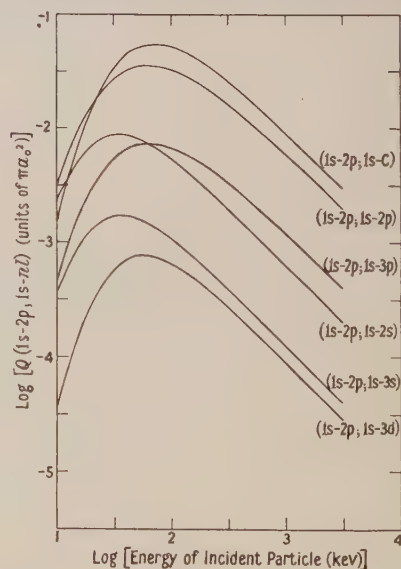
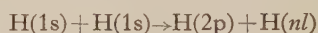


Figure 2. (Cross section, energy) curves for the collision



where nl represents 2s, 2p, 3s, 3p, 3d or C (the continuum).

when the azimuthal quantum numbers are such that the transitions are optically allowed, and that transitions involving the continuum ultimately predominate.

Since the small contribution that arises from $Q(1s-2s; 1s-nl)$ and $Q(1s-2p; 1s-nl)$ when n is greater than 3 can be neglected without causing more than a few per cent error, the results of the present paper together with those of the previous paper are sufficient to enable summations (3) yielding $Q_i(1s-2s; 1s-\Sigma)$ and $Q(1s-2p; 1s-\Sigma)$ to be evaluated. The $[\log(\text{cross section}), \log(\text{impact energy})]$ curves obtained are shown in figure 3, in which

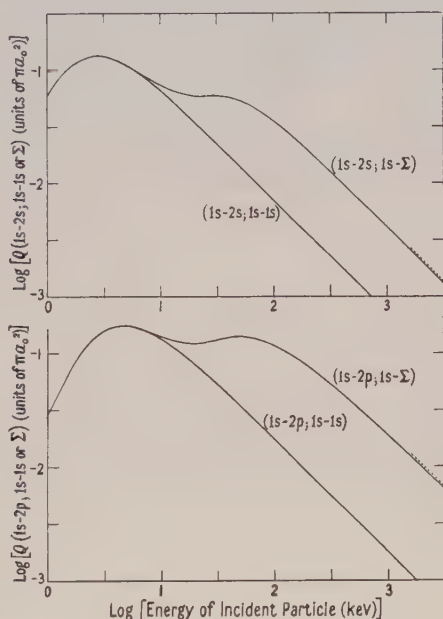


Figure 3. Comparison of the (cross section, energy) curves for collisions in which the *incident* atom is unaffected with those for collisions in which it is left in *any* state. The upper diagram refers to excitation of the *stationary* atom to the 2s state and the lower to excitation of the *stationary* atom to the 2p state. The broken lines represent the asymptotic behaviour of $Q(1s-2s; 1s-\Sigma)$ and $Q(1s-2p; 1s-\Sigma)$ as given by formulae (23) and (24) of the text.

is included, for the sake of comparison, the corresponding curves for $Q(1s-2s; 1s-1s)$ and $Q(1s-2p; 1s-1s)$. Single-transition collisions are naturally the more effective at low values of \mathcal{E} but, as can be seen, double-transition collisions become significant when \mathcal{E} reaches about 10 keV, and at high values of \mathcal{E} it is they which are the more effective. Because of this each of the final curves has two maxima, one due to single-transition collisions and the other to double-transition collisions. However, it should be noted that reliance cannot be placed upon the Born approximation in the lower part of the energy region concerned and consequently the first of the two may be at least partially suppressed in each case, so that the true curves may conceivably show but one broad maximum.

The asymptotes obtained from formulae (23) and (24) are represented in figure 3 by the broken lines. Clearly the curves lie close to them when \mathcal{E} is above some 1000 keV, so that the neglect of the higher discrete states is justified.

Formulae (25) and (26), which may be written more conveniently

$$\mathcal{Q}((1s)^2 - (1s, \Sigma')) \sim [82.8/\mathcal{E}] \pi a_0^2; \mathcal{Q}((1s)^2 - (\Sigma, \Sigma')) \sim [209.5/\mathcal{E}] \pi a_0^2, \dots\dots\dots(28)$$

provide a further illustration of the importance of double-transition collisions at high impact energies. It is to be noted that such collisions must have much less effect on the ionization cross sections than they have on the excitation cross sections considered, for while the ratio of $\mathcal{Q}((1s)^2 - \Sigma, \Sigma')$ to $\mathcal{Q}((1s)^2 - (1s, \Sigma'))$ (which depends mainly on the ionization cross sections) tends to 2.5_3 , the ratio of $\mathcal{Q}((1s)^2 - (2s, \Sigma))$ to $\mathcal{Q}((1s)^2 - (2s, 1s))$ and of $\mathcal{Q}((1s)^2 - (2p, \Sigma))$ to $\mathcal{Q}((1s)^2 - (2p, 1s))$ tend to 5.8_6 and 10.1_5 respectively.

REFERENCES

- BATES, D. R., and GRIFFING, G. W., 1953, *Proc. Phys. Soc. A*, **66**, 961.
 BETHE, H. A., 1930, *Ann. Phys., Lpz.*, **5**, 325.
 BOHR, N., 1948, *Kgl. Danske. Videnskab. Selskab, Mat-fys. Medd.*, **18**, 109.
 MOTT, N. F., and MASSEY, H. S. W., 1949, *Theory of Atomic Collisions*, 2nd Edn (Oxford: Clarendon Press).

On the Thick Target Bremsstrahlung Spectrum at Relativistic Energies

By K. PHILLIPS

Research Department, Metropolitan-Vickers Electrical Co. Ltd., Trafford Park, Manchester

*Communicated by Willis Jackson; MS. received 21st October 1953,
and in final form 24th February 1954*

Abstract. The bremsstrahlung energy distribution has been measured for 9 mev electrons striking a thick copper target. This method involves the energy measurement of the photo-protons produced in the ${}^2\text{H}(\gamma, n){}^1\text{H}$ reaction. The experimental results are compared with a theoretical distribution which is deduced from the thin target bremsstrahlung spectrum. By invoking the usual expressions for the energy loss by ionization and radiation of the incident electrons in the target reasonable agreement between experiment and theory is found.

IN recent years there have been several reports describing various methods of measuring the bremsstrahlung radiation produced by electrons with energies ranging from a few mev to several hundred mev. The interest in the energy distribution has been stimulated not only by the desire to verify existing theories of bremsstrahlung but also by the need for an accurate knowledge of the spectra for the application of electron accelerators in certain nuclear experiments. Induction accelerators were used by Wang and Wiener (1950), Koch and Carter (1950) and Phillips (1952) for energies up to 20 mev and synchronous acceleration by McDiarmid (1942) up to 70 mev, and by Powell, Hartsough and Hill (1951) up to 322 mev. Small but definite discrepancies have been brought to light, notably in the lower energy ranges. These differences are likely to be due to variations in the performance of particular accelerators. All the previously mentioned methods of acceleration are cyclic, and machines of this type tend to give thin target distributions. The usual method of allowing the electrons to strike the target is by deflecting the particles from their stable orbit, as a result of which the electrons may strike the target at grazing incidence. In this case little will be known about the effective target thickness, and its value will be dependent on the spiral pitch of the expanding (or contracting) orbit and also on the focusing action of the scattered electrons by the magnetic field, i.e. on the characteristics of the particular machine being used.

For instance, McDiarmid (1952) used a rod of tungsten about 0.5 cm diameter as a synchrotron target and yet his angular distribution measurements indicated a target thickness of the order of 0.05 to 0.1 cm.

The availability of an 8 mev linear accelerator being developed for x-ray therapy (Miller 1953) enabled these ambiguities to be avoided since in this case the electrons strike the target perpendicularly.

The present experiment measured the energy distribution of the bremsstrahlung produced in a thick copper target by electrons accelerated to 9 mev by a linear accelerator. Under the conditions for this experiment light loading and electron phasing gave an electron energy distribution with a peak at approximately 9 mev. The following points have been regarded as significant: (i) the copper target was $\frac{3}{8}$ in. thick, a thickness adequate to stop the beam of incident electrons;

(ii) the x-rays were collimated so that only the photons originating in the target and travelling in the forward direction were measured; (iii) the photodisintegration of the deuteron was chosen since the cross section had been determined by numerous workers over this energy region.

At energies above 3 mev the photodisintegration of the deuteron is principally through electric dipole capture; the previously determined cross sections are listed in the table. The energy of the incident photon is given by the equation

$$k = 2E_p + \text{binding energy (2.2 mev)}$$

where E_p is the energy of the proton.

Photon energy	$\sigma \times 10^4$ (barns)	References
2.75 (^{24}Na)	15.6 ± 1.0	Wilson, Collie and Halban (1949)
2.75 (^{24}Na)	16.0 ± 4.0	Russell, Sachs, Wattenberg and Fields (1948)
2.75 (^{24}Na)	14.5 ± 1.5	Snell, Barker and Sternberg (1949)
6.14 ($^{19}\text{F} + p$)	21.5 ± 1.2	Barnes, Stafford and Wilkinson (1950)
7.39 ($^9\text{Be} + p$)	18.4 ± 1.5	Barnes, Stafford and Wilkinson (1950)
8.14 ($^{13}\text{C} + p$)	16.4 ± 1.2	Barnes, Stafford and Wilkinson (1950)

A quarter-plate C2 Ilford emulsion, 100 microns thick, was exposed to the collimated bremsstrahlung for approximately 15 seconds. A heavy wax film ($C_n D_{n+2}$, $n \simeq 30$) 5 microns thick, supported on thin backing of 'Cellophane' and fastened to a metal frame, was fitted closely to the surface of the plate. A control plate with a paraffin wax target was exposed under similar conditions in order to estimate any possible background effects. The plates were developed in a solution of Azol and 1% potassium bromide.

Several square centimetres of emulsion were scanned using a Cooke, Troughton and Simms M4000 Type microscope, and about 500 proton tracks were measured in the heavy wax plate. Of these almost 30% were rejected on the grounds that their angle of dip in the emulsion did not lie within the limits of 5 to 45 degrees. The lower limit was fixed in order to reduce the error in energy measurement due to the range of the protons in the heavy wax target.

The number of photo-protons in the energy range 0 to 3 mev, produced by different photon energies from 3 to 8.5 mev, is shown in the histogram (figure 1). On the control plate only nine tracks were found for the corresponding area. The distribution of the protons rises rapidly as the proton energy approaches 1 mev. The drop at lower energies is undoubtedly due to the difficulty in finding all the short tracks. Figure 2 shows the photon spectrum obtained by suitable adjustment of the proton histogram so as to correct for the variation in the photoelectric cross section with photon energy. The dotted curve is a rough estimate of the spectrum which has been deduced by considering the processes by which an electron loses energy when it penetrates the target. The total rate of loss of energy is given approximately by the equation (Heitler 1946)

$$dE/dx = \alpha + \beta E$$

where α and β are constants and x is the thickness of the target. On the approximate assumption that the thin target spectrum varies inversely as the photon energy it can be shown that the number of photons for a thick target is given by

$$\frac{1}{\bar{k}} \ln \frac{\beta E_0 + \alpha}{\beta k + \alpha}$$

where E_0 is the energy of the incident electron and k is the energy of the photons.

It is usual to consider the variation of intensity with energy, which removes the emphasis on the lower energy end of the spectrum. Figure 3 shows a plot of the experimental results together with the theoretical curve normalized at 4.5 mev.

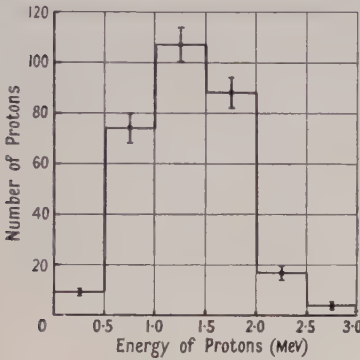


Figure 1. The distribution of photo-protons found in the C2 plate using deuterium wax target.

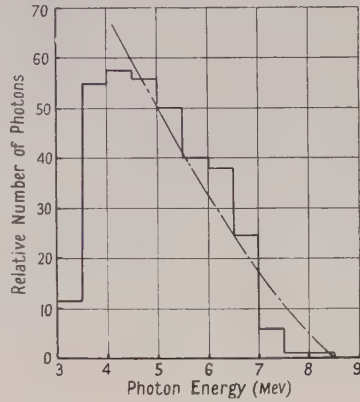


Figure 2. The experimental photon spectrum deduced from the number of photo-protons using previously determined ${}^2\text{H}(\gamma, n){}^1\text{H}$ cross sections. The chain-dotted curve is the calculated spectrum normalized at 4.75 mev.

For comparison the thin target intensity spectrum for 8.5 Mev electrons is also illustrated. The theoretical curve indicates the general shape of the spectrum, but the fit is obviously dependent on the point of normalization. Better agreement

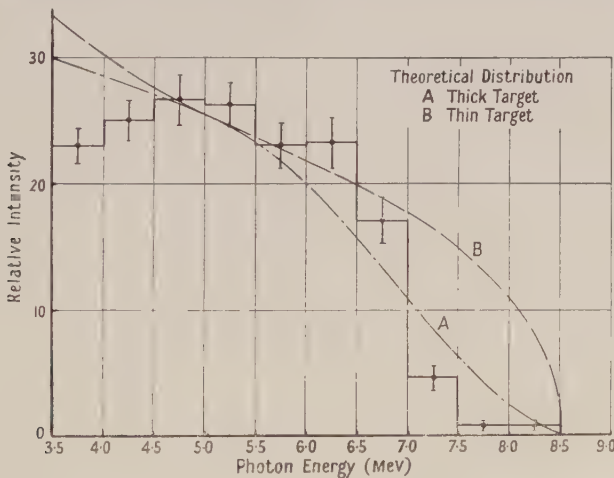


Figure 3. The intensity spectrum histogram. The errors are based on the number of photo-protons related to the respective energy intervals.

may be obtained in the middle energy range by normalizing at 6 mev. This would result, however, in much worse correlation at the higher energy end. Certain differences between the experimental and theoretical results may be due to approximations used in deducing the theoretical curve. For instance, the

'squaring off' of thin target bremsstrahlung spectrum, which has been done purely for convenience, would most likely increase the theoretical intensity at the upper limit. The ambiguity could only be resolved by carrying out exact numerical calculation of the radiation characteristic, but this would be rather laborious and is beyond the scope of the present work. Nevertheless it is interesting to compare these spectral characteristics with previously published experimental results for thinner targets, in particular the more rapid fall at the high energy tip of the spectrum, and the observation that there are relatively more quanta in the lower energy values than predicted by the theory. In the present case these differences cannot be attributed to multiple passage of the accelerated electrons through the target as with cyclic machines. Lawson (1952) has suggested that straggling may affect the forward spectrum for very thick targets, and even though an exact treatment of the phenomena is not possible it seems likely that straggling would cause some increase in the number of lower energy photons and a decrease at the tip of the spectrum.

ACKNOWLEDGMENTS

The author wishes to acknowledge the assistance given to him by Mr. C. W. Miller and Dr. A. Aiken of the Linear Accelerator Group, and by Mrs. D. Peberdy and Mrs. I. Johnson in connection with the scanning. He thanks Mr. F. R. Perry for his advice, and Dr. Willis Jackson, Director of Research and Education, and Mr. B. G. Churcher, Manager of Research Department, Metropolitan-Vickers Electrical Co. Ltd., for permission to publish this work.

REFERENCES

- BARNES, C. A., STAFFORD, G. H., and WILKINSON, D. H., 1950, *Nature, Lond.*, **165**, 69.
 HEITLER, W., 1946, *Quantum Theory of Radiation*, 2nd Edn (Oxford: University Press).
 KOCH, H. W., and CARTER, R. K., 1950, *Phys. Rev.*, **77**, 165.
 LAWSON, J. D., 1952, *Nucleonics*, **10**, 61.
 MCDIARMID, J. B., 1952, *Phil. Mag.*, **344**, 1003.
 MILLER, C. W., 1953, *Nature, Lond.*, **171**, 297.
 PHILLIPS, K., 1952, *Proc. Phys. Soc. A*, **65**, 57.
 POWELL, W. M., HARTSOUGH, W., and HILL, M., 1951, *Phys. Rev.*, **81**, 213.
 RUSSELL, B., SACHS, D., WATTENBERG, A., and FIELDS, R., 1948, *Phys. Rev.*, **73**, 545.
 SNELL, A. H., BARKER, E. C., and STERNBERG, R. L., 1949, *Phys. Rev.*, **75**, 1290 (A).
 WANG, P. K. S., and WIENER, M., 1950, *Phys. Rev.*, **78**, 1724.
 WILSON, R., COLLIE, C. H., and HALBAN, H., 1949, *Nature, Lond.*, **163**, 245.

The Second Born Approximation in Inelastic Collisions of Electrons with Atoms

By W. ROTHENSTEIN

Physics Departments, University College, London, and Battersea Polytechnic, London

Communicated by H. S. W. Massey; MS. received 1st April 1954

Abstract. The second approximation in Born's theory of collisions is worked out for the excitation of the 2p state of hydrogen and of the 2^1P state of helium from the corresponding ground states by electron impact. The method is not applicable to electron energies too close to the threshold. The correction introduced by the second approximation, which reduces the intensity of the small angle inelastic scattering and the total inelastic cross section by an amount increasing as the electron energy decreases, is of the correct sign and about the right magnitude, in the energy range to which it is applicable, to provide an explanation of the discrepancies between calculated and observed cross sections for excitation of optically allowed transitions.

§ 1. INTRODUCTION

THE validity of Born's first approximation for the calculation of the cross sections for excitation of atoms by electron impact has been discussed in relation to observed data by Bates, Fundaminsky, Leech and Massey (1950), (see also Massey and Burhop 1952, Chap. 3). While it is confirmed that the approximation is quite inadequate for dealing with slow collisions, the type of failure, broadly speaking, depends on whether the excitation involved is an optically allowed one or not. In the latter case the approximation frequently leads to a gross error at electron energies near the threshold, where the cross section is often quite large. For optically allowed excitations, such as from S to P states in helium, as well as for ionizing transitions, the cross section attains a maximum rather gradually as the electron energy increases from the threshold value to about four or more times that value. The first Born approximation, which is in good agreement with experiment at high energies, begins to fail at energies slightly above the observed maximum by overestimating the cross section by an amount which increases as the energy decreases. This leads to a predicted maximum at too low an energy, but at no time does the error grow much larger than a factor of two or so.

A major reason for the gross failure of Born's first approximation at energies near the threshold appears to be the use of plane waves to represent the motion of the electron relative to the atom in the transition matrix elements. This can be allowed for by an appropriate use of distorted instead of plane waves (Erskine and Massey 1952, Bransden and Dalgarno 1953, Massey and Moiseiwitsch 1954). The failure for optically allowed transitions cannot be accounted for in this way (Massey and Mohr 1933). The relatively small discrepancies in these cases suggest, however, that the second approximation in Born's method might be

adequate at least to indicate the way in which the first approximation is likely to begin to fail. This approximation has been previously investigated for elastic scattering (Massey and Mohr 1934) but never applied to any inelastic collisions. In this paper the method used by Massey and Mohr is extended to calculate the second Born approximation for the excitation of the 1s-2p transition in hydrogen and 1¹S-2¹P transition in helium. The method is not applicable at energies close to the threshold, but at higher energies it is found to give correctly the nature and order of magnitude of the observed deviation from the predictions of the first Born approximation.

§ 2. THE FIRST AND SECOND APPROXIMATIONS FOR HYDROGEN

The differential cross sections for elastic and inelastic scattering of a beam of electrons of wave number $k/2\pi$ by a hydrogen atom may be obtained from the solutions $F_0(\mathbf{r})$ and $F_n(\mathbf{r})$ of the coupled differential equations (Mott and Massey 1949, p. 137)

$$(\nabla^2 + k^2)F_0(\mathbf{r}) = 2m\hbar^{-2} \sum_n F_n(\mathbf{r}) V_{n0}(\mathbf{r}) \quad \dots\dots(1)$$

$$(\nabla^2 + k_n^2)F_n(\mathbf{r}) = 2m\hbar^{-2} \sum_s F_s(\mathbf{r}) V_{sn}(\mathbf{r}). \quad \dots\dots(2)$$

The potentials $V_{sn}(\mathbf{r})$ are given by

$$V_{sn}(\mathbf{r}) = \int V(\mathbf{r}, \mathbf{r}_a) \psi_s(\mathbf{r}_a) \psi_n^*(\mathbf{r}_a) d\tau_a \quad \dots\dots(3)$$

where $V(\mathbf{r}, \mathbf{r}_a)$ is the interaction energy between an electron of coordinates \mathbf{r} and the atom, whose proton is at the origin and electron at coordinates \mathbf{r}_a . By solving (1) and (2), subject to the condition that

$$F_0(\mathbf{r}) \sim \exp(ik\mathbf{n}_0 \cdot \mathbf{r}) + r^{-1} \exp(ikr) f_0(\theta, \phi) \text{ and } F_n(\mathbf{r}) \sim r^{-1} \exp(ik_n r) f_n(\theta, \phi),$$

in which \mathbf{n}_0 is a unit vector in the direction of the incident electron beam, the differential cross sections for elastic and inelastic scattering are given by $|f_0(\theta, \phi)|^2$ and $(k_n/k) |f_n(\theta, \phi)|^2$ respectively. Born's approximation is obtained by writing on the right-hand sides of equations (1) and (2) $F_0(\mathbf{r}) = \exp(ik\mathbf{n}_0 \cdot \mathbf{r})$ and $F_n(\mathbf{r}) = 0$ when $n \neq 0$, ignoring the perturbation of the incident wave by its interaction with the atom. The solutions are then (Mott and Massey 1949, p. 114):

$$F_0(\mathbf{r}) = \exp(ik\mathbf{n}_0 \cdot \mathbf{r}) - \frac{m}{2\pi\hbar^2} \int V_{00}(r_1) \frac{\exp\{ik|\mathbf{r} - \mathbf{r}_1|\}}{|\mathbf{r} - \mathbf{r}_1|} \exp(ik\mathbf{n}_0 \cdot \mathbf{r}_1) d\tau_1 \quad \dots\dots(4)$$

$$F_n(\mathbf{r}) = -\frac{m}{2\pi\hbar^2} \int V_{0n}(r_1) \frac{\exp\{ik_n|\mathbf{r} - \mathbf{r}_1|\}}{|\mathbf{r} - \mathbf{r}_1|} \exp(ik\mathbf{n}_0 \cdot \mathbf{r}_1) d\tau_1. \quad \dots\dots(5)$$

A second Born approximation may be obtained by substituting the solutions (4) and (5) instead of the unperturbed wave in the right-hand sides of equations (1) and (2) and resolving them. Equation (2), which corresponds to inelastic scattering, then becomes:

$$\begin{aligned} (\nabla^2 + k_n^2)F_n(\mathbf{r}) = & 2m\hbar^{-2} V_{0n}(\mathbf{r}) \exp(ik\mathbf{n}_0 \cdot \mathbf{r}) - \frac{m^2}{\pi\hbar^4} \sum_s V_{sn}(\mathbf{r}) \int V_{0s}(r_1) \\ & \times \frac{\exp\{ik_s|\mathbf{r} - \mathbf{r}_1|\}}{|\mathbf{r} - \mathbf{r}_1|} \exp(ik\mathbf{n}_0 \cdot \mathbf{r}_1) d\tau_1. \quad \dots\dots(6) \end{aligned}$$

At energies sufficiently high to write $k_s \simeq k$ in all terms of the series occurring in (6)

this series becomes $\sum_s V_{sn}(\mathbf{r}) V_{0s}(\mathbf{r}_1)$ and may be summed by using the expansions:

$$\psi_0(\mathbf{r}_a) V(\mathbf{r}_1, \mathbf{r}_a) = \sum_s a_s(\mathbf{r}_1) \psi_s(\mathbf{r}_a),$$

giving $a_s(\mathbf{r}_1) = \int \psi_0(\mathbf{r}_a) V(\mathbf{r}_1, \mathbf{r}_a) \psi_s^*(\mathbf{r}_a) d\tau_a = V_{0s}(\mathbf{r}_1)$

and $\psi_n^*(\mathbf{r}_a) V(\mathbf{r}, \mathbf{r}_a) = \sum_s b_s(\mathbf{r}) \psi_s^*(\mathbf{r}_a),$

giving $b_s(\mathbf{r}) = \int \psi_n^*(\mathbf{r}_a) V(\mathbf{r}, \mathbf{r}_a) \psi_s(\mathbf{r}_a) d\tau_a = V_{sn}(\mathbf{r}).$

Multiplying these two expansions, integrating over the coordinates (\mathbf{r}_a) , and using the orthonormal properties of the wave functions we have:

$$\int V(\mathbf{r}, \mathbf{r}_a) V(\mathbf{r}_1, \mathbf{r}_a) \psi_0(\mathbf{r}_a) \psi_n^*(\mathbf{r}_a) d\tau_a = \sum_s V_{sn}(\mathbf{r}) V_{0s}(\mathbf{r}_1),$$

which now may be used in (6):

$$\begin{aligned} (\nabla^2 + k_n^2) F_n(\mathbf{r}) &= 2m\hbar^{-2} V_{0n}(\mathbf{r}) \exp(ik\mathbf{n}_0 \cdot \mathbf{r}) \\ &\quad - \frac{m^2}{\pi\hbar^4} \iint V(\mathbf{r}, \mathbf{r}_a) V(\mathbf{r}_1, \mathbf{r}_a) \frac{\exp\{ik|\mathbf{r} - \mathbf{r}_1|\}}{|\mathbf{r} - \mathbf{r}_1|} \exp(ik\mathbf{n}_0 \cdot \mathbf{r}_1) \\ &\quad \times \psi_0(\mathbf{r}_a) \psi_n^*(\mathbf{r}_a) d\tau_a d\tau_1. \end{aligned} \quad \dots\dots (7)$$

To evaluate the double integral in (7) the origin is now transferred from the position of the proton to the position of the field point (\mathbf{r}) . The new polar coordinates are ρ, ϑ, η with the axes $\vartheta=0$ and $\eta=0$ parallel to the axes $\theta=0$ and $\phi=0$. If $\rho_0, \vartheta_0, \eta_0$ are the coordinates of the proton with respect to the new origin, then $\rho_0=r$, $\vartheta_0=\pi-\theta$ and $\eta_0=\phi+\pi$. Also $\mathbf{r}_a=\mathbf{r}+\boldsymbol{\rho}_a$ and $\mathbf{r}_1=\mathbf{r}+\boldsymbol{\rho}_1$, so that (7) becomes

$$(\nabla^2 + k_n^2) F_n(\mathbf{r}) = 2m\hbar^{-2} \{V_{0n}(\mathbf{r}) + v_{0n}(\mathbf{r})\} \exp(ik\mathbf{n}_0 \cdot \mathbf{r}) \quad \dots (8)$$

in which the additional potential $v_{0n}(\mathbf{r})$ is given by

$$\begin{aligned} v_{0n}(\mathbf{r}) &= -\frac{m}{2\pi\hbar^2} \iint V(\mathbf{r}, \mathbf{r}+\boldsymbol{\rho}_a) V(\mathbf{r}+\boldsymbol{\rho}_1, \mathbf{r}+\boldsymbol{\rho}_a) \frac{\exp\{ik(\rho_1 + \mathbf{n}_0 \cdot \boldsymbol{\rho}_1)\}}{\rho_1} \psi_0(\mathbf{r}+\boldsymbol{\rho}_a) \\ &\quad \times \psi_n^*(\mathbf{r}+\boldsymbol{\rho}_a) d\boldsymbol{\rho}_a d\boldsymbol{\rho}_1 \end{aligned} \quad \dots\dots (9)$$

where $d\boldsymbol{\rho}_a$ and $d\boldsymbol{\rho}_1$ are volume elements.

§ 3. THE 1s-2p TRANSITION IN HYDROGEN

In order to be able to carry out the integrations over the angular variables in (9) the polar axis is taken along \mathbf{n}_0 . This, however, necessitates dealing with the transitions to the " $\cos\theta_a$ " and " $\sin\theta_a \exp(\pm i\phi_a)$ " levels separately, which is normally avoided in Born's approximation by taking the polar axis along the change of momentum vector (Mott and Massey 1949, p. 225). The required wave functions are:

$$\psi_0 = -(Z^3/\pi)^{1/2} \exp(-Zr_a) = -(Z^3/\pi) \exp(-Z\rho_{0a}) \quad \text{where } r_a = |\mathbf{r} + \boldsymbol{\rho}_a| = \rho_{a0} \quad \text{and} \\ Z = a_0^{-1}$$

$$\begin{aligned} \psi_1 &= -\frac{1}{4} (Z^5/2\pi)^{1/2} \exp(-\frac{1}{2}Zr_a) \left\{ \begin{array}{l} r_a \cos\theta_a \\ 2^{-1/2} r_a \sin\theta_a \exp(\pm i\phi_a) \end{array} \right\} \\ &= -\frac{1}{4} (Z^5/2\pi)^{1/2} \exp(-\frac{1}{2}Z\rho_{0a}) \left\{ \begin{array}{l} r \cos\theta + \rho_a \cos\vartheta_a \\ 2^{-1/2} \{r \sin\theta \exp(\pm i\phi) + \rho_a \sin\vartheta_a \exp(\pm i\eta_a)\} \end{array} \right\}. \end{aligned}$$

The product of the interaction energies occurring in (9) is

$$\epsilon^4 \left(\frac{1}{r} - \frac{1}{\rho_a} \right) \left(\frac{1}{\rho_{01}} - \frac{1}{\rho_{1a}} \right) = -\epsilon^4 \left(-\frac{1}{r\rho_{01}} + \frac{1}{\rho_a\rho_{01}} + \frac{1}{r\rho_{1a}} - \frac{1}{\rho_a\rho_{1a}} \right).$$

Substitution in (9) gives

$$v_{01}(\mathbf{r}) = \left(\frac{1/8\sqrt{2}}{1/16} \right) \frac{m\epsilon^4 Z^4}{\pi^2 \hbar^2} (-I_1 + I_2 + I_3 - I_4) \dots\dots(10)$$

in which the integrals I_1, I_2, I_3 and I_4 correspond to the four terms in this product. The factors $1/8\sqrt{2}$ and $1/16$ apply to the " $\cos \theta_a$ " and each of the " $\sin \theta_a \exp(\pm i\phi_a)$ " levels respectively. The integral $I_1=0$ since the wave functions ψ_0 and ψ_1 are orthogonal. Each of the I_2, I_3 and I_4 is now subdivided into two parts $I_2' + I_2''$ etc., corresponding to the two parts of the wave function ψ_1 involving

$$\begin{cases} r \cos \theta \\ r \sin \theta \exp(\mp i\phi) \end{cases} \quad \text{and} \quad \begin{cases} \rho_a \cos \vartheta_a \\ \rho_a \sin \vartheta_a \exp(\pm i\eta_a) \end{cases}$$

Writing $\mu = \frac{3}{2}Z$ we have:

$$\begin{aligned} I_2' &= \iint \frac{g'(\mathbf{r}, \boldsymbol{\rho}_1, \boldsymbol{\rho}_a)}{\rho_a \rho_{01} \rho_1} d\boldsymbol{\rho}_a d\boldsymbol{\rho}_1 & I_2'' &= \iint \frac{g''(\mathbf{r}, \boldsymbol{\rho}_1, \boldsymbol{\rho}_a)}{\rho_a \rho_{01} \rho_1} d\boldsymbol{\rho}_a d\boldsymbol{\rho}_1 \\ I_3' &= \iint \frac{g'(\mathbf{r}, \boldsymbol{\rho}_1, \boldsymbol{\rho}_a)}{r \rho_{1a} \rho_1} d\boldsymbol{\rho}_a d\boldsymbol{\rho}_1 & I_3'' &= \iint \frac{g''(\mathbf{r}, \boldsymbol{\rho}_1, \boldsymbol{\rho}_a)}{r \rho_{1a} \rho_1} d\boldsymbol{\rho}_a d\boldsymbol{\rho}_1 \\ I_4' &= \iint \frac{g'(\mathbf{r}, \boldsymbol{\rho}_1, \boldsymbol{\rho}_a)}{\rho_a \rho_{1a} \rho_1} d\boldsymbol{\rho}_a d\boldsymbol{\rho}_1 & I_4'' &= \iint \frac{g''(\mathbf{r}, \boldsymbol{\rho}_1, \boldsymbol{\rho}_a)}{\rho_a \rho_{1a} \rho_1} d\boldsymbol{\rho}_a d\boldsymbol{\rho}_1 \end{aligned} \quad (11)$$

where $g'(\mathbf{r}, \boldsymbol{\rho}_1, \boldsymbol{\rho}_a) = \exp\{ik(\rho_1 + \mathbf{n}_0 \cdot \boldsymbol{\rho}_1) - \mu\rho_{0a}\} \begin{cases} r \cos \theta \\ r \sin \theta \exp(\mp i\phi) \end{cases}$

and $g''(\mathbf{r}, \boldsymbol{\rho}_1, \boldsymbol{\rho}_a) = \exp\{ik(\rho_1 + \mathbf{n}_0 \cdot \boldsymbol{\rho}_1) - \mu\rho_{0a}\} \begin{cases} \rho_a \cos \vartheta_a \\ \rho_a \sin \vartheta_a \exp(\mp i\eta_a) \end{cases}$

To evaluate these integrals the following expansions, recurrence laws and definite integrals are used:

$$\exp(ik\mathbf{n}_0 \cdot \boldsymbol{\rho}_1) = \left(\frac{\pi}{2k\rho_1} \right)^{1/2} \sum_{n=0}^{\infty} (2n+1) i^n J_{n+1/2}(k\rho_1) P_n(\cos \vartheta_1)$$

$$\rho_{01}^{-1} = \sum_{n=0}^{\infty} \gamma_n(r, \rho_1) P_n \cos \Theta_{01}$$

where $\gamma_n(r, \rho_1) = \begin{cases} \rho_1^n r^{-(n+1)} & \text{if } r > \rho_1 \\ r^n \rho_1^{-(n+1)} & \text{if } \rho_1 > r \end{cases}$

and a similar expansion for ρ_{1a}^{-1} .

$$\exp(-\mu\rho_{0a}) = -(r\rho_a)^{-1/2} \sum_{n=0}^{\infty} (2n+1) \zeta_n(r, \rho_a) P_n(\cos \Theta_{0a})$$

where $\zeta_n(r, \rho_a) = \begin{cases} \frac{\partial}{\partial \mu} \{K_{n+1/2}(\mu r) I_{n+1/2}(\mu \rho_a)\} & \text{if } r > \rho_a \\ \frac{\partial}{\partial \mu} \{K_{n+1/2}(\mu \rho_a) I_{n+1/2}(\mu r)\} & \text{if } \rho_a > r \end{cases}$

$$\cos \vartheta_a P_n(\cos \vartheta_a) = \frac{n+1}{2n+1} P_{n+1}(\cos \vartheta_a) + \frac{n}{2n+1} P_{n-1}(\cos \vartheta_a)$$

$$\sin \vartheta_a P_n(\cos \vartheta_a) = \frac{1}{2n+1} \{P_{n+1}^1(\cos \vartheta_a) - P_{n-1}^1(\cos \vartheta_a)\}$$

and similar recurrence laws for the angle θ

$$\iint P_s(\cos \Theta_{01}) P_n^m(\cos \vartheta_1) \exp(im\eta_1) \sin \vartheta_1 d\vartheta_1 d\eta_1 \\ = \frac{4\pi}{2n+1} P_n^m(\cos \vartheta_0) \exp(im\eta_0) \quad \text{if } s=n,$$

and 0 if $s \neq n$ with similar integrals for the other pairs of angles.

Finally by expressing the half integral order Bessel functions in terms of exponential functions the integrations over ρ_a and ρ_1 are carried out, and involve extensive use of the exponential integral function of complex argument. The definition of these functions in the complex plane was chosen to agree with that used in their tables of values. In every one of the integrals (11) the above recurrence relations for the Legendre polynomials must be used at some stage. It is therefore clear that $I_2 + I_3 - I_4$ is the sum of two expansions in

$$\begin{aligned} & \begin{cases} P_n(\cos \theta) \\ P_n^1(\cos \theta) \exp(\mp i\phi), \end{cases} \\ \text{the first starting with a term in } & \begin{cases} P_1(\cos \theta) \\ P_1^1(\cos \theta) \exp(\mp i\phi), \end{cases} \\ \text{the second with a term in } & \begin{cases} P_0(\cos \theta) \\ 0. \end{cases} \end{aligned}$$

On adding these expansions $I_2 + I_3 - I_4$ is expressed in the form $\Sigma I(r, P_n)$. The formulae, even for $I(r, P_0)$ and $I(r, P_1)$, are too complicated to be reproduced here.† It was found that at large values of r

$$I(r, P_n) \sim -\frac{16\pi^2 i}{k} \frac{\partial}{\partial \mu} \left[\frac{2}{\mu^6 r^1} + \frac{2(-1)^n(3\mu^4 + 6\mu^2 k^2 + 8k^4)}{\mu^4 r^1 (\mu^2 + 4k^2)^3} \exp(2ikr) \right] \begin{cases} (2n+1) P_n(\cos \theta) \\ 0 \end{cases} \\ + \frac{16\pi^2 i}{k} \frac{\partial}{\partial \mu} \left(\frac{12\delta_{1n}}{\mu^6 r^4} \right) \begin{cases} P_n(\cos \theta) \\ P_n^1(\cos \theta) \exp(\mp i\phi) \end{cases} + O(r^{-5}) \quad \dots\dots (12)$$

where δ_{1n} is the Kronecker δ .

Although $I_2 + I_3 - I_4 = \Sigma I(r, P_n)$, it must not be assumed that the asymptotic form of $I_2 + I_3 - I_4$ may be obtained by adding the asymptotic expansions of the $I(r, P_n)$. This arises from the fact that as r increases we require an increasing number of terms N to make

$$|I_2 + I_3 - I_4 - \sum_0^N I(r, P_n)| < \epsilon.$$

This increase of N with r more than offsets the improved accuracy of each of the asymptotic expansions (12). Ultimately as $r \rightarrow \infty$ $N \rightarrow \infty$ and the summation of the right-hand side of (12) diverges completely from $I_2 + I_3 - I_4$.

At small r it was found that

$$I(r, P_n) = O(r^{n-1}) \begin{cases} P_n(\cos \theta) \\ P_n^1(\cos \theta) \exp(\mp i\phi). \end{cases}$$

The additional potential $v_{01}(\mathbf{r})$ for the 1s-2p transition given by (10) and (11)

† Further details will be published in the form of a thesis to be submitted to the University of London.

must now be added to the matrix element $V_{01}(\mathbf{r})$ where

$$V_{01}(\mathbf{r}) = \int V(\mathbf{r}, \mathbf{r}_a) \psi_0(r_a) \psi_1^*(\mathbf{r}_a) d\tau_a = -\frac{\epsilon^2 Z^4}{\sqrt{2}} \left(\cos \theta \right. \\ \left. \times \frac{\partial}{\partial \mu} \left[\frac{2}{\mu^4 r^2} - \left(\frac{1}{\mu^2} + \frac{2}{\mu^3 r} + \frac{2}{\mu^4 r^2} \right) \exp(-\mu r) \right] \right). \quad \dots\dots(13)$$

The scattering amplitude $f_{01}(\theta, \phi)$ is obtained from

$$f_{01}(\theta, \phi) = -\frac{m}{2\pi\hbar^2} \int \exp\{i(\mathbf{k}\mathbf{n}_0 - k_{01}\mathbf{n}) \cdot \mathbf{r}'\} \{V_{01}(\mathbf{r}') + v_{01}(\mathbf{r}')\} d\tau' \quad \dots\dots(14)$$

where \mathbf{n} is a unit vector in the direction (θ, ϕ) . Denoting the change in momentum by the vector $K\mathbf{n} = (\mathbf{k}\mathbf{n}_0 - k_{01}\mathbf{n})$, and expanding $\exp(iK\mathbf{n} \cdot \mathbf{r}')$ in Bessel functions, (14) may first be integrated over (θ', ϕ') and then over r' as previously discussed when dealing with the other integrations. The result may be written in the form

$$f_{01}(\theta, \phi) = f_{01}^{(B)}(\theta, \phi) + f_{01}^{(C)}(\theta, \phi).$$

The Born amplitude is given by

$$f_{01}^{(B)}(\theta, \phi) = -2\sqrt{2}i \frac{Z^4}{a_0} \left\{ \frac{4\mu}{K(\mu^2 + K^2)^3} \right\} \left\{ (k - k_{01} \cos \theta)/K \right. \\ \left. - 2^{-1/2} k_{01} \sin \theta \exp(\mp i\phi)/K \right\}. \quad \dots\dots(15)$$

The uncorrected differential cross section is

$$(k_{01}/k) \sum |f_{01}^{(B)}|^2 = \frac{8Z^8}{a_0^2} (k_{01}/k) \left\{ \frac{16\mu^2}{K^2(\mu^2 + K^2)^6} \right\} \quad \dots\dots(16)$$

where the summation for the contributions arising from excitation of the three levels can be carried out by making use of the formula $K^2 = k^2 + k_{01}^2 - 2kk_{01} \cos \theta$ (Born 1926). The correction amplitude is

$$f_{01}^{(C)}(\theta, \phi) = -\frac{2\sqrt{2}}{a_0^2} Z^4 \left(\frac{1}{2^{-1/2}} \right) \sum_n \frac{\mathcal{J}(P_n)}{64\pi^3} \quad \dots\dots(17)$$

where $\mathcal{J}(P_n)$ results from the integration of $I(r', P_n)$ occurring in $v_{01}(\mathbf{r}')$ in (14) and the factors (1) and $(2^{-1/2})$ belong to the " $\cos \theta_a$ " and each of the " $\sin \theta_a \exp(\pm i\phi_a)$ " levels respectively. The corrected differential cross section is obtained again by summing over the three levels the formula

$$(k_{01}/k) \sum |f_{01}^{(B)}(\theta, \phi) + f_{01}^{(C)}(\theta, \phi)|^2. \quad \dots\dots(18)$$

The real and imaginary parts of $\mathcal{J}(P_0)$ and $\mathcal{J}(P_1)$ were calculated for electrons of $ka_0 = 2$ (54 volts) scattered by hydrogen after exciting the $2p(\cos \theta_a)$ level. At small angles they are all quite small compared with $f_{01}^{(B)}(\theta, \phi)$. Since the latter is purely imaginary, the contributions of the real parts of $\mathcal{J}(P_0)$ and $\mathcal{J}(P_1)$ in (18) are negligible. The imaginary parts converge rapidly as indicated in figure 1. This was also confirmed at other values of ka_0 . In the subsequent calculations only $\mathcal{J}(P_0)$ was therefore included and the correction was applied for electron scattering after excitation of the " $\cos \theta_a$ " level only. The correction for exciting the " $\sin \theta_a \exp(\pm i\phi_a)$ " levels has no zero-order contribution and was therefore ignored.

Figure 2 shows the corrections to be applied to the differential cross sections per unit θ . The corrections are quite small compared with Born's approximation at small angles, and decrease as the energy of the incident electrons increases. A final integration over all angles θ gives the total cross section (Elsasser 1927). This is shown in figure 3, where the calculations are extended to quite small

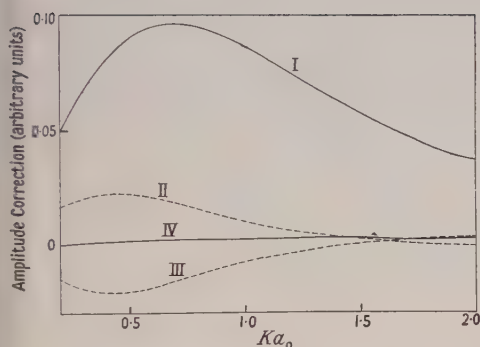


Figure 1. Imaginary parts of amplitude corrections at $ka_0=2$ for excitation of the $2p(\cos \theta_a)$ level of atomic hydrogen. The first-order corrections must be multiplied by $(k-k_{01} \cos \theta)/k$ before being applied to the Born amplitude.

I, zero order; II, first order (first part); III, first order (second part); IV, first order (total).

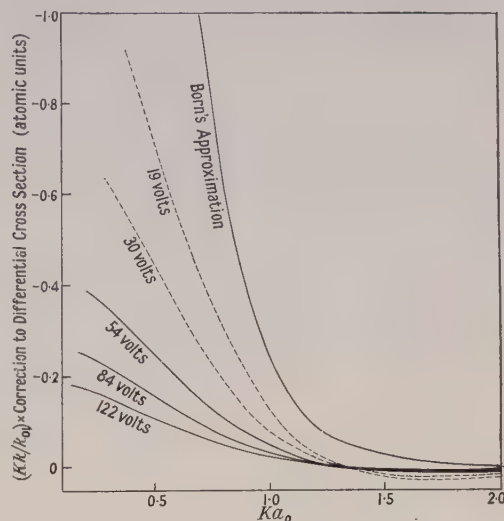


Figure 2. $(Kk/k_{01}) \times$ zero-order correction to differential cross section for inelastic scattering of electrons by atomic hydrogen after exciting the $2p$ level (broken line for very small values of ka_0).

$(2/k^2) \times$ area under graphs gives corrections to total cross sections in units of πa_0^2 . Born's approximation is also shown on the same scale, but refers to positive ordinates.

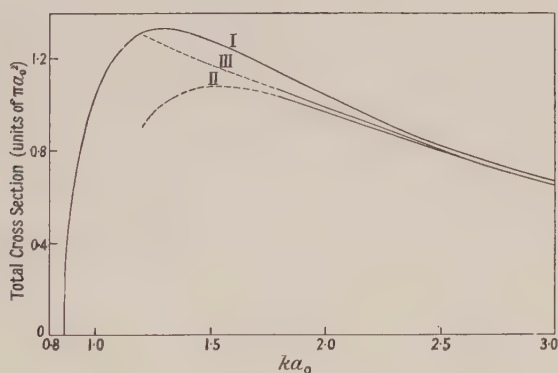


Figure 3. Total cross sections for the $1s-2p$ transition in atomic hydrogen by electron impact at different values of ka_0 .

I, Born's approximation; II, second approximation using all $k_s=k$ in the summation of the polarization corrections arising from different excited states; III, the same using all $k_s=k_1$ (broken line refers to very small energies). The energy of the incident electrons in electron volts is given by $13.5 (ka_0)^2$.

energies. In this region the approximation $k_s \simeq k$ for all terms in (6) is unlikely to be valid. To estimate the error inherent in this assumption the calculations were repeated replacing $k/2\pi$ by $k_i/2\pi$, the wave number which the scattered electron would have after losing the ionization energy to the hydrogen atom. By using k_i throughout in the evaluation of the additional potential (10) the rapid convergence of $\sum_n \mathcal{J}(P_n)$ will remain assured, and the correction is obtained from a system of coupled equations (1) and (2) in which all the wave numbers involved are reduced to the lowest one present, instead of being increased to the highest. The result is also indicated in figure 3. There is no very marked difference between the two methods above about 40 volts.

§ 4. THE 1S-2¹P TRANSITION IN HELIUM

Similar methods can be used for the 1S-2¹P transition in helium. The potential $V_{01}(\mathbf{r})$ is now given by

$$V_{01}(\mathbf{r}) = \iint V(\mathbf{r}, \mathbf{r}_a, \mathbf{r}_b) \psi_0(r_a, r_b) \psi_1^*(\mathbf{r}_a, \mathbf{r}_b) d\tau_a d\tau_b \dots\dots (19)$$

where the interaction energy $V(\mathbf{r}, \mathbf{r}_a, \mathbf{r}_b) = \frac{\epsilon^2}{|\mathbf{r} - \mathbf{r}_a|} + \frac{\epsilon^2}{|\mathbf{r} - \mathbf{r}_b|} - \frac{2\epsilon^2}{r}$

and the wave functions are (Eckart 1930)

$$\psi_0(r_a, r_b) = \psi_0(Z|r_a) \psi_0(Z|r_b)$$

and $\psi_1(\mathbf{r}_a, \mathbf{r}_b) = 2^{-1/2} \{ \psi_0(\gamma|r_a) \psi_1(\alpha|\mathbf{r}_b) + \psi_0(\gamma|r_b) \psi_1(\alpha|\mathbf{r}_a) \}$

with $Za_0 = 27/16$, $\gamma a_0 = 2.003$, $\alpha a_0 = 0.965$.

The uncorrected differential cross section becomes

$$\frac{16 Z^3 \alpha^5 c^2}{a_0^2} (k_{01}/k) \left\{ \frac{16 \mu^2}{K^2 (\mu^2 + K^2)^6} \right\} \dots\dots (20)$$

in which $\mu a_0 = (Z + \frac{1}{2}\alpha) a_0 = 2.17$ and $c^2 = Z^3 \gamma^3 \pi^{-2} [\int \exp \{ -(Z + \gamma) r_b \} d\tau_b]^2 = 0.978$.

The energy required for excitation is 21.2 volts giving

$$a_0^2 (k^2 - k_{01}^2) = 21.2/13.53 = 1.567$$

compared with $a_0^2 (k^2 - k_{01}^2) = 0.75$ in hydrogen. The ratio of these two quantities is the same as the ratio of the values of $\mu^2 a_0^2$ for helium $(2.17)^2$ and for hydrogen $(1.5)^2$. It becomes possible therefore to obtain the uncorrected differential and total cross sections in helium at wave numbers $(2.17/1.5)(k/2\pi)$ from the values in hydrogen at wave numbers $k/2\pi$ by direct proportion, since in (20) the values of μ and K (for fixed angles of scattering) are all $2.17/1.5$ times as great as the corresponding values in hydrogen.

The additional potential which must be added to $V_{01}(\mathbf{r})$ to obtain a second approximation is

$$\begin{aligned} v_{01}(\mathbf{r}) = & -\frac{m}{2\pi\hbar^2} \iiint V(\mathbf{r}, \mathbf{r} + \boldsymbol{\rho}_a, \mathbf{r} + \boldsymbol{\rho}_b) \\ & \times V(\mathbf{r} + \boldsymbol{\rho}_1, \mathbf{r} + \boldsymbol{\rho}_a, \mathbf{r} + \boldsymbol{\rho}_b) \\ & \times \frac{\exp \{ ik(\rho_1 + \mathbf{n}_0 \cdot \boldsymbol{\rho}_1) \}}{\rho_1} \\ & \times \psi_0(\mathbf{r} + \boldsymbol{\rho}_a, \mathbf{r} + \boldsymbol{\rho}_b) \psi_1^*(\mathbf{r} + \boldsymbol{\rho}_a, \mathbf{r} + \boldsymbol{\rho}_b) d\boldsymbol{\rho}_a d\boldsymbol{\rho}_b d\boldsymbol{\rho}_1. \dots\dots (21) \end{aligned}$$

The product of the interaction energies in (21) is

$$\epsilon^4 \left(\frac{1}{\rho_a} + \frac{1}{\rho_b} - \frac{2}{r} \right) \left(\frac{1}{\rho_{1a}} + \frac{1}{\rho_{1b}} - \frac{2}{\rho_{01}} \right)$$

and involves product terms of the type $\epsilon^4/\rho_n \rho_{1b}$ in addition to all the terms already discussed in the case of hydrogen. The latter terms can be obtained from the hydrogen calculations by direct proportion. The zero order contribution due to the new terms is added to this, and the remainder of the calculations carried out as previously. The results are shown in figures 4 and 5.

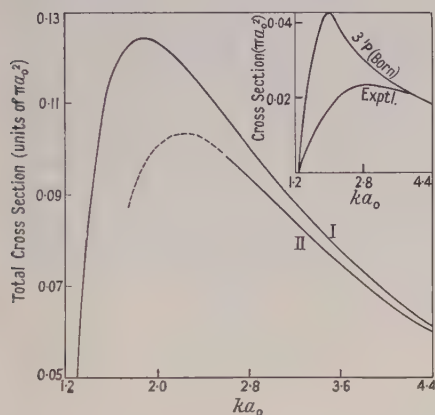


Figure 4. Total cross sections for 1^1S-2^1P transition in helium. I, Born's approximation; II, second approximation shown as broken line at very low energies. The energy of the incident electrons in electron volts is given by $13.5(ka_0)^2$.

In the inset the cross sections for the excitation of the 3^1P state are shown. The discrepancies between the values calculated by Born's first approximation and those obtained experimentally are of similar nature as the differences between the first and second approximations calculated for the excitation of the 2^1P state. Note that the vertical scale for the main graph begins at $0.05 \pi a_0^2$ and not at 0.

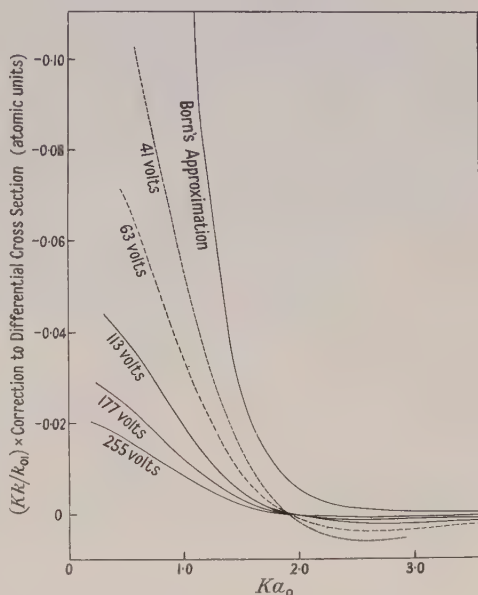


Figure 5. $(Kk/k_0) \times$ zero-order correction to differential cross sections for 1^1S-2^1P transition in helium. Born's approximation refers to positive ordinates.

§ 5. DISCUSSION AND CONCLUSION

The principal assumption in the above calculations is that the effect of the scattering field on the incident wave is small. In this respect the treatment may be compared with the approximate solutions for the currents in two loosely coupled circuits (A) and (B), each containing self inductance and resistance, with a source of alternating e.m.f. in (A) only. As a first approximation the effect of the current induced in (B) on circuit (A) is ignored. The solution for the current in (A) may then be used to obtain an approximate value of the current in (B), which in turn makes it possible to calculate the effect of (B) on (A) and hence to find a better approximation to the current in (A). In this way successive approximations to the current in either circuit are obtained.

In the present case Born's treatment gives approximate solutions for all the $F_s(\mathbf{r})$, which are then used to calculate the effect of the excitations of all states (s)

on the inelastic scattering corresponding to one particular state (n). It was found that this effect is in general small compared with Born's approximation at small angles of scattering and decreases with increasing energy of the incident electrons, which confirms the assumption that the incident wave is only slightly perturbed by its interaction with the atom under these conditions. The correction reduces the differential cross section at small angles.

At large angles of scattering the correction exceeds the first approximation (which decreases as K^{-14}) and can therefore in general not be regarded as accurate.

The correction to the total cross section includes the effect for all angles and will be a good estimate of this polarization, since in the final integration the main contribution comes from the small angle scattering. The approximation $k_s \simeq k$ for all excited states, made in the calculation of the correction term, introduces less error at higher electron energies than at lower, but an estimate made in the case of hydrogen indicates that the error is fairly small even at electron energies as low as 40 volts. The final calculations and graphs, like the ones for Born's approximation, have been continued below about 40 volts for hydrogen and 80 volts for helium to give a rough estimate of the order of magnitude of the correction.

The results discussed above and shown in figures 2 to 5 refer to zero-order corrections only. As indicated in figure 1, the first-order correction in the case of excitation of the " $\cos \theta_a$ " level is quite negligible. For the " $\sin \theta_a \exp(\pm i\phi_a)$ " levels the first-order correction is not so small, since the two parts of this correction shown in figure 1 have to be weighted differently on account of the change in the recurrence formula of the Legendre polynomials applying in this case. An estimate of the first-order correction indicated some further decrease in the total cross sections.

Although there is no direct observational evidence about the cross sections for excitation of either the 2p state of hydrogen or 2¹P state of helium, there seems little doubt that the correction introduced by the second Born approximation is of the right sign and about the magnitude which would be expected. In the inset of figure 5 a comparison of the observed excitation function of the 3¹P state of helium with that calculated by Born's first approximation is illustrated, it being assumed that above 400 eV electron energy the two agree (Massey and Burhop 1952, p. 150). It will be seen that the calculated values begin to deviate from the observed at about the energy indicated from the present calculations. The discrepancy also increases as the electron energy decreases at about the correct rate.

It seems then that, except quite close to the threshold, where the cross section is relatively small, introduction of the second Born approximation effects a very considerable improvement. Eventually, as the threshold is approached it would be necessary to take into account further approximations and the series may eventually diverge. However, for optically allowed transitions the cross section is small under these conditions and it is less important to be able to make accurate predictions.

ACKNOWLEDGMENTS

I am greatly indebted to Professor H. S. W. Massey for his interest and encouragement in this work and for the valuable advice he has frequently given me.

I would also like to thank Dr. H. R. Heath for the facilities he has provided at Battersea Polytechnic.

REFERENCES

- BATES, D. R., FUNDAMINSKY, A., LEECH, J. W., and MASSEY, H. S. W., 1950, *Phil. Trans. Roy. Soc. A*, **243**, 93.
- BORN, M., 1926, *Göttingen Nachr. Math. Phys. Klasse*, 146.
- BRANDEN, B. H., and DALGARNO, A., 1953, *Proc. Phys. Soc. A*, **66**, 268.
- ECKART, C., 1930, *Phys. Rev.* **36**, 878.
- ELSASSER, W., 1927, *Z. Phys.*, **45**, 522.
- ERSKINE, G. A., and MASSEY, H. S. W., 1952, *Proc. Roy. Soc. A*, **212**, 521.
- MASSEY, H. S. W., and BURHOP, E. H. S., 1952, *Electronic and Ionic Impact Phenomena* (Oxford : Clarendon Press).
- MASSEY, H. S. W., and MOHR, C. B. O., 1933, *Proc. Roy. Soc. A*, **139**, 187; 1934, *Ibid.*, **146**, 890.
- MASSEY, H. S. W., and MOISEWITSCH, B. L., 1954, *Proc. Roy. Soc. A*, in the press.
- MOTT, N. F., and MASSEY, H. S. W., 1949, *The Theory of Atomic Collisions* (Oxford : Clarendon Press).

Angular Distributions in the $^{10}\text{B}(\text{d}, \text{p})^{11}\text{B}$ Reaction

BY N. T. S. EVANS AND W. C. PARKINSON†

Cavendish Laboratory, Cambridge

MS. received 15th February 1954, and in amended form 12th April 1954

Abstract. Angular distributions of six proton groups from the reaction $^{10}\text{B}(\text{d}, \text{p})^{11}\text{B}$ were obtained using a scintillation counter spectrometer and an incident deuteron energy of 7.7 MeV. Distributions for the three longest range groups were also obtained at the additional deuteron energies of 6.2, 7.1 and 8.0 MeV. The results are largely compatible with the normal theory of deuteron stripping, and the five longest range proton groups appear to correspond to ingoing p-neutrons. The properties of the first excited state in ^{11}B are, however, in some doubt. Possible spin assignments for the lower levels of ^{11}B arising from excitation within the p-shell are considered and the corresponding relative values of the neutron capture probability are listed.

§ 1. INTRODUCTION

It is well known that the parities of the energy levels of a residual nucleus, together with some information about the spins, may be derived (Butler 1950) from a study of the stripping process for deuterons of energy about 10 MeV. This paper describes a study of the reaction $^{10}\text{B}(\text{d}, \text{p})^{11}\text{B}$ using 7.7 MeV deuterons from the Cambridge University cyclotron in conjunction with a scintillation crystal spectrometer. Tentative assignments of spins and parities for a number of levels of ^{11}B were made by Jones and Wilkinson (1952) as a result of a study of the $^7\text{Li}(\alpha, \gamma)^{11}\text{B}$ reaction, but, as they pointed out, an independent determination of the parities, particularly as obtained from the stripping reaction, would be of considerable interest.

In addition to determining the parities of a number of the levels, a preliminary investigation was made of the part played in the reaction by processes other than simple stripping.

§ 2. APPARATUS

2.1. Target Chamber

The deuteron beam was defined by two vertical slits, 2 mm and 5 mm wide respectively, placed 8 ft apart in the fringe field of the cyclotron magnet; these served to reduce the spread in energy of the beam. After passing through a focusing magnet, the beam was further collimated by a circular lead liner of 1 cm internal diameter located at the entrance of the target chamber (figure 1). The upper half of the chamber carried the proton detector and could be rotated, permitting measurements over a range $\pm 140^\circ$ with respect to the incident deuteron beam. The protons entered the counter through an aperture of 1 cm diameter and an aluminium window 0.0006 in. thick. The elastically scattered deuterons were stopped in lead foil of just sufficient thickness placed inside the target chamber in front of the window.

† On leave from the Department of Physics, University of Michigan.

The targets were prepared by allowing a slurry of amorphous boron and water to dry on backing foils of gold 0.000 05 in. thick. Targets both of commercial boron (19% ^{10}B) and of enriched boron (95% ^{10}B)[†] were used. The relative intensities of the proton groups measured in each case served as a check on the identification of those groups due to the $^{10}\text{B}(d, p)^{11}\text{B}$ reaction. The targets were thin enough to have no significant effect on the resolution.

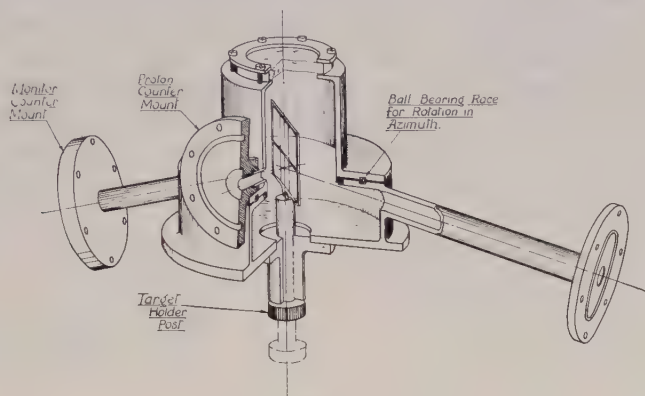


Figure 1. The scattering chamber.

The target could be displaced vertically so as to bring a similar foil without boron into the beam for background measurements. It could also be rotated about an axis perpendicular to the beam, although it was inclined at an angle of 20° for most measurements.

The deuteron beam was monitored by a second crystal counter which detected deuterons scattered elastically through an angle of 24° by the target nuclei. Their intensity was reduced to a suitable value by a lead stop 1 mm in diameter. The bottom and sides of the target chamber were lined with lead to stop the main deuteron beam and to reduce the background counting rate.

2.2. The Crystal Counters

The crystal was 1 cm in diameter and was approximately 0.040 in. thick so as to reduce the number of γ -rays detected. This thickness was sufficient to stop all protons with energies less than about 14 mev. Proton groups of higher energy were first slowed down by aluminium foils placed in front of the crystal. The crystal itself was cleaved in a dry box and immediately sealed in an air-tight Perspex holder by an aluminium foil 0.0006 in. thick.

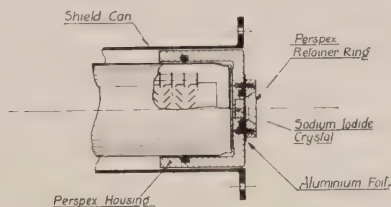


Figure 2. The NaI(Tl) crystal mounting.

The Perspex holder fitted over the end of the photomultiplier as shown in figure 2. An EMI 5311 photomultiplier was used because it gave the best energy

[†] We are indebted to the Atomic Energy Research Establishment, Harwell, for supplying us with the enriched ^{10}B .

resolution of the tubes available to us. Nine stages of electron multiplication were used, and the output taken from the ninth dynode in order to obtain positive pulses; the remaining dynodes were earthed.

A cathode follower, mounted at the base of the photomultiplier, and a matched coaxial cable fed the pulses into an amplifier with an integrating time constant of $0.2\ \mu\text{sec}$. The output pulses were displayed on a multi-channel kicksorter (Hutchinson and Scarrott 1951). The voltage supply of the photomultiplier was an electronically stabilized power pack. To reduce drift the counter was operated in the 'plateau' region, where the counting rate increases least rapidly with voltage. The plateau was located by plotting counting rate against counter voltage for γ -rays from a ^{134}Cs source. For the photomultiplier used the plateau occurred with 70 volts per stage, with four times this voltage between the photocathode and the first dynode. Under these conditions no noticeable drift occurred in the location of the proton groups.

The monitor counter consisted of a NaI(Tl) crystal cut to a thickness of approximately 0.05 in. and an RCA 5819 photomultiplier operating at 1120 v. The 5819 was used because of the change in counting rate with time of the EMI 5311 at high counting rates, due presumably to charge collecting on the dynode insulators. The output was taken from the tenth dynode and the pulses, after amplification, were recorded on a fast scaling unit.

§ 3. EXPERIMENTAL DETAILS

3.1. *Limitations on Resolution*

The resolution of the experimental arrangement is determined mainly by five factors: (i) the energy spread in the incident beam, (ii) the finite and non-uniform thickness of the target and backing, (iii) the change in proton energy over the finite range of angles covered by the detector, (iv) range straggling in the absorbers between the target and detector, (v) the inherent energy resolution of the detector. The first four factors produce a spread in energy of the protons reaching the crystal and result in a spread in amplitude of the detector voltage pulses which may be considerably greater than that due to the detector alone. It is of interest, then, to assess the relative contribution of each to the overall resolution.

The deuteron beam from the cyclotron has a spread in energy of the order of 5% to 10%. Without additional magnetic focusing this may be reduced only at the expense of beam intensity. The use of slits in the fringe field of the cyclotron magnet reduced the spread to approximately 2%, which represented a reasonable compromise.

The energy spread due to target thickness is a result of the stripping reaction occurring at different depths in the target and is easily calculated from the rates of energy loss (Aron *et al.* 1949) of deuterons and protons in the target and backing material. By using thin targets this effect was made negligibly small without undue sacrifice of counting rate. Also, because the targets were thin, their lack of uniformity contributed a negligible amount to the energy spread. It is perhaps worth noting that in this respect the crystal spectrometer has a decided advantage over a proportional counter telescope in that the former records all the pulses in a proton group, whereas the latter is normally used to obtain a differential range curve. Thus for measurements of a given statistical accuracy to be taken in the same total time, the energy spread due to the incident beam and target thickness may be reduced considerably with the crystal spectrometer.

The problem of detector geometry has been treated for a special case by Livingston and Bethe (1937). Recently Beach (1952) has treated the more general case. His results indicate that for our arrangement the energy spread resulting from the finite solid angle is of the order of 0.1% and is thus negligible.

The effect of range straggling in the aluminium absorbers can be estimated from the straggling curve given by Bethe (1949). For example, in completely stopping 13 mev protons the range straggling is about 1.7%. Since the protons are slowed down but not stopped in the aluminium, this value represents an upper limit.

The factors affecting the resolution of the combined crystal and photomultiplier have been treated by Garlick and Wright (1952). These are (i) the variation in intensity of successive light pulses reaching the photocathode due to imperfect crystals and to absorption and reflection in the crystal and optical system, (ii) variations due to the low photoelectric response and non-uniformity of the photocathode, and (iii) statistical fluctuations due to the finite number of photoelectrons produced per pulse. They have shown experimentally that the half-width of the output pulse does vary inversely as the square root of the number of photoelectrons per light pulse. Thus for a given crystal and optical system the inherent resolution of the detector varies inversely as the square root of the energy of the incident particle. Perhaps the greatest gain in counter resolution is to be made by improving the quality of the optical system and the photoelectron collection efficiency of the photomultiplier.

The important factors in the present measurements were energy spread of the deuteron beam, range straggling and detector resolution. Protons of 13 mev expending their whole range in the crystal produced voltage pulses the half-width of which was 10%, due almost entirely to the detector. (Considerable improvement in this figure should be possible by improving the optical system and by having a larger selection of photomultipliers from which to choose.) Because of the non-linearity of the range-energy curves, and the fact that the resolution of the detector varies inversely as the square root of the energy of the incident particle, the effective resolution can be improved by slowing down the proton groups before they enter the crystal. Two factors have to be considered, namely the variation of the half-width of the voltage pulses due to a given proton group, and the change in the mean separation of two groups, as absorber is added.

The voltage spread ΔV of a given group of mean pulse height V will be a minimum when the slope of the $[(\Delta V)^2, V]$ curve of the detector is equal and opposite to the slope of the $[(\Delta V)^2, V]$ curve obtained from all the other factors combined. A semiquantitative estimate of the spread can be made by assuming a range-energy relationship of the form $R = kE^{n/2}$. A value of $n = 3.5$ gives a reasonable fit to the curve for protons in aluminium down to approximately 4 mev. On the assumption that range straggling is gaussian, it can be shown that the spread in energy ΔE_{2s} for a proton group slowed down in aluminium to an energy E_2 from an initial energy E_1 is

$$\Delta E_{2s} = \frac{2}{n} \sqrt{\frac{2}{\pi}} \left\{ [(S_1 E_1)^2 - (S_2 E_2)^2 + 2(1 - 2/n)] \int_{R_2}^{R_1} \frac{S^2 E^2}{R} dR \right\}^{1/2}$$

where S_1 and S_2 are the values of range straggling of protons of energy E_1 and E_2 (and range R_1 and R_2) stopped completely in aluminium. It also follows that the spread in energy ΔE_2 at an energy E_2 due to an initial spread ΔE_1 at E_1 is

$$\Delta E_2 = \left(\frac{E_1}{E_2} \right)^{(n-2)/2} \Delta E_1.$$

The 2% spread in energy of the incident deuteron beam produced a spread ΔE_{1b} of the initial proton groups of almost 0.13 MeV which, after slowing down in foil to about 4 MeV, resulted in a value of $(\Delta E_{2b})^2$ approximately five times that due to range straggling. If ΔE_{2d} and E_2 are measured in MeV, then the spread due to the detector can be represented by $(\Delta E_{2d})^2 \simeq 0.12 E_2$. Thus the total energy spread $\Delta E_T \simeq [(\Delta E_{2b})^2 + (\Delta E_{2d})^2]^{1/2}$ was due mainly to the detector and to the non-homogeneity of the incident deuteron beam, and had a minimum of roughly 600 keV at about $E_2 = 4$ MeV.

The separation of two adjacent proton groups increases as absorber is added. As an example, a separation of 0.6 MeV between two groups near 13 MeV is increased to 1.5 MeV when the groups are slowed down to about 4 MeV. While it is possible to add just enough foil to stop the lower of the two groups completely, the high background counting rate due to γ -rays makes it impracticable to reduce the mean energy of the group under observation to less than about 4 MeV. This is not a serious drawback since the energy spread of the individual groups becomes rapidly worse below 4 MeV.

3.2. Experimental Procedure

Since it was observed that the widths of the proton groups remained very nearly constant for all angles of the proton counter up to 70° , the intensities of the groups at each angle were estimated from the heights of the peaks displayed on the kicksorter. As a check on this method the areas under the curves for each group were determined in several cases. Any errors due to possible secular changes in the apparatus were minimized by repeatedly covering a range of angles and combining the separately normalized angular distributions thus obtained. The monitor count was corrected for the different numbers of scattering centres in the background foil and the target foil. The correction factor was measured by alternating between the two foils a number of times while the cyclotron beam was held reasonably constant.

The differential cross sections and the angles of observation were converted to the centre-of-mass system. No corrections were made for the finite width of the deuteron beam or for the solid angle of the proton counter, as errors due to these were negligible compared with the statistical fluctuations in the counts. The proton counting rate was reduced below 100 per second to reduce kicksorter counting losses.

§ 4. RESULTS

The proton spectrum obtained with an enriched ^{10}B target is shown in figures 3 and 4. In figure 3 the proton groups Q_0 and Q_1 are not resolved, since the former has not come to rest in the crystal. The addition of 60 mg cm^{-2} of aluminium foil in front of the crystal resulted in the spectrum shown in figure 4. With the apparatus employed it was not possible to resolve groups Q_4 and Q_5 , or groups Q_8 , Q_9 and Q_{10} .

The observed angular distributions for the groups Q_0 , Q_1 , Q_2 , Q_3 , $Q_{4,5}$ and $Q_{8,9,10}$ are shown in figures 5–10, together with the theoretical distributions calculated from the 'modified' Butler formula (Butler and Salpeter 1952) using $r_0 = 6.0 \times 10^{-13}$ cm. (It might be noted that the use of the modified Butler formula requires essentially the same value of r_0 as the Huby formula (Bhatia *et al.* 1952).) The wave number of the neutrons was calculated from the value of $E_n = -(Q + \epsilon)$ rather than as given by Butler, since the modified form is not consistent with the original assumption of an infinitely heavy target nucleus.

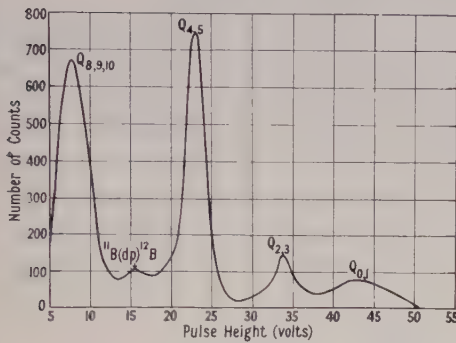


Figure 3. The proton spectrum obtained in the reaction $^{10}\text{B}(d, p)^{11}\text{B}$. Proton groups Q_0 and Q_1 are not resolved; the proton group Q_0 does not come to rest in the crystal.

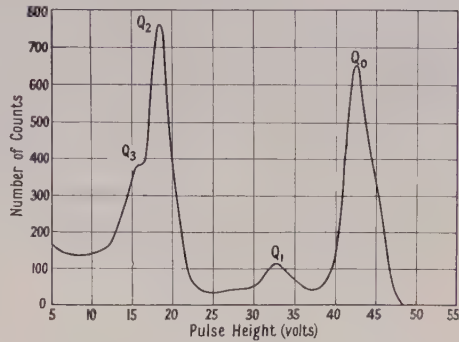


Figure 4. The proton spectrum obtained with 60 mg cm^{-2} of aluminium in front of the crystal. Proton groups Q_0 and Q_1 are both brought to rest in the crystal.

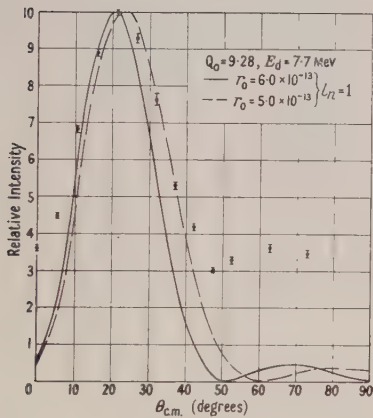


Figure 5. The angular distribution of protons in the centre-of-mass system for the ground state group Q_0 in the $^{10}\text{B}(d, p)^{11}\text{B}$ reaction.

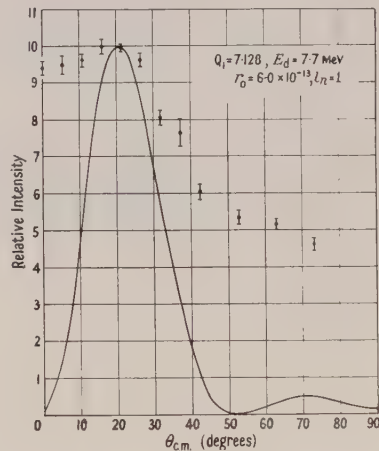


Figure 6. The angular distribution of proton group Q_1 in the $^{10}\text{B}(d, p)^{11}\text{B}$ reaction.

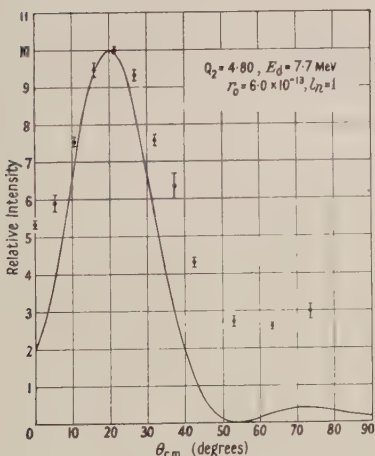


Figure 7. The angular distribution of proton group Q_2 in the $^{10}\text{B}(d, p)^{11}\text{B}$ reaction.

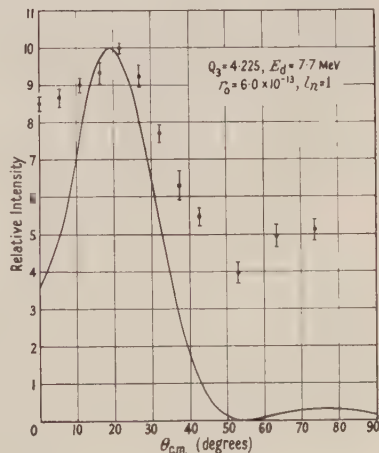


Figure 8. The angular distribution of proton group Q_3 in the $^{10}\text{B}(d, p)^{11}\text{B}$ reaction.

The data are summarized in the table. The measured levels are listed in column 1, with their respective excitation energies given in column 2. Column 3 lists the l -values assigned to the incoming neutron. For the unresolved levels the possibility of other l -values occurring can certainly not be excluded, nor should it be inferred that admixtures of $l_n = 3$ or $l_n = 5$ do not occur in the resolved levels.

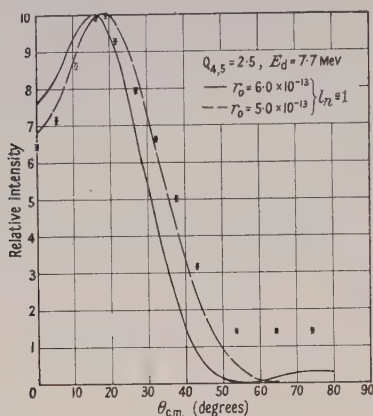


Figure 9. The angular distribution of proton groups $Q_{4,5}$ and Q_5 (unresolved) in the $^{10}\text{B}(\text{d}, \text{p})^{11}\text{B}$ reaction.

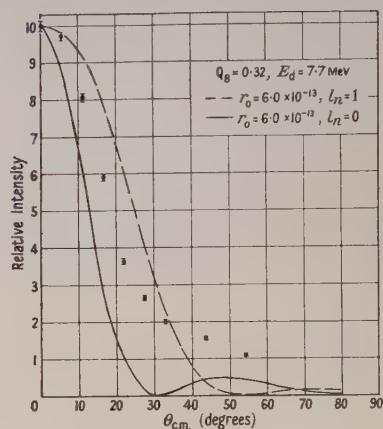


Figure 10. The angular distribution of proton groups Q_8 , Q_9 and Q_{10} (unresolved) in the $^{10}\text{B}(\text{d}, \text{p})^{11}\text{B}$ reaction.

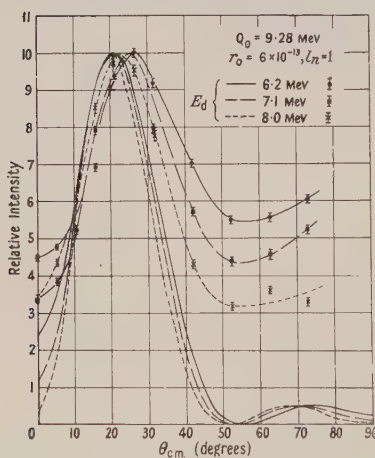


Figure 11. The angular distributions obtained for proton group Q_0 at deuteron bombarding energies of 6.2, 7.1 and 8.0 mev.

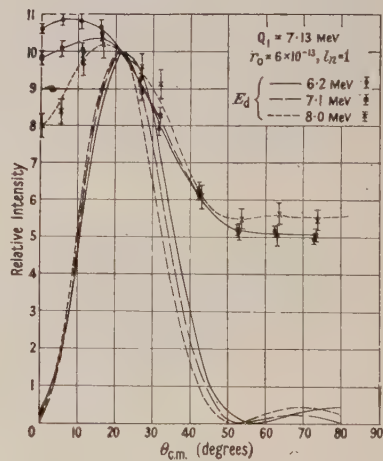


Figure 12. The angular distributions obtained for proton group Q_1 at deuteron bombarding energies of 6.2, 7.1 and 8.0 mev.

In addition to these results there was evidence for a proton group, presumably Q_7 , with an energy about 0.5 mev less than the Q_8 group, which appeared to correspond to an ingoing neutron for which $l_n = 1$. It was not resolved sufficiently, however, for any accurate angular distribution to be obtained.

No evidence was found for proton groups between $Q_{4,5}$ and Q_7 corresponding to the 7.30 mev (Van Patter *et al.* 1951) and 7.99 mev (Elkind and Sperduto 1953)

levels in ^{11}B . These levels are presumably very weak, the group corresponding to the 7.30 mev level perhaps being lost in the tail of $Q_{4,5}$ and that corresponding to the 7.99 mev level being masked by the ground state protons of the $^{11}\text{B}(d, p)^{12}\text{B}$ reaction.

Figures 11 to 13 show the angular distributions obtained for the groups Q_0 , Q_1 and Q_2 at deuteron energies of 6.2, 7.1 and 8.0 mev, together with the calculated distributions. Data taken at a deuteron energy of 6.7 mev for the three groups are intermediate to the data of 6.2 and 7.1 mev but, to avoid confusion, are not shown.

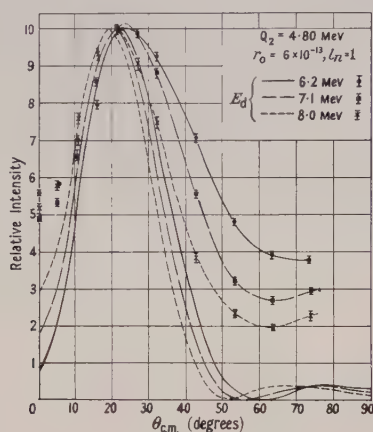


Figure 13. The angular distributions obtained for proton group Q_2 at deuteron bombarding energies of 6.2, 7.1 and 8.0 mev.

§ 5. DISCUSSION

In the table are listed the l -values associated with each level of ^{11}B for which a reliable measurement could be taken. The levels up to and including at least one member of the 6.8 mev doublet appear to have not only odd parity but some contribution of $l_n = 1$. Since the spin of ^{10}B in the ground state is 3, the existence in the (d, p) reaction of an $l_n = 1$ component, no matter how small, restricts the spin j_f of

(1) Group	(2) Excitation (mev)	(3) l_n -value	(4) Rel. int.	(5) Λ_{l_n}	(6) j_f (assumed)	$\frac{\Lambda_{l_n}}{2j_f+1}$	(7) j_f (assumed)	$\frac{\Lambda_{l_n}}{2j_f+1}$
Q_0	0	1	10.1	5.0	3/2	1.3	3/2	1.3
Q_1	2.14	1	2.3	0.9	1/2	0.45	7/2	0.12
Q_2	4.46	1	6.0	1.6	5/2	0.26	5/2	0.26
Q_3	5.03	1	2.23	0.5	3/2	0.13	3/2	0.13
$Q_{4,5}$	$\begin{cases} 6.76 \\ 6.81 \end{cases}$	1	35	5.7	7/2	—	1/2	—
$Q_{8,9,10}$	$\begin{cases} 8.93 \\ 9.19 \\ 9.28 \end{cases}$	0-1?	126	—	—	—	—	—

that level to $3/2 \leq j_f \leq 9/2$. Our results, therefore, cannot be reconciled with the tentative assignments made by Jones and Wilkinson (1952) from their study of the $^7\text{Li}(\alpha, \gamma)^{11}\text{B}$ reaction, in which they assign even parity to the second excited state and a spin 1/2 to the first excited state.

Odd parity is consistent with the shell model, provided these levels arise from excitation within the p-shell. The ground state configuration for ^{11}B is presumed to be $(p_{3/2})^7$, giving rise to a spin of $3/2$. A possible configuration for the first few excited states is $(p_{3/2})^6(p_{1/2})^1$. On this assumption Inglis (1953) has shown that for the first excited state a spin $1/2$ is to be expected on the basis of both pure j - j and intermediate coupling. Pure L - S coupling is unlikely since it would imply a spin $1/2$ for the ground state with the $3/2$ level lying close to it. With a value of about 5 for the intermediate coupling parameter a/K defined by Inglis the ordering of the first five levels is $3/2, 1/2, 5/2, 7/2, 3/2$. Thus the difficulty persists of reconciling spin $1/2$ for the first excited state with the interpretation of the data. It must be stressed that the character of the data for this state is unusual, and an assignment of $l_n = 1$ for the transition should be viewed with some doubt. Nevertheless it is difficult to believe that it contains no component less than $l_n = 2$.

A possible explanation is obtained by assuming ^{11}B to have the configuration $(p_{1/2})^4(p_{3/2})^3$. This implies an interchange of the ordering of the $p_{1/2}$ and $p_{3/2}$ sub-shells. In support of this questionable assumption it might be noted that Flowers (1952) in calculating the magnetic moment of the ^{11}B ground state, assuming j - j coupling between the nucleons, finds better agreement for the configuration $(p_{3/2})^5(p_{1/2})^2$ than for $(p_{3/2})^7$. Assuming a complete interchange to occur, the levels then arise from the coupling of three $p_{3/2}$ nucleons, for which the ordering as given by Inglis, and also as calculated by Edmonds and Flowers (1952) for a suitable range of force parameter, is $3/2, 7/2, 5/2, 3/2$ and $1/2$. This is not inconsistent with our results, since one member of the close doublet at 6.8 MeV could have a spin $1/2$, implying an $l_n = 3$ transition, which might be so weak as to be masked by the other member of the doublet having $l_n = 1$.

Following the procedure of Holt and Marsham (1953), the relative intensities of the various proton groups were determined and the neutron capture probabilities Λ_{l_n} calculated, using the expression of Bhatia *et al.* (1952). These are listed in columns (4) and (5) respectively of the table. The intensities used in the calculations were those obtained from the peaks of the angular distributions. For proper comparison the values of Λ_{l_n} should be divided by the statistical weight factor $2j_f + 1$ where j_f is the spin of the final state. Since states of similar constitution are expected to have similar neutron capture probabilities, with the values for single particle states being somewhat larger than those formed by excitation within the configuration, one might expect the value of $\Lambda_{l_n}/(2j_f + 1)$ for the ground state to be significantly larger than for the excited states arising from the $(p_{1/2})^4(p_{3/2})^3$ or $(p_{3/2})^6(p_{1/2})^1$ configurations. Further, these states would be expected to have approximately the same values of $\Lambda_{l_n}/(2j_f + 1)$. Column (6) of the table lists the sequence of j_f values expected for j - j coupling in the $(p_{3/2})^6(p_{1/2})^1$ configuration, together with the resulting values of $\Lambda_{l_n}/(2j_f + 1)$. Column (7) gives the corresponding quantities for the $(p_{1/2})^4(p_{3/2})^3$ configuration. While the results bear out the above remarks, there seems to be little to choose between the two configurations, although the scatter is less for $(p_{1/2})^4(p_{3/2})^3$. Little can be said about the $Q_{4,5}$ doublet since the relative contributions from the two levels are unknown, but it appears that one may be a single particle state.

The assumption of the $(p_{1/2})^4(p_{3/2})^3$ configuration still leads to difficulties when applied to the results of Jones and Wilkinson (1952). In the light of the parity determinations by the stripping reaction, their data can be interpreted,† though less

† Private communication. We are indebted to Drs. Wilkinson and Jones for many enlightening discussions.

well, as giving $5/2-$ for the 4.46 meV level, and $3/2-$ for the 6.81 meV level. However, the near absence of γ -transitions to the 2.14 meV level still requires them to assign it a spin of $1/2$ or $9/2$ or higher. The values $1/2$ or greater than $9/2$ would be at variance with our admittedly questionable conclusion that $l_n = 1$ for this level. The value $9/2$ is consistent with $l_n = 1$, but would be excluded by the Pauli principle if this level represents an excitation within the p-shell. In support of the assignment of spin $1/2$ to the first excited state, Thirion (1951) finds a $(p\gamma)$ coincidence ratio of unity between 90° and 180° in the $(d, p\gamma)$ reaction. One hesitates to place too much weight on these results, however, since the measurements were made at a deuteron energy of 790 keV, and the statistics are about 8%.

A striking feature of the data is the deviation from the theoretical angular distributions. The variation with deuteron energy, especially for the 2.14 meV level, is rather unexpected and may suggest some kind of interference effect. It is significant that the variation cannot be accounted for by the assumption of an isotropic 'background' due to compound nucleus formation. However, it is reasonable to believe that a more complete theory of (d, p) reactions, particularly one in which the interaction of the proton and nucleus is included, will give rise to interference terms.† The introduction of potential scattering of the proton by the nucleus (Horowitz and Messiah 1953) does not seem adequate to explain all these anomalies. It is possible that coulomb scattering may help to account for the relatively large cross section at high angles (Grant, private communication).

The variation with energy indicates that some uncertainty exists in the interpretation of stripping data. The angular distribution of Q_1 at 6.2 meV would hardly be interpreted as an $l_n = 1$ transition as is suggested by the data at 8.0 meV. A mixture of $l = 0$ and 2 does not improve the fit. While it is probable that such a variation is rare, it will be of interest to look for other cases. Transitions for which $l_n = 1$ are particularly suited for study since the angular distributions at small angles cannot contain $l_n = 0$ components and are not likely to be influenced by mixtures of higher l -values. Distributions for which the cross section at large angles is an appreciable fraction of the peak cross section can be expected to show the greatest energy dependence.

In the light of these results, any quantitative attempt to arrive at the purity of the nuclear states on the basis of admixtures of l -values (Bethe and Butler 1952, Parkinson *et al.* 1952) will have little significance until the effect is better understood.

The measurements are being extended, particularly to larger angles. The results will be reported in the future.

ACKNOWLEDGMENTS

To the members of the technical staff of the Cavendish cyclotron, in particular Messrs. Morley and Turner, who were most helpful throughout the course of this work, we express our appreciation.

† Interference may occur between the normal stripping amplitude and an 'exchange' amplitude, in which the proton in the deuteron exchanges with a proton in the nucleus. This possibility was pointed out to us by Dr. A. P. French. A preliminary analysis carried out by him indicates that such an effect can account for many of the observed deviations of stripping data from the theoretical distributions. While such a treatment can only be considered as a crude approximation to the true situation, it does indeed produce better agreement with experiments.

The financial aid of the Department of Scientific and Industrial Research is acknowledged by N.T.S.E.

The work described herein was carried out while one of us (W.C.P.) was on leave from the Department of Physics, University of Michigan. The support of the U.S. Educational Commission in the United Kingdom, and of the Graduate School of the University of Michigan is gratefully acknowledged. The many courtesies extended him by the members of the Cavendish Laboratory were much appreciated.

REFERENCES

- ARON, W. A., HOFFMAN, B. G., and WILLIAMS, F. C., 1949, Berkeley, University of California Radiation Laboratory Report, **121**.
BEACH, E. H., 1952, *Thesis*, University of Michigan,
BETHE, H. A., 1949, *Oak Ridge National Laboratory Report*, BVL-T7.
BETHE, H. A., and BUTLER, S. T., 1952, *Phys. Rev.*, **85**, 1045.
BHATIA, A. B., HUANG, K., HUBY, R., and NEWNS, H. C., 1952, *Phil. Mag.*, **43**, 485.
BUTLER, S. T., 1950, *Phys. Rev.*, **80**, 1095; 1951, *Proc. Roy. Soc. A*, **208**, 559.
BUTLER, S. T., and SALPETER, E. E., 1952, *Phys. Rev.*, **88**, 133.
EDMONDS, A. R., and FLOWERS, B. H., 1952, *Proc. Roy. Soc. A*, **215**, 120.
ELKIND, M. M., and SPERDUTO, A., 1953, *Phys. Rev.*, **91**, 463A.
FLOWERS, B. H., 1952, *Phil. Mag.*, **43**, 1330.
GARLICK, G. F. J., and WRIGHT, G. T., 1952, *Proc. Phys. Soc. B*, **65**, 415.
HOLT, J. R., and MARSHAM, T. N., 1953, *Proc. Phys. Soc. A*, **66**, 1032.
HOROWITZ, J., and MESSIAH, A. M. L., 1953, *Phys. Rev.*, **92**, 1326, *J. Phys. Radium*, **14**, 695.
HUTCHINSON, G. W., and SCARROTT, G. G., 1951, *Phil. Mag.*, **42**, 792.
INGLIS, D. R., 1953, *Rev. Mod. Phys.*, **25**, 390.
JONES, G. A., and WILKINSON, D. H., 1952, *Phys. Rev.*, **88**, 423.
LIVINGSTON, M. S., and BETHE, H. A., 1937, *Rev. Mod. Phys.*, **9**, 280.
PARKINSON, W. C., BEACH, E. H., and KING, J. S., 1952, *Phys. Rev.*, **87**, 387.
THIRION, J., 1951, *C. R. Acad. Sci., Paris*, **232**, 2418.
VAN PATTER, D. M., BUECHNER, W. W., and SPERDUTO, A., 1951, *Phys. Rev.*, **82**, 248.

Gaseous Reactions involving Positronium

BY H. S. W. MASSEY AND C. B. O. MOHR†

Department of Physics, University College, London

MS. received 5th March 1954

Abstract. The problems involved in providing a detailed interpretation of the processes involved in the ultimate fate of positrons slowed down in a gas are examined by considering the idealized case of a gas of atomic hydrogen. The processes leading to the formation and dissociation of positronium are considered as well as those which lead to the slowing down of a positronium pair in a gas and to the conversion of ortho- into para-positronium. It is shown that the rate of the latter process probably depends strongly on the kinetic energy of the pair. Elastic collisions of a pair, in its ground state, with gas atoms are determined almost completely by electron exchange interaction, but this is so strong that it cannot be taken account of in a weak coupling treatment.

§ 1. INTRODUCTION

IN recent years the study of the ultimate fate of a stream of positrons in a gas has been greatly extended and many interesting results have been obtained (for a review article see Deutsch 1953). It appears that most positrons, when emitted from a radioactive source into a gas at normal pressure, do not suffer annihilation by collision with atomic electrons before they have a high probability of capturing an electron from a gas atom to form positronium. If the captured electron has the opposite spin to the positron, forming para-positronium, the lifetime towards mutual annihilation is only about 10^{-10} sec, but if the spins are parallel, forming ortho-positronium, the lifetime is much longer, about 10^{-7} second. Furthermore, in the latter case annihilation leads to the emission of three γ -rays in contrast to the former, in which only two are emitted. It is therefore experimentally possible to distinguish ortho- from para-positronium decays from either the longer lifetime or the multiplicity of the γ -ray emission. This affords an opportunity to study the processes which can occur in a gas after ortho-positronium is formed. If conditions are adjusted so that the ortho-form is transformed into the para by collisions in the gas at a rate faster than the natural decay rate, it is possible to obtain information about the rate of the collision process concerned. This is of interest because it is a further source of information about slow collisions of systems of electronic mass in a gas. We are still far from understanding all the factors which determine the rates of such collisions. Comparison of theoretical estimates based on different approximations with the results of experiments on the quenching of ortho-positronium is likely to be a fruitful method of improving the accuracy of the available theories. It appears also, from experiments carried out to date, that there is some kind of inverse correlation between the efficiency of a gas in quenching ortho-positronium and the dielectric strength of the gas. In view of this it is worth while to carry out as detailed an analysis as possible of the reactions which influence the lifetime of

† Now at Physics Department, University of Melbourne, Australia.

a positron in a gas using both theoretical and experimental methods. As a first step from the theoretical side we examine in this paper the evidence about the rates of various processes involving production and loss of ortho-positronium, using simple approximations and mainly limiting our considerations to a gas of atomic hydrogen. This will be found to yield interesting results, and the analysis can later be improved and extended to other cases as the experimental work develops.

We may classify the processes involved under the following heads:

(a) Processes leading to formation of positronium by electron capture from neutral gas atoms.

(b) Processes leading to slowing down of the positronium by inelastic collisions with gas atoms.

(c) Elastic collisions of positronium with gas atoms. These determine the rate of slowing down when the kinetic energy is too small for inelastic collisions to occur.

(d) Exchange collisions with gas atoms in which the positronium electron changes place with an atomic electron, so converting ortho- into para-positronium.

(e) Conversion of ortho- to para-positronium by direct reversal of electron spin in a collision.

In a gas of atomic hydrogen these are the main possibilities—in helium the exchange quenching (d) cannot occur if spin-orbit interaction is negligible. The rate at which positronium, once formed, slows down is important, for it is probable that the quenching process (d) is strongly energy dependent, as will be seen below.

We now consider each of these processes separately.

§ 2. FORMATION OF POSITRONIUM

Provided its kinetic energy is sufficient, a positron has a finite chance of capturing an atomic electron into a bound state of positronium. The cross section for capture into a given state may be calculated, within the accuracy of Born's approximation, by a method exactly similar to that used by Bates and Dalgarno (1952) and by Jackson and Schiff (1953) for calculating the cross section for capture of electrons by protons from neutral hydrogen atoms. We first apply this method to the problem and then make approximate allowance for the fact that a slow positron is repelled by the field of a hydrogen atom so that the wave function for its motion relative to the atom has a considerably smaller amplitude in the region of the atom than the plane wave form assumed in Born's approximation.

We shall consider capture into the ground state in some detail, the corresponding cross sections for capture into excited states being then estimated somewhat less accurately.

2.1. *Capture into the Ground State.*

The cross section for capture of an electron by a positron of momentum $\mathbf{k}_i\hbar$ from a hydrogen atom, leading to formation of an ortho-positronium pair in its ground state with momentum $\mathbf{k}_f\hbar$, is given according to Born's approximation applied to rearrangement collisions (Mott and Massey 1949) by

$$Q_c^0 = \frac{3}{4} 2\pi \int_0^\pi |f_c^0(\theta)|^2 \sin \theta d\theta \quad \dots\dots(1)$$

where $\cos \theta = \mathbf{k}_i \cdot \mathbf{k}_f / k_i k_f$ and

$$f_c^0(\theta) = \frac{4\pi m e^2}{h^2} \iint \left(\frac{1}{r_1} - \frac{1}{r_2} \right) \psi_0(r_2) \chi_0^*(|\mathbf{r}_1 - \mathbf{r}_2|) \\ \times \exp i\{\mathbf{k}_i \cdot \mathbf{r}_1 - \frac{1}{2}\mathbf{k}_f \cdot (\mathbf{r}_1 + \mathbf{r}_2)\} d\tau_1 d\tau_2. \quad \dots\dots(2)$$

$\mathbf{r}_1, \mathbf{r}_2$ are the vectors joining the proton to the positron and electron respectively, m is the electron mass, $\psi_0(r_2)$ is the ground state wave function of the hydrogen atom and $\chi_0(|\mathbf{r}_1 - \mathbf{r}_2|)$ that of the relative motion of electron and positron in positronium. k_i and k_f are related by the energy condition

$$k_i^2 - \frac{1}{2}k_f^2 = \frac{8\pi^2 m}{h^2} (E_H - E_P) \quad \dots\dots(3)$$

where E_H is the energy of the ground state of hydrogen and E_P of positronium. Substituting the Bohr formulae for these energies gives

$$k_i^2 - \frac{1}{2}k_f^2 = e^2/2a_0^2. \quad \dots\dots(4)$$

The factor $\frac{3}{4}$ in (1) represents the chance that the positron and electron spins will be parallel.

In this formula the interaction energy has been taken in the post form but, provided ψ_0 and χ_0 are exact wave functions, the same result is obtained using instead the prior interaction $1/r_1 - 1/r_{12}$.

Writing for $\psi_0(r_2)$, $\chi_0(|\mathbf{r}_1 - \mathbf{r}_2|)$,

$$(\alpha^3/\pi)^{1/2} \exp(-\alpha r_2), \quad (\mu^3/\pi)^{1/2} \exp(-\mu|\mathbf{r}_1 - \mathbf{r}_2|) \quad \dots\dots(5)$$

respectively, in which $\alpha = 1/a_0$, $\mu = 1/2a_0$, and making the transformation to new integration variables ρ_1, ρ_2 , where $\rho_1 = \mathbf{r}_1 - \mathbf{r}_2$, $\rho_2 = -\mathbf{r}_2$, we have

$$f_c^0(\theta) = \frac{4\alpha^3\mu^3 m e^2}{h^2} \iint \left\{ \frac{1}{|\rho_1 - \rho_2|} - \frac{1}{\rho_2} \right\} \exp(-\alpha\rho_2 - \mu\rho_1) \\ \exp i\{\mathbf{k}_i \cdot \rho_1 - \mathbf{k}_f \cdot \rho_2\} d\rho_1 d\rho_2 \quad \dots\dots(6)$$

where

$$\mathbf{k}_1 = \mathbf{k}_i - \frac{1}{2}\mathbf{k}_f, \quad \mathbf{k}_2 = \mathbf{k}_i - \mathbf{k}_f. \quad \dots\dots(7)$$

The integral which occurs in (6) is of exactly the same form as that considered by Bates and Dalgarno (1952) and Jackson and Schiff (1953) in their calculations on capture of electrons from hydrogen atoms by protons. Two different methods were used by these authors to evaluate the integral. Bates and Dalgarno used an expansion in spherical harmonics of $\cos \delta (= \mathbf{k}_1 \cdot \mathbf{k}_2 / k_1 k_2)$, which converges quickly if k_1/μ , k_2/μ are both small compared with unity. Jackson and Schiff on the other hand showed that Feynman's parametrization technique (1949), which has been employed so successfully in calculating high order approximations in quantum electrodynamics, could be used to evaluate the integral analytically. The possibility of using Feynman's method for evaluating exchange integrals of the form (6) has also been pointed out independently by Corinaldesi and Trainor (1952). Both methods were used in the present work. The formulae given by Bates and Dalgarno for the successive terms in the harmonic expansion of $f_c^0(\theta)$ could be used immediately. In applying Feynman's method it was found more convenient for numerical calculation to use the formula

$$f_c^0(\theta) = \frac{32\alpha^4\mu^4\pi m e^2}{h^2} \left| \int_0^1 \frac{y(1-y)(P + Qy + Ry^2 + Sy^3 + Ty^4)}{(Dy - E)^3(Fy^2 + Gy + H)^{5/2}} dy - \frac{4}{(\alpha^2 + k_2^2)(\mu^2 + k_1^2)^2} \right| \\ \dots\dots(8)$$

where

$$\begin{aligned}
 D &= \alpha^2 - \mu^2 + k_2^2 - k_1^2, & E &= -(\mu^2 + k_1^2), & F &= -(\mathbf{k}_1 - \mathbf{k}_2)^2, \\
 G &= (\mathbf{k}_1 - \mathbf{k}_2)^2 + \alpha^2 - \mu^2, & H &= \mu^2, & P &= 3k_1^4 + 10k_1^2\mu^2 + 15\mu^4, \\
 Q &= (\alpha^2 - \mu^2 + k_2^2 - k_1^2)(30\mu^2 + 10k_1^2) + (k_1^2 - \mathbf{k}_1 \cdot \mathbf{k}_2)(40\mu^2 + 8k_1^2), \\
 R &= 32(k_1^2 - \mathbf{k}_1 \cdot \mathbf{k}_2)^2 - (\mathbf{k}_1 - \mathbf{k}_2)^2(20\mu^2 + 4k_1^2) + (\alpha^2 - \mu^2 + k_2^2 - k_1^2) \\
 &\quad \times (15\alpha^2 - 15\mu^2 + 15k_2^2 + 25k_1^2 - 40\mathbf{k}_1 \cdot \mathbf{k}_2), \\
 S &= (\mathbf{k}_1 - \mathbf{k}_2)^2(-20\alpha^2 + 20\mu^2 - 20k_2^2 - 12k_1^2 + 32\mathbf{k}_1 \cdot \mathbf{k}_2), \\
 T &= 8(\mathbf{k}_1 - \mathbf{k}_2)^4.
 \end{aligned}$$

The integral can be evaluated analytically but the final formula is very cumbersome and the chance of error is so considerable that it is quicker and safer to commence the numerical evaluation with the formula (8).

Having evaluated $f_c^0(\theta)$ for a given k_i , Q_c^0 is obtained by numerical integration from the formula (1).

The results obtained in this way are illustrated in figure 1. It will be seen that, as expected on general grounds, the cross section is of the order of atomic dimensions at the maximum occurring at a positron energy of 14 ev. It falls off quite rapidly at higher energies in a manner characteristic of capture processes.

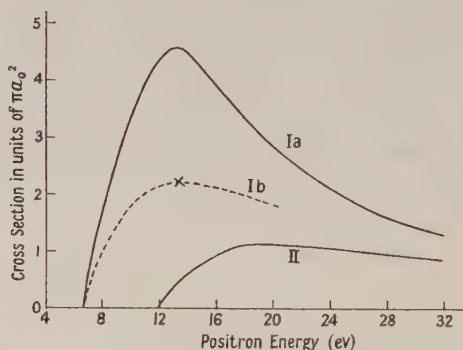


Figure 1. Cross sections for capture of electrons from hydrogen atoms by positrons.

- I. Capture into 1s level of positronium.
- Ia. Calculated by Born's approximation.
- Ib. Estimated curve, allowing for distortion of the incident positron wave. The cross indicates a calculated point allowing for distortion.
- II. Capture into 2s level of positronium; cross section multiplied by 5.

The subsequent career of a positronium pair depends quite markedly on the kinetic energy it possesses immediately after formation. In view of the importance of the velocity dependence of the capture cross section it is necessary to consider what effect the repulsion between the incident positron and the unperturbed atom will have. Positrons with an energy of 10 or so electron volts and zero angular momentum are quite strongly perturbed by this repulsion, but positrons with angular momentum are very little affected. To investigate the importance of the effects detailed calculations were carried out for 13.54 eV positrons with zero angular momentum about the proton. The wave equation for the relative motion of such positrons in the mean atomic field is

$$\frac{d^2f}{dr^2} + \left\{ k_1^2 - \frac{8\pi^2 me^2}{\hbar^2} \left(\frac{1}{r} + \frac{1}{a_0} \right) \exp \left(-\frac{2r}{a_0} \right) \right\} f = 0, \quad \dots\dots (9)$$

the wave function being given by f/r ; f must have the asymptotic form

$$f_0 \sim \exp(i\eta_0) \sin(k_1 r + \eta_0). \quad \dots\dots(10)$$

In the absence of any atomic field the phase shift η_0 is zero. The equation (9) was integrated numerically for $k_1 a_0 = 1$. It was found that $\eta_0 = -0.4$ radian and that f could be represented quite accurately by the empirical expression

$$f_0 = \exp(i\eta_0) \{ \sin(k_1 r - 0.4) + \exp(-1.6r) \sin 0.4 \}. \quad \dots\dots(11)$$

The plane wave $\exp(i\mathbf{k}_1 \cdot \mathbf{r}_1)$ in (2) must now be replaced by

$$\exp(i\mathbf{k}_1 \cdot \mathbf{r}_1) + (k_1 r_1)^{-1} \{ f_0(r_1) - \sin k_1 r_1 \}. \quad \dots\dots(12)$$

On the other hand the motion of the positronium pair relative to the proton is very well represented by a plane wave. Because of the coincidence of the mass and electrical centres in the positronium the mean interaction energy with the proton vanishes and the only effects arise from polarization of the positronium.

The form (12) was substituted for $\exp(i\mathbf{k}_1 \cdot \mathbf{r}_1)$ in (2) and the calculation carried out, working only to zero order in the harmonic expansion method. The resulting cross section, indicated in figure 1, is only about 0.5 of that in which distortion is ignored. As the distortion effect will decrease with increasing positron energy the maximum in the cross section energy curve will be considerably flattened. It is clear that in carrying out detailed calculations for cases of practical importance, such as capture in helium, distortion effects, which will be larger than in hydrogen, must be taken into account in order to obtain satisfactory capture cross sections.

2.2. Capture into Excited States

Calculations have been carried out, using the harmonic expansion method for capture into the 2s state of positronium. The resulting cross section is illustrated in figure 1 as a function of positron energy. It is only comparable with that for capture into the ground state at quite high positron energies. At these energies the cross section for ionization, or rather dissociation, of positronium by atom impact is as large as or larger than the capture cross section (see figure 2) so, on the average, permanent capture will only take place at much lower energies. Capture into excited states is therefore likely to be unimportant in deciding the ultimate fate of positrons in a gas.

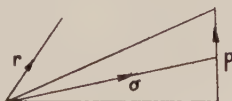


Figure 2. Illustrating coordinates used in formula (14).

§ 3. INELASTIC COLLISIONS OF POSITRONIUM WITH HYDROGEN ATOMS

After formation a positronium pair may have sufficient energy to undergo inelastic collision with the gas atoms. These may lead to excitation or ionization either of the atoms or the positronium. It is easy to see that, according to Born's approximation and neglecting electron exchange between the atom and the positronium, there is a vanishingly small probability of excitation or ionization of the gas atom, or of the positronium from the ground state to any even excited state. Thus for an inelastic collision with a hydrogen atom, involving discrete

excitation of either or both of the colliding systems, the cross section according to Born's approximation, ignoring exchange and treating the proton as of infinite mass, is given by

$$Q_{\text{in}} = 2\pi \int |f_{\text{in}}|^2 \sin \theta d\theta \quad \dots\dots(13)$$

where

$$f_{\text{in}} = \frac{4\pi me^2}{h^2} \iiint \left\{ \frac{1}{|\boldsymbol{\sigma} - \frac{1}{2}\mathbf{p}|} - \frac{1}{|\boldsymbol{\sigma} - \frac{1}{2}\mathbf{p} - \mathbf{r}|} - \frac{1}{|\boldsymbol{\sigma} + \frac{1}{2}\mathbf{p}|} + \frac{1}{|\boldsymbol{\sigma} - \mathbf{r} + \frac{1}{2}\mathbf{p}|} \right\} \\ \times \psi_i(\mathbf{r})\psi_f^*(\mathbf{r})\chi_i(\mathbf{p})\chi_f^*(\mathbf{p}) \exp(i\mathbf{K} \cdot \boldsymbol{\sigma}) d\boldsymbol{\sigma} d\mathbf{p} d\mathbf{r}. \quad \dots\dots(14)$$

In these expressions m is the electron mass, $\boldsymbol{\sigma}$, \mathbf{p} and \mathbf{r} are as indicated in figure 2. $\psi_i(\mathbf{r})$, $\psi_f(\mathbf{r})$ are the initial and final atomic wave functions, $\chi_i(\mathbf{p})$, $\chi_f(\mathbf{p})$ respectively those for the positronium. $\mathbf{K} = \mathbf{k}_i - \mathbf{k}_f$ where \mathbf{k}_i , \mathbf{k}_f are the initial and final wave vectors of the motion of the positronium relative to the atom. The integration over $\boldsymbol{\sigma}$ in (14) can readily be carried out using the well-known formula

$$\int \frac{\exp(i\mathbf{K} \cdot \mathbf{r}_1)}{|\mathbf{r}_1 - \mathbf{r}_2|} d\tau_1 = \frac{4\pi}{K^2} \exp(i\mathbf{K} \cdot \mathbf{r}_2) \quad \dots\dots(15)$$

and we find

$$f_{\text{in}} = \frac{32\pi^2 mi}{K^2 h^2} \int \sin(\frac{1}{2}\mathbf{K} \cdot \mathbf{p}) \chi_i(\mathbf{p}) \chi_f^*(\mathbf{p}) d\mathbf{p} \int \{1 - \exp(i\mathbf{K} \cdot \mathbf{r})\} \psi_i(\mathbf{r}) \psi_f^*(\mathbf{r}) d\mathbf{r}. \quad \dots(16)$$

Since $\sin(kr \cos \theta)$ contains only odd harmonics of $\cos \theta$ it follows that the integral over \mathbf{p} will vanish unless χ_i and χ_f have opposite symmetry for exchange of electron and positron in the positronium. This is of course a consequence of the fact that, in contrast to an atom, the centres of mass and charge in positronium are coincident.

These considerations do not apply when electron exchange between the atom and the pair is allowed for. Unfortunately it is difficult to carry out the calculations for this case even when the plane wave approximation for the wave functions of relative motion of atom and pair is assumed (see §4). It is probable that exchange interaction between atom and pair is quite large and will distort the relative plane waves to a serious extent. Experience with the corresponding calculations for excitation of atoms indicates that exchange is most important in dealing with s-s transitions and is relatively ineffective in s-p transitions. If this is also true for atom-positronium collisions we can assume that energy loss due to excitation of p states of hydrogen atoms is small. On the other hand loss by excitation of s states may be quite large for positronium energies near the threshold. Loss by excitation of the positronium is more important since the threshold energy is lower and the number of pairs which result from the capture process with sufficient energy will be greater. The position here is that the estimation of the importance of the excitation of s states must await a detailed calculation with full allowance for electron exchange, which is bound to be lengthy and difficult. By analogy with electron-atom collisions the loss by p state excitation can be estimated ignoring exchange. The cross section for the 2p and 3p excitations of positronium have been calculated in this way from the formula (13). The results are illustrated in figure 3. Experience with corresponding calculations for electron excitation of atoms indicates that the correct cross sections in such cases are somewhat smaller than the calculated to an extent which increases as the electron energy decreases (Bates, Fundaminsky, Leech and Massey 1951).

The broken curves in figure 3 represent an estimate of the correct cross sections based on this experience. The cross section for a combined excitation of the positronium and atom to 2p states, though finite, is about 40 times smaller than for the single excitation.

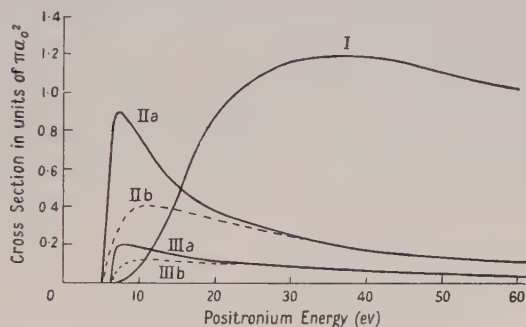


Figure 3. Cross sections for excitation of positronium by impact with hydrogen atoms.

- I. Cross section for ionization of the positronium (Born's approximation).
- II. Cross section for excitation of 2p state : a, Born's approximation ; b, estimated form of actual curve.
- III. Cross section for excitation of 3p state : a, Born's approximation ; b, estimated form of actual curve.

One other interesting case to consider is that of ionization of the positronium. Experience with calculations of cross sections for ionization of atoms by electrons suggests that here also exchange may be ignored, although the reason for this is somewhat obscure in view of the fact that s-s transitions are involved, at least at energies near the threshold. It was therefore considered worth while to use the formula (14), making the further approximation of representing the relative motion of electron and positron in the free state by a plane wave. The calculations, although tedious, are elementary and the results are illustrated in figure 3, in which the total ionization cross section is given as a function of positronium energy. It rises more slowly from the threshold than for excitation of atoms. This is because no contribution comes from excitation of s levels in the positronium continuum. Allowance for exchange may modify this, although there is little evidence for its importance in ionizing collisions between electrons and atoms.

§ 4. ELASTIC COLLISIONS OF POSITRONIUM WITH GAS ATOMS

As soon as the kinetic energy of a positronium pair in the ground state falls below 5.1 eV it can only lose energy through elastic collisions with gas atoms. Because of the coincidence between the mass and electric centres in normal positronium the direct interaction with a gas atom vanishes. There will, of course, be some polarization, but this is hardly likely to be effective except at very low energies. Nevertheless the elastic cross section may be quite large because there is quite a strong exchange interaction due to the possibility of electron exchange between the atom and the pair. This interaction is usually quite strongly energy dependent, increasing rapidly with decrease of the kinetic energy of the positronium—an effect which should be taken into account in interpreting the observed data on quenching, which is probably also strongly energy dependent (see § 5).

We shall begin by considering the exchange scattering by hydrogen atoms using the Born–Oppenheimer approximation, realizing that it is only likely to give a very rough indication. Because of this, the very involved calculations which are necessary to determine the cross section even to this crude approximation have not been carried out in full detail. Sufficient has been done to obtain the order of magnitude and to decide whether the approximation is likely to give results of any value.

If we denote the position vectors of the positron and the two electrons, relative to the proton, by $\mathbf{r}_1, \mathbf{r}_2, \mathbf{r}_3$ respectively, then, according to the Born–Oppenheimer approximation, the cross section for elastic scattering of a pair by a hydrogen atom is given by

$$Q_0 = 2\pi \int_0^\pi |f_0(\theta)|^2 \sin \theta \, d\theta, \quad \dots\dots (17)$$

where

$$f_0(\theta) = \frac{4\pi m e^2}{h^2} \iiint \left(-\frac{1}{r_1} + \frac{1}{r_3} - \frac{1}{r_{23}} + \frac{1}{r_{12}} \right) \psi(r_3) \chi(|\mathbf{r}_1 - \mathbf{r}_2|) \\ \times \psi^*(r_2) \chi^*(|\mathbf{r}_1 - \mathbf{r}_3|) \exp \frac{1}{2} i \{ k \mathbf{n}_i \cdot (\mathbf{r}_1 + \mathbf{r}_2) - k \mathbf{n}_f \cdot (\mathbf{r}_1 + \mathbf{r}_3) \} d\tau_1 d\tau_2 d\tau_3 \dots (18)$$

ψ is the ground state wave function of the hydrogen atom and χ of the positronium, as in (5); $k\mathbf{n}_i\hbar, k\mathbf{n}_f\hbar$ are the initial and final momenta of the positronium, $\mathbf{n}_i \cdot \mathbf{n}_f = \cos \theta$ and, in terms of the kinetic energy E of the positronium,

$$k^2 = 16\pi^2 m E / \hbar^2. \quad \dots\dots (19)$$

It is clear that the calculation of (18) involves the evaluation of very complicated three-centre integrals. To avoid this labour and yet obtain a good idea of the magnitude of Q_0 at different energies the following procedure was adopted. There is no difficulty in calculating the low energy limit of Q_0 . It was then assumed that each of the four coulomb interaction terms in (18) give contributions which vary in nearly the same way with energy. If this were true it would be only necessary to evaluate the energy variation of the contribution from that coulomb interaction for which the calculation is simplest—the term in $1/r_1$ in (18). This was the procedure adopted. Even for this term the complete integral is difficult to calculate, and attention was confined to the zero order terms only in the expansion of the plane wave terms in spherical harmonics. Thus the integral evaluated was

$$\iiint \exp - \{ \mu(r_3 + r_2) + \alpha(r_{12} + r_{13}) \} r_1^{-1} \frac{\sin \frac{1}{2} K r_1}{\frac{1}{2} K r_1} \frac{\sin k r_2}{k r_2} \frac{\sin k r_3}{k r_3} d\tau_1 d\tau_2 d\tau_3 \dots (20)$$

where $K = k |(\mathbf{n}_i - \mathbf{n}_f)|$.

Some justification for this procedure is provided by the work of Bates and Dalgarno (1952) for an analogous case—the capture of electrons into excited states by protons from hydrogen atoms. They pointed out that the energy variations of the contributions from the two coulomb interaction terms involved (as $1/r_1$ and $1/r_2$ in (2)), is nearly the same in the cases which have been worked out and, assuming it to be generally true, obtained cross sections for capture to a number of other excited states.

A rough check on the order of magnitude was also carried out by evaluating integrals of the form (20) arising from the other coulomb interaction terms, by double numerical integration.

The low velocity limit of the elastic cross section according to (18) is $230\pi a_0^2$, but the estimated decrease as the energy increases is very rapid. Thus at a positronium energy of 6.7 eV it is $25\pi a_0^2$ and at 27 eV, $0.4\pi a_0^2$. Even so the value at 6.7 eV is probably much too large. Thus if s-scattering alone occurred the maximum possible value of the cross section at 6.7 eV would be $4\pi a_0^2$. It is true that even with the approximate formula (20) there are some contributions from p, d... etc. scattering, but these are not likely to make the value at 6.7 eV more than six times the maximum s cross section. We must conclude that the exchange interaction must be regarded as a strong coupling and the elastic scattering calculated by solving an integro-differential equation either numerically or by a variational method. In either case the calculation would be formidable. For this reason it is best to consider particularly a case of practical importance such as elastic scattering in helium, a gas which, because of the lightness of its atoms, is a very suitable moderator for slowing down positronium to energies comparable with the gas kinetic. This is reserved for a later paper. Meanwhile it is clear that strong dependence of the elastic cross section on positronium energy may well occur. This is particularly relevant in relation to quenching by electron exchange.

§ 5. QUENCHING OF ORTHO-POSITRONIUM BY ELECTRON EXCHANGE

If an ortho-positronium pair on collision with a gas atom or molecule can exchange an electron with an atomic electron of opposite spin without appreciable energy transfer then the gas concerned will be an effective quencher.

An atom with an incomplete outer shell such as atomic hydrogen, an unsaturated molecule such as NO in which there is a single unpaired electron, a molecule such as O₂ in which the ground state is a triplet, or a metastable atom in a triplet state, such as the 2³S metastable state of helium, will all be effective quenchers from this point of view. The experiments of Deutsch and others (Deutsch 1953) have shown that this is so in practice for NO and O₂ though the quenching cross sections obtained are different in order of magnitude (10^{-16} cm² for NO, 10^{-19} cm² for O₂).

The quenching process is exactly similar to that which gives rise to elastic scattering. Except at very low energies (comparable with the energy difference between the singlet and triplet ground levels of positronium) the cross section for quenching of ortho-positronium in collision with a hydrogen atom will, according to the Born–Oppenheimer approximation, be $\frac{1}{4}$ of that of elastic scattering, this factor representing the chance that the spins will be appropriately oriented. This is not of quantitative value as we have pointed out that the approximation probably very much overestimates the cross section in the energy range of importance. Since the coupling is strong, however, it is likely that the cross section will be of the order πa_0^2 , at least at energies of a few eV. This is comparable with the observed cross section for NO but much larger than that for O₂. As the cross section for quenching, like that for elastic scattering, might well be strongly energy dependent it is important to remember that the observed cross sections are averages depending on the degree of moderation of the positronium energy. Experiments in which this is controlled in some definite way are essential in order to compare quenching cross sections. It must be admitted nevertheless that the big difference between the effectiveness of NO and O₂ in quenching is still somewhat surprising. The probable existence of other determining factors is

indicated by the observed effectiveness of Cl_2 as a quencher. Because of these interesting phenomena it is even more important to establish definitely how important direct exchange quenching is by suitable controlled experiments.

§ 6. QUENCHING OF ORTHO-POSITRONIUM BY DIRECT SPIN REVERSAL

There is no difficulty in estimating the cross section for conversion of ortho- into para-positronium by direct spin reversal in collision with an atom. It is only necessary to use the Breit form of the spin-orbit interaction with Born's approximation. The resulting cross section is utterly negligible under experimental conditions. It is possible that if the spin reversal due to spin-orbit interaction is associated also with exchange between the two colliding systems of two electrons which initially have the same spin, the cross section may be one or two orders of magnitude larger, for reasons similar to those which make exchange predominant in determining the elastic scattering of positronium. Even so the cross section for quenching by spin-reversal is not likely to exceed 10^{-22} cm^2 .

§ 7. CONCLUDING REMARKS

Although the calculations described above do not lead to results which can be checked directly, they indicate some of the difficulties which must be taken into account in providing a thoroughgoing theory of the ultimate fate of a positron in a gas. They also serve to point out the importance of carrying out experiments with controlled moderation of the positronium so that quenching cross sections can be referred to a definite mean energy of the positronium concerned. It seems clear that a careful study of quenching and moderation phenomena in positronium will provide very useful additional data to assist further development of the theory of the collisions of slow particles of electronic mass with gas atoms.

In view of the greater possibility of experimental work with helium a detailed theoretical investigation, taking into account as far as possible all the important complications pointed out above, is reserved for the case of positronium in this gas.

ACKNOWLEDGMENTS

We are indebted to Miss L. Fosgate and Miss J. Nicholson for carrying out some of the numerical calculations.

REFERENCES

- BATES, D. R., and DALGARNO, A., 1952, *Proc. Phys. Soc. A*, **65**, 919.
 BATES, D. R., FUNDAMINSKY, A., LEECH, J., and MASSEY, H. S. W., 1951, *Phil. Trans. Roy. Soc. A*, **243**, 93.
 CORINALDESI, E., and TRAINOR, R., 1952, *Nuovo Cim.*, **9**, 940.
 DEUTSCH, M., 1953, *Progr. Nucl. Phys.*, **3**, 131.
 FEYNMAN, R., 1949, *Phys. Rev.*, **76**, 769.
 JACKSON, J. D., and SCHIFF, H., 1953, *Phys. Rev.*, **89**, 359.
 MOTT, N. F., and MASSEY, H. S. W., 1949, *Theory of Atomic Collisions*, 2nd Edn (Oxford : University Press), Chap. VIII.

The van der Waals Energy of Two Helium Atoms

BY K. M. HOWELL

H. H. Wills Physical Laboratory, University of Bristol

*Communicated by N. F. Mott; MS. received 3rd December 1953,
and in amended form 13th April 1954*

Abstract. An expression is derived for the van der Waals energy of two helium atoms, exchange terms being neglected. This expression can be expanded as an asymptotic series in inverse powers of the internuclear distance. The first two terms in this series are compared with the dipole-dipole and dipole-quadrupole terms of previous workers.

§ 1. INTRODUCTION

THE aim of this paper has been to calculate in greater detail than previously the van der Waals interaction between two atoms when their electronic structure overlaps. The reason for doing this is that it is now believed that van der Waals forces play an important role in the cohesion between the ions of solids such as silver bromide and probably between the ions of metals such as copper where there is a full d-band. The usual treatment of these metals involves an expansion in ascending powers of $1/r$; while this is probably sufficient for the cohesive energy, it may give totally wrong results for the compressibility and elastic constants. The aim of this paper, therefore, was to calculate the forces using second-order perturbation theory but without making the above expansion. The approximation used is to replace all transitions of the atom by one of oscillator strength unity.

For simplicity we have made the calculation for a pair of helium atoms. The results show indeed that as soon as the overlap becomes considerable the exact expression bears little resemblance to the expansion, especially as regards the force and its gradient. Our general conclusion from this work is, therefore, that it would be risky to use calculated van der Waals forces in evaluating the elastic constants of solids.

§ 2. OUTLINE OF METHOD

In evaluating the interaction between two atoms one has to calculate integrals involving r_{12} , the distance between the electrons. Previously, workers expanded $1/r_{12}$ in powers of the reciprocal of the internuclear distance R and obtained an asymptotic series for the van der Waals energy. Here r_{12} is taken as the variable of integration, and terms involving other distances are expanded as functions of it. Different expansions are used over different regions of space where each is valid, so that the exact values of the integrals are found.

§ 3. THE PERTURBATION METHOD

Let ψ_n ($n=0, 1, 2, \dots$) be a set of normalized, orthogonal wave functions for the system in the unperturbed state and let a perturbation V be applied. If E_n are the energies corresponding to these wave functions, the sum of the first and second order perturbation energies is

$$\Delta E = V_{00} + \sum_{n=1}^{\infty} \frac{V_{0n} V_{n0}}{E_0 - E_n}$$

where

$$V_{mn} = \int \psi_m^* V \psi_n d\tau.$$

The term in the denominator depends on n but is replaced by an average value which is taken to be just E_0 , E_n being small compared with E_0 (Margenau 1939). This gives

$$\Delta E = V_{00} + \frac{1}{E_0} \sum_{n=1}^{\infty} V_{0n} V_{n0}.$$

By the rule of matrix multiplication

$$\sum_{n=0}^{\infty} V_{0n} V_{n0} = (V^2)_{00} = \int \psi_0^* V^2 \psi_0 d\tau;$$

the energy is therefore

$$\Delta E = V_{00} + \{(V^2)_{00} - (V_{00})^2\}/E_0. \quad \dots\dots(1)$$

This means that the van der Waals energy can be calculated using only the wave function of the ground state.

§ 4. APPLICATION TO HELIUM

The system consists of two helium atoms with electrons 1 and 2 on nucleus a and electrons 3 and 4 on nucleus b. The wave function of the i th electron is taken, following Slater, to be

$$\psi_{a0}(i) = k^3 2\pi^{-1/2} \exp(-kr_{ai})$$

where the subscript zero denotes the ground-state wave function. Writing all the quantities in atomic units, the interaction between the atoms is

$$V = \left(\frac{1}{r_{13}} + \frac{1}{r_{14}} + \frac{1}{r_{23}} + \frac{1}{r_{24}} - \frac{2}{r_{a3}} - \frac{2}{r_{a4}} - \frac{2}{r_{b1}} - \frac{2}{r_{b2}} + \frac{4}{r_{ab}} \right).$$

Previous methods depend on expanding V in inverse powers of the inter-nuclear distance R . This expansion is only valid if R is greater than the distance between electrons if the atoms were superimposed. However large R may be, this will not be satisfied in part of the region of integration, which is over all space. Because of this, the series obtained is divergent for all values of R (Brooks 1952, Roe 1952). It is, however, asymptotic to the exact value of the integral for large values of R .

The purpose of this paper is to give the exact values of the integrals and to compare the results with expressions given by other workers.

§ 5. EVALUATION OF INTEGRALS

The total unperturbed wave function of the system is

$$\psi_0 = \psi_{a0}(1)\psi_{a0}(2)\psi_{b0}(3)\psi_{b0}(4) = (k^6/\pi^2) \exp\{-k(r_{a1} + r_{a2} + r_{b3} + r_{b4})\}.$$

Several of the terms in the perturbation are equivalent, so the expressions for V and V^2 can be reduced to

$$V = \left(\frac{4}{r_{ab}} - \frac{8}{r_{a3}} + \frac{4}{r_{13}} \right)$$

$$V^2 = \left(\frac{16}{r_{ab}^2} - \frac{64}{r_{ab}r_{a3}} + \frac{32}{r_{ab}r_{13}} + \frac{48}{r_{a3}r_{a4}} + \frac{16}{r_{a3}^2} \right. \\ \left. - \frac{32}{r_{a3}r_{14}} - \frac{32}{r_{a3}r_{13}} + \frac{4}{r_{13}r_{24}} + \frac{8}{r_{13}r_{14}} + \frac{4}{r_{13}^2} \right),$$

It is convenient to abbreviate the integrals as follows:

$$C_1 = \int \psi_b(3) \frac{1}{r_{a3}} \psi_b(3) d\tau_3$$

$${}_2C_1 = \int \psi_b(3) \frac{1}{r_{a3}^2} \psi_b(3) d\tau_3$$

$$C_2 = \iint \psi_a(1) \psi_a(1) \frac{1}{r_{13}} \psi_b(3) \psi_b(3) d\tau_1 d\tau_3$$

$${}_2C_2 = \iint \psi_a(1) \psi_a(1) \frac{1}{r_{13}^2} \psi_b(3) \psi_b(3) d\tau_1 d\tau_3$$

$${}_bC_2 = \iint \psi_a(1) \psi_a(1) \frac{1}{r_{b1}r_{13}} \psi_b(3) \psi_b(3) d\tau_1 d\tau_3$$

$$C_3 = \iiint \psi_a(1) \psi_a(1) \frac{1}{r_{13}r_{14}} \psi_b(3) \psi_b(3) \psi_b(4) \psi_b(4) d\tau_1 d\tau_3 d\tau_4.$$

$$\text{Then } V_{00} = \frac{4}{R} - 8C_1 + 4C_2$$

$$(V^2)_{00} = \frac{16}{R^2} - \frac{64}{R} C_1 + \frac{32}{R} C_2 + 48C_1^2 + 16{}_2C_1 - 32C_1C_2 \\ - 32{}_bC_2 + 4C_2^2 + 8C_3 + 4{}_2C_2 \quad \dots\dots(2)$$

where $R = r_{ab}$.

All these integrals can be evaluated using a method given by Barnett and Coulson (1951); we find

$$C_1 = R^{-1} [1 - (1 + \frac{1}{2}x)e^{-x}]$$

$$C_2 = R^{-1} \left[1 - \left(1 + \frac{11}{16}x + \frac{3}{16}x^2 + \frac{1}{48}x^3 \right) e^{-x} \right]$$

$${}_2C_1 = kR^{-1} [(x+1)e^{-x} \{ \text{Shi } x + \frac{1}{2}\text{Ei}(-x) \} + \frac{1}{2}(x-1)e^x \text{Ei}(-x)]$$

$${}_2C_2 = kR^{-1} \left[\left(\frac{1}{24}x^3 + \frac{1}{4}x^2 + \frac{5}{8}x + \frac{5}{8} \right) e^{-x} \left\{ \text{Shi } x + \frac{1}{2}\text{Ei}(-x) \right\} \right. \\ \left. + \left(\frac{1}{48}x^3 - \frac{1}{8}x^2 + \frac{5}{16}x - \frac{5}{16} \right) e^x \text{Ei}(-x) - \frac{7}{24}x \right]$$

$${}_bC_2 = kR^{-1} [(x+1)e^{-x} \{ \text{Shi } x + \frac{1}{2}\text{Ei}(-x) - \frac{1}{2}\gamma - \frac{1}{2}\ln 2x \} \\ + \frac{1}{2}(x-1)e^x \{ \text{Ei}(-x) - \text{Ei}(-2x) \} - (\frac{1}{8}x^2 - \frac{3}{8}x)e^{-x}]$$

$$C_3 = kR^{-1} \left[(x+1)e^{-x} \{ \text{Shi } x + \text{Ei}(-x) - \gamma - \ln 2x + \frac{1}{2}\ln 3 \} + \frac{1}{2}(x-1)e^x \{ \text{Ei}(-x) \right. \\ \left. - 2\text{Ei}(-2x) + \text{Ei}(-3x) \} - \left(\frac{1}{4}x^2 - \frac{43}{36}x + \frac{28}{27} \right) e^{-x} + \left(\frac{1}{18}x + \frac{28}{27} \right) e^{-2x} \right]$$

where $x = 2kR$,

$$\text{Shi } x = \int_0^x \frac{\sinh t}{t} dt = \sum_{n=0}^{\infty} \frac{x^{2n+1}}{(2n+1) \cdot (2n+1)!} \quad (\text{Bretschneider 1861})$$

$$\text{Ei}(-x) = - \int_x^{\infty} \frac{e^{-t}}{t} dt = \gamma + \ln x + \sum_{n=1}^{\infty} \frac{(-1)^n x^n}{n \cdot n!} \quad (\text{Lowan 1940})$$

$$\gamma = 0.5772 \dots \quad (\text{Euler's constant}).$$

The following asymptotic expansions are used (Jahnke and Emde 1945)

$$\begin{aligned} \text{Shi } x &\sim \frac{e^x}{2x} \sum_{n=0}^{\infty} \frac{n!}{x^n}, \\ \text{Ei}(-x) &\sim - \frac{e^{-x}}{x} \sum_{n=0}^{\infty} (-1)^n \frac{n!}{x^n}, \\ e^{-x} &\sim 0. \end{aligned}$$

The expressions for the integrals can be checked by finding the limit as R tends to zero. These limits are given by the mononuclear integrals of Barnett and Coulson and are easily evaluated:

$$M_1 = k, \quad {}_2M_1 = 2k^2, \quad {}_bM_2 = \frac{3}{4}k^2, \quad M_2 = \frac{5}{8}k, \quad {}_2M_2 = \frac{2}{3}k^2, \quad M_3 = \frac{23}{54}k^2;$$

where, for example,

$${}_2M_2 = \iint \psi_a(1)\psi_a(1) \frac{1}{r_{13}^2} \psi_a(3)\psi_a(3) d\tau_1 d\tau_3.$$

Substituting these expressions for the integrals into those for V_{00} and $(V^2)_{00}$, equation (2), the equation (1) gives

$$\begin{aligned} \Delta E = R^{-1} &\left(4 + \frac{5}{4}x - \frac{3}{4}x^2 - \frac{1}{12}x^3 \right) e^{-x} \\ &+ \frac{R^{-2}}{E_0} \left[\left(\frac{1}{12}x^4 + \frac{1}{2}x^3 - \frac{11}{4}x^2 - \frac{11}{4}x \right) e^{-x} \text{Shi } x \right. \\ &+ \left(\frac{1}{24}x^4 - \frac{1}{4}x^3 - \frac{11}{8}x^2 + \frac{11}{8}x \right) e^x \text{Ei}(-x) \\ &+ \left(\frac{1}{24}x^4 + \frac{1}{4}x^3 + \frac{5}{8}x^2 + \frac{5}{8}x \right) e^{-x} \text{Ei}(-x) + 2(x^2 + x)e^{-x}(2\gamma + \ln 3 + 2\ln 2x) \\ &+ 2(x^2 - x)e^x \{ 2\text{Ei}(-2x) + \text{Ei}(-3x) \} + \left(4 - \frac{7}{12}x^2 \right) \\ &- \left(8 + \frac{521}{54}x + \frac{49}{18}x^2 - \frac{5}{6}x^3 \right) e^{-x} + \left(4 + \frac{521}{54}x + \frac{1757}{576}x^2 + \frac{7}{96}x^3 \right. \\ &\left. \left. - \frac{83}{192}x^4 - \frac{3}{32}x^5 - \frac{1}{192}x^6 \right) e^{-2x} \right]. \quad \dots\dots(3) \end{aligned}$$

There are two special cases, R small and R large.

$$\Delta E \rightarrow \frac{4}{R} - \frac{11}{2}k + \frac{5783}{432} \frac{k^2}{E_0} \quad \text{as } R \text{ tends to zero.}$$

The first term gives the energy of repulsion between two helium nuclei. The two constant terms represent the electronic interaction. In actual fact the exchange forces will mask these terms when the interatomic distance is small.

At large distances, an asymptotic series is obtained:

$$\Delta E \sim \frac{1}{E_0} \left(\frac{24}{k^4 R^6} + \frac{540}{k^6 R^8} + \frac{15750}{k^8 R^{10}} + \dots \right).$$

§ 6. COMPARISON WITH PREVIOUS WORK

Hylleraas (1929) carried out a variation calculation for one helium atom using the same wave function and gives the values $k=27/16$ and $E_0=(-729/128+4)$ to a first approximation. E_0 is twice the ionization potential for one helium atom. This value of E_0 , -1.6953 should be compared with the experimental value, -1.80711 . There is no justification for using the more accurate value of E_0 since only a simple wave function is used. In any case, the form of the curve of ΔE against R is not changed appreciably.

Substituting these values in the series for the energy, we find

$$-\Delta E \sim 1.746(R^{-6} + 7.90R^{-8} + 80.9R^{-10} + \dots). \quad \dots\dots(4)$$

If the experimental value of E_0 is used, the coefficient is 1.638 . Margenau (1939) gives $-\Delta E = 1.61(R^{-6} + 7.9R^{-8} + 30R^{-10} + \dots)$. It seems likely that the third term in Margenau's expression includes only the quadrupole-quadrupole terms. A dipole-octopole interaction also gives an R^{-10} term.

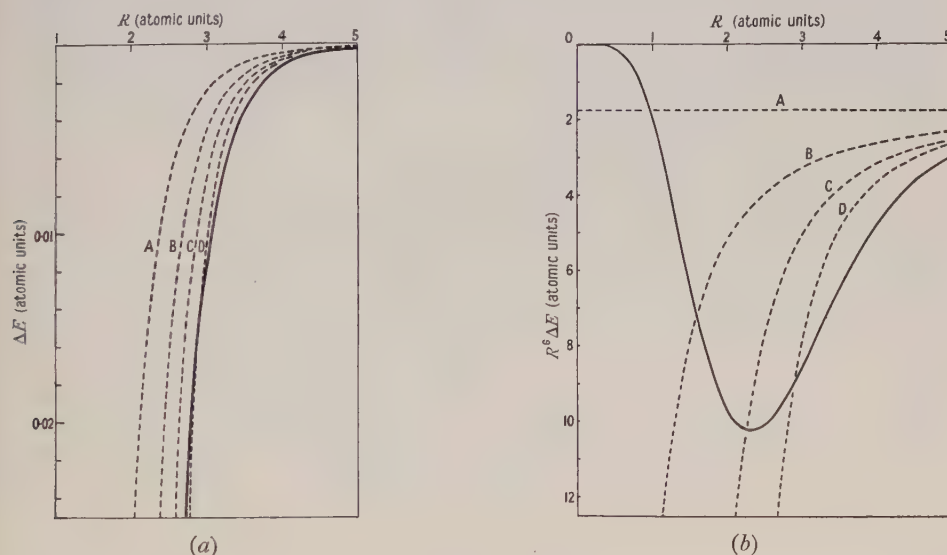


Figure 1. Variation of (a) ΔE and (b) $R^6\Delta E$ with R , the internuclear distance. The full line is that given by the expression (3) derived in this paper. The four dotted lines A, B, C and D are the approximations given by the first four partial sums of the asymptotic series (4).

In figure 1(a) the series (4) is compared with the original expression (3). The four curves A, B, C and D are given by one, two, three and four terms of the series (4). The energy ΔE is plotted against internuclear distance R . The second figure 1(b), where the quantity $R^6\Delta E$ is plotted against R , shows more clearly how the addition of more terms improves the approximation.

Within the limitations of the method the expression (3) obtained is correct. The graphs show that, as the atoms approach more closely, the series in inverse powers of R becomes a very poor approximation to it.

Adding the exchange energy to the expression (3) will therefore give the total interaction energy more accurately at small separations than has previously been given. There is a lower limit to the separation for which the total energy can be found this way. This is reached when the total energy is not given by the sum of

the van der Waals and exchange energies. The effect of including spin interactions and excited states then becomes important.

§ 7. NOTES ON THE APPROXIMATIONS USED

The use of Slater's wave function is to some extent justified by comparison with the results of previous work. Thus Slater and Kirkwood (1931), using a variation method, find a value 1.564 for the coefficient in equation (4). Their calculation also avoids the approximation of neglecting all the E_n compared with E_0 , which occurs in the perturbation method.

Second-order perturbation is used. The third-order energy will be proportional to $(V^3)_{00}$. The order of magnitude of this term is easily seen by using the expansion of the perturbation. The asymptotic value, like that of the first-order perturbation, is zero. Consequently the change in total energy on introducing third-order perturbation will be small and will involve only exponential terms.

§ 8. TOTAL INTERACTION ENERGY

According to Slater and Kirkwood (1931) there is a minimum in the total interaction energy at about 5.5 atomic units. From figure 1 it can be seen that the R^{-6} term gives only about 70% of the van der Waals energy at this distance. Taking the R^{-8} term as well raises this to about 90%. This difference will affect the position and depth of the minimum. In fact it will be deeper and shifted to shorter separations where the R^{-6} approximation is even worse.

Qualitatively this agrees with the conclusion reached by Keesom (1942) where the interaction energy of two helium atoms obtained by consideration of the second virial coefficient is compared with that given by different authors on theoretical grounds. However, the present work would appear to indicate a minimum in the energy about five times that given by Slater and Kirkwood and shifted to about 4.5 atomic units separation. This may indicate that the van der Waals energy derived here is not as accurate as would be expected or that the repulsive term is inaccurate at shorter separations. A third possibility is that it is already incorrect simply to add the two terms and that perhaps the second-order exchange interaction should be taken into account. The calculation then becomes very difficult and cumbersome.

ACKNOWLEDGMENTS

The author is grateful to Professor N. F. Mott for suggesting the problem and for his advice and encouragement since the work was started. Thanks are due to the Director, Atomic Energy Research Establishment, for permission to publish this work.

REFERENCES

- BARNETT, M. P., and COULSON, C. A., 1951, *Phil. Trans. A*, **243**, 221.
 BRETSCHNEIDER, C. A. 1861 *Z. Math. Phys.*, **6**, 127.
 BROOKS, F. C., 1952, *Phys. Rev.*, **86**, 92.
 HYLLEAAS, E. A., 1929, *Z. Phys.*, **54**, 347.
 JAHNKE, E., and EMDE, F., 1945, *Tables of Functions* (New York : Dover).
 KEESOM, W. H., 1942, *Helium* (Amsterdam : Elsevier).
 LOWAN, A. N., 1940, *Tables of Sine, Cosine and Exponential Integrals*, Vol. II (Federal Works Agency Work Projects Administration, New York) (sponsored by the National Bureau of Standards).
 MARGENAU, H., 1939, *Rev. Mod. Phys.*, **11**, 1.
 ROE, G. M., 1952, *Phys. Rev.*, **88**, 659.
 SLATER, J. C., and KIRKWOOD, J. G., 1931, *Phys. Rev.*, **37**, 682.

The Scattering and Polarization of Electrons by Gold

By C. B. O. MOHR AND L. J. TASSIE

Physics Department, University of Melbourne

Communicated by L. H. Martin; MS. received 24th March 1954

Abstract. Using semi-analytic methods, accurate calculations of phase shifts are carried out for an exponentially screened field for electrons with energies between 0.9 and 121 kev. Utilization of these values shows that screening has a relatively small effect on the scattering above 33 kev and on the polarization above 121 kev. The precise form of the field becomes important below 5 kev, where diffraction effects become marked. The polarization is a maximum near 120° , both for the screened and the unscreened field, in agreement with recent experiments, though near the maximum the experimental value is only about half the theoretical.

§ 1. INTRODUCTION

THE study of the scattering of electrons in gases and thin foils has led to much information about the interaction of electrons with atomic and nuclear fields. At energies below 1 kev, where investigations have been carried out on a number of elements (Massey and Burhop 1952), diffraction effects predominate, and these are found to depend on the range of the atomic field rather than on its precise form.

At energies above 1 mev the effect of screening of the nucleus by the atomic electrons is unimportant, but electron spin must now be taken into account. McKinley and Feshbach (1948) have calculated the scattering for all elements for 1, 2 and 4 mev electrons, using an unscreened coulomb field. At energies above 10 mev the finite size of the nucleus must also be taken into account in the calculations, which satisfactorily account for the observations.

In the range 1 kev to 1 mev, however, the situation is not so clear. Few accurate experiments on the large-angle scattering have been conducted in this region.† The most accurate measurements are those of Chase and Cox (1940) for 50 kev electrons in aluminium, and they agree with the Mott formula for coulomb scattering by a light element to within 5%. Calculations were carried out some time ago for the unscreened field of mercury (Bartlett and Watson 1940), and attempts were made to assess the importance of screening (Bartlett and Welton 1941, Mohr 1943). But quantitative predictions of the effect of screening require the determination of a large number of phase shifts to a degree of accuracy which was not at that time attained, and the results do little more than indicate below what angles of scattering the effect of screening becomes important. More recently Gunnarsen (1952), in connection with experiments in this laboratory, carried out a more accurate calculation for 1.07 mev electrons and positrons in mercury, and showed that the effect of screening at large angles was small.

† See note added in proof, p. 717.

This result suggests that for a certain range of energies below 1 mev the precise form of the atomic field is not important. Calculations were therefore extended to lower and lower energies, using in place of the usual Hartree field in numerical form an exponentially screened field together with such analytic procedures as could be devised to reduce the computational labour. Screening was found to be unimportant down to energies lower than previously thought.

With little further calculation one obtains the polarization of electrons by double scattering. For a scattering angle of 90° the polarization for gold is practically the same down to 25 kev for a screened field (Massey and Mohr 1941) as for an unscreened field (Bartlett and Watson 1940), and such experiments as have been carried out are in fair agreement with theory.

A maximum in the polarization for angles somewhat greater than 90° has been predicted (Mohr 1943), though the actual values given are little more than rough indications, since the polarization at angles other than 90° is more sensitive than the single scattering to small inaccuracies in the determination of the phases. The more accurate calculations of this paper confirm the increase beyond 90° , which is found to occur even for an unscreened field. The effect has recently been observed by Ryu *et al.* (1953).

§ 2. GENERAL THEORY

The cross section for scattering per unit solid angle in the direction θ of a beam of unpolarized electrons of rest mass m , velocity v and charge e is given by

$$I(\theta) = |f|^2 + |g|^2, \quad \dots\dots(1)$$

$$\text{where } 2ikf(\theta) = \sum [(l+1) \{\exp(2i\eta_l) - 1\} + l \{\exp(2i\eta_{l-1}) - 1\}] P_l(\cos \theta),$$

$$2ikg(\theta) = \sum \{\exp(2i\eta_{l-1}) - \exp(2i\eta_l)\} P_l^1(\cos \theta), \quad \dots\dots(2)$$

$$\text{and } k = 2\pi\gamma mv/\hbar, \text{ where } \gamma = (1 - v^2/c^2)^{-1/2}. \quad \dots\dots(3)$$

η_l is a phase shift such that $\sin(kr - \frac{1}{2}l\pi + \eta_l)$ is the asymptotic form of that solution of the differential equation

$$G_l'' + \{k^2 - l(l+1)r^{-2} - 8\pi^2 m \hbar^{-2} V(r)\} G_l = 0 \quad \dots\dots(4)$$

which vanishes at the origin, where $V(r)$ is the modified Dirac potential

$$\left. \begin{aligned} V &= \gamma Z_p e^2/r + Z_p^2 e^4/2m c^2 r^2 - 3\alpha'^2/4\alpha^2 + \alpha''/2\alpha, \\ \alpha &= 2\pi(E - V + mc^2)/\hbar c. \end{aligned} \right\} \quad \dots\dots(5)$$

E is the total energy, Z_p is the effective nuclear charge at a distance r , and the primes denote derivatives with respect to r .

The asymmetry in double scattering is given by

$$2\delta = 2|fg^* - f^*g|^2/(|f|^2 + |g|^2)^2. \quad \dots\dots(6)$$

For reasons given in § 1 an exponentially screened field was taken, the following expressions being used:

$$\text{One-term field: } Z_p = 79 \exp(-3r/a_0); \quad \dots\dots(7)$$

$$\text{Two-term field: } Z_p = 20 \exp(-1.3r/a_0) + 59 \exp(-6r/a_0) \dots\dots(8)$$

These fields are compared with the Hartree field for gold in figure 1. The two-term field was naturally chosen to give a better fit than the one-term field, but even the one-term field fits the true field better than the Fermi field.

§ 3. CALCULATION OF PHASE SHIFTS

The following procedure was adopted for computing the phase shifts. Firstly the phase shifts η_l were calculated for the effective potential (5) with neglect of the terms in Z_p^2 and α , i.e. for the Schrödinger potential

$$V = \gamma Z \epsilon^2 e^{-\lambda r}/r. \quad \dots\dots(9)$$

The Born approximation then gives the following formula for the phases

$$\eta_l^0 = (\gamma Z/ka_0) Q_l(1 + \lambda^2/2k^2), \quad \dots\dots(10)$$

from which still more accurate values may be obtained by applying a correction due to Pais (1946). The Q_l are spherical harmonics of the second kind which may be calculated for the lowest l from explicit expressions and then from the recurrence formula, and for the higher l from the asymptotic expansion.

The WKB method gives, assuming V small compared with $k^2 a_0^2$,

$$\eta_l^0 = (\gamma Z/ka_0) K_0 \{ \lambda(l + \frac{1}{2})/k \}. \quad \dots\dots(11)$$

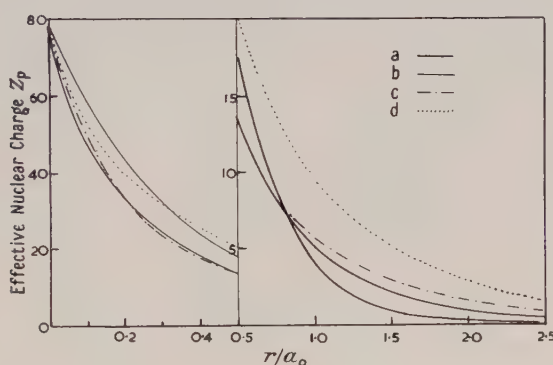


Figure 1. Variation with distance of the effective nuclear charge Z_p .

- a. Hartree field for gold.
- b. One-term field (equation (7)).
- c. Two-term field (equation (8)).
- d. Molière's three-term field approximating to the Fermi field, for gold.

Both formulae (10) and (11) were checked against accurate calculation of the phases by numerical integration of the modified radial equation (4) and by the WKB method with the Langer modification without the assumption of V small. Both methods were found to give results agreeing closely over the range of l for which either gave accurate values after the Pais correction was applied, viz. for all values of l except the first few. Since extensive tables of K_0 are available (*British Association Mathematical Tables*, 1937), the formula (11) is quick to apply even for a large number of l . To the results may be applied the Pais correction, which is small enough for easy interpolation, finally becoming negligible for large l .

For the first few values of l one would expect the spacing of the phases to be nearly the same for a screened field as for a coulomb field, for which the phases are easily calculated (Mott and Massey 1949 a). This fact allows the calculation of the phases to be extended to the lowest values of l .

Table 1 compares the phases obtained by the different methods. The WKB K_0 approximation with the Pais correction is seen to give reliable values down to fairly low l , below which the spacings of the coulomb values may be used. At lower

energies greater attention has to be paid to the lower order phases, many of which were calculated by numerical integration.

At lower energies the two-term field was used as well as the one-term field, but the necessary modification to the formulae (10) and (11) is obvious.

We may now discuss the necessary 'correction' to be added to these phases to allow for the effect of spin, i.e. for the use of the complete expression (5) for V . For a coulomb field the phases η_l and η_{-l-1} may be readily calculated (Mott and Massey 1949 b). They differ by a small amount from the phases η_l^0 for a coulomb field with neglect of spin. The difference is nearly the same as the corresponding difference for a screened field, the error being unimportant for small l , while for large l the difference is small in any case. The difference is added to the value of η_l^0 previously calculated, to give the required phases η_l and η_{-l-1} for a screened field with spin.

Table 1. Comparison of the phase shifts η_l^0 obtained by different methods for the one-term exponentially screened field (7) at $ka_0 = 100$.

l	Born Q_l approxn.	WKB K_0 approxn.	K_0 approxn. + Pais corrn.	Coulomb phase + 3.619	Numerical integration
0	4.107	4.221		3.922	3.936
1	3.131	3.148		3.148	3.154
2	2.645	2.652		2.693	2.687
5	1.894	1.895	1.869†	1.945	1.945
10	1.298	1.299	1.319	1.318	1.318
20	0.742	0.742	0.751	0.665	0.751
30	0.466	0.466	0.468		
40	0.305	0.305	0.305		

† As l decreases the Pais correction decreases again and finally changes sign. The method must be discarded when this decrease begins.

The accuracy of this procedure was checked here and there by a numerical calculation of the difference of $\eta_l - \eta_l^0$ for a coulomb and for a screened field, and similarly for $\eta_{-l-1} - \eta_l^0$, using the values of η_l^0 , η_l and η_{-l-1} for a coulomb and for a screened field given by the WKB method. The difference of the integrands is small and converges rapidly with increasing r .

The accuracy of the correction, and its utilization, are illustrated in table 2. The phases obtained in this work are estimated to be accurate to 0.01 in nearly all cases.

Table 2. Illustrating the accuracy of, and the use of, the 'correction' applied to the phase shifts η_l^0 for the Schrödinger potential in order to obtain the phase shifts η_l and η_{-l-1} for the Dirac potential for the one-term exponentially screened field (7) at $ka_0 = 100$.

l	η_l^0	η_l η_l^0		$\eta_{-l-1} - \eta_l^0$		η_l	η_{-l-1}
		Coulomb field	Screened field	Coulomb field	Screened field		
0	3.936	0.397	0.393	—	—	4.33	—
1	3.154	0.143	0.135	0.481	0.499	3.29	3.64
5	1.945	0.032	0.033	0.075	0.077	1.98	2.02

The phases were calculated individually up to $l = 30$ at the energies 0.87, 5.4, 33.0 and 121 keV energy, and thereafter at increasing intervals of l . They were

obtained for the energies 1.95 and 12.2 keV by interpolation of their differences from the values given by the K_0 approximation. The series (2) for f and g were then summed, usually in two ways as a check on the accuracy obtained. Firstly, the coefficients of the higher Legendre functions were fitted with an empirical formula involving the sum of terms of the form ae^{-ul} , and then an analytic formula for the sum was applied (Mohr 1943). Secondly, the successive groups of terms of the same sign were added, giving a series of single terms of alternating sign whose convergence was speeded by using the Euler transformation (Rosser 1951).

§ 4. THE ANGULAR DISTRIBUTION OF THE SCATTERING

The ratio R of the calculated scattering to the relativistic Rutherford scattering $Z^2\epsilon^4 \text{cosec}^4 \frac{1}{2}\theta / 4\gamma^2 m^2 v^4$ is given in figure 2 for a number of energies. The values

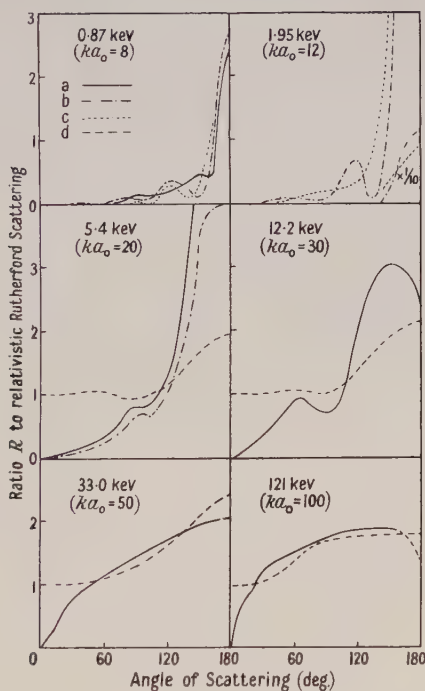


Figure 2.

- a. Screened field of gold (one-term field).
- b. Screened field of gold (two-term field).
- c. Screened field of gold (Thomas-Fermi field).
- d. Coulomb field of mercury.

were calculated at intervals of 30° , but it was frequently possible to interpolate at intervals of 15° using graphs of the real and imaginary parts of f and g . Smooth curves were then drawn through the points.

For 33.0 and 121 keV values were calculated at several angles less than 30° , and the resultant curve is seen to have slight kinks.[†] Such small fluctuations

[†] A detailed study has been made of the small angle scattering in a comparison of the results given by theories of multiple scattering. This appears in *Aust. J. Phys.*, 1954, 7, 217.

doubtless occur at other energies and at larger angles. At small angles, where g is negligible compared with f , the kinks occur near zeros of the real and the imaginary parts of f .

The values of R for the coulomb field of mercury are taken from Bartlett and Watson (1940), using interpolation where necessary for the particular energies required here. The values for 5.4 keV were calculated independently, as it is not possible to extrapolate so far below Bartlett and Watson's lowest energy of 24 keV. At the lowest two energies the values of R for a coulomb field oscillate rapidly with angle, and the effect of screening is overwhelming in any case, so there is no point in plotting them.

Screening is clearly important at large angles for energies as low as 33 keV. In other words the scattering is not at all critical to the form of the field down to 33 keV. At 5.4 keV screening produces large effects, but the fairly small difference between the two-term and the one-term field does not cause any great difference in the scattering except beyond 150° . At 1.95 and 0.87 keV diffraction effects are very marked, and they are obviously critical to the form of the field. It is worth noting that the form of the field is less important at still lower energies, where the diffraction effects are associated with the predominance of a very few spherical harmonics of low order (Massey and Burhop 1952). The curves for the Fermi field of mercury at the lowest two energies are taken from Henneberg (1933).

The two sets of phases are appreciably different for the one-term and two-term fields, and hence the strong similarity of the curves for 5.4 keV is an indication of the reliability of the present results. The curve for the one-term field would be expected to lie above the curve for the two-term field, especially at large angles, since the classical distance of closest approach is larger for the one-term field than for the two-term field for all but very large distances (see figure 1).

§ 5. THE ANGULAR DISTRIBUTION OF THE POLARIZATION

Figure 3 compares angular distributions of the polarization for the screened field with those for the coulomb field. Values of 2δ for the coulomb field are given explicitly only at 90° by Bartlett and Watson (1940), but their extensive tables of functions at intervals of 30° allow one to obtain values for these angles with little difficulty. Values for intermediate angles are best obtained by graphical interpolation, using graphs—not of the real and imaginary parts of f and g but of the amplitude and phase of $\delta^{1/2}$, which vary much more regularly. The screened field curves for 12.2, 33 and 121 keV electrons are for the one-term field, those for 1.95 and 5.4 keV electrons are for the two-term field.

The effect of screening is not marked at 121 keV except near the maximum of 2δ , but becomes important at 33 keV. Screening has more influence on the polarization than on the scattering, because of the occurrence of partial cancellation in the numerator of the expression (6) for 2δ .

The most important feature which emerges is that the polarization is a maximum near 120° , where it is appreciably larger than at 90° . This result cannot be due to inaccuracy in the screened field calculations, since it is given also by the more accurate coulomb field calculations. The recent experiments of Ryu *et al.* (1953) show a definite rise in 2δ as the angle increases from 90° to 135° in the range 60–130 keV, but their values near 120° are only about half the theoretical values. The discrepancy seems a little too large to attribute to the approximate field used

in the calculations. On the other hand due allowance was made in the experiments for the effect of plural scattering, the most important source of error.

At the lowest energies diffraction maxima occur at angles where $|f|^2 + |g|^2$ is a minimum, and since this quantity occurs in the denominator of the expression for 2δ , maximum values of 2δ will tend to occur at these angles. Such subsidiary maxima in 2δ are seen to occur for 5.4 and 1.95 keV electrons, though the actual values of 2δ are probably not reliable, owing to the particular sensitivity of 2δ to the form of the field at these energies.

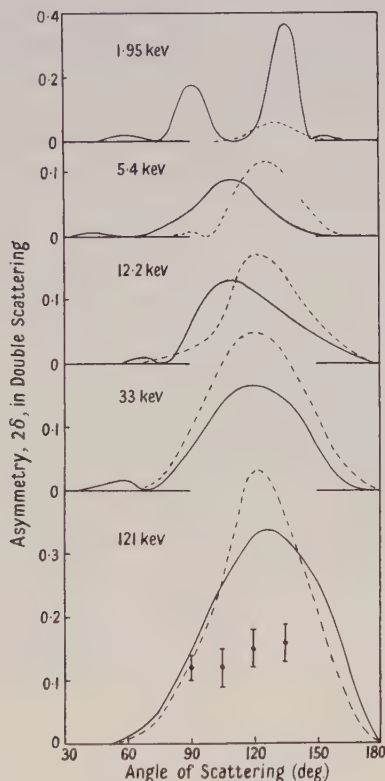


Figure 3. Full line: screened field of gold. Broken line: coulomb field of mercury. The experimental points are due to Ryu *et al.* at 100 keV.

For experiments in which the scattering angle is different at the two scatterers, comparison with theory can be made only if one knows whether the signs of $\delta^{1/2}$ at the two scattering angles are the same or opposite (Ryu 1952). The correct alternative may be ascertained immediately from figure 3; for it is clear that $\delta^{1/2}$ can change sign only when 2δ passes through a zero in the angular distribution. In other words, $\delta^{1/2}$ has the same sign between two adjacent zeros of 2δ .

Finally it may be mentioned that the extension of the calculations of Massey (1942) on the polarization of positrons by mercury to angles other than 90° shows that at no angle or energy does the value of 2δ for positrons become appreciable. There therefore appears to be little chance of detecting the polarization of positrons experimentally.

Note added in proof. We had overlooked the experiments of Kitzinger and Bothe, Kitzinger, and Paul and Reich, which indicate significant deviations

from coulomb scattering at angles for heavy elements for certain electron energies between 150 kev and 2.2 mev. Some doubt is cast on these results, however, by the recent work of Bayard and Yntema (1954, *Phys. Rev.*, **93**, 1412) at 1 mev, in which agreement is obtained with theoretical values to within $1\frac{1}{2}\%$. The latter authors give references to the former work.

REFERENCES

- BARTLETT, J. H., Jr., and WATSON, R. E., 1940, *Proc. Amer. Acad. Arts Sci.*, **74**, 53.
BARTLETT, J. H., Jr., and WELTON, T. A., 1941, *Phys. Rev.*, **59**, 281.
British Association Mathematical Tables, 1937 (Cambridge: University Press), vol. 6.
CHASE, C. T., and COX, R. T., 1940, *Phys. Rev.*, **58**, 242.
GUNNERSSEN, E. M., 1952, *Aust. J. Sci. Res. A*, **5**, 258.
HENNEBERG, W., 1933, *Z. Phys.*, **83**, 555.
MASSEY, H. S. W., 1942, *Proc. Roy. Soc. A*, **181**, 14.
MASSEY, H. S. W., and BURHOP, E. H. S., 1952, *Electronic and Ionic Impact Phenomena* (Oxford: University Press), Chap. 3, §2.
MASSEY, H. S. W., and MOHR, C. B. O., 1941, *Proc. Roy. Soc. A*, **177**, 341.
MCKINLEY, W. A., Jr., and FESHBACH, H., 1948, *Phys. Rev.*, **74**, 1759.
MOHR, C. B. O., 1943, *Proc. Roy. Soc. A*, **182**, 189.
MOTT, N. F., and MASSEY, H. S. W., 1949 a, *The Theory of Atomic Collisions*, 2nd Edn (Oxford: University Press), p. 53; 1949 b, *Ibid.*, p. 79.
PAIS, A., 1946, *Proc. Camb. Phil. Soc.*, **42**, 45.
ROSSER, J. B., 1951, *J. Res. Nat. Bur. Stand., Wash.*, **46**, 56.
RYU, N., 1952, *J. Phys. Soc. Japan*, **7**, 130.
RYU, N., HASHIMOTO, K., and NONAKA, I., 1953, *J. Phys. Soc. Japan*, **8**, 575.

A Method for the Solution of Nuclear Bound-State Problems

BY I. E. McCARTHY AND H. S. GREEN

University of Adelaide, South Australia

MS. received 20th April 1954

Abstract. It is shown that the Fredholm method for the solution of integral equations can be adapted to solve the covariant scattering equations for the proton-neutron system and the meson-nucleon system. A practical method is devised for obtaining the binding energies of the deuteron and hyperon in a fully covariant way. As a test of the method it has been applied to the corresponding non-covariant equation for the deuteron, and satisfactory numerical results are obtained.

§ 1. INTRODUCTION

MOST eigenvalue problems which arise in nuclear theory cannot be solved exactly. For non-relativistic calculations, requiring the solution of an integral equation equivalent to the Schrödinger equation, several approximate methods are already available, e.g. those due to Svartholm (1945) and Salpeter (1951), see also Salpeter and Goldstein (1953). But the covariant bound-state equations, which have been proposed on the basis of meson field theory, cannot be reduced to a form soluble by such methods without spoiling the covariance. Thus the Salpeter-Bethe equation for the deuteron (1951) is soluble by Salpeter's method only in non-relativistic approximation, and to solve the corresponding equation for the hyperon (V_1 or Λ -meson) Arnowitt and Deser (1953) and Fubini (1953) have had to adopt approximate non-covariant procedures.

The few attempts which have been made to solve the covariant equations in a covariant way have led to conclusions whose interpretation is rather obscure. Goldstein (1953), assuming a special (unrealistic) value for the binding energy, found an exact solution of the Salpeter-Bethe equation for a continuous range of values of the coupling constant, even after suitable boundary conditions were imposed. This result contradicts the possibility of a discrete energy level for the deuteron, but Goldstein has shown that the contradiction disappears if one introduces a cut-off energy in the virtual meson spectrum.

The method which will be suggested in this paper for solving the eigenvalue problems covariantly or non-covariantly is based on the Fredholm method for the solution of integral equations (see Hellinger and Toeplitz 1928). This method has already found applications to nuclear scattering problems (Jost and Pais 1951) and even bound-state problems (Fubini 1953) in non-covariant approximation. But difficulties have been encountered in applying the Fredholm method to the covariant equations; it is found, for example, that the integrals which arise are logarithmically divergent, like most of the 'unrenormalized' integrals of field theory. The purpose of this paper is to show how to remove these difficulties and adapt the method to practical computation, as a preliminary

step to solving the covariant equations. At the same time we have thought it worth while to test the accuracy of our procedure by applying it to a non-covariant problem where the answer is already known.

The method adopted for dealing with the divergences of the Fredholm solution is closely analogous to the renormalization method of current field theory; it has already been suggested by one of the authors (Green 1954), but has not so far been examined from the standpoint of mathematical rigour. The next section is therefore devoted to the mathematical procedure required to express the Fredholm solution in a meaningful form.

§ 2. THE FREDHOLM THEORY

The integral equations which we wish to consider are all of the type

$$\phi_r(k) = f_r(k) + \lambda \int K_{rs}(k, l) \phi_s(l) dl \quad \dots\dots (1)$$

where $f_r(k)$ and $K_{rs}(k, l)$ may be regarded as known, and the repetition of the suffix s implies summation over its admissible values. In the covariant equations k and l each stand for the four components of an energy-momentum vector, and the integration $\int \dots dl$ denotes integration over all four components of l . The above equation as it stands is characteristic of nuclear scattering problems, and the bound-state problems in which we are mainly interested are characterized by the vanishing of $f_r(k)$; but for the time being we shall allow $f_r(k)$ to remain.

For the neutron-proton system, which is one of those we shall specifically consider, $f_r(k)$ and $\phi_r(k)$ are bispinors, so that r and s both represent a pair of spinor suffixes, and $K_{rs}(k, l)$ is a compound Dirac matrix given by

$$(2\pi)^4 i K_{\alpha\bar{\epsilon}, \beta\eta}(k, l) = \{S_F(p-k)\gamma_5\}_{\alpha\bar{\epsilon}} \{S_F(p+k)\gamma_5\}_{\beta\eta} D_F(k-l) \quad \dots\dots (2)$$

where $S_F(q) = (\gamma \cdot q - m)^{-1}$ and $D_F(j) = (j^2 - \mu^2)^{-1}$. Here p is one half of the resultant energy-momentum vector of the system. For convenience in interpreting the singularities, variable imaginary parts are added to k_4 , l_4 and p_4 .

For the meson-nucleon system, on the other hand, $f_r(k)$ and $\phi_r(k)$ are both simple spinors, and $K_{rs}(k, l)$ is a Dirac matrix given by

$$(2\pi)^4 i K_{\alpha\beta}(k, l) = \{S_F(p-k)\gamma_5 S_F(p-k-l)\gamma_5\}_{\alpha\beta} D_F(l). \quad \dots\dots (3)$$

Here p is just the resultant energy-momentum vector of the system.

With either of these substitutions, equation (1) is of a type considerably more general than that to which the elementary Fredholm theory applies. Firstly, it is a set of simultaneous integral equations, and it involves four independent variables. Secondly, the kernel and one of the independent variables are complex. Thirdly, the range of integration of all four variables is infinite. For a discussion of the necessary generalizations of the elementary theory, and the associated literature, the reader is referred to §§ 12-13 of the treatise by Hellinger and Toeplitz already mentioned. Disregarding for the moment questions of convergence, Fredholm's solution of (1) can be expressed in the form

$$\phi_r(k) = f_r(k) + \{D(\lambda)\}^{-1} \int D_{rs}(\lambda; k, l) f_s(l) dl \quad \dots\dots (4)$$

where

$$D(\lambda) = 1 - \lambda u_1 + \frac{1}{2} \lambda^2 (u_1^2 - u_2) - \frac{1}{6} \lambda^3 (u_1^3 - 3u_1 u_2 + 2u_3) + \dots \quad \dots\dots (5)$$

and

$$D_{rs}(\lambda; k, l) = \lambda K_{rs}(k, l) - \lambda^2 \{u_1 K_{rs}(k, l) - K_{rs}^{(2)}(k, l) + \dots \quad \dots\dots (6)$$

where $K_{rs}^{(n)}(k, l)$ is the n th iterated kernel defined by

$$\left. \begin{aligned} K_{rs}^{(1)}(k, l) &= K_{rs}(k, l), \\ K_{rs}^{(n)}(k, l) &= \int K_{rq}(k, j) K_{qs}^{(n-1)}(j, l) dj, \end{aligned} \right\} \dots\dots (7)$$

and

$$u_n = \int K_{rr}^{(n)}(k, k) dk. \dots\dots (8)$$

In case a finite number of the u_n should diverge, they may be put equal to zero or any other constant without affecting the validity of the solution for all values of λ . On the other hand, it is necessary that all except a finite number of the u_n should converge; and this condition is not satisfied with either of the kernels (3) and (4), as we have defined them, with $D_F(k) = (k^2 - \mu^2)^{-1}$. To overcome this difficulty we shall assume instead that

$$D_F(k) = (\bar{k}^2 - \mu^2)^{-1} - (k^2 - M^2)^{-1} \dots\dots (9)$$

with the intention of allowing M to become infinite when it is convenient to do so. This is equivalent to adding a convergence factor $(\mu^2 - M^2)(k^2 - M^2)^{-1}$ to $D_F(k)$ as previously defined.

Bound-state problems, as distinct from scattering problems, require $f_r(k) = 0$. It is clear from (4) that a non-vanishing solution of equation (1) is then possible only if $D(\lambda) = 0$. We shall therefore be interested primarily from now on in the conditions under which $D(\lambda)$ can vanish.

The integrals u_n , defined by (8) in conjunction with (2) or (3), depend only on the value of $p = (p_4^2 - p_1^2 - p_2^2 - p_3^2)^{1/2}$. For large values of M they vary linearly with $\ln M$. This can be proved by changing the momentum variables from k, j etc. to $k' = k/M, j' = j/M$ etc. in the integral expression for $M(\partial u_n / \partial M)$, and verifying that one obtains a convergent integral v_n independent of p as M tends to ∞ . So one has

$$u_n(p) = v_n \ln(M/\mu) + w_n(p) \dots\dots (10)$$

where v_n is independent of p and M , and $w_n(p)$ approaches a limit as M tends to ∞ .

Now the coefficient of λ^n in the series expansion (5) of $D(\lambda)$ is

$$\sum' \frac{(-u_1)^{a_1}}{a_1!} \frac{(-\frac{1}{2}u_2)^{a_2}}{a_2!} \dots \frac{(-n^{-1}u_n)^{a_n}}{a_n!},$$

the summation Σ' extending over all integral values of the a_r such that $\sum_{r=1}^n r a_r = n$. Hence

$$D(\lambda) = \exp \left\{ - \sum_{r=1}^{\infty} r^{-1} u_r(p) \lambda^r \right\} \dots\dots (11)$$

provided the infinite series in the exponent converges. Since $D(\lambda)$ is an integral function of λ , the radius of convergence ρ of the power series $\Sigma r^{-1} u_r(p) \lambda^r$ must coincide with the least zero of $D(\lambda)$. If ρ_v and $\rho_w(p)$ are the radii of convergence of $\Sigma r^{-1} v_r \lambda^r$ and $\Sigma r^{-1} w_r(p) \lambda^r$, ρ will be identical with the smaller of ρ_v and $\rho_w(p)$, and therefore insensitive to the value of M , provided M is sufficiently large.

Even for λ less than ρ , $D(\lambda)$ will approach the value zero as M tends to ∞ . This is the explanation of Goldstein's result that, unless a convergence factor is added to the kernel of the Salpeter-Bethe equation, a solution exists for a continuous range of values of the coupling constant λ . The solution thus obtained obviously has nothing to do with bound states, however; the admissible solutions of the eigenvalue problem must be discrete values of λ depending on the value of p . Even with a convergence factor, a spurious solution of the problem will be obtained if it

should happen that $\rho_v < \rho_w(p)$, for then ρ_v is the least zero of $D(\lambda)$. Goldstein has solved the Bethe-Salpeter equation only for the single value $p=0$, so it is difficult to say whether his eigenvalue is spurious or not.

To ensure that only admissible eigenvalues will be obtained, the following procedure is suggested. Both $D(\lambda)$ and $D(\lambda; k, l)$ are multiplied by the factor

$$E(\lambda) = \exp \left\{ \sum_{r=1}^{\infty} r^{-1} u_r(p_0) \lambda^r \right\} \quad \dots\dots (12)$$

where p_0 is chosen to give the radius of convergence ρ_0 of the power series $\sum r^{-1} u_r(p_0) \lambda^r$ its maximum value. It should be noticed that $E(\lambda)$ tends to ∞ instead of 0 as λ tends to the smaller of ρ_0 and ρ_w , and is therefore not an integral function in general. The radius of convergence of the series

$$D(\lambda)E(\lambda) = 1 - \lambda u_1' + \frac{1}{2} \lambda^2 (u_1'^2 - u_2') - \frac{1}{6} \lambda^3 (u_1'^3 - 3u_1' u_2' + 2u_3') + \dots, \quad \dots\dots (13)$$

$$u_r'(p) = u_r(p) - u_r(p_0)$$

is ρ_0 . However, since ρ_0 is, by definition of p_0 , greater than $\rho_w(p)$, the series will converge for $\lambda = \rho_w(p)$.

Now $u_r'(p)$ tends to a finite limit as M tends to ∞ , so our object of eliminating M is now achieved. The only thing which remains is to specify the value of p_0 ; in this we are guided by physical considerations. As the value of the coupling constant increases, the binding energy increases, in the case of the proton-neutron system. It is true that for sufficiently large values of the coupling constant new bound states make their appearance, so that more than one coupling constant will allow the existence of a bound state with a given energy. But it is the least of these values (ρ_0) which gives the ground state this energy, so ρ_0 will increase monotonically with the binding energy $2(m - p_0)$. The correct value of p_0 is therefore the minimum value zero; the corresponding value of ρ_0 is either Goldstein's eigenvalue or infinity. Assuming that the hyperon is a metastable excited state of the meson-nucleon system, the situation is there somewhat different, for p_0 is complex, with an imaginary part inversely proportional to the lifetime of the state. As the coupling constant increases, the lifetime may be expected to increase and the excitation energy to decrease. Therefore ρ_0 will have its maximum value when $|p_0 - m|$ has its minimum value zero, i.e. when $p_0 = m$.[†] This choice of p_0 allows one to obtain $E(\lambda)D(\lambda)$ by applying standard renormalization procedures to the divergent integrals of $D(\lambda)$, without introducing a convergence factor at all.

§ 3. PRACTICAL DETERMINATION OF EIGENVALUES

We turn now to consider the practical problem of determining the least value $\rho_w(p)$ of λ which makes $E(\lambda)D(\lambda)$ vanish. Many methods exist for obtaining the zeros of the Fredholm denominator; these are well summarized in the recent monograph by Bückner (1952), but few, if any, of them are well adapted to problems of the type considered here. The method we shall suggest is based on the fact that ρ is the radius of convergence of the series.

$$-\ln \{D(\lambda)E(\lambda)\} = \sum r^{-1} u_r'(p) \lambda^r. \quad \dots\dots (14)$$

When $\lambda = \rho$, the dominant contribution to the right-hand side of this equation must

[†] The existence of a stable state of the meson-nucleon system, with rest energy less than m , is not inconceivable; but if it should occur, the respective roles of the nucleon and hyperon would be interchanged.

be $-\ln(1-\lambda/\rho) = \sum r^{-1}(\lambda/\rho)^r$. For sufficiently large values of r , therefore, one will have

$$\rho^r u_r'(p) = 1, \text{ very nearly.} \quad \dots\dots(15)$$

This determines ρ as a function of p , or, conversely, p as a function of ρ .

Since the labour required for the computation of $u_r'(p)$ increases extremely rapidly with r , it is essential, for the practicability of the method thus suggested for calculating eigenvalues, that a reasonably good value of ρ should be obtained from (15) when $r=2$, or 3 at most. As Ma (1954) has shown by means of an example, the result for $r=1$, is only mildly encouraging. But, as we shall show, also by means of examples taken from non-covariant theory, the numerical results for $r=2$ are already so good that the method can be regarded as a practical proposition.

§ 4. THE S-STATE OF THE DEUTERON

It is proposed to test the efficacy of the method just developed for solving nuclear eigenvalue problems by applying it to one of the corresponding non-relativistic problems : that of finding the binding energy of the deuteron.

The S-states of the neutron-proton system are described non-relativistically by the Schrödinger equation

$$\phi''(r) + k^2 \phi(r) = \lambda V(r) \phi(r) \quad \dots\dots(16)$$

where k^2 is the total energy, divided by \hbar^2/m , and $\lambda V(r)$ is the potential energy, divided by the same factor. The corresponding integral equation (cf. Jost and Pais 1951) is

$$\phi(r) = \exp(-ikr) - \exp(ikr) + \lambda \int_0^\infty K(r,s) \phi(s) ds \quad \dots\dots(17)$$

where $K(r,s) = \frac{1}{2}ik^{-1}V(s)[\exp\{ik(r+s)\} - \exp\{ik|r-s|\}] \quad \dots\dots(18)$

in the coordinate representation which is most convenient for our present purpose. For $V(r) = \mu r^{-1} \exp(-\mu r)$ (the Yukawa potential), or $V(r) = \mu^2 \{\exp(\mu r) - 1\}^{-1}$ (Hulthén's potential), the integrals u_n defined by analogy with (8) are all convergent, so that no regularization procedure is required and the binding energy can be obtained quite straightforwardly as a zero of $D(\lambda)$. This corresponds to the fact that a value of the binding energy can be found $(+\infty)$ which reduces $E(\lambda)$ to a mere constant and gives $u_r' = u_r$.

Let $D(\lambda) = 1 - \lambda f_1 + \lambda^2 f_2 - \lambda^3 f_3 + \dots, \quad \dots\dots(19)$

so that, according to (5),

$$f_1 = u_1, \quad f_2 = \frac{1}{2}(u_1^2 - u_2), \quad f_3 = \frac{1}{6}(u_1^3 - 3u_1 u_2 + 2u_3), \text{ etc.} \quad \dots\dots(20)$$

Then the approximation formula (15) will reduce to

$$u_2 \rho^2 = 1 \quad \dots\dots(21 a)$$

in the first approximation (discounting the case $r=1$), and

$$u_3 \rho^3 = 1 \quad \dots\dots(21 b)$$

in the next approximation. It is worth noticing that these prescriptions can be obtained independently as follows. Since ρ is a zero of $D(\lambda)$, it is also a zero of

$$e^{\alpha \lambda} D(\lambda) = 1 + (\alpha - f_1)\lambda + (\frac{1}{2}\alpha^2 - \alpha f_1 + f_2)\lambda^2 + \dots$$

Let α be chosen so as to make the coefficient of λ^2 vanish, i.e. so that

$$\frac{1}{2}\alpha^2 - \alpha f_1 + f_2 = 0. \quad \dots\dots(22)$$

Then one is left with the approximate equation

$$1 + (\alpha - f_1)\rho = 0. \quad \dots\dots(23)$$

Using (20) and (22), this is easily verified to be equivalent to (21 *a*). To obtain (21 *b*) in a similar way, α and β are chosen so as to make the coefficients of λ^2 and λ^3 vanish in the expansion of $\exp(\alpha\lambda + \beta\lambda^2)D(\lambda)$. Then one finds that (23) is equivalent to (21 *b*).

§ 5. RESULTS FOR THE YUKAWA AND HULTHÉN POTENTIALS

Substituting $V(r) = \mu r^{-1} \exp(-\mu r)$ in (17), one obtains for u_2

$$u_2 = -\frac{1}{4}(\mu/k)^2 \int_0^\infty dr \int_0^\infty ds (rs)^{-1} \exp\{-\mu(r+s)\} [\exp\{ik(r+s)\} - \exp\{ik|r-s|\}]^2. \quad \dots\dots(24)$$

For bound states k^2 is negative, so one substitutes

$$k = i\mu\epsilon. \quad \dots\dots(25)$$

Writing $r-s=u$ and $r+s=v$, and using the identity

$$\int_0^\infty v^{-1} \exp(-\theta v) \{1 - \exp(-\phi v)\} dv = \ln\{(\theta + \phi)/\theta\},$$

(24) reduces to

$$u_2 = \frac{1}{\epsilon^2} \left[\int_0^1 \left\{ \ln\left(\frac{1+2\epsilon-\epsilon t}{1+2\epsilon}\right) - \frac{1}{2} \ln\left(\frac{1+2\epsilon-2\epsilon t}{1+2\epsilon}\right) \right\} \frac{dt}{t} + \int_1^2 \left\{ \ln\left(\frac{1+\epsilon t}{1+2\epsilon}\right) - \frac{1}{2} \ln\left(\frac{1-2\epsilon+2\epsilon t}{1+2\epsilon}\right) \right\} \frac{dt}{t} \right]. \quad \dots\dots(26)$$

The integrals can be expressed in terms of the function

$$\text{Rl}(x) = \int_1^x (\xi-1)^{-1} \ln \xi d\xi$$

discussed and tabulated by Powell (1943). One has, in fact,

$$\begin{aligned} u_2 = \epsilon^{-2} & \left[\frac{3}{2} \text{Rl}(1+2\epsilon) - \text{Rl}(1+\epsilon) - \frac{1}{2} \text{Rl}(1-2\epsilon) \right. \\ & + \text{Rl}\left(\frac{1+\epsilon}{1+2\epsilon}\right) + \frac{1}{2} \text{Rl}\left(\frac{1-2\epsilon}{1+2\epsilon}\right) \\ & - \frac{1}{2} \ln 2 \ln(1+2\epsilon) - \frac{1}{2} \ln(1-2\epsilon) \{\ln 2 - \ln(1+2\epsilon)\} \\ & \left. - \frac{1}{2} \{\ln(1+2\epsilon)\}^2 \right] = 1, \quad \dots\dots(27) \end{aligned}$$

for $\epsilon \leq \frac{1}{2}$. The corresponding formula for $\epsilon > \frac{1}{2}$ can be obtained by using known properties of the Rl function. Using Powell's table, the following values of the coupling constant ρ were calculated from (21 *a*) for values of ϵ over the range generally used to fit experimental data. In the third row below are the corresponding values ρ_e determined from the variational formula

$$\rho_e = 1.680 + 2.2655\epsilon - 0.2456\epsilon^2 + 0.144\epsilon^3$$

(cf. Rosenfeld 1948).

ϵ	0.00	0.25	0.50	0.75	1.00	1.25	1.50
ρ	1.61	2.11	2.59	3.06	3.51	3.99	4.86
ρ_e	1.68	2.23	2.77	3.30	3.84	4.41	5.01

It will be seen that even in this first approximation the results are in satisfactory accord with those obtained otherwise.

As an additional check on the method we have computed values of ρ from (21 a) using the formula

$$u_2 = \frac{1}{4}\epsilon^{-2} [\{\Psi''(2\epsilon) + \frac{1}{6}\pi^2\} - \epsilon^{-1} \{\Psi'(2\epsilon) + C\}], \quad \dots\dots (28)$$

which was kindly derived for us by Dr. S. T. Ma using Hulthén's potential; $\Psi'(x)$ is the logarithmic derivative of the Γ -function (cf. Jahnke and Emde 1945). In this case the exact values ρ_e of ρ can be determined, and are given in the third row below.

ϵ	0.00	0.25	0.50	0.75	1.00	1.25	1.50
ρ	1.04	1.41	1.86	2.28	2.72	3.15	3.57
ρ_e	1.00	1.50	2.00	2.50	3.00	3.50	4.00

Again the values obtained from our first approximation formula are quite satisfactory.

As the equation (16) from which these results were derived is a non-relativistic approximation to the Salpeter-Bethe equation, there are grounds for believing that the method of §§ 2-3 will be equally successful in its application to the fully covariant equations. The result for the Salpeter-Bethe equation is virtually assured, while the close analogy between the deuteron and hyperon problems allows one to be reasonably optimistic with regard to the latter. Calculations are in progress in Australia directed to the solution of both equations.

REFERENCES

- ARNOWITT, R., and DESER, S., 1953, *Phys. Rev.*, **92**, 1061.
 BÜCKNER, H., 1952, *Praktische Behandlung von Integral-Gleichungen* (Berlin: Springer).
 FUBINI, S., 1953, *Nuovo Cim.*, **10**, 564.
 GOLDSTEIN, J. S., 1953, *Phys. Rev.*, **91**, 1516.
 GREEN, H. S., 1954, *Phys. Rev.*, **95**, in the press.
 HELLINGER, E., and TOEPLITZ, O., 1928, *Integralgleichungen* (Leipzig: Teubner); also in *Encyklopädie der Mathematischen Wissenschaften*.
 JAHNKE, E., and EMDE, F., 1945, *Tables of Functions* (New York: Dover).
 JOST, R., and PAIS, A., 1951, *Phys. Rev.*, **82**, 840.
 MA, S. T., 1954, *Aust. J. Phys.*, **7**, in the press.
 POWELL, E. O., 1943, *Phil. Mag.*, (7) **34**, 600.
 ROSENFELD, L., 1948, *Nuclear Forces* (Amsterdam: North-Holland Publishing Co.).
 SALPETER, E. E., 1951, *Phys. Rev.*, **84**, 1226.
 SALPETER, E. E., and BETHE, H. A., 1951, *Phys. Rev.*, **84**, 1232.
 SALPETER, E. E., and GOLDSTEIN, J. S., 1953, *Phys. Rev.*, **90**, 983.
 SVARTHOLM, N., 1945, *Binding Energies*, Dissertation, Lund.

LETTERS TO THE EDITOR

On the Propagation of Energy in Elastic Media

The aim of this note is to investigate the transformation properties of the velocity of energy propagation (shortly energy velocity) in elastic media.

The reasons for doing this are twofold:

(a) von Laue (1950) has suggested that the energy velocity should transform like the velocity of a particle. In the case of the electromagnetic field inside matter he has used this condition as the decisive factor to accept Minkowski's expression for the energy-momentum tensor of the electromagnetic field inside matter. Now, it would be of interest to see how far this condition is satisfied for the simpler case of the propagation of elastic stresses. If it is *not* satisfied (and we will show it is not), this might cast some doubt upon the validity of this criterion (or upon the correctness of the definition of energy velocity employed), since the commonly used energy-momentum tensor of the elastic body is very likely to be the correct one.

(b) If the energy velocity in an elastic medium does not transform like the velocity of a particle, the concept of the phonon is not a Lorentz-invariant concept; hence the representation of the elastic energy current as a stream of phonons will not, in general, hold for all frames of reference. (As far as the customary theories employing phonons are concerned, this is no objection at all, since they describe the physical situation staying permanently in the frame in which the body is at rest.)

Take then the energy-momentum tensor of the elastic body, $T_{ik} = T_{ki}$ of the form

$$\left(\begin{array}{c|c} p_{\alpha\beta} & \begin{array}{l} -ig_1 \\ -ig_2 \\ -ig_3 \end{array} \\ \hline \begin{array}{l} -iS_1 - iS_2 - iS_3 \end{array} & \omega \end{array} \right)$$

$\alpha, \beta = 1, 2, 3$; ω is the energy density, S_α the energy current, g_α the momentum density, $p_{\alpha\beta}$ the components of the stress. The velocity of light c is put equal to 1; $x_4 = it$. (The sign of the tensor is chosen so that in the rest frame $\omega > 0$. This entails that $p_{\alpha\beta} > 0$ are the components of the stress and not that of the pressure.)

The energy velocity w_α , a three-vector, is defined to be $w_\alpha = S_\alpha / \omega = iT_{4\alpha} / T_{44}$. It is easy to find the conditions that w_α should transform like a three-vector under Lorentz transformations. In general, of course, it will not. However, there is a much simpler way to proceed.

If we are able to show that there exists such a frame of reference in which w , the magnitude of w_α , tends to infinity, we have immediately demonstrated that w_α does not transform like the velocity of a particle, since for the latter w can reach at most the value $c = 1$.

Whether such a physical situation can actually be realized is not our present concern; if in principle such a frame exists, the transformation properties of w_α will *not* be that of a velocity, and this is our main interest.

We show now that, indeed, this is the case, for we can find a frame in which T_{44} goes to zero, while $T_{4\alpha}$ remains finite. From the transformation law of symmetric tensors of rank two we have $\omega = (\omega^0 - \beta^2 p_{11}^0)/(1 - \beta^2)$, where the zero index refers to the value of the quantities in the rest frame and β is the velocity of the frame. ω is zero if $\beta = \pm (\omega^0/p_{11}^0)^{1/2}$. This is real if p_{11}^0 is positive (a stress), and smaller than 1 if $p_{11}^0 > \omega^0$. (It is hardly necessary to mention that no matter will withstand stresses of this magnitude.)

In this frame $T_{41} = -iS_1 = ip_{11}^0$; thus $S_1 = -\beta p_{11}^0 \neq 0$. Consequently, w goes to infinity as the speed of the elastic body approaches the value $(\omega^0/p_{11}^0)^{1/2}$. For this speed the energy-density of the body is zero. For speeds higher than this it is *negative*.

To interpret this result physically we first observe that the existence of stresses (and not pressures) in the rest frame is necessary for the disappearance of the energy-density. This observation immediately leads us to the physical interpretation.

Suppose that in the rest frame at $t=0$ there are applied equal and opposite forces pulling at opposite ends of an elastic slab. The line of action of the forces is normal to the end surfaces. Equilibrium is maintained in this frame, and in all other frames as well. However, viewed from a moving frame of reference the two forces will begin to act at different times and, to maintain equilibrium, the body itself will do work against the acting force as long as the other force is not engaged. This work decreases the energy content of the body, hence the decrease in ω . If the acting force is sufficiently large, and the delay of sufficient duration, one may actually use up the total energy content of the body. In this frame ω vanishes. Imparting a bigger velocity to the frame we may increase the delay still more, thereby making ω actually negative.

The quantitative analysis is now exceedingly simple.

At $t=0$ in the rest frame forces $+F$ and $-F$ start to act on the opposite sides of a slab of elastic body. The sides of area A are at a distance l_0 from each other. The total energy of the body is E_0 . In a frame in which the body has the velocity β along the line of action of the forces ($c=1$), A and the forces retain their original values. E , the energy of the body, will be $E_0/(1 - \beta^2)^{1/2}$, while its length l shrinks to $l_0(1 - \beta^2)^{1/2}$. An observer in this frame will find that the two forces will start to act with a delay $\Delta t = \beta l_0/(1 - \beta^2)^{1/2}$. During this time the work done against F will be $F\beta\Delta t$. If the situation is to be such that this amount of work just consumes the energy content of the body, we have $F\beta\Delta t = E$. Substituting, we obtain $F\beta^2 l_0/(1 - \beta^2)^{1/2} = E_0/(1 - \beta^2)^{1/2}$. Dividing both sides by A and rearranging, we get $\beta^2 = (E_0/Al_0)(A/F) = \omega^0/p_{11}^0$, since $p_{11}^0 = F/A$. This is indeed the same expression for the critical velocity that we have already deduced by more sophisticated means.

Department of Physics,
University of Alabama,
Alabama, U.S.A.
6th May 1954.

N. L. BALAZS.

The Lattice Thermal Conductivity of Silver-Palladium Alloys at Low Temperatures

Although a number of measurements of the low temperature thermal conductivity of cupro-nickel alloys and other alloys of technical interest have been reported (listed by Olsen and Rosenberg 1953), comparatively little information is available on the lattice component of the thermal conductivity in alloys at low temperatures, and on the scattering processes which limit it. The data of Berman (1951) and Estermann and Zimmerman (1952) do indicate that at sufficiently low temperatures the lattice waves or phonons are scattered principally by free electrons, leading to a lattice conductivity κ_g , proportional to T^2 . One of us (Klemens 1954 b) has shown theoretically that the magnitude of κ_g can be deduced from the magnitude of the ideal electronic thermal resistivity W_i at low temperatures. The magnitude of κ_g to be expected if conduction electrons interact as strongly with transverse as with longitudinal waves, as was assumed by Makinson (1938), is about twenty times as great as that to be expected on the assumption of Bloch (1928) that the conduction electrons do not interact with the transverse waves.

Since it is of interest in the interpretation of the conduction properties of monovalent metals to know whether the electrons do interact with the transverse lattice waves (Klemens 1954 a) we have measured the thermal conductivity κ at temperatures between 2° and 160°K of a series of silver-palladium alloys ranging from 2% to 30% palladium concentration. The apparatus and procedure used for the measurements have been described previously (White 1953 a).

The total thermal conductivity is given by

$$\kappa = \kappa_g + \kappa_e \quad \dots\dots(1)$$

where the electronic thermal resistivity is

$$1/\kappa_e = W_e = W_0 + W_i, \quad \dots\dots(2)$$

W_0 is the residual thermal resistivity and W_i is the ideal thermal resistivity. At helium temperatures $W_i \ll W_0$ and $\kappa_g \propto T^2$, so that $1/W_0$, which is proportional to T , can be deduced by plotting κ/T against T . Having found W_0 and assuming for W_i the values previously obtained (White 1953 b) for a rod of pure strained silver, we can deduce κ_e and hence κ_g .

We have also measured the electrical resistance of wires of the same alloys, and found that the ideal electrical resistivity $\rho_i = \rho - \rho_0$, ρ_0 being the residual electrical resistivity, for these alloys differs at room temperature from ρ_i for pure silver by less than 2%, thus suggesting that it is valid to identify W_i with the value for pure silver.

The residual thermal resistance W_0 should be related to the residual electrical resistance ρ_0 by

$$W_0 = \rho_0/LT \quad \dots\dots(3)$$

where L is the Lorenz number. The experimental value of ρ_0 for the wires differs from the value deduced from W_0 by a few per cent although both the thermal and electrical conductivity specimens were subjected to the same annealing conditions. This difference has been ascribed to the much greater deformation of the wires than the rods before annealing.

Figure 1, a logarithmic plot of κ_g against T , indicates that below 12°K κ_g is proportional to T^2 , as is to be expected if the scattering of phonons is mainly due to the conduction electrons. Additional scattering processes, leading to a different temperature dependence of thermal resistance, become apparent at higher temperatures. Figure 2 shows the variation of $W_g T^2$ with palladium concentration, together with the values for pure silver calculated by Klemens (1954 b) on the coupling schemes assumed by Makinson (1938) and Bloch (1928) respectively. The experimental results indicate that the conduction electrons interact with both longitudinal and transverse waves, though possibly less strongly with the latter.

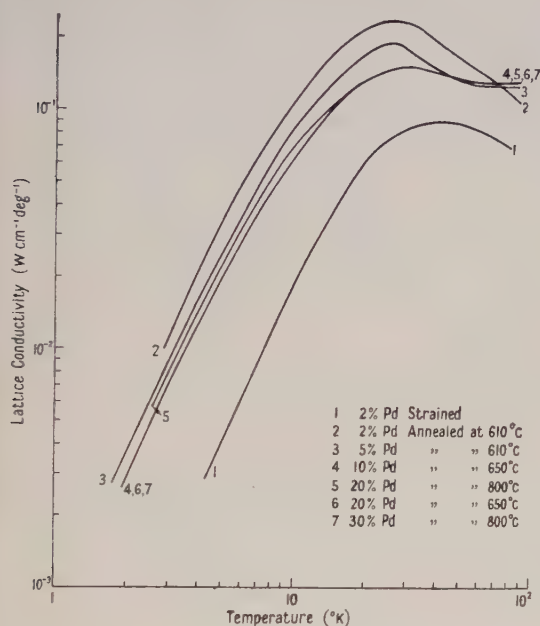


Figure 1. Lattice component of thermal conductivity of silver-palladium alloys.

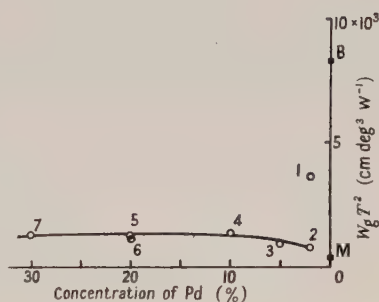


Figure 2. Variation of $W_g T^2$ for lowest temperatures with composition.

For a band of free electrons we would expect $W_g T^2$ to be independent of the electron concentration. The variation of $W_g T^2$ with palladium concentration below 10% palladium may be due to the approach of the Fermi surface to the zone boundary with increasing electron concentration. At high palladium content we would expect a marked increase in $W_g T^2$, resulting from the scattering of lattice waves by holes in the d-band. This has not been observed up to 30% palladium, in contrast to cupro-nickel alloys, which behave as if there are holes in the d-band for quite low concentrations of the transition element (Klemens 1954 b). It is also apparent from other properties (Coles 1952) that the system silver-palladium approximates better to the simple band theory of Mott (1935), which predicts holes for above 40% palladium, than the system copper-nickel.

It may be noted that the lattice conductivity in an unannealed 2% specimen is very much lower than for the corresponding annealed specimen, while the corresponding change in W_0 is only a few per cent, indicating that the

imperfections removed by annealing scatter lattice waves more strongly than free electrons. Further experiments are being made on the effect of strain, and the range of electron concentration is being extended by studying alloys of higher palladium content and silver-cadmium alloys.

A preliminary report on this work was presented by one of us (G.K.W.) at the International Conference on Low Temperature Physics at Houston, Texas, in December 1953. One of us (A.K.S.) is grateful to the Australian Commonwealth Government for a Fellowship under the Colombo Plan.

Division of Physics,
Commonwealth Scientific and
Industrial Research Organization,
Sydney, Australia.
4th May 1954.

W. R. G. KEMP.
P. G. KLEMENS.
A. K. SREEDHAR.
G. K. WHITE*.

* At present at the National Research Council, Ottawa.

BERMAN, R., 1951, *Phil. Mag.*, **42**, 642.

BLOCH, F., 1928, *Z. Phys.*, **52**, 555.

COLES, B. R., 1952, *Proc. Phys. Soc. B*, **65**, 221.

ESTERMANN, I., and ZIMMERMAN, J. E., 1952, *J. Appl. Phys.*, **23**, 578.

KLEMENS, P. G., 1954 a, *Proc. Phys. Soc. A*, **67**, 194; 1954 b, *Aust. J. Phys.*, **7**, 57.

MAKINSON, R. E. B., 1938, *Proc. Camb. Phil. Soc.*, **34**, 474.

MOTT, N. F., 1935, *Proc. Phys. Soc.*, **47**, 571.

OLSEN, J. L., and ROSENBERG, H. M., 1953, *Advances in Physics (Phil. Mag., Suppl.)*, **2**, 28.

WHITE, G. K., 1953 a, *Proc. Phys. Soc. A*, **66**, 559; 1953 b, *Ibid.*, **66**, 844.

The Difference in the Multiple Scattering of Electrons and Positrons

The various theories of multiple scattering are based on approximations to the single scattering which are identical for electrons and positrons. A finite, if small, difference in the multiple scattering is to be expected, and in fact a difference of the order of 10% has been observed for argon (Groetzinger *et al.* 1952). At the small angles of scattering concerned screening must be taken into account, but the exact method of phase shift analysis involves summation of series which are extremely slowly convergent at small angles, and it is difficult to obtain the small difference between the single scattering of electrons and positrons with any accuracy in this way, although the attempt has been made for gold (Mohr and Tassie 1954).

For light elements, however, it is possible to use the second Born approximation (Dalitz 1951) for the exponentially screened field $Ze^2r^{-1}\exp(-\lambda r)$. We are concerned with small angles of scattering θ , and with high energies for which the de Broglie wavelength $2\pi/k$ of the electrons is very small compared with the range $1/\lambda$ of the atomic field. Then the ratio of the scattering of electrons to the relativistic Rutherford scattering reduces to the result

$$R'_S = K^4(\lambda^2 + K^2)^{-2} \left\{ 1 - \beta^2 \sin^2 \frac{1}{2}\theta + \alpha\lambda(\lambda^2 + K^2)\beta^{-1}k^{-1}(\lambda^2 + \frac{1}{4}K^2)^{-1} \right. \\ \left. + \frac{1}{2}\alpha\beta k^{-2}(\lambda^2 + K^2)(\operatorname{cosec} \frac{1}{2}\theta \tan^{-1}(K/2\lambda) - \frac{1}{2}\pi) \right\} \dots\dots(1)$$

where $K = 2k \sin \frac{1}{2}\theta$, $k = 2\pi\gamma mv/h$, $\gamma = (1 - \beta^2)^{-1/2}$, $\beta = v/c$, $\alpha = Z/137$. The prime denotes the use of the second Born approximation, the suffix S the use of the screened field. The corresponding value R'_S^+ for positrons is given by changing the sign of α in (1).

The term $K^4(\lambda^2 + K^2)^{-2}$ is of course the result given by the first Born approximation. For a coulomb field $\lambda=0$, and (1) then reduces to the well known result (McKinley and Feshbach 1948):

$$R'_C = 1 - \beta^2 \sin^2 \frac{1}{2}\theta + \pi\alpha\beta \sin \frac{1}{2}\theta (1 - \sin \frac{1}{2}\theta). \quad \dots\dots (2)$$

For heavy elements the second Born approximation is not accurate, but we apply an approximate correction, based on the fact that we know the error in the approximation when applied to the coulomb field, the exact calculation having been carried out for electrons (McKinley and Feshbach 1948) and for positrons (Yadav 1952). While these exact values, denoted by R without a prime, have been calculated only for angles of 30° and greater, they may be extrapolated to small angles quite safely for positrons. For electrons the extrapolation is less certain, but the tabulated values of the constants A , B , etc. given by McKinley and Feshbach may be extrapolated with greater certainty, to give values of R_C^- at small angles. The curves of Feshbach (1952) for R_C^+/R_C^- may be used as a check.

We take the fractional error in the value given by the second Born approximation for the electron-positron difference to be the same for the screened field as for the coulomb field, i.e. we take

$$(R_S^- - R_S^+)/ (R_S'^- - R_S'^+) = (R_C^- - R_C^+)/ (R_C'^- - R_C'^+). \quad \dots\dots (3)$$

This ratio for angles less than 5° varies from about 0.9 for $\alpha=0.1$ to about 0.5 for $\alpha=0.6$ for energies above 1 MeV, the precise value depending slightly on the energy. The ratio increases to values above 1 at somewhat larger angles. It is possible, therefore, that the assumption made in (3) may give rise to errors for heavy elements, though the magnitude of the final results is still of interest; but the results for light elements should be fairly accurate.

Let us now consider the difference in the root mean square angle of scattering for electrons and positrons, which we denote by θ_{rms}^- and θ_{rms}^+ respectively. The mean θ_{rms} of these two angles is given on the theory of Molière (1948) by

$$\theta_{\text{rms}}^2 = \frac{1}{2} \theta_{\text{max}}^2 B$$

where $B - \ln B = 2 \ln (\theta_{\text{max}}/1.08 \theta_{\text{min}})$,

with $\theta_{\text{min}} = (1.13 + 3.76 \alpha^2 / \beta^2)^{1/2} / (0.885 Z^{-1/3} k a_0)$,

a_0 being the Bohr radius. θ_{max} is such that the total probability of single scattering through an angle greater than θ_{max} is 1, its value depending partly on the thickness of the scatterer.

The appropriate value to take for the constant λ determining the shielding is given by equating the range of the field $1/\lambda$ to $1/k\theta_{\text{min}}$ (Mohr and Tassie 1954). The final results are found, however, not to be very critical to the precise value chosen for λ .

We now have for the fractional difference in the value of θ_{rms} for electrons and positrons

$$\begin{aligned} (\theta_{\text{rms}}^- - \theta_{\text{rms}}^+) / \theta_{\text{rms}} &= \frac{1}{2} (\theta_{\text{rms}}^{-2} - \theta_{\text{rms}}^{+2}) / \theta_{\text{rms}}^2 \\ &= (\theta_{\text{rms}}^{-2} - \theta_{\text{rms}}^{+2}) / \theta_{\text{max}}^2 B. \end{aligned}$$

The last numerator may be calculated using the fact that

$$\theta_{\text{rms}}^2 = \int_0^{\theta_{\text{max}}} \theta^2 P(\theta) d\theta$$

where $P(\theta)$ is the probability of a single scattering through an angle between θ and $\theta + d\theta$. For small angles we have (Mott and Massey 1949)

$$P = 2\theta_{\max}^2 R_S d\theta/\theta^3,$$

so that

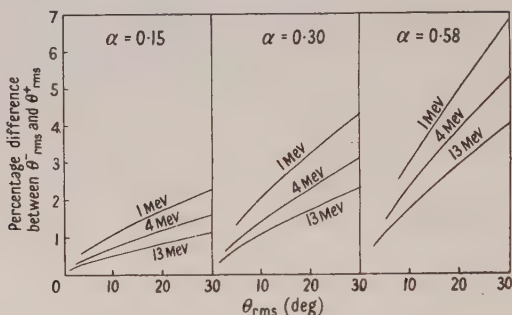
$$\theta_{\text{rms}}^2 = 2\theta_{\max}^2 \int_0^{\theta_{\max}} R_S d\theta/\theta.$$

Hence

$$(\theta_{\text{rms}}^- - \theta_{\text{rms}}^+)/\theta_{\text{rms}} = 2B^{-1} \int_0^{\theta_{\max}} (R_S^- - R_S^+) d\theta/\theta.$$

The value of $R_S^- - R_S^+$ having been calculated as a function of angle from (3), this integral is readily evaluated by numerical integration.

This quantity, multiplied by 100 to convert it to a percentage, is plotted as a function of θ_{rms} for certain energies and values of α in the figure. The percentage difference is seen to be quite small in most cases, and attempts to measure it should clearly be made with thickish foils, heavy elements and not too high energies.



The percentage difference between the root mean square angle of multiple scattering of electrons and positrons as a function of the root mean square angle for different energies and values of $\alpha = Z/137$.

The only direct measurements are those of Groetzinger *et al.* (1952) for argon ($\alpha = 0.13$) for energies in the range 0.3 to 2 mev, and corresponding values of θ_{rms} between 10° and 3° . The observed difference was about 10%, but the calculated difference is seen from the figure to be about 1%. This large discrepancy is difficult to understand, and experiments with other elements would be of interest.

Physics Department,
University of Melbourne,
Australia.
15th April 1954.

C. B. O. MOHR.

DALITZ, R. H., 1951, *Proc. Roy. Soc. A*, **206**, 509.

FESHBACH, H., 1952, *Phys. Rev.*, **88**, 295.

GROETZINGER, G., HUMPHREY, W., Jr., and RIBE, F. L., 1952, *Phys. Rev.*, **85**, 78.

McKINLEY, W. A., Jr., and FESHBACH, H., 1948, *Phys. Rev.*, **74**, 1759.

MOHR, C. B. O., and TASSIE, L. J., 1954, *Aust. J. Phys.*, **7**, No. 2.

MOLIÈRE, G., 1948, *Z. Naturf.*, **3a**, 78.

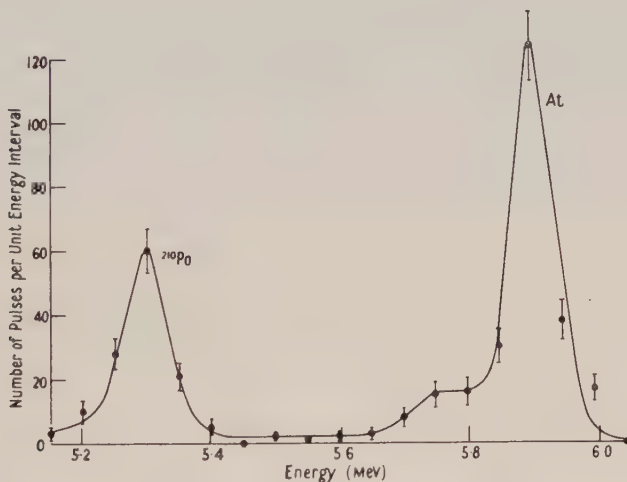
MOTT, N. F., and MASSEY, H. S. W., 1949, *The Theory of Atomic Collisions*, 2nd Edn. (Oxford: University Press), p. 195.

YADAV, H. N., 1952, *Proc. Phys. Soc. A*, **65**, 672.

The α -Activity induced in Gold by Bombardment with Ions of Carbon 13

The production of alpha-particle activity in gold bombarded by carbon ions was first reported by Miller *et al.* (1950). A 25-minute period ascribed to ^{205}At was found, and some evidence for the shorter lived ^{203}At was also obtained. Opportunity arose to repeat and extend these observations during some recent experiments (Burcham 1954) on the heavy ion bombardment of gold; the results are presented here.

Gold foils of thickness 15 microns were bombarded in the internal ^{13}C beam of the 60-inch Nuffield cyclotron of the University of Birmingham. The energy distribution of the ^{13}C ions is continuous up to a maximum of about 110 mev under the conditions of bombardment. Gross decay curves of the α -activity after bombardment were taken as described previously (Burcham 1954) by mounting the irradiated foil in an ionization chamber. Periods of 26.5 ± 1.0 minutes, 102 ± 10 minutes, and 8.6 ± 1 days were found. These periods are close to those tabulated for ^{205}At , ^{207}At and ^{206}Po . In order to confirm the presence of astatine isotopes, an irradiated foil was dissolved in lead at a temperature of about 350°C and volatile products were collected on a cooled silver foil mounted above the lead. The main component of α -activity found on the silver foil decayed with a period of about 25 minutes, and the energy of the group was found to be 5.90 ± 0.04 mev (see figure). The presence of a longer lived group of energy



Pulse size distribution for ^{210}Po and At.

5.73 ± 0.05 mev was also established. These observations, taken together with the periods found more accurately from the gross decay curve, confirm the production of ^{205}At and ^{207}At by the (^{13}C , 5n) and (^{13}C , 3n) reactions. The production of ^{206}Po was not confirmed chemically but the 8.6-day period is unambiguous; this isotope could be the electron-capture daughter of 2.6-hour ^{206}At formed by the (^{13}C , 4n) reaction. The 7-minute isotope ^{203}At was not detected, probably because the mean bombarding energy was too low to favour the (^{13}C , 7n) reaction.

With this interpretation of the observed activities it is possible to compare the yields of the 3n, 4n and 5n reactions under the conditions of this experiment.

The results of this comparison are shown in the table, together with similar information for the $^{14}\text{N} + \text{Au}$ reactions obtained in an earlier experiment (Burcham 1954). The figures give very roughly the saturation activity in disintegrations per minute for a bombarding current of 10^{-9} ampere; they may be in error by

(1)	(2)	(3)	(4)	(5)			
				3n	4n	5n	6n
$^{13}\text{C} + \text{Au}$	^{210}At	89	69	4600	56000	86000	—
$^{14}\text{N} + \text{Au}$	^{211}Em	91	80	—†	35000	22000	8000

(1) Reaction; (2) compound nucleus; (3) maximum excitation of compound nucleus (mev); (4) potential barrier in laboratory system (mev); (5) reaction yields.

† Note added in proof. Dr. Earl K. Hyde has kindly informed me that in similar experiments at Berkeley the production of ^{208}Em in the bombardment of gold by nitrogen ions has been observed.

as much as a factor of two. In compiling this table, figures for electron capture to α -branching ratios were taken from the article by Hollander, Perlman and Seaborg (1953); the α -branching of ^{206}Em and ^{205}Em was assumed to be small. Empirical masses given by Metropolis and Reitwiesner (1950) were used in calculating the excitation energy of the compound nucleus. Yields are given only for the activities which were actually observed; comparable amounts of other products, such as ^{208}At and ^{204}At which decay mainly by electron capture, would not have been detected in this experiment. The yields shown are, however, consistent with those expected on the assumption of evaporation of neutrons from compound nuclei whose minimum energy of excitation is determined by the Coulomb barrier traversed by the incident particle.

Department of Physics,
University of Birmingham.
7th April 1954.

W. E. BURCHAM.

BURCHAM, W. E., 1954, *Proc. Phys. Soc. A*, **67**, 555.

HOLLANDER, J. M., PERLMAN, I., and SEABORG, G. T., 1953, *Rev. Mod. Phys.*, **25**, 469.

METROPOLIS, N., and REITWIESNER, G., 1950, *Table of Atomic Masses*, U.S. Atomic Energy Commission Report No. NP1980.

MILLER, J. F., HAMILTON, J. G., PUTNAM, T. M., HAYMOND, H. R., and ROSSI, G. B., 1950, *Phys. Rev.*, **80**, 486.

Paramagnetic Resonance in Gadolinium Sulphate Octohydrate

We have recently investigated the paramagnetic resonance spectrum of single crystals of gadolinium sulphate octohydrate diluted with the isomorphous samarium salt in the ratio 1 : 200. The experiments have been conducted at room temperatures, and the samarium ions, because of their extremely short relaxation time, have an effect similar to that of a diamagnetic diluent (Bleaney, Elliott and Scovil 1951). The observed spectrum is thus that of gadolinium.

The structure of samarium sulphate octohydrate was studied by Zachariasen (1935) who found that there were eight ions per unit cell and that the space group was $A2/c$. In the paramagnetic resonance experiments two independent spectra are observed, indicating that there are two magnetically inequivalent

ions per unit cell. As is to be expected from the space group, the principal axes of one type of ion are related to those of the other by the two-fold rotation symmetry of the crystal, and the spectra observed with the magnetic field applied along corresponding axes are identical.

The observed spectra are consistent with a spin-Hamiltonian of the form

$$g\beta H \cdot S + B_2^0 P_2^0 + B_2^2 P_2^2 + B_4^0 P_4^0$$

where g is the spectroscopic splitting factor, β is the Bohr magneton, H is the magnetic field, S is the spin operator, the P 's are functions of the spin operators defined as in Bleaney and Stevens (1953) (for instance $P_2^2 = S_x^2 - S_y^2$), and the B 's are numerical coefficients. At the wavelength used, 3.378 cm, the spectrum observed with the magnetic field applied along the x -axis of the Hamiltonian extends from 2440 to 4440 gauss, the y -spectrum extends from 360 to 6600, and the z -spectrum from 380 to 7030 gauss. The half-width of the lines at half intensity is 12 gauss.

Analysis of the spectra in terms of the above Hamiltonian leads to the following values of the coefficients (in units of 10^{-4} cm^{-1})

$$3B_2^0 = 1265 \pm 10; \quad 3B_2^2 = 380 \pm 50; \quad 60B_4^0 = -13 \pm 3.$$

If the centre values of the coefficients given above are taken, the calculated positions of lines agree with the observed to within 80 gauss except in the case of the lowest-field line of the y -spectrum where the discrepancy is 150 gauss. In the case of the x - and y -spectra, exact solution of the secular equation by numerical methods is necessary, and we have solved it for the energy levels at a number of fields; the levels at other fields have been obtained by interpolation with the result that the calculated line positions are accurate only to ± 20 gauss. Our measurements do not determine the g -value to better than 1%, but since it is expected to be little affected by the nature of the crystalline field we have simply taken 1.99, which is the nearest round number to the values found for the ethylsulphate (Bleaney *et al.* 1951) and the double nitrate (Trenam 1953).

The zero-field levels predicted from the above values of the coefficients are doublets at 0, 0.20 ± 0.02 , 0.48 ± 0.03 and $0.82 \pm 0.03 \text{ cm}^{-1}$. It should be remarked that our measurements do not determine whether the coefficients, and consequently the zero-field levels, have the signs stated or the reverse signs. But measurements of the specific heat of concentrated gadolinium sulphate octohydrate at low temperatures which were made by Benzie and Cooke (1950) and other workers, and which were interpreted in terms of a quadruplet level lying between two doublets, indicated that the quadruplet was nearer to the lower doublet. We have therefore made the choice of sign which brings the mean position of the two intermediate zero-field doublets nearest to the lowest doublet. It is interesting to notice that according to our work the mean position of the intermediate levels is separated from the upper and lower levels by amounts in the ratio 5 : 3.55, which is to be compared with the ratio 5 : 3 used in interpreting the specific heat measurements; and that our choice gives the same sign to the largest coefficient B_2^0 as was found in the ethylsulphate and the double nitrate.

The principal axes of the Hamiltonian have been found by searching for those directions of applied field at which the lines are at extrema for changes of the field direction. The y -axis for one type of ion is inclined at 38° to the

b -axis of the crystal, and its projection on the ac plane lies along the c -axis; the z -axis is inclined at 55° to the b -axis, and its projection on the ac plane is inclined at 152° to the c -axis and at 90° to the a -axis. (The b -axis, which is the two-fold axis, is perpendicular to the ac plane; the monoclinic angle is 118° .) The x -axis is perpendicular to the y - and z -axes to within the experimental error of 1° . The lines of the spectra do not go to extrema at the same directions of field but at individual directions which show a scatter of 3° about the mean directions which are quoted above. The reason for this behaviour is not at present understood.

Preparations are being made to study the spectrum at a wavelength of 10 cm. When measurements made at this and at other wavelengths become available it will be possible to make a closer determination of the coefficients in the spin-Hamiltonian.

It is a pleasure to acknowledge the stimulating interest which has been shown by Drs. B. Bleaney and K. W. H. Stevens in the work reported above.

University of Otago,
Dunedin, New Zealand.
1st June 1954.

G. S. BOGLE.
V. HEINE, JR.

BENZIE, R. J., and COOKE, A. H., 1950, *Proc. Phys. Soc. A*, **63**, 213.

BLEANEY, B., ELLIOTT, R. J., and SCOVIL, H. E. D., 1951, *Proc. Phys. Soc. A*, **64**, 933.

BLEANEY, B., ELLIOTT, R. J., SCOVIL, H. E. D., and TRENAM, R. S., 1951, *Phil. Mag.*, **42**, 1062.

BLEANEY, B., and STEVENS, K. W. H., 1953, *Rep. Prog. Phys.*, **16**, 108 (London: Physical Society).

TRENAM, R. S., 1953, *Proc. Phys. Soc. A*, **66**, 118.

ZACHARIASEN, W. H., 1935, *J. Chem. Phys.*, **3**, 197.

REVIEWS OF BOOKS

Geometrical Mechanics and de Broglie Waves, by J. L. SYNGE. Pp. vi + 167. (Cambridge: University Press, 1954.) 25s.

It is not generally realized that Hamilton's contributions to dynamics were a product of his theory of geometrical optics. The earlier theory is indeed in some respects the more elegant since Hamilton's Optics is symmetrical in all coordinates whereas the customary formulation of Hamilton's Dynamics accords time a preferential role. One might therefore suspect that if the ideas of special relativity, in particular the concept of Minkowskian space, had been current at the time, Hamilton would have applied his optical theory to dynamics substantially without change. It is this task which Professor Synge sets out to fulfil in this entertaining little book.

The prescription is carried out meticulously, and this is somewhat to be regretted since the strange terminology of Hamilton's Optics masks familiar dynamical concepts and the examples, transplanted from optics, are distinctly uncomfortable in their new surroundings. If one compares Synge's 'optical' theory of particle dynamics with that which we may obtain from Hamilton's principle by replacing time by proper time (regarding x , y , z and t all as 'dependent' variables), we find that the 'medium function', 'slowness function' and 'slowness vector' are pseudonyms for the Lagrangian function, Hamiltonian function and momentum vector.

The author emphasizes that certain relations and phenomena which we normally associate with wave theory appear in a purely 'geometrical' theory. Thus the velocity of the action surfaces associated with an assembly of trajectories bears just the same relation to the particle velocity as phase velocity bears to the group velocity; but a physicist would of course object that the former yields no *physical* information while the latter does. A similar, but more serious, objection may be set against the treatment of refraction through a hole which shows that incident action surfaces emerge as spheres, since wave theory indicates that such refraction takes place only if the diameter of the hole is small compared with the wavelength of the 'radiation'; no such criterion appears in Synge's theory since both dimensions are taken to be zero.

The more interesting and more important part of the book is given to a method of 'primitive quantization'. This is the analogue of the approximate method used in optics of constructing wave patterns by setting up surfaces normal to an appropriate assembly of rays and then assuming that such surfaces have the same 'phase' if the optical distance between them (measured along any ray) is an integral number of free-space wavelengths: two action surfaces (which we may now identify with 'de Broglie waves') are supposed to have the same quantum-mechanical phase if the action difference (measured along any space-time trajectory) is an integral multiple of Planck's constant. This is an attractively simple rule which embraces the original de Broglie hypothesis and which is found to yield accurately the fine structure of the hydrogen spectrum. This is at first sight rather surprising, but the same formula was after all established by Sommerfeld by applying the Wilson-Sommerfeld quantization rule to a relativistic model of the hydrogen atom.

Most physicists will wish to know the relationship between Synge's 'primitive quantization' and other, more familiar, rules. This question the author does not investigate, which is a pity, for the answer is most instructive. It is clear from the author's comparison with the Klein-Gordon equation that the phase varies in the same way as that of the W.K.B. solution of this equation. When applied to orbital motion, the method is *identical* with the Wilson-Sommerfeld rule; this we may see as follows. The trajectories of a multiply periodic dynamical system may be enumerated by parameters which include an appropriate number of cyclic parameters θ , ϕ , etc. The adiabatic invariants, which according to the Wilson-Sommerfeld theory take values nh , may be written as

$$\oint d\theta p_r \frac{\partial x_r}{\partial \theta}, \text{ etc.},$$

where r enumerates all space-time coordinates. Synge's method is effectively to describe geometrically an assembly of trajectories by allowing such cyclic parameters to take all values and then to specify that the quantum-mechanical phase should be single-valued over configuration space. This implies that the action is to change by nh as one moves around contours such as that formed by varying θ and keeping all other parameters fixed, which is seen to be precisely the Wilson-Sommerfeld rule. Of the two formulations, Synge's is to be preferred as the simpler and more general.

The book is stated to be intended "for those who enjoy seeing a subject of considerable physical interest built up mathematically from a very simple basis, clearly stated". Judged in the spirit of this intention, the book may be recommended.

P. A. STURROCK.

Graphs of the Compton Energy-Angle Relationship and the Klein-Nishina Formula from 10 kev to 500 mev, by ANN T. NELMS. National Bureau of Standards (Circular 542). (Washington: U.S. Department of Commerce, 1953.) 55 cents.

This booklet is a compilation of some eighty full-page graphs giving the relationships between photon energy, electron energy, cross section and angle in the Compton Klein-Nishina process for a very wide range of photon energies. It is prefaced by a brief discussion of the Klein-Nishina formula. The diagrams are beautifully reproduced and very convenient in use. This booklet should prove very useful to all those who use or study high-energy x-rays and γ -rays, a category of people which to-day extends beyond the ranks of physicists alone.

S. DEVONS.

Nuclear Moments, by N. F. RAMSEY. Pp. x+169 (New York: John Wiley; London: Chapman and Hall, 1953.) 40s.

Following the great advance in electronics during the war, research based on nuclear moment measurements has increased immensely, and the methods are now extensively applied to the study of molecular, chemical, liquid and solid state problems as well. This book is based on the author's section on 'Nuclear Moments and Statistics' in Volume 1 of *Experimental Nuclear Physics*, edited by E. Segrè, and it summarizes the whole field in a manner which as is complete as can be expected in a book of this size.

The first two chapters are devoted to the quantum mechanical calculation of the energy associated with the electric and magnetic interactions between the nuclei and the electrons in atoms and molecules. This is followed by well presented, concise accounts of the experimental techniques of measuring nuclear moments and the methods of correcting the results for magnetic shielding and resonance shifts. A table of moments for stable nuclei, complete up to 1952, is included. The last part of this section is devoted to the significance of nuclear moments in nuclear theory.

The remainder of the book is concerned with the methods of applying the experimental techniques used for nuclear moment measurements to the study of the nature of chemical bonds, locations of atoms in molecules, electron distributions in molecules, the shape of the vibrational potential in molecules, molecular association and dissociation in liquids, chemical exchange, excitation of hindered rotation in solids, strains in solids, crystal structure, electron distributions in metals and other chemical and solid state properties.

Over 700 references to recent and old papers are given and there is a good author and subject index. Although the book is somewhat advanced for use by students, because of the nature of the quantum mechanics, it provides an excellent summary of an extensive subject and it should be of great use to research workers in the fields mentioned above.

K. SMITH.

Elementary Introduction to Molecular Spectra, by BORGE BAK. Pp. vi + 125. (Amsterdam : North-Holland Publishing Co., 1954.) 18s.

The interpretation of molecular spectra is built up on a foundation of rather involved quantum theory including quantum mechanics. The writer of any textbook on the subject is therefore faced with difficult decisions of where to start his explanations, and the resulting compromise will largely be a matter of taste. A treatment of molecular spectra, including polyatomic molecules, microwave, Raman, infra-red, visible and ultra-violet spectra, starting with the theory of the hydrogen wave functions and including time-dependent quantum-mechanical perturbation theory on the theoretical side, and some discussion of techniques on the experimental side, this is certainly a bold undertaking in a book of 125 pages. Accepting this task as given, one must admire the skill with which the author has fulfilled it, and it seems almost unfair to complain that the handling of the theory is occasionally a little superficial. Assuming Bohr's frequency relation (p. 13) and hence deriving the insufficiency of classical laws (p. 14), this does not seem very logical. Normal coordinates and normal vibrations are used on p. 20 and p. 51, and in some detail on p. 84, but what they really mean is not explained until p. 86. Franck and Condon's principle is stated in the wrong way often found in chemistry books ; it is not the time of the electron transition which is short compared with the period of vibration (in fact, it is very long compared with the latter), but the electronic period.

The book is written in a lively, often colloquial style. For those who are engaged in work on molecular spectra it will be most valuable as a summary of the essential theoretical relations and of the basic facts. Students and newcomers to the field of molecular spectroscopy will welcome the book as a most readable introduction.

H. G. KUHN.

CONTENTS OF SECTION B

Prof. R. WHIDDINGTON. Physics in the University and the Nation	601
Prof. R. W. DITCHBURN and Dr. G. A. J. ORCHARD. The Polarization of Totally Reflected Light	608
Mr. R. BULLOUGH and Dr. B. A. BILBY. Uniformly Moving Dislocations in Anisotropic Media	615
Mr. R. LAWRENCE, Dr. A. F. GIBSON and Dr. J. W. GRANVILLE. On the Current Gain of Germanium Filamentary Transistors	625
Dr. C. A. HOGARTH. Current Multiplication Processes in n-Type Germanium Point-Contact Transistors	636
Research Notes :	
Dr. D. H. PARKINSON and Mr. J. E. QUARRINGTON. The Resistance-Temperature Characteristics of Leaded Brass Wires at Helium Temperatures	644
Mr. P. RANSOM and Dr. F. W. G. ROSE. On the Relation between the Sum of Donor and Acceptor Concentration and Lifetime in Single Crystal Germanium	646
Letters to the Editor :	
Dr. H. K. HENISCH and Mr. P. M. TIPPLe. A Note on the Effect of Temperature Gradients at Point Contacts on Germanium	651
Reviews of Books	653
Contents of Section A	656

The Cooling of a Gas by Radiation*

By ERNEST BAUER† AND TA-YOU WU‡

* Institute of Mathematical Sciences, New York University

‡ Division of Physics, National Research Council, Ottawa, Canada

MS. received 15th March 1954

Abstract. We consider a gas composed of atoms having two electronic states. Transitions between these two states can take place by collisions, and by emission or absorption of radiation. When the radiative transition probabilities are small compared with those due to collisions, a 'temperature' may be defined for the translational motion. We formulate the general problem for the case where the total concentration of the gas depends on the space coordinates in a given way, and the possibility of the 'imprisonment' of the radiation emitted is taken into account. In this case the problem leads to a pair of coupled integro-differential equations, from which the 'temperature' and the concentration of atoms in the excited state are obtained as functions of space and time. Neglecting the imprisonment of the resonance radiation and the spatial variation of the temperature, we have made calculations for the case when the energy difference between the two states is of the order kT , for a number of values of the ratio between radiative and collisional transition probabilities. The results are applied to the problem of the cooling of the atmospheric gas at high altitudes (100 km) at night, as a result of the magnetic dipole transitions between the components of the 3P state of the oxygen atom.

§ 1. INTRODUCTION

IN a recent paper, Bates (1951) suggested that magnetic dipole transitions between the components of the 3P state of the oxygen atom could lead to a significant cooling of the upper atmosphere in that region where oxygen atoms are abundant, i.e. about 100 km above the earth. The (inverted) triplet state in question has splittings of the order 0.02 eV, which are of the order of the gas kinetic energy at these altitudes, so that the number of atoms in excited states of the triplet will be large; and thus, while the transition probabilities of the $^3P_0-^3P_1$, $^3P_1-^3P_2$ transitions are small (10^{-5} – 10^{-4} sec $^{-1}$; see Pasternack 1940), yet the total number of transitions per unit volume per second may be large and so may be the total energy transferred in this way.

These considerations are limited by the assumption of a Boltzmann distribution, which is valid only for a system in thermodynamic equilibrium, and by the neglect of the possibility that the radiation emitted will be absorbed by other atoms, leading to the familiar problem of the 'imprisonment of resonance radiation'. The purpose of the present work is to formulate the problem of the cooling of a gas by the emission of radiation without assuming the Boltzmann distribution for the atoms in various states and without neglecting the effect of

* This work was supported in part by Contract No. AF-19(122)-463 with the United States Air Force through sponsorship of the Geophysics Research Directorate of the Air Force Cambridge Research Center, Air Research and Development Command.

imprisonment of the radiation, and to carry out numerical calculations appropriate for application to the upper atmosphere when the effect of imprisonment of the radiation is neglected as a first approximation.

To simplify the calculations, we shall consider a gas composed of atoms having two electronic states 1 and 2, and distributed in space in a given manner (such as the gas in the atmosphere). Transitions between these two states can take place by collisions and by emission or absorption of radiation. In a collisional transition, energy is transferred between the translational and electronic modes of the atom; in a radiative transition an atom may emit a quantum $h\nu_{21}$ of radiation, or it may absorb a quantum $h\nu_{21}$ that has been emitted by another atom in the gas. We shall assume that there is no incident radiation from an external source having a frequency ν_{21} , so that the radiation energy of this frequency comes only from quanta emitted by atoms in the system. These quanta will eventually be lost to the system after undergoing a series of absorptions and re-emissions by other atoms in traversing the gas. The problem now is to study the change of state of the system, starting with suitable initial conditions. At time $t=0$ our gas is in statistical equilibrium at a given temperature T_0 as a result of collisions alone. Then, for $t>0$, we 'switch on' the radiative transitions, so that there is a net loss of energy from the system for $t>0$, and we now ask the following question: at what rate is energy lost from the system?

The behaviour of the system obviously depends on the spatial distribution of the atoms, and on the values of the collisional and radiative cross sections. Let the average cross section for gas kinetic collisions be σ_0 , and let those for excitation and de-excitation of the state 2 by collisions be σ_{12} and σ_{21} respectively, and let the Einstein A coefficient for the 2-1 transition be A_{21} . Let the total number density of the gas be N and the average velocity of the atoms be v . In the extreme case where

$$A_{21} \gg Nv\sigma_{21}, \quad \dots\dots(1)$$

the excited atoms in state 2 are removed by emission of radiation as soon as they are excited by collisions. The rate of loss of energy of the system is governed by the rate of collisional excitation (which is a function of time), and by the effect of the 'imprisonment' of the radiation in the gas. In this case, the distribution of the atoms in the two states 1 and 2, which varies with time, will not be given by the Boltzmann theorem at all since the departure from thermodynamic equilibrium is so great that it is not meaningful to speak of a 'temperature'. In the other extreme, where

$$A_{21} \ll Nv\sigma_{21}, \quad \dots\dots(2)$$

the rate of loss of energy by radiation is so small that one may regard the system as undergoing a continuous transition through states which differ only slightly from the equilibrium state.

These extreme cases can be treated easily, but are not general enough for our purpose. In the present work we shall consider the case where

$$A_{21} \ll Nv\sigma_0, \quad \dots\dots(3)$$

which is less stringent than (2), since in general $\sigma_0 > \sigma_{21}$, and usually $\sigma_0 \gg \sigma_{21}$. Under the condition (3), the frequency of elastic collisions is high compared with that of emission of radiation, so that the atoms make enough collisions to redistribute their kinetic energy of translation between radiative transitions. In this case, it is possible to assume that while the distribution of the atoms in the two

electronic states 1 and 2 may deviate greatly from the Boltzmann distribution, yet the translational degrees of freedom may be characterized by a 'temperature' T , defined by the kinetic energy of the atoms. On this assumption, the problem will be to find the 'temperature' T and the ratio N_2/N_1 of the numbers of atoms in the two states 2 and 1 as functions of time and space for certain initial and boundary conditions.

§ 2. FORMULATION OF THE GENERAL PROBLEM

We consider a gas species of number density $N=N(\mathbf{r})$ that has two states, a ground state 1 and an excited state 2, of densities $N_i(\mathbf{r}, t)$, ($i=1, 2$):

$$N(\mathbf{r}) = N_1(\mathbf{r}, t) + N_2(\mathbf{r}, t). \quad \dots\dots(4)$$

We shall define an effective temperature $T=T(\mathbf{r}, t)$ in terms of the total kinetic energy per unit volume. It is convenient to deal with the case when there are other gas atoms present in addition to the gas species we are concerned with primarily; these other atoms enter into the thermal collisions, but do not participate in any way in the radiative processes. (In the problem under consideration, there would be nitrogen molecules present as well as oxygen atoms.) Accordingly, the total number density of all particles will be $X(\mathbf{r})$, which may be greater than $N(\mathbf{r})$. Thus the total kinetic energy per unit volume is

$$3kTX/2, \quad \dots\dots(5)$$

which serves to define the effective temperature T .

Let the collisional cross sections for the excitation and de-excitation of the state 2 be $\sigma_{12}(v)$ and $\sigma_{21}(v)$, where v is the relative velocity of the colliding particles. There will also be radiative effects specified by the rates $B_{12}\rho(\nu_{12}; \mathbf{r}, t)$ and $\{A_{21} + B_{21}\rho(\nu_{21}; \mathbf{r}, t)\}$, where A, B are Einstein coefficients and ρ is the radiation energy density.

2.1. Collisional Transitions

In a state of equilibrium we have

$$N_i = N_i^0(\mathbf{r}), \quad T = T^0(\mathbf{r}), \quad \dots\dots(6)$$

and

$$N_2^0(\mathbf{r})/N_1^0(\mathbf{r}) = (g_2/g_1) \exp \{-\epsilon_{21}/kT^0(\mathbf{r})\}, \quad \dots\dots(7)$$

where the level splitting ϵ_{21} is given by

$$\epsilon_{21} = \frac{1}{2}M_R v_0^2 = h\nu_{21}. \quad \dots\dots(8)$$

M_R is the reduced mass of the colliding particles, and g_1, g_2 are the statistical weights of the states 1 and 2.

If X is the total number density of particles that may excite or de-excite our atom, the rate of increase of N_2 due to collisions is

$$\left(\frac{\partial}{\partial t} N_2\right)_{\text{coll}} = N_1 X \int_{v_0}^{\infty} dv v f(v) \sigma_{12}(v) - N_2 X \int_0^{\infty} dv v f(v) \sigma_{21}(v), \quad \dots\dots(9)$$

where $f(v)$ is the velocity distribution function.

The two cross sections σ_{12}, σ_{21} are not independent, but are related atomic properties. In particular, if we define two velocities v, v' , related by

$$v^2 = v'^2 + (2/M_R)\epsilon_{21} = v'^2 + v_0^2, \quad \dots\dots(10)$$

then the ratio $\sigma_{12}(v)/\sigma_{21}(v')$ depends only on atomic properties such as v, v', g , etc., and not on macroscopic quantities like the temperature. On account of this

fact, we may calculate this ratio of cross sections from the principle of detailed balance for conditions of statistical equilibrium, and be sure that the result will still hold when there is no statistical equilibrium.

The condition of detailed balance is

$$N_1\sigma_{12}(v)f(v)v\,dv = N_2\sigma_{21}(v')f(v')v'\,dv', \quad \dots\dots(11)$$

where the conditions (7), (10) must be satisfied. Equation (10) gives the result $v\,dv = v'\,dv'$. If we substitute a Maxwellian function for the velocity distribution function $f(v)$

$$f(v) = 4\pi(M_R/2\pi kT)^{3/2}v^2 \exp\{-M_R v^2/2kT\}, \quad \dots\dots(12)$$

then equation (11) leads to the result

$$\sigma_{12}(v)/\sigma_{21}(v') = (g_2/g_1)(v'/v)^2. \quad \dots\dots(13)$$

Substituting (13) in (9), we get^{†‡}

$$\left(\frac{\partial}{\partial t} N_2\right)_{\text{coll}} = XF(T) \left[N - N_2 \left(1 + \frac{g_1}{g_2} \exp\left(\frac{\epsilon_{21}}{kT}\right) \right) \right], \quad \dots\dots(14)$$

where

$$F(T) = \int_{v_0}^{\infty} dv v f(v) \sigma_{12}(v). \quad \dots\dots(15)$$

Neither the precise form nor even the numerical value of $\sigma_{12}(v)$ is known, but in view of the Boltzmann factor in $f(v)$ the precise form does not much matter as long as we can make a reasonable estimate of σ close to the threshold v_0 . If we put

$$\sigma_{12}(v) = \begin{cases} 0, & v < v_0, \\ \sigma, & v > v_0, \end{cases} \quad \dots\dots(16)$$

then

$$F(T) = 2\sigma(2kT/\pi M_R)^{1/2} (1 + \epsilon_{21}/kT) \exp(-\epsilon_{21}/kT). \quad \dots\dots(17)$$

2.2. The Escape of Energy by Radiation§

The rate of decrease of $N_2(\mathbf{r}, t)$ due to emission of the quantum $h\nu_{21}$ is

$$N_2(\mathbf{r}, t)\{A_{21} + B_{21}\rho(\nu_{21}; \mathbf{r}, t)\} \equiv N_2(\mathbf{r}, t)\gamma(\mathbf{r}, t), \quad \dots\dots(18)$$

where ρ is the radiation energy density of frequency ν_{21} , measured per unit frequency range. Instead of calculating this rate by evaluating the density ρ due to the radiation emitted by other atoms in the system, we proceed as follows.

Let the absorption cross section of radiation of frequency ν be k_ν , so that the radiation intensities $I_0(\nu)$, $I_s(\nu)$, measured a distance s apart, are related by

$$I_s(\nu) = I_0(\nu) \exp(-k_\nu N_1 s). \quad \dots\dots(19)$$

k_ν is some function of frequency ν , the precise form depending on the mechanism responsible for the line shape. Let $P(\nu)$ be the intensity distribution of the spectral line, so normalized that

$$\int_{\text{SL}} d\nu P(\nu) = 1, \quad \dots\dots(20)$$

where SL indicates that the integration extends over the whole of the spectral line.

[†] It is clear that in equilibrium, substituting (7) in (14) yields $(\partial N_2/\partial t)_{\text{coll}} = 0$, as must be the case.

[‡] In writing down equation (14), we assume the form (12) for $f(v)$, which implies equilibrium conditions. Since we have made the restriction (3) and have assumed the possibility of defining a temperature T in (5), the use of (12) in obtaining (14) is a consistent assumption.

[§] For the formulation of a similar but less general problem, see Holstein (1947, 1951).

Now $\Gamma(\xi, t)$, the probability that a quantum of radiation traverses a distance $\xi = |\mathbf{r} - \mathbf{r}'|$ before being absorbed, is

$$\Gamma(\xi, t) = \int_{\text{SL}} d\nu P(\nu) \exp \left\{ -k_\nu \int_0^\xi d\xi N_1(\xi, t) \right\}. \quad \dots\dots(21)$$

The number of quanta emitted in the volume element $d\mathbf{r}'$, and directed into the solid angle dS/ξ^2 , per second, is

$$\frac{dS}{4\pi\xi^2} N_2(\mathbf{r}', t) \gamma(\mathbf{r}', t) d\mathbf{r}', \quad \dots\dots(22)$$

and thus the number of quanta Λ that are absorbed in the volume element $d\xi = dS d\xi$ is

$$\Lambda = - \frac{dS}{4\pi\xi^2} N_2(\mathbf{r}', t) \gamma(\mathbf{r}', t) d\mathbf{r}' \frac{\partial \Gamma(\xi, t)}{\partial \xi} d\xi. \quad \dots\dots(23)$$

The number of quanta absorbed per unit volume element per second at \mathbf{r} due to radiation coming from all space is

$$\frac{1}{d\xi} \int d\mathbf{r}' \Lambda,$$

which is

$$- \frac{1}{4\pi\gamma} \int d\mathbf{r}' N_2(\mathbf{r}', t) \gamma(\mathbf{r}', t) \frac{\partial \Gamma(\xi, t)}{\partial \xi}. \quad \dots\dots(24)$$

$G(\mathbf{r}, \mathbf{r}'; t)$, the probability that a quantum emitted at \mathbf{r}' is absorbed in unit volume at \mathbf{r} , is given by

$$G(\mathbf{r}, \mathbf{r}'; t) = G(\mathbf{r}', \mathbf{r}; t) = \frac{-1}{4\pi\xi^2} \frac{\partial \Gamma(\xi, t)}{\partial \xi}. \quad \dots\dots(25)$$

Thus, from equations (18), (24), (25), the net rate of change of $N_2(\mathbf{r}, t)$ due to radiative processes is

$$\left(\frac{\partial}{\partial t} N_2 \right)_{\text{rad}} = -N_2(\mathbf{r}, t) \gamma(\mathbf{r}, t) + \int d\mathbf{r}' N_2(\mathbf{r}', t) \gamma(\mathbf{r}', t) G(\mathbf{r}, \mathbf{r}'; t), \quad \dots\dots(26)$$

and combining this with (14), the total rate of change of $N_2(\mathbf{r}, t)$ is given by

$$\begin{aligned} \frac{\partial}{\partial t} N_2 = & XF(T) [N - N_2 \{1 + (g_1/g_2) \exp(\epsilon_{21}/kT)\}] - N_2 \gamma(\mathbf{r}, t) \\ & + \int d\mathbf{r}' N_2(\mathbf{r}', t) \gamma(\mathbf{r}', t) G(\mathbf{r}, \mathbf{r}'; t), \quad \dots\dots(27) \end{aligned}$$

which is one of our fundamental equations.

This differential-integral equation can be simplified somewhat if we neglect the induced emission of radiation compared with the spontaneous emission, so that equation (18) gives

$$\gamma(\mathbf{r}, t) = A_{21} = \text{constant}. \quad \dots\dots(28)$$

This neglect is justified if there is no incident radiation from an external source, and if ρ arising from the atoms in the system is small. Using (28), equation (27) becomes

$$\begin{aligned} \frac{\partial}{\partial t} N_2 = & XF(T) [N - N_2 \{1 + (g_1/g_2) \exp(\epsilon_{21}/kT)\}] - N_2 A_{21} \\ & + A_{21} \int d\mathbf{r}' N_2(\mathbf{r}', t) G(\mathbf{r}, \mathbf{r}'; t). \quad \dots\dots(29) \end{aligned}$$

However, equation (29) still contains two unknown functions, $N_2(\mathbf{r}, t)$ and $T(\mathbf{r}, t)$, and thus to solve the problem we need another equation, which is furnished from the definition (5) of the effective temperature T .

2.3. Energy Balance and the 'Temperature' T

The kinetic energy per unit volume of the gas is $3kTX/2$. This is changed only by collisions and not by radiative transitions, because the radiative processes by themselves change only N_2 and N_1 but do not change the kinetic energy. Hence, the variations of the temperature at any given position and time are determined by the condition

$$\frac{\partial}{\partial t} \left\{ \frac{3}{2} kTX \right\} + \epsilon_{21} \left(\frac{\partial}{\partial t} N_2 \right)_{\text{coll}} = 0,$$

and from equation (14) this reduces to

$$\frac{\partial}{\partial t} \left\{ \frac{3}{2} kTX \right\} + \epsilon_{21} XF(T) [N - N_2 \{ 1 + (g_1/g_2) \exp(\epsilon_{21}/kT) \}] = 0. \quad \dots\dots (30)$$

In equations (29), (30) we have two coupled non-linear integro-differential equations which, together with the appropriate boundary conditions, will specify the two functions $N_2(\mathbf{r}, t)$ and $T(\mathbf{r}, t)$.

§ 3. SOLUTION OF A SIMPLIFIED PROBLEM

The solution of the two equations (29), (30) in their full generality presents considerable difficulties. In the present work, as a first approximation to the solution, we neglect the effect of imprisonment of resonance radiation by putting $G(\mathbf{r}, \mathbf{r}', t) = 0$. It is clear that this will give an over-estimate of the rate of energy loss due to radiation for the present problem since in this case all quanta radiated are immediately lost, there being now no mechanism for retaining them within the system.

To reduce the complications still further, we take the total densities N , X as absolute constants, so that there is now no space dependence left in the problem. Thus, our basic equations obtained from (29) and (30) are

$$\frac{\partial}{\partial t} N_2 + [XF(T) \{ 1 + (g_1/g_2) \exp(\epsilon_{21}/kT) \} + A_{21}] N_2 = XNF(T), \quad \dots\dots (31)$$

$$\frac{\partial}{\partial t} \{ 3kTX/2 \} + \epsilon_{21} XF(T) [N - N_2 \{ 1 + (g_1/g_2) \exp(\epsilon_{21}/kT) \}] = 0, \quad \dots\dots (32)$$

where now N_2 and T are functions of time only, and all other quantities (X , N , g_1 , g_2 , ϵ_{21} , A_{21}) are constants.

We now wish to solve the problem of equations (31) and (32) for $t > 0$ with the following initial conditions†

$$T = T_0, \quad \partial T / \partial t = 0, \quad \text{at } t = 0. \quad \dots\dots (33)$$

In order to solve the problem of (31)–(33), we introduce the following dimensionless variables and constants:

$$\left. \begin{aligned} n = N_2/N, \quad x = \epsilon_{21}/kT, \quad \tau = c_0 t, \quad XF(T) = c_0 \phi(x) \\ g = g_1/g_2, \quad \mu = 2N/3X, \quad \lambda = A_{21}/c_0. \end{aligned} \right\} \quad \dots\dots (34)$$

where c_0 is a constant of the order of the reciprocal of the time between two excitational collisions.

† Substituting (33) in (31) and (32), we find that at $t = 0$ we have $N_2 = N_2^0$ of equation (7), and also $\partial N_2 / \partial t = -A_{12} N_2$. Both these results are eminently reasonable, and show that the initial conditions (33) are satisfactory for describing how radiative 2–1 transitions disturb the initial statistical equilibrium.

In this new notation, the problem is

$$\frac{\partial}{\partial \tau} n + [\lambda + \phi(x)(1 + ge^x)]n = \phi(x), \quad \dots\dots\dots(35)$$

$$\frac{\partial}{\partial \tau} (1/x) + \mu\phi(x)[1 - n(1 + ge^x)] = 0, \quad \dots\dots\dots(36)$$

to be solved for $\tau > 0$ with the initial conditions

$$x = x_0, \quad \partial x / \partial \tau = 0, \quad \text{at} \quad \tau = 0. \quad \dots\dots\dots(37)$$

We shall take

$$\phi(x) = e^{-x}, \quad \dots\dots\dots(38)$$

as an approximation, bearing in mind that while the precise form of $F(T)$ is not known, yet an approximation such as (38) does yield the basic, exponential, T -dependence of equation (17).

3.1. Solution of the System (35)–(37)

A standard way of solving two coupled equations is to eliminate one of the two dependent variables; here it is clearly convenient to eliminate n rather than x . If we carry out the elimination, we get

$$n = \left\{ 1 + \frac{\partial}{\partial \tau} \left(\frac{1}{x} \right) / \mu\phi(x) \right\} / (1 + ge^x), \quad \dots\dots\dots(36')$$

and

$$\begin{aligned} \frac{d^2x}{d\tau^2} + \left(\frac{dx}{d\tau} \right)^2 \left\{ -\frac{2}{x} + \frac{1}{1 + ge^x} \right\} + \frac{dx}{d\tau} \left\{ \lambda + g + e^{-x} + \frac{\mu gx^2}{1 + ge^x} \right\} \\ - \lambda \mu x^2 e^{-x} = 0. \quad \dots\dots\dots(39) \end{aligned}$$

Thus the problem is reduced to the solution of equation (39) with the initial conditions (37). The independent variable τ only appears as $d/d\tau$, so that it is clearly convenient to transform (39) so as to make $dx/d\tau$ (or some function of it) the dependent, and x the independent variable; and in particular because the coefficient of $(dx/d\tau)^2$ in (39) is $-(2/x) + \text{a small quantity } \{= 1/(1 + ge^x)\}$, we introduce the new dependent variable

$$y = y(x) = \frac{1}{x^2} \frac{dx}{d\tau} \quad \dots\dots\dots(40)$$

which has the merit of making the y^2 term small ($y^2/(1 + ge^x)$). We now neglect this y^2 term and discuss the solution of†

$$\left. \begin{aligned} y \, dy/dx + yJ(x) - K(x) &= 0, \quad x^2J(x) = \lambda + g + e^{-x} + \frac{\mu gx^2}{1 + ge^x}; \\ x^2K(x) &= \lambda \mu e^{-x}, \end{aligned} \right\} \quad (41)$$

with the initial condition

$$y = 0 \quad \text{at} \quad x = x_0. \quad \dots\dots\dots(42)$$

† Calculations have been made and they show that the neglect of the y^2 term does not produce any significant changes, either in the general character of the solution or in its numerical values, for the range of parameters used here.

This equation (41) has been integrated numerically for the following values of the parameters:†

$$x_0 = \frac{1}{2}, \quad g = 2, \quad \mu = \frac{1}{4}, \quad \lambda = 1, \quad 10^{-3}, \quad 10^{-5}, \quad 10^{-7}, \quad \dots \quad (43)$$

A detailed discussion of the solution of equation (41) is given elsewhere (Bauer and Wu 1954); y rises very sharply just above x_0 (in fact, dy/dx is ∞ at $x = x_0$) to a maximum at x_1 , and then falls off to zero as x tends to infinity; beyond the maximum $y(x)$ may be approximated by $\eta(x)$, defined as

$$\eta(x) = K(x)/J(x). \quad \dots \quad (44)$$

Once we have y as a function of x , we can find $\tau(x)$ from equation (40), as

$$\int_{x_0}^x dx / \{x^2 y(x)\},$$

and then inversion gives $x = x(\tau)$. A transformation now gives the temperature T as a function of time t . Figure 1 gives $T(t)$ for $T(0) = 300^\circ\text{K}$, $\sigma = 10^{-16} \text{ cm}^2$ and a number of values of the Einstein coefficient A_{21} . The table gives T (10 hours) for $T(0) = 300^\circ\text{K}$ and various values of σ and A_{21} .

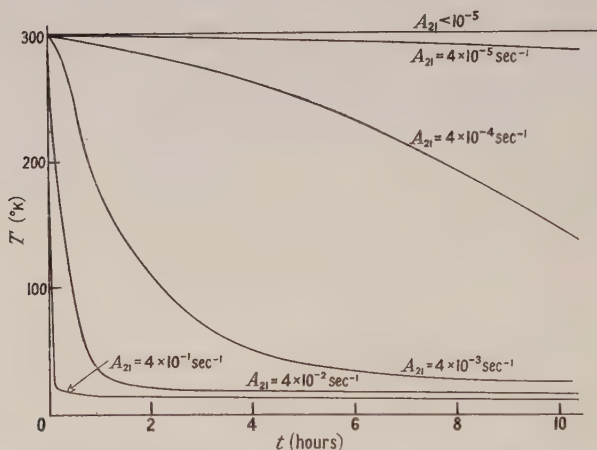


Figure 1. Nocturnal cooling: final temperatures. Starting from an initial temperature of 300°K , the temperature is given as a function of time for $\sigma = 10^{-16} \text{ cm}^2$ and various values of the Einstein coefficient A_{21} . See also table.

It is of interest and importance to see the extent to which the ratio N_2/N_1 of the concentration of the two states deviates from the Boltzmann expression (7) for equilibrium distribution. If we denote again as in (6) the equilibrium value by a superscript 0, we have from (34)

$$\frac{N_2(t)}{N_2^0(t)} = \frac{n(x)}{n^0(x)},$$

† For the theory and the calculation to be valid, the condition (3) must be satisfied. As λ in (34) is $\lambda = (A/X) \int \sigma_{12} v f(v) dv$, the condition (3) in terms of λ becomes $\lambda \ll \sigma_0/\sigma_{12}$. While the value $\lambda \sim 1$ is still permissible if $\sigma_0 \gg \sigma_{12}$, the case $\lambda = 1$ and $\sigma = 10^{-16} \text{ cm}^2$ in the table does not very well satisfy the above condition, and is hence included in parentheses in the table only for comparison.

and from (7), $n^0(x) = 1/(1 + ge^x)$. Hence, from (35)

$$\frac{N_2(t)}{N_2^0(t)} = 1 - y(x)e^x/\mu, \\ \simeq 1 - \eta(x)e^x/\mu = (g + e^{-x})/(\lambda + g + e^{-x}) \quad \dots\dots(45)$$

for $x > x_1$. Asymptotically, for large x (i.e. large t),

$$N_2/N_2^0 \rightarrow g/(\lambda + g). \quad \dots\dots(45')$$

Nocturnal Cooling

(a) The radiative transition probability A_{21} (in sec^{-1}) for different values of the cross section σ and the parameter λ . (N.B. $A_{21} = 4 \times 10^{-5} \text{ sec}^{-1}$ is a reasonable value (Pasternack 1940).)

λ	1	10^{-3}	10^{-5}	10^{-7}
$\sigma \text{ (cm}^2\text{)}$				
10^{-16}	(400)	0.4	4×10^{-3}	4×10^{-5}
10^{-18}	4	4×10^{-3}	4×10^{-5}	4×10^{-7}
10^{-20}	0.04	4×10^{-5}	4×10^{-7}	4×10^{-9}

(b) The overnight drop in temperature. The temperature listed (in $^\circ\text{K}$) as a function of σ and λ is the temperature after 10 hours of radiative cooling, starting from an initial temperature $T_0 = 300^\circ\text{K}$. See also figure 1.

λ	1	10^{-3}	10^{-5}	10^{-7}
$\sigma \text{ (cm}^2\text{)}$				
10^{-16}	(7.4)	12	27	288
10^{-18}	9.9	27	288	299.9
10^{-20}	16	288	299.9	300

Thus it is seen that there will be appreciable deviation from the Boltzmann distribution if λ is not too small compared with g . Figure 2 gives the ratio $N_2(t)/N_2^0(t)$ for $g=2$ and various values of A_{21} and σ for which λ has the same value 1.

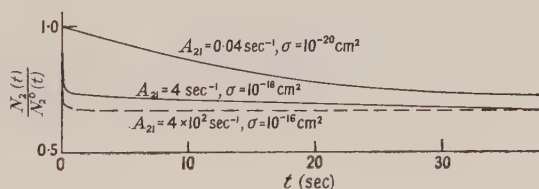


Figure 2. Disturbance of the equilibrium occupation numbers due to radiative processes. The ratio of the actual number density N_2 excited state 2 to that predicted from the Boltzmann theorem for the appropriate temperature (N_2^0 of equation (7)) is listed as a function of time, for the case $\lambda=1$, for a number of values of the cross section σ , and hence of the Einstein coefficient A_{21} .

§ 4. APPLICATION TO THE UPPER ATMOSPHERE

We shall apply the calculations of the preceding section for the simplified model to those regions of the upper atmosphere where there are oxygen atoms. Here we have a triplet state $^3P_{0,1,2}$ with the following energy difference and transition probabilities (Pasternack 1940):

$^3P_0 - ^3P_1$	$\nu = 68 \text{ cm}^{-1}$	$A = 1.68 \times 10^{-5} \text{ sec}^{-1}$.
$^3P_1 - ^3P_2$	$\nu = 158.5 \text{ cm}^{-1}$	$A = 8.8 \times 10^{-5} \text{ sec}^{-1}$.

If we consider the transition ${}^3P_1-{}^3P_2$ alone, and for that region of the atmosphere where the total particle density X is $\sim 3 \times 10^{13} \text{ cm}^{-3}$ (corresponding to an altitude of about 100 km), the appropriate values of the parameters are $g = 5/3$, $\mu \simeq 1/4$, $x_0 = 0.77$, which are comparable with those in (43). The value of the collisional cross section σ of equation (16) is not known, and accordingly calculations have been carried out for three values of σ , namely 10^{-16} , 10^{-18} , 10^{-20} cm^2 . The value 10^{-18} cm^2 may perhaps be a plausible one; corresponding to it, the value of c_0 of (34) is $\sim 4 \times 10^2 \text{ sec}^{-1}$. We are primarily interested in the cooling of gas over night, so that we want to see how the temperature changes in a time of the order of 10 hours. From the results given in the table, it is seen that the fall in temperature is about 30° . Thus, at this altitude, the cooling by radiation over night is not too great. This result is a consequence of the small values of A_{21} and the ratio N/X^\dagger . For high altitudes where the relative concentration of oxygen atoms becomes greater (i.e. larger μ in equation (36)), the effect of radiative cooling due to the transition in the 3P of the oxygen atom is somewhat greater.

The above result is obtained without considering the effect of the imprisonment of the radiation. It is clear that taking this into account will decrease the rate of cooling. In the particular problem of the atmosphere discussed above, this effect can be expected to be small. But in similar problems where the transition probability A is large, it is then necessary to work with the equations (29) and (30).

REFERENCES

- BATES, D. R., 1951, *Proc. Phys. Soc. B*, **64**, 805.
 BAUER, E., and WU, TA-YOU, 1954, *Research report CX-14*, Division of Electromagnetic Research, Institute of Mathematical Sciences, New York University.
 HOLSTEIN, T., 1947, *Phys. Rev.*, **72**, 1212; 1951, *Ibid.*, **83**, 1159.
 PASTERNAK, S., 1940, *Astrophys. J.*, **92**, 129.

† In fact, for this and lower altitudes, a good approximation to the result of the preceding section could have been obtained directly from the ratio of the energy radiation for unit volume of the gas in 10 hours (calculated on the assumption of a Boltzmann distribution at the initial temperature) and the thermal energy density of the gas. For the constants in (43), this comes out to be 0.55%, leading to a fall of 16° in temperature, instead of the 12° shown in the table.

Gamma Radiation from the Reaction $^{11}\text{B}(\text{p}, \gamma)^{12}\text{C}$

By P. J. GRANT, F. C. FLACK, J. G. RUTHERGLEN
AND W. M. DEUCHARS

Department of Natural Philosophy, The University, Glasgow

MS. received 15th March 1954

Abstract. The angular distributions of the 16.1, 11.7 and 4.4 mev γ -rays from the reaction $^{11}\text{B}(\text{p}, \gamma)^{12}\text{C}$ have been determined at a number of bombarding energies. The angular distribution of the 16 mev radiation is shown to be consistent with the accepted assignment of $J=2^+$ to the resonance at $E_p=163$ kev, and shows interference involving a higher level having $J=1^-$ which is identified with the broad resonance at $E_p=1390$ kev. The angular distribution of the 11.7 mev radiation shows interference between the resonances at 680 and 1390 kev and suggests the assignment $J=2^+$ to the 680 kev resonance.

§ 1. INTRODUCTION

EXPERIMENTS on the excitation functions, angular distributions and angular correlations of the γ -radiations from the reaction $^{11}\text{B}(\text{p}, \gamma)^{12}\text{C}$ have been made by a number of investigators (Ajzenberg and Lauritsen 1952, see also Huus and Day 1953, Jenkins *et al.* 1953, Gove and Paul 1953). In view of the apparent lack of agreement between some of these measurements we have made careful determinations, at a number of bombarding energies, of the angular distributions of the 16.1, 11.7 and 4.4 mev γ -rays. The apparatus and method employed were those previously described (Rutherglen *et al.* 1954) except that a larger sodium iodide crystal was used (a cylinder $1\frac{3}{4}$ in. diam. \times 2 in.).

§ 2. THICK TARGET MEASUREMENTS

γ -radiation was excited from a thick target of natural boron by bombardment with 350 kev molecular hydrogen ions ($E_p=175$ kev) so that the main contribution to the γ -radiation came from the 163 kev resonance. The angular distributions of the three γ -ray components were determined and the results are shown in table 1. The theoretical distributions were calculated for the capture of p-wave

Table 1

E_γ (mev)	Experiment	Theory
4.43	$I_0/I_{90}=1.16 \pm 0.02$	$W(\theta) \sim 1 + (0.16 \pm 0.02) \cos^2 \theta$
11.7	$W(\theta) \sim 1 + (0.26 \pm 0.01) \cos^2 \theta$	$W(\theta) \sim 1 + (0.23 \pm 0.02) \cos^2 \theta$
16.1	$I_0/I_{90}=1.08 \pm 0.03$	$W(\theta) \sim 1 + (0.34 \pm 0.02) \cos^2 \theta$

protons by $^{11}\text{B}(J=\frac{3}{2}^-)$ to form a level in $^{12}\text{C}^*$ with $J=2^+$, assuming a ratio $F=0.42 \pm 0.02$ (Thomson *et al.* 1952) for the relative participation of 'channel spins' 2 and 1. The cascade was assumed to be $2^+(\text{M1})2^+(\text{E2})0^+$ while the direct transition was calculated for $2^+(\text{E2})0^+$.

The distributions of the 4.43 and 11.7 mev γ -rays are in good agreement with the predicted functions. The result for the 16.1 mev radiation, which is in agreement with that of Kern *et al.* (1951), does not immediately appear to fit into this scheme.

It was suggested by Biedenharn *et al.* (1951) that the 16.1 and 11.7 meV radiations might come from different resonances. We have measured simultaneously the thick target excitation functions in the range $E_p = 150$ keV to $E_p = 200$ keV and find that the two show resonance at the same energy, and that the resonance width is the same, within the experimental error of ± 1 keV.

Another explanation would be that no 16 meV radiation is emitted at the 163 keV resonance, the apparent effect being caused by the simultaneous detection of an 11.7 meV and a 4.43 meV γ -ray. Such events would have an angular distribution in reasonable agreement with the experimental observation, and we therefore examined this possibility closely.

The measured intensity of the 16 meV relative to the 11.7 meV radiation was $7 \pm 2\%$, this figure being obtained from the pulse height spectrum beyond the peak due to the 11.7 meV radiation by fitting a curve whose shape was appropriate to a γ -ray energy of 16 meV. The efficiency of detection of the 4.43 meV radiation was about 1/120 (a geometrical factor of the order of 1/60 and an intrinsic efficiency of the order of 50%), but in calculating the intensity of addition effects this figure must be further reduced by a factor of approximately 2 since a 16 meV 'coincidence' peak could be produced only by the simultaneous occurrence of a pulse in the peak of the 4.43 meV pulse height distribution and in that of the 11.7 meV distribution. It is thus clear that the contribution to the observed 16 meV radiation from addition effects cannot exceed about 0.5% of the intensity of the 11.7 meV radiation.

These calculations were confirmed by measuring the apparent intensity of 4.14 meV cross-over γ -ray transitions from a source of ^{24}Na .

It is known that the reaction $^{11}\text{B}(p, \alpha)^8\text{Be}$ shows strong interference effects in the region of the 163 keV resonance (Thomson *et al.* 1952), and this suggests that the apparent discrepancy between the expected and experimental distributions of the 16 meV radiation has a similar explanation. At this point it is relevant to consider the results of Huus and Day (1953) and of Beckman *et al.* (1953). These are given in table 2. From this table we see that for $E_p \simeq 160$ keV

Table 2

E_{res} (keV)	F (keV)	$\sigma_{12}(10^{-6} \text{ bn})$	$\sigma_{16}(10^{-6} \text{ bn})$	$\sigma_{\alpha_0}(10^{-3} \text{ bn})$
163	7.5†	138	5.5	0.2
680	322	48.5	< 2.3	< 0.2
1390	1270	18.0	35.1	6.0

† Amended figure from Hunt and Jones (1953).

the tail of the broad resonance at 1390 keV will be relatively much more important for the 16 meV than for the 12 meV radiation, the resonance cross section ratio $\sigma_{1390}/\sigma_{163}$ being 50 times larger for the 16 meV radiation than for the other. We are here neglecting the 680 keV resonance, which produces little, if any, ground-state radiation. The assignment of $J = 1^-$, formed by S-wave protons, to the 1390 keV resonance is plausible from the figures in the table and is supported by the results of Thomson *et al.* who postulated a broad level with $J = 1^-$ to explain the interference effects in the angular distribution of the long-range α -particles from $^{11}\text{B}(p, \alpha)^8\text{Be}$.

§ 3. DETAILED ANALYSIS

The calculated expression for the angular distribution of the 16 MeV γ -radiation from a thin boron target is

$$W(\theta) \sim \frac{\lambda^2}{4\pi^2} \Gamma_1(E) \left\{ \frac{72}{7R_A^2} (1 + \frac{1}{3} \cos^2 \theta) + \frac{2a^2 p^2}{R_B^2} + \frac{2\sqrt{6}ap \cos \eta}{R_A R_B} \cos \theta \right\}.$$

The suffix A refers to the 163 keV resonance ($J=2^+$) and B to the 1390 keV resonance ($J=1^-$), $R = [(E - E_r)^2 + \frac{1}{4}\Gamma^2]^{1/2}$ where Γ is the total width of the resonance; $p^2 = \Gamma_0(E)/\Gamma_1(E)$ where $\Gamma_0(E)$ and $\Gamma_1(E)$ are the energy-dependent parts of the proton widths for protons of $l=0$ and $l=1$; a^2 is a constant related to the ratio of the peak yields at the 1390 and 163 keV resonances, $\eta = \alpha - \beta - \delta_A + \delta_B$, where $\delta = \tan^{-1} \Gamma/E - E_r$ and α, β are the intrinsic phases of the two resonances. Of the constants occurring in this expression only the term $\alpha - \beta$ in η is arbitrary, the others being fixed by the results of Huus and Day (§2), by the energy dependence of the proton widths (Christy and Latter 1948) and by the resonance factors.

In order to make a comparison with the experimental result the expression must be integrated over the target thickness. This has been done graphically, making the assumption that the stopping power of boron is independent of proton energy over the effective energy range of the integration. If $\alpha - \beta$ is set equal to 90° the thick target distribution for $E_p = 175$ keV becomes

$$W(\theta) \sim 1 - 0.18 \cos \theta + 0.32 \cos^2 \theta \quad \dots\dots (1)$$

so that $I_0/I_{90} = 1.14$, in fair agreement with the experimental result. Instead of being treated as a free parameter, $\alpha - \beta$ may be calculated by the dispersion theory of Wigner and Eisenbud (1947). The value obtained (apart from an uncertainty of π) is $\alpha - \beta = -30^\circ$. Using the value 150° for $\alpha - \beta$ the thick-target angular distribution becomes $W(\theta) \sim 1 - 0.11 \cos \theta + 0.32 \cos^2 \theta$. The calculated angular distribution is thus rather insensitive to the choice of $\alpha - \beta$, fair agreement with experiment being obtained over a wide range of values.

The angular distribution apparatus is incapable, for mechanical reasons, of reaching angles greater than 120° to the proton direction. Some additional measurements have, however, been made at 60° and 120° and these are shown in figure 1 together with the more accurate original determinations. The experimental points have been normalized to $I_{90} = 1$ and the curve is given by equation (1).

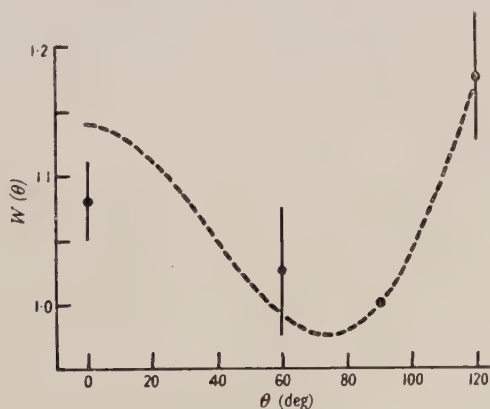


Figure 1. $^{11}\text{B}(p, \gamma)^{12}\text{C}$. 16 MeV γ -ray.

In view of the roughness of some of the approximations, the agreement with the experimental points is good. Further confirmation of the preceding arguments comes from angular distribution measurements on the 16 mev radiation from a thick target bombarded with protons of 500 kev energy. The radiation in that case was found to be isotropic within 3%.

§4. THIN TARGET EXPERIMENTS

Thin (20–30 kev) targets were made by the evaporation *in vacuo* of amorphous boron on to a thin backing of tantalum or copper. Thicker (up to 100 kev) and less uniform targets were made by painting a thin paste of amorphous boron in alcohol on to similar backings. The angular distribution of the 12 mev γ -ray component was determined at a number of proton energies between 400 and 680 kev. Typical curves are shown in figure 2(a) and (b). All the curves may

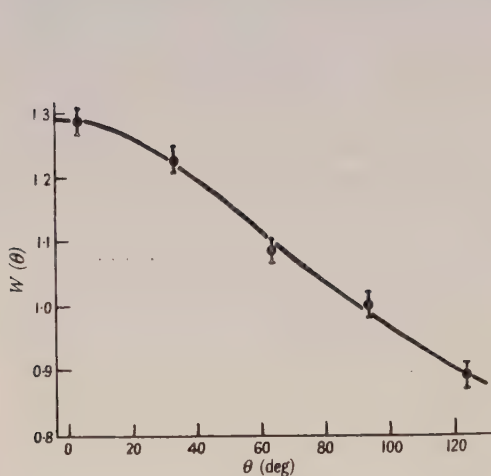


Figure 2 (a). $^{11}\text{B}(\text{p}, \gamma)^{12}\text{C}$.
Effective E_p 400 kev.
Angular distribution of 12 mev γ -ray.
 $W(\theta) \sim 1 + 0.18 \cos \theta + 0.11 \cos^2 \theta$.

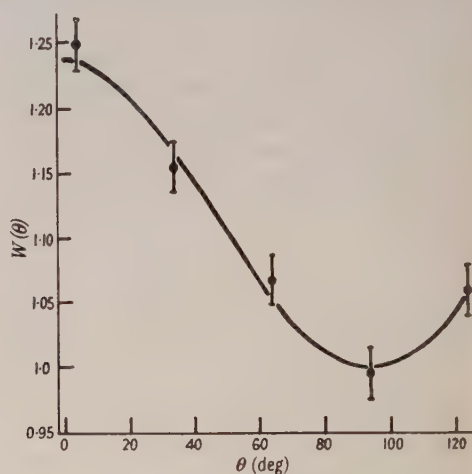


Figure 2 (b). $^{11}\text{B}(\text{p}, \gamma)^{12}\text{C}$.
Effective E_p 650 kev.
Angular distribution of 12 mev γ -ray.
 $W(\theta) \sim 1 + 0.02 \cos \theta + 0.22 \cos^2 \theta$.

be expressed in the form $W(\theta) \sim 1 + a_1 \cos \theta + a_2 \cos^2 \theta$ where both a_1 and a_2 vary with energy, a_1 falling from about 0.2 at 400 kev to zero near 680 kev, and a_2 rising from about 0.12 at 400 kev to 0.2 near 680 kev (figure 3). From this it follows that the 680 kev resonance cannot be formed by the capture of S-wave protons and that interference is occurring with another level of opposite parity.

§5. DISCUSSION

We shall assume that the 680 kev resonance arises from the capture of p-wave protons by $^{11}\text{B}(J = \frac{3}{2}^-)$: $l \geq 2$ may be rejected (see Beckman *et al.*). It can therefore have $J = 0, 1, 2, 3$ all with even parity. The theoretical coefficients of $\cos^2 \theta$ at resonance then have the following values:

$$\begin{array}{ll} J=0, & a_2=0; \\ J=2, & 7/11 > a_2 > -21/47; \end{array} \quad \begin{array}{ll} J=1, & 1/13 > a_2 > -1/67; \\ J=3, & a_2 = -9/28. \end{array}$$

We see that only a state $J = 2^+$ is capable of giving a coefficient a_2 of the correct size and sign.

It seems reasonable to ascribe the term in $\cos \theta$ to interference with the $J=1$ -resonance at 1390 keV. Calculations have been made similar to those in § 3, and by fitting the theoretical coefficient of $\cos^2 \theta$ to the experimental one near the resonance energy of 680 keV, where the effect of the 1390 keV resonance is relatively unimportant, we obtain the value $F=0.45 \pm 0.05$ for the relative participation of 'channel spins' 2 and 1. Using this figure and adjusting the phase angle $\alpha - \beta$ to make a_1 vanish near the resonance, it is possible to calculate a_1 and a_2 at all energies.

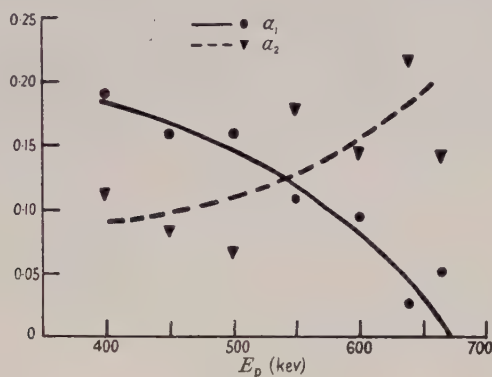


Figure 3. $^{11}\text{B}(p, \gamma)^{12}\text{C}$. 12 MeV γ -ray.
 $W(\theta) \sim 1 + a_1 \cos \theta + a_2 \cos^2 \theta$.

The agreement with experiment is not very good, the calculated values of a_1 and a_2 being consistently higher than the experimental ones. For example, at a proton energy of 400 keV the calculated values have become too high by about 60% for a_1 and 30% for a_2 .

It is disappointing that a better fit cannot be obtained, but the following points should be noted:

(a) The resonance cross-section data of Huus and Day have been used without making any allowance for the possible contribution from d-wave protons to the peak cross section at the 1390 keV resonance. At this resonance the proton energy is approaching the barrier height, therefore the barrier penetrability factors used to find the constants in our calculation are rather uncertain.

(b) No allowance has been made for the broad level indicated by the rise in the γ -ray yield above 2.2 MeV proton energy (Huus and Day 1953) which may still have an appreciable effect even at energies of the order of 500 keV.

(c) Owing to the rapid increase in the barrier penetration with rising energy there may still be an appreciable contribution from the 163 keV resonance at energies of the order of 400 keV. This effect will be exaggerated by any non-uniformity in the target thickness.

Objection may be raised to the assignment of $J=2^+$ to the 680 keV resonance level on the grounds that the emission of both ground state γ -radiation and α -particles to the ground state of ^8Be should occur. If we adopt the naive view that the 163 and 680 keV resonances are similar (both having $J=2^+$ and $F \sim \frac{3}{7}$), and that the cross sections for different modes of disintegration are roughly proportional, then we would expect the ground-state γ -ray cross section at the

680 keV resonance to be $\sigma_{16} \sim 1.9 \times 10^{-6}$ bn. This is below the limit of observation set by Huus and Day. Similarly we would expect a ground-state α -particle cross section $\sigma_{\alpha_0} \sim 0.07$ mbn. This is less than the limit of intensity given by Beckman *et al.*

It appears that the assignment of $J=2^+$ to the 680 keV resonance provides the best fit with our own and other data. Clearly, further detailed investigation is necessary at higher energies than 700 keV (the highest energy available to us) before this assignment can be regarded as definitely established.

ACKNOWLEDGMENTS

One of us (F.C.F.) wishes to acknowledge the award of an Imperial Chemical Industries Research Fellowship and one (W.M.D.) the receipt of a grant from the Department of Scientific and Industrial Research during the course of this work.

REFERENCES

- AJZENBERG, F., and LAURITSEN, T., 1952, *Rev. Mod. Phys.*, **24**, 321.
BECKMAN, O., HUUS, T., and ZUPANČIČ, C., 1953, *Phys. Rev.*, **91**, 606.
BIEDENHARN, L. C., ARFKEN, G. B., and ROSE, M. E., 1951, *Phys. Rev.*, **83**, 586.
CHRISTY, R. F., and LATTE, R., 1948, *Rev. Mod. Phys.*, **20**, 185.
GOVE, H. E., and PAUL, E. B., 1953, *Phys. Rev.*, **91**, 463.
HUNT, S. E., and JONES, W. M., 1953, *Phys. Rev.*, **89**, 1283.
HUUS, T., and DAY, R. B., 1953, *Phys. Rev.*, **91**, 599.
JENKINS, G. L., COCHRAN, L. W., KERN, B. D., and HAHN, T. M., 1953, *Phys. Rev.*, **91**, 915.
KERN, B. D., MOAK, C. D., GOOD, W. M., and ROBINSON, G. P., 1951, *Phys. Rev.*, **83**, 211.
RUTHERGLEN, J. G., GRANT, P. J., FLACK, F. C., and DEUCHARS, W. M., 1954, *Proc. Phys. Soc. A*, **67**, 101.
THOMSON, D. M., COHEN, A. V., FRENCH, A. P., and HUTCHINSON, G. W., 1952, *Proc. Phys. Soc. A*, **65**, 745.
WIGNER, E. P., and EISENBUD, L., 1947, *Phys. Rev.*, **72**, 29.

Short Range Forces and Nuclear Energy Levels in the Neighbourhood of ^{208}Pb

By D. M. BRINK

Clarendon Laboratory, Oxford

*Communicated by M. H. L. Pryce; MS. received 28th December 1953,
and in amended form 24th May 1954*

Abstract. The lowest excited states of nuclei differing by two particles from the double closed shell of ^{208}Pb , can be classified in terms of two-particle configurations. For a two-particle configuration, this paper gives an expansion for the matrix elements of a short range central interaction potential of any exchange type, as a power series in the range of the potential. It is shown that, in any configuration and with forces of range consistent with low energy proton neutron scattering data, the zero range approximation for the matrix elements is good for Wigner or Bartlett forces. For Majorana and Heisenberg forces the zero range approximation is fair for states of highest spin, but is inadequate for the states of lowest spin. Calculations, applied to ^{210}Bi (RaE), indicate that the β decaying state of this nucleus has spin 0, 1 or possibly 2 and odd parity.

§ 1. INTRODUCTION

IN a recent paper Pryce (1952) has attempted to predict and classify the excited states of nuclei in the neighbourhood of ^{208}Pb theoretically on the basis of the shell model of Haxel, Jensen and Suess (1949) and of Mayer (1949, 1950). According to the shell model ^{208}Pb is a spherically symmetrical structure consisting of a double closed shell of 82 protons and 126 neutrons. Pryce assumes that the lower energy levels of ^{209}Pb and of ^{209}Bi are approximately those of a single particle moving in the central field of a ^{208}Pb core. Similarly the lowest levels of ^{210}Pb , ^{210}Bi and ^{210}Po are those of two particles moving in the same central field and interacting by some given law of nuclear force. This interaction is treated as a perturbation on the levels of two non-interacting particles in the field of the ^{208}Pb core.

Pryce makes a calculation of the interaction energy of the two extra nucleons using a nuclear force of zero range. In order to study the effect of the range of the nuclear force on the interaction energy, this calculation has been extended to include forces of range short compared with the nuclear radius. In the zero range approximation, central forces of the ordinary and coordinate exchange type give identical^[1] values for the interaction energy of the two extra nuclear particles. The differences which appear if the forces are not of zero range have been investigated. Tensor forces are not considered here.

§ 2. MATRIX ELEMENTS OF THE INTERACTION ENERGY

In the following sections we consider the energy levels of a two-particle system in a central nuclear field. If the two particles do not interact they will move in orbits characterized by total angular momentum quantum numbers j_1

and j_2 . The angular momenta of the two particles will couple to give a resultant total angular momentum quantum number I , with z -component M . We can write the wave function of the two-particle system in this state as $|j_1 j_2, IM\rangle$. If the two particles are identical we must use the antisymmetrized wave function $N(|j_1 j_2, IM\rangle - |j_2 j_1, IM\rangle)$. Here N is a normalizing factor taking the value $1/\sqrt{2}$ if $j_1 \neq j_2$. If $j_1 = j_2$ and I is even $|j_1 j_2, IM\rangle$ is itself antisymmetrical.

The interaction energy of the two particles in the state $|j_1 j_2, IM\rangle$ is given to the first order of perturbation by the matrix element $\langle j_1 j_2, IM | U | j_1 j_2, IM \rangle$, where U is the potential energy of the interaction. The wave function of the system without interaction may not, however, be a good approximation to the stationary state of the interacting system. In this case configuration interaction must be considered, requiring the calculation of matrix elements of the type $\langle j_1' j_2', IM | U | j_1 j_2, IM \rangle$.

We will use a central two-body interaction potential of the following exchange type:

$$U = V(r_{12})(w + mP_x + hP_\tau + bP_\sigma)$$

where r_{12} is the internucleon distance, w , m , h and b are constants such that $w + m + b - h = -1$; P_x is the coordinate exchange operator, P_σ is the spin exchange operator and $P_\tau (= -P_\sigma P_x)$ the isotopic spin exchange operator.

When evaluating matrix elements of exchange potentials it is convenient to work in the LS coupling scheme. Explicit expressions for the transformation coefficients from jj to LS coupling scheme are given by Pryce (1952) and Blin-Stoyle (1953).

Each term in the above potential can be written as a product of a spin and a coordinate operator. In the LS representation a matrix element of a term in the potential breaks up into the product of a spin matrix element and a coordinate matrix element. The spin matrix element has the value unity for a Wigner or a Majorana force and, for a Bartlett or Heisenberg force, takes the value 1 in a triplet spin state and -1 in a singlet state. For a coordinate exchange potential the coordinate matrix element has the form

$$\langle l_1' l_2', LM | VP_x | l_1 l_2, LM \rangle,$$

where $l_1 (= j_1 \pm \frac{1}{2})$ etc. are the orbital angular momentum quantum numbers of the single particle states and reduces to $(-)^{l_1 + l_2 - L} \langle l_1' l_2', LM | V | l_1 l_2, LM \rangle$. Thus the calculation of matrix elements of an interaction potential of any exchange type reduces to the calculation of coordinate matrix elements of a function of internucleon distance.

2.1. Coordinate Matrix Elements

The coordinate matrix element $\langle l_1' l_2', LM | V | l_1 l_2, LM \rangle$ of a function V of internucleon distance is independent of the magnetic quantum number. By averaging over all values of the magnetic quantum number we obtain an expression for the matrix element independent of the axis of quantization. If we denote the value of the matrix element by $F(L)$, then

$$F(L) = \frac{1}{2L+1} \sum_{M=-L}^L \langle l_1' l_2', LM | V | l_1 l_2, LM \rangle.$$

We now make a transformation to a coordinate representation of the state vectors of the two-particle system. The wave functions will be products of a

radial component and an angular component consisting of appropriate linear combinations of spherical harmonics.

Thus we have

$$\langle \mathbf{r}_1, \mathbf{r}_2 | l_1 l_2, LM \rangle = \phi_1(r_1) \phi_2(r_2) \sum_m C(l_1 l_2 L, m M - m) Y_{l_1}^m(\theta_1 \phi_1) Y_{l_2}^{M-m}(\theta_2 \phi_2). \quad \dots (1)$$

The phases of the spherical harmonics are chosen to agree with the work of Racah (1942) and Condon and Shortley (1935). $C(l_1 l_2 L, m M - m)$ is the usual vector coupling coefficient. The matrix element $\langle \mathbf{r}_1, \mathbf{r}_2 | l_1' l_2', LM \rangle$ can be similarly expressed replacing l_1 and l_2 by l_1' and l_2' and ϕ by ψ in the radial wave functions.

Introducing the density function

$$\rho_L(\mathbf{r}_1, \mathbf{r}_2) = \frac{1}{2L+1} \sum_{M=-L}^L \langle l_1' l_2', LM | \mathbf{r}_1, \mathbf{r}_2 \rangle \langle \mathbf{r}_1, \mathbf{r}_2 | l_1 l_2, LM \rangle \quad \dots (2)$$

the expression for $F(L)$ reduces to a double integral over the coordinates \mathbf{r}_1 and \mathbf{r}_2 of the two nucleons,

$$F(L) = \iint V(|\mathbf{r}_1 - \mathbf{r}_2|) \rho_L(\mathbf{r}_1, \mathbf{r}_2) d\mathbf{r}_1 d\mathbf{r}_2. \quad \dots (3)$$

The density function is independent of the z axis of the coordinate representation and depends only on the magnitudes of the vectors \mathbf{r}_1 and \mathbf{r}_2 and on the angle between them. In order to evaluate the integral in (3) in an approximate form, suitable for short range forces, we make a transformation to relative coordinates.

Put

$$\mathbf{r}_2 - \mathbf{r}_1 = \mathbf{s} \quad \text{and} \quad \rho_L(\mathbf{r}_1, \mathbf{r}_2) = \rho_L'(\mathbf{r}_1, \mathbf{s})$$

then

$$F(L) = \iint V(s) \rho_L'(\mathbf{r}, \mathbf{s}) d\mathbf{r} d\mathbf{s}. \quad \dots (4)$$

Now expand $\rho_L'(\mathbf{r}, \mathbf{s})$ as a power series in \mathbf{s} and put this expansion into the integral for $F(L)$. $V(s)$ is a function of s only, and because of this symmetry, terms arising from odd powers of s_x , s_y or s_z will vanish on integration over \mathbf{s} . Using identities of the form

$$\int V(s) s_x^{2n} d\mathbf{s} = \frac{4\pi}{2n+1} \int V(s) s^{2n+2} ds,$$

the expression for $F(L)$ reduces to

$$\left. \begin{aligned} F(L) = & 4\pi \int V(s) s^2 ds \int \rho_L'(\mathbf{r}, 0) d\mathbf{r} \\ & + \frac{4\pi}{3!} \int V(s) s^4 ds \int [\nabla^2 \rho_L'(\mathbf{r}, \mathbf{s})]_{\mathbf{s}=0} d\mathbf{r} \\ & + \frac{4\pi}{5!} \int V(s) s^6 ds \int [(\nabla^2)^2 \rho_L'(\mathbf{r}, \mathbf{s})]_{\mathbf{s}=0} d\mathbf{r} \\ & + \text{higher terms.} \end{aligned} \right\} \quad \dots (5)$$

In the integrals $\int [(\nabla^2)^n \rho_L'(\mathbf{r}, \mathbf{s})]_{\mathbf{s}=0} d\mathbf{r}$, ∇^2 is the Laplacian operating on \mathbf{s} in the density function. The first two of these integrals are evaluated in the Appendix,

$$4\pi \int \rho_L'(\mathbf{r}, 0) d\mathbf{r} = P_0(L) \int \psi_1^*(r) \psi_2^*(r) \phi_1(r) \phi_2(r) r^2 dr, \quad \dots (A5)$$

reducing to the results of Pryce (1952) in the special case $l_1 = l_1'$ and $l_2 = l_2'$; and

$$4\pi \int [\nabla^2 \rho_L'(\mathbf{r}, \mathbf{s})]_{\mathbf{s}=0} d\mathbf{r} = P_1(L) \int \psi_1^*(r) \psi_2^*(r) \phi_1(r) \phi_2(r) dr \\ - P_0(L) \int \frac{d}{dr} (\psi_1^*(r) \phi_1(r)) \frac{d}{dr} (\psi_2^*(r) \phi_2(r)) r^2 dr. \quad \dots (A6, 7, 11)$$

Higher terms can be evaluated by similar methods.

2.2. Expressions for Matrix Elements in the jj Representation

We will specialize in the case where $j_1' = j_1$ and $j_2' = j_2$ and calculate explicit expressions for the matrix elements of the nucleon-nucleon interaction potential in the jj representation. Only the first two terms in the expansion for the coordinate matrix element will be retained.

For convenience write

$$I_0 = R^3 \int \psi_1^2(r) \psi_2^2(r) r^2 dr \\ I_{10} = R^5 \int \psi_1^2(r) \psi_2^2(r) dr \\ I_{11} = R^5 \int \frac{d}{dr} (\psi_1^2(r)) \frac{d}{dr} (\psi_2^2(r)) r^2 dr.$$

Here R is a scale factor equal to the nuclear radius and introduced so that I_0 , I_{10} and I_{11} depend only on the form of the radial wave functions and not on the nuclear radius. Also let us write

$$a_s = \langle I0, I | j_1 j_2, I \rangle P_0(I), \quad b_s = \langle I0, I | j_1 j_2, I \rangle P_1(I), \\ a_t = \sum_{L=I-1}^{I+1} \langle L1, I | j_1 j_2, I \rangle P_0(L), \quad b_t = \sum_{L=I-1}^{I+1} \langle L1, I | j_1 j_2, I \rangle P_1(L).$$

The matrix elements occurring here are the transformation coefficients from LS to jj coupling. Subscripts s and t distinguish the singlet and triplet parts of the interaction. The quantities defined refer only to Wigner and Bartlett forces. Corresponding quantities for a coordinate exchange force will be indicated by a superscript M . The coordinate exchange operator has no effect in the zero range approximation. Thus $a_t^M = a_t$, $a_s^M = a_s$.

The matrix elements of the interaction energy can be written in terms of the second and fourth moments of the interaction potential and the quantities defined above, containing the dependence on I and on the nuclear radius. We can separate the effect of coordinate exchange by writing the interaction potential as

$$U(r) = V(r)(w + bP_\sigma) + V(r)P_\sigma(m - hP_\sigma).$$

The interaction energy matrix element then splits into two terms. The first arises from the Wigner and Bartlett interactions, and the second from the interactions containing coordinate exchange.

$$E_{12} = \langle j_1 j_2, IM | U | j_1 j_2, IM \rangle = (w + b)E_{12}^0 + (m - h)E_{12}^M.$$

Here

$$E_{12}^0 = \left[\frac{I_0}{R^3} \int V(r) r^2 dr - \frac{I_{11}}{R^5} \int V(r) r^4 dr \right] (a_t + \epsilon a_s) + \frac{I_{10}}{R^5} \int V(r) r^4 dr (b_t + \epsilon b_s), \quad (6)$$

with $\epsilon = (w - b)/(w + b)$.

E_{12}^M has a similar expression with b_t^M , b_s^M and ϵ^M replacing b_t , b_s , and ϵ . In this case $\epsilon^M = (m+h)/(m-h)$. In these expressions ϵ and ϵ^M are factors containing the spin dependence of the force and take the value 1 if there is no spin dependence and -1 for spin exchange forces.

Blatt and Jackson (1949) have interpreted low energy scattering data in terms of a well depth parameter s and an intrinsic range b , which can be simply related to any particular interaction potential. The values of these parameters, determined from the binding energy of the deuteron and from low-energy scattering data, depend only weakly on the shape of the potential assumed, so we will express the moments of the potential occurring in (6) in terms of s and b . For a square well potential b is the radius of the well in centimetres and if V_0 is the depth of the well, $V_0 = 102 \times 10^{-26} s b^{-2}$ Mev. For a Yukawa well $V(r) = -\{U_0 \exp(-r/\beta)\}/(r/\beta)$, $b = 2.12\beta$ cm, and $U_0 = 312 \times 10^{-26} s b^{-2}$ Mev. Substituting these values in the expressions for the moments of the potentials we get

$$\int V(r)r^2 dr = 34 \times 10^{-26} s b \text{ for both Yukawa and square well potentials, and}$$

$$\int V(r)r^4 dr = 3.4 \times 10^{-26} s b^3 \text{ (square well)}$$

$$= 7.56 \times 10^{-26} s b^3 \text{ (Yukawa well).}$$

Hence we get the interaction energy expressed in terms of s and b ,

$$E_{12}^0 = - \frac{34 \times 10^{-26} s b}{R^3} \left[\left(I_0 - \frac{0.1b^2 I_{11}}{R^2} \right) (a_t + \epsilon a_s) + \frac{0.1b^2 I_{10}}{R^2} (b_t + \epsilon b_s) \right]$$

for a square well potential and

$$E_{12}^0 = - \frac{34 \times 10^{-26} s b}{R^3} \left[\left(I_0 - \frac{0.22b^2 I_{11}}{R^2} \right) (a_t + \epsilon a_s) + \frac{0.22b^2 I_{10}}{R^2} (b_t + \epsilon b_s) \right]$$

for Yukawa well. There are similar expressions for the coordinate exchange term E_{12}^M . E_{12} is given in Mev and R and b are measured in centimetres. It is seen that the dependence of the interaction energy on the intrinsic range of the potential is very much stronger for a Yukawa interaction than for a square well interaction. The binding energy of the deuteron and low energy neutron-proton scattering data suggests a value $s = 1.3$ and $b = 2.4 \times 10^{-13}$ cm. The nuclear radius in the neighbourhood of ^{208}Pb is of the order of 8×10^{-3} cm. Thus we get an estimate for $34 \times 10^{-26} s b/R^3 = 0.2$ Mev.

§ 3. MATRIX ELEMENTS FOR PARTICULAR CONFIGURATIONS

By application of first-order perturbation theory, the dependence of the splitting of a two-particle configuration on the total angular momentum quantum number I has been investigated for three particular configurations of interest in the level structure of ^{210}Bi , namely $(i_{11/2}, i_{13/2})$, $(g_{9/2}, h_{9/2})$ and $(g_{9/2}, i_{13/2})$. The matrix elements of the interaction potential have been computed using the expressions derived in § 2.2 for a square well neutron-proton interaction.

The overlap integrals of the radial wave functions I_0 , I_{10} and I_{11} have been estimated using wave functions for a square well of sufficient depth to accommodate the k orbital level. The exact form chosen for the radial wave functions is, however, not important. Wave functions for a harmonic oscillator will give results identical to within 10%, provided a suitable value is given to the parameter

describing the radius of the well. The values of the radial overlap integrals calculated from square well wave functions are given in table 1. Table 2 gives values of the parameters a_s , a_t , b_s and b_t for both ordinary and coordinate exchange forces in each of the above three configurations.

Table 1. Overlap Integrals of Radial Wave Functions

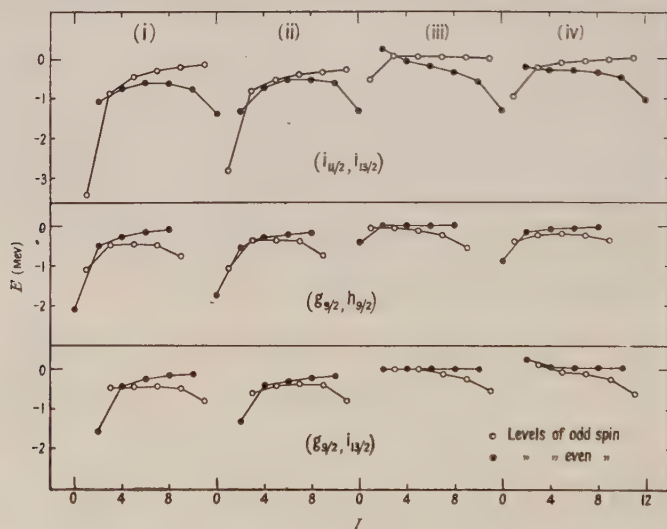
	$(i_{11/2}, i_{13/2})$	$(g_{9/2}, h_{9/2})$	$(g_{9/2}, i_{13/2})$
$I_0 = I_0^M$	3.5	2.1	2.1
$I_{10} = I_{10}^M$	5.5	3.6	3.6
I_{11}	100	-30	-30
I_{11}^M	100	170	170

In order to illustrate the effect of range and exchange on the proton-neutron interaction energy, E_{12} has been computed for all possible I -values in each of the three configurations $(i_{11/2}, i_{13/2})$, $(g_{9/2}, h_{9/2})$ and $(g_{9/2}, i_{13/2})$. The following cases have been considered:

- (i) A zero range force with no spin dependence.
- (ii) A Wigner force with $b/R=0.2$.
- (iii) A Majorana force with $b/R=0.2$.
- (iv) A Rosenfeld mixture giving saturation of nuclear binding energies (Rosenfeld 1948)

$$U(r) = V(r)(0.13 - 0.46P_\sigma - 0.93P_\pi - 0.26P_\tau),$$

again with $b/R=0.2$. The results are given in graphical form in the figure with E_{12} plotted against I . The energy scale corresponds to choosing the interaction parameter $34 \times 10^{-26} sb/R^3 = 0.2$ MeV in agreement with low-energy scattering data. The small value of the ratio $b/R=0.2$ corresponding to an intrinsic range



Dependence of the interaction energy E_{12} in ^{210}Bi on the nuclear spin I for the three configurations considered, and for four types of central potential.

- (i) Zero range force, no spin dependence.
- (ii) Wigner force, $b/R=0.2$
- (iii) Majorana force, $b/R=0.2$
- (iv) Rosenfeld mixture, $b/R=0.2$

Table 2. Angular Coefficients

Configuration I	0	1	2	3	4	5	6	7	8	9	10	11	12
a_s	0	0	0.006	0	0.115	0	0.182	0	0.273	0	0.431	0	0.985
a_t	4.846	4.846	1.655	1.273	0.973	0.714	0.732	0.463	0.640	0.303	0.662	0.174	1.067
b_s	3.23	3.23	-4.75	7.05	-8.53	10.38	-11.48	12.74	-13.11	13.51	-12.49	11.34	-5.91
b_t	-132.46	-132.46	63.51	-1.16	0	8.45	-8.79	12.06	-11.9	13.23	-11.79	11.22	-5.28
b_s^M	-3.23	-3.23	-4.75	-7.05	-8.53	-10.38	-11.48	-12.74	-13.11	-13.51	-12.49	-11.34	-5.91
b_t^M	-678.46	-678.46	-331.54	-199.77	-144.16	-108.48	-83.56	-64.88	-49.64	-37.51	-26.57	-17.82	-7.52
a_s	0	0.050	0	0.120	0	0.210	0	0.395	0	0.859			
a_t	5.00	2.525	1.212	0.999	0.629	0.699	0.373	0.640	0.202	0.955			
b_s	0	-1.21	3.64	-4.78	6.29	-6.99	8.60	-7.56	7.25	-3.82			
b_t	-120	-2.42	20.00	-5.15	8.67	-6.39	10.50	-7.15	7.60	-3.44			
b_s^M	0	-3.74	-3.64	-5.77	-6.29	-7.69	-8.60	-8.20	-7.25	-4.77			
b_t^M	-370	-245.05	-131.52	-82.76	-57.77	-42.57	-31.39	-21.00	-12.80	-6.11			
a_s			2.203	0	0.870	0	0.518	0	0.327	0	0.183	0	
a_t			1.468	1.061	0.174	0.891	0.049	0.877	0.018	1.040	0.007	1.950	
b_s			-41.12	48.95	-34.72	26.63	-18.26	12.67	-7.67	3.92	-0.88	0	
b_t			-17.62	-7.44	30.81	-31.60	32.68	-29.61	27.79	-24.03	19.68	-9.36	
b_s^M			-218.81	-48.95	-55.78	-26.63	-24.24	-12.67	-9.61	-3.92	-1.69	0	
b_t^M			-155.66	-115.10	-48.91	-59.19	-36.73	-41.34	-28.75	-30.55	-19.65	-17.94	

of $b = 1.6 \times 10^{-13}$ cm is chosen because of the essential inadequacy of the expansion (6) for larger b .

For Wigner forces with $bR = 0.2$ it is seen that forces of zero range give a good approximation to the interaction energy E_{12} as calculated by the more accurate expressions given in §2.2. In each configuration, when the range of the forces is taken into account, the magnitude of the interaction energy is reduced for the states of lowest spin, while the states of highest spin are not much affected. These conclusions can be expected to hold for intrinsic ranges up to 2.4×10^{-13} cm, the value given by low-energy scattering experiments. For longer ranges than this, higher terms in the series for the coordinate matrix element must be considered and the method rapidly becomes unworkable.

In the case of Majorana forces the expansion as far as the second term of the series can be expected to give a fair approximation to the interaction energy for the states of highest I in the configurations considered. For states of lowest I , however, the magnitudes of the matrix elements of the interaction potential are much reduced, even for an intrinsic range as short as $b = 1.6 \times 10^{-13}$ cm. For ranges longer than this, and in particular for ranges of the order of $b = 2.4 \times 10^{-13}$ cm predicted from scattering experiments, the zero range approximation to the value of the matrix element is completely inadequate and the expansion as a power series in the range of the potential is no longer useful. In all cases the effect of the finite range of the potential is to reduce the interaction energy in the states of low total angular momentum I , but for Majorana forces this effect is much stronger than for Wigner forces.

The effect of a spin exchange term in the interaction potential has been investigated by Pryce (1952) for forces of zero range. If a spin exchange component is included in the interaction potential, states in which the spins of the two particles are most nearly parallel are not affected, while the magnitude of the interaction energy is reduced for states in which the spins tend to be antiparallel, provided the spin exchange force is attractive in the triplet state. This result can be simply expressed in terms of the Nordheim number. If the two particles have total angular momentum quantum numbers j_1 and j_2 and orbital angular momentum quantum numbers l_1 and l_2 we define this number as $N = (j_1 - l_1) + (j_2 - l_2)$. If N is odd the state of maximum I corresponds to parallel alignment of spins and the interaction energy is unaffected by the inclusion of a spin exchange term in the force, while it is reduced in the state of minimum I . For N even the state of minimum I is unaffected and the interaction energy in the state of maximum I is reduced. These conclusions are not altered when the finite range of the nuclear force is included in the calculations. For N odd the Nordheim rule (Nordheim 1950) predicts that in any configuration a state of high angular momentum should have the lowest energy, and the state of lowest I should have the lowest energy for N even. This rule will hold for the configurations considered above provided the nuclear forces contain coordinate and spin exchange components of sufficient strength.

§4. APPLICATION TO THE LEVELS OF ^{210}Bi

4.1. Mass 209 Isobars

Following Pryce (1952) we consider ^{209}Pb or ^{209}Bi as a system consisting of a single neutron or proton moving in a central field produced by the double

closed shell core of 126 neutrons and 82 protons. Some of the single particle levels can be classified by considering the experimental knowledge of the ground and low excited states of these nuclei.

The shell model gives $h_{9/2}$, $f_{7/2}$, $f_{5/2}$, $p_{3/2}$, $p_{1/2}$ and $i_{13/2}$ as low states of the 83rd proton in ^{209}Bi . The ground state spin is $9/2$ so we assume the lowest level to be the $h_{9/2}$ state. The inelastic scattering of 2.5 mev neutrons indicates levels at 0.85 mev and 1.58 mev; but no spin assignments can at present be made to these states (Poole 1953, Eliot, Hicks, Beghian and Halban, private communication). Analogy with the closed shell of 82 neutrons would suggest that the first excited state of ^{209}Bi is the $f_{7/2}$ level.

The lowest group of states of ^{209}Pb is $g_{9/2}$, $i_{11/2}$, $g_{7/2}$, $d_{5/2}$, $d_{3/2}$ and $k_{15/2}$, where the $k_{15/2}$ level may be strongly depressed by spin orbit coupling. ^{209}Bi is formed by the beta decay of ^{209}Pb . The ft -value of the beta transition is compatible with a first-forbidden transition, $\Delta I=0$ or 1 and a change of parity. The maximum energy of the beta particles is 0.6 mev and there are no gamma-rays observed in the process (Wapstra 1950). Thus the beta decay of ^{209}Pb must be simple, all transitions leading to the ground state of ^{209}Bi . The ground state of ^{209}Bi having spin $9/2$ and odd parity, the lowest level of ^{209}Pb may be the $g_{9/2}$ or $i_{11/2}$ state.

Information about the excited states of ^{209}Pb is available from the reaction $^{208}\text{Pb}(d, p)^{209}\text{Pb}$ (Harvey 1953). Proton groups are observed corresponding to the ground state and excited states at 0.75, 1.56, 2.03 and 2.54 mev. The reaction cross section for the 0.75 mev level is small compared with the cross section for the other levels. This may indicate a large orbital angular momentum transfer and suggests that this level may be the $i_{11/2}$ or $k_{15/2}$ state. If it is the $i_{11/2}$ state then the formation of the $k_{15/2}$ state would probably not be detected in the $^{208}\text{Pb}(d, p)^{209}\text{Pb}$ reaction; but this state may still be quite low. The neutron binding energy determined from the above reaction is 3.87 mev.

In the following theoretical discussion of the low levels of ^{210}Bi it is necessary to assume that the low levels of ^{209}Bi and ^{209}Pb can be adequately described by single particle wave functions. This assumption is in line with the postulates of the shell model, particularly as ^{208}Pb is a double closed shell nucleus, but is open to question. For instance the magnetic moment of ^{209}Bi indicates that the ground state of this nucleus has a more complicated structure consisting of a superposition of a number of independent particle states.

4.2. The Lower Levels of ^{210}Bi

^{210}Bi exists in two isomeric states, a beta decaying state of low spin, in the following referred to as β , formed in the beta decay of ^{210}Pb (RaD); and a long-lived alpha decaying state denoted by α . The state α probably has a high spin. It is formed following slow neutron capture in ^{209}Bi (Neumann, Howland and Perlman 1950). Goldhaber and Hill (1953) give the energy of α , estimated from a closed cycle, as 25 ± 45 kev below the state β . The binding energy of the last neutron in ^{210}Bi , obtained from a closed cycle, is 4.54 mev (Kinsey, Bartholomew and Walker 1951). Comparing this with the neutron binding energy in ^{209}Pb (3.87 mev) we obtain a value of approximately 0.67 mev for the proton-neutron interaction energy in both the isomeric states of ^{210}Bi .

Recent work by Fred, Tomkins and Barnes (1953) indicates that the level β has either $I=0$ or a small magnetic moment (<0.18 nuclear magnetons).

Preliminary experiments made using an atomic beam method favour a spin $I = 1$ (Smith, private communication). Theoretical studies of the shape of the beta spectrum from RaE are consistent with the assignment $I = 0$ or 1 with odd parity (Petschek and Marshak 1952, Yamada 1953, Rose and Osborn 1954).

The gamma-ray spectrum following the capture of thermal neutrons in ^{209}Bi consists of a broad line of maximum energy 4.17 mev indicating transitions to a group of states within an energy range of about 70 kev (Kinsey, Bartholomew and Walker 1951). This group of states lies about 0.37 mev above the isomeric ground states α and β of ^{210}Bi , as shown by the difference between the neutron binding energy and the maximum gamma-ray energy following the neutron capture. The neutron capture state should have spin $I = 4$ or 5 and odd parity. Thus the group of states reached by the 4.17 mev gamma emission can have spins in the range $I = 2$ to $I = 7$ if the gamma-rays correspond to electric dipole, magnetic dipole or electric quadrupole transitions. States formed in this group following gamma radiation from the neutron capture state would decay by a cascade of soft gamma-rays to one of the states α or β . Neither of the states α or β is reached strongly by direct gamma transitions from the capture state.

The reaction $^{209}\text{Bi}(d, p)^{210}\text{Bi}$ shows levels in ^{210}Bi with neutron binding energies of 4.16, 2.52, 1.95 and 1.40 mev (Harvey 1953). These levels should be compared with the states found in ^{209}Pb with the $^{208}\text{Pb}(d, p)^{209}\text{Pb}$ reaction. The relevant levels in ^{209}Pb have neutron binding energies of 3.87, 2.31, 1.84 and 1.27 mev. The reaction cross sections for the various levels show a similar correspondence. This correspondence of levels and cross sections has been interpreted by Pryce (1952) and Harvey (1953) as indicating that these 'levels' found in ^{210}Bi are the unresolved configurations formed by a proton in the ground state and the captured neutron in states corresponding to the independent particle states of ^{209}Pb . It should be noted that the neutron binding energy deduced by this method corresponds to the value obtained from the gamma-ray energies following slow neutron capture in ^{209}Bi . Thus it is probable that the group of states reached by gamma emission from the slow neutron capture state is the same as the lowest group of states reached in the $^{209}\text{Bi}(d, p)^{210}\text{Bi}$ reaction.

$^{210}\text{Pb}(\text{RaD})$ decays by beta emission to an excited state of ^{210}Bi . The transition energy is low, probably about 18 kev, and the ft -value ($\log ft = 5.5$, Bannermann and Curran 1952) is consistent with an allowed or first-forbidden transition. The excited state of ^{210}Bi formed in this beta transition decays to the state β by gamma emission. Formerly, about six soft gamma rays following the beta decay had been reported, of which the strongest and most energetic had an energy of 46.7 kev. The level diagram to account for these gamma rays was extremely complicated, requiring five or six levels of low spin very close together near the β state. More recent work by Wu, Boehm and Nagel (1953) confirms only the 46.7 kev gamma ray and suggests that the other gamma rays previously reported were spurious. They estimate that the 46.7 kev gamma ray is emitted following $92 \pm 5\%$ of the beta transitions and suggest that the remainder of the transitions go directly to the β state. This work indicates that there is only one level of low spin near the β state. Measurements on the ratio of the L conversion line intensities suggest that the 46.7 kev gamma ray is an M1 transition. The β state of ^{210}Bi having odd parity, the 46.7 kev excited state should have spin $I = 0$ or 1 and odd parity.

We will now consider possible classifications of the low levels of ^{210}Bi consistent with the above experimental information on the basis of a two-particle model. We have concluded from the calculated proton-neutron interaction energy matrix elements given above that a good estimate of proton-neutron interaction energies for the state of highest spin in any configuration is given by the zero range approximation to the interaction potential. For these states we can calculate the proton-neutron interaction energy from the expression

$$E_{12} = -U_0 I_0 (a_t + \epsilon a_s), \quad \dots\dots(7)$$

where I_0 is the radial overlap integral defined above and

$$U_0 = 34 \times 10^{-26} sb/R^3 = 0.2 \text{ Mev}$$

for nuclear forces consistent with low-energy proton-neutron scattering data. The above work also shows that it is difficult to make an accurate estimate of the matrix elements of the proton-neutron potential starting from a short range approximation for the states of low spin in any configuration. The results indicate, however, a possible theoretical basis for Nordheim's rule in a two-particle configuration. We will use this rule to make estimates of the interaction energy for such states. It appears from the diagram of energy levels given above that the interaction energy is small for states of spin intermediate between the maximum and minimum values. In the following work values of a_s and a_t are taken from Pryce (1952).

We have seen that beta-decay data are consistent with the assignment of the $g_{9/2}$ or $i_{11/2}$ single-particle configurations to the ground state of ^{209}Pb . Let us first assume the ground state of ^{209}Pb to be the $g_{9/2}$ level. Then the lowest two-particle configuration in ^{210}Bi would be the $(g_{9/2}, h_{9/2})$. This configuration is split by proton-neutron interaction and the levels of spin 0 and spin 9 depressed. The diagram of levels given for the $(g_{9/2}, h_{9/2})$ configuration shows that for a Rosenfeld mixture of range 1.6×10^{-13} Mev the interaction energy is approximately 1 Mev in the state with spin $I=0$ and 0.3 Mev in the state with spin $I=9$. A natural choice of parameters could give an interaction energy in the state $I=0$ of 0.7 Mev indicated by experiment and it is possible that the state $(g_{9/2}, h_{9/2})_{I=0}$ corresponds to the experimental state β . The state $(g_{9/2}, h_{9/2})_{I=9}$ could correspond to the experimental state α if depressed by configuration interaction with states $(i_{11/2}, h_{9/2})_{I=9}$ and $(i_{11/2}, f_{7/2})_{I=9}$.

Assigning the $g_{9/2}$ level to the ground state of ^{209}Pb the 0.75 Mev excited state is probably the $i_{11/2}$ level. Also it is probable that the 0.8 Mev excited state in ^{209}Bi corresponds to the $f_{7/2}$ proton level. Making these identifications in ^{209}Pb and ^{209}Bi , we then have the $(g_{9/2}, f_{7/2})$ and $(i_{11/2}, h_{9/2})$ configurations lying close together at an excitation of about 0.8 Mev in ^{210}Bi before the proton-neutron interaction is considered. The proton-neutron interaction in each of the two states $(g_{9/2}, f_{7/2})_{I=8}$ and $(i_{11/2}, h_{9/2})_{I=10}$ is about 1.4 Mev as calculated from (7) using square well wave functions to estimate I_0 . Thus both these states might be expected to lie at about 0.1 Mev above the $(g_{9/2}, h_{9/2})_{I=0}$ state. Configuration interaction would push one of them down, which could then correspond to the experimental state α .

There are three possible low-lying states of spin $I=1$, namely $(g_{9/2}, h_{9/2})_{I=1}$, $(g_{9/2}, f_{9/2})_{I=1}$, $(i_{11/2}, h_{9/2})_{I=1}$. All these states have odd parity and would be expected to lie close together at about 0.5 Mev above the $(g_{9/2}, h_{9/2})_{I=0}$ state before

configuration interaction is considered. Configuration mixing could bring one state of spin $I=1$ close to, above or below, the $(g_{9/2}, h_{9/2})_{I=0}$ state. This doublet would then correspond to the state β and the 46.7 keV excited state. The present work cannot distinguish between the two possibilities for the spin of β , but an assignment of $I=0$ or $I=1$ is consistent with the predictions of the model. There may be a low-lying state of spin $I=2$ formed from the above three configurations. All these states have odd parity.

The group of levels reached by gamma emission following neutron capture in ^{209}Bi , should be the group of levels in the $(g_{9/2}, h_{9/2})$ configuration with intermediate spins $I=2$ to $I=7$. The group of states with neutron binding energy 4.16 MeV formed in the $^{209}\text{Bi}(d, p)^{210}\text{Bi}$ reaction corresponds to the formation of ^{210}Bi in the $(g_{9/2}, h_{9/2})$ configuration. The probability of reaching a state of spin I with this reaction should be proportional to $2I+1$ if the interaction between the 83rd proton and the incoming neutron is small. The total number of states in the $(g_{9/2}, h_{9/2})$ configuration is 100, so the state of this configuration with spin $I=0$ would be formed with probability 0.01 and the state with $I=1$ with probability 0.03. Thus the state β of ^{210}Bi would not be reached strongly in the $^{209}\text{Bi}(d, p)^{210}\text{Bi}$ reaction. Similar considerations show that the experimental state α should not be reached with probability greater than 0.2 in the (d, p) reaction on ^{209}Bi .

Another possible low configuration in ^{210}Bi is $(g_{9/2}, i_{13/2})$ with even parity. The Nordheim rule predicts that the proton-neutron interaction energy in the states $I=1$ and $I=2$ of this configuration should be less than 0.6 MeV. The state $(i_{11/2}, i_{13/2})_{I=2}$ would lie at about 0.7 MeV above the $(g_{9/2}, i_{13/2})_{I=2}$ level and configuration interaction could push the latter down; but the matrix element of the configuration interaction, $[0.4 - 6(b/R)^2]$ MeV, is too small to increase the binding energy by more than 0.5 MeV. It therefore seems unlikely that a state of spin $I=2$ and even parity could lie close to the experimental isomeric state β .

A similar classification cannot be made corresponding to the assignment $i_{11/2}$ to the ground state of ^{209}Pb . In this case the experimental state α would be the level $(i_{11/2}, h_{9/2})_{I=10}$. But the proton-neutron interaction energy in the state $(g_{9/2}, h_{9/2})_{I=0}$ would be expected to be less than in the state $(i_{11/2}, h_{9/2})_{I=10}$ so the former state should lie at least 0.75 MeV above the latter. The state $(i_{11/2}, h_{9/2})_{I=1}$ would be the experimental state β , but there is no other low-lying state of spin $I=0$ or 1 which could correspond to the 46.7 keV excited state.

4.3. Discussion

The increased quantity of experimental evidence available since Pryce's (1952) paper was written has simplified very much the theoretical task of classifying the low levels of ^{210}Bi . Now that the experimental gamma-ray spectrum following the beta decay of ^{210}Pb has been reinvestigated and simplified it is no longer necessary to postulate large splitting of high configurations to account for a number of closely spaced levels of low spin near the ground state. A much more natural assignment to the values of the various constants will explain the experimental picture. Pryce's calculations with zero range forces suggested that the ground state of ^{210}Bi should be a level of low spin. However, consideration of the effect of range and exchange properties of the nuclear forces has shown that the lowest state may be either of odd parity and low spin ($I=0, 1$), or high spin ($I=8, 9, 10$) in agreement with experiment.

The fact that single particle wave functions may not give a good approximation to the wave functions of ^{209}Pb and ^{209}Bi together with the inadequacy of the zero range approximation to nuclear forces and the first-order perturbation treatment make it difficult and unprofitable to make exact theoretical calculations on the two-particle model of ^{210}Bi . On the other hand the model can explain in a semi-quantitative way the observed level structure. It may be profitable to extend the application of the present model to neighbouring nuclei in the same semi-quantitative way as more experimental material becomes available. A study of the multipole orders of gamma rays and of angular correlations on cascades would assist in the assignment of spins and parities to the various observed levels.

APPENDIX

EVALUATION OF THE INTEGRALS OVER THE DENSITY FUNCTION

First we transform the expression (2) for the density function to a form more suitable for further calculation. Spherical harmonics of the same argument occurring in (2) can be coupled using vector coupling coefficients, and then the sum over vector coupling coefficients reduces to a Racah coefficient (Racah 1942). Putting $\psi_1^*(r_1)\psi_2^*(r_2)\phi_1(r_1)\phi_2(r_2) = R(r_1, r_2)$ the density function reduces to

$$\rho_L(\mathbf{r}_1, \mathbf{r}_2) = R(r_1, r_2)(-)^{L+l_1+l_1'} \times \sum_{J,N} [W(l_1 l_1' l_2 l_2', J L) Y_J^{N*}(\theta_1, \phi_1) Y_J^N(\theta_2, \phi_2) C(l_1 l_1', J) C(l_2 l_2', J)]. \quad \dots (A1)$$

The coefficient $C(l l', J)$ is closely related to the vector coupling coefficient and has the simple expression

$$\begin{aligned} C(l l', J) &= \left[\frac{(2l+1)(2l'+1)}{4\pi(2J+1)} \right]^{1/2} C(l l' J, 00) \\ &= 0 \quad \text{if } l+l'+J \text{ is odd,} \\ &= (-1)^{g-J} \left[\frac{(2l+1)(2l'+1)(2g-2J)!(2g-2l)!(2g-2l')!}{4\pi(2g+1)!} \right]^{1/2} \\ &\quad \times \frac{g!}{(g-J)!(g-l)!(g-l')!} \quad \text{if } 2g=l+l'+J \text{ is even.} \end{aligned}$$

The product $C(l_1 l_1', J) C(l_2 l_2', J)$ can be expanded as a series in the products $C(l_1 l_2, \lambda) C(l_1' l_2', \lambda)$ the coefficients in the expansion being Racah coefficients

$$C(l_1 l_1', J) C(l_2 l_2', J) = (-1)^{l_1+l_1'} \sum_{\lambda} (2\lambda+1) W(l_1 l_1' l_2 l_2', J \lambda) C(l_1 l_2, \lambda) C(l_1' l_2', \lambda). \quad \dots (A2)$$

The expansion (A2) follows from the definition of the Racah coefficient in terms of vector coupling coefficients, and from the relation connecting $C(l_1 l_2, \lambda)$ with the vector coupling coefficient $C(l_1 l_2 \lambda, 00)$. Finally (A1) and (A2) give

$$\begin{aligned} \rho_L(\mathbf{r}_1, \mathbf{r}_2) &= R(r_1, r_2)(-1)^{L+l_1+l_1'+l_2} \sum_{J,N} [(2\lambda+1) W(l_1 l_1' l_2 l_2', J L) W(l_1 l_1' l_2 l_2', J \lambda) \\ &\quad \times C(l_1 l_2, \lambda) C(l_1' l_2', \lambda) Y_J^{N*}(\theta_1, \phi_1) Y_J^N(\theta_2, \phi_2)]. \quad \dots (A3) \end{aligned}$$

The integrals to be evaluated are of the form

$$4\pi \int [(\nabla^2)^n \rho_L'(\mathbf{r}, \mathbf{s})]_{\mathbf{s}=\mathbf{0}} d\mathbf{r}$$

where ∇^2 is the Laplacian operating on \mathbf{s} in the density function $\rho_L'(\mathbf{r}, \mathbf{s})$. Transforming back to non-relative coordinates this term becomes

$$4\pi \int [(\nabla_2^2)^n \rho_L(\mathbf{r}_1, \mathbf{r}_2)]_{\mathbf{r}_1=\mathbf{r}_2} d\mathbf{r}_1 \quad \dots\dots (A4)$$

where ∇_2^2 is the Laplacian operating on \mathbf{r}_2 in the density function $\rho_L(\mathbf{r}_1, \mathbf{r}_2)$.

We now go on to consider how the integrals (A4) may be evaluated and so calculate the first few terms of the series (5) for $F(L)$. In the first term of the series we have the integral $4\pi \int \rho_L(\mathbf{r}, \mathbf{r}) d\mathbf{r}$. Substituting the expression (A3) for $\rho_L(\mathbf{r}_1, \mathbf{r}_2)$ and carrying out the integration we get

$$\begin{aligned} 4\pi \int \rho_L(\mathbf{r}, \mathbf{r}) d\mathbf{r} &= (-1)^{l_1+l_1'+l_2'} \int R(r, r) r^2 dr \sum_J (2J+1)(2\lambda+1) W(l_1 l_1' l_2 l_2', J, L) \\ &\quad \times W(l_1 l_1' l_2 l_2', J, \lambda) P_0(\lambda) \\ &= P_0(L) \int R(r, r) r^2 dr. \quad \dots\dots (A5) \end{aligned}$$

Equation (A5) follows from the orthogonality relation for Racah coefficients (Racah 1942). Here

$$P_0(L) = 4\pi C(l_1 l_2, L) C(l_1' l_2', L) = 0$$

unless $l_1 + l_2 + L$ and $l_1' + l_2' + L$ are both even.

The second term in the series for $F(L)$ contains the integral

$$4\pi \int [(\nabla_2^2 \rho_L(\mathbf{r}_1, \mathbf{r}_2)]_{\mathbf{r}_1=\mathbf{r}_2} d\mathbf{r}_1.$$

We can write the Laplacian in the form

$$\nabla^2 = \frac{1}{r^2} \frac{\partial}{\partial r} \left(r^2 \frac{\partial}{\partial r} \right) - \frac{1}{r^2} \mathbf{L}^2,$$

where \mathbf{L}^2 is the square of the orbital angular momentum operator of the second particle. Putting this form of the Laplacian into $4\pi \int [(\nabla_2^2 \rho_L(\mathbf{r}_1, \mathbf{r}_2)]_{\mathbf{r}_1=\mathbf{r}_2} d\mathbf{r}_1$ the integral splits into the sum of two parts. The first reduces to

$$-P_0(L) \int \frac{d}{dr} (\psi_1^*(r) \phi_1(r)) \frac{d}{dr} (\psi_2^*(r) \phi_2(r)) r^2 dr \quad \dots\dots (A6)$$

on integration by parts. The second part is

$$P_1(L) \int R(r, r) dr \quad \dots\dots (A7)$$

with

$$\begin{aligned} P_1(L) &= (-1)^{L+l_1'+l_2'+1} \sum_J P_0(\lambda) (2\lambda+1)(2J+1) J(J+1) \\ &\quad \times W(l_1 l_1' l_2 l_2', J, L) W(l_1 l_1' l_2 l_2', J, \lambda). \quad \dots\dots (A8) \end{aligned}$$

$P_1(L)$ is not yet in a form suitable for computation because the Racah coefficients have complicated sum expressions and are not tabulated for high values of the angular momentum quantum numbers. The expression for $P_1(L)$ may be

simplified, however, by using a recurrence relation for Racah coefficients. This recurrence relation, obtained by specialization of parameters from a formula given by Biedenharn, Blatt and Rose (1953), is

$$W(l_2 J 1 l_2', l_2 l_2') W(l_1 J L l_2', l_1' l_2) \\ = \sum_{\lambda} (2\lambda + 1) W(l_1 \lambda J l_2', l_2 l_1') W(1 \lambda l_2' l_1', L l_2') W(l_1 \lambda l_2 1, l_2 L),$$

or using symmetry relations for Racah coefficients (Racah 1942)

$$W(l_1 l_1' l_2 l_2', J L) W(l_2 1 J l_2', l_2 l_2') \\ = \sum_{\lambda} (-1)^{L+\lambda} (2\lambda + 1) W(l_1 l_1' l_2 l_2', J \lambda) W(1 \lambda l_2' l_1', L l_2') W(1 \lambda l_2 l_1, L l_2).$$

Now (A 9)

$$W(l_2 1 J l_2', l_2 l_2') = -2 \left[\frac{(2l_2 - 1)! (2l_2' - 1)!}{(2l_2 + 2)! (2l_2' + 2)!} \right]^{1/2} [J(J+1) - l_2(l_2+1) - l_2'(l_2'+1)]$$

and putting

$$\Delta(\lambda, L) = W(1 \lambda l_2' l_1', L l_2') W(1 \lambda l_2 l_1, L l_2) \left[\frac{(2l_2 + 2)! (2l_2' + 2)!}{(2l_2 - 1)! (2l_2' - 1)!} \right]^{1/2} \\ - \frac{l_2(l_2+1) + l_2'(l_2'+1)}{2L+1} \delta(\lambda, L).$$

(A 9) gives

$$J(J+1) W(l_1 l_1' l_2 l_2', J L) = \sum_{\lambda} (-1)^{L+\lambda+1} (2\lambda + 1) \Delta(\lambda, L) W(l_1 l_1' l_2 l_2', J \lambda). \quad \dots (A 10)$$

Substituting (A 10) in (A 8) and using the orthogonality relations for Racah coefficients we obtain an expression for $P_1(L)$

$$P_1(L) = \sum_{\lambda=L-1}^{L+1} (2\lambda + 1) \Delta(\lambda, L) P_0(\lambda). \quad \dots (A 11)$$

The coefficients $\Delta(L, \lambda)$ have the following simple form and can be easily evaluated

- (i) $\Delta(L, \lambda) = \Delta(\lambda, L).$
- (ii) $\Delta(L, \lambda) = 0$ unless $\lambda + 1 \geq L \geq \lambda - 1$ and $\left. \begin{matrix} (l_1 + l_2) \\ (l_1' + l_2') \end{matrix} \right\} \geq L \geq \left\{ \begin{matrix} (l_1 - l_2) \\ (l_1' - l_2') \end{matrix} \right\}.$
- (iii) $\Delta(L, L-1) = \frac{(2L-2)!}{(2L+1)!} [(L+l_1+l_2+1)(L+l_1-l_2)(L+l_2-l_1) \\ \times (l_1+l_2-L+1)(L+l_1'+l_2'+1)(L+l_1'-l_2') \\ \times (L+l_2'-l_1')(l_1'+l_2'-L+1)]^{1/2},$
 $\Delta(L, L) = \frac{2(2L-1)!}{(2L+2)!} [\{l_1(l_1+1) - l_2(l_2+1)\} \{l_1'(l_1'+1) - l_2'(l_2'+1)\} \\ - L(L+1) \{l_1(l_1+1) + l_2(l_2+1) + l_1'(l_1'+1) + l_2'(l_2'+1)\} \\ + \{L(L+1)\}^2].$

ACKNOWLEDGMENTS

The author wishes to thank Professor M. H. L. Pryce for suggesting the problem, for encouragement and advice throughout the work and for helpful criticism of the manuscript. Grateful acknowledgment is also made to the Rhodes Trustees for the award of a Scholarship.

REFERENCES

- BANNERMAN, R. C., and CURRAN, S. C., 1952, *Phys. Rev.*, **85**, 134.
BIEDENHARN, L. C., BLATT, J. M., and ROSE, M. E., 1953, *Rev. Mod. Phys.*, **24**, 251.
BLATT, J. M., and JACKSON, J. D., 1949, *Phys. Rev.*, **76**, 18.
BLIN-STOYLE, R. J., 1953, *Proc. Phys. Soc. A*, **66**, 729.
CONDON, E. U., and SHORTLEY, G. H., 1935, *Theory of Atomic Spectra* (Cambridge : University Press).
FRED, M., TOMKINS, F. S., and BARNES, R. F., 1953, *Phys. Rev.*, **92**, 1324.
GOLDHABER, M. and HILL, R. D., 1953, *Rev. Mod. Phys.*, **24**, 231.
HARVEY, J. A., 1953, *Canad. J. Phys.*, **31**, 278.
HAXEL, O., JENSEN, J. H. D., and SUESS, H. E., 1949, *Phys. Rev.*, **75**, 1766.
KINSEY, B. B., BARTHOLOMEW, G. A., and WALKER, W. H., 1951, *Phys. Rev.*, **82**, 380.
MAYER, M. G., 1949, *Phys. Rev.*, **75**, 1969 ; 1950, *Ibid.*, **78**, 16, 22.
NEUMANN, H. M., HOWLAND, J. J., and PERLMAN, I., 1950, *Phys. Rev.*, **77**, 720.
NORDHEIM, L. W., 1950, *Phys. Rev.*, **78**, 294.
PETSCHKE, A. G., and MARSHAK, R. E., 1952, *Phys. Rev.*, **85**, 698.
POOLE, M. J., 1953, *Phil. Mag.* **44**, 1398.
PRYCE, M. H. L., 1952, *Proc. Phys. Soc. A*, **65**, 773.
RACAH, G., 1942, *Phys. Rev.*, **62**, 438.
ROSE, M. E. and OSBORN, R. K., 1954, *Phys. Rev.*, **93**, 1315.
ROSENFELD, L., 1948, *Nuclear Forces* (Amsterdam : N. Holland Publ. Co.), 243.
WAPSTRA, A. H., 1950, *Phys. Rev.*, **86**, 562.
WU, C. S., BOEHM, F., and NAGEL, E., 1953, *Phys. Rev.*, **91**, 319.
YAMADA, M., 1953, *Prog. Theor. Phys.*, **10**, 252.

Approximate Nuclear Density Distributions in Light Elements

By K. M. GATHA, G. Z. SHAH AND N. J. PATEL

Department of Physics, M. G. Science Institute, Ahmedabad, India

MS. received 8th December 1953, and in amended form 4th May 1954

Abstract. With a suitable transformation of parameters, it is found that the experimental angular distributions for the nuclear scattering of 340 mev nucleons by light elements can be reasonably represented by a characteristic angular distribution. Within the region of validity of the first Born approximation, the radial distribution method has been used to determine the corresponding characteristic nuclear density distribution for light elements.

§ 1. INTRODUCTION

THE experimental observations and the corresponding theoretical considerations on the scattering of high energy nucleons by nuclei can be expected to provide valuable information about nuclear structure. In this connection, the theoretical investigations have been carried out by making use of the optical model of the nucleus, employing the concept of a partially transparent nucleus (Serber 1947). The nuclear scattering of 90 mev neutrons has been accounted for on this basis by assuming a uniform density distribution within the nucleus (Fernbach, Serber and Taylor 1949). Similarly, approximate interpretations have been obtained for the nuclear scattering of 280 mev neutrons (Fernbach 1951) and 340 mev protons (Gatha and Riddell 1952).

As a result of the above investigations, it has become clear that the assumption of a uniform nuclear density distribution is inadequate for a correct interpretation of the nuclear scattering of high energy nucleons. First of all, the nuclear radii required to correlate the experimental data at various energies appear to diminish with increasing energy (Mathur and Gatha 1953). Secondly, for the nuclear scattering of 340 mev protons, the theoretical differential cross sections vanish at the minima (Gatha and Riddell 1952) in contrast to the experimental angular distributions (Richardson, Ball, Leith and Moyer 1952). To avoid these difficulties an exponential tail has been attached to the uniform model (Jastrow and Roberts 1952). Also to correlate the nuclear shell structure with the nuclear density distribution a gaussian tail has been proposed (Born and Yang 1950, Yang 1951). However, no detailed investigations are available to confirm the validity of these models for the nuclear scattering of high energy nucleons. Moreover, the dependence of the nuclear size on the nuclear mass number becomes somewhat arbitrary for such models.

The above investigations on the nuclear scattering of high energy nucleons have been based on the correlation method. In this method the parameters of a conceptual nuclear density distribution are obtained by correlating the corresponding theoretical and experimental angular distributions. However, within the region

of validity of the first Born approximation, one can use the radial distribution method (Waser and Schomaker 1953). In the present investigation we have employed such a method for determining the nuclear density distributions on the basis of the experimental angular distributions for the scattering of 340 mev protons by light nuclei (Richardson, Ball, Leith and Moyer 1952).

As a reasonable approximation, we have assumed that the nuclear radial parameter is proportional to the cube root of the nuclear mass number. As a result, we have been able to obtain a characteristic angular distribution for several light elements. For extrapolating such an experimental angular distribution beyond the experimental range we have used the criterion of positiveness for the corresponding density distribution (Hauptman and Karle 1950). Finally, we have obtained a characteristic density distribution for such light elements.

§ 2. OPTICAL MODEL OF THE NUCLEUS

In the optical model for a semi-transparent nucleus, one characterizes the nuclear matter by a complex refractive index,

$$n = 1 + k_1/k + i(K/2k) \quad \text{.....(1)}$$

where the various parameters are given by

$$k = (E^2 - \mu^2 c^4)^{1/2} / \hbar c \quad \text{.....(2)}$$

where E is the energy of the incoming nucleon, μ is the reduced mass of the incoming nucleon and neglecting the effect of the exclusion principle

$$k_1 = (\pi \rho / k) \{f_{nn}(0) + f_{np}(0)\} \quad \text{.....(3)}$$

$$K = \frac{1}{2} \rho \{\sigma_{nn} + \sigma_{np}\} \quad \text{.....(4)}$$

where ρ is the nuclear density and

$f_{nn}(0), f_{np}(0)$ are the forward scattering amplitudes for (n, n) and (n, p) scattering respectively, and

σ_{nn}, σ_{np} are the scattering cross sections for (n, n) and (n, p) scattering respectively.

We have also used the parameters $k'_1 = k_1 \rho^{-1}$ and $K' = K \rho^{-1}$. We have calculated K' by assuming $\sigma_{nn} \simeq \sigma_{np}$ and taking the extrapolated experimental value of about 26 mbn for σ_{np} giving $K' \simeq 26 \times 10^{-27} \text{ cm}^2$. Since the nucleon-nucleon scattering experiments do not provide the forward scattering amplitudes, one obtains them by correlating some model for the process with the angular distributions within the experimental range. A model based on tensor interactions (Christian and Hart 1950, Christian and Noyes 1950) gives $k'_1 \simeq 20 \times 10^{-27} \text{ cm}^2$, while a model based upon a hard core nucleon (Jastrow 1951) gives $k'_1 \simeq 9 \times 10^{-27} \text{ cm}^2$. In the present investigation we have determined $k'_1 \simeq 8 \times 10^{-27} \text{ cm}^2$ on the basis of the normalization of the nuclear density which agrees with Jastrow's model.

The complex potential can now be simply written as

$$V = -\{(E^2 - \mu^2 c^4)/E\} n' \rho \quad \text{.....(5)}$$

where

$$n' = k'_1/k + i(K'/2k).$$

The above expression is based upon the assumptions $k_1/k \ll 1$, $K/2k \ll 1$, and $V^2/(E^2 - \mu^2 c^4) \ll 1$ for both the real and the imaginary parts. On the basis of the

density distributions and potentials obtained during the present investigation, we have found that these assumptions are fully justified. The effects due to the spin of the nucleon can be regarded as negligible (Gatha and Riddell 1952).

§ 3. THE RADIAL DISTRIBUTION METHOD

Within the region of validity of the first Born approximation, the scattering amplitude is given by

$$sf(s) = -(2\mu/\hbar^2) \int_0^\infty r V(r) \sin(sr) dr \quad \dots\dots(6)$$

where $f(s)$ = the scattering amplitude,

$$s = 2k \sin \frac{1}{2}\theta.$$

The radial distribution method consists in making the Fourier inversion of this integral, giving

$$r V(r) = -(\hbar^2/\pi\mu) \int_0^\infty s f(s) \sin(sr) ds \quad \dots\dots(7)$$

which leads to

$$r \rho(r) = N \int_0^\infty s |f(s)| \sin(sr) ds \quad \dots\dots(8)$$

where

$$N = \hbar^2 E / \pi \mu |n'| (E^2 - \mu^2 c^4).$$

A problem of great interest in the radial distribution method is the extrapolation of the experimental scattering data beyond the experimental range. Various methods are available for this purpose (Waser and Schomaker 1953). For the sake of its inherent simplicity, we have used the functional extrapolation method in our present approximate investigation. This consists of using a set of simple functions to represent the scattering amplitude within the experimental range. These functions are then assumed to represent the scattering amplitude beyond the experimental range, provided the functions are such as to yield positive density distributions only (Hauptman and Karle 1950). We have found it possible to use gaussian functions for this purpose.

§ 4. THE CHARACTERISTIC ANGULAR DISTRIBUTION

During the previous investigations on the nuclear scattering of nucleons of lower energy it has been found that for a uniform density distribution $R \propto A^{1/3}$, where R is the nuclear radius and A is the nuclear mass number. This suggests that in this investigation we introduce a parameter $r' = rA^{-1/3}$. Introducing a corresponding parameter $s' = sA^{1/3}$, we can write

$$r' \rho(r') = N \int_0^\infty s' |g(s')| \sin(s'r') ds' \quad \dots\dots(9)$$

where

$$\rho(r') = \rho(r) \text{ and } |g(s')| = |f(s)|/A.$$

At this stage we assume that a characteristic nuclear density distribution $\rho(r')$ exists for light elements. A consequence of this assumption would be the existence of a corresponding characteristic angular distribution $|g(s')|$ for these elements. Now it is well known that

$$|f(s)| = \{(1 - \beta^2) \sigma(s)\}^{1/2} \quad \dots\dots(10)$$

where $\beta = v/c$.

Since the available experimental data on the nuclear scattering of 340 mev protons (Richardson, Ball, Leith and Moyer 1952) has been obtained for $\theta \geq 5^\circ$, and since the coulomb effects are entirely insignificant in this region for light elements, we have taken these data to represent the nuclear scattering of 340 mev nucleons in general. In figure 1 we have plotted against s' the values of $g(s')$ calculated from these data for carbon and aluminium. An average smooth curve which can be represented by a set of simple functions has been drawn approximately through all these points as shown in figure 1. We have also plotted $g(s')$ for magnesium and silicon and found that these points also lie approximately along the same curve. Since we are interested in the present investigation in an

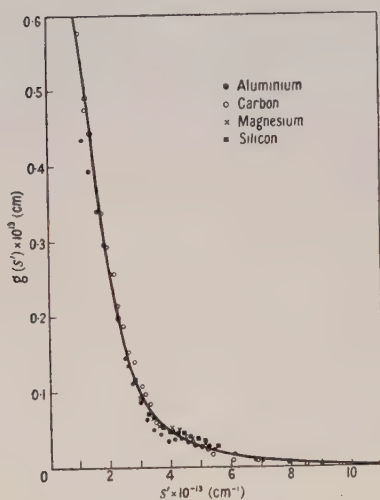


Figure 1. The characteristic angular distribution for light elements.

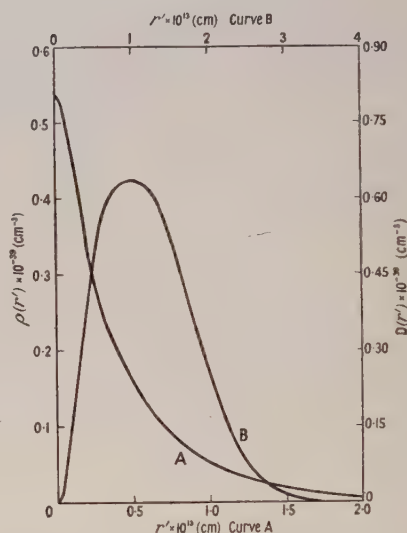


Figure 2. The characteristic density distribution for light elements.
A : $\rho(r')$. B : $D(r') = 4\pi r'^2 \rho(r')$.

approximate density distribution only, we have neglected the small minima and maxima indicated by the experimental points. Thus within the limits of these approximations, we can conclude that a characteristic angular distribution exists for these light elements. Therefore we can expect that a corresponding characteristic density distribution also exists for the light elements.

We have found that the characteristic angular distribution can be represented by

$$g(s') = \sum_{p=1}^3 a_p \exp(-b_p s'^2) \quad \dots\dots(11)$$

where

$$\begin{aligned} a_1 &= 0.01 \times 10^{-13} \text{ cm}; & b_1 &= 0.01 \times 10^{-26} \text{ cm}^2; \\ a_2 &= 0.11 \times 10^{-13} \text{ cm}; & b_2 &= 0.07 \times 10^{-26} \text{ cm}^2; \\ a_3 &= 0.66 \times 10^{-13} \text{ cm}; & b_3 &= 0.34 \times 10^{-26} \text{ cm}^2. \end{aligned}$$

It may be noted that all these coefficients are positive and therefore the gaussian functions would give only positive Fourier transforms.

§ 5. THE CHARACTERISTIC DENSITY DISTRIBUTION

Introducing $g(s')$ from equation (11) into equation (9) we obtain

$$\rho(r') = N \sum_{q=1}^3 \alpha_q \exp(-\beta_q r'^2) \quad \dots\dots(12)$$

where

$$\begin{aligned} \alpha_1 &= 3.77 \times 10^{26} \text{ cm}^{-2}; & \beta_1 &= 28.94 \times 10^{26} \text{ cm}^{-2}; \\ \alpha_2 &= 2.94 \times 10^{26} \text{ cm}^{-2}; & \beta_2 &= 3.83 \times 10^{26} \text{ cm}^{-2}; \\ \alpha_3 &= 1.50 \times 10^{26} \text{ cm}^{-2}; & \beta_3 &= 0.75 \times 10^{26} \text{ cm}^{-2}. \end{aligned}$$

The normalization integral for the nuclear density, in terms of our parameters takes the form

$$4\pi \int_0^\infty \rho(r') r'^2 dr' = 1. \quad \dots\dots(13)$$

Introducing $\rho(r')$ from equation (12) into equation (13) gives

$$N = 0.066 \times 10^{13} \text{ cm}^{-1}.$$

This leads to $|n'| = 3.43 \times 10^{-40} \text{ cm}^3$. Since at 340 mev, $k = 4.35 \times 10^{13} \text{ cm}^{-1}$, we obtain $k_1'^2 + K'^2/4 = 226 \times 10^{-54} \text{ cm}^4$. Now taking $K' \simeq 26 \times 10^{-27} \text{ cm}^2$ as obtained from the nucleon-nucleon scattering experiments, we obtain $k_1' \simeq 8 \times 10^{-27} \text{ cm}^2$ which is close to the value $k_1' \simeq 9 \times 10^{-27} \text{ cm}^2$ as obtained from the hard core nucleon model (Jastrow 1951), rather than to the value $k_1' \simeq 20 \times 10^{-27} \text{ cm}^2$ as obtained from the tensor interaction model (Christian and Hart 1950, Christian and Noyes 1950) for the nucleon-nucleon interaction. However, we believe that a more exact treatment will be required before this result can be fully confirmed. In figure 2 we have plotted $D(r') = 4\pi r'^2 \rho(r')$ and $\rho(r')$ against r' .

§ 6. THE CHARACTERISTIC ELECTROSTATIC ENERGY

Assuming that the proton density distribution is also given by the distributions obtained above, an elementary derivation gives the electrostatic energy, excluding the self-energies of protons as

$$E = Z(Z-1) A^{-1/3} E' \quad \dots\dots(14)$$

where

$$E' = 2\pi^{5/2} N^2 e^2 \sum_{q=1}^3 \sum_{q'=1}^3 \alpha_q \alpha_{q'} / \{\beta_q (\beta_q + \beta_{q'})^{3/2}\}.$$

Defining the mirror nuclei by $Z = \frac{1}{2}(A \pm 1)$ and assuming that the mass difference of a set of such nuclei is given by the difference of the respective electrostatic energies, we obtain

$$\Delta E = (A-1) A^{-1/3} E' \quad \dots\dots(15)$$

where $E' = 0.55 \text{ mev}$.

This value is close to $E' = 0.59 \text{ mev}$ obtained empirically (Elliott and King 1941). The theoretical derivations of E' have been so far based upon the assumption of a uniform density distribution within the nucleus of the radius given by $R \simeq 1.5 \times A^{1/3} \times 10^{-13} \text{ cm}$. Some calculations have also been made using some central core models. However, in all these calculations the parameters for the nuclear size have been used to obtain an agreement with the empirical results. Such models with these parameters do not appear to be consistent with the requirements of the nuclear scattering of high energy nucleons. On the other

hand, we have first determined the nuclear density distribution completely from the nuclear scattering of high energy nucleons. We now find that this density distribution is reasonably consistent with the requirements of the mass differences for the mirror nuclei.

§ 7. THE VALIDITY OF THE METHOD

A very important assumption in the present treatment is the validity of the first Born approximation for this problem. There appears to be no reliable criterion for testing such a validity. However, in our present approximate investigation we have assumed such a validity on the basis of the following considerations :

(1) Expressing the complex potential as $V = V_1 + iV_2$, we obtain

$$2E |V_1(r')| / (E^2 - \mu^2 c^4) = 0.16 \quad \text{and} \quad 2E |V_2(r')| / (E^2 - \mu^2 c^4) = 0.28$$

at $r' = 0$ and these ratios diminish rapidly with increasing r' . The smallness of these ratios compared with unity leads us to believe that the first Born approximation will be at least approximately valid for our problem, although it remains to be investigated whether the higher Born approximations make any significant contributions.

(2) To test the validity of the first Born approximation for the scattering at different angles (Mott and Massey 1949), we have obtained

$$\begin{aligned} E |V_1(1/k\theta)| / (E^2 - \mu^2 c^4) \theta &\simeq 0.04 \times A^{1/3} \\ \text{and} \quad E |V_2(1/k\theta)| / (E^2 - \mu^2 c^4) \theta &\simeq 0.06 \times A^{1/3} \end{aligned}$$

where $\theta \simeq A^{-1/3}(130^\circ)$, that is $\theta \simeq 57^\circ$ for carbon and $\theta \simeq 43^\circ$ for aluminium. These ratios diminish rapidly with decreasing values of θ . The smallness of these ratios compared with unity within practically the entire experimental range can also be taken as a criterion for an approximate validity of the first Born approximation.

Another important assumption in this investigation concerns the existence of an approximate characteristic density distribution for the light elements. Apart from other reasons, the approximate nature of this assumption is also apparent from the small deviations of the experimental angular distributions for different elements from the characteristic angular distribution. Moreover, as a result of a straightforward derivation we obtain for the elastic cross section $\sigma_e \propto A^{4/3}$. The values of σ_e calculated by integrating the experimental angular distributions (Richardson, Ball, Leith and Moyer 1952) do not appear to obey such a law. However, such an integration requires extrapolation of the $\sigma(\theta)$ curve below the minimum experimental angle. This introduces considerable arbitrariness in the values of σ_e . On the basis of our density distribution we obtain $\sigma_e = 97$ mbn and $\sigma_e = 286$ mbn as against Richardson's values $\sigma_e = 98$ mbn and $\sigma_e = 201$ mbn for carbon and aluminium respectively. Since our investigation also involves an extrapolation for small angles and since most of the contribution to σ_e comes from that region, any agreement between the theoretical and the experimental results cannot be regarded as significant. However, the disagreement for aluminium may also be due to the approximate nature of our assumption regarding the existence of a characteristic density distribution for the light elements.

§ 8. CONCLUSION

Within the limits of the approximations we have employed, we can conclude that the radial distribution method establishes the existence of a characteristic nuclear density distribution for the light elements which is reasonably described by the curve in figure 2. We believe that the results of the present investigation may help in the selection of more appropriate functions to represent the nuclear density distributions for the correlation method.

REFERENCES

- BORN, M., and YANG, L. M., 1950, *Nature, Lond.*, **166**, 399.
CHRISTIAN, R. S., and HART, E. W., 1950, *Phys. Rev.*, **77**, 441.
CHRISTIAN, R. S., and NOYES, H. P., 1950, *Phys. Rev.*, **79**, 85.
ELLIOTT, D. R., and KING, L. D. P., 1941, *Phys. Rev.*, **60**, 489.
FERNBACH, S., 1951, *The Scattering of High Energy Neutrons by Nuclei* (unpublished dissertation, Physics Department, University of California, Berkeley, pp. 16-18).
FERNBACH, S., SERBER, R., and TAYLOR, T. B., 1949, *Phys. Rev.*, **75**, 1352.
GATHA, K. M., and RIDDELL, R. J., Jr., 1952, *Phys. Rev.*, **86**, 1035.
HAUPTMAN, H., and KARLE, J., 1950, *Phys. Rev.*, **77**, 491.
JASTROW, R., 1951, *Phys. Rev.*, **81**, 165.
JASTROW, R., and ROBERT, J. E., 1952, *Phys. Rev.*, **85**, 757.
MATHUR, A. L., and GATHA, K. M., 1953, *Proc. Phys. Soc. A*, **66**, 773.
MOTT, N. F., and MASSEY, H. S. W., 1949, *The Theory of Atomic Collisions* (Oxford: University Press), p. 126.
RICHARDSON, R. E., BALL, W. P., LEITH, C. E., Jr., and MOYER, B. J., 1952, *Phys. Rev.*, **86**, 29.
SERBER, R., 1947, *Phys. Rev.*, **72**, 1114.
WASER, J., and SCHOMAKER, V., 1953, *Rev. Mod. Phys.*, **25**, 671.
YANG, L. M., 1951, *Proc. Phys. Soc. A*, **64**, 632.

Intensity Distribution among Nitrogen Bands in the Auroral Spectrum

BY M. E. PILLOW

Northern Polytechnic, London

MS. received 24th March 1954

Abstract. The factor $p = [\int \psi_v \psi_{v'} dr]^2$, occurring in transition probabilities between vibrational levels, has been calculated for a number of transitions of nitrogen molecules. Intensities obtained from these values have been used to investigate the distribution of intensities among bands in auroral spectra.

§ 1. INTRODUCTION

THE various band systems of nitrogen form a large part of the spectrum of the aurora, and a comparison of observed intensities with calculated values has been attempted by several workers in order to obtain information about the excitation processes occurring. Bates (1949) compared observed intensities of the N_2^+ First Negative group and the N_2 Second Positive group bands in high and low latitude aurorae with the results of his own calculations. Pearse (1953) used approximate values for theoretical and observed intensities in the N_2 Vegard-Kaplan system to indicate differences between the spectra of the aurora and the night sky, and Seaton (1954) used calculations made by Nicholls (1950) together with observations by Vegard and Kvifte (1952 and earlier) to detect the wavelength variation of absorption in the atmosphere.

The calculated transition probabilities used in these cases were either found by one of the earlier approximations, which allow quite large errors for the higher v -values, or were limited to low values of v , as in Bates' work, by the complexity of the calculations. It seemed desirable, therefore, to extend the range of the calculated probabilities, and hence the theoretical basis of the comparison with observation. A form of distortion method for plotting vibrational wave functions from a Morse potential function (Pillow 1951) has already been shown to be fairly reliable over a wide range of vibrational levels, and has therefore been applied here to the systems of N_2 (First and Second Positive and Vegard-Kaplan). For N_2^+ (First Negative group) the values used are some calculated before by a similar method and now extended. While this work was in progress, tables of values for these systems, using rather more elaborate methods but the same molecular constants (those quoted by Herzberg 1950), and still based on the Morse potential function, were published in instalments by Jarman, Fraser and Nicholls (1953, 1954) and by Jarman and Nicholls (1954). Their full tables were still not available when these calculations were complete, and no use could therefore be made of them. Satisfactory agreement between the sets of values furnishes a check on the deduction of the wave functions from the potential function. Only comparison with experiment can decide whether the potential function is suitably chosen.

Values of $p = [\int \psi_v \psi_{v'} dr]^2$ have been calculated for the transitions

N_2	$c^3\Pi - b^3\Pi$	(Second Positive group)
	$b^3\Pi - a^3\Sigma$	(First Positive group)
	$a^3\Sigma - x^1\Sigma$	(Vegard-Kaplan)
N_2^+	$b^2\Sigma - x^2\Sigma$	(First Negative group)

and also for the transitions from the ground level of nitrogen, $x^1\Sigma$, to the excited states $c^3\Pi$ and $b^3\Pi$ of Second Positive group and First Positive group, which are of importance in the discussion of causes of excitation. These p -values are given, with other results, in tables 1-6.

Table 1. N_2 Second Positive Group

v'	v''	0	1	2	3	4	5	6	7	8
0	0-47 ₀ 100(100)	0-35 ₀ 59(59)	0-15 ₃ 20(21)	0-06 ₁ 6(8)	0-02 ₇ 2(?)	0-00 ₃				
1	0-37 ₅ 104(A)	0-02 ₇ 6(4)	0-19 ₈ 34(20)	0-20 ₅ 28(14)	0-13 ₆ 15(8)	0-05 ₄ 4	0-02 ₁ 1(3)	0-00 ₇ 0(?)		
2	0-12 ₄	0-34 ₃ 98(A)	0-01 ₁ 2(?)	0-07 ₄ 13(?)	0-19 ₃ 28(3)	0-16 ₅ 19(3)	0-08 ₉ 8(?)	0-03 ₉ 3(?)	0-00 ₉	
3	0-02 ₃	0-26 ₀	0-21 ₄ 62(A)	0-08 ₈ 21(3)	0-00 ₇ 2(?)	0-13 ₀ 20(?)	0-18 ₁ 22(?)	0-13 ₂ 13(?)	0-07 ₇ 5	0-03 ₅
4	0-00 ₄	0-06 ₁	0-35 ₀	0-08 ₂ 24	0-13 ₄ 32(?)	0-00 ₀ 0(?)	0-06 ₁ 10	0-15 ₀ 19(?)	0-10 ₄ 8(?)	0-04 ₀ 2

Upper line: values of $p = [\psi_v \psi_{v''} dr]^2$.

Lower line: intensities on an arbitrary scale, calculated for uniform population of levels.

Numbers in brackets represent intensities measured by Petrie and Small (1953).

(A): definitely identified; (?): possibly present, but masked by other features.

Comments. Along any one progression the measured intensities agree very closely with those calculated, with the exception of (1, 6), which is discussed later. The apparently missing band (1, 5) is almost coincident with a band of N_2 First Negative group. The table indicates which of the doubtful bands are likely to be really present.

Table 2. N₂ First Positive Group

v''	0	1	2	3	4	5	6	7	8	9
0	0-33 ₀	0-31 ₅	0-19 ₀	0-09 ₄	0-04 ₆	0-01 ₉	0-00 ₆			
1	0-39 ₁ 100(100)	0-00 ₁	0-11 ₁	0-18 ₉	0-15 ₇	0-10 ₆	0-05 ₀			
2	0-22 ₁ 98(35)	0-19 ₄ 54(A)	0-09 ₄	0-00 ₁	0-07 ₂					
3	0-04 ₃ 33(A)	0-30 ₅ 143(A)	0-04 ₄ 13(3)	0-14 ₄	0-02 ₁					
4	0-01 ₁ 12(A)	0-16 ₀ 120(12)	0-31 ₄ 156(29)	0-00 ₁ 4	0-08 ₁					
5	0-00 ₁	0-04 ₂ 60(0-9)	0-25 ₂ 198(12)	0-17 ₇ 94(15)	0-04 ₇ 16	0-02 ₄				
6	0-00 ₀	0-01 ₀ 17	0-07 ₄ 89(1-1)	0-27 ₀ 223(9)	0-08 ₃ 46(A)	0-08 ₅ 32(?)				
7		0-01 ₂ 20	0-01 ₂ 20	0-15 ₁ 183(1-3)	0-28 ₅ 247(6)	0-01 ₀ 6(1-8)	0-11 ₆ 44(?)			
8				0-03 ₁ 53(?)	0-21 ₀ 264(1-3)	0-25 ₂ 228(3)	0-00 ₀ 0(A)			
9					0-05 ₇ 100(?)	0-31 ₀ 404(1-1)	0-23 ₁ 220(1-8)	0-01 ₉ 13(1-3)		
10						0-11 ₀ 199	0-33 ₀ 444(1-1)	0-10 ₆ 104(A)		
11						0-02 ₂ 53	0-18 ₃ 340(?)	0-32 ₁ 449(0-9)	0-04 ₆ 48(A)	
12							0-04 ₂ 104	0-26 ₀ 494(?)	0-26 ₉ 389(A)	0-00 ₂ 21

Upper line: values of $p = [\psi_0 \psi_0' dr]^2$.

Lower line: intensities on an arbitrary scale, calculated for uniform population of levels.

Numbers in brackets represent intensities measured by Petrie and Small (1953).

Bands marked (A): definitely identified; bands marked (?): possibly present, but masked by other features.

Comments. The agreement between numerical values of calculated and observed intensities is discussed later, and is found to have some wavelength dependence. The only noticeable discrepancy between theory and observation in this system is in the sequence of bands (7, 5), (8, 6), (9, 7), whose measured intensities, though weak, are not as low as the calculations would suggest. This may have significance as showing another emission in this region, but the apparent discrepancy must not be given undue weight.

Table 3. N₂ Vegard-Kaplan System

v'	v''	0	1	2	3	4	5	6	7	8	9	10	11	12	13	14	15	16
0	0.000	0.004	0.020	0.052	0.108	0.159	0.188	0.176	0.140	0.090	0.042	0.025	0.010	0.002	0.000			
									51(A)	18(A)	8(?)	2						
1	0.002	0.018	0.061	0.102	0.114	0.074	0.012	0.005	0.069	0.146	0.179	0.134	0.099	0.053	0.015	0.006	0.003	
										100(A)	93(A)	53(A)	28(A)	11	2			
2	0.007	0.043	0.094	0.093	0.034	0.000	0.040	0.075	0.053	0.007	0.013	0.085	0.134	0.157	0.102	0.053	0.022	
											8	27(A)	30(A)	25(A)	11(?)	4(A)	1	
3	0.016	0.069	0.092	0.039	0.000	0.033	0.069	0.020	0.005	0.053	0.064	0.022	0.003	0.057	0.120	0.163	0.117	
												12	1	19(?)	28(A)	28(A)	14	
4	0.030	0.081	0.063	0.003	0.027	0.046	0.013	0.004	0.049	0.029	0.001	0.044	0.071	0.026	0.001	0.054	0.153	
													37	10	0	12	24	
5	0.048	0.102	0.028	0.002	0.051	0.018	0.004	0.046	0.021	0.002	0.039							
6	0.063	0.056	0.004	0.033	0.037	0.000	0.030	0.026	0.002									
7	0.081	0.055	0.003	0.050	0.019	0.014	0.032	0.000	0.029									
8	0.092																	
9	0.104																	
10	0.110																	

Upper line: values of $p = [\psi_{v'}\psi_{v''} d\tau]^2$.

Lower line: intensities on an arbitrary scale, calculated for uniform population of levels.

Bands marked (A): definitely identified; bands marked (?): possibly present, but masked by other features.

No values for intensities are given by Petrie and Small.

Comments. In general, those bands appear which are indicated by theory. In one of their papers (1952) Petrie and Small discuss a number of bands which may be obscured by other features. The whole system is, of course, weaker than others occurring in the same region.

Table 4. N_2^+ First Negative Group

v''	0	1	2	3	4	5	6	7
v'								
0	0.67 ₀ 100(100)B	0.22 ₇ 24(30)B	0.07 ₇ 5(6)	0.01 ₈ 1(2)				
1	0.29 ₁ 63(10)B	0.24 ₄ 38(7)B	0.26 ₀ 28(6)B	0.13 ₆ 10(2)	0.04 ₄ 2(0.8)			
2	0.04 ₃ 13(?)	0.42 ₀ 91(2)B	0.07 ₀ 11(0.4)	0.20 ₉ 24(?)	0.20 ₅ 16(A)B	0.09 ₅ 5(0.2)		
3	0.00 ₂	0.11 ₀ 32(?)	0.41 ₇ 93(1)B	0.02 ₈ 4	0.13 ₄ 16	0.19 ₈ 16(0.6)		
4	0.00 ₂		0.19 ₁ 57(?)	0.30 ₆ 69(?)	0.00 ₀ 0	0.09 ₂ 11(?)	0.19 ₇ 17(0.4)	0.14 ₈ 9(0.2)
5					0.36 ₀ 81(?)	0.01 ₁ 2	0.04 ₃ 5	0.17 ₀ 14(0.2)

Upper line: values of $p = [\int \psi_{v'} \psi_{v''} dr]^2$.

Lower line: intensities on an arbitrary scale, calculated for uniform population of levels.

Numbers in brackets represent intensities measured by Petrie and Small (1953).

Bands marked (A): definitely identified; bands marked (?): possibly present, but masked by other features; bands marked (B): observed by Barbier in low latitude aurorae.

Comments. Many doubtful bands are in the region of N_2 Second Positive group bands. The (3, 4) band is noted by Vegard and Kvitte as being present.

Table 5. Excitation of $N_2C^3\Pi$ state (upper state of N_2 Second Positive group) from ground state of N_2

Values of $p = [\int \psi_{v'} \psi_{v''} dr]^2$ for $v'' = 0$

v'	0	1	2	3	4	5
p	0.45 ₇	0.31 ₂	0.14 ₈	0.05 ₅	0.02 ₅	0.00 ₅

Table 6. Excitation of $N_2B^3\Pi$ state (upper state of N_2 First Positive group) from ground state of N_2

Values of $p = [\int \psi_{v'} \psi_{v''} dr]^2$ for $v'' = 0$

v'	0	1	2	3	4	5	6
p	0.04 ₄	0.11 ₂	0.16 ₂	0.17 ₆	0.17 ₆	0.12 ₀	0.08 ₇
v'	7	8	9	10	11	12	
p	0.05 ₀	0.03 ₀	0.02 ₁	0.01 ₆	0.00 ₄	0.00 ₂	

§2. CALCULATED INTENSITIES AND OBSERVED BANDS

If the vibrational levels of the upper state of a transition were uniformly populated the intensity in emission of a band of origin ν could be regarded as proportional to $p\nu^4$, the electronic transition moment being treated as constant. Using the calculated values of p , the values of $p\nu^4$ have been obtained, and expressed on an arbitrary scale, for the bands of the four systems which are relevant to the examination of auroral spectra.

Vegard and Kvifte (1952) published the results of extensive observations on the aurora, and suggested identifications of a large number of features; in many cases there are two or more suggestions for the same wavelength. Petrie and Small (1952) made measurements covering the range from about 3100 to 4800 Å, and later (1952, 1953) made further measurements, up to about 9000 Å, using much greater dispersion, so that identifications are a great deal more definite. They have also given integrated intensities for the bands where these could be established with sufficient accuracy. In the tables given here bands identified and measured by Petrie and Small, and some noted by Barbier (1947) in low latitude aurorae, are shown with the calculated intensities, and a few doubtful cases are discussed. Petrie and Small themselves give fuller discussion of doubtful and blended features.

§3. NUMERICAL COMPARISON OF INTENSITIES: POPULATION RATES OF EXCITED STATES

Where the measured intensities are given, direct comparison with theory can be made, and the relative populations of the excited levels estimated. Petrie and Small treated some of their results in this way, using approximate theoretical values.

If I is the measured intensity of a band of origin ν , and $p = [\int \psi_{\nu'} \psi_{\nu''} dr]^2$ the value of $\log(I/p\nu^4)$ can be plotted against wavelength λ . Ideally the graph should consist of a set of straight lines, all parallel to the λ -axis, and separated by amounts determined by the relative population rates of the excited levels. A suitable shift $f(\nu')$ can bring all the lines into coincidence, and the population of the ν' level is proportional to the $-f(\nu')$ th power of 10. This is essentially what was done by Seaton with the results of Vegard and Kvifte but with the ratio reversed. In that case the slope of the lines is considerable, and is probably attributable largely to the effects of atmospheric extinction.

Using the newly calculated p -values, and a greater number of the measured bands, including a few of the Vegard-Kaplan system, this trend in the measurements of Vegard and Kvifte has been definitely confirmed, and is shown in figure 1, for the range 3000–5000 Å. The individual progressions are not shown separately, but the shifts used to bring them together in the case of N_2 Second Positive group

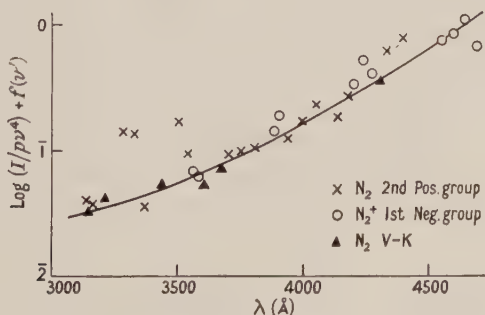


Figure 1. Measurements by Vegard and Kvifte.

are 0, 0.2, 0.4, 0.6 for the levels $v' = 0, 1, 2, 3$, and these would correspond to populations in the ratio 1, 0.6, 0.4, 0.25 for these levels. For N_2^+ First Negative group the relative shifts are 0, 0.8, 1.0, 1.2, giving populations for $v' = 0-3$ in the ratio 1, 0.16, 0.10, 0.06. Only two levels, $v' = 0, 1$, of the Vegard-Kaplan system are sufficiently reliably represented to be included, and these appear to have populations in the ratio of about 1 : 0.4.

The tables and photograph published by Vegard and Kvifte show the difficulty of ascribing an intensity measurement to one band only, and this can account for the scatter among the points of any one progression, and for the few bands which are unduly strong. The average slope of the graph represents a change in the ratio of measured to calculated intensity in this wavelength range of something like 40 : 1, whereas, apart from the few outstanding discrepancies, the scatter represents an uncertainty in the ratio of only about 1.4 : 1. Seaton attributes this slope mainly to the effect of atmospheric extinction. There is also the possibility of a systematic effect due to the calibration of the intensity scale.

The results for N_2 Second Positive group given first by Petrie and Small (1952) are now treated in the same way. Here allowance was made by the observers for atmospheric extinction arising from several causes. Relative shifts of 0, 0.25, 0.5, 0.75, corresponding to population rates for the $v' = 0, 1, 2, 3$, levels of 1, 0.56, 0.32, 0.18, gives the graph of figure 2. Excluding for the moment the (3, 2) and (0, 4) bands, the slope of the line is very much smaller, representing a systematic variation in the ratio of measured to calculated intensity of not more than 2.5 : 1 over the wavelength range 3000–4500 Å. Of the two bands which lie off the line, the (3, 2) band, which appears too weak, is at the extreme end of the measured range, so that the significance of the low value is doubtful. Neither Vegard and Kvifte nor Petrie and Small in their later work give a numerical value for its intensity. Laboratory observations indicate a higher value for it. The (0, 4) band has a high intensity, almost certainly due to the inclusion of the H_γ emission at this wavelength. The intensity, 2.0 on the scale used, is too high by a factor of about 2, suggesting that an intensity value 1.0 should be allotted to the band and 1.0 to the hydrogen line.

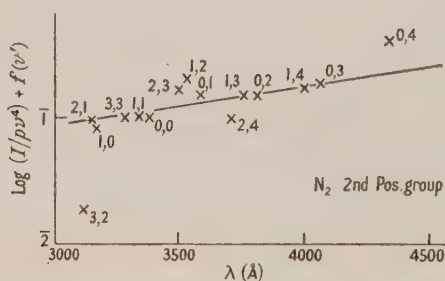


Figure 2. Measurements by Petrie and Small (1952).

Nicholls, in a private communication to Seaton, suggests that the neglect of the effect of varying internuclear distance on the electronic transition moment is likely to introduce a wavelength trend in the direction actually obtaining. The great reduction in line slope in this case as compared with the last indicates that atmospheric absorption was responsible for the greater part of that slope. The much smaller trend remaining may possibly be due to the effect mentioned by Nicholls. In any case, the detection of irregularities and the calculation of population rates can be carried out independently of this systematic variation.

The fuller publication by Petrie and Small in 1953 of intensities measured at much greater dispersion makes it possible to examine on a comparable scale the three systems N_2 Second Positive group, N_2 First Positive group, and N_2^+ First Negative group.

Figure 3 shows the results plotted for the range 3000–5500 Å.

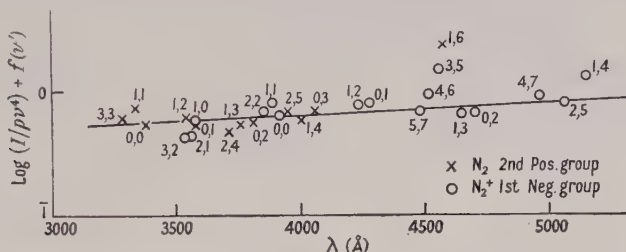


Figure 3. Measurements by Petrie and Small (1953) in the range 3000–5500 Å.

For N_2 , Second Positive group only the $v' = 0, 1$ progressions are here represented by any appreciable number of bands, so that the population rates of the remaining levels are somewhat uncertain. The rates appear to be 1, 0.5, 0.1, 0.1 for $v' = 0, 1, 2, 3$. The intensity of the (1, 6) band is too great by a factor of about 3, when compared with theory, and also seems to be too great when compared with laboratory results. Vegard and Kvitte suggest that other features exist here, and the high intensity makes this likely.

The results for N_2^+ First Negative group indicate population rates for the levels 0–5 of 1, 0.18, 0.032, 0.016, 0.016, 0.013. Here again the higher levels are represented by only a few bands, so that conclusions should not be too readily drawn; but it does appear that the upper levels are fairly evenly, though thinly, populated. The (3, 5) band is unexpectedly intense, and Petrie and Small suggest blending here. It is noteworthy that it lies close to the (1, 6) band of N_2 Second Positive group mentioned above.

In the measurements of intensity for N_2 First Positive group bands, several levels are represented by one band only, and population rates for the low and high levels cannot, therefore, be determined with any certainty. The points corresponding to levels $v' = 4-9$ are all brought on to one (curved) line by relative shifts of 0.15 v' , and the (2, 0), (10, 6), (11, 7) bands, although the only representatives of their progressions, agree with this scheme. The (7, 5) and (9, 7) bands, which lie off the line, have been discussed earlier.

There is a considerable wavelength variation of the ratio of measured to calculated intensity in the red region. Figure 4 shows on a smaller scale, and without the individual band numbers, all the range of measurements by Petrie and Small, and this trend is marked in the region beyond 6000 Å. This may be connected with the allowance for absorption, or with calibration, or Nicholls' suggestion about the electronic moment, mentioned before, may have some bearing here.†

The high latitude auroral measurements made by different observers at different times appear, after any wavelength trend has been discounted, to give excitation rates of the same order. The distributions are not generally thermal in type.

† It is of interest to note that laboratory measurements made by Nicholls, and just received (private communication), show a very similar trend, though less pronounced.

One more set of measurements should be mentioned. Barbier's measurements on N_2^+ First Negative group in low latitude aurorae, when treated in the same way, require progression shifts of 0, 0.2, 0.3, 0.4, indicating populations for the $v'=0, 1, 2, 3$ levels in the approximate ratio 1, 0.63, 0.5, 0.4. This corresponds to a much higher degree of excitation than is shown by the same system in high latitude aurorae, as Barbier pointed out.

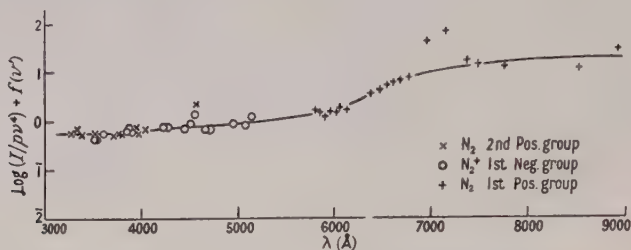


Figure 4. Measurements by Petrie and Small (1953).

§ 4. CONCLUSION

At present there are not available measurements on auroral bands made systematically at different times or in different places under the same instrumental conditions. Such measurements, compared with the same calculated values for the intensities, would show whether there is variation from time to time in population rates, in atmospheric absorption, or in the relative strengths of various features. As an example of the last effect, we may consider the H_γ line. If this varies in strength in a manner different from the (0, 4) band of N_2 Second Positive group the irregularity noted in figure 2 should indicate this variation. Such an effect can in fact be found when the results of Vegard and Kvitte are compared with those of Petrie and Small, but from photographs taken under different conditions, and calibrated differently, no safe conclusion on the point can be drawn.

The comparisons made here show how much information can be obtained from measured intensities, and indicate the value of further systematic observations.

ACKNOWLEDGMENTS

The writer is indebted to Dr. R. W. B. Pearse and to Dr. M. J. Seaton for discussions and suggestions.

REFERENCES

- BARBIER, D., 1947, *Ann. Geophys.*, **3**, 227.
 BATES, D. R., 1949, *Proc. Roy. Soc. A*, **196**, 217.
 HERZBERG, G., 1950, *Spectra of Diatomic Molecules* (New York: Van Nostrand).
 JARMAIN, W. R., FRASER, P. A., and NICHOLLS, R. W., 1953 and 1954, University of Western Ontario, Department of Physics, Contract No. A.F.19(122)-470. *Scientific Reports*, Nos. 8 and 10.
 JARMAIN, W. R., and NICHOLLS, R. W., 1954, *Canad. J. Phys.*, **32**, 201.
 NICHOLLS, R. W., 1950, *Phys. Rev.*, **77**, 421.
 PEARSE, R. W. B., 1953, Geophysical Research Papers, *Proceedings of 1951 Conference on Auroral Physics*.
 PETRIE, W., and SMALL, R., 1952, *J. Geophys. Res.*, **57**, 51; 1952, *Astrophys. J.*, **116**, 433; 1953, *Canad. J. Phys.*, **31**, 911.
 PILLOW, M. E., 1951, *Proc. Phys. Soc. A*, **64**, 772.
 SEATON, M. J., 1954, *J. Atmos. Terr. Phys.*, **4**, 285.
 VEGARD, L., and KVIFTE, G., 1952, *Geofys. Publ.*, **18**, 3.

The Self-Consistent Field for Au^+

By W. G. HENRY

The Division of Applied Chemistry, National Research Council, Ottawa, Canada

MS. received 5th May 1954

Abstract. The results are presented of the calculation of the self-consistent field, without exchange, for Au^+ .

§ 1. INTRODUCTION

THE limited, mutual, solid solubility in the copper-silver alloy system has been deduced by a quantum mechanical calculation (Arafa 1949). This was the first successful application of quantum mechanics to an alloy system in which the components differ markedly in atomic size. In the calculation the self-consistent fields, without exchange, for Cu^+ (Hartree 1933) and Ag^+ (Black 1934-1935) were taken as an approximation to the fields of the solvent and solute atoms. The author concludes his paper by remarking that it would be a searching test of the method to apply the procedure to the copper-gold alloy system. It was with this in mind that the self-consistent field of Au^+ was calculated.

§ 2. METHOD OF CALCULATION

The details of the method of the self-consistent field may be found in papers by Hartree (1928 and later). These papers and others have been reviewed by Hartree (1946). The determination of the field involves the numerical solution of (Hartree 1934),

$$(d^2/d\rho^2)(Pr^{-1/2}) + [2Er^2 + 2rZ_p - (l + \frac{1}{2})^2](Pr^{-1/2}) = 0 \quad \dots\dots(1)$$

where $\rho = \ln r$, $Z_p = -rV$ the effective nuclear charge for potential. E is the energy of the electron in the central field $V = V(r)$; V , E and r are all in atomic units; $P = r\psi$ where ψ is the wave function for an electron in a central field, and l is the azimuthal quantum number. Z_p is related to Z , the effective nuclear charge, by

$$dZ/d\rho = Z_p - Z. \quad \dots\dots(2)$$

The first approximation to Z was made in a manner analogous to that described by Manning and Millman (1936) using the results for Cs^+ (Hartree 1934) and Hg (Hartree 1935) for all groups $(1s)^2$ to $(4d)^{10}$ and the results for Hg and W (Manning and Millman 1936) for all groups $(4f)^{14}$ to $(5p)^6$. For the $(5d)^{10}$ group it was assumed that a plot of the contribution to Z against ρ would be displaced to values of ρ slightly larger than those of the corresponding $(5d)^{10}$ group in Hg^{2+} .

The numerical solution of equation (1) was carried out by methods developed by Hartree (1932-1933) for second order differential equations with the first derivative not present. The parameter E was varied until a reasonably asymptotic solution was obtained. The tabulated values of $Pr^{-1/2}$ have been smoothed to the usual asymptotic form (Manning and Millman 1936). The numerical solution of equation (2) was carried out by the usual methods (Scarborough 1950). The same integration constants were used in the calculation of P/r^{l+1} as those employed by Hartree for Hg to facilitate comparison.

Table 1. Radial Wave Functions, Au^+ . Table of P/r^{l+1}

\ln (1000 r) $=P$	(1s)	(2s)	(2p)	(3s)	(3p)	(3d)	(4s)	(4p)	(4d)	(4f)	(5s)	(5p)	(5d)
0	2.338	2.337	0.061	2.336	0.061	0.0003	2.336	0.061	0.0003	0.00000	2.336	0.061	0.0003
$0^{4/12}$	2.677	2.673	0.099	2.672	0.099	0.0007	2.672	0.099	0.0007	0.00000	2.672	0.099	0.0007
$0^{8/12}$	3.028	3.020	0.159	3.018	0.159	0.0016	3.017	0.159	0.0016	0.00000	3.017	0.159	0.0016
1	3.366	3.346	0.255	3.344	0.254	0.0036	3.342	0.254	0.0036	0.00001	3.343	0.254	0.0036
$1^{4/12}$	3.647	3.609	0.405	3.644	0.402	0.0081	3.602	0.402	0.0081	0.00004	3.603	0.402	0.0080
$1^{8/12}$	3.823	3.742	0.631	3.730	0.626	0.0180	3.727	0.626	0.0180	0.00012	3.728	0.626	0.0174
2	3.825	3.653	0.960	3.627	0.950	0.0394	3.619	0.950	0.0394	0.00036	3.620	0.950	0.0376
$2^{2/12}$	3.739	3.491	1.171	3.454	1.156	0.0578	3.443	1.156	0.0578	0.00063	3.443	1.156	0.0550
$2^{6/12}$	3.586	3.234	1.415	3.182	1.393	0.0842	3.167	1.392	0.0842	0.00110	3.166	1.392	0.0800
$2^{10/12}$	3.363	2.871	1.691	2.800	1.659	0.1218	2.780	1.656	0.1217	0.00191	2.778	1.656	0.1156
$2^{14/12}$	3.071	2.397	1.995	2.302	1.947	0.1747	2.276	1.941	0.1744	0.00329	2.273	1.941	0.1656
3	2.717	1.814	2.318	1.691	2.246	0.2481	1.658	2.235	0.2474	0.00562	1.654	2.235	0.2349
$3^{2/12}$	2.316	1.136	2.645	0.982	2.537	0.3483	0.942	2.519	0.3468	0.00951	0.937	2.518	0.3293
$3^{6/12}$	1.889	0.390	2.956	0.207	2.792	0.4824	0.161	2.764	0.4794	0.01594	0.155	2.761	0.4552
$3^{10/12}$	1.463	-0.380	3.223	-0.583	2.977	0.6574	-0.630	2.932	0.6518	0.02648	-0.637	2.926	0.6190
$3^{14/12}$	1.065	-1.120	3.415	-1.317	3.049	0.8799	-1.360	2.980	0.8693	0.04336	-1.364	2.970	0.8254
$3^{18/12}$	0.719	-1.763	3.500	-1.910	2.962	1.153	-1.938	2.860	1.133	0.06991	-1.937	2.846	1.075
$3^{22/12}$	0.441	-2.242	3.442	-2.271	2.676	1.474	-2.268	2.532	1.436	0.1108	-2.259	2.511	1.363
4	0.246	-2.503	3.240	-2.322	2.168	1.831	-2.267	1.974	1.763	0.1722	-2.247	1.942	1.673
$4^{1/12}$	0.180	-2.542	3.080	-2.215	1.832	2.017	-2.126	1.611	1.927	0.2129	-2.099	1.572	1.827
$4^{5/12}$	0.125	-2.519	2.885	-2.018	1.446	2.203	-1.891	1.198	2.084	0.2616	-1.856	1.153	1.974
$4^{9/12}$	0.084	-2.438	2.660	-1.735	1.018	2.383	-1.567	0.745	2.228	0.3194	-1.524	0.694	2.107
$4^{13/12}$	0.057	-2.304	2.411	-1.375	0.558	2.552	-1.165	0.265	2.351	0.3874	-1.114	0.209	2.219
$4^{17/12}$	0.035	-2.125	2.145	-0.951	0.080	2.703	-0.702	-0.225	2.445	0.4665	-0.644	-0.284	2.302
$4^{21/12}$	0.024	-1.912	1.871	-0.481	-0.401	2.830	-0.200	-0.705	2.502	0.5575	-0.137	-0.764	2.348
$4^{25/12}$	0.016	-1.676	1.597	0.013	-0.867	2.926	0.314	-1.153	2.513	0.6609	0.378	-1.208	2.348
$4^{29/12}$	0.009	-1.430	1.332	0.506	-1.300	2.985	0.808	-1.545	2.470	0.7768	0.869	-1.591	2.294
$4^{33/12}$	0.005	-1.185	1.083	0.973	-1.682	3.001	1.250	-1.858	2.366	0.9049	1.301	-1.889	2.180
$4^{37/12}$	0.003	-0.952	0.857	1.389	-1.997	2.971	1.607	-2.070	2.197	1.044	1.641	-2.079	2.002
$4^{41/12}$	0.001	-0.740	0.658	1.732	-2.231	2.893	1.852	-2.165	1.961	1.192	1.860	-2.144	1.758
5	—	-0.555	0.490	1.985	-2.376	2.768	1.963	-2.132	1.659	1.347	1.936	-2.073	1.451
$5^{1/12}$	—	-0.401	0.353	2.139	-2.429	2.599	1.928	-1.967	1.297	1.506	1.858	-1.865	1.087
$5^{5/12}$	—	-0.281	0.249	2.191	-2.392	2.391	1.745	-1.676	0.885	1.665	1.626	-1.528	0.677
$5^{9/12}$	—	-0.188	0.169	2.147	-2.274	2.153	1.425	-1.275	0.437	1.818	1.255	-1.081	0.237
$5^{13/12}$	—	-0.122	0.112	2.019	-2.089	1.895	0.991	-0.788	-0.030	1.960	0.773	-0.553	-0.214
$5^{17/12}$	—	—	0.112	1.831	-1.831	1.635	0.635	-0.247	-0.495	2.085	0.221	0.0	-0.654

Table of P/r^{l+1}

4 ⁶ / ₁₂	—	0.695	1.300	1.825	5.490	9.035	6 ⁴ / ₁₂	0.440	1.440	2.665	4.450	1.835	5.565	7 ⁸ / ₁₂	2.450
4 ⁷ / ₁₂	—	0.535	0.975	1.825	5.480	8.700	6 ⁵ / ₁₂	0.285	0.970	1.900	3.540	1.825	5.555	7 ⁹ / ₁₂	1.895
4 ⁸ / ₁₂	—	0.390	0.700	1.820	5.440	8.285	6 ⁶ / ₁₂	0.170	0.610	1.280	2.725	1.800	5.510	7 ¹⁰ / ₁₂	1.425
4 ⁹ / ₁₂	—	0.275	0.480	1.815	5.350	7.780	6 ⁷ / ₁₂	0.090	0.355	0.810	2.025	1.735	5.385	7 ¹¹ / ₁₂	1.035
4 ¹⁰ / ₁₂	—	0.180	0.310	1.790	5.195	7.185	6 ⁸ / ₁₂	0.045	0.190	0.475	1.445	1.625	5.160	8	0.725
4 ¹¹ / ₁₂	—	0.110	0.190	1.735	4.950	6.510	6 ⁹ / ₁₂	0.020	0.095	0.260	0.990	1.470	4.805		
5	—	0.065	0.110	1.650	4.605	5.765	6 ¹⁰ / ₁₂	0.005	0.040	0.125	0.645	1.275	4.330	8 ¹ / ₁₂	0.490
5 ¹ / ₁₂	—	0.035	0.060	1.520	4.170	4.975	6 ¹¹ / ₁₂	—	0.015	0.050	0.395	1.055	3.755	8 ² / ₁₂	0.315
5 ² / ₁₂	—	0.015	0.030	1.360	3.645	4.170	7	—	0.005	0.015	0.225	0.825	3.125	8 ³ / ₁₂	0.195
5 ³ / ₁₂	—	0.005	0.010	1.165	3.070	3.380	7 ¹ / ₁₂	—	—	0.005	0.115	0.615	2.485	8 ⁴ / ₁₂	0.110
5 ⁴ / ₁₂	—	—	0.005	0.950	2.475	2.640	7 ² / ₁₂	—	—	—	0.055	0.430	1.885	8 ⁵ / ₁₂	0.060
5 ⁵ / ₁₂	—	—	—	0.740	1.900	1.980	7 ³ / ₁₂	—	—	—	0.020	0.280	1.360	8 ⁶ / ₁₂	0.030
5 ⁶ / ₁₂	—	—	—	0.545	1.385	1.420	7 ⁴ / ₁₂	—	—	—	0.005	0.175	0.930	8 ⁷ / ₁₂	0.010
5 ⁷ / ₁₂	—	—	—	0.375	0.950	0.970	7 ⁵ / ₁₂	—	—	—	—	0.100	0.600	8 ⁸ / ₁₂	0.005
5 ⁸ / ₁₂	—	—	—	0.240	0.615	0.630	7 ⁶ / ₁₂	—	—	—	—	0.055	0.365	—	—
5 ⁹ / ₁₂	—	—	—	0.145	0.370	0.385	7 ⁷ / ₁₂	—	—	—	—	0.025	0.205	—	—
5 ¹⁰ / ₁₂	—	—	—	0.080	0.205	0.220	7 ⁸ / ₁₂	—	—	—	—	0.010	0.105	—	—
5 ¹¹ / ₁₂	—	—	—	0.040	0.105	0.120	7 ⁹ / ₁₂	—	—	—	—	0.000	0.050	—	—
6	—	—	—	0.020	0.050	0.060	7 ¹⁰ / ₁₂	—	—	—	—	—	0.020	—	—
6 ¹ / ₁₂	—	—	—	0.005	0.020	0.030	7 ¹¹ / ₁₂	—	—	—	—	—	0.005	—	—
6 ² / ₁₂	—	—	—	—	0.010	0.015	8	—	—	—	—	—	—	—	—
6 ³ / ₁₂	—	—	—	—	0.000	0.005		—	—	—	—	—	—	—	—

Table 3. Values of $\epsilon = -2E$ and $I = \int_0^\infty P^2 dr$ for Au⁺

(1s) ²	(2s) ²	(2p) ⁶	(3s) ²	(3p) ⁶	(3d) ¹⁰	(4s) ²	(4p) ⁶	(4d) ¹⁰	(4f) ¹⁴	(5s) ²	(5p) ⁶	(5d) ¹⁰
5410	897.0	864.0	209.5	193.7	163.95	44.20	37.125	24.45	7.660	6.815	4.600	1.155
0.003214	0.02950	0.04052	0.1358	0.1583	0.1823	0.5521	0.6592	0.7035	0.8486	2.838	3.986	8.195

 ϵ I

To begin the calculation it was assumed that the initial approximations for all the groups $(1s)^2$ to $(3d)^{10}$ were within the allowed limits of error. The $(4f)^{14}$ shell was treated first and the maximum difference between the estimated and calculated Z found to be nowhere greater than 0.025 electron. Attention was then turned to the outer groups. The maximum difference for the $(5s)^2$ group was found to be 0.015 electron. The $(5d)^{10}$ group was then brought into approximate self-consistency and the $(5p)^6$ group adjusted to bring the maximum difference for this group to 0.015 electrons. In all, ten approximations were required to bring the maximum difference between the estimated and calculated Z for the $(5d)^{10}$ group, which was 'overstable' (Hartree 1933), to 0.025 electron. All groups were then recalculated using the corrected field.

§ 3. RESULTS

The maximum difference between the estimated and calculated contributions to Z for any one group is 0.025 electron. The maximum difference between the calculated and estimated contributions to Z from all groups is 0.050 electron which occurs at $\rho = 4.0$ where the total Z is comparatively large. The results are summarized in the accompanying tables.

ACKNOWLEDGMENTS

The author wishes to thank Miss A. R. Graves for her part in the carrying out of the computations.

REFERENCES

- ARAFA, M. K. I., 1949, *Proc. Phys. Soc.*, **62**, 238.
 BLACK, M. M., 1934-1935, *Mem. Manchr. Lit. Phil. Soc.*, **79**, 29.
 HARTREE, D. R., 1928 a, *Proc. Camb. Phil. Soc.*, **24**, 89; 1928 b, *Ibid.*, **24**, 111; 1932-1933, *Mem. Manchr. lit. phil. Soc.*, **77**, 91; 1933, *Proc. Roy. Soc.*, **141**, 282; 1934, *Ibid.*, **143**, 506; 1934, *Phys. Rev.*, **46**, 738; 1935, *Proc. Roy. Soc.*, **149**, 210; 1946, *Rep. Progr. Phys.*, **11**, 113.
 MANNING, M. F., and MILLMAN, J., 1936, *Phys. Rev.*, **49**, 848.
 SCARBOROUGH, J. B., 1950, *Numerical Mathematical Analysis* (Baltimore : Johns Hopkins), p. 244.

The Electronic Spectra of Aromatic Molecules I: Benzenoid Hydrocarbons

BY M. J. S. DEWAR† AND H. C. LONGUET-HIGGINS‡

† University of London, Queen Mary College

‡ University of London, King's College

MS. received 7th April 1954

Abstract. Certain regularities observed in the spectra of benzenoid hydrocarbons by Clar and by Klevens and Platt are interpreted in terms of the l.c.a.o. molecular orbital theory on the assumption that electron repulsion mixes together only configurations which are degenerate when overlap is neglected. The frequency and intensity relationships between Clar's α , p , β and β' bands find a simple interpretation in this scheme, and the near ultra-violet spectra of benzene, naphthalene and anthracene are interpreted in the light of this theory.

§ 1. INTRODUCTION

THE visible and near ultra-violet spectra of aromatic hydrocarbons are of considerable theoretical interest, for several reasons. First, the main bands in these spectra undoubtedly correspond to π - π electronic transitions, and existing theories of unsaturated molecules stand or fall by their success in describing the behaviour of the π -electrons. Secondly, the aromatic hydrocarbons form a convenient series of molecules for comparative study; and thirdly, their spectra, which have been observed and studied in some detail by Clar (1941) and by Klevens and Platt (1949), show some remarkable regularities which represent a challenge to theoretical analysis.

The main experimental findings are as follows. The spectrum of an aromatic hydrocarbon usually contains four main regions of absorption, which from their intensity must be due to singlet-singlet transitions. These bands are called α , p , β and β' by Clar, and 1L_b , 1L_a , 1B_b and 1B_a by Platt (1949). The last three increase in frequency in the order $p < \beta \leq \beta'$, and are relatively intense, having oscillator strengths f of the order of 0.1, 1.5 and 0.5 respectively. The α band, on the other hand, is invariably weak ($f \simeq 0.005$) and usually occurs at longer wavelengths, though in some cases it underlies the p band, or appears between p and β . The p and α bands almost invariably show marked vibrational structure, but the β and β' bands rarely exhibit such structure. And finally, there is a remarkable relation, pointed out by Clar, between the wavelength maxima of the weak α band and the very strong β band, namely

$$\lambda_\alpha/\lambda_\beta \simeq 1.3. \quad \dots\dots(1)$$

This relation holds for a wide range of hydrocarbons of most diverse types.

Let us see now whether these results are intelligible in terms of the l.c.a.o. molecular orbital theory. This theory describes the ground state by the configuration

$$(\psi_1)^2(\psi_2)^2 \dots (\psi_{m-1})^2(\psi_m)^2$$

there being $2m$ π -electrons altogether; and an obvious supposition is that the

four bands α , p , β , β' correspond to excitation of one electron from one or other of ψ_{m-1} , ψ_m to one or other of ψ_{m+1} , ψ_{m+2} , the lowest unoccupied orbitals. The corresponding transition energies, namely $(\epsilon_{m+1}, \epsilon_{m+2}) - (\epsilon_m, \epsilon_{m-1})$, can be expressed as differences between molecular orbital energies, and the results so obtained show quite good correlation with experiment, particularly $\epsilon_{m+1} - \epsilon_m$ with the frequency of the p band (Coulson 1948, Platt 1950); but in other respects the simple treatment is inadequate. First, it requires all four transitions to be strongly allowed, whereas the α -band is invariably weak. Secondly, the vibrational structures of the bands are unexplained; and thirdly, Clar's rule (equation (1)) receives no theoretical interpretation.

These difficulties appear in an acute form in benzene, where the simple treatment, based on real molecular orbitals, predicts four degenerate allowed transitions; in actual fact the spectrum is of the normal type, except that the β and β' bands coincide. In this case, however, the reasons for the failure of the simple theory are known. The theory fails because it does not allow adequately for the mutual repulsion of the electrons. This repulsion splits the fourfold degenerate excited level into a twofold degenerate level, transitions to which are allowed, and two non-degenerate levels, transitions to which are forbidden if the ring has D_{6h} symmetry. The α and p bands nevertheless appear (since vibrations can destroy the symmetry), but with much lower intensity than the β , β' band. (A similar situation must occur in all symmetrical cyclic polyenes with $4n+2$ π -electrons, but the higher members of the series are unknown.)

This resolution of the difficulties for benzene and the cyclic polyenes has led Platt (1949), and more recently Moffitt (1954), to an interpretation of the spectra of the 'cata-condensed' hydrocarbons, that is, aromatic hydrocarbons derived from cyclic polyenes by the formation of additional transannular bonds (see figure 1). Platt suggested that the general pattern of the bands may be rather

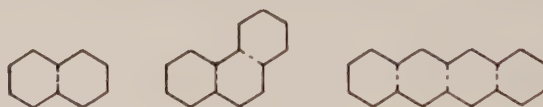


Figure 1.

little affected by the introduction of the cross-links, apart from the removal of the β , β' degeneracy, and that the low intensity of the band arises from the same factors that operate in benzene itself. Extending Platt's ideas, Moffitt (1954) has given a more quantitative account of the spectra of cata-condensed hydrocarbons by the l.c.a.o. method but still retaining the so-called 'perimeter approximation'.

However, the characteristic spectral pattern of aromatic hydrocarbons is not limited to the cata-condensed systems, and we have been considering the problem from a related but different standpoint which seems to throw light on the electronic transitions of alternant hydrocarbons in general (Coulson and Longuet-Higgins 1947). Our treatment concurs exactly with the accepted theory of the benzene spectrum (Goepfert-Mayer and Sklar 1938), but it seems to be more generally applicable than the perimeter approximation. It has the additional advantage of showing rather more clearly the extent to which the simple m.o. treatment of such systems is valid.

§2. ALTERNANT HYDROCARBON MOLECULES

As has already been remarked, in order to understand the details of electronic spectra it may be necessary to take into account electronic repulsion (Longuet-Higgins 1948). This repulsion has the effect of mixing together different electronic configurations of the same symmetry, so that it is not strictly correct to describe an electronic state as one in which there are so many electrons in ψ_1 , so many in ψ_2 , and so on. The importance of configurational interaction, however, would seem to depend very considerably upon individual circumstances, and Moffitt has distinguished two types of interaction that can occur.

First there is interaction between configurations of equal energy and the same symmetry. Electron repulsion mixes such configurations extensively and splits the degeneracy between them. This type of interaction Moffitt calls first-order. On the other hand we have second-order interactions between configurations of relatively unequal energy; this will produce much smaller effects and may be neglected in a first-order treatment. In the cyclic polyenes the first excited configuration is fourfold degenerate, so we have first-order configurational interaction, which is why the molecular orbital theory fails so badly unless electron repulsion is taken into account. However, as we shall see immediately, a similar situation arises not only in the cyclic polyenes but in any alternant hydrocarbon.

In the simple l.c.a.o. treatment (neglecting overlap) the molecular orbitals of an alternant hydrocarbon appear in pairs, with energies $\alpha \pm \epsilon_r$ where α is the coulomb integral for a carbon 2p orbital (Coulson and Rushbrooke 1940). The orbitals ψ_{m-1} , ψ_m , ψ_{m+1} , ψ_{m+2} will then have energies

$$\psi_{m+2}: \alpha + \epsilon_2$$

$$\psi_{m+1}: \alpha + \epsilon_1$$

$$\psi_m: \alpha - \epsilon_1$$

$$\psi_{m-1}: \alpha - \epsilon_2.$$

The energies of the first four excited configurations relative to the ground state will therefore be

$$\begin{aligned} (\psi_m^{-1}\psi_{m+1}) &: 2\epsilon_1 \\ (\psi_m^{-1}\psi_{m+2}), (\psi_{m-1}^{-1}\psi_{m+1}) &: \epsilon_1 + \epsilon_2 \\ (\psi_{m-1}^{-1}\psi_{m+2}) &: 2\epsilon_2. \end{aligned}$$

These relations are, diagrammatically,

$$\begin{array}{rcl} \chi_4 = (\psi_{m-1}^{-1}\psi_{m+2}) & \text{-----} & 2\epsilon_2 \\ \chi_3 = (\psi_{m-1}^{-1}\psi_{m+1}) & \left. \vphantom{\begin{array}{c} \chi_4 \\ \chi_3 \end{array}} \right\} & \\ \chi_2 = (\psi_m^{-1}\psi_{m+2}) & \text{=====} & \epsilon_1 + \epsilon_2 \\ \chi_1 = (\psi_m^{-1}\psi_{m+1}) & \text{-----} & 2\epsilon_1 \\ \chi_0 = \text{ground state} & \text{-----} & 0. \end{array}$$

The second configuration will therefore be doubly degenerate, and we shall expect first-order configurational interaction between χ_2 and χ_3 , but not, as a rule, between χ_1 and χ_4 . We may draw the preliminary conclusion that χ_1 and χ_4 represent reasonably well the wave functions of two excited singlet states Ψ_1 and Ψ_4 ; but that there will also be two other singlet states Ψ_2 and Ψ_3 whose wave functions must be mixtures of χ_2 and χ_3 , of the form

$$\Psi_2 = \chi_2 \cos \theta + \chi_3 \sin \theta$$

$$\Psi_3 = -\chi_2 \sin \theta + \chi_3 \cos \theta.$$

If, as we are supposing, the energies of χ_2 and χ_3 are identical, then we shall have

$$\Psi_2 = \sqrt{\frac{1}{2}}(\chi_2 + \chi_3)$$

$$\Psi_3 = \sqrt{\frac{1}{2}}(\chi_2 - \chi_3)$$

and if, as we shall show later, the transition moments $\int \chi_0 M \chi_2 d\tau$ and $\int \chi_0 M \chi_3 d\tau$ are equal in magnitude and direction, then the transition $\Psi_0 \rightarrow \Psi_3$ will be very weak, and $\Psi_0 \rightarrow \Psi_2$ very strong. Finally, if the electron repulsion integral

$$\sum_{i < j} \int \chi_2 \frac{e^2}{r_{ij}} \chi_3 d\tau$$

is denoted by γ , then the energies of these transitions will be split according to the equation

$$E(\Psi_3) - E(\Psi_0) = \epsilon_1 + \epsilon_2 - \gamma$$

$$E(\Psi_2) - E(\Psi_0) = \epsilon_1 + \epsilon_2 + \gamma$$

so that we shall have two associated transitions, one weak and one strong, separated by a gap of 2γ .

This situation is just that which is found in practice. The remarkable frequency relationship (1) discovered by Clar suggests that the α and β bands are in fact due to the associated transitions $\Psi_0 \rightarrow \Psi_3$ and $\Psi_0 \rightarrow \Psi_2$, the intensity of the latter being derived at the expense of the former. The p band is interpreted as due to the transition $\Psi_0 \rightarrow \Psi_1$, as its energy is found to be well correlated with calculated values of $2\epsilon_1$; and this leaves the β' band to be associated with the transition $\Psi_0 \rightarrow \Psi_4$. It remains, therefore, to show that

$$\int \chi_0 M \chi_2 d\tau = \int \chi_0 M \chi_3 d\tau$$

and to show that $\gamma > 0$, as it must be if the α band is to appear at longer wavelengths than the β band.

The peculiar property of an alternant hydrocarbon is that its atoms can be divided into two sets, 'starred' and 'unstarred', such that no two atoms in the same set are directly linked. A pair of molecular orbitals with energies $\alpha \pm \epsilon$ may then be written in the l.c.a.o. forms

$$\psi = \Sigma^* c_r \phi_r + \Sigma^0 c_s \phi_s$$

$$\psi' = \Sigma^* c_r \phi_r - \Sigma^0 c_s \phi_s$$

where the first sum is taken over the atomic orbitals ϕ_r of the starred atoms, and the second sum over the atomic orbitals ϕ_s of the unstarred atoms (Longuet-Higgins 1950). In short, the atomic orbital coefficients in such a pair of molecular orbitals are equal at the starred atoms and opposite at the unstarred atoms.

But ψ_m, ψ_{m+1} form such a pair, and so do ψ_{m-1}, ψ_{m+2} . It follows that
if $\psi_m = \Sigma^* a_r \phi_r + \Sigma^0 a_s \phi_s$ and $\psi_{m-1} = \Sigma^* b_r \phi_r + \Sigma^0 b_s \phi_s$
then $\psi_{m+1} = \Sigma^* a_r \phi_r - \Sigma^0 a_s \phi_s$ and $\psi_{m+2} = \Sigma^* b_r \phi_r - \Sigma^0 b_s \phi_s$.

Now $\chi_0 \rightarrow \chi_2$ and $\chi_0 \rightarrow \chi_3$, being one-electron transitions, have moments given by

$$\int \chi_0 M \chi_2 d\tau = e \int \psi_m \mathbf{r} \psi_{m+2} d\tau$$

$$\int \chi_0 M \chi_3 d\tau = e \int \psi_{m-1} \mathbf{r} \psi_{m+1} d\tau$$

where \mathbf{r} is the position vector of a point in the space of integration. Writing $\psi_{m-1}, \psi_m, \psi_{m+1}, \psi_{m+2}$ in the above forms, and neglecting overlap between atomic orbitals, we find that both these expressions reduce to the same expression, namely

$$\Sigma^* a_r b_r e \int \phi_r \mathbf{r} \phi_r d\tau - \Sigma^0 a_s b_s e \int \phi_s \mathbf{r} \phi_s d\tau$$

and this shows that the two transition moments are equal in magnitude and direction:

To calculate γ , defined as

$$\gamma = \sum_{i < j} \int \chi_2 \frac{e^2}{r_{ij}} \chi_3 d\tau,$$

it is necessary to write down explicit expressions for χ_2 and χ_3 . These are

$$\chi_2 = \sqrt{\frac{1}{2}} \{ |\psi_{m-1} \bar{\psi}_{m-1} \psi_m \bar{\psi}_{m+2}| - |\psi_{m-1} \bar{\psi}_{m-1} \bar{\psi}_m \psi_{m+2}| \}$$

$$\chi_3 = \sqrt{\frac{1}{2}} \{ |\psi_m \bar{\psi}_m \psi_{m-1} \bar{\psi}_{m+1}| - |\psi_m \bar{\psi}_m \bar{\psi}_{m-1} \psi_{m+1}| \}$$

where the expressions $|\dots|$ are ordinary Slater determinants, and the electrons in the lower orbitals are omitted from consideration. The orthogonality of the molecular orbitals enables us to reduce γ to the simpler form

$$\begin{aligned} \gamma = & 2 \iint \psi_{m-1}(1) \psi_{m+1}(1) \frac{e^2}{r_{12}} \psi_{m+2}(2) \psi_m(2) d\tau_1 d\tau_2 \\ & - \iint \psi_{m-1}(1) \psi_m(1) \frac{e^2}{r_{12}} \psi_{m+2}(2) \psi_{m+1}(2) d\tau_1 d\tau_2. \end{aligned}$$

If this expression is expanded, neglecting atomic orbital overlap, it becomes

$$\begin{aligned} \gamma = & \iint \rho(1) \frac{e^2}{r_{12}} \rho(2) d\tau_1 d\tau_2 + \iint \sigma(1) \frac{e^2}{r_{12}} \sigma(2) d\tau_1 d\tau_2 \\ & - 6 \iint \rho(1) \frac{e^2}{r_{12}} \sigma(2) d\tau_1 d\tau_2 \end{aligned}$$

where $\rho(1) = \Sigma^* a_r b_r \phi_r^2(1)$ and $\sigma(1) = \Sigma^0 a_s b_s \phi_s^2(1)$.

In this expression the first two integrals represent the coulombic self-energies of charge distributions; ρ and σ are therefore large and positive, the largest contribution coming from terms of the type

$$a_r^2 b_r^2 \iint \phi_r^2(1) \frac{e^2}{r_{12}} \phi_r^2(2) d\tau_1 d\tau_2.$$

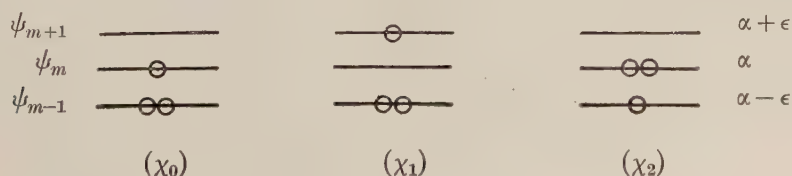
In the third integral, however, there are no terms of this type, since ρ and σ refer to different sets of atoms. The terms in this integral will therefore be of varying sign and individually smaller; so we may conclude beyond any reasonable doubt that γ will be a positive quantity. This shows that Ψ_3^* will be lower in energy than Ψ_2^* , and hence that the weaker of the two transitions will occur at longer wavelengths than the stronger. Unfortunately it does not seem possible to explain why in general

$$\frac{E(\Psi_2^*) - E(\Psi_0^*)}{E(\Psi_3^*) - E(\Psi_0^*)} \simeq 1.3;$$

but the present argument does show why $\lambda_\alpha/\lambda_\beta > 1$, which is the essential point.

§ 3. ALTERNANT HYDROCARBON RADICALS

The situation in alternant hydrocarbon radicals such as benzyl or triphenyl methyl is analogous in many respects to that in the normal hydrocarbon molecules. The three lowest electronic configurations are:



χ_0 represents the ground state configuration; χ_1 and χ_2 are the degenerate configurations $(\psi_m^{-1}\psi_{m+1})$ and $(\psi_{m-1}^{-1}\psi_m)$. The corresponding wave functions are

$$\begin{aligned}\chi_0 &= |\psi_{m-1}\bar{\psi}_{m-1}\psi_m| \\ \chi_1 &= |\psi_{m-1}\bar{\psi}_{m-1}\psi_{m+1}| \\ \chi_2 &= |\psi_{m-1}\psi_m\bar{\psi}_m|.\end{aligned}$$

Now ψ_m , being a non-bonding molecular orbital, may be written in the form $\psi_m = \sum^* a_r \phi_r$, the summation being confined to the starred atoms only; and ψ_{m+1} , ψ_{m-1} , being conjugate orbitals, have the related forms

$$\psi_{m\pm 1} = \sum^* b_r \phi_r \pm \sum^0 b_s \phi_s.$$

Hence $\int \chi_0 M \chi_1 d\tau = e \int \psi_m \mathbf{r} \psi_{m+1} d\tau = \sum^* a_r b_r e \int \phi_r \mathbf{r} \phi_r d\tau$

and $\int \chi_0 M \chi_2 d\tau = -e \int \psi_{m-1} \mathbf{r} \psi_m d\tau = -\sum^* a_r b_r e \int \phi_r \mathbf{r} \phi_r d\tau.$

The transition moments from χ_0 to χ_1 and χ_2 are therefore equal and opposite. But χ_1 and χ_2 , being degenerate, will be split by electron repulsion into their sum and difference; and the magnitude of this splitting is determined by the repulsion integral

$$\begin{aligned}\gamma &= \sum_{i < j} \int \chi_1 \frac{e^2}{r_{ij}} \chi_2 d\tau = - \iint \psi_{m-1}(1) \psi_m(1) \frac{e^2}{r_{12}} \psi_{m+1}(2) \psi_m(2) d\tau_1 d\tau_2 \\ &= - \iint \rho(1) \frac{e^2}{r_{12}} \rho(2) d\tau_1 d\tau_2 \quad \text{where} \quad \rho = \sum^* a_r b_r \phi_r^2.\end{aligned}$$

γ is therefore a negative quantity; and of the two wave functions $\Psi_1 = (\chi_1 + \chi_2)/\sqrt{2}$ and $\Psi_2 = (\chi_1 - \chi_2)/\sqrt{2}$ the former will have the lower energy. We therefore anticipate that the longest wavelength band in the electronic spectrum will be the weak transition $\Psi_0 \rightarrow \Psi_1$, and that at rather shorter wavelengths there will be a much more intense band arising from the associated transition $\Psi_0 \rightarrow \Psi_2$.

§ 4. THE POLYACENES

We shall now, by way of illustration, apply these ideas to benzene, naphthalene and anthracene. The pioneer theoretical work on the polyacenes was done by Coulson, who used the l.c.a.o. method, including overlap but neglecting configurational interaction. Here we are neglecting overlap and taking into account the consequent first-order configurational interaction; so, as will appear, our interpretations differ from his in certain respects, though we agree with him in the assignment of the p-bands.

One possible choice of real molecular orbitals for benzene is illustrated in figure 2; the dotted lines indicate nodal planes perpendicular to the plane of the molecules. ψ_2 and ψ_3 are degenerate, and so are ψ_4 and ψ_5 .

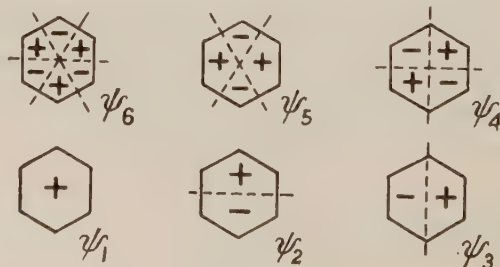


Figure 2.

The configurations $(\psi_2^{-1}\psi_5)$ and $(\psi_3^{-1}\psi_4)$ therefore combine together, as well as $(\psi_2^{-1}\psi_4)$ and $(\psi_3^{-1}\psi_5)$. The resulting wave functions, and their symmetries, are given in table 1. The usual interpretation of the observed spectrum, due to Goeppert-Mayer and Sklar (1938), is that the three lowest electronic transitions are to the B_{2u} , B_{1u} and E_{1u} states respectively; this interpretation is consistent with the relative intensities of the bands, and is supported by a further piece of evidence discussed in a later paragraph.

It should be noted, however, that the mean energies of the pairs $(\psi_2^{-1}\psi_5) \pm (\psi_3^{-1}\psi_4)$ and $(\psi_2^{-1}\psi_4) \pm (\psi_3^{-1}\psi_5)$ are not equal, as our simple theory predicts. Thus it cannot be strictly accurate to regard the energy of a one-electron excitation as a difference of one-electron energies.

Table 1. Electronic Spectrum of Benzene

Frequency (cm^{-1})	Oscillator strength (f)	Name (Clar)	Wave function	Assignment Symmetry
54500	0.69	β, β'	$\left\{ \begin{array}{l} (\psi_2^{-1}\psi_5) - (\psi_3^{-1}\psi_4) \\ (\psi_2^{-1}\psi_4) + (\psi_3^{-1}\psi_5) \end{array} \right\}$	E_{1u}
48000	0.10	p	$(\psi_2^{-1}\psi_5) + (\psi_3^{-1}\psi_4)$	B_{1u}
38000	0.002	α	$(\psi_2^{-1}\psi_4) - (\psi_3^{-1}\psi_5)$	B_{2u}

In naphthalene the orbitals $\psi_4, \psi_5, \psi_6, \psi_7$ are as shown in figure 3. Again the dotted lines denote nodal planes.

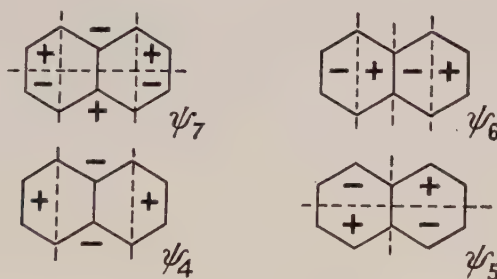


Figure 3.

On our assumptions the configurations $(\psi_4^{-1}\psi_6)$ and $(\psi_5^{-1}\psi_7)$ combine together but $(\psi_4^{-1}\psi_7)$ and $(\psi_5^{-1}\psi_6)$ do not. The resulting interpretation of the ultra-violet spectrum is indicated in table 2.

Table 2. Electronic Spectrum of Naphthalene (Klevens and Platt 1949)

Frequency (cm^{-1})	Oscillator strength (f)	Name (Clar)	Present assignment Wave function	Symmetry
60000	0.6	β'	$(\psi_4^{-1}\psi_7)$	B_{2u}
[52500	0.20]	—	—	—
45500	1.70	β	$(\psi_4^{-1}\psi_6) + (\psi_5^{-1}\psi_7)$	B_{1u}
34500	0.18	p	$(\psi_5^{-1}\psi_6)$	B_{2u}
32000	0.002	α	$(\psi_4^{-1}\psi_6) - (\psi_5^{-1}\psi_7)$	B_{1u}

The symbol B_{1u} indicates a transition moment parallel to the long axis of the molecule, and B_{2u} indicates a moment parallel to the central bond. The above

assignments of the four principal bands agree with those of Platt and Moffitt; the experimental evidence for the directions of polarization of these bands is inconclusive at present.

In addition to the α , p , β and β' bands there is a region of absorption around $52\,500\text{ cm}^{-1}$ which Platt has tentatively interpreted as a distinct band due to a symmetry-forbidden transition. The hypothesis that this band is due to a π -electron transition would be difficult to reconcile with the present theory.

When we come to anthracene the situation resembles that found in benzene, as there is an 'accidental' degeneracy in the second highest occupied m.o. and the second lowest unoccupied m.o. The forms of the orbitals ψ_5 to ψ_{10} are depicted in figure 4.

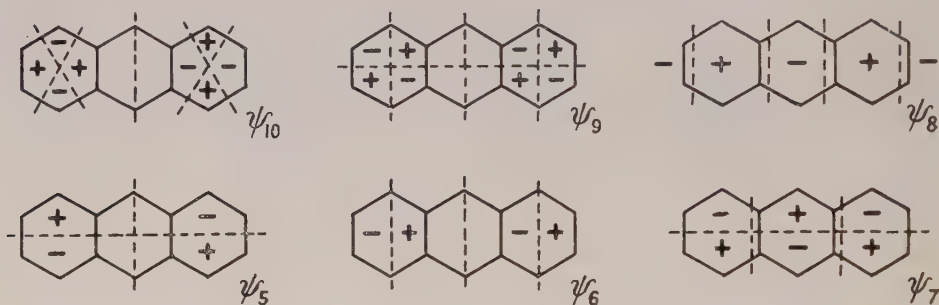


Figure 4.

The orbitals ψ_5 and ψ_6 are degenerate, with energy equal to that of ψ_2 and ψ_3 in benzene, which they closely resemble; and there is a corresponding resemblance between the degenerate pair ψ_9 , ψ_{10} and the benzene orbitals ψ_4 , ψ_5 .

The allowed single-electron transitions from ψ_5 , ψ_6 , ψ_7 , to ψ_8 , ψ_9 , ψ_{10} are:

$$\begin{array}{ll} (\psi_7^{-1}\psi_8), (\psi_6^{-1}\psi_9), (\psi_5^{-1}\psi_{10}) & \text{(transverse)} \\ \text{and} & \\ (\psi_7^{-1}\psi_9), (\psi_6^{-1}\psi_8) & \text{(longitudinal).} \end{array}$$

Owing to the degeneracy, electron repulsion will lead to strong interaction between $(\psi_6^{-1}\psi_9)$ and $(\psi_5^{-1}\psi_{10})$, and between $(\psi_6^{-1}\psi_8)$ and $(\psi_7^{-1}\psi_9)$. The resulting excited singlet states are given in table 3.

Table 3. Electronic Spectrum of Anthracene (Platt 1949)

Frequency (cm^{-1})	Oscillator strength (f)	Name	Present assignment Wave function	Symmetry
54000	0.65	β'	$(\psi_5^{-1}\psi_{10}) - (\psi_6^{-1}\psi_9)$	B_{2u}
45500	0.28	α'	$(\psi_5^{-1}\psi_{10}) + (\psi_6^{-1}\psi_9)$	B_{2u}
39000	2.3	β	$(\psi_6^{-1}\psi_8) + (\psi_7^{-1}\psi_9)$	B_{1u}
[28000]	0.002]	α	$(\psi_6^{-1}\psi_8) - (\psi_7^{-1}\psi_9)$	B_{1u}
26000	0.10	p	$(\psi_7^{-1}\psi_8)$	B_{2u}

The assignment of the p , α and β bands requires no comment, except that the data for the α band are based on inference, as it is obscured by the much stronger p band in the same region. On the other hand, the upper state of the β' band at $54\,000$ will not be $(\psi_6^{-1}\psi_9)$, but will involve also the configuration $(\psi_5^{-1}\psi_{10})$. Detailed analysis, along the same lines as for benzene, shows that, of the combinations $(\psi_5^{-1}\psi_{10}) \pm (\psi_6^{-1}\psi_9)$, that with the negative sign has the higher energy and greater intensity. This leads to the assignments given in table 3.

Our interpretation of the β' band agrees with Platt's in polarization; however, we regard the α' band as a weak transverse transition, whereas Platt suggested that it was electronically forbidden. Our assignments are supported by the following additional argument. The configurations $(\psi_6^{-1}\psi_9)$ and $(\psi_5^{-1}\psi_{10})$ are closely analogous to the benzene configurations $(\psi_3^{-1}\psi_4)$ and $(\psi_2^{-1}\psi_5)$, as can be seen by comparing the forms and energies of the orbitals involved. These configurations would therefore be expected to combine in the same manner in both molecules, giving bands of nearly the same frequencies and intensities. Comparison of tables 1 and 3 shows that the p and β bands in benzene are imitated in anthracene by the α' and β' bands, the intensity of the anthracene α' band being rather greater than that of the benzene p band, as might be expected from the higher symmetry of the latter molecule. It may be noted that this analogy would disappear if the assignments of the α and p bands in benzene were reversed, and this fact lends further support to the Goeppert-Mayer-Sklar assignment.

§ 5. DISCUSSION

The present interpretation of aromatic hydrocarbon spectra depends on two rather drastic assumptions, namely (i) that the l.c.a.o. approximation, neglecting overlap, is adequate for calculating the energies of excited configurations and their transition moments from the ground state, and (ii) that electron repulsion mixes together only configurations which are degenerate according to assumption (i). For these reasons our interpretations of the polyacene spectra differ somewhat from those given by Coulson (1948). More recent quantitative work by various authors (cf. Jacobs 1949) has taken configurational interaction into account, but the precise conclusions reached seem to depend sensitively on certain electron repulsion integrals about whose evaluation there is some dispute. It is difficult to know how much reliance to place on such calculations, and we therefore prefer a more heuristic approach by which we can obtain at least a qualitative insight into the regularities observed by the experimentalists. Of these regularities we attach particular significance to the extreme weakness of the α bands and the success of the simple l.c.a.o. theory in correlating the frequencies of the p bands in a series of hydrocarbons (Dewar 1952). These two phenomena receive a quite simple explanation on the present scheme. Again, the observed association between the α and β bands is immediately understandable if their upper states arise from the splitting of two 'conjugate' configurations; and lastly, the analogy between the p , β bands of benzene and the α' , β' bands of anthracene is simply accounted for on the present theory.

In conclusion it seems worth while to mention one interesting feature of the wave functions which we have used for the upper electronic states of aromatic hydrocarbons. This is that they all give rise to a uniform distribution of the π -electrons over the unsaturated framework. It is quite easy to see that this is true of the states $(\psi_m^{-1}\psi_{m+1})$ and $(\psi_{m-1}^{-1}\psi_{m+2})$ since these are obtained by transferring an electron from a bonding m.o. to the corresponding antibonding m.o., with numerically equal a.o. coefficients. It is slightly different with the configurations $(\psi_m^{-1}\psi_{m+2})$ and $(\psi_{m-1}^{-1}\psi_{m+1})$; in the former the electron density at atom r exceeds that in the ground state by $b_r^2 - a_r^2$, and in the latter by $a_r^2 - b_r^2$. But if the configurations are assigned equal weight (either 1:1 or 1:-1) in the wave function, then these quantities exactly cancel, and the electron density at every atom is the same as in the ground state, where it is known to be uniform. This uniformity of electron distribution suggests that the best molecular orbitals to use

in forming our excited state wave functions may be quite good approximate solutions of the equations of the self-consistent field (Roothaan 1951), and this circumstance leads us to place more reliance on these wave functions than would be justified by the rather drastic assumptions from which they were originally obtained.

ACKNOWLEDGMENTS

We are greatly indebted to Dr. W. Moffitt for letting us see his forthcoming paper in manuscript; his distinction between first- and second-order configurational interaction formed the starting-point of the work in this paper.

REFERENCES

- CLAR, E., 1941, *Aromatische Kohlenwasserstoffe*, 1st Edn (Berlin : Springer).
COULSON, C. A., 1948, *Proc. Phys. Soc.*, **60**, 257.
COULSON, C. A., and LONGUET-HIGGINS, H. C., 1947, *Proc. Roy. Soc. A*, **192**, 16.
COULSON, S. A., and RUSHBROOKE, G. S., 1940, *Proc. Camb. Phil. Soc.*, **36**, 193.
DEWAR, M. J. S., 1952, *J. Chem. Soc.*, p. 3532.
GOEPPERT-MAYER, M., and SKLAR, A. L., 1938, *J. Chem. Phys.*, **6**, 645.
JACOBS, J., 1949, *Proc. Phys. Soc.*, **62**, 710.
KLEVEN, H. B., and PLATT, J. R., 1949, *J. Chem. Phys.*, **17**, 470.
LONGUET-HIGGINS, H. C., 1948, *Proc. Phys. Soc.*, **60**, 270; 1950, *J. Chem. Phys.*, **18**, 265.
MOFFITT, W., 1954, *J. Chem. Phys.*, **22**, in the press.
PLATT, J. R., 1949, *J. Chem. Phys.*, **17**, 484; 1950, *Ibid.*, **18**, 1168.
ROOTHAAN, C. C. J., 1951, *Rev. Mod. Phys.*, **23**, 61.

Inelastic Heavy Particle Collisions Involving the Crossing of Potential Energy Curves

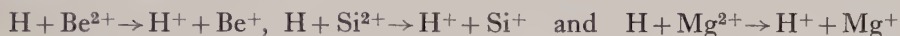
I: Charge transfer from H atoms to Be^{2+} , Si^{2+} and Mg^{2+} ions

BY D. R. BATES AND B. L. MOISEWITSCH

Department of Applied Mathematics, The Queen's University of Belfast

MS. received 15th March 1954; read at the Meeting of the Physical Society at Dublin, March 1954

Abstract. The charge transfer processes

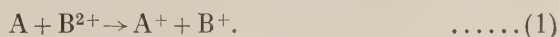


are investigated using the Landau-Zener formula for the transition probability arising from the pseudo-crossing of the potential energy curves of the initial and final systems. These pseudo-crossings occur at internuclear distances of 5.8_1 , 9.6_4 and 18.9_2 atomic units respectively (allowance being made for the effect of polarizability). It is found that the corresponding values of the energy separation due to the interaction between the initial and final states are $8.6_0 \times 10^{-1}$, $1.0_2 \times 10^{-1}$ and $2.3_4 \times 10^{-5}$ ev. The cross sections associated with the three processes are calculated over a wide range of impact energies.

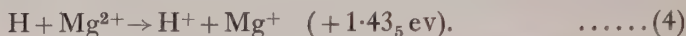
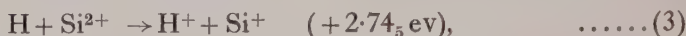
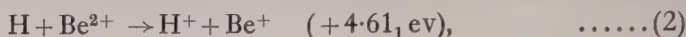
§ 1. INTRODUCTION

As has long been known, the pseudo-crossing of potential energy curves provides a means by which a transition can occur in a slow encounter between two heavy systems. In 1932 Landau and Zener independently developed simple treatments giving a formula for the cross section associated with such an inelastic collision. Slightly later in the same year Stueckelberg obtained essentially the same formula by a more rigorous method and further extended the theory. A recent survey (Bates and Massey 1954) of the general position has shown that there is a great need for detailed calculations as little quantitative information is available on the cross sections of the several types of collisions to which the Landau-Zener formula is applicable, earlier investigations (Magee 1940, 1952, Bates and Massey 1943) being mainly of an exploratory qualitative character. It is the purpose of the present series of papers to satisfy this need at least partially by carrying out calculations on as many examples as possible of each type of collision. Naturally, preference will be given, where practicable, to processes which either are of direct interest in some connection or are suitable for study in the laboratory; but, as is usual in the applications of quantum mechanics, the computational labour involved sets a limit to what can be achieved, and to provide representative data on a sufficient number of processes of the various types it is necessary to treat some which in themselves are unlikely to be of importance.

The first paper of the series is concerned with charge transfer from neutral atoms to doubly charged ions



Owing to the coulomb repulsion between the resulting singly charged ions there is usually a pseudo-crossing of potential energy curves for processes of this type which are *exothermic*; and moreover the internuclear separation at which this occurs can readily be determined unless the degree of exothermicity is so great that the crossing point lies in the region where the potential energy curves are distorted from their asymptotic forms. For the sake of simplicity A was taken to be an H atom and B^{2+} to be a Be^{2+} , Si^{2+} or Mg^{2+} ion so that the processes are



With this choice an important range of values of the energy difference† ΔE is covered. The fact that the transferred electron enters a p-orbital in the case of process (3) whereas it enters an s-orbital in the cases of processes (2) and (4) is, to be sure, an undesirable feature of the set since it may complicate the pattern of the results; but it is considered that any such complication is likely to be of only a minor character.

§ 2. THEORY

If the potential energy curves $U_i^0(R)$ and $U_f^0(R)$, associated with $(A + B^{2+})$ and $(A^+ + B^+)$ respectively, intersect at an internuclear separation R_X when the interaction between the initial and final states is neglected then because of this interaction there is a certain probability that particles which approach along the first curve recede along the second after the encounter. This probability may conveniently be designated \mathcal{P}_l , the subscript indicating the quantum number describing the angular momentum of the colliding particles about their centre of mass. If the influence of potential energy curves other than the two directly concerned is negligible the Landau-Zener formula gives that

$$\mathcal{P}_l = 2P_l(1 - P_l), \quad \dots\dots(5)$$

where

$$P_l = \exp(-w) \quad \dots\dots(6)$$

and

$$w = \pi^2 \{ \Delta U(R_X) \}^2 / \hbar v_l(R_X) \left| \frac{d}{dR} (U_i^0 - U_f^0) \right|_{R=R_X}, \quad \dots\dots(7)$$

$\Delta U(R_X)$ being the difference between the true potential energy curves $U_i(R_X)$ and $U_f(R_X)$, and $v_l(R_X)$ being the radial component of the velocity of relative motion both measured at the crossing point. It should be noted that the Landau-Zener formula is based on the assumption that it is only in the immediate neighbourhood of the crossing point that there is an appreciable chance of a transition from one potential energy curve to the other. This assumption is unjustified in cases where $\Delta U(R_X)$ is a considerable fraction of ΔE .

The cross section may be expressed as

$$Q = p \frac{\pi}{k_i^2} \sum_l (2l+1) \mathcal{P}_l, \quad \dots\dots(8)$$

with

$$k_i^2 = 8\pi^2 M E_i / \hbar^2, \quad \dots\dots(9)$$

† The energy differences cited were obtained from the data in the compilation of Charlotte Moore (1949). All the systems are unexcited. Capture into the $2p\ ^2P$ term of Be^+ is also exothermic but it is only so by 0.65_3 ev, and consequently the crossing occurs at such a large internuclear separation ($\sim 42a_0$) that the process does not proceed at an appreciable rate.

p being the probability that the particles approach along the specified potential energy curve†, E_i being the initial kinetic energy of relative motion and M being the reduced mass (cf. Mott and Massey 1949). Replacement of the summation by an integral and use of (5), (6) and (7) yields

$$Q = 4\pi R_X^2 p(1 + \lambda) \int_1^\infty \exp(-\eta x) \{1 - \exp(-\eta x)\} x^{-3} dx, \quad \dots (10)$$

$$\text{where} \quad \lambda = \{U_i(\infty) - U_i(R_X)\}/E_i, \quad \dots (11)$$

$$\text{and} \quad \eta = 2\pi^3 M \Delta U(R_X)^2 / k_1 h^2 (1 + \lambda)^{1/2} \left| \frac{d}{dR} (U_i^0 - U_f^0) \right|_{R=R_X} \quad \dots (12)$$

The internuclear separation at the crossing can of course be determined from the potential energy curves. If it is sufficiently large for the asymptotic forms of these to be adopted the equation to be solved is simply

$$e^2 \left\{ \frac{1}{R_X} + \frac{a_1}{R_X^3} + \frac{a_2}{R_X^4} \right\} = \Delta E, \quad \dots (13)$$

where

$$\left. \begin{aligned} a_1 &= 2\alpha_1(A) - \alpha_1(A^+) - \alpha_1(B^+) \\ a_2 &= 2\alpha_2(A) - \frac{1}{2}\alpha_2(A^+) - \frac{1}{2}\alpha_2(B^+) \end{aligned} \right\} \quad \dots (14)$$

in which the α_1 's are the coefficients of the inverse cube terms of the potentials and the α_2 's are the polarizabilities, the species being as indicated. Moreover in these circumstances

$$\frac{d}{dR} (U_i^0 - U_f^0) = e^{-2}(1 + \mu)(\Delta E)^2, \quad \dots (15)$$

$$\text{with} \quad \mu = \frac{e^4}{R_X^4 (\Delta E)^2} \left(a_1 + \frac{2a_2}{R_X} \right). \quad \dots (16)$$

Substitution in (12) gives

$$\eta = 247 \cdot 2 \left[\frac{M^{1/2} \{\Delta U(R_X)\}^2}{E_i^{1/2} (\Delta E)^2} \right] (1 + \lambda)^{-1/2} (1 + \mu)^{-1} \quad \dots (17)$$

in which the energies $\Delta U(R_X)$, E_i and ΔE are measured in electron volts and the reduced mass M is on the ^{16}O -scale. It may be remarked that the dimensionless quantities λ and μ are usually much smaller than unity.

§ 3. EXPRESSION FOR THE ENERGY SEPARATION

Regarding the nuclei as stationary and representing the complete electronic wave function Ψ by a linear combination of χ_i and χ_f , the zero-order wave functions describing the systems $(A + B^{2+})$ and $(A^+ + B^+)$, it may be seen from the variational theorem (cf. Coulson 1952) that if R_X^0 is the internuclear distance at which the potential energy curves intersect in the *absence of polarization* then

$$|\Delta U(R_X^0)| = 2 |H_{if}(R_X^0) - S_{if}(R_X^0) H_{ff}(R_X^0)| / \{1 - |S_{if}(R_X^0)|^2\}, \quad \dots (18)$$

$$= 2 |H_{fi}(R_X^0) - S_{fi}(R_X^0) H_{ii}(R_X^0)| / \{1 - |S_{fi}(R_X^0)|^2\} \quad \dots (19)$$

where the H's are the matrix elements of the hamiltonian operator \mathcal{H} and

$$S_{if}(R_X^0) = S_{fi}^*(R_X^0) = \int \chi_i^* \chi_f d\tau. \quad \dots (20)$$

† For the processes considered here p is therefore unity.

From the definition of R_X^0 it is obvious that $H_{ii}(R_X^0)$ and $H_{ff}(R_X^0)$ are equal. Owing to the action of the coulomb field there is actually strong polarization so that if Ψ were represented, as it should be, by a linear combination of not merely χ_i and χ_f but also χ_i' and χ_f' , the wave functions of the excited states, the coefficients of these latter would be quite large. These excited states must be taken into account in the calculation of the potential energy curves and of the internuclear distance R_X at which the crossing in fact occurs. This is done effectively in equations (13) and (15) above. Their *direct* influence on the vital energy separation is slight provided the polarization energies

$$p_i(R_X) = -2\alpha_2(A)e^2/R_X^4, \quad p_f(R_X) = -\{\alpha_2(A^+) + \alpha_2(B^+)\}e^2/2R_X^4, \quad \dots (21)$$

are much less than the excitation energies; for if this condition is satisfied application of the variational theorem gives in place of (18) and (19) the approximate formulae

$$|\Delta U(R_X)| = 2|H_{if}(R_X) - S_{if}(R_X)\{H_{ff}(R_X) + p_f(R_X)\}|/\{1 - |S_{if}(R_X)|^2\} \quad \dots (22)$$

$$= 2|H_{fi}(R_X) - S_{fi}(R_X)\{H_{ii}(R_X) + p_i(R_X)\}|/\{1 - |S_{fi}(R_X)|^2\}. \quad \dots (23)$$

Since the integrals involved are very sensitive to the internuclear distance the replacement of R_X^0 by R_X is important. Though the additional terms $p_i(R_X)$ and $p_f(R_X)$ are small their inclusion is significant in that it preserves detailed balancing.

Processes (2), (3) and (4) can be regarded as involving simply the transfer of a single electron from an orbital around one *passive* closed core to an orbital around another. Denoting the initial and final wave functions of this *active* electron by $\phi(\mathbf{r}_a|n_a)$ and $\phi(\mathbf{r}_b|n_b)$, where \mathbf{r}_a and \mathbf{r}_b are the position vectors with respect to the two nuclei, it may be easily seen that formula (22) reduces to

$$|\Delta U(R_X)| = 2|s(\rho - p_f) - \sigma|/(1 - s^2)_{R=R_X}, \quad \dots (24)$$

with

$$\left. \begin{aligned} s &= \int \phi(\mathbf{r}_a|n_a)\phi(\mathbf{r}_b|n_b) d\tau, & \rho &= \int \phi(\mathbf{r}_b|n_b)^2 r_a^{-1} d\tau, \\ \sigma &= \int \phi(\mathbf{r}_a|n_a)\phi(\mathbf{r}_b|n_b) r_a^{-1} d\tau, \end{aligned} \right\} \quad \dots (25)$$

the wave functions being taken to be real and all quantities being in atomic units (e^2/a_0 for energy). The corresponding result obtained from (23) is different in form but is of course completely equivalent.

It is apparent physically that the one-electron approximation used in deriving formula (24) is valid if the binding energies of the inner electrons are much greater than the binding energy of the outer electron and if the crossing point lies far outside the core. The approximation may also be justified mathematically. Consider, for example, process (2) in which three electrons are concerned. The change in the wave function representing either of the passive electrons is very slight indeed (cf. Moiseiwitsch 1954) and may be neglected without appreciable error. Let this wave function be $\phi(\mathbf{r}_b|1s, \text{Be})$, and let the initial and final wave functions of the active electron be $\phi(\mathbf{r}_a|1s, \text{H})$ and $\phi(\mathbf{r}_b|2s, \text{Be})$ respectively. Forming the suitably symmetrized combinations representing the three electrons, substituting in formula (22) and writing

$$t = \int \phi(\mathbf{r}_a|1s, \text{H})\phi(\mathbf{r}_b|1s, \text{Be}) d\tau, \quad \dots (26)$$

it may be seen that the previous result is unaltered except that the factor $1/(1-s^2)$ is replaced by

$$(1-t^2)^{1/2}/(1-s^2-t^2) \quad \dots\dots(27)$$

and the quantity σ is replaced by

$$\sigma - t \int \phi(\mathbf{r}_b|1s, \text{Be})\phi(\mathbf{r}_b|2s, \text{Be})r_a^{-1} d\tau. \quad \dots\dots(28)$$

Both corrections are clearly insignificant in the circumstances mentioned above, the first because the compactness of $\phi(\mathbf{r}_b|1s, \text{Be})$ causes t to be very small, the second because in addition this wave function and $\phi(\mathbf{r}_b|2s, \text{Be})$ are orthogonal so that the integral occurring in (28) almost vanishes.

§ 4. DETAILED CALCULATIONS AND RESULTS

4.1. Using the wave function given by Biermann and Lübeck (1946) the coefficient of the inverse cube term in the expansion of the Si^+ -potential is calculated to be 2.8_5 atomic units. None of the other potentials contain such a term.

Wentzel (1926) and Waller (1926) have shown that the polarizability of an H atom is 4.5 atomic units. The polarizabilities of the complex systems involved can be derived from the associated transition matrix elements using the standard quantal relationship (cf. Mott and Sneddon 1948). Some of the required matrix elements have been computed by Biermann (1946); the remainder were read from the tables of Bates and Damgaard (1949). It is found that the polarizabilities of Be^+ , Si^+ and Mg^+ ions are (in atomic units) approximately 24, 12 and 34 respectively.

Substitution in equations (13) and (14) yields the values of R_X displayed in table 1.

Since the main contribution to the integrals appearing in the formula for $\Delta U(R_X)$ comes from rather large radial distances special care must be exercised with the wave functions. In the case of hydrogen there is happily no uncertainty. Several authors have obtained an approximation to $\phi(\mathbf{r}_b|2s, \text{Be})$ by representing it as

$$N(1-cr_b)\exp(-\gamma r_b), \quad \dots\dots(29)$$

in which N is a normalization factor, c is chosen so that the orthogonality requirement is met, and γ is a varied parameter. The calculations give the ionization energy to be 17.90 eV in quite good agreement with the observed 18.21 eV (cf. Moiseiwitsch 1954). As the radial distances which are of importance in this particular instance are not unduly extreme the wave function was judged to be acceptable and adopted. The position regarding $\phi(\mathbf{r}_b|3p, \text{Si}^+)$ and $\phi(\mathbf{r}_b|3s, \text{Mg}^+)$ is quite satisfactory for accurate computations on them have been carried out by Biermann and Lübeck (1946) who used a core potential containing a polarizability parameter which was adjusted so as to give the correct ionization energies. In the original paper the wave functions are presented in numerical form. It was found convenient to fit them in the customary manner by a series of exponentials multiplied by powers. Neglecting the angular part and the external factor they tend asymptotically to

$$r_b^{n^*-1}\exp[-(2\epsilon)^{1/2}r_b], \quad \dots\dots(30)$$

in which n^* is the *effective* principle quantum number, ϵ is the ionization energy and all quantities are in atomic units. To ensure as much accuracy as possible at large radial distances a term of this form was included in the fitting series.†

† Actually the precise form given was not used. For the $(3p, \text{Si}^+)$ and $(3s, \text{Mg}^+)$ orbitals n^* is 1.82_4 and 1.90_2 respectively: but little error is caused by taking them to be exactly 2 in each instance and this was done since the calculations are thereby greatly eased.

With the ϕ 's as described the integrations in formula (25) for s , ρ and σ may be performed analytically. The resulting expressions are somewhat cumbersome and need not be displayed since they are simply combinations of the J -functions of Coulson (1942) and may thus be recovered without difficulty.

Table 1 shows the separation energies, $\Delta U(R_X)$, finally obtained. As would be expected they fall off extremely rapidly as R_X , the internuclear distance at the crossing point, increases. Going from one process to another naturally

Table 1. Basic Data relating to the Collision Processes studied

Process	Orbitals of active electron		ΔE	R_X	$\Delta U(R_X)$
	Initial	Final	(ev)	(a_0)	(ev)
(2)	1s(H)	2s(Be ⁺)	4.61 ₁	5.8 ₁	$8.6_0 \times 10^{-1}$
(3)	1s(H)	3p(Si ⁺)	2.74 ₅	9.6 ₄	$1.0_2 \times 10^{-1}$
(4)	1s(H)	3s(Mg ⁺)	1.43 ₅	18.9 ₂	$2.3_4 \times 10^{-5}$

involves changes in all the parameters. The dependence of $\Delta U(R_X)$ on R_X may, however, be isolated by considering the different processes separately. It is found that an increment δR_X (measured in atomic units) causes $\Delta U(R_X)$ to diminish by the factor

$$\exp(-a\delta R_X), \quad \dots\dots(31)$$

where a is about 0.9 for each of the three processes. However, this is not a serious matter as the values used for the R_X 's should lie very close indeed to the true values.

In table 2 the values of the various quantities occurring in formula (24) for $\Delta U(R_X)$ are given separately. It will be noted that there is little cancellation between the $s(\rho - p_f)$ and the σ terms which is fortunate as severe cancellation would render the calculations scarcely feasible; and it will be noted too that sp_f , the polarizability correction, is small or even negligible.

Table 2. Further Basic Data relating to the Collision Processes studied

Process	s	ρ (rydbergs)	p_f (rydbergs)	σ (rydbergs)
(2)	$-7.67_1 \times 10^{-2}$	$+3.44_5 \times 10^{-1}$	$-2.1_1 \times 10^{-2}$	$-5.94_8 \times 10^{-2}$
(3)	$-9.44_5 \times 10^{-3}$	$+2.14_0 \times 10^{-1}$	$-1.3_8 \times 10^{-3}$	$-5.79_7 \times 10^{-3}$
(4)	$+3.91_0 \times 10^{-6}$	$+1.05_7 \times 10^{-1}$	$-2.6_5 \times 10^{-4}$	$+1.27_1 \times 10^{-6}$

4.2. Having determined the basic parameters the evaluation of the cross sections from formula (10) is a trivial task since the required integral has been tabulated by Placzek (1946). In presenting the results it is thought most convenient to take the independent variable to be \mathcal{E} , the *impact energy of the doubly charged ion* (the neutral atom being regarded as at rest). The cross sections for processes (2)† and (3), $Q(\text{H}, \text{Be}^{2+}; \text{H}^+, \text{Be}^+)$ and $Q(\text{H}, \text{Si}^{2+}; \text{H}^+, \text{Si}^+)$ are shown as

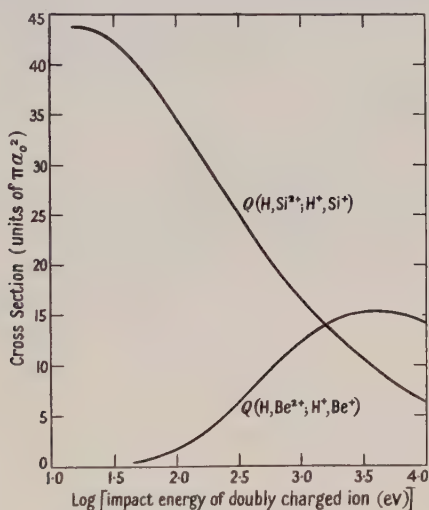
† In the case of process (2) $\Delta U(R_X)$ is perhaps rather large compared with ΔE but in the case of processes (3) and (4) no uncertainty arises from this cause.

functions of \mathcal{E} in the figure, a semi-log scale being used; that for process (4) is described by the simple formula

$$Q(\text{H}, \text{Mg}^{2+}; \text{H}^+, \text{Mg}^+) = 4.6 \times 10^{-4} \mathcal{E}^{-1/2} (\pi a_0^2)^{\dagger}, \quad \dots\dots (32)$$

in which \mathcal{E} is measured in ev. The three illustrate the remarkable range of cross section energy curves that can arise from curve-crossing.

According to the Landau-Zener formula all the cross sections eventually fall off inversely as the square root of the impact energy. It should, however, be remembered that this formula is only applicable when the velocity of relative motion is much less than the orbital velocity of the bound electrons.[‡] Momentum transfer is for example ignored. It must cause the ultimate fall off to be extremely rapid (cf. Bates and Dalgarno 1952). The treatment also required that $E(R_X)$, the relative kinetic energy at the crossing point, should be far greater than $\Delta U(R_X)$ §; but since $\Delta U(R_X)$ is usually small the restriction imposed on the \mathcal{E} -range is not of major importance in the present connection.



Cross section-energy curves for



Some mention has already been made of the possible inaccuracies in the calculations. If the estimated value of $\Delta U(R_X)$ for any process were, say, f times the true value a given cross section would occur, not at the predicted impact

† There are of course similar simple formulae for the other two cross sections but these are less useful since they are only valid at high impact energies whereas (32) is valid down to minute impact energies.

‡ The energies at which Be^{2+} , Si^{2+} and Mg^{2+} ions have the same velocity as the electron of the hydrogen atom are 2.24×10^5 , 6.95×10^5 and 6.03×10^5 ev respectively. In the figure, cross sections are given up to impact energies of 10^4 ev but this limit is rather arbitrarily chosen and may not be justified.

§ Each of the curves in the figure begins at an impact energy corresponding to a relative energy arbitrarily chosen to be about five times the separation energy. Further work is needed to determine the least acceptable factor between these last.

energy, but at an impact energy equal to f^{-4} times this† (cf. formulae (10) and (17)); however, provided $\Delta U(R_X)$ is not too large a fraction of ΔE the peak cross section should be correct since the value of R_X is not in doubt. Thus though the horizontal scale of the theoretical cross section–impact energy curves may be in error the vertical scale should in general be reliable. The reverse is usually the case with the corresponding experimental curves. Theoretical and experimental work should therefore complement each other admirably.

Table 3. Rate Coefficient for Process (3)

Temperature ($^{\circ}\text{K}$)	1000	2000	4000	8000	16000	32000
$\kappa(\text{H}, \text{Si}^{2+}; \text{H}^+, \text{Si}^+)(10^{-9} \text{ cm}^3 \text{ sec}^{-1})\ddagger$	(1.7)	(2.4)	(3.5)	4.8	6.1	7.5

† The bracketed values are unreliable as collisions in which condition (33) is not properly satisfied make an appreciable contribution.

Instead of the cross section it is often desirable to know the associated rate coefficient. This rate coefficient κ is obtained by averaging the product of the velocity of relative motion and the corresponding cross section over a Maxwellian distribution. Table 3 gives the computed values of $\kappa(\text{H}, \text{Si}^{2+}; \text{H}^+, \text{Si}^+)$ for various temperatures between 1000°K and 32000°K ; $\kappa(\text{H}, \text{Mg}^{2+}; \text{H}^+, \text{Mg}^+)$ is found to be constant and equal to $1.1 \times 10^{-14} \text{ cm}^3 \text{ sec}^{-1}$ down to very low temperatures. Since the Landau–Zener formula may only be used when

$$E(R_X) \gg \Delta U(R_X), \quad \dots\dots(33)$$

the calculation of $\kappa(\text{H}, \text{Be}^{2+}; \text{H}^+, \text{Be}^+)$ would require a refinement of the theory.

ACKNOWLEDGMENTS

We wish to thank Dr. A. Dalgarno for helpful discussions.

REFERENCES

- BATES, D. R., and DALGARNO, A., 1952, *Proc. Phys. Soc. A*, **65**, 919.
 BATES, D. R., and DAMGAARD, AGNETE, 1949, *Phil. Trans. Roy. Soc. A*, **242**, 101.
 BATES, D. R., and MASSEY, H. S. W., 1943, *Phil. Trans. Roy. Soc. A*, **239**, 269; 1954, *Phil. Mag.*, **45**, 111.
 BIERMANN, L., 1946, *Nachr. Akad. Wiss. Göttingen, Math.-Phys. Kl.*, **2**, 116.
 BIERMANN, L., and LÜBECK, K., 1946, *Z. Astrophys.*, **25**, 113.
 COULSON, C. A., 1942, *Proc. Camb. Phil. Soc.*, **38**, 210; 1952, *Valence* (Oxford: Clarendon Press).
 LANDAU, L., 1932, *Z. Phys. Sowjet*, **2**, 46.
 MAGEE, J. L., 1940, *J. Chem. Phys.*, **8**, 687; 1952, *Discussions of the Faraday Society*, **12**, 33.
 MOISEWITSCH, B. L., 1954, *Proc. Phys. Soc. A*, **67**, 25.
 MOORE, CHARLOTTE, 1949, *Atomic Energy Levels* (Washington: National Bureau of Standards).
 MOTT, N. F., and MASSEY, H. S. W., 1949, *Theory of Atomic Collisions* (2nd Edn) (Oxford: Clarendon Press).
 MOTT, N. F., and SNEDDON, I. N., 1948, *Wave Mechanics and its Applications* (Oxford: Clarendon Press).
 PLACZEK, G., 1946, *The Functions $E_n(x)$* (Chalk River: National Research Council of Canada).
 STUECKELBERG, E. C. G., 1932, *Helv. Phys. Acta*, **5**, 370.
 WALLER, I., 1926, *Z. Phys.*, **38**, 635.
 WENTZEL, G., 1926, *Z. Phys.*, **38**, 518.
 ZENER, C., 1932, *Proc. Roy. Soc. A*, **137**, 696.

† If $\Delta U(R_X)$ is very small it is better to say that the calculated cross section is f^2 times too large.

Coulomb Effects in Stripping Reactions

By J. YOCCOZ

Department of Theoretical Physics, University of Liverpool

*Communicated by R. Huby; MS. received 23rd February 1954,
and in final form 27th April 1954*

Abstract. The coulomb effect in (d, p) and (d, n) stripping reactions at low energies is investigated. It is shown that the angular distribution is flattened, the absolute cross section is decreased, and that the coulomb field contributes to the polarization of the spins of the particles. The calculations are valid for light nuclei only.

§ 1. INTRODUCTION

THE theory of the (d, p) and (d, n) reactions has been given by several authors since the original papers by Butler (1951) and Bhatia, Huang, Huby and Newns (1952). So far the coulomb field has been neglected except by Serber (1947), who takes it into consideration, but only for very high deuteron kinetic energies. Several experiments have, however, been performed with deuteron kinetic energies below the coulomb barrier, and have shown that the (d, p) and (d, n) reactions can still be accounted for partly by a stripping mechanism. It is the object of this paper to show how the coulomb field modifies the results of the previous theories, in § 2 for the angular distribution and in § 3 for the polarization of the spins of the particles. We give in § 4 some numerical results.

§ 2. ANGULAR DISTRIBUTION

We consider only the case in which one particle (proton or neutron) is captured in a state of definite orbital angular momentum l . The target nucleus is supposed to be infinitely heavy and, in this section, the particles to be spinless. The passage to the realistic case can be made in the usual way.

We use the following notation: \mathbf{r}_p , \mathbf{r}_n , $\mathbf{R} = \frac{1}{2}(\mathbf{r}_p + \mathbf{r}_n)$ and $\mathbf{r} = \mathbf{r}_p - \mathbf{r}_n$ refer to the radius vectors of the proton, the neutron, the centre of mass of the system neutron-proton, and the relative coordinates respectively; \mathbf{k}_d , \mathbf{k}_p and \mathbf{k}_n are the wave vectors of the deuteron, proton and neutron free waves; t is a parameter related to the binding energy E of the captured particle by the relation $\hbar^2 t^2 = 2ME$, M being the mass of the particle; θ is the angle between \mathbf{k}_n (or \mathbf{k}_p) and \mathbf{k}_d . Gerjuoy (1953) and Horowitz and Messiah (1953), have shown that Butler's formula for the angular distribution in the (d, n) reaction can be put into the alternative form

$$\sigma(\theta) \propto \sum_{m=-l}^{m=+l} |I_l^m(\theta)|^2$$

$$I_l^m(\theta) = \int_{r_p > R_0}^* \exp(-i\mathbf{k}_n \cdot \mathbf{r}_n) \psi_l^m(\mathbf{r}_p) V_{np}(\mathbf{r}) \psi_d(\mathbf{r}_p, \mathbf{r}_n) d\mathbf{r}_p d\mathbf{r}_n \quad \dots (1)$$

where $\psi_d(\mathbf{r}_p, \mathbf{r}_n)$ is the incident deuteron wave function, $\psi_l^m(\mathbf{r}_p)$ is the proton wave function in the bound state, with quantum numbers E , l , $l_z = m$; $V_{np}(\mathbf{r})$

is the interaction potential between proton and neutron, and R_0 is a parameter of the order of the nuclear radius. There is a similar formula for the (d, p) reaction.

We can take the coulomb field into account by making the following modifications to (1):

(i) $\psi_d(\mathbf{r}_p, \mathbf{r}_n)$ in first approximation is equal to $F_d(\mathbf{R})\chi(\mathbf{r})$, where $F_d(\mathbf{R})$ is the coulomb wave function of a particle of mass $2M$ and incident wave vector \mathbf{k}_d , and $\chi(\mathbf{r})$ is the internal wave function of the deuteron. The deuteron polarization is neglected. Studies of the Oppenheimer-Phillips process (Oppenheimer and Phillips 1935, Volkoff (1940) have shown that the polarization is negligible when the deuteron kinetic energy W is greater than $B - I$, where B is the coulomb barrier, and I the binding energy of the deuteron. The polarization is thus always negligible for the light nuclei for which $B \sim I$, the main effect of the coulomb field being the scattering implicit in $F_d(\mathbf{R})$. For the heavy nuclei this approximation will be valid only for W of the order of B or greater.

(ii) In the (d, n) case $\psi_l^m(\mathbf{r}_p)$ takes into account the coulomb field.

(iii) In the (d, p) case the plane wave $\exp(-i\mathbf{k}_p \cdot \mathbf{r}_p)$ is replaced by $F_p(\mathbf{r}_p)$, the coulomb wave function of a proton with incident wave vector $-\mathbf{k}_p$.

The coulomb field can be taken into account in Butler's theory in its original form if we replace the various free particle wave functions by the corresponding coulomb wave functions. This does not give a result formally identical with that obtained by our procedure just described, based on (1), but it can be shown by arguments similar to those of Horowitz and Messiah (1953) that the two methods are equivalent in so far as the polarization of the deuteron is neglected.

We use the following integral representation of the coulomb wave function with incident vector \mathbf{k} :

$$F(\mathbf{x}) = -\Gamma(1+i\alpha) e^{-\alpha\pi/2} (2\pi i)^{-1} \oint (-u)^{-i\alpha-1} (1-u)^{i\alpha} \exp[ikux + i\mathbf{k} \cdot \mathbf{x}(1-u)] du, \quad \dots (2)$$

the integration path being a closed loop starting from $u=1$ and encircling $u=0$ in the positive sense. The constant α is equal to MZe^2/h^2k , M being the mass of the particle. Provided ψ_l^m refers to a negative energy state of the captured particle, it is possible to reverse the order of integration of u and of the spatial coordinates in (1), and we have, in the (d, n) case,

$$I_l^m(\theta) = -\Gamma(1+i\alpha_d) \exp(-\alpha_d\pi/2) \cdot (2\pi i)^{-1} \oint (-u)^{-i\alpha_d-1} (1-u)^{i\alpha_d} H_l^m(u, \theta) du \quad \dots (3)$$

$$H_l^m(u, \theta) = \int_{r_p > R_0} \exp(-i\mathbf{k}_n \cdot \mathbf{r}_n) \psi_l^{m*}(\mathbf{r}_p) V_{np}(\mathbf{r}) \chi(\mathbf{r}) \cdot \exp[ik_d u R + i\mathbf{k}_d \cdot \mathbf{R}(1-u)] d\mathbf{r}_p d\mathbf{r}_n. \quad \dots (4)$$

$H_l^m(u, \theta)$ will be calculated using the Horowitz-Messiah approximation, which is equivalent to neglecting the range of the V_{np} interaction (see Appendix I):

$$H_l^m(u, \theta) \simeq A \int_{r_p > R_0} \exp(-i\mathbf{k}_n \cdot \mathbf{r}_p) \psi_l^{m*}(\mathbf{r}_p) \exp[ik_d u r_p + i\mathbf{k}_d \cdot \mathbf{r}_p(1-u)] d\mathbf{r}_p. \quad \dots (5)$$

Choosing a system of coordinates in which Oz lies along $\mathbf{p}_0 = \mathbf{k}_d - \mathbf{k}_n$ and Ox is in the plane defined by \mathbf{k}_d and \mathbf{k}_n , and putting $q = k_d u$, $\mathbf{p} = \mathbf{k}_d(1-u) - \mathbf{k}_n$, $\psi_l^m(\mathbf{r}_p) = \psi_l(\mathbf{r}_p) Y_l^m(\omega_p)$, we have

$$H_l^m(u, \theta) \simeq i A \sqrt{(8\pi)\Theta(lm)} B_l(u, \theta). \quad \dots (6)$$

Θ , defined by Condon and Shortley (1951), is a function of the angle between \mathbf{p} and \mathbf{p}_0 , and

$$B_l(u, \theta) = \int_{R_0}^{\infty} r_p^2 j_l(pr_p) \psi_l(r_p) \exp(iqr_p) dr_p. \quad \dots\dots(7)$$

For the (d, p) reaction we have, similarly,

$$I_l^m(\theta) = \Gamma(1 + i\alpha_d) \Gamma(1 + i\alpha_p) \exp\{-\pi(\alpha_d + \alpha_p)/2\} (-2\pi i)^{-1} \oint (-u)^{-i\alpha_d-1} (1-u)^{i\alpha_d} du \\ \times (-2\pi i)^{-1} \oint (-v)^{-i\alpha_p-1} (1-v)^{+i\alpha_p} dv \times H_l^m(u, v, \theta). \quad \dots\dots(8)$$

$$H_l^m(u, v, \theta) \simeq A_l^i \sqrt{(8\pi)\Theta(lm)} A_l(u, v, \theta), \quad \dots\dots(9)$$

$$A_l(u, v, \theta) = \int_{R_0}^{\infty} r_n^2 j_l(pr_n) \psi_l(r_n) \exp(iqr_n) dr_n; \quad \dots\dots(10)$$

with now $\mathbf{p} = \mathbf{k}_d(1-u) - \mathbf{k}_p(1-v)$, $\mathbf{p}_0 = \mathbf{k}_d - \mathbf{k}_p$, $q = k_d u + k_p v$. The approximations involved in the evaluation of A_l and B_l are considered in Appendix II.

The integrals of the form

$$I = (-2\pi i)^{-1} \oint (-u)^{-i\alpha-1} (1-u)^{i\alpha} f(u) du$$

are computed in the following way. $f(u)$ is an analytical function of u , without singularities. The integration path can be chosen as close as we wish to the segment (0,1) of the real axis. Therefore we approximate $f(u)$ by a polynomial

$$P_n(u) = \sum_{r=0}^{r=n} \beta_r u^r$$

such that $P_n(u_i) = f(u_i)$ for a set of real u_i between 0 and 1. If we define the quantities A_{ri} to be such that

$$\beta_r = \sum_{i=0}^{i=n} A_{ri} f(u_i)$$

and we write

$$K_r = (-1)^r \Gamma(1 + i\alpha) [\Gamma(r+1) \Gamma(1 + i\alpha - r)]^{-1} \\ = (-1)^r i\alpha(i\alpha - 1) \dots (i\alpha - r + 1)(r!)^{-1} \quad \dots\dots(11)$$

it is found that

$$I \simeq \sum_{i=0}^{i=n} g_i f(u_i), \quad \dots\dots(12)$$

where

$$g_i = \sum_{r=0}^{r=n} A_{ri} K_r.$$

For the purpose of computation we used $u_i = i/n$, with $n = 4$ or 5 . The approximations were checked and found fairly good. The double integral can be treated in the same way. Equations (3)–(8) show that $I_l^m(\theta)$ can be looked on as the average, with appropriate weights, of terms H_l^m closely related to the matrix elements I_l^m of Butler's theory, \mathbf{k}_p and \mathbf{k}_d being replaced by $\mathbf{k}_p(1-v)$ and $\mathbf{k}_d(1-u)$, where $0 \leq v \leq 1$ and $0 \leq u \leq 1$. The difference arises chiefly from the isotropic term e^{iqr} in the integrals A_l and B_l . If we confine ourselves to the (d, n) reaction, to replace \mathbf{k}_d by $\mathbf{k}_d(1-u)$ is to take into account the reduction by the coulomb field of the kinetic energy of the incident deuteron. The important factor in the angular distribution is the magnitude of the vector $\mathbf{p} = \mathbf{k}_d(1-u) - \mathbf{k}_n$. For $u=1$ the angular distribution is isotropic. For $u=0$ we have Butler's distribution. So we can expect a flattening of the angular distribution by this effect of the coulomb field. On the other hand, deflection of the deuterons by the coulomb field appears through the isotropic factor e^{iqr} and leads also to a flattening.

In the (d, p) reaction the integral A_l involves values of r greater than those involved in B_l , and so the deuteron wave function is less distorted. But we have to average over the effective \mathbf{k}_p (for $v=1$ the distribution is again isotropic) and coulomb deflection of the protons (q is larger than in the (d, n) case). It turns out from the numerical cases investigated that the flattening is greater in the (d, p) case than in the (d, n) case.

§ 3. POLARIZATION OF THE SPINS OF THE PARTICLES

Newns, with Huby (1953), and Horowitz and Messiah (1953) have shown that the spins of the outgoing particles can be polarized. Our purpose here is to show that, even when all refinements of Butler's theory other than the coulomb effect are neglected, the polarization is not zero. We restrict ourselves to the (d, n) case, and we suppose that the proton is captured in a state of definite orbital angular momentum l and total angular momentum $j=l\pm\frac{1}{2}$. The incident deuterons are supposed to be unpolarized. The polarization P_x is defined as $(N_+ - N_-)/(N_+ + N_-)$, where N_+ and N_- denote the number of particles having the x component of the spin equal to $\frac{1}{2}$ and $-\frac{1}{2}$ respectively. P_y and P_z are defined in a similar way. In the system of coordinates used above, a straightforward calculation leads to the following results: $P_x = P_z = 0$, in agreement with the general results, while

$$P_y = \pm 4[3(2j+1)]^{-1} \left[\sum_{\mu>0} \{(l+\frac{1}{2})^2 - \mu^2\}^{1/2} \mathcal{J}(I_l^{\mu+\frac{1}{2}*}(\theta) I_l^{\mu-1/2}(\theta)) \right] \left[\sum_m |I_l^m(\theta)|^2 \right]^{-1} \dots\dots(13)$$

μ , the z component of j , can take all values between $\frac{1}{2}$ and j . The sign + refers to the case $j=l+\frac{1}{2}$, — to $j=l-\frac{1}{2}$. We note that $P_y=0$ in the following cases: (i) for $l=0$ there is no polarization if the particle is captured in an s state; (ii) if the $I_l^m(\theta)$ all have the same phase, or if only one $I_l^m(\theta)$ contributes to the angular distribution; this is always the case for $\theta=0$ or π , and in Butler's theory.

§ 4. NUMERICAL RESULTS

The following numerical results are given only as illustrations of the influence of the coulomb field.

(i) Angular Distribution

(a) (d, n) reaction.

We have used data from the experiments of Pruitt, Hanna and Swartz (1952) on the ${}^9\text{Be}(\text{d}, \text{n}){}^{10}\text{B}$ reaction in which W (laboratory) = 0.94 mev, $k_d = 2.3 \times 10^{12} \text{cm}^{-1}$, $k_n = 4.6 \times 10^{12} \text{cm}^{-1}$, $R_0 = 5 \times 10^{13} \text{cm}$, $\alpha_d \simeq 1$, and have calculated the differential cross sections for $l=0, 1$ and 2 . Figures 1 to 3 give $\sigma_n(\theta)$ (differential cross section with coulomb field) and $\sigma(\theta)$ (differential cross section on Butler's theory). The scales for $\sigma_n(\theta)$ and $\sigma(\theta)$ are different, and the curves are made to coincide at $\theta=0^\circ$ for $l=0$ and 1 , and at $\theta=90^\circ$ for $l=2$. We have for the correspondence between the scales

$$\begin{aligned} l=0, \quad \sigma_n(0^\circ) &= 0.07\sigma(0^\circ) && \text{(figure 1)} \\ l=1, \quad \sigma_n(0^\circ) &= 0.14\sigma(0^\circ) && \text{(figure 2)} \\ l=2, \quad \sigma_n(90^\circ) &= 0.14\sigma(90^\circ) && \text{(figure 3).} \end{aligned}$$

We see that the coulomb field cannot explain the strong backward maximum observed by Pruitt, Hanna and Swartz. The coulomb effect is a flattening, as

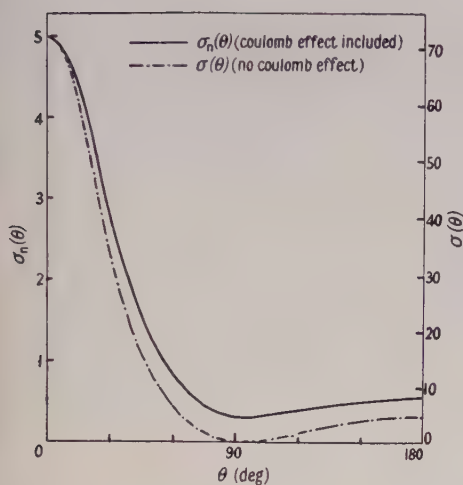


Figure 1. Angular distribution calculated for the (d, n) reaction ($l=0$).

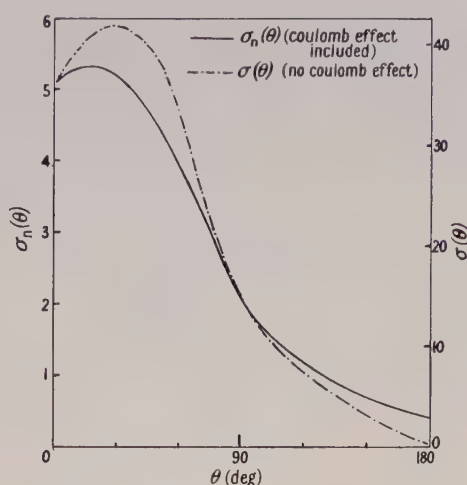


Figure 2. Angular distribution calculated for the (d, n) reaction ($l=1$).

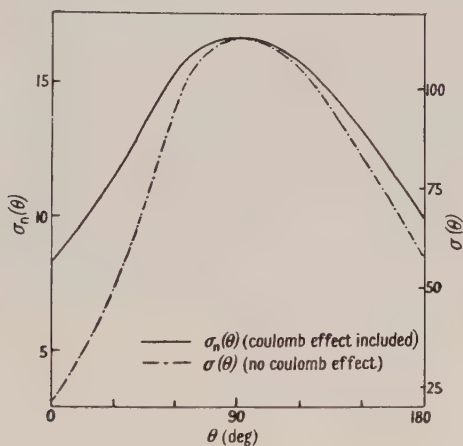


Figure 3. Angular distribution calculated for the (d, n) reaction ($l=2$).

expected, and a slight displacement of the maximum. Other numerical investigations have shown that the displacement can take place either towards larger or towards smaller angles. The zeros of the Butler formula are eliminated. The absolute magnitude of the cross section is strongly reduced. The ratio $\sigma_n(\theta)/\sigma(\theta)$ is equal to $\pi\alpha_d \exp(-\pi\alpha_d)\rho(\alpha_d, \theta)[\sinh \pi\alpha_d]^{-1}$, with

$$\rho(\alpha_d, \theta) = \left[\sum_m \left| \sum_i g_i H_l^m(u_i, \theta) \right|^2 \right] \left[\sum_m |H_l^m(0, \theta)|^2 \right]^{-1}.$$

$\rho(\alpha_d, \theta)$ is of the order of magnitude of $|g_i|^2$ and $\sigma_n(\theta)/\sigma(\theta)$ of the penetration factor.

(b) (d, p) reaction

The calculations are made for $l=0$, with $W=1.6$ mev ;

$$k_d = k_p = k_n = 4 \times 10^{12} \text{ cm}^{-1}, \quad \alpha_d = 1, \quad \alpha_p = 0.5.$$

we give in figure 4 $\sigma_p(\theta)$, $\sigma_n(\theta)$ and $\sigma(\theta)$, i.e. the cross sections for the (d, p) reaction, the (d, n) reaction with coulomb field and Butler's cross section respectively.

$\sigma_p(\theta)$ and $\sigma_n(\theta)$ are in the same units, while $\sigma_p(0^\circ) = 0.16\sigma(0^\circ)$ and $\sigma_n(0^\circ) = 0.18\sigma(0^\circ)$. The curves show that the flattening is more important in the (d, p) reaction than in the (d, n) reaction for the reasons mentioned above. The ratios $\sigma_n(\theta)/\sigma(\theta)$ and $\sigma_p(\theta)/\sigma(\theta)$ are of the same order of magnitude. This will not be true if the polarization of the deuteron becomes important, i.e. for the heavy nuclei ($Z > 20$).

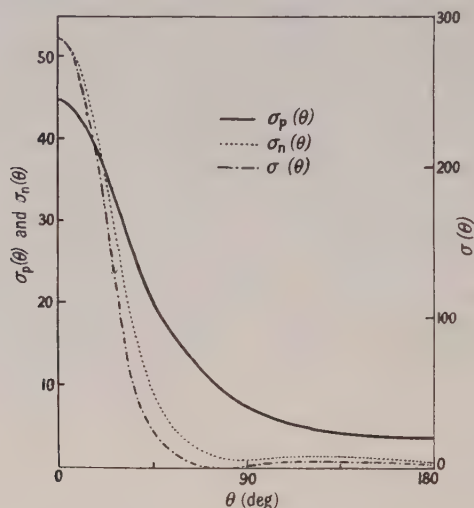


Figure 4. Angular distribution calculated for the (d, p) reaction ($l=0$).

(ii) Polarization of the Spins of the Particles

The following table, corresponding to the (d, n) reaction reported above, shows that the polarization can be of the same order of magnitude as the polarization calculated by Newns (1953) and Horowitz and Messiah (1953), but of the opposite sign.

	θ ($^\circ$)	30	60	90
$P_y(l=1)$;	$j=1/2$	+0.38	+0.36	+0.32
	$j=3/2$	-0.19	-0.18	-0.16

§ 5. CONCLUSIONS

We see that the coulomb effect on the angular distribution, in the range of deuteron kinetic energies considered, is small. This result is compatible with the results of Serber (1947), if extrapolated. The strong backward maximum reported by Pruitt, Hanna and Swartz (1952) at very low deuteron energies is not explained by the coulomb field. The absolute magnitude of the cross section is decreased. We emphasize that these calculations hold for light nuclei only, the polarization of the deuteron by the coulomb field being always neglected.

ACKNOWLEDGMENTS

The author wishes to thank Dr. R. Huby for guidance and for many valuable discussions and Professor H. Fröhlich for giving facilities to work in his department. He also wishes to thank Professor F. Joliot-Curie in whose laboratory this work, was begun, and the French Centre National de la Recherche Scientifique for financial support.

REFERENCES

- BHATIA, A. B., HUANG, K., HUBY, R., and NEWNS, H. C., 1952, *Phil. Mag.*, **43**, 485.
 BUTLER, S. T., 1951, *Proc. Roy. Soc. A*, **208**, 559.
 CONDON, E. U., and SHORTLEY, G. H., 1951, *Theory of Atomic Spectra* (Cambridge : University Press), p. 51.
 GERJUOY, E., 1953, *Phys. Rev.*, **91**, 645.
 HOROWITZ, J., and MESSIAH, A. M. L., 1953, *J. Phys. Radium*, **14**, 12, 695.
 NEWNS, H. C., 1953, *Proc. Phys. Soc. A*, **66**, 477.
 OPPENHEIMER, J. R., and PHILLIPS, M., 1935, *Phys. Rev.*, **48**, 500.
 PRUITT, J. S., HANNA, S. S., and SWARTZ, C. D., 1952, *Phys. Rev.*, **87**, 534.
 SALPETER, E. E., and GOLDSTEIN, J. S., 1953, *Phys. Rev.*, **90**, 983.
 SCHIFF, L., 1949, *Quantum Mechanics* (New York : McGraw-Hill), p. 77.
 SERBER, R., 1947, *Phys. Rev.*, **72**, 1008.
 VOLKOFF, G. M., 1940, *Phys. Rev.*, **57**, 866.
 WHITTAKER, E. T., and WATSON, G. N., 1940, *Modern Analysis* (Cambridge : University Press).

APPENDIX I

For the (d, n) reaction Horowitz and Messiah put

$$\int_{r_p > R_0} \exp(-i\mathbf{k}_n \cdot \mathbf{r}_n) \psi_l^m(\mathbf{r}_p) V_{np}(\mathbf{r}) \exp(+i\mathbf{k}_d \cdot \mathbf{R}) \chi(\mathbf{r}) d\mathbf{r}_p d\mathbf{r}_n \\ \simeq 4\pi\hbar^2 M^{-1} \int_{r_p > R_0} \exp(-i\mathbf{k}_n \cdot \mathbf{r}_p) \psi_l^m(\mathbf{r}_p) \exp(i\mathbf{k}_d \cdot \mathbf{r}_p) d\mathbf{r}_p \quad \dots\dots(14)$$

where $\chi(r)$ is set equal to $e^{-\alpha r/r}$. Actually the left-hand side is equal to

$$f(s) \times \int \exp(-i\mathbf{k}_n \cdot \mathbf{r}_p) \psi_l^m(\mathbf{r}_p) \exp(i\mathbf{k}_d \cdot \mathbf{r}_p) d\mathbf{r}_p \quad \dots\dots(15)$$

where

$$f(s) = \int \exp(-i\mathbf{s} \cdot \mathbf{r}) V_{np}(\mathbf{r}) \chi(\mathbf{r}) d\mathbf{r} \quad \text{and} \quad \mathbf{s} = \mathbf{k}_n - \mathbf{k}_d/2. \quad \dots\dots(16)$$

Disregarding the constant factors, we see that the Horowitz-Messiah approximation is good as long as $f(s)$ varies slowly compared with the other integral. $f(s)$ was computed by Salpeter and Goldstein (1953), and varies, for the Yukawa potential, from 1 to 0.7 as s increases from 0 to $9 \times 10^{12} \text{ cm}^{-1}$. Thus, if there is a wide variation in s , $f(s)$ could be used as a correcting factor, dependent on u in the coulomb case, but it can never lead to a backward maximum.

APPENDIX II

Calculation of A_l and B_l .

(1) For $r > R_0$, $\psi_l(r_n) = h_l^{(1)}(itr_n)$, and hence

$$A_l = \int_{R_0}^{\infty} \exp(iqr_n) h_l^{(1)}(itr_n) j_l(pr_n) r_n^2 dr_n, \quad \dots\dots(17)$$

where $h_l^{(1)}(x)$ and $j_l(x)$ are the Hankel and Bessel functions defined by Schiff (1949).

We obtain the following recurrence formula:

$$(2l-2)A_l = (2l-1)iA_{l-1}(t^2 + q^2 - p^2)t^{-1}p^{-1} - 2lA_{l-2} \\ + \exp(iqR_0)R_0^2 \left[\frac{h_l^{(1)}(itR_0)}{it} (lj_{l-2}(pR_0) - (l-1)j_l(pR_0)) \right. \\ \left. + \frac{j_{l-1}(pR_0)}{p} (lh_{l-2}^{(1)}(itR_0) - (l-1)h_l^{(1)}(itR_0)) - iq \frac{h_{l-1}^{(1)}(itR_0)}{it} \frac{j_l(pR_0)}{p} \right], \quad \dots\dots(18)$$

$$A_0 = -\exp(-tR_0 + iqR_0)[p \cos pR_0 + (t - iq) \sin pR_0][t p \{p^2 + (t - iq)^2\}]^{-1} \dots\dots\dots (19)$$

$$A_1 = R_0^2 \exp(iqR_0) h_1^{(1)}(itR_0) j_0(pR_0) + (it + q)p^{-1}A_0 \\ - qt^{-2}p^{-2} \int_{R_0}^{\infty} \exp\{-(t - iq)r\} \sin pr \, dr/r. \dots\dots\dots (20)$$

$$(2) \quad B_l = \int_{R_0}^{\infty} \exp(iqr_p) \psi_l(r_p) j_l(pr_p) r_p^2 \, dr_p. \dots\dots\dots (21)$$

Actually $\psi_l(r_p) = r^{-1} W_{-4\pi^2 M Z e^2 / \hbar^2 t, l + \frac{1}{2}}(2tr_p)$, $W_{-\beta, l + \frac{1}{2}}$ being the Whittaker function defined by Whittaker and Watson (1940). Using an integral representation,

$$B_l = (2t)^{l+1} [\Gamma(l+1+\beta)]^{-1} \int_0^{\infty} y^{l+\beta} (1+y)^{-\beta} b_l(y) \, dy \dots\dots\dots (22)$$

where

$$b_l(y) = \int_{R_0}^{\infty} \exp(iqr_p) j_l(pr_p) \exp\{-t(1+2y)r_p\} r_p^{l+2} \, dr_p. \dots\dots\dots (23)$$

$b_l(y)$ can be evaluated in terms of elementary functions. We can use

$$\psi_l(r_p) \simeq Ch_l^{(1)}(it'r_p),$$

C and t' being defined in such a way that $\psi_l(r_p)$ and $Ch_l^{(1)}(it'r_p)$ are equal for two values of r_p in the neighbourhood of R_0 ($r_p = R_0$ and $r_p = 2R_0$ for example). So $Ch_l^{(1)}(it'r_p)$ is a good approximation in the region of r_p important for the integral B_l . When l increases, t' defined above tends rapidly to the value t , the coulomb potential being less important if there is a strong centrifugal potential. The only parameter is t' , and $\psi_l(2R_0)/\psi_l(R_0) = h_l^{(1)}(2it'R_0)/h_l^{(1)}(it'R_0)$ can be calculated by the WKB approximation. For example, if $\beta = 0.465$, $t = 4.30 \times 10^{12} \text{ cm}^{-1}$, and $R_0 = 5 \times 10^{13} \text{ cm}$, then for $l=0$, $t' = 4.82 \times 10^{12} \text{ cm}^{-1}$; $l=1$, $t' = 4.62 \times 10^{12} \text{ cm}^{-1}$; $l=2$, $t' = 4.35 \times 10^{12} \text{ cm}^{-1}$.

A New Method for the Production of Active Nitrogen and its Application to the Study of Collision Effects in the Nitrogen Molecular Spectrum

By C. R. STANLEY

Department of Physics, Imperial College, London

MS. received 7th May 1954

Abstract. The source described employs a high tension arc and can operate at comparatively high pressures. The afterglow spectrum is that of the Lewis-Rayleigh glow at low pressures, but is modified at the higher pressures. Reasons are given for interpreting this modification as due to exchanges of vibrational energy occurring in collisions between nitrogen molecules.

A modification is made to Mitra's theory of active nitrogen.

§ 1. INTRODUCTION

THE existence of an active modification of nitrogen was reported by Lord Rayleigh in the Bakerian Lecture for 1911 and shown to be associated with the afterglow of nitrogen observed previously by Warburg (1884) and studied in some detail by P. Lewis (1900).

In these early experiments, and in the majority of the studies reported subsequently, the active nitrogen was produced by a condensed discharge at nitrogen pressures of the order of 10^{-1} mm Hg. Rayleigh and others have also found the electrodeless discharge effective for certain purposes, but it is limited to lower pressures than is the condensed discharge and is considerably less efficient. By using a tube the walls of which had been specially conditioned by previous running of the discharge for several days with a small admixture of oxygen, Kaplan (1932) was able to obtain an afterglow with an uncondensed discharge. However, this source gave rise to a different type of afterglow phenomenon with which we shall not be concerned in this paper.

In the following pages a new source of active nitrogen is described. This source functions at pressures from a few mm Hg up to at least an atmosphere. Its efficiency at the higher pressures, as estimated from the intensity of the afterglow, is comparable with that of the condensed discharge source at low pressures. Some of the more important properties of the active gas at these higher pressures are examined, and some results are presented which seem to show the source to be useful for the study of the effect of collisions on the nitrogen molecular spectrum.

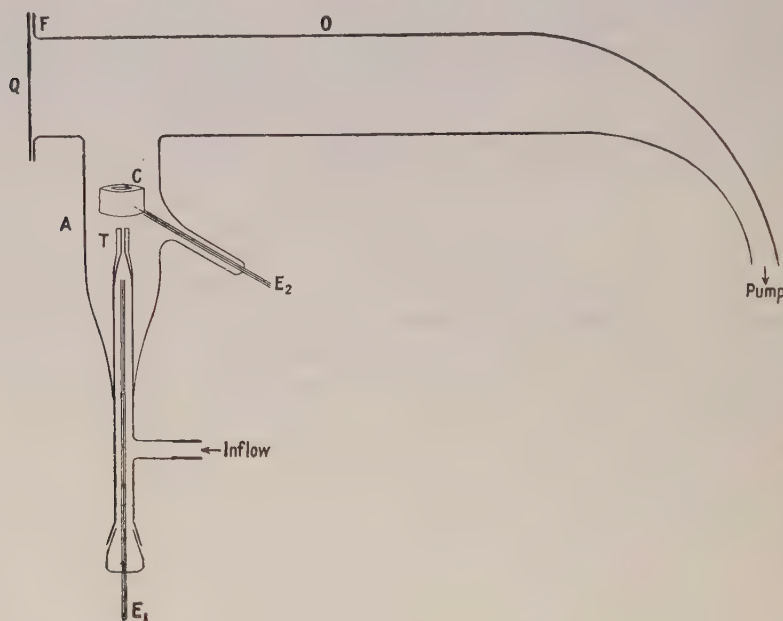
§ 2. DESCRIPTION OF THE APPARATUS

The essential features of the apparatus are an arc chamber, in which the active nitrogen is generated by means of a high tension quartz capillary arc, and a long observation vessel in which the properties of the active gas can be examined.

The details are depicted in the figure. O is the observation vessel, consisting of a glass tube some 6 cm in diameter and 30 to 40 cm long. It is made long to obtain a considerable depth of glowing gas and consequently greater intensity in

the spectral image. It terminates in a 'Wood horn' to prevent reflection of light back along the tube.

Spectrographic observation of the afterglow is made through the quartz window Q which is affixed to the tube by sealing wax. It was found in preliminary experiments that sealing wax is acted upon by the active nitrogen and is liable to contaminate the spectrum. To avoid this, the tube is provided with a broad ground glass flange F and the sealing wax is confined to the outer rim of this flange; thus the activity is removed before the gas reaches the wax. Water cooling (not shown) is necessary to prevent the wax from melting.



A high tension capillary arc source of active nitrogen.

A is the arc chamber for the production of the active nitrogen. A high voltage a.c. arc is maintained in the quartz capillary tube T between the tungsten electrodes E_1 and E_2 . The optimum dimensions of the capillary tube vary with the conditions of the experiment, but for most purposes a bore of 1 to 2 mm and a length of 1 to 1.5 cm have been found suitable. The arc length can be varied by advancing or withdrawing the electrode E_1 . A cap C for the electrode E_2 can be inserted via the window Q, and is found to prevent instability under certain of the experimental conditions.

The arc is operated from a 230 volt a.c. supply via a transformer giving 5 to 10 kv and up to 500 ma. The arc current is readily controlled by a variable resistance in the transformer primary circuit.

The nitrogen supply is obtained from a cylinder and for good results needs purification. Water vapour is particularly troublesome as it has a strong quenching action: it is removed by a train of liquid air traps designed to offer a large cold surface area with as little flow impedance as possible. Oxygen also has a quenching

action and must not be present in appreciable quantity; the requirement here can be largely met by using cylinders of 'oxygen-free' nitrogen, but even with this an improvement can be effected by passing the gas through a long quartz tube containing copper turnings at about 800°C. Other impurities, such as carbon dioxide and hydrogen, are detrimental not so much through their quenching action as through the consequent contamination of the afterglow spectrum, and it is difficult to remove them satisfactorily. In all respects it has been found advantageous to avoid rubber tubing in the supply line.

§ 3. THE SPECTRUM OF THE AFTERGLOW AT LOW PRESSURES

The identity of the afterglow was at first based on the similarity of its spectrum, as observed in a direct-vision spectroscope, to that of the Lewis-Rayleigh glow, there being three prominent broad 'bands' in the green, yellow and red respectively, and apparently no other features. This was confirmed by photographing the spectrum on small dispersion glass and quartz instruments: the α bands of the N_2 First Positive system and the β and γ bands of NO were readily identified on the resulting spectrogram, and there appeared to be no other nitrogen band or line. This is exactly as described by Fowler and Strutt (1911) for the spectrum of the afterglow of nitrogen.

On the first spectrograms which were obtained with a preliminary apparatus, there were seen in the ultra-violet and blue regions many broad diffuse bands that could not be identified with the small dispersion used. (It was not practicable to use larger dispersion as the glow was very faint in this earlier apparatus.) It was suspected that these bands might be connected with the sealing wax used for affixing the quartz observation window, for the glow was most concentrated near the wax seal. Hence in the new apparatus—designed primarily to give a brighter glow—the sealing wax was kept out of contact with the activated gas in the manner described in § 2. It was then found that the unidentified bands disappeared, leaving the NO β and γ bands, the OH (0, 0) and (1, 0) bands, the (0, 0) and (1, 1) bands of NH and, at higher pressures, some of the CN violet system.

§ 4. THE SPECTRUM OF THE AFTERGLOW AT HIGHER PRESSURES

The efficiency of the source as compared with that of the condensed discharge is most marked at the higher pressures. The spectrum at these higher pressures differs markedly from the low-pressure spectrum; as the pressure is increased from a few mm Hg, the other bands of the N_2 First Positive system appear in addition to the α bands, and their intensity, relative to that of the α bands, continues to increase until, at pressures approaching an atmosphere, the markedly anomalous intensity distribution so characteristic of the low-pressure glow, has given way to a much more uniform distribution somewhat similar to that of an ordinary positive column low-pressure discharge spectrum.

This is illustrated in the Plate, which is a reproduction of photographs taken on Ilford Astra III plates with a Hilger glass prism instrument of medium dispersion: (a) shows the spectrum of the glow at low pressure (1.4 mm Hg), while (b) refers to a pressure of 500 mm Hg. It can be seen that in (a) the emission is largely confined to the bands with $v' = 6$ and 10, 11, 12; and of these, the $v' = 11$ emission is much the most intense. In (b) there is seen to be a marked decrease in intensity of the $v' = 11$ bands, while bands with lower v' values, many of which

cannot be seen at all in (a), are now quite bright. The change has been followed throughout the intermediate pressures and is quite gradual.

The possibility that the spectrograms might be contaminated by stray light from the exciting discharge was ruled out: a screen was interposed which admitted light only from the observation window, and the observation vessel was terminated by a blackened 'Wood horn' to minimize the reflection. As a final check, 'blank' photographs were taken with the exciting arc on but the observation chamber made dark, either by preventing admission of the activated gas or by injecting a trace of moist air to quench the glow.

§ 5. DISCUSSION

A change in the intensity distribution throughout a band system implies a change in the distribution of vibrational energy among the molecules in the excited electronic state. This may arise in a variety of ways which can be classified under one of two heads: (I) There may be a change in the relative rates of entry into the vibrational levels of the excited state, such as would arise from a redistribution of vibrational energy in the *lower* state or from alterations in the mechanism or conditions of excitation. (II) There may be some disturbance modifying the relative exit rate from the vibrational levels of the upper state; exchange of vibrational energy in collisions with other molecules is the only instance of this likely to be found in the sources discussed here.

Feast (1950) reported a redistribution of vibrational intensity in the N_2 Second Positive system emitted by a high voltage arc at atmospheric pressure, as compared with the same system emitted by the positive column of an ordinary low-pressure discharge. This he attributed to vibrational de-activation resulting from the high collision rate obtaining in the arc, i.e. to process (II). However, the results, as presented, seem to admit of alternative interpretation. Feast gives no reason for excluding the possibility of process (I); indeed, the precise mechanism of excitation in arcs and other discharges is not known with any certainty. On the one hand, collisions with electrons are doubtless responsible for a large part of the excitation, and in view of the small mass of an electron compared with that of a molecule, one would expect the Franck-Condon principle to be applicable so that the relative entry rate would be determined by the vibrational distribution in the lower state. On the other hand, if molecular ions play any part in the excitation, there is likelihood of direct vibrational excitation, so that the relative entry rate into the vibrational levels of the upper state may depend on the concentration and velocity of the molecular ions as well as on the vibrational distribution in the lower state. Thus, if the part played by molecular ions changes in going from low-pressure discharge to high-pressure arc conditions, there will be a consequent change in the vibrational intensity distribution of the radiated band systems.

Furthermore, the only theoretical work bearing on this appears unfavourable to Feast's interpretation. Zener (1931), on the basis of certain assumptions which seem justifiable for the N_2 molecule, has calculated that the chance of vibrational energy exchange between an excited N_2 molecule and one in the ground state, is of the order of 10^{-4} in a collision at room temperature. If we take 5×10^9 per second as the collision frequency of N_2 molecules at atmospheric pressure and room temperature and 10^{-8} second as the mean lifetime of the excited state, then there are seen to be only 50 collisions during this lifetime, so that, according to Zener's calculations, only about five per thousand excited molecules would suffer a change

in vibrational energy, a proportion too small to produce a visually detectable change in the spectral intensity distribution.

The nature of active nitrogen and the mechanism of production of the afterglow are still matters of considerable doubt—see, for instance, the recent discussions by Mitra (1953) and by Oldenberg (1953)—but in comparison with electrical arcs and discharges there are a number of definite simplifications which permit a more reliable interpretation of experimental observations. It seems fairly certain from these discussions by Mitra and Oldenberg that electrons and molecular ions play no part in the excitation of the afterglow, and in any case there is no electrical field present. Furthermore, there is not the variation of pressure and lack of definition of temperature that is found in arcs and discharges; indeed, both temperature and pressure can be made reasonably uniform.

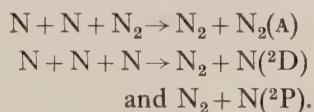
Whatever the type of collision that leads to the emission of the afterglow, the final result of any single collision can only depend on (i) the relative velocities of the collision partners and (ii) the nature of the collision partners. Consequently the average result of *all* the collisions can only depend on (i) the velocity distribution, and (ii) the nature and proportion of the particles concerned; in particular there can be no dependence on collision rate or pressure except via (i) or (ii).

Due to the uniformity of temperature and the absence of an electric field, the velocity distribution will be a function of temperature alone and not of pressure.

It remains therefore to consider whether or not (ii) varies with pressure, and for this some definite suppositions must be made regarding the mechanism of excitation of the afterglow, for it is obvious that with some mechanisms there would be pressure dependence of (ii) and with others there would not.

According to Mitra (1953), dissociative recombination of electrons and N_2^+ ions in the discharge produces metastable 2P and 2D nitrogen atoms. These lose their excitation energy and become ordinary nitrogen atoms in the ground state 4S . The afterglow then arises in the manner suggested by Gaydon (1947) from the recombination of two 4S nitrogen atoms colliding on a $^5\Sigma_g^+$ potential curve—a process which, according to Cario and Reinecke (1949), accounts satisfactorily for the afterglow and also for the reduction in the brightness of the glow with increasing temperature. Thus only one kind of particle is involved in the final excitation of the afterglow, and consequently the possibility of a variation in the proportion of the particles taking part does not arise.

According to Oldenberg, the primary particles are nitrogen atoms in (presumably) the ground state. Three-body collisions taking place between a pair of these nitrogen atoms and another particle result in excitation of the third particle and the formation of a nitrogen molecule, and since resonance is not effective in this type of collision, any degree of excitation of the third particle (up to the energy of dissociation of nitrogen) is possible; in particular, there will be produced metastable nitrogen molecules in the $A^3\Sigma_u^+$ state of 6.2 eV and metastable nitrogen atoms in the 2P and 2D states of 3.57 eV and 2.38 eV respectively, i.e.



Excitation of the afterglow then takes place by the transfer of the excitation energy from the metastable atoms to the A state molecules, which are thus raised to the $B^3\Pi_g$ state, as in the original theory of Cario and Kaplan.

Clearly the proportion of metastable $N_2(A)$ molecules may vary with pressure, since their rate of production depends on the concentration of inert N_2 molecules, while that of the metastable atoms does not. But in the Cario and Kaplan mechanism the functions of the metastable atoms on the one hand, and of the metastable molecules on the other, are complementary, so that a variation in their relative proportions will alter only the rate of reaction and not the relative entry rate into the vibrational levels of the $N_2(B)$ state.

The ratio of 2D atoms to 2P atoms is more important. Since they are produced by the same type of collision, their relative rate of *production* will be independent of pressure. Their loss, however, may be either (a) via collisions with $N_2(A)$ molecules or (b) by radiative transition to the ground state. Now the rates of loss via (a) are, for both 2D and 2P atoms, proportional to the concentration of $N_2(A)$ molecules, which depends on the total pressure, while the rates via (b) depend only on the radiation transition probabilities. So the net effect is variation with pressure of the relative rate of loss of 2D and 2P atoms.

However, it can be seen that for each metastable atom lost via (a) there will be one photon radiated in the nitrogen First Positive system, while for each atom lost via (b) there will be one photon radiated in the corresponding atomic line. It follows that the proportion of metastable atoms disappearing via (b) will be indicated experimentally by the ratio of the corresponding nitrogen line intensities to the First Positive band system intensity. In the literature there appears to be no report of the observation of either line, and in the present experiments a careful inspection was made in the regions concerned (3466 Å and 5200 Å) but there was no sign of any atomic line at any of the pressures used. It is therefore concluded that loss via (b) is negligibly small, so that the variation with pressure of the relative rate of loss of 2D and 2P atoms will also be negligible. It follows that the ratio of the concentrations of 2D and 2P atoms will be sensibly independent of pressure.

Summing up, it is seen that on either Mitra's (1953) theory or Oldenberg's theory there can be no change with pressure, of the relative vibrational entry rate into the $N_2(B)$ state, provided that the temperature is held constant. That is to say, process (I), as a possible explanation of the results presented in this paper, is excluded—the variation of temperature with pressure was considered by the author to be negligible in the present apparatus, at least to a first approximation, and this has been confirmed by more precise work which will be reported later.

§ 6. CONCLUSIONS

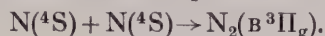
It would seem then that the results should be explained as arising from process (II), i.e. the exchange of vibrational energy occurring in collisions between the excited nitrogen molecules and the other molecules present.

If this is so, then the value of the order 10^{-4} , for the chance of such an exchange, suggested by Zener's calculations, must be too small. A similar conclusion would follow from Feast's observations on the spectrum of the high voltage arc in nitrogen, if one were to accept his interpretation of them. But in this source, as probably in all electrical discharge sources, conditions are too complicated for the results to be interpreted without ambiguity.

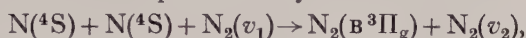
Because of the comparative simplicity of the conditions, together with the fact that a high collision rate is obtainable, the new source would seem to be useful for studying collisional energy exchanges quantitatively.

§ 7. A MODIFICATION TO MITRA'S (1953) THEORY

The opportunity is taken to draw attention to an omission in Mitra's theory. The essential mechanism in the production of the afterglow is the inverse pre-dissociation of two ^4S nitrogen atoms colliding on a $^5\Sigma_g^+$ potential curve, after the suggestion of Gaydon. The reaction is represented by Mitra as



This requires the approach of two ^4S nitrogen atoms with the same relative velocities as they might have had in the pre-dissociation process, and from geometrical considerations alone the probability of the reaction would be vanishingly small. The probability could be made finite only by the presence of a third body sufficiently massive to take part in a redistribution of energy and momentum. The most likely third body would, of course, be an ordinary nitrogen molecule, and the reaction should therefore be represented by



v_1, v_2 denoting the initial and final velocities of the inert molecule.

If the concentration of the active particles be denoted by n , and the pressure of the inert nitrogen by p , then the intensity I of the afterglow can be written

$$I = c(T)n^2p$$

where $c(T)$ is a parameter depending on the temperature. Accordingly we should expect the glow intensity to vary (i) as the cube of the concentration, when the volume of the activated gas as a whole is changed, (ii) as the square of the concentration of the active particles when the inert gas pressure is held constant, (iii) directly as the pressure when the concentration of active particles is held constant.

These are the three relations obtained experimentally by Rayleigh. The reaction proposed by Mitra does not lead to them: Mitra's suggested explanation for the variation of afterglow intensity with temperature is based on the necessity for the recombining atoms to have just the right relative velocity, and is scarcely plausible when one realizes the necessity for a third body.

This modification to Mitra's theory does not affect the considerations in § 5.

ACKNOWLEDGMENTS

I wish to express my thanks to Professor R. W. B. Pearse and Mr. W. R. S. Garton for their constant encouragement and for reading this paper, and to Sir George Thomson for his interest in the experimental work. I am indebted to the Department of Scientific and Industrial Research for the provision of a research grant, and to the Trustees and the University of London for the award of the William Gilles Research Fellowship.

REFERENCES

- CARIO, C., and REINECKE, L. H., 1949, *Abh. Braunschw. Wiss. Ges.*, **1**, 8.
 FEAST, M. W., 1950, *Proc. Phys. Soc. A*, **63**, 563.
 FOWLER, A., and STRUTT, R. J., 1911, *Proc. Roy. Soc. A*, **85**, 377.
 GAYDON, A. G., 1947, *Dissociation Energies* (London: Chapman and Hall).
 KAPLAN, J., 1932, *Phys. Rev.*, **42**, 807.
 LEWIS, P., 1900, *Astrophys. J.*, **12**, 8.
 MITRA, S. K., 1953, *Phys. Rev.*, **90**, 516.
 OLDENBERG, O., 1953, *Phys. Rev.*, **90**, 727.
 RAYLEIGH, Lord (STRUTT), 1911, *Proc. Roy. Soc. A*, **85**, 219.
 WARBURG, E., 1884, *Arch. Sci. Genève* (3), **12**, 504.
 ZENER, C., 1931, *Phys. Rev.*, **37**, 556.

The Specific Heat of Metals at Low Temperatures

BY M. J. BUCKINGHAM† AND M. R. SCHAFFROTH‡

Department of Theoretical Physics, University of Liverpool

Communicated by H. Fröhlich; MS. received 11th May 1954

Abstract. The free energy of an electron gas interacting with lattice vibrations is calculated. The linear term in the low-temperature specific heat contains a factor depending on the strength of the interaction. The result is compared with recent experiments and suggestions for new investigations are discussed.

§ 1. INTRODUCTION AND DISCUSSION

IN its simplest form the theory of metals is based on the assumption that the electrons are free, apart from their interaction with the lattice vibrations. Fröhlich (1950) discussed this interaction with the help of perturbation theory in terms of an interaction parameter F . He found that when F is greater than a critical value F_0 the normal distribution is unstable, and identified this state of the metal as superconducting.

When $F < F_0$, and the metal is normal, the lattice interaction still has important effects, notably an alteration in the density of energy levels near the surface of the distribution. This was pointed out some time ago (Buckingham 1951, quoted hereafter as I) and was suggested as an explanation for the anomalous behaviour observed in the low-temperature specific heat of certain metals. The qualitative discussion in I showed that an effect of the observed order of magnitude could be expected, although the temperature dependence of the specific heat was not of the same character as that shown by existing measurements. Recent experimental work, however, shows this discrepancy to be spurious owing to errors in the earlier observations, so that there is now support for the main features of the theory.

It is the principal object of the present paper to determine, in a more quantitative way than in I, the influence of the lattice interaction on the specific heat of normal metals. This is achieved by employing a perturbation formalism (Schafroth 1951, quoted as II) for calculating the free energy of the electron-lattice system. The general formalism is presented in some detail in the next section as a useful approach for studying the thermodynamic behaviour of a perturbed system.

The method has the great advantage that the expressions obtained are regular, no singularities arising from vanishing energy denominators. It is then easy to show that the use of principal values by Fröhlich (1950), in his perturbation theory calculation, was justified. The expression obtained for the free energy due to the electron-lattice interaction is separated into two terms, one depending on the electron distribution alone and one on the phonon distribution. The two terms are discussed separately; that arising from phonon excitations is interpreted as a change in the free energy of the lattice due to a renormalization of the sound velocity. At zero temperature this reduces to the renormalized phonon interaction discussion by Fröhlich (1952). From the point of view of the specific heat this term is taken account of automatically in the empirical lattice specific heat contribution (cf. detailed discussion in § 2).

† Now at Department of Physics, Duke University, Durham, North Carolina, U.S.A.

‡ Now at School of Physics, University of Sydney, Australia.

The other term, which depends on the electron distribution only, is our main concern here, and the calculations of the next section show that the free energy of the electron distribution is considerably modified by the presence of the lattice interaction. We take the Fermi energy ζ_0 to be large compared with kT and $k\theta$, where T and θ are the absolute and Debye temperatures respectively. It is then found that the unperturbed free energy of the N electrons, ϕ_0^{el} , is increased by a factor $1+f$ when the interaction is taken into account. To first order in the interaction constant F ,

$$f = r(\nu)F\{1 + g(T/\theta')\} \quad \dots\dots (I)$$

where ν is the number of free electrons per atom, and

$$\theta' = \begin{cases} \theta, & \\ (4\nu)^{1/3}\theta; & \end{cases} \quad r(\nu) = \begin{cases} (\frac{1}{2}\nu)^{1/3}, & 4\nu > 1 \\ 2\nu; & 4\nu < 1. \end{cases}$$

The function $g(t)$ vanishes at $t=0$ and approaches -1 as $t \rightarrow \infty$. Thus we see that the free energy and hence the specific heat is increased by a factor $1+r(\nu F)$ at low temperatures, and approached the unperturbed value at high temperatures, confirming the same conclusion reached in I. The actual temperature dependence of f contained in the factor $1+g(T/\theta')$ is given in the form of integrals, which cannot be evaluated in closed form. It is shown however that $1+g(t)$ first rises for small t and then decreases to approach zero asymptotically from above. This feature also emerged in figure 2 of I, where the energy level density first increases near ζ_0 before falling away to the unperturbed value.

The effect of coulomb interaction on the electronic specific heat of metals has been discussed recently by Pines (1953). The effect is not great, and for sodium leads to a value of the order of 0.8 of the free electron value. Since this effect is independent of temperature in the range we consider, it can be regarded as included in the 'unperturbed' value and will be ignored.

Current investigations by Hill and Smith† and by Parkinson† on the specific heat of sodium do not confirm the hump at about 7° reported by Pickard and Simon (1948), and presumably due to some fault in their apparatus. The discrepancy, remarked on in I, between the shapes of the observed and theoretical curves at the lowest temperatures does not now arise. The preliminary results obtained by Parkinson indicate a linear specific heat dependence on temperature, for which the coefficient γ has a value between one and two times the free electron value γ_0 . This would imply a value for $(\frac{1}{2})^{1/3}F$ between 0 and 1, comparable with the value ~ 0.2 estimated from high temperature conductivity measurements.

At temperatures of the order of the Debye temperature, θ , it is not possible to determine γ/γ_0 since the lattice specific heat cannot be calculated with sufficient accuracy. For higher temperatures, $\theta \ll T \ll \zeta/k$, the lattice specific heat is constant and equal to the equipartition value, so that the total specific heat is again linear. In this region $f=0$, and a comparison between the high and very low temperature linear specific heats permits in principle a direct determination of the factor $1+f$ for $T=0$. It is of interest in this connection that Manning and Chodorow (1939) have calculated the electronic specific heat for tungsten and tantalum; agreement with the observed high-temperature values of γ is good, whereas the observed low-temperature value for tantalum is about four times as great. While the theory presented here cannot be applied quantitatively

† Private communications.

to an electronic structure as complicated as that of tantalum, the large value of γ at low temperatures may well be due to this effect of lattice interaction.

The modification to the electronic energy level distribution near the Fermi level should lead to observable effects in other low temperature properties as well as the specific heat.

The soft x-ray emission spectra of metals reflects directly the properties of the energy level distribution (Skinner 1939). At low temperatures and sufficiently fine resolution there should be a peak in the spectrum just before the edge of the emission band. Skinner (1940) has observed a small bump, of the type expected, in the spectrum of sodium at the temperature of liquid oxygen. The conditions of these experiments, in which the resolution was about 0.05 eV, are just at the limit of observability of the effect, so that a quantitative analysis is not possible. However, the magnitude of the observed effect is consistent with the present theory, which is also supported by the fact that the bump disappeared at higher temperatures. The explanation offered at the time of the experiments, namely an overlapping of bands, seems most unlikely in the case of sodium.

Other properties of simple metals, whose measurement at low temperatures would be of interest in connection with the present theory, include the Pauli paramagnetism, the spectral and energy distribution of photoelectrons, and the Hall constant. For example, the observed paramagnetic susceptibility of sodium at room temperature is in good agreement with the free electron value of 0.65×10^{-6} c.g.s. units. The theory implies that at low temperatures this value should be increased by the factor $1+f$, so that the experimental investigation of this point would be of great value.

§ 2. CALCULATIONS

We use the formalism of perturbation theory on the density matrix as developed in II. There the following analogue of the Taylor expansion for matrix functions was given. In the representation in which the operator Λ_0 is diagonal,

$$\Lambda_0 |n\rangle = \lambda_n |n\rangle, \quad \dots\dots (1)$$

the matrix elements of a function $F_0(\Lambda_0 + \epsilon\Lambda_1)$ of a perturbed operator are given by

$$\begin{aligned} \langle n | F_0(\Lambda_0 + \epsilon\Lambda_1) | n' \rangle &= \langle n | 1 | n' \rangle F_0(\lambda_n) + \epsilon \langle n | \Lambda_1 | n' \rangle F_1(\lambda_n, \lambda_{n'}) \\ &+ \epsilon^2 \sum_{n''} \langle n | \Lambda_1 | n'' \rangle \langle n'' | \Lambda_1 | n' \rangle F_2(\lambda_n, \lambda_{n''}, \lambda_{n'}) + O(\epsilon^3). \end{aligned} \quad \dots\dots (2)$$

Here $F_k(x_0, \dots, x_k)$ are the difference quotients of $F_0(x_0)$ given by

$$F_k(x_0, \dots, x_k) = \sum_{i=0}^k \frac{F_0(x_i)}{\prod_{j \neq i} (x_i - x_j)}. \quad \dots\dots (3)$$

They are symmetrical functions in their variables and have the following property for confluent arguments

$$(\lambda \leq k) \lim_{\substack{x_1 \rightarrow x_0 \\ \vdots \\ x_\lambda \rightarrow x_0}} F_k(x_0, x_1, \dots, x_k) = \frac{1}{\lambda!} \frac{\partial^\lambda}{\partial x_0^\lambda} F_{k-\lambda}(x_0, x_{\lambda+1}, \dots, x_k) \quad \dots\dots (4)$$

which ensures that for a Λ_1 simultaneously diagonal with Λ_0 , (2) goes over into the usual Taylor series.

This theorem is applied to the calculation of the free energy of a perturbed system in the following way. The free energy ϕ is determined by

$$\text{Tr } e^{\alpha(\phi-H)} = 1, \quad (\alpha = 1/kT) \quad \dots\dots(5)$$

Let the Hamiltonian be of the form

$$H = H_0 + \epsilon H_1, \quad \dots\dots(6)$$

where the eigenstates $|n\rangle$ of the free Hamiltonian are known:

$$H_0|n\rangle = E_n|n\rangle. \quad \dots\dots(7)$$

We wish to find the free energy up to terms of the order ϵ^2 . We put therefore

$$\phi = \phi_0 + \epsilon\phi_1 + \epsilon^2\phi_2 + \dots \quad \dots\dots(8)$$

Calling then

$$F_0(\phi-H) \equiv e^{\alpha(\phi-H)} \quad \dots\dots(9)$$

we can apply (2) with $\Lambda_0 = \phi_0 - H_0$, $\Lambda_1 = \phi_1 - H_1 + \epsilon\phi_2$. (5) thus becomes, writing for simplicity $\langle n|1|n'\rangle\phi_1 \equiv \langle n|\phi_1|n'\rangle$,

$$\begin{aligned} 1 = & \sum_n F_0(\phi_0 - E_n) + \epsilon \sum_n \langle n|\phi_1 - H_1|n\rangle F_1(\phi_0 - E_n, \phi_0 - E_n) \\ & + \epsilon^2 \left\{ \sum_n \langle n|\phi_2|n\rangle F_1(\phi_0 - E_n, \phi_0 - E_n) \right. \\ & + \sum_{nn'} \langle n|\phi_1 - H_1|n'\rangle \langle n'|\phi_1 - H_1|n\rangle \\ & \times F_2(\phi_0 - E_n, \phi_0 - E_{n'}, \phi_0 - E_n) \} \quad \dots\dots(5') \end{aligned}$$

which yields

$$\sum_n F_0(\phi_0 - E_n) = 1, \quad \dots\dots(10)$$

$$\sum_n \langle n|\phi_1 - H_1|n\rangle F_1(\phi_0 - E_n, \phi_0 - E_n) = 0, \quad \dots\dots(11)$$

$$\begin{aligned} & \sum_n \langle n|\phi_2|n\rangle F_1(\phi_0 - E_n, \phi_0 - E_n) \\ & + \sum_{nn'} \langle n|\phi_1 - H_1|n'\rangle \langle n'|\phi_1 - H_1|n\rangle F_2(\phi_0 - E_n, \phi_0 - E_{n'}, \phi_0 - E_n) = 0. \quad \dots\dots(12) \end{aligned}$$

(10) expresses the definition of the zero-order free energy. (11) defines the first-order perturbation of the free energy. For the frequent case that H_1 has no diagonal elements—as for our problem—it simply reduces to $\phi_1 = 0$. Restricting ourselves to this case and using (9) and (4), we can rewrite (12) as

$$\alpha\phi_2 = \sum_{nn'} |\langle n|H_1|n'\rangle|^2 \left[\frac{\alpha(E_n - E_{n'}) + (1 - \exp[\alpha(E_n - E_{n'})])}{(E_n - E_{n'})^2} \right] \exp\{\alpha(\phi_0 - E_n)\}. \quad \dots\dots(13)$$

The advantage of the present method is apparent here: instead of the usual energy denominators of perturbation theory the expansion of the free energy contains regular expressions only, like the one in the square brackets; no ambiguities of the kind occurring in perturbation theory on the energy levels in an unsuitable representation arise here.†

† The fact that perturbation theory on the free energy is valid even for systems with a degeneracy where perturbation theory on the Hamiltonian is not directly applicable was first noticed by Peierls (1933).

For our present application we take H_0 to describe a system of N free electrons and a phonon gas in a periodicity volume G :

$$H_0 = \sum_{\mathbf{k}, \sigma} \epsilon_{\mathbf{k}} n_{\mathbf{k}, \sigma} + \sum_{\mathbf{w}} \hbar |\mathbf{w}| s N_{\mathbf{w}}. \quad \dots\dots (14)$$

$n_{\mathbf{k}, \sigma}$ is the occupation number operator of an electron state with momentum $\hbar \mathbf{k}$ and spin σ ; $N_{\mathbf{w}}$ the occupation number operator for a phonon of wave number \mathbf{w} ; $w = |\mathbf{w}|$; s is the velocity of sound, which for the moment may depend on \mathbf{w} : $s = s(\mathbf{w})$. This gives for ϕ_0 the sum of the well-known free energies

$$\left. \begin{aligned} \phi_0^{\text{el}} &= -\frac{\pi^2}{4} N \frac{(\hbar T)^2}{\zeta_0} \left[1 + O\left(\frac{\hbar T}{\zeta}\right) \right] \\ \phi_0^{\text{ph}} &= 3\nu^{-1} N \hbar k T \left(\frac{T}{\theta}\right)^3 \int_0^{\theta/T} dx x^2 \log(1 - e^{-x}). \end{aligned} \right\} \quad \dots\dots (15)$$

(in Debye approximation).

ζ_0 is the Fermi energy at $T=0$, given by

$$\zeta_0 = \frac{\hbar^2 k_0^2}{2m}, \quad \text{also} \quad N = 2 \frac{2k_0^3}{3(2\pi)^2} G. \quad \dots\dots (16)$$

We shall work in the representation in which $N_{\mathbf{w}}$ and $n_{\mathbf{k}, \sigma}$ are diagonal; $N_{\mathbf{w}}$ runs over all positive integers, $n_{\mathbf{k}, \sigma}$ over 0 and 1. ϵH_1 describes the interaction between electrons and phonons; its matrix elements M are taken to be

(a) for emission of a phonon:

$$N_{\mathbf{w}} \rightarrow N_{\mathbf{w}} + 1, \quad n_{\mathbf{k}, \sigma} \rightarrow n_{\mathbf{k}, \sigma} + 1, \quad n_{\mathbf{k}+\mathbf{w}, \sigma'} \rightarrow n_{\mathbf{k}+\mathbf{w}, \sigma'} - 1$$

$$|M|^2 = D(\mathbf{w})(N_{\mathbf{w}} + 1)(1 - n_{\mathbf{k}, \sigma})n_{\mathbf{k}+\mathbf{w}, \sigma'};$$

(b) for absorption of a phonon:

$$N_{\mathbf{w}} \rightarrow N_{\mathbf{w}} - 1, \quad n_{\mathbf{k}, \sigma} \rightarrow n_{\mathbf{k}, \sigma} - 1, \quad n_{\mathbf{k}+\mathbf{w}, \sigma'} \rightarrow n_{\mathbf{k}+\mathbf{w}, \sigma'} + 1,$$

$$|M|^2 = D(\mathbf{w})N_{\mathbf{w}}n_{\mathbf{k}, \sigma}(1 - n_{\mathbf{k}+\mathbf{w}, \sigma'});$$

(c) for all other processes:

$$|M|^2 = 0.$$

Here $D(\mathbf{w})$ is an interaction constant given by

$$D(\mathbf{w}) = \frac{1}{G} \frac{4}{3} \frac{F \hbar s(\mathbf{w})}{n} \zeta_0 w, \quad (nG = N/\nu) \quad \dots\dots (17)$$

in Fröhlich's notation. Inserting this into (13) we get

$$\phi_2 = \phi_2^{\text{a}} + \phi_2^{\text{b}},$$

where, for example,

$$\begin{aligned} \phi_2^{\text{a}} &= 2 \sum_{(N_{\mathbf{w}})} \sum_{(n_{\mathbf{k}})} \sum_{\mathbf{w}, \mathbf{k}} D(\mathbf{w}) \cdot (N_{\mathbf{w}} + 1)(1 - n_{\mathbf{k}})n_{\mathbf{k}+\mathbf{w}} \\ &\times \exp \left[\alpha \left(\phi_0 - \sum_{\mathbf{k}'} n_{\mathbf{k}'} \epsilon_{\mathbf{k}'} - \sum_{\mathbf{w}} N_{\mathbf{w}} \hbar s w \right) \right] \\ &\times \left[\frac{\epsilon_{\mathbf{k}+\mathbf{w}} - \epsilon_{\mathbf{k}} - \hbar s w + \alpha^{-1} \{ 1 - \exp \alpha (\epsilon_{\mathbf{k}+\mathbf{w}} - \epsilon_{\mathbf{k}} - \hbar s w) \}}{(\epsilon_{\mathbf{k}+\mathbf{w}} - \epsilon_{\mathbf{k}} - \hbar s w)^2} \right] \end{aligned}$$

(the factor 2 comes from the summation over spins). As the bracket is independent of the occupation numbers $N_{\mathbf{w}}$ and $n_{\mathbf{k}}$, the sum over $(N_{\mathbf{w}})$ and $(n_{\mathbf{k}})$ can be carried out. The effect of this is simply to replace $N_{\mathbf{w}}$ and $n_{\mathbf{k}}$ by their thermal

equilibrium values:

$$\left. \begin{aligned} \phi_2^a &= 2 \sum_{\mathbf{w}, \mathbf{k}} D(\mathbf{w}) (\bar{N}_{\mathbf{w}} + 1) (1 - \bar{n}_{\mathbf{k}}) \bar{n}_{\mathbf{k}+\mathbf{w}} \left[\frac{x + \alpha^{-1}(1 - e^{\alpha x})}{x^2} \right] \\ \phi_2^b &= 2 \sum_{\mathbf{w}, \mathbf{k}} D(\mathbf{w}) \bar{N}_{\mathbf{w}} \bar{n}_{\mathbf{k}} (1 - \bar{n}_{\mathbf{k}+\mathbf{w}}) \left[\frac{-x + \alpha^{-1}(1 - e^{-\alpha x})}{x^2} \right] \end{aligned} \right\} \dots\dots (18)$$

with $x \equiv \epsilon_{\mathbf{k}+\mathbf{w}} - \epsilon_{\mathbf{k}} - \hbar s \mathbf{w}$, where

$$\bar{N}_{\mathbf{w}} = [\exp(\alpha \hbar s \mathbf{w}) - 1]^{-1}, \quad \dots\dots (19)$$

$$\bar{n}_{\mathbf{k}} = [1 + \exp \alpha(\epsilon_{\mathbf{k}} - \zeta)]^{-1}. \quad \dots\dots (20)$$

The two terms in (18) can then be collected under one sum $\Sigma_{\mathbf{w}, \mathbf{k}}$; using the fact that from (19), (20)

$$(\bar{N}_{\mathbf{w}} + 1)(1 - \bar{n}_{\mathbf{k}}) \bar{n}_{\mathbf{k}+\mathbf{w}} \cdot \exp \alpha(\epsilon_{\mathbf{k}+\mathbf{w}} - \epsilon_{\mathbf{k}} - \hbar s \mathbf{w}) = \bar{N}_{\mathbf{w}} \bar{n}_{\mathbf{k}} (1 - \bar{n}_{\mathbf{k}+\mathbf{w}})$$

(18) simplifies to

$$\phi_2 = 2 \sum_{\mathbf{w}, \mathbf{k}} D(\mathbf{w}) \frac{(\bar{N}_{\mathbf{w}} + 1)(1 - \bar{n}_{\mathbf{k}}) \bar{n}_{\mathbf{k}+\mathbf{w}} - \bar{N}_{\mathbf{w}} \bar{n}_{\mathbf{k}} (1 - \bar{n}_{\mathbf{k}+\mathbf{w}})}{\epsilon_{\mathbf{k}+\mathbf{w}} - \epsilon_{\mathbf{k}} - \hbar s \mathbf{w}} \quad \dots\dots (21)$$

which is still regular at the zero of the denominator. (The fact that the extra terms in the brackets in (18) actually cancel in the end is not accidental; their only purpose in the earlier formulae is to keep the brackets regular however the terms (a) and (b) be evaluated.)

Next we wish to split up the sum in (21) into terms involving the phonon distribution $\bar{N}_{\mathbf{w}}$ and terms depending only on the electronic distribution $\bar{n}_{\mathbf{k}}$. By doing this our summand ceases to be regular. But as we know that the total expression (21) is regular we can choose an *arbitrary* way of defining the summation over the pole in the separate sums, provided that the total of these so defined sums reduces to (21). A convenient definition of singular integrals is the principal value and this has the required property. Thus we write

$$\phi_2 = 2 \sum_{\mathbf{w}, \mathbf{k}}^P D(\mathbf{w}) \frac{\bar{N}_{\mathbf{w}}(\bar{n}_{\mathbf{k}+\mathbf{w}} - \bar{n}_{\mathbf{k}})}{\epsilon_{\mathbf{k}+\mathbf{w}} - \epsilon_{\mathbf{k}} - \hbar s \mathbf{w}} + 2 \sum_{\mathbf{w}, \mathbf{k}}^P D(\mathbf{w}) \frac{\bar{n}_{\mathbf{k}+\mathbf{w}}(1 - \bar{n}_{\mathbf{k}})}{\epsilon_{\mathbf{k}+\mathbf{w}} - \epsilon_{\mathbf{k}} - \hbar s \mathbf{w}}. \quad \dots\dots (22)$$

Note. It is easily seen that the first sum goes to zero with vanishing temperature (see below); therefore at $T=0$ the change in energy of the electron gas due to its interaction with the phonons (which equals ϕ_2 at $T=0$) is given by the second term. This justifies the use of principal values in this problem by Fröhlich (1950).

We first discuss the terms involving the phonon distribution $\bar{N}_{\mathbf{w}}$. They can be written

$$\phi_2^{\text{ph}} = 2 \sum_{\mathbf{w}} \bar{N}_{\mathbf{w}} \hbar s \mathbf{w} \delta s(\mathbf{w}) \quad \dots\dots (23)$$

with

$$\delta s(\mathbf{w}) = \frac{2D(\mathbf{w})}{\hbar s \mathbf{w}} \sum_{\mathbf{k}}^P \frac{\bar{n}_{\mathbf{k}+\mathbf{w}} - \bar{n}_{\mathbf{k}}}{\epsilon_{\mathbf{k}+\mathbf{w}} - \epsilon_{\mathbf{k}} - \hbar s \mathbf{w}}. \quad \dots\dots (24)$$

(23) can be interpreted as the change in the free energy due to a variation $\delta s(\mathbf{w})$, equation (24), in sound velocity. If we insert into (24) for $\bar{n}_{\mathbf{k}+\mathbf{w}}$ and $\bar{n}_{\mathbf{k}}$ the zero-temperature distributions, $\delta s(\mathbf{w})$ goes over into $\delta_0 s(\mathbf{w})$, the change in sound-wave interaction at absolute zero discussed by Fröhlich (1952). Writing then

$$\delta s = \delta_0 s + \delta_1 s \quad \dots\dots (25)$$

we shall consider the effects of δ_0 and δ_1 separately.

The contribution to ϕ_2^{ph} due to $\delta_0 s$ will not be calculated here for the following reason. Its contributions are important in the same region ($T \sim \theta$) where the Debye approximation fails. If one knows experimentally the spectrum $s_{\text{exp}}(\mathbf{w})$ of the sound velocity, then this should be taken to be $s_{\text{exp}}(\mathbf{w}) = s(\mathbf{w}) + \delta_0 s(\mathbf{w})$, i.e. $\delta_0 s(\mathbf{w})$ then represents an unobservable renormalization. If, however, the lattice specific heat is calculated from a true lattice theory, then $\delta_0 s(\mathbf{w})$ should be evaluated from (24) for the same model of the lattice; the Debye approximation would here be misleading as $\delta_0 s$ strongly depends on the lattice type. We shall therefore omit this contribution to the free energy, taking it for granted that it has been accounted for in the first way.

The contribution due to $\delta_1 s(\mathbf{w})$ can be worked out, in the Debye approximation (taking s as constant), to give a correction

$$\delta\phi = -\frac{\pi^2}{4} \nu F \left(\frac{kT}{\zeta_0} \right)^2 \phi_0^{\text{ph}}. \quad \dots\dots(26)$$

This is clearly negligible in our approximation, so that ϕ_2^{ph} is fully accounted for by the above 'renormalization' terms.

We now turn to the terms not involving the phonon distribution with which we are mainly concerned, i.e.

$$\phi_2^{\text{el}} = 2 \sum_{\mathbf{w}, \mathbf{k}}^{\text{P}} D(\mathbf{w}) \frac{\bar{n}_{\mathbf{k}+\mathbf{w}}(1-\bar{n}_{\mathbf{k}})}{\epsilon_{\mathbf{k}+\mathbf{w}} - \epsilon_{\mathbf{k}} - \hbar s w}. \quad \dots\dots(27)$$

These give rise to a change of the free energy of the free electrons by a temperature independent factor at low temperatures ($T \ll \theta$). We wish, however, to get some idea of their behaviour at high temperatures ($T \gtrsim \theta$, but $kT \ll \zeta_0$). This again depends upon the lattice, but as we wish only a qualitative picture we shall evaluate it in the Debye approximation; i.e. we put $s(\mathbf{w}) = \text{constant}$, and cut off the phonon spectrum at $w = w_0$, given by

$$\hbar s w_0 = k\theta. \quad \dots\dots(28)$$

We wish to evaluate (27) under the assumptions

$$kT \ll \zeta_0, \quad k\theta \ll \zeta_0, \quad \dots\dots(29)$$

the relative magnitude of T and θ remaining open. It is convenient to write for the Fermi distribution the following expression, valid for $kT \ll \zeta_0$:

$$\bar{n}(\epsilon) \equiv \{\exp[\alpha(\epsilon - \zeta)] + 1\}^{-1} = \theta(\zeta - \epsilon) - \int_{-\infty}^{+\infty} d\xi g(\xi) \delta'(\epsilon - \zeta - \xi) \quad \dots\dots(30)$$

where

$$\theta(x) = \begin{cases} 1 & x \geq 0, \\ 0 & x < 0; \end{cases} \quad \dots\dots(30')$$

$$g(\xi) = \int_{|\xi|}^{\infty} d\epsilon \frac{1}{e^{\alpha\epsilon} + 1}, \quad \dots\dots(30'')$$

$$\int_{-\infty}^{+\infty} d\xi g(\xi) = \frac{1}{6} \pi^2 (kT)^2,$$

and $\delta(x)$ is Dirac's δ -function, $\delta'(x)$ its derivative. When inserting this into (27) we will consistently neglect terms of the order kT/ζ_0 and $k\theta/\zeta_0$ relative to the others. The result then appears as the first term in a power series in kT/ζ with coefficients being functions of T/θ . The leading term for $T \ll \theta$ results when $g(\xi)$ is replaced by $\frac{1}{6} \pi^2 (kT)^2 \delta(\xi)$.

Inserting (30) into (27) we get three terms. The first involves the product of two θ -functions and represents the self-energy of an assembly of electrons with given ζ ; it is temperature dependent only through ζ . Now this self-energy is of the order $N\zeta 2ms/\hbar k_0$ (Frohlich 1950); a change in ζ of the order of $\delta\zeta = (\mathbf{k}T)^2/\zeta$ gives, therefore, a change in the free energy of the order

$$N \frac{2ms}{\hbar k_0} \frac{(\mathbf{k}T)^2}{\zeta} \sim N \frac{\mathbf{k}\theta}{\zeta} \frac{(\mathbf{k}T)^2}{\zeta}$$

which is of the negligible order $\mathbf{k}\theta/\zeta$ compared with ϕ_0^{el} .

The second term arises from the cross-products between θ -functions and δ' -functions in (30) and reads, upon replacing sums by integrals,

$$\phi_{2a}^{\text{el}} = \frac{CG^2}{(2\pi)^6} \int_{-\infty}^{+\infty} d\xi g(\xi) I(\xi) \quad \dots\dots(31)$$

with

$$I(\xi) = 2 \int d^3\mathbf{k} \int d^3\mathbf{w} w \frac{\delta'(\epsilon_{\mathbf{k}+\mathbf{w}} - \zeta - \xi)}{\epsilon_{\mathbf{k}+\mathbf{w}} - \epsilon_{\mathbf{k}} - \hbar^2 w \sigma(k)/2m}, \quad \dots\dots(31')$$

where we have put $D(\mathbf{w}) = Cw$ and where

$$\frac{\hbar}{2ms} \sigma(k) = \begin{cases} +1 & |\mathbf{k}| \equiv k > k_0, \\ -1 & k < k_0. \end{cases}$$

This yields easily

$$I(\xi) = 8\pi^2 \left(\frac{2m}{\hbar^2}\right)^3 \int_0^{w_0} dw w^2 \int_{|k_1-w|}^{k_1+w} dk k \frac{1}{(k_1^2 - k^2 + \sigma(k)w)^2}$$

where $k_1^2 = 2m(\zeta + \xi)/\hbar^2$. The evaluation of this integral is straightforward; care has to be taken for $2k_1 = w_0$, where the singular line $k^2 = k_1^2 + \sigma(k)w$, which gives the main contribution, leaves the domain of integration. This makes it necessary to distinguish between the two cases $2k_0 < w_0$ and $2k_0 > w_0$.

For the case $w_0 > 2k_0$ we get, neglecting all terms which are of the relative order $\mathbf{k}T/\zeta$ or $\mathbf{k}\theta/\zeta$,†

$$I(\xi) = 4\pi^2 \left(\frac{2m}{\hbar^2}\right)^3 \frac{w_0^2}{k_0} \frac{\zeta}{\hbar s k_0} \left\{ 1 + \frac{\xi^2}{(\mathbf{k}\theta)^2} \log \left| \frac{\xi^2 - (\mathbf{k}\theta)^2}{\xi^2} \right| \right\} \quad \dots\dots(32)$$

and similarly for $w_0 < 2k_0$.

If we define

$$\mathbf{k}\theta' = \min [\hbar s w_0, 2\hbar s k_0],$$

$$\text{i.e.} \quad \theta' = \begin{cases} \theta & (w_0 < 2k_0) \\ 2(\frac{1}{2}\nu)^{1/3}\theta & (w_0 > 2k_0) \end{cases} \quad \dots\dots(33)$$

$$\text{and} \quad r(\nu) = \begin{cases} (\frac{1}{2}\nu)^{1/3} & (w_0 < 2k_0) \\ 2\nu & (w_0 > 2k_0), \end{cases} \quad \dots\dots(33')$$

inserting I (32) into (31) gives

$$\phi_{2a}^{\text{el}} = \phi_0^{\text{el}} r(\nu) F\{1 + f_a(T/\theta')\} \quad \dots\dots(34)$$

with

$$f_a(t) = \frac{4}{\pi^2} \int_0^\infty dx \frac{1}{e^x + 1} \left\{ t^2 x^3 \log \frac{1 - t^2 x^2}{t^2 x^2} - 2x - \frac{1}{t} \log \left| \frac{1 - tx}{1 + tx} \right| \right\}. \quad \dots\dots(35)$$

† Actually, for $w_0 \sim 2k_0$ these terms get somewhat more important, being then of the order of $\max \left[\frac{\mathbf{k}\theta}{\zeta} \log \frac{\mathbf{k}\theta}{\zeta}, \frac{\mathbf{k}T}{\zeta} \log \frac{\mathbf{k}T}{\zeta} \right]$, though still negligible.

The remaining third term, ϕ_{2b}^{el} , in the evaluation of (27), which is obtained by inserting the second term in (30) for both $\bar{n}_{\mathbf{k}}$ and $\bar{n}_{\mathbf{k}+\mathbf{w}}$, is evaluated similarly and gives

$$\phi_{2b}^{\text{el}} = \phi_0^{\text{el}} r(\nu) F f_b(T/\theta') \quad \dots\dots (36)$$

with

$$f_b(t) = \frac{24}{\pi^2} t^2 \int_0^\infty dx_1 \int_0^\infty dx_2 \frac{1}{(1 + \exp x_1)(1 + \exp x_2)} \\ \times \left\{ (x_1 + x_2)^2 \log \left| \frac{(x_1 + x_2)^2 - t^{-2}}{(x_1 + x_2)^2} \right| - (x_1 - x_2)^2 \log \left| \frac{(x_1 - x_2)^2 - t^{-2}}{(x_1 - x_2)^2} \right| \right\}. \\ \dots\dots (37)$$

Thus finally, writing $g(t) = f_a(t) + f_b(t)$ where $f_a(t)$ and $f_b(t)$ are given by (35) and (37), we obtain

$$(\phi_0 + \phi_2)^{\text{el}} = \phi_0^{\text{el}} [1 + r(\nu) F \{1 + g(T/\theta')\}]. \quad \dots\dots (38)$$

This contains the result (I) of § 1,

It remains to study the behaviour of $g(t)$ for low and high temperatures.

(a) *Low temperatures.* Expansion of $g(t)$ in powers of t yields

$$g(t) = \frac{9\pi^2}{5} t^2 |\log t| - K t^2 \quad \dots\dots (39)$$

where K is essentially given by a transcendental double integral which cannot be evaluated exactly. It can, however, easily be shown that $K > 8$, this being a very inaccurate lower limit (probably $K \gtrsim 20$).

(b) *High temperatures.* For $t \rightarrow \infty$, $g(t)$ tends to -1 , showing thus that for $T \gg \theta$ the effect of the lattice interaction on the electronic free energy is smeared out, as was to be expected. The actual asymptotic expansion again cannot be given in closed form. It is, however, easy to conclude that $g(t) + 1$ is positive for large t , so that the magnitude of the free energy is never decreased by the lattice interaction.

ACKNOWLEDGMENT

We wish to express our appreciation to Professor H. Fröhlich for his interest in this work.

REFERENCES

- BUCKINGHAM, M. J., 1951, *Nature, Lond.*, **168**, 281.
 FRÖHLICH, H., 1950, *Phys. Rev.*, **79**, 845; 1952, *Proc. Roy. Soc. A*, **215**, 291.
 MANNING, M. F., and CHODOROW, M. I., 1939, *Phys. Rev.*, **56**, 787.
 PEIERLS, R., 1933, *Z. Phys.*, **80**, 763.
 PICKARD, G. L., and SIMON, F. E., 1948, *Proc. Phys. Soc. A*, **61**, 1.
 PINES, D., 1953, *Phys. Rev.*, **92**, 626.
 SCHAFROTH, M. R., 1951, *Helv. Phys. Acta*, **24**, 645.
 SKINNER, H. W. B., 1939, *Rep. Progr. Phys.*, **5**, 257 (London: Physical Society); 1940, *Phil. Trans. Roy. Soc. A*, **239**, 95.

The Thermal Conductivity of Germanium and Silicon at Low Temperatures

By H. M. ROSENBERG

The Clarendon Laboratory, Oxford

Communicated by K. Mendelssohn; MS. received 24th May 1954

Abstract. The thermal conductivity of a single crystal of Ge and a polycrystalline specimen of Si have been measured in the range 2 to 100°K. Both specimens were very pure. The results indicate that, at low temperatures at least, the lattice waves are not scattered by the conduction electrons, but that their mean free path is limited either by the size of the specimen (for the germanium) or by the crystallite size (for the silicon).

§ 1. INTRODUCTION

THERE are two main reasons why it is of interest to measure the thermal conductivity of germanium and silicon. The first is that their crystal structure is the same as that of the diamond lattice. The thermal conductivity of diamond has recently been measured very carefully (Berman, Simon and Ziman 1953). Their experiments show that the maximum conductivity is much lower than one would expect theoretically, and also that this maximum is not as sharp as that found in other crystals, but that it has been flattened into a plateau. Therefore experiments on germanium and silicon are of interest to see whether a similar effect occurs in these elements.

The second reason for these experiments was to see whether in very pure semiconductors any effect due to the presence of conduction electrons could be detected. Electrical resistance measurements at low temperatures indicate that the number of current carriers must be very small, and so it is very unlikely that they can make any detectable contribution to the heat flow. Nevertheless, there might still be a sufficient number of carriers to scatter the lattice waves and in this way to decrease the thermal conductivity, since the measurement of thermal conductivity is an extremely sensitive method of detecting the scattering of phonons.

The behaviour of the thermal conductivity of dielectric crystals at low temperatures is now well established and the temperature dependence of this conductivity is explained very satisfactorily by the theory as developed by Peierls (1929, 1935). In this, the probability of phonon-phonon scattering, and hence the thermal resistance, decreases exponentially as the temperature is decreased. Below a certain temperature, however, the mean free path of the phonons becomes equal to the diameter of the specimen and cannot increase any more. This, together with the T^3 dependence of the specific heat, causes the thermal resistance to start to increase again at lower temperatures and to be proportional to T^{-3} .

Thus the thermal resistance shows a minimum at low temperatures, below which the conductivity is limited by the size of the specimen. A fuller review of the theory and its experimental verification is given by Berman (1953).

§2. THE SPECIMENS

The germanium specimen, Ge 1, was a single crystal about 1 cm long and with a rectangular cross section of 1.2 mm by 0.6 mm. It had a resistivity of 60 ohm cm at room temperature, indicating a very high degree of purity. Thermal contact was made at two points along the specimen by soldering annealed copper wires to it, using lactic acid as flux (Mitchell 1954).

The silicon specimen, Si 1, was prepared from a long thin needle of high purity silicon very kindly presented by Messrs. Johnson, Matthey. This was polycrystalline and was composed of fairly large crystallites which were about 0.2 mm in size. The sample was ground down until its cross section was about 1.5 mm square. It was about 1 cm long. It was then nickel-plated so that thermal contacts could be soldered to it. The unwanted nickel was dissolved off with acid.

The specimens were mounted so that one end was in contact with the helium container of a Simon expansion liquefier. A small electric heater was attached to the other end and the temperature gradient along the specimen was measured by two helium gas thermometers. Further details of the experimental procedure will be given in another paper by Rosenberg. Thermal conductivity measurements were taken from 2 to 100°K. The temperature differences varied from about 0.1 degree at the lower temperatures to about 1 degree at the higher temperatures.

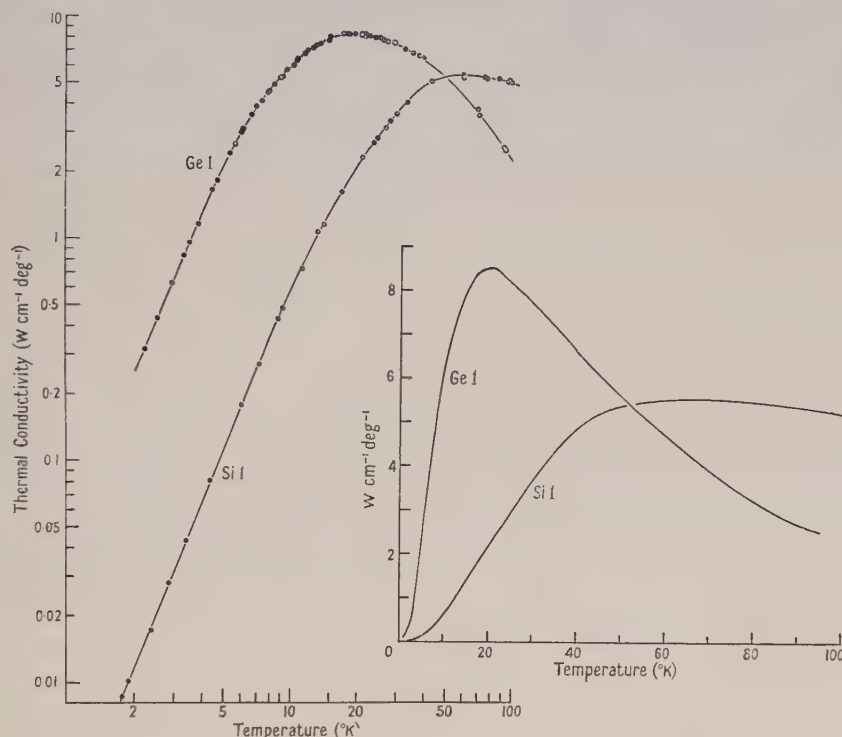
§3. RESULTS AND DISCUSSION

The graphs of thermal conductivity against temperature which were obtained in these experiments are shown on a logarithmic scale in the figure. The inset shows the same points plotted on a linear scale. The general form is that which one would expect from a pure dielectric crystal. At low temperatures the graphs are linear, indicating that the conductivity is proportional to a power of T . This power is 2.4 for the germanium and 2.5 for the silicon. These are less than the T^3 dependence predicted by the theory. Whilst this may be due to an oversimplification in the theoretical development, it should also be borne in mind that the specific heats of the diamond lattice elements are not strictly proportional to T^3 . All of them show a minimum in the value of the Debye θ (Hill and Parkinson 1952).

At higher temperatures the thermal conductivity of both specimens passes through a maximum, although for the silicon this was only just within the experimental range. Whilst the peak of the germanium curve might not be quite so sharp as that of other crystals it certainly does not show the peculiar plateau exhibited by diamond. The general form of the germanium curve is similar to that found by Estermann and Zimmerman (1951), but the conductivity of their specimen was much lower, as it was much less pure than ours.

The mean free path of the phonons has been calculated from the values of the thermal conductivity in the liquid helium region. For germanium the specific heat data of Estermann and Friedberg (1951) have been used ($\theta = 280^\circ$). The value of the mean free path comes out to be approximately 0.52 mm. This is approximately the same as the smallest dimension of the specimen (0.6 mm), indicating that in this region the conductivity is indeed being limited by the

specimen size. For silicon the specific heat measurements of Keesom and Pearlman (1952) have been used ($\theta = 668^\circ$). In this case the mean free path of the phonons was found to be approximately 0.13 mm. Whilst this is much smaller than the size of the specimen (1.5 mm square), it is about the same size as the dimensions of the crystallites of which the specimen was composed (~ 0.2 mm). In the silicon, therefore, it seems likely that the mean free path of the phonons is being limited by the dimensions of the crystallites. A single crystal specimen of silicon would probably give a much higher conductivity.



The thermal conductivity of the germanium and silicon specimens in the range 2 to 100°K plotted on a logarithmic scale. The inset shows the same curves plotted on a linear scale.

Thus the experimental results seem to be explained quite satisfactorily, at the lower temperatures at least, by assuming that the heat transport is by the lattice waves. These appear only to be scattered by the boundaries of the specimen or crystallites. The experiments provide no evidence that electrons play any noticeable part in the scattering process. It is not possible to be so specific about the higher part of the temperature range, but from a comparison of the general form of the curves with those obtained from other dielectric crystals it does not seem that electron scattering can be appreciable in this region either.

ACKNOWLEDGMENTS

I should like to thank Dr. K. Mendelssohn for the interest he has taken in this work, and Mr. E. L. Simmons for his advice and help in the preparation of the specimens.

REFERENCES

- BERMAN, R., 1953, *Advances in Physics* (*Phil. Mag.*, Suppl.), **2**, 103.
BERMAN, R., SIMON, F. E., and ZIMAN, J. M., 1953, *Proc. Roy. Soc. A*, **220**, 171.
ESTERMANN, I., and FRIEDBERG, S. A., 1951, Carnegie Inst. of Technology, O.N.R. Tech. Report No. 8.
ESTERMANN, I., and ZIMMERMAN, J. E., 1951, Carnegie Inst. of Technology, O.N.R. Tech. Report No. 6.
HILL, R. W., and PARKINSON, D. H., 1952, *Phil. Mag.*, **43**, 309.
KEESOM, P. H., and PEARLMAN, N., 1952, *Phys. Rev.*, **85**, 730.
MITCHELL, W. M., 1954, *J. Sci. Instrum.*, **31**, 147.
PEIERLS, R., 1929, *Ann. Phys., Lpz.*, **3**, 1055; 1935, *Ann. Inst. Poincaré*, **5**, 177.

The Emission of Light in the Passage of Alpha Particles through Gases

By A. WARD

Natural Philosophy Department, Glasgow University

MS. received 1st February 1954

Abstract. The emission of light from the tracks of α -particles in the gases argon, helium, nitrogen and methane has been studied using a photomultiplier. The specific emission along the track has been measured together with the total number of photons which are produced in the range 3000–6000 Å. The total number of emitted photons is found to be independent of pressure in the monatomic gases argon and helium, but varies with pressure in nitrogen and in mixtures of methane with argon or helium. The variation with pressure is explained by a simple theory of quenching by collision. The lifetime of the excited states responsible for the emission is estimated to be less than 10^{-6} second. The recombination of the ions is shown to play no appreciable part in the production of the photons.

§ 1. INTRODUCTION

FROM the earliest days of radioactivity the emission of light has been observed from gases near strong sources of α -particles. Similar effects are noticed in the residual gases and vapours of high tension accelerators and cyclotrons. With the advent of the highly sensitive photomultiplier having a sensitivity curve not very different from that of the eye and a far higher detection efficiency for transient light pulses, this emission can be investigated quantitatively with weak sources of α -particles (Grun and Schopper 1952, Auderbert and Lormeau 1949, 1950). The present paper describes experiments upon the emission of these photons during the passage of α -particles through the gases argon, helium, nitrogen and methane.

§ 2. THE VARIATION OF LIGHT EMISSION ALONG THE TRACK OF THE α -PARTICLE

Figure 1 shows an apparatus designed to measure the variation of light emission along the track of an α -particle as it slows up and stops in the gas. A clean polonium source was made from stock solution by deposition on silver and waxed on to a lead block at the top of the chamber. The particles travelled down the mid-section, passed through a thin aluminium window into a small chamber 3 mm in depth and were finally stopped in a piece of clean crystalline quartz forming the bottom plate of the chamber. The gas to be investigated was introduced into the chamber through a copper pipe and the light produced along the α -particle tracks passed through the crystalline quartz and was detected by an E.M.I. photomultiplier type 5311 placed immediately below. No liquid paraffin or similar usual coupling medium was inserted between the quartz and the glass envelope of the photomultiplier in case the ultra-violet emission from the gas might be converted to visible photons which would have produced spurious counts in the multiplier. The photomultiplier was followed by an amplifier, discriminator and

scaler. Air at known pressure introduced into the mid-section provided variable absorption in the path of the α -particles, while the aluminium window served as a vacuum seal and also prevented light from the mid-section reaching the photomultiplier. This method of absorption was adopted in preference to the use of foils in order to avoid the possibility of light from the room reaching the photomultiplier between readings. It had previously been found that if this occurred a temporary increase resulted in the noise current from the photo-cathode having the same pulse height distribution as the signals due to photon emission from the gas in the chamber. Crystal quartz was observed to scintillate feebly under α -particle bombardment, but the necessary correction for this effect was determined by introducing methane (a non-scintillating gas) into the chamber and repeating the observations. To estimate the range distribution of the particles reaching the chamber, as the pressure of air in the mid-section was varied, separate experiments were made with a ZnS screen above the quartz.

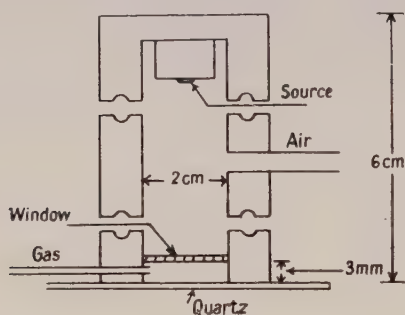


Figure 1.

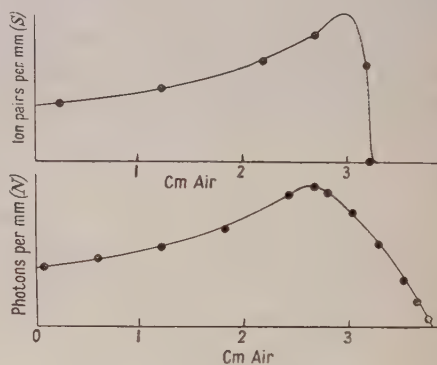


Figure 2.

A determination of the specific emission of photons by helium under α -particle bombardment is shown in figure 2, and for comparison the Bragg curve of ionization. Since the polonium source was weak it was not possible to collimate the α -particles and the spread in the α -particle ranges had a half-width of 5% of the mean range. This is not quite enough to explain the long tail in the specific emission curve. However, the difference between the calculated and observed spreads is small, and it would be unwise to lay any emphasis on it. The variation of emission along the track in air was found to be similar to that for helium.

It is concluded that the specific ionization and the specific emission of photons in the visible spectrum follow each other closely.

§ 3. THE NUMBER OF PHOTONS EMITTED IN THE VISIBLE SPECTRUM

Although the photon emission from the gases has a line spectrum (Ortner and Salim 1952) it is convenient to express it in terms of N_e , the equivalent number of photons of a wavelength at the peak of the sensitivity curve of the photomultiplier which would produce the same number of photo-electrons from the photo-cathode as the total emission from the gas when a polonium α -particle is fully absorbed. To estimate N_e a tungsten lamp was placed forty yards away from the photomultiplier, thus allowing the whole photo-cathode to be irradiated by a known random flux of photons. These photons produced pulses in the scaler in the same

way as the photons produced by α -particles absorbed in gases in close proximity to the photo-cathode and allowed a calibration of the number of counts in the scaler in terms of the number of photons falling on the photo-cathode. It is easily seen that

$$N_e = \frac{\theta n}{\epsilon} \frac{S'}{S} \frac{E_\alpha}{E} \frac{1}{M}, \quad \dots\dots(1)$$

where n is the number of equivalent photons emitted by the lamp in the visible spectrum in one second, θ is the fraction of the number of equivalent photons produced by the lamp which fell upon the window of the multiplier, ϵ is the efficiency of collection of the light produced by the α -particles in the gas, S'/S is the ratio of the counting rates on the scaler for the α -induced gas emission and the lamp respectively, E/E_α is the fraction of α -particle energy absorbed in the gas, and M is the number of α -particles absorbed per second. For equation (1) to hold it is necessary to keep E so small that rarely does the same α -particle cause the emission of more than one photo-electron from the photo-cathode. It was verified that this condition was satisfied by comparing the pulse height distribution from the lamp with that from the α -particles absorbed in the gases. It was also confirmed that single photons were responsible for the pulses produced in the photomultiplier by the lamp by plotting the counting rate on the scaler against the inverse square of the distance D between the lamp and the photo-cathode. A linear relationship was observed up to and beyond the counting rates encountered in the gas experiments. The evaluation of n was facilitated by using a high lamp temperature because the cross integration between the emission spectrum of the lamp and the sensitivity curve of the photomultiplier is more accurate under this condition. To avoid saturation of the photomultiplier from such a bright light D was kept very large and it is believed that n was measured to within a factor of two. For the calculations ϵ was evaluated by blackening the walls of the α -particle chamber and estimating the average solid angle subtended by the photo-cathode to the gas. Some error in the evaluation of ϵ will remain owing to the fact that the photons from the gases do not all pass normally through the surface of the quartz. Furthermore, the photons passing obliquely into the photo-cathode are more likely to produce photo-electrons than are those which pass through the surface normally. The photomultiplier used in these experiments had a sensitivity of ten equivalent photons per emitted electron.

The table shows the values obtained for N_e for different gases at atmospheric pressure by substitution of the above measured quantities into equation (1). For comparison, the corresponding figure for an anthracene crystal is included (Birks 1953). The actual number of highly excited states produced in the gases must

Gas	Nitrogen	Argon	Helium	Methane	Anthracene crystal
N_e	150	250	1000	—	9000

by our definition of N_e be greater than the numbers given in this table. Owing to the uncertainties involved these figures should only be taken as a guide in experiments using photomultipliers with response curves similar to that used by the author. It was found that the scintillations from air produced almost the same counting rate on the scaler as did those from nitrogen. This would suggest that the scintillations from air are due to the nitrogen component alone, in agreement with the results of Grun and Schopper.

§ 4. THE LIFETIME OF THE EXCITED STATES AGAINST EMISSION

In the absence of any converter, the ultra-violet light from the metastable states in a gas would be expected to contribute little to the counting rates in these experiments. The probable lifetime τ is likely to be of the order of 10^{-8} second corresponding to optically excited states. To verify this would require a refined coincidence technique but it is comparatively easy to show that the lifetime is less than 10^{-6} second.

At low gas pressures very rarely will more than one electron be liberated from the photo-cathode per α -particle, even when the gas chamber has highly reflecting walls. At high pressures, however, the table shows that each α -particle can release several electrons from the photo-cathode. If CR , the minimum differentiation time constant in the amplifier, is 10^{-6} second and $\tau \sim 10^{-8}$ second one large pulse corresponding to the integration of several electron pulses will result, whereas if $\tau \sim 10^{-4}$ second there will be several pulses whose average height corresponds to emission of a single electron. With CR set at 10^{-6} second the average height V of the pulses due to one electron was measured by exposing the photomultiplier to a tungsten lamp and obtaining the plateau on the discriminator. (To obtain a plateau it is essential to use a photomultiplier with a low noise level.) V can then be taken as the value of the signal pulse in volts at which the counting rate on the scaler equals one half the counting rate on the plateau. It was found that the average pulse height from air, argon and helium coincided with V at low pressures but rose, with no indication of flattening off, as the pressure was increased. The counting rate approached but did not exceed the number of α -particles per second.

§ 5. THE VARIATION OF EFFICIENCY WITH PRESSURE

It was found that the amount of light emitted from nitrogen, for the same amount of α -particle energy absorbed, varied with the pressure. This variation is shown as the broken line in figure 3. An almost identical curve was obtained for

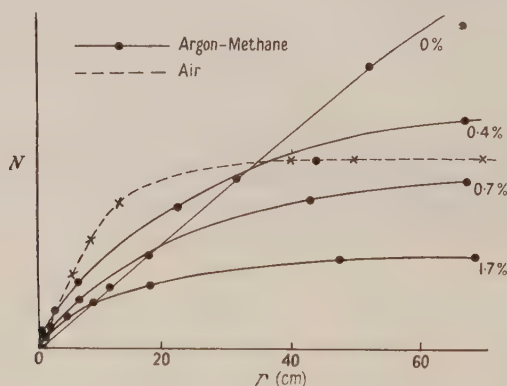


Figure 3.

air. This curve was obtained using a chamber whose dimensions were small compared with the range of the α -particles from a bare source of polonium, at the highest pressures used. The efficiency of collection of the light emitted was low to avoid the possibility that one α -particle might cause the emission of more than one photo-electron from the photo-cathode. As has already been explained, this allows N the counting rate on a scaler following a pulse-height discriminator to be

taken as directly proportional to the number of photons emitted from the tracks of the α -particles. It can be seen from figure 3 that N increases linearly with pressure, below 10 cm Hg, but above this value the curve flattens off.

Factors which might be thought to be responsible for the form of this curve include oxidation of the source, de-excitation on the walls of the chamber, self-absorption by the nitrogen and the emission of densely ionizing short range particles by the source. The effects of such factors were examined by turning the source away from the multiplier, changing radically the shape of the chamber and painting it inside, introducing an air gap between the chamber and the photo-cathode, and covering the source with an aluminium foil of stopping power equivalent to a pressure of 10 cm of air. None of these control experiments were found to affect the observed variation of N with pressure. In addition, the same curve was obtained by plotting the increase in the current flowing through the photomultiplier as the pressure was varied.

It is natural to attribute the saturation with pressure of the observed variation of photon emission to de-excitation of excited molecules (quenching) by collision with unexcited molecules. The application of the simple theory of optical quenching to this problem leads to the result that N (the counting rate in the scaler, which is proportional to the rate of emission of quanta from the gas) varies with pressure according to the relation

$$N = Kp(1 + kp)^{-1}, \quad \dots\dots(2)$$

where $kp = \tau n_e/n_0$, τ is the lifetime of the excited states involved, n_e is the number of collisions per second in the gas, n_0 is the mean number of collisions before quenching occurs and K is a constant independent of pressure. According to equation (2) there should be a linear dependence between N^{-1} and p^{-1} . The experimental observations are in approximate accord with this result, but there is some indication that processes other than collision quenching may also have to be taken into account in order to explain the pressure variation precisely. However, by assuming that most of the variation with pressure of the photon emission from the optically excited states is due to quenching an approximate value for n_0 can be obtained from equation (2).

The value of n_0 obtained in this way for the diatomic gas nitrogen is of the order unity when τ is taken to be of the order of 10^{-8} second. It is interesting to note that similar values for n_0 are found for the quenching of the mercury resonance line by organic vapours (Mott and Massey 1949).

It had already been found that the light output from the monatomic gases argon and helium increased linearly with pressure up to one atmosphere, the highest pressure used. Therefore as a further test of the simple theory outlined above, the variation with pressure of the light output from argon or helium was investigated when they contained small concentrations of methane, which is known to quench by collision excited states in argon (Curran and Craggs 1949).

The results for argon-methane mixtures are shown as the full lines in figure 3. Similar results were obtained for helium-methane mixtures. It was verified that methane did not appreciably absorb the photons from argon or helium by separate experiments in which a chamber containing methane was interposed between the gaseous scintillator and the photomultiplier. If the value of τ for the argon excited states is taken to be of the order 10^{-8} second, n_0 for collisions of excited argon molecules with methane molecules is again of the order unity. It can be seen that at low pressures the curves rise above the straight line for pure argon

suggesting that at low pressures the relatively long-lived ultra-violet emitting metastable argon states are sensitized by the methane and contribute to the emission in the visible spectrum. A similar effect is observed in some well-known fluorescent liquids, and figure 4 compares the behaviour of a xylene-terphenyl mixture (Kallmann and Furst 1951) with that of argon-methane at low pressures

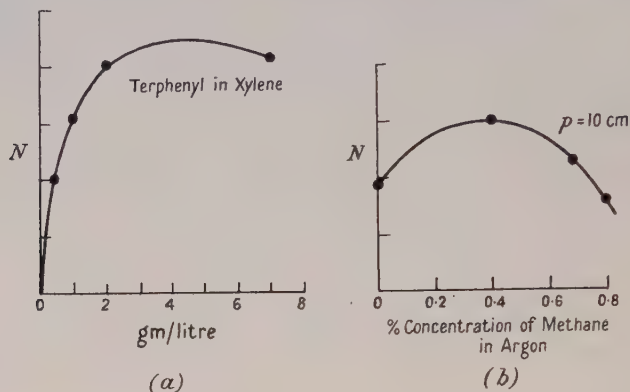


Figure 4.

§ 6. THE CONTRIBUTION TO THE EMISSION BY THE RECOMBINATION OF IONS

Since approximately one half of the α -particle energy absorbed in the gas appears as ion pairs which can be collected by an external field, it might be expected that an appreciable fraction of the light coming from the gas is due to the recombination of such ions.

To estimate this fraction, a gas chamber was constructed with two electrodes to remove the ions from the gas before appreciable recombination had occurred. A strong α -particle source was collimated so that the α -particles were restricted to a path roughly equidistant from the electrodes. The 'view' of the photomultiplier was limited to the gas in the immediate vicinity of the α -particle tracks. It was verified that sufficient voltage was applied between the electrodes to obtain the saturation current corresponding to little recombination of ions in the gas. The counting rate of the scaler was taken as a measure of the number of photons per second leaving the chamber.

In experiments of the above nature with helium and nitrogen, it was found that switching the collecting voltage on and off made no appreciable difference to the counting rate on the scaler. It is concluded that the contribution to the emission, made by the recombination of the ions responsible for the Bragg curve of ionization, is negligible.

REFERENCES

- AUDERBERT, R., and LORMEAU, S., 1949, *C. R. Acad. Sci., Paris*, **228**, 318; 1950, *Ibid.*, **230**, 956.
 BIRKS, J. B., 1953, *Scintillation Counters* (London: Pergamon Press), p. 79.
 CURRAN, S. C., and CRAGGS, J. D., 1949, *Counting Tubes* (London: Butterworths Scientific Publications), p. 45.
 GRUN, A. E., and SCHOPPER, E., 1952, *Z. Naturf.*, **6a**, 698-700.
 KALLMANN, H., and FURST, M., 1951, *Nucleonics*, **8**, 32.
 MOTT, N. F., and MASSEY, H. S. W., 1949, *Theory of Atomic Collisions* (Oxford: Clarendon Press), 2nd Edn, p. 283.
 ORTNER, G., and SALIM, S., 1952, *Nature, Lond.*, **169**, 1060.

RESEARCH NOTES

Intensities in Band Systems of O₂ :
³Σ_u⁺-¹Σ_g⁺ (Broida-Gaydon System) and
¹Σ_g⁺-³Σ_g⁻ (Atmospheric System)

BY M. E. PILLOW

Northern Polytechnic, London

MS. received 2nd June 1954

IN a recent study of oxygen afterglows, Broida and Gaydon (1954) observed, for the first time in emission, the Herzberg bands of O₂, ³Σ_u⁺-³Σ_g⁻. When suitable *v'* values had been assigned, most of the bands measured were found to fit into this system not only in wavelength but also in intensity (Pillow 1953). There were observed, however, a number of bands which did not fall readily into the scheme, and from consideration of their wavelengths Broida and Gaydon suggested that most of these could be attributed to a transition between the upper state ³Σ_u⁺ of the Herzberg bands and the upper state ¹Σ_g⁺ of the atmospheric bands. To test this identification the intensity distribution to be expected for the band system corresponding to this transition is here investigated.

The calculated intensities are shown in the table, equal distribution among the excited levels being assumed. In plotting the wave functions for the highest levels of the ³Σ_u⁺ state some extrapolation is required, and numerical results are given therefore only up to *v'* = 8, over which range they may be considered as a reliable guide to the probable intensity distribution.

Table 1. O₂: Broida-Gaydon System: Intensities in emission, on an arbitrary scale, assuming uniform population of vibrational levels of upper scale.

<i>v'</i>	<i>v''</i> 0	1	2	3	4
0	(4568)	(4881)	(5232)	(5631) 1	(6085) 2
1	(4412)	(4704)	(5027) 1	(5393) 4	(5807) 5
2	(4272)	(4545) 1	(4848) 3	(5187) 6	(5569) 9
3	(4146)	(4402) 2	(4686) 5	(5003) 10	(5357) 10
4	(4033) 1	(4275) 5	(4543) 10†	(4839) 14†	(5170) 10
5	(3932) 2	(4162) 9	(4415) 15‡	(4695) 18‡	(5005) 8
6	(3843) 7	(4062) 15‡	(4302) 21‡	(4568) 16‡	(4861) 5
7	(3764) 17	(3974) 23†	(4204) 27‡	(4457) 14	(4736) 2
8	(3696) 37†	(3899) 36†	(4120) 31†	(4363) 11	(4630)

† Bands observed by Broida and Gaydon.

‡ Bands overlapped by other features, and possibly or probably present.

The observed bands which, it seems, can with reasonable certainty be attributed to this system are :

Observed $\lambda(\text{\AA})$	Identification Band	$\lambda(\text{\AA})$	Observed $\lambda(\text{\AA})$	Identification Band	$\lambda(\text{\AA})$
3699	(8, 0)	3697	4124	(8, 2)	4120
3905	(8, 1)	3899	4546	(4, 2)	4542
3977	(7, 1)	3974	4835	(4, 3)	4839
4008	?(10, 2)	3998			

A number of theoretically strong bands are probably present on the plate, but cannot be confirmed definitely as they would nearly coincide with Herzberg bands, or would lie in a region where identification is difficult. These overlapped bands are indicated in the table. Other bands considered by Gaydon as possibly or probably present are (9, 0), (9, 1), (9, 2), (10, 1), and perhaps (11, 0), though apparently not (10, 0). These would agree generally with the trend of the main intensity parabola. The bands (4, 4), (3, 3), (3, 4), (2, 4), and others which might be expected to arise from the levels $v'=0, 1, 2$, are outside the observed wavelength range.

The presence of many bands in this and in the Herzberg system arising from the higher vibrational levels of the $^3\Sigma_u^+$ state indicates a high, and non-thermal, vibrational excitation of this state, as would be expected in a product of a recombination process not too strongly metastable.

Very nearly all the features observed by Broida and Gaydon can be accounted for by admitting the existence of the system $^3\Sigma_u^+ - ^1\Sigma_g^+$, in addition to the Herzberg system, and there seems to be sufficient agreement between calculated intensities and observed bands to confirm the identity of the new system.

Intensities have also been calculated for the atmospheric bands $^1\Sigma_g^+ - ^3\Sigma_g^-$ involving one of the same electronic states as the system just considered. These bands are well known in absorption, and have also been obtained in emission, the most extensive observations being those made by Herman, Hopfield, Hornbeck and Silverman (1949), on the flame of exploding CO and O₂.

Table 2. O₂: Atmospheric Bands: Intensities in emission on an arbitrary scale, assuming uniform population of vibrational levels of upper state.

v'	v''	0	1	2	3	4
0		(7619) 100†	(8647) 5†	(9968)		
1		(6882) 12	(7708) 80†	(8740) 9†		
2		(6287) 1	(6969) 22	(7802) 70†	(8842) 13†	(9823) 1
3			(6369) 3	(7058) 28	(7899) 54†	(8948) 15
4			(5875)	(6456) 6	(7152) 34	(8002) 37†

Wavelengths given are for band origins.

† Bands observed by Herman and others working between 7200 Å and 8800 Å.

The bands corresponding to higher v' values are faint, indicating a fairly rapid falling-off of population of levels with increasing v' . Precise measurements of intensity were not made.

The emission of this system in the air-glow is discussed by Chamberlain (1954).

Table 3. O₂: Atmospheric Bands: Intensities in absorption, together with approximate visual estimates compiled by Pearse and Gaydon (1950).

Band	0, 0	1, 0	2, 0	3, 0	4, 0
<i>I</i> (calc)	100	9	0.38	0.013	0.009
log <i>I</i> (calc)	2.00	0.95	1.58	2.12	3.94
<i>I</i> (vis) (approx)	10	8	3	1	0

There is a roughly linear relation between the logarithm of the calculated intensity and the approximate estimates, as would be expected for the one progression if there are no outstanding irregularities in the atmospheric absorption.

The (1, 1) band has also been observed, with low intensity of the same order as that of (3, 0). If the distribution among vibrational levels in the ground state is thermal, which is to be expected in the unexcited atmosphere, the lowest temperature that would permit the (1, 1) band to appear comparable with the rest is of the order of 240°K, which is not unreasonable.

REFERENCES

- BROIDA, H. P., and GAYDON, A. G., 1954, *Proc. Roy. Soc. A*, **222**, 181.
 CHAMBERLAIN, J. W., 1954, *Astrophys. J.*, **119**, 328.
 HERMAN, R. C., HOPFIELD, H. S., HORNBECK, G. A., and SILVERMAN, S., 1949, *J. Chem. Phys.*, **17**, 220.
 PEARSE, R. W. B., and GAYDON, A. G., 1950, *Identification of Molecular Spectra* (London: Chapman and Hall).
 PILLOW, M. E., 1953, *Proc. Phys. Soc. A*, **66**, 1064.

The Yield Curve of the ${}^7\text{Li}(p, \gamma){}^8\text{Be}$ Reaction

By P. C. PRICE

Cavendish Laboratory, Cambridge

*Communicated by E. S. Shire; MS. received 15th March 1954,
and in amended form 17th June 1954*

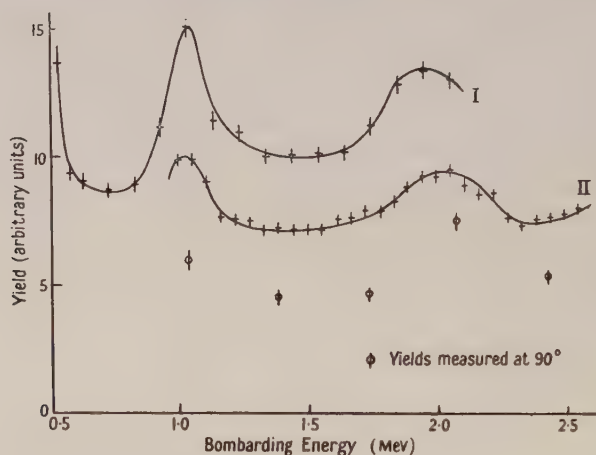
THE absolute yield of high-energy quanta from the ${}^7\text{Li}(p, \gamma){}^8\text{Be}$ reaction has been studied at bombarding energies up to 650 kev by Bonner and Evans (1948), and a more accurate estimate of the cross section at the 441 kev resonance has been made by Fowler and Lauritsen (1949). Bair *et al.* (1952) have published a relative yield curve in the range 1.8 to 5.2 mev. I have been able to calibrate the latter experiment in terms of the former by examining the yield curve from 0.5 to 2.5 mev. The only published yield curves for high-energy quanta covering any part of this range are the work of Hudson *et al.* (1940) and of Kraus (1954); the former is not very accurate and is unreliable above the neutron threshold, and the latter, which was not published when this work was undertaken, extends only up to 1.5 mev.

The radiation produced by proton capture at the 441 kev resonance consists of 17.6 and 14.8 mev quanta (Walker and McDaniel 1948). These are sufficiently high in energy to be detected in a NaI(Tl) crystal and photomultiplier tube biased so that pulses due to neutrons and to γ -rays from the reactions of protons

with likely target contaminants are not counted. A 1-inch crystal was used, and suitable bias conditions were obtained by examining the spectrum from the $^{19}\text{F}(\text{p}, \gamma)^{20}\text{Ne}$ and $^{19}\text{F}(\text{p}, \alpha, \gamma)^{16}\text{O}$ resonance at 669 kev on a Hutchinson-Scarrott kicksorter (Hutchinson and Scarrott 1951). The bias was set to exclude completely γ -rays of less than 10 mev energy.

The experiment was performed with the Cavendish electrostatic generator, using a thin target prepared by evaporating natural lithium on to a molybdenum backing. The evaporation did not take place inside the target chamber, so the target probably consisted mainly of lithium carbonate. The thickness of the target was first measured at the 441 kev resonance and found to be about 40 kev. A yield curve was then taken at 0° between 0.5 and 2.0 mev. The voltage scale was calibrated using the narrow $^{19}\text{F}(\text{p}, \alpha, \gamma)^{16}\text{O}$ resonances below 1.3 mev, using both the H^+ and the H_2^+ beams.

This yield curve is shown in the figure (curve I). A resonance at about 1 mev is indicated and another possible one at 2 mev. A second yield curve (II) was taken at the same angle from 1.0 to 2.5 mev to examine the nature of the rise in yield at 2 mev. To reduce the likelihood of fluorine contamination the fluorine target was removed from the target chamber and the voltage scale



obtained by examining the 1 mev resonance with both the H^+ and the H_2^+ beams. It was assumed for definiteness that this resonance occurs at 1.03 mev, the position of the resonance in $^7\text{Li}(\text{p}, \text{p}', \gamma)^7\text{Li}$ observed by Brown *et al.* (1951). This assumption is supported by Kraus (1954), who has examined the yield curves of both reactions simultaneously.

Curves I and II show that a resonance of half-width about 150 kev occurs at about 1 mev, and that a broad resonance or group of resonances is found at about 2 mev. The figure also shows the relative yields at 90° obtained at five values of the bombarding energy; these indicate that the 1 mev and 2 mev peaks are not due merely to changes in the angular distribution of the radiation.

The 2 mev resonance is not found in the yield curve of Bair *et al.*, but their statistics in this energy region are not very good. They only claim that in their experiment a resonance 3% of the intensity of the 441 kev resonance would easily have been detected; the height of the 2 mev peak above its background is only 0.6% of that intensity.

These resonances do not seem adequate to explain the high level of radiation, and Wilkinson (1954) has discussed the possibility of special mechanisms in this reaction, using the present results to calibrate the yield curve of Bair *et al.* (1952). To effect this calibration a value for the mean cross section between 1.8 and 2.4 mev of $0.14 \times 10^{-27} \text{ cm}^2$ is used, assuming the peak cross section at 441 kev to be $6.0 \times 10^{-27} \text{ cm}^2$ (Fowler and Lauritsen 1949).

Hill and Shoupp (1948) observed an increase in the yield of high energy γ -rays at about 1.8 mev, but they do not give any quantitative results. The discovery of the 1 mev resonance in this reaction was reported by Kraus (1953), shortly after this work had been completed, and he has since published a full study of this resonance (Kraus 1954).

ACKNOWLEDGMENTS

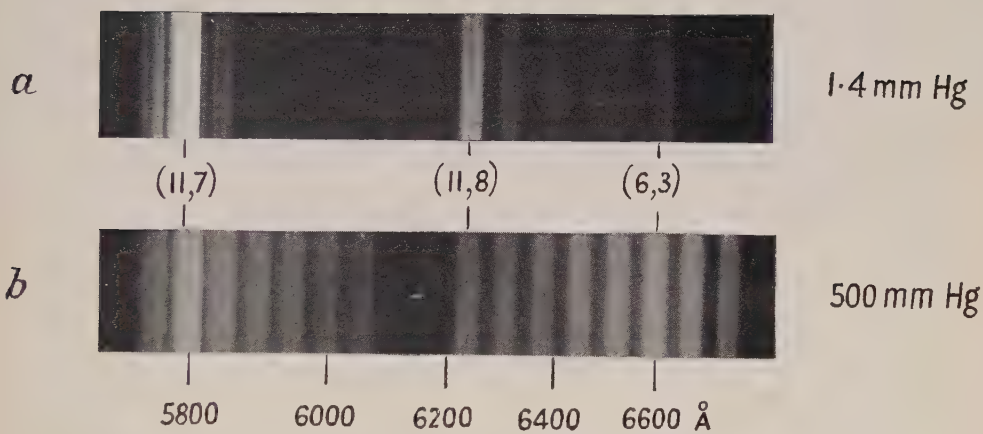
I have to thank Dr. D. H. Wilkinson for suggesting this experiment and for his advice, Mr. E. S. Shire for his interest and support, and Mr. R. H. M. Lamb for making the lithium target. I am obliged to Trinity College, Cambridge, for a Senior Scholarship and to the Department of Scientific and Industrial Research for a maintenance grant.

REFERENCES

- BAIR, J. K., WILLARD, H. B., SNYDER, C. W., HAHN, T. M., KINGTON, J. D., and GREEN, F. P., 1952, *Phys. Rev.*, **85**, 946.
BONNER, T. W., and EVANS, J. E., 1948, *Phys. Rev.*, **73**, 666.
BROWN, A. B., SNYDER, C. W., FOWLER, W. A., and LAURITSEN, C. C., 1951, *Phys. Rev.*, **82**, 159.
FOWLER, W. A., and LAURITSEN, C. C., 1949, *Phys. Rev.*, **76**, 314.
HILL, J. E., and SHOUPP, W. E., 1948, *Phys. Rev.*, **73**, 931.
HUDSON, C. M., HERB, R. G., and PLAIN, G. J., 1940, *Phys. Rev.*, **57**, 587.
HUTCHINSON, G. W., and SCARROTT, G. G., 1951, *Phil. Mag.*, **42**, 792.
KRAUS, A. A., 1953, *Phys. Rev.*, **92**, 1085; 1954, *Ibid.*, **93**, 1308.
WALKER, R. L., and McDANIEL, B. D., 1948, *Phys. Rev.*, **74**, 315.
WILKINSON, D. H., 1954, *Phil. Mag.*, **45**, 259.

CONTENTS OF SECTION B

	PAGE
Prof. J. B. BIRKS and Dr. G. T. WRIGHT. Fluorescence Spectra of Organic Crystals	657
Mr. A. E. CARTE. Heat Flow in the Transvaal and Orange Free State	664
Mr. G. S. BRINDLEY. The Order of Coincidence Required for Visual Threshold	673
Miss J. P. A. TILLET. A Study of the Impact on Spheres of Plates	677
Mr. R. CADE. Contributions to the Theory of Electrostatic Forces on Immersed Bodies	689
Mr. G. SAXON. A Theory of Electron Beam Loading in Linear Accelerators	705
Prof. SYDNEY CHAPMAN. A Monochromatically Ionized Layer in a Non-Uniformly Recombinant Atmosphere; with Applications to the D and E Ionospheric Regions	717
Research Notes :	
Dr. F. E. HOARE, Dr. J. S. KOUVELITES, Dr. J. C. MATTHEWS and Mr. J. PRESTON. The Temperature Variation of Susceptibility of Tantalum	728
Letters to the Editor :	
Mr. R. SCOTT. Transient Heat Flow in Anisotropic Strata	731
Reviews of Books	732
Contents of Section A	736



Spectrum of the afterglow of active nitrogen: (*a*) at low pressure, (*b*) at high pressure.

Les Méthodes Optiques d'Orientation Atomique et leurs Applications

PAR A. KASTLER

École Normale Supérieure, Laboratoire de Physique, Université de Paris

9th Holweck Lecture, delivered 13th May 1954; MS. received 21st June 1954

Résumé. La méthode optique d'orientation atomique est située parmi l'ensemble des méthodes proposées et mises en oeuvre. L'excitation optique sélective des sous-niveaux Zeeman d'un niveau atomique excité se manifeste dans l'état de polarisation de la lumière de résonance optique. En excitant des atomes avec de la lumière de résonance polarisée circulairement, on peut également produire une population sélective des sous-niveaux Zeeman de l'état fondamental. Les applications des atomes ainsi orientés sont leur utilisation pour des expériences de résonance magnétique sur l'état excité et sur l'état fondamental, la possibilité d'orienter des noyaux atomiques et enfin la production d'électrons polarisés par effet photoélectrique des atomes orientés.

Mr. President, dear colleagues,

It is for me a very great honour to have been awarded the Holweck prize and I am very grateful to the Council of the Physical Society. As the last French Holweck prize-winner of this decade for which the prize was established, and as actual President of the Société Française de Physique, I want to be the interpreter of the deep thanks of the French physicists to the Physical Society of Great Britain and to its Foreign Secretary Professor E. N. da C. Andrade for the initiative and the foundation of the Holweck prize.

This prize was founded to honour the memory of Fernand Holweck, who was one of our greatest physicists and a man who gave his life for the liberation of our country. The prize came in an epoch when French scientists, in spite of the liberation, felt depressed by the stagnation of scientific work in France during the occupation and by their intellectual isolation from other countries. While scientific work in the Allied nations had been activated by the war problems and the struggle for victory, it had been paralysed in our country, and this state of things inclined us to despondency.

In creating the Holweck prize and in stipulating that it should be given alternately to a French physicist by your Society and to a British physicist by our Society you showed us that in spite of our delay in scientific activity you had for us a feeling of equality and so you helped us to restore in our minds the self-reliance which we had lost, and for this we are so deeply grateful. Now the Holweck prize will be awarded again next year to a British physicist and then the first decade will come to the end. We all desire deeply that the bonds of friendship it established between our two societies may continue during further decades. The Council of the Société Française de Physique is proposing that for the next decade the grants may be taken in charge by our Society and we hope that you will agree with this proposal.

The subject of my lecture is to deal with "optical methods of atomic orientation and applications of this orientation". If I have to tell you of some work to which I contributed I am conscious that I could only do this through the constant help of my masters, my colleagues, my pupils and through constant stimulation coming from foreign colleagues. I am especially indebted for a great part of the inspiration and results of which I want to speak to my young friend Jean Brossel, who had the chance to improve his knowledge in physics in England and in the United States.

INTRODUCTION

L'ÉTAT quantique d'un atome est caractérisé par un certain nombre de vecteurs \mathbf{L} , \mathbf{S} , \mathbf{i} , \mathbf{F} qui représentent des moments cinétiques en unités \hbar : \mathbf{L} résultante des moments orbitaux, \mathbf{S} résultante des moments de spin électronique, $\mathbf{J} = \mathbf{L} + \mathbf{S}$, \mathbf{i} moment nucléaire et $\mathbf{F} = \mathbf{J} + \mathbf{i}$.

Lorsqu'un état donné J (ou F) est différent de zéro, l'atome est paramagnétique (si $J = 0$ et $i \neq 0$ le paramagnétisme est purement nucléaire) et peut exister dans $2J + 1$ (ou $2F + 1$) sous-niveaux magnétiques différents m_J (ou m_F) qui correspondent à des orientations quantifiées différentes du moment cinétique et du moment magnétique de l'atome dans l'espace.

En absence de champ extérieur ces sous-niveaux possèdent la même énergie, et à l'état d'équilibre thermique chacun de ces sous-niveaux est peuplé par le même nombre d'atomes. On dit que les niveaux sont 'dégénérés' et les propriétés de l'ensemble des atomes présentent le caractère d'isotropie. Nous dirons que les atomes sont 'orientés' lorsqu'une différence de population importante existe entre ces sous-niveaux magnétiques.

Une telle orientation plus ou moins prononcée peut être obtenue soit sous l'influence d'un champ directeur, champ magnétique ou champ électrique cristallin, soit—comme nous le verrons—par une irradiation optique anisotrope. L'agitation thermique (les chocs dans un fluide, les ondes thermoélastiques dans un réseau cristallin) produit un effet de désorientation. Pour réduire cette désorientation il faut soit opérer sur la matière condensée à très basse température, soit agir sur la matière à un état de densité très faible où les chocs sont rares (gaz sous faible pression ou jet atomique). On peut donc classer les méthodes d'orientation en quatre groupes suivant le procédé directeur et suivant l'état de la matière utilisée:

- | | |
|-----------------------|--|
| A. Méthode magnétique | $\begin{cases} \nearrow 1. \text{ Solide à très basse température.} \\ \searrow 2. \text{ Jet atomique.} \end{cases}$ |
| B. Méthode optique | $\begin{cases} \nearrow 1. \text{ Solide à très basse température.} \\ \searrow 2. \text{ Jet atomique ou gaz raréfié.} \end{cases}$ |

La méthode A 1 utilise la répartition d'équilibre thermique dans un champ magnétique. Celle-ci est régie par la loi de Boltzmann:

$$n_2/n_1 = \exp \{ -(W_2 - W_1)/kT \}$$

où $W_2 - W_1$ est la différence d'énergie entre deux niveaux quantiques qui sont ici des niveaux d'orientations différentes dans le champ. Si μ est le moment

Letters to the Editor

Section A

A Possible Variation of the Rate of Local Penetrating Showers, by J. G. DARDIS and C. B. A. McCUSKER.

The Elastic Scattering of 125 MeV Electrons by Beryllium, by K. M. GATHA, N. J. PATEL and P. F. PATEL.

The Total Cross Sections for the Nuclear Scattering of High Energy Nucleons, by K. M. GATHA and G. Z. SHAH.

Radiative Transitions in j - j Coupling, by G. R. SATCHLER.

Section B

Measurements on some Semiconducting Compounds with the Zinc-Blende Structure, by F. A. CUNNELL, J. T. EDMOND and J. L. RICHARDS.

the recoil motion. Details are given of the application of some of the methods to the measurement of the half-lives of the levels of ^{16}O at 6.13 mev (E3 transition), 6.9 mev (E2) and 7.1 mev (E1), with the following results:

$$\begin{array}{ll} 6.13 \text{ mev, } 5 \times 10^{-12} \leq \tau \leq 10^{-11} \text{ sec,} & 6.9 \text{ mev, } \tau \leq 1.2 \times 10^{-14} \text{ sec,} \\ & 7.1 \text{ mev, } \tau \leq 8 \times 10^{-15} \text{ second.} \end{array}$$

The Angular Correlation of Annihilation Radiation, by K. L. ERDMAN.

Abstract. The departure from exact 180° angular correlation of quanta resulting from positrons annihilating in various materials has been measured. This provides data as to the momenta of the centres of mass of the annihilating electron-positron pairs. It does not appear possible to account for the data on the assumption that the positron achieves thermal energy by lattice collisions before annihilating, so that such measurements may not be simply related to the momentum distribution of the more loosely bound electrons in the absorbing substance.

Plasma Oscillations in a Periodic Potential: the One-Zone Theory, by J. HUBBARD.

Abstract. The collective description of electron interactions in the presence of a periodic potential is investigated. It is shown that there is a reformulation of the problem which lends itself to a treatment closely resembling the free electron case. This treatment is carried through, and it is shown that the results are formally very similar to those for free electrons. For a parabolic band the main effect of the potential is to replace the electronic mass m by the effective mass m^* . The present theory applies only to the electrons in one Brillouin zone, and cannot be used when there is substantial overlapping of the occupied levels of this zone.

The [110] Magnetostriction of some Single Crystals of Iron and Silicon-Iron, by E. W. LEE.

Abstract. Using the results of a previous paper by the author on the shape of magnetization curves, the magnetostriction of single crystals of iron parallel to the [110] direction have been calculated as functions of intensity of magnetization and field strength, using the Néel model of domain structure. It is found that the magnetostriction is dependent on crystal width in a manner analogous to that found for the magnetization curves. Measurements on three crystals of Si-Fe show good agreement with their calculated behaviour. It is shown that in general the domain vectors in the demagnetized state are not uniformly distributed along all the easy axes and the distribution varies from one crystal to another. The actual distribution is evaluated in the two cases where it is found possible.

The Angular Correlation of Successive γ -Rays in ^{60}Ni at Low Temperatures, by H. R. LEMMER and M. A. GRACE.

Abstract. The angular correlation of the γ -rays excited in the decay of ^{60}Co has been measured in a paramagnetic crystal at 288°K and at 20°K to eliminate the influence of relaxation phenomena. No significant difference between the measurements was observed, each giving the full angular correlation. This is discussed in relation to the interpretation of nuclear orientation measurements.

Inelastic Collisions between Heavy Particles—III: Excitation of Helium Atoms in Fast Encounters with Hydrogen Atoms, Protons and Positive Helium Atoms, by B. L. MOISEWITSCH and A. L. STEWART.

Abstract. Born's approximation is used to calculate the cross sections for the processes $H(1s) + He(1s^2) \rightarrow H(2s, 2p, 3s, 3p, 3d \text{ or } C) + He(1s 2p^1P)$

where C represents the continuum. It is found that these *double* transition collisions are collectively much more effective at high impact energies than the simple single transition collision $H(1s) + He(1s^2) \rightarrow H(1s) + He(1s 2p^1P)$ which is also investigated.

Born's approximation is further used to calculate the cross sections for the processes $He^+(1s) \text{ (or } H^+) + He(1s^2) \rightarrow He^+(1s) \text{ (or } H^+) + He(1s 2p^1P)$ double transitions being here found to be unimportant.

An Investigation of the (γ, n) Reaction in Cu, Zn and Ag, by D. ST. P. BUNBURY (Research Note).

Phase of Matrix Elements in Nuclear Reaction and Radioactive Decay, by R. HUBY (Research Note).

Section B

The Effect of Intense Magnetic Fields on Electroluminescent Powder Phosphors, by A. N. INCE.

Abstract. The effect of intense magnetic fields on electroluminescent powder phosphors is investigated to furnish information which should be helpful in developing a theory of the mechanism of electroluminescence. No quenching effect was observed even for magnetic field intensities as high as 1.3×10^5 oersteds. The significance of this result is discussed.

Mechanisms of Creep in a Precipitation Hardened Alloy, by G. C. E. OLDS.

Abstract. The binary alloy 97% copper–3% silver was selected as the most ideal alloy for research on the creep process in a precipitation hardened alloy. A heat treatment was devised which gave a slightly overaged Widmanstätten structure of high internal hardness and maximum stability. Wires of the alloy were subjected to deformation over a range of constant stresses at temperatures from 100°C to 300°C. Two mechanisms of transient creep were observed and were found to be complementary. The first mechanism occurred at the lower temperatures giving creep strain proportional to $\ln(\text{time})$, whilst the second mechanism in which creep was proportional to $(\text{time})^{1/3}$ appeared and became dominant at higher temperatures. A quasi-viscous creep mechanism was also observed which at high temperatures was more important than the transient process. The linear nature of the quasi-viscous creep was limited by a critical time, and was believed to be governed by the plastic deformation which occurred on loading. The three mechanisms observed agree with some theoretical analyses which have been put forward.

The Effect of Particle Shape Variations on the Coercivity of Iron Oxide Powders,
by W. P. OSMOND.

Abstract. A gaussian distribution function for the variation of the axial ratio m of powder particles is suggested as the explanation for the measured values of the coercivity of γ -ferric oxide powders being less than the theoretical values for particles of the observed mean shape factor \bar{m} . Superposition of the theoretical hysteresis loops for 20 packets of equal volume, each assumed to consist of particles with one value only of m , approximating to such a distribution gives values of bulk coercivity in very close agreement with measured values for two particular examples of widely different mean shape factors. In the light of these results explanations are offered of some other observed values for this oxide, and it is suggested that this mechanism may account in part for results obtained by Weil some years ago for precipitated ferronickels.

Thermoelectric and Galvanomagnetic Effects in Lead Selenide and Telluride, by
E. H. PUTLEY.

Abstract. Measurements of the thermoelectric power and the Peltier, Nernst, Ettingshausen and Righi-Leduc effects are described. It is shown that the behaviour of these effects is in accordance with the expectations of standard semiconductor theory. The coefficients are also calculated from the known values of the Hall coefficient and conductivity of the specimen and good agreement is obtained between the measured and calculated galvanomagnetic coefficients. From observation of the Peltier effect an estimate of the thermal conductivity is obtained. Comparison of the measured and calculated value of the thermoelectric power enabled the effective mass of carriers in PbSe to be estimated.

The Hall Coefficient, Electrical Conductivity and Magneto-Resistance Effect of Lead Sulphide, Selenide and Telluride, by E. H. PUTLEY.

Abstract. The experimental procedure and results are described for measurements of the Hall coefficient and electrical conductivity of single crystals and natural specimens of PbS, PbSe and PbTe over the temperature range 77–1000°K. Some measurements at 20°K are also described. The magneto-resistance effect was also measured on some specimens at a number of temperatures between 20°K and 300°K.

At high temperatures all specimens show intrinsic behaviour. This will be discussed in detail in a subsequent paper but the behaviour in the extrinsic range, the temperature dependence of the mobility and irreversible effects found at high temperatures are discussed. It is concluded that the general behaviour of the effects considered can be accounted for by the usual semiconductor model.

Ferromagnetic Properties of Oxidized Mn_2Sb , by G. D. ADAM and K. G. STANDLEY (Research Note).

Electrical Conductivity of some Condensed Aromatic Hydrocarbons, by D. O. NORTHROP and O. SIMPSON (Research Note).

An Apparatus for Heat-Treatment and Quenching Small Specimens in a Vacuum from High Temperatures, by T. H. SCHOFIELD (Research Note).

SECRETARY-EDITOR,
PHYSICAL SOCIETY,
1 LOWTHER GARDENS,
PRINCE CONSORT ROAD,
LONDON S.W.7.

ORDER FORM 24

(issued October 1954)

To be returned to the Physical Society **NOT LATER THAN 1st November 1954**
Please supply 1 reprint of each of the following when published

Section A	Section B
ABRAHAM, COHEN and ROBERTS	INCE
BAYMAN and ROSS	OLDS
BOYD and MORRIS	OSMOND
BRANDEN, DALGARNO and KING .. .	PUTLEY (Thermoelectric) .. .
DEVONS, MANNING and BUNBURY .. .	PUTLEY (Hall coefficient) .. .
ERDMAN	
HUBBARD	
LEE	Research Notes
LEMMER and GRACE	ADAM and STANDLEY
MOISEWITSCH and STEWART	NORTHROP and SIMPSON
	SCHOFIELD
Research Notes	
BUNBURY	
HUBY	

I participate in the £1 1s. reprint scheme.

I enclose.....vouchers.

Please delete as necessary.

NAME (BLOCK CAPITALS)

ADDRESS

.....

.....

A Nuclear Emulsion Study of the Radioactive Decay of Actinium X (^{223}Ra), by
B. F. BAYMAN and M. A. S. ROSS.

Abstract. A nuclear emulsion method has been used to obtain the absolute intensity of the conversion electron spectrum following the radioactive decay of AcX. The results have been used in conjunction with the other available knowledge about the decay to show that in the level scheme of An there are three strong transitions having energies of 144, 154 and 268 kev and probably a fourth of 122 kev, all of which are either pure M1 or M1 with only a small admixture of E2. All four of these transitions probably go directly to the ground state of An. Estimates of the absolute intensities of these transitions and of several other less strong transitions have been made, and it is shown that the absolute intensity of K x-ray fluorescence is at least 0.3 and probably 0.5 quanta per disintegration.

An R.F. Probe for the Mass-Spectrometric Analysis of Ion Concentrations, by
R. L. F. BOYD and D. MORRIS.

Abstract. It has become increasingly evident of recent years that a detailed study of the processes occurring in gas discharges often requires a means of analysing and studying separately the various ionic species. This is true even in the case of the inert gases.

This paper describes the development, and analyses the action, of a versatile probe which can readily be moved radially into and out of a discharge tube and which is able to distinguish between ions (positive or negative) of various masses. With this instrument it is therefore now possible to make probe studies on a particular species of ion in the presence of others.

Basically the instrument is a very small 12 stage linear accelerator which discriminates in favour of ions of a particular mass-charge ratio passing through its sampling orifice. It is of high sampling efficiency and this, together with its mobility and the absence of a magnetic field, gives it certain pronounced advantages over the magnetic method of analysis.

Electron Capture: IV—Capture from Helium Atoms by Fast Protons, by B. H
BRANSDEN, A. DALGARNO and N. M. KING.

Abstract. A modified Born approximation is used to calculate the cross sections for capture of electrons from helium atoms by fast protons and for capture from hydrogen atoms by helium ions. A comparison is made with experimental data and it is shown that the Brinkman-Kramers approximation is inadequate. The theoretical results lend support to the data of Hasted and Stedeford and cast serious doubts on the accuracy of the data of other experimentalists.

Measurement of γ -Transition Lifetimes by Recoil Methods, by S. DEVONS,
G. MANNING and D. ST. P. BUNBURY.

Abstract. Methods of utilizing the recoil motion of excited nuclei produced in disintegrations, to obtain estimates of the half-lives of excited states are described. They involve measurement either of the distance moved by the recoiling nucleus before radiation occurs, or of the small Doppler shift in frequency produced by

THE PHYSICAL SOCIETY

1 Lowther Gardens, Prince Consort Road, London S.W.7

ABSTRACT BOOKLET 24

This booklet gives abstracts of papers accepted since the printing of Abstract Booklet 23. These abstracts are thus circulated before the paper has gone to press, whereas the reprints themselves are not printed until the month of publication in the *Proceedings*, usually 2–3 months after acceptance.

Those eligible to order reprints immediately are

- (a) Fellows and Students of the Society and general subscribers to the *Proceedings* who have purchased voucher books.
- (b) Fellows and Students of the Society who have paid the annual subscription of £1 1s. *Note:* This reduced rate is *not* available to general subscribers.

Members and subscribers may obtain 10s. voucher books (containing vouchers for five reprints) at any time. Reprints are **not** obtainable in any other way.

Users of reprint vouchers should attach the appropriate number of vouchers to their order form. The enclosed order form should be completed by marking with ticks the papers required and should be returned **not later than 1st November**. A slightly later date of receipt will be accepted for long distance overseas subscribers **only**.

A list of Letters to the Editor which have been accepted for publication since the printing of Abstracts Booklet 23 is given for information only. **Reprints will not be available.**

Note. Please be sure your name and address are entered on the form and your requirements indicated, otherwise your order cannot be executed.

All papers in Lists 1–21 have now been published. Reprints of papers covered by these Lists will have been despatched by mid-October; any outstanding orders should be queried as soon as possible after this date.

October 1954

Section A

The Binding Energies of ^3H and ^4He , by G. ABRAHAM, L. COHEN and A. S. ROBERTS.

Abstract. The binding energies of ^3H and ^4He are calculated as part of an attempt to solve the 'consistency' problem of light nuclei. A phenomenological two-body interaction, with central and tensor forces of different range, is assumed, the parameters being taken from a recent paper by Feshbach and Schwinger. The inclusion of additional sets of D-states in the wave functions is found to have a very appreciable effect on the binding energies. A rough calculation shows that the contribution of spin-orbit forces may not be negligible. Without a more extensive investigation into the effects of the additional D-states and the effect of spin-orbit forces, it is impossible to conclude that the interaction used leads to a satisfactory solution of the 'consistency' problem.

magnétique de l'atome, égal à $-g\mu_B J$ (g =facteur de Landé, μ_B =magnéton de Bohr), l'énergie d'orientation est égale à $-\mu H \cos \theta$ et la différence de population entre deux niveaux m_J voisins devient $n_2/n_1 = \exp(-g\mu_B H/kT)$. Dans le cas des ions paramagnétiques et en particulier des ions du groupe du fer où le moment de spin est seul orienté par le champ ($g=2$), on obtient des orientations notables à basse température, orientation pratiquement complète, c'est à dire concentration des atomes dans le niveau le plus bas ($m_J = -J$), à la température de l'hélium liquide. Cette orientation se manifeste dans les propriétés magnétiques: la susceptibilité paramagnétique de la substance approche de sa valeur de saturation. Elle se manifeste également dans les propriétés optiques: disparition dans le spectre d'absorption de certaines composantes Zeeman, augmentation d'intensité d'autres composantes provenant des niveaux Zeeman les plus bas, enfin polarisation rotatoire paramagnétique liée à ces variations d'intensité (voir les travaux de Jean Becquerel et de ses collaborateurs (Becquerel 1934, 1943)).

En réalisant des températures encore plus basses et en utilisant des champs internes, magnétiques ou électriques, plus intenses que les champs artificiels extérieurs, des orientations nucléaires importantes ont été récemment obtenues par cette méthode à Oxford et à Leiden (Simon, Rose et Jauch 1951, Blin-Stoyle, Grace et Halban 1953).

La méthode A2 est appliquée dans la célèbre expérience de Stern et Gerlach qui permet la séparation magnétique des atomes dont l'orientation spatiale est différente. Le développement de cette méthode et son application à l'étude des phénomènes de résonance magnétique par Rabi et ses élèves sont trop connus (Kellog et Millman 1946, Ramsey 1953) pour qu'il soit nécessaire de les rappeler ici.

Quant aux méthodes optiques, la première B1—qui consiste à irradier par de la lumière polarisée un solide à basse température contenant des ions paramagnétiques fluorescents (ions de terres rares)—n'a pas encore été essayée. A la condition d'être mise en oeuvre à des températures suffisamment basses (hélium liquide) où les temps de relaxation spin-réseau sont devenus nettement plus longs que les durées de vie des niveaux optiquement excités, des résultats positifs sont à prévoir. L'intérêt de cette méthode serait de nous renseigner sur les mécanismes de relaxation entre niveaux optiquement excités.

La suite de notre exposé va être consacré à l'étude de la dernière méthode B2 et à l'évocation de quelques unes de ses applications.

ORIENTATION DES ATOMES DANS UN ETAT OPTIQUEMENT EXCITÉ

Cette méthode est basée sur le fait que l'excitation optique des atomes par un faisceau lumineux convenablement orienté et polarisé conduit à une population sélective des sous-niveaux Zeeman de l'état optiquement excité. Cette sélection se reflète dans l'anisotropie d'intensité et dans la polarisation de la lumière réémise par résonance optique ou par fluorescence (Mitchell et Zemansky 1934, Pringsheim 1949). Cette polarisation est très sensible aux chocs et à des champs extérieurs de direction arbitraire aussi faible que le champ terrestre. Il est donc nécessaire de travailler sur des vapeurs à très faible pression ou sur des jets atomiques et dans un champ magnétique de direction convenable, à moins de réaliser une compensation rigoureuse du champ terrestre. Si ces

conditions sont observées, il est possible d'obtenir une sélectivité totale des sous-niveaux Zeeman de l'état optiquement excité. Voici quelques exemples :

(i) Excitation de la vapeur de mercure par de la lumière de résonance 2537 Å polarisée rectilignement. La figure 1 indique la structure Zeeman des niveaux atomiques qui interviennent et de la raie pour les isotopes pairs du mercure dépourvus de spin nucléaire et qui forment 70% du mélange naturel.

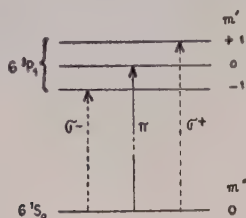


Figure 1 a. Schéma Grottrian.

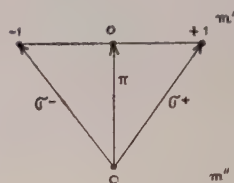


Figure 1 b. Schéma Heisenberg.

Figure 1. Composantes Zeeman de la raie 2537 Å de l'atome Hg.

Nous utiliserons deux modes de représentation ayant chacun ses avantages. Le schéma Grottrian (figure 1 a) est conforme à l'échelle d'énergie. Les sous-niveaux Zeeman sont séparés verticalement. La schéma Heisenberg (figure 1 b) étale les niveaux Zeeman horizontalement de façon à placer sur une même verticale des niveaux de même m_J . Dans cette représentation une transition $\pi (\Delta m = m' - m'' = 0)$ est représentée par une flèche verticale, une transition $\sigma^+ (\Delta m = m' - m'' = +1)$ par une flèche inclinée vers le haut à droite, une transition $\sigma^- (\Delta m = m' - m'' = -1)$ par une flèche inclinée vers le haut à gauche. L'inclinaison des flèches correspondant aux composantes Zeeman nous renseigne donc immédiatement sur l'état de polarisation de celles-ci. Rappelons qu'une composante Zeeman π correspond à un vecteur électrique vibrant parallèlement au champ magnétique, des composantes Zeeman σ^+ et σ^- à des vibrations circulaires dans le plan perpendiculaire au champ et dont le sens de rotation est celui du courant magnétisant (σ^+) ou le sens inverse (σ^-).

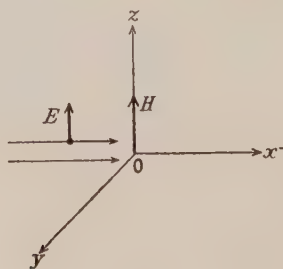


Figure 2.

Considérons un trièdre trirectangle $Oxyz$, la cellule de résonance étant en O , un champ magnétique H dirigé suivant Oz , et irradiions les atomes Hg par de la lumière se propageant suivant Ox et polarisée rectilignement avec son vecteur électrique E parallèle à Oz . Cette orientation de vecteur électrique correspond à la composante Zeeman π qui sera seule excitée et donnera des atomes excités au sous-niveau Zeeman $m_J = 0$ de l'état 6^3P_1 . Ces atomes ne pourront réémettre que la seule composante Zeeman π . Un observateur situé sur Oy observera

une lumière de résonance complètement polarisée, un observateur placé sur Oz observera une intensité d'émission nulle. Avec le mercure naturel on a observé des degrés de polarisation atteignant 85%, mais si on répétait l'expérience avec un isotope pair pur, par exemple ^{198}Hg , il est certain qu'on atteindrait 100% de polarisation, la polarisation imparfaite étant due à la présence des 30% d'isotopes impairs ^{199}Hg et ^{201}Hg conformément à la structure Zeeman des composantes hyperfines de leur raie de résonance.

(ii) Un deuxième exemple de sélection par excitation optique est fourni par l'excitation par échelons de l'atome de mercure. Comme l'a montré Fuchtbauer l'irradiation simultanée par les raies 2537 Å et 4358 Å permet d'atteindre le niveau excité 7^3S_1 , point de départ de l'émission de fluorescence du triplet visible 4046–4358–5461 Å (figure 3). La figure 4 montre la structure

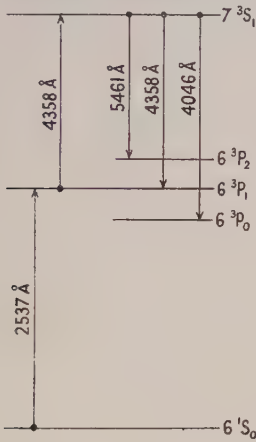


Figure 3. Diagramme des niveaux d'énergie de l'atome Hg intervenant dans l'excitation par échelon.

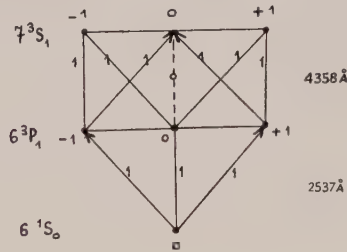


Figure 4. Schéma Zeeman de l'excitation par échelon en lumière naturelle du niveau 7^3S_1 de l'atome Hg.

Zeeman des 2 raies excitatrices. Ici l'irradiation, suivant Ox , par les deux raies 2537 et 4358 Å en lumière naturelle en présence d'un champ magnétique parallèle à Ox , permet d'exciter sélectivement le sous-niveau Zeeman $m_J=0$ de l'état 7^3S_1 , et cette sélection se manifeste par une polarisation caractéristique des trois radiations de fluorescence (Kastler 1936, 1946).

(iii) L'atome de sodium va nous fournir un troisième exemple : l'irradiation de la vapeur de sodium par la raie jaune formée du doublet D_1 (5896 Å), D_2 (5890 Å) porte l'atome Na du niveau fondamental $3^2\text{S}_{1/2}$ au niveau excité $3^2\text{P}_{1/2}$, $3^2\text{P}_{3/2}$. La figure 5 indique la structure Zeeman des niveaux et des raies. Les schémas montrent qu'une excitation en lumière naturelle ou en lumière polarisée rectilignement ne produit pas d'orientation intéressante à l'état excité, mais une irradiation en lumière polarisée circulairement (σ^+) permet d'exciter exclusivement les niveaux Zeeman $m_J>0$. Hanle (1927) a montré que dans ces conditions les atomes émettent, dans une direction parallèle à celle du faisceau lumineux excitateur, de la lumière dont la polarisation circulaire est complète. Nous pouvons dire que l'excitation en lumière circulaire fournit des atomes excités dont les moments magnétiques sont dirigés dans le même sens, et pour l'état $3^2\text{P}_{1/2}$ la saturation paramagnétique est atteinte. Il est vrai que le schéma simple que nous venons d'envisager ne s'applique qu'en présence d'un champ

magnétique suffisamment élevé pour découpler du spin électronique le spin nucléaire dont nous avons fait abstraction. Lorsque le champ magnétique est faible il faut tenir compte de la structure hyperfine des raies excitatrices. Dans ce cas la discussion est un peu moins simple, mais en revanche l'orientation atomique réalisée par l'excitation en lumière circulaire s'accompagne d'une orientation nucléaire analogue à celle obtenue dans les solides à très basse température.

ORIENTATION DES ATOMES À L'ÉTAT FONDAMENTAL PAR POMPAGE OPTIQUE

Réexaminons la figure 5. Par excitation optique de l'atome de sodium en lumière circulaire droite nous avons obtenu un peuplement sélectif des sous-niveaux Zeeman de l'état 3^2P excité. Les atomes excités retourneront à l'état normal en émettant les composantes Zeeman issues des niveaux excités. Les nombres inscrits à côté de ces composantes représentent les probabilités de passage correspondantes. L'excitation par D_1 , σ^+ fait passer des atomes de l'état $m_J = -1/2$ du niveau fondamental à l'état $m_J = +1/2$ du niveau $3^2P_{1/2}$. Ces atomes excités retomberont à l'état fondamental suivant le jeu des probabilités de passage: deux tiers d'entre eux retourneront à l'état de départ $m_J = -1/2$ par émission de la composante Zeeman σ^+ , mais un tiers ira vers l'état $m_J = +1/2$ du niveau fondamental par émission d'une composante Zeeman π . Nous pouvons appliquer des considérations analogues à l'excitation par D_2 , σ^+ . En définitive grâce à l'excitation optique un certain nombre d'atomes à l'état fondamental aura transité de l'état $m_J = -1/2$ vers l'état $m_J = +1/2$. Nous avons réalisé une pompe optique (Kastler 1950, 1951). La pompe optique est une pompe qui fuit, puisqu'un certain nombre d'atomes élevés au niveau excité revient à l'état de départ, il n'empêche qu'en principe, au bout d'une illumination infinie, tous les atomes se seront concentrés à l'état $m_J = +1/2$.

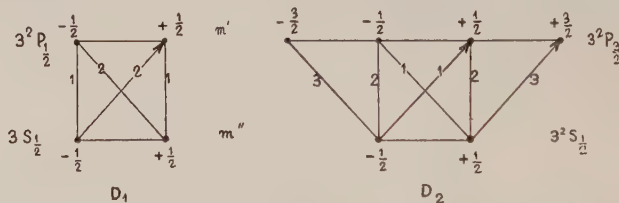


Figure 5. Schémas Zeeman des raies D_1 et D_2 de l'atome Na. Les nombres inscrits à côté des transitions sont proportionnels aux probabilités de passage.

Quel est le degré d'orientation qu'on peut obtenir au bout d'un temps d'illumination court, avec les intensités des sources lumineuses dont nous disposons? L'expérience nous a montré qu'en illuminant un jet atomique de sodium sur un parcours de 20 à 30 cm (ce qui correspond à un temps d'illumination d'environ 10^{-4} seconde) avec la lumière d'une lampe à sodium Philips commerciale, il est possible d'atteindre des degrés d'orientation notables, de l'ordre de 30 à 40% (Brossel, Kastler et Winter 1952, Cagnac 1953, Hawkins et Dicke 1953). Nous pouvons définir le degré d'orientation par le rapport $d = (n_+ - n_-)/(n_+ + n_-)$, n_+ étant le nombre d'atomes de l'état $m_J = +1/2$ et n_- celui à l'état $m_J = -1/2$ du niveau fondamental.

Mais ici se pose une question: Comment mettre en évidence l'orientation des atomes du jet? On pourrait songer à utiliser ce jet d'aimants atomiques pour produire une force électromotrice induite dans un circuit voisin et il est

probable que les méthodes modernes de détection électronique seraient assez sensibles pour mettre en évidence une telle force électromotrice qu'on pourrait d'ailleurs moduler. Nous avons préféré employer une méthode de détection optique dont voici le principe: Considérons encore une fois la figure 5 et supposons que la concentration des atomes à l'état $m_J = +1/2$ soit totale. Illuminons le jet avec de la lumière de résonance polarisée rectilignement de façon à n'exciter que les composantes Zeeman π et analysons la lumière σ réémise à l'aide d'un analyseur circulaire. La lumière réémise ne contiendra que des composantes σ^+ . Si au contraire les atomes du jet ne sont pas orientés, les intensités I_{σ^+} et I_{σ^-} des deux composantes circulaires de sens inverse sont égales. La différence relative $\rho = (I_{\sigma^+} - I_{\sigma^-}) / (I_{\sigma^+} + I_{\sigma^-})$ fournit donc une mesure du degré d'orientation des atomes. Une méthode photométrique différentielle permet d'enregistrer directement la différence $I_{\sigma^+} - I_{\sigma^-}$ (figures 6 et 6 a).

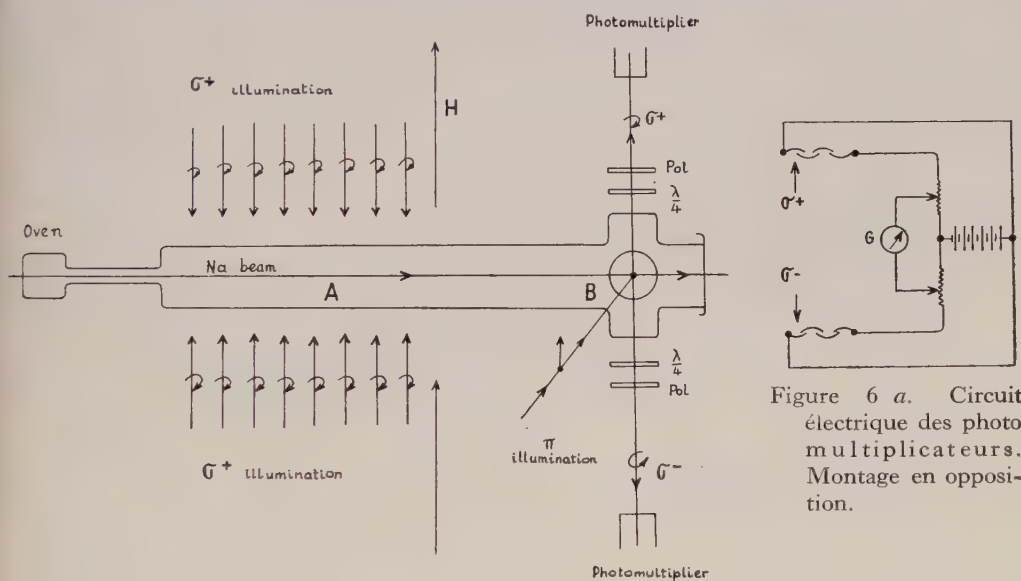


Figure 6. Schéma du montage de pompage optique. A, Région d'orientation. B, Région de détection.

APPLICATION DES ATOMES ORIENTÉS

Nous allons maintenant envisager les applications des atomes orientés. Nous considérerons successivement trois domaines d'application: (i) utilisation des atomes orientés pour des expériences de résonance magnétique, (ii) orientation des noyaux atomiques, (iii) production d'électrons polarisés.

(i) Les transitions de résonance magnétique sont des transitions spectrales entre sous-niveau magnétiques d'un même niveau atomique. Provoquées par un champ magnétique de haute fréquence répondant à la condition de résonance $\nu = \Delta E/h$ elles ont pour effet d'égaliser les populations des niveaux qu'elles font communiquer. La résonance magnétique désoriente les atomes orientés. Elle est donc détectée optiquement par la modification d'intensité et l'état de polarisation de la lumière de résonance optique (Brossel et Kastler 1949, Brossel et Bitter 1952, Brossel 1952). Cette méthode mise en oeuvre par Jean Brossel

sous la direction du professeur F. Bitter à M.I.T. lui a permis d'étudier la résonance magnétique du niveau optiquement excité 6^3P_1 de l'atome de mercure et de vérifier dans tous les détails les formules théoriques qui régissent le phénomène de résonance magnétique. Les figures 7 et 8 montrent des courbes

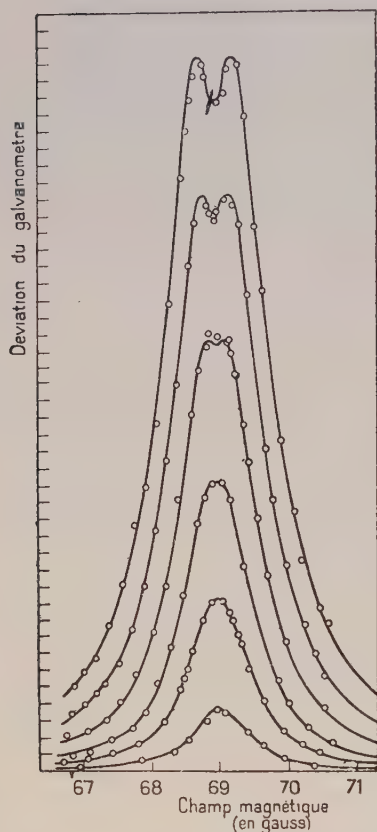


Figure 7. Courbes de résonance de l'état excité 6^3P_1 de l'atome Hg, isotopes pairs. En ordonnée I_σ (d'après Brossel 1952.)

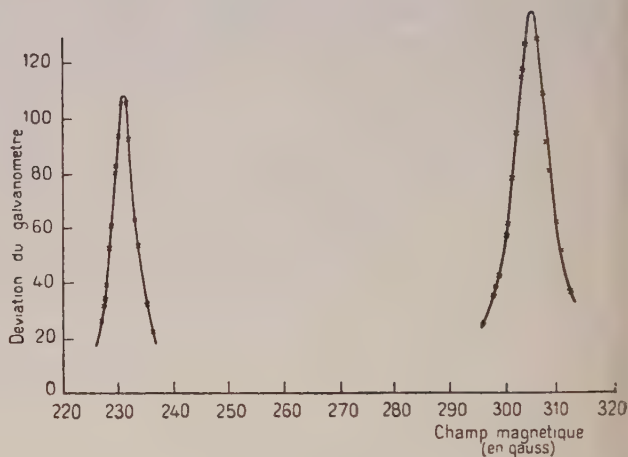


Figure 8. Courbes de résonance de l'état excité 6^3P_1 de l'atome Hg, isotope 201 ($i=3/2$) (d'après Brossel 1952).

Transitions : $F=3/2$, $m_F : +\frac{3}{2} \leftrightarrow +\frac{1}{2}$ et $-\frac{1}{2} \leftrightarrow -\frac{3}{2}$.

de résonance obtenus par Brossel pour les isotopes pairs et pour l'isotope ^{201}Hg . Le spin nucléaire modifie complètement la fréquence de résonance dans un champ magnétique faible. A partir de la largeur des courbes de résonance il a été possible de déterminer la durée de vie du niveau 6^3P_1 qui a été trouvée égale $1,55 \cdot 10^{-7}$ seconde à 1% près pour tous les isotopes de mercure. Récemment cette expérience a été reprise à Paris par Blamont et Brossel (1954) en superposant au champ magnétique un champ électrique qui lui est parallèle. Il a été ainsi possible de mettre en évidence l'effet Stark du niveau 6^3P_1 qui se manifeste par un dédoublement de la courbe de résonance dans un champ électrique de l'ordre de quelques kilovolts par cm (figure 9). L'effet est trop faible pour être accessible aux méthodes de la spectroscopie optique.

La méthode optique a été appliquée par P. Sagalyn à M.I.T. à l'étude de la résonance magnétique du niveau $3^2P_{3/2}$ de l'atome de sodium. Cet auteur a pu

mesurer des intervalles hyperfins et a montré que le noyau ^{23}Na possède un moment électrique quadrupolaire non nul et positif. Ce résultat malgré sa faible précision [$Q = (1 \pm 0,6) \cdot 10^{-25} \text{ cm}^2$] permet des conclusions importantes sur la structure du noyau ^{23}Na (Sagaly 1954, Moszkowski et Townes 1954).

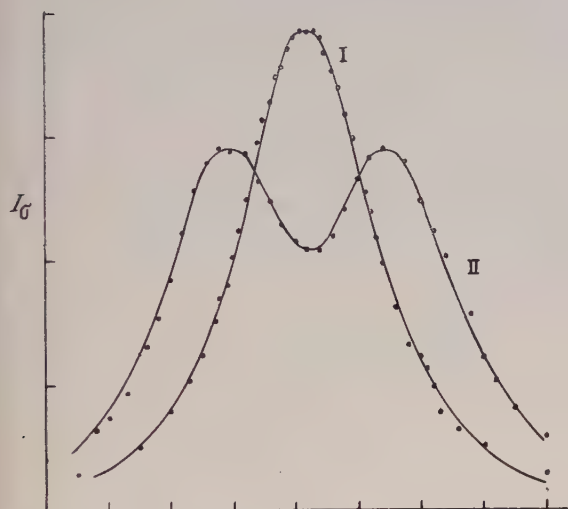


Figure 9. Effet Stark du niveau 6^3P_1 de l'atome Hg. En ordonnée I_σ , en abscisse le champ magnétique H .
 Courbe I : sans champ électrique.
 Courbe II : avec un champ électrique de 50 000 volts/cm $E \parallel H$ (d'après Blamont et Brossel 1954.)

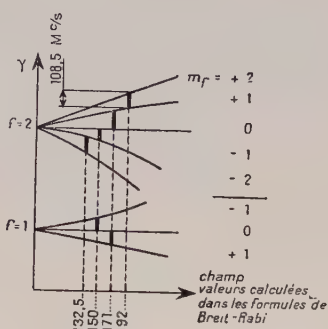


Figure 10. Effet Zeeman de la structure fine de l'état fondamental $3^2S_{1/2}$ de l'atome de sodium.

Récemment Series à Oxford a pu étudier par la méthode optique la résonance magnétique du niveau $5^2P_{3/2}$ de l'atome de potassium, par illumination de la vapeur de potassium avec la deuxième raie de résonance $\lambda = 4047 \text{ Å}$ (communication privée). Il est d'ailleurs possible de combiner la méthode d'orientation optique dans un état excité avec la méthode de détection de Rabi, et Rabi lui-même (1952) a fait des tentatives pour étudier ainsi la résonance magnétique d'un état optiquement excité.

L'orientation des atomes de sodium à l'état fondamental par pompage optique des atomes d'un jet a permis d'étudier la résonance magnétique de l'atome de sodium à l'état fondamental et de contrôler l'influence de la structure hyperfine sur cette résonance. Les quatre minima de résonance prévus (figure 10) ont été observés (figure 11), mais à notre surprise des résonances intermédiaires très fines sont apparues lorsque l'amplitude du champ de radiofréquence a été augmentée. De telles résonances, observées également par Kusch grâce à la méthode de Rabi, correspondent à l'interaction de plusieurs quanta électromagnétiques avec l'atome (Brossel, Cagnac et Kastler 1953, 1954, Kusch 1954, Besset, Horowitz, Messiah et Winter 1954).

(ii) Une deuxième application de l'orientation atomique est l'orientation nucléaire. Lorsque, comme c'est le cas de l'atome ^{23}Na , le niveau électronique fondamental est paramagnétique ($J \neq 0$), le spin nucléaire i est couplé avec le vecteur J et l'orientation atomique, par pompage optique, réalise simultanément

une orientation nucléaire. Nous projetons de répéter l'expérience avec des atomes de sodium radioactifs ^{22}Na ($i=3$) où l'orientation nucléaire doit se manifester par une anisotropie du rayonnement γ émis. Le calcul montre que dans ce cas le nombre de désintégrations dans un jet atomique est insuffisant à moins de recourir à des doses dangereuses de produits radioactifs. Il faut opérer sur la vapeur et la question est de savoir s'il est possible d'éviter que des atomes de sodium radioactifs ne s'incruster dans les parois du récipient.

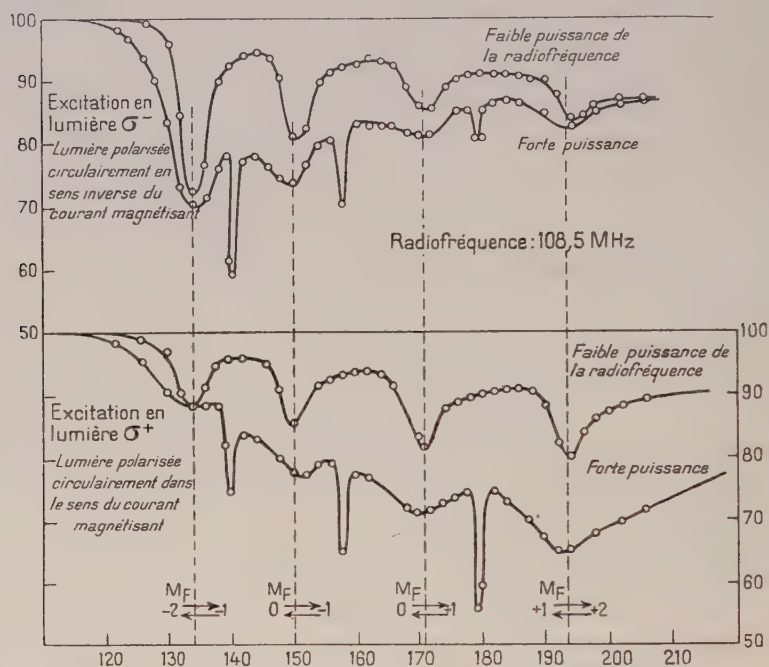


Figure 11. Courbes de résonance magnétique de niveau fondamental de l'atome de sodium. En abscisse, le champ magnétique directeur. En ordonnée, le signal de résonance $I_{\sigma^+} - I_{\sigma^-}$ (d'après Brossel, Cagnac et Kastler, 1953).

(iii) Enfin une dernière application des atomes orientés est la production d'électrons polarisés ou orientés par effet photoélectrique. Le premier qui semble avoir fait des tentatives dans ce sens est le Professeur Dicke à Princeton University en produisant l'effet photoélectrique sur des atomes orientés dans un état optiquement excité, mais le nombre d'électrons obtenus ainsi est faible car la proportion d'atomes excités est petite. L'orientation des atomes à l'état fondamental permet de produire l'effet photoélectrique directement sur l'état fondamental. Pour des atomes de sodium des radiations ultraviolettes de longueur d'onde inférieure à 2412 \AA sont nécessaires pour détacher des électrons. Les règles de sélection qui régissent l'effet photoélectrique (niveau supérieur dans la bande du spectre continu) sont les mêmes que celles qui régissent les transitions spectrales de l'effet Paschen-Back: $\Delta S = 0$. L'état de polarisation de la lumière qui produit l'effet photoélectrique est sans influence sur le moment de spin \mathbf{S} , elle ne modifie que le moment orbital \mathbf{L} . Ces règles ont été établies par la théorie quantique (Sauter 1931). Elles sont d'ailleurs évidentes dans le cas des atomes

ayant un seul électron de valence : les conditions d'effet Paschen-Back exigent que la séparation des niveaux Zeeman produite par le champ extérieur soit supérieur à l'intervalle de multiplet. Ces conditions sont bien réalisées pour la transition qui détache l'électron de l'atome, car le niveau fondamental de départ est, dans le cas des atomes alcalins, un niveau de spin pur ($J = S = 1/2$, $L = 0$) et l'intervalle de multiplet des niveaux 2P tend vers zéro lorsque le nombre quantique principal du niveau d'arrivée tend vers l'infini. Un champ magnétique très faible convenablement orienté suffit donc pour réaliser les conditions d'effet Paschen-Back. Il en résulte plusieurs conséquences : (i) Il n'est pas possible d'obtenir des électrons orientés en faisant agir sur des atomes non orientés de la lumière polarisée circulairement produisant l'effet photoélectrique. (ii) Il faut orienter préalablement le spin électronique des atomes. L'état de polarisation de la lumière qui produit l'effet photoélectrique est sans importance. On peut donc utiliser de la lumière naturelle intense et des faisceaux de grande ouverture. Mais il ne suffit pas de produire des électrons polarisés, il faut savoir reconnaître leur état de polarisation ce qui est sans doute plus difficile. On peut utiliser dans ce but la diffusion sur des atomes étudiée par Mott (Mott 1929, 1932, Sauter 1933). Mais ce sont là des projets d'avenir et il convient d'arrêter ici cette vue d'ensemble sur les problèmes liés à la production et à l'application des atomes orientés.

BIBLIOGRAPHIE

- BECQUEREL, J., 1934 et 1943, *Notice sur les travaux scientifiques* (Paris : Hermann).
- BESSET, C., HOROWITZ, J., MESSIAH, A., and WINTER, J., 1954, *J. Phys. Radium*, **15**, 251.
- BLIN-STOYLE, R. J., GRACE, M. A., and HALBAN, H., 1953, *Progr. Nucl. Phys.*, **3**, 63.
- BLAMONT, J., et BROSEL, J., 1954, *C. R. Acad. Sci., Paris*, **238**, 1487.
- BROSEL, J., 1952, *Ann. Phys., Paris*, **7**, 622.
- BROSEL, J., and BITTER, F., 1952, *Phys. Rev.*, **86**, 308.
- BROSEL, J., CAGNAC, B., et KASTLER, A., 1953, *C. R. Acad. Sci., Paris*, **237**, 984; 1954, *J. Phys. Radium*, **15**, 6.
- BROSEL, J., et KASTLER, A., 1949, *C. R. Acad. Sci., Paris*, **229**, 1213.
- BROSEL, J., KASTLER, A., et WINTER, J., 1952, *J. Phys. Radium*, **13**, 668.
- CAGNAC, J., 1953, *diplôme d'études supérieures*, Paris E.N.S.
- HANLE, W., 1927, *Z. Phys.*, **41**, 164.
- HAWKINS, W. B., and DICKE, R. H., 1953, *Phys. Rev.*, **91**, 1008.
- KASTLER, A., 1936, *Ann. Phys., Paris*, **6**, 663; 1946, *Physica*, **12**, 619; 1950, *J. Phys. Radium*, **11**, 255; 1951, *Physica*, **17**, 191.
- KELLOGG, J. B. M., and MILLMAN, S., 1946, *Rev. Mod. Phys.*, **18**, 323.
- KUSCH, P., 1954, *Phys. Rev.*, **93**, 1022.
- MITCHELL, A. C. G., and ZEMANSKY, M. W., 1934, *Resonance Radiation and Excited Atoms* (Cambridge : University Press), Chap. 5.
- MOSZKOWSKI, S. A., and TOWNES, C. H., 1954, *Phys. Rev.*, **93**, 306.
- MOTT, N. F., 1929, *Proc. Roy. Soc. A*, **124**, 425, **125**, 222; 1932, *Ibid.*, **135**, 429.
- PRINGSHEIM, P., 1949, *Fluorescence and Phosphorescence* (New York : Interscience), pp. 63-78.
- RABI, I. I., 1952, *Phys. Rev.*, **87**, 379.
- RAMSEY, N. F., 1953, *Nuclear Moments* (New York : Wiley), Chap. 3D.
- SAGALYN, P., 1954, *Phys. Rev.*, **94**, 885.
- SAUTER, F., 1931, *Ann. Phys., Lpz.*, **11**, 454; 1933, *Ibid.*, **18**, 61.
- SIMON, A., ROSE, M. E., and JAUCH, J. M., 1951, *Phys. Rev.*, **84**, 1155.

Investigations of Atomic and Molecular Absorption Spectra III: Ultra-Violet Absorption Spectra of Indium Vapour

BY W. R. S. GARTON

Department of Astrophysics, Imperial College, London

MS. received 26th May 1954

Abstract. By use of a King furnace the absorption spectra of In vapour in the near and vacuum ultra-violet have been observed. Fourteen new absorption lines of the In I^b spectrum have been found in the Schumann region, and the normal sharp and diffuse series extended. Classification of the strongest of the vacuum ultra-violet lines leads to an amendment of the sp^2 term assignments of McCormick and Sawyer in the isoelectronic spectrum of Sn II .

§ 1. INTRODUCTION

THE observations, here reported, of the ultra-violet absorption spectra of atomic indium, have been made in the course of a programme of work, of which the general aims and main experimental details are explained in paper I of this series (Garton 1952). A brief note (Garton 1950) reported some initial results for indium.

The ground state of the In atom is $5s^2 5p^2 P^0_{1/2, 3/2}$, and the series spectrum, with its term system built on the $5^1 S_0$ ground state of the ion, was summarized and extended by Paschen (1938). Recent work of Meggers and Murphy (1952) has yielded new infra-red lines of the series spectrum, and enabled location of the $5^2 F^0$ and $6^2 F^0$ terms.

The In I^b spectrum arises from the configurations $5s5pml$ ($l=s, p, d, \dots$), the terms of which converge to the $5s5p^1, ^3 P^0$ levels of In II ; the highest of the latter levels lying 109704 cm^{-1} above the ground state of the neutral atom, the whole I^b spectrum will lie at wavelengths greater than 911 \AA . The I^b configurations combining optically with the ground term are $5s5pmp$, each of which, for m greater than 5, gives eighteen levels; in the case of the lowest I^b configuration, $5s5p^2$, the number of levels is limited by the Pauli principle to eight, viz. in Russell-Saunders notation, $^4 P$, $^2 S$, $^2 P$, $^2 D$.

Included in Paschen's (1938) list, are the I^b terms $5s5p^2 ^4 P$, $^2 D$, $5s5p6s ^4 P^0$, of which the first-named was originally placed by Sawyer and Lang (1929) and Lansing (1929), and is certainly established; the other two terms are tentative, and it is doubtful if $sp^2 ^2 D$ can be separately distinguished from the $s^2 d ^2 D$ series which it perturbs.

By examination of the absorption spectra of indium in the quartz ultra-violet and Schumann region, it has now been possible to locate the remaining terms $^2 S$ and $^2 P$ of $5s5p^2$ and several of the $5s5pmp ^2 S_{1/2}$ terms, and to extend considerably the ordinary S and D series.

§ 2. EXPERIMENTAL

The absorption spectra were photographed with a 1-metre normal-incidence vacuum grating, in the range 1070–2200 Å, and with a Hilger medium-quartz spectrograph in the range above 2100 Å. With either a hydrogen tube or a Lyman-continuum 'flash-tube' (Garton 1953) providing the background continuum, sets of graduated exposures were obtained with the small King furnace at a succession of temperatures up to 1500°C. In all cases a slow current of helium, purified over copper oxide and liquid-air-cooled charcoal was maintained within the furnace envelope. Wavelength measurements were made with reference to various emission and absorption lines inevitably superimposed on the Lyman continuum, and arising from traces of impurity or the disintegration products of the silica capillary used. The quartz-region plates were measured with reference to iron and copper lines as listed by Harrison (1939).

§ 3. RESULTS AND DISCUSSION

3.1. *Schumann Region*

Figure 1 (Plate) is a reproduction of a typical set of exposures, obtained with the Lyman continuum as background, at the succession of furnace temperatures indicated.

At the long wavelength end of the 1250° and 1400° pictures, the higher members of the $5^2P^0_{1/2}-m^2S_{1/2}$ and $5^2P^0_{1/2}-m^2D_{3/2}$ series can be seen converging to the common limit near 2143 Å. The region of strong continuous absorption represents, of course, the ionization continuum beyond that limit. The absorption coefficient of this drops quickly towards shorter wavelengths, and is evidently low at 1800 Å. Apart from these features, there are present fourteen absorption lines, marked A to N, representing combinations of the ground doublet term with i^b terms.

The most striking feature of the spectra is the isolated group of five intense lines between 1760 and 1640 Å; these lines show considerable auto-ionization broadening, which is particularly marked in the 1757 Å line. The other i^b lines, all of which lie below 1400 Å, are considerably weaker.

Wavelengths, wave numbers, intensities, characters and classifications of the lines are given in table 1, together with the positions of the newly identified levels, measured upward from the ground level. The intensity figures are estimated on an arbitrary scale, with 100 for the strongest line, and are judged largely from order of appearance with rising vapour pressure. This visual estimate takes as much or more account of line-breadth as of central intensity. Moreover, absorption lines starting on $5^2P^0_{3/2}$ are at a disadvantage, since that level lies some 0.25 volt above $5^2P^0_{1/2}$. For these reasons the intensity figures bear little relation to relative f -values.

From table 1 the lines B to E form the PP' multiplet, lines A, J, M, N are assigned to the series $5^2P^0_{3/2}-5s5pmp^2S_{1/2}$ ($m=5-8$); lines F and G form a pair exhibiting the ground-term interval, and presumably their upper level 'X' belongs to $5s5p6p$. The latter level has no obvious correlation with any of those of sp^2 . Four lines are unclassified, the only significant point amongst them being that K and G show a difference of 2475 cm^{-1} , closely resembling

$$5s5p(^3P_2-^3P_1)=2478\text{ cm}^{-1}$$

in In II; this suggests that K starts on $5^2P^0_{1/2}$, in which case another level can be placed at 77068 cm^{-1} .

The grounds for the assignments of table 1 are as follows. Of the strong group A to E, the line A is most affected by auto-ionization; its upper state is therefore taken to be $5s5p^2^2S_{1/2}$. The remaining four lines then form the PP' multiplet, and are relatively less diffuse as expected from Shenstone's rules (1931). Lines J, M and N are also diffuse, and together with A appear to form a series converging on $5s5p^3P^0_2$ In II, if we assume their common lower state to be $5^2P^0_{3/2}$. This convergence is in accord with Hund's scheme. The absence of the combinations of the supposed $spp^2S_{1/2}$ levels with $5^2P^0_{1/2}$ calls for explanation, especially as regards the missing companion $5^2P^0_{1/2}-spp^2S_{1/2}$ of the intense line A. In *LS* coupling the missing line would have half the intensity of $5^2P^0_{3/2}-spp^2S_{1/2}$, and would be relatively stronger in absorption because of the low population of $5^2P^0_{3/2}$.

Table 1. Schumann Region Absorption Lines

Line	$\lambda_{\text{vac}}(\text{\AA})$	$\nu_{\text{vac}}(\text{cm}^{-1})$	<i>I</i>	Classification
A	1757.3	56905	100UU	$5^2P^0_{3/2}-5s5p^2^2S_{1/2}$
B	1740.9	57442	10U	$5^2P^0_{3/2}-5s5p^2^2P_{1/2}$
C	1711.1	58442	100u	$5^2P^0_{3/2}-5s5p^2^2P_{3/2}$
D	1676.2	59657	50U	$5^2P^0_{1/2}-5s5p^2^2P_{1/2}$
E	1648.7	60652	100u	$5^2P^0_{1/2}-5s5p^2^2P_{3/2}$
F	1381.7	72377	0s	$5^2P^0_{3/2}-\text{'X'}$
G	1340.6	74593	2s	$5^2P^0_{1/2}-\text{'X'}$
H	1333.4	74996	0s	
I	1323.5	75555	1s	
J	1319.5	75784	2U	$5^2P^0_{3/2}-5s5p6p^2S_{1/2}$
K	1297.5	77068	0s	
L	1232.5	81138	0s	
M	1213.0	82438	0u	$5^2P^0_{3/2}-5s5p7p^2S_{1/2}$
N	1172.5	85487	0u	$5^2F^0_{3/2}-5s5p8p^2S_{1/2}$

$$5s5p^2^2P_{1/2}=59657\text{ cm}^{-1}$$

$$^2P_{3/2}=60652$$

$$^2S_{1/2}=59118$$

$$5s5p6p^2S_{1/2}=77997$$

$$7p^2S_{1/2}=84651$$

$$8p^2S_{1/2}=87700$$

$$\text{'X'}=74593$$

In *jj* coupling the following argument leads to the expectation that the combinations with $5^2P^0_{1/2}$ will be absent. We may suppose the In I^b terms formed by addition of the s-electron to terms of $5pmp$ In II; in *jj* coupling terms of $5pmp$ with $J=0$ can be obtained from $5p_{1/2}mp_{1/2}$ and $5p_{3/2}mp_{3/2}$, and the *LS* labels of these would be 1S_0 , 3P_0 . Now in Sn I, the 1S_0 terms of pp configurations converge to $5^2P^0_{3/2}$ of Sn II (Meggers 1940), and are therefore to be correlated with $5p_{3/2}mp_{3/2}$. On adding the s-electron it is thus a fair presumption that in $5s5pmp$ of In I, $^2S_{1/2}$ is to be correlated with $5s5p_{3/2}mp_{3/2}$, so that with progressive change from *LS* to *jj* conditions, the combinations $5^2P^0_{1/2}-spp^2S_{1/2}$ will disappear, and the $5^2P^0_{3/2}-spp^2S_{1/2}$ series will converge on $5s5p^3P^0_2$, as found. Moreover, the large breadths of the $^2S_{1/2}$ levels will operate to decrease the central intensities of the absorption lines, and thus accelerate the weakening of the $5^2P^0_{1/2}$ combinations with increasing departure from *LS* conditions. It will be noted that, amongst the weaker lines below 1400\AA , the ground-term interval appears only once; this again

is to be anticipated with approach to jj coupling. Identification of the unclassified lines must await experiments with a longer absorbing path, which should yield further lines.

It will be seen from figure 1 that the absorption coefficients from the ground into the strongly auto-ionizing levels $sp^2 2P$, $2S$ are high, for example, much greater than that to the ionization continuum at the $5^2P^0_{1/2}$ limit. Short of a determination of the integral of the absorption coefficient over the lines, it is somewhat hazardous to make statements regarding the relative f -values of these transitions as compared with those of the series spectrum and ionization continuum, since it is well known that a broad line can be mistakenly regarded as more intense than a sharp one, for lack of adequate resolving power. However, as indicated in Part I of this series, there are grounds for believing correct an impression obtained from inspection of the absorption spectra, that a large part of the oscillator strength of the In atom is associated with the I^b lines.†

3.2. Isoelectronic Spectra

For the spectra isoelectronic with In I extensive observations and analysis exist only for Sn II, in which McCormick and Sawyer (1938) have identified long series and made assignments for all the terms of $5s5p^2$; identification of $2S$ and $2P$ of the latter was made from the group of five lines listed in table 2, classified as shown in the second column, the component $5^2P^0_{1/2}-sp^2 2P_{1/2}$ being considered absent. Apart from intensities, which are not comparable for reasons mentioned, the Sn II line group is closely similar to the In I group A to E; accordingly, the amendment of the Sn II classifications shown in the third column is suggested. The screening constants obtained from Sommerfeld's regular-doublet formula applied to $5s5p^2 \Delta^2P$ gives 34.6 and 31.1 respectively for In I and Sn II.

Table 2. Sn II $5^2P^0-5s5p^2 2P$, $2S$ Combinations

λ (Å)	Classification	
	McC & S	Suggested amendment
1180.51	$5^2P^0_{1/2}-sp^2 2P_{3/2}$	$5^2P^0_{1/2}-sp^2 2P_{3/2}$
1223.70	$-sp^2 2S_{1/2}$	$-sp^2 2P_{1/2}$
1243.00	$5^2P^0_{3/2}-sp^2 2P_{3/2}$	$5^2P^0_{3/2}-sp^2 2P_{3/2}$
1290.86	$-sp^2 2S_{1/2}$	$-sp^2 2P_{1/2}$
1316.59	$-sp^2 2P_{1/2}$	$-sp^2 2S_{1/2}$

Partial analyses of Sb III have been made by Lang (1930) and Lang and Vestine (1932), and of Te IV by Rao (1931). It does not seem possible to find analogues of the In A to E group in the published line lists, and application of the doublet laws indicates that, of the sp^2 terms named in these spectra, only $2D$ falls in the place expected; further experimental work on these spectra is needed.

3.3. Near Ultra-Violet

Exposures on the medium-quartz spectrograph, with the hydrogen-continuum as background, gave good photographs of the $5^2P^0_{1/2}-m^2S_{1/2}$, and $5^2P^0_{1/2}-m^2D_{3/2}$ absorption series up to $m=24$ and 30 respectively (Figure 2, Plate); previous emission spectra (Paschen 1938) had reached $m=15$. The use of higher dispersion

† Note added in proof. The impression that large f -values often attach to 'Beutler lines' strongly broadened by auto-ionization (cf. Garton 1952) receives support from recent measurements of Marr (*Proc. Roy. Soc. A*, 1954, **224**, 83) on TII; he finds $f=0.52$ for $\lambda 1610\ 6^2P^0_{1/2}-6s6p^2 2D_{3/2}$ against 0.20 for the strongest resonance line.

for the wavelength measurements was not possible at the time since the speculum-metal gratings available had very low speed at the short-wavelength end of the quartz region. As it is, the results given in tables 3 and 4 are accurate to 0.02 Å.

Discounting the poorly visible last line ($m=24$) of table 3, the series fits to $\pm 0.7 \text{ cm}^{-1}$, a Ritz formula $\nu = A - R/n^{*2}$, with

$$n^* = m - 3.72697 + 0.29910/m^2,$$

$$A = 46670.5 \pm 0.7 \text{ cm}^{-1}.$$

Paschen's (1938) limit $5^2P^0_{1/2} = 46669.93 \text{ cm}^{-1}$, based on the 2F series is thus substantially confirmed.

Table 3. In I $5^2P^0_{1/2}-m^2S_{1/2}$ Series

m	$\lambda_{\text{air}} (\text{\AA})$	$\nu_{\text{vac}} (\text{cm}^{-1})$	m	$\lambda_{\text{air}} (\text{\AA})$	$\nu_{\text{vac}} (\text{cm}^{-1})$
13	2202.19	45395.1	19	2163.82	46200.0
14	2190.81	630.9	20	61.22	255.6
15	82.38	807.1	21	59.05	302.1
16	75.98	941.9	22	57.18	342.2
17	70.99	46047.4	23	55.66	374.9
18	67.03	131.6	24	54.37	402.6

Table 4. In I $5^2P^0_{1/2}-m^2D_{3/2}$ Series

m	$\lambda_{\text{air}} (\text{\AA})$	$\nu_{\text{vac}} (\text{cm}^{-1})$	m	$\lambda_{\text{air}} (\text{\AA})$	$\nu_{\text{vac}} (\text{cm}^{-1})$
11	2211.14	45211.4	21	2156.69	46352.7
12	2197.39	494.3	22	55.22	384.3
13	87.38	702.5	23	54.00	410.6
14	79.85	860.3	24	52.89	434.5
15	74.07	982.2	25	51.93	455.2
16	69.52	46078.6	26	51.13	472.5
17	65.88	156.1	27	50.41	488.1
18	62.89	219.9	28	49.78	501.7
19	60.44	272.3	29	49.20	514.2
20	58.40	316.0	30	48.68	525.5

The 2D series is less regular, presumably owing to perturbation by $5s5p^2^2D$, and there is little point in fitting an elaborate series formula.

The only other significant feature of the near ultra-violet spectra is the presence of the $5^2P-5s5p^2^4P$ group as five sharp absorption lines, thus confirming the earlier identification.

REFERENCES

- GARTON, W. R. S., 1950, *Nature, Lond.*, **166**, 150; 1952, *Proc. Phys. Soc. A*, **65**, 268; 1953, *J. Sci. Instrum.*, **30**, 119.
 HARRISON, G. R., 1939, *M.I.T. Wavelength Tables* (New York: John Wiley).
 LANG, R. J., 1930, *Phys. Rev.*, **35**, 445.
 LANG, R. J., and VESTINE, E. H., 1932, *Phys. Rev.*, **42**, 233.
 LANSING, W. D., 1929, *Phys. Rev.*, **34**, 597.
 McCORMICK, W. W., and SAWYER, R. A., 1938, *Phys. Rev.*, **54**, 71.
 MEGGERS, W. F., 1940, *J. Res. Nat. Bur. Stand.*, **24**, 153.
 MEGGERS, W. F., and MURPHY, R. J., 1952, *J. Res. Nat. Bur. Stand.*, **48**, 334.
 PASCHEN, F., 1938, *Ann. Phys., Lpz.*, **32**, 148.
 RAO, K. R., 1931, *Proc. Roy. Soc. A*, **133**, 220.
 SAWYER, R. A., and LANG, R. J., 1929, *Phys. Rev.*, **34**, 712.
 SHENSTONE, A. G., 1931, *Phys. Rev.*, **38**, 873.

Galvomagnetic and Thermomagnetic Effects in a Plasma

By A. A. WARE

Associated Electrical Industries Ltd., Research Laboratories, Aldermaston, Berks.

*Communicated by D. R. Chick; MS. received 17th March 1954,
and in amended form 14th June 1954*

Abstract. The analysis of Davydov and of Tonks and Allis has been repeated to obtain the electrical and energy transport equations for a plasma subject to a magnetic field in which the isotropic part of the distribution is assumed Maxwellian but in which the momentum transfer due to electron self-interactions can be neglected. The validity of the various simplifying assumptions is considered. The exact coefficients have been evaluated and because of their unwieldy nature simpler approximate expressions are suggested and compared with the correct coefficients. The galvomagnetic and thermomagnetic effects are considered and it is shown that in addition to the Hall effect the Ettingshausen effect may also be important in laboratory discharges. The latter is suggested as a possible cause of the retrograde motion of an arc spot in a transverse magnetic field.

§ 1. INTRODUCTION

THE theoretical work which has been done on the velocity distribution of electrons in a non-uniform plasma, subject to a magnetic field, has so far been directed mainly at evaluating the forward and transverse diffusion coefficients and the associated electrical and thermal conductivities. Using the Lorentz method of solving Boltzmann's equation, Davydov (1937) and Tonks and Allis (1937) have determined these coefficients for the case in which the isotropic part of the distribution function is Maxwellian, but in which the electron self-interactions can be neglected in the momentum balance equations. The more general case in which the positive and negative particles in the gas are of comparable mass and in which the self-interactions cannot be neglected, has been treated by Chapman and Cowling (1939) and Cowling (1945) using the Chapman-Enskog method of solution. The results for the electron component of a completely ionized gas using this method have been evaluated by Landshoff (1949).

The coefficients of the terms in the transport equations obtained by Davydov, and by Tonks and Allis are of an unwieldy form since they involve the exponential integrals $\text{erf}(x)$ and $\text{Ei}(x)$. Tonks (1939) has compared the forward and transverse diffusion coefficients with the approximate but much simpler expressions obtained by mean free path theory and has shown that the latter are a sufficiently good approximation for most gas discharge applications. In this paper similar approximations are suggested for the thermal diffusion coefficients and the energy transfer coefficients. It has been found that good approximations are possible with quite simple expressions.

The galvomagnetic and thermomagnetic effects are implicitly contained in the transfer equations in the above papers, but they have not been studied as such, and apart from the Hall effect no attempt has been made to consider their importance in the behaviour of a discharge in a magnetic field. A considerable amount of theoretical work has of course been done on the theory of these effects in solid conductors, with which the effects are normally associated (see for example Sommerfeld and Frank 1931). The results are not immediately applicable to a plasma since they are based on a Fermi distribution for the electron velocities, but the method of treatment is essentially similar. From the point of view of statistics the plasma will resemble a semiconductor, but, since the magnitude and sign of the galvo- and thermomagnetic effects depend on the variation of the electron free path with velocity, the effects in the two media may be widely different.

In this paper the same assumptions are made as in the work of Davydov and of Tonks and Allis. Their equations for the transport of charge and energy are used to demonstrate the galvo- and thermomagnetic effects. The derivation of these transport equations is outlined so that the various simplifying assumptions and their limits of validity can be indicated. The importance of these magnetic effects in laboratory discharges is considered.

Using Cartesian coordinates, a simple problem is considered in which an electric field Z is applied to the plasma in the z direction and a magnetic field H in the y direction. The plasma is assumed uniform in these two directions. In the x direction, however, there are assumed to be density and temperature gradients and also a further component of electric field, X .

The various field vectors are therefore:

$$\left. \begin{aligned} \mathbf{E} &\equiv X, 0, Z & \mathbf{H} &\equiv 0, H, 0 \\ \nabla n &\equiv dn/dx, 0, 0 & \nabla T &\equiv dT/dx, 0, 0 \end{aligned} \right\} \dots\dots(1)$$

where n and T are the electron density and temperature.

The above orientation of the vectors is by no means the most general but it is sufficient for the demonstration of the galvomagnetic and thermomagnetic effects.

§ 2. THE VELOCITY DISTRIBUTION FUNCTION

As in previous work the assumption is made that the electron velocity distribution is approximately isotropic so that a good approximation to the distribution function is obtained by taking the first two terms in an expansion in spherical harmonics (see Morse, Allis and Lamar 1935, Davydov 1937). Thus

$$f = f_0(x, y, z, c) + \left(\frac{1}{c}\right) \mathbf{c} \cdot \mathbf{f}_1(x, y, z, c) \dots\dots(2)$$

where $f du dv dw dx dy dz$ is the number of electrons in the element of phase space $dx dy dz du dv dw$; u, v, w are the components of the particular electron velocity \mathbf{c} . This assumption is justified provided:

(i) $Ee\lambda \ll 3kT/2$, where λ is the electron mean free path for collisions with other types of particles in the plasma, and $3kT/2$ the mean random energy of the electrons. This relation will be true even for large electric fields if the electrons lose the energy they gain from the electric field mainly by collision with the other particles of the plasma. The average energy lost by an electron

in such a collision is small compared with its total energy. This is roughly true even if inelastic collisions are numerous since on the average at optimum electron energies at least three to four elastic collisions will be made per inelastic encounter. (The assumption will be made later however, that the inelastic collision frequency is small compared with the frequency of elastic collisions, a condition which is true for most laboratory discharges.) The random energy of the electrons must therefore build up until the small fraction lost per collision is comparable with $Ee\lambda$ and condition (i) will be satisfied. The electrons will lose their energy in this way if λ is small compared with the dimensions of the containing discharge tube. In addition the spatial variation of \mathbf{E} must be sufficiently slow to enable the electrons to attain the appropriate mean energy.

(ii) $\lambda/n|\nabla n| \ll 1$. If this is not satisfied then clearly appreciably more electrons will approach a point with velocity \mathbf{c} from the high density side than will approach with velocity $-\mathbf{c}$ from the low density side.

(iii) $\lambda/T|\nabla T| \ll 1$, for the same reasons as (ii). These conditions are considered again in §3.

In the case considered there is no drift motion in the y direction, so that

$$f = f_0 + \frac{u}{c}f_x + \frac{w}{c}f_z \quad \dots\dots(3)$$

where f_x and f_z are the components of \mathbf{f}_1 .

The fundamental equation which f must satisfy is Boltzmann's equation (see Chapman and Cowling 1939, p. 46) and with the particular field vectors chosen this takes the form

$$u \frac{\partial f}{\partial x} - \frac{e}{m} [X - wH] \frac{\partial f}{\partial u} - \frac{e}{m} [Z + uH] \frac{\partial f}{\partial w} = \left(\frac{\partial f}{\partial t} \right)_{\text{coll}} \quad \dots\dots(4)$$

where steady state conditions are assumed and $(\partial f/\partial t)_{\text{coll}}$ is the rate of change of f due to collisions. Electromagnetic units are used and $-e$ has been taken as the electronic charge.

Following the method of Davydov, equation (4) can be resolved into three component equations which give respectively the conservation of energy, and momentum components in the x and z directions, for electrons with velocity magnitude in the range dc . These are:

$$\frac{c}{3} \frac{\partial f_x}{\partial x} - \frac{Xe}{3mc^2} \frac{\partial(c^2 f_x)}{\partial c} - \frac{Ze}{3mc^2} \frac{\partial(c^2 f_z)}{\partial c} = \frac{mN}{Mc^2} \frac{\partial(c^2 Q f_0)}{\partial c} + \Delta_1 \quad \dots\dots(5)$$

$$\frac{c^2 \partial f_0}{3 \partial x} - \frac{Xec}{3m} \frac{\partial f_0}{\partial c} - \frac{\omega c}{3} f_z = -\frac{c^2}{3\lambda} f_x + \Delta_2 \quad \dots\dots(6)$$

$$-\frac{Zec}{3m} \frac{\partial f_0}{\partial c} + \frac{\omega c}{3} f_x = -\frac{c^2}{3\lambda} f_z + \Delta_3 \quad \dots\dots(7)$$

where ω is written for He/m . The first terms on the right-hand sides of these three equations are the rates of change of energy and momentum components due to elastic collisions between electrons and the neutral gas atoms or molecules. The Δ terms represent the contributions due to all other types of collisions made by the electrons. N is the density of gas atoms, M the mass of an atom and Q its cross section for momentum transfer for electrons with velocity c . λ is the mean free path $1/NQ$.

The assumption is made that the frequency of collisions with positive ions is small compared with frequency of collisions with neutral atoms (i.e. that only a small fraction of the gas is ionized). Secondly the contributions due to inelastic collisions are neglected. This leaves only the electron self-interactions to contribute to the Δ terms.

Experimental evidence suggests that in many laboratory discharges, in which the electron density is not too low, the form of f_0 is Maxwellian; and therefore in the subsequent work this will be taken to be the case. From the point of view of the theory developed here this amounts to assuming that the two parts of Δ_1 (due to electron self-interactions) are the most important terms in equation (5). The solution for f_0 obtained by equating Δ_1 to zero is the Maxwellian function. On the other hand, the electron self-interactions will be neglected in the momentum balance equations (terms Δ_2 and Δ_3). These two assumptions will be compatible provided

$$\tau_{en} \ll \tau_{ee} \ll M\tau_{en}/m \quad \dots\dots(8)$$

where τ_{en} , τ_{ee} are the mean collision intervals for electron-neutral atom and electron-electron collisions. $M\tau_{en}/m$ is the order of magnitude of the time taken for an electron to lose by collisions with neutral atoms a total amount of energy equal to its mean energy. If the condition (8) is true the electron self-interactions will be more important than electron-neutral atom collisions as far as energy transfer is concerned but less important for momentum transfer.

It has been suggested that partially organized electron oscillations occur in the plasma of a discharge and that these play a major role in the maintenance of a Maxwellian distribution of velocities (Gabor 1952). Unfortunately this does not increase the range of validity of the above assumptions since such interactions are likely to contribute to the terms Δ_2 and Δ_3 as well as to Δ_1 . In fact such oscillation may account for observed diffusion currents across a magnetic field: being many times larger than those predicted by the formulae of Tonks and Allis and of Davydov (see Guthrie and Wakerling 1949). In general, it must be assumed that any form of plasma oscillations will invalidate the transport formulae derived here.

Following Davydov, the terms Δ_2 and Δ_3 are neglected and the Maxwellian function is taken for f_0 . Equations (6) and (7) then yield the solutions for f_x and f_z :

$$f_x = \frac{-\lambda f_0}{1 + (\omega\lambda/\bar{c})^2} \left\{ \left[\frac{Xe}{kT} + \frac{1}{n} \frac{dn}{dx} + \frac{(mc^2 - 3kT)}{2kT^2} \frac{dT}{dx} \right] + \left(\frac{\omega\lambda}{c} \right) \frac{Ze}{kT} \right\} \quad \dots\dots(9)$$

$$f_z = \frac{-\lambda f_0}{1 + (\omega\lambda/\bar{c})^2} \left\{ - \left(\frac{\omega\lambda}{c} \right) \left[\frac{Xe}{kT} + \frac{1}{n} \frac{dn}{dx} + \frac{(mc^2 - 3kT)}{2kT^2} \frac{dT}{dx} \right] + \frac{Ze}{kT} \right\} \quad \dots\dots(10)$$

Before proceeding it is worth noting that these equations justify the assumption that $|\mathbf{f}_1| \ll f_0$ and that therefore f is approximately isotropic provided conditions (i), (ii) and (iii) of §2 are satisfied. At first sight it might appear that the conditions could be made less stringent by introducing the reduced mean free path $\lambda/[1 + (\omega\lambda/\bar{c})^2]$ instead of λ where \bar{c} is the mean random velocity. This may be true in certain circumstances but it is not true in general. Thus if the 'forces' are balanced such that $f_x = 0$,

$$\left[\frac{Xe}{kT} + \frac{1}{n} \frac{dn}{dx} + \left(\frac{mc^2 - 3kT}{2kT^2} \right) \frac{dT}{dx} \right] = - \frac{\omega\lambda}{c} \frac{Ze}{kT}$$

whence:

$$f_z = -\frac{\lambda f_0}{1 + (\omega\lambda/c)^2} \left[\left(\frac{\omega\lambda}{c} \right)^2 \frac{Ze}{kT} + \frac{Ze}{kT} \right] = -\frac{Ze\lambda}{kT} f_0$$

and $|f_z| \ll f_0$ only if $Ze\lambda/kT \ll 1$, which is condition (i).

From equations (9) and (10), the components of the electron current density I_x , I_z and of the energy transport due to the electrons W_x , W_z are obtained directly by means of the integrals:

$$\left. \begin{aligned} I_x &= -4\pi e \int_0^\infty \frac{c^3}{3} f_x dc & I_z &= -4\pi e \int_0^\infty \frac{c^3}{3} f_z dc \\ W_x &= 2\pi m \int_0^\infty \frac{c^5}{3} f_x dc & W_z &= 2\pi m \int_0^\infty \frac{c^5}{3} f_z dc \end{aligned} \right\} \dots\dots(11)$$

In addition to f_0 the one further quantity in (9) and (10) which may be a function of c is λ , the mean free path, and some assumption must be made as to the variation of λ with velocity before the above integrals can be evaluated. Since the various terms depend on different powers of λ the variation of λ with velocity can affect not only the magnitude but the signs of the components of \mathbf{I} and \mathbf{W} , as will be seen below.

It is important to point out that even for constant λ the terms in (9) and (10) due to the various 'forces'—the electric force, the magnetic ponderomotive force, the concentration and temperature gradients—depend on different powers of c , with the exception of the terms due to the concentration gradient and the electric field. It is because of this that, with the one exception, it is not possible to produce a balance between any two of the 'forces' without thermal or electric effects resulting. In other words it is not possible to get a balance such that say both I_x and W_x are zero if only two of the 'forces' are acting (with the one exception). If $I_x = 0$, $W_x \neq 0$ or if $W_x = 0$, $I_x \neq 0$, so that either a heat flow or a current is set up. If there are boundary effects this may set up a third 'force'. Once there are three 'forces' it is possible to get a balance such that both I_x and W_x are zero. In this form of equilibrium however, there is still not a Maxwellian velocity distribution. f_x is zero for at most only two distinct values of c ; for other values of c , f_x will be sometimes positive and sometimes negative.

§ 3. TRANSPORT FORMULAE FOR CONSTANT MEAN FREE PATH

For the purpose of demonstrating the thermomagetic effects the transport equations (11) will be integrated for the case of λ constant with respect to electron velocity. The method of integration has been indicated by Tonks and Allis and yields the transport formulae

$$I_x = neD \left\{ \alpha_1 \left(\frac{Xe}{kT} + \frac{1}{n} \frac{dn}{dx} \right) + \alpha_2 \frac{1}{T} \frac{dT}{dx} + \beta_1 \frac{Ze}{kT} \right\} \dots\dots(12)$$

$$I_z = neD \left\{ -\beta_1 \left(\frac{Xe}{kT} + \frac{1}{n} \frac{dn}{dx} \right) - \beta_2 \frac{1}{T} \frac{dT}{dx} + \alpha_1 \frac{Ze}{kT} \right\} \dots\dots(13)$$

$$W_x = -n(2kT)D \left\{ \gamma_1 \left(\frac{Xe}{kT} + \frac{1}{n} \frac{dn}{dx} \right) + \gamma_2 \frac{1}{T} \frac{dT}{dx} + \delta_1 \frac{Ze}{kT} \right\} \dots\dots(14)$$

$$W_z = -n(2kT)D \left\{ -\delta_1 \left(\frac{Xe}{kT} + \frac{1}{n} \frac{dn}{dx} \right) - \delta_2 \frac{1}{T} \frac{dT}{dx} + \gamma_1 \frac{Ze}{kT} \right\} \dots\dots(15)$$

where

$$\alpha_1 = 1 - h^2 + h^4 \exp(h^2) \text{Ei}(h^2) \quad \dots\dots(16)$$

$$\alpha_2 = \frac{1}{2} + \frac{1}{2}h^2 + h^4 - (h^2 + \frac{3}{2})h^4 \exp(h^2) \text{Ei}(h^2) \quad \dots\dots(17)$$

$$\beta_1 = \frac{1}{2}\pi^{1/2}h[1 - 2h^2 + 4h^3 \exp(h^2) F(h)] \quad \dots\dots(18)$$

$$\beta_2 = \frac{1}{2}\pi^{1/2}h[2h^2 + 2h^4 - 4(h^2 + \frac{3}{2})h^3 \exp(h^2) F(h)] \quad \dots\dots(19)$$

$$\gamma_1 = 1 - \frac{1}{2}h^2 + \frac{1}{2}h^4 - \frac{1}{2}h^6 \exp(h^2) \text{Ei}(h^2) \quad \dots\dots(20)$$

$$\gamma_2 = \frac{3}{2} - \frac{1}{4}h^2 - \frac{1}{4}h^4 - \frac{1}{2}h^6 + \frac{1}{2}(h^2 + \frac{3}{2})h^6 \exp(h^2) \text{Ei}(h^2) \quad \dots\dots(21)$$

$$\delta_1 = \frac{1}{2}\pi^{1/2}h[\frac{3}{4} - \frac{1}{2}h^2 + h^4 - 2h^5 \exp(h^2) F(h)] \quad \dots\dots(22)$$

$$\delta_2 = \frac{1}{2}\pi^{1/2}h[\frac{3}{4} - h^4 - h^6 + 2(h^2 + \frac{3}{2})h^5 F(h)] \quad \dots\dots(23)$$

$$\text{Ei}(h^2) = \int_{h^2}^{\infty} \frac{\exp(-x)}{x} dx, F(h) = \frac{1}{2}\pi^{1/2}\{1 - \text{erf}(h)\} = \int_h^{\infty} \exp(-x^2) dx,$$

D is the diffusion coefficient $\lambda\bar{c}/3$, and $h = 2\omega\tau/\pi^{1/2}$, where τ is the mean collision interval λ/\bar{c} , and \bar{c} is the mean random velocity $(8kT/\pi m)^{1/2}$. With the exception of δ_1 and δ_2 , which are a factor of two greater, these coefficients are identical with those obtained by Davydov.[†]

The coefficients are plotted against h in the figures 1(a)–4(a). The only exceptions to the general pattern of these curves are α_2 and β_2 , the coefficients

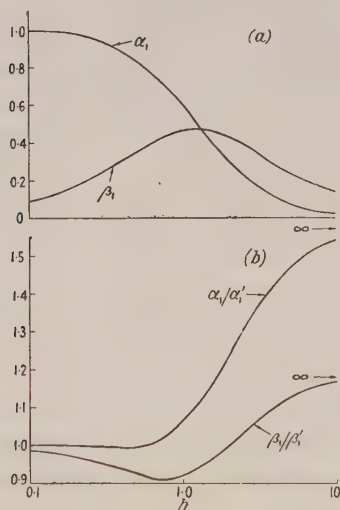


Figure 1.

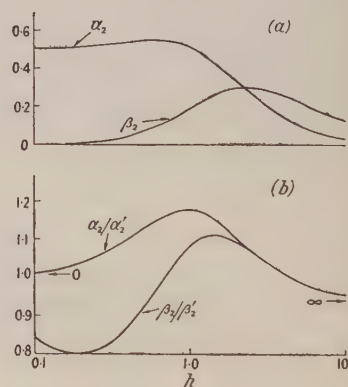


Figure 2.

for forward and transverse thermal diffusion. Unlike the other forward coefficients α_2 is not decreased by a magnetic field for values of h between 0 and 1, in fact it is slightly increased. Only for values of h greater than unity is the thermal diffusion reduced. This effect is due to the fact that thermal diffusion is the resultant of two drift motions. Fast particles ($mc^2 > 3kT$) have a mean drift

[†] The coefficients α_1 , α_2 , etc., satisfy Onsager's reciprocal relations if \mathbf{W} is replaced by the heat flow vector $\mathbf{W} - (3kT/2)\mathbf{l}$.

in the direction of the heat flow whereas slow particles drift in the opposite direction, since the concentration gradient is negative for the former and positive for the latter. For the particular variation of λ with c chosen (λ constant) the drift of the fast particles predominates. With small magnetic fields the decrease in the motion of the slow electrons is greater than the decrease in the motion of the fast electrons and hence the resultant mean diffusion is increased. With large magnetic fields the diffusion of both sets of electrons is substantially reduced and in this case the resultant is decreased.

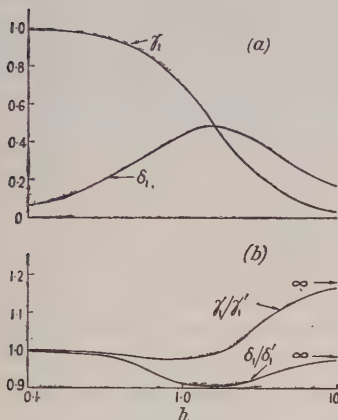


Figure 3.

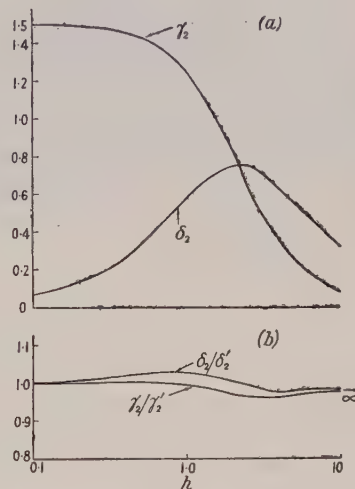


Figure 4.

Again at small h , although in the forward direction the drift of the slow electrons is appreciably less than that of the fast electrons, because the magnetic field has more effect on the slow particles the transverse components are nearly equal. Since the transverse components are also in opposite directions the resultant transverse thermal diffusion is small. As a result β_2 is much less than the other transverse coefficients for small h . At larger magnetic fields the drift of the fast particles becomes more important and β_2 is of the same order as the other coefficients.

§ 4. APPROXIMATE FORMULAE

It is obvious that the coefficients given by equations (16)–(23) make the transport equations extremely unwieldy for use in a particular diffusion or conduction problem. Because of this, Tonks (1939) has used the much simpler coefficients

$$\alpha_1' = \frac{1}{1 + (\omega\tau)^2}, \quad \beta_1' = \frac{\omega\tau}{1 + (\omega\tau)^2}. \quad \dots\dots(24)$$

These are the coefficients obtained by approximate mean free path derivation of the current transport equations, and as Tonks has pointed out they are moderately good approximations for α_1 and β_1 over the whole range $0 \leq h \leq \infty$ (see figure 1(b); the worst error is 57% for α_1 at large h). Because of the errors involved in the various simplifying assumptions which must be made in most gaseous discharge problems these formulae are sufficiently good approximations in most cases.

On the same basis approximate formulae have been sought for the other six coefficients, and it has been found possible to get very good approximations with expressions of the same form as α_1' and β_1' . These are:

$$\left. \begin{aligned} \alpha_2' &= \frac{\frac{1}{2}}{1 + \frac{1}{5}(\omega\tau)^2}, & \beta_2' &= \frac{5(\omega\tau)^3/2}{1 + 10(\omega\tau)^2 + 2(\omega\tau)^4}, \\ \gamma_1' &= \frac{1}{1 + \frac{1}{2}(\omega\tau)^2}, & \delta_1' &= \frac{3\omega\tau/4}{1 + \frac{1}{2}(\omega\tau)^2}, \\ \gamma_2' &= \frac{\frac{3}{2}}{1 + \frac{1}{4}(\omega\tau)^2}, & \delta_2' &= \frac{3\omega\tau/4}{1 + \frac{1}{4}(\omega\tau)^2}. \end{aligned} \right\} \dots\dots(25)$$

The ratios α_2/α_2' , β_2/β_2' , ... etc., are plotted in figures 2(b)–4(b). It is seen that the errors involved are never greater than 20%. (γ_2 and δ_2 are remarkably good approximations, the maximum error being about 3%.) The transverse coefficient for thermal diffusion β_2' has a somewhat different form to that of the other transverse coefficients because of the different variation with h described above

§ 5. THERMOMAGNETIC EFFECTS

Returning to the equations (12)–(15) these can be regarded as the general form of the transport equations for all possible variations of mean free path with electron velocity if D and the coefficients α , β , γ , δ are taken as arbitrary functions of the temperature and magnetic field. With the aid of these equations the galvomagnetic and thermomagnetic effects can be identified as follows. (The coefficients in each case are defined by analogy with the definition for solid conductors.)

(a) The Galvomagnetic Effects—Applied Forces Z and H

In the presence of the magnetic field H (parallel to Oy), the electric field Z produces a longitudinal current parallel to Oz , ($neD\alpha_1Ze/kT$), and a transverse current ($neD\beta_1Ze/kT$) parallel to the x axis. The latter is the *Hall current* and if X_0 is the transverse electric gradient required to reduce I_x to zero the *Hall coefficient* is given by:

$$R = X_0/I_x H. \quad \dots\dots(26)$$

(The coefficient is called the adiabatic coefficient if the condition $W_x=0$ is applied, and the isothermal coefficient if the condition is $dT/dx=0$.)

In addition the applied forces produce a longitudinal energy flow ($-2nD\gamma_1Ze$) and the transverse energy flow ($-2nD\delta_1Ze$). If the balancing field X_0 is acting, in general $-\gamma_1X_0 \neq \delta_1Z$ and there is a resultant transverse energy flow W_x . This is the *Ettingshausen effect*. If $(dT/dx)_0$ is the temperature gradient required to reduce W_x to zero the *Ettingshausen coefficient* is given by

$$P = \frac{(dT/dx)_0}{I_x H}. \quad \dots\dots(27)$$

A plasma with uniform density n is assumed throughout these definitions. The transport equations show that a density gradient behaves similarly to an electric field and hence such a gradient in the presence of a magnetic field will produce effects similar to the galvomagnetic effects.

(b) *The Thermomagnetic Effects—Applied Forces dT/dx and H*

The applied forces (dT/dx , H) produce a longitudinal current $neD\alpha_2 T^{-1} dT/dx$ parallel to the applied force dT/dx (thermal diffusion), and also a transverse current $-neD\beta_2 T^{-1} dT/dx$ in the z direction, which is the *Nernst effect* (transverse thermal diffusion). The *Nernst coefficient* is given by

$$Q = \frac{-Z_0}{H dT/dx} \quad \dots\dots(28)$$

where in this case Z_0 is the transverse field required to reduce I_z to zero. (As with the Hall effect there are adiabatic and isothermal coefficients.)

The forces produce also a forward energy flow ($-2nD\gamma_2 k dT/dx$) parallel to dT/dx and a transverse energy flow ($2nD\delta_2 k dT/dx$) in the z direction. Again, in general, $\gamma_1 Z_0 e/kT \neq \delta_2 T^{-1} dT/dx$ and there is a resultant transverse heat flow. This is the *Righi-Leduc effect* and the coefficient is

$$S = \frac{-(\partial T/\partial z)_0}{H \partial T/\partial x} \quad \dots\dots(29)$$

where $(\partial T/\partial z)_0$ is the temperature gradient which would have to be introduced to make W_z zero.

The negative signs in the definitions (28) and (29) are merely due to the particular orientation chosen for the applied forces dT/dx , H . The expressions for P , Q , R and S in terms of the component coefficients α , β , γ , δ have been evaluated by Sommerfeld and Frank (1931) and will not be given here. In most gas discharge problems the transport equations will be more useful than the coefficients P , Q , R and S .

§ 6. THE IMPORTANCE OF GALVOMAGNETIC AND THERMOMAGNETIC EFFECTS IN LABORATORY DISCHARGES

The primary effect involved in most cases of gas discharges subject to a magnetic field is the Hall effect and this has received considerable attention in the treatment of such problems. Rather surprisingly, however, no consideration appears to have been given to the Ettingshausen effect which must be associated with the Hall effect. A simple estimate will therefore be made of its order of magnitude in a typical low pressure discharge.

The two thermomagnetic effects are produced by a temperature gradient. For these to be important the quantity $T^{-1} \Delta T$ must be comparable in magnitude with Ee/kT . Now the types of discharges in which the magnetic effects in general will be important are essentially low pressure discharges where τ is sufficiently large to give $\omega\tau$ an appreciable magnitude. Except for extremely low pressures the order of magnitude of Ee/kT is rarely less than 10^{-1} cm^{-1} , whereas in such discharges no appreciable temperature gradients appear to have been observed. The reason for the absence of temperature gradients in such discharges is probably the fact that the ambipolar diffusion currents to the walls carry sufficient energy (kinetic and ionization energies) to dissipate most of the energy generated by the discharge currents. Allowing also for radiation, only a small fraction of the energy has to be removed by normal heat conduction. This plus the high heat conductivity of the electrons means that only very small temperature gradients are set up. These considerations suggest that the thermomagnetic effects will rarely be important in laboratory discharges.

The Ettingshausen Effect and Discharges in a Transverse Magnetic Field

A simple idealized discharge is considered in which a current I_z is produced by an applied electric field Z in the z direction. The discharge is assumed uniform in the y direction and subject to a magnetic field applied in this direction. The discharge is assumed non-uniform in the x direction. The appropriate vectors are therefore those chosen in (1) and the appropriate transport equations for the x direction—i.e. the transverse direction normal to both Z and H —are equations (12) and (14) (it being assumed for the moment that the condition λ constant with respect to c applies).

By eliminating X and the concentration gradient from these two equations:

$$W_x = -2kT \frac{\gamma_1}{\alpha_1} \frac{I_z}{e} - n(2kT)D \left\{ \left(\gamma_2 - \gamma_1 \frac{\alpha_2}{\alpha_1} \right) \frac{1}{T} \frac{dT}{dx} + \left(\delta_1 - \gamma_1 \frac{\beta_1}{\alpha_1} \right) \frac{Ze}{kT} \right\}. \quad \dots\dots(30)$$

In most practical cases the transverse current I_x is small and if this term and the temperature gradient term are neglected, equation (30) reduces to

$$W_x = -n(2kT)D \left\{ \delta_1 - \gamma_1 \frac{\beta_1}{\alpha_1} \right\} \frac{Ze}{kT}. \quad \dots\dots(31)$$

The approximate formulae (25) for the coefficients are introduced giving

$$W_x = \frac{1}{2}nkT \left(\frac{\omega\tau}{1 + \frac{1}{2}(\omega\tau)^2} \right) \mu Z \quad \dots\dots(32)$$

where μ is the electron mobility De/kT .

Thus even when I_x is negligibly small and the temperature gradient is zero, there is still a transverse heat flow. This is of course the Ettingshausen effect. Its magnitude is $nkTV$ where V is written for the velocity $\frac{1}{2}\omega\tau\mu Z/[1 + \frac{1}{2}(\omega\tau)^2]$. This is the same heat flow as would occur if all the electrons were travelling with a velocity V in the x direction each carrying the energy kT . For appreciable magnetic fields V is a substantial velocity. For $\omega\tau = 1$ it is equal to a third of the electron drift velocity parallel to the discharge current I_z .† For $\omega\tau \gg 1$ it is equal to Z/H which in most cases is still a substantial velocity: for example, for $Z = 1 \text{ v cm}^{-1}$ and $H = 100 \text{ G}$, Z/H is 10^6 cm sec^{-1} , and for $n = 10^{12}$ and T corresponding to 3 eV, W_x is 0.5 w cm^{-2} .

From these considerations it is clear that the Ettingshausen effect constitutes an appreciable heat flow which is likely to be comparable with the other energy currents in the gas such as that parallel to the discharge current I_z . The rise in temperature which this effect will lead to on the side of the discharge towards which the heat is flowing, will be governed by the facility with which the extra energy can be dissipated by such processes as extra ionization, heat losses to a wall, conduction in the longitudinal direction, etc. From the magnitude of the Ettingshausen heat flow however, it seems likely that in some cases it will play an appreciable part in deciding the character of the discharge.

Retrograde Motion of Arc Spots

It is seen from equation (32) that for the particular case where the mean free path λ is assumed constant with respect to electron velocity, W_x is positive. In other words the heat flow is in the opposite direction to the force acting on the discharge current I_z given by Ampère's law which in this case is in the

† That the drift velocity in the z direction I_z/ne is μZ follows directly from eqns. (12), (13) and (24), when $I_x = dT/dx = 0$.

negative x direction. This fact calls to mind the experimental observation that low pressure arc spots subject to a transverse magnetic field move in the opposite direction to the Ampère force. The theoretical explanation of this retrograde motion is uncertain. Thermomagetic effects in the metal have been suggested (Smith 1942) but this has not been generally accepted (Gallagher 1950, Yamamura 1950). Space charge effects and diffusion effects have also been suggested (Gallagher 1950, Yamamura 1950, Longini 1947, Himler and Cohn 1948), but no consideration has been given to the possibility of the Ettingshausen effect occurring in the discharge immediately above the arc spot. The above considerations suggest that this effect may be important.

If the mechanism of the spot is the direct transfer of energy from electrons in the gas to electrons in the metal leading to thermionic emission, since the Ettingshausen effect causes one side of the discharge to become hotter than the other, the position of the arc spot will move in this direction. This is the direction of retrograde motion. On the other hand, the Hall effect tends to push the electrons in the discharge in the 'correct' direction, and by means of the space charge generated, this force is shared with the positive ions. (The resultant force on the electrons plus the positive ions is the Ampère force.) The Ampère force and Ettingshausen effect therefore oppose each other, the former acting on the discharge column and the latter affecting the position of the hot spot.

The Ampère force is proportional to the product of the arc current and the magnetic field, and is independent of the pressure. The Ettingshausen effect however, is dependent on the pressure through the mean collision interval τ in the factor $\omega\tau/(1 + \frac{1}{2}\omega^2\tau^2)$. This factor also gives the variation with magnetic field through ω , and since the electric field Z will not vary much with current, the Ettingshausen effect will be relatively independent of the current. At high pressure and small magnetic fields ($\omega\tau \ll 1$), therefore, the Ettingshausen effect will be small and the Ampère force will predominate. The Ettingshausen effect has a maximum at $\omega\tau = \sqrt{2}$, and at low pressures and large magnetic fields, it again becomes small, and the Ampère force will again predominate. For intermediate values of $\omega\tau$ the Ettingshausen effect will predominate. Lastly, an increase in current for constant pressure and magnetic field will favour the Ampère force. These qualitative conclusions agree with the observed motion of arc spots with variation of pressure, magnetic field and current (see Smith 1942, Gallagher 1950).

In addition, it has been observed experimentally (Smith 1948, Cobine and Gallagher 1949) that if the cathode is heated so as to become thermionically emitting, the direction of motion of the arc changes to the correct direction. This effect is also in agreement with the above explanations since in these circumstances the cathode spot is not dependent on the heat received from the gas above the spot, and will be free to move in the correct direction. Lack of experimental information on the pressure and electron temperature in the arc immediately above the spot prevents a quantitative check of the theory.†

§ 7. THE EFFECT OF THE VARIATION OF MEAN FREE PATH WITH VELOCITY

If in equations (9) and (10) for f_x and f_z the mean free path, instead of being assumed constant, is taken as a function of c , it is clear that the relative magnitude of the various terms in the integrals (11) will be altered. Thus, for example, if λ is proportional to c , in equation (9) the magnetic ponderomotive force term

† See Note Added in Proof.

is proportional to the same power of c as the electric field and concentration gradient terms. Hence a balance is possible between these 'forces' at all velocities and there will be no Ettingshausen effect. If λ varies more rapidly than linearly with c then the Ettingshausen heat flow is reversed and is in the same direction as the Ampère force. Similar considerations show that thermal diffusion, the Nernst effect and the Righi-Leduc effect are also dependent in sign and magnitude on the variation of λ with velocity. The Hall effect is dependent only in magnitude on the variation of λ .

The variation of mean free path with velocity is therefore a fundamental factor in deciding the magnitude of these effects, i.e. in deciding the value of the coefficients in the transport equations. Care must therefore be exercised in applying equations (12)–(25), which are good approximations only when the electron mean free path can be assumed approximately constant over the velocity range for which the distribution function has appreciable magnitude. Lastly, as discussed in §2, it should be noted that in general the presence of plasma oscillations will invalidate these transport equations.

ACKNOWLEDGMENTS

The author wishes to thank Sir George Thomson for many stimulating discussions and Dr. T. E. Allibone for permission to publish this paper.

REFERENCES

- CHAPMAN, S., and COWLING, T. G., 1939, *The Mathematical Theory of Non-Uniform Gases* (Cambridge : University Press).
- COBINE, J. D., and GALLAGHER, C. J., 1949, *Elect. Engr.*, **68**, 469.
- COWLING, T. G., 1945, *Proc. Roy. Soc. A*, **183**, 453.
- DAVYDOV, B., 1937, *Phys. Z. Sowjet*, **12**, 269.
- GABOR, D., 1952, *Proc. Roy. Soc. A*, **213**, 73.
- GALLAGHER, C. J., 1950, *J. Appl. Phys.*, **21**, 768.
- GUTHRIE, A., and WAKERLING, R. K., 1949, *The Characteristics of Electrical Discharges in Magnetic Fields* (New York : McGraw-Hill).
- HIMLER, G. J., and COHN, G. I., 1948, *Elect. Engr.*, **67**, 1148.
- LANDSHOFF, R., 1949, *Phys. Rev.*, **76**, 904.
- LONGINI, R. L., 1947, *Phys. Rev.*, **72**, 184.
- MORSE, P. H., ALLIS, W. P., and LAMAR, E. S., 1935, *Phys. Rev.*, **48**, 412.
- SMITH, C. G., 1942, *Phys. Rev.*, **62**, 48; 1948, *Ibid.*, **73**, 543.
- SOMMERFELD, A., and FRANK, N. H., 1931, *Rev. Mod. Phys.*, **3**, 1.
- TONKS, L., 1939, *Phys. Rev.*, **56**, 360.
- TONKS, L., and ALLIS, W. P., 1937, *Phys. Rev.*, **52**, 710.
- YAMAMURA, S., 1950, *J. Appl. Phys.*, **21**, 193.

NOTE ADDED IN PROOF.

Recently two further mechanisms which will give retrograde motion of arc spots have been suggested by Robson and Von Engel (1954) and by St. John and Winans (1954). The former is based on the effect of the local self-magnetic field at the arc spot and the latter on the effect of the space charges and the magnetic field on the motion of the positive ions. These mechanisms and that suggested above predict different variation of spot velocity with arc current, but the experimental results are not sufficiently definite to decide between the mechanisms. Thus at high pressures near where the transition to forward motion occurs, an increase in current favours forward motion (Gallagher 1950, St. John and Winans 1954), but at low pressures an increase in current increases the retrograde velocity (Gallagher 1950, St. John and Winans 1954).

ROBSON, A. E., and VON ENGEL, A., 1954, *Phys. Rev.*, **93**, 1121.

ST. JOHN, R. M., and WINANS, J. G., 1954, *Phys. Rev.*, **94**, 1097.

The Beta Rays of Thallium 204

By J. C. KNIGHT†, T. H. BRAID‡ AND H. O. W. RICHARDSON||

† University of Edinburgh

‡ Palmer Physical Laboratory, Princeton University, U.S.A.

|| University College, Exeter

MS. received 11th June 1954, and in amended form 5th July 1954

Abstract. The β -spectrum of ^{204}Tl has been measured using thin evaporated sources in a spheroidal field β -spectrometer. The end-point was found to be at 766 ± 2 kev. Small deviations were found from the unique shape of spectrum predicted for a first-forbidden transition with a spin change of two units. The deviations extend up to about 400 kev.

The possibility that the decay is second forbidden and that the ground state of ^{204}Tl has even parity is noted.

§ 1. INTRODUCTION

THE β -decay of ^{204}Tl resembles that of radium E in that no γ -transition seems to be present. There is a weak decay by electron capture to ^{204}Hg , which has been estimated by der Mateosian and Smith (1952) to occur in 1.5 ± 0.5 per 100 disintegrations. The β -ray end-point has been found by Lidofsky, Macklin and Wu (1952), using a magnetic spectrometer, to be at 765 ± 10 kev, in agreement with the 766 ± 2 kev found in the present work. They concluded that the spectrum shape agreed with the theoretical shape for a first-forbidden transition with a spin change of 2 units and a parity change. There was, however, an excess of β -rays below 150 kev which is not explained because the theoretical shape is definite and cannot be adjusted. The present measurements do not extend to low energies but they show a small excess of slow β -rays which can be traced to energies as high as 400 kev.

Smith (1952) has shown that this shape of spectrum can be explained as a second-forbidden transition with a spin change of two units and no parity change, because contributions from several matrix elements can be adjusted to fit a variety of shapes. Both these degrees of forbiddenness give the ground state of ^{204}Tl a spin $I=2$. A state of odd parity can easily be explained on the shell model by, for example, assigning the odd proton and odd neutron to $s_{1/2}$ and $f_{5/2}$ states, respectively. The difficulties of explaining a state of even parity are considerably greater.

§ 2. PREPARATION OF SOURCES

The spectra were obtained from disc sources of 2 mm diameter made by condensation *in vacuo* of thallium on to $40 \mu\text{g cm}^{-2}$ nylon films which had been painted with an almost invisible layer of colloidal graphite to prevent source charging. The condensed deposits were transparent and had a metallic lustre, and their uniformity was verified by traversing a small aperture across each source and counting the collimated β -rays which passed through. The deposits

were protected by thin covering films of formvar about $10 \mu\text{g cm}^{-2}$ in thickness. The metal was prepared by electrolysing a sulphate solution made from 100 mg of active Tl_2O_3 supplied by Atomic Energy of Canada Ltd.

The source thicknesses were estimated roughly on the assumption that the specific activity of 100 mc g^{-1} quoted by the suppliers was correct. One estimate was made by counting the total β -activity of the source over a known solid angle, and this value was checked by comparing the area of the β -spectrum found in the spectrometer with the area found for the F-line of thorium B from a source of the same diameter. The absolute intensity of the thorium (B + C) source was found by counting the α -rays with a thin-window proportional counter.

The thicknesses found for the sources A and B were 0.11 and 0.028 mg cm^{-2} . These figures should be multiplied by a path factor of $\sec 74^\circ$ (3.63) to allow for the increased path in the source due to the small glancing angle between its surface and the focused sheaf of β -rays.

§ 3. THE SPECTROMETER

A spheroidal field spectrometer was used with the baffles placed in the positions illustrated elsewhere (Richardson 1952, figure 1 B). The selected sheaf of rays was emitted at a mean angle of 74° to the axis of the spheroid. The ring-slit of 9 cm radius was 1.7 mm wide, giving a resolution of 3%.

The ring window round the Geiger tube was covered with nylon of 0.3 mg cm^{-2} and the filling mixture was alcohol vapour (at about 1.5 cm pressure) and argon (added to a total of 11 cm). The magnetic field was measured by a spinning coil mechanism similar to that of Hedgran, Siegbahn and Svartholm (1950) using the centroids of the A, F and M lines of Th (B + C + C') for calibration.

§ 4. THE SPECTRA

The values of $y_1 = k_1(N/f)^{1/2}$ and $y_2 = k_2(N/fC_{1T})^{1/2}$ are plotted in curves 1 and 2 of the figure against ϵ , the electron energy (including rest energy) in units of $mc^2 = 510.96 \text{ kev}$. N is the number of β -particles found per second in a momentum interval of fixed width and k_1 and k_2 are convenient normalizing constants. Values of f were taken from the U.S. National Bureau of Standards Tables (1952). C_{1T} is the correction factor of Konopinski and Uhlenbeck (1941) for a first-forbidden transition with $\Delta I = \pm 2$, in which only the matrix element $\sum_{ij} B_{ij}$ can contribute.

$$C_{1T} = \sum_{ij} |B_{ij}|^2 \left(\frac{1}{12} L_0 (\epsilon_0 - \epsilon)^2 + \frac{3}{4} L_1 \right)$$

$$L_0 = \frac{g_0^2 + f_{-2}^2}{2p^2 F^2} ; \quad L_1 = \frac{g_1^2 + f_{-3}^2}{2p^2 F \rho^2} .$$

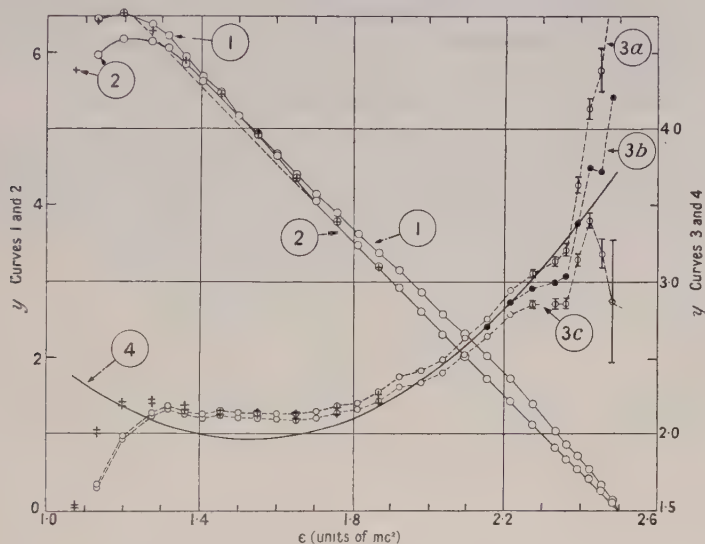
Values of L_0 and L_1 were obtained from the tables of Rose, Perry and Dismuke (1953). L_0 varies slowly with ϵ and differs slightly from the approximation $(1 + S)/2$ used in the explicit formula of Konopinski and Uhlenbeck for C_{1T} .

By fitting a straight line to y_2 by the method of least squares, using the points above 450 kev weighted inversely as their squared statistical errors, the end-point is found at $\epsilon_0 = 2.4992 \pm 0.002$ ($W_0 = 766 \pm 1 \text{ kev}$). The probable errors are computed from the deviations from the straight line, assuming the momentum calibration to be exact. Errors in the calibration would perhaps increase the probable error to $\pm 2 \text{ kev}$.

In curves 3 and 4 of the figure the deviation from the C_{IT} type of spectrum is shown by the more sensitive method of plotting against ϵ :

$$y_3 = k_3 N / f(\epsilon_0 - \epsilon)^2 \quad \text{and} \quad y_4 = k_4 C_{IT}.$$

y_3 depends on the choice of ϵ_0 and is plotted for the three values 2.505, 2.501 and 2.4972. In y_4 the value chosen for ϵ_0 is 2.500.



Energy spectra: curve 1, $y = k_1(N/f)^{1/2}$; curve 2, $y = k_2(N/fC_{IT})^{1/2}$. Correction factors: (a) unique first-forbidden factor, curve 4, with $\epsilon_0 = 2.50$, $y = k_4 C_{IT}$; (b) experimentally observed factors, curves 3a, 3b and 3c, $y = k_3 N / f(\epsilon_0 - \epsilon)^2$ with $\epsilon_0 = 2.4972$, 2.501 and 2.505 respectively. Circles: source A, 0.11 mg cm⁻². Crosses: source B, 0.028 mg cm⁻².

§ 5. DISCUSSION

The experiments show more β -rays between 400 kev and 100 kev than are predicted by the C_{IT} spectrum. The fall in the curve below 100 kev is due partly to window absorption and partly to source absorption. The latter must be present because the fall is greater than that found by Saxon (1951) for window absorption in nylon.

It seems unlikely that the small surplus of β -rays above 200 kev can be due to back-scattering or source thickness distortion because the sources A and B gave similar spectra above 250 kev. However, there is a little uncertainty due to the presence of the covering film and to the unusually low glancing angle of emission. The surplus of β -rays never exceeds 5%, so that its reality, which would indicate second forbiddenness, is not established beyond final question.

Second forbiddenness would require the ground state of ^{204}Tl to have even parity, which would be unusual for a heavy odd-odd nucleus in which the odd neutron and odd proton normally belong to configurations of opposite parity.

Another puzzling feature of the ^{204}Tl β -decay is the apparent absence of β -excitation of the 374 kev $2+$ level of the daughter nucleus ^{204}Pb . This has been discussed by de Shalit and Goldhaber (1953). These authors and Bohr and Mottelson (1953) note that the long γ -ray lifetime of the $2+$ state of ^{204}Pb

suggests that it is a nearly pure neutron state in which the protons bound in the stable 82 shell are not excited. A β -decay to such a state would be very weak. Support for this view of the $2+$ state has been obtained by Frauenfelder, Lawson and Jentschke (1954), who find its magnetic moment to be very small.

ACKNOWLEDGMENT

We wish to thank Professor Feather for his interest in the work, which was largely carried out at Edinburgh.

REFERENCES

- BOHR, A., and MOTTELSON, B. R., 1953, *Kgl. Danske Vidensk. Selsk. Mat.-fys. Med.*, **27**, No. 16.
- FRAUENFELDER, H., LAWSON, J. S., and JENTSCHKE, W., 1954, *Phys. Rev.*, **92**, 1126.
- HEDGRAN, A., SIEGBAHN, K., and SVARTHOLM, N., 1950, *Proc. Phys. Soc. A*, **63**, 960.
- KONOPINSKI, E. J., and UHLENBECK, G. E., 1941, *Phys. Rev.*, **60**, 308.
- LIDOFKY, I., MACKLIN, P., and WU, C. S., 1952, *Phys. Rev.*, **87**, 204 and 391.
- DER MATEOSIAN, E., and SMITH, A., 1952, *Phys. Rev.*, **88**, 1186.
- NATIONAL BUREAU OF STANDARDS, 1952, *Tables for the Analysis of Beta Spectra*, Washington.
- RICHARDSON, H. O. W., 1952, *J. Sci. Instrum.*, **29**, 93.
- ROSE, M. E., PERRY, C. L., and DISMUKE, N. M., 1953, *Tables for the Analysis of Allowed and Forbidden Beta-transitions*, Oak Ridge National Laboratory, Report O.R.N.L.-1459.
- SAXON, D., 1951, *Phys. Rev.*, **81**, 639.
- DE SHALIT, A., and GOLDBABER, M., 1953, *Phys. Rev.*, **92**, 1211.
- SMITH, A. M., 1952, *Phil. Mag.*, **111**, 915.

The Deviations of Nuclear Magnetic Moments from the Schmidt Lines

BY R. J. BLIN-STOYLE† AND M. A. PERKS

Department of Mathematical Physics, The University, Birmingham

Communicated by R. E. Peierls; MS. received 1st June 1954

Abstract. It is shown that the deviations of nuclear magnetic moments from the Schmidt lines can be accounted for in terms of simple interconfigurational mixing. In particular it has been found possible to explain the large deviation of ^{209}Bi .

§ 1. INTRODUCTION

ATTEMPTS to account for the considerable deviations of the nuclear magnetic moments of odd A nuclei from the Schmidt values predicted for the single particle model (SPM) of the nucleus can be conveniently divided into three categories.

In the individual particle model of the nucleus the various nuclear properties are attributed to all those nucleons which are outside closed shells; in particular for light and medium heavy nuclei assuming strong spin-orbit coupling and using the concept of charge independence it is possible to account partially for the deviations in the magnetic moments from the Schmidt values (e.g. Flowers 1952a). According to this model, however, the magnetic moment of a nucleus consisting of a double closed shell and one odd nucleon should not deviate from the SPM value. This is certainly true for ^{17}O where the deviation $\mu_c = 0.02$ nuclear magneton (n.m.); on the other hand ^{209}Bi , which consists of the very stable ^{208}Pb and an odd proton, has a magnetic moment deviating by 1.4 n.m. from the SPM value. So far no explanation has been given for this discrepancy.

The collective model of the nucleus proposed by Bohr (1953) attempts to account for nuclear properties in terms of a collective motion of the nucleons in the form of quantized surface waves. By this mechanism it has been found possible to account to some extent for the deviations of the magnetic moments of a large number of nuclei; again, however, ^{209}Bi is predicted to have a small deviation from the SPM value.

Finally a number of authors have attempted to account for the deviations in terms of interaction effects which, loosely speaking, modify the intrinsic nucleon moments. In particular the magnetic moment anomalies of $\pm \frac{1}{4}$ n.m. for ^3H and ^3He have been fairly satisfactorily explained using meson theoretical methods (Villars 1947). For heavier nuclei, however, it seems that any deviation in the magnetic moment due to interaction effects will be of the same order of magnitude as that for ^3H and ^3He and therefore much too small to account for the observed deviations.‡

† Now at the Clarendon Laboratory, Oxford.

‡ This point, together with other aspects of the problem, is discussed by Ross (1952).

In the present paper an attempt is made to explain the overall behaviour of nuclear magnetic moments in terms of simple interconfigurational mixing in the individual particle model of the nucleus. It is found that certain types of admixed configurations give a large contribution to the magnetic moment and that, by assuming a simple form for the internucleon interaction, it is possible to account quantitatively for the deviations of nuclear magnetic moments (including ^{209}Bi) from the Schmidt value.

§ 2. INTERCONFIGURATIONAL MIXING

There is necessarily a very large number of configurations which can be admixed with the SPM configuration and which will cause a deviation in the magnetic moment of a nucleus from the Schmidt value. However, if the amplitudes of the admixed configurations are small, then from the point of view of the magnetic moment the most important admixtures are those giving contributions to the magnetic moment linear in the amplitude. In the present paper it is shown that those admixtures which contribute in this way do, in fact, have small amplitudes, so that second-order effects can be neglected. Further, work in progress indicates that the amplitudes of other admixed configurations are also small. For the above reasons no further account is taken of second-order contributions. Under these circumstances it is convenient to describe the mixing for a nucleus of spin j in terms of a wave function of the form

$$\Psi_j = \chi_j + \sum_p \alpha_p \phi_{p,j} \quad \dots\dots(1)$$

where χ_j corresponds to the SPM configuration and the $\phi_{p,j}$ represent admixed configurations, such configurations being characterized by the variable p . Further, according to the individual particle model of the nucleus, χ_j and $\phi_{p,j}$ can be expanded in terms of single particle wave functions in jj -coupling.

The magnetic moment of the nucleus (in nuclear magnetons) is then obtained by calculating the expectation value of the operator $\sum_n (g_s^n \sigma^n + g_l^n L^n)$ using the above wave function, the summation being taken over all nucleons in the nucleus. g_s^n and g_l^n are the spin and orbital g -factors for the n th nucleon and σ^n and L^n are the appropriate spin and orbital angular momentum operators. Thus

$$\mu = \frac{j}{m} \langle \Psi_j^m | \sum_n (g_s^n \sigma_z^n + g_l^n L_z^n) | \Psi_j^m \rangle \quad \dots\dots(2)$$

where the nuclear wave function is constructed to represent a state in which the total angular momentum j has a component m along the axis of quantization.

If all the α_p are zero then the Schmidt value for the magnetic moment is obtained. On the other hand a large deviation from this value is to be expected if terms linear in the α_p are non-vanishing. Since the magnetic moment operator is a single particle operator, the condition for this is that χ_j and $\phi_{p,j}$ must differ at most by one single particle state and that then the orbital state must be the same. The only possible type of admixed configuration which satisfies this condition is one in which a single nucleon is transferred from a state $l_{j=l+\frac{1}{2}}$ to $l_{j=l-\frac{1}{2}}$, and it is the effect of such admixtures which will be considered in the remainder of the paper.

For spin $\frac{1}{2}$ nuclei it has been shown by Blin-Stoyle (1953 a) that, using a short-range interaction between nucleons for this type of interconfigurational mixing, corrections to the magnetic moment of the right sign and magnitude are obtained.

In particular, it is shown that the magnetic moments of $p_{1/2}$ nuclei should not deviate appreciably from the Schmidt value, whereas $s_{1/2}$ nuclei will in general deviate considerably from this value.

When configurational mixing is considered in relation to nuclei with spin j greater than $\frac{1}{2}$ it is apparent that several possibilities exist for the form of the admixed configuration according as $j = l - \frac{1}{2}$ or $l + \frac{1}{2}$. (i) If $j = l - \frac{1}{2}$, then admixed configurations in which one of the odd (O) nucleons in the state $l_{j'=l+\frac{1}{2}}$ is excited to the $l_{j=l-\frac{1}{2}}$ state will give a linear contribution to the magnetic moment except in the case that the $j = l - \frac{1}{2}$ shell consists of one hole when the Pauli principle forbids such an admixed state. Similarly (ii) if $j = l + \frac{1}{2}$, then admixed configurations in which a $l_{j=l+\frac{1}{2}}$ O nucleon is excited to the $l_{j'=l-\frac{1}{2}}$ state will contribute except in the case that the $j = l + \frac{1}{2}$ shell consists of one particle only, when the Pauli principle again forbids the admixture. Finally (iii a) for both $j = l - \frac{1}{2}$ and $j = l + \frac{1}{2}$ there is the possibility, as with spin $\frac{1}{2}$ nuclei, that an O or E (even) nucleon is excited from a state $l'_{j'=l+\frac{1}{2}}$ to $l'_{j'=l-\frac{1}{2}}$ or (iii b) that an E nucleon is excited from $l_{j=l+\frac{1}{2}}$ to $l_{j'=l-\frac{1}{2}}$.

In the work which follows it transpires that the largest contribution to the magnetic moment arises when there is the greatest number of cross terms both in the calculation of μ and α_p . This occurs when the admixed configurations are of type (i) or (ii) above because of the large number of terms arising from the antisymmetrization of the wave functions. Also for type (iii) admixtures excitation of an O nucleon is found to be more important than excitation of an E nucleon.

For the purposes of calculation it has been assumed that in the unperturbed state the even nucleons are coupled to spin zero. Thus the calculations apply rigorously to all spin $\frac{1}{2}$ nuclei and those in which the E nucleons form closed shells or sub-shells. In other cases the proper procedure is to solve the secular problem for the shell model ground state and then to consider admixtures to this state. However, if the ground state has a large contribution from the state in which the E nucleons are coupled to spin zero (as is frequently the case (Flowers 1952 b)), then the treatment presented will still be a reasonable approximation.

§ 3. CONFIGURATIONAL MIXING OF TYPE (i)

We consider here $j = l - \frac{1}{2}$ nuclei for which configuration mixing of type (i) is possible (i.e. the calculations do not apply to nuclei having only one hole in the $l_{j=l-\frac{1}{2}}$ shell). The calculation is formulated in terms of three particles, two of which in the SPM are in the state $l_{j'=l+\frac{1}{2}}$ coupled to spin zero and one of which is excited to the same state as the odd nucleon in the admixed configuration. This treatment will be rigorously valid only when there is a single nucleon in the $j = l - \frac{1}{2}$ state; in other cases the corrections which should be applied will, however, be of second order, and all such terms are ignored in the following calculations.

Thus, symbolically,

$$\chi_j \sim [(l_{j'})_0^2(l_j)_j]_j \quad \text{and} \quad \phi_{j,j} \sim [(l_{j'}l_j)_j(l_j)_j]_j$$

where $j = l - \frac{1}{2}$, $j' = l + \frac{1}{2}$ and the admixed configurations are now characterized by the angular momentum J to which j and j' are coupled.

Suitably antisymmetrized functions are then

$$\chi_j^m(1, 2, 3) = \frac{P}{2\sqrt{3}} \sum_{m'} c_{0m'-m'}^{0j'} \psi_{j'}^{m'}(2) \psi_{j'}^{-m'}(3) \psi_j^m(1), \quad \dots\dots(3)$$

$$\phi_{J,j}^m(1, 2, 3) = N_J P \sum_{\mu\sigma} c_{\mu\mu-\sigma\sigma}^{Jj'} c_{m\mu m-\mu}^{Jj} \psi_{j'}^{\mu-\sigma}(2) \psi_j^{\sigma}(3) \psi_j^{m-\mu}(1) \quad \dots\dots(4)$$

where P is the usual particle permutation operator taking values ± 1 according as the permutation is even or odd. The normalization factor N_J is given by

$$N_J = (6 - 6C_J)^{-1/2} \quad \dots\dots(5)$$

where

$$C_J = (2J + 1)W(j'jjj; JJ). \quad \dots\dots(6)$$

The magnetic moment of the nucleus to first order in the amplitude of the admixture is obtained by substituting (1), (3) and (4) into (2) and dropping all second-order terms in α_J .

The correction μ_c to the SPM value of the magnetic moment is then given by

$$\mu_c = \sum_J \alpha_J \mu_J \quad \dots\dots(7)$$

where

$$\mu_J = \frac{2j}{m} \langle \chi_j^m | \sum_{n=1}^3 (g_s^n \sigma_z^n + g_l^n L_z^n) | \phi_{J,j}^m \rangle.$$

Substituting from (3) and (4), after some manipulation the expression for μ_J reduces to

$$\mu_J = \frac{(g_l - g_s)}{(j+1)} \left(\frac{2j(2j+1)}{1-C_J} \right)^{1/2} [\delta_{J1}/\sqrt{3} - (-)^J (2J+1)^{1/2} W(j'jjj; 1J)] \quad \dots\dots(8)$$

where C_J is given by (6) and g_s and g_l are the spin and orbital g -factors for the O nucleons.

In order to calculate the α_J we use a delta function for the form of the inter-nucleon interaction and take account of the singlet and triplet interactions in the manner set out by Pryce (1952). Of course, for this particular case when all the nucleons considered are of the same type, the interaction will only take place in the singlet state and the inter-nucleon potential can be taken to have the form $V(\mathbf{r}) = A_s \delta(\mathbf{r})$ where A_s is the strength of the singlet interaction. Now by first-order perturbation theory we have

$$\alpha_J = - \langle \chi_j | V | \phi_{J,j} \rangle / \Delta E = - M_J / \Delta E \quad \dots\dots(9)$$

where ΔE (always positive) is the energy difference between the SPM and the admixed configurations (the spin-orbit splitting energy in this case). On substituting for $V(\mathbf{r})$, χ_j and $\phi_{J,j}$ the following expression is obtained for M_J :

$$M_J = - \left[\frac{2(2J+1)}{(1-C_J)(2j+1)(2j'+1)} \right]^{1/2} \sum_i (-)^i (2i+1) W(j'jjj; J1) \mathfrak{A}_{i;jj'j} \quad \dots\dots(10)$$

where

$$\mathfrak{A}_{i;jj'j} = A_s \int \psi_{i;jj'}^*(\mathbf{p}, \mathbf{q}) \delta(|\mathbf{r}_p - \mathbf{r}_q|) \psi_{i;jj}(\mathbf{p}, \mathbf{q}) d\tau_p d\tau_q.$$

Here, $\psi_{i;jj'}(\mathbf{p}, \mathbf{q})$ is a wave function representing nucleons p and q in the single particle states $\psi_j(p)$ and $\psi_{j'}(q)$ coupled to give a total spin i , and similarly for $\psi_{i;jj}(\mathbf{p}, \mathbf{q})$. Rewriting these wave functions in an LS coupling scheme, we find

$$\mathfrak{A}_{i;jj'j} = 2\epsilon_s \langle jj'i | i0 \rangle \langle jj'i | i0 \rangle P(i; ll) \quad \dots\dots(11)$$

where $\langle jjj | iLS \rangle$ are jj - LS transformation coefficients for spin $\frac{1}{2}$ particles (see e.g. Blin-Stoyle 1953 b). $P(i; ll)$ is related to the angular integral in the matrix element and is given by

$$P(i; ll) = \frac{(2l-i)!}{(2l+i+1)!} \left[\frac{(2l+1)! i! (\frac{1}{2}i+l)!}{(l-\frac{1}{2}i)! [(\frac{1}{2}i)!]^2} \right]^2 \quad \text{if } i \text{ is even}$$

$$= 0 \quad \text{if } i \text{ is odd,}$$

ϵ_s is the singlet interaction energy and can be expressed in terms of the single particle radial functions by

$$\epsilon_s = A_s \int |R_{nl}(r)|^4 r^2 dr.$$

The final expression for the correction to the magnetic moment is from (7), (8) and (10) (and noting that $j' = j+1$),

$$\mu_c = \frac{2(g_s - g_l)}{\Delta E(j+1)} \left[\frac{j}{2j+3} \right]^{1/2} \left[- \sum_i \frac{(2i+1)W(1i)\mathfrak{A}_i}{1-3W(11)} \right. \\ \left. + \sum_{ji} (-)^j \frac{(2J+1)(2i+1)W(1J)W(Ji)\mathfrak{A}_i}{1-(2J+1)W(JJ)} \right] \quad \dots\dots(12)$$

where $W(ab) \equiv W(j'jjj; ab)$ and $\mathfrak{A}_i \equiv \mathfrak{A}_{i;jj'j}$.

In (12) J can take all integral values from 1 to $2l$ and i can take all even integral values from 2 to $2l-2$.

It is convenient to express μ_c in the form $\mu_c = A_j^l \xi_l$ where A_j^l is known and $\xi_l (= \epsilon_s/\Delta E)$ depends primarily on l but also on n , and is expected to vary in an indeterminate manner from nucleus to nucleus.

The values taken by A_j^l for odd proton and odd neutron nuclei are given in table 1. The application of these results to particular nuclei will be considered in §5.

Table 1. Values of A_j^l for $j = l - \frac{1}{2}$

l	j	Odd proton	Odd neutron
2	3/2	-2.21	1.83
3	5/2	-2.91	2.42
4	7/2	-3.26	2.70
5	9/2	-3.36	2.79

§ 4. CONFIGURATIONAL MIXING OF TYPE (ii)

We now consider those $j = l + \frac{1}{2}$ nuclei which have more than a single particle in the $l_{j=l+\frac{1}{2}}$ state. The calculation is again formulated in terms of three particles, all three of which in the SPM are in the same state $l_{j=l+\frac{1}{2}}$ with two coupled to zero angular momentum, whilst in the admixed configuration one of these particles is excited to the $l_{j'=l-\frac{1}{2}}$ state. Thus, symbolically

$$\chi_j \sim [(l_j)_0^2(l_j)_j]_j \quad \text{and} \quad \phi_{j,j} \sim [(l_j l_{j'})_0(l_j)_j]_j$$

where $j = l + \frac{1}{2}$, $j' = l - \frac{1}{2}$ and the admixed configuration is now characterized by the angular momentum J to which j and j' are coupled.

Suitably antisymmetrized wave functions are constructed as for $j = l - \frac{1}{2}$ nuclei and the calculation for μ_c goes through in a similar fashion to give for the correction to the magnetic moment

$$\mu_c = \sum \alpha_J \mu_J,$$

where

$$\mu_J = (g_l - g_s) \left[\frac{2(2j-1)}{(1-C_J)(j+1)} \right]^{1/2} [\delta_{J1}/\sqrt{3} - (2J+1)^{1/2} W(j'jjj; 1J)] \dots\dots (13)$$

and $\alpha_J = -M_J/\Delta E$. Here

$$M_J = \frac{1}{2j+1} \left[\frac{2(2J+1)}{1-C_J} \right]^{1/2} \sum_i [(2i+1)W(j'jjj; Ji) - \delta_{Ji}] \mathfrak{F}_{i:jj'j} \dots\dots (14)$$

and $\mathfrak{F}_{i:jj'j}$ is given by (11) with $j' = l - \frac{1}{2}$.

The final expression for the correction to the magnetic moment is then

$$\mu_c = \frac{4(g_s - g_l)}{\Delta E(2j+1)} \left[\frac{(2j-1)}{(j+1)} \right]^{1/2} \left[\sum_i \frac{(2i+1)W(1i) \mathfrak{F}_i}{1-3W(11)} + \sum_i \frac{(2i+1)W(1i) \mathfrak{F}_i}{1-(2i+1)W(ii)} - \sum_{Ji} \frac{(2J+1)(2i+1)W(1J)W(Ji) \mathfrak{F}_i}{1-(2J+1)W(JJ)} \right] \dots\dots (15)$$

In (15) J can take all integral values from 1 to $2l$ and i can take all even integral values from 2 to $2l$.

Again it is convenient to express μ_c in the form $A_j^l \xi_l$ where A_j^l is known and ξ_l is the parameter already introduced. The values obtained for the A_j^l are given in table 2.

Table 2. Values of A_j^l for $j = l + \frac{1}{2}$

l	j	Odd proton	Odd neutron
1	3/2	3.62	-3.00
2	5/2	5.11	-4.24
3	7/2	4.43	-3.68
4	9/2	5.04	-4.18

§ 5. COMPARISON WITH EXPERIMENTAL VALUES FOR μ_c

Before a comparison between theory and experiment can be made it is necessary to obtain some estimate for the magnitude of the parameter $\xi_l = \epsilon_s/\Delta E$. Since ϵ_s is certainly negative and ΔE is always positive, it is clear from inspection of tables 1 and 2 that the calculated corrections to the magnetic moments will have the correct sign, i.e. inwards from the Schmidt lines. In principle ϵ_s could be calculated by assuming some radial dependence for the single particle wave functions and an appropriate value for A_s . However, in view of the approximation of a delta-function interaction (particularly bad for light nuclei) and uncertainty in the form of the radial dependence of the nucleon wave functions, the value obtained is likely to be in considerable error. Furthermore, there is generally some uncertainty as to the magnitude of the spin-orbit splitting.

In one case, however, a reasonable estimate can be made for ξ_l . For ^{209}Bi ($h_{9/2}$ odd proton nucleus) the assumption of a delta function for the inter-nucleon interaction is a reasonable approximation, and Pryce (1952) has estimated for this case that $-\epsilon_s \sim 0.5 - 1.0$ mev. In addition, the spin-orbit splitting ΔE for $l=5$ is well known to be about 2 mev, so that $-\xi_5 \sim 0.25 - 0.5$. To explain the observed deviation in the magnetic moment a value $\xi_5 = -0.43$ is required, which is in satisfactory agreement with the theoretical prediction.

For other nuclei it is more satisfactory to treat ξ_l as a parameter which, since it depends mainly on l , should have approximately the same value for $j = l - \frac{1}{2}$ and $j = l + \frac{1}{2}$ nuclei and should also be roughly independent of whether the nucleus is an odd proton or odd neutron type.

Considering all those nuclei whose magnetic moments can be treated by the above methods, values of ξ_l have been chosen to fit the experimentally observed mean deviations in the magnetic moments. The values of ξ_l so obtained are $\xi_1 = -0.38$, $\xi_2 = -0.26$, $\xi_3 = -0.20$, $\xi_4 = -0.24$, $\xi_5 = -0.43$. In figures 1 and 2 it can be seen that the general trend of the derivations is reproduced using these five parameters.

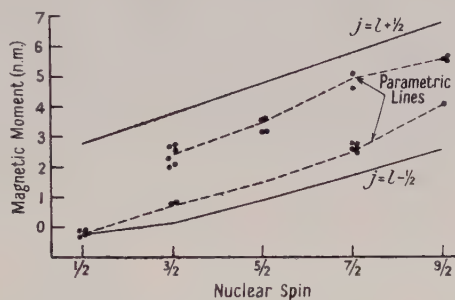


Figure 1. Schmidt diagram for odd proton nuclei.

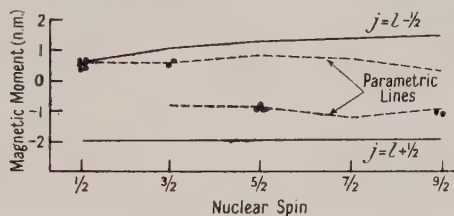


Figure 2. Schmidt diagram for odd neutron nuclei.

As pointed out earlier in the paper, the deviations of nuclei with one particle in a $j = l + \frac{1}{2}$ state or one hole in a $j = l - \frac{1}{2}$ state cannot be explained by this mechanism. Nevertheless there are some nuclei of this type which do deviate considerably from the Schmidt lines. There are two possible reasons for this. Firstly, throughout the paper the distribution of nucleons in the various levels has been taken to be that given by Klinkenberg (1952), and it is certain that in a number of cases the configurations given are not, in fact, correct. Secondly, there can be first-order contributions to the magnetic moment from inter-configurational mixing of the type (iii) mentioned in §2: (a) when an O or E nucleon is excited from a state $l'_{j'=l'+\frac{1}{2}}$ to $l'_{j''=l'-\frac{1}{2}}$, both of the states being different from that l_j of the odd particle, and (b) when an E nucleon is excited from $l_{j=l+\frac{1}{2}}$ to $l_{j'=l-\frac{1}{2}}$. The magnitude of the deviation in the magnetic moment resulting from this type of admixture is considered in the following paragraph.

§ 6. CONFIGURATIONAL MIXING OF TYPE (iii)

For this type of mixing the results given by Blin-Stoyle (1953) apply; thus

$$\mu_0^{(x)} = -M_1^{(x)} \mu_1 / \Delta E \quad \dots\dots(16)$$

where x = O or E according as the excited 'core' nucleons are of the odd or even type and ΔE is the spin-orbit splitting between the states $j' = l' + \frac{1}{2}$ and $j'' = l' - \frac{1}{2}$. μ_1 is given by

$$\mu_1 = 2(g_1 - g_s) \left[\frac{2jl'}{3(j+1)(2l'+1)} \right]^{1/2} \quad \dots\dots(17)$$

where g_s and g_l are the spin and orbital g -factors for the excited core nucleons. ($l' = l$ and $x = E$ in case (iii b)).

$$M_1^{(x)} = - \left[\frac{6}{(2j+1)(2j'+1)} \right]^{1/2} \sum_i (-)^{j'+j''-i} (2i+1) W(j' j'' j j; 1i) \mathfrak{F}_{i: j j' j''}^{(x)} \dots (18)$$

$$\text{and} \quad \mathfrak{F}_{i: j j' j''}^{(O)} = 2\epsilon_S \langle j j' i | i i 0 \rangle \langle j j'' i | i i 0 \rangle P(i; l') \dots (19)$$

$$\mathfrak{F}_{i: j j' j''}^{(E)} = \epsilon_S \langle j j' i | i i 0 \rangle \langle j j'' i | i i 0 \rangle P(i; l') + \epsilon_T \sum_y \langle j j' i | i y 1 \rangle \langle j j'' i | i y 1 \rangle P(y; l') \dots (20)$$

Here $\epsilon_{S,T} = A_{S,T} \int |R_{nl}(r) R_{n'l'}(r)|^2 r^2 dr$ where A_T is the triplet interaction strength.

Using the above relations, it can be shown that

$$2\epsilon_S M_1^{(E)} = (\epsilon_S - \epsilon_T) M_1^{(O)} \dots (21)$$

so that in calculations it is sufficient to evaluate only $\mathfrak{F}_{i: j j' j''}^{(O)}$ which is considerably simpler in form than $\mathfrak{F}_{i: j j' j''}^{(E)}$.

For purposes of computation it is more satisfactory to express $\mathfrak{F}_{i: j j' j''}^{(O)}$ in terms of Racah coefficients which are already tabulated. Thus after some algebra we can write for $\mu_c^{(O)}$

$$\mu_c^{(O)} = (g_l - g_s) \frac{\epsilon_S}{\Delta E} \frac{j(2j'-1)}{j'(j+1)} \sum_i (2i+1) |W(j' j'' j j; 1i)|^2 P(i; l') \quad \text{for } j = l - \frac{1}{2} \dots (22)$$

$$\mu_c^{(O)} = (g_s - g_l) \frac{\epsilon_S}{\Delta E} \frac{2j'-1}{j'} \sum_j (2i+1) |W(j' j'' j j; 1i)|^2 P(i; l') \quad \text{for } j = l + \frac{1}{2} \dots (23)$$

and by (21)

$$\mu_c^{(E)} = \frac{\epsilon_S - \epsilon_T}{2\epsilon_S} \frac{(g_s - g_l)_E}{(g_s - g_l)_0} \mu_c^{(O)} \quad \text{for } j = l \pm \frac{1}{2}. \dots (24)$$

The correction to the magnetic moment is again most conveniently written in the form $\mu_c = C_{j j' j''}^{ll'} \eta_{ll'}$, where for a given type of admixture $C_{j j' j''}^{ll'}$ has a definite value and where $\eta_{ll'} = (\epsilon_S / \Delta E)$ is again treated as a parameter whose order of magnitude and sign are known.

Comparison with experiment.

If we assume, following Pryce (1952), that $\epsilon_T = \frac{3}{2}\epsilon_S$, then equation (24) reduces to the following form:

$$\begin{aligned} \mu_c^{(E)} &= 0.3 \mu_c^{(O)} && \text{for an odd neutron nucleus} \\ \mu_c^{(E)} &= 0.2 \mu_c^{(O)} && \text{for an odd proton nucleus} \end{aligned}$$

which indicates that admixtures of states of E nucleons are less important than admixtures of states of O nucleons. Thus, since it is generally possible to admix an O nucleon state we shall not further consider E nucleon admixtures. Further, in view of the uncertainty in the correct value of $\eta_{ll'}$, it has not been thought worth while to present detailed results for individual nuclei. The overall situation can be stated as follows. The values of $|C_{j j' j''}^{ll'}|$ obtained for the different possible admixtures vary between 0.7 and 1.2 for $j = l - \frac{1}{2}$ nuclei and between 1.6 and 2.4 for $j = l + \frac{1}{2}$ nuclei, in agreement with the experimental observation that $j = l + \frac{1}{2}$ nuclei have generally larger deviations than $j = l - \frac{1}{2}$ nuclei. In addition, the sign

of $C_{jj',j''}^{ll'}$ is always such as to give a deviation in the magnetic moment in the required direction. Values of $\eta_{ll'}$ between -0.2 and -0.5 then suffice to explain the observed deviations. It is satisfactory that these values of $\eta_{ll'}$ are of the same order of magnitude as the parameters $\xi_l (= \eta_{ll})$ introduced in § 5.

§ 7. DISCUSSION

It is apparent from the foregoing calculations that the magnetic moment of a nucleus is very sensitive to admixtures of certain types of configurations, namely those which lead to first-order contributions to the magnetic moment. In particular the moment can be expected to deviate considerably from the Schmidt value when there is more than one nucleon in a $j = l + \frac{1}{2}$ state or more than one hole in a $j = l - \frac{1}{2}$ state. Furthermore, even if these conditions are not satisfied, there can still be an appreciable deviation resulting from admixtures of other types of configuration.

In certain cases, however, the distribution of nucleons among the various single particle states is such that no type of admixture can lead to a contribution to the magnetic moment linear in the amplitude of the admixture. Under these circumstances it is to be expected that the magnetic moment will lie close to the Schmidt value. The condition for this is that the nucleus should consist of doubly closed shells in both the LS and jj sense plus or minus an odd nucleon. The only nuclei which satisfy this condition (other than $p_{1/2}$ nuclei, which should have a small deviation in any case) are ^{17}O , ^{17}F , ^{41}Ca , ^{39}Ca , ^{39}K . Of these nuclei only the magnetic moments of ^{17}O and ^{39}K are known, and their deviations are particularly small, being 0.02 and 0.27 n.m. respectively (the latter value results from a hyperfine structure optical measurement and may be in error). On the other hand a nucleus like ^{209}Bi , which has doubly closed shells in the jj sense only, plus an odd proton, has a magnetic moment considerably different from the single particle value.

It is apparent that these first-order deviations in the nuclear magnetic moments, which result from mixing of the two components of a spin-orbit doublet, can be attributed to a breakdown in the pure jj -coupling model of the nucleus. The situation is now one of intermediate coupling, but approached from the jj extreme rather than the more usual approach from pure LS coupling (e.g. Lane 1953).

The calculations presented in this paper have been carried only to first order, terms of order α_J^2 being neglected. More correctly, the wave function describing the state of the nucleus should have the form

$$\Psi_j = [1 - \sum_J \alpha_J^2]^{1/2} \chi_j + \sum_J \alpha_J \phi_{J,j}$$

leading to a reduction in the first-order correction to the magnetic moment by a factor $[1 - \sum_J \alpha_J^2]^{1/2}$. However, since the magnitude of α_J is never greater than 0.2 and is usually less than 0.1 , this correction factor is small. Further, if second-order terms are not neglected then the correction to the magnetic moment will have the form

$$\mu_0 = \alpha^2 (\mu^{(2)} - \mu_{\text{SP}}) + \alpha (1 - \alpha^2)^{1/2} \mu^{(1)}$$

where $\mu^{(2)}$ represents second-order contributions from admixed configurations, $\mu^{(1)}$ represents first-order contributions and μ_{SP} is the Schmidt value. It is generally found that both the terms in the first bracket contribute in such a way as to increase the deviation and so compensate for the reduction in the first-order terms. This argument also applies to admixtures which do not contribute to $\mu^{(1)}$.

ACKNOWLEDGMENTS

The authors wish to thank Professor R. E. Peierls for helpful discussions during the course of this work. One of them (M.A.P.) is indebted to the Department of Scientific and Industrial Research for a grant.

REFERENCES

- BLIN-STOYLE, R. J., 1953 a, *Proc. Phys. Soc. A*, **66**, 1158; 1953 b, *Ibid.*, **66**, 729.
BOHR, A., 1953, *K. Danske Vidensk. Selsk. Mat. Fys. Medd.*, **27**, No. 16.
FLOWERS, B. H., 1952 a, *Phil. Mag.*, **43**, 1330; 1952 b, *Proc. Roy. Soc. A*, **214**, 515.
KLINKENBERG, P. F. A., 1952, *Rev. Mod. Phys.*, **24**, 63.
LANE, A. M., 1953, *Proc. Phys. Soc. A*, **66**, 977.
PRYCE, M. H. L., 1952, *Proc. Phys. Soc. A*, **65**, 773.
ROSS, M., 1952, *Phys. Rev.*, **88**, 935.
VILLARS, F., 1947, *Phys. Rev.*, **72**, 257; *Helv. Phys. Acta*, **20**, 476.

X-Ray Measurements on Lithium at Low Temperatures

By E. A. OWEN AND G. I. WILLIAMS

University College of North Wales, Bangor

MS. received 4th May 1954

Abstract. The paper gives the results of x-ray measurements on the variation of the lattice parameter of lithium with temperature. The mean thermal coefficient of expansion of lithium varies from 3.5×10^{-5} at -914°C to 4.7×10^{-5} at 20°C . The expansion of the material over this range of temperature is closely represented by the equation $a_t = a_0(1 + \alpha t + \beta t^2 + \gamma t^3)$ where $a_0 = 3.4992 \text{ kx}$; $\alpha = 4.6640 \times 10^{-5}$; $\beta = 3.8791 \times 10^{-8}$; $\gamma = -11.445 \times 10^{-11}$. After deformation at liquid air temperature lithium is found to contain a face-centred cubic structure as well as a body centred cubic structure, which confirms the findings of C. S. Barrett. The lattice parameters of these structures at -194°C were found to be 3.4760 kx (body-centred cubic) and 4.370 kx (face-centred cubic). After annealing the material at room temperature and afterwards obtaining its x-ray pattern at liquid air temperature the body-centred cubic structure remained alone.

§ 1. INTRODUCTION

AFTER the development of a low-temperature x-ray camera (Owen and Williams 1954) suitable for the investigation of small plates of material and the accurate measurement of the temperature of the specimen between room and liquid-air temperature when the specimen was simultaneously oscillated and rotated in the x-ray beam, it was decided to investigate the expansion of lithium in this range of temperature, as only few observations have been carried out on the material at these low temperatures. The x-ray camera was such that the temperature of the specimen could be maintained constant at any value for a length of time far exceeding the period necessary to obtain a good photographic record of the x-ray pattern. Values of the lattice parameters of lithium at room temperature have been determined by Aruja and Perlitz (1940), Lonsdale (1945), Hume-Rothery (1945) and Simon and Bergmann (1930), the latter having determined the expansion of lithium in bulk from liquid-air to room temperature whilst Lonsdale determined the lattice parameter at the two extreme temperatures for a single-crystal specimen of lithium of 98.5% purity.

§ 2. MATERIAL

The lithium specimens used in this investigation were prepared from a lump of the material, kept under paraffin, the purity of which was 99.92%; the impurities were as follows: sodium, potassium and magnesium, each not more than 0.01%, calcium 0.05%.

Since lithium tarnishes very rapidly if exposed to the atmosphere, all operations such as cutting, moulding, etc. were performed under paraffin. For examination in plate form flat discs about 6 mm in diameter and about 1 mm thick were prepared. After being allowed to anneal at room temperature for three hours the specimen was removed from the paraffin and to prevent oxidation its surfaces were quickly

covered with a layer of Apiezon L grease before being mounted in the specimen holder of the camera, a sheet of glass 0.2 mm thick being inserted between the specimen and the copper backing plate to cut off reflections from the copper. It was arranged that an annulus of the material was irradiated by the incident x-ray beam.

§ 3. EXPERIMENT

Several x-ray diffraction photographs were taken with the lithium plate after annealing at room temperature but the patterns obtained were not satisfactory in that the high-angle reflections were weak and indistinct even after ample exposure had been given. It was evident that better annealing conditions were necessary; the specimens, covered with grease and sealed off in an evacuated glass tube, were therefore annealed for 12 hours in a water bath maintained at 90°C. Employing unfiltered cobalt $K\alpha$ radiation patterns were obtained which were sufficiently clear for measurement and to apply the Lu-Chang (Lu and Chang 1941) extrapolation, the resulting lattice parameter value being 3.5025 kx at 18°C, which agrees with that obtained by Lonsdale and Hume-Rothery. To obtain reflections at higher Bragg angles copper radiation was used; since the reflections in the pattern were not well defined and, with a disc specimen, extended over only a limited range of reflecting angles, it was decided to attempt to obtain a full pattern at room temperature with a Debye-Scherrer camera of effective radius 55.63 mm, by means of which a fibre specimen could be rotated in the x-ray beam. After several attempts, a satisfactory specimen was made by using a mould consisting of four polished steel quadrants which fitted together to form a cylinder with a central hole about 0.8 mm diameter along its length. This method of preparing specimens had been successfully employed in the laboratory for other problems (Owen and Williams 1947). The specimens produced in this way were fairly uniformly cylindrical. They could be mounted in the fibre specimen holder of the Debye-Scherrer camera showing very little wobble on rotation. The x-ray patterns obtained with these specimens could be measured satisfactorily and the Nelson and Riley (1945) extrapolation applied. These measurements yielded consistent values of the lattice parameter of lithium at room temperature.

Satisfactory results at room temperature having been obtained, x-ray exposures with lithium in plate form were made on the low-temperature camera. Here, however, the specimen could not be placed in direct contact with the copper backing plate carrying the thermocouple junction because of the interposed glass sheet, and the temperature of the specimen was therefore deduced from the lattice parameter of silver: a semi-circular disc of silver was placed alongside a semi-circular disc of lithium in the specimen holder and exposed simultaneously in the x-ray beam, as in the double-specimen technique referred to in the paper describing the low-temperature camera (Owen and Williams 1954). It was arranged that the 'mean' reflecting surface of each specimen was as near as possible in the same plane and over the centre of the camera. That this was successfully achieved is shown by the Lu-Chang (1941) extrapolation graph, the inclination of which to the $\cos \phi$ axis was small.

§ 4. CHANGE OF LATTICE PARAMETER WITH TEMPERATURE

Many photographs were taken at different temperatures in the range from -194°C to room temperature. The temperatures recorded by the thermocouple agreed closely with the temperatures deduced from the lattice-parameter

measurements of silver, in spite of the fact that the glass sheet intervened between the specimen and the copper backing plate to which the thermocouple was attached.

The variation of the lattice parameter of lithium with temperature is shown in figure 1. The expansion of lithium over the range from -194°C to $+20^{\circ}\text{C}$ is

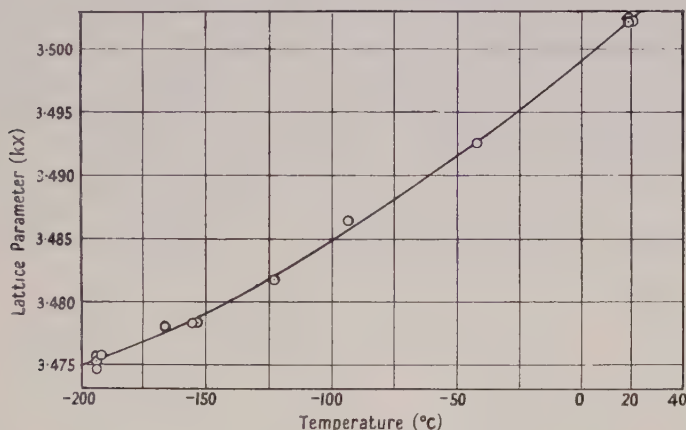


Figure 1. Variation of the lattice parameter of lithium with temperature.

closely represented by the equation $a_t = a_0(1 + \alpha t + \beta t^2 + \gamma t^3)$ where $a_0 = 3.4992 \text{ kx}$; $\alpha = 4.6640 \times 10^{-5}$; $\beta = 3.8791 \times 10^{-8}$; $\gamma = -11.445 \times 10^{-11}$. The mean coefficients of expansion $\alpha [\equiv (a_t - a_0)/a_0 t]$ at different temperatures are given in table 1.

Table 1. Mean Coefficients of Expansion of Lithium

Temp. ($^{\circ}\text{C}$)	$\alpha \times 10^5$	Temp. ($^{\circ}\text{C}$)	$\alpha \times 10^5$	Temp. ($^{\circ}\text{C}$)	$\alpha \times 10^5$
+20	4.7 ₁	-90	4.2 ₂	-170	3.6 ₆
-30	4.5 ₇	-110	4.0 ₉	-190	3.5 ₃
-50	4.4 ₆	-130	3.9 ₆	-194	3.4 ₉
-70	4.3 ₃	-150	3.8 ₁		

The results of previous workers are summarized in table 2. The values of the lattice parameters in the table against Simon and Bergmann were calculated from their measurements on the material in bulk assuming the value of the lattice parameter at 20°C to be that found in the present investigation. It will be observed there is good agreement between all the values. The present results confirm

Table 2. Summary of Lattice Parameters of Lithium in kx Units

Source	Temperature ($^{\circ}\text{C}$)							
	+20.	-30	-60	-100	-140	-180	-183	-194
Aruja & Perlitz	3.5017	—	—	—	—	—	—	—
Lonsdale	3.5023	—	—	—	—	—	3.4762	—
Hume-Rothery	3.5023	—	—	—	—	—	—	—
Simon & Bergmann	3.5025	3.4946	3.4899	3.4845	3.4801	3.4769	—	—
Present work	3.5025	3.4944	3.4899	3.4847	3.4802	3.4765	3.4763	3.4755

Lonsdale's values at 20°C and -183°C , and the lattice parameter values between room temperature and -180°C , deduced from the thermal-expansion curve of Simon and Bergmann, agree closely with the present values with the exception of the value at -180°C where the difference 0.0004 kx is just

outside the limit of experimental accuracy. On the whole the agreement is very satisfactory; the slight differences that are found may probably be accounted for by the different degrees of purity of the specimens.

§ 5. LOW-TEMPERATURE TRANSFORMATION

A low-temperature transformation in lithium has been discovered by Barrett (1947) and confirmed by Barrett and Trautz (1948). They also confirmed the results of previous observers that lithium does not transform spontaneously from its normal body-centred cubic structure when its temperature is lowered to that of liquid air, but they found that when lithium is suitably cold-worked at liquid-air temperature and examined at that temperature two forms of lithium co-exist: a face-centred cubic structure as well as the body-centred cubic structure is present, showing that only part of the material is converted into the new structure. The purity of the lithium originally used was 99.45% and the results were later confirmed with material of 99.86% purity.

The low-temperature camera now available was very suitable to examine this transformation further and to determine with fair accuracy the lattice parameters of the two structures. For the purpose a lithium specimen measuring approximately 3 mm cube was prepared and compressed at room temperature between steel plates, reducing the thickness by about 20%. Then the specimen was put into liquid air and by kneading it in different directions in the jaws of a pair of insulated pliers it was brought back approximately to a cubic shape. By a special arrangement the specimen was compressed between two steel plates whilst it was immersed in liquid air and a reduction in thickness of 70% produced. The compression was carried out slowly in stages, the whole operation taking about two minutes to perform. The specimen, after compression, was stored in liquid air until x-ray exposures could be started. Although lithium tarnishes readily at room temperature, specimens stored in liquid air retain their bright metallic surfaces; after storage for 50 hours in liquid air the surfaces remained untarnished.

When the specimen is being mounted on the camera liquid air flows continuously over it and the specimen holder; it is accurately positioned by means of a template which is also precooled. A special technique was followed in order to mount the specimen with its mid-plane over the centre of the camera. During the x-ray exposure the specimen is rotated in its own plane and oscillated about a vertical diameter in its mid-plane whilst being kept bathed in liquid air. It is so arranged that an annulus of the surface is irradiated by the x-ray beam. Copper radiation filtered through 0.025 mm of nickel was used and exposures up to two and a half hours at liquid-air temperature had to be made to obtain a satisfactory record of the diffraction pattern.

§ 6. RESULTS WITH COMPRESSED MATERIAL

As stated above all the specimens were compressed, mounted on the apparatus and photographed whilst they were immersed in liquid air. In each case the reduction in thickness on compression was 70%. The following is typical of the sequence of operations carried out on each specimen; compressed, stored for 17 hours in liquid air, photographed with filtered copper radiation, the exposure lasting about two and a half hours and the x-ray beam falling at an angle of incidence of 44° on the surface of the specimen. The slot of the camera cassette did not allow the reflections at angles lower than the (200) reflection to

appear on the film; these were recorded on a second piece of film mounted inside the cassette but could only be used to examine the quality of the reflection. The following is a description of the diffraction patterns recorded on the film:

Body-centred cubic structure		Face-centred cubic structure	
Reflection	Intensity	Reflection	Intensity
(110)	Strong	(111)	Medium
(200)	Medium	(200)	Very faint
(211)	Very strong	(220)	Medium
(220)	Medium	(311)	Medium
(310)	Medium	(222)	Faint
(222)	Medium	(400)	} Not visible
(321)	Strong	(331)	
(400)	Very faint	(420)	
(411)	Medium, diffuse	(422)	} Just visible
(420)	Medium, diffuse	[(333)]	
		[(511)]	

The specimen was allowed to reach room temperature and remain at this temperature for 40 minutes, when it was again immersed in liquid air and a diffraction photograph taken. The pattern obtained now did not show any face-centred cubic reflections, but all the body-centred cubic reflections were present and a new effect was observed, namely, some of the reflections were split into two. The specimen was again brought to room temperature and remained at this temperature for a further 17 hours. It was then immersed in liquid air and again photographed; the split reflections remained and the characteristics of the pattern were exactly the same as before, and as described below.

The same phenomenon was observed with other specimens treated similarly. The films reproduced in figure 2 (Plate) will illustrate the effects observed. The first pattern (*a*) is that obtained with unfiltered copper radiation and a specimen of undistorted lithium at liquid-air temperature; it shows only body-centred cubic reflections. The second pattern (*b*) is that obtained with filtered copper radiation and with lithium compressed at liquid-air temperature; it shows a mixture of body-centred and face-centred cubic structures. The third pattern (*c*) was also obtained with filtered copper radiation after the compressed specimen

Body-centred cubic structure		Remarks
Reflection	Intensity	
(110)	Strong	Unresolved into α_1 and α_2 components
(200)	Strong	Unresolved; split into two
(211)	Very strong	Unresolved; split into two
(220)	Medium	Unresolved
(310)	Strong	Unresolved; split into two
(222)	Faint	Unresolved
(321)	Strong	Unresolved
(400)	Faint	Unresolved
(411)	Strong	Resolved
(420)	Strong	Resolved

had been allowed to anneal for about 40 minutes at room temperature and its temperature afterwards reduced to liquid-air temperature; this shows all the body-centred cubic reflections with some split into two.

The lattice parameters of the two structures found together after compression at liquid-air temperature were measured. They had the following values at -194°C : $a_{\text{bcc}} = 3.4760 \text{ kx}$, $a_{\text{fcc}} = 4.370 \text{ kx}$.

The value of the lattice parameter of the body-centred cubic structure agrees closely with the value of the lattice parameter of the same structure when present alone. The transformation of the material thus takes place in part only, and the portion that is not transformed is not affected by the presence of the transformed material.

The splitting of the reflections from certain planes needs further consideration before a final explanation of the phenomenon can be offered. The main characteristics of the pattern when the splitting of the reflections occurs are (i) the (110) and (220) reflections are not split: the former is strong and the latter is of medium intensity; (ii) in all the x-ray patterns observed after deformation of lithium at liquid-air temperature, annealing at room temperature and lowering the temperature again to that of liquid air—these processes occurring in sequence—the same reflections, namely (200), (211) and (310) are split; (iii) the components of the split reflections are well resolved and sharply defined (see figure 2(c)).

Several possible explanations of the splitting were considered. A slightly distorted body-centred cubic structure producing a body-centred tetragonal structure will not explain the effect because other reflections in addition to those observed should be split. Neither is it explained on the assumption that it is due to an oxidized layer, because the reflections from this layer would be distinguishable from those from the body of the material. The patterns showing the effect were obtained after the material had been annealed at room temperature, that is, after recrystallization had taken place. Also the variation of the intensities of the reflections in the pattern indicates the presence of preferred orientations, as would be expected in recrystallized material after deformation. These considerations coupled with the fact that a comparatively thick specimen (about 1 mm thick) had been used to obtain a satisfactory diffraction photograph, provide the more likely explanation because planes in large crystals well separated from each other in depth of material come in turn into positions for reflection as the specimen is simultaneously oscillated and rotated. Furthermore, since the x-ray beam makes an angle of about 45° with the surface of the specimen, the effective thickness is about 1.5 mm, thus increasing the possible separation of the crystals. Also, since in recrystallized material after deformation the crystals have definite orientations, this will probably account for the limited number of reflections that show the effect. Further observations with the x-ray beam falling on the specimen surface at different angles of incidence would be desirable; the present authors will not have an opportunity to do this.

REFERENCES

- ARUJA, E. and PERLITZ, H., 1940, *Phil. Mag.*, **30**, 55.
BARRETT, C. S., 1947, *Phys. Rev.*, **72**, 245.
BARRETT, C. S., and TRAUTZ, O. R., 1948, *Trans. Amer. Inst. Min. (Metall.) Engrs*, **175**, 579.
HUME-ROTHERY, W., 1945, *Phil. Mag.*, **30**, 799.
LONSDALE, K., 1945, *Phil. Mag.*, **36**, 798.
LU, S. S., and CHANG, Y. L., 1941, *Proc. Phys. Soc.*, **53**, 517.
NELSON, J. B., and RILEY, D. P., 1945, *Proc. Phys. Soc.*, **57**, 176.
OWEN, E. A., and WILLIAMS, G. I., 1954, *J. Sci. Instrum.*, **31**, 49.
OWEN, E. A., and WILLIAMS, R. W., 1947, *Proc. Roy. Soc. A*, **188**, 509.
SIMON, F., and BERGMANN, R., 1930, *Z. Phys. Chem. B*, **8**, 268.

On Feynman's Theory of Liquid Helium

By H. N. V. TEMPERLEY†

The Brace Laboratory of Physics, The University of Nebraska, Lincoln, Nebraska, U.S.A.

MS. received 29th May 1954

Abstract. It is shown that Feynman's proof of the existence of a generalized Bose-Einstein condensation in liquid helium can be carried through on the basis of fewer and less restrictive assumptions than he actually makes. The underlying physical idea proves to be very similar to those put forward by a number of other workers. His treatment using a Bijl wave function is also examined, and it is concluded that the resulting energy-spectrum may very well be nearly correct, in spite of the fact that it does not agree numerically with that assumed in the present form of the Landau-Khalatnikov theory. Some serious difficulties in the latter theory seem to call for an adjustment of the parameter Δ to a *larger* value. This is in just the direction needed to improve the agreement with Feynman's theory.

§ 1. INTRODUCTION

IN a series of papers Feynman (1953 a, b, c, 1954) has approached the liquid helium problem along two distinct lines.

A. He proves (1953 a, b) that, if certain assumptions are granted, liquid helium may be expected to show a transition that is a direct generalization of that shown by the perfect gas model. In the Appendix we show that the assumptions actually made by Feynman (1953 b) and by Chester (1954) can be weakened considerably. Virtually all that need actually be assumed is: (a) a plausible generalization of the 'Kirkwood approximation', (b) an assumption that, in the limit of a very large assembly, the function $S(K)$, the Fourier transform of the two-atom distribution function, has a singularity at $K=0$, the singularity being of any type that justifies replacing, for example, equation (32) by (32a) in Feynman's paper (1953 b).

The conditions under which assumptions such as (a) can be made are not accurately known, even for a classical liquid. Assumption (b) seems to require that the interatomic forces are 'not too large', but no precise criterion has been obtained except for models of 'one-particle' type.

B. Feynman (1954) shows that A. Bijl's (1940) assumption, that the wave functions of the assembly can be satisfactorily represented by the expression

$$\phi \sum_i \exp(i\mathbf{K} \cdot \mathbf{r}_i) \quad \dots\dots(1)$$

(where ϕ is the wave function describing the ground state), leads to an energy spectrum that is 'best possible' in the sense that the energy for a given K is *lower* for an exponential function in (1) than for any other function. This is

$$E(K) = \hbar^2 K^2 / 2mS(K) \quad \dots\dots(2)$$

† Present address : National Bureau of Standards, Washington, D.C., U.S.A.

(where $S(K)$ is the Fourier transform of the two-atom distribution function). This spectrum, using present knowledge about $S(K)$ from neutron diffraction, turns out to be qualitatively very like the energy spectrum introduced semi-empirically by Landau (1947). Since Feynman could not obtain quantitative agreement with Landau's empirically determined value of the parameter Δ (the smallest energy of a 'roton'), he concluded (1954) that the wave function (1) is not sufficiently good over the whole of the important range of K . In this paper we shall show that the contrary assumption, namely that the spectrum (2) is substantially correct, is perfectly tenable in our present state of knowledge, and further, that this assumption removes some very serious difficulties confronting the Landau theory in its present form, as developed by further papers (Landau and Khalatnikov 1949 a, b, Khalatnikov 1950, 1952).

§2. RELATIONSHIPS BETWEEN FEYNMAN'S THEORY OF THE TRANSITION AND THE IDEAS OF SOME OTHER WORKERS

Feynman's interpretation of the transition of the liquid in terms of a certain property of the two-atom distribution function introduces an idea that is hard to formulate in concrete terms. Perhaps this is not surprising; after all, the transition itself must be a consequence of the fact that the He *atoms* have to be considered from their *wave* aspect. In the *nearly perfect* gas the transition may be attributed to an 'apparent attraction' between atoms in the same quantum state (Bijl, de Boer and Michels 1941, Mott 1949). It can also be described as an 'apparent attraction' between atoms in ordinary space (Matsubara 1951), or as an increase in the 'local density as seen from the location of a particular atom' (in the sense defined by London 1943)†. Yet another description of what is probably the same effect is due to Penrose (1951), who shows that the assumption that the Schrödinger representative of the density matrix does not vanish as $|\mathbf{r} - \mathbf{r}'| \rightarrow \infty$ would lead to the two-fluid picture of He II as a consequence. (Penrose's discussion is based on a 'one-atom' model, but clearly implies the same idea of attraction between atoms of equal momentum, and is not hard to relate to the discussion based on the distribution function for two atoms.) Another attempt to put into concrete form these correlations in momentum between small numbers of atoms was made by Temperley (1952 b, 1953), who introduced the idea of 'small' clusters in liquid He. All these ideas seem to be different 'pictorial' descriptions of a typically wave-mechanical effect. See also Mikura (1954).

The contentions of all these workers may be summed up in the claim that it is possible for the interaction energy to be large enough to cause liquefaction, and yet not so large that the 'statistical attraction' is altogether masked. For the extremely crude model of liquid He, in which we consider two interacting atoms moving in a smoothed potential representing their interactions with all the other atoms, we should expect the effect of the 'statistical attraction' to become unimportant as soon as the interaction between the pair was a few times the critical value needed for the formation of a bound level, because the two typical atoms would then spend nearly all their time in close proximity in any case. If, as is the case with He atoms, the interaction energy is of about the critical value, the two

† For interactions of the type and strength actually occurring between He atoms (about sufficient to lead to a bound state between two isolated atoms) the *signs* of these effects become uncertain.

forms of 'attraction' are of comparable importance. No similar *quantitative* criterion has yet been set up for the many-atom model. As Feynman's (1953 b) paper does show some promise of leading to this, it seems important to know exactly *what* assumptions *are* required in order to carry through his proof of the existence of a transition, and this question is considered in the Appendix.

§ 3. RELATIONSHIPS BETWEEN FEYNMAN'S PROPOSED WAVE FUNCTION AND OLDER MODELS

Feynman (1954) gives arguments to show that a wave function such as (1) is competent to give an approximate description of three types of situation: a few atoms 'following one another round a ring', an atom moving through the liquid and 'pushing others aside', or an atom moving in a 'cell' representing the effect of the rest of the liquid. His arguments could equally well be applied to a fourth model, an atom moving in a spatially periodic potential representing the smoothed effect of the remaining atoms. The third and fourth models were considered by other workers (Temperley 1947, Fraser 1950, Prigogine and Philipott 1952, 1953 a, b, c, Buckthought 1953, Mikura 1954), and are capable of describing various properties of the liquid, but it is difficult, in any concrete case, to determine the 'best' choice of the adjustable constants. As Feynman (1954) suggests, these diverse models *may* really be different approximate descriptions of the same thing, the typical 'local reshuffling' of molecules that must constantly occur in any liquid. Indeed, wave function (1) may perhaps be the long-sought 'physical model' of the liquid state, as it differs, in essential particulars, from both crystal and gas. In the rest of this paper we shall examine the hypothesis that (2) *does* represent a reasonable approximation to the energy spectrum of liquid He. The fact that the wave function (1) gives rise to an energy spectrum of the desired type does *not, by itself*, enable us to come to any conclusion about the probable accuracy of (1), nor to decide whether or not this wave function is accurate enough for the calculation of transport effects. To see this we need only notice that a spectrum very similar to (2) results from the model of a 'Hooke's law' solid, with a suitable choice of elastic moduli, even though the corresponding wave functions are completely different from the set (1). (For a description of the 'solid-like' wave functions see, for example, Temperley 1952 a.) We shall leave aside the difficult question whether it is more correct to calculate mean free paths using the method of Landau and Khalatnikov (1949 a, b), based directly on the energy spectrum together with quantum hydrodynamical considerations, or whether it is better to use perturbation calculations based directly on the wave function (1). In this paper we shall take the position that, even if the Landau-Khalatnikov process *is* the more correct one, it is still possible to accept the energy spectrum (2) as being nearly right. Put in another way, we shall criticize Feynman (1954) for making too gloomy an appraisal of his own theory.

§ 4. SOME CONSEQUENCES OF ACCEPTING EQUATION (2) AS CORRECT

The spectrum (2) calculated by Feynman (1954) does not differ greatly from a pure Debye spectrum (without 'cut-off'). Now it has always seemed to the writer that the only proper way to interpret the complete specific heat curve of liquid He is to analyse it as a normal Debye-like curve, with a typical λ -point anomaly *superposed* upon it, instead of adjusting the parameter Δ so as to account for the

whole of the extra observed specific heat, which is what Landau did (1947). In particular, the fact that the specific heat of He I suggests practically the same Debye temperature as we calculate from the observed velocity of sound c_1 , using a 'phonons only' model (Dingle 1952), taken in conjunction with the fact that the 'low temperature' portion of the specific heat curve of He II (below 0.6°K) suggests a very similar Debye temperature, seems to be decidedly more than an accident, and this is also consistent with the idea of describing both liquids by means of a single Debye-like spectrum such as (2). (In this paper we use the terms 'phonon' and 'roton' merely as convenient means of describing various parts of the spectrum (2), which is the sense in which Feynman (1954) and Landau (1947) also use these terms.)

We already run into difficulties in trying to explain even the equilibrium properties of liquid He by means of Landau's (1947) spectrum. Any such spectrum, if interpreted consistently according to Bose statistics, leads, as is well known, to a specific heat curve without any falling portion, and hence to much too large a value for He I. To avoid this difficulty, Landau (1941, 1947) was forced to assume, entirely *ad hoc*, that his spectrum, or at all events the 'roton part of it', breaks down completely at the transition temperature, and he supposed that this happens because of the interactions of the rotons and phonons. Such an occurrence is not *a priori* impossible (though it is hard to see why analogous effects should not occur in a solid lattice described by a Debye-like spectrum), but two very definite objections to such a hypothesis can be made: (a) Feynman's physical arguments (1954) for the wave function (1) apply quite as well to the He I as to the He II region, and, for that matter, almost equally well to any 'simple' liquid. Moreover, some Debye-like model *does* seem to be wanted for ordinary liquids (not to mention He I), see Frenkel (1946), yet Landau's assumption would mean that the applicability of a spectrum such as (2) to a liquid is, in practice, restricted to the one case of He II for which the numbers of excitations are small in the liquid region of temperatures. (b) A much more satisfactory theory of the transition is already available on the lines indicated by Feynman (1953 b), and it had already been established (Temperley 1952 a) that analogues of Bose-Einstein condensation can be found for certain many-body models.

Further objections to choosing a value of the constant Δ to be of the order of $k \times 10^\circ\text{K}$ appear when we consider the transport data. Let us provisionally accept the Landau Khalatnikov (1949 a, b) method of calculating mean free paths as correct. It is now necessary to point out that they altogether neglect certain relatively simple types of process, whose existence has been pointed out by quite a number of workers (Kramers 1952, Dingle 1952, Temperley 1952 a, Feynman 1954, Price 1954). Examples of such processes are: (a) The analogue for a liquid of 'Umklapp' processes. Since a liquid has short distance order only, such an effect, corresponding to Bragg reflection, may be 'smeared out' in comparison with what occurs in a solid, but this does *not* mean that it is altogether negligible. (b) Two phonons with nearly parallel directions of propagation can combine to form a third without violating the conservation laws. These three-phonon processes ought to be considered *before* invoking higher order ones. Unless their effect can definitely be shown to be negligible compared with the higher order ones, the good agreement with experiment shown by the Landau-Khalatnikov theory in its present form, Khalatnikov (1952), must be considered to be based on the

cancellation of two errors (a wrong choice of constants plus the neglect of certain low-order processes). This situation can perhaps be eventually rectified by a further revision of the Landau (1947) spectrum, probably including an increase in the value of Δ , a step that also seems to be called for by the above considerations based on the specific heat.

§ 5. THE λ -TRANSITION

We do not yet know in detail how to incorporate a theory of the λ -transition into Feynman's (1954) theory based on wave function (1), though it is quite easy to state the problem of statistical mechanics that is involved. We know (Temperley 1952 a, Feynman 1953 b), that an analogue of Bose-Einstein condensation could occur in a many-particle type of assembly for essentially the same reason that makes it possible in a one-particle type of assembly, namely that, even in a very large assembly, we must always allow in some way for the fact that a finite number of molecules is present.

There are at present two quite distinct statistical-mechanical methods of allowing for the finite number of molecules in an assembly. Unfortunately they are *not* equivalent, and the present problem seems to call for some new process intermediate between the two. The general problem of finding such procedures is being studied, as it will almost certainly be relevant to certain other difficult questions concerned with liquids, such as the 'communal entropy' problem. The two methods at present available are as follows: (a) We can limit the total number of *modes* in the energy spectrum. The use of a 'cut-off', chosen so that the total number of modes is equal to $3N$, is familiar in the Debye theory of specific heats, and has been shown to be nearly correct by later, more accurate investigations. In the present problem Ziman (1953) has proposed, but only as a rough approximation, a process practically equivalent to limiting all integrations to a spherical region of K -space. (b) We can limit the number of *excitations* in the assembly. In a one-particle type of model the total number of excitations is just N , and there is an obvious extension of this to cases in which a certain excitation refers always to a definite number of elementary particles, as in a theory of Mayer type (1940). This process is usually carried out by means of a 'selector variable' technique (or the practically equivalent method of an undetermined multiplier related to the chemical potential).

As Feynman (1954) points out, in the perfect gas case the ground state wave function is just a constant. Method (b) is then entirely correct, as each excitation in (2) then refers to *one* atom, but this definitely ceases to be true in other cases. (One excitation involves more than one atom to an extent that probably depends on the magnitude of K .) Method (a) is reasonable for a solid lattice, and possibly for ordinary liquids, but is obviously much too crude for use in the present context. It merely results in the specific heat approaching a finite value at 'high' temperatures, and *removes altogether* the transition that we are looking for. Method (b) is reasonable for small interactions, and, in conjunction with a spectrum such as (2), can be made to give a transition of approximately the observed type, but, as we have seen, spectrum (2) *without* a cut-off process of the type called for in method (a) completely fails to describe the He I region of the specific heat. Thus again we seem to require some combination of these two methods. Similar remarks seem to apply to the calculation of ρ_n , the 'density of normal fluid'.

§ 6. CONCLUSION

The fact that the energy spectrum (2) cannot be yet combined with existing theory in a way that gives agreement with experiment does *not* prove that this spectrum is wrong. Existing theory is incomplete in certain respects—quite enough to account for the difficulties noted by Feynman (1954).

ACKNOWLEDGMENTS

This paper was written during my tenure as a Visiting Professor at the University of Nebraska. I wish to thank Professor R. P. Feynman and Dr. P. J. Price for helpful discussions and correspondence.

REFERENCES

- BIJL, A., 1940, *Physica*, **7**, 869.
 BIJL, A., DE BOER, J. H., and MICHELS, A., 1941, *Physica*, **8**, 655.
 BUCKTHOUGHT, K., 1953, *Canad. J. Phys.*, **31**, 932.
 CHESTER, G. V., 1954, *Phys. Rev.*, **93**, 1412.
 DINGLE, R. B., 1952, *Advances in Physics (Phil. Mag. Suppl.)*, **1**, 111.
 FEYNMAN, R. P., 1953 a, *Phys. Rev.*, **90**, 1116; 1953 b, *Ibid.*, **91**, 1291; 1953 c, *Ibid.*, **91**, 1301; 1954, *Ibid.*, **94**, 262.
 FRASER, A. R., 1950, *Fellowship Thesis*, University of Cambridge.
 FRENKEL, J., 1946, *Kinetic Theory of Liquids* (Oxford: University Press).
 KHALATNIKOV, I. M., 1950, *J. Exp. Theor. Phys.*, **20**, 243; 1952, *Ibid.*, **23**, 8.
 KRAMERS, H. A., 1952, *Physica*, **18**, 653.
 LANDAU, L. D., 1941, *J. Phys., Moscow*, **5**, 71; 1947, *Ibid.*, **11**, 91.
 LANDAU, L. D., and KHALATNIKOV, I. M., 1949 a, *J. Exp. Theor. Phys.*, **19**, 637; 1949 b, *Ibid.*, **19**, 709.
 LONDON, F., 1943, *J. Chem. Phys.*, **11**, 203.
 MATSUBARA, T., 1951, *Progr. Theor. Phys., Osaka*, **6**, 714.
 MIKURA, Z., 1954, *Progr. Theor. Phys., Osaka*, **11**, 25.
 MAYER, J. E., and MAYER, M. G., 1940, *Statistical Mechanics* (New York: Wiley).
 MOTT, N. F., 1949, *Phil. Mag.*, **40**, 61.
 PENROSE, O., 1951, *Phil. Mag.*, **42**, 1373.
 PRICE, P. J., 1954, Report of Watson Computing Laboratory, New York.
 PRIGOGINE, I., and PHILIPOTT, J., 1952, *Physica*, **18**, 729; 1953 a, *Ibid.*, **19**, 227; 1953 b, *Ibid.*, **19**, 235; 1953 c, *Ibid.*, **19**, 508.
 TEMPERLEY, H. N. V., 1947, *Oxford Conference on Liquid Helium*; 1952 a, *Proc. Phys. Soc. A*, **65**, 490; 1952 b, *Ibid.*, **65**, 619; 1953, *Ibid.*, **66**, 995.
 ZIMAN, J. M., 1953, *Proc. Roy. Soc. A*, **219**, 257.

APPENDIX

Removal of some of the Assumptions made in Feynman's Treatment of the Generalized Bose-Einstein Transition

The problem studied by Feynman (1953 a, b) reduces to that of finding a workable method of estimating the integral in his equation (7) (1953 b), which is

$$\int \dots \int \sum_P \exp \left[\frac{-m'}{2\beta\hbar^2} \sum_i (\mathbf{z}_i - P\mathbf{z}_i)^2 \right] \rho_N(\mathbf{z}_1, \mathbf{z}_2, \dots, \mathbf{z}_N) d^N \mathbf{z}_i \dots \dots (A 1)$$

where \mathbf{z}_i is the vector specifying the position of the i th atom, $P\mathbf{z}_i$ is the vector into which \mathbf{z}_i is changed by the effect of the permutation P acting on the N atoms, and $\rho_N(\mathbf{z}_1, \mathbf{z}_2, \dots, \mathbf{z}_N)$ is proportional to the probability of finding the first atom near the end of \mathbf{z}_1 and atom 2 simultaneously near the end of \mathbf{z}_2 etc. The work of evaluating (A 1) can be arranged in a way that enables us to take over nearly

unchanged the mathematical results used by Mayer and others (see, for example, Mayer and Mayer 1940, Chap. 13 and Appendix 11) for the expression of the configuration integral in terms of cluster integrals. Consider, for example, the contribution to (A1) from the permutation represented by the cycles (123)(45)(67). This is

$$\int \dots \int \phi_{12}\phi_{23}\phi_{31}\phi_{45}\phi_{67}\rho_N(\mathbf{z}_1, \mathbf{z}_2, \dots, \mathbf{z}_N) d\mathbf{z}_1 \dots d\mathbf{z}_N \quad \dots\dots (A 2)$$

where ϕ_{12} stands for $\exp [(-m'/2\beta\hbar^2)(\mathbf{z}_1 - \mathbf{z}_2)^2]$ etc.

To evaluate (A 2) we make a 'generalized Kirkwood approximation' by assuming ρ_N to be proportional to

$$\rho_2(\mathbf{z}_1, \mathbf{z}_2)\rho_2(\mathbf{z}_2, \mathbf{z}_3)\rho_2(\mathbf{z}_3, \mathbf{z}_1)\rho_2(\mathbf{z}_4, \mathbf{z}_5)\rho_2(\mathbf{z}_6, \mathbf{z}_7)\rho_{N-7}(\mathbf{z}_8 \dots \mathbf{z}_N). \quad \dots\dots (A 3)$$

The integration over the coordinates of the $N-7$ atoms unaffected by this permutation can be carried out at once, leading simply to a factor proportional to V^{N-7} , while the remainder of the integral (A2) factorizes into $f_2^2 f_3$, where

$$\left. \begin{aligned} f_2 &= \int \dots \int \phi_{45}\rho_2(\mathbf{z}_4, \mathbf{z}_5) d\mathbf{z}_4 d\mathbf{z}_5 = \int \dots \int \phi_{67}\rho_2(\mathbf{z}_6, \mathbf{z}_7) d\mathbf{z}_6 d\mathbf{z}_7 \\ f_3 &= \int \dots \int \phi_{12}\phi_{23}\phi_{31}\rho_2(\mathbf{z}_1, \mathbf{z}_2)\rho_2(\mathbf{z}_2, \mathbf{z}_3)\rho_2(\mathbf{z}_3, \mathbf{z}_1) d\mathbf{z}_1 d\mathbf{z}_2 d\mathbf{z}_3 \end{aligned} \right\} \dots\dots (A 4)$$

the higher f_s 's involving longer cycles. Since all the coordinates range over the same volume V , all possible configurations of the atoms concerned are allowed for in the f_s 's, each one of which depends only on the *length* s of the corresponding cycle and not at all on the *numbering* of the atoms in it. In practice, configurations in which two atoms are far apart contribute little to the f_s 's, because the corresponding ϕ is small, while overlapping configurations also contribute very little because ρ_2 is then very small.

The definitions in (A4) differ slightly from Feynman's own definition of the f_s 's (1953 b, equation (24)), but avoid the difficulties he finds when s equals 1 or 2. (We have not yet given *our* definition of f_1 , but we now put it equal to V .) We can now complete the theory on exactly the lines indicated by Feynman (1953 b), except that, in his equation (26), we must replace $\Gamma^s(K)$ by $\Gamma^{s-1}(K)$, and in his equations (27) and (28) we consequently have $p(0)=1$. Each possible permutation contributes to (A1) a product of powers of the f_s 's corresponding to the *numbers* of cycles of each length into which the permutation is decomposed, so that the contribution of each permutation depends only on its 'type', and the evaluation is completed by using the well-known expression for the number of permutations of N objects of a given permutation type.

The 'factoring' of a permutation into *non-overlapping* cycles is closely related to the fact that, in the development of Mayer's theory, each term in the configuration integral corresponds to a distinct method of connecting points in a plane into *non-overlapping groups*. Integration over the coordinates of the atoms in any one group (or cycle) can then be carried out quite independently of the positions of the remaining atoms. If we include all possible terms in the configuration integral, *all* interactions have already been taken into account, and it is redundant to introduce interactions between clusters. The argument is readily modified to apply to the present treatment. Integration over the coordinates of the atoms in any one polygon can, without any qualms, take place independently of any other polygons, and it is unnecessary to include self-crossing polygons in the definition of the f_s 's as

Feynman does. Since the polygons do *not* overlap, integrals like (A 2) can be *factored*.

We conclude that the passage from equation (7) to equations (27) and (28) in Feynman's (1953 b) paper requires the 'generalized Kirkwood approximation' (A3) as the only assumption, some of the other assumptions made by Feynman not being needed. We agree entirely with Feynman (1953 b) and Matsubara (1951) that the transition results from the behaviour of terms corresponding to *long* permutation cycles.

Many of the mathematical complications dealt with by Mayer and Mayer (1940) arise from the necessity of providing for cases in which some of the cluster integrals are negative. In an expression such as (A 2), all the 'polygon integrals' into which it can be factored are necessarily positive, and the method of steepest descents used by Feynman (1953 b) then leads to correct results.

As explained in the text (p. 901), a further assumption about the behaviour of $S(K)$ as $K \rightarrow 0$ (in the limiting case of a large assembly of constant density) seems to be required before the existence of a transition can be definitely inferred. (We recall that *not all* 'one-particle' models lead to a transition.)

The Vibrational and Rotational Excitation of Molecular Hydrogen by Electron Impact

BY T. R. CARSON

Department of Applied Mathematics, Queen's University of Belfast

Communicated by D. R. Bates; MS. received 15th June 1954; read at the Spring Meeting of the Physical Society in Dublin, March 1954

Abstract. The Born approximation is applied to the collision of electrons with normal hydrogen molecules. Cross sections are calculated for collisions accompanied by the vibration-rotation transitions $0, 0 \rightarrow n, l$ ($[n=0, 1]$, $[l=0, 2, 4]$) for incident electron energies between 0 and 250 eV. Special attention is given to the choice of the interaction potential, the form of which has a marked effect upon the pure vibrational excitation function in the low-energy region where a sharp peak appears. The rotational excitation does not show the same sensitivity. Elastic scattering is also treated and the results are in satisfactory agreement with those of previous workers.

§1. INTRODUCTION

COMPARATIVELY little attention has been paid to the possibility of the excitation of molecular vibrations and rotations through electron collisions. Experiments by Bailey (1932) and others provide indirect evidence that in passing through a molecular gas electrons with insufficient energy to cause electronic transitions suffer energy losses far in excess of what would be expected if only elastic collisions took place. This has been interpreted by some as due to excitation of vibration and rotation, but lack of data on the probability of such inelastic collisions makes a quantitative appraisal of the position impossible.

Quantum mechanical calculations have been carried out, for the case of hydrogen, by Massey (1935) and Wu (1947), who considered only the excitation of a single vibrational quantum. From an analysis of the experimental data Bennett and Thomas (1942) have concluded that rotational excitation may be quite important in removing energy from very slow electrons. In hydrogen there are no low electronic states (appreciable electronic excitation not occurring until the electron energy reaches 8.8 eV, when excitation of the repulsive $^3\Sigma_u$ state begins).

Apart from providing much needed information, an investigation of the excitation of rotation and vibration by electron collisions is of some interest in itself. In view of the large ratio of the colliding masses, a small cross section for energy transfer by this means is to be expected from purely dynamical considerations. The present paper is devoted to calculations of cross sections for the vibrational and rotational excitation of hydrogen. For completeness elastic collisions, being a special case, are also included in the discussion.

§2. GENERAL THEORY

The solution of the general integro-differential equation describing the scattering of an electron by a molecule is complicated by the lack of spherical symmetry of the interaction potential. In the case of a diatomic molecule the potential is symmetrical only about the line joining the two nuclei, and the scattering amplitude therefore depends upon the direction of this axis relative to the path of the incident electron. For sufficiently high electron energies the distortion of the incident wave by the attractive potential of the molecule is small, so that Born's approximation may be employed. Neglecting exchange, and considering the centre of mass of the molecule to be at rest, we can then write for the differential cross section for scattering through an angle θ into the solid angle $d\omega$

$$I_{\text{if}}(\theta) d\omega = \frac{K_f}{K_i} \frac{4\pi^2 \mu^2}{h^4} |\mathcal{M}_{\text{if}}|^2 d\omega \quad \dots\dots(1)$$

$$\text{with} \quad K_f^2 = 8\pi^2(E - E_f)/h^2, \quad K_i^2 = 8\pi^2(E - E_i)/h^2, \quad E = E_i + \frac{1}{2}\mu v^2,$$

$$\mathcal{M}_{\text{if}} = \iiint \Psi_i \Psi_f^* \exp(i\mathbf{K}\mathbf{r} \cdot \mathbf{n}) V(\mathbf{r}, \mathbf{R}) d\mathbf{r} d\tau \quad \dots\dots(2)$$

in which E is the total energy of the composite system; v is the velocity of the incident electron and μ its reduced mass; E_i and E_f are the initial and final energies of the scatterer; K and \mathbf{n} are defined by $K\mathbf{n} = K_i\mathbf{n}_i - K_f\mathbf{n}_f$, \mathbf{n}_i and \mathbf{n}_f being unit vectors in the direction of the incident and the scattered electron, respectively; \mathbf{r} is the position vector of the electron with respect to the centre of the molecule; \mathbf{R} is the relative position vector of the nuclei and τ represents the aggregate of molecular electronic coordinates; Ψ_i and Ψ_f are the total wave functions for the molecule in its initial and final states; and $V(\mathbf{r}, \mathbf{R})$ is the interaction potential for the electron in the field of the molecule (cf. Mott and Massey 1949).

For a collision which does not result in a change of the electronic state of the molecule the integration over the coordinates τ may be performed immediately, yielding

$$\mathcal{M}_{\text{if}} = \iint \Phi_i(\mathbf{R}) \Phi_f^*(\mathbf{R}) \exp(i\mathbf{K}\mathbf{r} \cdot \mathbf{n}) V(\mathbf{r}, \mathbf{R}) d\mathbf{R} d\mathbf{r} \quad \dots\dots(3)$$

where now Φ_i and Φ_f are the initial and final nuclear wave functions.

§3. THE INTERACTION POTENTIAL

If the potential field of a homonuclear diatomic molecule may be split into two similar parts, each centred about a nucleus

$$V(\mathbf{r}, \mathbf{R}) = U(|\mathbf{r} + \frac{1}{2}\mathbf{R}|) + U(|\mathbf{r} - \frac{1}{2}\mathbf{R}|), \quad \dots\dots(4)$$

then (3) may be written in the form

$$\mathcal{M}_{\text{if}} = 2 \int \cos\{\frac{1}{2}\mathbf{K}\mathbf{n} \cdot \mathbf{R}\} \Phi_i \Phi_f^* d\mathbf{R} \int U(|\mathbf{s}|) \exp(i\mathbf{K}\mathbf{n} \cdot \mathbf{s}) d\mathbf{s}. \quad \dots\dots(5)$$

When the mutual interaction of the constituent atoms is negligible the form of U will be independent of R and the molecule can be regarded as two separate scattering centres. An inspection of (5) shows that as the cosine tends to unity the integral will vanish on account of the orthogonality of Φ_i and Φ_f , so that in this case (i.e. for low energies) it is not permissible to neglect any possible dependence of U on R . The importance of this fact was first pointed out by Massey (1935).

For a single hydrogen atom, U has the form

$$U(r_1) = (1 + r_1) \{ \exp(-2r_1) \} / r_1$$

where r_1 is the distance from the nucleus. In the presence of another atom, as in a molecule, this is modified to

$$U(r_1) = (1 + Zr_1) \{ \exp(-2Zr_1) \} / r_1 \quad \dots\dots (6)$$

where Z assumes the role of a screening parameter or effective nuclear charge. Wang (1928), using a variational treatment, has shown that Z is not constant but is a function of R , the internuclear distance. Starting at the value unity for infinite separation, it first decreases slightly as the atoms approach and then increases again fairly rapidly, taking the value 1.166 at the equilibrium distance R_0 , in the region of which the variation is practically linear. It is only in this region that the nuclear wave functions are of appreciable magnitude, so that, following Massey, we may expand Z about R_0 in a series

$$Z = Z_0 + (R - R_0)Z_0' + \dots \quad \dots\dots (7)$$

where $Z_0 = Z(R_0) = 1.166$; $Z_0' = (\partial Z / \partial R)_{R=R_0} = -0.23$; $R_0 = 1.40$. Derivatives higher than the first may be neglected. Inserting (7) in (6) gives, to the same approximation,

$$U(r_1) = \{ \exp(-2Z_0 r_1) \} \left\{ Z_0 + \frac{1}{r_1} - Z_0'(1 + 2Z_0 r_1)(R - R_0) \right\}. \quad \dots\dots (8)$$

A calculation of the molecular field based on this formula is in good agreement with the results obtained by Moiseiwitsch† using the full Wang function. The field does not, however, include a quadrupole term, which defect may be serious in the very low energy region (cf. Stein *et al.* 1954).

The interaction potential used by Wu (1947) was a spherically symmetric one, viz.

$$V(r) = -\frac{2}{1+S} \frac{\exp(-2Z_0 r)}{r} (1 + Z_0 r)$$

with $S = (1 + Z_0 R + \frac{1}{3} Z_0^2 R^2) \exp(-2Z_0 R)$. Quantitatively this function does not accurately reproduce the molecular field calculated by more refined methods: it has, for example, a single pole at the centre of the molecule whereas the true field has two poles centred on the nuclei.

Returning to equation (8), \mathcal{M}_{if} now becomes

$$\mathcal{M}_{if} = 8\pi \int \Phi_i \Phi_f^* \{ A + B(R - R_0) \} \cos(\frac{1}{2} K \mathbf{R} \cdot \mathbf{n}) d\mathbf{R} \quad \dots\dots (9)$$

where $A = (8Z_0^2 + K^2)(4Z_0^2 + K^2)^{-2}$, $B = -64Z_0^3 Z_0'(4Z_0^2 + K^2)^{-3}$.

§ 4. MOLECULE AS A LINEAR VIBRATOR

We will first consider the scattering produced by a molecule whose symmetry axis is fixed in space. This is not a hypothetical situation, for a trivial calculation shows that the molecule can only turn through a very small angle during the effective collision time associated even with slow incident electrons. We can therefore regard it as a linear vibrator, but since in practice we have randomly orientated molecules, it is necessary to average the cross sections initially obtained.

The most convenient wave functions available are those for the simple harmonic oscillator modified to the needs of the present problem by adjusting the parameters so that they reproduce, as far as possible, the spectroscopically determined

† We wish to thank Dr. B. L. Moiseiwitsch for making his results available to us prior to publication.

molecular constants (cf. Herzberg 1950). In this approximation the n th vibrational state is represented by

$$\Phi_n = \mathcal{N}_n \{ \exp(-\frac{1}{2}x^2) \} H_n(x) \quad \dots\dots (10)$$

$$\text{with} \quad x = \alpha^{1/2}(R - R_0), \quad \alpha = 4\pi M\nu_0/h, \quad \mathcal{N}_n = \left\{ \frac{(\alpha/\pi)^{1/2}}{2^n n!} \right\}^{1/2},$$

M being the reduced mass for the system and ν_0 the fundamental frequency.

The matrix element \mathcal{M}_{if} given in (9) may be evaluated by writing $\frac{1}{2}K\mathbf{R} \cdot \mathbf{n} = pR$ where $p = \frac{1}{2}\{K_i \cos \theta_i - K_f \cos \theta_f\}$, θ_i , ϕ_i and θ_f , ϕ_f being the angles defining \mathbf{n}_i and \mathbf{n}_f in spherical polar coordinates with the line of nuclei as polar axis. Then we have

$$K^2 = K_i^2 + K_f^2 - 2K_i K_f \{ \cos \theta_i \cos \theta_f + \sin \theta_i \sin \theta_f \cos \phi \} \quad \dots\dots (11)$$

where $\phi = \phi_i - \phi_f$. Thus, for a collision in which the first vibrational level is excited,

$$\mathcal{M}_{01} = \frac{\pi}{\alpha} \{ \exp(-p^2/8\alpha) \} \{ Ap \sin pR_0 + B(1 - p^2/4\alpha) \cos pR_0 \} \quad \dots\dots (12)$$

and the averaged total cross section is

$$\begin{aligned} \overline{\mathcal{Q}}_{01}(K_i) &= \frac{a_0^2}{4\alpha^2} \frac{K_f}{K_i} \iiint \exp\left(-\frac{p^2}{4\alpha}\right) \\ &\times \left\{ Ap \sin pR_0 + B\left(1 - \frac{p^2}{4\alpha}\right) \cos pR_0 \right\}^2 d \cos \theta_f d \cos \theta_i d\phi \quad \dots\dots (13) \end{aligned}$$

a_0 being the radius of the first Bohr orbit.

§ 5. MOLECULE AS A VIBRATING ROTATOR

In the preceding section we have treated the scattering by a molecule considered as a one-dimensional oscillator. Such a treatment suffices so long as we are only interested in vibrational excitation, but it is of course inadequate if we wish to investigate the probability of excitation of the molecule to any particular rotational level for a given simultaneous vibrational transition. This could be done by combining the vibrational wave functions above with the wave functions for a free rotator (that is, the surface harmonics $Y_{l,m}(\xi, \eta)$), obtaining

$$\Phi_n = \mathcal{N}_n' \exp(-\frac{1}{2}x^2) H_n(x) Y_{l,m}(\xi, \eta) \quad \dots\dots (14)$$

where now

$$\mathcal{N}_n' = \{R_0^2 + (n + \frac{1}{2})/\alpha\}^{-1/2} \mathcal{N}_n.$$

However, more accurate nuclear wave functions have been given by Fues (1926). These are obtained by solving the wave equation for the internuclear potential:

$$U(R) = -D + 2\pi^2\nu_0^2 MR_0^2(1 - 2/\rho + 1/\rho^2) \quad \dots\dots (15)$$

where $\rho = R/R_0$, and D , ν_0 , M , R_0 are the depth of the potential curve, fundamental frequency, reduced molecular mass and equilibrium distance, respectively. The radial wave functions are

$$R_{n,l}(\rho) = N_{n,l} \rho^{a-1} \exp(-\frac{1}{2}b\rho) L_{k+n}^k(b\rho) \quad \dots\dots (16)$$

with

$$N_{n,l} = \frac{2^a \gamma^{2a+1}}{(a+n)^{a+1}} \left[\frac{\Gamma(n+1)}{\{R_0 \Gamma(2a+n)\}^3} \right]^{1/2}$$

$$a = \frac{1}{2} + \{\gamma^2 + (l + \frac{1}{2})^2\}^{1/2}$$

$$b = 2\gamma^2/(a+n), \quad k = 2a-1$$

$$\gamma = 4\pi^2\nu_0 MR_0^2/h;$$

in which n and l are the vibrational and rotational quantum numbers and $L_{k+n}^k(b\rho)$ is the associated Laguerre polynomial indicated. Since γ is a large number (~ 36) a and b , and therefore the wave function, are practically independent of l . The complete nuclear wave function can now be written

$$\Phi_{n,l,m}(\rho, \xi, \eta) = R_{n,l}(\rho) Y_{l,m}(\xi, \eta).$$

Returning to equation (9), we can evaluate \mathcal{M}_{if} by expanding the cosine in the form

$$\cos\{\tfrac{1}{2}K\mathbf{R}\cdot\mathbf{n}\} = \sum_0^{\infty} (-1)^r (4r+1) S_{2r+\frac{1}{2}}(\tfrac{1}{2}KR) P_{2r}(\cos\xi) \dots\dots (17)$$

$S_r(x)$ denoting the spherical Bessel function $(\pi/2x)^{1/2} J_{r+1/2}(x)$ and $P_{2r}(\cos\xi)$ the Legendre polynomial.

This gives for the transition $n_1 l_1 m_1 \rightarrow n_2 l_2 m_2$

$$\begin{aligned} \mathcal{M}_{12} = & 8\pi \int_0^{2\pi} \int_{-1}^{+1} \sum_0^{\infty} (-1)^r (4r+1) P_{2r}(\cos\xi) Y_{l_1 m_1}(\xi, \eta) Y_{l_2 m_2}(\xi, \eta) d\cos\xi d\eta \\ & \times \int_0^{\infty} S_{2r+\frac{1}{2}}(\tfrac{1}{2}KR) R_{n_1 l_1}(R) R_{n_2 l_2}(R) \{A + B(R - R_0)\} R^2 dR, \dots\dots (18) \end{aligned}$$

where $K^2 = K_i^2 + K_f^2 - 2K_i K_f \cos\theta$, θ being the angle of scattering. It is at once evident from (18) that \mathcal{M}_{12} will be zero unless $m_1 = m_2$, and l_1 and l_2 have the same parity, i.e. the rotational quantum number can change only by an even integer.

§ 6. RESULTS AND DISCUSSION

6.1. Elastic Scattering

The elastic scattering of electrons by hydrogen molecules already has a considerable literature and it is not therefore intended to dwell on it here in any detail (cf. Massey and Burhop 1952). In the present connection elastic scattering arises as a special case when the changes in the vibrational and rotational quantum numbers are both zero. The angular distributions so obtained are in good agreement with the results of previous authors, but fail to show the rise observed beyond 90° for all electron energies—a failure generally attributed to the inadequacy of the Born formula. A very slight rise is found, however, for energies greater than about 70 volts. In figure 1, curve A,

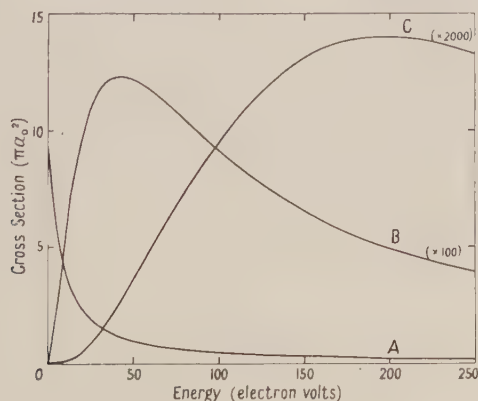


Figure 1. Elastic and rotational excitation cross sections of H_2 :
A, elastic; B, $l=0 \rightarrow l=2$; C, $l=0 \rightarrow l=4$.

the total elastic cross section is plotted as a function of the electron energy. It will be seen that as the electron energy is decreased the cross section approaches the finite low-velocity limit of $9.1\pi a_0^2$. Fisk (1936) has carried out calculations for slow electrons using a method analogous to that of Allis and Morse (1931) for atoms, obtaining a low-velocity limit of about twice this value, and at the same time resolving a Ramsauer effect below 1 ev. At high energies the calculations are in good agreement, the present theory giving for the asymptotic form of the cross section $(3.66/K_1^2)\pi a_0^2$.

6.2. Inelastic Scattering

The excitation of vibrational and rotational levels of the molecule may take place either separately or simultaneously. In figure 1, curves B and C, we have plotted as a function of the electron energy the cross sections for pure rotational excitation from the ground state ($n=0, l=0$) for transitions in which $\Delta l=2, 4$. ($\Delta l=0$ of course corresponds to an elastic collision.) These transitions correspond to energy changes of 0.044 and 0.144 ev respectively. The associated cross sections are much less than the elastic cross sections, the maximum values being smaller by successive factors of 10 and 20. The positions of the maxima are also of interest, occurring as they do at electron energies of 40 and 200 volts approximately. The cross sections increase rapidly until the maxima are reached, where, as the electron energy is increased, they begin to fall off again, taking the asymptotic forms $(0.73/K_1^2)\pi a_0^2$ and $(0.13/K_1^2)\pi a_0^2$ respectively.

In figure 2 we display in a similar fashion the excitation functions for the same rotational transitions accompanied by a vibrational transition $\Delta n=1$ ($n=0 \rightarrow n=1$). The energy changes involved here are 0.513, 0.555 and 0.650 ev respectively. In the case of $\Delta l=0$ (vibrational change only) there is a sharp peak at about 1.2 ev (which we shall return to in the next section) together with a second broader maximum in the region of 38 ev. The curves for $\Delta l=2$ and $\Delta l=4$ exhibit characteristics similar to the corresponding curves in the case $\Delta n=0$, but in contrast to that case the cross section for $\Delta l=2$ is of the same order of magnitude as that for $\Delta l=0$ except at very low energies. The cross section for $\Delta l=4$, however, is much smaller. Again the positions of the maxima are noteworthy, occurring this time in the regions of 25 and 120 ev. As before, the asymptotic forms vary as K_1^{-2} with proportionality constants 0.032, 0.026 and 0.0036 (in units πa_0^2).

6.3. Discussion

The rotational excitation cross sections present little difficulty in interpretation. In every case the maximum occurs far beyond the threshold energy, and it would indicate that the controlling factor is the amount of angular momentum rather than energy brought up by the incident electron. Owing to the large mass ratio, and the rapid decrease of the interaction with increasing impact parameter, this condition can only be fulfilled by going to high electron energies. The explanation of the detailed form of pure vibrational excitation curve is less obvious. Although the Born approximation is not expected to give reliable results at very low energies, the significance of the sharp peak cannot be lightly dismissed. In figure 2, curve A, the cross section for the same transition ($\Delta n=1, \Delta l=0$) has been plotted again, calculated this time without the inclusion in the interaction potential V of the term in $\partial Z/\partial R$. The curve so obtained

has a single maximum in the same position as the second maximum of the first curve (at approximately 38 volts). The peak in the vibrational excitation function can therefore be attributed to the variation of the effective nuclear charge with internuclear distance.[†] In the energy region below 38 volts the cross section is due almost entirely to the contribution from this effect. With increasing energy the predominance diminishes rapidly, and beyond the second maximum its contribution to the total cross section becomes inappreciable. This explains in a satisfactory manner how, in the low energy region, the explicit dependence

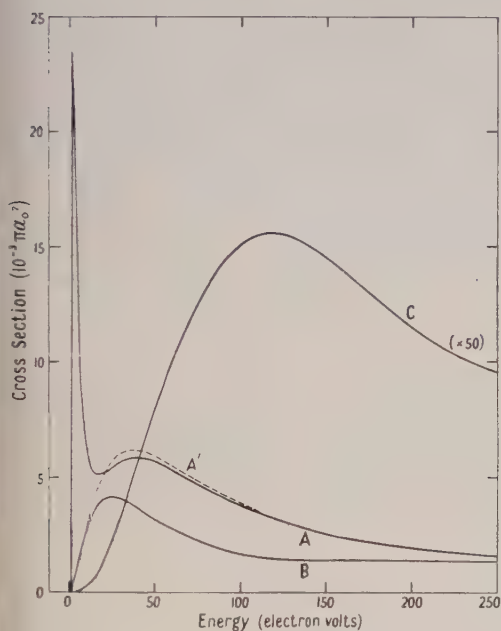


Figure 2. Vibration-rotation excitation cross sections of H_2 for vibrational transition $n=0 \rightarrow n=1$. A, $l=0 \rightarrow l=0$; B, $l=0 \rightarrow l=2$; C, $l=0 \rightarrow l=4$, allowing for variation of effective nuclear charge with nuclear separation; A', $l=0 \rightarrow l=0$, neglecting variation of effective nuclear charge.

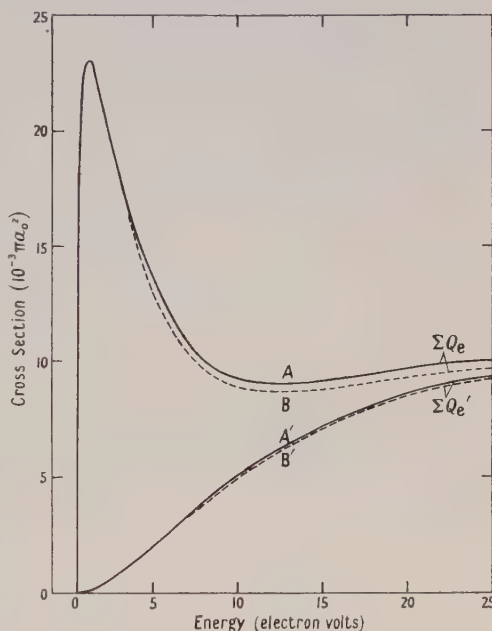


Figure 3. Comparison of vibrational excitation cross section for linear oscillator with that for rotating vibrator summed over rotational states: A, B allowing for variation of effective nuclear charge; A', B' neglecting variation of effective nuclear charge.

of V on R can increase the cross section by a considerable factor, and it also shows that the same is not true for higher energies.

From the foregoing it seemed advisable to investigate the effect in relation to the other collision processes. This has been done, and the results show that in no other case does the contribution to the cross section from the term in $\partial Z/\partial R$ amount to more than a few per cent of the total, throughout the entire energy range considered.

The results discussed so far are those based on the theory of §5 using the vibrating-rotator model for the molecule. We shall now consider the effect of

[†] The magnitude of the cross section at the peak is rather uncertain, for it is approximately proportional to $(Z_0')^2$ and the derivative Z_0' is far from being well determined.

suppressing the rotational degrees of freedom as was done in §4. Since the information obtained in this way is not so rich in detail and the computational labour is formidable, a much smaller range of energies (0–30 volts) has been covered. The calculations do, nevertheless, provide valuable comparison data. Only the vibrational transition $n=0 \rightarrow n=1$ has been treated in this manner, and the excitation function so obtained is plotted in figure 3 as curve A. This curve is to be compared with the sum of the excitation functions shown in figure 2 which is plotted as curve B. Curves A' and B' correspond to A and B but with the value of $\partial Z/\partial R$ taken as zero. We thus see that the linear oscillator model of the molecule reproduces all the characteristics of the vibrating-rotating model, summed over the rotational quantum number.

Morse (1953) has shown that the energy lost to the excitation of rotation-vibration of a molecule by an electron is of the same order of magnitude as that lost through momentum transfer in an elastic collision. An analysis of the cross sections presented here supports this conclusion. At low velocities more energy is lost to the excitation of the $0, 0 \rightarrow 1, 0$ transition than to the other inelastic transitions. Above 12 volts the rotational excitation $0, 0 \rightarrow 0, 2$ is the most effective in absorbing energy. On the basis of these results it is quite impossible to explain the large fractional energy losses observed for slow electrons in molecular gases.

ACKNOWLEDGMENT

The author has pleasure in thanking Professor D. R. Bates for suggesting this problem and for his continued assistance throughout the course of the work, and the Ministry of Education for Northern Ireland for a research grant.

REFERENCES

- ALLIS, W. P., and MORSE, P. M., 1931, *Z. Phys.*, **70**, 567.
 BAILEY, V. A., 1932, *Phil. Mag.* (7th Series), **13**, 993.
 BENNETT, W. H., and THOMAS, L. H., 1942, *Phys. Rev.*, **62**, 41.
 FISK, J. B., 1936, *Phys. Rev.*, **49**, 167.
 FUES, E., 1926, *Ann. Phys., Lpz.*, **80**, 367.
 HERZBERG, G., 1950, *Molecular Spectra and Molecular Structure*, Vol. I (London: Macmillan).
 MASSEY, H. S. W., 1935, *Trans. Faraday Soc.*, **31**, 556.
 MASSEY, H. S. W., and BURHOP, E. H. S., 1952, *Electronic and Ionic Impact Phenomena* (Oxford: Clarendon Press).
 MORSE, P. M., 1953, *Phys. Rev.*, **90**, 51.
 MOTT, N. F., and MASSEY, H. S. W., 1949, *The Theory of Atomic Collisions* (Oxford: Clarendon Press).
 STEIN, S., GREGORY, E., and HOLSTEIN, I., 1954, *Phys. Rev.*, **93**, 934.
 WANG, S. C., 1928, *Phys. Rev.*, **31**, 579.
 WU, TA-YOU, 1947, *Phys. Rev.*, **71**, 111.

The Photo-Ionization Cross Section of Lithium

By A. L. STEWART

Department of Applied Mathematics, The Queen's University of Belfast

*Communicated by D. R. Bates; MS. received 14th May 1954,
and in amended form 2nd July 1954*

Abstract. The photo-ionization cross section of lithium is calculated using Hartree-Fock wave functions. Good agreement is obtained between the dipole length and dipole velocity formulae for the cross section over the wavelength range considered, 2300 Å–1800 Å. The mean value at the spectral head is found to be $1.16 \times 10^{-18} \text{ cm}^2$, considerably smaller than either of the previous theoretical estimates by Hargreaves (1929) and by Trumphy (1929). The cross section curve rises on the short wavelength side of the series limit, as was found by Hargreaves.

§ 1. INTRODUCTION

MEASUREMENTS of the photo-ionization cross section of atomic lithium have been made recently by Tunstead (1953). The cross section is found by him to be $2.5 \pm 1.0 \times 10^{-18} \text{ cm}^2$ at the spectral head (2300 Å), and to fall off towards shorter wavelength approximately as $\lambda^{3.5}$. This is at variance with the theoretical results of Hargreaves (1929) who evaluated the quantal dipole length formula for the cross section using wave functions derived by the self-consistent field method. He found the cross section to be $2.9 \times 10^{-18} \text{ cm}^2$ at the spectral head, rising to a maximum at 1930 Å and falling off thereafter. No such maximum was obtained by Trumphy (1929), whose calculations agree with the measurements of Tunstead in that they give a cross section proportional to $\lambda^{3.5}$ on the short wavelength side of the spectral head (where, however, they give it to be $3.7 \times 10^{-18} \text{ cm}^2$).

The differences between the two sets of calculations and the measurements reduce the confidence that can be placed in any one of them. Optical transition probabilities are in general sensitive to the detailed nature of the wave functions involved and hence the extent of the agreement between theory and experiment provides a useful criterion for the accuracy of these. Seaton (1951) has shown that in the case of sodium the theory can reproduce the main features of the experimental results if Hartree-Fock wave functions are used. In this paper a similar calculation is carried out for lithium.

§ 2. THEORY

With the initial wave function Ψ_i normalized to unit density and the final wave function Ψ_f normalized to represent a core function of unit density together with a wave of unit amplitude at infinity the photo-ionization cross section for ejection of a bound electron into the continuum with velocity v is given by the standard quantal formula

$$a_v = \frac{32\pi^4 m^2 e^2}{3h^3 c} \frac{1}{\omega_i} \sum_i \sum_f v \left| \int \Psi_i^* \left(\sum_j \mathbf{r}_j \right) \Psi_f d\mathbf{r} \right|^2 \dots\dots(1)$$

where ω_i is the weight of the initial level, ν is the frequency of the incident radiation, \mathbf{r}_j is the position vector of the j th electron and e , m , c and h have the customary meanings; the summations Σ_i and Σ_f are over the initial and final states respectively (cf. Bates 1946a).

Equation (1) expresses the cross section in terms of the familiar dipole length matrix element, but we can equally well express it in terms of the dipole velocity or dipole acceleration matrix elements by means of the identities (Chandrasekhar 1945),

$$\int \Psi_i^* \left(\sum_j \mathbf{r}_j \right) \Psi_f d\mathbf{r} = \frac{h}{4\pi^2 m \nu} \int \Psi_i^* \sum_j \nabla_j \Psi_f d\mathbf{r} \quad \dots\dots(2)$$

$$= \frac{1}{4\pi^2 m \nu^2} \int \Psi_i^* \left(\sum_j \nabla_j V \right) \Psi_f d\mathbf{r}, \quad \dots\dots(3)$$

where V is the potential energy term in the Schrödinger equation. The use of separable wave functions considerably simplifies the expressions for the absorption cross section, and for the alkali metals (cf. Seaton 1951) it reduces to

$$a_\nu = 8.55 \times 10^{-19} (I + \epsilon) \mathcal{C}_p \sigma^2 \text{ cm}^2 \quad \dots\dots(4)$$

in which I is the ionization potential and ϵ is the energy of ejection of the electron, both in rydbergs; \mathcal{C}_p is a factor allowing for the distortion of the core, and σ is a quantity which depends on whether the dipole length L , velocity v or acceleration A formula is employed, being given by

$$\sigma(L) = \int_0^\infty P(ns|r) r P(\epsilon p|r) dr \quad \dots\dots(5)$$

$$\sigma(v) = \frac{2}{I + \epsilon} \int_0^\infty P(ns|r) \left\{ \frac{1}{r} P(\epsilon p|r) + \frac{d}{dr} P(\epsilon p|r) \right\} dr \quad \dots\dots(6)$$

$$\sigma(A) = \frac{4Z}{(I + \epsilon)^2} \int_0^\infty P(ns|r) \frac{1}{r^2} P(\epsilon p|r) dr \quad \dots\dots(7)$$

where r is in atomic units, the P 's are the radial wave functions indicated, $P(ns|r)$ being normalized in the usual manner and $P(\epsilon p|r)$ being normalized to have an asymptotic amplitude of $\epsilon^{-1/4}$ and Z is the atomic number of the system concerned. Formula (7) takes the simple form stated because the terms in (3) which arise from the mutual interactions of the electrons cancel to zero and we can write

$$\sum_j \nabla_j V = 2Z \sum_j \frac{\mathbf{r}_j}{r_j^3}.$$

The acceleration matrix element now only differs from the dipole length integral in the radial part and is reduced in the same way when separable wave functions are introduced.

§ 3. THE WAVE FUNCTIONS FOR LITHIUM

Hartree-Fock radial wave functions $P(1s|r)$ for the Li^+ ion, and $P(2s|r)$ for the Li atom series electron, have been published by Fock and Petrashen (1935). The corresponding radial function for the free electron $P(\epsilon p|r)$ is a solution of the equation

$$\left[\frac{d^2}{dr^2} + \frac{6 - 4Y_0(1s, 1s|r)}{r} - \frac{2}{r^2} + \epsilon \right] P(\epsilon p|r) + \frac{2}{3} \frac{Y_1(1s, \epsilon p|r)}{r} P(1s|r) = 0 \quad (8)$$

where we have used the well-established notation of Hartree (1946-47). This equation was solved by the method of Fox and Goodwin (1949), the exchange term being initially taken as zero or some other suitable value and successively improved.

With $P(2s|r)$ and $P(\epsilon p|r)$ carefully tabulated and the latter suitably normalized (cf. Bates and Seaton 1949) it is a simple task to evaluate σ by any of the alternate formulae. However, in computing $\sigma(L)$ the function $P(2s|r)$ given by Fock and Petrashen was considered insufficiently accurate at large radial distances. For large r one may use the Coulomb potential and the experimental term value in the equation for $P(2s|r)$ and solve in terms of a rapidly converging series (cf. Bates and Damgaard 1949). This solution was fitted to the function of Fock and Petrashen at $r=5.2a_0$, making it possible to tabulate $P(2s|r)$ to four significant figures over the range required.

As the core is only slightly distorted by the series electron \mathcal{C}_p was taken to be unity.

§ 4. RESULTS AND DISCUSSION

4.1. The integrals $\sigma(L)$, $\sigma(v)$ and $\sigma(A)$ have been evaluated using the experimental ionization potential, 0.3964 rydberg, and the photo-ionization cross section derived for a series of values of ϵ , the energy of ejection of the photo-electron, near the spectral head. No serious problems due to cancellation of the positive and negative parts of the integrals arose. The quantity $1-D$ (see Bates 1947), equal to the ratio of the value of the radial integral to whichever is the larger, the positive or the negative part of the integral, takes the values 0.288, 0.375 and 0.530 in the case of $\sigma(L)$, $\sigma(v)$ and $\sigma(A)$ respectively evaluated at the spectral head.† As a result the integrals should not be unduly sensitive to small changes in the wave functions. The results are compared with previous theoretical and experimental determinations in the table, these last being taken from a graph in the paper by Ditchburn, Jutsum and Marr (1953).

The Photo-Ionization Cross Section of Lithium using
Hartree-Fock Wave Functions

	a_v in units 10^{-18} cm^2					
$\epsilon =$	0	0.02	0.04	0.06	0.08	0.10
Evaluated by						
Dipole length	1.20	1.29	1.35	1.40	1.43	1.45
Dipole velocity	1.13	1.21	1.26	1.30	1.32	1.34
Dipole acceleration	34.0	26.7	21.1	16.7	13.3	10.6
Hargreaves (1929)	2.9	3.0	3.1	3.2	3.2	3.1
‡ Trumpy (1929)	3.7	3.7	3.7	3.6	3.5	3.4
Experiment	2.5	2.4	2.2	2.0	1.8	1.5

‡ The results cited here are taken from a diagram in Trumpy's original paper covering a wide wavelength range (see comments in main text).

† For comparison it may be mentioned that in the case of sodium Seaton (1951) gives 0.082 and 0.111 for the quantity $1-D$ using the dipole length and dipole velocity formulae respectively. In spite of the comparatively high sensitivity thus indicated, Seaton obtains, as has already been mentioned, good agreement with the measured cross sections. This is highly suggestive, for the calculations described in the present paper are based on the same approximations as he adopted.

If we ignore the absurdly high cross section given by the dipole acceleration formula the agreement between the absorption curves deduced from $\sigma(L)$ and $\sigma(v)$ is very encouraging. The shape of both these curves is similar to that of Hargreaves (1929) who used 'self-consistent' field wave functions. Thus the main effect of the introduction of exchange is the reduction in the magnitude of the cross section by a factor of 2.5 approximately, a reduction comparable with the corresponding reduction found by Seaton (1951) in the case of sodium.

The rise in the cross section with decrease in wavelength near the spectral head might at first seem disturbing in view of the agreement between the theoretical calculations of Trumphy (1929) and the experiments of Tunstead (1953), the absorption curve falling off with wavelength as $\lambda^{3.5}$ near the series limit in both cases. However, it must be borne in mind that both the bound and free wave functions employed by Trumphy are rather crude, the former being merely a product of an exponential and a simple polynomial in r and the latter an unmodified Coulomb wave function. In any event his results appear to be in error. His analysis can be very rapidly checked using the formula derived by Bates (1946b). It is found that the values he gives for the cross section should be multiplied by a factor of 1.2. This does not affect the shape of the curve, but it is found that his formula does in fact yield an increase in the cross section with increasing energy of the incident radiation, the maximum, however, being quite near the spectral head.† All of the theoretical calculations on lithium thus favour an absorption curve with the maximum cross section shifted from the spectral head towards shorter wavelengths, as was first found by Hargreaves. The cross sections obtained with the Hartree-Fock wave functions should be the most reliable. It is probably best to take a mean of the dipole velocity and dipole length results.

4.2. The dipole acceleration formula has not received a very wide application. It was first used by Chandrasekhar (1945) to determine the photo-ionization cross section for H^- with a very accurate variational ground state wave function (including r_{12} terms) and a plane wave approximation to the continuum state. The agreement between all three cross section formulae was found to be good. In his work on helium Huang (1948) has used wave functions of comparable accuracy to those used by Chandrasekhar for H^- but, because of his incorrect choice of $Z=1$ in the dipole acceleration formula (see formula (7) of this paper), his published results must be multiplied by a factor of 4, and when this is done they are in good agreement with the cross sections he has derived using the length and velocity formulae.

Such good agreement between the three cross section formulae cannot be expected when Hartree-Fock wave functions are used. Nevertheless the magnitude of the cross sections in the case of the acceleration formula applied to lithium (see table) was surprising. It was thought interesting to apply the acceleration formula to sodium‡ at the spectral head. The value obtained is $1.2 \times 10^{-15} \text{ cm}^2$ which is far larger than the values $1.0 \times 10^{-19} \text{ cm}^2$ and $0.7 \times 10^{-19} \text{ cm}^2$ computed by Seaton (1951) using the length and velocity formulae respectively.

† Seemingly Trumphy did not carry out computations close enough to the spectral head to detect the effect.

‡ I acknowledge, with thanks, my indebtedness to Dr. M. J. Seaton for supplying me with the Hartree-Fock wave functions for the sodium continuum and for some helpful comments on the acceleration formula.

The reason for this discrepancy becomes apparent if one attempts to derive a relation between the velocity and acceleration matrix elements using separable wave functions. The differential equations obeyed by the wave functions Ψ_i and Ψ_f which we adopted differ from the exact Schrödinger equations only in certain small terms, R_i and R_f respectively, but the derivation of the relation under discussion requires the neglect of terms such as

$$\int \Psi_i^* \sum_j \nabla_j R_f d\mathbf{r}$$

and, as may easily be demonstrated in specific cases, such terms are not small. The acceleration formula may thus give very inaccurate cross sections.

ACKNOWLEDGMENTS

My sincere thanks are due to Professor D. R. Bates for suggesting this problem and for his help and encouragement.

REFERENCES

- BATES, D. R., 1946 a, *Mon. Not. R. Astr. Soc.*, **106**, 432; 1946 b, *Ibid.*, **106**, 423; 1947, *Proc. Roy. Soc. A*, **188**, 350.
 BATES, D. R., and DAMGAARD, A., 1949, *Phil. Trans. Roy. Soc. A*, **242**, 101.
 BATES, D. R., and SEATON, M. J., 1949, *Mon. Not. R. Astr. Soc.*, **109**, 698.
 CHANDRASEKHAR, S., 1945, *Astrophys. J.*, **102**, 223.
 DITCHBURN, R. W., JUTSUM, P. J., and MARR, G. V., 1953, *Proc. Roy. Soc. A*, **219**, 89.
 FOCK, V., and PETRASHEN, M. J., 1935, *Phys. Z. Sowjet*, **8**, 547.
 FOX, L., and GOODWIN, E. T., 1949, *Proc. Camb. Phil. Soc.*, **45**, 373.
 HARGREAVES, J., 1929, *Proc. Camb. Phil. Soc.*, **25**, 75.
 HARTREE, D. R., 1946-47, *Rep. Progr. Phys.*, **11**, 113 (London : Physical Society).
 HUANG, S.-S., 1948, *Astrophys. J.*, **108**, 354.
 SEATON, M. J., 1951, *Proc. Roy. Soc. A*, **208**, 418.
 TRUMPY, B., 1929, *Z. Phys.*, **54**, 372.
 TUNSTEAD, J., 1953, *Proc. Phys. Soc. A*, **66**, 304.

Radiations from Water under Alpha-Particle Bombardment

By E. W. T. RICHARDS

Atomic Energy Research Establishment, Harwell, Didcot, Berks.

MS. received 15th December 1953, and in amended form 15th June 1954

Abstract. Experiments are described in which quanta emitted by water under alpha-particle bombardment have been detected. Differentiation between light pulses arising from liquid water and any gas present above the water surface has been accomplished by utilizing the difference in their times of duration. From measurements made of the absorption of the quanta from water by various gases an upper limit of the wavelength of 1900 Å is suggested. The importance of quantum emission in radiation chemical experiments is discussed but, owing to the apparently very high absorption coefficient of the water, it is difficult to assess the contribution from this phenomenon.

§ 1. INTRODUCTION

IN recent years considerable work has been carried out on the problems connected with scintillations from liquids when subjected to nuclear particle bombardment. It has been shown that when some pure solvents are subjected to alpha-particle bombardment photons are emitted (Belcher 1951). Some evidence of such photon emission has been reported in the case of water (Dee and Richards 1951, Belcher 1953), and the purpose of these experiments was to investigate this phenomenon further.

It has been shown that in liquid only a small percentage of the theoretical number of ion pairs produced by the passage of an alpha-particle can be collected by means of an electrostatic field (Jaffé 1913, Richards 1953). In view of this, and of the relatively large chemical effects produced by alpha-particle bombardment, the possibility of photon emission becomes of considerable interest. Such a process might well explain the production of radicals necessary for chemical reactions in a volume which, though small compared with the bulk of the liquid, was large compared with the original column; in this way the probability of radical combination was reduced. It was decided to investigate water as many chemical experiments have been carried out using it as a solvent, and as it is probably an important factor in most biological experiments. As is well known, the overall efficiency of water as a scintillator must be low since it cannot be used for counting purposes; it has been suggested that this is because water has a high coefficient of absorption for the radiations produced. In an attempt to overcome this difficulty in previous experiments thin water films supported by quartz slides were used. This technique involved the problem of differentiating between the quantum emission from water and that arising from the quartz (Birks and King 1953), which has created doubts as to the validity of the experiments. In the experiments described in this paper the water surface actually under alpha-particle bombardment was observed, thus allowing sufficient water to be used to stop the alpha-particles.

§ 2. EXPERIMENTAL TECHNIQUES

The experiments consisted in observing the light pulses emitted by a water surface under alpha-particle bombardment. Since it is impossible to eliminate all gases from over a water surface and the use of a thin alpha-window was undesirable due to photon emission from thin films (Richards and Cole 1951) it was necessary to differentiate between the light pulses from the gas and those from the liquid. This was effected by making use of the difference in duration of the light pulses emitted by the two media. Some information about the frequencies of the quanta emitted by water was obtained by filtering the radiations through different gases. Owing to the wavelengths involved and to the apparently low quantum efficiency of water, it proved impossible to use a spectrograph.

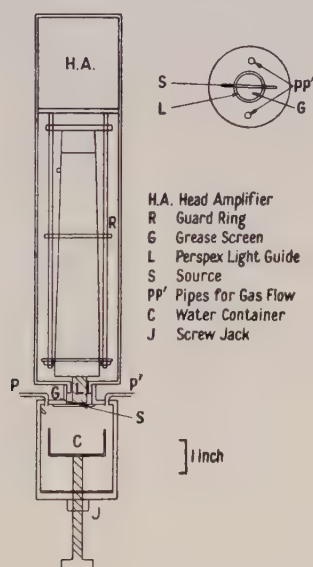


Figure 1.

§ 3. APPARATUS

Figure 1 shows the general design of the photomultiplier assembly used in these experiments. The apparatus consisted of an eleven-stage EMI photomultiplier, type VX 5045, which was fitted with a Perspex light guide, the free end of which was thinly coated with Apiezon M grease to act as a scintillation screen for ultra-violet light. A light-tight metal chamber, fitted with a water container whose position could be adjusted by means of a screw jack, could be attached to the photomultiplier case. Provision was made to enable any desired gas to be passed between the water surface and the end of the light guide. A head amplifier was mounted directly on to the base of the photomultiplier and suitable precautions taken to reduce 'background noise' to a minimum. The signals so produced were then fed into an amplifier of conventional design having a gain of up to 10^5 and fitted with variable integration and differentiation time constants. The pulses were analysed by means of a discriminator and single-channel pulse-amplitude analyser.

The alpha-particle source was 15 mc of polonium mounted on a platinum foil 2 cm long, 2 mm wide and 0.01 inch thick. This was mounted inside a small collimator made of aluminium on a thin Perspex strip across the end of the light guide. All water used in these experiments was triply distilled immediately prior to use to reduce the possibility of any scintillations being caused by impurities. Unfortunately, due to experimental difficulties it was impossible to conduct experiments free from dissolved gases.

For the investigation of light pulses emitted by gases, an internally polished aluminium tube was fitted on to the photomultiplier assembly (figure 2). One

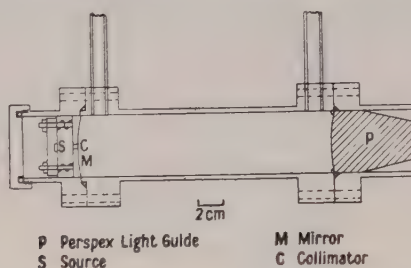


Figure 2.

end of this tube was fitted with a Perspex light guide and the other with a collimator so designed that no alpha-particle emitted from the source mounted immediately outside the cylinder could strike the walls. Provision was made for evacuating and filling the cylinder with any desired gas.

§ 4. EXPERIMENTAL PROCEDURE

Since water has low efficiency as a scintillator it was first necessary to adjust the time constants in the amplifier to their optimum values for differentiation between light pulses from water and those from the gas volume above the liquid surface. This was accomplished by making use of the jack incorporated in the water container. The liquid surface was first lowered so that no alpha-particles emitted by the source could strike the liquid, and the counting rate was recorded. The liquid level was then raised until it was 1 mm from the source and the counting rate was again noted. This procedure was repeated until the optimum settings for the time constants were found. Dry air at 5°C was passed over the water surface for 1½ hours before readings were taken in order to reduce the water vapour concentration as much as possible; the counting rate was recorded both with the surface of the water 1 mm from the source and in the lowered position. The experiment was repeated with various other gases flowing over the water surface. The effect of water vapour was also studied by stopping the flow of cold dry air and allowing the temperature of the apparatus to rise, at the same time noting any change in the counts recorded. With this method any effects on the grease screen and other parts of the apparatus due to emanations from the source were eliminated since these were independent of the position of the water surface and hence made the same contribution to the counting rates for both positions of the water surface. The possibility that x-rays arising from the alpha-particles in the water might produce changes in the counting rate was eliminated by blackening one end of the Perspex light guide and repeating measurements.

A further differentiation measurement was obtained by determining the optimum value of the time constants for pulses obtained from gases. For this purpose the aluminium cylinder was mounted on the photomultiplier case and the source placed in the collimator. The cylinder was evacuated and filled with the gas under investigation at a pressure of 2 cm Hg and the counting rate noted for various settings of the time constants.

§ 5. RESULTS

The counting rates observed from the water surface and from dry air, using the same time constants, are shown in figure 3. It will be noted that under the

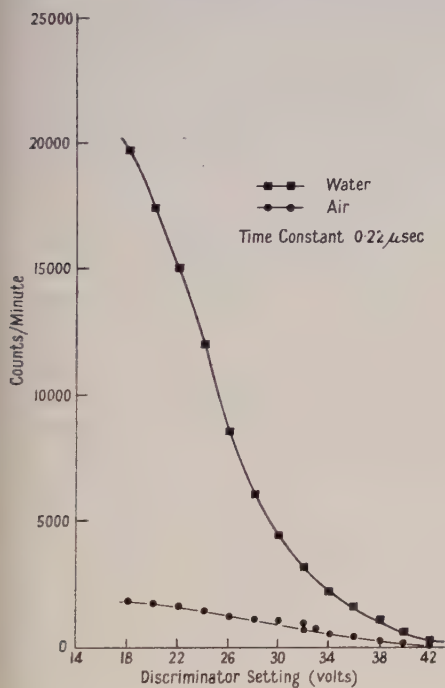


Figure 3. Counting rates for air and water.

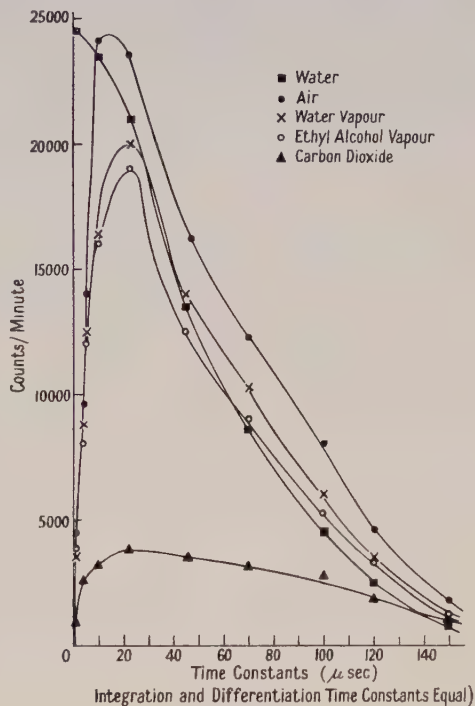


Figure 5. Comparison of pulse duration for gases and water.

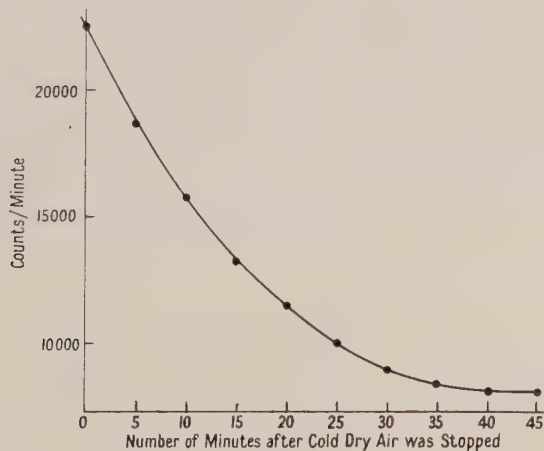


Figure 4. Effect of water vapour on counting rate.

conditions chosen water is a considerably more efficient scintillator than air. The maximum pulse heights recorded were of the order of four times noise level, but, as can be seen, the counting rate was considerably less than the rate of bombardment of the surface by alpha-particles. This fact may be due in part to the poor geometry for light collection of the apparatus which was necessary for observing the surface actually under bombardment, and in part to absorption by the water.

When ethyl alcohol or carbon dioxide were passed over the liquid surface no change in counting rate was observed for the two positions of the water level. The effect of water vapour is shown in figure 4, and it will be seen that at 18°C a 1 mm air gap saturated with water vapour absorbs about 66% of the emitted light. This value was confirmed by experiments in which the air over the water surface was not previously cooled and dried. It would appear therefore that the radiations emitted from the water are absorbed by ethyl alcohol vapour, carbon dioxide and water vapour and so must have a wavelength of less than 1900 Å. Further, the blackening of one end of the Perspex light guide eliminated all counts to the water and the gas, and so eliminated the possibility that the difference in counting rates was due to x-rays.

Further confirmation that the pulses recorded in the previous experiments were due to emission from the water was obtained from the duration of the light pulses arising for gases. Figure 5 shows the counting rates observed from gases for different settings of the time constants of the amplifier. It will be seen that by utilizing the appropriate values of the time constants a large measure of differentiation may be obtained. It would appear from the results obtained that light pulses from gases have a duration of up to 10^{-5} second. Whilst this time is large compared with known lifetimes for excited atoms it must be remembered that some of the excited states will most probably be formed by the recombination of ions, and it is therefore the recombination time which will control the maximum duration of the pulse. The duration of pulses from liquids from the same evidence is not greater than 10^{-7} second. However, the method used is not capable of any great accuracy since allowance must be made for the time constants in the head amplifier which in this case were of the order of 10^{-7} second.

§ 6. CONCLUSIONS

From the experiments described it would appear that when a water surface is bombarded with alpha-particles quanta are emitted. From the absorption of the various gases used above the liquid surface the wavelength of the light must be less than 1900 Å. Since water has a strong absorption band in this region no reliable estimate can be made of the efficiency of the original quantum emission process, and it is therefore very difficult to assess the importance of this process in radiation chemistry. It would appear unlikely that this light is produced by means of the well-known Čerenkov effect since the alpha-particles from polonium have less than the critical velocity for this process in water.

REFERENCES

- BELCHER, E. H., 1951, *Nature, Lond.*, **167**, 314; 1953, *Proc. Roy. Soc. A*, **216**, 90.
- BIRKS, J. B., and KING, J. W., 1953, *Proc. Phys. Soc. B*, **66**, 81.
- DEE, P. I., and RICHARDS, E. W. T., 1951, *Nature, Lond.*, **168**, 736.
- JAFFÉ, G., 1913, *Ann. Phys., Lpz.*, **42**, 303.
- RICHARDS, E. W. T., 1953, *Proc. Phys. Soc. A*, **66**, 631.
- RICHARDS, E. W. T., and COLE, J. F. I., 1951, *Nature, Lond.*, **167**, 286.

The Photo-Ionization of Neon

By M. J. SEATON

Department of Physics, University College, London

Communicated by H. S. W. Massey; MS. received 30th June 1954

Abstract. Previous calculations of the photo-ionization cross section of neon have been extended to wavelengths just beyond the L_1 edge at 256 Å. The absolute value of the calculated cross section is found to be in reasonable agreement with the experimental results of Lee and Weissler and of Ditchburn and Marr, but compared with the calculated results the experimental curve rises more steeply just beyond the threshold and falls more rapidly at higher energies.

THE photo-ionization cross section of neon has been calculated by Bates (1939) using wave functions calculated without inclusion of exchange and the usual dipole length formula† and by Seaton (1951a) using exchange wave functions and both the dipole length and dipole velocity formulae. Laboratory measurements of the cross section have been made recently by Lee and Weissler (1953) and independently by Ditchburn and Marr (unpublished). The two experimental determinations are in good agreement. The wavelength range covered by the laboratory measurements is greater than that for which calculations were originally made. The results of further calculations, made in order to extend the comparison between theory and experiment, are described in the present note.

From the first ionization threshold at 573 Å to the L_1 edge at 256 Å it is necessary to consider the two transitions $2p \rightarrow kd$ and $2p \rightarrow ks$, $k/2\pi$ being the wave number of the ejected electron. Beyond the L_1 edge the $2s \rightarrow kp$ transition must also be considered. The corresponding calculated cross sections will be denoted by $a_v(nl \rightarrow kl \pm 1)$. The various contributions may be discussed separately; detailed formulae quoted by Seaton (1951a) will not be repeated.

(i) $2p \rightarrow kd$. At the threshold $a_v(2p \rightarrow kd)$ was first calculated using Hartree-Fock wave functions for both the bound electrons and for the ejected electron. It was found that the radial function for the d wave was not far different from the corresponding coulomb field radial function. The calculations were then repeated using an analytic approximation to the bound wave function together with the coulomb radial function for the ejected electron, use being made of a general formula due to Bates (1946a). This calculation gave results which differed by 5% or less from the results of the first calculation. For energies beyond the threshold the results obtained using the general formula were adopted

† Comparison between the dipole length and dipole velocity formulae is of little significance using non-exchange functions; the two formulae give identical results if both bound and ejected electron wave functions are calculated in the same central field and if the theory ϵ_{nl} parameters are used in place of the observed energies. It may be noted, however, that in the work of Bates the wave functions for the ejected electron were calculated in the field of O^+ .

after multiplying by a constant close to unity to give agreement with the more exact threshold calculation. These results have now been extended to shorter wavelengths.

(ii) $2p \rightarrow ks$. Exchange calculations were made at the threshold and, slightly less accurately, at energies corresponding to wavelengths of 458 and 381 Å. At the higher energy the $2p \rightarrow ks$ transition was found to contribute less than 10% to the total cross section. Extrapolation of the matrix elements, bearing in mind the way in which the ks radial functions vary with energy, indicates that $a_v(2p \rightarrow ks)$ remains small for still higher energies. In consequence a detailed calculation scarcely seems justified. The simple approximation was adopted of assuming constant ratios $a_v(2p \rightarrow ks)/a_v(2p \rightarrow kd)$ for wavelengths less than 381 Å.

(iii) $2s \rightarrow kp$. The general expression for the cross section is

$$a_v(2s \rightarrow kp) = 1.71 \times 10^{-18} (I_{2s} + \epsilon_{kp}) |\sigma(2s \rightarrow kp)|^2 \text{ cm}^2 \quad \dots\dots(1)$$

(Bates 1946 b), ϵ_{kp} being the energy of the ejected electron and I_{2s} the relevant ionization potential, both measured in rydbergs (13.54 eV). The matrix elements are given by

$$\sigma(2s \rightarrow kp | L) = \int_0^\infty P(2s)rP(kp) dr \quad \dots\dots(2)$$

$$\sigma(2s \rightarrow kp | V) = \frac{2}{(I_{2s} + \epsilon_{kp})} \int_0^\infty P(2s) \left\{ \frac{1}{r} P(kp) + \frac{d}{dr} P(kp) \right\} dr \quad \dots\dots(3)$$

for the dipole length and dipole velocity formulae respectively, the radial functions $P(kp)$ being normalized to asymptotic amplitude $\epsilon_{kp}^{-1/4}$ and r being in atomic units.

Hartree-Fock functions $P(kp)$ have been calculated previously (Seaton 1951 b) for an electron in the field of $1s^2 2s^2 2p^6 \text{Na}^+$, and found to give Na photo-ionization cross sections in satisfactory agreement with experiment (Ditchburn, Jutsum and Marr 1953). These functions should not be far different from the corresponding function in the field of $1s^2 2s^2 2p^6 \text{Ne}^+$. The Na functions were therefore used to calculate $a_v(2s \rightarrow kp)$ for Ne.

The final results are shown in the figure. Compared with the experimental curve drawn by Lee and Weissler the experimental curve drawn in the figure

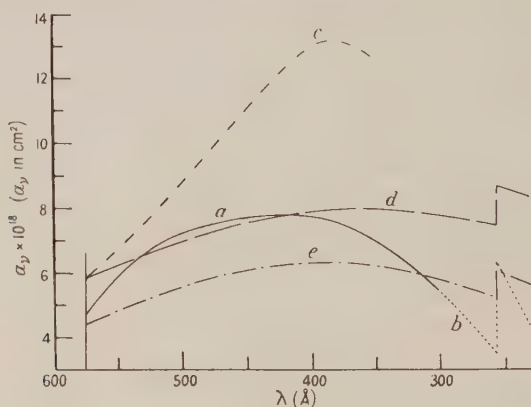


Photo-ionization cross section of Ne as a function of wavelength. *a*, *b*, experimental results; *c*, theory, non-exchange wave functions; *d*, theory, exchange wave functions, dipole length formula; *e*, theory, exchange wave functions, dipole velocity formula.

shows a_v to be smaller at the threshold and to increase more rapidly just beyond the threshold. However, our curve appears to be in better agreement with the experimental points plotted by Lee and Weissler and is confirmed by the measurements of Ditchburn and Marr. The dotted part of the experimental curve is stated by Lee and Weissler to be of a lower accuracy than the full-line curve, and in particular the magnitude of the discontinuity at the L_1 edge is uncertain by a factor of 2 (Weissler, private communication).

It is seen that the exchange theory gives reasonable results for the absolute magnitude of the cross section but does not give such satisfactory results for the shape of the curve. Comparison between the exchange and non-exchange calculations emphasizes the sensitivity of the calculated results to details of the wave functions. It has been remarked previously (Seaton 1951a) that the agreement between the exchange and non-exchange results at the threshold must be regarded as largely fortuitous. Bearing in mind both the experimental uncertainties and also the error arising from the use of the kp radial function for Na, the calculated magnitude of the L_1 discontinuity may be regarded as being in reasonable agreement with the experimental value.

It is possible that polarization effects are important in determining the exact behaviour of the cross section close to the threshold. In this connection it is of interest to note that Mott and Massey (1949) suggest that neglect of polarization is probably responsible for a comparatively minor discrepancy between exchange theory and experiment for the scattering of very slow electrons by He. For the higher energies it is probable that the error arising from the use of a coulomb kd wave is greater than at lower energies; as the wave function becomes more compact potential and exchange distortion might be expected to become more important. It may be noted that the less satisfactory agreement between theory and observation at the higher energies does not arise from the approximations used for $a_v(2p \rightarrow ks)$; if the true value of $a_v(2p \rightarrow ks)$ were smaller than the estimated value the calculated curve would not be altered significantly, while if it were greater the discrepancy between theory and experiment would be increased.

ACKNOWLEDGMENTS

The author is indebted to Professor G. L. Weissler and to Professor R. W. Ditchburn for their comments on the experimental results, and to Professor Ditchburn and Dr. G. V. Marr for permission to refer to their experimental results in advance of publication.

REFERENCES

- BATES, D. R., 1939, *Mon. Not. R. Astr. Soc.*, **100**, 25 ; 1946 a, *Ibid.*, **106**, 423; 1946 b, *Ibid.*, **106**, 432.
DITCHBURN, R. W., JUTSUM, P. J., and MARR, G. V., 1953, *Proc. Roy. Soc. A*, **219**, 89.
LEE, Po, and WEISSLER, G. L., 1953, *Proc. Roy. Soc. A*, **220**, 71.
MOTT, N. F., and MASSEY, H. S. W., 1949, *Theory of Atomic Collisions*, 2nd Edn (Oxford : Clarendon Press), p. 219.
SEATON, M. J., 1951 a, *Proc. Roy. Soc. A*, **208**, 408; 1951 b, *Ibid.*, **208**, 418.

Emission of Electron-Positron Pairs from Light Nuclei

III : γ -Transitions in the Reaction $^{15}\text{N}(p, \gamma)^{16}\text{O}$

By G. GOLDRING

Imperial College of Science and Technology, London

Communicated by S. Devons; MS. received 15th April 1954 and in amended form 11th June 1954

Abstract. In two recent papers by the author in cooperation with Devons and with Lindsay, investigations of internally produced pairs in various nuclear reactions in solid targets have been reported. In this paper an apparatus is described for the investigation of internal pairs produced in a ^{15}N gas target by proton bombardment. A search was made for a cascade transition from the 13.05 mev level in ^{16}O through the 6.06 mev level to the ground state, but no indication for such a reaction could be found.

§ 1. INTRODUCTION

THE ground state of the ^{16}O nucleus, and the first excited state (at 6.06 mev excitation energy) have the same angular momentum, the same parity and the same isotopic spin (0^+ and $T=0$) (Hornyak *et al.* 1940); we therefore expect all nuclear reactions leading to the ground state to be accompanied, where energetically possible, by a similar reaction leading to the first excited state. A study of the branching ratios of related reactions of this type is of interest because it furnishes some information on the relation of the wave functions for the two states. The analysis is most straightforward for electromagnetic transitions where the dependence of emission probability on quantum energy is well known. In the following an experiment will be described in which an attempt is made to measure the relative probabilities of the γ -transitions to the ground state of ^{16}O and to the 6.06 mev state, from the resonance level excited in the reaction $^{15}\text{N}(p, \gamma)^{16}\text{O}$ with protons of 1.05 mev energy.

At this proton energy, in addition to the proton capture γ -transition (13.05 mev) to the ground state of ^{16}O , much more intense γ -radiation of 4.47 mev energy is produced by the process $^{15}\text{N}(p, \alpha)^{12}\text{C}^*$. For the neighbouring, sharper, resonance levels at proton energies of 0.898 and 1.21 mev, only this latter γ -radiation from $^{12}\text{C}^*$ is present. (Details of the resonance levels are shown in the table which is compiled from the results of Shardt, Fowler and Lauritsen (1952).)

E_R (Mev)	E_0 (Mev)	Γ (kev)	$Y(4.47)$	$Y(13.05)$
0.898	12.95	2.2	11.3	
1.05	13.05	150	16.7	1
1.21	13.24	22.5	55	

E_R is the energy of the bombarding protons, E_0 is the excitation energy of the ^{16}O compound nucleus, Γ is the total width of the level, $Y(4.47)$, $Y(13.05)$ are the numbers of quanta emitted from a thick target per incident proton, arbitrarily normalized.

At all three resonances, the γ -radiation will be accompanied by internal conversion electron-positron pairs, and if, in addition to the direct 13.05 mev γ -transition, a cascade transition through the 6.06 mev level of ^{16}O occurs,

then there will be an additional contribution to the pairs from the monopole transition ($0, + \rightarrow 0, +$) from the 6.06 Mev to the ground state of ^{16}O .

The small value of the conversion coefficient for pair creation in γ -transitions, together with the characteristic angular correlation of the monopole pairs (Devons, Goldring and Lindsey 1954), makes the detection of the latter a very sensitive method of measuring the preceding γ -transition. In particular, if quite a small fraction of the transitions from the 1.05 Mev resonance are via the 6.06 Mev level of ^{16}O , then the angular correlation of the pairs at this resonance will be markedly different from that at the other two resonances. In fact, as described below, no appreciable difference was found, which enables one to place an upper limit to the relative number of γ -transitions, from the 1.05 Mev resonance, to the ground state and 6.06 Mev levels of ^{16}O .

§ 2. APPARATUS

The electron-positron detectors were two electron counter telescopes set in coincidence. Nitrogen gas enriched to 67% in ^{15}N was used as a target and bombarded through a mica window 0.7 mg cm^{-2} thick. The target assembly is shown in figure 1. The wall thickness of the tube containing the ^{15}N was 0.003 inch in the region near the target, A. In order to avoid radiations from Al

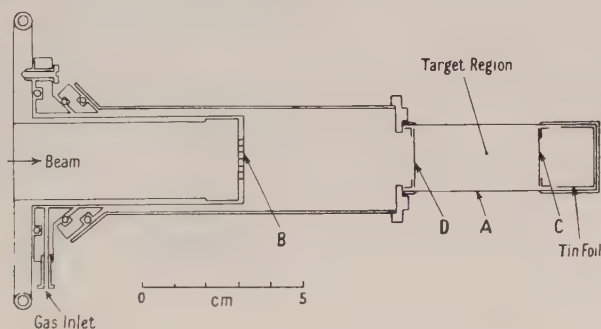


Figure 1.

bombarded by protons the window holder was copper plated, and the rear wall of the target chamber was lined with tin foil. Proton bombardment of both copper and tin gave rise to soft x-rays which were recorded in the electron counters. These counts were eliminated by placing tin foil absorbers of 25 mg cm^{-2} over the front counters, and of 12 mg cm^{-2} over the rear counters. The counters were arranged with one telescope fixed with respect to the target, and the other one could be rotated about an axis coinciding with the axis of the beam. The axes of both telescopes were in the plane through the centre of the target chamber perpendicular to the beam.

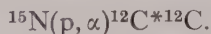
§ 3. EXPERIMENTAL PROCEDURE

As a preliminary check, a CaF_2 target evaporated on Al foil 0.2 mg cm^{-2} thick, was placed at the centre of the target chamber, and pairs were produced by the reaction $^{19}\text{F}(p, \alpha\pi)^{16}\text{O}$, with proton energy 840 keV. The angular correlation of the pair emission was found to be $1 + 0.85 \cos \theta^\dagger$. The calculated correlation for the geometry used is $1 + 0.96 \cos \theta$; the difference was interpreted

† Similar results were obtained by Devons and Lindsey (1949), using the same general arrangement.

as due to scattering. This amount of scattering was not considered excessive for the present measurements.

In order to obtain enough yield from the broad 1.05 mev level it was desirable to have the target as thick and as concentrated in space as possible, i.e. a high gas pressure; on the other hand care must be taken to avoid the 0.898 mev and the 1.21 mev levels which give rise to other γ -radiations from the reaction



This was accomplished as follows: a mica absorber 1 mg cm^{-2} thick was placed at the position C (figure 1). When the 1.05 mev level was investigated, the proton energy and the gas pressure (about 5 cm) were adjusted so that the 1.05 mev voltage region would be at the centre of the target chamber, the 0.898 mev region well inside the mica absorber, and the 1.21 mev region inside the mica window, B. An additional absorber of Dutch metal, 0.3 mg cm^{-2} thick, was inserted in position D in order to concentrate the effective target region towards the centre of the target chamber, and so reduce the radiation from remote parts.

The excitation curve for electrons and positrons, measured in a single counter-telescope, is shown in figure 2, curve 1. The lower peak appears double because,

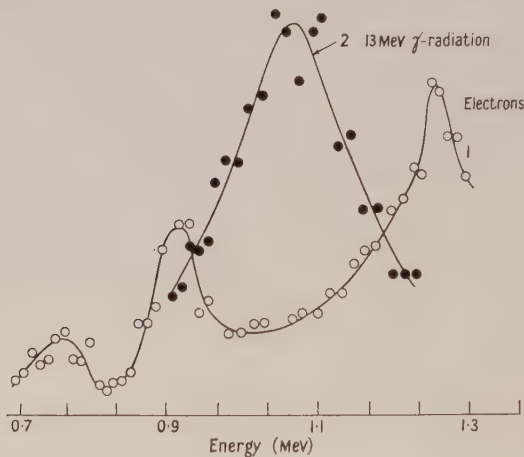


Figure 2.

as the proton energy is increased the level is excited first in the region between the window B and the absorber D and then in the central region of the chamber. The difference in height between the two maxima is interpreted as being due to the fact that the field of view of the counter-telescopes is limited to a region in the neighbourhood of its axis. This also permits us to assume that most of the externally produced electrons recorded by the counter-telescopes originate in either the wall of the target chamber or in the front wall of the front counter. On this assumption one would expect the contribution from externally produced pairs to the total number of counts in the telescope to be only of the order of 10%, most of the counts being due to internal pairs. This was verified in the following way: a copper absorber 0.2 mm thick was inserted in front of the telescope, and the number of telescope counts was found to be slightly reduced. Had the counts been due to external electrons, they should have increased about threefold.

The width of the two lower peaks in curve 1 is due to straggling of the protons in the gas, the window and the Dutch metal absorber, and also to the non-uniformity of the window.

The position of the 1.05 mev level cannot be distinguished on curve 1. To locate this level, a lead radiator was placed in front of one of the telescopes and a brass absorber 2mm thick (enough to stop the electrons produced by the 4.47 mev radiation) was inserted between the front and the rear counters. Curve 2 of figure 2, gives the number of coincidence counts per single count in the front counter; it follows very closely the excitation curve for the 13.05 mev radiation.

§ 4. MEASUREMENTS

The expected monopole pairs from the 6.06 mev level in ^{16}O must be discriminated against the background of conversion pairs from the 4.47 mev level in ^{12}C . A fairly good approximation to the angular correlations in both processes is obtained by neglecting the rest mass of the electron in comparison with the transition energy. The angular correlation in the E2 transition in ^{12}C is given in this approximation by Goldring (1953, §3):

$$f_{\text{E}2}(\theta) = \frac{2}{3u} + \frac{1}{90} - \frac{8}{90}u, \quad u = 1 - \cos \theta,$$

and the monopole pair angular correlation is given by $f_0(\theta) = 2 - u$. The ratio $f_0/f_{\text{E}2}$ has a flat maximum at $u = 4 - \sqrt{8}$. At $u = 1$ ($\theta = \pi/2$) the value of $f_0/f_{\text{E}2}$ is not much different from the maximum value, whereas the total yield of pairs is greater, and the discrimination against scattered electrons considerably better than at $u = 4 - \sqrt{8}$. The telescopes were therefore set at $\theta = \pi/2$ and the number of coincidence counts per single telescope count (denoted by η) was measured at the 0.898 mev level and at the 1.05 mev level, and also at the 840 kev level in the reaction $^{19}\text{F}(\text{p}, \alpha\pi)^{16}\text{O}$, with the CaF_2 target described above. The coincidence counts were corrected for random coincidences and for background counts, determined by replacing the heavy nitrogen with air. The results, arbitrarily normalized, were:

$$\left. \begin{array}{l} \text{for the 0.898 mev level } \eta_1 = 1 \pm 0.15 \\ \text{for the 1.05 mev level } \eta_2 = 1.1 \pm 0.15 \\ \text{from a CaF}_2 \text{ target } \eta_3 = 5.6 \pm 0.2 \end{array} \right\} \dots\dots(1)$$

The accuracy of the measurements was limited by the fact that a considerable fraction of the background was due to external electrical disturbances and could not be established accurately. The location of the two levels by means of the curves in figure 2 is not very accurate, and the uncertainty from this source has been incorporated in the errors in (1). Another source of error derives from the fact that whereas the radiations from the 0.898 mev level and the $^{19}\text{F} + \text{p}$ level originate in a sharply defined region, the 1.05 mev level is spread almost uniformly over the length of the target chamber between the absorbers C and D (figure 1). This error is, however, relatively unimportant.

§ 5. INTERPRETATION

The relative coincidence rates η_1, η_3 in (1) refer to pair emission from the 4.47 mev level in ^{12}C and from the 6.06 mev level in ^{16}O respectively. For η_2 we have:

$$\eta_2 = \frac{\eta_1\epsilon + \eta_3\chi\delta}{\epsilon + \chi\delta}, \quad \dots\dots(2)$$

where ϵ is the pair conversion coefficient for the 4.47 meV γ -radiation, χ is the ratio of the number of 13.05 meV quanta to the number of 4.47 meV quanta emitted at the ^{16}O resonance level, and δ is the branching ratio for the cascade transition through the 6.06 meV level in ^{16}O and the direct transition to the ground state. The small contribution of conversion pairs from the direct 13.05 meV γ -transition or competing cascade γ -transitions, and also from the 13.05–6.06 meV γ -transition has been ignored in (2).

For the branching ratio δ we get:

$$\delta = \frac{\epsilon}{\chi} \frac{\eta_2 - \eta_1}{\eta_3 - \eta_2} \dots\dots (3)$$

From (1) we see that $\eta_2 - \eta_1$ is not larger than approximately 0.3. Using the values $\epsilon = 1.3 \times 10^{-3}$ (Rose 1949), $\chi = 0.07$ (cf. the table above), we get from (2) and (3) $\delta < 1.3 \times 10^{-3}$.

The dependence of the transition probability $T(l)$ for electromagnetic 2^l -pole radiation, on the transition energy $\hbar\omega$ is given by $T(l) \sim (\hbar\omega)^{2l+1} M$ (Blatt and Weisskopf 1952, p. 595) where M is the square of the absolute value of the nuclear matrix element as defined by Blatt and Weisskopf. For the transitions under investigation $\omega_1/\omega_2 = 7.15/13.05 = 0.55$ so that

$M_1/M_2 < 0.01$ if the transitions are dipole radiations,

$M_1/M_2 < 0.025$ if the transitions are quadrupole radiations.

It is extremely improbable that the transitions are of higher order of forbiddenness than E2, because the branching ratio for γ and α emission is large in the 13.05 meV level as compared with the 12.51 meV, 12.95 meV levels which have been established as 2 (Kraus *et al.* 1953), and which therefore decay by M2 γ -emission.

It should be noted that according to the single particle model $M_1/M_2 \sim 1$ (Blatt and Weisskopf 1952, p. 627), whereas according to the liquid drop model, $M_1/M_2 \sim \omega_2/\omega_1 \sim 2$ (Blatt and Weisskopf 1952, p. 628), which makes the discrepancy even larger.

ACKNOWLEDGMENTS

I would like to express my deep gratitude to Professor S. Devons for suggesting this problem, and for his continual interest in this work. My thanks are also due to the Hebrew University for a research grant which made this work possible.

REFERENCES

- BLATT, J. M., and WEISSKOPF, V. F., 1952, *Theoretical Nuclear Physics* (New York: John Wiley.)
 DEVONS, S., and GOLDRING, G., 1954, *Proc. Phys. Soc. A*, **67**, 413.
 DEVONS, S., GOLDRING, G., and LINDSEY, G. R., 1954, *Proc. Phys. Soc. A*, **67**, 134.
 DEVONS, S., and LINDSEY, G. R., 1949, *Nature, Lond.*, **164**, 539.
 GOLDRING, G., 1953, *Proc. Phys. Soc. A*, **66**, 341.
 HORNYAK, W. F., LAURITSEN, T., MORRISON, P., and FOWLER, W. A., 1950, *Rev. Mod. Phys.*, **22**, 291.
 KRAUS, A. A., FRENCH, A. P., FOWLER, W. A., and LAURITSEN, C. C., 1953, *Phys. Rev.*, **89**, 299.
 ROSE, M. E., 1949, *Phys. Rev.*, **76**, 678.
 SHARDT, A., FOWLER, W. A., and LAURITSEN, C. C., 1952, *Phys. Rev.*, **86**, 527.

The Absorption Spectrum of Bismuth Selenide and Bismuth Telluride in the Region 2900–2200 Å

By C. B. SHARMA

Lucknow University, Lucknow, India

MS. received 19th March 1954

Abstract. Several new band systems have been observed in the absorption spectra of BiSe and BiTe molecules in the vapour state at high temperatures (1000° to 1300°C). All the band systems lie in the quartz ultra-violet region. The band-heads have been analysed and the following constants obtained :

Molecule System	Å	ν_0	ω_0''	$\omega_0''x_0''$	ω_0'	$\omega_0'x_0'$
BiSe I	2900–2700	35617.5	264.7	0.40	304.00	2.00
BiSe II	2350–2200	44425	264.7	0.40	316.00	2.00
BiTe I	2942–2814	—	208.5	0.52	—	—
BiTe II	2454–2382	—	208.5	0.52	—	—
BiTe III	2390–2315	42870	208.5	0.52	164.40	0.40
BiTe IV	2374–2279	43116	208.5	0.52	263.00	0.96
BiTe V	2276–2200	—	208.5	0.52	—	—

§ 1. INTRODUCTION

IN continuation of his previous work on SbS, SbSe and SbTe molecules the author (1953) has studied the absorption spectra of BiSe and BiTe molecules in the vapour state at high temperatures. No previous data are available on these molecules. Several new band systems have been observed and analysed.

In some of the measurements the absorption bands of the diatomic molecule Bi_2 were also observed but they were accounted for since they are well known from the studies made by Nakamura and Shidei (1935), Almy and Sparks (1933). Fortunately they do not interfere with the present measurements.

§ 2. EXPERIMENTAL

The experimental arrangement was the same as described by the author in his paper on SbSe and SbTe molecules. A mixture of equal amounts of pure bismuth and selenium or tellurium was kept in a silica tube which was placed in a graphite vacuum furnace. The band systems were well developed at about 1000–1200°C. No rotational structure was resolved on a medium quartz spectrograph.

§ 3. RESULTS

3.1. BiSe Molecule

Two new band systems have been observed and the band-heads measured. Both the systems are degraded to the violet.

System I.

System I lies in the region $\lambda = 2891\text{--}2712\text{ Å}$. The wave numbers fit well with the formula

$$\nu (\text{cm}^{-1}) = 35617.5 + (304.0 u' - 2.0 u'^2) - (264.7 u'' - 0.4 u''^2),$$

where $u = v + \frac{1}{2}$.

Table 1

λ (Å)	Int.	v'	v''	λ (Å)	Int.	v'	v''
2890.2	2	0	4	2800.0	7	2	2
2868.8	5	0	3	2782.0	10	1	0
2865.4	5	1	4	2779.5	7	2	1
2848.5	8	0	2	2759.3	10	2	0
2844.3	3	1	3	2757.2	4	3	1
2826.3	10	0	1	2737.3	3	3	0
2823.2	5	1	2	2735.3	9	4	1
2805.2	9	0	0	2712.8	7	6	2
2802.6	6	1	1				

System II.

System II lies in the region $\lambda = 2318\text{--}2200$ Å. The wave numbers fit well with the formula

$$\nu (\text{cm}^{-1}) = 44425 + (316.0 u' - 2.0 u'^2) - (264.7 u'' - 0.4 u''^2)$$

where $u = v + \frac{1}{2}$.

Table 2

λ (Å)	Int.	v'	v''	λ (Å)	Int.	v'	v''
2317.5	3	0	5	2240.3	6	4	4
2303.6	3	0	4	2233.2	10	1	0
2289.7	5	0	3	2230.9	8	2	1
2275.8	9	0	2	2229.0	7	3	2
2273.4	5	1	3	2227.2	7	4	3
2262.3	10	0	1	2217.8	8	2	0
2259.8	8	1	2	2216.0	8	3	1
2255.5	4	3	4	2214.2	8	4	2
2249.0	10	0	0	2212.6	6	5	3
2246.7	7	1	1	2203.2	3	3	0
2244.2	8	2	2	2201.3	6	4	1
2242.2	6	3	3				

3.2. *BiTe Molecule*

Five new band systems have been observed which are all degraded to the violet. Systems II, III and IV overlap. In systems I, II and V the number of bands is small and hence no satisfactory analysis could be made.

System I.

This system lies in the region $\lambda = 2942\text{--}2814$ Å. The band-heads with their intensities are 2944.0 (7), 2926.1 (8), 2908.8 (8), 2891.8 (7), 2875.0 (10), 2871.4 (9), 2854.5 (10), 2835.5 (9), 2817.6 (?).

System II.

System II lies in the region $\lambda = 2454\text{--}2382$ Å.

Table 3

λ (Å)	Int.	v'	v''	λ (Å)	Int.	v'	v''
2453.5	3	0	6	2405.6	10	0	2
2441.2	4	0	5	2393.8	10	0	1
2429.3	7	0	4	2382.1	9	0	0
2417.4	8	0	3				

System III.

System III lies in the region $\lambda = 2390\text{--}2315 \text{ \AA}$. The wave numbers fit well with the formula

$$\nu(\text{cm}^{-1}) = 42870 + (164.4 u' - 0.4 u'^2) - (208.5 u'' - 0.52 u''^2)$$

where $u = v + \frac{1}{2}$.

Table 4

$\lambda (\text{\AA})$	Int.	v'	v''	$\lambda (\text{\AA})$	Int.	v'	v''
2390.0	3	0	5	2344.5	7	0	1
2378.5	5	0	4	2335.5	8	1	1
2367.2	6	0	3	2333.2	4	0	0
2355.9	7	0	2	2324.3	8	1	0
2348.7	7	2	3	2315.5	3	2	0

System IV.

System IV lies in the region $\lambda = 2374\text{--}2279 \text{ \AA}$. The band-heads fit well with the formula

$$\nu(\text{cm}^{-1}) = 43116 + (263.0 u' - 0.96 u'^2) - (208.5 u'' - 0.52 u''^2)$$

where $u = v + \frac{1}{2}$.

Table 5

$\lambda (\text{\AA})$	Int.	v'	v''	$\lambda (\text{\AA})$	Int.	v'	v''
2373.3	5	0	5	2311.6	10	2	2
2362.3	6	0	4	2309.0	10	3	3
2350.8	7	0	3	2306.3	3	4	4
2339.8	8	0	2	2303.1	10	1	0
2336.5	8	1	3	2300.6	10	2	1
2333.7	4	2	4	2297.9	8	3	2
2331.0	4	3	5	2295.3	8	4	3
2328.4	4	0	1	2289.4	9	2	0
2325.3	8	1	2	2287.1	8	3	1
2322.6	6	2	3	2284.5	7	4	2
2319.9	8	3	4	2281.8	5	5	3
2317.3	3	0	0	2279.3	4	6	4
2314.2	8	1	1				

System V.

System V lies in the region $\lambda = 2276\text{--}2208 \text{ \AA}$. The number of bands is too small for complete analysis. These wavelengths and intensities are 2276.5 (5), 2264.4 (3), 2250.9 (4), 2244.0 (7), 2235.0 (10), 2228.4 (7), 2218.6 (6), 2208.4 (6).

§ 4. DISCUSSION

The conditions of formations of these molecules appear to be very critical. In absorption the bands appear at about 800°C but are best photographed between 1000 and 1200°C .

Considering the data for PbSe, PbTe and Bi₂ molecules it is expected that the value of ω_e'' in the ground state for BiSe and BiTe molecules should be of the same order. This is confirmed by the results obtained here.

Jevons (1944) discussed the trends of coefficients of IV–VI groups and V–V group molecules and showed a two-fold parallelism between the two groups. The data for V–VI groups molecules also show similar trends. ω_e'' shows a decrease,

as expected, with increasing number of electrons. $\omega_e''\mu^{1/2}$ which governs the force constant remains almost constant for the BiO, BiS, BiSe and BiTe molecules.

Molecule	Number of electrons	ω_e''	$\omega_e''\mu^{1/2} \times 10^{-9}$
BiO	91	695.9	2.5
BiS	99	386.0	2.6
BiSe	117	264.7	2.6
BiTe	135	208.5	2.4

ACKNOWLEDGMENTS

I take pleasure in expressing my thanks to Sir K. S. Krishnan for his guidance and encouragement and to Dr. D. Sharma for his helpful suggestions.

REFERENCES

- ALMY, G. M., and SPARKS, F. M., 1933, *Phys. Rev.*, **44**, 365.
 JEVONS, W., 1944, *Proc. Phys. Soc. A*, **56**, 211.
 NAKAMURA, G., SHIDEI, T., 1935, *Jap. J. Phys.*, **10**, 11.
 SHARMA, C. B., 1953, *Proc. Phys. Soc. A*, **66**, 1109.
 SUR, P. K., 1951, *Indian J. Phys.*, **25**, 65.

RESEARCH NOTES

Vibrational Transition Probabilities of Diatomic Molecules: III

BY P. A. FRASER†

Department of Physics, University of Western Ontario, London, Canada

Communicated by R. W. Nicholls; MS. received 28th June 1954

IN two previous communications (Fraser and Jarman 1953, Jarman and Fraser 1953, to be referred to as I and II respectively) an approximate analytic method of evaluating vibrational overlap integrals was presented. It will be recalled that the basis of the approximation was the replacement of α_1 and α_2 of the two Morse potentials each by some mean α , analytic evaluation of the overlaps then following. Parameters depending on α_1 and α_2 were adjusted to correspond to the new α . When the changes in α_1 and α_2 were small, any compensation to improve the overlap integrals was rightly ignored, and when the changes were large, the ' r_e -shift' method was introduced in II to provide a compensation, with considerable success.

The purpose of this note is to present for these latter cases a more rational improvement based on first-order perturbation theory.

The following nomenclature will be used throughout: 'new potentials' for the adjusted potentials; 'original potentials' (meaning clear); 'approximate overlap integrals', written $(v', v'')_0$; and 'improved overlap integrals' (v', v'') for overlap integrals presumably closer to those of wave functions in the original potentials than are the approximate overlap integrals. Notation is otherwise the same as in I.

It is possible to write

$$U_i(r - r_{ei}) = U'_i(r - r_{ei}) + \delta U_i(r - r_{ei}), \quad i = 1, 2 \quad \dots\dots(1)$$

where U_i are the Morse potentials and U'_i are the new potentials. δU_i may be considered as a perturbation on U'_i giving U_i , and through perturbation theory it is possible to express the wave functions in U_i in terms of the wave functions in U'_i . This is a convenient possibility, since overlap integrals of wave functions in U'_1 and U'_2 are amenable to analytic integration. The difference of the original and new potentials was calculated to the first non-vanishing term, and found to be

$$\delta U_i = D'_i \frac{(\alpha - \alpha_i)}{\alpha} x_i^3, \quad i = 1, 2 \quad \dots\dots(2)$$

where D'_i is the dissociation energy of the potential U'_i , $D'_i = (\omega_e)_i^2/4(\omega_e x_e)_i$, and where $x_i = \alpha(r - r_{ei})$.

To apply perturbation formulae matrix elements of x_i^3 are required. They are not available in the literature; however, matrix elements of x_i are available (Infeld and Hull 1951, Herman and Shuler 1953). Since the matrix elements of x_i^3 were required to be known but approximately, they were evaluated from the 'cube' of the x_i matrix, terms of order $K_i'^{-3/2}$ only being retained, where

† Now at Department of Physics, University College, London.

$K'_i = (\omega_e)_i / (\omega_e x_e)_i'$. This is the lowest order term appearing in any matrix element of x_i^3 . To this order the only non-vanishing matrix elements are $(v | x_i^3 | v-3)$, $(v | x_i^3 | v-1)$, $(v | x_i^3 | v+1)$, and $(v | x_i^3 | v+3)$, where v is the vibrational quantum number of the v th level in potential U_i' . For example, to this order

$$(v | x_i^3 | v-3) = (v | x_i | v-1)(v-1 | x_i | v-2)(v-2 | x_i | v-3).$$

Using the approximation

$$(v | x_i | v-1) \simeq \left[\frac{v}{K'_i - v} \right]^{1/2} \quad \dots\dots(3)$$

it is easily found that

$$(v | x_i^3 | v-3) \simeq \left[\frac{v(v-1)(v-2)}{(K'_i - v)^3} \right]^{1/2}, \quad \dots\dots(4)$$

$$(v | x_i^3 | v-1) \simeq 3 \left[\frac{v}{(K'_i - v)} \right]^{3/2} \quad \dots\dots(5)$$

with obvious changes for the other two matrix elements.

Finally, using the formulae of first-order perturbation theory and making a zeroth approximation to the energy difference denominators (that is, dropping the quadratic term), the following is obtained for the improved overlap integral:

$$\begin{aligned} (v', v'') = (v', v'')_0 &+ \frac{(\alpha - \alpha_1)}{\alpha} \frac{K_1}{4} \left\{ \frac{1}{3} \left[\frac{v'(v'-1)(v'-2)}{(K_1 - v')^3} \right]^{1/2} (v'-3, v'')_0 \right. \\ &+ 3 \left[\frac{v'}{K_1 - v'} \right]^{3/2} (v'-1, v'')_0 - 3 \left[\frac{v'+1}{K_1 - v' - 1} \right]^{3/2} (v'+1, v'')_0 \\ &- \left. \frac{1}{3} \left[\frac{(v'+3)(v'+2)(v'+1)}{(K_1 - v' - 3)^3} \right]^{1/2} (v'+3, v'')_0 \right\} \\ &+ \frac{(\alpha - \alpha_2)}{\alpha} \frac{K_2}{4} \left\{ \text{as brace above with } (K_1 \rightarrow K_2), \right. \\ &\left. v' \rightarrow v'', (v'-3, v'')_0 \rightarrow (v', v''-3)_0, \text{ etc.} \right\}. \quad \dots\dots(6) \end{aligned}$$

The K_1 and K_2 in the above are the *adjusted* values, the prime having been dropped to correspond to the final notation of I. The improved overlap integral is thus given by a linear combination of approximate overlap integrals which are obtained by the methods of I and the second part of II. In practice it is often possible, and proper, to neglect the outer terms in the braces, bearing in mind that this is an approximate calculation. They should be retained only when the inner terms give effectively nothing. Order of magnitude calculation with neglected terms show that the approximations made to δU_i and to the matrix elements are such that the results are good to quantum number 6 for $|\alpha - \alpha_i|/\alpha$ up to 10%. The formula, incidentally, gives an indication of the accuracy of the approximate method of I and II for any particular case.

It can never be emphasized too strongly that one must be thoroughly consistent about phases of the wave functions in applications of perturbation theory. If the formulae of I and II for approximate overlap integrals are used, there will be no trouble—the factors $(-1)^{v'+v''}$ must be included. The matrix elements of x_i^3 were calculated with the same phase convention.

The method has been successfully applied to nine bands of the CN violet system and the results shown in the table. Values of the overlaps for this system calculated numerically were available for comparison since they were used in the justification of the ' r_e -shift' method of II. The molecular constants and mean α used are as in table 1 of II. The method is being used at this laboratory

to make any necessary improvements to tables of overlaps calculated by the method of I.

CN, $B^2\Sigma^+ \rightarrow X^2\Sigma^+$ (Violet) Vibrational Overlap Integrals

$v' \backslash v''$	0	1	2
0	0.95 ₅	-0.28 ₄	0.08 ₆
	0.95 ₉	-0.27 ₃	0.07 ₂
	(0.95 ₈)	(-0.27 ₃)	(0.07 ₄)
1	0.29 ₃	0.86 ₇	-0.37 ₈
	0.28 ₁	0.88 ₇	-0.34 ₉
	(0.28 ₁)	(0.88 ₇)	(-0.34 ₇)
2	0.04 ₂	0.40 ₃	0.78 ₂
	0.03 ₃	0.37 ₂	0.83 ₃
	(0.03 ₄)	(0.37 ₀)	(0.83 ₁)

The three lines in each group indicate respectively: approximate overlap integral; improved overlap integral; overlap integral from numerical integration.

The research reported in this note has been sponsored by the Geophysics Research Directorate, Air Force Cambridge Research Centre, Air Research and Development Command, under Contract No. AF 19(122)-470.

REFERENCES

- FRASER, P. A., and JARMAN, W. R., 1953, *Proc. Phys. Soc. A*, **66**, 1145.
 HERMAN, R. C., and SHULER, K. E., 1953, *J. Chem. Phys.*, **21**, 373.
 INFELD, L., and HULL, T. E., 1951, *Rev. Mod. Phys.*, **23**, 21.
 JARMAN, W. R., and FRASER, P. A., 1953, *Proc. Phys. Soc. A*, **66**, 1153.

The Detection of Electron Pairs in a Cloud Chamber with Internal Counters

By P. J. CAMPION† AND W. T. DAVIES

The Clarendon Laboratory, Oxford

MS. received 23rd June 1954

WHEN studying, by means of a random sampling cloud chamber, the emission of electron pairs from a solid source which emits in addition single electrons and γ -rays, it is frequently difficult and sometimes impossible to decide whether paired tracks constitute a true electron pair or are associated by chance.

The difficulty is more acute than for the case of pair production in gases by γ -rays when the origin of the pair is usually clearly visible. Under these circumstances the main problem is to distinguish between true pairs and cases of large-angle single scattering of electrons. This can be satisfactorily achieved by using sufficiently well collimated beams of γ -rays.

With solid sources, on the other hand, the origin of the tracks may be unobservable because of light scattered from droplets condensed on the concentration of ions in the neighbourhood of the source; or, if observable, it may be common to several tracks.

† Now at Atomic Energy of Canada, Ltd., Chalk River, Ontario, Canada.

A method of indicating the tracks of contemporaneous particles is thus a desirable feature of cloud chamber technique.

Hodson, Loria and Ryder (1950) in a comprehensive paper have shown that the expansion of a Wilson chamber can be controlled by the discharge of an internal proportional counter forming part of the active volume of the chamber and operating in coincidence with externally placed counters. We have extended this technique to the control of the expansion by the coincident discharge of two internal proportional counters so that if, for example, a source emitting electron pairs is placed in a suitable position relative to the counters the expansion can be induced by paired particles.

The essential parts of the counter system are visible in the photograph (Plate).

A and A' denote the wire anodes which are of 42 s.w.g. platinum. A horizontal, earthed brass rod of diameter approximately 1.5 mm is mounted 1 cm above and below each wire and serves to limit the vertical depth of the sensitive region of the counter. A 3 mm thick brass septum S, the full depth of the chamber, effectively screens one counter electrically from the other and also reduces the chance of both counters being traversed by a single particle. There is a gap of 8.5 cm between the free end of S and the wall of the chamber at the point where electrons enter through a thin mica window W. This allows the source to be placed close to the window without restricting unduly the solid angle within which electron pairs may be observed to trigger the chamber.

In operation the chamber is taken through two or three cleaning cycles during which there is no voltage on the counter wires. When cleaning is complete and conditions are thermally steady a voltage sufficient to operate the counters in the proportional region is applied. When a coincident discharge occurs a pulse generator removes this voltage within 5 μ sec. The expansion itself occurs about 10 msec later.

The photograph also shows a 4.45 mev pair from $^{12}\text{C}^*$ produced by the reaction $^9\text{Be}(\alpha, n)^{12}\text{C}^*$ in a source placed outside the chamber.

The particles triggering the chamber are clearly indicated by droplets condensed upon the beads of ionization X and X' which surround the intersection of the horizontal projection of the tracks with the counter wires. These beads arise from the positive ions created in the discharge.

The sign of the particles is indicated and their momentum determined by applying an axial magnetic field of 550 gauss with the usual arrangement of Helmholtz coils.

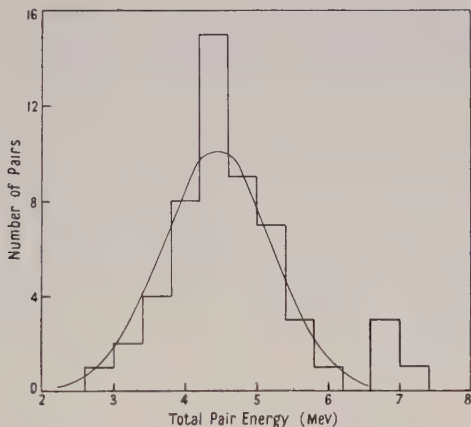
Thus 1 is the positron and 2 the electron of the pair. A second positron, 3, has clearly traversed the chamber after removal of the counter voltage and may have been associated with the faintly visible electron, 4.

The unambiguous identification of the pair particles removes a further drawback of the cloud chamber method as applied to the study of pair production. Previously, it has been customary to use as a condition of acceptance of the tracks as a genuine pair, the agreement, within arbitrarily close limits, of the measured energy with the mean energy of a large number of cases or with the expected energy, where this was known by other methods. This leads to the rejection or false pairing of tracks of particles which have suffered multiple scattering in excess of an arbitrary value.

In a preliminary test of the system we have filled the chamber with a mixture of 5 parts argon and 1 part helium by volume, at a total pressure of about 60 cm Hg,

and used ethyl alcohol as the stabilizing and condensing vapour. The r.m.s. spread in the projected radius of curvature due to multiple scattering is then approximately 20%. To this must be added an error of about 5% in the curvature measurements themselves.

A comparison between measurements on 56 triggered pairs and the distribution to be expected from the same number of 4.45 mev pairs which have undergone multiple scattering in the gas-vapour mixture is given in the figure. The smooth



curve is calculated from Bethe's treatment of multiple scattering curvature (Bethe 1946) taking the average value for the individual track length as 15 cm. We make the simplifying assumption that energy is divided equally between the components of the pair.

It is evident that the spread in measured energy is reasonably well accounted for by the multiple scattering in the tracks and the errors of measurement. Its magnitude makes the interpretation of the four triggered, higher-energy pairs somewhat uncertain. However, their occurrence is in agreement with the previous observations of Davies and Harries (1952) using a randomly operated cloud chamber in which air at about 60 cm Hg was used as filling so that the multiple scattering was appreciably less.

By increasing the magnetic field to 1000 gauss, and replacing the argon filling by a lighter gas at higher pressure, it is hoped to reduce the multiple scattering error to a value comparable with the error in curvature measurement while keeping a sufficient value of ionization density and diffusion coefficient to allow electron tracks to be measured. Modifications to the coils and chamber to permit of this being done are almost complete.

In conclusion we may mention that the yield of pairs from beryllium bombarded by alpha-particles from 80 mc of polonium is 1 in 5 triggered expansions. This may be compared with 1 pair in 20 expansions for a randomly operated chamber and 200 mc of polonium. Discussion of this yield will be given elsewhere.

REFERENCES

- BETHE, H. A., 1946, *Phys. Rev.*, **70**, 821.
DAVIES, W. T., and HARRIES, G. H., 1952, *Proc. Phys. Soc. A*, **65**, 564.
HODSON, A. L., LORIA, A., and RYDER, N. V., 1950, *Phil. Mag.*, **319**, 826.

The Resolving Time of an Internal Counter Controlled Wilson Chamber

BY P. J. CAMPION† AND W. T. DAVIES

The Clarendon Laboratory, Oxford

MS. received 23rd June 1954, and in amended form 16th July 1954

IN the preceding note (Campion and Davies 1954) we have described the use of two internal proportional counters operated in coincidence to detect electron-positron pairs in a cloud chamber. In this note we show that the resolving time of a chamber controlled by one or more internal proportional counters can be considerably shorter than with other methods of control or operation.

To obtain the highest degree of time discrimination in a random sampling Wilson chamber one must limit the sensitive time—i.e. the interval after the expansion during which condensation can occur and the droplets grow to visible size—and arrange that the gas mixture shall have a high diffusion coefficient for ions so that the diffuseness of the tracks of particles traversing the gas before the expansion shall be as marked as possible. It is not feasible, however, to achieve a resolving time of less than about 0.04 sec by these measures. Moreover, any improvement in this direction on the higher values generally used is at the cost of a proportionately decreased yield of experimental data. Decreasing yield also sets a practical limit to a reduction in the proportion of chance associated events by the use of weak sources.

When a Wilson chamber is controlled by counters the selected particles traverse the gas before supersaturation and the resulting tracks are diffuse. When external counters are used (Blackett and Occhialini 1933) or there is an internal ionization chamber (Cohen 1951) the age of a track must be deduced solely from its diffusion breadth, which is proportional to $\sqrt{(D\tau)}$ where D is the diffusion coefficient for ions of the gas filling and τ the time interval between transit of the particle and the onset of supersaturation. Under favourable conditions two non-contemporaneous tracks may be resolved if the ratio f of their widths is about 0.7 (Wilson 1951). If one of the two particles concerned is assumed to trip the counter system the resolving time is clearly $(1/f^2 - f^2)\tau_e$, where τ_e is the delay between triggering and expansion. Taking a value of 0.01 sec for τ_e we find a resolving time of about 0.015 second.

In the case of a chamber controlled by an internal counter working in the proportional region we may study the appearance of the bead of ionization surrounding the counter wire at the triggering point. The radial expansion of the bead in the high field near the counter wire is very much greater than the broadening of a track by diffusion in the same time interval. This method of control should therefore, as was first pointed out by Hodson *et al.* (1950), bring about a considerable reduction in resolving time.

To investigate the resolution obtainable a collimated beam of alpha particles was made to traverse an internal counter consisting of a thin platinum wire as anode and a hexagonal arrangement of wires forming an open cage cathode.

† Now at Atomic Energy of Canada, Ltd., Chalk River, Ontario, Canada.

The arrangement was similar to that described by Hodson *et al.* (1950). The e.h.t. was removed electronically after the receipt of a pulse. The minimum time required for the removal of the e.h.t. was $5\mu\text{sec}$, although this figure was later reduced by circuit modifications. The removal could also be delayed by known times ranging from microseconds to milliseconds.

A series of photographs was taken showing alpha particles triggering the internal proportional counter in which the removal of the e.h.t. was delayed by known amounts, and the results compared with those obtained using the minimum delay possible (i.e. $5\mu\text{sec}$). At $50\mu\text{sec}$ delay the discharge bead had expanded into a ring of diameter sufficient for its hollow nature to be recognized in a photograph by visual inspection. We may take such recognition to be a suitable criterion of resolution. By using microphotometer techniques to detect the expansion of the discharge the resolvable time interval between two discharges could be reduced still further.

As an example we show photographs (a), (b), (c) (see Plate). In (a) the e.h.t. was removed within $5\mu\text{sec}$ and in (b) within $200\mu\text{sec}$. In obtaining these two photographs no special precautions such as reducing the light intensity were taken to enable the two peaks in the horizontal projection of the discharge ring to be more easily distinguished. The radial expansion of the bead is readily apparent. In (c) the delay was only $50\mu\text{sec}$ and the illumination was reduced slightly in order to allow a photometric analysis of the discharge. The expanded nature of the bead is, however, still clearly visible on the negative without use of photometry. A slight asymmetry about the counter wire is due to gas motion during the expansion.

The radial spread of the bead is chiefly determined by the motion of the positive ions during the time interval between passage of the particle and removal of the voltage. It depends to some extent on diffusion and on motion due to self-repulsion during the expansion time of the chamber. Calculation shows that the last factor is insignificant, while a comparison between the bead and the breadth of the α -particle track in photograph (c) indicates that the limit of resolution set by diffusion will be appreciably less than $50\mu\text{sec}$. The above photographs were taken under favourable conditions for resolution which may not occur in a practical application such as the one described in the preceding note. However, even in this case a delay of $200\mu\text{sec}$ may be taken as a conservative figure for visual resolution, an improvement of about 100 times over a randomly operated chamber or one controlled by external counters or internal ionization chambers.

Since the e.h.t. was removed within $5\mu\text{sec}$ of the detection of a coincidence it follows that a particle traversing the counter at a time later than this will not produce a discharge bead. Hence, in the above pair experiment some confusion will arise only when an unassociated particle traverses the chamber in the interval between $200\mu\text{sec}$ before or $5\mu\text{sec}$ after the pair. With the source strength actually employed this was very unlikely and no photograph had to be rejected because of such confusion.

ACKNOWLEDGMENTS

Our thanks are due to Professor Lord Cherwell for his interest in this work, to Dr. A. L. Hodson for supplying us with details of his apparatus, and to the Nuffield Foundation for the award of a Research Fellowship to one of us (P.J.C.).

REFERENCES

- BLACKETT, P. M. S., and OCCHIALINI, G. P. S., 1933, *Proc. Roy. Soc. A*, **139**, 699.
 COHEN, M. J., 1951, *Rev. Sci. Instrum.*, **22**, 966.
 HODSON, A. L., LORIA, A., and RYDER, N. V., 1950, *Phil. Mag.*, **319**, 826.
 WILSON, J. G., 1951, *The Principles of Cloud Chamber Technique* (Cambridge: University Press).

The Reaction ${}^9\text{Be}(d, {}^3\text{He}){}^8\text{Li}$

By M. M. WINN

Department of Physics, University of Birmingham

Communicated by W. E. Burcham; MS. received 29th May 1954

§ 1. INTRODUCTION

THE radioactive nucleus ${}^8\text{Li}$ ($\tau_{1/2} = 0.85$ sec) is easily identified as a reaction product because of its characteristic decay by the emission of high-energy beta particles followed by breakdown of residual ${}^8\text{Be}$ nucleus into two alpha particles. Production of ${}^8\text{Li}$ in the reactions ${}^6\text{Li}(t, p)$, ${}^7\text{Li}(n, \gamma)$, ${}^7\text{Li}(d, p)$, ${}^9\text{Be}(\gamma, p)$ and ${}^{11}\text{B}(n, \alpha)$ (Ajzenberg and Lauritsen 1952) by photodisintegration of boron (Sheline 1952) and by high-energy spallation (Barkas and Tyren 1953) has already been established. Evidence has now been obtained for production of this nucleus in the bombardment of beryllium by 20 mev deuterons. This is ascribed to the ${}^9\text{Be}(d, {}^3\text{He}){}^8\text{Li}$ reaction for which the calculated Q -value is -11.37 ± 0.07 mev, corresponding to a threshold deuteron energy of 13.9 mev.

§ 2. EXPERIMENTAL METHOD

The apparatus is shown in figure 1. 20-mev deuterons from the 60 inch Nuffield cyclotron were extracted into a shielded room. The energy of the deuterons could be varied by interposing aluminium absorber foils in the path of the beam. The stopping power of these foils was calculated from

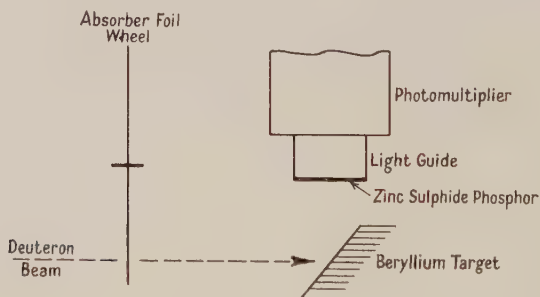


Figure 1. Apparatus.

the range-energy curves given by Aron, Hoffman and Williams (1951). ${}^8\text{Li}$ was detected by observing the decay alpha particles rather than the beta particles because of the high background of gamma radiation near the cyclotron. According to the kinematics of the reaction the nucleus ${}^8\text{Li}$ is projected into a cone whose semi-angle increases from 0° at the threshold to 46° for incident

deuterons of 20 mev. The alpha particles from the ^8Be decay have a most probable energy of about 1.5 mev and can only be observed if the ^8Li nucleus stops in or near the surface of the target; this was therefore held at 45° to the beam. The alpha particles were detected by a zinc sulphide screen viewed through a short light guide by an EMI type 6262 photomultiplier tube. The pulses were fed through an integral discriminator to the recording equipment.

An oscillator of period T seconds controlled the equipment. The cycle of activation and counting was repeated in a regular manner with a period of $16T$ seconds, the beam being on for the first half of this period and the counter for the second half. The beam was switched on and off by applying suitable voltages to the cathode of the cyclotron ion source. The photomultiplier tube was blocked during the 'beam on' period. The counting period was divided into eight equal channels each of T seconds; pulses were displayed in these channels on an oscillograph and photographed. Counts from each channel were accumulated over a number of separate activations.

The apparatus was tested by producing ^8Li from the $^7\text{Li}(d, p)$ reaction using a thin target of lithium oxide on tantalum backing. The channel duration T was set at 0.675 second (on and off times 5.4 sec) and the target bombarded with 3×10^{-9} amp of 19.3 mev deuterons. Delayed alpha particles of 0.88 ± 0.2 sec half-life were observed (figure 2, curve B). A small time independent background remained when the lithium was replaced by a target of stainless steel.

§ 3. RESULTS

A thick beryllium target was bombarded with 4×10^{-9} amp of 19.3 mev deuterons, using a channel duration setting $T=0.360$ second. Heavy particle decay of 0.84 ± 0.04 second half-life was observed; this is shown in figure 2, curve A. A blank decay curve was taken as before by replacing the beryllium by stainless steel. This is shown in figure 2, curve C.

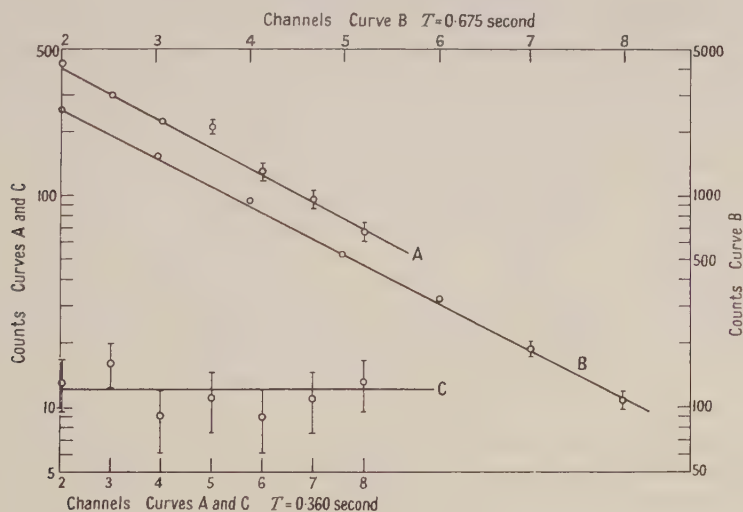


Figure 2. Decay curves for : A, ^8Li from $^9\text{Be}(d, ^3\text{He})$; B, ^8Li from $^7\text{Li}(d, p)$; C, background, deuterons on stainless steel.

A rough yield curve for production of the 0.84-second activity from beryllium bombarded by deuterons was drawn by plotting the total number of counts per coulomb, recorded in the 'beam off' periods, as a function of the deuteron energy. This is given in figure 3 and shows that the observed yield curve is consistent with the calculated threshold. The shape of the curve above the threshold is difficult to interpret, since it is dependent on the proportion of alpha particles from ^8Be counted. This is a function of the incident deuteron energy and cannot be easily calculated.

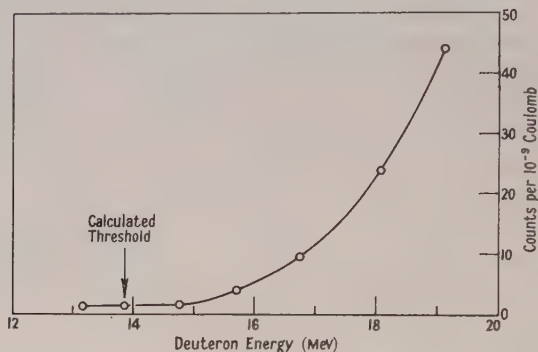


Figure 3. Yield curve.

ACKNOWLEDGMENTS

The author wishes to thank Professor P. B. Moon for his interest and for making the necessary laboratory facilities available for this work. Thanks are due to Professor W. E. Burcham for helpful discussions on many phases of the work, to Mr. W. T. Link who calibrated and mounted the aluminium absorber foils, and to Mr. W. Hardy and the cyclotron staff for the bombardments.

REFERENCES

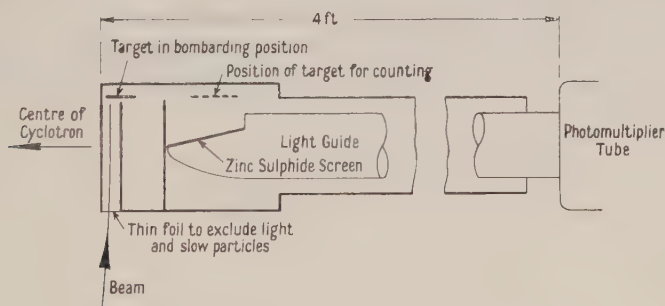
- AJZENBERG, F., and LAURITSEN, T., 1952, *Rev. Mod. Phys.*, **24**, 321.
 ARON, W. A., HOFFMAN, B. G., and WILLIAMS, F. C., 1951, *Range-Energy Curves* (U.S. Atomic Energy Commission Report, AECU-663).
 BARKAS, H. W., and TYREN, H., 1953, *Phys. Rev.*, **89**, 1.
 SHELINE, R. K., 1952, *Phys. Rev.*, **87**, 557.

LETTERS TO THE EDITOR

Short-Lived Alpha Emitters produced by ^3He and Heavy Ion Bombardments

The Birmingham cyclotron produces external beams of deuterons, protons and alpha particles. Internal beams of $^3\text{He}^{2+}$, $^{14}\text{N}^{6+}$ and $^{16}\text{O}^{6+}$ are available; these however cannot at present be extracted efficiently due to the incorrect shimming of the magnet fields used in their acceleration (Fremlin 1953, Walker *et al.* 1954). Reactions caused by the above particles are interesting as they may lead to the production of neutron deficient isotopes, including certain alpha emitters with periods in the 0.1 to 60 second region. This note reports the results of preliminary work on a number of reactions in which the alpha decay of the product nucleus was followed inside the vacuum chamber of the cyclotron.

A special internal probe was constructed (see figure), the inside end of which carried a target holder which could be moved in and out of the beam electro-mechanically. In the 'out' position the target faced a zinc sulphide screen on the end of a four-foot light guide leading to a magnetically shielded photomultiplier tube (type 6260). A master oscillator provided the timing for bombardment and counting. For the first three periods of the oscillator the



Probe for detection of short-lived alpha emitters.

target was moved in and bombarded. On the fourth period it moved in front of the detector and a signal turned off the cyclotron radio-frequency supply. The alpha activity on the target was then counted for six oscillator periods, the pulses from the photomultiplier being passed through a stepping relay switch to six separate scalers. The cycle of ten periods was repeated until a sufficient number of counts from the decay had been recorded. The activities identified are shown in the table. Evidence for the $\text{Li} + ^3\text{He}^{2+}$ reactions is inconclusive due to difficulty of separating 0.6 and 0.85 second activities, (corresponding respectively to ^8B and ^8Li) in the presence of a rather uncertain background of photomultiplier noise pulses.

Target	Bombarding particle	Energy (MeV)	Beam current $\times 10^{-9}$ A	Half-lives observed	Reactions	References and Remarks
Li	d	15	2	0.88 ± 0.05 sec	${}^7\text{Li}(d, p){}^8\text{Li}$	To test apparatus
Be	d	18	10	0.80 ± 0.13 sec	${}^9\text{Be}(d, {}^3\text{He}){}^8\text{Li}$	Winn (1954)
Bi	α	28	10	0.22 ± 0.03 sec	${}^{209}\text{Bi}(\alpha, n){}^{212}\text{At}$	Segrè (1948)
Pb	α	28	10	$\left\{ \begin{array}{l} 0.5 \pm 0.1 \text{ sec} \\ 27.0 \pm 5.0 \text{ sec} \end{array} \right.$	$\left\{ \begin{array}{l} {}^{208}\text{Pb}(\alpha, n){}^{211}\text{Po} \\ {}^{208}\text{Pb}(\alpha, n){}^{211}\text{Po}^* \end{array} \right.$	$\left\{ \begin{array}{l} \text{Leininger } et al. \\ (1951) \text{ and} \\ \text{Speiss}(1951) \end{array} \right.$
Au	${}^{14}\text{N}^{6+}$	~ 80	20	7.0 ± 1.0 min	${}^{197}\text{Au}({}^{14}\text{N}, xn)?\text{Em}$	Burcham (1954)
Li	${}^3\text{He}^{2+}$	13	50	0.6 to 0.9 sec	One or more of ${}^6\text{Li}({}^3\text{He}, n){}^8\text{B}$; ${}^7\text{Li}({}^3\text{He}, 2n){}^8\text{B}$ ${}^7\text{Li}({}^3\text{He}, 2p){}^8\text{Li}$	See below

The author would like to thank Professor W. E. Burcham for his helpful advice, Mr. K. G. Stephens for his work on the probe design and Mr. D. R. Sweetman for assistance with the ${}^3\text{He}$ circulation system. The bombardments were made by Mr. W. Hardy and the staff of the Nuffield cyclotron.

Physics Department,
The University,
Birmingham, 15.
29th May 1954.

M. M. WINN.

BURCHAM, W. E., 1954, *Proc. Phys. Soc. A*, **67**, 555.

FREMLIN, J. H., 1953, *Phil. Mag.*, **44**, 141.

LEININGER, R. F., SEGRÈ, E. G., and SPEISS, F. N., 1951, *Phys. Rev.*, **82**, 334 (A).

SEGRÈ, E. G., 1948, as reported by SEABORG, G. T., and PERLMAN, I., 1948, *Rev. Mod. Phys.*, **20**, 585.

SPEISS, F. N., 1954, *Phys. Rev.*, **94**, 1292.

WALKER, D., FREMLIN, J. H., LINK, W. T., and STEPHENS, K. G., 1954, *B. J. Appl. Phys.*, **5**, 157.

WINN, M. M., 1954, *Proc. Phys. Soc. A*, **67**, in the press.

Consistency of Nuclear Radii from Electron Scattering and Coulomb Energy Data

The recent experiments on electron scattering can be explained on the basis of a uniform charge model taking a radius approximately equal to†

$$R_{\text{scatt}} = 1.0 \times 10^{-13} A^{1/3} \text{ cm.} \quad \dots\dots(1)$$

On the other hand, the energy differences of mirror nuclei indicate for the radius a value

$$R_c = 1.45 \times 10^{-13} A^{1/3} \text{ cm} \quad \dots\dots(2)$$

which seems hard to reconcile with (1). This shows the inadequacy of the uniform density model.

† Experiments on the x-ray spectrum of μ -mesonic atoms also indicate nuclear radii closer to (1) than to (2).

A number of alternative models have been suggested by different authors (Wilson 1952 and references cited therein). In this connection Bitter and Feshbach (1953) and Cooper and Henley (1953) have recently given some general arguments showing that no positive definite charge distribution exists which can give a smaller radius for scattering and a bigger one for coulomb energy. According to their argument, the most favourable situation occurs in the uniform density model; and since the above discrepancy lies in that model itself, the position would appear quite hopeless.

One of us (Vachaspati 1954) has recently given a theory of the electron scattering, taking a model for which the charge density is given by

$$Ze\rho = Ze \left[-(C-1)\delta^3(\mathbf{r}) + \frac{CB^2}{4\pi} \frac{e^{-Br}}{r} \right]. \quad \dots\dots(3)$$

Since the electron scattering is fairly insensitive to the details of the nuclear model, one can use the calculations made there to find scattering cross sections on different models by suitably choosing B and C . It is shown there that this model would give almost the same differential cross section as the uniform model with radius R_{scatt} if one assumes

$$C = 1.75, \quad (BR_{\text{scatt}})^2 = 14.8. \quad \dots\dots(4)$$

It is interesting that this model represents a nucleus with $3Ze/4$ negative charge at the centre and $7Ze/4$ positive charge outside, the concentration of the latter decreasing outwards.

Now the coulomb energy of a nucleus is given by

$$E = \frac{1}{2} Z^2 e^2 \int \int \frac{\rho(\mathbf{x})\rho(\mathbf{y})}{|\mathbf{x}-\mathbf{y}|} d^3x d^3y. \quad \dots\dots(5)$$

If one substitutes for ρ the value given in (3) one finds, after an easy calculation, that

$$E = \frac{1}{2} Z^2 e^2 (1 - \frac{1}{2}C) CB. \quad \dots\dots(6)$$

Comparing with the case of the uniform charge model, where the energy is $\frac{3}{5} Z^2 e^2 / R_c$, we now see that the effective coulomb radius is

$$R_c = \frac{6}{5} \frac{1}{(1 - \frac{1}{2}C)CB}. \quad \dots\dots(7)$$

Multiplying both the numerator and the denominator of (7) by R_{scatt} we get

$$R_c = \alpha R_{\text{scatt}} \quad \dots\dots(8)$$

where

$$\alpha = \frac{6}{5} \frac{1}{(1 - \frac{1}{2}C)C(BR_{\text{scatt}})}. \quad \dots\dots(9)$$

If we now use the values of C and (BR_{scatt}) given in (4), we readily find $\alpha = 1.43$. Substituting this in (8) we see that, on the basis of the density distribution (3), the coulomb energy radius is bigger than, and is in fact 1.43 times, the scattering radius. This is in remarkable agreement with the values (1) and (2).

Physical Research Laboratory,
Ahmedabad 9,
India,
7th April 1954.

VACHASPATI,
S. M. SHAH.

- BITTER, F., and FESHBACH, H., 1953, *Phys. Rev.*, **92**, 837.
COOPER, L. N., and HENLEY, E. M., 1953, *Phys. Rev.*, **92**, 801.
VACHASPATI, 1954, *Phys. Rev.*, **93**, 502.
WILSON, R. R., 1952, *Phys. Rev.*, **88**, 350.

REVIEWS OF BOOKS

Science in Progress. Sigma Xi National Lectureships, edited by GEORGE A. BAITSELL. 7th Series, 1949 and 1950, pp. ix+512; 8th Series, 1951 and 1952, pp. xiv+285. (New Haven: Yale University Press; London: Oxford University Press, 1951, 1953.) \$6.00 each volume.

As Sterne might have remarked: "They order these matters better in America". Doubtless many British scientists are moved by motives of piety; doubtless this often results in admirable popular accounts of contemporary research; but no enterprising editor collects them into annual volumes such as are the subject of this notice. The two volumes under review consist of 22 lectures delivered before the Sigma Xi Society. They are well illustrated (221 figures) and cover most branches of Science. Few specialists are likely to learn much from the articles dealing with their own field, but most scientists will find in these articles information invaluable in the discussions on the general application and purpose of Science which so frequently arise in modern democracy.

For example the two excellent articles on "Atomic Energy" as well as giving a good account of reactors along conventional lines treat the power problem as a whole and discuss biological and other means of making use of solar energy. As Professor Harrington Daniels remarks: "Atomic energy for military purposes was developed with the aid of two billion dollars in three war years under conditions of centralized authority and secrecy. It would be interesting to see what could be done with two million dollars in three years for the greater utilization of solar energy."

The mathematician is catered for in an article by Professor Artin on the theory of braids and its relationship to group theory.

Many of the biological articles are of the type which interest the amateur biophysicist. Professor Muller devotes over seventy pages to an account of "Radiation damage to the Genetic Material" while Professor Harvey's article on luminescent organisms shows some interesting oscillographic studies of the flash of the firefly. What subject of discussion could be more appropriate for the physicist and his lass as they survey the wonders of nature beneath a tropical moon?

These volumes are well worthy of consideration for inclusion in any library which has to serve the needs of undergraduates reading Natural Science. They are well produced, reasonably priced and are prefaced by useful biographical notes on the authors.

C. H. COLLIE.

Scientific Papers presented to Max Born on his Retirement from the Tait Chair of Natural Philosophy in the University of Edinburgh, by Sir EDWARD APPLETON *et al.* Pp. vi+94. (Edinburgh: Oliver & Boyd.) 12s. 6d.

This collection of short papers written by some of his friends and published as a tribute to Professor Born on the occasion of his leaving Edinburgh may be divided into two classes as follows: six of the essays are straightforward and four are controversial.

The first of the six is a condensed but very interesting discussion by Sir Edward Appleton on the relations between geomagnetism and various ionospheric phenomena, leading up to an account of the substantial simplification which is achieved by plotting the F2 layer critical frequency against the geomagnetic latitude.

There are brief articles by Professor Courant on the method of characteristics and the classification of non-linear partial differential equations, by Professor Weyl on the extension of a theorem of Lagrange to an arbitrary field, and by Professor von Kármán and S. Penner on constant pressure deflagration. Professor Schrödinger contributes a cautious discussion of possible relations between relativity and quantum theory and shows that by limiting speculation to a moderate amount he *cannot* derive the well-known relation between the radii of the nucleus and the universe and the so-called number of nucleons in the universe. Dr. P. Jordan compares Boltzmann statistics and the uncertainty principle in physics with Mendelian inheritance and mutations in biology. Possible relations between rare mutations and evolution are discussed in some detail, but the reviewer is quite incompetent to comment on what appear to him to be fundamental assumptions.

The four controversial papers deal with the probability interpretation of quantum theory which was originally due to Professor Born. These articles by Professors Einstein and Landé, M. L. de Broglie and Dr. Bohm are unfortunately one-sided. It is true that Landé takes a view opposite to the others, but the general effect is to suggest that the usual interpretation of quantum mechanics is wrong, and that we must find some way of describing physical systems which gives more information than the wave function. As this is opposed to the views of Niels Bohr and his school, it is a pity that the latter's views are not represented (a few relevant paragraphs in Jordan's article on biology are hardly to be counted).

Einstein states that quantum mechanics describes ensembles of systems, not individual systems, and that in this sense the wave function gives an incomplete description of the individual system. He does not add that, for all physical systems which have been suggested, it has been shown that the wave function gives as complete a description as is self-consistent. de Broglie suggests that there is a singular solution of the wave equation such that the motion of the singularity gives the classical motion of the particle, but to obtain this singular solution he has to abandon the linear wave equation. The difficulties so created, and the lack of definiteness, both in the mathematics and in the physical ideas, would appear to many to be strong arguments in favour of the simple idea of Bohr and Heisenberg that the usual wave function describes all that anyone can ever find out about a physical system, and therefore the wave function provides the answers to all the meaningful questions about the system which can be asked. Bohm tries to discuss the results of measurements without reference to the eigenstates or the eigenvalues of the appropriate linear operators, and his statements as a result suffer in clarity.

The article by Landé tries to carry the war into the territory of Einstein, de Broglie and Bohm, his thesis being "that it is futile in principle to search for hidden causes behind any distribution which satisfies the rules of probability, whether the distribution occurs in a classical or a quantum-theoretical investigation". The main line of his argument can be indicated by quoting

his remark: "a deterministic derivation of irreversibility from reversible deterministic mechanics is an impossibility". This, however true, is not the point at issue in the discussion about the interpretation of quantum theory. Classical mechanics gives differential equations describing the trajectory of a single particle; quantum mechanics gives differential equations which describe operators associated with the particle, and the expectation values of the operators tell all that can be stated about the trajectory. Thermodynamical effects do not appear to enter the discussion to a first approximation.

It will be interesting to know what Professor Born may have to say about this symposium.

J. HAMILTON.

Physics and Applications of Secondary Electron Emission, by H. BRUINING. Pp. xii + 178. (London: Pergamon Press, 1954.) 25s.

Apart from its fundamental interest in the physics of metals, secondary emission has to-day an enormous number of practical applications, especially in modern electronic equipment. The result is that the literature on the subject is extensive and is rapidly expanding; this applies both to the academic and technological papers. The present book is one of a series of monographs which report on research, and help to bring together the vast amount of data now being published. A modern book on secondary electron emission is necessary and the present work, by Dr. H. Bruining, of the Philips Research Laboratory, Eindhoven, himself an authority, is to be welcomed.

A very wide field is covered in 178 pages. A chapter is devoted to experimental methods of measurement of secondary emission and this is followed by two chapters which review previous results on secondary electron emission from metals and metal compounds. A short chapter is devoted to the variation of secondary emission yield caused by external absorption of ions and atoms, a field of increasing importance; but it is unfortunate that it has not been found possible to include mention of the most recent work in this particular field. Two important chapters are then devoted to theories of electron emission, and the last three deal with applications and these will be particularly valuable to electronic engineers.

The author gives an account of published data and of the theories which have been proposed to account for them. When these are not entirely satisfactory, or when the data themselves are not self-consistent, the author simply states the facts, and this makes the book a valuable work of reference. An extensive list of references is given of important papers up to 1952. The book, should prove extremely useful, especially to those working on electronics, and can be strongly recommended.

F. LLEWELLYN JONES.

Handbook of Elliptic Integrals for Engineers and Physicists, by P. F. BYRD and M. D. FRIEDMAN. Pp. xii + 355. (Berlin: Springer-Verlag, 1954.) DM. 36 (DM. 39.60 bound in linen).

The authors have collected together for easy reference a very large number of important formulae to facilitate the evaluation of a class of integrals often met with in applied mathematics and physics. They are not concerned with the formal theory of elliptic functions but content themselves with clear definition

and the inclusion of enough theory to make the book useful to those who have not met these functions before. In all there are about 3000 formulae and integrals.

The reader is introduced to the three kinds of elliptic integral, Jacobi's elliptic functions and their inverses and to Jacobi's zeta function, all of which are defined and exhibited graphically. A few conformal mappings involving these functions are also given.

A large section is devoted to the classification of integrals involving the square root of a cubic or a quartic or of certain simple polynomials of higher degree. There are also lists of single and multiple integrals of various combinations of Jacobi's elliptic functions; integrals involving trigonometric or hyperbolic functions, which can be evaluated in terms of elliptic functions, are also dealt with. Another section of the book is concerned with integrals and derivatives with respect to the modulus or argument, and with series and product expansions. Weierstrassian elliptic functions and theta functions are considered in an appendix.

At the end of the book tables are given of the complete and incomplete elliptic functions of the first and second kinds, and also of the zeta function.

A. N. GORDON.

BOOK NOTICES

Inter-relations between the Terrestrial Atmosphere and Cosmic Radiation, by P. K. BHATTACHARYA. Pp. iv + 50. (Calcutta: Indian Physical Society, 1952.)

A new Periodic Table of the Elements, based on the Structure of the Atom, by S. I. TOMKEIEFF. Pp. 30. (London: Chapman and Hall, 1954.) 10s.

CONTENTS OF SECTION B

	PAGE
Dr. J. A. LEE and Dr. G. V. RAYNOR. The Lattice Spacings of Binary Tin-Rich Alloys	737
Dr. R. L. INGRAHAM. Taylor Instability of the Interface between Superposed Fluids—Solution by Successive Approximations	748
Dr. P. T. NETTLEY. The Approach to the Steady State in Gaseous Thermal Diffusion and its Application to Determining the Dependence of Gas Diffusivity on the Concentration Ratio	753
Dr. D. G. AVERY, Dr. D. W. GOODWIN, Mr. W. D. LAWSON and Dr. T. S. MOSS. Optical and Photo-Electrical Properties of Indium Antimonide	761
Dr. J. E. ALLEN and Dr. P. C. THONEMANN. Current Limitation in the Low-Pressure Mercury Arc	768
Dr. T. S. MOSS. The Interpretation of the Properties of Indium Antimonide	775
Mr. P. E. DOUGLAS. The Vapour Pressure of Calcium : I	783
Dr. D. H. TOMLIN. The Vapour Pressure of Calcium : II	787
Corrigendum (TILLET)	794
Reviews of Books	795
Contents of Section A	800

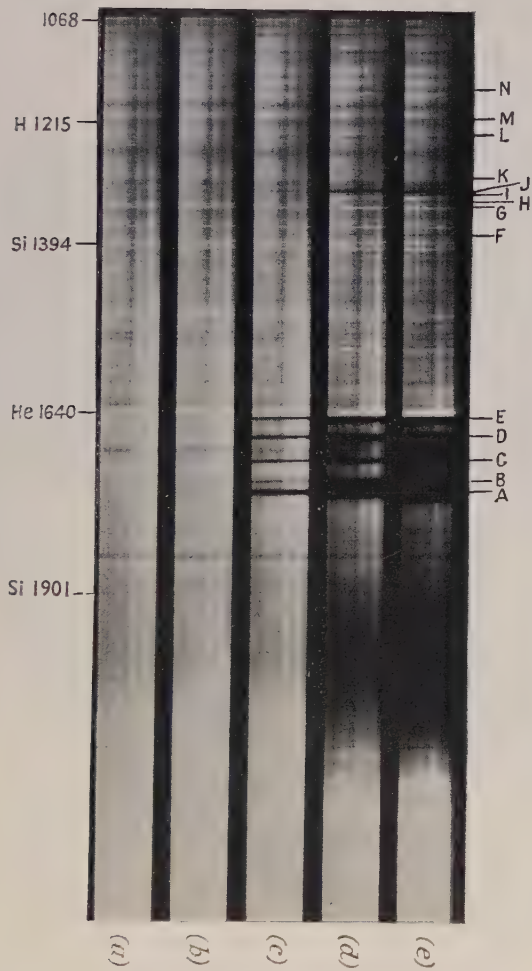


Figure 1.

Schumann region absorption spectrum of In vapour.
(a) 20°; (b) 900°; (c) 1100°; (d) 1250°; (e) 1400°C.

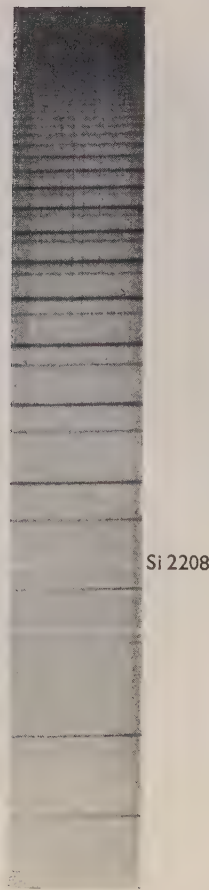


Figure 2.

In I sharp and diffuse
series in absorption.

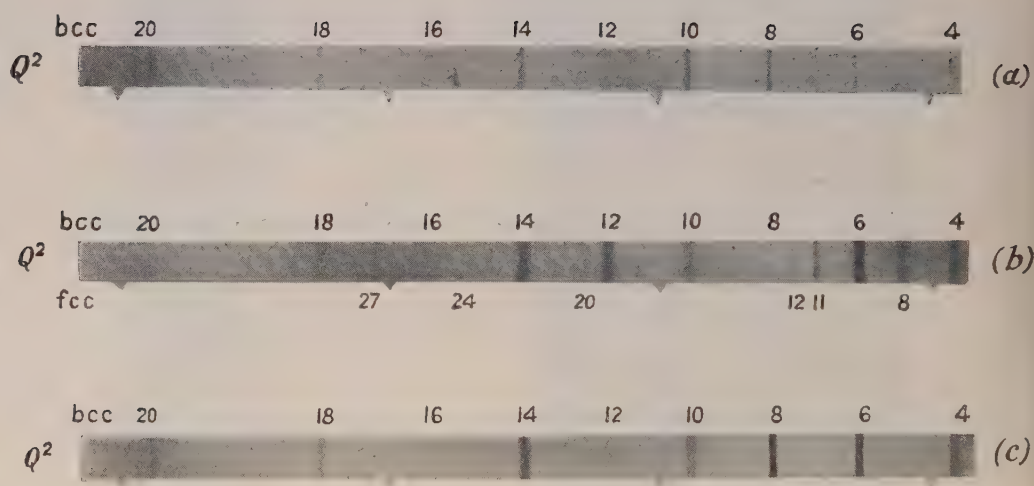
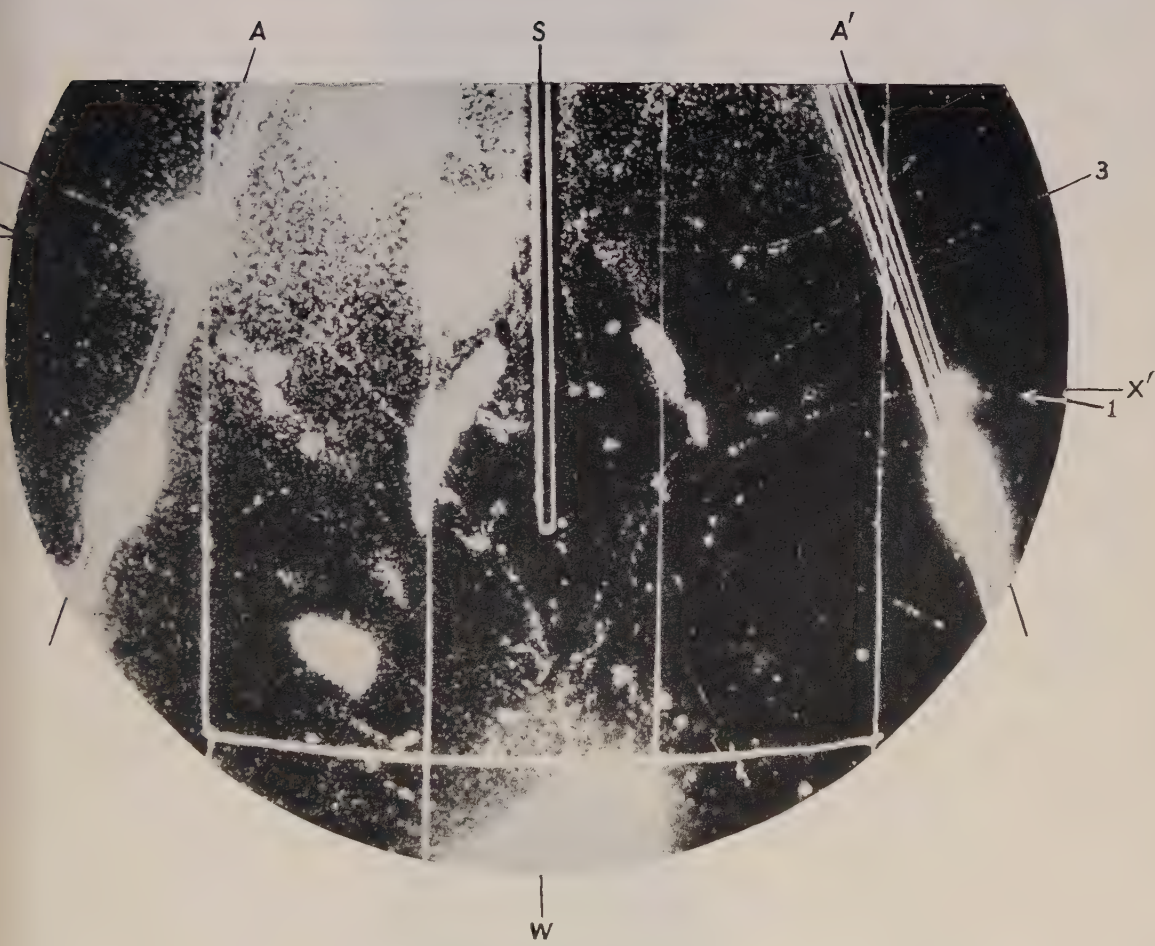
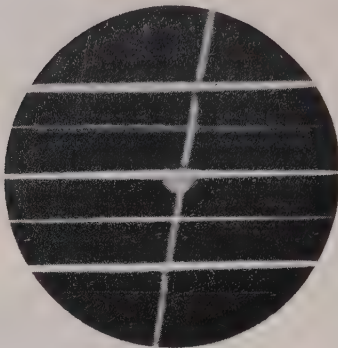


Figure 2. Illustrating the effect of deforming lithium at liquid-air temperature.

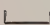
- (a) Lithium at -194°C . Body-centred cubic structure. Unfiltered copper radiation.
 (b) Lithium at -194°C after deformation at -194°C . Mixture of body-centred cubic and face-centred cubic structures. Filtered copper radiation. (c) Lithium, after (b) above, allowed to anneal at room temperature and then cooled to -194°C . Body-centred cubic structure with some reflections split in two. Filtered copper radiation.

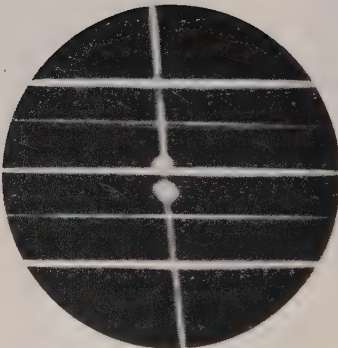


Scale  1 cm



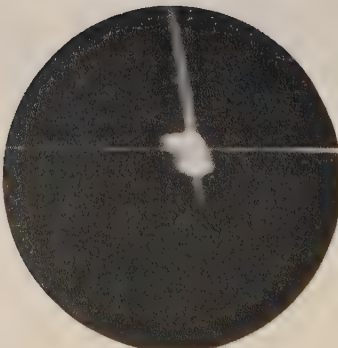
(a)

 1 cm



(b)

 1 cm



(c)

The Scattering of Nucleons by Alpha Particles—the s-Phases

By S. HOCHBERG, H. S. W. MASSEY AND L. H. UNDERHILL

University College, London

MS. received 22nd June 1954

Abstract. The s-phase shifts for scattering of neutrons and of protons by alpha particles have been calculated over the energy range 0–4 mev. A central interaction between nucleons of gaussian form has been assumed, the constants being consistent with the binding energy of the deuteron and alpha particle. The resonating group structure method has been employed to provide integro-differential equations for the wave functions which describe the scattering. These equations are internally consistent in that the functions used to describe the resonating groups are only assumed to satisfy the usual variational integral condition in terms of the alpha particle binding energy. The s-phases were determined by accurate numerical solutions of the equations. Very good agreement was obtained with the phases derived from analysis of observed data both for neutron and for proton scattering, provided the internucleonic forces were taken to be of symmetrical exchange character. The work is a necessary preliminary to an investigation of the p-phases in terms of an internucleonic spin-orbit interaction.

§ 1. INTRODUCTION

THE first observation of the anomalous scattering of alpha particles by protons was made by Chadwick and Bieler in 1921 (see also Mohr and Pringle 1937) and the first measurement of the scattering of neutrons by helium nuclei was made years later by Staub and Tatel (1940). These measurements first directed attention to the possibility that the p-phase shifts for nucleon-alpha particle collisions are split. Further, more extensive, measurements by Barschall and Kanner (1940) with 25 mev neutrons were analysed by Wheeler and Barschall (1940) and found to provide definite evidence of a wide splitting. The possibility that non-central forces of the tensor kind can give a sufficiently large splitting has been discounted since Dancoff (1940) estimated that they would be quite inadequate. Attention was therefore drawn to the possibility that strong spin-orbit interactions exist between nucleons and subsequent work has been directed to obtaining information about these interactions. In 1949 Critchfield and Dodder carried out a phase analysis of the data obtained by Freier, Lampi, Sleator and Williams (1949) on the scattering of protons with energies ranging from 0.95 to 3.88 mev. They found that the data were consistent with contributions from s, $p_{1/2}$ and $p_{3/2}$ phase shifts but were naturally unable to tell whether the p doublet was normal or inverted. The analysis was later extended by Dodder and Gammel (1952) to cover the extended proton energy range (5.81 and 9.48 mev) studied experimentally by Adair (1952) and by Kreger, Kerman and Jentschke (1952). Polarization measurements carried

out by Heusinkveld and Freier (1952) by studying the double scattering of protons by helium nuclei decided definitely that the doublet is inverted. Similar measurements and analyses carried out with neutrons (Huber and Baldinger 1952, Seagrave 1953) have led to substantially the same conclusions.

Although it was realized at the outset that the observed doublet splitting is most readily understood if the internucleonic interaction includes a spin-orbit coupling term (Rosenfeld 1948) there has been no theoretical work up to the present which attempts to determine the magnitude of this term. Hochberg (1953), Burgel (reference by Huber and Baldinger 1952) and Sack, Biedenharn and Breit (1954) have examined the possibility of representing the results in terms of a central nucleon-alpha particle interaction to which a spin-orbit term is added, but it is desirable to attempt a more fundamental approach, relating the scattering to the fundamental interactions. It is true that in a five-body problem of this kind many-body forces may be important—whether they are necessary or not is a matter for investigation. We have therefore commenced a study of nucleon-alpha-particle scattering in terms of two-body interactions. The first aim is to examine whether the s-phases can be calculated assuming a reasonable central interaction. The first attempt in this direction was made by Nogami in 1942. He assumed a gaussian interaction between nucleons but made very drastic approximations in carrying out the calculation of the s-phases.

In the present paper we report the results obtained using a similar two-body gaussian interaction to that assumed by Nogami, but with a much more accurate method of calculation. The phases have been obtained for both n- α and p- α collisions and the agreement with observation is so good as to encourage the belief that extension of the work to the p-phases, including spin-orbit interaction, will be profitable in yielding information about this non-central term.

When this work was nearly complete we became aware of the independent work on n- α scattering carried out by Bransden and McKee. They used nearly the same interaction but worked with an integro-differential equation to describe the scattering which is less consistent in its derivation than the one used in the present work. Furthermore they obtained the phases by a variational method whereas we obtained them by accurate numerical solution of the integro-differential equation concerned. There are quite considerable differences in the results obtained.

§ 2. GENERAL FORMULAE

We consider first neutron collisions. Using the number 1 to represent the coordinates of the incident neutron, 2 and 3 the neutrons in the helium nucleus and 4 and 5 the nuclear protons, the wave equation for the combined system may be written

$$\left[\frac{\hbar^2}{M} \{ \nabla_{45}^2 + \frac{3}{4} \nabla_{3,45}^2 + \frac{2}{3} \nabla_{2,345}^2 + \frac{5}{8} \nabla_{1,2345}^2 \} + E - \sum_{\text{all pairs}} \mathcal{V}_{ij} \right] \Psi = 0 \quad \dots\dots(1)$$

where the suffix 1,2345 means that the coordinates concerned are those of particle 1 relative to the centre of mass of the particles 2, 3, 4 and 5, etc. For the calculation of the s-phase shift it is not necessary to take into account the spin orbit interaction as it gives a vanishing contribution to this phase. We therefore write

$$\mathcal{V}_{ij} = (mM + \hbar H + bB + w)V(r_{ij}) + \frac{e^2}{r_{ij}} \epsilon_{ij} \quad \dots\dots(2)$$

where M , H and B are the usual Marjorana, Heisenberg and Bartlett operators, m , h , b and w numerical constants such that

$$\begin{aligned} m + h + w + b &= 1, \\ m + w - (h + b) &= x, \end{aligned} \quad \dots\dots(3)$$

where x is the ratio of the 1S to the 3S interaction in the deuteron and $\epsilon_{ij}=1$, if i, j are protons and zero otherwise.

Following the method of resonating group structure we now seek a solution of equation (1) of the form

$$\begin{aligned} \Psi = & \alpha(1)\chi(\widetilde{23}, \widetilde{45})F(1)\phi(-1) + \alpha(2)\chi(\widetilde{31}, \widetilde{45})F(2)\phi(-2) \\ & + \alpha(3)\chi(\widetilde{12}, \widetilde{45})F(3)\phi(-3) \quad \dots\dots(4) \end{aligned}$$

where $\phi(-1)$ is the space wave function of an alpha particle cluster in which all particles except neutron 1 are included. $\chi(\widetilde{23}, \widetilde{45})$ is the spin function for an alpha particle cluster, i.e.

$$\chi(\widetilde{23}, \widetilde{45}) = \{\alpha(2)\beta(3) - \alpha(3)\beta(2)\}\{\alpha(4)\beta(5) - \alpha(5)\beta(4)\}. \quad \dots\dots(5)$$

The function (4) is antisymmetric for interchange of the protons and of any pair of neutrons. In each term of (4) the function F represents the motion of the neutron relative to the alpha particle. To obtain an integro-differential equation from which to determine F we substitute (4) in (1), multiply on the left by $\alpha(1)\chi(\widetilde{23}, \widetilde{45})\phi^*(-1)$, sum over spins and integrate over the configuration space of the alpha particle 2345. If we further suppose that the functions ϕ , while not being necessarily exact solutions of the alpha particle ground state equation, are nevertheless good variational approximations, we may also use the relation

$$\begin{aligned} \sum_{\text{spins}} \int \phi^*(-1)\chi(\widetilde{23}, \widetilde{45}) \left[-\frac{\hbar^2}{M} \{\nabla_{45}^2 + \frac{3}{4}\nabla_{3,45}^2 + \frac{3}{3}\nabla_{2,345}^2\} + \sum_{\text{all pairs}} \mathcal{V}_{ij} \right] \\ \times \phi(-1)\chi(\widetilde{23}, \widetilde{45})d\tau_{-1} = E_\alpha \end{aligned} \quad \dots\dots(6)$$

where E_α is the (negative) energy of an alpha particle in its ground state. This gives, after a little elementary algebra,

$$\begin{aligned} [\nabla_1^2 + k^2 - (4w + 2b - m - 2h)] \int U_{12} |\phi(-1)|^2 d\tau_{-1} F(1) \\ = (4m + 2h - w - 2b) \int \phi^*(-1) U_{12} F(2) \phi(-2) d\tau_{-1} \\ - 3(m + w) \int \phi^*(-1) \{U_{23} + U_{13} + U_{45}\} F(2) \phi(-2) d\tau_{-1} \\ + \int \phi^*(-1) \{\nabla_2^2 - \kappa^2 - C_{45}\} F(2) \phi(-2) d\tau_{-1} \\ + \int \phi^*(-1) F(2) \{\frac{8}{5}\nabla_{45}^2 + \frac{6}{5}\nabla_{3,45}^2 + \frac{16}{15}\nabla_{1,345}^2\} \phi(-2) d\tau_{-1} \quad \dots\dots(7) \end{aligned}$$

where

$$U_{ij} = \frac{8M}{5\hbar^2} V_{ij}, \quad k^2 = \frac{8M}{5\hbar^2} (E - E_\alpha), \quad \kappa^2 = -\frac{8M}{5\hbar^2} E, \quad C_{45} = \frac{8M}{5\hbar^2} \frac{e^2}{r_{45}}. \quad \dots\dots(8)$$

If we now choose as coordinates the vectors

$$\begin{aligned} \mathbf{r} = \mathbf{r}_1 - \frac{1}{4}(\mathbf{r}_2 + \mathbf{r}_3 + \mathbf{r}_4 + \mathbf{r}_5), \quad \mathbf{p}_2 = \mathbf{r}_2 - \frac{1}{3}(\mathbf{r}_3 + \mathbf{r}_4 + \mathbf{r}_5), \\ \mathbf{p}_3 = \mathbf{r}_3 - \frac{1}{2}(\mathbf{r}_4 + \mathbf{r}_5), \quad \mathbf{p}_4 = \mathbf{r}_4 - \mathbf{r}_5, \end{aligned} \quad \dots\dots(9)$$

and write

$$\mathbf{r}' = \mathbf{r}_2 - \frac{1}{4}(\mathbf{r}_1 + \mathbf{r}_3 + \mathbf{r}_4 + \mathbf{r}_5) = -\frac{1}{4}\mathbf{r} + \frac{15}{16}\mathbf{p}_2 \quad \dots\dots(10)$$

(7) may be written in the standard form

$$[\nabla^2 + k^2 - W(r)]F(\mathbf{r}) = \int K^a(\mathbf{r}, \mathbf{r}')F(\mathbf{r}')d\mathbf{r}', \quad \dots\dots(11)$$

where

$$\begin{aligned} W(r) &= (4w + 2b - m - 2b) \int |\phi(\mathbf{p}_2, \mathbf{p}_3, \mathbf{p}_4)|^2 U(|\mathbf{r} - \frac{3}{8}\mathbf{p}_2|) d\mathbf{p}_2 d\mathbf{p}_3 d\mathbf{p}_4, \\ K^a(\mathbf{r}, \mathbf{r}') &= \left(\frac{16}{15}\right)^3 \left[\{(4m + 2h - w - 2b)U(|\mathbf{u} - \mathbf{v}|) - \kappa^2\} \right. \\ &\quad \times \iint \phi^*(\mathbf{u}, \mathbf{p}_3, \mathbf{p}_4)\phi(\mathbf{v}, \mathbf{p}_3, \mathbf{p}_4) d\mathbf{p}_3 d\mathbf{p}_4 - 3(m + w) \\ &\quad \times \iint \phi^*(\mathbf{u}, \mathbf{p}_3, \mathbf{p}_4) \{U(|\mathbf{u} - \frac{2}{3}\mathbf{p}_3|) + U(|\mathbf{v} - \frac{2}{3}\mathbf{p}_3|) + U(\rho_4)\} \phi(\mathbf{v}, \mathbf{p}_3, \mathbf{p}_4) d\mathbf{p}_3 d\mathbf{p}_4 \\ &\quad + \left(\frac{16}{15}\right)^2 \iint \{ \phi^*(\mathbf{u}, \mathbf{p}_3, \mathbf{p}_4) \nabla_v^2 \phi(\mathbf{v}, \mathbf{p}_3, \mathbf{p}_4) + \phi(\mathbf{v}, \mathbf{p}_3, \mathbf{p}_4) \nabla_u^2 \phi(\mathbf{u}, \mathbf{p}_3, \mathbf{p}_4) \\ &\quad + \frac{1}{2} \nabla_u \phi^*(\mathbf{u}, \mathbf{p}_3, \mathbf{p}_4) \cdot \nabla_v \phi(\mathbf{v}, \mathbf{p}_3, \mathbf{p}_4) \} d\mathbf{p}_3 d\mathbf{p}_4 \\ &\quad \left. + \iint \phi^*(\mathbf{u}, \mathbf{p}_3, \mathbf{p}_4) \left(\frac{6}{5} \nabla_{\rho_3}^2 + \frac{8}{5} \nabla_{\rho_4}^2 - U(\rho_4) \right) \phi(\mathbf{v}, \mathbf{p}_3, \mathbf{p}_4) d\mathbf{p}_3 d\mathbf{p}_4 \right] \quad \dots\dots(12) \end{aligned}$$

where

$$\mathbf{u} = \frac{16}{15}\mathbf{r}' + \frac{4}{15}\mathbf{r}, \quad \mathbf{v} = \frac{4}{15}\mathbf{r}' + \frac{16}{15}\mathbf{r}. \quad \dots\dots(13)$$

Since $K^a(\mathbf{r}, \mathbf{r}') = K^{a*}(\mathbf{r}', \mathbf{r})$ the integral operator in (11) is Hermitian as it must be.

In obtaining the equation (11) we have not assumed that the functions ϕ satisfy the wave equation for the alpha particle. If they are exact solutions the kernel K^a can be reduced to the form K^b where

$$\begin{aligned} K^b(r, r') &= \left(\frac{16}{15}\right)^3 \left[\{(4m + 2h - w - 2b)U(|\mathbf{u} - \mathbf{v}|) + \left(\frac{32}{15}k^2 + \frac{17}{15}\kappa^2\right)\} \right. \\ &\quad \times \iint \phi^*(\mathbf{u}, \mathbf{p}_3, \mathbf{p}_4)\phi(\mathbf{v}, \mathbf{p}_3, \mathbf{p}_4) d\mathbf{p}_3 d\mathbf{p}_4 + (m + w) \\ &\quad \times \iint \phi^*(\mathbf{u}, \mathbf{p}_3, \mathbf{p}_4) \left\{ \frac{1}{3}U(|\mathbf{u} - \frac{2}{3}\mathbf{p}_3|) + \frac{1}{3}U(|\mathbf{v} - \frac{2}{3}\mathbf{p}_3|) + \frac{17}{3}U(\rho_4) \right\} \\ &\quad \times \phi(\mathbf{v}, \mathbf{p}_3, \mathbf{p}_4) d\mathbf{p}_3 d\mathbf{p}_4 \\ &\quad + \iint \left\{ \frac{128}{1225} \nabla_u \phi(\mathbf{u}, \mathbf{p}_3, \mathbf{p}_4) \cdot \nabla_v \phi(\mathbf{v}, \mathbf{p}_3, \mathbf{p}_4) \right. \\ &\quad \left. - 17\left(\frac{4}{15}\right)^2 \phi(\mathbf{u}) \left(\frac{9}{8} \nabla_{\rho_3}^2 + \frac{3}{2} \nabla_{\rho_4}^2 \right) \phi(\mathbf{v}) \right\} d\mathbf{p}_3 d\mathbf{p}_4 \Big]. \quad \dots\dots(14) \end{aligned}$$

The equation used by Bransden and McKee (1954) is intermediate between (12) and (14), both of which are Hermitian. In deriving (12) it is not assumed that the functions ϕ are exact solutions of the alpha-particle wave equation, but in obtaining (14) this assumption is made and used twice to reduce the equation to the symmetrical (Hermitian) form (14). Bransden and McKee used the assumption only once as they did not work with a symmetrical equation. When the functions ϕ are only variational wave functions it is more consistent to work with our equation (12). As will be seen below, substantially different results are obtained if equation (14) or that of Bransden and McKee is used instead.

There is no difficulty in obtaining the corresponding equations for incident protons. We find in place of equation (11)

$$[\nabla^2 + k^2 - W(r) - W^c(r)]F(r) = \int [K(\mathbf{r}, \mathbf{r}') + K^c(\mathbf{r}, \mathbf{r}')]F(\mathbf{r}') d\mathbf{r}' \quad \dots\dots(15)$$

where

$$\begin{aligned} W^c(r) &= 2 \int \int \int |\phi(\mathbf{p}_2, \mathbf{p}_3, \mathbf{p}_4)|^2 C(|\mathbf{r} - \frac{3}{4}\mathbf{p}_2|) d\mathbf{p}_2 d\mathbf{p}_3 d\mathbf{p}_4, \\ K^c(\mathbf{r}, \mathbf{r}') &= (\frac{16}{15})^3 \int \int \phi^*(\mathbf{u}, \mathbf{p}_3, \mathbf{p}_4) \{C(\mathbf{p}_4) - C(|\mathbf{u} - \mathbf{v}|) - C(|\mathbf{u} - \frac{2}{3}\mathbf{p}_3|) \\ &\quad - C(|\mathbf{v} - \frac{2}{3}\mathbf{p}_3|)\} \phi(\mathbf{v}, \mathbf{p}_3, \mathbf{p}_4) d\mathbf{p}_3 d\mathbf{p}_4. \end{aligned} \quad \dots\dots(16)$$

The kernels K^a , K^b , K^c can be expanded in the form

$$K = (4\pi r r')^{-1} \sum (2l+1) k_l(r, r') P_l\left(\frac{\mathbf{r} \cdot \mathbf{r}'}{r r'}\right) \quad \dots\dots(17)$$

and if we expand $F(\mathbf{r})$ in the form

$$F(\mathbf{r}) = r^{-1} \sum f_l(r) P_l(\cos \theta), \quad \dots\dots(18)$$

we obtain, for incident neutrons,

$$\frac{d^2 f_l}{dr^2} + \left\{ k^2 - W(r) - \frac{l(l+1)}{r^2} \right\} f_l = \int k_l^{a, b}(r, r') f_l(r') dr'. \quad \dots\dots(19a, b)$$

In the present calculation we are concerned only with f_0 for the spin-orbit interaction which we have ignored will have an important influence on all other cases. We require therefore a solution of (19) with $l=0$ which has the asymptotic form

$$f_0 \sim \sin(kr + \eta_0). \quad \dots\dots(20)$$

The corresponding equation for incident protons is

$$\frac{d^2 f_0}{dr^2} + \{k^2 - W(r) - W^c(r)\} f_0 = \int [k_0(r, r') + k^c(r, r')] f_0(r') dr' \quad \dots\dots(21)$$

and we require a solution with the asymptotic form

$$f_0 \sim \sin(kr - n \log 2kr + \zeta_0 + \delta_0) \quad \dots\dots(22)$$

where

$$n = \frac{2e^2 M}{\sqrt{5} \hbar^2 k}, \quad \zeta_0 = \arg \Gamma(1 + in), \quad \text{and } W^c(r) \sim \frac{2nk}{r} = \frac{0.11126}{r}. \quad \dots\dots(23)$$

§ 3. FORMS ASSUMED FOR INTERACTION POTENTIALS AND NUCLEAR WAVE FUNCTIONS

In order to make the calculations practicable it is necessary to assume an internucleonic interaction of gaussian form viz.

$$V(r_{ij}) = A \exp(-\beta r_{ij}^2). \quad \dots\dots(24)$$

For the same reasons it is necessary to approximate to the function ϕ by a simple gaussian form which was taken as

$$\begin{aligned} \phi(\mathbf{p}_2, \mathbf{p}_3, \mathbf{p}_4) &= N \exp \{ -\alpha (r_{23}^2 + r_{24}^2 + r_{25}^2 + r_{34}^2 + r_{35}^2 + r_{45}^2) \} \\ &= N \exp \{ -\alpha (3\rho_2^2 + \frac{8}{3}\rho_3^2 + 2\rho_4^2) \}. \end{aligned} \quad \dots\dots(25)$$

In order to be consistent with (6) it is necessary to choose a range $\beta^{-1/2}$ for the interaction V for which use of a trial function of the form (25) gives a good

approximation to the binding energy of the alpha particle. The following numerical values were chosen

$$\beta = 0.2657 \times 10^{26} \text{ cm}^{-2}, \quad A = -45 \text{ mev}, \quad x = 0.6 \quad \dots\dots (26)$$

for which ϕ with $\alpha = 0.0789 \times 10^{26} \text{ cm}^{-2}$ gives a binding energy for the alpha particle of -26.68 mev compared with the correct value -28.2 mev . The values of A and β are consistent with the binding energy of the deuteron but evidence from other low-energy two-body observational data supports a shorter range than we have assumed. On the other hand it must be remembered that we are dealing here with a purely central force, in which some equivalent central representation of the tensor force is implicit. It by no means follows that this equivalent central force is the same for a four-body problem as for the two-body one. This is already apparent from a study of the binding energy of the alpha particle in which tensor forces are included—the tensor force is relatively less effective in producing binding than in the two-body case. We therefore began with the assumptions (26) and were fortunate in that no further modifications were required—the phases η_0 and δ_0 calculated with them agree very well with those obtained by phase analysis of the experimental data.

§ 4. METHOD OF CALCULATION

The functions $W(r)$, $W^c(r)$, $k_0^a(r, r')$, $k_0^b(r, r')$ were easily evaluated by substituting the forms (24) and (25) for V and ϕ respectively. The calculation of $k_0^c(r, r')$ was a little tedious as the final integration involved had to be carried out numerically.

There is an important difference to be noted at the outset between the forms of the solutions of the equations (19a) and (19b) respectively.

The complete solution of (19a) which is finite throughout space, vanishes at the origin and has the required asymptotic form can be written

$$f^a(r) = A\chi(r) + g^a(r)$$

where

$$g^a(r) \sim \sin(kr + \eta_0), \quad \chi(r) = r \exp(-16ar^2/5) \quad \dots\dots (27)$$

and A is an arbitrary constant. This is because the substitution of $r^{-1}\chi(r)$ for F in the resonating group form (4) causes Ψ to vanish identically for all values of the variables if the form (25) is assumed for ϕ . The existence of the redundant solution $A\chi(r)$ complicates the practical evaluation of the phase η_0 . Thus it is uncertain whether a good approximation can be obtained by representing the integro-differential equation by a set of simultaneous algebraical equations in the usual way. Such a set of equations gives a unique solution whereas the exact equation possesses an infinite set of solutions of the form (27). It cannot be assumed that the unique solution, obtained from the simultaneous equations, which has been accidentally selected by the choice of intervals in setting up differences will really give a good approximation to η_0 . Speaking loosely it may well be that the selected solution is an approximation to one of the infinite set (27) in which A is so large that the error, though small for the function as a whole, is nevertheless relatively very great in the small part represented by $g^a(r)$.

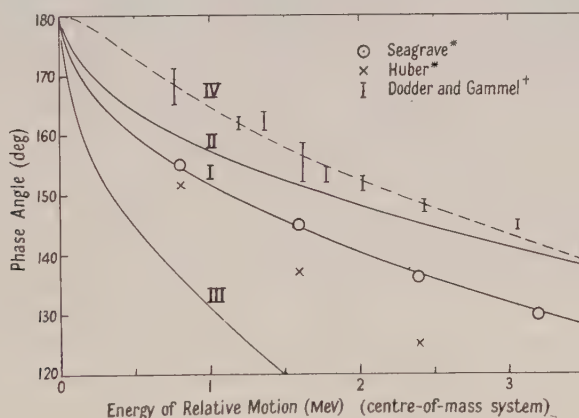
On the other hand the alternative iterative method of solution for equation (19a) must be carried out with care in order that the series of iterations should not tend to converge to the redundant solution $\chi(r)$. To avoid this an orthogonality condition can be imposed before commencing a further iteration at each stage.

Thus if $f_n^a(r)$ is the function obtained by solving (19a) with $g_{n-1}^a(r)$ substituted for $f^a(r)$ on the right-hand side, the next approximation is obtained replacing $g_{n-1}^a(r)$ by $g_n^a(r)$ where

$$g_n^a(r) = f_n^a(r) - \chi(r) \int_0^\infty f_n^a(r) \chi(r) dr / \int_0^\infty \chi^2(r) dr.$$

In this way it is assumed that the iterated solutions converge to a function $f^a(r)$ in which A is negligibly small. This procedure was used in solving (19a) and found to be very satisfactory.

The equation (19b) is exactly equivalent to (19a) only if the functions ϕ are exact solutions of the alpha particle ground state wave equation corresponding to an energy E_α . As remarked earlier it is inconsistent to use (19b) if approximate functions ϕ are employed. Under these circumstances the equation (19b), unlike (19a), has a unique solution and may be solved to sufficient accuracy by the difference method which leads to simultaneous algebraic equations. It is true, however, that if ϕ is a good approximation to the true alpha particle function, the tendency for a redundant solution to appear may be reflected in a marked instability in any method of successive approximation to the solution. Equation (19b) was solved for one or two cases by the difference method and it was found that the rapidity of convergence depended rather strongly on the size of interval chosen. As will be seen from the figure the phases obtained from (19b) differ considerably



Comparison of observed and calculated zero order phase shifts η_0 and δ_0 for n- α and p- α scattering respectively.

Curve I	η_0	calculated using symmetrical exchange forces and eqn 19 (a).
Curve II	η_0	„ „ Serber „ „ „ „ „
Curve III	η_0	„ „ symmetrical „ „ „ „ „ 19 (b).
Curve IV	δ_0	„ „ „ „ „

* selected points from Seagrave's analysis of observed data and Huber's analysis of his observations respectively.

† δ_0 derived from observed data by Dodder and Gammel with limits of error indicated.

from those from (19a). Since the derivation of the latter equation is consistent with the properties of the assumed approximate bound state functions while that of the former is not, most attention was devoted to obtaining solutions of (19a) for different cases.

To obtain the phase energy curve for n- α collisions η_0 was calculated by accurate solution of (19a) as described above for two selected neutron energies

(0.566 and 3.2 MeV). The phase is initially arbitrary to an extent $n\pi$. Since the solution f^a of (19a) which satisfies the orthogonality condition described above, has one additional node near the origin as compared with the corresponding plane wave solution we have made η_0 tend to π as k tends to zero.

Using these phases the constants a and r_0 in the effective range formula

$$k \cot \eta_0 = -\frac{1}{a} + \frac{1}{2} r_0 k^2, \quad \dots\dots(28)$$

were determined. The applicability of the formula was checked by calculating r_0 independently from the formula

$$\frac{1}{2} r_0 = \frac{1}{\{\psi(0)\}^2} \left[\int_0^\infty [\psi^2(r) - f^2(r)] dr + \int_0^\infty \int_0^\infty f(r) J(r, r') f(r') dr dr' \right] \quad \dots\dots(29)$$

where $k^a(r, r') = H(r, r') + k^2 J(r, r')$ and $\psi(r)$ is the asymptotic form of f , using the lower energy solution. The resulting value of r_0 agreed with that derived from the calculated phases to 0.5%.

A similar procedure was adopted for p- α collisions, the only complication being the need to allow in the effective range formula for the effect of the Coulomb field. Equation (28) must be replaced by (Bethe 1949)

$$2nk \left[\Re \frac{\Gamma'(1+in)}{\Gamma(1+in)} + C - \log n \right] + (2\pi n/e^{2\pi n} - 1) k \cot \delta_0 = -\frac{1}{a} + \frac{1}{2} r_0' k^2. \quad \dots(30)$$

r_0' could be evaluated by an expression similar to (29) but owing to the difficulty of tabulating the asymptotic form of the function it was regarded as sufficient to check that r_0' and r_0 were nearly the same.

§ 5. RESULTS AND DISCUSSION

The phases η_0 , δ_0 were calculated as a function of nucleon energy assuming (i) symmetrical and (ii) Serber exchange forces. The figure illustrates the comparison with observation.

It will be seen that very good agreement is obtained between the values of η_0 calculated assuming symmetrical exchange forces and those deduced from the analysis of the observed n-d scattering data due to Seagrave (1953). This agreement is seen to be much less satisfactory if Serber exchange forces are assumed. A different η_0 -energy curve has been obtained by Huber and Baldinger (1952) from analysis of his observations. It will be seen that this does not agree with the curves calculated for either symmetrical or Serber exchange forces.

A further check with observation is provided from the value of the cross section in the low energy limit. Reference to the table shows that again there is

Low Energy Limit of the n- α Elastic Cross Section (in 10^{-24} cm²)

Observed		0.78
Calculated by method of this paper	{ symmetrical exchange forces Serber exchange forces	0.794
(eqn 19 a) assuming		0.509
Calculated by variational approximation	{ symmetrical exchange forces Serber exchange forces	0.50
(Bransden and McKee) assuming		0.19

very good agreement between the observed value (Hibdon and Muelhouse 1951) and that calculated assuming symmetrical exchange forces—much better than with Serber forces. It is of interest also to compare our results in this connection with those of Bransden and McKee who calculated the phases using the Hulthén-Kohn variational method and a trial function of the form employed

by Swan (1953) in his calculations on n - ^3H collisions. It will be seen that very considerable differences exist between their results and those obtained by the accurate numerical method of this paper. These differences persist throughout the nuclear energy range considered. It is not clear whether the differences are due to inaccuracy in the variational method of Bransden and McKee or their use of a less consistent integro-differential equation to represent the scattering than our equation (19a).

The agreement between the calculated phases assuming symmetrical exchange forces and observed data persists also for p - α collisions as may be seen by reference to the figure in which the calculated phases δ_0 are compared with those obtained by Critchfield and Dodder (1949) from an analysis of observed data.

It is difficult to say how much weight can be attached to the better agreement obtained when symmetrical instead of Serber exchange forces are assumed. The magnitude of the errors introduced by the use of the resonating group method with gaussian α particle wave functions is difficult to assess. Errors due to neglect of polarization of the α particle by the colliding nucleon are not likely to be very serious for such a firmly bound structure but the gaussian functions may not be sufficiently good approximations to the unperturbed α particle functions. Nevertheless, it is clearly worth while to extend the work to the first order phases assuming again symmetrical exchange central forces to which a spin-orbit interaction of adjustable strength is added. Comparison with the $p_{1/2}$ and $p_{3/2}$ phases obtained from analysis of observed data should give a good indication of the strength of the internucleonic spin-orbit interaction if it is responsible for the level splitting. This work is now being undertaken.

ACKNOWLEDGMENTS

Throughout this work we have had the benefit of many discussions with Dr. R. A. Buckingham, Mr. L. Castillejo and Dr. P. Swan. Much assistance in carrying out the numerical computations was afforded by Miss L. Fosgate, Miss J. Nicholson, Miss J. Turner and Miss M. J. Lambeth. An accurate numerical solution of one of the equations for the n - α scattering was carried out for us, as a check, by the Scientific Computing Service. We are indebted to the Central Research Fund of London University for a grant which covered the cost of this check.

One of us (L.H.U.) wishes to thank the University of Wales for the award in the first instance of a Studentship and later of a Fellowship, and another (S.H.) wishes to thank the University of London for a Hoover Postgraduate Studentship.

REFERENCES

- ADAIR, R. K., 1952, *Phys. Rev.*, **86**, 155.
BARSCHALL, H. H., and KANNER, M. H., 1940, *Phys. Rev.*, **58**, 590.
BETHE, H. A., 1949, *Phys. Rev.*, **76**, 38.
BRANDEN, B. H., and McKee, J. S., 1954, *Phil. Mag.*, **45**, 869.
CHADWICK, J., and BIELER, E. S., 1921, *Phil. Mag.*, **42**, 923.
CRITCHFIELD, C. L., and DODDER, D. C., 1949, *Phys. Rev.*, **76**, 602.
DANCOFF, S. M., 1940, *Phys. Rev.*, **58**, 326.
DODDER, D. C., and GAMMEL, J. L., 1952, *Phys. Rev.*, **88**, 520.
FREIER, G., LAMPI, E., SLEATOR, W., and WILLIAMS, J. H., 1949, *Phys. Rev.*, **75**, 1345.
HIBDON, C.T., and MUELHAUSE, C. O., Atomic Energy Commission Report, ANL 4680.

- HUISINKVELD, M., and FREIER, G., 1952, *Phys. Rev.*, **85**, 80.
HOCHBERG, S., 1953, *Thesis*, University of London.
HUBER, P., and BALDINGER, E., 1952, *Helv. Phys. Acta*, **25**, 435.
KREGER, W. E., KERMAN, R. O., and JENTSCHKE, W. K., 1952, *Phys. Rev.*, **86**, 593.
MOHR, C. B. O., and PRINGLE, G., 1937, *Proc. Roy. Soc. A*, **160**, 190.
NOGAMI, M., 1942, *Proc. Phys. Math. Soc. Japan*, **24**, 26.
ROSENFELD, L., 1948, *Nuclear Forces, Part II* (Amsterdam: North-Holland Publishing Co.), p. 365.
SACK, S., BIEDENHARN, L. C., and BREIT, G., 1954, *Phys. Rev.*, **93**, 321.
SEAGRAVE, J. D., 1953, *Phys. Rev.*, **92**, 1222.
STAUB, H., and TATEL, H., 1940, *Phys. Rev.*, **58**, 820.
SWAN, P., 1953, *Proc. Phys. Soc. A*, **66**, 238, 740.
WHEELER, J. A., and BARSCHALL, H. H., 1940, *Phys. Rev.*, **58**, 682.

On the Neutron Spectrum for $v^{-\alpha}$ Absorption Cross Section

By B. DAVISON† AND M. E. MANDL

Atomic Energy Research Establishment, Harwell, Berks.

Communicated by B. H. Flowers; MS. received 4th June 1954

Abstract. An approximate expression is found for the neutron absorption energy spectrum in an infinite medium consisting of atoms of mass number M , for which scattering is assumed isotropic in the centre-of-mass system and $\sigma_a/\sigma_{sc} \propto v^{-\alpha}$, where α is a positive constant. The accuracy of certain useful types of integral over the resulting spectrum is examined.

§ 1. INTRODUCTION

IN neutron transport theory one often wants to know certain integrals over the neutron absorption energy spectrum, rather than the details of the neutron absorption energy spectrum itself. In many cases the form of these integrals is such that their accuracy depends upon that with which we can determine the probability for a neutron to be absorbed before reaching energy E , rather than upon the accuracy of the neutron spectrum itself. It is therefore of interest to examine those cases where the probability for a neutron to be absorbed before reaching energy E can be calculated with much greater accuracy than its derivative with respect to energy.

Placzek (1946) has evaluated the exact solution of the integral equation for the stationary energy distribution in an infinite non-capturing medium, assuming isotropic scattering in the centre-of-mass system; and has given an approximate solution for the case of $\sigma_a \propto 1/v$ with σ_{sc} constant, which is valid after a few collision intervals and as long as the capture probability per collision is sufficiently small. His solution for the spectrum breaks down for low energies; but this is one of the cases where the probability of survival can be calculated with much greater accuracy than the spectrum itself. The above problem is a particular case of the more general situation where $\sigma_a/\sigma_{sc} \propto v^{-\alpha}$, where α is a positive constant.

By a similar method we determine an approximate solution for the more general case, which is still finite at low energies. The accuracy of certain useful types of integrals over the resulting energy spectrum is then examined. The assumption that $\sigma_a/\sigma_{sc} \propto v^{-\alpha}$ is not very restrictive, since in many substances it is possible to subdivide the energy range into fairly wide sub-ranges with a different value of α in each.

§ 2. THE INTEGRAL EQUATION FOR THE NEUTRON SPECTRUM

We consider an infinite homogeneous medium in which N_0 neutrons per second of energy E_0 are produced per unit volume. We suppose that the medium consists of atoms of mass number M , with absorption and scattering cross sections $\sigma_a(E)$ and $\sigma_{sc}(E)$, respectively, for neutrons of energy E .

† Now at the Department of Mathematical Physics, The University, Birmingham.

The integral equation for the spectrum of neutrons slowed down by collisions in such a medium was derived by Placzek (1946), using a slightly different notation.

If $p(E)$ is the probability for a neutron released at energy E_0 to survive absorption at least to the energy E , the probable number of neutrons absorbed in the energy interval $(E-dE, E)$ is $N_0 p'(E) dE$ and the probable number of neutron collisions in this interval is

$$N_0 \frac{\sigma_{sc}(E) + \sigma_a(E)}{\sigma_a(E)} p'(E) dE, \quad \text{where} \quad p'(E) = \frac{dp(E)}{dE}.$$

If a neutron of energy E' has a scattering collision (assumed isotropic in the centre-of-mass system) at a nucleus of mass number M , it can have all energies between E' and $\{(M-1)/(M+1)\}^2 E'$ with equal probability after such a collision, i.e. the probability of its resulting energy being in the interval $(E-dE, E)$ is

$$\frac{(M+1)^2 dE}{4M E'} \quad \text{if} \quad E' > E > \left(\frac{M-1}{M+1}\right)^2 E'$$

and zero otherwise. Considering the number of neutrons having collisions in the interval $(E-dE, E)$, we must have, writing E_1 for $\{(M+1)/(M-1)\}^2 E$,

$$N_0 \frac{\sigma_{sc}(E) + \sigma_a(E)}{\sigma_a(E)} p'(E) dE = \frac{(M+1)^2}{4M} \int_E^{E_1} N_0 \frac{\sigma_{sc}(E')}{\sigma_a(E')} p'(E') \frac{dE}{E'} dE' \\ + \begin{cases} N_0 & \text{if } E-dE < E_0 < E \\ 0 & \text{otherwise.} \end{cases} \quad \dots\dots(1)$$

Taking the neutron velocity $v = \sqrt{2E}$ for the new independent variable, and putting $p'(E) = G(v)$, $k = (M+1)/(M-1)$, we obtain

$$\frac{\sigma_{sc}(v) + \sigma_a(v)}{\sigma_a(v)} G(v) = \frac{2k^2}{k^2 - 1} \int_v^{kv} \frac{\sigma_{sc}(v')}{\sigma_a(v')} G(v') \frac{dv'}{v'} + \frac{\delta(v - v_0)}{v_0} \quad \dots\dots(2)$$

where $\delta(v - v_0)$ is the Dirac δ -function.

As no neutron can survive to zero energy in a medium for which $\sigma_a(v)/\sigma_{sc}(v)$ does not tend to zero† as v becomes small, we shall have $p(0) = 0$, while clearly $p(E_0) = 1$. Hence we have

$$\int_0^{E_0} p'(E) dE = 1 \quad \text{or} \quad \int_0^{v_0} v G(v) dv = 1. \quad \dots\dots(3)$$

Placzek evaluated the exact solution of equation (2) for the case where $\sigma_{sc}(v)/\{\sigma_{sc}(v) + \sigma_a(v)\}$ is independent of v , and also showed that, for $v < v_0/k^n$ where n is 2, or at most 3, this exact solution is practically indistinguishable from the appropriately normalized solution $G_1(v)$ of the homogeneous equation obtained by omitting the δ -function term from equation (2), v now varying from zero to infinity.

In many integrals over the neutron spectrum the contribution from the range $v_0/k^n \leq v \leq v_0$ is so insignificant that it is possible to ignore the deviation of $G(v)$ from $A_1 G_1(v)$ for this small range. The normalization integral is an example of this; and for the cases which arise in practice we can determine the normalization coefficient A_1 by

$$\int_0^{v_0} v A_1 G_1(v) dv = 1. \quad \dots\dots(4)$$

† If $\sigma_a(v)/\sigma_{sc}(v) \rightarrow 0$ as $v \rightarrow 0$, there would be an accumulation of neutrons of zero energy, and mathematically this would not correspond to a steady state. Of course, in practice, the assumption that $\sigma_a(v)/\sigma_{sc}(v) \rightarrow 0$ as $v \rightarrow 0$ would be unrealistic.

§ 3. APPROXIMATE SOLUTION FOR $\sigma_a(v)/\sigma_{sc}(v) \propto v^{-\alpha}$.

We now consider in detail the homogeneous equation, putting $\sigma_a(v)/\sigma_{sc}(v) = (v^*/v)^\alpha$, where v^* is a constant.† Putting $v^\alpha = w$, the homogeneous equation becomes

$$(w + w^*) G_1(w) = \frac{2k^2}{\alpha(k^2 - 1)} \int_w^{k^2 w} G_1(w') dw'. \quad \dots\dots(5)$$

A series solution of this equation for large values of w , obtained by a generalization of Placzek's method, is

$$G_1(w) = \frac{C}{2\omega^{-\alpha} + 1} \left\{ 1 + \sum_{n=1}^{\infty} \left(-\frac{w^*}{w} \right)^n \prod_{j=1}^n \left[1 - \frac{2}{\alpha j + 2} \frac{k^{\alpha j + 2} - 1}{k^{\alpha j} (k^2 - 1)} \right]^{-1} \right\} \quad \dots\dots(6)$$

where C is a normalization constant. However, it is more convenient for numerical work to use the formula

$$\log G_1(w) = \log C - \left(\frac{2}{\alpha} + 1 \right) \log w + \sum_{n=1}^{\infty} B_n \left(-\frac{w^*}{w} \right)^n \quad \dots\dots(7)$$

where the coefficients B_n in equation (7) are determined from equation (6) by taking logarithms and re-expanding in terms of $-w^*/w$. In particular,

$$B_1 = \left[1 - \frac{2}{\alpha + 2} \frac{k^{\alpha + 2} - 1}{k^{\alpha} (k^2 - 1)} \right]^{-1}. \quad \dots\dots(8)$$

As the series solution (6) converges for $w > w^*$ but diverges for $w < w^*$, the series (7) must also diverge‡ for $w < w^*$.

We now examine the error involved in terminating the series (7) at the term $n = 1$.

§ 4. THE NATURE OF THE APPROXIMATE SOLUTION

If we terminate the series (7) at the term $n = 1$, we obtain the approximate solution

$$G_2(w) \equiv C_0 (w^{1+2/\alpha})^{-1} \exp(-B_1 w^*/w). \quad \dots\dots(9)$$

To examine the error involved in using $G_2(w)$ for $G_1(w)$ we examine the dependence of C_0 upon w which would make $G_2(w) \equiv G_1(w)$, i.e.

$$G_1(w) = C_0(w) (w^{1+2/\alpha})^{-1} \exp(-B_1 w^*/w). \quad \dots\dots(10)$$

One expects that if $G_2(w)$ is a good approximation for $G_1(w)$, then $C_0(w)$ will not depend much upon w . We now show that $C_0(w)$ decreases monotonically with increasing w , so that we need examine only its end-values.

Substituting (10) in equation (5), we have

$$C_0(w) = \left[\frac{2k^2}{\alpha(k^2 - 1)} \int_w^{k^2 w} \frac{C_0(w')}{(w')^{1+2/\alpha}} \exp\left(-B_1 \frac{w^*}{w'}\right) dw' \right] / \left[\frac{w + w^*}{w^{1+2/\alpha}} \exp\left(-B_1 \frac{w^*}{w}\right) \right] \quad \dots\dots(11)$$

$$> \left[\int_w^{k^2 w} \frac{C_0(w')}{(w')^{1+2/\alpha}} \exp\left(-B_1 \frac{w^*}{w'}\right) dw' \right] / \left[\int_w^{k^2 w} \frac{1}{(w')^{1+2/\alpha}} \exp\left(-B_1 \frac{w^*}{w'}\right) dw' \right] \quad \dots\dots(12)$$

† v^* has a simple physical meaning—it is the velocity at which absorption and scattering are equally probable.

‡ In fact it may also diverge for some part of $w > w^*$, for although $G_1(w)$ cannot vanish for any real w (from its physical interpretation), if it vanishes for some complex $w = w'$, then $\log G_1(w)$ will have a singularity at $w = w'$ and the series (7) will diverge for all $w < |w'|$.

by direct integration for $k > 1$ and $w^*/w > 0$. That is, $C_0(w)$ decreases on the average over any interval $w < w' < k^\alpha w$. To prove that $C_0(w)$ decreases monotonically it is now necessary to prove that $dC_0(w)/dw \neq 0$ for any real positive w . Clearly $dC_0(w)/dw < 0$ for sufficiently large w ; hence if $C_0(w)$ has any extrema for finite w , the one for the largest w (w_1 say) must be a maximum. This implies at least one minimum within $(w_1/k^\alpha, w_1)$. However, if such a minimum does exist, differentiating equation (11) and applying it at $w = w_1$ and at the nearest minimum of $C_0(w)$, we obtain two difference relationships which can easily be shown to be incompatible with the existence of the two stationary values. This completes the proof that $C_0(w)$ decreases monotonically.

§ 5. THE ERROR IN $\int_v^\infty v' G_1(v') dv'$.

We can examine the error involved in using $G_2(v)$ for $G_1(v)$ in the integral

$$\int_v^\infty v' G_1(v') dv',$$

which is the approximate expression used for $1 - p(v)$, by examining the ratio

$$F(v) \equiv \left[\int_v^\infty v' G_1(v') dv \right] / \left[\int_v^\infty v' G_2(v') dv' \right]$$

or

$$F(w) \equiv \left[\int_w^\infty \frac{C_0(w')}{\alpha w'^2} \exp \left(-B_1 \frac{w^*}{w'} \right) dw' \right] / \left[\int_w^\infty \frac{C_0}{\alpha w'^2} \exp \left(-B_1 \frac{w^*}{w'} \right) dw' \right]. \quad \dots\dots(13)$$

Hence, like $C_0(w)$, $F(w)$ decreases monotonically with increasing w , so that we need only examine it at $w = 0$ and $w = \infty$.

To avoid specifying C_0 at this stage, we consider

$$H(v) \equiv \left[\int_v^\infty v' G_1(v') dv' \right] / [1 - \exp \{ -B_1 (v^*/v)^\alpha \}] \propto F(w). \quad \dots\dots(14)$$

Since $G_1(v)$ should, in any case, be normalized so that

$$\int_0^\infty v' G_1(v') dv' = 1,$$

we see that $H(0) = 1$.

Multiplying equation (5) by w^η and integrating over all w , putting

$$M(\eta) \equiv \int_0^\infty w^\eta G_1(w) dw, \quad \dots\dots(15)$$

we obtain

$$w^* M(\eta) = \left\{ \frac{2}{\alpha(\eta+1)} \frac{k^2 - k^{2-\alpha(\eta+1)}}{k^2 - 1} - 1 \right\} M(\eta+1) \quad \dots\dots(16)$$

and, from the normalization of $G_1(w)$, $\alpha^{-1} M(2\alpha^{-1} - 1) = 1$. Since $M(\eta)$ is regular in the neighbourhood of $\eta = 2\alpha^{-1} - 1$,

$$M(2\alpha^{-1} - 1 - \epsilon) = \alpha + O(\epsilon).$$

From (6), $M(2\alpha^{-1} - \epsilon) = C/\epsilon + \text{terms which remain finite as } \epsilon \rightarrow 0$.

Substituting these results in (16) gives

$$C = w^* \left[\frac{1}{2} - \frac{\log k}{k^2 - 1} \right]^{-1} \quad \dots\dots(17)$$

on taking the limit as $\epsilon \rightarrow 0$. Hence

$$H(v) \rightarrow \left[\alpha B_1 \left(\frac{1}{2} - \frac{\log k}{k^2 - 1} \right) \right]^{-1} \text{ as } v \rightarrow \infty. \quad \dots\dots(18)$$

For small $k - 1$ this limit is approximately

$$1 - \frac{\alpha}{3}(k-1) + \frac{\alpha}{36}(3\alpha+8)(k-1)^2 + \dots \quad \dots\dots(19)$$

We see that, for small $k - 1$, $H(v)$ (and therefore, also, $F(v)$) has only a small variation with v . Thus it is not necessary to use the same normalization for $G_2(v)$ as for $G_1(v)$, and a small range of normalization coefficients C_0 is suitable.

If $G_2(v)$ is normalized in the same way as $G_1(v)$, i.e.

$$\int_0^\infty v G_2(v) dv = 1,$$

there is no error in $F(v)$ for $v = 0$, and the relative error in $F(v)$ is less than

$$\frac{\alpha}{3}(k-1) - \frac{\alpha}{36}(3\alpha+8)(k-1)^2 + \dots \quad \dots\dots(20)$$

for all v . Alternatively, if C_0 is fixed so that $F(v) = 1$ for $v \rightarrow \infty$, the relative error in $F(v)$ is less than

$$\frac{\alpha}{3}(k-1) + \frac{\alpha}{36}(\alpha-8)(k-1)^2 + \dots \quad \dots\dots(21)$$

for all other v . Thus, for C_0 within this range, the relative error produced by using $G_2(v)$ for $G_1(v)$ in

$$1 - p(v) = \int_v^\infty v' G_1(v') dv'$$

is less than the expression (21) for all v .

§ 6. THE ERROR IN $\int_v^\infty v' G_1(v') \phi(v') dv'$.

The error in integrals of the type

$$\int_v^\infty v' G_1(v') \phi(v') dv',$$

where $\phi(v)$ is non-negative and increases monotonically with v , can be estimated as follows. Since

$$\int_v^\infty v' G_1(v') \phi(v') dv' = \phi(v) \int_v^\infty v' G_1(v') dv' + \int_v^\infty \frac{d\phi(v')}{dv'} \int_v^{v'} v'' G_1(v'') dv'' dv'$$

and, with the above restrictions on $\phi(v)$, the two terms are of the same sign, the relative error in using $G_2(v)$ for $G_1(v)$ in integrals of this type is not greater than the relative error in using $G_2(v)$ for $G_1(v)$ in

$$\int_v^\infty v' G_1(v') dv'.$$

Many of the integrals used in transport theory are found to be of this type, e.g. $\phi(v) \propto \exp \{-c L_s^2(v)\}$, where L_s is the slowing-down length from velocity v_0 to velocity v , and c is a constant.

§ 7. EXTENSION TO MORE THAN ONE ENERGY RANGE

For clarity we discuss the case where there are two energy ranges only, with $\alpha = \alpha_1$ for $v_1 \leq v \leq v_0$ and $\alpha = \alpha_2$ for $v_2 \leq v \leq v_1$.

The normalization can be determined in various ways, as in § 5, but using the principle that the spectrum for $v \geq v_1$ must be independent of the cross sections for $v < v_1$ we obtain the following normalization equations:

$$A_1 \int_{v_0}^{\infty} v G_1(v) dv = 1$$

$$A_2 \int_0^{v_1} v G_2(v) dv + A_1 \int_{v_1}^{v_0} v G_1(v) dv = 1$$

where $A_1 G_1(v)$ and $A_2 G_2(v)$ are the approximate solutions (9) for the two energy ranges.

One easily sees that this produces a spectrum discontinuous at $v = v_1$, which cannot be correct; but the relative discontinuity can be shown to be

$$\frac{\alpha_1 B_1(x_1)}{\alpha_2 B_2(x_2)} - 1 \simeq \frac{1}{3}(\alpha_1 - \alpha_2)(k-1) + \frac{1}{36}(\alpha_1 - \alpha_2)(\alpha_1 - 3\alpha_2 - 8)(k-1)^2 + \dots$$

for small $k-1$, and this is usually quite small.

REFERENCE

PLACZEK, G., 1946, *Phys. Rev.*, **69**, 423.

Radiations from the Proton Bombardment of ^{23}Na

By F. C. FLACK†, J. G. RUTHERGLEN AND P. J. GRANT

Department of Natural Philosophy, The University, Glasgow

MS. received 16th June 1954

Abstract. The excitation functions and absolute yields of the reactions $^{23}\text{Na}(\text{p}, \gamma)^{24}\text{Mg}$ and $^{23}\text{Na}(\text{p}, \alpha)^{20}\text{Ne}$ have been measured for proton energies between 250 and 700 kev. Resonances for the emission of γ -radiation were found at 310, 515, 593 and 679 kev, and for α -particle emission at 287, 338 and 593 kev. The spectrum of γ -radiation was measured at each resonance together with the relative intensities of the γ -rays. A decay scheme is given which has been verified by γ - γ coincidence measurements.

§ 1. INTRODUCTION

BURLING (1941) has studied the yield of γ -radiation from the reaction $^{23}\text{Na}(\text{p}, \gamma)^{24}\text{Mg}$ for proton energies up to 2 mev. The resonances up to 500 kev and their yields have been measured by Tangen (1946). Determinations of the γ -ray spectrum at the resonance produced by protons of 310 kev have been made by Casson (1953), Turner (1953) and by Nelson, Geer and Carlson (1954).

Investigations of the competing reaction $^{23}\text{Na}(\text{p}, \alpha)^{20}\text{Ne}$ have been carried out by Freeman and Baxter (1948) and by Freeman (1950) for proton energies in the range 400 kev to 1 mev.

In the present paper a description is given of measurements of the thin-target excitation functions and absolute yields of α - and γ -radiation from the two reactions, together with the energy spectrum of the γ -rays at each resonance between proton energies of 250 and 700 kev. A decay scheme is given which has been confirmed by measurements of γ - γ coincidence spectra.

I. EXCITATION FUNCTIONS

§ 2. γ -RAY MEASUREMENTS

The γ -rays produced by the bombardment of sodium chloride targets, 5 to 10 kev thick, deposited on to a copper backing, were detected by a cylindrical sodium iodide crystal, $1\frac{3}{4}$ in. diam \times 2 in. long, and photomultiplier, the pulses being amplified and fed through a discriminator to a scaler. When studying the excitation function the discriminator and scaler were set to count all pulses corresponding to energies greater than 2.5 mev, in order to reduce the effects of background γ -radiation. Using the yield of the 6.13 mev γ -radiation from $^{19}\text{F}(\text{p}, \alpha\gamma)^{16}\text{O}$ at 340 kev, corrected to zero bias, to provide the intensity calibration, the absolute yield of the highest energy γ -ray (10.6 mev) was determined at each resonance. Knowledge of the spectra at the various resonances (see § II) then enabled the number of γ -rays leaving the resonant state to be found.

† Now at Department of Physics, University College of the South West, Exeter.

§ 3. α -PARTICLE MEASUREMENTS

A magnetic spectrometer similar to that described by Rutherglen and Smith (1953) was used to separate α -particles from the scattered protons. The α -particles were detected by a zinc sulphide scintillation screen and a photomultiplier. A discriminator was used to reject the residual background of small pulses from protons scattered round the spectrometer. By measuring, at the peak field setting, the α -particle counting rate versus the discriminator bias the α -particle yield at zero bias was determined. Energy and intensity calibration was effected by making similar measurements on the α -particles from $^{19}\text{F}(\text{p}, \alpha)^{16}\text{O}^*$ at the 340 kev resonance.

§ 4. RESULTS

The energies and integrated yields of resonances for α -particle and γ -ray emission are shown in table 1. Correction of the voltage scale was made by comparison with the standard resonances in $^{19}\text{F}(\text{p}, \alpha\gamma)^{16}\text{O}$. The energies are believed to be accurate to ± 1.5 kev and the absolute yields to within 20%

Table 1

E_{res} (kev)	$Y/10^{10}$ protons (NaCl target)		
	Y_{α}	Y_{γ} (10.5 mev)	Y_{γ} Total from top level
287	0.2		<0.005
310	<0.02	0.13	0.37
338	0.17		<0.01
515	<0.04	0.115	0.16
593	84	0.10	0.35
679	<0.13	0.16	1.09

Of the resonances shown in table 1, those at 287 and 338 kev have not previously been reported, probably due to their low intensity. It was verified that they were not due to contaminants in the target by measurement of the Q -value, which agreed exactly with that from the known resonance at 593 kev. A careful examination of the two reactions near 600 kev showed that both α -particles and γ -rays were resonant at the same proton energy of 593 kev within the experimental error of ± 1 kev.

II. γ -RAY SPECTRA

§ 5. METHOD

The γ -ray spectrometer consisted of the large single crystal of sodium iodide with photomultiplier tube. Pulses from the photomultiplier, after amplification, were fed into a 100 channel pulse amplitude analyser (Hutchinson and Scarrott 1951). Spectra were taken, at 90° and 180° to the proton direction, at all the γ -ray resonances listed in table 1, each spectrum being obtained by measurements at two gain settings of the amplifier to provide reasonable resolution at both high and low energies. A fixed monitor counter was used to normalize the runs at different gain settings.

Apart from variations in the relative intensities at different resonances, the same components appeared in all spectra. Typical results are shown in figure 1.

It will be seen that the γ -ray spectrum is complex and therefore in order to make possible a detailed analysis it is necessary to know accurately the pulse

THE PHYSICAL SOCIETY

1 Lowther Gardens, Prince Consort Road, London S.W.7

ABSTRACT BOOKLET 25

This booklet gives abstracts of papers accepted since the printing of Abstract Booklet 24. These abstracts are thus circulated before the paper has gone to press, whereas the reprints themselves are not printed until the month of publication in the *Proceedings*, usually 2-3 months after acceptance.

Those eligible to order reprints immediately are

- (a) Fellows and Students of the Society and general subscribers to the *Proceedings* who have purchased voucher books.
- (b) Fellows and Students of the Society who have paid the annual subscription of £1 1s. *Note:* This reduced rate is *not* available to general subscribers.

Members and subscribers may obtain 10s. voucher books (containing vouchers for five reprints) at any time. Reprints are **not** obtainable in any other way.

Users of reprint vouchers should attach the appropriate number of vouchers to their order form. The enclosed order form should be completed by marking with ticks the papers required and should be returned **not later than 1st December**. A slightly later date of receipt will be accepted for long distance overseas subscribers **only**.

A list of Letters to the Editor which have been accepted for publication since the printing of Abstract Booklet 24 is given for information only. **Reprints will not be available.**

Note. Please be sure your name and address are entered on the form and your requirements indicated, otherwise your order cannot be executed.

All papers in Lists 1-22 except that by Price have now been published. Reprints of papers covered by these Lists will have been despatched by mid-November; any outstanding orders should be queried as soon as possible after this date.

November 1954

Guthrie Lecture

The abstract of the Lecture, by Sir Geoffrey Taylor, appears on page 6.

Section A

Inelastic Collisions between Heavy Particles: IV—Contribution of Double-Transitions to certain Cross Sections including that associated with the Ionization of Hydrogen Atoms in Fast Encounters with other Hydrogen Atoms,
by D. R. BATES and G. W. GRIFFING.

Abstract. Born's approximation is used to calculate the cross sections associated with the processes



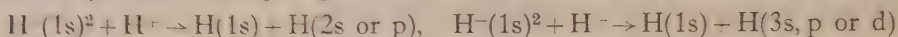
and



where C represents the continuum. These cross sections and others calculated in papers I and II are combined to yield the cross section for excitation to the third quantum level, the cross sections for ionization and the total cross section for all inelastic collisions. Both single and double transitions are taken into account. The ratio of the electron loss cross section to the electron capture cross section is computed.

Inelastic Heavy Particle Collisions Involving the Crossing of Potential Energy Curves: III—Charge Transfer from Negative Ions of Atomic Hydrogen to Protons, by D. R. BATES and J. T. LEWIS.

Abstract. The Landau-Zener formula for the transition probability arising from the pseudo-crossing of potential energy curves is applied to the processes



and $\text{H}(1s) + \text{H}(3s, p \text{ or } d) \rightarrow \text{H}(1s) + \text{H}(2s \text{ or } p)$ allowance being made for the effect of the orbital degeneracy. Cross sections and rate coefficients are given over a wide range of impact energies and temperatures. The calculations show that the electron transferred in slow encounters between H^- and H^- ions falls mainly into the third quantum level. Recombination thus leads to the emission of the first Balmer line. The de-activation process studied is of interest in that it provides an illustration of a type of mechanism whereby electronic energy can readily be converted into translational energy in thermal collisions.

An Extension of the Analysis of the Yttrium Spectrum, by L. F. H. BOVEY.

Abstract. Nineteen lines of the yttrium spectrum have been found in the region 9400–11500 Å and have been assigned to term combinations in the Yt I and Yt II spectra.

The magnetic Susceptibility of Potassium Manganicyanide, by A. H. COOKE and H. J. DUFFUS.

Abstract. The magnetic susceptibility of potassium manganicyanide has been measured at temperatures from 4.2°K to 300°K. The susceptibility, which at room temperature approximately follows Curie's law, approaches a temperature-independent value at very low temperatures. This behaviour is compared with the theoretical prediction of Kotani.

The Coulomb Scattering of High-Energy Electrons and Positrons by Nuclei, by R. M. CURR.

Abstract. The Mott cross section for the Coulomb scattering of high-energy electrons and positrons by atomic nuclei has been expressed by McKinley and Feshbach in terms of series in powers of $Z^{-1/3}$, up to terms in Z^4 where Z is the atomic number of the scattering nucleus. The coefficients of these series, which were evaluated numerically, have been recalculated and some minor errors corrected. Further coefficients have been calculated to enable application of the method to heavy elements and the resulting cross section, expressed as a ratio to the Rutherford cross section, is given in the form of a single power series.

Theory of (d, p) and (d, n) Reactions: II—Coulomb Corrections and Numerical Results, by I. P. GRANT.

Abstract. The results of an earlier publication are generalized to take account of the effect of the Coulomb field on the differential cross section in a deuteron

ORDER FORM 25

(issued November 1954)

To be returned to the Physical Society **NOT LATER THAN 1st December 1954**

Please supply 1 reprint of each of the following when published

Section A

BATES and GRIFFING
 BATES and LEWIS
 BOVEY
 COOKE and DUFFUS
 CURR
 GRANT
 McMURRAY and COLLIE
 PATTENDEN
 POPLE
 SIDA
 SWIATECKI
 TOMITA
 WEALE
 WOLFE

Section B

BANBURY and HOUGHTON
 CADE
 LONAPPAN.. .. .
 LOW
 SCHALLAMACH
 TAYLOR

Research Notes

GREENOUGH and SMITH
 WALLER (Symmetry of)
 WALLER (Note on)

Please cancel my order for

ADAM and STANDLEY
 (Booklet 24)

Research Notes

ADAM and STANDLEY.. .. .
 BREITENBERGER
 GREENLEES
 HUSAIN
 SHAW
 SRIVASTAVA

I participate in the £1 1s. reprint scheme.

I enclose.....vouchers.

Please delete as necessary.

NAME (BLOCK CAPITALS)

ADDRESS

.....

.....

SECRETARY-EDITOR,
PHYSICAL SOCIETY,
1 LOWTHER GARDENS,
PRINCE CONSORT ROAD,
LONDON S.W.7.

Section B

Measurements of Injection Ratio of Point Contacts on Germanium, by P. C. BANBURY and J. HOUGHTON.

Abstract. Measurements are reported of injection ratio γ on various specimens of n-type germanium. γ was found to be insensitive to the nature of the contact material, to the contact thrust, and to the carrier concentration of the germanium over the limited range investigated. In all cases measured, γ decreased with increasing emitter current over the range 0.5 to 30 mA. A slight decrease of γ with increasing humidity of the ambient air was also observed.

An Electrostatic Problem, Involving a Non-Linear Fluid Dielectric, by R. CADE.

Abstract. An approximate calculation is made of the electrostatic couple on an anisotropic dielectric sphere influenced by a uniform field and immersed in a slightly non-linear fluid dielectric. The non-linearity is contained in a term in the dielectric constant proportional to the square of the field strength, and may arise from an intrinsic property of the dielectric or through electrostriction. These alternatives are discussed in the light of numerical values for the couple, and the possibility of experimental application is considered. The problem has paramagnetic and steady-current analogues, and the results are adapted to these problems.

Thermal Expansion of Potassium Chlorate, by M. A. LONAPPAN.

Abstract. The principal coefficients of expansion and the orientation of the ellipsoid of expansion have been determined for potassium chlorate for the ranges 30 to 90, 90 to 150 and 150 to 200°C. An x-ray method was used and the expansion coefficient in the directions normal to the various planes in the zones [100], [010] and [001] were determined by recording the zero layer of the rotation photographs taken about the three axes in a Unicam high temperature camera. The values of α_{22} and α_{33} are nearly equal (~ 30 to 40×10^{-6}) whereas the value of α_{11} ($\sim 130 \times 10^{-6}$) is much higher than both. The direction of the greatest expansion coefficient is found to be almost perpendicular to the plane of the oxygen atoms according to Zachariasen's structure. The expansion coefficients along a , b and c axes and the rate of change of the monoclinic angle with temperature are also given, using which the lattice dimensions of the crystal at any temperature can be determined.

Modulation of the Surface Conductance of Germanium and Silicon by External Electric Fields, by G. G. E. Low.

Abstract. A method is described which enables the modulation of surface conductance by capacitively applied electric fields to be investigated on single crystal specimens. Experimental results are given for n-type and p-type germanium and for p-type silicon. The observed conductance changes and their time dependence provide information concerning the surface barrier and the relaxation phenomena associated with departure from electronic and ionic equilibrium.

On the State of Solid Hydrogen, by K. TOMITA.

Abstract. Co-operative appearance of the rotation of hydrogen molecules in the solid phase is described using a semi-classical theory. The order of magnitude of the restriction to the rotation which is experienced by a molecule at the lowest temperature is estimated to be about 4°K using several different types of experiments, and the results are in reasonable agreement with each other. For the case of pure ortho-hydrogen a calculation of the potential energy and the anisotropy based on intermolecular forces is carried out in the Appendix.

Alpha-Gamma Angular Correlations and Internal Conversion Measurements in ThCC'' and ThC'D, by J. W. WEALE.

Abstract. The angular correlation between all γ -rays leading to ThC' ground state and the ThC'D α -rays has been measured and found isotropic, in agreement with theory. The angular correlation between the 6.04 mev α -ray and the 40 kev γ -ray in ThCC'' has been measured and found anisotropic, the best fit being the curve $W(\theta) = 1 - (0.22 \pm 0.05) \cos^2 \theta$. Spin assignments of 1 or 2, 4 and 5 are deduced for the levels ThC (ground), ThC'' (40 kev) and ThC'' (ground) respectively. The total internal conversion coefficient of the 40 kev ThCC'' γ -ray has been measured and a value for the L-shell conversion coefficient of $\alpha_L = 15.7 \pm 1.6$ is deduced. This is in much better agreement with theoretical prediction than previous measurements.

The Theory of the Reflectivity of Metals, by R. WOLFE.

Abstract. The reflectivity of an ideal metal is calculated for infra-red light by a quantum-mechanical method. It is assumed that the conduction electrons in the metal absorb light by a photoelectric process which takes place near the surface, that these electrons behave as if they are free and that the light within the metal decays according to the formula given by the classical skin effect. Two types of wave functions are assumed for the electrons, corresponding to the assumptions of specular and diffuse reflection of the electrons at the surface of the metal. The absorptivity ($1 - R$, where R is the reflectivity) in the case of specular electron reflection is found to be $A_s = (Ne^2/2\pi m v^2) v_0^3/c^3$ for diffuse reflection, $A_D = \frac{3}{4} v_0/c$. These results are the same as those obtained by Holstein and by Dingle using different methods which are essentially classical. Since A_D gives the better agreement with experiment, it is concluded that the 'diffuse reflection' wave functions are a better approximation to the exact electronic wave functions than the 'specular reflection' wave functions which have been used in previous work on the photoelectric effect and reflectivity.

Ferromagnetic Properties of Oxidized Mn₂Sb, by G. D. ADAM and K. J. STANDLEY (Research Note).

On Source Scattering in Angular Correlation Experiments with Soft Electrons, by E. BREITENBERGER (Research Note).

Levels of ²⁴Mg from the ²⁷Al(p, α)²⁴Mg Reaction, by G. W. GREENLEES (Research Note).

Electron Scattering in Photographic Emulsions, by A. HUSAIN (Research Note).

Scattering of 14.3 mev Neutrons by the ⁴He Nuclei, by D. F. SHAW (Research Note).

Performance of Hot Wire Thermal Diffusion Columns, by R. C. SRIVASTAVA (Research Note).

stripping reaction. The results, which are expressed in analytical form, have been compared in detail with the observations in two reactions using ^9Be as target nucleus at low energies.

The Radium Equivalent of ^{24}Na Sources and the Photodisintegration Cross Section of Deuterium, by W. R. McMURRAY and C. H. COLLIE.

Abstract. A stable β -detecting proportional counter has been constructed and used in the $\beta\gamma$ coincidence method to calibrate a Curie chamber substandard for ^{24}Na γ -ray sources. The mg Ra equivalent of ^{24}Na is found to be $0.333 \pm 1.5\%$ mc. This calibration leads to a revised value of the deuterium photodisintegration cross section at 2.76 mev (15.05 ± 0.5 barns).

The Slow Neutron Cross Section of Scandium, by N. J. PATTENDEN.

Abstract. The neutron total cross section of scandium oxide has been measured from 0.0015 ev to 5000 ev. A resonance in scandium was observed at (3600 ± 200) ev, with $\Gamma \sim 180$ ev, and at lower energies the cross section varied in a way which could be explained by the existence of a level with parameters $E_r = -(130 \pm 30)$ ev, $\Gamma_n^\circ = (0.84 \pm 0.25)$ ev and $\Gamma_a = (0.25 \pm 0.1)$ ev.

The Electronic Spectra of Aromatic Molecules: II—A Theoretical treatment of excited States of Alternant Hydrocarbon Molecules bases on Self-Consistent Molecular Orbitals, by J. A. POPLE.

Abstract. The theoretical treatment of the electronic spectrum of benzenoid hydrocarbons recently given by Dewar and Longuet-Higgins (Part I) is generalized so that full account is taken of electron interaction. The method is based on the use of a self-consistent molecular orbital function for the ground state and corresponding functions for excited states. It is found that all the general features of the method of Part I carry over, although certain accidental degeneracies are removed. Approximate numerical calculations based on the new method give support to the assignments made by Dewar and Longuet-Higgins.

The detachment of Electrons from Negative Hydrogen Ions by Impact with Neutral Atoms, by D. W. SIDA.

Abstract. Born's approximation is applied to calculate the cross section for detachment of an electron from a negative ion of hydrogen in collision with a helium atom as a function of the energy of the ion. The results are compared with observed data and show agreement to within a factor of two or so over an energy range from 100 to 20 000 electron volts.

The Effect of a Potential Gradient on the Density of a Degenerate Fermi Gas, by W. J. SWIATECKI.

Abstract. By studying the properties of a degenerate gas in a linearly varying potential a modified relation is derived between density and potential which replaces the usual $\rho = \text{const. } V^{3/2}$, takes into account explicitly the presence of potential gradients and can be used in regions of negative kinetic energy. When combined with Poisson's equation this gives a modified Thomas-Fermi differential equation. The resulting change in the density distribution of electrons in an atom is most marked in the outer regions, where the new equation leads to an $r^{-2} \exp(-r/a)$ decrease of density for a neutral atom. Applications to nuclear surface problems are mentioned.

On the Abrasion of Rubber, by A. SCHALLAMACH.

Abstract. The following theoretical results on the abrasion of rubber have been deduced from a few simple assumptions concerning the initiation of the surface damage. The abrasion is proportional to the normal load, independent of the particle size of the abrasive if the particles are polyhedral, and proportional to their mean radius of curvature if they can be approximated to hemispheres. The spacing of the abrasion pattern is proportional to the cube root of the normal load, proportional to the two-thirds power of the particle size on an abrasive with polyhedral particles, and directly proportional to the particle size on an abrasive with hemispherical particles.

These predictions have been reasonably well confirmed by experiment.

Diffusion and Mass Transport in Tubes, by G. I. TAYLOR (Guthrie Lecture).

Abstract. When soluble matter is introduced into a solvent flowing slowly through a capillary tube it is dispersed longitudinally by a process which involves both the variation in fluid velocity over the cross section of the tube and radial diffusion by molecular agitation. Measurements of longitudinal dispersion provide a new means for measuring diffusion coefficients. Results obtained by this method will be given.

The stability of solutions contained in vertical tubes when the density increases upwards also depends on radial diffusion. Measurements of the equilibrium density gradient can be used as another new method for determining diffusion coefficients.

The mechanics of dispersion in turbulent flow through a pipe can be discussed by a method which is analogous to that used for streamline flow. The results of this calculation are compared with experiments in which brine was injected into water flowing in 3.8 inch and 40 inch pipes, and the subsequent dispersion along the pipe was measured. Similar comparisons are made with American measurements in long pipe lines.

Information Faults in Cold-Worked Metals, by G. B. GREENOUGH and E. M. SMITH (Research Note).

Symmetry of Vibrating Square Membrane, by MARY D. WALLER (Research Note).

Note on Surface Vibrations of a Circumscribed Liquid, by MARY D. WALLER (Research Note).

Letters to the Editor

The Infra-red Luminescence of Solid Halogens, by M. J. DUMBLETON.

Absolute Calibration of Neutron Counters with Po- α -Be, by G. N. HARDING.

Dislocations and the Biot-Savart Law, by E. KROENER.

Nuclear Shell Structure, by M. H. L. PRYCE. This Letter consists of an amendment to the paper of the same title which was published in *Reports on Progress in Physics*, 17, 1 (1954). Reprints will be sent free to holders of this volume, if a stamped and addressed envelope is enclosed with the application.

height distributions expected from single γ -rays of the appropriate energies. Line shapes were measured for γ -rays from the following nuclear reactions and radio-isotopes: $^{11}\text{B}(\text{p}, \gamma)^{12}\text{C}$ (4.43 and 11.8 Mev), $^{13}\text{C}(\text{p}, \gamma)^{14}\text{N}$ (8.06 Mev), $^{19}\text{F}(\text{p}, \alpha\gamma)^{16}\text{O}$ (6.13 Mev); ^{24}Na (1.38 and 2.76 Mev), ThC'' (2.62 Mev) and

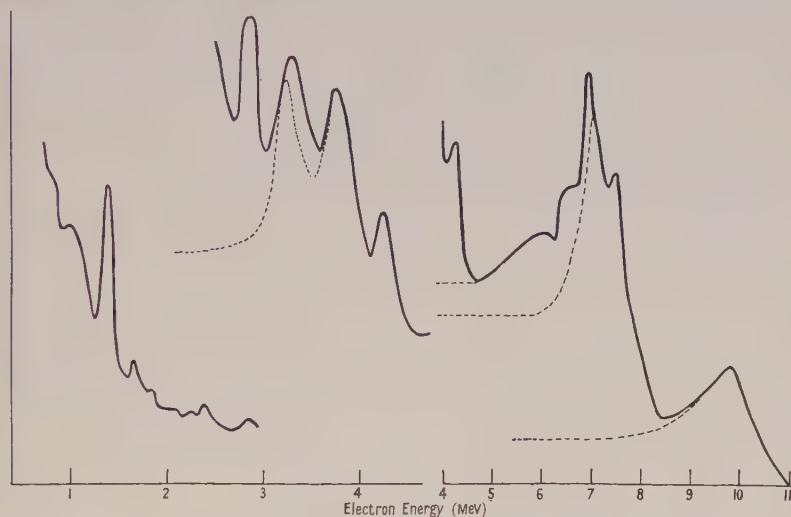


Figure 1.

^{22}Na (1.28 Mev). In the cases of $^{11}\text{B}(\text{p}, \gamma)^{12}\text{C}$ and ^{24}Na the subtraction of the higher energy γ -ray was carried out by assuming that the flat region below the group of peaks remained horizontal down to zero pulse height. This assumption was verified in each case by calculating the relative intensities of the two γ -rays, which are in cascade, from the areas under the separated curves. After allowance had been made for the variation of detection efficiency with γ -ray energy the intensities of the two γ -rays were found in each case to be equal within 10%.

Figure 2 shows some line shapes from single γ -rays normalized so that the peak corresponding to the escape of both annihilation quanta is at the same point. It was found that the low-energy tail of the measured distribution for the 8.06 Mev γ -ray from $^{13}\text{C}(\text{p}, \gamma)^{14}\text{N}$ did not interpolate smoothly between the

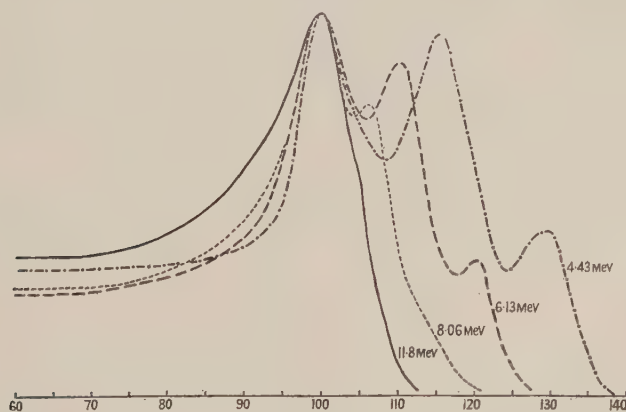


Figure 2.

curves for the 11.8 and 6.13 mev radiations. Subtraction of the interpolated from the experimental line shape yielded a curve corresponding roughly to a γ -ray of energy approximately 5.6 mev with an intensity $9 \pm 2\%$ of that of the 8.06 mev radiation. These figures are in good agreement with the values of 5.8 mev and 7% given by Barnes *et al.* (1952) and help to confirm the reliability of the method. The curve could, however, equally well correspond to a γ -ray from ^{19}F contamination ($6.13 \text{ mev} \simeq 5.65 + m_0c^2$) (see e.g. Clegg and Wilkinson 1953). We have therefore used the interpolated curve in the region below the peak, rather than the experimental distribution, to provide the standard distribution for a γ -ray of energy approximately 8 mev.

Intensities in a complex spectrum may be compared by measuring the areas under the separated single curves but this is often difficult where several γ -rays, not widely differing in energy, are involved. It was found convenient to construct curves of the quantity A/PH where P is the pulse height for a given peak, H is the number of counts per unit pulse height interval at the peak and A is the area under the curve. Figure 3 shows this quantity plotted for the three peaks of electron energy E_γ , $E_\gamma - m_0c^2$ and $E_\gamma - 2m_0c^2$ as a function of γ -ray energy using the line shapes from the standard γ -rays. Use of these curves enables the area under a curve to be determined from a knowledge of P and H only.

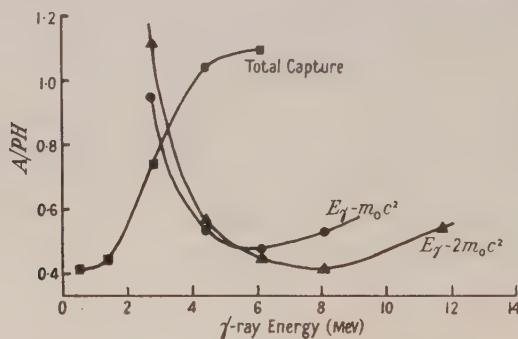


Figure 3.

§ 6. RESULTS

Table 2 shows the γ -ray energies and intensities observed at the different resonances. The intensities were measured at 90° to the proton beam but the integrated intensities in the table have been derived from a knowledge of the angular distributions of the individual components (to be presented in a later paper). The energies are thought to be accurate to within 1% for the more intense and 4% for the weak components, while the intensities are believed accurate to within 20%.

It will be noted that in no case is there evidence for a direct transition to the ground state of ^{24}Mg , which would have involved the emission of a γ -ray of about 12 mev, the Q -value being 11.69 ± 0.04 mev (Li 1952, Feather 1953).

§ 7. DECAY SCHEME

On the basis of the energy and intensity measurements of the preceding section and the known first excited state of ^{24}Mg at 1.38 mev it is possible to construct a decay scheme which provides a good account of all the experimental data. This is shown in figure 4.

Table 2

Reson. energy E_{res}	^{24}Mg E_{exc}	E_{γ}	Rel. Int.	Interpretation	
0.310	11.99	10.5	1.0	11.99	→ 1.38
		7.75	1.5	11.99	→ { 4.24 4.14?
		6.75	0.35	11.99	→ 5.26
		4.24	1.3	4.24	→ 0
		4.0	0.27	5.26	→ 1.38
		2.88	0.44	4.24	→ 1.38
				4.14?	→
		1.38	1.8	1.38	→ 0
		10.8	1.0	12.18	→ 1.38
		8.1	0.24	12.18	→ { 4.24 4.14?
0.515	12.18	7.1	0.12	12.18	→ 5.26
		4.23	0.15	4.24	→ 0
		2.86	0.06	4.24	→ 1.38
				4.14?	→
		1.38	1.2	1.38	→ 0
		10.8	1.0	12.27	→ 1.38
		8.09	1.9	12.27	→ { 4.24 4.14?
		7.01	0.61	12.27	→ 5.26
0.593	12.27	4.24	1.27	4.24	→ 0
		3.93	0.3	5.26	→ 1.38
		2.86	1.0	4.24	→ 1.38
				4.14?	→
		1.38	2.0	1.38	→ 0
		1.64	0.8	$^{20}\text{Ne}^*$	→ ^{20}Ne
		10.9	1.0	12.34	→ 1.38
		8.15	3.9	12.34	→ { 4.24 4.14?
		7.09	1.9	12.34	→ 5.26
		5.5	0.7	5.26	→ 0
0.679	12.34	4.23	2.8	4.24	→ 0
		3.91	1.0	5.26	→ 1.38
		2.84	1.4	4.24	→ 1.38
				4.14?	→
		1.38	3.2	1.38	→ 0
		1.6		$^{20}\text{Ne}^*$	→ ^{20}Ne

All energies are in Mev.

In this connection it is necessary to consider the levels of ^{24}Mg deduced from other experiments. The β -decay of ^{24}Na proceeds almost entirely to a level at 4.14 Mev which subsequently decays by the successive emission of γ -rays of 2.76 and 1.38 Mev. The 4.24 Mev γ -ray shown in the table cannot be the cross-over transition from the 4.14 Mev β -decay level since it is known that the cross-over does not occur to an extent greater than about 10^{-6} of the intensity of the cascade transition (Beghian *et al.* 1951). The energy of 4.24 Mev is, however, in excellent agreement with the energy of a level in ^{24}Mg found by inelastic scattering of protons (Hausman *et al.* 1952), while the same γ -ray is observed in the β^+ -decay of ^{24}Al (Glass *et al.* 1953, Breckon *et al.* 1954).

It would seem likely that the 2.86 Mev γ -ray arises from a transition between the 4.24 and 1.38 Mev levels although the presence of a component of 2.76 Mev

(4.14 \rightarrow 1.38) would be difficult to detect in intensity up to 50% of the 2.86 MeV γ -ray. It is thus not certain whether the 4.14 MeV level plays any part in the various cascade transitions observed.

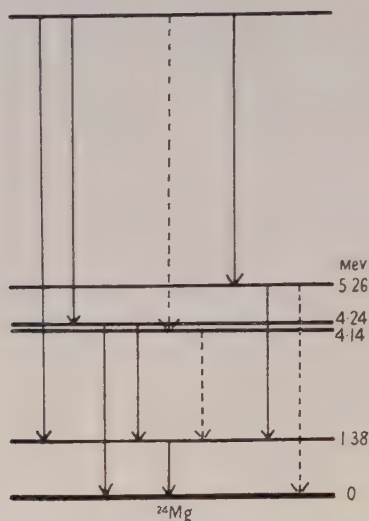


Figure 4.

§ 8. COINCIDENCE MEASUREMENTS

Confirmation of the proposed decay scheme was obtained by coincidence measurements using a second sodium iodide crystal spectrometer (with the same size of crystal) in conjunction with that already described. A pair of discriminators on the output from one spectrometer enabled the main peak region of any given γ -ray to be separated from the remainder of the spectrum. The pulses from this energy band, after shaping, were made to trigger a coincidence gate on the pulse amplitude analyser which made it sensitive for about $4\mu\text{sec}$ after the arrival of the gating pulse. The pulses from the other spectrometer were delayed by $2\mu\text{sec}$ and then applied to the analyser. When interpreting the coincidence spectra, allowance must be made for the fact that if the 'gating' pulse is due to γ -rays other than those of the highest energy in the spectrum, the 'tails' of the components of higher energy, falling in the accepted pulse-height band, contribute unwanted coincidence pulses.

The coincidence measurements at each resonance showed the same general features. Figure 5 shows the pulse-height spectrum in coincidence with the 10.6 MeV γ -ray at the 310 keV resonance. It is clearly due to a single γ -ray of 1.38 MeV, the shape for a known single γ -ray of 1.28 MeV (following the positron decay of ^{22}Na) being drawn for comparison. This observation is in direct contradiction to the results reported by Turner and supports the simple decay scheme shown in figure 4.

Measurements on the 8 MeV γ -ray revealed that it is in coincidence with the 4.24 MeV radiation and also with the γ -ray (or γ -rays) of about 2.8 MeV, the competing cascades being comparable in intensity. This again is in accord with the simple decay scheme and the intensity figures in table 2.

When the selected energy band covered the 1.38 mev peak the coincidence spectrum showed the 7 mev γ -ray enhanced in intensity relative to the 8 mev radiation, compared with the ratio observed in the single spectrometer. This helps to confirm that the 7 mev radiation feeds the 5.26 mev level which in turn decays mainly via a γ -ray of 3.9 mev in cascade with one of 1.38 mev.

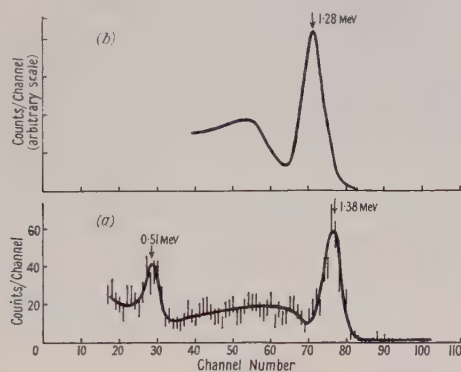


Figure 5. (a) Pulse-height spectrum of γ -radiation in coincidence with 10.6 mev γ -ray from $^{23}\text{Na}(p, \gamma)^{24}\text{Mg}$ at 310 kev resonance. (b) Pulse-height spectrum of 1.28 mev γ -ray from ^{22}Na decay.

§ 9. DISCUSSION

The decay scheme given in figure 4 provides a good account of all the observed γ -ray energies and intensities. It will be noted in table 2 that the three γ -rays of highest energy all vary in energy as the bombarding energy changes, thus definitely establishing that each is the first member of its cascade.

It is possible that the existence of the level in ^{24}Mg at 5.26 mev provides an explanation of the very weak ($\sim 1/2000$) high-energy γ -radiation reported as approximately 4 mev (Cavanagh and Turner 1951) and as approximately 3.8 mev (Beghian *et al.* 1951) which is observed in the β -decay of ^{24}Na . The transition $5.26 \rightarrow 1.38$ corresponds to an energy of 3.88 mev while the corresponding β -spectrum would have an energy of 0.27 mev. For the same type of β -transition as the observed one the intensity should be 0.025 of the main spectrum. If the low-energy spectrum is one degree more forbidden than the main spectrum this figure will be reduced by a factor of between 10 and 100, in agreement with the observed intensity. If the main spectrum is an allowed one this would suggest assigning odd parity to the 5.26 mev level. A full discussion of spin and parity assignments will, however, be deferred to a later paper presenting the results of γ -ray angular distribution and γ - γ angular correlation studies of the reaction.

ACKNOWLEDGMENTS

We would like to thank Dr. G. W. Hutchinson for a number of helpful discussions.

One of us (F.C.F.) wishes to acknowledge the award of an Imperial Chemical Industries Research Fellowship during the course of this work.

REFERENCES

- BARNES, C. A., CARVER, J. H., STAFFORD, G. H., and WILKINSON, D. H., 1952, *Phys. Rev.*, **86**, 359.
- BEGHIAN, L. E., BISHOP, G. R., and HALBAN, H., 1951, *Phys. Rev.*, **83**, 186.
- BRECKON, S. W., HENRIKSON, A., MARTIN, W. M., and FOSTER, J. S., 1954, *Canad. J. Phys.*, **32**, 223.
- BURLING, R. L., 1941, *Phys. Rev.*, **60**, 340.
- CASSON, H., 1953, *Phys. Rev.*, **89**, 809.
- CAVANAGH, P. E., and TURNER, J. F., 1951, *Phil. Mag.*, **42**, 636.
- CLEGG, A. B., and WILKINSON, D. H., 1953, *Phil. Mag.*, **44**, 1269.
- FEATHER, N., 1953, *Advances in Physics* (Phil. Mag. Suppl.), **2**, 141.
- FREEMAN, J. M., 1950, *Proc. Phys. Soc. A*, **63**, 668.
- FREEMAN, J. M., and BAXTER, A. S., 1948, *Nature, Lond.*, **162**, 696.
- GLASS, N. W., JENSEN, L. K., and RICHARDSON, J. R., 1953, *Phys. Rev.*, **90**, 320.
- HAUSMAN, H. J., ALLEN, A. J., ARTHUR, J. S., BENDER, R. S., and MCDOLE, C. J., 1952, *Phys. Rev.*, **88**, 1296.
- HUTCHINSON, G. W., and SCARROTT, G. G., 1951, *Phil. Mag.*, **42**, 792.
- LI, C. W., 1952, *Phys. Rev.*, **88**, 1038.
- NELSON, E. B., GEER, E. H., and CARLSON, R. R., 1954, *Bull. Amer. Phys. Soc.*, **29**, 62.
- RUTHERGLEN, J. G., and SMITH, R. D., 1953, *Proc. Phys. Soc. A*, **66**, 800.
- TANGEN, R., 1946, *K. Norske Vidensk. Selsk. Skr.*, No. 1.
- TURNER, O. H., 1953, *Aust. J. Phys.*, **6**, 380.

Theory of (d, p) and (d, n) Reactions

I: General Theory Ignoring Coulomb Effects

BY I. P. GRANT

Clarendon Laboratory, Oxford

MS. received 12th February 1954, and in amended form 30th April 1954

Abstract. The differential cross section for the (d, p) process is evaluated using a Green's function technique. Elastic scattering of the proton by an average central potential well is taken into account. A later specialization to the case of a harmonic oscillator potential gives a result similar to that of Horowitz and Messiah but having a closed form. Compound nucleus formation is discussed and it is shown that the (d, p) cross sections for different angular momentum transfers l_n and j_n are always additive. Polarization of the emitted particles is considered.

§1. INTRODUCTION

THE importance of (d, p) and (d, n) reactions as a tool for the determination of characteristics of nuclear states (spins, parities and, to a lesser degree, widths for nucleon emission) and of nuclear radii has been the cause of a number of attempts to clarify Butler's original deduction (1951) of the angular distribution and cross section (see, for example, Gerjuoy (1953), where a list of other references may be found). These treatments all predict the same type of angular distribution characteristic of the orbital angular momentum of the nucleon absorbed by the target nucleus. In most experiments this can be assigned unambiguously, but the values of other nuclear parameters inferred from the data (radii and level widths) are often in disagreement with those obtained by other means (Birmingham Conference 1953).

These discrepancies can be attributed to several causes, such as the theoretical neglect of compound nucleus formation of the Coulomb interaction, and of elastic scattering of the emitted nucleon. This last effect was considered by Horowitz and Messiah (1953) using a hard sphere potential for the scattering, and resulted in slight improvements in the shape of the theoretical angular distribution and in the values obtained for nuclear radii and level widths.

In this paper we report an attempt at formal investigation of the deviations from the simple theory of (d, p) and (d, n) reactions based on a Green's function technique. The interaction of the emitted particle with the target nucleus is discussed, and expressions are given for a scattering potential having a harmonic oscillator shape. Compound nucleus formation is considered formally, and it is shown that the property of incoherence of scattering amplitudes corresponding to different orbital angular momenta of the absorbed nucleon, which is characteristic of the stripping mechanism, holds for compound nucleus transitions also.

In a subsequent communication the distortion due to the Coulomb field will be discussed. The application of the results of the present investigation to

the interpretation of experimental data will be deferred to this latter communication owing to the importance of Coulomb corrections for experiments at low bombarding energies.

§ 2. FORMAL THEORY

For definiteness we consider the reaction $A(d, p)B$. We use a notation essentially that of Bhatia *et al.* (1952), though with slight differences which will be stated at the appropriate points.

We wish to solve the Schrödinger equation

$$(H - E)\Psi = 0 \quad \dots\dots(1)$$

(where the Hamiltonian $H = T + H_A + V_n + V_p + V_{np}$, T being the total kinetic energy operator in the centre-of-mass system, H_A the Hamiltonian for the internal motion of A , and V_n , V_p and V_{np} the respective interaction potentials of neutron and proton with A and with each other) for a stationary scattering state Ψ describing a reaction starting from the ground state of A , with quantum numbers α , j_A and m_A , and going to some state of B described by quantum numbers β , j_B and m_B ; α and β denote any quantum numbers necessary for the complete description of the nuclear states apart from the spins j_A and j_B . We write

$$\Psi = \Psi_0 + \Psi_1 \quad \dots\dots(2)$$

which at large distances from the scattering centre represents an incident beam of deuterons

$$\Psi_0 \xrightarrow{\text{large } r_p} \psi_0 = \chi_d(\mathbf{s}, \sigma_n, \sigma_p) \exp\left\{\frac{1}{2}i\mathbf{k}_d \cdot (\mathbf{r}_n + \mathbf{r}_p)\right\} \chi_A(\alpha, j_A, m_A; \xi) \quad (\mathbf{s} = \mathbf{r}_n - \mathbf{r}_p)$$

together with a part outgoing in protons (Ψ_1). We shall ignore Coulomb effects and other possible final channels.

Let us consider now a process resulting in a state of the final nucleus $\chi_B(\beta, j_B, m_B; \mathbf{r}_n, \sigma_n, \xi)$. The probability amplitude for a scattered proton at a point \mathbf{r}_p with spin unspecified is

$$A(\mathbf{r}_p, \sigma_p) = \int \chi_B^* \Psi d\mathbf{r}_n d\sigma_n d\xi \xrightarrow{\text{large } r_p} \frac{\exp(ik_p r_p')}{r_p'} f(\theta_p \phi_p) \chi_p(\sigma_p). \quad \dots\dots(3)$$

Strictly speaking the wave function (2) should be properly antisymmetrized with respect to all the particles, so that (3) implies a summation over all protons involving direct and exchange terms. The former involves only that proton belonging to the incident deuteron ('stripping' term), and the second includes the effect of what is usually termed compound nucleus formation. Thus we can write down the flux of protons at infinity

$$v_p |f^s(\theta_p \phi_p) + f^c(\theta_p \phi_p)|^2 \quad \dots\dots(4)$$

using the decomposition of the amplitude described above.

We cannot obtain an analytical expression for f^c , but we shall obtain one for f^s using standard Green's function methods. We decompose Ψ_1 in the corresponding way to (4),

$$\Psi_1 = \Psi_1^s + \Psi_1^c \quad \dots\dots(5)$$

and from (1), (2) and (5) we see that

$$(H - E)\Psi_1^s = -(H - E)(\Psi_0 + \Psi_1^c). \quad \dots\dots(6)$$

For large r_p , Ψ_1^s satisfies the Schrödinger equation in which there is no interaction between the outgoing proton and the other particles. Rewriting (6) in the form

$$(T + H_A + V_n - E)\Psi_1^s = -(H - E)(\Psi_0 + \Psi_1^c) - (V_p + V_{np})\Psi_1^s \quad \dots\dots(7)$$

we see that a solution for Ψ_1^s outgoing in the protons can be constructed in the symbolic form

$$\Psi_1^s = \psi_1 - G(H - E)\Psi_0 - G(V_p + V_{np})\Psi_1^s - G(H - E)\Psi_1^c \quad \dots\dots(8)$$

where $(T + H_A + V_n - E)\psi_1 = 0. \quad \dots\dots(9)$

G is the outgoing Green's function for a free proton and nucleus B, so that

$$(T + H_A + V_n - E)G(x, x') = \delta(x - x'). \quad \dots\dots(10)$$

x denotes the aggregate of coordinates required for the specification of the system. Explicitly (cf. Gerjuoy 1953)

$$G(x, x') = \sum_{\beta, j_B, m_B} g(E - E_\beta) \chi_B(\beta, j_B, m_B; \mathbf{r}_n, \sigma_n, \xi) \\ \times \chi_B^*(\beta, j_B, m_B; \mathbf{r}_n', \sigma_n', \xi') \chi_p(\sigma_p) \chi_p^*(\sigma_p') \quad \dots\dots(11)$$

the summation over the states β, j_B and m_B of the final nucleus being taken over both discrete and continuous levels. $g(E - E_\beta)$ is the free space Green's function for the proton

$$g(E - E_\beta) = -\frac{1}{4\pi} \frac{2M_p^*}{\hbar^2} \frac{\exp\{ik_p |\mathbf{r}_p' - \mathbf{r}_p''|\}}{|\mathbf{r}_p' - \mathbf{r}_p''|}. \quad \dots\dots(12)$$

Equation (8) is exact. To solve it we adopt an iterative procedure, and ignore the overlap with final configurations in our first approximation

$$\Psi_1^s \simeq \psi_1 - G(H - E)\Psi_0. \quad \dots\dots(13)$$

Assuming that this is sufficiently accurate for our purposes we have

$$\Psi = \Psi_0 + \Psi_1^c + \psi_1 - G(H - E)\Psi_0. \quad \dots\dots(14)$$

We can now estimate the amplitude f^s of (4). Firstly, the contribution from Ψ_0 will vanish at large distances unless the final configuration contains inelastically scattered deuterons (which we decided to ignore). Secondly, a simple argument due to Gerjuoy (1953) shows that the contribution from ψ_1 vanishes also. For reasons of space this is omitted here. Taking the limit of large distances r_p , we see that (14) yields

$$f^s(\beta, j_B, m_B; \theta_p \phi_p) \\ = -\frac{1}{4\pi} \frac{2M_p^*}{\hbar^2} \int \exp(-i\mathbf{k}_p \cdot \mathbf{r}_p') \chi_B^*(\beta, j_B, m_B; \mathbf{r}_n, \sigma_n, \xi) \chi_p^*(\sigma_p) (H - E)\Psi_0 dx \quad \dots\dots(15)$$

where we have made the quantum numbers explicit in the definition of the amplitude f^s .

§ 3. EVALUATION OF INTEGRALS

We denote by $I^s(\beta, j_B, m_B; \sigma_p; \theta_p \phi_p)$ the integral occurring in (15). We shall drop the quantum numbers β, j_B and m_B unless ambiguity arises by so doing.

We shall substitute ψ_0 for Ψ_0 in this integral (see §2). This is equivalent to ignoring the complicated structure of Ψ_0 within the nuclear radius r_0 . The result of performing this substitution is

$$I^s = \int \exp(-i\mathbf{k}_p \cdot \mathbf{r}_p') \chi_B^*(\mathbf{r}_n, \sigma_n, \xi) \chi_p^*(\sigma_p) (V_n + V_p) \exp\{\frac{1}{2}i\mathbf{k}_d \cdot (\mathbf{r}_n + \mathbf{r}_p)\} \\ \times \chi_d(\mathbf{s}, \sigma_n, \sigma_p) \chi_A(\xi) dx. \quad \dots\dots(16)$$

This is a sum of two terms of which the first is just the Born approximation matrix element evaluated by Bhatia *et al.* (1952). We shall state their result first, and then extend the technique to the evaluation of the second ('scattering') term. For a given final state they found

$$I^{\text{Born}} = \sum_{l_n m_n \mu_n} \langle \beta, j_B, m_B | V_n | \alpha, j_A m_A, l_n m_n, \frac{1}{2}\mu_n \rangle C(\frac{1}{2} \frac{1}{2} 1; \mu_n \mu_p) g_{l_n}^{m_n} \dots\dots(17)$$

where C is a Wigner coefficient. The nuclear matrix element is defined as the integral

$$\int \chi_B^*(\mathbf{r}_n, \sigma_n, \xi) V_n(\mathbf{r}_n, \sigma_n, \xi) \chi_A(\xi) Y_{l_n}^{m_n}(\theta_n \phi_n) \chi_{\mu_n}(\sigma_n) d\mathbf{r}_n d\sigma_n d\xi. \quad \dots\dots(18)$$

If the axis of quantization of l_n , the orbital angular momentum of the captured neutron, is taken in the direction of the recoil momentum $\mathbf{k} = \mathbf{k}_d - (M_A/M_B)\mathbf{k}_p$, then

$$g_{l_n}^{m_n} = \delta_{m_n, 0} [4\pi(2l_n + 1)]^{1/2} i^{l_n} G(q) j_{l_n}(kR) \quad \dots\dots(19)$$

where R is a mean radius at which exterior quantities dependent on r_n are evaluated. We expect R to be approximately equal to r_0 , the nuclear radius. j_l is the spherical Bessel function defined by Schiff (1949), $\mathbf{q} = \frac{1}{2}\mathbf{k}_d - \mathbf{k}_p$, and

$$G(q) = 4\pi \int_0^\infty j_0(qs) \psi(s) s^2 ds. \quad \dots\dots(20)$$

Assuming the 'zero-range' approximation

$$\psi(s) = \left(\frac{\gamma}{2\pi}\right)^{1/2} \frac{e^{-\gamma s}}{s}$$

($\gamma = 0.2317 \times 10^{-13} \text{ cm}^{-1}$, cf. for example Squires 1952) we have

$$G(q) = \frac{2(2\pi\gamma)^{1/2}}{\gamma^2 + q^2}. \quad \dots\dots(21)$$

The second part of (16), denoted by I^{scatt} , is treated similarly. We write

$$I^{\text{scatt}} = \sum_{l_n m_n \mu_n} V(l_n m_n, \frac{1}{2}\mu_n) \langle l_n m_n, \frac{1}{2}\mu_n | \phi_p(\mathbf{r}_p, \sigma_p) | 1, \mu_d \rangle_{r_n=R} \quad \dots\dots(22)$$

where $V(l_n m_n, \frac{1}{2}\mu_n)$ is independent of \mathbf{r}_p . We define the product $V\phi_p$ by

$$V(l_n m_n, \frac{1}{2}\mu_n) \phi_p(\mathbf{r}_p, \sigma_p) = \langle \beta, j_B, m_B | V_p | \alpha, j_A m_A, l_n m_n, \frac{1}{2}\mu_n \rangle \\ = \int \chi_B^*(\mathbf{r}_n, \sigma_n, \xi) V_p(\mathbf{r}_p, \sigma_p, \xi) \chi_A(\xi) Y_{l_n}^{m_n}(\theta_n \phi_n) \\ \times \chi_{\mu_n}(\sigma_n) d\mathbf{r}_n d\sigma_n d\xi \quad \dots\dots(23)$$

and

$$\begin{aligned} \langle l_n m_n, \frac{1}{2} \mu_n | \phi_p(\mathbf{r}_p, \sigma_p) | 1, \mu_d \rangle_{r_n=R} = & \left\{ \int Y_{l_n}^{m_n*}(\theta_n \phi_n) \chi_{\mu_n}^*(\sigma_n) \right. \\ & \times \chi_{\mu_p}^*(\sigma_p) \exp(-i \mathbf{k}_p \cdot \mathbf{r}_p) \cdot \phi(\mathbf{r}_p, \sigma_p) \\ & \left. \times \chi_d(\mathbf{s}, \sigma_n, \sigma_p) \exp\left\{\frac{1}{2} i \mathbf{k}_d \cdot (\mathbf{r}_n + \mathbf{r}_p)\right\} \cdot d\mathbf{r}_p d\omega_n d\sigma_p d\sigma_n \right\}_{r_n=R} \dots\dots (24) \end{aligned}$$

where analogously to Bhatia *et al.* we have replaced r_n in terms involving exterior quantities by R .

To estimate (24) we employ a mean two-body potential $\bar{\phi}(r_p)$ dependent only on the separation r_p of the proton from the target nucleus A . As in the evaluation of I^{Born} , it is convenient to use the neutron as origin for the integration over the proton coordinates, so that the integrand of (24) must be expressed in terms of \mathbf{s} and \mathbf{r}_n . We take \mathbf{k} as axis of quantization. Thus if

$$\bar{\phi}(r_p) = \sum_{\lambda \mu} \zeta_\lambda(r_n, s) Y_\lambda^{\mu*}(\theta_n \phi_n) Y_\lambda^\mu(\theta_s \phi_s) \dots\dots (25)$$

we find

$$\begin{aligned} \langle l_n m_n, \frac{1}{2} \mu_n | \bar{\phi}(r_p) | 1, \mu_d \rangle_{r_n=R} = & [4\pi(2l_n+1)]^{1/2} i^{l_n} G(q) C(\frac{1}{2} \frac{1}{2} 1; \mu_n \mu_d - \mu_n) \\ & \times \sum_l \left(\frac{2l+1}{2l_n+1} \right) i^{l-l_n} j_l(kR) \sum_\lambda (2\lambda+1)^{1/2} (-i)^\lambda M_\lambda(q) \\ & \times C(\lambda l_n; 0, 0) C(\lambda l_n; 0 m_n) Y_\lambda^{m_n*}(\theta_q \phi_q) \dots\dots (26) \end{aligned}$$

where θ_q, ϕ_q are the polar angles of \mathbf{q} with respect to \mathbf{k} and

$$M_\lambda(q) = [G(q)]^{-1} \int_0^\infty j_\lambda(qs) \zeta_\lambda(R, s) \psi(s) s^2 ds. \dots\dots (27)$$

We must make an explicit choice of potential $\bar{\phi}(r_p)$ if this is to be of any practical use. We use the attractive potential well

$$\begin{aligned} \bar{\phi}(r_p) = & -[1 - (r_p/R)^2] & r_p \leq R \\ & = 0 & r_p > R. \end{aligned}$$

Then $\zeta_0 = 4\pi \left(\frac{s}{R}\right)^2, \quad \zeta_1 = -\frac{8\pi}{3} \left(\frac{s}{R}\right), \quad \zeta_2 = 0 \text{ for } \lambda > 1 \quad s \leq 2R$
 $\zeta_\lambda = 0 \quad \text{for all } \lambda \quad s > 2R$

where r_n has been replaced by R throughout. This gives

$$M_\lambda(q) = [G(q)]^{-1} \int_0^{\alpha R} j_\lambda(qs) \zeta_\lambda(R, s) \psi(s) s^2 ds \dots\dots (28)$$

when αR is some average radius ($< 2R$). This approximation is forced upon us by our choice of a bounded potential well. The effective value of α is not expected to depend strongly on the angle of scattering.

We can now write down the complete matrix element

$$\begin{aligned} I^s = & \sum_{j_n l_n m_n \mu_n} C(\frac{1}{2} \frac{1}{2} 1; \mu_n \mu_d - \mu_n) C(l_n \frac{1}{2} j_n; m_n \mu_n) C(j_A j_n j_B; m_A m_B - m_A) \\ & \times [4\pi(2l_n+1)]^{1/2} i^{l_n} G(q) B_\beta(j_n l_n) \\ & \times \left\{ j_{l_n}(kR) \delta_{m_n, 0} + \lambda(j_n l_n) \left[M_0(q) j_{l_n}(kR) \delta_{m_n, 0} - \frac{3M_1(q)}{2l_n+1} \sqrt{\left(\frac{4\pi}{3}\right)} Y_1^{m_n*}(\theta_q, 0) \right. \right. \\ & \times \{ (l_n j_{l_n-1}(kR) - (l_n+1) j_{l_n+1}(kR)) \delta_{m_n, 0} \\ & \left. \left. + \sqrt{[\frac{1}{2} l_n(l_n+1)] [j_{l_n-1}(kR) + j_{l_n+1}(kR)]} \delta_{m_n, \pm 1} \} \right] \right\}. \dots\dots (29) \end{aligned}$$

Here we have chosen the x -axis so that it lies in the plane of the reaction and so that ϕ_q vanishes. The reduced matrix element $B_\beta(j_n l_n) = \langle \beta, j_B \parallel V_n \parallel \alpha j_A j_n(l_{n\frac{1}{2}}) \rangle$ is defined by

$$\langle \beta, j_B m_B | V_n | \alpha, j_A m_A, l_n m_n, \frac{1}{2} \mu_n \rangle = \sum_{j_n} C(l_{n\frac{1}{2}} j_n; m_n \mu_n) C(j_A j_n j_B; m_A, m_B - m_A) \\ \times \langle \beta j_B \parallel V_n \parallel \alpha j_A j_n(l_{n\frac{1}{2}}) \rangle \quad \dots\dots(30)$$

and

$$\lambda(j_n l_n) = \langle \beta j_B \parallel \alpha j_A j_n(l_{n\frac{1}{2}}) \rangle / \langle \beta j_B \parallel \phi_n' \parallel \alpha j_A j_n(l_{n\frac{1}{2}}) \rangle$$

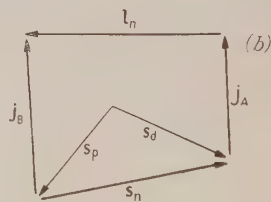
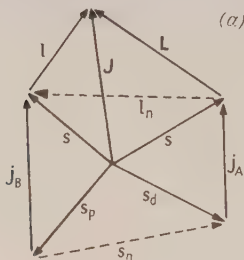
where the numerator is just the reduced matrix element of the unit operator. In defining $\lambda(j_n l_n)$ we have made the assumption that a good approximation to (23) is obtained by writing $V_p = U\phi_p(\mathbf{r}_p, \sigma_p)$ where U is the potential well-depth, and that $V_n = U\phi_n'$ where ϕ_n' is the corresponding well-shape for the neutron.

§ 4. COMPOUND NUCLEUS FORMATION

In this section we shall consider formally the formation of a compound nucleus. A formal expression for the amplitude for the production of protons with a given spin component may be written down using the group-theoretical properties of angular momentum eigenfunctions (cf. Biedenharn and Rose 1953)

$$I^c = \sum_{\substack{LSJ\Pi \\ lsm}} i^{L-l} (2L+1)^{1/2} C(j_A 1 S; m_A \mu_d) C(LSJ; 0M) \mathcal{S}(J\Pi; \alpha LS; \beta ls) \\ \times C(lsJ; M-m m) C(j_{B\frac{1}{2}} s; m_B \mu_p) Y_l^{M-m}(\theta_p \phi_p). \quad \dots\dots(31)$$

\mathcal{S} is the scattering matrix for the compound nuclear process, for which the vector diagram is given in figure 1(a). This vector diagram can be compared with that for the stripping process shown in figure 1(b). The angular momenta corresponding to the l_n and s_n of the stripping process (s_n is the spin of the neutron)



Angular momentum diagrams for (d, p) process

- (a) passing through a compound nuclear state of angular momentum \mathbf{J} ;
(b) assuming a stripping mechanism.

are shown by broken lines in figure 1(a). In this context they have the character of resultants only—for example $\mathbf{s}_n = \mathbf{s}_d - \mathbf{s}_p$, and so can take on the magnitudes $1/2$ and $3/2$, whereas in the stripping case s_n is the spin of the neutron and can take the value $1/2$ only.

Since we sum in (31) over a variety of compound states leading to the same final level we might expect that (31) could be written in a form similar to (29) involving only the initial and final states and the angular momentum transfers l_n and j_n ,

$$I^c = \sum_{\substack{j_n l_n s_n \\ m_n \mu_n}} C(s_{n\frac{1}{2}} 1; \mu_n \mu_d - \mu_n) C(j_A j_n j_B; m_A m_B - m_A) [4\pi(2l_n+1)]^{1/2} \\ \times i^{l_n} B_\beta(j_n l_n) \mathcal{S}_{l_n}^{m_n}(j_n)^c. \quad \dots\dots(32)$$

This can be done by standard techniques (Biedenharn and Rose 1953) with the result

$$\mathcal{J}_{l_n}^{m_n}(j_n)^c = (-)^{j_n - s_n} \left[\frac{2j_n + 1}{3\pi(2j_B + 1)} \right]^{1/2} \times \sum_{LSJ\Pi l_s} (-)^{J-S} (2J+1) [(2L+1)(2S-1)(2s+1)]^{1/2} \times i^{L-l-l_n} C(Ll l_n; 0 m_n) W(LS l_s; J l_n) X(s S l_n; j_B j_A j_n; \frac{1}{2} 1 s_n) \times [\mathcal{O}(J\Pi; \alpha LS; \beta l_s) B_\beta(j_n l_n)] Y_l^{m_n*}(\theta_p \phi_p) \quad \dots\dots (33)$$

where W is the Racah coefficient and the X coefficient is defined by Fano (1951). The phase factor i^{L-l-l_n} will be real since $L-l-l_n$ must be even by conservation of parity.

§ 5. THE DIFFERENTIAL CROSS SECTION

We are now in a position to write down the complete formal expression for the differential cross section. From (4), (15), (29) and (32) we obtain, on performing a statistical average over initial spin states and on summing over final spin states,

$$\frac{d\sigma}{d\omega} = \frac{M_p^* M_d^*}{4\pi^2 \hbar^4} \frac{k_p}{k_d} \sum_{s_B} \sum_{s_A} \frac{1}{3(2j_A + 1)} |I^s + I^c|^2, \quad \dots\dots (34)$$

which reduces by virtue of the orthogonality properties of Wigner coefficients to

$$\frac{d\sigma}{d\omega} = \frac{M_p^* M_d^*}{2\pi \hbar^4} \frac{k_p}{k_d} \sum_{s_B} \left(\frac{2j_B + 1}{2j_A + 1} \right) \sum_{l_n} |B_\beta(j_n l_n)|^2 |\mathcal{J}_{l_n}^{m_n}(j_n)|^2 \quad \dots\dots (35)$$

and the amplitude $\mathcal{J}_{l_n}^{m_n}(j_n)$ is made up of two terms $\mathcal{J}_{l_n}^{m_n}(j_n)^s$ and $\mathcal{J}_{l_n}^{m_n}(j_n)^c$, of which the latter is defined in (39). \mathcal{J}^s is defined in the same way as \mathcal{J}^c . The sum over s_n is of course purely formal for the terms \mathcal{J}^s as only those terms for which $s_n = \frac{1}{2}$ contribute.

Thus the complete differential cross section can be written as the sum of three terms,

$$\frac{d\sigma}{d\omega} = \left(\frac{d\sigma}{d\omega} \right)_{\text{strip}} + \left(\frac{d\sigma}{d\omega} \right)_{\text{Cpd}} + \left(\frac{d\sigma}{d\omega} \right)_{\text{Int}} \quad \dots\dots (36)$$

corresponding to stripping, compound nucleus formation, and interference terms respectively. In fact, selecting a given final state β, j_B , we see that

$$\left(\frac{d\sigma}{d\omega} \right)_{\text{strip}} = \frac{M_p^* M_d^*}{2\pi \hbar^4} \frac{k_p}{k_d} \left(\frac{2j_B + 1}{2j_A + 1} \right) \sum_{j_n m_n} |B_\beta(j_n l_n)|^2 |\mathcal{J}_{l_n}^{m_n}(j_n)^s|^2, \quad \dots\dots (37)$$

with $|\mathcal{J}^c|^2$ replaced by $|\mathcal{J}^s|^2$ and $2\text{Re}(\mathcal{J}^{s*}\mathcal{J}^c)$ in the case of the compound nucleus and interference terms. Explicitly

$$\sum_{m_n} |\mathcal{J}_{l_n}^{m_n}(j_n)^s|^2 = G^2(q) \cdot \left[\left| j_n(kR) - \lambda(l_n l_n) \right. \right. \\ \times \left[M_0(q) j_{\frac{1}{2}}(kR) - \frac{3M_1(q)}{2l_n + 1} \cos \theta_{\frac{1}{2}}(l_n j_{n-1}(kR) - (l_n + 1) j_{n+1}(kR)) \right] \Big|^2 \\ \left. + \frac{1}{2} l_n(l_n + 1) |\lambda(j_n l_n) \frac{3M_1(q)}{2l_n + 1} \sin \theta_{\frac{1}{2}}(j_{\frac{1}{2}-1}(kR) + j_{\frac{1}{2}+1}(kR))|^2 \right] \dots\dots (38)$$

§ 6. PRODUCTION OF POLARIZED PARTICLES

The polarization vector \mathbf{P}_p which is the expectation value of σ_p has components in an arbitrary coordinate system

$$P_z = \pm \frac{2}{3} \frac{\sum_{s_n} \{ |B_\beta(j_n l_n)|^2 \} / \{ 2j_n + 1 \} \sum_{m_n} m_n | \mathcal{J}_{l_n}^{m_n}(j_n)^s |^2}{\sum_{s_n} |B_\beta(j_n l_n)|^2 \sum_{m_n} | \mathcal{J}_{l_n}^{m_n}(j_n) |^2} \dots\dots (39a)$$

(\pm corresponding to $j_n = l_n \pm \frac{1}{2}$) and

$$P_x = \pm \frac{2}{3} \frac{\sum_{s_n} [\{ |B_\beta(j_n l_n)|^2 \} / \{ 2j_n + 1 \}] \sum_{\mu} [(l_n + \frac{1}{2})^2 - \mu^2]^{1/2} \text{Re} [\mathcal{J}_{l_n}^{\mu-1/2}(j_n) \cdot \mathcal{J}_{l_n}^{\mu+1/2}(j_n)]}{\sum_{s_n} |B_\beta(j_n l_n)|^2 \sum_{m_n} | \mathcal{J}_{l_n}^{m_n}(j_n) |^2} \dots\dots (39b)$$

$$P_y = \pm \frac{2}{3} \frac{\sum_{s_n} [\{ |B_\beta(j_n l_n)|^2 \} / \{ 2j_n + 1 \}] \sum_{\mu} [(l_n + \frac{1}{2})^2 - \mu^2]^{1/2} \text{Im} [\mathcal{J}_{l_n}^{\mu+1/2}(j_n) \cdot \mathcal{J}_{l_n}^{\mu-1/2}(j_n)]}{\sum_{s_n} |B_\beta(j_n l_n)|^2 \sum_{m_n} | \mathcal{J}_{l_n}^{m_n}(j_n) |^2} \dots\dots (39c)$$

where the incident deuterons are assumed unpolarized.

With a choice of axes as in § 3, the amplitudes $\mathcal{J}_{l_n}^{m_n}(j_n)$ are real save for a common factor i^{l_n} , and it may be easily verified that the resultant polarization vanishes when compound nucleus terms are ignored. However, when the Coulomb field is taken into account, some of the components of \mathbf{P}_p may be expected to be non-vanishing, since $i^{l_n} \mathcal{J}_{l_n}^{m_n}(j_n)^s$ will no longer be real.

§ 7. DISCUSSION

In the preceding paragraphs we have considered the corrections to the simple (d, p) differential cross section which are due to the elastic interaction of the emitted particle with the nucleus. The result is dependent on nuclear structure through the constant $\lambda(j_n l_n)$, and it should be possible to correlate the value of this constant obtained experimentally with the predictions of nuclear models. This is in contrast to the model of Horowitz and Messiah (1953), which gives a result dependent on the size of the nucleus but not on the structure.

In considering the interaction of the proton with the nucleus we omitted two sets of terms. The first arises from the fact that the wave function Ψ should be completely antisymmetrical in all the nucleons, and that we have singled out those terms which give the direct scattering of the proton originally bound in the deuteron, and have ignored those corresponding to proton exchange. The second set arise from higher order approximations to the solution of the integral equation (8) than we have considered in (13). They correspond to transitions involving intermediate states. Both sets of terms are part of what is usually described as the contribution of the compound nucleus. The fact that the simple stripping theory gives a very good account of the angular distribution in (d, p) reactions suggests either that the effect of the neglected terms is small, or that they have a similar form to those due to the stripping mechanism. This latter possibility is suggested by the result of § 4, but it is not possible at present to decide which of them is valid.

ACKNOWLEDGMENTS

The author would like to thank Dr. R. J. Blin-Stoyle for advice on this problem, Dr. L. A. Radicati for reading the manuscript and Mr. G. R. Satchler for many interesting discussions. He also thanks the Department of Scientific and Industrial Research for a maintenance grant.

REFERENCES

- BHATIA, A. B., HUANG, K., HUBY, R., and NEWNS, H. C., 1952, *Phil. Mag.*, **43**, 485.
BIEDENHARN, L. C., and ROSE, M. E., 1953, *Rev. Mod. Phys.*, **25**, 729.
BUTLER, S. T., 1951, *Proc. Roy. Soc. A*, **208**, 559.
FANO, U., 1951, *National Bureau of Standards Report* 1214.
GERJUOY, E., 1953, *Phys. Rev.*, **91**, 645.
HOROWITZ, J., and MESSIAH, A. M. L., 1953, *J. Phys. Radium*, **14**, 695.
Report of the Birmingham Conference on Nuclear Physics, July 1953, p. 41.
SCHIFF, L. I., 1949, *Quantum Mechanics* (New York : McGraw-Hill), p. 77.
SQUIRES, G. L., 1952, *Progress in Nuclear Physics* (London : Pergamon Press).

The D-D Reaction

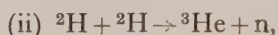
By W. M. FAIRBAIRN†

Department of Mathematical Physics, University of Birmingham

Communicated by R. E. Peierls; MS. received 9th July 1954

Abstract. The two reactions ${}^2\text{H}(\text{d}, \text{p}){}^3\text{H}$ and ${}^2\text{H}(\text{d}, \text{p}){}^3\text{He}$ are examined under the assumption that they proceed via a stripping process. Coulomb effects are ignored. The angular distribution of the protons from the ${}^2\text{H}(\text{d}, \text{p}){}^3\text{H}$ reaction, and the variation with bombarding energy of the forward cross section are used for the comparison between the theoretical predictions and the experimental data. The agreement which is found is sufficiently good to justify the assumption that the reactions proceed partly via a stripping process. Stripping becomes the predominant process for bombarding energies greater than 5 mev (lab.).

WHEN deuterium is bombarded with deuterons two of the possible reactions are



and both of these reactions could proceed via a stripping process. In this paper we investigate such a hypothesis and consider to what extent it is justifiable.

Experimental results on the angular distributions of the products from the D-D reaction are now available up to a value of 20 mev for the bombarding energy. At very low energies (below about 5 mev) a theoretical description of the reaction has been given under the assumption that all four nucleons interact with each other (Beiduk *et al.* 1950), and it has been reasonably successful in explaining the angular distributions. However at higher energies the forward maxima in the angular distributions indicate that reactions (i) and (ii) may proceed predominantly via a stripping process. Such a conclusion might seem surprising for such a light nucleus as the bombarded deuterium, but it has been shown that the stripping process is important in the ${}^3\text{H}(\text{d}, \text{n}){}^4\text{He}$ reaction (Butler and Symonds 1951).

Since we neglect the effect of Coulomb forces the two reactions (i) and (ii) are considered together, but for the sake of clarity we deal only with the ${}^2\text{H}(\text{d}, \text{p}){}^3\text{H}$ reaction. There is one essential difference between the analysis of this reaction and the analysis of the 'normal' stripping process (Butler 1951) and that is the identity of the bombarding and the bombarded particles. Because of this the reaction can proceed in two ways: either the bombarded deuteron can strip off a neutron from the bombarding deuteron or the bombarding deuteron can pick up a neutron from the bombarded deuteron. Both possibilities give a free observable proton and, because the probability for either occurring is the same, in the centre-of-mass system the angular distribution of the protons must be symmetrical about 90° .

† Now at Department of Mathematics, University of Glasgow.

The wave functions for the system must be symmetrical in the deuteron coordinates (since they are particles with integral spin), and antisymmetrical in the neutron and the proton coordinates (since nucleons have half-integral spin). Therefore in the centre-of-mass system the initial configuration is represented by the wave function

$$\begin{aligned} \Psi_{M_1 M_2}(\mathbf{r}_{n1}, \mathbf{r}_{n2}, \mathbf{r}_{p1}, \mathbf{r}_{p2}) &= \exp \{i\mathbf{K} \cdot (\mathbf{r}_{n1} + \mathbf{r}_{p1})/2\} \phi(\mathbf{r}_{p1} - \mathbf{r}_{n1}) \chi_1(M_1) \\ &\times \exp \{-i\mathbf{K} \cdot (\mathbf{r}_{n2} + \mathbf{r}_{p2})/2\} \phi(\mathbf{r}_{p2} - \mathbf{r}_{n2}) \chi_1(M_2) \\ &+ \exp \{-i\mathbf{K} \cdot (\mathbf{r}_{n1} + \mathbf{r}_{p2})/2\} \phi(\mathbf{r}_{p1} - \mathbf{r}_{n2}) \chi_1(M_2) \\ &\times \exp \{i\mathbf{K} \cdot (\mathbf{r}_{n2} + \mathbf{r}_{p1})/2\} \phi(\mathbf{r}_{p2} - \mathbf{r}_{n1}) \chi_1(M_1) \\ &- \exp \{i\mathbf{K} \cdot (\mathbf{r}_{n2} + \mathbf{r}_{p1})/2\} \phi(\mathbf{r}_{p1} - \mathbf{r}_{n2}) \chi_1(M_1) \\ &\times \exp \{-i\mathbf{K} \cdot (\mathbf{r}_{n1} + \mathbf{r}_{p2})/2\} \phi(\mathbf{r}_{p2} - \mathbf{r}_{n1}) \chi_1(M_2) \\ &- \exp \{-i\mathbf{K} \cdot (\mathbf{r}_{n2} + \mathbf{r}_{p1})/2\} \phi(\mathbf{r}_{p1} - \mathbf{r}_{n2}) \chi_1(M_2) \\ &\times \exp \{i\mathbf{K} \cdot (\mathbf{r}_{n1} + \mathbf{r}_{p2})/2\} \phi(\mathbf{r}_{p2} - \mathbf{r}_{n1}) \chi_1(M_1), \quad \dots\dots(1) \end{aligned}$$

where $\mathbf{r}_{n1}, \mathbf{r}_{n2}$ are the position vectors of the neutrons, $\mathbf{r}_{p1}, \mathbf{r}_{p2}$ are the position vectors of the protons, $2\hbar\mathbf{K}$ is the relative momentum of the two deuterons which have magnetic quantum numbers M_1 and M_2 . $\chi_1(M)$ is the spin wave function for a particle of spin 1, and $\phi(\mathbf{r}_p - \mathbf{r}_n)$ is the internal wave function for the deuteron. (At present we take M_1 and M_2 as fixed but finally we require to sum and average over these quantum numbers.) (1) can be written as

$$\begin{aligned} &\sum_{\mu_{n1}\mu_{n2}\mu_{p1}\mu_{p2}} \iint d\mathbf{k}_{p1} d\mathbf{k}_{p2} \exp(i\mathbf{k}_{p1} \cdot \mathbf{r}_{p1}) \exp(i\mathbf{k}_{p2} \cdot \mathbf{r}_{p2}) \chi_{\frac{1}{2}}(\mu_{n1}) \chi_{\frac{1}{2}}(\mu_{n2}) \chi_{\frac{1}{2}}(\mu_{p1}) \chi_{\frac{1}{2}}(\mu_{p2}) \\ &\times \{C_{\frac{1}{2}\mu_{n1}\frac{1}{2}\mu_{p1}}^{1M_1} C_{\frac{1}{2}\mu_{n2}\frac{1}{2}\mu_{p2}}^{1M_2} \phi_T(\frac{1}{2}\mathbf{K} - \mathbf{k}_{p1}) \phi_T(-\frac{1}{2}\mathbf{K} - \mathbf{k}_{p2}) \\ &\times \exp \{i(\mathbf{K} - \mathbf{k}_{p1}) \cdot \mathbf{r}_{n1}\} \exp \{i(-\mathbf{K} - \mathbf{k}_{p2}) \cdot \mathbf{r}_{n2}\} + \text{three similar terms}\}, \quad \dots(2) \end{aligned}$$

where $\chi_{\frac{1}{2}}(\mu)$ is the spin wave function for a particle of spin $\frac{1}{2}$, $C_{b\beta c\gamma}^{a\alpha}$ are the usual Clebsch-Gordan vector coupling coefficients, and $\phi_T(\mathbf{Q}) = \int \phi(\mathbf{r}) \exp(i\mathbf{Q} \cdot \mathbf{r}) d\mathbf{r}$.

The proton which is observed in the reaction is either p1 or p2, and therefore the tritium nucleus produced has either p2 or p1 as one of its constituent nucleons. If p1 is taken to be the observed proton then near the boundaries

$$\begin{aligned} (a) \quad &|\mathbf{r}_{n1} - \frac{1}{3}(\mathbf{r}_{n1} + \mathbf{r}_{n2} + \mathbf{r}_{p2})| = r_0 \\ (b) \quad &|\mathbf{r}_{n2} - \frac{1}{3}(\mathbf{r}_{n1} + \mathbf{r}_{n2} + \mathbf{r}_{p2})| = r_0 \end{aligned}$$

the triton wave function reduces to the product of a wave function for a deuteron and a wave function for a neutron (n1 near boundary (a), and n2 near boundary (b)). Outside these boundaries the wave function is an exponentially decreasing function of the radial coordinate of the neutron. For example, near boundary (a) the 'interior' wave function is

$$\begin{aligned} \Phi_{m\mu_{p1}}(\mathbf{r}_{n1}, \mathbf{r}_{n2}, \mathbf{r}_{p1}, \mathbf{r}_{p2}) &= \sum_{M_2\mu_{n1}} \int d\mathbf{k}_{p1} \exp(i\mathbf{k}_{p1} \cdot \mathbf{r}_{p1}) \chi_{\frac{1}{2}}(\mu_{p1}) \\ &\times \exp \{-i\mathbf{k}_{p1} \cdot (\mathbf{r}_{n1} + \mathbf{r}_{n2} + \mathbf{r}_{p2})/3\} \phi(\mathbf{r}_{p2} - \mathbf{r}_{n2}) \\ &\times \chi_1(M_2) \chi_{\frac{1}{2}}(\mu_{n1}) u_{jm\mu_{p1}}^{M_2\mu_{n1}} \{\mathbf{k}_{p1}, \mathbf{r}_{n1} - \frac{1}{3}(\mathbf{r}_{n1} + \mathbf{r}_{n2} + \mathbf{r}_{p2})\} \\ &\dots\dots(3) \end{aligned}$$

where j and m are the spin and the magnetic quantum number of the triton state: outside the boundary (a) the wave function (4) is the same as (3) except that the function $u_{jm\mu_{p1}}^{M_2\mu_{n1}}$ is replaced by an exponentially decreasing function of $|\mathbf{r}_{n1} - \frac{1}{3}(\mathbf{r}_{n1} + \mathbf{r}_{n2} + \mathbf{r}_{p2})|$.

If p_2 is the observed proton we have similar wave functions near and outside the boundaries

$$(c) \quad |\mathbf{r}_{n1} - \frac{1}{3}(\mathbf{r}_{n1} + \mathbf{r}_{n2} + \mathbf{r}_{p1})| = r_0$$

$$(d) \quad |\mathbf{r}_{n2} - \frac{1}{3}(\mathbf{r}_{n1} + \mathbf{r}_{n2} + \mathbf{r}_{p1})| = r_0.$$

Following the approach of Butler (1951) we write in (3)

$$u_{jm\mu_{p1}}^{M_2\mu_{n1}}(\mathbf{k}_{p1}, \mathbf{R}) = \sum_{l_{n1}m_{n1}l_1m_{l1}} B_{jm\mu_{p1}}(\mathbf{k}_{p1}) C_{l_1m_{l1}1M_2}^{jm} C_{l_{n1}m_{n1}1\mu_{n1}}^{I_1m_{I1}} Y_{l_{n1}m_{n1}}(\theta_{n1}, \phi_{n1}) \\ \times k_{n1} a_{l_{n1}}^{jI_1}(k_{p1}) \{h_{l_{n1}}^{(1)}(k_{n1}R) + b_{l_{n1}}^{jI_1}(k_{p1}) h_{l_{n1}}^{(2)}(k_{n1}R)\} \quad \dots\dots (4)$$

where $\mathbf{R} = \mathbf{r}_{n1} - \frac{1}{3}(\mathbf{r}_{n1} + \mathbf{r}_{n2} + \mathbf{r}_{p2})$, $l_1 = l_{n1} + \frac{1}{2}$, $m_{l1} = m_{n1} + \mu_{n1}$, $Y_{lm}(\theta, \phi)$ are the normalized spherical harmonics with the phases given by Condon and Shortley (1951), $h_{l_n}^{(1), (2)}(KR)$ are the spherical Hankel functions as defined by Schiff (1949), $-3\hbar^2 k_{n1}^2/4M_n = E_n$, the binding energy of the neutron in the triton, M_n being the neutron mass. For the wave function outside the boundary we replace

$$B_{jm\mu_{p1}}(\mathbf{k}_{p1}) a_{l_{n1}}^{jI_1}(k_{p1}) \{h_{l_{n1}}^{(1)}(k_{n1}R) + b_{l_{n1}}^{jI_1}(k_{p1}) h_{l_{n1}}^{(2)}(k_{n1}R)\}$$

by

$$A_{jm\mu_{p1}}^{I_1l_{n1}}(\mathbf{k}_{p1}) h_{l_{n1}}^{(1)}(k_{n1}R).$$

The wave functions (2), (3), (4) and their derivatives are matched at the boundaries (a)–(d) by a method rather similar to that used by Butler (1951). For details the reader is referred to Fairbairn (1953), and here only the final result is stated. The differential cross section $\sigma_s(\theta_p, \phi_p)$ in the $^2\text{H}(\text{d}, \text{p})^3\text{H}$ reaction is given by

$$\sigma_s(\theta_p) = \frac{(2j_s + 1)k_{ps}}{K} \sum_{l_n m_n} N_{l_n}^{j_s}(k_{ps}, r_0) \\ \times |F_{l_n}(\theta_p) Y_{l_n m_n}(\theta_{z_1}, \phi_{z_1}) + (-1)^{l_n} F_{l_n}(\pi - \theta_p) Y_{l_n m_n}(\theta_{z_2}, \phi_{z_2})|^2, \quad \dots\dots (5)$$

where s denotes the state of ^3H which is formed (spin j_s), $N_{l_n}^{j_s}(k_{ps}, r_0)$ is independent of θ_p , $\mathbf{Z}_1 = \mathbf{K} - \frac{2}{3}\mathbf{k}_{ps}$, $\mathbf{Z}_2 = \mathbf{K} + \frac{2}{3}\mathbf{k}_{ps}$,

$$F_{l_n}(\theta_p) = \phi_T(\frac{1}{2}\mathbf{K} - \mathbf{k}_{ps}) \{j_{l_n}(Z_1 r_0) \frac{\partial}{\partial r_0} h_{l_n}^{(1)}(i\kappa_s r_0) - h_{l_n}^{(1)}(i\kappa_s r_0) \frac{\partial}{\partial r_0} j_{l_n}(Z_1 r_0)\},$$

$\kappa_s^2 = -k_{ns}^2 = 4M_n E_{ns}/3\hbar^2$, $F_{l_n}(\pi - \theta_p)$ is $F_{l_n}(\theta_p)$ with \mathbf{k}_{ps} replaced by $-\mathbf{k}_{ps}$ and Z_1 replaced by Z_2 . The ground state ($s=0$, say) of the triton has spin $\frac{1}{2}$ and even parity and the added neutron must have $l_n=0$, $I=\frac{1}{2}$. Using this in (5) we obtain

$$\sigma_0(\theta_p) = \frac{8\pi C^2 k_{p0}}{K \kappa_0^2 r_0^2} \exp(-2\kappa_0 r_0) N_{\frac{1}{2}, 0}^{\frac{1}{2}}(k_{p0}, r_0) \\ \times \left\{ \left[\frac{\kappa_0}{Z_1} \sin Z_1 r_0 + \cos Z_1 r_0 \right] \left[\frac{1}{\frac{1}{4}K^2 + k_{p0}^2 + a^2 - Kk_{p0} \cos \theta_p} \right. \right. \\ \left. \left. - \frac{1}{\frac{1}{4}K^2 + k_{p0}^2 + (a+b)^2 - Kk_{p0} \cos \theta_p} \right] \right. \\ \left. + \text{term with } \theta_p \rightarrow (\pi - \theta_p), Z_1 \rightarrow Z_2 \right\}, \quad \dots\dots (6)$$

where we have taken

$$\phi(\mathbf{r}_p - \mathbf{r}_n) = C \{ \exp(-a|\mathbf{r}_p - \mathbf{r}_n|) [1 - \exp(-b|\mathbf{r}_p - \mathbf{r}_n|)] / |\mathbf{r}_p - \mathbf{r}_n| \}.$$

Since

$$Z_1^2 = K^2 + 4k_{p0}^2/9 - (4Kk_{p0} \cos \theta_p)/3$$

$$Z_2^2 = K^2 + 4k_{p0}^2/9 + (4Kk_{p0} \cos \theta_p)/3$$

$\sigma_0(\theta_p)$ is symmetrical about $\theta_p = 90^\circ$.

Because of the loose structure of the bombarded nucleus in this reaction the radius r_0 is not well defined. In the present calculations the value $r_0 = 4 \times 10^{-13}$ cm has been used. The Q -value for the reaction is 4.034 mev and figures 1 and 2 show the comparison between experimental cross sections and those predicted by (6). The experiments were performed at 7.94 mev (Burrows *et al.* 1951) and at 19.1 mev (R. G. Freemantle, private communication, 1954), both energies being given in the laboratory system.

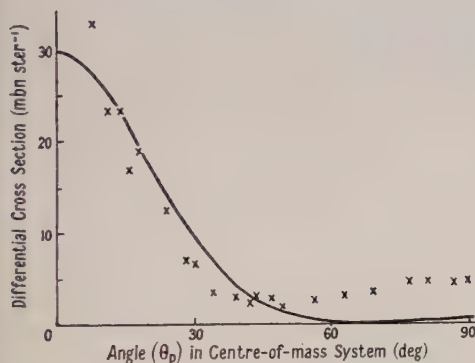


Figure 1. Comparison between the theoretical curve (magnitude in arbitrary units) and the experimental points for 7.94 mev (laboratory) incident deuterons.

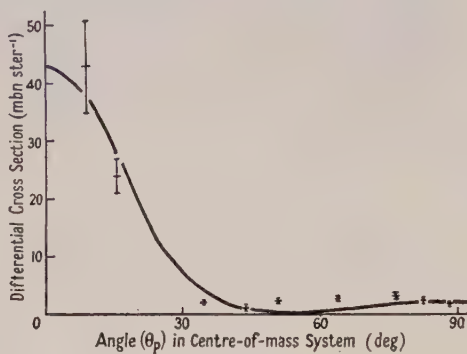


Figure 2. Comparison between the theoretical curve (magnitude in arbitrary units) and the experimental points for 19.1 mev (laboratory) incident deuterons.

An examination of the curves in figures 1 and 2 shows that formula (6) reproduces the main features of the experimental angular distribution. The cross sections found experimentally are symmetrical about 90° as expected. Experimental results at lower bombarding energies have also been analysed but the agreement is not so good as in the two cases shown. This is true also for the ${}^2\text{H}(d, n){}^3\text{He}$ reaction. The probable reason for the discrepancy is the neglect throughout the work of Coulomb forces: in the D-D reaction a bombarding energy of 8 mev in the lab. system is equivalent to only 4 mev in the centre-of-mass system and at such low energies Coulomb effects are non-negligible.

As a further test of the assumption of a stripping process we examine the variation in the cross section as the bombarding energy is increased. Since the forward and the backward scattering are equal a good estimate of this value can be made even although measurements cannot be taken at either of these two positions. The variation of $\sigma_0(\theta_p = 0)$ as given by formula (6) is shown in figure 3: the experimental variation is shown in figure 4. We see that below an energy of about 6 mev the two curves differ considerably. The low cross sections at these lower energies are presumably due to the effects of Coulomb forces which will decrease the cross sections through the mutual repulsion of

the deuterons. At the higher energies the curves are more alike, but it cannot be said that the theoretical predictions give exactly the experimental variation.

The qualitative agreement which has been found between the experimental data and the theoretical predictions is sufficiently good to justify the assumption that the D-D reaction proceeds partly via a stripping process. As the bombarding energy is increased the stripping process becomes predominant. It should be added that in an analysis of the angular distributions from the reactions (i) and (ii) between laboratory energies of 2 mev and of 11 mev a better fit could be obtained

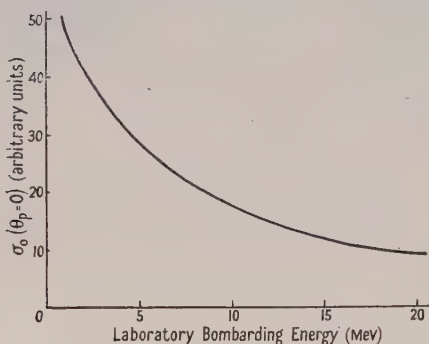


Figure 3. Theoretical variation with bombarding energy of the forward (or backward) scattering.

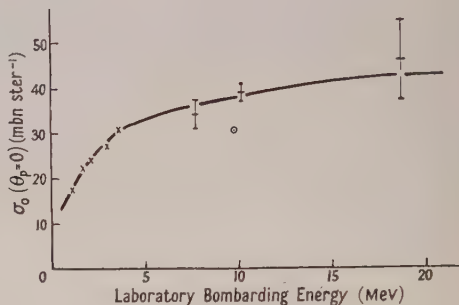


Figure 4. Experimental variation with bombarding energy of the forward (or backward) scattering: points below 6 mev given by Blair *et al.* (1948) and Hunter and Richards (1949); at 9.94 mev by Leiter *et al.* (1950) (probable error stated to be large); at 10.3 mev by Allred *et al.* (1951).

if an effect is introduced which interferes destructively with the pure stripping effect. Such an effect has been found by Horowitz and Messiah (1953 a) who alter the assumptions of the stripping process to include the proton-nucleus interaction. Since such an interaction must be present in the D-D reaction at the lower energies it is likely that the polarization of the protons and of the neutrons from the D-D reaction at low energies (see, for example, Baungartner and Huber 1952) can be explained in this way (Horowitz and Messiah 1953 b).

ACKNOWLEDGMENTS

The author wishes to thank Professor R. E. Peierls for suggesting this problem, and to acknowledge the receipt of a Department of Scientific and Industrial Research maintenance allowance.

REFERENCES

- ALLRED, J. C., PHILLIPS, D. D., and ROSEN, L., 1951, *Phys. Rev.*, **82**, 782.
 BAUNGARTNER, E., and HUBER, P., 1952, *Helv. Phys. Acta*, **25**, 626.
 BEIDUK, F. M., PRUETT, J. R., and KONOPINSKI, E. J., 1950, *Phys. Rev.*, **77**, 622.
 BLAIR, J. M., FREIER, G., LAMPI, E., SLEATOR, W., and WILLIAMS, J. H., 1948, *Phys. Rev.*, **74**, 1599.
 BUTLER, S. T., 1951, *Proc. Roy. Soc. A*, **208**, 559.
 BUTLER, S. T., and SYMONDS, J. L., 1951, *Phys. Rev.*, **83**, 858.
 BURROWS, H. B., GIBSON, W. M., and ROTBLAT, J., 1951, *Proc. Roy. Soc. A*, **209**, 489.

- CONDON, E. V., and SHORTLEY, G. H., 1951, *Theory of Atomic Spectra* (Cambridge : University Press).
- FAIRBAIRN, W. M., 1953, *Thesis*, University of Birmingham.
- HOROWITZ, J., and MESSIAH, A. M. L., 1953 a, *J. Phys. Radium*, **14**, 695; 1953 b, *Ibid.*, **14**, 731.
- HUNTER, G. T., and RICHARDS, H. T., 1949, *Phys. Rev.*, **76**, 1445.
- LEITER, H. A., RODGERS, F. A., and KRUGER, P. G., 1950, *Phys. Rev.*, **78**, 663.
- SCHIFF, L. I., 1949, *Quantum Mechanics* (New York : McGraw-Hill).

NOTE ADDED IN PROOF

Mr. R. G. Freemantle has informed the author that the estimate given in figure 4 for the value of $\sigma_0(\theta_p=0)$ at 19.1 mev should be multiplied by 0.93. Also the experimental angular distribution for the ${}^2\text{H}(d, n){}^3\text{He}$ reaction at 19.1 mev is in reasonable agreement with the distribution which is calculated from (6) with the roles of proton and neutron interchanged and with the Q -value 3.28 mev. Unfortunately measurements have not yet been taken at small enough angles for any detailed comparisons to be made. The author is grateful to Mr. R. G. Freemantle for informing him of these results prior to publication.

The Sidereal Correlation of Extensive Air Showers

By F. J. M. FARLEY AND J. R. STOREY

Auckland University College, Auckland, New Zealand

MS. received 21st June 1954

Abstract. About 3×10^5 extensive air-shower events were recorded at Auckland (altitude 40 m, latitude 37° S.) with 3 counter trays at the corners of a 4 m triangle, each of sensitive area 2360 cm^2 , in the period February 1951 to February 1952. The results show a solar diurnal amplitude of $(1.45 \pm 0.25)\%$ with maximum at (2.7 ± 0.6) hours local solar time and a sidereal diurnal amplitude of $(1.10 \pm 0.26)\%$ with maximum at (19.8 ± 0.9) hours local sidereal time (standard errors). By introducing the concept of antisidereal time (there are 364.2 antisidereal days per year) an allowance is made for the seasonal amplitude modulation of the solar diurnal variation. When this correction is applied, the true sidereal diurnal amplitude becomes $(1.43 \pm 0.38)\%$ with maximum at (17.6 ± 1.0) hours local sidereal time. The results indicate a maximum in the cosmic ray intensity when the galactic plane is overhead.

§ 1. INTRODUCTION

THE results of experimental attempts to detect a sidereal variation of cosmic rays can be expected to depend on (a) the energy of the primary rays to which the apparatus responds, and (b) the effective polar diagram of the apparatus regarded as a receiver of primaries. Low-energy primaries will have their directions altered by the magnetic fields of the earth and sun, and will be deviated more often by galactic fields, so that we must expect the directional effects to be small: high-energy primaries should have the greatest sidereal variation. The polar diagram of the receiver becomes important if an attempt is made to detect point sources of cosmic rays. A point source will show up better against an isotropic background if the polar diagram is narrow.

The two criteria of high primary energy and narrow polar diagram both point to the extensive air showers as the cosmic ray phenomenon most likely to show a sidereal variation. By recording extensive air showers at sea level we select the highest primary energy ($\sim 10^{14} \text{ ev}$), and the polar diagram is narrow ($\pm 20^\circ$) because of atmospheric absorption.

The results of previous experimental studies are as follows. For sea-level ionization (primary energy $\sim 10^{10} \text{ ev}$, medium polar diagram) no sidereal variation has been established (Hogg 1950). For meson intensity at sea level (primary energy $\sim 10^{10} \text{ ev}$, wide polar diagram) there are two rather contradictory results: Duperier (1946) reports a sidereal amplitude 0.21% with maximum at 21 hours local sidereal time, while Elliot and Dolbear (1951) find an amplitude 0.02% with maximum at five hours local sidereal time. For meson intensity underground (primary energy $\sim 10^{13} \text{ ev}$, medium polar diagram) the 10% increase reported by Sekido *et al.* (1951) under 1200 metres water equivalent (m.w.e.) can equally well be ascribed to statistical fluctuations. Barrett and Eisenberg (1952) under 1600 m.w.e.

find less than 2%, and Sherman (1953) under 840 m.w.e. finds less than 0.5% sidereal diurnal amplitude. For extensive air showers, however, Hodson (1951) finds a barely significant sidereal diurnal amplitude ($1.15 \pm 0.61\%$) with maximum at 23.5 hours local sidereal time, and Daudin and Daudin (1952), using counter trays of area 2300 cm^2 separated by 80 m at the Pic du Midi, altitude 2860 m, report an amplitude ($0.39 \pm 0.13\%$) with maximum at 22 hours local sidereal time. All errors quoted in this paper are standard deviations. Earlier work on time variations of cosmic rays is reviewed by Dauvillier (1951).

All the observations on high energy primaries made so far have been in the Northern Hemisphere, a circumstance which would be favourable for detecting the Compton-Getting effect (maximum at latitude 47° N.) (Compton and Getting 1935), but unfavourable if the greatest intensity comes from the direction of the galactic centre. In the latter case we would expect a maximum effect at latitude 26° S. ; the effect would be reduced in the Northern Hemisphere, particularly in the case of extensive air showers, because of the narrow polar diagram for reception.

We have made observations of extensive air showers at Auckland (latitude 37° S. , altitude 40 m) and have included as part of the apparatus an arrangement of counters for which the effective polar diagram for primaries is reduced to $\pm 10^\circ$.

§ 2. APPARATUS

The polar diagram of an extensive air-shower recorder regarded as a detector of primary cosmic rays can be controlled at sea level because (a) the direction of the shower axis is thought to preserve the direction of the incident primary, and (b) electrons of energy E mev deviate from the shower axis by a root mean square angle $15/E$ radians (Rossi and Greisen 1941). In our equipment we select electrons of median energy 100 mev (r.m.s. deviation about 7°) and ensure that they arrive vertically within $\pm 7^\circ$ (between half-intensity points) by means of a coincidence system enclosed in a lead wall to eliminate side showers. This lead collimator, 6 ft 2 in. high, has walls 6 in. thick and encloses a space 36 in. \times 15 in. in horizontal section, the long axis lying North and South. Coincidences between counter trays at the bottom and top of the collimator are then due to vertical electrons in the showers, and more rarely to penetrating particles. By including a 4 in. aluminium absorber we set a lower limit to the energy (55 mev) so that the median energy is of order 100 mev, and thus ensure that the coincidence events are due to showers with their axes vertical in the E-W plane within $\pm 10^\circ$ (between half-intensity points). Extensive air showers are selected by requiring that two further trays spaced 4 m from the lead collimator are also triggered.

Figure 1 is a sketch of the equipment. The five trays are identical, each containing ten geiger counters, separately quenched by external trigger circuits, the sensitive area of each tray being 2360 cm^2 . A coincidence between the outlying trays 1 and 2 and tray 3 at the top of the collimator records the extensive showers with the usual $\pm 20^\circ$ polar diagram and a counting rate 50 per hour. A simultaneous count in tray 4 (in the collimator but above the aluminium absorber) indicates the presence of a near vertical electron in the shower. The 1234-coincidences have a bias towards vertical showers, counting rate 18 per hour. If tray 5 is also triggered, the near vertical electron has passed through the absorber so that the 12345-coincidences correspond to nearly vertical showers, as already explained, the counting rate being 8 per hour.

The coincidence events are recorded on a 20-pen operation recorder with clockwork drive (Esterline-Angus Company, Inc.), both individually and after scaling by 10. Subsidiary traces indicate that the mains voltage is within $\pm 5\%$ of its nominal value, and check the counting rates of the individual trays.

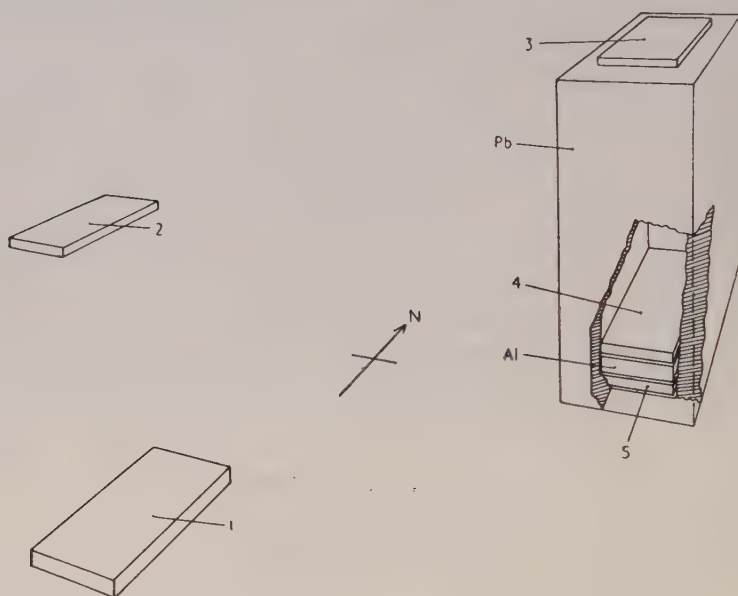


Figure 1. Apparatus.

1, 2, 3, 4 and 5, counter trays. Pb, lead wall. Al, aluminium absorber.

§ 3. OBSERVATIONS AND RESULTS

Records are taken for a year from February 1951 to February 1952, and the coincidence events tabulated for half-hour intervals. The results for the 123-coincidences will be discussed first.

Averaging the results and plotting against solar time we obtain figure 2. There is a clearly visible solar diurnal variation which apparently correlates with ground temperature. A least-squares fit to the points gives an amplitude $(1.45 \pm 0.25)\%$ for the 24-hour component with maximum at (2.7 ± 0.6) hours solar time. The apparent temperature coefficient is -0.51% per $^{\circ}\text{C}$.

Regrouping the results to obtain the mean intensity for half-hourly intervals of sidereal time we obtain figure 3. Inspection shows a significant 24-hour sidereal variation, which by least-squares analysis has amplitude $(1.10 \pm 0.26)\%$ with maximum at (19.8 ± 0.9) hours local sidereal time. These figures differ slightly from the results quoted in our preliminary note (Farley and Storey 1954), through the correction of an arithmetical error; moreover we are now quoting standard deviations instead of probable errors.

§ 4. DETAILED ANALYSIS OF THE DATA

We have fitted to the half-hourly values of 123-coincidence intensity I the expression

$$I = I_0 + [A + 2B \cos 2\pi(t + \phi_2)] \cos 2\pi(Nt + \phi_1) + C \cos 2\pi\{(N+1)t + \phi_3\}. \dots (1)$$

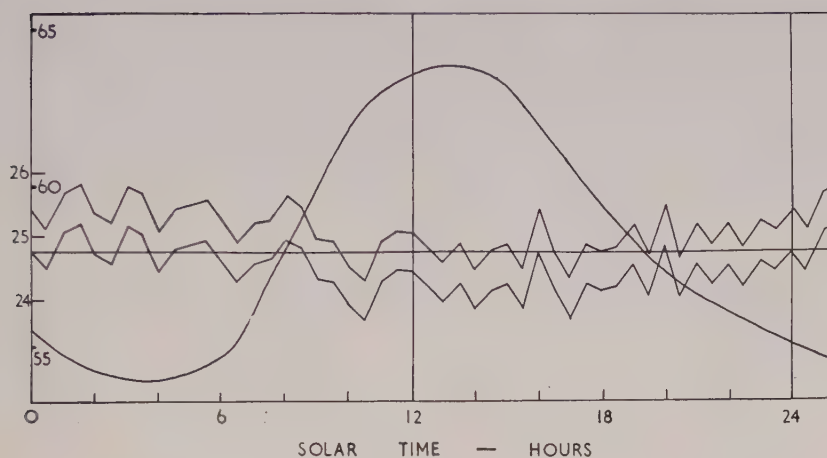


Figure 2. 123-coincidences (counts/half hour), and ground level temperature ($^{\circ}\text{F}$), versus solar time. The limits of error indicated by the two lines are \pm standard deviation of the individual counts.

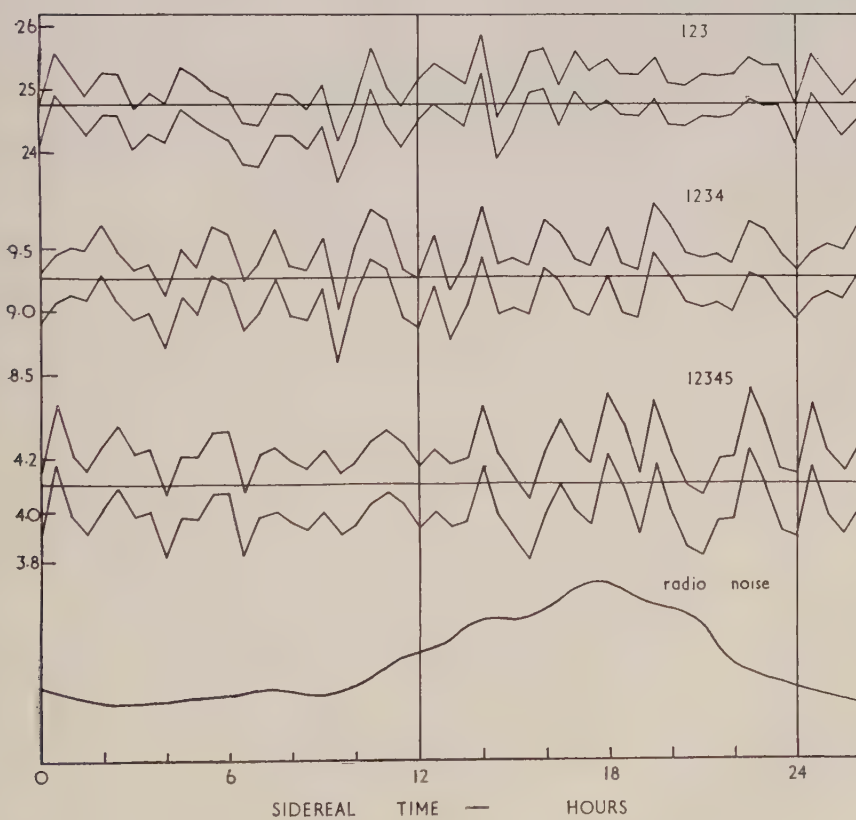


Figure 3. Coincidences (counts/half hour), and radio noise, versus local sidereal time.

In this formula the unit of time t is one year, time zero being 00.00 hours on 22nd September, the day in which solar and sidereal times coincide. The first term is the mean intensity I_0 . The second represents the solar diurnal variation of mean amplitude A with a seasonal variation in amplitude specified by B and ϕ_2 ; the third term represents the sidereal diurnal variation of amplitude C , there being $(N+1)$ sidereal days in the year. The times for the maxima of the diurnal variations and of the seasonal modulation term are determined by the phases ϕ_1 , ϕ_2 and ϕ_3 .

We have assumed that the solar diurnal effect has a seasonal variation in amplitude but not in phase. This is a reasonable assumption; in any case it is not profitable to consider an unknown variation in the phase because it cannot be disentangled from the sidereal effect.

It is well known that the seasonal variation of the solar diurnal effect can give rise to an apparent sidereal variation when the intensities are grouped according to corresponding intervals of sidereal time and averaged over the year. Our approach to this problem is to express the modulated solar variation, of frequency N , as an unmodulated 'carrier', plus 'sidebands' of frequency $(N+1)$ and $(N-1)$. The first sideband is of sidereal frequency and interferes with the estimation of the true sidereal effect C , ϕ_3 . The correction can be found however by evaluating the second sideband of frequency $(N-1)$; it has the same amplitude as the first, and the phases are uniquely related. This is called the 'antisidereal' component. We therefore rewrite equation (1) as follows:

$$I = I_0 + A \cos 2\pi(Nt + \phi_1) + B \cos 2\pi\{(N-1)t + \phi_1 - \phi_2\} \\ + B' \cos 2\pi\{(N+1)t + \phi_1 + \phi_2\} + C \cos 2\pi\{(N+1)t + \phi_3\}. \quad \dots\dots(2)$$

$B' = B$, but it is convenient to label the terms by distinctive amplitude symbols so that we can label the vectors in figure 4 to correspond.

The last two terms of sidereal frequency combine thus:

$$B' \cos 2\pi\{(N+1)t + \phi_1 + \phi_2\} + C \cos 2\pi\{(N+1)t + \phi_3\} = D \cos 2\pi\{(N+1)t + \phi_4\}. \\ \dots\dots(3)$$

The terms in A , B and D are orthogonal when a year's results are analysed. We can therefore analyse separately for the solar, sidereal and antisidereal components as though the others were absent. The procedure is as follows: To find A and ϕ_1 we have grouped the year's results according to corresponding half-hourly intervals of solar time to yield 48 half-hourly values I_s for the mean solar day. A least-squares fit then gives A and ϕ_1 . To obtain the error in the least-squares assignment we have calculated the 48 residuals Z_s and evaluated $(1/45) \sum Z_s^2 = \sigma^2$, which is the variance of the values I_s about the assigned diurnal variation. We divide by 45 instead of 48 because three parameters have been fitted. The variance of A is then $\sigma^2/24$ and the variance of ϕ_1 is $\sigma^2/24.4^2$ radians.

The standard deviation σ has been compared with the value σ' to be expected if the statistics of the counts was the only source of error, the larger of the two being used to estimate the probable standard errors. To check that the residuals Z_s are uncorrelated we have evaluated $d = \sum (Z_s - Z_{s-1})^2 / \sum Z_s^2$. A value less than 1.5 would indicate a correlation (Durbin and Watson 1951).

Similarly, to obtain D and ϕ_4 we have grouped the results according to sidereal time and repeated the procedure. To find the modulation term B , ϕ_2 we have grouped the results according to corresponding intervals of 'antisidereal time';

that is, the time for which there are $N - 1$ days per year. The least-squares fit then gives B and $\phi_1 - \phi_2$, from which ϕ_2 can be found.

The true sidereal variation C , ϕ_3 is then found by subtraction, using equation (3).

The results with standard errors are given in the table. The diurnal amplitudes are given as percentages of the mean I_0 . The time for the maximum of the diurnal variation is expressed in solar, sidereal or antisidereal time as the case may be. σ and σ' are given as intensities and are directly comparable with I_0 .

	Diurnal amplitude %	Time of maximum (hr)	σ from residuals	σ' from statistics	d
Solar A	1.45 ± 0.25	2.7 ± 0.6	0.279	0.304	2.20
Apparent sidereal D	1.10 ± 0.26	19.8 ± 0.9	0.309	0.304	2.05
Antisidereal B	0.78 ± 0.25	3.2 ± 1.2	0.304	0.304	2.25
True sidereal C	1.43 ± 0.38	17.6 ± 1.0	—	—	—

$$I_0 = 24.744$$

1234-coincidences,
apparent sidereal 0.52 ± 0.41 19.7 ± 3.0

12345-coincidences,
apparent sidereal 0.52 ± 0.61 20.7 ± 4.5

The errors in the two terms B' and D , subtracted to give C , are independent and can therefore be combined using the usual rules. The uncertainty in the time for the maximum of A adds to the error in C and has been included fully in the estimated probable errors of C and ϕ_3 .

Comparison of the values for the standard deviations σ and σ' show that the statistics of the counting accounts for the whole of the variance of the results. Variations due to temperature and barometric effects have apparently averaged out over the year.

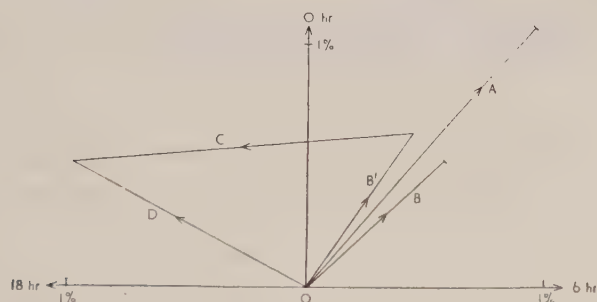


Figure 4. Harmonic dial.

A , solar diurnal variation; B , antisidereal; B' , reflection of B in line A ;
 C , true sidereal; D , apparent sidereal.

The relations between the terms in equations (2) and (3) are displayed on the harmonic dial, figure 4. In effect this represents the relation between the harmonic vectors near time zero, when solar, sidereal and antisidereal times coincide. As the year progresses the solar vector A remains fixed, the antisidereal vector B rotates clockwise, and the sidereal vectors B' and C with their resultant D rotate anticlockwise. D shows the apparent sidereal effect with its maximum at 19.8 hr sidereal time. After correcting for the influence of the solar seasonal modulation this becomes C , the true sidereal effect, with its maximum at 17.6 hr sidereal time.

The solar diurnal amplitude is the resultant of **A**, **B** and **B'**. It varies from a maximum of $(3.01 \pm 0.57)\%$ in September to a minimum of $-(0.11 \pm 0.57)\%$ in March. This large variation is surprising and suggests that the antisidereal correction has been overestimated.

It is clear, however, that the effect of correcting for the solar seasonal effect has been to increase rather than to decrease the sidereal variation and to alter its phase. Allowing even a large error in the determination of **B**, it is hardly conceivable that the solar seasonal modulation alone could account for the observed sidereal vector **D**. This confirms the existence of a true sidereal variation.

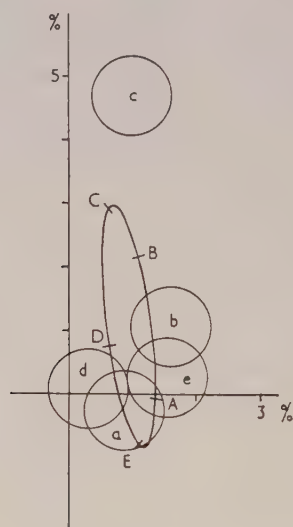


Figure 5. Harmonic dial.

Ellipse gives locus of equation (1) during the year. *a, b, c, d, e*, experimental points with circles of error. *A, B, C, D, E*, corresponding points from equation (1).

The magnitude and phase to be assigned to the sidereal diurnal component are presumably the corrected values C, ϕ_3 . If, however, the correction has been too large the sidereal amplitude will be smaller and the phase nearer to that of the vector **D**. But on the whole we must expect that the correlated values C, ϕ_3 will give a better estimate than D, ϕ_4 , and we therefore adopt the value $(1.43 \pm 0.38)\%$ with a maximum at (17.6 ± 1.0) hours local sidereal time.

To check our assignments of amplitudes and phases to equation (1) we have divided the year's results into 5 groups and determined the apparent solar diurnal variation for each group. The results are plotted on the solar harmonic dial, figure 5, together with the ellipse obtained from equation (1). Small letters indicate the experimental points plotted with circles of error, while the corresponding positions on the ellipse are marked in capital letters. The agreement is not exact, but suggests that the assignments are broadly correct. Though point *c* is well off the ellipse, we note that the mean of *b* and *c* would come very close to its theoretical position. Also there is a definite anticlockwise circulation of the experimental points, confirming the existence of a true sidereal component.

The existence of a 12-hour sidereal component is required by some theories of cosmic ray acceleration. We have analysed our data for such an effect and find

an apparent amplitude $(0.41 \pm 0.25)\%$ with maximum at (2.0 ± 2.3) hours local sidereal time.

§ 5. DISCUSSION

Further evidence that we are observing a true sidereal variation is obtained by comparing our results (in the Southern Hemisphere) with those of Daudin and Daudin (1952) and Hodson (1951) (Northern Hemisphere). If the observed sidereal variations are due solely to the seasonal modulation of the solar diurnal variation (assumed the same in both hemispheres) we should expect the apparent sidereal variation observed in the two hemispheres to differ in phase by 180° (Compton and Getting 1935). In fact, however, the variations obtained at the three stations are in phase and the maxima coincide in local sidereal time almost within the probable error. For this comparison we have used our uncorrected figures and have estimated the error in the time of maximum for the other stations from the quoted errors in amplitude, with the following result:

Manchester (lat. 53° N.): maximum at 23.5 ± 2.0 hours
Pic du Midi (lat. 43° N.): maximum at 22.0 ± 1.3 hours
Auckland (lat. 37° S.): maximum at 19.8 ± 0.9 hours.

This gives further grounds for believing that the variation observed is a genuine sidereal effect and is not a residuum due to seasonal changes in the solar diurnal effect.

Although the times of the maxima at Auckland and the Pic du Midi do not agree exactly, at both places the local maximum coincides very closely with the time at which the Milky Way is overhead (22 hours at the Pic du Midi, 17.7 hours at Auckland). This suggests that cosmic rays come preferentially from regions of high star density in the galactic plane. An examination of figure 3 shows, however, that the intensity does not rise sharply when the galaxy crosses the meridian; instead there is a broad maximum lasting for about 8 hours.

At Auckland our corrected maximum (17.6 hours) coincides with the time at which the centre of the galaxy crosses the meridian (17.7 hours). The declination of the galactic centre being -26° , it passes daily within 11° of the vertical at Auckland, but only within 69° of the vertical at the Pic du Midi. Any effect due to cosmic rays coming from this direction would therefore be much stronger in Auckland than in Europe. Because the apparatus used at the various stations has been different it is difficult to make an exact comparison, but the evidence suggests that the sidereal amplitude is larger in the Southern Hemisphere.

It thus appears that the direction from which we receive the maximum cosmic ray intensity lies in the galactic plane. The direction within the plane can in principle be found by experiments at several latitudes. The present meagre data suggest that this direction lies in the southern celestial hemisphere, and the direction of the galactic centre is a possibility.

In this connection it is interesting to compare our results with the radio noise signals from the direction of the galactic centre, observed at the same latitude and with a similar polar diagram. The results of Shain (1951) obtained at Sydney (lat. 34° S.) on 18.3 mc/s with a vertical aerial, polar diagram 17° between half-power points, are shown in figure 3. There is a broad correlation between the curves of shower intensity and radio noise. But this suggests merely that both radio noise signals and cosmic rays are emitted from the regions of high star density near the galactic plane.

§ 6. POINT SOURCES OF COSMIC RAYS

So far we have discussed only the 123-coincidence events. The results for 1234- and 12345-coincidences plotted against sidereal time are also shown in figure 3. The sidereal variation, while still present, is less in these cases, and less significant because of the smaller number of events. The results of the least-squares analysis are given in the table. Inspection of the curves gives no evidence of point sources of cosmic rays.

If a point source of cosmic rays passes overhead, the relative increase in intensity should be three times as great for the 5-fold as for the 3-fold coincidences because the area under the polar diagram is reduced to one third. This advantage is however largely off-set by the 6-fold decrease in counting rate, which results in a 2.4 times increase in statistical fluctuations.

From the absence of significant peaks on the curves we deduce that, if a point source exists, less than 10^{-4} of the total cosmic ray flux as registered by our equipment appears to come from it. This means that, if point sources exist, the diffusion of primary trajectories before they reach the earth (for primaries of the energy range selectively received by the experimental arrangement) must be large enough to prevent any strengthening of selection by the arrangement involving angular discrimination.

ACKNOWLEDGMENTS

We are indebted to the University of New Zealand Research Committee for a grant covering the major cost of the apparatus, and one of us (J.R.S.) for a Research Fellowship.

We wish to thank Dr. G. S. Watson of the University of Melbourne for advice on statistical methods, Dr. C. A. Shain for information about galactic radio noise, and Professor P. W. Burbidge for his continued interest and encouragement.

The name antisidereal was suggested to us by G. Cocconi.

REFERENCES

- BARRETT, P. H., and EISENBERG, Y., 1952, *Phys. Rev.*, **85**, 674.
 COMPTON, A. H., and GETTING, I. A., 1935, *Phys. Rev.*, **47**, 817.
 DAUDIN, A., and DAUDIN, J., 1952, *C. R. Acad. Sci., Paris*, **234**, 1551.
 DAUVILLIER, A., 1951, *Cah. Phys.*, **35**, 1.
 DUPERIER, A., 1946, *Nature, Lond.*, **158**, 196.
 DURBIN, J., and WATSON, G. S., 1951, *Biometrika*, **38**, 159.
 ELLIOTT, H., and DOLBEAR, D. W. N., 1951, *J. Atmos. Terr. Phys.*, **1**, 205.
 FARLEY, F. J. M., and STOREY, J. R., 1954, *Nature, Lond.*, **173**, 445.
 HODSON, A. L., 1951, *Proc. Phys. Soc. A*, **64**, 1061.
 HOGG, A. R., 1950, *J. Atmos. Terr. Phys.*, **1**, 56.
 ROSSI, B., and GREISEN, K., 1941, *Rev. Mod. Phys.*, **13**, 240.
 SEKIDO, Y., MASUDA, T., YOSHIDA, S., and WADA, M., 1951, *Phys. Rev.*, **83**, 658.
 SHAIN, C. A., 1951, *Aust. J. Sci. Res. A*, **4**, 258.
 SHERMAN, N., 1953, *Phys. Rev.*, **89**, 25.

Note on the Relation between certain Forbidden Beta Transitions and the Nuclear Spin Orbit Interaction

BY G. N. FOWLER

University of Manchester

*Communicated by L. Rosenfeld; MS. received 15th June 1953,
and in amended form 22nd July 1954*

Abstract. The second-forbidden beta decay matrix element A_{ij} is given in terms of the nuclear spin orbit potential strength u and another second-forbidden beta decay matrix element R_{ij} . The result is used, together with the predictions of the Mayer shell model for the single particle configurations, to obtain an estimate of u from the decay of ^{99}Tc for two types of space dependence of the spin orbit potential. The result is in reasonable agreement with that found from a study of the stationary states of ^5He .

§ 1. INTRODUCTION

IN the case of second-forbidden beta transitions which satisfy the selection rules $\Delta J = 2$ and no parity change, the non-vanishing matrix elements include R_{ij} and A_{ij} . (For the definition of the various symbols reference should be made to Konopinski and Uhlenbeck (1941) whose notation and units are used throughout.)

In the following note A_{ij} is expressed in terms of R_{ij} and certain nuclear parameters including the spin orbit potential strength u . Since A_{ij} and R_{ij} may be obtained by explicit calculation for particular cases, once a definite choice of nuclear wave functions has been made, we can find an estimate of u . In both calculations appeal is made to the Mayer nuclear shell model. The particular cases selected are the decays of ^{99}Tc and ^{36}Cl for which the matrix elements in question have been calculated by Smith (1952). The values of u obtained in this way are compared with that given by Hughes and Le Couteur (1950), using a corrected value of the ^5He level splitting. Reasonable agreement is found.

§ 2. CALCULATION OF A_{ij} IN TERMS OF R_{ij} AND u

A method proposed by Pursey (1951) for first-forbidden transitions has been applied to our case, the second-forbidden transitions.

The method is based on the following nuclear Hamiltonian:

$$\begin{aligned}
 H = & - \sum_{s=1}^A (\boldsymbol{\alpha} \cdot \mathbf{p})^s + \frac{1}{2} \beta^s \{ (1 + \tau_3^s) M_n + (1 - \tau_3^s) M_p \} \\
 & + \frac{1}{2} \sum_{s=1}^A \sum_{k \neq s}^A \{ V_o + \boldsymbol{\tau}^s \cdot \boldsymbol{\tau}^k V_e - (\boldsymbol{\sigma}^s + \boldsymbol{\sigma}^k) \cdot (\mathbf{r}^s - \mathbf{r}^k)_{\Lambda} (\mathbf{p}^s - \mathbf{p}^k) V_s \\
 & + \frac{1}{2} (1 - \tau_3^s) (1 - \tau_3^k) V_o \} \dots\dots(1)
 \end{aligned}$$

where V_o , V_e , V_c , and V_s are the ordinary, charge exchange, Coulomb and spin orbit potentials respectively. No tensor force of the usual type has been included since it is found to give a negligible contribution to the result (cf. Pursey (1951)).

For the exchange term, which does not materially affect the results, a Yukawa-type space dependence has been assumed with strength $V = 100 \text{ mc}^2$ and range χ given by $\chi = r_0^{-1}$, when the nuclear radius is given by $R = r_0 A^{1/3}$.

For the spin orbit potential strength we assume two of the forms which are usually considered (cf. Hughes and Le Couteur 1950), viz.

$$(i) \quad V_s = \frac{u \exp(-\kappa r)}{2\kappa r}, \quad \dots \quad (ii) \quad V_s = \frac{-u}{2\kappa_1 r} \frac{\partial}{\partial(\kappa_1 r)} \left(\frac{\exp(-\kappa_1 r)}{r} \right),$$

where we take the values of κ and κ_1 used by Hughes and Le Couteur, namely $\kappa^{-1} = 1.5 \times 10^{-13} \text{ cm}$ and $\kappa_1^{-1} = 1.1 \times 10^{-13} \text{ cm}$. It should be noted that Hughes and Le Couteur used the notation σ instead of the more usual $\frac{1}{2}\sigma$. In order to facilitate comparison with their results we have introduced a factor $\frac{1}{2}$ in (i) and (ii). Finally, the form of the spin orbit term has been chosen to satisfy the requirements of charge independence, with the omission of a term multiplied by $\tau^i \cdot \tau^k$ (cf. Avery and Blanchard (1951)). Such a term would give a contribution of order $(N-Z)A^{-1}$ when we average over the nuclear core (see below). In view of the rather approximate nature of the calculation it has not seemed worth while to include this term.

One now calculates the commutator of the Hamiltonian with

$$\frac{1}{2} \sum_{s=1}^A (\tau_1 - i\tau_2)^s (r_i r_j)^s.$$

When it is assumed that the nucleus consists of a single external transforming particle together with a spin saturated core, the resulting expression may be averaged over the particles of the core. This gives A_{ij} as a function of R_{ij} , u and another beta decay matrix element, T_{ij} . This latter may be eliminated using the relativistic angular momentum operator of Dirac: (cf. Pursey 1951)

$$k = \beta(\sigma \cdot \mathbf{l} + 1), \quad \dots \dots (2)$$

whose eigenvalues are given by $\mp(j + \frac{1}{2})$ for $j = l \pm \frac{1}{2}$. It can be shown that

$$[k, \mathbf{r}] = -i\beta\sigma_{\wedge} \mathbf{r}, \quad \dots \dots (3)$$

from which one finds

$$[k, r_i r_j - \frac{1}{3}\delta_{ij}(r^2)] = -i\beta(r_i(\sigma_{\wedge} \mathbf{r})_j + r_j(\sigma_{\wedge} \mathbf{r})_i). \quad \dots \dots (4)$$

Taking matrix elements of both sides gives, in the non-relativistic approximation,

$$\int \beta = -1, \quad (f|\beta T_{ij}|i) = -(f|T_{ij}|i) = i\epsilon(f|R_{ij}|i) \quad \dots \dots (5)$$

$$\epsilon = k_f - k_i. \quad \dots \dots (6)$$

The final result is

$$(f|A_{ij}|i) = i[W_i - W_f - M_n + M_p + (N-Z)A^{-1}F_e(R) + Z\alpha/R + \epsilon F_s(R)](f|R_{ij}|i). \quad \dots \dots (7)$$

Here

$$F_s(R) \simeq \frac{3}{2}Au(\kappa R)^{-3}((\kappa R)^{-1} - 3(\kappa R)^{-3}) \text{ in case (i)} \\ \simeq \frac{3}{4}Au(\kappa_1 R)^{-3}((\kappa_1 R)^{-1} + 2(\kappa_1 R)^{-2} - 4(\kappa_1 R)^{-3}) \text{ in case (ii)} \quad \dots \dots (8)$$

$$F_e(R) \simeq -30A(\chi R)^{-3}((\chi R)^{-1} - (\chi R)^{-2}). \quad \dots \dots (9)$$

Equation (7) is the basic formula for the estimation of u from beta decay data.[†] However, in order to arrive at such an estimate this will be supplemented by an explicit calculation of A_{ij} and R_{ij} for the two special cases discussed below.

§ 3. EXPLICIT CALCULATION OF A_{ij} AND R_{ij}

For the cases $^{99}\text{Tc} \rightarrow ^{99}\text{Ru}$ and $^{36}\text{Cl} \rightarrow ^{36}\text{A}$ the matrix elements in question have been calculated by Smith (1952), who finds $A_{ij}/R_{ij}=0$ in both cases. Here the nuclear wave functions used are those found from the Mayer nuclear shell model.

One should add here that the result $A_{ij}/R_{ij}=0$ in these cases depends upon the fact that harmonic oscillator functions were used for the single particle wave functions. However, the success of the Mayer model leads one to expect that the best wave functions in the single particle approximation will not differ very much from harmonic oscillator functions. Thus at any rate the condition $A_{ij} \ll R_{ij}$ should hold good, and this is all we need for the following argument.

(a) $^{99}\text{Tc} \rightarrow ^{99}\text{Ru}$.

The ft value for this decay corresponds to a second-forbidden transition and the selection rules may be inferred from the following information on the nuclear states involved. The odd proton of the parent nucleus is assigned to the $g_{9/2}$ level from spin and magnetic moment measurements. The assignment of the odd neutron of the product nucleus to a $d_{5/2}$ level is not so unambiguous but from magnetic moment measurements on ^{95}Mo and ^{97}Mo the odd neutron in these nuclei has been assigned to this level. In addition, from Klinkenberg's (1952) tables the $d_{5/2}$ shell appears to fill steadily from ^{91}Zr with one $d_{5/2}$ neutron to ^{97}Mo with five. It follows that the selection rules for the decay are $\Delta J=2$, no. On this evidence, Mayer, Moszkowski and Nordheim (1951) predict the transition of a $d_{5/2}$ neutron to a $g_{9/2}$ proton. It is then found from equations (6) and (7) that $\epsilon = -2$ and $u \sim 27 \text{ mc}^2$ for case (i) and $\sim 155 \text{ mc}^2$ for case (ii). Here the assumption that the nucleus consists of a spin-saturated core together with a single external nucleon may be justified by the fact that the extra core nucleons are in shells of high angular momentum for which one would expect the Mayer pairing energy to be effective in causing the cancellation of the nuclear spins in pairs.

(b) $^{36}\text{Cl} \rightarrow ^{36}\text{A}$.

In this case the ft value again corresponds to a second-forbidden decay and the measured value of the spin of the parent nucleus is 2 units. Since the product is an even-even nucleus one should assign to it a spin of zero; furthermore, in this region of the shell model no change of parity is allowed in beta transitions so that the decay again satisfies the selection rules $\Delta J=2$, no.

The transition assumed by Smith (1952) is that of a $d_{3/2}$ neutron to an $s_{1/2}$ proton. This gives from equations (6) and (7) $\epsilon = -3$ and $u \sim 8 \text{ mc}^2$ and $\sim 50 \text{ mc}^2$, in cases (i) and (ii) respectively. However, according to Klinkenberg, the Mayer

[†] An expression which is in some respects similar to (7) has been derived for first-forbidden transitions by Ahrens and Feenberg (1952) using a similar commutation procedure but avoiding the use of a single particle model, relying instead on the semi-empirical nuclear energy surface. They claim good agreement with Pursey's results but on examination it becomes clear that this depends on the fact that Pursey used a value for the spin orbit potential strength which is fifteen times too small when more recent experimental results on the level splitting of ^5He are taken into account.

shell model predicts a $d_{3/2}$ neutron \rightarrow $d_{3/2}$ proton transition which would give $\epsilon = 0$ and therefore $T_{ij} = 0$. In addition it may be shown using the operator k as in §2 that

$$(f | \beta A_{ij} | i) = (\epsilon - (l_f^2 - l_i^2)/(k_f + k_i)) (f | A_{ij} | i) \quad \dots\dots(10)$$

so that for a $d_{3/2}$ neutron \rightarrow $d_{3/2}$ proton transition $\beta A_{ij} = 0$ also. Thus the only matrix elements that could play a role would be A_{ij} and R_{ij} . According to Longmire, Wu and Townes (1949), however, the combination of A_{ij} and R_{ij} occurring in the second-forbidden polar vector interaction cannot fit the observed energy spectrum. Some modifications of the initial configuration of Klinkenberg would therefore seem to be necessary and that of Smith is the most plausible. The choice $d_{3/2} \rightarrow s_{1/2}$ implies, however, that the interactions of the nucleons which occupy the unfilled shells of ^{36}Cl must be significant and so the assumption that the nucleus consists of a single particle outside a spin-saturated core must be considered rather doubtful. Accordingly, little weight should be attached to the value of u obtained from this case.

Before proceeding further one may note that the ratios $|T_{ij}/R_{ij}|^2$ obtained from equation (5) agree with the results of Smith in both cases, which provides a check of his results.

§ 4. COMPARISON WITH u FOUND FROM ^5He DATA

An independent method of obtaining u is available from a study of the stationary states of nuclei, in particular of ^5He , and calculations have been carried out in this case, in sufficient detail to permit a comparison to be made, by Hughes and Le Couteur (1950). These authors obtain values for u of 4 and 12 mc^2 in the two cases, based on an observed level splitting in ^5He of 0.64 mc^2 . They also try to show that these values of u are consistent with the level splittings observed in those heavier nuclei which have one nucleon outside closed shells.

However, more recent experimental work, although it does not give an unambiguous value for the level splitting of ^5He , is certainly inconsistent with the level splitting used by Hughes and Le Couteur. In the light of the available evidence Ajzenberg and Lauritsen (1952) took 5.2 mc^2 as the most reasonable value for the level splitting. Still more recent work by Adair (1953) on ^{17}O may be interpreted as confirming this value, although some measurements on the scattering of high energy neutrons by ^4He by Seagrave (1953) seem to be more consistent with the much larger value of 12 mc^2 suggested by Dodder and Gammel (1952). It is not appropriate here to give a more detailed analysis of these experiments and the value of 5.2 mc^2 for the level splitting will be adopted. This leads to values of u of 33 and 99 mc^2 on correcting the results of Hughes and Le Couteur. In addition, it has been shown by Avery and Blanchard (1951) for a potential of the form (1), that when the differing angular momenta of the single external nucleon and of the closed shells are taken into account values of u of the order of 50 mc^2 are found from the data concerning heavier nuclei. On comparing these results with those obtained from the decay of ^{99}Tc , one finds general agreement as to order of magnitude in either case, but, perhaps better agreement with a potential of the form (1).

ACKNOWLEDGEMENTS

Thanks are due to Professor L. Rosenfeld for his interest and encouragement and to the Department of Scientific and Industrial Research for a grant.

REFERENCES

- ADAIR, R. K., 1953, *Phys. Rev.*, **92**, 1491.
AHRENS, T., and FEENBERG, E., 1952, *Phys. Rev.*, **86**, 64.
AJZENBERG, F., and LAURITSEN, T., 1952, *Rev. Mod. Phys.*, **24**, 326.
AVERY, L., and BLANCHARD, C. H., 1951, *Phys. Rev.*, **81**, 35.
DODDER, D. C., and GAMMEL, J. L., 1952, *Phys. Rev.*, **88**, 520.
HUGHES, J., and LE COUTEUR, K. J., 1950, *Proc. Phys. Soc. A*, **63**, 1219.
KLINKENBERG, P. F. A., 1952, *Rev. Mod. Phys.*, **24**, 63.
KONOPINSKI, E. J., and UHLENBECK, G. E., 1941, *Phys. Rev.*, **60**, 308.
LONGMIRE, C., WU, C. S., and TOWNES, C. H., 1949, *Phys. Rev.*, **76**, 695.
MAYER, M. G., MOSZKOWSKI, S. A., and NORDHEIM, L. W., 1951, *Rev. Mod. Phys.*, **23**, 315.
PURSEY, D. L., 1951, *Phil. Mag.*, **42**, 1193.
SEAGRAVE, J. D., 1953, *Phys. Rev.*, **92**, 1222.
SMITH, A. M., 1952, *Phil. Mag.*, **43**, 915.

Inelastic Heavy-Particle Collisions Involving the Crossing of Potential Energy Curves

II : Charge Transfer from H-atoms to Al^{3+} , B^{2+} , Li^{2+} and Al^{2+}

By A. DALGARNO

Department of Applied Mathematics, The Queen's University of Belfast

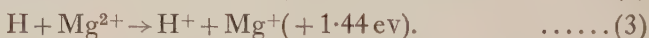
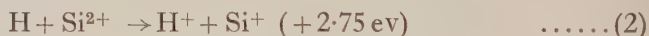
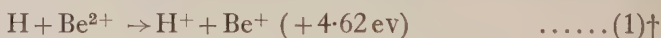
Communicated by D. R. Bates; MS. received 21st May 1954

Abstract. The charge transfer processes $\text{H} + \text{Al}^{3+} \rightarrow \text{H}^+ + \text{Al}^{2+}({}^2\text{S} \text{ and } {}^2\text{P})$, $\text{H} + \text{B}^{2+} \rightarrow \text{H}^+ + \text{B}^+({}^1\text{P})$, $\text{H} + \text{Li}^{2+} \rightarrow \text{H}^+ + \text{Li}^+({}^3\text{S} \text{ and } {}^1\text{S})$ and $\text{H} + \text{Al}^{2+} \rightarrow \text{H}^+ + \text{Al}^+$ are investigated using the Landau-Zener formula for the transition probability arising from the pseudo-crossing of the potential energy curves of the initial and final systems. These pseudo-crossings occur at nuclear separations of 3.34, 6.58, 11.1, 8.88, 20.9 and 5.29 atomic units respectively and the corresponding energy separations due to the interaction between the initial and final states are 5.18, 1.25, 5.69×10^{-3} , 1.24×10^{-1} , 2.12×10^{-6} and 1.54 eV. The cross sections associated with the six processes are calculated over a wide range of impact energies.

The relationship between energy excess and energy separation is briefly discussed in an appendix.

§ 1. INTRODUCTION

THE need for detailed estimates of the cross sections of various heavy-particle collision processes has been pointed out recently by Bates and Massey (1954), and this paper is a continuation of a programme initiated to supply such information. The first paper of the series (Bates and Moiseiwitsch 1954, to be referred to as I) used the Landau-Zener formula to investigate the reactions



The initial ion has in each case a closed shell configuration and the final ion is in its ground state. The crossing points of the potential energy curves of the initial and final systems are at internuclear distances of $5.8a_0$, $9.6a_0$ and $18.9a_0$ respectively (a_0 being 5.29×10^{-9} cm).

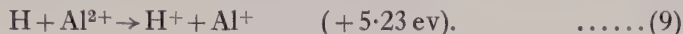
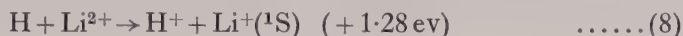
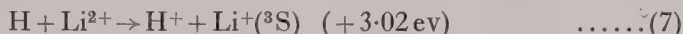
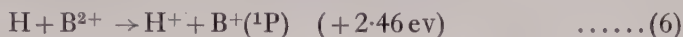
The first two reactions considered in this paper are



Throughout, the energy excesses have been computed using the tables prepared by Moore (1949). Reactions (4) and (5) are similar to (1), (2) and (3), but in (4)

[†] When no spectroscopic designation is given, the system is in its ground state.

the crossing point occurs at a much smaller internuclear distance and in (5) the final state is excited. The remaining reactions considered here are



In all of these the initial ion has a configuration consisting of a single electron outside a closed shell and, except in the last, the final ion is excited. With (7) and (8) there are neighbouring perturbing levels whose effect has been quantitatively examined.

These reactions have been chosen for investigation since they cover a wide range of energy excesses and so provide representative data for a considerable variety of reactions.

Results for the six reactions are given in the form of cross sections over a wide range of impact energies and, where possible, as rate coefficients over a wide range of temperatures.

§ 2. THEORY

The theory of processes involving a pseudo-crossing (Zener 1932, Landau 1932, Stueckelberg 1932) has been adequately described in paper I, and only the essential formulae need be given here. If $U_i(R)$ and $U_f(R)$ denote the potential energies of the initial and final systems at a nuclear separation R of a reaction



with crossing point at R_X , energy separation $\Delta U(R_X)$ eV and initial energy of relative motion E_i eV, then its cross section is given by

$$Q = 4\pi R_X^2 p(1+\lambda) \int_1^\infty \exp(-\eta x) \{1 - \exp(-\eta x)\} x^{-3} dx \quad \dots\dots(11)$$

where p is the probability that the particles approach along the specified potential energy curve, $\lambda = [U_i(R_\infty) - U_i(R_X)]/E_i$ and η is given by

$$\eta = 247.2 \left[\frac{M^{1/2} \{\Delta U(R_X)\}^2}{E_i^{1/2} \Delta E^2} \right] (1+\lambda)^{-1/2} (1+\mu)^{-1} \quad \dots\dots(12)$$

with

$$(1+\mu)\Delta E^2 = e^2 \frac{d}{dR} (U_i - U_f)_{R=R_X}, \quad \dots\dots(13)$$

M being the reduced mass on the ^{16}O scale. Bates and Moiseiwitsch (paper I) have given a simple expression for μ when B is a doubly charged positive ion, A is a neutral atom and R_X is large:

$$\mu \sim \frac{e^4}{R_X^4 \Delta E^2} (a_1 + 2a_2/R_X) \quad \dots\dots(14)$$

where

$$a_1 = 2\alpha_1(\text{A}) - \alpha_1(\text{A}^+) - \alpha_1(\text{B}^-), \quad \dots\dots(15)$$

the α_1 's being the coefficients of the R^{-3} term in the expansion of the potential of a unit charge in the field of the atom indicated, and

$$a_2 = 2\alpha_2(\text{A}) - \frac{1}{2}\alpha_2(\text{A}^+) - \frac{1}{2}\alpha_2(\text{B}^-), \quad \dots\dots(16)$$

the α_2 's being the polarizabilities of the atom indicated. Slight modifications are necessary when B is a trebly charged ion. Equation (15) is replaced by

$$\alpha_1 = 3\alpha_1(A) - 2\alpha_1(A^+) - \alpha_1(B^-) \quad \dots\dots(17)$$

and equation (16) by

$$\alpha_2 = \frac{9}{2}\alpha_2(A) - 2\alpha_2(A^+) - 2\alpha_2(B^-). \quad \dots\dots(18)$$

§ 3. THE ENERGY SEPARATION

If Ψ_i is the initial wave function and Ψ_f the final wave function, the energy separation is obtained from a consideration of the energies of the systems described by $\Psi_i + \lambda\Psi_f$ (cf. paper I). Simple expressions for the energy separation may be obtained provided that the adopted wave function of either the initial or the final system is an exact solution of the wave equation at infinite separation of the nuclei. If we assume that the final wave function is exact for infinite separation, then the formulae given in paper I for the case when B is a doubly charged ion with a closed shell configuration and A a neutral atom consisting of one electron outside a closed shell remain valid when B is trebly charged apart from the difference in polarization energy. Denoting the initial and final wave functions of the active electron by $\phi(\mathbf{r}_a | n_a)$, $\phi'(\mathbf{r}_a | n_b)$ where \mathbf{r}_a , \mathbf{r}_b are the position vectors of the electron with respect to the two nuclei, the energy separation is given by

$$|\Delta U(R_X)| = 2 |S(\rho - p_f) - \sigma| / (1 - S^2)_{R=R_X} \quad \dots\dots(19)$$

with

$$S = \int \phi(\mathbf{r}_a | n_a) \phi'(\mathbf{r}_b | n_b) d\mathbf{r}, \quad \rho = \int \phi'(\mathbf{r}_b | n_b)^2 r_a^{-1} d\mathbf{r}$$

$$\sigma = \int \phi(\mathbf{r}_a | n_a) \phi'(\mathbf{r}_b | n_b) r_a^{-1} d\mathbf{r}$$

and

$$p_f = -2 \{ \alpha_2(A^+) + \alpha_2(B^-) \} / R_X^4. \quad \dots\dots(20)$$

The expression for the energy separation is rather more complicated when B has a configuration consisting of a single electron outside a closed shell since the symmetry of the atomic wave functions must be taken into account. Denoting the (orthogonal) initial and final wave functions of the lone passive electron by $\chi(\mathbf{r}_b | m_b)$, $\chi'(\mathbf{r}_b | m_b')$, where $\chi'(\mathbf{r}_b | m_b') \neq \phi'(\mathbf{r}_b | n_b)$, the energy separation is given by

$$|\Delta U(R_X)| = \frac{2 | \{ST + S'T'\} \{ \rho + \rho' - p_f \} - \{ (T\sigma + S\tau) \pm (T'\sigma' + S'\tau') \} |}{\{1 - (ST \pm S'T')^2\}} \quad \dots(21)$$

evaluated at $R = R_X$, the plus sign corresponding to B^- a singlet, the minus sign corresponding to B^- a triplet, where

$$S' = \int \phi(\mathbf{r}_a | n_a) \chi'(\mathbf{r}_b | m_b') d\mathbf{r},$$

$$T' = \int \chi(\mathbf{r}_b | m_b) \phi'(\mathbf{r}_b | n_b) d\mathbf{r}$$

$$\rho' = \int \chi'(\mathbf{r}_b | m_b')^2 r_a^{-1} d\mathbf{r},$$

$$\sigma' = \int \phi(\mathbf{r}_a | n_a) \chi'(\mathbf{r}_b | m_b') r_a^{-1} d\mathbf{r}$$

$$\tau = \int \chi(\mathbf{r}_b | m_b) \chi'(\mathbf{r}_b | m_b') r_a^{-1} d\mathbf{r},$$

$$\tau' = \int \phi'(\mathbf{r}_b | n_b) \chi(\mathbf{r}_b | m_b) r_a^{-1} d\mathbf{r}$$

$$\text{and } T = \int \chi(\mathbf{r}_b | m_b) \chi'(\mathbf{r}_b | m_b') d\mathbf{r};$$

p_f is given by (20) if B is trebly charged and by

$$p_f = -\frac{1}{2} \{ \alpha_2(A^+) + \alpha_2(B^-) \} / R_X^4$$

if B is doubly charged. When $\chi'(\mathbf{r}_b|m_b') \equiv \phi'(\mathbf{r}_b|n_b)$ (21) must be replaced by

$$\Delta U(R_X) = 2^{3/2} |ST(2\rho - p_f) - (T\sigma + S\tau)| / (1 - 2S^2T^2)_{R=R_X} \dots\dots (21a)$$

The expressions (21) and (21a) may be used only when the closed shell electrons are unaltered during the reaction and when R_X is large. Unless the passive electron orbital is considerably altered during the reaction, or is identical to the final orbital of the active electron, $S'T'$, $T'\sigma'$, $S'\tau'$ can usually be ignored.

Formulae (21) and (21a) have been obtained using what may be termed the 'post' form of the energy separation. In the case of reactions (7) and (9) (for which the smallest and largest values of R_X arise) the prior form has also been used making the assumption that the *initial* wave function is exact at infinite internuclear distance. The difference between the post and prior forms was found in each case to be less than 3%. This close agreement is at first sight rather surprising; it is due essentially to the fact that the energy separation depends more sensitively on the wave function of the hydrogen atom (which is known exactly) in regions close to the nucleus of the colliding ion than on the wave function of the ion in regions close to the proton (although the ion wave function must also be known with some accuracy). In collisions not involving a single-electron atom serious difficulties may arise.

§ 4. DETAILED CALCULATIONS AND RESULTS

Wentzel (1926) and Waller (1926) have calculated the polarizability of hydrogen to be 4.5 atomic units. The other polarizabilities required were calculated using the well-known expression (cf. Mott and Sneddon 1948) for α_2 in terms of dipole transition matrix elements, these being obtained from the tables of Bates and Damgaard (1949).† The values for $\text{Al}^{2+} (^2\text{S} \text{ and } ^2\text{P})$, $\text{Li}^+ (^3\text{S} \text{ and } ^1\text{S})$, and Al^+ are 14, 3, 38, 83 and 13 atomic units respectively.‡ The value for $\text{B}^+ (^1\text{P})$ is small but was not required since the R^{-4} term in (14) and (21) is negligible compared with the R^{-3} term.

The electron wave functions used were all linear combinations of products of exponentials and powers of the distance of the electron from the nucleus. Those for $\text{Al}^{3+} (^1\text{S})$, $\text{Al}^{2+} (^2\text{S})$ and $\text{Al}^+ (^1\text{S})$ were obtained by fitting to the numerical values given by Katterbach (1953) and Biermann and Harting (1943); for B^{2+} , B^+ , Li^+ the variational wave functions of Morse, Young and Haurwitz (1935) were employed (see also Coulson and Duncanson 1944); and Li^{2+} is hydrogenic. No wave function was available for $\text{Al}^{2+} (^2\text{P})$, but the coulomb approximation of Bates and Damgaard (1949) should be quite accurate for this state up to distances quite close to the nucleus. A series was fitted to the coulomb approximation values and found to be very nearly normalized, indicating good accuracy.

The integrals involved in (19) and (21) have all been tabulated by Coulson (1942) and were easily computed.§ Various quantities of interest in connection with the reactions studied here (and with those studied by Bates and Moiseiwitsch) are collected in table 1.

† Although this method of evaluating the dipole matrix elements is not very accurate for many two-electron systems, the approximation should suffice, the polarization energy being a small (even negligible) correction term.

‡ It is to be expected in general that α_2 is large for metastable excited states but small for excited states which can combine optically with the ground state.

§ The available tables (Mulliken, Rieke, Orloff and Orloff 1949 and Craig, Maccoll, Nyholm, Orgel and Sutton 1954) do not contain sufficient significant figures for our purpose.

Table 1. Basic Data relating to the Collision Processes so far studied

Reaction	Orbit†	ΔE (ev)	R_X (a_0)	S_{if}	$\Delta U(R_X)$ (ev)	X^\ddagger
(4)	3s	14.84	3.3 ₄	$4.5_9 \times 10^{-1}$	5.1 ₈	38
(9)	3s	5.23	5.2 ₉	$9.8_1 \times 10^{-2}$	1.5 ₄	83
(1)	2s	4.61	5.8 ₁	$7.6_7 \times 10^{-2}$	$8.6_0 \times 10^{-1}$	65
(5)	3p	8.16	6.5 ₈	$8.1_4 \times 10^{-2}$	1.2 ₅	101
(7)	2s	3.02 ₂	8.8 ₈	$1.1_8 \times 10^{-2}$	$1.2_4 \times 10^{-1}$	94
(2)	3p	2.74 ₅	9.6 ₄	$9.4_4 \times 10^{-3}$	$1.0_2 \times 10^{-1}$	104
(6)	2p	2.45 ₇	11.0 ₇	$9.8_8 \times 10^{-4}$	$5.6_9 \times 10^{-3}$	66
(3)	3s	1.43 ₅	18.9 ₂	$3.9_1 \times 10^{-6}$	$2.3_4 \times 10^{-5}$	113
(8)	2s	1.28 ₃	20.8 ₈	$4.6_8 \times 10^{-7}$	$2.1_2 \times 10^{-6}$	92

† Final orbital active electron.

‡ Parameter—cf. appendix.

Reactions (5), (6) and (9) are straightforward applications of the equations given earlier, but (4), (7) and (8) require special considerations and will be described separately.

4.1. $\text{Al}^{3+} + \text{H} \rightarrow \text{Al}^{2+} (^2\text{S}) + \text{H}^+$

Because of the high energy excess, the crossing point is small and the approximate equations of § 2 cannot be used. In particular, the closed shell electrons must be taken into account. The calculation is quite lengthy and will not be presented here; it leads to a crossing point at $3.34a_0$, which differs only slightly (due to cancellation between U_i and U_f) from the value $3.30a_0$ obtained when the inner electrons are ignored. Provided the inner electrons are unaltered during the reaction and it suffices to take $\Psi_i + \lambda\Psi_f$ as the wave function of the combined system*, equation (21) is still appropriate, giving an energy separation of 5.18 ev. This is so large that the Landau-Zener formula is not applicable (cf. paper I), but it is of interest to record that the cross section obtained is very small, being only $10^{-5}\pi a_0^2$ for an impact energy of 1 kev. In general it is to be expected that cases in which R_X is small (i.e. ΔE is large) are associated with very low cross sections.

4.2. $\text{Li}^{2+} + \text{H} \rightarrow \text{Li}^+ (^3\text{S} \text{ and } ^1\text{S}) + \text{H}^+$

The crossing points are at internuclear distances of 8.8_8a_0 and $20.9a_0$ respectively, and the energy separations computed using equation (21) are $1.2_4 \times 10^{-1}$ ev and $2.1_2 \times 10^{-6}$ ev. However, there are neighbouring levels which, though they do not interfere directly, their crossing points being at very large internuclear distances, may perturb those levels whose separations we require (cf. figure 1). Their effect is most directly examined by choosing as wave functions of the combined system

$$\Psi_i + \lambda\Psi_f + \mu\Psi_{f'}$$

where $\Psi_{f'}$ represents the other possible end products. For $\text{Li}^+ (^3\text{S})$ the most important perturbing level is that associated with $\text{Li}^+ (^3\text{P})$. Taking $\Psi_{f'}$ as its wave function and minimizing the system energy, a secular equation of degree three in the energy is obtained:

$$\begin{vmatrix} E - H_{ii} & ES_{if} - H_{if} & ES_{if'} - H_{if'} \\ ES_{if} - H_{if} & E - H_{ff} & ES_{ff'} - H_{ff'} \\ ES_{if'} - H_{if'} & ES_{ff'} - H_{ff'} & E - H_{f'f'} \end{vmatrix} = 0 \quad \dots (22)$$

where the H 's and S 's are the matrix elements of the total Hamiltonian and unity respectively. Numerical solution of (22) (a variational wave function being used

* This, of course, is not so since exchange between the colliding systems is becoming important.

for $\text{Li}^+(^3\text{P})$) shows that the energy separation is altered by less than 2%. The smallness of the effect is due to cancellation, both levels being shifted in the same direction. Similar conclusions hold for $\text{Li}^+(^1\text{S})$, the perturbing level being that associated with $\text{Li}^+(^1\text{P})$ (cf. figure 1).†

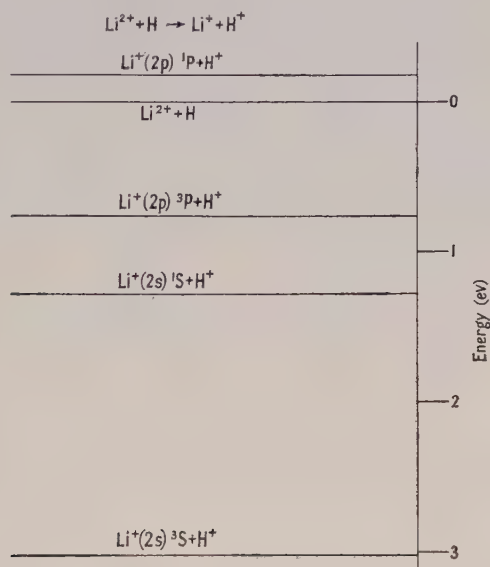


Figure 1. Energy levels in eV of $\text{Li}^{2+} + \text{H}$, $\text{Li}^+ + \text{H}^+$ for infinite nuclear separation.

4.3. Cross Sections and Rate Coefficients

The cross sections of processes (5), (7) and (9) are shown graphically in figure 2 as a function of the impact energy ϵ of the incident ion, the labelling being the

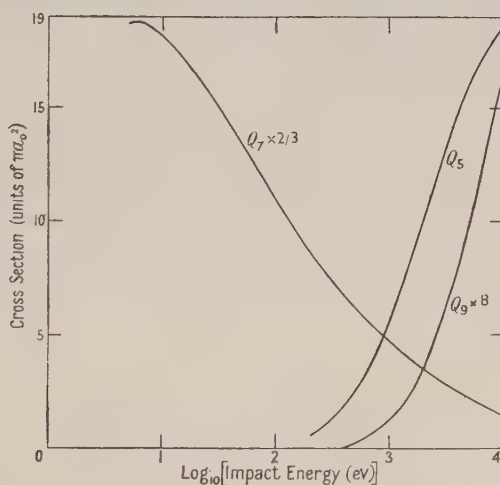


Figure 2. Cross sections for reactions (5), (7) and (9) in units of πa_0^2 as functions of the impact energy of the colliding ion.

† It may be noted that the perturbing level can be ignored provided that

$$\left| \frac{H_{if}^2}{H_{ii} - H_{ff'}} - \frac{H_{ff'}^2}{H_{ff} - H_{ff'}} \right|_{R=R_X} \ll \Delta U(R_X).$$

corresponding equation number. The cross sections of (6) and (8) are accurately represented by

$$Q_6 = 0.54\epsilon^{-1/2}(\pi a_0^2)$$

$$Q_8 = 1.03 \times 10^{-6}\epsilon^{-1/2}(\pi a_0^2),$$

in which ϵ is in eV. A discussion of the energies for which the Landau-Zener method may be used is given in paper I. The rate coefficient K_7 of process (7) is given in table 2 for temperatures between 1000°K and 32000°K on the assumption of a Maxwellian velocity distribution; K_8 is constant and equal to $1.6 \times 10^{-17} \text{ cm}^3 \text{ sec}^{-1}$ down to very low temperatures and K_6 is constant and equal to $2.0 \times 10^{-11} \text{ cm}^3 \text{ sec}^{-1}$ for temperatures greater than 1000°K. Since the Landau-Zener formula is only applicable when $E_i \gg \Delta U(R_X)$, it is not possible to compute rate coefficients for (4), (5) and (9).

Table 2. Rate Coefficient for Reaction (7)

T (°K)	1000	2000	4000	8000	16000	32000
K_7 ($10^{-9} \text{ cm}^3 \text{ sec}^{-1}$)	0.48	1.03	1.7 ₈	2.8 ₃	4.1 ₂	5.3 ₁

ACKNOWLEDGMENTS

The author is indebted to Professor D. R. Bates for suggesting this investigation and to Professor Bates and Dr. B. L. Moiseiwitsch for useful discussions.

APPENDIX

During the course of this series accurate values of the energy separation have been computed for nine reactions corresponding to energy excesses ranging from 1.28 eV to 14.84 eV. The significant quantity is not ΔE itself but rather $Z \cdot \Delta E \sim R_X$ where Z is the charge of the final ion. In table (1), $\Delta U(R_X)$, R_X and the overlap S_{if} of the colliding systems are compared.

Magee (1940) has suggested that

$$X = \Delta U(R_X) R_X / S_{if} \quad \dots\dots (23)$$

is approximately constant provided R_X is not too large; he estimates X to be about 10. Examination of the entries in the last column of the table reveals that (23) is remarkably successful, though a better value for X would be, say, 75.

This large value of X has considerable significance. Thus high energy separations, and consequently low cross sections, must be anticipated even when the energy excess of the reaction is not very great.

REFERENCES

- BATES, D. R., and DAMGAARD, A., 1949, *Phil. Trans. Roy. Soc. A*, **242**, 101.
 BATES, D. R., and MASSEY, H. S. W., 1954, *Phil. Mag.*, **45**, 111.
 BATES, D. R., and MOISEWITSCH, B. L., 1954, *Proc. Phys. Soc. A*, **67**, 805.
 BIERMANN, L., and HARTING, H., 1943, *Z. Astrophys.*, **22**, 81.
 COULSON, C. A., 1942, *Proc. Camb. Phil. Soc.*, **38**, 210.
 COULSON, C. A., and DUNCANSON, W. E., 1944, *Proc. Roy. Soc. Edinb. A*, **62**, 37.
 CRAIG, D. P., MACCOLL, A., NYHOLM, R. S., ORGEL, L. E., and SUTTON, L. E., 1954, *J. Chem. Soc.*, 354.
 KATTERBACH, K., 1953, *Z. Astrophys.*, **32**, 165.
 LANDAU, L., 1932, *Z. Phys. Sowjet*, **2**, 46.

- MAGEE, J. L., 1940, *J. Chem. Phys.*, **8**, 687.
MOORE, C., 1949, *Atomic Energy Levels* (Washington : National Bureau of Standards).
MORSE, P. M., YOUNG, L. A., and HAURWITZ, E. S., 1935, *Phys. Rev.*, **48**, 948.
MOTT, N. F., and SNEDDON, I. N., 1948, *Wave Mechanics and its Applications* (Oxford : Clarendon Press).
MULLIKEN, R. S., RIEKE, C. A., ORLOFF, D., and ORLOFF, H., 1949, *J. Chem. Phys.*, **17**, 1248.
STUECKELBERG, E. C. G., 1932, *Helv. Phys. Acta*, **5**, 370.
WALLER, I., 1926, *Z. Phys.*, **38**, 635.
WENTZEL, G., 1926, *Z. Phys.* **38**, 518.
ZENER, C., 1932, *Proc. Roy. Soc. A*, **137**, 696.

RESEARCH NOTES

On Antiferromagnetism in Metals

By R. H. TREDGOLD †

Physics Department, University of Nottingham

Communicated by L. F. Bates; MS. received 14th July 1954

§ 1. INTRODUCTION

It has been pointed out by Slater (1951) that the solution of the Hartree-Fock equations for electrons in a periodic potential might, under certain circumstances, lead to a ground state having an antiferromagnetic character. This idea has been taken up by Lidiard (1953, 1954) who extended it to formulate a phenomenological theory of the antiferromagnetic behaviour of chromium and manganese observed by Shull and Wilkinson (1953). However, a quantitative quantum mechanical treatment of this problem has not yet been carried out although a preliminary discussion has been given by Pratt (1953). It thus seems desirable to examine a simple model of a metal in an attempt to determine if circumstances exist in which the ground state is antiferromagnetic.

§ 2. THE GROUND STATE FOR A SIMPLE MODEL

The model considered here is similar to the one discussed by Pratt (1953) and consists of a linear chain of hydrogen-like atoms in which the atomic wave functions are approximated to by expressions of the form $\exp(-\frac{1}{2}\beta^2 r^2)$, the value of β being chosen to minimize the unperturbed energy. Although such a linear chain model would obviously lead to delusive results if studied from a statistical point of view there seems no reason to suppose that it should not yield qualitatively correct information about the ground state of a system involving atomic wave functions having spherical symmetry. Wannier (1937) functions may be constructed from the atomic functions in the usual way and will be denoted by $a(x-n\alpha)$ where $n\alpha$ is the coordinate of the n th atom and α is the lattice constant. One may then choose one electron wave function of the form

$$b_+(x, k) = \frac{1}{N^{1/2}} \sum_n a(x-n\alpha) \left[\frac{\lambda}{\sqrt{2}} \exp \{in\alpha(k - \pi/\alpha)\} + (1 - \frac{1}{2}\lambda^2)^{1/2} \exp(in\alpha k) \right] \dots\dots(1)$$

associated with + spin states and

$$b_-(x, k) = \frac{1}{N^{1/2}} \sum_n a(x-n\alpha) \left[\frac{\lambda}{\sqrt{2}} \exp \left\{ i(n+1)\alpha \left(k - \frac{\pi}{\alpha} \right) \right\} + (1 - \frac{1}{2}\lambda^2)^{1/2} \exp \{i(n+1)\alpha k\} \right] \dots\dots(2)$$

where

$$-\frac{\pi}{2\alpha} \leq k \leq +\frac{\pi}{2\alpha}$$

associated with - spin states. Here N is the number of atoms in the chain and will be assumed to be so large that end effects may be neglected; λ is a parameter

† Now at Physics Department, University of Maryland, U.S.A.

to be determined by the variational principle. It is of interest to note that if $\lambda=0$ one has the conventional collective electron description of the ground state of the linear chain and it may easily be shown that there will not be a resultant spin moment appearing on any one atom. If $\lambda=1$ each atom will show a spin moment of 1 Bohr magneton and there will be an antiferromagnetic structure.

Since the case of narrow energy bands is of primary interest in the present context a value of $\alpha=4.714$ atomic units was chosen for investigation and it was then found that the overlap integral had the value 0.044 and it was thus justifiable to neglect terms of the order of the square of the overlap integral in the calculation of the energy. To this approximation it is a straightforward process to calculate the energy using a single determinant wave function. The integrals occurring may all be evaluated in closed form by the method proposed by Boys (1950). It is found that part of the expression for the energy is independent of λ and, of course, of the arrangement of the spins and will accordingly be neglected here. The remaining part of the energy per atom expressed in atomic units will be denoted by E' .

Minimizing the energy with respect to λ one then finds that

$$\lambda^2 = 0.9030 \quad \dots\dots(3)$$

and $E' = -0.6005. \quad \dots\dots(4)$

This may be compared with the ferromagnetic case in which

$$E' = -0.5984 \quad \dots\dots(5)$$

and the conventional collective electron case ($\lambda=0$) in which

$$E' = -0.4244. \quad \dots\dots(6)$$

It may thus be seen that for the model under discussion the ground state is antiferromagnetic having an effective atomic moment of 0.9030 Bohr magneton and that the conventional collective electron description is seriously in error. It should be pointed out that the energies given in equations (4) and (5) are obtained from a large factor common to both expressions and very much smaller factors differing in the two expressions. Thus the small apparent energy difference is significant. It is interesting to note that the non-degenerate band considered does not have a ferromagnetic ground state, thus agreeing with the predictions of Slater, Statz and Koster (1953).

§ 3. DISCUSSION

The above discussion lends support to the view that any material having a narrow partly filled energy band and not exhibiting ferromagnetism will show antiferromagnetic properties at sufficiently low temperatures and thus supports the views expressed by Lidiard (1954) on the ground states of chromium and manganese. However, his treatment of the statistical problem of antiferromagnetism in these metals is open to certain criticism. His theory contains three parameters which are determined from the effective magnetic moment per atom extrapolated to 0°K, the transition temperature, and the value of the magnetic susceptibility at this temperature. Using these parameters he predicts the height of the anomalous peak in the specific heat at the transition temperature. In particular he finds that for manganese $\Delta C_p = 0.0033 \text{ cal mol}^{-1} \text{ deg}^{-1}$ and goes on to conclude that this quantity will be too small to be measurable. However,

Shomate (1945) has made very careful measurements of the specific heat of α -manganese (the allotropic form studied by Shull and Wilkinson (1953)). Using his results one finds that the anomaly in the specific heat at the transition temperature (94°K) is larger by a factor of one hundred than that predicted by Lidiard and is given approximately by $\Delta C_p = 0.37 \text{ cal mol}^{-1} \text{ deg}^{-1}$. In view of the limitations of the collective electron approximation in its application to statistical treatments of exchange dependent phenomena (Tredgold 1954) this discrepancy seems hardly surprising.

§ 4. THE RARE EARTHS

Since the rare earth elements share with the transition elements the characteristics of narrow partially filled energy bands and since only two of them, gadolinium and dysprosium (Trombe 1953), appear to be ferromagnetic it seems probable that some of the others should be antiferromagnetic at low temperatures. The case of manganese illustrates the fact that antiferromagnetism in a metal is not necessarily associated with a peak in the susceptibility-temperature curve, but that it may give rise to a measurable anomaly in the specific heat. Parkinson, Simon and Spedding (1951) have detected low temperature anomalies in the specific heats of cerium, praseodymium and neodymium and although these authors appear to favour an explanation of these phenomena based on Stark splitting, they point out that the shape of the anomalous peaks obtained would be more consistent with an explanation based on some form of cooperative phenomena.

Unfortunately the only unequivocal method of detecting antiferromagnetism is by means of neutron diffraction studies and until these materials are available in larger quantities it will be impossible to carry out such experiments.

ACKNOWLEDGMENT

I should like to thank Professor L. F. Bates for his continued interest and encouragement.

REFERENCES

- BOYS, G. F., 1950, *Proc. Roy. Soc. A*, **200**, 542.
LIDIARD, A. B., 1953, *Proc. Phys. Soc. A*, **66**, 1188; 1954, *Ibid.*, **224**, 161.
PARKINSON, D. H., SIMON, F. E., and SPEDDING, F. H., 1951, *Proc. Roy. Soc. A*, **207**, 137.
PRATT, G. W., 1953, *Quarterly Progress Report Solid State and Molecular Theory Group*, Jan. 1953 (Massachusetts Institute of Technology).
SHOMATE, C. H., 1945, *J. Chem. Phys.*, **13**, 326.
SHULL, C. G., and WILKINSON, M. K., 1953, *Rev. Mod. Phys.*, **25**, 100.
SLATER, J. C., 1951, *Phys. Rev.*, **82**, 538.
SLATER, J. C., STATZ, H., and KOSTER, G. F., 1953, *Phys. Rev.*, **91**, 1323.
TROMBE, F., 1953, *C.R. Acad. Sci., Paris*, **231**, 591.
TREDGOLD, R. H., 1954, *Proc Phys. Soc. A*, **67**, 221.
WANNIER, G. H., 1937, *Phys. Rev.*, **52**, 191.

Riesz Potential and the Elimination of Divergences from Quantum Electrodynamics: III

By L. S. KOTHARI

Tata Institute of Fundamental Research, Apollo Pier Road, Bombay 1

MS. received 14th July 1954

IN an earlier paper (Kothari 1954 b, referred to as II) we obtained a generalization of the Dirac equation and the Feynman function S_F in the β -plane† and showed how the divergence arising in quantum electrodynamics from the photon self-energy could be eliminated. However, the final result obtained for the self-energy of a photon was not gauge-invariant but also contained the Wentzel term. The necessity for modifying the formalism was thus felt.

In the present note we briefly give a new generalization of S_F and show how a gauge-invariant photon self-energy can be obtained.

Let

$$\begin{aligned}\mathcal{S}^\beta(x) &= G(\beta) l_0^\beta \int_{\chi > m} (\chi - m)^{\beta-1} S_x(x) d\chi \\ &= G(\beta) l_0^\beta \int_{\chi > m} (\chi - m)^{\beta-1} (-i\nabla - \chi) D_x(x) d\chi \quad \dots\dots(1)\end{aligned}$$

where $G(\beta) = (\sin 2\pi\beta)/2\pi$.

It satisfies the equation

$$(i\nabla - m)\mathcal{S}^\beta(x) = l_0^{-1}\mathcal{S}^{\beta+1}(x), \quad \dots\dots(2)$$

and for $\beta \rightarrow 0$, $\mathcal{S}^0(x) = S(x)$.

From (1) it follows that

$$\mathcal{S}_F^\beta(x) = \frac{G(\beta)}{(2\pi)^2} \int_0^\infty g_\beta(t) dt \int \frac{(\mathbf{k} + \mathbf{m} + t)e^{-i[\mathbf{k}x]}}{k^2 - (m+t)^2} d^4k \quad \dots\dots(3)$$

where $t = \chi - m$ and we have replaced the weight factor $l_0^\beta(\chi - m)^{\beta-1}$ by

$$g_\beta(t) = \frac{1}{2}(l_0^\beta t^{\beta-1} + l_0^{\beta*} t^{\beta*-1}) \quad \dots\dots(4)$$

(see II).

As Feynman (1949) has pointed out, the Wentzel term arises if the electron in going round the photon self-energy loop changes its mass at the two photon vertices. In order to avoid this change in mass we substitute the function $\mathcal{S}_F^\beta(x)$ only for one electron line and for the other we take the usual S_F function, but referring to a particle of mass $m+t$. This prescription has to be followed for all closed electron loops. (It may be noted here that with the generalization of II, this prescription could not work.) The matrix element is then proportional to

$$J_{\mu\nu}^\beta = - \frac{G(\beta)e^2}{(2\pi)^2} \int_0^\infty g_\beta(t) dt \int \frac{\text{Sp}[(\mathbf{k} + \mathbf{m} + t)(\mathbf{k} + \mathbf{p} + m + t)]}{\{k^2 - (m+t)^2\}\{(\mathbf{k} + \mathbf{p})^2 - (m+t)^2\}} d^4k. \quad \dots\dots(5)$$

Evaluating the spur and introducing a Feynman variable we obtain

$$\begin{aligned}J_{\mu\nu}^\beta &= - \frac{G(\beta)e^2}{\pi^2} \int_0^\infty g_\beta(t) dt \int_0^1 dx \\ &\times \int \frac{(m+t)^2 g_{\mu\nu} + k_\mu p_\nu + k_\nu p_\mu - [kp]g_{\mu\nu} + 2k_\mu k_\nu - k^2 g_{\mu\nu}}{\{\hat{k}^2 + p^2 x + 2[kp]x - (m+t)^2\}^2} d^4k. \quad \dots\dots(6)\end{aligned}$$

† For notation see Kothari 1954 a, b.

The integral over k is divergent but that over t converges for $0 < \beta < 2$. After integrating twice over t by parts, integration over k can readily be carried out. We obtain

$$J_{\mu\nu}^{\beta} = -\frac{4iG(\beta)\epsilon^2}{\beta} \int_0^{\infty} \left\{ I_0^{\beta} \left(\frac{m}{\beta+1} + \frac{t}{\beta+2} \right) (m+t)t^{\beta-1} + \text{c.c.} \right\} dt \\ \times \int_0^1 \frac{x(1-x)(p^2 g_{\mu\nu} - p_{\mu} p_{\nu})}{\{(m+t)^2 - p^2 x(1-x)\}^2} dx. \quad \dots\dots (7)$$

The integral over t is convergent for $-2 < \beta < 0$. Integrating over t by parts once and then analytically continuing the whole expression to $\beta=0$ (Kothari 1954a), we get

$$J_{\mu\nu} = J_{\mu\nu}^0 = 2ie^2(p_{\mu} p_{\nu} - p^2 g_{\mu\nu}) \left[\frac{1}{6} \log \frac{1}{m^2 l_0^2} - \int_0^1 x(1-x) \log \left\{ 1 - \frac{p^2 x(1-x)}{m^2} \right\} dx \right], \quad \dots\dots (8)$$

which is gauge-invariant.

ACKNOWLEDGMENT

The author wishes to thank Dr. Horowitz for making available to him the facilities of the Department of Mathematical Physics, C.E.N. de Saclay, France, during his stay there.

REFERENCES

- FEYNMAN, R. P., 1949, *Phys. Rev.*, **76**, 769.
KOTHARI, L. S., 1954 a, *Proc. Phys. Soc. A*, **67**, 17; 1954 b, *Ibid.*, **67**, 201.

Ferromagnetic Properties of Oxidized Mn_2Sb

BY G. D. ADAM AND K. J. STANDLEY

The University, Nottingham

Communicated by L. F. Bates; MS. received 10th September 1954

THE purpose of this note is to report the existence of a ferromagnetic material to which the empirical formula Mn_2SbO has been tentatively assigned.

When finely powdered dimanganese antimonide, Mn_2Sb , is heated in air to temperatures between 200°C and 350°C , an increase in weight is obtained, while prolonged heating in argon or in nitrogen produces no such effect. A systematic examination of several samples showed that, within this temperature range, the maximum increase in weight which could be produced was $7.0 \pm 0.1\%$. For one gramme-molecule of Mn_2Sb (i.e., 231.6 g) this corresponds to an increase of 16.2 g and thus suggests the formula Mn_2SbO for the oxidized material. Further absorption of oxygen occurs at higher temperatures (500°C to 600°C) and the ferromagnetism then disappears; this is probably due to decomposition and the formation of uncombined oxides of manganese and antimony.

The intensities of magnetization I of Mn_2Sb and Mn_2SbO were determined at room temperature using an oscillation magnetometer of the type described by Griffiths and Macdonald (1951) while the Curie points θ were found by a simple oscillation method. For Mn_2Sb , $I = 172 \pm 10$ e.m.u. cm^{-3} and $\theta = 280 \pm 5^\circ\text{C}$, in agreement within experimental error with the values found by Guillaud (1943) and quoted by Bozorth (1951). For Mn_2SbO , $I = 355 \pm 20$ e.m.u. cm^{-3} and $\theta = 310 \pm 5^\circ\text{C}$. In addition, relative susceptibility measurements indicate that from 370°C to 500°C the $1/\chi$ -temperature curve for Mn_2SbO is linear, whereas Serres (1947) reported a marked curvature in the similar graph for Mn_2Sb .

If identical corresponding states curves are assumed for the two materials, the above data together with the measured density ratio of 0.82 yield $2.5 \mu_B$ for the moment per manganese atom in Mn_2SbO compared with $0.94 \mu_B$ found for the same quantity in Mn_2Sb by Guillaud. A ferrimagnetic disposition of manganese ions in $3d^5$ and $3d^7$ states accounts satisfactorily for the observed moment in Mn_2Sb , but the magnitude of the moment in Mn_2SbO shows a similar arrangement there to be improbable.

X-ray powder photographs of the oxidized material, obtained using Fe $K\alpha$ radiation, showed a complex pattern which is quite different from that of Mn_2Sb and which has not yet yielded to analysis. However, it seems likely that the crystal structure of Mn_2SbO has a symmetry lower than tetragonal.

The microwave resonance absorption in powdered specimens of Mn_2SbO was examined at a wavelength of 1.26 cm using the method and apparatus previously described (Adam and Standley 1953). In the temperature range 20 – 320°C , a constant spectroscopic splitting factor g of 2.10 ± 0.05 was obtained. The width of the absorption line increased slightly with temperature up to 150°C and thereafter decreased rapidly as the Curie temperature was approached, the mean values at 20°C and 300°C being 5000 and 1000 oersteds respectively. This behaviour is again quite different from that of Mn_2Sb ; similar measurements on this latter material revealed multiple absorption lines whose magnitude and position varied markedly with change in temperature.

Further work is in progress, particularly on the microwave absorption in Mn_2Sb , and results will be communicated later.

REFERENCES

- ADAM, G. D., and STANDLEY, K. J., 1953, *Proc. Phys. Soc. A*, **66**, 823.
BOZORTH, R. M., 1951, *Ferromagnetism* (New York: Van Nostrand) pp. 334–36.
GRIFFITHS, J. H. E., and MACDONALD, J. R., 1951, *J. Sci. Instrum.*, **28**, 56.
GUILLAUD, C., 1943, *Thèse*, Strasbourg.
SERRES, A., 1947, *J. Phys. Radium*, **8**, 146.

LETTERS TO THE EDITOR

Radiative Transitions in j - j Coupling

Observation of an angular correlation involving a γ -ray of mixed multipolarity gives the relative sign and magnitude of the competing transition matrix elements (Biedenharn and Rose 1953, to be referred to as BR). Here we give explicitly the single-particle matrix elements for arbitrary multipoles, in the j - j coupling scheme, ready for immediate application to correlation studies.

The real reduced matrix elements $(J_2 \parallel L \parallel J_1)$, defined as in BR, are normalized so that the lifetime for a transition of E Mev from a state of spin J_1 to one of J_2 is

$$\tau = 5.205 \times 10^{-39} / E \Sigma_L (2 \parallel L \parallel 1)^2 \text{ sec.} \quad \dots\dots(1)$$

They have the conjugation property

$$(2J_2 + 1)^{1/2} (J_1 E_1 \parallel L \parallel J_2 E_2) = (-)^{J_2 - J_1 - L - 1} (2J_1 + 1)^{1/2} (J_2 E_2 \parallel L \parallel J_1 E_1). \quad \dots\dots(2)$$

The intensity ratio of $2^{L'}$ -pole to 2^L -pole is δ^2 , where $\delta = (2 \parallel L' \parallel 1) / (2 \parallel L \parallel 1)$, is the parameter in angular correlation formulae (BR, eqn 70).

The static moments are given by the diagonal elements

$$\left. \begin{aligned} \mu &= -[3J(J+1)]^{1/2} (J \parallel M1 \parallel J) k \\ Q &= 4[15J(2J-1)(J+1)(2J+3)]^{1/2} (J \parallel E2 \parallel J) / e k^2. \end{aligned} \right\} \quad \dots\dots(3)$$

We separate the contributions due to the charge (c) and spin (s) so that $(2 \parallel L \parallel 1) = (2 \parallel L(c) \parallel 1) + (2 \parallel L(s) \parallel 1)$. In terms of the wave number $k = E(\text{Mev}) / 5.063 \times 10^{10} \text{ cm}^{-1}$, nuclear radius R (cm), and μ , the intrinsic magnetic moment in nuclear magnetons β , ($= e\hbar / 2Mc$), the single-particle elements for a nucleon jumping from orbit j_1 to j_2 are

$$\begin{aligned} (2 \parallel EL(c) \parallel 1) &= \omega(12) e' k^L R^L J(L) i^{l_1+l_2-L} (-)^{j_1-l_1+1/2} \\ &\quad \times C(j_1 j_2 L; \tfrac{1}{2} - \tfrac{1}{2}) [(2j_2 + 1)(L + 1) / 2L]^{1/2} [(2L + 1)!]^{-1} \dots\dots(4) \end{aligned}$$

$$\begin{aligned} (2 \parallel ML(c) \parallel 1) &= B(L-1) (-)^{j_1-l_1-1/2} W(j_1 l_1 j_2 l_2; \tfrac{1}{2} L) \\ &\quad \times \left[\frac{(L+l_2+l_1+1)(L+l_1-l_2)(L+l_2-l_1)(l_1+l_2-L+1)}{2L(L+1)(2L+1)(2L-1)} \right]^{1/2} \end{aligned}$$

.....(5)

$$\begin{aligned} (2 \parallel L(s) \parallel 1) &= -\sqrt{3} \mu B(\gamma) A(\gamma) X(j_1 j_2 L; l_1 l_2 \gamma; \tfrac{1}{2} \tfrac{1}{2} 1) \\ B(\gamma) &= -\beta k^\gamma R^\gamma J(\gamma) i^{l_1+l_2-\gamma} C(l_1 l_2 \gamma; 00) \\ &\quad \times [(2j_2 + 1)(2l_1 + 1)(2l_2 + 1)]^{1/2} [(2\gamma + 1)!]^{-1} \end{aligned}$$

.....(6)

where $\gamma = L$, $A(\gamma) = (2L+1)^{1/2}$, for EL , and $\gamma = L-1$, $A(\gamma) = (L+1)^{1/2}$, for ML ; $\omega(12)$ is the sign of $(E_1 - E_2)$ and e' the effective nucleon charge (Bohr and Mottelson 1953). Expressions for the analogous tensor operators in β -decay have been given by Rose and Osborn (1954). Their $T(\mathbf{r}, \mathbf{p})$, $T(\mathbf{r}, \boldsymbol{\sigma})$ correspond to our $L(c)$, $L(s)$; they give explicitly the X coefficients needed in (6). The vector addition coefficients $C(abc; 00)$ are defined in BR, the $C(j_1 j_2 L; \frac{1}{2} - \frac{1}{2})$ tabulated by de-Shalit (1953) and the Racah W 's by Biedenharn (1952).

It is not sufficient to take for the radial integral

$$R^J(\gamma) = \int u_1(r) u_2(r) r^{\gamma+2} dr,$$

the 'uniform density' value $J(\gamma) = 3/(\gamma + 3)$, since we also require its sign; for this, oscillator functions may be used (Talmi 1952).

We note that δ for $EL + M(L + 1)$ mixtures is independent of nuclear radius and radial integrals.

For M1 and E2 the elements are very simple

$$\begin{aligned}(j'l \parallel M1 \parallel j'l) &= -k[(j+1)/3j]^{1/2}\mu(jl)\beta \\ (j+1, l \parallel M1 \parallel j'l) &= -(2\mu - \epsilon)k\beta[(2j+3)/12(j+1)]^{1/2} \\ (j_2 \parallel E2(c) \parallel j) &= \frac{1}{16}\omega(12)a(j_2j)e'k^2R^2J(2)[(2j+3)/5j(j+1)]^{1/2}\end{aligned}$$

where $a(j_2j) = -[(2j-1)/3]^{1/2}$ if $j_2=j$; or $i^{l_2-l_1}(j+2)^{-1/2}$ if $j_2=j+1$; $\mu(jl)$ is the Schmidt value of the magnetic moment and $\epsilon=1$ for a proton, 0 for a neutron.

The nuclear states in general will have a number of neutrons and protons in unclosed shells. The *sign* of δ for competing radiations is still given by the relative sign of the two single-particle elements, but the magnitudes of the elements will be modified by an angular momentum coupling factor. Publication of the detailed formulae, which involve fractional parentage theory, must, however, await completion of a study of empirical data. Lane and Radicati (1954) considered $j^{n-1}j_0 \rightarrow j^{n-1}j_1$ transitions, but the 'spin' parts of their formulae are valid only for M1. The operator for other multipoles includes a 'space' factor, $r^l Y_l^m$.

To emphasize the importance of this coupling we consider here two nucleons in the transition $J_1(j_1j) \rightarrow J_2(j_2j)$, when

$$(2 \parallel L \parallel 1) = g(-)^{J_2-L+j_1-j}[(2J_2+1)(2j_1+1)]^{1/2}W(j_1J_1j_2J_2; jL)(j_2 \parallel L \parallel j_1). \dots (7)$$

For a like pair (2N or 2P), $g=1$ if j, j_1, j_2 are all different, $g=\sqrt{2}$ if $j_1=j$ or $j_2=j$, and $g=2$ if $j_1=j_2=j$. For an unlike pair (N + P), $g=1$, and if $j_1=j_2$, there is a term like (7) for each particle.

Then for the two $L=5$ transitions: (i) $7(\frac{13}{2} \frac{3}{2}) \rightarrow 2(\frac{13}{2})^2$ and (ii) $7(\frac{13}{2} \frac{3}{2}) \rightarrow 2(\frac{3}{2})^2$, although the same element $(\frac{13}{2} \parallel 5 \parallel \frac{3}{2})$ is involved, (ii) is favoured over (i) by a factor 700 in intensity, and (i) is reduced to 1/2000 the single particle value!

Clarendon Laboratory,
Oxford.

G. R. SATCHLER.

1st June 1954; in revised form 7th September 1954.

BIEDENHARN, L. C., 1952, *Tables of Racah Functions* (Oak Ridge National Laboratory Report 1098).

BIEDENHARN, L. C., and ROSE, M. E., 1953, *Rev. Mod. Phys.*, **25**, 729.

BOHR, A., and MOTTELSON, B. R., 1953, *Dan. Mat. Fys. Medd.*, **27**, No. 16.

DE-SHALIT, A., 1953, *Phys. Rev.*, **91**, 1479.

LANE, A. M., and RADICATI, L. A., 1954, *Proc. Phys. Soc. A*, **67**, 167.

ROSE, M. E., and OSBORN, R. K., 1954, *Phys. Rev.*, **93**, 1326.

TALMI, I., 1952, *Helv. Phys. Acta*, **25**, 185.

A Possible Variation of the Rate of Local Penetrating Showers

During the course of an experiment on the development of the nucleon cascade in lead what may be a variation with solar time in the rate at which penetrating showers occur has been observed.

The apparatus (McCusker, Messel, Millar and Porter 1953), consisted of five trays of Geiger-Müller counters, A, B, C, D and E. Each tray contained 12 counters. Each of the counters was 50 cm long and 3.8 cm in diameter. The counters of trays A and B were in contact and those of tray A had their axes at right angles to those of tray B. Trays C and D were vertically beneath tray B. Tray C was separated from B by 10 cm of Pb and 60 cm of air. Tray D was separated from tray C by a further 5 cm of Pb. These last two trays were shielded at their sides and ends by 15 cm of Pb. A mass of lead 4 ft \times 4 ft in area and of varying thickness could be placed over tray A and the local penetrating showers were produced in this. Tray E, which was unshielded, was placed at a horizontal distance of 2 m from the centre line of the other trays.

The criterion for a penetrating shower was the discharge of at least two counters in each of trays B, C and D. If tray E was also triggered the event was classed as an extensive penetrating shower, if not, as a local penetrating shower. So far the time of arrival of 10 337 local and 1569 extensive penetrating showers has been recorded. The table gives the rate per hour of local penetrating showers for each

Hours (G.M.T.)	01-05	05-09	09-13	13-17	17-21	21-01
Rate of local penetrating showers per hr.	1.62 ± 0.038	1.60 ± 0.037	1.43 ± 0.038	1.60 ± 0.037	1.64 ± 0.038	1.52 ± 0.037
Rate of μ -mesons per min.	150.7 ± 0.75	148.2 ± 0.75	149.5 ± 0.75	150.1 ± 0.75	149.8 ± 0.75	149.7 ± 0.75

of the four hour periods beginning 0100 to 0500 G.M.T. This rate is an average for various thicknesses of lead above tray A from 20 cm to 82.5 cm. All the individual runs show the same effect, but, of course with much greater statistical errors. The average rate for the period 09-13 hours differs from that of the average rate for 01-09 and 13-21 hours by 4.4 standard deviations. The lowest rate recorded was 1.30 ± 0.07 for the period 10 to 11 hours, the highest 1.71 ± 0.08 for 04-05 hours. It thus seems that the effect is statistically established. It may, however, (since it is a variation with solar time) be due to some natural phenomenon not connected with cosmic radiation but which affects the apparatus, or to some man-made effect. Attempts have been made to discover some such cause. So far, none has been found. The a.c. input voltage and various other voltages have been continuously recorded but none shows a wave form similar to the curve for the local showers or one 180° out of phase with it. With the counter high tension below starting potential the rate for all hours is exactly zero. Various μ -meson rates through the apparatus have been monitored and show no time variation outside the small statistical error (one such rate is given in the table). The extensive penetrating showers show no variation outside the statistical error. Thus while it cannot yet be taken as certain that the effect is not spurious there seems some probability that it is not.

If it is real, it seems likely that it is connected with very high energy primaries since in the first place many of the showers detected must be due to nucleon primaries on the apparatus of at least 100 kmev and secondly several observers have found no such variation for primaries of 10^{13} – 10^{15} ev (Barrett, Cocconi, Eisenberg and Greisen 1954, Elliott 1953).

Finally if the effect is real it must be large, for a not inappreciable part of the recorded local shower rate is due to the (constant) μ -meson contamination.

We are greatly indebted to Dr. G. Cocconi for sending us his results before publication.

Dublin Institute for Advanced Studies.
30th July 1954.

J. G. DARDIS.
C. B. A. McCUSKER.

BARRETT, P., COCCONI, G., EISENBERG, Y., and GREISEN, K., 1954, *Phys. Rev.*, in the press.
ELLIOTT, H., 1953, *Proc. Bagnères Conference* (Toulouse: Imprimerie Universitaire), p. 18.
McCUSKER, C. B. A., MESSEL, H., MILLAR, D. D., and PORTER, N. A., *Phys. Rev.*, 1953, **89**, 1172.

REVIEWS OF BOOKS

Electricity and Magnetism for Degree Students, by S. G. STARLING. 8th Edn.

Revised in collaboration with the author by A. J. WOODALL. Pp. viii + 650.

(London: Longmans, Green & Co., 1953.) 30s.

It is now over 40 years since the first edition of this book appeared. There can hardly have been another textbook in the whole range of physics which has been in such constant use in all this time. Students of today use it as their predecessors did. It owes its success to its insistence on the fundamental principles of the subjects of electricity and magnetism. The original author is now joined by a younger colleague as a collaborator and both continue Starling's original idea of keeping the experimental aspect of the subject in the foreground, but they stress the need to express it with the aid of mathematics, not however with too difficult a use of that branch of knowledge.

The content of this work is well known. It has been found of great use by students in all universities, colleges and schools in their degree courses, including Honours courses. It makes no claim to specialization in any part, but supplies a firm basis for those who may later become specialists. The subject has grown in the past forty years beyond all expectation, but the author has not allowed himself to be turned aside from his original purpose in order to give a disproportionate space to a popular new discovery. The task of pruning and grafting has not been easy, and in the present edition the difficulty of choice and extent of new additions must have been great. Opinions on this question are bound to differ amongst teachers and students, but on the whole no serious adverse criticism will be made on this account, especially as addition is not possible without making the book cumbersome as a textbook for students.

A number of more recent topics have been touched upon, and readers are directed to fuller accounts by means of references.

There are some points concerning notation and presentation which may be considered with advantage in preparing another edition. In applying Kirchhoff's laws in networks it would be an improvement to introduce the method of Maxwell's circular currents. The old notation which uses (P , Q , R) and (α , β , γ) for intensity components in Maxwell's equations should now be replaced by the more usual E 's and H 's. The general use of complex quantities in alternating current theory would shorten the work and lighten the burden of the reader. It will also prepare him for the general method adopted in all more advanced work. The short paragraph on the M.K.S. system in the chapter on units and dimensions could with advantage be expanded. Finally, the quadrant electrometer needs a more realistic treatment.

H. T. FLINT.

The Physics of Experimental Method, by H. J. J. BRADDICK. Pp. xx + 404.

(London: Chapman and Hall, 1954.) 35s.

It has always been true of the experimental sciences, and particularly of physics, that advances in the knowledge of fundamental processes have been closely linked with technical improvements in the basic apparatus available to the experimenter. This is well shown by the outstanding progress in the present century, which has been undoubtedly due in no small measure to the gradual development of vacuum technology and high voltage electrical engineer-

ing, to the arrival on the scene of the radio valve and the corresponding emphasis on high-frequency circuit techniques, and to the availability of a wide range of instruments for the detection of radiations of all kinds.

It is unfortunately rather uncommon in University courses for the student to meet with more than incidental references to such technical matters. Such references as do occur are chosen partly by custom, partly because of the closeness of the subjects to pure physics, and partly by the criterion of how conveniently they can be used by a lecturer as illustrations of physical principles. From the postgraduate point of view the situation is often just as unsatisfactory. With three short years in hand and an original contribution to physics expected, a Ph.D. student is usually more interested in starting his experiments than in indulging in a critical survey of the properties and limitations of the materials, techniques and instruments available to him, however beneficial such a survey might be in the long run. Such information is normally picked up in a rough and ready fashion during the course of his work, more often than not by making mistakes and so wasting time.

Dr. Braddick in his book brings together successfully much of this basic practical knowledge, and by discussing at the same time the fundamental principles involved makes it easy to appreciate and remember. The range covered is, as would be expected, quite wide. The author begins by giving an account of the mathematical treatment of results, statistical methods, errors, curve fitting etc., with a useful appendix on numerical methods. Following this are chapters on the mechanical design of apparatus and on the properties of the materials normally used, such as metals, alloys, solders, magnetic materials, plastics, glasses etc., containing much useful data. Next come vacuum techniques, electrical measurements, electronics (covering the normal circuits used in laboratory practice), optical systems, and photography. A very interesting chapter follows in which fluctuation phenomena are discussed in connection with the inherent limits of measurement, illustrated by noise in electrical circuits, fluctuations in galvanometer readings, and the detection of weak light beams by the photocell and electrometer triode. The last chapter is concerned with the special techniques used in nuclear physics, including ionization chambers, Geiger counters, scintillation counters, the cloud chamber, and the photographic emulsion as a means of particle detection.

The treatment throughout is directed at giving an experimenter who has a problem to solve some guidance in the choice of instruments, the design of apparatus, and the assessment of errors and limitations. In this way it becomes less a reference book and more a handbook, a collection of information and principles which should be (and eventually will be) known by any successful research worker in physics, and indeed in many allied fields.

As to the author's choice of subject matter, it would be fair to say that most of the topics will be of use at some time or another to a physicist. The only noticeable omissions concern the methods of thin film production, i.e. windows, thin targets and surface films, and the practical details of sources of emission such as cathodes, ion sources etc. In these particular cases the availability of either the window or current of particles is often a vital factor in the feasibility of a proposed experiment.

The book is remarkably free from errors considering the amount of information it contains, and is well supplied with references for further reading.

R. LATHAM.

Microwave Spectroscopy, by M. W. P. STRANDBERG. Pp. viii + 140. (London: Methuen, 1954.) 9s. 6d.

The main part of this Methuen Monograph consists of a concise theoretical treatment of the microwave spectra of gases. Considerable acquaintance with quantum mechanical methods is assumed, but given that, the various steps are clearly set out and show how the energy levels and intensities can be calculated. The treatment covers the Stark and Zeeman effects, interaction with the nucleus and the spectra of oxygen and ammonia as well as the rotational spectra. There is no mention of experimental results, nor does the author discuss the quantities which can be measured by this technique. The second part contains some comments on experimental methods, using one particular arrangement as an example. Although there are some points of interest in this part, the general impression is of a rather hastily compiled set of notes. A full page photograph of a piece of waveguide with a mica-lead seal hardly adds anything to a description and certainly adds to the cost and detailed circuit diagrams should more properly be published elsewhere. In fact the book as a whole is badly balanced and it is not at all clear for what class of readers it was designed. Those starting work in the subject may find it of some use, but it certainly does not fulfil the aim of the series "to supply science students at University level with a compact statement of the modern position in each subject." A better plan would have been to expand the theoretical part and omit the second part. There are two useful tables of reduced energy values and of line strengths.

J. H. E. GRIFFITHS.

Microwave Spectroscopy, by W. GORDY, W. V. SMITH and R. F. TRAMBARULO. Pp. xii + 446. (New York: John Wiley; London: Chapman and Hall, 1953). 64s.

Microwave spectroscopy is a post-war subject and started with the very great advantage of well-developed techniques and instruments. The result is that a large number of papers has been published and a great deal of accurate information has been obtained in the last few years. Some review articles have been published on particular branches, but this is the first book and is much to be welcomed. As the authors say, it is not so much a book on a subject as on the applications of a technique and as is usual in such a book, some applications receive better treatment than others. In this case, of the two main branches, that of gaseous spectroscopy is favoured at the expense of spectroscopy of the solid state, including magnetic resonance phenomena.

The book is written in a style suitable for the ordinary physicist or chemist who is not an expert. The theoretical results are given as formulae which are easily applicable to particular cases and no derivations are given except where simple treatments, such as the vector model, can be used. Experts in this field will also find the book useful, mainly because of the great amount of information collected together in a readily accessible form.

The scope of the book is best shown by considering the individual chapters. After a brief introduction there is a long and useful chapter on instruments and experimental methods. In places this may be difficult to understand for those who are not accustomed to microwave techniques and terms. However, there are plenty of references, although many of these are to the Radiation Laboratory Series which is not so readily available in this country as in the

U.S.A. It is good to see a discussion of the ultimate sensitivity included in this chapter. Then follow the main chapter on the spectra of gases, a chapter on the Stark and Zeeman effects and one on shapes and intensities of lines. These are clearly written and bring out the main features of the various cases. The chapter on the spectra of solids and liquids, which follows, is not so satisfactory. Paramagnetic resonance is now too large a subject to be treated in one chapter and this one seems to be based on rather early information. Many of the results are mentioned, but they are not put together in such a way as to give a clear account of the subject. There follow three interesting chapters in which are discussed the various quantities which can be measured by means of microwave spectroscopy. These are nuclear properties such as spin, magnetic moment and quadrupole moment, the electrical properties of molecules such as dipole moments, and molecular structure constants such as bond lengths and angles. The final brief chapter is on applications to other fields and includes a discussion of the possibility of using a molecular absorption line as a standard of time and of applications to astronomy.

There are 97 pages of tables and references. The tables include various molecular and nuclear data which have been obtained by microwave techniques and some of the functions required for the analysis of gaseous spectra. References are given at the end of each chapter and also at the end of the book, arranged by subject in order of date of publication. While all this information is valuable, the book would have been more useful had some of this space been used to expand the chapters on experimental methods and on the spectroscopy of solids.

In all, this is a useful book and most physicists and physical chemists will find something of interest in it.

J. H. E. GRIFFITHS.

Progress in Cosmic Ray Physics, Vol. II, edited by J. G. WILSON. Pp. xi+322. (Amsterdam: North-Holland Publishing Company, 1954.) 86s.

Progress in Cosmic Ray Physics is published with the aim of providing a regular series of up-to-date reviews of those aspects of cosmic radiation "in which advances of broad significance are now being made". The first volume was published in 1952 and covered work done up to the beginning of the year 1951 in nine main fields of activity. The present volume gives the general position at the end of 1952 in five topics of current interest, namely, "The Nuclear Interactions of Stopped μ -Mesons" by R. D. Sard and M. F. Crouch, "The Heavy Unstable Particles" by the editor, "The Penetrating Component in the Upper Atmosphere" by the late E. G. Dymond, "The Development of a Nucleon Cascade" by H. Messel, and "Particle Identification with Photographic Emulsions" by L. Voyvodic. All these subjects except the one by the editor are different from those treated in Volume I. Evidently the editor considers (rightly) that the new unstable particles are of such great interest at present as to call for an article in each volume.

One's general reaction to this volume and to the previous one is very favourable, and it is undoubtedly true that a real need is being met. Although the reader's judgment of a particular article is coloured by his personal knowledge of the subject, each article should serve not only to enlighten but also to stimulate. The articles in the present volume measure up to these

standards in varying degrees but the reviews of Sard and Crouch and of Voyvodic deserve special mention as being particularly good.

Dymond's article is a careful and thorough survey of a narrow field of work by one who was very experienced in the art of balloon-flying. It can be recommended to all who contemplate work at very high altitudes. The present writer is not competent to judge Messel's article on nucleon cascades, but a close study leaves the impression that the author might have concentrated more on the general results, which are undoubtedly correct, and might have omitted much of the mathematical detail. The editor's review of the new particles was, unfortunately, written just before a very fruitful period of great advances and before agreement had been reached on the nomenclature. In consequence, this article is somewhat out of date and employs a symbolism much of which is rather different from the one now in use. Such difficulties must inevitably arise when the rate of advance is so rapid.

The general editor and the publishers are to be congratulated on the speed and excellence of production of the new volume, and it is to be hoped that this high standard will be maintained in future volumes in this series.

G. D. ROCHESTER.

Atomic Energy: a Survey, edited by J. ROTBLAT. Pp. viii+72. (London: Atomic Scientists' Association, 1954.) 6s. 6d. bound, 4s. 6d. paper.

This short book contains the published versions of lectures given before the University of London by nine distinguished members of the Atomic Scientists' Association in January and February 1954. The question whether scientists bear a particular responsibility for the misuse of scientific discoveries has often been debated. The views of the Association on this subject are definite and almost certainly correct. Its members believe that scientists have the same status as ordinary citizens when decisions of policy are taken, but that they have a special responsibility to inform their fellow-citizens and to place the issues clearly before them.

The lectures printed here, although necessarily rather condensed, are certainly very successful in presenting an accurate, balanced and up-to-date picture of atomic energy in Britain. Sir John Cockcroft, in describing the work of research at Harwell, shows how many problems in pure and applied science and in engineering have to be solved before large-scale release of nuclear power can be made feasible. This explains, what is not immediately obvious to an outsider, why Harwell is so large. Incidentally, his account provokes the speculation that all this research may well have a marked effect on technology quite outside the field of nuclear energy; for example, the intense efforts to develop liquid metal cooling, and the investigations into the properties and uses of formerly rare metals such as zirconium, must surely have a great influence on many branches of engineering.

Professor F. E. Simon's contribution on power from atomic energy is possibly the most interesting in the book, partly because it is expressed with such force. Great Britain is severely taken to task for wasting coal, and is told that she will not remain a first class industrial nation unless she reforms, and unless she also develops new sources of power. It is suggested that nuclear energy should be made to provide about 15 000 megawatts in something like 20 years. In

addition, the export of nuclear power plants should be a major factor in maintaining the balance of payments.

The effect of the development of atomic warfare on medicine is discussed by Dr. Loutit and Dr. Pochin. The first deals with the hazards peculiar to the new group of industries which has been created, and gives good reasons for hoping that the tragic mistakes made during the industrial revolution will not be repeated. Dr. Pochin describes some of the contributions which radio-isotopes have made to medical research, to diagnosis and to treatment.

The three lectures devoted to atomic warfare are less successful, even though Professor Frisch's explanation of the physical principles of atomic and hydrogen bombs is probably the most brilliantly written of all the contributions. He makes estimates of the damage caused by single weapons, but was evidently not asked to assess the destruction and confusion which would be caused by a full-scale attack on a nation such as ours. This, indeed, is not a task for which a physicist is particularly qualified. In the months since these lectures were delivered Civil Defence has become an exceedingly controversial subject. The public would be much helped by a sober and impartial explanation of the task which Civil Defence has to face, and the Atomic Scientists' Association would be a most suitable body to give it. If the Association has the courage of its convictions it will not be deterred by the danger of becoming involved in controversy.

The last lectures, by Professor Kathleen Lonsdale and Sir George Thomson, put forward two points of view on moral issues. Atomic warfare is a subject which has often appeared to be too much for professional moralists; the scientific amateurs represented here must not therefore be blamed if they have failed to agree on a solution.

W. J. W.

Ferromagnetic Domains, by K. H. STEWART. Pp. xii+176. (Cambridge : University Press, 1954.) 25s.

The concept of ferromagnetic domains, introduced nearly fifty years ago, has since remained indispensable in the qualitative interpretation of the behaviour of ferromagnetic materials. Even as a vaguely formulated hypothesis it proved invaluable as a stimulus to experimental and theoretical investigation. Many false trails were followed, but during the thirties there was a gradual approach to a more precise knowledge of the physical character of domains, and a better appreciation of the factors involved in their formation. On the slowly laid foundations, building proceeded very rapidly after the war. This book describes something of what has been accomplished.

After an opening chapter introducing the hypothesis of domains and outlining the reason for their occurrence, fairly full accounts are given of magneto-crystalline anisotropy, and of magnetostriction and the effect of stresses on magnetic properties. The three main chapters of the book deal with domain arrangements, particularly in single crystals, and with the direct evidence about these arrangements provided by powder pattern experiments; with the energies and widths of domain walls; and with the hindrances to boundary movements due to strains and inclusions. The last two chapters survey time-dependent magnetic effects and the thermal changes accompanying magnetization.

The book, it is stated in the preface, "attempts to give a coherent outline of the fundamentals of domain behaviour but not to give detailed consideration

to all parts of the subject". The author has succeeded in doing what he set out to do. The arrangement is good, the presentation is clear, and mention is made of virtually all the recent relevant work up to the time of writing. Yet somehow the book is disappointing. This is partly not so much because it goes over ground which has been largely covered in general articles and reviews but because it does so in much the same way. There is a lack of that detail and critical discussion which may be expected in a book, but not necessarily in a review. To dismiss details of the experimental techniques for the study of domain patterns to a bare reference is surely surprising in a book specifically on ferromagnetic domains. A fuller discussion would be expected of the quantitative discrepancies between theoretically calculated and observed boundary spacings, and of the difficult but important problem of the relation between exchange effects and domain boundary energy. The relevance of domain effects to magnetization curves is stressed, but very little is said about the detailed properties of particular materials. The treatment of the effects of internal stresses and inclusions by Becker and Kersten is fully described, and Néel's criticisms are mentioned, but there is little more about Néel's own treatment than the quotation of his formulae for coercivity.

The seven plates of domain patterns, admirable though they are, afford minor irritation. They are all from one laboratory, and so are not fairly representative of widespread work in this field; and the plates themselves bear no reference to the source nor to the text pages where they are mentioned.

Reference has been made to some typical omissions. To draw attention in a review to what is not in a book is ungracious and in general reprehensible. From the author's preface, however, it is to be presumed that most such omissions are deliberate rather than accidental. In a developing field it is often the uncertain, the insecurely established and the obscure which call for particular consideration, for these are the growing points. Within his self-imposed limits the author has written an eminently sound book; but if he had been less disciplined and more adventurous, he might, at the modest cost of a few mistakes and errors of judgment, have written a book of much greater value.

E. C. STONER.

Theorie der Chemischen Bindung, by H. HARTMANN. Pp. vii+357. (Berlin: Springer, 1954.) DM. 46.80, 49.80.

Professor Hartmann sets out to provide a complete account of the wave-mechanical theory of chemical binding, making no assumption except the existence of a wave equation. The policy which he has chosen to adopt is to develop the fundamental theory first; about one-third of the book is devoted in this way to an account of group theory and its representations, spin operators, perturbation theory, secular determinants and variation theory. After this an account of the Kepler problem leads naturally to the Periodic Table of the elements, the Heitler-London theory and its later developments in terms of hybridization and the valence state. This is followed by 40 pages on the molecular-orbital theory, leading to molecular complexes and another 40 pages devoted to the field of aromatic compounds. The book concludes with a short account of the theory of metals, and of the semi-empirical calculation of activation energies in reactions.

As will be seen from the above, the author has contrived to include a vast amount of material. The writing is clear, and, apart from difficulties due to compression, easy to follow. If it is necessary to classify books of this kind into those which are basically formal and those which are basically chemical, this one falls into the first category. It would appear to be most suitable for students of mathematics and physics who have already acquired some general knowledge of quantum theory and are prepared to face its applications. A good deal of the introductory material is scarcely detailed enough to be used without a fair amount of additional study.

The author has read very widely, and gives good references at the bottom of each page. But there is no author index and only a rather sketchy subject index. It would be worth while to extend these in any subsequent edition.

In view of the rather formal approach which the author has adopted it is not surprising that he says practically nothing about the hydrogen-bond, or the three-electron bond. But it is a pity that there is scarcely any reference to molecular spectroscopy (without which the molecular-orbital method loses much of its charm), or to the recent applications of the Hartree-Fock equations by the Chicago and Cambridge groups. Some people may think that there is a certain lack of balance in giving numerical details for a large number of aromatic hydrocarbons, some of which do not even exist, when there is no mention of configuration interaction and no guidance about the choice of fundamental parameters for dealing with heteronuclear aromatics. However, it is unreasonable to expect everything in 350-odd pages, and this is certainly a useful addition to current literature on the chemical bond. Much of the early work on this problem was done in Germany, particularly by Hund, Hückel, Heitler and London. The present book is all the more welcome in that it signals a revival of interest in that country in molecular architecture.

C. A. COULSON.

CONTENTS OF SECTION B

	PAGE
Mr. W. S. S. BLASCHKE. Field Aberrations in Wide Aperture Optical Systems .	801
Dr. B. D. SAKSENA and Mr. L. M. PANT. Cathodo-Luminescence of MgO .	811
Mr. J. R. COOK and Mr. K. A. MAHMOUD. Luminescence Characteristics of Some Scintillating Crystals	817
Dr. R. O. GANDY. Out-of-Focus Diffraction Patterns for Microscope Objectives	825
Dr. G. C. E. OLDS. Mechanisms of Creep in a Precipitation Hardened Alloy .	832
Research Notes :	
Dr. J. WOODS. The Secondary Electron Emission of Sodium and Zinc .	843
Mr. T. H. SCHOFIELD. An Apparatus for Heat-Treatment and Quenching Small Specimens in a Vacuum from High Temperatures	845
Letters to the Editor :	
Dr. F. A. CUNNELL, Mr. J. T. EDMOND and Dr. J. L. RICHARDS. Measure- ments on some Semiconducting Compounds with the Zinc-Blende Structure	848
Reviews of Books	850
Contents of Section A	856

The Time Coherence of Associated Cosmic Ray Particles

BY V. C. OFFICER AND P. J. ECCLES

Physics Department, University of Melbourne, Australia

Communicated by L. H. Martin ; MS received 14th June 1954

Abstract. Short reaction time Geiger counters have been used at sea level to study the time coherence of associated cosmic ray particles under 18 cm of Pb, and also in air. A 50-channel hodoscope has been used to identify the events giving coincidences between two 138 cm² trays of these counters separated by 15 cm in a horizontal plane. No evidence was found for delays between associated particles of the order of 2×10^{-8} sec, as reported by Robinson using spark counters, although the counter resolving time of 1.4×10^{-8} sec should have allowed detection of the effect. Multiple hits by particles on the Geiger counter trays were found to give modified counter reaction time distributions, and it is suggested that a similar effect could occur in spark counters. A theory which accounts for the behaviour of both spark and Geiger counters under multiple hit conditions has been developed.

§ 1. INTRODUCTION

THE possible existence of an interesting new cosmic ray effect was revealed by Robinson (1953 b), while making short time interval measurements with parallel plate spark counters. He used two spark counters, unshielded or shielded with 18 cm of lead, and separated horizontally by distances up to 21 cm. He found a broadening of the distribution of relative reaction times† which could be interpreted as due to a difference of mean value about 2×10^{-8} sec between the arrivals of associated particles. It was difficult to explain these delays in view of the strong spatial decoherence of the coincidences ; but two suggestions were made. Small velocity differences between pairs of penetrating μ -mesons originating higher than 1 km above the apparatus could give rise to the delays, but scattering would make it difficult for the mesons to conform to the decoherence curve observed. Robinson calculated that both the r.m.s. scattering angle and the angular spread at formation for particles of likely energy would exceed 1° , whereas their observed close spacing at sea level would not allow an angular separation greater than 2×10^{-2} degree. Alternatively some sort of decay process was suggested.

In the present experiment it was considered that the improved Geiger counters should be capable of detecting the new effect. Their relative reaction time distribution, roughly triangular in shape with extremes at $\pm 4.5 \times 10^{-8}$ sec and standard deviation of 1.4×10^{-8} sec, should be modified significantly by an effect which increased the width of the spark counter distribution at half height by 2×10^{-8} sec,

† The absolute reaction time of a counter is the interval between the passage of an ionizing particle and the appearance of a detectable output signal. The relative reaction time of two counters is the interval between the output signals when the counters are simultaneously traversed by ionizing particles.

and increased the extremes from about the Geiger counter value to $+8$ and -9×10^{-8} sec. Further, it was hoped that the type of event responsible for the delay could be identified by means of the 50-channel hodoscope, and that the group of delayed events thus isolated would provide a time interval distribution undiluted by spurious phenomena.

§ 2. APPARATUS

2.1. Short Reaction Time Counters

Research done by one of us† has led to a considerable reduction in Geiger counter reaction times. In order to produce faster counters previous workers have suggested or tried large wire diameter, small cathode diameter, low filling pressure and high overvoltage. Success is achieved when this list is amended to include small wire diameter and high filling pressure. This is probably explained by the recent discovery (references in § 5.1) that electron drift velocities in practical quenching mixtures are roughly independent of the electric field to pressure ratio over its important range, together with the fact that thin wires and high pressures in small diameter counters allow high overvoltages to be used. Ethyl formate gave better performance as quenching agent than alcohol or ethylene.

The counters have cathodes of nickel tube 4.6 mm in inside diameter with walls 0.003 in. thick, and the sensitive length is 30 cm. The anode wires are of 0.002 in. diameter tungsten terminated in Monel capillary tubes 1.7 mm in outer diameter and rounded at the ends. These capillary tubes pass through skirted glass spacers and tension is maintained in the wires by means of tungsten springs. Ten of these counters are mounted side by side in one Pyrex glass envelope 6 cm in diameter. The processing includes outgassing of the nickel by induction heating, and the filling is a 9:1 mixture of argon and ethyl formate at a total pressure of 28.5 cm of Hg. With this filling the starting voltage is 970 v and a working voltage of 1120 v is used. An external quenching circuit is provided for each tray of counters to ensure long life.

In the present experiment a tray consisted of one unit of ten counters, but trays of up to thirty counters have been used with only slight deterioration of performance. Figure 2(a) shows a relative reaction time distribution for trays of ten and a distribution for trays of thirty is given by Officer and Eccles (1954). In that investigation on the rare delayed particles in extensive air showers end effects were important, and these are described both for the present fast counters and a more easily constructed Maze type, which, however, has a more serious end effect.

2.2. The Experimental Arrangements

The timing apparatus which is similar to that described earlier (Officer 1951) uses a spiral time base generated from a 1 Mc/s crystal oscillator and displayed on a 908 BCC cathode ray tube operated at 7.5 kv. The pulses from the two counter trays, after separate amplification, different delays, and clipping to $0.1 \mu\text{sec}$, are mixed, and undergo a further delay before exciting a crystal damped ringing circuit which provides brilliance modulating pulses to the cathode ray tube. The amplification and delaying are carried out with an overall band width of 15 Mc/s. When an event selector pulse triggers the main brightening pulse, bright dashes 2.2×10^{-8} sec long are produced on the spiral trace and automatically photographed.

† V.C.O.

The event selector is a Rossi coincidence circuit with a resolving time of approximately $1\mu\text{sec}$, supplied with input pulses from taps on the two timing channel amplifiers. The time intervals are read by projecting the photographs on to a vernier reading circle centred on the electronically marked spiral centre, and measuring between the sharp trailing edges of the bright dashes.

The hodoscope uses glass cathode Maze counters 1.8 cm in inside diameter and 60 cm long, connected to conventional Regener circuits, 50 channels in all. The pattern of counters, fired by a cosmic ray event which also actuates the event selector, is displayed on an array of 50 neon lamps and photographed at the same time as the cathode ray tube picture is taken. The films are correlated by means of message registers included in each photograph.

Three main counter arrangements were used. In arrangement I, figure 1(a), the location of the timing trays A and B was similar to that used by Robinson for his spark counters (15 cm apart, 6 cm under 18 cm of Pb), except that here the

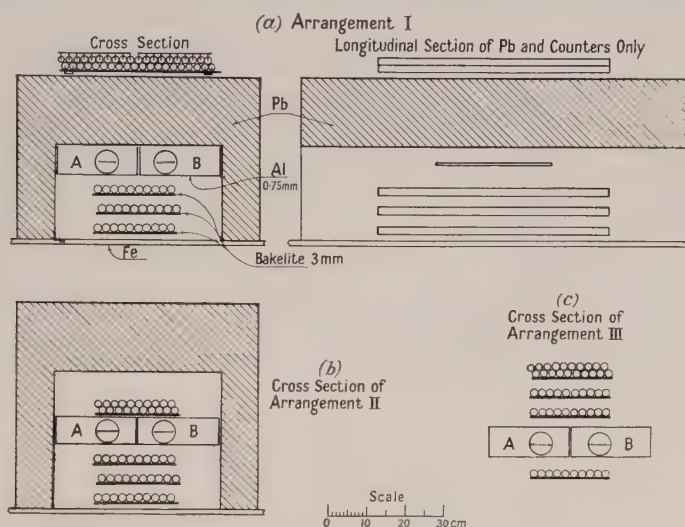


Figure 1. Cross sections of counter arrangements.

counters were 4.5 cm below the lead. This small difference is not likely to do more than reduce slightly the sensitivity to events giving secondary particles radiating from points in the bottom layers of the lead. The reduction would result from demanding wider angle, less abundant secondaries, but would tend to be compensated by the smaller absorption of soft wide angle secondaries in the 0.003 in. nickel cathodes compared with that in the 1/16 in. copper plates of the spark counters. The 30 cm long counter trays are longer than the spark counters which are only 11.5 cm in length, but the widths are similar. To give some information on the phenomena incident on the apparatus a double layer of hodoscope counters was placed on top of the lead. The remaining 30 hodoscope channels were connected to three layers of counters under the timing trays.

In arrangement II, figure 1(b), the distance between the timing trays and the bottom of the lead was 17 cm in order to accommodate a double layer of hodoscope counters. This double layer gave improved information on the nature of the events discharging the timing trays, but the greater distance below the lead gave increased sensitivity to secondary particles generated in the lead.

Arrangement III, figure 1(c), was unshielded except for a thin roof of iron and gypsum† 8 ft above the apparatus. Robinson's corresponding arrangement was 6 ft below a concrete roof 100 g cm^{-2} thick. The four layers of hodoscope counters above the timing trays provided another point of difference, but knock-on events produced in these layers could usually be recognized, and there was too little matter present for energetic electrons or photons to multiply appreciably.

To obtain relative reaction time distributions for the counters uninfluenced by any genuinely delayed events, the two timing trays were given a vertical separation of 35.5 cm. If a particle traversed both these trays as well as a lower tray covered with 16 cm of Pb the event was recorded, thus ensuring that only fast particles were used. In two of these tests five layers of ten hodoscope counters were placed between the timing trays to enable events other than single particle tracks to be rejected, but there were so few of these events and their effect on the time interval distribution was so slight that the precaution was not taken in later tests.

§ 3. RESULTS

3.1. Arrangement I

The distribution of 1422 time intervals measured with arrangement I is shown in figure 2(b), and is to be compared with the counter relative reaction time or simply the counter distribution in figure 2(a), both normalized to 500 observations.

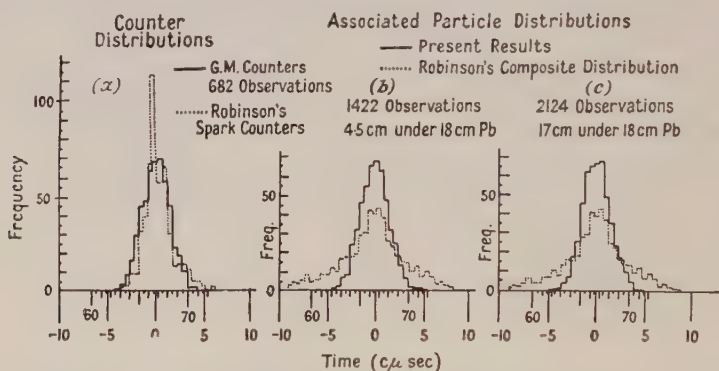


Figure 2. Time interval histograms for associated particles and counter relative reaction times normalized to 500 observations. The class boundaries are taken from the observed time scale which includes an artificial pulse separating delay. Robinson's histograms are superimposed on the present ones with time origins coinciding.

The counter distribution contains 682 observations, half of which were taken before the runs with arrangements I and II and half afterwards. Its standard deviation of $(1.38 \pm 0.04) \times 10^{-8}$ sec is not significantly different from $(1.47 \pm 0.03) \times 10^{-8}$ sec for the associated particle distribution. In addition the extremes do not show the increased spread expected on the basis of Robinson's results.

We could immediately conclude that associated particles with mutual delays of the order of 2×10^{-8} sec are not present under thick lead in the expected abundance, if it were not for the possibility that our somewhat different geometry may have caused a large dilution with unwanted events. The analysis of the hodoscope pictures provided the information required to settle this point.

† 0.6 g cm^{-2} of iron and 1.0 g cm^{-2} of gypsum.

3.2. Classification of Hodoscope Pictures

As far as the limited resolving power of the hodoscope would allow, the pictures were identified with known cosmic ray phenomena. Table 1 shows the result of this analysis and a selection of hodoscope records is shown in figure 3.

Table 1. Analysis of Associated Particle Results with Arrangement I

(All times are in centimicroseconds)

Nature of picture and interpretation	No. of events†	% of events	Rate (events/hr)	Time interval distributions	
				Mean	Standard deviation
Single track through A or B. μ -meson plus knock-on electron. (Occasional extra secondary between A and B.)	247	21.0	7.0 ± 0.4	-0.04 ± 0.09	1.46 ± 0.07
At least 2 secondaries apparently from bottom of Pb required.					
Knock-on showers from μ -mesons.					
(a) Small no. of secondaries.	393	46.5	15.4 ± 0.7	0.01 ± 0.08	1.51 ± 0.05
(b) Many secondaries widely spread.					
Tracks not resolved.	50			0.05 ± 0.23	$1.6_2 \pm 0.1_6$
(c) ≥ 25 counters under A and B hit.					
Tracks not resolved. Very many secondaries widely spread.	57			$0.15 \pm 0.1_9$	$1.4_5 \pm 0.1_4$
(d) Many hits on A; few on B.					
Knock-on shower core hit A.	22			$0.7_8 \pm 0.3_4$	$1.5_8 \pm 0.2_4$
(e) Many hits on B; few on A.					
Knock-on shower core hit B.	24			$-1.0_6 \pm 0.3_0$	$1.4_8 \pm 0.2_1$
(d) and (e) together.	46			$-0.1_8 \pm 0.2_6$	$1.7_8 \pm 0.1_9$
Hodoscope blank or a hit above Pb only. Very oblique meson plus knock-on electron or single meson.	210	17.9	5.9 ± 0.4	$0.1_7 \pm 0.1_0$	$1.5_1 \pm 0.07$
Hits on layer directly below A and B only. Very oblique knock-on showers.	104	8.8	2.9 ± 0.3	$-0.1_2 \pm 0.1_3$	$1.2_9 \pm 0.09$
Isolated hits on two lower layers.					
Photons hit hodoscope and oblique events implied for A and B.	30	2.5	0.9 ± 0.2	$-0.2_8 \pm 0.2_1$	$1.1_3 \pm 0.1_5$
≥ 3 hits above Pb. Air showers with penetrating component.	15	1.3	0.4 ± 0.1	0.4 ± 0.3	$1.3_4 \pm 0.2_4$
Tracks project back to point well inside Pb. Local penetrating showers.	4	0.3	0.1 ± 0.1	$-0.2, -0.7, -0.6, 0.2$	Actual time intervals
≥ 2 associated penetrating particles roughly parallel.	9	0.8	0.3 ± 0.1	$0.0, -1.6, 0.1, 1.7, 2.7, 30.6, 1.9, 0.5, -1.4$	
μ -meson decays in Fe base plate.	4	0.3	0.1 ± 0.1	$-37.2, -0.8_2, -0.2, -1.8$	
Miscellaneous.	7	0.6	0.2 ± 0.1	$0.2, -3.5, -0.7, -1.6, -2.0, 1.3, -3.5$	
Total events (mean taken as origin).	1422	100	33.2 ± 0.9	0.00 ± 0.04	1.47 ± 0.03

† These numbers do not sum to 1422 because 16 mm film magazine trouble caused the loss of some pictures.

‡ One interval was outside the range of measurement.

Nuclear disintegrations in the bottom of the lead could have been included among the possible interpretations of some of the classes of hodoscope pictures in addition to those given in table 1, but their numbers will be small.

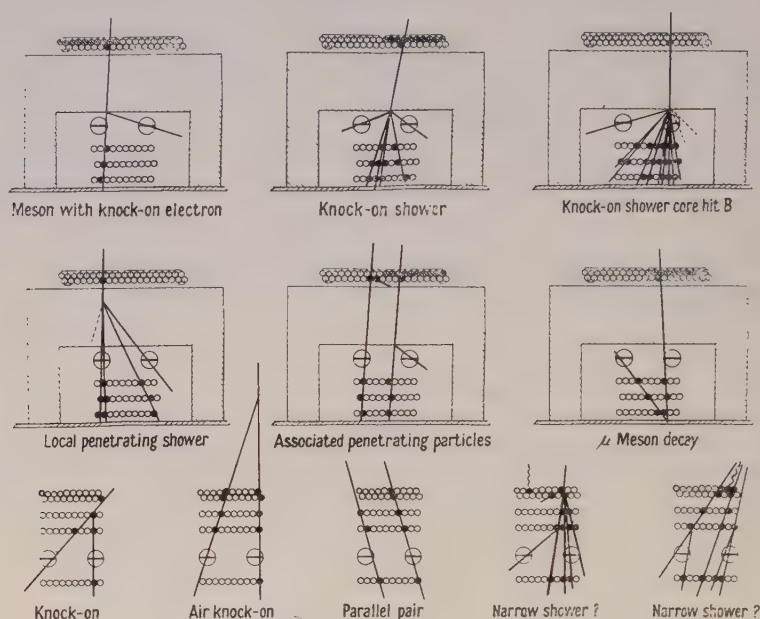


Figure 3. Some events recorded by the hodoscope with possible interpretations. Counters connected in parallel are shaded when hit whereas individually connected counters are blackened.

3.3. Discussion of the Hodoscope Groups

Associated penetrating particles which have been regarded as a possible source of mutually delayed particles are seen to provide no evidence for them. One very large interval of 30.6×10^{-8} sec is included in the group but it is probably due to an accidental coincidence, and is in any case much greater than the expected effect. Three other large intervals were observed, two with type 3 events and one with type 2(a), but most of the accidentals gave only one pulse on the time base. This occurred because the time base could not be triggered until the last pulse arrived, and there was pulse delay sufficient only to put the first pulse 30×10^{-8} sec down the trace after overcoming the event selector and trace brightening delays. The total number of recognizable accidentals was 18 compared with 8 estimated from the approximate resolving time and counting rates.

An inspection of table 1 reveals that no group of events shows an effect of the magnitude expected. In fact most of the events are not of a type that would be expected to give delayed particles. Even if a delayed particle did arise, possibly due to a decay process, it would have to hit a timing tray unaccompanied by a prompt particle to be recognized as delayed.

There is, however, a significant difference between the standard deviation $(1.7_8 \pm 0.1_9) \times 10^{-8}$ sec of group 2(d) plus (e) and $(1.38 \pm 0.04) \times 10^{-8}$ sec of the counter distribution. Also the shifts in the mean values of groups (2d) and 2(e), $(0.7_8 \pm 0.3_4) \times 10^{-8}$ sec and $-(1.0_6 \pm 0.3_0) \times 10^{-8}$ sec respectively, are significant.

The asymmetry of groups 2(d) and 2(e) is shown clearly in the histograms of figure 4(a). In § 5 it will be shown that these results can be accounted for by the influence of multiple hits on the reaction times of the timing trays.

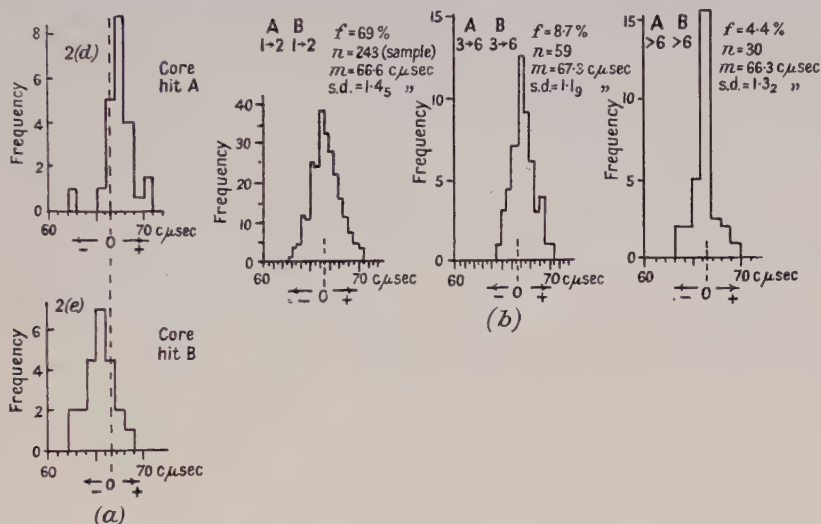


Figure 4 (a). Time interval histograms obtained with arrangement I for knock-on shower cores hitting trays A or B, and normalized to the same area.

Figure 4 (b). Time interval histograms taken from the knock-on shower group for arrangement II, and normalized to the same area. The approximate numbers of hits on trays A and B are shown. n is the number of observations in the histogram, and f the abundance within the knock-on shower group, itself 51% of the total events. m is the histogram mean and s.d. its standard deviation.

3.4. Arrangement II

The distribution of 2124 observations collected at 52 ± 1 per hr with arrangement II is shown in figure 2(c). Again the standard deviation of $(1.43 \pm 0.02) \times 10^{-8}$ sec is not significantly different from that of the counter distribution. Due to the increased distance below the lead of the timing trays, the knock-on shower group was larger with this arrangement, but the extra layers of counters immediately below the lead allowed a more detailed analysis of this group, and at the same time greatly reduced the number of pictures in which very oblique events had to be inferred. In figure 4(b) the effect of increasing numbers of hits on both trays A and B is shown. The histograms become more peaked for the higher multiplicities in qualitative agreement with the predictions of § 5.1. The highly asymmetrical multiplicities showed the same tendencies as groups 2(d) and 2(e), but the numbers of events were very small.

3.5. Arrangement III

The results for 954 observations with the unshielded arrangement III are shown in table 2. This run is not as reliable as the others. It was made earlier with an almost exhausted argon-alcohol filling in the timing counters. The counter distributions before and after the run show that some change in counter performance occurred†. However, it should be possible to compare the distributions

† There can be no doubt about the performance of the counters freshly filled with an ethyl formate-argon mixture as used in the other two runs, as they have since been used for 1850 hours in another cosmic ray experiment without detectable deterioration.

for the different classes of events as they would all be affected equally. Also the nature and abundance of the events seen in the hodoscope are of interest, showing as they do the difference between the phenomena in air and below the lead. A selection of hodoscope pictures is included in figure 3.

Table 2. Analysis of Associated Particle Results with Arrangement III

(All times are in centimicroseconds)						
Time interval distributions						
	Mean	Standard deviation	$\frac{1}{2}$ width at $\frac{1}{2}$ height	No. of events	% of events	Rate (events/hr)
Counter distribution before run.	-0.3_7 $\pm 0.2_3$	2.2_1 $\pm 0.1_6$	2.5	95		
Counter distribution after run.	-0.9_7 $\pm 0.1_2$	2.04 ± 0.08	2.7	297		
Total events recorded by hodoscope (Mean taken as origin and recognizable accidentals removed).	0.00 ± 0.07	2.18 ± 0.05	1.8	867	100	38.2 ± 1.3
Nature of picture and interpretation						
1. Forked tracks. Meson plus knock-on electron. Several V tracks, probably electron pairs, included.		1.8_6 $\pm 0.1_7$	1.7	58	6.7	2.6 ± 0.3
2. Single track through A or B. Meson knocks low energy electron into a timing counter but not into hodoscope.		2.3_0 $\pm 0.1_7$	2.0	97	11.2	4.3 ± 0.4
3. Blank. Mostly oblique mesons with knock-on electrons. A few nuclear disintegrations.		2.0_6 $\pm 0.1_1$	2.5	161	18.6	7.1 ± 0.6
4. Large numbers of counters fired. Air showers. Rate < calculated extensive shower rate.		2.0_0 $\pm 0.2_3$	2.3	37	4.3	1.6 ± 0.3
5. Single track through A or B with a more complicated event striking other tray. Local showers and some extensive showers.		2.1_6 $\pm 0.1_7$	1.7	82	9.4	3.6 ± 0.4
6. Pictures suggesting incident electrons and photons. Local showers and some extensive showers.		2.5_0 $\pm 0.1_7$	2.0	112	12.9	4.9 ± 0.5
7. Narrow, frequently diverging band of counters fired. Narrow showers?		1.9_7 $\pm 0.1_7$	0.5	65	7.5	2.9 ± 0.4
8. Some counters fired in layers adjacent to A and B only. Mostly oblique narrow showers. A few nuclear disintegrations.		2.2_6 $\pm 0.1_2$	1.5	168	19.4	7.4 ± 0.6
9. Parallel pairs of tracks.		2.0_0 $\pm 0.1_5$	2.7	87	10.0	3.8 ± 0.4

§ 4. CONCLUSIONS RELATING TO COSMIC RAY EFFECTS

The information provided by the hodoscope pictures in air and below lead suggests that Robinson's corrections for events other than associated penetrating particles were too small, and that associated penetrating particles or some unknown phenomena do not form a large fraction of the coincidences. In air the narrow shower and local shower contributions (Wei 1950, Wei and Montgomery 1950) are important, and the rate of parallel pairs of particles is about an order of magnitude higher than that of associated penetrating particles. Most of these parallel pairs of particles cannot have more than one member penetrating, and could consist of a μ -meson plus a knock-on electron from the air some distance above the apparatus, or in some cases air shower particles. Some tracks diverged sufficiently to allow a point of origin to be assigned somewhere between the apparatus and the roof, or in the roof.

Below the lead the major contribution comes from knock-on showers, even with the timing trays as close as 4.5 cm to the bottom of the lead. This is supported by recent cloud chamber observations by Pfofzer (1953) who found that 5.3% of μ -mesons emerging from 15 cm of Pb were accompanied by knock-on showers, and 6.3% by knock-on electrons. It is not easy to calculate the coincidence rate expected from knock-on showers with our geometry, but only 0.36% of the showers emerging from the 600 cm² comprising the area of the separated timing trays and the area between them, need be detected to account for the observed rate of 15.4 per hr.

The events comprising the major contributions are of such a nature that they would not be expected to give rise to appreciably delayed particles, and the less abundant events show no evidence for delays of the expected size.

§ 5. MULTIPLE HIT EXPLANATION OF SPARK AND GIEGER COUNTER RESULTS

5.1. *Geiger Counters*

When a counter or tray of counters is hit by several particles simultaneously, the first pulse to reach the detection level is the one recorded by the experimental arrangements considered. This means that the shortest of several randomly chosen absolute reaction times is effective, provided there is no interaction between the developing discharges, and that the hits are random in space in cases where the reaction time depends on the part of the counter hit. In Geiger counters the major source of reaction time is the drift time of the electrons from their point of liberation by an ionizing particle to the neighbourhood of the anode wire. When wide band amplification is used, the time required for the build-up of sufficient charge for detection is usually considered short by comparison with the drift time, and relatively free from fluctuation. For the present small diameter counters this may not be a good approximation but it will serve for the present purpose. No electron drift velocity measurements in ethyl formate-argon mixtures are available, but measurements in ether, butane, and alcohol-argon mixtures (Stevenson 1952, Colli and De Leonardis 1953) show an approximately constant drift velocity under the conditions found over most of the drift path in our counters. Ethyl formate is assumed to give a similar result and the absolute reaction time distribution for one hit at a time on a Geiger counter is therefore taken as a rectangle.

If, as shown previously by Officer (1951), $F(t)$ and $W(t)$ are two absolute reaction time distributions, the distribution of the shortest of a pair of reaction times, one from each distribution, is given by

$$Z(\tau) = F(\tau) \int_{\tau}^T W(t) dt + W(\tau) \int_{\tau}^T F(t) dt \quad \dots\dots(1)$$

where T is the maximum reaction time, and the distribution of the difference between a pair of reaction times, one from each distribution, is given by

$$Y(\tau) = \int_{0 \text{ or } -\tau}^{T-\tau \text{ or } T} F(t) W(t+\tau) dt \quad \dots\dots(2)$$

where the first pair of limits is to be taken with τ positive and the second with τ negative.

With $F(t) = 1/T$ up to $t = T$ and zero beyond, it follows that the absolute reaction time distribution for n simultaneous hits on a Geiger counter tray is

$$Z_n(\tau) = n(T-\tau)^{n-1}/T^n \quad \dots\dots(3)$$

and $Y_{r,n}$, the relative reaction time distribution for r hits on one tray and n on the other, follows from equation (2). The $Y_{1,n}$ and $Y_{2,n}$ families of curves take the form of figure 5 when $T = 5 \times 10^{-8}$ sec. It now seems reasonable to conclude that the histograms for groups 2(d) and 2(e) of table 1, showing significant shifts in their mean values, are made up of curves from these families.

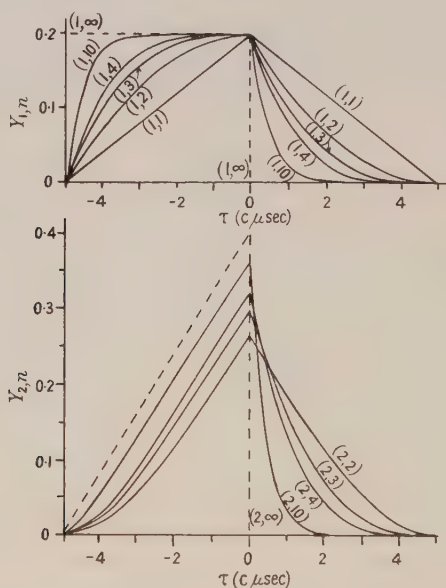


Figure 5. Relative reaction time distributions calculated for multiple hits on two trays of Geiger counters.

When no record is kept of which counter tray received the most hits, the appropriate symmetrical distribution can be constructed by taking the mean values of $Y_{r,n}$ for corresponding positive and negative values of τ . Several families of these curves are shown in figure 6. The significant broadening of group 2(d) plus (e) of table 1 can now be explained if hits of the type $(1, n)$ were

frequent. The peaking that occurs with many hits on each tray would not be so extreme in practice, because fluctuation in the time required to build up sufficient charge for detection has been neglected in this simple theory. The fact that there would not always be an electron liberated at the point on the cosmic ray track closest to the anode wire would also cause a modification of the curves.

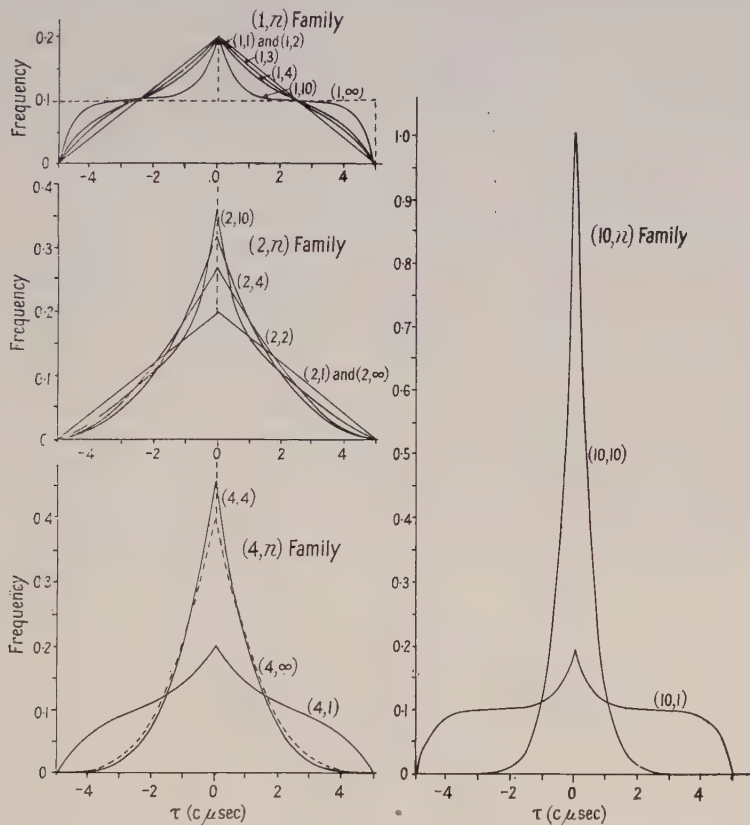


Figure 6. Relative reaction time distributions calculated for multiple hits on two indistinguishable trays of Geiger counters. The $(10, \infty)$ curve is almost coincident with the $(10, 10)$ curve.

The small difference between the counter distribution and the large knock-on shower distribution 2(a) of table 1, can be understood when it is realized that most of these events involve small numbers of hits on the timing trays, even when a large cascade passes between the trays, since half the cascade particles emerging from lead are on the average contained within a cone of semi-vertical angle about 26° (Juritz and Mohr 1947). However, at first sight the groups 2(b) and 2(c) having large numbers of secondaries widely spread, should give peaked distributions. These events are probably large cascade showers which emerge from the lead near the end of their development, and therefore have their particles well scattered. In some cases the shower may be dense enough to fire most of the 2 cm diameter hodoscope counters, but not dense enough to score many hits on both timing trays close under the lead. There will be other cases which give compensating broadening and narrowing effects, namely those with many hits on one tray and only one on the other, and many hits on both.

5.2. Spark Counters

We now consider the effect of multiple hits on spark counter reaction time distributions. The result is very different from the Geiger counter case due to the vast difference between the shapes of the two absolute reaction time distributions. It is not easy to calculate the spark counter absolute distribution directly, but it can be obtained by substituting the relative distribution given in figure 2 by Robinson (1953a) for $Y(\tau)$ in equation (2), and finding a $F(t) = W(t)$ that satisfies equation (2) and agrees with the general shape of experimental formative time lag distributions. It is found that an absolute distribution

$$\text{and } \left. \begin{aligned} F(t) &= A[(T-t+a)^{-1} - (T+a)^{-1}] \text{ for } 0 < t < T \\ F(t) &= A[(t-T+a)^{-1} - (T+a)^{-1}] \text{ for } T < t < 2T \end{aligned} \right\} \dots\dots(4)$$

where the normalizing factor $A = \frac{1}{2} [\ln(T+a)/a - 1 + a/(T+a)]^{-1}$, the fitting parameter $a = 0.1$ and $T = 5$ the average formative time lag[†], time being measured in centimicroseconds, transforms to the approximately exponential relative distribution given by Robinson. It also has a shape compatible with experimental formative time lag distributions (Kachickas and Fisher 1953). The average formative time lag chosen, 5×10^{-8} sec, is the smallest value that will give a spread in the relative distribution similar to that found by Robinson. The distribution is the same shape as the positive half of the one labelled (1, ∞) in figure 7.

It can then be shown that the absolute distribution for n simultaneous hits on a spark counter is given by

$$Z_n(\tau) = nA[(T-\tau+a)^{-1} - (T+a)^{-1}] \left[\frac{1}{2} + A \left(-\ln \frac{a}{T-\tau+a} - \frac{T-\tau}{T+a} \right) \right]^{n-1} \text{ for } 0 < \tau < T$$

$$\text{and } Z_n(\tau) = nA^n[(\tau-T+a)^{-1} - (T+a)^{-1}] \left[\ln \frac{T+a}{\tau-T+a} - \frac{2T-\tau}{T+a} \right]^{n-1} \text{ for } T < \tau < 2T.$$

Multiple sparks have been observed in spark counters by Bella and Franzinetti (1953), but for the present argument it would not be necessary for a spark to develop fully at every point hit in the counter. According to Bella and Franzinetti spark development could begin at all points struck if they were separated by more than about 0.4 mm, but it is possible that the first spark to reach a stage in development that causes a large reduction in gap voltage would quench the others.

Several relative distributions shown in figure 7 have been calculated numerically for n hits on one counter and r on the other, each counter receiving equal treatment on the average. The shapes of the distributions for many hits on both counters contrast sharply with those for Geiger counters and with the (1, 1) distribution for spark counters. Although the (r , ∞) distributions will never occur in practice, they serve to indicate how the higher multiplicity members of the curve families will develop. For positive values of τ they are in fact identical with the absolute distributions for r hits. It can be seen that combination of distributions with more than three hits on at least one of the counters could give rise to the spread shown by Robinson's associated particle results. It remains to be shown how multiple hits could occur with sufficient frequency both in the air and below the lead.

[†] The formative time lag is usually taken as the time a potential difference must be maintained across a gap containing a steady supply of primary ions, before it breaks down, but here it is identical with the absolute reaction time which will differ from the formative time lag as usually defined only in so far as this is affected by the magnitude of the primary ionization.

It seems reasonable that in Robinson's experiment as in ours the largest group of events under the lead will be knock-on showers. The angular spread of the majority of particles in these cascades as they emerge from the lead is small, so that in some cases one counter would be hit by many of the particles and the other by very few. However, with parallel plate spark counters there is a source of equivalent multiple hits in oblique particles, and with the counters close under the lead almost all of the knock-on shower, or knock-on electron hits, will be oblique in at least one counter. If we assume that all electrons liberated within one photon mean free path from a primary electron contribute to the same spark, we obtain the result that initiating electrons must be separated by at least 0.4 mm parallel to the plates before they can give rise to separate spark developments.

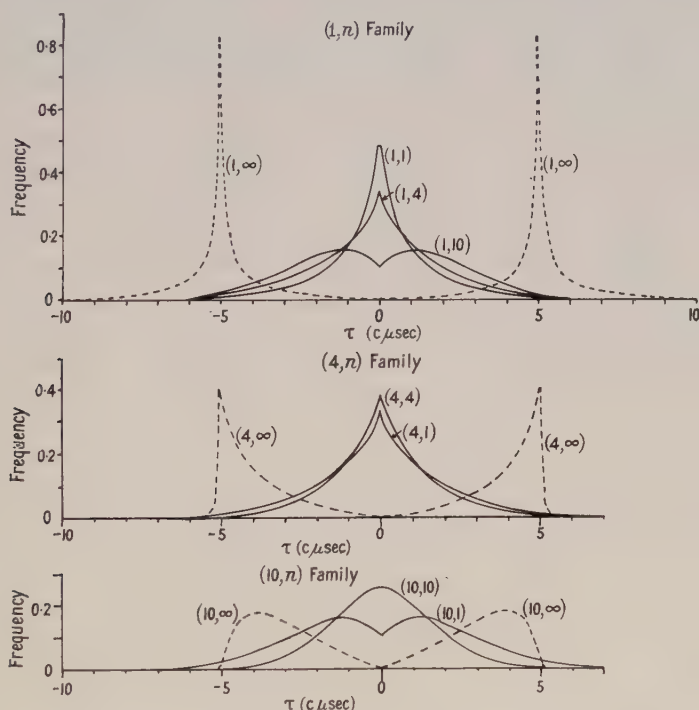


Figure 7. Relative reaction time distributions calculated for multiple hits on two indistinguishable spark counters. The broken curves for τ positive are the same as the absolute reaction time distributions.

This is based on the mean free path of avalanche breeding photons in alcohol vapour, 640^{-1} cm at n.t.p., found by Alder, Baldinger, Huber and Metzger (1947), and is supported by the work on multiple sparks of Bella and Franzinetti (1953), who found that 0.4 mm agrees better with experiment than 0.8 mm for the minimum spacing. From the geometry of the parallel plate spark counters 6 cm under the lead and separated by 15 cm, it can be seen that shower particles, radiating from a point on the under surface of the lead and crossing the 2 mm gap between the plates should seldom give rise to an equivalent multiple hit of less than 6 in at least one counter, and multiplicities should frequently be as high as 10†. This is so, even

† The corresponding multiplicities in the Geiger case would be 2 and 3 and the effect small, and since the individual drift distances would be correlated geometrically the effect would be even smaller.

when a dead layer next to the anode plate 0.3 mm[†] thick (Bella and Franzinetti 1953) is taken into account, but will be reduced slightly for minimum ionizing particles by fluctuation in the electron spacing along the track.

In the unshielded case, narrow showers, local showers, and extensive air showers as well as oblique phenomena should provide the multiple hits.

ACKNOWLEDGMENTS

We are indebted to Mr. G. F. Mauldon, who carried out most of the construction of the hodoscope, and it is a pleasure to thank Professor L. H. Martin for his continued interest and support. Part of the cost was met from funds provided by the Commonwealth Scientific and Industrial Research Organisation.

REFERENCES

- ALDER, F., BALDINGER, E., HUBER, P., and METZGER, F., 1947, *Helv. Phys. Acta*, **20**, 73.
BELLA, F., and FRANZINETTI, C., 1953, *Nuovo Cim.*, **10**, 1461.
COLLI, LAURA, and DE LEONARDIS, MARIA TERESA, 1953, *J. Appl. Phys.*, **24**, 255.
JURITZ, J. W. F., and MOHR, C. B. O., 1947, *Proc. Roy. Soc. A*, **190**, 426.
KACHICKAS, G. A., and FISHER, L. H., 1953, *Phys. Rev.*, **91**, 775.
OFFICER, V. C., 1951, *Aust. J. Sci. Res. A*, **4**, 526.
OFFICER, V. C., and ECCLES, P. J., 1954, *Aust. J. Phys.*, **7**, 410.
PFOTZER, G., *Z. Naturf.*, 1953, **8**, 353.
ROBINSON, E., 1953 a, *Proc. Phys. Soc. A*, **66**, 73 ; 1953 b, *Ibid.*, **66**, 79.
STEVENSON, A., 1952, *Rev. Sci. Inst.*, **23**, 93.
WEI, J. P. N., 1950, *Phys. Rev.*, **79**, 670.
WEI, J. P. N., and MONTGOMERY, C. G., 1950, *Phys. Rev.*, **80**, 480.

[†] A rough correction has been made for the fact that the pressure is 50% higher in Robinson's counters than in Bella and Franzinetti's.

The Angular Correlation of Successive γ -Rays in ^{60}Ni at Low Temperatures

BY H. R. LEMMER AND M. A. GRACE

Clarendon Laboratory, Oxford

MS. received 26th July 1954; and in final form 13th September 1954

Abstract. The angular correlation of the γ -rays excited in the decay of ^{60}Co has been measured in a paramagnetic crystal at temperatures of 288°K and 20°K in order to determine the influence of relaxation phenomena. No significant difference between the measurements was observed, each giving the full angular correlation. This result is discussed in relation to the interpretation of nuclear orientation measurements.

§ 1. INTRODUCTION

WHEN two or more radiations in succession are emitted by a nucleus, their directional correlation will depend, in general, on the angular momenta carried away in the transitions and on the spins of the nuclear levels involved. Consequently the method of angular correlation of γ -rays in a cascade has been used by many authors (see, for instance, Deutsch 1951, Frauenfelder 1953) for investigating the multipole character of γ -radiation and the spins of nuclear states. The form of this angular correlation will depend strongly on the purity of the transitions and therefore the method provides a sensitive means of measuring the phase difference and amplitude ratios for competing multipole orders. This theory has been developed for a γ -ray cascade where the nuclear system can be regarded as being free from disturbing extra-nuclear fields. The influence of external fields on angular correlations has been calculated by Goertzel (1946), Alder (1951) and Abragam and Pound (1953) and experimentally these effects have been demonstrated by the Zürich group working on the γ -rays of ^{111}Cd (Aeppli *et al.* 1951). The object of the present experiments was to see whether any influence by atomic fields on the angular correlation of the γ -rays of ^{60}Ni could be detected in paramagnetic crystals. This information is valuable not only because it provides information on the hyperfine structure coupling in the intermediate state and on the lifetime of this nuclear state but also because it is important for the interpretation of nuclear orientation experiments.

§ 2. NUCLEAR ORIENTATION

Daniels, Grace and Robinson (1951) have shown that nuclei may be oriented by extra-nuclear fields and this orientation has been detected by observation of the characteristic anisotropic distribution of radiation. So far experiments have been confined to measurement of the angular distribution of γ -radiation from a subsequent state rather than the β -radiation from the oriented state†; the angular distribution gives information on the degree of orientation of this γ -ray emitting

† Only in the rare cases where the β -spectrum shows a forbidden form will it be valuable to observe the angular distribution of the β -particles directly (see Blin-Stoyle, Grace and Halban 1953).

state, whence the degree of orientation of the initial state and the character of the previous emission processes which produce effective reorientation due to angular momentum changes may be inferred. However, these conclusions may not be valid if there is any subsequent perturbation of the nucleus due to coupling with external fields. The processes which could cause disturbance in a nuclear orientation experiment will also interfere with angular correlation measurements. Some of the possible causes of such an altered angular correlation will now be enumerated and their influence on angular correlation on the one hand and on nuclear orientation on the other will be considered.

§ 3. POSSIBLE CAUSES OF DISTURBED CORRELATION

Since the orientation experiments were performed with ^{60}Co (figure 1) in a single paramagnetic crystal† it is convenient to restrict discussion of some possible causes of altered angular correlations to this case. These are:

(i) If the hyperfine structure separation (ΔE) of the nuclear substates of the intermediate level, of mean lifetime T_1 , is such that $T_1\Delta E \lesssim 1$, then the intermediate nuclear state will be perturbed and the angular correlation may deviate from the undisturbed correlation (see, for instance, Frauenfelder 1953). This

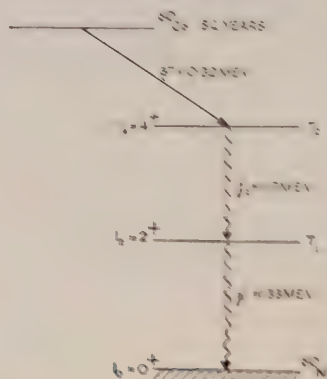


Figure 1. Decay scheme of ^{60}Co .

criterion will be valid if this hyperfine structure field arising from the paramagnetism of the ion remains fixed over the period of the nuclear transition. The degree of attenuation of the angular correlation produced by such coupling has been discussed both by Alder (1951) and by Abragam and Pound (1953).

(ii) Under conditions where the electron spin relaxation time T_e is not large the hyperfine structure field will change its direction with time due to exchange of energy with the lattice or other components in the crystal. The angular correlation will then depend on a function containing the term $T_e T_1 (\Delta E \hbar)^2$. When this term is of the order of unity attenuation will, in general, be observed; when it is negligible the full correlation will be found. Thus the absence of disturbance of the angular correlation may not indicate that $T_1 \Delta E \hbar$ is small but rather that the relaxation time T_e is short.

(iii) Following the β process the atom will be for a time T_p in an excited or ionized state which may cause changes in the electric or magnetic fields at the

† Copper Tutton salt 1% ^{60}Co , 12% ^{64}Cu , 87% ^{66}Zn $\text{SO}_4 \cdot \text{Rb}_2\text{SO}_4 \cdot 6\text{H}_2\text{O}$

nucleus. If these fields change with time then transitions between the nuclear substates may be induced and the angular correlation will be altered. If these fields are sensibly constant over the lifetime T_1 then the arguments of sections (i) and (ii) will apply.

(iv) If the nucleus recoils under the emission of γ_2 from its lattice position through changing fields, then as in process (iii) transitions between the nuclear states may be induced and the angular correlation altered.

These processes may also disturb nuclear orientation measurements. If an angular correlation experiment is carried out under the conditions of orientation experiments and no disturbing influence is detected, then it may be concluded that no perturbation of the intermediate state will occur in nuclear orientation measurements. For this reason it was decided to make angular correlation measurements on ^{60}Co in a paramagnetic crystal, identical with those used in orientation experiments, at a temperature of 20°K . Although this temperature is higher than those employed in orientation experiments, yet it is sufficiently low both to make the relaxation time long ($\simeq 10^{-8}$ sec deduced from line width values obtained in paramagnetic resonance experiments on stable cobalt) compared with the lifetime of the nuclear states ($< 10^{-10}$ sec), and to cause only the lowest electronic doublet to be populated. Under these conditions the hyperfine structure field is effectively fixed along the tetragonal axis of the ion. This in turn is fixed with respect to the crystalline axes. Further decrease of temperature is only expected to increase this relaxation time without introducing new disturbing phenomena.

§ 4. DESIGN OF EXPERIMENT

In order to avoid the difficulty of applying corrections to the measured angular correlation for such effects as the finite aperture of the detectors, the source dimensions and scattering in the source material (these have been discussed in detail by Lawson and Frauenfelder 1953, Walter, Huber and Zünti 1950, Rose 1953, Church and Kraushaar 1952) the measurements were compared with that found for a metal source. Lawson and Frauenfelder (1953) had earlier shown that within the accuracy of their experiment (± 0.001) a metal source showed the full angular correlation.

Two principal measurements of the angular correlation were performed: (a) in a single crystal of magnetically dilute cobalt Tutton salt at room temperature, (b) in the same crystal at 20°K . In experiment (a), since the spin-lattice relaxation time is 10^{-12} sec or shorter, continuous change in orientation of the electron spin and hence of the magnetic field at the nucleus occurs (Abragam and Pound 1953) and it is probable that only processes (ii)–(iv) can operate. At 20°K (as discussed earlier) this relaxation time should be so long that process (i) can operate; thus in experiment (b) all processes should take part.

§ 5. THE EXPERIMENTAL EQUIPMENT

A pair of scintillation counters (EMI Type 6260 photomultipliers fitted with 1 in. cube, dry mounted NaI(Tl) crystals), set up on a robust spectrometer table as in figure 2, formed the essentials of the equipment; NaI(Tl) crystals were chosen as they permitted good energy discrimination. The source was rigidly attached to the moving counter but moved in relation to the counter fixed in space. Careful control of the temperature of the equipment ensured constancy

of the single channel and coincidence counting rates (approximately 10^3 sec^{-1} and 10 sec^{-1} respectively) to within 1% over a period of 10 hours and to within $\frac{1}{4}\%$ over periods of about 30 minutes. The high voltage supply to the phototubes remained constant to about $1/10^4$.

A value for the resolving time of the coincidence circuit of $0.3 \mu\text{sec}$ was selected so that loss of coincidences arising from the finite emission time of the phosphor would not be greater than 5%. The source strength was then chosen so that the random coincidence rate was not greater than 30% of the total coincidence counting rate. Stability of the coincidence resolving time was shown to be better than 1% over periods of the order of days.

The elimination of radiation scattered from one crystal to the other is important in angular correlation measurements and was achieved by the use of lead cones

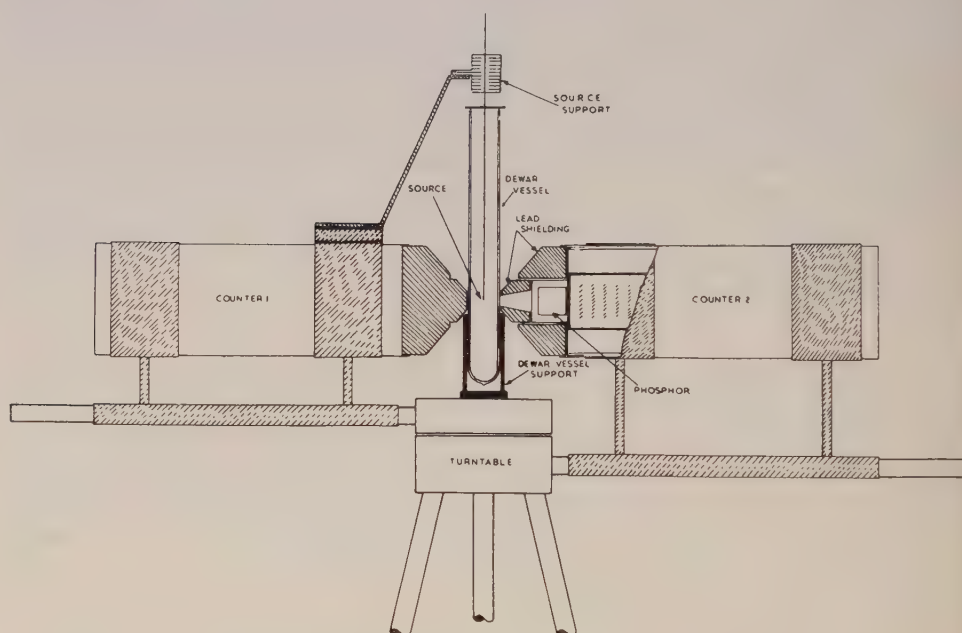


Figure 2. Diagram of counters and source mounting.

(minimum thickness 1.5 cm). In addition the detectors were biased at the photopeak for annihilation radiation and at this value the detection efficiency for 0.37 MeV quanta is negligible: this energy corresponds to that of degraded 1.3 MeV quanta scattered through 90° , the minimum angle through which quanta can be scattered in one detector and still reach the second detector. At the same time the detection efficiency for annihilation radiation originating in source contamination or internal pair creation is effectively reduced. The efficiency of this screening and discrimination was tested by observing coincidences using a source (^{59}Fe) of non-coincident γ -rays of the same energy as those from ^{60}Co . In the absence of scattering from one counter to the other the coincidence rate will correspond to the resolving time T_R of the coincidence set. These agreed to within 0.25% and it is concluded that no scattered radiation was being detected.

§ 6. SOURCES

The crystal of Tutton salt (dimensions $\frac{1}{2} \text{ mm} \times 1 \text{ mm} \times 1 \text{ mm}$) was grown from a solution containing ^{60}Co irradiated in metallic form in the Chalk River pile. In this crystal two types of cobalt ion can be identified, their axes of symmetry (tetragonal axes) being inclined at an angle of 74° to each other (Bleaney *et al.* 1954). The magnetic K_1 axis is the internal bisector of this angle. Since this represents the effective direction of the internal field, the maximum disturbance of the angular correlation should be observed when it is perpendicular to the plane of the γ -ray detectors. For this reason the crystal, cemented to a 2 mm diameter glass rod, was mounted with its K_1 axis coincident with the axis of rotation. The magnetic K_2 axis is perpendicular to these two axes of symmetry and in this direction one counter was fixed; the other counter moved in the K_2K_3 plane perpendicular to K_1 .

In the experiments at 20°K the crystal in the same mounting was immersed in a small Dewar vessel of 1 mm wall thickness (absorption $< 1\%$) containing liquid hydrogen. No effect due to scattering of the radiation in the Dewar vessel could be detected.

The cobalt metal source (approximate dimensions $\frac{1}{2} \times \frac{1}{2} \times \frac{1}{2} \text{ mm}$) was prepared by irradiating cobalt metal sponge in the Atomic Energy Research Establishment, Harwell pile and was mounted on a thin aluminium peg.

§ 7. PROCEDURE

In the absence of disturbing influences, the number of coincidences observed with an angular separation θ between the detectors is expected to be proportional to

$$W(\theta) = 1 + \frac{1}{8} \cos^2 \theta + \frac{1}{24} \cos^4 \theta$$

for a pure E2-E2 cascade such as occurs in ^{60}Ni . The maximum difference in coincidence rate should be observed when θ is changed from 0° or 180° to 90° or 270° . In order to obtain good statistics in a given measuring time observations were confined to these angles. Readings were taken with the counters at 90° , 180° and 270° of single channel and coincidence counting rates over successive 10 min periods and the counter positions changed each time a reading was taken. In this way small variations in the counter efficiency were compensated. Identity of the readings at 90° and 270° gave confidence that the apparatus was symmetrical in its behaviour.

Since the background both in the single channel counting rates and in the coincidence counting rates was negligible ($< 0.2\%$) the angular correlation ϵ where $\epsilon = [W(0) - W(\pi/2)] / W(\pi/2)$ was evaluated by normalizing the coincidence rate $N_c(\theta)$ to the two single channel rates $N_1(\theta)$, $N_2(\theta)$: this takes account of any changes of solid angle or changes of efficiency due to the influence of residual magnetic fields on the photomultipliers. Thus

$$W(\theta) = [N_c(\theta) / 2N_1(\theta)N_2(\theta) - T_R]$$

where T_R is the coincidence resolving time. In any single series of runs consisting of 40 individual readings of $W(\theta)$ the agreement was good and showed that the principal cause of deviation was statistical fluctuation in the coincidence counting rate. In the same way the values of ϵ obtained in different sets of 40 readings agreed well with each other within statistical deviation and the errors quoted are consequently the statistical counting errors based on the total number of

counts. The values of ϵ uncorrected for the finite aperture of the counters were:

Metal source	$= 0.143 \pm 0.002$
Crystal source at room temperature	$= 0.142 \pm 0.003$
Crystal source at 20°K	$= 0.144 \pm 0.005$

It was not possible to determine the angular resolution correction accurately because of the cubic form of the scintillation crystals. However, an approximate value was obtained by the method of Lawson and Frauenfelder (1953) in which a narrow pencil of ^{60}Co radiation is swept across the face of the scintillation crystal and the dependence of counter sensitivity on the position of the beam on the crystal determined. The value of ϵ is reduced from the theoretical value of 0.167 to 0.142 when this correction is applied. The value of ϵ obtained for the metal source is in excellent agreement with this and it was therefore assumed that the value of 0.143 ± 0.002 represented the full angular correlation.

§ 8. INTERPRETATION OF RESULTS

From the close agreement between the values for ϵ , both for the crystalline source at 288°K and 20°K and the metallic source, it is concluded that ϵ for the crystalline source at 20°K cannot be smaller than the theoretical angular correlation (0.167) by more than 0.005. Thus one can conclude that no significant nuclear reorientation takes place in the intermediate state T_1 . Since no other disturbing phenomena are expected to appear as the temperature is lowered to nuclear orientation temperatures ($\sim 0.01^\circ\text{K}$) one may infer that no reorientation of the intermediate state T_1 will take place during nuclear orientation measurements.

It can also be concluded from experiments that less than 0.005, 0.167, i.e. 3%, of the nuclei lose their orientation due to recoil under the first γ -ray emission (process iv). Furthermore it is inferred that negligible disturbance arises from time dependent perturbations due to the excitation or ionization of the atom (process iii). From the upper limit (0.005) to the destructive effect of the internal field on the angular correlation one may deduce something about the values of the hyperfine structure coupling and the lifetime of the excited state. Thus Alder (1951) has shown that an external magnetic field applied in a direction perpendicular to the plane of observation causes the angular correlation function to assume the form $W(\theta) = 1 + G_2 b_2 \cos 2\theta + G_4 b_4 \cos 4\theta$ for the case where the counters have the same sensitivity to the two γ -rays. This treatment is valid when the nuclear spin is coupled directly to the magnetic field and the atomic shell exercises no effect. G_r are attenuation coefficients of the form $[1 + (r\omega T_\gamma)^2]^{-1}$ where $\hbar\omega = \Delta E$ the separation of neighbouring nuclear levels by the applied field. For values of $G \sim 1$ and $b_r < 1$ it can be shown that $\Delta\epsilon/\epsilon \sim 1 - G_2$. This treatment also describes the processes which occur in a strongly anisotropic paramagnetic crystal at a temperature so low that only the lowest electronic state is populated and the electron spin relaxation time is long compared with the other times involved. In this case the energies of the nuclear substates can be described by a spin Hamiltonian of the form

$$\mathcal{H} = A S_z I_z + B(S_x I_x + S_y I_y)$$

with $B = 0$. This is approximately true for this Tutton salt at 20°K in which $A \gg B$ (Bleaney and Ingram 1951).

From the measurements of the angular correlation at 20°K we conclude that $1 - G_2 \leq 0.03$ where in this case $G_2 \simeq [1 + (AT_\gamma/\hbar)^2]^{-1}$. The approximation lies in the fact that $B \neq 0$ and also that the axis of symmetry of each ion is inclined

at an angle of 37° to the K_1 axis. Hence $T_1 \leq 9.2 \times 10^{-13}/A$ where A is in cm^{-1} . Now A represents the strength of the coupling between the hyperfine structure field in the residual ion and the magnetic moment of the excited state of ^{60}Ni . Since the Ni ion represents an impurity in the crystal lattice and is not normally found there, no values for the hyperfine structure field are known. However, since rearrangement of the outermost electron shell (3d) of the ion is expected to take times of the order of optical lifetimes ($\sim 10^{-8}$ sec) it seems plausible that no great change in the hyperfine structure field will occur during the β^- decay process. The nuclear moment of this state is not known but if one uses the value of 0.029 cm^{-1} for A (this is the value for stable ^{59}Co (Bleaney *et al.* 1954)) it is found that T_1 must be less than about 3×10^{-11} second. This limit is in accord with present knowledge of such E2 transitions in even-even nuclei (Bohr and Mottelson 1953) which suggests that values of lifetime from 10 to 100 times smaller than this figure might be expected. A direct determination of T_1 by Bay, Henri and McLernon (1953) gave a value of less than 2×10^{-10} second. Our figure can only be regarded as an order of magnitude calculation because of the uncertainty in the assumptions which have been made.

§ 9. CONCLUSIONS

Within the limitations of the measurements the undisturbed angular correlation of the γ -rays from ^{60}Co in a paramagnetic crystal is observed both at 288°K and at 20°K . Thus influences due to coupling with the ionic field, excitation of the ion in the β process and phenomena associated with the nuclear recoil are too small to be detected. From this we conclude that no disturbance of the intermediate state T_1 will occur in nuclear orientation experiments on ^{60}Co in this crystal.

ACKNOWLEDGMENTS

We are greatly indebted to Dr. Halban for many stimulating discussions and we wish to thank Lord Cherwell for extending to us the facilities of the Clarendon Laboratory.

REFERENCES

- ABRAGAM, A., and POUND, R. V., 1953, *Phys. Rev.*, **92**, 943.
 AEPPLI, H., ALBERS-SCHÖNBERG, H., BISHOP, A. S., FRAUENFELDER, H., and HEER, E., 1951, *Phys. Rev.*, **84**, 370.
 ALDER, K., 1951, *Phys. Rev.*, **84**, 369.
 BAY, Z., HENRI, V. P., and MCLERNON, F., 1953, *Phys. Rev.*, **90**, 371 (A).
 BLEANEY, B., and INGRAM, D. J. E., 1951, *Proc. Roy. Soc. A*, **208**, 143.
 BLEANEY, B., DANIELS, J. M., GRACE, M. A., HALBAN, H., KURTI, N., and ROBINSON, F. N. H., 1954, *Proc. Roy. Soc. A*, **221**, 170.
 BLIN-STOYLE, R., GRACE, M. A., and HALBAN, H., 1953, *Progress in Nuclear Physics*. (London: Pergamon Press), Vol. 3, p. 73.
 BOHR, A., and MOTTELSON, B., 1953, *Dan. Mat. Fys. Medd.*, **27**, No. 16.
 CHURCH, E. L., and KRAUSHAAR, J. J., 1952, *Phys. Rev.*, **88**, 419.
 DANIELS, J. M., GRACE, M. A., and ROBINSON, F. N. H., 1951, *Nature, Lond.*, **168**, 780.
 DEUTSCH, M., 1951, *Rep. Progr. Phys.*, **14**, 196.
 FRAUENFELDER, H., 1953, *Annu. Rev. Nuclear Science*, **2**, 129.
 GOERTZEL, G., 1946, *Phys. Rev.*, **70**, 897.
 LAWSON, J. S., and FRAUENFELDER, H., 1953, *Phys. Rev.*, **91**, 649.
 RCSE, M. E., 1953, *Phys. Rev.*, **91**, 610.
 WALTER, M., HUBER, O., and ZÜNTI, W., 1950, *Helv. Phys. Acta*, **23**, 697.

Plasma Oscillations in a Periodic Potential : The One-Zone Theory

By J. HUBBARD

Department of Mathematics, Imperial College, London S.W.7

Communicated by S. Raimes; MS. received 27th July 1954

Abstract. The collective description of electron interactions in the presence of a periodic potential is investigated. It is shown that there is a re-formulation of the problem which lends itself to a treatment closely resembling the free electron case. This treatment is carried through, and it is shown that the results are formally very similar to those for free electrons. For a parabolic band the main effect of the potential is to replace the electronic mass m by the effective mass m^* . The present theory applies only to the electrons in one Brillouin zone, and cannot be used when there is substantial overlapping of the occupied levels of this zone.

§ 1. INTRODUCTION

THE plasma oscillation theory recently introduced by Bohm and Pines (Bohm and Pines 1953, to be referred to as BP) promises to be a valuable theoretical scheme for the treatment of interactions in electron gases. One of the most interesting applications of the theory is to the conduction electrons of metals. However, in a metal there is the additional complication of the periodic potential. An important problem is, therefore, to determine the modification required to Bohm and Pines' theory in such a potential.

It is proposed to show in this paper that there is a re-formulation of the problem which lends itself to a treatment closely resembling that of BP. We shall carry through this treatment and show that the results are formally very similar to the free electron case.

In the theory of the present paper there are two important restrictions. The first of these is the neglect of the interactions of electrons in different zones. We shall, in fact, treat only the electrons in one zone, and shall call this the one-zone theory. This restriction is made for two reasons: firstly to avoid in the present paper some of the complexities of the multi-zone case, secondly because the present theory as it stands is quantitatively applicable to some metals and can give useful qualitative information in other cases.

The second restriction is the assumption that the effect of inter-zone transitions on the collective behaviour is small enough to be treated by perturbation theory. This should be so, provided (i) we can choose k_c (see § 2) so that $k_c \ll K_{\min}$ where K_{\min} is the shortest of the reciprocal lattice vectors apart from $\mathbf{K}=0$; (ii) that there is no substantial overlapping of the occupied part of the zone.

§ 2. RE-FORMULATION OF THE PROBLEM

The problem of n electrons moving in the periodic potential $V(\mathbf{r})$ of a crystal and interacting via their Coulomb fields is the eigenvalue problem for the Hamiltonian

$$H = \sum_{i=1}^n \left[\frac{1}{2m} \mathbf{p}_i^2 + V(\mathbf{r}_i) \right] + \sum_{i \neq j} \sum_{\mathbf{k}} \frac{2\pi e^2}{k^2} \exp \{ i \mathbf{k} \cdot (\mathbf{r}_i - \mathbf{r}_j) \} \quad \dots\dots (1)$$

where \mathbf{p}_i and \mathbf{r}_i are the momentum and position vectors of the i th electron. Here we have expanded the interaction in Fourier series; we assume the system as a whole is electrically neutral, and have therefore cancelled the term with $\mathbf{k} = 0$ in the interaction with $n\bar{V}$ where \bar{V} is the mean strength of the potential (the term with $\mathbf{k} = 0$ in the Fourier expansion of $V(\mathbf{r})$), and have then written $V'(\mathbf{r}) = V(\mathbf{r}) - \bar{V}$. In the rest of this paper we shall drop the prime on Σ_k' , its presence being understood.

We now split up the second term of (1) and write

$$H = \sum_i \left[\frac{1}{2m} \mathbf{p}_i^2 + V'(\mathbf{r}_i) \right] + \sum_{i,j} \sum_{\mathbf{k} < k_c} \frac{2\pi e^2}{k^2} \exp \{ i\mathbf{k} \cdot (\mathbf{r}_i - \mathbf{r}_j) \} - \sum_{\mathbf{k} < k_c} \frac{2\pi n e^2}{k^2} + H_{s.r.}, \quad \dots\dots(2)$$

$$H_{s.r.} \equiv \sum_{i \neq j} \sum_{\mathbf{k} > k_c} \frac{2\pi e^2}{k^2} \exp \{ i\mathbf{k} \cdot (\mathbf{r}_i - \mathbf{r}_j) \}. \quad \dots\dots(3)$$

We hope to be able to choose k_c so that $H_{s.r.}$ represents a weak, short-range interaction which can be treated as a perturbation; we can therefore drop this term from the Hamiltonian. The long-range part of the interaction which we have retained will bring about the collective behaviour of the system and will be treated in terms of plasma oscillators.

The present theory applies to one zone; the independent electron wave functions $\psi_{\mathbf{k}}(\mathbf{r})$ of this zone will satisfy an equation of the form

$$H_0(\mathbf{p}, \mathbf{r})\psi_{\mathbf{k}} \equiv \left[\frac{1}{2m} \mathbf{p}^2 + V'(\mathbf{r}) \right] \psi_{\mathbf{k}} = E(\hbar \mathbf{k})\psi_{\mathbf{k}}. \quad \dots\dots(4)$$

If we ignore the exclusion principle for the moment, the independent electron approximation to the wave function for the whole crystal will be

$$\Phi(\mathbf{r}_1, \boldsymbol{\sigma}_1; \dots \mathbf{r}_n, \boldsymbol{\sigma}_n) = \psi_{\mathbf{k}_1}(\mathbf{r}_1) u_{s_1}(\boldsymbol{\sigma}_1) \dots \psi_{\mathbf{k}_n}(\mathbf{r}_n) u_{s_n}(\boldsymbol{\sigma}_n), \quad \dots\dots(5)$$

where $\boldsymbol{\sigma}_i$ is the spin vector of the i th electron, $\mathbf{k}_1, s_1, \dots \mathbf{k}_n, s_n$ are the wave vectors and spin quantum numbers ($s_i = \pm 1$) of the occupied states, and the u_{s_i} are the spin functions. We now introduce the Wannier functions (Wannier 1937, Slater 1949, Adams 1952),

$$\phi(\mathbf{r}) = N^{-1/2} \sum_{\mathbf{k}} \psi_{\mathbf{k}}(\mathbf{r}), \quad \dots\dots(6)$$

where the sum is over the whole zone and N is the number of atoms in the crystal. It can be shown (Wannier 1937) that

$$\psi_{\mathbf{k}}(\mathbf{r}) = N^{-1/2} \sum_{\mathbf{R}} \exp(i\mathbf{k} \cdot \mathbf{R}) \phi(\mathbf{r} - \mathbf{R}), \quad \dots\dots(7)$$

where the sum is over all lattice vectors \mathbf{R} .

We can now write (5) in the form

$$\Phi = N^{-n/2} \sum_{\mathbf{R}_1, \mathbf{R}_2, \dots \mathbf{R}_n} \sum_{\alpha_1, \alpha_2, \dots \alpha_n} \{ \exp [i(\mathbf{k}_1 \cdot \mathbf{R}_1 + \dots + \mathbf{k}_n \cdot \mathbf{R}_n)] \delta_{s_1, \alpha_1} \dots \delta_{s_n, \alpha_n} \} \\ \times \phi(\mathbf{r}_1 - \mathbf{R}_1) u_{\alpha_1}(\boldsymbol{\sigma}_1) \dots \phi(\mathbf{r}_n - \mathbf{R}_n) u_{\alpha_n}(\boldsymbol{\sigma}_n), \quad \dots\dots(8)$$

where in the summation the α_i 's take the values $\alpha_i = \pm 1$. Equation (8) gives the independent electron approximation to the crystal wave function; a generalization of (8), capable of taking into account correlation effects, is

$$\Phi = \sum_{\mathbf{R}_1, \mathbf{R}_2, \dots \mathbf{R}_n} \sum_{\alpha_1, \alpha_2, \dots \alpha_n} \Psi(\mathbf{R}_1, \mathbf{R}_2, \dots \mathbf{R}_n; \alpha_1, \alpha_2, \dots \alpha_n) \\ \times \phi(\mathbf{r}_1 - \mathbf{R}_1) u_{\alpha_1}(\boldsymbol{\sigma}_1) \dots \phi(\mathbf{r}_n - \mathbf{R}_n) u_{\alpha_n}(\boldsymbol{\sigma}_n) \quad \dots\dots(9)$$

where Ψ is an as yet unknown function.

It is the assumption of the form (9) for Φ which defines the one-zone theory. This form should be suitable provided that the conditions mentioned in the introduction are satisfied.

To determine Ψ we use a generalization of the method given in the appendix to Slater's paper (1949). We substitute Φ from (9) into $(H-E)\Phi=0$, where H is obtained from (2) by omitting $H_{s,r}$, multiply by

$$\phi^*(\mathbf{r}_1 - \mathbf{R}_1') \dots \phi^*(\mathbf{r}_n - \mathbf{R}_n') u_{\alpha_1}^*(\sigma_1) \dots u_{\alpha_n}^*(\sigma_n),$$

integrate over $\mathbf{r}_1, \mathbf{r}_2, \dots, \mathbf{r}_n$ and sum over $\sigma_1, \dots, \sigma_n$. On carrying out the summation over the spin variables we obtain

$$\begin{aligned} 0 = & \sum_{\mathbf{R}_1, \mathbf{R}_2, \dots, \mathbf{R}_n} \Psi(\mathbf{R}_1, \mathbf{R}_2, \dots, \mathbf{R}_n; \alpha_1', \dots, \alpha_n') \int \phi^*(\mathbf{r}_1 - \mathbf{R}_1') \dots \phi^*(\mathbf{r}_n - \mathbf{R}_n') \\ & \times \left[\sum_i H_0(\mathbf{p}_i, \mathbf{r}_i) + \sum_{i,j} \sum_{k < k_c} \frac{2\pi\epsilon^2}{k^2} \exp\{i\mathbf{k} \cdot (\mathbf{r}_i - \mathbf{r}_j)\} - \sum_{k < k_c} \frac{2\pi n\epsilon^2}{k^2} - E \right] \\ & \times \phi(\mathbf{r}_1 - \mathbf{R}_1) \dots \phi(\mathbf{r}_n - \mathbf{R}_n) d\mathbf{r}_1 \dots d\mathbf{r}_n. \end{aligned} \quad \dots (10)$$

If $k_c \ll K_{\min}$ we can regard the second term in square brackets as a slowly varying function of the \mathbf{r}_i 's; since $\phi(\mathbf{r}_i - \mathbf{R}_i)$, $\phi(\mathbf{r}_j - \mathbf{R}_j)$ are strongly localized around \mathbf{R}_i , \mathbf{R}_j we can approximate this term by

$$\sum_{i,j} \sum_{k < k_c} \frac{2\pi\epsilon^2}{k^2} \exp\{i\mathbf{k} \cdot (\mathbf{R}_i - \mathbf{R}_j)\}.$$

On account of the orthogonality properties of Wannier functions the last three terms in square brackets then give a contribution

$$\left[\sum_{i,j} \sum_{k < k_c} \frac{2\pi\epsilon^2}{k^2} \exp\{i\mathbf{k} \cdot (\mathbf{R}_i' - \mathbf{R}_j')\} - \sum_{k < k_c} \frac{2\pi n\epsilon^2}{k^2} - E \right] \Psi(\mathbf{R}_1', \mathbf{R}_2', \dots, \mathbf{R}_n'). \quad \dots (11)$$

It is easily shown by the method used in Slater's paper that provided we regard $E(\hbar\mathbf{k})$ as a periodic function in \mathbf{k} -space, the first term in square brackets of (10) gives a contribution

$$\sum_i E\left(\frac{\hbar}{i} \frac{d}{d\mathbf{R}_i'}\right) \Psi(\mathbf{R}_1', \dots, \mathbf{R}_n').$$

We thus obtain from (10) the equation for Ψ :

$$\begin{aligned} & \left[\sum_i E(\mathbf{p}_i) + \sum_{i,j} \sum_{k < k_c} \frac{2\pi\epsilon^2}{k^2} \exp\{i\mathbf{k} \cdot (\mathbf{r}_i - \mathbf{r}_j)\} - \sum_{k < k_c} \frac{2\pi n\epsilon^2}{k^2} \right] \\ & \times \Psi(\mathbf{r}_1, \mathbf{r}_2, \dots, \mathbf{r}_n; \alpha_1, \dots, \alpha_n) = E\Psi \end{aligned} \quad \dots (12)$$

where $\mathbf{p}_i = \hbar\nabla_i/i$. The transition from the discrete variables \mathbf{R}_i' to the continuous variables \mathbf{r}_i of (12) has been discussed by Adams (1952). He finds that it is valid provided the slowly varying term does not lead to strongly localized bound states; as this condition is satisfied in the present case we feel justified in taking this step.

The result (12) is essentially the new formulation. It amounts to the eigenvalue problem for the operator in square brackets. This operator closely resembles

the Hamiltonian of BP (eqn (1)) and lends itself to the treatment applied to that Hamiltonian. In future we shall refer to this operator as our Hamiltonian.

We have finally to satisfy the exclusion principle. This requires that Φ be antisymmetric against the interchange of $(\mathbf{r}_i, \boldsymbol{\sigma}_i)$, $(\mathbf{r}_j, \boldsymbol{\sigma}_j)$. Though the form (9) for Φ was obtained by generalizing (8), which does not satisfy the exclusion principle, it is nevertheless quite easy to make the form (9) satisfy it. It is in fact sufficient that Ψ be antisymmetric against the interchange of (\mathbf{R}_i, α_i) , (\mathbf{R}_j, α_j) , for if we interchange $(\mathbf{r}_i, \boldsymbol{\sigma}_i)$, $(\mathbf{r}_j, \boldsymbol{\sigma}_j)$, we can also interchange the summation variables $\mathbf{R}_i, \alpha_i, \mathbf{R}_j, \alpha_j$, which then multiplies the right-hand side of (9) by -1 as required. This completes the re-formulation: Ψ is required to be an antisymmetric eigenfunction of the Hamiltonian in (12).

§ 3. TRANSITION TO THE COLLECTIVE DESCRIPTION

Here we shall follow the treatment of BP closely. We introduce the field variables q_k ($k < k_c$) and their canonically conjugate momenta p_k to describe the collective behaviour of the system. We can then show that the Hamiltonian

$$H = \sum_i E \left\{ \mathbf{p}_i + \sqrt{(4\pi\epsilon^2)} \sum_{k < k_c} q_k \hat{\mathbf{k}} \exp(i\mathbf{k} \cdot \mathbf{r}_i) \right\} - \frac{1}{2} \sum_{k < k_c} p_k p_{-k} - \sum_{k < k_c} \frac{2\pi n \epsilon^2}{k^2} \quad (13)$$

together with the subsidiary conditions

$$\Omega_k \Psi \equiv \left[p_k - i \left(\frac{4\pi\epsilon^2}{k^2} \right)^{1/2} \sum_i \exp(i\mathbf{k} \cdot \mathbf{r}_i) \right] \Psi = 0 \quad k < k_c \quad \dots\dots (14)$$

is equivalent to the Hamiltonian of (12). To do this we apply the inverse of the unitary transformation generated by

$$S = -i \sum_i \sum_{k < k_c} \left(\frac{4\pi\epsilon^2}{k^2} \right)^{1/2} q_k \exp(i\mathbf{k} \cdot \mathbf{r}_i), \quad \dots\dots (15)$$

and show, exactly as in BP, that the subsidiary conditions become $p_k \Psi = 0$, meaning that the transformed Ψ does not depend upon the q_k 's. Using this result we can show that the transformed Hamiltonian reduces to that of (12).

It is seen that, although we have introduced the extra variables q_k to describe the collective behaviour, we have also introduced just as many subsidiary conditions, thus restoring the correct number of degrees of freedom.

To proceed with the theory we have to expand the first term of (13) in terms of the q_k 's. This is not straightforward on account of the lack of commutativity of the terms in curly brackets. However, under the unitary transformation generated by S

$$\mathbf{p}_i \rightarrow \exp(-iS/\hbar) \mathbf{p}_i \exp(iS/\hbar) = \mathbf{p}_i + \sqrt{(4\pi\epsilon^2)} \sum_{k < k_c} q_k \hat{\mathbf{k}} \exp(i\mathbf{k} \cdot \mathbf{r}_i), \quad \dots\dots (16)$$

and therefore

$$E(\mathbf{p}_i) \rightarrow E \left\{ \mathbf{p}_i + \sqrt{(4\pi\epsilon^2)} \sum_{k < k_c} q_k \hat{\mathbf{k}} \exp(i\mathbf{k} \cdot \mathbf{r}_i) \right\}. \quad \dots\dots (17)$$

We can now evaluate the effect of the transformation on $E(\mathbf{p}_i)$ in another way; if S is small (corresponding to small amplitude plasma oscillations) we can use the expansion

$$E(\mathbf{p}_i) \rightarrow E(\mathbf{p}_i) + \frac{i}{\hbar} [E(\mathbf{p}_i), S] + \frac{1}{2!} \left(\frac{i}{\hbar} \right)^2 [[E(\mathbf{p}_i), S], S] + \dots\dots (18)$$

Evaluating the commutators we find

$$\begin{aligned}
 E \left\{ \mathbf{p}_i + \sqrt{(4\pi\epsilon^2)} \sum_{k < k_c} q_k \hat{\mathbf{k}} \exp(i\mathbf{k} \cdot \mathbf{r}_i) \right\} \\
 = E(\mathbf{p}_i) + \sqrt{(4\pi\epsilon^2)} \sum_{k < k_c} M_1(\mathbf{p}_i; \mathbf{k}) q_k \exp(i\mathbf{k} \cdot \mathbf{r}_i) \\
 + \frac{4\pi\epsilon^2}{2!} \sum_{k, k' < k_c} M_2(\mathbf{p}_i; \mathbf{k}, \mathbf{k}') q_k q_{k'} \exp\{i(\mathbf{k} + \mathbf{k}') \cdot \mathbf{r}_i\} \\
 + \frac{(4\pi\epsilon^2)^{3/2}}{3!} \sum_{k, k', k'' < k_c} M_3(\mathbf{p}_i; \mathbf{k}, \mathbf{k}', \mathbf{k}'') q_k q_{k'} q_{k''} \\
 \times \exp\{i(\mathbf{k} + \mathbf{k}' + \mathbf{k}'') \cdot \mathbf{r}_i\} + \dots, \quad \dots\dots (19)
 \end{aligned}$$

where

$$\begin{aligned}
 M_1(\mathbf{p}; \mathbf{k}) &= \frac{E(\mathbf{p}) - E(\mathbf{p} - \hbar\mathbf{k})}{\hbar k} = \hat{\mathbf{k}} \cdot \left[\nabla E(\mathbf{p}) - \frac{\hbar}{2!} \mathbf{k} \cdot \nabla \nabla E(\mathbf{p}) + \dots \right] \\
 M_2(\mathbf{p}; \mathbf{k}, \mathbf{k}') &= \frac{E(\mathbf{p}) - E(\mathbf{p} - \hbar\mathbf{k}) - E(\mathbf{p} - \hbar\mathbf{k}') + E(\mathbf{p} - \hbar\mathbf{k} - \hbar\mathbf{k}')}{\hbar^2 k k'} \\
 &= (\hat{\mathbf{k}} \cdot \nabla)(\hat{\mathbf{k}}' \cdot \nabla)E(\mathbf{p}) + \dots, \\
 M_3(\mathbf{p}; \mathbf{k}, \mathbf{k}', \mathbf{k}'') &= \frac{1}{\hbar^3 k k' k''} [E(\mathbf{p}) - E(\mathbf{p} - \hbar\mathbf{k}) - E(\mathbf{p} - \hbar\mathbf{k}') - E(\mathbf{p} - \hbar\mathbf{k}'') \\
 &\quad + E(\mathbf{p} - \hbar\mathbf{k} - \hbar\mathbf{k}') + E(\mathbf{p} - \hbar\mathbf{k} - \hbar\mathbf{k}'') \\
 &\quad + E(\mathbf{p} - \hbar\mathbf{k}' - \hbar\mathbf{k}'') - E(\mathbf{p} - \hbar\mathbf{k} - \hbar\mathbf{k}' - \hbar\mathbf{k}'')] \\
 &= (\hat{\mathbf{k}} \cdot \nabla)(\hat{\mathbf{k}}' \cdot \nabla)(\hat{\mathbf{k}}'' \cdot \nabla)E(\mathbf{p}) + \dots, \quad \dots\dots (20)
 \end{aligned}$$

and the general law of formation of the M_n 's can be inferred. We can now write our Hamiltonian (13)

$$\begin{aligned}
 H &= \sum_i E(\mathbf{p}_i) - \sum_{k < k_c} \frac{2\pi n \epsilon^2}{k^2} + \sqrt{(4\pi\epsilon^2)} \sum_i \sum_{k < k_c} M_1(\mathbf{p}_i; \mathbf{k}) q_k \exp(i\mathbf{k} \cdot \mathbf{r}_i) \\
 &\quad - \frac{1}{2} \sum_{k < k_c} p_k p_{-k} + 2\pi\epsilon^2 \sum_i \sum_{k, k' < k_c} M_2(\mathbf{p}_i; \mathbf{k}, \mathbf{k}') q_k q_{k'} \exp\{i(\mathbf{k} + \mathbf{k}') \cdot \mathbf{r}_i\} \\
 &\quad + \frac{(4\pi\epsilon^2)^{3/2}}{3!} \sum_i \sum_{k, k', k'' < k_c} M_3(\mathbf{p}_i; \mathbf{k}, \mathbf{k}', \mathbf{k}'') q_k q_{k'} q_{k''} \exp\{i(\mathbf{k} + \mathbf{k}' + \mathbf{k}'') \cdot \mathbf{r}_i\} + \dots \\
 &\quad \dots\dots (21)
 \end{aligned}$$

We now apply the *random phase approximation* (Bohm and Pines 1951, 1952, 1953). In the present case we apply it not only to the terms quadratic in the q_k 's but also to terms involving higher powers. A justification very similar to that given by BP for the free electron case can be given. We thus obtain

$$\begin{aligned}
 H &= \sum_i E(\mathbf{p}_i) - \sum_{k < k_c} \frac{2\pi n \epsilon^2}{k^2} + \sqrt{(4\pi\epsilon^2)} \sum_i \sum_{k < k_c} M_1(\mathbf{p}_i; \mathbf{k}) q_k \exp(i\mathbf{k} \cdot \mathbf{r}_i) \\
 &\quad - \frac{1}{2} \sum_{k < k_c} \left\{ p_k p_{-k} - 4\pi\epsilon^2 \sum_i M_2(\mathbf{p}_i; \mathbf{k}, -\mathbf{k}) q_k q_{-k} \right\} \\
 &\quad + \frac{(4\pi\epsilon^2)^{3/2}}{2} \sum_i \sum_{k, k' < k_c} M_3(\mathbf{p}_i; \mathbf{k}, \mathbf{k}', -\mathbf{k}') q_k q_{k'} q_{-k'} \exp(i\mathbf{k} \cdot \mathbf{r}_i) \\
 &\quad + \frac{(4\pi\epsilon^2)^2}{2^2} \sum_i \sum_{k, k' < k_c} M_4(\mathbf{p}_i; \mathbf{k}, -\mathbf{k}, \mathbf{k}', -\mathbf{k}') q_k q_{-k} q_{k'} q_{-k'} + \dots \quad \dots (22)
 \end{aligned}$$

From (20) it is seen that M_3 is of the order $\nabla\nabla\nabla E$ which we should expect to be small; therefore if the oscillator amplitudes q_k are small, we can treat the terms in M_3, M_4, \dots as perturbations. If we further neglect the third term of (22) and the subsidiary conditions, the eigenfunctions of H satisfying the exclusion principle are given, as in BP (eqn (21)), by

$$\Psi = \prod_{k < k_c} h_{n_k}(p_k) \exp \left[-\frac{|p_k|^2}{2\hbar\omega_{Pk}} \right] \text{Det} \{ \exp(i\mathbf{k}_1 \cdot \mathbf{r}_1) \delta_{s_1, \alpha_1}, \dots, \exp(i\mathbf{k}_n \cdot \mathbf{r}_n) \delta_{s_n, \alpha_n} \} \dots (23)$$

where h_n is the Hermite polynomial of order n , the n_k 's can take the values $0, 1, \dots$, the s_i 's are n spin quantum numbers and the \mathbf{k}_i 's are n wave vectors lying in the first Brillouin zone; for it can be shown from (23) and (9) that replacing \mathbf{k}_i by $\mathbf{k}_i + \mathbf{K}$ (\mathbf{K} reciprocal lattice vector) leads to the same wave function Φ .

ω_{Pk} is given by the dispersion relation

$$\begin{aligned} \omega_{Pk}^2 &= -4\pi e^2 \sum_i M_2(\hbar\mathbf{k}_i; \mathbf{k}, -\mathbf{k}) \\ &= \frac{4\pi e^2}{\hbar^2 k^2} \sum_i \{ E(\hbar\mathbf{k}_i + \hbar\mathbf{k}) + E(\hbar\mathbf{k}_i - \hbar\mathbf{k}) - 2E(\hbar\mathbf{k}_i) \} \\ &= 4\pi e^2 \hat{\mathbf{k}} \cdot \left\{ \sum_i \nabla \nabla E(\hbar\mathbf{k}_i) \right\} \cdot \hat{\mathbf{k}} + \dots \dots (24) \end{aligned}$$

If we average over the different directions \mathbf{k} we obtain

$$\overline{\omega_{Pk}^2} = \left\{ \frac{4\pi n e^2}{m^*} \right\}_{\text{av}} + \dots \dots (25)$$

where the average of m^* is over the occupied levels; this result agrees with that of Wolff (1953). An interesting point, noticed by Wolff, is that for a completely filled zone ω_{Pk} vanishes, as is easily seen from (24); thus a completely filled zone exhibits no collective behaviour (except possibly through inter-zone effects which we have neglected here).

The energy of the wave function (23) is, with the present approximations,

$$E = \sum_i E(\hbar\mathbf{k}_i) + \sum_{k < k_c} \left\{ \left(n_k + \frac{1}{2} \right) \hbar\omega_{Pk} - \frac{2\pi n e^2}{k^2} \right\}, \dots (26)$$

to which, to obtain the total energy of the electrons, we must add the contributions from the perturbations, in particular that from $H_{s.r.}$. In most metals $\hbar\omega_{Pk} \simeq 10$ eV and at normal temperatures the oscillators will be in the ground state ($n_k = 0$).

It should be noticed that the energy (26) and the dispersion relation (24) depend only upon the form of the energy surfaces $E(\hbar\mathbf{k})$; thus for a parabolic band with effective mass m^* the results will be the same as those obtained in BP with m replaced by m^* .

As in the free electron case the third term of (22) represents an oscillator-particle interaction which is too strong to be treated as a perturbation; in the next section we shall make a unitary transformation to remove this term.

§ 4. REMOVAL OF INTERACTION

We shall now show that a unitary transformation can be found which removes the interaction term of (22). The success of this method depends upon the smallness of the expansion parameter

$$\alpha = \left\langle \left(\frac{\mathbf{k} \cdot \nabla E(\mathbf{p}_i)}{\omega_{Pk}} \right)^2 \right\rangle_{\text{av}},$$

in which the average is over all electrons and over all oscillators \mathbf{k} . If we approximate the energy surfaces by a parabolic band with effective mass m^* we shall find $\alpha \simeq \beta^2/2m^*r_s$ (see BP). Since in nearly all cases $m^* > 1$, α will in general be smaller than in a free electron gas of the same density and will be a valid expansion parameter.

We follow BP in introducing the creation and destruction operators a_k, a_k^* defined by

$$q_k = \left(\frac{\hbar}{2\omega_k}\right)^{1/2} (a_k - a_{-k}^*), \quad p_k = i\left(\frac{\hbar\omega_k}{2}\right)^{1/2} (a_k^* + a_{-k}), \quad \dots\dots(27)$$

where ω_k is the oscillator frequency given by a new dispersion relation. Our Hamiltonian will now assume the form

$$H = H_{\text{part}} + H_{\text{coll}} + H_{\text{I}}, \quad \dots\dots(28)$$

where

$$H_{\text{part}} = \sum_i E(\mathbf{p}_i), \quad \dots\dots(29)$$

$$H_{\text{coll}} = \sum_{k < k_c} \frac{\hbar\omega_k}{2} (a_k a_k^* + a_k^* a_k) - \sum_{k < k_c} \frac{2\pi n \epsilon^2}{k^2} + \sum_{k < k_c} \left(\frac{\hbar}{4\omega_k}\right) (\omega_{Pk}^2 - \omega_k^2) (a_k a_k^* + a_k^* a_k - a_k a_{-k} - a_k^* a_{-k}^*). \quad \dots(30)$$

$$H_{\text{I}} = \sqrt{(4\pi\epsilon^2)} \sum_i \sum_{k < k_c} \left(\frac{\hbar}{2\omega_k}\right)^{1/2} \{M_1(\mathbf{p}_i; \mathbf{k}) a_k \exp(i\mathbf{k} \cdot \mathbf{r}_i) + \exp(-i\mathbf{k} \cdot \mathbf{r}_i) a_k^* M_1(\mathbf{p}_i; \mathbf{k})\} \quad \dots\dots(31)$$

and we have dropped for the moment the terms in M_3, M_4 , etc., which we treat as perturbations.

The unitary transformation we apply is a generalization of that used by BP and is generated by

$$S = -i\hbar \sum_i \sum_{k < k_c} \left(\frac{\hbar}{2\omega_k}\right)^{1/2} \{F(\mathbf{p}_i; \mathbf{k}) a_k \exp(i\mathbf{k} \cdot \mathbf{r}_i) - \exp(-i\mathbf{k} \cdot \mathbf{r}_i) a_k^* F(\mathbf{p}_i; \mathbf{k})\}, \quad \dots\dots(32)$$

where

$$F(\mathbf{p}; \mathbf{k}) \equiv \sqrt{(4\pi\epsilon^2)} \frac{M_1(\mathbf{p}; \mathbf{k})}{\hbar\omega_k + E(\mathbf{p} - \hbar\mathbf{k}) - E(\mathbf{p})}. \quad \dots\dots(33)$$

In transforming the Hamiltonian we use an expansion of the type (18); it is here we use α as an expansion parameter. If we write

$$H_a \equiv \sum_i E(\mathbf{p}_i) + \sum_{k < k_c} \frac{1}{2} \hbar\omega_k (a_k a_k^* + a_k^* a_k), \quad \dots\dots(34)$$

then it is easily found that $(i/\hbar)[H_a, S] = -H_{\text{I}}$. Thus, as in the free electron case,

$$H_a + H_{\text{I}} \rightarrow H_a + \sum_{n=1}^{\infty} \left(\frac{i}{\hbar}\right)^n [H_{\text{I}}, S]_n \left\{ \frac{1}{n!} - \frac{1}{(n+1)!} \right\}. \quad \dots\dots(35)$$

The leading term apart from H_a is $(i/2\hbar)[H_V, S]$. This can be evaluated straightforwardly. After using the random phase approximation, one obtains with some rearrangement†

$$\begin{aligned} \frac{i}{2\hbar} [H_V, S] = & \sqrt{(4\pi\epsilon^2)} \sum_i \sum_{k < k_c} (\hbar/4\omega_k) \{ M_1(\mathbf{p}_i + \hbar\mathbf{k}; \mathbf{k}) F(\mathbf{p}_i + \hbar\mathbf{k}; \mathbf{k}) \\ & - M_1(\mathbf{p}_i; \mathbf{k}) F(\mathbf{p}_i; \mathbf{k}) \} (a_k a_k^* + a_k^* a_k - a_k a_{-k} - a_k^* a_{-k}^*) \\ & - \sqrt{(4\pi\epsilon^2)} \sum_{i \neq j} \sum_{k < k_c} (\hbar/4\omega_k) [M_1(\mathbf{p}_i; \mathbf{k}) F(\mathbf{p}_j + \hbar\mathbf{k}; \mathbf{k}) \exp \{ i\mathbf{k} \cdot (\mathbf{r}_i - \mathbf{r}_j) \} \\ & - \exp \{ -i\mathbf{k} \cdot (\mathbf{r}_i - \mathbf{r}_j) \} M_1(\mathbf{p}_i; \mathbf{k}) F(\mathbf{p}_j + \hbar\mathbf{k}; \mathbf{k})] \\ & - \sqrt{(4\pi\epsilon^2)} \sum_i \sum_{k < k_c} (\hbar/4\omega_k) \{ M_1(\mathbf{p}_i; \mathbf{k}) F(\mathbf{p}_i; \mathbf{k}) \\ & + M_1(\mathbf{p}_i + \hbar\mathbf{k}; \mathbf{k}) F(\mathbf{p}_i + \hbar\mathbf{k}; \mathbf{k}) \}. \end{aligned} \quad \text{.....(36)}$$

If we now choose for our new dispersion relation

$$\omega_k^2 = \omega_{Pk}^2 + \sqrt{(4\pi\epsilon^2)} \sum \{ M_1(\mathbf{p}_i + \hbar\mathbf{k}; \mathbf{k}) F(\mathbf{p}_i + \hbar\mathbf{k}; \mathbf{k}) - M_1(\mathbf{p}_i; \mathbf{k}) F(\mathbf{p}_i; \mathbf{k}) \}, \quad \text{.....(37)}$$

then the zero order term in the expansion arising from the third term of (30) will just cancel the first term of (36) as in the free electron case. We can expand (37) in powers of α to give

$$\omega_k^2 = \omega_{Pk}^2 - \frac{8\pi\epsilon^2}{\hbar^4 k^2 \omega_{Pk}^2} \sum_i [E(\mathbf{p}_i + \hbar\mathbf{k}) - E(\mathbf{p}_i)]^3 + \dots \quad \text{.....(38)}$$

The second term of (36) represents a weak, attractive particle interaction which can be neglected for most purposes. The last term of (36) represents a change in the energy surfaces, corresponding to the change in effective mass in the free electron case. If we neglect all other terms in the expansion (which are of the order α^2), then our transformed Hamiltonian becomes

$$H = H_{\text{part}} + H_{\text{coll}} + H_{\text{r.p.}}, \quad \text{.....(39)}$$

where

$$\begin{aligned} H_{\text{part}} = & \sum_i E(\mathbf{p}_i) - \sqrt{(4\pi\epsilon^2)} \sum_i \sum_{k < k_c} (\hbar/4\omega_k) \\ & \times \{ M_1(\mathbf{p}_i + \hbar\mathbf{k}; \mathbf{k}) F(\mathbf{p}_i + \hbar\mathbf{k}; \mathbf{k}) + M_1(\mathbf{p}_i; \mathbf{k}) F(\mathbf{p}_i; \mathbf{k}) \} \\ = & \sum_i \left\{ E(\mathbf{p}_i) - 2\pi\epsilon^2 \sum_{k < k_c} \frac{[E(\mathbf{p}_i + \hbar\mathbf{k}) - E(\mathbf{p}_i)]^2}{\hbar^2 k^2 \omega_k^2} + \dots \right\} \\ \equiv & \sum_i E'(\mathbf{p}_i) \end{aligned} \quad \text{.....(40)}$$

where we have expanded in powers of α , and $E'(\hbar\mathbf{k})$ are the new energy surfaces;

$$H_{\text{coll}} = \sum_{k < k_c} \frac{\hbar\omega_k}{2} (a_k a_k^* + a_k^* a_k) - \sum_{k < k_c} \frac{2\pi n\epsilon^2}{k^2}; \quad \text{.....(41)}$$

$$\begin{aligned} H_{\text{r.p.}} = & \sum_{i \neq j} \sum_{k < k_c} \frac{8\pi\epsilon^2}{\hbar\omega_k} [\hat{\mathbf{k}} \cdot \nabla E(\mathbf{p}_i)] [\hat{\mathbf{k}} \cdot \nabla E(\mathbf{p}_j)] \exp \{ i\mathbf{k} \cdot (\mathbf{r}_i - \mathbf{r}_j) \} + \dots \\ & + \frac{(4\pi\epsilon^2)^{3/2}}{2} \sum_i \sum_{k, k' < k_c} M_3(\mathbf{p}_i; \mathbf{k}, \mathbf{k}', -\mathbf{k}') q_k q_{k'} q_{-k'} \exp (i\mathbf{k} \cdot \mathbf{r}_i) + \dots, \end{aligned} \quad \text{(42)}$$

† It should be mentioned that if the free electron energy $E = \mathbf{p}^2/2m$ is substituted in the last term of (36) it does not reduce exactly to the corresponding term of BP, eqn (54). The reason for this discrepancy is not yet clear; however, for the metals dealt with by Pines (1953) its effect on the total energy is quite negligible.

where we have expanded the first term of $H_{r,p}$, and have restored the terms in M_3, M_4 , etc. Strictly we should have transformed these terms also; however, if they can be treated as small perturbations, then the effects of the transformation, which are α times smaller, can be neglected.

We have thus succeeded in removing the oscillator-particle interaction apart from terms of $H_{r,p}$, which can be treated as a perturbation.

We must now investigate the effect of the transformation on our subsidiary conditions. The determination of the transformed Ω_k 's is quite straightforward using an expansion of the type (18); one obtains, to the order α^2 , using the dispersion relation (37),

$$\sum_i \frac{\hbar^2 \omega_k^2}{\hbar^2 \omega_k^2 - [E(\mathbf{p}_i) - E(\mathbf{p}_i - \hbar \mathbf{k})]^2} \exp(i\mathbf{k} \cdot \mathbf{r}_i) \Psi = 0; \quad k < k_c \quad \dots (43)$$

as the new subsidiary conditions. These subsidiary conditions act only on the particle coordinates; thus we have removed oscillator-particle coupling through the subsidiary conditions as well as in the Hamiltonian.

We shall consider the effect of the unitary transformation on our wave functions Ψ and Φ in the next section.

§ 5. THE COLLECTIVE DESCRIPTION

In this section we shall review the results of the previous work. By the unitary transformation we have succeeded in removing to a high order the coupling between particles and oscillators. If we neglect the subsidiary conditions we can take for our wave function the form (23) with ω_{Pk} replaced by ω_k . The corresponding energy will now be

$$E = \sum_i E'(\hbar \mathbf{k}_i) + \sum_{k < k_c} \left\{ (n_k + \frac{1}{2}) \hbar \omega_k - \frac{2\pi n \epsilon^2}{k^2} \right\} + E_{r,p}. \quad \dots (44)$$

where $E_{r,p}$ is the contribution to the energy from $H_{r,p}$.

In practically all cases of interest the oscillators will be in the ground state; in what follows we assume $n_k = 0$.

The calculation of $E_{r,p}$ is a straightforward perturbation calculation. The leading term of the first order perturbation is

$$\langle H_{r,p} \rangle = \frac{(4\pi\epsilon^2)^2}{4} \sum_i \sum_{k, k' < k_c} M_4(\hbar \mathbf{k}_i; \mathbf{k}, -\mathbf{k}, \mathbf{k}', -\mathbf{k}') \left(\frac{\hbar}{2\omega_k} \right) \left(\frac{\hbar}{2\omega_{k'}} \right) + \dots, \quad (45)$$

and the leading term of the second order perturbation is

$$H_{r,p}^{(2)} = \frac{(4\pi\epsilon^2)^3}{4} \sum_i \sum_{k, k' < k_c} \frac{|M_3(\hbar \mathbf{k}_i; \mathbf{k}, \mathbf{k}', -\mathbf{k}')|^2}{E(\hbar \mathbf{k}_i) - E(\hbar \mathbf{k}_i + \hbar \mathbf{k})} \left(\frac{\hbar}{2\omega_k} \right) \left(\frac{\hbar}{2\omega_{k'}} \right)^2 + \dots, \quad (46)$$

where we have neglected the small first term of (42). It is difficult to estimate the magnitude of these terms without reference to a specific set of energy surfaces, but it is thought that in general they will be small enough for the perturbation treatment to be valid.

To obtain the total energy of the electrons we must add to (44) two further terms which we shall discuss later. We must first investigate the form of our wave function Φ . In terms of the transformed Ψ it is given by

$$\Phi = \sum_{\mathbf{R}_1, \dots, \mathbf{R}_n} \sum_{\alpha_1, \dots, \alpha_n} U(q_k, \mathbf{R}_i) \Psi(q_k, \mathbf{R}_i) \phi(\mathbf{r}_1 - \mathbf{R}_1) \dots \phi(\mathbf{r}_n - \mathbf{R}_n) u_{\alpha_1}(\sigma_1) \dots u_{\alpha_n}(\sigma_n), \quad \dots (47)$$

where

$$U \equiv \exp(-iS/\hbar), \quad \dots (48)$$

and S is given by (32).

We can now regard Φ as a function of the variables q_k and the \mathbf{r}_i 's; the conditions (43) will imply a corresponding set of conditions on Φ . Though Ψ is separated, Φ is not so because the operator U mixes up the q_k 's and \mathbf{r}_i 's. However, the effects introduced by U are of the order α , and for many purposes may be neglected. If we do this and use the form (23) for Ψ , we can obtain after some rearrangement using (6),

$$\Phi = \exp \left[- \sum_{k < k_0} \frac{|p_k|^2}{2\hbar\omega_k} \right] \begin{vmatrix} \psi_{\mathbf{k}_1}(\mathbf{r}_1)u_{s_1}(\sigma_1) & \dots & \psi_{\mathbf{k}_n}(\mathbf{r}_n)u_{s_n}(\sigma_n) \\ \vdots & & \vdots \\ \psi_{\mathbf{k}_n}(\mathbf{r}_1)u_{s_n}(\sigma_1) & \dots & \psi_{\mathbf{k}_n}(\mathbf{r}_n)u_{s_n}(\sigma_n) \end{vmatrix} \dots \dots (49)$$

This bears a close resemblance to an independent electron wave function; one must bear in mind, however, the distortion produced by U , the subsidiary conditions and the perturbations $H_{s.r.}$, $H_{r.p.}$. Actually, for the ground state (or for any non-degenerate state), it is found on investigation that the form (23) satisfies the subsidiary conditions automatically.

We now use the wave function (49) to determine the perturbation energy due to $H_{s.r.}$. The neglect of U in obtaining (49) is, in this calculation, just equivalent to BP's neglect to transform $H_{s.r.}$. We obtain

$$\begin{aligned} \langle H_{s.r.} \rangle = & \sum_{i,j} \sum_{\mathbf{K} \neq 0} \frac{2\pi\epsilon^2}{K^2} \int \exp(i\mathbf{K} \cdot \mathbf{r}) \psi_{\mathbf{k}_i}^*(\mathbf{r}) \psi_{\mathbf{k}_i}(\mathbf{r}) d\mathbf{r} \int \exp(-i\mathbf{K} \cdot \mathbf{r}') \psi_{\mathbf{k}_j}^*(\mathbf{r}') \psi_{\mathbf{k}_j}(\mathbf{r}') d\mathbf{r}' \\ & - \sum_{i,j} \sum_{\mathbf{K}} \frac{2\pi\epsilon^2 \delta_{s_i s_j}}{|\mathbf{k}_i - \mathbf{k}_j + \mathbf{K}|^2} \left| \int \exp\{i(\mathbf{k}_i - \mathbf{k}_j + \mathbf{K}) \cdot \mathbf{r}\} \psi_{\mathbf{k}_i}^*(\mathbf{r}) \psi_{\mathbf{k}_j}(\mathbf{r}) d\mathbf{r} \right|^2 \end{aligned} \dots \dots (50)$$

where the \mathbf{K} 's are reciprocal lattice vectors. The second term of (50) is just the generalization of the exchange energy found by BP for a free electron gas; the first term represents a Coulomb energy. In the free electron case the background of positive charge just cancels out the mean electronic charge everywhere and there is no Coulomb energy. In the present case the potential produces a periodic variation in the charge density; there is then a corresponding Coulombic contribution to the energy, represented by the first term of (50) and the corresponding terms in the higher order perturbation energies. We have not yet calculated the second order perturbation $H_{s.r.}^{(2)}$, but presumably it will be of the same order as in the free electron case.

We have yet another term to add to the E given by (44). One of the assumptions we made at the outset was that the effect of inter-zone transitions on the collective behaviour could be treated as a perturbation. We have, then, to add in the corresponding perturbation energy. As these inter-zone effects are best treated by means of the multi-zone theory we leave further discussion over until this theory is presented.

Taking all these terms together, we obtain for the total electron energy

$$E = \sum_i E'(\hbar\mathbf{k}_i) + \sum_{k < k_0} \left\{ \frac{\hbar\omega_k}{2} - \frac{2\pi n\epsilon^2}{k^2} \right\} + E_{r.p.} + \langle H_{s.r.} \rangle + H_{s.r.}^{(2)} + E_{i.z.} \dots (51)$$

where the last term is the contribution to the energy of the inter-zone effects.

Finally we shall discuss the choice of k_c . Our initial aim was to solve the eigenvalue problem for (1). As a result of our calculations we have obtained the approximate wave function (49), containing k_c as a parameter, the corresponding energy E being given by (51). Then, regarding k_c as a variational parameter, the best choice of k_c will be that which minimizes E .

When such a choice of k_c has been made we have to verify that two conditions are satisfied if our theory is to be applicable. These are: (i) That k_c is large enough for $H_{s.r.}$ to be treated as a perturbation; if this condition is not satisfied by the best choice of k_c then the collective description is not very suitable for the treatment of the system. (ii) That the condition $k_c \ll K_{\min}$ is satisfied. If this condition is not satisfied it means that the multi-zone theory is more appropriate for the treatment of the system.

ACKNOWLEDGMENTS

I should like to express my thanks to Dr. S. Raimès for his advice and encouragement in this work. I am indebted also to the University of London for the award of a Postgraduate Studentship.

REFERENCES

- ADAMS, E. N., 1952, *Phys. Rev.*, **85**, 41.
BOHM, D., and PINES, D., 1951, *Phys. Rev.*, **82**, 625; 1952, *Ibid.*, **85**, 338; 1953, *Ibid.*, **92**, 609.
PINES, D., 1953, *Phys. Rev.*, **92**, 626.
SLATER, J. C., 1949, *Phys. Rev.*, **76**, 1592.
WANNIER, G. H., 1937, *Phys. Rev.*, **52**, 191.
WOLFF, P. A., 1953, *Phys. Rev.*, **92**, 18.

Inelastic Collisions between Heavy Particles

III : Excitation of Helium Atoms in Fast Encounters with Hydrogen Atoms, Protons and Positive Helium Ions

BY B. L. MOISEWITSCH AND A. L. STEWART[†]

Department of Applied Mathematics, The Queen's University of Belfast

Communicated by D. R. Bates; MS. received 19th July 1954

Abstract. Born's approximation is used to calculate the cross sections for the processes $H(1s) + He(1s^2) \rightarrow H(2s, 2p, 3s, 3p, 3d \text{ or } C) + He(1s2p^1P)$ where C represents the continuum. It is found that these *double* transition collisions are collectively much more effective at high impact energies than the simple single transition collision $H(1s) + He(1s^2) \rightarrow H(1s) + He(1s2p^1P)$ which is also investigated.

Born's approximation is further used to calculate the cross sections for the processes $He^+(1s)(\text{or } H^+) + He(1s^2) \rightarrow He^+(1s)(\text{or } H^+) + He(1s2p^1P)$

double transitions being here found to be unimportant.

§ 1. INTRODUCTION

IT was shown in papers I and II of this series (Bates and Griffing 1953, 1954) that, as compared with single transitions, double transitions give a large contribution to the cross section associated with the excitation of hydrogen atoms by fast encounters with other hydrogen atoms. The present paper is devoted mainly to a study of the analogous collision processes

$$H(1s) + He(1s^2) \rightarrow H(1s) + He(1s2p^1P) \quad \dots\dots(1)$$

$$H(1s) + He(1s^2) \rightarrow H(2s, 2p, 3s, 3p, 3d \text{ or } C) + He(1s2p^1P) \quad \dots\dots(2)$$

where C represents the continuum. In addition, the collision processes

$$He^+(1s) + He(1s^2) \rightarrow He^+(1s) + He(1s2p^1P) \quad \dots\dots(3)$$

$$H^+ + He(1s^2) \rightarrow H^+ + He(1s2p^1P) \quad \dots\dots(4)$$

are also investigated. The excitation of He atoms by He^+ ions is not influenced to a significant extent by double transitions which are therefore neglected.

§ 2. THEORY

2.1. In the first instance we consider a collision between a hydrogen atom and a helium atom, both particles being initially in their ground states. Ignoring the effects of exchange and making use of the Born approximation (Mott and Massey 1949) the cross section for the process in which the helium atom is excited to the $1s2p^1P$ state and the hydrogen atom is excited to the state with quantum numbers nl , is given by

$$Q(1s^2 - 1s2p^1P; 1s - nl) = \frac{8\pi^3 M^2}{K_i^2 h^4} \int_{K_{\min}}^{K_{\max}} |\mathcal{N}|^2 K dK \quad \dots\dots(5)$$

with $\mathcal{N} = \iint X(1s; \mathbf{p}) X^*(nl; \mathbf{p}) \exp(i\mathbf{R} \cdot \mathbf{K}) V(\mathbf{R}, \mathbf{p}) d\mathbf{p} d\mathbf{R} \quad \dots\dots(6)$

$$\mathbf{K} = \mathbf{K}_i - \mathbf{K}_f, \quad \mathbf{K}_i = 2\pi M\mathbf{v}_i/h, \quad \mathbf{K}_f = 2\pi M\mathbf{v}_f/h; \quad \dots\dots(7)$$

[†] Now at Westinghouse Research Laboratories, East Pittsburgh, Pa.

where M is the reduced mass, \mathbf{v}_i and \mathbf{v}_f are the initial and final velocities of relative motion, \mathbf{R} is the relative position vector of the nuclei of the two atoms and $\boldsymbol{\rho}$ is the position vector of the electron in the hydrogen atom relative to the proton, the X 's are the wave functions of the hydrogen atom in the states indicated, and $V(\mathbf{R}, \boldsymbol{\rho})$ is the interaction potential. If \mathbf{r}_1 and \mathbf{r}_2 are the position vectors of the two electrons in the helium atom relative to the alpha particle, then the interaction potential may be written

$$V(\mathbf{R}, \boldsymbol{\rho}) = e^2 \iint \phi^*(1s2p^1P; \mathbf{r}_1, \mathbf{r}_2) \left\{ \frac{2}{R} - \frac{2}{|\mathbf{R} + \boldsymbol{\rho}|} - \frac{1}{|\mathbf{R} - \mathbf{r}_1|} - \frac{1}{|\mathbf{R} - \mathbf{r}_2|} + \frac{1}{|\mathbf{R} + \boldsymbol{\rho} - \mathbf{r}_1|} + \frac{1}{|\mathbf{R} + \boldsymbol{\rho} - \mathbf{r}_2|} \right\} \phi(1s^2; \mathbf{r}_1, \mathbf{r}_2) d\mathbf{r}_1 d\mathbf{r}_2 \quad \dots\dots (8)$$

where the ϕ 's are the wave functions of the helium atom. The first two terms in the brackets under the integral sign in (8) give no contribution because of orthogonality.

It is necessary to use approximate wave functions in order to evaluate $V(\mathbf{R}, \boldsymbol{\rho})$. A suitable set of functions has been given by Morse, Young and Haurwitz (1935). Expressed in atomic units these functions are

$$\phi(1s^2; \mathbf{r}_1, \mathbf{r}_2) = w_1(\mathbf{r}_1)w_1(\mathbf{r}_2) \quad \dots\dots (9)$$

$$\phi(1s2p^1P; \mathbf{r}_1, \mathbf{r}_2) = \frac{1}{\sqrt{2}} \{w_2(\mathbf{r}_1)w_3(\mathbf{r}_2) + w_2(\mathbf{r}_2)w_3(\mathbf{r}_1)\} \quad \dots\dots (10)$$

where

$$w_1(\mathbf{r}) = \left(\frac{\alpha^3}{\pi}\right)^{1/2} \exp(-\alpha r) \quad \dots\dots (11)$$

$$w_2(\mathbf{r}) = \left(\frac{\beta^3}{\pi}\right)^{1/2} \exp(-\beta r) \quad \dots\dots (12)$$

$$w_3(\mathbf{r}) = \left(\frac{\gamma^5}{\pi}\right)^{1/2} r \cos \theta \exp(-\gamma r) \quad \dots\dots (13)$$

$$\text{and} \quad \alpha = 1.69, \quad \beta = 2.00, \quad 2\gamma = 0.97. \quad \dots\dots (14)$$

In the case of the single transition (1) we obtain from the integration formula of Bethe (1930) that

$$|\mathcal{N}| = 32\sqrt{2}\pi e^2 a_0^2 \frac{(\alpha^3 \beta^3)^{1/2}}{(\alpha + \beta)^3} \left\{ 1 - \frac{16}{(t^2 + 4)^2} \right\} |J| t^{-2} \quad \dots\dots (15)$$

$$\text{in which} \quad \mathbf{t} = \mathbf{K} a_0 \quad \dots\dots (16)$$

$$\text{and} \quad |J| = \left| \int w_1(\mathbf{r}) w_3(\mathbf{r}) \exp(i\mathbf{t} \cdot \mathbf{r}) d\mathbf{r} \right| \quad \dots\dots (17)$$

\mathbf{r} being now in units of a_0 , the radius of the first Bohr hydrogen orbit. From (5) it follows that

$$Q(1s^2 - 1s2p^1P; 1s - 1s) = \left[\frac{2^{10}}{s^2} \frac{\alpha^3 \beta^3}{(\alpha + \beta)^6} \int_{t_{\min}}^{t_{\max}} |J|^2 \left\{ 1 - \frac{16}{(t^2 + 4)^2} \right\}^2 t^{-3} dt \right] \pi a_0^2 \quad \dots\dots (18)$$

$$\text{where} \quad s^2 = \frac{1}{2} m v_i^2 / I_H \quad \dots\dots (19)$$

I_H being the ionization potential of hydrogen.

For the double transition collisions the orthogonality of the hydrogen wave functions leads to the result

$$|\mathcal{N}| = 32\sqrt{2}\pi e^2 a_0^2 \frac{(\alpha^3 \beta^3)^{1/2}}{(\alpha + \beta)^3} |I| |J| t^{-2} \quad \dots\dots (20)$$

$$\text{where} \quad |I| = \left| \int X(1s; \boldsymbol{\rho}) X^*(nl; \boldsymbol{\rho}) \exp(i\mathbf{t} \cdot \boldsymbol{\rho}) d\boldsymbol{\rho} \right| \quad \dots\dots (21)$$

Hence, for $n \neq 1$

$$Q(1s^2 - 1s2p^1P; 1s - nl) = \left[\frac{2^{10}}{s^2} \frac{\alpha^3 \beta^3}{(\alpha + \beta)^6} \int_{t_{\min}}^{t_{\max}} |I|^2 |J|^2 t^{-3} dt \right] \pi a_0^2. \dots (22)$$

The J integral defined by (17) is given by

$$|J| = \frac{32 \alpha^{3/2} \gamma^{5/2} (\alpha + \gamma) t}{\{t^2 + (\alpha + \gamma)^2\}^3} \dots (23)$$

while the I integrals defined by (21) are identical with those arising in the calculations described in paper I, expressions for them being given there for the $1s - 2s, 2p, 3s, 3p, 3d$ and C transitions.

The total cross section for the excitation of a helium atom to the $1s2p^1P$ state by a hydrogen atom is

$$Q(1s^2 - 1s2p^1P; 1s - \Sigma) = \sum_{nl} Q(1s^2 - 1s2p^1P; 1s - nl) \dots (24)$$

where the summation includes an integration over the continuum. A closed asymptotic formula for this cross section at sufficiently high energies may be obtained since in the high energy limit t_{\min} and t_{\max} can be taken to be zero and infinite respectively. Thus

$$Q(1s^2 - 1s2p^1P; 1s - \Sigma) \sim Q(1s^2 - 1s2p^1P; 1s - 1s) + \left[\frac{2^{10}}{s^2} \frac{\alpha^3 \beta^3}{(\alpha + \beta)^6} \int_0^\infty |J|^2 \sum_{\substack{nl \\ nl \neq 1s}} |I(1s - nl)|^2 t^{-3} dt \right] \pi a_0^2 \dots (25)$$

and since (cf. Bethe 1930)

$$\sum_{nl} |I(1s - nl)|^2 = 1 \dots (26)$$

it follows that

$$Q(1s^2 - 1s2p^1P; 1s - \Sigma) \sim \left[\frac{2^{11}}{s^2} \frac{\alpha^3 \beta^3}{(\alpha + \beta)^6} \int_0^\infty |J|^2 \left\{ 1 - \frac{16}{(t^2 + 4)} \right\} t^{-3} dt \right] \pi a_0^2 \dots (27)$$

$$\sim (0.310/s^2) \pi a_0^2. \dots (28)$$

2.2. In the case of high energy collisions between He^+ ions and He atoms, an analogous treatment to the one above for process (1) yields for the cross section corresponding to the process (3)

$$Q(1s^2 - 1s2p^1P; 1s - 1s) = \left[\frac{2^{10}}{s^2} \frac{\alpha^3 \beta^3}{(\alpha + \beta)^6} \int_{t_{\min}}^{t_{\max}} |J|^2 \left\{ 2 - \frac{16^2}{(t^2 + 16)^2} \right\} t^{-3} dt \right] \pi a_0^2. \dots (29)$$

Further, the asymptotic form for the total cross section in the high energy limit is given by the expression

$$Q(1s^2 - 1s2p^1P; 1s - \Sigma) \sim Q(1s^2 - 1s2p^1P; 1s - 1s) + \left[\frac{2^{10}}{s^2} \frac{\alpha^3 \beta^3}{(\alpha + \beta)^6} \int_0^\infty |J|^2 \left\{ 1 - \frac{16^4}{(t^2 + 16)^4} \right\} t^{-3} dt \right] \pi a_0^2. \dots (30)$$

It should be noted that whereas the integral occurring in (29) tends to an infinite value in the high energy limit, the integral in (30) remains finite. Consequently in this limit the ratio of the contribution from double transitions to that from single transitions tends to zero. The same is true in the low energy limit.

§ 3. RESULTS

The double transition cross sections $Q(1s^2 - 1s2p^1P; 1s - 2s, 2p, 3s, 3p, 3d \text{ or } C)$ for the collision of a hydrogen atom with kinetic energy \mathcal{E} and a helium atom at rest have been calculated using formula (22). The results are shown on a log-log scale in figure 1. They may be compared with the (cross-section-energy) curves for the analogous encounter of a hydrogen atom with another hydrogen atom which are displayed in figure 2 of paper II. The energy transferred to the internal motion is greater in the helium case and manifests itself, as would be expected, in a general reduction in the cross sections and a shift in the maxima of the cross-section curves towards higher impact energies. The rapid decrease of the cross sections with increase of the principal quantum number, for excitation of states with the same azimuthal quantum number, noted in paper II, is also observed. It is again apparent that, for given principal quantum numbers, the cross sections are, in general, greatest when the azimuthal quantum numbers are such that the transition is optically allowed and that the discrete transitions are smaller than those involving the continuum even at quite low impact energies.

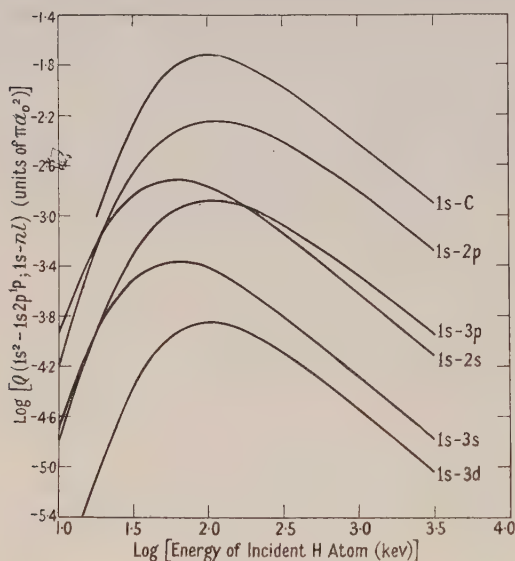


Figure 1. (Cross-section-energy) curves for the collision

$H(1s) + He(1s^2) \rightarrow H(nl) + He(1s2p^1P)$
 where nl represents $2s, 2p, 3s, 3p, 3d$ or C
 (the continuum).

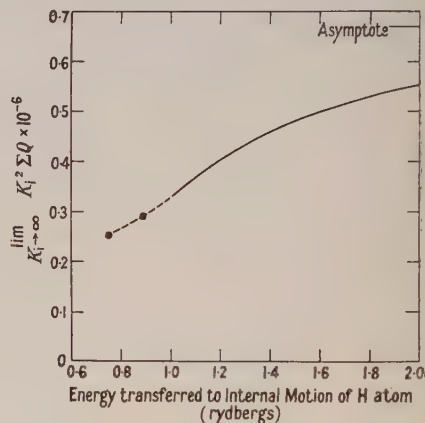


Figure 2. The quantity

$$\lim_{K_f \rightarrow \infty} \sum_{nl=1s}^{nl=n_f l_f \text{ or } \kappa} K_l^2 Q(1s^2 - 1s2p^1P; 1s - nl)$$

is plotted against $1 - 1/n_f^2$ or $1 + \kappa^2$ where $-1/n_f^2$ is the energy in rydbergs of the hydrogen atom in the level with principal quantum number n_f and κ^2 is the energy in rydbergs of the hydrogen atom in a state of the continuum.

The cross section $Q(1s^2 - 1s2p^1P; 1s - 1s)$, where the hydrogen atom remains unexcited, has been calculated from formula (18). This allows us to compute the total cross section $Q(1s^2 - 1s2p^1P; 1s - \Sigma)$ for inelastic collisions resulting in the excitation of the 1P level of helium, since the dominant contribution comes from the excitation of states of hydrogen with $n \leq 3$ and from the continuum. Comparing the total cross section thus obtained with that given by equation (28) we find that for infinite impact energy the neglect of the contribution from states with $n > 3$ gives rise to an error of only 6%. Though this is small it is nevertheless

larger than might have been anticipated from the rapid decrease in the cross sections with increase of principal quantum number. One might be tempted to attribute it in part to computational errors. This possibility can, however, be dismissed. The full line in figure 2 depicts the quantity

$$\lim_{K_I \rightarrow \infty} \left[K_I^2 Q(1s^2 - 1s 2p^1P; 1s - \Sigma) - K_I^2 \int_{\kappa}^{\infty} Q(1s^2 - 1s 2p^1P; 1s - \kappa) d\kappa \right]$$

as a function of $1 + \kappa^2$, where $\lim_{K_I \rightarrow \infty} K_I^2 Q(1s^2 - 1s 2p^1P; 1s - \Sigma)$ is given by (28), $Q(1s^2 - 1s 2p^1P; 1s - \kappa)$ is the cross section for the ejection of the hydrogen atom electron into the continuum with energy $\kappa^2 I_H$. The circles shown give the quantities

$$\lim_{K_I \rightarrow \infty} K_I^2 \sum_{nl=1s}^{nl=2p \text{ or } 3d} Q(1s^2 - 1s 2p^1P; 1s - nl)$$

plotted against the energy (in rydbergs) transferred to the hydrogen atom in a transition to the $n=2$ or $n=3$ level respectively; and, as can be seen, the curve through them joins smoothly to the curve associated with the continuum, as it should.

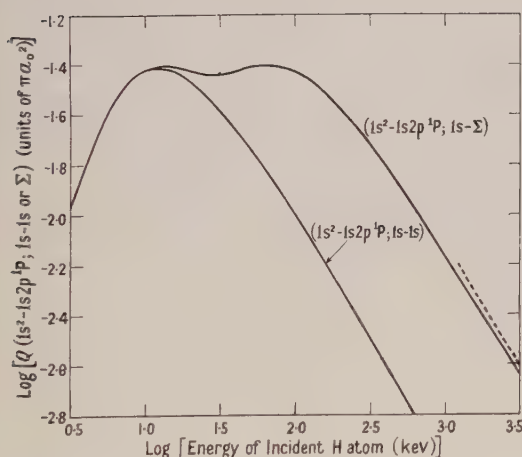


Figure 3. Comparison of the (cross-section-energy) curve for a collision in which the incident hydrogen atom is unaffected with that for a collision in which it is left in any state. The broken line represents the asymptotic behaviour of

$$Q(1s^2 - 1s 2p^1P; 1s - \Sigma)$$

as given by formula (28).

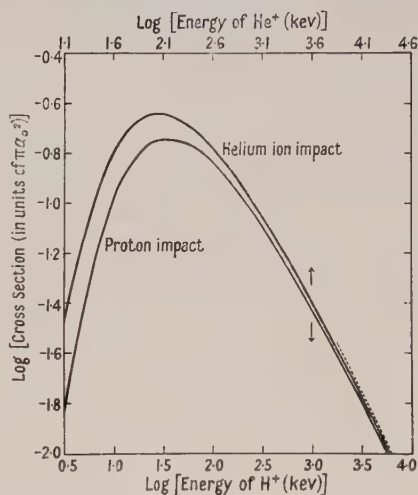


Figure 4. Comparison of the (cross-section-energy) curve for the collision of an He^+ ion with a helium atom, the ion remaining unaffected, with that for the collision of a proton with a helium atom, the helium atom being excited to the $1s 2p^1P$ level in both cases. The broken line represents the asymptotic behaviour of

$$Q(1s^2 - 1s 2p^1P; 1s - \Sigma)$$

as given by formula (30).

The (total cross-section-impact-energy) curve is plotted on a log-log scale in figure 3, where the dotted curve is the asymptote of the total cross section given by equation (28). Included is the curve for $Q(1s^2 - 1s 2p^1P; 1s - 1s)$ to demonstrate the contribution from single transition collisions. It can be seen that such collisions dominate at low values of \mathcal{E} but that when \mathcal{E} reaches about 20 kev

double transitions become significant and ultimately become of major importance. Thus to Born's approximation the total cross-section curve exhibits two maxima, one due to single transition collisions and the other to double transition collisions. Essentially the same shape of curve was obtained by Bates and Griffing (cf. paper I, figure 3) who, however, remark that, to a more accurate approximation in the lower part of the energy region concerned, the first maximum may be partially suppressed and that the true curve may conceivably show a single broad maximum.

The cross section $Q(1s^2 - 1s2p^1P; 1s - 1s)$ for process (3) (see formula (29)) is plotted on a log-log scale in figure 4, the abscissa representing the logarithm of the kinetic energy in kev of the He^+ ion, the neutral particle being considered at rest. The dotted curve is the asymptote of the total cross section $Q(1s^2 - 1s2p^1P; 1s - \Sigma)$ obtained from formula (30). It lies close to the single transition collision cross-section down to quite low impact energies so that the contribution from double transition collisions may, to a good approximation, be neglected. For the sake of comparison the cross section $Q(1s^2 - 1s2p^1P)$ for the encounter of a proton with a helium atom (process (4)) is included in figure 4, where it may be seen that it is only for very high energies that the He^+ ion may be taken as a single system of unit charge.† For moderate energies the screening of the nucleus by the electron is incomplete and as the impact energy tends to zero the He^+ ion behaves more and more as a single doubly charged system.

ACKNOWLEDGMENTS

It gives us great pleasure to thank Professor D. R. Bates for suggesting this problem and for useful discussions.

REFERENCES

- BATES, D. R., and GRIFFING, G. W., 1953, *Proc. Phys. Soc. A*, **66**, 961; 1954, *Ibid.*, **67**, 663.
 BETHE, H. A., 1930, *Ann. Phys. Lpz.*, **5**, 325.
 MORSE, P. M., YOUNG, L. A., and HAURWITZ, E. S., 1935, *Phys. Rev.*, **48**, 948.
 MOTT, N. F., and MASSEY, H. S. W., 1949, *Theory of Atomic Collisions*, 2nd Edn (Oxford: Clarendon Press).

† The abscissae are such that points on the two curves corresponding to equal velocities of relative motion lie on a vertical line.

Electron Capture—IV : Capture from Helium Atoms by Fast Protons

By B. H. BRANSDEN,[†] A. DALGARNO* AND N. M. KING^{†‡}

[†] Department of Physics, * Department of Applied Mathematics,
The Queen's University of Belfast

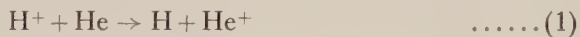
*Communicated by D. R. Bates; MS. received 8th June 1954 and in amended form
12th August 1954*

Abstract. A modified Born approximation is used to calculate the cross sections for capture of electrons from helium atoms by fast protons and for capture from hydrogen atoms by helium ions. A comparison is made with experimental data and it is shown that the Brinkman–Kramers approximation is inadequate. The theoretical results lend support to the data of Hasted and Stedeford and cast serious doubts on the accuracy of the data of other experimentalists.

§ 1. INTRODUCTION

EARLIER papers of this series (I, Bates and Dalgarno 1952, II, Dalgarno and Yadav 1953, III, Bates and Dalgarno 1953) have dealt with electron capture into the ground and excited states of hydrogen in collisions between protons and hydrogen atoms, as has an independent paper by Jackson and Schiff (1953). The total capture cross section calculated using the Born approximation agrees with that observed by Ribe (1951).

It was pointed out in these papers that the neglect of the nucleus–nucleus interaction term as in the work of Oppenheimer (1928), Brinkman and Kramers (1930) and Takayanagi (1952) was unjustified. For systems which possess more than one electron, an additional assumption involved in the use of the Brinkman–Kramers (BK) approximation is that the screening effect of the passive electrons on the perturbation may be ignored. It is desirable to examine the validity of this latter approximation for a simple reaction for which experimental comparison data are available; such a reaction (which has considerable intrinsic interest) is



comparison data being available up to an impact energy of 200 keV (Smith 1934, Meyer 1937, Keene 1949, Hasted and Stedeford 1954).

Since formidable computational difficulties are encountered, it has not been possible to evaluate exactly the Born approximation for process (1). However, the actual perturbation has been replaced by an ‘effective’ perturbation described by a variable parameter Z' . The sensitivity of the cross section to Z' is illustrated and an attempt made to select it to correspond as closely as possible to the correct interaction; it is concluded that whilst neglect of the screening effect of the passive electrons may be unjustified, useful results can be obtained by careful choice of Z' . The theoretical predictions are compared with experimental data.

[‡] Now at the Atomic Energy Research Establishment, Harwell, Berks.

§ 2. THEORY

2.1. Consider the rearrangement in which an electron is transferred from an orbital round a helium nucleus denoted by A to an orbital round a proton denoted by B. Let $\phi_i(\mathbf{r}_1, \mathbf{r}_2)$ be the wave function of the initial state of the helium atom, $\psi_f(\mathbf{r}_1)$ the wave function of the helium ion and $\chi_f(\mathbf{s}_1)$ the wave function of the hydrogen atom, where \mathbf{r} denotes the position vector of an electron from nucleus B, \mathbf{s} the position vector of an electron from nucleus A and the subscript 1 or 2 distinguishes the two electrons. Then, taking proper account of the identity of the electrons, the cross section for the process



is given in the Born approximation by (Mott and Massey 1949)

$$Q = \frac{8\pi^3 M^2}{h^4} \frac{v_f}{v_i} 2 \int_{-1}^{+1} |\mathcal{M}|^2 d(\cos \Theta), \quad \dots\dots(2)$$

with

$$|\mathcal{M}| = \left| \int \int \phi_i(\mathbf{r}_1, \mathbf{r}_2) \exp[i(\boldsymbol{\alpha} \cdot \mathbf{r}_2 + \boldsymbol{\beta} \cdot \mathbf{s}_2 + \boldsymbol{\gamma} \cdot \mathbf{r}_1)] \times \psi_f(\mathbf{r}_1) \chi_f(\mathbf{s}_2) V(\mathbf{r}_1, \mathbf{r}_2, \mathbf{s}_2) d\mathbf{r}_2 d\mathbf{s}_2 d\mathbf{r}_1 \right|, \quad \dots\dots(3)$$

where M is the reduced mass of the system, v_i and v_f are the magnitudes of the initial and final velocities of relative motion, Θ is the angle between unit vectors \mathbf{n}_i and \mathbf{n}_f parallel to these velocities and

$$\left. \begin{aligned} \boldsymbol{\alpha} &= -k_i \mathbf{n}_i \frac{M_A + m}{M_A + 2m} + k_f \mathbf{n}_f, \\ \boldsymbol{\beta} &= k_i \mathbf{n}_i - k_f \mathbf{n}_f \frac{M_B}{M_B + m}, \\ \boldsymbol{\gamma} &= -k_i \mathbf{n}_i \frac{m}{M_A + m} + k_f \mathbf{n}_f \frac{m}{M_A + 2m}, \end{aligned} \right\} \quad \dots\dots(4)$$

m , M_A and M_B being the masses of the electron, helium nucleus and proton respectively; and

$$\left. \begin{aligned} k_i &= \frac{2\pi}{h} v_i \frac{M_B (M_A + 2m)}{M_B + M_A + 2m}, \\ k_f &= \frac{2\pi}{h} v_f \frac{(M_B + m)(M_A + m)}{M_B + M_A + 2m}. \end{aligned} \right\} \quad \dots\dots(5)$$

The perturbation $V(\mathbf{r}_1, \mathbf{r}_2, \mathbf{s}_2)$ may be expressed in either of the forms

$$V_{\text{prior}} = \frac{Z_B e^2}{s_2} + \frac{Z_B e^2}{|\mathbf{r}_1 - \mathbf{r}_2 + \mathbf{s}_2|} - \frac{Z_A Z_B e^2}{|\mathbf{r}_2 - \mathbf{s}_2|}, \quad \dots\dots(6a)$$

$$V_{\text{post}} = \frac{Z_A e^2}{r_2} + \frac{Z_B e^2}{|\mathbf{r}_1 - \mathbf{r}_2 + \mathbf{s}_2|} - \frac{Z_A Z_B e^2}{|\mathbf{r}_2 - \mathbf{s}_2|} - \frac{e^2}{|\mathbf{r}_1 - \mathbf{r}_2|}, \quad \dots\dots(6b)$$

where $Z_A e$, $Z_B e$ and e are the charges of the helium nucleus, proton and electron respectively.

2.2. It has been proved by Jackson and Schiff (1953) that for the case of a single electron moving from one bare nucleus to another the cross section (2) obtained

using the prior interaction is identical to that obtained using the post interaction. This is, however, merely a special example of the more general result that the cross sections obtained using the prior and post interactions are identical provided that the atomic wave functions used are either exact (cf. Schiff 1949) or satisfy certain less stringent conditions (Bates, Fundaminsky, Leech and Massey 1950). In general when these conditions are not satisfied, the two forms of interaction will lead to different values of the cross section. As it is impossible to predict which interaction will provide the more accurate result (cf. Bransden 1954), it is better to use the form of V which presents the lesser complexity; accordingly the prior interaction (6a) has been used here.

2.3. It is customary in collision problems (and readily justifiable) to assume that the momentum change of the passive electron γ is zero. The matrix element then reduces to

$$|\mathcal{M}| = \int \int \phi_i(\mathbf{r}_1, \mathbf{r}_2) \exp[i(\boldsymbol{\alpha} \cdot \mathbf{r}_2 + \boldsymbol{\beta} \cdot \mathbf{s}_2)] \psi_f(\mathbf{r}_1) \chi_f(\mathbf{s}_2) \\ \times \left\{ \frac{Z_B e^2}{|\mathbf{s}_2|} + \frac{Z_B e^2}{|\mathbf{r}_1 + \mathbf{r}_2 - \mathbf{s}_2|} - \frac{Z_A Z_B e^2}{|\mathbf{r}_2 - \mathbf{s}_2|} \right\} d\mathbf{r}_1 d\mathbf{r}_2 d\mathbf{s}_2. \quad \dots\dots(7)$$

Considering capture from the ground state of helium into the ground state of hydrogen we take for the initial and final wave functions

$$\phi_i(\mathbf{r}_1, \mathbf{r}_2) = \frac{\lambda^3}{\pi a_0^3} \exp[-\lambda(r_1 + r_2)/a_0], \quad \lambda = 1.69; \quad \dots\dots(8)$$

$$\chi_f(\mathbf{r}) = (1/\pi a_0^3)^{1/2} \exp(-r/a_0), \quad \dots\dots(9)$$

$$\psi_f(\mathbf{r}) = (8/\pi a_0^3)^{1/2} \exp(-2r/a_0). \quad \dots\dots(10)$$

The integration over the coordinates of electron (1) may now be performed to give

$$|\mathcal{M}| = \frac{e^2}{\pi a_0^3} \lambda^{3/2} \frac{(8\lambda)^{3/2}}{(\lambda + 2)^3} \\ \times \int \int \exp\left\{-(\lambda r + s)/a_0\right\} + i(\boldsymbol{\alpha} \cdot \mathbf{r} + \boldsymbol{\beta} \cdot \mathbf{s}) \\ \times \left[\frac{1}{s} - \frac{1}{R} - \left\{ \frac{1}{2}(\lambda + 2) + \frac{1}{R} \right\} \exp\left\{ -\frac{(\lambda + 2)R}{a_0} \right\} \right] d\mathbf{r} d\mathbf{s}, \quad \dots\dots(11)$$

with $R = |\mathbf{r}_2 - \mathbf{s}_2|$, the distance between the helium nucleus and proton, and taking $Z_A = 2$, $Z_B = 1$.

2.4. The early calculations of Oppenheimer (1928) and Brinkman and Kramers (1930) ignored all terms of (11) except the $1/s$ term with the result that the integration could be carried out by elementary methods. The $1/R$ term presents considerable difficulty; it has been evaluated by Bates and Dalgarno (1953) using a series expansion and by Corinaldesi and Trainor (1952) and Jackson and Schiff (1953) using Fourier transforms (cf. Feynman 1949). Independently the authors had developed a third method which, though it has no advantages over the Feynman technique in its application to the integral considered here, may be useful for other integrals and is therefore described in an appendix. The integral involving the third term of the perturbation in (11) may be calculated by the use of either the second or third method, both leading to the same analytical formulae. The number of terms in the resulting expression is so great that to take account of all of them would take a prohibitive length of time and we have therefore used in place of the perturbation $1/R + \{ \frac{1}{2}(\lambda + 2) + 1/R \} \exp\{ -(\lambda + 2)R/a_0 \}$ an 'effective'

perturbation Z'/R . The decision as to the appropriate choice for Z' will be postponed until § 3, and we point out here merely that it is reasonable to assume that $1 < Z' < 2$ and that Z' tends to 2 as the impact energy tends to infinity. The matrix element is now

$$|\mathcal{M}| = \frac{e^2}{\pi a_0^2} \lambda^{3/2} \frac{(8\lambda)^{3/2}}{(\lambda+2)^3} \iint \exp \left[-\left(\frac{\lambda r + s}{a_0} \right) + i(\boldsymbol{\alpha} \cdot \mathbf{r} + \boldsymbol{\beta} \cdot \mathbf{s}) \right] \times \left\{ \frac{1}{s} - \frac{Z'}{R} \right\} d\mathbf{r} d\mathbf{s}. \quad \dots\dots (12)$$

Although by using either the second or third method the cross section can be obtained analytically, this proves to be so lengthy that it is generally more rapid to perform the two final integrations numerically (see Appendix).

2.5. By using the conservation of energy principle and the definitions (4), (5), it may be established that to sufficient accuracy

$$\alpha^2 = \frac{2M^2 p^2}{m^2 a_0^2} (1 + \cos \Theta) + \frac{1}{a_0^2} \left[\frac{1}{4p^2} \{p^2 + (a-b)^2\} \{p^2 + (a+b)^2\} - a^2 \right], \quad \dots\dots (13)$$

$$\beta^2 = \alpha^2 + (a^2 - b^2)/a_0^2, \quad \dots\dots (14)$$

$$\boldsymbol{\alpha} \cdot \boldsymbol{\beta} = -\alpha^2 - \frac{1}{2a_0^2} (a^2 - b^2) = -\beta^2 + \frac{1}{2a_0^2} (a^2 - b^2), \quad \dots\dots (15)$$

where $p = 2\pi m v_1 a_0 / \hbar$ and a^2/a_0^2 , b^2/a_0^2 are the binding energies of the active electron in the helium and hydrogen atoms respectively; in the system in which the helium atom is stationary, p^2 is m/M_1 times the initial kinetic energy of the proton, measured in rydbergs. Using (13), the integration over the scattering angle can be transformed into an integral over the energy; the upper limit of this integral may be taken as infinity (cf. paper I), whilst the lower limit is given by

$$(\alpha^2)_{\min} = \frac{1}{a_0^2} \left[\frac{1}{4p^2} \{p^2 + (a-b)^2\} \{p^2 + (a+b)^2\} - a^2 \right]. \quad \dots\dots (16)$$

The final expression for the cross section for the capture of an electron from a helium atom in its ground state by a proton into the ground state of a hydrogen atom becomes on writing $\alpha' = a_0 \alpha$, $\beta' = a_0 \beta$,

$$Q(1s-1s) = \frac{1}{2p^2} \lambda^3 \frac{(8\lambda)^3}{(\lambda+2)^6} \int_{(\alpha')^2_{\min}}^{\infty} d(\alpha')^2 \times \left| \frac{1}{\pi^2} \iint \exp \left[-(\lambda r + s) + i(\boldsymbol{\alpha}' \cdot \mathbf{r} + \boldsymbol{\beta}' \cdot \mathbf{s}) \right] \left(\frac{1}{s} - \frac{Z'}{R} \right) d\mathbf{r} d\mathbf{s} \right|^2, \quad \dots\dots (17)$$

in units of πa_0^2 ($\pi a_0^2 = 8.8 \times 10^{-17} \text{ cm}^2$). If the presence of the passive electron is ignored $(8\lambda)^3/(\lambda+2)^6$ is replaced by unity and Z' by 2. The Brinkman-Kramers approximation is immediately obtained by putting $Z' = 0$, the remaining integrations being elementary; if μ is the screening parameter occurring in the final wave function, then

$$Q_{\text{BK}}(1s-1s) = \frac{2^9 \lambda^5}{p^2} \frac{(8\lambda)^3}{(\lambda+2)^6} \frac{6}{5} \frac{1}{X^3 Y (2X + 4Y)}, \quad \dots\dots (18)$$

where

$$\left. \begin{aligned} X &= P^2 + \lambda^2 - a^2, \\ Y &= P^2 + \mu^2 - b^2, \\ P^2 &= \frac{1}{4p^2} \{p^2 + (a-b)^2\} \{p^2 + (a+b)^2\}, \end{aligned} \right\} \quad \dots\dots (19)$$

for capture into the ground state of hydrogen $\mu = b = 1$. We shall make use later of the Brinkman-Kramers approximations for capture into the excited 2s and 2p states of hydrogen.

$$Q_{\text{BK}}(1s-2s) = \frac{2^6 \lambda^5}{p^2} \frac{(8\lambda)^3}{(\lambda+2)^6} \left\{ \frac{6}{5} \frac{1}{X^2 Y (2X+4Y)} - 4\mu^2 \frac{7}{6} \frac{1}{X^4 Y (2X+5Y)} + 4\mu^4 \frac{8}{7} \frac{1}{X^6 Y (2X+6Y)} \right\}, \quad \dots\dots(20)^\dagger$$

$$Q_{\text{BK}}(1s-2p) = \frac{2^6 \lambda^5}{p^2} \frac{(8\lambda)^3}{(\lambda+2)^6} \left\{ \frac{7}{6} \frac{1}{X^4 Y (2X+5Y)} - \mu^2 \frac{8}{7} \frac{1}{X^6 Y (2X+6Y)} \right\}. \quad \dots\dots(21)^\dagger$$

In (20) and (21) $\mu = b = \frac{1}{2}$.

§ 3. THE 'EFFECTIVE' INTERACTION

In this section we shall discuss how best to choose Z' so that the cross sections derived from the matrix elements

$$I = \iint \exp[-(\lambda r + s) + i(\boldsymbol{\alpha} \cdot \mathbf{r} + \boldsymbol{\beta} \cdot \mathbf{s})] \times \left\{ \frac{1}{R} + \left(\frac{\lambda+2}{2} + \frac{1}{R} \right) e^{-(\lambda+2)R} \right\} d\mathbf{r} d\mathbf{s}$$

and \dots\dots(22)

$$I' = \iint \exp[-(\lambda r + s) + i(\boldsymbol{\alpha} \cdot \mathbf{r} + \boldsymbol{\beta} \cdot \mathbf{s})] \frac{Z'}{R} d\mathbf{r} d\mathbf{s} \quad \dots\dots(23)$$

are equal. It is readily established that

$$I_1 = \iint \exp[-(\lambda r + s) + i(\boldsymbol{\alpha} \cdot \mathbf{r} + \boldsymbol{\beta} \cdot \mathbf{s})] \frac{1}{R} d\mathbf{r} d\mathbf{s}, \quad \dots\dots(24)$$

$$I_2 = \iint \exp[-(\lambda r + s) + i(\boldsymbol{\alpha} \cdot \mathbf{r} + \boldsymbol{\beta} \cdot \mathbf{s})] \frac{1}{2} (\lambda+2) \exp[-(\lambda+2)R] d\mathbf{r} d\mathbf{s}, \quad \dots(25)$$

$$I_3 = \iint \exp[-(\lambda r + s) + i(\boldsymbol{\alpha} \cdot \mathbf{r} + \boldsymbol{\beta} \cdot \mathbf{s})] \frac{1}{R} \exp[-(\lambda+2)R] d\mathbf{r} d\mathbf{s} \quad \dots\dots(26)$$

are all positive, this following from inspection of their forms when the transforms described in the appendix are used. As $\{\exp(-x^2)\}(1+x^2) \leq 1$ it may be seen almost immediately that $I_2 + I_3 \leq I_1$. Thus the assertion

$$1 \leq Z' \leq 2 \text{ for all } \alpha, \beta \quad \dots\dots(27)$$

is rigorously true. It may be noted that if the problem were treated consistently as a one-electron problem, the appropriate choice of Z' would be 1.69 since the bound helium electrons move in a field approximately the same as that of a charge 1.69 e . (If the post interaction were used, a different Z' would be appropriate.)

Closer estimates of Z' may be obtained from a consideration of the cross sections resulting from putting the ratio m/M equal to zero in the integrands of I, I' † in which case they may be evaluated without undue difficulty. (The approximation

† These formulae are taken from an extensive unpublished list prepared by D. R. Bates and A. Dalgarno.

‡ This approximation gives the correct results when applied to the Brinkman-Kramers potential term $1/s$ alone.

is *not* equivalent to the assumption of zero momentum transfer for which also $(\alpha^2)_{\min}$ is zero.) Putting $\alpha + \beta = 0$ we obtain

$$I_1 = \frac{32\pi^2}{|\alpha|} \frac{1}{(\lambda^2 - 1)^3} \left[(\lambda^2 - 1) |\alpha| \left(\frac{\lambda}{\alpha^2 + 1} + \frac{1}{\alpha^2 + \lambda^2} \right) - 4\lambda \{ \arctan(|\alpha|) - \arctan(|\alpha|/\lambda) \} \right], \quad \dots\dots(28)$$

$$I_2 = \frac{32\pi^2}{|\alpha|} \frac{(\lambda + 2)}{(\lambda^2 - 1)^3} \left\{ (\lambda^2 - 1) |\alpha| \left(\frac{\lambda(\lambda + 2)}{[(\lambda + 3)^2 + \alpha^2]^2} + \frac{2(\lambda + 1)}{[4(\lambda + 1)^2 + \alpha^2]} \right) - 2\lambda |\alpha| \left(\frac{1}{(\lambda + 3)^2 + \alpha^2} - \frac{1}{4(\lambda + 1)^2 + \alpha^2} \right) \right\}, \quad \dots\dots(29)$$

$$I_3 = \frac{32\pi^2}{|\alpha|} \frac{1}{(\lambda^2 - 1)^3} \left[(\lambda^2 - 1) |\alpha| \left(\frac{\lambda(\lambda + 3)}{(\lambda + 3)^2 + \alpha^2} + \frac{2(\lambda + 1)}{4(\lambda + 1)^2 + \alpha^2} \right) - 4\lambda \{ \arctan \{ \alpha/(\lambda + 3) \} - \arctan \{ \alpha/(2\lambda + 2) \} \} \right]. \quad \dots\dots(30)$$

The values of Z' obtained using these formulae, in (11) and (17), are shown in figure 1. It is seen that the variation of Z' with energy is very slow, and that Z' tends to 2 as p^2 tends to infinity (cf. § 2.3). (The minimum in Z' is due to cancellation between the $1/s$ and the remaining perturbation terms of (17).) The cross sections calculated using (17)[†] and the values of Z' in figure 1 should correspond closely to the exact cross sections.

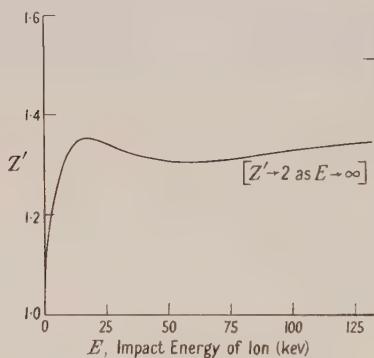


Figure 1. The effective charge parameter Z' as a function of E , the impact energy of the ion.

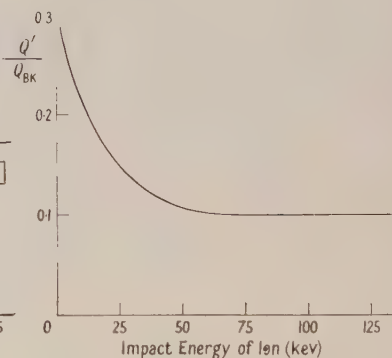


Figure 2. The ratio of Q' , the cross section for the reaction $H^+ + He(1s^2) \rightarrow H(1s) + He^+(1s)$ (calculated using the effective charge parameter Z' shown in figure 1), to the Brinkman-Kramers cross section Q_{BK} .

§ 4. RESULTS

The cross section for the process



obtained from (17) is a quadratic function of Z' :

$$Q(Z') = AZ'^2 - BZ' + C. \quad \dots\dots(32)$$

[†] The approximation of putting $m/M=0$ is no longer made.

A , B and C have been computed for $p^2 = 0.2$ to 5.0 and are given in table 1 while the minimum and maximum values of $Q(Z')$ § are included in table 2 where Z' is

Table 1. Cross Sections for Electron Capture $H^+ + He(1s) \rightarrow He^+(1s) + H(1s)$ expressed as a Function of Effective Charge Z' †

	$Q = AZ'^2 - BZ' + C$		
p^2 ‡	A	B	C
0.2	47.0	85.1	43.6
0.5	23.7	52.1	31.6
1.0	10.3	24.5	16.0
2.0	3.00	7.69	5.46
3.0	1.21	3.23	2.39
4.0	0.55	1.54	1.19
5.0	0.28	0.81	0.65

† In units of πa_0^2 ($8.8 \times 10^{-17} \text{ cm}^2$).

‡ Impact energy of ion = $24.97 p^2 \text{ kev}$.

Table 2. Cross Sections† for Electron Capture $H^+ + He(1s^2) \rightarrow He^+(1s) + H(1s)$

p^2 ‡	Q'	Q''	Q_{\max}	Q_{\min}	Q_{BK}
0	0	0	0	0	0
0.1	8	20.0	—	—	31.5
0.2	10.31	34.1	62.0	5.50	43.6
0.5	4.63	11.6	22.2	2.97	31.9
1.0	1.60	3.94	8.20	1.43	16.0
2.0	0.55	1.02	2.08	0.53	5.46
3.0	0.24	0.37	0.77	0.23	2.39
4.0	0.12	0.16	0.31	0.11	1.19
5.0	0.065	0.080	0.159	0.064	0.65
6.0	0.038	—	—	—	0.38
10.0	0.0067	—	—	—	0.067
14.0	0.0018	—	—	—	0.018
20.0	0.00038	—	—	—	0.0038

Q' cross section calculated with 'best' value of effective charge parameter Z' .

Q'' cross section calculated for $Z' = 1.69$.

Q_{\max} , Q_{\min} maximum and minimum possible values of the cross section.

Q_{BK} Brinkman-Kramers cross section.

† In units of πa_0^2 ($8.8 \times 10^{-17} \text{ cm}^2$).

‡ Impact energy = $24.97 p^2 \text{ kev}$.

restricted according to (27). It is seen that Q is rather sensitive to Z' for low energies but less so for the important high-energy region. The cross sections $Q(Z')$ with Z' as in figure 1, the one-electron approximation $Q(1.69)$ and the BK approximation $Q(0)$ are compared in table 2. The error is in general less than 5% but may occasionally be slightly greater. For high energies, the ratio $Q(Z')/Q_{\text{BK}}$ tends to a constant (cf. figure 2) as does the corresponding ratio for proton capture from hydrogen atoms (Jackson and Schiff 1953)¶ and this has been used to extrapolate $Q(Z')$ for $p^2 > 5$ (the extrapolated values are given in italics).

By making use of the principle of detailed balancing (cf. Massey and Burhop 1952) the cross section Q_r for the reaction



can be shown to be $\frac{1}{4}Q(Z')$.

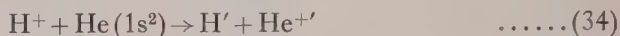
§ For many purposes it is sufficient to know the cross section lies between these limits.

¶ The constants are different in the two cases, being 0.10 for $H^+ + He$ and 0.66 for $H^+ + H$.

Finally it should be mentioned that some calculations on electron capture from helium by protons at very low energies have been carried out by Massey and Smith (1933) and Garstang (1952) using a perturbed stationary state method.

§ 5. COMPARISON WITH EXPERIMENTAL DATA

Experiments on capture from helium atoms by protons have been carried out by Smith (1934), Meyer (1937), Keene (1949), and Hasted and Stedeford (1955, in course of publication), and their results are illustrated in figure 3. The experimental cross sections include contributions from reactions



the dashes denoting excited states, but it is not easy to estimate their magnitude.

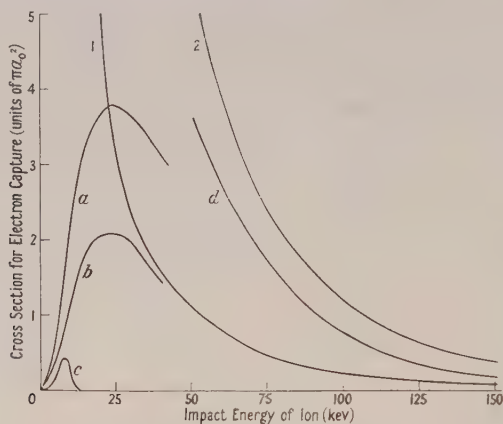


Figure 3. Cross sections for the reaction $\text{H}^+ + \text{He} \rightarrow \text{H} + \text{He}^+$.

Experimental cross sections: *a* Keene (1949), *b* Hasted and Stedeford (1955), *c* Smith (1933), *d* Meyer (1937).

Calculated cross sections: 1. The cross section found with the 'best' value of Z' (an allowance has been made for capture involving excited states). 2. The Brinkman-Kramers cross section, with no allowance for capture involving excited states.†

† The disagreement between the Brinkman-Kramers cross section and Meyer is thus rather more serious than is apparent from the graph.

However some calculations using formulae (20), (21) indicated that the ratio of the cross sections for (31) and (34) is much the same as in the case of electron capture from hydrogen by protons.‡ Assuming this to be so, a theoretical curve is obtained which may be directly compared with experiment. The results obtained taking the cross section for (31) as $Q(Z')$ and as Q_{BK} are illustrated in figure 3. Their magnitudes may be in error by a factor between one half and unity but the energy variation should be accurate.

Although there is considerable disagreement amongst the various experimenters, it appears that Q_{BK} is a gross overestimate. Keene and Hasted and Stedeford agree that the maximum cross section occurs at 25 keV whereas theory predicts a maximum at about 5 keV. The Born approximation will not be reliable below about 30 keV (cf. work on hydrogen) so that the discrepancy is not surprising. The theory agrees with Hasted and Stedeford for impact energies greater than

‡ This ratio varies but slowly with energy.

30 keV (though only a very limited comparison is possible and the agreement may merely be an apparent one) and indicates that Keene's results are too large by a factor of about two. Smith's results disagree considerably both with theory and with the results of the other experimenters. In the high-energy region (where the theory should be the most accurate) the results of Meyer are greater than those of theory by a large factor and must be considered suspect; in fact by no choice of Z' (with $1 < Z' < 2$) can Meyer's results be obtained.

It is not possible to draw firm conclusions about the accuracy of the one-electron approximation (cf. table 2) but the cross section $Q(1.69)$ appears to increase much too rapidly as it approaches its maximum. At high energies it may well be sufficiently accurate.

The predicted cross section for the reaction



taking account as before of the contributions from reaction involving excited states, is compared with the experimental data of Meyer (1937) and Keene (1949) in figure 4, where it is seen that the agreement is rather poor.† Although Meyer

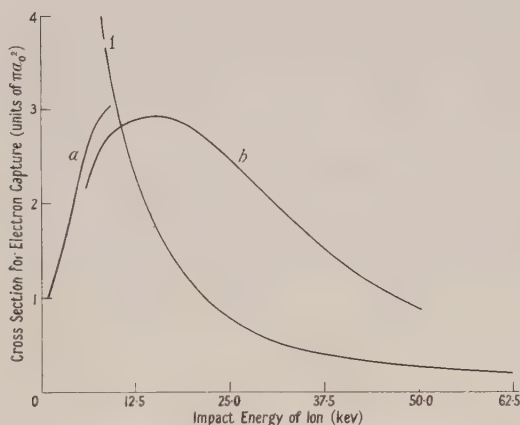


Figure 4. Cross sections for the reaction $\text{H} + \text{He}^+ \rightarrow \text{H}^+ + \text{He}$.

Experimental cross sections: *a* Keene (1949), *b* Meyer (1937).

Calculated cross sections: 1. The cross section found by applying the principle of detailed balancing to the cross section $Q(Z')$ (table 2), together with an allowance for capture involving excited states.

and Keene agree fairly well (where comparison is possible over only a limited range), in view of the discrepancies existing for the reverse reaction, their results need experimental confirmation before any conclusion can be made about the accuracy of the theory.

The cross section for (35) may be used in conjunction with the equilibrium measurements of Schnitzer (1953) on the neutralization of a helium ion beam in hydrogen to derive values for the loss cross section of helium atoms in hydrogen, but this is not worth while until the existing discrepancies between the theory and experiment have been resolved.

† It is most unlikely that the influence of molecular binding could be sufficient to bring about agreement.

§ 6. CONCLUSIONS

The modified Born approximation agrees with the most recent data for energies greater than 35 kev but only a very limited comparison is possible. Until more extensive measurements at high energies have been carried out to supplement the observations of Hasted and Stedeford and confirm or otherwise the results of Meyer, no firm conclusion can be drawn about the accuracy of the theoretical calculations.† Should their accuracy be confirmed, a calculation of the separate contributions of reactions involving excited states may then become profitable.

ACKNOWLEDGMENTS

It is a pleasure to record our indebtedness to Professor D. R. Bates for his encouragement throughout the course of this work. Our thanks are due to Dr. J. B. Hasted and J. B. H. Stedeford for allowing us to quote their results prior to publication and to the former for some interesting comments.

APPENDIX

The calculation of the nuclear interaction integral

The method will be described only for the coulomb integral

$$I|\alpha| = \int \int \exp[ar + bs + i(\alpha \cdot \mathbf{r} + \beta \cdot \mathbf{s})] \frac{1}{R} d\mathbf{r} d\mathbf{s} \quad \dots\dots (A1)$$

but it can be used equally well for integrals in which $1/R$ is replaced by more complicated functions of R . By making use of the transforms

$$\exp(-2\mathcal{K}x) = \int_0^\infty \exp[-(x^2\nu + \mathcal{K}^2/\nu)] \mathcal{K}(\pi\nu^3)^{-1/2} d\nu, \quad \dots\dots (A2)$$

$$x^{-1} = \int_0^\infty \exp[-x^2\nu] (\pi\nu)^{-1/2} d\nu, \quad \dots\dots (A3)$$

used by Edwards (1952) in another connection, it is easily established that

$$I = \frac{ab}{4} \int \int \int_{-\infty}^{\infty} (\pi^3 \lambda^3 \mu^3 \nu^3)^{-1/2} \exp\left[-\frac{1}{4}\left(\frac{a^2}{\lambda} + \frac{b^2}{\mu}\right)\right] J(\lambda, \mu, \nu) d\lambda d\mu d\nu \quad \dots\dots (A4)$$

with

$$J(\lambda, \mu, \nu) = \int \int \exp[-\lambda r^2 - \mu s^2 - \nu(r^2 + s^2 - 2\mathbf{r} \cdot \mathbf{s}) + i(\alpha \cdot \mathbf{r} + \beta \cdot \mathbf{s})] d\mathbf{r} d\mathbf{s} \quad \dots\dots (A5)$$

J is readily evaluated by standard methods (Watson 1944) to be

$$J(\lambda, \mu, \nu) = \pi^3 (\nu\lambda + \lambda\mu + \mu\nu)^{-3/2} \exp\left\{\frac{-(\nu + \mu)\alpha^2 + (\nu + \lambda)\beta^2 + 2\nu\alpha \cdot \beta}{4(\nu\lambda + \lambda\mu + \mu\nu)}\right\} \quad \dots (A6)$$

Combining (4) and (6) and making the substitutions

$$\nu = R^2 \cos^2 \theta, \quad \mu = R^2 \sin^2 \theta \cos^2 \phi, \quad \lambda = R^2 \sin^2 \theta \sin^2 \phi \quad \dots\dots (A7)$$

† *Note added in proof.* Recent unpublished results up to an energy of 200 kev by Dr. P. M. Stier and Mr. C. F. Barnett are in essential agreement with theoretical predictions. We are indebted to Dr. Stier for sending us a copy of the data before publication.

we obtain

$$I = 2ab\pi^{3/2} \int_0^\infty dR \int_0^\pi d(\cos\theta) \int_0^{2\pi} d\phi R^{-8} (\cos^2\theta \sin^2\theta + \sin^4\theta \cos^2\phi \sin^2\phi)^{-3/2} \\ \times (\sin^4\theta \sin^2\phi \cos^2\phi)^{-1} \times \exp \left\{ -\frac{1}{4R^2} \left[\frac{a^2}{\sin^2\theta \cos^2\phi} + \frac{b^2}{\sin^2\theta \sin^2\phi} \right. \right. \\ \left. \left. + (\alpha^2(\cos^2\theta + \sin^2\theta \sin^2\phi) + \beta^2(\cos^2\theta + \sin^2\theta \sin^2\phi) \right. \right. \\ \left. \left. + 2\alpha \cdot \beta \cos^2\theta)(\sin^4\theta \cos^2\phi \sin^2\phi + \cos^2\theta \sin^2\phi)^{-1} \right] \right\}. \quad \dots\dots (A 8)$$

The integration over R may be carried out using the formula (Watson 1944)

$$\int_0^\infty R^{-n} \exp(-\delta^2/R^2) dR = \Gamma(\frac{1}{2}(n-1))/2\delta^{n-1} \quad \dots\dots (A 9)$$

whilst that over $\cos\theta$ is elementary. We are left with an integration of the form

$$I = \int_{-1}^{+1} \mathcal{G}(\alpha, \beta, y) dy \quad \dots\dots (A 10)$$

where the substitution $y = \cos 2\phi$ has been used; \mathcal{G} is an algebraic function of y which may be integrated analytically in terms of elementary functions. However, the result is in general so lengthy that it is quicker to compute I numerically.

To complete the calculation of the capture cross section it remains then to square I and integrate with respect to α^2 . I is a function of the incident energy so the procedure must be followed for each energy value at which the cross section is required.

REFERENCES

- BATES, D. R., and DALGARNO, A., 1952, *Proc. Phys. Soc. A*, **65**, 919; 1953, *Ibid.*, **66**, 972.
 BATES, D. R., FUNDAMINSKY, A., LEECH, J. W., and MASSEY, H. S. W., 1950, *Phil. Trans. Roy. Soc. A*, **243**, 93.
 BRANSDEN, B. H., 1954, *Phys. Rev.*, **94**, 726.
 BRINKMAN, H. C., and KRAMERS, H. A., 1930, *Proc. Acad. Sci. Amst.*, **33**, 973.
 CORINALDESI, E., and TRAINOR, L., 1952, *Nuovo Cim.*, **9**, 940.
 DALGARNO, A., and YADAV, H. N., 1953, *Proc. Phys. Soc. A*, **66**, 173.
 EDWARDS, S. F., 1952, *Proc. Camb. Phil. Soc.*, **48**, 652.
 FEYNMAN, R. P., 1949, *Phys. Rev.*, **76**, 769.
 GARSTANG, R. H., 1952, *Phys. Rev.*, **87**, 495.
 JACKSON, J. D., and SCHIFF, H., 1953, *Phys. Rev.*, **89**, 359.
 KEENE, J. P., 1949, *Phil. Mag.*, **40**, 369.
 MASSEY, H. S. W., and BURHOP, E. H. S., 1952, *Electronic and Ionic Impact Phenomena* (Oxford: University Press).
 MASSEY, H. S. W., and SMITH, R. A., 1933, *Proc. Roy. Soc. A*, **142**, 142.
 MEYER, H., 1937, *Ann. Phys. Lpz.*, **30**, 635.
 MOTT, N. F., and MASSEY, H. S. W., 1949, *The Theory of Atomic Collisions*, 2nd Edn (Oxford: University Press).
 OPPENHEIMER, J. R., 1928, *Phys. Rev.*, **31**, 349.
 RIBE, F., 1951, *Phys. Rev.*, **83**, 1217.
 SCHIFF, L. I., 1949, *Quantum Mechanics* (New York: McGraw Hill).
 SCHNITZER, E., 1953, *Phys. Rev.*, **89**, 1237.
 SMITH, R. A., 1934, *Proc. Camb. Phil. Soc.*, **30**, 514.
 TAKAYANAGI, K., 1952, *Sci. Rep. Saitama Univ.*, **1**, 9.
 WATSON, E. N., 1944, *Theory of Bessel Functions*, 2nd Edn (Cambridge: University Press).

The Elastic Scattering of Electrons by the Excited 2s and 2p States of Atomic Hydrogen

By P. SWAN†

University College, London

Communicated by H. S. W. Massey ; MS. received 1st June 1954

Abstract. The elastic scattering of electrons by H2s and H2p has been evaluated in the electron energy range 3–100 ev, the approximate method of Länger being used for large scattering phase-shifts and Born's approximation for the small phases corresponding to large values of the orbital angular momentum l .

The total elastic cross sections for H2s and H2p are much larger than for the ground state H1s even at the lowest energy considered, the interpretation being that the long tails of the H2s and H2p potentials make the partial cross sections for waves of higher orbital angular momentum l very important compared with the partial S cross section.

The effect of electron exchange is small even at 3 electron volts energy, an increase in cross section of 8% resulting from its inclusion, so that its effect has been neglected at higher energies.

§ 1. INTRODUCTION

THE concentration of excited states in an ionized gas can become comparable with the concentration of normal atoms. It is therefore possible for elastic collisions with excited atoms to increase the total momentum transfer cross section and thereby reduce the electron mobility. This paper is concerned with the calculation of the elastic scattering cross section for the 2s and 2p states of excited atomic hydrogen.

In connection with the collisions of electrons with atomic hydrogen, calculations have been carried out for elastic scattering by H1s by Morse and Allis (1933) and Massey and Moiseiwitsch (1951), using iterative procedures and the variational methods of Hulthén and Kohn respectively. Exchange has been included but only S-waves have been taken into account, as use of the Born approximation shows that contributions to the total cross section from waves of higher orbital angular momentum l are small. Thus even at the relatively high energy of 100 ev, where the effect of P and D waves should be most obvious, the Born approximation total cross section neglecting exchange is only $0.458 \times 10^{-16} \text{ cm}^2$ as compared to an accurate partial S cross section of $0.359 \times 10^{-16} \text{ cm}^2$. The small effect of the P and D waves may be attributed to the absence of an appreciable tail to the H1s interaction potential:

$$V_0(r) = -\left(\frac{1}{r} + 1\right)e^{-2r}. \quad \dots\dots(1)$$

Atomic units are used throughout.

* Now at Physics Department, Melbourne University, Melbourne, Australia.

The partial cross section σ_l for waves of orbital angular momentum l are given by

$$\sigma_l = (2l+1) \sin^2 \eta_l \quad \dots\dots(2)$$

where

$$\sin \eta_l = - \int_0^\infty r V(r) j_{l+1/2}(kr) f_l(r) dr. \quad \dots\dots(3)$$

k is the wave number of the incident electron, $j_l(kr)$ is the spherical Bessel function, and $f_l(r)$ is the scattering solution to the wave equation describing the scattering of electrons by the H1s potential (1), exchange being neglected.

For r small

$$kr j_l(kr) \sim r^{l+1}, f_l(r) \sim r^{l+1},$$

but for $r \rightarrow \infty$,

$$kr j_l(kr) \sim \sin(kr - \frac{1}{2}l\pi), \quad f_l(r) \sim \sin(kr - \frac{1}{2}l\pi + \eta_l).$$

Thus for r small the integrand in equation (3) becomes rapidly smaller as l is increased, but for r large its magnitude depends on the size of the tail of $V(r)$.

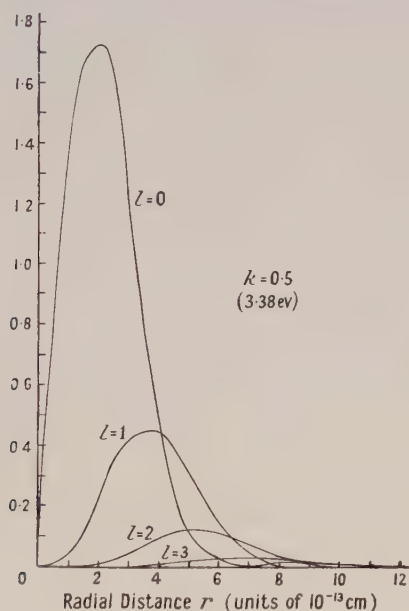


Figure 1. $-2r^2 j_l^2(kr) V(r)$ as a function of radial distance r , where $j_l(x)$ is the spherical Bessel function and $V(r)$ is the interaction potential between H2s and an incident electron,

$$V(r) = - \left(\frac{1}{r} + 0.75 + \frac{r}{4} + \frac{r^2}{8} \right) e^{-r}.$$

The area under each curve is equal to η_l/k in the Born approximation, where the wave number $k=0.5$ is in atomic units and η_l is the scattering phase.

Hence for the short-range H1s potential (1) with an asymptotic form for large r of e^{-2r} , η_l and σ_l are negligible for P, D and higher order interactions. However a potential asymptotic to $r^2 e^{-r}$ may result in large P and D phases even at energies of a few electron volts. This is illustrated in figure 1, where the integrand of (3), approximated by $-2r^2 j_l^2(kr) V(r)$ is plotted against r for the H2s potential

$$V(r) = - \left(\frac{1}{r} + \frac{3}{4} + \frac{1}{4}r + \frac{1}{8}r^2 \right) e^{-r} \quad \dots\dots(4)$$

for incident electron energies of 3.3823 eV ($k=0.5$) and 100 eV ($k=2.7187$).

In the Born approximation the area under each curve may be equated to the corresponding phase η_l assumed small, so that (4) leads to much larger scattering phases and partial cross sections than (1).

Further calculations have been performed by Erskine and Massey (1952) on the impact excitation of H2s by electrons, using distorted waves as determined by Hulthén's variational method with allowance for exchange. As this work takes account of incident S wave electrons only, it appears possible that the inclusion of P, D and higher waves will appreciably increase the excitation cross sections.

§ 2. DERIVATION OF THE WAVE EQUATION

In atomic units the appropriate wave equation describing a hydrogen atom plus an incident electron is

$$\left[\nabla_1^2 + \nabla_2^2 + \left(k^2 + 2E_1 + \frac{2}{r_1} + \frac{2}{r_2} - \frac{2}{r_{12}} \right) \right] \Psi = 0, \quad \dots\dots(5)$$

where the total wave function Ψ is given for singlet and triplet scattering respectively by the forms

$$\Psi = \phi(r_1)F(r_2) \pm \phi(r_2)F(r_1). \quad \dots\dots(6)$$

$\phi(r)$ is the wave function of the 2s or 2p state of atomic hydrogen, $F(r)$ is the scattering wave function, and E_1 is the energy of H2s or H2p. The ground state equations for H2s or H2p are given by

$$\left(\nabla^2 + 2E_1 + \frac{2}{r} \right) \phi(r) = 0. \quad \dots\dots(7)$$

From (5), (6) and (7), and employing Green's theorem, one obtains finally

$$[\nabla^2 + k^2 - 2V_{11}(r)]F(\mathbf{r}) \pm \int_0^\infty K_{11}(\mathbf{r}, \mathbf{r}')F(\mathbf{r}')d\mathbf{r}' = 0 \quad \dots\dots(8)$$

where

$$K_{11}(\mathbf{r}, \mathbf{r}') = \left(k_1^2 - \frac{2}{r_{12}} \right) \phi^*(\mathbf{r}')\phi(\mathbf{r}), \quad V_{11}(r) = \int \left(\frac{1}{r_{12}} - \frac{1}{r} \right) \phi^*(\mathbf{r}')\phi(\mathbf{r})d\mathbf{r}', \quad k_1^2 = k^2 - 2E_1. \quad \dots\dots(9)$$

To reduce (8) to radial form we make the usual expansions in terms of spherical harmonics:

$$F(\mathbf{r}) = \frac{1}{r} \sum_l f_l(r) P_l(\cos \theta), \quad K(\mathbf{r}, \mathbf{r}') = \sum_l \frac{(2l+1)}{4\pi r r'} P_l(\cos \vartheta) K_{11}^l(r, r') \quad \dots\dots(10)$$

where

$$K_{11}^l(r, r') = 2\pi r r' \int_0^\pi P_l(\cos \vartheta) \sin \vartheta d\vartheta K(\mathbf{r}, \mathbf{r}'). \quad \dots\dots(11)$$

One thus obtains:

$$\left[\frac{d^2}{dr^2} + k^2 - \frac{l(l+1)}{r^2} - 2V_{11}(r) \right] f_l(r) \pm \int_0^\infty K_{11}^l(r, r') f_l(r') dr' = 0. \quad \dots\dots(12)$$

§ 3. FIELD FOR ELECTRON INTERACTION WITH H2s

The wave function for the 2s state is $\phi(r) = (r-2)e^{-r/2}$; the potential $V_{11}(r)$ is then

$$V_{11}(r) = -\left(\frac{1}{r} + \frac{3}{4} + \frac{1}{4}r + \frac{1}{8}r^2 \right) e^{-r}. \quad \dots\dots(13)$$

The corresponding kernels for S and P wave scattering are

$$\begin{aligned} K_{11}^0(r, r') &= \frac{1}{8} r r' (r-2)(r'-2) e^{-(r+r')/2} [k_1^2 - 2\gamma_0(r, r')], \\ K_{11}'(r, r') &= -\frac{1}{12} r r' (r-2)(r'-2) e^{-(r+r')/2} \gamma_1(r, r'), \end{aligned} \quad \dots\dots (14)$$

where

$$\begin{aligned} \gamma_n(r, r') &= r^n / r'^{n+1} \quad (r > r') \\ &= r^n / r'^{n+1} \quad (r < r'). \end{aligned} \quad \dots\dots (15)$$

§ 4. SPHERICALLY SYMMETRICAL FIELD FOR ELECTRON INTERACTION WITH H2p

The wave functions of the 2p state comprise

$$\phi_1(\mathbf{r}) = r \sin \theta e^{i\phi} e^{-r/2}, \quad \phi_{-1}(\mathbf{r}) = r \sin \theta e^{-i\phi} e^{-r/2}, \quad \phi_0(\mathbf{r}) = r \cos \theta e^{-r/2},$$

corresponding to the magnetic quantum numbers $m=1, -1, 0$ respectively. The potentials and kernels derived from these are not spherically symmetrical, but depend on the angular coordinate θ of the iteration parameter. Thus one finds:

$$\begin{aligned} m = \pm 1, \quad V_{11}(r) &= -\left(\frac{1}{r} + \frac{3}{4} + \frac{1}{4}r + \frac{1}{24}r^2\right) e^{-r} \\ &\quad - \left[\frac{6}{r^3} - \left(\frac{6}{r^3} + \frac{6}{r^2} + \frac{3}{r} + 1 + \frac{1}{4}r + \frac{1}{24}r^2\right) e^{-r}\right] P_2(\cos \theta), \\ m = 0, \quad V_{11}(r) &= -\left(\frac{1}{r} + \frac{3}{4} + \frac{1}{4}r + \frac{1}{24}r^2\right) e^{-r} \\ &\quad + \left[\frac{12}{r^3} - \left(\frac{12}{r^3} + \frac{12}{r^2} + \frac{6}{r} + 2 + \frac{1}{2}r + \frac{1}{12}r^2\right) e^{-r}\right] P_2(\cos \theta), \\ m = \pm 1, \quad K_{11}^0(r, r') &= \frac{1}{24} r^2 r'^2 e^{-(r+r')/2} \left[k^2 - 2\gamma_0(r, r') + \frac{2}{5} \gamma_2(r, r') P_2(\cos \theta)\right], \\ m = 0, \quad K_{11}^0(r, r') &= \frac{1}{24} r^2 r'^2 e^{-(r+r')/2} \left[k^2 - 2\gamma_0(r, r') - \frac{4}{5} \gamma_2(r, r') P_2(\cos \theta)\right], \\ m = \pm 1, \quad K_{11}'(r, r') &= -\left[\frac{1}{60} \gamma_1(r, r') \cos \theta\right. \\ &\quad \left.+ \frac{1}{560} \gamma_3(r, r') (3 - 2 \cos^2 \theta) \cos \theta\right] r^2 r'^2 e^{-(r+r')/2}, \\ m = 0, \quad K_{11}'(r, r') &= -\left[\frac{1}{15} \gamma_1(r, r') \cos \theta\right. \\ &\quad \left.- \frac{1}{280} \gamma_3(r, r') (3 - 2 \cos^2 \theta) \cos \theta\right] r^2 r'^2 e^{-(r+r')/2}. \end{aligned} \quad \dots\dots (16)$$

Following McDougall (1932), one may find a spherically symmetric average field for H2p by assuming the distribution

$$\phi^* \phi = \frac{1}{3} (\phi_1^* \phi_1 + \phi_{-1}^* \phi_{-1} + \phi_0^* \phi_0). \quad \dots\dots (17)$$

From (16) and (17) average potentials and kernels are found:

$$V_{11}(r) = -\left(\frac{1}{r} + \frac{3}{4} + \frac{1}{4}r + \frac{1}{24}r^2\right) e^{-r}, \quad \dots\dots (18)$$

$$K_{11}^0(r, r') = \frac{1}{24} r^2 r'^2 e^{-(r+r')/2} [k^2 - 2\gamma_0(r, r')],$$

$$K_{11}'(r, r') = -\frac{1}{30} r^2 r'^2 e^{-(r+r')/2} \gamma_1(r, r') P_1(\cos \theta). \quad \dots\dots (19)$$

Spherical symmetry is thus obtained for $V_{11}(r)$ and $K_{11}^0(r, r')$, but $K_{11}'(r, r')$ and in fact kernels for $l \geq 1$ remain unsymmetrical; thus exchange cannot easily be taken into account for collisions of electrons with H2p except for S-wave scattering. Both the 2s potential (13) and the 2p potential (18) are very much larger than the ground state potential, but the 2s potential possesses a larger tail than the 2p potential, so that the cross section for the former should be rather larger than for the latter.

§ 5. EVALUATION OF THE SCATTERING

A few $l=0$ phase-shifts for the scattering of electrons by H2s have been given by Erskine and Massey (1952). The calculations are in the energy range 3.4–74.4 eV and are carried out both with and without exchange, the variational methods of Hulthén and Kohn being employed. Calculations were extended by the writer up to 100 eV energy with the variational method, but it soon became apparent that Hulthén's method, already complicated for $l=0$ scattering, becomes more and more impractical for higher l . The alternative of evaluating the phase-shifts by numerical integration is not useful either, because the long range of the potential fields (13) and (18) means that even at energies of a few electron volts the wave function has a number of nodes within the field range, so that a large number of steps, actually approaching 100, must be taken in the numerical integration. The inclusion of exchange would make the work very tedious indeed.

The practical method chosen to find the phase-shifts was Länger's approximation (1937), exchange being neglected:

$$\eta_l = \int_{r_1}^{\infty} [k^2 - 2V_{11}(r) - (l + \frac{1}{2})^2/r^2]^{1/2} dr - \int_{r_0}^{\infty} [k^2 - (l + \frac{1}{2})^2/r^2]^{1/2} dr, \dots (20)$$

where r_1 and r_0 are the zeros of the integrands respectively. Take R as some large value of r at which the two integrands of (20) are effectively equal; then (20) becomes

$$\begin{aligned} \eta_l = \frac{1}{4}\pi + \frac{1}{2}l\pi - \left[k^2 - \frac{(l + \frac{1}{2})^2}{R^2} \right]^{1/2} R - (l + \frac{1}{2}) \sin^{-1} \left(\frac{l + \frac{1}{2}}{kR} \right) \\ + \int_{r_1}^R \left[k^2 - 2V_{11}(r) - \frac{(l + \frac{1}{2})^2}{r^2} \right]^{1/2} dr. \dots (21) \end{aligned}$$

The expressions (20) or (21) are formally valid when the phase-shifts are not small, provided the potential is large and does not vary much in a wavelength. The latter condition excludes the treatment of collisions with energies of less than several electron volts, in which region the method fails. A comparison of the S-wave phases for electron scattering by H2s obtained by Hulthén's variational method, Länger's approximation and numerical integration is given in table 1. With the exception of the values at 70 eV and 100 eV the results obtained by Hulthén's method and numerical integration are taken from a table due to Erskine and Massey (1952). Exchange is neglected. Within the energy range 3–100 eV Länger's approximation gives 2–4% accuracy, but at lower energies leads to too large a value as one knows the phase at zero energy to be an integral multiple of π , clearly π in this case.

Table 2 shows the dependence of phase-shift η_l on orbital angular momentum l at six electron energies in the range 3–100 eV for collisions with H2s and H2p.

The higher order phases were evaluated even when very small, as the $(2l+1)$ weighting factor in the partial cross section expression (2) can render their contributions to the total cross section appreciable.

Table 1. Phase-shifts η_0 calculated by Hulthén's variational method, numerical integration and Länger's approximation for H2s

Electron energy (ev)	Electron wave number (atomic units)	Hulthén's method	Länger's approximation	Numerical integration
0.0338	0.050	—	4.179	—
0.541	0.200	—	3.621	—
3.382	0.500	2.745	2.800	2.709
9.343	0.831	2.219	2.274	2.210
20.302	1.225	1.812	1.861	1.819
43.980	1.803	1.438	1.486	1.426
70	2.2746	1.236	1.269	—
74.396	2.345	1.213	—	1.169
100	2.7187	1.088	1.135	—

Table 3 shows the total cross section σ for elastic collision of electrons with H2s and H2p together with the S-wave partial cross sections σ_0 and the Born approximation total cross sections σ (B.O.) as found from

$$\sigma(\text{B.O.}) = 2\pi \int_0^\pi |f(\theta)|^2 \sin \theta d\theta$$

where

$$f(\theta) = - \int_0^\infty \frac{\sin kr}{kr} 2V_{11}(r)r^2 dr. \quad \dots\dots(22)$$

It is clear that the S-wave partial cross section is a very bad underestimate of the scattering at all energies considered, although in the vicinity of zero energy it must approach in magnitude the total cross section. The Born approximation cross section becomes a reasonable estimate above an electron energy of about 50 ev ($k \sim 2$); at 3.4 ev it is 2.5 times too large but at 100 ev is only 1.06 times the correct figure for scattering by H2s. The corresponding ratios for H2p are 2.2 and 1.16 at 3.4 ev and 100 ev respectively. Figure 2 shows the cross sections found by Länger's method and the Born approximation plotted against k , together with the cross section for scattering by H1s.

The effect of electron exchange has not so far been taken into account. Erskine and Massey (1952) have treated it as regards the S-wave collisions with H2s, finding it to be appreciable only at low energies of the order several electron volts and decreasing with electron energy. As the contribution of exchange as represented by the integral term in (12),

$$\pm \int_0^\infty K_{11}^l(r, r') f_l(r') dr', \quad \dots\dots(23)$$

is velocity dependent, this effect might be expected; actually Fundaminsky (1949) has shown exchange effects to fall off with increase of energy in the Born approximation.

For an electron wave with orbital angular momentum l it is clear on physical grounds that exchange decreases in importance for increasing l as it takes place within a limited distance of the atom whereas the interaction distance increases

Table 2. Phase-shifts η_l tabulated against orbital angular momentum l and electron wave number k for H2s and H2p

l	$k=0.500$		$k=0.831$		$k=1.213$	
	2s	2p	2s	2p	2s	2p
0	2.8002	2.8054	2.2738	2.0897	1.8611	1.7322
1	1.2262	1.0481	1.0565	1.0125	0.8989	0.9432
2	0.3756	0.1880	0.4850	0.4403	0.6755	0.5159
3	0.0645	0.0305	0.2760	0.1592	0.4450	0.3250
4	0.0068	0.0030	0.1345	0.0662	0.2572	0.1908
5			0.0519	0.0252	0.1590	0.1130
6			0.0019		0.0801	0.0441
7					0.0450*	0.0130
8					0.0256	
9					0.0156*	
10					0.0074	
11					0.0022	
l	$k=1.803$		$k=2.2746$		$k=2.7187$	
	2s	2p	2s	2p	2s	2p
0	1.4858	1.3593	1.2694	1.1988	1.1353	1.0487
1	0.8250	0.9441	0.7770	0.8700	0.7461	0.8459
2	0.6364	0.4863	0.5970	0.3652	0.5687	0.4017
3	0.4620	0.3250	0.4370	0.2650	0.4150	0.3210
4	0.3000	0.2289	0.3101	0.2017	0.3193	0.2582
5	0.2180	0.1760	0.2490	0.1570	0.2700	0.2090
6	0.1610	0.1440	0.1981	0.1229	0.2376	0.1652
7	0.1135*	0.0840	0.1600*	0.1013*	0.1902	0.1245*
8	0.0673	0.0518	0.1285	0.0818	0.1502	0.1009
9	0.0513*	0.0325	0.1000*	0.0604*	0.1184	0.0806*
10	0.0390	0.0180	0.0769	0.0438	0.0958	0.0603
11	0.0293*	0.0108	0.0560*	0.0309*	0.0765	0.0460*
12	0.0202*	0.0061	0.0387*	0.0220*	0.0614	0.0365
13	0.0121		0.0281*	0.0156	0.0480	0.0300*
14	0.0060*		0.0207	0.0107	0.0379*	0.0243*
15	0.0019		0.0150*	0.0080*	0.0291*	0.0196
16			0.0110*	0.0058*	0.0219*	0.0149*
17			0.0080	0.0039*	0.0163	0.0106*
18			0.0058	0.0029	0.0124	0.0065
19			0.0045*	0.0023*	0.0095*	0.0050*
20			0.0035*	0.0018*	0.0074*	0.0030*
21			0.0029	0.0014	0.0059*	0.0022
22			0.0021		0.0045	
23			0.0019*		0.0036	
24			0.0014		0.0027*	
25			0.0011		0.0020*	
26					0.0015	

* The values in heavy type were found using Langer's approximation, the rest either by Born's approximation (valid for small phases) or in, the case of asterisked values, by graphical interpolation.

with l . For $r, r' \rightarrow 0$ one may show the radial dependence of $K_{11}^l(r, r')$ in (23) to be

$$K_{11}^l(r, r') \sim r^{l+1} r'^{l+1} \gamma_l(r, r')$$

and

$$f_l(r) \sim r^{l+1}, \quad \dots\dots\dots (24)$$

Table 3. Cross sections σ_0 for S-wave scattering by H2s and H2p, total cross sections σ , and Born approximation total cross sections $\sigma(\text{B.O.})$ as a function of wave number k , in units of 10^{-16} cm^2

k	Electron collisions with H2s			Electron collisions with H2p		
	σ_0	σ	$\sigma(\text{B.O.})$	σ_0	σ	$\sigma(\text{B.O.})$
0.500	1.584	49.05	123.59	1.537	35.92	79.12
0.831	2.977	32.27	48.03	3.856	20.64	32.05
1.213	2.330	15.04	24.33	2.338	12.86	18.44
1.803	1.079	8.463	11.109	1.038	6.500	7.412
2.2746	0.6224	5.707	6.733	0.5456	3.406	4.923
2.7187	0.3928	4.262	4.530	0.3586	2.895	3.349

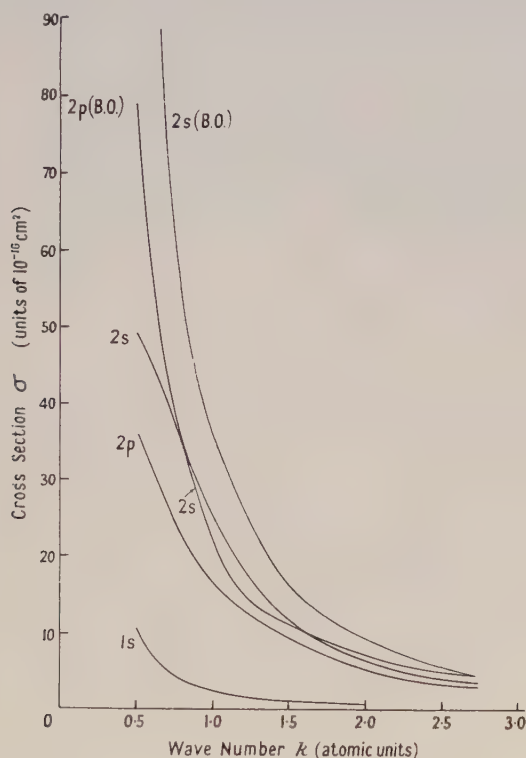


Figure 2. Cross sections in units of 10^{-16} cm^2 for the elastic scattering of electrons by H2s and H2p as calculated using Langer's approximation and Born's approximation (B.O.) respectively and of electrons by H1s. $k^2=1$ corresponds to an electron energy of 13.529 eV.

As the kernel falls off exponentially with r and r' , then the contribution to (23) must come chiefly from the region of small r' , so that the importance of the exchange term (23) falls off rapidly with increasing l . In practice this means that only the S and P phases need be corrected for exchange.

This was done for the S and P wave scattering by H2s for a wave number $k=0.5$. The wave equation (12) was first solved without exchange by numerical integration, and the effect of exchange included by an iteration process. The results obtained for the non-exchange, singlet (symmetric) and triplet (anti-symmetric) scattering are given in table 4.

Table 4. Non-exchange, singlet and triplet scattering phases η_l and partial cross sections σ_l (units of 10^{-16} cm²) for electron scattering by H2s at $k=0.5$ (3.38 ev)

l	Non-exchange		Singlet		Triplet	
	η_l	σ_l	η_l	σ_l	η_l	σ_l
0	2.768	6.695	2.451	20.40	3.114	0.0382
1	1.2262	133.56	1.270	137.56	1.5778	150.79
2	0.3756	33.82	0.3756	33.82	0.3756	33.82

The effect of exchange is included for $l=0, 1$ but neglected for higher l , where it will make only a small correction to already relatively small partial cross sections.

Taking the total cross section as

$$\sigma = \frac{1}{4}\sigma_S + \frac{3}{4}\sigma_T \quad \dots\dots(25)$$

one finds an exchange cross section at 3.380 ev of 53.06×10^{-16} cm², as compared with a non-exchange value of 49.05×10^{-16} cm², so that exchange has increased σ by only 8.2%. In view of the previous argument, it therefore appears justifiable to neglect exchange at higher energies for electron scattering by H2s, and also for the similar case of H2p.

Further calculations are being carried out on the elastic scattering of electrons by the 1s2s and 1s2p states of helium.

ACKNOWLEDGMENT

I would like to thank Professor H. S. W. Massey for the interest he has taken throughout the work.

REFERENCES

- ERSKINE, G. A., and MASSEY, H. S. W., 1952, *Proc. Roy. Soc. A*, **212**, 521.
 FUNDAMINSKY, A., 1949, *Ph.D. Thesis*, University of London.
 LÄNGER, R., 1937, *Phys. Rev.*, **51**, 669.
 MASSEY, H. S. W., and MOISEWITSCH, B. L., 1951, *Proc. Roy. Soc. A*, **205**, 483.
 MCDUGALL, J., 1932, *Proc. Camb. Phil. Soc.*, **28**, 341.
 MORSE, P. M., and ALLIS, W. P., 1933, *Phys. Rev.*, **44**, 269.

A Cloud Chamber Study of some Aspects of the Geiger Discharge*

By P. J. CAMPION†

Clarendon Laboratory, Oxford

MS. received 23rd July 1954

Abstract. An expansion type cloud chamber controlled by an internal counter has been used to study the discharge formed in the latter when operated in the Geiger and transitional regions. Both ethyl and iso-amyl alcohols have been used at their saturation vapour pressures as the combined condensant and quenching agent, together with argon or helium at various total pressures below one atmosphere. Significant differences in the behaviour of the counter are observed for the two alcohols, which can be attributed to the difference in the proportion of quenching agents in the two cases. The photographic evidence shown supports the accepted theory of Geiger counter operation.

§ 1. INTRODUCTION

THE control of the expansion of a Wilson chamber by means of an internal counter has been reported by Hodson, Loria and Ryder (1950) and by Cohen (1951). The former authors have demonstrated the use of the device for the observation of the proportional discharge, and Fireman and McHaney (1950) have made use of the Geiger discharge although their experimental arrangement did not permit of its observation.

In adapting this type of chamber to detect internal pair formation (Campion and Davies 1954) we have taken the opportunity to extend the work of Hodson *et al.* to the study of the discharge produced in the internal counter when operated in the Geiger and transitional regions.

§ 2. THE APPARATUS

The counter anode consisted of a fine platinum wire (0.05 mm radius) mounted along a diameter of the glass ring of the cloud chamber, in a manner similar to that described by Hodson *et al.* In some experiments the anode was surrounded by a hexagonal arrangement of wires forming an open cage cathode assembly, while for experiments involving photometric analysis of the discharge this cage was removed. In the latter case the clearing field wires situated just below the roof of the chamber were earthed.

The chamber was 22 cm in diameter by 6 cm deep and was actuated by a main valve based on a design by Chu and Valley (1948). The time delay between the passage of an ionizing particle which triggered the counter and the occurrence of supersaturation was approximately 10 msec. Since it was not practicable to

* Part of the material here presented formed a paper read by the author before the conference on Ionization Phenomena in Discharges, held at Oxford, June 1953.

† Now at Atomic Energy of Canada Ltd., Chalk River, Ontario.

bake out the cloud chamber in order to remove adsorbed impurities, the chamber was pumped out for several hours before filling. Ethyl or iso-amyl alcohol was used as the condensant and argon or helium as the gas filling at various total pressures below one atmosphere. Commercially available gases were considered to be sufficiently free from electronegative impurities for the work, but as a precaution against the possible presence of water or oil vapours the gas selected was passed through a coil of copper tubing immersed in liquid air before entering the chamber. The alcohols were dried by standard methods and redistilled before use.

Pulses from the counter anode were fed into an amplifier-discriminator circuit, and thence to a gate which transmitted pulses only when the chamber had completed its cleaning cycle and was ready for a main expansion. A pulse selected by these circuits was used to initiate the following events: (a) remove the e.h.t. from the counter, (b) to trigger the main valve release circuit, and (c) to remove the general clearing field (approximately 50 v cm^{-1}) from across the chamber.

The minimum time required for the completion of (a) from the instant of an ionizing event in the counters was about $1 \mu\text{sec}$. This represented the delay inherent in the valve circuits. The removal of the e.h.t. could be further delayed by known amounts by means of a calibrated delay line for short delays ($1 \mu\text{sec}$), or by univibrator circuits for delays up to 15 msec.

§ 3. EXPERIMENTAL RESULTS

3.1. *The Normal Geiger Discharge*

In Plate I(a) we show a typical Geiger discharge in an argon and ethyl alcohol (saturation vapour pressure $\sim 40 \text{ mm Hg}$) mixture at a total pressure of 60 cm Hg. The e.h.t. (2340 v) was removed within $3 \mu\text{sec}$ after the receipt of the pulse and the discharge has spread the whole length of the counter. The discharge is confined to a region very close to the wire and is uneven. This was characteristic of discharges taken with ethyl alcohol as the quenching agent and may be due to statistical fluctuations in the density of the ion sheath. The triggering electron in Plate I(a) can just be observed. The track of the initiating particle is not always visible in the succeeding plates since a light beam only 5 mm in depth was used and the track may therefore not be illuminated.

Plate I(b) shows the effect of delaying the removal of the e.h.t. across the counter. Here the voltage remained on for 5.8 msec, and it is seen that the discharge has travelled out radially under the influence of the electric field. A discharge which occurred prior to the opening of the gate is also visible on the photograph. The object marked A in Plate I(a), and visible in some succeeding plates is a holder for a weak polonium source. It is evident that the sheaths have a finite thickness, a point which will be discussed in more detail later.

Photographs of discharges in argon and iso-amyl alcohol (saturation vapour pressure 2 mm Hg) mixtures at the same total pressure are shown in Plates I(c) and (d). In Plate I(c) the e.h.t. was removed $3 \mu\text{sec}$ after the pulse whilst in Plate I(d) the removal was delayed by 13 msec. We observe that using iso-amyl alcohol the discharge is initially more uniform and occupies a somewhat greater volume. This indicates that the discharge propagating photons have a longer mean free path in this case, due mainly to the lower vapour pressure of the

quenching agent. The starting potential for Geiger action using iso-amyl alcohol was considerably less than that required for ethyl alcohol; and the e.h.t. applied across the counter in Plates I(c) and (d) was 1300 v.

An attempt was made to detect the 'giant' pulses observed by Curran and Rae (1947) and others, by suitably biasing the pulse height discriminator. A collimated beam of α -particles from a source in an earthed holder situated 5 cm from the counter wire was directed radially at the latter which in this case was surrounded by the cathode cage. The conditions were thought to be favourable for the production of giant pulses. However, the heights of pulses observed with this arrangement were uniform to within 20% and were indistinguishable from those produced by a γ -ray source. The photographs of discharges initiated by α -particles also showed them to be normal apart from somewhat enhanced beads of ionization at the point at which the particle traversed the counter. This is evidently due to the larger number of primary electrons reaching the wire but the increase in the ionization due to this cause must be small compared with the total ionization produced in the discharge. The photographs of Plate III were

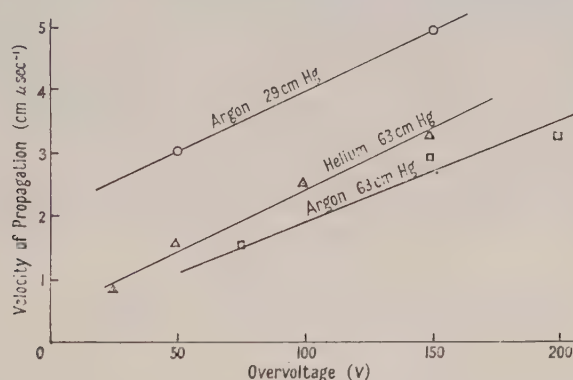


Figure 1. Velocity of propagation of Geiger discharges as a function of overvoltage.

taken with a similar experimental arrangement to that described in this paragraph but using a rather poorly collimated beam of α -particles. Although the counter was in fact operated in the transitional region (see § 3.6) the discharges show similar beads to those referred to here.

We must conclude, therefore, that favourable conditions for the production of giant pulses were not obtained and we are thus unable to comment on their mechanism.

3.2. The Velocity of Propagation of the Discharge

When the e.h.t. was removed with the minimum delay the Geiger discharges in argon and iso-amyl alcohol mixtures were observed to spread some 3 to 10 cm along the wire, depending on the overvoltage used. A calibrated delay line was introduced to increase the delay by known small amounts and hence using a difference technique, the velocity of propagation of the discharge could be determined.

The results using iso-amyl alcohol are shown in figure 1 where the measured velocity is plotted as a function of overvoltage for different total pressures and gas fillings. The values quoted for the overvoltage may appear to be high compared with the results of some other workers. This is due to the criterion

adopted for defining the Geiger threshold voltage, namely that voltage at which counts could just be detected by the recording system when adjusted for normal Geiger counting. This occurred at about 40 volts before that voltage at which the pulses became uniform in height. The experimental points represent the average velocity obtained from about ten measurements for each delay setting, although considerable fluctuations were observed in individual measurements. Similar fluctuations have been reported by Mortier and Roose (1954) and Saltzmann and Montgomery (1950) in measurements of the velocity of propagation using more conventional techniques. The method has not been applied to fillings using ethyl alcohol as the quenching agent, although an estimate made in the course of experiments using a fast quenching circuit described by Picard and Rogozinski (1953) is in agreement with the conclusions of the above workers that the velocity of propagation is much greater.

3.3. *The Ion Distribution within the Space Charge Sheath*

The fact that the positive ion space charge sheath has a significant width at least by the time it has travelled outwards a centimetre or so has been demonstrated in Plates I (b) and (d). Den Hartog and Muller (1949) and more recently Wilkinson (1952) have reached this conclusion from theoretical considerations. Wilkinson derives an expression for the time distribution of the number of ions arriving at a given point (the cathode). If we assume that we have radial geometry and that the space charge sheath is formed very close to the counter anode, it may be shown (see appendix) that the corresponding spatial distribution for the ion density, ρ , at any instant, within the boundaries of the sheath, is given by

$$\rho = 1/4\pi eKt \quad \dots\dots(1)$$

when e is the charge carried by an ion and K the mobility. Hence we see that at any time t after formation of the sheath ρ is independent of x so long as $x_1 > x > x_2$, where x_1, x_2 are the radii of the boundaries of the sheath. A rough qualitative check of this result was obtained by a photometric analysis of the negatives of such photographs as Plates I (b) and (d), having first determined the characteristic density-log (exposure) curve for the emulsion used. The method assumes that the amount of scattered light entering the camera is proportional to the ion density. Confirmation of the validity of this assumption is provided by the work of Bower (1938) on the distribution of ionization along an α -particle track. As a check on the optical system we have carried out a similar experiment with comparable results.

In these experiments the hexagonal open cage cathode was removed and the clearing field wires earthed. The counter could therefore be represented by a wire midway between two parallel earthed planes. However, if observations are confined to sheaths not far distant (about 1 cm) from the wire a cylindrical field distribution may be assumed as a good approximation. A shallow light beam of 5 mm depth was used in order to study that part of the sheath in the median plane. Neglecting the curvature of the boundaries of the sheath under these conditions it is evident from equation (1) that the expected distribution should be rectangular.

The results of some typical distributions obtained are shown in figures 2 and 3. The ordinates in both sets of distributions represent the amount of scattered light in arbitrary units and therefore, according to the above assumption, the ion

density within the illuminated portion of the space charge sheath. The full curves represent distributions obtained in an argon and ethyl alcohol mixture at a total pressure of 60 cm Hg and the broken curves those obtained using an argon and iso-amyl alcohol mixture at the same total pressure. The distributions shown in figure 2 were obtained using a delay of 2.65 msec; those in figure 3 with a delay of 13 msec (broken curve) and 14.2 msec (full curve). Strictly, therefore, the distributions in figure 3 cannot be assumed to occur under conditions of radial geometry. They are included however since they illustrate the difference between the two argon-alcohol mixtures even more markedly than those in figure 2.

In the argon and ethyl alcohol mixture the distribution has almost the expected shape. In this present discussion the motion of the sheath during the expansion time of the chamber, when the counter anode is effectively earthed, has been neglected. It has been shown (Campion 1954) that during this time the trailing edge remains practically stationary, under the conditions of the present experiment,

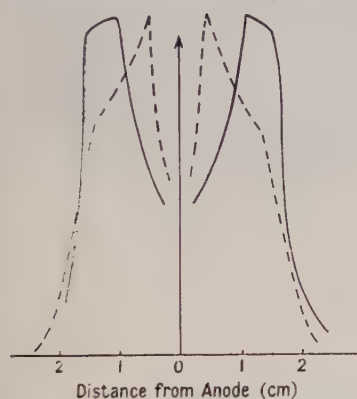


Figure 2. The ion density within the space charge sheath at a time 2.65 msec after formation, as a function of radial distance from the anode.

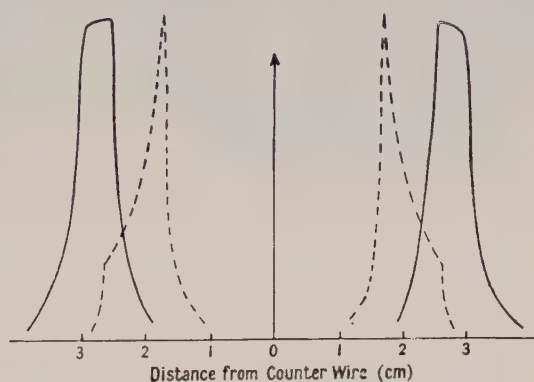


Figure 3. The ion density within the space charge sheath at approximately 13.5 msec after formation, as a function of radial distance from the anode.

whilst the leading edge continues to expand under the influence of the space charge behind it, but in opposition to the induced charge on the wire. This expansion may account qualitatively at least for the slight deviation from a true rectangular distribution towards the leading edge. For iso-amyl alcohol the distribution is definitely not rectangular, having a sharp peak at the trailing edge of the sheath. The difference may be explained in terms of the dependence of the initial distribution of ionization on the mean free path of the discharge propagating photons. In the case of ethyl alcohol, where the proportion of quenching agent is high, the mean free path is probably of the order of the critical radius (viz. that radius at which appreciable multiplication sets in), and the ionization is therefore confined to a small volume of radius a few times that of the wire. With iso-amyl alcohol the mean free path is much greater owing to its lower saturation vapour pressure, and the initial distribution can no longer be regarded as concentrated in an infinitely thin cylinder as is assumed in the derivation of equation (1) but must, owing to the weaker photon absorption, extend some distance beyond the critical radius.

3.4. Beaded Counters

The effect of beads placed on the anode of the counter was investigated to see if by this means the Geiger discharge could be limited, with a view to the possible use of a segmented counter as a coincidence arrangement to detect electron-positron pairs. By feeding the output of the counter-amplifier system into a pulse height discriminator set to record the simultaneous discharge of two or more segments it was hoped to record coincident particles. In order to determine the size of bead required to arrest the discharge five glass beads increasing in diameter from 1.25 mm to 4.93 mm were sealed on to the wire at equal intervals, thus forming the segmented counter. A weak polonium source was placed opposite the first segment and the chamber filled with argon and iso-amyl alcohol at 60 cm Hg. A short run revealed that the discharge was stopped only by the largest bead, Plate II (a). A similar run using argon and ethyl alcohol at the same total pressure showed that in this case the discharge was limited by the smallest bead, Plate II (b). This of course confirms the supposition put forward earlier that the mean free path of the propagating photons is much longer in the iso-amyl alcohol case.

Although an experimental arrangement using a beaded Geiger counter showed two coincident discharges when a suitable bias was applied to the discriminator, it was not possible to detect pair particles owing to the relatively high frequency with which a single electron discharged two segments.

3.5. The Effect of Electric Wind

In order to remove any hairs or dust particles from the counter anode the wire was first cleaned with alcohol and then flashed *in situ* prior to filling the chamber. Despite this procedure electric wind discharges were occasionally observed and we now discuss the effect of this phenomenon on the Geiger discharge.

De Vries (1946) observes that no additional spurious discharges are produced if dust particles are placed on the wire or if the wire is deliberately beaten or puckered. Wilkinson (1950) comments that other workers find evidence to the contrary. However, no evidence was found in the present investigation to suggest that these point discharges gave rise to Geiger discharges. This negative result rests on more than 100 photographs in which the spread of the Geiger discharge was limited to a few cm by the rapid removal of the working voltage. If electric wind discharges give rise to a Geiger discharge one would expect the arrested Geiger discharge to centre around the electric wind point in an appreciable fraction of the photographs. This was not the case, the (arrested) discharges being distributed at random along the wire.

Several observations were made of the interaction between a Geiger discharge spreading along the anode and a point discharge. Depending on the magnitude of the point discharge and the overvoltage a Geiger discharge either passes the point or is stopped by it—the point thus acting as a bead.

It appeared that if a Geiger discharge at a low overvoltage was arrested by a point it might, under suitable conditions, allow the discharge to pass at higher voltages, there being an intermediate stage in which some discharges were arrested while others were not. Plate II (c) shows a Geiger discharge arrested by an electric



(b)



(d)

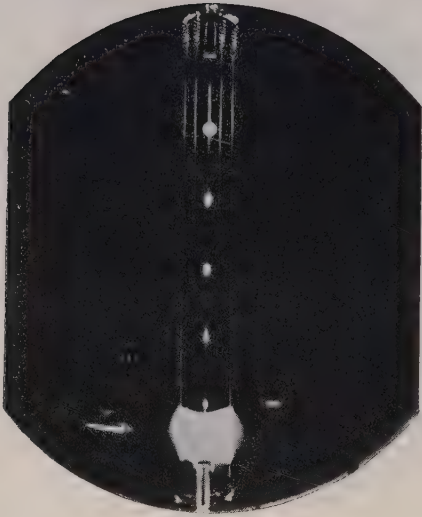


(a)



(c)

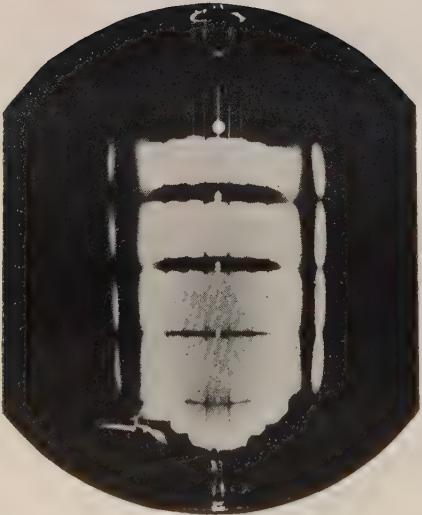
PLATE I.



(b)



(d)



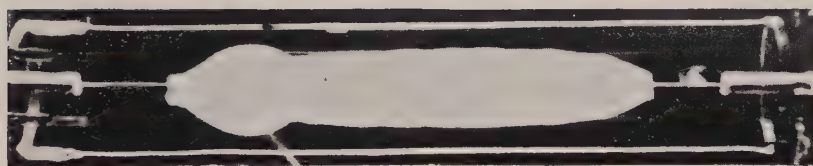
(a)



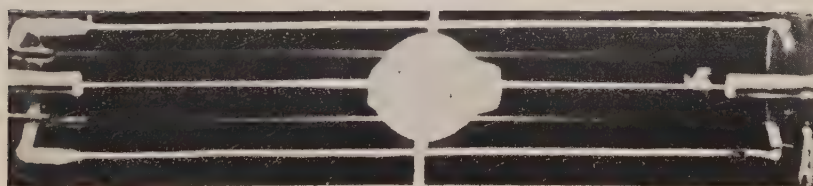
(c)



(a)



(b)



(c)

PLATE III.

wind point, whilst in Plate II (*d*), taken under the same conditions, the Geiger discharge has passed beyond the point leaving a characteristic spherical distortion in the discharge. This sphere may be explained in terms of a large concentration of positive ions created at the point. These ions then expand under their own self repulsion to form the observed sphere.

Discharges that are arrested by points give rise to pulses of reduced height. We have here therefore one explanation of the difference in pulse heights that is occasionally observed in some otherwise normal Geiger counters.

3.6. *The Transitional Region*

The type of discharge obtained when the internal counter is operated in the proportional region has been photographed by Hodson *et al.* (1950), and consists of a small bead of ionization localized around the point at which the triggering particle traverses the counter. As the e.h.t. across the counter was increased the bead, whilst still retaining a roughly spherical shape, was observed to grow in size owing to the greater amount of gas amplification, until a voltage was reached at which the discharge began to spread along the wire. Between this point (i.e. the end of the region of limited proportionality) and that at which the discharge travelled the whole length of the counter each time (i.e. the beginning of the Geiger region) there was a transitional region which extended for about 40 volts in the case of counters filled with iso-amyl alcohol and argon, and was characterized by large fluctuations in the spread of the discharge due to its statistical nature. Three photographs taken consecutively and under the same conditions are shown in Plate III (*a*), (*b*) and (*c*). In the first the discharge has spread more or less equally in both directions. The second shows that the discharge has spread mainly in one direction before being extinguished, and the third shows very little spread at all. The e.h.t. remained on the counter wire for 40 μ sec after the receipt of the pulse so that the discharges were not quenched externally.

Fenton and Fuller (1949) have previously noted the existence of such a transitional region, whilst Wilkinson (1950) has given a theoretical treatment for it. These authors attribute the region to the onset of avalanche breeding by photons resulting in a spread of the discharge along the wire and this is confirmed by the cloud chamber observations presented here.

§ 4. CONCLUSION

The observations presented here confirm the generally accepted theory of Geiger counter action. The cloud chamber makes it easier to visualize the operation of these counters, particularly those of the beaded type, and to study the behaviour of the space charge sheath subsequent to its formation. It provides a means of measuring the velocity of propagation of the discharge along the wire. Finally, from the observation of the behaviour of a Geiger discharge in the presence of point discharges, it suggests an explanation of the non-uniform pulse height sometimes obtained. Certain features still remain obscure, particularly the mechanism by which giant pulses are produced, and it is hoped that this phenomenon may, under suitable conditions, be observed in the cloud chamber and that this technique may aid the elucidation of this problem.

ACKNOWLEDGMENTS

The above work was carried out during the tenure of a grant from the Ministry of Education to whom the author is indebted. The author takes pleasure in thanking Dr. W. T. Davies for his continual interest and advice throughout the course of this work.

APPENDIX

For radial geometry, Wilkinson (1952) gives the fraction g of the sheath within a radius x at a time t as

$$t = \frac{(x^2 - r_1^2) \ln(r_2/r_1)}{2KV(1 + gm)}, \quad \dots\dots(1)$$

whence

$$\left(\frac{dg}{dx}\right)_t = \frac{x \ln(r_2/r_1)}{KVmt} \quad \dots\dots(2)$$

where r_1, r_2 are the radii of the internal and external electrodes of the counter, K the mobility of the ions, V the voltage on the wire and m is the ratio q/Q . q is the charge developed in the gas per unit length and Q is the charge on the wire per unit length required to maintain a voltage V across the counter, i.e. $Q = V/2 \ln(r_2/r_1)$. If $\rho(xt)$ is the ion density per unit volume at a radius x and time t , then by definition

$$g = \frac{1}{N} \int_{r_1}^x 2\pi x \rho(xt) dx$$

where N is the total number of ions in the sheath per unit length, i.e. $N = q/e$ where e is the charge on an ion. We have therefore

$$\left(\frac{dg}{dx}\right)_t = 2\pi x \rho / N \quad \dots\dots(3)$$

and equating (2) and (3) we find

$$\begin{aligned} \rho &= \frac{N \ln(r_2/r_1)}{2\pi K V m t} \\ &= 1/4\pi e K t \end{aligned}$$

which is a constant at any given instant. This result is dependent on the assumption, implicit in equation (1), that all the ions are born in an infinitely thin cylinder at the surface of the inner electrode.

REFERENCES

- BOWER, J. C., 1938, *Proc. Camb. Phil. Soc.*, **34**, 450.
 CAMPION, P. J., 1954, *Thesis*, University of Oxford.
 CAMPION, P. J., and DAVIES, W. T., 1954, *Proc. Phys. Soc. A*, **67**, 941.
 CHU, F. H., and VALLEY, G. E., 1948, *Rev. Sci. Instrum.*, **19**, 496.
 COHEN, M. J., 1951, *Rev. Sci. Instrum.*, **22**, 966.
 CURRAN, S. C., and RAE, E. R., 1947, *J. Sci. Instrum.*, **24**, 233.
 FENTON, A. G., and FULLER, E. W., 1949, *Proc. Phys. Soc. A*, **62**, 32.
 FIREMAN, E. L., and MCHANEY, G. M., 1950, *Rev. Sci. Instrum.*, **21**, 813.
 DEN HARTOG, H., and MULLER, F. A., 1949, *Physica*, **15**, 789.
 HODSON, A. L., LORIA, A., and RYDER, N. V., 1950, *Phil. Mag.*, **41**, 826.
 MORTIER, P. A. C., and ROOSE, J. F., 1954, *Proc. Phys. Soc. B*, **67**, 161.
 PICARD, E., and ROGOZINSKI, A., 1953, *J. Phys. Radium*, **14**, 304.
 SALTZMANN, H., and MONTGOMERY, C. G., 1950, *Rev. Sci. Instrum.*, **21**, 548.
 DE VRIES, H., 1946, *Physica*, **11**, 433.
 WILKINSON, D. H., 1950, *Ionization Chambers and Counters* (Cambridge : University Press); 1952, *Rev. Sci. Instrum.*, **23**, 463.

RESEARCH NOTES

Phase of Matrix Elements in Nuclear Reactions and Radioactive Decay

BY R. HUBY

Department of Theoretical Physics, The University of Liverpool

MS. received 18th August 1954

THE purpose of this note is to point out an error in the phase of matrix elements in nuclear reactions, which has been transmitted through several recent papers.

A formula for a differential cross section or an angular correlation contains, in addition to known 'geometrical' factors, certain unknown 'nuclear' factors such as scattering-matrix elements, reduced widths, or matrix elements of a perturbing Hamiltonian. The number of variable parameters on which these quantities depend can be reduced by the use of some general theorems, e.g. the unitarity and symmetry properties of the scattering matrix, the reality of reduced widths (Wigner and Eisenbud 1947), and the reality of decay matrix elements (e.g. Lloyd 1951). Most of these properties depend on invariance under time-reversal, and are only valid if the representation used is correctly phased. The principles involved are well known, but unfortunately the paper by Wigner and Eisenbud (1947), which has been taken as the basis of most later work on nuclear reactions, contains a slip in the normalization of the wave function. As a result, published formulae contain in principle errors of phase, which, however, cancel out in most cases of interest, but could sometimes lead to discrepancy with observable quantities.

The proofs of the theorems mentioned above involve applying the time-reversal operator K (Wigner, 1932) to an angular momentum eigenstate $|j, -m\rangle$. We have:

$$K|j, m\rangle = \alpha(j) i^{2m} |j, -m\rangle, \quad \dots\dots (1)$$

where $\alpha(j)$ can be varied by multiplying the vectors $|j, m\rangle$ by an arbitrary phase factor independent of m . It is desirable to choose $\alpha(j)$ so that the form of (1) is invariant under addition of angular momentum. That is, let us consider two separate state-spaces, with angular momenta (j_1, m_1) , (j_2, m_2) respectively, such that the combined system has eigenstates of total angular momentum (J, M) given by

$$|j_1, j_2, J, M\rangle = \sum_{m_1, m_2} (j_1, j_2, m_1, m_2 | j_1, j_2, J, M) |j_1, m_1\rangle |j_2, m_2\rangle, \quad \dots (2)$$

where $(j_1, j_2, m_1, m_2 | j_1, j_2, J, M)$ is a vector-addition coefficient. We require that, if $|j_1, m_1\rangle$, $|j_2, m_2\rangle$ conform to (1), then $|j_1, j_2, J, M\rangle$ should do likewise. It is found that, when we use the conventional, real representation of the vector-addition coefficients (Wigner 1931), this requirement is satisfied by making

$$\alpha(j) = i^{-2j}, \quad \dots\dots (3)$$

so that (1) becomes

$$K|j, m\rangle = (-1)^{j-m} |j, -m\rangle. \quad \dots\dots (4)$$

In the case that $|j, m\rangle$ represents a spherical harmonic, we must adopt $(i^j Y_l^m)$, where Y_l^m is the usual function of Condon and Shortley (1935).

This mode of phasing the representation $|j, m\rangle$ was adopted by Biedenharn and Rose (1953), to establish the reality of the matrix elements of the perturbing Hamiltonian in calculating angular correlations. However, Wigner and Eisenbud adopted instead $\alpha(j) = -1$ for nuclear reactions, but one stage of their calculations relies in effect on the invariance of (1) under addition of angular momentum, which is actually not fulfilled in their representation. Their paper thus requires correction by the substitution of state-vectors phased according to (4), in place of those corresponding to $\alpha(j) = -1$. The principal general results are, of course, not affected by this phase change. However, in calculating the differential cross section, it is necessary to expand a plane wave e^{ikz} in spherical harmonics, and the expansion coefficients do depend on the phase of the latter. The eventual effect is that the differential cross section formula (42) of Wigner and Eisenbud becomes:

$$d\sigma^{ss'} = \frac{\pi}{(2j_s + 1)k_s^2} \sum_{\nu\nu'} \left| \sum_{l'l'm'} (2l+1)^{1/2} i^{l'-l} \right. \\ \left. \times \{(-)^l U_{s\nu l 0; s'\nu' l' m'} - \delta_{s\nu l 0; s'\nu' l' m'}\} P_{l'm'}(\Omega_{s'}) \right|^2 d\Omega_{s'}, \quad \dots\dots (5)$$

the various formulae which define the quantities appearing here being left unaltered.

It may be most useful to discuss the changes which this entails in the angular distribution formulae of Blatt and Biedenharn (1952). There are two alternative ways of correcting the formulae:

(i) All the wave functions and modes of expansion may be left unchanged, so that all formulae remain correct except those which express properties of the scattering matrix elements $S_{\alpha's'l'; \alpha sl}^J$. However, if we write

$$S_{\alpha's'l'; \alpha sl}^J = i^{l'-l} \bar{S}_{\alpha's'l'; \alpha sl}^J, \quad \dots\dots (6)$$

then it is $\bar{S}_{\alpha's'l'; \alpha sl}^J$ (instead of $S_{\alpha's'l'; \alpha sl}^J$) which has the properties described by Blatt and Biedenharn, viz. it is symmetrical, and is given by their equation (5.6) in terms of real, reduced widths.

(ii) For all the basic orbital angular momentum eigenfunctions defining the representation, one substitutes ($i^l Y_l^m$) in place of Y_l^m . This will alter many more of the equations than method (i), but has the advantage that the statements made by Blatt and Biedenharn about the scattering matrix elements $S_{\alpha's'l'; \alpha sl}^J$ will remain correct. Let us consider what happens to a formula such as Blatt and Biedenharn (4.6), which expresses the cross section, expanded in spherical harmonics, as a function of the scattering matrix elements $S_{\alpha's'l'; \alpha sl}^J$ and the geometrical coefficients $Z(l_1 J_1 l_2 J_2, sL)$. It turns out that the correct formula is obtained if we drop from the Z coefficients the factor $i^{l_1 - l_2 + L}$ contained in their definition (Biedenharn, Blatt and Rose 1952). In fact, it appears that the 'natural' Z coefficients for nuclear reaction formulae are those without the phase factor just mentioned, and that the latter has only intruded as a result of the error of Wigner and Eisenbud.

Many other papers on nuclear reactions which derive ultimately from that of Wigner and Eisenbud must contain phase errors in principle.

It remains to consider the practical importance of the phase correction. From the method of correction (i) above, which affects only the properties of the scattering matrix, it is clear that the correction can be disregarded when the matrix elements are treated as completely unknown, complex quantities, to be adjusted to experiment. Otherwise, however, following method (ii), and in accordance with

equation (6), we must apply to each scattering matrix element $S_{\alpha's'l'; \alpha sl}^J$ of Blatt and Biedenharn a correction factor $i^{l'-l}$. The cross section being quadratic in the scattering matrix elements, this means that a term in the cross section corresponding to interference between (i) a transition leading from a channel l_1 to a channel l_1' and (ii) a transition leading from a channel l_2 to a channel l_2' requires a correction factor $i^{(l_1'-l_1)-(l_2'-l_2)}$. Considerations of parity show that this factor can only be ± 1 , but the change of sign can certainly occur in interference terms between channels of different l . Even so, however, use of the uncorrected formulae would only rarely lead to disagreement between theory and observation. To illustrate this, let us consider the symmetry property of the scattering matrix as utilized by Blatt and Biedenharn for reduction of the number of parameters. This is most apt for dealing with a collision in which no change of energy can occur, i.e. we have only elastic scattering, with possible change of s and l . It follows from parity conservation that in such a case the correction (6) cannot affect the symmetry of the scattering matrix, which can only be upset in reactions involving change of internal parity. On the other hand, actual discrepancy between theory and observation would probably result if one attempted, for example, to utilize the symmetry of the scattering matrix, employing the uncorrected formulae, in analysing the cross sections of all the possible processes, and the inverses, which occur on bombarding A with a , when there exists one other open channel $B+b$ with change of internal parity.

As a general rule, it is advisable always to use angular momentum eigenstates phased according to (4).

The following derivation of the symmetry of the scattering matrix S from a more general property may help to clarify matters. The general property is:

$$\langle \phi | S | \psi \rangle = \langle K\psi | S | K\phi \rangle, \quad \dots (7)$$

for any states $|\phi\rangle, |\psi\rangle$. If we write, in the notation of Blatt and Biedenharn,

$$S_{\alpha's'l'; \alpha sl}^J = \langle \alpha', s', l', J, M | S | \alpha, s, l, J, M \rangle$$

and assume that the bra and ket both satisfy (4), then (7) becomes

$$\langle \alpha', s', l', J, M | S | \alpha, s, l, J, M \rangle = \langle \alpha, s, l, J, -M | S | \alpha', s', l', J, -M \rangle,$$

which, because of the invariance of S under rotation, yields

$$S_{\alpha's'l'; \alpha sl}^J = S_{\alpha sl; \alpha's'l'}^J.$$

ACKNOWLEDGMENT

I am very grateful to have had the benefit of Professor Wigner's advice in the matters relating to his paper with Eisenbud.

REFERENCES

- BIEDENHARN, L. C., BLATT, J. M., and ROSE, M. E., 1952, *Rev. Mod. Phys.*, **24**, 249.
 BIEDENHARN, L. C., and ROSE, M. E., 1953, *Rev. Mod. Phys.*, **25**, 729.
 BLATT, J. M., and BIEDENHARN, L. C., 1952, *Rev. Mod. Phys.*, **24**, 258.
 CONDON, E. U., and SHORTLEY, G. H., 1935, *Theory of Atomic Spectra* (Cambridge: University Press).
 LLOYD, S. P., 1951, *Phys. Rev.*, **81**, 161.
 WIGNER, E. P., 1931, *Gruppentheorie* (Vieweg; Braunschweig); 1932, *Göttingen Nachr.*, **31**, 546.
 WIGNER, E. P., and EISENBUD, L., 1947, *Phys. Rev.*, **72**, 29.

An Investigation of the (γ , n) Reaction in Cu, Zn and Ag

BY D. ST. P. BUNBURY

Physics Department, Imperial College

Communicated by S. Devons; MS. received 27th August 1954

MOST of the experimental studies carried out so far on the giant resonances observed in photodisintegration processes have made use of the bremsstrahlung spectrum obtained from an electron accelerator. Owing to the continuous nature of the spectrum, the energy resolution obtainable with the method is relatively poor. Recently, however, Goldemberg and Katz (1953), using very careful control of the energy of a betatron, have shown that the excitation functions of the (γ , n) reaction in several light elements up to and including fluorine show a number of distinct breaks which they interpret as due to excitation levels of the nuclei irradiated.

The present note describes an attempt to find out whether a similar fine structure could be observed in the (γ , n) excitation functions of heavier elements. The method employed depended on the variation with angle of the energy of the 17.6 mev line from the reaction ${}^7\text{Li}(p, \gamma){}^8\text{Be}$ due to the Doppler effect. At the 440 kev resonance, where the γ -radiation is known to be emitted isotropically (Devons and Lindsey 1950), the energy shift amounts to ± 65 kev at 0 and 180° to the proton beam respectively.

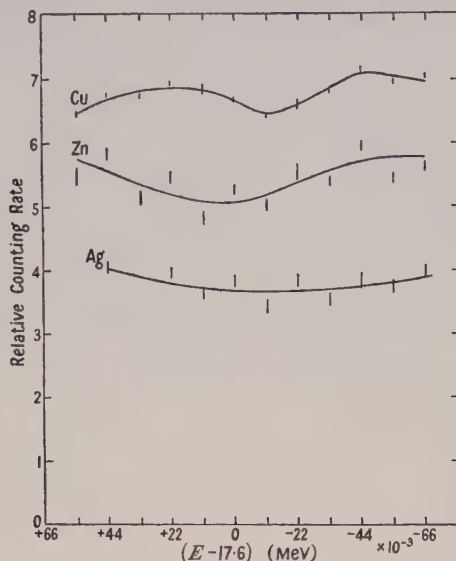
The elements studied were in the form of sets of twelve identical cylinders, 2 in. long and with inside diameter $\frac{1}{2}$ in. and wall thickness $\frac{1}{16}$ in. These were simultaneously irradiated on a jig which held them at equal distances (2 in.) from the target and spaced at equal intervals of $\cos \theta$ with respect to the incident proton beam. After irradiation for a period of the order of one half-life of the resulting activity, the cylinders were transferred to a set of thin-walled Geiger counters. This procedure was repeated until sufficient counts were accumulated. The relative efficiencies of the counters were determined by repeating the experiment with all the cylinders irradiated in the 90° plane with respect to the proton beam. As an additional precaution the counters were interchanged after each irradiation so that in each run every cylinder was used the same number of times with each counter.

The energy resolution obtained by this method was limited mainly by the finite angle subtended at the target by the cylinders, and is of the order of ± 10 kev.

Practical considerations limited the use of this method to three elements: Cu, Zn and Ag. In the case of Cu and Zn, the peak of the giant resonance lies close to 17.6 mev (Montalbetti, Katz and Goldemberg 1953); in the case of Ag, on the other hand, excitation will be due mainly to the broad 14.8 mev γ -ray, and any fine structure is therefore expected to be largely smoothed out. In each case the observed activity is almost entirely due to a single isotope.

The figure shows the results obtained. The cross section for the reaction ${}^{63}\text{Cu}(\gamma, n){}^{62}\text{Cu}$ as a function of energy shows fluctuations which are well outside the statistical error. That for Zn also shows a similar variation, although the result is somewhat more uncertain. Since the shapes of these curves differ from

each other and from that obtained with Ag, the results cannot be ascribed to either deviations from isotropy of the γ -ray or variations of solid angle subtended at the target.



Relative (γ , n) cross sections as a function of energy. The vertical scale is arbitrary, and different for the three curves. The alternation of points above and below the line in the lower two curves is due to an inaccuracy in the centring of the target.

I would like to thank Professor S. Devons for suggesting this experiment and for his continued interest. I am also grateful to Dr. G. Goldring for a number of helpful discussions.

REFERENCES

- DEVONS, S., and LINDSEY, G. R., 1950, *Proc. Phys. Soc. A*, **63**, 1202.
 GOLDBERG, J., and KATZ, L., 1953, *Phys. Rev.*, **92**, 852.
 MONTALBETTI, R., KATZ, L., and GOLDBERG, J., 1953, *Phys. Rev.*, **91**, 659.

Levels of ^{24}Mg from the $^{27}\text{Al}(p, \alpha)^{24}\text{Mg}$ Reaction

BY G. W. GREENLEES†
 Cavendish Laboratory, Cambridge

MS. received 9th September 1954

IN the course of a study of inelastic scattering by levels in Mg and Al, observations have been made of the charged particle reaction products emitted at 90° from an Al target bombarded by 6.5 mev protons from the Cavendish cyclotron. The target was an Al foil of 0.256 mg cm^{-2} . The reaction products observed were alpha-particles from the $^{27}\text{Al}(p, \alpha)^{24}\text{Mg}$ reaction and protons elastically and inelastically scattered by Al. These were detected using photographic emulsions (Ilford E1). Alpha-particle and proton tracks in the emulsion

† Now at the Physics Department, University of Birmingham.

could be distinguished by inspection. The scattered particles were separated using a subsidiary magnet; this avoided portions of the plate having too high a track density for measurement.

The range spectrum for α -particles shows three groups of lengths 10, 23 and 31 microns. The three groups give Q values of 1.61 ± 0.04 mev, 0.23 ± 0.03 mev and -2.57 ± 0.04 mev, corresponding to levels in ^{24}Mg at 0, 1.38 and 4.18 mev. The first two Q values have been measured by Donahue *et al.* (1953), who give 1.594 ± 0.002 mev and 0.228 ± 0.003 mev. The apparent single level in ^{24}Mg at 4.18 mev, corresponding to the third group, is presumably an unresolved doublet. This doublet is well known (cf. Endt and Kluyver 1954) and has been observed in the $^{27}\text{Al}(p, \alpha)$ reaction by Reilley *et al.* (1952), who found Q values corresponding to levels of ^{24}Mg at 4.11 and 4.21 mev.

In the present experiments the differential cross sections were estimated using the proton elastic differential cross section which was known from other experiments. The values obtained were 0.16 barns/steradian (1.61 mev), 0.61 barns/steradian (0.23 mev) and 0.15 barns/steradian (-2.57 mev). The errors in these are estimated as $\pm 20\%$.

REFERENCES

- DONAHUE, D. J., JONES, K. W., MCELLESTREM, M. T., and RICHARDS, H. T., 1953, *Phys. Rev.*, **89**, 824.
 ENDT, P. M., and KLUYVER, J. C., 1954, *Rev. Mod. Phys.*, **26**, 95.
 REILLEY, E. M., ALLEN, A. J., ARTHUR, J. S., BENDER, R. S., ELY, R. L., and HAUSMAN, H. J., 1952, *Phys. Rev.*, **86**, 857.

On Source Scattering in Angular Correlation Experiments with Soft Electrons

By E. BREITENBERGER†

Cavendish Laboratory, Cambridge

MS. received 30th August 1954

IN correlation experiments with soft conversion electrons or β -particles the inevitable electron scattering in the source material can cause serious errors. The possible falsifications of the angle of emission may be estimated from a nomogram given by Walter, Huber and Zünti (1950) and are found to be quite appreciable at energies of less than a few hundred kev. Calculation of suitable corrections seems impossible because in the usual plane, inhomogeneous sources the individual observed electrons have traversed different layers of matter, and have begun their paths at different angles with respect to the plane of the source. As regards detection of scattered electrons by the movable counter (e.g. in e-e or β -e correlations) the situation is still more complicated, the observations taking place at several angles with respect to the plane of the source.

By a simple extension of an argument which is due to Frankel (1951) one can, however, derive a safe upper limit to the expected scattering effects, and devise a counting method which eliminates their insidious angular dependence.

† Now at Department of Physics, University of Malaya, Cluny Road, Singapore 10.

Consider a simple model case: a perfectly centred point source, surrounded by a massive spherical scatterer. The spherical symmetry of this problem permits a straightforward treatment. Assuming first that only one of the two radiations is a soft electron, the number of genuine coincidences observed by two infinitely small counters is proportional to

$$W^*(\omega)d\Omega_1d\Omega_2 = d\Omega_1 \left[\int \int W(\theta)d\Omega S(\sigma) \right] d\Omega_2 \quad \dots\dots(1)$$

where ω is the angle between the counters, $W(\theta) = \sum a_n P_n(\cos \theta)$ the original correlation function, and $S(\sigma)$ the multiple scattering function. $S(\sigma)d\Omega_2$ gives the probability that an electron is scattered from a given direction through the angle σ into the element of solid angle $d\Omega_2$. The integration extends over the whole sphere.

We develop the scattering function into Legendre polynomials:

$$S(\sigma) = \frac{1}{4\pi} \sum (2m+1) G_m P_m(\cos \sigma) \quad \dots\dots(2)$$

with $G_0 = 1$; note that S is normalized to unity over the unit sphere. If, as usual, $S(\sigma)$ decreases monotonically with σ , the coefficients G_1, G_2, \dots are smaller than one but positive. For isotropic scattering $G_1 = G_2 = \dots = 0$. In the limiting case of no scattering S behaves like a Dirac delta so that all $G_m = 1$. After insertion of (2) in (1) the integration can be performed and yields (Frankel 1951)

$$W^*(\omega) = \sum a_n G_n P_n(\cos \omega). \quad \dots\dots(3)$$

If the other radiation is a soft electron too, the reduction process repeats itself and we obtain

$$W^{**}(\omega) = \sum a_n G_n' G_n'' P_n(\cos \omega), \quad \dots\dots(4)$$

the primes referring to the two scattering functions. The finite size of the detectors can now be taken into account in the usual way.

The conditions of an actual experiment can often be approximated, to some degree, in terms of this idealized example. Thus, if the fixed counter detects scattered electrons from a source the plane of which is normal to the centre-to-counter vector, the set-up can be represented by a point source behind a plane parallel scattering foil, and the requisite G_n can be taken from the explicit scattering function for normal electron incidence on that foil. Obviously this comparison will be the more accurate the feebler the scattering and the smaller the counter. The thickness of the fictitious scattering foil will have to be chosen according to circumstances; taking it equal to the actual thickness of the source one will in general obtain safe lower limits to the G_n .

Application of the spherical model to the case of electron detection by the movable counter requires approximate spherical symmetry of the source. One could, for instance, stick twelve plane sources on to the faces of a little regular dodecahedron. This arrangement still has the fault that some of the sources are always nearly parallel to the plane of revolution of the movable counter, and thus give rise to scattering effects which are hard to assess. But one can also replace the spherical scatterer of the model, without significant change of the G_n in (3) and (4), by a short cylinder, and accordingly arrange the twelve sources with cylindrical symmetry about the axis of revolution. It is readily seen that they need not all be there together: one may count on one source at a time, and finally add up all counts taken at one detector position. If one avoids, for each

source, to count at those angles at which the detector sees the source almost edgewise, the G_n can again be taken, *faute de mieux*, from the scattering function for electrons incident normally on a plane foil. Choosing the foil about 1.5 times as thick as the actual sources will yield fair lower limits of the G_n'' for approximately homogeneous sources. Note that this same thickness has to be used to obtain the G_n' for the electrons counted in the fixed detector. Note also that the sources had better be placed *into* the axis of revolution (successively, like the compartment walls in a capsule of poppy) in order to avoid large decentring errors (cf. Breitenberger 1954b).

Appropriate scattering functions have been given by several authors (see Spencer 1953). The older formulae of Goudsmith and Saunderson (1940), though not very accurate (Molière 1948, cf. Yang 1951), are well suited for the present purpose. They give the coefficients of (2) in the form $G_n = \exp(-S_n t)$, where t is the foil thickness in cm. Numerical values of the S_n (in Born approximation for a Wentzel potential $Ze^2 \exp(-r/a)/r$) are given below for (a) beryllium, (b) carbon of density 0.8 (e.g. formvar) and (c) aluminium, the three most important source backing materials of low Z .

E (kev)		20	30	50	100	200	500
(a)	$n=2$	1005	477	191	59.2	19.2	4.50
	4	1320	706	321	110	39.2	10.0
(b)	$n=2$	701	337	135	42.9	13.8	3.39
	4	824	467	212	77.5	27.4	7.40
(c)	$n=2$	4350	2120	860	276	90.3	22.4
	4	3780	2410	1210	460	169	47.1

For intermediate energies one can use linear interpolation on $(S_n)^{1/4}$.

The following numerical examples refer to e-e correlation experiments which it is hoped to publish shortly (cf. Breitenberger 1954a). (1) Electron energies 23 and 35 kev, activity deposited carrier-free on beryllium films of about 3000 Å; taking $t=4500$ Å one finds $G_2'G_2''=0.945$. (2) Energies 51 and 82 kev, activity embedded carrier-free in aluminium films of about 2200 Å; taking $t=3500$ Å gives $G_2'G_2''=0.955$ and $G_4'G_4''=0.935$.

REFERENCES

- BREITENBERGER, E., 1954 a, *Nature, Lond.*, **173**, 737; 1954 b, *Phil. Mag.*, **45**, 497.
 FRANKEL, S., 1951, *Phys. Rev.*, **83**, 673.
 GOUDSMITH, S., and SAUNDERSON, J. L., 1940, *Phys. Rev.*, **57**, 24.
 MOLIÈRE, G., 1948, *Z. Naturf.*, **3a**, 78.
 SPENCER, L. V., 1953, *Phys. Rev.*, **90**, 146.
 WALTER, M., HUBER, O., and ZÜNTI, W., 1950, *Helv. Phys. Acta*, **23**, 697.
 YANG, C. N., 1951, *Phys. Rev.*, **84**, 599.

LETTERS TO THE EDITOR

Nuclear Shell Structure

In a recent review article (Pryce 1954) I gave an erroneous account of some early work on nuclear shell structure. I quoted the numbers 2, 8, 18, 32, 50 and 126, not all of which are nowadays regarded as 'magic numbers', as having been proposed by Guggenheimer (1934) to correspond to shell closures. In fact this list is due to Elsasser (1934), where it appears in his Table 1. Elsasser also shows a plot of stable nuclei ((N, Z) plot), taken from Guggenheimer, on which he superposes arrows to indicate these numbers. I was misled by the arrows, appearing as they do on a diagram ascribed to Guggenheimer, into supposing that the numbers were also due to him.

The list, as I quoted it, is incomplete, and should also contain 82. Elsasser, in a note added in proof, suggests that 116 (as well as 126) is a shell closure.

Guggenheimer, in his papers, presents evidence which can be interpreted as shell closures at 50, 82 and 126.

I am grateful to Dr. Guggenheimer for drawing my attention to my error, and I sincerely regret having misrepresented his pioneer work.

H. H. Wills Physical Laboratory,
Bristol.

M. H. L. PRYCE.

14th October 1954.

ELSASSER, W., 1934, *J. Phys. Radium*, **5**, 389.

GUGGENHEIMER, K. M., 1934, *J. Phys. Radium*, **5**, 253, 475.

PRYCE, M. H. L., 1954, *Rep. Progr. Phys.*, **17**, 1 (London: Physical Society).

The Elastic Scattering of 125 MeV Electrons by Beryllium

Recently, the differential scattering curve for the elastic scattering of 125 mev electrons by beryllium has been experimentally obtained (Hofstadter, Fechter and McIntyre 1953). Several one parameter functions for the nuclear charge density distribution have been employed (Schiff 1953) to correlate these experimental data. The theoretical calculations are properly based on the first Born approximation. The parameters of the proposed functions have been obtained by comparing the theoretical and the experimental diffraction patterns. However, it has been found that only a pure gaussian function and a modified exponential function provide reasonable values for the nuclear electrostatic energy.

Now, we have proposed (Gatha, Shah and Patel 1954) the following characteristic nuclear density distribution for light elements to account for the nuclear scattering of high energy nucleons :

$$\rho(r') = \sum_{q=1}^3 \alpha_q \exp(-\beta_q r'^2) \quad \dots\dots(1)$$

where $r' = r A^{-1/3}$ while

$$\alpha_1 = 0.25 \times 10^{39} \text{ cm}^{-3}$$

$$\beta_1 = 28.94 \times 10^{26} \text{ cm}^{-2}$$

$$\alpha_2 = 0.19 \times 10^{39} \text{ cm}^{-3}$$

$$\beta_2 = 3.83 \times 10^{26} \text{ cm}^{-2}$$

$$\alpha_3 = 0.1 \times 10^{39} \text{ cm}^{-3}$$

$$\beta_3 = 0.75 \times 10^{26} \text{ cm}^{-2}$$

It has also been shown that this density distribution naturally turns out to be consistent with the requirement of the nuclear electrostatic energy. Therefore, it would be of some interest to determine whether it can naturally correlate the experimental data on the nuclear scattering of 125 mev electrons by beryllium.

It has been shown by one of us (Mathur and Gatha 1953) that for a non-singular electrostatic potential, the scattering amplitude in the first Born approximation is given by

$$f(\theta) = -\frac{8\pi E Z e^2}{(\hbar c)^2 A s^3} \int_0^\infty \rho(r) \sin(sr) r dr \quad \dots\dots(2)$$

where, $s = 2k \sin \frac{1}{2}\theta$ while the other symbols have the usual meanings. For the above density distribution one obtains

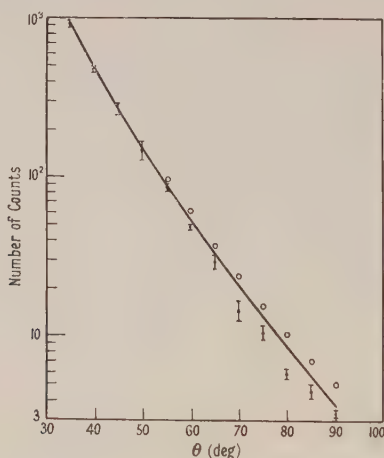
$$f(\theta) = -\frac{2\pi^{3/2} E A^{2/3} Z e^2}{(\hbar c)^2 s'^2} \sum_{q=1}^3 (\alpha_q / \beta_q^{3/2}) \exp(-s'^2 / 4\beta_q) \quad \dots\dots(3)$$

where $s' = s A^{1/3}$. One also has

$$\sigma(\theta) = (1 - \beta^2 \sin^2 \frac{1}{2}\theta) |f(\theta)|^2 \quad \dots\dots(4)$$

where $\beta = v/c$.

We have used the above expressions and calculated the theoretical diffraction pattern for the nuclear scattering of 125 mev electrons by beryllium. This diffraction pattern is shown in the figure, together with the experimental patterns with and without the empirical corrections. It can be seen that there is a reasonable agreement between the theoretical and experimental patterns. The slight deviations at large angles may perhaps be due to the inelastic scattering and other competing processes (Rose 1948).



The diffraction pattern for the nuclear scattering of 125 mev electrons by Be : (1) The full curve represents the theoretical pattern normalized at 35°. (2) The points with errors represent the uncorrected experimental data. (3) The circles represent the empirically corrected data.

Thus we conclude that the proposed nuclear density distribution is approximately consistent with the requirement of the nuclear scattering of high energy electrons.

M.G. Science Institute,
Navarangpura,
Ahmedabad, 9,
India.

8th August 1954.

K. M. GATHA.
N. J. PATEL.
P. F. PATEL.

- GATHA, K. M., SHAH, G. Z., and PATEL, N. J., 1954, *Proc. Phys. Soc. A*, **67**, 773.
HOFSTADTER, R., FECHTER, H. R., and MCINTYRE, J. A., 1953, *Phys. Rev.* **92**, 978.
MATHUR, A. L., and GATHA, K. M., 1953, *Proc. Phys. Soc. A*, **66**, 773.
ROSE, M. E., 1948, *Phys. Rev.*, **73**, 279.
SCHIFF, L. I., 1953, *Phys. Rev.*, **92**, 988.
-

The Absolute Standardization of the 2.615 Mev γ -rays of ThC'' and the Cross Section for the Photo Disintegration of the Deuteron at this Energy

MILLIGRAMME RADIUM EQUIVALENT OF ThB AND OF ThC''

Whilst intercomparing our radium standard (N.P.L. certificate C.2521) against the Paris substandard (Institut du Radium) we discovered that an error had been made in the interpretation of the intensity of our standard (Marin, Bishop and Halban 1953). The N.P.L. certificate quoted the radium content in milligrammes, and not the effective value of the source on their ionization chamber as we believed. Therefore, the effective value of the standard on our Curie chamber is not $1.01 \times 1.062/1.050 = 1.021$ mc as we stated, but $1.01/1.05 = 0.961$ mc. This value agrees with the one found 0.960 ± 0.003 mc, from the intercomparison with the Paris substandard.

The mg radium equivalent of ThB is now 1.15 ± 0.01 mc instead of the value 1.083 ± 0.016 mc, quoted before. The error is smaller, because we have reduced the uncertainty of 1%, due to the accuracy of the N.P.L. calibration, to 0.3%. The value of the mg radium equivalent of ThC'' becomes 0.407 ± 0.007 mc, instead of the previous value 0.384 ± 0.009 mc.

Substituting this value in the measurements of the cross section for photo-disintegration of the deuteron we find $\sigma = (13.0 \pm 0.29) \times 10^{-28}$ cm².

We would like to express our thanks to Madame I. Joliot Curie and Monsieur J. Lecoine (Institut du Radium, Paris) for making a calibrated radon source available to us.

Clarendon Laboratory,
Parks Road,
Oxford.
14th August 1954.

P. MARIN.
G. R. BISHOP.
H. HALBAN.

MARIN, P., BISHOP, G. R., and HALBAN, H., *Proc. Phys. Soc. A*, 1953, **66**, 608.

REVIEWS OF BOOKS

Relativity : The Special and the General Theory, by ALBERT EINSTEIN. Translated by ROBERT W. LAWSON. 15th Edition, revised and enlarged. Pp. x+165. (London : Methuen.) 12s. 6d.

This is the book that, in its earlier editions, gave many of us our first acquaintance with relativity theory. Probably there is still no better introduction. The publishers and Mr. R. W. Lawson, the original translator, are doing good service in keeping it available.

The main text and the three original appendices are reprinted without change. This is as it should be; for new readers will want the satisfaction of having a great little book in the form in which its reputation was established. But in any case the book stands in need of practically no revision. This is not to say that Einstein's theory of relativity is all that can ever be desired. But the book is concerned in the first place with a simplified presentation of considerations that any satisfactory theory must take into account. For the rest, it is Einstein's theory to which it is an introduction and not some as yet unformulated superseding theory.

The present edition contains also a brief appendix on the expanding universe, which has appeared in other recent editions, together with a longer new appendix now appearing for the first time. This is on "Relativity and the problem of space" and (in the prefatory note to this edition) Einstein describes it as "a presentation of my views on the problem of space in general and on the gradual modifications of our ideas on space resulting from the influence of the relativistic viewpoint." While I think that the view which it expresses is what has become the orthodox interpretation of relativity theory, actual statements of the view are quite hard to find. The present careful formulation is therefore very welcome. Particular attention may be called to the explanation (on p. 155) of the difference between the interpretation of the case of 'flat' space-time in general relativity and in special relativity. Practically the same explanation was given by Eddington (*Mathematical Theory of Relativity* (1924), p. 16; *Space Time and Gravitation* (1923), ch. X). This concerns one of the main aspects of the theory involved in the question as to whether it deals adequately with the problem of *inertia*. Opinions differ as to its adequacy in this respect. But, although Einstein does not discuss the question here, the interpretation he gives contains the answer to the cruder forms in which criticism of the theory has sometimes been framed.

In reviewing a book by Einstein at the present time one might be expected to say something on recent debates about the extent to which he was anticipated by other writers. But a work of elementary exposition is not a suitable starting-point for discussing this. Besides, the debates have not been about Einstein's own claims but about the historical accuracy of others in ascribing particular discoveries to him. It may, indeed, be remarked that in the present book Einstein himself makes more explicit reference to the contributions of others than seems to be common practice in purely expository writing.

Without, therefore, entering upon any detailed analysis, it may however be appropriate here to make one general comment. Parts of relativity theory were

discovered by others before Einstein and a good deal of the mathematical formulation of the theory may also be ascribed to others. Nevertheless, there seems to be little doubt that it was Einstein's own work that gave the theory its fundamental and comprehensive physical significance. I think that the view of Einstein's work as being pre-eminent in its effect upon physical thought is still the correct view.

The present is the fifteenth edition of a book that can be expected to see a number of further editions. It is to be hoped that in future editions the dates of the text, the appendices, and the translator's footnotes will be inserted.

W. H. McCREA.

Nuclear Physics, by W. HEISENBERG. Pp. ix + 225 (London: Methuen, 1953).

Translated from the German by Frank Gaynor and Amethe von Zeppelin with the assistance of W. Wilson, F.R.S. 12s. 6d.

I suppose most nuclear physicists have at one time or another been faced with the task of presenting their subject to an audience of 'intelligent laymen' and therefore know how difficult it can be to describe the concepts and experimental bases of modern nuclear physics in a form that is intelligible, and yet does not vulgarize or distort the subject. This little book, based originally on a series of lectures given under the auspices of the Association of German Electrical Engineers, is a real masterpiece in the art of presentation. The subject matter is well selected and written in a form that sustains the interest throughout.

The book commences with a summary of the development of the atomic theory from earliest times and leads on through an account of the early history of radioactivity to our present conception of the nucleus and its constituents. A chapter on the normal states of atomic nuclei is followed by a masterly account of nuclear forces in which difficult concepts such as those of exchange forces and the meson theory of nuclear forces are introduced in an elementary but clear manner. After a chapter on nuclear reactions there is a description of the tools of nuclear physics including an account of the construction of accelerators and of methods of detection and measurement of high energy particles. A final chapter deals with applications of nuclear physics in the production of atomic energy and in the use of isotopes in industry, medicine and research and this is followed by an appendix consisting of a reprint of an article in *Nature* on atomic energy research in Germany during the war. A useful series of tables of nuclear data concludes the book.

The production maintains a high technical standard throughout and altogether it is one of the best elementary expositions of modern nuclear physics that has yet appeared.

E. H. S. BURHOP.

Progress in Metal Physics 5, edited by B. CHALMERS and R. KING. Pp. vii + 324. (London: Pergamon Press, 1954.) 60s.

The new volume in the *Progress in Metal Physics* series contains articles on Fracture (N. J. Petch), the Plastic Deformation of Single Crystals (R. Maddin and N. K. Chen), the Structure of Liquid Metals (B. R. T. Frost), Precipitation (H. K. Hardy and T. J. Heal) and Solidification (Ursula M. Martius). Such articles as these, compiled from material drawn from a great mass of published work, are difficult to put together and require much laborious organization,

A tribute should be paid to those who take on such tasks, for metal physics would be all the poorer to-day without the results of their work as embodied in the five volumes of this series.

The articles in the present volume are fairly formidable even by previous standards. The report on precipitation runs to 137 pages with 350 references. Its value to many will be great indeed, but it hardly constitutes the kind of review the Editors have in mind in their Foreword. Can someone who is not active in the field read this review through and obtain a fair appraisal of the present situation? It is a complex account of theory, technique and experiment with some of the characteristics of a catalogue, and whilst it is to be admired for its comprehensiveness, the subject is surely altogether too large for a progress article. In other words, it becomes simply a very good reference source. Now an article in such a book as this should, in the first place, be readable. It should be illuminated by a point of view, and it should be most rigorously pruned of material not directly relevant to the exposition: ample references will take care of the rest. One does not want a sequence of abstracted summaries, but cohesion and even conjecture; in fact, one wants to be aware of the progress and aware of the direction in which this progress is heading, the whole being held together by some central framework. Certain articles have achieved this in the past, and they have all been both readable and worthy works of reference: Cottrell on Dislocations (Vols. 1 and 4), Nowick on Internal Friction (Vol. 4), and the Polygonization articles (Vol. 2) come to mind, and there are others.

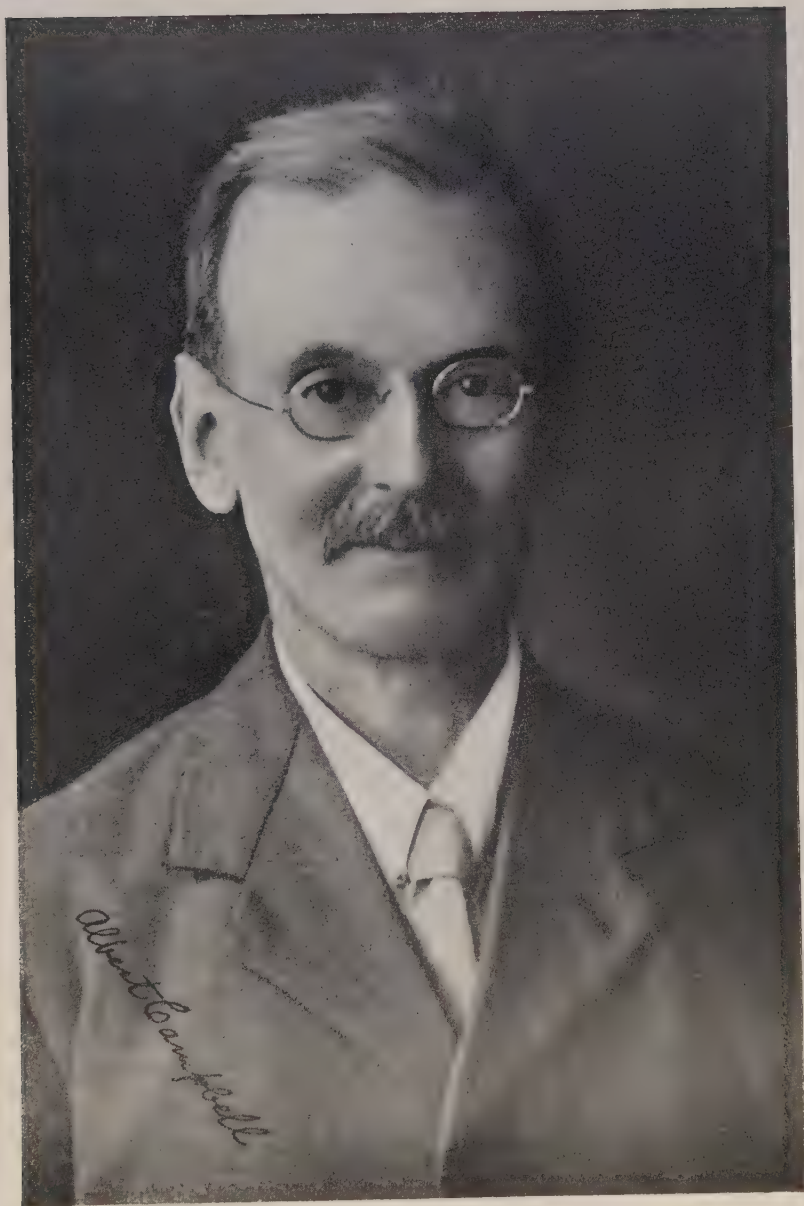
In the present volume, the fracture article fills a vacancy in this progress series. It is neatly compiled and very welcome. The consideration of the geometry of crystal deformation is usefully confined to crystallographic effects and particularly treats problems which have only recently been taken up as important—the heterogeneity of the glide process and composite slip for instance. The article gains by this limitation of viewpoint, as, in a way, does the article on solidification, which is severely confined to a consideration of some of the variables determining the mode of solidification. It does seem, however, to be quite inconclusive, and surely the whole question of nucleation and growth has received by now a disproportionate representation in this series, with the rate-process review (Vol. 2), the recrystallization and grain growth review (Vol. 3), and the nucleation review (Vol. 4), while other important subjects, such as fatigue, find no place among any of the thirty-four articles published so far. The liquid metals review introduces a new subject to the series, and reveals the inadequacy (indeed the naïvety) of the theoretical approaches to date. It would be interesting to see what a theoretical physicist, working on the subject, could have produced as a progress article of this nature. Fortunately, the emphasis is here on the experimental results, and as (for some reason) the subject rarely achieves a comprehensive review, the present article is all the more useful on that account.

To sum up; a valuable volume, more prosaic than its predecessors in its general style, but a worthy addition to the reference value of this series.

A. J. KENNEDY.

BOOK NOTICE

Nuclear Reactors for Industry and Universities, edited by E. H. WAKEFIELD.
Pp. ix+95. (Pittsburgh: Instruments Publishing Co., 1954.)



ALBERT CAMPBELL.



F. C. CHALKLIN.



REGINALD STANLEY CLAY.



ROBERT STEWART WHIPPLE.

OBITUARY NOTICES

HERBERT STANLEY ALLEN

Herbert Stanley Allen, the fifth son of Rev. Richard Allen, a Methodist minister, was born at Bodmin, Cornwall on 29th December 1873. During his early education at Kingswood School, Bath, he already showed great promise of a distinguished career. He was a Senior Prefect of the School and gained the distinction of taking the first place for all England in the London Matriculation Examination and in the Senior Cambridge Local Examination.

At Trinity College, Cambridge, which he entered in 1893, he was awarded a First Class in the second part of the Natural Sciences Tripos. He then went to Aberystwyth where he spent a short time in a temporary post as assistant lecturer before returning to Cambridge as a research worker under Professor J. J. Thomson. In 1900 he went to Renfrew to take charge of Lord Blythswood's Physical Laboratory. In 1905 he was appointed to the staff of the Physics Department in King's College, London, where in 1909 he was awarded the degree of D.Sc. for his work on the photoelectric effect.

In 1907 he married Miss Jessie Macturk whom he had met in Renfrew. They settled in New Malden, Surrey, where both their children were born and where they stayed until he was appointed lecturer in Professor Barkla's Department in Edinburgh University in 1920. There he became a Reader. After spending three years in Edinburgh he was appointed to the Chair of Natural Philosophy in The United College of St. Salvator and St. Leonard in the University of St. Andrews.

H. Stanley Allen was, for nearly fifty years, a member of the Physical Society. He took an active interest in the Society and between 1916 and 1921 he was a Member of Council and Honorary Papers Secretary. The Society received with deep regret the news of his death on 27th April 1954.

He was elected to the Fellowship of the Royal Society of Edinburgh when he took up his post in that city. He was awarded the Makdougall-Brisbane Medal and served on the Council. Election to the Fellowship of the Royal Society followed in 1930. This honour he shared with his brother Edgar Johnston Allen who was for many years director of the Marine Biological Laboratory at Plymouth. When, in 1944, he retired from the Chair of Natural Philosophy, the University of St. Andrews elected him Professor Emeritus and conferred on him the honorary degree of LL.D., fitting tributes to his devoted service to the University and to the cause of science.

His enthusiasm for research led him into many branches of physics among which may be mentioned photoelectricity, the Zeeman effect, spectroscopy, x-rays and radioactivity. In St. Andrews he was chiefly interested in the quantum theory and its applications to spectroscopy, especially to the band spectrum of hydrogen. Apart from publishing many research papers he was the author or joint author of a number of books. The first of these, published in 1913, was his *Photoelectricity*, based largely on lectures delivered in London and including an account of his own work on photoelectric fatigue.

The representation of physical phenomena merely in terms of a mathematical expression was, to Professor Allen, unsatisfying, and in his writing he always

tried to adopt the middle course between a purely mathematical treatment on the one hand and a purely descriptive treatment on the other. Whenever possible he tried to picture a physical model in terms of which the nature of the processes involved might be envisaged. 'This 'middle course' he mentions in the preface to *The Quantum and its Interpretation* (1928), a book which did not profess to be a treatise on the quantum but rather to be "an attempt to deal with the baffling problem of the nature of the quantum". This book was in the press just when the results of the earliest experiments on electron diffraction were being published. At that time much thought was directed to the dilemma of particles versus waves, a subject in which Allen was intensely interested and one which forms the theme of *Electrons and Waves* which appeared in 1932. In this book which is in a more descriptive vein he expressed his faith in an ultimate explanation of this dilemma. "Truth", he says, "is great, and will prevail".

Allen and Moore's *Text Book of Practical Physics*, first published in 1916, earned a well-merited popularity and by 1948, when the third edition appeared, it had passed through frequent reprinting. In *A Text Book of Heat* (1939), written in collaboration with his nephew, R. S. Maxwell, he adopted the historical method of presentation which is not so common as it deserves to be in scientific text books today. He had a gift for lucid exposition which was no less apparent in his lectures than in his writing; he spared no effort to make his meaning clear and, above all, to be accurate.

In his youth he was fond of cycling and walking; he and Mrs. Allen spent many happy holidays on the Continent. In later years he enjoyed motoring with his family in the Highlands of Scotland although he himself never mastered the art of driving. Professor Allen was naturally shy and retiring. He was always ready to help others with encouragement and advice; his personal qualities and the inspiration of his teaching won for him the respect and affection of his students and of his more immediate associates. It was only those who knew him most intimately who could appreciate the kindness which lay behind his quiet dignity of manner.

There are many who mourn the death of one who so unsparingly devoted himself to his life's work. Professor Allen died in the Black Isle, Ross-shire, at the home of his daughter Mrs. G. S. M. Walker with whom he spent the last year of his retirement.

D. JACK.

ALFRED BLACKIE

Alfred Blackie was born in 1882 at Crowborough, Sussex. He was educated at Tonbridge School, and Peterhouse, Cambridge. He obtained a First Class Honours Natural Sciences Tripos in 1903, and was awarded the Wiltshire prize for Mineralogy and Geology. Subsequently in 1905 he took the Mechanical Sciences Tripos.

His first post was on the teaching staff of the Royal Naval College, Dartmouth, an association which he very much treasured. In 1907 he joined the Physics Division of the National Physical Laboratory. His special knowledge of crystallography was of value in an investigation into the spontaneous changes of crystalline form that silica undergoes on prolonged heating at high temperature.

While at the N.P.L. he also devised a means, subsequently used in the Indian survey, of determining the corrections for the variation with height of the refractive index of the atmosphere.

As a territorial officer in the Artists Rifles he was mobilized on the outbreak of war, and from 1914 to 1919 served with the Royal Engineers on Coast Defence in Southern Ireland and on the Channel coast, with the rank of Captain.

On demobilization in 1919 he joined the newly founded Fuel Research Station of D.S.I.R. at Greenwich under its first Director—Sir George Beilby. In charge of the Physics Department he was responsible for developing a number of ingenious instruments, and methods of measurement of radiation and temperature, which proved of great value in the work of the Station. In research work on domestic heating he undertook fundamental work on the relationship of the optical density of smoke and its mass concentration, and on methods of reducing smoke. His advice was sought during World War II on smoke production for camouflage purposes. Before his retirement in 1947 he was responsible for designing a unique calorimeter building at the Fuel Research Station, containing 4 rooms, 12 ft. by 12 ft. by 9 ft., each a calorimeter equipped to measure completely and accurately the heat emission of a domestic heating appliance.

His work was marked by a care and accuracy which is the hall mark of the true physicist. His wide knowledge in the field of natural science was a help to all his colleagues. He was a Life Fellow of the Physical Society, and a Founder Fellow and Life Member of the Institute of Physics.

His interests were wide. He enjoyed foreign travel; he had a great love of nature, and specialized in Lepidoptera. He was a charming companion and friend, always willing to help those in need. Although not robust in health, he insisted on joining the Home Guard, and served as a Captain in the 23rd County of London Battalion. He died after a short illness in his 72nd year.

A. C. M.

ALBERT CAMPBELL

Albert Campbell, one of the oldest Fellows of the Physical Society, a Vice-President from 1910 to 1912, for many years a frequent contributor to the *Proceedings*, and the Duddell Medallist for 1925, died at Cambridge on 6th February at the age of ninety-one. He will probably be best remembered for his pioneer work on electrical measurements at the National Physical Laboratory, in particular his primary standard of mutual inductance and his alternating current bridges, but those who met him will long retain lively recollections of a highly original personality with qualities that aroused the warmest feelings on all sides.

He was born at Ballynagard House near Londonderry, the third son of Thomas Callender Campbell, J.P., who seems to have been a man of some enterprise with varied interests that must have done much to stimulate in his son the taste for practical scientific work. At Ballynagard he ran a mill for scutching the flax grown in the neighbourhood, grew gooseberries in quantity to supply a Glasgow jam-maker, and later, by way of producing a fertilizer as a substitute for imported Peruvian guano, set up the necessary plant, including

a mill for grinding bones, and a complete installation for synthesizing sulphuric acid by the lead chamber process. The "manure works", wrote Albert, "served the country for many years", but the family had the option of giving up the lease of the house and land every seven years, and "in 1898 we used this option, dismantling the manure works and taking down the tall chimney. We got a site nearer town, where we built the house Ballynatrua partly with material salvaged from the manure works". Albert's interests were to run on different lines, but it is possible to discern something of the same pattern in them.

When he left the N.P.L. in 1918 he went back to Ballynatrua, and it was there that he made his last and best absolute determination of the ohm, and from there he published it in what must be one of the shortest papers ever printed in the *Proceedings of the Royal Society*. In a private letter (Nov. 28, 1924) he gave a few more details. "The result came out 1.0005_4 , but the probable error is at least ± 0.0001 , for my time measurements are inadequate. I used a 100 c/s fork which I had tested before leaving Teddington, but I checked it with a phonic wheel and a 100-year-old 8-day clock which belonged to my great-grandmother."

But to return to his beginnings: he received his early education at Derry Academy, Queen's College, Belfast, and Edinburgh University. The link with Edinburgh no doubt came from his mother's family, who were Callenders of Leith. His first paper was a note on the Peltier effect, presented to the Royal Society of Edinburgh in 1882, presumably while he was still a student under Professor Tait at Edinburgh University. In the following year he proceeded to Cambridge; he was admitted at Corpus Christi College in October 1883, became a Foundation Scholar in 1884, headed the Senior Optimes in Part I of the Mathematical Tripos, 1886, and got a Second in the Natural Sciences Tripos, 1887. His energy at this time had clearly not been all devoted to work for the Tripos, for his second paper on the Peltier effect was published in July 1887, and he mentions that the experiments were carried out in Professor Tait's laboratory and later continued in his own laboratory at Ballynagard. However, he had not yet discovered the line of work that he was to make his own. He became a science master at various schools, took a short course in electrical engineering at the Central Technical College, South Kensington, and then in 1893, at the instigation of Alexander Russell, he joined the staff of Faraday House. Here he found himself in his element; he took part in the teaching work and supervised the testing and thus acquired an insight into the scientific problems of the rapidly growing electrical industry. Original work on instruments and measurements and on the electrical and magnetic properties of materials immediately followed, and by the time he left Faraday House he had published about a dozen papers, no less than five being read before the Physical Society between 1896 and 1901. However, his best-known work was to follow.

In 1901 Glazebrook entrusted him with the task of building up in the newly-founded National Physical Laboratory a section for the measurement of the basic quantities encountered in alternating-current practice—inductance, capacitance, frequency, etc. He started from zero and during the next eighteen years gradually developed instruments and methods of measurement that were recognized as amongst the best of their kind in the world. The original Campbell primary standard of mutual inductance still forms the ultimate reference standard for the country, and the standards employed in several other

national laboratories are based upon it. The Campbell inductometer or variable standard of mutual inductance was at one time a key-instrument, in almost every laboratory and test-room concerned with a.c. measurements, and his vibration galvanometer, his constant-inductance rheostat, and later his a.c. potentiometer became also very widely used.

Most of his instruments were made with his own hands. He found great satisfaction in such work and even made his own galvanometers and resistance boxes, though he was not a skilled mechanic in the ordinary sense of the term. He brought fine craftsmanship to bear on the vital part of an instrument, but everything else would be of the most primitive construction, and to any user but their maker the auxiliary mechanical adjustments were often almost comically crude.

This was all of a piece with his general character, which was one of extreme simplicity. Looking back, one associates most of his colleagues with brilliant careers; of Campbell no such thought is possible; one sees only a single-minded devotion to an ideal, not perhaps formulated explicitly, but unmistakably including simplicity as an essential element. It appeared not only in his instrument design but also in his gardening and music, which seemed to rank as the counterparts of his scientific work, his devotion to truth as he saw it in the one being matched by that to beauty in the others. He had very strong feelings about things that to him did not ring true, and he expressed them with force and wit. They might be anything from a part of an instrument showing a waste of labour or material, a pointless bit of administrative routine, or "the hideous wobble of the professional singer" (vibrato). A characteristic remark in gentler vein occurs in some memories of his childhood. Of his father, "He was a constructive gardener, not like my Mother, who was mainly a destructive one. She loved *tidying up*".

Such a personality could not fail to find much that was uncongenial in a large highly organized semi-industrial laboratory, and as the National Physical Laboratory continued to expand there came a point where Campbell felt that he would be better outside (though to the last his interest in the N.P.L. was always that of one who belonged to it). He was unmarried; his wants were simple and he estimated that he could manage to live without his salary, so he went back to Ireland and lived with his mother at Ballynatrua. He set up there his own laboratory and continued his work. His determination of the ohm there has already been mentioned.

On his mother's death in 1925 he decided to move to Cambridge. He packed up his laboratory and library (in 150 boxes!) and continued to work for about a year in lodgings while he had a house built to meet his own requirements. The 'base line' was a 2-metre scale distance that, following his N.P.L. practice, he required in the principal room for his galvanometers. A treadle lathe stood on one side and on the other a doorway led into the greenhouse where he raised his seedlings. In this setting he steadily followed his chosen course to the end.

It is not possible to give in a few words an adequate impression of his total achievement. Much of it was summarized in the articles he wrote in Ireland for Glazebrook's *Dictionary of Applied Physics*, Vol. 2. He was urged to expand these into a book but heavy literary work did not greatly appeal to him and it was a relief to him when he found in Dr. E. C. Childs a man with whom he could collaborate. It is a satisfaction to note that the book was published in 1935.

His closing years were uneventful. He was no longer to be met at scientific meetings but occasionally appreciative fellow workers from as far afield as the United States and Japan would seek him out, an informal scientific honour that one felt to be peculiarly appropriate.

L. HARTSHORN.

FRANCIS CECIL CHALKLIN

The tragic death of Frank Chalklin at the age of fifty-one came as a profound shock to his many friends. He was Professor of Physics at Canterbury University College, New Zealand, and had applied for the vacant chair of physics at University College, Hull. The authorities at Hull desired an interview and arranged for Chalklin to fly to England for this purpose. He duly embarked on the Qantas-B.O.A.C. Constellation air liner which crashed at Kallang airport on 13th March, 1954, there being no survivors among the thirty-one passengers. He had left his home in high spirits and the end was mercifully sudden.

Frank Chalklin was born on 15th November 1902, at Hadlow, near Tonbridge, of Kentish stock on both sides of the family, and his affection for his native county was very strong. He went to Judd School, Tonbridge, which he left in 1919 with high distinctions. He then studied at King's College, London, and after graduating in 1923 carried out research in the Wheatstone Laboratory, then under the guidance of Sir Owen Richardson. The subject of his early investigations was the excitation levels of very soft x-rays, on which three papers by Richardson and Chalklin appeared in the *Proceedings of the Royal Society*. The experience which Chalklin obtained in these early days, both in experiment and theory, stood him in good stead during his whole research career, for very soft x-rays and allied subjects remained his great laboratory interest throughout his life. The method used in the King's College experiments was a photoelectric one, but Chalklin subsequently turned to vacuum spectroscopy, with which he had outstanding success. For his work under Richardson he was awarded the Ph.D. in 1926.

From 1927 to 1930 he was at the University of Sheffield as junior lecturer under Professor S. R. Milner, whence he came to London to take up the post of lecturer on the physics staff at University College. Here he speedily established his position both as a teacher and as an original worker. His unselfishness and integrity made him both loved and respected: nothing was too much trouble if he thought that duty demanded it. Quiet and unassuming, he had beneath the surface unshakable standards to which he remained true. He was thorough and dependable in everything that he did, with no tricks for seeking the popularity which he nevertheless obtained. At University College, in conjunction with his wife, an accomplished physicist, he developed his first vacuum spectrometer, making use of a narrow ruled grating at grazing incidence. With this apparatus outstanding results were obtained in the neighbourhood of 50 \AA , a region then almost unexplored. He speedily became an acknowledged leader in this field, his discussion of his results showing a command of the theoretical aspect of his subject. In 1938 he published, with collaborators, in our *Proceedings* an account of a new vacuum spectrograph with a concave grating, designed for the spectral region 15 to 1000 \AA . His work with this instrument was brought to an end by the war, which saw the destruction of the

University College Physics Laboratory. During this period at University College he was awarded the London D.Sc. and made Reader in Physics of the University.

The war years he spent at the University College of Wales, Aberystwyth, whither part of the physics department of University College had emigrated. Here he won golden opinions by his knowledge, tact and assiduity. The responsibility exercised a maturing influence. As soon as he returned to the desolation at London in 1944 he threw himself wholeheartedly into aiding with the work of restoration and speedily had his own research started again, as witness a considerable paper on intensity measurements in the very soft x-ray region which appeared in the *Proceedings of the Royal Society* in 1948. At this time Chalklin was already in New Zealand, having been appointed to his Canterbury chair in 1946.

In New Zealand he set to work with his accustomed energy and with a full measure of success. He started research there by building, with his research students, the necessary apparatus, including the Geiger counter spectrograph for soft x-rays described in our *Proceedings* in 1951. He worked with system, laying the foundations surely for a solid school. In 1951 he was elected Fellow of the Royal Society of New Zealand and he had made himself greatly loved. The very full attendance at the memorial service held in the Cathedral at Christchurch bore witness to the respect in which he was held as a man and as a scientist.

Frank Chalklin had a very happy home life. In 1928, while he was at Sheffield, he married Letitia (Letty) Pulley Davies, who, as already recorded, helped him as collaborator in some of his best work and in less learned ways no less. There are three children, the eldest, a boy, now reading history at Oxford, and two girls, the youngest born in New Zealand. He was a very human character, much concerned with cricket, and himself a player of lawn tennis and badminton. Farming, too, was in his blood and in New Zealand the Chalklins had a small farm, run by a manager but the object of his expert interest. This notice can fitly conclude with some words which he himself wrote, just before his death, on his conception of a professor's task. They indicate well the man. "The basic duty is, of course, to maintain a good standard of undergraduate teaching. And I also hold the orthodox view that the university is still the best place for performing fundamental pure research and indeed has the duty of conducting it. I conform also with the view that the teaching is likely to be uninspired in departments in which research is neglected. The professor would seem to have the duty of encouraging his staff in this direction and, in particular, of helping young staff members to get the habit of research early in their careers. Their research record enables them to compete for posts in other universities as well as to secure promotion in their own. And movement between universities is stimulating to the individual and to the department. Finally, I believe that it is a duty to make the department a happy place for staff and students and that the senior and research students should be encouraged to look upon their department as their home."

E. N. DA C. ANDRADE.

REGINALD STANLEY CLAY

The death, on 10th April 1954, of Dr. R. S. Clay at the age of 85 years, removes a much respected figure from scientific circles in London.

Reginald Stanley Clay was born at Portsmouth and was educated in the first instance at Tollington Park College. He took the degree of B.Sc. (London) in 1889, and afterwards went to St. John's College, Cambridge, where he read Mathematics, becoming 21st Wrangler in 1892. Two years' experience as Physics Master at Mill Hill School was followed by his appointment in 1897 as head of the Physics Department at Birkbeck College. He was awarded the degree of D.Sc. (London) in 1900, the title of his thesis being 'On the application of Maxwell's curves to three-colour work, with especial reference to the inks to be employed, and to the determination of suitable light filters'. However, he seemed to incline to the fields of teaching and administration, rather than to the exclusive pursuit of science, and in the same year he accepted the post of principal of Wandsworth Technical College. Only two years later he was appointed Principal of the Northern Polytechnic Institute.

His position now allowed him the opportunity to wield a great influence in the development of the many sides of educational work in London, by no means exclusively concerned with science and technology. For example he was an active member of the National Council for Domestic Studies; he was Chairman of the Governors of the North London Collegiate School for Girls; and he became a member of various societies with cultural interests. From 1907 to 1911 he acted as secretary of the Association of Technical Institutes. A lifetime of social service was the outward expression of his Christian faith. He was a member of a Congregational Church, and became a Mason in the Ophthalmos Lodge in 1929.

His major scientific interest lay in the field of Optics, and his book on *Practical Light*, published in 1911, was widely used and valued. He joined the Optical Society in its early days, and took a large share in its elevation (during the 1914-18 war) from a minor status into that of a leading scientific Society. He served on its Council, and was President from 1927 to 1929. His Presidential Address dealt with the History of the Stereoscope. He was a keen participant in the discussions (sometimes rather heated) by which the members accomplished a good deal of their mutual education in optical matters. But Clay's urbane manner and charming smile never failed him. His numerous duties left him little time for continuous research, and he published comparatively little in this period beyond occasional brief descriptions of apparatus, but he was almost the ideal member and critic. Many were the occasions when some ingenious piece of equipment made by his own hands was brought to a meeting for exhibition. He was uniformly kind in his encouragement of younger workers, many of whom had cause to be grateful for his hospitality and constructive hints.

He took much interest (as representing the Optical Society) in the formation of the Institute of Physics, being a Founder Fellow in 1918. He was elected to the Board in 1920, and served the Institute in various capacities during the remainder of his life, i.e. as Examiner and as Chairman of the Advisory Board

for the *Journal of Scientific Instruments*, to which he was a frequent contributor of short articles describing various tools and processes. He was also a member of the Council of the British Optical Association, and was its President in 1927; and he acted for many years as Examiner for this body.

He became a member of the Physical Society in 1925, and later of the Optical Group, in which he took a great interest. He was welcome and honoured at all social events in connection with these bodies.

His retirement from the Northern Polytechnic in 1931 gave him more leisure to pursue his favourite studies. Somewhat before this time, he had become acquainted with Thomas Henry Court, and had begun to collaborate with him in historical studies of optical instruments, especially the microscope. (He was already a member of the Royal Microscopical Society, of which he served as President in 1937.) The most noteworthy product of this friendship was the *History of the Microscope*, written in collaboration with Court, and published in 1932. Clay himself had for some time been collecting old instruments, and in the end brought together a very representative set in which the period from A.D. 1670 to 1850 was represented by three hundred and twenty-eight microscopes. It is not surprising that the study of these, together with Court's own magnificent collection, made the foundation for a most authoritative book. The Clay collection was acquired in 1943-44 for the Ashmolean Museum, Oxford.

In 1936 he joined the Board of the United Kingdom Optical Company Ltd., at Mill Hill, and was associated with this firm in various ways till his death. During the war of 1939-45 he had much to do with the Admiralty Research Laboratory at Teddington, acting as liaison officer between this and various Service depots.

One of his greatest pleasures in more recent years was his membership of the Royal Institution; he was a regular listener to the Friday evening discourses, and took the greatest interest in the demonstrations. His faculties seemed undimmed and his memory keen; his delight in science as great as ever. It was difficult to believe that he was approaching his 86th year. He suffered only a short illness.

He married Theodora Tilley, who died in 1952. They had a son and two daughters.

The passing of a man such as this marks an epoch in the development of the Physical Sciences. At its beginning, the keen amateur could hold his own and take an important part; at its end, the Scientific Society largely reflects an aspect of professional duty. Is there any room for the non-specialist? It seems certain that, without the spirit of such people, Science might prove to be one of the biggest of human disappointments.

L. C. MARTIN.

FRANK KENNETH GOWARD

Frank Kenneth Goward, whose untimely death occurred on 10th March 1954, occupied a post of Senior Principal Scientific Officer at the Atomic Energy Research Establishment, Harwell. Born on 30th August 1919, he received his early education at Queen Elizabeth's Grammar School, Wakefield, and from there went up to St. John's College, Cambridge, in 1938 on an open scholarship. After graduating in honours physics in 1940 he joined a group of physicists working on the radar chain stations in the early years of the war. With this experience behind him he joined the Telecommunications Research Establishment at Malvern towards the end of 1942. From then until the end of the war he was concerned with research and development of centimetre aerial systems and rapidly established a reputation as an authority in this field.

When the war finished there was intense interest in this country and in the United States in methods of particle acceleration using radio-frequency fields. Frank Goward was quick to realize that experimental verification of the new principles of synchrotron acceleration could most readily be obtained by conversion of an existing betatron, and in collaboration with D. E. Barnes was the first to accelerate electrons by this method to an energy of 8 mev. Higher energy synchrotrons soon came into operation in other laboratories and Goward played a leading part in the design of Britain's largest electron accelerators at Glasgow and Oxford Universities, and in several 30 mev machines built at the Atomic Energy Research Establishment. Using the latter machine Goward and his team made a number of notable contributions to fundamental nuclear research in their photodisintegration work using photographic plate techniques.

In 1951, Goward was chosen to represent Great Britain at an international conference held under the auspices of Unesco to discuss the formation of an international laboratory for Nuclear Research. Arising from this he was largely responsible for drawing together an international team of scientists to examine the problems of design of a 15 kmev proton synchrotron. The activities of the group entered a new and exciting phase in mid-1952 after Goward and the group leader Dr. Dahl brought back from America information of the new principle of alternating gradient focusing. In 1953 Goward was given leave of absence from Harwell and moved to Geneva with his family to take up his duties as deputy group director of the proton synchrotron team for C.E.R.N. (the Central European Laboratory for Nuclear Research). Not many months afterwards he became seriously ill and his wife brought him back to this country for specialist treatment. His colleagues will remember Frank Goward for his irrepressible sense of fun and good humour.

W. WALKINSHAW.

FRANK LLOYD HOPWOOD

The death on 2nd May 1954 at the age of 70 of Professor F. L. Hopwood, one of the oldest members of the Physical Society and for many years a member of its Council, is a great loss to medical physics of which he was a leading authority.

Born in 1884 in Cheshire, Frank Lloyd Hopwood received his education at Hawarden Grammar School, the University College of North Wales, Bangor, and the Royal College of Science, and finally at the University College London, where he received his D.Sc. degree in 1919. He joined the staff of St. Bartholomew's Hospital in 1906 and was teaching physics to the students at the Medical College there. In 1920 he became Physicist to the Hospital, and in 1924 was appointed to the Chair of Physics at the Medical College of St. Bartholomew's Hospital, a post he held until his retirement in 1949, when the University of London conferred on him the title of Professor Emeritus.

During the First World War Hopwood worked with Sir William Bragg on submarine detection problems. Ever since then he maintained an interest in ultrasonics, and he pursued research in this subject and published several papers even after his retirement; an interesting feature of this research being that it was carried out by means of a kitchen tap and sieve. He also maintained a close interest in nuclear physics and it was in his laboratory that the Szilard-Chalmers process and the production of neutrons by x-rays in the photonuclear effect were discovered in 1934. But most of his interest lay in the fields of medical physics and radiology, in which he carried out a great deal of pioneering work. He played an important part in setting up the Strangeways Laboratory in Cambridge and in the installation of the million-volt x-ray machine at Barts, the first to be used for super-voltage therapy. In recent years he devoted a great deal of energy to the installation at Barts of the 15 mev linear accelerator.

Apart from the direct contributions he has made to radiotherapy, he has been very active in the organization and coordination of cancer research. He was a founder-member of the British Empire Cancer Campaign, and until his death he was a member of its Grand Council and its Honorary Secretary. He was a past President and Silvanus Thompson Medallist of the British Institute of Radiology, Honorary Member of the Faculty of Radiologists, and for many years Secretary to the British Committee for Radiological Units.

All these outside activities did not detract from his devotion to Barts, which he served with the utmost loyalty and where he was loved and admired by students and colleagues. During the Second World War, when the Pre-Clinical School was evacuated to Queens' College, Cambridge, Hopwood was appointed Vice-Dean, a post he held until his retirement. He was mainly responsible for the excellent relationships that existed between the two Colleges during the seven years of evacuation, and in recognition of this the University of Cambridge conferred on him the Honorary Degree of M.A., and Queens' College elected him an Honorary Member.

A tribute to the memory of Professor Hopwood would not be complete without a reference to his remarkable personality. He was a big man both

physically and mentally. He had a great sense of humour and an inexhaustible store of anecdotes; he was a charming companion, tolerant, tactful and generous. He was always available to give advice, help and comfort, and there were many who leaned on his wisdom, experience and sympathy. He had a gift of infecting people with his own enthusiasm and vitality. Many of the leading authorities in medical physics are either his former pupils or people whom he introduced and inspired to enter into this new field. He managed to stimulate an interest in physics, and in science in general, in many thousands of medical students who passed through his hands. He will be greatly missed by his former students, his colleagues and his friends.

J. ROTBLAT.

JOHN EDWARD LENNARD-JONES

In a brief obituary notice to a specialized journal it is impossible to do justice to all the aspects of the varied life and work of John Edward Lennard-Jones, mathematician, physicist, theoretical chemist, civil servant and administrator. Nor indeed can space be found there for a full record of his achievements and of the distinctions he received in recognition of his services. A fuller biography will doubtless appear elsewhere.

Faced with the task of selection, I inevitably recall the years 1925 to 1932 when we were close and intimate colleagues, a period also when in the prime of early manhood, Lennard-Jones was maturing from a state of marked promise as a researcher and teacher to that of high distinction and reputation.

Coming to the University of Bristol from Manchester and Cambridge, where he had already attracted attention by his estimation of molecular fields from gaseous viscosity, from the equation of state and from crystal measurements, he here developed the pattern of so much of his subsequent work and career. The investigations he then carried out on the lattice properties of crystals and the processes of adsorption and diffusion on surfaces, in terms of interatomic forces, will find a permanent place in the literature. Moreover in this period he started to develop the molecular orbital technique for the study of diatomic molecules, which in its extension to more complex molecules has proved to be of so particular an interest to chemists. Indeed it is only three months ago that the eighteenth paper under the heading 'Molecular Orbital Theory of Chemical Valency' was published from the Cambridge Laboratory where he held the Plummer Chair of Chemistry from 1932 until a year ago.

In the light of its importance to-day, it is interesting to recall the status of the subject of theoretical physics in 1925 when Bristol initiated a readership in it and invited Lennard-Jones to fill the appointment. Departments of Applied Mathematics were, of course, well known: but I am not aware of any permanent senior post at that time designed for a theorist working within the framework of a Physics Laboratory in a University of this country. Indeed, the very term 'theoretical physicist' was not then in use in Britain.

Two years after his arrival, the Henry Herbert Wills Physical Laboratory was completed, and a chair, the first in this subject in the country, was created for him. By then he had already begun to throw himself with all his drive and enthusiasm into the project of creating in a provincial centre a new school of theorists and experimenters, trained together, and working in daily contact and

close co-operation. When he left for Cambridge five years later, having helped in the meantime to secure substantial endowments for the Wills Laboratory from the Rockefeller Foundation and from Mr. Melville Wills, who endowed his chair, his pioneering work in its formative years had already borne fruit. Moreover, by his example, the conception behind the scheme was beginning to catch on in other centres. Indeed, when he himself was invited in 1932 to Cambridge as the first theorist to fill the Plummer Chair, he was again chosen to break fresh ground, though this time in a department of Chemistry.

At Bristol also, I remember his early interest in administration, as a member of Senate and for two years as Dean of the Faculty of Science. He seemed even then to enjoy with others the task of framing policy ; and the work also gave opportunity for the exercise of his orderly mind in matters of detail and procedure.

With the advent of war it was therefore not surprising to find him by 1942 in high office as Chief Superintendent of the Armament Research Establishment, and later as Chief Scientific Officer and Director General of Scientific Defence Research in the Ministry of Supply.

But the war over and in Cambridge again, re-established in an atmosphere of active research and academic influence, he might have been expected to have remained content in such pleasant and friendly surroundings. It therefore required courage and initiative on his part to be prepared to take up the challenge of a new task by accepting an invitation to become Principal of the University College of Staffordshire at this early stage in its life. How sad it is to record his death at the early age of 60, only a year after he and his wife had taken up their residence there.

One final word : readers of the literature, seeking his papers prior to 1925, will find them under the heading J. E. Jones. On his marriage to Kathleen Mary Lennard, daughter of the late Alderman Lennard of Leicester, he changed his name by deed poll. Thus arose the familiar abbreviation L-J, by which he was so often addressed or spoken of, to the end of his life, by an ever increasing circle of friends and fellow workers.

A. M. TYNDALL.

ROBERT STEWART WHIPPLE

Robert Stewart Whipple, born on 1st August 1871 was the son of G. M. Whipple, the Superintendent of Kew Observatory, and so was brought up in an environment in which scientific instruments played an important part. After leaving King's College School in 1888, he served as an Assistant in Kew Observatory under Dr. Charles Chree for eight years.

For a short time he was Assistant Manager to Mr. L. P. Casella, and two years later joined Sir Horace Darwin as a personal assistant. Mr. Horace Darwin, as he was then, had founded the Cambridge Scientific Instrument Company eighteen years earlier, and it was in connection with this Company that R. S. Whipple was to spend the remainder of his life. He was made Joint Managing Director in 1909 and served in this capacity up to his retirement in 1935. From then until 1949 he was the Chairman of the Board of Directors.

While his specialized early work was on the measurement of temperature, he was at all times interested in all types of scientific instruments. In a paper

on "Thermometers and Pyrometers" (1904) he says "one cannot help being struck with the interdependence of all branches of scientific work". This consciousness was to remain with him all his life. The interest in thermometry was coupled with an early realization of the importance of temperature measurement in industry, and later his interest turned to the control of temperature in industry. Radiation pyrometry was little used in this country until Whipple introduced it, and his zeal caused him to press for its adoption in industry up and down the country. He secured the rights of manufacture in this country of the Féry pyrometer for the Cambridge Instrument Company. He invented the Whipple Temperature Indicator for use with electrical resistance thermometers, and it is still in considerable use.

While he was a first-class physicist, much of his success was due to his practical outlook. For example, in a paper on "Pyrometry as applied to the making of pottery" (1913), in assessing the requirements for a successful pyrometer installation for pottery making, he put them in the order (i) simplicity, (ii) durability, and (iii) accuracy. In the same paper he said "... it is essential to assure the fireman that the purpose of the installation is to help him in his work".

This brings to mind his outstanding personal quality—a kindliness and gentleness of manner resulting from a sympathetic character. There are many young scientists who have been encouraged by a kind word from R. S. Whipple.

He served on many committees. He was President of the Optical Society, and was Treasurer of this Society for ten years, and a Vice-President for three years. He served for twenty-one years on the Board of the Institute of Physics, of which he was a Founder Member, and the Institute owes much to his generosity. He was one of the Founder Members of the Physical Society Club. He served the Royal Institution, as Visitor and Manager, and he was a Member of the Institution of Electrical Engineers, and served on its Council. He delivered the Faraday Lecture of that body in 1936. He was twice elected President of the Scientific Instrument Manufacturers' Association. He presided over Section A of the British Association in 1939.

His interest in all types of scientific instruments caused him to make a collection of historical scientific instruments and books; he gave this valuable collection to the University of Cambridge, together with a large sum of money for further purchases of books and apparatus. This formed the nucleus of a Museum of the History of Science, opened in 1951 as the "Whipple Museum". It is in large measure due to him that the History and Philosophy of Science is now a subject for the Natural Sciences Tripos.

He served his locality also, taking much interest in the Highgate Literary and Scientific Institution of which he was President for 16 years, and one of his last acts just before his death was to found a trust for the advancement of the sciences and arts especially in North London. Here again his breadth of outlook was shown by the latitude he left to the trustees.

He was, as a foreigner once described him, "un homme plus que gentil". To meet him was to respect him, to know him was to love him.

A. C. MENZIES.

MAURICE EDMOND JOSEPH GHEURY DE BRAY

We record with regret the death of M. E. J. Gheury de Bray who had been a fellow of the Physical Society from 1933 until he resigned through ill health in 1950. During the late 1940's Gheury de Bray compiled for his own use a comprehensive subject index of volumes 1-10 of the Physical Society's *Reports on Progress in Physics*. He presented the Physical Society with a copy of the Index, and this was published by the Society in 1953.

FRED HARRISON

We record with regret the death on 1st May of Fred Harrison, who had been a member of the Physical Society since 1893, and was thus one of the Society's oldest members.

CONTENTS OF SECTION B

	PAGE
Sir. GEOFFREY I. TAYLOR. Diffusion and Mass Transport in Tubes (Guthrie Lecture)	857
Mr. A. N. INCE. The Effect of Intense Magnetic Fields on Electroluminescent Powder Phosphors	870
Mr. W. P. OSMOND. The Effect of Particle Shape Variations on the Coercivity of Iron Oxide Powders	875
Dr. A. SCHALLAMACH. On the Abrasion of Rubber	883
Research Notes :	
Mr. D. C. NORTHROP and Dr. O. SIMPSON. Electrical Conductivity of Some Condensed Aromatic Hydrocarbons	892
Dr. MARY D. WALLER. Symmetry of Vibrating Square Membrane	895
Dr. MARY D. WALLER. Note on Surface Vibrations of a Circumscribed Liquid	899
Reviews of Books	900
Obituary Notices :	
HERBERT STANLEY ALLEN	905
ALFRED BLACKIE	906
ALBERT CAMPBELL	907
FRANCIS CECIL CHALKLIN	910
REGINALD STANLEY CLAY	912
FRANK KENNETH GOWARD	914
FRANK LLOYD HOPWOOD	915
JOHN EDWARD LENNARD-JONES	916
ROBERT STEWART WHIPPLE	917
MAURICE EDMOND JOSEPH GHEURY DE BRAY	919
FRED HARRISON	919
Contents of Section A	920
Subject Index, Section B, Vol. 67	921
Index of Authors (with Titles), Section B, Vol. 67	927
Index to Reviews of Books, Section B, Vol. 67	933

PROCEEDINGS OF THE PHYSICAL SOCIETY

SECTION A, 1954—VOLUME 67

SUBJECT INDEX

	PAGE
Absorption, continuous, of light in calcium vapour (R)	190
Absorption of light by indium vapour (L)	196
Absorption, optical, in metals and semiconductors, theory	74
Absorption spectra, atomic and molecular : III—ultra-violet spectra of In vapour	864
Absorption spectrum of BiSe and BiTe in region 2900–2200 Å	935
Absorption spectrum of bismuth oxide	44
Absorption spectrum of lutetium (R)	291
Absorption spectrum of thulium (R)	476
Absorption, ultra-violet, of In vapour	864
Air showers, extensive, sidereal correlation of	996
Alkali metals, free electron diamagnetism and susceptibilities (R)	464
Alloys, Ag–Pd, lattice thermal conductivity at low temperatures (L)	728
Alloys, substitutional, volume changes in (R)	388
Alpha-activity induced in gold by bombardment with ions of ^{13}C (L)	733
Alpha activity induced in gold by bombardment with nitrogen ions (R)	555
Alpha emitters, short-lived, produced by ^3He and heavy ion bombardments	949
Alpha-particle bombardment, radiations from water under	922
Alpha-particles, binding energy of	323
Alpha-particles, light emission in passage through gases	841
Alpha-particles, scattering of nucleons by : the s-phases	957
Alpha standardization, absolute, with liquid scintillators (L)	297
Aluminium monofluoride, triplet electronic states of (L)	94
Angular correlation experiments with soft electrons, source scattering (R)	1108
Angular correlation functions, electron-neutrino, in theory of beta-decay	117
Angular correlation of successive γ rays in ^{60}Ni at low temperatures	1051
Angular distributions in $^{10}\text{B}(\text{d}, \text{p})^{11}\text{B}$ reaction	684
Angular momenta, coupling, in reaction $^{27}\text{Al}(\text{p}, \gamma)^{28}\text{Si}$ (L)	392
Antiferromagnetism, collective electron (L)	295
Antiferromagnetism in metals (R)	1018
Aromatic molecules, electronic spectra : I—Benzenoid hydrocarbons	795
Atomic orientation, optical methods (Holweck Lecture)	853
Auger effect and negative meson capture	57
Auroral spectrum, intensity distribution among nitrogen bands in	780
Band spectra, ultra-violet, of CCl and SiCl (R)	186
Band structure of silicon (L)	562
Band system, beta, of NS molecule, rotational analysis	365
Band system, E–x, of SiS and dissociation energy of SiS (L)	95
Band systems of O_2 , intensities : Broida–Gaydon, and atmospheric	847
Bands, infra-red, auroral, of ionized nitrogen, excitation conditions (R)	188
Beta-decay, theory, electron-neutrino angular correlation functions in	117
Beta rays of thallium 204	881
Beta transitions, forbidden, and nuclear spin-orbit interaction	1005
Binding energy of alpha-particle	323
Bismuth 207, decay, and energy levels of ^{207}Pb	540
Bismuth oxide, absorption spectrum of	44
Bismuth selenide and telluride, absorption spectrum in region 2900–2200 Å	935
Bombardments, ^3He and heavy ion, producing short-lived emitters	949
Born approximation, second, in inelastic collisions of electrons with atoms	673
Bose–Einstein functions	632
Bremsstrahlung spectrum, thick target, at relativistic energies	669

	PAGE
Calcium vapour, continuous absorption of light in (R)	190
Celestial bodies, red-shift formula, interpretation (L)	193
Celestial bodies, red-shifts in spectra of (L)	192
Cloud chamber with internal counters, for detection of electron pairs	941
Cloud chamber study of Geiger discharge	1095
Cloud chamber study of internal pairs from $^{12}\text{C}^*$	153
Cloud chamber, <i>see also</i> Wilson chamber.	
Cobalt 57, disintegration (R)	280
Cohesive energy of metallic sodium, and correlation energy in metals	52
Collective electron antiferromagnetism (L)	295
Collective electron approximation, exchange interaction in	221
Collisions, inelastic, of electrons with atoms, second Born approximation	673
Collisions, inelastic, between heavy particles: II—double transitions associated with encounters between hydrogen atoms	663
Collisions, inelastic, between heavy particles: III—excitation of He atoms in fast encounters with H atoms, protons and positive He ions	1069
Collisions, inelastic heavy particle, involving crossing of potential energy curves: I—charge transfer from H atoms to Be^{2+} , Si^{2+} and Mg^{2+} ions	805
Collisions, inelastic heavy particle, involving crossing of potential energy curves: II—charge transfer from H-atoms to Al^{3+} , B^{2+} , Li^{2+} and Al^{2+}	1010
Condensation, Mayer theory, tested against simple model of imperfect gas	233
Correlation energy in metals and cohesive energy of metallic sodium	52
Cosmic radiation, ionization intensity and specific ionization in air at sea level	421
Cross section, photo-ionization, <i>see</i> Photo-ionization.	
Cosmic radiation, positive temperature coefficient (R)	637
Cosmic ray particles, associated, time coherence	1037
Coulomb effects in stripping reactions	813
Coulomb energy and electron scattering data, showing consistency of nuclear radii	950
Coulomb forces, and isotopic spin: excited states of light nuclei	39
Coupling, intermediate studies: II—radiative transitions in light nuclei	167
Coupling, j - j , radiative transitions in (L)	1024
Cross section for photodisintegration of deuteron at 2.615 Mev, and absolute standardization of rays of ThC'' (L)	1113
Cross sections, absorption, for 134 Mev protons	125
Cross sections, absorption, neutron spectrum for	967
Cross sections for reaction $^7\text{Li}(\gamma, p)^6\text{He}$ at 17.6 and 14.8 Mev and first excited state of ^6He (R)	469
Cross sections, (d, p) scattering, absolute magnitudes	273
Decay of ^{207}Bi and energy levels of ^{207}Pb	540
Decay of ^{203}Pb and energy levels of ^{203}Tl	254
De-excitation of helium metastable atoms in helium (R)	276
Deuteron bombardment of oxygen (L)	564
Diatomic molecules, vibrational transition probabilities: III	939
Discharge, Geiger, cloud chamber study of	1095
Discharges, hollow-cathode, KHF_2 , and ultra-violet spectrum of excited diatomic hydride	68
Disintegration of cobalt 57 (R)	280
Disintegration of MsTh_2 , lens spectrometer study	265
Disintegration of ^{233}Pa , lens spectrometer study	397
Dissociation energy of SiS , and E-x band system of SiS in emission (L)	95
Eckart and Bargmann potentials for investigation of triplet neutron-proton scattering in low energy region	111
Editorial	1
Elastic media, propagation of energy in (L)	726
Electron affinities of atomic fluorine, oxygen and lithium	25
Electron capture: IV—capture from helium atoms by fast protons	1075

	PAGE
Electron impact, vibrational and rotational excitation of molecular hydrogen by . . .	909
Electron-neutrino angular correlation functions in theory of beta-decay . . .	117
Electron pairs, detection in cloud chamber with internal counters . . .	941
Electron-photon showers, three-dimensional theory . . .	158
Electron-positron pairs, emission from light nuclei : I—monopole transition in ^{16}O	134
Electron-positron pairs, emission from light nuclei : II—transitions in ^8Be , ^{10}Be and ^{16}O . . .	413
Electron-positron pairs, emission from light nuclei : III—transitions in reaction $^{15}\text{N}(\text{p}, \gamma)^{16}\text{O}$. . .	930
Electron scattering and coulomb energy data, showing consistency of nuclear radii	950
Electron scattering by nuclei and spectroscopic isotope shifts (L) . . .	393
Electronic spin in semiconductors, chemical approach to treatment (L) . . .	294
Electronic states in metallic lithium, calculation of eigenvalues by cellular method .	2
Electronic states, triplet, of aluminium monofluoride (L) . . .	94
Electrons, elastic scattering of, by beryllium (L) . . .	1111
Electrons, elastic scattering of, by excited 2s and 2p states of atomic hydrogen .	1086
Electrons, free, applicability of free-electron network model to metals . . .	608
Electrons and positrons, difference in multiple scattering (L) . . .	730
Electrons, scattering and polarization by gold . . .	711
Electrons in solids, momentum distribution : results for some metals using Thomas-Fermi method . . .	9
Elements, light, approximate nuclear density distributions . . .	773
Emission spectra, ultra-violet, of gaseous monofluorides of gallium and indium .	528
Emission spectrum, E-x, of SiS and dissociation energy of SiS (L) . . .	95
Energy, <i>see also</i> Nuclear energy.	
Energy levels in ^{10}B and ^8Be (R) . . .	467
Energy levels of ^{207}Pb and decay of ^{207}Bi . . .	540
Energy levels of ^{203}Tl and decay of ^{203}Pb . . .	254
Energy levels of triatomic molecules . . .	351
Energy, propagation in elastic media (L) . . .	726
Exchange interaction in collective electron approximation . . .	221
Excitation conditions for infra-red auroral bands of ionized nitrogen (R) . . .	188
Excitation of hydrogen atoms in fast encounters . . .	663
Excitation, vibrational and rotational, of molecular hydrogen by electron impact .	909
Ferromagnetic anisotropy coefficient, etc., for nickel, calculation of . . .	505
Ferromagnetic crystals, inelastic magnetic scattering of neutrons from . . .	85
Ferromagnetic crystals, scattering of slow neutrons by . . .	248
Ferromagnetic exchange problem, self-consistent spin-wave theory for . . .	33
Ferromagnetic properties of oxidized MnSb_2 (R) . . .	1022
Ferromagnetic resonance, in colloidal nickel, temperature dependence (L) . . .	648
Ferromagnetism, Hesisenbergs's theory, modified form . . .	148
Feynman's theory of liquid helium . . .	901
Field, self-consistent, for Au^+ . . .	789
Fission rate, spontaneous, of ^{240}Pu (L) . . .	646
Forces, short range, and nuclear energy levels in neighbourhood of ^{208}Pb . . .	757
Free-electron network model, applicability to metals . . .	608
Gadolinium sulphate octohydrate, paramagnetic resonance in (L) . . .	734
Galvanomagnetic and thermomagnetic effects in a plasma . . .	869
Gamma radiation from reaction $^{27}\text{Al}(\text{p}, \gamma)^{28}\text{Si}$. . .	101, corr. 197
Gamma radiation from reaction $^{11}\text{B}(\text{p}, \gamma)^{12}\text{C}$. . .	751
Gamma-rays of ThC' , 2.615 mev, absolute standardization and photodisintegration cross section of deuteron (L) . . .	1113
Gamma-rays, resonant scattering in ^{63}Cu and ^{56}Fe . . .	601
Gas, cooling by radiation . . .	741
Gas, dissociating, non-equilibrium thermodynamics of thermal transpiration of (R)	639
Gas, imperfect, simple model, and Mayer theory of condensation . . .	233
Gases, contaminating, effect on energy per ion pair in helium (R) . . .	640

	PAGE
Gases, light emission in passage of α -particles through	841
Geiger discharge, cloud chamber study of	1095
Gold, α -activity induced by bombardment with ions of ^{13}C (L)	733
Gold, α -activity induced by bombardment with nitrogen ions (R)	555
Gold, scattering and polarization of electrons by	711
Gyromagnetic ratio, etc., for nickel, calculation	505
Half-lives of ^{25}Al and ^{26}Al , measurements, and determination of resonant energies for proton capture by ^{24}Mg and ^{25}Mg	443
Heat flow, inertia, in liquid helium II	485
Heavy water, traces of light water in, nuclear method of estimation	520
Heisenberg's theory of ferromagnetism, modified form	148
Helium atoms, electron capture from, by fast protons	1075
Helium atoms, excitation in fast encounters with hydrogen atoms	1069
Helium atoms, two, van der Waals energy of	705
Helium, effect of contaminating gases on energy per ion pair (R)	640
Helium 4, scattering of 15.7 mev electrons by	657
Helium 6, first excited state, and cross sections for reaction $^7\text{Li}(\gamma, p)^6\text{He}$ at 17.6 and 14.8 mev (R)	469
Helium metastable atoms, de-excitation in helium (R)	276
Holweck lecture, 9th	853
Hydride, diatomic, ultra-violet spectrum, excited in KHF_2 hollow-cathode discharges	68
Hydrogen atoms, excitation of helium atoms by, in fast encounters	1069
Hydrogen atoms, fast encounters, double transitions	663
Hydrogen, molecular, vibrational and rotational excitation by electron impact	909
Hydrogen molecular ion, properties: IV—oscillator strengths of transitions connecting lowest even and lowest odd σ -states with higher σ -states	533
Hyperfine structures in atomic spectrum of calcium	450
Indium antimonide, electrical properties at low temperatures (R)	385
Indium vapour, absorption of light by (L)	196
Indium vapour, ultra-violet absorption spectra	864
Internal pairs from $^{12}\text{C}^*$, cloud chamber study	153
Ionization by relativistic μ -mesons in oxygen	331
Ionization chambers, integrating, statistical errors at background intensities	431
Ionization, cosmic ray, in air at sea level	421
Isomerism in ^{46}Ti (R)	286
Isotope shift, spectroscopic, and nuclear deformations	622
Isotope shifts in atomic spectra of tin and cadmium (L)	478
Isotope shifts in atomic spectrum of calcium	181
Isotope shifts, spectroscopic, and electron scattering by nuclei (L)	393
Isotopic spin and coulomb forces: excited states of light nuclei	39
Lead 203, decay, and energy levels of ^{203}Tl	254
Lead 205, search for (R)	283
Lead 207, energy levels, and decay of ^{207}Bi	540
Lead sulphide, selenide and telluride, molar heats in temperature range 20–260°K	569
Light, absorption by indium vapour (L)	196
Light, continuous absorption in calcium vapour (R)	190
Light, emission, in passage of α -particles through gases	841
Light nuclei, emission of electron-positron pairs from: I—monopole transition in ^{16}O	134
Light nuclei, emission of electron-positron pairs from: II— γ -transitions in ^8Be , ^{10}Be and ^{16}O	413
Light nuclei, emission of electron-positron pairs from: III— γ -transitions in reaction $^{14}\text{N}(p, \gamma)^{16}\text{O}$	930
Light nuclei, excited states in	39

	PAGE
Light nuclei, radiative transitions—study in intermediate coupling	167
Liquid helium, Feynman's theory	901
Liquid helium II, inertia of heat flow	485
Liquid helium 3, possible model	495
Lithium, metallic, calculation of eigenvalues of electronic states by cellular method	2
Lithium, photo-ionization cross section	917
Lithium, x-ray measurements at low temperatures	895
Low temperatures, angular correlation of successive γ -rays in ^{60}Ni	1051
Low temperatures, electrical properties of indium antimonide (R)	385
Low temperatures, lattice thermal conductivity of Ag-Pd alloys	728
Low temperatures, specific heat of metals	828
Low temperatures, thermal conductivity of Ge and Si	837
Low temperatures, x-ray measurements on lithium	895
Lutetium, absorption spectrum (R)	291
Magnetic fields, static, in general relativity	225
Magnetic moments, <i>see also under</i> Nuclear.	
Magnetic susceptibilities, principal, of maleic acid molecule $\text{HOOC}\cdot\text{HC} : \text{CH}\cdot\text{COOH}$ (R)	643
Magnetic susceptibility, and diamagnetism of alkali metals (R)	464
Magnetic susceptibility of nitric oxide in clathrate compound	525
Magnetostriction, saturation, approach to (R)	381
Maleic acid molecule $\text{HOOC}\cdot\text{HC} : \text{CH}\cdot\text{COOH}$ (R)	643
Matrix elements, phase, in nuclear reactions (R).	1103
Mayer theory of condensation tested against simple model of imperfect gas	233
Meson capture, negative, and Auger effect.	57
Meson theory, elimination of divergences from, and Riesz potential	580
Mesons, <i>see also</i> Mu-mesons.	
Mesothorium 2, disintegration, lens spectrometer study	265
Metallic conductivity, use of perturbation theory in, justification	206
Metallic lithium and sodium, nuclear magnetic resonance	217
Metals, antiferromagnetism (R)	1018
Metals, applicability of free-electron network model	608
Metals, magneto-resistance effect at high frequencies	305
Metals, momentum distribution of electrons in, using Thomas-Fermi method.	9
Metals, monovalent, thermal conductivity (L)	194
Metals and semiconductors, theory of optical absorption	74
Metals, specific heat at low temperatures	828
Metals, thermal conductivity (R)	290
Mn_2Sb , oxidized, ferromagnetic properties (R)	1022
Molar heats of lead sulphide, selenide and telluride in temperature range 20–260°K	569
Molecular ion, hydrogen, properties : IV—oscillator strengths of transitions connecting lowest even and lowest odd σ -states with higher σ -states.	533
Molecular orbitals, approximate : I— $1\sigma_g$ and $2p\sigma_u$ states of H_2^+	343
Molecular orbitals, approximate : II— $2p\pi_u$ and $3d\pi_g$ states of H_2^+	457
Molecules, aromatic, <i>see</i> Aromatic molecules.	
Molecules, triatomic, energy levels	351
Momentum distribution of electrons in solids : results for some metals using Thomas-Fermi method	9
Momentum distribution in nuclei (R)	288
Multilayers, consisting of a few monolayers, x-ray diffraction from.	315
Mu-mesons, anomalous scattering of (R)	559
Mu-mesons, relativistic, ionization by, in oxygen	331
Neon, photo-ionization	927
Neutron scattering, inelastic magnetic, from ferromagnetic crystal	85
Neutron spectrum for $\nu^{-\alpha}$ absorption cross section	967
Neutron transport theory, two-group perturbation theory in	615

	PAGE
Neutrons, 15.7 mev, scattering by ^4He	657
Neutrons, slow, scattering by ferromagnetic crystals	248
Nickel, calculation of first ferromagnetic anisotropy coefficient, gyromagnetic ratio and spectroscopic splitting factor	505
Nickel, colloidal, ferromagnetic resonance, temperature dependence (L)	648
Nitric oxide, in clathrate compound, magnetic susceptibility	525
Nitrogen, active, method of production, and application to study of collision effects in N_2 spectrum	821
Nitrogen bands, in auroral spectrum, intensity distribution	780
Nitrogen, ionized, infra-red auroral bands, excitation conditions (R)	188
Nitrogen ions, to induce α -activity in gold by bombardment (R)	555
Nuclear bound-state problems, method of solution	719
Nuclear deformations and spectroscopic isotope shift	622
Nuclear density distributions, approximate, in light elements	773
Nuclear energy levels and short range forces in neighbourhood of ^{208}Pb	757
Nuclear levels, statistics of	586
Nuclear magnetic moments, deviations from Schmidt lines.	885
Nuclear magnetic resonance in metallic lithium and sodium	217
Nuclear radii, consistency, from electron scattering and Coulomb energy data	950
Nuclear reactions, phase of matrix elements in (R)	1103
Nuclear shell structure (L)	1111
Nuclei, electron scattering by, and spectroscopic isotope shifts (L)	393
Nuclei, momentum distribution in (R)	288
Nucleons and electrons, high energy, scattering by carbon (L)	92
Nucleons, scattering by alpha-particles : the s-phases	957
Obituaries	1117
Optical absorption in metals and semiconductors, theory	74
Optical constants of tin below superconducting transition temperature (R)	386
Optical methods of atomic orientation and their applications (Holweck lecture).	853
Optical systems, wide aperture, field aberrations in	801
Oxygen, deuteron bombardment (L)	564
Paramagnetic resonance in gadolinium sulphate octohydrate (L)	734
Particles, heavy inelastic collisions between : II—double transitions associated with encounters between hydrogen atoms	663
Particles, heavy, inelastic collisions between : III—excitation of He atoms in fast encounters with H atoms, protons and positive He ions	1069
Particles, inelastic heavy, collisions involving crossing of potential energy curves : I—charge transfer from H atoms to Be^{2+} , Si^{2+} and Mg^{2+} ions.	805
Particles, inelastic heavy, collisions involving crossing of potential energy curves : II—charge transfer from H-atoms to Al^{3+} , B^{2+} , Li^{2+} and Al^{2+}	1010
Penetrating showers, local, possible variation of rate (L)	1026
Perturbation theory for one-dimensional wave equation (R)	383
Perturbation theory, two-group, in neutron transport theory	615
Perturbation theory, use in metallic conductivity, justification	206
Photodisintegration, <i>see also</i> Cross section.	
Photodissociation of spectrum of NO and pressure broadening in (R)	474
Photo-ionization cross section of lithium	917
Photo-ionization of neon	927
Photon-electron showers, three-dimensional theory	158
Plasma, galvanomagnetic and thermomagnetic effects	869
Plasma oscillations in periodic potential : one-zone theory	1058
Plutonium 240, spontaneous fission rate (L)	646
Polarization of 10.4 mev ray in reaction $^{27}\text{Al}(\text{p}, \gamma)^{28}\text{Si}$ (L)	481
Polarization and scattering of electrons by gold	711
Positronium, gaseous reactions involving	695
Positrons and electrons, difference in multiple scattering (L)	730
Positrons from ^{25}Al , end point energy, measurement (L)	479

	PAGE
Potential, periodic, plasma oscillations in: one-zone theory	1058
Proton bombardment of ^{23}Na , radiations from	973
Proton capture by ^{24}Mg and ^{25}Mg below 550 kev, determination of resonant energies and measurement of half-lives of ^{25}Al and ^{26}Al	443
Protons, 134 mev, absorption cross sections	125
Quantum electrodynamics, elimination of divergences from, and Riesz potential: I	17
Quantum electrodynamics, elimination of divergences from, and Riesz potential: II	201
Quantum electrodynamics, elimination of divergences from, and Riesz potential: III (R)	1021
Radiation, <i>see also</i> Gamma radiation.	
Radiation, cooling of gas by	741
Radiative capture and stripping reactions (R)	471
Radiative transitions in j - j coupling (L)	1024
Reaction $^{27}\text{Al}(\text{p}, \alpha)^{24}\text{Mg}$, levels of ^{24}Mg from (R)	1107
Reaction $^{27}\text{Al}(\text{p}, \gamma)^{28}\text{Si}$, coupling of angular momenta (L)	392
Reaction $^{27}\text{Al}(\text{p}, \gamma)^{28}\text{Si}$, γ -radiation from	101, corr. 197
Reaction $^{27}\text{Al}(\text{p}, \gamma)^{28}\text{Si}$, polarization of 10.4 mev γ -ray (L)	481
Reaction, $^{10}\text{B}(\text{d}, \text{p})^{11}\text{B}$, angular distributions	684
Reaction $^{11}\text{B}(\text{p}, \gamma)^{12}\text{C}$	751
Reaction $^9\text{Be}(\text{d}, ^3\text{He})^6\text{Li}$	946
Reaction $^7\text{Li}(\text{p}, \gamma)^8\text{Be}$, yield curve	849
Reaction (γ , n) in Cu, Zn and Ag (R)	1106
Reactions, D-D	990
Reactions, (d, p) and (d, n) theory: I—general theory ignoring coulomb effects	981
Reactions, gaseous, involving positronium.	695
Reactions, <i>see also</i> Stripping.	
Red-shift formula, Freundlich's, interpretation (L)	193
Red-shifts in spectra of celestial bodies (L)	192
Relativistic energies, thick target bremsstrahlung spectrum at	669
Relativity, general, static magnetic fields in.	225
Resonance, paramagnetic, <i>see</i> Paramagnetic resonance.	
Riesz potential and elimination of divergences from meson theory	580
Riesz potential and elimination of divergences from quantum electrodynamics: I	17
Riesz potential and elimination of divergences from quantum electrodynamics: II	201
Riesz potential and elimination of divergences from quantum electrodynamics: III (R)	1021
Rotational analysis of β -band system of NS molecule	365
Scattering, anomalous, of μ -mesons (R)	559
Scattering, elastic, of electrons by excited 2s and 2p states of atomic hydrogen	1086
Scattering, elastic, of 125 mev electrons by beryllium (L)	1111
Scattering of high energy nucleons and electrons by carbon (L)	92
Scattering, multiple, of electrons and positrons, difference in (L)	730
Scattering, neutron, inelastic magnetic, from ferromagnetic crystal.	85
Scattering of nucleons by α -particles: the s-phases	957
Scattering and polarization of electrons by gold	711
Scattering, resonant, of gamma-rays in ^{63}Cu and ^{56}Fe	601
Scattering of slow neutrons by ferromagnetic crystals.	248
Scattering, source, in angular correlation experiments with soft electrons (R)	1108
Scattering, triplet neutron-proton, in low energy region using Eckart and Bargmann potentials	111
Scattering, <i>see also</i> Neutrons.	
Scintillators, liquid, absolute alpha standardization with (L)	297
Self-consistent field for Au^+	789
Semiconductors, electronic spin in, chemical approach to treatment (L)	294
Semiconductors and metals, theory of optical absorption in	74

	PAGE
Showers, electron-photon, three-dimensional theory	158
Showers, <i>see also under</i> Air, Penetrating.	
Silicon, band structure (L)	562
Sodium 23, radiations from proton bombardment of	973
Specific heat of metals at low temperatures	828
Spectra, electronic, of aromatic molecules : I—benzenoid hydrocarbons	795
Spectra, red-shifts (L)	192
Spectrometer, scintillation pair, modified (R)	644
Spectrometer study of disintegration of MsTh_2	265
Spectrometer study of disintegration of ^{233}Pa	397
Spectroscopic isotope shifts and electron scattering by nuclei (L)	393
Spectroscopic splitting factor, etc., for nickel, calculation	505
Spectrum, <i>see also</i> Absorption, Auroral Spectrum.	
Spectrum, atomic, of calcium, hyperfine structures	450
Spectrum, atomic, of calcium, isotope shifts in	181
Spectrum, atomic, of tin and cadmium, isotope shifts in (L)	478
Spectrum, bremsstrahlung, <i>see</i> Bremsstrahlung.	
Spectrum, N_2 , collision effects in, application of new source of active nitrogen to study	821
Spectrum of NO , pressure broadening in, and its photo-dissociation (R)	474
Spin-orbit interaction, nuclear, and forbidden beta transitions	1005
Spin-wave theory, self-consistent, for ferromagnetic exchange problem	33
Statistics of nuclear levels	586
Stripping reactions, Coulomb effects in	813
Stripping reactions and radiative capture (R)	471
Superconducting transition temperature, optical constants of tin below (R)	386
Tellurium 203, energy levels, and decay of ^{203}Pb	254
Temperature coefficient, positive, of cosmic radiation (R)	637
Tensors, spherical, in physics	239
Thallium 204, beta rays	881
Thermal conductivity of Ge and Si at low temperatures	837
Thermal conductivity, lattice, of Ag-Pd alloys at low temperatures (L)	728
Thermal conductivity of metals (R)	290
Thermal conductivity of monovalent metals (L)	194
Thermodynamics, non-equilibrium, of thermal transpiration of dissociating gas (R)	639
Thomas-Fermi method for determining momentum distribution of electrons in some metals	9
Thomas-Fermi methods, extended (R)	378
Time coherence of associated cosmic ray particles	1037
Titanium 46, isomerism in (R)	286
Transition probabilities, vibrational, of diatomic molecules : III	939
Ultra-violet spectrum of diatomic hydride excited in KHF_2 hollow-cathode discharges	68
Ultra-violet, <i>see also</i> Absorption.	
Van der Waals energy of two helium atoms	705
Vibrational transition probabilities of diatomic molecules : III	939
Water, heavy, traces of light water in, nuclear method of estimation	520
Water, radiations from, under α -particle bombardment	922
Wave equation, one-dimensional, perturbation theory for (R)	383
Wilson chamber, internal counter controlled, resolving time	944
Wilson chamber, <i>see also</i> Cloud chamber.	
X-ray diffraction from built-up multilayers consisting of only a few monolayers	315
X-ray measurements on lithium at low temperatures	895
Yield curve of $^7\text{Li}(p, \gamma)^8\text{Be}$ reaction.	849

INDEX OF AUTHORS (WITH TITLES)

	PAGE
Abraham, G. : Absolute magnitudes of (d, p) scattering cross sections	273
Adam, G. D., and Standley, K. J. : Ferromagnetic properties of oxidized Mn_2Sb (R)	1022
Alburger, D. E., and Grace, M. A. : The disintegration of cobalt 57 (R)	280
Alston, M. H., Crewe, A. V., Evans, W. H., Green, L. L., and Willmott, J. C. : The scattering of 15.7 mev neutrons by ^4He	657
Bagguley, D. M. S., and Harrick, N. J. : The temperature dependence of ferromagnetic resonance in colloidal nickel (L)	648
Balazs, N. L. : On the propagation of energy in elastic media (L)	726
Ballinger, R. A., and March N. H. : Extended Thomas-Fermi methods (R)	378
Barclay, F. R., Galbraith, W., Glover, K. M., Hall, G. R., and Whitehouse, W. J. : The spontaneous fission rate of ^{240}Pu (L)	646
Barrow, R. F., and Caunt, A. D. : The ultra-violet spectrum of a diatomic hydride excited in hydrogen-potassium fluoride hollow-cathode discharges	68
Barrow, R. F., Drummond, G., and Walker, S. : A note on the ultra-violet band spectra of CCl and SiCl (R)	186
Barrow, R. F., Drummond, G., and Zeeman, P. B. : Rotational analysis of the β band system of the NS molecule	365
Barrow, R. F., Jacquest, J. A. T., and Thompspon, E. W. : The ultra-violet emission spectra of the gaseous monofluorides of gallium and indium	528
Barrow, R. F., with Dodsworth, P. G. : Triplet electronic states of aluminium monofluoride (L)	94
Barrow, R. F., with Robinson, S. J. Q. : The E-X band system of SiS in emission and the dissociation energy of SiS (L)	95
Barton, J. C. : Note on the positive temperature coefficient of the cosmic radiation (R)	637
Basson, J. K., and Steyn, J. : Absolute alpha standardization with liquid scintillators (L)	297
Bates, D. R., Darling, R. T. S., Hawe, S. C., and Stewart, A. L. : Properties of the hydrogen molecular ion : IV—oscillator strengths of the transitions connecting the lowest even and lowest odd σ -states with higher σ -states	533
Bates, D. R., and Griffing, G. W. : Inelastic collision between heavy particles : II—contributions of double-transitions to the cross sections associated with the excitation of hydrogen atoms in fast encounters with other hydrogen atoms	663
Bates, D. R., and Moiseiwitsch, B. L. : Inelastic heavy particle collisions involving the crossing of potential energy curves : I—charge transfer from H atoms to Be^{2+} , Si^{2+} and Mg^{2+} ions	805
Bauer, Ernest and Wu, Ta-You : The cooling of a gas by radiation	741
Bell, D. G., Hensman, R., Jenkins, D. P., and Pincherle, L. : A note on the band structure of silicon (L)	562
Bishop, G. R., with Marin, P., and Halban, H. : The absolute standardization of the 2.615 mev γ -rays of ThC'' and the cross section for the photo disintegration of the deuteron at this energy (L)	1113
Bisset, D. C., and Iball, J. : X-ray diffraction from built-up multilayers consisting of only a few monolayers	315
Blackman, M., and Khan, I. A. : The intensity of high angle Kikuchi bands (R)	553
Blin-Stoyle, R. J., and Perks, M. A. : The deviations of nuclear magnetic moments from the Schmidt lines	885
Bodmer, A. R. : Spectroscopic isotope shift and nuclear deformations	622
Bogle, G. S., and Heine, V. : Paramagnetic resonance in gadolinium sulphate octohydrate (L)	734
Bonnor, W. B. : Static magnetic fields in general relativity	225
de Borde, A. H. : The Auger effect and negative meson capture	57
Born, Max : On the interpretation of Freundlich's red-shift formula (L)	193
Bovey, L. F. H., and Garton, W. R. S. : The absorption spectrum of lutetium (R)	291
Bovey, L. F. H., and Garton, W. R. S. : The absorption spectrum of thulium (R)	476

	PAGE
Braid, T. H., with Knight, J., and Richardson, H. O. W. : The beta rays of thallium 204	881
Bransden, B. H., Dalgarno, A., and King, N. M. : Electron capture : IV—capture from helium atoms by fast protons	1075
Breitenberger, E. : On source scattering in angular correlation experiments with soft electrons	1108
Bridge, N. K., and Howell, H. G. : The absorption spectrum of bismuth oxide	44
Brink, D. M. : Short range forces and nuclear energy levels in the neighbourhood of ^{208}Pb	757
Brinkley, T. A., with Titterton, E. W. : Cross sections for the reaction $^7\text{Li}(\gamma, p)^6\text{He}$ at 17.6 and 14.8 mev and the first excited state of ^6He (R)	469
Brodie, the late W. D. : Lens spectrometer study of the disintegration of MsTh_2	265, corr. 394
Brodie, the late W. D. : Lens spectrometer study of the disintegration of ^{233}Pa	397
Buckingham, M. J., and Schafroth, M. R. : The specific heat of metals at low temperatures	828
Bunbury, D. St. P. : An investigation of the (γ, n) reaction in Cu, Zn and Ag (R)	1106
Burch, P. R. : Cosmic radiation : Ionization intensity and specific ionization in air at sea level	421
Burch, P. R. : Statistical errors at background intensities in integrating ionization chambers	431
Burcham, W. E. : The α -activity induced in gold by bombardment with nitrogen ions (R)	555
Burcham, W. E. : The α -activity induced in gold by bombardment with ions of carbon 13	733
Burhop, E. H. S. : The de-excitation of helium metastable atoms in helium (R)	276
Campion, P. J. : A cloud chamber study of some aspects of the Geiger discharge	1095
Campion, P. J., and Davies, W. T. : The detection of electron pairs in a cloud chamber with internal counters (R)	941
Campion, P. J., and Davies, W. T. : The resolving time of an internal counter controlled Wilson chamber (R)	944
Carson, T. R. : The vibrational and rotational excitation of molecular hydrogen by electron impact	909
Cassels, J. M., and Lawson, J. D. : Absorption cross sections for 134 mev protons	125
Caunt, A. D., with Barrow, R. F. : The ultra-violet spectrum of a diatomic hydride excited in hydrogen-potassium fluoride hollow-cathode discharges.	68
Chartres, B. A., and Messel, H. : Three-dimensional theory of electron-proton showers	158
Churchill, J. L. W., with Hunt, S. E., and Jones, W. M. : Measurements of the end point energy of positrons from ^{25}Al (L)	479
Churchill, J. L. W., with Hunt, S. E., Jones, W. M., and Hancock, D. A. : The determination of the resonant energies for proton capture by ^{24}Mg and ^{25}Mg below 550 kev, and measurement of the half lives of ^{25}Al and ^{26}Al	443
Clark, A. C. : The binding energy of the alpha particle	323
Clunie, J. : On Bose-Einstein functions	632
Cooke, A. H., and Duffus, H. J. : The magnetic susceptibility of nitric oxide in a clathrate compound.	525
Coulson, C. A. : Note on the applicability of the free-electron network model to metals	608
Crawford, J. H., Jr., and Holmes, D. K. : A chemical approach to the treatment of electronic spin in semiconductors (L).	294
Crewe, A. V., with Alston, M. H., Evans, W. H., Green, L. L., and Willmott, J. C. : The scattering of 15.7 mev neutrons by ^4He	657
Dalgarno, A. : Inelastic heavy-particle collisions involving the crossing of potential energy curves : II—charge transfer from H-atoms to Al^{3+} , B^{2+} , Li^{2+} and Al^{2+}	1010
Dalgarno, A., with Bransden, B. H., and King, N. M. : Electron capture : IV—capture from helium atoms by fast protons	1075

	PAGE
Dalgarno, A., and Poots, G. : Approximate molecular orbitals : I—the $1s\sigma_g$ and $2p\sigma_u$ states of H_2^+	343
Dardis, J. G., and McCusker, C. B. A. : A possible variation of the rate of local penetrating showers (L)	1026
Darling, R. T. S., with Bates, D. R., Hawe, S. C., and Stewart, A. L. : Properties of the hydrogen molecular ion : IV—oscillator strength of the transitions connecting the lowest even and lowest odd σ -states with higher σ -states	533
Davies, W. T., with Campion, P. J. : The detection of electron pairs in a cloud chamber with internal counters (R)	941
Davies, W. T., with Campion, P. J. : The resolving time of an internal counter controlled Wilson chamber (R)	944
Davison, B., and Mandl, M. E. : On the neutron spectrum for v^{-2} absorption cross section	967
Deuchars, W. M., with Grant, P. J., Flack, F. C., and Rutherglen, J. G. : Gamma radiation from the reaction $^{11}B(p, \gamma)^{12}C$	751
Deuchars, W. M., with Rutherglen, J. G., Grant, P. J., and Flack, F. C. : γ -radiation from the reaction $^{27}Al(p, \gamma)^{28}Si$	101, corr. 197
Devons, S., and Goldring, G. : Emission of electron-positron pairs from light nuclei : II—transitions in 8Be , ^{10}B and ^{16}O	413
Devons, S., Goldring, G., and Lindsey, G. R. : Emission of electron-positron pairs from light nuclei : I—monopole transition in ^{16}O	134
Dewar, M. J. S., and Longuet-Higgins, H. C. : The electronic spectra of aromatic molecules : I—benzenoid hydrocarbons	795
Ditchburn, R. W., and Orchard, G. A. J. : The polarization of totally reflected light	608
Dodsworth, P. G., and Barrow, R. F. : Triplet electronic states of aluminium monofluoride (L)	94
Donovan, B. : The magneto-resistance effect in metals at high frequencies	305
Donovan, B., with March, N. H. : Free electron diamagnetism and susceptibilities of the alkali metals (R)	464
Drummond, G., with Barrow, R. F., and Walker, S. : A note on the ultra-violet band spectra of CCl and $SiCl$ (R)	186
Drummond, G., with Barrow, R. F., and Zeeman, P. B. : Rotational analysis of the band system of the NS molecule	365
Duffus, H. J., with Cooke, A. H. : The magnetic susceptibility of nitric oxide in a clathrate compound	525
Eccles, P. J., with Officer, V. C. : The time coherence of associated cosmic ray particles	1037
Elcock, E. W. : Collective electron anti-ferromagnetism (L)	295
Emel�us, K. G., with Stewart, D. T., and Gribbon, P. W. F. : Excitation conditions for the infra-red auroral bands of ionized nitrogen	188
Erskine, G. A. : The effect of contaminating gases on the energy per ion pair in helium (R)	640
Evans, N. T. S., and Parkinson, W. C. : Angular distributions in the $^{10}B(d,p)^{11}B$ reaction	684
Evans, W. H., with Alston, M. H., Crewe, A. V., Green, L. L., and Willmott, J. C. : The scattering of 15.7 mev neutrons by 4He	657
Fairbairn, A. R., with Gaydon, A. G. : Pressure broadening in the spectrum of NO and its photodissociation (R)	474
Fairbairn, W. M. : The deuteron bombardment of oxygen (L)	564
Fairbairn, W. M. : The D-D Reaction	990
Farley, F. J. M., and Storey, J. R. : The sidereal correlation of extensive air showers	996
Finlay-Freundlich, E. : Red-shifts in the spectra of celestial bodies (L)	192
Flack, F. C., Rutherglen, J. G., and Grant, P. J. : Radiations from the proton bombardment of ^{23}Na	973

	PAGE
Flack, F. C., with Grant, P. J., Rutherglen, J. G., and Deuchars, W. M. : Gamma radiation from the reaction $^{11}\text{B}(\text{p}, \gamma)^{12}\text{C}$	751
Flack, F. C., with Rutherglen, J. G., Grant, P. J., and Deuchars, W. M. : γ -radiation from the reaction $^{27}\text{Al}(\text{p}, \gamma)^{28}\text{Si}$	101 corr. 197
Fletcher, G. C. : Calculations of the first ferromagnetic anisotropy coefficient, gyromagnetic ratio and spectroscopic splitting factor for nickel	505
Fowler, G. N. : Electron-neutrino angular correlation functions in the theory of beta decay	117
Fowler, G. N. : Note on the relation between certain forbidden beta transitions and the nuclear spin orbit interaction	1005
Fraser, P. A. : Vibrational transition probabilities of diatomic molecules : III (R)	939
Galbraith, W., with Barclay, F. R. : The spontaneous fission rate of ^{240}Pu (L)	646
Garton, W. R. S. : Investigations of atomic and molecular absorption spectra : III—ultra-violet absorption spectra of indium vapour	864
Garton, W. R. S., with Bovey, L. F. H. : The absorption spectrum of thulium (R)	476
Gatha, K. M., Patel, N. J., and Patel, P. F. : The elastic scattering of 125 mev electrons by beryllium (L)	1111
Gatha, K. M., Shah, G. Z., and Patel, N. J. : Approximate nuclear density distributions in light elements	773
Gatha, K. M., with Shah, G. Z., and Patel, N. J. : Scattering of high energy nucleons and electrons by carbon (L)	92
Gaydon, A. G., and Fairbairn, A. R. : Pressure broadening in the spectrum of NO and its photodissociation (R)	474
Ghosh, S. K., Jones, the late G. M. D. B., and Wilson, J. G. : Ionization by relativistic μ -mesons in oxygen	331
Glover, K. M., with Barclay, F. R., Galbraith, W., Hall, G. R., and Whitehouse, W. J. : The spontaneous fission rate of ^{240}Pu (L)	646
Goldring, G. G. : Emission of electron-positron pairs from light nuclei : III— γ -transition in the reaction $^{15}\text{N}(\text{p}, \gamma)^{16}\text{O}$	930
Goldring, G., with Devons, S., and Lindsey, G. R. : Emission of electron-positron pairs from light nuclei : I—monopole transition in ^{16}O	134
Grace, M. A., with Alburger, D. E. : The disintegration of cobalt 57 (R)	280
Grace, M. A., with Lemmer, H. R. : The angular correlation of successive γ -rays in ^{60}Ni at low temperatures	1051
Grant, I. P. : Theory of (d, p) and (d, n) reactions : I—general theory ignoring coulomb effects	981
Grant, P. J. : The coupling of angular momenta in the reaction $^{27}\text{Al}(\text{p}, \gamma)^{28}\text{Si}$ (L)	392
Grant, P. J., Flack, F. C., Rutherglen, J. G., and Deuchars, W. M. : Gamma radiation from the reaction $^{11}\text{B}(\text{p}, \gamma)^{12}\text{C}$	751
Grant, P. J., with Flack, F. C., and Rutherglen, J. G. : Radiations from the proton bombardment of ^{23}Na	973
Grant, P. J., with Hughes, I. S. : Polarization of the 10.4 mev gamma-ray in the reaction $^{27}\text{Al}(\text{p}, \gamma)^{28}\text{Si}$	481
Grant, P. J., with Rutherglen, J. G., Flack, F. C., and Deuchars, W. M. : γ -radiation from the reaction $^{27}\text{Al}(\text{p}, \gamma)^{28}\text{Si}$	101 corr. 197
Green, H. S., with McCarthy, I. E. : A method for the solution of nuclear bound-state problems	719
Green, L. L., with Alston, M. H., Crewe, A. V., Evans, W. H., and Willmott, J. C. : The scattering of 15.7 mev neutrons by ^4He	657
Greenlees, G. W. : Levels of ^{24}Mg from the $^{27}\text{Al}(\text{p}, \alpha)^{24}\text{Mg}$ reaction (R)	1107
Gribbon, P. W. F., with Stewart, D. T., and Emel��us, K. G. : Excitation conditions for the infra-red auroral bands of ionized nitrogen (R)	188
Griffing, G. W., with Bates, D. R. : Inelastic collisions between heavy particles : II—contributions of double-transitions to the cross sections associated with the excitation of hydrogen atoms in fast encounters with other hydrogen atoms	663
Gupta, M. P. : The principal magnetic susceptibilities of the maleic acid molecule $\text{HOOC.HC} : \text{CH.COOH}$ (R)	643

	PAGE
ter Haar, D., and Ross, A. W.: Volume changes in a substitutional alloy (R)	388
Halban, H., with Marin, P., and Bishop, G. R.: The absolute standardization of the 2.615 mev γ -rays of ThC'' and the cross section for the photo disintegration of the deuteron at this energy (L)	1113
Hall, G. R., with Barclay, F. R., Galbraith, W., Glover, K. M., and Whitehouse, W. J.: The spontaneous fission rate of ^{240}Pu (L)	646
Hall, M. E.: The inertia of heat flow in liquid helium II	485
Hancock, D. A., with Hunt, S. E., Jones, W. M., and Churchill, J. L. W.: The determination of the resonant energies for proton capture by ^{24}Mg and ^{25}Mg below 550 kev, and measurement of the half lives of ^{25}Al and ^{26}Al	443
Harrick, N. J., with Bagguley, D. M. S.: The temperature dependence of ferromagnetic resonance in colloidal nickel (L)	648
Harries, G.: A cloud chamber study of internal pairs from $^{12}\text{C}^*$	153
Hatton, J., and Rollin, B. V.: The electrical properties of indium antimonide at low temperatures (R)	385
Hawe, S. C., with Bates, D. R., Darling, R. T. S., and Stewart, A. L.: Properties of the hydrogen molecular ion: IV—oscillator strengths of the transitions connecting the lowest even and lowest odd σ -states with higher σ -states	533
Heine, V., with Bogle, G. S.: Paramagnetic resonance in gadolinium sulphate octohydrate (L)	734
Henry, W. G.: The self-consistent field for Au^+	789
Hensman, R., with Bell, D. G., Jenkins, D. P., and Pincherle, L.: A note on the band structure of a silicon (L)	562
Hindmarsh, W. R.: Spectroscopic isotope shifts and electron scattering by nuclei (L)	393
Hindmarsh, W. R., Kuhn, H. G., and Ramsden, S. A.: Isotope shifts in the atomic spectra of tin and cadmium (L)	478
Hird, B., and Whitehead, C.: A modified scintillation pair spectrometer (R)	644
Hochberg, S., Massey, H. S. W., and Underhill, L. H.: The scattering of nucleons by alpha-particles—the s-phases	957
Holmes, D. K., with Crawford, J. H., Jr.: A chemical approach to the treatment of electronic spin in semiconductors (L)	294
Howell, H. G., with Bridge, N. K.: The absorption spectrum of bismuth oxide	44
Howell, K. M.: The van der Waals energy of two helium atoms	705
Hubbard, J.: Plasma oscillations in a periodic potential: the one-zone theory	1058
Huby, R.: Phase of matrix elements in nuclear reactions and radio-active decay (R)	1113
Hughes, I. S., and Grant, P. J.: Polarization of the 10.4 mev gamma-ray in the reaction $^{27}\text{Al}(p,\gamma)^{28}\text{Si}$	481
Hunt, S. E., Jones, W. M., and Churchill, J. L. W.: Measurements of the end point energy of positrons from ^{25}Al (L)	479
Hunt, S. E., Jones, W. M., Churchill, J. L. W., and Hancock, D. A.: The determination of the resonant energies for proton capture by ^{24}Mg and ^{25}Mg below 550 kev, and measurement of the half lives of ^{25}Al and ^{26}Al	443
Iball, J., with Bisset, D. C.: X-ray diffraction from built-up multilayers consisting of only a few monolayers	315
Ilakovac, K.: Resonant scattering of gamma-rays in ^{63}Cu and ^{58}Fe	601
Jacquest, J. A. T., with Barrow, R. F., and Thompson, E. W.: The ultra-violet emission spectra of the gaseous monofluorides of gallium and indium	528
Jenkins, D. P., with Bell, D. G., Hensman, R., and Pincherle, L.: A note on the band structure of silicon (L)	562
Jones, the late G. M. D. B., with Ghosh, S. K., and Wilson, J. G.: Ionization by relativistic μ -mesons in oxygen	331
Jones, W. M., with Hunt, S. E., and Churchill, J. L. W.: Measurements of the end point energy of positrons from ^{25}Al (L)	479
Jones, W. M., with Hunt, S. E., Churchill, J. L. W., and Hancock, D. A.: The determination of the resonant energies for proton capture by ^{24}Mg and ^{25}Mg below 550 kev, and measurement of the half lives of ^{25}Al and ^{26}Al	443

	PAGE
Jones, H., and Schiff, B.: Nuclear magnetic resonance in metallic lithium and sodium	217
Jutsum, P. J.: The continuous absorption of light in calcium vapour (R)	190
Kastler, A.: Les méthodes optiques d'orientation atomique et leurs applications (9th Holweck Lecture)	853
Kelly, F. M., Kuhn, H. G., and Pery, Anne: Hyperfine structures in the atomic spectrum of calcium	450
Kemp, W. R. G., Klemens, P. G., Streedhar, A. K., and White, G. K.: The lattice thermal conductivity of silver-palladium alloys at low temperatures (L)	728
Khan, I. A., with Blackman, M.: The intensity of high angle Kikuchi bands (R)	553
King, N. M., with Bransden, B. H., and Dalgarno, A.: Electron capture: IV—capture from helium atoms by fast protons	1075
Klemens, P. G.: The thermal conductivity of monovalent metals (L)	194
Klemens, P. G., with Kemp, W. R. G., Streedhar, A. K., and White, G. K.: The lattice thermal conductivity of silver-palladium alloys at low temperatures (L)	728
Knight, J. C., Braid, T. H., and Richardson, H. O. W.: The beta rays of thallium 204	881
Kothari, L. S.: Riesz potential and the elimination of divergences from quantum electrodynamics: I	17
Kothari, L. S.: Riesz potential and the elimination of divergences from quantum electrodynamics: II	201
Kothari, L. S.: Riesz potential and the elimination of divergences from quantum electrodynamics: III (R).	1021
Kothari, L. S.: Riesz potential and the elimination of divergences from meson theory	580
Kuhn, H., with Kelly, F. M., and Pery, Anne: Hyperfine structures in the atomic spectrum of calcium	450
Kuhn, H. G., with Hindmarsh, W. R., and Ramsden, S. A.: Isotope shifts in the atomic spectra of tin and cadmium (L)	478
Lane, A. M., and Radicati, L. A.: Studies in intermediate coupling: II—radiative transitions in light nuclei	167
Lang, J. M. B., and Le Couteur, K. J.: Statistics of nuclear levels.	586
Lawson, J. D., with Cassels, J. M.: Absorption cross sections for 134 mev protons	125
Le Couteur, K. J., with Lang, J. M. B.: Statistics of nuclear levels	586
Lee, E. W.: The approach to saturation magnetostriction (R)	381
Lemmer, H. R., and Grace, M. A.: The angular correlation of successive γ -rays in ^{60}Ni at low temperatures	1051
Lindsey, G. R., with Devons, S., and Goldring, G.: Emission of electron-positron pairs from light nuclei: I— π -monopole transition in ^{16}O	134
Longuet-Higgins, H. C., with Dewar, M. J. S.: The electronic spectra of aromatic molecules: I—benzenoid hydrocarbons	795
Majumdar, S. Datta: Energy levels of triatomic molecules	351
Makinson, R. E. B.: The thermal conductivity of metals (R).	290
Mandl, M. E., with Davison, B.: On the neutron spectrum for τ γ absorption cross section	967
March, N. H.: Momentum distribution of electrons in solids: results for some metals using the Thomas-Fermi method	9
March, N. H.: On momentum distribution in nuclei (R)	288
March, N. H., with Ballinger, R. A.: Extended Thomas-Fermi methods (R)	378
March, N. H., and Donovan, B.: Free electron diamagnetism and susceptibilities of the alkali metals (R)	464
Marin, P., Bishop, G. R., and Halban, H.: The absolute standardization of the 2.615 mev γ -rays of ThC'' and the cross section for the photo disintegration of the deuteron at this energy (L)	1113
Marr, G. V.: A note on the absorption of light by indium vapour (L)	196
Marshall, W.: Inelastic magnetic scattering of neutrons from a ferromagnetic crystal	85

	PAGE
Massey, H. S. W., and Mohr, C. B. O. : Gaseous reactions involving positronium	695
Massey, H. S. W., with Hochberg, S., and Underhill, L. H. : The scattering of nucleons by alpha-particles—the s-phases	957
McCarthy, I. E., and Green, H. S. : A method for the solution of nuclear bound-state problems	719
McCrum, N. G., and Shiffman, C. A. : The optical constants of tin below the superconducting transition temperature (R).	386
McCusker, C. B. A., with Dardis, J. G. : A possible variation of the rate of local penetrating showers (L)	1026
Messel, H., with Chartres, B. A. : Three-dimensional theory of electron-proton showers	158
Mohr, C. B. O. : The difference in the multiple scattering of electrons and positrons (L)	730
Mohr, C. B. O., and Tassie, L. J. : The scattering and polarization of electrons by gold	711
Mohr, C. B. O., with Massey, H. S. W. : Gaseous reactions involving positronium	695
Moiseiwitsch, B. L. : On the electron affinities of atomic fluorine, oxygen and lithium	25
Moiseiwitsch, B. L., and Stewart, A. L. : Inelastic collisions between heavy particles : III—excitation of helium atoms in fast encounters with hydrogen atoms, protons and positive helium ions	1069
Moiseiwitsch, B. L., and Stewart, A. L. : Approximate molecular orbitals : II—the $2p_u$ and $3d_g$ states of H_2^+	457
Moiseiwitsch, B. L., with Bates, D. R. : Inelastic heavy particle collisions involving the crossing of potential energy curves : I—charge transfer from H atoms to Be^{2+} , Si^{2+} and Mg^{2+} ions	805
Murdoch, H. S., and Webb, A. J. : Isomerism in ^{46}Ti (R)	286
Officer, V. C., and Eccles, P. J. : The time coherence of associated cosmic ray particles	1037
Owen, E. A., and Williams, G. I. : X-ray measurements on lithium at low temperatures	895
Parkinson, D. H., and Quarrington, J. E. : The molar heats of lead sulphide, selenide and telluride in the temperature range $20^\circ K$ to $260^\circ K$	569
Parkinson, W. C., with Evans, N. T. S. : Angular distributions in the $^{10}B(d, p)^{11}B$ reaction	684
Patel, N. J., with Gatha, K. M., and Patel, P. F. : The elastic scattering of 125 mev electrons by beryllium (L)	1111
Patel, N. J., with Gatha, K. M., and Shah, G. Z. : Approximate nuclear density distributions in light elements	773
Patel, N. J., with Shah, G. Z., and Gatha, K. M. : Scattering of high energy nucleons and electrons by carbon (L)	92
Patel, P. F., with Gatha, K. M., and Patel, N. J. : The elastic scattering of 125 mev electrons by beryllium (L)	1111
Perks, M. A., with Blin-Stoyle, R. J. : The deviations of nuclear magnetic moments from the Schmidt lines	885
Pery, Anne : Isotope shifts in the atomic spectrum of calcium	181
Pery, Anne, with Kelly, F. M., and Kuhn, H. G. : Hyperfine structures in the atomic spectrum of calcium	450
Phillips, K. : On the thick target bremsstrahlung spectrum at relativistic energies	669
Pillow, M. E. : Intensity distribution among nitrogen bands in the auroral spectrum	780
Pillow, M. E. : Intensities in band systems of O_2 : $^3\Sigma_u^+ - ^1\Sigma_g^+$ (Broida-Gaydon system) and $^1\Sigma_g^+ - ^3\Sigma_g^-$ (Atmospheric system) (R)	847
Pincherle, L., with Bell, D. G., Hensman, R., and Jenkins, D. P. : A note on the band structure of silicon (L)	562
Poots, G., with Dalgarno, A. : Approximate molecular orbitals : I—the $1s\sigma_g$ and $2p\sigma_u$ states of H_2^+	343
Prescott, J. R. : The decay, of ^{203}Pb and the energy levels of ^{203}Tl	254
Prescott, J. R. : The decay of ^{207}Bi and the energy levels of ^{207}Pb	540
Prescott, J. R., with Shaw, P. F. D. : A search for ^{203}Pb (R)	283

	PAGE
Price, P. C. : The yield curve of the ${}^7\text{Li}(p, \gamma){}^8\text{Be}$ reaction (R)	849
Price, P. J. : Perturbation theory for the one-dimensional wave equation (R)	383
Pryce, M. H. L. : Nuclear shell structure (L)	1111
Quarrington, J. E., with Parkinson, D. H. : The molar heats of lead sulphide, selenide and telluride in the temperature range 20°K to 260°K	569
Radicati, L. A. : Isotopic spin and coulomb forces : II—excited states of light nuclei	39
Radicati, L. A., with Lane, A. M. : Studies in intermediate coupling : II—radiative transitions in light nuclei	167
Raimes, S. : Correlation energy in metals and the cohesive energy of metallic sodium	52
Ramsden, S. A., with Hindmarsh, W. R., and Kuhn, H. G. : Isotope shifts in the atomic spectra of tin and cadmium	478
Rastogi, R. P., and Srivastava, R. C. : Non-equilibrium thermodynamics of thermal transpiration of a dissociating gas (R)	639
Reid, G. C. : Energy levels in ${}^{10}\text{B}$ and ${}^8\text{Be}$ (R)	466
Richards, E. W. T. : Radiations from water under alpha-particle bombardment	922
Richardson, H. O. W., with Knight, J. C., and Braid, T. H. : The beta rays of thallium 204	881
Robinson, S. J. Q., and Barrow, R. F. : The E-X band system of SiS in emission and the dissociation energy of SiS (L)	95
Rollin, B. V., with Hatton, J. : The electrical properties of indium antimonide at low temperatures (R)	385
Rose, M. E. : Spherical tensors in physics	239
Rosenberg, H. M. : The thermal conductivity of germanium and silicon at low temperatures	837
Ross, A. W., with ter Haar, D. : Volume changes in a substitutional alloy (R)	388
Rothenstein, W. : The second Born approximation in inelastic collisions of electrons with atoms	673
Rutherglen, J. G., Grant, P. J., Flack, F. C., and Deuchars, W. M. : γ -radiation from the reaction ${}^{27}\text{Al}(p, \gamma){}^{28}\text{Si}$	101, corr. 197
Rutherglen, J. G., with Flack, F. C., and Grant, P. J. : Radiations from the proton bombardment of ${}^{23}\text{Na}$	973
Rutherglen, J. G., with Grant, P. J., Flack, F. C., and Deuchars, W. M. : Gamma radiation from the reaction ${}^{11}\text{B}(p, \gamma){}^{12}\text{C}$	751
Satchler, G. R. : Some remarks on radiative capture and stripping reactions (R)	471
Satchler, G. R. : Radiative transition in j - j coupling (L)	1024
Schafroth, M. R. : Self-consistent spin-wave theory for the ferromagnetic exchange problem	33
Schafroth, M. R., with Buckingham, M. J. : The specific heat of metals at low temperatures	828
Schiff, B. : A calculation of the eigenvalues of electronic states in metallic lithium by the cellular method	2
Schiff, B., with Jones, H. : Nuclear magnetic resonance in metallic lithium and sodium	217
Seaton, M. J. : The photo-ionization of neon	927
Shah, G. Z., with Gatha, K. M., and Patel, N. J. : Approximate nuclear density distributions in light elements	773
Shah, G. Z., Patel, N. J., and Gatha, K. M. : Scattering of high energy nucleons and electrons by carbon (L)	92
Shah, S. M., with Vachaspati : Consistency of nuclear radii from electron scattering and coulomb energy data (L)	950
Sharma, C. B. : The absorption spectrum of bismuth selenide and bismuth telluride in the region 2900 – 2200 Å	935
Shaw, P. F. D., and Prescott, J. R. : A search for ${}^{205}\text{Pb}$ (R)	283
Shiffman, C. A., with McCrum, N. G. : The optical constants of tin below the superconducting transition temperature (R)	386
Squires, G. L. : The scattering of slow neutrons by ferromagnetic crystals	248

- Squires, G. L. : A nuclear method for the estimation of traces of light water in heavy water 520
- Sreedhar, A. K., with Kemp, W. R. G., Klemens, P. G., and White, G. K. : The lattice thermal conductivity of silver-palladium alloys at low temperatures (L) 728
- Srivastava, R. C., with Rastogi, R. P. : Non-equilibrium thermodynamics of thermal transpiration of a dissociating gas (R) 639
- Standley, K. J., with Adam, G. D. : Ferromagnetic properties of oxidized Mn_2Sb 1022
- Stanley, C. R. : A new method for the production of active nitrogen and its application to the study of collision effects in the nitrogen molecular spectrum. 821
- Stewart, A. L. : The photo-ionization cross section of lithium 917
- Stewart, A. L., with Bates, D. R., Darling, R. T. S., and Hawe, S. C. : Properties of the hydrogen molecular ion : IV—oscillator strengths of the transitions connecting the lowest even and lowest odd σ -states with higher σ -states. 533
- Stewart, A. L., with Moiseiwitsch, B. L. : Inelastic collisions between heavy particles: III—excitation of helium atoms in fast encounters with hydrogen atoms, protons and positive helium ions 169
- Stewart, A. L., with Moiseiwitsch, B. L. : Approximate molecular orbitals : II—the $2p_u$ and $3d_g$ states of H_2^+ 457
- Stewart, D. T., Gribbon, P. W. F., and Emeléus, K. G. : Excitation conditions for the infra-red auroral bands of ionized nitrogen (R) 188
- Steyn, J., with Basson, J. K. : Absolute alpha standardization with liquid scintillators (L) 297
- Storey, J. R., with Farley, F. J. M. : The sidereal correlation of extensive air showers 996
- Swan, P. : The elastic scattering of electrons by the excited 2s and 2p states of atomic hydrogen 1086
- Synge, J. L. : Geometrical mechanics and de Broglie waves 737
- Tait, J. H. : Two-group perturbation theory in neutron transport theory. 615
- Tassie, L. J., with Mohr, C. B. O. : The scattering and polarization of electrons by gold 711
- Temperley, H. N. V. : On Feynman's theory of liquid helium 901
- Temperley, H. N. V. : The Mayer theory of condensation tested against a simple model of the imperfect gas 233
- Temperley, H. N. V. : A possible model of liquid He_3 495
- Thompson, E. W., with Barrow, R. F., and Jacquest, J. A. T. : The ultra-violet emission spectra of the gaseous monofluorides of gallium and indium 528
- Tidman, D. A. : The anomalous scattering of mesons (R) 559
- Titterton, E. W., and Brinkley, T. A. : Cross sections for the reaction ${}^7\text{Li}(\gamma, p){}^6\text{He}$ at 17.6 and 14.8 mev and the first excited state of ${}^6\text{He}$ (R) 469
- Tredgold, R. H. : A modified form of Heisenberg's theory of ferromagnetism 148
- Tredgold, R. H. : On the exchange interaction in the collective electron approximation 221
- Tredgold, R. H. : On antiferromagnetism in metals 1018
- Turner, J. S. : Investigation of triplet neutron-proton scattering in the low energy region using the Eckart and Bargmann potentials 111
- Underhill, L. H., with Hochberg, S., and Massey, H. S. W. : The scattering of nucleons by alpha-particles—the s-phases 957
- Vachaspati and Shah, S. M. : Consistency of nuclear radii from electron scattering and Coulomb energy data (L) 950
- Walker, S., with Barrow, R. F., and Drummond, G. : A note on the ultra-violet band spectra of CCl_4 and SiCl_4 (R) 186
- Ward, A. : The emission of light in the passage of alpha particles through gases 841
- Ware, A. A. : Galvomagnetic and thermomagnetic effects in a plasma 869
- Webb, A. J., with Murdoch, H. S. : Isomerism in ${}^{46}\text{Ti}$ (R) 268

	PAGE
White, G. K., with Kemp, W. R. G., Klemens, P. G., and Sreedhar, A. K. : The lattice thermal conductivity of silver-palladium alloys at low temperatures	728
Whitehead, C., with Hird, B. : A modified scintillation pair spectrometer (R)	644
Whitehouse, W. J., with Barclay, F. R., Galbraith, W., Glover, K. M., and Hall, G. R. : The spontaneous fission rate of ^{240}Pu (L)	646
van Wieringen, J. S. : Justification of the use of perturbation theory in metallic conductivity	206
Williams, G. I., with Owen, E. A. : X-ray measurements on lithium at low temperatures	895
Willmott, J. C., with Alston, M. H., Grewe, A. V., Evans, W. H., and Green, L. L. : The scattering of 15.7 mev neutrons by ^4He	657
Wilson, J. G., with Ghosh, S. K., and Jones, the late G. M. D. B. : Ionization by relativistic μ -mesons in oxygen	331
Winn, M. M. : The reaction $^9\text{Be}(\text{d}, ^3\text{He})^8\text{Li}$ (R)	946
Winn, M. M. : Short-lived alpha emitters produced by ^3He and heavy ion bombardments (L)	949
Wolfe, R. : On the theory of optical absorption in metals and semiconductors	74
Wu, Ta-You, with Bauer, Ernest : The cooling of a gas by radiation	741
Yoccoz, J. : Coulomb effects in stripping reactions	813
Zeeman, P. B., with Barrow, R. F., and Drummond, G. : Rotational analysis of the β band system of the NS molecule	365

INDEX TO REVIEWS OF BOOKS

	PAGE
Allen, N. C. B., and Martin, L. H. : <i>Excercises in Experimental Physics</i>	97
Appleton, Sir Edward, et al. : <i>Scientific Papers presented to Max Born on his Retirement from the Tait Chair of Natural Philosophy in the University of Edinburgh</i>	952
Baitsell, George A. (Ed.) : <i>Science in Progress</i> (7th and 8th Series)	952
Bak, Borge : <i>Elementary Introduction to Molecular Spectra</i>	739
Bickley, W. G. : <i>Bessel Functions and Formulae</i>	567
Bleuler, E., and Goldsmith, G. J. : <i>Experimental Nucleonics</i>	653
Braddick, H. J. J. : <i>The Physics of Experimental Method</i>	1028
Bruining, H. : <i>Physics and Applications of Secondary Electron Emission</i>	954
Byrd, P. F., and Friedman, M. D. : <i>Handbook of Elliptic Integrals for Engineers and Physicists</i>	944
Chadwick, Sir James : <i>Radioactivity and Radioactive Substances</i>	299
Chalmers, B. (Ed.) : <i>Progress in Metal Physics</i> , Vol. 3	97
Chalmers, B., and King R. (Ed.) : <i>Progress in Metal Physics</i> , Vol. 5	1115
Chaundy, T. W., Barrett, P. R., and Batey, C. : <i>The Printing of Mathematics</i>	566
Corson, E. M., <i>Introduction to Tensors, Spinors, and Relativistic Wave-Equations</i>	300
Editions de la Revue d'Optique Théorique et Instrumentale, 1953 : <i>Les Applications de la Mecanique Ondulatoire a l'Étude de la Structure des Molecules</i>	483
Einstein, Albert : <i>Relativity : The Special and the General Theory</i>	1114
Feenberg, E., and Pake, G. E. : <i>Notes on the Quantum Theory of Angular Momentum</i>	301
Flügge, W. : <i>Four-Place Tables of Transcendental Functions</i>	566
Fowler, R. G. : <i>Introduction to Electric Theory</i>	395
Frisch, O. R. (Ed.) : <i>Progress in Nuclear Physics</i> , Vol. 3	567
Gaydon, A. G., and Wolfhard, H. G. : <i>Flames : Their Structure, Radiation and Temperature</i>	482
Gordy, W., Smith, W. V., and Trambarulo, R. F. : <i>Microwave Spectroscopy</i>	1030
Hartmann, H. : <i>Theorie der chemischen Bindung</i>	1034
Heisenberg, W. : <i>Nuclear Physics</i>	1115
Institute of Physics : <i>Static Electrification: a Symposium held by the Institute of Physics in London, 25th-27th March 1953. British Journal of Applied Physics Supplement, No. 2</i>	483
Jaynes, E. T. : <i>Ferroelectricity</i>	199
Koller, L. R. : <i>Ultraviolet Radiation</i>	299
McLachlan, N. W. : <i>Complex Variable Theory and Transform Calculus</i>	302
Nelms, Ann T. : <i>Graphs of the Compton Energy-Angle Relationship and the Klein-Nishina Formula from 10 keV to 500 MeV. (N.B.S. Circular 542).</i>	738
Parrish, W., Ekstein, M. G., and Irwin, B. W. : <i>Data for X-Ray Analysis. Vol. II : Tables for Computing the Lattice Constant of Cubic Crystals</i>	99
Parrish, W., and Irwin, B. W. : <i>Data for X-Ray Analysis. Vol. I : Charts for solution of Bragg's Equation (d versus θ and 2θ)</i>	99
Ramsauer, Carl : <i>Grundversuche der Physik in historischer Darstellung. Vol. I : Von den Fallgesetzen bis zu den electrischen Wellen</i>	198
Ramsey, N. F. : <i>Nuclear Moments</i>	738
Rotblat, J. (Ed.) : <i>Atomic Energy : a Survey</i>	1032

	PAGE
Sachs, Robert G. : <i>Nuclear Theory</i>	652
Segrè, E. (Ed.) : <i>Experimental Nuclear Physics</i> , Vols. 1 and 2	650
Starling, S. G. : <i>Electricity and Magnetism for Degree Students</i>	1028
Stewart, K. H. : <i>Ferromagnetic Domains</i>	1033
Strandberg, M. W. P. : <i>Microwave Spectroscopy</i>	1030
Synge, J. L. : <i>Geometrical Mechanics and de Broglie Waves</i>	737
Thomas, T. S. E. : <i>Physical Formulae</i>	299
United States Department of Commerce, National Bureau of Standards : <i>Tables of 10^x (Antilogarithms to the base 10)</i> . (Applied Mathematics Series No. 27)	482
United States Department of Commerce, National Bureau of Standards : <i>Graphs of the Compton Energy-Angle Relationship and the Klein-Nishina Formula from 10 keV to 500 MeV</i> . (N.B.S. Circular 542)	738
Westphal, W. H. : <i>Physikalisches Wörterbuch</i>	655
Wilson, A. J. C. (Ed.) : <i>Structure Reports for 1945-1946</i> , Vol. 10	483
Wilson, J. G. (Ed.) : <i>Progress in Cosmic Ray Physics</i> , Vol. II. (The price of this book, which was given as £4 6s., is now £3)	1031

THE PHYSICAL SOCIETY

1 Lowther Gardens, Prince Consort Road, London S.W.7

ABSTRACT BOOKLET 26

This booklet gives abstracts of papers accepted since the printing of Abstract Booklet 25. These abstracts are thus circulated before the paper has gone to press, whereas the reprints themselves are not printed until the month of publication in the *Proceedings*, usually 2–3 months after acceptance.

Those eligible to order reprints immediately are

- (a) Fellows and Students of the Society and general subscribers to the *Proceedings* who have purchased voucher books.
- (b) Fellows and Students of the Society who have paid the annual subscription of £1 1s. *Note:* This reduced rate is *not* available to general subscribers.

Members and subscribers may obtain 10s. voucher books (containing vouchers for five reprints) at any time. Reprints are **not** obtainable in any other way.

Users of reprint vouchers should attach the appropriate number of vouchers to their order form. The enclosed order form should be completed by marking with ticks the papers required and should be returned **not later than 1st January**. A slightly later date of receipt will be accepted for long distance overseas subscribers **only**.

A list of Letters to the Editor which have been accepted for publication since the printing of Abstracts Booklet 25 is given for information only. **Reprints will not be available.**

Note. Please be sure your name and address are entered on the form and your requirements indicated, otherwise your order cannot be executed.

All papers in Lists 1–23 except that by Morris have now been published. Reprints of papers covered by these Lists will have been despatched by mid-December; any outstanding orders should be queried as soon as possible after this date.

December 1954

Section A

The Electrical Conductivity of Cadmium Oxide at Low Temperatures, by J. A. BASTIN and R. W. WRIGHT.

Abstract. Measurements of the variation of conductivity with temperature in the range 1–250°K together with similar measurements by Wright in the range 100–700°K are compared with the theoretical expression for the conductivity in an ionic crystal derived by Howarth and Sandheimer. The comparison gives the number of free electrons and the characteristic temperature for each specimen. The resistance at zero temperature is discussed in relation to impurity scattering and crystalline boundary resistances.

The Effects of Finite Nuclear Size on Bremsstrahlung Production, by S. J. BIEL and E. H. S. BURHOP.

Abstract. Calculations have been made of the bremsstrahlung spectrum emitted in different directions following electron–nuclear collisions, allowing for the finite distribution of the nuclear charge.

Calculations were carried out for charge distributions of the uniform shape, spherical shell, gaussian and exponential forms, as well as for a uniform spherical case with a distribution falling off exponentially at the surface. In each case the parameter of the distribution was chosen to agree with the elastic scattering data of 16 mev.

The modification of the angular distribution obtained from the Bethe-Heitler formula for a point nucleus is large for electron energies above 20 mev.

On the Validity of the Weizsäcker Inhomogeneity Correction term, by R. BERG and L. WILETS.

Abstract. An investigation is made of Weizsäcker's correction to the Thomas-Fermi statistical treatment, of the many-body problem. Numerical solutions of Weizsäcker's equation were obtained for the isotropic harmonic oscillator and the step potential in plane symmetry. These particular potentials were chosen as approximations to nuclear potentials. In the case of the harmonic oscillator, the error in the energy is an order of magnitude greater than for the Thomas-Fermi equation, but a reduction in the magnitude of the Weizsäcker correction term by a factor of $1/8$ gives substantial improvement over the Thomas-Fermi solution. The step potential also shows that the Weizsäcker term is too great, but the reduction factor necessary to give substantial improvement is between $1/2$ and 1 . It is concluded that the Weizsäcker correction term is not reliable as such, but that a reduction in the magnitude of the term may give plausible solutions for the density. The reduction factor depends, however, upon the form of potential.

The Effect of Radiative Corrections on a Charged Spin $\frac{1}{2}$ Particle in a Constant Magnetic Field, by A. H. DE BORDE.

Abstract. As an alternative approach to the problem of determining magnetic moments, the S matrix formalism for a Dirac particle in an electromagnetic field is re-expressed as an integral equation of the Feynman type for a one electron wave function. For a constant magnetic field, the equation reduces to a differential equation which may be solved for the energy eigenvalues in a non-relativistic approximation with arbitrary radiative correction terms. Providing conditions resulting from gauge invariance are satisfied, application of charge renormalization shows that the cyclotron frequency is unaltered in all orders. The magnetic moment derived is the same as that derived direct from the S matrix.

On the Identification of X-Ray Satellites, by D. J. CANDLIN.

Abstract. The wave-numbers of K α satellites from $Z = 19$ to $Z = 42$ are calculated with analytical wave functions, and the spectroscopic terms from which the observed lines are derived are identified.

The Temperature Dependence of Magnetostriction in a Nickel Crystal, by W. D. CORNER and G. H. HUNT.

Abstract. From a single crystal of nickel two specimens have been prepared in the form of prolate spheroids whose major axes lie along the [100] and [111] crystallographic directions. By the use of a special capacitance bridge arrangement described elsewhere the longitudinal magnetostriction of each specimen has been measured over the temperature range -180°C to 360°C .

The results obtained indicate that at low temperatures the magnetostriction below saturation varies with magnetization approximately in the manner given

ORDER FORM 26

(issued December 1954)

To be returned to the Physical Society **NOT LATER THAN 1st January 1955**
Please supply 1 reprint of each of the following when published

Section A

BASTIN and WRIGHT
BIEL and BURHOP
BERG and WILETS
DE BORDE
CANDLIN
CORNER and HUNT
GRANT, RUTHERGLEN,
 FLACK and HUTCHINSON
GREENLEES
HURLEY
IHSAN
JACOBS
LANE III
LANE IV
MURRELL and
 LONGUET-HIGGINS
OWEN and WILSON
POTTS
SEATON
STEWART
TREACY

Section B

ARTHUR, BARDSLEY, BROWN
 and GIBSON
COOK
FRANCIS
FRANKS, GEACH and
 CHURCHMAN
HUGHES and SPURR
JONES
DE KLERK and MUSGRAVE
LITTLE and SMITH
NARASIMHAN
ROESLER
ROESLER and TWYMAN
WRIGHT

Research Notes

HALLIDAY and HIRST
ROBERTS and TILLMAN

Research Notes

Mohr

NOTE.—The Guthrie Lecture by Sir Geoffrey Taylor, which appeared in Abstract Booklet No. 25 is being published in the December issue of the *Proceedings*, Section B. It may be obtained either under the £1 1s. reprint scheme or by separate order, price 1s. 3d. unbound or 2s. 9d. in grey paper covers, post free.

I participate in the £1 1s. reprint scheme.

I enclose vouchers.

Please delete as necessary.

NAME (BLOCK CAPITALS)

ADDRESS

.....

.....

SECRETARY-EDITOR,

PHYSICAL SOCIETY,

1 LOWTHER GARDENS,

PRINCE CONSORT ROAD,

LONDON S.W.7.

by the domain treatment suggested by Heisenberg, and that with increasing temperature there is a steady departure from the calculated values. The saturation magnetostriction was found to depend on temperature in a way which did not correspond to any known theory.

Angular Distributions and Angular Correlations in the Reaction $^{23}\text{Na}(\text{p}, \gamma)^{24}\text{Mg}$,
by P. J. GRANT, J. G. RUTHERGLEN, F. C. FLACK and G. W. HUTCHINSON.

Abstract. The angular distributions and angular correlations of the more intense γ -ray components in the reaction $^{23}\text{Na}(\text{p}, \gamma)^{24}\text{Mg}$ have been determined at four resonances. Those at proton energies of 310 kev, 515 kev and 679 kev are assigned $J=2(-)$, $J=1(+)$ and $J=3(+)$ formed by p-, s- and d-wave protons respectively. The resonance at 593 kev has $J=2(-)$ formed by p-wave protons and is therefore distinct from that in the (p, α) reaction at this energy. The level in ^{24}Mg at 4.24 mev is assigned $J=2(+)$ and that at 5.26 mev $J=3$, probably with odd parity.

Excitation Functions for the Scattering of Protons and Deuterons by Be and Mg,
by G. W. GREENLEES.

Abstract. Absolute differential cross sections are given for the elastic and inelastic scattering by magnesium of protons with energies between 3.0 and 6.5 mev and of deuterons with energies between 4.0 and 7.8 mev. These were taken at an angle of 70° in the laboratory coordinates. Similar cross sections are given for protons scattered elastically and inelastically by beryllium at 90° . The levels giving rise to inelastic scattering have Q values of -1.37 ± 0.04 mev and -2.43 ± 0.05 mev for magnesium and beryllium respectively. The marked difference of excitation function for protons and deuterons is noted and a discussion of possible mechanisms involved is given.

On the Method of Atoms in Molecules, by A. C. HURLEY.

Abstract. The method of atoms in molecules is investigated in detail for the case of covalent-ionic resonance in the ground state of the hydrogen molecule. It is shown that the method is reliable if, and only if, different orbitals are used to approximate atomic and ionic states of the same molecule.

An Investigation of $^7\text{Li}(\text{d}, \text{n})^8\text{Be}$ and $^{11}\text{B}(\text{d}, \text{n})^{12}\text{C}$ Nuclear Reactions, by M. A. IHSAN.

Abstract. The energy levels of ^8Be and ^{12}C have been studied by means of the (d, n) reaction using deuterons of energy 686 kev. Evidence of levels in ^8Be was found at 2.98, and 7.53 mev. Investigation of energy levels of ^{12}C has shown energy peaks at 4.40, 7.63 and 9.72 mev respectively. The angular distribution of neutrons from the $^{11}\text{B}(\text{d}, \text{n})^{12}\text{C}$ reaction also has been investigated.

The Effect of $3\text{p}\pi$ Electrons: Energy Levels of Ethylene, by J. JACOBS.

Abstract. The usual LCAO MO method for obtaining wave functions of organic molecules with double bonds uses only $2\text{p}\pi$ atomic orbitals. As a refinement we include $3\text{p}\pi$ atomic functions in the basic molecular orbitals. Detailed calculations are made for ethylene, taking into account the interaction of configurations of like symmetry. The first excitation energy is calculated to be 8.7 ev, a much improved value compared with that obtained with only $2\text{p}\pi$ orbitals. The implication for MO theory is that in any refined treatment the higher energy atomic orbitals can no longer be ignored. A list of newly computed atomic integrals is given.

Study of Intermediate Coupling.—20—The authors discuss, by A. M. LANE. *Abstract.* The method of a previous paper is applied to the analysis of the spectra of the ^{16}O nucleus in terms of an intermediate coupling shell-model of the nucleus. It is shown that, within the projected uncertainties, all observed data are consistent with the predictions of the model. The mean value of the intermediate coupling parameter λ is about 7. It is an incidental result, suggested by the theory developed by Gell-Mann, that the shell-interaction mixture must be rather flat-topped, but squares are plotted based on the ^{16}O Fermi spectrum.

Study of Intermediate Coupling.—21—*Further results on the Nuclei ^{12}C and ^{14}N .* by A. M. LANE.

Abstract. The results reported in a previous paper on the nuclei ^{12}C and ^{14}N are extended to three more. On the nucleus ^{12}C the allowed mirror transition has been examined in greater detail, and is shown to be in excellent agreement with the previous results. The same properties of the nuclei have been calculated with different assumptions about the central force between nucleons. It is found that the previous results are not very much changed, even when the central force has been taken to be a simple Yukawa potential. Some discussion is given about the spin-parity states of ^{12}C and ^{14}N . In particular the application of the 'unique vector' assignment scheme, and its justification, is considered.

The Chemical Shifting of Atomic Spectra.—22—*The Effect of Inductive Substituents* by J. H. WILSON and W. C. FOSBERY, *Abstracts.*

Abstract. The chemical interpretation of aromatic hydrocarbon spectra in Part I of the series is used as a basis for examining the effects of inductive substituents on aromatic hydrocarbons. It is shown that of the four main bands in the ultraviolet spectrum, the π band of Claz is the most sensitive to substituent and evidence is given for the π band increase and the π band decrease at the adjacent bands for various positions of substitution in benzene. The theoretical results are shown to be in reasonable agreement with available data in the fluorobenzenes.

Measurement of the Momentum Spectrum of γ -Rays at Sea Level: I—The Momentum Range 5×10^6 – 2×10^7 eV c^{-1} . by B. G. OWEN and J. G. WILSON.

Abstract. The cosmic momentum spectrum near sea level in 57°N geomagnetic latitude has been measured for small defined angles of collection near the vertical direction. Results are given covering the momentum range 5×10^6 $\text{eV c}^{-1} < p < 2 \times 10^7$ eV c^{-1} , which are based on the measurement of about 10,000 trajectories.

Combinatorial Solution of the Triangular Ising Lattice by R. B. Potts.

Abstract. The combinatorial method of Kac and Ward is used to derive the partition function of an infinite two-dimensional triangular Ising lattice. The result agrees with that obtained by algebraic methods.

One Electron $2s$ – $2p$ Transitions in H and $3s$ – $3p$ Transitions in Na Produced by Proton Impact by M. J. SEATON.

Abstract. Relative cross sections for $2s$ – $2p$ transitions in H produced by electron and by proton impact are required in certain astrophysical problems. In calculating these cross sections it is necessary to allow for strong coupling effects.

Such effects are also important 3s 3p transitions in Na produced by electron impact, for which experimental results are available.

The total cross section Q is the sum of components Q' arising from the components of the incident wave with angular momenta $\hbar|l(l+1)|^{1/2}$. For these a limiting value $Q'(\text{max})$ is set by the requirement of charge conservation. The approximation adopted is to calculate the Q' using the Bethe approximation, to accept the values obtained if $Q'(\text{Bethe}) < \frac{1}{2}Q(\text{max})$ and to put $Q' = \frac{1}{2}Q'(\text{max})$ if $Q'(\text{Bethe}) \geq \frac{1}{2}Q'(\text{max})$. The conditions for the validity of this approximation are examined, some use being made of an exactly soluble schematic model. It is considered that the final results for the H transitions should be correct to within $\pm 20\%$. The results obtained for electron collisions with Na are found to be in good agreement with experiment, the approximation used being considerably superior to the Born approximation at low energies.

Electron Excitation Functions of Infra-Red Nitrogen Spectra, by D. T. STEWART.

Abstract. The relative excitation functions of lines and bands in the near infra-red spectrum of nitrogen have been determined using photographic photometry. The maximum of intensity of the (2, 0) and (3, 1) Meinel bands of N_2^+ occurs at 60 v while that of the Ni lines at 8200 Å resulting from the $3s^4\text{P}-3p^4\text{p}^0$ transition occurs at 90 v.

The Spin, Energy and Lifetime of ^8Be , by P. B. TREACY.

Abstract. Coincidences are used in studying the $^{11}\text{B}(\text{p}, \alpha)^8\text{Be}(\alpha)^4\text{He}$ reaction to infer directional correlations between successively emitted α -particles. From this the spin of the ground state of ^8Be is found to be zero and its breakup energy 90 ± 5 kev. The absence of any measurable loss of kinetic energy in the ^8Be nucleus when recoiling into a dense material enables us to place an upper limit on its half-life of 4×10^{-15} sec, which confirms the assignment of zero spin.

Positronium Formation in Gases and its Pressure Dependence, by C. B. O. MOHR (Research Note).

Section B

Carrier Extraction in Germanium, by J. B. ARTHUR, W. BARDSLEY, M. A. C. S. BROWN and A. F. GIBSON.

Abstract. It is well known that the density of current carriers (electrons and holes) in a germanium crystal can be increased by injection from a rectifying contact. The purpose of this paper is to show that large changes in carrier concentration can be obtained in near-intrinsic germanium by the reverse of injection, namely extraction. This technique allows some new fundamental experiments to be made and, by way of example, an experiment on the drift mobility of carriers in intrinsic germanium is described.

Photoconductivity and Conductivity in Calcium Tungstate Crystals, by J. R. COOK.

Abstract. In view of earlier contradictory published results on the photoconductivity of crystalline calcium tungstate, this effect has been examined using artificial single crystals and an intense ultra-violet source. Photoconductivity has been demonstrated, with a space charge build up of long relaxation time. This latter is probably linked with the long duration phosphorescence previously

reported in this material. The evidence produced indicates that calcium tungstate is an intrinsic semiconductor with an activation energy of 2.1 e.s.u. The photoconductive properties are in approximate agreement with the assumption of an exponential trap distribution if a variation of capture cross section with temperature is postulated.

The Growth of Electrodeless discharges in Hydrogen, by G. FRANCIS.

Abstract. Measurements have been made on the starting potential, current, and rate of growth of current of electrodeless discharges in hydrogen. The gas was contained in cylindrical glass or quartz vessels placed between plane parallel electrodes. The wavelength was varied from 50 m to 6×10^6 m (frequency range 6 Mc/s to 50 c/s), and the gas pressure from 1 to 76 mm Hg.

At short wavelengths the starting potential and current are low, and the discharge develops slowly. At a critical 'cut off' wavelength the starting potential rises abruptly and then remains almost constant to the longest wavelengths. At wavelengths just greater than cut-off the current is large, grows rapidly and flows continuously: at all longer wavelengths a smaller current flows in a brief pulse which occurs near each peak of the applied field, and is of constant height and shape.

The growth of the pulses is thought to be due to ionization in the gas, and electron emission from the walls of the vessel by photons. A pulse ceases when wall and space charges sufficiently reduce the field in the gas.

Pulses occur so regularly that electrons must be left over from one pulse to enable the next to start. They are loosely bound on the 'anode' wall at the end of one pulse and easily pulled off when the field reverses. This emission occurs in quite small fields (< 1000 v cm⁻¹), and is distinct from normal field emission.

This idea has been tested using alternating square wave fields of very long period, and by removing the wall charges.

Lamellar Defects in Single Crystals of Silicon, by J. FRANKS, G. A. GEACH and A. T. CHURCHMAN.

Abstract. Otherwise perfect single crystals of silicon have been shown to contain lamellar defects lying on (111) and (123) planes. Similar lamellae may be introduced by plastic deformation.

An Experimental Investigation of Non-metallic Wear, by G. HUGHES and R. T. SPURR.

Abstract. The rate of wear of a non-metallic substance is shown to be given by the equation $W = KI_s/P$ (where W is the wear per unit sliding distance, L the load and P the hardness) over a wide range of sliding conditions provided the variation of the hardness of the specimen with temperature is taken into account.

Growth of Lead Fluoride Crystals from the Melt, by D. A. JONES.

Abstract. The application of Stockbarger's technique to the growth of PbF₂ crystals is described. The melting point of PbF₂ was found to be $822^\circ\text{C} \pm 2^\circ\text{C}$, and owing to its fairly high vapour pressure at this temperature, the crystals were grown in an atmosphere of oxygen-free nitrogen at a pressure of 2 to 10 mm of mercury. The crystal structure was found to be of the fluorite type, and the lattice constant 5.942 ± 0.001 Å at 18°C. Refractive indices are given for various wavelengths in the visible spectrum. The transmission limits, defined as the wavelength at which a specimen of thickness 1 cm absorbs 50% of the incident radiation, are 11.6 μ and 2800 Å.

Internal Conical Refraction of Transverse Elastic Waves in a Cubic Crystal,
by J. DE KLERK and M. J. P. MUSGRAVE.

Abstract. A general method for obtaining the elastic wave surface appropriate to any aeolotropic medium is here used to investigate the behaviour of transverse plane waves of normal (1, 1, 1) in a cubic crystal. It is shown that the conditions for internal conical refraction prevail; this prediction has been verified experimentally.

High-frequency Ionic Conductivity of KCl Solutions, by V. I. LITTLE and V. SMITH.

Abstract. A differential method is described for measuring the ionic conductivity of potassium chloride solutions at 3×10^9 c/s. The results reveal that a strong dispersion region exists at concentrations below 0.5 normal, which may be explained in terms of the perturbations by the applied field of a shell of water molecules surrounding the ion at a mean distance of 6 Å.

Temperature Dependence of the Dielectric Constant of Diamond, by P. T. NARASIMHAN.

Abstract. The temperature dependence of the dielectric constant of diamond has been measured over the temperature range 50–200°C. The value of $(1/\epsilon)(d\epsilon/dT)$ over this range is $+1 \times 10^{-5}$. Details of the method of measuring the temperature coefficient of dielectric constant are also given. The magnitude and sign of $(1/\epsilon)(d\epsilon/dT)$ for diamond has been theoretically calculated using Maxwell's relationship and Kramers–Heisenberg theory. The agreement between theoretical and experimental values is extremely good.

Some Applications of Fourier Series in the Numerical Treatment of Linear Behaviour, by F. C. ROESLER.

Abstract. Earlier work is here continued. Certain functional relations common to various phenomenological theories, like the theory of linear visco-elasticity and the theory of linear electrical networks, may be written as integral equations of the convolution type. As the circular functions are eigenfunctions of the convolution type kernels, such equations can be solved by Fourier expansion. A number of possible applications of such Fourier expansions are indicated and the relevant details are worked out. The method centres on the evaluation of the eigenvalues for each kernel. The examples discussed refer to the theory of visco-elasticity and include the determination of the relaxation spectrum either from the dynamic elasticity as a function of frequency or from the stress relaxation as a function of time.

An Iteration Method for the Determination of Relaxation Spectra, by F. C. ROESLER and W. A. TWYMAN.

Abstract. The determination of relaxation spectra involves the numerical solution of certain linear, convolution-type integral equations of the first kind. A simple iteration method is shown by which some such equations may be solved. In the limit this is equivalent to the exact solution by means of Fourier integrals. If only moderate accuracy is required, the iteration method is sometimes less laborious than the use of Fourier series, proposed earlier, and in any case it involves only elementary arithmetical operations.

As one illustration, the relaxation spectrum of polyisobutylene is found from the damping, for the whole domain over which published data are available. In the rubber-glass transition region the results agree well with those previously obtained for this region by use of Fourier series. As a second illustration, successive approximations to a fictitious single line spectrum are shown.

Absolute Quantum Efficiency of Photofluorescence of Anthracene Crystals, by G. T. WRIGHT.

Abstract. The fluorescence characteristics of organic crystals differ appreciably from those of the emitting molecules due to self-absorption of the molecular radiation. These differences are investigated and properties of the fluorescence of the crystals are related to the corresponding properties of the molecular fluorescence; the equations developed are made the basis of an experimental determination of molecular quantum efficiencies of photofluorescence for the crystalline state. This method avoids the considerable errors involved in a direct measurement which are occasioned by having to integrate numerically over the whole sphere of emission inside an optically anisotropic crystal the fluorescence intensity that is measured directly only within a certain solid angle external to the crystal.

The method developed is particularly applicable to crystalline anthracene which has considerable overlap of absorption and fluorescence spectra. Experimental data for this substance are presented. These include the molecular and crystal fluorescence spectra and decay times; the latter are found to be 5.0 ± 0.2 m μ sec and 14.0 ± 0.3 m μ sec respectively. The molecular quantum efficiency of photofluorescence of crystalline anthracene at a temperature of 290 K is found to be 0.88 ± 0.02 which is reduced, by the effects of self-absorption of fluorescence, to a quantum efficiency for the crystal of 0.64 ± 0.02 ; efficiencies of photoluminescence are found to be the same within the limits of experimental error.

The Examination of Oxide Films by Reflection Electron Microscopy, by J. S. HALLIDAY and W. HIRST (Research Note).

The Barrier Height of Point-Contact Germanium Diodes Inferred from Measurements of the Voltage Dependence of Capacitance, by F. F. ROBERTS and J. R. TILLMAN (Research Note).

Letters to the Editor

Section A

Paramagnetism of Caesium Titanium Alum, by B. BLEANEY, G. S. BOGLE, A. H. COOKE, R. J. DUFFUS, M. C. M. O'BRIEN and K. W. H. STEPHENS.

Nuclear Spins and Ratio of Magnetic Moments of Europium 151 and 153, by B. BLEANEY and W. LOW.

Resolving Time of an Internal Counter Controlled Wilson Chamber, by P. J. CAMPION and W. T. DAVIES.

The Absolute Standardization of the 2.015 MeV γ -Rays of $^{232}\text{ThC}''$ and the Cross Section for the Photo Disintegration of the Deuteron at this Energy, by P. MARIN, G. R. BISHOP and H. HALBAN.

Section B

The Infra-Red Luminescence of Solid Halogens, by M. J. DUMBLETON.

On the Differential Analyser Solution of the Water Bells Problem, by G. N. LANCE and E. C. DELAND.

THE PHYSICAL SOCIETY

1 Lowther Gardens, Prince Consort Road, London S.W.7

ABSTRACT BOOKLET 23

This booklet gives abstracts of papers accepted since the printing of Abstract Booklet 22. These abstracts are thus circulated before the paper has gone to press, whereas the reprints themselves are not printed until the month of publication in the *Proceedings*, usually 2–3 months after acceptance.

Those eligible to order reprints immediately are

- (a) Fellows and Students of the Society and general subscribers to the *Proceedings* who have purchased voucher books.
- (b) Fellows and Students of the Society who have paid the annual subscription of £1 1s. *Note:* This reduced rate is *not* available to general subscribers.

Members and subscribers may obtain 10s. voucher books (containing vouchers for five reprints) at any time. Reprints are **not** obtainable in any other way.

Users of reprint vouchers should attach the appropriate number of vouchers to their order form. The enclosed order form should be completed by marking with ticks the papers required and should be returned **not later than 1st October**. A slightly later date of receipt will be accepted for long distance overseas subscribers **only**.

Note. Please be sure your name and address are entered on the form and your requirements indicated, otherwise your order cannot be executed.

All papers in Lists 1–20, except those by Sharma (19) and Owen and Williams (20), have now been published. Reprints of papers covered by these Lists will have been despatched by mid-September; any outstanding orders should be queried as soon as possible after this date.

September 1954

Section A

A Cloud Chamber Study of Some Aspects of the Geiger Discharge, by P. J. CAMPION.

Abstract. An expansion type cloud chamber controlled by an internal counter has been used to study the discharge formed in the latter when operated in the Geiger and transitional regions. Both ethyl and iso-amyl alcohols have been used at their saturation vapour pressures as the combined condensant and quenching agent, together with argon or helium at various total pressures below one atmosphere. Significant differences in the behaviour of the counter are observed for the two alcohols, which can be attributed to the difference in the proportion of quenching agents in the two cases. The photographic evidence shown supports the accepted theory of Geiger counter operation.

On the Neutron Spectrum for $v^{-\alpha}$ Absorption Cross Section, by B. DAVISON and M. E. MANDL.

Abstract. An approximate expression is found for the neutron absorption energy spectrum in an infinite medium consisting of atoms of mass number M , for which scattering is assumed isotropic in the centre-of-mass system and $\sigma_a/\sigma_{sc} \propto v^{-\alpha}$, where α is a positive constant. The accuracy of certain useful types of integral over the resulting spectrum is examined.

The D-D Reaction, by W. M. FAIRBAIRN.

Abstract. The two reactions ${}^2\text{H}(\text{d}, \text{p}){}^3\text{H}$ and ${}^2\text{H}(\text{d}, \text{p}){}^3\text{He}$ are examined under the assumption that they proceed via a stripping process. Coulomb effects are ignored. The angular distribution of the protons from the ${}^2\text{H}(\text{d}, \text{p}){}^3\text{H}$ reaction, and the variation with bombarding energy of the forward cross section are used for the comparison between the theoretical predictions and the experimental data. The agreement which is found is sufficiently good to justify the assumption that the reactions proceed partly via a stripping process. Stripping becomes the predominant process for bombarding energies greater than 5 MeV (lab.).

On the Relation between Certain Forbidden Beta Transitions and the Nuclear Spin Orbit Interaction, by G. N. FOWLER.

Abstract. The second forbidden beta decay matrix element A_{ij} is given in terms of the nuclear spin orbit potential strength u and another second forbidden beta decay matrix element, R_{ij} . The result is used, together with the predictions of the Mayer shell model for the single partial configurations, to obtain an estimate of u from the decay of ${}^{99}\text{Tc}$ for two types of space dependence of the spin orbit potential. The result is in reasonable agreement with that found from a study of the stationary states of ${}^5\text{He}$. Moreover, the special type of second forbidden tensor interaction which involves A_{ij} and T_{ij} alone is discussed, but it is found that in no case does this interaction lead to a value of u consistent with that found from the decay of ${}^{99}\text{Tc}$.

Theory of (d, p) and (d, n) reactions: I—General Theory ignoring Coulomb Effects, by I. P. GRANT.

Abstract. The differential cross section for the (d, p) process is evaluated using a Green's function technique. Elastic scattering of the proton by an average central potential well is taken into account. A later specialization to the case of a harmonic oscillator potential gives a result similar to that of Horowitz and Messiah but having a closed form. Compound nucleus formation is discussed and it is shown that the (d, p) cross sections for different angular momentum transfers l_n and j_n are always additive.

There is no polarization of the emitted particles in the model proposed.

Molecular Ions in Discharges in the Inert Gases, by D. MORRIS.

Abstract. The relative wall-currents of molecular and atomic ions have been measured in hot-cathode d.c. discharges in several of the inert gases. The radio-frequency mass spectrometer probe was used for this investigation and results were taken over a range of pressures up to 1 mm Hg and tube currents from 50 to 500 mA. From a study of the results the probable formation process for the molecular ions is found to be that involving collisions between normal atoms and atoms in highly excited states.

ORDER FORM 23

(issued September 1954)

To be returned to the Physical Society NOT LATER THAN 1st October 1954

Please supply 1 reprint of each of the following when published

Section A

Section B

CAMPION
DAVISON and MANDL
FAIRBAIRN
FOWLER
GRANT
MORRIS
OFFICER and ECCLES
SEATON
SWAN

BLASCHKE
COOK and MAHMOUD
DOUGLAS
GANDY
MOSS
SAKSENA and PANT
TOMLIN

Research Note
WOODS

Research Notes

CAMPION and DAVIES
(Detection of ...)
CAMPION and DAVIES
(Resolving Time ...)
KOTHARI
TREDGOLD
WINN

Letters to the Editor

SPIERS
WINN

I participate in the £1 1s. reprint scheme.

I enclose.....vouchers.

Please delete as necessary.

NAME (BLOCK CAPITALS)

ADDRESS

.....
.....

SECRETARY-EDITOR,

PHYSICAL SOCIETY,

1 LOWTHER GARDENS,

PRINCE CONSORT ROAD,

LONDON S.W.7.

The Interpretation of the Properties of Indium Antimonide, by T. S. MOSS.

Abstract. The data given in a paper by Avery, Goodwin, Lawson and Moss on the optical properties of InSb are analysed and precise values for the position and temperature dependence of the absorption edge are given.

The variation of the position of the absorption edge with impurity concentration is explained by the very low effective mass of the conduction electrons, which is estimated by three methods to be about 0.03 of the free electron mass.

Cathodo-Luminescence of MgO, by B. D. SAKSENA and L. M. PANT.

Abstract. The cathodo-luminescence spectra of different samples of MgO—fresh, previously exposed to cathode rays, heated in a Bunsen and oxy-coal-gas flame etc.—show different characteristics. For the fresh crystal we get a strong band with peak at 4550–4400 Å which weakens in intensity as the crystal receives increasing previous exposure to cathode rays. At the same time three bands in the red yellow region get increasingly stronger. On heating the exposed crystal, the previous condition (the same as that of the fresh crystal) is restored except for an increase of luminescence in the ultra-violet. The phosphorescence and the fluorescence spectra are the same for the fresh crystal, but for the crystal heated after previous exposure to cathode rays the fluorescence spectrum extends farther into the ultra-violet than the phosphorescence spectrum. The spectra of heated samples also show marked differences from the spectrum of the fresh crystal, and in the case of the sample heated in an oxy-coal-gas flame a new band at 2450 Å is obtained which disappears on continued cathode-ray bombardment.

The Vapour Pressure of Calcium: II, by D. H. TOMLIN.

Abstract. Further determinations of the vapour pressure of solid calcium have been carried out by a similar application of the Knudsen effusion method to that described in the companion paper by Douglas, but with radiochemical analysis of the condensed deposits. It is concluded from the good agreement with the results of Douglas and of Pilling that vapour pressure data for the temperature range 800°K to 900°K are now well established, and that the results of Rudberg are in error. The matching of the results with those of Hartmann and Schneider for liquid calcium, when extrapolation is made to the melting point is discussed. Agreement in this respect remains incomplete.

The Secondary Electron Emission of Sodium and Zinc, by J. WOODS (Research Note).

A Proposed Notation for Quantized Angular Momenta, by J. A. SPIERS (Letter).
Short-lived Alpha Emitters Produced by ^3He and Heavy Ion Bombardments, by
M. M. WINN (Letter).

Section B

Field Aberrations in Wide Aperture Optical Systems, by W. S. S. BLASCHKE.

Abstract. It is shown how the considerations which lead to the sine condition may be simply extended to take into account the aberrations which depend on the square of the field but include all powers of the aperture. In this way the relations known in primary aberration theory between pupil and image aberrations are re-interpreted and extended. The formulae are used to evaluate the field aberrations of a wide angle high numerical aperture flat field objective and comparison is made with the result of accurate trigonometrical calculation.

Luminescence Characteristics of some Scintillating Crystals, by J. R. COOK and K. A. MAHMOUD.

Abstract. The phosphorescence observed during the period 2 to 400 μsec following the absorption of gamma-ray photons has been studied in crystals of sodium iodide and potassium iodide (thallium activated) and calcium tungstate. The integrated light output is found to vary with temperature over the range -180°C to $+15^\circ\text{C}$ in a complex manner differing with each crystal. On the other hand, the decay time of the after pulses is to a first approximation temperature independent, with a decay constant in these particular crystals of around 15 μsec . It is concluded that a temperature dependent dissipative process occurs at some time during the initial decay, and is followed by the decay to a ground state with a time constant independent of temperature.

The Vapour Pressure of Calcium: I, by P. E. DOUGLAS.

Abstract. The vapour pressure of calcium in the temperature range 800°K–920°K has been measured by the Knudsen effusion method. Calcium metal was heated in a specially designed nickel crucible, and the vapour which effused through a narrow slit aperture into a well-defined solid angle was condensed and determined chemically. The vapour pressure p in mm Hg was found to be related to the absolute temperature T by the relation $\log_{10} p = 9.59 - 10089/T$.

Out-of-focus Diffraction Patterns for Microscope Objectives, by R. O. GANDY.

Abstract. Formulae are derived for the diffraction pattern at the image plane of an out-of-focus point source, and an out-of-focus line source. The lens considered is an idealization of a microscope objective; it is assumed to be a flat-field anastigmat and to subtend a small angle at the image, but no restriction is placed on the angle subtended at the object. A discussion is given of the assumptions required both for deriving and for applying the formulae, and some indication is given of the effect of the differences between practice and theory.

The Time Coherence of Associated Cosmic Ray Particles, by V. C. OFFICER and P. J. ECCLES.

Abstract. Short reaction time Geiger counters have been used at sea level to study the time coherence of associated cosmic ray particles under 18 cm of Pb, and also in air. A 50-channel hodoscope has been used to identify the events giving coincidences between two 138 cm² trays of these counters separated by 15 cm in a horizontal plane. No evidence was found for delays between associated particles of the order of 2×10^{-8} sec, as reported by Robinson (1953), using spark counters, although the counter resolving time of 1.4×10^{-8} sec should have allowed detection of the effect. Multiple hits by particles on the Geiger counter trays were found to give modified counter reaction time distributions, and it is suggested that a similar effect could occur in spark counters. A theory which accounts for the behaviour of both spark and Geiger counters under multiple hit conditions has been developed.

The Photo-Ionization of Neon, by M. J. SEATON.

Abstract. Previous calculations of the photo-ionization cross section of neon have been extended to wavelengths just beyond the L_1 edge at 256 Å. The absolute value of the calculated cross section is found to be in reasonable agreement with the experimental results of Lee and Weissler and of Ditchburn and Marr, but compared with the calculated results the experimental curve rises more steeply just beyond the threshold and falls more rapidly at higher energies.

The Elastic Scattering of Electrons by Excited 2s and 2p States of Atomic Hydrogen, by P. SWAN.

Abstract. The elastic scattering of electrons by H2s and H2p has been evaluated in the electron energy range 3–100 ev, the approximate method of Länger being used for large scattering phase-shifts and Born's approximation for the small phases corresponding to large values of the orbital angular momentum l .

The total elastic cross sections for H2s and H2p are much larger than for the ground state H1s even at the lowest energy considered, the interpretation being that the long tails of the H2s and H2p potentials make the partial cross sections for waves of higher orbital angular momentum l very important compared to the partial S cross section.

The effect of electron exchange is small even at 3 electron volts energy, an increase in cross section of 8% resulting from its inclusion, so that its effect has been neglected at higher energies.

The Detection of Electron Pairs in a Cloud Chamber with Internal Counters, by P. J. CHAMPION and W. T. DAVIES (Research Note).

The Resolving Time of an Internal Counter Controlled Wilson Chamber, by P. J. CHAMPION and W. T. DAVIES (Research Note).

Riesz Potential and the Elimination of Divergences from Quantum Electrodynamics: III, by L. S. KOTHARI (Research Note).

On Antiferromagnetism in Metals, by R. H. TREDGOLD (Research Note).

The Reaction ${}^9\text{Be}(d, {}^3\text{He}){}^8\text{Li}$, by M. M. WINN (Research Note).

